Y 3. At 7: 16/20-16

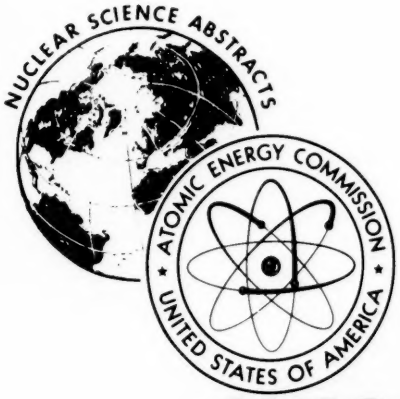

NUCLEAR SCIENCE ABSTRACTS

OCT 21 1966

Volume 20 Number 16

Abstracts 28871–30959

August 31, 1966

MIAMI UNIVERSITY LIBRARY

UNITED STATES ATOMIC ENERGY COMMISSION
Division of Technical Information

USAEC DEPOSITORY LIBRARIES

Collections of USAEC reports are maintained in the libraries of the organizations listed below for reference use by the general public. Facilities for making photocopies are available. The USAEC also makes available through these libraries atomic energy reports of countries other than the U. S. that are abstracted in *Nuclear Science Abstracts*.

ALABAMA
Auburn, Auburn University
ALASKA
College, University of Alaska
ARIZONA
Tucson, University of Arizona
ARKANSAS
Fayetteville, University of Arkansas
CALIFORNIA
Berkeley, University of California
Davis, University of California
Los Angeles, University of California
San Diego, Public Library
Stanford, Stanford University
COLORADO
Boulder, University of Colorado
Denver, Public Library
CONNECTICUT
New Haven, Yale University
DELAWARE
Newark, University of Delaware
DISTRICT OF COLUMBIA
Washington, Library of Congress
FLORIDA
Coral Gables, University of Miami
Gainesville, University of Florida
Tallahassee, The Florida State University
GEORGIA
Atlanta, Georgia Institute of Technology
HAWAII
Honolulu, University of Hawaii
ILLINOIS
Chicago, John Crerar Library
Chicago, University of Chicago
Evanston, Northwestern University
Urbana, University of Illinois
INDIANA
Bloomington, Indiana University
Lafayette, Purdue University
IOWA
Ames, Iowa State University
KANSAS
Manhattan, Kansas State University
KENTUCKY
Lexington, University of Kentucky
Louisville, University of Louisville
LOUISIANA
Baton Rouge, Louisiana State University
New Orleans, Tulane University
MARYLAND
Baltimore, Johns Hopkins University
College Park, University of Maryland
MASSACHUSETTS
Cambridge, Harvard University
Cambridge, Massachusetts Institute of Technology
MICHIGAN
Ann Arbor, University of Michigan
Detroit, Public Library
East Lansing, Michigan State University
MINNESOTA
Minneapolis, University of Minnesota
MISSISSIPPI
State College, Mississippi State University
MISSOURI
Kansas City, Linda Hall Library
Rolla, University of Missouri School of Mines and Metallurgy
St. Louis, Washington University
MONTANA
Bozeman, Montana State College
NEVADA
Las Vegas, Nevada Southern University
Reno, University of Nevada
NEW JERSEY
Princeton, Princeton University
Teaneck, Fairleigh Dickinson University
NEW MEXICO
Albuquerque, University of New Mexico
NEW YORK
Albany, The University of the State of New York
Buffalo, State University of New York at Buffalo
Ithaca, Cornell University
New York, Atomic Industrial Forum, Inc.
New York, Columbia University
New York, New York University
Rochester, University of Rochester
Schenectady, Union College
Syracuse, Syracuse University
Troy, Rensselaer Polytechnic Institute
NORTH CAROLINA
Charlotte, Public Library of Charlotte and Mecklenburg County
Durham, Duke University
Raleigh, North Carolina State College
NORTH DAKOTA
Grand Forks, University of North Dakota
OHIO
Cincinnati, University of Cincinnati
Cleveland, Public Library
OHIO (CONT.)
Columbus, Ohio State University
Toledo, University of Toledo
Youngstown, Youngstown University
OKLAHOMA
Norman, University of Oklahoma
Stillwater, Oklahoma State University
OREGON
Corvallis, Oregon State University
Portland, Reed College
PENNSYLVANIA
Philadelphia, University of Pennsylvania
Pittsburgh, Carnegie Library
University Park, Pennsylvania State University
PUERTO RICO
Rio Piedras, University of Puerto Rico
RHODE ISLAND
Providence, Brown University
SOUTH CAROLINA
Columbia, University of South Carolina
TENNESSEE
Knoxville, University of Tennessee
Memphis, Public Library
Nashville, Joint University Libraries
Oak Ridge, Oak Ridge Associated Universities
TEXAS
Austin, University of Texas
College Station, Texas A & M University
Dallas, Southern Methodist University
Houston, Rice University
Lubbock, Texas Technological College
San Antonio, Public Library
UTAH
Salt Lake City, University of Utah
VIRGINIA
Blacksburg, Virginia Polytechnic Institute
Charlottesville, University of Virginia
Norfolk, Old Dominion College
WASHINGTON
Pullman, Washington State University
Seattle, University of Washington
WEST VIRGINIA
Morgantown, West Virginia University
WISCONSIN
Madison, University of Wisconsin
Milwaukee, Public Library
WYOMING
Laramie, University of Wyoming

Volume 20, Number 16, August 31, 1966

NUCLEAR SCIENCE ABSTRACTS

A semimonthly publication of the USAEC Division of Technical Information, Edward J. Brunenkant, Director.
Published by the USAEC Division of Technical Information Extension, Robert L. Shannon, Extension Manager.

Nuclear Science Abstracts covers the international literature on nuclear science and technology and provides the only comprehensive abstracting and indexing of this body of information. Published twice each month since 1947, *NSA* covers technical reports of the U. S. Atomic Energy Commission and its contractors, technical reports of U. S. Government agencies and other governments, universities, industrial and research organizations, as well as patents, books, and journal literature on a world-wide basis. Nearly 350,000 abstracts have appeared in *NSA* through Volume 19. The subject matter covered in *NSA* is described in issue Number 1 and in TID-4552, *Subject Scope of Nuclear Science Abstracts*, available free from the U. S. Atomic Energy Commission, Division of Technical Information Extension, P. O. Box 62, Oak Ridge, Tennessee 37830.

Abstracts are arranged according to a number of subject categories and subcategories. Definitions of categories appear in issues Number 1 and 13. If the language of the original item is not English, the language will be indicated. Translations are not abstracted where an abstract of the original item has appeared in *NSA*.

INDEXES TO NSA

Corporate author, personal author, subject, and report number indexes appear in each issue and are cumulated quarterly, semiannually, and annually. Multi-volume cumulations have been issued as indicated on the following page. Report number indexes for all volumes (1–18) were issued at the end of Vol. 18. At the end of Vol. 19, the indexes for Vols. 1–15 were reissued to include additional public availability information. This cumulation will be a permanent shelf item and will not be reissued. Report number indexes for Vol. 19 are included as a cumulation beginning with Vol. 16.

AVAILABILITY OF PUBLICATIONS ABSTRACTED

The public availability of all U. S. Atomic Energy Commission reports is indicated in the report number indexes. The availability of other reports, when known, is also indicated. The availability of some unnumbered reports is given in the abstract.

Dissertations abstracted in *Dissertation Abstracts* and included in *NSA* are available from University Microfilms, Inc., 315 N. First Street, Ann Arbor, Michigan 48103.

Most of the published literature abstracted in *NSA* is on deposit at the Library, Oak Ridge Associated Universities, Oak Ridge, Tennessee, (a USAEC depository library) and is available through interlibrary loan. When requesting papers from this source, it is important that *NSA* volume and abstract number be cited.

HOW TO OBTAIN NUCLEAR SCIENCE ABSTRACTS

NSA is available on an exchange basis to universities, research institutions, industrial firms, and publishers of scientific information. Inquiries should be directed to the U. S. Atomic Energy Commission, Division of Technical Information Extension, P. O. Box 62, Oak Ridge, Tennessee 37830.

Government agencies may obtain *NSA* free of charge.

NSA is available to the general public on a subscription basis from the Superintendent of Documents, U. S. Government Printing Office, Washington, D. C. 20402, as follows:

For the 24 regular issues, $30.00 domestic, $37.00 foreign. A single issue costs $1.75, plus 25 per cent for foreign mailing. Domestic rates apply to the United States, Canada, Mexico, and Central and South American countries except Argentina, Brazil, Guyana and French Guiana, Surinam, and British Honduras. Foreign rates apply to the countries excepted above and to all other countries throughout the world.

For the quarterly, semiannual, and annual indexes, $22.00 domestic, $25.00 foreign.

Multivolume subject and author indexes are available as follows:

Vols. 1–4 (1948–1950) Johnson Reprint Corporation, 111 Fifth Avenue, New York, N. Y. 10003, $30.00.

Vols. 5–10 (1951–1956) Superintendent of Documents, U. S. Government Printing Office, Washington, D. C. 20402, $5.25.

Vols. 11–15, Subjects, Superintendent of Documents, U. S. Government Printing Office, Washington, D. C. 20402, $19.00.

Vols. 11–15, Personal Authors, Superintendent of Documents, U. S. Government Printing Office, Washington, D. C. 20402, $14.25.

Vols. 11–15, Corporate Authors, Superintendent of Documents, U. S. Government Printing Office, Washington, D. C. 20402, $2.50.

Cumulative Report Number Index, Vols. 1–15, Revised, is available from the Superintendent of Documents, U. S. Government Printing Office, Washington, D. C. 20402, $4.00.

Cumulative Report Number Index, Vols. 16–19, is available from the Superintendent of Documents, U. S. Government Printing Office, Washington, D. C. 20402, $2.50.

Annual Indexes are available separately from the U. S. Government Printing Office as follows:

Vol. 16, Subject and Authors, $9.75.
Vol. 17, Subject and Authors, $12.25.
Vol. 18, Subject and Authors, $12.50.
Vol. 19, Subject and Authors, $12.50.

ACKNOWLEDGMENTS

Agreements between the United States Atomic Energy Commission and the following organizations with regard to providing continuing services and specific literature coverage for *Nuclear Science Abstracts* are gratefully acknowledged:

American Institute of Physics; Atomic Energy of Canada Limited; Atomic Energy Research Establishment, United Kingdom; European Atomic Energy Community (EURATOM); Gmelin Institute; International Atomic Energy Agency; Japan Atomic Energy Bureau — Japan Atomic Energy Research Institute; Netherlands Patent Office; Reactor Centrum Nederland.

TABLE OF CONTENTS

Volume 20, Number 16, August 31, 1966

Category	*Page*
BIOLOGY AND MEDICINE	3503
General	3503
Ecology	3504
Metabolism, Tissue Distribution, and Toxicology	3504
Radiation Effects on Biochemicals	3507
Radiation Effects on Tissues	3511
Radiation Effects Therapy and Countermeasures	3526
Radiation Hazards and Protection	3528
Radiotherapy and Radiodiagnosis	3529
CHEMISTRY	3532
Analytical Procedures	3532
Inorganic and Physical Chemistry	3541
Organic Chemistry	3552
Radiation Chemistry	3553
Radiochemistry	3563
Separation Processes and Procedures	3564
ENGINEERING	3570
General	3570
Applications of Nuclear Explosions	3570
Facilities and Equipment	3570
Heat Transfer and Fluid Flow	3571
Materials Testing	3572
Protective Structures	3573
Space Propulsion	3573
Vacuum Engineering	3574
GEOLOGY, METEOROLOGY, AND MINERALOGY	3575
General	3575
Meteorology	3575
Natural Radioactivity and Fallout	3575
Techniques and Equipment	3580
Thorium and Uranium Minerals	3581
HEALTH AND SAFETY	3583
INSTRUMENTATION	3588
General	3588
Radiation Detection	3592
Radiation Effects	3599
ISOTOPE TECHNOLOGY	3600
Industrial Applications	3600
Power Application	3603
Separation and Production	3603
MATHEMATICS AND COMPUTERS	3604
METALS, CERAMICS, AND OTHER MATERIALS	3605
General	3605
Corrosion	3608
Fabrication	3610
Properties and Structure	3615
Radiation Effects	3631
PHYSICS	3635
General	3635
Accelerators	3636
Astrophysics and Cosmology	3639
Atomic Physics	3645
Cosmic Radiation	3649
Direct Energy Conversion	3652
Elementary Particles and Radiations	3653
Field Theory, Scattering Theory, and Symmetries	3662
Fluid Physics and Thermodynamics	3671
Geophysics	3675
Gravitation, Quantum Mechanics, and Relativity Theory	3680
Low Temperature Physics	3681
Neutron Physics	3689
Nuclear Properties and Reactions	3691
Plasma Physics and Thermonuclear Processes	3715
Shielding	3745
Solid State Physics	3747
REACTOR TECHNOLOGY	3753
General	3753
Auxiliaries and Components	3754
Criticality Studies	3758
Design and Feasibility	3761
Fuels	3761
Power and Power-Breeder Reactors	3762
Process Heat Reactors	3768
Production Reactors	3768
Propulsion and Space	3768
Research and Test Reactors	3769
WASTE DISPOSAL AND PROCESSING	3771
GENERAL AND MISCELLANEOUS	3773
CORPORATE AUTHOR INDEX	INDEX-1
PERSONAL AUTHOR INDEX	INDEX-8
SUBJECT INDEX	INDEX-55
REPORT NUMBER INDEX	INDEX-140

STAFF OF NUCLEAR SCIENCE ABSTRACTS

MANAGING EDITOR

John W. Norris

ASSISTANT MANAGING EDITOR

Donald D. Davis

ASSOCIATE EDITORS

Lawrence T. Whitehead
David E. Bost
Robert C. Kelly
Lee M. Thompson

SUBJECT INDEX EDITOR

Everett J. Hoffman

EVALUATORS

William D. Matheny
John H. Mitchell
Mary H. Newman

ABSTRACTORS

F. S. Armstrong (AECL)
Jane G. Buchanan
D. Lamar Cason
Bennie G. Di Bona
Helen G. Donald
James R. Dulaney
Wells L. Green
Mary Catherine Grissom
Fernando J. Hamilton
Phyllis C. Hansen
Carolyn D. Houston
Rose V. Jermain
Betty L. McDowell
Jean F. Peckham
Mona H. Raridon
Julia S. Redford
Francis L. Sachs
Lila B. Smith
Charles E. Stuber
Martha J. Thomas
Anne G. Ward
David C. West
Milton O. Whitson
Gabriel O. Ycaza

SUBJECT HEADING SPECIALIST

Robert E. Upchurch

CORPORATE AUTHOR SPECIALIST

Clara L. Fox

DESCRIPTIVE CATALOGING SPECIALIST

J. Paul Meredith

SCHEDULING AND PUBLISHING COORDINATOR

Brainard L. Patton

Communication concerning the editorial policy and content of *NSA* should be addressed to the Managing Editor, *Nuclear Science Abstracts*, AEC Division of Technical Information Extension, P. O. Box 62, Oak Ridge, Tennessee 37830.

Use of funds for printing this publication approved by the Director of the Bureau of the Budget, June 28, 1966.

Volume 20, Number 16 August 31, 1966

NUCLEAR SCIENCE ABSTRACTS

BIOLOGY AND MEDICINE

General

28871 (EUR-2636.f,i) NUCLEAR MEDICINE: ANNUAL REPORT, 1964. (Brussels Univ. (Belgium). Pisa Univ. (Italy)). Apr. 1966. 56p. (In French and Italian). Dep. mn.

Progress in nuclear medicine at the University of Brussels and the University of Pisa is reported on: design and construction of a whole-body counter; the study of dynamic models and their functions by the convolution method; erythropoietin measurement as an assessment of anemia in irradiated subjects; detection of tumors and their metastases by external counting using iodine-131-labeled fibrinogen; in vitro diagnosis of the hormonodependence of breast cancer; cerebral blood flow measurements using ^{85}Kr; determination of coronary blood-flow rate by methods using ^{86}Rb and ^{85}Kr separate measurement of renal clearance by external counting; measurement of glomerular filtration and the effect of tracer deiodination on this measurement; measurement of intestinal absorption of the triglycerides, albumin, and xylose; a dynamic model for iodine metabolism; measurement of insulinemia; studies of the action of insulin on tissues; determination by neutron activation of the ionic composition of the intracellular medium in the child; metabolism measurement in vivo by external counting of iodine-131-labeled albumin as a function of the iodine labeling intensity, in vivo measurement of amino acid metabolism and in vitro determination of glucose metabolism. (H.G.D.)

28872 FLUORESCENCE STUDIES ON DEUTERATED CHLORELLA VULGARIS. Ghosh, Ashish K. (Univ. of Illinois, Urbana); Govindjee; Crespi, H. L.; Katz, J. J. Biochim. Biophys. Acta, 120: 19-22(May 12, 1966).

Chlorella vulgaris grown in 99.8% heavy water show absorption spectra similar to the absorption spectra shown by those grown in ordinary water; there appears to be a minor shift of about 1 mμ towards shorter wavelengths in the blue and the red absorption bands, and a slight increase in chlorophyll b to a and carotenoids to chlorophyll a ratios in the heavy-water cells. Fluorescence (emission) spectra of deuterated Chlorella show an emission peak which is shifted about 2.0 mμ towards shorter wavelengths. In addition, the ratio of fluorescence at the main peak to fluorescence at 730 mμ is lower in the heavy-water cells, suggesting that they might have more of chlorophyll a_1 fluorescence. The yield of fluorescence is about 20–30% higher in deuterated Chlorella (measured at the emission peak). The excitation spectra of fluorescence show that the energy transfer from chlorophyll b to chlorophyll a 670 is almost 100% in both deuterated and ordinary hydrogen cells. (auth)

28873 VARIATION OF ANTIGENIC CHARACTERISTICS BETWEEN DIFFERENT MOUSE LYMPHOMAS INDUCED BY THE MOLONEY VIRUS. Klein, George; Klein, Eva; Haughton, Geoffrey (Karolinska Institutet Medical School, Stockholm). J. Nat. Cancer Inst., 36: 607-21 (Apr. 1966).

A number of mouse lymphomas induced by the Moloney viral agent were compared with regard to their sensitivity to the rejection response of syngeneic mice preimmunized with Moloney virus-containing materials, their susceptibility to the cytotoxic action of sera from resistant syngeneic animals, their ability to release virus as estimated by the mouse antibody production test, and their concentration of tumor-specific cell surface antigen as judged by the indirect fluorescent-antibody test and by absorption and inhibition experiments. The different parameters studied varied between different lymphomas, whereas individual lymphomas showed characteristic and well-reproducible patterns of behavior. All lymphomas examined carried the specific transplantation antigen characteristic for this system, though in different quantities. With one notable exception, there was a rough parallelism between immunosensitivity in vitro and in vivo. Immunosensitivity appeared related to the concentration of surface antigen, as judged by fluorescence and absorption. Immunoresistant tumors do exist that carry specific surface antigens, as measured by the fluorescence and absorption tests, which emphasizes the necessity to distinguish between antigenicity and immunosensitivity. The amounts of infectious virus released from known numbers of irradiated cells in vivo appeared to be independent of the concentration of surface antigen in the same tumor. These results do not critically distinguish between the possibility that cellular antigenicity is due to the release of infectious virus, or, alternatively, that a new cellular antigen appears independently of virus maturation, as in other antigenic virus-induced tumor systems. Passage of antigenic tumors in preimmunized mice did not lead to the selection of antigenic-loss variants or immunoresistant sublines. (auth)

28874 NUCLEAR HEMATOLOGY. Szirmai, E. (ed.). New York, Academic Press, 1965. 604p. $22.50.

Seventeen chapters on hematology and hematopoiesis are included. Separate abstracts were prepared for eight of the chapters. The remaining chapters consist of discussions of historical development of nuclear hematology, electron microscopy, and those aspects of hematology that utilize labeling with radioisotopes for the study of the morphology, physiology, and pathology of blood cells and blood forming organs. (H.G.D.)

For abstracts of individual chapters see: 28875, 28876, 28893, and 28981–28985.

28875 PROBLEMS OF BONE MARROW TRANSPLANTATION IN RADIATION DAMAGE. Szirmai, E. (Institution of Nuclear Engineers, London). pp 457-83 of Nuclear Hematology. Szirmai, E. (ed.). New York, Academic Press, 1965.

Experimental and theoretical problems of bone marrow transplantation are reported. Preservation, survival, and dosage of preserved hematopoietic cells, technical problems of bone marrow transfusions, bone marrow transfu-

sions after whole-body irradiation, and shielding procedures of organs are discussed. (H.G.D.)

28876 NUCLEAR HEMATOLOGY: BASED ON EXPERIENCE WITH ATOMIC EXPLOSIONS. Watanabe, Susumu (Hiroshima Univ.). pp 485-537 of Nuclear Hematology. Szirmai, E. (ed.). New York, Academic Press, 1965.

Hematological disorders in survivors of nuclear explosions are surveyed. Because of the fragmentary nature of knowledge about radiation injuries in man, hematological investigations of the populations in Hiroshima and Nagasaki exposed to atomic explosions and of the Japanese fisherman injured by a thermonuclear explosion on Bikini Atoll are important in clarifying radioinduced carcinogenesis and the somatic effects of radiation. (H.G.D.)

Ecology

Refer also to abstract 28925.

28877 (NYO-1918-124) BIOLOGICAL, CHEMICAL, AND RADIOCHEMICAL STUDIES OF MARINE PLANKTON. VOLUME I. Ketchum, Bostwick H.; Ryther, John H. (Woods Hole Oceanographic Institution, Mass.). Sept. 30, 1965. Contract AT(30-1)-1918. 178p. Dep. mn. CFSTI $5.00 cy, $1.00 mn.

Chemical and physical data obtained on 11 oceanographic cruises and stations occupied between Montauk Point, Long Island and Bermuda between July 1958 to July 1961 are reported. Methods used for determining temperature, chlorinity, chlorophyll a, dissolved oxygen, inorganic nutrients (inorganic phosphate, nitrate, nitrite, and ammonia), and silicates in sea water are described. (P.C.H.)

28878 (NYO-1918-138) BIOLOGICAL, CHEMICAL, AND RADIOCHEMICAL STUDIES OF MARINE PLANKTON. VOLUME II. Ketchum, Bostwick H.; Ryther, John H. (Woods Hole Oceanographic Institution, Mass.). May 1966. Contract AT(30-1)-1918. 192p. Dep. mn. CFSTI $5.00 cy, $1.00 mn.

Studies on the biology and chemistry of marine plankton populations are reported. The primary objective was to obtain an understanding of population dynamics in terms of the control exerted on them by physical and biological forces and their influence on the environment. Generally the studies were on: carbon cycle and distribution of carbon compounds in the ocean; relation between pigments and their decomposition products to phytosynthesis; biology of nitrifying bacteria; culture and nutrition of phytoplankton; oceanic distribution and taxonomic composition of phytoplankton; and physical, chemical, and biological factors influencing the swarming of salps. Data are tabulated. (P.C.H.)

28879 ^{90}Sr PLAQUES FOR BETA RADIATION STUDIES. Menhinick, Edward F. (Oak Ridge National Lab., Tenn.). Health Phys., 12: 973-9(July 1966). (ORNL-P-1180).

Strontium-90-yttrium-90 sources were developed for use in studies of the effects of environmental contamination on ecological systems. The ^{90}Sr was mixed with sodium silicate for application on the 13 in.-diameter plaques. The sodium silicate dried into a hard glossy surface that held the isotope well. Each plaque was placed in the recess of an aluminum disc, which was fitted into a plywood tray. The preparation of 75-mc, 750-mc, and 7500-mc sources with wood, glass, lead, or concrete shielding is described. (C.H.)

28880 ENDOGENOUS FORMATION OF CARBON MONOXIDE AND ITS IMPORTANCE IN A CLOSED ECOLOGICAL SYSTEM. Tiunov, L. A.; Kustov, V. V. Kosm. Issled., 4: 144-50(Jan.-Feb. 1966). (In Russian).

A literature survey is given on the endogenous formation of carbon monoxide and its oxidation and fixation in animal and plant tissues. The significance of these processes in ecological cycles, which can be modeled in systems for the support of life on spaceships, is pointed out. 67 references. (tr-auth)

28881 EFFECTS OF IRON ON THE ^{91}Y BEHAVIOR IN A TURFY-MEADOW SOIL. Molchanova, I. V. (Inst. of Biology, Ural Div., Academy of Sciences, USSR). Nauch. Dokl. Vyssh. Shkoly, Biol. Nauk, No. 2, 201-4(1965). (In Russian).

In studies in vitro on the effect of iron on the sorption of ^{91}Y on turfy meadow soil, both ^{56}Fe and ^{59}Fe were used. In dynamic experiments a 20-cc column was filled within a 5:1 mixture of soil and sand. With 20 cc of flowing water, 90 to 95% of the yttrium was sorbed in the presence of 10^{-8} M ^{56}Fe but only 70 to 75% in the absence of iron. The distribution of the yttrium on the column was somewhat different in the two cases. Under static conditions, 95 to 97% of the yttrium was sorbed when alone, independently of pH, but when ^{59}Fe was present in 10^{-6} M concentration, yttrium sorption decreased significantly. An increase in the iron concentration up to 10^{-4} M was accompanied by a sharp decrease in yttrium sorption. With a difference in the yttrium and iron concentrations of 2 to 3 orders of magnitude, apparently finely dispersed yttrium colloids are sorbed on colloidal iron, and the mobility of the yttrium depends on the iron mobility. (TTT)

28882 WHOLE-BODY COUNTING—AN ENVIRONMENTAL MONITORING TOOL. Abee, H. H. Nucl. Safety, 7: 229-31; 235(Winter 1965-1966).

Several papers on the use of whole-body counters in the evaluation of population exposure to environmental radioactive materials are reviewed. The advantages and limitations of whole-body counters for this application are discussed. (G.O.Y.)

28883 UPTAKE OF ^{131}I FROM THE SOIL AS RELATED TO ROOT DISTRIBUTION AND PHENOLOGY IN SAGEBRUSH VEGETATION [Thesis]. Price, Keith Robinson. Pullman, Wash., Washington State Univ., 1965. 92p.

The spatial distribution of sagebrush roots (Artemisia tridentata subsp. tridentata) and some of its associates in shrub-steppe habitats of Benton County, Washington, were studied by an ^{131}I soil-injection technique. Phenological, climatic, and edaphic records were made to facilitate interpretation of iodine uptake. The maximum number of sagebrush plants showing root uptake of ^{131}I from the upper meter of soil occurred during the month of April at a time just after the start of shoot growth and when leaf moisture contents were triple those observed during the fall season. All the associated perennial species tested showed a similar preferential period for root uptake of ^{131}I. The possibility of differences in sagebrush rooting habits among four different communities was studied. Important environmental differences between the three major study sites included elevation, precipitation, and air and soil temperatures. Root systems were investigated by determining whether the leaves of plants were radioactive from root uptake of ^{131}I injected into the soil at depths of 2, 4, 6, 8, and 10 dm. Samples were collected from plants at various distances, up to about 4 m, from the point of injection. Root systems of sagebrush plants in the Artemisia/Agropyron stand had a maximum lateral extent of 28 dm at 4 dm deep and probably another maximum greater than 10 dm deep. Plants of the Artemisia/Poa stand indicated maximums of 28 and 32 dm at 4 and 8 dm in depth, respectively. Similar results were obtained from the Artemisia/Bromus community where maximums were 26 and 28 dm at 4 and 8 dm in depth, respectively. Considering all three stands, sagebrush plants shorter than 3 dm or taller than 9 dm had lateral roots less than 20 dm long, whereas, those plants 6 to 9 dm in height had lateral roots extending 20 to 32 dm. Sagebrush plants of the Artemisia-Grayia/Poa stand had their roots restricted to a loamy sand layer comprising the upper 6 dm of the profile, where the maximum lateral extent was 12 dm. Grayia roots extended not only farther laterally (43 dm), but also extended into sand beneath the loamy sand layer to a depth of at least 10 dm. (TCO)

Metabolism, Tissue Distribution, and Toxicology

Refer also to abstracts 29024, 29451, and 29459.

28884 EFFECT OF URANIUM NITRATE ON THYROID GLAND OF ALBINO RAT IN CHRONIC EXPERIMENT. Zidrashko, T. M.; Golovin, D. I. Ark. Anat. Gistol. Embriol., 44: No. 5, 63-7(1963). (In Russian).

The effect of uranium salt on the thyroid gland was studied in chronic experiments on albino rats. Morphological and functional study of the thyroid gland was performed with the help of the radioactive iodine. More prolonged administration of uranium into the organism of the animal affects the morphological pattern of the thyroid gland. Deep changes in the organ resemble the picture of the parenchymatous goiter. A fall in the functional activity of the thyroid gland caused by a lasting application of uranium changes the morphological characteristics of the organ. (tr-auth)

28885 METABOLISM OF TRANSURANIC ELEMENTS. Debois, Jean-M. (Univ., Louvain, Belg.). Belgicatom, Ass. Belge Develop. Pac. Energ. At., Bull. Inform., 11: No. 60, 13-17(Feb. 1966). (In Dutch).

The toxicity and metabolism of the transuranium elements are reviewed. Special aspects of the metabolism of ^{237}Np, Pu, ^{241}Am, Cm, and ^{252}Cf are discussed. The resorption and inhalation of Pu are considered in some detail. (J.S.R.)

28886 CHARACTERISTICS OF CATECHOLAMINE METABOLISM IN ACUTE ^{210}Po LESIONS. Moroz, B. B.; Grozdov, S. P.; Petrovnina, E. N. Byull. Eksp. Biol. Med., 61: No. 3, 59-63(Mar. 1966). (In Russian).

Levels of catecholamines and the degree of their proteinization in the blood, myocardium, and adrenals were determined in rabbits with acute radiation sickness caused by injection of ^{210}Po. An increase was noted in the secretion of adrenaline in the initial period of the disease. Adrenaline synthesis was reduced and oxidation intensified at late periods. Adrenaline appeared in the blood and myocardium. Reduction of catecholamine proteinization was observed, especially during experiments in which the body was loaded with exogenous adrenaline. (A.G.D.)

28887 CONCENTRATION OF ^{137}Cs IN BEEF. Danbara, Hiroshi; Mitsuhashi, Toshihiko (National Inst. of Animal Industries, Chiba, Japan). Chikusan Shikensho Kenkyu Hokoku, No. 7, 1-5(Oct. 1964). (In Japanese).

A radiological investigation was carried out on beef. Twelve dairy cattle (female and male) were sacrificed; six different parts of the muscle were sampled from each of ten carcasses, and ten other different parts of the muscles were obtained from two other carcasses. After the muscle was ashed and treated with phosphoammonium molybdate, Cs-137 was measured in the form of cesium chloroplatinate by a β detecting method. The concentration of Cs-137 in the muscles was found, in most cases, to be 10 to 20 $\mu\mu$C/kg (in fresh weight) and in a few to be 40 to 50 $\mu\mu$C/kg (in fresh weight). These cattle had been fed conventional feed without grass or hay. In the case of feeding grass or hay, about 30 $\mu\mu$C Cs-137/kg (in fresh weight) was detected in the muscles. However, a difference was not observed either among the muscles or between the sexes. The concentration of Cs-137 in beef was found to be variable when the cattle were fed different contaminated feed materials such as beet pulp, grass, or hay. (auth)

28888 BODY DISTRIBUTION AND ELIMINATION OF ^{35}S-LABELED 2-MERCAPTOPROPYLAMINE IN MICE. Kalistratov, G. V.; Romantsev, E. F. Farmakol. Toksikol., 27: 364-7(1964). (In Russian).

Intraperitoneal $MeCH(^{35}SH)CH_2NH_2$ was deposited less in irradiated mice than in controls. The distribution was measured in kidneys, spleen, brain, liver, lungs, smooth muscle, stomach, heart, muscles, and blood. Metabolism products included disulfide, taurine, and $H_2NCH_2CH_2SO_2H$. $MeCH(SH)CH_2NH_2$ alters the balance between inorganic and etherified S in the urine. (C.H.)

28889 MEASUREMENT OF THE KINETICS OF CALCIUM METABOLISM IN CHILDREN AND ADOLESCENTS UTILIZING NONRADIOACTIVE STRONTIUM. Root, Allen W.; Bongiovanni, Alfred M.; Eberlein, Walter R.; Michie, Alexander J. (Children's Hospital, Philadelphia. Univ. of Pennsylvania, Philadelphia). J. Clin. Endrocrinol. Metab., 26: 537-44(May 1966).

Studies of the kinetics of calcium metabolism utilizing nonradioactive strontium as a tracer for calcium are reported in normal children and in children with diseases affecting mineral and skeletal metabolism. In 15 children without evidence of abnormality of calcium or bone metabolism the exchangeable pool of strontium, the turnover rate and the bone deposition rate of strontium increased with the age and surface area of the subject, reaching a maximum in the adolescent and decreasing thereafter to the adult range. An expanded exchangeable pool of strontium and increased turnover and bone deposition rates were observed in children with hyperthyroidism and polyostotic fibrous dysplasia. Children with either vitamin D sensitive or vitamin D resistant rickets had enlarged exchangeable strontium pools while the turnover and bone deposition rates fell within the normal range for their age and body size. In children with hypopituitarism, osteogenesis imperfecta and after prolonged treatment with glucocorticoids, the exchangeable pool of strontium and the turnover and bone deposition rates were found to be decreased. The exchangeable strontium pool turnover and bone deposition rates were normal in children with aseptic necrosis of the femoral head, cerebral palsy, nonparalytic poliomyelitis and congenital infantile hypoparathyroidism. An adolescent male who fractured his femur and developed hypercalcemia secondary to immobilization was studied serially. The initial investigation revealed a decreased exchangeable pool of strontium and a decreased bone deposition rate. With ambulation the serum calcium concentration returned to normal and there was a progressive increase in the exchangeable strontium pool. The turnover rate increased transiently after mobilization and then returned to its initial value. The bone deposition rate increased acutely after mobilization and remained constant in subsequent studies. (auth)

28890 EFFECTS OF ANDROGENS, ESTROGENS, AND CORTICOIDS ON STRONTIUM KINETICS IN MAN. Eisenberg, Eugene (Univ. of California, San Francisco). J. Clin. Endrocrinol. Metab., 26: 566-72(May 1966).

The effects of estrogens, androgens, and corticoids on kinetics of stable strontium metabolism were evaluated. The rapidly miscible pool volume, bone deposition rate and urinary excretion rate were determined before and after treatment of 67 subjects with androgens and estrogens, 44 subjects with corticoids and 34 subjects with placebos. Androgens and estrogens decreased urinary excretion rates and estrogens tended to decrease bone deposition. They thus appear to be anticatabolic for bone instead of anabolic, as previously thought. Estrogens may also be anti-anabolic. Corticoids did not decrease bone deposition rates, but did uniformly increase urinary excretion rates. They thus do not appear to be anti-anabolic for bone, as previously thought. Correction of bone deposition rates for fecal excretion rates did not affect the results. These studies did not reveal whether the changes in urinary excretion rates induced by both gonadal and glucocorticoid steroids were attributable to effects on the kidney, on the bone, or both. (auth)

28891 MOVEMENT OF RADIOACTIVE CALCIUM IN BRAIN SLICES AND INFLUENCE ON IT OF PROTOVERATRINE, OUABAIN, POTASSIUM CHLORIDE AND COCAINE. Fujisawa, Hisao; Kajikawa, Kozo; Ohi, Yoshihiro; Hashimoto, Yuichi; Yoshida, Hiroshi (Osaka Univ.). Jap. J. Pharmacol., 15: 327-34(Dec. 1965).

The movement of ^{45}Ca in brain cortex as affected by protoveratrine, ouabain, KCl, and cocaine, was examined in guinea pigs. Addition of azide and omission of glucose resulted in an increase in ^{45}Ca influx attributed to metabolic depression, an increase not significantly influenced by addition of cocaine. Protoveratrine, ouabain, or a high concentration of KCl caused an increase in ^{45}Ca influx into brain slices. The increase caused by protoveratrine and ouabain was completely blocked by cocaine while that by KCl was partially blocked. Efflux of ^{45}Ca from brain slices was reduced by replacing normal Ringer by Ca-free Ringer

solution containing EDTA. There was an increase in ^{45}Ca efflux from brain slices on addition of protoveratrine, ouabain, KCl or azide both in normal Ringer and in Ca-free Ringer solution. Cocaine largely prevented the increased efflux of ^{45}Ca caused by protoveratrine and ouabain, but the increased efflux of ^{45}Ca caused by KCl was only partially inhibited and that by azide did not seem to be affected significantly by addition of cocaine. The role of calcium in membrane permeability and the action mechanisms of these drugs are discussed on the basis of these findings. (BBB)

28892 BALNEOLOGICAL STUDIES USING ^{59}Fe. Furudate, Masayori (Hokkaido Univ., Sapporo, Japan). Nippon Onsen Kiko Butsuri Igakkai Zasshi, 28: 130-46 (Dec. 1964). (In Japanese).

The following aspects of balneological studies on mice using ^{59}Fe were investigated: the organ distribution of Fe following percutaneous absorption of the Fe by bathing; the effects of serial bathing on the concentration of ^{59}Fe in the organ following percutaneous absorption, gastrointestinal administration, and intramuscular injection; and the autoradiography of the skin bathed in bath water labeled with ^{59}Fe. For organ distribution studies, the lower half of the body of mice were immersed in the water with precautions to see that the mice did not drink the water; and immediately after immersion, the animals were washed to remove contaminating ^{59}Fe from the skin. After time periods of from 3 to 24 hours after bathing, the animals were sacrificed by decapitation. Immediately thereafter blood was collected from the neck, and the liver, spleen, kidney, muscle, and vertebral bone were removed. Following dry combustion of the organs, the radioactivity of each organ was measured with a scintillation counter. The results of the measurements provided evidence of the percutaneous absorption of radioactive iron into the body. The results of the experiments on serial bathing varied greatly due to individuality for bathing periods of 7 days or less; however, a "Habitual Phenomenon" or defense mechanism was seen in the groups treated with serial bathing of 14 days. Autoradiography of the skin bathed in water labeled with ^{59}Fe showed the highest concentration of radioactivity in the epidermal portion with the density decreasing gradually with approach to the corium. (TCO)

28893 NUCLEAR HEMATOLOGY AND BLOOD TRANSFUSION. Sachs, Volkmar (Univ. Kiel). pp 443-55 of Nuclear Hematology. Szirmai, E. (ed.). New York, Academic Press, 1965.

Nuclear hematology is reviewed in reference to the relationship between immune hematology and transfusion serology. Two types of hemotherapy for radiation injuries are described; elimination of radioactive contamination in tissues by exchange transfusion and transfusion therapy for acute and chronic radiation syndromes. The role of radioactive tracers and extracorporeal irradiation of blood in hematologic diagnosis, therapy, and research are discussed. (H.G.D.)

28894 ^{210}Po CONTENT OF HUMAN TISSUES IN RELATION TO DIETARY HABIT. Hill, C. R. (Inst. of Cancer Research, Belmont, Eng.). Science, 152: 1261-2 (May 27, 1966).

Concentrations of ^{210}Po, a natural fallout nuclide, in human placentas collected in northern Canada ranged up to 27.8 picocuries per 100 grams, or 80 times the average United Kingdom value. High levels are related to the inclusion of reindeer or caribou meat in the diet, and a correlation exists between the concentrations of ^{210}Po and ^{137}Cs in the placentas. (auth)

28895 EFFECT OF CHRONIC ADMINISTRATION OF EXCESS OF NICOTINIC ACID TO RABBITS ON INCORPORATION OF RADIOACTIVE ACETATE IN CHOLESTEROL AND ON TISSUE MICROSTRUCTURE. Shushevich, S. I.; Kuzminskii, P. N. (Inst. of Biochemistry, Academy of Sciences, Ukrainian SSR, Strazhesko Inst. of Clinical Medicine, Kiev). Ukr. Biokhim. Zh., 38: 33-8(1966). (In Ukrainian).

Prolonged (two months) introduction into the organism of rabbits of large quantities of nicotinic acid (150 mg/kg), in contrast to single or short-period administration (5 days), caused decrease in liver cholesterol (the free fraction by 21.9% and the esterified fraction by 30.6%) and in the specific radioactivity (by 27.3 and 32.6%, respectively). Pathohistological and histochemical investigations of the internal organs of rabbits receiving large doses of nicotinic acid revealed slight changes in liver composition (a slight decrease in neutral lipids and an increase in glycogen and ribonucleic acid), but did not reveal changes in the cellular structure of the liver and other organs. (auth)

28896 THE TOXICITY OF ^{90}Sr IN THE MONKEY SKELETON. CONSIDERATIONS OF RELATIONSHIP OF TOTAL RADIATION DOSE, DOSE-RATE, DOSE-TIME, PRODUCT AND BIOLOGICAL INJURY [Thesis]. Goeksel, Selahattin Adil. Rochester, N. Y., Univ. of Rochester, 1962. 175p.

Studies of the skeletal retention and distribution of ^{90}Sr in adult Rhesus monkeys following oral or intravenous administration were made. Determinations of the amount of ^{90}Sr transferred to baby monkeys through milk from mothers given ^{90}Sr orally during part of the lactation period were also made. Three lactating young adult female monkeys were fed 500 μC of carrier-free ^{90}Sr solution over an ingestion period of 30 days. Seven days later and several times up to 320 days, body burdens were determined by whole body bremsstrahlung counts. Analysis of retention data determined the constants of the "power function retention" equations. The three baby monkeys were nursed by their mothers until they were 6 months of age. The body burdens were determined several times by whole body bremsstrahlung counts from seven days to 320 days after the last ^{90}Sr feeding to the mothers. The power function analysis of the retention data of the babies showed two distinct components, the first component with a small slope (−0.009 to −0.114) represented the period before weaning and the second component with a much steeper slope represented the period after weaning. In intravenous injection studies four young male monkeys were given 45 or 90 μC of ^{90}Sr as single injections. Their ^{90}Sr burdens were also determined several times by whole body counts up to 150 days. The retention data were treated in the same fashion and the constants of the power function retention equations were determined. The distribution of the ^{90}Sr in components of the monkey skeleton as well as along the length of some bones (the femur, humerus and ribs) and the vertebral column was also studied after sacrifice of the four intravenously injected monkeys. Assuming that the bones in monkey skeleton have geometrical configurations resembling those of tablets, spheres or cylinders and by making use of the ^{90}Sr distribution data in monkey sleleton and the dimensional bone measurements done in monkey skeletons, it was possible to calculate the fraction of the $^{90}Sr-^{90}Y$ beta energy absorbed in monkey skeleton as 76 percent for an adult and 63 percent for a baby monkey of 6 months of age. The equations of the dose-rate, dose and the dose-time products to the skeleton have been developed and these quantities are calculated for three female monkeys and their babies, used in the milk transfer experiment. (TCO)

28897 THORIUM INHALATION STUDIES [Thesis]. Boecker, Bruce Bernard. Rochester, N. Y., Univ. of Rochester, 1962. 285p.

In an investigation of the distribution and excretion patterns of thorium following inhalation of thorium chloride, emphasis was placed on the effect of the size of the initial lung thorium burden on the subsequent distribution and excretion patterns. Groups of 20 rats were exposed to thorium chloride aerosols containing ^{234}Th (UX_1) as a tracer, and the size of the initial lung burden was varied mainly by increasing the concentration of carrier thorium in the aerosol generator solution. The retention of the inhaled thorium was followed for 4 to 90 days post-exposure with whole-body counting and serial sacrifice, and the thorium excretion was followed by collection of urine and feces. Soon after exposure, a fraction of the thorium in the lungs was absorbed into the body and the largest portion of this absorbed fraction was deposited in the skeleton. Following this initial uptake, the organ thorium burdens remained

approximately constant or decreased with time after exposure. The remaining thorium burden in the lungs decreased with time after exposure and was accompanied by excretion of thorium predominantly in the feces. The size of the initial lung thorium burden was varied by a factor of 1.1×10^5. Over this range, the fraction of the lung thorium burden that was absorbed did not appear to be affected by the variation, and this was also true for the thorium urinary and fecal excretion patterns. For comparison, a group of rats was exposed to a thorium citrate complex aerosol. The amount of initial absorption was increased by a factor of about 2 over that observed for a companion thorium chloride exposure but once the initial phase was completed, the thorium behaved in a similar manner for both groups. The thorium chloride results were compared with those reported for plutonium nitrate aerosols and several similarities were noted. (TCO)

Radiation Effects on Biochemicals

See also CHEMISTRY — Radiation Chemistry

Refer also to abstract 29037.

28898 (CEA-R-2910) EVALUATION PAR RESONANCE PARAMAGNETIQUE ELECTRONIQUE DU NOMBRE DE RADICAUX LIBRES PRODUITS DANS L'OS DE RAT IRRADIE. (Evaluation by Electronic Paramagnetic Resonance of the Number of Free Radicals Produced in Irradiated Rat Bone). Marble, Georges; Valderas, Ramon (Commissariat a l'Energie Atomique, Fontenay-aux-Roses (France). Centre d'Etudes Nucleaires). Mar. 1966. 14p. Dep. mn.

The number of long half-life free radicals created by γ irradiation in the bones of the rat was determined from the electronic paramagnetic resonance spectrum. This number decreased slowly with time (calculated half life: 24 days). It was proportional to the dose of γ radiation given to the rat. The method could find interesting applications in the field of biological dosimetry. (auth)

28899 ROENTGEN IRRADIATION EFFECTS ON MOUSE PROTEINS. Sassen, A.; Kennes, F.; Maisin, J. R. (Centre d'Etude de l'Energie Nucleaire, Mol, Belg.). Acta Radiol. Therapy, Phys., Biol., 4: 97-112(Apr. 1966).

Serum protein changes in whole-body x irradiated mice are described. A correlation was found between the decrease in the γ globulins concentrations and the x ray dose. Some change in the immunoelectrophoretic pattern was evident as early as at 6 to 8 hours. Certain abnormal alterations in the protein pattern of irradiated mice appear to be related to infection. (auth)

28900 CHANGES IN CELLULAR PERMEABILITY INDUCED BY LOW-DOSE X IRRADIATION. Srb, Vladimir (Kralove Medical Univ., Czechoslovakia). Biologia, 20: 877-82(1965). (In Czech).

Effects of x radiation on cell permeability were studied in epidermal tissues of Allium cepa exposed to various doses (25, 50, 100, or 250 R). A 1% light green stain in a solution of 0.5 KNO_3 and 1 m glycerin were used to establish effects on permeability. Results showed radiation effects on cell permeability and a different plasmolysis period in epidermal cells of irradiated and nonirradiated onions by using nonelectrolytes. Latent effects were confirmed from the standpoint of small difference radiation effects between the various doses used. An important conclusion, however, of a later report is that doses of 25 and 50 R affect cell permeability in comparison with the nonirradiated controls. The conclusion that cell permeability is more radiosensitive in comparison to plasma lipoproteins and cell membranes was manifested by early effects in external permeability. (tr-auth)

28901 ESR STUDY ON IRRADIATED SULFUR-CONTAINING AND SULFUR-FREE PYRIDOXINE DERIVATIVES. Moenig, H.; Koch, R. (Univ., Freiburg i. B.). Biophysik, 3: 11-21(1966). (In German).

Equal radical states were found for pyridoxine and some sulfur-containing pyridoxine derivatives both after uv irradiation and after x irradiation at 20°C. An unpaired electron probably occurs in the methyl group of position 4 or 5. In the derivatives which contain sulfur in the form of sulfhydryl, a radical migration to the sulfur occurs. Therefore, the radical state on the sulfur of the 4-mercapto pyridoxine was formed faster than in the case of the 5-mercaptopyridoxine. The disulfide bond of pyrithioxine is more stable than the sulfhydryl bond of the mercaptopyridoxine. If the sulfur is present in the form of a thioether (4,5-methylene sulfide pyridoxine), a radical of the alkyl type that does not migrate to the sulfur is produced. The ESR studies show that the formation and the time behavior of the radicals are dependent not only on their immediate surroundings but also on the total structure of the molecules. (tr-auth)

28902 DIRECT AND INDIRECT RADIATION EFFECTS ON ENZYMES IN THE CELL. Pauly, Helmut; Pfister, Helmut; Rajewsky, Boris (Max Planck-Institut fuer Biophysik, Frankfurt am Main). Biophysik, 3: 36-9 (1966). (In German).

The x radiation-induced inactivation of lactate dehydrogenase in rat liver and invertase in yeast was investigated. The inactivation was almost equal in moist living cells and in dried cells although a contribution of the indirect radiation effect was observed in moist cells. (tr-auth)

28903 TEMPERATURE DEPENDENCE AND ACTIVATION ENERGY IN DIRECT RADIATION EFFECTS. Pauly, Helmut (Max Planck-Institut fuer Biophysik, Frankfurt am Main). Biophysik, 3: 40-3(1966). (In German).

The temperature dependence of dry irradiated enzymes was explained using the Eyring statistical theory of reaction velocity. It was shown that one must introduce temperatures different from the environmental temperature and often a very high reaction temperature and reaction time. On this basis it is not possible generally to calculate the activation energy. (tr-auth)

28904 DIFFUSION OF SOME NUCLEOTIDES INTO OUTER MEDIUM FROM NON-IRRADIATED AND GAMMA-IRRADIATED EUGLENA CELLS. Matsuoka, Saburo Gifu Univ., Japan). Bull. Inst. Chem. Res., Kyoto Univ., 44: 57-65(Ján. 1966).

When non-irradiated Euglena cells were suspended in distilled water and incubated for several hours, some ultraviolet absorbing substances diffused out of the cells into distilled water. The amount of these substances increased according to cell concentration and to incubation temperature. When the cells were exposed to 0.5, 1, and 2×10^5 R gamma-rays, respectively, and then were incubated as above, similar ultraviolet absorbing substances diffused in large quantity out of the irradiated cells. The total amount of these diffused-out substances was rather small as compared with the total amount of acid soluble ultraviolet absorbing substances in the cells, that is, about 10.1% during a 3-hr incubation period after irradiation. It increased according to the irradiation dosage given. When these diffused-out substances from both non-irradiated and irradiated cells were investigated with Dowex-1-formate column, it was found that they contained some nucleosides and nucleotides, and also that they changed in composition before and after the irradiation. That is, uridine monophosphate, guanosine monophosphate, and uridine diphosphate were recognized only after the irradiation. R-substance, AMP, and ATP markedly increased in quantity after the irradiation. Contrary to this, some nucleosides, GTP, and uridine compounds decreased in amount after the irradiation. (auth)

28905 EFFECT OF IONIZING RADIATIONS ON THE ELECTROPHORETIC MOBILITY OF MAMMALIAN CELLS. Stein, G.; Seaman, G. V. F.; Mehrishi, J. N.; Simon-Reuss, I. (Cambridge Univ., Eng.). Int. J. Radiat. Biol., 10: 251-9(1966).

The effects of x and γ radiations on the electrophoretic mobility of a variety of mammalian cell-lines, including

embryonic and L-strain mouse fibroblasts, monkey kidney cells, human amnion, human red cells, and also the Davidson, DiVita, Ehrlich-Landschütz and Lettré strains of murine ascites-tumor cell, are reported. The suspensions of cells were prepared in a number of ways under various experimental conditions. The effects of the presence of low concentrations of cupric and zinc ions and of EDTA during these studies are also presented. In no instance did irradiation of the cells with low doses, up to circa 1000 rads, produce statistically significant changes in their electrophoretic characteristics. The results are compared with those obtained in a previous investigation, and it is concluded that infection of the cells used then may have been responsible for the observed effects. Doses of about 2000 rads produced a decrease in electrophoretic mobility of tumor cells, but not of red blood cells. (auth)

28906 PRODUCTION OF LONG-LIVED FREE RADICALS BY IRRADIATION IN THE BONES OF RAT MEASURED BY R.P.E. Valderas, Ramon; Marble, Georges (CEN, Fontenay-aux-Roses, France). Int. J. Radiat. Biol., 10: 283-5(1966). (In French).

The bones of rats were exposed to ^{60}Co γ radiation and the number of free radicals induced was measured by electron spin resonance techniques during the next 24 hr. A linear relation was demonstrated between radiation dose and the number of long-lived free radicals produced. (C.H.)

28907 HISTOCHEMICAL INVESTIGATION OF GLYCOGEN IN THE RABBIT RETINA. Melik-Mus'yan, A. B. Izv. Akad. Nauk Arm. SSR, Biol. Nauki, 17: No. 12, 71-8 (1964). (In Russian).

In the normal rabbit retina the distribution of glycogen is irregular and related to the physiological state. The greatest deposition of glycogen in the normal retina was in the region corresponding to the ganglionic cells, layer of nerves, Muller's fibers, and receptor layer. Irradiation of only the head at 1000 to 5000 R caused an immediate increase in glycogen consumption. (C.H.)

28908 RADIATION DAMAGES IN DEOXYRIBONUCLEOPROTEINS AT THE MOLECULAR AND SUPERMOLECULAR LEVELS. Tseitlin, P. I.; Spitkovskii, D. M.; Gorin, A. I.; Ivannik, B. P.; Kulikova, L. G.; Luchkina, L. A.; Martynov, E. V.; Ryabchenko, N. I.; Usakovskaya, T. S. (Inst. of Experimental Biology, Moscow). Izv. Akad. Nauk SSSR, Ser. Biol., No. 2, 197-211(Mar.-Apr. 1966). (In Russian).

A study of damages at the level of deoxyribonucleoprotein (DNP) super-molecular structures was made to gain insight into structural rearrangements occurring in chromosomes exposed to irradiation. The method of separation of DNA strands and that of isolation and testing of one-stranded DNA were used to show that the number of single breakages in the two-stranded DNA increased in proportion to the irradiation dose. The total amount of such damages in the irradiated DNA fell as compared to that of DNP and nuclei exposed to irradiation. Calculations of paired breakages in the DNA leading to its depolymerization indicated that there are no grounds to expect a drop in the DNA molecular weight at doses below 10^4 rad, the number of single breakages reaching, however, the value of several dozen. Absorption spectra and dispersion curves of the DNA optic rotation did not undergo changes at doses below the above value. At the same time melting curves were dose dependent, thus indicating the development of latent damages in the DNA secondary structure in response to x irradiation. Irradiation at doses below 10^3 rad caused single breakages in a small number of DNA molecules only. This brought about no changes in physico-chemical properties of the DNA or DNP as a whole, though it certainly may have some biological effect. Therefore, there are practically no grounds to believe that the effect of low irradiation doses that manifests in structural rearrangements of chromosomes can be related to changes in DNA macromolecules. However, quantitative changes in the DNP properties in response to irradiation doses of the order of 10 rad and less appear to be associated with the breakdown of intermolecular bonds of the protein-protein type localized in one of the fractions of the DNP protein component. This was proven by studies regarding the radiosensitivity of DNP supermolecular structures, isolated from nucleoproteins with a progressively decreasing protein amount. An establishment of the mechanism of this phenomenon paves the pathway for an understanding of radiation damages in chromosomes. (P.C.H.)

28909 EFFECT OF γ-RAYS FROM ^{60}Co ON CERTAIN METABOLIC PROCESSES IN PEA PLANTS. Tselishchev, S. P.; Ivanova, G. F.; Shmel'kova, N. I.; Lin, Hung-Hsi. Izv. Timiryazevsk. Sel'skokhoz. Akad., No. 4, 87-95(1965). (In Russian).

The growth of plants from pea seeds irradiated with 25,000 R was greatly depressed. This was attributed to the breakdown of all the metabolic processes. The extent of breakdown was a function of the physiological state and age. Radiation caused essential changes in the N metabolism both in the aerial and root portions of the plant. This was manifested by the increase of low molecular weight N compounds and by the retardation of protein synthesis. In irradiated plants, an increase in free amino acids occurred, coupled with a change in their proportions, as compared to that found in nonirradiated plants. A sharp increase in dicarboxylic acids and their amides was noted after irradiation. Irradiation of seeds caused a 15–20% drop in DNA and RNA in the root meristems, in the roots and in the aerial portions. The nucleotide composition was not changed. Carbohydrate metabolism was affected, especially in young plants, and a drop in the reducing sugar content was noted. (C.H.)

28910 PHOTOCHEMISTRY OF URIDYLYL-(3′ → 5′)-URIDINE. Brown, I. H.; Freeman, K. B.; Johns, H. E. (Univ. of Toronto). J. Mol. Biol., 15: 640-62(Feb. 1966).

When ^{32}P-labeled UpU (uridylyluridine) was uv irradiated with monochromatic light in the wavelength range from 225 to 289 mμ, three isomeric dimers, UpU^1, UpU^2, and UpU^3, and hydration photoproducts could be separated by paper chromatography. The initial yields of UpU^1, UpU^2, and UpU^3, respectively, were in the ratio of 6 : 2 : 1 after 265-mμ irradiation. At each wavelength there was a maximum amount of dimer that can be formed. This maximum was 4.4% at 225 mμ, 30% at 254 mμ, and 33% at 280 mμ. The dose required to produce 90% of the maximum amount of dimer increased with wavelength from 0.2 μE/cm^2 at 225 mμ to 6.4 μE/cm^2 at 280 mμ. A mathematical analysis of dose-effect curves was used to determine cross sections for the production of photoproducts from UpU, and for the reversal of the dimers to UpU. The cross sections can be used to predict the reaction for low doses, sufficient to produce about 90% of the maximum amount of dimers, but not for higher doses because of unknown side reactions. The phosphodiester bond of the dimers is not hydrolyzed by ribonuclease and diesterases from spleen and snake venom. At pH 9.3 the dimers undergo a reversible split between the $N_{(3)}$ and $D_{(4)}$ positions of the ring. (BBB)

28911 EXAMINATION OF THE RADIOSENSITIVITY OF THE RED CELL CATALASE IN VITRO. Zseboek, Z.; Hernady, T. Magyar Radiol., 18: 68-71(Apr. 1966). (In Hungarian).

Experimental data are presented that show patients receiving x ray treatment or in animal experiments the usual doses produce no radiation injury in the red cell catalase. Principles are discussed. (C.H.)

28912 EXPERIMENTAL STUDIES ON THE INFLUENCE OF HORMONES IN X-IRRADIATED ANIMALS. PART III. STUDIES ON THE INFLUENCE OF HORMONES UPON HEME SYNTHESIS IN X-IRRADIATED RABBITS. Kawasaki, Sho (Kyoto Univ.). Naika Hokan, 12: 561-70 (Oct. 1965). (In Japanese).

Studies were made to confirm a decreased erythropoiesis in x irradiated rabbits and to determine the effects of hormones or other humoral factors on the decreased erythropoiesis. Erythropoiesis was studied by measuring the ratio of incorporation of ^{14}C-glycine into heme by red blood cell precursors in vitro. It is suggested that a factor, which

stimulates heme synthesis, was present in the homologous rabbit serum as well as the autologous one. On the contrary, Krebs-Ringer's solution halted heme synthesis. Bone marrow cells were markedly decreased in number in the rabbits irradiated with 800 R. The activity of heme synthesis by a definite number of the bone marrow cells was reduced. The activity of heme synthesis by bone marrow of a normal rabbit was decreased when it was incubated together with the serum from the rabbit irradiated with 800 R. Such a depressing effect upon heme synthesis was confirmed in the serum of 3 out of the 7 irradiated rabbits. The decreased heme synthesis of irradiated rabbits treated with thyroxine recovered earlier than that of the irradiated rabbits treated with other hormones or of the non-treated irradiated rabbits. In normal rabbits given ACTH or estradiol, heme synthesis by a definite number of bone marrow cells was depressed. This fact was noted especially in the rabbits treated with estradiol. (auth)

28913 GAMMA-RAY THERMOLUMINESCENCE IN NUCLEIC ACID CONSTITUENTS. **Singh, B. B.; Charlesby, A. (Royal Military Coll. of Science, Shrivenham, Eng.). Photochem. Photobiol., 5: 63-73 (Jan. 1966).**

The following constituents of DNA and RNA, as well as DNA and RNA preparations, were examined for γ thermoluminescence intensity after exposure to ^{60}Co at 77°K: adenine, adenosine, adenylic acid (5-phosphate), polyadenylic acid, guanine, guanosine, guanylic acid, D-ribose, cytosine, thymine, uracil, uridine, and uridylic acid. The thermoluminescence glow curve from adenine and guanine was a single peak at 110°K. Thymine also gave a narrow peak at this temperature followed by a long tail at the higher temperature.side. Cytosine gave two peaks, α at 135 and β at 180°K; a previously reported third peak at about 115°K was not satisfactorily reproduced. The uracil glow curve also had a single peak and DNA, RNA, and D-ribose gave similar curves. The temperatures at which these peaks occurred are shown. The addition of sugar and sugar-phosphate groups to the base-molecules affected only the amount of light emitted. The thermoluminescence emission spectra lay in the same wavelength region as the uv-induced phosphorescence, suggesting a triplet-singlet transition. The spectral content of DNA thermoluminescence seemed to be superposition of contributions from its constituents. An attempt was made to explain the phenomenon as a result of electron-cation recombination. (BBB)

28914 PHOTOIONIZATION AND BIPHOTONIC PROCESSES OF NUCLEIC ACIDS DERIVATIVES IN FROZEN SOLUTIONS. **Helene, Claude; Santus, Rene; Douzou, Pierre (Museum d'Histoire Naturelle, Paris). Photochem. Photobiol., 5: 127-33 (Jan. 1966).**

In alcoholic solutions at 77°K, purine, adenosine, guanosine were characterized by their fluorescence and phosphorescence spectra and the lifetime of the phosphorescent triplet state. The intensity of phosphorescence was lowered on irradiation with uv light. The decrease followed an exponential law in an interval where the phosphorescence intensity was lowered by a factor of about two. The fluorescence intensity remained practically constant. A relation was derived by designating by τ the time of irradiation needed to reduce the phosphorescence intensity by a factor of two and by I the intensity of radiation. In the three compounds tested it was observed that the rate constant k of phosphorescence quenching ($k = 0.69/\tau$) is proportional to I^p, where p is about 1.6. The relation did not change with variations of the concentration between 10^{-4} and 10^{-3}M. After irradiating the solution for a time τ at 77°K, warming it to room temperature, and refreezing to 77°K, about 90% of the initial phosphorescence intensity could be restored. If the irradiated sample was kept at 77°K in the dark for half an hour, there was no increase in the phosphorescence intensity. In aqueous solution, the phosphorescence intensity of purine, adenosine, and guanosine was quenched by uv irradiation and did not differ from the behavior in alcoholic solutions. Photosensitization of alcohol occurred. A biphotonic absorption process involving the lowest triplet state is suggested. The formation of radicals by these processes led to a decrease of the phosphorescent triplet-state population of the molecules tested. Some consequences for the photochemistry of nucleic acids are discussed. (BBB)

28915 DETERMINATION OF AMINO ACID QUANTUM EFFICIENCIES BY DIFFERENCE SPECTROPHOTOMETRY. **Dunlop, J. I. (Wool Industries Research Association, Leeds, Eng.). Photochem. Photobiol., 5: 227-9 (Jan. 1966).**

Difference spectra were produced by exposing amino acid solutions to uv radiation. The difference spectra produced by uv irradiation are unique for each amino acid and in particular cases use might be made of the forms of the difference spectra to determine the quantum efficiencies of the photolyses. The difference spectra of tyrosine and tryptophan solutions irradiated in the wavelength region of 254 to 320 mμ are shown. The amino acid solutions were irradiated at three different wavelengths, 254, 260 to 280, and 280 to 300 mμ and the absorption coefficients at these wavelengths were calculated from the spectrophotometric curves of the samples. The difference spectra are characterized by a broad maximum at ~300 mμ by a minimum between 260 and 280 mμ, the position and inverted shape of which approximate to the spectra of the original amino acids. The appearance of these features is explained by: a general decrease in the optical density of the irradiated sample at wavelengths less than 350 mμ due to the formation of new chemical species, and a reduction of the optical density in the 260 to 280 mμ region due to loss of tyrosine or tryptophan from the irradiated sample, producing the observed minimum. The minimum feature is of interest because its magnitude represents the amount of amino acid that disappears from the irradiated sample due to photolytic decomposition. The magnitude of this feature can be estimated by extrapolating through the smooth curve of the 300-mμ maximum through the minimum. The optical density difference between the extrapolation and the minimum can then be converted to moles of amino acid and the quantum efficiency calculated. (BBB)

28916 KINETICS OF THE UV-INDUCED DIMERIZATION OF THYMINE IN FROZEN SOLUTIONS. **Fuechtbauer, Walter (Univ., Wuerzburg, Ger.); Mazur, Peter. Photochem. Photobiol., 5: 323-35 (Apr. 1966). (ORNL-P-1614).**

Dimerization of thymine during uv irradiation at 2537 Å readily occurred in liquid solutions of DNA, thymine dinucleotides, and polynucleotides, but thymine itself dimerized only when solutions were irradiated while frozen or dried. Attempts made to explain the role of freezing and drying include hypotheses claiming a special interaction between ice and thymine and those suggesting that the dimerization is just a consequence of the physical clumping of thymine during freezing or drying. Data required to determine the mechanism of dimerization are the state of thymine solutions at subzero temperatures (whether completely solid or not) and the quantum yield for the reaction. Experiments were performed to estimate the quantum yield for dimerization in frozen solutions and the contribution of radiation scattered by the ice. The eutectic point of aqueous thymine solutions was found to be −0.02°C. Since the irradiation of frozen solutions is always carried out at lower temperatures, dimerization must occur in the solid state. Activation energies and quantum yields for dimer formation were determined by irradiating 1-mm layers of thymine solution at −5 to −70°C for various lengths of time. As expected, the activation energy was zero. After measuring the amount of radiation scattered by samples of ice, the extreme values for the quantum yield were found to be 0.73 and 4.08. The lower limit assumed that all the scattered light was absorbed by thymine; the upper limit assumed that none was absorbed. Since the theoretical maximum quantum yield is 2, the best estimate of the quantum yield is considered to be between 1 and 2. (BBB)

28917 COLLAGEN AND HEXOSAMINE CHANGES IN SUBCUTANEOUS GRANULOMA IRRADIATED LOCALLY WITH A ^{60}Co SOURCE. **Nimni, Marcel E.; Lyons, Charles; Bavetta, Lucien A. (Univ. of Southern California, Los**

Angeles). Proc. Soc. Exp. Biol. Med., 122: 134-7(May 1966). (USC-113P13-1).

Radioactive capsules containing 1 mC of ^{60}Co when imbedded in subcutaneous induced granulomas, significantly decreased the amount of collagen present. This decrease is due mainly to a change in the rate of synthesis, as judged by the considerable drop in the amount of soluble collagen precursors present in the irradiated granulomas. Hexosamine concentration in developing granuloma was not significantly affected by irradiation. The necrotic skin above the granulation tissue in the irradiated animals showed an increase in total collagen, presumably of a relative nature due to a depletion of soluble tissue constituents. The rate of synthesis at this site was decreased as judged by a drop in soluble collagen precursors extractable by isotonic NaCl solution. (auth)

28918 CHANGES IN FAT AND GLYCOGEN CONTENTS IN PARAMECIUM CAUDATUM AFTER UV TREATMENT. Samoilova, K. A. Tsitologiya, 5: 546-53(1963). (In Russian).

Fat and glycogen accumulations were observed in paramecia on the first day post-irradiation with 2537 Å uv. Increase in these substances was dose-dependent. It is suggested that the fat and glycogen increases resulted from interference with the cellular oxidation reaction. (TCO)

28919 NUCLEIC ACID CONTENT IN THE GUINEA PIG BRAIN IN DYNAMICS OF ACUTE RADIATION SICKNESS. Kucherenko, N. E.; Sopin, E. F. (Shevchenko State Univ., Kiev). Ukr. Biokhim. Zh., 38: 50-4(1966). (In Ukrainian).

The method of quantitative paper chromatography was used together with ultraviolet spectrophotometry to study the RNA and DNA compositions of the guinea pig brain in the normal state and in the dynamics of acute radiation sickness. The composition of RNA and DNA was studied on separate preparations isolated from brain tissue. As a result of the studies changes were found in the nucleotide composition of RNA and in the ratio of nitrogenous bases of brain DNA of guinea pigs affected by acute radiation sickness. These changes consisted, chiefly, in a decrease in the quantity of uridylic acid in RNA and of thymine and guanine in brain DNA of animals with acute radiation sickness as compared with the normal state. (auth)

28920 RADIATION ASPECTS OF GENETIC CELL DIFFERENTIATION AND THE PROBLEM OF MALIGNANT GROWTH. Dubinin, N. P.; Goldman, I. L. Vestn. Akad. Med. Nauk SSSR, 20: No. 3, 53-68(1965). (In Russian).

Radiation effects produced on the human leukocyte cell nuclei in a blood culture were studied. It was shown that following irradiation there occurs a complex set of nuclear changes, such as structural mutations of chromosomes, binuclear state, aneuploidy, and polyploidy. A heretofore unknown phenomenon of paradiploid aneuploidy was also demonstrated. A complex analysis was made of all types of nuclear changes and the mechanism underlying their radiation-induced origin. The role of radiation in carcinogenesis is discussed. (C.H.)

28921 EFFECT OF IONIZING RADIATION ON VITAMIN C METABOLISM. Danetskaya, E. V.; Lebedeva, M. A. Vop. Pitaniya, 24: No. 3, 17-22(1965). (In Russian).

Rats and guinea pigs were irradiated with a single x ray dose of 100 R and the urinary excretion of ascorbic acid content in blood and adrenals were measured at intervals for 38 days. In rats, the content in the urine increased after 1 day nearly 300%, and continued at a high level thereafter for 38 days, while the blood level dropped 20%, and the adrenals showed a nearly 10% gain. In guinea pigs, which are unable to synthesize ascorbic acid, the urinary content showed a 60% drop for a 15-day period. Rats were irradiated for 427 days with a daily dose of 0.05 R from ^{60}Co, and the ascorbic acid content in urine, blood, liver, spleen, adrenals, brain, and small intestines was measured. Some of the rats were on a folic acid-deficient diet, as were some of the controls. The urinary excretion of rats receiving folic acid was much higher than in the folic acid-deficient rats. The ascorbic acid content in the liver of the experimental rats was consistently lowered during the entire experimental period. (C.H.)

28922 RED CELL CARBONIC ANHYDRASE FOLLOWING X IRRADIATION [Thesis]. OKunewick, James Philip. Los Angeles, Univ. of California, 1965. 93p.

Investigations were carried out to determine whether or not there is a radiation-induced reduction in the overall activity of red cell carbonic anhydrase that could result in an upset of the carbon dioxide balance in the blood, thus leading to a toxic condition. Measurements of carbonic anhydrase activity of lysed whole red cells following in vivo x irradiation at 500 and 2000 R showed that the overall activity of the enzyme is unaffected by either sublethal or supralethal doses of this magnitude. Measurements of radio-zinc incorporation by blood cells following 560 R showed a significant depression in zinc uptake in vivo following total-body x irradiation. This depression was in part related to post-irradiation leukopenia and in part to a lowered level of zinc in the erythrocyte. Comparisons of in vivo radio-zinc incorporation in the carbonic anhydrase obtained from the red cells of irradiated rats with that of controls indicates that this depression is probably not related to carbonic anhydrase. Studies of the in vivo incorporation of ^{14}C-labeled serine into red cells and their carbonic anhydrase following x irradiation showed that while the production of protein, as measured by the uptake of this labeled amino acid, is significantly reduced by irradiation in both the whole cell and the fraction obtained in the extraction of carbonic anhydrase, the radio-carbon uptake is markedly higher in the carbonic anhydrase fraction than in the whole cells. Thus it seems that synthesis of the material contained in the carbonic anhydrase fraction may be carried out independently of the synthesis of the major red cell protein, hemoglobin. Furthermore, it is possible that carbonic anhydrase synthesis proceeds at least for a limited time in some of the younger cells of the circulating blood. (Dissertation Abstr.)

28923 PROTEIN SYNTHESIS IN EHRLICH MOUSE ASCITES TUMOR CELLS IN VITRO, AND THE EFFECT OF X IRRADIATION THEREON [Thesis]. Drewes, Patricia Ann. Los Angeles, Univ. of California, 1965. 204p.

The amino acid composition of the blood plasma of mice bearing Ehrlich ascites tumor was compared with that of normal mice. The presence of the tumor lowered the amino acid concentrations in the plasma and decreased the ratio of essential to non-essential amino acids. The amino acid composition of the ascitic fluid showed a very different profile from that of the plasma, having larger amounts of proline, glycine, glutamic and aspartic acids, but only one-tenth as much glutamine. Analysis of the fluid after contact with the tumor cells for 2½ hours at 25°C, showed a greatly decreased ratio of essential to non-essential amino acids. An in vitro incubation system for the linear incorporation of ^{14}C-labelled amino acid into the protein of the tumor cells for over an hour was developed. An incorporation rate of about 19×10^{-3} μmoles leucine/mg protein/hour was achieved. The complete system consisted of washed tumor cells, Krebs-Ringer phosphate buffer, pH 7.25, and adequate amounts of glucose and all twenty amino acids required for protein synthesis. Measureemtns of the change in total protein over an hour showed the complete system to support the net synthesis of protein. The increase in protein amounted to about 3-4% of the original amount. While a net increase in total protein was not observed in the incomplete system, incorporation did proceed, although at a decreased rate. The effect of in vitro x irradiation on the subsequent protein synthesis of Ehrlich tumor cells was investigated by means of both the incorporation procedure and determination of net increase in protein. A dose of 4000 R had no effect on protein synthesis. At 8000 R there was a slight inhibition of incorporation, followed by progressively increased inhibition at 12,000 and 16,000 R. The effect of these higher doses on total protein was to enhance the 3-4% net synthesis of protein another 1%. This effect was more short-lived in the case of the 16,000 R dose, since

30 min the protein level became constant. Since protein content reflects the net result of synthetic and degradative processes, the lowered incorporation and increased total protein indicated that x irradiation adversely affected protein degradation as well as synthesis. (TCO)

28924 INFLUENCE OF IONIZING RADIATION ON THE METABOLISM IN HUMAN ERYTHROCYTES. Voigt, E.-D. Berlin, Freie Univ., 1965. 39p. $2.00 Gmelin, AED-Diss. 65-249.

Erythrocyte suspensions were x irradiated in vitro with 800 R. No influence on glycolysis and oxidative glucose transformation was observed. The ATP breakdown activity of the erythrocytes decreases. K transport is not changed. (Gmelin Inst.)

Radiation Effects on Tissues

Refer also to abstracts 29402 and 29587.

28925 (AD-633024) AN ESTIMATE OF THE EFFECTS OF FALLOUT BETA RADIATION ON INSECTS AND ASSOCIATED INVERTEBRATES. Teresi, J. D.; Newcombe, C. L. (Naval Radiological Defense Lab., San Francisco, Calif.). Feb. 28, 1966. 88p. (USNRDL-TR-982). CFSTI $3.00 cy, $0.75 mn.

Three practical considerations were found to merit attention in the evaluation of the impact of fallout radiation on terrestrial insects and associated invertebrates. First, the relatively low dose levels that will affect developmental stages as compared to adult stages; second, the lower doses required to produce late mortality as compared to those required for early deaths; and third, the relatively low doses that will cause sterility. The calculated potential beta doses indicated that the dose level expected to sterilize a large majority of the organisms considered would be found in areas bounded approximately by the 50 R/hr at 1 hr gamma contour (4,600 beta rads accumulated in about 5 days) for a 1 MT burst, by the 100 R/hr at 1 hr gamma contour (5200 beta rads in about 5 days) for a 10 MT burst and by the 100 R/hr at 1 hr contour (5200 beta rads in about 14 days) for a 100 MT burst. (348 references). (auth)

28926 (AD-633469) STUDIES ON TRANSFER OF MYELOMA PROTEIN SYNTHESIS WITH RNA FROM C_3H PLASMA CELL TUMOR (X5563). I. IN VIVO INCUBATION OF RNA-TREATED CELLS. Chin, P. H.; Silverman, M. S. (Naval Radiological Defense Lab., San Francisco, Calif.). Apr. 5, 1966. 22p. (USNRDL-TR-1005). CFSTI $1.00 cy, $0.50 mn.

Lymphoid cells from normal C_3H mice were incubated in vitro with RNA isolated from the X5563 plasma cell tumor. The cells were subsequently injected into sublethally irradiated isogenic mice. Electrophoretic analysis of sera from these recipient mice showed the presence of a serum component having the same electrophoretic mobility as the γ myeloma protein synthesized by the tumor cells. The induced synthesis of this protein was relatively stable and persisted for approximately forty days. However, the protein was detected in sera from only a small percentage of the animals. Sera from mice injected with cells incubated with RNA isolated from normal lymphoid tissues did not contain the protein nor was it demonstrated in sera from normal or irradiated mice. (auth)

28927 (BNL-9647) EXTRACORPOREAL IRRADIATION OF THE BLOOD. Schiffer, L. M.; Chanana, A. D.; Cronkite, E. P.; Greenberg, M. L.; Joel, D. D.; Schnappauf, Hp.; Stryckmans, P. A. (Brookhaven National Lab., Upton, N. Y.). Oct. 27, 1965. Contract AT(30-2)-Gen-16. 28p. Dep. mn. CFSTI $2.00 cy, $0.50 mn.

The underlying principle and techniques of extracorporeal irradiation of the blood (ECIB) are described. The theoretical reasons for its use in the leukemias and in tissue and organ homotransplantation are discussed. At the present time, studies have reached the stage where it can be safely applied in a program to prevent or reverse rejection of human organs after homotransplantation. ECIB has significant potential usefulness in this field, but full evaluation remains to be performed. Limited studies of the treatment potentials of ECIB using γ or x radiation sources in acute myelocytic leukemia indicated that it may be useful in selected cases, but it is not recommended for general use, especially as the sole treatment. Further studies of its usefulness in chronic lymphocytic and chronic myelocytic leukemia are indicated because of favorable results in a small number of patients. Irrespective of its possible clinical usefulness, fuller use of this technique will increase the basic understanding of immune phenomena and normal and abnormal leukocyte kinetics in animals and man. (auth)

28928 (CONF-651109, pp 417-25) TECHNIQUES FOR DETERMINING THE PROTON DEPTH DOSE DISTRIBUTION IN PRIMATES. Mitchell, John C.; Hardy, Kenneth A.; Hurt, William D. (Aerospace Medical Div., Brooks AFB, Tex.).

The dosimetry work reported herein was conducted in support of an experimental program involving the irradiation of a large number of primates, Macaca mulatta, with 32-, 55-, 138-, 250-, 400-, and 2200-Mev protons. In each experiment, the primates were placed in special exposure cylinders and rotated in the proton beam. The primates used has an average cross-sectional diameter of about 10 cm and a body configuration similar to man. Because biological responses are greatly influenced by the depth dose distribution, rather extensive measurements and calculations were made to determine the dose pattern in the rotated primates. The results are presented of depth dose measurements obtained using a series of Lucite and Masonite phantoms and depth dose blocks embedded with glass rod microdosimeters and alanine dosimeters. (M.O.W.)

28929 (CONF-651109, pp 574-98) HIGH-DOSE HUMAN EXPOSURE FROM A 10-Mev LINEAR ACCELERATOR. Lanzl, Lawrence H.; Rozenfeld, Martin L. (Chicago Univ., Ill. Dept. of Radiology. Argonne Cancer Research Hospital, Chicago, Ill.); Tarlov, Alvin R. (Chicago Univ., Ill. Dept. of Medicine. Argonne Cancer Research Hospital, Chicago, Ill.).

The dosimetry and other aspects of an accident involving a large average current, 10-Mev linear accelerator are discussed. An industrial worker was accidentally exposed to radiations near and on the edge of a radiation beam consisting primarily of electrons, when he walked into the room in which the accelerator was in operation. The effects of the exposure are described. (M.O.W.)

28930 (CONF-651109, pp 601-16) ACUTE CELLULAR EFFECTS OF HEAVY CHARGED PARTICLE IRRADIATIONS. Lyman, John T. (Lawrence Radiation Lab., Univ. of California, Berkeley).

The results of heavy-ion irradiation of mammalian cells cultured in vitro are summarized. The radiations that most effectively inhibit colony-forming ability and produce chromosome aberrations are those that have rates of energy loss between 1000 and 2000 Mev-cm^2/g. The effect of modifiers such as oxygen, dose fractionation, chemical protection (cysteamine), and chemical sensitization (5-iododeoxyuridine), which affect the radiosensitivity of the cells exposed to lightly ionizing radiations, fail to modify the response, or modify it less when the cells are exposed to densely ionizing radiations. The dose-effect curves for mammalian cells exposed to radiations of differing rates of energy loss are not all necessarily the same shape; therefore the RBE values derived from the curves are generally a function of the level of damage being considered. Estimates of RBE values at low levels of radiation exposure are given for cells that receive acute exposures of densely ionizing radiation. Exposures at low dose rates may result in RBE values 3 to 4 times the values given. (auth)

28931 (CONF-651109, pp 624-35) SOME EFFECTS OF WHOLE-BODY IRRADIATION BY PROTONS ON PRIMATES. Lindsay, I. R.; Dalrymple, G. V. (Aerospace Medical Div., Brooks AFB, Tex.).

The results of radiation effects studies of 32- to 400-Mev proton irradiation of primates, Macaca mulatta, are presented. An RBE of unity for protons that penetrate the primate is estimated, based on mortality and hematological effects. (M.O.W.)

28932 INFLUENCE OF IONIZING RADIATION ON THE PROLINE CONTENT OF POTATO TUBERS. Jaarma, Maire (Univ. of Stockholm). Acta Chem. Scand., 20: 323-7(1966).

Proline contents in common Swedish potato varieties were determined by paper chromatography before and after irradiating the tubers. The results of the investigation indicated that there is a correlation between proline content and sprouting. It was also shown that there is an influence of γ rays on proline metabolism. The reason for the accumulation of proline in irradiated tubers is discussed. (auth)

28933 SOLUBILIZATION OF A CHOLINESTERASE FROM PLAICE MUSCLE BY BACTERIA. Lundin, S. J.; Bovallius, A. (Research Inst. of National Defence, Sundbyberg, Sweden). Acta Chem. Scand., 20: 395-402 (1966).

A bacterial strain, Cytophaga sp., incubated for 24 hr at 30°C on a water suspension of plaice (Pleuronectes platessa) muscle, liberated into the supernatant about 100% of the butyrylcholine splitting activity present in a muscle homogenate. The treatment allows a further purification of this cholinesterase from the muscle. (auth)

28934 INFLUENCE OF γ IRRADIATION ON β-FRUCTOFURANOSIDASE IN POTATO TUBERS. Jaarma, Maire (Univ. of Stockholm). Acta Chem. Scand., 20: 592-4(1966).

Crude "invertase" preparations were isolated from irradiated and nonirradiated potato tubers and enzyme activities of these preparations were determined. No "invertase" activity was observed in freshly harvested control tubers; in tubers stored for a year, there was, however, a marked increase of activity. In tubers irradiated immediately or a few months after harvest and analyzed a short time after irradiation, no "invertase" activity could be shown. In batches of the same tubers, stored for a year or more after irradiation, an "invertase" activity was observed, which was about 50% of the activity in the preparations from the corresponding control tubers. (M.C.G.)

28935 INFLUENCE OF γ IRRADIATION ON UDPGLUCOSE-FRUCTOSE GLUCOSYLTRANSFERASE IN POTATO TUBERS. Jaarma, Maire (Univ. of Stockholm). Acta Chem. Scand., 20: 594-6(1966).

In order to determine if the marked increase of sucrose in potato tubers, caused by ionizing radiation, could be related to changed activity of "transferase," this enzyme was isolated from γ-irradiated, and corresponding non-irradiated tubers. The activities of the isolated enzyme preparations were determined. In control tubers there was a pronounced decrease of enzyme activity after prolonged storage. In irradiated tubers, however, particularly one month or more after irradiation, the activity of the isolated "transferase" was about twice the activity of this enzyme from the corresponding control tubers. (M.C.G.)

28936 THE EFFECT OF REPEATED EXPOSURE TO LASER BEAMS. CASE REPORT WITH NINE MONTHS' PERIOD OF OBSERVATION. Goldman, L.; Richfield, D. F. Acta Dermato-Venereol., 44: 264-8(1964).

The hazards of lasers in industry and research, with special reference to their use in range finders, welding and drilling apparatus, and signalling devices are discussed. Each laser must be in a laser-restricted area which only authorized persons may enter, and general rules for these areas are given. The maximum permitted exposure of personnel to laser energy shall be as follows: (a) for a laser pulse of duration between 10^{-8} and 5×10^{-3} seconds, the energy density falling upon the retina of the eye shall not exceed 10^{-2} joules/cm^2; (b) the total laser energy incident upon the retina during any period of 1.0 seconds shall not exceed 10^{-1} joules/cm^2; (c) the total laser energy incident upon any part of the body other than the eye for 1.0 seconds shall not exceed 10^{-1} joules on any cm^2. The duties of persons in charge of lasers are detailed. Appendices show how to calculate energy density at the retina and set out requirements for special safety spectacles. (auth)

28937 THE EFFECT OF ERYTHEMAL REACTION CAUSED BY ULTRAVIOLET IRRADIATION ON MAST CELL DEGRANULATION IN THE SKIN. Valtonen, E. J.; Jaenne, J.; Siimes, M. Acta Dermato-Venereol., 44: 269-72(1964).

The effect of ultraviolet radiation on the degranulation of the mast cells in the skin of mice was investigated. The external ear of the mouse provided the skin to be investigated; the other ear served as a control. Specimens were taken from 22.5 minutes up to 24 hours after the beginning of the irradiation. It was observed that the mast cells decreased up to 55% of the control value, with a maximum of degranulation corresponding well with the maximum point of erythema. Some possible mechanisms for this occurrence are discussed. (auth)

28938 VARIATION IN RADIOSENSITIVITY OF MICE WITH TIME OF DAY. Nelson, Richard F. (Albert Einstein Coll. of Medicine, New York). Acta Radiol. Therapy, Phys., Biol., 4: 91-6(Apr. 1966).

Using 400 Swiss Webster male mice, 14 weeks old, an investigation was undertaken to determine their variation in sensitivity to radiation as a function of the time of day as measured by their death rate. Twelve groups were exposed to 800 R with 280 kv x rays at two-hour intervals. Using chi square tests, the night group as a whole appeared more sensitive than the day group as a whole. The variations within the day and night groups were not considered to be significant. (auth)

28939 THE ROLE OF SYMPATHETIC INFLUENCES IN THE GENESIS OF STRESSED ORGANISM REACTIONS TO IONIZING RADIATION. Kandror, V. I. (All-Union Inst. of Experimental Endocrinology, USSR). pp 91-5 of Adrenalin i Noradrenalin. Grashchenkov, N. I. (ed.). Moscow, Izdatel'stvo Nauka, 1964. (In Russian).

Male rats were given 5 to 500 μC of ^{24}Na per rat weighing 250 g. The total amount of catecholamines was determined by a colorimetric absorption method. An increase in catecholamine concentration of the internal medulla of the adrenal gland was observed one hour after the beginning of the irradiation with 500 μC of ^{24}Na per rat (473 ± 30.3 μg of catecholamine/g compared to 371 ± 23.7 μg of catecholamine/g in the controls). No changes could be seen at this time in the cortical layer of the adrenal gland. Changes in the cortical layer were observed about 5 hrs after introduction of the radioactive ^{24}Na. Thus, the ascorbic acid concentration decreased to 346 mg % compared to 412 mg % in the controls. The gland weight increased 224 μg/g compared to 155 μg/g in the controls. Both parts of the adrenal system showed these changes at as low as 50 μC of ^{24}Na per rat weighing 250 g. A dose as low as 0.02 μC per 1 g body weight showed no changes in the cortical layer, but still gave an increase in catecholamine concentration in the adrenals of 473 μg/g compared to 371 μg/g in the controls. Thus, it is concluded that the sympathetic adrenal system responded more readily to radiation stress than the hypophysis, adrenal, cortical system. It is presumed that the catecholamines play a mediatory role in the stress reactions of the organism to the effects of radiation. (TTT)

28940 DISTURBANCE IN CATECHOLAMINE METABOLISM INDUCED BY IONIZING RADIATION AND ITS EFFECTS ON ORGANISM REACTION TO RADIATION. Graevskaya, B. M.; Shchedrina, R. N. (Inst. of Genetics, Academy of Sciences, USSR). pp 246-9 of Adrenalin i Noradrenalin. Grashchenkov, N. I. (ed.). Moscow, Izdatel'stvo Nauka, 1964. (In Russian).

Mice were given lethal doses of 600 and 2000 R. It was found that the catecholamine content in the adrenals decreased the first few days after irradiation, mainly at the expense of the free adrenaline (A). The dehydroadrenaline (DA) level increased significantly. On the second and third days after the irradiation, the total catecholamine content

in the adrenals increased; the level of adrenaline decreased somewhat; the amount of DA (the reversibly oxidizable form of adrenaline) and of adrenaline-like substances (ALS) increased sharply and exceeded the normal value by a factor of about seven. A dose of 600 or 2000 R led to a gradual fall in the catecholamine level of the blood and liver. Noticeable amounts of free adrenaline appeared. A histochemical analysis of the medullary layer of the adrenals showed that a 600 R dose led to a decrease in the number of adrenaline-producing cells. The number of cells secreting nonadrenaline (NA) did not change substantially. At doses of 600 and 2000 R an increase in the total amount of adrenaline in the adrenals was accompanied by a decrease in liver glycogen level, and conversely, a fall in adrenaline concentration was paralleled by an increase in liver glycogen content. Mice with the highest catecholamine content in the adrenals were found to be the most resistant to the effects of irradiation. (TTT)

28941 ALTERATIONS IN THE CONTENT OF ADRENALINE-LIKE SUBSTANCES IN THE BLOOD OF DOGS DURING ACUTE AND SUB-ACUTE RADIATION SICKNESS. Kuznetsova, N. E. (Inst. of Neurology, Academy of Medical Sciences, USSR). pp 250-4 of Adrenalin i Noradrenalin. Grashchenkov, N. I. (ed.). Moscow, Izdatel'stvo Nauka, 1964. (In Russian).

Dogs were given a single, whole-body, lethal, x-ray dose of 600 R and a sublethal dose of 300 R. The content of adrenaline-like substances (ALS) was determined by a colorimetric absorption method. The relative content of unoxidized adrenaline and ALS was estimated from the specificity coefficient K_s. The ALS content in the controls varied from 0 to 17 μg % with an average of 6.0 ± 2.9 μg %. The K_s value for the controls varied from 0.3 to 2.4% with an average of 1.1 ± 0.37%. The content of dehydroadrenaline varied from 0 to 7 μg % with an average of 2.0 ± 1.9 μg μg %. Thus, the content of unoxidized adrenaline and of its reversibly oxidized forms was low. A dose of 300 or 600 R led to an increased ALS content and an increased value of K_s on the first day after irradiation. Then with a 600 R dose the ALS content was found to be low on subsequent periods after the irradiation. This behavior could be interpreted as a sign of exhaustion of the sympathetic adrenal system. With a sublethal dose of 300 R, the ALS content was increased on the 3rd to 7th day after irradiation. The value of K_s was high at 2 to 7.5, that is, the content of unoxidized adrenaline increased. At later periods the ALS content rose in most dogs. Repeated stimulation of the sympathetic adrenal system was a necessary component of the recovery processes taking place in the surviving dogs. (TTT)

28942 EFFECT OF IONIZING RADIATIONS ON THE PROPAGATION OF ROOT-KNOT NEMATODES, MELOIDOGYNE INCOGNITA CHITWOOD. Ishibashi, Nobuyoshi (Saitama Agricultural Experiment Station, Japan); Taguchi, Shigetoshi. Annot. Zool. Jap., 38: 182-9(Dec. 1965).

Sweet-potato roots infected with root-knot nematodes were irradiated with gamma rays at various stages of nematode development. The egg production of nematodes was estimated, and the effects of radiation on the propagation of the nematodes was studied. Following irradiation with 10 kR or more, larvae in early developmental stages, i.e., in less than 3 days after entry to host plants, were highly sensitive to radiation and failed to reach maturity and to lay eggs. With advancement of development, the nematodes became resistant to the rays as far as the number of eggs produced concerned. However, the development of embryos produced from nematodes irradiated in advanced stages was retarded. Males increased after irradiation during early stages. If plants were irradiated with 10 kR or more of gamma and/or x rays prior to the penetration of nematodes, the number of nematodes entering the roots was markedly decreased. (auth)

28943 INFLAMMATION AND PENETRATING IONIZING RADIATION. Kraevskii, N. A.; Ivanov, A. E. Ark. Patol., 25: No. 8, 3-14(1963). (In Russian).

A survey of literature data is presented pertinent to the peculiarities of the inflammatory reaction development in conditions of isolated irradiation and against the background of radiation sickness. Emphasis is placed on pathologico-anatomical data. (86 references.) (C.H.)

28944 THE EFFECT OF COLD AND ULTRAVIOLET RAYS ON THE MAST CELL SYSTEM. Solov'ev, Yu. N.; Demina, D. M. Ark. Patol., 26: No. 8, 63-8(1964). (In Russian).

Data are presented on the morphological and quantitative changes in the mast cell system of the subcutaneous connective tissue induced in rats by the action of cold, ultraviolet rays and a combination of both factors. Cold, a combination of cold with ultraviolet rays, and short wave ultraviolet radiation in erythematous doses considerably increased degranulation of most cells. A supposition is put forward on the transforming role played by mast cells in the process of interaction of corticoid hormones and connective tissue. (C.H.)

28945 REACTIONS OF HEMATOPOIETIC SYSTEM IN GUINEA PIGS TO CHRONIC EFFECTS OF IONIZING RADIATION IN SMALL DOSES. Toroptsev, I. V.; Sokolova, N. V.; Teterina, V. I.; Sorokina, V. A. (Tomsk Medical School, USSR). Arkh. Patol., 27: No. 8, 10-17(1965). (In Russian).

A study is presented on guinea pigs fractionally irradiated with the RYM-3 apparatus (a dose of 10 to 12 R). Irradiation was carried out up to the time of the animal death. Chronic radiation sickness accompanied by deep leukopenia, thrombocytopenia, and anemia developed in all the cases. In two cases of 22 there developed a picture of acute hemocytoblastosis by the 390th and the 417th days of the experiment (total doses of 2,122 R and 2,302 R). Acute reticulosis was seen in one case. In four cases a state of approaching erythroleukemia was observed. Foci of extramedullary hemopoiesis were revealed in the internal organs (spleen, lung, lymph nodes, liver, adrenal glands). (auth)

28946 ON THE ROLE OF ADIPOSE CELLULAR TISSUE IN THE REPAIR OF ACUTE RADIATION INJURIES OF THE SKIN. Afrikanova, L. A. Arkh. Patol., 27: No. 8, 18-24(1965). (In Russian).

In analogous experiments with x-irradiation of an area of the skin on the back with soft rays in doses of 5,000 R (rats and mice) and 10,000 R (mice), (30 kV, 15 mA, filter 0.1 mm aluminum, dose rate 1,533 R per minute), it was revealed that the repair processes in the zone of affliction differed in rats and mice. Whereas in the majority of the mice the acute radiation necrosis focus terminated in the formation of a scar at periods of up to two months, in ⅔ of the rats there developed protracted ulcers of the skin. This was largely caused by the difference in the structure of the skin and of subcutaneous adipose tissue in rats and mice. The differences in the depth of radiation necrosis and in the sources of the form producing processes for the scar tissue were associated with these peculiarities. The unfavorable course of the repair process becomes unfavorable when the formation of a scar replacing the skin defect occurs in complete absence or in the presence of but poorly developed subcutaneous adipose cellular tissue. (auth)

28947 UNCOUPLING OF OXIDATION AND PHOSPHORYLATION IN THE MITOCHONDRIA OF GREEN PLANTS AFTER X-RAY IRRADIATION. Kalacheva, V. Ya.; Sisakyan, N. M. (Bakh Inst. of Biochemistry, Moscow). Biochemistry (USSR) (Engl. Transl.), 30: 737-41 (July-Aug. 1965).

Translated from Biokhimiya, 30: 858-63(July-Aug. 1965).

The influence of the conditions of isolation, washing, and incubation of the mitochondria on the uncoupling of oxidation and phosphorylation in irradiated peas (Pisum sativum) was investigated. It was found that when oxidative phosphorylation is measured under conditions of maximum phosphorylating efficiency, a decrease in quotient P/O (with succinate and α-ketoglutarate as the oxidation substrates) can be detected only at radiation doses of 10 kR. The removal of certain activators of phosphorylating oxidation from the isolation medium and the use of the method of preincubation

of the mitochondria in the absence of an oxidation substrate permit the detection of a more distinct decrease in the P/O quotient immediately after irradiation of the plants even in a dose of 5 kR. (M.C.G.)

28948 GENETIC RECOMBINATION OF BACTERIOPHAGE ΦX174 IN SPHEROPLASTS. Jansz, H. S.; Van Rotterdam, C.; Cohen, J. A. (National Defense Research Organization TNO, Rijswijk, Netherlands). Biochim. Biophys. Acta, 119: 276-88(May 19, 1966).

In a system of host-range mutants of bacteriophage ΦX174, genetic recombination was shown to occur, not only between mutant phages in intact bacterial cells, but also when spheroplasts were infected with DNA isolated from the mutants. The recombination frequency in spheroplasts was of the same order of magnitude as that in bacteria. Lethal damage by ultraviolet and x irradiation of DNA only slightly affected its ability to induce recombinants; however, chain breaks induced by deoxyribonuclease treatment abolished the recombining faculty of the DNA. (auth)

28949 SIMULTANEOUS RESYNTHESIS OF DNA AND 50-S RIBOSOMAL RNA IN ULTRAVIOLET-IRRADIATED ESCHERICHIA COLI. Brdar, B.; Drakulic, M.; Kos, E. (Inst. Ruder Boskovic, Zagreb). Biochim. Biophys. Acta, 119: 362-72(May 19, 1966).

The effect of the ultraviolet irradiation of 2 different strains of Escherichia coli on the synthesis of ribosomal RNA has been investigated during the inhibition of DNA synthesis and after the resumption of DNA synthesis either spontaneously or by photo-reactivation. The synthesis of 50-S ribosomes and 23-S RNA was partially inhibited during the whole period of the inhibition of synthesis of DNA after ultraviolet irradiation. After removal of the block in the synthesis of DNA, spontaneously or by photo-reactivation, a normalization of the synthesis of 50-S ribosomes and of 23-S RNA also took place. During the permanent inhibition of DNA synthesis in the irradiated or photo-reactivated E. coli K 12 meth$^-$ relaxed strain, growing without methionine, the synthesis of 23-S RNA was also permanently inhibited to the extent of about 40% as compared with the unirradiated control. The above results could be explained by postulating 2 coincident, but independent, enzymic repair mechanisms, acting at the level of DNA and of RNA. Alternatively, the resynthesis of DNA and of 23-S RNA after ultraviolet-irradiation followed by photo-reactivation, could be metabolically related processes. (auth)

28950 CYBERNETIC STUDIES ON RADIATION EFFECTS ON YEAST CELLS. I. REPRODUCTION OF IDEAL HOMOGENEOUS AND SYNCHRONOUS CELL POPULATIONS. Pohlit, W.; Domke, A. (Max Planck-Institut fuer Biophysik, Frankfurt am Main). Biophysik, 3: 44-64(1966). (In German).

Cybernetic investigations of radiation effects on living yeast cells were carried out in which the effect of regulating and controlled processes in the cell during the radiation reaction were quantitatively considered. The reproduction of individual cells in homogeneous and synchronized populations was theoretically investigated. Several possibilities for the experimental determination of lag times both in liquid media and on agar surfaces were given, from which the scattering of the population could be determined. Pseudo lag times could arise through very small concentrations, through contribution of avital cells, through changes of state of the agar surfaces and through the occurence of cell groups following a long separation time. The pseudo lag time simulates a delayed cell division. These possibilities were treated quantitatively. (tr-auth)

28951 LASERS AND ULTRASONICS. Smart, Desmond; Ingram, H. Vernon; Manson, Neil (Univ. of Newcastle upon Tyne, Eng.). Brit. Med. J., 1: 859(Apr. 2, 1966).

Some aspects of hazards involved in the generation of ultrasonics in the focal zone of a ruby laser beam are discussed. Of the known possible hazards of laser radiation are the undesirable effects from ultrasonic waves generated by the laser beam. In the clinical range of retinal phototherapy (0.05–0.5 J) such effects may be disregarded. Experimentally, neurological changes have been reported in rats treated with laser energy of the order of 100 J. In rabbits, because of the large dispersion and attenuation when doses of this range are used, no neurological symptoms are produced. It is unlikely, therefore, that neurological changes could result in humans with the clinical laser dose energy referred to. In two and a half years of clinical experience with instruments designed on the basis of these studies, no undesirable retinal or other pathological change has been seen. With high energy lasers in experimental situations retro-ocular changes and alterations in the clear media can be produced. These changes were induced by doses far in excess of the energy range available for retinal laser phototherapy. The fact that a laser will produce electromagnetic disruption of molecules is simply demonstrated with a high energy laser beam in air or in biological material. This is evident from the alterations induced in cell metabolism, which are different from those produced by mechanical or thermal damage. There do not appear to be unexpected deleterious phenomena, since from the laser-induced changes in the cell regime it is possible to predict with remarkable accuracy the observed post-operative course of a laser lesion. No concern should be given in taking advantage of this technique for prophylactic or other retinal work because of fears of side-effects of ultrasonics or electromagnetic phenomena. It is because a chorioretinal change is induced electromagnetically that the lesion can be so easily sited and limited in extent. (BBB)

28952 CORRELATION OF SEXES IN THE OFFSPRING OF FEMALE AND MALE RATS IRRADIATED AT DIFFERENT PERIODS OF THEIR ONTOGENESIS. Pozhidaev, E. A. (Inst. of Experimental Medicine, Academy of Medical Sciences, USSR). Byull. Eksp. Biol. Med., 60: No. 11, 92-5(Nov. 1965). (In Russian).

In irradiation of female gametes in a dose of 50 R a decrease in the age of females is accompanied by a trend toward an increase in their offspring of the number of males from 45.5% (in irradiation of 50 to 90-day-old females) to 54.5% (in irradiation of females in the antenatal period at a fetal age of 10 to 17 days). The difference between these values is significant. In irradiation of adult females in a dose of 600 R, the correlation of sexes in their offspring is close to that in the control. The irradiation of males at different ante- and postnatal periods in a dose of 50 R and of adult males in a dose of 600 R as well as the crossbreeding of males irradiated in a dose of 600 R with females irradiated with the same dose, did not influence the correlation of sexes in their offspring. A certain prevalence of males in the offspring was obtained in experiments with irradiation of adult males in a dose of 1,000 R. However, the difference as compared to control falls short of being significant. An increase in the number of males in the offspring of female rats irradiated in the antenatal period possibly testifies to a very early predetermination of sex in mammals. (auth)

28953 NUCLEIC ACID SYNTHESIS IN X-IRRADIATED THYMOCYTES. Myers, D. K.; Skov, Kirsten (Atomic Energy of Canada Ltd., Chalk River, Ont.). Can. J. Biochem., 44: 839-52(June 1966).

The rate of incorporation of thymidine into the deoxyribonucleic acid (DNA) of rat thymocytes in vitro was not immediately affected by low doses of x radiation, but became progressively more inhibited as the irradiated cells were incubated at 37°C for periods of up to 6 hours. Ribonucleic acid (RNA) synthesis deteriorated almost at the same rate as DNA synthesis after x irradiation in vitro, but protein synthesis was slightly more resistant. Addition of 10 to 50 mM nicotinamide to the irradiated cell suspensions tended to retard the development of this inhibition, particularly at low temperatures, but high concentrations of nicotinamide were also toxic to these cells. The inhibition of DNA synthesis by x irradiation appeared to follow a qualitatively similar pattern in thymus, spleen, and regenerating liver in vivo. In addition to the inhibition resulting from degenerative processes in the irradiated

cells, DNA synthesis in vitro was directly inhibited by 20 to 30 kR x radiation. The effects of radiation on DNA synthesis paralleled to some extent its effects on the gel-forming capacity of the deoxyribonucleoprotein from the thymus cells. It is suggested that the normal synthesis of both RNA and DNA in thymocytes depends on the integrity of the deoxyribonucleoprotein. (auth)

28954 METABOLISM OF SERUM PROTEINS IN RATS UNDER SEVERAL CONDITIONS. **Hiratsuka, Satoshi (Kyushu Univ., Fukuoka). Fukuoka Igaku Zasshi, 56: 669-87(July 1965). (In Japanese).**

The metabolism of serum protein fractions was observed by comparing the ^{14}C-glycine uptake (determined by specific activity) of each fraction of the serum and tissue proteins. The rats were divided into six groups, including a control group, according to whether they received: 1. acute carbon tetrachloride intoxication; 2. subacute carbon tetrachloride intoxication; 3. irradiation with ^{60}Co in a single large dose; 4. irradiation with ^{60}Co in repeated small doses; or were 5. phlebotomized. The level of serum albumin decreased in each group except the last, and the level of serum globulin increased in every group; an increase of α-globulin in 1 and 3, whereas in 2 and 4 an increase of γ-globulin was noticed. The specific activity of serum protein changed similarly as serum albumin, e.g., the specific activity was raised in 3 and 5 but decreased in 1, 2 and 4. The specific activity of α-globulin was raised in each group except 4, and the specific activity of γ-globulin increased in 2, 3 and 5 and decreased in the other group. The specific activity of β-globulin changed irregularly. In group 1, a decreased incorporation of $^{14}C-2-$glycine was noticed in the microsome in each tissue, so that a decreased synthesis of proteins takes place in this condition. The labeling of the cell sap proteins was also raised in the liver and the spleen. The labeling of γ-globulin in the cell sap increased only in the liver, and decreased in the other organs. As compared with 1, a different alteration of protein synthesis was noted in 2, in which an increase of protein synthesis took place in the spleen and the bone marrow; because an increase of the labeling was observed in the microsome as well as γ-globulin in the cell sap in the spleen and the bone marrow, and also in the cell sap proteins in each tissue except the bone marrow. In group 3, an increase of the incorporation of $^{14}C-2-$glycine was confirmed in the microsome fraction in every tissue. In group 4, however, a decreased incorporation was noticed. These findings suggest that the mode of the irradiation influences the disturbance in protein synthesis. In 3 the labeling of the cell sap proteins was raised in each tissue except the bone marrow, though the labeling of γ-globulin in the cell sap variably changed. In 4, however, the proteins as well as γ-globulin in the cell sap were labeled irregularly among the tissues. (auth)

28955 STABILITY OF DROSOPHILA CHROMOSOMES TO RADIOACTIVE DECAY OF INCORPORATED ^{32}P. **Lee, William R.; Oden, Carol K.; Bart, Carol A.; Debney, Carole W.; Martin, Robert F. (Univ. of Texas, Austin). Genetics, 53: 808-22(May 1966).**

Transmutation of ^{32}P to ^{32}S and the accompanying energy released by steric changes in the molecule and recoil of the ^{32}S nucleus were separated from the mutagenic effect of accompanying beta radiation by storage of ^{32}P-labeled spermatozoa in unlabeled Drosophila females. Because of the high energy of the ^{32}P beta particle, only a negligible dose is received by sperm from beta radiation during storage. Mature sperm containing DNA labeled with ^{32}P was obtained from 2-day-old males that had been fed ^{32}P as larvae. Females recently mated to ^{32}P labeled males were divided into two groups. One group was allowed to produce progeny immediately. The other was first stored on sugar agar media at 18°C for 3 weeks to inhibit oviposition, and then permitted to oviposit freely on cornmeal media. The mutation rates of progeny of the two groups were compared to measure additional genetic damage, if any, caused by ^{32}P decay in sperm during the storage period. Incorporation of ^{32}P was determined by counting spermatozoa microscopically, washing with cold trichloroacetic acid, and determining the radioactivity with a liquid scintillation detector. The average number of ^{32}P disintegrations during storage per X chromosome euchromatin was 35 and the minimum estimate was 11. There was no significant change during storage in the rate either of chromosome breakage (as measured by loss of the marker B^S on the marked $B^S \cdot Y$ chromosome) or of sex-linked recessive lethals that could be attributed to transmutation and recoil. By combining the minimum increase in mutation rate that could have been detected statistically with the minimum estimate of ^{32}P disintegrations, it was concluded that less than one ^{32}P disintegration in 2,000 in the X chromosome will produce a complete recessive lethal. (auth)

28956 EQUILIBRIA FOR INVERSIONS INDUCED BY X RAYS IN ISOGENIC STRAINS OF DROSOPHILA PSEUDOOBSCURA. **Sperlich, Diether (Rockefeller Univ., New York). Contract AT(30-1)-3096-5. Genetics, 53: 835-42(May 1966).**

Strains of Drosophila pseudoobscura made isogenic for their second and third chromosomes were x irradiated; nine inversions (one of them double) were induced in chromosome III and four in chromosome II. Experimental populations were made carrying the induced inversions, with initial gametic frequencies of 25%. In six of the populations the induced inversions were eliminated, or were close to elimination, within a year; three populations were lost by contamination (including one with inversions both in the second and in the third chromosomes); and in two remaining populations the inversions established balanced equilibria. These two heterotic inversions are the more remarkable since they are lethal, or at least semilethal, in homokaryotypes. Induced heterotic mutants, as well as heterotic position effect, could explain these heterotic inversions. (auth)

28957 ACATALASEMIC AND HYPOCATALASEMIC MOUSE MUTANTS. **Feinstein, Robert N.; Howard, Judith B.; Braun, Joann T.; Seaholm, John E. (Argonne National Lab., Ill.). Genetics, 53: 924-33(May 1966).**

Screening of 12,306 mice, progeny of x irradiated sires, uncovered at least five partially dominant mutations for low blood catalase and two others that may by further genetic analysis prove to be mutants. One of the mutants appears comparable to the human acatalasemics reported, the heterozygote showing approximately 50% of normal catalase, and the homozygote showing only a trace of catalase in the blood, perhaps 1% of normal. The other four established mutant lines have no known human counterpart; the heterozygote is approximately 65% of normal, and the homozygote, 20%. The five mutants are in all probability alleles, although it is possible they are closely linked nonalleles. (auth)

28958 PIGMENT MUTATIONS IN ANACYSTIS NIDULANS INDUCED BY NITROSOMETHYLUREA. **Stoletov, V. N.; Zhevner, V. D.; Garibyan, D. V.; Shestakov, S. V. (Lomonosov Moscow State Univ.). Genetika, No. 6, 61-6(Dec. 1965). (In Russian).**

Lethal and mutagenic effect of uv, x rays, and nitrosomethylurea were studied on the obligate photoautotrophic blue-green alga Anacystis nidulans. Dependence of cell survival on varying doses of these mutagenic factors was investigated. Ultraviolet and x rays do not induce pigment mutations in A. nidulans, while nitrosomethylurea causes a mutagenic effect. When nitrosomethylurea was used, the yellow-green colony mutants, sectoral yellow-green mutants with affected synthesis of phycocyanine, and a bluish-green mutant with low contents of carotenoids and high contents of phycocyanine, were obtained. The rate of appearance of induced yellow-green mutants was higher than that of bluish-green mutants. Under treatment with varying doses of nitrosomethylurea the dependence of the rate of yellow-green mutations on cell survival is of a linear character. (auth)

28959 MUTAGENIC ACTION OF EXTRACTS FROM VARIOUS ORGANS OF IRRADIATED MICE. **Kerkis,**

Yu. Ya.; Yasnova, L. N.; Urzhenko, A. V. (Inst. of Cytology and Genetics, Academy of Sciences, Novosibirsk, USSR). Genetika, No, 6, 110-14(Dec. 1965). (In Russian).

The effect of salt-water extracts from various organs of x-irradiated mice on chromosome aberrations in corneal cells of normal mice was studied. The injection of the brain extract resulted in an essential increase of the number of chromosome aberrations (0% in the control and 0.29% upon injection of the extract from irradiated animals). Extracts from other organs and from in vitro irradiated brain of mice had no effect. It is evident that the integrity of a living organism plays an important role in the formation of mutagenic factors in it during x-irradiation of mice. (auth)

28960 EXPERIMENTAL MUTATIONS IN CEREALS (WHEAT, BARLEY, OATS) INDUCED BY IONIZING RADIATIONS. Zarubailo, T. Ya.; Kislyuk, M. M.; Kozhushko, N. N. (All-Union Inst. Plant Breeding, Leningrad). Genetika, No. 6, 132-6(Dec. 1965). (In Russian).

Dry wheat and barley seeds were given a neutron or gamma dose of 5, 10, 15, and 20 kR. The dose to the shoots was 0.5, 0.9, 1.2, 1.5 or 2.0 kR. The most effective neutron flux in producing viable mutants was 1×10^{10} to 1×10^{11} neutrons/cm^2. The most effective ^{60}Co gamma dose was 15 kR for the dry seed, and 1.5 kR for the shoot. Repeated gamma irradiation gave the highest percent of viable mutants (0.97%). Soft spring wheat (Diamond variety) showed the greatest variability in mutations. On irradiating with ^{60}Co gamma rays, the relative mutation frequencies were 47% with changes in spike beardedness, 21% with changes in spike color, 16% with changes in grain color, and 16% with changes in the structure of the plant spike. The changes in spike beardedness and color depended significantly on the dose. Thus, a dose of 780 R gave mutations with changes in beardedness in 6.4% of the cases, and with changes in spike color in only 0.9% of the cases. On the other hand, a dose of 550 R gave mutations with changes in spike color in 4.1% of the cases, and with changes in spike beardedness in only 0.3% of the cases. (TTT)

28961 RECOVERY FROM X-RAY-INDUCED SUB-LETHAL DAMAGE IN SACCHAROMYCES CEREVISIAE CELLS OF DIFFERENT PLOIDY. Bacchetti, Silvia; Elli, Raffaella; Falchetti, Roberto; Mauro, Francesco; Sacchi, Ada (Univ., Rome). Int. J. Radiat. Biol., 10: 213-21(1966).

Experiments of x ray dose fractionation were performed on a polyploid series (from 2n to 4n) of yeast cells, in order to check for the recovery from sub-lethal damage and to investigate whether there is a correlation between kinetics of recovery and ploidy. Cells in a resting state or in log phase of growth were used. The data obtained show that recovery takes place in all the tested strains and display a similar type of kinetics, independently from the degree of ploidy. In the case of resting cells we get a curve describing only the recovery process, while, when growing cells are used, this curve is modified by the concomitant progression of the cells toward division. In this latter case, the value of complete recovery is attained by the three strains in different time intervals, probably related to the specific rates of growth. (auth)

28962 RADIOTHERAPEUTIC EFFECTS ON MAMMALIAN TUMOUR CELLS. 1. MODIFICATION OF LEUKAEMIA L1210 GROWTH KINETICS WITH X-IRRADIATION. Johnson, Ralph E.; Hardy, Walter G.; Swain, Robert W. (National Cancer Inst., Bethesda, Md.). Int. J. Radiat. Biol., 10: 243-9(1966).

The effect of x irradiation on the growth kinetics of mammalian tumor cells has been examined using the murine leukemia L1210 system. After single doses of radiation, the surviving cells were found to have decreased virulence compared with single normal leukemic cells as measured by the survival-time of recipient mice. Studies on cloned sub-lines demonstrated their capacity for continuous division resulting in death of inoculated animals, although the rate of proliferation determined from growth curves was significantly slower. These in vivo experiments confirm the in vitro observations that ionizing radiation produces a type of non-lethal hereditable damage which results in modification of cell-growth rates. (auth)

28963 RELATIVE BIOLOGICAL EFFICIENCY OF A BEAM OF 20-Mev ELECTRONS AS A FUNCTION OF DEPTH. Wambersie, A.; Dutreix, A.; Dutreix, J.; Lellouch, J.; Moustacchi, E.; Tubiana, M. (Institut Gustave-Roussy, Villejuif, France). Int. J. Radiat. Biol., 10: 261-75(1966). (In French).

The Relative Biological Efficiency (RBE) of a 20 Mev electron beam has been evaluated as a function of depth in an irradiated medium, using survival of bacteria (E. coli) and diploid yeast (Saccharomyces cerevisiae) as biological tests. The doses were determined by means of chemical dosimetry. Ferrous sulfate was irradiated at different depths in Perspex cells. The thickness of the layer of $FeSO_4$ solution was 2 mm to reduce, in the detector volume, the dose inhomogeneity due to sharp gradient of the dose in depth. The bacteria and the yeast were irradiated under the same geometrical conditions. The RBE was determined for the bacteria at four different depths (corresponding to per cent doses 95, 83, 37 and 24) and for the yeast at two depths (per cent doses 80 and 37), the biological efficiency at the level of 100 per cent was taken as the reference. For both biological systems no significant variation in biological efficiency was found with depth. Moreover, we found no difference in RBE between 20 Mev electrons, 20 Mv photons, and ^{60}Co. The variation in depth-dose curves according to the type, diameter, and correction factors obtained with ionization measurements from a high-energy electron beam could probably explain the variability of published results. (auth)

28964 CONTENT OF CATECHOLAMINES OF HEART AND SUPRARENALS OF RAT AFTER IRRADIATION WITH X-RAYS. Cession-Fossion, A.; Beaumariage, M. L. (Univ., Liege). Int. J. Radiat. Biol., 10: 277-82(1966). (In French).

Local x irradiation at high level (10 to 40 kR) does not change the noradrenaline content of the rat's heart during the 80 min following irradiation; it increases the adrenaline content of the suprarenals of the same rats. Chronic irradiation (200 R per day for 43 days) does not change the noradrenaline content of the rat's heart. The hypertensive action of catecholamines and tyramine in the rat is increased after a total body dose of 0.5 or 1 kR, but if the dose is 2 kR or more, the reaction to these amines is smaller than normal. (auth)

28965 EFFECT OF FRACTIONAL IRRADIATION ON ADSORPTION AND ANTIBODIES FORMATION BY THE RETICULAR AND ENDOTHELIAL SYSTEMS. Stepanyan, E. D.; Petrosyan, R. A. Izv. Akad. Nauk Arm. SSR, Biol. Nauki, 18: No. 3, 27-34(1965). (In Russian).

Rabbits were irradiated with doses of 100, 300, and 600 R and 6 hours later were immunized with 1-ml injections of dead brucellosis antigens. The irradiation sharply suppressed the sorptive power of the reticuloendothelial system. Phagocytosis was initially suppressed and then stimulated. Irradiated and immunized rabbits were subjected to second irradiations after 1, 4, 8, and 12 days. The suppression of antibody formation and reticuloendothelial adsorption diminished as the interval between the two irradiations increased. (D.E.B.)

28966 EFFECT OF X-IRRADIATION ON THE YIELD OF POTATOES. Avakyan, V. A.; Gukasyan, L. A.; Sisakyan, I. Sh. (Inst. of Roentgenology and Oncology, Erevan). Izv. Akad. Nauk Arm. SSR, Biol. Nauki, 18: No. 5, 52-6(1965). (In Russian).

Potato tubers were x irradiated with 100, 500, 1000, and 2000 R before and after sprouting. The irradiation decreased yield of nonsprouted potatoes to 23.9 to 56.2% and of the sprouted to 8.1 to 42.4%. Sprouting tubers after irradiation with small doses (100 to 500 R) increased the yield up to 12.5 to 14.4%. Doses of 2000 R reduced the yield. (C.H.)

28967 CHANGE IN CHEMICAL COMPOSITION WHEN PLANTS ARE IRRADIATED AT VARIOUS PERIODS OF ONTOGENESIS DEPENDING ON CLIMATIC FACTORS. Zhunusov, R. S. Izv. Akad. Nauk Kaz. SSR, Ser. Biol. Nauk, 3: 65-70(1965). (In Russian).

The reaction of plants to irradiation depends on the growth phase. Protein content is increased in beans by irradiation during the budding phase; starch yield is increased in potatoes by irradiation during the period of tuber formation. The weight of root crops and sugar yield from sugar beets are increased by irradiation at the beginning of sugar accumulation. Irradiation seems to intensify the normal metabolic processes, which are determined by the growth condition. (TCO)

28968 SYNERGISTIC EFFECTS OF IONIZING RADIATION AND VIBRATION UPON THE ANIMAL ORGANISM. L'vova, T. S. Izv. Akad. Nauk SSSR, Ser. Biol., No. 3, 355-61(May-June 1966). (In Russian).

Exposure of mice to vibration of 70 cps frequency 4 and 24 hours prior to irradiation decreased their mortality by 10 to 20% and increased their average longevity by 10 to 40% as compared with control animals that were subjected to irradiation alone. Vibration applied 5 days prior to irradiation increased the mortality and decreased average longevity. Exposure to vibration 4 and 24 hours and 5 days after irradiation decreased the mortality of mice by 15 to 38% and increased the average longevity of test animals. Preliminary 1-hour exposure of animals to 700 cps vibration produced no noticeable modifying effect on the development and results of radiation damage. Vibration of 700 cps applied a day after irradiation exerted no effect while that applied 5 days after irradiation promoted radiation disease. (auth)

28969 ULTRAVIOLET MUTAGENESIS IN BACTERIOPHAGE T4. I. IRRADIATION OF EXTRACELLULAR PHAGE PARTICLES. Drake, John W. (Univ. of Illinois, Urbana). J. Bacteriol., 91: 1775-80(May 1966).

Ultraviolet-(uv) irradiation of extracellular T4 phage particles induces about 2×10^{-4} r mutations per lethal hit. The mutants largely escape detection unless the irradiated phages are plated with very soft overlay agar. Multiplicity reactivation is not a prerequisite for mutagenesis. A much higher frequency of base pair substitution-type mutants is induced than is found in the spontaneous background, but sign mutants are also induced. Nearly half of the mutants map into previously identified uv hot spots. The rII mutants induced extracellularly are very similar to those induced to those induced intracellularly. The mutants also appear to result from direct radiation effects upon the bacteriophage deoxyribonucleic acid. (auth)

28970 BIOLOGIC EFFECTS OF HUMAN RADIATION EXPOSURE. REPORT OF A CRITICALITY ACCIDENT. Fuqua, P. A.; Norwood, W. D.; Marks, S. J. Occup. Med., 7: 85-93(Mar. 1965).

The results of extensive clinical and laboratory studies conducted over a period of 2 years on 3 employees exposed to radiation in a criticality accident are presented. The estimated whole-body doses ranged from 19 to 123 rems of mixed gamma and neutron radiation. Evidence of temporary radiation effects was obtained only in the gonads and hematopoietic system. The gonadal effects consisted of impaired spermatogenesis and increased gonadotrophin excretion. Hematologic effects included transitory bone marrow damage, a mild decline in the lymphocyte count in 1 case, and the production of morphologically aberrant blood cells. A significant increase in chromosome aberrations in the circulating leukocytes occurred. No ocular damage or increase in the urinary excretion of amino acids was observed. (Pub. Health Abstr.)

28971 EFFECTS OF COSMIC FLIGHT IN SATELLITE VOSKHOD ON TRADESCANTIA PALUDOSA MICROSPORES. Delone, N. L.; Egorov, B. B.; Antipov, V. V. Kosm. Issled., 4: 156-61(Jan.-Feb. 1966). (In Russian).

Stems and flowers of Tradescantia paludosa were mixed in special containers on the satellite Voskhod. Fixation of pollens was carried out four times after landing: 2¼, 24, 48, and 120 hrs. In addition, the buds were fixed 1.5 hrs before landing. The sensitivity of the phases in microspores of Tradescantia paludosa to the action of cosmic-flight factors turned out to be varied. The analysis was carried out according to two criteria of sensitivity: reconstruction of the chromosomes and impairment of the mechanism of mitosis in the cells. (tr-auth)

28972 SIMULATION OF THE BIOLOGICAL EFFECTS OF THE DEPTH DOSE FROM A MONOENERGETIC FLUX OF PROTONS. Morozov, V. S.; Shashkov, V. S.; Davydov, B. I. Kosm. Issled., 4: 172-4(Jan.-Feb. 1966). (In Russian).

Experiments were carried out to determine the change of biological effectiveness of particles during their passage through tissue until stopping. Mice were placed in rows perpendicular to the axis of a monochromatic 120-Mev proton beam and were irradiated with a dose of 1600 rad at a dose rate of 50 rad/min. Half of the animals received an intraperitoneal injection of the radioprotective agent AET at a dose of 150 mg/kg 15 to 20 min before irradiation. The survival percentage after 5 and 30 days and the average duration of life of animals dying within 30 days were determined as functions of row, for both the injected and the control groups. The protective effect of AET was significant, except for the 3rd and 4th rows, corresponding to a tissue depth of 8 to 10 g/cm^2. (M.J.T.)

28973 EFFECTS OF β IRRADIATION OF SKIN ON CANCEROGENESIS CAUSED BY 7,12-DIMETHYLBENZ-α-ANTHRACENE. Turusov, V. S. (Inst. of Experimental and Clinical Oncology, Academy of Medical Sciences, USSR). Med. Radiol., 10: No. 12, 47-50(Dec. 1965). (In Russian).

In experiments on mice-hybrids ($C_{57} \times$ CBA F_1) it was shown that local irradiation of the skin performed directly before the application of a concentrated solution of dimethylbenzanthracene inhibited the restoration of tissular injuries and reduced the incidence of tumors caused by the chemical cancerogen. It was suggested that radioinduced inhibition of chemical carcinogenesis might be attributed to damage to epithelial proliferation and interrelationships with underlying tissues. (H.G.D.)

28974 CERTAIN BIOCHEMICAL INDICES IN INNERVATION DISTURBANCES OF THE MOTOR APPARATUS INDUCED BY IONIZING RADIATION. Sadchikova, E. N. (Inst. of Industrial Hygiene and Occupational Diseases, Moscow). Med. Radiol., 10: No. 12, 63-6(Dec. 1965). (In Russian).

A total of 73 people were subjected to clinical testing after being exposed to repeated external or internal doses of radiation. Group I contained 33 people who showed no changes in the functional state of the muscle. Group II contained 40 people who showed motor innervation changes. No change in aldolase content could be detected in either of these groups as compared to the controls. The content of creatinine in the blood serum and in the urine was normal for both groups. The creatinine content in the urine was 160 mg/day for Group II, 85 mg/day for Group I, and 60 mg/day for the controls. The aminotransferase content in Groups I and II also did not significantly exceed the normal value. The creatinuria observed in the irradiated people was thought to be a result of the suppression of the creatinkinase enzyme which catalyzes the transfer of phosphate in muscle from ATP to creatine. (TTT)

28975 DETERMINATION OF THE 17-KETOSTEROID AND OF THE 11-OXYCORTICOID IN THE IRRADIATED GUINEA PIG. Rava, G. (Ospedale Miulli, Acquaviva, Italy). Minerva Radiol., Fisioterap. Radiobiol., 10: 638-40(Dec. 1965). (In Italian).

A considerable increase of the 11-oxycorticoid and 17-ketosteroid excretion was observed from the first day in a group of guinea pigs x irradiated with a single 600 R dose on the adrenal region. This increase persisted from 4 to 10 days. It was followed by a rapid drop of the initial values in all animals except the values of the urinary output of the hormones, which remained high. The period in which the excretion of the hormones remained constant is thought to

represent the period of greatest reaction for the purpose of restoring a balance in the formation and excretion of steroid hormones. (tr-auth)

28976 CHANGES IN THE LYMPHOCYTES OF THE LATEROCERVICAL LYMPH NODES OF CAVIA COBAYA AFTER X IRRADIATION. AN ULTRASTRUCTURAL STUDY, WITH REFERENCE ESPECIALLY THE PARACENTRIOLAR REGION. Nicolato, A. (Univ., Pavia, Italy). Minerva Radiol., Fisioterap. Radiobiol., 11: 209-18(Apr. 1966). (In Italian).

A sub-microscopical investigation was made of the injuries caused by x-irradiation in the lymphocytes of guinea pig lymph nodes. The severe morphologic changes in the nucleus and in the components of the centrosomal area of the cytoplasm, especially the mitochondria and Golgi's structures, are described. The particular sensitivity to the effect of ionizing radiations of the part of the nucleus that faces the centrosome is stressed, and the hypothesis is suggested that substances capable of affecting the nucleus are set free by the injured mitochondria and Golgi's structures. (auth)

28977 INCREASE IN FREQUENCY OF ULTRAVIOLET-INDUCED MUTATION BROUGHT ABOUT BY THE COLICINE FACTOR, col I IN SALMONELLA TYPHIMURIUM. Howarth, Sheila (Univ. of Otago, Dunedin, New Zealand). Mutat. Res., 3: 129-34(Apr. 1966).

It was previously demonstrated that bacteria carrying the colicine I factor are more resistant to the lethal effect of uv radiation than non-colicinogenic strains. Results of experiments are described which show that the mutagenic effect of uv is increased in these colicinogenic bacteria, as measured by the frequency of reversion to prototrophy of auxotrophic mutants. (auth)

28978 EXPERIMENTAL STUDIES ON THE INFLUENCE OF HORMONES IN X-IRRADIATED ANIMALS, PART I. STUDIES ON THE INFLUENCE OF HORMONES AND OF REMOVAL OF ENDOCRINE GLANDS UPON SURVIVAL AND HEMATOLOGY IN X-IRRADIATED ANIMALS. Kawasaki, Sho (Kyoto Univ.). Naika Hokan, 12: 533-44 (Oct. 1965). (In Japanese).

The effects of various hormones on radiosensitivity and recovery from radiation injury in mice were studied. Mice were given various hormones before or after lethal doses of whole body x irradiation. Following irradiation, the survival time and change in body weight were measured. The survival time and blood counts were investigated in the Wistar Strain albino rats deprived of respective endocrine gland, followed by x irradiation with or without administration of the hormone. ACTH, given before or after, especially after x irradiation, increased the survival rate of the irradiated rats. Cortisone, given before or after x irradiation, shortened the survival time of the irradiated mice, whereas DOCA did not significantly modify the survival time of the irradiated mice. The adrenalectomized mice were more sensitive to x irradiation than normal mice. The decreased survival rate was improved, when the adrenalectomized mice were treated with cortisone after x irradiation. Thyroxine given prior to x irradiation protected significantly against x-ray lethality. When given after x irradiation, it was effective for recovery from radiation damage. Thyroidectomized rats were more sensitive to x irradiation than normal rats, so that their survival time was shortened. Replacement with thyroxine after x irradiation was ineffective in prolonging the survival time. Sex hormones had no protective effect against radiation injury, but were effective for recovery from radiation damage. These findings were confirmed by the decreased mortality and recovery of reduced body weight in the rats that were given the hormones after x irradiation. (auth)

28979 RADIATION CONTROL CONCENTRATION CHANGES OF FREE AMINO ACID IN THE BLOOD PLASMA OF MAN. Ladner, H. A.; Hahn, K. (Univ., Freiburg i. B.). Naturwissenschaften, 53: 226(1966). (In German).

The effects of radiotherapy on the concentration of free amino acids in blood plasma were studied in patients having gynecological tumors. To determine the radiation effects, free amino acids in normal women were also determined. The amino acids were measured 10 days after the beginning of the radiation treatment and at the end of the radiation series. The results showed that in the tumor patients there was a significantly lower amino acid concentration before the irradiations. At the end of the irradiation series, a decrease of the amino acid concentrations could be detected in the blood plasma. (J.S.R.)

28980 THE EFFECTS OF GAMMA (^{60}Co) IRRADIATION ON THE POLLEN GERMINATION OF PINUS DESIFLORA AND PINUS THUNBERGII. Fujimoto, Yoshiyuki; Watanabe, Misao; Anma, Yoshiteru (Shizuoka Prefecture Forrest Experimental Station, Hamakita, Japan). Nippon Ringaku Kaishi, 46: 389 94(Dec. 1964). (In Japanese).

In experiments carried out in May 1963 and April 1964, pollen samples of Japanese red and black pines were irradiated using a ^{60}Co source up to dosage levels of 150 kC under various conditions. Up to 75 kC no significant effects were observed on the pollen germinability; however, the growth of the pollen tube deteriorated with increasing dosage. Both the pollen germination and the growth of pollen tube decreased remarkably with doses up to 150 kr after being stored in a refrigerator at 5°C for 11 months. The germinability of pollen stored at room temperature was reduced after 11 months but pollen stored in a refrigerator at 5°C for 11 months showed vigorous germination. More remarkable responses were shown by pollen samples attached to the cut twigs than those shed from the twigs. The pollen tube length growth generally appeared to be more sensitive to γ irradiation than the percentage of pollen germination. (OID)

28981 ACUTE RADIATION EFFECTS: DAMAGE OF HEMATOPOIESIS. Haley, Thomas J. (Univ. of California, Los Angeles). pp 265-73 of Nuclear Hematology. Szirmai, E. (ed.). New York, Academic Press, 1965.

Investigations of the effects of acute whole-body exposure to ionizing radiations and the variation of sensitivity in animal species are reviewed. Changes in the cellular content of the peripheral blood depend upon the radiosensitivity of the precursor cells for any one cellular group, upon their ability to recover from the initial injury, and upon their life span or rate of utilization as mature cells. General effects of irradiation on leukocytes, lymphocytes, monocytes, granulocytes, erythrocytes, and thrombocytes are discussed and the total sequence of events involved in acute hematopoietic radiation death is tabulated. Regeneration of the hematopoietic system is dose dependent. When larger doses are counteracted by the administration of bone marrow, recovery usually occurs within 6 to 12 weeks. Because a number of drugs can produce the same type of hematopoietic injury as that associated with the radiation syndrome, film badge or ionization chamber dosimetry is more dependable than that derived from examination of hematological changes. (H.G.D.)

28982 TOTAL-BODY IRRADIATION INJURY: A REVIEW OF THE DISORDERS OF THE BLOOD AND HEMATOPOIETIC TISSUES AND THEIR THERAPY. Mathe, Georges (Hopital Paul Brousse, Villejuif, France). pp 275-338 of Nuclear Hematology. Szirmai, E. (ed.). New York, Academic Press, 1965.

Immediate consequences of blood or hematopoietic system irradiation are reviewed. Morphological, biochemical, and functional effects of acute external irradiations are described, and etiology and recovery from hematological and hematopoietic disturbances are considered. From results of studies of chronic external radiation effects, it is concluded that a threshold dose is required for a leukopenic effect. However, anemia and hematopoietic disorders may appear after chronic exposure to small doses. Internal irradiation of hematologic and hematopoietic tissues is usually characterized by a more gradual occurrence than of external exposure. Experimental results with ^{32}P, ^{89}Sr, ^{90}Sr, ^{198}Au, ^{140}Ba, ^{140}La, ^{91}Y, ^{131}I, ^{239}Pu, ^{210}Po, Ra, and ^{24}Na are cited. (H.G.D.)

28983 EFFECT OF IRRADIATION ON IMMUNITY. Mathe, G. (Hopital Paul Brousse, Villejuif, France).

pp 339-56 of Nuclear Hematology. Szirmai, E. (ed.). New York, Academic Press, 1965.

Fundamental concepts of immunity and effects of irradiation on immunity and para-immune defenses are reviewed. Practical applications of the effect of irradiation on immunity are considered with emphasis on the possibility of preconditioning the body with irradiation for the acceptance of a homograft. (H.G.D.)

28984 CHRONIC RADIATION EFFECTS: DAMAGE OF HEMATOPOIESIS. Betz, E. H. (Univ. of Liege). pp 357-77 of Nuclear Hematology. Szirmai, E. (ed.). New York, Academic Press, 1965.

The effects of radiation of hematopoiesis are discussed in view of the conditions under which irradiation is performed, since hematopoietic lesions produced by γ, x, or neutron irradiation do not appear to be qualitatively different. Effects of single dose, fractionated, and chronic irradiation on hematopoiesis are reviewed. (H.G.D.)

28985 EFFECTS OF RADIATIONS ON THE COAGULATION OF BLOOD. Iossifides, Ioulios A.; Geisler, Philip H. (Jefferson Medical Coll., Philadelphia). pp 379-442 of Nuclear Hematology. Szirmai, E. (ed.). New York, Academic Press, 1965.

Radioinduced alterations of blood coagulation patterns are reviewed. Major changes in the normal processes of blood coagulation are caused by penetrating energies such as γ or x rays or neutrons. Experimental evidence indicates that the fundamental response of the coagulation apparatus is basically similar in animals and humans. Radiation effects on the various components of the clotting mechanism are discussed. (H.G.D.)

28986 THE POSSIBILITY OF REVIVAL AND FEATURES PECULIAR TO THE DEVELOPMENT OF RADIATION SICKNESS IN MACACUS RHESUS IRRADIATED DURING AGONY AND CLINICAL DEATH. Lapin, B. A. (Inst. of Experimental Pathology and Therapy, Academy of Medical Sciences, Sukhumi, USSR); Negovskii, V. A.; Novikova, M. I.; Semenov, L. F.; Soboleva, V. I. Patol. Fiziol. Eksp. Terap., 10: 22-8(Jan.-Feb.). (In Russian).

A possibility of revival and peculiarities of radiation sickness were studied in Macacus rhesus irradiated during agony and clinical death caused by general desanguination. Gamma-ray irradiation of monkeys during agony and clinical death had no effect on the process of revival. Irradiation during clinical death lead to the development of radiation sickness in the revived animals. However, irradiation during the minimal vital activity (agony, clinical death) produced a weaker effect than in normal physiological conditions. (auth)

28987 STERILIZATION OF BONE TISSUES WITH THE HELP OF GAMMA RADIATION IN POLAND. Ostrowski, K. (Medical Academy, Warsaw); Aleksandrowicz, J.; Zarnowiecki, K.; Grzelewski, L. Postepy Tech. Jadrowej, 9: 466-8(1965). (In Polish).

Various methods of sterilization are described with emphasis on the use of the ^{60}Co γ radiation for the sterilization of bone tissues used for grafts. (TCO)

28988 INFLUENCE OF DEUTERATION ON CIRCULATING ANTIBODY LEVELS IN THE MOUSE. Siegel, Benjamin V.; Morton, Jane I. (Univ. of Oregon, Portland). Proc. Soc. Exp. Biol. Med., 122: 305-7(May 1966).

Depressed serum antibody levels were observed in mice drinking 30% D_2O continuously, starting 17 days before immunization with BSA in complete Freund's adjuvant. Adjuvant-induced increases in body weight were also diminished in these animals. Ten days pretreatment with heavy water did not, however, alter the response to BSA. In another group of mice pretreated with heavy water for 7 days, primary agglutinin levels to sheep red cells were normal in the continuously deuterated mice for the first 2 weeks following immunization, diminishing thereafter. The extent of heavy water pretreatment required suggests that mere equilibration of body fluids and exchangeable tissue hydrogens with 30% D_2O does not result in depressed antibody levels. Only after substantial deuterium was incorporated by synthesis into non-exchangeable sites were circulating antibody titers observed to be diminished. (auth)

28989 EFFECT OF FAST NEUTRONS ON DNA SYNTHESIS IN SEEDLINGS. Tokarskaya, V. I.; Kuzin, A. M. (Inst. of Biological Physics, Moscow). Radiobiologiya, 6: 3-8(1966). (In Russian).

Dry pea seeds were irradiated with fast neutrons at 1, 3, and 10 krad, and the absorption of ^{14}C in 4 to 7 day old seedlings grown from the irradiated seeds was studied. In seeds irradiated with fast neutrons at 1 to 10 krad, ^{14}C was found in 4 to 7 day old seedlings. Under neutron irradiation, the rate of DNA synthesis dropped 90% (compared with the control samples). Gamma irradiation of the seeds at the same dosage lowered DNA synthesis in the seedlings by 30%. Unlike gamma irradiation, neutron irradiation lowered high polymer DNA yield by 50% to 60%. It is concluded that under γ irradiation, the destruction of DNA is largely due to the damage to cytoplasm metabolism, while under neutron irradiation, the cells are damaged owing to the disruption of the adenine structure in DNA. The DNA synthesis rate as a function of dosage and kind of irradiation is graphed. (CFSTI)

28990 DOSE-RESPONSE RELATIONSHIP FOR EPITHELIAL CELLS OF SKIN. Withers, H. Rodney (Mount Vernon Hospital, Northwood, Eng.). Radiology, 86: 1110-11(June 1966).

A method was developed for cloning epithelial cells of mouse skin. The method was used to establish dose-survival curves and to study the kinetics of recovery at the cellular level in skin. The experiments were performed on the mouse back to simulate the situation in radiotherapy using 29 kvp or 150 kvp x radiation in doses from 900 to 2,300 rads under conditions of hyperboric oxygen and anoxia. Fractionation experiments were performed with 29 kvp. After an initial rapid recovery, attributed to intracellular repair, fluctuations in the recovery curve were observed for 18 to 24 hr, attributed to progression of a synchronized population of survivors through the division cycle, followed by a steady rise in recovery between 24 and 72 hrs post-radiation, attributed to cellular proliferation. (C.H.)

28991 RADIATION-INDUCED MUTATIONS AND THEIR REPAIR. Witkin, Evelyn M. (State Univ. of New York Downstate Medical Center, Brooklyn). Science, 152: 1345-53(June 3, 1966).

A discussion of how bacteria reduce the mutagenic effects of ultraviolet light by repairing DNA damage by the radiation is presented. (B.G.D.)

28992 CHANGES IN CHOLESTEROL LEVEL IN BLOOD FOLLOWING IRRADIATION. Bukhman, N. D. (Scientific Research Inst. for Radiation Protection, Leningrad). pp 263-9 of Trudy Vtoroi Nauchnoi Konferentsii po Voprosy Problema Zhira V Pitanii. Kadykov, B. I. (ed.). Leningrad, VNIIZh, 1962. (In Russian).

White rats were given an x ray dose of 100 r, and the cholesterol level in the blood was determined colorimetrically at 3 hrs and 1, 3, 5, 10, 15, and 20 days after the irradiation. The rats were maintained on a synthetic diet containing potato starch as carbohydrate, casein as protein, and refined sunflower oil as a source of fat. Various amounts of phosphatide concentrate obtained from the sunflower oil were also fed to the white rats (0.1, 1.5 and 2.0 g per kg of body weight). The cholesterol level in the rats given 0.1 g of phosphatide concentrate per kg of body weight varied from 130 to 200 mg % with an average value of 172 mg %. The average dropped to 130 mg % 3 hours after irradiation, and remained at 109 to 130 mg % up to the 15th day after the irradiation. Then the cholesterol level returned to its initial level on the 20th day after irradiation. The behavior of the cholesterol level was similar in white rats who obtained 1.5 and 3.0 g of phosphatide concentrate per kg of body weight. The rats given no phosphatide concentrate showed an incomplete recovery in the blood cholesterol level 20 days after irradiation with an average value of only 148 mg %. These studies showed that a dose of 100 R could disturb the lipid exchange in the body, and that

phosphatide had a tendency to restore the lipid metabolism to normalcy. (TTT)

28993 THE INFLUENCE OF A VARIABLE FAT CONTENT DIET ON THE COURSE OF RADIATION SICKNESS. Nesterin, M. F. (Inst. of Dietetics, Academy of Medical Sciences, Moscow). pp 270-4 of Trudy Vtoroi Nauchnoi Konferentsii po Voprosy Problema Zhira V Pitanii. Kadykov, B. I. (ed.). Leningrad, VNIIZh, 1962. (In Russian).

A study was made of the effect of a diet containing different amounts of unsaturated fatty acids on the state of the secretory function of the intestine in dogs irradiated with x rays. The dogs were maintained on a diet which contained 30% fat according to the calorie count. The fat given to the dogs was in the form of beef fat, sunflower oil, or linoleic acid, and as a concentrate containing about 8% arachidic acid (a fatty acid containing four double bonds). The dogs were given an x ray dose of 400 R. The clinical picture showed that the general state was more satisfactory and recovery was faster in dogs fed the arachidic acid concentrate as the source of fat in the diet. These dogs also showed a smaller and more constant secretory flow in the intestine after irradiation. All the irradiated animals showed the presence of blood in the intestinal secretion, but the amount of blood was the least in the animals fed the arachidic acid concentrate. The content of enterokinase in the intestinal juice was clearly higher in dogs fed with the arachidic acid concentrate. It is noted that 3 out of 7 dogs on the beef diet perished, while none of the four dogs on the arachidic acid ration died. Highly unsaturated fats seemed to increase the resistance of the organism to radiation sickness. (TTT)

28994 THE INFLUENCE OF A CHEMICAL UPTAKE OF RADIOACTIVE SUBSTANCES ON THE LIPID AND CHOLESTEROL LEVELS IN BLOOD. Zapol'skaya, N. A.; Fedorova, A. V. (Scientific Research Inst. of Radiation Protection, Leningrad). pp 275-82 of Trudy Vtoroi Nauchnoi Konferentsii po Voprosy Problema Zhira V Pitanii. Kadykov, B. I. (ed.). Leningrad, VNIIZh, 1962. (In Russian).

A total of 3×10^{-3} microcuries of ^{90}Sr per rat was administered daily via the gastrointestinal tract. The concentrations of total lipids, neutral fat, and cholesterol in the blood were determined before innoculation with ^{90}Sr and at various periods after innoculation. The cholesterol level reached a minimum of 45.8% of the control value on the 20th day after innoculation, and then rose gradually until it approached the initial value on the 60th day after innoculation. The total lipid content attained a minimum of 65.2% of the controls on the 5th day, and then increased gradually to its original value on the 60th day after innoculation. The neutral fat content decreased to 70.1% of the controls, and regained its initial value on the 20th day after innoculation. The total dose accumulated over 60 days was calculated to be 9.5 rads. The observations were repeated on administering 8×10^{-3} and 2×10^{-4} microcuries of ^{90}Sr per rat. The results showed a decrease in blood cholesterol level to 42% of the controls on the 10th day after innoculation with 8×10^{-3} microcuries of ^{90}Sr. Then the cholesterol level increased, but did not regain its original value 3 months after innoculation. The accumulated dose was 10 rads over the 3 month period. The lipoid phosphorous content showed an increase. The observations were again carried out with the use of radioactive glucose tagged with ^{14}C. A similar behavior was observed on replacing 0.003 microcuries of ^{90}Sr by 1.0 microcuries of ^{14}C. The cholesterol content dropped, and the lipoid phosphorous content increased. (TTT)

28995 THE INFLUENCE OF VARIOUS DIETS AND X RADIATION ON THE CHOLESTEROL LEVEL IN TISSUES. Sherman, L. G. (Scientific Research Inst. of Radiation Protection, Leningrad). pp 283-90 of Trudy Vtoroi Nauchnoi Konferentsii po Voprosy Problema Zhira V Pitanii. Kadykov, B. I. (ed.). Leningrad, VNIIZh, 1962. (In Russian).

Groups of rats were given an x ray dose of 100 R, and the cholesterol content in various tissues were determined 3 hours, 72 hours, 7 days and 14 days after the irradiation. Three hours after the irradiation the cholesterol content decreased by 41% in the liver and by 66% in the pancreas. At 72 hours after irradiation the cholesterol content had decreased by 56% in the liver, by 44% in the testicles, and by 79.6% in the adrenals. The cholesterol level increased somewhat in the lungs, aorta, and heart muscle. Most of the cholesterol values tended to return to normal 14 days after the irradiation. Significant reductions in the cholesterol content of the liver, pancreas, heart, intestines, lungs, aorta, kidneys, spleen, testicles, blood, and brain tissues were observed in irradiated rats which were on a diet including cocoanut oil, cocoanut oil + 5% cholesterol, or refined sunflower oil + 5% cholesterol. It was not clear why the decreases in cholesterol level in various tissues were different. The highest concentration of cholesterol in the controls was found in the adrenal glands which apparently are a cholesterol depot. (TTT)

28996 ON THE PROBLEM OF EXPERIMENTAL ARTERIOSCLEROSIS IN WHITE RATS EXPOSED TO WHOLEBODY X IRRADIATION. Lavrent'ev, L. N. (Scientific Research Inst. of Radiation Protection, Leningrad). pp 291-8 of Trudy Vtoroi Nauchnoi Konferentsii po Voprosy Problema Zhira V Pitanii. Kadykov, B. I. (ed.). (In Russian).

Groups of white male rats which were maintained on three different diets were given an x ray dose of 103.7 R. Diet I consisted of 18% casein, 30% cocoanut oil, 52% starch according to calorie count, a salt mixture, yeasts, and vitamins A and D. Diet II had the same composition with 5% cholesterol added to the cocoanut oil. Diet III contained sunflower oil + 5% cholesterol instead of the cocoanut oil. The unirradiated rats on diet I showed a weight increase of 136 g in the first six months, and 41 g in the second six months. With diet II the weight increases were 123 and 63 g for the first and second six month periods respectively. With diet III the weight increases were 110 g and 17 g respectively. The irradiated rats on diets I and II showed no weight increases in the second six month period. The weight increase was slight with diet III. A histological study showed no pathological changes in rats on diet I. On the other hand, unirradiated rats on diets II and III showed a thickening of the aortic wall due to lipid deposition. Atherosclerotic changes were observed in the aorta. Massive lipid plates were deposited between the outer and middle shells of the aorta. Lipid deposition was observed in large blood vessels of internal organs. Atherosclerotic changes were observed in irradiated rats kept on diets II and III, but more intensive resorption of lipids by macrophages was frequently observed. Neutral fats, cholesterol, and fatty acids in the form of small drops were found in the lipid deposits. (TTT)

28997 AUTORADIOGRAPHIC STUDY OF THYMUS GLAND IN ACUTE IRRADIATION SICKNESS AFTER ADMINISTRATION OF ^{35}S-LABELLED METHIONINE. Khussar, Yu. Uch. Zap. Tartusk. Gos. Univ., No. 134, 224-31 (1963). (In Russian).

The intensity and dynamics of metabolism of sulphur-containing proteins (with the help of ^{35}S-labeled methionine) were studied in the thymus of 46 adult albino rats suffering from accute irradiation sickness. Total single exposure to x ray at doses of 800 R was used. The intensity of metabolism in the cortical substance fell to its minimum within 1 to 4 days following irradiation. At the same time the maximum destruction of lymphocytes was observed. On the 21th day after irradiation the metabolic level approached the initial value. The changes in medullar substance and connective tissue of the organ were less significant. (tr-auth)

28998 CHOLESTEROL PROTEIN BLOOD COMPLEXES OF DOGS IN RADIATION INJURY. Polosukhina, T. I.; Alshanova, T. M. (Alma-Ata State Medical Inst., USSR). Ukr. Biokhim. Zh., 38: 3-8(1966). (In Russian).

The effects of a single total radiation of the head of a dog with x rays in doses of 1000 Roentgen units upon the cholesterol protein complexes of blood of the experimental animal were studied. It was found that even 24 hours after irradiation there was an increase in cholesterol

content bound with protein in the serum of the arterial blood of the dog. The source of cholesterol is to a great extent the intestine itself. In contrast to the normal animals the liver of the experimental animals retained cholesterol protein complexes from the blood coming into it. (auth)

28999 INFLUENCE OF GAMMA-RAYS ON THE CONTENT OF VARIOUS FORMS OF ASCORBIC ACID AND REDUCED GLUTATHIONE IN COTTON PLANTS. Nazirov, N. N. Uzb. Biol. Zh., 9: No. 1, 5-10(1965). (In Russian).

The rapidly maturing relatively radioresistant variety, 1306-DB, and the later maturing radiosensitive variety, C-1622, were studied. The dry seeds and shoots of 1306-DB contained considerably more ascorbic acid, but later on the content was reduced, while the content of reduced glutathione grew proportionally. In the 1st days of germination, the cotyledonous leaves of the cotton plant were richer than the rootlets in ascorbic acid and relatively poor in glutathione. This difference subsequently disappeared. The maximum quantity of ascorbic acid was observed during the initial periods of life of the plant, and then gradually decreased, and did so faster and more smoothly in 1306-DB. Irradiation of air-dried seeds with γ rays (10 kR) led to a decrease in free ascorbic acid in C-1622, while the bound ascorbic acid was increased and total ascorbic acid remained unchanged. In 1306-DB, the content of both forms of ascorbic acid decreased. Immediately after irradiation (10 kR) of germinating seeds of 1306-DB ascorbic acid decreased and reduced glutathione increased. These changes were reversible. (C.H.)

29000 EFFECT OF STRONTIUM ON THE FUNCTIONAL STATE OF THE THYROID GLAND IN DOGS. Yusupov, A. A. Uzb. Biol. Zh., 9: No. 2, 5-8(1965). (In Russian).

Seven male dogs were administered 1 μC of ^{90}Sr or an equivalent amount of ^{90}Y orally. The 7 treated dogs and 3 controls were then injected subcutaneously with 1 μC of ^{131}I. During the first 6 to 8 days after the injection no differences were apparent, but several days later the treated dogs developed leukocytosis followed by leukopenia. Symptoms of radiation sickness appeared in 20 days, and two dogs died after 29 days. Maximum ^{131}I uptake appeared 8 hours after injection in the Sr-treated dogs and 24 hours after injection in the controls. Histological examinations revealed smaller thyroids of solid consistency and enlarged follicles with thick colloid surrounded by low epithelial cells in the Sr-treated dogs. (D.E.B.)

29001 THERMAL AND ANAPHYLACTOID EDEMA IN ACUTE RADIATION SICKNESS. Dorofeev, V. M.; Polushkin, B. V.; Tsyran, N. I. (Inst. of Medical Radiology, Obninsk, SSSR). Vestn. Akad. Med. Nauk SSSR, 20: No. 9, 78-83(1965). (In Russian).

The paws of rats were scalded in 55°C water for 20 seconds 2, 4, and 8 days after the rats had been exposed to 680- and 750-R of gamma radiation from a ^{60}Co source at 77 R/sec. The extent of edema and serotonin content of blood were followed. Analyses and comparisons were then made of the effects of preliminary administrations of iprazid, 5-hydroxytryptophan, indopan, or secrotonin on edema and blood serotonin in healthy rats and rats with acute radiation sickness. (TCO)

29002 MUTAGENIC EFFICIENCY OF INTERMEDIATE NEUTRONS. Troitskii, N. A.; Bylinskii, A. F.; Filippovich, A. S. Vestsi Akad. Navuk BSSR, Ser. Biyal. Navuk, No. 4, 124-6(1965). (In Russian).

The efficiency of fractionated doses of intermediate neutrons with mean energy of 200 kev with respect to chromosome breakage and phage induction exceeds that of reversion formation. The RBE was determined to be: for intermediate neutrons for ~100 for chromosome breaks in onion; ~0.6 for reversions in E. coli K-12; and ~45 for prophage induction in E. coli K-12. (tr-auth)

29003 EFFECT OF X-IRRADIATION ON THIAMINE PHOSPHORYLATION. Savitskii, I. V.; Rozanov, A. Ya., Pozdnyakova, L. E. Vop. Med. Khim., 8: 592-8(Nov.-Dec. 1962). (In Russian).

A decreased ability of x irradiated animals to utilize thiamine is evidenced by diminished accumulation of injected thiamine-^{35}S in liver and thin guts of white mice. The phosphorylation of injected thiamine was inhibited, as shown by a decrease in phosphate esters accumulation in liver and guts, of irradiated mice after thiamine-^{35}S injection. (tr-auth)

29004 HEAT RESISTANCE OF RABBIT BLOOD SERUM IN CONTINUOUS AND DISCONTINUOUS ULTRAVIOLET RADIATION. Krivova, A. A.; Madievskii, Yu. M. (State Medical School, Kharkov). Vop. Med. Khim., 9: 463-9(Sept.-Oct. 1963). (In Russian).

The dynamics of alterations in rabbit total blood plasma proteins, estimated by the time of their heat coagulation, in continuous and discontinuous ultraviolet radiation was studied. Blood serum proteins content shows phasic alterations within 10 per cent from the initial protein level. Heat resistance in impulse radiation depends on doses and interruption duration. Heat resistance effects in interruptions from 1 to 30 seconds have a phasic character and proved to be lower, while in 120 seconds interruptions the effect was more distinct as compared with the influence of the same dose of continuous radiation. (tr-auth)

29005 METABOLISM OF EXOGENOUS ACTH IN NORMAL AND IRRADIATED RATS. Bagramyan, E. R. (All-Union Inst. of Experimental Endocrinology, Moscow). Vop. Med. Khim., 10: 265-9(May-June 1964). (In Russian).

The quantity of ACTH in blood was determined by its ability to lower the concentration of ascorbic acid in adrenals of hypophisectomized rats. It was found that the ACTH injected into irradiated rats disappears from the blood with the same velocity as from the blood of normal animals. Complete disappearance of ACTH was observed within 45 minutes. Similarity in the rate of disappearance of exogenous ACTH from the blood of both normal and irradiated animals shows that there is no significant difference in the metabolism of ACTH in irradiated animals as compared with normal. (tr-auth)

29006 SECONDARY DISEASE IN IRRADIATED ANIMALS TREATED WITH BONE MARROW. Tumanyan, M. A.; Izvekova, A. V. (Inst. of Epidemiology and Microbiology, Academy of Medical Sciences, USSR). Zh. Mikrobiol. Epidemiol. Immunobiol., No. 10, 76-80(Oct. 1965).

Mice irradiated with lethal doses of gamma rays and treated with homologous bone marrow developed a secondary disease. Use of the method of passive anaphylaxis revealed that the disease arose from an unusual immunological situation, the simultaneous occurrence of two conflicting reactions, host against transplant and transplant against host. The symptoms of the secondary disease, especially the morphological changes in the liver and other organs, are similar to the changes characteristic of anaphylactic shock. These changes plus the increased sensitivity to infection suggest that the secondary disease and anaphylactic reaction have a common mechanism of action. (CFSTI)

29007 THE EFFECT OF IONIZING RADIATION ON NUCLEAR REORGANIZATION PROCESSES IN PARAMAECIUM PUTRINUM. I. NUCLEAR PROCESSES IN IRRADIATED CONJUGANTS. Kovaleva, N. E.; Yankovskii, A. V. (Inst. of Cytology, Leningrad). Zh. Obshch. Biol., 26: 176-89(Mar.-Apr. 1965). (In Russian).

A method is presented for comparing nuclear reorganization during conjugation in Paramaecium putrinum under normal conditions and after x irradition (75kR). The nonlethal exposure was usually during late prophase of the first progamic division of the micronucleus, but in some cases radiation treatment was administered in the early prophase. In all stages of progamic divisions of the micronucleus the chromosomes show a tendency to fuse into dense clots. The spindles are like elongated ribbons wound into spirals, particularly in the first progamic division of the micronucleus. The number of nuclei emerging from the second and third progamic divisions of the micronucleus varies greatly. A varying number of nuclei participate in the formation of the syncaryon, and fusion is more incom-

plete than complete. Only rarely does the syncaryon proceed to postzygotic division; in exconjugants the syncaryon usually does not synthesize RNA and does not divide during cell division. A new viable macronucleus may develop from fragments of the old macronucleus which increase their ploidy in the exconjugants. (CFSTI)

29008 RADIATION INJURY OF THE THYMUS IN MICE, AND METHODS OF EVALUATING IT. Rass, I. T. (Inst. of Animal Morphology, Moscow). Zh. Obshch. Biol., 26: 224-9(Mar.-Apr. 1965). (In Russian).

Two widely used morphological criteria for evaluating radiation injury after various doses of radiation are presented: the number of cells stained with eosin in a drop of a cell suspension; and the number of cells with pycnotic nuclei in a smear. Both criteria allow observation of radiation injury of thymocytes after only 50 R. As the dose is increased to 200 R, the number of stained cells and the number of cells with pycnotic nuclei both increase. At doses of 50 to 100 R the percentage of stained cells is higher than the percentage of pycnoses, but beginning with 200 R, it is lower. With a further increase in the dose to 2,000 to 4,000 R, the number of stained and pycnotic cells does not increase; about 35% of all the cells are stained with eosin and about 70% are pycnotic. Supravital staining, then, does not reveal all the cells injured by radiation and can result in mistaken conclusions. Counting cells with pycnotic nuclei therefore appears a more accurate method of evaluating radiation injury in cells of the thymus. (CFSTI)

29009 CHANGES IN THE CONDITIONED REFLEX ACTIVITY OF DOGS UNDER THE INFLUENCE OF SMALL DOSES OF RADIOACTIVE ^{24}Na FOLLOWING PRELIMINARY ADMINISTRATION OF ALCOHOL. Shal'nev, B. I. (Sechenov Medical Inst., Moscow). Zh. Vysshei Nerv. Deyatel'nosti im. I. P. Pavlova, 15: 445-52(1965). (In Russian).

Male dogs were investigated by the method of motor-conditioned reflexes with food enforcement and freedom of movement in a chamber. Three types of nervous activity were established: balanced (A), impulsive (B), and weak (C). One group was given ^{24}Na in sausage meat with $NaHCO_3$ (3 times at monthly intervals and twice at a 2-week interval). A second group consisted of 3 type A; one, the control, received 30 ml of 96% EtOH with 150 ml milk; 2 dogs received the same amount of alcohol 20 min prior to internal irradiation with 5 μC/kg. In 40 days, the experiment was repeated. Functional neural disturbances were observed in all of group-1 with 0.26 to 0.38 rad energy uptake. The C type revealed damages of both differentiations and positive reflexes for an extended period, the B type (with impairment of a single differentiation) exhibited slight changes, and the A type exhibited changes of short duration with disinhibition of one differentiation and preservation of the other. The most characteristic change was demonstrated in weakening of the internal inhibition process. Frequent disinhibition of the differentiations and weakening of the inhibition ability were noted, especially in type C. This impairment occurred 2 to 3 days after ^{24}Na administration and lasted for 12 to 25 days. The control (group 2), exhibited only temporary (1–2 days) weakening of the internal inhibition, demonstrated in partial disinhibition of the differentiation followed by distinct inhibitory systems. Group-2 irradiated without EtOH, revealed only slight changes in the reflexes in response to weak stimuli and preserved the differentiation. The part (with EtOH) soon revealed a parabiotic state in the cerebral cortex detected in the loss of the individual conditioned reflexes, impairment of the internal inhibition process, and the appearance of the paradoxical and ultraparadoxical phases. These impairments appeared to be caused by the latent EtOH action in combination with the ionization effect on the brain. The indicated ^{24}Na action was not sufficient to produce similar changes alone. (C.H.)

29010 INFLUENCE OF IONIZING RADIATION ON THE LIVER BLOOD CIRCULATION OF RABBITS. Zwanzger, G. Munich, Univ., 1964. 43p. $2.00 Gmelin, AED-Diss. 64-1049.

Blood circulation in rabbit liver was determined from ^{198}Au clearance of the plasma. Clearance was increased significantly after irradiation of the head-neck area with 850 R x radiation. No increase was found after whole-body irradiation with the same dose. (Gmelin Inst.)

29011 SURVIVAL TIMES OF RABBITS AFTER IRRADIATION OF THE LEFT UPPER BRAIN HEMISPHERE. Gernhardt, C. Munich, Univ., 1964. 22p. $2.00 Gmelin, AED-Diss. 64-1048.

The upper brains of 7 rabbits were x irradiated with 37 to 70 kR. Survival times are given. Sensitivity to sound and light was studied. Bioelectrical activity before death was determined. (Gmelin Inst.)

29012 HISTOPATHOLOGICAL EFFECTS AFTER X IRRADIATION OF DEVELOPING CHICK EMBRYOS. STATISTICAL ANALYSIS. Onken, K. O. Heidelberg, Univ., 1965. 123p. $2.00 Gmelin, AED-Diss. 65-278.

Chick embryos were x irradiated with doses of from 20 to 2000 R. Mortality rates as a function of dose and development time are given. The occurrence of malformations was also studied. (Gmelin Inst.)

29013 MORPHOLOGY OF BOVINE EPIDIDYMAL SPERMATOZOA AFTER X-IRRADIATION OF TESTES [Thesis]. Gillette, Edward LeRoy. Fort Collins, Colo., Colorado State Univ., 1965. 111p.

Two-year-old Hereford bulls were used for a study of morphology of epididymal sperm before and during a period of 12 to 133 days following testicular exposure to 800 R of 70-kev x rays. Smears of spermatozoa from 6 areas of the head of the epididymis, 3 areas of the body, and 3 areas of the tail of the epididymis were examined. In some cases, spermatozoa of the lower vas deferens and the ampulla were examined. Tissues from these same areas were also examined histologically. Following irradiation, all degrees and types of defective spermatozoa were seen throughout the epididymis. These were generally the same types observed prior to irradiation and were increased in number after irradiation. The distribution of the various types within the epididymis was approximately the same before and after irradiation with the exception of spermatozoa with abnormal heads. The proximal droplets moved to a more distal position or were lost completely by the time the spermatozoa progressed through the head of the epididymis. The distal droplets were nearly all removed by the time the spermatozoa passed through the tail of the epididymis. Tail and middle piece abnormalities occurred in highest numbers in the body and tail of the epididymis. When abnormalities of heads of spermatozoa increased following irradiation there were always fewer numbers in the tail of the epididymis than in the head. The histologic appearance corresponded to an earlier description of the histology of the bovine epididymis. Macrophages were not numerous even during times when great numbers of abnormal spermatozoa were present in the lumen of the epididymis. These did not appear to be present in sufficient numbers to account for the degree of cell removal indicated by the decrease in numbers of spermatozoa with abnormal heads observed to take place with passage of spermatozoa through the body and tail of the epididymis. (Dissertation Abstr.)

29014 RECOVERY OF THYMECTOMIZED CHICKENS FROM INDUCED IMMUNOLOGICAL UNRESPONSIVENESS [Thesis]. Chaperon, Edward Alfred. Madison, Wis., Univ. of Wisconsin, 1965. 73p.

It was postulated that development of immunologically competent cells in the bursa may be somehow thymus-dependent. The method used to test this hypothesis involved the destruction or functional inhibition of immunologically competent cells in conjuction with surgical removal of the thymus. This was done specifically by injecting large doses of antigen into young chickens, thereby inducing a state of tolerance to that antigen, or non-specifically with sublethal doses of total-body x ray. In both cases, if bursal function or regeneration by bursal-

derived tissue is thymus-dependent, thymectomized birds would be expected to require longer to recover immune competence, as measured by precipitin response to soluble protein antigens and rejection of skin homografts, than their respective controls. The results show that thymectomy in young chickens augments the effect of a large dose of bovine serum albumin in causing decreased responsiveness to this antigen. Animals so treated showed a lower precipitin response than unoperated massively injected birds when challenged at six weeks, or failed to recover immune competence at twelve weeks as indicated by a delayed antigen clearance, longer induction period, and lower mean peak titer. Total-body irradiation in adult chickens resulted in virtual elimination of the precipitin response for at least one week, with almost complete recovery by fourteen weeks following irradiation. This recovery was found to be eliminated or significantly delayed in neonatally thymectomized chickens irradiated as adults. However, these birds were able to reject skin homografts. The findings indicate that the thymus plays a significant part in the development of the immune system in chickens. (TCO)

29015 PHYSIOLOGICAL RESPONSES AND IMPLICATIONS OF THEIR GENETIC TRANSMISSION AFTER EMBRYONIC X IRRADIATION OF THE DOMESTIC FOWL [Thesis]. Muller, Harry Dierks. Fort Collins, Colo., Colorado State Univ., 1965. 103p.

Sensitivity of the avian embryo to x irradiation fluctuated during development, decreasing from initiation of development through day 12, increasing from day 13 to day 18, and decreasing again through day 21. Morphological modifications were evident in embryos that succumbed to the irradiation insult. Post-hatching body weights of irradiation survivors were significantly lighter than those of controls. Depression in growth rate was partially dependent on embryo age at exposure. Female survivors of embryonic irradiation exposure demonstrated depressed levels of ovulation rate. Male survivors of embryonic irradiation failed to demonstrate any depression in fertilizing capacity, testes weights, seminiferous tubule development, or sperm quality. Artificial mating of survivor individuals produced progeny at levels comparable to those demonstrated by control matings. Body weights, growth patterns, and reproductive potentials of progeny of survivors are discussed. (TCO)

29016 SIGNIFICANCE OF PIGMENTS IN RADIATION RESISTANCE OF MICROCOCCUS RADIODURANS [Thesis]. Krabbenhoft, Kenneth Louis. Corvallis, Oreg., Oregon State Univ., 1965. 130p.

Microorganisms resembling M. radiodurans were isolated from ground beef and pork sausage as well as from beef hides and water from Cox Creek (Albany, Oregon). The presence of NZ-Case (a tryptic digest of casein) in the isolation medium produced more luxuriant growth than TGYM medium but the radiation sensitivity of M. radiodurans increased ten-fold in the former medium and the degree of pigmentation was less. Subsequent studies using thin-layer chromatography indicated that the less resistant strain was lacking two of the eight pigments present in the more resistant culture. The degree of resistance was inversely related to the concentration of NZ-Case in the growth medium at all of the levels tested. At the highest level of NZ-Case used (0.5 percent), the LD_{30} dose was 350 krads as compared to 700 krads when TGYM was the growth medium. The resistance to ultraviolet radiation was also reduced. Removal of NZ-Case from the growth medium resulted in a return of the high level of resistance and the reappearance of the missing pigments. A possible role of the pigments in the radiation resistance of this organism was thus suggested and described. In this role the pigments would serve as scavengers of toxic ions and radicals produced by radiation and thus protect the functionally important lipids and lipoproteins of the cell membranes from being altered with resultant release of cellular enzymes. Spectral analysis of the eight pigments indicated that they were all closely related and were tentatively identified as lycopene, hydroxy lycopene, or dihydroxy lycopene. None of the pigments absorbed in the ultraviolet range. Pigments obtained from cells grown in NZ broth had the same spectral characteristics but were present in reduced concentrations. (Dissertation Abstr.)

29017 NATURAL RESISTANCE MECHANISMS TO NEOPLASTIC DISEASES IN MICE [Thesis]. Oshiro, Lyndon Satoru. Salt Lake City, Univ. of Utah, 1963. 124p.

The hypothesis has been established that in a system involving white mice (albino Mus musculus) and Ehrlich ascites tumor (EAT) a mechanism of normal resistance exists against the establishment of the neoplasm. The degree of resistance can be significantly increased by intravenous (iv) immunization with a sublethal dose of viable tumor cells. The role played by living cells in the induction of increased resistance was investigated. Whole-body x irradiation at varying intervals after iv injection with EAT cells did not result in increased incidence of lung tumors in mice. The experimental results obtained did not support the hypothesis that dormant tumor cells mediate some mechanism by which living cells induce increased resistance to subsequent tumor challenge. Indirect evidence for the existence of cellular defenses in natural resistance was exhibited by x-irradiated animals. Whole-body irradiation (300 R) of normal mice 4 days prior to intraperitoneal or subcutaneous challenge with EAT cells resulted in depressed resistance compared to nonirradiated animals. Irradiation of immunized mice, to the same extent as normal mice, did not depress resistance to challenge with EAT cells, indicating the role of humoral defenses in induced resistance. The effects of factors other than radiation on the viability of tumor cells and the resistance of mice to the cells are also discussed. (TCO)

29018 THE INDUCTION OF EXTRAMUTATIVE RADIATION EFFECTS ON PERICLINAL CHIMERAS WITH KNOWN CONSTITUTION OF PELARGONIUM ZONALE AIT., EUPHORBIA PULCHERRIMA WILLD., AND ABUTILON HYBRIDUM HORT. Poetsch, J. Potsdam, Paedagogische Hochschule, 1964. 214p. $2.00 Gmelin, AED-Diss. 64-1053.

The LD_{50} of Pelargonium zonale and Abutilon hybridum for single and fractionated 80-kv x irradiations were determined. Several x-ray effects, such as growth stimulation and depression, coloration, and branching were studied. Properties of varieties produced by somatic mutations are described. (143 references.) (Gmelin Inst.)

29019 EXPERIMENTAL STUDIES WITH ANIMALS ON GERM INJURY WITH IONIZING RADIATION. Kreft, R. Muenster, Ger., Univ., 1965. 36p. $2.00 Gmelin, AED-Diss. 65-267.

The gonads and germ cells of 33 rabbits were x irradiated with 100 R. No significant effects were observed. (Gmelin Inst.)

29020 UL'TRAFIOLETOVOE OBLUCHENIE ZHIVOTNYKH. (Irradiation of Animals with Ultraviolet Rays). Melyukov, A. N. Moscow, Izdatel'stvo Kolos, 1964. 192p.

The reduction of ultraviolet radiation during the fall and winter months affects the well-being and productivity of domestic animals, leading toward the development of D-avitaminosis. The low quality of hay, silage, and other winter fodder contributes to this effect. Exposure to uv radiation was found to be generally beneficial, improving the metabolic processes, stimulating the glands of internal secretion, increasing the immunological resistance, and causing an overall improvement in the health and work performance of the animals. The biological effects of uv radiation are reviewed in detail, describing the advantages of various artificial sources, such as mercury-quartz, mercury-tungsten lamps, fluorescent tubes, etc. Determination of the effective dose for various domestic animals is discussed, reviewing the results of large-scale tests and drawing practical conclusions for animal husbandry. The importance of this type of irradiation for the veterinary medicine is also mentioned. The economic importance of the irradiation method is illustrated on detailed numerical examples. Safety problems and industrial hygiene considerations are also pointed out. (TTT)

29021 EFFECTS OF X RAYS ON EXCITATION CONDUCTION OF NERVES OF COLD BLOODED ANIMALS. Zimmermann, M. Karlsruhe, Ger., Technische Hochschule, 1965. 73p. $2.00 Gmelin, AED-Diss. 65-256.

The action potentials of x irradiated nerves were measured. In order to obtain reproducible results the distance between the irradiated zone and the electrodes was at least 15 mm. Dose-effect curves are explained by the safety factor of excitation conduction and its biological variability. (Gmelin Inst.)

29022 THOROTRAST TUMORS. QUANTITATIVE STUDIES OF THE DOSE-EFFECT PROBLEM AND OF THE INFLUENCE OF SPLENECTOMY ON THOROTRASTOSIS. Wenz, W. Heidelberg, Univ., 1963. 190p. $2.00 Gmelin, AED-Diss. 63-818.

Data on 76 malignant tumors produced by thorotrast in 300 rats given 25 to 1000 mg ThO_2 are analyzed. Results indicate that deposition in organs depends on quantity. Small quantities are resorped in the spleen, larger quantities in liver and bone marrow. Time delay between injection and tumor incidence is 1.5 to 2.5 years. Survival times of rats with splenectomy before injection are reduced. (Gmelin Inst.)

29023 RADIOPROTECTION OF SACCHAROMYCES CEREVISIAE BY CYSTAMINE [Thesis]. Stuart, Bruce Owen. Rochester, N. Y., Univ. of Rochester, 1962. 262p.

Aqueous suspensions of Saccharomyces cerevisiae were exposed to x-ray doses of 0 to 80 kiloroentgens, in the presence or absence of 1×10^{-2}M cystamine. These irradiations were performed under conditions of oxygen or nitrogen saturation, with the suspending media at either pH 6.5 or pH 4.0. It was found that radiation damage to the cell membrane, as evidenced by increased rates of potassium leakage, was greatly reduced by the presence of cystamine during irradiation in oxygen. Cells irradiated in nitrogen without cystamine showed a much smaller degree of increased potassium leakage, but there also seemed to be some slight additional protection in this gas by cystamine. Yeast irradiated without cystamine in oxygen at pH 4.0 showed leakage rates much higher than those of yeast in suspension at pH 6.5; no pH effect was observed in the degree of protection offered by cystamine. There was very little increased methylene blue staining of cells after irradiation at these doses, indicating that membrane damage resulting in increased potassium leakage was fairly specific. Displacement of a large percentage of surface bound cystamine from the cells by competing cations (Mn^{++} and Ca^{++}), showed no change in the degree of protection, suggesting that the mechanism of radiation protection may be a radical scavenging action of cystamine in the extracellular media. Cystamine did not show a protective effect towards the ability of irradiated yeast to form visible colonies perhaps because of a lack of penetration of the compound into the cell in sufficient amounts to protect cell growth mechanisms. (Dissertation Abstr.)

29024 METABOLISM OF PROTECTANT DOSES OF L-CYSTEINE BY RAT AND GUINEA PIG WITH REFERENCE TO POST-IRRADIATION TAURINURIA [Thesis]. Hewitt, Roger Roy. Rochester, N. Y., Univ. of Rochester, 1963. 81p.

Rats have been shown to exhibit post-irradiation hypertaurinuria, whereas guinea pigs do not. The metabolism of large doses of cysteine was investigated in both rat and guinea pig in order to examine the possibility that the difference in post-irradiation urinary taurine excretion is based on interspecies metabolic differences. Cysteine was selected because it is generally thought to be a taurine precursor, and it has been shown to be a radiation protectant in rats and mice. The effect of subsequent irradiation on the metabolism of large cysteine doses also were studied in the rat. Chemical analyses of urinary taurine and sulfate were done in all experiments. Data pertinent to the study were also obtained by measurements of radioactivity in various fractions of urinary sulfur excreted after the administration of cysteine-^{35}S. It was concluded that the guinea pig has less than one-tenth the capacity of the rat to convert cysteine to taurine. The conversion of cysteine to sulfate was also less in the guinea pig than in the rat, but this difference was less marked than in the case of taurine. Cysteine appeared to be much more toxic to the guinea pig than to the rat. The possibility that conversion of cysteine to cystine may account for the increased sensitivity of the guinea pig to cysteine was discussed. Conversion of cysteine to taurine to the same extent by the rat, with or without subsequent irradiation, and the equal specific activities in the two cases, was offered as evidence that cysteine prevents losses of body taurine in response to irradiation. (Dissertation Abstr.)

29025 PATHO-PHYSIOLOGIC ASPECTS OF RADIATION NEPHRITIS [Thesis]. Maier, John Gail. Rochester, N. Y.; Univ. of Rochester, 1963. 187p.

Irradiation of the canine kidney with a single, localized exposure to x rays produced physiological and pathological alterations related to absorbed dose. Functional studies indicated hypertension, proteinuria, hematuria, diuresis, decreased urinary concentration, diminished excretory function, nitrogen retention, and anemia. Morphological findings revealed an arteriolonephrosclerosis. The degree of functional and morphological changes within 6 months at 500, 1,000 and 2,000 rad irradiation to single or bilateral kidneys in situ and single kidneys having subcutaneous exteriorization were correlated. (Dissertation Abstr.)

29026 STUDIES OF THE EFFECTS OF MODERATE LEVELS OF X IRRADIATION UPON THE RENAL HEMODYNAMIC FUNCTIONS OF THE DOG [Thesis]. Maillie, Hugh David. Rochester, N. Y., Univ. of Rochester, 1963. 187p.

Certain physiological responses to a moderate level of x-ray exposure were examined. The physiological parameters chosen were those concerning renal hemodynamics: glomerular filtration rate (GFR), effective renal plasma flow (ERPF), and maximum tubular excretion of PAH (Tm_{PAH}). Acute studies were made in which individual animals were irradiated to doses at or near to the median lethal level of either whole-body or lower-body x irradiation. Such animals served as their own controls and the value of the pertinent parameters was noted both before and following irradiation. It was noted that a consistently significant increase in the ERPF occurred within the first 48 hours of such exposures. Such increases were not noted beyond two days post-irradiation. Animals that survived acute whole-body radiation also showed significant decreases in Tm_{PAH}, which eventually returned to normal. Such responses are interpreted to be dependent upon an irradiation of the kidney area. Latent effects studies were made in which the renal functions of normal dog populations were compared with those of populations of dogs that had survived median lethal levels of either whole-body or lower-body x irradiation for periods of 0.7 to 1.2 years. The only significant difference noted among these populations were a decreased Tm_{PAH} in dogs that survived approximately 750 R lower-body x radiation for about one year. (Dissertation Abstr.)

29027 MUTANTS OF ESCHERICHIA COLI PARTIALLY RESISTANT TO BACTERIOPHAGE T1 [Thesis]. Carta, Guy Rodney. New Brunswick, N. J., Rutgers State Univ., 1965. 99p.

Mutants exhibiting an intermediate type of resistance to bacteriophage T1 were isolated from ultraviolet irradiated cultures of Escherichia coli B/r—a radiation-resistant strain. These mutants have previously been described as partially resistant (B/r/1p). Partially resistant strains were prototropic, and exhibited the usual wild-type sensitivity to streptomycin and sodium azide. Additionally, they were able to ferment lactose, arabinose, xylose, and galactose but not maltose. The mutants differed from the parent sensitive strain in their response to T1 and did not show cross resistance to T5. A test of the model B/r/1p strain indicated the absence on a spontaneously or ultraviolet light inducible prophage. Phage T1 propagated on a B/r/1p culture was not altered with respect to its host range or plaque

morphology. On the basis of studies made, it was concluded that a B/r/1p cell is genetically stable; however, it may exist in either of two phenotypic states with respect to its response to T1, one receptive and the other refractory. The transition from the receptive to refractory states or vice versa is in part or totally dependent on the cells physiological state as determined by the growth phase. Receptive and refractory cells react toward phage somewhat as typically sensitive and resistant bacteria respectively. Hypotheses presented provide possible explanations for the transitions in phenotype of B/r/1p cells and concern the nature of the genetic determinants that might control the variable phenotypes encountered. (TCO)

29028 EFFECTS OF CUPFERRON ON THE FREQUENCY OF X-RAY INDUCED CHROMOSOMAL ABERRATIONS IN TRADESCANTIA PALUDOSA [Thesis]. Davis, Herbert Larkin Jr. Atlanta, Emory Univ., 1965. 79p.

The effects of cupferron (ammonium salt of n-nitrosophenylhydroxylamine) on radiation damage in Tradescantia paludosa microspores was investigated. Inflorescences were irradiated in helium at an intensity of 50 R/min for 8 min for a total dose of 400 R. The toxicity of cupferron was determined using concentrations ranging from 2 to 10^{-6} molar. Concentrations of 10^{-2} molar or greater proved to be toxic to inflorescences as shown by loss of turgor, bleaching of the leaves, and sterility of the microspores. Cupferron solutions of 10^{-1}, 10^{-2}, 10^{-3}, and 10^{-4} molar did not produce any radiomimetic effects in microspores examined 96 hours after treatment. Pretreatment with various concentrations of cupferron ranging from 10^{-1} to 10^{-6} molar resulted in a reduction in the number of chromosomal aberrations observed. Pretreatment in a 10^{-3} molar cupferron solution for periods of time ranging from 15 to 240 minutes showed that the cupferron could affect the aberration yield in 15 minutes and could produce the maximum reduction after 30 minutes pretreatment. The greatest reduction in aberration frequency was produced by 10^{-3} molar cupferron, which resulted in 0.15 ± 0.02 aberrations per cell compared to 0.24 ± 0.02 observed in the control experiment. A pre- and posttreatment cupferron effect demonstrated that the action of cupferron was on recovery. The results of experiments with anoxia and inhibition of the cytochrome system suggest that cupferron is stimulating respiration thus making more energy available for recovery. The effect of cupferron on respiration is thought to be produced by ammonia. An experiment with 10^{-3} molar ammonium chloride resulted in the same aberration frequency as that produced by 10^{-3} molar cupferron. Cupferron was used in combination with DNP, DMSO, and ATP but did not act synergistically with any of the other chemicals. DMSO in a concentration of 2% produced a reduction of aberrations to a level of 0.13 ± 0.02 compared to a control of 0.24 ± 0.02. (Dissertation Abstr.)

29029 INJURY AND RECOVERY OF THE HEMATOPOIETIC SYSTEM IN DOGS EXPOSED TO VARYING DOSES OF X-IRRADIATION DELIVERED TO THE UPPER, LOWER, AND WHOLE BODY IN A MANNER SIMULATING SOME OF THE POSSIBLE EXPOSURES DURING MANNED SPACE TRAVEL [Thesis]. Odland, Lawrence Thomas. Rochester, N. Y., Univ. of Rochester, 1962. 395p.

One hundred and sixteen registered beagles were randomly distributed to 23 groups, each differing in dose and method of exposure to ionizing radiation (1000 kvp unfiltered). Fifty animals were given whole-body exposures, as a single dose, and as the same dose divided into four equal fractions and given at regular intervals of time, i.e., 12-24-48 hours. Thirty were given lower-body exposures, as single and divided doses, and 21 upper-body exposures again singly and divided. Ten animals were sham exposed, and five received 225 R whole-body exposures 30 days postsplenectomy. Each animal was studied for sixty days postexposure, unless death intervened, by clinical observation and changes in selected hematological parameters including plasma iron clearance rates, red cell uptake of radioiron, and red cell and plasma volumes. Protection of a portion of the body greatly increased the dose of x ray necessary to cause lethality. Except for lymphocyte changes, the impairment of various parameters considered was greater after upper than lower body exposures, and in some cases (neutrophils) recovery was sooner and more complete. Changes in these same parameters after whole-body exposures where doses did not exceed 300 R were greater than those after upper body. Plasma iron clearance rates detected any pattern or schedule of exposures within 24 hours after single (or fourth, in case of fractionation) provided the total dose exceeded 150 R, and was given as a single dose to whole, lower, or upper body, or as fractionated dose to whole and upper body. In no animal did death occur at a time when the plasma iron clearance rate was at or near control values. In this respect it served as a better predictor of survival than white blood cell and differential counts. In general, iron uptake by red cells 10 days after injection of tracer dose of ^{59}Fe was of little aid in sorting out individual dogs that had received lethal doses. Splenectomized animals responded qualitatively in much the same manner as those in possession of the spleen, and given the same dose of x ray, but recovery was more rapid. Clinically, they experienced much less morbidity. It was found that lymphocyte numbers reach their maximum depression within 24 hours post-exposure, and the drop is nearly independent of dose or method of exposure, once the total exceeds 150 R. On the basis of platelet numbers, venous blood hematocrits, and erythrocyte sedimentation rate, determined 14 days post-exposure, it was possible to differentiate the animals that received lower body exposures from those given upper- or whole-body x irradiation. Comments on the implications of these findings with regard to military and civilian defense planning, and manned space travel are presented. (TCO)

29030 PHYSIOLOGICAL STUDY OF DEGENERATIVE AND AGING CHANGES IN RATS AS INFLUENCED BY EXPOSURE TO IONIZING RADIATIONS [Thesis]. Sproul, James Andrew Jr. Rochester, N. Y., Univ. of Rochester, 1962. 120p.

Long-Evans rats were injected intravenously with 10 μC/kg body weight of polonium-210. Quantitative studies of some of the physiologic changes commonly associated with the aging process were made over the course of several months. The results indicate that rats exposed to internal radiation from polonium alpha particles show a significant increase in blood pressure, an increase in hair depigmentation, a slight decrease in urinary specific gravity, and an increased rate of cataractogenesis. These manifestations of an acceleration of the aging process are related to cumulative radiation dose. The findings are compatible with the view that the development of the aging syndrome is markedly accelerated and can be measured quantitatively by the physiologic end points studied. (Dissertation Abstr.)

29031 RELATION OF CHROMOSOMAL BRIDGES AT ANAPHASE TO EXCHANGES AT METAPHASE: RADIATION STUDIES [Thesis]. Sarda, Ram Prasad. Gainesville, Fla., Univ. of Florida, 1965. 100p.

Tradescantia microspores and dry (approximate water content, 2.5%) dormant seeds of barley were irradiated with uranium-fission fast neutrons (average energy of a spectrum, slightly greater than 0.53 Mev) and high-voltage (250 or 300 kvp) x rays. Late anaphases of the first cycle of mitotic cell division after irradiation were analyzed for the presence of dicentric bridges and acentric fragments. Experimental results demonstrate that anaphase bridges do not show a simple linear relationship with dose as is reported in the literature but exhibit a parabolic curve at high doses, as was predicted by Conger, with fast neutrons as well as x rays in both the plant materials studied. Similarly the normal anaphases (anaphase with no bridge or a fragment) versus dose curve is bowl-shaped on a semilogarithmic paper and not linear. It is concluded that a gradual increase in the number of bridges (about linearly with dose) is observed as damage due to increasing dose of radiation increases until the effective sites for bridges are saturated at which time such a curve reaches its maxi-

mum height. Later at higher doses the number of bridges versus dose curve starts its decline until yield of bridges reaches zero. This fact leads to the conclusion that an estimation of radiation-induced damage from anaphase bridge studies is subject to inherent errors especially at the larger doses, and previous ideas concerning the anaphase bridges (or per cent of cells with bridges) versus dose curve as well as normal anaphases (anaphase without a bridge, or anaphase without a bridge or a fragment) versus dose curve need to be modified. (Dissertation Abstr.)

29032 ADRENALIN I NORADRENALIN. (Adrenaline and Noradrenaline). Grashchenkov, N. I. (ed.). Moscow, Izdatel'stvo Nauka, 1964. 312p.

The catecholamines and their role in regulating body functions are discussed in a series of papers presented at a conference in Moscow on Dec. 1 to 3rd, 1962. The material is organized into three sections. The first section deals with the physiology and biochemistry of the catecholamines. Here the interaction of catecholamine with specific receptors, and the effects of various inhibitors and regulators are discussed. The second section deals with catecholamine exchange in human pathology. Disturbances in catecholamine metabolism after irradiation or during various stages of atherosclerosis are discussed in this section. The third section deals with the study of catecholamines in biological liquids. Methods of determination and types of analytical equipment are presented. Fluorescence and colorimetric absorption methods of analysis are emphasized. (TTT)

Radiation Effects Therapy and Countermeasures

Refer also to abstracts 28875 and 29241.

29033 THE USE OF PRESERVED HEMATOPOIETIC TISSUES FOR TREATMENT OF MICE LETHALLY IRRADIATED WITH GAMMA RAYS UNDER HIGH DOSE RATE. II. EFFECT OF PRESERVED HOMOLOGOUS BONE MARROW. Hama, Masaharu (Kyoto Univ.). Bull. Inst. Chem. Res., Kyoto Univ., 44: 11-36(Jan. 1966).

Mice were irradiated lethally with gamma rays under high dose rate and were treated with preserved homologous bone marrow. The homologous bone marrow was preserved in 15% glycerol-Tyrode's solution or 10% dimethylsulfoxide TC 199 at −80°C as long as 360 days. 5×10^6 and 10×10^6 homologous bone marrow cells suspended in 15% glycerol-Tyrode's solution and preserved for 90 and 360 days, respectively, retained their ability to protect lethally irradiated mice from death. Homologous bone marrow cells (10×10^6) suspended in 10% DMSO-TC 199 retained the ability when the period of preservation was less than 270 days. (auth)

29034 THE USE OF PRESERVED HEMATOPOIETIC TISSUES FOR TREATMENT OF MICE LETHALLY IRRADIATED WITH GAMMA RAYS UNDER HIGH DOSE RATE. III. EFFECT OF PRESERVED HOMOLOGOUS FETAL LIVER. Hama, Masaharu (Kyoto Univ.). Bull. Inst. Chem. Res., Kyoto Univ., 44: 37-56(Jan. 1966).

Mice were irradiated lethally with gamma rays under high dose rate and were treated with preserved homologous fetal liver. The homologous fetal liver was suspended in 15% glycerol-Tyrode's solution or 10% dimethyl-sulfoxide TC 199 solution and preserved at −80°C as long as 360 days. The homologous fetal liver cells which were preserved as long as 360 days could protect the lethally irradiated mice. (auth)

29035 MODIFICATION OF HEMATOPOIETIC CELL TRANSPLANTATION IN MICE IRRADIATED WITH GAMMA RAYS UNDER HIGH DOSE RATE. II. APPLICATION OF METHOTREXATE FOR SUPPRESSION OF IMMUNE RESPONSE. Adachi, Kazushige (Kyoto Univ.). Bull. Inst. Chem. Res., Kyoto Univ., 44: 103-16(Jan. 1966).

The early administration of methotrexate (MTX) was effective for suppression of homograft response in mice lethally gamma-irradiated and transplanted with homologous bone marrow (HBM), but survival rate thus obtained was still less than that when isologous bone marrow (IBM) was transplanted. The effect of MTX for suppression of homograft response in the mice lethally irradiated and transplanted with homologous spleen cells (HSC) was not satisfactory. MTX for suppression of homograft response in the mice sublethally irradiated and treated with HBM or HSC was highly effective. The possible mechanism of MTX for suppression of homograft response was discussed. (auth)

29036 MODIFICATION OF HEMATOPOIETIC CELL TRANSPLANTATION IN MICE IRRADIATED WITH GAMMA RAYS UNDER HIGH DOSE RATE. III. ALTERATION OF MIDLETHAL DOSE KILLING EFFECT. Adachi, Kazushige (Kyoto Univ.). Bull. Inst. Chem. Res., Kyoto Univ., 44: 117-22(Jan. 1966).

AET protected mice supralethally irradiated with gamma rays under high dose rate were treated with isologous bone marrow (IBM) or homologous bone marrow (HBM). The combined use of AET and IBM was effective for saving the mice exposed to supralethal irradiation, but most of the AET protected and HBM treated ones died after the 21th post-irradiation day. The AET protected and gamma-irradiated donor HBM could not prevent delayed death. (auth)

29037 A STUDY OF FREE-RADICAL REACTIONS DURING AN EXPOSURE OF MODEL SYSTEMS TO IRRADIATION AND THE ROLE OF RADICALS IN THE RADIATION DAMAGE. Emanuel, N. M.; Burlakova, E. B.; Kruglyakova, K. E.; Sapezhinskii, I. I. (Inst. of Chemical Physics, Moscow). Izv. Akad. Nauk SSSR, Ser. Biol., No. 2, 183-96(Mar.-Apr. 1966). (In Russian).

The process of oxidative recombination of radicals of irradiated proteins was studied. Free radicals were found to participate in many reactions (e.g., formation of peroxide radicals, transfer of oxidation chain, and exchange reactions with inhibitors). The investigations provided data on the Roentgen- and photochemiluminescence of protein aqueous solutions. Kinetic studies demonstrated that the luminescence occurred due to reactions of peroxide radicals of irradiated proteins. The after-luminescence parameters were significantly affected by radioprotectors. Reactions of free radicals played an important role in the radioinduced DNA degradation. Chemiluminescence of irradiated DNA solutions was studied in parallel with the decomposition of DNA peroxidases. The chemiluminescence appeared to be related to the decomposition of the cytosine perioxidase. A study of the action of different inhibitors upon the DNA post-irradiation degradation allowed the conclusion to be made that derivatives of gallic acid, phenylethylamine, and oxypyridine drastically reduced the effect of irradiation, the gallic acid and oxypyridine derivatives remaining efficient after irradiation as well. Electron microscope data concerning the propyl gallate protective action are also given. A correlation was established between the survival of animals and the anti-radical activity of inhibitors in free radical reactions. There exists a linear relationship between these two values. The data indicate an important role of free radicals in the process of radiation damage. (auth)

29038 MECHANISM OF RECOVERY OF THE REGENERATIVE CAPACITY INHIBITED BY X IRRADIATION. Polezhaev, L. V. (Inst. of Animal Morphology, Moscow). Izv. Akad. Nauk SSSR, Ser. Biol., No. 2, 254-65(Mar.-Apr. 1966). (In Russian).

X irradiation that suppressed the regenerative capacity of axolotl limbs caused serious damage in the nucleic metabolism of irradiated tissues, brought about inhibition of their ability to dedifferentiate and to form embryonic type cells of the regeneration blastema, and gave rise to suppression of the ability of morphogenesis, to the reduction but not a complete inhibition of the mitotic activity, and appearance of atypical mitoses. An experimentally

induced recovery of the regenerative capacity suppressed by x irradiation restored all the above phenomena. Injections of high-polymeric freshly prepared RNA helped to prolong considerably the life span of the animals after their total irradiation and development of radiation sickness. (auth)

29039 SOME RESULTS AND TASKS IN THE STUDY OF RADIOPROTECTIVE MECHANISMS. Graevskii, E. Ya. (Inst. of Animal Morphology, Moscow). Izv. Akad. Nauk SSSR, Ser. Biol., No. 3, 376-82(May-June 1966). (In Russian).

It is suggested that an increase in the radioresistance of biological objects under the action of radiation protectors does not occur in connection with their direct effect but due to an elevated content of sulfhydryl groups caused by them. Radioprotective agents (anoxia, aminothiols, serotonin) bring about a distinct rise of the amount of thiol groups in the mouse spleen and Ehrlich ascite carcinoma cells. Modified resistance of the animal causes corresponding changes in the content of sulfhydryl groups. During irradiation of Ehrlich ascite carcinoma with the homogenate of anoxia-protected spleen reduces the radiation damage of the cell chromosome apparatus. A discussion is given on possible pathways to increase the level of sulfhydryl groups in protected biological objects and on mechanisms of their radioprotective effect. The content of endogenous sulfhydryl groups in biological objects is supposed to determine also natural differences in their radiosensitivity. (auth)

29040 RADIATION DAMAGE OF PROTEIN MOLECULES AND MOLECULAR PROTECTIVE MECHANISMS. Eidus, L. Kh. (Inst. of Biological Physics, Moscow). Izv. Akad. Nauk SSSR, Ser. Biol., No. 3, 383-92(May-June 1966). (In Russian).

Modern concepts of the molecular mechanisms of the action of chemical protectors are reviewed. Principal results of the research are presented. The idea is advanced that the protective effect is closely associated with the interference of oxygen. Protector molecules in the solution undergo radiolysis, the products of which have damaging or restoring effect, depending on their donor-acceptor properties. Reacting with these short-living products, oxygen deprives them of their reactivity, thus producing a protective or damaging effect. Therefore, the protection efficiency depends on the properties of radiolysates rather than on protectors themselves. This appears to account for a sharp difference that is frequently observed in protective properties of two substances of the same column that differ very little from each other. A new physical mechanism of chemical protection is based on adsorption of protective molecules by biological materials. The mechanism prevents manifestation of latent damage. (H.G.D.)

29041 RADIOMIMETIC PROPERTIES OF 2-AMINOPURINE IN ESCHERICHIA COLI. Zampieri, Antonio; Greenberg, Joseph (Palo Alto Medical Research Foundation, Calif.). J. Bacteriol., 91: 1773-4(May 1966).

A radioresistant mutant (R_4) of Escherichia coli strain S was found to be resistant to 2-aminopurine. The composition of the post-treatment plating medium and temperature of incubation did not influence the sensitivity of R_4 to 2-aminopurine. However, strain S was much more sensitive to 2-aminopurine when plated on tryptone-agar than on minimal glucose-salts-agar. Strain S was also more sensitive when the post-treatment incubation was at 37°C than at 45°C. When E. coli strain S was treated with sufficient 2-aminopurine to permit only 10^{-5} survivors, 67% of the survivors were resistant to ultraviolet light and to radiomimetic compounds. 2-Aminopurine induced filaments in radiation-sensitive, but not radiation-resistant, strains of E. coli. It is concluded that 2-aminopurine, a base analogue which induces transition mutations, is radiomimetic in several properties. (auth)

29042 HEMATOPORPHYRIN AND SURVIVAL TEST OF THE PAN-IRRADIATED MOUSE. IN VIVO EXPERIMENTATION OF A SELECTIVE RADIOSENSITIZER. Cittadini, G. (Univ., Siena, Italy). Minerva Radiol., Fisioterap. Radiobiol., 10: 623-9(Dec. 1965). (In Italian).

The relations between the hematoporphyrin dose administered and the radiobiological effect obtained were examined using the survival test in whole-body irradiated mice. The possibility of the existence of sex-linked differences was also investigated. Four well-marked areas in which the effect of the drug differs were demonstrated with respect to the relationship of hematoporphyrin administered and radiobiological effect. It was possible to attribute a well defined role to sex in the response of animals pretreated with hematoporphyrin. A working hypothesis derived from the data obtained is presented. (tr-auth)

29043 EXPERIMENTAL STUDIES ON THE INFLUENCE OF HORMONES IN X-IRRADIATED ANIMALS. PART II. STUDIES ON THE INFLUENCE OF HORMONES AND OF REMOVAL OF ENDOCRINE GLANDS UPON IRON METABOLISM IN X-IRRADIATED RATS. Kawasaki, Sho (Kyoto Univ.). Naika Hokan, 12: 545-59(Oct. 1965). (In Japanese).

Studies were made to determine the validity of plasma iron turnover rate ($T\frac{1}{2}V$) and ^{59}Fe uptake into red blood cells (%RU) as indexes of erythropoiesis in x-irradiated rats of Wistar strain. The effects of hormones upon radiation injury were investigated by use of these indexes. X-irradiated rats treated with various hormones or those rats deprived of respective endocrine gland followed by x-irradiation were used. In the rats given 50 to 300 R radiation, an erythropoietic depression in response to the radiation dose was found quantitatively by $T\frac{1}{2}V$, or %RU. The depression reached a maximum 24 hrs after irradiation of each dose. The data suggest that radioactive-Fe tracer studies are useful as an early indicator of radiation injury and its recovery. In rats given 300 R x radiation, the serum iron concentration elevated slightly 1 to 2 days after irradiation, and then recovered to normal rapidly; therefore the serum iron level was a less sensitive index of radiation injury than $T\frac{1}{2}V$, or %RU. The protective effect of ACTH against x irradiation was noted, but no effect was demonstrated for recovery of radiation injury. Cortisone did not show any ameliorating effect on radiation injury. No difference was noted in $T\frac{1}{2}V$ or %RU between the irradiated, adrenalectomized rats and the irradiated, non-adrenalectomized rats. Thyroxine was found to be effective for both protection against and recovery from radiation injury. The thyroidectomized rats proved to be more sensitive to x irradiation than normal rats. Testosterone did not show any protective effect on radiation injury but showed the effect on its recovery. In gonadectomized male rats, recovery from radiation injury was more prolonged than in normal rats. The erythropoietic activity was depressed by estrogen administration in normal rats. In the irradiated rats treated with estrogen, radiation injury was increased and its recovery was delayed, as compared with the non-treated, irradiated rats. There was no difference in radiation injury between the oophorectomized rats and normal rats. (auth)

29044 THE EFFECT OF ACTH OF HYPOPHYSIS ON THE CYTOLYTIC ACTIVITY OF THE BLOOD AND OF ORGANS OF IRRADIATED RATS. Aleksandrova, M. F. Probl. Endokrinol. Gormonoterap., 8: No. 2, 35-8(Mar.-Apr. 1962). (In Russian).

Investigations demonstrated that a single ACTH administration to healthy rats, as well as irradiation, is accompanied by increased leukolytic activity of the blood and organs. ACTH administration to irradiated rats reduced the lysis of hepatic cells and leukocytes. The action of ACTH on the leukolytic activity of the blood and of the organs of irradiated rats varied depending on the time of its administration after irradiation. (tr-auth)

29045 NEW WAYS OF STUDYING CHEMICAL PROTECTION AGAINST GENETIC CHANGES. Zhukov-Verezhnikov, N. N.; Volkov, M. N.; Rybakov, N. I.; Saksonov, P. P.; Kozlov, V. A.; Konstantinov, P. A.; Antipov, V. V.; Dobrov, N. N.; Aniskin, E. D. Probl. Kosm. Biol., 4: 445-50(1965). (In Russian).

Aminothiols and some pyrimidine analogs were tested for their ability to block development of infectious phage from prophage after induction of E. coli K-12(λ) with x rays. Experimental and control samples were subjected to x-irradiation (15,000 R) and then cultured on agar. 2-Mercaptopropylamine hydrochloride was most effective; cultures treated with it produced 119 times fewer phage particles than control samples. Other good inhibitors of induced phage formation were 2-(γ-aminopropyl) disulfide dihydrobromide, sodium diethyldithiocarbamate, and ammonium dithiocarbamate, which reduced phage production 76.3 to 70.1 times. Less effective were the salts of β-mercaptoethylamine. Data show the essential connection between the chemical structure of the tested preparations and their ability to block the development of infectious phage. The antigenetic effect of β-mercaptoethylamine preparations is determined by their acid radicals as well as by their base. It may be possible to obtain even more effective preparations of this compound by forming salts with other acids. The failure of 3-(β-aminoethyl)isothiuronium hydrobromide to produce an antigenetic effect is especially interesting. (TCO)

29046 ADENOSINE TRIPHOSPHATE: PROTECTION AGAINST RADIATION-INDUCED CHROMOSOME LOSS IN DROSOPHILA. Mittler, Sidney; U, Raymond (Northern Illinois Univ., DeKalb). Contract AT(11-1)-1081. Science, 152: 1087-8(May 20, 1966).

Injection of 5 milligrams of adenosine triphosphate per milliliter into adult Drosophila melanogaster X^{c2} yB/sc^{8}y^{+} 4 to 8 hours old either immediately before or after administration of 2000 R of x rays protected those cells in spermatogenesis which were in or near meiosis from the loss of the ring X or the y^{+} portion of Y chromosome. The loss of the chromosomes was determined by appearance of exceptional XO males in the offspring. (auth)

29047 PROTECTIVE ACTION OF CYSTAMINE ON THYROID GLAND TISSUES IN CASE OF ACUTE RADIATION DISEASE. Khussar, Yu. P. Tsitologiya, 5: 91-3 (1963). (In Russian).

The injection of cystamine-HCl (100 mg/kg 1% sterile solution) intraperitoneally 20 to 30 min before irradiation decreased the primary irradiation damage in rats and increased the regeneration of the thyroid gland after x irradiation (1000 R). (C.H.)

29048 CHANGE IN THE ACTIVITY OF GLUCOSOPHOSPHATE–ISOMERASE AND ALDOLASE UNDER THE EFFECT OF A RADIOMIMETIC NEMBUTAL PREPARATION. Vasyutinskaya, E. M. (Research Lab. for Sanitary Chemistry, Odessa). Ukr. Biokhim. Zh., 38: 148-54(1966). (In Ukrainian).

Considerable changes in the activity of glucosophosphate-isomerase and aldolase-under the effect of a radiomimetic nembutal preparation were found in rat tissue. The principal change is that of increase in activity. Of the two investigated enzymes the most regular changes under the effect of nembutal were noted in the activity of serum aldolase. The changes in the activity of this enzyme of the serum under the effect of a radiomimetic nembutal preparation and of roentgen rays differ perceptibly in their tendencies. On introducing the radiomimetic, enhancement of activity is noted; on irradiation, inhibition. The specific differences in the experimental animals affect both the time when the changes in activity arise and their intensity. In rats these changes are more pronounced. (auth)

29049 RECOVERY OF CELLS FROM PRIMARY CYTOGENETIC INJURIES. Tsarapkin, L. S.; Poryadkova, N. A.; Labzina, N. G.; Alekseeva, S. I.; Pyatenko, V. S. (Inst. of Medical Radiology, Obninsk, SSSR). Vestn. Akad. Med. Nauk SSSR, 20: No. 9, 26-32(1965). (In Russian).

Experiments were performed on pea seeds and shoots. Pea seeds with a water content of 12 to 18% were subjected to ^{60}Co γ irradiation at a dose of 15 kR. The radioprotective effects of various chemical and biological agents were evaluated. In shoots, cysteine exerted a protective influence on actively metabolizing cells only when used before irradiation. However, ATP and yeast extract diminished the number of injured cells independently of the time of action. EDTA and $CaCl_2$ intensified the effect of injury independently of the time of use. In work involving the testing of the chemical substances on the cells of Ehrlich ascites carcinoma, streptomycin reduced, and oxidized oleic acid and EDTA increased the number of ascites cells with chromosomal aberrations. (C.H.)

29050 LOSS OF HYPOTENSIVE ACTIVITY BY DERIVATIVES OF 5-HYDROXYINDOLE WHEN ANIMALS ARE IRRADIATED. Grinev, A. N.; Il'yuchenok, T. Yu.; Lepekhin, V. P.; Shadurskii, K. S. (Inst. of Medical Radiology, Obninsk, SSSR). Vestn. Akad. Med. Nauk SSSR, 20: No. 9, 55-8(1965). (In Russian).

Results are presented of studies of derivatives of 5-hydroxyindole of the 5-hydroxytryptamine (serotonin) type. The effects of the compounds on hypotensive activity was evaluated in rats irradiated with 300 and 600 rad. (C.H.)

29051 THE THERAPEUTIC EFFECTIVENESS OF ANTIBIOTICS ON THE BACKGROUND OF RADIOPROTECTIVE CYSTAMINE ACTION DURING SEVERE RADIATION SICKNESS. Tumanov, G. V.; Bakanidze, I. G.; Zatyuryukin, V. G.; Kugot, P. L.; Lomteva, E. V. Voenno-Med. Zh., No. 3, 64-7(Mar. 1965). (In Russian).

Five groups of rabbits (10 in each group) were given an x ray dose of 1100 R. All the rabbits in group I died with an average survival time of 10.3 days. Groups II, III, and IV were given penicillin, streptomycin, and penicillin G three hours after the irradiation over a period of 14 days. Streptomycin was the most effective in prolonging the survival time to 17.1 days. The blood picture was also improved compared to the control group. Hence, group V was given streptomycin and cystamine which was administered 30 minutes before irradiation. In group V the survival time increased to 25.3 days, and 3 out of 10 of the rabbits survived beyond the 10 to 11 month period. The surviving animals appeared normal except for changes in the peripheral blood. The antibiotics improved the survival time by combatting infection. The use of the radioprotective agent cystamine further improved the results. (TTT)

29052 THE THERAPEUTIC EFFECT OF SINGLE OR MULTIPLE GRAFTS OF HOMOLOGOUS MARROW AND ANTIBIOTICS UPON DOMESTIC RABBITS AFTER VARYING AMOUNTS OF X-RAY. Chang, Tsung-hsien. Yuan Tzu Neng, No. 1, 43-50(1965).

One-hundred and fifteen male rabbits weighing 2 to 3 kg each were subjected to x irradiation at doses of 900 coulombs ($LD_{50/30}$) and 1,200 coulombs ($LD_{100/30}$) through a Cu–Al filter at a distance from the source to the dorsal skin of 60 cm at 900 coulombs and 52 cm at 1,200 coulombs. The radiation intensity was 13.8 and 18.5 coulomb/min, respectively, for an interval of 65 minutes. The results showed that no marrow grafts were necessary and the application of antibiotics was sufficient to tide the rabbits over the crisis of radiation sickness after a dose of 900 coulombs ($LD_{50/30}$). The application of both marrow grafts and antibiotics increased the survival rate when rabbits were treated with 1,200 coulombs ($LD_{100/30}$), since rabbits may die of infection if no antibiotics are used in addition to marrow grafts after 1,200 coulombs. Injection of marrow once on the second day after radiation or injection of the same amount of marrow on the 2nd, 3rd, and 4th day after radiation had essentially the same effect on survival, both producing favorable convalescence. However, injection of a large amount of marrow in a single dose induced serious reactions, so that it was safer to inject at three successive times. (CFSTI)

Radiation Hazards and Protection

See also HEALTH AND SAFETY.

29053 (NP–15951) DATA FROM RADIATION PROTECTION PROGRAMS. Volume 4, Number 2, February 1966. (Department of National Health and Welfare, Ot-

tawa (Ontario). Radiation Protection Div.). 41p. Dep. mn.

Procedures used by the Radiation Protection Division to ensure that exposure of radiation workers and of the general public will remain within the acceptable limits as defined by the guides are discussed. Guide levels in radiation protection programs are considered. Data are presented on: Canadian fallout data for January 1966; ^{137}Cs activity in seal samples; and reactor environment monitoring for January 1966. A selected list of 10 divisional reports and bulletins available to the public on request is included. (H.G.D.)

29054 (NP-16119) THE ASSESSMENT OF THE POSSIBLE RADIATION RISKS TO THE POPULATION FROM ENVIRONMENTAL CONTAMINATION. (Medical Research Council, London (England)). 1966. 16p. Dep. mn. BIS $0.30. HMSO 1s. 9d.

Possible hazards to the population of the United Kingdom from environmental contamination from nuclear weapon testing or other sources are reviewed in terms of the possible incidence of certain types of harmful effect, for example leukemia. An estimate of the total doses that will arise from fallout from all weapons that were tested up to the end of 1965 are estimated, along with risks that may be associated with these doses. The applicability of remedial measures against fallout is also discussed. Data on the irradiation of bone marrow due to the incorporation of ^{90}Sr into bone are appended. (P.C.H.)

29055 ON THE ANTILEUCOPENIC ACTION OF MARINAMYCIN IN THE CASE OF X-RAY IRRADIATION. Soeda, Momoe; Mitomi, Mamoru (Japan Defense Agency, Tokyo). Nippon Saikingaku Zasshi, 18: 227-33(June 1963). (In Japanese).

A single intravenous injection of 1.0 to 2.0 mg of marinamycin (M2) 2 to 4 hr before whole-body x irradiation (182 R) protected rabbits from leukopenia. With the same dose of irradiation, three prior intravenous injections of adenine sulfate (10 mg each time) showed similar results. The natural recovery from leucopenia in rabbits irradiated with 182- or 300-R doses took the same time, 73 days. The injection of 5.0 mg M2, 2 hr or 48 hr prior to irradiation (300 R) prevented acute leukopenia, but did not show the same effect as when given 24 hr prior to irradiation. Administration of M2 after the irradiation (300 R) provided the same rapid recovery effect from leukopenia. Administration of benzyl kinetin prior to the whole-body irradiation (300 R) did not prevent leukopenia. The leukopenia caused by the administration of the anticancer antibiotics carcinophilin and mitomycin C was also prevented by M2 treatment. (BBB)

29056 CALCULATION OF DOSES IN X AND GAMMA IRRADIATIONS THROUGH SCREENS. Berlovskii, A. Ya.; Fain, E. A.; (Khar'kov Regional Oncological Clinic). Vop. Onkol., 12: No. 2, 91-3(1966). (In Russian).

It was found that the effective dose under a grid at any depth can be expressed in the following form: $D_{eff} = (D_0/100)\,[\alpha_{S_0} - \alpha_0\,(1 - \eta_\lambda)]$. Here D_0 is the dose in air at a point just above the grid. The term α_{S_0} is the relative percent dose at a depth x for an area S_0, which is the area of the open part of the grid. The term α_0 is the relative percent dose at a depth x with no grid openings. The term η_λ is a gamma transmission factor that depends on the grid material: $n_\lambda = (S_0/S) + (S - S_0)/KS$. S is the total grid area, and K is the attenuation factor. The dose is given in roentgens. The distribution of depth dose under a grid is shown graphically. An example was calculated for a lead grid 10×15 in size with $S = 150$ cm^2, $S_0 = 80$ cm^2, and a value of $\eta_\lambda = 0.6$ for x rays. The effective dose at a depth of 10 cm is $0.336\ D_0$. The skin dose was also calculated. (TTT)

29057 TEMPERATURE EFFECT ON CYSTEAMINE ACCUMULATION IN CELLS AND ITS RADIOPROTECTING ACTIVITY. Graevskii, E. Ya.; Konstantinova, M. M.; Nekrasova, I. V.; Tarasenko, A. G. (Inst. of Animal Morphology, Moscow). Zh. Obshch. Biol., 25: 298-301(1964). (In Russian).

The temperature dependence of the radioprotective properties of cysteamine (effective at 37° and ineffective at 0°) seems to indicate a chemical nature for the interaction between cysteamine and cell substrates. (TCO)

29058 METHOD OF EVALUATING RADIATION RISKS FOR MANNED SPACE FLIGHTS. Billingham, John (Ames Research Center, Moffett Field, Calif.); Robbins, Donald E.; Ewing, David. 29p. (CONF-660212-6). ORAU. Gmelin, AED-CONF-66-016-6.

From Radiation Research Society, 14th Annual Meeting, Coronado, Calif.

Problems concerning an evaluation of the hazard from doses of ionizing radiation during manned space flights are discussed. A method is given for statistically combining solar flare data with assessments of the likelihood for biological responses. This approach is aimed at synthesizing radiophysical and radiobiological data so that the interfaces between radiation, crew safety, and mission success can be better related to other hazards during mission planning. (auth)

Radiotherapy and Radiodiagnosis

Refer also to abstract 28927.

29059 (TID-22860) OXYGEN SATURATION OF TUMOR CELLS TO INCREASE THE EFFECT OF INTERNAL RADIATION. Grady, Edgar D.; Nolan, Thomas R.; Grady, Charlotte; Daughtrey, William (Piedmont Hospital, Atlanta, Ga.). [1965]. Contract AT(40-1)-3096. 18p. Dep. mn. CFSTI $1.00 cy, $0.50 mn.

Intra-arterial injection of a suspension of radioisotopes sized 50 to 100 microns led to homogeneous trapping of the radioactive particles in the area supplied by the artery injected. Seventy-one patients with advanced cancer were treated by intravascular injection of ^{90}Y particles as $^{90}Y_2O_3$. One third of these patients had apparent control of the disease from 3 to 40 months and another third were helped for various periods. Modifications of the method are under study in animals. Results are reported from a study in rabbits with lung tumor that showed that animals exposed to high pressure oxygen (90% oxygen at 3 atmospheres absolute) twice daily for 10 days gave a better response to treatment with $^{90}Y_2O_3$ particles than did rabbits without exposure to hyperbaric oxygen. (15 references.) (C.H.)

29060 TANDERIL IN THE TREATMENT OF RADIATION CYSTITIS. Johannessen, Steen (Centralsygehuset, Slagelse, Denmark). Acta Radiol. Therapy, Phys., Biol., 4: 81-5(Apr. 1966).

Ten patients were given Tanderil to prevent discomfort due to radiation cystitis produced by radioactive ^{182}Ta treatment of malignant tumors of the urinary bladder. The results achieved were excellent as regards tenesmus and satisfactory as to bladder capacity since only one patient had a significant reduction. Tanderil probably deserves a trial in ^{60}Co teletherapy of vesical tumors. (auth)

29061 EFFECTS OF DIFFERENT PARAMETERS ON DOSE DISTRIBUTIONS IN ^{60}Co PLANAR ROTATION. Tsien, K. C.; Cunningham, J. R.; Wright, D. J. (Temple Univ., Philadelphia). Acta Radiol. Therapy, Phys., Biol., 4: 129-54(Apr. 1966).

The effects of different parameters on dose distributions in ^{60}Co γ planar rotation were studied with the use of a digital computer. The parameters considered were field size, angle of rotation, position of the center in the phantom, shape and size of the phantom, and the penumbra of the beam. On the basis of the results obtained, the conditions under which the rotation technique can be most advantageously used are discussed. (auth)

29062 EXPERIENCES WITH "INFUSION UROGRAPHY" IN CHILDREN. Lodin, H.; Widman, H. Ann Radiol., 9: 48-53(1966).

A dilution of the amount of radiographic contrast medium with the same amount of glucose or rheomacrodex does not give a better filling of the renal pelvis and the ureters than

the same amount of undiluted contrast medium. The greater amount of contrast medium injected seems to be the only factor responsible for the satisfactory filling of pelvis and ureters. This generally makes compression superfluous. The results obtained show that renal investigations in children can preferably be performed with 2 ml of 60% urografin per kg body weight and with compression in selected cases. Such a method has the advantages of providing a more physiological examination since a kinematographical registration of physiological conditions is possible, an adequate comparison of both the pelvis and ureters is possible on repeated examinations, if the infusion method does not seem to give a good morphological evaluation, compression can be applied 15 min after contrast injection, simultaneous cystography and possibilities of limited urethrography, and children can be easily handled and there are no recorded complications. (auth)

29063 THE RADIOISOTOPE NEPHROGRAM WITH ^{125}I-LABELED HIPPURAN IN INFANCY AND CHILDHOOD. Fendel, H.; Feine, U. (Univ., Tuebingen, Ger.). Ann. Radiol., 9: 54-65(1966).

The radioactive nephrogram has been widely used in investigation of adult renal function and on its own has proved very valuable. Substances containing iodine-131 by reason of gamma radiation emitted, need a thick lead protective screen. Apparatus of this kind makes it very difficult to compare both kidneys at the same time in geometrically favorable conditions in the unweaned child and young infant. This inconvenience is overcome by the use of iodine-125. Radioactive nephrograms have been carried out with hippuran-iodine-125 in unweaned and older children suspected of having renal disease, with the use of radioactive scintillation counters adjusted to the measurement of iodine-125. Results are described. Indications and importance of irradiation are discussed. (auth)

29064 PROBLEMS IN THE DESIGN AND SELECTION OF TECHNICAL PARAMETERS FOR THERAPY UNITS. Sinitsyn, R. V. Med. Radiol., 10: No. 12, 3-10(Dec. 1965). (In Russian).

The throughput capacity ν of a teletherapy irradiation unit can be expressed as the number of people irradiated per unit time as follows: $\nu = 1/[(D/I) + t_l]$. Here D is the average dose to the tumor; I is the dose rate, and t_l is the time lost in arranging the patient before and after the irradiation. The efficiency n of machine time use is plotted as a function of the ratio of lost time to irradiation time. The ratio I/D is plotted as a function of lost time t_l for various values of efficiency of machine time use (n = 0.6, 0.7, 0.8, and 0.9). The source activity can be estimated from the relation $C = I/K_\gamma F^2$. Here I is the optimum dose rate; K_γ is the gamma constant of the isotope, and F is the source-to-skin distance. Formulas are given for estimating the integrated dose to a tumor. The relative errors in estimating the dose are presented. (TTT)

29065 SCANNING OF LIVER, SPLEEN AND BONE MARROW WITH COLLOIDAL ^{99m}Tc. Atkins, H. L.; Richards, P.; Schiffer, L. (Brookhaven National Lab., Upton, N. Y.). Nucl. Appl., 2: 27-32(Feb. 1966).

The physical characteristics of ^{99m}Tc, including a short half life of 6 hr and a nearly monochromatic gamma emission of 140 kev, make it an excellent agent for scintillation scanning. Because of the short half life and absence of significant beta emission, large amounts of activity may be used with the radiation dose to the patient kept very low. Possibilities thus exist for greater resolution through optimal design of collimation and for more rapid scans because of better counting statistics. A colloid of this isotope was prepared by passing hydrogen sulfide through a solution of 1N HCl containing pertechnetate. This colloid, with an average blood disappearance half time of 2.5 min, proved useful in performing scintillation scans of liver, spleen, and bone marrow. A specially designed collimator of 721 holes provided resolution comparable to the commercially available 31-hole collimator but with a sensitivity considerably greater than the 19-hole collimator. Maximum count rates over the liver were 75,000 to 100,000 counts/min following administration of 10 mC of the colloid intravenously. Modification of a commercially available scanner was made by bypassing the contrast enhancement circuits and doubling the speed in order to exploit the high count rates. Count rates over bone marrow are maximally $1/10$ to $1/15$ of the liver count, and spleen count rates fall in between liver and bone-marrow rates. Estimation of spleen size and extent of functioning marrow are possible in addition to detection of space-occupying disease of the liver. (auth)

29066 LABELED COMPOUNDS IN MEDICAL DIAGNOSIS. Bayly, Russell J. (Radiochemical Centre, Amersham, Eng.). Nucleonics, 24: No. 6, 46-53(June 1966).

The use of labeled compounds in medical diagnosis is reviewed from a biochemical viewpoint. These medical uses are considered under 4 categories: for studying the physical location or migration of the compound, for studying the biochemical fate of the compound administered to the patient, for studying the biochemical fate of the compound added to isolated tissue, and for assaying biochemicals from isolated tissue or body fluids. Radiation hazards and purity and stability of labeled compounds are discussed. (M.C.G.)

29067 POSITIONING CIRCUIT FOR ANATOMICAL MARKING ON GAMMA-CAMERA SCINTIPHOTOS. Scrimger, J. (Univ. of Toronto); Poole, G. Phys. Med. Biol., 11: 325-8(1966).

Electronic equipment is described that was developed for marking anatomical features on a γ camera scintiphoto. The anatomical features are marked on a grid when the patient is in the final position and at the end of the photograph the coordinates of the feature can be seen on the grid and the appropriate settings made on the capacitors. Anatomical features outside the field of view of the camera can be recorded on the film. The system is stable and reproducible. (C.H.)

29068 DANGER OF UNINTENTIONAL DIAGNOSTIC IRRADIATION OF THE FETUS IN ROUTINE X-RAY PRACTICE. Sedlacek, F. (Roentgenabteilung des Militaerkrankenhauses, Ruzomberok, Czechoslovakia). Radiol. Diagn., 7: 109-22(1966). (In German).

Out of the 716 women in fertile age x rayed in the years 1959 through 1961 and in whom the genetically important regions were subjected to radiation (cholecystography, urography, investigations of gastro-intestinal tract, etc.), 15 were in the first ten weeks of pregnancy. The pregnancy was not known and the treating physician had sometimes misinterpreted the typical complaints. The course of pregnancy and the health of the new-born were followed. The number of observations is too small to allow statistical conclusions regarding damage due to radiation of the fetus. (auth)

29069 EVALUATION OF FRACTIONATED TOTAL-BODY IRRADIATION IN PATIENTS WITH LEUKEMIA AND DISSEMINATED LYMPHOMAS. Johnson, Ralph E. (National Cancer Inst., Bethesda, Md.). Radiology, 86: 1085-9(June 1966).

Total 2 Mev x ray doses exceeding the single dose LD_{50} may be administered with relative safety by employing fractionated treatment schedules. The usefulness of total-body irradiation in chronic leukemia has been confirmed, and fractionated schedules have been evaluated in patients with disseminated lymphoma, with objective improvements being observed. These preliminary results warrant a continued investigation of total-body irradiation in patients having generalized involvement with radiosensitive malignant disease. (auth)

29070 AUTOMATIC DEPTH-DOSE ACQUISITION SYSTEM. Fitzgerald, Lawrence T.; Bruno, Fred P.; Mauderli, Walter (Univ. of Florida, Gainesville). Radiology, 86: 1107-9(June 1966).

The scanning system described is being employed to acquire data for use with computer programs in treatment planning. As a by-product, isodose curves can be

obtained from the measured data with a digital x-y plotter attached to the computer. Measurements have been completed on over 300 radiation fields for a ^{60}Co teletherapy unit. Any radiation field up to 20 × 20 cm may be scanned to a depth of 30 cm, and 1,860 data points measured and punched on IBM cards within fifteen minutes. The computer can plot all the isodose curves for any field size in approximately five minutes. (auth)

29071 PLANNING OF RADIOTHERAPY FACILITIES. REPORT OF A JOINT IAEA/WHO MEETING. World Health Organ., Tech. Rep. Ser., No. 328, 1-44(1966).

Guiding principles for the planning of radiotherapy facilities are presented. Topics discussed include the relationship of the radiotherapy services to other hospital services, staff requirements and qualifications, choice of equipment, radiological protection, and the use of radioisotopes. (C.H.)

29072 RADIOPHOSPHORUS IN THE TREATMENT OF CERTAIN SKIN DISEASES. Chou, Mao-heng; Tung, Shao-hua; Wu, Pao-sun; Chao, Hui-yang; Chin, Wei-ch'iao (First Shanghai Medical Coll.). Yuan Tzu Neng, No. 2, 182-4 (1965).

Because of the weak penetrating power of β rays, ^{32}P has been used for the treatment of superficial diseases of humans. In the present work, 250 cases were treated clinically with ^{32}P in different dosages and the results were analyzed. In the first group of patients (including neurodermatitis, chronic eczema and others), each patient received 7 to 8 treatments at a dosage of 25 R. Among 114 cases so treated, 35.97% were completely cured, 39.47% were better than 50% cured, and 12.28% showed different degrees of improvement. The effectiveness of this method of treatment was thus 87.72%. In the second group of patients, the treatment also involved 7 to 8 sessions of radiation, but at higher dosages (50 to 100 roentgens). The rate of effectiveness among 125 patients in this group was 90.40%, including 58.40% completely cured, 15.20% significantly improved, and 16.80% somewhat improved. Based on the results of these clinical experiments, the authors suggest that the proper dosage for localized neurodermatitis and eczema would be 50 to 100 R for 7 to 8 treatments. (ATD)

29073 INVESTIGATIONS OF INTEGRAL DOSES IN SECTION RADIOGRAPHY. Staehli, G. Munich, Univ., 1964. 55p. $2.00 Gmelin, AED-Diss. 64-1051.

Integral doses for normal and section radiography were determined from isodose distributions. Results indicate that doses for both exposure types are approximately equal. (Gmelin Inst.)

29074 GYNAECOLOGICAL INDIVIDUAL RADIUM DOSIMETRY IN SITU USING X RAY STEREOSCOPY. Werhahn, P. Duesseldorf, Medizinische Akademie, 1963. 77p. $2.00 Gmelin, AED-Diss. 63-816.

A simple method for determination of the γ dose from radium is given. Location of the source is determined from stereoscopic x ray photography and dose distributions are determined from isodose curves by graphic methods. (Gmelin Inst.)

29075 PRODUCTION OF RADIOACTIVE GOLD PREPARATIONS FOR MEDICAL PURPOSES. Schneider, V. (Kernforschungszentrum, Karlsruhe, Ger.). pp 142-5 of Atomstrahlung in Medizin und Technik. Munich, Verlag Karl Thiemig KG, 1964. (In German).

Radiogold is widely used in medicine to destroy malignant tumors. However, previous methods yielded colloidal Au particles that were too small for medical purposes. The method described for obtaining larger Au particles involves producing colloidal inactive Au seeds of 50 Å and then dropping the radiogold solution into a gelatin solution that contains the germinating seeds. Under reducing and stabilizing actions of gelatin, the inactive seeds grow to large active Au particles that are of uniform size and are easier to use in localized applications. The application of radiogold suspensions and the insertion of very small particles of radiogold metal is extremely dangerous because ^{198}Au emits not only the therapeutically desirable γ radiation of 0.41 Mev but also β particles of 0.96 Mev maximum energy. The powerful β radiation causes necroses, which destroy both malignant and healthy tissues, but the use of radiogold grains, covered with a Pt coating that shields against the β radiation, eliminates this action. (OID)

29076 CHANGES IN VAGINAL SMEARS AFTER THERAPEUTIC IRRADIATION. Leung, K. T. Heidelberg, Univ., 1965. 37p. $2.00 Gmelin, AED-Diss. 65-279.

Changes in vaginal smears of 60 patients after therapeutic irradiation were studied by cytologic methods. Changes were observed even after more than 5 years after the last irradiation. Results indicate that hormone treatment is effective for vaginal skin regeneration. (Gmelin Inst.)

29077 RADIOTHERAPY PHANTOM. Alderson, Samuel Weir (to Alderson Research Labs., Inc.). British Patent 1,025,962. Apr. 14, 1966. Filed Dec. 13, 1962.

A dummy copy of the human body and its method of fabrication from a human skeleton and a moldable plastic material having substantially the same average atomic number and/or the same average specific gravity as human soft tissue is described. The skeleton components are impregnated with a plastic material to match the radiation absorption characteristics of the bone marrow, and the skull portion of the skeleton is filled with a moldable plastic having substantially the same average atomic number and specific gravity as the human skull. At least two components are included within the moldable plastic torso section to simulate the human lungs. The dummy can be dissected with a power saw to allow the positioning of radiation detectors at any desired point and then may be clamped together again with scarcely any air space between sections. The positioning of detectors inside the dummy permits the calculation of radiation doses at various internal positions within a patient. (B.L.M.)

CHEMISTRY

Analytical Procedures

See also Separation Processes and Procedures

Refer also to abstract 29363.

29078 (AD–633252) NEUTRON AND GAMMA-RAY SPECTROSCOPY AND ACTIVATION ANALYSIS. Final Report, January 1, 1961–January 1, 1966. Rasmussen, Norman C.; Thompson, Theos J. (Massachusetts Inst. of Tech., Cambridge). Feb. 1966. Contract AF19(604)-7492. 176p. (MITNE–70; AFCRL–66-135). CFSTI $5.00 cy, $1.00 mn.

The preparation of lithium-drifted solid-state γ detectors, with active volumes between 0.5 and 17 cm^3, is described. The energy resolution of these detectors is 0.5% FWHM for ^{137}Cs γ rays and 0.13% for the 7-Mev capture γ rays in iron. The experimental facility at the MIT reactor for using these detectors to study capture γ rays is described. The Ge(Li) detector is used in conjunction with two large NaI crystals. This system of detectors is operated as a triple coincidence pair spectrometer to study γ rays with energies above 2 Mev and in anticoincidence for Compton reduction when studying the spectrum below 2 Mev. Preliminary results for the spectrum of Fe and Mn are presented. A 6-m bent-crystal spectrometer and a pair scintillation spectrometer were used to study the capture γ spectrum of ^{45}Sc, ^{191}Ir, ^{193}Ir, ^{103}Rh, ^{161}Dy, ^{164}Dy, and ^{165}Ho. The results of these measurements were used to help construct proposed energy level schemes in ^{46}Sc, ^{165}Dy, and ^{166}Ho. Some additions to present level schemes of ^{104}Rh and ^{162}Dy are suggested. A technique for the nondestructive analysis of spent reactor fuel using Ge(Li) γ spectrometers is described. The fuel elements are scanned and the concentrations of three fission products, ^{137}Cs, ^{134}Cs, and ^{95}Zr, are determined from the intensity of emitted γ rays. The ratios of the intensities of these fission products are used to determine burnup, flux, and irradiation time of fuel. A comparison of the results of this method with independently determined results showed agreement within ±10% in all cases for the MIT reactor fuel studied. An improved method for determining fast neutron spectra is described. As an example of the application of this method, measurements of the fast flux of the MIT reactor medical therapy beam are reported. The method uses threshold foil data and computes the spectrum using a weighted orthonormal and a weighted orthonormal polynomial method. A code was also developed for calculating fast neutron dose in hydrogenous material. A technique using prompt activation analysis for the determination of boron and lithium is described. Samples are internally mounted inside a gas flow proportional counter. The counter is then placed in a thermal neutron flux of 10^8 neutrons/cm^2sec and α rays from the (n,α) reaction are detected. The method is capable of determining boron and lithium in the levels of 1 ppM. Fast neutron activation analysis using the (n,2n) reaction was investigated. Preliminary work indicated that about 10^{-6} to 10^{-7} gms of N, F, K, Zn, Ga, Br, Mo, and Ag can be detected using 2 NaI crystals in coincidence to detect annihilation radiation from the induced positron activities. (auth)

29079 (AERE-M-1736) THE γ-RAY SPECTRA OF PITCHBLENDE AND MONAZITE OBTAINED WITH A LITHIUM-DRIFT GERMANIUM DETECTOR. Williams, D. (Atomic Energy Research Establishment, Harwell (England)). Apr. 1966. 14p. Dep. mn. BIS $0.50. HMSO 2s. 6d.

The γ-spectra of pitchblende and monazite were obtained using a lithium-drift germanium detector of 1cc volume and having a resolution of 3 kev f.w.h.m. at 60 kev. The spectrum from pitchblende is compared with spectra from radium and uranium oxide. A tentative analysis of the results is given and it appears likely that the enhanced resolution obtained with this measurement system will provide a means of uranium dis-equilibrium determination for minerals. (auth)

29080 (IDO–14676) BURNUP DETERMINATION OF NUCLEAR FUELS. Project Report for the Quarter, October 1–December 31, 1965. Maeck, William J.; Abernathey, Robert M.; Rein, James E. (eds.) (Phillips Petroleum Co., Idaho Falls, Idaho. Atomic Energy Div.). May 1966. Contract AT(10-1)-205. 28p. Dep. mn. CFSTI $2.00 cy, $0.50 mn.

The main emphasis during this period was devoted to the development of an isotope dilution, mass spectrometric analysis method for ruthenium and the determination of the absolute thermal fission yields of stable and long lived isotopes of ruthenium for ^{233}U and ^{235}U. The average values, determined on two each of dissolved, standard ^{233}U and ^{235}U burnup capsules, are given. (M.O.W.)

29081 (NP-14705) POVEDENIE TSEZIYA-137 V KHODE ANALIZA PROB ATMOSFERNYKH OSADKOV. (Behavior of Cesium-137 During Analysis of Atmospheric Precipitation Samples). Gedeonov, L. I.; Gritchenko, Z. G.; Zhilkina, M. I. (U.S.S.R. Sovet Ministrov. Gosudarstvennyi Komitet po Ispol'zovaniyu Atomnoi Energii). 1963. 19p. Dep. mn.

The behavior of ^{137}Cs during analysis of atmospheric precipitation specimens using HCl, HNO_3, HCl + HF, and HNO_3 + HF was studied using a γ spectrometer. Studies were also made of ^{137}Cs distribution in successive treatments by aqua regia and 5 and 6N HCl. Complete dissolution of macro impurities of the specimen and ^{137}Cs as a component in radioactive fallout was achieved by HCl + HNO_3 and HNO_3 + HF. (R.V.J.)

29082 (SGAE-CH–27/1966) EIN BEITRAG ZUR QUANTITATIVEN AKTIVIERUNGSANALYTISCHEN REINHEITSBESTIMMUNG VON SELTENERDOXYDEN. (A Report on Quantitative Activation Analytical Purity Determination of Rare Earth Oxides). Bildstein, H.; Auer-Welsbach, H.; Manhartsberger, H. (Oesterreichische Studiengesellschaft fuer Atomenergie G.m.b.H., Seibersdorf). 1966. 11p. Dep. mn.

A quantitative trace determination of europium in gadolinium, praseodymium in neodymium, and lutetium in ytterbium could be obtained by activation of the samples and subsequent separation on the cation exchanger Dowex 50W × 8. A complete separation of Eu and Gd and Pr and Nd could be obtained in aqueous ammonium α-hydroxyisobutyrate solution. For separation of Yb and Lu, ammonium lactate can be used. The positions of the elution peaks in each case were reproducible. By means of this method, the residual impurities could be determined at the following concentrations: 0.065 μg of $EuP_{1.5}$/mg $GdO_{1.5}$, 1.2 μg $PrO_{1.83}$/mg $NdO_{1.5}$, and 1.5 μg $LuO_{1.5}$/mg $YbO_{1.5}$. (tr-auth)

29083 (UCRL–14767) ANALYTICAL CHEMISTRY SECTION PROGRESS REPORT, JANUARY 1–DECEMBER 31, 1965. Harrar, J. E. (comp. and ed.) (Lawrence Radiation Lab., Univ. of California, Livermore). Contract W-7405-eng-48. 35p. Dep. mn. CFSTI $2.00 cy, $0.50 mn.

Developments in studies on vacuum analysis equipment and methods, instruments analysis, and solution analysis are reported. Besides various equipment and methods that are described, determination is given for: sulfur in organic compounds; trace impurities in ultrapure gases; yttrium and lanthanides in rock; carbon in high purity titanium; tin in catalyst; and iron and copper in copper ore leach solution. (P.C.H.)

29084 SIGNIFICANCE OF PHOSPHORESCENCE IN THE MEASUREMENT OF LOW-ENERGY BETA ISOTOPES WITH LIQUID SCINTILLATOR AND SINGLE-CHANNEL COUNTER. Fodor-Csanyi, P.; Levay, B. (Electrochemistry Research Group, Hungarian Academy of Sciences). Acta Chim. Acad. Sci. Hung., 47: 343-66(1966).

The role of phosphorescence was studied in the measurement of soft beta emitters (mainly tritium and ^{14}C) by liquid scintillation techniques using a single-channel counter. It was found that the most serious problems encountered in the use of a single-channel counter, mainly in the determination of tritium, arise as a consequence of the phosphorescence on glass bottles and of the solvents. The lowest measurable activity and the number of measurements that can be carried out in one day are determined by the decay rate of the phosphorescence and by the intensity of residual phosphorescence. There is no significant difference between the phosphorescence of sample containers made of various glasses: the initial phosphorescence was, with any of these, on the order of magnitude of 10^6 counts/100 sec, and even after a day it remained as high as several thousand counts/100 sec. No considerable differences were found in the phosphorescence of various solvents (toluene, xylene, dioxane, and ethyl alcohol); however, the purity of the solvents had a marked effect. Techniques for reducing phosphorescence (discrimination and the use of an optical filter), when applied separately, did not bring about satisfactory results. Discrimination involves, even in the case of the ^{14}C isotope, a decrease in efficiency, and requires several hours of storage in the dark; in the case of tritium, the use of this method is entirely impossible. The phosphorescence of scintillation grade toluene can be totally cancelled by the use of an optical filter. In this manner, the intensity of the phosphorescence is decreased to such an extent that it becomes possible to measure tritium after a dark storage of 2 hr, and the capacity of the measuring device is increased ten times. The lowest detectable activity level is decreased by 20% and the measuring efficiency is decreased by 20 to 25%. By the simultaneous use of the optical filter and discrimination, ^{14}C-containing samples can be measured after a dark storage of half an hour, and the intensity of the residual phosphorescence is 80 counts/100 sec. With containing a scintillator it was found that in the presence of the optical filter and a scintillator emitting at a suitable wavelength (e.g., p-terphenyl), the intensity of observed phosphorescence increased compared to that of the empty bottle. The portion of the phosphorescence of glass outside of the sensitivity range of the photocathode is absorbed by the solvent and the scintillator, and it is emitted at a new wavelength characteristic of the scintillator. The latter wavelength is within the measuring range. As a consequence of the introduction of phosphorescence, it is not reasonable to study the phosphorescence of the sample container and of the solvent independently from the scintillator solution, and when choosing the appropriate scintillator and optical filter, the possibility of the introduction of phosphorescence must be taken into consideration. In order to decrease this effect, it is preferable to use a scintillator that emits in the range of shorter wavelengths, together with a filter that is transparent with respect to the scintillator. Scintillators emitting in the range of longer wavelengths are apt to introduce a higher proportion of the phosphorescence of the bottle into the measuring range, and the intensity of phosphorescence is higher at higher wavelengths. An optical filter may completely cancel only phosphorescence at wavelengths higher than its own limit of transmission on the high wavelength side. (auth)

29085 IMPROVEMENTS IN ^{14}C ASSAY OF ORGANIC COMPOUNDS BY DRY COMBUSTION. Hamada, Masayuki; Kawano, Eiko (Radiation Center of Osaka Prefecture). Anal. Chem., 38: 943-5(June 1966).

Modifications in the dry combination procedures and coupling system for ^{14}C-labeled compounds, which allow reduction of nitrogen oxides in a stream of nitrogen and to a low background counting system are described. Results of the assay of various ^{14}C-labeled compounds are presented. During evacuation after measurements, it is desirable to heat the counting tube to 120°C to reduce background. (F.J.H.)

29086 SPECTROFLUORIMETRIC TRACE DETERMINATION OF TERBIUM(III) WITH POTASSIUM OXALATE. Alberti, Giulio; Massucci, Maria Antonietta (CNEN, Rome. Univ., Rome). Anal. Chim. Acta, 35: 303-8(July 1966).

Potassium oxalate acts as a specific reagent in enhancing the fluorescence intensity of terbium in aqueous solutions. Maximum fluorescence intensity is obtained by irradiating (at 255 mμ) terbium(III) dissolved in 0.01M potassium oxalate solution at pH 7.8. The enhancement and quenching phenomena caused by other lanthanides, errors in the determination, and various examples of spectrofluorimetric analysis of traces of terbium in mixtures with other lanthanides are described. The sensitivity of the method is 5×10^{-2} μg/ml of terbium. (auth)

29087 DETERMINATION OF TRACE COPPER IN HIGH-PURITY ARSENIC BY NEUTRON ACTIVATION. Nizet, G.; Fouarge, J.; Duyckaerts, G. (Univ., Liege). Anal. Chim. Acta, 35: 370-5(July 1966). (In French).

The determination of traces of copper (<ppM) in arsenic is impossible by nondestructive γ spectrometry because of the similarity in the half lives and spectra of the two isotopes used. The proposed separation and decontamination of copper are based on the following operations: bromine attack, hydrolysis, precipitation of barium arsenate, anion exchange, separation of copper as sulfide and recovery by electrolysis. Amounts of copper in the range from 20 to 100 ng can be determined. (auth)

29088 STUDY OF THE MACROSCOPIC DISTRIBUTION OF OXYGEN IN A STEEL ROD BY NEUTRON-ACTIVATION AND VACUUM-FUSION TECHNIQUES. van Wyk, Justus M. (South African Iron and Steel Industrial Corp., Pretoria); Cuypers, Marc Y.; Fite, Lloyd E.; Wainerdi, Richard E. Analyst, 91: 316-23(May 1966).

The distribution of oxygen was determined along the length of a steel rod. Neutron-activation and vacuum fusion techniques were used alternatively, and the relevant pieces of apparatus and methods are described. The over-all average oxygen content determined by neutron-activation analysis was 129 ppM, in excellent agreement with 128 ppM found by vacuum fusion. The results further showed the continuity between the two sets of results, and also a definite inhomogeneity in the macroscopic distribution of oxygen. (auth)

29089 NEWER METHODS FOR THE SEPARATION AND CONTINUOUS MEASURING OF ^{14}C-COMPOUNDS IN THE GASEOUS PHASE. Drawert, F.; Bachmann, O. (Forschungsinstitut fuer Rebenzuechtung Geilweilerhof, Siebeldingen/Pfalz, Ger.). Angew. Chem., 75: 717-22 (Aug. 7, 1963). (In German).

Radiometric methods are similar to gas chromatographical methods and both methods can be used continuously. A combination of these methods is promising because the total gas volume and the radioactive components can be determined simultaneously. In order to apply gas radiochromatography, labeled compounds must be converted into suitable volatile substances, and this can be carried out by methods described by F. Drawert and others (Ange. Chem. 72: 555, 1960). The use of detectors and measuring instruments, depending on the substance and type of activity, is described, and it was emphasized that the substances separated by gas chromatographical methods must always be converted into the same chemical compound for radiometric measurements. The application of the method using ^{14}C-labeled alcohols, aldehydes, esters, and organic acids is illustrated by examples taken from viticultural research and chemical investigations of grape juice fermentation and wine analysis. It was found that a mixture of hydrogen with methane or helium with methane was very good for carrying and counting and reproducible results were obtained when the gas chromatographically separated compounds were converted to either $^{14}CH_4$ or $^{14}CO_2$. (OID)

29090 CHEMICAL ANALYSIS USING THE METHOD OF HEAVY ION SCATTERING AT LARGE ANGLES. Karamyan, S. A.; Shukurov, Ya. At. Energ. (USSR), 20: 56-7(Jan. 1966). (In Russian).

Analytical methods based on scattering of β or γ radiation or on activation by fast or thermal neutrons may be

used only if the percentage of the element to be determined is low; they also require long time periods for the determination. The method involving wide-angle scattering of charged particles overcomes this disadvantage but requires the use of high-intensity monoenergetic beams. The energy resolution of α particles and ^{14}C and ^{40}Ar ions is presented graphically. Heavy ions represent α promising tool for elementary analysis, even for isotopic determinations. At an energy resolution of 0.5 to 1% and using the scattering of ^{12}C ions, the presence of elements differing by 5 mass units may be detected in the mass range of about 200. If the energy is decreased, proportionally thinner targets must be used. For ^{12}C, the optimum energy is within the range from 10 to 20 Mev. In mixtures containing mostly light elements, such as Si, as little as 10^{-3} to 10^{-4} per weight of heavy elements, with A ~ 200, may be detected using an exposure time of about 5 minutes and an ion current of 1 microamp. In tests with $^{12}C^{4+}$ ion beams, accelerated in the cyclotron to 80 Mev, the ion scattering was recorded with surface-barrier Si detectors and a 1.5% resolution for the α line of ^{241}Am was achieved. Experiments with targets containing Au and CsI yielded results in agreement with theoretical predictions. (TTT)

29091 SPECTROPHOTOMETRIC DETERMINATION OF FLUORINE WITH A PAC–Th COMPLEX. Toei, Kyoji; Hayami, Tadashi; Miyata, Haruo; Shimoishi, Yasuaki (Okayama Univ., Japan). Bull. Chem. Soc. Jap., 39: 638 (Mar. 1966).

It was found that the thorium complex of PAC, [2-(1,8-dihydroxy-3,6-disulfo-2-naphthylazo)-phenoxyacetic acid], can be used in the spectrophotometric determination of microgram quantities of fluoride ions, and that the sensitivity of the thorium complex towards fluoride ions is almost twice that of the thorium neo-thorin complex. The determination was based on the bleaching effect of the fluoride ions on the thorium complex. (M.C.G.)

29092 HIGH-FREQUENCY TITRIMETRIC STUDY OF THE REACTION BETWEEN THORIUM AND ALKALI MOLYBDATE. Mittal, M. L.; Dube, S. S. (Government Coll., Kota, India). Bull. Chem. Soc. Jap., 39: 1064-5 (May 1966).

The reaction between Th^{4+} and MoO_4^{2-} ions was investigated by means of high-frequency titrations of thorium nitrate with sodium molybdate by both direct and reverse methods in 30% ethanolic media. Both direct and reverse titrations yielded well-defined breaks and suggested the formation of normal thorium molybdate, $ThO_2 \cdot 2MoO_3$. The accuracy and reproducibility of the titrations were found to be excellent. The results of high-frequency titrations agreed with those obtained by other electrometric methods. (F.J.H.)

29093 THE INTERACTION OF THORIUM(IV) WITH PYROCATECHOL-3,5-DISULFONATE AT A 1:1.5 MOLAR RATIO. Murakami, Yukito; Martell, Arthur E. (Kyushu Univ., Fukuoka. Illinois Inst. of Tech., Chicago). Bull. Chem. Soc. Jap., 39: 1077-9(May 1966).

A study was made of the 1 : 1.5 thorium(IV)-pyrocatechol-3,5-disulfonate system by means of potentiometric measurements to clarify the nature of the dinuclear thorium chelate. Potentiometric titration curves are shown. A sharp inflection region was observed at m = 3.0 and it was concluded that the 1 : 1 metal chelate is nearly completely formed at this point. From the appearance of a second inflection at ~m = 4.0, it was assumed that a simple intramolecular olation reaction takes place. (M.C.G.)

29094 FLUOROMETRIC DETERMINATION OF YTTRIUM WITH 5,7-DICHLOROOXINE; DETERMINATION OF YTTRIUM IN XENOTIME ORE. Shigematsu, Tsunenobu (Kyoto Univ.); Nishikawa, Yasuharu; Hiraki, Keizo. Bunseki Kagaku, 15: 493-8(May 1966). (In Japanese).

Optimum conditions for the fluorometric determination of yttrium by 5,7-dichlorooxine were investigated, and the method was developed for the direct determination of yttrium in xenotime ore. A 250 to 500 mg portion of an ore sample was treated for 2 to 3 hours with 30 to 40 ml of hot concentrated H_2SO_4. The solution was diluted to 50 to 100 ml with water, and any insoluble residue was filtered. Sixty ml of 1N oxalic acid was added to the solution and the pH was adjusted to 2.2. After standing for several hours, the precipitate was ignited to obtain the total amount of rare earth oxide, which was found to be 25 to 50 mg. It was dissolved in HCl and diluted with water to adjust the concentration to 10 μg total rare earths oxide per ml. A 0.5 to 1.0 ml portion of the solution was transferred to a 100 ml beaker. To it were added 0.25 ml of 0.2% 5,7-dichlorooxine, 20 ml of water, and 5 ml of 20% NH_4Cl solution. The yttrium chelate was extracted with 25 ml of chloroform at pH 9.5, and the fluorescence intensity of the extract was measured. Yttrium contents of xenotime and fergusonite samples were 20.29 to 29.81% as Y_2O_3. (auth)

29095 DIRECT SPECTROGRAPHIC DETERMINATION OF SMALL CONCENTRATIONS (0.001 percent) OF LANTHANUM AND NEODYMIUM IN PURE CERIUM OXIDE. Radwan, Zofia; Strzyzewska, Bozena (Inst. for Nuclear Research, Warsaw). Chem. Anal. (Warsaw), 11: 191-3 (1966). (In Polish).

The operating conditions of an optical spectrograph are described (in both English and Polish, in tabular form) for attainment of sensitivities of 10 to 250 mg/g of La and 25 to 250 mg/g of Nd in cerium oxide, with a coefficient of variation of 21% for La and 22% for Nd. The present method was not successful for Pr determinations because the analytical lines were weak. (TTT)

29096 URANYL COMPLEXES WITH PHENOLIC LIGANDS. VI. COMPLEXES WITH KOJIC AND MECONIC ACIDS. Sommer, L.; Kurilova-Navratilova, L.; Sepel, T. (Purkyne-Univ., Brno). Collect. Czech. Chem. Commun., 31: 1288-1314(Mar. 1966). (In German).

The equilibrium of the complex formation of UO_2^{2+} ions with 3-hydroxy-5-hydroxy-methyl-4-pyrone (kojic acid) and 2,6-dicarboxy-3-hydroxy-4-pyrone (meconic acid) in solutions was investigated spectrophotometrically. The constants of some equilibria were calculated. The suitability of these reagents for uranyl determination was shown. (tr-auth)

29097 STUDY OF THE THERMAL DECOMPOSITION OF TRIHYDRATED LUTETIUM IODATE BY THERMOGRAVIMETRY, DIFFERENTIAL THERMAL ANALYSIS, AND INFRARED ABSORPTION SPECTROGRAPHY. Harmelin, Mireille (ENSCP, Paris). Compt. Rend., Ser. B, 262: 620-3(Feb. 28, 1966). (In French).

The existence of the lutetium iodate anhydride $Lu(IO_3)_3$ and of the paraperiodate $Lu_5(IO_6)_3$ were shown as stable intermediary phases arising during the heating of the trihydrate. The final term of the calcination up to 1000°C is the oxide Lu_2O_3. The infrared absorption spectra recorded between 4000 and 200 cm^{-1} are described and discussed. (tr-auth)

29098 MEASURING THE ACTIVITY OF TRITIATED WATER PREPARATIONS BY MEANS OF A FLOW COUNTER. Lenskii, L. A. Dokl. Mosk, Sel'skokhoz, Akad., No. 89, 362-9(1963). (In Russian).

Preliminary experiments showed that tritium water samples (1 ml) could be counted on a flow counter, if the sample were placed at a distance of less than 5 mm from the counter window. The length of the voltage plateau was about 400 v. A count was run on tritium solutions having specific activities of 0.545, 1.090, 1.635, 2.18, 2.725, 3.270, 3.815, 4.360, 8.00, 11.1, and 13.7 μC/ml. The steel counting cups were 7 mm high, 2 mm deep, and 29 mm internal diameter. The count rate was directly proportional to the tritium concentration in the water. It was estimated that only 4% of the counts originated from evaporation of tritium water vapor, while 96% of the counts came from a surface layer 0.7 mg/cm^2 thick. A counting efficiency of about 4% was obtained at a specific activity of 2.0 μC/ml. This efficiency is about the same as that obtained with ^{32}P, ^{35}S, ^{45}Ca, and ^{14}C on an end-window counter. Residual activity was removed by blowing gas through the counter for 3 to 5 minutes. A background count must be taken before taking a tritium water count. (TTT)

29099 RADIOCHEMICAL TESTS OF INDUSTRIAL WASTE WATER. I. SIMPLE DETERMINATION OF ADDED ^{131}I IN THE WATER FOR THE STUDIES OF WASTE DISTRIBUTION. Kametani, Katsuaki; Urakubo, Goro (National Hygienic Lab., Tokyo). Eisei Kagaku, 11: 65-6(Mar. 1965). (In Japanese).

A simple and rapid method for the determination of ^{131}I added in water is proposed. The method consists of precipitation of ^{131}I as AgI, redissolution in 50% NaI and γ measurement with a well-type scintillation counter. Although the recovery was not very satisfactory, the method may be useful for investigating the distribution of industrial waste in a river. (auth)

29100 METHOD FOR DETERMINING HYDROGEN IN MAGNOX Al 80 AND MAGNOX Zr 55 BY VACUUM SUBLIMATION. Colombo, A. (EURATOM, Ispra, Italy). Energ. Nucl. (Milan), 13: 251-6(May 1966). (In Italian).

A vacuum sublimation method for determining hydrogen in Magnox Al 80 and Magnox Zr 55 is described. Using a commercial vacuum fusion instrument for the determination of gases in metals, samples are sublimed in a graphite crucible heated at 1000°C, and the gases extracted during the process are analyzed by gas chromatography. With samples weighing 50–100 mg, Magnox with hydrogen content ranging from a few ppm to some hundred ppm has been analyzed. The sensitivity of the method is about 1 ppm hydrogen. (auth)

29101 CONTENT OF RARE EARTHS IN THE STANDARD IGNEOUS ROCKS G-1, W-1, AND G-B. Aleksiev, E.; Boyadjieva, R. (Geological Inst., Sofia). Geochim. Cosmochim. Acta, 30: 511-13(May 1966).

The results of determinations of rare earth elements in granite G-1, diabase W-1, and Bulgarian granite G-B are given. The x-ray fluorescence method was used after chemical enrichment of the samples. (auth)

29102 USE OF A STANDARD IN THE SOLID PHASE FOR QUANTITATIVE ARGON DETERMINATION BY THE METHOD OF ISOTOPE DILUTION. Artemov, Yu. M.; Knorre, K. G.; Strizhov, V. P. (Vernadskii Inst. of Geochemistry and Analytical Chemistry, Moscow). Geokhimiya, No. 3, 349-51(Mar. 1966). (In Russian).

Data are given to show that additions of argon in the solid phase may be used as a standard in the isotopic dilution determination of argon. (tr-auth)

29103 DETERMINATION OF TRACE SALT BY BREMSSTRAHLUNG X-RAYS, INDUCED BETA PARTICLES, AND PRECISION ANALYSIS OF THE MEASUREMENTS. Chiaki, Hideo (Central Research Inst. of Electric Power Industry, Tokyo). Gijutsu Kenkyusho Shoho, 1964: No. 64045, 1-12 (Oct. 1964). (In Japanese).

A new technique using absorptiometry and reflectometry of fluorescent x rays (Cl–K, or Si–K was developed for determining the amount of salt deposited on a glass plate. A tritium–zirconium target was used as the x ray source. Characteristics of the gas-flow proportional counters constructed and the statistical fluctuations in counting the soft x rays were investigated both experimentally and theoretically. It was found that optimum conditions for determining salt deposits from 0.01 to 0.1 mg/cm^2 by the x ray fluorescent method within the variation coefficient of 10% were the 10 minutes' counting time and a maximum counting rate of 400 cpsec. (auth)

29104 MASS SPECTROMETRIC EVIDENCE FOR H_3O, HD_2O, AND D_3O. Melton, C. E.; Rudolph, P. S. (Oak Ridge National Lab., Tenn.). J. Catalysis, 5: 387-9(Apr. 1966).

It was previously postulated that H_3O is an important intermediate in the radiolysis of aqueous solutions, and it was predicted from thermochemical considerations that hydrogen-excess radicals such as H_3O may be stable. Furthermore, mass spectrometry revealed an ion beam at mass 19 not explained on the basis of an isotopic contribution. Evidence is reported that the ion beam observed at M/E = 19 is in fact H_3O^+; the progenitor is neutral H_3O, which is formed by a heterogeneous reaction on the walls of the ion source. Samples of either H_2O or D_2O were introduced into the instruments in the pressure range of 10^{-9} to 10^{-8} torr. The ions, HD_2O^+ and D_3O^+ were not observed in the absence of the ionizing electron beam or at very low electron energy. Qualitative appearance potential measurements showed that the ionization potential of D_3O was about 1 ev lower than that of D_2O. Wall reactions of D_2O^* to form D_3O^+ were ruled out because of the low concentration of D_2O^*. Furthermore, the walls were made negative with respect to the ion repeller to prevent the possible evolution of ions from the surface. A second possible origin of the ions, ion-molecule reactions with D_2O^+ or some other abundant ion from D_2O, was also eliminated. Under the experimental conditions and pressures of 2 to 30 × 10^{-9} torr the abundance of secondary ions from ion-molecule reactions was many orders of magnitude too low to explain the observed abundance of the new species. In addition to this evidence, the intensity ratios, HD_2O^+/DHO^+ and D_3O^+/D_2O^+ were measured as a function of the electric-field strength within the ionization chamber. No change in these ratios was observed for changes in the electric-field strength from about 0 to 20 v cm^{-1}. This proved that HD_2O^+ and D_3O^+ are not produced by ion-molecule reactions since the abundance of secondary ions is sensitive to changes in the electric-field strength within the ionization chamber. A third possible origin of the ions, dissociative ionization of a dimer evolving from the surface, although apparently unlikely, could not be ruled out. Evidence from these experiments is consistent with the formation of neutral H_3O by a surface reaction. The lifetime, with respect to spontaneous decomposition, of H_3O in the gas phase must be at least 10^{-6} sec (transit time from the surface to the electron beam). (BBB)

29105 RADIO GAS CHROMATOGRAPHY PEAK ANALYZER. Pearson, Richard Jr.; Fink, William C.; Gordus, Adon A. (Univ. of Michigan, Ann Arbor). J. Gas Chromatogr., 3: 381-3(Nov. 1965).

Disadvantages of present methods used to determine radioactivity quantitatively in effluent fractions from gas chromatography columns are cited. A simple inexpensive method of determining the activities was developed. The pulses from a radioactivity detector are fed simultaneously into an electronic (log-scale) rate meter (a lab survey meter suffices) and into an electronic scaler with at least four electronic decades. An auxiliary circuit is actuated every time the scaler reaches 10, 10^2, 10^3, and 10^4 total accumulated counts. This auxiliary circuit produces a pulse whose height depends on the number of counts it represents. The duration of the pulse is sufficiently long so as to register reproducibly on a pen recorder with a full scale response time of 1 sec. When two or more pulses occur simultaneously (e.g., at 10^3, which corresponds to the triggering of the 10, 10^2, and 10^3 output recording pulses) only the largest output is recorded. The output from the rate meter is fed to one pen and the output from the auxiliary circuit to a second pen of a two-pen recorder. The only uncertainties in this method are those associated with the statistics of radioactivity and the measurement of the time intervals chosen to encompass the peak. This latter uncertainty, however, only affects the value of the background count to be subtracted and this is usually small in comparison with the activity of the peak. The recovery times of the electronic components and typical scintillation or proportional counters would not introduce a detectable error unless the counting rates were at least 10^5 cpm. The electronic circuits were designed for use with transistorized scalers. (BBB)

29106 SAMPLE FURNACE FOR EXPERIMENTS ON NEUTRON SCATTERING. Oehme, H.; Hauschild, J. (Kernforschungszentrum, Karlsruhe, Ger.). Kerntechnik, 8: 205-8(May 1966). (In German).

A special high-vacuum sample furnace for neutron diffraction experiments was designed and operated up to sample temperatures of about 1000°C. The only structural

material in the neutron beam is vanadium, of which the coherent scattering amplitude is practically zero. Therefore, the scattering curves of the samples are not disturbed by interference effects from the furnace. The furnace is equipped with a high-vacuum pump and a safety and control unit and is designed for automatic operation over long periods. Temperature control gives a very constant sample temperature. Some operational experience is reported. (auth)

29107 ANALYSIS OF CHROMIC SALT SOLUTIONS BY MEANS OF β-RAY BACKSCATTERING. Blazej, A.; Toelgyessy, J.; Uher, M. (Slovenska Vysoka Skola Technika, Bratislava). Leder, 14: (Jan. 1963). (In German).

The method developed for analyzing chrome liquors of various compositions is based on β backscattering of Cr atoms. Backscattering was determined from the backscattering factor (R- the ratio of the backscattered radiation to the incident radiation), which depends on the atomic number, the incident energy, layer thickness, and concentration of the backscattered atoms. By keeping all other factors constant, the Cr^{3+} content can be calibrated by using a Geiger counter to measure the intensity of the incident and backscattered radiation. ^{204}Tl was used as the β source, and the backscattered electrons were counted by a specially constructed Geiger counter connected to a recorder. The effects of the presence of cations (Na^+, K^+, Ca^{2+}, Mg^{2+}, Al^{3+}, and Fe^{3+}), anions (Cl^-, SO_4^{2-}, oxalates, formates), skin proteins, and tanning agents on R are discussed. For continuous backscattering measurements which are required in a large chrome tannery, a ^{90}Sr β source and an ionization chamber for the R measurement are preferred. (OID)

29108 OXYGEN DETERMINATION IN HIGH-MELTING METALS, THEIR ALLOYS, AND REFRACTORY MATERIALS. Lassner, E. (Metallwerk Plansee AG, Reutte/Tyrol). pp 511-24 of Metals for the Space Age. Plansee Proceedings, 1964. Benesovsky, F. (ed.). Reutte/Tyrol, Metallwerk Plansee AG, 1965. (In German).

Following a comparative description of the methods of oxygen determination in metals in general and the vacuum degassing methods in particular, optimum analysis conditions for powders and solid specimens as determined by means of the Exhalograph EA-1, are described for: Ta, Nb, Mo, W, TiC, WC, and cemented carbides. (auth)

29109 SIMULTANEOUS SPECTROPHOTOMETRIC DETERMINATION OF THORIUM AND THE RARE EARTHS WITH XYLENOL ORANGE. Mukherji, Anil K. (Drexel Inst. of Tech., Philadelphia). Microchem. J., 11: 243-54 (June 1966).

A spectrophotometric method is described for the determination of microgram amounts of thorium and rare earths using Xylenol Orange. Thorium forms a colored complex (λ_{max} 576 mμ) with the reagent at 2 pH and the rare earths do not. At 6 pH, however, both thorium and the rare earths form complexes and the absorbances are additive. The concentration range for determination of effects of pH, time, reagent, and interferences are discussed. Reproducibility was excellent with an average error of ±1.2%. (auth)

29110 STUDY OF BETA BACKSCATTERING FOR APPLICATION IN ANALYTICAL CHEMISTRY. Jirkovsky, Rudolf (Montanhochschule, Ostrava, Czechoslovakia). Mikrochim. Acta, No. 1-2, 186-95(1966). (In German).

The application of the β scattering for the nondestructive analysis of metallurgical materials is discussed. The applications for determination of ash in coals, taking account of the moisture content and the grain size, are described in which 20 mC $^{90}Sr-^{90}Y$, and simple equipment are employed. Numerous other possibilities of using this method are indicated. (auth)

29111 RAPID COLORIMETRIC DETERMINATION OF BERYLLIUM IN Al–Mg–Be ALLOYS. Ishiguro, Yoshio (Government Industrial Research Inst., Nagoya, Japan); Niimi, Yoshinobu. Nagoya Kogyo Gijutsu Shikensho Hokoku, 15: 8-13(Jan. 1966). (In Japanese).

A colorimetric method for determining beryllium based on the absorption maximum at 580 mμ in alkaline solution of the reddish blue water-soluble chelate with arsenazo I was studied. The absorbance obeyed Beer's law within the concentration range of 0 to 0.6 ppM of beryllium, and the complex had a molar extinction coefficient of 1×10^4. The composition of the beryllium complex with arsenazo I was investigated by the continuous variation method, and the ratio of beryllium to arsenazo I was found to be 1:2 at pH 12.2, and 1:1 at pH 5. Using this method, the amount of beryllium contained in Al–Mg–Be alloys (within the range of 0.1–5%) can be determined rapidly and accurately. (auth)

29112 ACTIVATION ANALYSIS OF ALKALI HALIDES BY PHOTONUCLEAR REACTION. Abe, Shigeki (Yamagata Univ., Yonezawa, Japan). Nippon Kagaku Zasshi, 87: 426-32(May 1966). (In Japanese).

Based on results of photoactivation of alkali halides, methods for nondestructive determination of chloride in sodium bromide and iodide in sodium chloride or bromide were developed. Alkali halides were irradiated for 10 min or an hour with 20-Mev bremsstrahlung generated from a linear electron accelerator. The induced radioactivities, composed mainly of ^{34m}Cl, ^{80m}Br, ^{80}Br, ^{126}I, and ^{18}F, which were produced by (γ,n) reactions, were measured by a multichannel pulse-height analyzer. The γ spectrum of the chloride showed a prominent ^{34m}Cl photopeak at 0.15 Mev and decayed with a half life of 33 min. In the γ spectrum of the bromide, the intense photopeaks of $^{80m}Br-^{80}Br$ at 0.51 and 0.61 Mev were observed. In the iodide, the ^{126}I photopeaks of 0.38, 0.51, 0.67, 0.74, and 0.86 Mev were observed, all of which decayed with a half life of 13 days. For analyses of halide contents, the photopeak activities vs. the weight ratio of halides were plotted and the linear relationships were obtained. The content of chlorine in bromide samples and iodine in chloride or bromide samples can be analyzed up to 50%, respectively. (auth)

29113 SPECTROCHEMICAL ANALYSIS OF ZIRCONIUM AND ITS ALLOYS. I. SPECTROGRAPHIC DETERMINATION OF IMPURITIES IN ZIRCALOY-2. Nishizaki, Kyoji; Matsumura, Tetsuo; Miwa, Hisayoshi (Kobe Steel Ltd., Japan). Nippon Kinzoku Gakkaishi, 30: 94-8(1966). (In Japanese).

A spectrographic method for the simultaneous determination of trace elements (Al, Co, Mg, Mn, Mo, Pb, Ti and V) in zircaloy-2 is described. The technique has two advantages from a viewpoint of spectrochemical analysis, that is, the simple preparation of standard samples and the high sensitivity. A mixture of the oxide sample and graphite powder containing Y_2O_3 as an internal standard was arced for 15 sec in a 7 amp dc arc, with sufficient sensitivity and high precision. The density of spectra obtained was measured by an automatic recording microphotometer, and then converted into the relative intensity by means of special calculator respectra. The coefficient of variation was from 5 to 20% in the analytical concentration range from 5 to 200 ppM. (auth)

29114 SPECTROCHEMICAL ANALYSIS OF ZIRCONIUM AND ITS ALLOYS. II. SPECTROGRAPHIC DETERMINATION OF HAFNIUM IN ZIRCONIUM BY THE POWDER-SPARK TECHNIQUE. Takao, Zenichiro; Miyoshi, Satoshi; Kamigaito, Ichiro; Kawaguchi, Takehiko (Kobe Steel Ltd., Japan). Nippon Kinzoku Gakkaishi, 30: 186-90 (1966). (In Japanese).

In the production and quality control of Zr and its alloys, it is the most important problem to determine trace Hf rapidly and accurately because of its high absorption cross section for thermal neutrons. The method for the determination of Hf in reactor-grade Zr and also in commercial grade Zr is described. The metal was converted into the oxide by chemical treatment. Sample electrodes were prepared by coating with a thin layer of oxide powder on the flat top of a 5 mmϕ graphite rod. The analysis was performed with the 3.4-meter Ebert mounted grating spectrograph using Raiskii spark excitation. Analysis of several unknown samples containing 100 ppM Hf, determined independently by other physical methods, showed good agree-

ment. The precision was 3% for 0.20 to 5.00% Hf and 8% for 40 to 600 ppM Hf. (auth)

29115 SPECTROCHEMICAL ANALYSIS OF ZIRCONIUM AND ITS ALLOYS. III. SPECTROGRAPHIC DETERMINATION OF HAFNIUM IN ZIRCONIUM BY THE POINT-TO-PLANE SPARK TECHNIQUE. Matsumura, Tetsuo; Kudo, Yasuo; Kawaguchi, Takehiko (Kobe Steel Ltd., Japan). Nippon Kinzoku Gakkaishi, 30: 191-5(1966). (In Japanese).

A spectrographic method for determination of trace Hf in Zr and its alloy was developed and the discharge of a high voltage condensed spark was employed for exciting the solid sample. The optimum condition of excitation to detect trace Hf less than 100 ppM was investigated. By using Raiskii spark excitation, the required sensitivity and reproducibility were obtained. With some modifications in the excitation condition and with the addition of a low speed emulsion, the method was also applied to the determination of Hf in the percent range. The analysis was carried out on the line pairs-Hf 2641.4Å/Zr2653.6Å in the ppM range and Hf 2641.4Å/Zr 2761.9Å in the percent range. The precision of the method was ±2 to ±12% at the level of 100 ppM and ±5% at the level of 2 to 3%. The method offers an increase in speed and improved stability as compared with most of the previous methods for the determination of Hf by means of excitation of the oxides. (auth)

29116 ACTIVATION ANALYSIS FOR CHLORINE IN PETROLEUM PRODUCTS AND RELATED MATERIALS. Braier, H. A.; Mott, W. E. (Gulf Research and Development Co., Pittsburgh). Nucl. Appl., 2: 44-7(Feb. 1966).

A photoneutron source of improved design, with a larger and more uniform thermal-neutron flux than designs previously described in the literature, permits instrumental analysis of chlorine to 0.05 ppM with good accuracy and reproducibility. The satisfactory analyses of more than 1200 samples by the method described proved its suitability for routine use by technicians. (auth)

29117 BORON ASSAY IN STAINLESS STEEL. Bermanis, H. L. (General Electric Co., Cincinnati). Nucl. Appl., 2: 48-50(Feb. 1966).

Borated stainless steel is frequently used in critical experiments for special measurements and to simulate reactor components. The validity of such measurements depends on the accuracy with which the boron density in the steel is known and on the uniformity of the boron dispersion in the steel. A technique is described for measuring the boron inventory in two different borated stainless steels by means of a sensitively instrumented subcritical test assembly. The results compared favorably with monochromatic neutron transmission measurements and with classical chemical analyses. Absolute calibration of the test assembly for boron was accomplished by means of steel coupons to which measured amounts of powdered elemental boron were added. (auth)

29118 USE OF NEUTRON GENERATORS IN ACTIVATION ANALYSIS. Strain, J. E. Progr. Nucl. Energy, Ser. IX, 4: 137-57(1965).

A survey was made of the applications of the 100- to 400-kv neutron generator to activation analysis. Results indicated that there are areas in which this method can compete with routine chemical methods. However, only a few elements can be determined by this method at concentrations of less than 100 ppM. With an automated system coupled directly to a computer, it is possible with a single irradiation to determine several components in a few seconds, exclusive of the time necessary for irradiation and counting. Uses of the neutron generator in mineralogy, process control, and as a teaching device or research tool in neutron-activation analysis and nuclear physics are described. Generator construction and health physics considerations are discussed. (M.C.G.)

29119 INSTRUMENT AND CHEMICAL ANALYSIS ASPECTS OF ELECTRON MICROANALYSIS AND MACROANALYSIS. PROGRESS IN NUCLEAR ENERGY. SERIES IX. ANALYTICAL CHEMISTRY. VOLUME 5. Elion, Herbert A. (GCA Corp., Bedford, Mass.). Progr. Nucl. Energy, Ser. IX, 5: 1-244(1966).

The present and future state of the electron analysis field, centering about the evolution of scanning electron analysis is surveyed. An attempt is made to give the analyst a working knowledge of its principles, operation, and capabilities. Improvements in and applications of electron optical systems, electron lenses, x-ray optics, and detectors are noted. The combination of electron, x-ray, and light energies as they interact with the specimen under examination is discussed. Specific methods of micro- and macroanalysis are considered in some detail. (J.G.B.)

29120 SEPARATION PROCESS FOR GENERAL USE IN ACTIVATION ANALYSIS. PART II. Gebauhr, W. (Siemens Schuckert Werke AG, Erlangen, Ger.). Radiochim. Acta, 5: 8-14(Mar. 1966). (In German).

Special chemical considerations in the separation scheme are discussed briefly. The sequence of the discussion follows that of the grouping of the separation process or general chemical analytical groups. The results of test analyses in which activities in a pure radiochemical form were added to a carrier mixture are given. (J.S.R.)

29121 EVALUATION OF ACTIVITY DETERMINATION OF BIOLOGICAL MATERIALS WITH AN ELECTRONIC COMPUTER. Hoffmann, W.; Kusemann, D. (Farbwerke Hoechst AG, Frankfurt am Main). Radiochim. Acta, 5: 49-50(Mar. 1966). (In German).

Since evaluation of activity determination of biological materials requires considerable calculation time, a program was developed for evaluation of these determinations on the IBM-705. The program is synchronized with a liquid scintillation spectrometer with 2 to 3 channels and an automatic zero effect subtraction so that the net impulse is expressed. The channel ratio method is used for determination of the counting yield. Formulas are presented for determination of the percentage activity in organs, blood, or excretions and the amount of the introduced pharmaceutical in the sample. (J.S.R.)

29122 LOSS OF ^{137}Cs AND POTASSIUM BY DRY ASHING AND HYDROCHLORIC ACID TREATMENT OF TOTAL DIET SAMPLES. Akaishi, Jun; Iwamoto, Junko; Fujita, Minoru (Japan Atomic Energy Research Inst., Tokyo). Radioisotopes (Tokyo), 15: 103-8(1966). (In Japanese).

Loss of ^{137}Cs and potassium by dry ashing and by hydrochloric acid treatment was studied on large amounts of total diets. Total diets were collected from 1963 to 1965 and samples for 2 or 5 days were treated as a whole. In this study, radioactive cesium was not added to the samples as a tracer, but fallout ^{137}Cs contained in them was used to check the recovery. The amounts of both ^{137}Cs and ^{40}K were determined by gamma spectrometry. Ashing at 600°C for 10 hours gave several per cent of loss for ^{137}Cs, and no loss for potassium. In the process of dry ashing for 2 to 20 hours, no significant difference was found between 450 and 600°C. By the hydrochloric acid (1 : 1) treatment of the ashed sample, 90 to 80% of ^{137}Cs was leached out but 10 to 20% remained in the residue, while potassium was dissolved perfectly. (auth)

29123 STUDY ON A RADIO PAPER PARTITION CHROMATOGRAPHY OF ORGANIC HALOGEN COMPOUNDS BY NEUTRON IRRADIATION: A QUALITATIVE APPROACH. Kim, You-sun; Chae, Song-cha (Atomic Energy Research Inst., Seoul. Ewha Womens Univ., Seoul). Ta Han Hua Hsueh Hui-Chih, 8: No. 2, 47-56(June 1964).

When a developed paper partition chromatogram was irradiated in the pneumatic tube system of the Korean research reactor (neutron flux: 1.5×10^{12} n/sq cm/sec) qualitative confirmation of the developed spot on the chromatogram was possible. In the case of organic halogen compounds (chloro-acid, chloro-ester, iodide, and fluoride) spot analysis was possible whereas the same spot did not give the distinct coloring with common coloring reagents. Filter paper thickness calibration and activity calibration induced by irradiation of the components of the

filter paper, which were a source of erroneous interpretation of the spot, were searched and an average filter paper calibration method and filter paper activity were improvised to obtain a good qualitative analysis of the spot. The use and applicability of this method for the analysis and identification of an organic halogen compound were evaluated. As the filter paper phase an ordinary phase (Whatmann no. 1. filter paper) and reversed phase (liquid paraffin impregnated) were used. (auth)

29124 PULSE-ANALYSIS METHOD OF LIGHT ELEMENTS. I. FUNCTIONAL REPRESENTATION OF PULSE-HEIGHT DISTRIBUTION. Shimizu, Ryuichi; Murata, Kenji; Shinoda, Gunji. Technol. Rep. Osaka Univ., No. 16, 255-64 (Oct. 1965).

The acceptability of the Weibull function as a functional representation of pulse-height distributions of the light elements is discussed. By comparing with the experimental result it is shown that the Weibull function describes the empirical data of Be, B, C, O-pulse-height distribution quite well. And the linear relation between the shape parameter of the Weibull function and the photon energy of the light element characteristic radiation is found. As a practical applicability of the Weibull function an approach to extend Dolby's pulse-analysis method to the light elements is mentioned. (auth)

29125 ABSORPTION-SPECTROPHOTOMETRIC DETERMINATION OF RARE EARTHS IN TRIBUTYLPHOSPHATE EXTRACTS. Mishchenko, V. T.; Lauer, R. S.; Efryushina, N. P.; Poluektov, N. S. (Inst. of General and Inorganic Chemistry, Academy of Sciences, Ukrainian SSR). Ukr. Khim. Zh., 31: 1189-97(1965). (In Russian).

The absorption spectra of tributyl phosphate complexes with Pr, Nd, Sm, Eu, Gd, Dy, Ho, Er, and Yb were investigated. It was established that during complex formation in tributyl phosphate solution the majority of the absorption band maxima are displaced to the side of increased wavelength by 1 to 10 mμ. The displacement of some absorption peaks, for example Er, to smaller wavelengths was also observed. The heights of the peaks of rare earth absorption bands are often increased 1.1 to 3.5 times and more. The conditions for determination of Pr, Nd, Sm, Ho, and Er in mixtures of rare earth elements of the cerium and yttrium subgroups in TBP were worked out for concentrated solutions of the rare earth elements up to 130 mg/ml and for different concentrations of the solutions of TBP and other solvents. The sensitivity of the method in mg/ml of the oxide was 0.03 for Nd, 0.04 for Ho and Er, 0.06 for Pr, and 0.18 for Sm. (tr-auth)

29126 NEW TYPE OF HIGH-FREQUENCY MASS SPECTROMETER WITH TWO ELECTRODES. Gautherin, G.; Lejeune, C.; Septier, A. (Univ., Paris, Orsay, France). Vide, 22: 120-31(Mar.-Apr. 1966). (In French).

The principle of a new type of mass spectrometer using a HF electric field (of frequency f) generated between two parallel plates, in which ions are injected parallel to the median plane, was studied. The spectra are obtained by sweeping the frequency. For each mass there exists a whole series of resonance frequencies permitting the transmission, but it is possible to eliminate higher order spectra. By reducing the luminosity it is possible to attain a resolving power of about 200. A low resolution prototype for the analysis of hydrogen ions, produced by a duoplasmatron source and accelerated under 30 to 40 kv, was built and successfully used. Possible applications as a helium leak detector or spectrometer for residual gases are envisaged since the whole system is light and compact. (auth)

29127 DETERMINATION OF THE ASH CONTENT OF BITUMINOUS COAL BY γ-IRRADIATION WITH ^{170}Tm. Koch, Siegfried; Windelband, Rolf (Technische Univ., Dresden). Wiss. Z. Tech. Univ. Dresden, 13: 23-30(1964). (In German).

The gravimetric determination of bituminous coal has 2 very serious drawbacks; therefore, this method was replaced in many cases by the radiometric method, e.g., for measuring relatively large volumes of coal from the attenuation of the penetrating γ intensity. Since the ash components have a higher atomic number than the ash-free components, the intensity of the penetrating radiation decreases with increasing ash content, i.e., the greater the decrease the lower the photon energy. A 1-C ^{170}Tm low-energy source was used, which emitted 84-kev gammas in addition to β radiation of 968-kev maximum energy. A study was made to determine to what extent collimation of the radiation beam, thickness of the penetrated layer, and the spectrum of the recorded radiation affected the measuring sensitivity. Best results were obtained with measurements restricted to the 52-kev characteristic x-ray emission emitted by ^{170}Tm as a result of the interaction of the γ rays and atoms of the radioactive preparation. By reducing the diameter of the collimator boring and increasing the thickness of the layer of coal penetrated, the measuring sensitivity was increased, and the error was reduced to ±1% for an ash content of 15%. (OID)

29128 THE FLUORESCENT MEASUREMENT OF NEGLIGIBLE AMOUNTS OF URANIUM IN WASTE WATER. Liu, Lun-yu; Chang, Yuan-chin. Yuan Tzu Neng, No. 1, 60-4(1965).

Fluorescent analysis is a sensitive method for measuring negligible amounts of uranium, especially in waste water. The intensity of fluorescence produced from excited uranium compounds under the influence of ultraviolet rays, x-rays or cathode rays, is directly proportional to the uranium content. A 0.5 mm platinum wire, one end of which was made into a small ring, 3 to 4 mm in dia, a type-24 pH meter, a portable fluorimeter or ultraviolet lamp, a doubly connected air pump, and a standard uranyl nitrate solution (10 μg/ml) were used. In order to eliminate any possible error, 18 pearlite balls were made containing 0, 0.25, 0.5, 1.0, 2.0, 3.0, 5.0, 8.0, 10, 12, 15, 18, 20, 25, 30, 40, 50, and 100 μg of uranium, respectively. Under the oxidizing flame of an alcohol lamp at 700°C, the fluorescence of the pearlite ball reached a maximum in three minutes, after which the color became yellow. The effect of interfering elements on the fluorescent analysis was tested and tabulated, showing that interference appears in the measurement of uranium fluorescence when the content of interfering iron is over 10 mg, that of niobium and magnesium is over 5 mg, or that of copper, lead, and manganese is below 5 mg. Activated charcoal was used to eliminate the interference and the best absorption was obtained at pH 5. Activated charcoal was found to absorb the negligible amounts of uranium in waste water, which could thus be separated from the interfering elements after desorption by means of Na_2CO_3. By means of fluorescent analysis, negligible concentrations of uranium, as low as 10^{-6}, not only in waste water but in natural water, can be measured easily and promptly with satisfactory results. (ATD)

29129 MICRODETERMINATION OF RARE EARTHS IN URANIUM COMPOUNDS BY A SPECTROGRAPHIC METHOD. Teng, Po. Yuan Tzu Neng, No. 2, 97-108 (1965).

The recovery of rare earths using the tributyl phosphate CCl_4 extraction system was >94%. During the hydroxide precipitation process, the recovery rate reached 95%. For the spectrographic determination of rare earths, a crater-type graphite electrode (electrode height 1 to 3 mm) was used as a spark source and an atmosphere of CO_2 maintained around the arc to suppress the cyanogen bands. High sensitivity and reproducibility were achieved when the electrode was treated with a drop of 3% polystyrene solution; the distance between the two electrodes at the beginning was 1.5 mm and 9 amperes of alternating current were applied to excite the spectrum for 20 sec. No interference with the rare earths spectrum was produced by 125γ of Na, 100γ of Pb, or 10γ of Al, Fe, and Mg. Interference due to 10γ of Ca and Th could be avoided by carrying out the NH_4OH precipitation under the protection of sulfonyl salicylic acid. The presence of 20γ of K prevents the interference due to 50γ of P and increases the intensity of the spectral lines. The maximum sensitivity of this method was found to be only 0.05γ of Sm, 0.005γ of Eu,

0.16γ of Dy, and 0.06γ of Er. The relative error was approximately 10 to 15%. (ATD)

29130 COLORIMETRIC MICRO-DETERMINATION OF URANIUM BY MEANS OF EDTA-NITROSONAPHTHOL-AZOARSINE I. Hu, Kuo-chen. Yuan Tzu Neng, No. 4, 346-8(1965).

The V. I. Titov method is discussed and the Titov process reviewed. Some modifications are recommended. For color development the optimum pH is 5, compared with the earlier recommended pH of 4 to 8. The color is stable and does not produce any interfering yellow coloration at this pH; precipitation of uranium is optimum at pH 8.2 instead of 6.8 to 8; at this pH, the EDTA-nitroso-naphthol separates the uranium from most of the interfering elements. Iridium, cobalt, and traces of iron can be precipitated by carbonization. This method is said to deviate from the carbonization volumetric method by 7%, and the method is noted for its efficient elimination of the interfering minerals. (ATD)

29131 SIMPLE METHOD FOR ^{15}N DETERMINATION. Guenther, H.; Floss, H. G.; Simon, H. (Technische Hochschule, Munich). Z. Anal. Chem., 218: 401-8(1966). (In German).

A method for measuring the ^{15}N content of organic and inorganic compounds is given. The substances are combusted with CuO and CaO at 650°C in an evacuated glass tube and the nitrogen formed is analyzed in a mass spectrometer. (auth)

29132 PAPER ELECTROPHORESIS OF STEROIDS. PART I. COMPARATIVE STUDY USING RADIOACTIVE AND SPECTROPHOTOMETRIC TECHNIQUES. Abdel-Wahab, M. F.; Bishara, R. H. (MERR Center for Arab Countries, Cairo. GOPCA, Giza, United Arab Republic). Z. Anal. Chem., 219: 183-7(1966).

A radiochemical method for the identification of some steroids on electropherograms is described. A comparison between this method and another modified spectrophotometric method is given. The radiochemical method can be used for quantitative work; the relationship between the concentration of the hydrazones and the radioactivity gained by the steroids is linear. This technique was concluded to be superior to any colorimetric one, it needs less reagents and is not as time consuming. (auth)

29133 ANALYSIS OF RARE EARTH ALLOYS IN NON-AQUEOUS SOLUTIONS. Kreshkov, A. P.; Yarovenko, A. N.; Milaev, S. M. (Mendeleev Chemical Engineering Inst., Moscow). Zavodsk. Lab., 32: 396-7(1966). (In Russian).

A rapid method for the analysis of alloys of the rare earth elements was developed. It was based on their dissolution in hydrobromic acid and subsequent differential titration of the compounds obtained in methanol–acetone media with standard benzene–methanol solutions of tetraethylammonium hydroxide. (tr-auth)

29134 QUANTITATIVE SPECTRAL DETERMINATION OF YTTRIUM AND RARE EARTH ELEMENTS OF YTTRIUM SUBGROUP IN ORES AND MINERALS. Karpenko, L. I.; Fadeeva, L. A.; Bel'tyukova, S. V. (Lab. of General and Inorganic Chemistry, Academy of Sciences, Ukrainian SSR). Zavodsk. Lab., 32: 424-6(1966). (In Russian).

A method for the quantitative spectrographic determination of Gd, Tb, Dy, Ho, Er, Tm, Yb, Lu, and Y in solutions of rare earth mixtures obtained from ores and minerals is described. The method is based on the comparative intensity of the spectral lines of given rare earth elements and a comparison element, scandium, during spectral excitation in a discharge of high-voltage condensed sparks. The mean error of the determination is 8 to 10%. (tr-auth)

29135 ORGANIC COPRECIPITANTS. PART 23. COPRECIPITATION OF PROTACTINIUM(V) IN THE FORM OF ANIONIC COMPLEXES AND COMPLEXES WITH REAGENTS OF THE ARSENAZO GROUP. Kuznetsov, V. I.; Fisenko, L. P.; Akimova, T. G. pp 49-54 of Radiokhimicheskie Metody Opredeleniya Mikroelementov. Moscow-Leningrad, Izdatel'stvo Nauka, 1965. (In Russian).

A preparation of ^{233}Pa, which is a β and γ emitter, was used. A study of the effects of acidity on the extent of coprecipitation of Pa with induline chloride and rhodamine B from HCl, HBr, HI, and HSCN solutions showed that Pa precipitates best from concentrated HCl (11 M), in which it is present as an anion, and to a lesser extent from the other acids. A practically complete coprecipitation of Pa with arsenazo I also requires the presence of crystal violet. With arsenazo II and III, crystal violet is required in weakly acid solutions, and rhodamine B in more acid ones (0.1–6 M HCl). Heavier organic molecules of the precipitant (arsenazo) are more suitable for the coprecipitation. The general pattern of coprecipitation of Pa present in solutions in various states is presented. Depending upon the species in which Pa exists in the solution, the most complete coprecipitation is ensured by the mechanism which is most suitable for the given species of Pa. (CFSTI)

29136 DERIVATIVE NEUTRON ACTIVATION ANALYSIS OF ZINC [Thesis]. Harmison, Lowell Thomas. College Park, Md., Univ. of Maryland, 1965. 88p.

Derivative neutron activation analysis was applied to the determination of less than microgram quantities of zinc. The analysis involves the chelation of the metal ion, the separation of the complex from excess chelating agent, and subsequent activation of the complex. An aqueous solution of zinc was treated with a chloroform solution of the dibromoxine reagent (57-dibromo-8 quinolinol. The zinc was extracted from the aqueous phase into the chloroform. The zinc chelate (R_f: 0.8) was then separated from the excess reagent (R_f: 1.0) and the contaminants by paper chromatography. After separation, the chromatograms were activated for eight hours in the University of Maryland pool-type nuclear reactor with a flux of about 10^{11} $n/cm^2/sec$. The induced ^{82}Br activity was counted, after allowing for the decay of short-lived isotopes, with a well-type NaI crystal and a single-channel spectrometer. The counting was semi-integral, covering the major 0.777-Mev energy peak of ^{82}Br. The results show that trace quantities of zinc can be quantitatively determined in the range from 0.25 to 1.4 μg with an accuracy of approximately ±15% over the detection range. The lower detection limit is below the one μg sensitivity that can be obtained with the standard chemical zinc dithizone analysis. In terms of direct neutron activation, it represents an even greater increase in sensitivity, because the theoretical sensitivity of zinc-65 under identical conditions would be approximately 200 μg. With higher neutron fluxes greater sensitivity would appear possible. In summary, the determination of an element by neutron activation analysis is no longer limited by its unique nuclear properties when the particular element can be incorporated into a derivative molecular complex containing activable atoms with optimum nuclear properties. (Dissertation Abstr.)

29137 INSTRUMENTAL ACTIVATION ANALYSIS USING NEUTRON CAPTURE AND DELAYED GAMMA-RAY SPECTROMETRY [Thesis]. Isenhour, Thomas Lee. Ithaca, N. Y., Cornell Univ., 1965. 100p.

Two approaches to greater resolution in activation analysis are advanced. The first is full utilization of resolution based on half-life. Three computer programs were developed, which compute the optimum irradiation and decay times for maximum selectivity of desired radioactive signals in any mixture regardless of its complexity. Program OPTIMIZE computes optimum values for a single element in a mixture. Program OPTIPLOT graphically presents the effects of using different irradiation times with optimized decay times for groups of elements and Program MULTIOPT seeks a single irradiation time with individual decay times for determining a group of elements. The three programs are combined into master program AARDVARK, which, by referring to a library tape containing nuclear parameters and reference gamma spectra, can evaluate the feasibility of applying either single-element and/or multielement activation analysis to any sample. The second method developed is the quantitative use of neutron-capture gamma rays. These

prompt gamma rays are more abundant in most cases than the delayed gamma rays produced by radioactive decay. A high speed thermal neutron chopper was designed, which produces a "square wave" neutron beam. A signal from the chopper gates a multichannel scintillation spectrometer in alternate memory modes thereby allowing individual recording of the gamma spectra produced during the two halves of the cycle. The subtraction of these spectra results in a net spectrum of prompt gamma rays without contribution from delayed gamma rays and other interferences. Since high-cross-section reactions result in a greatly attenuated neutron beam, the rate of gamma-ray production is an asymptotic function of concentration. To permit accurate quantitative measurements an internal standard system was developed in which the ratio of two gamma signals is a function of the concentration ratio between the standard and unknown. The study of prompt gamma radiation is concluded with a comparison between the sensitivity of delayed and prompt gamma-ray activation analysis. (Dissertation Abstr.)

29138 NEW DEVELOPMENTS IN NEUTRON ACTIVATION SYSTEMS FOR ANALYSIS OF OXYGEN IN STEEL. Wood, D. E.; Jessen, P. L.; Jones, R. E. (Kaman Nuclear, Colorado Springs, Colo.). 38p. (CONF-660201-2). ORAU.

Conference on Analytical Chemistry and Applied Spectroscopy, Pittsburgh.

Neutron activation analysis of oxygen in steel was previously proven fast, reliable, and accurate on a laboratory basis. Developments in neutron generators and pneumatic transfer systems made the technique suitable for routine quality control applications by technicians with minimum training. Sealed-tube fast neutron generators were developed with outputs in the range of 10^{10} to 10^{11} neutrons/second to eliminate the hazard associated with handling tritiated titanium targets in pumped accelerators. Neutron flux monitoring is achieved with a transfer standard in a second transfer tube. Sample and standard are rotated on two axes to ensure identical irradiation. Comparison with single rotation, no rotation, and remote flux monitors indicated an order of magnitude improvement in reproducibility. Standard deviations of 1% for high-oxygen samples are routinely measured. Long-term calibration stability is better than 3%. Measurements at low levels (around 10 ppm) were improved by reducing the "blank" value due to the carrier bottle from the equivalent of 60 ppm in steel to 10 ppm equivalent for samples of uniform size. (auth)

29139 FAST-NEUTRON ACTIVATION ANALYSIS USING SMALL ACCELERATORS. Hull, R. L. (Humble Oil and Refining Co., Baytown, Tex.). 6p. (CONF-640513-1). ORAU.

From American Petroleum Institute's Div. of Refining, 29th Midyear Meeting, Session on Activation Analysis, St. Louis.

Elemental analysis performed by radioactivation using accelerator-produced fast neutrons combined with rapid gamma spectrometry using multichannel pulse height analyzers offers many advantages in speed, reduced sample handling, and sample preservation. Approximately 20 elements of interest to the petroleum industry may be determined by this technique, many of them at concentrations of a few hundred parts per million. The equipment used and results of analyses for barium, oxygen, chlorine, antimony, silicon, titanium, and aluminum are described. (auth)

29140 LUNAR AND PLANETARY SURFACE ANALYSIS USING NEUTRON ACTIVATION. Cuypers, M. Y.; Hislop, J. S.; Kuykendall, W. E.; Wainerdi, R. E. (Texas Agricultural and Mechanical Univ., College Station). 27p. (CONF-660207-9). ORAU. Gmelin, AED-CONF-66-011-13.

From Symposium on Radioisotope Applications in Aerospace, Dayton, Ohio.

The 14-Mev neutron activation analysis technique was used for the determination of silicon, iron, aluminum, magnesium, and oxygen in granites and basalts. A prototype system for lunar surface analysis was developed and utilized to investigate the feasibility of the technique. The principle of operation involved the use of a rotating assembly for alternately positioning the neutron generator and the gamma detector directly above the surface to be analyzed. Results are based on the analyses of decay curves and gamma spectra obtained by multiple counting of irradiated samples. (auth)

29141 REQUIREMENTS OF A GENERAL ANALYTICAL LABORATORY IN PURE MATERIALS RESEARCH. Adler, S. J. (Radio Corp. of America, Princeton, N. J.). 10p. (CONF-651004-13). ORAU.

From 9th Conference on Analytical Chemistry in Nuclear Technology, Gatlinburg, Tenn.

In determining crystalline imperfections, a general analytical laboratory should utilize almost exclusively broad techniques based mainly on direct observations. The electronic behavior of "as-grown," pure single crystals in great part depends upon point defects, especially those caused by impurities. Optical emission and solids mass spectrography were found to be useful for obtaining a broad survey of low-level impurities; however, their shortcomings require the use of supplemental techniques, including tracer methodology and specific element analysis (i.e., oxygen). Line defects, i.e., dislocations, are receiving increasing attention with respect to their effects on crystal growth and their interactions with point defects; electron microscopy and special x-ray topographic techniques are suited for directly observing these defects. In order to study other defects, which may arise in the early or intermediate stages of crystal growth, a general analytical laboratory should have available a host of additional techniques, including optical microscopy, micro-radiography, electron probe analysis, and x-ray diffraction. Information other than that pertaining to crystal defects is often required for adequate characterization of a pure material; such additional information may require determination of stoichiometry, valence states, and detailed structure (crystallography). The impact of computer programming on materials analysis is discussed, including automatic data collection and reduction, and time-averaging of data, which is limited by a poor ratio of signal-to-noise. (auth)

29142 MONITORING OF GASEOUS CONTAMINANTS IN THE ATMOSPHERE USING RADIOACTIVE CLATHRATE TECHNIQUES. Klainer, Stanley M. (Tracerlab/Research, Waltham, Mass.). 10p. (CONF-660207-14). ORAU. Gmelin, AED-CONF-66-011-8.

From Symposium on Radioisotope Applications in Aerospace, Dayton, Ohio.

An instrument was developed using radioactive clathrate techniques to detect certain reactive gases when present in the atmosphere in the ppM range. Fluorine, chlorine, chlorine trifluoride, sulfur dioxide, nitrogen oxide, nitrogen dioxide, amines, and ozone are some of the gases that are measurable by this technique. The use of clathrates for gas analysis is categorized as an inverse radioactive tracing technique. This may be defined as a process in which the constituent to be analyzed undergoes a chemical reaction that results in the release of an active tracer gas whose concentration is proportional to the original species to be analyzed. The major advantage of this system is that it permits sub ppM sensitivities to be obtained in a portable dry chemical system. (auth)

29143 DETERMINATION OF ^{18}O BY BOMBARDMENT WITH ALPHA PARTICLES AND DETECTION OF LIBERATED NEUTRONS. Amiel, Saadia; Nir, Aharon (to Yeda Research and Development Co. Ltd.). U. S. Patent 3,247,380. Apr. 19, 1966. Priority date June 6, 1961, Israel.

A method is described for the nondestructive quantitative measurement of ^{18}O in solid, liquid, or gaseous samples. The sample is irradiated with α-particles having an energy of from 4 to 9 Mev, and the liberated neutrons are counted. The method is applicable to the continuous determination of ^{18}O in a gas chromatogram, and apparatus for this application of the method is described in detail. (B.L.M.)

Inorganic and Physical Chemistry

Refer also to abstracts 29635, 29770, 29774, and 30268.

29144 (IS–1355) PARTIAL MOLAL HEAT CAPACITIES OF SOME AQUEOUS RARE-EARTH CHLORIDE SOLUTIONS AT 25 DEG C. Jones, K. C.; Spedding, F. H. (Ames Lab., Iowa State Univ. of Science and Tech.). Nov. 1965. Contract W-7405-eng-82. 85p. Dep. mn. CFSTI $3.00 cy, $0.75 mn.

An adiabatic calorimeter was designed and built to measure the specific heats of aqueous solutions at 25°C with a precision of at least 0.05%. Specific heats were determined for a number of aqueous solutions of lanthanum, neodymium, dysprosium, erbium, and ytterbium chlorides at 25°C. The concentration range covered was from 0.1 molal to saturation (approximately 4.0 molal). From the specific heat data, apparent molal heat capacities were calculated for each of the rare-earth chloride solutions. The apparent molal heat capacity results for each salt were expressed as a function of the square root molality by means of a fourth degree polynomial equation. Partial molal heat capacities of the solute and solvent were calculated for each rare-earth salt from these polynomial equations. The apparent molal heat capacity data obtained indicate the rare earths may be divided into two subgroups at moderate concentrations, with the heavy rare earths belonging to one group and the light rare earths to another. This behavior was qualitatively explained by assuming that the heavy rare-earth ions have a lower coordination number for water than the light ones, and evidence to support this assumption was presented. The partial molal heat capacities showed possible evidence for complex-ion formation near saturation. (74 references.) (P.C.H.)

29145 (NP–16047) INTERIM REPORT ON THE BONDING REACTION MECHANISM IN CHEMICALLY BONDED ZrO_2. PHASE II. Edlin, V. (Douglas Aircraft Co., Inc., Santa Monica, Calif. Missile and Space Systems Div.). Aug. 10, 1964. 16p. (SM–45974).

Studies were made on the chemical reactions and bond mechanism involved in the low temperature, 400°F (205°C), bonding of zirconia (ZrO_2). Chemical bond phenomena were investigated by means of petrographic analysis and stoichiometric studies. The results led to the determination of the chemical reactions occurring for ZrO_2 bonded with monofluorophosphoric acid (H_2PO_3F). The bonding reaction was produced by the formation of zirconium tetrafluoride (ZrF_4) and subsequent reaction with a phosphate radical to form the bonding medium zirconium pyrophosphate (ZrP_2O_7). It was determined that ZrP_2O_7 produced without the presence of the fluoride ion is a relatively weak bonding medium for ZrO_2. Chemical bonding of magnesia (MgO) at the same temperature, based upon bonding reactions similar to that employed with ZrO_2, produced apparently strong bodies of MgO. (auth)

29146 (SC-R-66-885) REACTION RATES FOR HIGH-TEMPERATURE AIR. Carnicom, Mina L. (Sandia Corp., Albuquerque, N. Mex.). May 1966. Contract AT(29-1)-789. 53p. Dep. mn. CFSTI $3.00 cy, $0.50 mn.

The reaction rate values used in the field of high-temperature (≥1000°K) reactions of nitrogen and oxygen species were compiled and are presented in tabular forms for comparison. Included are radiative processes and reactions involving neutral and/or charged particles. An attempt was made to trace the rate values to their origin publications. Also included is a list of the air models considered by several investigators. (111 references). (auth)

29147 (UCRL–14901-T) RELAXATION PHENOMENA AND CHEMICAL CROSS SECTION. Alder, B. J. (Lawrence Radiation Lab., Univ. of California, Livermore). May 13, 1966. Contract W-7405-eng-48. 25p. Dep. mn. CFSTI $1.00 cy, $0.50 mn.

By following molecular trajectories on the computer it was possible to obtain much greater detail about molecular behavior in simple systems than is feasible experimentally. These studies, consequently, allow the validity of various theoretically proposed mechanisms to be evaluated. With respect to relaxation phenomena in fluids, it could be shown that the concept of an activation barrier to molecular flow is invalid. Instead, the van der Waals description of a fluid, in which the attractive part of the intermolecular forces is treated as a weak perturbation, led to remarkably accurate results. Comparison of the theory to experimental transport coefficients in dense systems of the rare gases was made by taking into account that the repulsive part of the intermolecular potential is soft. The chemical cross-section calculations are illustrated for the simplest possible case of the exchange reaction of hydrogen atoms with hydrogen molecules. These calculations involve in the first place an accurate quantum mechanical evaluation of the potential energy surface, which confirm the existence of a barrier, although of smaller height and width than earlier and cruder calculations. With the given potential surface, the trajectories for classical particles leading to a reaction were evaluated as a function of the relative velocity and of the vibrational and rotational state of the particles. Finally, it could be shown that a quantum mechanical calculation of the trajectories would not significantly affect the reaction rate predicted on a classical basis. (auth)

29148 FLUORIDE AND SULFATE COMPLEXES OF NEPTUNIUM(IV). Ahrland, Sten; Brandt, Lars (Univ. of Lund, Sweden). Acta Chem. Scand., 20: 328-46(1966).

The complexes formed by neptunium(IV) with sulfate and fluoride ions were investigated by means of cation exchange, and, in the case of fluoride, potentiometric measurements (using the Fe^{3+}/Fe^{2+} electrode). All measurements were performed in a 4M perchloric acid medium, and at a temperature of 20°C. For the sulfate system, the stability constants of the first two complexes were determined; further complexes were not formed within the range of ligand concentrations covered by the cation exchange method. Also for the fluoride system, only the constants of the first two complexes could be determined by this method, but an extension of the range was achieved by the emf measurements. These yielded reliable values for the constants of the second and third complexes, and an approximate constant for the fourth complex as well. For the second constant, the two methods employed gave concordant results. As expected for a four-valent ion, both the sulfate and, especially, the fluoride complexes were very strong. A feature of the fluoride system is that the second complex has an unusually narrow range of existence. (auth)

29149 VAPOR PRESSURE OF SOLID D_2O. Kiss, I.; Jakly, G.; Illy, H. (Central Research Inst., for Physics, Budapest). Acta Chim. Acad. Sci. Hung., 47: 379-84 (1966).

The vapor pressure of solid D_2O was measured in the temperature range from −40 to 0°C. The results showed, contrary to the anomaly observed by Johannin-Gilles and Johannin, an increase in the relative vapor pressure difference between H_2O and D_2O with decreasing temperatures. The HDO vapor pressure at temperatures below 0°C determined from the vapor pressure measured on a H_2O and D_2O mixture with 50 at % D concentration was found to obey the rule of the geometrical mean. (auth)

29150 CRYSTAL STRUCTURE OF THORIUM NITRATE PENTAHYDRATE BY X-RAY DIFFRACTION. Ueki, Tatzuo; Zalkin, Allan; Templeton, David H. (Univ. of California, Berkeley). Acta Crystallogr., 20: 836-41 (June 10, 1966). (UCRL–16438).

Crystals of $Th(NO_3)_4 \cdot 5H_2O$ are orthorhombic, space group Fdd2, a = 11.182, b = 22.873, and c = 10.573 Å, and Z = 8. Thorium has three water molecules and eight oxygen atoms from four nitrate ions as neighbors in a highly polar arrangement. All hydrogen atoms are in hydrogen bonds 2.71 to 2.96 Å in length. Average bond distances are: Th–O (water) 2.46 Å, Th–O (nitrate) 2.57 Å, N–O (next to Th) 1.27 Å, and N–O (terminal) 1.22 Å. An error of about 0.05 Å is made in the position of the thorium atom if anomalous dispersion ($\Delta f'' = 9$) is neglected. (auth)

29151 CRYSTAL STRUCTURE OF THORIUM NITRATE PENTAHYDRATE BY NEUTRON DIFFRACTION. Taylor, J. C.; Mueller, M. H.; Hitterman, R. L. (Argonne National Lab., Ill.). Acta Crystallogr., 20: 842-51(June 10, 1966).

The crystal structure of thorium nitrate pentahydrate, $Th(NO_3)_4 \cdot 5H_2O$, was determined by neutron diffraction. It is orthorhombic, space group Fdd2, with a = 11.191 ± 0.007, b = 22.889 ± 0.015, and c = 10.579 ± 0.007 Å. A total of 1642 independent reflections with $2\theta < 122°$ (λ = 1.065 Å) were used. The structure was solved from the three-dimensional Patterson function and refined by the full-matrix least-squares method to R = 4.3% with the use of a statistical weighting scheme. Eleven oxygen atoms are bound to the thorium atom, eight from four bidentate nitrate groups and the other three from water molecules. The Th–O (water) distances, 2.438 and 2.473 Å, are shorter than the Th–O (nitrate) distances, 2.528 to 2.618 Å. The nitrate groups are planar and the N–O distances are significantly different within the group. The structure is tied together by a simple hydrogen-bond scheme in which the hydrogen bonds are either "strong" water–water hydrogen bonds (2.70 Å) or "weak" water–nitrate oxygen hydrogen bonds (2.90 to 2.95 Å). (auth)

29152 INFLUENCE OF METAL IONS ON THE HYDROLYSIS OF POLYPHOSPHATES. van Steveninck, J. (Lab. of Medical Chemistry, Leiden). Biochemistry, 5: 1998-2002(June 1966).

The influence of some metal ions on the hydrolytic degradation of polyphosphates was studied. Uranyl salts catalyze the hydrolysis of polyphosphates. A number of metal ions (e.g., uranyl and nickel (II) ions) change the rate of hydrolysis presumably by changing the conformation of the polyphosphate chains. The influence of metal ions on the hydrolysis of pyrophosphate is different from the influence of these ions on the hydrolysis of larger polyphosphates. The possible relationship between these effects and the influence of some metal ions on enzymatic reactions involving polyphosphates is briefly discussed. (auth)

29153 TRANSFER OF THE OXYGEN ATOM OF WATER IN AN AQUEOUS SOLUTION OF IRON AND COPPER SULFATES. Suzuki, Nobutake; Hotta, Hiroshi; Hashimoto, Hitoshi (Japan Atomic Energy Research Inst., Takasaki). Bull. Chem. Soc. Jap., 39: 422-5(Mar. 1966).

When an ^{18}O-enriched aqueous solution of ferrous, ferric, and cupric sulfates was heated between 130 and 200°C, the ^{18}O content decreased in the order of $Fe^{2+} > Fe^{3+} < Cu^{2+}$ in water; and it increased in the sulfate group and in the molecular oxygen of the gaseous phase. A transfer of oxygen from water to the sulfate group was also observed, even in a nitrogen atmosphere. The oxygen transfer was promoted in all the cases in the presence of molecular oxygen, and it increased further in the presence of benzene. Since the exchange reaction of oxygen does not occur between water and sulfate ions, these facts may be attributed to the reactions between water and the thermal decomposition products of the sulfate group, and between water and the hydrogen peroxide produced. The peroxy species, produced by oxidation of the decomposition products, are more reactive in such a transfer of oxygen, since the reaction is promoted in the presence of oxygen. The peroxides in the autoxidation of benzene seem also to be reactive in it. (auth)

29154 COPRECIPITATION BEHAVIOR OF STRONTIUM WITH CALCIUM OXALATE BY PRECIPITATION FROM A HOMOGENEOUS SYSTEM. Matsui, Masakazu (Kyoto Univ.). Bull. Chem. Soc. Jap., 39: 581-5(Mar. 1966).

The coprecipitation of strontium with calcium oxalate was studied using dimethyloxalate to precipitate calcium from a homogeneous solution. The effects of the coprecipitation conditions on the distribution coefficients were investigated in the fractional precipitation process of calcium-strontium oxalate mixtures. Regardless of the pH value, the concentration of acetic acid and other factors, the coprecipitation curves of strontium showed similar shapes in almost all cases. It appeared to be an anomalous system, because an increase in the fraction of the calcium precipitated tended to decrease the distribution coefficients. It was concluded that two coprecipitation mechanisms are involved in the coprecipitation system; one is surface adsorption on fine crystals, while the other is a normal systematic type. When the adsorption part was removed, it was found that the modified system obeyed the Doerner and Hoskins logarithmic distribution law and that the coefficient gave nearly a constant, 0.1. (auth)

29155 ORGANIC COMPOUNDS OF URANIUM. PART I. REACTIONS OF URANIUM PENTAETHOXIDE WITH β-KETOESTERS. Bhandari, A. M; Kapoor, R. N. (Univ. of Jodhpur, India). Can. J. Chem., 44: 1468-71(June 15, 1966).

Reactions between these two substances were studied in various stoichiometric ratios in benzene. All the derivatives were dark brown liquids or pasty solids with the viscosity increasing as more ethoxy groups were replaced. These derivatives could be distilled under reduced pressure. In each, uranium was found to be pentavalent. (F.S.A.)

29156 KINETICS OF THE HOMOGENEOUS ISOTOPE EXCHANGE BETWEEN ISOPROPYL CHLORIDE AND CHLORIDE IONS IN DIMETHYLFORMAMIDE. Elias, Horst; Strecker, Helmut (Technische Hochschule, Darmstadt, Ger.). Chem. Ber., 99: 1019-25(1966). (In German).

The kinetics of the homogeneous isotope exchange between ^{36}Cl-labeled isopropyl chloride and tetrabutylammonium chloride were studied in dimethylformamide between 75 and 100°C. Analysis was by precipitation with $AgNO_3$ after suitable periods of time, followed by measurement of the activity of the AgCl formed. A second-order rate constant of 17.4×10^{-4} (±2%) was found for the exchange at 100°C; there was a small contribution from a first-order reaction ($k = 2.0 \times 10^{-7}$). The rate constant was 4.71×10^{-4} (±2%) at 85°C and 1.79×10^{-4} (±2%) at 75°C. The enthalpy of the reaction was calculated to be 22.9 ± 0.3 kcal/mole, and the entropy −9.9 ± 0.8 eu/mole. Isopropyl chloride produced chloride ions by a small-yield side reaction in dimethylformamide. (BBB)

29157 KINETICS OF THE HOMOGENEOUS ISOTOPE EXCHANGE BETWEEN CYCLOALKYL CHLORIDES AND CHLORIDE IONS IN DIMETHYL SULFOXIDE. Elias, Horst; Krutzik, Siegfried (Technische Hochschule, Darmstadt, Ger.). Chem. Ber., 99: 1026-31(1966). (In German).

The kinetics of the homogeneous isotope exchange between ^{36}Cl-labeled cyclopentyl chloride, cyclohexyl chloride, cycloheptyl chloride, and cyclooctyl chloride and LiCl in dimethyl sulfoxide were measured. Tables of rate constants are presented for the reaction of cyclopentyl chloride between 45 and 100°C, cyclohexyl chloride between 102 and 140°C, cycloheptyl chloride between 60 and 120°C, and cyclooctyl chloride between 60 and 120°C. Extrapolated second-order rate constants at 25°C, enthalpies of reaction, and entropies of reaction were found to be as follows: cyclopentyl chloride, $(9.53 \pm 0.48) \times 10^{-7}$, 23.2 ± 0.2 kcal/mole, −7.9 ± 0.4 eu/mole; cyclohexyl chloride, $(6.10 \pm 0.30) \times 10^{-9}$, 27.8 ± 0.5 kcal/mole, −2.1 ± 0.4 eu/mole; cycloheptyl chloride, $(4.72 \pm 0.24) \times 10^{-7}$, 23.4 ± 0.2 kcal/mole, −8.6 ± 0.5 eu/mole; and cyclooctyl chloride, $(4.97 \pm 0.25) \times 10^{-8}$, 25.7 ± 0.2 kcal/mole, −5.4 ± 0.2 eu/mole. Analysis was performed by precipitation of the reaction mixture with $AgNO_3$, followed by measurement of the activity of the AgCl. (BBB)

29158 A CLASS OF NEW SULFIDE COMPOUNDS OF RARE EARTHS AND SILVER OF THE TYPE $AgTS_2$. Ballestracci, Regis (CEN, Grenoble, France). Compt. Rend., Ser. C, 262: 1253-6(Apr. 18, 1966). (In French).

The sulfide $YbAgS_2$ has a tetragonal structure with the space group $I\,4_1md$. The environment of the rare earth ions constitutes an almost regular octahedron, but the octahedric vicinity of the Ag ion is very deformed. The other ternary sulfides from Sm to Yb and Y have a mono-

clinic structure corresponding to a deformation of a double cell of the $YbAgS_2$ cell. This deformation increases with the radius of the rare earth. Some of these compounds also have a disordered structure of the NaCl type. (tr-auth)

29159 HYDROLYSIS OF URANIUM–THORIUM–CARBON ALLOYS RICH IN CARBON. Besson, Jean; Blum, Pierre L.; Del Litto, Bernard (CEN, Grenoble, France). Compt. Rend., Ser. C, 262: 1265-7(Apr. 1966). (In French).

The gases formed during hydrolysis of uranium–thorium–carbon systems containing an excess of free graphite contain a quantity of methane proportional to the concentration of uranium in these alloys. The formation of methane appears to be connected to the presence of monocarbide in these alloys, placing in doubt the existence of a pseudobinary system UC_2–ThC_2. (tr-auth)

29160 THORIUM ORTHOPHOSPHATES. Molodkin, A. K.; Balakaeva, T. A.; Kuchumova, A. N. (Kurnakova Inst. of General and Inorganic Chemistry, Academy of Sciences, USSR). Dokl. Akad. Nauk SSSR, 165: 573-4 (Nov. 21, 1965). (In Russian).

Attempts to synthesize some thorium phosphate complexes from saturated aqueous solutions of phosphoric acid and of sodium, potassium, and ammonium phosphates gave the hydrates of $Th_3(PO_4)_4$, $NaTh_2(PO_4)_3$, $NaTh(PO_4)(OH)_2$, $(NH_4)_2Th(PO_4)_2$, and $KTh(PO_4)(OH)_2$. As the phosphate concentration in the solution was increased, the thorium concentration decreased, becoming zero at the extreme of $PO_4^{3-}/Th^{4+} = 1.33$. Further increase in the phosphate in the liquid phase did not affect the amount of thorium precipitate on the solid phase composition. In the PO_4^{3-}/Th^{4+} range 1.33 to 2.5, the electric conductivity decreased sharply with no change in the thorium concentration in solution. No other thorium phosphates were observed in the systems studied. However, in nitrate systems, mixtures of 70% aqueous solutions of thorium nitrate with 20-fold excess of saturated solutions of sodium or ammonium tertiary phosphates and secondary potassium phosphate formed white, easily filterable compounds shown to be the hydrates of $(NH_4)_2Th(PO_4)_2$, $NaThPO_4(OH)_2$, and $KThPO_4(OH)_2$. All the synthesized thorium complexes were stable in air, insoluble in water or organic solvents, and decomposed by heat at 450°C. (TTT)

29161 DETERMINATION OF THE FACTORS AFFECTING THE SELECTIVE PENETRATION OF SODIUM PENTACHLOROPHENOLATE IN WOOD BY RADIOACTIVATION ANALYSIS. Gheorghe, M.; Catrina, J.; Constantinescu, O. (Inst. de Cercetari Forestiere, Bucharest). Drevar. Vysk., No. 3, 113-25(1964). (In German).

By research, using radioactivation analysis, into the factors that could influence the selective penetration of the ions of sodium pentachlorophenolate for impregnation of wood, it was established that the pH of the solution represents one of the factors, but not an essential one. The selectivity is no specific phenomena for the sodium pentachlorophenolate. It is impossible to draw a rigorous conclusion on addition of borax and soda into the impregnating solution. (auth)

29162 X-RAY L_{III} SPECTRA OF GADOLINIUM ABSORPTION IN HYDRIDES. Vainshtein, E. E.; Bril, M. N.; Staryi, I. B.; Kost, M. E. (Inst. of General and Inorganic Chemistry, Academy of Sciences, USSR. Inst. of Geochemistry and Analytical Chemistry, Academy of Sciences, USSR. Odessa Teacher's Inst.). Fiz. Metal. Metalloved., 21: 138-40(Jan. 1966). (In Russian).

Gadolinium metal is hydrogenated in a vacuum at 400°C for 30 minutes and subsequently heated to give products of the following composition: $GdH_{2.7}$, $GdH_{2.4}$, $GdH_{2.2}$, $GdH_{1.8}$, $GdH_{1.6}$, and $GdH_{1.4}$. The L_{III}-absorption spectra of these hydrides are presented and compared with the spectrum of the oxide. The fine structure and energy position coincide for the five hydrides. The absorption spectra of Gd are identical to the spectra of La and Ce. Hence, the valence state of the metal in the di- and trihydrides is the same. The maximum in the L_{III}-absorption spectrum in the hydrides is shifted by ~0.5 ev towards the long wavelength side compared to the metal oxide. Thus, the type of chemical bonding in the hydrides apparently does not depend on the lattice type (cubic or hexagonal). (TTT)

29163 OXIDATION OF LANTHANUM HEXABORIDE IN AIR AT 800 AND 1000 C. Hsu, Hsiao-pai; Kuo, K'o-hsin. Hua Hsueh Hsueh Pao, 31: 271-6(1965).

The rate of oxidation of lanthanum hexaboride was investigated by determining the extent of oxidation of different specimens at definite time intervals after dissolving their surface oxide layers with dilute hydrochloric acid. The experimental results may be summarized by the following relation: $\mu = atk$, where μ is the extent of oxidation, t is the time of oxidation, and a and k are constants at a given temperature. It was found that k = 0.75 and 0.95 at 800 and 1000°C, respectively. (ATD)

29164 RARE EARTH TUNGSTEN BRONZES. Ostertag, Werner (Wright-Patterson Air Force Base, Ohio). Inorg. Chem., 5: 758-60(May 1966).

Cubic rare earth tungsten bronzes of the formula $M_{0.1}WO_3$ where M stands for the rare earth elements Ce, Pr, Nd, Sm, Eu, Gd, Tb, Dy, Ho, Er, Tm, Yb, and Lu were prepared. The bronzes were obtained by a solid-state reaction at 1100°C with quenching to room temperature. The lattice parameters a_0 were found to decrease from $Ce_{0.1}WO_3$ (α = 3.828 Å) to $Lu_{0.1}WO_3$ (α = 3.788 Å). The extension of the homogeneity range of the cubic phase of Eu_xWO_3 and Gd_xWO_3 was studied by x-ray-diffraction methods. The value of x was found to range from 0.085 to 0.16. Susceptibility measurements were carried out on all bronzes between 290 and 80°K. Measurements indicate that the rare earth ions account for the magnetic moment exhibited by these compounds. All rare earth ions are present in the trivalent state. (auth)

29165 PREPARATION OF CURIUM HYDROXIDE SOL-GEL SPHERES AS AN INTERMEDIATE TO CmO_2 MICROSPHERE PREPARATION. Baybarz, R. D. (Oak Ridge National Lab., Tenn.). Inorg. Nucl. Chem. Lett., 2: 129-32(May 1966). (ORNL-P-2143).

A sol-gel procedure was developed to produce spheres of curium oxide for incorporation into irradiation targets. The curium sol was produced by precipitation of the hydroxide from a nitric acid solution with NH_4OH. Sufficient 0.1M HNO_3 was added to the precipitate to give a NO_3^- to curium mole ratio of 0.15 to 0.25. The slurry was stirred and heated at 50 to 70°C for 1 to 2 hr, during which it became a thin sol. The maximum sol concentration achieved was about 100g Cm/l, at which concentration ^{244}Cm has a power level of 300 w/l. The sol is then cast into gel particles by introducing small droplets of sol into a countercurrent flowing column containing a drying agent. The resulting gel microspheres are in the form of a free-flowing powder. They are calcined quickly. (M.C.G.)

29166 FORMATION OF AZIDES OF PRASEODYMIUM (III) AND NEODYMIUM(III). Gutmann, V.; Leitmann, O.; Schuetz, R. (Technische Hochschule, Vienna). Inorg. Nucl. Chem. Lett., 2: 133-5(May 1966).

It was found that triazides and tetrazidometallates are formed in nonaqueous media. Anhydrous perchlorates of Pr(III) and Nd(III) were prepared in dimethylsulfoxide and trimethylphosphate. The solvated cations were found to react with chloride and azide ions in solutions of trimethyl phosphate. (M.C.G.)

29167 PHASE DIAGRAM OF THE SYSTEM Sc_2O_3–Cr_2O_3. Tresvyatskii, S. G.; Pavlikov, V. N.; Lopato, L. M. (Inst. for Problems of Materials, Ukrainian SSR). Izv. Akad. Nauk SSSR, Neorg. Mater., 2: 269-74(1966). (In Russian).

Phase transformations in the Sc_2O_3–Cr_2O_3 system were studied in samples subjected to heat treatment in a high-temperature furnace in an argon atmosphere. A photographic investigation was made by the conventional method with penetrating and reflected light; in the latter case with the use of etching in a melt of $KHSO_4$ at 200°C for 2 to 3 min. An x-ray investigation was also made. Infrared spec-

tra of the alloys were obtained over an interval from 400 to 700 cm^{-1}. The change in the oxide content during heat treatment was monitored by conventional chemical analysis. A phase diagram based on the experimental results, a table showing the x-ray results, and microphotos of the samples are presented. The existence of a compound that melts at 2130 ± 30°C was observed. The probable composition of this compound is: Cr_2O_3/Sc_2O_3 = 1:3 or 1:4. The initial oxides form solid solutions based on chromium oxide with a specific solubility of chromium oxide in scandium oxide of 10 mole %. With a decrease in temperature, the specific solubility decreases to 17 mole % scandium oxide and 5 mole % chromium oxide. (ATD)

29168 REACTION OF MANGANESE AND SCANDIUM OXIDES IN AIR. **Komissarova, L. N.; Pokrovskii, V. I.; Shaplygin, I. S. (Moscow State Univ.). Izv. Akad. Nauk SSSR, Neorg. Mater., 2: 275-80(1966). (In Russian).**

The mole % content of scandium oxide in the samples varied from 0 to 100%, the calcining temperature from 700 to 1100°C, and the calcining time from 2 to 100 hours. The starting samples were prepared by precipitation of scandium and manganese hydroxides by a mixture of $NH_4OH + H_2O_2$ from nitric acid solutions. The samples were calcined in a platinum boat at 700 to 1500°C and then quenched in liquid nitrogen. An x-ray analysis was made of the samples. Thermal analyses were also made. The magnetic susceptibility was determined by the Faraday method. A phase diagram of the system, constructed from experimental data, is presented. The existence of a compound with the composition $ScMnO_3$ and three types of cubic solid solutions, based on Sc_2O_3, Mn_2O_3, and a cubic modification with the composition Mn_3O_4 was established. The compound $ScMnO_3$ crystallized in a hexagonal lattice; its specific magnetic susceptibility was $18.0 \pm 0.5 \times 10^{-6}$ abs. el. units/gram; at 1350 ± 20°C it decomposed with the formation of solid solutions based on Sc_2O_3 and the cubic modification Mn_3O_4. The solubility of Mn_2O_3 in scandium oxide changed only slightly with temperature and was from 17 to 20 mole %; the solubility of Sc_2O_3 in cubic Mn_3O_4 rose sharply from 10.5 mole % at 1200°C to 30.0 mole % at 1500°C. It is shown that scandium oxide does not form compounds or a wide range of solid solutions with MnO, NiO, CoO, CdO, and ZnO. (ATD)

29169 COMPLEX ALLOYS BASED ON MOLYBDENUM DISILICIDE AND BORON CARBONITRIDE. **Lapshov, Yu. K. (Inst. for Problems of Materials, Ukrainian SSR). Izv. Akad. Nauk SSSR, Neorg. Mater., 2: 303-7(1966). (In Russian).**

Samples with a boron carbonitride content of 15, 30, and 40 wt % were tested. The $MoSi_2$ powders, with a particle size of 46 μ, had the following chemical composition: total silicon, 34%; bound silicon, 31.3%; free silicon, 1.5%; molybdenum, 64%; and iron, ~0.5%. Pressed rods were cut into pieces of the required length and dried at 150° for 150 to 200 min. After drying, the samples were sintered in a tubular graphite furnace in a hydrogen atmosphere. After sintering, determinations were made of the pycnometric density and the porosity of the systems by hydrostatic suspension. The optimum sintering temperature for these systems was found to be 1150°C and the optimum sintering time 60 min. A study was made of the influence of the duration of the holding time on the oxidation process of the systems at 1200°C; it was established that the increase in weight of the samples for 560 minutes was 2.234 mg/cm^2 for a composition of 70% $MoSi_2$ and 30% boron carbonitride, 0.541 mg/cm^2 for a composition of 60% $MoSi_2$ and 40% boron carbonitride, and 0.930 mg/cm^2 for pure molybdenum disilicide. A study was made of the dependence of the specific electric resistance on temperature. It was found that the electric resistance of the systems decreases with increasing temperature and reaches 30 ohm-cm at 1300°C for a system with 30% boron carbonitride, and 58 ohm-cm for a system with 40% boron carbonitride. At the same time, the specific electric resistance of pure molybdenum disilicide is 0.5 ohm-cm at 1300°C. (ATD)

29170 NEW DOUBLE OXIDES OF URANIUM AND TUNGSTEN. **Rozanova, O. N.; Trunov, V. K.; Kovba, L. M. (Moscow State Univ.). Izv. Akad. Nauk SSSR, Neorg. Mater., 2: 319-20(1966). (In Russian).**

A study was made of the possibility of forming new compounds by the reaction of uranium dioxide with tungsten anhydride and uranyl tungstate. The investigation was made by x-ray methods. Stoichiometric mixtures of the starting substances were calcined in evacuated and sealed quartz ampoules. An x-ray photo of a sample with the empirical formula $UO_2 + 2WO_3$, calcined at 1000°C for 40 hours, was identical with that for thorium tungstate. The lattice parameters of $U(WO_4)_2$ are close to those of $Th(WO_4)_2$. Details of the x-ray investigation of $U(WO_4)_2$ are given. The isostructure of $Th(WO_4)_2$ and $U(WO_4)_2$ makes it possible to settle the question of the valence state of uranium and tungsten in these compounds. In the reaction of uranium dioxide and uranyl tungstate (1000°) the compound U_2WO_8 was formed, which is isostructural with U_2MoO_8. It must be noted that these double oxides, at a calcining temperature of 1000°C, slowly decompose with the formation of the U_xWO_3 and $(U,W)O_{2+x}$ phases. (ATD)

29171 THE HEAT OF FORMATION OF GASEOUS URANIUM FLUORIDES. **Godnev, I. N.; Sverdlin, A. S. (Ivanov Chemical-Technological Inst., USSR). Izv. Vyssh. Ucheb. Zaved., Khim. Khim. Tekhnol., 9: 40-3(1966). (In Russian).**

The heats of formation ΔH_{298} of uranium fluoride UF_n in the gaseous state were estimated for n = 1, 2, 3, 4, and 5. These values were found to be −440 for UF_5, −336 for UF_4, −257 for UF_3, −141 for UF_2, and −20 kcal/mol for UF in the ordinary standard state. The initial data for UF_6 and UF_4 were used in making the estimates by two methods whose results were averaged. In the first method the heat of formation of the gaseous fluorides UF_n from F (gas) and U (gas) was plotted as a function of n. In the second method the heat of removal was estimated for the reaction: UF_n (gas) → UF_{n-1} (gas) + F (gas) + H_n as a function of n. The agreement between the two methods was satisfactory. (TTT)

29172 ULTRASONIC ATTENUATION AND RELAXATION TIMES IN WATER VAPOR AND HEAVY WATER VAPOR. **Yamada, Kazunari; Fujii, Yahei (Ship Research Inst., Tokyo). J. Acoust. Soc. Amer., 39: 250-4(Feb. 1966).**

Determination was made of the thermal relaxation time in water vapor necessary for energy transfer between the external degrees of freedom and the vibrational degree of freedom with the lowest characteristic temperature. Earlier measurements in H_2O vapor by the so-called direct method in the range of the ratio ω/p (angular frequency/pressure) from 1 to 50 Mcps/atm gave the vibrational relaxation time to be from 0.8 to 2.0×10^{-8} sec by assuming the excess relaxational attenuation to be almost wholly owing to vibrational relaxation. In the search for a relaxation peak in the excess absorption, an apparatus of the direct-method type was constructed for measurements over the range of ω/p where the presence of the peak was predicted. Ultrasonic attenuation in water vapor and heavy-water vapor was measured over the range of ω/p from 10 to several hundred radian Mcps/atm at 137°C. The resulting vibrational relaxation time at 1 atm for H_2O vapor was about $(8 \pm 2.5) \times 10^{-9}$ sec and that in D_2O vapor about $(7.0 \pm 1.0) \times 10^{-9}$ sec. (BBB)

29173 INFRARED ABSORPTION OF Ce^{3+} IN LaF_3 AND OF CeF_3. **Buchanan, R. A.; Rast, H. E.; Caspers, H. H. (Naval Ordnance Lab., Corona, Calif.). J. Chem. Phys., 44: 4063-5(June 1, 1966).**

The infrared absorption spectra of Ce^{3+} in LaF_3 and of CeF_3 were observed in the region from 3 to 6 μ. The four absorption lines for Ce^{3+} in LaF_3 at 2160, 2240, 2635, and 2845 cm^{-1} that persist at liquid-helium temperature were identified as transitions originating on the ground Stark component of the $^2F_{5/2}$ and terminating on the four Kramers-degenerate Stark levels of the $^2F_{7/2}$. Observation of the temperature dependence of the spectrum revealed two additional transitions beginning on a $^2F_{5/2}$ Stark level 150

cm^{-1} above the ground state and ending on the two lowest levels of the $^2F_{\frac{5}{2}}$. The results were essentially the same for CeF_3 and were in substantial agreement with the results of temperature-dependent studies of the magnetic susceptibility and Faraday rotation of CeF_3 and tysonite. (auth)

29174 NIOBIUM–Al_2O_3 REACTIONS YIELDING CONDENSED AND VOLATILE PRODUCTS. Grossman, L. N. (General Electric Co., Pleasanton, Calif.). Contract NObs-90496. J. Chem. Phys., 44: 4127-31(June 1, 1966).

A mass-spectrometric and thermogravimetric study of the equilibrium interaction between Al_2O_3 and Nb between 1800 and 2200°K was conducted. The reaction proceeds principally as $Al_2O_3 + 3Nb \rightarrow 2Al(g) + 3NbO(s)$; two secondary reactions of about equal importance under neutral conditions are $Al_2O_3 + Nb \rightarrow Al_2O(g) + NbO_2(g)$ and $Al_2O_3 + 2Nb + \frac{1}{2}O_2 \rightarrow Al_2O(g) + NbO_2(g) + NbO(s)$. The latter reaction can dominate under oxidizing conditions. The weight loss caused by the gaseous reaction products is about one hundred times the weight loss caused by the evaporation of alumina under neutral conditions. Calculations show that yttria and some other oxides can be used with Nb at high temperatures with no significant reaction. (auth)

29175 VIBRATIONAL SPECTRUM OF HYDRAZINE-d_4 AND A RAMAN STUDY OF HYDROGEN BONDING IN HYDRAZINE. Durig, J. R.; Bush, S. F.; Mercer, E. E. (Univ. of South Carolina, Columbia). J. Chem. Phys., 44: 4238-47(June 1, 1966).

The infrared spectra of liquid, solid, and gaseous tetradeuterated hydrazine were measured from 250 to 4000 cm^{-1}. Fine structure was resolved for three of the perpendicular fundamental bands of the assumed symmetric top. The Raman spectra of liquid hydrazine and tetradeuterated hydrazine were recorded and depolarization values measured. A complete vibrational analysis based on band type, position, and depolarization values is given, which satisfies the product rule for both the a and b vibrational symmetry species. The intensity of the 3189-cm^{-1} band of hydrazine was studied as a function of temperature. ΔH^0 for H-bond formation in hydrazine was found to be −1450 cal/mole. The relative intensity of the 3189-cm^{-1} band to that of the 3260-cm^{-1} band was studied as a function of concentration in dimethylsulfoxide and indicated that part of the intensity of the 3189-cm^{-1} band arises from a vibrational mode of the hydrazine monomer. (auth)

29176 ENERGY THRESHOLD FOR $D + H_2 \rightarrow DH + H$ REACTION. Kuppermann, Aron; White, John M. (California Inst. of Tech., Pasadena). J. Chem. Phys., 44: 4352-4(June 1, 1966).

The value obtained for the threshold energy for the reaction $D + H_2 \rightarrow DH + H$ was 0.33 ± 0.02 ev. The method used consisted of photolyzing a mixture of DI or DBr plus H_2 with monochromatic light and determining the wavelength dependence of the resulting $[DH]/[D_2]$ concentration ratio. (M.C.G.)

29177 MUONIUM CHEMISTRY. Mobley, R. M.; Bailey, J. M.; Cleland, W. E.; Hughes, V. W.; Rothberg, J. E. (Yale Univ., New Haven). J. Chem. Phys., 44: 4354-5(June 1, 1966).

Two methods for studying muonium chemistry are described. The first involves the use of a magnetic resonance transition between two hyperfine-structure magnetic substates of muonium. The second involves the measurement of the polarization of muons as a function of time and of impurity concentration by use of a precision digital time analyzer following the scintillation counters for the positrons. Cross sections for muonium collisions with NO, O_2, and C_2H_4 are presented. (M.C.G.)

29178 ABSORPTION, DEGASSING, AND SOLUTION EQUILIBRIUM IN THE NITROGEN–NIOBIUM SYSTEM AT ULTRAHIGH VACUUM AND HIGH TEMPERATURE. Pasternak, R. A.; Evans, B.; Bergsnov-Hansen, B. (Stanford Research Inst., Menlo Park, Calif.). J. Electrochem. Soc., 113: 731-5(July 1966).

In the nitrogen-niobium system, sorption at high constant temperature and low pressure follows approximately the parabolic rate law $S/S_0 = 1 - (c/c_e)^2$, where S is the sticking probability at the nitrogen concentration c in the metal, S_0 the initial sticking probability, and c_e the saturation concentration. This rate law can be explained by a reversible reaction mechanism: nitrogen is adsorbed atomically on the essentially clean metal surface at a rate that is proportional to pressure but independent of temperature; it then transfers rapidly into the bulk and distributes itself uniformly by fast diffusion. In the reverse reaction nitrogen recombines on the surface at a rate that is proportional to the square of the nitrogen atom concentration in the bulk. The observed degassing rates at both constant and variable pressure can be explained by the same mechanism. (auth)

29179 STUDIES IN COMPLEX FORMATION OF METAL IONS WITH TROPOLONES. PART III. SPECTROPHOTOMETRIC STUDIES ON COMPLEXES OF MOLYBDENUM(VI), THORIUM(IV), AND ZIRCONIUM(IV) WITH α-CARBOXY-β-METHYLTROPOLONE. Dutt, Yag; Singh, R. P. (Delhi Univ.) J. Indian Chem. Soc., 43: 107-10(1966).

The composition of zirconium, thorium, and molybdenum complexes with α-carboxy-β-methyltropolone at different pH values was studied using Job's method of continued variations at different wave lengths. Both zirconium and molybdenum form 1:1 and 1:2 complexes, whereas thorium forms 1:1, 1:2, and 1:3 complexes with this reagent with increasing pH values. (auth)

29180 SPECTROPHOTOMETRIC STUDY OF THE CHELATES OF AMMONIUM AURINTRICARBOXYLATE WITH SCANDIUM, YTTRIUM, AND LANTHANUM. Munshi, Kailash N.; Sangal, Satendra P.; Dey, Arun K. (Univ. of Allahabad, India). J. Indian Chem. Soc., 43: 115-18(1966).

The formation of a pink color produced by the interaction of ammonium aurintricarboxylate (Aluminon) and scandium, yttrium, or lanthanum was studied to determine the composition, stability, and other characteristics of the chelates formed. The absorbance curves of the complexes showed maxima at 535 mμ in all the chelates. The compositions of the chelates were established by three different methods. The apparent stability constants of the chelates were estimated as 104.4 to 104.9 for scandium, 104.4 to 104.6 for yttrium, and 104.1 to 104.5 for lanthanum at pH 5.5 and at 25°C. The chelates were stable over a wide range of pH (4.5 to 8.5). The maximum color formation was attained at pH 5.5 when the mixtures contained greater than 4-fold excess of the reagent with respect to the metal solution and the color intensity remained unaltered even after keeping the mixture for 12 hours at the room temperature. A tentative suggestion was made for the position of the chelate ring in the chelates. (auth)

29181 SPECTROPHOTOMETRIC AND CONDUCTOMETRIC STUDY OF UO_2(II) COMPLEX OF QUINIZARIN-2-SULPHONIC ACID. Joshi, D. P.; Jain, D. V. (Meerut Coll., India). J. Indian Chem. Soc., 43: 119-24(1966).

UO_2^{2+} forms, with quinizarin-2-sulfonic acid, a water-soluble, blackish violet complex in the ratio of 1:1 between pH 3.95 and 4.50. The complex is stable between pH 3.09 and 6.0 and has maximum absorbance at 470 mμ. The molecular extinction coefficient, ε, is 5.968×10^2 at 570 mμ and 4.814×10^2 at 580 mμ and ionic concentration of 0.1 (NaCl). (auth)

29182 MECHANISM OF BROMINE EXCHANGE IN THE BROMINE–GRAPHITE LAMELLAR COMPOUNDS. Salzano, F. J.; Aronson, S. (Brookhaven National Lab., Upton, N. Y.). J. Inorg. Nucl. Chem., 28: 1343-53(June 1966). (BNL-9456).

The rates of exchange of normal and radioactive bromine in bromine–graphite were studied at temperatures of 20 to 45°C. A range of natural graphite flake sizes from 50 to 2000 μ were used to prepare the compounds. The dependence of the rate of exchange on particle size, a, changed abruptly from $1/a$ at large particle sizes to $1/a^2$ at small particle sizes. The apparent activation energy varied by a factor of three over the temperature range investigated. A mechanism of exchange is proposed, which explains the

observed particle size dependence, temperature dependence, and the form of the rate curves in terms of two consecutive surface processes and the structural features of the natural graphite flakes. (auth)

29183 MASS-SPECTROMETRIC STUDIES AT HIGH TEMPERATURES. X. SUBLIMATION PRESSURES OF SCANDIUM(III), YTTRIUM(III), AND LANTHANUM(III) TRIFLUORIDES. Kent, R. A.; Zmbov, K. F.; Kana'an, A. S.; Besenbruch, G.; McDonald, J. D.; Margrave, J. L. (Rice Univ., Houston, Tex.). J. Inorg. Nucl. Chem., 28: 1419-27(June 1966).

Sublimation pressures of ScF_3, YF_3, and LaF_3 were measured by mass spectrometric and semimicrobalance studies via the Knudsen and Langmuir techniques. The mass spectrometric work established $ScF_3(g)$, $YF_3(g)$, and $LaF_3(g)$ as the major vapor species over their respective solid trifluorides. For ScF_3 the results are represented by: $\log P_{atm} = -(1.938 \pm 0.042) \times 10^4/T + 9.43 \pm 0.33$, $(1172 < T < 1402°K)$; for YF_3 by $\log P_{atm} = -(2.185 \pm 0.030) \times 10^4/T + 9.77 \pm 0.23$, $(1256 < T < 1434°K)$; and for LaF_3 by $\log P_{atm} = -(2.02 \pm 0.02) \times 10^4/T + 8.20 \pm 0.15$, $(1200 < T < 1434°K)$. The errors quoted are standard deviations from the least-square fits. The heat of sublimation for ScF_3 at 1290°K is 89 ± 3 kcal mole^{-1}; for YF_3 at 1332°K, $\Delta H° = 100 \pm 3$ kcal mole^{-1}; and for LaF_3 at 1324°K, $\Delta H°$ is 92 ± 2 kcal mole^{-1}. (auth)

29184 THE BEHAVIOUR AND STRUCTURE OF URANYL NITRATE IN ORGANIC SOLVENTS. III. INVESTIGATIONS OF ANHYDROUS URANYL NITRATE SOLUTIONS IN KETONES BY CONDUCTIVITY METHOD. Jezowska-Trzebiatowska, B.; Ernst, S. (Wroclaw Univ. Inst. of Physical Chemistry, Wroclaw). J. Inorg. Nucl. Chem., 28: 1435-40(June 1966).

Results of conductance measurements on anhydrous uranyl nitrate solutions in acetone, methylethylketone, methylisobutylketone, and n-heptanone-2 are presented. Anhydrous uranyl nitrate in ketonic solutions behaves as a very weak 1:1 electrolyte: $UO_2(NO_3)_2 \rightleftharpoons UO_2NO_3^+ + NO_3^-$. The results obtained were analyzed by the Fuoss-Kraus method. The ratios K_A/Λ_0^2 were obtained (K_A = association constant). From the Walden's rule $\Lambda_{0\eta_0}$ = constant, the limiting molar conductivities $\Lambda_{0\,molc}$ were found, and from the ratios K_A/Λ_0^2 the association constants, ΔG and Bjerrum's parameters were calculated. Similar calculations were made for the data previously obtained from conductivity studies on uranyl nitrate hexahydrate solutions in acetone, methylethylketone, and methylisobutylketone. Comparing the results obtained for anhydrous uranyl nitrate and hexahydrate uranyl nitrate solutions in these ketones it was obvious that the anhydrous compound is a weaker electrolyte than the hexahydrate. (auth)

29185 ISOTOPE EFFECT IN THE ELECTROMIGRATION OF SODIUM IONS IN FUSED SODIUM NITRATE. Saito, Nobufusa; Tomita, Isao; Okada, Isao (Tokyo Univ.). J. Nucl. Sci. Technol. (Tokyo), 3: 140-3(Apr. 1966).

The isotope effect of sodium ions in countercurrent electromigration (Klemm's method) was investigated for a system of fused sodium nitrate labelled with the radioactive nuclide ^{22}Na. Two runs were made (Experiments A and B, respectively). In Experiment A, the fused salt chain, Al(cathode)-$NaNO_3$-Pt(anode) was electrolyzed for 20 hr at 340°C with a current density of 1.3 A/cm^2 in the separating tube. In Experiment B, electrolysis was carried out for 67 hr at 380°C with a current density of 1.5 A/cm^2 in the separating tube. After electromigration, a change was observed in the specific activity of sodium in the separating tube. The elementary process separation factor, defined as the ratio of the mobilities of the isotopic ions, i.e., V_{Na-22}/V_{Na-23}, was calculated to be 1.0023 for Experiment A and 1.0017 for B. The mass effect for sodium ion in fused sodium nitrate was calculated to be -0.045 ± 0.006 (standard deviation). (auth)

29186 CHEMISORPTION OF ETHYLENE ON YTTRIUM OXIDE. Krasil'nikova, M. K.; Topchieva, K. V. (Moscow State Univ.). Kinet. Kataliz, 6: 1118-21(Nov.-Dec. 1965). (In Russian).

The chemisorption of ethylene by samples of yttrium oxide, exposed to different processing temperatures in a vacuum, was investigated. By the adsorption method and the electron conductivity method it was found that water inhibits the centers activated for ethylene chemisorption. A hypothesis on the existence of some types of charged forms of chemisorbed ethylene was expressed. (tr-auth)

29187 KINETIC ISOTOPE EFFECTS ACCOMPANYING OXIDATION OF CO, H_2, AND CH_4. Zielinski, Mieczyslaw (Warsaw Univ.). Nucl. Appl., 2: 51-4 (Feb. 1966).

A simple apparatus is used for separation of the components of a mixture of CO, H_2, and CH_4. The separation of CO and CH_4 by selective oxidation with CuO was studied with $^{14}CH_4$. The ^{13}C isotope fractionation during the oxidation of CO with I_2O_5 and with CuO, and during the elevated temperature oxidation of CH_4 with CuO, and the tritium fraction during the oxidation of tritiated hydrogen with CuO are reported. (auth)

29188 ISOTHERMAL REACTION OF URANIUM WITH STEAM BETWEEN 400 AND 1600 DEG C. Wilson, R. E.; Barnes, C. Jr.; Koonz, R.; Baker, L. Jr. Nucl. Sci. Eng., 25: 109-15(1966).

Isothermal studies of the kinetics of the reaction of metallic uranium with steam by a volumetric method are reported. The reaction $U + 2H_2O \rightarrow UO_2 + 2H_2$, $\Delta H = -142$ kcal/mole at 1133°C, could be described accurately by the following parabolic rate law between 600 and 1200°C: $V^2 = (1.95 \pm 0.8) \times 10^5\, t[\exp(-18{,}600 \pm 750)/RT$, where V is the volume of H_2 evolved in milliliters at STP per square centimeter, t is the time in minutes, R is the gas constant, 1.987 cal/(mole deg K), and T is the absolute temperature in degrees Kelvin. Between 1200 and 1600°C the following parabolic rate law described the experimental results: $V^2 = (1.59 \pm 0.5) \times 10^6\, t[\exp(-25{,}000 \pm 1000)/RT]$, although it was likely that an activation energy somewhat greater than 25 kcal/mole should be used for extrapolation to short reaction times or higher reaction temperatures. The reaction at 400°C followed a linear rate, while at 500°C the reaction was complicated by effects of the transition from a linear reaction at low temperatures to a parabolic reaction at higher temperatures. The oxide formed at 600°C and above was a glossy black UO_2 which did not flake off until the samples were cooled after exposure. Oxide formed at 400°C was a brown colloidal material that was continually washed from the sample. Reaction rates with an alloy containing 1 at. % aluminum (1130 ppm) and one containing 105 ppm aluminum did not differ significantly from those found with unalloyed uranium. (auth)

29189 NONISOTHERMAL REACTION OF URANIUM WITH WATER BY THE CONDENSER DISCHARGE METHOD. Baker, Louis Jr. Nucl. Sci. Eng., 25: 116-30(1966).

A combined experimental and theoretical study of the reaction of solid wires and molten particles of uranium with water is reported. The experiments were performed by the condenser-discharge method that had been developed for studies of the zirconium-water reaction. The uranium-water reaction was studied with initial metal temperatures from 660 to 4000°C with 30- and 60-mil wires in water at 25°C and in water at 100°C. Wires heated to the melting point of uranium, 1133°C, reacted to a maximum of about 4% in 25°C water and 7% in 100°C water. Wires heated above the melting point formed molten particles whose mean diameter decreased continuously with increasing metal temperature. At initial metal temperatures approaching 4000°C, 45% uranium-water reaction occurred in 25°C water, and 100% reaction occurred in 100°C water. The experimental results are explained in terms of a two-step reaction scheme in which the reaction rate is initially controlled by the rate of gas-phase diffusion of water vapor toward the hot metal particles and of hydrogen, generated by reaction, away from the particles. At a later time, the reaction becomes controlled by the parabolic rate law, resulting in cooling and quenching of the reaction. Initial control of the reaction by gas-phase diffusion was shown to be responsible for the important effects of particle

size and water temperature on the reaction and the relative unimportance of metal temperatures at values greater than about 1500°C. The mathematical model of the reaction of molten metal spheres with water, which was originally developed to explain the reaction of zirconium with water, was also applied to the uranium-water reaction. Good agreement between experimental and calculated extents of reaction was found for metal temperatures below the melting point using the experimental parabolic rate equation reported in the previous paper for temperatures between 600 and 1200°C. At metal temperatures above the melting point, the results were correlated with the following parabolic rate equation: $V^2 = 8.69 \times 10^6\ t[\exp(-30{,}000/RT)]$, where V is the volume hydrogen generated in milliliters at STP per square centimeter, t is the time in minutes, R is the gas constant in calories per mole per degree Kelvin, and T is the temperature in degrees Kelvin. The results calculated from this equation corresponded very well with the observed values. The rate equation obtained by differentiating the above equation is recommended for inclusion in reactor accident models in which the effect of uranium-water or steam reaction is to be included. (auth)

29190 DIFFUSION OF FISSION PRODUCTS IN OVERLAPPING CHEMICAL REACTIONS. MATHEMATICAL BASIS. Laser, M.; Kirchner, H. (Institut fuer Chemische Technologie, Juelich, Ger.). Nukleonik, 8: 230-4(May 1966). (In German).

It is concluded from previous investigations on the mass transport of fission products in graphite that no pure diffusion exists, but that it is superimposed by one or more reactions. Previous studies on the theory of diffusion with superimposed reactions are summarized and expanded by a specific determination. The equations obtained are used to evaluate the diffusion, when the pure diffusion is superimposed by a reversible first- or second-order reaction or an irreversible reaction. (tr-auth)

29191 DEUTERON MAGNETIC RESONANCE IN SINGLE CRYSTALS OF ND_4Cl AND ND_4Br. Hovi, V.; Pyykkoe, P. (Univ. of Turku, Finland). Phys. Kondens. Mater., 5: 1-4(1966).

The deuteron quadrupole coupling constant in ND_4Cl and ND_4Br were measured. The results are 179.9 ± 2.0 and 180.0 ± 2.0 kHz, respectively. From the temperature dependence of the line width in ND_4Cl for the d-c magnetic field along [100] the hindered rotation potential barrier of the ND_4^+-ion was found to be 5.1 kcal/mole. In crystals containing moisture a narrow line component was observed, which is probably due to the formation of an eutectic solution. (auth)

29192 PARAMAGNETIC RESONANCE OF Er^{3+} IN Y_2O_3. Schaefer, G.; Scheller, S. (Technische Hochschule, Darmstadt, Ger.). Phys. Kondens. Mater., 5: 48-57(1966). (In German).

The paramagnetic resonance absorption of trivalent erbium in single crystals of Y_2O_3 on sites of crystal field symmetry C_{3i} and C_2 was investigated at 4.2°K and 9.2 kMc/s. The values of the g-tensors and those of the hyperfine structure parallel to the axes of crystalline fields are: $g_{||} = 12.176$, $g_\perp = 3.319$, $A = 426.4 \times 10^{-4}$ cm^{-1}, and $g_z = 12.314$, $g_x = 1.645$, $g_y = 4.892$, and $A_z = 433.2 \times 10^{-4}$ cm^{-1} for the C_{3i}-ions and the C_2-ions, respectively. For ions on sites of symmetry C_2 the principal axes of g in the plane perpendicular to z are found ±2° beside the [100]-directions. This is different from the results on Yb^{3+} in Y_2O_3. The dependency of g on the angle of rotation is determined for the (001), (110), and (111) planes. (auth)

29193 DIFFUSION OF TRITONS IN NH_4F-DOPED ICE SINGLE CRYSTALS. Dengel, O.; Jacobs, E.; Riehl, N. (Technische Hochschule, Munich). Phys. Kondens. Mater., 5: 58-9(1966). (In German).

The diffusion coefficient of tritons in ice was measured as a function of the concentration of NH_4F. The absolute value of the diffusion coefficient as well as the activation energy of diffusion were found to be independent of the doping within the error limits. The value found for the activation energy amounts to Q = 14.5 ± 1.0 kcal/mole. (auth)

29194 L-UNCOUPLING EFFECTS ON THE ELECTRON-PARAMAGNETIC-RESONANCE SPECTRA OF $^{14}N^{16}O$ AND $^{15}N^{16}O$. Brown, Robert L.; Radford, H. E. (National Bureau of Standards, Washington, D. C.). Phys. Rev., 147: 6-12(July 8, 1966).

High-resolution paramagnetic-resonance spectra were obtained for the molecules $^{14}N^{16}O$ and $^{15}N^{16}O$ in the $J = \frac{3}{2}$ and $J = \frac{5}{2}$ rotational levels of the $^2\Pi_{\frac{1}{2}}$ ground state at X-band and S-band microwave frequencies. The results are: $g_J(^{14}N^{16}O; J = \frac{3}{2}) = 0.777246 \pm 0.000018$, $g_J(^{15}N^{16}O; J = \frac{3}{2}) = 0.778072 \pm 0.000020$; $g_J(^{14}N^{16}O; J = \frac{5}{2}) = 0.316648 \pm 0.000045$; and $g_J(^{15}N^{16}O; J = \frac{5}{2}) = 0.317617 \pm 0.000040$ for the molecular g factors. The measured g factors were compared with those calculated from the theory of magnetic effects on Λ-type doubling previously developed by Radford. Somewhat improved values for the Λ-type doubling frequencies and nuclear hyperfine-structure coupling constants were also obtained. (auth)

29195 CHELATE FORMATION OF AMERICIUM AND CURIUM WITH NITRILOTRIACETIC ACID. Eberle, S. H.; Ali, Sameh Abdel Hadi (Technische Hochschule, Karlsruhe, Ger. Kernforschungszentrum, Karlsruhe, Ger.). Radiochim. Acta, 5: 58-9(Mar. 1966). (In German).

The chelate formation equilibrium of Am and Cm was investigated by an ion exchange method in the system metal(III)–nitrilotriacetic acid–0.1M NH_4ClO_4. The stability constants of the chelates prepared were calculated. The stability constants of Am(III) are $4.8 \pm 0.2 \times 10^{11}$ and $2.93 \pm 0.15 \times 10^{20}$. The stability constants of Cm(III) are $8.6 \pm 0.2 \times 10^{11}$ and $8.8 \pm 0.3 \times 10^{20}$. (J.S.R.)

29196 ACTIVITY COEFFICIENTS IN MULTICOMPONENT SYSTEMS. III. COMPUTATION OF ACTIVITY COEFFICIENTS OF URANYL NITRATE IN MAGNESIUM, CALCIUM, STRONTIUM, AND ZINC NITRATE SOLUTIONS. Vdovenko, V. M.; Ryazanov, M. A. Radiokhimiya, 7: 545-53(1965). (In Russian).

By a method developed earlier, the activity coefficients of uranyl nitrate in the four systems $UO_2(NO_3)_2$–$Mg(NO_3)_2$–H_2O, $UO_2(NO_3)_2$–$Ca(NO_3)_2$–H_2O, $UO(NO_3)_2$–$Sr(NO_3)_2$–H_2O, and $UO_2(NO_3)_2$–$Zn(NO_3)_2$–H_2O were calculated at 25°C. It is shown that, within the limits of error, the Harned rule is fulfilled with respect to uranyl nitrate. It is also shown that the magnitude of the Harned coefficient is a characteristic salting-out capacity of the second nitrate. (tr-auth)

29197 COMPLEX FORMATION OF URANYL ION WITH SALICYLIC ACID. III. STUDIES OF THE COMPOSITION AND REGIONS OF SEDIMENTATION FORMED IN URANYL SALICYLATE SOLUTIONS. Paramonova, V. I.; Platunova, N. B. Radiokhimiya, 7: 554-63(1965). (In Russian).

Potentiometric titration was used to show that in uranyl salicylate solutions, two completely different precipitates can be formed as a function of the precipitation conditions. Analysis of the precipitates showed that one can be represented as a nonsoluble complex compound of uranyl ions and salicylic acid. The molar ratios of the components are, $[UO_2^{2+}]:[Sal^{2-}]:[K^+] = 1:3:1$. The formula assumed for this compound is $KH_3[UO_2Sal_3]$. The second precipitate can be represented as a nonsoluble hydrolysis product. The ratio of uranyl and potassium in the hydrolysis precipitate varies with the precipitation conditions. On the basis of an analysis of the mother solution the solubility product of the complex $KH_3[UO_2Sal_3]$ was evaluated as 4×10^{-21}. Curves of the dependence of $pC_{\Sigma UO_2^{2+}} \times C_{\Sigma H_3Sal}$ on the pH and $pRC^2_{\Sigma H_3Sal}$ on the pH were constructed and these make it possible to determine the range of existence of the complex and hydrolysis precipitates. (tr-auth)

29198 KINETICS OF U(IV) OXIDATION IN CARBONATE SOLUTION BY ATMOSPHERIC OXYGEN. Kanevskii, E. A.; Goncharov, I. V.; Rengevich, V. B. Radiokhimiya, 7: 579-85(1965). (In Russian).

It is shown that the velocity of oxidation of U(IV) in

carbonate–bicarbonate solution by atmospheric oxygen is determined by the speed of dissolution of molecular oxygen. Under the same conditions the rate of oxidation of Cu(I) is 100 times faster. The oxidation kinetics of U(IV) in carbonate–bicarbonate solution by atmospheric oxygen with precipitation of cupric ammonium complexes was investigated. The velocity of the process can be expressed by the equation $W = K[Cu^{2+}]_0^{0.5} + W_H$. The mechanism assumed for the oxidation of U(IV) in alkaline solutions with catalytic participation of Cu(II) was examined and found to explain the experimental data obtained. (tr-auth)

29199 CATALYTIC ACTION OF COPPER AMMONIATE DURING OXIDATION OF URANIUM DIOXIDE BY ATMOSPHERIC OXYGEN. Kanevskii, E. A.; Goncharov, I. V.; Rengevich, V. B. Radiokhimiya, 7: 585-9(1965). (In Russian).

It was established that the velocity of the catalytic oxidation and dissolution of uranium dioxide in carbonate-bicarbonate solutions in the presence of copper ammoniate can be expressed by the equation $W = KS[Cu(II)]_0^x$ where $x \cong 0.5$, i.e., close to the exponent in the kinetic equation in the case of catalytic oxidation of uranium pentacarbonate. (tr-auth)

29200 PHYSICO-CHEMICAL INVESTIGATION OF SOLID PHASES OF $NH_4F–UO_3–H_2O$ SYSTEMS. Opalovskii, A. A.; Batsanov, S. S.; Kuznetsova, Z. M. Radiokhimiya, 7: 589-96(1965). (In Russian).

Physico-chemical investigations of the solid phase of the $NH_4F–UO_3–H_2O$ system are reported. It is shown that during the interaction of uranium trioxide with aqueous solutions of ammonium fluoride two separate compounds, $NH_4(UO_2)_2(OH)_4F$ and $(NH_4)_3UO_2F_5$, are formed as a function of the concentration of the ammonium fluoride. The two compounds were studied by chemical, thermographic, x-ray, and crystallochemical-analytical methods. (tr-auth)

29201 DECOMPOSITION OF ZIRCONIUM SILICATE WITH POTASSIUM FLUOSILICATE. Catoiu, E.; Segarceanu, T. Rev. Chim. (Bucharest), 17: 193-6(Apr. 1966). (In Rumanian).

The results of zirconium silicate decomposition tests by treatment with potassium fluosilicate are given and the parameters of the process are discussed. The process is apparently based on the property of K_2SiF_6 of decomposing under heat to KF and SiF_3, which is the attack agent of zirconium silicate. The ZrF_4 formed unites with the KF set free to rebuild the hexafluorinated complex on the basis of the minimum structure change. A decomposition yield of 95% was reached in the case of some concentrates with 40% ZrO_2. (auth)

29202 SPECTROPHOTOMETRIC STUDY OF THE URANYL NITRATE–SALICYLALDOXIME SYSTEM. Kiss-Imreh, Gabriela; Szekely, Zoltan; Ripan, Raluca (Academie Filiale, Cluj). Rev. Roum. Chim., 11: 47-51(Jan. 1966). (In French).

A spectrophotometric study of the U(VI)–salicylaldoxime system in the visible region established that UO_2^{2+} reacts with salicylaldoxime in aqueous solutions to form an orange complex at pH = 3.40 to 12.60 with a maximum stability at pH = 8.60. By means of a logarithmic method this stoichiometric ratio between the components (salicylaldoxime/UO_2^{2+} = 1) and the instability constant of the complex formed ($k_n = 2.1 \pm 0.3 \times 10^{-3}$) were determined. (tr-auth)

29203 BIS-ACETYLACETONE-ETHYLENEDIIMINES OF ZIRCONIUM AND THORIUM. Macarovici, Const. Gh.; Perte, Eugenia; Motiu, Emilia (Academie Filiale, Cluj). Rev. Roum. Chim., 11: 59-66(Jan. 1966). (In French).

Some complexes of $ZrOCl_2 \cdot 8H_2O$ and $Th(NO_3)_4 \cdot 4H_2O$ with acetylacetone–ethylenediimine were synthesized. Their solubilities in water and in different organic solvents were determined qualitatively and the thermograms were traced. In addition to the acetylacetone–ethylenediimine of Zr and Th, internal chelates were also obtained, which contained two monovalent inorganic anions. The most probable structure of these complexes was deduced. (tr-auth)

29204 REFRACTOMETRIC INVESTIGATION ON THE FORMATION OF COMPLEX SAMARIUM HALOGENIDES IN AQUEOUS SOLUTION. Spacu, P.; Albescu, Ileana (Institut fuer Anorganische Chemie, Bucharest). Rev. Roum. Chim., 11: 79-83(Jan. 1966). (In German).

Results of refractometric investigations of systems of the type $SmX_3–Me^1X$(Me^1 = Na, K, Rb, and Cs, and X = Cl and Br) in concentrated solutions are reported. The following compounds were detected: $NaSmCl_4$, $KSmCl_4$, Rb_2SmCl_5, Cs_2SmCl_5, $NaSmBr_4$, $KSmBr_4$, $RbSmBr_4$, Na_2SmBr_5, K_2SmBr_5, Rb_2SmBr_5, and K_3SmBr_6. (tr-auth)

29205 STUDIES ON THE LIGAND FIELD THEORY. I. AN IMPROVED WEAK FIELD SCHEME. Tang, Au-chin (Kirin Univ., Changchun, China); Sun, Chia-chung; Kiang, Yuan-sun; Deng, Zung-hau; Liu, Jo-chuang; Chang, Chian-er; Yan, Go-sen; Goo, Zien; Tai, Shu-shan. Sci. Sinica (Peking), 15: 610-44(May 1966).

An improved weak field coupling scheme in the ligand field theory is proposed. On using the basis functions $\psi^1_{\Gamma\gamma}$ of the irreducible representations of both the three-dimensional rotation group and the point group as the one-electron orbitals, the wave functions and terms of d^n configurations are classified according to the irreducible representations of the following groups: SU_{2l+1}, R_{2l+1}, R_3, and the point group, and the new Clebsch-Gordan coefficients $(l_1l_2\Gamma_1\Gamma_2|l\Gamma)$ and their related V coefficients $V(l_1l_2l/\Gamma_1\Gamma_2\Gamma)$ are defined, by virtue of which we can apply the Wigner-Eckart theorem to the calculation of the matrix elements. In this scheme, the classification of the wave functions and terms is clear and complete. The new V coefficients enable the calculation of the matrix elements to be simplified to the calculation of the reduced matrix elements of the three-dimensional rotation group. All the calculations are straightforward and standardized. New coefficients of fractional parentage $[d^{n-1}(S'\xi'L'\Gamma')d\Gamma''|\}d^nS\xi L\Gamma]$ are defined. They may also be used in the calculation of matrix elements. Like Racah's method in the calculation of the atomic terms, these calculations are also standardized. Based on this improved weak-field scheme, it is easier to find the relationships between the weak-field and strong-field schemes. The results are to be reported later. To facilitate the tabulation, the orthogonal and symmetry properties of the new V coefficients are studied. More than 220 of them and all the c.f.p. of the $d^3–d^5$ configurations have been calculated and tabulated for consultation. (auth)

29206 ROLE OF SCAVENGERS IN GAS-PHASE RECOIL TRITIUM REACTIONS. Urch, D. S.; Welch, M. J. (Queen Mary Coll., London). Trans. Faraday Soc., 62: 388-92(Feb. 1966).

The effect of various scavengers upon the distribution of labeled products from the reaction of recoil-tritium atoms with gaseous hydrocarbons is discussed. In particular, it is shown that different yields of labeled alkyl halides produced in the presence of bromine or iodine and that oxygen markedly affects the amount of ethylene-t formed from ethane. A reaction scheme involving a triplet state C_2H_5T molecule is postulated to explain the latter observation. It is concluded that the role of scavengers in hot atom reactions is more involved than was assumed up to now. (auth)

29207 KINETIC STUDIES OF MODERATELY RAPID ISOTOPIC EXCHANGE REACTIONS. Beronius, Per (Royal Inst. of Tech., Stockholm). Trans. Roy. Inst. of Technol., Stockholm, No. 239, 1-28(1964).

In order to test the so-called "integral method" the kinetics of the isotopic exchange between methyl iodide and iodide ions were investigated in ethyl alcohol and acetone as solvent media at half-times of exchange ranging from 0.1 to 900 sec. The analytical precision was ~±3% standard deviation for the single velocity coefficient at half-times exceeding a few seconds. No significant systematic errors were observed. (auth)

29208 COMPLEXING OF SERINE WITH SOME RARE EARTH ELEMENTS IN AQUEOUS SOLUTIONS. Panasyuk, V. D.; Golub, V. A. (Inst. of Physical Chemistry, Acad-

emy of Sciences, Ukrainian SSR). Ukr. Khim. Zh., 31: 1025-31(1965). (In Russian).

The complexing of La, Ce, Pr, Nd, Sm, and Eu by serine was followed by pH-potentiometric titration at an ionic strength of 0.1. The equilibrium concentration of serine addend was calculated in order to determine the complexing functions and the instability constants from the data. Only complexes with a 1:1 ratio of metal to addend were detected. The instability constants were found to be 4.0×10^{-4} for the La complex, 2.5×10^{-4} for Ce, 1.9×10^{-4} for Pr, 1.7×10^{-4} for Nd, 1.5×10^{-4} for Sm, and 1.3×10^{-4} for the Eu complex. The stability of the rare earth complex increased continuously from lanthanum to europium. (TTT)

29209 TEMPERATURE EFFECT ON THE YIELD AND COMPOSITION OF HEXANITROCOBALTIC RARE EARTHS MIXED WITH POTASSIUM. Aleksandrov, G. P.; Shevchenko, Yu. V. (Inst. of Geology and Geochemistry of Natural Fuels, Academy of Sciences, Ukrainian SSR). Ukr. Khim. Zh., 31: 1040-5(1965). (In Russian).

The reaction of a mixture of rare earth and cobalt nitrates with potassium nitrite gave a mixed hexanitrocobaltate salt of the following composition: $mKR[Co(No_2)_6] \cdot nK_4[Co(NO_2)_6]$, where R stands for La, Ce, Pr, Nd or Sm. A salt with a Co/La ratio of 2 was obtained at 0°C and at high concentrations of initial reactants of 343 g/l of $La(NO_3)_3$, 610 g/l of $Co(NO_3)_2$, and 1270 g/l of KNO_2. On increasing the temperature from 30 to 90°C, the amount of $K_2[Co(NO_2)_4]$ in the solid phase increased, and the amount of mixed salt decreased at the same time from about 80% at 30°C, to 50% at 60°C, and to 15% at 90°C. (TTT)

29210 POLAROGRAPHIC STUDY OF RARE EARTH ELEMENTS ON A BACKGROUND OF FUSED POTASSIUM ACID SULFATE. Panchenko, I. D.; Penkalo, I. I. (Inst. of General and Inorganic Chemistry, Academy of Sciences, Ukrainian SSR). Ukr. Khim. Zh., 31: 1203-6(1965). (In Russian).

A polarographic study of the rare earth oxides was carried out on a background of fused potassium acid sulfate using rotating disc electrodes. The half-wave potentials for reduction of the oxides were determined. The separation potentials of rare earth elements in the fused electrolyte differ significantly from each other; for instance, the difference between the separation potentials of La and Eu is 0.7 v. It was found that the limiting diffusing current is directly proportional to the concentration of the oxide studied. From the limiting diffusing current the coefficients of diffusion of the La, Gd, Y, Ce, and Eu ions were calculated. The thickness of the diffusing salt in the fused potassium acid sulfate was determined to be approximately 2×10^{-3} cm. (tr-auth)

29211 VOLATILIZATION OF URANIUM FISSION PRODUCTS IN HYDROGEN, NITROGEN, AND OXYGEN. Roeder, Erhard; Herrmann, Guenter (Univ., Mainz). Z. Anal. Chem., 219: 93-102(1966). (In German).

The volatilization of the fission products germanium, arsenic, molybdenum, ruthenium, cadmium, tin, antimony, and tellurium from neutron-irradiated uranium oxide in flowing hydrogen, nitrogen, or oxygen of atmospheric pressure was investigated between 900 and 1500°C. At 1500°C most of these elements were volatilized with high yield within one hour. (auth)

29212 PREPARATION AND STRUCTURE OF THE RARE EARTH TITANATES AND OF EUROPIUM(II) ZIRCONATE. Holzapfel, H.; Sieler, J. (Karl-Marx-Univ., Leipzig). Z. Anorg. Allg. Chem., 343: 174-80(1966). (In German).

The titanates of the rare earth metals (Ln = La, Ce, Pr, Nd, Gd, and Eu) were prepared by heating Ln_2O_3 and Ti_2O_3 in silica capsules in vacuo at 1150°C. They have a distorted perovskite lattice. Europium titanate and europium zirconate are cubic with a = 7.810 ± 0.002 and 4.099 ± 0.002 Å, respectively. Europium zirconate is isomorphic with the analogous strontium compound. (auth)

29213 STUDIES ON RARE EARTH TRICHLOROACETATES. I. THERMAL BEHAVIOR IN AIR AND IN NITROGEN ATMOSPHERE. Mathur, B. S.; Bhat, T. R. (Atomic Energy Establishment, Trombay, India). Z. Anorg. Allg. Chem., 343: 220-4(1966).

Trichloroacetates of La, Ce, Pr, Nd, Sm, Eu, Gd, Tb, Dy, Ho, Er, Tm, Yb, Lu, and Y were prepared and their composition determined. Decomposition of these compounds was studied by thermogravimetry in air and in a nitrogen atmosphere followed by chemical analysis. In all cases the anhydrous chloride was first formed. This remained stable in nitrogen, while in air the oxychloride and subsequently the oxide were formed at higher temperatures. (auth)

29214 PREPARATION AND SOME PROPERTIES OF ANHYDROUS SCANDIUM NITRATE AND ITS SOLVATES. Komissarowa, L. N.; Puschkina, G. J.; Chramejewa, N. P.; Spitzin, V. I. (Moscow State Univ.). Z. Anorg. Allg. Chem., 344: 76-85(Apr. 1966). (In German).

Several methods for the preparation of anhydrous scandium nitrate were checked. $Sc(NO_3)_3$ was best obtained from the interaction of $ScCl_3$ with liquid N_2O_4 and N_2O_5. The appropriate reaction conditions are also described for preparing the solvates $Sc(NO_3)_3 \cdot nN_2O_4$ (n = 1 to 2). These nitrates are crystalline and very hygroscopic, with a covalent-ionic metal to nitrate bond. Whereas the solvates are decomposed just above 20°C, the anhydrous nitrate is stable up to 105°C. At higher temperatures, the anhydrous nitrate gives basic compounds $Sc_2(NO_3)_4$, $ScONO_3$, and $Sc_4O_5(NO_3)_2$. (auth)

29215 FREE ENERGIES OF FORMATION OF SOME INORGANIC FLUORIDES BY SOLID STATE ELECTROMOTIVE FORCE MEASUREMENTS. Heus, R. J.; Egan, J. J. (Brookhaven National Lab., Upton, N. Y.). Z. Phys. Chem. (Frankfurt), 49: 38-43(Apr. 1966). (BNL-9899).

The free energies of formation of ThF_4, AlF_3, NiF_2, PbF_2, CoF_2, and UF_3 were determined by emf measurements. The following cells were operated: $Mg,MgF_2(s)/CaF_2(s)/ThF_4,Th(s)$; $Th,ThF_4(s)/CaF_2(s)/AlF_3,Al(s)$; $U,UF_3(s)'CaF_2(s)/AlF_3,Al(s)$; $Th,ThF_4(s)/CaF_2(s)/NiF_2,Ni(s)$; $Al,AlF_3(s)/CaF_2(s)/PbF_2(s),Pb(l)$; and $Al,AlF_3(s)/CaF_2(s)/CoF_2,Co(s)$. They yielded the following free energies at 600°C: $\Delta G^0_{ThF_4} = -436.2$, $\Delta G^0_{AlF_3} = -305.7$, $\Delta G^0_{NiF_2} = -126.8$, $\Delta G^0_{PbF_2} = -130.9$, $\Delta^0_{CoF_2} = -129.6$, and $\Delta G^0_{UF_3} = -310.5$ kcal. Experimental details and difficulties are discussed. (auth)

29216 MIXED CONDUCTION IN ThO_2 AND ThO_2–Y_2O_3 SOLUTIONS. Lasker, M. F.; Rapp, Robert A. (Ohio State Univ., Columbus). Contract AT(11-1)-1440. Z. Phys. Chem. (Frankfurt), 49: 198-21(May 1966).

A dilute solution model was developed for prediction of the partial ionic and electronic conductivities, as well as ionic transference numbers, in doped ThO_2 electrolytes. Total conductivity measurements were carried out between 800 to 1100°C for "pure" ThO_2 and $ThO_2-Y_2O_3$ solutions over a wide range of oxygen chemical potentials. Galvanic cell measurements were made to separate the total conductivity into partial ionic and partial electronic conductivities. Although $\sigma_\oplus$ was in agreement with the predictions of the dilute solution theory for all electrolyte compositions, σ_{ion} exhibited a maximum with increasing Y_2O_3 concentration. No significant excess electron conductivity was indicated for any $ThO_2-Y_2O_3$ composition at oxygen partial pressures as low as those for $Cr-Cr_2O_3$ equilibrium coexistence. With increasing $YO_{1.5}$ content in $ThO_2-Y_2O_3$ electrolytes, the P_{O_2} range for exclusive ionic conduction was extended to higher P_{O_2}; although no experimental data are available, the dilute solution theory predicts that the P_{O_2} range for exclusive ionic conduction would also be extended to lower P_{O_2} with increasing Y_2O_3 concentration. (auth)

29217 THE STABILITY OF METAL-ALLOY BOND IN RARE EARTHS PHTHALOCYANINES. Shklover, L. P.; Plyushchev, V. E. (All-Union Research Inst. for Chemical Reagents and Pure Chemical Substances, USSR). Zh. Fiz. Khim., 39: 2924-6(Dec. 1965). (In Russian).

The electron absorption spectra of solutions of rare

earth phthalocyanines in α-bromonaphthalene were examined in the visible range. The displacement of the position of the most intense absorption maximum λ_1 in the spectra of these solutions as a function of the sequence of element numbers N in the series from praseodymium to lutetium can be described by the equation $\lambda = 4.4205\underline{N} + 24838/\underline{N}$, in mμ. The short wave displacement of position λ_1 with increases of N is explained by the increase of the stability of the rare earth phthalocyanine. (tr-auth)

29218 THORIUM TETRASULFATE COMPOUNDS. Molodkin, A. K.; Skotnikova, G. A.; Ivanova, O. M. (Kurnakov Inst. of General and Inorganic Chemistry, USSR). Zh. Neorg. Khim., 10: 2441-8(Nov. 1965). (In Russian).

The tetrasulfate complexes of thorium $(NH_4)Th(SO_4)_4 \cdot 2H_2O$, $K_4Th(SO_4)_4 \cdot 2H_2O$, $Rb_4Th(SO_4)_4$, and $Cs_4Th(SO_4)_4 \cdot H_2O$ and the complex $Na_{10}Th_2(SO_4)_9 \cdot 5H_2O$ were prepared and some of their properties (behavior with reagents, density, index of refraction, electric conductivity of aqueous solutions, and thermal stability) were investigated. The internal structure was considered and some coordination formulas for the tetrasulfate complexes are proposed. (auth)

29219 SOLUBILITY OF AMMONIUM PLUTONYL PHOSPHATE COMPOUNDS IN AQUEOUS SOLUTIONS. Denotkina, R. G.; Shevchenko, V. B.; Moskvin, A. I. Zh. Neorg. Khim., 10: 2449-52(Nov. 1965). (In Russian).

The solubility of ammonium plutonyl phosphates in aqueous solutions was determined in the pH interval from 1.0 to 6.4. From experimental data on the solubilities, the solubility products of ammonium plutonyl phosphates and of dibasic plutonyl phosphates were calculated to be $2.3 \pm 1.2 \times 10^{-27}$ and $2.8 \pm 1.3 \times 10^{-13}$, respectively. The instability concentration constants of $NH_4PuO_2PO_4$ and PuO_2HPO_4 were calculated as 3.7×10^{-22} and 6.8×10^{-9}. On the basis of the solubility products calculated for $NH_4PuO_2PO_4 : 3H_2O$ and PuO_2HPO_4 it was found that ammonium plutonyl phosphate behaves as a slightly soluble compound formed during the interaction of PuO_2^{2+} ions with phosphoric acid. (tr-auth)

29220 HYDROLYSIS OF RARE EARTH METAL DICARBIDES. Kosolapova, T. Ya.; Kaminskaya, O. V.; Kovalenko, N. A.; Pustovoit, L. T. Zh. Neorg. Khim., 10: 2453-6(Nov. 1965). (In Russian).

Gaseous products from the hydrolysis of dicarbides of yttrium, lanthanum, cerium, praseodymium, neodymium, and gadolinium were investigated. It was established that the following hydrolysis products appear: acetylene, hydrogen, ethylene, and ethane. The electron structure of metals forming the carbides appears to determine the quantity of acetylene and hydrogen formed. (tr-auth)

29221 1,10-PHENANTHROLINETHENOYLTRIFLUOROACETONE COMPLEXES OF RARE EARTH ELEMENTS. Kononenko, L. I.; Tishchenko, M. A.; Vitkun, R. A.; Poluektov, N. S. Zh. Neorg. Khim., 10: 2465-70(Nov. 1965). (In Russian).

The formation in aqueous ethanol solutions of ternary complexes of rare earth complexes with 1,10-phenanthroline–thenoyltrifluoroacetone was investigated by the turbidimetric method. By means of molar ratios in isomolar series methods it was established that under these conditions the nonsoluble complexes are formed with the component ratios RE : PHEN : TTA = 1 : 1 : 3. The ternary complexes of La, Nd, Sm, Eu, Dy, and Y were separated and analyzed for the rare earth, 1,10-phenanthroline, and TTA contents. It was established that the general formula of the compound is $Me(C_{12}H_8N_2)(O_2C_3H \cdot CF_3 \cdot C_4H_3S)_3$. It was established that the ternary complexes of Sm and Eu have nuclear fluoresence after irradiation with long-wave ultraviolet light. The luminescence spectra of the $^5D_0 - {}^7F_2$ band of europium in the ternary complexes were different from the luminescence spectrum of simple europium thenoyltrifluoroacetone. (tr-auth)

29222 COMPLEX FORMATION OF RARE EARTHS WITH ETHYLENEDIAMINETETRAACETIC ACID. Verenikin, V. B.; Astakhov, K. V.; Malanichev, F. G. Zh. Neorg. Khim., 10: 2471-6(Nov. 1965). (In Russian).

By use of a series of isomolar solutions and a series of solutions with constant central ion content and variable addends it was established that at a pH of 4 to 6 the Pr^{3+}, Nd^{3+}, Sm^{3+}, and Er^{3+} ions form complexes with ethylenediaminetetraacetic acid with the ratio rare earth ion : EDTA = 1 : 1. Investigation of a series of solutions with constant addend content and variable central ion (Nd^{3+}) content showed the formation of complexes of the composition 1 : 1 only at pH_4. Polynuclear complexes were not formed. The method for calculation of the size of the instability constant of the complexes formed with rare earth ions, on the basis of spectrophotometric data, is reported. Calculation of the size of the acidolysis constant and the instability constant of ytterbium complexes with EDTA is described. (tr-auth)

29223 FORMATION AND THERMAL DISSOCIATION OF YTTRIUM FLUORIDES AND CARBONATES. Fridman, Ya. D.; Moshkina, V. A.; Gorokhov, S. D.; Nitsevich, E. A. Zh. Neorg. Khim., 10: 2477-83(Nov. 1965). (In Russian).

The thermal dissociation of carbonates and fluorides was investigated by thermogravimetric, thermographic, and x-ray analyses. The results obtained indicated that yttrium carbonate decomposes in the temperature interval from 155 to 700°C according to the scheme $Y_2(CO_3)_3 \cdot 3H_2O \rightarrow Y_2(CO_3)_3 \rightarrow Y_2O_3 \cdot 0.2CO_2 \rightarrow Y_2O_3$. Yttrium fluoride decomposes in the temperature interval from 450 to 800°C in accordance with the scheme $YF_3 \rightarrow YOF \rightarrow Y_2O_3$ with the formation of intermediate products. Results of the interaction of yttrium fluoride with sodium carbonate showed that in the temperature interval from 550 to 700°C the interaction in the system obeys the summary equation $2YF_3 + 3Na_2CO_3 \rightarrow Y_2O_3 + 6NaF + 3CO_2$. In the temperature interval from 800 to 850°C, with excess concentrations of sodium carbonate, an interaction of Na_2CO_3 with yttrium oxide occurred during which the compound $NaYO_2$ is probably formed. (tr-auth)

29224 THERMAL DISINTEGRATION OF NITRATES OF CERIUM, NEODYMIUM, AND GADOLINIUM. Chizhikov, D. M.; Rabinovich, B. N.; Subbotina, E. A. Zh. Neorg. Khim., 10: 2527-34(Nov. 1965). (In Russian).

Investigations of the thermal decomposition of the nitrates of cerium, neodymium, and gadolinium showed that the dehydration process of cerium nitrate proceeds in the temperature interval from 75 to 130°C, of neodymium nitrate in two stages at 80 to 150 and 150 to 300°C, and of gadolinium nitrate in the temperature interval from 100 to 300°C. The formation of the oxide during the thermal decomposition of the nitrates was observed for cerium nitrate at 170°C, for neodymium nitrate at 300°C, and for gadolinium nitrate at 400°C. These data were confirmed by x ray and magnetometric studies of the decomposition products. (tr-auth)

29225 NEODYMIUM AND ERBIUM BROMIDE COMPLEXES. Mal'kova, T. V.; Shutova, G. A.; Yatsimirskii, K. B. (Ivansvsk Inst. of Chemistry and Tech., USSR). Zh. Neorg. Khim., 10: 2611-14(Dec. 1965). (In Russian).

The systems $Nd^{3+} - Br^-$ and $Er^{3+} - Br^-$ were investigated by differential spectrophotometric analysis. The formation of 1- and 2-coordination complex compounds was established. The stability constants of these compounds were determined as $\beta_1 = 1.56 \pm 0.69 \times 10^{-1}$ and $\kappa_2 = 5.31 \pm 0.018 \times 10^{-4}$ for $NdBr^{2+}$ and $NdBr_2^+$ and $\beta_1 = 2.63 \pm 0.19 \times 10^{-1}$ and $\kappa_2 = 4.03 \pm 0.01 \times 10^{-3}$ for $ErBr^{2+}$ and $ErBr_2^+$. The applicability of the differential spectrophotometric method was shown and the system with step-wise complex formation was investigated. (tr-auth)

29226 THORIUM PENTA- AND HEXASULFATE COMPOUNDS. Molodkin, A. K.; Skotnikova, G. A.; Ivanova, O. M. (Kurnakov Inst. of General and Inorganic Chemistry, USSR). Zh. Neorg. Khim., 10: 2675-83 (Dec. 1965). (In Russian).

Some penta-and hexasulfate complexes of thorium $(NH_4)_6Th(SO_4)_5 \cdot 3H_2O$, $Cs_6Th(SO_4)_5 \cdot 3H_2O$, and $(NH_4)_8Th(SO_4)_6 \cdot 2H_2O$ were prepared and some of their properties (density, reaction with reagent, electric conductivity of aqueous solution, and index of refraction) were investigated. The inter-

nal structure of the compounds was considered and some coordination formulas are proposed. It was established that thorium sulfates do not interact with the sulfates of divalent metals. (tr-auth)

29227 PRESSURE AND COMPOSITION OF SATURATED VAPOR IN NaCl–$LaCl_3$ SYSTEM. Novikov, G. I.; Tolmacheva, V. D. Zh. Neorg. Khim., 10: 2712-16(Dec. 1965). (In Russian).

By the boiling point method, data on the pressure of saturated vapor in the NaCl – $LaCl_3$ system were obtained in the temperature interval from 1100 to 1350°C. Analysis of the condensate made it possible to determine the gross composition of the vapor. From the experimental data and the mass-spectrometric determination of the vapor composition, it was concluded that the vapor, aside from the simple form, contains the complex $NaLaCl_4$. By the characteristic thermodynamic equation $(NaLaCl_4) \rightarrow (NaCl) + (LaCl_3)$ the following results were obtained: $\Delta H^0_{1500°K} = 69.8 \pm 2.5$ kcal/mol and $\Delta S^0_{1500°K} = 32.8 \pm 1.8$. (tr-auth)

29228 CERIUM NITRILOTRIACETATES. Verenikin, V. B.; Astakhov, K. V. Zh. Neorg. Khim., 10: 2753-9 (Dec. 1965). (In Russian).

The formation of complexes of cerium with nitrilotriacetic acid was studied by the ion exchange method. The formation of cerium ions with anions of nitrilotriacetic acid HX^{2-} of two complex compositions 1 : 1 and 1 : 2 was established. Determination of the sign of the charge of the complexes indicated the formulas CeX and CeX_2^-. The sizes of the acidolysis constant and instability constant were calculated. The agreement of the values of the instability constant of the 1 : 1 complex with the values obtained by others using polarographic and potentiometric methods is shown. (tr-auth)

29229 HEAT OF FORMATION OF SOME THORIUM, PROTACTINIUM, URANIUM, NEPTUNIUM, AND AMERICIUM HALIDES. Maslov, P. G.; Maslov, Yu. P. Zh. Obshch. Khim., 35: 2112-15(1965). (In Russian).

The heats of formation, $-\Delta H^0_f$, of the halides PaX_4, PuX_4, AmX_4, (X = F, Cl, Br, and I), NpI_4, UH_4, PuH_3, and UH_3 in the solid state at 25°C were found with a precision of ±(2 to 10) kcal/mol or 2 to 5%. It is shown that the heat of formation of ThI_4, 131 kcal/mol, reported previously is probably wrong and that this value probably is 154 ± 2 kcal/mol. The heats of formation were calculated for a large group of mixed halides of Th, Pa, U, Np, Am, and Pu in the solid phase at 25°C. The precision was 1 to 5%. (tr-auth)

29230 TEMPERATURE EFFECTS ON ELECTRON POLARIZATION VARIATIONS IN ORDINARY AND HEAVY WATER MOLECULES. Frontas'ev, V. P.; Shraiber, L. S. (Saratov State Univ., USSR). Zh. Strukt. Khim., 6: 512-21(July-Aug. 1965). (In Russian).

The effects of temperature on electron polarization in ordinary and heavy water were investigated and the anomalous behavior of the polytherm of electron polarization of the total molecule was detected. This is in contrast to ordinary liquids with densely packed molecules in which the polytherm of electron polarization of the molecule is almost linear. The polarization polytherms of H_2O and D_2O at temperatures from 55 to 65°C have minima. For D_2O this minimum is displaced 5 to 10°C to the higher temperatures in comparison with H_2O, but the D_2O molecule has less polarization. The anomalous behavior of the polytherm of electron polarization of the molecule of ordinary and heavy water is connected with the structural characteristic change of water under temperature effects. Data on the precise changes of the refraction of H_2O and D_2O according to the four spectral lines (C, D, E, and F) in the temperature interval from 2.5 to 94°C are reported. (tr-auth)

29231 CERTAIN CRYSTALLOCHEMICAL PROPERTIES OF CUBIC-SHAPED HYDRATED URANIUM TETRAFLUORIDE. Bakakin, V. V.; Gagarinskii, Yu. V.; Borisov, S. V.; Zadneprovskii, G. M.; Durasova, S. A. (Inst. of Inorganic Chemistry, Academy of Sciences, Siberian SSR). Zh. Strukt. Khim., 6: 563-70(July-Aug. 1965). (In Russian).

The discrepancy between calculated and experimental density of cubic $UF_4 \cdot \underline{n}\ H_2O$ and the anomalous pattern of the density change with relation to $\underline{n}$ are related to the non-integral number of the quantity of formula units in the cell and its decrease with increases of $\underline{n}$, which indicates the presence of defects in the anion shell and corresponding deficiencies of cations. (tr-auth)

29232 STABILITY CONSTANTS OF RARE EARTHS WITH SOME CARBOXYLIC ACIDS [Thesis]. Schoeb, Virginia Rowland. Ames, Iowa, Iowa State Univ. of Science and Tech., 1965. 90p.

The stepwise formation constants for complexes between yttrium, lanthanum, and the rare earths, except promethium, and the ligands quinate, mandelate, and dilactate were measured at 25°C and the ionic strength of 0.1M ($NaClO_4$). They were determined potentiometrically using a Beckman research pH meter. Optimum values of the successive equilibrium constants were computed via a least squares technique using an IBM 7074 computer. The presence of hydroxyl groups enhances the stability of rare-earth quinates over rare-earth 1-hydroxycyclohexane-carboxylates. The mandelates in solution could be nine-coordinated in the case of the light rare earths and either eight- or nine-coordinated in the case of the heavy rare earths, with mandelate acting bidentately throughout. Dilactic acid seems to be at least a tridentate ligand if not a pentadentate ligand. (Dissertation Abstr.)

29233 MATHEMATICAL STUDY OF GAS-PHASE HOT-ATOM REACTIONS [Thesis]. Hsiung, Chi-hua Wu. Ann Arbor, Mich., Univ. of Michigan, 1962. 205p.

Mathematical models are developed to describe the various processes associated with chemical reactions activated by nuclear processes. The primary activation is described in terms of a momentum transfer to an atom in a molecule and there is derived an equation that can be used to calculate the minimum energy that must be imparted to the atom so that it will dissociate from the molecule. The minimum net recoil energy required for carbon-halogen bond rupture, the kinetic energy of the recoiling radicals, and the internal energy of the radical originally bonded to the activated atom are calculated for a series of simple alkyl halides. The extent of molecular dissociation following ^3H and ^{14}C beta-decay recoil is evaluated, using the above model, for HT, T_2, $^{14}CO_2$, $^{14}C_2H_6$, and tritiated alkanes. The calculated percents of bond rupture are in good agreement with mass-spectral experimental observations. A mathematical model is presented for calculating the percent of the hot atoms that react with thermal-energy molecules. There are calculated (1) the hot-atom energy ranges in which stable compounds can be formed, (2) the energy degradation that results from collisions of the hot atoms with the thermal-energy molecules, (3) the probability that a thermal molecule colliding with a hot atom in a reactive energy range will form a particular chemical product, and (4) the percent yield of a product in (a) pure systems, (b) inert-gas moderated systems, and (c) systems consisting of more than one reactive species. Calculated yields are found to compare favorably with experimental data available in the literature for reactions of (1) tritium, formed by the $^3He(n,p)^3H$ reaction, with CH_4, CD_4, C_2H_6, CH_3F, CH_2F_2, CHF_3, CF_4, and CH_4 + He, CD_4 + He, H_2 + D_2 mixtures, (2) ^{80}Br, formed by the $^{79}Br(n,\gamma)^{80}Br$ reaction, with CH_4, C_2H_6, and CH_4 + inert-gas mixtures, (3) ^{128}I, formed by the $^{127}I(n,\gamma)^{128}I$ reaction, with CH_4, CD_4, CHF_3, C_2H_6, C_3H_8, and CH_4 + inert-gas mixtures. (Dissertation Abstr.)

29234 INVESTIGATION OF THE INTERACTIONS THAT OCCUR BETWEEN RADIONUCLIDES AND AEROSOLS IN THE RESPIRABLE SIZE RANGE [Thesis]. Craig, Douglas Kenneth. Rochester, N. Y., Univ. of Rochester, 1964. 262p.

It has been reported in the literature that radioactive nuclides are usually subject to rapid and irreversible adsorption at surfaces. Aerosols, whether pre-existing in the atmosphere or generated in a nuclear incident, represent

such surfaces and it is to be expected that radionuclides that escape into the environment will become attached to them. The relationship between adsorbed activity and aerosol particle size was investigated for an important fission product under carefully controlled laboratory conditions. A labeled iron oxide aerosol was allowed to interact with radionuclides consisting of molecular sodium iodide with specific activities of from 0.15 to 15 mC ^{131}I/mg NaI. The Goetz Aerosol Spectrometer was used to characterize the adsorption of NaI molecules onto the aerosol as a function of particle size. Relative radionuclide-aerosol concentrations were varied from 3×10^2 to 3×10^5 molecules per particle and mean interaction times by a factor of about 2.5. The following conclusions were drawn: although considerable quantities of the radionuclide did become attached to the aerosol, the adsorption process was not irreversible; variation of the experimental conditions over the above range did not significantly affect the results; and the adsorbed activity was proportional to a function $D(I)^Z$, where D(I) is the aerosol diameter and $2 \leq Z \leq 3$ over the approximate size range $0.06 < D(I) \leq 0.65\ \mu$ and possibly up to particle diameters as large as 1.2 μ, the inference being that adsorbed activity would be proportional to the true surface area under equilibrium conditions. (Dissertation Abstr.)

29235 CHEMISTRY OF SELENIUM, TELLURIUM AND POLONIUM. **Bagnall, K. W. Topics in Inorganic and General Chemistry. Monograph 7. New York, Elsevier Publishing Co., 1966. 207p. $13.00.**

Existing knowledge on the chemistry of selenium, tellurium, and polonium is reviewed. Topics covered included: the discovery and uses of the elements; separation, purification, and determination; elements, hydrides, and other derivatives; oxides, oxo-acids, sulfides, and sulfur-oxo-acids; halides; salts formed with oxo-acids; and carbon compounds. Crystallographic data are presented in tabular form. (M.C.G.)

Organic Chemistry

Refer also to abstract 30906.

29236 APPLICATION OF A NEW METHOD TO SYNTHESIS OF RADIOACTIVE SODIUM 3,5-DIIODOFLUORESCEIN (3,5-^{131}I). **Kato, Sadatake; Kurata, Kunio (Dainabot Radioisotope Labs., Ltd., Chiba, Japan). Chem. Pharm. Bull. (Tokyo), 13: 1252-4(1965).**

A method to increase the radioactive yield in a substitutional reaction was developed and applied to the preparation of sodium 3,5-diiodofluorescein (3,5-^{131}I). In this method radioisotopes of inert form are converted to active form by isotopic exchange and reused for the reaction. The radioactive yield was increased from 43% to 70%. (auth)

29237 RACEMIZATION AND ISOTOPIC EXCHANGE WITH Na ^{35}SCN OF 4-CHLOROBENZHYDRYL THIOCYANATE IN BORDERLINE NUCLEOPHILIC SUBSTITUTION. **Tonellato, Umberto; Ceccon, Alberto (Univ., Padua). Gazz. Chim. Ital., 96: 71-82(Jan.-Feb. 1966). (In Italian).**

Organic thiocyanates of the benzhydryl series isomerize to isothiocyanates by an ionization mechanism. This racemization was examined by an isotope exchange technique. Use of the ^{35}SCN$^-$ ion in a kinetic study of the racemization of 4-chlorobenzhydryl thiocyanate in acetonitrile and acetone at 70°C suggested an intramolecular ionization path via nondissociated intermediates as the main mechanism involved. In the presence of Na^{35}SCN, two different routes contribute to the racemization: the intramolecular route just referred to and a second one that involves inversion caused by a nucleophilic displacement by the ^{35}S end of the ^{35}SCN$^-$ ion. The contribution to the racemization rate of the latter path is equal to $2k_2$ [NaSCN], where k_2 is the bimolecular rate constant of the isotopic exchange measured with Na^{35}SCN. On the basis of results obtained the nature of borderline nucleophilic substitution is discussed. (BBB)

29238 INVESTIGATION OF LUMINESCENCE OF ACETYL ACETONATES OF SAMARIUM, EUROPIUM, AND TERBIUM. **Movsesyan, M. E.; Gevorkyan, V. A.; Safaryan, F. P.; Mezhlumyan, P. G. (Erevan State Univ.). Izv. Akad. Nauk Arm. SSR, Ser. Fiz. Mat. Nauk, 18: No. 4, 101-5(1965). (In Russian).**

In view of the possibility of obtaining a large quantum yield from organic complexes of rare-earth elements, acetylacetonate complexes were synthesized with Sm, Eu, and Tb by means of a technique described by B. B. Anufriyev and A. N. Zaydel' (ZhETF, v. 24, no. 1, 1953, 114). The absorption of the solutions of the complexes of the rare-earth elements was investigated with the aid of a quartz spectrophotometer (SF-4). A spectrograph (ISP-73) and photographic photometry were employed in the visible region. The samples were cooled with nitrogen vapor. The absorption spectra showed the presence of two absorption regions with a slight contribution from the rare-earth ion. The luminescent spectra obtained at −185C showed strong luminescence for the Sm complex (especially at 6435 Å), which became stronger with decreasing temperature. In the case of Eu, only a few luminescence lines were observed at room temperature, but more at −185C. The Tb acetyl acetonate had intense luminescence at room temperature, especially at 5420, 5446, and 5472 Å. Lowering the temperature caused line shifts and a redistribution of the luminescence intensity. The data on the various lines are tabulated. (ATD)

29239 FAR-INFRARED SPECTRA OF CRYSTALLINE ACETYLENES C_2H_2 AND C_2D_2. **Anderson, A.; Smith, William Hayden (Princeton Univ., N. J.). J. Chem. Phys., 44: 4216-19(June 1, 1966).**

The far-infrared spectra of polycrystalline films of acetylene and fully deuterated acetylene were recorded at 77°K, using a commercial Michelson interferometer. Two sharp bands were observed for each crystal, and the frequency change on deuteration led to their assignment as translational lattice modes. From these and other spectroscopic results, deductions concerning the crystal structure, which was not directly measured at this temperature, were made, and it was concluded that the most likely factor group is of D_{2h} symmetry with two molecules per unit cell on C_{2h} sites, a structure similar to those of crystalline carbon disulfide and the halogens. (auth)

29240 PHYSICAL AND CHEMICAL PROPERTIES OF HYDROXYFLAVONES. V. DEUTEROXYFLAVONES FROM ACETOXYFLAVONES BY IMIDAZOLE-CATALYZED DEACETYLATION. **Looker, J. H.; Kagal, S. A.; Edman, J. R. (Univ. of Nebraska, Lincoln). J. Heterocycl. Chem., 3: 61-6(Mar. 1966).**

A purification method for hydroxyflavones, in which the acetate was hydrolyzed in aqueous ethanol or methanol in the presence of catalytic amounts of imidazole, was modified for the formation of a mono- or bis-deuteroxyflavone. Hydrolysis of monoacetoxyflavones was carried out either in deuterioethanol–deuterium oxide or deuteriomethanol–deuterium oxide mixtures at reflux temperature. The monodeuteroxyflavone resulted in all instances. Because of previous unsuccessful attempts at preparation of 5-deuteroxyflavone, this substance was subjected to detailed study. 7-Deuteroxyflavone, prepared from interaction of 7-acetoxyflavone with deuterioethanol–deuterium oxide, gives a deuterium analysis in reasonable agreement with theory. In addition, the infrared spectrum contained bands associated with the OD stretching mode, but was virtually transparent in the 2500–2900 cm^{-1} region. Spectra of the other monodeuteroxyflavones were also virtually transparent in the OH-stretching region, but contained bands corresponding to the OD-stretching mode. All infrared spectra were devoid of ester carbonyl stretching bands. Satisfactory results were obtained in preparing the four 5,n-bis-deuteroxyflavones only if the hydrolysis of the diacetate was effected in deuteriomethanol–deuterium oxide. When deuterioethanol–deuterium oxide was used, the hydrolysis products had wide melting ranges. Comparison of spectra of appropriate monohydroxyflavones and monodeuteroxyflavones permitted assignment of δ (OH) bands in four hydroxyflavone spectra. (BBB)

29241 SYNTHESIS OF POTENTIAL ANTIRADIATION AGENTS. PART I. SOME RHODANINE DERIVATIVES. Mamdapur, V. R.; Choughuley, A. S. U.; Chadha, M. S. (Atomic Energy Establishment, Trombay, India). J. Indian Chem. Soc., 42: 825-30(Dec. 1965).

Thiazoline and thiazolidine derivatives were previously tested as radioprotective agents and some of these were reported to be effective. The corresponding rhodanines may also possess radioprotective activity and in view of this, several rhodanine derivatives were synthesized. Some α- and β- unsaturated acids and their epoxides on treatment with ammonium dithiocarbamate furnished rhodanine derivatives. Structural proof is provided by their conversion to the corresponding diones and in some cases by synthesis through independent routes. (auth)

29242 ^{14}C ISOTOPE EFFECTS IN THE BECKMANN REARRANGEMENT. Glover, I. T.; Raaen, V. F. (Oak Ridge National Lab., Tenn.). J. Org. Chem., 31: 1987-8 (June 1966).

^{14}C isotope effects in the rearrangment of methylene-labeled phenyl-2-propanone oxime and phenyl-1-labeled acetophenone oxime investigated by Yukawa and Kawakami were re-examined. Their findings of relatively large reverse isotope effects were not substantiated. Within the limits of experimental error no isotope effect was observed in the reaction of methylene-labeled and carbonyl-labeled phenyl-2-propanone oxime. (M.C.G.)

29243 WILZBACH TRITIATION OF AN ALKYNE-2 ACID WITH HIGH SPECIFIC ACTIVITY. Kasang, G.; Wenzel, M. (Freie Univ., Berlin). Naturwissenschaften, 53: 199-200(1966). (In German).

It is shown that in the direct Wilzbach labeling of an alkyne-(2)-acid practically no hydration reactions occur and therefore high specific activities can be produced. Octyne-(2)-acids-(1) were enriched. The sample analyzed by thin-layer chromatography showed little ^{3}H-labeled octyne and no ^{3}H-labeled octane acids. (J.S.R.)

29244 SYNTHESIS OF 5-BROMOURACIL-^{82}Br BY ISOTOPIC EXCHANGE METHOD. Pyun, Hyung-chick; Kim, Jae-rock (Atomic Energy Research Inst., Seoul). Ta Han Hua Hsueh Hui-Chih, 8: No. 2, 39-42(June 1964). (In Korean).

In order to eliminate the presence of a considerable amount of impurities in 5-bromouracil-^{82}Br obtained by means of bromination with $^{82}Br_2$, the isotopic exchange method was investigated. Bromide-82 ion such as $NH_4{}^{82}Br$ or $H^{82}Br$ undergoes no isotopic exchange with 5-bromouracil-Br. The exchange rates between $NH_4{}^{82}Br$ and Br_2 as well as $^{82}Br_2$ and 5-bromouracil-Br were too fast to be determined. The result indicated that this method can be used in the production of pure 5-bromouracil-^{82}Br. It was also found that the use of reducing agent to maintain ^{82}Br as bromide form was unnecessary on $NH_4{}^{82}Br$ production from the reactor. (OID)

29245 HYDROGEN ISOTOPE EXCHANGE REACTIONS OF NONBENZOID AROMATICS. II. THE REACTIVITY OF SUBSTITUTED AZULENES IN ELECTROPHILIC H-D EXCHANGE. Weiss, C.; Engewald, W.; Mueller, H. (Karl-Marx-Univ., Leipzig). Tetrahedron, 22: 825-33 (Mar. 1966). (In German).

The relative reactivity to electrophilic attack of these compounds was measured by acid-catalyzed H-D exchange. The exchange rates were measured for position 3 of 22 substituted azulenes in a 0.1N solution of CH_3COOD in CH_3OD at 100°C. The relative reactivity of the 1-substituted azulenes follow strictly the Hammett equation. It was assumed that the substitution constant (σ) values for 1-substituents are the same as in the m-position of benzene. From the lg k/k_0-σ-plot ($\rho = -4.35$) the σ_m values for the thiocyano and the phenylazomethine groups were 0.53 ± 0.07 and 0.35 ± 0.03, respectively. The reactivity of azulenes depended not only on the substituent but also on its position in the azulene system. A linear correlation was found between the logarithm of the relative rates and the basicity for the various methylazulenes and for the 1-substituted azulenes protonated on position 3 by acids. (BBB)

29246 SYNTHESES OF ISOTOPICALLY LABELED COMPOUNDS. PART III. SYNTHESIS OF THE ISOTOPICALLY LABELED INSECTICIDES 1605-C-14 AND LURGO-P-32. T'u, T'ung-yuan; Yao, Tu-ch'ing; Tung, Hui-chen. Yuan Tzu Neng, No. 1, 56-9(1965).

Insecticide 1605-^{14}C was produced experimentally from

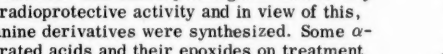

and $CH_3{}^{14}CH_2OH$

The

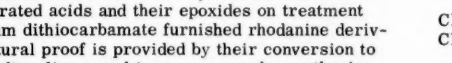

was prepared from S, PCl_3, and HO-⬭-NO_2 and reacted with $CH_3{}^{14}CH_2OH$ (prepared from $Ba^{14}CO_3$) to produce 1605-^{14}C in 67% yield and with a recovery of 60% of the radioactivity. Chemical analysis of the purified product ($C_{10}H_{15}O_3NPS$) showed 5.01% N and 10.64% P (theoretical content: N 4.81%, P 10.64%). Another insecticide, Lurgo-^{32}P, was prepared by a modified Dauterman's method. The process involved the reaction of $Na_2H^{32}PO_4$ with P and S for the production of $^{32}P_2S_5$, which was then reacted with methanol and ammonia to yield a product that was mixed with $ClCH_2CONHCH_2$ to produce the insecticide $CH_2OCH_2OPSSCH_2CONHCH_2$. The yield was 75 to 77% and the radioactivity recovered calculated on the basis of $Na_2H^{32}PO_4$ was 26.4%. Chemical analysis of the final product showed that it contained 12.89% P and 6.09% N (theoretical content: P 13.51%, N 6.1%). The results of paper chromatography and autoradiography indicated that the experimental products were identical with the commercial insecticides. (JPRS)

29247 EXPERIMENTAL INVESTIGATION OF CHEMICAL REACTIONS INVOLVING MUONIUM. Babaev, A. I.; Balats, M. Ya.; Myasishcheva, G. C.; Obukhov, Yu. V.; Roganov, V. S.; Firsov, V. G. (Inst. of Theoretical and Experimental Physics, USSR). Zh. Eksp. Teor. Fiz., 50: 877-89(Apr. 1966). (In Russian).

The asymmetry coefficients in the angular distribution of positrons emitted in $\mu-e$ decays were measured for a number of compounds and their binary mixtures. The rate constants for the interaction of atomic muonium and matter were computed on the basis of the results obtained. The method of competing acceptors for parallel reactions was employed with the aim of increasing the accuracy of the measurements and elucidating the mechanism of the processes. The variations of the asymmetry coefficients with the magnetic field strength were measured for a number of compounds. The data are discussed within the framework of the picture of chemical reactions of muonium. (auth)

Radiation Chemistry

See also BIOLOGY AND MEDICINE — Radiation Effects on Biochemicals Radiation Effects on Tissues

29248 (BNL-9672) THE PHOTOCHEMICAL DECOMPOSITION OF SODIUM BROMATE. Herley, P. J.; Levy, P. W. (Brookhaven National Lab., Upton, N. Y.). Nov. 1, 1965. Contract AT(30-2)-Gen-16. 4p. (CONF-660701-1). Dep. mn. CFSTI $1.00 cy, $0.50 mn.

From International Symposium on Reaction Mechanisms of Inorganic Solids, Aberdeen, Scotland.

The photolytic decomposition of normal and irradiated $NaBrO_3$ was investigated using a high-pressure mercury lamp. It was concluded that the decomposition proceeds from a site that acquires a second excitation while still

excited from a previous excitation. Reaction mechanisms are suggested. (P.C.H.)

29249 DECAY OF RADIATION INDUCED RADICALS AND THE YIELD OF THERMOLUMINESCENCE. Sanner, Tore; Pihl, Alexander (Norsk Hydro's Inst. for Cancer Research, Oslo). Acta Chem. Scand., 20: 266-8(1966).

An empirical relation between results obtained with thermoluminescence measurements and electron spin resonance (ESR) spectroscopy for some biochemicals are presented. (M.C.G.)

29250 THERMAL AND RADIATION OXIDATIONS OF BENZENE TO PHENOL IN AQUEOUS SOLUTIONS CONTAINING METAL IONS AT ELEVATED TEMPERATURES. VII. THE MECHANISMS OF PHENOL FORMATION AS STUDIED BY STABLE ISOTOPES. Hotta, Hiroshi; Suzuki, Nobutake; Abe, Toshihiko (Japan Atomic Energy Research Inst., Takasaki). Bull. Chem. Soc. Jap., 39: 417-22(Mar. 1966).

When benzene was oxidized to phenol in an ^{18}O-enriched aqueous solution of iron and copper sulfates, the ^{18}O was much concentrated to phenol. The ^{18}O content depended on the kind of metal ion and on the temperature. This suggested that the oxygen in the phenol produced is donated not only by the molecular oxygen, but also by the water. Therefore, it is assumed for the termination process that phenol is formed by the ionic reactions. When an equimolar mixture of benzene and benzene-d_6 was oxidized, the isotope effect of hydrogen, k_H/k_D, as estimated from the isotopic composition of the phenol produced, was about 1.2. This value seemed to be small for the hydrogen abstraction reaction of radicals. The main reaction of the propagation process was concluded to be the abstraction reaction of hydrogen by phenyl peroxide. In this experiment, it was also found that phenol exchanges hydrogen with water. The rate constant of the exchange reaction was estimated by Bateman's equation. The rate constant was the highest in the ferric sulfate solution. (auth)

29251 PHOTOLYSIS OF cis-2-BUTENE AND ITS IMPLICATIONS FOR RADIATION CHEMISTRY. Hatano, Yoshihiko; Shida, Shoji (Tokyo Inst. of Tech.). Bull. Chem. Soc. Jap., 39: 456-9(Mar. 1966).

The direct photolysis at 1849 Å and the mercury-photosensitized reaction at 2537 Å of cis-2-butene were studied in the gas phase at room temperature. It may be considered that the excited singlet state of cis-2-butene is formed in the former, and that the excited triplet state of cis-2-butene is formed in the latter. Trans-2-butene is predominantly produced in the latter, while decomposition products (e.g., hydrogen, methane, ethane, ethylene, propylene, etc.) predominate in the former. The rates of the formation of all the products are pressure-independent in the former, while in the latter those of all products except trans-2-butene decrease rapidly with an increase in the initial pressure. The rate of trans-2-butene formation in the latter, however, increases gradually with an increase in the initial pressure until it becomes constant above 100 mm Hg. By comparing the pressure dependence and the product distribution of these two reactions with the results of the radiolysis of liquid cis-2-butene, it was concluded that the excited triplet state of cis-2-butene contributes chiefly to the formation of trans-2-butene in the radiolysis, while the excited singlet state of cis-2-butene contributes chiefly to the decomposition products. (auth)

29252 RADIATION-INDUCED ADDITION OF HYDROGEN CHLORIDE TO ETHYLENE. Terakawa, Akira; Nakanishi, Jun; Hirayama, Toru (Central Research Lab., Tokyo). Bull. Chem. Soc. Jap., 39: 892-8(May 1966).

Ethyl chloride and n-butyl chloride were selectively prepared by the ^{60}Co gamma-induced addition of hydrogen chloride to ethylene. The G values of consumed ethylene reached 35,000. The reaction was presumed to be a vapor-phase radical chain reaction, and the proposed reaction mechanism showed a good agreement with experimental results. The activation energies for the production of ethyl chloride and n-butyl chloride were calculated from the rate constants to be 6.94 and 8.95 kcal/mol, respectively. (auth)

29253 RADIOLYSIS OF AQUEOUS SOLUTIONS OF POTASSIUM IODIDE. Sawai, Takeshi; Shinozaki, Yoshiharu; Meshitsuka, Gisuke (Tokyo Metropolitan Isotope Research Center). Bull. Chem. Soc. Jap., 39: 951-5(May 1966).

The radiolysis of potassium iodide aqueous solutions was studied in order to elucidate the contribution of the hydrated electrons to the radiolysis mechanisms. Deaerated and aerated solutions were irradiated by ^{60}Co γ rays under various conditions, and the yields of iodine, hydrogen peroxide, hydrogen, and oxygen were determined. The pH dependences of the initial yields of iodine and hydrogen peroxide in the deaerated solutions were different from the results obtained in aerated solutions. These results can be explained by assuming the hydrogen atoms and hydrated electrons to be the reducing species. The radiolysis mechanisms of the potassium iodide aqueous solutions are discussed. The rate constant of the reaction of hydrated electrons for iodine was calculated to be 5.9×10^{10} m^{-1} sec^{-1}. (auth)

29254 RADICAL YIELDS IN THE RADIOLYSIS OF NEUTRAL AQUEOUS SOLUTIONS. Sawai, Takeshi (Tokyo Metropolitan Isotope Research Center). Bull. Chem. Soc. Jap., 39: 955-60(May 1966).

Determination of the yields of two reducing species and OH radicals in the radiolysis of neutral aqueous solutions was undertaken using deaerated 2-propanol aqueous solutions containing potassium nitrate or hydrogen peroxide as electron scavengers. Irradiation was carried out with ^{60}Co γ rays, and the hydrogen, nitrite ion, acetone, hydrogen peroxide, and pinacol so produced were analyzed. The hydrogen yield decreased on the addition of hydrogen peroxide or nitrate ions. The yield of hydrogen atoms was found to be 0.61 ± 0.03 by subtracting the molecular yield of hydrogen from the total hydrogen yield in the solutions containing enough scavengers. The yield of nitrite ions increased with an increase in the concentration of nitrate ions and decreased with an increase in the concentration of acetone and with a decrease in the pH value. The acetone yield increased sharply with an increase in the quantity of nitrate ions and reached a plateau value in the concentration range of nitrate ions higher than 1×10^{-2} M. In the presence of potassium nitrate of 1×10^{-2} M, pinacol was not formed, and the yield of hydrogen peroxide was less than the molecular yield of hydrogen peroxide. On the basis of these results, radiolysis mechanisms were elucidated and the yields of the hydrated electron and the OH radical of a neutral solution were found to be 2.77 ± 0.03 and 3.0, respectively. The relative rate constants, $k_{H+NO_3^-}/k_{H+(CH_3)_2CHOH}$ and $k_{e^-aq+(CH_3)_2CO}/k_{e^-aq+NO_3^-}$, were found to be 0.18 and 0.78. (auth)

29255 EFFECTS OF ^{60}Co γ RADIATION ON AMIDONE. EVOLUTION OF THE STRUCTURAL STATE OF THE AMIDONES OF MAIZE AND POTATOES IRRADIATED DRY AND MOIST. Charbonniere, Robert; Guilbot, Andre. Compt. Rend., Ser. C, 262: 545-8(Feb. 14, 1966). (In French).

The x-ray diffraction spectra of the amidones of maize and potatoes irradiated in the dry and hydrated states by ^{60}Co indicate that the irradiation, up to a dose of 75 Mr alters only partially their physical structure. The water intervening in the structure of hydrated amidones exercises a protective effect against the effect of radiation. The physical bonds that determine the structure of these amidones appear more fragile to radiation in the case of the amidone of potatoes. (tr-auth)

29256 RADIOLYSIS OF HEXACHLOROCYCLOPENTADIENE. Rabovskaya, N. S.; Kogan, L. M. (Moscow State Univ. All-Union Scientific-Research Inst. of Chemical Protection of Plants, USSR). Dokl. Akad. Nauk SSSR, 165: 337-40(Nov. 11, 1965). (In Russian).

Studies on the gamma radiolysis of hexachlorocyclopentadiene showed that the chlorine atom is removed and

united with another molecule of the irradiated substance; the resulting radicals recombine and other atoms of chlorine are split off. The studies were made with a ^{60}Co source (1.95×10^{16} to 3.82×10^{16} ev/ml sec). The color of the compound changed from yellow to dark brown, and at 15.7×10^{22} ev/ml it was very viscous. As the dose increased the reaction rate decreased. The radiochemical yield was 5 molecules per 100 ev at 5% conversion. Among the products formed was white crystalline cyclo-C_5Cl_8 (20 to 30%); viscous, red, oily $C_{10}Cl_{10}$ (50%), and yellow crystalline (possibly) $C_{10}Cl_{10}$ (1 to 2%). Under other conditions $C_{15}Cl_{12}$ was obtained. The product compounds were identified by chemical analyses and infrared spectra. Detailed structural equations are given to indicate the reactions that take place. (TTT)

29257 STEADY STATE IN THE RADIOLYSIS OF NEUTRAL AQUEOUS SOLUTIONS OF OXYGEN. Kabakchi, S. A.; Shubin, V. N.; Dolin, P. I. (Inst. of Electrochemistry, Academy of Sciences, USSR). Dokl. Akad. Nauk SSSR, 165: 601-3(Nov. 21, 1965).

The radiolysis reaction in water solutions of oxygen irradiated with ^{60}Co gamma rays reached steady state at a dose of 5×10^{19} ev/ml. With initial oxygen concentrations of 1.4×10^{-3} and 2.8×10^{-4} M, the steady-state hydrogen peroxide concentration plotted as a function of the square root of the irradiation rate was approximately linear up to about 2×10^{8} ev/ml sec and then leveled off; the hydrogen concentration increased similarly and then dropped. A similar plot of the $[O_2]/[H_2O_2]$ ratio was almost hyperbolic in shape, reaching limiting values of 2.75 and 1.85, respectively, for the two oxygen concentrations mentioned. The results indicate different mechanisms of radiolysis at different dose rates. At a constant dose rate of 2.95×10^{6} ev/ml sec but different initial oxygen concentrations, log plots of the steady-state hydrogen peroxide and hydrogen concentrations vs the oxygen concentration were close to the theoretical curves calculated according to Ershler (Dokl. Akad. Nauk 129: 866 (1959)). (TTT)

29258 CORRELATION BETWEEN THE ISOMERIC EFFECT IN SZILARD-CHALMERS RECOIL AND THE CHEMICAL CONSTITUTION OF THE TARGET STUDIED ON 13 Co(III) COMPLEXES. Lazzarini, E. (Centro Studi Nucleari E. Fermi, Milan). Energ. Nucl. (Milan), 13: 233-7(May 1966).

Experiments were carried out to ascertain if ^{60}Co and ^{60m}Co, formed by (n, γ) reaction, have different behaviors in their Szilard-Chalmers recoil. It was found that the ratio of their retentions (percent of radioactive atoms in the original chemical form) is different from 1 and dependent on the chemical constitution of the irradiated target. As result of a systematic investigation carried out on 13 cobalt(III) complexes, it was deduced that a correlation exists between the retention ratio ρ and the splitting Δ of d-orbitals of Co atom, due to the ligand field. The correlation line is $\rho = (0.641 \pm 0.074) \cdot 10^{-4}\ \Delta - 0.114$ where Δ, given in cm^{-1}, is measured by means of the following optical absorption transition $(t_{2g})^6\ ^1A_{1g} \rightarrow (t_{2g})^5\ (e_g)^1\ ^1T_{1g}$. Possible interpretations of the effect are discussed. (auth)

29259 ISOTOPIC EXCHANGE IN THE SOLID STATE AND THERMAL ANNEALING OF RECOIL DAMAGE IN COBALT COMPLEXES: A NEW MODEL. Nath, Amar; Khorana, S.; Mathur, P. K.; Sarup, S. (Atomic Energy Establishment Trombay, Bombay). Indian J. Chem., 4: 51-6(Feb. 1966).

Isotopic exchange was studied in cobalt complexes doped with radio-Co^{2+}. Bis-indenyl cobalt(III) nitrate and cyanocobalamin hardly undergo any exchange, while tris-acetylacetone cobalt(III), sodium ethylenediaminetetraacetato Co(III) tetrahydrate and tris-dipyridyl cobalt(III) perchlorate trihydrate exhibit considerable exchange. The influence of specific activity of dopant and of dehydration, crushing and x-irradiation on thermal exchange in doped dipyridyl complex was also investigated in detail. The "variable-depth electron trapping" model suggested earlier is elaborated to explain both isotopic exchange and annealing of recoil damage in the solid state. The multicomponent exponential annealing (and isotopic exchange) can be explained by virtue of release of electrons from variable-depth traps formed and populated by fragmentation and effect of spray of Auger electrons in the recoil track, and by the effect of extraneous radiation during reactor irradiation in the bulk. The free electrons in the conduction band, lifted from traps or valence band, are captured by the "dopant" or recoil species, viz. radio-Co^{2+}, giving Co^{+} in the excited state which exchanges instantaneously with a neighboring chelate molecule resulting in an increase in retention. An attempt was also made to interpret other existing data in literature on thermal annealing, radiation annealing and isotopic exchange on the basis of this model. (auth)

29260 RADIOLYTIC OXIDATION OF NAPHTHALENE IN AERATED ORGANIC SOLVENTS. Rao, N. B. S. N.; Rao, P. S.; Reddy, M. P. (National Chemical Lab., Poona). Indian J. Chem., 4: 244-6(May 1966).

Radiolysis of solutions of naphthalene in alcohol, acetic acid, and tetrahydrofuran, with and without water, led to the formation of naphthols in low yields. Metal ions of the oxidation-reduction type, viz. Fe^{2+}, Fe^{3+}, Ce^{4+}, Hg^{2+}, and UO^{2+}, reduced the yields, presumably by intercepting the OH and HO_2 radicals in a chain reaction. Increase in the reaction temperature enhanced the naphthol yields slightly. (auth)

29261 SEPARATION OF RECOILING CHROMIUM(II) ION FROM NEUTRON-IRRADIATED CHROMIUM(III) ION BY THE DYNAMIC EXTRACTION METHOD USING ION-EXCHANGER. Matsuura, T.; Sasaki, T. (Rikkyo Univ., Yokosuka, Japan). Inorg. Nucl. Chem. Lett., 2: 111-15 (Apr. 1966).

A dynamic technique using an ion exchanger to study recoil phenomena was applied to investigations of recoiling Cr(II) from neutron irradiated chromic compounds. Oxalic acid was used to separate Cr(II) from Cr(III). It was found that a substantial amount of $^{51}Cr(II)$ is produced from Cr(III) ions. Both the separable yield and the enrichment factor by the dynamic method were somewhat higher than those by the static method. (M.C.G.)

29262 APPROXIMATE VALUES OF THE RATE CONSTANTS OF RADIATION-INDUCED REACTIONS OF HYDROGEN ATOMS AND HYDROXYL RADICALS IN AQUEOUS SOLUTIONS. Pikaev, A. K.; Glazunov, P. Ya.; Spitsyn, Vikt. I. (Inst. of Physical Chemistry, Academy of Sciences, USSR). Izv. Akad. Nauk SSSR, Ser. Khim., No. 3, 401-8(1965).

A method of evaluating the absolute rate constants of radioinduced reactions involving H and OH radicals is described, based on the use of two independent methods of kinetic treatment of experimental data obtained by studying the radiolysis of aqueous sulfuric acid solutions of ferrous sulfate containing oxygen and subjected to pulses of electron radiation. The mechanism of radiolytic oxidation of Fe^{2+} ions at high rates of the absorbed dose was examined. The decrease in the yield of Fe^{3+} is attributed to the competition of the reactions H + OH, Fe^{2+} + OH and H + O_2. Absolute values of the reaction rate constants were determined: $k_{Fe^{2+}+OH} = 2.7 \times 10^{8}$; $k_{H+O_2} = 5.3 \times 10^{9}$; and $k_{H+OH} = 4.5 \times 10^{10}$/mole · sec. On the basis of literature data on the relative constants and absolute values obtained, the rate constants of a series of radioinduced reactions of H and OH radicals were estimated. (ATD)

29263 EFFECT OF AN ELECTRIC FIELD ON LIQUID-HYDROCARBON RADIOLYSIS. Gusynin, V. I.; Tal'roze, V. L. Izv. Akad. Nauk SSSR, Ser. Khim., No. 7, 1313(1965).

Application of a d-c electric field across samples of liquid saturated hydrocarbons being irradiated with fast electrons was found to cause a sharp increase (up to 100%) in the rate of formation of hydrogen. Irradiation was performed with 1.6-Mev electrons at dose rates of about 10^{3} to 10^{5} R/sec at room temperature; the electric field intensity was (0.5 to 3) 10^{4} v/cm. Turning off the electric field caused the rate of formation of hydrogen to drop back to its initial value. Application of an a-c field had no effect. Control experiments excluded all trivial explanations.

Further experiments will be conducted to elucidate the nature of the phenomenon. (ATD)

29264 REACTION INTERMEDIATES IN THE RADIOLYSIS OF ALKYL HALIDES AT 77 DEG K. Claridge, R. F. C.; Willard, J. E. (Univ. of Wisconsin, Madison). Contract AT(11-1)-32. J. Amer. Chem. Soc., 88: 2404-7 (June 5, 1966).

To investigate reaction intermediates in the radiolysis of alkyl halides, the spectra of C_2H_5I, $n\text{-}C_4H_9I$, $i\text{-}C_4H_9I$, $n\text{-}C_5H_{11}I$, $n\text{-}C_4H_9Br$, and $n\text{-}C_4H_9Cl$ in the glassy state at 80°K were determined in the 3000 to 8000-Å region immediately after exposure to γ-irradiation. The iodides all showed essentially the same four absorption peaks. The growth and decay characteristics of the peaks indicated that they represent four different species and that there are short-lived precursors that are not seen. The fact that the bromides and chlorides showed different spectra than the iodides indicated that the absorption peaks are due to halogen-containing species. The 4050-Å peak, which grew with a first-order half life following irradiation, was tentatively assigned to I_2^-, and the 7500-Å peak to $(RI)_n^+$. Other growth and decay patterns occurring as a function of time, bleaching, and temperature are discussed and compared with information on trapped radicals obtained from ESR measurements. (auth)

29265 SUBSTITUTION REACTION OF 3-ev TRITIUM ATOMS WITH METHANE. Chou, C. C.; Rowland, F. S. (Univ. of California, Irvine). J. Amer. Chem. Soc., 88: 2612-13(June 5, 1966).

Photolysis of ^3HBr was used to produce 3-ev tritium and both abstraction and substitution reactions of the tritium with methane were observed. Results indicated that the yield ratio of abstraction and substitution reactions is approximately 3.5 to 4.0 for 3-ev atoms in methane and depends to some extent on the ratio of scavenger molecule to methane. (M.C.G.)

29266 XENON-SENSITIZED RADIOLYSIS OF PROPANE. Bone, L. I.; Sieck, L. W.; Futrell, J. H. (Wright-Patterson Air Force Base, Ohio). J. Chem. Phys., 44: 3667-72(May 15, 1966).

The xenon-sensitized radiolysis of propane was investigated in the presence and absence of small amounts of ion and free radical interceptors. From an analysis of mixtures of deuterated propanes and a knowledge of radical disproportionation yields in the scavenged and unscavenged systems it is possible to construct a complete quantitative kinetic analysis for the decomposition. Ion titration methods demonstrate that the neutralization of $C_3H_7^+$ ions occurs heterogeneously in the system investigated and leads quantitatively to the production of equivalent yields of isopropyl radicals and hydrogen atoms. (auth)

29267 MAIN-CHAIN SCISSION AND ESR SPECTRA OF IRRADIATED POLYTETRAFLUOROETHYLENE OXIDE. Barnaba, P.; Cordischi, D.; Site, A. Delle; Mele, A. (CNEN, Rome. Univ., Rome). J. Chem. Phys., 44: 3672-7(May 15, 1966).

The chief effect of ionizing radiation on polytetrafluoroethylene oxide (PTFEO) is to incude main-chain scission. The ESR spectrum of the irradiated polymer in vacuum consists of two components. The stable spectrum is attributed to the $-CF_2-CF_2-O^{\cdot}$ and $-O-\dot{C}F-CF_2-O-$ radicals. The former radical decays slowly at room temperature, the latter is unchanged even after several weeks. The unstable spectrum disappears in a few hours and its structure is uncertain. Tentatively this spectrum is assigned to the $-O-CF_2-CF_2^{\cdot}$ radical. Admission of air to the irradiated polymer gives rise to a spectrum formed of a symmetric singlet assigned to $-CF_2CF_2-OO^{\cdot}$ radical and an asymmetric signal. A $G_{fracture} = 1.8$ was calculated from viscosity data. (auth)

29268 POSITRON ANNIHILATION IN MATERIALS UNDER IONIZING RADIATION. Tao, S. J. (New England Inst. for Medical Research, Ridgefield, Conn.); Green, J. H. J. Chem. Phys., 44: 4007-9(May 15, 1966).

Positron-annihilation lifetime spectra in tritiated water and ice are described, and the effect of irradiation products on positron-annihilation rates in a medium is estimated. In a liquid medium the interference mainly comes from stable products accumulated during irradiation and in a solid medium from free radicals frozen in the lattice. It is also indicated that care must be taken in preparing samples for positron-annihilation experiments to avoid excessive radiation damage to the medium by the positron source. (auth)

29269 THE γ RADIOLYSIS OF CARBON SUBOXIDE. Blake, A. R.; Hodgson, K. E. (Berkeley Nuclear Labs., Gloucestershire, Eng.). J. Chem. Soc., No. 5, 533-4 (1966).

The γ radiolysis of carbon suboxide was investigated. The products are a polymer, with a structure similar to that of thermal suboxide polymers, and carbon monoxide. It is suggested that the polymer is formed by an ionic chain mechanism. (auth)

29270 SOLUTE EFFECTS IN THE RADIOLYSIS OF CYCLOHEXANE SOLUTIONS. PART II. ELECTRON SCAVENGING BY NITROUS OXIDE AND AROMATIC COMPOUNDS. Sherman, Warren V. (Soreq Nuclear Research Center, Yavne, Israel). J. Chem. Soc., No. 5, 599-602(1966).

The gaseous products of γ radiolysis, at relatively low dose, of solutions of nitrous oxide in cyclohexane were determined as a function of concentration. The results clearly indicated that nitrous oxide can scavenge a precursor of molecular hydrogen, and that this precursor is the electron. Nitrous oxide may be used as a specific scavenger of electrons produced in the radiolysis of cyclohexane, and the relative electron affinities, EA_{N_2O}, of a number of aromatic hydrocarbons were determined. In most cases the values were directly related to the gas-phase electron affinities, determined by Lovelock's method. A comparison was made between other studies of the effect of solutes on $G(H_2)$ and the effects of nitrous oxide. (auth)

29271 NOVEL VALENCE STATES OF THALLIUM AS STUDIED BY PULSE RADIOLYSIS. Cercek, B.; Ebert, M.; Swallow, A. J. (Christie Hospital and Holt Radium Inst., Manchester, Eng.). J. Chem. Soc., No. 5: 612-15 (1966).

The absorption spectra of Tl^{2+} and Tl_2^+ in aqueous solutions were obtained using the technique of pulse radiolysis. The formation and reactions of the species were studied under a variety of conditions, and rate constants for the following reactions were obtained: $OH + Tl^+ \rightarrow OH^- + Tl^{2+}(7.6 \pm 1) \times 10^9$ l mole^{-1} sec^{-1}; $2Tl^{2+} \rightarrow Tl^+ + Tl^{3+}(2.3 \pm 0.8) \times 10^9$ l mole^{-1} sec^{-1} at zero ionic strength; $Tl^{2+} + HO_2 \rightarrow Tl^+ + H^+ + O_2(2.5 \pm 1) \times 10^9$ l mole^{-1} sec^{-1}; $Tl^{2+} + H_2O_2 \rightarrow Tl^+ + H^+ + HO_2(2.8 \pm 0.8) \times 10^7$ l mole^{-1} sec^{-1}; $Tl + Tl^+ \rightleftharpoons Tl_2^+ + K_6 = k_F/k_B = 2.3 \times 10^3$ l mole^{-1}; and $Tl_2^+ + Tl^{2+} \rightarrow 3Tl^+(4.4 \pm 0.9) \times 10^9$ l mole^{-1} sec^{-1} at zero ionic strength. (auth)

29272 RADIATION DAMAGE TO TBP–KEROSENE SOLVENT. II. EFFECT ON EXTRACTION BEHAVIOR OF URANIUM AND THORIUM AND ON THEIR LOADING EFFECT. Tsujino, Takeshi; Ishihara, Takehiko (Japan Atomic Energy Research Inst., Tokyo). J. Nucl. Sci. Technol. (Tokyo), 3: 144-9(Apr. 1966).

Radiation damage to 30 vol % TBP/kerosene was investigated to determine changes in the extraction behavior of uranium and thorium with the solvent irradiated up to 10^8 R in nitrate system and similarly in the stripping behavior with 0.01 N nitric acid. The effect on uranium and thorium was discernible only with irradiations reaching 10^8 R. Changes in the behavior of fission products present in company with uranium or thorium were found to be similar to the case where they existed free of uranium or thorium. At irradiations below 10^7 R, uranium and thorium manifested loading effect, but it disappeared when irradiation reached 10^8 R. Calculation of one-stage decontamination factors of fission products from uranium and thorium confirmed deterioration of the power of separation with irradiation, and the degree of deterioration was determined quantitatively. The decontamination factor for $^{95}Zr-^{95}Nb$ was decreased to $1/2000$ by irradiation to 10^8 R,

while the same dosage of irradiation had little effect for $^{106}Ru-^{106}Rh$. Physical properties such as density, viscosity, emulsification tendency and phase separation time were also observed to be affected by irradiation to 10^8 R. (auth)

29273 EFFECTS OF IONIZING RADIATION ON TWO GELATIN FRACTIONS. III. CARBONYL GROUP ANALYSES AND ELECTRON SPIN RESONANCE STUDIES. Prusak, Leonard P. (Johnson and Johnson, New Brunswick, N. J.); Sciarrone, Bartley J. J. Pharm. Sci., 55: 407-13(Apr. 1966).

Low-temperature alcohol fractionation of acid-treated pigskin gelatin yielded 2 distinct fractions having different average molecular weights and characteristic acid/base binding properties. Intrinsic viscosity studies on these fractions showed a higher molecular weight (173,000) fraction, F-I, and a lower (86,000) fraction, F-II. For electron spin resonance studies, film strips of F-I and F-II were submitted to the scanned beam of the 3-Mev Van de Graaff accelerator. The resulting average absorbed doses were 0.46, 0.67, 1.71, and 3.12 Mrad. Carbonyl group formation was obtained by the difference between control and irradiated solutions. In the irradiated solutions the number of carbonyl groups formed per g of protein was directly proportional to the dose. In irradiated films of F-I and F-II there was less carbonyl formation than in 1 and 5% solutions, and a proportional relation to the logarithm of the dose was seen. It appeared that carbonyl groups were formed at the same rate in the 2 gelatin fractions despite widely different average molecular weights. Electron spin resonance studies showed a typical doublet of 25 G line separation obtained for all irradiated samples. A 32% increase in radiation dose from 0.461 to 0.679 Mrad elicited a 56% increase in free radicals in F-I and a 78% increase in F-II. A further increase of 60% in radiation produced 69% more free radicals in F-I, but only a 50% increase in F-II, the latter indicating a downward trend in free radical formation despite a 2.5-fold increase in energy. A further 45% increase in irradiation produced 71% more free radicals in F-I and a 75% increase in F-II. In both films, therefore, the higher the dose absorbed, the greater the excess of unpaired electrons. Data showed that radical concentration is proportional to the three-halves power of the radiation dose. It was concluded that increases in molecular weight in irradiated dilute gelatin solutions could be attributed to cross-linking through covalent and weak hydrogen bonds. (BBB)

29274 RADIATION-INDUCED SOLID-STATE COPOLYMERIZATION OF MALEIC ANHYDRIDE AND ACENAPHTHYLENE. Shimizu, Akira; Hayashi, Koichiro (Osaka Labs.). J. Polym. Sci. Pt. A-1, 4: 1291-1301 (May 1966).

Radioinduced solid-state copolymerization of the maleic anhydride–acenaphthylene system was carried to study solid-state polymerization of vinyl compounds in a binary system. Melting point measurements confirmed that the binary monomer system forms a eutectic mixture in the solid state. The solid-state polymerization of these monomers proceeded at maximum rate at the eutectic composition, and the polymerization products consisted of a mixture of polyacenaphthylene and 1:1 maleic anhydride–acenaphthylene alternating copolymer. Since the 1:1 copolymer was obtained in solution polymerization also and maleic anhydride did not homopolymerize in the solid state, it was concluded that the solid-state copolymerization of maleic anhydride and acenaphthylene occurs in a liquid-like state at the boundary of the two monomer crystals. (auth)

29275 INITIATION AND PROPAGATION IN γ-RADIATION-INDUCED POLYMERIZATION OF ETHYLENE. Machi, Sueo; Hagiwara, Miyuki; Gotoda, Masao; Kagiya, Tsutomu (Japan Atomic Energy Research Inst., Gumma). J. Polym. Sci., Pt. A-1, 4: 1517-29(June 1966).

The initiation and propagation reaction in γ-induced polymerization of ethylene was studied by the two-stage irradiation method, i.e., a first state in which initiation and propagation occur at a high dose rate, and a second stage where only the growth of polymer radical occurs. The rate of initiation was calculated from the amount of polymerized monomer and the degree of polymerization as the rate of increased in the number of polymer chains. The initiation rate is shown to be proportional to the ethylene density in the reactor and dose rate. G_R of radical formation was found to be about 1.6 at 30°C at a dose rate of 2.5×10^4 rad/hr and was almost independent of ethylene density but decreased slightly with increasing irradiation dose rate. The lifetime of the growing polymer chain radical is shown to be long at normal temperature. The absolute propagation rate is proportional to the square of ethylene fugacity and depends on dose rate to some extent. For chain growth, irradiation at a low dose rate is necessary. The apparent activation energy for the propagation reaction is −9 kcal/mole. (auth)

29276 KINETICS OF RADIATION-INDUCED ISOTOPE EXCHANGE BETWEEN DEUTERIUM AND SILICA GEL HYDROXYL GROUPS. Dolidze, G. M.; Kirtadze, M. G.; Kolbanovskii, Yu. A.; Lukyanov, A. T.; Polak, L. S.; Pustyl'nikov, L. M.; Tsetskhladze, T. V. (Inst. of Physics, Academy of Sciences, Georgian SSR. Inst. of Oil Technological Chemical Synthesis, Academy of Sciences, USSR. Kazakh State Univ., USSR). Kinet. Kataliz, 6: 1003-9 (Nov.-Dec. 1965). (In Russian).

The kinetics of the radioinduced isotopic exchange of D_2 with the OH groups on silica gel were studied. A kinetic equation, describing the experimental data, was formulated; the equation was numerically evaluated by the final difference method. The number of exchangeable hydroxyl groups on the surface was determined as 1.2×10^{14} cm^{-2}. A mechanism for the radioinduced isotopic exchange was proposed. (tr-auth)

29277 RADIOLYSIS OF CONCENTRATED AQUEOUS SOLUTIONS OF ISOPROPYL ALCOHOL IN THE PRESENCE OF OXYGEN. Saraeva, V. V.; Bkhattachariya, Sudkhindra Natkh (Moscow State Univ.). Kinet. Kataliz, 6: 1102-5 (Nov.-Dec. 1965). (In Russian).

During a study of the radiolytic process in aqueous solutions of isopropyl alcohol (0.01 to 13M), it was established that in neutral and acid solutions in the presence of oxygen the formation of products occurs as the result of direct and indirect effects of the radiation. Chains were not developed. For 1M solutions and very high concentrations of alcohol in the presence of 0.01M $HClO_4$ and oxygen, the development of chain processes was observed. Temperatures, dose output, and solution composition are factors regulating the development of chains. (tr-auth)

29278 RADIATION-INDUCED CATALYTIC CONVERSION OF METHANOL AT A SMALL SURFACE COVERAGE. Vladimirova, V. I.; Zhabrova, G. M.; Kadenatsi, B. M. (Inst. of Chemical Physics, Academy of Sciences, USSR). Kinet. Kataliz, 6: 1112-13(Nov.-Dec. 1965). (In Russian).

The radiocatalytic conversion of methanol was studied in adsorbing layers on the surface of silica gel at 20°C and with the priming of 0.007 to 1.5 monolayers. By comparison with the results obtained on the homogeneous radiolysis of methanol it is shown that the region of small primings of the catalyst surface is the most effective for radiation catalytic properties. (tr-auth)

29279 PULSE-RADIOLYSIS STUDIES ON THE REACTIVITY OF CATALASE WITH HYDRATED ELECTRONS AND FREE OH RADICALS. Henglein, A.; Karmann, W.; Roebke, W.; Beck, G. (Hahn-Meitner-Institut fuer Kernforschung, Berlin). Makromol. Chem., 92: 105-13 (1966). (In German).

The absolute bimolecular reaction rate constants of hydrated electrons and OH radicals with low-molecular-weight compounds, studied by pulse radiolysis, are on the order of 10^9 to 10^{11} $mole^{-1} \cdot l \cdot sec^{-1}$. That is, the reactions are extremely rapid, and depend essentially only on the diffusion rate of the reactants. Comparison was made of macromolecular reactions with free OH radicals and electrons using intense radiation for μsec periods as provided by 1.5-Mev electrons accelerated by the Van de Graaff generator. Catalase reacted with the hydrated electron and the OH radical in aqueous solutions with rate constants of 3.7×10^9 and 8.3×10^{10} $mole^{-1} \cdot l \cdot sec^{-1}$, re-

spectively. The reaction of ·OH with catalase was diffusion controlled, although part of the amino acids of catalase did not react at every collision with an OH radical under isolated conditions. A diffusion coefficient of 2.3×10^{-5} $cm^2 \cdot sec^{-1}$ of the OH radical was derived from the measurements. The results are discussed with respect to the radiolysis of catalase in aqueous solutions and the influence of catalase on the radiation sensitivity of biological systems. It was postulated that fast but not exclusively diffusion-controlled reactions of small radicals with monomers may become diffusion controlled if the reaction partner is a macromolecule consisting of the same kind of base units. (BBB)

29280 PAIRWISE TRAPPING IN γ-IRRADIATED SODIUM NITROPRUSSIDE. McNeil, D. A. C.; Raynor, J. B.; Symons, M. C. R. (The Univ., Leicester, Eng.). Mol. Phys., 10: 297(1966).

The main paramagnetic species detected by electron spin resonance spectroscopy in γ-irradiated sodium nitroprusside crystals were identified as the anion $[Fe(CN)_5NO]^{3-}$. For a random orientation of the crystal, the two magnetically distinguishable ions in the unit cell give rise to two hyperfine triplets. These are flanked by pairs of satellite lines of relatively low intensity each pair being centered on one of the main triplets. From the maximum of the outermost pair (278 gauss at room temperature) and using a point dipole model, the separation between magnetic centers is estimated to be 5.8 Å. (B.G.D.)

29281 THE ELECTRON SPIN RESONANCE OF IRRADIATED GLYCINE AT 77 DEG K. Collins, M. A.; Whiffen, D. H. (National Physical Lab., Teddington, Eng.). Mol. Phys., 10: 317-25(1966).

The electron spin resonance spectrum of the radical $\dot{C}H(NH_3^+)CO_2^-$, I, trapped in irradiated glycine has been reexamined at 77°K and the hyperfine couplings obtained when the $-NH_3^+$ ceases to rotate. The individual hydrogens are clearly identified by reference to the x-ray structure. Improved values are obtained for the room temperature couplings of this radical. There is also, after irradiation at 77°K, a spectrum consisting of two broad lines tentatively attributed to one of the molecular ions; the species giving rise to this spectrum changes irreversibly into I on warming above 77°K. (auth)

29282 STUDIES ON FREE RADICALS PRODUCED BY IRRADIATION. II. ESR SPECTRA OF γ-IRRADIATED POLYCRYSTALLINE POWDERS OF SOME FLUORINE-CONTAINING COMPOUNDS. Iwasaki, Machio; Toriyama, Kazumi. (Government Industrial Research Inst., Nagoya, Japan). Nagoya Kogyo Gijutsu Shikensho Hokoku, 14: 330-7(Sept. 1965). (In Japanese).

The powder spectra of γ-irradiated salts and amides of some fluorinated carboxylic acids were interpreted on the basis of the spectral shapes of the α-fluorine hyperfine-coupling line. Because of the large anisotropy of α-fluorine coupling tensor, it was possible to observe the shoulders corresponding to the maximum principal value of the coupling tensor. The separation between the wing patterns and the wing hyperfine structures made it possible to identify the radical species produced. The probable radicals were the ones formed by the removal of the atoms attached to the α-carbon. (auth)

29283 DOSE ESTIMATION OF ELECTRON BEAM BY GLASS METHOD. Hayakawa, Kiyoshi; Nunome, Keichi (Government Industrial Research Inst., Nagoya, Japan). Nagoya Kogyo Gijutsu Shikensho Hokoku, 14: 338-45(Sept. 1965). (In Japanese).

Several factors that seem to affect the reproducibility of absorbed energy measurements when irradiation was carried out by electrons from a 6 Mev linear accelerator are discussed. The cobalt glass for gamma dosimetry and the ordinary microscope slides were adopted as secondary dosimeters, and the relationship between the ^{60}Co gamma exposure dose and the optical density increase in the range of 350 to 500 mμ was obtained on both glasses. The piled glasses moving at a constant speed were irradiated by the scanned beam of the electrons from the linear accelerator, the absorbed dose and the variation in absorbed dose due to the depth were estimated from their extents of coloration, and the results were compared with the calculated value based on the conventional method. The feasibility of the above method in the estimation of the absorbed dose for electron irradiations is discussed. (auth)

29284 ELECTRON SPIN RESONANCE OF IRRADIATED THIOPHENE 2-CARBOXYLIC ACID. Eda, Bunzo (Government Industrial Research Inst., Nagoya, Japan); Whiffen, David H. Nagoya Kogyo Gijutsu Shikensho Hokoku, 14: 442-6(Dec. 1965). (In Japanese).

ESR absorption of γ-irradiated 2-thiophenecarboxylic acid was measured at 35,000 Mc/sec on a superheterodyne spectrometer. The spectrum of an irradiated single crystal heated for 40 minutes at 90°C showed two large couplings, which were nearly isotropic but always different from each other. The couplings were attributed to two hydrogen atoms attached to position 5 in the thiophene ring. The two isotropic coupling constants, 78 and 90 Mc/sec, show that there is no plane of symmetry to the radical and suggest that the ring is buckled. The spectrum obtained from 5-deutero 2-thiophenecarboxylic acid clearly showed that the deuterium occupied one of the two large coupling positions in about equal proportions and that this radical does have the >CHD group at position 5. There is also a coupling whose isotropic part is 24 Mc/sec. It has the characteristic anisotropy of an α-hydrogen attached to a carbon atom with spin population of 0.37 in a pure p-orbital. From the spectral analysis, it was concluded that the coupling arises from a proton located at position 4. In addition to these couplings, there was a small coupling which was not always clearly resolved. The 6 Mc/sec isotropic coupling, however, indicated a spin density of ±0.09 at position 3. The three principal values were all of the same sign and a negative spin population was strongly indicated, in accord with the electronic structure. The g-shift gave an indication of the spin population on the sulphur atom, and this was confirmed by a Hückel π-electron calculation. (auth)

29285 COBALT-60 GAMMA RADIOLYSIS OF DEUTERIUM–OXYGEN MIXTURES. Kubose, Don A. (Naval Radiological Defense Lab., San Francisco). Nature, 210: 897-901(May 28, 1966).

An investigation of the ^{60}Co γ radiolysis of mixtures of oxygen and deuterium was undertaken to determine whether any other product, such as deuterium peroxide, would be formed, and to gain further insight into the mechanism of the oxidation reaction. (B.G.D.)

29286 YIELDS AND RATE CONSTANTS OF THE PRECURSORS OF HYDROGEN IN THE RADIOLYSIS OF n-PROPANOL. Basson, R. A.; Van Der Linde, H. J. (Atomic Energy Board, Pretoria). Nature, 210: 943-4 (May 28, 1966).

The formation of hydrogen in irradiated n-propanol in the presence of a scavenger is investigated in order to correlate differences in percursor yields with the polarity of the medium. (B.G.D.)

29287 RADIATION-INDUCED cis-trans ISOMERIZATION OF STILBENE IN METHANOL SOLUTION. Torikai, Ayako; Fueki, Kenji; Kuri, Zen'ichiro (Univ. of Nagoya, Japan). Nippon Kagaku Zasshi, 87: 391-4(May 1966). (In Japanese).

The cis-trans isomerization of stilbene induced by γ rays in methanol solution was investigated in the concentration range from 2×10^{-5} to 2×10^{-3} mol/l of stilbene. The isomerization of trans-stilbene to cis-stilbene was observed with the formation of side products, but the isomerization of cis-stilbene to trans-stilbene rarely occurred, although side products were formed in this case. The G-value for the formation of cis-stilbene from trans-stilbene was estimated to be 0.02 to 1.0 in the concentration range studied. Addition of small amounts of benzene, piperidine, and carbon tetrachloride had little effect on the radioinduced reaction of trans-stilbene. In the presence of ferric chloride, both the rate of the isomerization and side product formation were reduced. In the solid state, the isomerization of trans-stilbene to cis-stilbene did not occur. The results

indicated that free radical intermediates rather than excited or ionic species may play a major role in the isomerization. The side products formed were identified with bibenzyl-type compounds. (auth)

29288 RADIATION GRAFTING OF METHYL METHACRYLATE ONTO LIGNIN. Koshijima, Tetsuo; Muraki, Einosuke (Government Industrial Research Inst., Osaka). Nippon Mokuzai Gakkaishi, 10: 110-13(June 1964). (In Japanese).

Direct radiation grafting was studied using HCl lignin of softwood (Pinus desiflora) (N) and hardwood (Betula tauschii) (L). A mixture of monomer-lignin (3:1) or (10:1) was irradiated with an 1,000-c ^{60}Co source at room temperature in an O_2-free atmosphere. The lignin-methyl methacrylate system showed a maximum grafting rate of 24.1% in (N) and 9.5% in (L) at 1.02×10^5 R/hr after 5 hr and no grafting was observed with styrene or vinyl acetate. The inhibition period of grafting increased with decreasing dosage rate. At 1.02×10^5 R/hr the maximum grafting rate rose to 38% when the lignin was acetylated with acetic anhydride and pyridine. This higher rate resulted from the partially methylated lignin treated with diazomethane. It was concluded that: graft copolymerization onto lignin might be possible when the phenolic hydroxyl was protected; grafting was poor with fully acetylated lignin; and aliphatic alcohol hydroxyl in lignin molecule may play an important part in the grafting of lignin. Surface grafting was expected to occur predominantly in the present case. (OID)

29289 EPR IN NEUTRON-IRRADIATED DPPH. Van Itterbeek, A.; Witters, J.; Van Audekercke, R.; Nihoul, J. (Instituut voor Lage Temperaturen en Technische Fysica, Leuven, Belg.). Physica, 32: 494-6(Feb. 1966).

The influence of neutron irradiation on diphenylpicrylhydrazyl as measured by paramagnetic resonance at low temperatures is reported. The observed effects include a considerable increase in the number of spins and in the linewidth and a small but significant change in g-values. (auth)

29290 EFFECT OF STABILIZERS ON IRRADIATED POLYPROPYLENE. Nechitaylo, N. A.; Sanin, P. I.; Gol'denberg, A. L.; Polak, L. S. Plast. Massy, No. 7, 7-13(1965).

Polypropylene (Mw ~224,000) was irradiated with a ^{60}Co source in ampoules at about 10^{-3} mm Hg. The stabilizers chosen were phenyl-β-naphthylamine (Neozone D), 2-mercaptobenzimidazole, and barium di-n-octadecyldithiophosphate; for comparison, experiments were made with ionol. Thermograms were recorded automatically with a Kurnakov pyrometer, and the temperatures of the thermal effects observed were studied in relation to the irradiation dose and the content of stabilizers. The endothermic effects on the heating curves correspond to the melting of the polymer samples, and the exothermic ones to the reactions of oxidation of polypropylene. The degree of oxidation was determined by infrared spectroscopy from the content of carbonyl compounds. On the basis of the quantity of carbonyl groups formed in the various experiments, the most effective oxidation inhibitors are phenyl-β-naphthylamine and ionol. The intrinsic viscosity of the samples was studied as a function of the irradiation dose. The protection coefficients, energy transfer factors, and intrinsic viscosities of polypropylene irradiated in air were determined. The number of breaks in the primary molecular chain caused by the ionizing radiation was correlated with the reciprocal molecular weight. The addition of 2% ionol is sufficient to prevent cross-linking in the polymer at a dose of 70 MR. At 160 and 250 MR, 5 and 8% ionol, respectively, is needed to prevent gel formation. (CFSTI)

29291 EFFECT OF NUCLEAR RADIATION ON THE ACTIVITY OF VANADIUM CATALYST IN THE REACTION OF SULFUR DIOXIDE OXIDATION. Kozak, Zdzislaw; Akerman, Karol. Przem. Chem., 45: 189(Apr. 1966). (In Polish).

The activity of the $V_2O_5-Ag_2SO_4-SiO_2$ catalyst in SO_2 oxidation by air was examined before and after activation [$^{109}Ag(n,\alpha)^{110m}Ag$]. Measurements showed that the result of neutron activation was a decrease of the catalyst activity. (auth)

29292 USE OF THE FINKELSTEIN REACTION FOR MEASURING PARTIAL ORGANIC RETENTION DURING IRRADIATION OF ALKYL BROMIDES IRRADIATED BY NEUTRONS. Ledrut, J. H. T.; Point, J. J. (Centre de la Faculte Polytechnique, Mons, Belg.). Radiochim. Acta, 5: 59-60(Mar. 1966). (In French).

It is shown that the Finkelstein reaction can be used to measure partial organic retentions after neutron irradiation of alkyl bromides. The irradiated alkyl bromide is washed in a solution of NaI. Under the conditions described, C_2H_5Br, CH_2Br_2, and 1,2-$C_2H_4Br_2$ react with NaI by the Finkelstein reaction to give insoluble NaBr. 1,1-$C_2H_4Br_2$, $CHBr_3$, $C_2H_3Br_3$, and $C_2H_2Br_4$ do not react. The sum of the retentions can be measured directly in the form of C_2H_5Br, CH_2Br_2, and 1,2-$C_2H_4Br_2$. The technique is simple and rapid. (J.S.R.)

29293 RADIOLYSIS OF ACETYLENE IN SOLUTION. III. EFFECTS OF γ RADIATION ON THE AQUEOUS SOLUTION OF ACETYLENE; THE ROLE OF HYDROGEN AND OXYGEN UNDER DYNAMIC CONDITIONS. Fiti, Maria; Tudor, Lucia (Institut de Physique Atomique, Bucharest). Rev. Roum. Chim., 10: 1151-9(Nov. 1965). (In French).

The role of hydrogen and oxygen in radiolytic processes occurring in aqueous solutions of acetylene during bubbling of these gases and acetylene in tetradistilled water was studied during irradiation. Results obtained made possible a better understanding of the complex mechanism of the processes of oxidation and polymerization occurring in this system. The experimental conditions that totally surpress radiolytic polymerization, the conditions for activation of the oxidation in the presence of oxygen, and the conditions for activation of the polymerization in the presence of hydrogen were also determined. The results obtained with respect to the nature and the yield of the radiolysis products were used for elaboration of hypotheses explaining the reaction mechanism. (tr-auth)

29294 STUDIES OF GRAFT COPOLYMERIZATION ONTO VISCOSE RAYON. III. GRAFT COPOLYMERIZATION OF ACRYLONITRILE BY SIMULTANEOUS IRRADIATION METHOD OF ^{60}Co γ-RAY. Imamura, Rikizo (Kyoto Univ.); Washijima, Shigeo. Sen'i Gakkaishi, 21: 349-57(July 1965). (In Japanese).

Graft copolymerization of viscose rayon was accomplished by irradiating the rayon immersed in an aqueous solution of acrylonitrile with ^{60}Co. The effects of various factors were examined, such as time of irradiation, temperature, liquor ratio, denier of rayon, the monomer concentration, and pH value of monomer solution. Also, using the effect of the degree of swelling of fiber for various kinds of rayon samples was examined, and the percentage of grafting was found to be proportional to this property of fiber in solution system. Microphotograph of the cross section of grafted rayon (percentage of grafting 53.4%) showed a uniform distribution of graft polyacrylonitrile. Also, graft polyacrylonitrile was isolated by the acid hydrolysis method. Its intrinsic viscosity was measured and found to be nearly equal to that of homopolymer. The x-ray diffraction pattern of the graft rayon was found to be composed of the pattern of cellulose II and that of polyacrylonitrile. This suggests that graft polyacrylonitrile deposits in amorphous region and is crystallized. The practical properties of grafted rayon were measured; tensile strength, elongation, and degree of crimping increased and tenacity decreased subject to the percentage of grafting. (auth)

29295 γ-RADIOLYSIS OF WATER VAPOR IN THE PRESENCE OF NH_3 AND O_2. Anderson, A. R.; Knight, B.; Winter, J. A. (Atomic Energy Research Establishment, Harwell, Eng.). Trans. Faraday Soc., 62: 359-70(Feb. 1966).

Measurements of H_2 production from pure water vapor as a function of dose indicate that, like liquid water, it is essentially stable to γ radiation. The net yield of H_2 is very low leading to a mean integral value of $G(H_2) \sim 0.007$ but the amount of H_2 obtained depends critically on the care taken in cleaning the cells and admitting the water, and it is concluded that previously published yields are all integral values obtained under a variety of conditions.

Measurement of the primary yields in the presence of NH_3 and of $NH_3 + O_2$ gives $g(OH) = 6.6 \pm 0.2$, $g(H) = 5.7 \pm 0.2$, $g(H_2) = 0.47 \pm 0.01$, but no distinction can be made between yields of electrons and H atoms. Primary processes of ionization and charge recombination are considered in view of earlier postulates, together with physical evidence which demonstrates the stability of ion clusters in water vapor even at low pressures. It is suggested that, under certain conditions in the vapor phase, charge neutralization of the H_3O^+ ion leads to the same yield of radicals as in liquid water. (auth)

29296 EFFECTS OF γ RADIATION ON THE STRUCTURE OF EPOXY RESINS AND RESIN-BASE METALLIC POLYMERS. Khimchenko, Yu. I.; Ul'berg, Z. R.; Prikhod'ko, G. P.; Ivanova, E. I.; Kobakchi, A. M.; Meleshevich, A. P.; Natanson, E. M. (Pisarzhevskii Inst. of Physical Chemistry, Academy of Sciences, Ukrainian SSR). Ukr. Khim. Zh., 31: 1164-7(1965). (In Russian).

By the method of infrared spectroscopy it was found that irradiation with doses of 4×10^8 rad decreases the concentration of the epoxy group in the nonsolid purified epoxy resin ED-5 by 23 to 25%. The introduction of colloidal copper and lead led to a very sharp reduction of the epoxy group during irradiation at doses of 4×10^8 rad. This indicated that in irradiation processes the colloidal metals cause an increase of molecular weight of the resins because of the opening up of the epoxy ring. The decrease in per cent concentration of the epoxy group is accompanied by an increase of the integral intensity of the 1720 cm^{-1} band, characterizing the valence oscillation of the carbonyl group. (tr-auth)

29297 X-RAY STUDY OF EPOXIDO-DIANIC ED-5 RESIN IRRADIATED WITH ^{60}Co GAMMA RAYS AND METALLOPOLYMERS ON ITS BASE. Klochkov, V. P.; Shpigun, A. A.; Ul'berg, Z. R.; Prikhod'ko, G. P.; Ivanova, E. I.; Kabakchi, A. M.; Meleshevich, A. P.; Natanson, E. M. Ukr. Khim. Zh., 32: 366-70(1966). (In Russian).

During irradiation of epoxido-dianic ED-5 resin clearly expressed structures appeared. Under the action of high-energy irradiation, finely dispersed copper accelerated the regulating effect in epoxido-dianic ED-5 resin. Under the action of irradiation in the binary system ED-5 + 6% Cu, a sharp increase in the degree of ED-5 crystallinity was observed. The mutual effect of ^{60}Co irradiation and colloidal lead on the structure formation of ED-5 and its interaction with metals was much weaker than in the case of copper systems. (tr-auth)

29298 SYNTHESIS OF HIGH MOLECULAR COMPOUNDS BY RADIATION POLYMERIZATION METHODS. Ivanov, V. S. Usp. Khim., 35: 93-120(Jan. 1966). (In Russian).

The polymerization of various monomers is reviewed according to their classes. The polymerization of olefine hydrocarbons such as ethylene, propylene, isobutylene, and some higher olefines; the polymerization of diene hydrocarbons such as divinyl and isoprene; the polymerization of halogen derivatives such as tetrafluoroethylene, vinyl chloride, and perfluorobutadiene; and the polymerization of unsaturated carboxylic acids and their derivatives such as acrylic acid, methacrylate, and acrylamide are considered. The polymerization of vinyl ethers and of the vinyl derivatives of heterocyclic compounds is discussed. Other classes of compounds include allyl monomers, acetylene monomers, carbonyl compounds, unsaturated nitriles, isocyanates, cyclic monomers, and compounds containing silicon or phosphorous. The type of radiation, dose, dose rate, G-value, effect of impurities, and the molecular weight of the product are given for each compound where this information is available (352 references). (TTT)

29299 RADICAL FORMATION IN RADIOLYSIS OF HARD RUBBER. Kozlov, V. T.; Tarasova, Z. N. (Scientific-Research Inst. of Tire Industry, USSR). Vysokomol. Soedin., 8: 943-8(May 1966). (In Russian).

Using ESR methods the formation of radicals at low temperature (−196°C) during radiolysis of rubbers NK, SKI-3, nairit A, SKD, SKS-30 ARM, SKMS-30 ARKM and SKEP was studied. All radicals with the exception of SKEP are the allylic type. In SKEP alkyl radicals are formed. Superposition of NK and SKI spectra shows that in NK the more probable is the cleavage of H atoms from C_4 and in SKI from C_1, which could be attributed to less regular SKI structure. The ESR spectra in the initial and in crosslinked (up to 1.2×10^{20} links/gram) rubber are identical. The curves of radical accumulation with dose were determined, and the radiation yields (G_R) were found on the initial linear parts of the curves. They form the series: $G_{R(SKEI)} = 0.55 > G_{R(NK,SKI)} = 0.28 > G_{R(XK)} = 0.20 > G_{R(SKD)} = 0.19 > G_{R(SKMS)} = 0.113 > G_{R(SKS)} = 0.096$. It could be assumed that this series of G values corresponds qualitatively to the E_1 series taking into account that at proximate values of E_1, the geometry (symmetry) of electron clouds plays an important role in the decomposition into radicals. (auth)

29300 RADIATION-INDUCED POLYMERIZATION OF TETRAFLUOROETHYLENE AND ACRYLONITRILE AT 4.2 K. Bruk, M. A.; Gromov, V. F.; Chernyak, I. V.; Khomikovskii, P. M.; Abkin, A. D. Vysokomol. Soedin., 8: 961-2(May 1966). (In Russian).

Polymers of tetrafluoroethylene or acrylonitrile were prepared by bulk radioinduced polymerization of the monomers at 4.2°K. Molten monomer samples were frozen at a given rate in liquid nitrogen, placed in a cryostat with liquid helium, and irradiated. Defrosting of the samples was conducted under conditions that excluded post-polymerization. It is assumed that in the course of polymerization of the monomers at low temperatures the bulk temperature of the samples does not determine the character of the polymer chain formation, which takes place in "hot" regions. The polymer chains grow before relaxation of the vibration excitation of molecules in "hot" regions has time to occur. It is also assumed that polymerization follows the cooperative mechanism that does not require activation for the addition of individual monomer molecules. (auth)

29301 RADIOCHEMICAL PROPERTIES OF CERTAIN PEPTIDES. Sanaev, B.; Yanova, K. G.; Sharpatyi, V. A.; Ibragimov, A. P.; Margolin, D. D.; Maslov, B. V. (Karpov Inst. of Physics and Chemistry, Moscow). Zh. Fiz. Khim., 39: 2510-14(Oct. 1965). (In Russian).

The radicals H and OH play a predominant role in the radiolytic decomposition of aqueous solutions of dipeptides. The radicals formed from the dipeptides both during the radiolysis of aqueous solution and in the polycrystalline form have basically the same structure. (tr-auth)

29302 RADIOLYSIS OF ISOOCTYL AND HEPTYL HYDROPEROXIDE SOLUTIONS IN HYDROCARBONS. Romantsev, M. F.; Saraeva, V. V.; Mishchenko, O. A. Zh. Fiz. Khim., 39: 2599-2602(Oct. 1965). (In Russian).

During the radiolysis of tertiary isooctyl and secondary heptyl hydroperoxides in hydrocarbons, dialkyl peroxides and alcohols are formed. The decomposition of two molecules of ROOH yields one molecule of ROOR and two molecules of alcohol. Carbonyl compounds are not formed. Investigation of the dependence of the decomposition yield of the hydroperoxide on concentration showed that the hydroperoxide in the concentration interval from 1.8×10^{-4} to 5.6×10^{-3} M at 0°C appears as the acceptor of radicals formed during the radiolysis of the hydrocarbon. The decomposition yield of ROOH and the formation of products depend little on the temperature. The activation energy of this process is ≈0.7 kcal/mol. In the presence of oxidation products (carbonyl compounds and alcohols) the RO radicals, products of the decomposition of ROOH, are not completely consumed in the formation of ROOR, but partially participate in other processes. (tr-auth)

29303 EFFECTS OF γ- AND ULTRAVIOLET RAYS ON COPPER GLYCOCOL. Shagisul, G. A.; Tanova, L. A.; Il'yukevich, L. A.; Budyrko, L. I. (Belorussian State Univ., USSR). Zh. Fiz. Khim., 39: 2730-4(Nov. 1965). (In Russian).

The radiolysis at high γ doses and photolysis of dilute aqueous solutions of Cu^{2+} complexes of glycocoll are accompanied by oxidation-reduction conversions with forma-

tion of cupric salts. The reaction yields were calculated and hypotheses on the mechanism of the process are given. (tr-auth)

29304 RADIATION EFFECTS ON THE CATALYTIC ACTIVITY OF PLATINUM DURING HYDROGENATION. Krylova, I. V.; Filonenko, A. P.; Kobozev, N. I. Zh. Fiz. Khim., 39: 2742-4(Nov. 1965). (In Russian).

The irradiation of platinum catalyst using a quartz mercury vapor lamp led to an increase of the activity during hydrogenation of cyclohexenes. In the reduction of nitro groups and also in the decomposition of hydrogen peroxide, preliminary irradiation of platinum led to a reduction of catalytic activity. (tr-auth)

29305 RADIATION EFFECTS ON FORMATION OF FREE RADICALS IN FROZEN $CH_3OH + CCl_4$ SOLUTIONS. Roginskii, V. A.; Kotov, A. G.; Pshezhetskii, S. Ya. (Karpov Inst. of Physics and Chemistry, Moscow). Zh. Fiz. Khim., 39: 2892-5(Dec. 1965). (In Russian).

The formation of radicals in frozen CCl_4-CH_3OH solutions by γ radiation was investigated. The dependence of the radical yield on the composition of the solution is characterized by a maximum during which the nature of the superadditive radicals coincides with the HCl yields. A mechanism for the reaction occurring in irradiation fields is proposed. It explains the formation of superadditive radicals by reactions of H atoms with CCl_4 molecules and of Cl atoms with CH_3OH molecules. The accumulation of radicals and the formation of H_2, CO, CH_4 was examined in solutions with different concentrations. The results obtained agree satisfactorily with the process mechanism proposed. (tr-auth)

29306 INHIBITING EFFECTS OF SOME SOLID IMPURITIES ON RADIATION CHEMISTRY PROCESSES. Lukhovitskii, V. I.; Tsingister, V. A.; Lagucheva, R. M.; Karpov, V. L. (Karpov Inst. of Physics and Chemistry, Moscow). Zh. Fiz. Khim., 39: 3083-4(Dec. 1965). (In Russian).

The heterogeneous inhibition effect of solid impurities containing metals of a variable valence in the lowest valence state (Fe^{2+}) on homogeneous radiation chemical processes was detected. Explanation of this effect on the basis of contemporary hypotheses on the mechanism of radiation-chemical processes is not possible. (tr-auth)

29307 RADIATION CHEMISTRY OF CARBOHYDRATES. VI. RADIOLYSIS OF AQUEOUS SOLUTIONS OF β-METHYL-, β-PHENYL-, AND β-BENZYL-D-GLUCOSIDES. Kochetov, N. K.; Kudryashov, L. I.; Chlenov, M. A. Zh. Obshch. Khim., 35: 2246-51(1965). (In Russian).

The decomposition yields of β-methyl-, β-phenyl-, and β-benzyl-D-glucosides and the formation of glucose during their radiolysis were determined. The effect of the aglycon structure on the stability of the glucoside bond under γ irradiation in β-methyl-, β-phenyl-, and β-benzyl-D-glucosides was detected. A possible mechanism for the radiation-chemical hydrolysis of the glucosides is suggested in which the participation of the solvated electron was assumed. During the radiolysis of all the glucosides investigated, acids were formed as secondary products; therefore, oxidizing hydrolysis did not occur. (tr-auth)

29308 PREPARATION OF ION-EXCHANGE MEMBRANE BY PRE-IRRADIATION METHOD. Kochergins-kaya, L. L.; Rosenblyum, N. D.; Stasyuk, Kh. A.; Zhitkova, L. G.; Breger, A. Kh. Zh. Prikl. Khim., 38: 2662-5 (Dec. 1965). (In Russian).

It was found that the pre-irradiation method can be used to produce homogeneous ion-exchange membranes. The exchange capacity, the electric conductivity, and mechanical strength were guaranteed by the use of suitable polymers, the nature and quantity of the grafted monomers, and the presence of introducible inorganic groups. (tr-auth)

29309 ELECTRON PARAMAGNETIC RESONANCE STUDIES OF THE FORMATION OF PEROXIDE RADICALS IN IRRADIATED PALMITIC ACID AND POTASSIUM PALMITATE. Revina, A. A.; Karasev, A. L. (Inst. of Electrochemistry, Academy of Sciences, USSR). Zh. Strukt. Khim., 6: 556-62(July-Aug. 1965). (In Russian).

The EPR spectra of palmitic acid, tripalmitin, and potassium palmitate, exposed to γ irradiation at 77°K in a vacuum, were investigated. The radicals formed were identified and their conversion in a vacuum during temperature increases to 300°K was investigated. The formation kinetics in the irradiated palmitic acid and potassium palmitate of peroxide radicals from radicals of different structures was studied at p_{O_2} = 730 to 750 mm Hg and a difference in the reduction capacities of the original radicals was detected. It was established that the characteristic of the process is the increase of the total concentration of the radicals together with the formation of the $RO_2^{\cdot}$ radicals. The kinetics of the formation of the $RO_2^{\cdot}$ in irradiated potassium palmitate at 195°K was studied as a function of p_{O_2} and it is shown that the first stage of the oxidation process is formation of unstable nonparamagnetic complexes $(2R^{\cdot},O_2)$, which are slowly converted to $RO_2^{\cdot}$ and $R^{\cdot}$. (tr-auth)

29310 ELECTRON SPIN RESONANCES IN X-IRRADIATED SILVER NITRATE [Thesis]. Mosley, Wilbur Clanton Jr. University, Ala., Univ. of Alabama, 1965. 69p.

Four paramagnetic species were identified by electron spin resonance in single crystals of silver nitrate x-irradiated at 77°K. The principal values and corresponding principal axes of the g tensors and hyperfine tensors were determined. An eight-line spectrum (four doublets) due to Ag^{2+} is described by a spin Hamiltonian with principal g values of 2.3098, 2.0455, and 2.0879 ± 0.0005 and principal hyperfine values of 98.1, 70.5, and 56.0 ± 1.0 Mc/sec. A twelve-line spectrum (four triplets) characteristic of stationary NO_2 molecules was observed in previously irradiated pure crystals and crystals doped with silver nitrite. The principal g values are 1.9982, 2.0033, and 2.0094 ± 0.0005; the principal values of the hyperfine tensor describing the coupling to a single nitrogen nucleus are 135.1, 143.1, and 195.1 ± 1.0 Mc/sec. A spectrum consisting of two weak singlets with principal g values of 2.0046, 2.0084, and 2.0134 ± 0.0005 is tentatively assigned to NO_3. A twenty-four line spectrum (four sestets) is believed to be due to $AgNO_3^-$. The principal values of the g tensor are 2.000, 2.002, and 2.007 ± 0.001; the principal values of the hyperfine tensor that describes the coupling to a single silver nucleus are 38, 41 and 47 ± 2 Mc/sec; the principal values of the hyperfine tensor that describes the coupling to a single nitrogen nucleus are 100, 104, and 189 ± 2 Mc/sec. The spectra due to Ag^{2+} and $AgNO_3^-$ disappear upon warming to 140°K. The intensity of the spectrum due to NO_2 increases markedly as the spectrum due to Ag^{2+} disappears. Warming to 240°K causes the spectrum due to NO_2 to disappear. Only the weak singlets due to NO_3 are observable at room temperature. Since the production of NO_2 depends on the presence of nitrite in the crystal, the experiments indicated that nitrite is formed only above 200°K and is not a direct product of the decay of Ag^{2+} or $AgNO_3^-$. (Dissertation Abstr.)

29311 ELECTRON SPIN RESONANCE STUDIES OF SELF-RADIOLYSIS OF ^3H-LABELED SOLID AMINO ACIDS AND DICARBOXYLIC ACIDS. Lassmann, G. Leipzig, Univ., 1965. 90p. $2.00 Gmelin, AED-Diss. 65-268.

Formation of radicals by self-radiolysis of amino acids and dicarboxylic acid molecules by ^3H β decay was studied. Radicals produced by β radiation gave the same electron resonance spectra as those by γ radiation. Radical formation as a function of temperature was investigated. Energy for the production of 1 stabilized radical is 20 to 100 ev, depending on compound type. (Gmelin Inst.)

29312 EFFECT OF RADIATION ON THE SYNTHESIS OF AMMONIA [Thesis]. West, Roger Karl. Ithaca, N. Y., Cornell Univ., 1965. 83p.

Gamma radiation from ^{60}Co with an average energy of 1.25 Mev was applied to the synthesis of ammonia in the presence and absence of catalysts. The non-catalytic batch production of ammonia at a rate of 9.5×10^{-6} mole/l-hr at 250 psig, 40°C, and a dose rate of 2.4×10^6 rad/hr con-

firmed the results of earlier studies. The G-value was 0.66 molecules NH_3 per 100 ev absorbed. Dose rates were measured with the Frick ferrous sulfate dosimeter. Changes in temperature from 40 to 350° had no effect on the rate. Conversely, the rate was directly proportional to the pressure over the range of 70 to 315 psia. Below 70 psia a nonlinear dependence of rate on total pressure was suggested by the data. The effect of composition and dose rate were also investigated. The continuous synthesis in an Inconel flow reactor packed with a typical industrial triply promoted iron catalyst exhibited the dependence on temperature, pressure, and space velocity usually found in catalysts of that type. At 450°, 1,000 psig, and about 50 cc (25°, 1 atm)/min g-catalyst, a radiation dose rate of 1.8×10^5 rad/hr produced no change in the rate of ammonia production after two hours. Further studies at lower temperatures at 1,000 psig showed no effect of radiation as well. Thus, no effect on either the equilibrium concentration or the rate of reaction was produced by the radiation. Any primary changes in the catalyst were probably lost rapidly by electron flow through the metal. (Dissertation Abstr.)

29313 EFFECTS OF GAMMA RADIATION ON THE VISCOELASTIC PROPERTIES OF POLYMERS [Thesis]. Traeger, Richard Kieth. Albuquerque, N. Mex., Univ. of New Mexico, 1965. 195p.

Three styrene-butadiene and three silicone rubbers were irradiated in a cobalt-60 source to doses of 0 to 200 Mrads. The dynamic shear properties, the hardness values, and the crosslink densities were determined for the irradiated materials. The styrene-butadiene rubbers consisted of peroxide-cured, unfilled Ameripol 1009 (23% styrene plus divinyl benzene), Ameripol 1500 (23% styrene), and Ameripol 1013 (43% styrene). The silicone rubbers were peroxide-cured, silica-filled systems of a dimethyl polymer Silastic 50, a methyltrifluoropropyl polymer Silastic LS63, and an experimental high-aromatic-content polymer X3-0272. Hardness and the crosslink densities of the styrene-butadiene rubbers were increased by the irradiation. Storage moduli of all specimens increased significantly. Loss moduli of the low-styrene-content polymers increased on irradiation to about 50 Mrads and then remained constant on further irradiation exposure. The high-styrene-content Ameripol 1013 continued to show increasing loss modulus with irradiation indicating that the styrene was limiting the scissioning radiation effects. The loss tangent curves of the rubbers were lowered in height and the maxima were widened as a result of the radiation. The relaxation spectra were increased in magnitude and extended to longer times. Hardness of all the silicone rubbers increased during radiation exposure. Significant changes in the crosslink density were only noted for the dimethyl polysiloxane. The crosslink density changes were again noted in the dynamic properties in which the moduli of the dimethyl material were significantly increased, the moduli of the methyltrifluoropropyl polymer were changed slightly, and the moduli of the aromatic containing system were not affected. Loss tangents were lowered by the irradiation but no maximum was found in the loss tangent curves for these rubbers. Relaxation spectra were increased in magnitude but not extended to longer times as was the case in the styrene-butadiene rubbers. (Dissertation Abstr.)

29314 I. CHARGE TRANSFER IN THE RADIOLYSIS OF LIQUID XENON HEXANE SOLUTIONS. II. POSITIVE ION CHEMISTRY IN SOLID METHANE [Thesis]. Davis, Donald Robert. Los, Angeles, Univ. of California, 1966. 142p.

Possible charge transfer from xenon ion to hexane was studied in liquid xenon containing from 0.043 to 0.1 mole fraction hexane, and irradiated at −78°. The distribution of dimer and hexene products is independent of the hexane mole fraction even though more than 90% of the products are formed by energy transfer in the most dilute solutions studied. The yields correspond to essentially 100% efficient energy transfer. A mechanism involving charge transfer seems best able to account for the experimental results although transfer of energy from neutral excited xenon atoms to hexane cannot be completely excluded. The polymerization of solid methane was studied at 77°K. A detailed analysis of the yield and properties of the polymer was carried out for samples receiving doses corresponding to between 0.04 and 1.5% conversion. Each of the following properties of the polymer was found to be independent of the dose and dose rate. It contains from about 13 to 26 carbon atoms per molecule; the average molecular weight and composition is equivalent to $C_{20}H_{40}$. Many hundreds of different hydrocarbon isomers contribute to the polymer yield, and individual isomers increase linearly with dose. Each molecule contains an average of 8 methyl groups and has few if any unbranched chains containing four or more carbon atoms. A small amount of unsaturation and rings seems to be present in the polymer. The yield is 0.32 methane molecules converted to polymer per 100 ev absorbed, and the induction dose, if any, is less than 1 Mrad or 0.01% conversion. Addition of air, xenon, nitric oxide, and carbon tetrachloride has little or no influence on the polymer yield, except that air leads to formation of heavy molecules containing oxygen. A chain mechanism carried by carbonium ions explains a wide variety of experimental results. The high molecular weight of the polymer may be thermodynamically inconsistent with a chain reaction, however, and the energy required for the formation of heavy hydrocarbons may be supplied by a mechanism involving charge transfer. This research supports the hypothesis that positive ion chemistry is important in the radiolysis of condensed alkanes. (Dissertation Abstr.)

29315 STUDY OF WATER RADIOLYSIS AND HYDROGEN PEROXIDE FORMATION USING RADIOACTIVE ^{15}O. Halko, A.; Ovadia, J. 17p. (CONF-660212-1). ORAU. Gmelin, AED-CONF-66-016-5.

From Radiation Research Society, 14th Annual Meeting, Coronado, Calif.

Mechanisms in the radiolysis of water were studied using ^{15}O as tracer. A 15-Mev electron beam was used in the irradiation. Production of H_2O_2 in water irradiated in the presence of oxygen was determined. The results did not support the existence of a molecular reaction. The peroxide was derived entirely from interaction of O_2^- rather than the recombination of OH radicals. (M.C.G.)

29316 TECHNIQUE FOR GAMMA RADIATION GRAFT POLYMERIZATION. Hargreaves, G. (Naval Air Engineering Center, Philadelphia). 7p. (CONF-660214-1). ORAU. Gmelin, AED-CONF-66-039-1.

From American Chemical Society, 1st Middle Atlantic Regional Meeting, Philadelphia.

A method was developed for producing grafts by ionizing radiation without the attendant degradation of other methods. The fibrous substrate is not irradiated; only the monomer to be grafted passes through the irradiation chamber. Gamma radiation from ^{60}Co at a dose rate of ~0.94 Mrad per hour was used. Nylon fabric and acrylonitrile and acrylic acid monomers were studied. This technique can be adapted to large-scale use. (M.C.G.)

29317 FISSION RECOIL SYNTHESIS. Steinberg, M. (Brookhaven National Lab., Upton, N. Y.). New York, American Inst. of Chemical Engineers, 1966, Preprint 26D, 57p., $0,50. (CONF-660506-3). ORAU.

From American Inst. of Chemical Engineers, Nuclear Engineering Div. Symposium, Columbus, Ohio.

The use of fission fragment recoil energy in synthesis of chemical compounds is discussed. Fixation of nitrogen for production of fertilizers, ozone synthesis, carbon dioxide decomposition, decomposition of water vapor, hydrogen peroxide synthesis, hydrazine synthesis, and hydrogen cyanide synthesis are considered. Reactor physics and fuel development for use in fissiochemonuclear processes are discussed. Contamination problems, inpile loop construction and operation, and economics are considered. (M.C.G.)

29318 THERMOLUMINESCENT EMISSION OF IRRADIATED RARE EARTH IONS IN CaF_2. Merz, J. L.;

Pershan, P. S. (Harvard Univ., Cambridge, Mass.). 13p. (CONF-660107-7). ORAU. Gmelin, AED-CONF-66-003-6.

From American Physical Society Meeting, New York.

The thermoluminescent emission of x-irradiated CaF_2:$(RE)^{3+}$ ions was studied between 77 and 440°K. Remarkable similarities were observed between the glow curves from different rare earth ions. A photoelectric method was devised to record the spectra of the individual glow peaks at low intensity and high resolution (less than 1 A°). Measurements of $CaF_2:Gd^{3+}$ 0.03% showed that the emission spectrum from the low-temperature peaks was identical to the fluorescence of trivalent gadolinium ions in cubic sites. However, high-temperature thermoluminescence was identical to fluorescence from sites of tetragonal symmetry. A model can be proposed to explain this. An electron deficient center, or a self-trapped hole, diffuses to the site of a divalent rare earth ion, capturing an electron and leaving an excited trivalent rare earth ion. Decay of this ion results in the observed thermoluminescence. For the low temperature peaks, this center must leave the rare earth in a cubic site; for example, a V_k center would have this property. At high temperatures the tetragonal spectra could result from the diffusion of F^0 atoms. (auth)

29319 FISSIO-CHEMICAL PROCESS AND EQUIPMENT. (to Union Stock Yard Transit Co.). British Patent 1,027,479. Apr. 27, 1966. Filed July 29, 1964.

A fissiochemical process is described in which the fuel composed of liquid reactants mixed with finely divided particles of nuclear fuel uniformly distributed through the liquid is passed through a critical volume where nuclear fission results to release sufficient energy in fission fragments to cause reaction of the liquid reactants to form gaseous reaction products. The gaseous reaction products are separated from the remaining liquid reactants in which the fissionable material remains distributed, and this suspension is then recycled through the critical volume. The process is specifically described for the production of hydrazine from liquid ammonia. (B.L.M.)

29320 PROCESS OF COATING THE EXTERIOR SURFACE OF ARTICLES WITH A POLYMERIZABLE COATING MATERIAL SUBJECTED TO HIGH ENERGY IONIZING IRRADIATION. Burlant, William J. (to Ford Motor Co.). U. S. Patent 3,247,012. Apr. 19, 1966. Filed May 1, 1963.

A process for continuously coating the exterior surface of an article consists of applying a liquid film of free flowing, polymerizable coating material to the article and polymerizing the material in situ by passing a beam of polymerization effecting electrons through the film. The polymerizable coating is substantially free of non-polymerizable solvent, and the preferred coating material is a solution of an unsaturated polyester resin in vinyl monomers. The energy of the electron beam and the spacing of the electron source from the coated article are so maintained that the polymerization is substantially equal throughout the coating to yield an evenly cured polymerized coating. (B.L.M.)

29321 ISOMERIZATION OF TRANS POLYMERS OF CONJUGATED DIENES BY HIGH ENERGY PARTICLE RADIATION. Anderson, Herbert R. Jr. (to Phillips Petroleum Co.). U. S. Patent 3,247,088. Apr. 19, 1966. Filed July 11, 1961.

Irradiation of a solid vulcanized rubbery polymer of conjugated dienes containing unsaturation of the trans-1,4 variety with a high energy beam in an inert atmosphere resulted in the isomerization of at least a part of the trans-1,4 structures to the cis-1,4 structures. The high energy beam can be alpha particles, protons, or electrons; but the energy of the beam, preferably electrons, must be at least 1 Mev and ranging as high as 1 Bev. The beam current may be varied from 0.1 to 1000 μamp for a period of time ranging from about 0.5 to 60 min for irradiation. (B.L.M.)

29322 RUBBER PRODUCTS RESISTANT TO RADIATION DAMAGE. Anderson, Herbert R. Jr. (to Phillips Petroleum Co.). U. S. Patent 3,247,160. Apr. 19, 1966. Filed Dec. 19, 1960.

A natural or synthetic vulcanized rubber was patented that is resistant to ionizing radiation effects, which usually deteriorates the rubber vulcanizates. Certain halogenated organic compounds of which 1,4-di(2-chloroethyl)benzene, 1,3-di(iodomethyl)benzene, fluoromethylbenzene, and 2-methyl-5-fluorobenzoxazole are examples are incorporated into the rubber to serve as radiation damage inhibitors. (B.L.M.)

29323 RADIATION RESISTANT LUBRICATING OIL. Barry, Edward G. (to Socony Mobil Oil Co., Inc.). U. S. Patent 3,249,542. May 3, 1966. Filed July 20, 1962.

A mineral lubricating oil containing a small amount (0.5 to 5 wt %) of a substituted thiuram sulfide and with good resistance to radiation deterioration such as increasing viscosity was developed. (B.L.M.)

Radiochemistry

See also Separation Processes and Procedures

29324 ELECTROSTATIC COLLECTING OF RADIUM A AND A PROPERTY OF THE β EMISSION OF RADIUM E FORMED FROM THE COLLECTED RADIUM A. Dubois, Emmanuel; Roche, Jean; Andanson, Pierre (Univ. Paris, Clermont-Ferrand, France). Compt. Rend., Ser. B., 262: 784-5 (Mar. 14, 1966). (In French).

The variation of the β emission with the atomic number of the acceptor conductor is due to the selective effect of the backscattering of β particles. (tr-auth)

29325 BEHAVIOR OF RECOIL ATOMS IN THE DECAY OF ^{219}Rn AND ^{220}Rn IN GASES. Schwarz, E.; Denschlag, H. O.; Hermann, G. (Univ., Mainz). Radiochim. Acta, 5: 53-4(Mar. 1966). (In German).

It was previously recorded that in the decay of ^{222}Rn in methane volatile ^{212}Pb compounds are formed and up to 38% of the lead remains in the gaseous state. Additional studies were made with ^{220}Rn and ^{219}Rn in methane, hydrogen, and nitrogen. The results showed that less than 1% of the lead formed remained in the gaseous state. The distribution of the ^{219}Rn daughter products in an electric field were also investigated. The results are tabulated. (J.S.R.)

29326 STRUCTURE ELUCIDATION AND IDENTIFICATION OF ORGANIC SUBSTANCES BY "ELECTRON BURNING." PART II. "ELECTRON BURNING" OF MENTHOL. Schildknecht, H.; Penzien, K. (Univ., Heidelberg). Z. Anal. Chem., 219: 102-21(1966). (In German).

The behavior of menthol during "electron burning" was studied and it was found that this method is also useful in the elucidation of the structure of terpenoids. In addition to the loss of the isopropyl group a fragmentation product, 2,5-dimethylcyclohexanol, and a ring-cleavage product, 2,6-dimethyloctanal-8, were also observed. For elucidation of the mechanism of "electron burning," it was important to know that isomerization with formation of the isomers of the most stable configuration is possible. "Electron burning" and mass spectrometry of methol were compared. In both cases primary radicals are formed. With "electron burning" these radicals react intermolecularly with the H(T) atoms, the OH(OT) radicals, and the tritium-water, in mass spectrometry they are stabilized by intramolecular fragmentation. (auth)

29327 USE OF β DECAY OF BROMINE ISOTOPES AS A POSSIBLE METHOD FOR SYNTHESIS OF KRYPTON COMPOUNDS. Murin, A. N.; Nefedov, V. D.; Kirin, I. S.; Grachev, S. A.; Gusev, Yu. K.; Shapkin, G. N. Zh. Obshch. Khim., 35: 2137-40(1965). (In Russian).

The possibility of using the chemical changes occurring during the β decay of bromine isotopes for synthesis of the fluorides and oxides of krypton is suggested. A method for the analysis of krypton compounds is proposed. (tr-auth)

Separation Processes and Procedures

See also Analytical Procedures
ISOTOPE TECHNOLOGY — Separation and Production

29328 (ANL–7066) REMOVAL OF PLUTONIUM HEXAFLUORIDE FROM CELL EXHAUST AIR BY HYDROLYSIS AND FILTRATION. Kessie, R. W.; Ramaswami, D. (Argonne National Lab., Ill.). Dec. 1965. Contract W-31-109-eng-38. 70p. Dep. mn. CFSTI $3.00 cy, $0.75 mn.

The fluoride volatility process for recovering fissionable plutonium from spent reactor fuel as the volatile plutonium hexafluoride (PuF_6) requires a demonstrated ability to contain the highly toxic plutonium. Experimental studies indicated that at low concentrations of PuF_6 and moisture, the hydrolysis reaction rate is directly proportional to both the partial pressure of the PuF_6 and moisture and to the area of the solid surfaces available for reaction. Adsorbed PuF_6 and HF reduce the reaction rate at partial pressures greater than 0.001 mm Hg. At high concentrations of PuF_6 and moisture, the reaction proceeds rapidly in the gas phase to produce a finely dispersed product PuO_2F_2. Most of the particles are smaller than 0.1 micron. With air containing excess moisture, the fraction of released plutonium penetrating two high-efficiency filters in series amounted to between 10^{-9} and 10^{-6} at a filter-media velocity of 1.0 cm/sec. Filter efficiency was increased by the agglomeration of particles before filtration and by loading effects of the collected particles on the filters. When an excess of moisture is available, agglomeration effects tend to limit the maximum discharge rate of plutonium, and loading effects tend to limit the maximum total quantity of plutonium that can be discharged from a single filter. Design criteria of practical air clean-up systems are presented. (auth)

29329 (ANL–7128) DESIGN AND OPERATION OF A PILOT-PLANT GETTERING SYSTEM OF TITANIUM-METAL SPONGE FOR REMOVAL OF NITROGEN FROM ARGON. Kyle, M. L.; Arntzen, J. D.; Coleman, L. F. (Argonne National Lab., Ill.). Jan. 1966. Contract W-31-109-eng-38. 41p. Dep. mn. CFSTI $2.00 cy, $0.50 mn.

A pilot-plant scale unit designed to demonstrate the removal of low concentrations (less than 1%) of nitrogen from large, relatively pure volumes of inert gases was constructed and operated. The system utilized titanium-metal sponge at a temperature of 900°C as the gettering agent for removal of the nitrogen impurity. Gas preheaters and regenerative heat exchangers were used to obtain better utilization of the titanium sponge and to provide heat economy. The pilot-plant unit operated at a flow rate of 10 cfm of argon containing 100 to 1000 ppM nitrogen for a period of about 1800 hr. Operation of the system was terminated because of the deterioration of the shaft seals on the gas-circulating blower. This deterioration is believed to be the result of prolonged exposure of these seals to a low-water, low-oxygen-concentration atmosphere. During the 1800 hr of system operation, all equipment items except the blower performed their design functions well. The pilot-plant unit successfully demonstrated the usefulness and relative economy of titanium-metal sponge as a gettering agent for nitrogen impurity in argon. The performance of the equipment is assessed, and recommendations for design of large, inert-gas purification systems are presented. (auth)

29330 (EURAEC–1601) REPROCESSING OF IRRADIATED FUELS. Quarterly Report No. 22, July 1–September 30, 1965. (Centre d'Etude de l'Energie Nucleaire, Mol (Belgium)). Contract 00-65-7RCIB(RD). 29p. (EUR–2819). Dep. mn. CFSTI $2.00 cy, $0.50 mn.

Work Performed under United States–Euratom Joint Research and Development Program.

Studies were made on the use of chlorine trifluoride, at low temperature, as a fluorinating agent for the production of uranium hexafluoride. In this case the plutonium remains in the residue and is transformed into a hexafluoride by fluorine at around 550°C. Particular attention was paid to direct attack on compact UO_2. Thermogravimetric studies revealed the existence of a solid reaction intermediary, probably on oxyfluoride or complex fluoride of uranium. The same research also showed that at 100°C the compact UO_2 structure may give rise to an induction period; this was longest for monocrystalline UO_2. The direct attack tests on compact UO_2 in a fluid bed were concerned with studying the influence of the presence of alumina and fissium on the reaction rate. These additives generally cause the rate to fall, especially at 100°C. The various observations made led to the conclusion that the very high transformation capacities expected from the chlorine trifluoride cycle will be affected by the high burnup ratios and the presence of alumina; however, these effects do not seem liable to limit the practical application of the process. The behavior of various fission products during direct attack on UO_2 with ClF_3 was examined on a tracer scale. The elimination of Ru, Nb, Te, Np, and probably Tc as well, at the same time as the elimination of uranium, was a function of the reaction temperature. Normal progress is reported on plutonium volatilization, decladding, chemical attack on uranium carbide, conversion of plutonium fluoride into an oxide in a molten salts medium, detection of traces of fluorinating agents, and the chemical resistance of the ventilation filters. (auth)

29331 (KAPL-M–6554) A PROCEDURE FOR THE QUANTITATIVE RECOVERY OF ^{233}Pa FROM IRRADIATED THORIA. Stricos, D. P. (Knolls Atomic Power Lab., Schenectady, N. Y.). Apr. 13, 1966. Contract W-31-109-eng-52. 14p. Dep. mn. CFSTI $1.00 cy, $0.50 mn.

A procedure is presented for the dissolution of irradiated thoria, quantitative separation of the Pa-233 formed in the irradiation, and gamma counting of the isolated protactinium. Samples were dissolved by heating in 12M HCl–0.04M HF under reflux. Fifteen gram samples were solubilized in about one day; fifty gram samples required about one week. Protactinium was isolated by an anion exchange technique using Dowex 1 × 8 resin. The separated Pa-233 was then gamma counted in polyethylene counting bottles. The recovery of Pa-233 was greater than ninety-eight per cent as was demonstrated with synthetic samples. (auth)

29332 (ORNL-P-1811) DEVELOPMENT AND APPLICATIONS OF MINERALS IN RADIOACTIVE WASTE DISPOSAL. Tamura, Tsuneo (Oak Ridge National Lab., Tenn.). [1966]. Contract W-7405-eng-26. 35p. (CONF-660601-2). Dep. mn. CFSTI $2.00 cy, $0.50 mn.

From International Clay Conference, Jerusalem, Israel.

The use of clay minerals and allied materials in radioactive waste disposal is considered. The rationale behind the development of these applications and the implications of the experimental results in understanding reactions of radiocesium and radiostrontium in ground disposal operations are also discussed. Radiocesium-clay mineral reactions are treated in great detail. The data support the hypothesis that clay mineral structure is the dominant factor in radiocesium sorption from radioactive waste solutions. Information on the sesquioxides, common constituents in soil and clay mineral systems, is also included because they complicate the absorption behavior of radionuclides in soils. (P.C.H.)

29333 (RT-CHI–(65)33) STUDI SULLA FILTRABILITA E SUI TEMPI DI COALESCENZA DI SOLUZIONI DI ANN–HNO_3–Hg^{+2}–SiO_2 COLLOIDALE IN PRESENZA DELLE FASI ORGANICHE TCAN–SOLVESSO 100 E TBP–SHELLSOL T. (Studies on Filterability and Coalescence Time of Colloidal Solutions of ANN–HNO_3–Hg^{2+}–SiO_2 in Presence of Organic Phases TCAN–Solvesso 100 and TBP–Shellsol T). Beone, G.; Moccia, A. (Comitato Nazionale per l'Energia Nucleare, Rome (Italy)). Sept. 1965. 27p. Dep. mn.

The results of the clarification of acid or acid-deficient solutions with low uranium concentration, containing colloidal silicon dioxide, are described together with the results of tests on the coalescence time of the organic phases TCAN–Solvesso 100 and TBP-Shellsol T. The variation of coalescence time and of the type of interface following irradiation of the organic phase and the aging of the aqueous solution are also described. Gelatin (100 ppM at 80°C), followed by centrifuging, was used to coagulate the silica in the acid solutions, while in the acid-deficient solutions the silica was separable per se by centrifuging. (tr-auth)

29334 THE SYNERGISTIC EFFECT ON THE EXTRACTION OF $^{233}U(VI)$ BY DI-BUTYLPHOSPHATE (DBP) AND TRI-BUTYLPHOSPHATE (TBP) OR TRI-OCTYL PHOSPHINEOXIDE (TOPO). Liem, Djiet Hay; Dyrssen, David (Royal Inst. of Tech., Stockholm). Acta Chem. Scand., 20: 272-4(1966).

The extraction of carrier-free $^{233}U(VI)$ from aqueous 0.10M H_2SO_4 solutions at 25°C into hexane or carbon tetrachloride by dibutyl phosphate in the presence of tributyl phosphate or trioctylphosphine oxide is reported. Results indicated that the synergistic effect in the systems may be described, in some cases, as an addition reaction and in other cases as a substitution reaction. (M.C.G.)

29335 CHEMISTRY OF PROTACTINIUM. I. THE PREPARATION OF ^{233}Pa AND THE PURIFICATION OF ^{231}Pa. Suzuki, Shin; Inoue, Yasushi (Tohoku Univ., Sendai). Bull. Chem. Soc. Jap., 39: 490-7(Mar. 1966).

Many methods, such as the co-precipitation method, the solvent-extraction method, and the ion-exchange method, were previously proposed for the separation and the purification of protactinium. However, these methods have some defects for the separation of ^{233}Pa produced by the thermal neutron irradiation of thorium dioxide and the purification of commercial ^{231}Pa, when an attempt is made to study the chemistry of protactinium. A combined method of solvent extraction and anion exchange was investigated. The conditions for TBP extraction of protactinium from a hydrochloric acid solution and the method for its final purification by anion exchange are described. (auth)

29336 SEPARATION OF ^{90}Sr AND ^{90}Y BY PAPER ELECTROPHORESIS WITH VERY DILUTE HYDROCHLORIC ACID BACKGROUND ELECTROLYTE. Kawamura, Shoichi; Izawa, Masami (National Inst. of Radiological Sciences, Chiba, Japan). Bull. Chem. Soc. Jap., 39: 624-5(Mar. 1966).

The successful use of 10^{-3}N HCl as the background electrolyte for the separation of ^{90}Sr and ^{90}Y by paper electrophoresis is reported. The R_D value of ^{90}Y in 10^{-3}N HCl is 0, while ^{90}Sr migrates to the cathode. The migration distance of ^{90}Sr in a free solution was calculated to be 22 cm. (M.C.G.)

29337 SEPARATION OF AMERICIUM AND CURIUM BY EXTRACTION CHROMATOGRAPHY USING A HIGH-MOLECULAR-WEIGHT QUATERNARY AMMONIUM NITRATE. Horwitz, E. P.; Orlandini, K. A.; Bloomquist, C. A. A. (Argonne National Lab., Ill.). Inorg. Nucl. Chem. Lett., 2: 87-91(Apr. 1966).

A rapid method for separating Am(III) from Cm(III) by extraction chromatography using a quaternary ammonium nitrate (aliquat-336 nitrate) is described. The activities of eluate fractions were determined by standard scintillation counting techniques. Approximately 2 hr were required for a complete separation and recovery. Greater than 99% of the Cm and Am were recovered in a radiochemically pure state. (M.C.G.)

29338 RADIOCHEMICAL SEPARATION OF ^{18}F FROM REACTOR IRRADIATED GOLD AND URANIUM. Wilkniss, P.; Born, H. J. (Technische Hochschule, Munich). Int. J. Appl. Radiat. Isotop., 17: 304-6(May 1966). (In German).

Methods for the separation of ^{18}F from reactor-irradiated gold and uranium are described. The methods are based on distillation of the fluorine, but preliminary processing to reduce the contamination of the fluorine with other elements is necessary. (J.S.R.)

29339 THE EXTRACTION OF URANIUM(VI) FROM HYDROCHLORIC ACID SOLUTIONS BY TRI-N-OCTYLAMINE. Sato, Taichi (Shizuoka Univ., Hamamatsu, Japan). J. Inorg. Nucl. Chem., 28: 1461-7(June 1966).

The partition of uranium(VI) between hydrochloric acid solutions and solutions of tri-n-octylamine (TOA) in organic solvents was investigated under different conditions, and infrared studies were made of the organic phase. (auth)

29340 SORPTION OF CERTAIN TRANSPLUTONIUM IONS ON AMORPHOUS ZIRCONIUM PHOSPHATE. Horwitz, E. P. (Argonne National Lab., Ill.). J. Inorg. Nucl. Chem., 28: 1469-78(June 1966).

The sorption of tracer concentrations of Am(III), Cm(III), Bk(IV), and Cf(III) on amorphous zirconium phosphate with a PO_4/Zr mole ratio of 1.34 was investigated. Tracer Ce(III), Eu(III), and U(VI) were also included in the study. The distribution coefficients were investigated at 75°C as a function of time and nitric acid concentration. Small separation factors were found for ions with the same charge; large separation factors were found for Bk(IV)/Cm(III), and U(IV)/Am(III). The phosphate hydrolysis of amorphous zirconium phosphates with varying PO_4/Zr mole ratios was studied between 1 and 10^{-3}M nitric acid concentrations at 75°C. Spectrophotometric and neutron activation analysis techniques were used to detect small concentrations of phosphate ion. (auth)

29341 THE GAMMA IRRADIATION FACILITY OF THE FRANKFURT RESEARCH REACTOR. Egelhofer, J. A.; Pluntke, A.; Wensel, A. (Johann-Wolfgang-Goethe-Univ., Frankfurt am Main). Kerntechnik, 8: 210-12(May 1966). (In German).

A pneumatic system for sample irradiation with gamma rays from the Frankfurt research reactor recombiner is described. Only materials that are not radiation sensitive were used. The radiation dose rate is determined by means of an ionization chamber at the same distance from the recombiner as the irradiation capsule. (auth)

29342 SEPARATION OF TRACES OF MANGANESE AND COBALT FROM IRON. Muzzarelli, R. A. A. (Univ. of Sherbrooke, Quebec). Microchem. J., 11: 223-8(June 1966).

Traces of manganese and cobalt compounds were separated from iron by paper chromatography using ethyl ether. Tracer studies were made of the efficiency of the method. Iron could be easily collected by prolonging the chromatography and allowing the solvent front to proceed past the extremity of the strip and drop into a collector. Manganese and cobalt remained adsorbed on a very small area of paper and could be recovered by elution using NH_4SCN or by destruction of the small amount of cellulose. (M.C.G.)

29343 PAPER ELECTROPHORESIS OF COMPLEXES OF RARE EARTHS WITH HYDROXYAMINO ACIDS. Jokl, V.; Majer, J.; Scharf, H.; Kroll, H. (Komensky Univ., Bratislava). Mikrochim. Acta, No. 1-2, 63-76(1966). (In German).

The rare earths form 1 : 1 and 1 : 2 chelates with N,N-bis-(2-hydroxyethyl)glycine(BHG) and with N-2-hydroxyethyl-iminodiacetic acid (HIDA). Their composition and approximate stabilities were determined by a paper electrophoretic method. HIDA-complexes of the rare earths appeared to be very useful for their electrophoretic separation. In a 0.05 molar (about 1%) solution of HIDA with a pH of 2 to 2.5, it is possible to separate completely the light rare earths Sc–Y–La–Ce–Pr–Nd–Sm–Eu–Gd–Tb. The reasons for a perfect separation of Pm from Nd and Sm are given too. In the group of the erbium earths, it is possible to separate Dy(Ho)–Er–Tm, but the separation Dy–Ho and Tm–Yb–Lu fails. The approximate stability constants of the mentioned complexes and the electrophoretic separation factors are given. (auth)

29344 USE OF SILICA GEL IN INORGANIC ANALYSES. SEPARATION OF THORIUM FROM ZIRCONIUM. Dolezal,

J.; Petrekova, J.; Sulcek, Z. (Charles Univ., Prague. Zentralinstitut fuer Geologie, Prague). Mikrochim. Acta, No. 1-2, 248-56(1966). (In German).

The sorption of thorium and zirconium on silica gel from EDTA and tartaric acid was followed. At pH 7 and in the presence of tartaric acid, the zirconium passes through the silica gel column, whereas Th(IV) is sorbed quantitatively. This finding was employed for the separation of thorium from zirconium in a concentration ratio of 1:200. Because Zr(IV) is quantitatively sorbed from 0.5N HCl, while the sorption of Th(IV) is practically zero from this medium, Zr(IV) can be separated from a considerable excess of Th(IV) in this way. The separation is still quantitative at a ratio of 1:1000. (auth)

29345 CONCENTRATION OF RADIONUCLIDES IN SEA WATER BY METAL SULFIDE-ION EXCHANGE RESINS. Watari, Kazuo (National Inst. of Radiological Sciences, Japan); Tsubota, Hiroyuki; Koyanagi, Taku; Izawa, Masami. Nippon Genshiryoku Gakkaishi, 8: 182-5(Apr. 1966). (In Japanese).

Radionuclides present in sea water were concentrated by metal sulfide-ion exchange resins. The resins were prepared by converting a cation exchange resin of hydrogen form to a certain metal form, the metal sulfides being made up by adding thioacetamide, hydrogen sulfide, or ammonium sulfide. Alternatively, an anion exchange resin of sulfur form was used to make metal sulfide-anion exchange resin. The prepared resins have the same properties as metal sulfides (color, chemical stability, etc.) and as ion exchange resins. Experiments were carried out by batch method, 50 ml of sea water containing radionuclides being shaken with 0.5 g of air-dried resin. ^{144}Ce, ^{95}Zr, A and ^{106}Ru were adsorbed quantitatively on both resins. ^{85}Sr and ^{137}Cs were adsorbed with the metal sulfide-cation exchange resin to about 35 and 15%, respectively, but were not adsorbed with the metal sulfide-anion exchange resin. The resins could be used for concentrating radionuclides in natural waters and in any solution even acidic solution, because of the high stability of the resin. (auth)

29346 SURFACE CONCENTRATION CHANGES DURING DISTILLATION OF LIQUID METALS. Walsh, W. J.; Burnet, George. Nucl. Sci. Eng., 25: 227-35(July 1966). (IS-1047).

To learn more about liquid metal distillation as it might be applied to nuclear fuel recovery and reprocessing, liquid metal distillations involving the tin-zinc, cadmium-bismuth, and indium-zinc binary systems were conducted in an evacuated chamber. An x ray fluorescence spectrometer provided a continuous chemical analysis of the distilling surface during each run. This information was used to evaluate the validity of various theories and assumptions concerning surface depletion, oxide contamination, and turbulence effects. The existence of a large surface depletion effect in nonturbulent metal distillations was proven. However, the level of turbulence necessary to eliminate concentration gradients was found to be much lower than that assumed by some designers of commercial equipment. The presence of surface oxides was often an important factor in determining the enrichment and rate of distillation. The Langmuir-Knudsen theory was shown to be unreliable when liquid diffusion or surface oxide resistances were significant. A more complete approach involving the principles of transport phenomena was developed. An analytical solution was derived for the nonturbulent case and was tested using the spectrometer data. (auth)

29347 EFFECTS OF STRUCTURE AND SUBSTITUENT GROUP ELECTRONEGATIVITY ON THE EXTRACTION PROPERTIES OF ORGANIC COMPOUNDS. II. EFFECT OF THE ELECTRONEGATIVE GROUP. Rozen, A. N.; Nikolotova, Z. I.; Petrov, K. A.; Skotnikov, A. S.; Teterin, E. G. Radiokhimiya, 7: 517-33(1965). (In Russian).

The extraction of uranyl nitrate and nitric acid with phosphates containing electronegative groups (C_6H_5, $ClCH_2$, $ClCH_2CH_2$, and CCl_3) in the series TBP–TOPO was studied at three temperatures. The extraction decreased more strongly as the chlorine atoms increased and when the chlorine atoms were located on the phosphate atoms. The infrared spectra of the compounds and their solvate with uranyl nitrate were measured. The scale of electronegativity of the electronegative groups found was made more precise. It is shown that removal of the chlorine from the phosphate atoms of the electronegative group decreases in accordance with theory in a geometric progression. The effective electronegativity of the groups was calculated. It was confirmed that the relation of the excess effective electronegativity of electronegative radicals $\Delta X_{eff} = X_{eff} - X_a$ to excess spectral electronegativity $\Delta X = X - X_a$ (X_a is the electronegativity of exchangeable alkyl radicals) is approximately constant for all the compounds studied and approaches 2. It is shown that the effective electronegativity, found in the extraction of the uranyl nitrate, also well describes extractive capacity with respect to nitric acid. For 2 compounds containing C_6C_5, $ClCH_2$, and $ClCH_2CH_2$, the thermal effects showed, in general (with alkyl compounds of TBP–TOPO series), a dependence on the electronegativity sum without introduction of the effective electronegativity. The divergence of the effective electronegativity from the spectral electronegativity for these compounds was indicated by means of entropy factors. Some aspects of the dependence of the selectivity of the extraction on the structure of the extractant are discussed. It is shown that the Gammet-Taft equation can be determined from equations containing electronegativity. The later can be also be used for description of the reacting capacities of organic compounds. (tr-auth)

29348 DECONTAMINATION OF WATERS CONTAINING ^{90}Sr AND ^{90}Y WITH GYPSUM AND BENTONITES. Galea, V.; Birsan, E. T.; Uray, Ildiko (Medical-Pharmaceutical Inst., Cluj. Inst. of Hygiene and Labor Safety, Cluj). Rev. Chim. (Bucharest), 16: 318-20(July 1965).

The decontaminating capacities of raw gypsum, commercial superphosphate, and some Rumanian bentonites are reported. The tests also considered the quantity of decontaminating agent, various proportions in mixtures of the substances, the presence of salts often found in surface waters, and the pH. Best results were obtained with raw gypsum, especially for fluoridated water; bentonites were found to be most effective as mixtures of two types. (JPRS)

29349 SEPARATION OF ^{90}Sr AND ^{90}Y IN THE PRESENCE OF CALCIUM BY PAPER CHROMATOGRAPHY. Baez, Juan N.; Nussis, Nicolas; Farias, Nestor. Rev. Fac. Ing. Quim., Univ. Nac. Litoral, Santa Fe, Arg., 32: 211-19(1963). (In Spanish).

The influence of calcium on the mobility of yttrium when ^{90}Sr is separated from ^{90}Y by paper chromatography was studied. An isopropyl alcohol–pyridine–acetic acid–water solvent was used with volumetric proportions of 8:8:1:4 and several series of tests were performed with different types of paper. The system did not permit the separation of ^{90}Sr from ^{90}Y when carrier was absent. The separation was possible if yttrium carrier or appropriate quantities of calcium were added. The presence of increasing quantities of calcium in the samples to be separated, produced an increase of the R_f value for yttrium without affecting the corresponding value for strontium, thus making it possible to separate ^{90}Y from ^{90}Sr without using yttrium carrier. In the presence of isotopic carriers of both nuclides, the method allows efficient separation of ^{90}Sr and ^{90}Y; in this case the addition of variable quantities of calcium, up to 20 times higher than that of the strontium present, does not produce noticeable variations in the values of R_f for strontium and yttrium. (auth)

29350 INFLUENCE OF CERTAIN IONS ON THE ADSORPTION OF URANIUM BY ION EXCHANGE RESINS. Tataru, Sever. Rev. Roum. Chim., 10: 1143-9(Nov. 1965) (In French).

The effects of the anions CO_3^{2-}, Cl^-, and SO_4^{2-} on the adsorption of uranium by the strong-base-type ion exchange resin AV-17 were examined under dynamic conditions. The presence of these anions in alkaline solutions of uranyl carbonate caused a decrease of the adsorption capacity for

uranium both with respect to the adsorption of these anions on the resin and to the partial elution of the uranium adsorption. The exchange capacities were determined up to the "leak." In the case of a resin having the OH^- form initially, the decrease of the capacity could also be caused by the increase in pH during adsorption since the uranium is precipitated under these conditions as the uranate, which is not adsorbed by the resin. (tr-auth)

29351 STUDIES ON FOCUSING CHROMATOGRAPHY SEPARATION OF ^{239}Np FROM NEUTRON-IRRADIATED URANIUM. Oyoshi, Akira; Oyoshi, Emiko; Shinagawa, Mutsuaki. Technol. Rep. Osaka Univ., No. 16, 343-56 (Oct. 1965).

Neptunium-239 was separated by means of focusing chromatography from uranyl salt irradiated by slow neutrons. On the basis of these data the electrophoretic property of the element was investigated. The three typical modes of focusing to form neptunium bands were observed; i.e., the first migrated toward the anode as a complex anion, the second remained at the area where the sample was spotted and the last migrated toward the cathode as a cation. The band of cationic neptunium showed the highest purity of almost 100% among bands of the three kinds. (auth)

29352 SORPTION AND SEPARATION OF ZIRCONIUM AND HAFNIUM ON NATIVE ANIONITES. Vinarov, I. V.; Shulgina, N. S. (Inst. of General and Inorganic Chemistry, Academy of Sciences, Ukrainian SSR). Ukr. Khim. Zh., 31: 1219-22(1965). (In Russian).

The conditions for sorption of zirconium and hafnium on the native anionites AN-2F, EDE-10P, AD-16, and AD-17 were investigated. The most complete sorption, up to 100%, took place in dilute hydrochloric solutions on the weakly basic anionites AN-2F and EDE-10P in the OH^- form. Selective sorption of zirconium occurred with the use of the weakly basic resin AV-16. The concentration of HfO_2 in $(Zr,Hf)O_2$ in equilibrium hydrochloric solutions was almost doubled, from 29 to 54.5%, and the Hf yield was 55 to 60%. During the sorption from hydrofluoric solution and subsequent dilution with different salts or sulfuric acid, enriched concentrations of Hf were obtained from the eluent. The most effective elution agent was 1N sulfuric acid using the AD-16 resin with the mean enrichment of the concentration attaining 50% during direct Hf yields of 69%. The possibility of the partial separation of Zr and Hf on anionites of native manufacture, particularly the basic resin AV-16, was investigated and the conditions for the separation were studied. (tr-auth)

29353 ELIMINATION OF BOTH PHOSPHORUS ISOTOPES ^{31}P AND ^{32}P FROM DOMESTIC WASTE WATER. Haltrich, Walter. Wasser, Luft Betrieb, 9: 798-9(1965). (In German).

Radioactive ^{32}P can be eliminated from waste water with the help of activated sludge methods in certain ranges. Active purification processes increase the elimination. Activated sludges serve as oxygen-deficient phosphates for the sludge liquor. Results of investigations are summarized. (TCO)

29354 RELATION BETWEEN THE CHEMICAL STRUCTURE OF ALKYL DIBUTYL PHOSPHONATES AND THE CHARACTERISTICS OF URANIUM AND THORIUM EXTRACTION. Shih, Li-lan; Chang, Tseng-jui; Yuan, Ch'eng-yeh. Yuan Tzu Neng, No. 3, 239-44(1965).

The distribution coefficients and the degree of separation during extraction of uranium and thorium by alkyl dibutyl phosphonates having the same number of carbon atoms but different structures were studied. The relation between the alkyl group structure and the extraction characteristics, as well as the effect of the solvent, were also investigated with the infrared spectrum taken into consideration. It is pointed out that the effectiveness of extracting uranium and thorium by alkyl dibutyl phosphonates is determined chiefly by the charge density on the acyloxy phosphorus atom, but that the effect of steric hindrance should not be neglected. Based on the distribution coefficients during uranium and thorium extraction, the most effective extracting agent can be selected. It was also found, from a study of the infrared spectra of alkyl dibutyl phosphonates combined with uranyl nitrate or thorium nitrate, that the binding of metals is due to the acyloxy phosphorus atoms, and has nothing to do with the methoxy group. The characteristic frequency of the phosphorous-oxygen bond in the infrared spectrum does not change significantly when the alkyl phosphonate is transferred from an inert solvent to an alkaline solvent, but does change in an acid solvent. The use of chloroacetophenone as a solvent had a greater effect on the dipole moment of the phosphorus-oxygen bond of the phosphonate than on that of the carbon-oxygen bond. (ATD)

29355 CHROMATOGRAPHIC ANALYSIS AND LIQUID-LIQUID EXTRACTION. Ts'ai, Ch'i-hsiu; Chou, Hsing-ch'uar; Yuan, Ch'eng-yeh. Yuan Tzu Neng, No. 4, 334-41 (1965).

The relation between chromatographic separation and liquid-liquid extraction, as well as variations in the R_f value of uranium due to different factors were studied. TBP, DBBP, BDBP, and TBPO complexes were used as the fixed phase; nitric acid as the developing agent; and ethane, n-butyl acetate, and chloroform as the solvents. The R_f values of uranium decreased in the order TBP > DBBP > BDBP > TBPO, which agreed with the corresponding increase in extraction coefficient E_a^0 when the same complex was used as the extraction liquid. When TBP and DBPP were used, E_a^0 and $(1/R_f - 1)$ were linearly proportional at a given nitric acid concentration. By using 0.01, 0.05, 0.1, 0.25, and 0.5M solutions of the complexes, the log plots of E_a^0 and $(1/R_f - 1)$ could be linearly related with a slope close to 1. The HNO_3 concentration also affected the R_f value, but the minimum value of R_f did not correspond to the maximum value of E_a^0. When TBP and DBBP were used, the R_f value increased with temperature but the opposite result was obtained when BDBP and TBPO complexes were used; the $(1/R_f - 1)$ versus 1/T relation was linear. The solvent had little effect on the R_f value; this was different from the liquid-liquid extraction method, in which the solvent affected the E_a^0 significantly. (ATD)

29356 USE OF HIGH-VOLTAGE ELECTROPHORESIS FOR THE SEPARATION OF RADIONUCLIDES. Baechmann, K. (Technische Hochschule, Darmstadt, Ger.). Z. Anal. Chem., 218: 321-38(1966). (In German).

The separation of alkali, alkaline earth, and rare earth elements, actinides and some other elements by high-voltage electrophoresis is discussed. These examples are the basis of general considerations on the optimum conditions for electrophoretic separations. (auth)

29357 SEPARATION SCHEME FOR ISOLATION OF Pu, Np, Zr, Nb, Mo, Tc, Te, AND U FROM FISSION-PRODUCT SOLUTIONS. Markl, Ilse; Bobleter, O. (Oesterreichische Hochschule, Vienna. Univ., Vienna). Z. Anal. Chem., 219: 160-73(1966). (In German).

A procedure was developed and proved to be quantitative for the total separation of Zr, Nb, Mo, and Tc by anion exchange in hydrochloric acid solutions using known single separations of Zr, Nb; Zr, Mo; and Mo, Tc. Utilizing hydrochloric acid solutions containing alcohol as eluents, a method for the separation of Zr, Nb, Mo, Tc, and U was developed. Highly concentrated hydrochloric acid solutions of these elements are added to the resin column and eluted sequentially with mixed solvents of decreasing over-all acidity. Tc is not desorbed with hydrochloric acid or mixtures of hydrochloric acid and alcohol; it is removed from the column with nitric acid. Investigations indicated that the separation of Zr, Nb, Mo, Tc, U, and Te is possible. Experiments to include Np in the sequential separation scheme developed, did not yield satisfying results because of the similarity of the elution curves of Zr(IV) and Np(V). The eluted Zr was contaminated with Np and required further purification. Based on measurement of the distribution coefficients of Np(V) in hydrochloric acid solutions, which show a maximum of adsorption at low concentrations of hydrochloric acid a method for the separation of Zr from Np was developed. The elements in 1.3M HCl solutions were added to the resin column; Zr was not absorbed. The elution was continued with 1.3M HCl solution

to remove Np, which was eluted only with larger volumes of this acid. Since Pu can be removed from the resin column with highly concentrated hydrochloric acid solutions prior to the other elements, the sequential separation scheme makes possible the isolation of Pu, Np, Zr, Nb, Mo, Tc, Te, and U from fission product mixtures. (auth)

29358 ADSORPTION OF NEPTUNIUM(V) ON ANION EXCHANGERS FROM AQUEOUS AND ALCOHOL-CONTAINING HCl SOLUTIONS OF DIFFERENT MOLARITY. Markl, Ilse; Bobleter, O. (Oesterreichische Hochschule, Vienna. Univ., Vienna). Z. Anal. Chem., 219: 173-7 (1966). (In German).

Lewatit M 500 anion exchange equilibrium studies on Np^{5+} in hydrochloric acid solutions (acid concentrations ranging from 0.1M to concentrated HCl solution) showed strong adsorption from 9 to 12M HCl solution and a small maximum of the distribution coefficient at low concentrations of hydrochloric acid. Investigations of the anion exchange behavior of Np^{5+} in hydrochloric acid solutions containing 50, 65, and 80 vol % of ethanol showed a maximum of adsorption at low concentrations of hydrochloric acid. The extent of adsorption increased with increasing percentage of alcohol in the mixtures. (auth)

29359 SOLVENT EXTRACTION OF PRODUCTS OF URANYL NITRATE HYDROLYSIS BY α-n-AMYLPYRIDINE-N-OXIDE. Mikhailov, V. A.; Torgov, V. G. (Inst. of Inorganic Chemistry, Academy of Sciences, Siberian SSR). Zh. Neorg. Khim., 10: 2780-6(Dec. 1965). (In Russian).

It is shown that α-alkylpyridine-n-oxides, and particularly α-n-amylpyridine-N-oxide, in contrast to tributyl phosphate, extracts into the organic phase products from the hydrolysis of uranyl nitrate. The hydroxy form extracted seems to dissolve nitrouranic acid of the composition $UO_2(OH)NO_3 \cdot 2P_YO_X$. The equilibrium constants of this process were evaluated. (tr-auth)

29360 EFFECTS OF POROUS STRUCTURE OF LIGNIN CARBONS ON URANIUM SORPTION. Kuzin, I. A.; Plachenov, T. G.; Aleksandrova, N. S.; Taushkanov, V. P. (Leningrad Technological Inst.). Zh. Prikl. Khim., 38: 2026-30(Sept. 1965). (In Russian).

Investigations of the effect of the porous structure of lignin carbon on its sorptive capacity for acids and uranium from acetate solutions, ammonium rhodanide, and oxalic acid showed that the capacity of the lignin carbon is determined basically by the size of the surface pores with radii of 5.8 to 30 Å. (tr-auth)

29361 EXTRACTION OF URANIUM AND CERTAIN ASSOCIATED ELEMENTS WITH DI-2-ETHYLHEXYLPYROPHOSPHORIC ACID (D2EHPPA). Laskorin, B. N.; Smirnov, V. F. Zh. Prikl. Khim., 38: 2439-43(Nov. 1965). (In Russian).

An investigation was made of the effect of the molecular weight of alkylpyrophosphate, its concentration in the organic phase, and the concentrations of the element being extracted and of phosphoric acid in the liquid phase on the value of the distribution coefficient for uranium, thorium, iron, and aluminum between their phosphoric acid solutions and a solution of di-2-ethylhexylpyrophosphoric acid in n-hexane. The reextraction of uranium and thorium from the organic phase are considered. The dependence of extraction of uranium (VI) by alkylpyrophosphoric acid on the number of atoms in the alcohol is shown. The extraction was carried out in a 0.1 molar solution of alkylpyrophosphate in n-hexane. It is shown that with an increase in the number of oxygen atoms in the alkyl radical the degree of uranium extraction in the organic phase somewhat decreases, which is evidently connected with the coextraction of the hydroxyl group. With a change in the molar ratio (alcohol to phosphoric anhydride) the extraction of uranium (VI) at first increased, attained a maximum at 1.0 to 1.4, and then fell. To investigate the effect of the concentration of di-2-ethylhexylpyrophosphoric acid on the extraction of uranium (VI), a 5M solution of phosphoric acid containing 0.47 g/liter uranium (VI) and a solution of di-2-ethylhexylpyrophosphoric acid in n-hexane was used. Results indicated that with an increase in the initial concentration of di-2-ethylhexylpyrophosphoric acid in the organic phase, the magnitude of the distribution coefficient increased. Results of experiments on the effect of the concentration of phosphoric acid in the liquid phase on the extraction of uranium (VI), uranium (IV), thorium (IV), iron (III), and iron (II) by a 0.05 molar solution of di-2-ethylhexylpyrophosphoric acid in n-hexane are shown. Equations connecting the magnitude of the distribution coefficient of uranium (VI) and thorium (IV) with the concentration of di-2-ethylhexylpyrophosphoric acid in the organic phase and the concentration of phosphoric acid in the liquid phase are included. (ATD)

29362 FUNDAMENTALS OF THE SEPARATION OF A MIXTURE OF HYDROGEN AND CARBON DIOXIDE BY GASEOUS DIFFUSION [Thesis]. Primrose, Russell Adrian. Blacksburg, Va., Virginia Polytechnic Inst., 1965. 184p.

A gaseous diffusion column was designed, constructed, and its operation tested with a system of electrolytic hydrogen and carbon dioxide. The column contained one diffusion unit with two 6-inch-diameter barrier areas. The flow rates of the hydrogen-carbon dioxide mixture were varied from 0 to 15 cubic feet per hour. Vacuum on the system was varied from 0 to 25 inches of mercury. Composition of the feed mixture was held constant at 50 mol % hydrogen and 50 mol % carbon dioxide. Temperature of the system varied with the surroundings from 75 to 85°F. Barrier materials were of 0.008-in.-thick fiber glass called Dexiglas mat obtained from Dexter and Sons, and 0.018-in.-thick fiber glass Ultra Efficient Filter media mat obtained from Mine Safety Appliance Company. The separation obtained could be adequately represented as a combination of gaseous diffusion and adsorbed flow. Agreement of observed values was within five per cent with an estimate of gaseous diffusion using Weller and Steiner's equation plus a value for adsorbed flow from a modified version of Russell's equation. The separation of hydrogen from carbon dioxide in the equipment as constructed increased as the pressure increased from 10 to 20 in. of mercury for flow rates of one to ten cubic feet per hour for the gaseous mixture. A permeability apparatus was constructed and operated with a system of carbon dioxide and hydrogen. Composition of the feed mixture was either pure electrolytic hydrogen, pure carbon dioxide, or a mixture of 50 mol % hydrogen and 50 mol % carbon dioxide. Temperature of the system varied with the surroundings from 25 to 28°C. Barrier materials of 0.008-in.-thick Dexiglas, 0.001-in.-thick polystyrene from Dow Chemical Company, 0.001-in.-thick cellulose acetate supplied by Celanese Corporation, and silicone rubber obtained from General Electric Company, Silicone Division, were used in this investigation. The permeation of a mixture of carbon dioxide and hydrogen is in direct relationship with the adsorption of that mixture onto a powdered sample of the barrier material. (Dissertation Abstr.)

29363 SEPARATION AND DETERMINATION OF TRACES OF STRONTIUM IN CALCAREOUS MEDIA [Thesis]. Brandt, Peter Juergen. Charlottesville, Va., Univ. of Virginia, 1965. 116p.

The conditions of pH for the separation of calcium, strontium, and magnesium by ion exchange chromatography on Dowex 50W-X8 cation exchange resin, using ethylene glycol-bis-(β-aminoethylether)-N + N′-tetraacetic acid (EGTA) were calculated. The calculated pH conditions were tested by carrying out distribution experiments on ion exchange columns using ^{85}Sr and ^{45}Ca radioistope tracers. The experimental results were generally found to agree well with the calculated values. The method was found to be applicable to virtually any strontium-containing calcareous medium except those containing barium, which cannot be separated from strontium by this method. The passage of a solution of calcium, strontium, and magnesium containing 0.05M NH_4-EGTA and buffered to pH 6.2−6.3 with 0.02M NH_4-maleate through a column of Dowex 50W-X8 cation exchange resin results in the complete absorption of the last

two cations, while calcium is quantitatively recovered in the effluent. Elution of this column with 0.05M NH_4-EGTA buffered to pH 7.7–8.0 with 0.02M NH_4-barbital yields a strontium fraction contaminated with small amounts of magnesium and considerable amounts of alkali metal ions. Further purification and enrichments were achieved by lowering the pH of the EGTA-containing strontium fraction to pH 4.5–5.0 with acetic acid and allowing it to flow through a small volume of Dowex A-1 chelating resin. The polyvalent metal ions were recovered from the chelating resin by elution with 1M HCl or $HClO_4$. The eluate obtained the strontium, up to 200 μg magnesium and traces of sodium and potassium in high concentrations of chloride or perchlorate ions, respectively. A radiation buffer method was developed, which allowed the flame photometric determination of 3–10 ppM strontium in solutions containing ammonium-EGTA. The concentration of strontium in various samples was determined and, when available, compared with values reported in the literature. The reproducibility of the combined ion-exchange separation and flame analysis varied from 1.2 to 2.0% relative standard deviation. Recovery of added strontium was in the range of 98–99%. (TCO)

29364 RELATIVE PROBLEMS OF THE DESIGN OF PILOT PLANTS FOR REPROCESSING BY VOLATILIZATION. Schmets, J.; Heremans, R.; Pierini, G. (Centre d'Etude de l'Energie Nucleaire, Brussels). 18p. (In French). (CONF-650964–2; BLG–358). ORAU.

From Symposium on Design and Construction Problems of Pilot Plants for Recycling Irradiated Fuels, Turin.

Irradiated fuel reprocessing by volatilization emphasizes some problems that affect the concept of reprocessing pilot plants. Criticality, inventory, installation capacity, instrumentation, waste disposal, remote handling, shielding, and safety problems have particular characteristics that necessitate research. In some cases suitable solutions have been found. In other cases, the solutions should result from operation of cold or hot technological units in several laboratories, and also from research on several specific aspects of fluorine chemistry. (auth)

29365 MONOALKYL PHOSPHORIC ACID EXTRACTION OF CESIUM AND STRONTIUM VALUES. Schmitt, J. M. (to U. S. Atomic Energy Commission). U. S. Patent 3,258,315. June 28, 1966.

A method was developed for selectively removing cesium and strontium values from an aqueous solution containing these values. The aqueous solution is contacted with an organic solution of a monoalkylphosphoric acid and the equilibrium pH of the aqueous solution is adjusted to a value of 1 to 5. Cesium is preferentially extracted at a pH of 1 to 2 and strontium is preferentially extracted at a pH of 2 to 5. (AEC)

ENGINEERING

General

Refer also to abstracts 29395 and 29622.

29366 (TID–22970, pp 375-91) INSTRUMENTATION LABORATORY. (Massachusetts Inst. of Tech., Cambridge).

Research is summarized on epoxy insulation, gyro damping fluids, lubricants for vacuum environments, Be corrosion, radiation effects on optical materials, organic coatings, organic materials for spacecraft, BeO stability, ceramic electric motor parts, potting compounds, adhesives, flame-spray fabrication of gyro wheel rims, ball-bearing surface coating, ball-bearing materials and gas-bearing materials. (J.R.D.)

29367 (TRG-Report–1089) MECHANIZED STRUCTURAL ANALYSIS: A USER'S GUIDE TO THE GRID-FRAME PROGRAM. Jobson, D. A.; Enderby, J. A.; Ellington, J. P. (Reactor Group, United Kingdom Atomic Energy Authority, Risley (England)). Sept. 16, 1965. 40p. Dep. BIS $1.10. HMSO 5s. 6d.

An investigation was made to enable engineers who may have no experience of computers to use a U.K.A.E.A. program GRID-FRAME, which was written in Fortran IV for an IBM 7090. GRID-FRAME will carry out a complete linear elastic analysis of most skeletal structures which initially lie in one plane, when subjected to any three-dimensional system of joint loads. The program will deal with anything from a simple beam to a structure of 600 members, and calculates the distorted shape under specified loads and restraints from a definition of the members and the connections between them. It takes into account member extension, bending, shear and twisting, where appropriate, printing out the forces and couples associated with each, together with the nodal point deflections and rotations. (auth)

29368 POWER SUPPLY SYSTEM FOR THE SIEMENS-SCHUCKERT RESEARCH CENTER. Baisch, Roderich; Linzmaier, Josef; Stier, Robert; Zieten, Willy. Siemens Z., 39: 1296-1303(Dec. 1965). (In German).

The high- and low-voltage circuits, the switching station, the safety system, and the emergency current supply of the power system of the Siemens-Schuckert Research Center are discussed. (G.O.Y.)

29369 TELEMETERING FROM MAGNETICALLY SUSPENDED ROTORS [Thesis]. Robinson, Thomas Kneeland Jr. Charlottesville, Va., Univ. of Virginia, 1965. 94p.

Methods were developed for the measurement of the temperature of magnetically suspended rotors and for the measurement of electrical potential differences generated in certain types of centrifuged solutions. The temperature measurements were accomplished by means of a radio telemetering device installed inside the rotor. Temperature was sensed by means of a thermistor, which controlled the pulse repetition rate of a blocking oscillator, with the latter used for amplitude modulation of a radio-frequency carrier. The device may be used to measure temperatures associated with the rotor to within ±0.01°C at rotor speeds up to 300 rps. Small electrical potential differences were measured by capacitively coupling the source contained in the moving rotor to a fixed measuring system, using the moving rotor for d-c to a-c conversion. A potentiometer arrangement was employed in which a variable d-c potential difference was introduced into the rotor to balance the unknown emf, with the occurrence of this balance detected by means of the coupling system mentioned above. Potential differences less than 2 mv may be measured to within ±25 μv using this method. (Dissertation Abstr.)

Applications of Nuclear Explosions

29370 (PNE–3003) APPLICATION OF THE PLOWSHARE PROGRAM OF NUCLEAR EXCAVATION ON EXPERIMENTATION TO HIGHWAY CONSTRUCTION. (National Academy of Sciences–National Research Council, Washington, D. C.). Apr. 1966. 14p. Dep. mn. CFSTI $1.00 cy, $0.50 mn.

Results obtained from experiments on excavation by nuclear explosions in the Nevada Test Site were evaluated. It was concluded that additional tests be carried out, with particular emphasis given to highway applications. The objectives of blasting for highway construction and current status of nuclear excavation research are also discussed. Radiation hazards associated with the application are briefly mentioned. (P.C.H.)

Facilities and Equipment

Refer also to abstract 29872.

29371 (AWRE-E–1/66) A FACE-ON VERTICAL BLAST LOADING SIMULATOR FOR STRUCTURAL RESPONSE STUDIES. Clare, R. (Atomic Weapons Research Establishment, Aldermaston (England)). Feb. 1966. 32p. Dep. mn. BIS $1.40. HMSO 7s. 0d.

A vertical blast simulator which produces a reflected blast overpressure of 13 to 400 psi with a duration of 20 to 24 ms is described. Examples of the pressure-time records obtained are given and are compared with that of a "classic" blast wave. (auth)

29372 (TID–22978) COSTS OF LARGE FOSSIL FUEL FIRED POWER PLANTS. (Jackson and Moreland, Boston, Mass.). Apr. 30, 1966. Contract W-7405-eng-26. 137p. (J and M–636). Dep. mn. CFSTI $4.00 cy, $1.00 mn.

Forty eight plant variations were investigated to reflect effects of size, alternate fuels, type of construction, and first unit on a site versus an addition to existing facility. Cost factors are included and discussed as a basis for adjusting the estimates to a particular plant concept. Data are presented either in the form of curves or tabulations for easy reference. Among items considered are variations in construction costs versus geographical regions, site conditions such as profile, seismology, geology, and availability of water. Methods are provided to readily estimate lifetime plant capacity factor and also levelized fixed charges. In designing a specific facility, capital costs are balanced against applicable fuel and operation and maintenance costs. The optimized capital costs vary primarily with fuel cost and annual fixed charges on capital costs. In determining the specific thermal cycles for this study, annual fixed charges were taken at 12% and the fuel cost at 25 cents which is within the price range a recent market analysis indicates large nuclear units will be able to compete in 1970. (M.O.W.)

29373 PLANT FOR THE ELECTROLYTIC REFINING OF NUCLEAR METALS. Wurm, Joseph G. (to EURATOM). Canadian Patent 731,126. Mar. 29, 1966. Priority date Sept. 13, 1962, Germany.

High frequency induction is the heat source for the metal electrolysis vessel which is enclosed by a translucent quartz tube having suitable seals at the top and bottom. This tube is filled with an inert gas or maintained at a vacuum to prevent oxidation of the purified metal. The bottom of the electrolysis vessel is the cathode with the temperature high enough to keep the purified metal as liquid during the process. The multiple anodes are the desired metal in the impure state. A molten salt of the metal forms the elec-

trolyte. A cooling coil built into the wall of the vessel maintains a layer of solid salt on the wall to prevent corrosion. The cycle of operation is outlined. (AECL)

Heat Transfer and Fluid Flow

See also PHYSICS — Fluid Physics and Thermodynamics

29374 (ANL–7190, pp 156–66) LIQUID METAL HEAT TRANSFER RESEARCH PROGRAM. (Argonne National Lab., Ill.).

Research on the thermodynamic properties of liquid metals during single-phase flow, two-phase flow, and boiling flow in forced convection systems is summarized. Information is included concerning two-phase adiabatic flow of Na, boiling Na test facility, liquid-metal loop heater development, heat exchanger analyses, and methods of predicting reactor coolant-channel temperatures. (J.R.D.)

29375 (ANL–7190, pp 193–200) EDUCATION—RESEARCH ACTIVITIES. (Argonne National Lab., Ill.).

Summaries of investigations are presented on relations of steam voids to sinusoidal power modulation in thin-walled boiling water coolant channels, heat transfer instabilities near critical points of fluids, vertical two-phase flow mechanics, density disturbance propagation in air-water flow, and oscillations in natural-circulation two-phase-flow boiling loops. (J.R.D.)

29376 (BAW–3238–9) BURNOUT FOR FLOW INSIDE ROUND TUBES WITH NONUNIFORM HEAT FLUXES. (Babcock and Wilcox Co., Lynchburg, Va. Atomic Energy Div.). May 1966. Contract AT(30-1)-3238. 114p. (EURAEC–1640). Dep. mn. CFSTI $4.00 cy, $0.75 mn.

Work Performed under United States–Euratom Joint Research and Development Program.

An experimental and analytical investigation was made to determine how irregular heat flow through reactor channels affects the operating conditions that cause burnout (critical heat flux). Experimental work on tubular specimens with four axial power shapes was completed. Annular specimens with five power shapes are now being tested, and an effort to correlate the experimental data with empirical and analytical models is being made. The data and results from the tubular test sections are presented. The experimental parameters were chosen to cover a range of design conditions for nuclear power reactors. The test sections were nominally 0.446-inch ID tubes 72 inches long with water flowing inside; the tubular geometry was chosen in order to compare the results with the industry's past experiments, most of which were performed with tubes and uniform heat flux. The analysis presents observations regarding critical heat flux location and magnitude along with equations which evaluate the effect of operating parameters on critical heat flux location and magnitude. (M.O.W.)

29377 (BAW–3238–11) NONUNIFORM HEAT GENERATION EXPERIMENTAL PROGRAM. Quarterly Progress Report No. 10, October–December 1965. (Babcock and Wilcox Co., Lynchburg, Va. Atomic Energy Div.). Contracts AT(30-1)-3238; 59-3090. 32p. (EURAEC–1554). Dep. mn. CFSTI $2.00 cy, $0.50 mn.

Work Performed under United States–Euratom Joint Research and Development Program.

During this period, data were obtained on an annular test section having both surfaces heated. The experiments through December included all parameters, but the time permitted evaluating only the 1500 psia data before the end of the quarter. An additional task, a feasibility study of an analytical burnout model, was completed. (auth)

29378 (NYO–3304–7) INVESTIGATION OF BOILING FLOW REGIMES AND CRITICAL HEAT FLUX. Quarterly Progress Report, September 16–December 15, 1965. Report No. 625. Bergles, A. E.; Clawson, L. G.; Roos, J. P., Bourne, J. G. (Dynatech Corp., Cambridge, Mass.). Feb. 1, 1966. Contract AT(30-1)-3304. 23p. Dep. mn. CFSTI $1.00 cy, $0.50 mn.

The design details of the steam loop were completed and major components are being procured. The operating characteristics of the steam loop are discussed. Preliminary tests were made with an electrical probe which measures the characteristics of the annular liquid film. The data indicate that the mean film thickness decreases with increased steam quality and increased total flow rate. In addition, the liquid film disappears as the critical condition is approached. The operational checkout of the traversing isokinetic sampling probe was completed. The results for centerline sampling of adiabatic single-phase flow are in good agreement with generalized velocity profile data. Only a few of the two-phase sampling data points can be considered correct due to leaks which developed after extended periods of operation. The film probe and the sampling probe have indicated that the high quality flow pattern is characterized by an annular liquid film and a core with entrained liquid, thereby establishing that this flow pattern is spray annular. (auth)

29379 (SAN–1011) ANALYTICAL AND EXPERIMENTAL STUDY OF TRANSIENT HEAT TRANSFER FOR EXTERNAL FORCED CONVECTION. Report No. TS-66-1. Soliman, Moustafa (California Univ., Berkeley. Coll. of Engineering). Jan. 1966. Contract AT(11-1)-34. 237p. Dep. mn. CFSTI $6.00 cy, $1.25 mn.

Thesis.

An exact solution, for the wall heat flux, is presented for the problem of transient forced-convection heat transfer when the velocity profile is linear and the shear stress varies very slowly along the wall (Transient Lévêque Problem). The surface temperature undergoes a step jump with time. The solution is obtained by double Laplace transformation methods. Asymptotic expressions are presented for the solution at small and large times. Next, an approximate analysis is presented to predict the transient local and mean wall temperatures of a flat plate cooled on both sides by a steady incompressible turbulent flow of Prandtl number unity. The plate is heated by a uniform heat source which undergoes either a step jump or an exponential rise with time ($q_0 e^{t/t_0}$). The effect of the thermal capacity of the plate is included. Experimental data are presented for the transient mean wall temperatures of thin metallic ribbons simulating the analytical model and cooled by a flow of water. (M.O.W.)

29380 (TID–22967) A STUDY OF CONVECTION BOILING INSIDE CHANNELS. Progress Report. Ferrell, J. K. (North Carolina State Univ., Raleigh). Dec. 31, 1964. Contract AT(40-1)-2950. 34p. Dep. mn. CFSTI $2.00 cy, $0.50 mn.

Experimental and analytic studies were made to determine the effects of the pertinent variables upon two-phase single component frictional and contraction-expansion pressure losses. The frictional pressure drop relationships are to be determined for both horizontal and vertical, heated and unheated, channel surfaces. Work during this period was devoted primarily to (1) evaluation of the experimental results obtained from the uniform cross section, uniformly heated channel, and (2) preparation of the experimental apparatus for studying two-phase flow through channels of non-uniform cross section. (M.O.W.)

29381 ADVANCES IN HEAT TRANSFER. VOLUME 3. Irvine, Thomas F. Jr.; Hartnett, James P. (eds.). Advance. Heat Transfer, 3: 1-313(1966).

Review articles by five authors are presented on recent developments in heat transfer research. The effect of free-stream turbulence on heat transfer rates is evaluated in detail. Theories that permit calculation of heat and mass transfer in turbulent boundary layers are presented. Fundamental aspects of forced convection heat transfer in symmetrical ducts when the fluid is a liquid metal are surveyed. Improved prediction methods suitable for engineering analysis and design are discussed. An analysis of heat transfer in a radiating media and a review of the literature pertaining to specific convection-radiation interaction problems is

presented. Methods for measuring and calculating dilute gas transport properties are critically surveyed. (J.G.B.)

29382 THERMAL INVESTIGATIONS ON ROD-CLUSTER ELEMENTS (EXPERIMENTAL METHODS AND RESULTS). Stiefel, U. (Eidgenoessiche Technische Hochschule, Wuerenlingen, Ger.). Neue Tech., 8: 55-68 (1966). (In German).

For the conception of gas- or superheated steam-cooled power reactor, EIR has been engaged in experimental work in order to evaluate the thermodynamical phenomena of rod-cluster fuel elements. The problems investigated, the test facilities and some of the results are discussed. (auth)

29383 HIGHLIGHTS OF THE 8TH NATIONAL HEAT TRANSFER CONFERENCE. Miller, David. Power Reactor Technol., 8: 228-44(Fall 1965).

Some studies on heat exchangers, packed beds, desalinization, and loss-of-coolant accidents are summarized. Some more fundamental studies of boiling and condensation, two-phase flow, pressure drop, radiation, and thermophysical properties are also considered. (G.O.Y.)

29384 FLUID FRICTION, HEAT TRANSFER, TURBULENCE, AND INTERCHANNEL FLOW STABILITY IN THE TRANSITION FROM TURBULENT TO LAMINAR FLOW IN TUBES [Thesis]. Bankston, Charles A. Jr. Albuquerque, N. Mex., Univ. of New Mexico, 1965. 286p.

The interchannel stability limits for multiple tube gas heaters with constant heat rate and pressure drop were determined experimentally for tubes 450 diameters long with uniform heating of normal hydrogen at exit to inlet temperature ratios up to 8.9. Stability limits are defined for inlet Reynolds numbers less than 3000. For greater Reynolds numbers, instabilities will not occur at temperature ratios less than 8.9. Local heat transfer coefficients and friction factors are reported for gaseous normal hydrogen in the range of Reynolds numbers from 600 to 13,000 with wall to bulk temperature ratios to 2.25. The local friction factors are found to be strongly influenced by transverse temperature gradients in the laminar and transition flow regimes. The effect of transverse gradients, or heat rate, on the heat transfer coefficients in the laminar regime is small, but the heating rate does have an important effect on the character of the transition region. At high heating rates the laminar character of the heat transfer correlation is extended to local bulk Reynolds numbers considerably in excess of the isothermal critical value. Turbulent intensities are reported for isothermal and heated flows of helium in similar tubes. These measurements confirm the transition from turbulent to laminar flow in a heated gas flow with constant section. In heating of a gas in a smooth straight tube the local flow will be laminar if the local bulk Reynolds number is less than 2000. The local heat transfer and friction results are expected to be of value in improving the determination of stability limits for other systems, and they may also find application in the design of heat exchangers. (Dissertation Abstr.)

29385 HYDRAULIC CHARACTERISTICS OF A BOILING WATER CHANNEL WITH NATURAL CIRCULATION [Thesis]. Spigt, Cornelis Ludovicus. Eindhoven, Netherlands, Technische Hogeschool, 1966. 158p.

The hydraulic characteristics of a single coolant channel of simple annular geometry in a boiling water nuclear reactor were studied, emphasis on stability characteristics The experimental part was restricted to the operation under conditions of natural circulation. The range of independent variables was: pressures of 2.03 to 30.7 ata (30 to 450 lbs/in.^{2}), channel powers of 10 to 465 kw, subcooling temperatures of 0 to 43°C, and a hydraulic diameter of 16.16 and 25.03 mm. The range of dependent variables was: inlet velocities of 0 to 1.4 m/sec, exit qualities of 0 to 25%, and uniform heat fluxes of 0 to 180 w/cm^2. The pressurized and atmospheric boiling water loops, the two test sections, and the power supply are described. The measuring, recording, and analyzing equipment are reviewed. Special attention was paid to the measurement of the void fraction in a two-phase system under steady as well as under transient conditions. The results obtained by the two methods used, γ attenuation and impedance, were compared and good agreement is reported. The analysis of boiling noise in terms of spectral power density and autocorrelation was used in determining the onset of hydraulic instabilities. Autocorrelation, cross-correlation, and noise rejection techniques were used to characterize the severe flow oscillations and to express the stability of the steady state in terms of transfer functions. In the analysis of signals use was made of digital as well as analog computers. In the presentation of results obtained in steady states, the influence of channel power, system pressure, subcooling, and hydraulic diameter is shown on the recirculation flow rate, the exit void fraction, and longitudinal void and pressure distribution. An analysis was made in terms of the slip ratio, S, and the two-phase friction multiplier, R. The void fraction and the two-phase friction loss data were plotted as a function of the Martinelli and Nelson correlator. The void fraction data were also plotted in the "weighted mean velocity-average volumetric flux density" plane proposed by Zuber and Findlay. From this plot it could be deduced that flat profiles for the velocity or concentration distribution are present under the operating conditions reported. During operation, it was possible to distinguish between three types of flow oscillations with frequencies of roughly .03, 1, and 15 cps. Systematic research was carried out on the 1 cps flow oscillations only. After accepting a criterion for defining the onset of the hydraulic oscillations, the influence of system pressure, subcooling hydraulic diameter on the instability threshold channel power was systematically examined. It was found that the effect of increased subcooling on the onset of severe hydraulic oscillations at low subcooling rates was opposite to that at high subcooling rates. The character of these oscillations was studied by making recordings during hydraulic oscillations of the relevant physical quantities, such as, for instance, the void fraction along the height, the inlet mass flow, etc. Results of transfer function measurements from channel power to inlet mass flow and local void fraction are presented. Characteristic for all these transfer functions was the occurrence of a sharp resonance peak when the instability threshold was approached. It is shown that there exists a relationship between the character of the transfer function and the onset of spontaneous flow oscillations. The influence on the two of the operating conditions is similar. Burnout channel powers and heat fluxes are presented for various values of system pressure and subcooling. Nearly all the burnouts were obtained under unstable flow conditions. General equations were derived describing the performance characteristics of a boiling system under steady-state and nonsteady-state conditions. Special attention was paid to the formulation of boundary conditions and the introduction of pressure effects into the equations. The dynamic equations were linearized by assuming small disturbances from the steady state. By applying an open-loop analysis, stability criteria were derived for detecting the onset of flow oscillations in natural as well as forced circulation boiling systems. The equations were numerically integrated by means of a digital computer. Preliminary results of calculations were reported for the operating and geometry conditions as considered in the experimental program. Fairly good agreement was obtained between theoretically and experimentally obtained quantities of the steady-state performance, the instability threshold power, and the character of the hydraulic oscillations. (auth)

Materials Testing

29386 (ANL–7074) CORRELATION OF THE HEAT TRANSFER PROPERTIES AND ULTRASONIC TRANSMISSION PROPERTIES OF BONDS. di Novi, Roberta Ann (Argonne National Lab., Ill.). Feb. 1966. Contract W-31-109-eng-38. 21p. Dep. mn. CFSTI $1.00 cy, $0.50 mn.

Two types of bonds, mechanical bonds in the form of copper braze-bonded specimens and roll bonds in the form

of Borax fuel-plate sections, were investigated. The thermal-pulse method was utilized for measuring the thermal properties and a through-transmission method was employed for the ultrasonic measurements. The amplitude of the transmitted ultrasonic pulse decreased with a decrease in the heat transfer properties of the copper braze-bonded specimens. This relation was strongly frequency-dependent; the rate of loss of ultrasonic transmission decreased as the wavelength decreased. Unless a definite relation was established between the thermal conductivity and the ultrasonic transmission of each particular bonded fuel-plate section, it was not possible to predict the exact heat transfer properties from the ultrasonic properties. (W.L.G.)

29387 MAGNETIC METHODS FOR MEASURING THE MAXIMUM TEMPERATURE OF IRRADIATED SAMPLES. **Marth, W. (Kernforschungszentrum, Karlsruhe, Ger.); Stoelzl, D.; Sizmann, R. Kerntechnik, 8: 208-10(May 1966). (In German).**

The maximum temperature reached by a sample during irradiation in a reactor can be determined by the temperature dependence of the remanent magnetization of added small ferromagnetic indicators. Two procedures are discussed. On the Curie-point method the magnetization of an indicator vanishes when the sample temperature exceeds the Curie point of this indicator. In the remanence method below the Curie point the decrease of the magnetization of an indicator is a measure for the maximum temperature reached by the sample. (auth)

29388 IONIZING GAMMA-DEFECTOSCOPY FOR LEAD CONTAINERS. **Abrams, I.; Veveris, O.; Kalis, Kh. (Inst. of Physics, Academy of Sciences, Latvian SSR). Latv. PSR Zinat. Akad. Vestis, Fiz. Tek. Zinat. Ser., No. 6, 19-26(1965). (In Russian).**

A method was developed for ionizing γ defectoscopy with cylindrical γ-ray sources. The method was used for defectoscopy of lead containers for the storage and transport of radioactive drugs. The sensitivity limit of the method was computed. (auth)

29389 ULTRASONIC INSPECTION OF CRITICAL COMPONENTS AND WELDMENTS FOR PRESSURE AND NUCLEAR VESSELS. **Drouillard, Thomas F. (Illinois Inst. of Tech., Chicago). Mater. Eval., 24: 299-308 (June 1966).**

The nondestructive testing program described includes the inspection of base materials, in-process inspection, and the present methods employed in weld inspection. Several examples are presented demonstrating the application of ultrasonic testing in solving fabrication problems. One of these is the inspection of weld deposit cladding for lack of bond and for weld defects. (auth)

29390 COMMON RADIATION SOURCES FOR CRUDE STRUCTURE TESTS. **Becker, E. (Technische Hochschule, Magdeburg, Ger.). Technik (Berlin), 18: 793-9 (Dec. 1963). (In German).**

Flaws in working pieces can be detected by γ emitters, which have relatively long half lives and high specific activities such as ^{60}Co, ^{192}Ir, ^{137}Cs, and ^{170}Tm. Methods of attaining the maximum specific activity by neutron bombardment and the effective activity of a cylindrical radiation source in the direction of the cylinder axis are discussed. Tabular data are given for wire and flaw detectabilities for ^{170}Tm, ^{192}Ir, ^{137}Cs, and ^{60}Co for various test materials, widths, films, and foil combinations. From these data, the most advantageous range of application for steel foils and steel plates (from 2 to 160 mm) is diagrammed for the γ sources mentioned above. An extension of the ^{60}Co range can be obtained with ^{24}Na whose $E_\gamma = 2.7$ Mev can penetrate steel plates up to 200 mm, but its short half life of 15 hr makes it applicable only near a reactor. (OID)

29391 BETA-BACKSCATTER TECHNIQUES FOR THE MEASUREMENT OF LAYER THICKNESS IN A MULTILAYER COATING. **Semmler, R. A.; Spalek, J.; Loewe, W. E. (ITT Research Inst., Chicago). 23p. (CONF-660322-1). ORAU. Gmelin, AED-CONF-66-018-4.**

From Society for Nondestructive Testing, Spring Convention, Los Angeles.

Several beta-backscatter techniques were used to determine the thickness of individual layers in a multilayer coating. These methods include: measurement of total backscatter at several different source energies, analysis of the energy distribution of the backscattered electrons using a single monoenergetic source, and measurement of electron backscatter as the energy of the incident monoenergetic electrons is continuously varied. All three methods were used to measure layer thicknesses in two-layer coatings. The first method was used with a three-layer coating. Simulated coatings using metal foils in the 1 to 10 mil range were used in the experiments. A refined instrument to measure layers less than 1 mil using lower energy electrons is currently being constructed. This design is based largely on the first method but uses the third method for the top layer and some spectrum analysis to isolate those regions of the backscattered spectrum that convey the most information. (auth)

Protective Structures

29392 DESIGN VALUES FOR LIVESTOCK FALLOUT SHELTERS. pp 295-6 of American Society of Agricultural Engineers. 1965.

Design criteria are presented for fallout shelters for domestic animals. Factors considered include water and food requirements, ventilation, space requirements, radiation attenuation requirements, and emergency power supplies. (C.H.)

Space Propulsion

See also **ISOTOPE TECHNOLOGY — Power Application**
REACTOR TECHNOLOGY — Propulsion and Space

29393 APPLICATION OF BERYLLIUM ON THE AGENA. **Rebholz, M. J. (Lockheed Missiles and Space Co., Sunnyvale, Calif.). J. Spacecraft Rockets, 3: 715-22(May 1966).**

An extensive development and qualification testing program was undertaken to obtain design information on cross-rolled sheet beryllium for the Agena D spacecraft. Curved Be panels were used as structural skins and doors for a weight reduction redesign. Two major problem areas were curved panel buckling allowables and panel edge attachment allowables. The studies and tests conducted to develop edge attachment allowables for the Be panels are reported. Various rivets, bolts, and screws were tested using simple lap joints. Several methods of locally increasing the panel edges to reduce high bearing stresses were also investigated. Based on these tests, the final attachment design used No. 10 titanium screws in combination with integral edge thickening of the panels produced by selective chemical milling. In addition, exploratory testing of adhesive bonded and brazed joints was conducted, and such joints proved to be satisfactory for certain applications. The use of Be sheet now available, with better and more consistent properties, permits its increased utilization in light weight aerospace structures. (auth)

29394 RESEARCH ON ELECTRIC DRIVES FOR SPACE VEHICLES. **Au, Guenther F. (Institut fuer Strahlantriebe, Braunschweig, W. Ger.). Sci. Ind. Spatiales, 1: Nos. 7-8, 69-73(1965). (In German).**

Current and projected work handled in the Institute for Jet Propulsion of the DFL in Braunschweig covering electrostatic ion-propulsion and an electromagnetic drive are reviewed; these are being purposefully shaped up into a space-travel project. Essential experiments are to be carried out with a larger ion-drive recently constructed in a simulation apparatus 5-m long and 2-m in diameter, to give practical flight application. The measuring devices adapted thereto are briefly described. Lastly, a study is

made of a nuclear-electric payload transporter with a nuclear energy source and an electric drive, which holds great promise of useful possibilities for numerous missions. (auth)

29395 IMPROVEMENTS IN THERMAL ENGINES, FOR EXAMPLE GAS TURBINE ENGINES, JET PROPULSION UNITS, AND ENGINES POWERED BY NUCLEAR REACTORS. Kershaw, Herbert Arthur. British Patent 1,029,840. May 18, 1966. Filed Oct. 25, 1961.

A thermal engine is patented that includes at least one motive fluid heating chamber in which continuous combustion takes place and which receives compressed air for combustion from a jet type air compressor. A heat exchanger is connected within the motive fluid chamber and is supplied with fluid at a high temperature by a nuclear reactor. The heating chamber is provided with a compressed air inlet and a gas outlet conduit at opposite ends. The air compressor that supplies air to the combustion chamber consists of an air entraining chamber having an air inlet and an air forcing throat leading to the compressed air inlet of the motive fluid heating chamber. An air induction nozzle is provided in the entraining chamber adjacent to the air inlet of the chamber and in line with the throat. Fluid transfer means connect the outlet end of the motive fluid heating chamber with the induction nozzle for transferring part of the motive fluid from the heating chamber directly to the induction nozzle to effect air entrainment in the compressor. (B.L.M.)

Vacuum Engineering

29396 PRESENT LIMITS OF DEVICES FOR THE PRODUCTION OF LOW PRESSURES. Amoignon, J. (Centre d'Etudes et de Production des Gaz, Vitry-sur-Seine, France). Vide, 21: No. 121, 1-10(Jan.-Feb. 1966). (In French).

Within the framework of a general review, the various devices for the production of low pressures are summarized. Their present limits are outlined and the problems of the contamination of pumps and vacuum enclosures is discussed in detail. (tr-auth)

GEOLOGY, METEOROLOGY, AND MINERALOGY

General

Refer also to abstract 30805.

29397 (NAS-NRC-1276) GEOCHRONOLOGY OF NORTH AMERICA. Nuclear Science Series Report No. 41. (National Academy of Sciences–National Research Council, Washington, D. C.). 1965. 326p. National Academy of Sciences, Washington, D. C. $6.00.

The present status of geochronological methods is discussed, and compilations are given for Precambrian data and Phanerozoic data. 144 references are given for the compilations. (P.C.H.)

29398 THERMOLUMINESCENCE AS A FUNCTION OF CLIMATE AND TEMPERATURE. Ronca, L. B.; Zeller, E. J. (Univ. of Kansas, Lawrence). Contract AT(11-1)-1057. Amer. J. Sci., 263: 416-28(May 1965).

The theory of thermoluminescence as a function of temperature was tested by measuring the natural thermoluminescence of samples of limestone collected from several climatic areas. The agreement between the theory and the experimental results is satisfactory. It is concluded that in nonpolar regions of the world, with average erosion rates and average geothermal gradient, the number of electrons responsible for the 230°C glow-curve peak for calcite is in equilibrium with the average temperature of the hottest month. In polar areas the equilibrium is not reached, as frigid conditions have not existed in the area for the necessary length of time. Samples from Victoria Land, Antarctica, indicate that a climate which did not exceed 0°C in its warmest month existed in the area for more than one million years. It should be noted, however, that certain samples collected very near present sealevel at Marble Point show a much shorter duration for frigid conditions. In these cases it is probable that the collecting sites were inundated during the interglacial periods and the contact with the relatively warmer sea water produced the observed effect. (auth)

29399 CHEMICAL STUDIES OF MINERALS CONTAINING RARER ELEMENTS FROM THE FAR EAST DISTRICT. LX. THALENITE FROM SUISHOYAMA, KAWAMATA-MACHI, FUKUSHIMA PREFECTURE, JAPAN. Nagashima, Kozo (Tokyo Univ.); Kato, Akira. Bull. Chem. Soc. Jap., 39: 925-8(May 1966).

Chemical studies of thalenite from Suishoyama pegmatite, Fukushima Prefecture, showed its composition to be very close to the ideal formula, $Y_2Si_2O_7$, and a selective distribution pattern of rare earths belonging to the thortveitite-type as defined by Goldschmidt and Thomassen. The x-ray powder studies disclosed a metamict state hitherto unknown in this species, and the original state could be recovered by thermal treatment. Optical and other properties include: color, colorless to light gray; luster, resinous; optical properties, $\alpha = 1.709 \pm 0.002$, $\beta = 1.716 \pm 0.002$, $\gamma = 1.723 \pm 0.002$, $(-)2V \sim 70°$, and $\rho < \nu$; specific gravity, 4.16; and hardness, 6½. Chemical analysis indicated: SiO_2, 30.68%; Al_2O_3, 0.10%; Fe_2O_3, 0.17%; ΣY_2O_3, 64.89%; UO_2, 1.12%; ThO, 0.20%; CaO, 0.35%; MnO, 0.38%; MgO, 0.33%; Na_2O, 0.02%; $H_2O(+)$, 1.56%; and $H_2O(-)$, 0.11% for a total of 99.91%. (auth)

29400 CALIBRATION OF THERMOLUMINESCENCE MEASUREMENTS. Hutchison, Charles Strachan (Univ. of Malaya, Kuala Lumpur). New Zeal. J. Sci., 8: 431-45(Sept. 1965).

Geological applications of the thermoluminescence of minerals require that the natural thermoluminescence be first drained before the specimen is subjected to increasing measured doses of ionizing radiation for the establishment of a calibration curve. The standard method of drainage has been by heating, but recent proposals have been made that ultraviolet radiation may be preferable. Both methods are described and their effects compared and discussed. The thermoluminescence, as subsequently measured, varies considerably depending on which method is used. Ultraviolet drainage is shown to give more reliable results, and, despite the more difficult technique involved, it is recommended that all future calibrations be performed using this as the standard method. In archaeological applications of thermoluminescence measurements, calibration is obtained by using what is called a "specific glow" of the specimen. This method is described and discussed in comparison with the calibration curve technique. (auth)

29401 RADIOISOTOPES IN OCEANOGRAPHIC RESEARCH. Pedrick, Robert A.; Magin, George B. Jr. Nucleonics, 24: No. 6, 42-4(June 1966).

Sources of radioactivity are reviewed. Measuring techniques are described. The Deep-Water Isotopic Current Analyzer is discussed along with instruments for sediment density measurements, activation analysis, oxygen content determinations, and beach sediment movement measurements. (M.C.G.)

Meteorology

See also Site Survey and Selection

Refer also to abstract 30221.

29402 ON THE POSSIBILITY OF WEATHER PREDICTION ON THE BASIS OF MEASUREMENT OF DIMINUTION OF THE ELECTRICAL CONDUCTIVITY OF THE AIR. POLARIZATION EFFECTS OF NEUTRINOS, AND THEIR BIOLOGICAL EFFECT. Ankara, Said-Ali (Univ. of Ankara). Neue Phys., 4: 97-119(1964-65). (In German).

Observations on the electric conductivity of the air indicated that a decrease of 8.10^{-5} esu/sec indicated a strong change in the weather in 24 hr. Use of this method over an extended period of several months indicates an accuracy of 88% in prediction of weather. This suggests that the conductivity of the air is based on production of neutrinos by the sun and the ionization which such particles produce. It is also suggested that physiological factors associated with changes in the weather (rheumatic pain, etc.) may also be due to modifications in the absorption of such polarizing radiation by the body. Examples of acceleration or intensification of biological processes by irradiation with neutrinos, particularly in viruses, are suggested. The sole radiation absorbed by organisms at great depths in the sea is neutrino radiation, whose polarization effects may account for a part of the biological activity of such species. (BBB)

29403 SUMMARY OF MEASUREMENTS OF DISPERSION FROM QUASI-INSTANTANEOUS SOURCES. Slade, D. H. (Weather Bureau, Washington, D. C.). Nucl. Safety, 7: 225-9; 234-5(Winter 1965–1966).

A tentative estimate of the magnitude of dispersion from a quasi-instantaneous source is obtained from the available experimental data. (G.O.Y.)

Natural Radioactivity and Fallout

See also HEALTH AND SAFETY

29404 (CEA-R-2880) MESURE DE L'INTENSITE TOTALE D'IONISATION AU VOISINAGE DU SOL ET SEPARATION DE SES DIFFERENTES COMPOSANTES. (Measurement of the Total Ionization Intensity Near the Ground and Separation of the Various Components). Grevet, Philippe (Commissariat a l'Energie Atomique, Fontenay-aux-Roses (France). Centre d'Etudes Nucleaires). 1966. 56p. Dep. mn.

Thesis. Submitted to Paris Univ., France.

An investigation was made to measure the total amount of ion-pairs produced in the air per unit time and unit volume. It is possible, furthermore, by using continuous recording to study the variations in the ionization due to α, β, and γ radiation at a height of one meter. The apparatus which was developed consists of two chambers of 120 liters: one, hermetically sealed detects the γ component, the other with a circulation of the ambient air detects the α and γ; it is thus possible by difference to evaluate the α component. The chambers and the associated electronic equipment were designed for continuous operation in the open air. Another chamber without walls can be used for measuring directly the total ionization intensity and from this an approximate calculation may be made of the β component. A series of recordings was made near Saclay where the natural radioactivity level is moderate, and in regions of low and high activity (near the sea and in the CEA's mining divisions). It was thus possible to show the variation in the γ component as a function of the geographic position of the measurement (from 3.7 to 6.3 l/cm^3/sec), the very large variations of the α component at a given place with changing meteorological conditions (from 1.5 to 45 l/cm^3/sec at Saclay for example) and the far smaller variations in the β component. (auth)

29405 (NP-14694) VOPROSY GLOBAL'NOGO RADIOAKTIVNOGO ZAGRYAZNENIYA VOD MIROVOGO OKEANA. (Problems of Overall Radioactive Contamination of the Waters of the Oceans). Bogorov, V. G.; Popov, N. I. (U.S.S.R. Sovet Ministrov. Gosudarstvennyi Komitet po Ispol'zovaniyu Atomnoi Energii). 1963. 10p. Dep. mn.

Radioactive contamination of the Atlantic and Pacific Oceans from waste disposal and fallout is estimated. Concentrations of ^{90}Sr in sea water and ^{90}Sr uptake by fish and marine organisms are discussed. The hazards posed by human consumption of contaminated fish are pointed out. (R.V.J.)

29406 (NP-14719) VYPADENIE Ce^{141}, Ce^{144}, Zr^{95} + Nb^{95} I Sr^{90} NA TERRITORII SSSR VO VTOROI POLOVINE 1962 G. (Fallout of ^{141}Ce, ^{144}Ce, ^{95}Zr + ^{95}Nb and ^{90}Sr on U.S.S.R. Territories in the Second Half of 1962). Malakhov, S. G.; Davydov, E. N.; Karagod, N. A. (U.S.S.R. Sovet Ministrov. Gosudarstvennyi Komitet po Ispol'zovaniyu Atomnoi Energii). 1963. 9p. Dep. mn

Radiochemical and γ-spectrometric analyses were made of the content of ^{141}Ce, ^{144}Ce, ^{95}Zr–^{95}Nb, and ^{90}Sr in fallout over various regions of the U.S.S.R. during the third and fourth quarters of 1962. Diagrams and tables were constructed to show seasonal fallout variations and latitudinal distribution of radioisotopes in European and Asiatic parts of the U.S.S.R. (R.V.J.)

29407 (AEC-tr-6666) GLOBAL FALLOUT PRODUCTS OF NUCLEAR EXPLOSIONS. Lavrenchik, V. N. Translation of Global'noe Vypadenie Produktov Yadernykh Vzryvov, Atomizdat, Moscow, 1965. 192p. Dep. mn. CFSTI $5.00 cy, $1.00 mn.

The quantitative relationships involved in the formation of fission products during nuclear explosions are reviewed and the important products formed in the fission of ^{235}U, ^{238}U, ^{239}Pu, and ^{232}Th by neutrons of various energies are tabulated. An evaluation of the spectrum of neutrons originating in nuclear and thermonuclear bombs is included. The interactions of neutrons with air, water, and soil are considered briefly, and a comparison is made of various sources of activity originating during a burst. Methods used for determining the date of formation of radioactive products are presented and basic methods of collecting and analyzing fallout samples are described. The process of the formation of radioactive aerosols and the behavior of radioactive aerosols in the atmosphere and in space are discussed. Equations for use in forecasting radioactive fallout from tropospheric or stratospheric fallout are included. A brief summary of contemporary concepts of the harmful biological effects of fallout radioactivity is also included. (173 references.) (C.H.)

29408 MEASUREMENTS OF ENVIRONMENTAL RADIOACTIVITY AT VALENCIA DURING 1964. Catala, J.; Garcia, A.; Diez, R.; Perez, R. (Facultad de Ciencias, Valencia). An. Real Soc. Espan. Fis. Quim. (Madrid), Ser. A, 62: 75-8(Mar.-Apr. 1966). (In Spanish).

The results are presented of measurements of the activity of atmospheric air, rain water, and settled dust carried out at Valencia during 1964. The general level of activity is relatively low and the only singular point is the detection of the first Chinese atomic bomb test, carried out in October 1964. (auth)

29409 TRITIUM CONTENT IN ATMOSPHERIC FALLOUT OVER MOSCOW DURING 1962–1963. Yakimenko, L. M.; Kuznets, E. D.; Tsionskii, V. M. At. Energ. (USSR), 20: 84-5(Jan. 1966). (In Russian).

Natural tritium is oxidized and usually found on the ground as the radioactive component of rainwater, amounting to several T units (1 T unit is defined as 1 tritium atom per 10^{18} hydrogen atoms). As the result of the atmospheric thermonuclear tests, the T level increased by 2 orders of magnitude and at times it reached several thousands of T units. The factors that affect the T level of rainwater include the distance of the point from the site of the explosion, the distance from large oceanic masses, geographic location, and meteorological conditions. Fission products may reside long periods in the upper layers of the atmosphere. The T level of precipitations collected in Moscow was systematically determined, starting in December 1961. The samples were first enriched by a three-stage electrolytic process, the deuterium content determined by the drop method, and the tritium determined by its activity in hydrogen, obtained by decomposing the water in vacuum over Mg amalgam. The reproducibility of the method was ascertained by α analyzing the same tap water samples repeatedly. The error of the measurements was ±10% and its sensitivity was 20 ± 10 T units. The tritium content of collected snow and rainwater samples increased from 523 in December 1961 to 5890 in July 1963, reaching values between 618 and 1125 T units in December 1963. (TTT)

29410 ACCUMULATION OF RADIOISOTOPES IN JUNIPERUS VIRGINIANA L. Pittillo, J. Dan; Plummer, Gayther L. (Univ. of Georgia, Athens). Bull. Ga. Acad. Sci., 23: 95-104(Sept. 1965).

Concentrations of fallout radioisotopes in components of juniper trees growing in highland and lowland granitic outcrops or in woodlands were determined. Computer analysis showed radioactivities decreased in order from ^{144}Ce to ^{106}Ru, ^{54}Mn, ^{137}Cs, ^{40}K, and ^{95}Zr. Juniper twigs often showed higher activities than leaves. Because new shoots are added each year and older leaves may remain on the stem for several years, the longer exposure period of the older parts would allow more accumulation. Bark generally had much less γ activity than that of other external parts, i.e., leaves and twigs. Radioactivities of ^{137}Cs, ^{54}Mn, and ^{40}K in woody tissues of juniper indicated that more fallout isotopes were present than the naturally occurring ^{40}K. Manganese-54 concentrations were considerably greater in sapwood than heartwood from outcrop junipers. Outcrop juniper contained more ^{137}Cs in the heartwood than sapwood. Juniper on the outcrops had higher concentrations of radioisotopes per g dry weight than those of woodlands. One explanation may be the greater exposure of outcrop trees to rainfall than the more protected woodland trees, but a better explanation might be greater absorption by outcrop trees due to less mineral availability in the poorly developed outcrop soils. Foliar absorption may be the primary mode of entry for some radioisotopes, whereas others enter primarily through the roots. Data from juniper are compared with 1962 data from spruce. (TCO)

29411 PHYSICAL DATA ON RADIOACTIVE DEBRIS RESULTING FROM NUCLEAR EXPLOSIONS AND WORLD EXPERIENCE WITH ATMOSPHERIC FALLOUT. Santholzer, Vilem (Charles Univ., Hradec Kralove, Czechoslovakia). Cesk. Cas. Fys., 16: 228-41(1966). (In Czech).

The fundamental characteristics of radioactive debris, its size, density, etc., are explained. A survey is given of information about the collection of atmospheric fallout, the transport and falling-out of debris, the composition of at-

mospheric fallout and some nuclides occurring in the biosphere as a consequence of atomic explosions. Special attention is paid to the period of megaton nuclear tests in 1961–1962 and to the period after they had been stopped. (auth)

29412 THORIUM AND URANIUM ISOTOPES IN SEA-WATER AND SEDIMENTS. Somayajulu, B. L. K.; Goldberg, E. D. (Univ. of California, San Diego, La Jolla). Earth Planet. Sci. Lett., 1: 102-6(May 1966).

Thorium concentrations in three open Pacific Ocean water samples had values of $n \times 10^{-10}$ grams/liter, concentrations similar to those previously measured in the Atlantic. Radioactive disequilibrium exists between the dissolved forms of ^{228}Th and ^{232}Th and the dissolved, excess unsupported ^{228}Th apparently is introduced by the input of ^{228}Ra from the particulate phases containing ^{232}Th. The $^{230}Th/^{232}Th$ ratios in seawater are similar to those taken from the surface sediments in the same area. Differences in the $^{230}Th/^{232}Th$ ratios in barite and foraminifera extracted from the same levels in sediments are suggestive of differences in the ratio between surface and deep ocean waters. (auth)

29413 SINGLE-SAMPLE POTASSIUM-ARGON AGES USING THE OMEGATRON. Crasty, R. L.; Mitchell, J. G. (Cambridge Univ., Eng.). Earth Planet. Sci. Lett., 1: 121-2(May 1966).

A method of potassium-argon age determination is suggested, in which the sample is irradiated with neutrons and the $^{40}Ar/^{39}Ar$ ratio is subsequently measured. Determination of the neutron absorption of the sample involves irradiation of samples of known ages and measurement of the relative abundances of the resultant argon isotopes. Relative abundances of the argon isotopes are determined using a standard argon extraction line in conjunction with the omegatron. (A.G.W.)

29414 PRELIMINARY INVESTIGATION OF THE SOURCE OF LEAD AND STRONTIUM IN DEEP GEOTHERMAL BRINES UNDERLYING THE SALTON SEA GEOTHERMAL AREA. Doe, B. R.; Hedge, C. E.; White, D. E. (Geological Survey, Denver. Geological Survey, Menlo Park, Calif.). Econ. Geol., 61: 462-83(May 1966).

A radiogenic tracer study was made of lead and strontium in deep geothermal brines, salt from brine, and the upper Quaternary rhyolite domes near the Salton Sea in the Imperial Valley, California. Data on the brines and rhyolite glasses were compared to those from Quaternary Colorado River and Tertiary sediments of the area. The brines sampled contained ~100 ppM Pb, sufficient for consideration as a possible ore-forming fluid. The isotopic data indicated that 80 to 100% of the strontium and 50 to 100% of the lead in these brines were acquired from associated sediments. The isotopic compositions of lead and strontium in the Quaternary rhyolite glasses were distinctly different from those of the sediments and brines. The strontium data suggested that the rhyolite glasses were derived from basaltic or gabbroic material but may have attained as much as 40% of their strontium from upper crustal rocks such as the sediments analyzed. (auth)

29415 THORIUM, URANIUM AND POTASSIUM CONCENTRATIONS IN GRANITES AND GNEISSES OF THE RUM JUNGLE COMPLEX, NORTHERN TERRITORY, AUSTRALIA. Heier, K. S.; Rhodes, J. M. (Australian National Univ., Canberra. Bureau of Mineral Resources, Canberra, Australia). Econ. Geol., 61: 563-70(May 1966).

The concentrations of thorium, uranium, and potassium were determined in the granites and gneisses of the Rum Jungle Complex. The arithmetic means of all the rocks analyzed are 10.3 ppM U and 45.7 ppM Th. This is more than twice the average concentrations of these elements in granites of similar major element composition reported in the literature. High concentrations of thorium and uranium are also found in the "younger granites" within this area. It is demonstrated that the Rum Jungle Complex and the surrounding area is a thorium, uranium province. The sediments that can be demonstrated in parts to be derived from material similar to the granites of the Rum Jungle Complex would inherit the high concentrations of uranium and thorium. Subsequent separation of thorium and uranium with concentration of uranium in structurally favorable zones took place during a period of low-grade metamorphism. This may have resulted from mobilization of the uranium occurring dispersed throughout the sediments or by mobilization and leaching of the basement granites. (auth)

29416 DEPOSITION OF ATMOSPHERIC FALLOUT BY PRECIPITATION IN A SUBCLOUD LAYER. Chalov, P. I.; Tsevelev, M. A. (Inst. of Physics and Mathematics, Academy of Sciences, USSR). Fiz. Atmos. Okeana, 2: 205-7(1966). (In Russian).

Radioactive fallout was investigated by establishing three stainless steel sampling stations with a collecting area of 0.38 m^2 on the side of a mountain at 2070, 2477, and 2689 m above sea level. The horizontal distance between sampling points was 550 m between the two lowest points and 370 m between the two highest points. The water samples were evaporated and the beta activity was determined in the residue. The type of cloud formation had an effect on the rate of fallout. With stratocumulus clouds fallout was consistently observed in the rain. The total radioactive fallout was higher at the lower altitudes. It was concluded that although fission product fallout by atmosphere precipitation does take place, the effect is quite variable. (TTT)

29417 THE DEPENDENCE OF THE RADIOACTIVITY AND THE CONTENT OF CHEMICAL ELEMENTS ON THE MECHANICAL COMPOSITION OF SEDIMENTARY ROCKS. Kovalevskii, A. K. (Buryat Complex Scientific-Research Inst., Academy of Sciences, Ulan-Ude, USSR). Geokhimiya, No. 3, 362-8(Mar. 1966). (In Russian).

The relation between radioactivity and clays in rock fractions of less than 0.01 or 0.02 mm was established for sedimentary rocks of the Western Siberian lowlands. The comparative natural fluctuations of the radioactivity from this relation reached ±4 to 10%. The actual deviations were substantially misrepresented by errors in the analysis. The presence of a close relation between the radioactivity and the clay of mountain rocks can be used for geological mapping of lithological varieties of rocks differing in their mechanical composition. In some cases the use of the relation between radioactivity and clay of the rocks can exclude the effects of the nonhomogeneity of the mechanical properties of mountain rocks. The presence of a clear dependence of the concentration of the series of chemical elements in sedimentary rocks on their clays, particularly concentrations of zinc, nickel, manganese, and cobalt, can be used to obtain concentrates. The presence of a close relation between the radioactivity and a series of geochemical parameters studied and between the radioactivity and the clays of sedimentary rocks confirmed that sufficiently tight interactions occur between some chemical elements to permit their use in practical prospecting in geochemical studies. (tr-auth)

29418 ON THE DISTRIBUTION OF THE URANIUM AND THORIUM CONTENT IN EFFUSIVE AND INTRUSIVE FORMATIONS OF THE NORTHEASTERN BALKHASH FORELAND. Kazmin, V. N. (Central Kazakhstan Geological Dept., Karaganda, USSR). Geokhimiya, No. 3, 369-73(Mar. 1966). (In Russian).

The distribution of uranium and thorium in effusive and intrusive formations of the region does not contradict the hypothesis on their normal distribution. Thorium at the boundary of each group has a comparatively lower dispersion and a smaller coefficient of variation than the uranium. The distribution of uranium and thorium, their mean concentration in all effusive carbonate formations, and their distribution in intrusive formations of all ages is practically the same in spite of the different composition of these formations. The intrusive formations of the Permian and carbonaceous periods are sharply differentiated from each other with respect to the distribution and mean concentration of uranium and thorium. The mean concentration of uranium and thorium for the area investigated is 1.5 to 2 times less than the mean concentration of these elements in rocks around Vinogradov. (tr-auth)

29419 URANIUM IN TRAPS OF THE SIBERIAN PLATFORM. Masaitis, V. L.; Abramovich, I. I.; Dodin, D. A.; Smyslov, A. A. (All-Union Scientific-Research Inst. of Geology, Leningrad). Geokhimiya, No. 5, 511-24 (May 1966). (In Russian).

The average uranium content in traprock formations of the Siberian platform depends on the petrochemical type of the parent magma, which formed as a result of selective fusion of the mantle matter at different depths. By their uranium content the Siberian traps are on the whole close to tholeitic basalts of other regions of the Earth and strongly differ from highly radioactive alkaline basaltoids of mesocenozoic activation zones. (auth)

29420 ARTIFICIAL RADIOACTIVITY IN RAIN-BORNE DUST AND IN RAIN WATER OBSERVED IN CALCUTTA DURING 1962. Das, S. K.; Chatterjee, S. D. (Jadavpur Univ., Calcutta). Indian J. Meteorol. Geophys., 15: 487-8 (1964).

The total maximum β-activity was of the order of 0.5 mμC per liter of rain water. (Indian Sci. Abstr.)

29421 STATISTICAL ERRORS IN DETERMINING CONCENTRATIONS OF RADIOACTIVE ELEMENTS IN ROCKS USING γ-THRESHOLD AND DIFFERENTIAL SPECTROMETERS. Balyasnyi, N. D.; Kogan, R. M.; Mishenko, V. M.; Renne, O. S.; Fridman, Sh. D. Izv. Akad. Nauk SSSR, Fiz. Zemli, No. 4, 89-97(1966). (In Russian).

Gamma count rates at a given energy threshold or in a given energy interval can be used to estimate the amounts of elements such as radium, thorium, and potassium in soils and rocks. The errors are due to the instability of the spectrometer energy scale, the statistics of radioactive decay, and the variation in activity concentrations with depth. With a 1% energy scale drift it was calculated that the error in determining the uranium concentration is 100% at a U/Th ratio of 0.1, and that the error is 30% at a U/Th ratio of 1.0. The error in determining thorium was 15% at a U/Th ratio of 1, and 100% at a U/Th ratio of 10. Thus, drift introduces considerable error in determining low concentrations of an element. With a NaI crystal 70 mm in diameter and 50 mm high at a counting time of 1 minute, the statistical counting error was 100%, for a uranium concentration of 10^{-3}% and a thorium concentration of 0.1%. The statistical counting error for Th was 45% at a Th concentration of 10^{-3}% and a U concentration of 0.1%. The errors in determining uranium were high with a variation of Th concentration with depth. Thus, the error was 115% at a Th/U of 10 with a threefold variation of Th with depth (m = 3). The error was 500% at m = 6. (TTT)

29422 RADIOACTIVE FALLOUTS FROM THE THREE NUCLEAR EXPLOSIONS OF LATE 1964 AND THE EARLY 1965. Murayama, N. Kishocho Kenkyu Jiho, 17: 246-58 (Apr. 1965). (In Japanese).

Radioactive fallout caused by the low-yield nuclear explosion in the Takla Makan desert on October 16, 1964 was surveyed in Japan. Radioactive debris was transferred through such lower altitudes as several kilometers. The first arrival of debris on the ground was dry, while wet fallout arrived after the lapse of 3 days. Highly active and short-lived giant particles were detected at one day. The β decay curve had a definite angle at about 260 hours after the production time. Observations suggested that scatter of values of radioactivity concentrations in air or in rain came from the existence of an extremely active single particle in the radioactive fallout in its early period. Radioactive fallout caused by the underground nuclear explosion in Semipalatinsk on January 15, 1965 was also surveyed. Radioactive debris was carried through lower altitudes such as the 850 mb level, with 5 days of elapsed time. The debris had a considerably long half life. Surveys of radioactive fallout from the second Chinese nuclear detonation on May 14, 1965 were supplemented. This fallout was characterized by the delayed arrival of the radioactive cloud through the middle troposphere and an extremely small number of highly radioactive giant particles as compared with the October 16, 1964 case. (auth)

29423 STUDIES ON FALLOUT PARTICLES. V. Mamuro, Tetsuo; Yoshikawa, Kazuko; Matsunami, Tadao; Fujita, Akira (Radiation Center of Osaka). Nippon Genshiryoku Gakkaishi, 8: 242-8(May 1966). (In Japanese).

Two distinct types of radionuclide fractionation were discerned in the highly radioactive fallout particles originating from the first Chinese nuclear test explosion of 16 October 1964. The first type is similar to the fractionation observed in the highly radioactive fallout particles from the large-scale airbursts carried out by the U.S.S.R. in the autumn of 1961 and 1962. The radiochemical composition of the particles fractionated according to this type was invariably highly enriched in $^{95}Zr + {}^{95}Nb$ and depleted in ^{103}Ru, and more or less enriched or depleted in most other nuclides. The particles of the second type were highly enriched in ^{103}Ru and depleted in $^{95}Zr + {}^{95}Nb$. This second type of fractionation was never observed in the Russian particles examined. Fractionation factors were measured for some of the present Chinese samples. It was found that the particles having markedly high activity among the 300 particles collected were all fractionated according to the second type, and that the others were fractionated in different degrees, some being of the first, and others being of the second type. Such difference in fractionation behavior between the Chinese and the Russian particles might be attributed to the fact that the former were produced in a small-scale land surface and the latter in large-scale airbursts. (auth)

29424 RADIOACTIVITY OF CERTAIN ORGANISMS FOUND AT THE BOTTOM OF THE NORWEGIAN SEA FLOOR. Fedorov, A. F.; Kilezhenko, V. P. Okeanologiya, 3: 123-6(1963). (In Russian).

Benthic samples were collected by the trawler Sigsbi at seven stations in the north, east, and southern parts of the Norwegian Sea. The radioactivity of 39 of the larger benthic forms was investigated after drying to constant weight at 100 to 120°C. The concentration coefficients varied from 1.14 to 7.25. The beta activity of the dry residue was counted on a large disk with an area of 60 cm^2 to avoid self-absorption errors. The radioactivity of the samples was a factor of 10 higher at 3 of the stations than it was at the other four stations. A significant amount of a 10 to 12 day short-lived contamination was detected at two of the stations showing high activities. (TTT)

29425 RADIOCHEMICAL COMPOSITION OF IRON–MANGANESE CONCRETIONS AND MANGANESE ORES. Efimova, E. I.; Nikolaev, D. S. Radiokhimiya, 7: 603-14 (1965). (In Russian).

A radiochemical investigation was made of the iron–manganese concretions from the Barents and Kara Seas, the Gulf of Riga, the Gulf of Finland, and of manganese ore samples from Nikopolsk and Chiatursk Strata. The concentration of uranium, ^{230}Th, radium, and thorium were determined. The concentration of uranium found in the concretions and manganese ores studied was analogous to the uranium concentrations in concretions from the Pacific and Indian Oceans. With the exception of concretions from the Barents Sea, very poor in radium, all the investigated concretions had approximately the same radium concentrations as concretions from the ocean. Very low concentrations of thorium and ^{230}Th were observed in the concretions and manganese ores. A sharp displacement of the radioactive equilibrium between uranium, ^{230}Th, and radium was established both in the concretions and in the strata. The size of the ratios Ra/U and $^{230}Th/U$ greatly exceeded the equilibrium value. The sample of manganese ore was characterized by equilibrium ratios of the radioactive elements. The ratios established between the radioactive elements and the phenomenon of radium migration from the concretions to the exterior exclude the possibility of reliable calculations of the concretion age. (tr-auth)

29426 ON THE FORMS IN WHICH CAN BE FOUND RADIOACTIVE ELEMENTS IN IRON–MANGANESE CONCRETIONS. Nikolaev, D. S.; Efimova, E. I. Radiokhimiya, 7: 614-22(1965). (In Russian).

Published data on the form on uranium, thorium, ^{230}Th, and radium, in iron–manganese concretions were ex-

amined. Ocean water appeared to be the enrichment source of the radioactive elements in the iron–manganese concretions. The transition mechanism of uranium, thorium, ^{230}Th, and radium from the water to the iron–manganese concretions in the aging period leads to sorption on suspensions, especially on iron and manganese hydroxides during their precipitation on the bottom. The subsequent secondary migration of radium from the internal layers of the concretions to the mud and sea water agreed with the radium surplus in ocean water. An hypothesis on the degree of time dependence obeying the linear equation between the concentrations of thorium, ^{230}Th, and radium and the residence time of suspensions in aqueous solutions is presented. If this hypothesis can be experimentally confirmed, then there would be a very effective method available for establishment of the time of occurrence of suspensions in water strata and, therefore, ideas on the speed and direction of mobility of the water mass in reservoirs. (tr-auth)

29427 DETECTION AND MEASUREMENT OF RADIOACTIVITY IN PULP. **Tinnis, Walentin (Kymmene Co., Kuusankoski, Finland). TAPPI, 48: 391-5(July 1965).**

Investigations begun after World War II showed that radioactive contamination of x-ray and photographic materials was caused by low-energy beta rays and that contamination of the raw material came from air and process water. The radioactivity of the photographic paper and its pulp can be determined autoradiographically or with a sensitive radiation detector. Since 1960 the Kymmene Co. has made measurements of the specific radioactivity of the bleached sulfite pulp produced. In 1960 beta radioactivity was about 30; it is now a little below 500 pC/m^2 of pulp. (557 pC/m^2 of pulp is set as an acceptable maximum at the demonstrable fog density of x-ray film.) The process water has varied between 200 and 780 pC/m^3 for mechanically purified water, and between 10 and 180 pC/m^3 for chemically purified water. Radioactivity of the pulp has been shown to be caused principally by cerium-144, ruthenium-106, and cesium-137, as well as zirconium-95 and niobium-95. (Public Health Eng. Abstr.)

29428 RADIOLOGICAL HEALTH DATA AND REPORTS. Volume 7, Number 1. Public Health Service, Washington, D. C., Jan. 1966. 56p. GPO $0.50.

Data are presented on fallout radioactivity in samples of milk, other foods, total diet, surface waters, and precipitation collected throughout the U.S. and throughout the Americas during 1965. Data are included on the ^{131}I content in bovine thyroids collected from Jan. through June, 1965. Environmental levels of radioactivity during the first half of 1965 are reported for the Union Carbide Nuclear Company, Oak Ridge, Tenn., and Paducah, Ky., and the Goodyear Atomic Corp., Piketon, Ohio. Data are included on three U.S. underground nuclear tests announced by the Atomic Energy Commission during Dec. 1965. Separate abstracts were prepared for three sections of this report. (C.H.)

For abstracts of individual sections see: 29429, 29430, and 29472.

29429 THE APPEARANCE OF ^{131}I AND ^{140}Ba–La IN FALLOUT DUE TO THE SECOND CHINESE NUCLEAR TEST. Johnson, James E.; Wilson, Daniel W.; Ward, Gerald M. (Colorado State Univ., Fort Collins). Radiol. Health Data Rep., 7: 1-2(Jan. 1966).

Fresh fission product debris of the May 14, 1965 Chinese nuclear device test was detected at Fort Collins Colo., on May 25. Levels of ^{131}I in milk reached a peak of 130 pCi/liter on June 5. Barium–lanthanum-140 was not detected in milk samples. The expected spring increase of ^{137}Cs was observed in forage and milk samples. (auth)

29430 GAMMA ACTIVITY IN SURFACE AIR: 80TH MERIDIAN NETWORK, JANUARY–MARCH 1965. Krey, Philip W. (U. S. Atomic Energy Commission, New York). Radiol. Health Data Rep., 7: 3-9(Jan. 1966).

Monthly measurements of gamma activity during the first quarter of 1965 are presented for stations in both hemispheres along the 80th meridian W. Latitude profiles of the results for the first 3 months of 1965 show maxima at midlatitudes for both hemispheres, a low near the equator, and a minimum at Chacaltaya, Bolivia. Comparison of first-quarter profiles for 1964 and 1965 indicates generally similar shapes, although gamma activity decreased sharply in the Northern Hemisphere in early 1965. Average concentrations for the hemispheres show spring maxima and evidence of the mainland Chinese nuclear test of October 16, 1964, as well as different trends in the two hemispheres. (auth)

29431 RADIOLOGICAL HEALTH DATA AND REPORTS. Volume 7, Number 2. Public Health Service, Washington, D. C., Feb. 1966. 84p. GPO $0.50.

Data are presented on environmental levels of radioactivity from fallout in samples of milk, selected foods, total diet, precipitation, and surface waters throughout the United States, and at representative Canadian and Pan American locations during 1965. Data are included on the radioactivity of Minnesota municipal water supplies and environmental levels of radioactivity at the Hanford Works, Pinellas Peninsula Plant, Fla., Savannah River Plant, and Shippingport Atomic Power Station, Penna., during the first half of 1965. Three underground nuclear tests were announced by the Atomic Energy Commission during Jan. 1966 and brief data are included. Separate abstracts have been prepared for three sections. (C.H.)

For abstracts of individual sections see: 29432, 29433, and 29473.

29432 ^{137}Cs IN MILK, MEAT, AND MAN IN NORWAY, 1962–1965. Madshus, Kjell; Stromme, Aksel; Koren, Kristian. Radiol. Health Data Rep., 7: 61-3(Feb. 1966).

Studies in Norway indicate regular seasonal patterns of ^{137}Cs concentrations in milk with a general increase in mean concentration from 75 pCi/liter in 1962 to 300 pCi/liter in 1965 in spring milk. Increases in ^{137}Cs body burdens from 16.0 to 80.9 nanocuries, observed from March 1963 through October 1964, roughly paralleled increases in milk concentrations of ^{137}Cs for this period. Results of analyses for ^{137}Cs in lamb and beef ranging from 0.3 to 23.7 nCi/kg of meat are given, but no trends are indicated. Lamb showed higher concentrations than beef. (auth)

29433 ^{90}Sr IN FOOD: A SUMMARY OF RESULTS ON SELECTED FOODS IN THE UNITED STATES, JULY 1962–OCTOBER 1963. Setter, Lloyd R.; Smith, Donald; Spector, Mozart (Public Health Service, Washington, D. C.). Radiol. Health Data Rep., 7: 64-78(Feb. 1966).

Strontium-90 content and ^{90}Sr, Ca, ratios are summarized for nine staple foods sampled during a six-consecutive quarter household survey which began in July 1962. The data are grouped into six broad geographical regions of production insofar as possible. Strontium-90 concentrations in whole milk and evaporated milk showed regional differences and observable trends in a 3- or 6-month period; ^{90}Sr concentrations in bread had similar but less pronounced trends. Regional trends in ^{90}Sr were least discernible for potatoes, eggs, meat, fruit, and oleomargarine, due in part to the low ^{90}Sr content per unit weight and presumably to interregional shipment of food and feed. Foods such as cabbage, potatoes, and fruit had ^{90}Sr/Ca ratios greater than those for whole milk and evaporated milk. (auth)

29434 RADIOLOGICAL HEALTH DATA AND REPORTS. Volume 7, Number 3. Public Health Service, Washington, D. C., Mar. 1966. 69p. GPO $0.50.

Data are presented on environmental levels of radioactivity from fallout in samples of milk, representative diets, precipitation, surface waters, and atmosphere throughout the United States and selected sites in Canada and Pan America during 1965. Data are included on gross β activity in California water supplies during the first half of 1965 and the content of ^{137}Cs, ^{89}Sr, and ^{90}Sr in muscle, rumen contents, and bone of Alaskan caribou and reindeer sampled from 1963 through 1965. Results of environmental radiation monitoring at Argonne National Lab., Lamont Ill., Atomics International, Canoga Park, Calif., and the National Reactor

Testing Station, Idaho Falls, Idaho, during the first half of 1965 and at the Feed Materials Production Facility, Weldon Spring, Mo., during 1964. Data are summarized for two underground nuclear tests announced by the Atomic Energy Commission during February 1966. Separate abstracts have been prepared for three sections. (C.H.)

For abstracts of individual sections see: 29474–29476.

29435 $^{230}Th/^{238}U$ AND $^{234}U/^{238}U$ AGES OF ELEVATED PLEISTOCENE CORAL REEFS AND THEIR GEOLOGICAL IMPLICATIONS [Thesis]. Veeh, Hans Herbert. San Diego, Calif., Univ. of California, 1965. 103p.

Unrecrystallized fossil corals occurring in their growth positions between 2 and 9 m above mean low tide at many locations in the Pacific and Indian Oceans were dated by the $^{230}Th/^{238}U$ and $^{234}U/^{238}U$ methods. Where possible, live corals were also collected and analyzed for their U and Th isotopes. The U contents of the corals were determined fluorimetrically; the $^{234}U/^{238}U$ activity ratios, and the Th concentrations were ascertained by alpha spectroscopy. The $^{230}Th/^{238}U$ ages of the fossil corals range from 90,000 ± 20,000 to 160,000 ± 40,000 years B.P. and the $^{234}U/^{238}U$ ages range from 80,000 ± 50,000 to 180,000 ± 60,000 years B.P. Absence of ^{230}Th in recent corals, independent of location, shows that the assumptions made for the age determinations are reasonable. An average U concentration of 2.4 parts per million in the recent corals, in comparison with an average 2.6 parts per million in the fossil corals, suggests that most of the U occurring in the fossil corals is of primary origin. The absence of ^{232}Th in the corals confirms the assumption that the ^{230}Th found in the fossil corals arose solely by radioactive decay of its parent U. Control samples of pre-Pleistocene material showed radioactive equilibrium between the various members in the ^{238}U decay chain. Both the internal consistency of the ages, within the limits of experimental error, and the agreement between the $^{230}Th/^{238}U$ and $^{234}U/^{238}U$ ages, strongly support the general validity of these ages. If the assumptions made are correct, the ages obtained for the elevated reefs define the time when the corals were growing in a sea that stood between 2 and 10 m higher, relative to the sample locations, than at present. The similarity of the $^{230}Th/^{238}U$ ages of Pleistocene coral reefs with like elevations above sea level in many localities suggests a eustatic sea level stand between 2 and 10 m higher than now at about 120,000 ± 20,000 years B.P., possibly during an interglacial stage of the Pleistocene. (Dissertation Abstr.)

29436 ABUNDANCE AND DISTRIBUTION OF SCANDIUM IN COMMON ROCKS AND PARTICLE COMPETITION IN NUCLEAR DE-EXCITATION [Thesis]. Norman, Jack Clifford. Madison, Wis., Univ. of Wisconsin, 1965. 79p.

The Sc, Fe, Co, and Cr contents of more than 60 common rocks were determined by instrumental neutron activation analysis (INAA). Comparison of the results of INAA with the results of other methods indicates that Sc and Fe may be determined with an accuracy of about ±10% and Co with an accuracy of about ±20%. Cr contents found by INAA are erratically higher than those found by other methods, probably because of interference from Th in the rocks. The Sc content decreases with igneous rock type in the order basic, ultrabasic, acid. No significant correlation was found between the Sc and Fe contents of igneous rocks. A good correlation of the Sc and Fe contents of sedimentary rocks was found, indicating that Sc is precipitated with $Fe(OH)_3$ in the formation of sediments. No correlation of the rare-earth elements with Sc was found. The effects of proton and alpha-particle competition on neutron emission leading to the formation of the isomeric pair $^{87,87m}Y$ were estimated using statistical model calculations. The angular-momentum distributions of the residual nuclei are substantially changed by the competing particles, but proton and alpha emissions are such rare events that they do not appreciably affect the isomeric cross-section ratios. (Dissertation Abstr.)

29437 ESTESTVENNAYA RADIOAKTIVNOST' RASTENII I POCHV. (Natural Radioactivity of Plants and Soils). Grodzinskii, D. M. Kiev, Naukova Dumka, 1965. 216p.

Data on the natural radioactivity of plants and soils and its significance in plant life and soil fertility are summarized. Methods of studying natural radioactivity and of determining U, Ra, Th, Po, and other natural radioelements in plants and soils are discussed. The nature of radioactivity of various types of plants and regional soils and the radiation field produced by this radioactivity in the biosphere are described. New data are included on the biophysical and biochemical processes on which the effects of radioactivity on growth depend. The role of radioactivity in the origin of life on earth and in the evolution of species is shown. The physiological role of natural radioactivity, the significance of the radioactive properties of an element essential to plant nourishment, potassium, and practical uses of naturally radioactive elements are discussed. (tr-auth)

Techniques and Equipment

Refer also to abstract 30950.

29438 (CONF-650652) RADIOCARBON AND TRITIUM DATING. Proceedings of the Sixth International Conference Held at Washington State University, Pullman, Washington, June 7–11, 1965. Chatters, Roy M. (comp.) (Washington State Univ., Pullman); Olson, Edwin A. (comp.) (Whitworth Coll., Spokane, Wash.). Contract AT(45-1)-353. 800p. Dep. mn. CFSTI $8.00 cy, $3.25 mn.

Seventy-three papers are included on: radiocarbon processing and counting; radiocarbon dating in New World Archeology; radiocarbon dating in European Archeology; radiocarbon dating in general archeology; tree rings and radiocarbon dating; preparation and counting of tritium; tritium and radiocarbon in the atmosphere and ocean; carbon-14 and tritium in hydrology; and radiocarbon dates in geologic chronologies. Invited addresses on: natural radiocarbon and tritium in retrospect and prospect; problems in the establishment of a carbon-14 and tritium laboratory; and the impact of radiocarbon dating upon archeology are also included. (P.C.H.)

29439 DETERMINATION OF ISOTOPE RATIOS AND MODEL AGES OF BOLIVIAN ANDES LEAD ORES. Stahl, Wolfgang J. Geochim. Cosmochim. Acta, 30: 515-23 (May 1966). (In German).

The lead isotope ratios and the model ages of 23 lead ore samples from the region of the Bolivian Andes are reported. The model ages cover a period of 400×10^6 years and indicate a regional concentric convergent decrease in age. Concordances in the model ages are discernible along tectonic lines of disturbances. An estimation of errors to the Holmes-Houtermans age model is included. (auth)

29440 SOLAR SIMULATION TESTING OF THE NUCLEAR TEST DETECTION SPACECRAFT. Goldman, K. L.; Glenn, E. E.; Lehr, S. N.; Norris, J. E. (TRW Systems, Redondo Beach, Calif.). Contract AF04(695)-36. J. Spacecraft Rockets, 3: 658-66(May 1966).

A test program for solar simulation of the nuclear test detection satellite was carried out in three steps, a full-scale engineering model development test, 10-day full-scale operational qualification test of the prototype spacecraft, and 7-day operational acceptance test of each flight spacecraft. The value of the composite test program was demonstrated through comparison and application of test data and, ultimately, through successful launch and performance in orbit of twin flight spacecraft. The model test provided accurate, early verification of spacecraft thermal control design and flight instrumentation performance. The data obviated more extensive spacecraft testing and were useful in evaluating solar simulation performance and the interaction with spacecraft configuration. The prototype test provided valuable data on spacecraft performance not otherwise obtainable except by flight testing. Limitation in spacecraft operation under solar simulation conditions could be determined, thereby allowing modifications to the flight spacecraft. Finally, solar simulation of the flight spacecraft provided excellent indication of performance in orbit and was useful in demonstrating reliability. (auth)

29441 THE IONIUM/URANIUM METHOD FOR THE DETERMINATION OF THE AGE OF RECENT VOLCANIC MINERALS. Cerrai, E. (CISE, Milan); Lonati, R. Dugnani; Gazzarrini, F.; Tongiorgi, E. Rendic. Soc. Mineral. Ital., 21: 47-62(1965). (In Italian).

An ionium/uranium method for the determination of the age of minerals is proposed. It is based on the determination of uranium chemically and of ionium (^{230}Th) by γ spectrometry. If a chemical separation of thorium from uranium and other α-emitting descendants is performed, the method gives sufficiently precise results. The details of the determination of U, Th, and ^{230}Th in zirconia and ilmenite are reported. The procedure consists of decomposition of the mineral, separation of the uranium from the other elements and its quantative determination, separation of the thorium from the other elements, and γ spectrometry of the thorium for determination of the ^{230}Th activity. The ^{230}Th/U ratio in the zirconia and ilmenite in concentrates was measured and the results graphed. (J.S.R.)

29442 METHOD OF COMPENSATING FOR THE IRON CASING EFFECT IN RADIOACTIVE WELL LOGGING. Caldwell, Richard L. (to Socony Mobil Oil Co.). U. S. Patent 3,246,152. Apr. 12, 1966. Filed Sept. 14, 1961.

A method of obtaining a radioactive log of an iron cased borehole that is free from both background and iron interference includes the irradiation of a synthetic environment with primary radiation to produce a secondary radiation representative of the background and the iron contribution. The secondary radiation so produced is detected to yield a first function representative of this secondary radiation. The borehole is then irradiated with primary radiation, and a second function representative of the secondary radiation detected within the borehole is obtained. The two functions are compared to obtain a log free from background radiation including the effect of the iron casing. (B.L.M.)

29443 SHIELDING SYSTEM FOR A CHLORINE LOGGING APPARATUS. Reed, Dale H.; Dunlap, Henry F.; Pritchett, William C. (to Atlantic Refining Co.). U. S. Patent 3,246,157. Apr. 12, 1966. Filed July 12, 1962.

A shielding array for a chlorine logging apparatus reduces borehole effects, does not interfere with neutrons entering the formation, prevents source originating gamma rays from reaching the detector, absorbs thermal neutrons in a manner to produce minimum borehole effects, and reduces to the minimum detection of gamma rays in the chlorine energy spectrum that originate from captures other than in the formation of interest. The chlorine logging sonde has a neutron source at the lower end and a scintillation crystal and a photomultiplier tube located above the source. The shielding array consists of a lead shield positioned between the source and the scintillation crystal, a bismuth shield having a longitudinal dimension less than the lead shield positioned above the adjacent to the lead shield, and a boron shield located in a groove in the outside portion of the sonde encircling the scintillation crystal and having an outside diameter substantially equal to that of the sonde. The boron shield may be replaced by two boron shields, located between the bismuth shield and the scintillation crystal and the second located outside the sonde at least opposite the crystal. (B.L.M.)

29444 NEUTRON GENERATING DISCHARGE TUBE. Frentrop, Arthur H. (to Schlumberger Well Surveying Corp.). U. S. Patent 3,246,191. Apr. 12, 1966. Filed Mar. 23, 1961.

A neutron generator is described that is small enough in diameter to permit its introduction into a cased or uncased deep well and short enough in length for convenient source-detector spacing for well logging operations. The source section of the generator comprises an envelope containing an ionizable gas and having oppositely disposed openings. A pair of magnetic members each disposed in one of the openings have electrically conductive confronting surfaces and are sealed in gas-tight relationship at the envelope openings to define the cathode electrodes. A magnetic annulus surrounds the envelope and has opposite portions disposed in flux linking relation to the magnetic members to provide a flux path with the magnetic members. An annular anode electrode is supported within the envelope and is composed of a material capable of absorbing and emitting the ionizable gas. The target section of the generator includes a target within the envelope that is adapted to react with ions of the ionizable gas when a high potential is applied to the target. This target is supported within the envelope in sealed relation with respect to the electrodes and the filament. (B.L.M.)

29445 SCINTILLATION-TYPE WELL LOGGING DEVICE WITH TWO CRYSTALS RESPONDING SEPARATELY TO THERMAL NEUTRONS AND GAMMA RAYS. Hall, Hugh E. Jr. (to Texaco Inc.). U. S. Patent 3,247,377. Apr. 19, 1966. Filed Apr. 12, 1962.

A neutron well logging apparatus is described for quantitatively determining the presence of hydrogen in liquid-filled earth formations traversed by the borehole in which a thermal neutron component is introduced into the response of the neutron-gamma log in order to produce a log that is more nearly indicative of the hydrogen content. The thermal neutron response and the gamma radiation are detected by a scintillation type radiation detector. The detector is made up of two luminophor elements: the first of which is sensitive to gamma radiation, for example a TlI_3 activated NaI crystal, and the second luminophor which surrounds the first and which is sensitive to thermal neutrons, for example an Eu activated LiI crystal. Preferably, in actual use, the relative volumes of the two luminophor elements are in a predetermined relationship such that an increase in the response of the gamma detecting luminophor due to the presence of chlorine nuclei in formations adjacent to the borehole is substantially compensated by a decrease in the response of the thermal neutron detector. Thus the overall response of the detector is substantially independent of the chlorine content of the formations. (B.L.M.)

29446 METHOD OF CHLORINE LOGGING IN A NON-FERROUS ENVIRONMENT. Caldwell, Richard L.; Salaita, George N. (to Socony Mobil Oil Co., Inc.). U. S. Patent 3,247,381. Apr. 19, 1966. Filed Dec. 29, 1960.

The sensitivity of a well logging system suitable for chlorine logging is improved to enable discrimination between salt-water-saturated and oil-saturated formations by limiting the range of recorded gamma rays to those having energies of from about 4.6 to 6.3 Mev. To prevent interference from iron, a non-ferrous environment is provided by making the housing of the logging tool of Al, Mg, Zr, or Be. It is also preferable that the borehole be cased with Al. (B.L.M.)

Thorium and Uranium Minerals

29447 INVESTIGATION OF RARE-EARTH CARBONATES USING INFRARED SPECTROSCOPY. Akhmanova, M. V.; Orlova, L. P. (Vernadskii Inst. of Geochemistry and Analytical Chemistry, Moscow). Geokhimiya, No. 5, 571-8(May 1966). (In Russian).

The infrared spectra of rare earth carbonates (F-bastnaesite, OH-bastnaesite, thorium bastnaesite, and parisite), which were investigated at various ignition temperatures (200 to 600°C) showed the presence of OH groups in bastnaesite, confirmed the irreversibility of structural changes in these minerals caused by ignition and revealed an analogous character of changes in the unignited thorium bastnaesite, which was exposed to the action of α decay of the thorium contained in this bastnaesite. (auth)

29448 ON THE PARAGENETIC POSITION OF URANIUM PITCHBLENDE IN THE HYDROTHERMAL DEPOSITS OF THE WEST ERZGEBIRGE. Harlass, Eberhard; Schuetzel, Heinz Z. Angew. Geol., 11: 569-81(Nov. 1965). (In German).

Various concepts of the formation of metal deposits in the ore-bearing mountains of Saxony, the Saxo-Bohemian

Erzgebirge, are discussed. Carbonate veins, which can be taken as equivalent of neither the eba- nor the uq-formation, are assumed to be the carriers of the primary mineralization of uranium. The mineralization of these veins is subdivided into two stages: the quartz-pitchblende-calcite formation (kku), and the dolomite-selenide formation (dse). In both of them pitchblende is found; that from the dolomitic formation is an ascendant mobilizate as well as a remainder from the kku-formation. The selenium associated with uranium is economically important. Sulfide minerals are only found sporadically. Oxides of trivalent iron and a large-area metasomatism of magnesium are typical of the pitchblende-carbonate veins. It was suggested that uranium was transported in hydrothermal springs in the hexavalent stage as an uranyl carbonate complex and, owing to changes undergone in the physico-chemical medium, was separated in a tetravalent form as a result of interactions with the country rock and by pressure release (escape of CO_2). The mineralization of uranium in the entire process of mineralization of the West Erzgebirge is reviewed and it is emphasized that the metal content of the ore-bearing granitic magmas is substantially determined by the character of the country rock assimilated with it. (BBB)

29449 OBRAZOVANIE EKZOGENNYKH MESTOROZHDENII URANA I METODY IKH IZUCHENIYA. (Origin of Uranium Exogenous Deposits and Methods for Their Exploration). Danchev, V. I.; Strelyanov, N. P.; Shilovskii, P. P. Moscow, Atomizdat, 1966. 248p.

The characteristics of natural processes leading to the formation of the basic types of exogenous deposits of uranium are presented. The most important methods of field, office, and laboratory investigations usually applied to solve problems of the origin and the regularities of localization of uranium mineralization are described. The separate methods are illustrated by examples of their practical use. For the deposits examined, the multistage character of the formation of their ore deposits is clearly pointed out. (tr-auth)

HEALTH AND SAFETY

See also BIOLOGY AND MEDICINE — Radiation Hazards and Protection
GEOLOGY, METEOROLOGY, AND MINERALOGY — Natural Radioactivity and Fallout

Refer also to abstracts 29142 and 29234.

29450 (ISO–270) CRITICALITY SAFETY OF FISSILE MATERIALS IN THE CHEMICAL PROCESSING DIVISION. Reed, P. E. (Isochem Inc., Richland, Wash.). Apr. 1, 1966. Contract AT(45-1)-1851. 12p. Dep. mn. CFSTI $1.00 cy, $0.50 mn.

Procedures for: off-site shipment of fissile materials; receiving fissile materials from off-site; posting and labeling fissile materials; and requirements for use of the chemical fissile materials symbol are listed. Shipments of radioactive materials must conform to the applicable federal and state regulations that are not included in the procedures. (P.C.H.)

29451 (NYO–2598-29) THE LOSS OF ORGANIC AND INORGANIC MATERIALS FROM ABOVE-GROUND PLANT PARTS, WITH ESPECIAL REFERENCE TO DECONTAMINATION OF PARTS UTILIZED FOR FOOD. Progress Report. Tukey, H. B. Jr. (Cornell Univ., Ithaca, N. Y. Dept. of Floriculture and Ornamental Horticulture). [1966]. Contract AT(30-1)-2598. 19p. Dep. mn. CFSTI $1.00 cy, $0.50 mn.

Leaching is defined as the loss of organic and inorganic metabolites from fruit, flowers, foliage, and stems by the leaching action of aqueous solutions including rain, dew, and mist. Results are summarized from studies of factors that influence leaching of plants in which radioisotopes were used as tracers. A mechanism for the leaching of cations was developed that is compatible with current theories of ion translocation. The recycling of leached nutrients in the same plant or other plants was demonstrated. The findings were applied in studies of the decontamination of food plants of radioactive fallout, with emphasis on the removal of ^{90}Sr from the fruit of beans, peas, and tomatoes and lettuce foliage. A series of studies were made to evaluate the extent of leaching and recycling of leached metabolites in plants in tropical environments in conjunction with other feasibility studies related to the proposed construction of a canal in Central America with atomic devices. (C.H.)

29452 (ORNL–3721(Suppl.3)) SAFETY ANALYSIS OF RADIONUCLIDE RELEASE TO THE CLINCH RIVER. Final Progress Report No. 3. Cowser, K. E.; Snyder, W. S. (Oak Ridge National Lab., Tenn.). May 1966. Contract W-7405-eng-26. 122p. Dep. mn. CFSTI $4.00 cy, $0.75 mn.

One of the principal objectives of the Clinch River Study has been the evaluation of radiation dose equivalents to populations downstream from operations at the Oak Ridge National Laboratory. Evaluation was based on long-term monitoring data (1944 to 1963) and the identification of critical exposure pathways and population groups. Knowledge of water utilization downstream indicates that the important avenues of exposure from discharge of low-level contaminated waste water to the Clinch River include consumption of contaminated water and fish, consumption of agricultural produce that may be irrigated with river water, exposure to contaminated water and bottom sediments during recreational and industrial use of the water, and exposure to buildup of sludge and deposits in water systems utilizing river water. The major sources of exposure are currently the ingestion of contaminated water and fish. Mathematical models were developed for internal dose calculations and include the differences in intake and in size of the critical organ as a function of the individual's age. It was found that the skeleton of man received the largest exposure and ^{90}Sr was responsible for more than 99% of the dose equivalent. Based upon realistic but conservative assumptions, the estimated total doses from internal and external sources (20 year period) received by the skeleton of critical population groups, the 18-year-old individuals (in 1944) utilizing the Clinch River and the 14-year-old individuals (in 1944) utilizing the Tennessee River were 3.2 Rem and 0.45 Rem, respectively. These values are about a factor of 10 less than permissible limits established by ICRP and FRC. Methods of calculation are presented, and examples are given for the transfer of ^{90}Sr and ^{137}Cs to man by irrigation water. If irrigation is practiced on the Clinch River in the future, it may become the dominant exposure pathway. It is noteworthy that in 1962 and 1963 fallout from nuclear tests contributed the same quantity of the critical radionuclide, ^{90}Sr, to the Clinch River as did purposeful releases from the laboratory. (auth)

29453 (RL-SEP–590) DESIGN CRITERIA, PLUTONIUM BUY-BACK FACILITY. Borgeson, M. E.; Nelson, D. C. (General Electric Co., Richland, Wash. Hanford Atomic Products Operation). Sept. 3, 1965. Contract AT(45-1)-1350. 20p. Dep. mn. CFSTI $1.00 cy, $0.50 mn.

Design criteria for receiving and repackaging for storage or shipment of power-reactor-grade plutonium separated and purified as a nitrate are described. The criteria are based on available information that the material will be shipped in 10 l bottles and containers. The facilities include: shipping container handling mechanisms, receiving and dispensing facilities having container transfer mechanisms, liquid transfer equipment, balances for determining product and container weights, and equipment for taking liquid samples for accountability. (P.C.H.)

29454 (SC-CR–66-2010) PARTICLE FALLOUT AND DISPERSION IN THE ATMOSPHERE. Quarterly Report No. 2, September 1–November 30, 1965. Hage, K. D.; Brown, P. S. (Travelers Research Center, Inc., Hartford, Conn.). Dec. 1965. Contract AT(29-1)-789; Subcontract 48-2417. 51p. Dep. mn. CFSTI $3.00 cy, $0.50 mn.

For Sandia Corp., Albuquerque, N. Mex.

Progress is described on the development of an atmospheric fallout model to be used to estimate particulate concentrations in the air and on the earth's surface for particles released at any altitude up to 90 km. The particle size range of interest is 1 to 200 microns in diameter. The model is being programmed to be run on a CDC-3600 computer. Preliminary specifications and coding for the program were completed for all but one major component of the model. (auth)

29455 THE RADIOACTIVITY IN RAIN WATER, SETTLED DUST AND ACTIVATED SLUDGE OBSERVED AT KAGOSHIMA DISTRICT. [PART] XIII. Kitahara, Keid; Akiyama, Takashi (Kagoshima Univ., Japan). Acta Med. Univ. Kagoshima., 7: 131-5(Aug. 1965).

A report is made of the radioactivities measured in the Kagoshima district during 1964 (the year of the Chinese atom bomb test) for rain water, settled dust, and activated sludge. Rain water and settled dust samples were collected each day except Sundays. The settled dust was collected by means of gummed acetate paper, which was ashed for the radioactivity measurements. The radioactive sludge samples were collected every week from a sewage treatment plant and centrifuged to obtain sludges, which were burned to ashes for the radioactivity measurement. The radioactivities in rain water were below 50×10^{-10} C/m^2 throughout the year, showing no influence of the Chinese nuclear detonation. For the settled dust, the total cumulative radioactivity was 336.49×10^{-10} C/m^2 for October, in contrast to

a value below 30×10^{-10} C/m^2 for the other months (excluding April, 78.21×10^{-10} C/m^2). This clearly showed the influence of the Chinese test. The radioactivities in the sludge were approximately 2×10^{-10} C/g of ash throughout the year, showing no influence of the nuclear detonation. (TCO)

29456 ROUTINE DOSIMETRY WITH ^{182}Ta AND ^{192}Ir WIRES. Hall, E. J.; Oliver, R.; Shepstone, B. J. (Churchhill Hospital, Oxford). Acta Radiol. Therapy, Phys., Biol., 4: 155-60(Apr. 1966).

Data sheets were prepared of the γ dose distribution around wires of ^{182}Ta and ^{192}Ir. A computer was programed to perform the calculations, which included an allowance for oblique filtration in the platinum screen. (auth)

29457 LASER HAZARD. Zaret, M. M. Arch. Environ. Health, 10: 629-30(Apr. 1965).

Generalized statements as to the parameters of human hazard from lasers may prove of limited value when applied to specific laser systems. Commercially available laser generating devices which may produce recognizable retinal burns from as small a quantity of incident laser radiation as 1 millijoule/cm^2 in a 0.5 millisecond burst from a ruby laser are described. Three accidental exposure cases free of serious sequelae are mentioned. Need for supervisory industrial hygiene and medical cooperation in preventive programs is stressed. (auth)

29458 MULTIPOINT CONTROL OF RADIATION LEVELS. Zhernov, V. S.; Murashov, E. P.; Ryzhov, N. V.; Skatkin, V. M. At. Energ. (USSR), 20: 82-4(Jan. 1966). (In Russian).

The tendency toward centralization and automation of control systems extends to the continuous collection of radiation dose data from operating personnel while working. Cathode-ray tubes were found suitable for such centralized collection of radiation safety information. Continuous and simultaneous indication of the radiation levels from several locations, e.g., in the form of vertical lines, the lengths of which are proportional to the dose level, allows a rapid and convenient survey of the situation at any given moment. The system requires suitably placed individual senders, connection systems, and a central control room provided with amplifiers and scanners. A multichannel count-rate device is used, with a linear, rather than logarithmic measuring system. Care was taken to eliminate interaction between channels. (TTT)

29459 STUDIES ON THE PREVENTION OF CONTAMINATION OF MILK BY FALLOUT. I. ON THE DECREASE OF ^{90}Sr SECRETED INTO MILK BY HIGH-LEVEL CALCIUM FEEDING. Danbara, Hiroshi; Miyamoto, Susumu (Hokkaido National Agricultural Experiment Station, Japan). Chikusan Shikensho Kenkyu Hokoku, No. 7, 13-19(Oct. 1964). (In Japanese).

The results of experiments designed to decrease the Sr-90 concentration in milk of cows fed "the contaminated feed" containing fission products of the Nuclear Test are reported. Two cows were used as test animals and were fed Ca-supplemented feed (Ca content 3 to 5 times higher than the conventional feed) prepared by adding $CaCO_3$ to the conventional feed. One cow was used as the control. The feeding experiments covered a period of 5 months, and the milk was assayed for Ca and Sr-90 every 15 days. The Sr-90 content in the milk from test cows was found to be moderately lower than in the control one. The same feeding experiments were conducted at Hokkaido, Chiba, and Kyushu to re-confirm the findings. (TCO)

29460 RADIATION CONTROL FOR RADIOACTIVE FACILITIES. Yoshida, Yoshikazu (Japan Atomic Energy Research Inst., Tokyo). Genshiryoku Kogyo, 11: No. 10, 11-17(Oct. 1965). (In Japanese).

Radiation control carried out in the Japan Atomic Energy Research Institute is described in detail, with emphasis on that for JPDR (Japan Power Demonstration Reactor). The radiation control procedures consist of: control areas and entrance-exit radiation control, environmental (or air) contamination; monitoring of radioactive waste water; monitoring of radioactive exhaust gas; and radiation-exposure control for personnel working in the controlled areas. For other radioactive facilities, descriptions are given for measuring; tritium accumulating in the heavy water of JRR-2 and JRR-3 reactors; activation of structural materials of linear and Van de Graaff accelerators; and external exposures due to β rays. The duties in the JAERI Radiation Control Section are also described. (TCO)

29461 EFFECT OF DETERGENTS ON THE PENETRATION OF ^{90}Sr THROUGH ANIMAL SKIN. Khodyreva, M. A. Gig. Truda Prof. Zabolev., 8: No. 10, 14-18(1964). (In Russian).

After applying a ^{90}Sr solution to untreated rabbit skin and to skin rubbed with ammonium carbonate, 3% potassium permanganate, ammonium carbonate again, 5% oxalic acid, and 3% hydrochloric acid, the skin permeability was evaluated by determining the radioactivity in blood, internal organs, and bone ash. The rate of ^{90}Sr penetration through treated skin was 1.5 times the rate for untreated skin. (TCO)

29462 ^{54}Mn IN FRESHWATER CLAMS. Gabay, Jack J.; Dapolito, John A.; Sax, N. Irving (New York State Dept. of Health, Albany). Health Phys., 12: 968-70(July 1966).

Manganese-54 was found in clams (genus Lampsillis) from Lake Ontario. Analysis of soft tissues, shell, and clam juice showed that ^{54}Mn is concentrated by this species in both soft tissue and shell, with the higher concentration in soft tissue. (C.H.)

29463 AVAILABILITY OF FALLOUT ^{137}Cs TO DAIRY CATTLE FROM DIFFERENT TYPES OF FEED. Stewart H. F. (Colorado State Univ., Fort Collins); Ward, Gerald M.; Johnson, James E. J. Dairy Sci., 48: 709-13(June 1965).

The transfer coefficient (^{137}Cs secreted daily per liter of milk as a percentage of total daily ^{137}Cs intake) for individual cows ranged from 0.25 to 0.72 and was found to be closely related to the crude fiber content of the diet. The correlation coefficient between transfer coefficient and crude fiber intake for 5 cows was -0.66. The average percentage of dietary ^{137}Cs found in the milk, urine, and feces of three cows was 7.4, 13.5, and 81.5. The results reported here suggest that fallout ^{137}Cs in dairy cattle feeds is considerably less available than suggested by studies with tracers. (Public Health Eng. Abstr.)

29464 DISTRIBUTION OF RADIONUCLIDES IN DAIRY PRODUCTS FROM TWO MILK PROCESSING PLANTS. Reavey, Thomas C. (Northeastern Radiological Health Lab., Winchester, Mass.). J. Environ. Health, 27: 809-17 (Mar.-Apr. 1965).

A study was undertaken to obtain information on the distribution of ^{90}Sr, ^{131}I and ^{137}Cs in milk and milk products. For ^{131}I, whole milk contributes an estimated 90% of the total intake from dairy products, with only 10% coming from the various products derived from milk. For ^{90}Sr and ^{137}Cs, whole milk contributes about 80% of the total intake from dairy products. (Pub. Health Abstr.)

29465 AIR LOCKS FOR SAFE ESCAPE IN NUCLEAR REACTORS. Hanffstengel, K. v.; Kober, K. J.; Marterstock, R. (Battelle-Institut e.V., Frankfurt am. Main). Kerntechnik, 8: 201-5(May 1966). (In German).

It is advised that personnel air locks be provided in nuclear reactors with an operating mechanism that ensures consecutive phases of motional action so that special elements for interlocking the two doors and the pressure-equalizing valves are not required. Rectangular sliding doors permit a very quick passage through the air lock. If the air lock is used, additional protection can be provided for escaping persons by a sealable room situated in front of the air lock inside the containment. The door of this room should not be part of the interlocking mechanism of the air lock. (auth)

29466 RADIOACTIVE FALLOUT PARTICLES FROM A NUCLEAR DETONATION IN CHINA. Mamuro, Tetsuo

(Radiation Center of Osaka Prefecture). Mizu Shori Gijutsu, 6: No. 8, 9-14(Aug. 1965). (In Japanese).

The results of an investigation on radioactive fallout particles from a nuclear detonation in China in October, 1964, are described. Radioactive fallout reached the Osaka area 50 hours after the detonation. Large radioactive particles were detected by filtration of the air through a large filter paper and examination of the filter paper by an autoradiograph. The beta activities, particle sizes, shapes, and colors were examined and compared with those of radioactive particles from larger nuclear detonations in Soviet Russia (1961 and 1962). The radioactivities of large particles from China reached a maximum of 130 $\mu\mu$C with diameters of 20 μ. The differences in size, color, and shape between the particles in China and those in Soviet Russia were attributed to the fact that the detonations in Soviet Russia were carried out in the atmosphere on a large scale, while that in China was near the surface of the earth. In both cases, particles larger than 20 μ in diameter were hardly detected, which agrees well with the accepted view that particles smaller than 20 μ are carried away by atmospheric movement while others larger than 20 μ fall mainly under the influence of gravity. (auth)

29467 SAMPLING AIRBORNE RADIOIODINE IN ORGANIC COMPOUNDS. Whittaker, E. L.; Bretthauer, E. W. (Southwestern Radiological Health Lab., Las Vegas, Nev.). Nucl. Appl., 2: 55-6(Feb. 1966).

Conventional air-sampling techniques were adapted to include the quantitative collection of iodine from airborne carbon–iodine bonded compounds. A high-frequency electric spark is used to rupture the organic bond and the resulting ionic and molecular forms of iodine are sorbed on an ion-exchange resin. A gamma spectrometer was used to measure ratioactivity and determine recovery. (M.C.G.)

29468 POLICIES AND PROCEDURES USED IN THE UNITED STATES FOR DECONTAMINATING HOT CELLS. Carr, W. H. Nucl. Safety, 7: 212-14; 216-17(Winter 1965–1966).

A survey of decontamination policies and procedures in the United States is summarized. (G.O.Y.)

29469 WHY AND HOW OF NUCLEAR ACCIDENT DOSIMETRY. Vallario, Edward J.; Wasson, Hodge R. (Atomic Energy Commission, Washington, D. C.). Nucl. Safety, 7: 218-25; 234(Winter 1965–1966).

The basic parameters that should be considered for an effective nuclear accident dosimetry program are discussed. Several dosimeters are described, and their use is discussed. (G.O.Y.)

29470 PROGRESS SUMMARY OF NUCLEAR SAFETY RESEARCH AND DEVELOPMENT PROJECTS. Murphy, C. M. Nucl. Safety, 7: 247-57; 267-9(Winter 1965–1966).

The most significant developments in the safety-related projects that are sponsored by the AEC Division of Reactor Development and Technology are summarized. (D.C.W.)

29471 CRITICALITY STUDIES WITH PLUTONIUM SOLUTIONS. Lloyd, R. C.; Richey, C. R.; Clayton, E. D.; Skeen, D. R. Nucl. Sci. Eng., 25: 165-73(1966). (BNWL-SA-232).

A series of criticality experiments were performed with plutonium (4.6% ^{240}Pu) nitrate solution in stainless steel spheres of 11.5-, 14-, and 15.2-in. diam. Reflectors of water, concrete, paraffin, and stainless steel were used; experiments were also performed on the 15.2-in. sphere unreflected. The spheres were made critical with plutonium concentrations varying from 24 to 435 g Pu/liter and molarity varying from 0.2 to 7.7. The minimum critical volumes for $Pu(NO_3)_4$ in water containing 4.6% ^{240}Pu were determined to be about 22 and 11 liters, respectively, for bare and reflected spheres at a concentration of 175 g Pu/liter. The effect of a 0.030-in. cadmium shell or a 4-in. air gap between the reflector and the vessel reduced the reflector worth to that of a nominal reflector (1-in. of water or less) for the concentrations of plutonium measured. Comparisons were made between experimental and theoretical results using multigroup diffusion theory. (auth)

29472 RADIOCARBON IN THE ENVIRONMENT. Drobinski, J. C. Jr. (Northeastern Radiological Health Lab., Winchester, Mass.). Radiol. Health Data Rep., 7: 10-12 (Jan. 1966).

Analyses of various samples collected since July 1962 indicate that radiocarbon levels in man and most of his foods have increased about 20 to 30 percent above 1950 levels. This compares to a carbon-14 increase in surface air on the order of 40 to 70 percent. (auth)

29473 PROGRESS ON METHODS FOR REDUCING ^{90}Sr IN WHEAT AND MILLED PRODUCTS. Anderson, R. A.; Pfeifer, V. F. (Dept. of Agriculture, Peoria, Ill.). Radiol. Health Data Rep., 7: 57-60(Feb. 1966).

Various simple cleaning techniques were applied to four varieties of Kansas hard red winter wheat, to determine their effectiveness in removing ^{90}Sr. As much as 73 percent of the ^{90}Sr content in wheat and 80 to 83 percent in bran was removed by washing with dilute phosphoric or citric acid. This treatment also produced substantial reductions in the ^{90}Sr content of flour. (auth)

29474 VARIABILITY OF FLUID MILK CONSUMPTION AND ITS RELATIONSHIP TO RADIONUCLIDE INTAKE. Thompson, J. C. Jr. (New York State Veterinary Coll., Ithaca. Cornell Univ., Ithaca, N. Y.). Radiol. Health Data Rep., 7: 139-44(Mar. 1966).

Using Federal milk marketing order statistics and population estimates for market areas, average monthly fluid milk consumption estimates were derived for cities located in areas covered by the Public Health Service Pasteurized Milk Network. The average per capita milk consumption for 67 cities in July 1962 was found to be 0.302 liters per day, which compared well with the Bureau of the Census estimate of 0.297 liters per day for the same month. Establishment of a comparative milk consumption-radionuclide level network is described for the 38 cities which participate in both collection of the milk order statistics and the PHS milk monitoring system. This method is useful for determining regional and temporal variations in average milk consumption. Widespread geographic variations in radionuclide intakes are apparent from a summary of data for these cities, ranging to as high as sixfold for ^{90}Sr and fifteenfold for ^{137}Cs between stations. The estimates indicate that the average intake of ^{90}Sr and ^{137}Cs are approximately 70 percent less than estimates based on an assumed milk consumption of 1 liter per day. It is emphasized, however, that the averages include portions of the population whose milk intake is considerably greater than the average. These represent the critical elements in public health planning if large releases of radioactivity should occur. (auth)

29475 ^{137}Cs IN FOOD: A SUMMARY OF RESULTS ON SELECTED FOODS IN THE UNITED STATES, JULY 1962 TO OCTOBER 1963. Setter, Lloyd R.; Smith, Donald; Spector, Mozart (Public Health Service, Washington, D. C.). Radiol. Health Data Rep., 7: 145-56(Mar. 1966).

Cesium-137 content and cesium-137 to potassium ratios are summarized for nine staple foods sampled during a survey conducted for six consecutive quarters from July 1962 through October 1963. Insofar as possible, the results have been grouped by the six broad geographical production regions that were previously used for comparing ^{90}Sr data for the same samples. The general trend of the ^{137}Cs to potassium ratios was similar to the ^{90}Sr to calcium ratios previously reported, being generally higher in fruits and vegetables than in milk; however, the lowest ratios were found in lettuce, cabbages, potatoes, and eggs. It was noted that the region-to-region variations of ^{137}Cs concentrations were greater than those of ^{90}Sr for whole milk, evaporated milk, bread, apples, and oranges. (auth)

29476 GROSS ALPHA RADIOACTIVITY OF HUMAN BONES AND TEETH. Rothe, William E. Radiol. Health Data Rep., 7: 204-5(Mar. 1966).

Bone sections from 51 cadavers and molar teeth from 75 persons were analyzed for total α activity during 1964 and 1965. No significant difference in total α activity was found in samples from American and German subjects. (C.H.)

29477 NEW EXPERIMENTAL DATA ON THE DECONTAMINATION OF PROTECTIVE CLOTHING. Boenzi, D.; Branca, G. Riv. Ing. Nucl., 3: 807-14(May-Aug. 1965). (In Italian).

After some considerations on the present state of decontamination, the results of a study for the purpose of preparing a mixture with a large action spectrum, capable of removing from cotton tissues, fission products, uranium, and thorium simultaneously were reported. The decontaminating capacity of the mixture (sodium lauryl sulfate, Antarox DM-970, sodium hexametaphosphate, sulfosalicylic acid, and sodium nitrate in equal parts) was compared with the decontaminating capacity of some commercial products. The results obtained were interpreted as a function of the various mechanisms effecting the contamination. In particular, if decontamination is bound to an ion exchange process, a new washing technique is proposed. The technique consists in substituting a batch treatment for a single-column treatment, allowing radioactivity to be eluted with acid solutions of convenient composition. (tr-auth)

29478 SAFETY MEASURES WITH REGARD TO THE USE OF RADIOISOTOPES AND THE PROPOSAL FOR NEW DETECTING EQUIPMENT FOR BETTER PERSONAL SAFETY. Branca, F. Paolo. Securitas, 50: 21-38 (May 1965).

The harmful effects of ionizing radiations on the body are reviewed, and a table based on recent statistics gives data regarding the harm suffered by the body in proportion to the amounts absorbed. Some details are given to assist in characterizing radioactive sources, screening, and instruments. A new type of apparatus that is able to safeguard workers exposed to ionizing radiations is also described. (Public Health Eng. Abstr.)

29479 ON THE DEPOSITION VELOCITY OF ^{131}I. Ito, Shozo (Japan Meteorological Agency, Tokyo). Tenki, 12: 231-5(July 1965). (In Japanese).

According to experiments on ^{131}I, the characteristic velocity to control its deposition is related to the frictional velocity due to the shearing stress. A method is reported for estimating the frictional velocity in urban districts, using the available data from the meteorological observations and of the statistical results on the frequency of occurrence of different deposition velocities in each season, obtained in connection with the stratospheric condition of the atmosphere. By means of observation of the wind velocity (U) at a given height (Z), the frictional velocity (V) can be expressed by $V = KU(Z)/(\ln^Z/Z_0 + \beta/L(Z-Z_0))$, where L is the stability length; β, the empirical constant; and Z_0, the roughness constant. When the average wind velocity is fixed, the frictional velocity is, in general, increased in the less stable air layers and the deposition velocity is increased. Since the amount of deposition, however, depends both on the distance and the deposition velocity, the amounts of deposition cannot be compared only by considering the deposition velocities. Conversions to the frictional velocity and deposition velocity were made by the statistics of the average wind velocity in each season (January, April, July, and October) of 1959. (auth)

29480 LASER SYSTEMS: CODE OF PRACTICE. London, Ministry of Aviation, 1965. 15p.

The hazard of lasers in industry and research is considered with special reference to their use in range finders, welding and drilling apparatus, and signalling devices. Each laser must be a "laser-restricted area" which only authorized persons may enter, and general rules for these areas are given. The maximum permitted exposure of personnel to laser energy shall be as follows: for a laser pulse of duration between 10^{-8} and 5×10^{-3} seconds, the energy density falling upon the retina of the eye shall not exceed 10^{-2} joules/cm^2; the total laser energy incident upon the retina during any period of 1.0 seconds shall not exceed 10^{-1} joules/cm^2; the total laser energy incident upon any part of the body other than the eye for 1.0 seconds shall not exceed 10^{-1} joules on any cm^2. The duties of persons in charge of lasers are detailed. The calculation of energy density at the retina and the requirements for special safety spectacles are explained. (auth)

29481 DAMAGING EFFECTS OF UNDERWATER NUCLEAR EXPLOSION (REVIEW). Zherbin, E. A.; Besyadovski, R. A.; Ivanov, K. V.; Rumyantsev, A. P. Voenno-Med. Zh., No. 2, 68-72(Feb. 1966). (In Russian).

The main harmful factors of an underwater nuclear explosion are the shock wave, penetrating gamma radiation, and radioactive contamination. Abdominal injuries, and, more rarely, chest injuries are encountered as a result of the shock wave. The high g values encountered in shock waves can cause damage to the bones and other parts of the body. A gamma dose of 1000 rads causes death within a few hours. Medical aid may have to be rendered in 10% of the cases even at absorbed doses of 50 to 100 rads. Radioactive contamination can cause skin damage at doses of 2 to 200 $\mu C/cm^2$. Inhalation of aerosol radioactivity is discussed. (TTT)

29482 PROJECTED REQUIREMENTS IN RADIATION DOSIMETRY. Motz, J. W. (National Bureau of Standards, Washington, D. C.). 25p. (CONF-660212-3). ORAU. Gmelin, AED-CONF-66-016-2.

From Radiation Research Society, 14th Annual Meeting, Coronado, Calif.

Dosimetry measurements must be carried out with many different types of dosimeters in many different radiation fields involving electrons, neutrons, protons, mesons, or photons having a wide range of flux densities and energies extending from the ev to the Bev region. The readings of the different dosimeters obtained in these radiation fields must be related to a parameter of the field or to a specific radiation effect in a system of interest. A procedure, which is based on the determination of fluence response functions for the different dosimeters or the systems of interest with monoenergetic radiation beams of known fluences, is proposed to meet this need. The fluence response function gives the dependence on the particle energy (or on any other field parameter such as the particle direction, the flux density, or the type of particle) of the response of the irradiated system per unit fluence of the incident radiation. These functions provide a quantitative criterion for introducing and distinguishing the dual concepts of a "field" and an "effects" dosimeter, such that the reading of the "field" dosimeter may be directly related to the fluence of the radiation field, and the reading of the "effects" dosimeter may be directly related to a specific radiation effect in a system of interest. Such relationships may be achieved with less experimental difficulty and greater accuracy by the proposed procedure than by the conventional procedure, which requires measurements of the dosimeter response per unit dose as a function of the incident particle energy. (auth)

29483 PROTECTIVE LIGHTWAY FOR FALLOUT SHELTERS. Chieffe, John F. U. S. Patent 3,246,564. Apr. 19, 1966. Filed Apr. 26, 1962.

A subterranean lightway is provided for redirecting sunlight into a fallout shelter during the daylight hours while fully protecting the shelter interior from the adverse effects of radiation. A primary hollow shaft is positioned with one end to receive the daylight, and a secondary hollow shaft communicates at an angle and is interconnected with the opposite end of the primary shaft. The shafts pass through the radiation shielding material and are of such relative length that the radiation entering the one end of the primary shaft is intercepted by the shielding material. Light reflecting means are disposed at the interconnection of the two shafts for redirecting light from the primary into the secondary shaft. Removable transparent protective means are associated with the primary shaft for sealing it against the entry of fallout material. The shafts are of sufficient dimensions that they may be used for the movement of personnel into and out of the shelter. (B.L.M.)

29484 DETECTING CONTAMINATION ON SURFACES. Anderson, John Lynde (to Cleanometer Corp.) U. S. Patent 3,247,385. Apr. 19, 1966. Filed Dec. 21, 1961.

A process for detecting contamination held by a surface consists of exposing the surface to be tested to a gaseous

radioactive-labeled material, effecting the retention of some of the material by the contaminant, removing unretained material, determining the radioactive emission from the surface to be tested, and similarly measuring the emission from under control conditions in the absence of any contamination. A comparison of the radioactive emission from the test surface and the control conditions gives a measure of the contamination. Material labeled with the gamma-emitter ^{131}I is preferable for this process. (B.L.M.)

INSTRUMENTATION

General

Refer also to abstracts 29598 and 30754.

29485 (EUR-2799.e) DIGITAL COMPARATORS FOR HANDLING OF DATA FROM NUCLEAR EXPERIMENTS. Colling, F. (European Atomic Energy Community, Geel (Belgium). Central Nuclear Measurements Bureau). Mar. 15, 1966. 40p. Dep. mn.

Two digital comparators for binary or binary coded decimal information were built and tested. The comparator stages for all bits are cascaded and identical, so that they can be used as standard units in building block systems. The operation time of the 20-bit three-state transistor comparator is about 90 ns per bit for the slowest comparison. With a 10-bit window comparator, containing two two-state comparators with tunnel diodes as threshold elements, a minimum comparison speed of about 6 ns per stage (bit) was reached. This characteristic can be improved up to one order of magnitude, if necessary, when fast tunnel diodes are used. For data handling purposes two-state comparators should be preferred because of their possible simplicity and speed. A maximum flexibility in application is given in addition. Three state comparators, also by combination of two-state comparators, can be used with advantage for regulation purposes as for instance gain stabilization. (auth)

29486 (NASA-CR-54964) ULTRASONIC TEMPERATURE MEASURING DEVICE. Third Quarterly Progress Report. Carnevale, E. H.; Lynnworth, L. C.; Klaidman, S. L. (Parametrics, Inc., Waltham, Mass.). Apr. 1966. Contract NAS3-7981. 24p.

Piezoelectric and magnetostrictive transducers at both high and low frequencies were evaluated. In addition, the design of the capsule for the radiation test was agreed upon. Analysis of radiation effects eliminated iridium as a possible sensor material. Calculations indicated that Nb, Mo, and Re can be safely tested ultrasonically, without a hot cell, within two months after irradiation. Preliminary tests were conducted at high temperatures in an r-f oven. This oven is one of several being considered to provide a high temperature carbon free environment in which radiation effects on sound velocity can be measured. Additionally, construction of an automatic pulsing and receiving unit has begun. (auth)

29487 (UCRL-16632) "DO-IT-YOURSELF" LOCK-IN AMPLIFIERS, RADIO AND AUDIO FREQUENCY. Lamers, Kenneth W. (Lawrence Radiation Lab., Univ. of California, Berkeley). Jan. 14, 1966. Contract W-7405-eng-48. 71p. Dep. mn. CFSTI $3.00 cy, $0.75 mn.

Two specific lock-in amplifiers, one designed for radio frequency, the other for audio, are described. In view of the general utility of these amplifiers, included are detailed schematics, photographs, templates, and other data useful in duplicating either unit. (M.O.W.)

29488 (WANL-TME-948) THERMOCOUPLE PROGRAM TO INVESTIGATE RELATIVE ERROR. Collier, G. (Westinghouse Electric Corp., Pittsburgh, Pa. Astronuclear Lab.). Sept. 15, 1964. Contract SNP-1. 15p. Dep. mn. CFSTI $1.00 cy, $0.50 mn.

In the use and design of thermocouples it is desirable to know the true and the measured temperature to determine the relative error. A theoretical model was derived for this purpose. The model and computer program for making the calculations are included. (M.O.W.)

29489 SOME THEORETICAL CONSIDERATIONS OF ION OPTICS OF THE MASS SPECTROMETER ION SOURCE. I. MATHEMATICAL ANALYSIS OF ION MOTION. Naidu, P. S. (Univ. of British Columbia, Vancouver, Can.); Westphal, K. O. Brit. J. Appl. Phys., 17: 645-51(May 1966).

The equation of trajectory of a charged particle in a two-dimensional electric field and a normal magnetic field was derived from the basic equations of motion. A series of paraxial approximations reduced the nonlinear trajectory equation to a linear inhomogeneous ordinary differential equation. This equation was used to compute the ion trajectories in the multiple-slit ion source of the mass spectrometer. The effect on the ion trajectories of the various components such as repeller field plate, exit slit plate, deflector plates and the source magnetic field, was evaluated. (auth)

29490 SOME THEORETICAL CONSIDERATIONS OF ION OPTICS OF THE MASS SPECTROMETER ION SOURCE. II. EVALUATION OF ION BEAM TRANSMISSION EFFICIENCY. Naidu, P. S. (Univ. of British Columbia, Vancouver, Can.); Westphal, K. O. Brit. J. Appl. Phys., 17: 653-6(May 1966).

The mathematical theory of the motion of ions in the ion source was applied to evaluate the ion beam transmission efficiency. In the absence of any repeller field, ions from a narrow horizontal strip of width equal to that of the exit slit are withdrawn. On the other hand, in the presence of a repeller field the ion withdrawal space consists of two star-shaped figures connected by a narrow canal. The dimensions of the star-shaped figures are comparable with the widths of the entrance slit, which is about ten times the width of the exit slit. When the ion withdrawal space is a maximum, the transmission efficiency is a maximum. The repeller field for a maximum ion withdrawal space is about 0.32 per cent of the accelerating field. The mass discrimination for heavy ions due to a weak source magnetic field (a few hundred gauss) is negligible. (auth)

29491 ERROR IN DENSITY MEASUREMENT OF COMPRESSED STOCK COAL BY A BACK-SCATTERING GAMMA-RAY DENSITY METER. Ono, Hironori; Machida, Tadao (Central Research Inst. of Electric Power Industry, Tokyo). Gijutsu Kenkyusho Shoho, 1964: No. 64062, 1-19 (Feb. 1964). (In Japanese).

The γ-ray density meter investigated consists of a probe (44 mm in dia., 620 mm in length), containing a radioactive source (^{137}Cs, 10 mC.), lead block shield (188 mm in length), Mullard MX-120 GM counter and preamplifier; an external main amplifier; a scaler; and a high voltage source. The probe is inserted into the access tube and beaten deep into the compressed stock coal. The gamma rays from the source are Compton-scattered by the surrounding coal. This scattering serves as a measure of the density of the stock coal. The error in the density measurement is caused mainly by the following eight factors: statistical fluctuation of the radioactivity of the source used; deviation of the working curve; fluctuation of the thickness of the access tube; position of the probe in the access tube; space between the access tube and the surrounding coal; bias of the detector response to the inhomogeneity of the coal density; difference in the conditions between the calibration and field measurements; and non-linearity of the electronic counting circuit. The main drawbacks of the method in the field measurements were found to be the inconvenience and difficulty of beating the access tube deep into the stock coal and the poor reproducibility. (auth)

29492 AUTODYNE NUCLEAR MAGNETIC RESONANCE PICKUPS. Dekabrun, L. L.; Kil'yanov, Yu. N.; Mkrtchyan, A. R. (Inst. of Chemical Physics, Academy of Sciences, USSR). Izv. Akad. Nauk Arm. SSR, Ser. Fiz. Mat. Nauk, 18: No. 3, 134-42(1965). (In Russian).

An analysis is presented of the stabilizing action of active negative feedback on autodyne pickups for the investigation of solids by the NMR method. In such applications, autodyne pickups have certain advantages over

others, but must be stabilized when the signal voltage is low, such as is the case with solid-state NMR. The transients in an autodyne pickup with stabilized amplitude are calculated, and the modifications that must be introduced in the pickup circuit to ensure stability are described. Empirical means of selecting the autodyne circuit and its parts to obtain maximum sensitivity are suggested, since a theoretical analysis of this problem is impossible. A schematic diagram of a pickup with stable operation at less than 0.005 volt on the resonant circuit is presented. The diagram is shown. The circuit has been thoroughly tested and proved itself in practical investigations of several natural compounds by the NMR method. (ATD)

29493 DOUBLE FOCUSING IN MASS SPECTROMETERS WITH AN INHOMOGENEOUS MAGNETIC FIELD. **Starodubtsev, S. V.; Pozharov, S. L.; Chernov, I. G. (Nuclear Physics Inst., Academy of Sciences, Uzbek SSR). Izv. Akad. Nauk Uz. SSR, Ser. Fiz.-Mat. Nauk, No. 4, 40-4(1965). (In Russian).**

The use of an inhomogeneous magnetic field in mass spectrometry markedly enhances the dispersion and resolving power of instruments without changing the radius of ion trajectory and the slit width of source and receiver. However, owing to the presence of initial kinetic energies in the ions and the distribution of potentials in the ion source, the ions in the beam may get scattered with respect to energies and the lines may widen. This effect may be eliminated by adding a specially selected electrostatic field. FISHER (Zs. f. Physik, 133, 1952, 455) has described a mass spectrometer with first-order double focusing with combined electrostatic and magnetic fields. Such combining involves difficulties due to the need to overcome the boundary-field effect; moreover, it is not always convenient to have the receiver and source in the magnetic-field region. Hence, an investigation was made of the conditions for first-order double focusing in the central plane for a tandem-type mass spectrometer with an inhomogeneous magnetic field and a homogeneous electrostatic field, with both fields deflecting the ion beam in the same direction. The formula for double focusing in such directions and speeds is derived, and a particular example is presented, showing how the difficulties involved in this solution can be overcome. (JPRS)

29494 ON THE CHARACTERISTICS OF THE HOT CATHODE MAGNETRON GAGE FOR THE MEASUREMENT OF ULTRAHIGH VACUUM. PART 1. **Nakao, Fusafumi (Matsushita Electric Industrial Co., Ltd., Japan). Shinku, 9: No. 2, 49-59(Feb, 1966). (In Japanese).**

In order to extend the low-pressure limit of the hot cathode ionization gage, it is necessary to increase the ratio of ion current to x-ray photocurrent. Two types of hot cathode magnetron gage, the Lafferty type and the coaxial type, were fabricated and their characteristics were measured. Under normal operating conditions, these magnetron gages are operated in a magnetic field with an intensity 2.5 times stronger than the cutoff value for the Lafferty gage and 2 times stronger than the cutoff value for the coaxial gage. A very low level of electron emission was used to obtain a stable operation in accordance with Lafferty's suggestion. The characteristics of both types of gages are compared and discussed. The ion current in the coaxial gage is more sharply risen up to a flattening region than in the Lafferty gage. For the characteristics of the gas ionization probability by electron impact, the position of maximum ion current in the coaxial gage was shifted to lower anode voltage than in the Lafferty gage. Other characteristics of both types of gages were essentially the same in operation. The positive ion emission from the cathode was suppressed by a careful construction of the filament on the axis of the cylindrical anode for both the magnetron gages. The measured sensitivity and x-ray photocurrent indicated that the linear relationship between the pressure and ion current may be established. Ion currents of magnetron gages for Lafferty type and coaxial type decreased linearly with a pressure ranging from 5×10^{-6} to 10^{-12} torr and from 1×10^{-6} to 10^{-12} torr, respectively. The measured pumping speeds of these gages were found to be one-tenth as large as that of the conventional ionization gage under normal operating conditions. (auth)

29495 TEMPERATURE MEASUREMENTS IN STUDIES OF THE COMBUSTION OF SOLID FUEL PARTICLES. **Finaev, Yu. A. Vestsi Akad. Navuk BSSR, Ser. Fiz. Tekh. Navuk, No. 3, 55-6(1965). (In Russian).**

Recently developed platinum-rhodium/platinum thermocouples were tested for resistance to heat and accuracy in high-temperature measurements from 460 to 1110°C. Two test thermo-couples were placed simultaneously in an electric furnace: the hot junction of one was left bare and that of the other was encased in a thin quartz sleeve with a closed end. The bare thermocouple consistently registered a higher temperature than the cased one (from 13 deg in the 1100° range of 24 deg at about 870°, and 20 deg at about 470°). The differences in readings are attributed to the different thermal characteristics of platinum and quartz. Errors in measuring temperatures in a gas can be reduced by increasing the heat transfer from the gas to the thermocouple. This is accomplished by decreasing the diameter of the junction, which action increases the coefficient of heat transfer and decreases the error due to radiation. Measurement error due to leakage of heat through the leads is practically eliminated by pushing back the electrode coverings about 30 diameters to allow the gas to flow against the electrodes. Another small error is due to the catalytic effect of platinum. Measurements of temperatures of burning solid fuel particles in the range of 1000°C were within 2% error. (CFSTI)

29496 MASS SPECTROMETER REMOVABLE HEAD FOR NECESSARY SENSITIVITY FOR LEAK DETECTION IN ULTRA-HIGH VACUUM SYSTEMS ATTAINING 10^{-8} TO 10^{-12} TORR. **Bargery, J.; Jalenques, F. Vide, 22: 167-70(Mar.-Apr. 1966). (In French).**

A mass spectrometer head attachment and control equipment specially designed for an ultra-high vacuum leak detector is described. This unit is derived from a standard Centronic leak detector mass spectrometer and was used in testing large vacuum chambers, ultra-high vacuum systems, and accelerators. (auth)

29497 APPLICATION OF THE STRAIGHT LINE METHOD COUPLED WITH THE METHOD OF INTEGRAL TRANSFORMATIONS TO THE PROBLEM OF ELECTROSTATIC FIELDS WITH AXIAL SYMMETRY. **Martynovich, T. L.; Korduba, B. M. Zh. Vychisl. Mat. Mat. Fiz., 5: 1120-4(Nov.-Dec. 1965). (In Russian).**

An approximation method is outlined for the calculation of electrostatic fields for axially symmetric electron lenses. The physical problem is expressed by the Poisson equation, which with certain boundary conditions can be described as a Dirichlet boundary value problem. The straight line method is applied to the z-coordinate such as the Poisson equation takes on a form which, after simplifications, yields a set of n-independent differential equations of the zeroth-order Bessel type. A solution is obtained making use of Fourier series. Neglecting the electrode thickness and assuming the system grounded an expression is obtained which is then applied to the case of an electro-optical system with three cylindrical electrodes, symmetric with respect to the z = 0 plane. The solution leads to a set of algebraic equations of the 22nd order for determining the unknown charge density $q_6(\alpha)$. (L.B.S.)

29498 METODY YADERNOGO MAGNITNOGO REZONANSA. (Nuclear Magnetic Resonance Methods). **Shumilovskii, N. N.; Skripko, A. L.; Korol', V. S.; Kovalev, G. V. Fizicheskie i Fizikokhimicheskie Metody Kontrolya Sostava i Svoistv Veshchestva. (Physical and Physico-Chemical Methods for Determining the Composition and Properties of Materials). Moscow and Leningrad, Izdatel'stvo Energiya, 1966. 140p.**

The essence of the NMR phenomenon is examined, and relations determining the parameters of the signals are presented. Variations of block schemes of NMR spectrographs and analyzers are shown, and the separate subassemblies of the apparatus are considered. Domestic and

foreign NMR spectrographs and analyzers are described. Special attention is given to the use of the NMR method for measuring humidity. A survey of the analytical uses of NMR spectroscopy is presented. (tr-auth)

29499 ADVANCES IN ELECTRONICS AND ELECTRON PHYSICS. VOLUME 21. Marton, L. (ed.). New York, Academic Press, 1965. 355p.

Topics discussed in this volume are the polarization of electron beams and the measurement of the g-factor anomaly of free electrons, fast ion scattering against metal surfaces, kinetic ejection of electrons from solids, scanning electron microscopy, high-speed magnetic-core memory technology, and physical foundations of plasma applications for generation and amplification of microwaves. (B.G.D.)

29500 PLAZMENNYE I ELEKTRONNYE USILITELI I GENETRATORY SVCH. (Plasma and Electron uhf Amplifiers and Generators). Bernashevskii, G. A.; Bogdanov, E. V.; Kislov, V. Ya; Chernov, Z. S. Moscow. Izdatel'stvo Sovetskoe Radio, 1965. 96p.

Methods of generating and amplifying uhf oscillations using a rotating electron current and an electron-ion plasma penetrated by an electron beam are considered. The principles of using a plasma for uhf generation and amplification and the interactions of the oscillations with an electron beam are examined. Results of theoretical and experimental studies of plasma amplifiers and generators are presented. Centrifugal electrostatic focusing of rotating electron currents and the amplifiers and generators constructed using this focusing are described. The stability of the electron current during focusing is analyzed. Studies of traveling-wave return-wave tubes with central electrostatic focusing are discussed. The processes of h-f grouping in a rotating electron current are examined in the linear and nonlinear approximations, and it is shown that space-charge self-grouping of electrons is possible. (M.J.T.)

29501 POWER-SUPPLY CIRCUITS (Engineering Materials). (Oak Ridge National Lab., Tenn.). (CAPE-1337).

2 drawings.

The inexpensive, Regulated Power Supply/Q-2295/ has overload protection, however, it must be used in a laboratory since a temperature compensation factor is not included. It is a 24-v d-c supply of 100-ma mp current. The Battery Power Supply and Calibration Adapter Circuit/Q-2298/ is used with a 350 Ω strain-gauge transducer. Four Mallory tubes, 1.34-v Hg batteries, 14,000-ma mp-hr are used. The useful life of the batteries must be at least 800 hr. (For details, see TID-4100). (J.F.P.)

29502 WIND RECORDING SYSTEM /Q-2506/ (Engineering Materials). (Oak Ridge National Lab., Tenn.). (CAPE-1343).

1 drawing.

This circuit is given for the Health Physics wind recording control box. The box controls an anemometer 97-3102A-10SL-2P; a velocity recorder 97-3102A-14S-2P; an E-A 0-1 ma recorder; an Electronic Control Systems, Inc., Model 100 magnetic amplifier; a direction recorder 97-3201A-10SL-3P; and a Belford Instrument Co., AP 1 meter 220 μ a d-c. (For details, see TID-4100). (J.F.P.)

29503 LOW LEVEL EMITTED LIGHT MEASURING SYSTEM /Q-2528/ (Engineering Materials). (Oak Ridge National Lab., Tenn.). (CAPE-1348).

4 drawings.

This sensitive photometer system is used in evaluating commercially available instruments and watch dials containing radioactive materials. It can be used on dial sizes from ½ in. to 5 in. in dia with varying luminescence properties. A 3-in. type-6363 photomultiplier tube with peak response at 4400 A (S-11 response) is the photometer detector. It is mounted in a 6-in.-in-dia cylindrical Al housing. The cylindrical chamber is mounted in an Al rectangular box for mechanical protection and for shielding from the room light. The h-v power supply is a PRL Electronics, Inc., Model DP-1447 HV and the readout instrument is an E-H Research Laboratories electrometer amplifier, Model 202. (For details, see TID-4100). (J.F.P.)

29504 NUCLEAR MEASUREMENTS, 1963. 6 Reports, Presented at the 43rd Annual Meeting, January 13–17, 1964. Highway Research Record Number 66. Jackson, Earle W. (ed.). Highway Research Board of the National Academy of Sciences - National Research Council Publication 1250. Washington, D. C., Highway Research Board of the National Academy of Sciences - National Research Council, 1965. 88p. $1.80. (CONF-378).

The conference includes 6 papers. Separate abstracts were prepared for five papers. The other paper on the use of nuclear methods for measuring mineral filler and asphaltic content of bituminous concrete is briefly summarized. (J.F.P.)

For abstracts of individual papers see: 29505–29509.

29505 EFFECTS OF TYPE OF MATERIAL ON NUCLEAR DENSITY MEASUREMENTS. Kuehn, S. H. (National Inst. for Road Research, Pretoria). pp 1-14 of Nuclear Measurements, 1963. Jackson, Earle W. (ed.). Highway Research Record 66. Washington, D. C., Highway Research Board of the National Academy of Sciences - National Research Council, 1965.

Laboratory and field investigations were carried out to improve the practical application of the nuclear method for moisture content and density control in highway construction. Various factors were studied, including the effective depth of measurement and effects of source energy and soil type on density measurements. Two methods are described for the possible elimination of the effect of soil type in practical density measurements. In the first, direct transmission is used as an auxiliary test to normal backscatter measurements. In the second method, introduction of an air gap between the surface probe and the soil surface is used to obtain a count ratio which, when plotted against density, gives a positive slope relation independent of soil type for densities up to 400 pcf. (auth)

29506 NUCLEAR MEASUREMENT OF SOIL PROPERTIES. Ralston, H. H.; Anday, M. C. (Virginia Council of Highway Investigation and Research, Charlottesville). pp 15-33 of Nuclear Measurements, 1963. Highway Research Record 66. Jackson, Earle W. (ed.). Washington, D. C., Highway Research Board of the National Academy of Sciences - National Research Council, 1965.

Results of the investigation of three commercially available nuclear devices for the measurement of soil density and moisture contents are presented. The investigation was divided into three phases: an equipment and geometry evaluation, including precision testing of the device itself, depth and area of influence determinations, and evaluation of the effect of air voids under the probes; an attempt to calibrate the devices on representative subgrade and base-course materials from construction projects in Virginia; and field testing of the devices on construction projects throughout the state. Densities and moisture contents obtained with the nuclear devices were compared with those obtained by conventional water-balloon methods. (auth)

29507 FIELD EVALUATION OF NUCLEAR GAGES USED IN COMPACTION CONTROL OF EMBANKMENTS. Worona, Valentin; Gunderman, William. pp 34-50 of Nuclear Measurements, 1963. Highway Research Record 66. Jackson, Earle W. (ed.). Washington, D. C., Highway Research Board of the National Academy of Sciences - National Research Council, 1965.

Nuclear moisture-density gages under actual field conditions were evaluated. A preliminary evaluation of one Nuclear-Chicago d/M system showed favorable results, hence a more extensive study was conducted with eleven additional nuclear gages. A complete d/M system was assigned to each Pennsylvania's engineering districts and used on varied construction and soil types. These gages were used in the field for one full year, and the results were compared to the sand-cone method for determining soil density and the oven-drying and speedy moisture methods of determining moisture content. Test results were compiled and tabulated by IBM 650 data processing machine. Tabulations were requested to isolate variables affecting correlation of nuclear to sand-cone results.

These variables are soil type, soil gradation, construction type (embankment, soil cement, subbase, etc.) and different d/M systems. Standard deviations were computed for series of grouped tests to determine the repeatability of both methods for measuring moisture and densities of construction materials. (auth)

29508 LABORATORY AND FIELD EVALUATION OF NUCLEAR SURFACE GAGES FOR DETERMINING SOIL MOISTURE AND DENSITY. Weber, William G. Jr. (California Division of Highways, Sacramento). pp 51-72 of Nuclear Measurements, 1963. Highway Research Record 66. Jackson, Earle W. (ed.). Washington, D. C., Highway Research Board of the National Academy of Sciences - National Research Council, 1965.

A laboratory evaluation of the nuclear surface gages for determining soil moisture and density was conducted using eight soils from various areas of California. A calibration curve was developed for each soil and all calibration curves were compared. The volume of soil being measured was determined. The reproducibility and other characteristics of the nuclear gages were studied. The nuclear gages were used on ten projects under construction and the nuclear readings were compared to conventional tests. The results of this evaluation program indicated that individual calibration curves would be required for the various soils encountered. (auth)

29509 DETERMINATION OF ASPHALT CONTENTS IN A PAVING MIXTURE BY THERMAL NEUTRONS. Varma, Man Mohan; Reid, George W. (Tufts Univ., Medford, Mass.). pp 73-83 of Nuclear Measurements, 1963. Highway Research Record 66. Jackson, Earle W. (ed.). Washington, D. C., Highway Research Board of the National Academy of Sciences - National Research Council, 1965.

The purpose of this research was to determine the feasibility of measuring the asphalt content of bituminous paving by the neutron bombardment-counting technique. The correlation of neutron count and asphalt percentages depends primarily on the chemical content of the asphalt. Because the chemistry of asphalt is that of a variable mixture, it can be expected that data collected will fluctuate to some degree with changes in the asphalts tested. (auth)

29510 SEMICONDUCTOR RADIATION DETECTOR MEASUREMENTS OF GASEOUS DIFFUSION COEFFICIENTS. Mistler, T. E. (Westinghouse Atomic Products Division, Pittsburgh); Mingle, J. O. New York, American Inst. of Chemical Engineers, 1966, Preprint 29B, 23p., $0.50. (CONF-660506-2). ORAU.

From American Inst. of Chemical Engineers, Nuclear Engineering Div. Symposium, Columbus, Ohio.

The feasibility of measuring gaseous diffusion coefficients using a tracer technique in a modified Ney-Armistead cell containing a semiconductor detector was demonstrated. Measurements were made at 20°C in the transition pressure range using CO_2 tagged with ^{14}C. The experimentally determined self-diffusion coefficients agreed within 5% with the theories of Bosanquet and Wheeler at pressures from 50 to 400μ. Sources of error and possible refinements of the apparatus are considered. (A.G.W.)

29511 IMPROVEMENTS IN AND RELATING TO ELECTRIC CONNECTORS. Buckland, Ernest Clifford (to M. B. Metals Ltd.). British Patent 1,026,751. Apr. 20, 1966. Filed Apr. 20, 1961.

An electrical connector of the type suitable for use in unusual places as in a nuclear reactor comprises first and second separable members. One of the members has a plug portion adapted to enter a socket portion on the other member. One of the portions has a number of contact members spaced in the direction of entry of one portion into the other portion. The contacts on one portion have a generally cylindrical contact-making surface, and the contacts in the other portion are each formed of an elongated member such as a wire or the like shaped to extend in use around the surface of the cooperating contact in the one portion and to present a resilient non-cylindrical contact-making surface so that contact between cooperating contact-making surfaces is established at a number of spaced points. A plug and cavity-type modification of the connector is described also. (B.L.M.)

29512 IMPROVEMENTS IN AND RELATING TO ELECTRICAL COUPLING DEVICES. Buckland, Ernest Clifford (to M.B. Metals Ltd.). British Patent 1,026,752. Apr. 20, 1966. Filed Mar. 30, 1962.

An electrical coupling member is provided for attachment to the end of a round element, such as a reactor fuel element, having a shoulder or the like adjacent but spaced from the end of the round element for providing electrical coupling at high working temperatures, of the order of several hundred degrees, and in conditions which do not permit ready access to the coupling and associated parts. The coupling member includes a body portion having electrical connections in it and a split or interrupted sleeve. The split or interrupted ends have inturned portions spaced around the sleeve for engagement with the retention upon the shoulder. Adjacent to the other end of the sleeve is a screw threaded portion. The coupling member also includes a threaded ring for engaging the body portion. The ring serves to retain the inturned portion of the sleeve around the shoulder and to retain the sleeve upon the body. An intermediate member that is adapted to make plain face to face engagement with the end of the fuel element may be included in the coupling assembly. (B.L.M.)

29513 IMPROVEMENTS IN OR RELATING TO VACUUM GAGES. Lloyd, Owen (to United Kingdom Atomic Energy Authority). British Patent 1,027,350. Apr. 27, 1966. Filed Aug. 14, 1963.

A vacuum gage for investigating the pressure of a gas comprises an electron gun that can be caused to emit an electron beam, an electrically conductive chamber having an apertured end plate through which the electron beam passes into the chamber, and means for immersing the chamber in a magnetic field that is generally parallel to the beam path, and of such strength that ions resulting from ionization of the gas by the beam remain in the beam. An electrostatic probe is positioned within the chamber adjacent to the beam path, and means are provided to determine the time interval between voltage transients of the probe. The voltage transients occur each time a virtual cathode is created within the chamber, and after an interval which is dependent upon the gas pressure, the virtual cathode disappears and another of the transients occurs. (B.L.M.)

29514 IMPROVEMENTS IN OR RELATING TO TEMPERATURE RECORDERS. Thurlbeck, Arthur (to United Kingdom Atomic Energy Authority). British Patent 1,028,192. May 4, 1966. Filed Jan. 22, 1963.

A self-contained temperature recorder suitable for use in a reactor or other remote site for temperature measurements over a prolonged period of time is described. The recorder comprises a bimetallic strip that carries at one end a recording stylus and is fixed at the other end to a carriage, a reference stylus connected to the carriage, a revolvable drum with a surface adapted to receive tracings from both styli, and a lead screw with driving means. The screw driving means moves the carriage parallel to the longitudinal axis of the drum so that the styli can record traces on the drum. Driving means are provided also for revolving the drum, and the driving means for both the screw and the drum are linked so as to be driven by the same source of motive power, a weight situated above the recorder whose potential energy is transmitted to the driving means by way of a lever and a crank. (B.L.M.)

29515 SAFETY DEVICES FOR USE WITH RADIOACTIVE MEASURING APPARATUS. Schutz, Gerhard; Seltmann, Hans (to Veb Vakutronik). British Patent 1,028,556. May 4, 1966. Filed Feb. 26, 1964.

A safety device for use with radioactive measuring apparatus comprises a radiation-permeable plate situated between a radiation emitter and a channel for receiving material to be measured and safety means connected to the plate by means of which an electrical circuit is actuated when a foreign body moves towards the radiation

source and impinges upon the plate. The radiation-permeable plate is electrically nonconductive and may be coated with an electrically conductive coating. When a foreign body impinges on the plate, the electrically conductive coating is damaged to open a circuit and actuate an alarm. (B.L.M.)

29516 DEVICE FOR PRODUCING A MODULATED BEAM OF BETA OR X-RADIATION. Handel, Neil E. (to Industrial Nucleonics Corp.). U. S. Patent 3,247,376. Apr. 19, 1966. Filed May 5, 1961.

An apparatus for producing a modulated beam of beta or x rays includes a collimated beta ray emitting source for producing a narrow beam of beta rays and a radiation absorbing shield having an aperture positioned in the path of the beta ray beam. A magnetic field of continuously varying intensity is produced in the path of and perpendicular to the beta beam to continuously deflect the beam across the aperture in the radiation absorbing shield to produce a modulated beam emanating through the aperture. A target comprised of a material in which the beta particles will undergo radiative collisions with the nuclei to produce x radiation may be placed in the path of the modulated beta ray beam to produce a modulated x radiation beam. (B.L.M.)

29517 RADIALLY COLLIMATING WINDOW FOR WELL-TOOL ORIENTING INSTRUMENTS. Brady, Franklin P. (to Schlumberger Well Surveying Corp.). U. S. Patent 3,247,384. Apr. 19, 1966. Filed Oct. 16, 1962.

A window design is described for a well tool orienting instrument comprising a cylindrical pressure housing, a gamma ray source, and a gamma ray detector spaced longitudinally apart. Shielding opaque to gamma radiation is disposed between and about the source and detector and defines a pair of open windows extending respectively from the source and the detector radially to the interior wall of the housing. The source and detector windows each have a rectangular shape elongated in the direction of the housing a width of about $^5/_{16}$ in. A strip of material selected from the group consisting of Ta, W, and Mo is mounted in at least the detector window in a radial plane bisecting the window, and the strip is substantially coextensive with the dimensions of the detector window and has a thickness of about $^1/_{64}$ in. This arrangement serves to enhance the angular resolution of the instrument for more accurate orientation in a radial plane. (B.L.M.)

Radiation Detection

Refer also to abstracts 28882, 29469, 29841, 29956, and 29969.

29518 (BNWL-SA-27) PULSED REACTOR TESTS OF DOSIMETERS. Bramson, P. E.; Endres, G. W. R. (Battelle-Northwest, Richland, Wash. Pacific Northwest Lab.). June 7, 1965. Contract AT(45-1)-1830. 11p. Dep. mn. CFSTI $1.00 cy, $0.50 mn.

Hanford Criticality Dosimeters, Personnel Beta-Gamma Film Badge Dosimeters and several types of experimental silicon diode neutron dosimeters were exposed to seven unshielded pulsed reactor bursts of between 0.24×10^{16} to 2×10^{16} fissions per burst. The exposures were made at the Sandia Pulsed Reactor Facility. Reported neutron doses between 40 and 2700 rads and the actual measurements were in agreement to within ±15% for the Hanford Criticality Dosimeter and to within ±25% for the criticality section of the Personnel Beta-Gamma Film Badge Dosimeter. The special silicon diodes were able to measure the fast neutron dose with an accuracy of about ± 15%. The small base width (0.040") diodes provided good results to about 2500 rads. The large base width (0.07") diodes gave the best results between 20 and 200 rads. Glass rod dosimeters formulated from "high atomic number" glass provided measurements of the gamma dose agreeing to within ± 30% of the reported dose. The errors stated for both the neutron dose exposures and the gamma photon exposures include any fundamental differences in absolute calibration that may exist between Hanford and the Sandia Pulsed Reactor Facility. Each of the routine radiation monitoring instruments currently used at Hanford was tested for response to a single 0.1 μsec duration pulse of 600-kev x-rays from a Flash x-ray unit. Only the G.M. instruments failed to give a good indication that a radiation pulse occurred. (auth)

29519 (BNWL-SA-31) A SYSTEM FOR CRITICALITY VERIFICATION. Rising, F. L. (Battelle-Northwest, Richland, Wash. Pacific Northwest Lab.). June 7, 1965. Contract AT(45-1)-1830. 10p. Dep. mn. CFSTI $1.00 cy, $0.50 mn.

Occasionally, a criticality alarming system will sound a false alarm. After such an alarm, a prompt verification is desired to assist in planning building reentry and the myriad of emergency actions that need to be taken. A fast neutron detector system is used to provide this verification at Pacific Northwest Laboratories of Battelle Memorial Institute. The neutron sensitive detector was chosen to eliminate the changes in gamma background that arise from time to time due to the normal transfer of radioactive materials. The system is capable of detecting a criticality of about 10^{15} fissions shielded by eight inches of normal concrete at a distance of seven hundred feet. The equipment is not alarming and is used only to verify an occurrence. The absence of a verification is never accepted as an indication of a false criticality alarm. The instrument is powered by rechargeable batteries continuously trickle-charged by a line-powered battery charger. The recorder is hand wound and spring driven. This system provides for several hours of continuous operation following a power failure. The recorder can be placed at the detector position or wired to a central control point. In addition to confirming the occurrence of a criticality event, the instrument also indicates through the recorded record whether the reaction is a continuing one or a single burst occurrence. The equipment also provides information to indicate if more than one burst occurred. The basic electronic design was adopted from research work completed by the Hanford Nucleonics Instrumentation group, and is used with a scintillation detector as aerial survey equipment. (auth)

29520 (CLOR-45/D) ^{90}Sr-^{90}Y MEASUREMENTS USING SILICON COUNTERS. Dabrowski, A.; Jagusztyn, M.; Roman, J. (Centralne Laboratorium Ochrony Radiologicznej, Warsaw (Poland)). 1966. 18p. Dep.

Large-area silicon surface-barrier detector with a guard-ring was constructed and used for low-level ^{90}Sr-^{90}Y beta assay. The counting efficiency was of about 41 percent and the background count was less than 1.5 cpm. The counter has proved to be well suited for routine use under ordinary laboratory conditions. (auth)

29521 (CONF-651109, pp 213-23) HIGH-ENERGY PARTICLE SPECTROMETRY USING ACTIVATION DETECTORS. Dolias, M.; Benezech, G.; Bricka, M. (Commissariat a l'Energie Atomique, Cadarache (France). Centre d'Etudes Nucleaires).

A simplified spectrometer using activation detectors was earlier developed for nuclear accidents dosimetry. The method of spectral indexes, particularly, allows a simple exploitation and the rapid collection of spectra, fluxes, and doses. A model was developed for computer computations for high energy particle spectrometry. This model is described. (M.O.W.)

29522 (CONF-651109, pp 286-305) INFERENCE OF ACCELERATOR STRAY NEUTRON SPECTRA FROM VARIOUS MEASUREMENTS. O'Brien, Keran; Sanna, Robert; McLaughlin, James (Health and Safety Lab., New York Operations Office (AEC), N. Y.).

Neutron spectra measurements were made with nuclear track emulsions and with Bonner's spectrometer of the neutrons penetrating the 2.5 meters of earth and concrete of the H-10 target at the BNL AGS. The two measurement techniques were compared. (M.O.W.)

29523 (CONF-651109, pp 639-46) USE OF PERSONAL MONITORING NEUTRON FILM NEAR THE 50-Mev INJEC-

TOR OF THE ZGS. Steele, Thomas A. (Argonne National Lab., Ill.).

The purpose of this investigation was to determine the usefulness of Kodak personal monitoring neutron track film, Type A, around the proton linac at Argonne National Laboratory's Zero Gradient Synchrotron. In order for this to be accomplished, knowledge of the stray neutron spectrum and the neutron film spectral sensitivity was required. The effect of shielding on the stray neutron spectrum and the dose rates are discussed along with the potential hazard and interpretation of a neutron exposure. (auth)

29524 (CONF-651109, pp 647-52) PULSE-SHAPE DISCRIMINATION APPLIED TO FAST NEUTRON DOSIMETRY. Roesch, W. C.; Nichols, L. L. (Battelle-Northwest, Richland, Wash. Pacific Northwest Lab.).

An investigation was made of the use of pulse-shape discrimination with a large organic scintillation crystal in neutron dosimetry. The scintillations due to recoil protons were distinguished from those due to electrons by their pulse shape. Then different ways of correlating the resulting pulse height spectra with the neutron dose were investigated. (M.O.W.)

29525 (CONF-660209-9) HIGH-RESOLUTION MUONIC X-RAY STUDIES. Devons, S. (Columbia Univ., New York). [nd]. Contract AT(30-1)-Gen-72. 26p. Dep. mn. CFSTI $2.00 cy, $0.50 mn.

From Conference on Intermediate Energy Physics, Williamsburg, Va.

A review of investigations of muonic x-ray spectra and of the accuracy needed for these measurements is presented. The response of lithium-drifted germanium detectors for these investigations is discussed. Muonic x-ray spectra is given for the following nuclei: ^{142}Nd, ^{144}Nd, ^{146}Nd, ^{209}Bi, and ^{238}U. (M.O.W.)

29526 (INP-444/PL) SEMICONDUCTOR SYSTEM FOR CHARGED PARTICLE IDENTIFICATION. Chwaszczewska, J.; Freindl, L.; Karcz, W.; Przyborski, W.; Slapa, M. (Institute of Nuclear Physics, Krakow (Poland)). Jan. 1966. 16p. Dep.

A system consisting of two semiconductor counters of types "dE/dx" and "E" was built to separate particles from nuclear reaction. The properties of this system were checked by detection of products of reaction induced by 24.8-Mev alpha particles and 12.4-Mev deuterons on Au, C, and Ca nuclei. (auth)

29527 (ITEF-341) TOCHNOST VOSSTANOVLENIYA TRAEKTORII CHASTITSY V ISKPOVOI KAMERE. (Accuracy of Particle Trajectory Location in a Spark Chamber). Bayukov, Yu. D.; Zaitsev, Yu. M.; Leksin, G. A.; Sokolova, L. N. (Gosudarstvennyi Komitet po Ispol'zovaniyu Atomnoi Energii SSSR, Moscow. Institut Teoreticheskoi i Eksperimental'noi Fiziki). 1965. 12p. Dep. mn.

An accuracy of particle trajectory location as a function of the point position on a spark through which extrapolated lines are drawn is investigated. It is shown that the location of the point least removed from the trajectory of the particle — the alignment point — depends on the work conditions of the spark chamber and it is practically identical for the particles crossing the chamber at different angles. It is found that the mean square deviation at the point close to the alignment point is 0.2 mm for the particles crossing the chamber perpendicularly to the plates. It is proved that the straight line drawn by the least squares method is really the trajectory of the particle within the limits of the accuracy of the experiment. (auth)

29528 (LA-3456) CALCULATION OF THE PULSE-HEIGHT RESPONSE OF Ge(Li) SEMICONDUCTOR COUNTERS. Fry, Edward S.; Palms, John M.; Day, Robert B. (Los Alamos Scientific Lab., Univ. of California, N. Mex.). Jan. 21. 1966. Contract W-7405-eng-36. 33p. Dep. mn. CFSTI $2.00 cy, $0.50 mn.

A Monte Carlo calculation was used to determine the pulse-height response of Ge(Li) detectors to gamma rays. A set of runs for three different crystal sizes and six different energies was made. The crystals were cylinders of length A and diameter A, where A was successively given the values 1 cm, 1 in., and 3 in. The source was a point source 10 cm from the end of the crystal, and the gamma-ray energies in Mev were 0.279, 0.412, 0.6616, 1.114, 2.7535, and 4.432. In addition to spectrum plots, there are plots of intrinsic efficiency vs energy and photo fraction vs energy for three crystal sizes. (auth)

29529 (RPI-328-56, pp 94-112) FAST NEUTRON SPECTRUM PROGRAM. (Rensselaer Polytechnic Inst., Troy, N. Y.).

The overall experimental arrangement and instrumentation for fast spectrum measurements are described and some of the preliminary results of the calibration of the detectors are described. Preliminary measurements of fast spectra from lead and uranium are described. (M.O.W.)

29530 (SCL-DR-65-13) A TIME-INTERVAL MEASURING CIRCUIT. Smith, E. E. (Sandia Corp., Albuquerque, N. Mex.). May 1966. Contract AT(29-1)-789. 10p. Dep. mn. CFSTI $1.00 cy, $0.50 mn.

Supersedes SCL-TM-65-87.

An experimental circuit was developed for measuring the time interval between two events with an accuracy and resolution of ±2 nanoseconds. The device occupies a volume of less than 1 cubic foot. A simple microammeter can be used for readout. (auth)

29531 (UCRL-16715) FLUCTUATIONS OF ENERGY LOSS IN SEMICONDUCTOR DETECTORS. Maccabee, Howard D.; Raju, Mudundi R.; Tobias, Cornelius A. (Lawrence Radiation Lab., Univ. of California, Berkeley). Feb. 17, 1966. Contract W-7405-eng-48. 8p. (CONF-660304-12). Dep. mn. CFSTI $1.00 cy, $0.50 mn.

From Institute of Electrical and Electronics Engineers, Scintillation and Semiconductor Counter Symposium, Washington, D. C.

Significant fluctuations and broadening of the energy-loss spectrum are expected in certain cases of passage of charged particles through "thin" detectors. Experimental measurements of this phenomenon (by use of lithium-drifted silicon detectors) are in good agreement with the rigorous theory of Vavilov, as tabulated by Seltzer and Berger. (auth)

29532 (NASA-TT-F-389, pp 518-25) RECORDING CHARGED PARTICLES WITH AN ENERGY OF 0.1-10 kev WITH A SPHERICAL ELECTROSTATIC ANALYZER. Vernov, S. N.; Mel'nikov, V. V.; Savenko, I. A.; Savin, B. I.; Pervaya, T. I. Translated from Issledovaniya Kosmicheskogo Prostranstva. Trudy Vsesoyuznoy Konferentsii po Fizike Kosmicheskogo Prostranstva. Izdatel'stvo, Nauka, Moscow, June 10-16, 1965.

The design and characteristics of spherical electrostatic analyzers, and the results of experiments on the satellites Kosmos-12, Kosmos-15, and Elektron-2 are discussed. (B.G.D.)

29533 CORRECTIONS FOR THE GRAPHICAL METHOD FOR RECONSTRUCTION OF EVENTS PRODUCED IN THE INTERIOR OF BUBBLE CHAMBERS. Senent, F.; Gil, G. (Facultad de Ciencias, Valencia). An. Real Soc. Espan. Fis. Quim. (Madrid), Ser. A, 62: 99-107(Mar.-Apr. 1966). (In Spanish).

The use of Borelli's graphical method for the reconstruction of events photographed in bubble chambers gives rise to systematic errors. A way of reducing these errors without impairing neither the usefulness nor ease of application of the original method is presented. (auth)

29534 PARTICLE DETECTORS. 1. NUCLEAR EMULSIONS. Herz, A. J.; Lock, W. O. CERN Cour., 5: 83-7(May 1966).

The use of nuclear emulsions as particle detectors is outlined. Topics discussed are its history, advantages and disadvantages, and present and future applications. An example of this technique for particle detection for the Λ^0 magnetic moment experiment at CERN is presented. (B.G.D.)

29535 RATEMETER CHARACTERIZED BY FAST RESPONSE AND LOW RIPPLE FOR VARIABLE FLOW MEASUREMENTS. Azzoni, A.; Dotti, D. (CISE, Milan). Energ. Nucl. (Milan), 13: 238-42(May 1966). (In Italian).

Flow measurements were carried out by means of a small turbine, determining the frequency of unipolar standardized pulses triggered by rotation of the turbine itself. In order to measure rapidly variable low flows, a ratemeter was designed so that it could follow the fast frequency variations with a low ripple. The ratemeter uses a filter including a resistive nonlinear element characterized by a dead zone. (auth)

29536 FAST CIRCUITS FOR NEUTRON DETECTION. Ryu, Norio (Hiroshima Univ.). Hiroshima Daigaku Kogakubu Kenkyu Hokoku, 13: No. 2, 1-6(Jan. 1966). (In Japanese).

To detect fast neutrons by the reaction T(d,n)He, fast circuits, that is, amplifier, divider, discriminator, and linear gate were designed for photomultiplier pulses caused by the light in a plastic scintillator. Using transistors of very wide gain band-width (around 1000 Mc) to set up the fast circuits is a more recent practice than using vacuum tubes, because of the transistors' good stability and simplicity. Ezaki diodes (tunnel diodes) also play an important role on the discrimination of the pulses and the formation of rectangular pulses without jitter. Since the rise time and the width of the pulses used were 6 n-sec and 30 n-sec, respectively, the circuits described were enough to analyze within 10 n-sec coincidence. If these circuits are used to analyze pulses of about 1 n-sec in rise time, the fact that a small distortion may appear must be taken into account. (auth)

29537 FAST DOUBLE OR TRIPLE COINCIDENCE CIRCUIT. Hasai, Hiromi (Hiroshima Univ.). Hiroshima Daigaku Kogakubu Kenkyu Hokoka, 13: No. 2, 7-10(Jan. 1966). (In Japanese).

As one of the fast pulse circuits, a fast triple coincidence circuit was designed for experiments of neutron scattering. The input circuit has a discriminator that selects the input pulses with a bias level of more than 0.7 volt. This bias level is set by the Esaki diodes. The two pulses are mixed after being amplified by transistors. When two pulses are mixed, pulses are clipped by the delay line of 5 n-sec. Then, the coincidental width is 10 n-sec. The mixed pulses are fed into an amplifier and are discriminated again by the Esaki diodes. A univibrator circuit is used to obtain outputs of sufficient pulse height. A switch is provided to allow selection of the circuit as a double or triple coincidence by a switch. (auth)

29538 REGISTRATION OF SECONDARY-ELECTRON CURRENT WITH A SCINTILLATION COUNTER (BY THE METHOD OF MEASURING THE TOTAL CURRENT). Arifov, U. A.; Kogan, V. I.; Khalikov, A. Kh. Izv. Akad. Nauk Uz. SSR, Ser. Fiz.-Mat. Nauk, No. 3, 29-31(1965). (In Russian).

A method previously investigated (Izv. AN UzSSR, Seriya Fiz.-Mat. Nauk, 1965, no. 2, 16) for the measurement of secondary-emission current, by counting the current pulses produced at the output of a photomultiplier when the secondary electrons strike a scintillator, is improved by using an oscilloscope to record the total current from the photomultiplier output and by bombarding the target with a modulated primary ion beam. The equipment and the experimental procedure are described in detail. Although the results are still tentative, it is concluded that the sensitivity of the method (up to 1×10^{-15} amperes) is higher than that of an electrometer, and the method offers also advantages of higher speed and insensitivity to a strong light background. A shortcoming of the method is the need for a high vacuum (on the order of 10^{-9} mm Hg). (ATD)

29539 MULTI-VELOCITY CORRECTIONS IN THE THEORY OF NEUTRON-DETECTING FOILS. Williams, M. M. R. (London Univ.). J. Nucl. Energy: Pt. A and B, 20: 345-54(May 1966).

The accuracy of the one-velocity, average cross section, approach in the theory of neutron detecting foils is assessed. This is achieved by treating the full energy-dependent Boltzmann equation and forming a variational functional for the foil activation. The use of simple but realistic trial functions enables this functional to be reduced to tractable integrals. In the case of graphite, at room temperature or above, it is concluded that the one-velocity method is adequate. However, for moderators with rapidly varying scattering cross sections in the thermal region—water, for example, discrepancies arise which cannot be neglected. Also for cold moderators (i.e. temperature around 100°K or less), particularly crystalline ones, the effect of the Bragg cut off and the corresponding increase of the mean free path below this, can lead to a large increase in the foil activation. This effect is not predicted by the one-velocity approximation. (auth)

29540 STEADY-STATE RESPONSE OF SILICON RADIATION DETECTORS OF THE DIFFUSED p-n JUNCTION TYPE TO X RAYS. II. PHOTODIODE MODE OF OPERATION. Scharf, Karl; Sparrow, Julian H. (National Bureau of Standards, Washington, D. C.). J. Res. Nat. Bur. Stand., 70A: 181-91(Mar.-Apr. 1966).

The response to x rays of silicon radiation detectors of the p-n junction type was investigated with special consideration of their dependence on the applied voltage. In agreement with theory, the photocurrent, I_g, was found to consist of a voltage-independent part mainly determined by the average diffusion length of minority carriers in the base layer, and a voltage-dependent part, which is proportional to the width of the depletion region, w. Due to the voltage dependence of w, I_g increased with increasing voltage applied, but its relative change produced by different voltages was independent of exposure rate and quality of radiation. Exposure rate and energy dependence of I_g expressed in relative values were thus independent of applied voltage. Silicon radiation detectors, used as photodiodes could therefore be useful for monitoring of radiations at exposure rates larger than 1 R/min, taking advantage of the possibility of increasing current sensitivity by increasing the voltage and of increasing the voltage signal by increasing the load resistance R_L. There were, however, limitations in increasing v and R_L because of the increasing noise with increasing dark current and some dependence of measured current signals on R_L. The temperature coefficient of I_g was positive and independent of R_L, but showed some small voltage dependence. In the temperature range between 25 and 50°C, the average temperature coefficient was approximately 0.35 percent per degree centigrade. A value of the average diffusion length of minority carriers in the base layer was derived from the measured voltage dependence of I_g. (auth)

29541 LIQUID SCINTILLATORS BASED ON MEDICINAL PARAFFIN FOR USE IN WHOLE-BODY COUNTERS. Barnaby, C. F.; Jasani, B. M. (London Univ.). J. Sci. Instrum., 43: 220-3(Apr. 1966).

The measurement of the scintillation efficiencies of a number of mixtures based on medicinal paraffin is described. It is shown that it is possible to choose mixtures having efficiencies comparable to the best liquid scintillator and better than plastic scintillator. A mixture suitable for use in whole-body counters is recommended. This makes the construction of a highly sensitive whole-body counter possible at a comparatively small cost. (auth)

29542 METHODS OF CALCULATING THE PULSE HEIGHT DISTRIBUTION AT THE OUTPUT OF A SCINTILLATION COUNTER. Gale, H. J.; Gibson, J. A. B. (Atomic Energy Research Establishment, Harwell, Eng.). J. Sci. Instrum., 43: 224-8(Apr. 1966). (AERE-R-5067).

A systematic approach was made to the prediction of the pulse height distribution at the anode of the photomultiplier in a scintillation counter arising from a distribution of electrons in the scintillator. Iterative procedures were developed for use with a digital computer to calculate the distribution exactly. A more convenient continuous algebraic function was derived and applied to extend the method to

higher input energies. The derived function is simple and is significantly more accurate than the usual Gaussian representation, particularly for small numbers of electrons. These methods were developed to explain the pulse-height distributions observed with low and higher energy beta emitters in a liquid scintillation counter. The method can, however, be applied to any scintillation counter where the electron distribution in the scintillator is known. (auth)

29543 GAIN VARIATIONS IN SOME CHANNEL MULTIPLIERS. Smith, D. G. (Univ. of Leicester, Eng.). J. Sci. Instrum., 43: 270-1(Apr. 1966).

Three distinct types of gain variation observed in channel multiplier samples are described, and possible mechanisms of these variations are suggested. (auth)

29544 NUCLEAR ELECTRONS: RELAY-CONTROLLED PULSE GENERATOR FOR TESTING NUCLEAR ELECTRONICS. Lauch, J.; Nachbar, H. U. (Hahn-Meitner-Institut fuer Kernforschung, Berlin). Kerntechnik, 8: 221-3(May 1966). (In German).

A pulse generator for checking and calibrating linear amplifiers and pulse-height analyzers is described. It generates exponential decay pulses like those produced by radiation detectors. The generator is triggered by a mercury relay, which is energized by line power. The rise time is adjustable in steps between 4 and 300 nsec and the decay time constant in the range of 1 to 200 μsec. The amplitude can be varied between 0 and ±12v, and at normal laboratory conditions the drift rate is less than 2×10^{-4} per 8 hr. (auth)

29545 RADIOFREQUENCY MASS SPECTROMETER FOR THE "ELECTRON" SATELLITES. Zarkhin, B. I.; Istomin, V. G.; Rafal'son, A. E.; Slutskii, M. E. Kosm. Issled., 3: 768-81(Sept.-Oct. 1965). (In Russian).

A small-size mass spectrometer intended for measuring the ion and neutral composition of the atmosphere on satellites is described. A special feature of the device is the use of a regime of alternating delay potential, giving it to a large degree insensitivity to the gas-separation background (in the region of mass numbers from 4 to 34 amu) and preventing the registration of spurious mass peaks. The range of the device is from 1 to 34 amu, and the resolution is of the order of 20 in the region M = 20. The sensitivity is of the order of 10/cm^3 for ion analysis and of the order 1×10^{-10} mm Hg for analysis of the neutral component. (tr-auth)

29546 TESTING OF A DRILLED-HOLE SCINTILLOMETER EMBEDDED IN PLASTIC BY MEANS OF A POINT SOURCE OF RADIATION AND A RADIOACTIVE LIQUID. Vasvari, G. Magyar Tud. Akad. Kozp. Kem. Kut. Int. Kozlem., 8: 83-92(1964).

The value as a detector of the "drilled-hole" scintillometer embedded in plastic was investigated. A point source of radiation with ^{60}Co or ^{134}Cs and the γ-rays of ^{131}I radioactive liquid were used. The background of the scintillometer was measured an attempts were made to reduce it. The total detecting efficiency was established in all the three cases. Further studies revealed how the distance between the radiation sources and the bottom of the hole influenced the efficiency and the signal/noise ratio. The curves plotted as the function of this distances showed maxima at constant high voltage; it is proved that the maxima are the result of the co-operation of the double system consisting of the scintillometer and electron multiplier tube. Thus, the signal/noise ratio is markedly altered by the high voltage, and around the maximum it is relatively little influenced by the distance. The experiments were made using a Du Mont 6292 photoelectron multiplier, and an EMG utility scaler of subdivision 512 which was modified to an input sensitivity of 20 mv. (auth)

29547 SOME NOTES ON THE PRACTICAL APPLICATIONS OF GLASS DOSIMETRY. Sugimoto, Emiko; Kaneko, Masahito; Anzai, Ikuro; Yoshizawa, Yasuo (Tokyo Univ.). Nippon Genshiryoku Gakkaishi, 8: 25-7(1966). (In Japanese).

Some practical problems associated with the use of Toshiba FD-P8-1 (8 × 8 × 4.7 mm) phosphate glass dosimeters in monitoring are discussed. Since these dosimeters were to be used in medical work, the performance in the mR range up to 100 mR was evaluated. The precision in dose measurements increased from 27% at 10 mR to 7.5% at 50 mR. The predose readings averaged 395 mR with 11.3%. The dose response was linear at least up to 60 mR. The slope of the response curve was steeper than that of the Sm glass response which is supplied as standard. Considerable error resulted from switching the fluorimeter between the sensitivity ranges. The dosimeters could be used with satisfactory results as long as the predose value was below 600 mR. The relative response of the bare glass to ^{226}Ra and ^{137}Cs radiation was greater than to ^{60}Co radiation. When a 1 mm Sn filter was interposed, the response to ^{226}Ra was lowered but that to ^{137}Cs was increased. (TTT)

29548 A FET PREAMPLIFIER FOR COOLED SEMICONDUCTOR DETECTORS. Sakai, Eiji; Kumahara, Tadashi (Japan Atomic Energy Research Inst., Tokyo). Nippon Genshiryoku Gakkaishi, 8: 257-60(May 1966). (In Japanese).

29549 NUCLEAR TRANSDUCERS. Roux, D. P. Nucl. Safety, 7: 179-84(Winter 1965–1966).

Two techniques that were developed to avoid the effects of gamma radiation in ionization chambers intended for neutron-flux measurements are discussed, together with some limitations of fission counters for use in reactors. In-core ionization chambers, self-powered neutron detectors, and self-regenerating neutron detectors are described and are evaluated as in-core neutron monitors. (D.C.W.)

29550 CHARGE-CARRIER COLLECTION FROM INSIDE AND OUTSIDE THE SPACE-CHARGE REGION. Basso, Michael J. Nucl. Sci. Eng., 25: 152-6(1966).

A theoretical and experimental study of the collection of charge carriers produced within and outside the space-charge region of a p-n-type solid-state radiation detector by an incident energetic alpha particle of 4.98-Mev energy is described. The depth of the space-charge region was made smaller by a variable forward-bias voltage externally applied. The magnitude of the applied voltage was smaller than the barrier potential. Measurements were made of the number of collected carriers from inside and outside the space-charge region as the depth of space-charge region was varied over the range of the incident alpha particle. The measured results show agreement with the theoretical considerations. Alpha-particle energies of 4.67, 3.87, 2.98, and 2.31 Mev were also investigated, but are not reported because results were analogous to that shown for 4.98 Mev. The collection efficiency of the detector was also investigated and is given, independent of the particle energy, as a function of the applied bias voltage. (auth)

29551 METHODS FOR HIGH ENERGY EXPERIMENTS ON HEAVY NUCLEI USING MICA DETECTORS. Brandt, Reinhard (Max-Planck-Institut fuer Kernphysik, Heidelberg. CERN, Geneva). Nukleonik, 8: 235-9(May 1966). (In German).

It is shown that 18-Mev protons leave no etchable traces in mica. Negligibly small etchable traces (A > 30) are produced by the interaction with impurities in mica for $<10^{13}$ p/cm^2. A mica-pack-("sandwich")-method was developed in which a very thin metal layer (about 10 μg/cm^2 uranium on 200 μg/cm^2 aluminum) was pressed between two mica foils. These packs were irradiated and the particle traces were etched out in an acid bath. Single traces were observed under an ordinary optical microscope, which were produced by spallation phenomena. Further, two traces spacially associated with one another were seen, which result from a fission phenomena. Occasionally three associated traces were observed, whose origin is possibly a nuclear three-body fission process. The mica-pack method is suitable for determining the fission interaction cross section as a function of energy and mass more exactly than previous determinations. (tr-auth)

29552 MEASUREMENT OF α PARTICLES BY USE OF A p-n JUNCTION SEMICONDUCTOR DETECTOR. Uemura, Teiji (Industrial Research Inst., Osaka Prefecture). Osaka Furitsu Kogya-Shoreikan Hokoku, No. 36, 11-15 (July 1965). (In Japanese).

A commercial p-n junction detector was used to observe the energy spectra of α particles from ^{210}Po and ^{237}Np. The use of a single channel pulse-height analyzer was not suitable for measuring the narrow line width since the counting rates were too low in a small window width. Spectrum from a collimated ^{210}Po source measured with a multichannel pulse-height analyzer was obtained with a resolution of 1.6% in air. For the uncollimated source, the spectrum was unsymmetrical and resolution was poor. (auth)

29553 DOSE RATE MEASUREMENTS OF LOW-LEVEL X-RAYS HAVING LESS THAN 35 kev ENERGIES. Hayashi, Satoshi; Hayashi, Miyoko (Osaka Public Health Inst.). Osaka-Furitsu Koshueisei Kenkyusho Kenkyu Hokoku, No. 2, 49-53(Mar. 1965). (In Japanese).

The dose rates from ionizing electromagnetic radiations are usually measured by ordinary survey meters, which were calibrated with radioisotopes emitting high-energy radiations such as Ra, Co, or Cs. Considerable errors occur when these meters are used to measure monochromatic or polychromatic and low-level (more than the background) radiations, having low energies (less than 35 kev). The stray radiations from television receivers and x-ray diffractometers were measured by converting the count rates of the commercial end-window type GM-counter (for β-counting) to the radiation dose rates. The procedure and conversion chart employed for this purpose are given. Discussions are presented on the selection of the suitable GM-counter, its geometric factors, the upper and lower limits, and the precision of the method. (auth)

29554 ELECTRON MULTIPLICATION PROCESS IN PROPORTIONAL COUNTERS. Gold, Raymond; Bennett, Edgar F. (Argonne National Lab., Ill.). Phys. Rev., 147: 201-13(July 8, 1966).

The electron multiplication process in proportional counters was investigated by observing the counter response to single electrons in a manner similar to the original experiment of Curran, Cockroft, and Angus. The single-electron pulse-height spectrum was measured over a range of anode voltages for a number of different argon-methane counter gas mixtures. The behavior of the gas amplification as a function of anode voltage is used as a criterion to determine proper proportional counter operation. The single-electron pulse-height spectrum obtained in the present measurements is not constant but depends upon the average final number of electrons in the avalanche. This behavior is attributed to the fact that the electron branching process in proportional counters is non-Markovian. Two non-Markovian branching models are introduced and the asymptotic behavior of these models is compared with experimental results. (auth)

29555 SMALL NEUTRON BEAM CHOPPER. Whittemore, W. L. (General Atomic Div., General Dynamics Corp., San Diego, Calif.). Rev. Sci. Instrum., 37: 742-5 (June 1966).

A simplified variable-speed rotating mechanical beam chopper was developed for reactor neutron spectrum measurements and for use in conjunction with a crystal spectrometer for inelastic neutron scattering measurements. Neutron pulses are produced with a time jitter which is small compared to the time between pulses, the rotor speed during runs of several hours being constant to at least 5%. Rotor designs for beam sizes of 1.59 × 4.45 cm were successfully used for neutrons with energies up to 1.0 ev and with a transmission of about 80%. (auth)

29556 SYSTEM FOR SUPPRESSING LARGE, NON-STATISTICAL NOISE BURSTS IN DIGITAL AVERAGING. Goodman, L. S.; Salter, F. O. (Argonne National Lab., Ill.). Rev. Sci. Instrum., 37: 769-71(June 1966).

A device which eliminates the effect of noise bursts that exceed the average signal rate of digital data by more than a chosen, preset amount was designed and constructed and is described. (auth)

29557 USE OF A DELAYED DEVELOPMENT PROCESS IN FILM DOSIMETRY. Kubal, I. (Inst. for Nuclear Research, Czechoslovakian Academy of Sciences, Prague). Zh. Nauch. Prikl. Fotogr. Kinematogr., 11: 90-4(Mar.–Apr. 1966). (In Russian).

The development of overexposed film can be slowed down by the addition of antifogging substances such as benzotriazole (BTA) or mercaptobenzothiazole (MCBT). The use of BTA at 0.25 g/l prolongs the development time 30 to 60 minutes, and also increases the contrast. With slow development the film behaves as though it were desensitized. The addition of 3 g of BTA per liter of developer can decrease the sensitivity by a factor of 100. The development is carried out without danger of fogging. The BTA is added directly to the developer. Slow development can be used to determine irradiation doses up to 100 R on very sensitive x ray film. Two films are ordinarily carried for dosimetry purposes. If one film is overexposed, the other can be developed with the addition of BTA. (TTT)

29558 MAGNETIC SPECTROMETER WITH FIELD ALTERATIONS. Tarantin, N. I. Zh. Tekh. Fiz., 36: 139-46(Jan. 1966). (In Russian).

The dispersion and focusing qualities of magnetic particle spectrometers in which the otherwise uniform magnetic field is altered in intensity within limited regions, each bounded by four half-planes with a common edge parallel to the direction of the field are discussed. The field is assumed to be uniform within each region of altered field. The electron optics problem is treated in detail and equations are derived with the aid of which one can so determine the shapes and locations of the altered field regions and the magnitudes of the field alterations as to optimize the performance of the spectrometer. The dispersion of the altered field spectrometer is compared with that of a variable field spectrometer in which the magnetic field strength is proportional to R^{-n}, where R is the distance from the axis. The dispersion of a properly designed altered field spectrometer having m altered field regions is equal to that of a variable field spectrometer with $n = (m^2 - 1)/m^2$. In a real spectrometer the magnetic field strength will not change discontinuously at the boundary of an altered field region but will vary continuously throughout a narrow region in the vicinity of the boundary plane. These transition regions do not significantly affect the optical properties of the instrument in the plane perpendicular to the magnetic field, but they provide axial focusing and with proper design can improve the performance of the spectrometer. It is concluded that the performance of an altered field spectrometer would be at least equal to that of the best contemporary variable field spectrometers, and that the altered field instrument is much simpler to construct since the required field alterations can be realized with the aid of relatively simple shims and cuts in the pole pieces. (ATD)

29559 ON THE POSSIBILITY OF DETERMINING EXTREMELY SMALL QUANTITIES OF ^{37}Ar AND TRITIUM. Viktorov, S. V.; Kocharov, G. E.; Naidenov, V. O. (Ioffe Physicotechnical Inst., Leningrad). Zh. Tekh. Fiz., 36: 199-201(Jan. 1966). (In Russian).

Small proportional counters were constructed and tested with the view to their possible use for determining small quantities of ^{37}Ar and ^{3}H in the gaseous state. The counters were from 0.1 to 2.7 cm^3 in volume and were filled with argon and methane at 1 atm. The counters were shielded with 360 g/cm^2 of concrete, 20 cm of iron, and/or 2.5 cm of mercury. The background due to penetrating cosmic rays was reduced by connecting the proportional counter in anticoincidence with a pair of plastic scintillation counters. The background of an 0.1 cm^3 counter was so far reduced that not a single count was recorded during a period of 27 hours in the energy region of the 2.8 kev ^{37}Ar Auger line, although during the same period some 29 counts were recorded at other energies. It was possible reliably to detect the presence of 1.7×10^6 atoms of ^{3}H in a counter of 1.06 cm^3 volume. These results do not represent the limits of the capabilities of the counters described. (ATD)

29560 STUDIES OF THE ENERGY DEPENDENCE OF THE EFFICIENCY OF A MULTIPLE PLATE ION CHAMBER FOR RELATIVE ACTIVITY MEASUREMENTS OF γ EMITTERS. Zimmermann, W. Leipzig, Univ., 1965. 102p. $2.00 Gmelin, AED-Diss. 65-270.

The design of a multiple plate ion chamber for γ measurements is described. Various electrode configurations are studied. The chamber can be made energy independent for primary energies between 0.6 and 1.2 Mev. (Gmelin Inst.)

29561 EXO- AND CHEMICAL ELECTRON EMISSION. Fintelmann, D. Jena, Ger., Univ., 1964. 85p. $2.00 Gmelin, AED-Diss. 64-1068.

Theories of exo-electron emission mechanisms are reviewed. Design of a proportional counter for electron detection is described. Energy distributions and decay curves of various substances are given. Results indicate that exoemission and chemical emission are very similar. (Gmelin Inst.)

29562 TABLE OF ABSOLUTE DETECTION EFFICIENCIES OF CYLINDRICAL SCINTILLATION GAMMA-RAY DETECTORS INCLUDING CORRECTION COEFFICIENTS TO TAKE INTO ACCOUNT THE FINITE EXTENSION OF PLANE SOURCES. Grosjean, Carl C.; Bossaert, Walter. Ghent, University of Ghent, 1965. 544p.

A table of results of computer calculations of absolute detection efficiencies of cylindrical scintillation NaI(Tl) detectors for isotropic point gamma-ray sources situated on the symmetry axis, as well as correction factors permitting the evaluation of detection efficiencies for extended plane gamma sources of arbitrary shape, is presented. Results for 64 commercially available crystal sizes, 18 source-to-crystal distances, and 22 gamma energies are included. The formulas and methods used in the computations are described, and some examples of practical applications are shown. (M.J.T.)

29563 GAMMA DOSIMETER G-M PROBE /Q-2521/ (Engineering Materials). (Oak Ridge National Lab., Tenn.). (CAPE-1346).

1 drawing.

Flat response for γ radiation is obtained with this equipment. The dosimeter is $16^{15}/_{32}$ in. long. The small portion of the instrument containing the Amperex 18509/02 G-M tube has a tin shield .368 in. OD and .265 in. ID which is wrapped in a .010-in.-thick lead foil. This is contained in a .392-in. ID, .425-in. OD fluorothene jacket fitted with a stainless steel case $^{7}/_{16}$-in. OD. The remainder of the instrument has a $^{1}/_{2}$-in. OD, $^{3}/_{8}$-in. ID polyethylene case which contains a $^{3}/_{8}$-in. OD stainless steel liner with a .035-in. thick wall. (For details, see TID-4100). (J.F.P.)

29564 GAMMA ION CHAMBER FOR IN-CELL MONITORING /Q-2500/ (Engineering Materials). (Oak Ridge National Lab., Tenn.). (CAPE-1341).

2 drawings.

This ion chamber is sensitive to γ radiation and is used in in-cell monitoring. The approximate γ sensitivity is 4×10^{-12} amps/r/hr. The chamber is fabricated of .025-in. thick brass and it is $^{59}/_{64}$ in. OD and $2^{5}/_{32}$ in. long. The chamber housing is constructed of .035 in. thick stainless steel 1 in. OD and 4 in. long. It is xenon filled to 1 atmospheric pressure (absolute). (For details, see TID-4100). (J.F.P.)

29565 PARALLEL PLATE GAMMA ION CHAMBER - 100 cc /Q-2523/ (Engineering Materials). (Oak Ridge National Lab., Tenn.). (CAPE-1347).

1 drawing.

This parallel plate ion chamber is sensitive to γ radiation. The approximate γ sensitivity is 1×10^{-11} amps/r/hr. It is fabricated of $^{1}/_{16}$ in. thick Al and is $5^{5}/_{8}$ in. OD and 2 in. deep. The collector is $2^{3}/_{4}$ in. OD Al $^{1}/_{16}$ in. thick and the h-v electrode is 3 in. in dia, $^{1}/_{16}$ in. thick Al. The chamber is N filled to 1 atmospheric pressure (absolute). (For details, see TID-4100). (J.F.P.)

29566 NEUTRON TIME-OF-FLIGHT MEASURING SYSTEM /Q-2520/ (Engineering Materials). (Oak Ridge National Lab., Tenn). (CAPE-1345).

5 drawings.

This measuring system is used to obtain reliable data from a neutron time-of-flight spectrometer. The system includes a time-to-pulse-height converter, line drive and gate with power supply for a photomultiplier tube, and a fast and slow coincidence for a time interval meter driver. (For details, see TID-4100). (J.F.P.)

29567 4096-CHANNEL 50-Mc/s SERVO STABILIZED ANALOG-TO-DIGITAL CONVERTER. Gere, E. A.; Miller, G. L. (Bell Telephone Labs., Inc., Murray Hill, N. J.). 23p. (CONF-660304-14). ORAU. Gmelin, AED-CONF-66-020-12.

From Institute of Electrical and Electronics Engineers, Scintillation and Semiconductor Counter Symposium, Washington, D. C.

A 4096-channel 50-Mc discharge converter stabilized by reference to pulse generator signals is described. Since the converter operates independently of a computer, it employs an output buffer. The system can be used as a window amplifier free of the problem of differing pulse shapes. The effect of thermal transients on system performance is considered. Integral linearity is 0.13% and channel width equality is ±1% for the top 96% of the range. (A.G.W.)

29568 TIME RESOLUTION MEASUREMENTS WITH FAST PHOTOMULTIPLIERS. Bertolini, G.; Cocchi, M.; Mandl, V.; Rota, A. (Joint Nuclear Research Center, Ispra, Italy). 15p. (CONF-660304-13). ORAU. Gmelin, AED-CONF-66-020-8.

From Institute of Electrical and Electronics Engineers, Scintillation and Semiconductor Counter Symposium, Washington, D. C.

A comparison of experimental data and theoretical predictions on time resolution limits of fast photomultipliers was performed. XP 1020 photomultipliers were used and measurements were done with a fast electronic system built in the laboratory. This system was tested with a ^{60}Co source; the best time resolutions achieved over a period of two hours were 164 psec at f.w.h.m. A hydrogen discharge lamp was built, which produced short light pulses whose shape is determinated by a sampling method. Several light intensities were used to simulate different energy losses in plastic scintillators and time resolution measurements were performed for different threshold settings of the discriminator. The results of these measurements were compared to theoretical data calculated by means of a statistical model of the photomultiplier. Good agreement was found assuming a photoelectronic yield of one photoelectron per 2.5 kev in Naton 136 plastic scintillator and a single electron response (SER) variance of 500 psec. (auth)

29569 RECTIFICATION PROCESS AT METAL-SILICON SURFACE BARRIERS. Walter, F. J.; Boshart, R. R. (Nuclear-Chicago Corp., Oak Ridge, Tenn.). 25p. (CONF-660304-10). ORAU. Gmelin, AED-CONF-66-020-3.

From Institute of Electrical and Electronics Engineers, Scintillation and Semiconductor Counter Symposium, Washington, D. C.

Explanations for the rectification at metal-semiconductor contacts are considered. They range from those that attribute the establishment of the diffusion potential (V_d) entirely to work function differences to those that presume a major role for adsorbed gases and surface states. By making direct (differential capacitance) measurements of the barrier height (V_d) and E-I characteristics during fabrication, and as a function of ambient and surface treatment, it is shown that it is possible to rank the variables for the type of etched silicon surfaces commonly used for radiation detector fabrication in the following order of importance: (1) surface treatment, (2) adsorbed gases, and (3) work function. It is also shown that the high reverse currents observed in Au–Si structures before exposure to air are directly correlated with a small V_d and that the V_d associated with various surface treatments agrees with the results of Buck.

Preliminary work with liquid metal contacts supported the assumption of a secondary role for the work function. A theoretical model based on surface states and interfacial layers of finite thickness is presented to explain the behavior of metal contacts on etched silicon surfaces, including the fact that many metals (e.g., Al) were observed to form both rectifying and non-rectifying contacts on etched Si. (auth)

29570 IMPROVEMENTS IN OR RELATING TO THE MEASUREMENT OF CONCENTRATION OF LIQUID COMPONENTS OF A MIXTURE OF LIQUIDS BY NUCLEAR RADIATION. Bell, Eric Brayton (to Saunders Roe and Nuclear Enterprises Ltd.). British Patent 1,028,197. May 4, 1966. Filed Sept. 14, 1963.

A concentration measuring device for liquid components of a mixture of liquids includes a radiation source, radiation detector, and a member buoyant in the liquid. Either the source or detector can be mounted on the buoyant member, or the buoyant member can regulate the depth of flow through a chamber containing the radiation source that emits radiations through at least a part of the regulated depth towards the detector. During measurement, the mass of liquid between the source and detector is maintained constant, and the amount of radiation received by the detector determines the component concentrations of the liquid substantially independent of density changes in the liquid. (B.L.M.)

29571 RADIATION SOURCE MEASURING APPARATUS HAVING AUTOMATIC BACKGROUND SUBTRACT MEANS. Stoddart, Hugh F.; Williams, James B.; Hindel, Robert; Burnham, Charles A. (to Miles Laboratories, Inc.). U. S. Patent 3,246,150. Apr. 12, 1966. Filed Nov. 24, 1961.

Detecting and computing apparatus is described that is effective to detect, count, compute, and so measure the level of gamma radiation of a source. The measurement is automatically corrected for a predetermined background radiation level regardless of the counting time selected. The apparatus includes provision for selection of a number of preset counting times in which the activity of the sample counted is indicated as net counts/min regardless of the counting time selected. Provision is made for both counting of total activity and of specific activity. A nonblocking ratemeter in the apparatus operates continuously whether or not the digital counting circuit is actuated and provides an over-load indication to prevent inadvertent miscounting of a high activity sample. (B.L.M.)

29572 AUTOMATIC SAMPLE CHANGER FOR RADIOACTIVE SAMPLES. Frank, Richard B.; Kus, Joseph E.; Rowan, Floyd R. (to Nuclear-Chicago Corp.). U. S. Patent 3,246,156. Apr. 12, 1966. Filed Apr. 15, 1963.

Means are described for using an automatic sample changing system to select the samples to be counted and those to be by-passed. The operation of the system is readily altered to permit great flexibility of use of the system by a large number of people. A single signaling member constitutes a plug that is inserted in the conveyor in a manner similar to the operation involved in inserting a sample by its presence or absence and serves to produce the counting or the by-passing of an entire following group of samples of any desired length. The end of any group is signaled by the absence of a sample in the receptacle immediately following the last sample in a given group since the actuation of the counting cycle programming means takes place only when a sensor detects the presence of a sample. (B.L.M.)

29573 RADIATION DETECTION DEVICE WITH AN INTENSIFIER SCREEN. Erikson, Herman E. (to Polaroid Corp.). U. S. Patent 3,247,378. Apr. 19, 1966. Filed May 25, 1962.

A device is provided for the detection and measurement of x rays and gamma radiation that when attached to the lens of a camera, e.g., a Polaroid Land Model 150, provides a simple and highly efficient dosimeter. The device comprises means opaque to acting light for defining a chamber with an opening at one end and with means opposite the open end for admitting radiation from a radioactive source into the chamber. Between the radiation-admitting means and the open end is positioned a visible light-emitting means that may be made up of one or a number of intensifier screens. Filters for the visible light are positioned between the visible light-emitting means and the open end of the chamber and so co-operate with the visible light-emitting means as to be capable of converting admitted radiation to a pattern of visible light having areas of graduated levels of intensity. (B.L.M.)

29574 RADIATION DOSIMETER. Shurcliff, William A. (to Polaroid Corp.). U. S. Patent 3,247,379. Apr. 19, 1966. Filed Oct. 21, 1952.

A dosimeter is patented that combines an ordinary dosimeter with at least two modifying elements that compensate for the direction of the incident radiation with respect to the wearer and for the shielding effects of the body of the wearer. The dosimeter includes a detecting element composed of a material, which, when subjected to a dose of penetrative radiation, provides a response by reason of the aggregate effect of the dose; and the response is functionally related to the dose. The first modifying element has a surface area that is contiguous with one area of the detecting element, has a modifying coefficient of at least one, and is composed of a material having an atomic number of at most 15. The second modifying element has a surface area that is contiguous with substantially all the remaining areas of the detecting element, has a modifying coefficient of at most one, and is composed of a material having an atomic number of at least 30. In a detector of this type, the quotient of the modifying coefficient of the second modifying element divided by the modifying coefficient of the first modifying element is a constant within the range of 0.3 to 0.8. (B.L.M.)

29575 NUCLEAR RADIATION DETECTING MEANS AND TRANSMISSION SYSTEM CONNECTING SAME TO REMOTE INDICATOR MEANS. Stone, Leonard R.; Muskovac, Nicholas G.; Cook, James E. (to Republic Steel Corp.). U. S. Patent 3,248,546. Apr. 26, 1966. Filed Jan. 15, 1964.

A nuclear radiation indicating system for providing indications at a point remote from the point of radiation detection is described with particular application to operation of a metallurgical furnace. The system is very stable in its operational characteristics and readily permits the detection of radiation intensity at a relatively inaccessible point and its direct transmission through low impedance transmission circuits in a simple and reliable manner to a distant point for observation, use, direct calibration, and monitoring. The system avoids the use of any vacuum tube except a Geiger radiation detection tube to give reliable radiation indications over prolonged operational periods without the need for close supervision, frequent recalibration, or maintenance. (B.L.M.)

29576 POCKET DOSIMETER USING A PHOSPHOR AND PHOTOCATHODE. Pawar, Vijay N. (to Bendix Corp.). U. S. Patent 3,249,755. May 3, 1966. Filed Aug. 29, 1962.

An apparatus is described that is capable of changing detected radiation to a measurable current. The apparatus uses a phosphor for changing the absorbed radiation energy into photons, and then uses a photocathode material for changing the photons into electrons that can be measured in the conventional manner with electrometers. The apparatus is energy independent and is capable of operating over a wide range of rates of radiation intensities without showing saturation effects. A glass coating is provided over the phosphor to prevent evaporation and preserve the vacuum around the electrometer, to provide a base for the photocathode, and to prevent interaction between the phosphor and the photocathode. The thickness and properties of the phosphor and photocathode material are matched to obtain optimum efficiencies for measuring particular radiation, such as gamma and x rays. The apparatus can be used to detect fast neutrons by using an hydrogenous radiator for

first converting the neutrons into protons that activate the phosphor to give the photon yield that in turn impinges on the photocathode coating to get electrons. The apparatus may be used with a radiation rate meter for measuring instantaneous rate of radiation or with a dosimeter for measuring the accumulated radiation dose. (B.L.M.)

Radiation Effects

29577 (CEA-R-2959) FIABILITE DE TRANSISTORS AU SILICIUM, A STRUCTURE PLANE, SOUMIS AU RAYONNEMENT γ DU ^{60}Co. (Reliability of Planar Silicon Transistors Exposed to ^{60}Co γ Rays). Blin, Andre; Le Ber, Jacques (Commissariat a l'Energie Atomique, Saclay (France). Centre d'Etudes Nucleaires). Mar. 1966. 76p. Dep. mn.

Results are presented from investigations on the reliability of silicon planar transistors, irradiated by the ^{60}Co γ rays. The variation of the average values of the parameters of the lots under test is considered. Then, a more complete statistical study is carried out (distribution of the values of the parameters within the lots; research of correlations, etc.). It is clearly stated and shown that evaluation of the degradation of the gain of transistors depends on: the conditions of measurement (voltage, current), after irradiation, the polarization of the elements during irradiation, and the origin of manufacture of the lots under test (4 manufacturers). Difficulties met to predict the behavior of the transistors under radiation stress were discussed, and an attempt was made to define practical rules for design engineers. (auth)

29578 (EUR-2649.e) IN-PILE APPLICATION OF STRAIN GAGES: PRELIMINARY RESULTS. Weltevreden, P. (European Atomic Energy Community, Ispra (Italy). Joint Nuclear Research Center). Nov. 15, 1965. 26p. Dep. mn.

An investigation was made to establish limits on the use of resistance strain gauges in a radioactive environment. To this extent a number of strain gauges is attached to a tube-section in various compensating arrangements. The tube section is mounted inside an irradiation rig and subsequently introduced in a reflector position of a CP-5 type reactor. A detailed description of the irradiation device is given and the data are summarized in the form of strain gauge parameters versus integrated neutron flux. Definite conclusions concerning irradiation stability are given and the continuation of the irradiation program is outlined. (auth)

29579 (NAA-SR-11887) ENERGY DEPENDENCE OF NEUTRON AND GAMMA RADIATION DAMAGE IN SILICON. Robinson, M. N.; Davies, N. F.; Kimble, S. G. (Atomics International, Canoga Park, Calif.). May 25, 1966. Contract AT(11-1)-Gen-8. 54p. Dep. mn. CFSTI $3.00 cy, $0.50 mn.

Silicon transistors were irradiated in fission and water-moderated fission neutron spectra, and in several different gamma spectra. Predictions of displacement damage from a point defect model are compared with damage constants from experimental measurements of the common-emitter current gain. Significant agreement is demonstrated between a spectrum normalization scheme, based upon this damage model, and the experimental results. Base current measurements also confirm an analytical neutron-gamma damage equivalence. It is concluded that test irradiations of silicon devices in water-moderated fission neutron and gamma spectra may be directly applied to SNAP payload evaluations. (auth)

29580 SIGNAL PRODUCED IN A MONOPOLE ANTENNA BY THE GAMMA FLUX FROM A NUCLEAR EXPLOSION. Taylor, C. D. (Sandia Corp., Albuquerque, N. Mex.); Duncan, R. H. IEEE (Inst. Elec. Electron. Eng.) Trans. Antennas Propagation, AP-14: 45-8 (Jan. 1966).

A transient signal is induced in a receiving antenna, or probe, by the high-density γ flux emitted from a nuclear explosion. When an object is irradiated by this flux, it becomes positively charged because of electrons being scattered from it by virtue of the Compton effect. An attempt is made to explain the transient signal produced in an irradiated antenna by considering the temporal charging of the antenna to be exciting the receiving circuit. A monopole antenna is considered to be bombarded by a flux of γ rays propagating normally to the axis of the antenna. As a result of this bombardment, electrons are scattered from the antenna, thus charging the antenna positively. This induces a current in the load impedance of the antenna, appearing as if the antenna were receiving a transient r-f signal. An expression for the time-dependent voltage across the load impedance of the antenna is obtained by considering that every electron scattered from the antenna never returns and that the antenna impedance and capacitance are their free-space values. The accuracy and range of validity of the results could be greatly improved if the antenna impedance and capacitanee were known for antennas in proximity to a moving charge distribution. To measure the r-f signal from a nuclear explosion accurately, it is necessary to know the effects on the antenna, or probe, produced by the γ flux from the nuclear explosion. From the results obtained it should be possible to estimate these effects under most conditions. (BBB)

ISOTOPE TECHNOLOGY

Industrial Applications

Refer also to abstracts 28932, 28934, 28935, and 29317.

29581 (AD–633785) POTENTIAL APPLICATIONS OF RADIOISOTOPES IN THE NAVY. Gardner, L. B.; Hanna, A. E.; Stanton, H. E. (Naval Civil Engineering Lab., Port Hueneme, Calif.). May 1966. 35p. (R–445). CFSTI $2.00 cy, $0.50 mn.

Potential applications of isotopic devices and techniques within the Naval Shore Establishment were studied. Radiation characteristics, general applications of isotopic devices, and specific problem areas are discussed. Recommendations are included for the use of surface density and moisture gages in the inspection of compacted earth, and for additional work in the determination of the thickness of in-place steel sheet piling and the thickness and density of concrete. (auth)

29582 (MIT–3343-26) SIMULTANEOUS RADIATION-HEATING TREATMENT OF PRECOOKED MARINE PRODUCTS. Final Report, February 1, 1965–February 28, 1966. Goldblith, S. A.; Nickerson, J. T. R. (Massachusetts Inst. of Tech., Cambridge). May 1966. Contract AT(30-1)-3343. 52p. Dep. mn. CFSTI $3.00 cy, $0.50 mn.

Radiation effects on cooked fish sticks and scallops while holding at 150°F and lobster meat and blue crab meat while holding at 140°F were evaluated. Controls were also prepared and evaluated. When very low count (aerobic bacterial count) lobster or crab meat was available, irradiation at 125,000 rad while holding at 32°F was found to be a good method of extending the refrigerated storage life. Very good refrigerated storage life extension of lobster and crab meat, moderately contaminated with bacteria, was obtained by irradiating at 125,000 rad while holding at 140°F. Organoleptic tests indicated that irradiation of lobster or crab meat at 125,000 rad, either while holding at 32 or 140°F, has little effect on the taste of these products, at the start or after refrigerated storage. Spoilage of lobster meat or crab meat because of the growth of anaerobic bacteria during refrigerated storage was not observed. The same was true for increases in clostridia. (P.C.H.)

29583 (TID–22515) APPLICATION OF RADIATION-PASTEURIZATION PROCESSES TO PACIFIC CRAB AND FLOUNDER. Final Summary, November 1964–October 1965. Miyauchi, David; Spinelli, John; Pelroy, Gretchen; Stoll, Nancy (Bureau of Commercial Fisheries, Seattle, Wash. Technological Lab.). Nov. 1965. Contract AT(49-11)-2058. 131p. Dep. mn. CFSTI $4.00 cy, $1.00 mn.

Progress is reported on investigations of the application of ^{60}Co γ rays at substerilization doses to selected Pacific Coast fishery products to extend the shelf life of the fresh products at above-freezing refrigerated temperatures. The rate of production of trimethylamine (TMA), total volatile bases (TVB), and volatile acids (VAN) was studied in fish irradiated at 0, 0.1, 0.15, 0.2, 0.3, and 0.4 megarad and stored at 33, 42, 50, and 72°F. Studies on fish-tissue nucleotides show that measurements of these compounds or their corresponding nucleosides and free bases serve as useful indicators of fish freshness. Methods for the measurement of these compounds have been both evaluated and developed so that their measurement could routinely be made in modest quality-control laboratories. The rates of nucleotide degradation and hypoxanthine accumulation have been determined on English sole, petrale sole, Pacific ocean perch, lingcod, true cod, and rockfish. The introduction of nitrogen after the fish are irradiated in a vacuum protected the product from subsequent off-color and rancidity, but carbon dioxide did not. Treatment of halibut steaks, Pacific ocean perch, English and petrale sole fillets with mixtures of sodium tripolyphosphate and salt prior to irradiation showed that the formation of drip was almost completely retarded even after 35 days of storage and that a product stored for 4 weeks closely resembles the pre-irradiation product. The contribution of the existing microflora to the observed spoilage patterns of radiation-pasteurized petrale sole fillets was appraised by determining the incidence of organisms possessing certain hydrolytic enzymes that are known to produce malodorous breakdown products in spoiling food. Post-irradiation storage conditions were shown to have a strong influence on the composition of the microflora. The spoilage flora of irradiated fillets stored under oxygen-permeable film consisted of Achromobacter and strongly aerobic yeasts; whereas the spoilage flora of vacuum-packed samples were predominantly lactic acid bacteria, and no yeast were found. The effect of various storage temperatures on the shelf life as determined by sensory, chemical, and bacteriological indices was also studied. The spoilage of the 0.1-megarad and 0.15-megarad samples at 42°, 50°, and 72°F was very similar to that of the control samples in the time and type of spoilage. The spoilage of the samples irradiated at 0.2 megarad and higher was different from the control samples. (auth)

29584 (TID–22991) MARINE PRODUCTS DEVELOPMENT IRRADIATOR FACILITY LOCATED AT BUREAU OF COMMERCIAL FISHERIES, TECHNOLOGICAL LABORATORY, GLOUCESTER, MASSACHUSETTS. (Associated Nucleonics, Inc., Garden City, N. Y.). Feb. 15, 1964. Contract AT(30-1)-3181. 27p. (AN–147). Dep. mn. CFSTI $2.00 cy, $0.50 mn.

The Marine Products Development Irradiator (MPDI), which is currently under design and construction at Gloucester, Mass., is described. It is a semi-production fixed facility with the capability of processing approximately 2,000 lbs. per hour of product at a typical pasteurization dose of 250,000 rad. Its capabilities will include processing large amounts of foods, primarily seafoods, for shipping, storage, and other large-scale tests. It is generally a rectangular, one-story facility of slightly under 4,000 ft^2, divided into a general building area and an irradiation cell. Availability and economics are also discussed. (P.C.H.)

29585 GAMMA IRRADIATION OF FOOD. Wetherill, J. M. (Alberta Dept. of Public Health, Edmonton). Can. J. Public Health, 56: 521-4(Dec. 1965).

The effects of radiation on food are described covering such aspects as nutritional adequacy and safety of consumption. Applications of the radiation processing for specific foods and the dose rates required to prolong storage life or prevent sprouting of vegetables are discussed. Other uses are the eradication of insect pests and food parasites. Control of processors from a radiation safety standpoint is essential in view of the limited experience to date. (F.S.A.)

29586 THE INFLUENCE OF γ-RADIATION ON THE GASIFICATION OF LIGNITE. Haeusler, W. Energietechnik, 14: 175-6(Apr. 1964). (In German)

It was reported by Polish research workers that the irradiation of anthracitic coal with γ rays during gasification produced an increase in the fuel value of 83 to 100 kcal/cm^3. Tests were made to determine whether a similar increase in the calorific value could also be obtained in bituminous coal if the γ irradiation were directed towards the area of gasification. Laboratory-scale tests were made with an apparatus commonly used for gasification and fuel testing and with 16 ring-shaped ^{60}Co preparations (total activity of 400 mC) arranged around the gasification area. The dose rate, measured with a rod-shaped LiF-dosimeter, was 35 ± 5 r/hr. In the 2 series of experiments carried out at 770 and 700°C, gasification was observed with and without γ irradiation. Results showed that at 770°C, immediately upon impact of the γ rays, the CO content increased by 4.7%

which correspond to a rise of 20% in the CO gas produced. At 700°C, the CO content increased by 4.8%, which corresponded to an increase of 40% in CO production. When the radiation source was removed, the CO content returned to its preirradiation value. The applied dose rate of 35 r/hr was very low. The reason is not known for the increase in CO production, but it is believed that the radiation produced catalytic centers, which changed the course of the gasification. (OID)

29587 POSSIBILITY OF CONTROL OF TERMITES WITH ATOMIC WASTE. Kurir, A. (Institut fuer Forstentomologie und Forstschutz, Vienna). Holzforsch. Holzverwert., 15: 67-70(Sept. 1963). (In German).

It is proposed that radioisotopes, as waste fission products, might be used in the field to exterminate termite colonies. Because of the increasing availability of this material it might be economically feasible under certain situations. Under the use envisioned, radioactive sources would be inserted in the ground to a depth of one to two meters near termite colonies. The object would not be to cause immediate death of the whole colony but to induce sterility in breeding male and female insects. This would gradually but generally lower fertility of the population and lead to eradication of the species in that locality. The γ emitter ^{60}Co and the β emitter ^{90}Sr are proposed especially for this application. A mobile ^{60}Co source would be preferable and would offer highly penetrating radiation. Possible hazards involved are discussed and it is pointed out that sealed sources could be used in unpopulated areas and that unsealed sources might lead to ground water contamination. Steel and lead source holders, which could be inserted into the ground are described and diagrammed. Means by which surface doses would be monitored to protect vertebrate wild life and humans are also considered. (BBB)

29588 THE EFFECT OF γ-RADIATION ON LEATHERS TANNED BY VARIOUS METHODS. Strakhov, I. P.; Shifrin, I. G.; Levenko, P. I. Izv. Vyssh. Ucheb. Zaved., Tekhnol. Legkoi Prom., No. 2, 93-9(1963). (In Russian).

The action of ^{60}Co γ radiation on the physical and mechanical properties of leathers tanned by various methods is discussed. (OID)

29589 EFFECT OF STORAGE AT AMBIENT TEMPERATURE ON THE VOLATILE COMPONENTS OF IRRADIATED BEEF. Wick, E. L. (Massachusetts Inst. of Tech., Cambridge); Koshika, M.; Mizutani, J. J. Food Sci., 30: 433-40(May-June 1965).

Volatile components of beef irradiated at 5 megarad by concurrent radiation-distillation, by radiation just prior to distillation, and by radiation and storage at ambient temperature for 6 months before distillation were isolated and characterized. The total yield of odor isolate from stored beef was approximately 4.4 mg per lb (about 10 ppM), or about one-third of the yield obtained from freshly irradiated beef or from unirradiated beef. The n-alkanals and methional, major volatile components of freshly irradiated beef, are minor components of stored irradiated beef. n-Alkanols are present in relatively greater amount in odor concentrates of stored beef. n-Alkanes and 1-alkenes are volatile components of both stored and freshly irradiated beef, but are present in much smaller quantity in the stored product. (Public Health Eng. Abstr.)

29590 MODEL LEVEL-GAUGES. Andresen, E. G. (Staatliche Ingenieurschule Gauss, Berlin). Kerntechnik, 8: 213-17(May 1966). (In German).

The advantages of nuclear liquid-level gages in comparison with the conventional methods are discussed. In order to study the specific problems of these gages and their function under various operating conditions, two experimental arrangements were built, which will allow a number of investigations and measurements under various conditions. (auth)

29591 THE EFFECT OF γ-RADIATION ON CHROME-TANNED SHOE UPPER LEATHER. Strakhov, I. P.; Levenko, P. I.; Shifrin, I. G. (Inst. of Technology, Moscow). Kozh.-Obuvn. Prom., 5: No. 7, 20-5(July 1963). (In Russian).

Cr-tanned upper leather was irradiated by ^{60}Co γ rays to a total activity of 186,950 g-equiv Ra with 10^7, 10^6, and 10^5 rad. Test measurements of whole Cr-tanned upper leather and its tear resistance before and after irradiation showed that it was damaged greatly by irradiation with 10^7 rad, less damaged by 10^6 rad, and undamaged or even improved by 10^5 rad. Stretch measurements did not give correlating results. The results were explained by the formation and destruction of cross-linkages in Cr-tanned upper leather and this destruction was greater in pig leather than in other types of Cr-tanned upper leather. (OID)

29592 THE EFFECT OF SMALL DOSES OF γ-RADIATION ON SOME OF THE PHYSICAL-MECHANICAL PROPERTIES OF CHROMIUM-TANNED LEATHER. Strakhov, I. P.; Levenko, P. I.; Shifrin, I. G. (Inst. of Technology, Moscow). Kozh.-Obuvn. Prom., 5: No. 11, 24-9(Nov. 1963). (In Russian).

Irradiation at 10^7 rad of Cr-tanned goat leather lowered the tear resistance and the grain-crack resistance in air and at 300 mm. The original tear resistance and the grain-crack resistance were lowered at 10^{-4} mm by irradiation at 1.5×10^4, 10^5, and 10^6 rad. Approximately one-third of the strength loss was caused by ionized air, and the cross-linkages produced by tanning were affected very little. (OID)

29593 PRINCIPLES OF THE MOST IMPORTANT METHODS FOR USE OF RADIOACTIVE RADIATION SOURCES. Wiesner, L. (Isotopen-Studiengesellschaft eV, Karlsruhe, Ger.). Neue Tech., 8: 80-91(1966). (In German).

The principle of measurement methods and apparatus based on the application of radioactive sources are described. Indications are given as to what aspects should be considered, in measurement problems of all kinds, in the choice of the radiation source, and what accuracy of measurement can generally be achieved in practice. A description is given of the methods used for thickness, density, surface weight and level measurement. Measurement methods for gaseous media based on the ionization effect of nuclear radiation and of the application of radiation sources for continuous elementary operational analysis are treated. Finally, explanations are given of the various measurement and analysis possibilities resulting from the use of neutron sources. (auth)

29594 MEASURING DENSITY WITH THE NUCLEAR BACK-SCATTER METHOD. Taylor, Denis; Kansara, Mohan (Univ. Coll., Nairobi, Kenya). Nucleonics, 24: No. 6, 54-6(June 1966).

The performance of radiation, back-scatter gages in measuring the density of soils is discussed. Theoretical considerations are reviewed. Sensitivity and effects of soil moisture content and voids are discussed. (M.C.G.)

29595 APPLICATION OF X RAYS TO MEASURE POROSITIES AND SATURATIONS IN POROUS MEDIA. Norel, G. (Institut Francais du Petrole, Rueil-Malmaison, France). Rev. Inst. Franc. Petrole Ann. Combust. Liquides, 21: 212-26(Feb. 1966). (In French).

Detailed data, including theoretical considerations, mathematical formulations, instrumentation, techniques, and experimental results, are provided, which show that it is possible to make remote control measurements of porosities and degree of saturation by liquids of solids through absorption of x or γ rays. The principle of this measurement is based on the usual selective absorption laws of such radiations. The measurement process and application of this method are facilitated by the use of a radioactive source as radiation emitter. The choice and features of this source are defined according to the conditions imposed by the numerous applications made in the laboratory. Results obtained for porous clay discs, in the dry state or saturated with potassium iodide solutions, are presented to illustrate application of the technique. (BBB)

29596 GAMMA RADIOGRAPHY WITH A LARGE ^{60}Co SOURCE. Ishii, Yugoro; Kanno, Akira (Tokyo Inst. of

Tech.). Senpaku Gijutsu Kenkyujo, 2: No. 3, 35-48(Jan. 1965). (In Japanese).

A method for obtaining high quality radiographs with a 50 C cobalt-60 gamma-ray source equipment, was studied. Back scattering was satisfactorily reduced by a 3 mm back shielding plate of Pb in radiographs of less than 100 mm thick steel plates. Penetrameter sensitivity of radiographs of steel plates over 80 mm thickness was less than 1% with fine grain film at the condition of reduced scattered ray. (TCO)

29597 RADIATION PRESERVATION OF SEVERAL FRESH FRUITS AND VEGETABLES. Hayakawa, Akira; Umeda, Keiji; Shiroishi, Masahide (Ministry of Agriculture and Forestry, Tokyo). Shokuryo Kenkyusho Kenkyu Hokoku, No. 18, 200-3(Mar. 1964). (In Japanese).

The use of γ radiation for increasing the stability of fresh fruits was studied. Results obtained with a 400-C ^{60}Co source indicated that oranges irradiated with a dosage of 1.78×10^5 rep showed no significant changes in color or in constituents such as ascorbic acid, reducing sugar, and titrative acidity. With a dosage of 5.5×10^5 rep, persimmons showed a marked decrease in the quality of the astringent determined as tannic acid. The storage life of these fruits was prolonged when polyethylene bags were used before irradiation. With dosages of 1.28×10^4 to 6.4×10^5 rep, the storage life of matsutake was increased for at least 7 days. With dosages from (1.3 to 6.4) $\times 10^4$ rep chestnuts showed no decrease in organoleptic acceptability, and the possibility was also indicated of controlling insects in chestnuts by radiation. (OID)

29598 RADIOIZOTOPNYE PRIBORY V METALLURGII. (Radioisotopic Instruments in Metallurgy). Afanas'ev, V. N.; Latyshev, V. K.; Lyndin, V. V.; Felinger, A. K. Moscow, Izdatel'stvo Metallurgiya, 1966. 224p.

The physical principles for using radioisotopes and nuclear radiation for controlling the parameters of technological processes are presented, and a description is given of radioisotope devices for measuring the levels of liquid metals and of corrosive and friable materials in metallurgical apparatus, the thickness of hot and cold rolled sheets, and the pressure and flow rate of liquids and gases. Radiation safety problems in the metallurgical use of radioisotopes are considered. (M.J.T.)

29599 ACTIVATION DURING RADIATION CONSERVATION OF FOOD. Tuchscheerer, T. Karlsruhe, Ger., Technische Hochschule, 1965. 91p. $2.00 Gmelin, AED-Diss. 65-252.

Calculated activities of foodstuffs after γ irradiation are compared with experimental data. Agreement is satisfactory. In the energy range 0.05 to 10 Mev only the production of isomers has to be considered. For higher energies (γ,n) reactions are most important. Results indicate that the induced activities are not hazardous in comparison to maximum permissible levels of radioactive isotopes in food. (Gmelin Inst.)

29600 ELECTRON-SINGLE-SCATTER-GAGE: A NEW VACUUM GAGE FOR THE RANGE FROM 10^{-5} TORR TO 1 TORR. Schumacher, B. W.; Aruja, E.; Falckenberg, H. R. (Ontario Research Foundation, Toronto). 43p. (CONF-650643-2). ORAU.

From 3rd International Vacuum Congress, Stuttgart.

An electron beam or beta particles are fired through the vacuum space over a path length of about 50 cm. This primary beam is intercepted by a beam stop. The single-scatter in the acute forward direction of some of the electrons by the residual gas molecules is measured by scintillation counters or solid-state detectors. Scattering from anywhere in the beam path is counted, and no electron optics are employed. With an electron beam of 40, 60, or 80 kev the scatter-count for constant primary current (in the order of 10^{-12} A) was found to be a linear function of pressure between 0.1 torr and 10^{-5} torr. This agreed closely with predictions from scattering theory. With a beta-emitting isotope source, about 500 mC of ^{147}Pm, in a light-weight gage structure, a useful working range from 10^{-3} torr to 0.2 torr was found. An extension of the upper range limit to 10 torr and the lower one to 10^{-13} torr seems possible. These gages measure the vacuum in "free" space far from walls and structure elements of the gages themselves. There is no inherent outgassing or gettering effect. Details of the design theory and the experiments are discussed. (auth)

29601 ALPHA RADIATION GAGING TECHNIQUES AS APPLIED TO BASIS WEIGHT MEASUREMENT. Gray, Thomas A. 15p. (CONF-660213-1). ORAU. Gmelin, AED-CONF-66-042-1.

From Technical Association of the Pulp and Paper Industry, 51st Annual Meeting, New York.

Techniques for measurement of basis weight by alpha absorption were developed. It is particularly adaptable to measurement of lightweight material varying in weight between 3 and 60 g/m^2 or 1.5 to 25 lb/2000 ft^2. The properties of alpha sources, the absorption conditions of materials to be measured, and the principal characteristics of the detectors are considered. The differential measurement technique was utilized. Two identical combinations of source, ionization chamber, and absorbent were used and the ionization current resulting from each ionization chamber was compared. (M.C.G.)

29602 THE EFFECT OF IRRADIATION TEMPERATURE ON ORGANOLEPTIC, PHYSICAL AND CHEMICAL PROPERTIES OF BEEF. Harlan, Jerry W.; Kauffman, F. Leo; Heiligman, Fred (Army Natick Labs., Mass. Swift and Co., Chicago). 18p. (CONF-650902-24). ORAU. Gmelin, AED-CONF-65-235-6.

From American Chemical Society, 150th National Meeting, Atlantic City.

The effect of the temperature of irradiation on the chemistry and technology of amino acids, proteins, and meats was investigated in a number of laboratories. Electron spin resonance studies of amino acids and proteins showed the free radicals produced by irradiation at temperatures below $-80°C$ to be different from those observed at higher temperatures and a large temperature effect on the yields of primary radiochemical reactions of amino acids and peptides in aqueous solutions was found in chemical studies. The irradiation flavor intensity of enzyme-inactivated beef steaks was found to decrease linearly with irradiation temperature in the range from 20 to $-196°C$. The rate of decrease varied with irradiation dose. Physical and chemical properties of irradiated steaks, including tenderness, nonprotein nitrogen, and volatile mercaptan level were found to be temperature dependent. A process variable study on enzyme-inactivated steaks showed that an organoleptically superior radiation-sterilized steak can be produced by irradiating at liquid nitrogen temperatures in a vacuum and slowly warming to room temperature for storage. (auth)

29603 THE DEVELOPMENT OF RADIATION-STERILIZED SEAFOOD PRODUCTS. I. ENZYME INACTIVATED COD AND HALIBUT PATTIES. Sinnhuber, R. O. (Oregon State Univ., Corvallis); Landers, Mary K.; Yu, T. C.; Simon, Morris; Heiligman, Fred. 14p. (CONF-660609-2). ORAU.

From International Symposium on Food Irradiation Meeting, Karlsruhe, Ger.

Studies were made to develop radiosterilized seafood products that would withstand ambient storage for periods up to a year. The storage stability and the effect of antioxidants on radiosterilized seafood products were determined. Treatments were utilized that are known to improve flavor, such as vacuum packing and the use of charcoal packets to lessen radiation odors and flavors. Consumer-type preference panels were used to determine the quality of the products and the effect of various treatments. Storage changes were evaluated by objective tests, including thiobarbituric acid number, total volatile bases, pH, and color measurements. Results are presented in tables. Two radiosterilized products, enzyme-inactivated cod patties and enzyme-inactivated halibut patties, were developed. In the 6 months storage study, preference panels indicated

that the radiosterilized cod patties without antioxidant and with one of the antioxidants were preferred to the nonirradiated control after 6 months storage at 72°F. There was no significant difference in preferences for halibut patties after 6 months storage. In the 12 months storage study, the panels preferred the nonirradiated control samples to the irradiated samples for both cod and halibut. (M.C.G.)

29604 PROCEEDINGS OF THE FIFTH INTERNATIONAL PULP AND PAPER INSTRUMENTATION SYMPOSIUM, VANCOUVER, BRITISH COLUMBIA, MAY 18–23, 1964. Pittsburgh, Instrument Society of America, 1964. 122p. (CONF-640503).

Sixteen papers are presented on the uses of instruments in the paper industry. Instrumentation of efficiency, control, and measurement techniques, now and in the future, are discussed. One paper was previously abstracted for NSA. For abstract number see CONF-640503 in the Report Number Index. (J.G.B.)

29605 ILLUMINATED TELEPHONE DIAL. Greenslade, Walter Percival (to Ericsson Telephones Ltd.). British Patent 1,030,141. May 18, 1966. Filed Mar. 4, 1964.

In order to illuminate a telephone dial, a closed transparent arcuate tube containing tritium and having its inner wall coated with a phosphor that reacts with tritium to produce light is embedded in the plastic behind the part of the telephone dial assembly that bears the digits and letters. (B.L.M.)

Power Application

See also ENGINEERING — Space Propulsion

Refer also to abstract 30926.

29606 (ALO–3634–1) QUARTERLY PROGRESS REPORT OF RESEARCH AND DEVELOPMENT OF VACUUM FOIL-TYPE INSULATION FOR RADIOISOTOPE POWER SYSTEMS, FEBRUARY–APRIL 1966. Dunlay, J. B. (Thermo Electron Engineering Corp., [Waltham], Mass.). May 27, 1966. Contract AT(30-1)-3634. 30p. Dep. mn. CFSTI $2.00 cy, $0.50 mn.

The designs of the material compatibility screening and the planar thermal conductivity test assemblies were completed. Fabrication of the test assemblies was initiated. Preliminary designs of the cylindrical thermal conductivity and the edge heat loss test assemblies were established. (auth)

29607 UNDERSEA ROLE FOR ISOTOPIC POWER. Buck, K. E. (Aerojet-General Nucleonics, San Ramon, Calif.). Nucleonics, 24: No. 6, 38-41 (June 1966).

Uses of radioisotope power generators in navigational aids, fixed underwater networks, manned underwater platforms, and propulsion of small submersibles are discussed. Characteristics of radioisotopic heat sources are reviewed. The SNAP-7 series, SNAP-21 and SNAP-23, RIPPLE, URIPS, and SNAP-15A are described. Economics and reliability are considered. (M.C.G.)

29608 NUCLEAR POWER SYSTEMS FOR ADVANCED HIGH-POWERED COMMUNICATIONS SATELLITES. Gylfe, J. D. (North American Aviation, Inc., Canoga Park, Calif.). New York, American Inst. of Aeronautics and Astronautics, 1966, Paper No. 66-305, 32p., $1.50. (CONF-660517–1). ORAU.

From AIAA Communications Satellite Systems Conference, Washington, D. C.

A survey of the nuclear power systems that are considered to be most suitable for advanced, high-powered communications satellites and that can be available in the 1970 to 1975 time period is presented. The general criteria for communication satellite power systems are discussed and candidate power systems that might be expected to meet these criteria are identified. A description and summary of the major design and performance characteristics of reactor, radioisotope, and solar-photovoltaic power systems are presented and compared for a range of power levels up to ~20 kwe. A nuclear-powered communication satellite concept is described and compared with a typical solar-powered concept on a total mission cost basis. It is concluded that the reliability and lifetime criteria dictate the use of passive, thermoelectric power conversion equipment for the nuclear power systems that could be made available in the 1970–1975 time period, and that reactor-thermoelectric systems offer the most attractive power system for advanced, high-powered communication satellites, based on overall mission cost considerations. (auth)

Separation and Production

See also CHEMISTRY — Separation Processes and Procedures

29609 (NP–15947) SOME FUTURE REQUIREMENTS FOR LARGE-SCALE ISOTOPE IRRADIATION IN REACTORS. Gehem, L.; Lopez-Menchero, E. (European Company for the Chemical Processing of Irradiated Fuels, Mol (Belgium)). Feb. 1966. 15p. (ETR–178; CONF-650972–1). Dep. mn. CFSTI $1.00 cy, $0.50 mn.

From European Atomic Energy Society Symposium on Irradiation Experiments, The Hague.

The irradiation charges for different isotopes were compared and it was found that there are large differences in the contribution of the irradiation cost to the total cost per initial thermal watt. Consequently, a large scale isotope irradiation program could lead to a better overall neutron economy depending upon the isotope chosen for power generation. (P.C.H.)

29610 HIGH-SPECIFIC-ACTIVITY ^{198}Au LOW IN ^{199}Au. Lewis, R. E. (Oak Ridge National Lab., Tenn.). Nucl. Appl., 2: 33-5 (Feb. 1966).

^{198}Au with a specific activity of 370 C/g and containing <0.1% ^{199}Au was produced by the epithermal neutron-capture reaction, ^{197}Au(n,γ)^{198}Au. The secondary neutron-capture reaction, ^{198}Au(n,γ)^{199}Au, was greatly reduced by a thermal-neutron absorber, a cadmium capsule in which the samples of gold foil and gold-aluminum alloy were irradiated. High-specific-activity ^{198}Au with <0.1% ^{199}Au is especially useful for medical purposes. (auth)

29611 PROCESS FOR ISOTOPE CONCENTRATION. Glew, David N. (to Dow Chemical Co.). Canadian Patent 727,029. Feb. 1, 1966.

The flow sheet for this process indicates an exchange reaction between hydrogen sulfide or a hydrocarbon derivative and hot water, in which deuterium is removed from the water. In the next step gaseous hydrogen sulfide enriched in HDS or an equivalent hydrocarbon species runs through a "hydrate forming reactor" in which a solid hydrate enriched in HDO, results. In the next stage the hydrate is decomposed to give liquid water enriched in D_2O. Recycling is used to increase efficiency. In a variation of the method liquid hydrogen sulfide is used at a suitably low temperature. Numerical examples are given, which claim a considerably increased yield over the dual temperature exchange process. (F.S.A.)

MATHEMATICS AND COMPUTERS

29612 (ANL–7126) THE NUMERICAL INTEGRATION OF ORDINARY DIFFERENTIAL EQUATIONS OF VARIOUS ORDERS. Gear, C. W. (Argonne National Lab., Ill.). Jan. 1966. Contract W-31-109-eng-38. 34p. Dep. mn. CFSTI $2.00 cy, $0.50 mn.

Modified multistep predictor-corrector methods are described for general initial-value problems and new methods are introduced. These new methods are of degree 2k for k-step methods and require only one function evaluation. Equivalence classes of methods are discussed, and it is argued that the Nordsieck formulation is the best for high-accuracy problems, and that for low-accuracy problems either the Nordsieck formulation or versions of the new methods should be used. The direct application of the methods to higher-order equations is analyzed, and some numerical evidence is given to suggest that this application leads to faster and more accurate methods than the usual method of integrating a system of first-order equations. Some preliminary tests on the integration of singular families are mentioned. Finally, existence and convergence proofs are presented. (auth)

29613 (TRG-Report–1198) A GENERAL-PURPOSE MULTIPLE REGRESSION PROGRAMME FOR THE IBM 7090. Chatterley, F. J. (Reactor Group, United Kingdom Atomic Energy Authority, Sellafield (England)). Feb. 14, 1966. 12p. Dep. BIS $0.30. HMSO 1s. 9d.

The program accepts up to 25 variables and up to 2,000 values of each provided the total number of numbers read in is less than 10,000. Additional variables can be derived from those read directly. Means, standard deviations and correlations of the variables are all calculated. For each regression equation, the residual sum of squares and standard deviations and covariances of the coefficients are all available. Nonsignificant variables can be automatically eliminated. Details of the input data required and the output obtainable, together with mathematical definitions of all the quantities calculated, are included. (auth)

29614 GENERALIZED SPHERICAL FUNCTIONS FOR THE NONCOMPACT ROTATION GROUPS. Fischer, J.; Niederle, J.; Raczka, R. (International Center for Theoretical Physics Trieste, Italy). J. Math. Phys., 7: 816-21 (May 1966).

Special representations of arbitrary noncompact rotation groups labeled by one independent Casimir operator are considered. The explicit construction of the corresponding generalized spherical functions is given and the properties of these representations are discussed in detail. (auth)

29615 DIRECT METHODS OF QUALITATIVE SPECTRAL ANALYSIS OF SINGULAR DIFFERENTIAL OPERATORS. Glazman, I. M. New York, Daniel Davey and Co., Inc., 1965. 242p. (IPST–2146). Israel Program for Scientific Translations, Jerusalem, 1965.

Translated from Pryamye Metody Kachestvennogo Spektral'nogo Analiza Singulyarnykh Differentsial'nykh Operatorov.

The character of the spectrum of singular differential operators as dependent on the behavior of the coefficients of the corresponding differential operation is investigated. Direct methods of qualitative spectral analysis, for obtaining criteria of positions of parts of the spectrum, are presented, and their use is illustrated by examples, many connected with problems in quantum mechanics. The operator mainly considered is the Schroedinger operator. (M.J.T.)

METALS, CERAMICS, AND OTHER MATERIALS

General

Refer also to abstracts 29320, 29598, 29820, 30801, and 30903.

29616 (BMI–1738) PROGRESS RELATING TO CIVILIAN APPLICATIONS DURING JULY, 1965. Dayton, Russell W.; Paprocki, Stan J. (Battelle Memorial Inst., Columbus, Ohio). Aug. 1, 1965. Contract W-7405-eng-92. 39p. Dep. mn. CFSTI $1.00 cy, $0.50 mn.

Research and development progress is reported on reactor materials and components, ceramic fuels, radioisotope and radiation applications, coated-particle fuels, fluoride volatility processes, and gas cooled reactor materials. (J.R.D.)

29617 (EURAEC–1593) USE OF PLUTONIUM AS A FUEL IN NUCLEAR REACTORS. Quarterly Report No. 8, October 1–December 31, 1965. (Societe Belge pour l'Industrie Nucleaire, Brussels). Feb. 1966. Contract 001-64-1 TRUB. 120p. (EUR–2814; BN–6602-02). Dep. mn. CFSTI $4.00 cy, $0.75 mn.

Work Performed Under United States–Euratom Joint Research and Development Program.

The factors governing the selection of Incoloy 800 as cladding for UO_2–PuO_2 fuels are discussed. The development of the fabrication processes for vibratory-compacted fuel elements is described. Mechanical strength and ductility tests revealed that the ductility of the Incoloy 800 cladding was not effected by swaging. The localized heat surpluses caused by segregation of PuO_2 in the fuel elements were found to have a negligible effect on the thermal performance of the fuels. A process for separating fission products was adapted for the analysis of the burnup ratio of low-burnup fuels. Problems still exist due to the plutonium interference resulting from the inability to separate the plutonium from the fission products. Two methods were used for the theoretical interpretation of the space-time neutron distributions characteristic of subcritical lattice research with the pulsed neutron method. The first method employed spot kinetics, where it is assumed that neutron density can be separated into an amplitude function and a shape function, the first dependent on time and the second assumed independent of it. The remaining eigenvalue for neutron density is then a simple function of the effective multiplication factor of the medium in question, of the effective fraction of neutrons delayed, and of the lifetime of the prompt neutrons. The other method is based on nodal analysis where the medium is subdivided into core and reflector, for which time-dependent conservation equations are formulated. Resolution of the system gives two decay constant eigenvalues of different orders of magnitude. An experimental neutron study of the lattices formed by fuel rods from the Thetis reactor continued with an overflight of the lattices with volumetric water/oxide ratios of 2.6, 6.3, and 1.5. The 4.1 ratio lattice was then reloaded and void coefficient measurements and measurements of the effects of absorbents at the core boundary were effected. (W.L.G.)

29618 (GEAP–4982) SODIUM-COOLED REACTORS. FAST CERAMIC REACTOR DEVELOPMENT PROGRAM. Quarterly Report No. 16, August–October 1965. Breizy, C. E. (comp.) (General Electric Co., San Jose, Calif. Advanced Products Operation). Jan. 1966. Contract AT (04-3)-189. 69p. Dep. mn. CFSTI $3.00 cy, $0.75 mn.

Preliminary isothermal tests of UO_2–25 wt % PuO_2 fuel compatibility in Na at 750°C indicate the superiority of stoichiometric and hypostoichiometric fuel vs hyperstoichiometric fuel. Estimates of cladding strain rate in the low-burnup specimen (C3B) which was transient irradiated indicate that the observed cracking of the cladding probably was due to deformation after radiation embrittlement. Calculations were made to assess the desirability of employing a thermal-flux filter (Cd) to reduce the flux depression in the fuel sample when transient irradiated in TREAT. The calculations show that the resultant temperature profiles are not substantially different from those obtained in unfiltered irradiations. A study of temperature profiles and fission-gas-generation profiles in fuel in a thermal and in a fast flux were made. It was concluded that while the thermal-flux temperature profile could be made to approximate a fast-flux temperature profile, the gas-generation profiles in thermal and fast fluxes are quite different. Irradiation of a gap conductivity capsule was completed and preliminary information indicates that fuel center temperature is extremely sensitive to gap size. In addition, this experiment also indicated that interference fit gap sizes exhibit significantly less mechanical fuel-cladding interaction than comparable water-cooled fuel experiments. The solidus and the liquidus of the PuO_2–UO_2 system were measured and the anomalous maximum at 10 wt% PuO_2 as measured in earlier studies was shown to have been caused by a stoichiometry shift during the measurements. Fuel pin F1C, irradiated for short term at 16 kw/ft, was examined destructively. No significant axial fuel redistribution was observed. The structural changes which occurred (central void formation and grain growth) were as expected. The effects of current uncertainties in cross sections on the important nuclear design parameters of a large fast ceramic reactor were evaluated. Nuclear calculations were performed on a specified set of fast reactor cores and the results were submitted to ANL for comparison with similar results calculated by other fast reactor design groups. Results in both cases were presented at the International Conference on Safety, Fuels, and Core Design in Large, Fast Power Reactors at Argonne National Laboratory. Several structural modifications in type 316 stainless steel of interest to the radiation damage program were evaluated and the most promising modifications were selected. (W.L.G.)

29619 (NAA-SR–11813) ZONE MELTING OF URANIUM MONOCARBIDE. Ervin, G. Jr.; Smalley, A. K. (Atomics International, Canoga Park, Calif.). May 25, 1966. Contract AT(11-1)-Gen-8. 26p. Dep. mn. CFSTI $2.00 cy, $0.50 mn.

Two furnaces for float-zone melting are described briefly, and data on zone melting of UC are presented. Induction zone melting of UC in a He atmosphere does not cause much loss of U by preferential vaporization, and it was therefore possible to make use of the compositional changes along the length of the zone-melted rod to calculate distribution coefficients for excess U and C in UC. These distribution coefficients indicate the shape of the U–C phase diagram in the neighborhood of the melting point of UC. Electron beam zone melting in vacuum produced single crystals of UC, normally containing UC_2 as a second phase; but, at fast transverse rate, the evaporation of U was minimized and single-phase singly crystals of UC were produced. (auth)

29620 (NP–16046) SUMMARY OF LITERATURE AND BIBLIOGRAPHY ON THE RELATION BETWEEN WETTING AND BOILING MERCURY HEAT TRANSFER. SNAP-8 Technical Memorandum. Clark, L. T.; Parkman, M. F. (Aerojet-General Nucleonics, San Ramon, Calif.). Aug. 25, 1964. 46p.

A survey was made on basic phenomena that might affect the boiling of mercury. Studies are divided into three general areas of boiling, wetting, and surface tension. Interfacial phenomena are discussed as they are applicable to wetting by mercury. It was concluded that wetting is required for high heat fluxes in boiling, since non-wetting results in premature transition to film boiling. Wetting may be induced by proper surface preparation, extended boiling, and use of certain additives, such as alkali and alkaline earth metals. It was also concluded that the

microscopic aspects of wetting are important as well as the macroscopic. (67 references). (auth)

29621 (NUMEC-3524-17) DEVELOPMENT AND TESTING OF PuO_2–UO_2 FAST REACTOR FUELS. Progress Report, January 1–March 31, 1966. (Nuclear Materials and Equipment Corp., Apollo, Pa.). May 20, 1966. Contract AT(30-1)-3524. 25p. Dep. mn. CFSTI $1.00 cy, $0.50 mn.

The production of pellets for the EBR-II irradiation rods is continuing. The greater proportion of the coprecipitated and master blended fuel pellets have been produced. The production of the mechanically mixed fuel is underway and the necessary sintering trials continue. The apparent lack of correlation in sintering results between trial batches and production lots is most likely due to the difference in mixing techniques. Control of density is a persistent problem at the levels and limits considered necessary at this stage. Yields and materials losses encountered to date are tabulated. The metallography of UO_2-clad powder specimens heated to 1250°C for 24 hours indicates no reaction zone. The difference in PuO_2-UO_2 melting points under argon and N_2-6 vol % H_2 appears to be quite significant and details are presented. (W.L.G.)

29622 (TID-22970) RESEARCH IN MATERIALS SCIENCE AND ENGINEERING. Annual Report, 1965–66. (Massachusetts Inst. of Tech., Cambridge). Apr. 1966. Contract AT(30-1)-905. 440p. Dep. mn. CFSTI $7.40 cy, $2.00 mn.

Research and development are summarized in ten sections. Separate abstracts were prepared for six sections. Sections for which no abstracts were prepared are concerned with advanced electronics and laboratory central facilities listings. Information is also included concerning staff and academic personnel. (J.R.D.)

For abstracts of individual sections see: 29366, 29623, 29624, 29709, 30734, and 30735.

29623 (TID-22970, pp 121-256) METALLURGY AND MATERIALS SCIENCE. (Massachusetts Inst. of Tech., Cambridge).

Results of research on the physics of solids are presented. Information is also presented from research on physical metallurgy, x-ray and electron optics, high-temperature metallurgy, ceramics, minerals, surface chemistry, corrosion, electronic materials, and superconductors. (J.R.D.)

29624 (TID-22970, pp 257-329) MATERIALS ENGINEERING. (Massachusetts Inst. of Tech., Cambridge).

Research is reported on deformation, fracture, and mechanical properties of materials. Summaries of research are included on mechanical behavior of structural materials, surface properties and behavior of materials, cryogenics, materials chemical engineering, and radiation effects on materials. (J.R.D.)

29625 ANNEALING STUDIES OF BORON-DOPED GRAPHITE BY ELECTRON MICROSCOPY AND X-RAY DIFFRACTION. **Turnbull, J. A.; Stagg, M. S.; Eeles, W. T. (Berkeley Nuclear Labs., Eng.).** Carbon, 3: 387-92(Feb. 1966).

By heating amorphous boron near its melting point in a reactor grade graphite crucible it was possible to produce single crystals of graphite containing up to 4% boron. These crystals were studied before and after heat treatments by electron microscopy, x-ray diffraction and mass spectra. A model is proposed to explain the results which necessitates the boron occupying both interstitial and substitutional sites. The former caused a c-axis lattice parameter expansion, the latter causing a c-axis contraction and a-axis expansion. The interstitial population diffused after low temperature anneals of 1200°–1400°C while the substitutional boron 2% remained stable until 2000°C, when it diffused leaving behind a supersaturation of vacancies which precipitate as loops. Differences between vacancy loop distributions in specimens annealed before cleavage into thin foils and specimens cleaved after annealing lead to the conclusion that substitutional boron can diffuse along the c-axis in graphite. (auth)

29626 REACTION OF NUCLEAR GRAPHITE WITH WATER VAPOR. PART I. EFFECT OF HYDROGEN AND WATER VAPOR PARTIAL PRESSURES. Giberson, R. C.; Walker, J. P. (Battelle-Northwest, Richland, Wash.). Carbon, 3: 521-5(Feb. 1966).

The rate of oxidation of graphite by water vapor in the presence of hydrogen is given by: $R = (k_1 P_{H_2O})/(1 + k_2 P_{H_2}^{\frac{1}{2}} + k_3 P_{H_2O})$ which is different from that given previously by others. A mechanism, which yields this expression is proposed. It involves the dissociative adsorption of hydrogen on graphite and accounts for the experimental results. The mechanism is compatible with results of others and also for conditions where hydrogen is not deliberately added to the gas stream. (auth)

29627 NEUTRON RADIOGRAPHY. Bukarev, V. A.; Shtan, A. S. Defektoskopiya, No. 2, 65-72(1966). (In Russian).

A brief review is given on neutron radiography considering the most efficient operation of portable neutron generations. (tr-auth)

29628 AMPLIFICATION FACTOR OF LEAD SCREENS FOR ELECTRORADIOGRAPHY. Rakauskas, Yu. K. (Scientific-Research Inst. of Electrography, Vilnius, USSR). Defektoskopiya, No. 2, 72-8(1966). (In Russian).

The amplification factor of lead screens was measured, using Se photographic plates, as a function of the thickness, hardness, and x-ray emission of the lead screens and as a function of the translucence of an Al alloy on the Se plates. The amplification factor of the front and back lead screens increased proportionately with the emitted x-ray energy up to 200 Kv. (G.O.Y.)

29629 THERMAL TREATMENT OF URANIUM AND URANIUM–THORIUM OXIDES OBTAINED BY SOL-GEL PROCESS. Cogliati, G. (CNEN, Rome). Energ. Nucl. (Milan), 13: 243-50(May 1966). (In Italian).

The results of preliminary studies on the heat treatment of uranium dioxides and thorium-uranium oxides obtained by the sol-gel method are reported. These oxides show a microcrystalline structure and high densities with firing temperatures much lower than those generally required for sintering agglomerates of the correspondent crystalline powders. (auth)

29630 FLUIDIZED-BED DEPOSITION OF PROTECTIVE COATINGS ON REFRACTORY METALS. Chao, P. J. pp 301-15 of Metals for the Space Age. Plansee Proceedings, 1964. Benesovsky, F. (ed.). Reutte/Tyrol, Metallwerk Plansee AG. 1965.

The fluidized bed deposition of silicon onto refractory metals and their alloys to form oxidation-resistant silicide diffusion coatings was investigated and found to be both efficient and practical. Process parameters can be controlled to achieve specific results. Co-deposition of alloying elements with silicon was also found to be feasible. (P.C.H.)

29631 NONMETALLIC POWDERS COATED WITH TUNGSTEN AND MOLYBDENUM. Roberson, A. H.; Landsberg, A.; Block, F. E. pp 316-24 of Metals for the Space Age. Plansee Proceedings, 1964. Benesovsky, F. (ed.). Reutte/Tyrol, Metallwerk Plansee AG, 1965.

Methods used to coat MgO, Al_2O_3, ZrO_2, ZrC, and ZrB_2 particles with W and Mo are described, along with the compacts resulting from compacting and sintering the coated particles. The two methods include: hydrogen reduction of an oxide coating on a selected refractory powder; and concurrent reduction of W or Mo chloride by hydrogen and deposition of the metal on a fluidized bed of finely divided oxide powder. Although both methods produce a final product that may be pressed and sintered to produce dense, strong, compacts, the oxide process is favored. (P.C.H.)

29632 REACTIONS OF ZIRCONIUM–MOLYBDENUM ALLOYS WITH HYDROGEN AND WITH NITROGEN. Brauer, G.; Leibbrandt, F. (Univ., Freiburg, i. B.). pp 340-50 of Metals for the Space Age. Plansee Proceed-

ings, 1964. Benesovsky, F. (ed.). Reutte/Tyrol, Metallwerk Plansee AG, 1965. (In German).

Molybdenum alloys with 10, 30, 50, 70, and 90 at. % zirconium react with highly purified hydrogen by forming hydrides. In some of these alloys the hydrogenation which is strongly exothermic, already begins at ambient temperature. According to the composition of the Zr–Mo alloy, different hydride phases occur whose structure is currently being investigated. At 750°C, the alloys react with ammonia with formation of mixed zirconium–molybdenum nitrides. The constitution of these nitrides is also being investigated. A phase (Zr, Mo)N with sodium chloride-type lattice occurs preferentially. (auth)

29633 PROCESSES FOR THE DEGASSING OF NIOBIUM AND TANTALUM. Gebhardt, E.; Fromm, E.; Jakob, D. (Max-Planck-Institut fuer Metallforschung, Stuttgart). pp 421-37 of Metals for the Space Age. Plansee Proceedings, 1964. Benesovsky, F. (ed.). Reutte/Tyrol, Metallwerk Plansee AG, 1965. (In German).

The reactions responsible for the removal of nitrogen and oxygen during high-temperature vacuum degassing of solid niobium and tantalum are described. During the degassing of nitrogen-containing specimens, a decomposition of the mixed crystal phase and of any nitrides that are present takes place. Molecular nitrogen is liberated and removed by the vacuum system. Quantitative investigations of the equilibrium conditions, taking into account the equilibrium pressures, led to the establishment of the PVT diagrams of the systems Nb–N and Ta–N on the metal-rich side up to concentrations of approximately 30 at. % N. In addition to some thermodynamic data that were obtained in these investigations, relationships could be established for these systems that permit an estimation of the attainable residual nitrogen content if the sample temperature and the partial pressure of the recipient are known. The elimination of oxygen from niobium and tantalum is due to the evaporation of volatile oxides that are evidently formed during the separation process and which are condensed immediately on the cooled walls of the recipient. For the purpose of quantitative description of these degasification processes, a specific degasification half-period is given for the systems Nb–O and Ta–O. By means of these, it is possible to estimate the time after which the concentration of oxygen in a specimen of any shape has decreased to half the initial value if the temperature of the specimen is known. The activation energy of the degasification process could be determined for both systems. It is 130 and 132 kcal/mole, respectively, which is considerably higher than the magnitude of the activation energy of the diffusion process. Thus, it may be assumed that the process of separation of the volatile oxides from the specimen surface proceeds considerably more slowly than the diffusion of the oxygen atoms towards the specimen surface. (auth)

29634 ELECTRON-BEAM REFINING OF NIOBIUM. Kimura, Hirozo; Sasaki, Yasuo; Uehara, Sigeaki (National Research Inst. for Metals, Tokyo). Nippon Kinzoku Gakkaishi, 29: 924-30(1965). (In Japanese).

The removal process of oxygen, carbon, and nitrogen from niobium metal is studied quantitatively using a laboratory-scale electron beam melting furnace. Optical microscopic observation and hardness measurement of the ingots are carried out. The removal of carbon as CO is possible in the case of crude metal containing oxygen, according to the following reaction: Nb(O) + Nb(C) → Nb + CO, and the excess oxygen is removed as NbO. The removal of oxygen as NbO proceeds at a rate about four times faster than the loss of oxygen as CO. The addition of oxygen to crude metal is necessary to remove the excess carbon in niobium. The excess carbon is removed when oxygen is added to crude metal by oxidation. However, the addition of oxygen as niobium pentoxide to crude metal is not effective, since the oxide volatilizes abruptly in the melting process and does not cause decarburization. To obtain a high purity niobium, it is necessary to adjust the composition; the oxygen/carbon weight ratio in crude metal is desirable to be 4 ~ 5. Nitrogen is degassed gradually during the melting process. Gross pores are observed at the interface part between melted and sintered zones in the ingot. In an optimum condition, it is possible to obtain a high-purity niobium with gas impurities of less than 200 ppM and the hardness of 50 VHN. (auth)

29635 REDKOZETNI ELEMENTI. (Rare Earth Elements). Aleksiev, E. L. Sofia, Nauka Izkustvo, 1965. 154p.

The atomic structure, chemical, physical, and nuclear properties, and analytical determination of rare earth elements are surveyed. The geochemistry of rare earths is discussed, including their distribution in the earth's crust and the cosmos, their role in geochemical processes, and their incidence in certain geological formations, and the industry of prospecting for rare earths. Methods of obtaining rare earths, including enrichment, extraction, and separation processes, are described. The use of rare earth elements in metallurgy, nuclear technology, and the silicate industry is considered. (M.J.T.)

29636 INSULATING COATING FOR ELECTRICAL CONDUCTORS. Earl, John Alfred (to Physical Sciences Corp.). British Patent 1,023,325. Mar. 23, 1966. Filed Apr. 24, 1964.

An insulating vitreous coating and a method for its application to electrical conductors, particularly wires, that are exposed to particle bombardment in the field of a reactor without excessive deterioration of mechanical and electrical properties are described. The coating is comprised of 70 to 82 wt % PbO; 10 to 14 wt % SiO_2; 6 to 14 wt % Bi_2O_3; up to 2 wt % Al_2O_3; up to 2 wt % total of any of the oxides of Ce, Zr, Ti, and Mo; up to 6 wt % total of any of the oxides of Ba, La, Mg, Ca, Zn, Sr, and Be; and the balance, if any, consisting of any compatible components other than B_2O_3. (B.L.M.)

29637 PRODUCTION OF CURED RESIN BODIES BY RADIATION PRE-GELLING AND HOT CURING. Guenther, John Richard; Mesrobian, Robert B. (to Continental Can Co.). U. S. Patent 3,246,054. Apr. 12, 1966. Filed Apr. 6, 1962.

A method of preparing a shaped article includes impregnating a porous substrate selected from the group consisting of paper, glass, asbestos, felt, cotton, linen, and rayon cloths with a liquid consisting of a mixture of unsaturated polyester resin, styrene, and an effective amount of an organic-peroxide curing catalyst and exposing the impregnated substrate to about 1 megarad of beta radiation while moving the impregnated substrate past the source of radiation at the rate of about 30 ft/min to obtain a partially gelled product having a Barcol hardness of about 10. The irradiated substrate is then shaped mechanically and heated at a temperature ranging from 250 to 300°F for a period of 1 to 3 min to obtain a shaped article with the impregnant having a Barcol hardness of at least 40. The preferred resin is that obtained by the reaction of ethylene glycol and maleic anhydride. The curing catalyst is either benzoyl peroxide or tert-butyl perbenzoate. (B.L.M.)

29638 PROCESS FOR COATING RADIOACTIVE SPHEROIDS WITH PYROLYTIC GRAPHITE. Finicle, Robert L. (to Union Carbide Corp.). U. S. Patent 3,247,008. Apr. 19, 1966. Filed Dec. 18, 1962.

A process is described for coating radioactive spheroids with pyrolytic graphite at temperatures above the surface sintering temperature of the particles. The particles are heated to a temperature slightly below the surface sintering temperature in a suitable container and in an atmosphere composed of an inert gas and a gaseous hydrocarbon until the hydrocarbon cracks or pyrolyzes to deposit free carbon atoms on the surface of the radioactive particles. Once the initial layer of pyrolytic graphite has been deposited, the temperature is raised above the surface sintering temperature of the particles and the deposition is continued until the coating of the desired thickness is achieved. During both stages of the heating operation and during the cooling period, the particles are kept in motion by some

suitable means, such as a rotating capsule, fluidized bed, or vibrating surface. The process is applicable to the coating of radioactive materials for use as reactor fuels. (B.L.M.)

Corrosion

Refer also to abstracts 30794 and 30902.

29639 (EURAEC-1578) [MECHANICAL PROPERTIES OF STEELS]. Quarterly Report No. 5, October-December 1965. (Compagnie des Ateliers et Forges de la Loire, Paris (France). Departement des Recherches). Contract 033-64-9TEE-F(RD). 64p. (EUR-2807). Dep. mn. CFSTI $3.00 cy, $0.75 mn.

Work Performed under United States-Euratom Joint Research and Development Program.

Results of the continued stress corrosion testing of austenitic and austeno-ferritic stainless steels in various chloride solutions are reported. Observations made to date on the effects of the pH of the solution, silicon and molybdenum content of the steels, and the austeno-ferritic structure on the stress corrosion of steels are summarized. (W.L.G.)

29640 (NP-16048) COMPREHENSIVE CAVITATION DAMAGE DATA FOR WATER, MERCURY, AND LEAD-BISMUTH ALLOY INCLUDING CORRELATIONS WITH MATERIAL AND FLUID PROPERTIES. Technical Report No. 4. Garcia, R.; Hammitt, F. G.; Nystrom, R. E. (Michigan Univ., Ann Arbor. Lab. for Fluid Flow and Heat Transport Phenomena). May 1966. 83p.

Ultrasonic-induced cavitation studies were conducted in lead-bismuth alloy at 500 and 1500°F, in mercury at 70 and 500°F, and in water at 70°F for a wide variety of materials, including refractory alloys, steels, brasses, copper, nickel, plastics, etc. Comprehensive computer correlations of the cavitation damage data with applicable mechanical and fluid properties were carried out. The major conclusions of the study are: The tantalum-base alloys were the most cavitation resistant in all the tests except in mercury at 70°F, where the stainless steels were the most resistant. All materials tested in lead-bismuth at 500 and 1500°F, and all materials tested in mercury at 70 and 500°F sustained greater damage at the higher temperature with the exception of carbon steel. Corrosion effects in those regions where cavitation was absent were negligible in this investigation. Damage rates in mercury were 3 to 20 times greater than in water, depending upon the material. Hence, clearly no correlating equation which considers only the mechanical properties of the material can apply for both fluids. There is no single material mechanical property which can be used to correlate the damage, even if coupling parameters to account for fluid property changes are included in the correlation. In general, the best correlations include energy-type mechanical properties, strength-type properties, and fluid coupling parameters. No relatively simple single correlating equation applies well to all the data. This may indicate the insufficiency of the statically-determined mechanical and fluid properties for the correlation of cavitation damage which is known to be a highly transient process. (auth)

29641 (SC-DC-65-1691) FIRST ANNUAL PROGRESS REPORT ON THE COMBUSTION OF METALS, JULY 1, 1964-JUNE 30, 1965. Hansel, J. G.; Zwillenberg, M.; Mellor, A. M.; Sullivan, H. F.; Glassman, I. (Princeton Univ., N. J. Guggenheim Labs. for the Aerospace Propulsion Sciences). Aug. 1965. Contracts AT(30-1)-3451; 74-0336. 38p. Dep. mn. CFSTI $2.00 cy, $0.50 mn.

For Sandia Corp., Albuquerque, N. Mex.

The combustion of resistively heated metal wires or strips was examined in a controlled atmosphere chamber capable of operating at elevated or reduced pressures. Metals which burn primarily at the surface, such as tantalum, molybdenum, and zirconium, and metals which burn primarily in the vapor phase, such as calcium and magnesium, were studied. Various gaseous atmospheres were used, the components of which were oxygen, nitrogen, carbon dioxide, water vapor, and argon. Results are interpreted in terms of Glassman's hypotheses of metal burning. Preliminary experimentation on the determination of metal flame temperatures and of ignition processes on a flat flame burner is discussed. (auth)

29642 PHOSPHIDATION OF COMPACT ZIRCONIUM METAL. Freund, F. (Univ., Goettingen, Ger.); Gingerich, K. A. Ber. Deut. Keram. Ges., 43: 132-5(Feb. 1966). (In German).

Phosphidation of compact zirconium metal by phosphorus vapor at approximately 1 atm between 500 to 1000°C leads to the formation of hexagonal zirconium monophosphide layers. The outer more porous part is composed of randomly oriented crystals, while in the inner part the monophosphide crystals grow with their c-axis normal to the reaction interface. In the very beginning of the reaction and at the reaction interface phosphide/metal, a 2 to 3 microns thick subphosphide layer is formed, probably Zr_5P_3. (auth)

29643 THE EFFECT OF INCREASED NICKEL CONTENT ON THE INTERGRANULAR CORROSION OF ALLOY 20 Cb. Scharfstein, L. R.; Maniar, G. N. (Carpenter Steel Co., Reading, Pa.). Brit. Corros. J., 1: 36-41(July 1965).

It was found from previous work that increasing the nickel content from 28 to 33% eliminated stress corrosion cracking in sulfuric acid of a commercial niobium-stabilized Cr-Ni-Mo-Cu austenitic steel. This relatively small increase in nickel content, however, made the alloy more susceptible to intergranular corrosion. On the bases of x-ray and electron diffraction, electron microscopy, and corrosion tests, it was concluded that raising the nickel content increased the solubility of Nb(C,N) at 1065°C and also promoted the formation of deleterious carbides at lower temperatures. From this study an optimum annealing temperature of 980 to 1010°C for the alloy (Carpenter 20 Cb-3) was determined. (auth)

29644 STUDY OF THE ACTION OF OXYGEN ON TITANIUM, ZIRCONIUM, HAFNIUM, VANADIUM, NIOBIUM, AND TANTALUM IN POWDERED FORM. Davignon, Leon (Faculte des Sciences, Paris). Compt. Rend., Ser. C, 262: 1321-4(Apr. 25, 1966). (In French).

The action of oxygen, studied under identical conditions, made it possible to compare the reactivities of titanium, zirconium, hafnium, vanadium, niobium, and tantalum. The kinetics of the oxidation of niobium and of tantalum depended on an interphase process but for titanium it was controlled by a diffusion process. (tr-auth)

29645 KINETICS OF THE OXIDATION OF UN AND U(CO) IN CARBON DIOXIDE, STEAM, AND WATER AT ELEVATED TEMPERATURES. Antill, J. E.; Myatt, B. L. (Atomic Energy Research Establishment, Berks, Eng.). Corros. Sci., 6: 17-23(Jan. 1966).

The oxidation of dense compacts of UN and three uranium oxycarbides, $UC_{0.9}O_{0.1}$, $UC_{0.8}O_{0.2}$ and $UC_{0.7}O_{0.3}$, by carbon dioxide, steam, and water was studied over the temperature ranges 500-1000°C, 200-1000°C, and 80-300°C, respectively. Most of the reactions were identified, and the kinetics determined and compared with those for compacts of UC. The materials showed considerable resistance to steam at low temperatures (i.e., ≤350°C) and to water. Under other conditions the rates of oxidation were similar to those for UC. (auth)

29646 BOILING MERCURY CORROSION OF CERTAIN REFRACTORY METALS AND STAINLESS STEELS FROM 593 TO 703 DEG C. Fleitman, A. H.; Romano, A. J.; Klamut, C. J. (Brookhaven National Lab., Upton, N. Y.). Corrosion, 22: 137-42(May 1966).

Mercury corrosion of the refractory metals W, Mo, Ta, and Nb-1Zr was studied in natural circulation quartz loops with two-phase mercury at temperatures from 593 to 703°C. Three thousand hour tests on these materials indicate that Ta and W showed no attack or weight loss and could not be detected in the mercury. Mo and Nb-1Zr alloy were detected in trace amounts in the mercury. Similar tests in

quartz loops on types 304 and 410 stainless steel also were completed. Effectiveness of small additions of Ti to the mercury in preventing corrosion was evaluated. Results indicate that Ti when added to mercury is effective in reducing mass transfer of type 410 stainless steel but appears to increase both the depth of corrosion and weight loss of type 304. (auth)

29647 STUDIES ON THE OXYGEN GRADIENTS IN OXIDIZING METALS. IV. KINETICS OF THE OXIDATION OF HAFNIUM AT HIGH TEMPERATURES. Pemsler, J. P. (Kennecott Copper Corp., Lexington, Mass.). J. Electrochem. Soc., 113: 619-21(June 1966).

An attempt is being made to separate quantitatively the film growth and oxygen dissolution processes in hafnium oxidation and to gain insight into the film growth mechanism. Data for the total weight gain between 850 and 1400°C are given in the form of a logarithmic plot. Examination of cross sections of the oxidized spheres indicated that at all times and temperatures there is a high degree of irregularity of the film thickness. During film formation grain growth occurred in the metal and became pronounced at high temperatures and long times. (M.C.G.)

29648 OXIDATION OF OXYGEN-DEFICIENT ZIRCONIA AND ITS RELATIONSHIP TO THE OXIDATION OF ZIRCONIUM. Douglass, D. L. (General Electric Co., Pleasanton, Calif.); Wagner, Carl. Contract AT(04-3)-189. J. Electrochem. Soc., 113: 671-6(July 1966).

Upon heating black oxygen-deficient zirconia in oxygen of atmospheric pressure to 450 to 900°C, oxygen is taken up. The increase in the thickness $\Delta\xi_w$ of a white layer of virtually ideal composition with time t follows a parabolic rate law, $\Delta\xi_w^2/2t = k_p$. The rate constant k_p is about two orders of magnitude higher than Tammann's rate constant $k_T = (\Delta\xi_{oxide})^2/2t$ for the increase in thickness $\Delta\xi_{oxide}$ of a ZrO_2 layer during the oxidation of zirconium metal. Equations for the concentrations of ionic and electronic defects in zirconia as functions of the oxygen partial pressure are presented in order to derive theoretical equations for the rates of oxidation of oxygen-deficient zirconia and of zirconium metal. (auth)

29649 INVESTIGATIONS ON THE CORROSION OF ZIRCONIUM IN ELECTROLYTIC SOLUTIONS BY THE USE OF RADIONUCLIDES. Wertenbach, H.; Lieser, K. H. (Technische Hochschule, Darmstadt, Ger.). Kerntechnik, 8: 224-9(May 1966). (In German).

The corrosion of reactor grade zirconium in HCl, NH_4F–HCl, $FeCl_3$–HCl, and $CuCl_2$–HCl solutions was investigated at 20 and 97°C. ^{95}Zr, and in some cases, ^{59}Fe and ^{45}Ca, were added as tracers. In HCl solutions at 20°C no zirconium was carried from the solution to the surface of the zirconium plates. At 97°C an early stage of pitting was observed by autoradiography. In presence of NH_4F, $FeCl_3$, or $CuCl_2$ the zirconium was heavily attacked. While in NH_4F–HCl solutions no ^{95}Zr was carried to the surface of the zirconium plates, it could be domonstrated by following the deposition of ^{95}Zr that pitting occurs in presence of $FeCl_3$ or $CuCl_2$. (auth)

29650 PROTECTIVE LAYER PROBLEMS WITH HIGH-TEMPERATURE MATERIALS. Bueckle, H. (O.N.E.R.A., Paris). pp 31-60 of Metals for the Space Age. Plansee Proceedings, 1964. Benesovsky, F. (ed.). Reutte/Tyrol, Metallwerk Plansee AG, 1965. (In German).

The protective layer problems with high-temperature materials are illustrated in a review of the development of molybdenum protective layers. The operational conditions under which the protective layers would be used, the property of the molybdenum alloys and/or compounds, and the production methods are considered. (J.S.R.)

29651 PROTECTIVE COATINGS FOR NIOBIUM AND ITS ALLOYS. Hubbard, R. T. J.; Minton, C. D. T. (Imperial Metal Industries Ltd., Birmingham, Eng.). pp 444-59 of Metals for the Space Age. Plansee Proceedings, 1964. Benesovsky, F. (ed.). Reutte/Tyrol, Metallwerk Plansee AG, 1965.

The results of comparative evaluation of several different types of protective coating systems for niobium and niobium alloys are presented. Coating performance as determined by static oxidation tests is related to temperature and to the oxidation rate/temperature behavior of uncoated niobium alloys and niobium compounds. The effects of prolonged heating in air, vacuum, and other atmospheres upon subsequent oxidation performance of the coating are discussed. (auth)

29652 HIGH-TEMPERATURE OXIDATION MECHANISM ON 2.5 TIN–ZIRCONIUM ALLOY. Maekawa, Tatsuo; Ishii, Bunpei. (Mitsubishi Atomic Power Industries Inc., Omiya, Japan). Nippon Kinzoku Gakkaishi, 30: 270-4 (1966). (In Japanese).

The breakaway oxidation, mainly at 850°C, of Zr–2.5% Sn alloy in oxygen was investigated by thermogravimetric measurements, electron microscopic observations, electron-probe microanalysis and x-ray diffraction studies. On the post-breakaway stage, the oxidation kinetics was largely dependent on the pressure of oxygen. and the significant cracking of the oxide film was observed. The electron-probe microanalysis and x-ray diffraction studies indicated that the tin in the alloy was precipitated as the intermetallic compound of ZrSn at the oxide/metal interface, and suggested that the oxide film has a multilayer structure consisting of ZrO_2 and $(ZrSn)O_2$ layers. The mechanism of the heavy breakaway phenomena of the alloy at high temperature was discussed on the basis of the behavior of tin in the alloy, and it was concluded that stress between the layers of ZrO_2 and $(ZrSn)O_2$ induced the cracks of the oxide film and permitted the increased oxidation. (auth)

29653 THE EFFECT OF MOLYBDENUM ON THE OXIDATION OF TiC–Ni–Mo ALLOYS. Hachisuka, Takeji; Nishimura, Tomio; Kondo, Masao (Fujikoshi Ltd., Japan). Nippon Kinzoku Gakkaishi, 30: 296-301(1966). (In Japanese).

To investigate the oxidation behavior of TiC-base-alloys containing Mo, TiC–10 Ni and TiC–10 Ni–(2.5 to 18.57) Mo alloys were prepared by sintering. These alloys were exposed in still air at 600 to 1300°C. The oxidation process and the effect of Mo on oxidation were studied by weight gain, surface recession, x-ray diffraction, and microstructure observation of scales. The following results were obtained. Addition of Mo to TiC–10 Ni alloy increased the weight gain due to oxidation below 1100°C, which was most effective at 700 to 800°C. This effect was, however, decreased at higher temperatures and at 1300°C Mo increased in oxidation resistance reversely. From the results by x-ray diffraction, it appeared that at higher temperatures oxidation of Mo was suppressed to cause the appearance of metallic Mo in the scales and $NiO \cdot TiO_2$ was also increased, while at lower temperatures NiO was combined preferentially with $NiO \cdot MoO_3$ and decreased $NiO \cdot TiO_2$ content in the surface layer of scales. From measurements of the surface recession, it was found that the progress of oxidation of all alloys at 1000°C was parabolic and the parabolic rate constant increased in proportion with the Mo content. But at 1300°C, the surface layer of scales became porous and no parabolic relation was found in all the alloys. (auth)

29654 PERFORMANCE OF MILD STEEL IN D_2O MODERATOR-COOLANT IN THE HWCTR. McKibben, J. Malvyn (E. I. du Pont de Nemours and Co., Aiken, S. C.). Nucl. Appl., 2: 21-6(Feb. 1966).

The performance of mild steel was excellent during the three-year operation of the Heavy Water Components Test Reactor (HWCTR). Surfaces were covered uniformly with an adherent film of black oxide, and no significant pitting occurred. The total corrosion of mild steel test specimens was 3.1 mg/cm² after 6 months, and 5.5 mg/cm² after 33 months. The rate of iron release to the D_2O moderator-coolant was 0.16 mg/cm² per month during the first 6 months and approximately 0.04 mg/cm² per month, thereafter. No problems occurred because of particulate matter in the D_2O. The concentration of particulates in D_2O was approximately 80 parts per billion (ppb) during the

first two years of operation and was approximately 6 ppb during the last year. The purification system operated satisfactorily without a prefilter. The radiation intensity from typical primary circuit piping was approximately 30 mR/hr at 3 in. when reactor operation was terminated. (auth)

29655 THE PREPARATION OF TRICHLOROETHYLENE LABELED WITH ^{36}Cl AND ITS APPLICATION TO THE STUDY OF CORROSION. Silkos, O.; Wiesner, L.; Wagner, E. (Technische Hochschule, Hanover). pp 273-9 of Atomstrahlung in Medizin und Technik. Munich, Verlag Karl Thiemig KG, 1964. (In German).

In order to clean the surfaces of workpieces, Cl-containing solvents such as carbon tetrachloride or trichloroethylene are used in many cases. Extremely small residues of these substances may initiate metal corrosion, especially after the workpieces are heated. The detection and action of these residues were investigated by using chlorinated solvents labeled with ^{36}Cl. To determine quantitatively the corrosive effects of chlorinated solvents, various workpieces (ferritic steel with Cr, austenitic steel with Cr and Ni, and Ni–Cr and Ni–Cr–Ti–Al alloys) were immersed from 1 to 900 min in a solution of trichloroethylene containing 1 μC of ^{36}Cl and dried at 120°C to evaporate the solvent completely. The residual Cl was highest in ferritic, not as high in austenitic steel, and lowest in the alloys. In every material examined the chlorine content was proportional to the logarithm of the immersion time. One-half of the Cl could be removed by treatment with petroleum ether, and 80% could be removed by thorough scrubbing with water or acetone. (OID)

29656 KINETICS OF HIGH TEMPERATURE (> 2000°K) OXIDATION OF REFRACTORY MATERIALS: SUBSONIC STAGNATION-FLOW REACTOR STUDIES. Walsh, P. N. (Union Carbide Research Inst., Tarrytown, N. Y.); Quets, J. M.; Ladd, I. R.; Graff, R. A. New York American Inst. of Chemical Engineers, 1966, Preprint 1D, 27p. $0.50. (CONF-660506–4). ORAU.

From American Inst. of Chemical Engineers, Nuclear Engineering Div. Symposium, Columbus, Ohio.

The concept of utilizing a high-velocity gas stream impinging normally on a solid sample to enhance gas-solid mass transfer and thus substantially reduce diffusional inhibition of heterogeneous reactions rates is discussed. Two reactors based on this concept are described. Experimental data for the $W-CO_2$, $W-O_2$, and graphite-CO_2 reactions are used to illustrate the usefulness of these reactors in generating high-temperature kinetic data. In the stagnation-flow reactor a jet of reactive gas mixture impinges normally on a flat sample surface and the extent of surface reaction is determined by measuring the recession at the stagnation point. The surface temperature can be measured directly by an optical pyrometer sighted through a window at the upstream end of the nozzle. (M.C.G.)

29657 DEVELOPMENT OF ThO_2 PELLET FABRICATION. Beltram, C.; Forscher, F.; Vondra, B. L. (Nuclear Materials and Equipment Corp., Apollo, Pa.). 21p. (CONF-651101–75). ORAU. Gmelin, AED-CONF-65-332-40.

From 13th Conference on Remote Systems Technology, Washington, D. C.

A pellet fabrication process was developed for the production of more than 13,000 kgs of dense (95 ± 2% of theoretical) thoria pellets on a production basis. The thoria powder was produced from thorium nitrate tetrahydrate by the oxalate precipitation route. It was capable of being sintered to the required density after pressing to 6.1 ± 0.1 gm/cc and firing 4 to 8 hours at 1650 to 1750°C in a wet hydrogen atmosphere. (auth)

Fabrication

Refer also to abstracts 29727 and 30816.

29658 (ANL–6283) FABRICATION OF SPIKED-CORE FUEL ELEMENTS FOR THE EXPERIMENTAL BOILING WATER REACTOR. Final Report. Kramer, W. C.; McCuaig, F. D.; Beatty, R. A.; Bean, C. H.; Noland, R. A. (Argonne National Lab., Ill.). Nov. 1965. Contract W-31-109-eng-38. 63p. Dep. mn. CFSTI $3.00 cy, $0.50 mn.

In the modification of the Experimental Boiling Water Reactor to allow for a heat-dissipation capacity of 100 Mw(t), 28 of the original, slightly enriched, metal-fuel elements were replaced with elements containing highly enriched ceramic fuel. Of 35 fuel elements fabricated for this purpose, 32 contained a solid-solution ceramic fuel composed of 9.01 wt % UO_2 (93% ^{235}U), 9.07 wt % CaO, and 81.92 wt % ZrO_2 in the form of cylindrical pellets nominally 0.82 cm dia × 1.3 cm long. The three remaining elements contained a cermet fuel composed of a dispersion of 11.83 wt % U_3O_8 (with the uranium being 93% ^{235}U) in an 88.17 wt % matrix of X-8001 aluminum. The cermet fuel was nominally 0.82 cm dia × 122 cm long. All the fuel was jacketed in Zircaloy-2 tubing, except the rods comprising one cermet fuel element that had A-288 aluminum jackets. Commercial procurement and/or ANL fabrication of Zircaloy-2, type 304 stainless steel, and aluminum hardware for fuel-element components are discussed. Methods are reviewed covering fuel-rod fabrication, fuel-element assembly, and evaluation procedures. (auth)

29659 (COO–1518-3) FABRICATION OF TUNGSTEN ALLOY TUBING. Progress Report, February 2, 1966–May 1, 1966. Sowman, H. G.; Milner, A.; Rowenhorst, D. D. (Minnesota Mining and Mfg. Co., St. Paul). May 10, 1965. Contract AT(11-1)-1518. 15p. Dep. mn. CFSTI $1.00 cy, $0.50 mn.

W–26% Re tubing up to 11 in. long was fabricated. The feasibility of using prealloyed powders in the tube extrusion process was shown. Structures similar to those obtained from elemental powders were obtained. Tensile data obtained on W–26% Re alloys from sintered elemental powders gave ultimate tensile strength values of 175,000 psi and 9% elongation at room temperature. (auth)

29660 (GEAP–4960) SPECIFIC ZIRCONIUM ALLOY DESIGN PROGRAM. Quarterly Progress Report No. 10, Klepfer, H. H.; Jaech, J. L.; Blood, R. E. (General Electric Co., San Jose, Calif. Atomic Power Equipment Dept.), Oct. 1965. Contract AT(04-3)-189. 48p. (EURAEC–1538). Dep. mn. CFSTI $2.00 cy, $0.50 mn.

Work Performed under United States–Euratom Joint Research and Development Program.

Nonuniform distribution of coarse intermetallic compounds is detrimental to corrosion performance. Segregation and thus nonuniform intermetallic distribution result from processing in the two-phase alpha-plus-beta temperature region; this region was determined to be 800 to 900°C for the Zr–2 at. % Cr–0.16 at. % Fe alloy. Beta solution treatments of 6 hours at 1000°C or $\frac{1}{2}$ to $1\frac{1}{4}$ hours at 1050°C were found to be required to take large, 4μ, precipitates into solution. Precipitate coarsening during alpha annealing at temperatures of 760°C and below was found to be very slow. These results and corrosion test results on the alloy fabricated in twenty-six different ways were employed in specifying a tentative fabrication schedule for a second batch of fuel cladding. Tests in progress in high-pressure, refreshed steam (25 ppM O_2 + 3 ppM H_2) at 300, 400, and 500°C appear to show that up to 100 ppM, the nitrogen content of the alloy has no significant effect on corrosion. (auth)

29661 (HWS–8241(Rev.4)) WELDING OF STAINLESS STEEL FOR PROCESS QUALITY WELDS FOR MILDLY CORROSIVE RADIOACTIVE SERVICE. Kingsley, P. S. (General Electric Co., Richland, Wash. Hanford Atomic Products Operation). Apr. 10, 1963. Contract AT(45-1)-1350. 9p. Dep. mn. CFSTI $1.00 cy, $0.50 mn.

Specifications are given covering the requirements for fusion welding of process quality welds in stainless steel vessels, piping and piping systems, and other equipment for use in the chemical processing of highly radioactive, mildly corrosive materials. (W.L.G.)

29662 (HWS-8242(Rev.5)) WELDING OF STAINLESS STEEL FOR STRUCTURAL QUALITY WELDS FOR MILDLY CORROSIVE NON-RADIOACTIVE SERVICE. Kingsley, P. S. (General Electric Co., Richland, Wash. Hanford Atomic Products Operation). Apr. 5, 1963. Contract AT(45-1)-1350. 7p. Dep. mn. CFSTI $1.00 cy, $0.50 mn.

Specifications are given covering the requirements for fusion welding of structural quality welds in stainless steel vessels, piping and piping systems, and other equipment for use in the chemical processing of nonradioactive, mildly corrosive materials. (W.L.G.)

29663 (KAPL-M-6556) ASSESSMENT OF INHOMOGENEITY OF SOLID REACTOR FUELS BY FISSION-TRACK COUNTING. Covert, A. S.; Schultz, W. W. (Knolls Atomic Power Lab., Schenectady, N. Y.). Apr. 1966. Contract W-31-109-eng-52. 13p. Dep. mn. CFSTI $1.00 cy, $0.50 mn.

A new method for measuring homogeneity of U and/or Th in nuclear fuels was developed. The method was applied to mixed oxide fuels. Fission tracks in insulating materials are used as the basis for the measurement. Statistical methods of testing for randomness are suggested. (auth)

29664 (LA-DC-7745) FABRICATION AND PROPERTIES OF COPPER-BORON CARBIDE CONTROL MATERIAL FOR PHOEBUS II REACTOR. Sheinberg, H.; Keil, R. W. (Los Alamos Scientific Lab., Univ. of California, N. Mex.). [nd]. Contract W-7405-eng-36. 10p. Dep. mn. CFSTI $1.00 cy, $0.50 mn.

A feasibility study developed procedure for producing uniform, dense, stable sheet material of Cu-20, 40, and 50 vol % normal B_4C. The procedures were, with only slight modifications, translated to production operation to yield sheet from which Phoebus II control plates and end poison plates were made. (auth)

29665 (RSIC-482) MACHINING AND GRINDING OF NICKEL- AND COBALT-BASE ALLOYS. Olofson, C. T.; Gurklis, J. A.; Boulger, F. W. (Battelle Memorial Inst., Columbus, Ohio). Apr. 20, 1966. Contract DA-01-021-AMC-11651(Z). 144p. (NASA-TM-X-53446).

The state of the art of metal-removal operations for nickel- and cobalt-base alloys is reviewed. The methods currently employed for conventional machining, grinding, electrolytic, and chemical-machining processes are described. The precautions that should be taken to avoid troubles resulting from the characteristics typical of these alloys are pointed out. Nine machining, two grinding, two cutting, and two unconventional metal-removal operations are discussed separately. Other sections discuss the classification of these alloys and their general response to machining variables. (auth)

29666 (RSIC-484) JOINING OF NICKEL AND NICKEL-BASE ALLOYS. Vagi, J. J.; Monroe, R. E.; Evans, R. M.; Martin, D. C. (Battelle Memorial Inst., Columbus, Ohio). Apr. 20, 1966. Contract DA-01-021-AMC-11651(Z). 142p. (NASA-TM-X-53447).

The state of the art of the joining of nickel and nickel-base alloys that contain at least 50% nickel is reviewed. This report covers joining by welding, brazing, and soldering. Joining preparations, specific joining processes, joining dissimilar metals, and joint quality are discussed. (auth)

29667 (RSIC-509) MECHANICAL FASTENING OF NICKEL-BASE ALLOYS. Cheever, D. L.; Monroe, R. E.; Martin, D. C. (Battelle Memorial Inst., Columbus, Ohio). Apr. 20, 1966. Contract DA-01-021-AMC-11651(Z). 86p. (NASA-TM-X-53441).

The state of the art of mechanical fastening of nickel-base alloys is reviewed. The designing, forming, machining, assembling, and inspection of nickel-base joints are described in detail when the processes used are known to differ markedly from those processes used for common steel, aluminum, and copper alloys. (auth)

29668 (Y-NA-18) AVERAGE-RADIUS GAGE. Broome, F. H. (Union Carbide Corp., Oak Ridge, Tenn. Y-12 Plant). June 10, 1966. Contract W-7405-eng-26. 12p. Dep. mn. CFSTI $1.00 cy, $0.50 mn.

An inspection gage was developed that utilizes an electronic integrator to determine the average radius of a near-circular section to within ±25 microinches as the surface is rotated before a gaging head. The gaging unit is automatic in its operation, is simple to calibrate and check, and eliminates the need for averaging calculations to obtain a precise answer. The unit is relatively small, can be easily transported from one gaging setup to another, and is adaptable for use with commercially available, high-precision electronic measuring equipment. (auth)

29669 SPHERICAL PRESSED-GRAPHITE FUEL ELEMENTS FOR HIGH-TEMPERATURE REACTORS. Hrovat, M.; Spener, G. (Nuklear-Chemie und -Metallurgie GmbH, Wolfgang, Ger.). Ber. Deut. Keram. Ges., 43: 220-3(Mar. 1966). (In German).

Pressed spherical graphite fuel elements were developed which contain the fuel in the form of coated (U,Th)C particles within a thin pressed graphite shell. The spheres are pressed semihydrostatically as two-zone and three-zone elements and have a high strength and high thermal conductivity. They are also very isotropic and resistant to oxidation. (auth)

29670 MANUFACTURE OF NUCLEAR REACTOR FUEL ELEMENTS AND THEIR COATING WITH PYROLYTIC CARBON. Fleischhauer, G.; Hackstein, K.; Huschka, H.; Venet, P. (Nuklear-Chemie und -Metallurgie GmbH, Wolfgang, Ger.). Ber. Deut. Keram. Ges., 43: 231-8 (Mar. 1966). (In German).

Recently interest has grown in the use of coated particles as fuel and fertile elements in high temperature nuclear reactors. At NUKEM the following work was carried out aimed at the manufacture of nuclear fuel elements from fused carbides and their coating with pyrolytic carbon. The manufacture of Grunling particles composed of oxide and carbon can be carried out both by granulation and by sol-gel processes. After reacting the particles at 1400 to 2000°C to form the carbide, they are melted at about 2550°C. The coating of the particles was carried out in 1 kg charges through the pyrolysis of methane in a rotating furnace and a fluidized bed apparatus. A variety of types of layer could be produced at temperatures from 1400 to 2000°C. Particular advantages in economy and quality were attained by coating in vacuum. (auth)

29671 FLUIDIZED-BED COATING OF FUEL PARTICLES WITH PYROCARBON LAYERS. Koss, P. (Reaktorzentrum, Seibersdorf, Austria). Ber. Deut. Keram. Ges., 43: 239-45(Mar. 1966). (In German).

The fluidized bed coating of fuel particles with pyrolytic-carbon is described. By using porous plates instead of nozzles for the introduction of the coating gases into the reaction vessel, it was possible to obtain batch sizes of up to 5 kg. The structure of the coatings as a function of methane concentration and temperature was investigated. Methods for the evaluation of coated particles are described with special emphasis on surface contamination, fission product retention, and the formation of reaction zones in the coating (auth)

29672 A NEW METHOD FOR THE PRODUCTION OF RHENIUM IN POWDERED FORM. Amiel, Jean; Lecaille, Claude (Univ., Paris). Compt. Rend., Ser. C, 262: 1261-4(Apr. 18, 1966). (In French).

A study of the thermal decomposition of the rhenium(III) tetrammine chloride $Re(NH_3)_4Cl_3$ in a controlled atmosphere showed that it is possible to obtain, below 500°C, powdered rhenium with interesting morphological properties. Thermal decomposition was studied by comparison of the results obtained with thermogravimetric and differential thermal analyses and by study of the residues by x rays. Under a nitrogen atmosphere a plateau was observed near 285°C with a weight loss of 24 to 25%. The end of the reaction was placed near 450°C and corresponds to a weight loss of 49%.

Under hydrogen the reaction had the same shape but the plateau was shifted to 280°C and the end of the reaction to 370°C. Differential thermal analyses were made under nitrogen, hydrogen, and argon. Under nitrogen and argon there were 3 endothermal peaks. The similarities of the curves under nitrogen and argon show that the nitrogen does not take part in the reaction. X-ray analysis of the residues showed that the final product was metallic rhenium. The size of the crystallites obtained under H_2 and N_2 was determined and compared with the crystallite size of commercial rhenium powders prepared by high-temperature reduction of an alkaline perrhenate. A decrease in size was observed in the transition from commercial rhenium to powders prepared from $Re(NH_3)_4Cl_3$. (J.S.R.)

29673 SINTERING OF URANIUM OF EXTREMELY OXIDE-FREE SURFACE. Hampe, E. (Zentralinstitut fuer Kernforschung, Rossendorf, Ger.). Kernenergie, 9: 100-4(Mar. 1966). (In German).

Sintering studies of loose uranium powders are continued. The results obtained by using the same powder as before, but with a modified initial state now extremely free from oxide (0.01 per cent of oxygen), are presented. Using modified bending tests the formation of sintering bridges between the particles of the powder occurred at essentially lower temperatures (450°C upward) for the early sintering stage compared to the former results. The bending strength parabolically increased as a function of sintering time. The early sintering stage essentially based on the surface diffusion is followed by the late sintering stage at high temperatures, including the total gamma-phase range. The proceeding compression of the samples in this stage was studied by measuring the linear shrinkage. Shrinkage obeys a law $S = at^n$ with n about 0.5 and an activation energy of 33.8 kcal/gram-atom resulting from the Arrhenius equation. These values, in connection with the high compression rates observed, mean yield processes in the late stage of sintering. (auth)

29674 THE ELECTRON-BEAM MELTING OF REFRACTORY METALS. IV. THE ELECTRON-BEAM MELTING OF MOLYBDENUM MINOR ALLOYS. Takaai, Tetsuya (Hitachi Central Lab., Ltd., Tokyo). Nippon Kinzoku Gakkaishi, 29: 918-23(1965). (In Japanese).

The electron beam melting processes of molybdenum minor alloys were studied principally from the melting conditions and the spectroscopic analysis results. The electron beam melting of the molybdenum ingot with the alloying element addition was quite different from that of ingot making of pure molybdenum. That is, for example, by the melting of molybdenum ingot with 1.8 wt % zirconium addition, the frictional force between the ingot and the inner surface of the mould increased greatly during the melting, resulting in the ingot rotation and pronounced roughness of the melted ingot surface. The reason for such interruption is probably due to the coexistence of liquid and solid phases in the ingot during the melting, and it was verified that in a wider range of the coexistence temperature it becomes more difficult to make a good ingot. The result showed that the composition of alloyed carbon decreased to about the same level of carbon in pure molybdenum. On the other hand, about 99.8 ~ 99.9% alloyed titanium and about 95.5 ~ 96.6% alloyed zirconium were lost during the melting. Thus measured evaporation coefficient values 1.5 and 3.0 wt % titanium in molybdenum were 44.1 and 64.0, respectively, comparable to those calculated at 3500 and 3000°K. But the measured values of evaporation coefficient were 1.8 and 3.0 wt % zirconium in molybdenum, being about 100 and 250 times as large as the calculated values of 0.04 and 0.05. (auth)

29675 THE DEOXIDATION OF Mo DURING ARC MELTING AND THE EFFECT OF B ON THE WORKABILITY. Hosoda, Tadashi; Matoba, Toshio (Mitsubishi Metal Mining Co., Ltd., Japan). Nippon Kinzoku Gakkaishi, 30: 231-7(1966). (In Japanese).

The deoxidation process of Mo during arc melting was studied using, C, TiH, and B as deoxidizers. Emphasis was placed on the effects of B on the workability of Mo. The results are summarized as follows: The deoxidation reaction by C proceeds, based on the reaction C + O = CO. The over-addition of C is not effectively used for deoxidation but causes the precipitation of intergranular carbides. TiH is effective as deoxidizer. The intergranular precipitates which are made by the addition of TiH are fine and dispersed. (TiH + C) is more effective as deoxidizer. B is useful as deoxidizer and also very effective in grain refinement. Mo containing B has two kinds of intergranular precipitates. The one is granule-like which is made by low B addition, the other is stripe-like by high B addition. Both precipitates seem to dissolve Mo oxide precipitates and to contribute to strengthen grain boundaries. Mo containing B is very ductile. Even Mo which has high oxygen content (100 ppM) can be worked at a relatively low temperature (800°C). (auth)

29676 STUDIES ON THORIUM CARBIDES. PREPARATION OF THORIUM CARBIDES. Ishino, Toshio; Tamura, Hideo. Technol. Rep. Osaka Univ., No. 16, 315-24(Oct. 1965).

The preparation of the fine particle of thorium carbides was studied used with the closed reactor system. The progress of reactions were monitored by the measurement of pressure changes. It was found that thorium reacted with hydrogen at 00−500°C according to a equation, $Th + H_2 = ThH_2$, and produced thorium di-hydride, and after this reaction, ThH_2 reacted with hydrogen again at 250 ~ 225°C on cooling and produced Th_4H_{15}. The comminution of thorium is accomplished by the decomposition of Th_4H_{15} in vacuum. Both of ThC and ThC_2 were produced by the reaction between thorium fine powder prepared from thorium hydride and propane at 650 ~ 800°C, but it was estimated that ThC was produced more easily at high temperature than ThC_2. (auth)

29677 KINETICS OF COMBINED CARBOTHERMAL REDUCTION OF NIOBIUM AND TUNGSTEN. Kol'chin, O. P.; Sumarokova, N. V.; Vol'dman, M. A. Tsvetn. Metal., No. 4, 67-70(Apr. 1966). (In Russian).

Mixtures were made up to contain 5, 15, 30, and 39.7 wt % W in order to determine the conditions for the occurrence of the following reactions: $Nb_2O_5 + WO_3 + NbC \rightarrow Nb-W + CO$, $Nb_2O_5 + WC + NbC \rightarrow Nb-W + CO$, and $NbC + WO_3 \rightarrow Nb-W + CO$. In the presence of tungsten the reduction went to completion at 1200 and 1400°C. Niobium oxide was completely reduced on holding for 3 hours at 1700°C. The degree of reduction was computed from the amount of evolved carbon monoxide. The loss of any tungsten oxide due to sublimation was small. An intermediate niobium oxycarbide was formed. Above 1200°C only metallic tungsten or a niobium-tungsten alloy could be found. (TTT)

29678 REDUCTION OF TANTALUM FROM TANTALUM PENTOXIDE BY THE CARBOTHERMAL METHOD. Kolchin, O. P.; Berlin, I. K. Tsvetn. Metal., No. 8, 67-71 (1964).

To determine optimum technology for obtaining Ta from Ta_2O_5 by reduction with carbon, the effect of various factors involved in the preparation of TaC from Ta_2O_5 and in the subsequent reduction of the Ta_2O_5−TaC mixture was investigated. The initial raw material was Ta_2O_5 powder, with a particle size of 180 μ, containing 0.55% TiO_2, 0.07% Fe_2O_3, and 1.34% SiO_2. TaC powder containing from 5.1 to 6.2% C_{total} was prepared by mixing Ta_2O_5 with carbon black and heating the mixture at 1750 to 1800°C for 1.5 hr in a current of hydrogen. A mixture of Ta_2O_5 and TaC was then compacted and reduced in a vacuum of 0.001 mm Hg by heating to 900°C in 5 to 10 min, followed by heating to 1700°C in 5 min, holding at this temperature for 2 hr, and cooling in a vacuum. After reduction, the compacts were sintered at 2400°C for 2 hr and then at 2700°C in a vacuum of 0.005 to 0.0005 mm Hg. The best results were obtained with Ta_2O_5 powder with a particle size of less than 147 μ taken in an amount exceeding the stoichiometric by 2 to 3%, mixed for about 1 hr with TaC powder with particles ranging in size from 104 to 147 μ. The mixture was compacted in 10-mm cubes under a pressure of 1 t/cm^2, and the tantalum was reduced at 1700 to 1900°C or a higher temperature in

a vacuum of 0.01 mm Hg. The reduced metal was sintered in a vacuum of 0.005 mm Hg at 2400°C and then at 2700 to 2750°C, holding 2 to 3 hr at each temperature. Tantalum obtained under these conditions contained a few thousandths of one percent each of C and O, 0.006 to 0.011% N, less than $(1 \text{ to } 5) \cdot 10^{-3}$% each of Ti, Fe, Si, Mn, S, Al, P, Cu, and As, less than $1 \cdot 10^{-4}$% each of Sn, Pb, Sb, Bi, and Cd, $\sim 1 \cdot 10^{-4}$% H, and less than $3 \cdot 10^{-6}$% Zn. The yield of the sintered Ta was 95.0% of the amount contained in the Ta_2O_5. (ATD)

29679 CERTAIN PROBLEMS IN DYNAMIC AND STATIC PRESSING OF METALLIC POWDERS. Roman, O. V.; Bogdanov, A. P. Vestsi Akad. Navuk BSSR, Ser Fiz. Tekh. Navuk, No. 3, 72-7(1965). (In Russian).

Experiments were made in pressing sheets and plates from metallic powders by explosive techniques. Comparative data are obtained from evaluating ordinary "static" pressing and pressing with dynamic loads. Relations derived for determining the pressure required for static pressing (neglecting wall friction on the pressing form) can be used to determine the pressure required for matrixless dynamic pressing. Iron powder, sifted through an 016 sieve, was used to determine the dynamic coefficient that characterizes the behavior of the powder during dynamic pressing. The data obtained can be used to define the parameters for dynamic pressing of powdered metals. (CFSTI)

29680 METALS FOR THE SPACE AGE. Plansee Proceedings, 1964. Papers Presented at the Fifth Plansee Seminar, De Re Metallica, held June 22–26, 1964, Reutte/Tyrol. Benesovsky, F. (ed.). Reutte/Tyrol, Metallwerk Plansee AG, 1965. 884p. (CONF-517).

Fifty-two articles are included; separate abstracts were prepared for 37. Two articles on properties of Mo single crystals and high temperature chemistry of refractory carbides were previously abstracted in NSA as 18: 24133 and 19: 39139. The remaining 13 articles contain information on materials for space flight, technology of refractory metals, and studies of less commonly used metals that may be of interest to space technology. (P.C.H.)

For abstracts of individual papers see: 29108, 29630–29633, 29650, 29651, 29681–29690, 29756–29774, and 29820.

29681 HIGH-PRESSURE ISOSTATIC PRESSING AND PRESSURELESS SINTERING OF SOME METAL POWDER COMPACTS. Greenspan, J. (Army Materials Research Agency, Watertown, Mass.). pp 163-76 of Metals for the Space Age. Plansee Proceedings, 1964. Benesovsky, F. (ed.). Reutte/Tyrol, Metallwerk Plansee AG, 1965.

Isostatic pressing at relatively high pressures, that is, of the order of 150,000–175,000 psi, was examined with respect to compressibility of beryllium, iron, copper, and aluminum powder compacts. Pressure-porosity relationships are given. For beryllium the investigation included some studies of sintering, generally confined to temperatures below 1950°F (1066°C), and determinations of tensile strength. Beryllium compacts were compressible to approximately 91–92% of theoretical for a single pressing cycle, and up to 99% when annealed and recompacted. Iron, copper, and aluminum were compressible respectively to about 94, 96, and 99% for a single pressing cycle. The entire study was confined generally to commercially available powders with particle size designated as minus 200 mesh. (auth)

29682 FLOW TURNING OF REFRACTORY METALS. Machenschalk, R. (Metallwerk Plansee AG, Reutte/Tirol). pp 177-83 of Metals for the Space Age. Plansee Proceedings, 1964. Benesovsky, F. (ed.). Reutte/Tyrol, Metallwerk Plansee AG, 1965. (In German).

The method of flow turning and its advantages and possible applications are described. Necessary changes in procedure and equipment are discussed. The production of a tungsten nozzle is explained in detail. Finally, the attainable tolerances and the necessary mechanical treatment of components made from refractory metals by flow turning are described. (P.C.H.)

29683 COMPARISON OF PRESSED AND SINTERED AND ARC-CAST BILLETS FOR REFRACTORY METAL FORGINGS. Warga, J. J.; Evans, F. D.; Kotfila, R. J. (Aerojet General Corp., Sacramento, Calif.). pp 184-98 of Metals for the Space Age. Plansee Proceedings, 1964. Benesovsky, F. (ed.). Reutte/Tyrol, Metallwerk Plansee AG, 1965.

Comparisons were made of pressed, sintered, and arc-cast W and Mo billets for forging. It was concluded that pressed and sintered and arc-cast Mo forgings can be used interchangeably for engineering applications, provided that the impurity levels are comparable and the forging techniques employed for each type of material are similar. It was also concluded that pressed and sintered W only is suitable for forgings. All the Mo forgings investigated displayed anisotropy in mechanical properties; the anisotropy was most pronounced in the pressed and sintered material. In applications requiring directional uniformity of properties, therefore, the forging procedures should be carefully selected and controlled. (P.C.H.)

29684 SOME OBSERVATIONS ON THE INDIRECT SINTERING OF TUNGSTEN. Hargrave, D. P.; Cox, F. G. (Murex Ltd., Rainham, Essex, Eng.). pp 219-32 of Metals for the Space Age. Plansee Proceedings, 1964. Benesovsky, F. (ed.). Reutte/Tyrol, Metallwerk Plansee AG, 1965.

Preliminary investigations into the sintering of various sizes of tungsten compacts by indirect heating gave an interesting insight into some of the factors involved, showing that results obtained on small compacts can sometimes be misleading. The investigation involved the sintering of specimens for long periods at temperatures in excess of 2000°C and the design of a suitable furnace. Using this furnace, experiments were made on the effect of variation of compact size, compaction pressure, furnace atmosphere, particle size of powder, and various deoxidation techniques on the properties of the sintered compacts as assessed by density, oxygen content, and microstructure. (P.C.H.)

29685 DEVELOPMENT OF SILVER INFILTRATED TUNGSTEN NOZZLES FOR UNCOOLED ROCKET MOTORS. Matt, R. E.; Warga, J. J. (Aerojet-General Corp., Sacramento, Calif.). pp 233-55 of Metals for the Space Age. Plansee Proceedings, 1964. Benesovsky, F. (ed.). Reutte/Tyrol, Metallwerk Plansee AG, 1965.

The need for a solid rocket nozzle material that would operate at temperatures close to the melting point of tungsten led to the development of a sintered tungsten matrix with controlled density and porosity. Sintered tungsten matrices with densities below 75% of theoretical were found to be lacking in the strength required for performance; those matrices with densities above 85% theoretical lacked the interconnecting pores required for uniform infiltration. For successful manufacture of a silver infiltrated billet for solid rocket nozzles, it was found that the following sequences had to be closely controlled: selection and blending of tungsten powder; compaction of the shaped part; sintering of the compact; and infiltration of the sintered matrix. Investigations of the relationship between powder particle size, shape, and distribution and the resultant product led to the use of an irregularly shaped tungsten powder with an average particle size of 3 to 7 microns and a closely controlled distribution of fines and coarses. Subsequent compaction had to be closely controlled to avoid layering of the different particles. Sintering times and temperatures were found to be influenced by the atmosphere during sintering, the size of the billet, the distribution of powder particle sizes, the average particle size, and the chemistry of the powder. Infiltrability was found to be a function both of the matrix and the infiltrant. (auth)

29686 ELASTIC AND PLASTIC DEFORMATION OF DISPERSED PHASE-LIQUID PHASE SINTERED TUNGSTEN COMPOSITE MATERIALS. Krock, R. H. (P. R. Mallory and Co., Burlington, Mass.). pp 256-77 of Metals for the Space Age. Plansee Proceedings, 1964.

Benesovsky, F. (ed.). Reutte/Tyrol, Metallwerk Plansee AG, 1965.

The development of microstructure, elastic modulus, and tensile curves of a series of two phase, tungsten–nickel–iron composites were investigated over a wide temperature range. Sintering in the liquid phase was essentially complete in less than 10 minutes at 1460°C, although continued growth of the dispersed tungsten particles took place with increasing sintering time. Particle growth took place by agglomeration of particles in the liquid followed by volume diffusion. The size of the dispersed particles showed a fourfold increase over the initial tungsten particle size after 10 minutes sintering at 1460°C and increased with one-third power of time for progressive sintering. The elastic moduli of four tungsten composites as well as the constituent phases of the composites were tested from room temperature to 1000°K by a dynamic method using Rochelle-Salt piezo-electric transducers. The modulus of the matrix alloy which contained 53.2% Ni, 22.8% Fe, 24% W by weight was 19.3×10^6 psi and that of tungsten was 58.1×10^6 psi at room temperature. The composite elastic moduli exhibited higher values than that predicted by theory using the properties of the individual phases. From the elastic and plastic deformation data on W–Ni–Fe composite materials, it was concluded that composite properties need not simply be a compromise between the properties of the individual phases. (P.C.H.)

29687 FLUORIDE TUNGSTEN. Oxley, J. H.; Beidler, E. A.; Blocher, J. M. Jr.; Lyons, C. J.; Park, R. S.; Pearson, J. H. (Battelle Memorial Inst., Columbus, Ohio. Allied Chemical Corp., Morristown, N. J.). pp 278-300 of Metals for the Space Age. Plansee Proceedings, 1964. Benesovsky, F. (ed.). Reutte/Tyrol, Metallwerk Plansee AG, 1965.

One of the more interesting new space-age materials to be developed during the past few years is fluoride tungsten. It promises to be the forerunner of a class of products with new and unusual properties. A laboratory set up to produce small quantities of the granular product is described. The properties and purity of the granular material are discussed. The granules can be consolidated into billets and rolled to sheet or pressed into final shapes. Some previously disclosed properties of the consolidated tungsten are reviewed and uses are suggested. Recent developments are also described. (auth)

29688 PRODUCTION OF TUNGSTEN SHEET BARS BY ZONE REFINING OF CEMENTED TUNGSTEN-BASE ALLOYS. Parikh, N. M.; Arnold, S. V. (I. I. A. Research Inst., Chicago. Army Materials Research Agency, Watertown, Mass.). pp 325-39 of Metals for the Space Age. Plansee Proceedings, 1964. Benesovsky, F. (ed.). Reutte/Tyrol, Metallwerk Plansee AG, 1965.

Cemented tungsten–nickel–iron alloys of high tungsten content can be cold rolled substantially in form of sheet bars. Because of the solubility of tungsten in the matrix alloys and the lack of solubility of the matrix alloys in tungsten, it is possible to separate the two phases by a technique known as temperature gradient zone melting. Almost pure tungsten sheet bars can be made by this method with the use of ductile tungsten–nickel–iron as the starting raw material. The tungsten sheet bars prepared by this method can be hot rolled and subsequently cold rolled to a satisfactory wrought product. The details of an investigation based on these principles are described, and the feasibility of this process is reported. The operating parameters are discussed and the mechanical behavior of the tungsten prepared by this method was compared with those of tungsten prepared by conventional techniques. (auth)

29689 OXIDE–METAL COMPOUND CERAMICS. Ryshkewitch, E. (National Beryllia Corp., Haskell, N. J.). pp 823-30 of Metals for the Space Age. Plansee Proceedings, 1964. Benesovsky, F. (ed.). Reutte/Tyrol, Metallwerk Plansee AG, 1965.

Several methods of blend-uniting and joining such dissimilar construction materials as beryllium (or other refractory) oxide with tungsten (or some other refractory) metal or carbide to produce compound bodies of uniform or gradient composition, including pieces consisting of pure sintered beryllia at the one end, and pure sintered tungsten at the other are reported. Nozzles of rocket engines, nose cones of extra-atmosphere reentry missiles, and other responsible construction parts of low specific weight and high thermal and mechanical stability can successfully be made from such composites. (P.C.H.)

29690 SINTERED SEMICONDUCTORS FOR THERMOELECTRIC CURRENT GENERATION AND COOLING. Schreiner, H. (Siemens-Schuckertwerke, AG, Erlangen, Ger.). pp 831-44 of Metals for the Space Age. Plansee Proceedings, 1964. Benesovsky, F. (ed.). Reutte/Tyrol, Metallwerk Plansee AG, 1965. (In German).

Examples of materials for thermoelectric generators with operating temperatures of up to 600°C and materials for thermoelectric cooling plates are given. The aim of development in this field is to obtain materials with maximum thermoelectric efficiency over a wide temperature range ($z = a^2\sigma/\varkappa$) and for generators particularly, materials capable of operating continuously at maximum temperature without undergoing structural modification. In addition to the development of efficient materials, the electrical connection of the thermocouple components is an important technical problem. Of interest are further economic production and processing of the thermocouple components. Thus far, they have mostly been made by various melting methods, such as deposition or zone-refining in which single crystals or coarse-grained polycrystals were obtained. The components can also be made by powder metallurgical techniques by pressing, sintering, pressure-sintering, or hot pressing of the alloy powders or of powder mixtures and by extrusion of sintered materials. These methods are described by means of examples and the properties of the sintered thermocouple components are described. The structure of the sintered materials as compacted with that of material produced by a melting process is characterized by much smaller grain size. The structure of sintered thermoelectric materials is determined by the lamellar shape of the powder particles used as starting material. (P.C.H.)

29691 IMPROVEMENTS IN OR RELATING TO THE FORMING OF MATERIALS BY EXTRUSION. Green, Derek (to United Kingdom Atomic Energy Authority). British Patent 1,027,692. Apr. 27, 1966. Filed June 22, 1962.

An apparatus for the extrusion of material to form a tube comprises a container having a cylindrical bore, an extrusion die located at one end of the bore in the container, and a mandrel rigidly located in the bore of the container in line with the longitudinal axis of the extrusion die. The mandrel has an enlarged head fitted into the bore of the container. Means are provided in the bore of the container for positioning the mandrel longitudinally in the bore and for spacing the head of the mandrel from the extrusion die. A space for a tubular extrusion billet is defined inside the bore, around the mandrel, between the head of the mandrel and the extrusion die. A liquid is pressurized in the bore of the container on the side of the mandrel head remote from the die, and longitudinal passageways provided in the head of the mandrel allow this pressure in the liquid to be transmitted to liquid on the side of the mandrel head facing the die. (B.L.M.)

29692 IMPROVEMENTS IN OR RELATING TO THE PRODUCTION OF CARBONACEOUS BODIES CONTAINING CARBIDES. Moore, Norman Clement; Cowlard, Frederick Claud; Redfern, Bernard (to Plessey Co. Ltd.). British Patent 1,029,245. May 11, 1966. Filed July 14, 1961.

A process is described for the production of substantially impermeable carbonaceous bodies containing carbide that consists of mixing a phenol-aldehyde type resin with an element capable of forming a carbide to form a homogeneous mixture, heating the mixture in order to cure the resin, and then further heating the mixture at a temperature that is sufficiently high to bring about the formation

of the carbide and to carbonize an excess of the resin to form the vitreous carbon. The process is particularly useful for producing carbonaceous bodies containing UC and ThC. Alternatively, the resin may be pre-cured, finely powdered, and then mixed with the element capable of forming the carbide The mixture is then hot pressed to yield a body that is then carbonized. (B.L.M.)

29693 EXTRUSION APPARATUS. Green, Derek (to United Kingdom Atomic Energy Authority). U. S. Patent 3,243,985. Apr. 5, 1966. Filed Sept. 28, 1964.

An extrusion apparatus is described that has a resiliently yieldable non-metallic die and fluid pressure means for deforming the die radially inward into close embracement of the workpiece. (B.L.M.)

29694 NUCLEAR REACTORS OPERATING WITH SUBSTANTIALLY ISOTROPIC GRAPHITIZED BODIES. Martin, Samuel W.; Shea, Frederick L. Jr.; Juel, Leslie H. (to Great Lakes Carbon Corp.). U. S. Patent 3,245,880. Apr. 12, 1966. Filed Mar. 18, 1963.

Several methods are described for making graphitized bodies suitable for use in nuclear reactors as containers for fuel elements, fuel elements themselves, materials for reflector mantles, or as moderator elements. The formed graphitized bodies are prepared by pressing, molding, or shaping of materials that are already isotropic or that are capable of being made substantially isotropic by certain techniques employed in the fabrication procedure. The shaping of the carbonaceous material is followed by baking and graphitizing procedures that are described in detail. (B.L.M.)

29695 REFRACTORY BODIES AND METHOD OF MAKING SAME. Taylor, Kenneth M. (to Carborundum Co.). U. S. Patent 3,247,000. Apr. 19, 1966. Filed Oct. 16, 1961.

A method for making refractory bodies having high strength coupled with high resistance to thermal shock comprises the steps of preparing a raw batch consisting essentially of a finely divided mixture of 70–85 wt % alumina and 30–15 wt % of monoclinic zirconia, forming the batch into the body of desired shape and size, and sintering the body at a temperature of about 1400°C to provide a body having a porosity of between 3 and 13%. Alternatively, the body can be subjected to at least one controlled thermal shock that consists of rapidly heating the body to the sintering temperature and then rapidly cooling the body. (B.L.M.)

29696 PROTECTED REFRACTORY ARTICLES. Gerry, Ronald J. (to Norton Co.). U. S. Patent 3,249,460. May 3, 1966. Filed Mar. 7, 1961.

A refractory article having a low capture cross section for thermal neutrons was developed that includes a main body composed of graphite, a coating consisting essentially of SiC covering the outer surface of the graphite base, and an impervious protective glaze covering the SiC coating. The glaze consists essentially of a fused mixture of ZnO, Al_2O_3, Pb_3O_4, and SiO_2 in the proportions of 6–10, 2–6, 55–65, and 25–30 wt %, respectively. The SiC coating is applied in a thin layer to the formed graphite article, then a frit, which will provide the fused layer, is applied over the SiC layer. Firing of the resulting structure produces the protective glaze over the superimposed SiC layer. (B.L.M.)

Properties and Structure

See also CHEMISTRY — Inorganic and Physical Chemistry
PHYSICS — Solid State Physics

Refer also to abstracts 29393, 30790, 30792, and 30794.

29697 (AECL–2538) EFFECT OF TEMPERATURE ON THE MICRO-INDENTATION PROPERTIES OF ZIRCONIUM HYDRIDE. Ambler, J. F. R. (Atomic Energy of Canada Ltd., Chalk River (Ontario)). Mar. 1966. 12p. Dep. mn. AECL $0.50.

This investigation into the micro-indentation properties of zirconium hydride at temperatures up to 225°C, indicates that above 50°C zirconium hydride can deform plastically by at least 8%. This tends to support the idea that the restoration of the tensile properties of zirconium alloys containing orientated hydrides, which begins at approximately 50°C, is due to plasticity of the hydride flakes. The results obtained also indicate a much higher ultimate tensile strength for zirconium hydride than is given by tensile testing. (auth)

29698 (ANL–7101) ELASTICITY AND ANELASTICITY OF URANIUM OXIDES AT ROOM TEMPERATURE. Forlano, Roberto J. (Argonne National Lab., Ill. Illinois Univ., Urbana); Allen, Alfred W. (Illinois Univ., Urbana); Beals, Robert J. (Argonne National Lab., Ill.). Dec. 1965. Contract W-31-109-eng-38. 75p. Dep. mn. CFSTI $3.00 cy, $0.75 mn.

The elastic modulus of sintered compacts of stoichiometric uranium oxide at room temperature increases with increasing density. When the volume-fraction porosity is less than 0.1, either a linear or an exponential equation can be used to calculate the elastic trait as a function of density. When the volume-fraction porosity becomes greater than 0.1, a linear equation seems to be most suitable. The linear expression is given by $E = 2233.85(1-2.277P)$, and the exponential equation by $E = 2243.56e^{-2.52P}$; where E is the elastic modulus of porous polycrystalline uranium oxide, and P is the volume-fraction porosity. The elastic modulus of stoichiometric, nonporous uranium dioxide at room temperature was found by extrapolation to be 2243.56 ± 22.1 kilobars when the exponential equation was used, and 2233.85 ± 22.05 kilobars when the linear expression was used. Internal friction of $UO_{2.00}$ decreased sharply as the grain size increased. Other microstructural characteristics, namely, number, size, and position of pores also contribute to this behavior. In nonstoichiometric urania, the presence of a two-solid phase is the pre-eminent factor dictating the damping properties at room temperature. Young's modulus for nonstoichiometric uranium oxide at room temperature depends mainly on the history of the sample. Varying the oxidation and/or the rate of cooling will produce completely different results. When studying or specifying the elastic or anelastic trait of nonstoichiometric urania at room temperature, one must characterize the material not only by the oxygen-to-uranium atom ratio, but also by microstructure, particularly the number, location, and quantity of solid phases present and the type of porosity. In the oxidation range studied here, the ratio of UO_{2+x} to U_4O_9 (or U_4O_{9-y}) is advisable to relate properties at room temperature to uranium-oxygen content. (auth)

29699 (CONF-650674–1) THE DEPENDENCE ON MICROSTRUCTURE OF THE HIGH-TEMPERATURE PROPERTIES OF URANIUM OXIDE–MOLYBDENUM AND URANIUM OXIDE–TUNGSTEN CERMETS. I. ELECTRICAL RESISTIVITY. Amato, I.; Colombo, R. L.; Polin, F. (FIAT, Turin (Italy). Sezione Energia Nucleare). Apr. 9, 1965. Contract 002-63-9 CODI. 16p. (R–103). Dep. mn.

From International Conference on Mechanical and Physico-Chemical Properties of Refractories at High Temperature, Paris.

The electric conductivity of the $Mo-UO_2$ and $W-UO_2$ cermets was dependent upon the volume percent of metal, the fabrication process, and the temperature from 25 to 1300°C. (W.L.G.)

29700 (COO–1477-4) FRACTURE TOUGHNESS OF REACTOR PRESSURE VESSEL STEELS. DEVELOPMENT OF TEST PROCEDURES. [Period Covered]: May 1, 1965–May 1, 1966. Ripling, E. J.; Crosley, Phillip (Materials Research Lab., Inc., Richton Park, Ill.). May 31, 1966. Contract AT(11-1)-1477. 17p. Dep. mn. CFSTI $1.00 cy, $0.50 mn.

A tapered double cantilever beam specimen for fracture toughness testing was developed, and experimental compliance calibrations of the specimen were performed. The effect of side grooves was investigated with the testing of 7075-T651 and 2024-T351 aluminum alloys. The results indicate that the use of side grooves promotes plane strain fracturing, and that, when plane strain conditions are satisfied, measured values of fracture toughness are not affected by groove depth. A technique of alternating fatigue with increasing load testing was used for testing 5456-H321 aluminum alloy. Initiation of rapid fracture in specimens precracked in fatigue (rather than in increasing load) occurred at lower values of the crack extension force, indicating that this technique promotes plane strain fracturing. Very high loading rates were used for room temperature testing of A302-B specimens pre-cracked in fatigue. With pulse loading, crack arrests were obtained. The procedure offers the promise of yielding room temperature plane strain fracture toughness data, for fracture initiation and arrest of A302-B steel with specimens of a reasonable size. (auth)

29701 (EURAEC–1547) A STUDY ON PLASTIC FATIGUE EMBRITTLEMENT OF REACTOR VESSEL STEELS. Quarterly Report No. 8, October 1–December 31, 1965. (Centre National de Recherches Metallurgiques, Liege (Belgium)). Contract 005-63-12TEEB. 46p. (EUR–2689). Dep. mn. CFSTI $2.00 cy, $0.50 mn.

Work Performed under United States–Euratom Joint Research and Development Program.

Charpy V impact strength tests were performed on ASTM A302B, Ducol W30, and Soudotenax 56 steel samples that were previously subjected to cyclic plastic fatigue at 20 and 300°C. The results show that the increase in the transition temperature of samples exhibiting a crystallinity of 50% at the fracture surface is not a continuous function of the number of plastic fatigue cycles. Only a few cycles at 300°C were sufficient to cause an appreciable embrittlement of the steels. Rockwell B measurements were performed on samples that possessed a completely crystalline fracture from the Charpy test. The Rockwell B hardness maxima corresponded to the embrittlement maxima. Biaxial bend tests were performed to investigate the effects of prior strain-hardening on the fatigue life at 300°C. Two of the three steels showed an increase in their plastic fatigue properties at rupture. (W.L.G.)

29702 (EURAEC–1616) STUDY OF THE INFLUENCE OF INITIAL STRESS ON ISOTHERMAL STRESS-RELIEF TESTS. Special Report No. 9. (Chantiers de l'Atlantique Penhoet-Loire, Paris (France)). Mar. 10, 1966. Contract 054-61-12RDF. 13p. (EUR–2829). Dep. mn. CFSTI $1.00 cy, $0.50 mn.

Work Performed under United States–Euratom Joint Research and Development Program.

Results of stress-relaxation measurements performed at 650°C on low-alloy steel samples, which were deformed 0.2, 0.4, or 0.6% prior to testing, are reported. (W.L.G.)

29703 (KAPL–3112) THERMAL EXPANSION AND TEMPERATURE DEPENDENCE OF THE ELASTIC MODULI OF POLYCRYSTALLINE HAFNIUM. Washburn, D. F.; Blechinger, F. K. (Knolls Atomic Power Lab., Schenectady, N. Y.). Apr. 15, 1966. Contract W-31-109-eng-52. 17p. Dep. mn. CFSTI $2.00 cy, $0.50 mn.

Hafnium plate with a known texture was utilized for making measurements of the temperature dependence of the elastic moduli and for measuring the thermal expansion. The texture of the plate was moderately strong with the basal planes parallel to the rolling direction and the basal poles tilted at an angle of about 45° to the rolling plane. The $[11\bar{2}0]$ was aligned in the rolling direction. (auth)

29704 (MSAR-66-78) RESULTS OF MECHANICAL PROPERTIES TESTS OF 316 SS SPECIMENS IN 1200 F SODIUM CONTAMINATED WITH OXYGEN (~300 ppM). Topical Report No. 5. Andrews, R. C.; Hiltz, R. H.; Kirschler, L. H.; Rodgers, S. J.; Tepper, F. (MSA Research Corp., Evans City, Pa.). May 1966. Contract AT(11-1)-765. 116p. Dep. mn. CFSTI $4.00 cy, $0.75 mn.

The mechanical properties of one heat of type 316 stainless steel were measured in a dynamic sodium system contaminated with 300 ppM oxygen at 1200°F. The effects were evaluated by comparing these mechanical properties with the mechanical properties of the same heat in air, helium and low oxygen sodium. Some comparisons were also made with regard to a carburizing environment. Both as received and 4000-hour exposed material were tested. Creep, creep-rupture, and fatigue tests were conducted in the flowing sodium system, while tensile tests were conducted in air and helium at both room temperature and test temperature on exposed material. Impact tests were conducted in air at room temperature. Metallurgical techniques used in post-test evaluation of the specimens and tabs included carbon analyses, microhardness measurements, microprobe analyses, metallographic analyses, and standard x-ray diffraction. Sodium chemistry, cold trapping, and plugging indicator studies are discussed, as well as operation and post-test examination. (auth)

29705 (NAS-CR–54973) GENERATION OF LONG-TIME CREEP DATA ON REFRACTORY ALLOYS AT ELEVATED TEMPERATURES. Eleventh Quarterly Report, December 26, 1965–March 26, 1966. Sawyer, J. C.; Steigerwald, E. A. (TRW Equipment Labs., Thompson Ramo Wooldridge Inc., Cleveland, Ohio). Apr. 15, 1966. Contract NAS3-2545. 84p.

Creep data obtained on arc-cast and vapor-deposited W, TZC, TZM, and Nb-modified TZM Mo-base alloys, and T-222 Ta-base alloys are presented. (W.L.G.)

29706 (NASA-TM-X-53448) SURFACE TREATMENTS FOR NICKEL AND NICKEL-BASE ALLOYS. Jackson, C. M.; Hall, A. M. (Battelle Memorial Inst., Columbus, Ohio). Apr. 20, 1966. Contract DA-01-021-AMC-11651 (Z). 144p. (RSIC-513).

The state of the art in regard to selected surface treatments for nickel and nickel-base alloys is reported. The treatments covered are diffusion coating, electroplating, electroless plating, hard facing, surface treatment for purposes of lubrication, explosive hardening, peening, burnishing and planishing. Each treatment is described and its application to nickel and nickel-base alloys is discussed. Reasons for using the treatment are covered, as are the effects of the operations involved on appropriate properties of nickel and nickel-base alloys. Problem areas are defined and recommendations for research are made. (auth)

29707 (ORNL-TM–1457) MEASUREMENT OF MASS ATTENUATION COEFFICIENTS USING 50- TO 150-kvp X RAYS. Foster, Billy Evon (Oak Ridge National Lab., Tenn.). June 1966. Contract W-7405-eng-26. 58p. Dep. mn. CFSTI $3.00 cy, $0.50 mn.

Thesis. Submitted to Vanderbilt Univ., Nashville, Tenn.

Experimental determinations of the low-energy x-ray attenuation coefficients of some materials associated with nuclear technology were made to permit their use in homogeneity studies and various radiographic techniques. The materials examined were types 304 and 347 stainless steel, Zircaloy-2, type 1100 aluminum, and uranium–aluminum alloys of 7, 18.6, and 24.8 wt % U. A Norelco 150 x-ray unit was used as the source of radiation. The detector was a NaI(Tl) crystal, optically coupled to a photomultiplier tube. The equipment, its operation, and the experimental procedure are discussed in detail. Mass attenuation coefficients were determined as the summation of the fractional absorption caused by the significant constituent elements within the limits of predetermined energy ranges. (auth)

29708 (SC-DC–65-1744) COMPRESSIVE STRAIN RATE TESTS ON FOUR COMPOSITES. Phase I. Babcock, S. G.; Green, S. J.; Maiden, C. J. (General Motors Corp., Santa Barbara, Calif. Defense Research Labs.). Sept. 1965. Contracts AT(29-1)-789; 16-3381. 133p. Dep. mn. CFSTI $4.00 cy, $1.00 mn.

For Sandia Corp., Albuquerque, N. Mex.

The dynamic stress-strain relations in compression for four composite materials: phenolic nylon, phenolic carbon, phenolic asbestos, and phenolic refrasil were investigated. Each was tested over seven orders of magnitude of strain rate for two directions of interest. All four materials behaved in a nonlinear manner, showing at least some degree of strain rate sensitivity over the seven orders of magnitude. Each material was tested for repeatability under all test conditions, and the results are presented statistically. (auth)

29709 (TID–22970, pp 65-119) ELECTRIC, MAGNETIC, AND OPTICAL PROPERTIES OF MATERIALS AND APPLICATIONS TO DEVICES. (Massachusetts Inst. of Tech., Cambridge).

Summaries of research are presented: bond structures and electronic properties of materials, semiconductor materials and devices, preparation and properties of crystals, crystal structures, microwave and quantum magnetics, and mass spectroscopy. (J.R.D.)

29710 (TID–22986) PROPERTIES OF SOME REFRACTORY METALS. IV. EXPERIMENTAL TECHNIQUES EMPLOYED IN STRESS-RUPTURE AND CREEP MEASUREMENTS TO 3000 DEG C. McCullough, W. L.; Flagella, P. N. (General Electric Co., Cincinnati, Ohio. Nuclear Materials and Propulsion Operation). Apr. 29, 1965. Contract AT(40-1)-2847. 38p. (TM–65-5-10). Dep. mn. CFSTI $2.00 cy, $0.50 mn.

Equipment and techniques were developed for the measurement of refractory metal creep-rupture properties to 3000°C in hydrogen or inert atmospheres. The furnace, using a split tungsten tube as the heating element and heated resistively, is capable of operating at constant temperature continuously for hundreds of hours. Temperature control within 10°C is obtained by automatically maintaining a constant voltage to the heating element. Temperature is determined by sighting an optical pyrometer into a black-body tube located adjacent to the test specimen. The dead weight load, imposing the desired stress on the test specimen, is suspended below the furnace in the load shell which also contains the furnace atmosphere. Strain measurements are obtained using a special optical extensometer consisting of two parallel telemicroscopes. Each telescope is focused on a 0.005-inch-diameter hole, used as a fiducial mark, at either end of the specimen gage length. Creep data for arc-cast molybdenum at 2200°C, obtained with the optical extensometer, are presented demonstrating the excellent temperature control and reproducibility of test data obtained. (auth)

29711 (UCRL–11996) DISLOCATION DIPOLES IN DEFORMED MAGNESIUM OXIDE. Cass, Thomas Robert (Lawrence Radiation Lab., Univ. of California, Berkeley). Nov. 1965. Contract W-7405-eng-48. 142p. Dep. mn. CFSTI $4.00 cy, $1.00 mn.

The microscopic processes connected with the plastic deformation of magnesium oxide were investigated by a careful study of the dislocation substructures developed during deformation. However, the application of transmission electron microscopy, the experimental technique used, was limited because no complete theory of the diffraction contrast of dislocation dipoles was available. Thus, calculations of dislocation dipole contrast were made using the Dynamical Theory of Howie and Whelan. Besides this primary application of the computations the following auxiliary topics were treated: The transition from kinematical to dynamical diffraction conditions, differentiation between a narrow dipole and a single dislocation, determination of the nature, i.e., interstitial or vacancy, of a dipole, and determination of which surface a line defect lies closer to. In order to best utilize the results of the calculations, all experimental conditions were standardized. In particular, specimens were prepared from platelets diamond-sawed parallel to an active [110] slip plane, and observations were always made when only the [220] family of planes was responsible for the diffraction contrast. Almost all the visible damage was present in the form of dislocation dipoles; however, these dipoles often deviated greatly from the edge orientation. In fact, segments of pure screw dipole were observed. Their stability is evidence of the extremely high lattice friction stress in the cross-slip ([001]) plane. There was a spectrum of dipole widths and lengths; the narrowest visible dipole was estimated to have a spacing of about ten Burgers vectors. Many of the dipoles had orientation junctions along their length. Both interstitial and vacancy dipoles were present in the as-deformed crystal. Single edge dislocations were seldom observed, but screw portions had edge dipoles of varying widths spaced every few microns along their length. The effect on the dislocation substructure of a high stress on the cross-slip plane was similar to the effect of increasing the deformation temperature; fewer, wider dipoles were formed. All newly discovered features of the dislocation substructure were consistent with a model for dipole formation previously proposed by Washburn. The a priori assumption of the easy nucleation of unit jogs must be made in order to predict the high density of dislocation dipoles observed. (auth)

29712 (WANL-PR–(P)-009) DETERMINATION OF THE WELDABILITY AND ELEVATED-TEMPERATURE STABILITY OF REFRACTORY METAL ALLOYS. Ninth Quarterly Report, June 21, 1965–September 20, 1965. Lessmann, G. G.; Stoner, D. R. (Westinghouse Electric Corp., Pittsburgh, Pa. Astronuclear Lab.). Contract NAS3-2540. 68p. (NASA-CR–54923).

Room temperature and elevated temperature tensile properties of the Ta and Nb alloys were determined for both base metal and TIG welded specimens. Tests were run at 75, 1800, 2100, and 2400°F. Excellent tensile weld joint efficiencies near 100% were obtained for all alloys throughout the temperature range. The tensile data demonstrated that, on a density uncorrected basis, Ta alloys were generally stronger than Nb alloys and have greater stability with increasing temperature. Within respective alloy groups, the solid solution alloys are considerably weaker than those containing reactive element solute additions, which enhance strength by both dispersion and solid solution mechanisms. Most alloys displayed a failure mode transition between 1800°F, where fractures were primarily of the ductile shear type, and 2400°F where intergranular failures were predominant. In this respect, large weld grain sizes in either weld or base metal tended to result in lowering high temperature ductility. This was particularly apparent with Ta–10W. C129Y and D43Y exhibited extensive grain boundary separation throughout the base metal at the highest test temperature. Tensile elongation of the Y modified alloys was high, despite the gross separation of grain boundaries, because of small grain sizes. This advantage due to grain size could not be realized in welds, and weld tensiles failed with considerably less ductility. The weldability of T-111, T-222, and FS-85 was compared on the basis of sensitivity to contamination by oxygen. The sensible contamination limit for this investigation was identified as 1000 ppm oxygen. At this level both the weld and base bend transition temperatures exceeded 1000°F. T-111 and FS-85 are about equivalent in oxygen sensitivity. Above the threshold of about 4000 atomic ppM ductility decreases rapidly in T-111 and FS-85 with increasing contamination. The threshold for T-222 appears to be less than 2000 atomic ppM. Tensile results were obtained at two oxygen levels, as received and 500 wt ppM. Increasing the oxygen content produced higher strength and less ductile behavior at all test temperatures. The oxygen contamination strengthening effect on short time properties is most pronounced up to 1800°F, above which there is little difference between uncontaminated and contaminated properties. Room temperature ductility is low with contaminated T-111 and T-222 exhibiting less than 5% tensile elongation. The variation in strength and fracture location with testing temperatures indicate oxide precipitation strengthening reactions are occurring, either during the tensile test itself, as strain aging reactions, or during the preceding 50-hr diffusion anneal corresponding

to the tensile testing temperature. The tensile test results of the uncontaminated specimens are comparable to the general tensile test results for transverse welds in sheet specimens. Ultimate and yield strengths of T-111, T-222, and FS-85, in the two separate testing programs, are similar and a difference in tensile elongation can be attributed to the respective thermal treatments; the regular program welds were post-weld annealed and the contamination program material was heat treated 50 hr at various diffusion annealing temperatures prior to welding. (W.L.G.)

29713 (WANL-PR-(P)-010) DETERMINATION OF THE WELDABILITY AND ELEVATED-TEMPERATURE STABILITY OF REFRACTORY METAL ALLOYS. Tenth Quarterly Report, September 21, 1965–December 20, 1965. Lessmann, G. G.; Stoner, D. R. (Westinghouse Electric Corp., Pittsburgh, Pa. Astronuclear Lab.). Contract NAS3-2540. 25p. (NASA-CR-54975).

Long-time high-temperature aging studies conducted in ultra-high vacuum furnaces operating at approximately 10^{-10} torr pressure were initiated. Aging temperatures range from 1500 to 2400°F, while selected aging times extend to 10,000 hr. Base metal, TIG welds, and electron beam welds are included. All specimens were machined to final test configuration prior to aging to avoid accidental machining losses after the considerable investment of time and effort accrued during aging. 2700 bend specimens and 610 tensile specimens were prepared, inspected, and post weld annealed for the aging studies. The first phase of the oxygen contamination program was completed and all results except tensile test data are available. The weld restraint patch tests were completed and no tendency toward hot or cold cracking was observed as the oxygen content was increased. (W.L.G.)

29714 (WANL-TME-1031) PROPERTIES OF P-03 GRAPHITE. Kachur, V. (Westinghouse Electric Corp., [Pittsburgh, Pa.] Astronuclear Lab.). Jan. 12, 1965. Contract SNP-1. 82p. Dep. mn. CFSTI $3.00 cy, $0.75 mn.

P-03 graphite, a premium fine-grained material, was evaluated for NERVA reactor hardware. This grade is available both as regularly molded stock with a well-established fabrication technology and as semicommercial isostatically molded stock. Both versions of P-03 have a high and relatively uniform density in the 1.85 ± 0.03 g/cc range. The mechanical properties, are very promising for structural applications. Youngs modulus is in the $1.5-2 \times 10^6$ psi range. The thermal expansion coefficient, averaged between room temperature and 800°C, is between 2.3 and 3.3 microinches per inch per °F; for all types of P-03 at higher temperatures the coefficient increases to a somewhat greater value. Electrical resistivity was also determined; it shows good correlation with flexure strength. P-03 has a fine grained microstructure; the pores between coke particles are small in comparison with those of most other premium graphites. The large-scale structure is essentially free of such defects as cracks, voids, and inclusions. (auth)

29715 (WANL-TME-1287) THE EFFECT OF HYDROGEN AND TEMPERATURE ON MECHANICAL PROPERTIES OF THE Ti-5Al-2.5Sn ELI ALLOY. Nadler, R. A. (Westinghouse Electric Corp., [Pittsburgh, Pa.] Astronuclear Lab.). Sept. 1965. Contract SNP-1. 35p. Dep. mn. CFSTI $2.00 cy, $0.50 mn.

The effects of hydrogen content on the mechanical properties of the Ti-5Al-2.5Sn ELI alloy were investigated in the temperature range −320 to +200°F. In addition, the absorption of hydrogen by the alloy was studied to determine safe operating limits for the 0.020-inch thick core band. The data show that Ti-5Al-2.5Sn ELI can tolerate 300 ppM hydrogen at all temperatures investigated. It was established that the core band can safely be heated in hydrogen to 750°F for 3 hours and to 650°F for at least 5 hours during decay heating in NERVA reactors. The effects of pressure and radiation on the absorption of hydrogen during reactor operation were judged to be negligible. (auth)

29716 (WAPD-T-1819) SOME OBSERVATIONS ON ZIRCONIUM AND ITS ALLOYS BY TRANSMISSION ELECTRON MICROSCOPY. Katz, O. M. (Bettis Atomic Power Lab., West Mifflin, Pa.). Apr. 1966. Contract AT(11-1)-Gen-14. 64p. (CONF-650819-2). Dep. mn. CFSTI $3.00 cy, $0.75 mn.

From American Electron Microscopy Society, 23rd Annual Meeting, New York.

Structures obtained by cold-working Zr sheet and annealing Zircaloy-4 tubes are discussed. The most prominent slip mode is $\{10\bar{1}0\}\langle 11\bar{2}0\rangle$ even though some evidence of slip on $\{10\bar{1}1\}$ was found. Twinning on the $\{10\bar{1}2\}$ planes was observed. In the first stages of cold working, a subgrain boundary network is formed where the density of dislocations in the boundaries increases. For heavily worked material, the dislocations form dense tangled bands which in some areas form a cell structure. In Zircaloy-4 the intermetallic precipitates anchor the dislocations, increasing the strength. Upon recovery, there is a sharpening of subgrain boundaries and dislocation walls, and some reorientation seems to have started. (auth)

29717 SYSTEMS RHENIUM–ARSENIC, RHENIUM–ANTIMONY, RHENIUM–BISMUTH, RHENIUM–TELLURIUM, AND NIOBIUM–ANTIMONY–TELLURIUM. Furuseth, Sigrid; Kjekshus, Arne (Oslo Univ.). Acta Chem. Scand., 20: 245-50(1966).

Phase relationships in the systems Re−As, Re−Sb, Re−Bi, Re−Te, and Nb−Sb−Te were studied by means of x-ray diffraction, density, and magnetic susceptibility measurements. The structure type, lattice dimensions, and observed densities of the observed intermediate phases are: for Re_3As_7 Ir_3Ge_7-type, a = 8.7162 ± 0.0007 Å and d_{pycn} = 10.77 g cm^{-3}; for $ReTe_2$ a = 12.987 ± 0.007, b = 13.055 ± 0.006, and c = 14.271 ± 0.008 Å; and d_{pycn} = 8.50 g cm^{-3}; for $Nb_3(Sb,Te)_7$ Ir_3Ge_7-type, a = 9.8155 ± 0.0008 Å, and d_{pycn} = 8.16 g cm^{-3}. Re_3As_7, $ReTe_2$, and $Nb_3(Sb,Te)_7$ have diamagnetic susceptibilities. (auth)

29718 CRYSTAL STRUCTURE OF Eu_6O_4. Rau, Robert C. (General Electric Co., Cincinnati). Contract AT(40-1)-2847. Acta Crystallogr., 20: 716-23(June 10, 1966).

The crystal structure of trieuropium tetroxide, Eu_3O_4, was determined from single-crystal x-ray diffraction data. This compound, containing both divalent and trivalent europium ions, is isomorphous with $CaFe_2O_4$. It crystallizes in the orthorhombic system, space group Pnam. The unit cell has dimensions a = 10.085, b = 12.054, and c = 3.502 Å, and contains four formula units. The structure is layered along the short c axis, with all atoms on mirror planes at $z = 1/4$ and $z = 3/4$. Least-squares refinement of x and y positional parameters and isotropic temperature factors was based on 955 observed independent hk0 and hk1 reflections, and established the structure with a final R of 0.089. The coordination of oxygens around trivalent europium is sixfold, forming a distorted octahedron around each Eu^{3+} ion. Around divalent europium the coordination is eightfold, with each Eu^{2+} ion lying at the center of a triangular prism of six oxygen atoms. Two oxygen atoms lying out from the centers of two of the prism faces complete the coordination. (auth)

29719 CRYSTALLOGRAPHIC DATA FOR CERIUM–ZINC COMPOUNDS. Lott, Bryan G.; Chiotti, Premo (Ames Lab., Ames, Iowa). Acta Crystallogr., 20: 733-8 (June 10, 1966). (IS-1151).

Nine compounds were identified in the cerium-zinc system. The x-ray data obtained for CeZn and $CeZn_{11}$ were consistent with previously reported structures. The compound $CeZn_5$ is shown to be isostructural with $CaCu_5$ as previously reported but the lattice constants a = 5.4163 to 5.4069 Å and c = 4.2647 to 4.2757 Å, which correspond to the composition range $CeZn_{5.36}$ to $CeZn_{5.10}$, respectively, are significantly different. The unit cells and diffraction symmetries for all the remaining compounds except $CeZn_7$ were determined. Orthorhombic $CeZn_2$, a = 4.63, b = 7.54, c = 7.50 Å, is isostructural with $CeCu_2$. $CeZn_3$ and Ce_3Zn_{11}

are also orthorhombic with a = 4.62, b = 10.43, and c = 6.64 Å for $CeZn_3$ and a = 4.5215, b = 8.8855, and c = 13.463 Å for Ce_2Zn_{11}. $CeZn_{4.5}$ is hexagonal with a = 14.60, c = 14.11 Å. Ce_2Zn_{17} is shown to be isostructural with U_2Zn_{17}, space group R3m. Only x-ray data on powdered specimens of $CeZn_7$ were obtained. (auth)

29720 EVALUATION OF PHASES FOR STRUCTURE DETERMINATION BY NEUTRON DIFFRACTION. Karle, J. (Naval Research Lab., Washington, D. C.). Acta Crystallogr., 20: 881-6(June 10, 1966).

The formulas for phase determination often used for x-ray diffraction data are not immediately applicable to neutron diffraction data when atoms with both positive and negative scattering factors are present. A formula is presented from which normalized structure factors for the squared structure may be calculated from the normalized scattering data, as obtained from a neutron diffraction experiment. Since the squared structure is defined as the structure that scatters with the square of the scattering factor for each atom in the original structure, the computed structure factors for the squared structure always represent a positive structure and the formulas for phase determination used for x-ray data are applicable. Test calculations are presented. (auth)

29721 NOTE ON THE NINE-LAYER HEXAGONAL STRUCTURE OF YAl_3. Dagerhamn, T.; Westman, S. (Univ. of Stockholm). Acta Crystallogr., 20: 919-20 (June 10, 1966).

An investigation of an alloy prepared from components weighed out to correspond to the composition $YAl_{3.00}$ gave a = 6.195 and c = 21.129 Å with c/a = 3.411, from x-ray Guinier powder photograph data. Each layer was found to have the composition YAl_3, and the layer sequence was ... ABABCBCAC .... The space group is $R\bar{3}m$ with 36 atoms per hexagonal unit cell. The coordination of Al around Y(1) is quite regular and all 12 Y–Al distances are 3.10Å. The mean Y(2)–Al distance is 3.07Å. (M.C.G.)

29722 TABLE OF THE REAL PART OF THE DISPERSION CORRECTION FOR X-RAY SCATTERING. Saravia, Luis R.; Caticha-Ellis, S. (Instituto de Fisica, Montevideo). Acta Crystallogr., 20: 927-30(June 10, 1966).

A method was previously described (Acta Crystallogr., 15: 863(1962)) using the real part of the dispersion correction $\Delta f'$ in the x-ray atomic scattering factor for the solution of centrosymmetric crystal structures. A table is presented that includes the value of $\Delta f'$ for elements between Z = 20 and Z = 83 for 32 different Kα wavelengths ranging from 0.435 to 2.750 Å. (M.C.G.)

29723 LOW-TEMPERATURE ELECTRICAL RESISTIVITY OF LATTICE DEFECTS IN DEFORMED TUNGSTEN SINGLE CRYSTALS. Shukovsky, H. B.; Rose, R. M.; Wulff, J. (Massachusetts Inst. of Tech., Cambridge). Acta Met., 14: 821-30(July 1966).

The generation of vacancies and dislocations during plastic deformation of tungsten single crystals was studied using electrical resistivity measurements at low temperatures. An etch pit technique was used to determine the dislocation density N_D as a function of strain. The dislocation resistivity at low temperatures is found to obey the following relation: $\partial\rho_D/\partial N_D = 6.7 \times 10^{-11}\ \mu\Omega\text{-cm}^3$. The density of dislocations produced was found to be proportional to $\epsilon^{1.3}$ and also to the work done per unit volume in deforming the crystal $\int_0^{\epsilon_T}\sigma_T d\epsilon_T$ where σ_T and ϵ_T are the true stress and true strain respectively. The vacancy resistivity was found to vary as $\epsilon^{0.9}$ for strains of less than 2% and as $\epsilon^{1.9}$ between 2 and 8%. At higher strains the vacancy resistivity increases less strongly with increasing strain. The vacancy resistivity, and hence the vacancy concentration variation with strain, is consistent with both the moving jog and dislocation dipole recombination mechanisms of vacancy production if one considers the energy balance, fixed barrier, and growing barrier models. The temperature variation of the ideal resistivity of a typical unstrained crystal is in agreement with Berthel who reports a T^5 dependence for tungsten. (auth)

29724 INVESTIGATION OF THE MECHANISM OF THERMALLY ACTIVATED DEFORMATION IN TANTALUM AND TANTALUM-BASE ALLOYS. Arsenault, R. J. (Oak Ridge National Lab., Tenn.). Acta Met., 14: 831-8 (July 1966). (ORNL-P-1464).

The activation energy and activation volume of tantalum and tantalum-base solid-solution alloys were obtained from both constant stress (creep) tests and constant strain rate (tensile or compression) tests. These parameters were investigated as a function of stress, temperature, and interstitial concentration. The agreement between the activation parameters obtained from creep and tensile or compression tests supports many assumptions that have been made in the past about the differential technique. The functional dependence of the activation energy with changes in modulus (produced by an alloying element) is in agreement with that predicted from calculations of the energy of formation of a double kink over the Peierls' stress barriers. Electron-transmission micrographs show a predominance of screw dislocations in samples deformed at large effective stresses. This observation is explained in terms of a larger Peierls' stress of the screw dislocations. It is concluded that experimental results support the double-kink mechanism as the rate-controlling mechanism of low-temperature deformation in bcc metals. (auth)

29725 OBSERVATIONS OF DISLOCATIONS IN HIGH-ANGLE BOUNDARIES IN TUNGSTEN. Ryan, H. F.; Suiter, J. (CSIRO, Melbourne. Univ. of Melbourne). Acta Met., 14: 847-51(July 1966).

Field ion microscope observations of low angle twist boundaries in tungsten have enabled particular features in the micrographs to be identified with dislocations which constitute the boundary and are largely screw in character. Comparison with micrographs of high angle tilt boundaries in the same material shows that isolated dislocations of the same type are frequently present in such boundaries also. The direction of the dislocation line is very nearly [011] with an associated shear vector component of (a/2) [011]. (auth)

29726 THE ORIENTATION RELATIONSHIP AND GROWTH DIRECTION OF Mo_2C IN FERRITE. Dyson, D. J. (United Steel Co. Ltd., Rotherham, Eng.); Keown, S. R.; Raynor, D.; Whiteman, J. A. Acta Met., 14: 867-75(July 1966).

Thin foil electron microscopy and electron diffraction have enabled the Mo_2C/ferrite orientation relationship to be determined. Trace analysis has shown that the growth direction of Mo_2C is along [10.0] ≡ [11.0] which is parallel to $[100]_\alpha$. This direction is consistent with those determined from an analysis of the streaked Mo_2C reflections occurring from small precipitates, and is in good agreement with lattice misfit calculations. (auth)

29727 NEW CLASS OF HYPEREUTECTIC CARBIDE COMPOSITES. Kendall, E. G.; Slaughter, J. I.; Riley, W. C. (Aerospace Corp., El Segundo, Calif.). AIAA (Amer. Inst. Aeron. Astronaut.) J., 4: 900-5(May 1966).

Extremely high thermal shock resistance in the Group IV-A carbides (TiC, ZrC, HfC) has been achieved by the fabrication of carbide-graphite composites using vacuum arc melting and casting techniques. High purity materials were employed to ensure a low interstitial content. Gravity and skull casting have been employed to produce test shapes. The eutectic composition between the monocarbide and terminal graphite phase has been defined in each system. When carbon content exceeds the eutectic composition, the excess precipitates from the liquid as platelets within the eutectic matrix. Mechanical properties have been determined at room temperature on Ti–C and Zr–C materials. A sharp demarcation has been noted at the eutectic point where, in the Ti–C system, compressive strengths of 240,000 psi for hypoeutectic material decrease to 30,000 psi for hypereutectic material. Similarly, flexure strength drops from 30,000 to 10,000 psi. Thermal shock resistance was evaluated in both 200-kw and 5-Mw air arc tunnels at heating rates of 700, 1800, and 2400 Btu/ft^2/sec. No evidence of failure was noted in hypereutectic materials

within any of the three systems. In comparative testing with tungsten and graphite, HfC-C showed marked superiority by exhibiting no measurable recession whatsoever when exposed to a heat flux of 700 Btu/ft^2/sec. (auth)

29728 MODIFICATIONS OF NIOBIUM PENTOXIDE. Schaefer, Harald; Gruehn, R.; Schulte, F. (Univ., Muenster, Ger.). Angew. Chem. Int. Ed. Engl., 5: 40-52 (Jan. 1966).

The designation and characterization of the modifications (forms) of niobium pentoxide, their modes of formation, chemical and physical properties, structures, and thermal and thermochemical behavior are discussed. Crystal photographs of the T-, B-, H-, M-, N-, and P-forms of Nb_2O_5 are shown. Niobium pentoxide can be obtained in many different ways. If the solid oxide is heated at temperatures above 1000 to 1200°C, the H-form, which is stable under these conditions, is always produced. The forms of Nb_2O_5 prepared at lower temperatures are mostly metastable. The stoichiometric O/Nb ratio of 2.5 can be achieved by the combination of various octahedral linkages, and this is the reason for the multiplicity of the Nb_2O_5 structures. A discussion of the Nb_2O_5 structures from idealized geometrical points of view provides information on the possible structure variants and on relation between them. The absolute value of the enthalpy of formation of the Nb_2O_5 modifications decreases in the sequence B > T > H, while the molar volume increases in that sequence. Studies of the thermal and thermochemical behavior of the oxides showed that the thermal transformations observed depend on the history of the preparations. The conversions take place monotropically, and the transition temperatures are therefore due to kinetics. Observations made support the assumption that of all the forms, B-Nb_2O_5 has the highest absolute value of the enthalpy of formation. Consequently, B-Nb_2O_5 is thermodynamically stable at low temperatures. The conversion B → H can be observed at 750°C, while the reverse conversion is realized at 650°C. If the mean (700°C) is taken to be the equilibrium temperature, and if, in addition, an enthalpy of transformation of 2 kcal/mole is assumed for the B → H transformation the entropy increase is 2 cal. The increase in entropy can be understood on the basis of the structure. (BBB)

29729 THERMODYNAMIC OBSERVATIONS ON REACTIONS OF HIGH-MELTING CARBIDES IN THE TEMPERATURE REGION OF 2000 DEG C. Eberle, L.; Nixdorf, J.; Poeschel, E.; Rochow, H. (Battelle-Instituts e.V., Frankfurt am Main). Ber. Deut. Keram. Ges., 43: 146-61(Feb. 1966). (In German).

The criteria for the selection of materials for thermionic convertors is discussed. In view of the high service temperatures employed, the materials must be stable at high temperatures. The materials considered were the carbides of the elements of the 4th to 7th subgroup of the Periodic Table and the high-melting metals: Nb, Ta, Mo, W, Re, and Ir. There should be no reactions between these materials at service temperatures. Thermodynamic calculations and estimations give a rough guide in the choice of suitable material combinations. Evaporation and diffusion processes are discussed. (auth)

29730 TIME FACTOR IN THE GRAPHITE COATING PROCESS. Wege, E. (Ringsdorff-Werke GmbH, Bad Godesberg, Ger.). Ber. Deut. Keram. Ges., 43: 224-30 (Mar. 1966). (In German).

In the graphite coating process the apparent density, the bending strength, the electrical resistivity, and the separation of planes of stratification quickly tend to limiting values. The determining factor is the temperature. The limiting value of the strength is independent of the temperature above about 2300°C, but the other factors decrease with increasing temperature. While the structure of the intercrystalline phase is built up at relatively low temperatures, the crystalline ordering process requires higher temperatures. The electrical resistivity of the graphite particles is directly dependent on the degree of ordering and on the size of the crystallites, and is well suited to the determination of the state of the graphite coating. The logarithms of the ash and element contents of the carbon particles decrease in proportion to the square root of the coating time in the graphite coating process. Under the same conditions after equal times the ratio of instantaneous ash content to initial ash content is constant. At concentrations <5 to 10 ppM the rate of diffusion decreases more rapidly. (auth)

29731 EFFECT OF SURFACE EVAPORATION ON DIFFUSION MEASURED BY ISOTOPIC EXCHANGE REACTIONS. Dawson, D. K.; Barr, L. W.; Pitt-Pladdy, R. A. (Atomic Energy Research Establishment, Harwell, Eng.). Brit. J. Appl. Phys., 17: 657-62(May 1966).

The influence of evaporation on measurements of diffusion by the heterogeneous isotopic exchange technique was examined. A standard solution for diffusion involving moving boundaries was adapted and used to analyze the results. The measurements on bromine diffusion in potassium bromide show that evaporation of the crystal influences the diffusion measurements at surprisingly low temperatures. This conclusion also seems to apply to many of the reported isotopic exchange measurements and to measurements of fission gas diffusion made by the gas release method. Based on this study a criterion is suggested to decide when the solution with evaporation should be applied. It is further shown that if there is appreciable evaporation it is not in general correct to use the method of measuring diffusion coefficients on one specimen at successive temperatures. For this procedure to be used the velocity of evaporation and the diffusion coefficient must have the same temperature dependence. (auth)

29732 FUTURE OF REFRACTORY CERAMICS IN THE NUCLEAR FIELD. Houyvet, A. (Commissariat a l'Energie Atomique, Paris). Bull. Soc. Franc. Ceram., No. 64, 21-6(July-Sept. 1964). (In French).

Increasing use of refractory ceramic materials is discussed in terms of developments in the nuclear industry, which involve an increase in the operating temperatures of reactors. The materials used must therefore be increasingly refractory and various ceramic products are important. These applications are considered under the following headings: for fuels, uranium oxide and uranium carbide; for control materials and a large capture cross section, boron carbide and rare earth oxides; and for thermal insulators, pure oxides, which are of low absorbance in reactors, and heat-resistant insulating materials, which protect the large structures. The various forms of uranium oxides and carbides that are combined with ceramic materials are considered, along with special problems involved with each form. Ceramic materials required for nuclear reactor technology must be of high purity and the tolerance imposed on them in some instances is very precise. (BBB)

29733 STRUCTURAL STUDIES ON THE v.u.v./CO_2 OXIDATION OF GRAPHITE. Adamson, I. Y. R. (Glasgow Univ.); Dawson, I. M.; Feates, F. S.; Sach, R. S. Carbon, 3: 393-6(Feb. 1966).

A study was made on the changes that occur in the visible structure of graphite on exposure to vacuum ultraviolet irradiated carbon dioxide. Electron micrographs illustrate the main pattern of the oxidation process both in pure carbon dioxide and also with admixtures of small percentage of methane, carbon monoxide, or ketene. Oxidation is clearly visible and leads to removal of graphitic carbon from prismatic faces of the sample and from vacancy or impurity sites on the graphite surface. Deposition of an amorphous particulate material was also visible on the graphite surfaces, which in samples irradiated in pure CO_2 was less than that observed in the presence of 0.1% methane or 1% carbon monoxide. With the addition of 1% ketene neither gasification nor deposition was observed. These results are discussed in terms of the known structure and defect structure of graphite. (auth)

29734 THERMAL CREEP AND INELASTIC BEHAVIOR OF ARTIFICIAL GRAPHITE. Rappeneau, J.; Jouquet, G.; Guimard, M. (Centre d'Etudes Nucleaires, Saclay, France). Carbon, 3: 407-20(Feb. 1966). (In French).

The elastic moduli of French nuclear graphite were de-

termined from dynamic and static tests, and satisfactory agreement was obtained between the different methods of measurement. Analysis of the stress-strain curves under simple compression at room temperature confirmed the validity of the equations proposed by others. A probable effect of the stress rate on the magnitude of the strain was observed. Experiments on thermal creep, under simple compression in air at temperatures below 350°C and for periods of about 200 hr, led to the following empirical equation connecting the creep strain ϵ_c to time t: $\epsilon_c = \gamma \log t + \beta t^{\frac{1}{3}}$. The coefficient γ decreased when the apparent density of the graphite increased, and increased with the load and temperature. The secondary creep coefficient β appeared to be an increasing function of these three variables. (auth)

29735 DEFORMATION OF GRAPHITE LATTICES BY INTERSTITIAL CARBON ATOMS. Coulson, C. A. (Mathematical Inst., Oxford); Senent, S.; Herraez, M. A.; Leal, M.; Santos, E. Carbon, 3: 445-57(Feb. 1966).

Calculations were made of the self-energy of an interstitial carbon atom placed between the layers of an otherwise perfect graphite crystal. The position of minimum energy was confirmed to be directly above an atom in the one plane, and centrally placed below three atoms in the other plane. It is essential to allow for deformation of the layers up to two on each side of the interstitial. The maximum displacement of an atom near to the interstitial was about 0.6 Å. The most uncertain feature of the analysis was the form of the carbon–carbon repulsion potential. Various alternatives were compared, and the choice of a function due to Crowell was made. With this function the self-energy of an interstitial (i.e. energy difference between the interstitial situation and a perfect lattice with the extra atoms carefully removed) was about 2.32 ev, of which about 0.12 ev came from the deformation of second neighbor planes. The migration energy of an interstitial was estimated to be about 0.14 ev, and comparison was made with available experimental measurements. (auth)

29736 DEFORMATION AND FRACTURE OF PYROLYTIC CARBONS DEPOSITED IN A FLUIDIZED BED. Bokros, J. C. Price, R. J. (General Atomic Div, General Dynamics Corp., San Diego). Carbon, 3: 503-19(Feb. 1966).

The mechanical properties of pyrolytic carbon formed by the pyrolysis of hydrocarbon gas in a fluidized bed as related to structure, which in turn depends on the deposition conditions and subsequent heat treatment, were investigated. Carbons deposited from methane between 1350 and 1925°C were characterized according to their density, degree of preferred orientation, apparent crystallite size, and micrographic appearance (laminar, isotropic, or granular). Stress-strain fracture curves were obtained from room-temperature three-point bend tests on planar samples and the mode of fracture was investigated by optical microscopy and electron microfractography. Both the elastic modulus and the fracture stress decreased in progressing from laminar to isotropic to granular structures, whereas the fracture strain was highest in the isotropic deposits. Annealing at temperatures between 1700 and 2800°C was found to change greatly the properties of only the high-density laminar structures deposited from high methane concentrations, where the elastic modulus and fracture stress were reduced by annealing. The mechanical properties of the various carbons are discussed in terms of their structure. (auth)

29737 REVIEW OF DIFFUSION PROCESSES IN ZIRCONIUM AND ITS ALLOYS. Kidson, G. V. (Atomic Energy of Canada Ltd., Chalk River, Ont.). Electrochem. Technol., 4: 193-205(May-June 1966).

The results of self-diffusion and solute diffusion measurements in both the hcp and the bcc phases of zirconium and its alloys are critically reviewed. Those from the low-temperature hcp studies are relatively difficult to obtain, generally lack reproducibility, and are correspondingly inconclusive. Measurements in the bcc phase are more consistent and exhibit an unusual temperature dependence of the activation energies and frequency factors. Some theoretical models proposed to account for this are examined. (auth)

29738 PROPERTIES OF OBJECTS PRODUCED FROM LANTHANUM AND YTTRIUM HEXABORIDES BY SINTERING IN VACUUM. Meerson, G. A.; Manelis, R. M.; Telyukova, T. M. Izv. Akad. Nauk SSSR, Neorg. Mater., 2: 291-8(1966). (In Russian).

Previous literature data indicated that objects made of lanthanum boride sintered in a hydrogen atmosphere have a porosity of up to 8%, and with sintering in vacuum not less than 30%. Test samples were made of lanthanum boride and yttrium boride powders. Results of the pressing operation on these powders are exhibited in a series of curves and tables, as well as in microphotographs. Contrary to previously published data, the possibility of producing mechanically strong and sufficiently dense objects from lanthanum hexaboride (σ_{bend} equal to 960 kg/cm²) and yttrium hexaboride (σ_{bend} equal to 400 kg/cm²) by sintering previously pressed billets in a vacuum was demonstrated. The porosity of objects made of lanthanum hexaboride is of the order of 18 to 20%, and from yttrium hexaboride it is 30%. The objects permit polishing, electric sparking, and ultrasonic treatment without destruction. It was established that, with sintering under identical conditions, samples of lanthanum hexaboride obtained by reduction of lanthanum oxide with boron carbide have slightly less shrinkage and less density and strength than analogous samples made of lanthanum hexaboride produced by reduction of lanthanum oxide with boron. (ATD)

29739 CHANGES IN ELECTRIC CONDUCTIVITY AND RATE OF CREEP OF SINTERED CeO_2 CERAMIC DURING ITS REDUCTION. Poluboyarinov, D. N.; Shapiro, E. Ya.; Bakunov, V. S.; Akopov, F. A. (Chemico-technological Inst., Moscow). Izv. Akad. Nauk SSSR, Neorg. Mater., 2: 336-42(1966). (In Russian).

Investigations were carried out on samples prepared from cerium dioxide with a content of the base component of 99.7%. The main impurities were oxides of the rare earth elements. The cerium dioxide was ground in a steel mill by the "wet" method for 30 hours with subsequent purification from iron. Samples for determination of the rate of creep were in the form of small beams, and for determination of the electric conductivity in the form of disks. Calcining was done in an oxidizing atmosphere at 1500°C. The electric conductivity was determined in air over the temperature interval from 20 to 1100°C. The creep rate was determined in air and in an inert gas medium by measurement of the bending deformation of the sample with loading at four points. The experimental results are shown in a series of curves. It was found that during reduction, the properties of cerium dioxide ceramic change in a regular manner. The activation energy fell from 23 to 10 kcal/mole for electric conductivity, and from 92 to 39 kcal/mole for creep in the reduction of $CeO_{2.00}$ to $CeO_{1.90}$. The electric conductivity of CeO_2 was basically electronic. With reduction of CeO_2 to $CeO_{1.95}$ the mobility of the electrons increased by five orders of magnitude, and with further reduction to $CeO_{1.90}$ by another order of magnitude. Creep of stoichiometric CeO_2 was due to various factors but, according to the degree of reduction, the limiting factor was the process of diffusion voids. The diffusion coefficient for the oxygen ion in the reduction of $CeO_{2.00}$ to $CeO_{1.90}$ changed by one order of magnitude. (ATD)

29740 STRENGTH OF CERAMICS MADE OF PURE OXIDES. Matveev, M. A.; Matveev, G. M.; Kharitonov, F. Ya. (Chemico-Technological Inst., Moscow). Izv. Akad. Nauk SSSR, Neorg. Mater., 2: 395-402(1966). (In Russian).

Practical applications of the relationship between the thermal and mechanical characteristics of ceramic materials are discussed. The structural, mechanical, and thermophysical properties of a large number of ceramics made of pure highly refractory oxides are presented. The comparatively low strength of industrial ceramic materi-

als is due to the nonuniformity of their structure, the presence of nonuniformly distributed imperfect crystalline structures (dislocations, voids, foreign atoms) and grain boundaries, and to industrial defects (pores, chemical nonhomogeneity, etc.). This leads to a drop in the energy capacity of ceramics as a result of the nonhomogeneous character of the absorption of energy by different volumetric materials. From a comparison of the strength of monocrystalline oxides and monocrystalline aggregates of these oxides, it was found that the greater the strength of the bonds of the crystalline lattice, the greater the divergence between the strength of a single crystal and that of the oxide in the polycrystalline state. This permits the conclusion that the relative effect of the structural factor on strength decreases with a decrease in the specific energy capacity of the material. The optimum structural state of a given material is a structure that will assure the greatest uniformity in the absorption of energy by the crystalline lattice in the process of deformation of the ceramic material. (ATD)

29741 ROOM-TEMPERATURE THERMAL CONDUCTIVITY OF THE RARE-EARTH METALS GADOLINIUM, TERBIUM, AND DYSPROSIUM. Powell, R. W. (Purdue Univ., West Lafayette, Ind.). J. Appl. Phys., 37: 2518-19 (May 1966).

Previous research on the room-temperature conductivity of the rare-earth metals gadolinium, terbium, and dysprosium by Gallo (J. Appl. Phys., 36, 3410 (1965)) is discussed. A note added in proof from work by Powell and Jolliffe (Phys. Letters 14, 171 (1965)) is considered. It is suggested that the lower values given remove the need for any additional mechanism such as a bipolar thermal conductivity, at least on the basis of Gallo's analysis. This is shown by the tabulated data. (J.F.P.)

29742 MEASUREMENT OF DENSITIES AND ESTIMATION OF CRITICAL PROPERTIES OF THE ALKALI METALS. Dillon, I. G.; Nelson, P. A.; Swanson, B. S. (Argonne National Lab., Ill.). Contract W-31-109-eng-38. J. Chem. Phys., 44: 4229-38(June 1, 1966).

The vapor and liquid densities of the alkali metals rubidium, cesium, sodium, and potassium were measured from room temperature up to near the critical point by a method that utilizes radioactive isotopes of the alkali metals. Critical temperature and critical density were then estimated by several methods of correlation including those of Rowlinson, Cailletet and Mathias, and Kordes, and by a generalized correlation of reduced density versus reduced temperature. Critical temperatures of the alkali metals estimated by these correlating methods were as follows: 2573 ± 350°K for sodium, 2223 ± 600°K for potassium, 2093 ± 25°K for rubidium, and 2057 ± 40°K for cesium. Corresponding critical densities were: 0.206 ± 0.041 g/cc for sodium, 0.194 ± 0.37 g/cc for potassium, 0.346 ± 0.009 g/cc for rubidium, and 0.428 ± 0.012 g/cc for cesium. The critical temperature and critical density of lithium were estimated using the liquid-density data for lithium reported by Tepper and the generalized correlation of reduced density with reduced temperature. The estimated critical temperature of lithium was 3223 ± 600°K and the estimated critical density 0.120 ± 0.033 g/cc. The technique used in these measurements involved charging a metal capsule (molybdenum or molybdenum–tungsten alloy) with a calculated amount of alkali metal, sealing the capsule, and irradiating it in a thermal neutron flux to obtain a radioactive isotope of the metal being tested. The irradiated capsule was then placed in an insulated inductively heated high-temperature cell made of molybdenum–tungsten alloy. Gamma radiation emanating from the vapor and liquid regions in the capsule passed through the thin capsule wall (30 mil) and telescoping holes in the high-temperature cell to a sodium iodide crystal outside the furnace. The measured radiation was proportional to the density of the vapor or liquid. While this method of measurement was demonstrated on alkali metals, the technique is general and can be applied in many cases to measure vapor and liquid densities at high temperatures (up to 220°K) for metals, alloys, fused salts, and other materials. (auth)

29743 HIGH-TEMPERATURE HEAT CONTENTS AND RELATED THERMODYNAMIC FUNCTIONS OF EIGHT RARE-EARTH METALS: Sc, Gd, Tb, Dy, Ho, Er, Tm, AND Lu. Dennison, D. H.; Gschneidner, K. A. Jr.; Daane, A. H. (Ames Lab., Ames, Iowa). J. Chem. Phys., 44: 4273-82(June 1, 1966).

The high-temperature heat contents of scandium, gadolinium, terbium, dysprosium, holmium, erbium, thulium, and lutetium were measured from 0°C to at least the melting points of these metals. The specific heats, heats of transition, heats of fusion, and related thermodynamic functions were calculated. The smoothed values of $H_T^0 - H_{298.15}^0$, $(H_T^0 - H_{298.15}^0)/T$, S_T^0, and $-(F_T^0 - H_{298.15}^0)/T$ were tabulated at 100°C intervals. An examination of the entropies of transition and fusion of all of the measured rare earth metals showed that the entropy of the fcc (or hcp ⇌ bcc transition depends on the number of valence electrons and the entropy of fusion decreases with increasing rare earth size. The electronic dependence of the entropy of transformation was also observed to hold for other metals undergoing similar transformations. (auth)

29744 ON THE BONDING ENERGY IN CESIUM–GRAPHITE COMPOUNDS. Salzano, F. J.; Aronson, S. (Brookhaven National Lab., Upton, N. Y.). J. Chem. Phys., 44: 4320-6(June 1, 1966). (BNL–9768).

A model is proposed for the bonding of cesium in the cesium–graphite lamellar compounds. The model assumes that the compounds consist of layers of cesium ions situated between metal-like sheets corresponding to the graphitic layer planes. The bonding energy of the cesium to the graphite layers results from the electrostatic interaction of the cesium ions with the metal-like sheets and can be calculated by means of image-force theory. An independent value for the bonding energy was also derived from thermodynamic data on the basis of a semiempirical reaction mechanism. This mechanism resolves the heats of formation into three elementary energy parameters; the bonding energy of cesium to the adjacent graphitic layer planes; the energy to separate graphitic layer planes; and the energy of interaction of the cesium ions with neighboring layers of cesium ions. The values of the bonding energy of cesium obtained by the two methods are in good agreement. The energy to separate graphitic layer planes is compared to values obtained in other studies. (auth)

29745 PROPERTIES OF ANODIC FILMS FORMED ON REACTIVELY SPUTTERED TANTALUM. Gerstenberg, D. (Bell Telephone Labs., Inc., Murray Hill, N. J.). J. Electrochem. Soc., 113: 542-7(June 1966).

The technique of reactive sputtering was used for producing tantalum films with various concentrations of interstitial additives like oxygen, carbon, nitrogen, and hydrogen. A number of compounds between tantalum and these nonmetallic elements were also deposited. The dielectric properties of anodic films on the tantalum formed in an aqueous solution of citric acid were related to the composition of the tantalum. It was found that the capacitance density of 130v anodic films remains unaffected by the presence of oxygen and hydrogen, while it decreases as the atomic concentration of nitrogen and carbon in the tantalum increases. The dielectric constant, ϵ, of anodic films on Ta_2N is approximately 50% of the value of anodic Ta_2O_5 formed on pure tantalum. (auth)

29746 SEGREGATION COEFFICIENTS OF SOME RARE EARTH NIOBATES IN $SrMoO_4$. Brixner, L. H. (E. I. du Pont de Nemours and Co., Inc., Wilmington, Del.). J. Electrochem. Soc., 113: 621-3(June 1966).

Some relations between the ionic radii and the segregation coefficients for the $LnNbO_4$-type rare earth niobates in $SrMoO_4$ are shown. The segregation coefficient varied directly with the deviation of the rare earth ion size from that of Sr^{2+}. No crack-free crystals could be grown for the cases of cation size differences of around 15%. (M.C.G.)

29747 PEARLITE REACTION IN SOME URANIUM–CHROMIUM ALLOYS. Bar-Or, A. (Israel Atomic Energy Commission, Tel-Aviv). J. Inst. Metals, 94: 214-17 (June 1966).

Characteristic needles of chromium were found following the $\beta \rightarrow \alpha$ transformation in uranium–chromium alloys made from electrolytic pure uranium (E.P.U.), at temperatures in the upper α range. The fact that no similar needles were present in alloys containing chromium made from nuclear pure uranium (N.P.U.) is ascribed to the higher carbon content of the latter. The growth rate (G) of the eutectoid decomposition product in a series of chromium-containing E.P.U. alloys and also the dependence of the rate of growth on undercooling and chromium content varied from those found previously from N.P.U. alloys. No clear relationship between growth rate and interspacing of the needles in these alloys could be established, suggesting that the diffusion of chromium does not control growth. The lack of similarity between the rate of growth and the morphology of the chromium precipitate in the two types of alloy is attributed to the difference in the mode of nucleation of chromium, which affects the mechanism of growth of the decomposition product. It is suggested that the factor governing the growth of the eutectoid decomposition product in E.P.U. alloys is the growth of α, which is itself regulated either by a two-dimensional nucleation process, similar to the mechanism suggested previously as controlling the growth of the decomposition product in N.P.U. alloys or by another process in which the interspacing between needles does not play a major part. (auth)

29748 DIFFUSION OF CHROMIUM INTO NICKEL–THORIA ALLOYS. Fleetwood, M. J. (International Nickel Ltd., Birmingham, [Eng.]). J. Inst. Metals, 94: 218-23(June 1966).

Although nickel dispersion-hardened with 5% thoria possesses excellent stress-rupture properties between 1000 and 1200°C, the oxidation-resistance of the nickel–thoria alloys is inadequate above 800°C. The possibility of providing protection by means of a surface layer of an oxidation-resistant material was studied by examination of the behavior of an electrodeposited coating of chromium on a nickel–5% thoria alloy, at various temperatures. Electron-probe, x-ray micro-analysis was used to determine the rate of diffusion of chromium into the alloy and measurements were made of the total quantity of chromium diffused and the changes in surface concentration as a function of time and temperature of diffusion-treatment. In comparison with published data for the diffusion of chromium into nickel–chromium alloys, values of the coefficient of diffusion of chromium into nickel–5% thoria were high and the activation energy of diffusion was low, owing, probably, to the fine particle dispersion and high dislocation density in subgrain boundaries. The rapid diffusion imposed a severe limit upon the efficacy of chromium in protecting nickel–thoria alloys against high-temperature corrosion. The maximum temperature at which a nickel–chromium coating >100μm thick can provide reliable protection against oxidation and sulphidation for 1000 h is ~815°C. (auth)

29749 THE URANIUM–CARBON–NITROGEN SYSTEM. Katsura, Masahiro; Sano, Tadao (Osaka Univ.). J. Nucl. Sci. Technol. (Tokyo), 3: 194-9(May 1966).

In a previous work dealing with the equilibrium phase relations in the ternary system U–C–N a qualitative phase was constructed from thermodynamical calculations and experiments. In the thermodynamical calculations, it was assumed that the free energy of formation of the solid solution between UC and UN, i.e., $UC_{1-x}N_x$, is the sum of $(1-x)\Delta G^0(UC)$, $x\Delta G^0(UN)$ and a term for the entropy of mixing $RT\{x \log x + (1-x)\log(1-x)\}$, neglecting the heat of mixing. The same U–C–N system is considered statistico-thermodynamically, and the heat of mixing is evaluated from the results of several experiments. A value of about −1.3 kcal/mole was obtained as the heat of mixing corresponding to $\{2\varphi(C-N)-\varphi(C-C)-\varphi(N-N)\}N$, where $\varphi(C-N)$, $\varphi(C-C)$ and $\varphi(N-N)$ are the bond energies of C–N, C–C and N–N respectively. (auth)

29750 LORENZ NUMBER OF GRAPHITE AT VERY LOW TEMPERATURES. Holland, M. G.; Klein, C. A.; Straub, W. D. (Raytheon Research Div., Waltham, Mass.). J. Phys. Chem. Solids, 27: 903-6(May 1966).

It is demonstrated that by applying a strong magnetic field the electronic component in the low-temperature thermal conductivity of graphite can be removed, and thus the charge-carrier contribution at any field strength can be deduced unequivocally. Only basal-plane processes are considered. Thus the measurements reported were carried out with a primary charge or heat flow in the layer planes while the magnetic field was in the c-axis direction. Thermal and electric conductivity was measured as a function of temperature from 1.5 to 300°K and are shown. Also shown is the electronic thermal conductivity in the layer-plane direction of highly heat-treated pyrolytic graphite. It is concluded that throughout the liquid-helium temperature range there is a sizeable electronic component in the thermal conductivity of graphite which is related to layer-plane resistivity by the Wiedemann-Franz-Lorenz expression. (J.F.P.)

29751 GALVANOMAGNETIC PROPERTIES OF GRAPHITE AT LOW TEMPERATURES. Sugihara, Ko; Ono, Shusuke (Matsushita Electric Industrial Co., Ltd., Osaka). J. Phys. Soc. Jap., 21: 631-7(Apr. 1966).

A diagonal component of the magnetoconductivity tensor in graphite at 0°K is calculated as a function of magnetic field from 10^4 to 2.50×10^4 gauss by the use of the Slonczewski and Weiss model and the quantum theory of galvanomagnetic phenomena by Adams and Holstein. The Fermi level is calculated in the region of field intensity from 10^4 to 6.4×10^4 gauss. The theory is limited to the case 0°K but it is consistent with the features of the measurement made by Soule, McClure and Smith at 1.26°K qualitatively. The scattering potential used in this study is a quasidelta function with a finite force range of 6°A. For simplicity the trigonal symmetry of the bands (γ_3) is disregarded. (auth)

29752 MAGNETIC PROPERTIES OF RARE EARTH INTERMETALLIC COMPOUNDS IN Gd(Ag,Cd,In) AND Gd(Cu,Ag,Au) SYSTEMS. Sekizawa, Kazuko; Yasukochi, Ko (Nihon Univ., Tokyo). J. Phys. Soc. Jap., 21: 684-92(Apr. 1966).

Rare earth intermetallic compounds in Gd(Ag, Cd, In) and Gd(Cu, Ag, Au) systems are studied. Most of these compounds have the CsCl type of crystal structure. Magnetization measurements are made on these compounds to determine the type of the magnetic order and its relationship to the number of conduction electrons. GdAg, $GdAg_{0.9}In_{0.1}$, $GdAg_{0.2}In_{0.8}$, $GdAg_{0.1}In_{0.9}$, and GdIn in the Gd(Ag, In) system and GdCu, GdAg, $GdAg_{0.7}Au_{0.3}$, and $GdAg_{0.5}Au_{0.5}$ in the Gd(Cu, Ag, Au) system are antiferromagnetic at low temperatures. On the contrary, GdCd, $GdAg_{0.8}In_{0.2}$, $GdAg_{0.7}In_{0.3}$, $GdAg_{0.5}In_{0.5}$, and $GdAg_{0.3}In_{0.7}$ are ferromagnetic at low temperatures. GdCd has a very high Curie temperature of 262°K. In the Gd(Cu, Ag, Au) system, the Néel temperatures increases with the increase in the lattice constant. The remarkable difference in magnetic behavior between the Gd(Ag, Cd, In) system and the Gd(Cu, Ag, Au) system is considered to be associated with the fact that the number of conduction electrons plays a more important role in determining the magnetic behaviors than the interatomic separation. (auth)

29753 LOW TEMPERATURE RESISTIVITY, MAGNETIC SUSCEPTIBILITY, AND SUPERCONDUCTING TRANSITION TEMPERATURE IN LANTHANUM CONTAINING RARE-EARTH IMPURITIES. Sugawara, Tadashi; Eguchi, Hiroko (Tokyo Univ.). J. Phys. Soc. Jap., 21: 725-33(Apr. 1966).

The resistivities and the magnetic susceptibilities of lanthanum containing small amounts of other rare-earth metals are measured at low temperatures. Resistance minima are found at about 6.5°K in fcc La-Ce alloys and at about 5.8°K in hcp La-Ce alloys. The temperature at which the resistance minimum occurs is independent of the concentration of Ce. Any minimum has not been found in the alloys with solutes other than Ce. The observed resistivity of all the alloys contains a term proportional to

log T in accordance with the recent theories on the s-d or s-f resistivity due to Kondo and others. The magnetic susceptibilities of La-Ce, La-Pr, and La-Nd alloys are not inconsistent with the resistive behaviors of these alloys. The effective s-f exchange integrals for various rare-earth solutes have been calculated from the resistivity data and compared with those calculated from the change of the superconducting transition temperature of La due to added rare-earth metals. The agreement between the two is not good for heavy rare-earth solutes. The increment in the residual resistivity of La due to the solute seems to be explained mostly by the magnetic scattering. (auth)

29754 RADIATION BACKSCATTERING AND RADIATION-INDUCED X RAYS FOR MEASURING SURFACE COMPOSITION AND STRUCTURE. Berk, Sigmund (Frankfort Arsenal, Philadelphia). Mater. Eval., 24: 309-12(June 1966).

The use of promethium-147 beta backscattering to measure the thickness of plastic coatings on copper was determined. Backscattering radiation was also used to determine the structure and surface composition of copper specimens. A preliminary study of the use of beta-particle backscattering and beta-particle-induced x rays for measuring corrosion is described. (auth)

29755 STRUCTURE OF LIQUID METALS AND ALLOYS. Wilson, J. R. (Queen's Univ., Kingston, Ont.). Met. Rev., 10: 381-590(1965).

Properties and structure of liquid metals and alloys are discussed. Topics covered include: direct measurements of structure, thermodynamic properties, atomic transport properties, densities and and volumes of mixing, electronic properties, surface properties and melting, solidification, and supercooling. (596 references). (M.C.G.)

29756 RECENT DEVELOPMENTS IN THE TECHNOLOGY OF ARC-CAST MOLYBDENUM. Braun, H.; Semchyshen, M.; Barr, R. Q. (Climax Molybdenum Co., Zurich, Climax Molybdenum Company of Michigan, Detroit). pp 351-73 of Metals for the Space Age. Plansee Proceedings, 1964. Benesovsky, F. (ed.). Reutte/Tyrol, Metallwerk Plansee AG, 1965.

The technology of arc-cast molybdenum during the past three years has been identified with three important advancements: the development and commercial production of low carbon, unalloyed molybdenum with improved toughness; the commercial production of TZM alloy (Mo + 0.5% Ti + 0.01% Zr) sheet to meet rigid specifications; and the realization of superior high temperature properties by heat treating alloys of molybdenum containing titanium, zirconium, and carbon. The low carbon, arc-cast molybdenum has been processed to heavy forgings and rolled bars which exhibit ductile-brittle transitions well below room temperature and to plate and sheet which can be bent and formed readily at room temperature, exhibiting bend transition temperatures as low as –70°C. Special processing schedules have been designed for the production of quality controlled TZM sheet of a wide range of thickness, a narrow range of tensile properties and the capability of flanging at room temperature. The heat treatment of the TZM alloy has been successfully applied to increase the hardness and tensile strength of wrought bars, to raise the recrystallization temperature, and to extend to higher temperatures the useful properties of this versatile alloy. (auth)

29757 DETERMINATION OF BRITTLE-DUCTILE TRANSITION TEMPERATURES IN MOLYBDENUM AND TUNGSTEN. Kamoun, G.; Lachenaud, R. (Sud-Aviation, Courbevoie, France). pp 374-81 of Metals for the Space Age. Plansee Proceedings, 1964. Benesovsky, F. (ed.). Reutte/Tyrol, Metallwerk Plansee AG, 1965. (In French).

Specimens with small dimensions were selected in order to determine their behavior under multiaxial stress and in reduction of area. Two test methods were used: deep drawing of circular plate; and bending of small rectangular plate. The tests were carried out on different temperatures in the vicinity of the transition temperature on various commercial Mo and W grades and Mo–W alloys as well as on Mo sheet in the form of electron gun welding specimens having zones of different transition temperatures. In all cases there was a certain temperature below which the material was brittle and above which it was ductile. The methods used are characterized by simplicity and rapidity. (auth)

29758 HIGH-ENERGY-RATE FORMING OF MOLYBDENUM. van Wely, F. E.; Verbraak, C. A. (Metaalinstituut T. N. O., Delft, Netherlands). pp 382-93 of Metals for the Space Age. Plansee Proceedings, 1964. Benesovsky, F. (ed.). Reutte/Tyrol, Metallwerk Plansee AG, 1965.

The response of recrystallized polycrystalline molybdenum and molybdenum-single crystals to shock waves of 20–300 kbar was studied at different temperatures. At room temperature mechanical twinning seemed to be a common deformation mode. From the experiments with single crystals of different orientations it was concluded that shock deformation takes place by mechanical twinning in any orientation. It, therefore, is not possible to suppress mechanical twinning during shock loading of Mo by using sheet material with a definite texture. It was found, however, that at higher temperatures (200–300°C) shock-loaded Mo deforms by slip rather than mechanical twinning. To prove the absence of twins both microscopic and x-ray techniques were used. Moreover it was found that prior conventional deformation reduces the capacity for subsequent mechanical twinning during shock loading. By making use of this memory-effect, combined with elevation of temperature, high energy rate forming of Mo will be possible without undue deterioration of properties. (auth)

29759 PRECIPITATION HARDENING NIOBIUM–HAFNIUM–NITROGEN ALLOYS. Begley, R. T.; Godshall, J. L.; Stickler, R. (Westinghouse Electric Corp., Pittsburgh). pp 401-20 of Metals for the Space Age. Plansee Proceedings, 1964. Benesovsky, F. (ed.). Reutte/Tyrol, Metallwerk Plansee AG, 1965.

The response to heat treatment of the Nb–Hf–N alloys appears to follow classical precipitation hardening behavior. The high as-quenched hardness would seem to be due primarily to a high supersaturation with respect to nitrogen, although, considering the rapid overaging observed in this system, it is possible that some precipitation occurs during the quenching treatment. The hardness increase on aging apparently arises from the precipitation of a coherent nitride phase (HfN). At temperatures above 800 to 900°C, loss of coherency and coalescence of the precipitate occurred, resulting in pronounced softening. Further increase in aging temperature above 1400°C resulted in further growth of the precipitates and resolution of nitrogen in the matrix. The pronounced effect of the nitride phase on high temperature strength was illustrated by hot hardness data. A rapid decrease in hot hardness occurred at temperatures over 982°C (1800°F), but at temperatures up to at least 1315°C (2400°F) the hot hardness values were much higher than those of the low interstitial Nb-5 Hf binary alloy. The strength levels indicated by the hot hardness data were confirmed by the results of tensile tests. Even in the partially overaged condition (1 hour at 1200°C) the alloy exhibited tensile strengths superior to the best commercially available Nb alloys. However, the engineering application of the Nb-5 Hf–0.2N alloy would appear to be precluded by the low ductility values observed at both low and elevated temperatures. The low ductility appeared to be associated with nitride precipitation at grain boundaries. (auth)

29760 PROPERTIES, AVAILABILITY, AND APPLICATIONS OF TANTALUM-BASE ALLOYS. Torti, M. L.; Moore, J. H. pp 438-43 of Metals for the Space Age. Plansee Proceedings, 1964. Benesovsky, F. (ed.). Reutte/Tyrol, Metallwerk Plansee AG, 1965.

Data on the most important room and high temperature properties and availability of tantalum base alloys are tabulated. The properties generally include yield strength, ultimate tensile strength, elongation, and ductility. (P.C.H.)

29761 DEFORMATION PROPERTIES OF NIOBIUM. TRANSMISSION ELECTRON MICROSCOPE STUDY OF ITS PLASTIC DEFORMATION MECHANISM. Berghezan, A. pp 460-72 of Metals for the Space Age. Plansee Proceedings, 1964. Benesovsky, F. (ed.). Reutte/Tyrol, Metallwerk Plansee AG 1965.

Observations on dislocation structure that forms during deformation of thin niobium foils as observed by transmission electron microscopy are described. Dislocations structures in Nb samples deformed outside and inside the electron microscope were investigated. The movement and interaction of dislocations with one another or possibly with minute amounts of impurities are discussed. (P.C.H.)

29762 MECHANICAL PROPERTIES OF HIGH-PURITY NIOBIUM SINGLE CRYSTALS. Votava, E. pp 473-7 of Metals for the Space Age. Plansee Proceedings, 1964. Benesovsky, F. (ed.). Reutte/Tyrol, Metallwerk Plansee AG, 1965.

Using a new method for the direct production of high-purity and strain-free tensile specimens the mechanical properties of Nb single crystals were investigated at room temperature as a function of the orientation. All the crystals investigated showed pronounced yield points and the yield-point drop depends on the orientation. The (111) orientation has the smallest and the (110) orientation the largest yield-point drop. In addition, a tendency was observed for large yield-point drops along the line (110)–(112). Other results are also discussed. (P.C.H.)

29763 CURRENT COLUMBIUM ALLOY TECHNOLOGY IN THE UNITED STATES. Worcester, S. A.; Kieffer, B. F. pp 478-85 of Metals for the Space Age. Plansee Proceedings, 1964. Benesovsky, F. (ed.). Reutte/Tyrol, Metallwerk Plansee AG, 1965.

The development of niobium alloys with satisfactory strength, fabricability, and weldability for present day uses, such as space technology, is discussed. Some of the more important Nb alloys include: Nb–W–Zr–C; Nb–Mo–V–Zr; Nb–W–Zr; Nb–W–Hf–Y; Nb–Ta–W–Zr; and Nb–Hf–Ti. (P.C.H.)

29764 NEW TANTALUM, NIOBIUM, IMPREGNATED, OR SINTERED ALLOYS AND COMPOUND MATERIALS WITH GRAPHITE. Kieffer, R.; Nowotny, H.; Windisch, S. (Technische Hochschule, Vienna. Univ., Vienna). pp 486-510 of Metals for the Space Age. Plansee Proceedings, 1964. Benesovsky, F. (ed.). Reutte/Tyrol, Metallwerk Plansee AG, 1965. (In German).

During a search for new high-temperature materials, it was found that the group-V-A metals niobium and tantalum can replace W(Mo), if special infiltration techniques are employed. The methods of infiltration and fluid-phase sintering also permit the production of solid solutions of the group-V-A and VI-A metals at considerably lower temperatures than were previously thought necessary. The accelerating effect of metal additions, e.g., Al, Ni, Cr, Sn, Zn, and Be on the copper or silver infiltrant was investigated; Al, Ni, Cr, and Sn proved to be particularly efficient and economic. The infiltration of skeletons consisting of group V(A) and VI(A) metals with the corresponding Ni-eutectic is readily accomplished, resulting in solid solutions and compound materials with a structure analogous to that of W–Cu–Ni. The solid solutions (mixed crystals) produced by the different methods referred to above can be isolated by treatment with mineral acids. The occurrence of ternary phases in the systems Ta(Nb)–Cu–Ni and Ta(Nb)–Cu–Al is also reported. Infiltration tests using molten or dissolved salts of Nb, Ta, Mo, W, and Rh showed that Mo, W, and Rh in metallic form and Nb and Ta in form of the monocarbides can be incorporated in a quantity of 30–70 weight-% and possibly over, into porous graphite bodies with a resultant increase in compressive strength (skeleton within a skeleton). Infiltration of these materials with copper and silver was only superficial. With coarsely porous material, however, complete infiltration in the autoclave appears possible. Copper–silicon and especially molybdenum–silicon alloys wet graphite at elevated temperatures and the lastnamed results in partial infiltrations that form a good base for the adhesion of scaling resistant coatings. (auth)

29765 SOME PROPERTIES OF TUNGSTEN–RHENIUM ALLOYS. Kieffer, B. F.; Root, G. S.; Worcester, S. A. pp 571-6 of Metals for the Space Age. Plansee Proceedings, 1964. Benesovsky, F. (ed.). Reutte/Tyrol, Metallwerk Plansee AG, 1965.

Powder metallurgical and vacuum arc melting techniques were used to consolidate the tungsten–rhenium alloys prior to fabrication into sheet and wire. Wire of tungsten–rhenium alloys (up to 5% rhenium) shows remarkable ductility in the annealed condition, whereas, sheet of the same alloys shows a lack of ductility. The presence of sigma-phase in tungsten–rhenium alloys increases the brittle to ductile transition temperature. Tungsten–rhenium alloys in the range of 22 to 26% rhenium show some ductility even after recrystallization. Recrystallized arc-cast tungsten-25% rhenium sheet has a brittle to ductile transition temperature of 35°C, whereas, the powder metallurgical tungsten-25% rhenium sheet has a brittle to ductile transition temperature of 130°C. Arc-cast rhenium–tungsten alloys (up to 10% tungsten) result in high strength, ductile alloys. (auth)

29766 RESISTIVITIES AND LATTICE PARAMETERS OF SOME PALLADIUM AND NIOBIUM ALLOYS. Catterall, J. A.; Barker, S. M. (National Physical Lab., Teddington, Eng.). pp 577-87 of Metals for the Space Age. Plansee Proceedings, 1964. Benesovsky, F. (ed.). Reutte/Tyrol, Metallwerk Plansee AG, 1965.

Measurements were made of the resistivities and lattice-parameters of niobium–molybdenum and niobium–zirconium alloys, and of palladium-rich palladium–zirconium, palladium–niobium, and palladium–molybdenum alloys. The results are discussed in terms of possible models for the electronic structure indicated by recent work of others on the magnetic susceptibility and electronic specific heat. It is suggested that the model proposed previously for the electronic structure of palladium–uranium alloys may be applicable to some other systems. (auth)

29767 DEVELOPMENT OF BERYLLIUM FOR USE IN AIRCRAFT. Moore, A.; Lord, W. B. H. (Atomic Weapons Research Establishment, Aldermaston, Eng. Ministry of Defence, London). pp 588-612 of Metals for the Space Age. Plansee Proceedings, 1964. Benesovsky, F. (ed.). Reutte/Tyrol, Metallwerk Plansee AG, 1965.

A survey was made of the causes of brittleness in beryllium. Essentially there are two distinct problems. Above 200°C the metal is plastic but the plot of ductility-vs-temperature shows a minimum at 600°C whereas below 200°C the ductility-vs-temperature plot undergoes a marked transition and the polycrystalline metal shows no plasticity. The deformation characteristics were studied from –196 to 700°C in both poly- and single crystals ranging in purity from 99.975% (zone-refined and distilled metal), through commercial grades of 99.85 to 99.95%, to specific alloys containing up to 0.4% iron. Various effects of heat treatment on mechanical properties, including tensile, compression, and fatigue were studied and correlated with constitutional changes by x-ray diffraction, electron microscopy, and microprobe analysis. It was found that the mechanical properties above 200°C can be controlled and the ductility minimum at 600°C eliminated by appropriate overaging treatments. By contrast, the brittleness below 200°C cannot be altered by either purification or heat treatment. It was concluded that purification will be of little benefit in alleviating brittleness below 200°C and its only effect is to decrease the strength to an unsatisfactory level (~10,000 psi). Furthermore it is argued that optimum properties (ductility, impact strength, resistance to crack propagation) for any grade of purity can only be obtained by grain refinement and randomization. The relative merits, therefore, of fabricating beryllium parts by powder metallurgical and also by direct fabrication from a casting were compared. (P.C.H.)

29768 RECENT DEVELOPMENTS IN RHENIUM AND RHENIUM ALLOY TECHNOLOGY. Port, J. H. (Chase

Brass and Copper Co., Inc., Waterbury, Conn.). pp 613-35 of Metals for the Space Age. Plansee Proceedings, 1964. Benesovsky, F. (ed.). Reutte/Tyrol, Metallwerk Plansee AG, 1965.

Considerable progress has been made to recover greater quantities of rhenium, to evaluate and modify its properties, to study the effects of rhenium as an alloying addition to other refractory metals, and to develop satisfactory fabricating procedures for rhenium and rhenium alloys. Recent developments that have led to new alloys not previously available are discussed. Among the most significant of these was the development of tungsten–rhenium–thoria alloys for cathodes and platinum clad tungsten–rhenium and molybdenum–rhenium wire for grids in electron tubes. Properties, fabrication, and the application of these alloys are considered in detail. Significant progress also has been made in the fabrication of molybdenum–rhenium and tungsten–rhenium alloy tubing. The outstanding properties of these materials have led to their use for many high temperature applications including thermocouple sheaths, electron tube components, and heat exchanger tubes. The advantages of strength, ductility, high melting point, low vapor pressure, resistance to water cycle effect, and weldability of rhenium are shown for applications such as heaters. (P.C.H.)

29769 THERMAL DIFFUSION OF OXYGEN IN REFRACTORY METALS. Rieck, G. D.; Vogel, D. L. (Technological Univ., Eindhoven, Netherlands). pp 636-49 of Metals for the Space Age. Plansee Proceedings, 1964. Benesovsky, F. (ed.). Reutte/Tyrol, Metallwerk Plansee AG, 1965.

A discussion is given of thermal diffusion (Ludwig-Soret effect) of interstitial solutes in metals and its possible influence on the mechanical properties of the metal. The conditions are outlined for studying the effects in refractory metals in a quantitative way. In connection herewith a survey is given of the terminal solubilities of C, N, and O in groups IV A-, V A- and VI A-transition metals and an estimate is given of the rate of evaporation of oxygen (as an oxide) from niobium. The method by which thermal diffusion of oxygen in β-zirconium was determined is described. The heat of transport for this system was found to be at least 13.6 ± 2.0 kcal/mole. An estimation is given of the time required to give a rather large concentration gradient of oxygen in zirconium under specified conditions. In an experiment with niobium a decrease in oxygen content was found everywhere, most probably due to evaporation. (auth)

29770 DEVELOPMENT OF INTERMETALLIC COMPOUNDS FOR AEROSPACE APPLICATIONS. Beaver, W. W.; Stonehouse, A. J.; Paine, R. M. (Brush Beryllium Co., Cleveland). pp 682-700 of Metals for the Space Age. Plansee Proceedings, 1964. Benesovsky, F. (ed.). Reutte/Tyrol, Metallwerk Plansee AG, 1965.

The most interesting intermetallics for aerospace application have recently been studied in more detail, and a number of compounds not previously known have been discovered. The major systems of interest include Nb–Al, Ta–Al, W–Si, Ta–Si, Zr–Be, Nb–Be, Mo–Be, Ti–Be, and Ta–Be. Fabrication developments studies are described, showing that powder metallurgy methods such as sintering after vibration packing, isopressing or direct axial compaction, and modified ceramic processes, such as extrusion, slip casting, have proven most feasible. The correlations of type of materials, method of fabrication, and related hardware resulting are described. The principal advantages of these materials are good electrical and nuclear properties, oxidation resistance, and high strength-to-weight properties at elevated temperature, and high heat capacity and thermal conductivity. Recent research leading to elimination of the pest phenomena through structural modification and alloying is discussed. Studies of the failure mechanism leading to explanation why the phenomena take place only in certain systems and can be overcome in others are presented. Further research on obtaining improved impact resistance at low temperatures through purification, or structural modification by alloying, is described, including studies of new ternary or quaternary systems (i.e., Mo–Be–Si) showing promise for application at temperatures higher than 1700°C. (P.C.H.)

29771 FRICTION AND HARDNESS OF REFRACTORY COMPOUNDS. Brookes, C. A.; Atkins, A. G. (Cambridge Univ., Eng.). pp 712-21 of Metals for the Space Age. Plansee Proceedings, 1964. Benesovsky, F. (ed.). Reutte/Tyrol, Metallwerk Plansee AG, 1965.

The frictional properties, as a function of temperature, of some monocrystalline solids are detailed and discussed. It was found that the presence of metallic bonding may influence these properties, but that neither the onset of bulk plastic flow nor a rapid decrease in hardness with increasing temperature influence the magnitude of the coefficient of friction. Finally, the influence of temperature on the mutual indentation hardness of refractory compounds in polycrystalline form is outlined. The effect on hardness of rate of strain, time at maximum load, and internal porosity are briefly discussed. (auth)

29772 INVESTIGATION OF BORIDE COMPOUNDS FOR HIGH-TEMPERATURE APPLICATIONS. Kaufman, L.; Clougherty, E. V. (ManLabs, Inc., Cambridge, Mass.). pp 722-58 of Metals for the Space Age. Plansee Proceedings, 1964. Benesovsky, F. (ed.). Reutte/Tyrol, Metallwerk Plansee AG, 1965.

A comprehensive study was made of the properties of high purity well characterized samples of $TiBe_2$, ZrB_2, HfB_2, NbB_2, and TaB_2. Floating zone refining and high pressure hot pressing were used to prepare high density single crystal and polycrystalline material respectively. In addition, studies of the sintering mechanism of TiB_2 and powder purification by acid leaching and vacuum heating were performed. Properties measured included lattice parameters, x-ray thermal expansion, linear thermal expansion, electrical resistivity, microhardness, and thermal conductivity. These quantities were obtained for materials that satisfied stringent sample requirements for various experiments. Measurements were generally performed between 25 and 1000°C, although some properties were determined for temperatures up to 1700 to 2000°C. Thermal properties measured include specific heat, vapor pressure, and heat of vaporization. Phase boundary measurements were performed in the Zr–B system by electron microprobe analyses of diffusion couple and two phase alloy specimens and the current status of the phase diagrams of the diborides were reviewed and compared with theoretical calculations of the temperature-composition fields of stability of the diborides. Quantitative measurements of the rate of oxygen pickup of all the diborides were performed over the range 1200 to 1800°C. These measurements gave information on the oxidation resistance and mechanism of oxidation of these compounds. An integrated thermodynamic analysis of the diborides was performed for the diborides based on the Schottky-Wagner model of non-stoichiometric compound phases. This analysis permits computation of the vapor pressure and rates of evaporation of the elemental components of TiB_2, ZrB_2, HfB_2, NbB_2, and TaB_2 as a function of temperature and composition within the single phase diboride field. This treatment permits prediction of congruency and phase boundaries for each of these compounds as a function of temperature. (auth)

29773 GRAPHITE IN SPACE TRAVEL. Rubisch, O.; Vohler, O. (Siemens Plania AG, Meitingen, Ger.). pp 759-85 of Metals for the Space Age. Plansee Proceedings, 1964. Benesovsky, F. (ed.). Reutte/Tyrol, Metallwerk Plansee AG, 1965. (In German).

High resistence against cyclic thermal stresses combined with the extraordinarily high sublimation temperature make graphite particularly suitable as a high-temperature material. Above 1500°C (2732°F) graphite has the highest specific strength of all known materials. Pyrolytic graphite is distinguished by a particularly pronounced anisotropy, e.g., with respect to thermal conductivity which is an advantage for its use in thinwalled nozzles and other high-temperature applications. By

suitable production methods that were developed in recent years, graphites having the most diverse properties such as high-strength electrographite, low-density graphite, fiber-reinforced graphite laminates, and cloth can be produced. In order to improve the oxidation resistance at high temperature, compound materials of graphite and carbides and coatings of refractory carbides, silicides, oxides, and cermets were developed. By applying a double layer of TiC–$TiSi_2$, for example, oxidation can be inhibited for a certain length of time at a temperature of 1600°C (2912°F). (auth)

29774 THERMODYNAMIC CONSIDERATIONS IN THE SELECTION OF MATERIALS FOR HIGH-TEMPERATURE APPLICATIONS. Rudy, E.; Chang, Y. A. (Aerojet-General Corp., Sacramento, Calif.). pp 786-822 of Metals for the Space Age. Plansee Proceedings, 1964. Benesovsky, F. (ed.). Reutte/Tyrol, Metallwerk Plansee AG, 1965.

Conditional equations governing the phase-equilibria in ternary systems are discussed and applied to a number of ternary carbon systems of the refractory transition metals. The relative stabilities of the carbides derived from the phase diagrams are in good agreement with the data obtained by other methods. Values are presented for the free energies of formation of certain unstable binary phases in the group VI metal-carbon systems. These data include the stabilities of the cubic (Bl) phases in the systems Cr–C, Mo–C, and W–C, the stabilities of molybdenum and tungsten carbides exhibiting the structural characteristics of the chromium-carbides, and values for the free energies of formation of tungsten carbide type structures in the system chromium–carbon. The effects of the stability of these compounds on the high temperature phase behavior in refractory carbide systems are discussed. (auth)

29775 STUDY ON URANIUM ALLOYS. Nippon Genshiryoku Gakkaishi, 8: 195-208(Apr. 1966). (In Japanese).

Various tests were made on high purity binary uranium alloy specimens with 1 at. % Mo. These tests include: thermal cycling; high temperature hardness; thermal expansion; internal friction; creep; high temperature tensile test; metallography; and T-T-T curve determination. The results of similar tests carried out by different organizations were compared with each other. Metallographic tests were also made on 16 other binary uranium alloys prepared by arc melting. Photomicrographs thus obtained are reproduced and should prove useful in identifying the phases appearing in various uranium alloys. (P.C.H.)

29776 THE BEHAVIOR OF THE CRYSTALS AND THE VOIDS IN CENTRALLY HEATED UO_2 GREEN PELLETS. Taketani, Kiyoaki (Japan Atomic Energy Research Inst., Tokyo). Nippon Genshiryoku Gakkaishi, 8: 248-56(May 1966). (In Japanese).

Observations of the microstructure of centrally heated UO_2 green pellets indicate that the outer part usually has a sintered microstructure, but in the central part of the pellet the relation between grains and voids becomes very important. In the higher-temperature parts of the pellet, voids gather near the grain boundaries and form narrow and long voids along the temperature gradient in the pellet. When the edge of the void at higher temperature is heated to a certain temperature, molecules of UO_2 vaporize from this edge and condense at the lower-temperature edge of the void. Repetition of this phenomenon, leads to growth of columnar grains with (111) preferred orientation, and long voids are transformed in shape to lenticular voids. This phenomenon of the grain boundary void transformation is clearly revealed in transversal microstructures. Growth is observed at the low-temperature side of cracks in the pellet, despite prevailing temperatures too low to cause the above-mentioned phenomenon. This grain growth is assumed to be of the common pattern. (auth)

29777 REVIEW OF WORK ON BERYLLIUM AS CLADDING MATERIAL. Moroznmi, Shotaro (Tohoku Univ., Japan). Nippon Genshiryoku Gakkaishi, 8: 261-6(May 1966). (In Japanese).

Some recent studies related to the properties of beryllium as fuel cladding material for CO_2 gas-cooled reactors are described, together with developments on methods of working this metal. The need for improvements in the transverse ductility of tubular specimens, which call for further studies from the metallurgical standpoint, is emphasized. (auth)

29778 CONSIDERATION ON SOME PROPERTIES OF SINTERED WC–Co ALLOYS CONTAINING A SMALL AMOUNT AMOUNT OF TaC. Sugiyama, Masataka; Suzuki, Hisashi; Yamamoto, Takaharu; Hara, Akio; Kitano, Hitoshi. Nippon Kinzoku Gakkaishi, 29: 965-9(1965). (In Japanese).

WC–TaC–10% Co alloys containing 0.5, 1.0, 3.0% TaC (added in the form of a mixed carbide) and having various carbon contents were vacuum-sintered at 1375°C for 2 hr. The particle size of the WC powder used was controlled to obtain an approximately same grain size of carbides in the sintered alloys. Some properties of the as-sintered alloys and the effect of low-temperature annealing (at 800°C up to 50 hr) on them were studied as a function of the TaC and carbon contents. The main results are as follows: The properties of two phase alloys are remarkably influenced by their carbon contents and also by low temperature annealing when the carbon contents are lower, are substantially maintained in the alloys containing TaC. The composition of binder phase, width and position in the two phase range (a γ + TaC + WC three phase range) of the WC–TaC–10% Co alloys do not change by the addition of TaC. The alloys containing TaC are higher in hardness than the straight alloys, but the strength scarcely decreases. The aging rate at a low temperature is retarded in the alloys containing TaC. (auth)

29779 INFLUENCES OF TiC ON SOME PROPERTIES OF SINTERED WC–Co ALLOYS. Suzuki, Hisashi; Sugiyama, Masataka; Hayashi, Kozi (Tokyo Univ.). Nippon Kinzoku Gakkaishi, 29: 970-4(1965). (In Japanese).

WC–10% Co alloy and two series of WC–TiC–10%Co alloys with 0.64 and 1.28% TiC, having various carbon contents in the phase range free from the η and graphite phase, were vacuum-sintered mainly at 1375°C for 1.5 hr. Effects of the TiC addition to the sintered WC–10% Co alloys on their properties and, moreover, on their binder phase were studied, in detail by measuring their density, lattice constant of the binder phase, relative magnetic saturation, hardness, transverse-rupture strength, grain size of WC, etc. The experimental results obtained are as follows: The variation of general properties of the TiC containing alloys, due to a small change of the carbon content, is equal to that of straight WC–Co alloys. The value of magnetic saturation of the alloys and the lattice constant of the binder phase which are changeable according to their carbon content are also identical with the straight alloys. From this and the formation of the WC–TiC solid solution by the 0.15% TiC addition, it may be concluded that TiC is hardly soluble in the binder phase. In this respect, the behavior of TiC is almost similar to that of TaC. The width of the γ + carbides range and the position of the stoichiometric carbon content in that range are in good agreement with those of the straight alloys. It can be predicted that the addition of a small amount of TiC to the WC–Co alloys inhibits the recrystallization of the carbide phase, and consequently the alloys have finer WC grains and higher hardness than the corresponding alloys of TiC free compositions. Because of this finer structure, the rate of precipitation of the Co_3W type compound from the binder phase is accelerated when the low carbon alloys are annealed at low temperatures. The TiC addition makes the η-phase grain finer and improves its dispersion, so that the strength of the alloys even under the appearance of the η phase does not decrease abruptly. (auth)

29780 PROPERTIES OF A SINTERED WC-10 PERCENT Co ALLOY IN RELATION TO THE PARTICLE SIZE AND THE COMPOSITION OF THE BINDER-PHASE. Suzuki, Hisashi; Sugiyama, Masataka; Umeda, Takateru (Tokyo Univ.). Nippon Kinzoku Gakkaishi, 29: 974-9(1965). (In Japanese).

It has been reported that the composition of the binder-phase of two phase alloys changes remarkably from about 2 to 10% W due to a small change of their carbon content, so that the properties and the aging characteristics of cemented carbides are directly influenced by the composition. Some properties of cemented carbides affected by the particle size were investigated in close consideration of the composition of the binder phase. The properties such as hardness, strength, magnetic saturation, coercive force, and electrical resistivity of the alloys and the lattice parameter of binder phase, were measured. The results obtained may be summarized as follows: The value of coercive force is not only dependent upon the particle size, but also upon the tungsten content of the binder phase. Therefore, the determination of the mean particle size by a coercive force method is erroneous. The hardness and electrical resistivity decrease with increasing of the particle size and the carbon content. The transverse-rupture strength shows a maximum under the condition that the mean particle size is about 2.0 μ and the carbon content of WC is about 6.20% which is almost the maximum carbon content of the two-phase alloy. And as a condition to obtain a maximum strength, it is generally accepted in the two-phase alloy that the carbon content should be almost maximum, if the particle size is nearly equal to or less than about 2.0 μ, but in the case of a fairly coarser particle size it should be almost minimum. Both the lattice constant of the binder phase and the magnetic saturation of the alloy are not influenced by the particle size of WC, that was developed after sintering. Therefore, it is clear that the tungsten content in the solid binder phase has no relation to the particle size, provided that the carbon content of the alloy is invariable. But the rate of precipitation of Co_3W, when low carbon alloys are annealed at low temperatures, is sensitive to the particle size. A carbide structure of coarse and homogeneous particle size is desirable to stabilize the properties of low carbon alloys at a higher temperature. (auth)

29781 STUDIES ON THE MULTILAYER Nb–Sn SUPERCONDUCTING WIRE. Tachikawa, Kyoji; Fukuda, Satoshi (National Research Inst. for Metals, Tokyo). Nippon Kinzoku Gakkaishi, 29: 1125-30(1965). (In Japanese).

The multilayer Nb–Sn wire containing a continuous intermediate phase lengthwise was made by the following procedure. A small-diameter Nb tube was set concentrically in a large diameter Nb tube and molten Sn was poured into the empty space. This composite rod was cold drawn into a fine wire and then heated at elevated temperatures. By this heat treatment, Nb and Sn diffused each other and Nb–Sn intermediate phases were formed. The Nb–Sn intermediate phases were distinguished by the anodizing oxidation technique and their compositions were determined by an electron probe x-ray microanalyzer. Three intermediate phases, i.e., Nb_4Sn, Nb_3Sn_2 and Nb_2Sn_3, were found. The Nb_4Sn phase is formed above 900°C, the Nb_3Sn_2 phase is formed between 800°C and 925°C, and the Nb_2Sn_3 phase is formed below 850°C. At 950°C, the relation between the width of the Nb_4Sn phase x (μ) and the diffusion time t (hr) is represented approximately as $x \sim 7.5\sqrt{t}$. The highest superconducting transition temperature is obtained by the diffusion treatment between 950 and 1100°C. The superconducting to normal transition of the specimen begins at 17.8°K and finishes at 18.0°K. When the diffusion temperature is lowered below 950°C, the transition finishes at 17.5°K and the transition width of the specimen increases. (auth)

29782 PROPERTIES OF HIGH-ZIRCONIUM WROUGHT COPPER BASE ALLOYS. Sugiyama, Masataka; Suzuki, Hisashi; Kitano, Hitoshi; Sato, Testuo (Tokyo Univ.). Nippon Kinzoku Gakkaishi, 30: 32-7(1966). (In Japanese).

Cu-base binary alloys containing 0.3 to 3.0% Zr were studied from the viewpoint of dispersion and age hardenability. Two kinds of chill cast and water-cooled chill cast ingots (80 mmϕ × 170 mm) were prepared. They were first hot-rolled at about 850°C, subsequently solution-annealed at 880 to 890°C for 40 min, and finally 83% cold-reduced to plates 0.5 mm in thickness. Properties of these two series of specimens were examined as a function of aging conditions. The results obtained are as follows: Maximum values of hardness and tensile strength obtainable after aging at 400°C for 1 hr increase remarkably with increasing of the Zr content, but the softening temperature and the electrical conductivity decrease slightly. Compared with chill casting, water-cooled chill casting can reduce the Zr content in the alloys to attain definite properties, and also improves their heat resistivity. Accordingly, the water-cooled chill casting is essential in making high Zr–Cu-base alloys. For example, properties of the alloys containing 1.14 and 2.24% Zr and aged at 400°C are: 170 and 180 Hv in hardness, 55 and 60 kg/mm^2 in tensile strength, 80 and 75% IACS in electrical conductivity. The reason why this method is so effective may be explained by the fact that the refinement of the casting structure takes place during casting, namely, the dispersion of Cu_3Zr is improved with the reduced grain size. The dispersed particles are almost stable at a temperature below 900°C. (auth)

29783 ELECTRON BEAM MELTING OF REFRACTORY METALS. V. EFFECTS OF ALLOYING ELEMENTS ON THE DUCTILITY OF ELECTRON-BEAM-MELTED MOLYBDENUM. Takaai, Tetsuya (Hitachi, Ltd., Tokyo). Nippon Kinzoku Gakkaishi, 30: 38-42(1966). (In Japanese).

The effects of alloying elements on the ductility of electron-beam-melted Mo were studied mainly by the fractographic method, Charpy impact test, and electron diffraction technique. From the fractographs of brittle fractured ingots, it was known that the structure of the pure Mo ingot consisted of well collimated columnar crystal grains, and the fracture surfaces were principally columnar grain boundaries. Contrary to the above, the structures to which small amounts of Ca, Ti, and Zr were added showed the disappearance of the columnar grains, and the fracture surfaces were almost cleavage planes. The ductile-to-brittle transition temperatures (T_c) by the Charpy impact test were found between the liquid nitrogen temperature and 300°C. But no remarkable changes of T_c were observed in annealing in the temperature range of 1150 to 1400°C excepting Ti-added Mo and pure Mo which was worked to the test piece sizes by repeating the hot forging and heating. However, the transition temperature (T_c) were affected remarkably by grain sizes and $dT_c/d\ \ln(d^{-\frac{1}{2}}) = -1/\beta$ relations (d: grain size, β: constant) were also found for Mo. The calculated values of β were 1.2×10^{-3}/°C for pure Mo and C-added Mo, and 2.1×10^{-3}/°C for Ti added Mo. However, for equal grain sizes, T_c of the former was about 100 to 200°C higher than the latter. The electron diffraction results showed that the grain boundary inclusions were neither Ti oxide and carbide nor Mo oxide and carbide. From the above results, the author speculated that the grain boundary inclusions of Ti-added Mo consisted of a complex oxide of Ti and Mo, and the grain boundary brittleness due to the presence of a simple oxide or carbide of Mo was diminished. (auth)

29784 STUDIES OF HARD SUPERCONDUCTORS. I. SUPERCONDUCTING PROPERTIES OF Nb–Zr–Ti TERNARY ALLOYS. Doi, Toshio; Mitani, Masao; Umezawa, Tadashi (Hitachi, Ltd., Tokyo). Nippon Kinzoku Gakkaishi, 30: 133-8(1966). (In Japanese).

Nb–Zr–Ti ternary alloys of varying compositions were produced by levitation melting, and the critical temperature, critical current density vs applied magnetic field, electrical resistivity at 293 and 77°K were measured in addition to observations of the optical microscopic structure. The critical temperature of the Nb–30 at. % Zr alloy showed a maximum value of 10.9°K. Since over the wide composition range the critical temperature was found to be over 8°K, there is the possibility that these alloys can be used as solenoids for the superconducting magnet. Especially, the critical current density vs applied magnetic field of the Nb–40 at. %–10 at. % Ti alloy was favorable, and the critical current density at the applied magnetic field was 4.0×10^4, 2.7×10^4, and 1.5×10^4 amp/cm^2 at 60, 70,

and 80 kOe, respectively. In this experiment, the uniform cold working and heat treatment were carried out on the specimens. Therefore, further improvement in the properties of the alloys may be achieved by some other alternative treatment. (auth)

29785 STUDIES OF HARD SUPERCONDUCTORS. II. STUDY OF Nb–Zr–Ti PHASE DIAGRAM. Doi, Toshio; Ishida, Humihiko; Umezawa, Tadashi (Hitachi, Ltd., Tokyo). Nippon Kinzoku Gakkaishi, 30: 139-45(1966). (In Japanese).

Although the critical temperature and the critical field of hard superconductors are determined basically by the intrinsic properties of material, the critical current depends on the internal structure of material such as the magnitude of the localized internal stress due to the dislocation, precipitation, composition fluctuation, etc. Accordingly, a study of superconducting properties of Nb–Zr–Ti ternary alloys requires a phase diagram. A Nb–Zr–Ti ternary phase diagram at the temperatures of 570 to 1100°C, at which the eutectoid transformation and the two-phase decomposition occurred, was examined by means of microscopical and x-ray analysis. The isothermal sections at 1100, 900, 800, 700, and 570°C are shown. (auth)

29786 MICROHARDNESS AND PLASTIC DEFORMATION OF URANIUM DIOXIDE. Honda, Yutaka; Nagata, Sadayoshi; Takahashi, Shuichiro (Mitsubishi Atomic Power Industries, Inc., Japan). Nippon Kinzoku Gakkaishi, 30: 146-50(1966). (In Japanese).

The plasticity of fused UO_2 single crystals in the temperature range from room temperature to 500°C was examined by indenting a diamond pyramid indenter of a microhardness tester and by observing slip lines and dislocation etch pits with an optical- and an electron-microscope. The decrement of hardness of UO_2 crystals at elevated temperatures was larger than that of Al_2O_3 and of WC. Before the occurrence of cracks, slip lines appeared around the indentations of UO_2 crystals indented at room temperature. The domain of slip lines was widely spread when UO_2 crystals were indented at higher temperatures. Dislocation densities, which were determined by counting the number of etch pits near the indentations of UO_2 crystals indented at room temperature, 200, and 500°C, were $1.9 \times 10^7/cm^2$, $5.4 \times 10^7/cm^2$, and $2.1 \times 10^8/cm^2$, respectively, while $8.5 \times 10^6/cm^2$ in the as-received UO_2 crystals. Plastically deformed domain in the indented UO_2 crystals was recrystallized by annealing at 1500°C for 1 hr in hydrogen atmosphere, and the dislocation density decreased to $1.5 \times 10^7/cm^2$. (auth)

29787 STUDIES OF HARD SUPERCONDUCTORS. III. EFFECT OF COLD WORKING AND HEAT TREATMENT ON FIELD CRITICAL CURRENT CHARACTERISTICS OF Nb–25 AT. PERCENT Zr AND Nb–40 AT. PERCENT Zr–10 AT. PERCENT Ti ALLOYS. Doi, Toshio; Ishida, Humihiko; Umezawa, Tadashi (Hitachi Ltd., Tokyo). Nippon Kinzoku Gakkaishi, 30: 213-19(1966). (In Japanese).

The effects of cold working, final and intermediate heat treatments, and amounts of cold working before and after intermediate heat treatment on the applied magnetic field vs critical current density were examined on Nb–25 at. % Zr and Nb–40 at. % Zr–10 at. % Ti alloys at the magnetic field transverse to the transport current at 4.2°K. Although the critical current density of Nb–25 at. % alloy was greatly increased by cold working, there was little effect due to heat treatment. Where as the critical current density of Nb–40 at. % Zr–10 at. % Ti alloy increased slightly by cold working, but there was an increase of about 10^2 amp/cm² in the order of magnitude by heat treatment. The critical current density of Nb–25 at. % Zr alloy was 3×10^4 amp/cm² at 60 kOe, while that of Nb–40 at. % Zr–10 at. % Ti alloy was 9×10^4, 6×10^4 amp/cm² at 60, 70, and 90 kOe, respectively. It was made clear that the latter had extremely superior properties. (auth)

29788 STUDIES OF HARD SUPERCONDUCTORS. IV. EFFECT OF COLD WORKING AND HEAT TREATMENT ON THE CRITICAL CURRENT CHARACTERISTICS OF Nb–25 AT. PERCENT Zr AND Nb–40 AT. PERCENT Zr–10 AT. PERCENT Ti ALLOYS. Doi, Toshio; Ishida, Humihiko; Umezawa, Tadashi (Hitachi Ltd., Tokyo). Nippon Kinzoku Gakkaishi, 30: 220-5(1966). (In Japanese).

Study was made on Nb–25 at. % Zr and Nb–40 at. % Zr–10 at. % Ti alloys with respect to the relation between the internal structure and the critical current density, especially the effects of cold working and heat treatment on the critical current density when the tranverse magnetic field was applied. The principal cause assignable for the increase of critical current density of Nb–40 at. % Zr–10 at. % Ti alloy is to be sought in the increase of the localized internal stress due to precipitation. It can be considered that the above-mentioned effect in Nb–25 at. % Zr alloy is attributable to the increase of the localized internal stress due to the increase and rearrangement of dislocation textures. Although the precipitation contributes considerably to an increase of critical current density at low fields, the dislocation has a favorable effect even at high fields. It can be conceived that these effects are brought about since the flux density is high at a strong magnetic field and so the formation of flux bundles becomes easier. The flux bundle can only be trapped by tangled dislocations having a higher strain energy as the action of Lorentz force on the flux bundles are large. (auth)

29789 SUPERCONDUCTING Nb–10Zr ALLOY. Komata, Toranosuke; Ishihara, Katsumi; Tanaka, Mituo (Mitsubishi Electric Co. Ltd., Japan). Nippon Kinzoku Gakkaishi, 30: 241-6(1966). (In Japanese).

The effects of cold working and heat-treatment on the superconducting critical current of Nb–Zr wires containing about 10 wt % Zr were studied. Samples were electron-beam melted and forged at temperatures between 900 and 1150°C, and cold drawn into 0.25 mm dia wires. The cold workability of this alloy was so good that 10 mm dia rods were drawn into 0.25 mm dia wires without any intermediate heat-treatment. Superconducting critical currents, I_{c_1}, of short wire samples were measured as functions of applied vertical magnetic fields, H, up to 20 kOe at 4.2°K. The results show that I_c of Nb–10% Zr wire increases with increasing cold work, but that the improvement on H–I_c characteristics of the wire by heat-treatment is very small as compared with Nb–33% Zr wire. (auth)

29790 YIELDING AND STRAIN AGEING OF NIOBIUM CRYSTALS. Kim, H. C.; Pratt, P. L. (Imperial Coll. of Science and Tech., London). Phys. Status Solidi, 14: K151-5(Apr. 1, 1966).

Impurity effects on niobium single crystal mechanical properties are presented. The crystals, which were grown by an electron beam zone melting technique, showed a variation of resolved shear stress, hardness and electric resistivity ratio with the number of zone passes. Impurity effects on strain ageing are also shown. (J.F.P.)

29791 OBSERVATION OF THE LINEAR TERM AND THE H.F.S CONTRIBUTION TO THE HEAT CAPACITY BELOW 1 DEG K OF SOME DILUTE ALLOYS. Du Chatenier, F. J.; Miedema, A. R. (Kamerlingh Onnes Lab., Leiden). Physica, 32: 403-14(Feb. 1966).

The results are presented of measurements below 1°K on the heat capacity of some dilute alloys, clearly demonstrating a linear dependence on temperatures below 0.8°K for two Cu–Cr alloys and one Au–Fe alloy. The curves of the heat capacity versus temperature for the Mn alloys show minima at about 0.2°K, the increase at lower temperatures being due to hfs effects. The hfs parameters derived from the T^{-2} tail are considerably smaller than those for Mn in ionic crystals. (auth)

29792 LAVES PHASES IN SYSTEMS CONTAINING RHENIUM AND RARE-EARTH METALS. Savitskii, E. M.; Khamidov, O. Kh.; Tylkina, M. A. (Baikov Inst. of Metallurgy, Academy of Sciences, USSR). Soviet Phys.-Cryst. (Eng. Transl.), 10: 763-4(May-June 1966).

Translated from Kristallografiya, 10: 917-18(Nov.-Dec. 1965).

The interaction of rhenium with gadolinium, terbium, and

erbium was studied by physicochemical-analysis methods. Experimental results indicate the formation of intermetallic compounds $GdRe_2$, $TbRe_2$, and $ErRe_2$ of the $MgZn_2$ type. The cast and annealed alloys of these compounds show a system of lines typical of Laves phase of the $MgZn_2$ type. The crystal-lattice parameters of these compounds are presented. (B.G.D.)

29793 INVESTIGATION OF THE EFFECT OF INTERSTITIAL IMPURITIES ON THE STRUCTURE AND PROPERTIES OF TUNGSTEN SINGLE CRYSTALS. Savitskii, Ya. M.; Tsarow, G. L. Vestsi Akad. Navuk BSSR, Ser. Fiz. Tekh. Navuk, No. 2, 84-91(1965). (In Russian).

Tungsten single crystals, 4 mm in diameter and 250 mm long, were grown by electron-beam zone melting in a vacuum of $5(10)^{-5}$ mm Hg. The single crystals contained 0.0012%C and 0.001% each O_2 and N_2. To determine the effect of interstitial impurities on the structure and mechanical properties, the single crystals were artificially contaminated with carbon, oxygen, or nitrogen, vacuum homogenized at about 2000C for 8 hr, and then tested for mechanical strength at 25°C. It was found that after impregnation with C in a vacuum of $2(10)^{-6}$ mm Hg at 1300C for 6 hr, the carbon content in the crystals increased to 0.054%, i.e., almost 45 times. Carbon was present mostly in the form of finely dispersed carbides. Carbon increased the dislocation density from $1.2(10)^6$ to $1(10)^7/cm^2$, probably because of the relaxation of internal stresses resulting from the introduction of hexagonal W_2C carbide into the cubic lattice of W. The critical-cleavage stress and the yield strength at 25C increased from 15.7 to 34.1 and from 34.0 to 73 kg/mm^2, respectively. The microhardness increased only slightly, but the reduction of area decreased from 100 to 40%, and the NDT temperature rose from −196 to 0°C. This is ascribed to the formation of dislocation sources−carbides−in the presence of which the plastic deformation proceeds mainly on account of the multiplication of dislocations. Impregnation with oxygen at 1200C for 48 hr increased the O_2 content in crystals from 0.001 to 0.002% and decreased slightly (by 2.5 kg/mm^2) the critical-cleavage stress. Oxygen had no effect on the ductility of the crystals, but improved somewhat the dislocation density and distribution by reacting with and decreasing the amount of dispersed carbides, thereby ensuring a freer movement and subsequent annihilation of dislocations. Impregnation with nitrogen (at 2300C for 5 hr) brought about no changes in the structure or mechanical properties of the crystals. No nitrides were detected in the crystal structure and, if they were formed, they exist only at the surface or grain boundaries. (ATD)

29794 TERNARY OXIDES. V. INVESTIGATIONS ON THE SYSTEMS $PbO-Ta_2O_5$, $PbO-Nb_2O_5$, AND $PbO-U_2O_5$. REPORT ON THE CONSTITUTION OF TERNARY OXIDES WITH PYROCHLORE STRUCTURE. Kemmler-Sack, S.; Ruedorff, W. (Laboratorium fuer Anorganische und Analytische Chemie, Tuebingen, Ger.). Z. Anorg. Allg. Chem., 344: 23-40(Apr. 1966). (In German).

In the $PbO-Ta_2O_5$ system, in addition to the already known compound $PbTa_2O_6$, the following phases were identified by x-ray analysis: cubic $Pb_{1.5}Ta_2O_{6.5}$, stoichiometric, with a = 10.54 Å; a rhombohedral pyrochlor-type phase between $Pb_2Ta_2O_7$ (a = 10.71 Å, α = 88° 26′) and $Pb_{2.5}Ta_2O_{7.5}$ (a = 10.73 Å, α = 87° 58′); and a tetragonal phase $Pb_3Ta_2O_8$ (a = 10.62 Å, c = 10.86 Å). The existence of all the phases of $PbO-Nb_2O_5$ system already mentioned in the literature were confirmed. In the $PbO-U_2O_5$ system, only a single phase was found between $Pb_{1.5}U_2O_{6.5}$ and $Pb_{2.5}U_2O_{7.5}$. With increasing PbO content, a steady conversion from a cubic to a distorted rhombohedral structure occurred. The composition of the cation sublattice in the various compounds was found by density measurements to be quite different for the uranium compounds, than for the niobium and tantalum compounds. (auth)

29795 INVESTIGATION OF NICKEL−BERYLLIUM−BORON AND COBALT−BERYLLIUM−BORON SYSTEMS. Becher, H. J.; Neidhard, H. (Technische Hochschule, Stuttgart). Z. Anorg. Allg. Chem., 344: 125-39(May 1966). (In German).

A compound with the mean composition $[Ni_{0.63}Be_{0.37}][Be_{1.40}B_{0.60}]$ with the cubic C_{15} structure of $MgCu_2$ was found in the ternary system Ni−Be−B. The Ni atoms and part of the Be atoms were statistically distributed on the Mg sites of the $MgCu_2$ lattice and the rest of the Be atoms and the B atoms were on the Cu sites. The lattice constant had values between 5.762 and 5.772 Å. Another ternary compound with a still unknown structure had the mean composition $Ni_6Be_7B_3$. In the Co−Be system the existence of a phase with C_{15} structure could be established. The compound was formed at a Co : Be ratio of 1 : 8 to 1 : 12 from the molten components. At temperatures below 1150°C, a hexagonal Co−Be phase was observed in the same region of the system. Boron can occupy the Be positions of the cubic Co−Be phase, causing a lattice contraction up to 2.5%. The already known $CuBe_2$ and C_{15} structure, however, does not allow substitution by boron. (auth)

29796 SEARCH FOR A DEFECT MODEL FOR UO_2. Kroeger, F. A. (Univ. of Southern California, Los Angeles). Contract AF-AFOSR-986-66. Z. Phys. Chem. (Frankfurt), 49: 178-97(May 1966).

Experimental data for deviation from stoichiometry of UO_2 as $f(p_{O_2}, T)$ as available in the literature are presented and are discussed in terms of imperfection models in which ionized as well as non-ionized defects play a part. (auth)

29797 DISTRIBUTION OF ERBIUM IN MOLTEN Al−Cd, Al−Pb, AND Al−Bi ALLOYS. Bayanov, A. P.; Serebrennikov, V. V. (Tomsk State Univ., USSR). Zh. Fiz. Khim., 39: 2816-17(Nov. 1965). (In Russian).

The distribution coefficients of erbium in Al−Cd, Al−Pb, and Al−Bi systems were determined at 700°C. The values of the activity coefficients and of the excess partial molar isobar-isothermal potentials of erbium in aluminum were determined at 700°C. (tr-auth)

29798 BINARY URANIUM AND MOLYBDENUM OXIDES. Trunov, V. K.; Rozanova, O. N.; Kovba, L. M. (Moscow State Univ.). Zh. Neorg. Khim., 10: 2576-7 (Nov. 1965). (In Russian).

The system $UO_2-UO_3-MoO_3$ was investigated at 750°C. The samples were annealed, and x-ray phase analyses were made of the anneal product. The results are tabulated and show that in the $UO_3-UO_2-MoO_3$ system at 750°C only one new compound, U_2MoO_8, is formed. The crystalline data obtained from the x-ray study of U_2MoO_8 are tabulated. This compound crystallizes in the rhombic system with the parameters a = 6.7, b = 22, and c = 4.1Å. (J.S.R.)

29799 HIGH-TEMPERATURE X-RAY PHASE ANALYSIS OF URANIUM–OXYGEN SYSTEM FROM $UO_{2.50}$ TO $UO_{2.67}$. Rachev, V. V.; Smurova, V. S.; Kovba, L. M.; Ippolitova, E. A. Zh. Neorg. Khim., 10: 2796-2800(Dec. 1965). (In Russian).

The uranium−oxygen system was investigated by high-temperature x-ray phase analysis in the composition interval from $UO_{2.50}$ to $UO_{2.67}$ at temperatures from 20 to 900°C. It is shown that the homogeneity range of the U_3O_{3-x} phase is expanded with increasing temperature from $UO_{2.66}$ at 20°C to $UO_{2.63}$ at 950°C. The existence of the rhombic oxide $U_5O_{13\pm x}$, stable at all temperatures studied and having an outstanding homogeneity range, was shown. It was established that in the temperature interval from 20 to 1100°C the fluorite phase U_4O_{9+x} coexists with the oxide U_5O_{13-x}. The conditions for formation of β-U_3O_8 were determined. (tr-auth)

29800 WORK FUNCTION OF REFRACTORY-METAL CARBIDES IN CESIUM VAPORS. Bol'shov, V. G. (Ioffe Inst. of Physics and Tech., Leningrad). Zh. Tekh. Fiz., 36: 331-7(Feb. 1966). (In Russian).

The thermoelectric emission of TaC and ZrC treated in Cs vapor was studied in vacuum and in a cesium-vapor atmosphere. The results of the experiments demonstrate the volumetric character of the sorption of Cs by materials. (tr-auth)

29801 THERMIONIC PROPERTIES OF POLYCRYSTALLINE ZIRCONIUM, BERYLLIUM, AND SELECTED

ZIRCONIUM BERYLLIDES [Thesis]. Jerner, R. Craig. Denver, Univ. of Denver, 1965. 130p.

The thermionic emission properties of polycrystalline zirconium, beryllium, beryllium oxide, and selected zirconium beryllides were investigated. Cylindrical geometry was used in order to obtain high emitter-collector fields. A Richardson work function of 4.34 ± 0.04 ev and a value of the thermionic constant equal to 3500 amp/cm^2–°K^2 were determined for zirconium. An exact value of the Richardson work function of pure beryllium was not determined. However, results indicate that the work function of beryllium is probably about 3.20 ev. A Richardson work function of 3.80 ± 0.07 ev and a value of the thermionic constant equal to 31 amp/cm^2–°K^2 were determined for beryllium oxide. The work functions of the zirconium beryllides were found to increase from approximately 3.40 ev to about 3.85 ev as beryllium evaporated from the surface of the emitter. An anomalous region was observed in some of the Schottky plots in the transition from space-charge-limited to temperature-limited emission. (Dissertation Abstr.)

29802 SOME EFFECTS OF TEMPERATURE AND HEAT TREATMENT ON THE STRENGTH OF SINTERED WC-Co ALLOYS. Betser, A. A. (Israel Inst. of Tech., Haifa); Gurland, J. New York, American Society of Mechanical Engineers, 1966, Preprint No. 66-MD-17, 5p., $1.50. (CONF-660519–1). ORAU.

From Design Engineering Conference and Show, Chicago.

Experimental results are presented on the separate effects of elevated temperatures and quenching and annealing on the transverse rupture strength of sintered tungsten carbide. It was found that the fracture strength was little affected by temperatures up to 475°C for compositions ranging from 10 to 31 vol% of cobalt. The strength was slightly increased by rapid cooling from the sintering temperature in the range from 50 to 75 vol% of cobalt. The theoretical implications of these results are briefly discussed. (auth)

29803 URANIUM ALLOY DEVELOPMENT FOR NON-NUCLEAR APPLICATION. Progress Report No. 3. Skelly, H. M.; Dixon, C. F.; Spence, N. S. (Dept. of Mines and Technical Surveys, Ottawa). 24p. (CONF-650841–2). ORAU. Gmelin, AED-CONF-65-277-5.

From Conference of Metallurgists, Ottawa.

Work in the development of high-strength uranium-base alloys is reported. A procedure was established for the melting, alloying, and casting of small batches (about 1800 g) of experimental uranium alloys. Binary alloys of the following nominal compositions were prepared: U–1% Mo, U–2% Mo, U–3% Mo, U–1% Nb, U–2% Nb, U–3% Nb, U–2% V, U–3% V, U–0.5% Zr, U–2% Zr, U–0.5% Ti, and U–2% Ti. The quality of the resulting castings was assessed by chemical and x-ray fluorescence analyses, gamma radiography, and microexamination. The response of the alloys to various heat treatments was determined by hardness measurements, and the results showed that a large range of hardnesses can be obtained—from 264 to 677 VHN. The strength and hardness of the alloys were generally improved by heat treatment, but their ductility was seriously reduced. The highest mechanical properties in the as-cast condition were given by the U–3% Nb alloy, viz. 180 kpsi UTS, 157 kpsi 0.2% YS, 3.4% elongation, 370 kpsi compressive strength, 159 kpsi 0.2% compressive yield strength, and 412 VHN. The U–2% Mo alloy gave the highest heat-treated tensile properties, viz. 185 kpsi UTS, 180 kpsi 0.1% YS, and 1% elongation. The compressive strengths of the heat treated alloys were all in the range of 313 to 365 kpsi, except for the U–2% Zr alloy, which gave 452 kpsi. Densities ranged from 17.85 to 18.86 g/cm^3. (auth)

Radiation Effects

See also CHEMISTRY — Radiation Chemistry

Refer also to abstracts 29486, 30260, 30301, 30740, and 30742.

29804 (EURAEC–1637) URANIUM MONOCARBIDE SHAPING AND IRRADIATION. Quarterly Report 17 and 18, July 1, 1965–December 31, 1965. (Commissariat a l'Energie Atomique, Paris (France). Commissariat a l'Energie Atomique, Grenoble (France). Centre d'Etudes Nucleaires). 20p. (EUR–2839). Dep. mn. CFSTI $1.00 cy, $0.50 mn.

Work Performed under United States–Euratom Joint Research and Development Program.

Cylinders of UC enriched with 8% ^{235}U were irradiated for 1000 hr at 750°C in K–Na to a burnup of 1000 Mwd/t. A 0.2% decrease in density occurred with no apparent changes in the microstructure. The irradiated specimens appeared to have an increased susceptibility to atmospheric corrosion. (W.L.G.)

29805 (NUMEC–3432–21) IRRADIATION TESTING OF PuO_2–UO_2 FUELS. Quarterly Progress Report, January 1–March 31, 1966. (Nuclear Materials and Equipment Corp., Apollo, Pa.). May 31, 1966. Contract AT(30-1)-3432. 36p. Dep. mn. CFSTI $2.00 cy, $0.50 mn.

Photomicrographs of irradiated PuO_2–UO_2 fuels, prepared by five different procedures, are presented and discussed. A plot of fission gas release as a function of the fuel volume showing the effects of grain growth indicates that homogeneous and heterogeneous substoichiometric fuels behave similarily. There appears to be little difference in the fission gas release from coprecipitated and substoichiometric mechanically-blended mixtures operating at the same temperature. Mechanically-blended stoichiometric oxides showed significant grain growth in comparison to the other specimens, but very little difference in the amount of fission gas released. (W.L.G.)

29806 (ORNL-TM–1511) POSTIRRADIATION EXAMINATION OF HIGH BURNUP EGCR PROTOTYPE FUEL CAPSULES. Osborne, M. F.; Long, E. L. Jr.; Morgan, J. G. (Oak Ridge National Lab., Tenn.). June 1966. Contract W-7405-eng-26. 32p. Dep. mn. CFSTI $2.00 cy, $0.50 mn.

Results of the examination of nine fuel capsules which were irradiated in the Engineering Test Reactor (ETR) for periods of three to four years are presented. The irradiation capsules were prototypes of the fuel elements for the Experimental Gas-Cooled Reactor (EGCR), the construction of which has been discontinued. Some of the capsules were examined much more thoroughly than others. Only one of this group of nine capsules was found to have suffered a loss of cladding integrity. Three stainless steel containment vessels which had been exposed to nitrogen at high temperatures were examined; two of these vessels had experienced appreciable nitriding. (auth)

29807 (TRG-Report–325) GRAIN BOUNDARY HOLES IN IRRADIATED URANIUM. Chatwin, W. H.; Hyam, E. D. (Reactor Group, United Kingdom Atomic Energy Authority, Sellafield (England)). May 1, 1962. 30p. Dep. BIS $1.00. HMSO 5s.

Calder fuel elements do not develop detectable grain boundary cracking of the type which results from stress-induced bubble growth up to irradiation levels of 2800 Mwd/te; this is probably because the irradiation temperatures are relatively steady. Growth of grain boundary gas bubbles induced by the intergranular tensile stresses generated by severe thermal cycling during irradiation was shown to be responsible for the grain boundary cavitation and cracking previously observed in some specimens of uranium–½ at. % chromium alloy. The mechanism of this process is described in detail. The phenomenon provides one explanation of the pronounced tendency of irradiated uranium to develop grain boundary cracks, with accompanying decrease in apparent density, in certain circumstances in the α range. For irradiated uranium generally, the observations imply that similar intergranular cavitation and cracking, with accompanying changes in dimensions and density, can in principle be produced by any other conditions which cause intergranular tensile stresses (e.g. irradiation growth, $\alpha\beta$ cycling or external stressing as in a tensile or creep test) provided that these stresses

can be maintained for sufficient time at temperature for vacancy diffusion to occur. The little evidence available suggests that this type of structure may only develop under these conditions of thermal cycling at temperatures ≳490°C, for irradiation levels ~2000 Mwd/te, though it is possible that this temperature limit may be somewhat lower for higher irradiations. (auth)

29808 DIRECT OBSERVATION OF RADIATION DAMAGE PRODUCED IN COPPER, GOLD, AND ALUMINUM DURING ION BOMBARDMENTS AT LOW TEMPERATURES IN THE ELECTRON MICROSCOPE. Howe, L. M.; McGurn, J. F.; Gilbert, R. W. (Chalk River Nuclear Labs., Ontario, Can.). Acta Met., 14: 801-20(July 1966).

Copper, gold and aluminum foils were bombarded directly in the electron microscope with 100 kev O^- ions at temperatures as low as ~20°K. Visible defects appearing as spots, small irregular dislocation loops or complex tangles, depending upon the ion dose, were produced in all of the foils. Analysis of the images of the defects appearing as spots revealed that most of these particular defects are vacancy in character (i.e., represent depleted zones) and have a strain field which is not spherically symmetrical. Furthermore the results indicate that the strain field associated with the larger of these defects in the copper and gold foils has a principal component along either ⟨111⟩ or ⟨110⟩ directions which suggests that these larger defects are actually unresolved vacancy loops having a/3 ⟨111⟩ or a/2 ⟨110⟩ Burgers vectors; the a/3 ⟨111⟩ loops being the more numerous. Quenched and aged gold foils containing stacking-fault tetrahedra were also bombarded at temperatures as low as ~20°K. In the early stages of bombardment the tetrahedra collapsed into irregular shapes which still exhibited stacking-fault contrast or into triangular sessile dislocation loops lying on {111} planes. With increasing ion bombardment the collapsed tetrahedra decreased in size until they could no longer be distinguished from the radiation-produced defects. These results are consistent with a mechanism whereby interstitial atoms are gradually accumulated at the tetrahedra or at collapsed forms of the tetrahedra which encompass a stacking fault. However, interstitial atoms will not be freely migrating in gold at 20°K. It is suggested, therefore, that the accretion of interstitial atoms at the stacking-fault tetrahedra occurs as the result of collision chains and channeled atoms, which emanate from the region of the depleted zones, being defocused or dechanneled at the stacking faults. (auth)

29809 FURTHER RESULTS FROM RESEARCH ON STRESS-INDUCED VARIATIONS IN THE SPECTRAL DISTRIBUTION OF GAMMA RADIATION FROM ^{137}Cs TRANSMITTED BY GRAPHITIZED CARBON. Bujok, Jozef (Main Inst. of Mining, Katowice, Poland). Acta Phys. Pol., 29: 643-53(May 1966).

Results are presented from research on variations in the spectral distribution of gamma rays (^{137}Cs) transmitted by graphitized carbon, depending on the magnitude of vertical loads. These results supplement those published previously. (auth)

29810 BERYLLIUM OXIDE IN THE NUCLEAR INDUSTRY. Morize, P. Bull. Soc. Franc. Ceram., No. 64, 27-34(July-Sept. 1964). (In French).

The neutronic, chemical, mechanical, and thermal properties of pure beryllium oxide, which make it an important material for use in nuclear reactors as a moderator and a reflector, are discussed. The irradiation of this oxide by rapid neutrons, disturbing the crystalline network, affects its mechanical and thermal properties. Experimental results showed that these properties vary as a function of the quantity of neutrons received and of the irradiation temperature, thus limiting the practical field of use. The major applications, present or planned, of beryllium oxide in the nuclear field are reviewed. Use of BeO–UO_2 mixtures in fuel elements is considered in particular. (BBB)

29811 TENSILE FRACTURE STRAIN OF GRAPHITE DETERMINED DURING NEUTRON IRRADIATION. Jackson, J. L. (Battelle Memorial Inst., Richland, Wash.). Carbon, 3: 397-400(Feb. 1966).

Graphite, when used as a moderator material, is subjected to neutron damage gradients. These damage gradients can generate internal stresses which could lead to fracture. The strain that could be accumulated before fracture during irradiation for EGCR-type AGOT graphite was investigated. Strains were measured on parallel cut samples irradiated at 625 ± 25°C at a nominal strain rate of 0.13% per 10^{20} n/cm^2. Strains before fracture ranging from 0.37 to 0.42% were obtained, compared to strains at fracutre of 0.1 to 0.2% for unirradiated material. (auth)

29812 RADIATION EFFECTS IN GRAPHITE AT HIGH TEMPERATURE. Helm, J. W. (Battelle Memorial Inst., Richland, Wash.). Carbon, 3: 493-501(Feb. 1966).

Radiation-damage effects in various nuclear graphites were studied at neutron exposures ranging up to 1.6×10^{22} neutrons/cm^2 (E > 0.18 Mev) for irradiation temperatures of 425–1200°C. Graphites tested were conventional-coke graphites CSF and TSGBF; needle-coke graphites NC7, NC8, and TSX; and raw-coke graphites. Properties studied were length changes, coefficient of thermal expansion, microscopy, and strengths. For samples cut in the direction transverse to the extrusion axis, physical length changes at an irradiation temperature of 800°C showed a contraction followed by an expansion several times greater than the contraction. At 425 and 1200°C the transverse samples exhibited about the same contraction and the amount was more than that at 800°C. In the parallel direction, the samples continued to contract with increasing neutron exposure. The 800°C data again show the least contraction but the contraction at 1200°C was much greater than that at 425°C. The raw-coke graphites generally contracted less than the other types. The CTE of the less-graphitic material changed under neutron irradiation. (auth)

29813 IRRADIATION OF GRAPHITE IMPREGNATED WITH FURFURYL ALCOHOL. Engle, G. B.; Disselhorst, B. F.; Tully, G. R. Jr.; Wallace, W. P. (General Atomics Div., General Dynamics Corp., San Diego). Carbon, 3: 543-4(Feb. 1966). (GA–6670).

Dimensional changes induced by fast neutrons in graphite impregnated with furfuryl alcohol were studied. A series of impregnations on the pore structure of commercial grade graphite increased the density 4–7%. The irradiation experiments were carried out in a series of capsules in a test reactor. After a short irradiation at 450 or 750°C, little difference in dimensional stability was observed in the impregnated graphite. Thermal expansion changes were noted in the samples that were cut perpendicular but not in the samples cut parallel to extrusion. (J.G.B.)

29814 KINETICS OF ANNEALING IN IRRADIATED BARIUM NITRATE. Mohanty, S. R.; Upadhyay, S. R. (Banaras Hindu Univ., Varanasi, India). Indian J. Chem., 4: 57-9(Feb. 1966).

The kinetics of isothermal annealing in γ-irradiated barium nitrate was studied at different temperatures in the range 200–275°C. It is found that the process can be represented by the combination of one rapid first-order and one slow second-order reaction, each with a different energy of activation. It is considered that the damage fragments are of two kinds: Correlated NO_2^- ion and O atom pairs decay unimolecularly; and completely liberated NO_2^- ions and O fragments undergo random recombination bimolecularly. (auth)

29815 THEORY OF THE ADSORPTION EFFECT ON THE SURFACES OF SEMICONDUCTORS AND GELS DUE TO EFFECTS OF IONIZING RADIATION. Aronov, D. A.; Ablyayev, Sh. A.; Pilatov, U. U.; Shamasov, R. G. (Physicotechnical Inst., Academy of Sciencs, Uzbek SSR). Izv. Akad. Nauk Uz. SSR, Ser. Fiz.-Mat. Nauk, No. 5, 63-70(1965). (In Russian).

The electron theory of chemosorption is used to determine the sign of the adsorption effect as a function of the parameters of the semiconductor (or gel) and the experimental conditions. The case considered is limited to that of a strong absorption when the ionizing radiation generates electron-hole pairs near the surface. The expression for the adsorption effect, which determines its sign, is then ap-

plied to several special cases. It is shown that adsorption occurs more readily when volume recombination of carriers is low in comparison with surface recombination. This is the case of a gel with a strongly developed surface. Such effects have been observed experimentally in gels irradiated with slow electrons. (ATD)

29816 RADIATION BLISTERING: INTERFEROMETRIC AND MICROSCOPIC OBSERVATIONS OF OXIDES, SILICON, AND METALS. Primak, William; Luthra, Jagdish (Argonne National Lab., Ill.). J. Appl. Phys., 37: 2287-94(May 1966).

Photographs and descriptions of the phenomena are given. Most of the observations were of magnesium oxide, a few were of spinel and corundum. The fringe systems arising from a blister (two films on a substrate) are described. Results are given for miscellaneous H^+, D^+, He^+, and He^{++} bombardments, 0.025–4 Mev. Measurements are given of blister heights, diameters, shell thicknesses, and depths of cavities left after blister shells break away (exfoliate). Effects arising from superficial deposited films are described. Blistering was found on polycrystalline copper bombarded with H^+ or He^+ and on polycrystalline nickel with He^+ only. Blistering was not found on several other metals bombarded similarly. For the oxides, blistering was first noted at $\sim 3 \times 10^{17}$, while for the metals at $\sim 8 \times 10^{17}$. The effects of gas permeability, radiation expansion, and elastic moduli on blister growth are discussed. The dispersion of refractive index of magnesium oxide is given. (auth)

29817 METHOD OF UTILIZING NUCLEAR REACTIONS IN THE STUDY OF OXIDE LAYERS. Ollerhead, R. W.; Almqvist, E.; Kuehner, J. A. (Chalk River Nuclear Labs., Ontario). J. Appl. Phys., 37: 2440-4(May 1966).

The reaction $^{17}O(^3He,^4He)^{16}O$ was used to investigate the diffusion of oxygen into surface layers of zirconium oxide on zirconium metal under different conditions of time and temperature. The methods used are described in detail, and examples of typical results are given. This technique is generally applicable as a means of investigating the penetration of oxygen into materials up to a depth of about five microns. (auth)

29818 EFFECT OF VOID VOLUME VARIATION ON PRESSURE BUILDUP IN VIBRATORY-COMPACTED UO_2 FUEL ELEMENT. Kubota, Tadashi; Nohara, Tadahide; Takahashi, Shuichiro (Mitsubishi Atomic Power, Inc., Japan). J. Nucl. Sci. Technol. (Tokyo), 3: 125-30(Apr. 1966).

The effect of void volume variation on pressure buildup in a vibratory compacted UO_2 fuel element was studied. The apparatus and the experimental procedure for measuring void volume in vibratory compacted UO_2 fuel element are described. It is indicated from a comparison of the ratio of void volume to total inner volume of fuel element and the ratio of total inner volume of fuel element minus calculated volume of UO_2 to total inner volume of fuel element that no particle bonding occurred and also that no additional closed pores were generated during vibratory compaction. Thermal simulation experiments resulted in void volume decrease by microstructural changes such as sintering phenomena and densification. (auth)

29819 RADIATION DAMAGE CAUSED BY NEUTRONS IN METALS. Drittler, K. (Gesellschaft fuer Kernenergieverwertung in Schiffbau und Schiffahrt mbH, Geesthacht-Tesperhude, Ger.). Kerntechnik, 8: 217-21(May 1966). (In German).

The most important defects in the crystal lattices of metals, caused by irradiation with neutrons, are briefly discussed. The annealing of radioinduced defects is described. The influence of these microphysical processes on macrophysical properties is explained. The effects of radiation on swelling, hardening, and embrittlement as well as on changes of chemical reactions are discussed. (auth)

29820 BEHAVIOR OF REFRACTORY METALS IN RADIATION ENVIRONMENTS. Waldron, M. B.; Adam, J.; Eyre, B. L. (Atomic Energy Research Establishment, Harwell, Eng.). pp 859-79 of Metals for the Space Age, Plansee Proceedings, 1964. Benesovsky, F. (ed.). Reutte/Tyrol, Metallwerk Plansee AG, 1965.

Three main topics are discussed: radiation damage in molybdenum relevant to its use as a nuclear cladding material; compatibility problems in thermionic diodes consisting of UC–ZrC clad in refractory metals; and compatibility of PuC with refractory metals for possible application in SNAP devices. Irradiation of commercially pure molybdenum by neutrons or fission fragments produces hardening and raises the brittle-ductile transition. By continuing irradiation well beyond the threshold at which changes in mechanical properties occur to relatively high doses ($\sim 10^{20}$ nvt), point defect clusters were observed. On annealing in the temperature range 650–1100°C the clusters grow into dislocation loops which finally interact to form networks. All the loops were found to be interstitial in nature indicating that the annealing occurs by a process of coalescence. The interpretation of these results suggests the importance of interstitial impurities in the thermal recovery of properties in irradiated molybdenum. The compatibility of UC–ZrC with W, Ta, Mo, Nb, and Re was examined in the region 1800–2500°C. Tungsten, tantalum, and rhenium were found to have the best short-term stability in contact with the carbide. The observations are discussed in relation to thermodynamic and phase equilibria considerations. Compatibility studies between PuC and V, Zr, Nb, Mo, Ta, and W showed extensive reactions in all cases in the temperature range 1200 to 1400°C. It was concluded that the use of protective layers may be needed for the successful use of PuC in SNAP devices. (auth)

29821 MODIFICATION OF THE CONDUCTIVITY OF $Ni(OH)_2$ AND CdO BY IRRADIATION WITH NEUTRONS. Scharmann, A.; Euler, J. (Univ., Giessen, Ger. Varta AG, Frankfurt am Main). Naturwissenschaften, 53: 224 (1966). (In German).

The effects of reactor radiation on the electric conductivity of pure and commercial $Ni(OH)_2$ and pure CdO were studied on pressed-powdered samples. The neutron dose was 10^{14} to 10^{15} fast neutrons/cm^2. In pure $Ni(OH)_2$ an increase in the specific resistance of about 14 to 22% was established after irradiation. In technical nickel hydroxide the specific resistance increased by a factor of 2.3 to 2.8. In pure CdO the specific resistance decreased 10 to 15% after irradiation. (J.S.R.)

29822 RADIATION DAMAGE OF LOW-PERMEABILITY GRAPHITE AND HARD CARBON. Masuyama, Toshio (Nippon Carbon Co., Ltd., Japan). Nippon Genshiryoku Gakkaishi, 8: 185-94(Apr. 1966). (In Japanese).

Low permeability graphite and hard carbon were irradiated in a fuel hole of an experimental reactor. The radiation damage was studied through measurements of such factors as low temperature thermal conductivity, dimensional changes, and permeability. The temperature dependence of the thermal conductivity of hard carbon followed a glass like pattern. After irradiating and annealing at 1,200°C, the temperature dependence of thermal conductivity underwent a change suggesting the structure change caused by neutron bombardment. The relative intensity of diffracted x rays of hard carbon irradiated with high neutron flux at high temperatures showed different characteristics from artificial graphites. The treatment looked like graphitization of hard carbon by irradiation without high temperature heat treatment. (P.C.H.)

29823 GAMMA-INDUCED ELECTRICAL CONDUCTIVITY IN ALUMINA. Dau, Gary J.; Davis, Monte V. Nucl. Sci. Eng., 25: 223-6(July 1966).

Theoretical development for the gamma-induced production of conduction band electrons in alumina is presented. Consideration of charge carrier mobility limited investigations to crystals having ionic bonding. Because of the difficulty in evaluating theoretical constants, all were combined and considered to be independent of temperature and radiation. This constant was evaluated experimentally. A model

with a single trap depth was developed for predicting conductivity of ionic insulators as a function of temperature and radiation dose rate. The model is $\sigma(T,P) = \sigma(T) + PG \exp(-W/kT)(T)^{\frac{1}{2}}$, where the first term on the right represents ionic conductivity of material external to a radiation field and the second term describes radiation-induced conductivity. Term P represents gamma dose rate in roentgen per hour, G is an experimentally determined constant, and W represents the energy necessary to raise trapped electrons into the conduction band. The temperature dependence of the mobility is represented by $(T)^{\frac{1}{2}}$. Evaluation of experimental data for alumina gave W = 0.086 ± 0.014 eV and $G = 7.4 \times 10^{-21} (\Omega^{-1}cm^{-1}K^{\frac{1}{2}}R^{-1}h)$. (auth)

29824 RELEASE OF STORED ENERGY AND ELECTRIC RESISTIVITY CHANGES BELOW 65 DEG K IN NEUTRON-IRRADIATED COPPER. Heeger, D.; Rau, F.; Tischer, P.; Wenzl, H. Phys. Lett., 21: 393-4(June 1, 1966). (In German).

The release of stored energy and the corresponding change of electric resistivity are measured during the annealing from 10 to 65°K of copper irradiated at 4°K in the core of the Munich Research Reactor. The ratio of the stored energy to the change of electric resistivity was 28.0 ± 1.3 Ws/gμΩcm in agreement with the results after deuteron-irradiation. (auth)

29825 EMBRITTLEMENT OF REACTOR STRUCTURAL STEELS BY NEUTRON IRRADIATION. Kawasaki, Masayuki; Fujimura, Tadato (Atomic Energy Research Inst., Tokyo). Tetsu To Hagane, 51: 2328-35(Dec. 1965). (In Japanese).

An in-pile test rig was constructed for testing the embrittlement of steels by neutron irradiation. The test rig, experimental conditions available with the rig in a vertical experimental tube of JRR-2, and the results of the irradiation tests, including the post-irradiation V-notch Charpy tests on the A 302 B steel, its welded portion, and an aluminum killed steel, are described. (TCO)

29826 FAST NEUTRON IRRADIATION EXPERIMENTS WITH STRONTIUM TITANATE SINGLE CRYSTALS [Thesis]. Miner, George Kenneth. Cincinnati, Univ. of Cincinnati, 1965. 79p.

Fast-neutron irradiation damage was investigated in single crystals of strontium titanate. The emphasis was placed on relating changes in structure and electrical properties to the integrated fast-neutron flux and the direction of fast-neutron bombardment with respect to the crystallographic orientation of the samples. Four total integrated fast-neutron fluxes were used ranging from 10^{15} to 10^{19} neutrons/cm^2. The directions of bombardment were (100), (110) and (111). The structural effects were investigated with Laue back reflection, x-ray rocking curves, and x-ray absorption measurements. Examination of electrical properties was accomplished through resistivity and dielectric constant measurements. It was found that each of these parameters was changed by neutron irradiation. Most significant was the reduction of mosaic spread in each case. For isotropic neutron bombardment an increase in mosaic spread is usually observed. The reversal of this trend here was due to the almost unidirectional bombardment. Moreover, the reduction varied with orientation, an effect that can be explained with channelling. The results of the Laue investigations and the x-ray absorption measurements agreed with the change in mosaic spread. For each orientation the dielectric constant was reduced by bombardment, and the resistivity decreased for low dosages but exhibited some increase for additional bombardment. This could be explained by an increase in the number of carriers due to displaced atoms and a reduced mobility of carriers due to defects. There seems to be some correlation among the parameters examined corresponding to a better alignment of the mosaic blocks in the crystals. This better alignment could be accomplished by the displacement of atoms in the region between mosaic blocks. The number of carriers would increase due to these and other displacements. The decrease in the mobility of carriers for higher dosages could result from a large number of defects. (Dissertation Abstr.)

PHYSICS

General

29827 (UCRL-16824) CORRELATIONS OF PHOTONS FROM A THERMAL SOURCE. Ma, Shang-keng (Lawrence Radiation Lab., Univ. of California, Berkeley). Apr. 21, 1966. Contract W-7405-eng-48. 111p. Dep. mn. CFSTI $4.00 cy, $0.75 mn.

Thesis.

The amplitude and the intensity-correlation of photons from a model thermal source are studied. The objective is to express the photon correlation function in terms of the parameters describing the source. The source model is analyzed utilizing the temperature Green's function method. The power spectrum (line shape) is computed numerically for some special cases. General properties of temperature Green's functions are also studied. (auth)

29828 EMISSION OF A POINT CHARGED PARTICLE PASSING ALONG THE AXIS OF A SEMI-INFINITE WAVEGUIDE. Ayvazyan, Yu. M.; Sedrakyan, D. M. (TsNI Physico-Technical Lab., Armenian SSR). Izv. Akad. Nauk Arm. SSR, Ser. Fiz. Mat. Nauk, 18: No. 5, 83-9 (1965). (In Russian).

An expression is obtained for the angular distribution of the emission intensity of a point charged particle from a plane waveguide consisting of two semi-infinite flat plates, using Maxwell equations and the solutions of the d'Alembert equation. (L.B.S.)

29829 STUDY OF CHARGED PARTICLE MOTION IN A MAGNETIC DIPOLE FIELD IN AN EXTERNAL MAGNETIC FIELD BY THE STÖRMER METHOD. I. Shalimov, V. I.; Shvachunov, I. N. Kosm. Issled., 4: 208-20(Mar.-Apr. 1966). (In Russian).

The problem of the motion of charged particles in a magnetic-dipole field located in an external homogeneous magnetic field H_0 antiparallel to the magnetic-moment vector of the dipole, M, is solved by the Störmer method. It is shown that the shape and dimensions of the allowed and forbidden regions depend on the particle energy, even if the Störmer unit of length is used as the scale. There exists a threshold value of the particle energy, depending on the relation between H_0 and M, such that, if the particle energy is lower than the threshold, and only internal allowed regions exist for all values of the Störmer constant γ. If the particle energy is higher than the threshold, then there are external as well as internal allowed regions as functions of the values of γ, and they join at $\gamma = \gamma^-$, since the value of γ^* also depends on the particle energy. (tr-auth)

29830 INFLUENCE OF HIGHER SPACE FIELD HARMONICS ON ELECTRODYNAMIC FORCES AND THE JOULE LOSSES IN CONDUCTING LAYERS MOVING IN TRAVELING MAGNETIC FIELDS. Valdmanis, Ya. Ya.; Lielpeter, Ya. Ya.; Mikelson, Yu. Ya. (Inst. of Physics, Academy of Sciences, Latvian SSR). Latv. PSR Zinat. Akad. Vestis, Fiz. Tek. Zinat. Ser., No. 6, 27-33(1965). (In Russian).

Expressions of force density and the Poynting vector were obtained for a conducting layer located in a travelling magnetic field of a two-sided symmetrical inductor considering the higher harmonics and the motion of the layer. Curves of dependence of these expressions on the velocity of the layer for different electric and geometric parameter values were plotted. (auth)

29831 ELECTROMAGNETIC CAVITY RESONANCES IN ACCELERATED SYSTEMS. Yildiz, Asim; Tang, C. H. (Raytheon Co., Wayland, Mass.). Contract AF19(628)-4380. Phys. Rev., 146: 947-54(June 24, 1966).

Electromagnetic cavity-resonant frequencies in rotating systems are investigated through the covariant space-time formulation of the classical electromagnetic field theory in which the concept of the constitutive relation is introduced in a consistent manner. Three different types of rotating systems are considered: namely, (1) rotating cavity, stationary medium; (2) rotating cavity and medium; and (3) stationary cavity, rotating medium. In the most general form of the solution, it is shown that the electric and magnetic types of modes are coupled by the rotation. A set of coupled differential equations which describe the coupling is derived. Various relations for mode splitting are obtained on the basis of physical optics, and the customary approximations for geometrical optics are applied. It is found that the physical-optical approach leads to slight but interesting differences with respect to the existing earlier kinematical analysis by von Laue. (auth)

29832 ELECTROMAGNETIC SCATTERING FROM INHOMOGENEOUS DIELECTRICS OF FINITE EXTENT. Von Roos, Oldwig (Astrophysics Research Corp., Los Angeles). Phys. Rev., 146: 960-5(June 24, 1966).

A theory of scattering of electromagnetic waves from objects possessing an arbitrary space-dependent complex permittivity is developed. By means of two new variational principles, the analog of the so-called "augmented Born approximation" in quantum mechanics is derived. The theory is applied to the scattering of light from a homogeneous dielectric sphere in which case exact solutions are known. A comparison of the extinction coefficient as obtained from the exact solution to calculations within the augmented Born approximation show the latter to constitute an improvement over the Rayleigh-Gans approximation in many cases. (auth)

29833 TEMPERATURE-DEPENDENT LIFETIMES OF NONEQUILIBRIUM Fe^{3+} IONS IN CoO FROM THE MOESSBAUER EFFECT. Bhide, V. G.; Shenoy, G. K. (Inst. of Science, Bombay). Phys. Rev., 147: 306-10 (July 8, 1966).

The lifetime of the nonequilibrium Fe^{3+} state in a CoO: ^{57}Co source was determined in the temperature range 78 to 1000°K. The intensity of the ferrous state is highly temperature-dependent and was hardly detectable above 800°K. The width of the nuclear excited level of the nonequilibrium state is determined by the nuclear decay time τ and the atomic decay time $\theta(3)$. The expected changes in the linewidth of the nonequilibrium Fe^{3+} state in the Mössbauer spectra were observed. The observed deviation of the temperature variation of the hf magnetic field at the nuclei of both Fe^{2+} and Fe^{3+} ions from that expected by the molecular-field theory may be due to a possible biquadratic exchange interaction in CoO, with $j/J_2 \simeq 0.022$. (auth)

29834 ACCELERATION IN GENERALIZED COORDINATES. Della Torre, E.; Longo, C. V. (Rutgers Univ., New Brunswick, N. J.). Proc. IEEE (Inst. Elec. Electron. Eng., 54: 404(Mar. 1966).

A simple formula is presented for calculating the derivatives of unit vectors which describe the motion of particles in generalized coordinates. (B.G.D.)

29835 POLYPHASE CYLINDRICAL INDUCTOR WITH A MULTIPOLE FIELD. Fomin, A. A. Zh. Tekh. Fiz., 36: 186-90(Jan. 1966). (In Russian).

The magnetic field produced within a circular cylinder by a system of conductors parallel to the axis and equally spaced on the surface of the cylinder carrying equal currents with a constant phase difference between the currents in successive conductors is calculated. The calculation is based on an expression for the vector potential previously given, the result is expressed as a Fourier series in the azimuth. If the space outside the cylinder is filled with a ferromagnetic material with infinite permeability the field strength within the cylinder is doubled. If d is the phase difference between the currents in successive conductors and there are a total of N conductors in all, the number of phases is $\beta = 2\pi/d$, the number of pole pairs is $p = N/\beta$, and the field near the axis is proportional to r^p, where r is the distance from the axis. This rapid increase of field strength with distance from the axis is ad-

vantageous for the design of electrodynamic supports, electromagnetic crucibles, and magnetic traps. For fixed N, p is maximum when $\beta = 2$, and a two-phase system is recommended for the design of electrodynamic supports. (ATD)

29836 RADIATION OF A CHARGE MOVING ABOVE AN ANISOTROPICALLY CONDUCTING PLANE. Barsukov, K. A.; Naryshkina, L. G. (Moscow State Pedagogical Inst.). Zh. Tekh. Fiz., 36: 225-9(Feb. 1966). (In Russian).

The radiation of a charge moving above a plane with anisotropic conductivity is examined. The field of the moving charge and the spectrum and energy of the radiation are investigated. Special features of the conditions for radiation used in the calculation are evaluated. The forces acting on the charge from the direction of the radiation field are found. (tr-auth)

29837 INTERACTION BETWEEN ELECTROMAGNETIC WAVES AND TWO LEVEL SYSTEM. Krasovitskii, V. B.; Kurilko, V. I. Zh. Tekh. Fiz., 36: 401-4(Feb. 1966). (In Russian).

The problem of the reflection of a monochromatic wave of resonance frequency from a half-space filled with a nonlinear medium is considered. The coefficients of reflection and transmission, generalizing the Fresnel formulas for the case of a nonlinear medium, are obtained in the two-level approximation. The possibility of focusing electromagnetic energy owing to the nonlinearity of the medium is studied. The variation of the dimensions of the region of focusing with the parameters of the medium and the amplitude of the wave is found. (tr-auth)

29838 MANY-BODY THEORY. Kubo, Ryogo (ed.). 1965 Tokyo Summer Lectures in Theoretical Physics. Part I. Tokyo, Syokabo Publishing Co. New York, W. A. Benjamin, Inc., 1966. 165p. $6.75 W. A. Benjamin Inc., New York.

Separate abstracts were prepared for each of the ten papers included. (G.O.Y.)

For abstracts of individual papers see: 30186–30189, 30311–30313, 30511, 30780, and 30781.

29839 LA THEORIE DU POTENTIEL. Colloques Internationaux du Centre National de la Recherche Scientifique. Orsay, 22–26 Juin 1964. No. 146. (International Conference on the Theory of Potential, Orsay, June 22–26, 1964). Paris, Centre National de la Recherche Scientifique, 1965. 318p. (CONF-640632).

Papers (16) presented at the International Conference on Potential Theory are compiled. Abstracts for each paper are included in the table of contents. Some of the topics discussed are the transformation of Markov processes, the differences between the theory of martingales and the ergodic theory, Bessel potentials, maximal functions and capacities, the role of the minimax theorem in the fine theory of potential, some integral representations of superharmonic functions using reductions, Dirichlet's problem for second-order elliptical equations with discontinuous coefficients, and an axiomatic theory of harmonic functions. (G.O.Y.)

Accelerators

Refer also to abstract 30357.

29840 (CERN-66-16) THE 150-KJ CAPACITOR BANK FOR THE MAGNETIC HORN. Giesch, M.; van der Meer, S. (European Organization for Nuclear Research, Geneva (Switzerland)). Apr. 6, 1966. 16p. Dep. mn.

The construction and operation of the pulsed power supply of the magnetic horn, a 150 kJ capacitor bank is described. It has worked satisfactorily for more than 3 million CERN proton synchrotron cycles during the CERN Neutrino Experiment. (M.O.W.)

29841 (CONF- 651109) PROCEEDINGS OF THE USAEC FIRST SYMPOSIUM ON ACCELERATOR RADIATION DOSIMETRY AND EXPERIENCE, BROOKHAVEN NATIONAL LABORATORY, UPTON, NEW YORK, NOVEMBER 3–5, 1965. (Division of Operational Safety (AEC), Washington, D. C. Division of Research (AEC), Washington, D. C. Division of Biology and Medicine (AEC), Washington, D. C.). 662p. Dep. mn. CFSTI $6.75 cy, $2.75 mn.

Separate abstracts were prepared for 20 of the 38 included papers. For abstracts of the remaining 18 papers see papers under CONF 651109 in the report number index. (M.O.W.)

For abstracts of individual papers see: 28928–28931, 29521–29524, 29842–29851, 30719, and 30720.

29842 (CONF-651109, pp 20-33) RADIATION LEVELS IN AND AROUND NIMROD. Perry, D. R.; Shaw, K. B.

Radiation detection methods for monitoring Nimrod are briefly described. Measurements were made in the accelerator hall, through the accelerator shielding, and outside interlock areas. Induced radiation measurements were made. A brief description of results is presented. (M.O.W.)

29843 (CONF-651109, pp 34-56) RADIATION ENVIRONMENT AT THE ZERO GRADIENT SYNCHROTRON. Dvorak, Robert F.; Mundis, Robert L.; Wheeler, Robert V. (Argonne National Lab., Ill.).

The Argonne ZGS is completely covered with an earth shield with the exception of the wall between the accelerator enclosure and the separate experimental areas. In this instance, steel and high density concrete walls were constructed with channels to allow the extraction of secondary particle and proton beams. The structural and operating characteristics of the accelerator are fully described where they are directly related to the resulting radiation environment. Personnel warning and control systems are briefly mentioned and evaluated. A description and evaluation of the radiation environment, as measured to date, is emphasized. Principally, the accelerator enclosure, experimental areas, and the radiation environment outside the basic earth shield are discussed. (M.O.W.)

29844 (CONF-651109, pp 103-16) HEALTH PHYSICS SURVEY METHODS FOR THE MEASUREMENT OF STRAY RADIATION AROUND THE CERN HIGH-ENERGY ACCELERATORS. Baarli, J.; Sullivan, A. H. (European Organization for Nuclear Research, Geneva (Switzerland)).

The instruments and methods used for routine measurements of the dose equivalent of stray radiation around the CERN accelerators are described. The instruments used are such that independent estimations can be made of the dose equivalent from thermal neutron, fast neutron, nuclear interaction from high energy particles and gamma radiation together with the direct ionization by charged particles. These components are summed to find the total dose equivalent which may be divided by the absorbed dose, measured with a tissue equivalent ionization chamber, to obtain the apparent quality factor. Measurements with the instrument system indicate that wide variations in radiation composition can be found around an accelerator. The reasons for these variations are discussed, and it is shown that a large part of the dose can be due to neutrons originating from radiation escaping through weak parts of the machine shield. The estimations of the "apparent quality factor" of the radiations give values not inconsistent with those recommended by the ICRP. The limitations of the measurement system and the modifications that are necessary to make measurements of short burst radiation and of low levels of radiation are discussed. (auth)

29845 (CONF-651109, pp 117-42) METHODS AND EXPERIENCE ACQUIRED IN DOSIMETRY AT THE SATURNE SYNCHROTRON. Tardy-Joubert, Ph. (Commissariat a l'Energie Atomique, Saclay (France). Centre d'Etudes Nucleaires).

A brief description of the accelerator is given. The detectors used in conjunction with the radiation monitoring panel are briefly described, The use of BF_3 counters, threshold detectors, and neutron spectroscopy is briefly described. Other dosimetry methods are briefly described. (M.O.W.)

29846 (CONF-651109, pp 154-60) NEUTRON RADIATION MONITORING USING A ^{3}He SPECTROMETER. Sayres, A.; Lorio, P. M. (Columbia Univ., New York).

An investigation of the neutron radiation penetrating the shielding at the Columbia University 400 Mev Cyclotron, at the Nevis Laboratory, was undertaken with the following objectives: (1) To study the application of the ^{3}He fast neutron spectrometer with risetime discrimination to the field of neutron radiation monitoring. (2) To provide some information about the intensity of the high energy neutrons penetrating the existing shielding, because a modification of the cyclotron is being considered to increase the beam current and therefore the radiation produced by the accelerator. It is therefore necessary to evaluate the need for additional shielding. (3) To compare the relative response to various high energy neutron fluxes of a conventional commercial neutron survey meter, where the spectrum was investigated using the ^{3}He neutron spectrometer. A brief summary of results is presented. (M.O.W.)

29847 (CONF-651109, pp 181-98) DETERMINATION OF QUALITY FACTOR THROUGH THE UTILIZATION OF A BALANCED, TISSUE-EQUIVALENT, IONIZATION CHAMBER. Distenfeld, Carl H.; Markoe, Arnold M. (Brookhaven National Lab., Upton, N. Y.).

Accelerator dosimetry tends toward either specifying the field by way of its components or using a tissue equivalent chamber with a fail-safe Quality Factor (QF). This investigation attempts a third approach, the determination of QF directly. A Lucite, three-parallel plate ionization chamber was constructed with a common center electrode and two independent outer electrodes. This configuration allows the position of the center electrode to be manually adjusted to effect first order balance; vernier balance is obtained electronically through adjustment of one of the paired electrometers. The chamber can be pressurized to at least 10 atmospheres with a tissue equivalent gas mixture and, therefore, approximates tissue rad response. This ionization chamber is capable of detecting differences in LET of any radiation by operating on the principle of columnar recombination. One of the chambers is operated at low polarizing potential while the other is variable. The difference current between the two chambers is adjusted to zero for background levels and when sensing radiation this difference current is a measure of QF. In operation, the slope, with voltage, of the difference current is proportional to the QF of the radiation. This proportionality is, apparently, linear at 10 atm. over a range of QF from one to at least 7.5. This response was shown to be dose-rate independent. (M.O.W.)

29848 (CONF-651109, pp 199-212) TECHNIQUES OF FAST NEUTRON SPECTROMETRY WITH NUCLEAR EMULSIONS. Sanna, Robert; O'Brien, Keran; McLaughlin, James E. (Health and Safety Lab., New York Operations Office (AEC), N. Y.).

The development of neutron spectra from proton track measurements with emulsions was considered in 4 steps, namely: (1) Emulsion exposure to neutrons. (2) Emulsion processing. (3) Recoil proton track length measurements. (4) Data analysis to achieve the proton energy spectrum. (M.O.W.)

29849 (CONF-651109, pp 442-58) RADIATION PROTECTION PROBLEMS AT THE STANFORD TWO-MILE LINEAR ACCELERATOR. Jenkins, T. M.; McCall, Richard C.; Warren, Gary J. (Stanford Linear Accelerator Center, Stanford Univ., Calif.).

Radiation protection problems at SLAC are discussed in terms of the following: (1) prompt radiation from the accelerator; (2) residual radiation of accelerator parts; and (3) radiation not associated with the beam. (M.O.W.)

29850 (CONF-651109, pp 472-89) RADIATION HAZARDS PECULIAR TO A LINEAR ACCELERATOR MESON FACTORY. Knowles, H. B. (Yale Univ., New Haven, Conn.).

The radiation hazards pertaining to a meson factory linear accelerator are considered. The problems of shielding, activation and radiation damage in the target area do not differ significantly from those created by a cyclotron of equivalent beam energy and intensity, while these problems within the accelerator itself are different from those in circular machines. The linear geometry is advantageous in almost every way. Particular attention must be paid to the kinds of component adjustment or failure that might produce hazards to personnel and equipment. The mechanism of beam losses resulting from mismatch at the frequency transition, radio-frequency power failure, and focusing magnet failure are discussed together with the necessary precautions to be taken against these mishaps. These are related to the specific linear accelerator design envisaged by the Yale Design Study. (auth)

29851 (CONF-651109, pp 556-73) CAMBRIDGE ACCELERATOR FIRE OF JULY 5, 1965. (Cambridge Electron Accelerator, Mass.).

A detailed report of the explosion and fire at the Cambridge Electron Synchrotron on July 5, 1965, is presented. General guides for application in the review of safety at accelerator facilities are discussed. (M.O.W.)

29852 (INR-640/SLBAL/E) PHASE MOTION OF PROTONS IN A PROTON LINEAR ACCELERATOR WITH A PERTURBED AXIAL FIELD. Sura, J. (Institute of Nuclear Research, Warsaw (Poland)). Nov. 1965. 27p. Dep.

The effect of a modulation of the axial electric field on the phase acceptance in a proton linear accelerator is considered. The numerical solution of the equation of phase motion gives for a small modulating frequency a decrease of acceptance, which is comparable to that caused by the decrease of the level of flat field. (auth)

29853 (ORNL-3940) ELECTRONUCLEAR DIVISION ANNUAL PROGRESS REPORT FOR PERIOD ENDING DECEMBER 31, 1965. (Oak Ridge National Lab., Tenn.). May 1966. Contract W-7405-eng-26. 124p. Dep. mn. CFSTI $4.00 cy, $0.75 mn.

Separate abstracts were prepared for the 4 included chapters. (M.O.W.)

For abstracts of individual chapters see: 29854, 29855, 30353, and 30354.

29854 (ORNL-3940, pp 70-82) THE OAK RIDGE ISOCHRONOUS CYCLOTRON. (Oak Ridge National Lab., Tenn.).

During this year over 60% of the total operating time of the Oak Ridge Isochronous Cyclotron was scheduled for nuclear research; cyclotron operation was extended to the full 168 hr/week. Beams of protons at 11 to 65 Mev, deuterons at 21 to 40 Mev, alpha particles at 42 to 80 Mev, and ^{3}He at 25 to 52 Mev are routinely available to experimenters. Beam-on-target time averaged 75 hr/week. With the incorporation of a new 70-ton broad-range spectrograph into the system, resolution up to 1 part in 3000 is available. (M.O.W.)

29855 (ORNL-3940, pp 83-111) ADVANCED ACCELERATOR DEVELOPMENT. Denkins, R. F.; Fulmer, C. B.; Howell, L. N.; (and others) (Oak Ridge National Lab., Tenn.).

In advanced accelerator development the practicability of a very high current separated-orbit cyclotron facility to operate at proton energies up to 1000 Mev is being examined. In a study of the first-stage 12-sector 50-Mev SOC, a full-scale magnet sector is being assembled for magnetic field measurements and evaluation of fabrication tolerances. A prototype r-f cavity is also being fabricated for a detailed study of problems in ion acceleration. (M.O.W.)

29856 (UCRL-16829) MECHANICAL DESIGN OF A REGENERATIVE DEFLECTOR FOR THE BERKELEY 88-INCH CYCLOTRON. Elo, Don; Carneiro, A. R.; Bierlein, Fred; Wong, J. L. (Lawrence Radiation Lab., Univ. of California, Berkeley). Apr. 25, 1966. Contract W-7405-eng-48. 14p. (CONF-660510-5). Dep. mn. CFSTI $1.00 cy, $0.50 mn.

From International Conference on Isochronous Cyclotrons, Gatlinburg, Tenn.

Following the success of a test electrostatic regenerator unit in the Berkeley 88-in. cyclotron, a new regenerative deflection system was built. The system was comprised of a regenerator unit and an electrostatic channel. The regenerator unit was positioned opposite the dee near extraction radius. This unit having a positive voltage gives the last few accelerating internal beam orbits such a bump off their normal orbit paths that their turn-to-turn separation was increased at the entrance to the deflector channel. This separation decreased the amount of beam dumped on the septum and thus increased the efficiency of the deflector. The electrostatic channel consisted of three pairs of electrodes. Each end of each electrode was positioned remotely from the control room where its radial position was also read. This was made possible by the use of a flexible linear ball-bearing unit connected between the electrode end and a motor drive unit located outside the cyclotron vacuum barrier. This same motor unit also drove a system of selsyns for position readout. The entrance septum elevation was also remotely adjustable. The septum was mounted on a linear ball-bearing wedge driven by a unit similar to that used in positioning the electrodes. (auth)

29857 (UCRL-16839) THE OMNITRON: A VERSATILE MEDIUM-ENERGY SYNCHROTRON FOR THE ACCELERATION OF LIGHT AND HEAVY IONS. Ghiorso, Albert; Main, Robert M.; Smith, Bob H. (Lawrence Radiation Lab., Univ. of California, Berkeley). Apr. 26, 1966. Contract W-7405-eng-48. 13p. (CONF-660510-2). Dep. mn. CFSTI $1.00 cy, $0.50 mn.

From International Conference on Isochronous Cyclotrons, Gatlinburg, Tenn.

A novel guide-magnet configuration was devised which makes possible the acceleration of all charge-to-mass ratios from 0.04 to 1. A concentric storage ring, with the associated beam-switching equipment, allows for the extension of beam duty factor to essentially 100%. The storage ring can also be used in a bootstrap acceleration of heavy ions in which the ions are injected at low e/m, accelerated to a moderate velocity, stored while the accelerating ring returns to minimum field, stripped to maximum e/m, and reinjected for further acceleration. With a pressurized 2.5 Mv Cockcroft-Walton injector, the proposed system is capable of accelerating all ions from protons to uranium—to energies up to 1.5 Bev for protons and 0.3 to 0.5 Bev/nucleon for the heavier ions. Intensities of 10^{12} to 10^{13} nucleons/sec for the lighter ions ($M \leq 128$) are anticipated. The heavy-ion charge-exchange probabilities determine the vacuum requirements of this system. To minimize these requirements and to increase beam intensity, a 60/sec cycling rate was chosen. The vacuum requirements and the special r-f resonator and beam-switching problems attendant with the high cycling rate are discussed. (auth)

29858 CONTINUOUS OPERATION MICROTRON. Kapitsa, S. P. Elektron. Bol'shikh Moshchn., 4: 178-89 (1965). (In Russian).

The basic characteristics of the continuously operating microtron were reported. The calculations were based on investigations reported previously in which the microtron theory was presented and the experimental investigation of the pulse-operated microtron was given. (tr-auth)

29859 ELECTRON-BUNCHING ACCELERATOR. Kosarev, E. L. Elektron. Bol'shikh Moshchn., 4: 190-205(1965). (In Russian).

The results of the numerical calculation of the grouping of electrons in the oscillation fields E_{010} and E_{011} of a cylindrical resonator were reported. A bunching regime was obtained with dimensions of the electron bunch up to $1/100$ of the wavelength of the accelerating field with entrapment of this regime with $1/3$ all the electrons emitted. (tr-auth)

29860 STABILIZATION OF INTENSE COASTING BEAMS IN PARTICLE ACCELERATORS BY MEANS OF INDUCTIVE WALLS. Briggs, R. J.; Neil, V. K. (Univ. of California, Livermore). J. Nucl. Energy: Pt. C, 8: 255-69(May-June 1966). (UCRL-14407(Rev.1)).

A method for stabilizing a relativistic coasting beam against the negative mass instability is described. It is shown that a beam above the transition energy can be stabilized, even in the absence of a frequency spread in the beam, by making the wave impedance at the beam inductive. Several possible structures that can result in such an inductive impedance are described, and the case of a thin dielectric material positioned against the tank wall is analyzed in detail. The effect of the dielectric wall on the longitudinal and transverse resistive instabilities is considered. It is shown that the dielectric can also play an important role in the stability criteria for these resistive modes, and in some cases can make the requirements on the frequency spread for stability less stringent. Several numerical examples are given to illustrate the typical range of the parameters involved. (auth)

29861 MOMENTUM COMPACTION IN A CYCLIC ACCELERATOR. Arikawa, Tatsuo; Huke, Kazuo; Iwata, Giiti; Miyamoto, Goro; Takeda, Tatsuoki (Tokyo Univ.). J. Phys. Soc. Jap., 21: 823-4(Apr. 1966).

The addition of an appropriate electric guide field to a cyclic accelerator is inferred theoretically to give a very large momentum compaction factor and is proved to do so by a model test. (B.G.D.)

29862 STANFORD'S LONG, LONG BEAM. Dupen, D. W. New Sci., 30: 296-8(May 5, 1966).

The two-mile long electron accelerator at Stanford University is described. The design of this linear accelerator which accelerates electrons to 20 Bev is discussed, and some of the experiments for which it will be used are considered. (J.F.P.)

29863 LIQUID HYDROGEN TARGET FOR EXPERIMENTS OF HIGH-ENERGY NUCLEAR REACTIONS. Ohnuki, Yuji (Tohoku Univ., Sendai, Japan). Oyo Butsuri, 35: 128-31(Feb. 1966). (In Japanese).

A Mylar window type liquid hydrogen target was devised for experiments with an INS electron synchrotron. A commercial Dewar vessel was used as the reservoir of liquid H_2 and glass fiber superinsulation as the thermal shield. The loss rate of liquid H_2 was about 0.1 liter per hour with no liquid nitrogen cooling and no high vacuum insulation. (auth)

29864 ELECTRONS ACCELERATED TO THE 10- TO 20-Gev RANGE. Panofsky, W. K. H.; Neal, R. B. (Stanford Linear Accelerator Center, Calif.). Science, 152: 1353-5(June 3, 1966).

A report is presented on the first full-length operation of the Stanford Two-Mile Linear Accelerator. Overall performance, beam dynamics and breakup, energy measurement and future plans are discussed. (B.G.D.)

29865 HIGH-VOLTAGE ELECTROSTATIC SEPARATORS. Rohrbach, F. (CERN, Geneva). Vide, 21: No. 121, 52-74(Jan.-Feb. 1966). (In French and English).

A review of the most important problems involved in the design of electrostatic separators for high energy physics (bushings, insulators, electrodes, and vacuum tank) and an investigation of the most important parameters acting on the high voltage behavior of plane electrodes (structure, surface slate, shape, area, pressure and gap) are given. A possible theoretical explanation of the pressure effect is discussed by taking into account the sputtering phenomena. The behavior of different types of bushings and insulators for feeding and holding very high voltage in vacuum is considered. (auth)

29866 PROTON SCATTERING IN THE TUBE OF AN ELECTROSTATIC ACCELERATOR. Niedzwiedziuk, Kazimierz; Kasinski, Leszek; Malecki, Henryk. Zesz. Nauk. Uniw. Lodz., Ser. II, 9: 23-39(1961). (In Polish).

The best operating conditions for a 600-kev proton accelerator with regard to beam scattering due to gas pressure and the voltage applied to the accelerator tube, the

extracting voltage of the ion source, and the composition of the residual gas in the tube were evaluated. The loss distribution of the proton beam along the tube was also obtained. (D.C.W.)

29867 QUASILINEAR ACCELERATION OF PARTICLES BY A TRANSVERSE ELECTROMAGNETIC WAVE. Kolomenskii, A. A.; Lebedev, A. N. (Lebedev Inst. of Physics, Moscow). Zh. Eksp. Teor. Fiz., 50: 1101-6 (Apr. 1966). (In Russian).

A new mechanism of acceleration of charged particles by a plane electromagnetic wave is proposed which does not require the retarding systems characteristic for linear accelerators. Due to the action of a so-called synchronizing magnetic field with a special spatial dependence, the particle moves along such a trajectory that on the average the electric field does positive work on it. The relations between the particle energy and longitudinal coordinate and also the conditions which the synchronizing field must satisfy are determined. The time independence of the latter facilitates its realization and seems to ensure a high mean intensity of the accelerated particle beam. (auth)

29868 FOCUSING CHARACTERISTICS OF AN ELECTROSTATIC MIRROR WITH A CYLINDRICAL FIELD. Zashkvara, V. V.; Korsunskii, M. I.; Kosmachev, O. S. Zh. Tekh. Fiz., 36: 132-8(Jan. 1966). (In Russian).

Focusing of charged particles by the electrostatic field between two coaxial cylindrical electrodes is discussed. The ions are assumed to originate in a point source on the common axis of the electrodes and to enter and leave the interelectrode region through circular slots in the inner electrode. Charged particles with a certain energy, depending on their charge and mass, the potential difference between the electrodes, the radii of the electrodes, the distance between the slots in the inner electrode, and the position of the source, will be brought to a focus on the axis. It is proposed to employ such a system of electrodes to record the energy spectrum of charged particles by keeping fixed the positions of the source and detector and varying the potential on the electrodes. The focusing conditions are derived It is shown that not only first order, but also second order focusing occurs if the angle between the initial trajectory and the axis is 42° 20′. The second order aberrations and the effect of finite source size are also calculated, but only the results are discussed, and the calculations are not presented. The energy resolution can be improved by employing multiple focusing with suitable irises in the intermediate image planes to eliminate oblique trajectories. The linear dispersion in energy of the cylindrical capacitor is approximately equal to that of a 180° spherical analyzer of equal size. The quality of focusing is adequate for analysis of ion beams with an angular divergence of 360° in the radial plane and several degrees in the axial plane. (ATD)

29869 CAPTURE OF ELECTRONS INTO BETATRON ORBITS. Lobanov, Yu. N.; Tulinova, N. I. Zh. Tekh. Fiz., 36: 151-4(Jan. 1966). (In Russian).

The effect of injection current and duration of the injection pulse on the output of a betatron is investigated. Injection pulses as short as 10 nanosec were employed; with such short pulses electrons were injected into only about one-third of the circular orbit, so that any collective effects that might arise from interaction between successive turns of the injected beam were eliminated. When much longer injection pulses were employed (pulse durations up to 160 nanosec were investigated) the effects (if any) of such multiturn interactions would be present and might be identified. The inner and outer radii of the betatron chamber were 4.5 and 10.6 cm and the radius of the equilibrium orbit was 7.5 cm. The electrons were injected at energies of 1 to 2 kev; the injection phase was selected for maximum betatron output and corresponded to an initial orbit radius of 9 cm. When the pulse length was 11 nanosec the betatron output N was proportional to the injection current I (determined from the measured average injection current $\bar{I}$ and the duty cycle) for I less than 30 mamp and to I^2 for I between 35 and 70 mamp. The critical value $I_c = 30$ M mamp of I at which $d\log N/d\log I$ changed from 1 to 2 (injection energy 1 kev) agreed within a factor 2 or 3 with the value calculated by the formula of I. M. Samoylov (ZhETF, 39, 705, 1959). The value of I_c for an injection energy of 2 kev decreased from 43 to 4 mamp as the pulse duration was increased from 23 to 103 nanosec. When the injection current I was increased sufficiently the betatron output began to decrease with increasing I. The value I_{max} of I at which N assumed its maximum value N_{max} was in approximate agreement with the value calculated earlier, but decreased slightly with increasing pulse duration. The value of N_{max} depended significantly and nonmonotonically on pulse duration. (ATD)

29870 SHAPING OF SMALL BUNCHES IN A LINEAR ELECTRON ACCELERATOR. Ostrovskii, E. K. Zh. Tekh. Fiz., 36: 155-62(Jan. 1966). (In Russian).

Two methods for minimizing the extent in phase of the electron bunches at the output of high energy linear accelerator are discussed. The first method involves operating the constant phase velocity injection accelerator at a phase velocity below the optimum value for maximum capture and minimum energy spread. Under these conditions the velocity distribution in the injected bunch is such that the bunch decreases in length for a time during drift in field free space. By employing a drift tube of the proper length between the injector and the accelerator proper one can achieve minimum length of the injected bunches. For optimum results injection should take place somewhat before the bunching process in the drift tube is completed in order to compensate for a debunching action of the accelerator proper. An advantage of this technique is that the electrons in the drift tube have energies of several Mev and space charge effects can accordingly be neglected. The second method of minimizing the extent in phase of the output bunches involves operating the first section of the accelerator at a phase velocity equal to the velocity of the electrons in the injected bunch. This method is discussed in some detail and a numerical example was worked out with the aid of an electronic computer. The energy scatter arising in the bunching process is inconsiderable, and the technique can therefore be employed with moderate energy accelerators as well as with high energy accelerators. (ATD)

29871 PIERCE OPTICS OF A BEAM WITH FINITE PHASE VOLUME. Batalin, V. A. Zh. Tekh. Fiz., 36: 313-15(Feb. 1966). (In Russian).

The distribution of potential along the axis of a paraxial beam of charged particles required to keep constant the diameter of the beam having finite phase volume and propagating along the axis is obtained from the equation for the envelopes of the particle beam with self-consistent space-charge field. (tr-auth)

29872 MAGNETIC METHODS AND APPARATUS FOR MANIPULATING A BEAM OF CHARGED PARTICLES. Skala, Stephen F. (to Western Electric Co., Inc.). U. S. Patent 3,246,147. Apr. 12, 1966. Filed Nov. 29, 1963.

A method and apparatus are described for extending at least one dimension of the effective cross section of a collimated beam of charged particles so that the particles are bent through a constant angle and the strength of the magnetic field remains constant. The magnetic field is arranged in the path of the beam and is moved along the initial beam longitudinally of the beam to cause the bent portion of the beam to sweep over an elongated area. This technique offers a solution to the problem of irradiation of objects of troublesome geometry without the necessity of multiple radiation sources. (B.L.M.)

Astrophysics and Cosmology

Refer also to abstract 30222.

29873 (NASA-SP-100) SIGNIFICANT ACHIEVEMENTS IN SOLAR PHYSICS, 1958–1964. (National Aeronautics and Space Administration, Washington, D. C.). 1966. 96p. GPO $0.50.

A brief introduction to solar research is given. Various chapters discuss the following aspects of solar research:

instrumentation, mapping the suns u-v spectra, mapping the suns soft x-ray spectra, evidence of solar hard x-ray emission, corona, satellite monitoring of solar radiation, and the future flight program. (M.O.W.)

29874 (NASA-TT-F-389, pp 714-31) MEASUREMENT OF SOLAR X-RAY RADIATION INTENSITY BY MEANS OF THE SPACE STATION "ELEKTRON-2." Tindo, I. P. Translated from Issledovaniya Kosmicheskogo Prostranstva. Trudy Vsesoyuznoy Konferentsii po Fizike Kosmicheskogo Prostranstva. Izdatel'stvo, Nauka, Moscow, June 10–16, 1965.

Significant variations in a stream of soft x radiation from a quiet sun, as well as brief bursts of intensity, are reported from data acquired from the electron-2 satellite. (B.G.D.)

29875 (NASA-TT-F-389, pp 732-9) COSMIC-RAY GENERATION ON THE SUN. Charakhch'yan, A. N.; Charakhch'yan, T. N. Translated from Issledovaniya Kosmicheskogo Prostranstva. Trudy Vsesoyuznoy Konferentsii po Fizike Kosmicheskogo Prostranstva. Izdatel'stvo, Nauka, Moscow, June 10–16, 1965.

A discussion is presented on cosmic ray bursts and its relation to chromospheric flares on the sun. A study of proton energy spectrum in these bursts is also presented. Cosmic ray bursts generated on the back side of the solar disc are considered. (B.G.D.)

29876 INTERPRETATION OF OBSERVATIONS OF QUASI-STELLAR OBJECTS. McCrea, W. H. (London Univ.). Astrophys. J., 144: 516-33(May 1966).

Magnitudes and redshifts of quasi-stellar objects measured by Lynds, by Sandage, and by Schmidt are discussed on the supposition that the objects are "cosmological" sources in a model universe. The inferred intrinsic properties of the radiation emitted by the sources are considered; while the properties show considerable dispersion, they confirm that a single category is treated. This appears to be characterized by a very flat spectrum to which a good approximation is given by a formula used by Sandage; an attempt is made to synthesize a spectrum over the range about 6 to 26×10^{14} c. Evidence is encountered for distinguishing some five of the sources as a possible significant subset. Schmidt's concept of estimating the emitted flux at a particular emitted frequency is exploited; when this flux is plotted against redshift, the diagram is compatible with the existence of an envelope for brightest sources, and this may assist in discriminating between models. The absence of points in part of this and other diagrams is accounted for by the fact that the optical observations do not yet include sources with apparent magnitude fainter than about 18. Another instructive diagram shows the results of calculating how the observed sources would appear were they transferred to other distances in the model. The discussion illustrated for three particular cosmological models: the special-relativity model, the steady-state model, an evolutionary model used by Schmidt. The observations are not indisputably incompatible with any of these. General considerations and minor features make the last model possibly the least plausible. General considerations make the steady-state model plausible, but special features appear possibly unfavorable. The special-relativity model represents the observations quite plausibly. But this case can be regarded either as a particular cosmological model or as a description of a cosmically local phenomenon. It may be necessary to contemplate the possibility that the sources are not "cosmological." (auth)

29877 NATURE OF THE QUASI-STELLAR OBJECTS. Hoyle, F. (Cambridge Univ., Eng.); Burbidge, G. R. Astrophys. J., 144: 534-52(May 1966).

The origin of the quasi-stellar objects is discussed from two different points of view: (i) that they are objects at cosmological distances as has been commonly supposed, and (ii) that they are local objects situated at distance ~1–10 Mpc. The optical properties of the quasi-stellar objects are compared with the optical properties of galaxies associated with strong radio sources and Seyfert nuclei from both points of view. A discussion of (i), and on this basis it is argued that they are most probably the nuclei of galaxies which have reached a high-density phase at which time the formation of massive objects and their subsequent evolution has occurred. Apart from the suggestion of Terrell, little attention has been paid until now to the possibility that they are local objects, and so this is considered in considerable detail. A plausible case can now be made for supposing that they are coherent objects which have been ejected at relativistic speeds from the nuclei of galaxies at times when they erupt to give rise to strong radio sources and other phenomena. On this basis a likely candidate to give rise to the objects in the vicinity is NGC 5128 which is a powerful radio source in which at least two outbursts appear to have occurred. In this case some objects with blueshifts may be present. The fraction of such objects and the solid angle about NGC 5128 in which they lie is given as a function of the distance of NGC 5128, average speed of ejection, and time which has elapsed since the explosion. Calculations are also made of the redshift-magnitude relation to be expected in the local theory, and comparison is made with the relation in orthodox cosmology. Some of the problems associated with the hypothesis that the objects lie at cosmological distances have arisen through the observation of Dent of the radio emission from 3C 273B. This shows that at 8000 Mc the intensity has increased by about 40 per cent over the last 2 years, and that the spectrum is flat over the range 200–8000 Mc and may be flat over a wider range. It is shown that a model based on the synchrotron process is able to explain the form of the spectrum with the object at a cosmological distance provided that the following conditions prevail: the electron distribution is optically thin; the magnetic-field intensity depends on distance r from the center with the form $H = H_0(a/r)^n$; the electron energy spectrum is everywhere the same; the energy density of the electron distribution is of the form $W = W_0(b/r)^m$; (5) $n + m = 3$. Even with this model there is considerable difficulty in explaining a flat spectrum beyond 10^4 Mc. The difficulties associated with the model are somewhat reduced in the local theory. A number of programs are outlined which may permit a determination of whether the objects are at cosmological distances or are local. (auth)

29878 EXTENSION OF NON-THERMAL RADIO-SOURCE SPECTRA TO 8000 Mc/s. Dent, W. A.; Haddock, F. T. (Univ. of Michigan, Ann Arbor). Astrophys. J., 144: 568-86(May 1966).

The flux densities of thirty-five nonthermal radio sources were measured at a frequency of 8000 Mc (λ 3.75 cm). There are no previously reported flux densities for most of these sources above 3200 Mc. The antenna temperatures of the sources were measured by two independent procedures. Corrections were made for the finite angular size of the source, the variation of the antenna gain with its orientation, the linear polarization of the source, receiver response nonlinearities, and atmospheric extinction. The flux-density calibration was made relative to absolute measurements of Cas A, Tau A, and Cyg A by other observers. The radio-source spectra extended to 8000 Mc are presented using the lower-frequency flux-density measurements in the survey of Conway, Kellermann, and Long. Of the thirty-five sources studied only 17 per cent were found to have straight spectra; 63 per cent of the source spectra curved downward. Seven sources, or 20 per cent, had radio spectra that either became flatter with increasing frequency (e.g., 3C 273 and 3C 345) or had a pronounced upward turn in their centimeter-wave spectra (e.g., NGC 1275 and 3C 279). Quasi-stellar sources with such spectra are associated with rapidly variable radio emission. A general definition for a curvature index of radio-source spectra is proposed, and curvature indices of the observed sources were computed. A correlation between curvature index and spectral index was found as well as a correlation between curvature index and component separation of double radio sources. The latter correlation suggests that sources originate with flat radio spectra which then steepen to produce spectra typical of the majority of radio sources. This result and the observed double structure of some quasi-stellar sources suggests that double sources and their associated D galaxies may have evolved from a quasi-stellar phase. (auth)

29879 TEMPERATURE OF INTERGALACTIC MATTER. Gould, Robert J. (Univ. of California, San Diego, La Jolla); Ramsay, William. Astrophys. J., 144: 587-98 (May 1966).

The various processes which determine the temperature of intergalactic matter are considered. Heating by cosmic-ray ionization and dissipation of hydrodynamic turbulence are estimated, as well as cooling by inelastic electron collisions with H, He, and He^+, and by bremsstrahlung and recombination radiation. The effects of the presence of a "cosmic" abundance of helium in intergalactic space are significant because of the associated strong cooling for temperatures of 3×10^4 to 2×10^{5}°K. The effects of dielectronic recombination are included for helium. It is shown that heating by a universal cosmic-ray flux can maintain temperatures of $1-5 \times 10^{4}$°K against cooling by electron collisions with H, He, and He^+ for cosmic He/H abundance and local hydrogen densities of $10^{-4}-10^{-5}$ particles/cm^3. However, the relaxation time for hydrogen and singly ionized helium recombination is about ten times the cosmic expansion time of $\tau_E = 10^{17}$ sec for hydrogen densities of 10^{-5} cm^{-3} at these temperatures, while doubly ionized helium recombines in about 3×10^{17} sec. Thus, unless intergalactic matter exists in "clouds" in which the hydrogen density is ten times the usually assumed mean of 10^{-5} cm^{-3}, ionization steady-state conditions may not exist. Moreover, if the temperature of the intergalactic gas was initially greater than about 2×10^{5}°K, the cooling processes are not sufficient to cause an appreciable lowering of temperature in a time τ_E, so that such an initially hot intergalactic gas could remain hot. Dissipation of turbulent energy in a time $\ll \tau_E$ could produce an initially hot gas. Galaxy formation is considered briefly. It is suggested that an intergalactic gas at about 2×10^{5}°K is unstable to density condensations, due to the strong cooling by He^+ at lower temperatures; such thermal instabilities could result in the formation of galaxies and galaxy clusters. (auth)

29880 SIGNIFICANCE OF COHERENT PLASMA RADIOWAVE EMISSION FOR QUASI-STELLAR RADIO OBJECTS AND SUPERNOVAE REMNANTS. Ginzburg, V. L.; Ozernoi, L. M. (Lebedev Inst. of Physics, Moscow). Astrophys. J., 144: 599-610(May 1966).

The possibility of interpreting the radio waves from the "compact" long-wave radio source in the Crab Nebula and part of the radiation from quasi-stellar objects on the basis of the coherent plasma mechanism is discussed. This seems to be quite feasible for the "compact" source in the Crab, even when the effect of the magnetic field is not taken into account. The variable centimeter and decimeter waves from quasi-stellar objects may also be of a coherent plasma nature but apparently only if the effect of the magnetic field is taken into account. The problem of re-absorption of noncoherent magnetobremsstrahlung radiation in radio sources with a homogeneous or inhomogeneous field is analyzed. (auth)

29881 FREE-FREE EMISSION AS A SOURCE OF GALACTIC X RAYS. Manley, Oscar P. (American Science and Engineering, Inc., Cambridge, Mass.). Astrophys. J., 144: 628-34(May 1966).

The assumptions underlying a simple model for discrete galactic x-ray sources, viz., free-free emission from a hot, fully ionized, hydrogenic plasma were examined. It was found that, for internal consistency, some combinations of the model parameters must be constrained, i.e., the parameters cannot be prescribed arbitrarily. The interpretation of the currently available data relevant to Sco X-1 in terms of the simple model yields significant lower bounds on the distance, size, and mass of that x-ray source. In fact, it was shown that, on using a self-consistent model, it is possible to interpret the data relevant to Sco X-1 in terms of free-free emission from a tenuous cloud of hot hydrogenic plasma. The calculation indicates that Sco X-1 may be as close as 1 light-year. (auth)

29882 SKY NEAR THE BRIGHTEST X-RAY SOURCE IN SCORPIUS. Johnson, Hugh M. (Lockheed Missiles and Space Co., Palo Alto, Calif. Kitt Peak National Observatory, Tucson, Ariz.). Astrophys. J., 144: 635-8(May 1966).

The x-ray source in Scorpius is discussed in terms of a number of optical observations of the area near it. The source remains unidentified, although it may be present as a stellar or nebular image; otherwise it may be $1'-7'$ in diameter with such a low surface brightness that it is invisible. A distance of 50 – 100 pc is derived from the apparent association with nebulae that are concentrically arranged around it over an area of several hundred square degrees. The proper motion of IC 4592, a nearby reflection nebula, is observed. The current radiation of a visible hot plasma with an electron density $\geq 2 \times 10^5$ cm^{-3} in a volume $\geq 2 \times 10^{48}$ cm^3, or of an invisible hot plasma with a density of 700 to 1.3×10^4 cm^{-3} in a much larger volume, appears to be consistent with the x-ray and optical data. (auth)

29883 STELLAR CONVECTION ZONES, CHROMOSPHERES, AND ROTATION. Wilson, O. C. (Carnegie Institution of Washington, Washington, D. C. California Inst. of Tech., Pasadena). Astrophys. J., 144: 695-708 (May 1966).

An attempt is made to connect the rotations of main-sequence stars with their chromospheric properties and, hence, with the extent of their hydrogen convection zones. It is based on 10 Å/mm spectrograms of 308 stars, with $b-y \geq 0.240$, from the Strömgren-Perry catalog. On the zero-age main sequence it is found that rotational velocities of the order of V sin i ≥ 50 km/sec set in very abruptly at $b-y = 0.285$, and Kraft's observations show that this is true also in the Hyades. However, similar rotational velocities are found among the field stars at the upper edge of the main-sequence band among spectral types G0 – G5, and it is logical to suppose that these objects have evolved from the zero-age line near $b-y = 0.285$. A curve can be drawn in the $(b-y)-c_1$ plane which separates the large from the small rotations, and this curve, therefore, approximates the evolutionary track of stars originating at $b-y = 0.285$ on the zero-age line. This curve, which divides the larger from the smaller angular momenta, applies to the members of spectroscopic binary systems as well as to single stars. Stars showing emission at H and K have a strong concentration to the zero-age line and extend up the main sequence to $b-y = 0.30$. It cannot be stated definitely that stellar chromospheres terminate near this point, but the evidence indicates that it is quite possible that they do. If so, the close agreement between the onset of larger rotations and the termination of chromospheres is very suggestive of the braking mechanism described by Schatzman. The implication, then, is that deep hydrogen convection ends at $b-y = 0.285$ on the zero-age line (spectral type F4), and the observations show that the change from deep to shallow convection must occur within a mass range of the order of 5 per cent. (auth)

29884 STUDIES IN STELLAR EVOLUTION. IV. THE INFLUENCE OF INITIAL CONDITIONS ON PRE-MAIN-SEQUENCE CALCULATIONS. Bodenheimer, Peter (Univ. of California, Berkeley). Astrophys. J., 144: 709-22(May 1966).

The available observational material, both in support of, and in exception to, pre-main-sequence evolutionary tracks of the Hayashi type, is briefly reviewed. A method is described for starting calculations of evolutionary sequences with allowance for possible large variations in initial conditions. Detailed calculations of early pre-main-sequence evolution of a configuration of 2 $M_\odot$ are presented. The results show that the effects of variations in initial conditions during fully and partially convective evolutionary phases do not cause significant deviations from previously calculated Hayashi tracks. The deviations are, in general, smaller than those which can be expected on the basis of theoretical uncertainties in model atmospheres. (auth)

29885 MEASUREMENTS OF SOLAR MAGNETIC FIELDS. Sheeley, N. R. Jr. (California Inst. of Tech., Pasadena). Astrophys. J., 144: 723-32(May 1966).

Using the photographic technique of Leighton, high spatial resolution measurements of photospheric magnetic fields were obtained with the following chief results: Regarding sunspot groups as sources of magnetic flux and defining a "source flux" that may be determined uniquely for a sun-

spot group from flux measurements, a variation in source fluxes from group to group was found ranging from less than 0.2 SFU (1 SFU [solar flux unit] = 10^{21} Maxwells) for very "small" spot groups to more than 20 SFU for very "large" groups. This variation of source flux with sunspot group "size" is described by the rule-of-thumb $\Phi = 1.2\ A_m$, where Φ is the source flux in SFU and A_m is the group size in 10^{18} cm^2 defined as the maximum area attained by the sunspot group during its development. Zeeman photographs emphasize that as a bipolar magnetic region (BMR) develops in time and as its magnetic flux spreads over a progressively larger area, the flux density does not decrease smoothly from the vicinity of the source to the outer limit of detectable flux but is distributed in successively smaller bits and fragments. Moreover, measurements obtained from these Zeeman photographs reveal magnetic field strengths of 200–700 gauss in these bits and fragments, showing that fields of a few hundred gauss are not uncommon for small magnetic features even in quiet regions of the sun. Numbers of polar faculae were calibrated to give magnetic flux on the polar caps of the sun as a function of time during the period 1905–1964. The fluxes vary cyclicly with time approximately 90° out of phase with the variation of the sunspot number for the whole solar disk with time during the same period (provided the sunspot number is given a polarity corresponding to the magnetic polarity of the following sunspots of the relevant hemisphere). The maxima of the polar fluxes vary considerably from cycle to cycle (just as the maxima of the sunspot number vary considerably from cycle to cycle), maximum fluxes ranging from 6 to 21 SFU, with 12 SFU being a typical maximum polar flux during 1905–1964. These results are consistent with the hypothesis that emerging BMR's are the sources of all the flux on the solar surface, and that the random walk plus differential rotation is the dominant mechanism for the distribution of the flux provided by these sources. More important, these measurements provide a means of testing this hypothesis in more detail than has been possible heretofore. (auth)

29886 EVIDENCE FOR AN OSCILLATORY COMPONENT IN SOLAR GRANULATION BRIGHTNESS FLUCTUATIONS. Edmonds, Frank N.; McCullough, James R. (Univ. of Texas, Austin). Astrophys. J., 144: 754-62 (May 1966).

The evidence for an oscillatory component of continuum brightness fluctuations, secondary maxima in temporal autocorrelation functions and power spectra, is examined critically with the provisional conclusion that such a component is theoretically possible and probably does exist. This component, with periods distributed about 5 min, constitutes between 0.5 and 2 per cent of the total fluctuation power. The results from one analysis (725) suggest the coexistence of a second oscillatory component with periods distributed about 10 min, but the evidence is quite uncertain. There are also indications that the effects of spectral windows may be masking a stronger concentration of power of continuum brightness fluctuations to lower frequencies. (auth)

29887 INTEGRATED FLUX DISTRIBUTIONS IN NEUTRON CAPTURE IN STARS. Seeger, Philip A.; Fowler, William A. (Los Alamos Scientific Lab., N. Mex. California Inst. of Tech., Pasadena). Astrophys. J., 144: 822-4(May 1966). (LA-DC-7442).

The neutron capture process in stellar nucleosynthesis is considered. The value for the average number of neutrons captured by the seed nuclei exposed to the maximum integrated flux obtained from previous work is considered reasonable on the basis of possible sources of neutron and iron-group abundances in stars. It implies that light nuclei on which (α,n) occur are at most 100 times as abundant as the iron-group nuclei. It is noted that this value is adequate to produce the observed Pb abundance without appreciable cycling among the Pb isotopes having occurred. The neutron exposure distribution is also obtained from these calculations. (J.F.P.)

29888 LOCAL HYPOTHESIS FOR THE QUASI-STELLAR OBJECTS. Setti, G.; Woltjer, L. (Columbia Univ., New York). Astrophys. J., 144: 838-9(May 1966).

Lower limits on the masses of quasi-stellar objects are discussed. These are considered to make a local theory for the large observed red shifts improbable. The results for two quasi-stellar objects are listed. (J.F.P.)

29889 COLLAPSED STARS IN BINARIES. Zeldovich, Ya. B.; Guseynov, O. H. (Academy of Sciences, Moscow). Astrophys. J., 144: 840-1(May 1966).

Attention is drawn to collapsed stars in binaries. While an unambiguous proof of the existence of a collapsed star would be of great interest, it is noted that even a negative result is of some value: a comparison with the number of binaries with larger masses could provide some support to the conclusion that stars escape from collapsing. (J.F.P.)

29890 ABSORPTION LINES IN THE SPECTRA OF DISTANT SOURCES. Bahcall, John N.; Salpeter, E. E. (California Inst. of Tech., Pasadena. Cornell Univ., Ithaca, N. Y.). Astrophys. J., 144: 847-52(May 1966).

The properties of absorption lines that might appear in the continuum spectra of distant quasi-stellar sources, and deductions from these lines are outlined. Absorption by intergalactic gas in clusters of galaxies in the line of sight is considered, and a previous discussion of absorption lines caused by neutral hydrogen is extended to resonant absorption lines in other elements. A table of the spectral lines expected to be prominent in absorption is presented for various temperatures. It is shown that the identification of absorption lines with a common redshift appreciably different from that of the emitting quasi-stellar sources would be strong evidence for the hypothesis that the redshifts of these sources are cosmological. Also absorption features which could be formed by gas clouds near a quasi-stellar source which might lead to apparent variations in the observed wavelengths of emission lines are discussed. (J.F.P.)

29891 SOLAR NUCLEOSYNTHESIS OF EXTINCT ^{129}I. Rowe, M. W. (Univ. of Arkansas, Fayetteville). Earth Planet. Sci. Lett., 1: 97-8(May 1966).

It is pointed out that the recent finding of a lack of significant amounts of fissiogenic xenon in the presence of an excess of radiogenic ^{129}Xe in two Ca-rich achrondrites, Nakhla and Lafayette, is consistent with the view that ^{129}I could be produced in two different nucleosynthesis events. ^{244}Pu and ^{129}I could have been incorporated into the Nakhlitic parent material by galactic nucleosynthesis and decayed there. After the material was apparently outgassed to the extent that virtually all the excess fissiogenic Xe was lost, ^{129}I from solar nucleosynthesis could have been incorporated into the material and subsequently decayed to ^{129}Xe, which is finally detected in excess in the two Nakhlites. (A.G.W.)

29892 MASS SPECTRUM OF FISSION XENON IN THE PASAMONTE METEORITE. Eberhardt, P.; Geiss, J. (Univ. of Bern). Earth Planet. Sci. Lett., 1: 99-101(May 1966).

The xenon abundances determined by Rowe and Bogard in Pasamonte II are corrected for trapped as well as for spallation xenon, and the following mass spectrum for the fission component is obtained: ^{131}Xe = 33.5 ± 3; ^{132}Xe = 95 ± 5; ^{134}Xe = 91 ± 2.5; ^{136}Xe = 100. The correction for spallation xenon increases the ^{132}Xe yield considerably. The Pasamonte II fission spectrum differs from the spontaneous ^{238}U and thermal neutron ^{235}U fission spectrum, indicating that long-lived transuranic elements have contributed to the fission xenon. (auth)

29893 ISOTOPIC ABUNDANCE AND CONTENT OF SULFUR IN METEORITES. Kaplan, I. R.; Hulston, J. R. (McMaster Univ., Hamilton, Ont.). Geochim. Cosmochim. Acta, 30: 479-96(May 1966).

Twenty meteorites were studied in the iron (hexahedrites and octahedrites) and stony (enstatite achondrite, carbonaceous, enstatite, bronzite, and hypersthene chondrites) families. Troilite is the chief sulfur component of iron meteorites and the δ^{34}S ranges from 0 to +0.6‰ with respect to Canyon Diablo troilite. Stony meteorites contain a wide variety of sulfur compounds including water and acid-soluble sulfides, elemental sulfur, water- and acid-soluble sulfates, and unidentified components soluble

only in aqua regia. The $\delta^{34}S$ content of the isolated compounds varies from +2.5 to −5.5% with respect to Canyon Diablo. The weighted average for all components of each meteorite, however, falls within ±1% of Canyon Diablo. The ^{33}S distribution closely follows ^{34}S. The data strongly suggest that differentiations occurred in a closed system, corresponding to the meteorites or their parent body, and starting from a single source of sulfur. There is no evidence for biological activity in the meteorites, either from the distribution of sulfur compounds or from the isotope abundance data. (auth)

29894 27-DAY RECURRENCE TIME PATTERN OF Σ Kp AND THE GEOMETRY OF SOLAR PLASMA STREAMS. Sano, Yukizo Kakioka Magnet. Observ., Mem., 12: No. 1, 49-53(1965).

An illustration is given of the 27-day recurrence-time patterns of Σ Kp for the periods 1951 to 1953, and 1961 to 1963, with reference to the solar plasma velocity changes measured by the Mariner 2 spacecraft. Twenty-seven day recurrence tendencies of the solar plasma velocity, geomagnetic index Σ Kp and daily mean values of the geomagnetic H-component at Kakioka are plotted, and M-region streams and the trajectory of the Mariner 2 spacecraft are shown schematically. (Int. Aerospace Abstr.)

29895 POSSIBLE ANTIMATTER NATURE OF MICROMETEORS. Konstantinov, B. P.; Bredov, M. M. Belyaevskii, A. I.; Sokolov, I. A. Kosm. Issled., 4: 66-73(Jan.-Feb. 1966). (In Russian).

Considerations on the possible antimatter nature of comets and micrometeors of showers are expressed, and results of an experiment on the verification of this hypothesis are presented. (tr-auth)

29896 QUASARS—A MINORITY REPORT. Hunter, James H. Jr. (Yale Univ., New Haven); Sofia, Sabatino; Fletcher, Emery. Nature, 210: 346-8(Apr. 23, 1966).

The fundamental problem of the distances and luminosities of quasars is considered by using accepted procedures of classical astronomy. (B.G.D.)

29897 DISTRIBUTION OF QUASI-STELLAR RADIO SOURCES IN STEADY STATE COSMOLOGY. Sciama, D. W.; Saslaw, W. C. (Cambridge Univ., Eng.). Nature, 210: 348-52(Apr. 23, 1966).

The quasi-stellar radio sources are proposed to Be inside our own galaxy. It is suggested that some of quasi-stellar radio sources not measured will have essentially zero red shift, corresponding to the relatively very small velocities possessed by galactic objects. From this view the population of these sources is suggested to be not homogeneous, but consisting of two entirely different and unrelated components. The reason for introducing this possibility has to do with the relation between counts of quasi-stellar radio sources and the steady-state model of the universe. (B.G.D.)

29898 STRENGTH OF COSMIC RADIO SOURCES. Gold, Louis (Stevens Inst. of Tech., Hoboken, N. J.). Nature, 210: 927(May 28, 1966).

An attempt is made to account for the unusually high levels of radio emission from quasars and to explain, in particular, the spectral output from the substructures A and B of 3C-273. (B.G.D.)

29899 EXACT NONLINEAR ELECTROMAGNETIC WHISTLER MODES. Lutomirski, R. F. (Cornell Univ., Ithaca, N. Y.); Sudan, R. N. Phys. Rev., 147: 156-65 (July 8, 1966).

The nonlinear, relativistic equations of motion were solved exactly for an electron moving in a right circularly polarized wave which propagates along a static uniform magnetic field $B_0 e_z$. In the wave frame where the induction electric field disappears, two constants of the motion were found. With their aid, the particle trajectories were examined and the periods and amplitudes of oscillation in the z direction were obtained. In the absence of collisions, the exact solution of the relativistic Vlasov equation in the wave frame is an arbitrary function of the constants. The requirement of self-consistency imposed by Maxwell's equations is examined and, in particular, it is shown that sufficient arbitrariness remains that no dispersion relation exists for these waves. However, for less general distribution functions, a dispersion relation independent of wave amplitude may still exist. When it is required that the moments of the distribution be correct to first order in the amplitude of the wave, in analogy with the electrostatic case, the linearized distribution function is obtained together with a principal-value prescription for treating the usual singularity, and the transverse Van Kampen modes are also obtained. (auth)

29900 X RAYS IN ASTRONOMY. Stepien, Kazimierz Postepy Astron., 13: 13-16(Jan.-Mar. 1965). (In Polish).

A discussion of cosmic x-ray sources detected by rocket probes, with particular reference to the constellation of Scorpius and the Crab nebula is given. The creation of neutron stars from a supernova explosion and the mechanism of their radiation are examined. (Int. Aerospace Abstr.)

29901 X-RAY SPECTRA FROM THREE COSMIC SOURCES. Grader, R. J.; Hill, R. W.; Seward, F. D.; Toor, A. (Univ. of California, Livermore). Science, 152: 1499-1504(June 10, 1966). (UCRL-14732).

Three cosmic x-ray sources were observed from a water-launched rocket carrying two x-ray detectors to an altitude of 200 kilometers. The x-ray spectra, measured in the photon energy range between 1 and 40 kev, are all different. The sources in order of hardness of spectra are Cyg XR-1, Tau XR-1 and Sco XR-1. The intensity of Sco XR-1 decreased at low photon energies. The differences in spectra might be interpreted as evidence of different source mechanisms. (auth)

29902 COLLECTIVE PROCESSES IN GRAVITATING SYSTEMS. I. Lebedev, V. I.; Maksumov, M. N.; Marochnik, L. S. (Astronomical Inst., Academy of Sciences, Tadzhik SSR). Soviet Astron. AJ (Engl. Transl.), 9: 549-54(Jan.-Feb. 1966).

Translated from Astron. Zh., 42: 709-17(July-Aug. 1965).

Methods developed in plasma physics are used for the investigation of the dispersion equation of small oscillations in locally homogeneous segments of collisionless gravitating systems of particles. It is shown that such systems are unstable. A formula is derived for the calculation of the critical wavelength (in the sense of Jeans). Systems formed by two encountering interpenetrating "cold" and Maxwellian flows, and also "cold" and Maxwellian systems at rest, are considered. The instability is of an oscillatory character for wavelengths less than a certain λ_1, and thus differs from the aperiodic gravitational instability of a continuous medium. Application to the galaxy shows that in the circumsolar neighborhood the time in which instability develops is of the order of $\tau \sim 2\ (10)^8$ years. (auth)

29903 THEORY FOR TYPE II BURSTS OF SOLAR RADIO EMISSION. Zaitsev, V. V. (Gorkii State Univ.). Soviet Astron. AJ (Engl. Transl.), 9: 572-8(Jan.-Feb. 1966).

Translated from Astron. Zh., 42: 740-8(July-Aug. 1965).

Radio emission from shock waves propagated through the corona may be responsible for type II bursts. The amplitude of the plasma oscillations that develop in the shock front is determined. The radio intensity is computed for the first and second harmonics, representing stationary plasma oscillations. The splitting in the harmonic spectra due to electron drift in the shock front is discussed. The estimates agree satisfactorily with the results of burst observations. (auth)

29904 CORONAL SOLAR RADIATION IN THE CONTINUOUS SPECTRUM. Barkov, V. I. Soviet Astron. AJ (Engl. Transl.), 9: 579-82(Jan.-Feb. 1966).

Translated from Astron. Zh., 42: 749-53(July-Aug. 1965).

The radiative transfer equation is solved for a spherically symmetrical isothermal model of the solar corona. The flux of the coronal component of solar radio emission at $\lambda = 9.1$ cm is computed, assuming that electron density in the corona varies as indicated by the Bogorodskii-Khinkulova formula. (auth)

29905 INVESTIGATION OF A CHROMOSPHERIC LIMB FLARE. Polupan, P. N.; Yakovkin, N. A. (Kiev State Univ.). Soviet Astron. AJ (Engl. Transl.), 9: 590-8(Jan.-Feb. 1966).

Translated from Astron. Zh., 42: 764-74(July-Aug. 1965).

On the basis of a solution of the steady-state equations for the first six levels of the hydrogen atom the effective extent ($1.2(10)^7$ cm), electron concentration ($2.1(10)^{12}$), and temperature (7500°) of a chromospheric limb flare observed on July 27, 1961. In the computations an allowance was made for stimulated emission, ionization, and excitation of atoms by solar radiation and the radiation of the flare itself. Triple and photorecombinations were taken into account, as well as ionization and excitation by electron collision. The total energy emitted by hydrogen atoms for the above-mentioned flare thickness was approximately 15 ergs/cm^3· sec. (auth)

29906 FORMATION OF SUNSPOTS AND SOLAR MAGNETIC FIELDS. II. Romanchuk, P. R. (Kiev State Univ.). Soviet Astron. AJ (Engl. Transl.), 9: 599-605 (Jan.-Feb. 1966).

Translated from Astron. Zh., 42: 775-83(July-Aug. 1965).

Arguments in support of the outward transport of the magnetic fields of spots and bipolar regions into the corona are presented. This process is considered decisive for the formation of radially oriented coronal rays. The formation of corpuscular streams in the linear and fan rays of the corona is discussed. An hypothesis of the general magnetic field of the sun is proposed. It is postulated that this field is formed by the uniting of the magnetic fields of coronal rays which are caught up in the subphotospheric layers. In the process of joining of the magnetic fields, which takes place at the activity minimum, the coronal rays pass through different stages of development, being transformed from straight rays into intermediate-size and then into large and very large fan rays. The lines of force of the general field, lying in the surface layers of the sun, emerge at the poles and then are caught up in interplanetary space, thus forming polar rayed structures and very large equatorial fan rays. The polarity of the new solar magnetic field is determined by the polarity of those magnetic fields of bipolar regions which lie closest to the particular pole. The old general magnetic field is transported into interplanetary space by convective and corpuscular streams. It is shown that corpuscular streams identified with the upper parts of large and very large fan rays are geoactive. The lag in the maximum of geomagnetic disturbances in comparison with the maximum of solar activity is related to the lag in formation of the above-mentioned rays. (auth)

29907 ORIGIN OF JOVIAN RADIO EMISSION. Zheleznyakov, V. V. (Gorkii State Univ.). Soviet Astron. AJ (Engl. Transl.), 9: 617-25(Jan.-Feb. 1966).

Translated from Astron. Zh., 42: 798-809(July-Aug. 1965).

The hypothesis of the origin of the decameter radio emission of Jupiter, in which the source of the Jovian radio-emission bursts are plasma waves excited in the planetary ionosphere, is discussed. The simplest variant of the hypothesis, which does not take the Jovian magnetic field into account and ensures the generation of radio emission at frequencies $\omega \sim \omega_L$ where ω_L is the plasma frequency, is possible only for extremely small values of the recombination coefficient $\alpha_{eff} \sim 10^{-13}-10^{-14}$ cm^3 (necessary for creating an ionospheric electron concentration of $N \sim 10^7$ el/cm^3). However, in actuality α_{eff} cannot decrease below 10^{-12} cm^3, that is, below the value of the coefficient of radiative recombination. Allowance for a magnetic field makes it possible to decrease the value N and accordingly increase α_{eff} to reasonable limits; the necessary values of the frequency of radio emission in this case $\omega \approx \omega_H$ (ω_H is the gyrofrequency) are obtained when the strength of the magnetic field in the ionosphere is quite great (several oersteds). The observed characteristics of Jovian decameter radio emission can be explained if $N \sim 3\ (10)^5$ el/cm^3. In particular, this value N is adequate to explain the directional character of the Jovian bursts associated with the gyroresonance absorption of extraordinary radio emission in the upper layers of the planetary ionosphere (at the level where $\omega \approx 2\omega_H$). The predominant emission of extraordinary waves ensures a mechanism of transformation of plasma waves in the region of sharp decreases of density of ionospheric plasma of the shock-wave type. It is noted that plasma waves at the frequencies $\omega \approx \omega_H$ can be excited by the "anisotropy" of temperatures or by "two-stream" instability at schock-wave fronts. In conclusion arguments are given against the cyclotron mechanism and in favor of the synchrotron mechanism of Jovian decameter radio emission. (auth)

29908 FREQUENCY SPECTRUM OF THE SLOWLY VARYING COMPONENT OF SOLAR RADIO EMISSION. Abbasov, A. R. Vestn. Leningr. Univ., Ser. Mat., Mekhan. Astron., No. 1, 174-6(1966). (In Russian).

The results of a statistical treatment of daily radio observations at wavelengths near 3, 8, 10, and 15 cm, which were made in 1961, 1962, and 1963, are presented. The frequency spectrum of the S-component of the solar radio emission is derived. In the frequency spectrum, the maximum of the emission related to the sunspots is at $\lambda \sim 8$ cm and that of the flocculi is at $\lambda \geq 10$ cm. (G.O.Y.)

29909 ON THE THEORY OF THE ORIGIN OF ATOMIC NUCLEI OF OUR SOLAR SYSTEM. Suess, Hans E. (Univ. of California, San Diego, La Jolla). Z. Naturforsch., 21a: 90-2(Jan.-Feb. 1966). (In German).

In general, diffulties attached to the theories of element origins are overcome by the assumption that elements in our solar system represent mixtures of different kinds of nuclei that arose in various ways at various times and at various sites. There is, however, a basic objection to this assumption. Through selection of a suitable classification of the nuclear types it can be shown that in the given mass ranges the nuclear frequencies have a conspicuous relation with the nuclear binding energies determined by Mattauch et al., for example, with the binding energy of the last α particle. This relation is not quantitatively explainable at this time. (tr-auth)

29910 MEASUREMENTS OF SOLAR MAGNETIC FIELDS [Thesis]. Sheeley, Neil Rolfson Jr. Pasadena, Calif., California Inst. of Tech., 1965. 130p.

The photographic technique of Leighton was used to obtain high-resolution measurements of photospheric magnetic fields. Source fluxes, Φ (defined as the average of the absolute values of the total fluxes of positive and negative polarity in a bipolar magnetic region on the day when this average is largest), of bipolar magnetic regions (BMRs) were measured as a function of the size, A_m, of the associated sunspot activity. A_m is defined to be the area covered by all of the sunspots of a group (umbras plus penumbras of both leading and following parts) on the day when this area is largest. The source fluxes were found to satisfy $\Phi = 1.2\ A_m$ within about ±50%, where Φ is in solar flux units (1 SFU = 10^{21} maxwells) and A_m is in units of 10^{18} cm^2. Two BMRs were traced for the first few months following their birth. The development of each was semiquantitatively what one would expect if the random-walk plus solar differential rotation were the only means of flux transport on the solar surface. In quiet regions of the solar surface, magnetic flux is distributed in small bits and fragments, and in the quietest regions, in tiny points less than 3000 km in diameter. Measurements for eight small features yielded fluxes ranging from 0.05 SFU for the very small points to 0.4 SFU for typical network fragments. The corresponding magnetic fields ranged from 200 gauss for the points to 700 gauss for the network fragments. Polar faculae curves were calibrated to give magnetic flux on the polar caps of the sun as a function of time during the period 1905–1964. The principal conclusion is that these measurements are consistent with the hypothesis that all of the magnetism on the sun's surface originates in BMRs, and that it is gradually spread about the surface by the random-walk and differential rotation, eventually causing the cancellation and reversal of the polar fields. (TCO)

Atomic Physics

Refer also to abstracts 29525 and 30773.

29911 (COO–1112-21) A MEASUREMENT OF THE 2^3P FINE STRUCTURE OF ^4He. Lifsitz, Jacob Robert (Michigan Univ., Ann Arbor). 1965. Contract AT(11-1)-1112. 173p. Dep. mn. CFSTI $5.00 cy, $1.00 mn.

Thesis.

An accurate determination was made of the fine structure in the n = 2 triplet P-states of ^4He. The method used is an application of level-crossing spectroscopy, in which one detects a change in the angular distribution of resonance fluorescence in a magnetic field when the field value is such that a crossing occurs between a pair of excited state Zeeman sublevels. Four such crossings are studied in detail, at field values (in gauss) of: $H_A = 562.8$, $H_B = 578.5$, $H_C = 1227.4$, $H_D = 8280.0$. The magnetic field at which the altered scattering is observed is measured in terms of the nuclear magnetic resonance frequency of protons (deuterons) in $H_2O(D_2O)$. Using the solutions to the secular equations for the Zeeman effect, in conjunction with certain accurately known ratios of atomic and nuclear g-values, the extrapolation to the zero-field separations, $\epsilon_{12} = E(^3P_1) - E(^3P_2)$ and $\epsilon_{02} = E(^3P_0) - E(^3P_2)$, is effected. (M.O.W.)

29912 (ISS–66/6) THE SPECTRAL DISTRIBUTION OF PHOTONS SCATTERED BY ELECTRONS BOUND IN THE K SHELL. [PART] I. Di Lazzaro, M. A.; Missoni, G. (Istituto Superiore de Sanita, Rome (Italy). Laboratori di Fisica). Feb. 21, 1966. 39p. Dep. mn.

Several measurements of spectral distributions of 662-kev γ-rays scattered by K-shell electrons of gold and uranium are reported. The experimental results are compared with numerical values calculated from the expression of the cross section deduced from the Klein–Nishina formula. Finally, a new and more accurate calculation of the differential cross section is given. (M.O.W.)

29913 (ISS–66/7) THE SPECTRAL DISTRIBUTION OF PHOTONS SCATTERED BY ELECTRONS BOUND IN THE K SHELL. [PART] II. Di Lazzaro, M. A.; Missoni, G. (Istituto Superiore de Sanita, Rome (Italy). Laboratori di Fisica). Feb. 21, 1966. 80p. Dep. mn.

29914 (ISS–66/8) THE SPECTRAL DISTRIBUTION OF PHOTONS SCATTERED BY ELECTRONS BOUND IN THE K SHELL. [PART] III. Di Lazzaro, M. A.; Missoni, G. (Istituto Superiore de Sanita, Rome (Italy). Laboratori di Fisica). Feb. 21, 1966. 115p. Dep. mn.

29915 (JINR–P-2627) KULONOVSKOE POLE I NERELYATIVISTSKOE KVANTOVANIE PROSTRANSTVA. (Coulomb Field and Non-Relativistic Space Quantization). Mir-Kasimov, R. M. (Joint Inst. for Nuclear Research, Dubna (USSR). Lab. of Theoretical Physics). 1966. 15p. Dep. mn.

A possibility is considered of describing a hydrogen atom in terms of the p-space of constant curvature. An analogy with space quantization treated by Snyder is drawn. Different ways of projective introduction of metric into the p-space are investigated. (auth)

29916 (ORNL-TM–1458) SEMI-CLASSICAL MODEL OF THE PHOTOELECTRIC EFFECT IN METALS. Connor, W. G.; Ritchie, R. H. (Oak Ridge National Lab., Tenn.). June 1966. Contract W-7405-eng-26. 86p. Dep. mn. CFSTI $3.00 cy, $0.75 mn.

Thesis. Submitted by W. G. Connor to Vanderbilt Univ., Nashville, Tenn.

Photoemission from a bounded, free-electron-like metal was treated on the basis of separate semi-classical models of surface and volume photoemission processes. It is proposed that the surface photoeffect may be considered the inverse of the transition radiation process. The vectorial effect in surface photoemission is related to the complete polarization of transition radiation in the plane of emission. This model leads to the prediction that electron yield from a thin foil should depend upon the thickness of the foil in an oscillatory way. The volume photoeffect is described on a phenomenological basis, relating photoelectron yield from a given metal with the response of the metal to photons, the cascade-transport process of nascent photoelectrons in the metal, and the transmission probability of these electrons at the surface of the metal. Comparison of calculated yields with published experimental data reveals only fair agreement between the results of different experimenters and between these data and the present theory. Reasons for the discrepancies are discussed. (auth)

29917 (TID–22957) CONFIGURATION INTERACTION IN TWO- AND THREE-ELECTRON ATOMS. Brown, Robert Theodore (Michigan Univ., Ann Arbor). 1965. Contract AT(11-1)-1112. 147p. Dep. mn. CFSTI $4.00 cy, $1.00 mn.

Thesis.

A theory for configuration interaction was developed and used to determine the 2^2P-energy state of lithium. Comparisons were made with ground state determinations for two-electron atoms and the 2^2S-state of lithium. (M.O.W.)

29918 (UCRL–11670) CONSIDERATIONS AFFECTING THE DESIGN OF ATOMIC- AND MOLECULAR-BEAM APPARATUS. McColm, Douglas (Lawrence Radiation Lab., Univ. of California, Berkeley). May 17, 1965. Contract W-7405-eng-48. 25p. Dep. mn. CFSTI $1.00 cy, $0.50 mn.

Optimum design criteria for atomic- and molecular-beam apparatus are discussed, and signal strengths under a number of conditions are calculated. Signal strength and signal-to-noise ratios are shown graphically as functions of the design parameters. Vertical-slit geometries only are considered. (auth)

29919 (UCRL–14214) NEUTRALIZATION OF FAST HYDROGEN IONS COLLIDING WITH H_2, CO, CH_4, AND H_2O MOLECULES. Chambers, E. S. (Lawrence Radiation Lab., Univ. of California, Livermore). June 8, 1965. Contract W-7405-eng-48. 17p. Dep. mn. CFSTI $1.00 cy, $0.50 mn.

Fast neutral particle production cross sections, for H^+, H_2^+, and H_3^+ ions colliding with H_2, CO, CH_4, and H_2O molecules, were obtained by measuring the quantity of fast neutral particles produced. Ion energies ranged from 1 to 55 kev. Electron capture cross sections for H^+ increased in the order H_2, CO, CH_4, and H_2O. They extended at 10 kev from 8 $Å^2$ for H_2 to 14 $Å^2$ for H_2O. Similarly for H_2^+ the neutral production cross sections at 10 kev ranged from 8 $Å^2$ for H_2 to 19 $Å^2$ for H_2O. The H_3^+ cross section versus energy curves showed broad maxima. The position of these maxima increased in both intensity and energy with the various gases in the order H_2, CO, CH_4, and H_2O. Gryzinski's criterion for the energy of maximum cross section led to values approximating those observed. Calculations of electron capture as a function of energy, based on Gryzinski's approximation formulas, are compared with the present experimental results. (auth)

29920 (UCRL–14271) IONS AND DISSOCIATION PRODUCTS OBTAINED FROM A HYDROGEN RF ION SOURCE. Chambers, E. S. (Lawrence Radiation Lab., Univ. of California, Livermore). June 23, 1965. Contract W-7405-eng-48. 6p. Dep. mn. CFSTI $1.00 cy, $0.50 mn.

Low-intensity ions from an r-f-excited hydrogen ion source and their dissociation products from collision with H_2 molecules were investigated through the apparent mass range from 0 to 3.9. Along with the normally expected ions, the following were observed: H_3^{2+} and its dissociation products H_2^+ and H^+; H^+ from dissociation of H_2^+, H_3^+, H_5^+, OH^+ and O_2H^+; HD^+ from H_2D^+; B^{2+} from $B_2O_3^+$; and N^{2+}, N^{3+}, N^{4+}, N^{5+} from N_2^+. A number of additional ions were observed but not identified. (auth)

29921 MOLECULAR CONSTANTS AND THERMODYNAMIC FUNCTIONS OF SOME LINEAR SYMMETRICAL MOLECULES. Nagarajan, G. (Oklahoma State Univ., Stillwater). Acta Phys. Austr., 21: 355-65(1966).

A brief vibrational analysis of C_3, Si_3, Ge_3 and XeF_2 mole-

cules possessing a linear symmetrical structure is given. Mean-square amplitude quantities, generalized mean-square amplitudes (mean-square parallel amplitudes, mean-square perpendicular amplitudes and mean cross products) and mean amplitudes of vibration for the bonded and nonbonded atom pairs were calculated by the Cyvin's method and the values are reported at the temperatures T = 0, 298, and 500°K. The numerical values of the Bastiansen-Morino shrinkage effect are given at these temperatures. The statistical thermodynamic functions for the Si_3, Ge_3 and XeF_2 molecules were also calculated on the basis of a rigid rotator, harmonic oscillator model. (auth)

29922 ELECTROMAGNETIC PROPERTIES OF THE BARYON. HYPERFINE STRUCTURE OF HYDROGEN. Nambu, Y. (Univ. of Chicago). pp 87-93 of High Energy Physics. Takeda, Gyo (ed.). Tokyo, Syokabo Publishing Co. New York, W. A. Benjamin, Inc., 1966.

The discrepancy between the experimental and theoretical values of the correction to the hyperfine splitting of hydrogen for form-factor effects and two-photon-exchange effects is explained by two different approaches. (D.C.W.)

29923 INFLUENCE OF ELECTRON BINDING ON THE INCOHERENT SCATTERING OF LOW-ENERGY GAMMA RAYS. Rao, Ramana P. V.; Rao, J. Rama; Lakshminarayana, V. (Andhra Univ., Waltair, India). Indian J. Pure Appl. Phys., 4: 56-9(Feb. 1966).

The incoherent scattering cross sections (σ_b) in elements carbon, aluminum, copper and cadmium were determined at photon energies 280, 145, 129 and 100 kev and are compared with the corresponding integral-free-electron incoherent scattering cross sections (σ_f) calculated using the Klein-Nishina formula, to assess the influence of electron binding. The diminution of σ_b relative to σ_f is found to increase progressively with decreasing energy and increasing atomic number, thereby indicating the growing severity of binding effects in these two directions. The experimental values of the ratio (σ_b/σ_f) are compared with theoretical estimates of the same computed on the basis of the Thomas-Fermi atomic charge distribution. Fair agreement is noticed between the two ratios whenever the diminution in the value of the cross section due to binding effects does not exceed about 10 percent. In other cases, progressively increasing deviations between the two values of the ratio (σ_b/σ_f) are found towards decreasing energy and increasing atomic number. The deviations are attributed to systematic errors inherent in the theoretical estimates made on the basis of the Thomas-Fermi model. (auth)

29924 ABSOLUTE PHOTOELECTRIC CROSS SECTIONS OF 320 kev GAMMA RAYS. Parthasaradhi, K.; Lakshminarayana, V.; Swami, Jnanananda (Andra Univ., Waltair, India). Indian J. Pure Appl. Phys., 4: 87-8 (Feb. 1966).

Absolute photoelectric cross sections of 320-kev gamma rays in Pb, Pt and Ta were determined experimentally using a well-type plastic crystal scintillation spectrometer. It is found that the agreement between the experimental results and the values obtained from the recently developed theoretical expressions as well as with the interpolated values from the G. W. Grodstein's tables is satisfactory. (auth)

29925 ION SOURCE OF HYDROGEN IONS AT LOW GAS PRESSURES. Starodubtsev, S. V.; Muminov, V. A.; Babal'yants, V. F.; Abdurakhmanov, A. Kh. Izv. Akad. Nauk Uz. SSR, Ser. Fiz.-Mat. Nauk, No. 4, 79-80(1965). (In Russian).

A source in which the generated ions are drawn out in a direction perpendicular to the source is described. The frame of the source consists of two 590-mm steel rings connected by eight stainless steel tubes 14 mm in diameter and 1900 mm long. The anode and cathode are in the form of 0.5-mm tungsten wires suspended from insulated sleeves on the framing tubes. The wires are alternately incandescent and cold, and the potential difference applied to them ignites the discharge. The source assembly is placed in a vacuum chamber of approximately 600-l capacity evacuated with an oil-diffusion pump to 10^{-5} mm Hg. Hydrogen gas is fed in at a working pressure of $(2-4) \times 10^{-4}$ mm Hg. The discharge current ranged from 0.6 to 1 amp at an electrode potential on the order of 1.5 kv and a filament current of 32 amp, depending on the high negative potential applied to the collector. The latter was located 200 mm from the ion-production region. It is assumed on the basis of published data that at an arc current of 1 amp the percentage of H_1^+ ions reaches 90. The ion current varies linearly with the drawing voltage on the collector. (ATD)

29926 INDIVIDUAL EFFICIENCY CURVES FOR THE EXCITATION OF 2^3S AND 2^1S STATES OF HELIUM BY ELECTRON IMPACT. Cermak, V. (Univ. of Colorado, Boulder). J. Chem. Phys., 44: 3774-80(May 15, 1966).

Measurement of kinetic energy of electrons released in ionization of argon by helium atoms in metastable 2^1S and 2^3S states was applied for the determination of separated efficiency curves for the two states. No quenching in electric field or deflection in an inhomogeneous magnetic field was necessary. The ratio of the cross sections for the 2^1S and 2^3S states, excited by electron impact, was found larger than that determined in experiments in which secondary electron emission was used for detecting metastable atoms. This seems to indicate that the Penning ionization cross section for argon by helium atoms in the 2^1S state is larger than that by the atoms in the 2^3S state. (auth)

29927 RETARDING-POTENTIAL MEASUREMENT OF THE KINETIC ENERGY OF ELECTRONS RELEASED IN PENNING IONIZATION. Cermak, V. (Univ. of Colorado, Boulder). J. Chem. Phys., 44: 3781-6(May 15, 1966).

Kinetic energy of electrons released in ionization of N_2, CO, NO, COS, CO_2, C_2H_2, CH_4, C_2H_6, C_3H_8, and n-C_4H_{10} by means of helium atoms in metastable 2^1S and 2^3S states was measured and the energy of electronically excited ionic states determined. In N_2, CO, COS, and CO_2 all accessible excited states were populated probably by a Franck-Condon transition. Ionization of NO seems to proceed through preionization of the HeNO complex in which a part of internal energy is converted into kinetic energy of He and NO^+. In ionization of C_2H_2 and CH_4, energy which can be effectively stored in the $C_2H_2^+$ and CH_4^+ ions in the ground state was determined and the aspects of the dissociative ionization discussed. In ionization of C_2H_6, C_3H_8, and n-C_4H_{10}, more excitation energy is conferred on the ions than in ionization by charge transfer or electron impact. (auth)

29928 GROSS- AND PARTIAL-IONIZATION CROSS SECTIONS FOR ELECTRONS ON WATER VAPOR IN THE ENERGY RANGE 0.1-20 kev. Schutten, J.; de Heer, F. J.; Moustafa, H. R.; Boerboom, A. J. H.; Kistemaker, J. (FOM-Laboratorium voor Massascheiding, Amsterdam). J. Chem. Phys., 44: 3924-8(May 15, 1966).

Measurements are made on the gross-ionization cross sections for 0.1–20 kev electrons on water vapor at pressures of about 3×10^{-4} torr. The results are compared with the cross sections of H_2 and O_2. Within the experimental error of 15% no deviations are found from the additivity rule. The energy dependence of the cross section satisfies the Bethe-Fano-Platzman relation for collision-induced dipole transitions at energies exceeding 400 ev. A comparison is made with photoionization and inelastic electron-scattering cross sections. Some results are given on the partial cross sections for the production of fragment ions for 0.02–2-kev electrons on water vapor. (auth)

29929 PRIMARY AND AFTERGLOW EMISSION FROM LOW-TEMPERATURE GASEOUS NITROGEN EXCITED BY FAST ELECTRONS. Sebacher, Daniel I. (Langley Research Center, Hampton, Va.). J. Chem. Phys., 44: 4131-6(June 1, 1966).

Measurements were made of the primary and afterglow emission decay times of some of the emitting species in an expanded nitrogen flow when excited by a 10-kev electron beam. Both the first negative system of N_2^+ and the second positive system of N_2 were observed in the afterglow to persist for about 2×10^{-6} sec. The origin of the afterglow is explained by the possible transfer of energy from ground-state N_2^+ ions and secondary electrons to ground state N_2 molecules. This is substantiated by observations of the departure from a Boltzmann distribution of the rotational energies in the N_2 molecules. (auth)

29930 MEASUREMENT OF THE LIFETIMES OF THE n = 3 STATES OF H BY ELECTRON CAPTURE DURING FAST H^+ IMPACT ON GASES. Hughes, R. H.; Dawson, H. R.; Doughty, B. M. (Univ. of Arkansas, Fayetteville). J. Opt. Soc. Amer., 56: 830-1(June 1966).

In an attempt to obtain the relative cross sections for 3s, 3p, and 3d capture, an H^+ beam was allowed to enter a target-gas-filled and differentially pumped collision chamber of known length. After the partially neutralized beam left the chamber and entered an evacuated observation region, the intensity of Balmer radiation from the resulting fast atoms was measured as a function of the distance from the beam-departure aperture. A plot of the intensity of H_α emission from H^+ on N_2 vs distance from the beam-departure aperture is shown. The decay curve is the sum of three exponential decays. The time constants of the decay agree with the theoretical 3s, 3p, and 3d lifetimes. (A.G.W.)

29931 INVESTIGATION OF THE ELECTRON STATES OF ATOMS, MOLECULES, AND SOLIDS BY QUASIELASTIC KNOCK-ON OF AN ELECTRON BY A FAST ELECTRON (e,2e). Smirnov, Yu. F.; Neudachin, V. G. (Moscow State Univ.). JETP Lett. (USSR) (Engl. Transl.), 3: 192-3(Apr. 1, 1966).

Translated from Zh. Eksp. Teor. Fiz., Pis'ma Redaktsiya, 3: 298-301(Apr. 1, 1966).

Three examples (impulse approximation) are presented of investigations on the electronic states of atoms, molecules, and solids which make it possible to obtain the Fourier transform of the wave function of the knock-on electron and its binding energy. The examples are H_2 molecules, H_2^+ ions in state $1\sigma_g$; free electrons in a metal (plane waves), and strong coupling with the lattice (Bloch's sums). (B.G.D.)

29932 MEASUREMENT OF THE CROSS SECTIONS OF ION-ATOM COLLISIONS AT LOW ENERGIES BY THE METHOD OF OVERTAKING BEAMS. Belyaev, V. A.; Brezhnev, B. G.; Erastov, E. M. JETP Lett. (USSR) (Engl. Transl.), 3: 207-9(Apr. 15, 1966).

Translated from Zh. Eksp. Teor. Fiz., Pis'ma Redaktsiya, 3: 321-3(Apr. 15, 1966).

An experiment is described based on the principle of monochromatic particle beams crossed at a small angle (overtaking beams) for studying atom–ion collisions of the same substance. However, only one monokinetic atom–ion beam is utilized. The process chosen was resonance charge exchange of protons with hydrogen atoms and cross sections for these collisions were obtained. (B.G.D.)

29933 LONG-RANGE THREE-BODY FORCES BETWEEN HELIUM AND HYDROGEN ATOMS. Dalgarno, A.; Victor, G. A. (Queen's Univ., Belfast). Mol. Phys., 10: 333-7(1966).

The nonadditive contribution to the long-range interaction energy of three atoms A, B and C at large distances R_{ab}, R_{bc} and R_{ca} apart may be written $E(ABC) = \gamma(ABC)(1 + 3\cos\theta_a \cos\theta_b \cos\theta_c)/(R_{ab}R_{ac}R_{bc})^3$, where θ_a, θ_b and θ_c are the internal angles of triangle ABC. The values of γ(ABC) for triads selected from hydrogen and helium atoms are calculated. In atomic units they are respectively 21.64, 8.12, 3.80 and 1.49 for the mixtures H–H–H, H–H–He, H–He–He and He–He–He. (auth)

29934 ABSORPTION SPECTRA OF PtH AND PtD. Loginov, V. A. Opt. Spectros. (USSR) (Engl. Transl.), 20: 88(Jan. 1966).

Translated from Opt. Spektros., 20: 167(Jan. 1966).

The absorption spectra of PtH and PtD were obtained by exploding Pt wires electrically in H_2O and D_2O, respectively. A rotational analysis of the 0–0 band of the PtH radical referred to the transition $^2\Delta \rightarrow X^2\Delta$ was carried out. (B.G.D.)

29935 CROSSING AND ANTICROSSING SIGNALS OF THE ^1H AND ^2H ATOMS IN A UNIFORM MAGNETIC FIELD. Hiismaeki, P.; Jauho, P. (Inst. of Tech., Otaniemi, Finland). Phys. Lett., 21: 516-18(June 15, 1966).

The scattering cross section of polarized light at level crossings of 3483 and 5224 gauss was calculated paying special attention to the hyperfine interaction. The resulting formulas allow easy comparison with experiments. (auth)

29936 BINDING EFFECTS IN ELECTRONIC EXCITATIONS BY HEAVY CHARGED PARTICLES. Brandt, W.; Laubert, R.; Sellin, I. (New York Univ., N. Y.). Phys. Lett., 21: 518-19(June 15, 1966).

The ratios of K-shell x-ray production cross sections by He^+ and H^+ ions of 25 to 50 kev per amu energy in Al and Mg are found to be influenced strongly by additional binding of the target electrons at the time of excitation. (auth)

29937 MEASUREMENT OF THE GREAT POLARIZATION EFFECTS AT LOW-ENERGY ELECTRON SCATTERING. Jost, K.; Kessler, J. (Technische Hochschule, Karlsruhe, Ger.). Phys. Lett., 21: 524-5(June 15, 1966).

Experimental results on angular and energy dependence of the polarization of slow electrons scattered elastically by mercury are communicated. The theoretical predictions of the high polarization peaks prove valid down to energies of 180 ev. (auth)

29938 K^- MESONIC X RAYS AND THE $\bar{K}$-N SCATTERING LENGTHS. von Hippel, Frank; Douglas, John H. (Cornell Univ., Ithaca, N. Y.). Phys. Rev., 146: 1042-8 (June 24, 1966).

K^- mesonic x rays from helium have recently been observed and their energies and intensities measured. The strong-interaction effects on these lines appear to be an order of magnitude smaller than expected on the basis of simple considerations. A model for the strong K^--α interaction effects is discussed assuming dominance of two-body $\bar{K}$-N interactions and based upon the representation of the $\bar{K}$-N interactions by complex central Yukawa potentials adjusted to the experimental scattering lengths. For ranges associated with any known particle exchanges, the results, although very different from those obtained previously in Born approximation, still disagree by an order of magnitude with experiment. After considering various alternative explanations of this disagreement, it is noted that a $\bar{K}$-N scattering-length solution having a value for Im A_1 considerably smaller than that currently favored would allow agreement of our model with experiment. (auth)

29939 FINE AND HYPERFINE STRUCTURE OF THE 3^2P TERM IN LITHIUM. Budick, B.; Bucka, H.; Goshen, R. J.; Landman, A.; Novick, R. (Columbia Univ., New York). Contracts DA-36-039 SC-90789; DA-28-043 AMC-00099(E). Phys. Rev., 147: 1-5(July 8, 1966).

The fine and hyperfine structures of the 3^2p term in ^7Li were studied by the technique of level-crossing spectroscopy. A preliminary value for the fine-structure separation is $\Delta\nu = 2882.9 \pm 1.2$ Mc/sec. It is expected that the present technique can be extended to obtain a result that is reliable to a few parts per million. It is noteworthy that the fine-structure intervals in lithium are 8% and 12% smaller for the 2p and 3p levels, respectively, than the corresponding intervals in hydrogen. A theory is developed for interpreting the separation between hyperfine level crossings. Its application depends on a detailed knowledge of the core-polarization effects of the 3p electron. Evidence is presented indicating that the core-polarization effects in the np states (n = 2, 3) scale as $\langle 1/r^3 \rangle_{np}$ for the valence electron. Assuming this to be true, it is estimated that $a_e(3p) = -3.05(12)$ Mc/sec for ^7Li. The limited precision achieved so far in this work prevented observation of the ^7Li quadrupole interaction. (auth)

29940 COUPLED-STATE CALCULATIONS OF H^+-H SCATTERING. Wilets, L.; Gallaher, D. F. (Univ. of Washington, Seattle). Contract AT(45-1)-1388. Phys. Rev., 147: 13-20(July 8, 1966). (TID-22691).

The proton-hydrogen scattering problem was treated numerically under the following approximations: (1) The

protons describe straight-line classical trajectories; (2) the (spinless) electronic wave function is expanded in terms of a finite subset of traveling hydrogenic functions centered about either proton. The resulting set of coupled differential equations is solved without further approximation, except for numerical techniques. Most of the results reported include 1S, 2S, $2P_0$, and $2P_{\pm 1}$ states. A limited number of calculations include the 3S, $3P_0$, and $3P_{\pm 1}$ states. The 2P direct excitation and transfer excitation cross sections follow the trend of the experimental data of Stebbings et al., but are low by a factor of roughly 2. The calculations also agree qualitatively with the experiments of Everhart et al. on 3° total transfer probability, but are somewhat out of phase in respect to the oscillation of this quantity with energy. Large polarizations of the final 2P states are predicted. Limitations of the model are discussed; possible modifications and improvements are suggested. (auth)

29941 ATOMIC-BEAM STUDY OF THE STARK EFFECT IN THE CESIUM AND RUBIDIUM D LINES. Marrus, Richard; McColm, Douglas, Yellin, Joseph (Univ. of California, Berkeley). Contract W-7405-eng-48. Phys. Rev., 147: 55-9(July 8, 1966). (UCRL-16541).

Details of a new atomic-beam method for the study of the Stark effect in optical transition are presented. The method is then applied to a study of the transitions $6^2p_{\frac{1}{2},\frac{3}{2}} \rightleftharpoons 6^2s_{\frac{1}{2}}$ in cesium and $5^2p_{\frac{1}{2},\frac{3}{2}} \rightleftharpoons 5^2s_{\frac{1}{2}}$ in rubidium. The splitting by the electric field of the $p_{\frac{3}{2}}$ level into two levels is observed. It is shown that the characterization of the Stark effect in the ^2p levels by a simple scalar and tensor polarizability does not hold. Fine-structure effects giving rise to differences of the $^2p_{\frac{3}{2}}$ and $^2p_{\frac{1}{2}}$ radial functions are sufficiently strong that the Stark effect of the ^2p level must be expressed in terms of three parameters. If the polarizability $\alpha(n^2p_J m_J)$ is defined by the relation $\Delta W(n^2p_J m_J) = -\frac{1}{2}E^2\alpha(n^2p_J m_J)$, where E is the electric field and ΔW the induced energy shift, then the following values of the polarizabilities are deduced. For cesium, $\alpha(6^2p_{\frac{1}{2}}) = 187(29) \times 10^{-24}$ cm^3; $\alpha(6^2p_{\frac{3}{2}} \pm \frac{3}{2}) = 196(30) \times 10^{-24}$ cm^3; and $\alpha(6^2p_{\frac{3}{2}} \pm \frac{1}{2}) = 273(42) \times 10^{-24}$ cm^3. For rubidium $\alpha(5^2p_{\frac{1}{2}}) = 112(17) \times 10^{-24}$ cm^3; $\alpha(5^2p_{\frac{3}{2}} \pm \frac{3}{2}) = 102(15) \times 10^{-24}$ cm^3; and $\alpha(5^2p_{\frac{3}{2}} \pm \frac{1}{2}) = 148(23) \times 10^{-24}$ cm^3. The polarizabilities are compared with results deduced from Stone's recent oscillator-strength calculations for cesium and with values deduced from the method of Bates and Damgaard. (auth)

29942 ELECTRON-ALKALI ATOM SCATTERING: NONADIABATIC APPROACH. Mittleman, M. H. (Univ. of California, Livermore). Contract W-7405-eng-48. Phys. Rev., 147: 69-72(July 8, 1966). (UCRL-14591).

The nonadiabatic method of Temkin which was applied to electron-hydrogen scattering is generalized to the problem of electron-alkali scattering. A two-body equation is derived in which the core of the atom has the principal effect of modifying the two-body interaction and of excluding the two extra-core electrons from the occupied states of the core. This equation may be viewed as a generalization of the Bethe-Goldstone equation for the problem of scattering from a finite system. (auth)

29943 RESONANCES IN MULTICHANNEL SCATTERING. Mittleman, Marvin H. (Univ. of California, Livermore). Contract W-7405-Eng-48. Phys. Rev., 147: 73-6(July 8, 1966). (UCRL-14636).

The formalism of Feshbach as used by O'Malley and Geltman for finding resonances in elastic electron-hydrogen scattering is extended to more than one channel. A result of Feshbach's is rederived. It is found that resonances occur in all open channels at the same energy and with the same width. Infinities of "resonances" are found below the higher N levels in electron-hydrogen scattering, and recurrence relations determining the relative positions of the higher resonances are found. (auth)

29944 RESONANT ELECTRON CAPTURE IN SMALL-ANGLE COLLISIONS OF Ar^+ ON Ar AND Ne^+ ON Ne. Jones, P. R.; Eddy, N. W.; Gilman, H. P.; Jhaveri, A. K.; Van Dyk, G. (Univ. of Massachusetts, Amherst). Phys. Rev., 147: 76-85(July 8, 1966).

Measurements of the electron capture probability P_0 were made for single collisions of Ar^+ ions with neutral Ar atoms and Ne^+ ions with neutral Ne atoms, the latter measurements being an extension of work previously reported by this laboratory. The incident ions ranged in energy from 200 ev to 4 kev, the scattered particles being detected at angles ranging from 0.75° to 15° in the laboratory coordinates. A charge analysis of the scattered particles yielded values of P_0 as a function of the incident ion energy T and scattering angle θ; in both cases P_0 is found to oscillate rapidly as a function of θ, with some dependence upon T also. The periodicity of P_0 as a function of T and θ is consistent with a description of the collision wherein the electronic state of the ion-atom system changes adiabatically and is a superposition of symmetric and antisymmetric energy eigenstates of the diatomic molecular ion. The data are discussed in terms of this description, yielding empirical values of an integral I, defined as the energy difference ΔE between these two eigenstates, integrated over the collision path of relative motion. For the range of collisions studied, I varied from about 6 to 26 ev-Å in the case of Ar^+ on Ar, and from about 5 to 25 ev-Å in the case of Ne^+ on Ne. An approximate functional dependence of ΔE upon internuclear separation R is also obtained, although there is some evidence that ΔE may also depend upon the relative collision speed v in the case of the Ar^+-on-Ar collisions. It is proposed that the ΔE measured for the gentler collisions which produce no excitation of either atomic system is the energy difference between the Π_g and Π_u states of the quasi-molecule. (auth)

29945 CALCULATION OF THE COMPLEX ATOMIC SCATTERING AMPLITUDES FOR FAST ELECTRONS FOR EVALUATION OF ELECTION DIFFRACTION DIAGRAMS. Haase, Joachim (Univ., Kiel). Z. Naturforsch., 21a: 187-92(Mar. 1966). (In German).

The complex atomic scattering amplitudes of Ar and U were calculated by known methods at acceleration voltages of 40, 60, 80, 100, and 120 kv. The Thomas-Fermi-Dirac potentials were used as atomic potentials. The results were compared with the results of Karle and Bonham at 40 kv acceleration voltage. (tr-auth)

29946 LOW ENERGY ELECTRON-ATOM SCATTERING CROSS SECTION IN THOMAS-FERMI THEORY. Tietz, T. (Univ. of Lodz, Poland). Z. Naturforsch., 21a: 360-1(Mar. 1966).

The low energy electron-atom scattering cross section in Thomas-Fermi theory is discussed. The scattering length a for an approximate Thomas-Fermi potential was found. (J.S.R.)

29947 BREAKUP OF FAST NEGATIVE IONS IN INERT GASES. Lopantseva, G. B.; Firsov, O. B. Zh. Eksp. Teor. Fiz., 50: 975-8(Apr. 1966). (In Russian).

Breakup of weakly bound negative ions of the first group of the periodic system in inert gases is considered. Perturbation theory with a Fermi potential is applied in the calculations. The breakup cross section for a negative ion is found equal to the total elastic scattering cross section for slow free electrons on the corresponding atoms of inert gases when the electron velocities are equal to the relative velocity of the colliding atomic systems. (auth)

29948 DISSOCIATIVE CHARGE EXCHANGE AND IONIZATION IN COLLISIONS OF NEON ATOMS AND IONS WITH CARBON MONOXIDE. Ogurtsov, G. N.; Flaks, I. P. (Ioffe Physicotechnical Inst., Leningrad). Zh. Tekh. Fiz., 36: 117-22(Jan. 1966). (In Russian).

Cross sections for production of C^+, O^+, C^{2+}, O^{2+}, C^{3+}, CO^+, CO^-, C^-, and O^- ions in collisions between CO molecules and Ne atoms and Ne^+, Ne^{2+}, and Ne^{3+} ions accelerated in potentials from 3 to 30 kv were measured. The experimental apparatus and technique were described earlier. The cross sections for production of positive ions were measured with an accuracy of 15%; the cross sections for production of negative ions were measured with less accuracy. The results are presented graphically and are discussed. The total ionization cross section increased monotonically with incident particle velocity; total ionization

cross sections as large as 8×10^{-16} cm^2 were measured. The total ionization cross section was nearly independent of the charge on the incident particle; from this it is concluded that "potential ionization" processes are not significant. The cross sections for production of the various positive ions are discussed in terms of possible endothermic and exothermic reactions, and it is concluded that processes leading to the excitation of reaction products are more probable than the "potential ionization" processes previously detected. Cross sections for production of O^-, C^-, and CO^- ions were of the order of 10^{-18}, 10^{-19}, and 10^{-20} cm^2, respectively. The detection of CO^- ions with lifetimes exceeding 10^{-6} sec is significant, because the possibility of the existence of a stable CO^- ion has been disputed. (ATD)

29949 SOME APPLICATIONS OF THE SYMMETRIC DIRAC-COULOMB HAMILTONIAN [Thesis]. Chattarji, Dipankar. Durham, N. C., Duke Univ., 1965. 142p.

The problem of the Dirac electron in a Coulomb potential is reviewed. Properties of the symmetric Hamiltonian, which is an approximation to the Dirac-Coulomb Hamiltonian to order $(\alpha Z)^2/|K|$ and has two vector invariants $\vec{J}$ and $\vec{K}$, are discussed. Bound state solutions of the symmetric Hamiltonian are used to calculate x-ray scattering form factors of xenon. It is shown that relativistic effects cannot be ignored and the results are compared with Hartree-Fock values and experimental measurements. Angular momentum eigenfunctions corresponding to the continuum states of the symmetric Hamiltonian are obtained. It is shown that these are related to the exact Dirac continuum solutions by a simple mapping. Scattering solutions with the required boundary conditions are obtained and applied to the study of relativistic E1 bremsstrahlung for electrons. (Dissertation Abstr.)

29950 ENERGETIC AND ANGULAR STUDIES OF D_2H^+ FORMATION IN $D_2^+ - H_2$ COLLISIONS [Thesis]. Leventhal, Jacob Joseph. Gainesville, Fla., Univ. of Florida, 1965. 62p.

Measurements were made of the energy distributions and angular distributions of D_2H^+ formed in $D_2^+ - H_2$ collisions. The range of primary ion kinetic energy is 4 to 9 ev. The experimental method consists of directing a well-collimated, mass-analyzed and velocity-selected, D_2^+ ion beam into a reaction region containing H_2 gas at low pressure. An energy and mass analysis is then performed on the product D_2H^+ emerging from the reaction region at a fixed angle. The angular distributions are obtained by varying, stepwise, the fixed angle, and repeating the energy and mass analysis of the D_2H^+. It was found that the product D_2H^+ ions emerging from the reaction region have two distinct kinetic energies, corresponding to two distinct Q's for the reaction, one of which is positive and the other negative. There is a suggestion of fine structure superimposed on the two principal kinetic energy peaks, which is not clearly resolved, but is believed to correspond to further internal energy states of D_2H^+. It was also observed that the D_2H^+ ions formed in the exothermic process are more forward collimated than those product ions formed in the endothermic process. These results have permitted comparisons to be made with recent theoretical calculations concerning the bound states of the H_3^+ molecular ion. (Dissertation Abstr.)

29951 ENERGY AND ANGULAR DISTRIBUTION OF SECONDARY ELECTRONS PRODUCED BY 50- TO 200-kev PROTONS IN NITROGEN, OXYGEN, NEON, AND ARGON [Thesis]. Anderson, Jorge Carlos. Lincoln, Neb., Univ. of Nebraska, 1965. 102p.

The angular and energy distribution of electrons ejected from nitrogen, oxygen, neon, and argon by protons in the range 50–200 kev was investigated. The range of electron energies measured was from 1 to 500 ev for scattering angles from 10 to 160°. Electron energies were analyzed by a 127° electrostatic analyzer. At a scattering angle of 10°, all the gases have a differential cross section almost independent of electron energy over the region of 10 to 50 ev. For larger angles the cross sections follow approximately a law of the form e^{-bE_0}, where E_0 is the secondary electron energy and b is a constant. Argon deviates from this general behavior for scattering angles from 70° to 130° where a flat portion appears in the differential cross-section curves in the region of 150 ev. The cross sections integrated over electron energies fall off for increasing scattering angles and then fluctuate for larger angles. Neon seems to be the most regular of the gases investigated. The cross sections integrated over angles and electron energies are larger than those obtained by other methods. (Dissertation Abstr.)

29952 HOT ELECTRON RANGE IN THIN METAL FILMS. Brienza, M. J. (Univ. of Notre Dame, Ind.); Juenker, D. W. 35p. (CONF-660324-3; COO-274-69). ORAU. Gmelin, AED-CONF-66-036-1.

From 26th Annual Conference on Physical Electronics, Cambridge, Mass.

Some general aspects of hot electron transport and emission in thin films are treated in a calculation using classically exact optical considerations. It is shown that, for films deposited on transparent substrates, the ratio of photoemission currents for illumination from the front and rear can be used to determine the hot electron range without the usual approximations regarding uniformity of the work function and brevity of the optical attenuation length. The dependence of the emission ratio on film thickness is indifferent to the alternate interpretation of the range as a ballistic path or as a diffusion length. The method of data analysis suggested by the calculation was applied to measurements in vapor-deposited, unannealed films of Mo, Ta, and Re. In all three cases the electron ranges were less than the optical decay lengths for excitation wavelengths in the quartz ultraviolet. For Mo and Re the ranges were less than 4 mμ, and for Ta between 2 and 16 mμ. Absence of a vectorial effect in the photoemission from such films is taken as evidence that the short ranges observed are diffusion lengths. (auth)

29953 INELASTIC ELECTRON SCATTERING FROM H_2. Heideman, H. G. M.; Kuyatt, C. E.; Chamberlain, G. E. (National Bureau of Standards, Washington, D. C.). 8p. (CONF-651070–5). ORAU. Gmelin, AED-CONF-65-395-13.

From 18th Annual Gaseous Electronics Conference, Minneapolis.

In a study of inelastic scattering in H_2, energy loss spectra were measured for incident electron energies of 50.7, 30.7, 15.7, and 13.7 ev, and the excitation of some electronic states as a function of the incident energy was investigated. It was found that in the energy loss spectra at low incident energies loss peaks due to either or both of the $a^3\Sigma_g^+$ and $c^3\pi_u^+$ states, which are not observed at incident energies above ~20 ev, become very pronounced and much larger than the nearby $B^1\Sigma_u^+$ states. The excitation cross sections of the v = 0 and v = 1 vibrational levels of the $B^1\Sigma_u^+$ state show sharp and large resonances corresponding in energy with resonances in the total scattering. (A.G.W.)

Cosmic Radiation

See also Elementary Particles and Radiations
Nuclear Properties and Reactions

Refer also to abstracts 30079 and 30222.

29954 (NASA-TT-F-389, pp 657-77) PROBLEMS OF AND PROSPECTS FOR PRIMARY COSMIC-RAY RESEARCH. Ginzburg, V. L.; Kurnosova, L. V.; Razorenov, L. A.; Syrovatskii, S. I.; Fradkin, M. I. Translated from Issledovaniya Kosmicheskogo Prostranstva. Trudy Vsesoyuznoy Konferentsii po Fizike Kosmicheskogo Prostranstva. Izdatel'stvo, Nauka, Moscow, June 10–16, 1965.

A discussion of problems involving research into primary cosmic rays, including γ-radiation is presented. The discussion is presented in three sections; proton-nuclear component, electron-positron component of cosmic rays, and cosmic γ rays and x rays. (B.G.D.)

29955 (NASA-TT-F-389, pp 678-83) STUDIES OF PRIMARY COSMIC RADIATION ON THE SATELLITES "ELEKTRON-2" AND "ELEKTRON-4." Vernov, S. N.; Vakulov, P. V.; Zatsepin, V. I.; Logachev, Yu. I.; Okhlopkov, V. P.; Chudakov, A. E. Translated from Issledovaniya Kosmicheskogo Prostranstva. Trudy Vsesoyuznoy Konferentsii po Fizike Kosmicheskogo Prostranstva. Izdatel' stvo, Nauka, Moscow, June 10–16, 1965.

Experimental data on primary cosmic radiation, obtained on satellites elektron-2 and -4 from primary one gas discharge counters screened by 2.3 g cm^{-2} Al are examined. Intensity variations indicated by these results are the slow variations related to the 11 year cycle of solar activity, and rapid variations with a characteristic time on the order of two weeks. (B.G.D.)

29956 (NASA-TT-F-389, pp 684-91) STUDY OF COSMIC RAYS DURING FLIGHTS OF SPACECRAFTS-SATELLITES AND THE "KOSMOS" AES. Vasilova, R. N.; Nesterov, V. E.; Pisarenko, N. F.; Savenko, I. A.; Shavrin, P. I. Translated from Issledovaniya Kosmicheskogo Prostranstva. Trudy Vsesoyuznoy Konferentsii po Fizike Kosmicheskogo Prostranstva. Izdatel'stvo, Nauka, Moscow, June 10–16, 1965.

From measurements of time variations of cosmic rays on satellites and from measuring the cosmic ray equator, the performance of gas discharge counters in measuring cosmic radiation is discussed. (B.G.D.)

29957 (NASA-TT-F-389, pp 693-710) RESULTS DERIVED FROM STUDYING THE COSMIC RAY NUCLEAR COMPONENT ON THE SATELLITE "ELEKTRON-2." Blokh, Ya. L.; Dorman, L. I.; Kurnosova, L. V.; Logachev, V. I.; Platonov, G. F.; Razorenov, L. A.; Sinitsina, V. G.; Suslov, A. A.; Fradkin, M. I. Translated from Issledovaniya Kosmicheskogo Prostranstva. Trudy Vsesoyuznoy Konferentsii po Fizike Kosmicheskogo Prostranstva. Izdatel'stvo, Nauka, Moscow, June 10–16, 1965.

Observations of nuclei streams of primary cosmic rays for a long period of time are reported. Their changes as a function of solar activity are determined during the International Quiet Sun Year. Descriptions of the equipment on board the elektron-2 satellite are presented. (B.G.D.)

29958 COSMIC BLACK-BODY RADIATION, HIGH-ENERGY ELECTRONS, AND ORIGIN OF ISOTROPIC X-RAY AND GAMMA RADIATION. Fazio, G. G.; Stecker, F. W.; Wright, J. P. (Smithsonian Institution, Cambridge, Mass. Harvard Univ., Cambridge, Mass.). Astrophys. J., 144: 611-14(May 1966).

The inverse Compton x and gamma flux resulting from the interaction of high-energy electrons with an assumed cosmic black-body radiation at 3.5°K is calculated. The energy-dependent electron flux used is that observed in the vicinity of the earth. The theoretical results are compared with the appropriate experimental measurements. The x-ray flux cannot be explained locally by this effect as the gamma-ray flux would be excessive. It is also shown that the electron distribution used will not continue to be homogeneous and isotropic in space to distances much greater than the radius of the galaxy if the black-body radiation is universal. (auth)

29959 DAMPING OF INTERSTELLAR PLASMA WAVES BY THE COSMIC-RAY GAS. Tidman, Derek A. (Goddard Space Flight Center, Greenbelt, Md.). Astrophys. J., 144: 615-27(May 1966).

The propagation of waves in a thermal plasma that coexists with a tenuous gas of relativistic suprathermal particles is discussed. Low-frequency modes such as the magnetosonic and Alfvén wave experience a damping due to the suprathermal particles. Waves propagating in such regions as the interstellar medium or the plasma of a supernova remnant would be significantly damped by the cosmic radiation fluxes as a result of this mechanism. Although the decay of disturbances in the interstellar medium (produced, e.g., by stellar winds or old supernova remnants) would be hastened by this process, it is unlikely that it represents a significant energy transfer to the cosmic radiation. For the magnetosonic wave propagating directly across a magnetic field the damping has its origin in a cyclotron resonance between a wave of frequency ω ($\omega^2 \ll \Omega_{0i}^2$) and those relativistic particles for which $\Omega_i = (\Omega_{0i}/\gamma) \cong \omega$, where $\gamma = (1 - v^2/c^2)^{-\frac{1}{2}}$ and Ω_{0i} is the non-relativistic ion cyclotron frequency. (auth)

29960 DAILY VARIATION OF EXTENSIVE AIR SHOWERS. Ahababian, N.; Betev, B.; Kavlakov, S.; Sandor, T.; Somogyi, A. (Inst. of Physics, Sofia. Central Research Inst. of Physics, Budapest). pp 243-8 of International Conference on High-Energy Physics. Budapest, Central Research Inst. of Physics, 1963.

Extensive air showers were registered at the peak Musala (2930 m a.s.l.) in the Rela Mountains in Bulgaria during two periods, from March to Nov. 1960, and from Dec. 1961 to May 1962, in order to investigate both sidereal and the solar periodicity of the shower intensity. The measuring apparatus consisted of forty identical GM counters in four counter groups, and fourfold coincidences were registered with a resolving time of ~3 μsec. The mathematical method used for the determination of the root mean square amplitude of the daily variation is outlined. The results based on measurements during the first period are as follows: $a^2 = 36 \pm 56$ for the solar daily periodicity, and $\overline{a^2} = -1.6 \pm 36$ for the sidereal daily periodicity. (L.B.S.)

29961 COSMIC RAYS IN JULY OF 1961. Kuz'min, A. I.; Krymskii, G. F.; Skripin, G. V.; Chirikov, N. P.; Shafer, Yu. G.; Shafer, G. V. (Inst. of Cosmic Research and Aeronomy, Academy of Sciences, Siberian SSR). pp 263-77 of International Conference on High-Energy Physics, Budapest, Central Research Inst. of Physics, 1963. (In Russian).

Ground level and stratospheric measurements of cosmic mesons and neutrons at Yakutsk on July 9–20, 1961, are analyzed. The measurements are related to other galactomagnetic and solar phenomena that occurred successively during the same dates. The anisotropy of the cosmic showers is calculated, and the data obtained for 18 July are compared with data obtained at other European and American stations. (G.O.Y.)

29962 HIGH-ENERGY PARTICLE EVENT OBSERVED BY SPUTNIK III. Knuth, R. (Observatory for Ionospheric Research, Kuehlungsborn, Ger.). pp 292-6 of International Conference on High-Energy Physics. Budapest, Central Research Inst. of Physics, 1963.

Intensity measurements are reported of high-energy particles recorded between May 5 and Aug. 16, 1958, by Sputnik III at heights between 220 and 950 km. No remarkable changes in intensity occurred from May 5 to July 5, excluding the days around June 30. Strong enhancements were recorded in high geomagnetic latitudes ($\phi > 57°$) around July 7, reaching a maximum on July 8, and then decreasing with strong fluctuations to the normal value on about July 20. The observed increase is explained on the basis of solar cosmic rays emitted during the chromospheric flare of July 7. (L.B.S.)

29963 INVESTIGATION OF COSMIC RAY VARIATIONS IN YAKUTSK. Kuz'min, A. I.; Krasil'nikov, D. D.; Krymskii, G. F.; Skrypin, G. V.; Shafer, Yu. G. (Inst. of Cosmic Investigations and Aeronomy, Academy of Sciences, Siberian SSR). pp 299-306 of International Conference on High-Energy Physics. Budapest, Central Research Inst. of Physics, 1963. (In Russian).

A brief summary of the comprehensive report to the All-Union Congress of 1962 on the results of the first two years of study of cosmic ray variations at Yakutsk is presented. (G.O.Y.)

29964 INVESTIGATIONS OF THE SOFTER CORPUSCULAR PARTICLES BY MEANS OF COSMOS III AND COSMOS V. Mulyarchik, T. M. Kosm. Issled., 4: 95-104 (Jan.-Feb. 1966). (In Russian).

Estimates of the electron energy spectrum recorded on the satellites Cosmos-3 and Cosmos-5 were carried out from the ratios of the signals from electron detectors with

foils of various thicknesses at various accelerating voltages. It was shown that the contribution of electrons with energies E < 40 kev to the recorded signal was not everywhere the same. The ratio of the intensity of electrons with E < 40 kev to that of electrons with E > 40 kev varied roughly from 10^{-2} to 5. The basic contribution to the group with E < 40 kev is made by the soft electrons (E ~ 10 to 20 kev). The soft electrons appear chiefly at low invariant altitudes h_{min} in those cases when large real heights correspond to small values of h_{min}, i.e., over regions of central and southern Asia, the Indian Ocean, Indonesia, and the western part of the Pacific Ocean. Their intensity at heights of ~1000 km over the South Atlantic was substantially less than at analogous heights in the eastern hemisphere. The maximum electron intensity at E = 10 to 20 kev at a height of ~1500 km reached 10^7 particles cm²/sec/sterad. The sensitivity threshold of the apparatus corresponded to an intensity of ~5 × 10^5 particles/cm²/sec/sterad. (tr-auth)

29965 CASES OF TRANSIENT INCREASES OF FLUX OF HEAVY NUCLEI ACCOMPANIED BY BURSTS OF X RADIATION. Kurnosova, L. V.; Mandel'shtam, S. L.; Razorenov, L.A.; Tindo, I. P.; Fradkin, M. I. Kosm. Issled., 4: 170-2(Jan.-Feb. 1966). (In Russian).

A report is given of observations made on Electron-2 of short increases of the flux of the primary-cosmic-ray nuclear component with Z ≥ 15 associated with solar x-ray bursts, occurring at 2200 on Jan. 13 and 0215 on Feb. 14, 1964, and lasting about 16 min each. Results of measurements of the count rates due to the nuclear component and due to solar x radiation in the range 2 to 10 Å as functions of time are correlated for both instances. The probability that the observed phenomena are the results of statistical fluctuations or of chance coincidences of nuclear-component increases and x-ray bursts is analyzed. (M.J.T.)

29966 RECORDING COSMIC RAYS ON THE COSMOS-17 SATELLITE. Avdyushin, S. I.; Kogan, R. M.; Nazarova, M. N.; Pereyaslova, N. K.; Petrenko, I. E.; Svidskii, P. M. Kosm. Issled., 4: 268-79(Mar.-Apr. 1966). (In Russian).

Results are presented of measurements of the cosmic-ray intensity outside of the earth's radiation belts as a function of the L coordinate. The average value of the radiation intensity varies from 0.5 to 3.0/cm²/sec for charged particles and from 9 to 22/cm²/sec for gamma quanta. A high-latitude cut-off of the cosmic-ray spectrum is observed at rigidity R = 1.8 Bv. A cosmic- ray equator is constructed for altitudes from 400 to 600 km. Data are also presented of recordings of showers with divergence angles greater than 60°, arising in interactions of cosmic rays with the satellite body. The average characteristics of these showers are the following: particle density, 0.038/cm²; total number of particles, ~10^2; ratio of number of photons to number of particles, 11.3. (tr-auth)

29967 EVIDENCE FOR A SIDEREAL-TIME-DEPENDENT COSMIC-RAY SIGNAL. Ryan, D. F.; Acosta, V.; Buckwalter, G. L.; Carey, W. M. Jr.; Cowan, C. L.; Curtin, D. J. (Catholic Univ. of America, Washington, D. C.). Phys. Lett., 21: 475-7(June 1, 1966).

Data are presented for over 20,000 muon events produced by a neutral component of the cosmic rays which gives evidence of a strong dependence on sidereal time. The data presented cover the period from 11 May 1965 to January 1966. (auth)

29968 CONFIRMATORY EVIDENCE FOR A SIDEREAL-TIME-DEPENDENT NEUTRAL COMPONENT IN THE COSMIC RAYS. Buckwalter, G. L.; Cowan, C. L.; Ryan, D. F. (Catholic Univ. of America, Washington, D. C.). Phys. Lett., 21: 478-80(June 1, 1966).

Evidence is shown which tends to confirm a previously reported sidereal-time dependent signal in the cosmic rays. Results were obtained observing the production and decay of a muon. Anticoincidence techniques insure the muon was produced by a neutral. (auth)

29969 ASTRONOMICAL OBSERVATIONS OF HIGH-ENERGY GAMMA RAYS. Faudrowicz, Adam. Postepy Astron., 13: 3-12(Jan.-Mar. 1965). (In Polish).

Review of photon-flux measurements obtained by Explorer II (1961 N 1) and OSO-1 (1962 Z 1). The principles of operation of high-energy gamma-photon detectors on board these satellites are examined. The distribution of cosmic photons calculated by Milford is compared with Krushaav's results. (Int. Aerospace Abstr.)

29970 METHOD OF INDIVIDUAL LOCATION OF THE AXES OF EXTENSIVE AIR SHOWERS OF COSMIC RADIATION. Gawin, Jerzy; Hibner, Juliusz (Univ., Lodz, Poland). Zesz. Nauk. Uniw. Lodz., Ser. II, 17: 35-40 (1964). (In Polish).

A method is described for the determination of the location of the axes of individual extensive air showers using hodoscopic detectors for the electrons and the penetrating component. (G.O.Y.)

29971 EFFECTS OF DEPTH FLUCTUATION OF PRIMARY PROTON INITIAL INTERACTIONS ON RECORDING PENETRATING COMPONENTS IN WIDE ATMOSPHERIC SHOWERS. Zawadzki, Aleksander. Zesz. Nauk. Uniw. Lodz., Ser. II, 17: 47-51(1964). (In Polish).

It was shown that the direct correspondence between the value of the primary energy and the total number of high-energy muons is not valid if the penetrating component of the extensive showers contains low-energy muons and nucleons. The final effect of the fluctuation of the number of penetrating particles is much attenuated for low-energy nucleons. Thus the effect of the fluctuation of the penetrating component does not correspond to the fluctuation of the primary energy, nor does the number of penetrating particles represent an unequivocal measurement of this energy. (tr-auth)

29972 INVERSE COMPTON PHOTONS, COSMIC ELECTRONS, AND RELATED PROBLEMS IN PARTICLE ASTROPHYSICS [Thesis]. Felten, James Edgar. Ithaca, N. Y., Cornell Univ., 1965. 158p.

The history of the inverse Compton process (the generation of high-energy photons through scattering of thermal photons by fast electrons) in the astrophysical literature is briefly reviewed, and its importance on a cosmic scale is discussed. The theory of inverse Compton emission is presented in the Thomson approximation, and convenient formulas are developed for astrophysical applications. A similar but briefer treatment is given for synchrotron emission. Analogies are drawn between the two, with particular application to emission from the Galactic halo. Possible cosmic source regions for the observed diffuse or isotropic background component of cosmic x and gamma rays are listed: galactic halos, clusters of galaxies, the Metagalaxy. Data from radio and optical astronomy and cosmic-ray physics are used to derive dimensions and physical parameters for a series of source models. Magnetic trapping of electrons by ordered or diffusive fields is taken into account. Maximum plausible values are assumed for the electron densities in the various models, and theoretical Compton spectra are obtained. These are then corrected for effects of cosmic loss processes on the electron spectra. It is shown that the form of the Halo radio spectrum implies a disordered random-walk field with an escape time ~ 3 × 10^8 yr, B ~ 5 μg in the scattering centers, and N ~ 0.1 cm^{-3} for the mean gas density. The spectra are corrected also for cosmic absorption cutoffs, and the possibility of cosmological corrections is discussed. The corrected spectra are compared with experimental data on the photon flux from 1 kev to 100 Mev. It is found that the models of cosmic scale (R ~ ct_h) can provide a reasonable fit to the integrated intensities observed, but cannot reproduce the steep power-law dependence of the data in the range 100 kev−1 Mev. It is possible to revise the models to match these data provided certain unconventional assumptions are added. Three revised models are suggested. (TCO)

29973 INTERPLANETARY DIFFUSION MODEL FOR TIME BEHAVIOR OF INTENSITY IN A SOLAR COSMIC-RAY EVENT. Krimigis, Stamatios Mike. Iowa City, Iowa, Univ. of Iowa, 1965. 107p.

It is found possible to give a coherent interpretation of the time history of the intensity of several solar cosmic-

ray events in terms of a unified interplanetary diffusion model that assumes that the diffusion coefficient $D = M r^{\beta}$, where r is the heliocentric radial distance and M and β are parameters that may be dependent on particle energy E. The model is particularly successful in accounting for the decay phases. For the September 28, 1961, event, M varies as $E^{0.33}$ and, assuming spherical geometry, β is equal to one for $55 < E < 500$ Mev and decreases rapidly at lower energies. At r = 1 au the mean free path λ is about 0.081 au for $E \sim 200$ Mev and 0.15 for E = 23 Mev. The energy dependences of β and λ suggest 0.006 au as the order of magnitude of the scale size of irregularities in the interplanetary magnetic field. It is shown that large-angle scattering takes place for $E_p \gtrsim 150$ Mev. An upper limit to the density of scattering centers in interplanetary space is established at 3.5×10^5 $(au)^{-3}$. The total number of particles and the source spectrum is inferred. The diffusive mechanism becomes strongly dependent on energy at low energies. It is shown that in at least one case (5 February 1965) protons of energy $0.50 \leq E_p \leq 11$ Mev did not propagate according to the above picture. The possibility of nonspherical geometry of diffusion is considered as is the implication of the results with respect to the solar modulation of galactic cosmic radiation. Specifically, the galactic cosmic ray intensity in terms of the intensity observed at earth is computed and the 11-year solar modulation cycle is discussed. (Dissertation Abstr.)

Direct Energy Conversion

29974 (ANL-7190, pp 167-75) MAGNETOHYDRODYNAMICS. (Argonne National Lab., Ill.).

The potential of liquid-metal magnetohydrodynamic (MHD) cycles for central station power systems is evaluated. Data and discussion are included on efficiencies of binary cycles, MHD generator tests, end losses in MHD generators, two-phase nozzle experiments, and condensing injector studies. Results of investigations on production of a-c current using MHD generators are reported. Theoretical studies of electromagnetic field control of liquid metal condensation, and MHD generator heat transfer are reported. (J.R.D.)

29975 (GIC-3362-4) THERMOELECTRIC BISMUTH TELLURIDE IMPROVEMENT PROGRAM. Final Report. (General Instrument Corp., Newark, N. J. Thermoelectric Div.). [1965]. Contract AT(30-1)-3362. 74p. Dep. mn. CFSTI $3.00 cy, $0.75 mn.

A survey of the bismuth telluride alloys, involving changes in the bismuth antimony ratio, additions of various dopants to increase the power number at elevated temperatures was made. The Figure of Merit was also measured by measuring the thermal conductivity on those alloys which were optimized (as shown by the power number) in an attempt to correlate the power number with the Figure of Merit. Various additions were then made in order to increase the energy gap and change the temperature coefficient so that thermoelectric property will have a net gain in the Figure of Merit. (M.O.W.)

29976 (IPP-3/38) DER INNERE POTENTIALABFALL IN MHD-GENERATOREN. (The Internal Potential Drop in MHD Generators). Salvat, M. (Institut fuer Plasmaphysik, G.m.b.H., Garching (West Germany)). Apr. 1966. 14p. Dep. mn.

The finite length of the electrodes in MHD generators perturbes the potential distribution corresponding to an ideal case (i.e., to infinitely segmented electrodes). Hence the potential drop between the electrodes and thus the internal resistance of the generator increase. It is shown by means of simple physical arguments that the change of the potential drop and the corresponding increase of the internal resistance are expressible in the form

$$\frac{\Delta\varphi i^*}{\Delta\varphi^*} = \frac{Ri}{R} = \frac{1}{A + \beta D}$$

where $\Delta\varphi^*$ and R are the potential drop and the internal resistance, respectively; the subscript "i" denotes the "ideal" case, $\beta = \omega\tau$ is the Hall coefficient, A and D are two parameters which, as is shown are defined by the geometry and the relative position of the electrodes. (auth)

29977 (N-65-32716) SPACE ELECTRIC POWER SYSTEMS. American Institute of Aeronautics and Astronautics Short Lecture Series. Frankel, Philip (Lockheed-California Co., Burbank). Feb. 1964. 204p. (LR-17558).

A series of lectures on the state-of-the-art of important space power system components and concepts is presented. A review of the basic fundamental principles is included, and the various problems and proposed methods of solutions are illustrated by reference to typical spacecrafts and missions. Emphasis was placed on the problems of batteries, hydrogen-oxygen fuel cells, and thermionic and thermoelectric power generation. Basic research on magnetohydrodynamics (MHD), biochemical fuel cells, and the electrostatic generator is also briefly discussed. (auth)

29978 AMBIPOLAR POTENTIAL IN MAGNETOACTIVE COLD PLASMA. Mori, Ichiro; Suita, Tokuo (Osaka Univ.). J. Phys. Soc. Jap., 21: 815(Apr. 1966).

An application of ambipolar potential in magnetoactive cold plasma to power generation is considered, and also the effect of electric field on the diffusion coefficient is analytically studied. (B.G.D.)

29979 PHYSICAL PROCESSES IN MAGNETOHYDRODYNAMIC GENERATORS. Celinski, Z. (Inst. of Nuclear Research, Warsaw). Postepy Tech. Jadrowej Dodatek, No. 41, 61(1965). (In Polish).

This booklet discusses motion in electric and magnetic fields, electric conductivity of gas in magnetic fields, and types of MHD generators. An extensive bibliography of 310 papers is included. (NSA of Poland)

29980 LIQUID-METAL MHD TOPPING CYCLES. Petrick, Michael. Power Reactor Technol., 8: 199-209 (Fall 1965).

The coupling of a liquid-metal MHD generator to a liquid-metal-cooled reactor is briefly discussed, together with five types of cycles that have been proposed for liquid-metal MHD power systems. The results of some analyses of the efficiency of liquid-metal MHD cycles using Cs, Li, Hg, K, and Hg-K alloy as the working fluids are presented, along with the results of an analysis of overall plant efficiency. The status of liquid-metal MHD generators is summarized, and a comparison of liquid-metal and plasma MHD cycles is presented. (D.C.W.)

29981 REMOVAL OF ENERGY FROM A PLASMA OF A THERMOELECTRIC CONVERTER THROUGH THE DIFFUSION OF EXCITED ATOMS AND RESONANCE RADIATION. Baksht, F. G.; Moizhes, G. Ya.; Nemchinskii, V. A. Zh. Tekh. Fiz., 36: 324-30(Feb. 1966). (In Russian).

Calculations of energy losses from the Cs plasma in an arc-mode thermionic converter are carried out. An attempt is made to verify two assumptions made in previous studies of the cesium-atom ionization: (1) that the atomic electromagnetic radiation has only a weak effect on the step-ionization process and (2) that diffusion of excited atoms is insignificant, so that the concentration of excited atoms at each point is determined by the local temperature and the electron density. The energy loss via removal of radiation at the electrodes is calculated. It is found that the energy corresponding to the resonance transitions is insignificant in comparison to the energy given off by the electrons in the ionization process and that losses of about one-third of the ionization losses are caused by drifting of the excited atoms onto the electrodes. Losses caused by diffusion of excited atoms within the plasma volume are found to be insignificant. Numerical results are shown. (M.J.T.)

29982 IMPROVEMENTS IN AND RELATING TO MAGNETOHYDRODYNAMIC GENERATORS. (to Brown

Boveri and Co. Ltd.). British Patent 1,029,347. May 11, 1966. Priority date Nov. 29, 1963, Switzerland.

A magnetohydrodynamic generator is described that includes an open circuit for flow of the working gas and a closed circuit for flow of any element of the first to third group of the periodic system added to the working gas in elemental or compound form for increasing the electrical conductivity of the working gas. The closed circuit includes means for introducing the additional material into the working gas at the start of the open cycle and for recovering the material from the working gas at a point towards the end of the open cycle. A minimum quantity of the additional material is added sufficient to combine with all the sulfur oxides present in the working gas. Means are also included for at least partly removing the sulfur contained in the recovered additional material by purifying it before it is again mixed with the working gas. The sulfur is available in a form that enables it to be utilized commercially as technically pure H_2SO_4 or a fertilizer, and the return from the sale of these products helps offset the costs of the purifying and recovery plant for the additional material. (B.L.M.)

29983 MAGNETOHYDRODYNAMIC GENERATOR. Rosner, Manfred (to Aktiengesellschaft Brown, Boveri, and Cie). U. S. Patent 3,247,405. Apr. 19, 1966. Priority date Dec. 13, 1960, Switzerland.

A MHD generator for the production of electric power is described that combines the advantages of both the "open" and "closed"-type operating cycles for MHD generators while at the same time avoiding the disadvantages inherent with both types of operation. The hot working gas operates on an "open" cycle in that it is discharged as waste to the atmosphere after passing once through the gas channel of the generator. The additive, any element or compound selected from the first to the third group of the periodic table, but preferably Cs, to the working gas for increasing its electrical conductivity operates on a "closed" cycle in that it is added to the hot working gas in advance of that part of the gas channel in which the electrodes and magnetic field producing components are located and recovered from the working gas after it has passed the electrodes and magnetic field for recirculation through the gas channel and generator. (B.L.M.)

29984 CONSTRUCTION OF MHD ELECTRICAL POWER GENERATOR. Brill, Edward F.; Kaeser, Ernst K. (to Allis-Chalmers Mfg. Co.). U. S. Patent 3,248,578. Apr. 26, 1966. Filed Dec. 26, 1961.

An MHD generator for power production comprises a hollow steel body portion made of a stack of alternately arranged frame plates and yoke plates which are secured against displacement. Means are provided to secure the frame plates and yoke plates and their constituent pieces together in proper alignment and to prevent their displacement. The body portion of the generator supports an elongated magnetic coil, preferably fluid cooled, that is arranged within the passageway so as to surround the two elongated magnet poles. The body portion of the generator also supports insulating means and electrode means that are arranged within the passageway and define a tapered flow channel of rectangular configuration in the constricted part of the passageway where the magnet field is densest for the flow of high temperature, high velocity, electrically conductive gases or plasma. The gases or plasma are supplied to the narrow end of the flow channel through a water cooled nozzle by means such as a cyclone furnace. Heat resistant air supply means for supplying pressurized air are located along each side of the flow channel behind the inner end positions of electrode chutes and in front of the conductors that comprise the magnet coil. Electrical connections to each electrode are made directly to the electrode at the point where the chute leaves the body portion of the generator. Each pair of opposing electrodes of opposite polarity is adapted for electrical connection to a load device or for connection to means that convert the d-c power produced by the generator to a-c power of desired voltage. (B.L.M.)

Elementary Particles and Radiations

See also Field Theory, Scattering Theory, and Symmetries

Refer also to abstracts 29922, 30534, and 30535.

29985 (CONF-640509(Pt.1), Paper 1) POLE CONTRIBUTIONS TO N-N SCATTERING BELOW PION PRODUCTION. Bryan, R. (Paris Univ., Orsay (France). Laboratoire Joliot- Curie de Physique Nucleaire). 29p.

It is shown that the essential features of N-N scattering over the 0- to 300-Mev energy range are embodied in the one-meson-exchange terms due to the ω, ρ, η, π, and σ_0, where the latter symbol stands for a T = 0, J = 0^+ meson of mass near that of the neutrino. A detailed theoretical discussion is presented. (M.O.W.)

29986 (CONF-640509(Pt.1), Paper 2) π-N SCATTERING. Hamilton, J. (London Univ. (England). University Coll.). 35p.

The understanding of π-N scattering amplitudes up to the 1 Bev region is discussed in detail. Resonances, phase shifts, and Regge plots are discussed with respect to the scattering amplitudes. The resonances are also discussed in terms of SU(3). (M.O.W.)

29987 (COO–1261-4) SOME PRELIMINARY RESULTS OF AN ANALYSIS OF THE ANL–CERN SPARK CHAMBER PICTURES. Kim, Y. S.; Roberts, A.; Romanowski, T. A. (Argonne National Lab., Ill.). [1965]. Contract W-31-109-eng-38. 31p. Dep. mn. CFSTI $2.00 cy, $0.50 mn.

In order to study the feasibility of extracting Λ^0 and Σ^0 polarizations from the ANL-CERN pictures, 476 $2V^0$-events were analyzed and 152 ($\pi^- + p \rightarrow K_1^0 + \Lambda^0$) events and 28 ($\pi^- + p \rightarrow K_1^0 + \Sigma^0$) events at the incident beam momentum of 1.17 Bev/c were accepted. From these samples it was found that: $\langle \alpha_\Lambda P_\Lambda \rangle = +0.61 \pm 0.10$ and $\langle \alpha_\Lambda P_{\Sigma^0} \rangle = +0.08 \pm {}^{0.5}_{0.12}$. An examination of 96 $2V^0$-events from ^{12}C target indicates that the samples have about 20% ^{12}C (Fermi) contamination. (auth)

29988 (ITEF-356) RASPADY $\eta^0 = \pi^0 + e^+ (\mu^+) + (\mu^-)$ I NESOHRANENIE CP-CETNOST. ($\eta^0 \rightarrow \pi^0 + e^+ (\mu^+) + e^- (\mu^-)$ Decays and the Violation of CP Parity). Solov'ev, V. V. (Gosudarstvennyi Komitet po Ispol'zovaniyu Atomnoi Energii SSSR, Moscow. Institut Teoreticheskoi i Eksperimental'noi Fiziki). 1965. 8p. Dep. mn.

The spectra and the probabilities of the decays: $\eta^0 \rightarrow \pi^0 + e^+ (\mu^+) + e^- (\mu^-)$ are considered in connection with the possible violation of CP-parity. The estimates are given for two cases: (1) the violation of CP-parity is connected with the existence of X-interaction; and (2) CP-parity is violated in electromagnetic interaction. (auth)

29989 (ITEF–361) VPRUGOE RASSEYANIE PROTONOV DEITRONAMI NA BOL'SHIE UGLY. (Proton Elastic Scattering on Deuterons at Large Angles). Bayukov, Yu. D.; Vorob'ev, D. S.; Leksin, G. A.; Fedorov, V. B.; Khovanskii, V. D. (Gosudarstvennyi Komitet po Ispol'zovaniyu Atomnoi Energii SSSR, Moscow. Institut Teoreticheskoi i Eksperimental'noi Fiziki). 1965. 17p. Dep. mn.

The proton-deuteron 135.3° L.s. elastic scattering differential cross sections at the energies of incident protons 715 Mev (θ_{cm} = 157.5°), 1000 Mev (θ_{cm} = 160°), 3660 Mev (θ_{cm} = 169.5°) were measured and they are equal (26.3 ± 8.0) μ barn/ster, (17.7 ± 4.3) μ barn/ster, (3.1 ± 3.1) μ barn/ster, respectively in cms. The results are discussed within the frameworks of the pole graph with the neutron exchange. (auth)

29990 (JINR-P-2667) OBRAZOVANIE ELEKTRON-POZITRONNYKH PAR γ-KVANTAMI BOL'SHIKH ENERGII. (Formation of Electron-Positron Pairs by High-Energy γ Quanta). Bem, Ya.; Grishin, V. G.; Kistenev, E. P.

(Joint Inst. for Nuclear Research, Dubna (USSR). Lab. of High Energy). 1966. 6p. Dep. mn.

Photoproduction of (e^+e^-)-pairs by γ quanta (E_γ = 10–5000 Mev) was investigated with the help of a 24-liter propane bubble chamber. Experimental distributions in the quantity V (the ratio of the positron energy to that of a γ-quantum) agree with theoretical predictions. (auth)

29991 (ORNL-TM-1443) POSITRON ANNIHILATION IN METALS. Crowell, Julian; Ritchie, R. H. (Oak Ridge National Lab., Tenn.). June 1966. Contract W-7405-eng-26, 191p. Dep. mn. CFSTI $5.00 cy, $1.00 mn.

Thesis. Submitted by Julian Crowell to Vanderbilt Univ., Nashville, Tenn.

A theoretical study is made of the two-photon annihilation of positrons in metals in the approximation in which a metal is regarded as a free-electron gas in a smeared-out positive-charge background. The emphasis of the study is on calculations of the annihilation rate and on calculations of the static dielectric constant of an electron gas; although, some attention is also given to angular correlation, to the question of annihilation from a bound state, and to the question of whether the positron can be treated as a nonrecoiling particle in annihilation calculations. (M.O.W.)

29992 (UCRL-16717) ANTIPROTON ANNIHILATION AT REST IN DEUTERIUM [Thesis]. Kojoian, Gabriel (Lawrence Radiation Lab., Univ. of California, Berkeley). Feb. 21, 1966. Contract W-7405-eng-48. 89p. Dep. mn. CFSTI $3.00 cy, $0.75 mn.

The annihilation of antiprotons at rest in the LRL 15-inch deuterium-filled bubble chamber ($E_{center\ of\ mass}$ = 2.8137 Bev) is reported. The experiment was performed at the Bevatron. A total of 2071 events at rest were observed. The ratio of proton to neutron annihilations is 1.33 ± 0.07. The reaction $\bar{p}d \rightarrow 3\pi^- + 2\pi^+ + n\pi^0 + p$ was examined extensively. The number of neutral pions was determined and it was found that the deviation between the statistical model and the experimental data was not overwhelming. The measured pion momentum and multiplicity distributions are in agreement with the Lorentz-invariant phase-space model when one considers an interaction volume of $\Omega = \lambda\Omega_0$ where $\Omega_0 = \frac{4}{3}\pi(\hbar/m_\pi c)^3$, λ = 10, and m_π is the mass of the pion. The momentum distribution of the observed recoil proton showed a marked difference from the internal momentum distribution of the deuteron. Secondary effects were considered because final state pion-proton interactions were not the major contributors to the annihilation dynamics. Stars yielding K mesons accounted for a fraction (0.05 ± 0.01) of the total annihilation events observed. (auth)

29993 SERIES DEVELOPMENT OF THE SOLUTION OF AN EIGENVALUE PROBLEM. Lopez, Arturo (Centro Atomico Bariloche, Argentina). Acta Phys. Austr., 21: 237-44(1966).

In view of the divergencies of the field theory, the convergence of series developments of bound eigenfunctions in powers of the coupling constant is studied. Born approximation represents a suitable development in cases where an unperturbated state can be defined and in which the energy shift due to the interaction is finite. Another series development, at fixed energy, can be devised. This latter development leads necessarily to coefficients which represent nonregular functions in configuration space, nevertheless, those series converge to a regular function if the fixed energy coincides with an eigenvalue of the considered problem or, in cases where the energy of the systems is given, furnish an eigenvalue problem for the coupling constant. (auth)

29994 PHOTONUCLEAR INTERACTIONS OF HIGH-ENERGY MUONS. Paty, M.; Aguilar, R.; Senent, F. (Facultad de Ciencias, Valencia). An. Real Soc. Espan. Fis. Quim. (Madrid), Ser. A, 62: 93-7(Mar.-Apr. 1966). (In Spanish).

A proof of the validity of the Williams-Weizsäcker theory is given. The photonuclear cross-section was calculated as well as the total cross-section for muon-nucleon interaction. The interaction is also described, giving statistics of the produced particles. (auth)

29995 RADIATION FROM A STREAM OF ELECTRONS MOVING PARALLEL TO A METAL GRID LOCATED ON THE EDGE OF A UNIAXIAL CRYSTAL OF FINITE THICKNESS. Baregamyan, V. A.; Tret'yakov, O. A.; Chernyakov, E. I.; Shestopalov, V. P. (Erevan State Univ.). Izv. Akad. Nauk Arm. SSR, Ser. Fiz. Mat. Nauk, 18: No. 5, 90-6(1965). (In Russian).

A rigorous solution is given for the problem of radiation from a beam of electrons moving above the surface of an anisotropic dielectric of finite thickness with a grating. It is assumed that a grid made up of metal bands is applied to one of the surfaces of a plane-parallel layer of anisotropic dielectric material (a uniaxial crystal) with a given permeability. A formula is derived in the form of a Fourier series for the proper electromagnetic field of the electron beam. Conditions are determined under which radiation takes place in the crystal and in free space. (ATD)

29996 ELECTRON-POSITRON PAIR PRODUCTION DURING SCATTERING OF GAMMA QUANTA IN A NUCLEAR FIELD. Mukhtarov, A.; Nadzhafov, I.; Tenyakova, N. Izv. Akad. Nauk Azerbaidzh. SSR, Ser. Fiz.-Tekh. Mat. Nauk, No. 3, 74-80(1965). (In Russian).

The electron–positron pair production $\gamma + (Ze) \rightarrow (Ze)' + \gamma' + e_- + e_+$, which accompanies the scattering of γ quanta from nuclei, was studied in an attempt to determine the angular and energy distribution of the scattered particles. It was found that pair production during the scattering of γ quanta in the nuclear field differs from ordinary pair formation: in the latter case the formation of an electron-positron pair is forbidden, while in the first instance it has its highest value. A study of the correlation between the cross section and the angle indicated that the resonance character of the scattering is conserved only for angles close to 0 ; when the angle is increased, the resonance peaks disappear. The angular dependence of the polarization of the pair also has a resonance character. (TTT)

29997 CHECK ON T INVARIANCE IN THE $\pi^+ \rightarrow e^+ + \nu + \gamma$ DECAY. Vainshtein, A. I.; Ioffe, B. L. JETP Lett. (USSR) (Engl. Transl.), 3: 214-16(Apr. 15, 1966).

Translated from Zh. Eksp. Teor. Fiz., Pis'ma Redaktsiya, 3: 333-6(Apr. 15, 1966).

A possible check of time reversal invariance in the $\pi^+ \rightarrow e^+ + \nu + \gamma$ decay by observing the polarization of the γ quanta is discussed. (B.G.D.)

29998 DIFFERENTIAL CROSS SECTION OF CHARGE EXCHANGE OF 4.8-Gev/c π^- MESONS WITH PROTONS. Azimov, M. A. (Joint Inst. of Nuclear Research, Dubna, USSR); Basova, E. N.; Gulyamov, U. G.; Igamberdiev, K. R.; Kolesnik, V. G.; Pantuev, V. S.; Sil'vestrov, L. V.; Khachaturyan, M. N. JETP Lett. (USSR) (Engl. Transl.), 3: 216-19(Apr. 15, 1966).

Translated from Zh. Eksp. Teor. Fiz., Pis'ma Redaktsiya, 3: 336-40(Apr. 15, 1966).

Preliminary results are presented of the measurement of the differential cross section of the reaction $\pi^- + p \rightarrow n + \pi^0$ with the aid of a spark chamber and a total-absorption Cherenkov counter. (B.G.D.)

29999 CROSS SECTION OF QUARK GENERATION. Maksimenko, V. M.; Sisakyan, I. N.; Feinberg, E. L.; Chernavskii, D. S. (Lebedev Inst. of Physics, Moscow). JETP Lett. (USSR) (Engl. Transl.), 3: 219-21(Apr. 15, 1966).

Translated from Zh. Eksp. Teor. Fiz., Pis'ma Redaktsiya, 3: 340-4(Apr. 15, 1966).

The absence of quarks from p-N collisions in accelerators or cosmic rays has led to the conviction that their mass m_q is much higher than their generation threshold; it is further assumed that their generation cross section σ_q can not be much smaller than $\sim(10^{-3}-10^{-4})\sigma_0$, where $\sigma_0 \approx 30$ mb is the cross section of inelastic NN collision. It is shown that independent experiment and theory lead to $\sigma_q \sim \exp(-2\, m_q/\mu)$, where μ is the pion mass, so that any increase of m_q by an amount equal to m_N reduces σ_q by ~5 orders of magnitude. (B.G.D.)

30000 TWO-PION DECAY OF K_2^0 MESONS. Winter, K. pp 27-43 of Kolloquium Ueber β-Zerfall und Schwache

Wechselwirkungen. Heidelberg, Max-Planck-Instituts fuer Kernphysik, 1965. (In German).

Results are reported of the first of a series of experiments planned at CERN for investigating the two-pion decay of K_2^0, and which yield quantitative information for a phenomenological theory of the apparent violation of CP invariance. (L.B.S.)

30001 INTERACTION STRENGTHS OF THE NEUTRON AND PROTON. Daniel, H. (Max-Planck-Institut fuer Kernphysik, Heidelberg). pp 160-3 of Kolloquium Ueber β-Zerfall und Schwache Wechselwirkungen. Heidelberg, Max-Planck-Instituts fuer Kernphysik, 1965.

Evidence is accumulated to show that there is a universal difference in the interaction strengths of the neutron and proton. The interactions considered are weak interaction, strong interaction, and electromagnetic interaction. (J.S.R.)

30002 REVIEW OF FUTURE NEUTRINO EXPERIMENTS. Bienlein, J. K.; Schultze, K. pp 309-14 of Kolloquium Ueber β-Zerfall und Schwache Wechselwirkungen. Heidelberg, Max-Planck-Instituts fuer Kernphysik, 1965. (In German).

Possible future investigations on the neutrino to improve the knowledge of neutrino reactions are indicated. Those discussed are the increase of the rate of events, reactions of free nucleons, and elastic reactions. (J.S.R.)

30003 POSSIBILITY OF THE MEASUREMENT OF THE MUON POLARIZATION IN NEUTRINO EXPERIMENTS. Wachsmuth, H. W. pp 315-17 of Kolloquium Ueber β-Zerfall und Schwache Wechselwirkungen. Heidelberg, Max-Planck-Instituts fuer Kernphysik, 1965. (In German).

The possibility of detecting a transverse muon polarization in neutrino interactions by measurement of the asymmetric distribution of the decay electrons is considered. The experimental conditions necessary for the dectection of such muon polarization are indicated. (J.S.R.)

30004 NEUTRON-PROTON TOTAL CROSS SECTIONS NEAR 20, 24, AND 28 Mev. Groce, D. E.; Sowerby, B. D. (Australian National Univ., Canberra). Nucl. Phys., 83: 199-208(1966).

The neutron-proton total cross section is measured at three neutron energies in a good geometry transmission experiment using a pressurized gaseous sample. The resulting cross sections are 493.3 ± 2.4 mb at a laboratory neutron energy of 19.565 ± 0.026 Mev, 397.2 ± 1.7 mb at 23.951 ± 0.017 Mev and 337.6 ± 2.1 mb at 27.950 ± 0.013 Mev. (auth)

30005 NUCLEON-ANTINUCLEON ANNIHILATION IN THE QUARK MODEL. Rubinstein, H. R.; Stern, H. (Weizmann Inst. of Science, Rehovoth, Israel). Phys. Lett., 21: 447-9(June 1, 1966).

The consequences of the quark model are investigated for nucleon-antinucleon annihilation. A good qualitative and quantitative understanding is obtained for every feature of the reaction. Comparison with other theories is made. (auth)

30006 CURRENT ALGEBRAS AND GENERALIZED WARD-TAKAHASHI IDENTITIES. Raman, K.; Sudarshan, E. C. G. (Syracuse Univ., N. Y.). Phys. Lett., 21: 450-2 (June 1, 1966). (NYO-3399-64).

The general consequences of current algebras for many particle amplitudes are derived using generalized Ward-Takahashi indentities. Several applications are indicated. (auth)

30007 EXISTENCE OF AXIAL-VECTOR MESONS. Renner, B. (Cambridge Univ., Eng.). Phys. Lett., 21: 453-4(June 1, 1966).

Certain current algebra commutators can only be saturated if the existence of axial vector mesons is assumed. As possible candidates the $A_1(1072)$ and $K_c(1215)$ resonances are examined. (auth)

30008 CONSEQUENCES FROM THE VECTOR CURRENT CONSERVATION. Gribov, V. N.; Ioffe, B. L.; Shekhter, V. M. (Academy of Science, Moscow). Phys. Lett., 21: 457-9(June 1, 1966).

Assumptions necessary to derive the relation of Cabibbo and Radicati are analyzed. The expressions for the vector part of the amplitude of the process $\bar{\nu} + p \rightarrow n + l^+ + \gamma$ were obtained. (auth)

30009 INTERFERENCE EFFECTS BETWEEN N*(1236) AND K*(891) PRODUCTION IN THE $K^- + p \rightarrow K^- + \pi^+$ CHANNEL AT 1.45 Gev/c. Fridman, A. (Centre de Recherches Nucleaires, Strasbourg. Univ., Heidelberg); Maurer, G.; Michalon, A.; Schiby, B.; Strub, R.; Zech, G.; Cueer P. Phys. Lett., 21: 462-4(June 1, 1966).

The channel $K^-p \rightarrow K^-n\pi^+$ at 1.45 Bev/c is studied and a strong interference between N*(1,236) and K*(891) observed. By comparison with other data at the same energy the interference in the production $K^+p \rightarrow NK\pi$ can be explained by an isovector exchange. (auth)

30010 OBSERVATION OF THE REACTION $d + d \rightarrow {}^4He + 2\pi$ AT 1.69 Gev/c. Chapman, K. R. (Univ. of Birmingham, Eng.); Jafar, J. D; Martelli, G.; (and others). Phys. Lett., 21: 465-7(June 1, 1966).

The momentum spectrum of ^4He produced at 0^0 lab. by deuteron-deuteron collisions at 1.69 Bev/c, are measured to determine possible π-π resonances of low effective mass values. No significant deviations from phase space are found. The total cross sections for the reaction $d + d \rightarrow {}^4He + 2\pi$ is found to be $(0.6 \pm 0.2) \times 10^{-30}$ cm^2. (auth)

30011 NEGATIVE PION-PROTON ELASTIC SCATTERING AT 1.7 Gev/c. Allen, D. D.; Fisher, G. P.; Godden, G.; Kopelman, J. B.; Marshall, L.; Sears, R. (Univ. of Colorado, Boulder). Phys. Lett., 21: 468-70(June 1, 1966).

The differential elastic scattering cross section for 1.7 Bev/c π^- on protons is evaluated by analysis of Brookhaven 20'' bubble chamber film. Primary and secondary diffraction peaks are evident. These are discussed in terms of optical model parameters. (auth)

30012 C-PARITY VIOLATION AND NEUTRAL PARTICLES PRODUCTION IN COLLIDING ELECTRON-POSITRON BEAMS. Berestetsky, V. B. (Inst. of Theoretical and Experimental Physics, Moscow). Phys. Lett., 21: 554(June 15, 1966).

The possibility is considered of the production of a neutral vector meson pair via one virtual photon in electron-positron annihilation. (auth)

30013 ADDITIONAL RADIATIVE CORRECTION TO WIDE-ANGLE PAIR PRODUCTION. Lomon, E. L. (CERN, Geneva). Phys. Lett., 21: 555-7(June 15, 1966).

In pair photoproduction the reaction energy is inferred from the pair energy. The radiative correction arising from the shift of reaction energy is derived when the pair radiates an undetected photon. The effect is significant. (auth)

30014 BYERS-YANG MODEL FOR NN AND $\bar{N}N$ CHARGE EXCHANGE. Phillips, R. J. N. (Atomic Energy Research Establishment, Harwell, Eng.); Ringland, G. A. Phys. Lett., 21: 557-9(June 15, 1966).

The Byers-Yang model is compared with pn and $\bar{p}p$ charge exchange at 3.0 Bev/c. Although this model can give a reaction peak narrower than elastic scattering, it cannot reproduce the extremely narrow pn $\rightarrow$ np peak. The wide $\bar{p}p \rightarrow \bar{n}n$ peak may be explained if there is strong spin-flip. (auth)

30015 TWO-ION DECAY MODES OF THE K MESONS. Ferrari, E.; Mathur, V. S.; Pandit, L. K. (Univ. of Rochester, N. Y.). Phys. Lett., 21: 560-3(June 15, 1966). (UR-875-143).

An absolute determination of the $K \rightarrow 2\pi$ decay modes is made on the basis of the algebra of currents, in an attempt to test the current-current weak Hamiltonian and Cabibbo's universality for nonleptonic decays. (auth)

30016 ON THE K^+-K^0 MASS DIFFERENCE. Marshak, R. E.; Mathur, V. S.; Pandit, L. K. (Univ. of Rochester, N. Y.). Phys. Lett., 21: 563-7(June 15, 1966). (UR-875-142).

The electromagnetic mass difference between K^+ and K^0 is related to that between π^+ and π^0 by means of the algebra of currents and hypothesizing a partial conservation of the isovector electromagnetic current in analogy with PCAC. (auth)

30017 ON THE CONSISTENCY OF WOLF PION-PION PHASE SHIFTS WITH DISPERSION RELATIONS FOR FORWARD SCATTERING. Pisut, J. (Univ. Komenskeho, Brastislava). Phys. Lett., 21: 569-71(June 15, 1966).

It is shown that the Wolf pion-pion phase shifts are in reasonable agreement with dispersion relations for forward scattering. Some discrepancies are probably due to too large ρ-meson width. (auth)

30018 KN DISPERSION RELATIONS AND SYMMETRY GROUPS. Buccella, F. (Univ., Florence); Lusignoli, M.; Violini, G. Phys. Lett., 21: 572-4(June 15, 1966).

Two sum rules obtained from KN forward dispersion relations are discussed from the point of view of group theory. It is shown that the K meson coupling constants, which are incompatible with SU(3) invariance, are consistent with $(SU(4) \times SU(2))_W$, the group obtained from $SU(6)_W$, breaking SU(3). (auth)

30019 $p\bar{p}$ ELASTIC SCATTERING AT HIGH MOMENTUM TRANSFERS AND THE OREAR FORMULA. Bialas, A. (Jagellonian Univ., Krakow); Czyzewski, O. Phys. Lett., 21: 574-6(June 15, 1966).

It is shown that the Orear formula describes correctly the present data on pp elastic scattering at high momentum transfers. The result is consistent with models of Hagedorn, and Wu and Yang. (auth)

30020 SUM RULES FOR STRONG INTERACTIONS. De Alfaro, V. (Univ., Turin); Fubini, S.; Rossetti, G.; Furlan, G. Phys. Lett., 21: 576-9(June 15, 1966).

Sum rules for strong interactions are derived from analyticity and high-energy bounds for the scattering amplitudes of particles endowed with spin. Those bounds, much more stringent than for the spinless case, are strongly suggested by unitarity. (auth)

30021 EVIDENCE FOR A BOSON RESONANCE AT 1.63 Gev in π^-p INTERACTIONS AT THE INCIDENT MOMENTUM OF π^--MESONS 4.7 Gev/c. Vetlitsky, I. A.; Guszavin, V. M.; Kliger, G. K.; Kolganov, V. Z.; Lebedev, A. V.; Lomkazi, G. S.; Smoljankin, V. T.; Sokolov, A. P.; Sisoev, E. A. (Inst. for Theoretical and Experimental Physics, Moscow). Phys. Lett., 21: 579-81(June 15, 1966).

A new resonance in the $\pi^+\pi^-\pi^-$ system produced in the reaction $\pi^-p \rightarrow p\pi^+\pi^-\pi^-$ is found in 55 cm hydrogen bubble chamber photographs, with π^--momentum 4700 ± 30 Mev. The mass value is 1.63 ± 0.03 Bev. $\Gamma \approx 0.1$ Bev, isotopic spin $I \geq 1$, production cross section ~0.1 mb. (auth)

30022 SEARCH FOR AN ISOBAR OF ISOTOPIC SPIN $T = 5/2$. Banner, M. (Centre d'Etudes Nucleaires, Saclay, France); Detoeuf, J. F.; Fayoux, M. L.; Hamel, J. L.; Movchet, J.; Van Rossum, L.; Cheze, J.; Teiger, J.; Zsembery, J. Phys. Lett., 21: 582-4(June 15, 1966).

A mass spectrum of $(\pi^+\pi^-p)$, measured by a missing mass spectrometer, is presented in the reaction $\pi^-p \rightarrow \pi^-\pi^+\pi^-p$ at 1840 Mev/c momentum in the lab. This spectrum does not seem to show an effect characteristic of a resonance in the state of isotopic spin $T = 5/2$. (auth)

30023 ISOSPIN OF THE A MESONS. Abolins, M. A.; Carmony, D. D.; Lander, R. L.; Piccioni, O.; Xuong, Nguyen-Huu; Yger, P. M. (Univ. of California, San Diego, La Jolla). Contract AT(11-1)-GEN-10. Phys. Lett., 21: 584-6(June 15, 1966).

With a detailed computation, it is shown that the collisions of pions and deuterons occur quite often when the two nucleons are separated enough that they cannot interfere in the production of A_1, A_2 resonances. This strengthens the conclusion that the isospin of A_1,A_2 is one. (auth)

30024 INELASTIC Σ^-p INTERACTIONS AT LOW MOMENTA. Engelmann, R.; Filthuth, H.; Hepp, V.; Kluge, E. (Univ., Heidelberg). Phys. Lett., 21: 587-9(June 15, 1966).

The total cross sections for the two reactions $\Sigma^-p \rightarrow \Lambda n$ and $\Sigma^-p \rightarrow \Sigma^0 n$ in the momentum interval $105 \leq p_{\Sigma^-} \leq 165$ Mev/c are presented. For the process $\Sigma^-p \rightarrow \Lambda n$ the differential cross section and the Λ-polarization are given. (auth)

30025 THE π^+-π^- INTERACTION AS STUDIED IN 12- AND 18-Gev PION-NUCLEON REACTIONS. Jones, L. W.; Caldwell, D. O.; Zacharov, B.; Harting, D.; Bleuler, E.; Middelkoop, W. C.; Elsner, B. (CERN, Geneva). Contract N. 1224(23). Phys. Lett., 21: 590-4(June 15, 1966).

From a study of peripheral interactions wherein a negative pion of 12 or 18 Bev/c incident on a nucleon produced a pair of high-momentum pions, the pion-pion s-wave interaction was deduced. Normalizing to the ρ^0 production cross sections, a pion-pion cross section falling smoothly from 50 mb (300 Mev) to 20 mb (600 Mev) is observed. The forward-backward asymmetry is negative for low dipion masses. (auth)

30026 FURTHER RESULTS FROM THE INTERFERENCE OF K_S AND K_L IN THE $\pi^+\pi^-$ DECAY MODES. Alff-Steinberger, C.; Heuer, W.; Kleinknecht, K.; Rubbia, C.; Scribano, A.; Steinberger, J.; Tannenbaum, M. J.; Tittel, K. (CERN, Geneva). Phys. Lett., 21: 595-7(June 15, 1966).

Previous measurements on K^0 decay and the interference of K_L and K_S in the $\pi^+\pi^-$ decay modes were extended. It is found that the interference term has the predicted coefficient with an experimental uncertainty of about 15%, that the $K_L - K_S$ mass difference is ± (0.445 ± 0.034), the phase $\varphi = \varphi_\eta - \varphi_f$ is ± (1.41 ± 0.18) and no evidence is found for the lepton pair decays of K_L. With 90% confidence $\Gamma_{L,\mu^+\mu^-}/\Gamma_L < 2 \times 10^{-4}$ $\Gamma_{L,e^+e^-}/\Gamma_L < 1.6 \times 10^{-4}$. (auth)

30027 NEUTRON FORM FACTORS FROM A STUDY OF INELASTIC ELECTRON SPECTRA IN THE ELECTRO-DISINTEGRATION OF DEUTERIUM. Hughes, E. B.; Griffy, T. A.; Hofstadter, R.; Yearian, M. R. (Stanford Univ., Calif.). Phys. Rev., 146: 973-9(June 24, 1966).

Measurements of the ratio of the total inelastic electron-deuteron cross section to the elastic electron-proton cross section were made to an accuracy of about 3% for values of the square of the four-momentum transfer q^2 in the range 1.5 to 7.5 F^{-2}. These ratios were analyzed in terms of the form factors of the neutron using the "area method," and it is concluded that the corrections necessary to the simple sum rule given by Jankus are approximately equal in magnitude to those encountered in the use of the more familiar "peak method." A detailed comparison was made between the shapes of the observed inelastic electron-deuteron cross sections as a function of the scattered electron momentum and the shapes expected according to a theoretical treatment due to Durand. (auth)

30028 NUCLEON-NUCLEON TOTAL CROSS SECTIONS FROM 1.1 TO 8 Gev/c. Bugg, D. V. (Rutherford High Energy Lab., Chilton, Eng.); Salter, D. C.; Stafford, G. H.; George, R. F.; Riley, K. F.; Tapper, R. J. Phys. Rev., 146: 980-92(June 24, 1966).

Measurements were made of the total cross sections σ(p-p) and σ(p-d) over the laboratory momentum range 1.1 to 8 Bev/c, with relative errors of 0.1%. The absolute accuracies of these cross sections are limited to 0.3% by lack of information that will allow the Coulomb-nuclear interference to be calculated accurately. Values of the total cross sections σ(p-n) and $\sigma(I = 0)$ are deduced by assuming the Glauber correction. Structure is observed in σ(p-p) near a mass value of 2.75 Bev/c^2; its interpretation is discussed. $\sigma(I = 0)$ rises rapidly in the range 2.3 to 2.9 Bev/c^2, and this is attributed to the onset of strong inelastic scattering. (auth)

30029 CONVERSION OF GAMMA RAYS FROM THE DECAY $\eta^0 \rightarrow \pi^+ + \pi^- + \gamma$. Grossman, Ronald A.; Price, LeRoy R.; Crawford, Frank S. Jr. (Univ. of California, Berkeley). Contract W-7405-Eng-48. Phys. Rev., 146: 993-4(June 24, 1966). (UCRL-16684).

A search for electron pairs produced in hydrogen by the gamma rays from a sample of 33 kinematically determined events $\pi^+p \rightarrow \pi^+p\eta, \eta \rightarrow \pi^+\pi^-\gamma$ yielded one event, where 0.4 events were expected. A search for six-pronged events in the same 72-in. bubble-chamber film yielded three events. One event is an example of the internal-conversion process $\eta \rightarrow \pi^+\pi^-e^+e^-$, and gives an internal-conversion probability $\Gamma(\eta \rightarrow \pi^+\pi^-e^+e^-)/\Gamma(\eta \rightarrow \pi^+\pi^-\gamma) = 0.026$, based on one event.

(The other two events arise from ordinary Dalitz decays of π^0.) No example was found of $\pi^+p \rightarrow \pi^+p\pi^+\pi^-\pi^+\pi^-$, although the c.m. energy is 120 Mev above threshold. One event would have corresponded to a cross section of 0.35 μb. (auth)

30030 PHOTOPRODUCTION OF HYDROGEN OF ρ^0 MESONS BETWEEN THRESHOLD AND 6 Bev. Crouch, H. R. Jr. (Brown Univ., Providence); Hargraves, R.; Kendall, B.; (and others). Contract AT(30-1)-2262. Phys. Rev., 146: 994-1000(June 24, 1966). (NYO-2262-114).

Data are presented on the details of the interaction $\gamma + p \rightarrow p + \rho^0$ observed in a 12-in. hydrogen bubble chamber exposed to a bremsstrahlung photon beam of 6-Bev maximum energy at the Cambridge electron accelerator. The energy dependence of the cross sections, the production angular distributions, and the decay angular distributions of the ρ^0's are compared with the predictions of the one-pion-exchange (OPE) mechanism and with a diffraction or multiperipheral model proposed by Berman and Drell. These data, as well as a comparison with ω^0 and with $\rho^0 + N^*(1238)$ production, reject the OPE model and favor a diffraction mechanism. (auth)

30031 SEARCH FOR THE SPLITTING OF GAMMA-RAY PHOTONS IN THE ELECTRIC FIELD OF THE NUCLEUS. Adler, A. W.; Cohen, S. G. (Hebrew Univ., Jerusalem). Phys. Rev., 146: 1001-3(June 24, 1966).

A search was made for an effect predicted by quantum electrodynamics closely connected with vacuum polarization, namely, the splitting of gamma-ray photons in the electric field of the nucleus. The scattering of 1.1-Mev gamma rays from a 2-Ci source of ^{65}Zn in various target elements was investigated. The spectrum of the sum of the two photon pulses appearing simultaneously in two NaI(Tl) scintillating crystals, situated at backward angles with respect to the target, was recorded over long periods of time. Evidence for the production of photon pairs, whose energy sum is equal to that of the original incident photon, was obtained for copper and cobalt nuclei. For photon pairs produced in these nuclei, at average angles of 105° with respect to the incident photon direction, and of 130° with respect to each other, it is estimated that the differential cross section to be $(3 \pm 1)Z^2(\Delta w/mc^2)10^{-35}$ cm^2/(sr)^2, where Δw is the energy interval corresponding to one component of the pair. This is about six times larger than the value predicted theoretically by Shima. However, double Rayleigh scattering from bound electrons may also contribute to the splitting process, and no exact quantitative calculations of this have yet been made. (auth)

30032 ELECTROMAGNETIC MASSES OF PSEUDOSCALAR MESONS. Nieh, H. T. (Harvard Univ., Cambridge, Mass.). Phys. Rev., 146: 1020-2(June 24, 1966).

Based on a recently proposed generalization of the "tadpole" mode of Coleman and Glashow, the six electromagnetic mass splittings of baryons and pseudoscalar mesons are considered. With the inclusion of the "nontadpole" contributions calculated by Coleman and Schnitzer and by Socolow, the agreement between theory and experiment is satisfactory. (auth)

30033 ZERO-EFFECTIVE-RANGE ANALYSIS OF PION-NUCLEON REACTIONS NEAR THE η^0 PRODUCTION THRESHOLD. Dobson, Peter N. Jr. (Univ. of Hawaii, Honolulu). Phys. Rev., 146: 1022-5(June 24, 1966).

A two-channel scattering matrix, assuming zero effective range, was fitted to two sets of pion-nucleon phase shifts in the S_{11} channel. One of these, due to Cence, agrees well with the model, and implies a virtual bound state of the η^0-nucleon system at a mass of about 1460 Mev. The predicted η^0 production cross section is in reasonable agreement with experiment. (auth)

30034 POSSIBLE $N^*(1688) \rightarrow K^+\Lambda$ PRODUCTION IN 3-Bev $p + p \rightarrow K^+ + \Lambda + p$. Davis, Howard F. (Univ. of Washington, Seattle). Phys. Rev., 146: 1031-4(June 24, 1966).

There is some possible evidence of a B = 2, S = −1 hyperon-nucleon resonance with a mass of about 2.375 Bev. The data for this come from large-angle K^+ production in about 3-Bev proton-proton collisions. It is believed that part, if not all, of this effect may be due to the production and subsequent decay of the $N^*(1688) \rightarrow K^+ + \Lambda^0$ in the proton-proton collision. (auth)

30035 ONE-PARTICLE-EXCHANGE MODEL FOR BOOTSTRAP. Banyai, L.; Marinescu, N.; Novacu, V.; Rittenberg, V. (Inst. of Physics, Bucharest). Phys. Rev., 146: 1035-41(June 24, 1966).

A Cini-Fubini-like representation is assumed to describe low-energy meson-meson interaction. The spectral densities are determined by iteration from nonlinear integral equations given by unitarity. For bootstrap calculations, Breit-Wigner-type functions are proposed as a zero-order approximation. An approximate determination of the resonance parameters can be achieved through a best-fit condition between the zero and first-order approximations in the resonance region. Such calculations take into account crossing symmetry exactly but unitarity approximately. An application is given for the ρ-meson bootstrap and a symmetric-shaped amplitude is obtained with m_ρ = 450 Mev and Γ_ρ = 40 Mev. (auth)

30036 SUM RULE CONNECTING MESONIC AND PHOTONIC MATRIX ELEMENTS AND THE RATE FOR $\omega^0 \rightarrow \pi^0 + \gamma$. Gasiorowicz, S. (Univ. of Minnesota, Minneapolis). Contract AT(11-1)-1371. Phys. Rev., 146: 1067-71 (June 24, 1966). (COO-1371-26).

The Gell-Mann current-commutation relations are used to obtain a relation between matrix elements involving vector currents and matrix elements involving axial currents, in the infinite energy limit. This relation leads to a set of sum rules. One of these is used to calculate the rate for $\omega^0 \rightarrow \pi^0 + \gamma$ in terms of the ρ-meson width and the axial-current renormalization constant, under the assumption that only states with spin and parity $0^\pm$ and 1^- need be taken into account. The result, $\Gamma(\omega^0 \rightarrow \pi^0 + \gamma) = 1.2$ Mev, is in reasonable agreement with experiment. (auth)

30037 SUM-RULE CALCULATION OF THE ISOVECTOR FORM FACTOR. Gasiorowicz, S. (Univ. of Minnesota, Minneapolis). Phys. Rev., 146: 1071-4(June 24, 1966). (COO-1371-25).

A class of sum rules due to Fubini is rederived from a point of view that clarifies the assumptions made about the singularities of field operators. A calculation of the isovector magnetic moment is performed in the isobar approximation. The result $F_1^V(0) = 1/2$ emerges as a model-independent consistency condition, but the calculated value $F_2^V(0) = 3.64$ is in disagreement with the experimental value. (auth)

30038 "INCOHERENT DROPLET" MODEL OF HIGH-ENERGY LARGE-ANGLE SCATTERING. Huang, Kerson (Inst. for Advanced Study, Princeton, N. J.). Phys. Rev., 146: 1075-9(June 24, 1966).

The high-energy large-angle scattering between two hadrons is thought of as inco' erent scattering between two objects of complicated intern l structure. A model is proposed whereby the incoheren e is simulated by a simple recipe. Consequences of the model can be deduced simply. The salient feature of the re: ult is that transverse momentum transfer is strongly inhibited for kinematical reasons. Orear's empirical fit for large-angle p-p scattering is obtained. (auth)

30039 FORWARD ELASTIC SCATTERING AT HIGH ENERGY IN AN SU(3) REGGE-POLE MODEL. Barger, V.; Olsson, M. (Univ. of Wisconsin, Madison). Contract AT(11-1)-881. Phys. Rev., 146: 1080-91(June 24, 1966). (COO-881-57).

The total-cross-section data on $\pi^\pm p$, $K^\pm p$, $K^\pm n$, pp, $\bar{p}p$, pn, and $\bar{p}n$ for laboratory momenta in the range 5 to 20 Bev/c are analyzed in terms of a meson-exchange model. The dynamics of the theoretical model for the forward scattering amplitude are provided by the Regge-pole amplitudes of the contributing exchanges; the total cross sections are obtained by the optical theorem. The allowed neutral, zero-strangeness meson exchanges are classified as members of established SU(3) nonet or singlet multiplets. Certain

linear combinations of the total cross sections are used in the analysis in order to separate the contributions of different SU(3) multiplets according to signature under charge conjugation C. The odd-C exchanges are associated with the members [ρ^0(760), ϕ(1020), ω(783)] of the vector-meson nonet. The unitary-singlet Pomeranchuk Regge pole (P) and the Regge exchanges corresponding to the [A_2(1310), s_0(1525), f_0(1250)] members of the tensor nonet comprise the even-C exchanges. The residues of the Regge poles are related by SU(3) symmetry. The model is consistent with the experimental total cross sections. A statistical fit to the data yields information on f/d ratios, Regge-pole residues, and trajectory intercepts at zero-momentum transfer. These parameters are in turn used to predict the real parts of the forward elastic-scattering amplitudes. (auth)

30040 RADIATIVE DECAYS OF BOSONS AND SU(6)w SYMMETRY. Tripathy, Kishor C. (Univ. of Delhi). Phys. Rev., 146: 1107-9(June 24, 1966).

The rare decays of bosons were considered within the framework of the collinear group $SU(6)_W$. From the observed decay rate of $\omega \rightarrow \pi\gamma$, the other decay widths were computed. An estimation of $\rho \rightarrow \pi\pi\gamma$ and $\omega \rightarrow \pi\pi\gamma$ was given. From the known widths of $\pi \rightarrow 2\gamma$ and $\eta \rightarrow 2\gamma$, the η-X mixing parameter is determined and the decay rate of $X \rightarrow 2\gamma$ was predicted. (auth)

30041 PARITY-VIOLATING NONLEPTONIC DECAY AND THE CABIBBO CURRENT. Rosen, S. P. (Purdue Univ., Lafayette, Ind.); Pakvasa, S.; Sudarshan, E. C. G. Phys. Rev., 146: 1118-22(June 24, 1966). (NYO-3399-46).

In a current × current theory of weak interactions, the use of a Cabibbo-type current endows parity-violating nonleptonic decay with certain specific properties. These properties do not include octet dominance, but they are sufficient to forbid all $K \rightarrow 2\pi$ decays in the limit of SU(3)-conserving strong interactions. When electromagnetic corrections are taken into account, the decay modes $K_1^0 \rightarrow \pi^+\pi^-$ and $K^+ \rightarrow \pi^+\pi^0$ are allowed, but $K_1^0 \rightarrow 2\pi^0$ is still forbidden. Consequently the smallness of the rate for $K^+ \rightarrow \pi^+\pi^0$ relative to both modes of K_1^0 decay can be explained only by an appeal to medium-strong, SU(3)-breaking interactions. In the case of nonleptonic hyperon decay, the Cabibbo current × current interaction predicts two sum rules for parity-violating amplitudes. The recent results obtained by Sugawara and Suzuki from current commutation relations can be understood in terms of these sum rules, together with one simple constraint upon the effective hamiltonian. (auth)

30042 NEUTRON-PROTON MASS DIFFERENCE ACCORDING TO THE BOUND-STATE MODEL. Barton, G. (Univ. of Sussex, Brighton, Eng.). Phys. Rev., 146: 1149-58(June 24, 1966).

The proton must be heavier than the neutron according to any correct calculation treating them as pion-nucleon bound states whose masses are shifted because of one-photon-exchange corrections to the binding forces, and which takes into account no particles other than pions and nucleons. The reason is simply that only the neutron can contain two charged constituents, p and π^-, and that both the electric and the magnetic forces between these are attractive, thus binding the neutron more tightly. Dashen's previous calculation of this effect was based on an unreliable variant of the Dashen-Frautschi method for eliminating infrared divergences; the sources of the mistakes in that calculation are pointed out. On the basis of the pion-nucleon bound-state picture, a simple and physically well-based estimate of the Coulomb contribution to the mass splitting is given in terms of the pion and nucleon form factors; as compared with experiment it has the right order of magnitude but necessarily the wrong sign. The magnetic energy is more difficult to estimate, apart from its sign; but it is probably much smaller. It is concluded that a consistent calculation, if it is to be successful, must include other baryons and mesons. As a by-product simple dynamical interpretation of the fact that the neutron's charge form factor is very small is obtained. (auth)

30043 M1 PHOTO-EXCITATION $N \rightarrow N^*$ AND SU(6) SYMMETRY. Dalitz, R. H.; Sutherland, D. G. (Clarendon Lab., Oxford). Phys. Rev., 146: 1180-5(June 24, 1966).

A direct evaluation of the M1 amplitude for the photo-excitation $p \rightarrow N^{*+}$ is made from the π^0 photoproduction cross section at resonance, with result (1.28 ± 0.02) times the SU(6) prediction $2\sqrt{\mu_p}/3$. It is shown that the N* electro-excitation data also lead to the same value, within larger errors. There is pointed out a strong kinematic form-factor correction to this SU(6) prediction, which occurs in consequence of the N-N* mass difference arising from SU(6) symmetry-breaking interactions. The most direct phenomenological evaluation (based on the three-quark model for the baryonic states) for this correction would reduce the predicted M1 amplitude to $0.79 \times (2\sqrt{2}\mu_p/3)$. (auth)

30044 STUDY OF THE REACTIONS $p\bar{p} \rightarrow Y\bar{Y}$ BY REGGE-POLE EXCHANGE MODEL. Roy, D. P. (Tata Inst. of Fundamental Research, Bombay). Phys. Rev., 146: 1218-22(June 24, 1966).

The reactions $p\bar{p} \rightarrow \Lambda\bar{\Lambda}$, $p\bar{p} \rightarrow (\Lambda\bar{\Sigma}^0 + \bar{\Lambda}\Sigma^0)$ and $p\bar{p} \rightarrow \Sigma^+\bar{\Sigma}^-$ are studied using a Regge-pole exchange model. Only the contribution of the leading trajectory, which in this case is K*, is retained. In analogy with ρ, a linear trajectory is assumed for K* with a slope close to that of ρ, and the t dependence of the residues is neglected, after the threshold factor has been extracted out. The energy and angular dependence of the cross sections so obtained are in reasonable agreement with experiment. (auth)

30045 POLARIZATION MEASUREMENT OF THE 6-Gev COHERENT BREMSSTRAHLUNG FROM THE HAMBURG ELECTRON SYNCHROTRON. Criegee, L.; Lutz, G.; Schulz, H. D.; Timm, U.; Zimmermann, W. (Deutsches Elektronen Synchrotron, Hamburg). Phys. Rev. Lett., 16: 1031-3(June 6, 1966).

An experiment is described in which linear polarizations up to 70% are measured for a 6-Bev coherent Bremsstrahlung produced in diamonds suitably oriented by a high-precision goniometer. (B.G.D.)

30046 REFRACTION OF ELECTRON BEAMS BY INTENSE ELECTROMAGNETIC WAVES. Kibble, T. W. B. (Imperial Coll. of Science and Tech., London). Phys. Rev. Lett., 16: 1054-6(June 6, 1966).

The refraction of a beam of electrons passing through an electromagnetic wave, whose intensity is independent of time, is discussed. The electron in the wave is described by an effective potential energy $\frac{1}{2}\, m\mu^2c^2$, where μ^2 is the intensity parameter, and the wave appears like a medium of refractive index $(1 - \mu^2c^2/\nu^2)^{\frac{1}{2}}$. (B.G.D.)

30047 SEARCH FOR EVIDENCE OF A K^+K^+ RESONANCE. Erwin, A. R.; Walker, W. D.; Weinberg, A. (Univ. of Wisconsin, Madison). Phys. Rev. Lett., 16: 1063-6(June 6, 1966).

An examination of a sample of events of the type $K^+ + p \rightarrow K^+ + K^+ + \Lambda^0$ and $K^+ + p \rightarrow K^+ + K^+ + \Sigma^0$, which were produced in the 80 inch BNL hydrogen bubble chamber by a separated K^+ beam with mean momentum of 3.535 Bev/c, is presented. An investigation of the K^+K^+ resonance at 1280 Mev/c^2 is attempted. (B.G.D.)

30048 $SU(6)_W$ AND MESON RESONANCES OF EVEN PARITY. Capps, Richard H. (Northwestern Univ., Evanston, Ill.). Phys. Rev. Lett., 16: 1066-9(June 6, 1966).

A model stating that if the three-particle vertices involving the pseudoscalar and vector octet and singlet mesons are invariant to the group $SU(6)_W$, the one-M (-meson) exchange force may bootstrap the M as P-wave, MM bound states is discussed. In this model, there are forces in states of even orbital angular momentum that are of the same order as the P-wave forces. These even l forces will lead to predicted meson resonances of even parity. A list of the quantum numbers and relative coupling strengths of different decay modes of the predicted even-parity mesons is presented, and some of the results are compared with experiment. (B.G.D.)

30049 RECENT RESULTS ON STRANGENESS-ONE RESONANCES. Bishop, J. M.; Goshaw, A. T.; Erwin, A. R.; Thompson, M. A.; Walker, W. D.; Weinberg, A. (Univ. of Wisconsin, Madison). Phys. Rev. Lett., 16: 1069-72(June 6, 1966).

From investigation of K^+-proton interactions at an energy of 3.54 Bev/c in the 80-inch BNL bubble chamber, evidence for several resonances involving one K meson and two π mesons is reported. (B.G.D.)

30050 ELASTIC SCATTERING OF 14-Mev NEUTRONS BY DEUTERONS. Popova, A. M.; Stefan, Muscalu (Moscow State Univ.). Yadern. Fiz., 3: 813-16(May 1966). (In Russian).

An expression for the differential cross section in the elastic scattering of neutrons by deuterons was obtained, using the method of summing perturbation theory diagrams. The reaction amplitude in the calculations was presented as the sum of the impulse approximation amplitude and a function, approximating the contribution of diagrams, corresponding to multiple scattering in the reaction process and depending on the scattering angle and initial energy. The differential cross-section curves for the elastic scattering of neutrons by deuterons, constructed according to the obtained formulas, are compared with the experimental angular distribution of 14 Mev neutrons, elastically scattered by deuterons. (auth)

30051 RATIO OF THE REAL AND IMAGINARY PARTS OF THE p-d AND $\bar{p}$-d SCATTERING AMPLITUDES. Vernov, Yu. S. (Lebedev Inst. of Physics, Moscow). Yadern. Fiz., 3: 877-9(May 1966). (In Russian).

Dispersion relations are used to calculate the real part of the amplitude for zero-angle elastic scattering of protons and antiprotons on deuterons at high energies. (auth)

30052 CORRELATION FUNCTIONS OF RANDOM BREEDING-TYPE PROCESSES. Kozik, B. (Joint Inst. for Nuclear Research, Dubna, USSR). Yadern. Fiz., 3: 883-6(May 1966). (In Russian).

It is shown that the correlation functions of a very broad class of random processes are determined by a system of equations, the form of which coincides with the system of equations for the mathematical expectations of the considered random quantities, if their central second order momenta are given. This property of the correlation functions can be extended to the corresponding point processes, if the number of "breeding particles" is distributed over a continuous set of states. (auth)

30053 APPLICATION OF THE AUTOMATICAL IDENTIFICATION OF OBJECTS TO THE IDENTIFICATION OF HIGH-ENERGY PARTICLES. Golovin, B. M.; Kulyukina, L. A. (Joint Inst. for Nuclear Research, Dubna, USSR). Yadern. Fiz., 3: 887-91(May 1966). (In Russian).

The passage of a charged particle through a detecting system consisting of several detectors is simulated, using the random test method. The obtained ionization losses in several detectors are used to instruct an electronic computer to identify the charge of a particle. The dependences of the charge identification reliability on the value of the charge, the energy threshold of the detecting system, and the number of instruction points, are established. (auth)

30054 ON A RESONANCE IN THE e-p SYSTEM. Zazunov, L. G.; Sannikov, S. S. (Inst. of Physics and Tech., Academy of Sciences, Ukrainian SSR). Yadern. Fiz., 3: 892-4(May 1966). (In Russian).

The $e + p \rightarrow e + p$ scattering process is considered, taking the renormalizable weak interaction, leading to a resonance in the ep system, into account. An expression is found for the differential cross section of the considered process. Estimations of the cross section are given for electron energies of the order 2 Bev. It is shown that for large angles the contribution of the weak interaction is comparable with the Rosenbluth scattering. (auth)

30055 DECAYS IN A MIXED ENSEMBLE OF NEUTRAL K MESONS. Lyuboshits, V. L. (Joint Inst. for Nuclear Research, Dubna, USSR). Yadern. Fiz., 3: 895-902(May 1966). (In Russian).

The description of the decay properties of a mixed ensemble of neutral K-mesons with the help of the two-row density matrix method is considered. The case when the neutral K-meson is contained in a $K^0\bar{K}^0$ system is considered in detail. Interference effects in the decay of neutral K-mesons into two π-mesons, when CP-invariance is violated, are discussed from a new point of view. (auth)

30056 EXPERIMENTAL DETERMINATION OF THE $K_2^0 \rightarrow \pi^+\pi^-$ DECAY PROBABILITY IN A SLOPED K_2^0-MESON BEAM. Neagu, D.; Okonov, E. O.; Petrov, N. T.; Rusakov, V. A.; Takhtamyshev, G. G.; Wu, Tsung-fan (Joint Inst. for Nuclear Research, Dubna, USSR). Yadern. Fiz., 3: 903-6(May 1966). (In Russian).

A search was made for $K_2^0 \rightarrow 2\pi$ decay events in a sloped beam of K_2^0-mesons, which should take place if the antigravitation hypothesis is correct. It is found, that within the experimental errors the $K_2^0 \rightarrow 2\pi$-decay probabilities for a sloped and horizontal beam are the same and are equal to the calculated background of threebody K_2^0-decays, imitating K_1^0-decays. This result shows that the gravitational masses of the K^0- and $\bar{K}^0$-mesons have the same signs. The value of the relative $K_2^0 \rightarrow 2\pi$ decay probability $\leq 2.5 \cdot 10^{-3}$ is in agreement with the results of other authors. (auth)

30057 PHOTON BREMSSTRAHLUNG IN THE SCATTERING OF VECTOR MESONS ON EACH OTHER. Kondratyuk, L. A.; Masunov, E. S. Yadern. Fiz., 3: 907-9 (May 1966). (In Russian).

The differential and total cross sections of the process $W^+ + W^- \rightarrow W^+ + W^- + \gamma$ for ultrarelativistic vector mesons are calculated in the lowest order of the perturbation theory. It is shown that if the energy of the colliding W-mesons in their cms is less than a boundary energy, the unitary condition is not violated for the considered process. (auth)

30058 LEPTONIC DECAYS OF BARYONS IN THE UNIVERSAL V-A THEORY. Bokov, O. G.; Nguyen Van Hieu; Rerikh, K. V.; Tavkhelidze, A. N.; Khelashvili, A. A. (Joint Inst. for Nuclear Research, Dubna, USSR). Yadern. Fiz., 3: 910-17(May 1966). (In Russian).

The leptonic decays of baryons are systematically studied in the framework of the universal V−A theory of weak interactions. Expressions are obtained for the decay probability, the $\tilde{l}\nu$-angular correlation, the energy spectra of leptons and recoil baryons and the asymmetry parameters in the angular distribution of leptons and recoil baryons in the decay of polarized baryons. The contributions from all possible form factors were considered, taking their linear dependence on the momentum transfer into account. (auth)

30059 CALCULATION OF THE Σ^+- AND Σ^--HYPERON MASS DIFFERENCE BY THE DASHEN-FRAUTSCHI METHOD. Anselm, A. A.; Dyatlov, I. T. (Joint Inst. for Nuclear Research, Dubna, USSR). Yadern. Fiz., 3: 932-41 (May 1966). (In Russian).

The dispersion method is used to estimate the electromagnetic mass difference of the Σ^+- and Σ^--hyperons. The $\Sigma^\pm$-particles are considered as poles in the $\pi^\pm\Lambda$-scattering amplitudes. It is shown that the large value of the $\Sigma^\pm$-hyperon mass difference is related to the existence of electromagnetic transitions between the two nearby levels $\Lambda \rightleftharpoons \Sigma_0$. Using the SU(3)-symmetry and varying the badly known parameters in a plausible region, we obtain δM in the region -6.5 Mev to -8.5 Mev, in good agreement with the experimental value $\delta M_{exp} = -7.9$ Mev. (auth)

30060 MODIFIED SEPARATION METHOD FOR NUCLEAR POTENTIALS. Stocker, W. (Univ., Cologne). Z. Phys., 193: 310-17(1966).

In order to obtain a regular but energy-dependent nuclear potential, the following modification of the separation method of Moszkowski and Scott is used. The nuclear potential $v_c(r)$ is replaced by a long-range potential $v_1(r) = v_c(r)\,\Theta\,(r-d_0)$ together with a short-range energy dependent repulsion $v_s = h(k)\,\Theta\,(r_c-r)$, where d_0 is the separation distance for vanishing energy and r_c is the hard-core radius. The potential $v = v_s + v_1(r)$ is fitted to the S-wave scattering data and the binding energy of the deuteron.

h(k) turns out to be almost proportional to the scattering energy E_{rel} for energies $E_{rel} < 150$ Mev. (auth)

30061 EQUIVALENT NONLOCAL NUCLEON-NUCLEON POTENTIALS. Mittelstaedt, P.; Ristig, M. (Univ., Cologne). Z. Phys., 193: 349-57(1966).

The local nucleon-nucleon potential which contains a strong repulsive core is often replaced by an equivalent weak but nonlocal potential. Such potentials can be obtained by unitary transformations of the two-body hamiltonian. Necessary and sufficient conditions are derived which must be fulfilled by the unitary transformations in order to give equivalent potentials. Special examples of unitary transformations with this property are investigated. (auth)

30062 INDUCED SCATTERING OF PHOTONS ON PHOTONS. Varfolomeev, A. A. Zh. Eksp. Teor. Fiz., 50: 1024-35(Apr. 1966).

The cross section for scattering of photons by photons of a given frequency is calculated for the case when a third field of the same frequency is present. It is shown that for a certain spatial configuration of the fields the scattering cross section increases proportionally to the energy density of the third beam in the region of intersection of the first two beams. Some numerical results are presented. (auth)

30063 APPLICATION OF THE DECOMPOSITION METHOD TO RADIATION TRANSPORT EQUATIONS. Marchuk, G. I.; Sultangazin, U. M. Zh. Vychisl. Mat. Mat. Fiz., 5: 852-63(Sept.-Oct. 1965). (In Russian).

In dealing with the problem of radiation transport equations, it was found advisable to formulate the algorithm of decomposition of the integro-differential operator involved in the problem in terms of the simplest integral and differential operators. The method described by G. I. Marchuk and N. N. Yamenko (Solution of multidimensional kinetic equations by the decomposition method, (Dokl. AN SSSR, 1964, 157, No. 6, 1291-1292)) was very effective for the case of one-dimensional problems of the transport theory. It yielded fast convergence. A detailed study is given of a simple case of the problems involved in transport theory, namely the problem of isotropic dispersion of radiation in a plane-parallel medium. (ATD)

30064 HIGH ENERGY PHYSICS. Takeda, Gyo (ed.). 1965 Tokyo Summer Lectures in Theoretical Physics. Part II. Tokyo, Syokabo Publishing Co. New York, W. A. Benjamin, Inc., 1966. 126p. $5.75 W. A. Benjamin Inc., New York.

Separate abstracts were prepared for eight of the nine papers included. The other paper was previously abstracted in NSA (20: 11679). (G.O.Y.)

For abstracts of individual papers see: 29922, 30065–30067, and 30108–30111.

30065 NUCLEAR DEMOCRACY, REGGE POLES AND THE ANALYTIC S-MATRIX. Chew, G. F. (Univ. of California, Berkeley). pp 1-8 of High Energy Physics. Takeda, Gyo (ed.). Tokyo, Syokabo Publishing Co. New York, W. A. Benjamin, Inc., 1966.

The position of the analytic S-matrix theory of strong interactions is discussed in terms of nuclear democracy (against primacy of one elementary particle) and of Regge poles. (G.O.Y.)

30066 BOOTSTRAPPING WITH THE REGGE BOUNDARY CONDITION. Chew, G. F. (Univ. of California, Berkeley). pp 9-16 of High Energy Physics. Takeda, Gyo (ed.). Tokyo, Syokabo Publishing Co. New York, W. A. Benjamin, Inc., 1966.

A bootstrap model is described using the Mandelstam procedure supplemented by the assumption of second-degree analyticity. (D.C.W.)

30067 PRESENT STATUS OF WEAK INTERACTIONS. Marshak, R. E. (Univ. of Rochester, N. Y.). pp 35-66 of High Energy Physics. Takeda, Gyo (ed.). Tokyo, Syokabo Publishing Co. New York, W. A. Benjamin, Inc., 1966.

The SU_3 group, the Cabibbo angle, and the algebra of currents are discussed, together with the non-leptonic processes, CP violation, and some intermediate vector boson and high-energy neutrino experiments. 56 references. (G.O.Y.)

30068 THIRD-ORDER PERTURBATION CALCULATION OF DEUTERON PARAMETERS [Thesis]. Neumann, Herschel. Lincoln, Neb., Univ. of Nebraska, 1965. 77p.

An evaluation is presented of the usefulness of a perturbation-theoretic approach and harmonic oscillator-basis functions for calculating ground-state parameters for the deuteron. Various perturbation series and some refinements of them were calculated, all third-order terms being retained exactly. Binding energies, rms radii, D-state probabilities, and quadrupole moments were determined for deuteron systems described by several groupings of Gaussian central attractive, central repulsive, and tensor potentials, by use of variational wave functions based on perturbation-theoretic forms. It is shown that, if the perturbation series utilizes Rayleigh-Schrodinger energy denominators, nearly all sums over intermediate states can be performed analytically. It is found that even a quite flexible wave function of the type indicated above is of only modest quality for the deuteron. It is argued, from a combination of the results of the present study with those of previous authors, that although the oscillator-basis model is not particularly well suited to the deuteron, it must be reasonably satisfactory for the heavier ls-shell nuclei, even in second order. A rapid, accurate numerical procedure was devised to calculate binding energies and wave functions for two-channel coupled Schrodinger equations. The method is an extension of one previously given by Cooley for single-channel equations. For a given trial input energy and D-state/S-state relative normalization, "match-in-the-middle" wave function information is used to improve both the energy and the relative normalization. If coded for computers capable of sufficient precision, it is possible by this procedure to separate rounding and truncation errors and to extrapolate to zero mesh size. (Dissertation Abstr.)

30069 COMPOSITE-PARTICLE MODEL WITH APPLICATION TO Ω^- DECAY [Thesis]. Harte, John. Madison, Wis., Univ. of Wisconsin, 1965. 116p.

A composite-particle model is presented, which is particularly suited for the study of the long-range behavior of a composite system. The model is applied principally to calculate decay properties of the Ω^-. Electromagnetic properties of vector mesons and baryon isobars are also discussed, and the $\omega \rightarrow 2\pi$ decay rate is calculated. It is found that the model predicts Ω^- branching ratios and absolute rates that differ significantly from predictions based on phenomenological Rarita-Schwinger treatments of the Ω^-. In particular, the $\Omega^- \rightarrow \Xi\pi/\Lambda\bar{K}$ ratio is a crucial test of the theory. The ω and Ω^- are taken to be $\kappa\bar{\kappa}$ and $\Xi\bar{\kappa}$ bound states, respectively. Strong-binding effects are assumed to be described by a Green's function satisfying the Bethe-Salpeter equation and the Bethe-Salpeter wave functions are written in the form of a product of an appropriate asymptotic, non-relativistic wave function times a relative energy-dependent factor given by the product of the relativistic constituent particle propagators. Approximations that suggest this form are discussed in detail. The weak or electromagnetic interactions giving rise to the decay are treated in lowest order perturbation theory. Branching ratios for all important Ω^- decay channels, slightly cutoff-dependent absolute rates, and the p- to d-wave ratio for the non-leptonic decay modes are calculated. The $\omega \rightarrow 2\pi$ decay rate is calculated under the assumption of strong final state enhancement due to ω-ρ mixing, with the ω and ρ described by a Bethe-Salpeter Green's function in the $\kappa\bar{\kappa}$ channel. A comparison of this rate and the Ω^- decay properties with predictions using other models is made. A generalization of the model to a single resonance channel and to multi-channel problems is discussed. Finally, applications of the model to other vector meson electromagnetic decays and to baryon-isobar electromagnetic mass differences are suggested. (Dissertation Abstr.)

30070 STUDY OF LOW-ENERGY MESON-BARYON DYNAMICS [Thesis]. Golowich, Eugene. Ithaca, N. Y., Cornell Univ., 1965. 118p.

Formulas for low-energy, long-range forces in meson-

baryon scattering for partial waves S_{ℓ_2} to H_{ℓ_2} are derived. The internal symmetry SU(3) is used to both describe the scattering states and to fix values of those coupling constants that are at present experimentally inaccessible. The multiplets, j = 1 − baryon octet, j = 1 + decuplet, vector meson octet, j = 2 − Y_0^+ (1520) singlet, j = 2 − octet are the exchanged particles that generate the forces. The findings agree roughly with S-wave scattering lengths determined from experiment, substantiate the bootstrap scheme for generating Regge trajectories by means of elastic forces in meson-baryon scattering, and support the assignment to Y_0^+ (1520) as unitary singlet. If elastic forces are important in generating Y_1^+ (1765), then it belongs to the SU(3) multiplet, 8, and the remaining members of the octet are experimentally unobservable as resonances due to cancellations among the long-range forces brought on by mass-breaking effects. An approximation technique due to Balazs and used in dispersion relations which parameterizes the short-range effects of strong interactions, is studied. It is concluded that this method is potentially most useful in obtaining an estimate for the coupling constant of a bound state or resonance by fixing the output pole in the amplitude at the experimental position through a judicious selection of matching points. A generalization of the method to multi-channel processes is derived. The effect of introducing additional channels to a given problem is studied, and the phenomenon of mass splittings from the degenerate SU(3) model is considered. The former is done with matrix ND^{-1} calculations, both a first-order determinantal approximation and a full solution of a cutoff model. The study of mass-breaking effects implies that the assumptions of an approximately SU(3) invariant and crossing symmetric amplitudes are compatible and that the magnitudes of various exchange forces, which are taken to generate the low energy bound and resonant states, are consistent with experiment. (TCO)

30071 ANGULAR DISTRIBUTION AND POLARIZATION OF NEUTRAL HYPERONS PRODUCED IN ASSOCIATION WITH K^0 MESONS [Thesis]. Binford, Thomas Oriel. Madison, Wis., Univ. of Wisconsin, 1965. 104p.

The production properties of the interactions $\pi^- + p \rightarrow \Lambda^0 + \kappa^0$ and $\pi^- + p \rightarrow \Sigma^0 + \kappa^0$ were studied in a hydrogen bubble chamber at four incident pion momenta between 1128 and 1326 Mev/c. Expansion coefficients for the angular distributions and polarizations, $\sigma\alpha P$, are presented. These coefficients are compared with data at nearby energies. Angular distributions of $\pi^- + p \rightarrow \Lambda^0 + \kappa^0$ show that at the momenta above 1128 Mev/c, terms involving $\cos^3\theta$ and higher powers of $\cos\theta$ are small, but terms in $\sigma\alpha P$ including $\cos^2\theta$ are observed, indicating the presence of partial waves higher than p wave. In the reaction $\pi^- + p \rightarrow \Sigma^0 + \kappa^0$, a term in $\cos^3\theta$ appears at 1128 Mev/c and becomes strong at higher momenta. (Dissertation Abstr.)

30072 PROPERTIES OF Ξ^- AND Ξ^0 HYPERONS [Thesis]. Pjerrou, Gerald Michael. Los Angeles, Univ. of California, 1965. 198p.

The properties of the hyperons (Ξ^-) and hyperons (Ξ^0) were investigated by exposing a hydrogen bubble chamber to meson (K^-) beams of 1.80 and 1.95 Bev/c. The cross sections for hyperon (Ξ) production by various interactions were determined as well as the mean lives of the hyperons. The hyperon (Ξ^-) mass and the mass difference ($\Xi^- - \Xi^0$) were also measured. The spin of the hyperon (Ξ^-) was determined, and the properties of Ξ^* resonances were studied. (TCO)

30073 STUDY OF THE PARTIAL WAVE DISPERSION RELATIONS FOR PION-NUCLEON SCATTERING [Thesis]. Simmons, Leonard Micajah Jr. Ithaca, N. Y., Cornell Univ., 1965. 67p.

In an approximate calculation of the l^{th} partial-wave amplitude, the requirements of threshold and asymptotic consistency are shown to lead to the introduction of 2l-1 arbitrary parameters. This statement is independent of the method of solution. As an example, the p-state equations are solved numerically for pion-nucleon scattering by nucleon exchange. The results are extremely sensitive to the arbitrary parameter present. The conclusion is drawn that, while partial-wave dispersion relations may retain some usefulness for examining, in a qualitative fashion, the relative magnitudes of various forces, or for phenomenological purposes, they can not be used to calculate detailed properties of the amplitudes, such as the approximate positions and widths of resonances. (Dissertation Abstr.)

30074 PARTIAL-WAVE DISPERSION RELATIONS FOR PIONIC DISINTEGRATION OF DEUTERON [Thesis]. Vasavada, Kashyap. College Park, Md., Univ. of Maryland, 1965. 216p.

A dispersion theoretic approach is made within the framework of partial-wave dispersion relations to the pionic disintegration of the deuteron at low energies. The reaction amplitude is expressed in terms of six independent Lorentz-invariant scalar functions which are free from kinematical singularities, and the partial wave helicity amplitudes are obtained. Dispersion relations are written after removing kinematical singularities. After some approximations, the dispersion relations become soluble integral equations of the Omnes-Muskhelishvilli type. The contribution of the left-hand single nucleon exchange cuts is evaluated exactly. The left-hand anomalous contribution is evaluated approximately by replacing the cuts by poles in the appropriate channels. Analytic continuation in the deuteron mass gives the contribution of the right-hand anomalous cut. Part of the right-hand cut due to the two-proton intermediate state is taken into account by using the experimental energy-dependent phase-shift parameters for proton-proton scattering. The intermediate state containing two nucleons and one pion is effectively replaced by one particle and a resonance, and model amplitudes are used to evaluate the contribution. The results of this calculation are numerically evaluated on an IBM 7090 computer. For the angular distribution and the total cross section, a reasonable agreement is obtained with the results from low-energy experiments. (Dissertation Abstr.)

30075 MEASUREMENT OF K^+ DECAY BRANCHING RATIOS [Thesis]. Callahan, Andrew Charles. Madison, Wis., Univ. of Wisconsin, 1965. 106p.

The following four meson (K^+) decay branching ratios were measured: $B_{K\mu_3} = .0277 \pm .0018$, $B_{Ke_3} = .0394 \pm .0017$, $B_{K\pi_2} = .214 \pm .009$, and $B_\tau = .0554 \pm .0017$. A $K\mu_2$ branching ratio of .648 ± .009 is inferred using the τ' branching ratio of Bisi. The form factor ratio for $K\mu_3$ decay, $\xi = f_+/f_-$ is found, using the value of $B_{K\mu_3}/B_{Ke_3} = .70 \pm .05$, to have a real part $Re\xi = +.40 \pm .40$. This number depends on $Im|\xi| < 1$ and μ-e universality. Recent measurements on the $K\mu_3$ mode obtain $Re\xi = .50 \pm .32$ and $Im|\xi| < 1$. The agreement can be said to confirm μ-e universality, or put quantitatively $f_+(K\mu_3)/f_+(Ke_3) = .99 \pm .05$. (Dissertation Abstr.)

30076 MUON-NUCLEON INELASTIC INTERACTIONS [Thesis]. McNulty, Peter J. Buffalo, State Univ. of New York, 1965. 93p.

Previous experiments in which cosmic-ray muons were used for pion production indicated the existence of an anomalous non-electromagnetic interaction in addition to the Coulomb scattering. In the present experiment it is shown that the inelastic interactions can be explained in terms of pure electromagnetic interactions. This would imply that the muon would make an excellent probe for determining the nucleon structure. The muon would make an excellent replacement for the electron in scattering studies especially at high energies where bremsstrahlung effects make a monoenergetic electron beam much more difficult to obtain. Muons would, therefore, make an ideal probe in the search for a breakdown in electrodynamics at small distances. The virtual photon exchange in the electromagnetic interaction was analyzed. No evidence was found of interactions that could be attributed to longitudinally polarized virtual photons. Therefore, at this incident energy and at small angles, the cross section for the inelastic muon-nucleon interaction can be expressed solely in terms of the cross section for transversely polarized virtual photons, the limit of this latter cross section approaching the real photoproduction cross section as q^2 approaches zero. The semi-classical Williams-Weiszacker approach, therefore, is shown to be valid and its extensions in quantum electrodynamics to be in complete agreement with experi-

ment. Further studies of muon scattering at higher incident energies will be necessary to search for the possible breakdown of electrodynamics at small distances. Such studies would provide additional information on pion production in electromagnetic interactions and would allow a more quantitative determination of any contribution from longitudinally polarized virtual photons. (Dissertation Abstr.)

30077 CONTRIBUTIONS OF ELASTIC UNITARITY TO THREE-PION SCATTERING [Thesis]. Fleming, Gordon Neeld. Philadelphia, Univ. of Pennsylvania, 1964. 203p.

The three-pion channel has a purely elastic region and in this region the elastic scattering amplitude for three pions satisfies a purely elastic unitarity equation. Some consequences of this equation for a generalized version of the isobar model of three-pion scattering are investigated. Intermediate recoupling effects are considered, and it is shown that by retaining the recoupling terms in the elastic unitarity equation it is possible to satisfy Watson's theorem regarding terminal state interactions. The ρ-π scattering amplitude for the isoscalar $J = 1^-$ state is introduced, and further evaluation of the equations yields the result that if the forces are made strong enough to bind the ρ-π system at the mass of the ω, 5.6 μ, then the width of the ω is about 5 Mev. This agrees well with the present experimental data. (TCO)

30078 A_1 AND A_2 RESONANCE PRODUCTION IN 3.7-Bev/c π^--DEUTERIUM INTERACTIONS [Thesis]. Abolins, Maris Arvids. San Diego, Calif., Univ. of California, 1965. 114p.

Some of the properties of the A_1 and A_2 mesons, the bound states of a $\rho(I = 1, \pi\pi$ resonance with a mass of ~ 760 Mev) and a π meson, with masses of 1090 and 1310 Mev and widths of 150 and 80 Mev respectively, are studied. A ρ-π resonance can have isotopic spin 0, 1 or 2. Since the A_1 and A_2 were initially seen in singly charged states, the possibilities are reduced to I = 1 or I = 2. The production of the A_1 and the A_2 in reactions that differ only in the charges of the outgoing particles is investigated. In this way only charge independence of strong interactions need be assumed to predict the ratio of production in the doubly charged to the singly charged state. Two comparisons are made: (1) (a) $\pi^- + d \rightarrow p + p + A_{1,2}^-$ → $\rho^- + \pi^-$ with (b) $\pi^- + d \rightarrow p + n + A_{1,2}^-$ → $\rho^0 + \pi^-$; and (2) (a) $\pi^- + n \rightarrow p + A_{1,2}^-$ → $\rho^- + \pi^-$ with (b) $\pi^+ + p \rightarrow p + A_{1,2}^+$ → $\rho^0 + \pi^+$. The cross-section for 2(a) is deduced from a π^- d interaction and can be considered as a π^- n collision only in the approximation that the deuteron is made of two free nucleons with little mutual interaction. The validity of such an approximation is discussed quantitatively. The comparison of the cross-sections for 1(a) and 1(b) suggests an I = 1 assignment for both A_1 and A_2 but the evidence is not compelling. The ratio of σ(2a) and σ(2b), where 4 Bev/c π^+ p data are used for σ(2b), on the other hand, quite strongly indicates that I = 1 for both resonances. The production of A_1 and A_2 is investigated in the final state d + $\pi^+ + \pi^- + \pi^-$. No evidence is seen for the production of the A_2. The general peaking in the 3π mass spectrum around 1100 Mev, introduced by the momentum transfer restrictions due to the form factor of the deuteron, makes the detection of the A_1 very difficult. (TCO)

30079 INTERNATIONAL CONFERENCE ON HIGH-ENERGY PHYSICS, TIHANY, HUNGARY, SEPT. 25–30, 1962. Budapest, Central Research Institute of Physics, 1963. 325p. (CONF-620905).

In English and Russian.

Forty-three papers and five abstracts are included; separate abstracts were prepared for nine papers. Abstracts of thirty-four papers appeared previously in NSA as 15: 26258, 16: 21322, 33670, 17: 2193, 9200, 9319, 9362, 9374, 13097, 13425, 15084, 15137, 16934, 19029, 20803, 22466, 26269, 26463, 26464, 28171, 18: 857, 2617, 6005, 6008, 15183, 18601, 34616, 36351, 37976, 38082, 40287, 40551, 44551, and 44814. (L.B.S.)

For abstracts of individual papers see: 29960–29963, 30080–30083, and 30368.

30080 PERIPHERAL PROTON-NUCLEON INTERACTIONS AT 9 Gev. Novak, M.; Pernegr, J.; Simak, V. (Inst. of Physics, Prague). pp 60-9 of International Conference on High-Energy Physics. Budapest, Central Research Inst. of Physics, 1963.

An experimental determination was made of four-momentum transfer and isobar mass using the data concerning grey recoil protons in a sample of 150 proton-nucleon interactions. It is shown, on the basis of the OPE model, that the π-nucleon resonance T = 312 plays an important role in interactions that have recoil protons of energy lower than 200 Mev. (auth)

30081 ON THE PERIPHERAL MECHANISM IN THE $\pi^- + n \rightarrow p + \pi^- + \pi^-$ REACTION. Mihul, El. K. (Inst. of Atomic Physics, Bucharest). pp 76-9 of International Conference on High-Energy Physics. Budapest, Central Research Inst. of Physics, 1963.

One-pion production in π^--n interactions is investigated from the point of view of the interaction mechanism, considering both the statistical model and the one-meson approximation in the peripheral model. The ratio between the cross sections for $\pi^- + n \rightarrow p + \pi^- + \pi^- + \pi^0$ and $\pi^- + n \rightarrow p + \pi^- + \pi^-$ was calculated, and a marked contradiction between the results obtained by the two models was observed. It is noted that an experiment with a large propane chamber would be of interest in order to draw some conclusions with regard to the reaction mechanism for $\pi^- + n \rightarrow p + \pi^- + \pi^-$. (L.B.S.)

30082 CHARGE ASSYMETRY OF MESONS CREATED IN PROTON-NEUTRON INTERACTIONS. Rob, L. (FTJF, Prague). pp 80-4 of International Conference on High-Energy Physics. Budapest, Central Research Inst. of Physics, 1963.

Angular distributions of π^+ and π^- mesons produced in proton interactions with neutrons and protons in a nuclear emulsion stack were measured. 117 p-n interactions and 165 p-p interactions were found. Methods of measurement and identification of the fast and slow secondary particles are briefly discussed. The cms angular distributions from the p-n interactions exhibited a pronounced asymmetry; the coefficients were found to be $K(\pi^+) = +0.78 \pm 0.18$ and $K(\pi^-) = -0.75 \pm 0.40$. For p-p interactions, $K(\pi^-) = -0.001 \pm 0.180$ and $K(\pi^-) = -0.06 \pm 0.25$. (L.B.S.)

30083 EXPERIMENTAL SEPARATION OF INTERACTIONS WITH FREE PROTONS. Kopylova, D. K.; Lyubimov, V. B.; Nodgoretskii, M. I.; Rizaev, Kh.; Strel'tsov, V. N.; Trka, Z. (Joint Inst. for Nuclear Research, Dubna, USSR). pp 164a-164c of International Conference on High-Energy Physics. Budapest, Central Research Inst. of Physics, 1963. (In Russian).

A missing-mass criterion for separating the products of proton interactions is given. This criterion is verified experimentally from data obtained in meson(π^-)-p elastic scattering interactions at 6.8 Bev/c as well as from inelastic double-beam meson(π^-)-p peripheral interactions at 180 to 500 Mev/c. (G.O.Y.)

Field Theory, Scattering Theory, and Symmetries

See also Elementary Particles and Radiations

Refer also to abstract 30248.

30084 (CONF-640509(Pt.1)) INTERNATIONAL CONFERENCE ON THEORETICAL PHYSICS, MAY 28–JUNE 2, 1964. PART 1. (Bordeaux Univ. (France). Laboratoire de Physique Theorique). 132p. Dep. mn.

In English and French.

Separate abstracts were prepared for 4 of the 5 included papers. The remaining paper appeared previously in NSA as 20: 19459. (M.O.W.)

For abstracts of individual papers see: 29985, 29986, 30085, and 30086.

30085 (CONF-640509(Pt.1), Paper 3) PRODUCTION AND DECAY OF RESONANCES AT A FEW Gev. Jackson, J. D. (Illinois Univ., Urbana. European Organization for Nuclear Research, Geneva (Switzerland)). 37p.

Discussions are presented on quasi two-body processes, peripheral aspects of the production process, decay correlations, and collimation of the production process by absorption of low partial waves due to competing processes. (M.O.W.)

30086 (CONF-640509(Pt.1), Paper 4) METHODE D'APPROXIMATION DANS L'ETUDE DE LA DIFFUSION A HAUTES ENERGIES. (Approximation Method in the Study of Scattering at High Energies). Levy, M. (Paris Univ., Orsay (France). Laboratoire de Physique Theorique et Hautes Energies). 16p.

Several approximation methods for high energy scattering are discussed. The approximation methods are discussed for both large and small angle scattering. (M.O.W.)

30087 (IC-66/46) REGGE POLE BEHAVIOR IN AN SL(2,c) MODEL FIELD THEORY. Cocho, G.; Ar-Rashid, Harun (International Centre for Theoretical Physics, Trieste (Italy)). May 1966. 24p. Dep. mn.

A model SL(2,c) field theory proposed by Fronsdal was employed to evaluate a strong interaction vertex. Using this vertex function and an assumed mass spectrum of the exchanged SL(2,c) tower in a Feynman diagram, the high-energy and low momentum transfer part of the amplitude was extracted out. This shows characteristic Regge behavior and compares favorably with the proton-proton scattering data, although the numerical agreement is not considered significant in this model study. (auth)

30088 (IC-66/50) RENORMALIZED $\omega - \phi$ MIXING ANGLE AND $J^P = 1^-$ MESON DECAYS. Rivers, R. J. (International Centre for Theoretical Physics, Trieste (Italy)). May 13, 1966. 9p. Dep. mn.

Field-theoretic arguments are used to define a renormalized $\omega - \phi$ mixing angle and predictions are compared for the normalized and renormalized theories and experiment. The sensitivity of the predictions to the initial assumptions is briefly discussed. (auth)

30089 (IC-66/51) THE REPRESENTATIONS OF SL(n,C). Fronsdal, C. (International Centre for Theoretical Physics, Trieste (Italy)). May 1966. 59p. Dep. mn.

Separate detailed discussions are presented on the following: the group SL(n,C) and its algebra, generalities on representations, finite and infinite representations of the algebra, group representations, multipliers, generalized tensors, and reduction of product representations. (M.O.W.)

30090 (IC-66/52) CABIBBO ANGLE AND PARTIAL CONSERVATION OF AXIAL CURRENT. Krolikowski, W. (International Centre for Theoretical Physics, Trieste (Italy)). May 16, 1966. 8p. Dep. mn.

A partial conservation condition for the total hadronic axial weak current is written in such a way that it determines the Cabibbo angle in a close agreement with experiment. (auth)

30091 (JINR-P-2621) DINAMICHESKAYA SIMMETRIYA I SPEKTR MASS ADRONOV. (Dynamical Symmetry and Hadron Mass Spectrum). Stoyanov, D. Ts.; Todorov, I. T. (Joint Inst. for Nuclear Research, Dubna (USSR). Lab. of Theoretical Physics). 1966. 26p. Dep. mn.

The semidirect product of the Poincaré group with U(6,6) is considered in which the non-compact internal symmetry group U(6,6) is an invariant subgroup. The hadrons are classified in the "ladder" (unitary, infinite dimensional) representations of U(6,6). The mass-square operator is defined in terms of "dynamical" 4-momentum. A method of successive approximations is proposed for the calculation of its eigenvalues. The first approximation is in good agreement with experiment in the case of baryons while in the meson case the results are less satisfactory. (auth)

30092 (JINR-P-2700) NEKOTORYE VOPROSY KVANTOVOI TEORII SKALYARNOGO POLYA S TOCHECHNYMI ISTOCHNIKAMI. (Some Problems of Quantum Theory of Scalar Field With Point Sources). Shirokov, M. I. (Joint Inst. for Nuclear Research, Dubna (USSR). Lab. of Theoretical Physics). 1966. 18p. Dep. mn.

The mathematical and physical vacuum vectors are orthogonal in the model considered. In this case there are grounds not only physical but also mathematical for the introduction of the so-called "clothed" particle operators. It is shown that canonical representations with vacua are possible simultaneously for the "clothed" and "bare" operators. It turns out that the above orthogonality suggests the Fock-Tamm-Dancoff type of equations as a suitable apparatus for the solution of physical problems provided that the corresponding Fock amplitudes are properly defined. (auth)

30093 (JINR-P-2701) PREDSTAVLENIYA 189 I 405 GRUPPY SU(6) I KLASSIFIKATSIYA MEZONNYKH REZONANSOV 2^+, 1^+, 0^+. (Representations 189 and 405 of the Group SU(6) and Classification of Mesonic Resonances 2^+, 1^+, and 0^+). Enkovski, L.; Kukhtin, V. V.; Nguyen Van Hieu (Joint Inst. for Nuclear Research, Dubna (USSR). Lab. of Theoretical Physics). 1966. 34p. Dep. mn.

A possibility of classification of mesonic resonances 2^+, 1^+ and 0^+ in the framework of the group SU(6) is considered. The decomposition of the 189-plet and 405-plet of the group SU(6) into irreducible multiplets of its subgroups SU(3) ⊗ SU(2) and SU(4) ⊗ SU(2) is investigated, values of mixing coefficients between different unitary multiplets with the same spin are derived. C-parity of particles in the given multiplet is determined and relations between the decays constants of the type $2^+ \to 0^- + 0^-$, $0^+ \to 0^- + 0^-$ and $1^+ \to 0^- + \gamma$ are derived. (auth)

30094 (UCRL-14222) GENERAL PHENOMENOLOGICAL FORMALISM FOR REACTIONS WITH PARTICLES OF ARBITRARY SPIN. I. ROTATION INVARIANCE. Csonka, Paul L.; Moravcsik, Michael J.; Scadron, Michael D. (Lawrence Radiation Lab., Univ. of California, Livermore). [nd]. Contract W-7405-eng-48. 114p. Dep. mn. CFSTI $4.00 cy, $0.75 mn.

An investigation was made for describing a particle reaction containing an arbitrary number of particles with arbitrary spins, using only information supplied by rotation invariance, and of calculating the structure of the various experimental observables. Only three-dimensional formalisms were used: manifestly covariant formalisms are not discussed. It is shown that the M matrix of any complicated reaction can always be factorized into simple irreducible constituents, and that even the observables calculated from this M matrix can be factorized into observables pertaining to the constituent reactions. All M matrices are written in a space spanned by three mutually orthonormal rank-one momentum tensors, two of which are vectors and one a pseudovector. Two formalisms are explored in detail. One works in terms of spin tensors, the other of polarization tensors. Formulas are given once and for all for the traces of the spin tensors and the sum-rules for the polarization tensors. Examples are worked out to illustrate the results, and the mathematical background is supplied in appendices. To facilitate the practical use of the results, a set of step-by-step instructions is outlined whereby one can construct the M matrix and calculate any observable for any reaction. A program is now being prepared (and will be made available upon request) for a large class of electronic computers, which will calculate the expectation values of any spin observable in terms of the density matrix of the incoming particles and a complete set of arbitrary coefficients in the scattering matrix. (auth)

30095 DIAGONALIZATION OF HELICITY-CROSSING MATRICES. Kotanski, Andrzej (Jagellonian Univ., Krakow). Acta Phys. Pol., 29: 699-711(May 1966).

New scattering amplitudes, which are linear combinations of helicity amplitudes, are proposed. They correspond to definite projections of spins not on particle momenta but on

the normal to the scattering plane. Their spin crossing matrices are very simple, in each column and in each row there is exactly one non-zero element (of modulus one). Parity conservation implies simply vanishing of some amplitudes, the remaining ones being already linearly independent. (auth)

30096 ELECTROMAGNETIC FORM FACTOR NORMALIZATION. Galindo, A. (Facultad de Ciencias, Zaragoza, Spain); Pascual, P. An. Real Soc. Espan. Fis. Quim. (Madrid), Ser. A, 62: 109-13(Mar.-Apr. 1966).

Without using perturbation theory, the physical meaning of the electromagnetic form factors at $q^2 = 0$ is given. (auth)

30097 ON P, C, T TRANSFORMATIONS FOR DIRAC FIELDS. Galindo, A. (Facultad de Ciencias, Zaragoza, Spain); Pascual, P. An. Real Soc. Espan. Fis. Quim. (Madrid), Ser. A, 62: 115-18(Mar.-Apr. 1966).

The P, C, T, transformation laws for Dirac fields are analyzed as a consequence of the transformation of monoparticle states. From this analysis some inconsistencies contained in the usual treatment of these transformations are deduced. A solution to the problems encountered is given. (auth)

30098 REPRESENTATIONS OF GROUPS CONTAINING THE POINCARE GROUP. [PART] I. Hermann, Robert (Argonne National Lab., Ill.). Commun. Math. Phys., 2: 71-7(1966).

It is proved that in certain representations of the Poincaré group the mass operator must be identically zero. (auth)

30099 GROUP REPRESENTATIONS AND CREATION OPERATORS. Hermann, Robert (Argonne National Lab., Ill.). Commun. Math. Phys., 2: 78-93(1966).

A general formalism for describing unitary representations of non-compact semisimple groups is presented. It is applied to describe some general properties of representations of SU(6,6), of possible interest for the classification of elementary particles. (auth)

30100 ANALYTIC STRUCTURE IN λ OF THE S MATRIX FOR STRONGLY SINGULAR POTENTIALS. Jaksic, B. (Univ., Turin); Limic, N. Commun. Math. Phys., 2: 94-107(1966).

The asymptotic behavior in the λ-plane of solutions of the Schrödinger equation for scattering on singular potentials is investigated. The asymptotic behavior of the Jost functions and the S-matrix is obtained. Furthermore, the general analytic form in the λ-plane of the Jost functions and the S-matrix is established. Some properties of the distribution of poles of the S-matrix are proved. (auth)

30101 CONSERVED CURRENTS AND ASSOCIATED SYMMETRIES; GOLDSTONE'S THEOREM. Kastler, Daniel; Robinson, Derek W.; Swieca, Andre (Univ. of Illinois, Urbana). Commun. Math. Phys., 2: 108-20(1966).

In the framework of local field theory with translation symmetry, automorphisms connected with locally conserved currents are considered. It is shown that such automorphisms lead to symmetries, i.e., are implementable by unitary operators, whenever the smallest mass in the theory is non-zero. Therefore it is concluded that a spontaneously broken symmetry is possible only in the event that the smallest mass is zero. This establishes the theorem first conjectured by Goldstone. (auth)

30102 IRREDUCIBLE TENSORS FOR THE GROUP SU_3. Banyai, L.; Marinescu, N.; Raszillier, I.; Rittenberg, V. (Inst. of Physics, Bucharest). Commun. Math. Phys., 2: 121-32(1966).

The explicit determination of the matrix elements of the SU(3) irreducible tensors is carried out by a purely algebraic method. These expressions may be used to compute the Clebsch-Gordan coefficients by orthogonalisation. For the special case of (0,q) tensors simple formulas are derived. (auth)

30103 DIRAC MATRICES AND THE DIRAC MATRIX DESCRIPTION OF LORENTZ TRANSFORMATIONS. Macfarlane, A. J. (Syracuse Univ., N. Y.). Commun. Math. Phys., 2: 133-46(1966).

A new discussion of Dirac matrices and of the Dirac matrix description of Lorentz transformations is presented. The five anticommuting quantities $\gamma^J (J = 1, 2, 3, 0, 5)$ are treated on an equal footing and recognition of the rule for expressing the three-fold product $\gamma^J \gamma^K \gamma^L$ in terms of one- and two-fold products and of invariant five-space tensors g^{JK}, ϵ^{JKLPQ} allows all kinds of multiplication and trace laws for Dirac matrices to be derived systematically. The five-space formalism for Dirac matrices affords a very convenient vehicle for the Dirac matrix description of de Sitter transformations of a space with quadratic form $g_{KL}x^K x^L$. By considering the subset of these which leave the coordinate x^5 invariant, the Dirac matrix description of Lorentz transformations is obtained. Not only does this description give the well-known formula for any Lorentz transformation matrix L in terms of the matrix S, which enters the transformation law of a Dirac spinor $\psi(x)$ under L, it also gives an explicit and apparently new inverse formula expressing S in terms of L. (auth)

30104 S-MATRIX IN HEISENBERG'S REPRESENTATION. Medvedev, B. V.; Sukhanov, A. D. (Steklov Inst. of Mathematics, Academy of Sciences, USSR. Moscow Inst. of Radioelectronics and Mining Electromekhanics). Dokl. Akad. Nauk SSSR, 165: 305-8(Nov. 11, 1965). (In Russian.)

S-matrix representations in the form of functional operator resolution of asymptotic fields $\varphi_{in}(x)$ or $\varphi_{out}(x)$ are widely employed but the direct Heisenberg-type representation did not attract too much attention up to now. A method was therefore developed for deriving the S matrix in the Heisenberg representation on the basis of the existence of the so-called "half" S matrix $S_{in}(\sigma -)$. By this method, a unitary transformation into a new "out" representation may be accomplished directly, satisfying the requirements of relativistic covariance, independence from a concrete choice of space-like surfaces, finiteness and unitary character. The derivation showed that upon transition from the "in" representation to the Heisenberg representation, the functional dependence of the S matrix changes and the chronological ordering is transformed into an antichronological one. (TTT)

30105 ON THE PROBLEM OF MOMENTS IN THE QUANTUM FIELD THEORY. Gachok, V. P. (Inst. of Mathematics, Academy of Sciences, Ukrainian SSR). Dokl. Akad. Nauk SSSR, 165: 506-9(Nov. 21, 1965). (In Russian).

The condition of positive determinancy of the field theory may be identified by means of an infinite series of unequalities based on Wightman functionals. The singular character of such an expression is related to the self-conjugate nature of the field operators. A scheme is proposed for determining the required conditions, without recourse to the postulates of the theory, such as the Lorentz invariance, spectral nature or causality. The previously established condition, —namely that this question is related to the singularity of the problem of moments, —was satisfied and a unique solution was obtained for the problem of moments. (TTT)

30106 SYMMETRY OF ELEMENTARY PARTICLES IN NONUNIFORM GROUP THEORY. Novozhilov, Yu. V.; Terent'ev, I. A. (Zhdanov Leningrad State Univ.). Dokl. Akad. Nauk SSSR, 165: 530-3(Nov. 21, 1965). (In Russian.)

Extension of Poincaré groups lead to a single concept of space-time variables and internal group variables; the whole group may be considered as a product of Poincaré and internal symmetry groups. However, internal symmetry represents only a rough approximation that must await the development of an as yet nonexistent theory. Introduction of additional mechanisms leading to the breakdown of symmetry and based on unknown dynamic effects would render the theory purely phenomenological. The concept of the P(SU6) group which at statistical limits is transformed into SU6 was further broadened, assuming a strictly symmetrical character. This is not in contradiction with accepted concepts because limitations concerning equality of masses and supermultiplets are not involved. A determinant system was used for establishing the symmetry of elementary particles, whereby the role of the invariant spin has been taken into account. (TTT)

30107 CONTRIBUTION TO THE QUANTUM THEORY OF UNSTABLE ELEMENTARY PARTICLES. Khalfin, L. A. (Steklov Inst. of Mathematics, Leningrad). Dokl. Akad. Nauk SSSR, 165: 541-4(Nov. 21, 1965).

It was assumed that stable and unstable particles are equally elementary and their properties are independent of the manner by which they were obtained. The consequences of this and of the opposite assumptions were examined closely. Attention was given to the generation rather than to the decay of particles, considering schemes, such as $m_1 + m_2 \rightarrow m_3 + m$, $m \rightarrow m_4 + m_5$, $m \rightarrow m_6 + m_7$, whereby $m_4 + m_5 < m_6 + m_7$ and m_i represents the rest mass of the i-th particle. The study included consideration of the effect of the breakdown of the conservation laws and the principle of identity of similar particles and their effects. If the properties are dependent on the method of generation, and thus the particles are not elementary and the law of conservation of energy is valid, then the various decay channels represent decays of different particles; the quantum numbers, masses and lifetimes of these particles coincide but their new quantum numbers are different. If this assumption is correct, our current concept of elementary particles and weak interactions must be completely revised. (TTT)

30108 S-MATRIX AT VERY HIGH ENERGY. Van Hove, L. (CERN, Geneva). pp 17-26 of High Energy Physics. Takeda, Gyo (ed.). Tokyo, Syokabo Publishing Co. New York, W. A. Benjamin, Inc., 1966.

Some results concerning the high-energy behavior of the scattering amplitudes at fixed momentum transfer are presented. The results constitute some far-reaching generalizations of the Pomeranchuk theorem on total cross sections and are consequences of the analyticity of the scattering amplitude in the energy variable at fixed momentum transfer. (G.O.Y.)

30109 HIGH ENERGY BEHAVIOR OF THE FORWARD SCATTERING AMPLITUDE. Kinoshita, Toichiro (Cornell Univ., Ithaca, N. Y.). pp 27-34 of High Energy Physics. Takeda, Gyo (ed.). Tokyo, Syokabo Publishing Co. New York, W. A. Benjamin, Inc., 1966.

Several inequalities that are satisfied by the real part of the forward scattering amplitude are derived from the usual dispersion relations. (G.O.Y.)

30110 ALGEBRA AND SYMMETRIES. Ne'eman, Y. (Israel Atomic Energy Commission, Tel-Aviv. Tel Aviv Univ., Israel). pp 68-86 of High Energy Physics. Takeda, Gyo (ed.). Tokyo, Syokabo Publishing Co. New York, W. A. Benjamin, Inc., 1966.

Unitary spin and its dynamical extensions U(3) and U(6) are discussed. (G.O.Y.)

30111 MASS FORMULAE IN SU(3) AND SU(6). Glashow, S. L. (Univ. of California, Berkeley). pp 112-21 of High Energy Physics. Takeda, Gyo (ed.). Tokyo, Syokabo Publishing Co. New York, W. A. Benjamin, Inc., 1966.

The electromagnetic mass formulas and the "strong" mass formulas that result from assuming SU(3) and SU(6) symmetry of strong interactions are discussed. The $J = 2^+$ meson resonances are discussed in some detail. (G.O.Y.)

30112 ELECTROMAGNETIC INTERACTIONS IN THE QUARK MODEL. Baldin, A. M. (Joint Inst. for Nuclear Research, Dubna, USSR). JETP Lett. (USSR) (Engl. Transl.), 3: 171-3(Apr. 1, 1966).

Translated from Zh. Eksp. Teor. Fiz., Pis'ma Redaktsiya, 3: 265-8(Apr. 1, 1966).

Model representation concerning the quark structure of the particles rather than application of SU(6) symmetry to electromagnetic interactions is discussed. The component concerned with pseudoscalar mesons in the Lagrangian for the interaction between mesons and quarks is considered. (B.G.D.)

30113 ELECTRON SPECTRUM IN A ONE-DIMENSIONAL SYSTEM WITH RANDOMLY ARRANGED SCATTERING CENTERS. Bychkov, Yu. A.; Dykhne, A. M. (Inst. of Theoretical Physics, Academy of Sciences, USSR). JETP Lett. (USSR) (Engl. Transl.), 3: 202-4(Apr. 15, 1966).

Translated from Zh. Eksp. Teor. Fiz., Pis'ma Redaktsiya, 3: 313-16(Apr. 15, 1966).

A one-dimensional model is proposed, in which an exact solution to the problem of determining the spectral density of the energy levels of an electron moving in a random field can be obtained. (B.G.D.)

30114 THEORY OF WEAK INTERACTIONS. Stech, Berthold (Univ., Heidelberg). pp 1-26 of Kolloquium Ueber β-Zerfall und Schwache Wechselwirkungen. Heidelberg, Max-Planck-Instituts fuer Kernphysik, 1965. (In German).

An attempt is made to give an insight into the modern problems in the theory of weak interactions. The semi-phenomenological theory of weak interactions is given. The lepton decay, the use of form factors, the concept of universality, and axial vector currents are considered. (J.S.R.)

30115 RELATION BETWEEN THE POINCARE GROUP AND THE EXCEPTIONAL LIE GROUP G_2. Goodall, M. C. (Boston Univ.). Nature, 210: 932-3 (May 28, 1966).

In view of the known representations of the electromagnetic field F = (E,B) by quadratic or linear complexes in L_3, the corresponding physical interpretation to P_5 is investigated. (B.G.D.)

30116 VARIATIONAL VACUUM BOUNDARY CONDITIONS FOR A P_N APPROXIMATION. Davis, James A. Nucl. Sci. Eng., 25: 189-97(1966). (WAPD-T-1848)

Approximate vacuum boundary conditions for a P_N approximation are obtained by variational methods. Two stationary principles are proposed, one having what is called "odd" Marshak conditions as its natural boundary conditions, and the other having "even" Marshak conditions as its natural boundary conditions. The principles are valid for arbitrary geometry. The odd Marshak conditions are seen to be suitable for an odd-order P_N approximation and the even Marshak conditions for an even-order P_N approximation. The odd Marshak conditions are precisely the conditions obtained by Vladimirov from an extremum principle in which certain restrictions are imposed on the source and scattering. The present treatment contains no such restrictions. (auth)

30117 DYNAMICAL ORIGIN OF SU(6). Delbourgo, R.; Salam, A.; Strathdee, J. (International Center for Theoretical Physics, Trieste). Phys. Lett., 21: 455-7(June 1, 1966).

A relativistic dynamical model for massive quark-antiquark binding which gives rise to the rest symmetry $U(6) \otimes O(3)$ for the meson bound states is discussed. (auth)

30118 CURRENT ALGEBRAS AND MAGNETIC MOMENTS. Gatto, R. (Univ., Florence. Istituto Nazionale di Fisica Nucleare, Florence); Preparata, G.; Maiani, L. Phys. Lett., 21: 459-61(June 1, 1966).

The problem of baryon magnetic moments in current algebra is considered in a model employing local commutation rules and in an alternative model using only commutation rules of charges. (auth)

30119 SATURATION OF THE SU(3) ALGEBRA OF CURRENT DENSITIES. Oehme, R. (International Centre for Theoretical Physics, Trieste, Italy). Phys. Lett., 21: 567-9(June 15, 1966).

The SU(3) algebra of vector current densities is saturated with octet and decimet states of baryons at infinite momentum and finite momentum transfer. The results are consistent with those of collinear U(6). They are in good agreement with experiments. (auth)

30120 DIVERGENCE OF THE DISTORTED-WAVE BORN SERIES FOR REARRANGEMENT SCATTERING. Greider, K. R.; Dodd, L. R. (Univ. of California, Davis). Contract AT(11-1)-Gen-10. Phys. Rev., 146: 671-5 (June 17, 1966). (UCD-CNL-38).

The convergence of the Born-series solution for the exact, three-body scattering amplitude for rearrangement processes is investigated in the framework of the dis-

torted-wave formalism. An integral equation for the three-body scattering operator is derived, such that the inhomogeneous term is just the "direct" or the distorted-wave Born term. It is shown that the iterative solution to this integral equation diverges, since the kernel of the equation contains three-particle disconnected diagrams, and is therefore not completely continuous. As a consequence, the distorted-wave Born term must be questioned as the lowest order approximation to the exact amplitude. (auth)

30121 RIGOROUS SOLUTION OF THREE-BODY SCATTERING PROCESSES IN THE DISTORTED-WAVE FORMALISM. Dodd, L. R.; Greider, K. R. (Univ. of California, Davis). Contract AT(11-1)-Gen-10. Phys. Rev., 146: 675-86(June 17, 1966). (UCD-CNL-43).

General methods are developed for obtaining convergent solutions to the exact nonrelativistic three-body scattering amplitudes within the framework of the distorted-wave representation. A simplification of the Faddeev-Lovelace coupled integral equations is obtained when the mass of one particle is either much larger or much smaller than the other two. When this mass restriction applies, it is shown that each amplitude is determined by a single, tractable integral equation. The kernel of a typical equation is well-behaved and depends only on calculable, two-body operators. The inhomogeneous term consists of two parts, one of which is the usual distorted-wave Born term and the other, a term involving excitation of a set of two-body intermediate states. Applications are made to a variety of nuclear scattering processes, and the implications for the distorted-wave Born model discussed. (auth)

30122 CONSTRUCTION OF AN EQUIVALENT LAGRANGIAN FOR INTERACTING FERMION-BOSON FIELDS. Zimmerman, Robert L. (Univ. of California, Livermore). Phys. Rev., 146: 955-9(June 24, 1966).

The principal object of the present work is the derivation of a Lagrangian density $L_\phi(\psi,\bar{\psi})$ which is a function of only the fermion and antifermion fields and contains a boson state at mass μ. It is also required $L_\phi(\psi,\bar{\psi})$ to be equivalent to a theory with a Yukawa coupling plus a Matthews term in the limit that the wave-function renormalization constant Z_3 vanishes. The case is first considered where the Matthews term is neglected and it is shown that $L_\phi(\psi,\bar{\psi})$ is just the usual four-fermion theory. In the case where the Matthews term is not neglected, $L_\phi(\psi\bar{\psi})$ is derived in the case of strong coupling and weak coupling. The Lagrangian density is a highly nonlinear function of the fermion fields which, in the weak-coupling limit, reduces to the four-fermion theory as the Matthews term vanishes. (auth)

30123 BROKEN U(3) SYMMETRY AND SEMILEPTONIC WEAK INTERACTIONS. Nieh, H. T. (Harvard Univ., Cambridge, Mass.). Contract AF49(638)-1380. Phys. Rev., 146: 1012-20(June 24, 1966).

A phenomenological field theoretic model of U(3)-symmetry breakdown is proposed. It allows a unified treatment of both mass renormalization and field renormalization of the phenomenological fields associated with particles. Specifically, the renormalization effects on the semileptonic weak coupling constants were calculated. Based on the model, it is shown that the empirically observed damping factor for $|\Delta Y| = 1$ transitions cannot be explained by symmetry-breaking effects and therefore the Cabibbo angle is intrinsic to weak-interaction theory. From our calculation, a 20% renormalization effect was expected on all $|\Delta Y| = 1$ axial-vector coupling constants for baryon leptonic decays. This renormalization effect is supported by the present experimental information about the G_A/G_V ratio of lambda beta decay. To make a sharp test of the model, more accurate experimental data concerning the G_A/G_V ratios of the baryon leptonic decays are required. The model also reproduces the Ademollo-Gatto theorem on the nonrenormalization of the $|\Delta Y| = 1$ vector transitions and Okubo's speculated mass formulas for vector mesons. (auth)

30124 PERTURBATION METHODS IN DISPERSION THEORY. Kugler, M. (Columbia Univ., New York). Contract AT(30-1)-1932. Phys. Rev., 146: 1026-30 (June 24, 1966). (NYO-1932-105).

A complete perturbation method for N/D calculations in potential scattering is presented. This method agrees with the Dashen-Frautschi method in first order. It is shown that in cases where resonant states are shifted by the perturbation into bound states the effect is not of first order and the Dashen-Frautschi method is therefore inadequate. Some possible utilizations of the perturbation method are outlined. (auth)

30125 UNSUBTRACTED DISPERSION RELATIONS IN WEAK INTERACTIONS AND REGGEIZATION. Saito, Takesi (Univ. of California, Berkeley). Contract W-7405-Eng-48. Phys. Rev., 146: 1048-51(June 24, 1966). (UCRL-16628).

It was previously shown that in field theory there are two possible conditions under which an elementary particle lies on a Regge trajectory. The first is that the proper vertex function vanishes and that the proper vertex poles are not the poles of scattering amplitudes; the second, due to Kaus and Zachariasen, is that the form factor and Z_3 both vanish. It is shown that under the second condition, the pology approach (due to Bernstein et al.) and the original approach (due to Goldberger and Treiman) of obtaining the Goldberger-Treiman relation both fail. Therefore, this condition may be inadequate as a condition for Reggeization. (auth)

30126 W SPIN FOR ANY SPIN. Harari, H. (Stanford Linear Accelerator Center, Calif.); Horn, D.; Kugler, M.; Lipkin, H. J.; Meshkov, S. Contract NA-onr-7-66. Phys. Rev., 146: 1052-7(June 24, 1966).

The collinear group $SU(6)_W$ is used to discuss vertices, form factors, and other collinear processes in an SU(6) theory that is consistent with relativistic invariance. It leads, however, to a classification of the particles which is different from that of the "static" $SU(6)_S$. The general "W-spin" properties of an arbitrary spin state constructed from any number of basic spin-$\frac{1}{2}$ objects are discussed in detail. Explicit formulas for expressing the eigenstates of W^2 as linear combinations of ordinary spin states are given and some properties of the transformation matrices are discussed. The relation between W spin and ordinary S spin in the framework of the SU(2) ⊗ SU(2) algebra is generalized to an arbitrary Lie algebra of the form G ⊗ G. Some examples of such generalized W-type algebras are considered and the special case of $SU(6)_W$ and $SU(6)_S$ is discussed in detail. An explicit formula for calculating the $SU(6)_W$ properties of an arbitrary component of a representation of the nonchiral U(6) ⊗ U(6) is given. Some explicit transformation matrices between the eigenstates of W spin and S spin are shown. (auth)

30127 BOOTSTRAP CONDITIONS IN A SOLUBLE MODEL. Jin, Y. S.; Kang, Kyungsik (Brown Univ., Providence). Contract AT(30-1)-2262. Phys. Rev., 146: 1058-67(June 24, 1966). (NYO-2262-107).

A soluble model obtained by a slight extension of the Lee model is considered in a study of the bootstrap mechanism. By examining the general solution that is obtained by using properties of the Herglotz function, it is found that the bootstrap mechanism can be achieved if and only if two further restrictions in addition to the general requirements of analyticity, unitarity, and crossing symmetry are imposed on the solution. They are that (i) the scattering amplitude satisfies the asymptotic condition $\lim_{\omega\to\infty}\omega^{-2}t^{-1}(\omega) = 0$ and (ii) the scattering amplitude has no Castillejo-Dalitz-Dyson (C.D.D.) zeros. It is also proved that the condition (i) is equivalent to $\lim_{\omega\to\infty}\omega^{-1}D(\omega) = 0$ when $N(\omega) = 0(\omega^{-1})$ as $\omega \to \infty$ or $Z_3 = 0$ or the Levinson theorem holds, while condition (ii) is equivalent assuming the two familiar bootstrap equations based on the N/D method and implies in particular a nonpositive scattering length. Either of the conditions (i) and (ii) alone gives in general only an inequality between the mass and coupling constant, and it is therefore concluded that the possibility of the bootstrap mechanism depends in a very sensitive way on the low-energy behavior as well as the high-energy behavior of the scattering amplitude. It is further argued that destroying the crossing symmetry in the approximate solutions will not give any physically meaningful conditions for determining the parameters un-

less one introduces a subtraction or one C.D.D. zero in the Low equation. (auth)

30128 APPLICATION OF AN APPROXIMATE SOLUTION OF PARTIAL-WAVE DISPERSION RELATIONS TO YUKAWA POTENTIAL SCATTERING. Reinfelds, J. (George C. Marshall Space Flight Center, Huntsville, Ala.); Smith, J. Phys. Rev., 146: 1091-7(June 24, 1966).

The time-reversal symmetrization of the multichannel scattering amplitude proposed by Fulton and Shaw is used to construct the amplitude for nonrelativistic single-channel Yukawa potential scattering. It provides a modified determinantal method for the solution of the N/D equations. This amplitude is compared to the exact solution of the Schrödinger equation. It is found that the scattering lengths predicted by this method are qualitatively the same as those predicted by the full N/D equations and significantly better than the results of the determinantal method. The computational simplicity of the determinantal method has been retained and combined with the accuracy of the full N/D solution, which, with first-order Born approximation, gives quite a reliable picture of the qualitative features of the scattering. (auth)

30129 THREE-PARTICLE CONTRIBUTIONS TO ELASTIC SCATTERING. Grisaru, M. T. (Brandeis Univ., Waltham, Mass.). Phys. Rev., 146: 1098-1106 (June 24, 1966).

Equations such as those derived by Cook and Lee and by Ball, Frazer, and Nauenberg for taking into account the effects of production on the elastic scattering amplitude are re-examined. It is found that the conventionally defined partial-wave projection of the three-particle amplitude has a singularity in the space of partial energies of two of the particles, and that this singularity introduces some additional terms in the dispersion equations. These terms vanish in the sharp-resonance approximation but are otherwise present. (auth)

30130 MATRIX N/D METHOD WITH ARBITRARY INELASTICITY. Warnock, Robert Lee (Illinois Inst. of Tech., Chicago. Argonne National Lab., Ill.). Phys. Rev., 146: 1109-17(June 24, 1966).

The N/D method for n two-body channels is extended to allow arbitrary inelastic effects. The functions regarded as given are the left-cut discontinuities and the "absorption matrix." (The absorption matrix F is the term of the unitarity condition accounting for transitions between the n channels and any other open channels: $\mathrm{Im}T_+ = T_+\rho T_- + F$.) The procedure is based on a new D matrix, which is defined by means of generalized complex phase shifts. The basic equation is a singular but linear integral equation for ImD. The singular equation is related to an equivalent Fredholm equation. The method may provide a useful general framework in which to discuss absorptive corrections to the peripheral model of high-energy processes. It includes other ways of treating such corrections as special approximations. The technique may also be valuable as a tool in constructing a more rigorous bootstrap theory. A by-product of the investigation is an elegant parametrization of an n-channel submatrix of the entire S matrix. (auth)

30131 FINITE RANGE OF STRONG INTERACTIONS AND ANALYTICITY PROPERTIES IN MOMENTUM TRANSFER. Omnes, Roland (Centre de Recherches Nucleaires, Strasbourg). Phys. Rev., 146: 1123-9(June 24, 1966).

It is investigated how the finite range of strong interactions can be stated in terms of an experiment. It is found that it is equivalent to the fact that the probability of any process generated by strong interactions should decrease exponentially as a function of the impact parameter a. This impact parameter is defined by a translation of the initial wave packet in a direction normal to its mean velocity in the center-of-mass system. Because of the spreading of wave packets with time, it is necessary to consider wave-packets whose width in configuration space increases like $\sqrt{a}$. It is then shown that this property is equivalent to the analyticity of all absorptive parts due to different channels as functions of the momentum transfer inside an ellipse. Such analyticity properties are also valid for the amplitude of a two-body channel. The ellipse does not shrink to the physical region when the energy tends to infinity. (auth)

30132 DISPERSION RELATIONS FOR THREE-PARTICLE SCATTERING AMPLITUDES. I. Rubin, Morton (Univ. of Wisconsin, Madison); Sugar, Robert; Tiktopoulos, George. Phys. Rev., 146: 1130-49(June 24, 1966).

The scattering of three nonrelativistic spinless particles interacting via two-body Yukawa potentials is considered. The on-energy-shell T-matrix element is studied as a function of the total center-of-mass kinetic energy E for fixed physical values of the vectors $y_i = k_i(2m_iE)^{-\frac{1}{2}}$, $y_i' = k_i'(2m_iE)^{-\frac{1}{2}}$; i = 1, 2, 3, where k_1, k_2, k_3 and k_1', k_2', k_3' are the initial and final momenta of the particles, respectively, and m_1, m_2, m_3 are their masses. It is shown that T(E) [defined as a real analytic function: $T(E) = T^*(E^*)$] has no complex singularities in the E plane. Along the real E axis, apart from the expected unitarity branch cuts and the "potential" or left-hand cuts, three kinds of anomalous singularities are found. The first kind arises from the kinematical possibility of the particles undergoing a finite number (depending on the mass ratios) of successive binary collisions ("rescatterings") at arbitrarily large spatial separations. The other two kinds are associated with the existence of two-particle bound states. It is shown that the discontinuities of T(E) across the anomalous cuts can be explicitly expressed in terms of on-shell physical amplitudes. Accordingly, N/D equations are formulated for the determination of the amplitude. The connection between the rescattering singularities and the convergence of the partial-wave expansion of the amplitude is briefly discussed. (auth)

30133 REMARK ON THE MIXING MODEL OF INTERMEDIATE VECTOR BOSONS. Joshi, G. C.; Bhakar, B. S. (Univ. of Delhi). Phys. Rev., 146: 1159-60(June 24, 1966).

A model in which the intermediate vector bosons belong to a particular representation of SU(3) is investigated. It has been shown that, if in order to account for the $\Delta S = 1$ and $\Delta I = \frac{1}{2}$ rules, an additional Lagrangian is introduced, then the vector bosons coupled to the $\Delta S = 0$ and $\Delta S = 1$ octet currents mix in such a way that the $\Delta S = 1$ leptonic decays are suppressed, and the equality of the vector coupling constant of β decay and μ decay is maintained. (auth)

30134 UNSUBTRACTED DISPERSION RELATIONS IN WEAK INTERACTIONS AND UNITARY SYMMETRY. Nishijima, K.; Swank, L. J. (Univ. of Illinois, Urbana). Phys. Rev., 146: 1161-80(June 24, 1966).

In a series of papers a dynamical approach to weak interactions based on unsubtracted dispersion relations has been introduced and discussed. Emphasis has been placed on the possible existence of eigenvalue restrictions arising from the homogeneity of the basic equations for the weak-interaction amplitudes, and the selection rules resulting from the eigenvalue restrictions have been derived when strong interactions possess certain symmetries. The following topics are covered in this paper: the irreducibility theorem for the weak-interaction amplitudes, generalization of the Goldberger-Treiman relation, derivation of the Gell-Mann-Okubo and Coleman-Glashow mass formulas from weak interactions as eigenvalue restrictions or self-consistency conditions, and a new approach to nonleptonic decays based on the empirical solution of the leptonic decays. Comparison of the theory of nonleptonic decays with experiments indicates that the agreement is satisfactory. (auth)

30135 SPONTANEOUSLY BROKEN SYMMETRIES AND THE QUESTION OF MASSLESS PARTICLES IN A MODEL FIELD THEORY. Deshpande, N. G.; Bludman, S. A. (Univ. of Pennsylvania, Philadelphia). Phys. Rev., 146: 1186-94(June 24, 1966).

An example is given showing that the condition of broken symmetry can be formally satisfied without the presence of interacting massless particles. The model used is an extension of Zachariasen's model and is a relativistic generalization of the high-density electron gas. The model is defined by a sum of perturbation-theory diagrams and also by an equivalent Lagrangian. In this model, when the physical vacuum is not invariant under a certain continuous sym-

metry of the Lagrangian, massless particles must be present. If, however, a Yukawa interaction of infinite range is present, then these massless mesons decouple from all physical amplitudes. (auth)

30136 SYSTEMATIC ITERATIVE APPROACH TO THE PROBLEM OF SCATTERING ON SINGULAR POTENTIALS. Calogero, F. (Univ., Rome. Istituto Nazionale di Fisica Nucleare, Rome); De Stefano, M. B. Phys. Rev., 146: 1195-1201(June 24, 1966).

A systematic iterative approach for the evaluation of the partial-wave scattering amplitude, which is convergent both for regular and for singular potentials, is introduced and discussed. The singular potentials are assumed to be repulsive in the singular region. The convergence is proved for real $k > 0$ for regular and singular potentials for all partial waves, and for $k = 0$ for repulsive potentials for S waves (k being the momentum in the reference frame of the potential). In the latter case the convergence is monotonic. (auth)

30137 ALGEBRA OF CURRENTS AND FORM FACTORS AT FINITE MOMENTUM TRANSFER. Riazuddin; Lee, Benjamin W. (Univ. of Pennsylvania, Philadelphia). Phys. Rev., 146: 1202-8(June 24, 1966).

By using equal-time commutation relations of chiral $SU(3) \times SU(3)$ current components, and the partially conserved-axial-vector-current hypothesis, several relationships among the axial-vector and electromagnetic form factors and the pion electroproduction amplitude at nonzero momentum transfer are derived. In the approximation of retaining only the (3,3) resonance contribution to the pion electroproduction amplitude, an approximate identity of the isovector Dirac charge form factor and the axial-vector form factor is derived. Further sum rules for the isovector and isoscalar Pauli magnetic-moment form factors are obtained which are fairly well satisfied. The form factor for the induced pseudoscalar coupling is discussed. (auth)

30138 SCALAR DENSITIES IN CURRENT COMMUTATION RELATIONS AND THE PARTIALLY-CONSERVED-AXIAL-VECTOR-CURRENT HYPOTHESIS. Kawarabayashi, Ken (California Inst. of Tech., Pasadena); Wada, Walter W. Contracts AT(11-1)-68; AT(11-1)-1545. Phys. Rev., 146: 1209-17(June 24, 1966). (CALT-68-63).

In the theory of the $SU(3) \times SU(3)$ group for baryons and mesons, there exist eighteen scalar and pseudoscalar densities. Considering only the $SU(2) \times SU(2)$ subgroup, the pseudoscalar densities are equal to the divergences of the axial-vector currents and therefore can be interpreted as being proportional to the pion field on the basis of the partially-conserved-axial-vector-current hypothesis. An attempt is made to give physical interpretation to the scalar density by calculating the expectation value of its space integral with respect to nucleon states. It is found that this expectation value is small (at most, of the order of the pion mass), which is related to Adler's consistency condition on the pion-nucleon scattering amplitude implied by the PCAC hypothesis. Specific models that are consistent with the PCAC hypothesis, such as the gradient-coupling model and the σ-meson model, are examined on the basis of our result. (auth)

30139 BROKEN SYMMETRY, SUM RULES, AND COLLECTIVE MODES IN MANY-BODY SYSTEMS. Stern, H. (Univ. Libre, Brussels). Phys. Rev., 147: 94-101(July 8, 1966).

An investigation is made of the relationship between long-wavelength, low-frequency normal modes and broken symmetry in nonrelativistic many-body systems. In particular, the relationship between broken symmetry as manifested through the so-called Goldstone pole and the normal-mode structure is examined. Through the study of various models, it is shown that the structure of the normal modes is correlated to the Goldstone pole either completely, partially, or not at all, according to the class of symmetry of the hamiltonian of the system. For example, in the neutral superconductor, the hamiltonian has such low symmetry that although the Anderson modes restore the symmetry of the ground state, they have no relationship at all to the Goldstone pole. It is observed that as the symmetry decreases, a dynamical sum rule takes the place of such a correlation and in all systems a sum rule gives the normal-mode frequency ω. These sum rules also give the ω distribution of states through the Huang-Klein dispersion relation. (auth)

30140 PERSISTENT CURRENTS IN MANY-BOSON SYSTEMS. Grobman, Warren D. (Princeton Univ., N. J.); Luban, Marshall. Phys. Rev., 147: 166-84(July 8, 1966).

A theoretical study of persistent currents in liquid ^4He is given, in which a system of N interacting bosons confined to a cylindrical container is chosen as a model. It is argued that these currents are metastable and a general model-independent stability criterion valid for all temperatures is derived. In this formulation it is essential that there is a single-particle state φ_c with nonzero angular momentum l_c which is occupied by a macroscopic number [O(N)] of particles. The stability criterion is applied to the study of two soluble models, one, an independent-particle model studied for all temperatures, the other a quasiparticle model studied for $T = 0°K$. For both models persistent currents are possible at $T = 0$ provided that the interactions between particles are sufficiently strong and l_c does not exceed a characteristic critical value l_M. The quantity l_M is calculated for different choices of single-particle functions, and in particular for the solutions of a Hartree equation, which is relevant to a description of line vortices with quantized circulation. The density $\rho_c(T)$ of particles macroscopically occupying φ_c at a temperature T, as well as the critical temperature T^* above which no persistent currents are possible, are calculated for the independent-particle model. (auth)

30141 $\Delta S = 0$ BARYONIC CURRENT COUPLED TO THE MUONIC CURRENT. Pascual, P.; Pascual, Ramon (Facultad de Ciencias, Valencia). Phys. Rev. Lett., 16: 1057-8(June 6, 1966).

From experimental results, evidence is presented which rules out the hypothesis that the electronic current interacts with the strangeness-conserving baryonic current $\cos\theta\ (V_\mu^{(0)} + A_\mu^{(0)})$, but that the muonic current interacts with $\cos\theta\ (V_\mu^{(0)} - A_\mu^{(0)})$. (B.G.D.)

30142 EQUIVALENT REPRESENTATIONS IN SYMMETRIZED TENSORS. Tompkins, Donald R. (Louisiana State Univ., Baton Rouge). Phys. Rev. Lett., 16: 1058-60(June 6, 1966).

In many inquiries of detailed properties of group representations, tensor methods have not been used. The reason is that the basis of decomposed tensors has usually been implicit. The cause of this trouble is in a portion of a theorem given by Weyl, which states that if C is a Young symmetrizer, then the tensors CF form an irreducibly invariant subspace which is incorrect except for one dimensional representations. The correct method for constructing the irreducibly invariant subspaces is presented. (B.G.D.)

30143 CHIRAL ALGEBRA, CONFIGURATION MIXING, AND MAGNETIC MOMENTS. Gerstein, I. S.; Lee, B. W. (Univ. of Pennsylvania, Philadelphia). Phys. Rev. Lett., 16: 1060-2(June 6, 1966).

A model is presented for baryon states based on the chiral $U(3) \otimes U(3)$ algebra at infinite momentum. The possibility that the expectation values of the commutators of the time components of vector and axial-vector currents between stable octet baryons are saturated by single-particle states and observed resonances is considered. The magnetic moments of these states are also considered. (B.G.D.)

30144 MOTION OF ELEMENTARY CHARGED PARTICLES. Blau, R. (Microwave Associates, Inc., Burlington, Mass.). Proc. IEEE (Inst. Elec. Electron Eng.), 54: 402-4(Mar. 1966).

Includes reply by D. V. Geppert.

The difficulty arising from the generalization of the Coulomb field based on the concept of charge moving with the speed of light previously presented by Geppert (Proc. IEEE

53; 1775 (1965)) is discussed. A method in which this difficulty may be circumvented is presented. (B.G.D.)

30145 ELEMENTARY PARTICLES AND BOUND STATES. Ikeda, Mineo; Maekawa, Takayoshi; Miyachi, Yoshihiko; Senba, Kei; Shohno, Naomi. Sci. Rep. Res. Inst. Theoret. Phys., Hiroshima Univ., No. 4, 1-127(1965).

The problem of bound states is presented within the framework of the conventional quantum field theory, particularly the Sakata model utilizing as basic particles the fermions which have a four-fermion coupling. Topics included are the normal mode method, two-body system, integral equations and partial wave analysis, coupling, and application to the full symmetry theory of the Sakata model. (B.G.D.)

30146 CURRENT-GENERATED ALGEBRAS AND FORM FACTORS. Winternitz, P.; Makarov, A. A.; Matveev, V. A.; Nguyen Van Hieu; Smorodinskii, Ya. A.; Tkachev, L. G.; Uhlir, M. (Joint Inst. for Nuclear Research, Dubna, USSR). Yadern. Fiz., 3: 918-23(May 1966). (In Russian).

Relations following from the current-generated algebra are obtained for the vector and axial current form factors. (auth)

30147 CASIMIR OPERATORS FOR THE GROUPS U(n) AND SU(n). Perelomov, A. M.; Popov, V. S. (Inst. of Theoretical and Experimental Physics, State Atomic Energy Commission, USSR). Yadern. Fiz., 3: 924-31(May 1966). (In Russian).

A simple method of finding the eigenvalues of the invariant operators (Casimir operators) C_p of arbitrary order p is developed for the groups U(n) and SU(n). The connection between the U(n) and SU(n) Casimir operators is established. Explicit formulas are given for the operators C_p with $p \leq 6$. (auth)

30148 APPROXIMATE EQUATIONS FOR SCATTERING MATRIX ELEMENTS IN THE RELATIVISTIC THREE-BODY PROBLEM. Stoyanov, D. C.; Shelest, V. P. (Joint Inst. for Nuclear Research, Dubna, USSR). Yadern. Fiz., 3: 942-5(May 1966). (In Russian).

Approximate equations were obtained connecting the matrix elements of the amplitudes for various three-particle processes. The limit cases of strong and weak coupling in the two-particle bound states are considered. The suggested equations are more significantly simple than the previously obtained exact ones. (auth)

30149 PHENOMENOLOGY OF CERTAIN INELASTIC REACTIONS INVOLVING PARTICLES WITH SPIN. Zlotnikov, L. M.; Klepikov, N. P.; Shekhter, L. Sh. (Moscow State Univ. Saratov State Univ., USSR). Yadern. Fiz., 3: 951-6(May 1966). (In Russian).

The phenomenological scheme of reactions involving particles with spins $0, \frac{1}{2} \rightarrow 0, \frac{1}{2}$ and $\frac{1}{2}, \frac{1}{2} \rightarrow 0, \frac{1}{2}, \frac{1}{2}$ is considered. The construction of the reaction matrix for a given angle and energy is investigated for the first scheme. (auth)

30150 NONRELATIVISTIC THEORY OF SCATTERING ON A COMPOSITE PARTICLE WITH LOW BINDING ENERGY. Braun, M. A. (Leningrad State Univ.). Yadern. Fiz., 3: 957-64(May 1966). (In Russian).

Scattering on a composite particle with the binding energy tending to zero is considered in a nonrelativistic theory. It is shown that the scattering amplitude reduces to a simple expression, similar to the well-known impulse approximation. The elastic scattering contributes mainly at small angles; it is small in comparison with the inelastic one and can be expressed in terms of the zero-angle amplitude for scattering on the constituents. (auth)

30151 INFORMATION LOSS IN THE THEORY OF SMALL-ANGLE MULTIPLE SCATTERING. Ernst, Valentin (Univ., Munich). Z. Naturforsch., 21a: 359-60 (Mar. 1966). (In German).

An inversion of the theory of elastic small-angle multiple scattering to permit calculation of the effective cross sections ($\cos\theta$) from the directly measurable magnitudes $I^{in}(n)$, $I^{out}(n)$, N, and D was previously proposed. The inversion of the theory must depend on what information on differential cross sections can be obtained from the directly measurable magnitudes in the presence of multiple scattering. An answer to this question is outlined on the basis of a generalization of the Goudsmit-Saunderson form of the small angle multiple scattering. (J.S.R.)

30152 REGULARIZED DELTA FUNCTIONS. Bopp, Fritz (Univ., Munich). Z. Phys., 193: 119-33(1966). (In German).

In the Laurent Schwartz theory of distributions the integral $\int \delta(r)f(r)dr$ is only defined for a certain class of test functions. Unfortunately, in physics, test functions f(r) like $e^{ikr}/r, e^{-\kappa r}/r$, $\nabla(e^{ikr}/r)$ and so on are obtained, which do not belong to the Laurent Schwartz class. The class of test functions is extended so that it includes physically meaningful functions with poles of finite order in $r = 0$. For this purpose the Laurent Schwartz axiomatic method defining the δ-distribution is replaced by a constructive one considering $\delta(r)$ as a given set of sequences of functions. The redefined δ-function is proved to satisfy the equations, axiomatically assumed by Laurent Schwartz. Well defined and finite results even in the case of test functions with poles at $r = 0$ are obtained. The Fourier components of the new δ-function are given. It is also shown why the δ-function is Lorentz invariant. (auth)

30153 QUANTUM THEORY OF A PARTICLE WITH AN ELECTRIC AND MAGNETIC CHARGE. Tevikyan, R. V. (Inst. of Physics, Erevan). Zh. Eksp. Teor. Fiz., 50: 911-14(Apr. 1966). (In Russian).

The quantum theory of a spinor particle which simultaneously possesses an electric charge e and magnetic charge g is investigated. In this case the particle has an intrinsic magnetic moment e/2m and electric moment g/2m, the magnitudes of the electric and magnetic charges being arbitrary. Due to the presence of a scalar magnetic charge in the particle P and T parities are violated. (auth)

30154 VIOLATION OF SYMMETRY IN THE WIGHTMAN AXIOMATIC SCHEME. Vasil'ev, A. N. (Leningrad State Univ.). Zh. Eksp. Teor. Fiz., 50: 954-7(Apr. 1966). (In Russian).

The problem of violation of symmetry is formulated and analyzed within the framework of Wightman axiomatics on the basis of the concept of a set of dynamic equations introduced previously. Two possible types of symmetry violation are considered. Previous results are used for analyzing the possibility of both types of symmetry violation. (auth)

30155 BOSONS IN THE FIELD OF A PLANE ELECTROMAGNETIC WAVE. Borgardt, A. A.; Karpenko, D. Ya. (Dnepropetrovsk State Univ., USSR). Zh. Eksp. Teor. Fiz., 50: 1167-70(Apr. 1966). (In Russian).

The Kemmer equation is solved for the case of a plane-wave field. The solution is obtained by employing reducible representations of the Kemmer algebra and the projection operator technique. (auth)

30156 COMPOSITENESS CONDITIONS AND BROKEN SYMMETRY IN A MODEL FIELD THEORY [Thesis]. Deshpande, Nilendra Ganesh. Philadelphia, Univ. of Pennsylvania, 1965. 106p.

Two aspects of non-perturbative field theory, the distinction between composite elementary particles and the intrinsic breakdown of symmetry, are studied in the context of a solvable relativistic field theory, the Zachariasen model. Three alternative formulations of the Zachariasen model are discussed. The relation of the model to a more complete field theory and to other solvable field-theoretic models is discussed. In carrying out the renormalization, the method of summing perturbation graphs is preferred. With two couplings $\lambda_0\bar{B}B\bar{B}B$ and $g_0\bar{B}BA$, renormalization is carried out. The renormalized propagator and vertex function are obtained, and their properties are discussed. An LSZ approach to the Zachariasen model is given. General spectral representations for the 2- and 3-point functions are set up and include the possibility of a zero of the propagator and a pole of the vertex function. Formulas for Z_3 and $\delta\mu^2$ are derived in two particle approximations and are illustrated by specializing to the Zachariasen model. A

comparison is made with the dispersion-theory solution of the Zachariasen model. The occurrence of redundant zero in the N/D solution in the $Z_3 = 0$ limit and its relation to the removal of the CDD ambiguity is discussed. The distinction between a $Z_3 \neq 0$ elementary-particle theory and a bound-state theory or $Z_3 = 0$ limit of elementary-particle theory is discussed using Levinson's theorem on the high-energy behavior of phase shifts. A résumé of the Goldstone theorem, which asserts the existence of massless particles when a continuous symmetry of a Lagrangian is broken by a degenerate ground state, is given. The Lagrangian formulation of the Zachariasen model is used, and the model is solved. (TCO)

30157 PROOF THAT SCATTERING IMPLIES PRODUCTION IN QUANTUM FIELD THEORY [Thesis]. Aks, Stanley Oelaf. College Park, Md., Univ. of Maryland, 1965. 107p.

A proof of the necessity of production processes in quantum field theory is carried out in the axiomatic framework. It is shown that a field theory which is assumed to have a nontrivial scattering amplitude violates crossing symmetry, if production processes are absent. The proof is based on the rigorous analytic properties of the scattering amplitude, particularly the analyticity in the invariant scattering variables, s, t, and u. In the case of a scalar theory with pairing symmetry, the scattering amplitude is known to be analytic within the domain $|stu| < 7168m^6$, except for the cuts $s \geq 4m^2$, $t \geq 4m^2$, and $u \geq 4m^2$. Under the working assumption that production processes are null, it is shown that this domain can be enlarged by applying the elastic unitarity conditions beyond the (usual) elastic region. The domain is enlarged sufficiently to include the first Landau singularity of the absorptive part of the scattering amplitude. This singularity is not symmetric in s and t within the extended (symmetric) domain, and this is incompatible with the crossing symmetry of the scattering amplitude. In order to avoid a contradiction, it follows that the discontinuity across this Landau singularity must be null. It follows that the scattering amplitude must itself be null. Hence, if production processes are null, the scattering amplitude must be null as well. The proof is first given in the context of a scattering amplitude satisfying the Mandelstam representation and is then modified to include the somewhat more restrictive analytic properties that follow in the axiomatic framework. In the case of the Mandelstam representation, the proof is also carried out in the equal-mass case without pairing symmetry and in the unequal-mass case. (TCO)

30158 THRESHOLD BEHAVIOR IN N/D CALCULATIONS WITHOUT ARBITRARY PARAMETERS [Thesis]. Thomas, Bruce Robert. Ithaca, N. Y., Cornell Univ., 1965. 55p.

It is shown that the usual methods of enforcing the expected q^{2L} threshold dependence in N/D calculations of partial-wave amplitudes involve arbitrary parameters and the introduction of poles into the amplitude. An alternative solution is proposed in which there are no arbitrary parameters and in which the number of spurious poles is about half the usual number. The interpretation of these poles is discussed. The approximation of representing the unphysical cut by a finite sum of poles is employed throughout. It is shown that in this approximation the N/D method always yields a simple expression for the inverse amplitude. An explicit prescription for constructing the solution is given, and the $J = 3/2$ states of π-N scattering are considered as an example. (Dissertation Abstr.)

30159 CROSSING RELATIONS AND THE PREDICTION OF SYMMETRIES [Thesis]. Tambasco, Daniel James. Iowa City, Iowa, Univ. of Iowa, 1965. 66p.

A two-channel model proposed by Martin and McGlinn, which incorporates unitarity and general crossing symmetry, is extended. The point of the discussion is to see whether general crossing symmetry (along with unitarity) is sufficient to predict the strong interaction symmetries. As the basis for the generalization, the three-channel static model of Low is taken. The derivation of a Low-type equation is included, where initially eigenstates of energy and angular momentum are taken. The statement of general crossing symmetry consists in requiring that the crossing matrix A satisfy two conditions: (1) $A^2 = 1$, and (2) $\Sigma_j A_{ij} = 1$. It is found that there exist two distinct several-parameter sets of crossing matrices satisfying these conditions. The conclusions reached are those of Martin and McGlinn. Imposing crossing symmetry does not restrict the set of crossing matrices to any subsets corresponding to a particular symmetry. Included also is a derivation of the Low equation for the scattering of neutral pseudoscalar mesons from a static source with spin 1. (Dissertation Abstr.)

30160 HIGH ENERGY SCATTERING PROCESSES WITH CUTS IN THE ANGULAR MOMENTUM PLANE [Thesis]. Reichert, John Douglas. Pasadena, Calif., California Inst. of Tech., 1966. 128p.

The experimental consequences of Regge cuts in the angular momentum plane are investigated. The principal tool in the study is the set of diagrams originally proposed by Amati, Fubini, and Stanghellini. Mandelstam has shown that the AFS cuts are actually cancelled on the physical sheet, but they may provide a useful guide to the properties of the real cuts. Inclusion of cuts modifies the simple Regge pole predictions for high-energy scattering data. As an example, an attempt is made to fit high-energy elastic scattering data for pp, $\bar{p}p$, $\pi^{\pm}p$, and $K^{\pm}p$, by replacing the Igi pole by terms representing the effect of a Regge cut. The data seem to be compatible with either a cut or the Igi pole. (Dissertation Abstr.)

30161 TWO STUDIES OF DYNAMICAL CALCULATIONS IN TWO MESON SYSTEMS [Thesis]. Beder, Doug Stanley. Pasadena, Calif., California Inst. of Tech., 1965. 114p.

Dynamical calculations in dispersion theory relating to meson states are described. The first part discusses the bound-state pseudoscalar mesons, utilizing a pole model representation of the binding forces. In the one-channel pseudoscalar vector calculation, and in a calculation coupling this to the baryon-antibaryon channel, fairly modest forces suffice to produce a tightly bound state. However, the output coupling constants are much larger than those fed into the calculation, so that bootstrap self-consistency is not attained. It is also interesting that the baryon-antibaryon channel seems to be a very significant contributor to the dynamical generation of bound-state pseudoscalar mesons. The second part of this work considers electromagnetic mass splittings of mesons. In a dynamical scheme for generating the mesons, mass splittings of the derived multiplets arise both because of mass splittings of the particles participating in the relevant scattering channels, and, because of photon exchanges. A crude inelastic bootstrap calculation of the ρ vector meson is developed and then subject to electromagnetic perturbations. As a corresponding pseudoscalar meson bootstrap is not available, pseudoscalar and vector mass differences can be related here. A rough estimate for the ρ meson is $M\rho_0 - M\rho^+ \geq 11$ Mev. A yet cruder estimate of the K*(885) mass difference is $MK_0^* - MK_+^* \sim 5$ Mev. (Dissertation Abstr.)

30162 ON THE CONVERGENCE OF BORN SERIES FOR REARRANGEMENT COLLISIONS [Thesis]. Chen, Augustine Chen-hsin. New York, New York Univ., 1964. 77p.

The convergence of Born expansion for rearrangement collisions is discussed in the context of a one-dimensional model for a 3-body scattering problem in which exchange scattering takes place. The Born series diverges as expected since a bound state is involved in both the original and rearranged channels. To cure this divergence, the method of orthogonality constraint originally formulated for potential scattering involving a bound state is extended to rearrangement collisions. The method modifies the potential by projecting out the binding effect of the potentials strong enough to support a bound state and considering only the scattering effect of the potentials as the perturbation on a distorted wave orthogonal to the bound state. The modified Born series obtained by iterating the relevant Lippmann-Schwinger integral equation, the inhomogeneous term of which contains the orthogonalized

distorted wave, is shown to be convergent, provided resonances not associated with the bound state are absent. The convergence proof is given for a separable potential, as the mathematics involved is then tractable. However, the results can be extended to potentials that can in principle be expanded into or approximated by a sum of separable potentials. The results are shown also to be valid for the three-dimensional case provided the potential in momentum space is appropriately redefined. The relation between this method and the methods of Rotenberg and Weinberg is also discussed. (Dissertation Abstr.)

30163 REGGE POLES IN FIELD THEORY AND CRITERIA FOR ELEMENTARITY [Thesis]. Chester, Arthur Noble. Pasadena, Calif., California Inst. of Tech., 1965. 90p.

It is known that in the field theory description of the Compton scattering of nucleons by vector mesons the nucleon lies on a Regge trajectory. In this work it is found that the vector meson channel of the same theory exhibits no such Regge-like behavior. However, in electron-graviton scattering the spinor particle is again Reggeized. The various problems that arise when zero-mass mesons are used in the scattering are discussed, and it is shown that the Reggeization generally proceeds as in the massive case. A field theory of massive gravitons is discussed. The dynamical criterion of vanishing renormalization constants is applied to Reggeized particles and it is shown that this criterion successfully distinguishes an elementary Reggeized particle from a true dynamical state. This provides a dynamical test that can replace the postulate that a "bootstrapped" theory is characterized by the absence of Kronecker delta terms in all channels. Thus the one-to-one correspondence between dynamical particles and certain moving poles in the partial wave amplitudes may be recovered. Appendices B and C review the generation of Regge trajectories by iteration through unitarity and Mandelstam's treatment of Reggeization using the N/D equations. (Dissertation Abstr.)

30164 S-MATRIX THEORY OF ELECTROMAGNETIC INTERACTIONS [Thesis]. Chou, Tsu-teh. Iowa City, Iowa, Univ. of Iowa, 1965. 90p.

If the basic principles of the S-matrix theory are applied to electrodynamics, many results of quantum electrodynamics can be reproduced. However, an approximation scheme, different from that in the strong interaction, i.e., an expansion in powers of e, has to be used. The scattering amplitudes of various processes, not higher than fourth order, are found to be the same as obtained in quantum electrodynamics. Various finite contributions due to lowest order primitive divergent diagrams can also be shown to be equivalent. In most cases, the calculations in the S-matrix theory are more straightforward and less laborious. It is also conceptually more simple; the artificial and unphysical renormalization program does not appear at all. However, at the present stage, the S-matrix theory of electromagnetic interactions is still plagued by a number of fundamental problems. Higher order calculations would be quite difficult, if not impossible to make, since the dispersion relations do not appear to take simple forms. Bound-state problems remain to be investigated. The infrared problem has to be solved. The specific results obtained here show that for all fourth order processes (and lower) the pure S-matrix theory gives results completely equivalent to those of quantum electrodynamics. (Dissertation Abstr.)

Fluid Physics and Thermodynamics

See also Plasma Physics and Thermonuclear Processes

Refer also to abstracts 30263 and 30570.

30165 (BNL-9254) ON SOME MATHEMATICAL ASPECTS OF KINETIC MODEL EQUATIONS. Sirovich, Lawrence (Brown Univ., Providence, R. I. Div. of Applied Mathematics); Thurber, James K. (Brookhaven National Lab., Upton, N. Y.). [1965]. Contract AT(30-2)-Gen-16. 28p. Dep. mn. CFSTI $2.00 cy, $0.50 mn.

A class of integro-differential equations used in the kinetic theory of gases is investigated. Under relatively weak conditions the existence and uniqueness of solutions to the initial value problem for these equations are shown. Under somewhat stronger assumptions the validity of the application of Fourier-Laplace transforms to this problem is demonstrated. Finally the asymptotic approach to hydrodynamics is shown. (auth)

30166 (NYO-3326-13) ATOMIC MOTIONS IN MONATOMIC FLUIDS. Desai, Rashmikant Chimanlal (Cornell Univ., Ithaca, N. Y. Dept. of Engineering Physics). June 1966. Contract AT(30-1)-3326. 85p. Dep. mn. CFSTI $3.00 cy, $0.75 mn.

Thesis.

Van Hove's self correlation function, $G_s(\underline{r},t)$, for monatomic gases is studied within the kinetic approach initiated by Nelkin. Non-Gaussian corrections are calculated for three types of interatomic potentials: rigid sphere potential, Lenard Jones potential and exponential 6 potential. It is found that the behavior of non-Gaussian corrections for all the three potentials is qualitatively similar to that found for the single relaxation time kinetic model by Nelkin and Ghatak and to that found by Rahman from a high density molecular dynamics calculation. It is also found that the corrections are larger for higher densities and at low densities, the corrections increase almost by a factor of two when attractive forces are included. Fourier transforms of $G_s(\underline{r},t)$ are also studied. The intermediate scattering function, $X_s(\underline{\kappa},t)$ and the scattering law, $S_s(\underline{\kappa},\omega)$ are calculated for real monatomic gases. Using the spatial moments for liquid argon, as calculated by Rahman from molecular dynamics and using his delayed convolution approximation, the energy distribution of scattered neutrons and $S(\underline{\kappa},\omega)$ for liquid argon are calculated. Results are compared with the experiments of Chen et al., and it is shown that the recent neutron scattering experiments and the computer experiments are in semiquantitative agreement. Theoretical questions resulting from this conclusion are pointed out. (auth)

30167 (SC-DC-65-1916) NUMERICAL SOLUTIONS OF THE FLOW FIELD PRODUCED BY A PLANE SHOCK WAVE EMERGING INTO A CROSSFLOW. Tyler, Lynn D.; Zumwalt, Glen W. (Oklahoma State Univ., Stillwater). Aug. 1965. Contract AT(29-1)-789. 196p. Dep. mn. CFSTI $5.00 cy, $1.00 mn.

For Sandia Corp., Albuquerque, N. Mex.

An analysis was conducted to determine if there existed conditions for experimental blast simulation using a shock tube mounted on the side of a wind tunnel. The primary purpose of this study was to describe mathematically the phenomena of a plane shock propagating into a supersonic crossflow. A finite difference technique proposed by the Russian mathematician, Rusanov, was applied to the problems of a shock propagating from an opening into both a still and supersonic crossflow. The geometries of the openings used for the still medium problems were slit-like and circular while the opening geometry used in the crossflow problem was a long slit, i.e., the geometry was plane. A computer program, which applied the difference scheme to a 6000 point mesh, was written for a CDC 3600 computer. Results were obtained for a shock of strength 10.0 (i.e., pressure ratio) which propagated into both a Mach 2.0 and a Mach 5.0 crossflowing stream. Also, for shock strengths of 4.0 and 10.0, computations for propagation into a still medium from both of the above geometries were obtained. (auth)

30168 (SC-DC-66-1329) TRANSIENT FLOW FIELD ANALYSIS OF A PLANE BLAST WAVE INTERCEPTING A STATIONARY CONE AT ZERO ANGLE OF ATTACK. Jackomis, William N.; Zumwalt, Glen W. (Oklahoma State Univ., Stillwater). Aug. 1965. Contract AT(29-1)-789. 194p. Dep. mn. CFSTI $5.00 cy, $1.00 mn.

For Sandia Corp., Albuquerque, N. Mex.

A numerical analysis of the transient flow field caused

by a plane blast wave passing axially over a blunt-based stationary missile was performed. A determination of the various physical and thermodynamic parameters affecting the blast conditions from the time the blast wave intercepts the conical body nose until the quasi-steady base flow conditions is established was included. Whitham's axi-symmetric cone solution was used to predict the shock diffraction pattern past the forebody. This solution is shown to be in close agreement with experimental shock tube tests obtained from Sandia Corporation, Albuquerque, New Mexico. The shock wave configuration and transient flow properties obtained from this solution were adapted to provide initial conditions required for the base region analysis numerical techniques. The approach of Rusanov was adapted for the numerical technique. From this technique, the detailed pattern of shock waves interacting with the base region of a conical body up to the quasi-steady flow condition was obtained. The results of the transient analysis are compared with experimental results for the blast wave passage past a stationary cone with semi-apex angle of 13.347 degrees. In addition, the associated numerical solutions and computer programs are presented. A new approach concerning the initial shock wave representation was developed which utilizes several logical assumptions regarding the property gradients through the interior of the shock wave. The shock wave is represented, not as a finite discontinuity, but as a steep gradient of the flow properties ahead of and behind the wave. The results of the blast-base interaction solution were used to relate the blast passage with the formation of the separated flow region behind the body. The method of Zumwalt and Tang was adapted and is shown to provide a satisfactory approach to problems of this type. Thus, a continuous solution for this transient analysis was performed which should provide a strong foundation for extensions to more complex blast interaction problems. The analytical and numerical techniques utilized in this study are shown to yield excellent representations of the transient flow phenomena which occur as a result of a plane blast wave intercepting a stationary cone axially. (auth)

30169 (UCRL–14198) A COMPARISON OF ANALYTICAL AND NUMERICAL SOLUTIONS FOR THE SHOCK TUBE PROBLEM. Crowley, Barbara K. (Lawrence Radiation Lab., Univ. of California, Livermore). May 21, 1965. Contract W-7405-eng-48. 32p. Dep. mn. CFSTI $2.00 cy, $0.50 mn.

The classical shock tube problem is discussed. Derivation of an analytical solution from the Rankine-Hugoniot relations for an ideal gas across a plane shock are reviewed. A typical shock tube with large discontinuities is chosen and simulated on various numerical finite-difference calculations. These calculations are performed in the Eulerian, Lagrangian, and Eulerian-Lagrangian coordinate frames. The results of these calculations are shown and compared with the analytical solution. They indicate that the Lagrangian approach is worth considering for problems with large discontinuities in the initial conditions. (auth)

30170 (UCRL–14251) SHOCK COMPRESSION OF ARGON. Van Thiel, M.; Alder, B. J. (Lawrence Radiation Lab., Univ. of California, Livermore). June 14, 1965. Contract W-7405-eng-48. 37p. Dep. mn. CFSTI $2.00 cy, $0.50 mn.

Liquid argon was shock-compressed from two initial states at 86°K and 2 bars, and at 148.2°K and 70 bars. The highest pressure of 700 kbars and temperature of 13000°K were obtained by reflecting a shock wave with a pressure of 270 kbars from a tungsten wall. These shock loci allow a test of the interatomic potential over a wide region and show that the potential can be represented by a sum of pair interactions over a large pressure range. The pair potential is furthermore found to be considerably less repulsive at small interatomic distances than the twelve power repulsive law. In fact, an exponential form yields good results up to 360 kbars. Above this pressure range the reflected shock data require a large change in the potential form which is interpreted to be due to a pressure induced electronic transition to the conduction band. Calculations show that a discontinuity in the Hugoniot data at 50 kbars and 1200°K could be identified with the melting line. This temperature corresponds to three times the highest reduced melting temperature observed so far. (auth)

30171 WAVES IN A HEAVY, VISCOUS, INCOMPRESSIBLE ELECTRICALLY CONDUCTING FLUID OF VARIABLE DENSITY IN THE PRESENCE OF A MAGNETIC FIELD. Kothari, D. S. (Univ. of Udaipur, Rajasthan, India); Gupta, G. P.; Gandhi, J. M. Acta Phys. Austr., 21: 248-61(1966).

An equation, relating the growth rate n, and the wave number k, which characterizes the equalibrium of a heavy, viscous, incompressible stratified fluid of finite depth in the presence of a vertical magnetic field, derived by Hide, was studied. The properties of the magnetohydrodynamic waves generated under certain conditions were discussed in detail. (auth)

30172 ORIENTATION OF THE MAGNETIC FIELD IN RAYLEIGH-TAYLOR'S INSTABILITY. Gandhi, J. M. (Univ. of Rajasthan, Jaipur, India); Mathur, R. B. Acta Phys. Austr., 21: 350-4(1966).

It is shown that variational methods are not useful for tackling the problems of the equilibrium of a heavy non-viscous fluid in the presence of a magnetic field which is inclined at some angle to the direction of gravity. Variational principle only exists if the magnetic field is either parallel to the direction of gravity or perpendicular to it. (auth)

30173 HOLLOW-CATHODE GLOW DISCHARGE IN HYDROGEN AND THE NOBLE GASES. Sturges, D. J.; Oskam, H. J. (Univ. of Minnesota, Minneapolis). Contract AF19(604)-8072. J. Appl. Phys., 37: 2405-12(May 1966).

Properties of a discharge maintained between a planar anode and a cathode consisting of two parallel electrodes were studied in helium, neon, hydrogen, and helium–argon mixtures at pressures between 1 and 25 torr. The analysis of the data led to the following main conclusions: The enhancement of the discharge efficiency by the hollow-cathode effect does not vary widely between the gases tested. The presence of metastable excited atoms is not essential for a pronounced hollow-cathode effect to occur. The minimum distance for the cathodes at which the anode fall develops is a function of the cathode dimensions, and is simply related to changes in the electron concentration and average electron energy. The lowest observed cathode fall for a hollow-cathode discharge corresponded closely to the cathode fall of a normal plane-cathode discharge. The general nature of the hollow-cathode effect in the gases tested is sufficiently similar to allow simple design cirteria to be developed for plane-parallel hollow-cathode discharge tubes. (auth)

30174 FLOW AND SELF-DIFFUSION OF GASES IN CAPILLARIES. PART I. Lund, L. M.; Berman, A. S. (Oak Ridge Gaseous Diffusion Plant, Oak Ridge, Tenn.). J. Appl. Phys., 37: 2489-95(May 1966). (K-L–6077-IR).

A model is presented for describing transport under a partial pressure gradient (self-diffusion) as well as transport under a total pressure gradient in capillaries of arbitrary length-to-radius ratio over a pressure range extending from the free molecule to the continuum regimes. The model provides a unified description of the transport and yields the same results as existing theories in the limited ranges appropriate for their application. (auth)

30175 FLOW AND SELF-DIFFUSION OF GASES IN CAPILLARIES. PART II. Lund, L. M.; Berman, A. S. (Oak Ridge Gaseous Diffusion Plant, Tenn.). J. Appl. Phys., 37: 2496-2508(May 1966). (K-L–6077-2R).

A variety of experimental data on the pressure dependence of the flow of gases through capillaries is examined using the model presented previously. The model is found to provide a good description of flow and self-diffusion in capillaries of arbitrary length-to-radius ratio at pressures ranging from the near free molecule to the continuum regimes. Experimental free-molecule flows are found to differ from those predicted from existing theories based on the diffuse scattering of gas molecules by the capillary wall. The dif-

ferences, which in general cannot be explained by specular reflection, are found to depend on the geometrical structure of the surface, the length-to-radius ratio of the capillary, and on the gas being transported. For a given gas flowing through a capillary of given length-to-radius ratio, the slip contribution to the transport is found to be a monotonically increasing function of the ratio of observed-to-theoretical free-molecule transports. (auth)

30176 COMPUTATION AND MEASUREMENT OF HALL POTENTIALS AND FLOW-FIELD PERTURBATIONS IN MAGNETOGASDYNAMIC FLOW OF AN AXISYMMETRIC FREE JET. Otis, David R. (Univ. of California, Berkeley). J. Fluid Mech., 24: 41-63(Jan. 1966).

The interaction was observed between a supersonic free jet of partially ionized argon and the magnetic field of a coil concentric with the jet. Nominal values of the parameters were: Mach number, 3; Reynolds number, 1000; magnetic Reynolds number, 0.2; magnetic interaction parameter, 1; Hall parameter, 1. The jet was strongly channeled. Axial and radial electric fields were observed in the jet with a net rise in potential across the interaction. These observations were consistent with predictions based on the single fluid, macroscopic equations, and a simple slug flow model. The current equation was solved to second order in the Hall parameter giving a closed-form expression for the Hall potential which agreed with the experiments for weak fields. Flow perturbations were calculated for Mach numbers of 3.11, 6.08, and 10.05, neglecting Hall currents; the calculations are in qualitative agreement with the experiments and show Joule heating to be the main factor in perturbing the flow at high Mach numbers. (auth)

30177 STEADY-STATE EXOTHERMAL HYDROMAGNETIC DISCONTINUITY FOR AN ARBITRARILY ORIENTATED MAGNETIC FIELD. Kennedy, Lawrence A. (Northwestern Univ., Evanston, Ill.). J. Fluid Mech., 24: 177-89(Jan. 1966).

An exothermal hydromagnetic discontinuity in a perfectly conducting gas is studied for the case of an arbitrarily orientated magnetic field. The evolutionary modes and the manner of variation of the physical properties for such phenomena are determined. The Hugoniot adiabatic is obtained and analyzed. (auth)

30178 PRINCIPLE OF EXCHANGE OF STABILITIES FOR THE MAGNETOHYDRODYNAMIC THERMAL STABILITY PROBLEM IN COMPLETELY CONFINED FLUIDS. Sherman, Michael; Ostrach, Simon (Case Inst. of Tech., Cleveland). J. Fluid Mech., 24: 661-71(Apr. 1966).

The principle of exchange of stabilities (exchange principle) for the thermal stability problem has been proved by Pellew & Southwell for fluids bounded by two infinite, horizontal parallel planes. Chandrasekhar discussed the establishment of the exchange principle for the same geometry when the fluid is an electrical conductor and when an arbitrary oriented, uniform, external magnetic field is applied in the vertical direction. The exchange principle is examined for fluids completely confined in an arbitrary region with rigid bounding surfaces that are good electrical conductors with respect to the fluid. The uniform magnetic field is applied in an arbitrary direction. A generalized thermal boundary condition is imposed which includes the fixed temperature and prescribed heat-flux conditions as special cases. In the magnetohydrodynamic thermal stability problem, the exchange principle is found to be valid if the total kinetic energy associated with an arbitrary disturbance is greater than or equal to its total magnetic energy. In a special case it is demonstrated that a sufficient condition which will establish the exchange principle is $k \leq \eta$, where k is the fluid thermal diffusivity and η is the fluid electric resistivity. (auth)

30179 MAGNETOHYDRODYNAMIC DRAG ON AN OSCILLATING SPHERE. Motz, Robin O. (Columbia Univ., New York). J. Fluid Mech., 24: 705-20(Apr. 1966).

The case of a dielectric sphere executing small-amplitude oscillations in an incompressible, conducting fluid with a uniform magnetic field aligned along the axis of oscillation is studied. For the case of large Hartmann and Reynolds numbers, the MHD equations are linearized. Solutions correct to $O(R_m)$ are obtained for the velocity, pressure, current, and electric and magnetic fields in the fluid. The MHD drag on an oscillating dielectric sphere in mercury was experimentally determined in aligned fields to 0.8 Wb/m^2. The experimental results agree well with the theory. The theory and experiment were extended to include the régime where the perturbed velocity is not small compared with the velocity present in the absence of a magnetic field. The validity of using the inviscid velocity to compute the current is verified by measuring the angular dependence of the induced electric field. (auth)

30180 UNSTEADY SLIP FLOW OVER A FLAT PLATE UNDER TRANSVERSE MAGNETIC FIELD. Datta, Sunil (Univ. of Lucknow, India). J. Phys. Soc. Jap., 21: 794-9 (Apr. 1966).

The slip flow of an electrically conducting viscous fluid over a porous flat plate under uniform transverse magnetic field is investigated. The external velocity is time dependent and the cases of impulsive free stream and accelerated free stream are considered in detail. It is found that the velocity increases with slip parameter $\sqrt{\epsilon}$ while the skin friction and displacement thickness decrease with it. The graphs drawn indicate that the analysis is not applicable beyond certain value of $\sqrt{\epsilon}$. (auth)

30181 NUCLEAR SPIN RELAXATION IN LIQUID HYDROGEN. Miller, C. E. (National Bureau of Standards, Boulder, Colo.); Flynn, T. M.; Grady, T. K.; Waugh, J. S. Physica, 32: 244-51(Feb. 1966).

The proton longitudinal relaxation time, T_1, was measured in dilute solutions of orthohydrogen in parahydrogen over a range of temperature and composition. Below 1.75% orthohydrogen the temperature dependence of T_1 observed at higher concentration is reversed. This fact is interpreted in terms of an anisotropic intermolecular forces which is of longer range for ortho-ortho than for ortho-para pairs, in keeping with previous interpretations of T_1 in the gaseous state. (auth)

30182 A CONTRIBUTION TO THE PROBLEM OF THERMODYNAMIC SIMILARITY OF H_2O AND D_2O. Juza, J.; Kmonicek, V.; Sifner, O.; Schovanec, K. (Inst. of Thermomechanics, Prague). Physica, 32: 362-84(Feb. 1966).

The results of p-v-T measurements of D_2O in the region of 500 to 3500 bar, 80 to 350°C, and the results of measurements of the Joule-Thomson effect of H_2O and D_2O in that of 1.2 to 1.8 bar, 130 to 190°C are reported. An analysis and comparison with data of other investigators indicate that the measurements conducted in the region of high pressures are accompanied by limit errors of ± 15 bar, ± 0.2°C, ± 0.0015 cm^3/g, and that of the Joule-Thomson effect by a limit error of ± 0.03°C/bar. A presentation is made of Jůza's equation of state which very well describes the experimental data of H_2O in the investigated regions. The above information has been used for checking the validity of the Van der Waals theorem of corresponding states in the respective regions. The theorem was found to be valid within the limits of the errors of measurement in the region of the measured Joule-Thomson effect lying in the vicinity of the saturation line. Deviations exceeding the errors of measurement found to exist in the region of high pressures, were expressed in the equation of state by correction terms describing the real values within the limits of the errors of measurement. (auth)

30183 TURBULENT FLOW OF LIQUID METALS IN MAGNETOHYDRODYNAMIC CHANNELS OF CIRCULAR SECTION. Khozhainov, A. I. Zh. Tekh. Fiz., 36: 147-50(Jan. 1966). (In Russian).

A semi-empirical formula is derived for the flow resistance in turbulent magnetohydrodynamic flow in a channel of circular section as a function of the Hartman and Reynolds numbers. Four experimental points obtained previously in a 6.35-mm-diameter channel at Hartman numbers of 79 and 121 are compared with the theoretical formula, and good agreement is shown. Many experimental data on flow resistance at Hartman numbers from 0 to 60 of mercury in a 1-cm diameter tube of circular section with

insulating walls in a transverse magnetic field are presented graphically as a plot of the logarithm of the flow resistance against the logarithm of the Reynolds number and are discussed briefly. At low and moderate Hartman numbers the transition region from laminar to turbulent flow is narrower in tubes of circular section than in tubes of rectangular section. This is ascribed to a specific effect of the corners on the formation of turbulence. (ATD)

30184 ESTIMATES OF THE GREEN'S FUNCTION FOR THE HELMHOLTZ EQUATION. Andronov, V. D. Zh. Vychisl. Mat. Mat. Fiz., 5: 1006-23(Nov.-Dec. 1965). (In Russian).

A study is made of the exterior boundary value problem

$$(\Delta + k^2)U = -\delta(M - M_0),\ \frac{\partial u}{\partial n}\Big|_{M \in S} = 0,\ \sqrt{r}\left(\frac{\partial U}{\partial r} + ikU\right) \to 0 \text{ as}$$

$$\sqrt{x^2 + y^2} = r \to \infty$$

where D is a region bounded by a convex closed contour S of positive curvature and δ is the Dirac delta, $M \notin D + S$. The behavior of the solution as $k \to \infty$ is studied, obtaining an asymptotic formula for the solution of the given problem. (ATD)

30185 ONE-DIMENSIONAL SELF-SIMILAR MOTION OF THERMALLY AND ELECTRICALLY CONDUCTING GAS IN A MAGNETIC FIELD. Volosevich, P. P.; Levanov, E. I. Zh. Vychisl. Mat. Mat. Fiz., 5: 1096-1106(Nov.-Dec. 1965). (In Russian).

The one-dimensional, unsteady motion of an electrically conducting fluid was studied with special emphasis on thermal conductivity properties of the fluid. Both the thermal conductivity coefficient $\varkappa$ and the magnetic viscosity ν_m are assumed to be functions of the temperature and density. The self-similarity variable is given by $\lambda = r/At^n$, and a set of ordinary differential equations is obtained. Various special cases are discussed, such as the radial component of H is set equal to zero, or a sudden isothermal explosion is assumed, and the resulting simplified equations are integrated directly. For H (radial) = 0, the case of a plane piston is considered with a frozen magnetic field. The solution of the resulting equations shows the generation of temperature waves moving ahead of the piston and carrying isothermal magnetic shock waves. The analysis also shows that the magnetic field components, h_z and h_φ, are zero on the piston. (ATD)

30186 FLUCTUATION-DISSIPATION THEOREM AND BROWNIAN MOTION. Kubo, Ryogo (Tokyo Univ.). pp 1-16 of Many-Body Theory. Kubo, Ryogo (ed.). Tokyo, Syokabo Publishing Co. New York, W. A. Benjamin, Inc., 1966.

The relation of the fluctuation-dissipation theorem to a generalized theory of Brownian motion is demonstrated. The simplest example of classical Brownian motion in one dimension is treated. (D.C.W.)

30187 ELEMENTARY EXCITATIONS IN A HOMOGENEOUS BOSE LIQUID, WITH APPLICATION TO He II. Pines, David (Univ. of Illinois, Urbana). pp 36-64 of Many-Body Theory. Kubo, Ryogo (ed.). Tokyo, Syokabo Publishing Co. New York, W. A. Benjamin, Inc., 1966.

A brief survey of the present understanding of elementary excitations in homogeneous Bose liquids, especially in liquid He II, is presented. Some general considerations on excitations in an arbitrary Bose liquid at T = 0 are given, and the excitations found experimentally in He II at low temperatures and in the vicinity of the λ-point are discussed. (G.O.Y.)

30188 PROPERTIES OF LIQUID HELIUM-THREE. Brueckner, Keith A. (Univ. of California, San Diego, La Jolla). (Contract DA-31-124-ARO-D-257. pp 65-72 of Many-Body Theory. Kubo, Ryogo (ed.). Tokyo, Syokabo Publishing Co. New York, W. A. Benjamin, Inc., 1966.

A semi-phenomenological theory of liquid ^{3}He is outlined and is compared with the Landau theory and the Brueckner Gammel theory. The results of calculations of nine liquid properties by the semi-phenomenological theory are compared with experimental observations. (D.C.W.)

30189 NEW FORMULATION OF THE INHOMOGENEOUS ELECTRON GAS PROBLEM. Kohn, W. (Univ. of California, San Diego, La Jolla). pp 73-85 of Many-Body Theory. Kubo, Ryogo (ed.). Tokyo, Syokabo Publishing Co. New York, W. A. Benjamin, Inc., 1966.

An exact formal variational principle for the ground-state energy of an inhomogeneous electron gas in which the density $n(\vec{r})$ is the variable function is derived. Contained in this principle is a universal functional $F[n(\vec{r})]$ which governs the ground state of all electronic systems, regardless of the external potential in which the electrons are moving. The characteristics of this function are discussed at length. A generalization of the formalism to finite temperatures is discussed along with its application to the electronic specific heat of metals. Some elementary excitations in the ground-state "fluid" are also discussed. (G.O.Y.)

30190 STUDY OF NONLINEAR PHENOMENA IN THE PROPAGATION OF ELECTROMAGNETIC WAVES IN A WEAKLY IONIZED GAS [Thesis]. Chan, Tsiu Chiu. Pasadena, Calif., California Inst. of Tech., 1966. 100p.

Nonlinear phenomena in the propagation of electromagnetic waves in a weakly ionized gas externally biased with a magnetostatic field were studied. The study is restricted to the nonlinear phenomena arising from the interaction of electromagnetic waves in the ionized gas. The important effects of nonlinearity are wave-form distortion and generation of mixed frequencies. The wave-form distortion leads to cross modulation of one wave by a second amplitude-modulated wave. The nonlinear effects are assumed to be small so that a perturbation method can be used. Boltzmann's kinetic equation with an appropriate expression for the collision term is solved by expanding the electron distribution function into spherical harmonics in velocity space. In turn, the electron convection current density and the conductivity tensors of the nonlinear ionized gas are found from the distribution function. Finally, the expression for the current density and Maxwell's equations are employed to investigate the effects of nonlinearity on the propagation of electromagnetic waves in the ionized gas, and also on the reflection of waves from an ionized gas of semi-infinite extent. (Dissertation Abstr.)

30191 HALL CURRENTS AND ELECTRON TEMPERATURE EFFECTS IN MHD SHOCK WAVES [Thesis]. Leonard, Brian Phillip. Ithaca, N. Y., Cornell Univ., 1965. 129p.

The steady state structure of magnetohydrodynamic shock waves in a slightly ionized gas is discussed. In this model, the overall viscosity is primarily that of the neutral species, and the magnetic diffusivity is very much greater than both the viscous and thermal diffusivities. These properties lead naturally to the application of a singular perturbation technique for finding the structure of the magnetic layer, in which imbedded viscous and thermal sub-layers may appear in the form of discontinuities. Numerical solutions are obtained for a variety of typical scalar and tensor conductivity cases in which the transport parameters are assumed to be independent of species temperature variation. When the cyclotron frequency is significant compared with the collision frequency, Hall currents give rise to a spiraling magnetic field trajectory, as compared with the scalar conductivity solutions in which the magnetic field always remains in a single plane. The limiting cases of switch-on and switch-off shocks are discussed in addition to typical transverse and fast and slow oblique shocks. Some of the structures studied include a sub-shock at which the overall velocity and temperature exhibit discontinuities although the magnetic field is continuous. In cases not containing a sub-shock all variables are continuous. The criterion for the existence of a sub-shock is that both the upstream (ordinary gasdynamic) Mach number must be greater than unity and the downstream Mach number must be less than unity for a sub-shock to occur in the structure. A preliminary investigation is made of the electron temperature varia-

tion throughout an idealized fast shock containing a sub-shock. Both constant and square root temperature dependent transport parameter models are considered. The mechanisms involved in changing the internal energy of the electrons include compression of the electron gas through the sub-shock, electron thermal diffusion, collision relaxation, and Joule dissipation. When the neutral species is diatomic, very large electron temperatures may result in the electron shock layer, which is always much wider than the viscous sub-shock. Joule heating has the effect of raising the general level of electron temperature throughout the magnetic layer. (Dissertation Abstr.)

30192 PROPERTIES OF LIQUID ^{3}He [Thesis]. Campbell, Laurence Joseph. San Diego, Calif., Univ. of California, 1965. 169p.

It is shown that many of the properties of liquid ^{3}He at the lowest temperatures attained can be understood by introducing a hard-core repulsion into the interaction between ^{3}He atoms and using Brueckner's theory of Fermion systems to determine the ground-state energy. The attractive effects of the ^{3}He potential are extracted from the free scattering phase shifts for the usual 6-12 potential. The various properties are calculated as a function of the hard-core radius r with the result that the velocity of sound (compressibility), symmetry energy (susceptibility), thermal expansion coefficient, viscosity, thermal conductivity, and spin diffusion are all equal to the experimental values for a ± 4% variation of r about 1.8 Å. For this value of r, the binding energy is too positive and the effective mass is too small although both do attain their experimental values for r = 1.1 and 2.0 Å, respectively. The single-particle energy spectrum was chosen to satisfy the Van Hove particle separation theorem and to have a curvature corresponding to the experimental effective mass. The connection of this method with the Landau theory of Fermi liquids is derived and the advantage of the former in calculating the transport properties is explained. A self-consistent calculation of the single-particle energy spectrum using the 6-12 potential is also discussed, and its results are used to support the above one-parameter phenomenological theory. It is also shown how hole-hole interactions can be incorporated into Brueckner's theory and some results of doing so are presented for the case of a Fermi gas with hard-core repulsive interactions. (Dissertation Abstr.)

Geophysics

Refer also to abstract 29532.

30193 (LA–3409(Suppl.)) PROMPT AIR FLUORESCENCE EXCITED BY HIGH-ALTITUDE NUCLEAR EXPLOSIONS. PHOTOELECTRIC INSTRUMENTATION AND THE HIGH-ALTITUDE FLUORESCENCE (HAF), AND HIGH-ALTITUDE RESONANCE ABSORPTION CALCULATION (HARAC) CODES. Bennett, E. W.; Holland, R. F. (Los Alamos Scientific Lab., Univ. of California, N. Mex.). Sept. 1965. Contract W-7405-eng-36. 76p. Dep. mn. CFSTI $3.00 cy, $0.75 mn.

Details of the design, calibration, and use of the photoelectric "log box" detectors used to obtain air fluorescence data are given. Descriptions of the High Altitude Fluorescence (HAF) and High Altitude Resonance Absorption Calculation (HARAC) machine codes are presented. These descriptions are concerned mainly with assumptions, derivations, and some program features of the codes; no coding details are provided. The procedures used to obtain absorption cross sections for use in HARAC are described, including a discussion of the assumptions and the approximation used to account for the rotational structure. The importance of some neglected processes is discussed. (M.O.W.)

30194 (MIT–2241-16) A STUDY OF ENERGY SOURCES FOR THE THERMOSPHERE. Report No. 17. Mahoney, James R. (Massachusetts Inst. of Tech., Cambridge. Dept. of Meteorology). Jan. 15, 1966. Contract AT(30-1)-2241. 232p. Dep. mn. CFSTI $6.00 cy, $1.25 mn.

Thesis.

The importance of various sources and sinks of energy for the thermosphere is investigated in two separate but related studies. In one study a time-dependent model of solar heating, radiational cooling and conductive redistribution of energy from 80 to approximately 500 kilometers is used to investigate the relationships between various specifications of heating rates and resulting changes in thermospheric structure. It is found that the model is highly sensitive to changes in the various heating parameters (solar flux intensity, absorption cross-sections, coefficients of heat conduction and radiative cooling rates), and that the model results agree with the data for the thermosphere only for relatively limited ranges of these parameters. A parallel study of photoionization rates indicates that diurnal changes in neutral atmospheric structure are of primary importance in determining the spatial and temporal profiles of ion production. In the other study several detailed soundings of mesospheric winds (from 30 to 70 kilometers approximately) were used to estimate the magnitude of the vertical energy flux into the lower thermosphere which can be accomplished by small scale traveling wave motions. The analysis is hindered by the smoothing which was applied to the original wind data, but it is likely that the 80 to 105 kilometer region receives more energy by the dissipation of vertically propagating motions than by solar heating and conduction heating from above. (auth)

30195 (NASA-TT–F-389) SPACE RESEARCH. TRANSACTIONS OF THE ALL-UNION CONFERENCE ON SPACE PHYSICS. Skuridin, G. A.; Al'pert, Ya. L.; Krasovskii, V. I.; Shvarev, V. V. (eds.) Translation of Issledovaniya Kosmicheskogo Prostranstva. Trudy Vsesoyuznoy Konferentsii po Fizike Kosmicheskogo Prostranstva. Izdatel'stvo, Nauka, Moscow, June 10–16, 1965. 835p. (CONF-650672). CFSTI $8.35 cy, $3.50 mn.

Separate abstracts are prepared for 35 of the 82 papers presented. One paper was previously included in NSA as 20: 6209. 46 papers were in summary form and were not abstracted for NSA. (B.G.D.)

For abstracts of individual papers see: 29532, 29874, 29875, 29954–29957, and 30196–30223.

30196 (NASA-TT–F-389, pp 8-25) CERTAIN PROBLEMS OF UPPER ATMOSPHERE PHYSICS AND SPACE NEAR THE EARTH. Krasovskii, V. I. Translated from Issledovaniya Kosmicheskogo Prostranstva. Trudy Vsesoyuznoy Konferentsii po Fizike Kosmicheskogo Prostranstva. Izdatel'stvo, Nauka, Moscow, June 10–16, 1965.

A summary is presented on the phenomena related to the physics of the upper atmosphere and space near the earth. Some of the topics discussed are warming and circulation of the atmosphere, photochemical conversions and ionization, atmospheric emissions, atomic and allotropic composition, periodic and sporadic geomagnetic variations, aurorae polaris and outer corpuscular streams, and particularly the phenomenon of radiation zones or bands. (B.G.D.)

30197 (NASA-TT–F-389, pp 166-201) ALTITUDINAL-TIME DISTRIBUTION OF THE ELECTRON CONCENTRATION AND NONUNIFORM FORMATIONS OF THE OUTER IONOSPHERE. Al'pert, Ya. L.; Sinel'nikov, V. M. Translated from Issledovaniya Kosmicheskogo Prostranstva. Trudy Vsesoyuznoy Konferentsii po Fizike Kosmicheskogo Prostranstva. Izdatel'stvo, Nauka, Moscow, June 10–16, 1965.

Experimental results from studying the ionosphere by means of coherent radio waves emitted from an artificial earth satellite are presented. The difference, measured in these experiments, between Doppler frequency shifts of two coherent radio waves at any point on the earth's surface is directly related to the velocity components of the emitter, the electron concentration of the ionosphere, and its spatial-time changes. (B.G.D.)

30198 (NASA-TT-F-389, pp 202-24) BRIEF SURVEY OF THE RESULTS OF PHYSICAL EXPERIMENTS ON THE SATELLITE "KOSMOS-2" IN THE IONOSPHERE. Afonin,

V. V.; Breus, T. K.; Gdalevich, G. L.; Gorozhankin, B. N.; Gringauz, K. I.; Rybchinskii, R. E.; Shyutte, N. M. Translated from Issledovaniya Kosmicheskogo Prostranstva. Trudy Vsesoyuznoy Konferentsii po Fizike Kosmicheskogo Prostranstva. Izdatel'stvo, Nauka, Moscow, June 10–16, 1965.

A summary is presented of the experimental results obtained from the satellite Kosmos-2. In the latitude region from 49°N to 49°S and in the altitude range from ~212 to ~1550 km, the concentration of positive ions was measured. At altitudes from ~212 to ~600 km electron concentration and temperature were measured using Langmuir probes. Positive ion temperatures were determined with honeycomb-type ion traps. Data were obtained on the variations in photo emission from metals undergoing shortwave solar radiation in the altitude range close to the ionization peak of the f region of the ionosphere. The variations permitted estimation of the integral absorption of solar ultraviolet radiation in this ionospheric region. The orientation of a space vehicle relative to its velocity vector was determined by means of ion sensors. (B.G.D.)

30199 (NASA-TT-F-389, pp 248-58) ROCKET DATA ON THE BEHAVIOR OF ELECTRON CONCENTRATION IN THE IONOSPHERE AT ALTITUDES OF 100-300 km. Kazachevskaya, T. V.; Ivanov-Kholodnyi, G. S. Translated from Issledovaniya Kosmicheskogo Prostranstva. Trudy Vsesoyuznoy Konferentsii po Fizike Kosmicheskogo Prostranstva. Izdatel'stvo, Nauka, Moscow, June 10–16, 1965.

An attempt to draw conclusions regarding the laws followed by electron concentration changes (n_e) at altitudes of 100–300 km, based only on the results of direct rocket probes of the ionosphere is presented. All the results from rocket measurements of n_e were compared at different moments for different seasons. (B.G.D.)

30200 (NASA-TT-F-389, pp 273-6) ONE ANOMALY IN ELECTRON PITCH-DISTRIBUTIONS. Vaysberg, O. L.; Shuyskaya, F. K. Translated from Issledovaniya Kosmicheskogo Prostranstva. Trudy Vsesoyuznoy Konferentsii po Fizike Kosmicheskogo Prostranstva. Izdatel'stvo, Nauka, Moscow, June 10–16, 1965.

The satellite Kosmos-5 carried narrow-beam charged particle sensors for recording a directional intensity of electrons with energies >40 Mev. The satellite was not oriented, and rotated around its own axis, which was approximately perpendicular to the sensor axes. Employing the readings of the solar orientation recorders and the sensor data as supplementary readings, the orientation of these sensors was determined for 5 revolutions. The dependence of the directional intensity of electrons upon pitch angle for each time the plane perpendicular to the force line was intersected by the sensors was determined. (B.G.D.)

30201 (NASA-TT-F-389, pp 277-81) VARIATIONS IN THE SOFT COMPONENT OF THE ELECTRON ENERGY SPECTRUM. Mulyarchik, T. M. Translated from Issledovaniya Kosmicheskogo Prostranstva. Trudy Vsesoyuznoy Konferentsii po Fizike Kosmicheskogo Prostranstva. Izdatel'stvo, Nauka, Moscow, June 10–16, 1965.

An increase in electron energy recorded due to accelerating voltages in electron sensors carried on the satellites Kosmos-3 and Kosmos-5 leads to signal increase (positive modulation) for an energy of ≤30 kev and to signal decrease (negative modulation) for 50–150 kev energies. By combining the ratio of three sensor signals with the sign and magnitude of the modulation, the energy spectrum of the electrons recorded can be determined. (B.G.D.)

30202 (NASA-TT-F-389, pp 281-7) SPATIAL DISTRIBUTION OF DIFFERENT GROUPS OF TRAPPED CORPUSCLES BASED ON DATA FROM THE SATELLITES "KOSMOS-3" AND "KOSMOS-5." Temnyi, V. V. Translated from Issledovaniya Kosmicheskogo Prostranstva. Trudy Vsesoyuznoy Konferentsii po Fizike Kosmicheskogo Prostranstva. Izdatel'stvo, Nauka, Moscow, June 10–16, 1965.

From data obtained on satellites Kosmos-3 and Kosmos-5 envelopes were compiled in order to study the distribution of particle streams recorded. The envelopes determine the continuous change in trapped particle streams along the satellite's orbit. (B.G.D.)

30203 (NASA-TT-F-389, pp 288-91) MEASUREMENT OF SOFT ELECTRON STREAMS IN THE UPPER ATMOSPHERE AT ALTITUDES TO 500 km. Antonova, L. A.; Kazachevskaya, T. V. Translated from Issledovaniya Kosmicheskogo Prostranstva. Trudy Vsesoyuznoy Konferentsii po Fizike Kosmicheskogo Prostranstva. Izdatel'stvo, Nauka, Moscow, June 10–16, 1965.

Experiments are described which measure the streams of very soft electrons with energies of less than 0.1 kev in the upper atmosphere. Two methods that were used for these measurements were an open-type secondary-electron multiplier and a thermoluminescent phosphor $CaSO_4$(Mn) device which has valuable properties permitting absolute measurements in the shortwave region of the spectrum below 1350 Å. (B.G.D.)

30204 (NASA-TT-F-389, pp 375-86) STATE OF AND PROSPECTS FOR STUDYING THE RADIATION ZONES OF THE EARTH. Vernov, S. N. Translated from Issledovaniya Kosmicheskogo Prostranstva. Trudy Vsesoyuznoy Konferentsii po Fizike Kosmicheskogo Prostranstva. Izdatel'stvo, Nauka, Moscow, June 10–16, 1965.

A summary is presented on the present status of information regarding the radiation zones of the earth. The results of data acquired from satellites are discussed. The data include measurements on electron and proton energy, spatial, and time distribution and intensity variations through the radiation zones. The effects of solar wind are considered. The mechanism of accelerating particles in radiation zones is also considered. (B.G.D.)

30205 (NASA-TT-F-389, pp 386-425) PENETRATION PROCESSES INTO THE MAGNETOSPHERE OF THE EARTH, CAPTURE AND ACCELERATION OF SOLAR STREAM PARTICLES, AND THEIR ROLE IN THE DYNAMICS OF THE GEOMAGNETIC TRAP. Pletnev, V. D.; Skuridin, G. A.; Shalitov, V. P.; Shvachvonov, I. N. Translated from Issledovaniya Kosmicheskogo Prostranstva. Trudy Vsesoyuznoy Konferentsii po Fizike Kosmicheskogo Prostranstva. Izdatel'stvo, Nauka, Moscow, June 10–16, 1965.

A survey of recent studies which investigated the interconnection between geophysical phenomena occurring in circumterrestrial cosmic space from the point of view of the dynamics of a geomagnetic trap is presented. Topics discussed are the motion of charged particles in the magnetosphere (modified problem of Störmer), penetration of charged particles within the magnetosphere in the vicinity of neutral points, and capture of charged particles in the geomagnetic trap and their acceleration during the inverse phase of a magnetic storm. (B.G.D.)

30206 (NASA-TT-F-389, pp 426-42) ANOMALOUS DIFFUSION OF CHARGED PARTICLES IN THE RADIATION ZONES OF THE EARTH. Tverskoy, B. A. Translated from Issledovaniya Kosmicheskogo Prostranstva. Trudy Vsesoyuznoy Konferentsii po Fizike Kosmicheskogo Prostranstva. Izdatel'stvo, Nauka, Moscow, June 10–16, 1965.

The analysis of experimental data shows that the radiation zones of the earth contains several groups of rapid particles which differ in terms of their composition, energy spectrum, spatial distribution, and variations in time. These groups are soft electrons, heavy electrons in the outer zone, protons of the inner zone, and protons of the outer zone (including hard protons). It is shown that the basic mechanism by which electrons and protons are accelerated in the outer zone, and also the mechanism by which the inner zone is formed, is the transfer of particles across the drift envelopes. (B.G.D.)

30207 (NASA-TT-F-389, pp 442-53) THE FORMATION OF RADIATION ZONES AS A RESULT OF PARTICLE DRIFT IN THE DEPTHS OF THE MAGNETOSPHERE. Antonova, A. E.; Ershkovich, A. I.; Shabanskii, V. P. Translated from Issledovaniya Kosmicheskogo Prostranstva. Trudy Vsesoyuznoy Konferentsii po Fizike Kosmicheskogo Prostranstva. Izdatel'stvo, Nauka, Moscow, June 10–16, 1965.

The spatial distribution of particle intensity in the magnetosphere is considered by solving an equation of continuity, assigning definite mechanisms to the formation and destruction of particles. (B.G.D.)

30208 (NASA-TT-F-389, pp 457-63) COMPARISON OF SIMULTANEOUS MEASUREMENTS OF THE MAGNETIC FIELD AND POSITIVE ION STREAMS WITHIN THE EARTH'S MAGNETOSPHERE, PERFORMED ON THE SATELLITE "ELEKTRON-2." Gringauz, K. I.; Dolginov, Sh. Sh.; Bezrukikh, V. V.; Eroshenko, E. G.; Zhuzgov, L. N.; Musatov, L. S.; Solomatina, E. K.; Fastovskii, U. V. Translated from Issledovaniya Kosmicheskogo Prostranstva. Trudy Vsesoyuznoy Konferentsii po Fizike Kosmicheskogo Prostranstva. Izdatel'stvo, Nauka, Moscow, June 10–16, 1965.

The results derived from comparing data from several measurements performed with the charged particle trap and the magnetometer on the Elektron-2 satellite, as well as the K_p-indices characterizing the geomagnetic field perturbation based on data from simultaneous measurements performed at magnetic observations on the Earth are presented. This comparison indicates that there is a correlation between changes in the magnetic activity on the Earth's surface and changes in the geomagnetic field strength and positive ion streams at great distances from the Earth, within its magnetosphere, during the initial flight period of the satellite. (B.G.D.)

30209 (NASA-TT-F-389, pp 464-82) INVESTIGATION OF THE EARTH'S MAGNETOSPHERE IN THE RADIATION ZONE REGION (3-6R_E), FEBRUARY–APRIL 1964. Dolginov, Sh. Sh.; Eroshenko, E. G.; Zhuzgov, L. N. Translated from Issledovaniya Kosmicheskogo Prostranstva. Trudy Vsesoyuznoy Konferentsii po Fizike Kosmicheskogo Prostranstva. Izdatel'stvo, Nauk, Moscow, June 10–16, 1965.

Systematic measurements of the magnetosphere at distances of 3–6 R_E in the space of the outer radiation belt were acquired from the satellite Elektron-2. These measurements indicate that there is a quiet-day outer magnetic field associated with protons and electrons of the radiation zones. (B.G.D.)

30210 (NASA-TT-F-389, pp 499-517) STRUCTURE OF THE SOLAR CORPUSCULAR STREAM AND ITS INTERACTION WITH THE MAGNETOSPHERE OF THE EARTH. Kalinin, Yu. D.; Mogilevskii, E. I. Translated from Issledovaniya Kosmicheskogo Prostranstva. Trudy Vsesoyuznoy Konferentsii po Fizike Kosmicheskogo Prostranstva. Izdatel'stvo, Nauka, Moscow, June 10–16, 1965.

The manner in which the solar corpuscular stream transmits energy to the magnetosphere of the earth is discussed by comparison of probe and terrestrial observations. (B.G.D.)

30211 (NASA-TT-F-389, pp 535-50) RESULTS DERIVED FROM STUDYING THE GEOMETRIC POSITION AND PARTICLE COMPOSITION OF RADIATION ZONES OF THE EARTH BASED ON DATA FROM THE SATELLITES "ELEKTRON" AND "ELEKTRON-2." Vernov, S. N.; Chudakov, A. E.; Vakulov, P. V.; (and others). Translated from Issledovaniya Kosmicheskogo Prostranstva. Trudy Vsesoyuznoy Konferentsii po Fizike Kosmicheskogo Prostranstva. Izdatel'stvo, Nauka, Moscow, June 10–16, 1965.

Experimental results obtained on the quiet state of the radiation zones by the satellites Elektron-1 and -2 during February 1964 are presented. The analysis of these results was divided into the inner, intermediate, and outer regions encompassing the zone of spatial distribution of trapped radiation. (B.G.D.)

30212 (NASA-TT-F-389, pp 551-66) PRELIMINARY RESULTS DERIVED FROM CORPUSCLE INVESTIGATIONS ON THE SATELLITE "ELEKTRON-1." Bolyunova, A. D.; Vaysberg, O. L.; Gal'perin, Yu. I.; Potapov, B. P.; Temnyi, V. V.; Shuyskaya, F. K. Translated from Issledovaniya Kosmicheskogo Prostranstva. Trudy Vsesoyuznoy Konferentsii po Fizike Kosmicheskogo Prostranstva. Izdatel'stvo, Nauka, Moscow, June 10–16, 1965.

Preliminary results on the spatial distribution of soft and hard electrons and soft protons trapped by the geomagnetic field detected by the Electron-1 Satellite are presented. (B.G.D.)

30213 (NASA-TT-F-389, pp 566-8) POSSIBLE EXISTENCE OF A SOFT ELECTRON COMPONENT IN THE OUTER RADIATION ZONE AND ITS VARIATIONS. Bezrukikh, V. V.; Gringauz, K. I.; Musamov, L. S.; Solomatina, E. K. Translated from Issledovaniya Kosmicheskogo Prostranstva. Trudy Vsesoyuznoy Konferentsii po Fizike Kosmicheskogo Prostranstva. Izdatel'stvo, Nauka, Moscow, June 10–16, 1965.

A portion of the experimental results derived from measuring charged particle streams on the satellite Electron-2 by means of a charge particle trap is presented. (B.G.D.)

30214 (NASA-TT-F-389, pp 569-75) TIME CHANGES IN THE OUTER RADIATION ZONE OF THE EARTH BASED ON DATA FROM THE "ELEKTRON" SATELLITES. Kuznetsov, S. N.; Sosnovets, E. N.; Stolpovskii, V. G. Translated from Issledovaniya Kosmicheskogo Prostranstva. Trudy Vsesoyuznoy Konferentsii po Fizike Kosmicheskogo Prostranstva. Izdatel'stvo, Nauka, Moscow, June 10–16, 1965.

The outer radiation belt intensity variations on the nocturnal side of the earth are discussed by analysis of the experimental results from the Elektron-2 Satellite. (B.G.D.)

30215 (NASA-TT-F-389, pp 576-87) IRREGULAR HIGH-ENERGY ELECTRON STREAMS NEAR THE BOUNDARY OF THE RADIATION ZONES OF THE EARTH. Vernov, S. N.; Chudakov, A. E.; Vakulov, P. V.; Kuznetsov, S. N.; Logachev, Yu. I.; Sosnovets, E. N.; Stolpovskii, V. G. Translated from Issledovaniya Kosmicheskogo Prostranstva. Trudy Vsesoyuznoy Konferentsii po Fizike Kosmicheskogo Prostranstva. Izdatel'stvo, Nauka, Moscow, June 10–16, 1965.

The simultaneous study of high energy electron streams in the outer regions of the Van Allen radiation belts by the satellites Elektron-1 and Elektron-2 is discussed. (B.G.D.)

30216 (NASA-TT-F-389, pp 588-606) STUDY OF THE EARTH'S OUTER RADIATION ZONE AT LOW ALTITUDES DURING SPACECRAFT-SATELLITE FLIGHTS AND THE "KOSMOS" AES FLIGHTS BETWEEN 1960 AND 1963. Vernov, S, N.; Nesterov, V. E.; Pisarenko, N. F.; Savenko, I. A.; Tverskaya, L. V.; Shavrin, P. I. Translated from Issledovaniya Kosmicheskogo Prostranstva. Trudy Vsesoyuznoy Konferentsii po Fizike Kosmicheskogo Prostranstva. Izdatel'stvo, Nauka, Moscow, June 10–16, 1965.

The experimental results derived from the cosmic spacecraft-satellites and satellites in the Kosmos series pertaining to longitudinal intensity behavior, position of the outer radiation zone maximum, time variations, the space between radiation zones, and escapes from the outer radiation zones based on measurements at low altitudes are presented. (B.G.D.)

30217 (NASA-TT-F-389, pp 607-15) STUDY OF THE INNER AND ARTIFICIAL RADIATION ZONES OF THE EARTH AT LOW ALTITUDES IN 1960–1964. Nesterov, V. E.; Pisarenko, N. F.; Savenko, I. A.; Tel'tsov, M. V.; Shavrin, P. I.; Sharvina, K. N. Translated from Issledovaniya Kosmicheskogo Prostranstva. Trudy Vsesoyuznoy Konferentsii po Fizike Kosmicheskogo Prostranstva. Izdatel'stvo, Nauka, Moscow, June 10–16, 1965.

An analysis of experimental data obtained from the second and third satellites in 1960 and space crafts of the Kosmos series is presented. These results included data on the artificial zone off the coast of Brazil. The data included longitudinal behavior, spatial and time distributions and lifetimes of electrons and protons. (B.G.D.)

30218 (NASA-TT-F-389, pp 616-23) OUTER RADIATION ZONE OF THE EARTH AND BURSTS OF X-RAY RADIATION IN THE STRATOSPHERE. Vernov, S. N.; Lazutin, L. L.; Charakhich'yan, A. N.; Charakhch'yan, T. N. Translated from Issledovaniya Kosmicheskogo Prostranstva. Trudy Vsesoyuznoy Konferentsii po Fizike Kosmicheskogo Prostranstva. Izdatel'stvo, Nauka, Moscow, June 10–16, 1965.

A discussion is presented on the production of photons of braking radiation from electrons entering the upper atmosphere in an air layer of approximately 10–100 mg. An attempt to clarify the mechanisms by which electrons leave the radiation zones as a result of perturbations occurring in it is also presented. (B.G.D.)

30219 (NASA-TT-F-389 pp 623-9) MEASUREMENT RESULTS ON THE SATELLITE "KOSMOS-41" IN THE OUTER RADIATION ZONE. Vernov, S. N.; Savenko, I. A.; Tel'tsov, M. V.; Shavrin, P. I. Translated from Issledovaniya Kosmicheskogo Prostranstva. Trudy Vsesoyuznoy Konferentsii po Fizike Kosmicheskogo Prostranstva. Izdatel'stvo, Nauka, Moscow, June 10–16, 1965.

Measurement results of electron and proton distribution in radiation zones of the earth from radiometric apparatus carried by Kosmos-41 Satellite are presented. (B.G.D.)

30220 (NASA-TT-F-389, pp 633-52) THE OUTERMOST ZONE OF CHARGED PARTICLES. Gringauz, K. I.; Khokhlov, M. Z. Translated from Issledovaniya Kosmicheskogo Prostranstva. Trudy Vsesoyuznoy Konferentsii po Fizike Kosmicheskogo Prostranstva. Izdatel'stvo, Nauka, Moscow, June 10–16, 1965.

The results derived from studying zones of charged particles with comparatively low energies (from ~100 ev to 10–40 kev) located beyond the outer radiation zone are examined (including new data obtained from the satellites Elektron-2 and the space rocket Zond-2). (B.G.D.)

30221 (NASA-TT-F-389, pp 741-57) INTERPRETATION OF RADIATION DATA FROM METEOROLOGICAL SATELLITES. Kondrat'ev, K. Ya. Translated from Issledovaniya Kosmicheskogo Prostranstva. Trudy Vsesoyuznoy Konferentsii po Fizike Kosmicheskogo Prostranstva. Izdatel'stvo, Nauka, Moscow, June 10–16, 1965.

A survey of radiation data in satellite meteorology which have practical applications is presented. From these data investigation of problems such as energetics of atmospheric processes, identification of cloudiness, cloud temperatures and altitudes, troposphere humidity, and vertical movements in cloudiness can be attempted. (B.G.D.)

30222 (NASA-TT-F-389, pp 758-63) RADIATION SAFETY PROBLEMS IN SPACE FLIGHTS. Nesterov, V. E.; Pisarenko, N. F.; Savenko, I. A.; Shavrin, P. I. Translated from Issledovaniya Kosmicheskogo Prostranstva. Trudy Vsesoyuznoy Konferentsii po Fizike Kosmicheskogo Prostranstva. Izdatel'stvo, Nauka, Moscow, June 10–16, 1965.

A review of the three basic radiation dangers in space flights caused by primary cosmic radiation, radiation of the earth's radiation belts, and radiation generated during major chromospheric flares on the sun is presented. (B.G.D.)

30223 (NASA-TT-F-389, pp 817-21) INFLUENCE OF SATELLITES ON RADIATION INTENSITY IN THE RADIATION ZONES. Vakulov, P. V. Translated from Issledovaniya Kosmicheskogo Prostranstva. Trudy Vsesoyuznoy Konferentsii po Fizike Kosmicheskogo Prostranstva. Izdatel'stvo, Nauka, Moscow, June 10–16, 1965.

An investigation of the effect of satellites on the destruction of radiation zone particles is presented. The size of the satellite is determined which will appreciably decrease the number of particles. (B.G.D.)

30224 THE ASYMMETRICAL CONFIGURATION OF THE TRAPPED REGION AND SOME CORRELATED AERONOMICAL PHENOMENA. Shu, Yung-Lan; Hsieh, Liu-Hsiang (Institute of Geophysics and Meteorology, Shanghai). Acta Geophys. Sinica, 14: 73-84(June 1965). (In Chinese).

A study is made of the motions of the charged particles in a deformed magnetosphere in conjunction with certain asymmetrical phenomena. Under the action of the solar wind the magnetosphere boundary is generally deformed like a falling water drop. Because of the complexity of the motion of charged particles in a deformed magnetic field, the discussion is limited to the drifting surface with constant β defined by the guiding center of the drifting particles. The result of the calculation shows that the three-dimensional configuration of the trapped regions inside the magnetosphere is asymmetric with respect to the magnetic axis. The frontal part facing the sun is much larger than the rear. The results of the calculations are compared with the data of Explorer XIV, Injun I, Injun III, and the diurnal variation of auroras. The results are in good agreement with the experiments. The mean daily variation of the K index of 31 high-latitude stations were calculated for the relatively quiet magnetic period in the years 1957 through 1958. All of the data demonstrate the asymmetrical characteristics of the correlated phenomena inside the magnetosphere. (auth)

30225 QUESTION OF ANOMALOUS ABSORPTION IN THE POLAR CAP. Gachechiladze, R. G.; Khocholava, G. M. (Institut Geofiziki, Tiflis, Georgian SSR). Akad. Nauk Gruz. SSR, Soobshch., 39: 555-60(Sept. 1965). (In Russian).

Investigation of anomalous absorption occurring in the polar-cap regions during the chromospheric flare of July 7, 1958, is discussed. This absorption is attributed to a combination of high-energy protons and a lower-energy corpuscular flux. The anomalous ionization at altitudes from 60 to 70 km is calculated and found to be of the order of 1.8×10^3 cm^{-3}. Maps of the Δf_0F2 isolines are plotted for the purpose of studying the dynamics of the ionospheric perturbation in the F2 layer. (Int. Aerospace Abstr.)

30226 A NEW METHOD OF FORECASTING GEOMAGNETIC ACTIVITY AND ITS PRACTICAL TRY-OUT. Bednarova-Novakova, Bohumila (Czechoslovak Academy of Sciences, Prague). Geofysik. Sb., 12: 277-333(1964).

A description of a method for forecasting geomagnetic activity based on a detailed examination of the fine chromospheric structure and filaments in the sun as an indicator of the magnetic conditions in the layers is given. The method assumes 15 hypotheses concerning the behavior of filaments, coronal splitting, and cylindrical coronal formation. A table is presented in which 300 forecasts based on this method are listed and the results analyzed. Out of 445 days for which geomagnetic forecasts were made, 417 days or 94% were successful. (Int. Aerospace Abstr.)

30227 EFFECT OF NUCLEAR EXPLOSIONS ON THE ATMOSPHERIC POTENTIAL GRADIENT NEAR THE GROUND. Agarwala, K. S. Indian J. Meteorol. Geophys., 15: 437-8(1964).

Available data for the atmospheric potential gradient near the ground at Colaba (Bombay) and Poona were studied and discussed with reference to the ground deposition levels of mixed fission products in order to find out possible variations of the atmospheric potential gradient caused by nuclear explosions. There was no secular change in the atmospheric potential gradient due to nuclear explosions. This evidence is in disagreement with that from certain stations in Europe. (Indian Sci. Abstr.)

30228 EFFECT OF NUCLEAR EXPLOSIONS UPON THE IONOSPHERE. Mitra, S. N.; Sen Gupta, P. R. (AIR, New Delhi). J. Inst. Telecomm. Eng., 10: 323-40(1964).

An attempt was made to find out whether nuclear explosions (5 megatons and above) carried out by the USSR at Novaya Zemlya (75°N, 60°E) during 1961 and 1962 produced any noticeable effect upon the ionosphere. An analysis of hourly values of f_0F_2, following a nuclear detonation, given by 40 widely separated ionosonde stations situated on different geomagnetic and geographical coordinates revealed an isotropic spread, up to a distance of 8000 km from the source, of a disturbance-pattern in the shape of increase in electron density. The speed of the spread in the F_2-layer was found to lie between 230 and 580 m/sec, the most probable speed being 355 m/sec. Analysis of records of long-wave field strength continuously recorded at Delhi of Radio Tashkent on 164 kc/sec showed that a similar disturbance occurred in the D-region and the speed of propagation of this disturbance was found to lie between 390 and 1320 m/sec. A plausible explanation of the higher speed of the disturbance observed from analysis of the long-wave record is indicated. Out of 20 events for which long-wave records are avail-

able, effects of 13 events could be clearly seen. Marked relations between the intensity of the explosion and the relative increase in long-wave signal in db appeared to exist. Thus, the long-wave experiment appears to offer a reliable technique of obtaining information about nuclear detonations in the atmosphere and their intensities. In three instances a clear effect of the nuclear detonation on cosmic noise absorption (18.9 Mc/sec) was observed. (Indian Sci. Abstr.)

30229 OBSERVATIONS OF GEOMAGNETIC AND EARTH-CURRENT MICROPULSATIONS WITH PERIODS OF ABOUT 1 CPS. I. ON THE OBSERVING APPARATUS OF GEOMAGNETIC MICROPULSATIONS. Kawamura, Makoto; Kashiwabara, Shizuo Kakioka Magnet. Observ., Mem., 12: No. 1, 1-13(1965).

As one of the IQSY program observations of geomagnetic and earth-current micropulsations with periods ranging between 0.2 and 10 seconds were planned. The observing apparatus of short-period geomagnetic mircopulsations, pc-1, pc-2 and the shorter side of pi-1 (≤10 sec) are described. Those apparatus were installed at Memambetsu (43°55′N, 144°12′E) and Kanoya (31°25′N, 130°53′E) and used for continuous observations. (auth)

30230 DEVELOPMENT OF POLAR GEOMAGNETIC DISTURBANCE AND PCA EVENT ON FEBRUARY 11, 1958. Nagai, M. (Kakioka Magnetic Observatory, Ibaraki, Japan); Hakura, Y. Kakioka Magnet. Observ., Mem., 12: No. 1, 15-48(1965).

An investigation was made on the development of ionospheric and geomagnetic storms caused by solar corpuscular clouds emitted from a major flare that appeared at 21:08 UT on February 9, 1958. Several interesting characteristics are discussed in the analysis on the relation between the world-wide patterns of ionospheric disturbances and the corresponding current systems of geomagnetic storms, such as simultaneous occurrence of a peculiar polar disturbance with sudden development of PCA in the auroral zone far preceding the sudden commencement and appearance of the transient stage removed from S_p^q-field to DP(Pre SC)-field, unusual increase of ionization right before the onset of the sudden commencement over the whole polar cap, outstanding two-stepped expansions of the region of polar cap blackouts and equivalent current systems of two successive sudden commencements, and variations of directions of the straight currents flowing in the central part of the polar cap. (auth)

30231 MORPHOLOGICAL STUDY ON SUDDEN COMMENCEMENTS OF MAGNETIC STORMS AND SUDDEN IMPULSES. [PART] IV. Sano, Yukizo Kakioka Magnet. Observ., Mem., 12: No. 1, 55-76(1965).

The results of the morphological study on sudden impulses, si's, concerning a few characteristics of the horizontal disturbance vector changes in high latitudes, and their individual equivalent current systems at several successive stages are presented. These results are compared with the morphology of sudden commencements of magnetic storms, ssc's, which is obtained in previous work. It is found that si's differ slightly from ssc's in a character concerning the occurrence distribution of the polarity of the vector change, but are quite similar in the other characters. Various kinds of equivalent current systems of si's which show some great different features from each other are found. Of course, the ones which show a pronounced similarity to those of ssc's are also found. (auth)

30232 INVERTED SC IN THE LOW LATITUDE REGIONS. Yamaguchi, Yushin. Kakioka Magnet. Observ., Mem., 12: No. 1, 77-103(1965).

In the low and middle latitudes, the horizontal component of the main impulse of SC's usually increases. But, from some observatories, SC's of the decreasing horizontal component (inverted SC) are reported, though their frequencies are very small. The two inverted SC, observed at rather more observatories in the low and middle latitudes are examined somewhat in detail. The results show that one at 04h 59m, April 2nd, 1958 is a s.f.e. and the other at 07h 18m, Jan. 10th, 1960 would be better classified as Si (magnetic sudden impulse). The suitable classification of the rapid variations is often difficult, based on the record of only one station and this examination is made by means of the world wide data. It is suggested that the horizontal component of the main impulse of SC may always increase in the low latitude regions near Kakioka. (auth)

30233 RECORDS OF FISSION-GENERATED γ RADIATION DURING THE HIGH-ALTITUDE EXPLOSION OF JULY 9, 1962, OVER JOHNSTON ISLAND. Kukushkin, Yu. V.; Strelkov, A. S. Kosm. Issled., 4: 105-10(Jan.-Feb. 1966). (In Russian).

On the basis of the physical picture of the development of the cloud from the high-altitude nuclear burst and the movement of the charged gamma- and beta-active fission fragments captured in the geomagnetic field it is shown that the phenomenon of gamma-glow, observed during the American nuclear blast of July 9, 1962, on the Cosmos-5 satellite, can be explained by gamma emission of the fragments rising above the horizon. It is also shown that the observed effect can not be caused by radiation from the nuclear blast if the source is below the horizon. (tr-auth)

30234 ON RADIOACTIVITY OF COSMOS III AFTER THE EXPLOSION OF JULY 9, 1962. Bolyunova, A. D. Kosm. Issled., 4: 167-9(Jan.-Feb. 1966). (In Russian).

At the time of the July 9, 1962, thermonuclear explosion 400 km above Johnston Island, Cosmos-3 was at 600 km altitude, 44°S lat, and 3.1°W long. Six hr after the explosion, the satellite passed within 550 km of Johnston Island. About one full day after the explosion, the recording apparatus was switched on, and the radioactivity was measured to be about 2.6 times the average value for position and height (about 230 km). Results are given of the G-M count rates of the satellites Cosmos-3, Explorer-7, and Cosmos-17 as functions of L and of the decay of the excess count rate over cosmic-ray background for Cosmos-3 and Cosmos-5. The excess count rate measured on Cosmos-3 was found to be independent of longitude, magnetic-field intensity, L, and cosmic-ray background. The results suggest that the radiation source was either very widespread or was on the satellite itself; it is possible that the satellite picked up radioactive products in the contaminated upper atmosphere. (M.J.T.)

30235 STUDY OF THE RADIATION INTENSITY IN THE EARTH'S RADIATION BELTS BY THE COSMOS-17 SATELLITE. Kirdina, G. A.; Kulagin, Yu. M.; Malyshev, A. B.; Nazarova, M. N.; Svidskii, P. M.; Yudkevich, I. S. Kosm. Issled., 4: 257-67(Mar.-Apr. 1966). (In Russian).

Data are presented on the charged-particle fluxes in the earth's radiation belts, recorded by Geiger and scintillation counters at altitudes of 260 to 780 km from May 22 to 30, 1963. It was established that, according to the composition of the particles traversing a screen of ~1 g/cm^2, the inner radiation belt can be divided into two regions: at L from 1.15 to 1.6 the basic part of the flux is composed of electrons from nuclear explosions, and at L from 1.6 to 2.5, of protons. The flux of protons with energies $E_p > 30$ Mev has increased since 1958. In the space between the inner and outer radiation belts a narrow region was detected in which electrons with energies of $0.1 \leq E_0 \leq 1.5$ Mev were recorded. Stable fluxes of soft particles, apparently electrons with energies from 50 to 100 kev, were observed below the lower boundary of the inner belt. (tr-auth)

30236 MAGNETOMETRIC APPARATUS OF THE ELECTRON-2 SPACE STATION. Aleksanyan, L. M.; Eroshenko, E. G.; Zhuzgov, L. N.; Fastovskii, U. V. Kosm. Issled., 4: 302-10(Mar.-Apr. 1966). (In Russian).

A description is given of two three-component search-coil magnetometers with differing sensitivity, set up on the satellite Electron-2. The meteorological characteristics of the apparatus are presented, and an estimation of the accuracy of measurements of the earth's magnetic field at distances from 3 to 11.67 R_E is carried out. (tr-auth)

30237 SOLAR ACTIVITY AND PRESSURE VARIATIONS IN THE TROPOSPHERE. Kubyshkin, V. V. (Volgograd Pedagogical Inst.). Soviet Astron. AJ (Engl. Transl.), 9: 606-16(Jan.-Feb. 1966).

Translated from Astron. Zh., 42: 784-97(July-Aug. 1965).

A further development is made for investigations reported previously. The results of the study, based on application of the superposition-of-epochs method, are shown. Figures were constructed for "reference" meteorological stations for which data are available for the 14th-18th cycles of solar activity. All flocculi were used without separation into "working" and "nonworking" flocculi. Curves II_{un} corresponding to flocculi situated in the "unfavorable" solar hemisphere and those corresponding to "central" flocculi, for which $\Delta L_c \geq 7^d$ are given. The relations represented and especially the S.C. show an identical picture: virtually constant atmospheric pressure for flocculi of group II_{un} and a clearly expressed pressure maximum at the phase $\Delta t \approx 6^d$ for the flocculi of groups I and I_γ. As a result of the decreased role of the effects of successive disturbances, the I_γ curves in all cases indicate a considerably greater amplitude of pressure increase than the I curves. Curves are given for the change (increase) of atmospheric pressure occurring after the appearance of a chromospheric flare. A list of the flares used is given. This list is based on study and contains the clearest cases, when the mutual superposing of successive geomagnetic disturbances is minimal. The meteorological stations used for study of the pressure effect are divided into five groups on the basis of geographical and other considerations. A composite is made for all 28 stations and all flares. Here, as in all cases, there is a pressure increase, but the maximum is at the phase $+3^d - 4^d$, which coincides with geomagnetic data. Thus, the results of this study, based on a considerable amount of uniform data, confirm the conclusions drawn previously that corpuscular streams in actuality induce variations of atmospheric pressure even at the level of the earth's surface. (auth)

Gravitation, Quantum Mechanics, and Relativity Theory

Refer also to abstract 29615.

30238 (JINR-P-2691) O RELYATIVISTSKIKH VOLNOVYKH PAKETAKH V PROSTRANSTVE I VREMENI. 1. (On Relativistic Wave Packets in Space and Time. [Part] 1). Polubarinov, I. V. (Joint Inst. for Nuclear Research, Dubna (USSR). Lab. of Theoretical Physics). 1966. 26p. Dep. mn.

A special representation (picture of measurement) is introduced so that time in quantum mechanics should have equal rights with other space coordinates. The covariant form is obtained for the uncertainty relations for time—coordinate and energy—momentum. Minimizing packets are constructed in space and time. The dynamical properties of such packets are briefly considered. (auth)

30239 (JINR-P-2692) KVANTOVAYA TEORIYA TYAGOTENIYA V GAIZENBERGOVSKOM PREDSTAVLENII I V PREDSTAVLENII VZAIMODEISTVIYA. (Quantum Theory of Gravity in the Heisenberg Representation and Interaction Representation). Ogievetskii, V. I.; Polubarinov, I. V. (Joint Inst. for Nuclear Research, Dubna (USSR). Lab. of Theoretical Physics). 1966. 30p. Dep. mn.

The quantum theory of gravity is considered from the point of view of field theory. The Heisenberg representations and interaction representation are given. A general simple recipe for constructing the states, which satisfy the supplementary condition, is formulated in the interaction representation. The S-matrix structure is analyzed. (auth)

30240 (BNL-tr-67) THE NON-STEADY PROBLEMS OF QUANTUM MECHANICS AND THE LAPLACE TRANSFORM. Demkov, Yu. N. Translated for Brookhaven National Lab., Upton, N. Y., from Dokl. Akad. Nauk SSSR, 166: 1076-9(1966). 11p. Dep. mn. CFSTI $1.00 cy, $0.50 mn. JCL $1.60 fs, $0.80 mf.

There are not many cases known where the Shroedinger non-steady state equation $H(t)\psi = [H_0 + V(t)]\psi = i\partial\psi/\partial t$ with an energy operator, H, dependent on time can be solved accurately or brought to a solution of a steady state problem with operator, H_0, independent of time. It is shown that for a special, although a fairly wide class of operators V(t) of the type $V = |\varphi > \beta\kappa\varphi|$ the problem may be solved accurately as a contour integral using Dirac's notations). Thus, operator, V, must linearly depend on time and be a projection operator on a certain basis vector $|\varphi>$ in the space functions $|\psi>$. It is shown that the properties of the energy operator, H (in particular, the behavior of its eigenvalues with respect to time), are such in this case that in various specific problems, for example, in the collision theory, an operator of this type may be approximately substituted for the real energy operator. (M.O.W.)

30241 NOTE ON AN INTEGRAL CONSERVATION LAW IN GENERAL RELATIVITY. Biswas, P. K. (Indian Association for the Cultivation of Science, Calcutta). Acta Phys. Austr., 21: 273-7(1966).

From an integral conservation law due to J. L. Synge the following results are obtained: the total proper energy of a cloud of incoherent dust remains conserved, the total proper energy of a perfect fluid decreases by the amount of work it does by expansion. The motion is irrotational in both the cases. (auth)

30242 NOTE ON THE KINEMATICAL AND DYNAMICAL PRINCIPLES OF RELATIVITY. Podlaha, M. (National Technical Museum, Prague). Acta Phys. Austr., 21: 296-7(1966).

A previously formulated principle of relativity in which the Lorentz transformation was derived from the principles of time dilation and relativity is explained in more detail. (J.F.P.)

30243 TRANSFORMATION PROPERTIES OF THE ELECTROMAGNETIC FIELD. Mirman, R. (Long Island Univ., Brooklyn). Amer. J. Phys., 34: 427-30(May 1966).

The electromagnetic field transforms as an antisymmetric second-rank tensor under Lorentz transformations. Starting with the electric field and relativity, the assumptions required to obtain this result are considered, as well as how the existence of the magnetic field and some of its properties follow from the transformation law. (auth)

30244 SPHERICALLY SYMMETRIC MOTIONS IN GENERAL RELATIVITY. McVittie, G. C. (Univ. of Illinois Observatory, Urbana). Nature, 210: 930-1 (May 28, 1966).

Exact solutions of Einstein's equations of general relativity are presented which refer to a spherically symmetric mass of material in radial motion, which may be collapsing on to the central point (gravitational collapse) or be exploding from that point (spherical blast). (B.G.D.)

30245 GRAVITATIONAL SHIELDING AND ABSORPTION. Weber, J. (Univ. of Maryland, College Park). Phys. Rev., 146: 935-7(June 24, 1966).

The general theory of relativity is used to calculate gravitational shielding and absorption. These effects are analogous to the shielding of electromagnetic fields with the exception that in lowest order quadrupoles rather than dipoles are involved. Quasistatic shielding effects occur in the tides, and for some models the shielding effect is several percent of the applied field. The dynamic shielding is much too small to observe at this time. (auth)

30246 PERTURBATIONS IN THE SCHWARZSCHILD METRIC. Peters, P. C. (Univ. of Washington, Seattle). Phys. Rev., 146: 938-46(June 24, 1966).

Exact solutions of the general-relativistic field equations are known only for very simple physical systems. In order to obtain solutions of the field equations for more realistic systems, an expansion of the field equations about some known exact solution is considered, keeping only terms linear in the perturbation. The unperturbed metric is then chosen to be the Schwarzsohild metric, corresponding to the exterior of any spherically symmetric mass distribution, and the case is considered where the perturbing matter is not located close to the Schwarzschild radius. A discussion of the solution for a scalar Green's function in curved

space leads directly to an explicit expression for the perturbed metric in terms of the perturbing matter. (auth)

30247 IS THE GRAVITON A GOLDSTONE BOSON? Phillips, Peter R. (Washington Univ., St. Louis). Phys. Rev., 146: 966-73(June 24, 1966).

A theory is outlined in which Lorentz invariance is spontaneously violated, giving rise to a constant vector field λ^μ. The two quantities which are most simply related to λ^μ are the gravitational constant G and the decay rate of $K_2^0 \rightarrow 2\pi$, assuming that the latter will eventually show an energy dependence. Using a method suggested by Bjorken for electrodynamics, it is concluded that the model may support a graviton, and determine the order of magnitude of G. A simple argument relates the K_2^0 decay to G; the agreement with experiment is good. (auth)

30248 S-MATRIX POTENTIAL IN SCHROEDINGER ONE-DIMENSIONAL EQUATION. Faddeev, L. D. Tr. Mat. Inst., Akad. Nauk SSSR, 73: 314-36(1964). (In Russian).

A proof of the author's previous statements (Dokl. Akad. Nauk SSSR, 121: 63-6 (1958)) concerning the S-matrix potential, based on the one-dimensional Schrodinger equation $-y'' + q(x)y = k^2y$ for $-\infty < x < \infty$, is presented. The problem differs markedly from that involving the radial equation, although the methods used for the solution are quite similar. As a result of this derivation, the properties of the S matrix which satisfy certain specified boundary conditions are identified. (TTT)

30249 MOTION LAWS OF UNCLOSED QUANTUM SYSTEMS. Bausch, R. (Technische Hochschule, Aachen). Z. Phys., 193: 246-65(1966). (In German).

Starting from so-called dynamical mappings which map the set of density operators onto itself, a possibility is discussed for deriving stochastic equations of motion for quantum systems. Two simple applications are given, the relaxation of a nuclear spin, and a quantum-mechanical equation of motion for a damped harmonic oscillator. The method can also be used in quantum electrodynamics. This theory is usually considered as closed in the following sense that in any Feynman graph the external lines of which describe photons and electrons only contain also in the virtual states these two kinds of particles only. It seems to be more realistic to replace this postulate of nonexistence of other interactions by the weaker assumption that such interactions exist but are not completely known. In this way a modification of quantum electrodynamics is achieved for high energy processes. (auth)

30250 RADIATION OF ELECTROMAGNETIC WAVES BY AN ELECTRON SHEET MOVING ABOVE A DIFFRACTION GRATING. Tret'yakov, O. A.; Chernyakov, E. I.; Shestopalov, V. P. (Inst. of Mining Machine Construction, Automation, and Computing Tech., Kharkov). Zh. Tekh. Fiz., 36: 33-8(Jan. 1966). (In Russian).

The radiation of an infinite plane sheet of electrons moving at constant velocity parallel to a plane diffraction grating is discussed. The grating is assumed to consist of an infinite sequence of infinitely long rods of rectangular section with their axes in the x-y plane and parallel to the x axis of a rectangular Cartesian coordinate system xyz. The dimensions of the rods are assumed to be $2(L - d)$ in the y-direction and 2h in the z direction, and the rods are assumed to be separated by the distance 2d, so that the grating constant is L. The electrons are assumed to move in the plane $z = p$ with constant velocity in the y direction, and the density of the sheet is assumed to be proportional to $\exp[i(ky - ft)]$, where i is the imaginary unit, k and f are constants, and t is the time. The wave radiated by the electron sheet is diffracted by the grating. The diffracted wave is expanded in a series of partial waves and an infinite set of linear equations is derived for the expansion coefficients. These equations were solved with the aid of a computer for different values of the grating parameters, Poynting's vector was calculated for the case that only a single diffracted wave is radiated approximately normally to the grating, and the results are presented graphically. The calculations were checked by comparison with previous work for the case $h = 0$. It is shown that the maximum power is radiated when L/d is approximately 5, that resonant increase of the radiated power occurs when 2h is a multiple of half the wavelength, and that the radiated power increases rapidly with decreasing distance between the electron sheet and the grating. (ATD)

30251 GEOMETRODYNAMICS OF CYLINDRICAL SYSTEMS [Thesis]. Thorne, Kip Stephen. Princeton, N. J., Princeton Univ., 1965. 275p.

A complete presentation is given of the general relativity theory of cylindrical systems (systems invariant under rotations about an axis of symmetry and translations along the axis). Results scattered widely through the literature are brought together and unified by means of the concept of "C-energy," and a large number of new results are reported. The most important topics discussed are: (1) the way in which C-energy governs the statics and dynamics of cylindrical systems; (2) Levi-Civita's external gravitational field for static cylinders; (3) the hydrostatics and stability of cylinders composed of perfect fluid; (4) cylindrical gravitational radiation, including generalizations of the gravitational waves of Einstein and Rosen; (5) cylindrical cosmological models; (6) the gravitational collapse of cylindrical dust clouds, and the gravitational radiation they emit; (7) cylindrical electromagnetic systems; and (8) the resistance of electric and magnetic flux to gravitational collapse. (Dissertation Abstr.)

30252 ELECTROMAGNETIC RADIATION FROM EXTENDED SOURCES: A COVARIANT TREATMENT OF NON-RADIATING MODES [Thesis]. Kirkpatrick, Kim Allan. University Park, N. Mex., New Mexico State Univ., 1965. 72p.

The standard treatment of electromagnetic radiation is reviewed, and criticism is offered of the usual identification of the rate of radiation of momentum and energy out of the finite domain with the rate of loss of momentum and energy from the charge and current sources of the field. It is shown that this identification, when put in formally covariant form, is observer dependent. The work of Schild and of Rohrlich on the covariant definition of the radiation of momentum-energy from a point electric charge is reviewed. A definition of the total radiation of momentum-energy ΔP^k_{PQ} out of the finite domain due to current-charge sources within a certain space-time region R_{PQ} is offered, which is covariant and which overcomes the objections with regard to the usual treatment of radiation from sources. R_{PQ} is the space-time region enclosed by the future light cone with vertex at event P and the past light cone with vertex at Q, with P-Q timelike. Only Maxwell's equations, the usual interpretation of Poynting's theorem, and the connection of the field to the sources through the retarded potential are assumed. From this definition of radiation is obtained the necessary and sufficient condition that the sources lose no momentum-energy by radiation. Other equivalent conditions are then found. With the restriction to periodic sources Goedecke's criterion for non-radiation is re-derived. It is pointed out that the condition for non-radiation does not involve the charge density except as it is related to the current density through the equation of continuity. It is shown that the criteria for non-radiating charge oscillations given in the recent article of Perkins are sufficient but not necessary. (Dissertation Abstr.)

Low Temperature Physics

Refer also to abstract 29753.

30253 (CEA-R-2808) CONTRIBUTION A L'ETUDE DU COMPORTEMENT MAGNETIQUE IRREVERSIBLE DES SUPRACONDUCTEURS. (Contribution to the Study of the Irreversible Magnetic Behavior of Superconductors). Kuhn, Gerard (Commissariat a l'Energie Atomique, Grenoble (France). Centre d'Etudes Nucleaires). 1966. 116p. Dep. mn.

Thesis. Submitted to Grenoble Univ., France.

The influence of the presence of extended lattice defects on the magnetic behavior was studied for the case of type I superconductors, such as Re and Ta, and in a more quantitative manner for the type II superconductor niobium. In this case, measurements of the thermal conductivity have given an estimate of the relative concentration of lattice defects in each specimen. These measurements show that the larger the number of lattice defects, the more irreversible becomes the magnetization curve, and the larger becomes the values of the critical current, which is related by a simple model to the magnetization values. Finally, a study by transmission electron microscopy has confirmed on the one hand the diversity of the extended lattice defects and on the other hand has allowed the formulation of several hypothesis on their respective influence. (auth)

30254 (LA-DC-7209) A TRANSISTORIZED LIQUID-HELIUM TEMPERATURE REGULATOR. Lindsay, J. D. G. (Los Alamos Scientific Lab., Univ. of California, N. Mex.). [1963]. Contract W-7405-eng-36. 11p. Dep. mn. CFSTI $1.00 cy, $0.50 mn.

A transistorized temperature regulator that is capable of controlling the temperature of a liquid helium bath to better than ± 10 micro degrees for periods of 20 to 30 minutes is described. The circuit employs a carbon resistor as the temperature sensing element and achieves its temperature control by varying the current supplied to a 200 Ω heater located in the liquid helium bath. Both a null meter and a heater current meter are incorporated in the design so that regulator performance can be continuously monitored. (auth)

30255 (ORO-2430-28) SUPERCONDUCTING CIRCUITRY. Progress Report. Vail, Charles R.; Artley, John L. (Duke Univ., Durham, N. C. Dept. of Electrical Engineering). May 1966. Contract AT(40-1)-2430. 23p. Dep. mn. CFSTI $1.00 cy, $0.50 mn.

Research directed toward the application of thin-film materials on computer circuitry has proceeded in three broad areas: (1) electric and magnetic characteristics of cryogenic circuit elements; (2) adaptive superconducting logic; and (3) the development of optimum materials for thin-film devices. The projected experimental and analytical work on the use of thin-film superconductors in threshold logic computer elements was completed. A detailed discussion of progress in each of the above three areas is presented. (M.O.W.)

30256 SCATTERING OF SLOW NEUTRONS IN AN ACOUSTICAL FIELD: TOTAL SCATTERING CROSS SECTION. Fulinski, Andrzej (Jagellonian Univ., Krakow). Acta Phys. Pol., 29: 691-7(May 1966).

The total cross section for the scattering of slow neutrons by systems under acoustical (ultrasonic) field is calculated. It is found that the action of the field shifts the singularities of the cross section as the function of the initial energy of neutrons. As an example, the cross section for an ideal-gas scatterer is calculated, and it is found that the scatterer in the presence of the field cuts off the low-energy part of the incident neutron beam. The possibilities of use of other than acoustical oscillating field are also mentioned. However, in order to obtain noticeable effects, strong fields are needed. (auth)

30257 NEW DEVELOPMENTS IN CONNECTION WITH SUPERCONDUCTORS. Buckel, W. (Technische Hochschule, Karlsruhe, Ger.). Chem.-Ing.-Tech., 38: 505-8 (May 1966). (In German).

The conception of characteristic properties of superconductors has changed decidedly in the last ten years. Type II superconductors were not diamagnetically shielded in very high magnetic fields and remained without Ohmic resistance. Under certain conditions high magnetic fields can be maintained practically free from losses with type II superconductors, which can be particularly useful for modern methods of energy production. The main characteristics of these technically interesting materials are investigated. (tr-auth)

30258 SUPERCONDUCTING THIN-FILM TECHNOLOGY AND APPLICATIONS. Pritchard, J. Paul Jr. IEEE (Inst. Elec. Electron. Eng.), Spectrum, 3: 46-54(May 1966).

In the past two years, significant gains were made in cryogenic array technology and also in the necessary support areas. The problems peculiar to array fabrication are reviewed, experimental evidence of recent progress is cited and an attempt is made to project the likelihood of the emergence of various cryoelectronic data-processing systems. A review is given of basic characteristics of superconductive devices for logic and storage functions and their implications with respect to fabrication methods. (auth)

30259 PRESSURE EFFECTS ON THE TRANSITION TEMPERATURE OF SUPERCONDUCTORS. Ganguly, B. N.; Sinha, K. P. (National Chemical Lab., Poona). Indian J. Pure Appl. Phys., 4: 49-56(Feb. 1966).

A theoretical analysis of the pressure dependence of the transition temperature of superconducting systems was made. Additional perturbations over the Bardeen, Cooper and Schrieffer theory are invoked which can lead to intraband or interband scattering of electrons near the Fermi surface. Theoretical expressions relating the transition temperature as a function of pressure are derived. The theory predicts a decrease or an increase of the transition temperature with an increase of pressure depending on the relative magnitude of the parameters involved. Experimental results, obtained with appropriate systems showing a decrease or an increase in the transition temperature with an increase of pressure, were compared with those predicted by theory. The agreement between the experimental and theoretical results is satisfactory. (auth)

30260 EFFECT OF THERMAL-NEUTRON IRRADIATION ON THE SUPERCONDUCTING PROPERTIES OF Nb_3Al AND V_3Si DOPED WITH FISSIONABLE IMPURITIES. Bean, C. P.; Fleischer, R. L.; Swartz, P. S.; Hart, H. R. Jr. (General Electric Research and Development Center, Schenectady, N. Y.). Contract AF33(657)-117220. J. Appl. Phys., 37: 2218-24(May 1966).

The superconducting critical temperatures and current carrying capacities of Nb_3Al and V_3Si doped with small amounts of uranium and boron and subsequently irradiated with thermal neutrons are reported. While the critical temperatures are substantially unaffected, the critical current densities are dramatically increased by the internal fission of uranium in both materials. Samples of Nb_3Al containing 0.321 at. % uranium and V_3Si containing 0.19 at. % uranium irradiated with 1.7×10^{18} neutrons/cm^2 give superconducting critical current densities over 10^6 A/cm^2 at 30 kOe. The boron-doped samples, however, showed no effects arising from fission of boron. Two new experimental techniques were used in this investigation. First, uranium and boron analyses as well as information on homogeneity were determined by use of the Price-Walker nuclear track detectors. Secondly, the critical current measurements were made on 50-mg samples of 70-μ powders by a technique that measures the generation of odd-harmonic voltages caused by small alternating magnetic fields applied to the sample. (auth)

30261 MAGNETIC INSTABILITIES AND FLUX ANNIHILATION IN GROSSLY INHOMOGENEOUS SUPERCONDUCTORS. Blaugher, R. D.; Joiner, W. C. H. (Westinghouse Electric Corp., Baltimore). J. Appl. Phys., 37: 2351-4(May 1966).

Magnetic instabilities in the form of reversed field flux annihilation pulses were observed in a grossly inhomogeneous superconductor. The magnetic field values for which the instabilities are observed depend on the previous field history of the sample. In particular, the annihilation begins at lower values the higher the previous reversed field maximum, and the annihilation instabilities for a given field direction have as an upper limit the maximum field achieved in the opposition direction. The origin of this behavior, as well as the more common phenomenon of flux jumping, is discussed in terms of large-scale potential wells which trap large quantities of fluxoids. Magnetic instabilities are a result of a critical difference between the density of fluxoids within the well and the density of those outside. (auth)

30262 EDDY CURRENTS IN TYPE II SUPERCONDUCTORS INDUCED BY FAST-PULSED MAGNETIC FIELDS.

Boyd, R. G. (Univ. of California, Berkeley). J. Appl. Phys., 37: 2517-18(May 1966).

Hypotheses for transitions in superconductors are examined. Such transitions may be caused by eddy currents induced in the superconductor by the rapidly pulsed magnetic field, and will be much larger in the superconducting state than in the normal state. The hypotheses that the eddy currents may exceed the critical current of the specimen or that they may raise the temperature of the specimen through Joule heating so that at some field H, $T(\overline{x}) \geq T_c(H)$ throughout the specimen are considered. (J.F.P.)

30263 BROWNIAN MOTION IN A FERMI FLUID. Davis, H. Ted; Dagonnier, R. (Univ. Libre, Brussels). J. Chem. Phys., 44: 4030-5(May 15, 1966).

Using the quantum-mechanical Boltzmann equation the motion of a heavy ion (mass M) moving through a Fermi fluid of light particles [mass m, $\gamma = (m/M)^{\frac{1}{2}} \ll 1$] under the influence of an electric field is studied. Contrary to the classical case, it is found that the condition $\gamma \ll 1$ is not sufficient to ensure that the ion undergoes Brownian motion (i.e., its motion is characterized by a Fokker-Planck equation). The condition $\gamma\xi \ll 1$ must hold, where ξ^2 is the ratio of the Fermi energy to the temperature. When ξ is too large the ion will suffer large momentum changes upon colliding with the fermions and hence its motion will not be describable by a Fokker-Planck equation. In liquid ^{3}He there is a temperature region ($4° > T > 1°K$) in which a heavy ion experiences quantum-mechanical Brownian motion; the Fokker-Planck equation still holds but the friction coefficient contains quantum-mechanical effects. Using a formula for mobility and the mobility data of Meyer the effective mass of an ion in liquid ^{3}He is estimated to be about 20 times the mass of an ^{3}He atom. This is in agreement with the recent measurements of Dahm and Sanders in liquid ^{4}He. They have found the effective mass to be between 20 to 40 ^{4}He atoms. However, since only binary scattering events are accounted for in this mobility formula, its application to liquid ^{3}He should be taken with reservation. (auth)

30264 LATTICE STABILITY IN THE PHONONLESS MECHANISM OF SUPERCONDUCTIVITY. Balkarei, Yu. M.; Khomskii, D. I. (Lebedev Inst. of Physics, Moscow). JETP Lett. (USSR) (Engl. Transl.), 3: 181-3 (Apr. 1, 1966).

Translated from Zh. Eksp. Teor. Fiz., Pis'ma Redaktsiya, 3: 281-4(Apr. 1, 1966).

The conditions for lattice stability in a mechanism of superconductivity in the presence of electron-electron interactions are discussed. (B.G.D.)

30265 POSSIBLE EXPERIMENT FOR FINDING SUPERCONDUCTORS WITH DIFFERENT PAIR MULTIPLICITY. Akhtyamov, O. S. (Bashkir State Univ., Ufa, ASSR). JETP Lett. (USSR) (Engl. Transl.), 3: 183-5(Apr. 1, 1966).

Translated from Zh. Eksp. Teor. Fiz., Pis'ma Redaktsiya, 3: 284-7(Apr. 1, 1966).

An experiment is described for finding superconductors with different pair multiplicity by Josephson tunneling. (B.G.D.)

30266 STATE OF LIQUID HELIUM IN THE VICINITY OF THE λ LINE. Kiknadze, L. V.; Mamaladze, Yu. G.; Cheishvili, O. D. (Inst. of Physics, Academy of Sciences, Georgian SSR). JETP Lett. (USSR) (Engl. Transl.), 3: 197-200(Apr. 15, 1966).

Translated from Zh. Eksp. Teor. Fiz., Pis'ma Redaktsiya, 3: 305-9(Apr. 15, 1966).

The assertion that liquid helium should actually be either superfluid throughout or normal throughout in a vessel, in which the pressure P_0 at the lid and the temperature T are such that at a certain depth Z_λ the pressure corresponds to the λ line ($P_0 + \rho g z_\lambda = P_\lambda(T)$), is proved. (B.G.D.)

30267 ANOMALOUS BEHAVIOR OF $j_c(H,T)$ OF HEAT-TREATED Nb–75 PERCENT Zr ALLOYS. Goncharov, I. N.; Khukhareva, I. S. (Joint Inst. for Nuclear Research, Dubna, USSR). JETP Lett. (USSR)(Engl. Transl.), 3: 236-9(May 1, 1966).

Translated from Zh. Eksp. Teor. Fiz., Pis'ma Redaktsiyu, 3: 365-9(May 1, 1966).

An investigation of the critical current density as a function of temperature and magnetization of Nb–75% Zr wires is discussed. Measurements are made in the temperature interval from 1.5°K to T_c in a transverse magnetic field up to 80 kG. (B.G.D.)

30268 QUESTION OF SUPERCONDUCTIVITY IN ORGANIC MOLECULES. Paulus, K. F. G. Mol. Phys., 10: 381-9(1966).

Little (Phys. Rev., 134: A1416(1964)) has proposed that high temperature superconductivity should be possible in long substituted polyenes, with electronic virtual excitations in the substituents providing a mechanism for attractive forces between polyene electrons. This proposal is examined in detail, and in particular the question of screening of the coulomb interaction between electrons under these circumstances is discussed. Reasons are given why screening should not be taken into account. Explicit calculations for a number of substituted polyenes lead to the conclusion that the criterion for superconductivity is not satisfied in these systems. (auth)

30269 ROLE OF SURFACE CURRENTS IN THE MAGNETIZATION OF HYSTERETIC SUPERCONDUCTORS. Bertman, B.; Schweitzer, D. G. (Brookhaven National Lab., Upton, N. Y.). Phys. Lett., 21: 361-2(June 1, 1966). (BNL–9939).

Magnetization measurements were made on solid and hollow cylinders of a hysteretic low κ type II superconductor. The behavior was found to be qualitatively similar indicating a surface current contributes significantly to hysteresis. The symmetry observed in the limit of very thin walls is different from that previously reported. (auth)

30270 ORIENTATION DEPENDENCE OF THE RESISTIVE TRANSITION NEAR H_{c2} IN HIGH FIELD SUPERCONDUCTORS. Williamson, S. J.; Furdyna, J. K. (Massachusetts Inst. of Tech., Cambridge). Phys. Lett., 21: 376-8 (June 1, 1966).

Microwave experiments on Nb–10% Zr and Nb–25% Zr wires indicate an isotropic critical field H_{c2} although resistive measurements indicate an anisotropic critical field. The anisotropy may be attributed to surface superconductivity which has nucleated at grain boundaries inside the wires. (auth)

30271 TRANSITION TEMPERATURE OF SUPERCONDUCTORS WITH PARAMAGNETIC IMPURITIES. Crow, J. E.; Parks, R. D. (Univ. of Rochester, N. Y.). Phys. Lett., 21: 378-9(June 1, 1966).

The dependence of the superconducting transition temperature on the concentration of Gd spins is reported for the $La_{3-x}Gd_x$ In system. The results are compared with the predictions of the theory of Abrikosov and Gorkov and other experimental attempts to verify the theory. (auth)

30272 CRITICAL VELOCITIES IN SUPERFLUID He II. Craig, P. P. (Technische Hochschule, Munich. Brookhaven National Lab., Upton, N. Y.). Phys. Lett., 21: 385-6 (June 1, 1966).

A new critical velocity condition in He II of the form $v^3 d = B \ln(1 + C/v)$ is derived and compared with recent Leiden experiments. Good agreement is found over a range of 10^7 in channel size (d). (auth)

30273 SOME EXPERIMENTS ON THE DISTRIBUTION OF A DIRECT TRANSPORT CURRENT IN SHEETS OF TYPE-II SUPERCONDUCTORS. Druyvesteyn, W. F.; Staas, F. A.; Niessen, A. K. (Philips' Gloeilampenfabrieken, Eindhoven, Netherlands). Phys. Lett., 21: 387-8 (June 1, 1966).

Measurements are reported on sheets of type II superconductors carrying d-c currents perpendicular to an applied magnetic field. (B.G.D.)

30274 AUTOMATIC SUPERCONDUCTING FLUX PUMP. Laquer, H. L.; Carroll, K. J.; Hammel, E. F. (Los Alamos Scientific Lab., N. Mex.). Phys. Lett., 21: 397-8(June 1, 1966). (LA-DC–7720).

The design and operation of a simple self-switching and self-rectifying flux pump are discussed. The concept has been tested using a low temperature transformer and a 10 kOe, 30 A, Nb–Zr coil paralleled by a 45 A switching coil made from Pb–Sn solder. (auth)

30275 VISCOSITY COEFFICIENTS FOR LIQUID ^{3}He IN THE INTERVAL 0.36 TO 2.6 DEG K. Webeler, R. W. H., Hammer, D. C. (Lewis Research Center, Cleveland). Phys. Lett., 21: 403-4(June 1, 1966).

The torsional crystal technique was employed to determine the viscosity coefficients in liquid ^{3}He and the results of this investigation are compared with other data. (auth)

30276 MAGNETIC FIELD REPULSION BY A SUPERCONDUCTING SPLIT CYLINDER. Brown, C. R.; Daniels, B.; Matthews, P. W. (Univ. of British Columbia, Vancouver). Phys. Lett., 21: 405-6(June 1, 1966).

It is shown that the presence of a longitudinal split in a hollow cylinder of a superconductor makes little difference to the axial force on an approaching magnet, even though the split eliminates circular current loops. (auth)

30277 NEW EFFECT AT SUPERCONDUCTING CONTACTS. Pankove, J. I. (RCA Labs., Princeton, N. J.). Phys. Lett., 21: 406-7(June 1, 1966).

When two oxidized superconductors are in pressure contact, a current in excess of the normal single-particle tunnel current is obtained over a range of biases extending more than a decade beyond 2Δ. (auth)

30278 FLUX PINNING IN SUPERCONDUCTING NIOBIUM THIN FILMS. Hudson, W. R.; Jirberg, R. J.; Simmons, J. H. (Lewis Research Center, Cleveland). Phys. Lett., 21: 493-4(June 15, 1966).

The effect of flux pinning on the resistive behavior of superconducting niobium thin films was investigated. No resistive voltage, longitudinal or transverse, was observed below the upper critical field, H_{c2}, determined by a two coil technique. (auth)

30279 THE SUPERCONDUCTING TRANSITION TEMPERATURES OF Nb_6Sn_5 AND $NbSn_2$. Charlesworth, J. P. (Atomic Energy Research Establishment, Harwell, Eng.). Phys. Lett., 21: 501-2(June 15, 1966).

Superconducting transitions were found at 2.07° in Nb_6Sn_5 and 2.68°K in $NbSn_2$. Previously reported values are <0.3°K for Nb_6Sn_5 and 2.6°K for $NbSn_2$. (auth)

30280 INFLUENCE OF SURFACE CURRENTS ON THE ALTERNATING-CURRENT LOSS OF HARD SUPERCONDUCTORS. Ullmaier, H. A. (Oak Ridge National Lab., Tenn.). Phys. Lett., 21: 507-8(June 15, 1966). (In German).

The influence of surface currents on the alternating current losses in hard superconductors is shown. A formula which takes into account this influence is in good agreement with experimental results for Nb–25% Zr. (tr-auth)

30281 ULTRASONIC INVESTIGATION OF ENERGY-GAP ANISOTROPY IN SUPERCONDUCTING RHENIUM. Jones, C. K. (Westinghouse Research Labs., Pittsburgh); Rayne, J. A. Phys. Lett., 21: 510-11(June 15, 1966).

The attenuation of longitudinal waves propagating along the principal directions in pure rhenium was measured in the normal and superconducting states. The observed energy gap anisotropy is discussed in terms of the Garland model. (auth)

30282 EXPERIMENTAL THERMAL CONDUCTIVITY OF ^{3}He. Anderson, A. C.; Connolly, J. I.; Vilches, O. E.; Wheatley, J. C. (Univ. of Illinois, Urbana). Contract AT(11-1)-1198. Phys. Rev., 147: 86-93(July 8, 1966). (COO–1198-318).

The thermal conductivity of liquid ^{3}He at pressures of 0.11, 6.78, and 27.0 atm was measured down to 0.06°K. For each pressure the conductivity passes through a minimum, the temperature of the minimum decreasing with increasing pressure. At temperatures greater than $\frac{1}{2}$°K the thermal conductivity is nearly independent of pressure. The effect of pressure is to decrease the conductivity. The pressure effect increases monotonically down to the lowest temperature. (auth)

30283 LOW-TEMPERATURE HEAT CAPACITY OF LIQUID ^{3}He. Abel, W. R.; Anderson, A. C.; Black, W. C.; Wheatley, J. C. (Univ. of Illinois, Urbana). Contract AT(11-1)-1198. Phys. Rev., 147: 111-19(July 8, 1966). (COO–1198-328).

The heat capacity of pure ^{3}He was measured using a difference method from 6 to 50 m°K at 0.28 atm and from 4 to 30 m°K at 27.0 atm. In neither case is the ratio of heat capacity to temperature constant over the range of temperature of the measurements. Moreover, the high- and low-pressure heat capacities seem to have qualitatively different temperature dependences. The raw heat-capacity data down to a temperature [on the magnetic temperature scale valid for powdered cerium magnesium nitrate (CMN) in the form of a right circular cylinder with diameter equal to height] of 2 m°K at 0.28 atm and 4 m°K at 27.0 atm show no evidence for anomalous behavior. As a by-product of the measurements the heat capacity of the CMN cooling salt was also obtained. (auth)

30284 THEORY OF A SUPERFLUID FERMI LIQUID. II. COLLECTIVE OSCILLATIONS. Leggett, A. J. (Univ. of Illinois, Urbana). Phys. Rev., 147: 119-30(July 8, 1966).

The long-wavelength, low-frequency "collisionless" collective oscillations of a superfluid Fermi liquid are studied throughout the region $0 < T < T_c$ with the help of a field-theoretic formalism developed previously. It is found that any collective mode (other than the density fluctuation) that is possible in the normal phase persists below T_c as an oscillation of the normal component, but disappears at some finite temperature which in general depends on the Landau interaction parameters F_0, F_1, Z_0, etc. The behavior of the density-fluctuation mode depends critically on F_0; if the latter is negative, there is a well-defined collective oscillation only for $T \ll T_c$, while if it is small and positive, the oscillation is well defined for $T \ll T_c$ and $T - T_c \ll T_c$ but not in the intermediate region. If F_0 is large and positive, the density-fluctuation collective mode exists throughout the whole region $0 < T < T_c$ and its velocity is approximately temperature-independent. (auth)

30285 MEASUREMENTS OF THE MUTUAL-FRICTION PARAMETER B' IN ROTATING HELIUM II. Snyder, H. A.; Linekin, D. M. (Brown Univ., Providence). Phys. Rev., 147: 131-9(July 8, 1966).

The mutual-friction parameter B′ was measured in the temperature range 1.3 to 2.1°K with an error ranging from 20 to 100%. The method is to observe the removal of mode degeneracy by rotation of a resonator for second sound. The empirical temperature dependence of B′ is in good agreement with the kinetic model of Hall and Vinen; but the agreement with all published calculations of the roton-vortex-line scattering cross section is poor. The results are at variance with the predictions of Lin's equations of motion for rotating helium II but are in accord with the equations of Hall and Vinen. Some measurements on the attenuation of second sound in a rotating resonator when the angular frequency of rotation is modulated show that there is very little interaction between the different types of vortex motion in the resonator. (auth)

30286 STABILITY OF A LATTICE OF SUPERFLUID VORTICES. Fetter, A. L. (Stanford Univ., Calif.); Hohenberg, P. C.; Pincus, P. Contract AF 49(638)-1389. Phys. Rev., 147: 140-52(July 8, 1966).

Landau's superfluid hydrodynamics is applied to the vibration spectrum of a lattice of rectilinear vortices in both charged and neutral superfluid systems. The resulting vortex dynamics is identical with that of classical hydrodynamics: each vortex moves with the local superfluid velocity at its core. The only mode considered is one in which the vortices move without bending. This mode is unstable for all lattice structures in a neutral system (liquid helium II); in a charged system (type-II superconductors) the mode is unstable for a square lattice but stable for a triangular lattice. The corresponding long-wavelength dispersion relation is $\omega = (eB/mc)q^2\lambda d(\sqrt{3}/32\pi)^{\frac{1}{2}}$, where B is the

magnetic induction, λ is the London penetration depth, q is the wave number, and d is the lattice spacing. An elasticity theory of the lattice vibrations in the charged system is shown to predict identical results. These calculations agree qualitatively with those of de Gennes and Matricon but disagree with those of Abrikosov, Kemoklidze, and Khalatnikov; the discrepancies are discussed in detail. (auth)

30287 ENERGY OF A LATTICE OF QUANTIZED FLUX LINES. Fetter, Alexander L. (Stanford Univ., Calif.). Contract AF 49(638)-1389. Phys. Rev., 147: 153-5(July 8, 1966).

Analytic expressions are given for the magnetic flux density B and the Gibbs free energy G of a bulk type-II superconductor in an intermediate magnetic field H_0 ($H_{c1} \ll H_0 \ll H_{c2}$). Both square and triangular lattices are considered; the triangular lattice is confirmed as the more stable structure. (auth)

30288 SOUND MEASUREMENTS IN LIQUID AND SOLID ^{3}He, ^{4}He, AND ^{3}He-^{4}He MIXTURES. Vignos, James H.; Fairbank, Henry A. (Yale Univ., New Haven). Phys. Rev., 147: 185-97(July 8, 1966).

Using the ultrasonic pulse technique at a carrier frequency of 10 Mc/sec, the longitudinal velocity of sound was measured in liquid and solid ^{3}He, ^{4}He, and ^{3}He-^{4}He mixtures (0.0, 5.03, 25.0, 74.9, 98.00, 99.84% ^{3}He) in the temperature range from 1 to 4.2°K and the pressure range from 1 to 150 atm. An upper limit to the attenuation of sound in the region of the solid investigated is on the order of 0.3 to 0.7 cm^{-1}. Values of the adiabatic compressibility of the liquid along the melting curve of ^{4}He are given. The discontinuity in the propagation velocity at a first-order phase boundary was utilized to locate the solidification curves of these samples and also to investigate the bcc-hcp crystallographic transition in solid samples, including pure ^{4}He, similar to that observed in pure ^{3}He by Grilly and Mills. The triple points for this transition in ^{4}He are given by $T_l = 1.449 \pm 0.003$°K, $P_l = 26.18 \pm 0.05$ atm; $T_u = 1.778 \pm 0.003$°K, $P_u = 30.28 \pm 0.05$ atm. The upper triple points for the mixtures lie on a straight line connecting ^{3}He and ^{4}He in temperature-pressure space. In addition, by observing the peak in the attenuation of sound, it was possible to measure the λ line in ^{4}He and in the 5.0% and 25.0% ^{3}He liquid mixtures. The upper λ point for pure ^{4}He is given by $T_s = 1.765 \pm 0.003$°K and $P_s = 29.90 \pm 0.05$ atm. Comparison is made with existing data wherever possible. (auth)

30289 MICROWAVE ABSORPTION IN NORMAL-CONDUCTING FILMS ON SUPERCONDUCTING SUBSTRATES. Fanelli, Robert; Meissner, Hans (Stevens Inst. of Tech., Hoboken, N. J.). Phys. Rev., 147: 227-34(July 8, 1966).

The microwave absorption at 9.2 kMc/sec in films of gold and copper plated onto bulk tin was measured as a function of the temperature in the range $1.4 \leq T \leq 4.2$°K. The results are extrapolated to zero temperature, where they indicate the presence of an energy gap of 0.61×10^{-23} J at the surface of a 190-Å film of gold and at the surface of a 500-Å film of copper on tin. The normal bulk resistivity of the gold was estimated from d-c measurements as well as from the microwave data. The theory of the proximity effect, that is, the influence of adjoining normal and superconducting metals, as given by de Gennes and Werthamer, was applied to the measurements, and yielded an estimate for N(0)V for gold of 9×10^{-3}. Assuming that the sign of N(0)V is positive, this leads to a very low transition temperature. (auth)

30290 CALCULATION OF THE LOW-TEMPERATURE MICROWAVE RESISTANCE OF A THIN METAL FILM ON A BULK SUBSTRATE. Meissner, Hans (Stevens Inst. of Tech., Hoboken, N. J.). Phys. Rev., 147: 235-8(July 8, 1966).

A simple free-electron model is used to explain the experimentally observed low values of the effective resistivities derived from the low-temperature microwave absorption of metal films plated onto (normal-conducting) tin. In the limit of zero film thickness the calculation gives effective resistivity of $\rho = \rho_1 l_1 / 2\delta$, where $\rho_1 l_1$ is a material constant of the material of the film and δ is the anomalous skin depth in the base metal. Good agreement is obtained for gold films on tin. The experimental data for copper films on tin are much higher than expected from this model. The implications of these findings for the proximity effects in superconductivity, that is, for the influence of a normal metal on an adjoining superconductor and vice versa, are discussed. (auth)

30291 CRITICAL TEMPERATURES AND CRITICAL FIELDS OF MULTIPLE SUPERCONDUCTING AND NORMAL-CONDUCTING FILMS. Duffy, R. J.; Meissner, Hans (Stevens Inst. of Tech., Hoboken, N. J.). Phys. Rev., 147: 248-55(July 8, 1966).

The critical temperatures and critical magnetic fields were determined for a series of superposed normal and superconducting films. Both Cu–Sn and Au–Sn samples were investigated. The samples were prepared by vacuum-deposition methods or by electroplating. Thicknesses of the Sn films ranged from 160 to 2700 Å. The dependence of the critical temperature T_c of the multiple film on normal-metal thickness is compared with recent theories. Experimental evidence is given that the observed effects are true proximity effects, caused by the free exchange of electrons between the two metals, and that metallic diffusion alone is not responsible for the observed phenomena. The critical magnetic fields of both single and multiple films are compared with the microscopic theories. It is shown that at fields near the critical fields with the multiple film still superconducting the gap function Δ(r) and the magnetization are negligibly small on the normal side of the film. (auth)

30292 NONLINEAR SELF-COUPLING OF JOSEPHSON RADIATION IN SUPERCONDUCTING TUNNEL JUNCTIONS. Werthamer, N. R. (Bell Telephone Labs., Murray Hill, N. J.). Phys. Rev., 147: 255-63(July 8, 1966).

A study is made of the nonlinear feedback of the a-c tunneling current (first pointed out by Josephson) in a superconducting tunnel junction via the electromagnetic fields radiated by the current into the resonant-mode structure of the junction. The junction operating point is investigated, and a calculation is made of the d-c current drawn by a strongly self-coupled fundamental mode together with weakly self-coupled harmonic modes. Attention is directed to the frequency dependence of the tunneling-current amplitudes reported briefly by Riedel, as a tentative explanation of the bumps in current-voltage characteristics which have been observed at $eV = 2\Delta/(\text{integer})$, where 2Δ is the energy gap. (auth)

30293 a-c SUSCEPTIBILITY TRANSITION IN TYPE-II SUPERCONDUCTORS AND SURFACE CRITICAL CURRENTS. Bertman, B.; Strongin, Myron (Brookhaven National Lab., Upton, N. Y.). Contract AT(30-2)-Gen-16. Phys. Rev., 147: 268-72(July 8, 1966). (BNL-9857).

The a-c susceptibility transition below H_{c3} was investigated as a function of a-c field amplitude, in cylindrical samples of Pb–Bi alloys ($1 \leq \kappa \leq 5$). Converting the a-c fields to critical surface currents J_c permits comparison with the values calculated by Abrikosov and Park. The present results agree with those of Swartz and Hart, and of Rollins and Silcox. Although above H_{c2} the qualitative behavior is similar to the theoretical calculations, the magnitudes are found to be lower. At H_{c2} a sharp break is found in J_c, as reported previously. $J_c\kappa/H_c$ is found to be independent of κ within experimental error. Surface roughness and slight sample misalignment could have lowered the observed J_c. (auth)

30294 THERMAL CONDUCTIVITY OF THICK PURE LEAD FILMS FOR THE STUDY OF SURFACE SUPERCONDUCTIVITY. Seidel, T.; Meissner, Hans (Stevens Inst. of Tech., Hoboken, N. J.). Phys. Rev., 147: 272-9(July 8, 1966).

The differential thermal conductivity of lead films in a magnetic field parallel to the plane of the film was measured in the temperature range 1.2 to 4.2°K. The thicknesses of the films (from 2500 to 7000 Å) were selected so

that the expected volume of the superconducting surface regions is an appreciable volume fraction of the sample. The fraction of material remaining in the surface superconducting state just above the film's critical field is related to the measured thermal conductivity via a simple phenomenological model. The analysis allows a heuristic determination of the product of the thickness of the superconducting surfaces and the square of the order parameter at the surface. The results are compared with the recent calculations of Fink and Kessinger. Well defined values of H_c and H_{c3} are obtained. Some hysteresis is observed near H_c in a decreasing magnetic field, and the role of phonons in the heat transport is manifest, but its contributions above H_c is negligible when compared with the electronic contribution to the thermal conductivity. (auth)

30295 TEMPERATURE AND PURITY DEPENDENCE OF THE SUPERCONDUCTING CRITICAL FIELD, H_{c2}. II. Helfand, E.; Werthamer, N. R. (Bell Telephone Labs., Murray Hill, N. J.). Phys. Rev., 147: 288-94(July 8, 1966).

A rigorous gauge-invariant solution of the linearized Gor'kov equations is presented, yielding the complete temperature and electron-mean-free-path dependence of the upper critical magnetic field H_{c2} of a bulk type-II superconductor. Comparison is made with previously known results in special cases, and it is pointed out that localized approximations such as the "dirty," or the Ginzburg-Landau, limits represent the leading term in an asymptotic rather than convergent, expansion. (auth)

30296 TEMPERATURE AND PURITY DEPENDENCE OF THE SUPERCONDUCTING CRITICAL FIELD, H_{c2}. III. ELECTRON SPIN AND SPIN-ORBIT EFFECTS. Werthamer, N. R.; Helfand, E.; Hohenberg, P. C. (Bell Telephone Labs., Murray Hill, N. J.). Phys. Rev., 147: 295-302(July 8, 1966).

A previously obtained solution of the linearized Gor'kov equations for the upper critical magnetic field H_{c2} of a bulk type-II superconductor is extended to include the effects of Pauli spin paramagnetism and spin-orbit impurity scattering. To carry out the calculation, it is necessary to introduce an approximation which assumes that spin-orbit scattering is infrequent in comparison with spin-independent scattering. It is found that spin-orbit scattering counteracts the effects of the spin paramagnetism in limiting the critical field and improves agreement between theory and experiment. (auth)

30297 SUPERCONDUCTIVITY AND ELECTRONIC STRUCTURE IN THE ALLOY SYSTEM LEAD–THALLIUM. Claeson, T. (Univ. of California, San Diego, La Jolla). Phys. Rev., 147: 340-7(July 8, 1966).

The superconducting transition temperatures of Pb–Tl alloys covering the entire composition range were determined. The T_c's of the alloys are in general intermediate between those of Pb and Tl, except for samples in the concentration range 75–85 at.% Tl, for which the T_c's are lower. Two other features, a continuous change of slope of T_c versus composition, and a small peak structure in T_c, occur at about the 50 at.% composition. These features, which occur in the fcc (Pb) phase, might arise from a Brillouin-zone effect of the Merriam type. If the model for the Fermi surface in lead proposed by Anderson and Gold (based upon their de Haas-van Alphen data and using the orthogonalized plane-wave method) is employed, such an effect would be expected at the composition observed. On the other hand, an order-disorder transformation might contribute to the observed effects. A speculation regarding a connection between the electronic structure effect and a possible ordering process is made. Superconductivity behavior suggests an extension of the Pb solid solution, in a limited temperature interval, to higher Tl concentrations than those in the accepted phase diagram. The terminal solid solubility of Tl in Pb is found to be 88 ± 2 at.% at 25 and at 295°C. The solubility of Pb in α-Tl is 2.5 ± 1 at.% at 25°C; in β-Tl it is 5 ± 1 at.% at 295°C. The T_c's of a few Bi–Tl samples were also measured. Structure, similar to that at $Pb_{0.50}Tl_{0.50}$, appeared in the T_c curve at $Bi_{0.15}Tl_{0.85}$. (auth)

30298 SUPERCONDUCTING TRANSITIONS OF AMORPHOUS BISMUTH ALLOYS. Shier, J. S.; Ginsberg, D. M. (Univ. of Illinois, Urbana). Contract SD-131. Phys. Rev., 147: 384-91(July 8, 1966).

Measurements were made of the critical temperatures T_c of binary-alloy films composed of amorphous bismuth with lead, thallium, or antimony in concentrations up to 13 at.%. The curves showing T_c as a function of impurity concentration are nearly linear, as expected for a superconductor with no crystalline anisotropy. The slopes of the curves are not simply related to the valence or free-atom size of the impurity atoms. It is suggested that this may be explainable by extending Faber and Ziman's theory of the breakdown of Linde's rule for liquid alloys. The transitions of the films into the superconducting state are extremely sharp (~5 mdeg wide). This indicates strongly that the electromagnetic coherence length does not limit the sharpness of the transition. (auth)

30299 MEASUREMENTS OF THE ULTRASONIC ATTENUATION IN LIQUID ^{4}He AT LOW TEMPERATURES. Abraham, B. M.; Eckstein, Y.; Ketterson, J. B.; Vignos, J. H. (Argonne National Lab., Ill.). Phys. Rev. Lett., 16: 1039-42(June 6, 1966).

Preliminary measurements of the attenuation of ultrasound, $\alpha(\omega,T)$ in liquid ^{4}He at low temperatures and at frequencies of 30, 90, and 150 Mc, where ω is the angular frequency and T the absolute temperature, are presented. (B.G.D.)

30300 ULTRASONIC ATTENUATION IN PURE STRONG-COUPLING SUPERCONDUCTORS. Ambegaokar, Vinay (Cornell Univ., Ithaca, N. Y.). Phys. Rev. Lett., 16: 1047-8(June 6, 1966).

It is shown that a straightforward calculation of sound attenuation in pure strong-coupling superconductors is possible in the limit $ql \gg 1$, where q is the phonon wave number and l is the electron mean free path. (B.G.D.)

30301 INFLUENCE OF NEUTRON IRRADIATION ON THE SUPERCONDUCTIVE PROPERTIES OF TIN AND INDIUM FOILS. Van Itterbeek, A.; Van Poucke, L.; Nihoul, J.; Thys, W. (Instituut voor Lage Temperaturen en Technische Fysica, Louvain, Belg.). Physica, 32: 484-8(Feb. 1966).

Tin and indium foils were neutron-irradiated with a flux of approximately 1.9×10^{16} th.n/cm^2 at liquid nitrogen temperature. The influence of the irradiation on the superconductive properties was investigated. For the tin foils reproducible effects obtained were a decrease in the critical temperature from 0.004 to 0.011°K, and in the critical field. The residual resistance increased a few per cent. A measurable variation on the indium foils when irradiated in a similar way as the tin foils could not be found. A comparison with theory and experiments on tin alloys is given. It is shown that the decrease of the mean free path l by impurities and neutron irradiation influence T_c in a different way. (auth)

30302 SURFACE SUPERCONDUCTIVITY AT HIGH TEMPERATURES. Silvert, William (Michigan State Univ., East Lansing). Physics, 2: 153-63(Mar. 1966).

The possibility that surface superconductivity of the Ginzburg type might occur at high temperatures is investigated. The most likely effect is seen to be surface ordering brought about by resonance coupling through the impurity surface states. A mechanism is described by which the localized coherence which this requires can occur, giving transition temperatures orders of magnitudes higher than any now known. (auth)

30303 INDUCTANCE VS. CURRENT CHARACTERISTICS OF SUPERCONDUCTORS. Clorfeine, A. S.; Young, F. J. (Carnegie Inst. of Tech., Pittsburgh). Proc. IEEE (Inst. Elec. Electron. Eng.), 54: 415-17(Mar. 1966).

A calculation of the inductance-current curves of superconductors in analogy to the C-V curves of varactors is presented. (B.G.D.)

30304 HIGH-FREQUENCY RESIDUAL LOSSES IN SUPERCONDUCTORS. Haden, C. R. (Univ. of Oklahoma, Norman). Proc. IEEE (Inst. Elec. Electron. Eng.), 54: 417-18(Mar. 1966).

A flux trapping model is presented to describe the h-f residual losses in superconductors. The model is based on flux trapping of the r-f field at imperfections in the superconducting surface. (B.G.D.)

30305 FLUX ENTRY IN MACROSCOPIC SUPERCONDUCTING RINGS. Zimmerman, J. E.; Silver, A. H. (Ford Motor Co., Dearborn, Mich.). Solid State Commun., 4: 133-6(Mar. 1966).

Accurate measurements of the flux in a weakly connected superconducting ring of inductance L, as a function of applied field and critical current i_c, show the linear relation between current and field at low superconducting pair velocities and the existence of de-pairing at high pair velocities. Transitions between quantum states with the selection rule $\Delta k = \pm 1$ are either reversible or irreversible depending upon the value of $2eLi_c/h$. (auth)

30306 MEASUREMENT OF THE TEMPERATURES OF THE λ TRANSITION AND DENSITY MAXIMUM OF LIQUID ^{4}He. Peshkov, V. P.; Borovikov, A. P. (Inst. of Problems in Physics, Academy of Sciences, USSR). Zh. Eksp. Teor. Fiz., 50: 844-52(Apr. 1966). (In Russian).

The vapor pressure of ^{4}He at the λ point and the temperature difference between the λ point (T_λ) and the temperature of the density maximum of liquid ^{4}He ($T_{max\rho}$) were measured with high precision. The position of the λ point was determined from the shape of the specific-heat curve and the sharp change of heat transfer. The position of the density maximum was determined from the change of the nature of convection. The vapor pressure at the λ point was found to be $P_\lambda = 37.80 \pm 0.03$ mm Hg (0°C, g = 980.665 cm/sec^2), $T_\lambda^{(58)} = 2.1720 \pm 0.0003$°K, and the temperature difference $T_{max\rho} - T_\lambda = 0.0065 \pm 0.0005$°. (auth)

30307 VISUAL SOLIDIFICATION OF HELIUM ISOTOPE SOLUTIONS. Bereznyak, N. G.; Bogoyavlenskii, I. V. (Inst. of Physics and Technology, Academy of Sciences, Ukrainian SSR). Zh. Eksp. Teor. Fiz., 50: 853-5(Apr. 1966). (In Russian).

Solidification of helium isotopes and pure ^{4}He solutions in a glass ampoule was investigated, and a distinct difference between the two processes was found. The boundary layer between the liquid and solid phases was a finely dispersed mixture of small crystals and liquid. The ease of obtaining a solid phase of uniform composition can probably be explained by the special properties of the crystallization of the solution. (auth)

30308 A RESONANCE METHOD STUDY OF THE NATURE OF OSCILLATIONS OF HELIUM II NEAR THE SURFACE OF A VIBRATING DISC. Andronikashvili, E. L.; Gamtsemlidze, G. A.; Dzhaparidze, Sh. A. Zh. Eksp. Teor. Fiz., 50: 856-60(Apr. 1966). (In Russian).

It was found that during supercritical oscillations of a disc in helium II the region into which the supercritical (vortex) oscillation regime penetrates is much smaller than the region in which the liquid participates in the disc oscillations. The respective values of the penetration depth for a vortex and ordinary oscillation regime were measured in a temperature interval from 1.6 to 1.9°K. The effective density of the superfluid component involved in the supercritical oscillations was calculated. (auth)

30309 BOUNDARY CONDITIONS AND SURFACE SUPERCONDUCTIVITY. Zaitsev, R. O. Zh. Eksp. Teor. Fiz., 50: 1055-63(Apr. 1966). (In Russian).

The boundary conditions for the Ginzburg-Landau-Gorkov equations on the interface between two superconductors and between a superconducting and normal metal are found. In particular, the limiting cases of pure or very impure metals are considered. Boundary conditions for an arbitrary impurity concentration can also be derived by means of a simple generalization. The quasiclassical trajectory method employed can be used for determining the boundary condition for a plane or a rough surface. The critical field for a system consisting of a superconducting and normal metal is calculated; it slightly exceeds the second critical field H_{c2} of a massive superconductor. (auth)

30310 METHOD OF IMAGES IN MAGNETOSTATIC PROBLEMS INVOLVING A SPHERICAL SUPERCONDUCTIVE BOUNDARY. Beloozerov, V. N.; Levin, M. L. Zh. Tekh. Fiz., 36: 3-6(Jan. 1966). (In Russian).

It was previously shown that the magnetic field produced by a current flowing in a closed circuit every element of which is at the same distance from the center of a superconducting sphere is equal to the sum of the magnetic field produced in the absence of the superconducting sphere by the original current and that produced by a certain image current flowing in a circuit obtained from the original circuit by inversion in the sphere. This image technique is generalized to the case in which the elements of the circuit are not all at the same distance from the center of the sphere. In this case the image currents comprise a nonuniform current flowing in the image circuit obtained by inversion in the sphere and radial currents flowing between the center of the sphere and the elements of the image circuit. The total image current is solenoidal. This technique can also be applied to calculate the magnetic field within a spherical cavity with a superconducting wall. In this case the image circuit is outside the spherical cavity and the radial image currents flow between elements of the image circuit and infinity. This technique is illustrated with several simple examples, including calculation of the field of a point magnetic dipole in the presence of a superconducting sphere and the radiation of a magnetic dipole moving at nonrelativistic velocity past a superconducting sphere. (ATD)

30311 NEW MECHANISM FOR SUPERCONDUCTIVITY. Luttinger, J. M. (Columbia Univ., New York). pp 86-97 of Many-Body Theory. Kubo, Ryogo (ed.). Tokyo, Syokabo Publishing Co. New York, W. A. Benjamin, Inc., 1966.

A mechanism for superconductivity, which provides instability against Cooper pair formation, is outlined. It is found that a weakly interacting system of fermions cannot maintain a sharp Fermi surface down to the absolute zero of temperature, regardless of the form of the interaction. A criterion for superconductivity is also given. (G.O.Y.)

30312 BREAKDOWN OF THE QUASI-PARTICLE APPROXIMATION IN METALS. Schrieffer, J. Robert (Univ. of Pennsylvania, Philadelphia). pp 98-116 of Many-Body Theory. Kubo, Ryogo (ed.). Tokyo, Syokabo Publishing Co. New York, W. A. Benjamin, Inc., 1966.

An essentially exact solution to the one-phonon Green's function for the coupled-yield problem is derived and is applied to electron tunneling. It is shown that the static transport coefficients, electrical and thermal conductivities, spin diffusivity, etc., are all unaffected by the strong electron-phonon coupling, in spite of the apparent breakdown of the quasi-particle approximation at high temperatures. Strong-coupling superconductivity is also discussed in terms of this Green's function theory. (G.O.Y.)

30313 LANDAU-GINSBURG EQUATIONS AND THE PROPERTIES OF TYPE II SUPERCONDUCTORS. de Gennes, P. G. (Univ., Paris, Orsay). pp 117-33 of Many-Body Theory. Kubo, Ryogo (ed.). Tokyo, Syokabo Publishing Co. New York, W. A. Benjamin, Inc., 1966.

The Landau-Ginsburg equations are derived and are used to study the properties of type-II superconductors. (G.O.Y.)

30314 THEORY OF THE SUPERCONDUCTIVE ENERGY GAP AND THE THERMAL CONDUCTIVITY OF IMPURE TIN [Thesis]. Ulbrich, Carlton Wilbur. Storrs, Conn., Univ. of Connecticut, 1965. 96p.

The experimental results of Pearson for the thermal conductivity of normal and superconducting impure tin are explained theoretically. An integral expression is developed for the normal-state lattice thermal conductivity from the Boltzmann equation and includes the scattering of phonons by grain boundaries and by electrons. The latter scattering mechanism is assumed to be adequately described by the electron-phonon interaction of Pippard. A detailed numerical comparison to experiment is not made, but it is shown that the theory predicts the observed temperature dependence of the lattice conductivity. The theory of Bardeen, Rickayzen, and Tewordt for the ratio of the thermal conductivities in the normal and superconducting states is ex-

tended to account for anisotropy in the superconducting energy gap. The experimental results of other investigators for the energy gap as a function of crystal direction in pure tin are closely approximated by an algebraic function. This function is used to calculate theoretical curves for the ratio of the conductivities to which the pure sample data of Pearson are compared. The agreement between theory and experiment is good and does not require adjustment of the experimental data for the energy gap in order to obtain the agreement. By use of Green's function techniques an expression is derived which describes the energy gap as a function of crystal direction and impurity concentration. The result shows that a change in the average energy gap may be possible when the density of states is a function of crystal direction. The expression for the energy gap is consistent with Anderson's prediction that the anisotropy should be decreased with the addition of impurities. The comparison of the theory to the experimental results for the impure samples shows that the data lie slightly outside the range of the theoretical curves to which the pure sample data were compared. (TCO)

30315 SUPERCONDUCTING PROPERTIES OF HIGH-PURITY NIOBIUM [Thesis]. Stromberg, Thorsten Frederick. Ames, Iowa, Iowa State Univ., 1965. 105p.

The superconducting properties of high-purity niobium were investigated throughout the temperature range from 1.1°K to the transition temperature at 9.25°K. The results of these measurements show that niobium exhibits a reversible, but broad magnetic transition like that found in type-II superconductors. Analysis of the niobium data shows that H_c, the thermodynamic critical field, is linear in T^2 to one percent with $T_c = 9.25$°K and $H_0 = 1990$ gauss. The free energy shows approximate agreement with the BCS prediction. From low temperature H_c data a value for γ, the normal state electronic specific heat coefficient, is found to be 1.80×10^{-3} cal/mole°K^2. The temperature dependence of H_{c1} follows the function $H_{c1}(t) = 1735(1 - t^{2.14})$ to 1%. The magnetic moment in the region near H_{c_1} is a continuous function of applied field with a slope ten times smaller than the demagnetizing slope. Consequently, the transition is of second order. H_{c2} fits a function of the following form: $H_{c2}(t) = (1 - t^2)/(1 + t^2)$ to 5%. The GLAG theory of superconductivity predicts a temperature dependence at $T = 0$ for H_{c2} which is 30% smaller than the measured values. Presumably this discrepancy is due to the fact that niobium does not satisfy the locality condition ($\xi_0 \ll \lambda$) required by the GLAG theory. Only in a very restricted temperature range near T_c, where the locality condition can be satisfied, is there any agreement with theory. (Dissertation Abstr.)

30316 SUPERCONDUCTING TRANSITION TEMPERATURES OF ZIRCONIUM AND ZIRCONIUM ISOTOPES [Thesis]. Jones, Delbert Merle. Madison, Wis., Univ. of Wisconsin, 1965. 186p.

Measurements were made of the superconducting transition temperatures of several samples of both naturally occurring and isotopically enriched zirconium. The work was initiated to examine the deviation of the superconducting properties of a transition element from the isotope effect as predicted by the Bardeen-Cooper-Schrieffer theory ($T_c M^{1/2} = \text{const.}$). An a-c null-detection system operating at 96 cps was used to monitor the relative magnetic susceptibilities of the samples as a function of temperature and applied magnetic field, with a measuring field calculated to be less than 0.025 gauss. The necessary temperatures were obtained with the use of a ^{3}He cryostat which was designed and constructed for this project. Samples of ^{90}Zr, ^{92}Zr, and ^{94}Zr, produced by an iodide process and enriched to an isotopic concentration of more than 90% were measured and found to have transition temperatures in zero magnetic field at 0.560°, 0.558°, and 0.561°K, respectively. From the order of temperature in which the three isotopes became superconducting and from the small temperature separations between the transitions, it was concluded that there is no isotope effect in zirconium. Measurements were also made in small applied magnetic fields. The isotopes were found to have similar critical field curves, which were nearly parabolic and had initial slopes of 230 gauss/deg. Two samples of iodide process Zr of slightly lesser purity and having natural isotopic constitution were found to become superconducting at 0.525°K. A sample of sponge process Zr of considerably lesser purity became superconducting at 0.605°K, with behavior characteristic of a hard superconductor. (TCO)

30317 SUPERCONDUCTING COILS FOR SHIELDING IN SPACE [Thesis]. Englesson, George Anthony. Ames, Iowa, Iowa State Univ., 1965. 124p.

A shield was designed to protect man from the hazard of space radiation on interplanetary-exploration-colonization missions. The shielding is provided by a magnetic field generated by superconducting coils wound as a large-diameter toroid. The configuration approximates an infinite solenoid, and a field-free region is provided within the solenoid by winding two concentric coils with the same number of turns and allowing each to carry an equal but oppositely directed current. (TCO)

30318 SUPERCONDUCTIVITY IN THE TRANSITION METALS AT VERY LOW TEMPERATURES [Thesis]. Jensen, M. Anthony. San Diego, Calif., Univ. of California, 1965. 175p.

The results of an investigation of the occurrence of superconductivity in certain transition elements and alloys are presented. The experimental results are from the beginning and end of the transition metals. Most of the elements in these two regions aren't superconducting to the lowest temperatures reached (0.02°K), but many results were obtained on their alloys. These results are discussed in terms of the properties of all the transition metals and in terms of the theory presented for the transition temperature. It is concluded that the behavior (decrease) of superconductivity near Pd, Pt, and Rh is a real effect, which also manifests itself in a greatly enhanced spin susceptibility. Also, in this region the superconductivity, electronic specific heat, and spin susceptibility all seem to depend only on the electron density. The behavior (no superconductivity) near Sc, Y, and Lu may be affected by the presence of impurities. (Dissertation Abstr.)

30319 THEORY OF SOLID ^{3}He [Thesis]. Rosenwald, David. San Diego, Calif., Univ. of California, 1965. 106p.

A detailed investigation is made of the single-particle model calculation for solid ^{3}He at 0°K and under an external pressure at 30 atm. It is shown at the outset that this calculation gives a rigorous upper bound for the ground state enthalpy of the system, provided that the correct hamiltonian is used. The many-body wavefunction is taken to be a product of single-particle wavefunctions cubically symmetric about their respective lattice sites. In order to obtain the best product wavefunction of this type, the standard minimization principles are applied, and self-consistent equations are obtained, which are similar (but not identical) to the usual Hartree equations. These equations are then solved numerically to obtain the ground state energy of the system as a function of the volume. An improvement of only 8% is obtained in the calculated enthalpy by using cubically symmetric single-particle wavefunctions rather than spherically symmetric ones, and the calculated enthalpy is still significantly higher than the probable experimental value. Subsequently, to get better results for the ground state energy, pair correlations are included explicitly in the many-body wavefunction. It is then seen that the effects of pair correlations can be taken into account to first order by using a modified two-body potential in the single-particle model calculation. Several different forms are used for this modified potential, and the significance of the markedly improved energy results is discussed. (Dissertation Abstr.)

30320 STUDIES OF SOLID H_2–D_2 MIXTURES BY NUCLEAR MAGNETIC RESONANCE [Thesis]. de Castro, Elve Monteiro. Columbus, Ohio, Ohio State Univ., 1964. 161p.

Solid mixtures of H_2–D_2 were studied in several concentrations by NMR with a broad line spectrometer (CW) and the pulsed technique. In experiments with pure n-H_2 at

10 Mcps and 4.2°K the resonance line is narrower than a gaussian, has a linewidth of 5.7 gauss and is slightly asymmetric at an r-f field $H_1 \approx 7.5$ mgauss. At 1.10°K the λ-splitting of the H_2 resonance line shows the center line, two side peaks, and the two humps at 3.2, 39.8, and 76 gauss separation measured from peak to peak, respectively. The experiments with pure n-D_2 at 2.6 mcps show no λ-splitting above 1.10°K. The linewidth at 4.2°K was 1.66 gauss from peak to peak and very asymmetric compared with the n-H_2 line. The λ-splitting of D_2 was found below 2°K when an enriched sample of D_2 containing 80% para/ortho was used. The side peaks were 76.8 Kcps apart. Mixtures of normal H_2 with normal D_2 behaved very much like mixtures of ortho and para H_2. Concentrations above 95% H_2/D_2 show the same type of λ-splitting as pure H_2, and no significant change in the splitting distances was observed. The temperature T_λ of the transition decreases as the H_2 concentration decreases. At 10°K the resonance line is simple with a small broad tail of similar shape and amplitude in all concentrations. The broad tail at 4.2°K has larger amplitude for samples with lower concentrations of H_2. Below 4.2°K the tail increases very much in amplitude; the lineshape becomes composite and almost resolved at the lower concentrations of H_2. In all concentrations it was observed that the linewidth narrows with increasing the r-f field H_1. If these results are compared with the theory due to Provotorov, one obtains T_1' (the longitudinal relaxation time characteristic of the return to the equilibrium distribution of the dipolar energy) of the order of 0.4 T_1. (TCO)

30321 ELECTRONIC THERMAL CONDUCTIVITY AND OTHER PROPERTIES OF GAPLESS SUPERCONDUCTORS [Thesis]. Griffin, Peter Allan. Ithaca, N. Y., Cornell Univ., 1965. 205p.

Calculations of the decay of a heat current, a longitudinal sound wave, and the nuclear spin temperature in a superconducting alloy with a small concentration of paramagnetic impurities are discussed. The electronic thermal resistance arising from the electron-impurity scattering was computed starting from a Kubo formula, scattering-in terms due to ladder diagrams being included. The final expression for the thermal conductivity K_s may be examined analytically in several limits. Most of the discussion is based on the physically reasonable assumption that the exchange scattering time τ_S is much larger than the total scattering time due to the paramagnetic and nonmagnetic impurities. This is equivalent to assuming that the generalized mean free path in the gapless superconductor is equal to that in the normal metal. In this case, the quadrature for the ratio K_s/K_n is considerably simplified; in particular, it only depends on τ_S and $\Delta(T,\tau_S)$. In addition, the attenuation (α_s) of an ultrasonic longitudinal sound wave ($|q| > 1$) and the nuclear spin-lattice relaxation rate (R_s) are computed using a "Golden Rule" approach. The results for α_s complement the low-frequency results of Kadanoff and Falko. Analytic expressions for K_s, α_s and R_s are given for low temperatures and for $T \to T_c$. The slope (as a function of $t \equiv T/T_c$) of K_s is proportional to $1/\tau_S$ near T_c for small but finite concentrations; on the other hand, α_s and R_s are proportional to τ_S in the same region. Numerical calculations were made over the whole temperature range for several impurity concentrations ($\propto 1/\tau_S$). The onset of gaplessness [$\Delta(T,\tau_S)\tau_S < 1$] is not marked by any dramatic changes in the transport properties or their derivatives as a function of t. For convenience, the numerical values of $\Delta(T)$, $\omega_0(T)$ and the density of states $\rho(\omega)$ used in the calculations are included. The results, suitably reinterpreted, may also describe irreversible processes in thin, "dirty" films under the influence of magnetic fields, persistent currents, and rotations. (TCO)

Neutron Physics

See also REACTOR TECHNOLOGY — Criticality Studies

Refer also to abstract 30166.

30322 (BNL-947) NEUTRON THERMALIZATION AND DIFFUSION IN NONISOTHERMAL MEDIA. Sehgal, Bal Raj (Brookhaven National Lab., Upton, N. Y.). Oct. 1965. Contract AT(30-2)-Gen-16. 12p. Dep. mn. CFSTI $1.00 cy, $0.50 mn.

The effect of nonuniform temperature distribution on the stationary thermal neutron distribution is studied in an extended nonabsorbing, nonisothermal moderator medium. Expressions are derived for the neutron concentration diffusion coefficient and the neutron "thermal" diffusion factor which are valid for a general scattering law. Specific results are obtained for a hydrogen gas moderator and for a heavy gas moderator. The results for neutron distribution, the diffusion coefficient and the thermal diffusion factor are compared with those of previous studies. (auth)

30323 (ORNL-TM-1537) TRANSFER: A PROGRAM TO CALCULATE P_n MULTIGROUP SCATTERING MATRICES. Craven, C. W. Jr.; Lucius, J. L. (Oak Ridge National Lab., Tenn.). May 9, 1966. Contract W-7405-eng-26. 37p. Dep. mn. CFSTI $2.00 cy, 10.50 mn.

TRANSFER is a Fortran program which calculates multigroup scattering matrices in the P_n approximation for use in S_nP_n transport theory calculations and B_n spectral calculations. Pointwise total scattering cross sections and Legendre expansion coefficients of the angular distribution are reduced to narrow group averages by assuming a 1/E flux spectrum and numerically integrating the inscattering source term in the Boltzmann equation. The resulting multigroup transfer matrices are placed on punched cards. (auth)

30324 (RPI-328-56, pp 52-93) NEUTRON THERMALIZATION. (Rensselaer Polytechnic Inst., Troy, N. Y.).

Developments in each of the following areas are reported: space-dependent spectra in a multiplying media; investigation of mean emission times through time-of-flight spectrum measurements; 3 meter flight path for thermalization studies; preliminary time dependent spectra measurements in polyethylene and D_2O; analysis of thermalization in Be; re-entrant hole perturbation in water; computer codes development; and reactor kinetics. (M.O.W.)

30325 (RPI-328-56, pp 113-34) LOW-ENERGY NEUTRON INELASTIC SCATTERING. (Rensselaer Polytechnic Inst., Troy, N. Y.).

Operation of the new fast chopper neutron spectrometer is discussed. Preliminary results of differential scattering cross sections for 0.486-ev fast neutrons on polyethylene are given and compared with previous ones. Cross section measurements were also made for ZrH_2 by 0.238- to 0.570-ev neutrons. (M.O.W.)

30326 METHOD FOR NUMERICAL INTEGRATION OF THE NEUTRON TRANSPORT EQUATION IN SLAB GEOMETRY. Takeuchi, Kiyoshi; Kataoka, Iwao (Ship Research Inst., Tokyo). J. Nucl. Sci. Technol. (Tokyo), 3: 209-12 (May 1966).

A brief description is given of the mathematical procedures for direct integration of the neutron transport equation in slab geometry using the EOS code, and some results are given for carbon, water, and polyethylene. (L.B.S.)

30327 TIME-DEPENDENT THERMALIZATION IN MULTIPLYING SYSTEMS. Kaneko, Yoshihiko (Japan Atomic Energy Research Inst., Tokyo). J. Nucl. Sci. Technol. (Tokyo), 3: 212-15 (May 1966).

An analysis was made of the time-dependent neutron thermalization problem on a discrete eigenvalue model. It is concluded that the thermalization time constant in a multiplying system should be smaller than in a corresponding pure nonmultiplying system. The conclusion was substantiated by preliminary measurements made by the silver filter transmission method in which the thermalization time constant in a pure graphite system was compared with those in graphite moderated enriched uranium systems. (L.B.S.)

30328 P_1 ANALYTICAL SOLUTION OF THE ENERGY- AND SPACE-DEPENDENT TRANSPORT EQUATION FOR THERMAL NEUTRONS. Syros, Constantin (C.C.R.

Euratom, Ispra, Italy). Nucl. Sci. Eng., 22: 263-5(June 1965).

Starting from the fundamental theory given by Case a number of investigations are made in order to solve the transport equation with energy-dependent cross sections. (B.G.D.)

30329 SPIN POLARIZATION AND THE AGE OF NEUTRONS IN WATER. Goldsmith, Mark. Nucl. Sci. Eng., 25: 242-7(July 1966). (WAPD-T-1844; CONF-651101-39).

The effects of spin polarization on the slowing down of neutrons in water is investigated. Spin-dependent scattering cross sections are derived from a combination of resonance parameters, experimental phase shifts, and optical model calculations. It is shown that the effect of polarization on the age of neutrons slowing down from an unpolarized plane source in an infinite moderator may be rigorously obtained from the P-1 approximation to the transport equation. One finds that the age of fission neutrons slowing down in water would be decreased by 0.8% by polarizing collisions with oxygen below 2.6 Mev were it not for depolarizing collisions with hydrogen that reduce this figure to 0.2%. (auth)

30330 SLOW-NEUTRON SCATTERING BY WATER. McMurry, H. L.; Russell, G. J.; Burgger, R. M. Nucl. Sci. Eng., 25: 248-60(July 1966).

Experimental data on the slow-neutron (<0.1 ev) scattering of room-temperature water were obtained using the velocity selector at the Materials Testing Reactor. The data agree with the results of Haywood obtained using a slow-neutron velocity selector, with the results of Kottwitz and Leonard obtained using a triple-axis spectrometer, and with the results of Kirouac obtained using a linear accelerator plus phased chopper. There are marked differences from the results of Sakamoto and coworkers, who used cold neutrons and a rotating crystal spectrometer. An extension of the Nelkin model was devised that gives calculated results in good agreement with the MTR data, whereas the Nelkin model generally gives poor agreement. The new model treats water as a mixture of 10% of free molecules and 45% each of two aggregates in which the effective masses for H scattering are 75 and 150. Each aggregate has a set of vibrational modes with energies distributed in the range $0 < E \leq 0.125$ ev, and each H_2O molecule exhibits the internal modes with characteristic energies of 0.2, 0.45, and 0.46 ev. The amplitudes of the low-energy vibrations are selected so the calculated scattering agrees with the Materials Testing Reactor data. Total cross sections calculated on the new model and the Nelkin model agree quite well with the data. The new model gives values of the average cosine of the scattering angle that are closer to the data than those calculated by the Nelkin model, but the calculated results are always higher than the data. At very low neutron energies, the present Nelkin model calculations give total cross sections that are lower than those reported by Koppel and Young using essentially the same model. The reason for this is not known. (auth)

30331 THERMAL-NEUTRON SPECTRUM IN WATER WITH TEMPERATURE DISCONTINUITY. Saastamoinen, J. Nucl. Sci. Eng., 25: 261-5(July 1966).

The relaxation of the neutron spectrum near a temperature discontinuity is studied both theoretically and experimentally. The P_1 approximation and Nelkin's model for light water are used. When the temperature difference is 45°C, theoretical values of 4.5 and 4.6 mm for the relaxation lengths on the warmer and colder side of the discontinuity are obtained. The experimental value is about 2.3 mm. Thus, there is large disagreement between the experimental and theoretical results. The reason for this cannot be pinpointed, but the following explanations are possible: transport effects, inapplicability of Nelkin's model, and insufficient accuracy of the trial functions for flux and the treatment of its energy-dependence. (auth)

30332 SELF-ADJOINT VARIATIONAL PRINCIPLE FOR DERIVING VACUUM AND INTERFACE BOUNDARY CONDITIONS IN THE SPHERICAL HARMONICS METHOD. Toivanen, Timo. Nucl. Sci. Eng., 25: 275-84(July 1966).

By the technique of splitting the total directional flux into even and odd portions in angle, the stationary monoenergetic Boltzmann equation with arbitrary collision kernel and with arbitrary external directional source of a general geometry is symmetrized to a self-adjoint form. The continuity and boundary conditions for the resulting self-adjoint integro-differential equation are explicitly constructed. A variational principle is then set up by devising a self-adjoint Lagrangian whose minimum property is equivalent to the symmetrized Boltzmann equation with the associated continuity and boundary conditions. The developed variational principle contains no arbitrariness and is used for deriving unique variational boundary conditions for the P_1 approximation of the spherical harmonics method. It is shown, for a general geometry, that applying the semidirect variational method with an angle-independent trial function yields, without any physical reasoning, the correct P_1 differential equation and the corresponding no-return-current boundary condition. (auth)

30333 NEUTRON LIFETIME AND SLOWING-DOWN TIME CALCULATIONS IN BERYLLIUM. Ahmed, Feroz; Ghatak, A. K. (Univ. of Delhi). Nucl. Sci. Eng., 25: 298-300(July 1966).

The results of the calculations by numerically solving the Laplace-transformed diffusion equation employing a method similar to that of Ghatak and Krieger are reported, and the effects of the presence of large elastic scattering peaks on $\langle t \rangle_E$ are investigated. The calculations are performed for various sizes of the beryllium-moderated assembly to include normal absorption. These calculations give more insight into the trapping effect. (auth)

30334 INELASTIC SCATTERING CROSS SECTIONS FOR POLYETHYLENE AND WATER IN THE GAS TRANSITION REGION. Kirouac, G. J.; Moore, W. E.; Seemann, K. W. (Rensselaer Polytechnic Inst., Troy, N. Y.). Nucl. Sci. Eng., 25: 300-2(July 1966).

The double-differential cross section $\partial^2\sigma/(\partial\Omega\partial E)$ is reported for polyethylene and water at three incident neutron energies, 0.83, 1.0, and 1.8 ev. Data in this energy range demonstrate the transition of the inelastic-scattering cross section from bound-atom to gas-like behavior. (B.G.D.)

30335 COHERENT NEUTRON SCATTERING AMPLITUDES OF ^{10}B AND ^{11}B. Donaldson, R. E.; Groves, D. J.; Pearson, R. K. (Univ. of California, Livermore). Phys. Rev., 146: 660-1(June 17, 1966). (UCRL-14301).

The coherent neutron scattering amplitude of B_2O_3, highly enriched in ^{11}B, was measured by the multiple-refraction method. Combination with the coherent scattering amplitude of B measured by the mirror method yields: $a_{^{11}B\,coh} = +6.53 \pm 0.35$ F; $a_{^{10}B\,coh} = +1.4 \pm 1.5$ F. (auth)

30336 TIME EXPANSION OF CORRELATION FUNCTIONS AND THE THEORY OF SLOW NEUTRON SCATTERING. Nijboer, B. R. A.; Rahman, A. (Argonne National Lab., Ill.). Physica, 32: 415-32(Feb. 1966).

The velocity correlation function for a classical system of particles interacting with a two-particle potential is expanded in powers of t. The coefficients in this expansion are averages of derivatives of the interaction potential and can be expressed in terms of instantaneous two, three, etc., particle distribution functions. For the special case of a harmonic crystal these expressions reduce to the respective moments of the frequency distribution function. For liquid argon the range of values of t, for which the velocity correlation is well represented by the first few terms of its time expansion, is determined from a comparison with computer results. Similarly, the range of values of the momentum transfer is investigated, for which this time expansion leads to a useful representation of the incoherent scattering cross section for slow neutrons. For coherent scattering analogous formula are given, but no numerical comparison with the computer results were made. In addition, it is shown that the non-Gaussian behavior of $G_s(r,t)$ obtained from the computer results has considerable influence on the shape of the incoherently scattered slow neutron spectrum. It is pointed out that

slow neutron scattering with large values of momentum transfer can be used as an experimental technique for the determination of the mean square acceleration in any system. (auth)

30337 CLASSICAL DERIVATION OF EFFECTIVE DIFFERENTIAL SCATTERING CROSS SECTION FOR NEUTRONS IN A MONATOMIC GAS. Lieberoth, Juergen. Z. Phys., 193: 181-4(1966). (In German).

A simple, classical derivation on the effective differential scattering cross section concerning the scattering of neutrons in a monatomic gas is presented. (auth)

30338 ON THE GENERAL DISPERSION LAW OF THE LINEAR BOLTZMANN EQUATION. Joest, Karl-Heinz (Interatom, Bensberg, Ger.). Z. Phys., 193: 202-17(1966). (In German).

The conditions for the existence of particular solutions are investigated for the space- and time-dependent linear Boltzmann equation which describes the neutron field. The regular solutions correspond to a discrete spectrum of parameters. Therefore, such particular states can be isolated asymptotically in suitable experiments. The number of possible asymptotic neutron-field experiments is determined by the number of possible combinations of discrete parameter values corresponding to regular solutions. In the course of the analysis, two possible types of new experiments are found. These are the instationary exponential experiment and the neutron-wave experiment with damped excitation. The formulation of the problem is extended to include the energy dependence of neutron distribution functions. (auth)

30339 TIME-DEPENDENT MONOENERGETIC NEUTRON TRANSPORT IN TWO ADJACENT SEMI-INFINITE MEDIA [Thesis]. Erdmann, Robert C. Pasadena, Calif., California Inst. of Tech., 1966. 191p.

An exact solution to the monoenergetic Boltzmann equation is obtained for the case of a plane isotropic burst of neutrons introduced at the interface separating two adjacent, dissimilar, semi-infinite media. The method of solution used is to remove the time dependence by a Laplace transformation, solve the transformed equation by the normal mode expansion method, and then invert to recover the time dependence. The general result is expressed as a sum of definite, multiple integrals, one of which contains the uncollided wave of neutrons originating at the source plane. It is possible to obtain a simplified form for the solution at the interface, and certain numerical calculations are made there. The interface flux in two adjacent moderators is calculated and plotted as a function of time for several moderator materials. For each case it is found that the flux decay curve has an asymptotic slope given accurately by diffusion theory. Furthermore, the interface current is observed to change directions when the scattering and absorption cross sections of the two moderator materials are related in a certain manner. More specifically, the reflection process in two adjacent moderators appears to depend initially on the scattering properties and for long times on the absorption properties of the media. This analysis contains both the single infinite and semi-infinite medium problems as special cases. The results in these two special cases provide a check on the accuracy of the general solution since they agree with solutions of these problems obtained by separate analyses. (Dissertation Abst.)

30340 THERMAL NEUTRON DISTRIBUTIONS FROM AN ANISOTROPIC FAST NEUTRON SOURCE [Thesis]. Cohen, Martin Owen. New York, Columbia Univ., 1965. 143p.

A comparison is reported of calculated and measured thermal neutron density distributions from a point source of fast neutrons in water. Protons accelerated in a Van de Graaff generator produced, through the Li(p,n) reaction, a point source of neutrons of energy 3.36 Mev or less. Although the source is anisotropic a comparison with an isotropic source can be made by integrating detector response over all solid angle. The method employed provided automatic integration over all solid angles and eliminated flux depression effects. It involved activation of the manganese in a 1N solution of $MnSO_4$ contained in sections with spherical boundaries concentric about the source. The boundaries were made of lucite, too thin to perturb the fluxes significantly. The concentric spherical regions were immersed in a water-filled tank, the walls of which were at least 26 cm from the furthest region measured. After activation runs of about three hours, each region was separately drained and thoroughly stirred. Thus the averaging process over all solid angles was effected. The average specific activity of each region was then determined by counting with a NaI(Tl) gamma ray spectrometer. The average thermal neutron densities were measured in this manner, with better than 0.5% counting statistics, out to 46 cm, representing an attenuation of over four decades. The results were also interpreted to give the total neutron current passing through each of the spherical boundaries. A Fortran Monte Carlo code, MOCINGBIRD, was written to calculate the spatial distributions of averaged thermal neutron density. The experimental and Monte Carlo histograms of thermal neutron density agreed in shape to better than 8% over the whole range and in absolute measure to better than 10%. The average neutron age to absorption was determined from the manganese activity data. The overall agreement between the experimental and calculational results indicates that the important parameters associated with the attenuation and moderation of fast neutrons in water can be successfully calculated providing the cross sections are well known. (TCO)

Nuclear Properties and Reactions

Refer also to abstracts 29143, 29233, 29436, 29529, 29853, and 30249.

30341 (AECL-2529) AN APEX PROGRAM FOR THE ANALYSIS OF GAMMA-GAMMA ANGULAR CORRELATION DATA. Leigh, J. L. (Atomic Energy of Canada Ltd., Chalk River (Ontario)). Jan. 1966. 30p. (CRT-1231). Dep. mn. AECL $1.00.

A program to analyze γ-γ angular correlation data from the cascade decay of aligned nuclei was written in the APEX language for the AECL G-20 computer. Quadratic programming methods are used to determine the population parameters and multipole mixing ratios best fitting the data. Multipole contributions to the gamma rays may include dipole, quadrupole and octupole. The mixing ratios may be defined either as the ratio of L-pole amplitude to dipole amplitude or as the radio of L-pole amplitude to quadrupole amplitude. The program contains algorithms which search for good starting approximations to the parameters, carry out the fit and trace the variation of χ^2 in the region of the best fit. In addition a search for a minimum in χ^2 may be initiated from any desired starting approximation. (auth)

30342 (AERE-M-1670) ETA AND NEUTRON CROSS SECTIONS OF ^{235}U FROM 0.03 TO 200 ev. Brooks, F. D.; Jolly, J. E.; Schomberg, M. G.; Sowerby, M. G. (Atomic Energy Research Establishment, Harwell (England)). Feb. 1966. 17p. Dep. mn.

Measured values of eta, σ_T and σ_F and derived values of σ_C are given for ^{235}U from 0.03 to 200 ev. The averages of the cross sections and of eta and alpha have been calculated for a number of energy groups together with various ratios and integrals of these quantities which are of interest for reactor design studies. Comparisons are made between the results obtained in the present experiment and those from other laboratories. (auth)

30343 (COO-1371-30) ISOBARIC SPIN IN STRIPPING AND PICK-UP REACTIONS. Bayman, B. F. (Minnesota Univ., Minneapolis. School of Physics). [1965]. Contract AT(11-1)-1371. 23p. (CONF-660306-8). Dep. mn. CFSTI $1.00 cy, $0.50 mn.

From American Physical Society, Conference on Isobaric Spin, Tallahassee.

The reactions (d,t) and (d,He-3) on the same target are compared. The (d,t) reaction excites states with isobaric spin $T_A - \frac{1}{2}(\equiv T_<)$ and $T_A + \frac{1}{2}(\equiv T_>)$. The isobaric analogue

of each of the $T_>$ states should be excited by the (d,He-3) reaction. To compare the relative intensities with which pairs of analogue states are excited, an expansion of the target wave function in terms of states of the first A-1 nucleus, coupled to the last nucleon, is considered. (M.O.W.)

30344 (EUR-2779.e) NEUTOF: A PROGRAM TO CORRECT NEUTRON TIME-OF-FLIGHT SPECTRA. Verdan, G. (European Atomic Energy Community, Ispra (Italy). Joint Nuclear Research Center). Mar. 7, 1966. 32p. Dep. mn.

Under special consideration of the finite energy width of the incident neutrons and of the finite chopper burst-time, a correction computer program is being developed. Thanks to the free parameter choice it can be used for many inelastic and elastic neutron scattering problems. In the optional second section of the main program the generalized frequency distribution of the investigated solid can be calculated. The programs written in FORTRAN II are listed. (auth)

30345 (EUR-2798.e) ELASTIC SCATTERING OF NEUTRONS FROM NATURAL SILICON. Coppola, M.; Knitter, H.-H. (European Atomic Energy Community, Geel (Belgium). Central Nuclear Measurements Bureau). Mar. 26, 1966. 10p. Dep. mn.

Angular distributions of neutrons elastically scattered from natural Si were measured in the energy range between 0.57 and 2.28 Mev, using a fast neutron time-of-flight spectrometer. Corrections for beam attenuation and multiple scattering in the sample were performed. Differential cross section results were fitted with a Legendre polynomial expansion and the coefficients for the best fits are presented. (auth)

30346 (GEMP-411) NEUTRON CROSS SECTIONS FOR ^{244}Cm AND ^{238}Pu. Prince, A. (General Electric Co., Cincinnati, Ohio. Nuclear Materials and Propulsion Operation). Feb. 22, 1966. Contract AT(30-1)-3526. 65p. Dep. mn. CFSTI $3.00 cy, $0.75 mn.

Neutron cross sections for ^{244}Cm and ^{238}Pu were calculated from below thermal to 14 Mev. A discussion is presented for the possible neutron reactions, the theoretical assumptions made along with their justification and reasons for choosing certain recommended values. (auth)

30347 (IDO-17147, pp 13-28) NUCLEAR TECHNOLOGY. (Phillips Petroleum Co., Idaho Falls, Idaho. Atomic Energy Div.).

A preliminary comparison of the inelastic scattering in liquid lead yields qualitative agreement with a model that incorporates the idea of high-frequency collective modes of vibration. Detailed analysis is continuing. Studies were made of geometrical effects in boron trifluoride neutron detectors in a preliminary study of the effects of electric field inhomogeneity on pulse-height response. Void effects measurements designed to evaluate the reactivity worth of displaced water in the ARMF I showed (a) that reactivity worths of aluminum and water in the center location were not significantly affected by sample geometry over a large range of sample sizes and (b) that in the corner location, sample geometry effects were significant, but not large. The swelling of Be samples cut from MTR lattice piece LB-15, which was irradiated to 4.0×10^{21} fast n/cm^2 and containing 8.0 cc He/cc Be, is reported. An upper limit of $\approx$1 millibarn was measured for the thermal neutron capture cross section of ^{10}Be. The alpha spectrum of ^{227}Ac chemically separated from ^{231}Pa is shown. The sample holder for preparing and mounting wafer-thin radioactive samples for neutron cross-section experiments is described. (M.O.W.)

30348 (INP-446/PL) OBLICZANIE $\delta(\Theta)$ WEDLUG TEORII SILNEJ ABSORPCJI FRAHNA-VENTERA PROGRAMY DLA MASZYNY CYFROWEJ UMC-1. Computation $\delta(\Theta)$ According to the Strong Absorption Theory Given by Frahn and Venter. Programs for Computer UMC-1). Dudek, Alicja (Institute of Nuclear Physics, Krakow (Poland)). Jan. 1966. 71p. Dep.

The programs for computation of the differential cross sections for elastic scattering of charged particles in the presence of strong absorption are presented according to the theory given by Frahn and Venter both with and without consideration of the volume absorption. (auth)

30349 (JAERI-1102) PROCEEDINGS OF THE SEMINAR ON FAST-NEUTRON CROSS SECTIONS. (Japan Atomic Energy Research Inst., Tokyo). Aug. 1965. 110p. (In Japanese). Dep. mn.

A survey of data was made in order to discuss in detail the problem of neutron cross section data from the experimental and theoretical points of view. The data and their phases involved were discussed for the following: reactions leaving the discrete states of final nucleus, reactions leaving the continuous state of final nucleus, (n,γ) reactions and resonance phenomena, and nuclear fusion. (M.O.W.)

30350 (JINR-P-2682) OB UROVNYAKH SREDNEGO POLYA YADER. (On Average Field Levels of Nuclei), Kalinkin, B. N.; Grabovskii, Ya.; Gareev, F. A. (Joint Inst. for Nuclear Research, Dubna (USSR). Lab. of Theoretical Physics). 1966. 22p. Dep. mn.

A variant of an approximate solution of the Schrödinger equation with the Saxon-Wood potential is considered. Wave functions of one-particle analytical states are obtained, as well as some integrals of their combinations. The results can be applied to the theory of the nucleus and nuclear reactions. (auth)

30351 (N-65-14857) GAMMA FLUXES FROM CIRCULAR AND SPHERICAL SOURCES. Keith, Johnnie R.; Shelton, Frank H. (Kaman Nuclear, Colorado Springs, Colo.). May 15, 1964. 26p. (KN-691-64-5).

The direct (unscattered) delayed gamma fluxes from uniform disks and spheres of radioactive debris are considered for several configurations, and are compared with the flux from a point source of comparable magnitude. An approximation is also made of the buildup factor necessary to obtain the actual gamma flux from the direct gamma flux. Formulas are given for estimating the flux from (1) a point source of monoenergetic gamma rays in which the scattering and possible effects from an inhomogeneous atmosphere are not considered; (2) a plane uniform disk from the vertical symmetry axis and off-axis configuration; and (3) the delayed gammas emitted by fission products at one second after the fission process. All curves show that proximity to a disk containing 1 KT/km^2 of debris is necessary to receive fluxes much greater than 10^3 R/sec, while the dosage rate approaches infinity at the surface. However, if the disk is assumed to be a few kilometers thick, the maximum dosage rate obtainable from a fission density of 1 KT/km^2 is approximately 10^4 R/sec. (auth)

30352 (NASA-TR-R-240) BORON CROSS SECTIONS AS A SOURCE OF DISCREPANCY FOR CAPTURE CROSS SECTIONS IN THE kev REGION. Bogart, Donald (National Aeronautics and Space Administration, Cleveland, Ohio. Lewis Research Center). June 1966. 22p. CFSTI $1.00 cy, $0.50 mn.

Discrepancies in capture cross sections for gold from 80 to 200 kev are explained by changes in boron (nα) cross sections used to monitor neutron fluxes. These changes in boron cross sections are shown to improve agreement in capture data for iodine, indium, silver, antimony, and tantalum. Reexamination of the boron cross section measurements discloses that a modified long counter with considerable loss in efficiency below 200 kev was used, but its response was taken to be flat. Boron cross sections, corrected for long counter efficiency, depart significantly from an inverse neutron velocity variation (1/v) above ~80 kev. (auth)

30353 (ORNL-3940, pp 1-61) EXPERIMENTAL NUCLEAR PHYSICS. (Oak Ridge National Lab., Tenn.).

The nuclear physics research this year was chiefly concerned with direct reactions and their applications for the study of nuclear models. Nuclei of around mass 90 were most thoroughly investigated. The N = 28 nuclei were studied with deuteron interactions. Investigation of the optical model for 40-Mev protons was continued with the polarized proton beam. The inelastic scattering of polarized protons was studied. The optical model for the scattering of complex projectiles was investigated. In con-

tinuation of heavy-ion work on the tandem accelerator, fluctuations in the cross section and nucleon transfer reactions were the principal subjects for research. The major programming effort for the "multishell" shell-model code was completed, and the program is being extensively applied to problems of physical interest. The detailed study of alpha decay and gamma spectra of rare-earth radionuclides produced in ORIC was continued. (auth)

30354 (ORNL–3940, pp 62–9) NUCLEAR PHYSICS THEORY. (Oak Ridge National Lab., Tenn.).

In the past year the major programming effort for the "multishell" shell-model code was completed. The program is now being extensively applied to problems of physical interest. In connection with the general studies of nuclear structure, some effort has gone into relating the effective interaction used in the shell model (and extensions) to the "fundamental" nucleon-nucleon interaction. One method of attack is discussed. An application of a "fundamental" effective interaction to the calculation of the normal-parity spectrum of 1p-shell nuclei is presented. An attempt was made to find an optical potential for the scattering of nucleons from alpha particles. (M.O.W.)

30355 (ORNL-P–2084) IMPOSSIBLE LEGENDRE COEFFICIENTS. Irving, C. D.; Coveyou, R. R.; MacPherson, R. D. (Oak Ridge National Lab., Tenn.). [nd]. Contract W-7405-eng-26. 9p. (CONF-660303–30). Dep. mn. CFSTI $1.00 cy, $0.50 mn.

From American Physical Society, Conference on Neutron Cross Section Technology, Washington, D. C.

It has long been realized that Legendre polynomial expansions of differential cross sections can result in negative cross-section values due to the truncation of the infinite series. It is also possible that a given set of Legendre coefficients may result in negative cross sections because they do not represent any physically possible, everywhere positive angular distribution. The mathematical criteria that must be satisfied in order that there exist an everywhere positive distribution having a given set of Legendre coefficients are discussed. A check of Legendre coefficients from several published sources has revealed a surprisingly large number of instances where the coefficients are impossible. A computer program is offered which will examine a set of Legendre coefficients to determine if they can be derived from a possible distribution. (auth)

30356 (ORNL-TM–1448) POINT-SET REPRESENTATION OF ^{238}U CROSS SECTIONS; VALUES AND A FORTRAN PROGRAM FOR COMPUTATION. Webster, J. Wallace (Oak Ridge National Lab., Tenn.). June 1966. Contract W-7405-eng-26. 73p. Dep. mn. CFSTI $2.00 cy, $0.75 mn.

As part of the current effort in reactor analysis to obtain representations of cross sections as sets of values at discrete energy points rather than as sets of averaged values over broad intervals of the energy domain, a FORTRAN program is presented which computes total and capture cross sections of ^{238}U at specified energy points over a resonance. The resonance parameters and the temperature are input data. Using the data on the resonance parameters given in BNL-325, Second Edition, Supplement No. 2, Vol. III (Feb. 1965), and the above program, 862 point representations were computed for the cross sections of ^{238}U at a temperature of 300°K for neutron energy less than 1000 ev. The results are presented in the form of machine printouts as well as Calcomp plots. (auth)

30357 (RPI–328–56) LINEAR ACCELERATOR PROJECT. Progress Report, January 1966–March 1966. (Rensselaer Polytechnic Inst., Troy, N. Y.). Contract AT(30-3)-328. 144p. Dep. mn. CFSTI $4.00 cy, $1.00 mn.

Separate abstracts were prepared for 4 of the 5 included sections. The remaining section contained only a brief summary of 50-Mev electron radiation damage studies on germanium and silicon. (M.O.W.)

For abstracts of individual sections see: 29529, 30324, 30325, and 30358.

30358 (RPI–328–56, pp 1–48) NEUTRON CROSS SECTIONS. (Rensselaer Polytechnic Inst., Troy, N. Y.).

Developments are reported on each of the following areas of study: a new technique for measuring weak neutron scattering from resonances undergoing a strong fission and capture; cross-section measurements of fissile isotopes; total neutron cross section of ^{240}Pu; the parameters of the neutron resonances in ^{182}W, ^{183}W, ^{184}W, and ^{186}W; neutron radiative capture measurements at the R.P.I. electron LINAC; gamma spectra from radiative capture of thermal and resonance neutrons; high energy neutron inelastic scattering; measurement of neutron multiplicity from ^{235}U fission due to resonance energy neutrons; and measurements of neutron capture and fission cross sections for ^{233}U. (M.O.W.)

30359 (UCRL–16757) THE HYPERFINE-STRUCTURE ANOMALIES OF ^{198}Au AND ^{199}Au [Thesis]. Vanden Bout, Paul Adrian (Lawrence Radiation Lab., Univ. of California, Berkeley). Mar. 31, 1966. Contract W-7405-eng-48. 95p. Dep. mn. CFSTI $3.00 cy $0.75 mn.

The hyperfine-structure separations and nuclear magnetic moments of ^{198}Au (2.70d) and ^{199}Au (3.15d) were measured using the atomic-beam magnetic-resonance method. The ratio of the electronic g factor of gold to those of potassium and cesium was measured. Second-order corrections to the hyperfine structure are shown to be negligible. The nuclear results are interpreted in terms of the shell model of the nucleus with allowance for configuration mixing. The measurement of some ratios of alkali electronic g factors was also made. (M.O.W.)

30360 (WASH–1068) REPORTS TO THE AEC NUCLEAR CROSS SECTIONS ADVISORY GROUP MEETING HELD AT WASHINGTON, D. C., MARCH 24–25, 1966. Motz, H. T. (comp.) (Los Alamos Scientific Lab., Univ. of California, N. Mex.). Contract W-7405-eng-36. 233p. (EANDC(US)–85U; INDC(US)–3U). Dep. mn. CFSTI $6.00 cy, $1.25 mn.

Included are brief summaries of reports which were presented to the AEC Nuclear Cross Sections Advisory Group at the meeting on March 24–25, 1966, in Washington, D. C. These reports contain an informal statement of recent development, changes of emphasis, and preliminary data which are of importance to the cross section measurement program of the AEC. (M.O.W.)

30361 SCALAR INTERACTION AND CONFORMAL SPACE. Hafner, H.; Ionescu-Pallas, N. J. Acta Phys. Austr., 21: 290–5(1966).

One considers the space with indefinite metrics, conformal to Minkowskian space. The particle trajectories in this space are time oriented geodesics. The equations of movement formally coincide with those proposed for scalar interaction by O. Bergman which postulates a certain Lorentz-invariant Lagrange function. By extending Einstein's concept about the relation between physics and geometry, without making some conventional assertions, one equates the curvature scalar with a quantity proportional to the invariant density of field-charges. The insertion of a "cosmological constant" leads to the appearance of the short-range interactions of Yukawa type. One obtains a nonlinear field equation and one suggests the opportunity to use it in meson-theory. (auth)

30362 DIRECTIONAL CORRELATIONS OF GAMMA RAYS IN ^{147}Sm. Goworek, T.; Wawryszczuk, J. (Marie Curie-Sklodowska Univ., Lublin). Acta Phys. Pol., 29: 655–61(May 1966).

The directional correlation measurements of 7 cascades in ^{147}Eu to ^{147}Sm decay were performed. The spin of 799 kev level was found as 3/2. The mixing ratios of 602, 678, 862 kev and the sine of δ for the 76 and 121 kev transitions were determined. The multipolarity of 1256 kev transition is discussed. (auth)

30363 ENERGY LEVELS OF ^{8}Be PRODUCED IN THE $^{11}B(n,\alpha)^{8}Li \rightarrow {}^{8}Be$ PROCESS. Jaskola, M. (Inst. of Nuclear Research, Warsaw); Natanson, L.; Turkiewicz, J.; Osakiewicz, W. Acta Phys. Pol., 29: 673–7(May 1966).

The α particle spectrum of ^{8}Be produced by the β decay of ^{8}Li from the $^{11}B(n,\alpha)$ reaction was measured by the nu-

clear emulsion method. The 2.9 Mev state of ^{8}Be appears to be predominant. No evidence was found for the existence of other excited states of ^{8}Be in the 0–10 Mev range. (auth)

30364 INTERACTIONS OF 12.8-Gev PROTONS IN NUCLEAR EMULSIONS. III. INTERACTIONS WITH HEAVY NUCLEI OF THE EMULSION. Villar, E.; Gomez, J. L.; Tarrega, P.; Gil, D.; Lleo, A. (Facultad de Ciencias, Valencia). An. Real Soc. Espan. Fis. Quim. (Madrid), Ser. A, 62: 79-92(Mar.-Apr. 1966). (In Spanish).

The intranuclear cascades from 145 interactions produced by 13.8 Bev/c protons on the heavy nuclei of the emulsion in a strong magnetic field were studied. Angular distributions and both momentum and transverse momentum distributions of 264 secondaries are obtained. An energy balance of the interaction is given and results are compared with those found in the literature for other beam particles and energies. (auth)

30365 SHELL MODEL STUDIES OF 1f-SHELL NUCLEI. I. FRACTIONAL PARENTAGE COEFFICIENTS FOR NUCLEAR f^3 AND f^4 CONFIGURATIONS. Nagai, Hiroyuki (Kyushu Inst. of Tech., Fukuoka); Itaya, Mitsuo. Bull. Kyushu Inst. Technol., Math., Natur. Sci., No. 10, 41-6(Mar. 1963).

The orbital fractional parentage coefficients for the states of the nuclear f^3 and f^4 configurations in LS coupling are calculated. The method used is that developed by Jahn in connection with the nuclear d^3 and d^4 configurations in LS coupling, and later extended to the p^n configurations, with $2 \leq n \leq 12$, by Jahn and van Wieringen. Following the methods developed by Racah in connection with the atomic f-shell and later extended to the nuclear f^n configurations by Flowers, the orbital states of the f^3 and f^4 configurations are classified in terms of the irreducible representations of the groups U_7, R_7, G_2, and R_3 under the full reduction $U_7 \rightarrow R_7 \rightarrow G_2 \rightarrow R_3$. The classification of the states of the f^4 configuration in terms of the irreducible representations of U_7, R_7, G_2 and R_3 is given in tabular form together with the results obtained by Flowers. The calculations are much simplified by using a theorem of Racah which follows as a corollary to Schur's lemma. The orbital parentage coefficients for the f^3 and f^4 configurations so obtained are tabulated for convenience and completeness with the results obtained by Racah for the atomic f-shell. (auth)

30366 NEUTRON SEPARATION ENERGIES OF ^{143}Nd–^{144}Nd, ^{149}Sm–^{150}Sm, AND ^{164}Dy–^{165}Dy. Hughes, L. B.; Kennett, T. J.; Prestwich, W. V.; Wall, B. J. (McMaster Univ., Hamilton, Can.). Can. J. Phys., 44: 919-21(Apr. 1966).

Precise measurements of these energies can be obtained by a study of the total energy released as electromagnetic radiation following thermal neutron capture by detecting the gamma rays with a 6-cc Ge(Li) spectrometer. This technique complements measurements of (d,p) Q values and mass-spectrographic determinations. (AECL)

30367 PRODUCTION OF NUCLIDES IN THE REGION OF Z = 126 AND N = 184. Sikkeland, Torbjorn; Clarkson, Jack E.; Lebeck, Donald F.; Ghiorso, Albert (Univ. of California, Berkeley). Inorg. Nucl. Chem. Lett., 2: 141-8(May 1966).

Cross sections for various production schemes for superheavy nuclei are evaluated. Three types of reactions may give superheavy nuclei: fission following a fusion of two heavy nuclei such as $^{238}U + ^{238}U \rightarrow {}^{476}184$ (fission); grazing reactions, in which nucleons are interchanged between target nuclei and ions; and complete fusion of target nuclei and ions followed by neutron evaporation. The Jackson formula, modified for fission competition and angular momentum effects, was used to calculate the cross sections. Most of the cross sections were found to be of the order of 10^{-27} cm^2 (mb). (M.C.G.)

30368 TWO DECAYS OF MASS-SEVEN HYPERFRAGMENTS AND THE POSSIBLE BIASES IN SCANNING FOR HAMMER-LIKE HYPERFRAGMENT DECAYS IN EMULSION. Pniewski, J.; Pniewski, T.; Popov, S.; Zakrzewski, J. (Univ. of Warsaw). pp 146-50 of International Conference on High-Energy Physics. Budapest, Central Research Inst. of Physics, 1963.

Two decays of mass seven hyperfragments produced by 1.5 Bev/c meson (K^-) interactions on heavy emulsion nuclei are reported. One is identified as $_{\Lambda}Li^7$; for the other event the most probable interpretation is given to $_{\Lambda}He^7$. Two other events identified as helium hyperfragments, and probably as $_{\Lambda}He^5$, are discussed in connection with the possible biases in scanning for hammer-like decay of hyperfragments. (L.B.S.)

30369 COEFFICIENT OF β-RADIATION BACKSCATTERING FROM ALUMINUM BACKING IN 2π GEOMETRY. L'vova, M. A.; Bochkarev, V. V. Izmeritel. Tekh., No. 12, 45-7(Dec. 1965). (In Russian).

Measurements were carried out of the backscattering coefficients of beta particles from ^{14}C, ^{60}Co, ^{32}P, ^{35}S, ^{147}Pm, ^{204}Tl, and ^{90}Sr + ^{90}Y from Al backing in 2π geometry. Measurements were performed for thick backing, insuring saturation backscattering, and for finite thickness of the active layer. Results for saturation backscattering as a function of maximum beta energy are presented. Sources containing from 0.0001 to 0.02 μg of dry material show very little energy dependence of the backscattering, but sources containing about 3 μg of dry material show an increase of backscattering with beta energy. Backscattering coefficients determined as functions of layer thickness, including the effects of self-scattering and self-absorption of the sample, are given. (M.J.T.)

30370 PRODUCTION OF SLOW π^+ MESONS BY INTERACTION BETWEEN PROTONS OF 9-Bev ENERGY WITH PHOTOEMULSION NUCLEI. Azimov, S. A.; Aripov, R.; Gulyamov, U. G.; Rizaev, Kh. A. (Nuclear Physics Inst., Academy of Sciences, Uzbek SSR). Izv. Akad. Nauk Uz. SSR, Ser. Fiz.-Mat. Nauk, No. 4, 59-62(1965). (In Russian).

Certain aspects of the process of the formation of slow mesons, including subbarrier mesons, are investigated by exposing an emulsion plate to a beam of protons with 9-Bev energy in a synchrophasotron and tracking the paths of the identified π^+-mesons. It is shown that the formation of slow π^+-mesons cannot be explained by the standard mechanism of the evaporation of a strongly excited nucleus, a mechanism normally used to account for the emission of slow protons. The study resulted in the detection of 282 primary stars containing π^+-mesons with energies of up to 30 Mev. The search for and analysis of slow π^--mesons are continuing. (CFSTI)

30371 AZIMUTHAL ANGULAR DISTRIBUTION OF SLOW PARTICLES PRODUCED BY NUCLEAR INTERACTIONS WITH HEAVY EMULSION NUCLEI AT HIGH ENERGIES. Azimov, S. A.; Rasulkulov, M. S. (Nuclear Physics Inst., Academy of Sciences, Uzbek SSR). Izv. Akad. Nauk Uz. SSR, Ser. Fiz.-Mat. Nauk, No. 4, 70-2(1965) (In Russian).

Results are presented of an investigation of the azimuthal angular correlations of slow particles in the showers formed on the interaction between singly charged high-energy cosmic-ray particles and heavy emulsion nuclei ($n_g + n_h \geq 15$, $n_s \geq 15$) by a method better than that originally employed by the Polish scientists Bogdanowich and Ciok (Nucl. Phys., 40: 270(1963)) who investigated the distribution of the slow ("gray," n_g, and "black," n_h) particles formed by nuclear interactions with heavy emulsion nuclei in the presence of high energies. The slow particles for each shower were divided into "gray" and "black" tracks, calculating for each shower the Lorentz factor of the center-of-mass system as well as the azimuthal correlation of angular distribution of the slow particles β_c. On this basis and on the basis of the tabulated findings, it is established that, contrary to previous assumptions, all lines with a large number of slow particles displaying a generally high multiplicity of the generation of fast (n_0) particles cannot be regarded as central collisions between a fast particle and heavy nuclei. It is postulated that the azimuthal asymmetry of "gray" tracks is a consequence of an intranuclear cascade in the presence of noncentral nuclear interactions with heavy emulsion nuclei. (CFSTI)

30372 E2 TRANSITIONS FROM THE 3^+ LEVEL OF EVEN-EVEN NUCLEI. Begzhanov, R. B.; Rakovitskii, S. L.; Starodubtsev, S. V. (Inst. of Nuclear Physics, Academy of Sciences, Uzbek SSR). Izv. Akad. Nauk Uz., SSR, Ser. Fiz.-Mat. Nauk, No. 5, 36-48(1965). (In Russian).

A comparison is made on the basis of 98 references, of the position of 3^+ levels of even-even nuclei and the ratios of the given probabilities of transitions from this level to the lower 2_1^+, 4_1^+, levels with the predictions of various theories of the nucleus by Davydov and Filippov, Bohr, and Mottelson (see, e.g., Atomnaya Energiya [Atomic Energy], 1963, No. 14, 41), and by V. I. Belyak, D. A. Zaikin, (Izv. AN SSSR, Seriya Fizich. [Bulletin of the AS USSR, Physics Series], 25, 1163, 1961). Such a comparison was partially made earlier by Ye. P. Grigor'yev and M. P. Avotina (Izv. AN SSSR, Seriya Fizich. 24, 324, 1960). Because of the limited amount of data at the time concerning the 3^+ levels (only nine nuclei) and poor experimental accuracy of the numbers involved, these authors were not able to make pronouncements concerning the merits of the various theories. The present discussion shows that in spite of numerous favorable agreements, many experimental facts are still in disagreement with the above-mentioned nuclear theories. (CFSTI)

30373 MASS DISTRIBUTION IN THE FISSION OF ^{229}Th. Ravindran, N.; Flynn, K. F.; Glendenin, L. E. (Argonne National Lab., Ill.). J. Inorg. Nucl. Chem., 28: 921-4(Apr. 1966).

Yields for twenty-five mass chains in thermal-neutron-induced fission of ^{229}Th were measured radiochemically. The mass-yield curve was asymmetric with the light peak centered at mass 88 and the heavy peak centered at mass 140. The peak-to-valley ratio was about 500. No significant increase in yield in the region of symmetric fission was observed. (auth)

30374 α-DECAY OF ^{219}Fr AND ^{215}At. Graeffe, G.; Kauranen, P. (Univ. of Helsinki). J. Inorg. Nucl. Chem., 28: 933-6(Apr. 1966).

The α decay of ^{219}Fr and ^{215}At was studied by means of semiconductor detectors, recoil collection, and α-γ coincidence techniques. Four new fine structure α peaks in ^{219}Fr and one in ^{215}At were observed; γ rays were also measured and a decay scheme for ^{219}Fr was proposed. (auth)

30375 PARTIAL HALF LIFE FOR β-DECAY OF ^{36}Cl. Goldstein, G. (Oak Ridge National Lab., Tenn.). J. Inorg. Nucl. Chem., 28: 937-9(Apr. 1966). (ORNL-P-1284).

The partial half life for β decay of ^{36}Cl was determined with a high-specific-activity preparation of ^{36}Cl (32.6 atom per cent). Results by the specific activity method were $3.06 (\pm 0.02) \times 10^5$ years (liquid scintillation counting) and $3.10 (\pm 0.04) \times 10^5$ years ($4\pi\beta$ counting) in excellent agreement with the best previous value of $3.08 (\pm 0.03) \times 10^5$ years. (auth)

30376 ISOMERS OF ^{129}Sn. Chu, P.; Marinsky, J. A. (State Univ. of New York, Buffalo). J. Inorg. Nucl. Chem., 28: 1339-42(June 1966).

Evidence to indicate that the 1.0-hr isomeric state of ^{129}Sn reported in the literature does not exist is discussed. Its observation appeared to be an artifact of the chemical procedure employed. Experiments showed the presence of a 2.0-min ^{129}Sn activity instead. (auth)

30377 PHENOMENOLOGICAL NUCLEAR CLUSTER MODEL WITH SHELL STRUCTURE. Keller, K. (Univ. of Arizona, Tucson). J. Nucl. Energy: Pt. A and B, 20: 355-69(May 1966).

A phenomenological nuclear model is outlined which assumes that nucleons are correlated into α clusters and also have a shell structure. The shell structure is determined by an LS coupling scheme in which the intrinsic spins of the nucleons within an α cluster interact with each other, but not with the spins of nucleons outside the alpha. In order to apply a quantum-number scheme to α clusters, it is assumed that the alphas strongly interact and can be described by antisymmetric wave functions which lead to an exclusion principle. A possible quantum-number scheme showing the so-called magic numbers is given. The ground and excited state energies of the nucleons are assumed to depend on the radial and orbital angular momentum quantum numbers of the nucleons. The large binding energy of the α cluster causes the spatial subgrouping of the nucleons. A semi-empirical binding energy equation in terms of the α cluster aspect of the model is presented. This equation, which roughly accounts for the nucleons that are not in alphas, is used to interpret the main features of the chart of the nuclides. Some details of nuclear structure are considered in terms of the quantum-number scheme. The magnetic moments on several light nuclei are discussed on the basis of the angular momentum the alphas and extra nucleons might be expected to have. The possibility of other stable clusters, such as deuterons, tritons and ^{3}He, existing in nuclei is also considered. It is shown that deuterons and ^{3}He clusters probably do not occur in stable nuclei. The magnetic moments of ^{7}Li, ^{19}F, ^{23}Na, and ^{27}Al indicate that these nuclei have stable triton clusters. (auth)

30378 CALCULATION OF NEUTRON ACTIVATION CROSS SECTIONS FOR ^{51}V, ^{55}Mn, ^{63}Cu, ^{65}Cu AND ^{127}I IN THE 0.1 TO 14 Mev RANGE. Naguib, K.; Lukyanov, A. (Atomic Energy Establishment, Cairo). J. Nucl. Energy: Pt. A and B, 20: 373-5(May 1966).

A method of calculating the fast neutron radiative capture cross sections is presented and used to calculate the neutron activation cross sections of ^{51}V, ^{55}Mn, ^{63}Cu, ^{65}Cu, and ^{127}I nuclei in the energy range from 0.1 to 14 Mev. (auth)

30379 GAMMA-RAY SPECTRA OF FISSION PRODUCTS OBSERVED WITH LITHIUM-DRIFTED GERMANIUM DETECTORS. Takayanagi, Sei-ichi; Oi, Noboru; Kobayashi, Tetsuji; Sugita, Tohru (Tokyo Shibaura Electric Co., Ltd.). J. Nucl. Sci. Technol. (Tokyo), 3: 200-7(May 1966).

The γ-ray spectra of fission products from thermal neutron irradiation of natural U were observed with an encapsulated Li-drift-Ge γ-ray spectrometer. The spectra were recorded at various periods after irradiation—1, 2, 5, 12, 30, 250 days and 3 years. The γ-ray spectra of eight individual fission products including ^{239}Np were also studied. Due to the high resolution obtained with the detector, many nuclides were identified which would have been undetectable without resorting to chemical separation. (auth)

30380 NUCLEAR FISSION MODEL WITH CORE. Honda, Takao (Yamanashi Univ., Kofu, Japan). J. Phys. Soc. Jap., 21: 813(Apr. 1966).

A simple model is presented which can explain fission phenomena to some extent, as the first step of a phenomenological approach to the theory expected. This model assumes that the fission fragments have stiff cores with N = 50 ($A_C^L \sim 82$) and Z = 50 ($A_C^H = 128$) for the light and the heavy groups of the fragments respectively and only the parts outside of these cores are able to deform. (B.G.D.)

30381 PARITY NONCONSERVATION IN RADIATIVE TRANSITION OF ^{175}Lu. Lobashov, V. M.; Nazarenko, V. L.; Saenko, L. F.; Smotritskii, L. M.; Kharkevich, G. I. (Ioffe Inst. of Physics and Tech., Leningrad). JETP Lett. (USSR) (Engl. Transl.), 3: 173-6(Apr. 1, 1966).

Translated from Zh. Eksp. Teor. Fiz., Pis'ma Redaktsiya, 3: 268-74(Apr. 1, 1966).

An investigation is presented on the circular polarization of the γ quanta of ^{175}Lu, resulting from nucleon-nucleon interaction, and the 396-kev $^9/_2^- \rightarrow {}^7/_2^+$ transition with multipolarity E1 + M2, going to ground state. (B.G.D.)

30382 ON THE SIGN OF THE CHANGE OF THE CHARGE RADIUS OF THE ^{119}Sn NUCLEUS. Krizhanskii, L. M.; Rogozev, B. I.; Popov, G. V. JETP Lett. (USSR) (Engl. Transl.), 3: 248-9(May 1, 1966).

Translated from Zh. Eksp. Teor. Fiz., Pis'ma Redaktsiyu, 3: 382-4(May 1, 1966).

The nuclear-gamma-resonance spectroscopy method to investigate the behavior of $Ba(Ti,Sn)O_3$ solid solutions in the region of transition from the paraelectric into the

ferroelectric state is discussed. From an analysis of the data on the temperature dependence of the chemical shift in the absorption spectra of such solid solutions in the transition region, and from a comparison with similar data for $Ba(Ti,Fe)O_3$, conclusions are drawn concerning the sign of the change of the charge radius of the ^{119}Sn nucleus. (B.G.D.)

30383 INELASTIC SCATTERING OF 1-Mev PHOTONEUTRONS ON MEDIUM NUCLEI. Oehler, H.; Pose, H. (Institut fuer Experimentelle Kernphysik, Pirna-Copitz, Ger.). Kernenergie, 9: 95-100(Mar. 1966). (In German).

The inelastic scattering cross sections of cadmium, tin, antimony, and copper were determined by using a ^{24}Na + Be neutron source (E_n about 960 kev). A spherical symmetrical arrangement for carrying through the scattering experiments and using layers of different thickness allowed the effect of elastic and plural scattering to be eliminated as far as possible. The resolving power of the spherical ionization chamber used as the neutron spectrometer was about 15%. This fact permitted the separation of neutron groups and, herewith, the determination of cross sections of single excited levels of Cd and Sb. The most probable magnitudes of the spins were theoretically determined: $J = \frac{1}{2}$ for the 575 kev level of ^{121}Sb, and $J = \frac{3}{2}$ for the 540 kev level of ^{123}Sb. (auth)

30384 SOME SHELL-MODEL CALCULATIONS USING REALISTIC INTERACTIONS. Lee, C. W.; Baranger, E. (Univ. of Pittsburgh). Nucl. Phys., 79: 385-402(1966).

A shell-model calculation of ^{42}Ca, ^{92}Zr, and ^{16}O is described in which the nuclear states are assumed to belong to configurations involving two nucleons outside a closed shell and in which the residual interaction is taken to be Green's velocity-dependent potential and Tabakin's separable potential, both of which reproduce the free two-nucleon scattering data. The two potentials yield similar two-particle matrix elements. Some of the $J = 0$ diagonal matrix elements are small and even positive; some off-diagonal ones are large. The energy spectra of the nuclei are similar; configuration mixing is important. The agreement with experiment is very poor. This may be due to using these interactions as residual shell-model interactions. It is more probably due to not including core excitation in the calculation. (auth)

30385 GAMMA-RAY SPECTRA OF ^{124}Te, ^{164}Dy, ^{178}Hf AND ^{183}W FROM THE RADIATIVE CAPTURE OF NEUTRONS AT RESONANCES. Vogt, R. H. (Naval Research Lab., Washington, D. C.). Nucl. Phys., 82: 441-8 (1966).

Gamma spectra of ^{124}Te, ^{164}Dy, ^{178}Hf, and ^{183}W following radiative capture of neutrons at resonances in the energy region from 1 to 5 ev were obtained with NaI scintillation detectors using the sum-coincidence method and γ-γ coincidences. The spectra are interpreted as representing triple cascades to the ground state of ^{124}Te and double cascades to the ground or first excited states of ^{164}Dy, ^{178}Hf, and ^{183}W. (auth)

30386 RADIATIVE TRANSITION PROBABILITY FROM THE $3/2^+$ STATE TO THE $3/2^-$ STATE IN ^5He. Hoang, Tran Duc; Smith, Robert C. (Univ. of Ottawa). Nucl. Phys., 83: 9-16(1966).

The radiative transition probability from the $\frac{3}{2}^+$ state at 16.7 Mev to the $\frac{3}{2}^-$ ground state in ^5He is calculated using cluster-model wave functions. The excited state is assumed to have a triton-deuteron cluster structure and the ground state an alpha-particle-neutron structure. The result is found to be in quite close agreement with the experimental value, indicating that the cluster-model wave functions provide a good description of the ^5He nucleus. (auth)

30387 PROTON PICKUP FROM THE EVEN LEAD NUCLEI. Hinds, S. (Atomic Weapons Research Establishment, Aldermaston, Eng.); Middleton, R.; Bjerregaard, J. H.; Hansen, Ole; Nathan, O. Nucl. Phys., 83: 17-32 (1966).

Angular distributions of the Pb(t,α) reactions leading to states of ^{207}Tl, ^{205}Tl, and ^{203}Tl are measured at an incident triton energy of 13.5 Mev using the Aldermaston tandem accelerator and multi-angle magnetic spectrograph. The states of ^{207}Tl are probably single-proton hole states and were observed at excitations of 0 Mev $(3s_{\frac{1}{2}})^{-1}$; 0.35 Mev, $(2d_{\frac{3}{2}})^{-1}$; 1.34 Mev, $(1h_{\frac{11}{2}})^{-1}$; 1.67 Mev, $(2d_{\frac{5}{2}})^{-1}$, and 3.48 Mev possibly $(1g_{\frac{7}{2}})^{-1}$. For ^{205}Tl sixteen excited states were observed up to an excitation of 2.74 Mev, and for ^{203}Tl nine excited states were observed up to 1.69 Mev. The number of excited states observed in these two nuclei is in rough agreement with the prediction of the model of a single proton hole coupled to the states of the corresponding Pb cores. Some of the angular distributions for the three Tl isotopes have been analyzed using distorted wave methods and spectroscopic factors were extracted. These factors for the four lowest states of ^{207}Tl support the single-hole assignments and for the states of ^{205}Tl and ^{203}Tl are within the sum rule limits. The results are discussed on the basis of the above model. (auth)

30388 POSITRONS AND CONVERSION ELECTRONS FROM ^{90}Mo DECAY. Pettersson, H.; Baeckstroem, G.; Bergman, C. (Inst. of Physics, Uppsala). Nucl. Phys., 83: 33-45(1966).

Positron and conversion electron spectra from the ^{90}Mo decay are measured using a 50 cm radius, double-focusing spectrometer. The positron investigation showed one intense branch with an end-point energy of 1085 ± 4 kev. The standard error in the energy determinations of the 17 transitions ascribed to the ^{90}Nb nucleus varied between 10^{-4} and 10^{-3}. From $K/\Sigma L$ ratios the multipolarities of the 122 and 257 kev transitions were determined to be E2 and E3, respectively. Conversion coefficients for most transitions were obtained by combining the conversion intensities of this work with previously reported gamma intensities, and it was found that the majority of the transitions are of E1 or M1 character. On the basis of sum relationships for the transition energies and the intensities, a decay scheme is suggested. Tentative spin and parity assignments of all energy levels are given. (auth)

30389 POLARIZATION IN p-α SCATTERING FROM 17 TO 27 Mev. Weitkamp, W. G.; Haeberli, W. (Univ. of Wisconsin, Madison). Nucl. Phys., 83: 46-63(1966). (COO-7-0394).

The proton polarization in p-α scattering is measured for proton energies between 17.5 and 27 Mev at six laboratory scattering angles from 45 to 115°. The $^3He(d,p)^4He$ reaction was used as the source of polarized protons. The measured extremes of polarization at 17.5 Mev are −0.68 ± 0.03 at 75° and 0.92 ± 0.04 at 115°. The magnitude of the polarization decreases slowly with increasing energy except near 23 Mev, where an anomaly, attributed to the $\frac{3}{2}^+$ state in ^5Li, is observed. A phase shift analysis of all available p-α scattering data was made at 14.3, 17.5, 20.6, 26.1, 27.7, and 31.0 Mev. These phase shifts together with resonance parameters for the $\frac{3}{2}^+$ state obtained by analyzing the $^3He(d,p)^4He$ total cross-section data were used to calculate the energy dependence of the p-α polarization and the cross section near the resonance. The results are in good agreement with the measurements. (auth)

30390 SCATTERING OF NEUTRONS BY ALPHA PARTICLES. Hoop, B. Jr.; Barschall, H. H. (Univ. of Wisconsin, Madison). Nucl. Phys., 83: 65-79(1966). (COO-7-0393).

The differential cross section for the scattering of neutrons by α-particles is measured at neutron energies between 6 and 30 Mev. In the neighborhood of the resonance at 22.16 Mev neutron energy, measurements are performed at closely spaced neutron energies. The present data as well as earlier measurements of elastic scattering and total cross sections, and previous polarization measurements are fitted with phase shifts which are based largely on the p-α phase shifts of Weitkamp and Haeberli. Satisfactory fits are obtained for neutron energies up to 30 Mev, including the region of the 22.16 Mev resonance. The analyzing power of helium deduced from these phase shifts is presented in the form of a contour plot. (auth)

30391 STRIPPING ANALYSIS OF (d,p) ANGULAR DISTRIBUTIONS FROM THE $^{37}Cl(d,p)^{38}Cl$ REACTION. Rapaport, J. (Univ., Chile, Santiago); Buechner, W. W. Nucl. Phys., 83: 80-96(1966). (MIT-2098-172; MIT-2098-216).

The (d,p) reaction from a target enriched in ^{37}Cl was studied with a multiple-gap spectrograph and a Van de Graaff accelerator using a 7.5 Mev deuteron beam. A total of 37 states in ^{38}Cl were identified up to an excitation energy of 5.5 Mev. All showed an angular distribution characteristic of a stripping process. The ground state Q-value was measured to be 3.878 ± 0.010 Mev, in agreement with previous measurements. Transition strengths and values of the orbital angular momenta of the transferred neutrons were derived from the measurements by a zero-range, distorted wave, Born approximation analysis. (auth)

30392 SINGLE-PARTICLE ENERGY LEVELS IN A NILSSON WELL. Chi, Benjamin E. (Western Reserve Univ., Cleveland). Nucl. Phys., 83: 97-144(1966).

A comprehensive table of energy levels of a single particle in a Nilsson well is computed, using as a basis the coupled representation $|j,j_3\rangle$. The energy levels are also shown in graphs as a function of the nuclear deformation. Tables relating the various deformation parameters in common use and giving the energy levels for very small deformation are also presented. The decoupling parameter is also computed for all K = ½ states. (auth)

30393 THE REACTION $^{9}Be(d,\gamma)^{11}B$. Ziegler, B.; Buss, W.; Waeffler, H. (Max-Planck-Inst. for Chemistry, Mainz). Nucl. Phys., 83: 145-65(1966).

Radiative transitions $^{9}Be(d,\gamma)$ to the ground and excited states of ^{11}B were observed. Absolute cross sections and angular distributions were measured for deuteron energies from 0.4 to 1.4 Mev. The results indicate the predominance of a direct capture process, proceeding through a one-stage as well as a two-stage mechanism. There is evidence for a large contribution to the capture reaction by external capture. (auth)

30394 (n,p) CROSS SECTIONS OF SOME LOW-Z NUCLEI FOR 14.8-Mev NEUTRONS. Mitra, B.; Ghose, A. M. (Bose Inst., Calcutta). Nucl. Phys., 83: 157-65 (1966).

The (n,p) cross sections of ^{16}O, ^{19}F, ^{23}Na, ^{27}Al, ^{28}Si, ^{37}Cl, ^{51}V, and ^{52}Cr for 14.8 ± 0.1 Mev neutrons are measured respectively as 40.1 ± 2.7, 23.3 ± 2.8, 41.8 ± 3.8, 97 ± 10, 222 ± 12, 21.3 ± 2.1, 24.7 ± 2.2, and 82.8 ± 5.8 mb. Sources of systematic errors and the steps taken to control them are discussed. The results are compared with calculated values given by Erba et al. and Gardner and Levkovskii. (auth)

30395 THE EXCHANGE ENERGY OF SEMI-INFINITE NUCLEAR MATTER. Donnelly, I. J.; Naqvi, M. A. (Univ. of Sydney). Nucl. Phys., 83: 166-8(1966).

The local density approximation for calculating the exchange energy of semi-infinite nuclear matter is investigated for the case of the linear potential model. It is found to be adequate for all values of the slope of the potential. (auth)

30396 APPLICATION OF FANO-RACAH FORMALISM TO A KINEMATIC STUDY OF NUCLEAR REACTIONS. Dumontet, P.; Gaillard, P.; Lambert, M. (Institut d'Etudes Nucleaires, Alger, France). Nucl. Phys., 83: 169-80 (1966). (In French).

By means of the Fano and Racah formalism, general formulas are given for the angular distribution and polarization of particles of arbitrary spin which are emitted in a nuclear reaction with polarized beam and polarized target of arbitrary spins. (auth)

30397 FLUCTUATIONS OF DIFFERENTIAL POLARIZATION OF PARTICLES EMITTED IN NUCLEAR REACTIONS. Lambert, M.; Dumazet, G. (Institut d'Etudes Nucleaires, Alger, France). Nucl. Phys., 83: 181-98(1966). (In French).

It is shown that the tensor moments of polarization and differential polarization exhibit Ericson fluctuations. The cases where they are zero and the symmetry properties of the mean values are studied. The mean square deviations are calculated and compared. It is shown that the fluctuations of integrated cross sections are smaller than those of differential cross sections and the latter are smaller than those of components of differential polarization. It is also shown that when the beam or the target is polarized, or both, the fluctuations are then amplified. (auth)

30398 CORRECTIONS TO THE RANDOM-PHASE APPROXIMATION. da Providencia, J. (Univ., Coimbra) Nucl. Phys., 83: 209-31(1966).

Starting from the Green function formalism, corrections to the random-phase approximation are calculated by taking into account processes which lead to the renormalization of the free particle-hold propagator and two-body interaction and to the excitation of two quasi boson states. The corrections considered produce a conserving approximation because they satisfy an extension of the Thouless theorem. (auth)

30399 STRONG-COUPLING APPROXIMATION FOR DOUBLE STRIPPING REACTIONS. Stamp, A. P. (Nuclear Physics Lab., Oxford). Nucl. Phys., 83: 232-40(1966).

The strong coupling approximation is applied to mass exchange reactions. The zero-range approximation is made and the strong coupling and distorted wave Born approximations (DWBA) are compared. It is shown that the stripping peak is naturally predicted by the strong coupling approximation in cases where the cut-off DWBA must be used. (auth)

30400 EXCITED STATES OF ^{22}Na BY THE $^{20}Ne(^{3}He,p\gamma)^{22}Na$ REACTION. Maier, H. J.; Pelte, D.; Pronko, J. G.; Rolfs, C. (Univ., Freiburg i. B.). Nucl. Phys., 84: 1-12 (1966).

The gamma decay of the excited states of ^{22}Na below 4.40 Mev excitation was studied using the reaction $^{20}Ne(^{3}He,p\gamma)^{22}Na$ at a ^{3}He energy of 5.35 Mev. A gas target of spectroscopically pure neon gas was used. From these studies the branching ratios of gamma rays from states in ^{22}Na were deduced. Proton-gamma angular correlations with the proton counter at zero degrees yielded the following spin assignments: J(1.528) = 3, 5,(2); J(2.211) = 1; J(2.566) = 1, 2, 3, and J(3.947) = 1. Some evidence is given for the existence of the second T = 1 state near 1.96 Mev. (auth)

30401 SIGN AND MAGNITUDE OF THE CORIOLIS COUPLING BETWEEN THE $5/2^-[532]$ AND $7/2^-[523]$ ORBITALS IN ^{161}Tb. Zylicz, J.; Hansen, P. G.; Nielsen, H. L.; Wilsky, K. (Research Establishment, Roskilde, Denmark). Nucl. Phys., 84: 13-24(1966).

The decay of 3.6 min ^{161}Gd to levels in ^{161}Tb was reinvestigated by means of scintillation and Ge(Li) counters and γ-γ coincidence techniques with the aim of improving the energy and intensity data. A complete decay scheme is presented. The analysis is centered around the levels (kev (I^π)) 417($7/2^-$), 480($5/2^-$) and 586($7/2^-$). These three levels, which are unambiguously interpreted as belonging to the Nilsson orbitals $7/2^-[523]$ and $5/2^-[532]$, are populated with log ft values of 4.85, 6.2 and 5.95, respectively. The beta intensities together with the energies of these states require the assumption of a strong Coriolis interaction for which the intrinsic matrix element A_K takes the value −(23 ± 3) kev corresponding to 18% mixing of the $7/2^-$ states. The theoretical (Nilsson) result without corrections for pairing is −53 kev. (The sign of A_K relative to the product sign of the two beta decay matrix elements.) (auth)

30402 REACTIONS $^{7}Li+d$. Milone, C.; Potenza, R. (Univ., Catania, Italy). Nucl. Phys., 84: 25-36(1966).

The interactions of deuterons with ^{7}Li, producing two α-particles and a neutron in the final state are studied at E_d = 0.8 and 1 Mev. The spectra and the angular distribution of the α-particles and neutrons, and the angular correlation of the α-particles are measured. The two-dimensional display of α-particle pulses is studied. The contribution of the $^{7}Li(d,\alpha)^{5}He$ reaction to the α-spectra and the angular distribution of the α-particles from the decay of ^{5}He are obtained. (auth)

30403 DECAY SCHEME OF ^{123}Cs. D'Auria, John M.; Preiss, Ivor L. (Yale Univ., New Haven). Nucl. Phys., 84: 37-48(1966). (YALE-2726H-78).

The decay scheme of ^{123}Cs was studied via the decay of its precursor ^{123}Ba produced in heavy ion bombardments of natural indium. The ^{123}Cs isotope decays with a $T_{\frac{1}{2}}$ = 5.6 min via electron capture and beta decay (E_{max} = 2.6 Mev) to the 98 kev first excited state and ground state of ^{123}Xe. The 98 kev transition has a K-conversion coefficient of 0.80. The lifetime of the 98 kev state is ≤ 13 nsec. The positon-to-K-capture ratio for the excited state transition is 1.98. (auth)

30404 RATIO OF ASYMMETRIC TO SYMMETRIC FISSION IN FISSION OF ^{239}Pu BY NEUTRONS OF ENERGIES FROM 30 kev TO 14.7 Mev. Cuninghame, J. G.; Fritze, K.; Lynn, J. E.; Webster, C. B. (Atomic Energy Research Establishment, Harwell, Eng.). Nucl. Phys., 84: 49-61 (1966).

Radiochemical measurements were made of the peak-to-valley ratio of the mass yield curve for neutron induced fission of ^{239}Pu at neutron bombarding energies ranging from 30 kev to 14.7 Mev, and the results compared with similar measurements on ^{235}U. For both target nuclides, the ratios all show a similar nonlinear dependence on nuclear temperature at excitation energies below that at which intrinsic nucleonic levels become available. Once such levels are available, a more or less linear dependence on nuclear temperature is seen. This behavior suggests that the mass asymmetry is governed primarily by the transition state spectrum, at least at low energies, and calculations were made to check one of the experimentally measured ratios in ^{239}Pu fission. The calculations are based on the α_3 symmetries of the levels of the transition state spectrum up to 300 kev, beyond which present knowledge of the spectrum is too sketchy to allow further calculation. This limited calculation agrees moderately well with the trend in the experimental results and so, as far as it goes, supports the applicability of the channel theory of fission to the mass division. (auth)

30405 WEAK ALPHA AND ELECTRON-CAPTURE DECAY IN ^{208}Po AND ^{209}Po. Hagee, G. R. (Monsanto Research Corp., Miamisburg, Ohio. Univ. of Cincinnati); Lange, R. C.; McCarthy, J. T. Contract AT-33-1-GEN-53. Nucl. Phys., 84: 62-80(1966).

The weak alpha and electron-capture decay modes of ^{208}Po and ^{209}Po were investigated. Previously unobserved alpha groups were found at 4.22 Mev with 2.44×10^{-4}% abundance in ^{208}Po decay and at 4.11 and 4.31 Mev with 5.66×10^{-4}% and 1.46×10^{-4}% abundances, respectively, in ^{209}Po decay. The 4.617 Mev alpha group in ^{209}Po was measured explicitly and found to have 0.48% branching. Electron-capture branchings in ^{208}Po and ^{209}Po were measured as 1.81×10^{-3}% and 0.263%, respectively. Predominant electron-capture feeding in ^{208}Po populates a 921 kev level in ^{208}Bi. The log ft value of this transition was determined to be 13.7 in agreement with its assignment as a second-forbidden transition ($\Delta I = 2$, $\Delta\pi$ = NO). Gamma rays following electron-cature decay in ^{208}Po were found at energies of 65, 291, 534, 565, 599 and 865 kev. Measurements of internal conversion coefficients or K to L + M shell conversion electron ratios on the 291, 534, 565 and 599 kev transition in ^{208}Po or 263 and 900 kev transitions in ^{209}Po show them to be pure M1 or mixed M1 + E2 transitions. (auth)

30406 ENERGY LEVELS OF ^{63}Zn. Birstein, L.; Harchol, M.; Jaffe, A. A.; Tsukrovitz, A. (Hebrew Univ., Jerusalem). Nucl. Phys., 84: 81-90(1966).

The energy levels of ^{63}Zn were investigated by three different experimental techniques and some new low-lying states were found. The observed levels in ^{63}Zn have excitations of 190, 246, 627, 636, 649, (694) and 1061 kev. The relative yields of the reaction ^{63}Cu(p,n)^{63}Zn to some of these levels is compared with the predictions of the Hauser-Feshbach statistical model. Spin and parity assignments of $5/2^-$ and $1/2^-$ for the first two excited states respectively yield best agreement with the results. (auth)

30407 SHELL-MODEL CALCULATIONS ON ODD-PARITY LEVELS OF NUCLEI IN THE RANGE ^{33}S TO ^{41}Ca. Erne, F. C. (Rijksuniversiteit, Utrecht). Nucl. Phys., 84: 91-105(1966).

The shell model is used to investigate quantitatively some odd-parity levels of nuclei in the range ^{32}S–^{41}Ca. An inert ^{32}S core is assumed with a residual two-particle interaction of the outer nucleons. Only one nucleon is considered to be in the $1f_{\frac{7}{2}}$ shell, while the others are in the $1d_{\frac{3}{2}}$ shell. The interaction matrix elements are reduced to linear expressions in 14 parameters (i.e., 12 two-particle interactions and two binding energies to the core. The numerical results are presented as they are obtained from fitting the 14 parameters to 60 nuclear level energies. From the values of these parameters the energies and spins of about 240 levels are derived. Though the root mean square deviation of the calculated energies from the experimental energies is about 0.5 Mev, most of the level orders are calculated correctly. In addition, the energies of some 0^- levels are calculated from configurations containing two particles in the $1f_{\frac{7}{2}}$ shell. These level energies appear to have a larger spread around the experimental energies. An expansion of the matrix elements of the effective interaction of one nucleon in the $1d_{\frac{3}{2}}$ and one in the $1f_{\frac{7}{2}}$ shell in terms of interaction moments shows that the mean two-body interaction for the T = 0 case is attractive, with a significant quadrupole splitting; this agrees with a weak spin dependence of the effective nuclear forces. The mean two-body interaction for the T = 1 case is slightly repulsive, the octupole splitting being the most significant one. (auth)

30408 NON-LOCAL POTENTIAL FOR OPTICAL-MODEL ANALYSIS OF PROTON SCATTERING. Sood, P. C. (Univ. of Alberta, Edmonton). Nucl. Phys., 84: 106-12(1966).

The Perey-Buck local approximation for non-local potentials is applied to the case of protons to investigate the effects of introducing nonlocality. The procedure for including the Coulomb correction term arising from the nonlocality of the interaction gives rise to two different forms for the proton potential. The mathematical formulation and the evaluation of the parameters of the nonlocal potential for the optical model analysis of the proton scattering are carried out for both the forms. The departure from linear energy dependence of the equivalent local potentials is discussed assuming the validity of this approximation. An expression is derived for the calculation of the symmetry term in the optical-model potential for the nonlocal case corresponding to the determination of this term for the local case. (auth)

30409 STUDY OF THE REACTION ^{197}Au(n,γ)^{198}Au Johnson, L. V.; Hughes, L. B.; Kennett, T. J.; Prestwich, W. V. (McMaster Univ., Hamilton, Can.). Nucl. Phys., 84: 113-28(1966).

The gamma radiation from the ^{197}Au(n,γ)^{198}Au reaction was studied using a Ge(Li) spectrometer. A total of 80 gamma rays was observed and their intensity and energy determined. The neutron separation energy was found to be 6516 ± 5 kev. The decay modes of the first 44 levels were deduced from a detailed computer program incorporating low-energy crystal spectrometer data and the observed level structure. A calculation of the gamma-ray reduced widths indicates an anomalous strength maximum in transitions from the capture state to levels near the ground state. (auth)

30410 EXCITED STATES IN ^{82}Kr POPULATED BY DECAY OF 35-h ^{82}Br. Etherton, R. C.; Kelly, W. H. (Michigan State Univ., East Lansing). Nucl. Phys., 84: 129-49(1966).

The energy levels of ^{82}Kr populated by the negaton decay of 35 h ^{82}Br were studied. The internal conversion electron spectra were recorded with permanent magnet electron spectrometers and the singles and coincidence γ-ray spectra were recorded using both NaI(Tl) and Ge(Li) detectors. A total of 21 γ-ray transitions were identified. Excited states in ^{82}Kr were placed at 777, 1475, 1821, 2094, 2429, 2560, 2648, 2652 and 2832 kev. Angular correlation measurements

for eight of the prominent γ-γ cascades were made and the results used to make unique spin assignments for the 777, 1475, 1821, 2094 and 2648 kev states. Transitions from the 2832, 2652 and 2560 kev states and log ft values were used to place limits on the possible spin assignments for these states. (auth)

30411 TRANSVERSE INELASTIC FORM FACTORS IN ^{12}C FROM A CONTINUUM MODEL. Friar, James L. (Stanford Univ., Calif.). Contract AF 49(638)-1389. Nucl. Phys., 84: 150-60(1966).

The transverse inelastic form factors in ^{12}C, which appear in electron excitation of the giant resonance continuum states, were investigated. Using a particle-hole model the $J^\pi = 1^-$ form factor was calculated assuming the particle lies in the continuum. It was found that as momentum transfer increases the peak of the resonance shifts in energy. The integrated form factor was calculated and showed the characteristic dip with increasing momentum transfer. In addition, it was found to be roughly 70% of that calculated using bound state wave functions for the excited states. (auth)

30412 ODD-PARITY STATES OF ^{16}O WITH A REALISTIC NUCLEON-NUCLEON INTERACTION. Kallio, A. (Univ. of Minnesota, Minneapolis); Green, A. M. Nucl. Phys., 84: 161-76(1966). (COO-1371-21).

The effective interaction between nucleons on the Fermi surface of light nuclei is calculated with a realistic two-nucleon force having a hard core and tensor component. The relative S-state part of the effective force which corresponds to the Brueckner-Gammel-Thaler potential is shown to be very similar to the one obtained earlier for a simpler exponential S-state force, which however, fits the low-energy two-nucleon data. The effective force is used to calculate the properties of the odd-parity states of ^{16}O. It is found that the energies of 0^- states are particularly sensitive to the tensor part of the effective force. In general, the agreement with experiment is satisfactory. (auth)

30413 OPTICAL-MODEL ANALYSIS OF THE SCATTERING OF 24.7-Mev ALPHA PARTICLES. McFadden, Lynne; Satchler, G. R. (Oak Ridge National Lab., Tenn.). Nucl. Phys., 84: 177-200(1966). (ORNL-P-1880).

The measured elastic scattering of 24.7 Mev alpha particles from the nuclei O, Mg, Al, Si, Ca, Mn, Ni, Co, Cu, Ge, Zr, Ag, In, Sn, Hf, W, Au, Bi and U was analyzed using the optical model. Fits were obtained using a four-parameter Woods-Saxon potential. No marked improvement was found by using a more general potential. The fits for medium and heavy nuclei are good, but those for the lighter nuclei are noticeably poorer. Potential ambiguities were studied in some detail for Ni and Mg, and potentials with depths of about 150 Mev and 200 Mev were obtained for all the nuclei in addition to a more shallow potential. The medium-weight nuclei show a preference for the deep potentials, the light nuclei for the shallow ones. The behavior of the predicted scattering matrix elements is discussed also. (auth)

30414 STUDY OF BERYLLIUM WITH POLARIZED NEUTRONS OF ENERGY 2.60 TO 2.77 Mev. Schirmer, G.; Pose, H.; Haensgen, H. (Technische Univ., Dresden). Nucl. Phys., 84: 201-8(1966).

The polarization of neutrons scattered elastically by ^9Be was measured at 50° lab system from 2.60 to 2.77 Mev. In this interval the polarization varies very rapidly with energy. The experimental results are in good agreement with theoretical values assuming $4^-(l = 2)$ for the spin and parity of the level at 9.27 Mev in ^{10}Be. (auth)

30415 PROTON SCATTERING FROM ^{27}Al IN THE ENERGY RANGE FROM 3.5 to 11.3 Mev. Elliott, R. V.; Spear, R. H. (Australian National Univ., Canberra). Nucl. Phys., 84: 209-34(1966).

The scattering of protons from ^{27}Al was studied for proton energies from 3.5 to 11.3 Mev with an energy resolution of approximately 10 kev. Excitation functions were obtained at laboratory angles of 90° and 140° for groups corresponding to the ground and first six excited states of ^{27}Al. The validity of a fluctuation theory interpretation of the data was investigated; it is concluded that such an interpretation is valid for the upper part of the range but is questionable for the lower energies. The distortion of auto-correlation functions due to non-statistical variations in the reaction yield has been eliminated by calculating fluctuations with respect to an average cross section defined by using an averaging interval of 400 kev. An auto-correlation analysis indicates that the mean width of ^{28}Si levels participating in the reaction is approximately 34 kev at an excitation energy of 21.5 Mev. Estimates of level width based on the density of maxima in the excitation functions are in satisfactory agreement with this value. The present result is compared with ^{28}Si level widths reported by other authors. The significance of values for the normalized variances of the excitation functions determined from the auto-correlation analysis is discussed. The data show some evidence for the presence of intermediate structure of width and spacing of the order of several hundred kev. (auth)

30416 DECAY OF ^{141}Nd. PART II. Koehler, D. R.; Grissom, J. T. (Army Missile Command, Redstone Arsenal, Ala.). Nucl. Phys., 84: 235-8(1966).

The decay of ^{141}Nd activity resulting from 14 Mev neutron bombardment of ^{142}Nd was studied using a Li-drifted Ge detector with a resolution of 0.75%. Gamma rays are observed with energies of 1.293 Mev, 1.146 Mev, 1.126 Mev and 0.145 Mev to within ±1 kev. The results of this work strongly support the conclusions of a previous study for the existence of a level in ^{141}Pr at 1.126 Mev. (auth)

30417 FAST NEUTRON SCATTERING CROSS SECTIONS OF IRON. Jacquot, A.; Rousseau, C. (EURATOM, Geel, Belg.). Nucl. Phys., 84: 239-40(1966).

Elastic and inelastic neutron scattering cross sections for natural iron were measured absolutely in the energy range 0.45-2.28 Mev with an accuracy of better than ±6%. (auth)

30418 ZIRCONIUM(n,p) CROSS-SECTION MEASUREMENTS. Carroll, Edward E.; Stooksberry, Robert W. Nucl. Sci. Eng., 25: 285-90(July 1966). (WAPD-T-1730).

The $^{90}Zr(n,p)^{90}Y$ cross section is measured between 3.55 and 6.02 Mev and at 15 Mev by using an activation technique. The $^{91}Zr(n,p)^{91}Y$ cross section was measured between 4.32 and 6.02 Mev, and upper limits were set on the $^{92}Zr(n,p)^{92}Y$ and $^{94}Zr(n,p)^{94}Y$ cross sections at 6 Mev. (auth)

30419 TOTAL CROSS SECTIONS OF GADOLINIUM FOR FAST NEUTRONS. Wickstrom, C. J.; Potter, S. B.; Tiller, Hans. Nucl. Sci. Eng., 25: 291-3(July 1966).

The total neutron cross section of gadolinium is measured at neutron energies of 2.4, 3.0, 13.3, 13.9, 14.6, 15.2, and 15.7 Mev. The measured transmission values are corrected for in-scattering and multiple scattering effects. The total cross sections range from 5.0 to 6.3 b. (auth)

30420 UTILITY OF THE STATISTICAL TREATMENT OF RESONANCE ABSORPTION IN THE UNRESOLVED RESONANCE REGION. Dyos, M. W.; Stevens, C. A. (General Atomic Div., General Dynamics Corp., San Diego, Calif.). Nucl. Sci. Eng., 25: 294-6(July 1966).

In computing resonance integrals by statistical methods one has a knowledge of the average value of a resonance parameter (neutron width) over many resonances, but no information regarding the actual value of the parameter at any energy. From physical principles it is possible to assign a probability distribution of local-to-average widths and, by appropriate weighting with this distribution, physical quantities can be computed. The estimation of the confidence limits on these computations within the unresolved range is discussed in terms of s-wave neutrons only. (B.G.D.)

30421 ESTIMATE OF THE DECREASE IN THE EFFECTIVE RESONANCE INTEGRAL DUE TO RESONANCE OVERLAP. Keane, A. (Wollongong Univ. Coll., Australia). Nucl. Sci. Eng., 25: 296-8(July 1966). (AAEC-TM-296).

A simple model is investigated analytically which shows the range of validity of and the correction necessary to Rowlands' formula, which allows for the effect of resonance overlap in data preparation codes, and provides an alternative expression for those concentrations where Rowlands' formula has its greatest error. (B.G.D.)

30422 MOESSBAUER EFFECT MEASUREMENTS IN THE FIRST AND SECOND EXCITED STATES OF ^{155}Gd. Stevens, R. R. Jr.; Lee, Y. K.; Walker, J. C. (Johns Hopkins Univ., Baltimore). Phys. Lett., 21: 401-3(June 1, 1966).

Mössbauer studies in ^{155}Gd set a lower limit for lifetime of the first excited state of 0.22 nanoseconds. Observed quadrupole structure implies a spin of $\frac{1}{2}$ for the second excited state and quadrupole splitting of 9.3×10^{-7} ev for the ground state. (auth)

30423 COMPARISON OF THE EFFECTIVE TWO-NUCLEON INTERACTION IN $2s_{\frac{1}{2}}$-$1d_{\frac{5}{2}}$-SHELL NUCLEI WITH A SURFACE DELTA INTERACTION. Glaudemans, P. W. M. (Rice Univ., Houston, Tex.); Wildenthal, B. H.; McGrory, J. B. Phys. Lett., 21: 427-9(June 1, 1966). (TID-22835)

It is shown that the effective two-nucleon interaction in $2s_{\frac{1}{2}}$-$1d_{\frac{5}{2}}$-shell nuclei can be well approximated by a delta function which acts only at the nuclear surface. (auth)

30424 DIFFERENCE OF BINDING ENERGIES OF ^{3}H AND ^{3}He NUCLEI. Choudhury, S. Rai (Moscow State Univ.); Bhakar, B. S.; Bhasin, V. S. Phys. Lett., 21: 430-1(June 1, 1966).

Recent estimates of the difference of binding energies between ^{3}H and ^{3}He nuclei due to the Coulomb repulsion between the protons give a value which is insufficient by about 0.1 to 0.2 Mev from the experimental value. An attempt is made to explain this in terms of electromagnetic effect of a non-Coulombic nature. (auth)

30425 ABSENCE OF STRUCTURE IN THE FISSION CROSS SECTION OF ^{235}U IN THE NEUTRON ENERGY RANGE 380 TO 620 kev. Gilboy, W. B.; Knoll, G. F. (Kernforschungszentrum, Karlsruhe, Ger.). Phys. Lett., 21: 432-3(June 1, 1966).

The ^{235}U fission cross section is measured with high resolution by a time-of-flight method over the energy range 380–620 kev. In contrast to results recently obtained by another author, no evidence for immediate structure is found. (auth)

30426 REMARK ON F. MORINGO'S FORMULA FOR THE AMPLITUDE OF (d,n) COULOMB STRIPPING. Cejpek, J. (Purkyne Univ., Brno). Phys. Lett., 21: 433-4 (June 1, 1966).

An analytical formula for the (d,n) reaction on the Coulomb approximation is derived using some properties of the harmonic polynomials and the hypergeometric function. The formula is valid for any orbital momentum of the captured proton. Generalization to the (d,p) process is evident. (auth)

30427 POLARIZATION OF THE NEUTRONS FROM THE ^{15}N(d,n)^{16}O REACTION. Bruening, R. (Institut fuer Experimentalphysik, Hamburg); Buesser, F. W.; Niebergall, F.; Christiansen, J. Phys. Lett., 21: 435-6(June 1, 1966).

The polarization of the neutrons from the ^{15}N(d,n)^{16}O reaction was measured for deuterons energies from 1.6 to 3.0 Mev. Polarization values up to –0.463 were found. (auth)

30428 SHELL MODEL AND THE STOCHASTIC THEORY OF FISSION. Ramanna, R.; Ramamurthy, V. S. (Atomic Energy Establishment, Trombay, India). Phys. Lett., 21: 437-40(June 1, 1966).

By treating nuclear fission as a Markov process, the transition matrix is evaluated directly from ground state nuclear data without the introduction of any free mass dependent parameters, to give the observed mass distributions of several nuclei. It is also shown that there is some indication of a nonuniform charge distribution at the saddle point if shell corrections are introduced at the saddle point. (auth)

30429 RE-EXAMINATION OF THE SPIN OF THE ^{45}Sc 378-kev LEVEL. Schwartz, J. J.; Alford, W. Parker (Univ. of Rochester, N. Y.). Phys. Lett., 21: 441-2(June 1, 1966).

Stripping and angular correlation measurements indicate a spin and parity of $\frac{3}{2}^-$ for the 378 kev level of ^{45}Sc, rather than the previously suggested spin and parity of $\frac{5}{2}^-$. (auth)

30430 SPECTROSCOPIC INFORMATION ON SAMARIUM ISOTOPES FROM ANALOG-STATE EXPERIMENTS. Bassani, G.; Cassagnou, Y.; Levi, C.; Papineau, L. (CEN, Saclay, France). Phys. Lett., 21: 442-4(June 1, 1966).

Results on analog states of ^{149}Sm, ^{151}Sm, and ^{153}Sm observed by elastic and inelastic scattering of protons are presented. A possible location of the same $\frac{3}{2}^-$ state in odd samarium isotopes from 83 to 89 neutrons is proposed. (auth)

30431 EFFECT OF STRIPPING CHANNELS ON THE ELASTIC SCATTERING OF DEUTERONS. Rawitscher, G. H. (Max-Planck-Institut fuer Kernphysik, Heidelberg). Phys. Lett., 21: 444-6(June 1, 1966).

The elastic 11 and 12.8 Mev d-^{40}Ca cross section is calculated with the explicit inclusion of one stripping channel under various simplifying assumptions. The presence of the stripping channel gives rise to an apparent transparency of the nucleus to the incident deuterons. (auth)

30432 PRODUCTION OF ANTIPROTONS BY HIGH-ENERGY PHOTONS. Bertram, W. (Deutsches Elektronen-Synchroton, Hamburg); Carrol, J.; Eandi, R.; Huebner, R.; Kern, W.; Koetz, U.; Schmueser, P.; Skronn, H. J.; Buschhorn, G. Phys. Lett., 21: 471-5(June 1, 1966).

Experimental evidence is presented for the photoproduction of antiprotons on nitrogen and hydrogen by photons of energy 4.1–6.2 Bev. Yields and $\bar{p}/\pi$ ratios are given and compared to a simple one-nucleon-exchange model. (auth)

30433 SOME ANOMALIES IN THE REACTION ^{16}O(^{3}He,α_0)^{15}O. Bray, K. H.; Nurzynski, J.; Bourke, W. P. (Australian National Univ., Canberra). Phys. Lett., 21: 536-7(June 15, 1966).

Irregularities in the location of maxima and minima in the angular distributions of the reaction ^{16}O(^{3}He,α_0)^{15}O are reported. They are similar to those observed in elastic scattering. (auth)

30434 BINDING AND SATURATION OF NUCLEAR MATTER. Sprung, D. W. L. (McMaster Univ., Hamilton, Can.); Bhargava, P. C.; Dahlblom, T. K. Phys. Lett., 21: 538-41(June 15, 1966).

It is shown that the theory of Brueckner as modified by Bethe can give good agreement with experiment using modern potentials. The reference spectrum method including third-order corrections is a simple accurate way to treat the tensor force, which is shown to play an important role in saturation. (auth)

30435 NEGATIVE-PARITY LEVELS IN EVEN-EVEN MERCURY ISOTOPES. Petry, R. F.; Naumann, R. A.; Evans, J. S. (Princeton Univ., N. J.). Phys. Lett., 21: 541-3(June 15, 1966).

Two negative-parity levels were located in the nuclei ^{194}Hg, ^{196}Hg and ^{198}Hg at excitation energies of 1.6–1.9 Mev. These levels are populated by the electron-capture decay of the 7^+ isomeric states of ^{194}Tl, ^{196}Tl and ^{198}Tl. (auth)

30436 EXCITATION OF COLLECTIVE STATES IN ^{208}Pb BY INELASTIC ELECTRON SCATTERING. Peterson, G. A.; Ziegler, J. F. (Yale Univ., New Haven). Phys. Lett., 21: 543-5(June 15, 1966).

Inelastic electron scattering cross sections for the excitation of collective 2^-, 3^- and 4^+ states in ^{208}Pb were measured and compared with distorted-wave calculations in the momentum transfer range from 0.21 to 0.65 fm^{-1} for 70 Mev electrons. (auth)

30437 COUPLED-CHANNEL CALCULATION OF INELASTIC SCATTERING BASED ON A MICROSCOPIC NUCLEAR DESCRIPTION. Glendenning, N. K. (Univ. of California, Berkeley). Phys. Lett., 21: 549-50(June 15, 1966). (UCRL-16841).

The detailed shell model wave functions for ^{60}Ni are tested by comparing the predicted cross sections for 17.8 Mev protons exciting a number of levels, with experiment. It is concluded that the collective 2^+ state is moderately well represented but not the noncoherent levels, which present a much greater challenge to the structure theory. (auth)

30438 A J DEPENDENCE IN THE (^{3}He,α) REACTION CONFIRMING NEW SPECTROSCOPIC ASSIGNMENTS IN ^{14}N AND ^{13}C. Ball, G. C.; Cerny, J. (Univ. of California, Berkeley). Phys. Lett., 21: 551-3(June 15, 1966).

A J dependence was observed in the (^{3}He,α) reaction which confirmed the $(p_{3/2},p_{1/2})_{1^+}^{-1}$, $T=1$ state in ^{14}N at 13.72 ± 0.04 Mev and the lowest T = 3/2 state in ^{13}C at 15.108 ± 0.014 Mev. (auth)

30439 STRUCTURE OF THE ALPHA PARTICLE FROM ELASTIC ELECTRON SCATTERING. Frosch, R. F.; Rand, R. E.; Van Oostrum, K. J.; Yearian, M. R. (Stanford Univ., Calif.). Phys. Lett., 21: 598-600(June 15, 1966).

Elastic electron scattering from ^{4}He was studied at values of q^2, the 4 momentum transfers squared, ranging from 0.5 fm^{-2} to 10.0 fm^{-2}. Among the models which have been found to fit the new data are modified Gaussian distribution with a half density radius of 1.19 fm and a skin thickness of 1.61 fm. (auth)

30440 ISOSPIN QUINTUPLETS IN A = 16 NUCLEI. Leonardi, R.; Loncke, P.; Pradal, J. (Institut de Physique Nucleaire, Orsay, France). Phys. Rev., 146: 615-25 (June 17, 1966).

Two experimentally observed 0^+ and 2^+ levels of ^{16}O were interpreted as analogs of ^{16}O and ^{16}N states, each being considered as belonging to isospin quintuplets, although the corresponding levels were not observed in ^{16}F and ^{16}Ne. Such T = 2 levels can be theoretically understood in terms of two-particle–two-hole excitations. Two perturbation methods are proposed. The first one is based on the knowledge of the T = 1 odd-parity-state wave functions. The second, the higher random-phase approximation with unperturbed ground state (Tamm-Dancoff), leads to a diagonalization in the space of operators defined by coupling one hole-hole pair with one particle-particle pair. The results of the two methods are comparable and in satisfactory agreement with experiment. In fact, a complete fit is reached in method II with a Serber-Yukawa interaction potential, while a Rosenfeld mixture also gives a rather good agreement. (auth)

30441 MEASUREMENT OF THE SPIN-ROTATION PARAMETER β IN PROTON-^{4}He SCATTERING AT 48 Mev. Griffith, T. C.; Imrie, D. C.; Lush, G. J.; Robbins, L. A. (Univ. Coll., London). Phys. Rev., 146: 626-32 (June 17, 1966).

The spin-rotation parameter β was measured at nine scattering angles between 11 and 90° (lab) in proton-^{4}He elastic scattering at 48 Mev, using the polarized proton beam from the proton linear accelerator at the Rutherford High Energy Laboratory. The results are in good agreement with the predictions of the 40-Mev phase shift analysis of Giamati, Madsen, and Thaler. (auth)

30442 NEUTRON-DEUTERON POLARIZATION AT 22.7 Mev. Malanify, J. J.; Simmons, J. E.; Perkins, R. B.; Walter, R. L. (Los Alamos Scientific Lab., N. Mex.). Phys. Rev., 146: 632-7(June 17, 1966). (LA-DC-6721).

A measurement of the neutron-deuteron polarization function was made at E_N = 22.7 Mev over the angular range 44.5 to 158.8° cm. Neutrons with polarization approximately 0.5 were obtained from the T(d,n)^{4}He reaction at a deuteron energy of 6.6 Mev and a lab angle of 30°. Comparison is made to existing neutron data at 23.7 Mev and to proton data at 22 Mev. Agreement with the latter is good except near 130° cm where the value given here falls low. Theoretical comparisons do not exist in the energy range of this experiment. (auth)

30443 COULOMB CORRECTIONS TO THE BETA DECAY OF ^{14}O. Chen, Fei-Shian (Yale Univ., New Haven); Durand III, Loyal; McGee, Ian J. Phys. Rev., 146: 638-50(June 17, 1966).

The Coulomb corrections to the nuclear matrix element for the beta decay of ^{14}O, ^{14}O(β^+)^{14*}N, are reexamined using nuclear wave functions obtained from a variational calculation of the nuclear binding energies. The corrections so obtained are an order of magnitude larger than those obtained in perturbation theory, but are, nevertheless, too small to account for the 2% difference between the values of the vector beta-decay coupling constant determined from the decays of the muon and ^{14}O. The differences between the present calculation and the perturbation calculation are discussed in detail. (auth)

30444 INTERACTIONS OF ^{3}He PARTICLES WITH ^{9}Be, ^{12}C, ^{16}O, AND ^{19}F. Hahn, R. L.; Ricci, E. (Oak Ridge National Lab., Tenn.). Phys. Rev., 146: 650-9 (June 17, 1966). (ORNL-P-1936).

Excitation functions for reactions induced by ^{3}He particles in Be, C, O, and F were determined by irradiating thin foils of beryllium, mylar, teflon, and nylon with ^{3}He ions of energies from 3 to 10 Mev. The radioactive products were assayed by gamma spectrometry, and their decay curves fitted by least-squares analysis. The maximum cross sections (and corresponding ^{3}He energies) were ^{9}Be(^{3}He,n)^{11}C, 113 ± 11 mb (4.3 Mev); ^{12}C(^{3}He,n)^{14}O, 16.5 ± 1.8 mb (6.3 Mev); ^{12}C(^{3}He,d)^{13}N, 98.9 ± 12.2 mb (9.5 Mev); ^{12}C(^{3}He,α)^{11}C, 366 ± 26 mb (8.2 Mev); ^{16}O(^{3}He,p)^{18}F, 436 ± 44 mb (6.3 Mev); ^{16}O(^{3}He,α)^{15}O, 169 ± 17 mb (6.6 Mev); ^{19}F(^{3}He,α)^{18}F, 22.1 ± 2.0 mb (7.1 Mev); and ^{19}F(^{3}He,αn)^{17}F, 50.4 ± 5.0 mb (8.2 Mev). Results for some of these reactions, previously obtained by other workers, were in reasonable agreement with our data; in particular, the fine structure of the reaction ^{12}C(^{3}He,n)^{14}O was confirmed in these experiments. An integral excitation function, calculated from the differential data of Towle and Macefield for the ^{9}Be(^{3}He,n)^{11}C reaction, agreed with the integral data obtained in this work. The distorted-wave theory of direct reactions was used to compute excitation functions for comparison with integral data for (^{3}He,α) reactions on ^{12}C, ^{16}O, and ^{19}F, and for the (^{3}He,d) reaction on ^{12}C. The results of the comparison between theory and experiment indicate that a direct mechanism is operative in all the cases studied, except the ^{12}C(^{3}He,α)^{11}C reaction, which appears to proceed to a large extent by way of a compound-nucleus reaction. Thus, the integral data indicate that the primary mechanisms operative in the reactions (^{3}He,α) on ^{16}O and ^{19}F, and (^{3}He,d) on ^{12}C, are respectively direct pickup and stripping. (auth)

30445 DECAY OF THE 2.34- AND 2.71-Mev STATES OF ^{9}B. Wilkinson, D. H. (Brookhaven National Lab., Upton, N. Y. Nuclear Physics Lab., Oxford); Samples, J. T.; Alburger, D. E. Phys. Rev., 146: 662-70(June 17, 1966). (BNL-9872).

Proton emission from ^{9}B states at 2.34 and 2.71 Mev were investigated by populating the states in the ^{10}B(^{3}He,α)^{9}B reaction and by measuring α-p coincidences with a 2-dimensional pulse-height analyzer. The 2.34-Mev, $J^\pi = 5/2^-$ level decays less than 0.5% by proton emission to the ground state of ^{8}Be, while the 2.71-Mev level decays nearly 100% by this route. The 1f proton reduced width of the 2.34-Mev level for the ground state of ^{8}Be (in units of $\hbar^2/mR^2$) is then less than 5×10^{-3} when R has the value 4.35°F. The coincidence method clearly resolves the 2.71-Mev $J^\pi = 5/2^+$ state from the 2.34-Mev state and background, its excitation and width being 2.71 ± 0.03 Mev and 0.71 ± 0.06 Mev, respectively. These figures imply a 1d proton reduced width of the 2.71-Mev state for the ground state of ^{8}Be of about 0.7. (auth)

30446 INELASTIC-SCATTERING MODEL FOR (p,xn) AND (p,p(x-1)n) REACTIONS AT INTERMEDIATE ENERGIES. Saha, G. B.; Porile, N. T. (Purdue Univ., Lafayette, Ind.). Contract AT(11-1)-1505. Phys. Rev., 146: 687-91(June 17, 1966). (COO-1505-6).

A semiclassical model was developed to calculate isobaric ratios of (p,xn) to (p,p(x-1)n) reaction cross sections at energies of 40–100 Mev. It is assumed that these reac-

tions are due to inelastic or charge-exchange scattering processes in which sufficient excitation energy is transferred to the residual nuclei to lead by subsequent particle evaporation to the products of interest. Account is taken of some of the effects of the exclusion principle and of the motion of the struck target nucleons. However, the effects of refraction, reflection, and absorption of the incident and emitted nucleons, as well as that of the relative availability of different target nucleons, are assumed to cancel in the calculation of the isobaric ratio. The results are in moderately good agreement with the available experimental data in the above energy range. (auth)

30447 ELEMENTARY-PARTICLE TREATMENT OF MUON CAPTURE IN ^{16}O. Kim, C. W. (Univ. of Pennsylvania, Philadelphia). Phys. Rev., 146: 691-4(June 17, 1966).

The rate of the muon-capture process in ^{16}O that leads to the 2^- ground state of ^{16}N is calculated treating the initial and final nuclei as "elementary" particles. Nuclear form factors are evaluated on the basis of the conserved-vector-current and partially-conserved-axial-vector-current hypotheses using experimental data on the corresponding beta-decay and inelastic-electron-scattering processes. The resultant calculated rate $[\Gamma(\mu^- + {}^{16}O\ (0^+) \rightarrow {}^{16}N\ (2^-) + \nu_\mu)]_{theor} = (5.8 \pm 2.3) \times 10^3\ sec^{-1}$ is consistent with the measured value $[\Gamma(\mu^- + {}^{16}O\ (0^+) \rightarrow {}^{16}N\ (2^-) + \nu_\mu)]_{exper} = (6.3 \pm 0.7) \times 10^3\ sec^{-1}$ and is to be contrasted with a calculated rate of $(12 \pm 2) \times 10^3\ sec^{-1}$ obtained on the basis of a nuclear-model impulse-approximation approach. (auth)

30448 A-BINDING ENERGIES IN HEAVY HYPERFRAGMENTS ($35 \lesssim A \lesssim 80$). Bhowmik, B.; Chand, T.; Chopra, D. V.; Goyal, D. P. (Univ. of Delhi). Phys. Rev., 146: 703-7(June 17, 1966).

Analysis of 16 short-range ($\leq 10\mu$) hyperfragments, produced from 1.5-Bev/c K^- interactions in L_4 hypersensitized emulsions and decaying π^--mesonically, is presented. Of these, 9 are classified as due to the residual spallation products of silver and bromine nuclei, 5 as belonging to lighter species ($A \leq 20$), and 2 as ambiguous. The masses of the 9 spallation hyperfragments are determined using the "spallation model." It is concluded that for hyperfragments of masses $A \simeq 35$ to 80, the upper limits of B_Λ could vary from 21.9 to 24.5 Mev. (auth)

30449 EIGENCHANNEL THEORY OF NUCLEAR REACTIONS. Danos, Michael; Greiner, Walter (National Bureau of Standards, Washington, D. C.). Phys. Rev., 146: 708-12(June 17, 1966).

A method is proposed by which the eigenstates and the eigenvalues of the S matrix, i.e., the eigenchannels, can be directly computed from the nuclear problem, for example, from the shell model. The calculation of all cross sections, vis., partial and total cross sections, is then exceedingly simple. The characteristics of the eigenchannels are described and the relation with other reaction theories is briefly discussed. (auth)

30450 SCATTERING OF 40.5-Mev ALPHA PARTICLES BY ^{12}C, ^{13}C, ^{14}N, ^{15}N, ^{16}O, AND ^{18}O. Harvey, B. G. (Univ. of California, Berkeley); Meriwether, J. R.; Mahoney J.; de Nercy, A. Bussiere; Horen, D. J. Phys. Rev., 146: 712-22(June 17, 1966). (UCRL-16573).

Elastic and inelastic scattering of 40.5-Mev α particles from targets of ^{12}C, ^{13}C, ^{14}N, ^{15}N, ^{16}O, and ^{18}O was studied. Angular distributions were measured for a large number of excited states. It was found that the shape of the angular distribution depends on the nature of the single-particle transition involved. Six examples of quadrupole transitions involving promotion of a $p_{\frac{1}{2}}$ nucleon to the $p_{\frac{1}{2}}$ shell were found. Although the cross sections varied over a tenfold range, the shapes of the angular distributions remained very similar. Six examples of the dipole transition $p_{\frac{1}{2}} \rightarrow 2s_{\frac{1}{2}}$ and seven examples of the octupole transition $p_{\frac{1}{2}} \rightarrow d_{\frac{5}{2}}$ were also observed. The dipole transitions gave angular distributions of a characteristic and unusual shape. Excitation of the ^{14}N levels at 9.41, 9.71, 10.22, and 10.55 Mev suggests that they are all T = 0. The levels at 6.05, 6.70, 7.40, and 7.60 Mev were not observed; probably they do not exist. A weak level at 10.85 Mev and two strongly excited levels (or groups of levels) at 11.3 and 12.9 Mev were observed in ^{14}N. The angular distribution of particles scattered from the 4.45-Mev level of ^{18}O suggests strongly that this level is 1– rather than 3+. Several unnatural parity states were observed, but no states known to have isotopic spin different from the ground state. The angular distributions for several scattered particle groups were compared with distorted-wave Born approximation calculations and very approximate reduced transition probabilities for excitation of the levels were obtained. For the quadrupole and octupole excitations the results are in reasonably good agreement with values measured by electromagnetic methods. (auth)

30451 RADIATIVE MUON CAPTURE AND THE GIANT DIPOLE RESONANCE IN ^{40}Ca. Fearing, Harold W. (Stanford Univ., Calif.). Contract AF 49(638)-1389. Phys. Rev., 146: 723-33(June 17, 1966).

The photon spectrum and total rate for radiative muon capture in ^{40}Ca using the giant dipole resonance (GDR) model used by Foldy and Walecka to significantly improve theoretical calculations of ordinary muon capture rates are calculated. In this model the dipole parts of the nuclear matrix elements relevant for radiative muon capture are related to integrals over experimental photo-absorption cross sections in the region dominated by the giant dipole resonance. The remaining other multipole and velocity parts of the nuclear matrix elements are evaluated in the closure approximation using harmonic oscillator wave functions. Numerical results are presented for the photon spectrum as calculated in the GDR model for various values of the weak-interaction coupling constants and of the average maximum photon energy k_m which is used in the other multipole and velocity parts of the calculation. The most important effect of the GDR calculation is to reduce the dipole contribution to the capture rate, thus giving an absolute radiative rate some 40% lower and a relative rate (ratio of radiative and ordinary rates) some 20% lower than that obtained in the closure–harmonic-oscillator model. As a consequence, the GDR model requires a larger value of the induced pseudoscalar coupling constant g_p to reproduce a given spectrum that does the closure–harmonic-oscillator model. Finally, the results are compared with the data of Conversi et al., who found by interpreting their data in the closure–harmonic-oscillator model that $g_P = (13.3 \pm 2.7)g_A$, where g_A is the axial vector coupling constant. It is found that the GDR calculation requires $g_P = (16.5 \pm 3.1)g_A$ for a fit to the experiment, assuming $k_m = 88$ Mev and taking currently accepted values for the other coupling constants. Alternatively, by taking the Goldberger-Treiman value $g_P \cong 7g_A$ and varying the induced tensor coupling constant g_T a fit to the data was obtained for $g_T \gtrsim 35\ g_V$. As these results are quite sensitive to k_m, in addition results for other values of k_m are given. (auth)

30452 $^{42}Ca(d,p)^{43}Ca$ REACTION AT 7.0- AND 7.2-Mev BOMBARDING ENERGIES. Dorenbusch, W. E.; Belote, T. A.; Hansen, Ole (Massachusetts Inst. of Tech., Cambridge). Contract AT(30-1)-2098. Phys. Rev., 146: 734-8(June 17, 1966). (MIT-2098-214).

The $^{42}Ca(d,p)^{43}Ca$ reaction was studied at 7.00- and 7.20-Mev bombarding energies using the MIT-ONR electrostatic generator in connection with the multiple-gap spectrograph. Proton spectra were observed at 23 scattering angles from 7.5 to 172.5 deg with an overall energy resolution of 12 kev. Eighty transitions were observed up to an excitation energy of 5.0 Mev. Angular distributions showing stripping character were analyzed in the distorted-wave approximation to yield l_n values and spectroscopic strengths. A sum-rule analysis indicated that all of the available $1f_{\frac{7}{2}}$, $1d_{\frac{3}{2}}$, and 2p strengths were observed. The beginnings of the $1g_{\frac{9}{2}}$, $1f_{\frac{5}{2}}$, and $2d_{\frac{5}{2}}$ transitions were recorded. Anomalies observed in the angular distributions to the four lowest excited states are discussed. The results are compared with other data on ^{42}Ca and ^{43}Ca and are discussed in terms of the shell model with residual interactions. The data suggest that neither the neutron nor the proton $1d_{\frac{3}{2}}$ shell is filled in the ^{42}Ca ground state. (auth)

30453 HIGH-RESOLUTION STUDY OF THE ^{54}Fe(t, p)^{56}Fe REACTION. Cohen, Bernard L. (Univ. of Pittsburgh); Middleton, Roy. Phys. Rev., 146: 748-55(June 17, 1966).

The ^{54}Fe(t,p)^{56}Fe reaction was studied with 12-Mev incident tritons using the Aldermaston tandem Van de Graaff and multigap spectrograph. The angular distributions of the protons are characterized by sharp structure. For eight cases where the spin and parity of the final state are known, the position of the first maximum agrees very well with predictions of the plane-wave Born approximation. These positions were then used for assigning spins and parities to many other levels. The only known unnatural parity state is excited two orders of magnitude less strongly than the strongly excited states, and has an unusual angular distribution. The collective 3^- state (4.51 Mev) is the most strongly excited state in the spectrum; it is shown that this is very difficult to explain. Other very strongly excited states are the ground and first excited states, 1^- states at 5.19 and 7.06 Mev, and a 6^+ (or 7^-) state at 5.15 Mev. The spin and parity assignments of all states up to 4.5 Mev are discussed in the light of other evidence; the principal correction is to change the assignment of the 3.122-Mev state from 5^+ to 5^-. (auth)

30454 MUON CAPTURE IN HEAVY NUCLEI. Klein, R. (New York Univ.). Contract AT(30-1)-1480. Phys. Rev., 146: 756-60(June 17, 1966).

The systematics of muon capture rates in complex nuclei is discussed in the closure approximation. It is shown that for calculations in infinite nuclear matter, the nuclear ground state can be reasonably approximated by an infinite Fermi gas. The closure approximation and Fermi-gas model for the nuclear ground state are then used in an analysis of the experimental capture rates in a large number of nuclei. It is found that this procedure does allow one to satisfactorily interpret quantitatively the muon-capture rates in the heavier nuclei and that it is possible to interpret the analysis in a manner that is not inconsistent with a universal Fermi interaction. The possibility of using muon capture rates to determine a neutron-proton nuclear-radius difference is also explored but with negative results. (auth)

30455 STUDY OF LOW-LYING STATES OF ^{33}S. Becker, J. A.; Chase, L. F. Jr.; Fossan, D. B.; McDonald, R. E. (Lockheed Palo Alto Research Labs., Calif.). Phys. Rev., 146: 761-73(June 17, 1966).

The low-lying states of ^{33}S at 0.84, 1.97, 2.31, 2.94, and 3.22 Mev were studied using the charged-particle–gamma-ray angular-correlation method of Litherland and Ferguson. The ^{32}S(d,p)^{33}S reaction was used to populate the levels of ^{33}S, with an incident deuteron energy of 3.20 Mev. Charged particles were detected near 180° with respect to the incident beam direction using an annular solid-state counter, and gamma radiation was detected in a 10.2-cm × 10.2-cm NaI(Tl) crystal at angles between 0 and 90° relative to the beam direction. Coincident data were stored in a 64 × 64-channel 2-parameter pulse-height analyzer. Gamma-ray branching ratios are presented for the levels mentioned above, and also the 2.87-Mev level of ^{33}S. Spin assignments of $\frac{5}{2}$, $\frac{3}{2}$, $\frac{7}{2}$, and $(\frac{3}{2})$ were established for the levels of ^{33}S at 1.97, 2.31, 2.94, and 3.22 Mev, respectively, as well as a most probable assignment of positive parity for the 1.97-Mev level. Some gamma-ray mixing ratios are also presented. An upper limit for the mean lifetime of these latter states as well as the 0.84-Mev level of $\tau_m \leq 10^{-9}$ sec has been obtained. These results, combined with the results of previous investigations, lead to spin-parity assignments of $\frac{3}{2}^+$, $\frac{1}{2}^+$, $\frac{5}{2}(+)$, $\frac{3}{2}^+$, and $\frac{7}{2}^-$ for the ^{33}S levels at 0, 0.84, 1.97, 2.31, and 2.94 Mev, and support the $J = \frac{3}{2}$ assignment for the 3.22-Mev level. No evidence was obtained for the existence of a level in ^{33}S near 1.4-Mev excitation energy. (auth)

30456 LOW-INTENSITY BRANCHES IN THE ^{45}Ti DECAY. Porter, F. T.; Freedman, M. S.; Wagner, F. Jr.; Orlandini, K. A. (Argonne National Lab., Ill.). Phys. Rev., 146: 774-80(June 17, 1966).

The decay of ^{45}Ti (~100% electron capture and β^+ to the ^{45}Sc ground state) was reinvestigated with the Argonne toroidal-field beta spectrometers and with lithium-drifted germanium gamma detectors. New low-intensity branches to levels in ^{45}Sc at 725.1 ± 0.8 [149 ± 35], 1238 ± 1.5 [16 ± 6], and 1411.3 ± 0.9 [112 ± 30] kev were found. Numbers in brackets are the intensities for 10^5 decays. The 12.4-kev level in ^{45}Sc previously seen in the β decay of ^{45}Ca is also populated in the ^{45}Ti decay; its energy is $12.40^{+0.02}_{-0.01}$ kev and its intensity is [12 ± 3]. The intensity of the first-forbidden unique decay ($\frac{7}{2}^-$ to $\frac{3}{2}^+$) to the 12.4-kev state is not known because of the unknown amount of gamma branching to the 12.4-kev state from higher levels in ^{45}Sc, but from the observed 12.4-kev intensity, log $f_1t > 8.1$. No evidence was found for beta decay to the 376-kev level [<60] or to the 540-kev level [<9]. Log ft values for beta decays to the three states at 725, 1238, and 1411 kev are 6.3, 6.8, and 5.6, respectively. In general, to the other states, log ft values are greater than 7, with the exception of the 1660-kev state for which our gamma intensity limit yields log ft > 5.7. The available data are consistent with spin and parity assignments of $(\frac{3}{2}^+)$ for the 12.4-kev state and $(\frac{3}{2}^-)$ for the 376-kev state. The end point of the positron spectrum, 1044 ± 5 kev, indicates a total decay energy, ^{45}Ti → ^{45}Sc, of 2066 ± 5 kev, 20 to 40 kev higher than earlier measurements and in better agreement with reaction data, 2062 ± 4 kev. Our half-life measurement of 3.08 ± 0.01 h agrees with previous measurements. (auth)

30457 POLARIZATION IN THE ELASTIC SCATTERING OF PROTONS FROM CARBON AND NITROGEN. Steben, J. D.; Brussel, M. K. (Univ. of Illinois, Urbana). Phys. Rev., 146: 780-90(June 17, 1966).

The polarization of protons elastically scattered from nitrogen and carbon was measured using double-scattering techniques. The polarization was determined for nitrogen at a scattering angle of 40°_{cm} in the proton-energy interval 12.6 to 13.6 Mev. The polarization resulting from elastic proton scattering with nitrogen targets had a constant value of –0.60 ± 0.10 in the incident proton-energy interval 8.2 to 11.8 Mev. The polarization from carbon, however, varied markedly with energy at most scattering angles. [Example: $P(50^\circ_{lab}, 12.9 \text{ Mev}) = -0.8$, $P(50°, 13.2) = -0.4$, and $P(50°, 13.5) = -0.7$.] At numerous angles between 20 and 140°, polarization measurements from carbon covered the range of energies from 12.8 to 13.4 Mev. The angular distributions of polarization (and cross section) are in general quite sensitive to small changes in energy; the 12.95- and 13.25-Mev angular distributions even differ in shape significantly for $\theta > 90°$. The energy-averaged (12.8- to 13.4-Mev) angular distribution for the polarization of protons scattered from carbon was compared with optical-model calculations. (auth)

30458 LEVEL STRUCTURE IN ^{52}Cr POPULATED IN 5.7-DAY ^{52}Mn DECAY. Freedman, M. S.; Wagner, F. Jr.; Porter, F. T.; Bolotin, H. H. (Argonne National Lab., Ill.). Phys. Rev., 146: 791-8(June 17, 1966).

The energy-level structure in ^{52}Cr populated in the decay of 5.7-day ^{52}Mn was studied with a toroidal-field electron spectrometer and Ge(Li) detector. The decay is found to populate only the states at (Mev, $J\pi$, v = dominant seniority) (3.6177, 5+, 4), (3.1146, 6+, 2), (2.7688, 4+, 2), (2.3703, 4+, 4), and (1.4345, 2+, 2). Low upper limits set on the intensity of gamma rays of 2.65, 1.73, 1.465, 1.214, 1.18, 1.07, and 0.61 Mev previously reported in ^{52}Mn remove all evidence for the population by ^{52}Mn of states at 3.832, 3.161, and 2.648 Mev (the latter two known from nuclear reactions). All 9 possible transitions of multipolarity E2 or lower between known levels have been seen, including new weak gammas of 0.504 and 0.398 Mev. Conversion coefficients indicate strong M1 mixing only in the transition of 1.2474 Mev from the 3.6177- to the 2.7686-Mev state, for which $\Delta v = 0$, in agreement with seniority selection rule for half-filled shells; and E2 dominance in the 1.4345-, 1.3343-, 0.9358-, 0.8498-, 0.7443-, and 0.3460 Mev transitions. Seniority mixing coefficients in the two 4+ states deduced from gamma intensities agree with those derived from previously reported nuclear-reaction data. The ratio of electron capture to positron emission for decay to the 6+ state is 2.04, in good agreement with theory. (auth)

30459 $^{40}Ca(d,d)$, (d,d'), AND (d,p) REACTIONS WITH 12.8-Mev DEUTERONS. Niewodniczanski, H. (Inst. of Nuclear Physics, Krakow. Jagellonian Univ., Krakow); Nurzynski, J.; Strzalkowski, A.; Satchler, G. R. Contract W-7405-eng-26. Phys. Rev., 146: 799-803(June 17, 1966). (ORNL-P-1955).

Differential cross sections were measured for the $^{40}Ca(d,d)$, (d,d'), and (d,p) reactions initiated by 12.8-Mev deuterons. Inelastic scattering to the 3.35-Mev (0^+), 3.73-Mev (3^-), and 4.48-Mev (5^-) levels of ^{40}Ca, and (d,p) reactions feeding the ground ($\frac{7}{2}^-$), 1.97-Mev ($\frac{3}{2}^-$), and 2.47-Mev ($\frac{3}{2}^-$) levels of ^{41}Ca were observed. An optical-model analysis of the elastic scattering was made, and the potentials obtained were used in a distorted-wave study of the reactions. The collective model gave a good fit to the inelastic excitation of the 3^- and 5^- levels; it was necessary to use the complex form of interaction in order to obtain reasonable values of the deformation parameters. The effects of finite range and nonlocality were included in the deuteron-stripping analysis and yield reasonable agreement with the observed cross sections. The spectroscopic factors extracted when spin-orbit coupling is included in the deuteron optical potential are significantly less than the value unity expected. (auth)

30460 SCATTERING OF ALPHA PARTICLES BY ^{52}Cr, ^{53}Cr, AND ^{51}V. Meriwether, John R.; Gabrielli, Italo; Hendrie, David L.; Mahoney, Jeannette; Harvey, Bernard G. (Univ. of California, Berkeley). Contract W-7405-eng-48. Phys. Rev., 146: 804-10(June 17, 1966). (UCRL-16518).

The scattering of various-energy alpha particles by ^{52}Cr was studied. The spins and parities of most of the ^{52}Cr levels up to 7 Mev were either assigned or confirmed. The reduced transition probabilities B(EI)$_\downarrow$ for several levels were determined with the aid of the Austern-Blair model. Similar measurements with 50-Mev alpha particles on ^{53}Cr and ^{51}V were made and some evidence is considered for the description of ^{53}Cr as a ^{52}Cr core coupled to an odd neutron. (auth)

30461 LIMITS FOR LEPTON-CONSERVING AND LEPTON-NONCONSERVING DOUBLE BETA DECAY IN ^{48}Ca. der Mateosian, E.; Goldhaber, M. (Brookhaven National Lab., Upton, N. Y.). Contract AT(30-2)-Gen-16. Phys. Rev., 146: 810-15(June 17, 1966). (BNL-9791).

A search was made for double beta decay in ^{48}Ca using a new technique that involves the use of CaF_2 crystals as scintillation detectors. These crystals, enriched in either ^{48}Ca or ^{40}Ca, were used to detect ionizing particles originating within the crystals. The advantages of this technique are (1) a 4π geometry for a source without self-absorption and (2) good resolution which is independent of the relative angular and energy distribution of the two electrons. A lower limit of 2×10^{20} yr is placed on the lepton-nonconserving double beta decay without neutrinos. The determination of a lower limit for the Dirac-type double beta decay (with emission of two neutrinos) is complicated by impurities in the ^{48}Ca used. By resorting to the usual coincidence type of search for double beta decay, which makes the effect of the impurities negligible, a lower limit of 5×10^{18} yr was established for this process. This is comparable with the lower limit of the theoretical estimates. (auth)

30462 ELASTIC AND INELASTIC PROTON SCATTERING FROM ^{106}Pd AND ^{108}Pd. Robinson, R. L.; Ford, J. L. C. Jr.; Stelson, P. H.; Satchler, G. R. (Oak Ridge National Lab., Tenn.). Contract W-7405-eng-26. Phys. Rev., 146: 816-23(June 17, 1966). (ORNL-P-1940).

Angular distributions of elastically and inelastically scattered 12- and 13-Mev protons from ^{106}Pd and ^{108}Pd were measured for angles between 24 and 165°. Quadrupole and octupole deformation parameters, β_2 and β_3, were extracted from the experimental cross sections by means of the distorted-wave direct-interaction theory. They are: $\beta_2 = 0.25$ and $\beta_3 = 0.15$ for ^{106}Pd, and $\beta_2 = 0.23$ and $\beta_3 = 0.14$ for ^{108}Pd. These are consistent with values obtained through Coulomb-excitation studies. The octupole states were observed at 2.07 Mev in ^{106}Pd and 2.03 Mev in ^{108}Pd. Differential cross sections of the two-quadrupole phonon states were compared with the predictions of the coupled-channels theory as extended by Tamura. To achieve reasonable agreement between experiment and theory for excitation of the second 2^+ level, it was necessary to admix the one- and two-quadrupole phonon states. Energies and cross sections at one angle for a number of other levels below 3.2 Mev are also reported. (auth)

30463 GAMMA RAYS FROM SHORT-LIVED FISSION-FRAGMENT ISOMERS. Sund, R. E.; Walton, R. B. (General Atomic Div., General Dynamics Corp., San Diego, Calif.). Phys. Rev., 146: 824-35(June 17, 1966).

Measurements of the energy spectra of isomeric gamma rays from the neutron fission of ^{235}U and ^{239}Pu at a number of time intervals between 50 and 600 μsec showed six prominent gamma rays for both cases of fission. The intensities and half-lives for these gamma rays indicate that there are three fission-fragment isomers, each giving rise to a pair of gamma rays in cascade. The energies of the cascade gamma rays and the half-life for each isomer are 1260, 450 kev (80 μsec), 850, 250 kev (54 μsec), and 990, 710 kev (32 μsec). Absolute gamma-ray intensities were obtained by measuring the integral number of gamma rays above a fixed bias energy as a function of time and normalizing these data at 10 msec to the absolute intensities derived from the theoretical work by Griffin and the data of Fisher and Engle. The intensities of delayed gamma rays from photofission of ^{235}U, ^{239}Pu, and ^{238}U were also measured at early times, starting at 2 μsec after fission. An intense short-lived component with an apparent half-life of a few μsec was observed for all three cases of photofission. (auth)

30464 STUDY OF (p,n) REACTIONS BETWEEN 100 AND 400 Mev. Treytl, W. J.; Caretto, A. A. Jr. (Carnegie Inst. of Tech., Pittsburgh). Phys. Rev., 146: 836-40(June 17, 1966).

Excitation functions of (p,n) reactions were determined for proton energies between 100 and 400 Mev using targets of ^{45}Sc, ^{64}Ni, ^{103}Rh, ^{130}Te, and ^{186}W. The energy dependence of the cross sections was found to vary from $E^{-1.31}$ to $E^{-1.5}$ over this range of mass numbers. This variation is apparently related to the increase in attenuation of the incident and outgoing nucleon waves with increasing target mass number. The experimental cross sections were compared with Monte Carlo cascade calculations based on a simple model which did not take refraction of the incident protons into account and which made use of a square-well nuclear potential. Serious deviations were observed between the calculated and the experimental energy dependencies, indicating the necessity of employing a more sophisticated model than one based on simple intranuclear nucleon-nucleon cascades. (auth)

30465 NEUTRON TOTAL CROSS SECTION OF ^{242}Pu. Auchampaugh, G. F.; Bowman, C. D.; Coops, M. S.; Fultz, S. C. (Univ. of California, Livermore). Contract W-7405-Eng-48. Phys. Rev., 146: 840-3(June 17, 1966). (UCRL-12379; UCRL-12379(Rev.1)).

The neutron total cross section of ^{242}Pu was studied from 0.02 to 400 ev using the time-of-flight facility at the Livermore linear electron accelerator. Resonance parameters were determined for fourteen resonances, and the s-wave neutron strength function was found to be $(0.95 \pm 0.40) \times 10^{-4}$. The total cross section at 0.025 ev was found to be 38.9 ± 1.6 b. (auth)

30466 HIGH-ENERGY γ SPECTRA RESULTING FROM NEUTRON CAPTURE IN HAFNIUM ISOTOPES. Namenson, A.; Jackson, H. E.; Smither, R. K. (Argonne National Lab., Ill.). Phys. Rev., 146: 844-52(June 17, 1966).

The γ spectra resulting from thermal-neutron capture in targets of natural hafnium, enriched ^{177}Hf, and enriched ^{179}Hf were measured with lithium-drifted germanium detectors. The energies and intensities of 42 gamma lines in the range from about 5.5 to 7.6 Mev were determined and the transitions were identified with the reactions $^{177}Hf(n,\gamma)^{178}Hf$, $^{178}Hf(n,\gamma)^{179}Hf$, $^{179}Hf(n,\gamma)^{180}Hf$, or $^{180}Hf(n,\gamma)^{181}Hf$. The neutron separation energies were determined to be 7623 kev for

^{179}Hf, 6098 kev for ^{179}Hf, 7383 kev for ^{180}Hf, and 5693 kev for ^{181}Hf, the uncertainty in energy being ±3 kev in each case. The gamma spectrum of each final nucleus was used to identify 28 new levels, and to verify 14 previously known levels. Some of these levels are discussed. (auth)

30467 FURTHER STUDY OF NUCLEAR RESONANT SCATTERING USING NEUTRON-CAPTURE GAMMA RAYS. Ben-David, G.; Arad, B.; Balderman, J.; Schlesinger, Y. (Soreq Nuclear Research Center, Yavne, Israel). Phys. Rev., 146: 852-60(June 17, 1966).

The study of resonance scattering of neutron-capture gamma rays was extended using 22 capture gamma sources and 57 scattering targets. About 50 resonance-scattering events were observed in 23 elements and the effective cross sections evaluated. Some cases of complex spectra are described. The association of the scattering with nuclei in the region of closed shells is clearly shown. Problems of minimum observable cross sections are discussed and some further applications of the technique are suggested. (auth)

30468 INELASTIC ALPHA-PARTICLE EXCITATION IN THE EVEN TIN ISOTOPES. Baron, N. (Lewis Research Center, Cleveland); Leonard, R. F.; Need, John L.; Stewart, W. M. Contract AT(45-1)-1062. Phys. Rev., 146: 861-8(June 17, 1966). (RLO-1062-664).

Angular distributions were measured for elastic and inelastic alpha-particle scattering by isotopically enriched targets of ^{116}Sn, ^{118}Sn, ^{120}Sn, and ^{122}Sn using the 40-Mev alpha beam of the NASA 60-inch cyclotron. Two states of energies close to 1.2 and 2.4 Mev were the only strong excitations observed. The inelastically scattered groups of alpha particles were analyzed using a distorted-wave Born approximation (DWBA) and the nuclear vibrational model. The results of these calculations are in good agreement with the known spins and parities: 2^+ for the first excited state and 3^- for the second. DWBA calculations were also carried out for the 2^+ excitations using eigenfunctions of the pairing plus Q·Q potentials. The calculated cross sections show a tendency to decrease with increasing neutron number. The experimental trend is qualitatively similar but much less regular. The absolute cross sections calculated using only cloud configurations are short of experimental values by about a factor of 4 when the Gammel-Thaler 40-Mev proton-alpha interaction is used. The relation of this discrepancy to the contribution from extracloud configurations is discussed. (auth)

30469 NUCLEAR LEVELS OF ^{101}Ru POPULATED IN THE DECAY OF ^{101}Rh ISOMERS. Aras, Namik K.; O'Kelley, G. Davis; Chilosi, G. (Oak Ridge National Lab., Tenn.). Contract W-7405-eng-26. Phys. Rev., 146: 869-76(June 17, 1966). (ORNL-P-1888).

The decay properties of 4.3-day ^{101}Rh^m and 3.0-yr ^{101}Rh^g were investigated with the aid of p-i-n, lithium-drifted germanium gamma-ray detector and with a NaI(Tl) gamma-gamma coincidence spectrometer. Energies (and transition intensities) of the gamma rays from the decay of ^{101}Rh^m are 127.0 ± 0.3 (1.2), 180.1 ± 0.4 (0.9), 184.4 ± 0.5 (0.3), 233.4 ± 0.5 (0.4), 238.1 ± 0.4 (0.5), 306.8 ± 0.3 (100), 311 ± 1 (0.1), 331.9 ± 0.4 (0.06), 418 ± 1 (0.01), and 542.2 ± 0.5 (5.6) kev, and coincidence data require these transitions to be fitted into a level scheme in ^{101}Ru with energies at 127.0 ± 0.3, 306.8 ± 0.3, 311.0 ± 0.5, 545.2 ± 0.5, and 639 ± 1 kev. Gamma-ray energies (and transition intensities) observed in the decay of ^{101}Rh^g are 127.0 ± 0.3 (105), 198.4 ± 0.4 (100), 295.4 ± 0.4 (0.9), 325.4 ± 0.3 (21), and 422.4 ± 0.6 kev, which are consistent with excited states of ^{101}Ru at 127.0 ± 0.3, 325.4 ± 0.3, and 422.4 ± 0.6 kev. Possible spin assignments for the excited levels in ^{101}Ru are discussed. The half-life of ^{101}Rh^m was remeasured as 4.34 ± 0.01 days. (auth)

30470 HIGHER ORDER EFFECTS IN β-γ CORRELATIONS INVOLVING ALLOWED β TRANSITIONS. Cipolla, S.; Grabowski, Z. W.; Naser, H. M.; Steffen, R. M. (Purdue Univ., Lafayette, Ind.). Contract AT(11-1)-1420. Phys. Rev., 146: 877-82(June 17, 1966).

Higher order effects in allowed β transitions may be generated by the interference of the allowed Gamow-Teller components with second-forbidden components. In strongly hindered β transitions, this interference effect is expected to give rise to β-γ directional correlations with measurable anisotropies. The β-γ directional correlations of the hindered allowed β transition (log ft >8) in the deformed nuclei ^{152}Eu, ^{154}Eu, and ^{160}Tb were studied. The β-correlation factor A_2^β, which characterizes the β transition in the expression for the β-γ directional correlation $W(\theta) = 1 + A_2^\beta A_2^\gamma P_2(\cos\theta)$, was found to be vanishingly small in all cases, except that of ^{160}Tb. The results are: $A_2^\beta = -0.017 \pm 0.012$ for the 0.70-Mev β transition of ^{152}Eu (log ft = 10.6); $A_2^\beta = +0.016 \pm 0.020$ for the 0.20-Mev β transition of ^{152}Eu (log ft = 9.6); $A_2^\beta = 0.007 \pm 0.006$ for the 0.58-Mev β transition of ^{154}Eu (log ft = 10.0); and $A_2^\beta = +0.041 \pm 0.015$ for the 0.566-Mev β transition of ^{160}Tb (log ft = 8.1). A summary of β-γ directional correlation measurements on allowed β transitions is presented and the implications of the results are discussed. In most cases the experimental results suggest that the effects that cause the reduction of the allowed matrix elements are also operative in reducing the second-forbidden matrix elements. (auth)

30471 SOME NUCLEAR STATES OF ^{103}Rh. Potnis, V. R.; Nieschmidt, E. B.; Mandeville, C. E.; Ellsworth, L. D.; Agin, G. P. (Kansas State Univ., Manhattan). Phys. Rev., 146: 883-6(June 17, 1966).

The gamma rays emitted in de-excitation of ^{103}Rh following beta decay of ^{103}Ru were studied in a Ge(Li) detector and with coincident scintillation counters. Quanta were detected at energies of 53, 297, 445, 498, 557, and 610 kev with relative intensities of 0.41, 0.31, 0.40, 100, 0.87, and 7.35. The data also indicate the presence of a gamma ray at 65 kev. The K-shell conversion coefficient of the 53-kev gamma ray was measured to be 1.77 ± 0.03. A disintegration scheme for ^{103}Ru was proposed. (auth)

30472 PROTON SPECTRA FROM REACTIONS INDUCED BY 30.5-Mev ALPHA PARTICLES. Swenson, L. W. (Massachusetts Inst. of Tech., Cambridge. Franklin Inst., Swarthmore, Pa.); Gruhn, C. R. Contract AT(30-1)-2098. Phys. Rev., 146: 886-98(June 17, 1966). (MIT-2098-212).

The (α,p) reaction was studied at 30.5 Mev for the targets ^{27}Al, ^{48}Ti, ^{51}V, Fe, ^{59}Co, ^{58}Ni, ^{60}Ni, ^{61}Ni, ^{62}Ni, ^{63}Cu, ^{65}Cu, ^{67}Zn, ^{93}Nb, Mo, ^{103}Rh, Pd, ^{113}Cd, ^{114}Cd, ^{119}Sn, ^{120}Sn, ^{124}Sn, ^{181}Ta, ^{195}Pt, and ^{197}Au. Proton evaporation spectra were measured at 30, 60, 90, 120, and 150° up to excitation energies of 25 Mev in the residual nucleus. The spectra were compared with statistical-model predictions and the parameters α and T obtained. The lack of mass dependence of these parameters and the average low value of the level-density parameter $\alpha = 5.5$ Mev^{-1} add evidence for a nuclear-temperature anomaly. The anomaly is discussed in terms of recent intermediate-resonance models. (auth)

30473 DECAY OF ^{133}I TO LEVELS IN ^{133}Xe. Eichler, Eugene; Chase, John W.; Johnson, Noah R.; O'Kelley, G. Davis (Oak Ridge National Lab., Tenn.). Contract W-7405-eng-26. Phys. Rev., 146: 899-906(June 17, 1966). (ORNL-P-1829).

The decay of ^{133}I was studied by a combination of lithium-drifted germanium and scintillation-coincidence techniques. Radiations identified were: gamma rays of energies (and intensities) 250 (0.1), 263 (0.18), 340 (0.3), 360 (0.3), 422 (0.40), 509.8 (2.50), 529.4 (100), 617.0 (0.30) 679 (1.0), 706.8 (1.7), 768 (0.59), 821 (0.22), 856.0 (1.4), 875.3 (5.8), 912 (0.40), 1052 (0.72), 1062 (0.16), 1234 (1.7), 1297 (2.7), and 1350 kev (0.16); and beta rays of energies 1540, 1230, 890, and 500 kev. A ^{133}Xe level scheme was constructed with states at 233, 529.4, 679, 875.3, 1052, 1235, 1296.9, 1349.4, 1385.2, and 1591.4 kev. The ^{133}I half-life was remeasured as 20.8 ± 0.2 h. (auth)

30474 27.7-kev LEVEL IN ^{129}I AND SOME REMARKS ABOUT ITS USE IN MOESSBAUER EXPERIMENTS. Sanders, R.; de Waard, H. (Rijksuniversiteit, Groningen, Netherlands). Phys. Rev., 146: 907-11(June 17, 1966).

The properties of the first excited state of ^{129}I were studied with a mass-separated ^{129m}Te source. The energy of this state, as determined from the conversion-electron

spectrum, is $E_\gamma = 27.72 \pm 0.06$ kev. This differs considerably from the often quoted value of 26.8 kev, but it agrees very well with the value recently published by Bemis and Fransson. An accurate half-life value $T^{1/2} = 16.8 \pm 0.2$ nsec was determined from delayed βe^- coincidences. A total conversion coefficient $\alpha = 5.3 \pm 0.3$ was obtained from the relative intensities of the 27.7-kev gamma rays and the 27.4- kev x rays that accompany the isomeric transition in ^{129}Te. The contributions of these rays were separated by comparing Mössbauer spectra obtained with the 70-min and 33-day activities of ^{129}Te. Some remarks are made about the relative merits of these activities for use in Mössbauer source. (auth)

30475 ^{182}W(d,p)^{183}W REACTION AT 7.5 AND 12 Mev: AN INVESTIGATION OF THE STRIPPING PROCESS ON A DEFORMED HEAVY NUCLEUS. Siemssen, R. H.; Erskine, J. R. (Argonne National Lab., Ill.). Phys. Rev., 146: 911-25(June 17, 1966).

The ^{182}W(d,p)^{183}W reaction was studied at 7.5 and 12 Mev with a broad-range magnetic spectrograph. At 12 Mev, angular distributions were obtained from 5 to 145° for the transitions to the ground state and to the levels at excitations of 46, 99, 208, 292, 412, and 453 kev. In addition, the scattering of deuterons on ^{182}W and protons on ^{183}W was measured at 12 Mev. The elastic scattering was analyzed in terms of the nuclear optical model. A serious ambiguity in the deuteron parameters has been observed. For inelastic deuteron scattering leaving ^{182}W in its first excited state, a distorted-wave Born-approximation (DWBA) analysis based on a deformed complex potential leads to a deformation parameter $\beta = 0.23$ for ^{182}W. The angular distributions of the ^{182}W(d,p)^{183}W reaction were compared with DWBA calculations with different distorting potentials, and spectroscopic factors were extracted. The ratios of the experimental spectroscopic factors agree quite well with those predicted by the Nilsson model, when band mixing is included in the calculation of the theoretical spectroscopic factors. Absolute spectroscopic factors, on the other hand, may disagree by as much as a factor of 2–3. The data were also compared with the DWBA calculations of Penny and Satchler, which include "two-step" processes. The results indicate that "two-step" processes are probably unimportant for the reaction studied. (auth)

30476 NUCLEAR CHARGE DISTRIBUTION IN FISSION: ^{92}Y, ^{93}Y, ^{94}Y, AND ^{95}Y INDEPENDENT YIELDS. Norris, Andrew E.; Wahl, Arthur C. (Washington Univ., St. Louis). Phys. Rev., 146: 926-31(June 17, 1966).

The fractional independent yields of ^{92}Y, ^{93}Y, ^{94}Y, and ^{95}Y from thermal-neutron fission of ^{235}U were determined to be 0.0013 ± 0.0002, 0.016 ± 0.004, 0.08 ± 0.02, and 0.29 ± 0.08, respectively. The experimental method involved rapid separation of yttrium and strontium fission products by precipitation of yttrium hydroxide and subsequent radiochemical determination of the yttrium isotopes. Newly determined half-life values are 84 ± 5 sec for ^{94}Sr and 33 ± 6 sec for ^{95}Sr. Gaussian curves which satisfactorily represent the nuclear charge dispersion for A = 92, 93, 94, and 95 have standard deviations $\sigma = 0.58 \pm 0.02$, 0.56 ± 0.02, 0.56 ± 0.04, and 0.53 ± 0.02, respectively. The average value of σ for ten mass numbers (A = 91–95 and 139–143) is 0.59 ± 0.02. For the individual mass numbers, a singie Gaussian curve with $\sigma = 0.59 \pm 0.06$ (full width at half-maximum = 1.56 ± 0.12 charge units) gives a satisfactory representation of nuclear-charge dispersion. (auth)

30477 NUCLEAR CHARGE DISTRIBUTION IN FISSION: ^{92}Rb AND ^{93}Rb INDEPENDENT YIELDS. Wahl, Arthur C. (Washington Univ., St. Louis); Norris, Andrew E.; Ferguson, Robert L. Phys. Rev., 146: 931-4(June 17, 1966).

The fractional independent yields of ^{92}Rb and ^{93}Rb from thermal-neutron fission of ^{235}U were determined to be 0.62 ± 0.16 and 0.59 ± 0.08, respectively. These values agree with those predicted from Gaussian representations of nuclear charge dispersion for A = 92 and A = 93. Newly determined half life values are 4.1 ± 0.3 sec for ^{92}Rb and 5.1 ± 0.3 sec for ^{93}Rb. The experimental method involved rapid separation of rubidium and strontium fission products by adsorption of strontium on solid strontium carbonate and subsequent radiochemical determination of yttrium descendants. (auth)

30478 RADIATIVE CORRECTIONS TO ELECTRON-INDUCED PROCESSES. Kuo, P. K.; Yennie, D. R. (Univ. of Minnesota, Minneapolis. Cornell Univ., Ithaca, N. Y.). Phys. Rev., 146: 1004-11(June 24, 1966).

Radiative corrections are calculated for a class of electron-induced processes in which the final electron is not observed. The process can either be a nuclear excitation process or a production process in which a particle, e.g., a pion, is produced. The calculated radiative corrections are found to be considerably smaller than those of comparable processes in which the final electron is detected at some nonforward angle. The result also exhibits a linear logarithmic dependence on the initial electron energy if the ratio $E_{final}/E_{initial}$ is kept constant. (auth)

30479 RANGE OF PHOTOPARTICLE RECOIL ATOMS IN SOLIDS. Van Lint, V. A. J.; Wyatt, M. E.; Schmitt, R. A.; Suffredini, C. S.; Nichols, D. K. (General Atomic Div., General Dynamics Corp., San Diego, Calif.). Contract AF 33(616)-6795. Phys. Rev., 147: 242-8(July 8, 1966).

The ranges of atoms recoiling from photonuclear reactions in various elements were measured, utilizing foil-sandwich irradiations followed by standard radiochemical detection techniques. Different energy spectra of recoil atoms were achieved by varying the bremsstrahlung energy and the angle of emission relative to the incident photons. The results were compared with some theoretical calculations. An empirical best fit to the data, using the reduced vector range and energy, ρv and ϵ, given by Lindhard, is $\rho v = 2.4\epsilon^{0.74}$ for $\epsilon < 0.15$. (auth)

30480 INVESTIGATION OF ISOBARIC ANALOG STATES BY (p,n) REACTIONS FOLLOWED BY PROTON EMISSION. Yavin, A. I.; Hoffswell, R. A.; Jones, L. H.; Noweir, T. M. (Univ. of Illinois, Urbana). Phys. Rev. Lett., 16: 1049-50(June 6, 1966).

A new method for investigating proton-unstable isobaric analog states is presented. The reaction ^{91}Zr(p,n$\tilde{p}$)^{90}Zr is selected as a favorable example since ^{91*}Nb is proton unstable, but neutron stable. (B.G.D.)

30481 DISCREPANCIES IN PROTON-TRANSFER REACTIONS TO STATES WITH DIFFERENT ISOBARIC SPIN. Siemssen, R. H. (Argonne National Lab., Ill.); Morrison, G. C.; Zeidman, B.; Fuchs, H. Phys. Rev. Lett., 16: 1050-4(June 6, 1966).

The relative spectroscopic factors from (^{3}He,d) and (d,n) reactions to the low T = 0 and T = 1 states in the odd-odd nuclei ^{10}B, ^{14}N, and ^{26}Al are compared. It is shown that in each case a smaller value of the relative spectroscopic factor for the T = 1 states is deduced from the (d,n) reaction than from the (^{3}He,d) reaction, the spectroscopic factors being normalized to the T = 0 ground states. (B.G.D.)

30482 GAMMA DECAY OF LEVELS IN ^{40}Ca MEASURED WITH THE ^{39}K(p,γ)^{40}Ca REACTION. Leenhouts, H. P.; Endt, P. M. (Rijksuniversiteit, Utrecht). Physica, 32: 322-36(Feb. 1966).

In the proton-energy range $E_p = 500-2900$ kev fifty-three resonances were observed in the ^{39}K(p,γ)^{40}Ca reaction. The resonance energies and strengths were determined. The decay modes of most of the resonances and of fifteen lower excited states in ^{40}Ca were determined from single and coincidence gamma-ray spectra. (auth)

30483 TWO-NUCLEON EXCHANGE REACTIONS IN NUCLEAR STRUCTURE INVESTIGATIONS. Wiktor, S. (Inst. of Nuclear Physics, Krakow). Postepy Tech. Jadrowej, 9: 348-52(1965). (In Polish).

At first an outline of the results of the theory of stripping and pickup reactions is presented and the expression for cross section in Born approximation is written. Also the heavy particle stripping is presented. The applications of the reactions above in spectroscopy are described. Finally, account is taken of pairing forces. (auth)

30484 THE MODEL OF THE EXCITED CORE OF THE NUCLEUS. Strzalkowski, A. (Inst. of Nuclear

Physics, Krakow). Postepy Tech. Jadrowej, 9: 444-7 (1965). (In Polish).

This model proposed in 1957 by Lawson and Vretsky is presented, together with the energy level schemes for some pairs of nuclei, e.g., ^{202}Hg(core) and ^{203}Tl(odd nuclide). Angular distributions of elastic scattered protons and deuterons on such pairs of nuclides are compared. (auth)

30485 THE π^+-MESONIC DECAYS OF HYPERNUCLEI. Mayeur, C. (Univ. Libre, Brussels); Sacton, J.; Vilian, P.; (and others). Univ. Brux., Inst. Phys., Bull., No. 25, 1-21 (Mar. 1966).

Experimental results are presented on eleven π^+ decays of hypernuclei obtained in 11,000 K^- captures at rest in nuclear emulsions. Ten of the eleven were attributed to $_{\Lambda}He^4$ decay. (B.G.D.)

30486 PROBLEM IN STATISTICAL THEORY OF NUCLEAR FISSION. Yu, Chuan-tsan; Kuo, Chien-chung. Wu Li Hsueh Pao, 22: 111-14(Jan. 1966). (In Chinese).

In current statistical theories of nuclear fission the fission process is treated as a quasistable state, assuming that the size of the two fragments is controlled by the state just prior to fission. The number of fission modes is expressed as $N(A_L,A_H) \propto e^{2\sqrt{aE}}$, where $a = a_L + a_H$ is the sum of level densities of the light and heavy fragments, $E = E_L + E_H$ is the sum of the excitation energy of the light and heavy fragments and $A_L + A_H$ are the masses of the light and heavy fragments. Attempts at predicting two different modes of fission taking place simultaneously are refuted by experimental results; it is simply impossible to handle complicated mass distribution curves changing repeatedly from one, two and three peaks. Calculated kinetic energies of the fragments and from secondary neutron release differ from experimental data. The excitation energies E were therefore calculated from experimental data, assuming minimum deformation at the moment of fission; the level density a was also calculated on the basis of the experimental secondary neutron release from the fragments. When these values were substituted back into the above-indicated formula, it was found only equal fragments are favored. The inability of currently accepted theories to account for different fission modes occuring simultaneously is attributed to inadequate basic assumptions. (TTT)

30487 GAMMA RADIATION OF 12.3-YEAR ^{152}Eu. Dzhelepov, B. S.; Zhukovskii, N. N.; Maloyan, A. G. Yadern. Fiz., 3: 785-93(May 1966). (In Russian).

The γ spectrum of 12.3-year ^{152}Eu is investigated with the help of the magnetic spectrometers—photoritron and elotron. 29 γ lines were observed and their energy and relative intensities were measured with an accuracy higher than in previous papers. The 296, 360, 674, 720, 840, 1253 and 1454 kev γ lines were found for the first time. The α_K-values for 15 γ transitions were determined more precisely. The decay scheme of ^{152}Eu is given: the γ transition intensities and log ft values are obtained from the results. (auth)

30488 COULOMB EXCITATION OF LEVELS IN THE β- AND γ-VIBRATIONAL BANDS OF THE ^{152}Sm AND ^{186}W NUCLEI. Gangrskii, Yu. P.; Lemberg, I. Kh.; Nabichvrishvili, V. A. (Ioffe Inst. of Physics and Tech., Leningrad). Yadern. Fiz., 3: 794-7(May 1966). (In Russian).

The Coulomb excitation of nuclear levels in ^{152}Sm and ^{186}W was investigated using the method of coincidences between γ-quanta and inelastically scattered ^{14}N ions. The levels 0^+, 2^+ and 4^+ in the β-vibrational band and 2^+ in the γ-vibrational band of ^{152}Sm and also the levels 2^+ and 4^+ in the ^{186}W γ-vibrational band were excited. The values were determined of the reduced probability of the electric quadrupole transition from the ground state to the levels 2^+ of the β- and γ-vibrational bands in ^{152}Sm and ^{186}W. (auth)

30489 DETECTION OF A ^{113}Cd ISOMER BY MEANS OF THE γ RADIATION FROM ^{60}Co. Veres, A.; Ozhdyani, M. (State Atomic Energy Committee, Budapest). Yadern. Fiz., 3: 798-800(May 1966). (In Russian).

A ^{113}Cd isomer was found using a ^{60}Co source. The following values were determined from the experimental data: half-life ~14 years, activation cross-section $\sigma_m = 1.4 \cdot 10^{-32}$ cm^2 and partial level width at 1.1 Mev about $3.5 \cdot 10^{-5}$ ev. (auth)

30490 TOTAL NEUTRON CROSS SECTIONS FOR HEAVY EVEN-EVEN TIN ISOTOPES IN THE ENERGY REGION BELOW 10 kev. Adamchuk, Yu. V.; Moskalev, S. S.; Muradyan, H. V. Yadern. Fiz., 3: 801-3(May 1966). (In Russian).

Total neutron cross-sections were investigated for heavy even-even tin isotopes. The level parameters were determined taking the interference between resonance and potential scattering into account. The most probable values of the strength functions for ^{116}Sn, ^{118}Sn, ^{120}Sn, ^{122}Sn and ^{124}Sn are $0.46^{+0.41}_{-0.19}$, $0.36^{+0.38}_{-0.15}$, $0.12^{+0.20}_{-0.045}$, $0.49^{+0.62}_{-0.22}$ and $0.13^{+0.32}_{-0.06}$ respectively. The values are higher than the previously published experimental data. (auth)

30491 PAIRING CORRELATIONS AND THE MASSES OF SPHERICAL NUCLEI. Krainov, V. P. Yadern. Fiz., 3: 804-12(May 1966). (In Russian).

The influence of pairing correlations in nuclei with few nucleons above a completed shell is taken into account using Green function techniques. Pair energies are calculated using the universal pairing interaction of the finite Fermi system theory. A good agreement with experiments is obtained for nuclei in the region of Ca, Zr, Sn, Ba, and Pb. It is shown that the pairing occurs inside the nuclear volume, not only on the surface. The mixing of nucleons with respect to single-particle states, due to the pairing is calculated, taking into account the excitation of nucleons in the completed shell. The results are compared with the calculations of others. (auth)

30492 EQUALITY OF THE POLARIZATION AND ASYMMETRY IN INELASTIC SCATTERING. Inopin, E. V. Yadern. Fiz., 3: 817-19(May 1966). (In Russian).

It is shown, that the theorem on the equality of the polarization of initially unpolarized particles and the asymmetry in the scattering of a completely polarized beam, holds in adiabatical collisions of particles with spin $\frac{1}{2}$ on nuclei with arbitrary spin, leading to excited states of the nuclei. This result is the generalization to inelastic scattering of the corresponding theorem, previously proven for elastic scattering. (auth)

30493 INFLUENCE OF THE IDENTITY OF COLLIDING NUCLEI IN INELASTIC SCATTERING AT SUB-BARRIER ENERGIES. Dalidchik, F. I.; Sayasov, Yu. S. (Inst. of Chemical Physics, Academy of Sciences, USSR). Yadern. Fiz., 3: 820-32(May 1966). (In Russian).

A general theory of inelastic processes is developed for the scattering of identical nuclei. Features of the angular distributions of collision products in semiclassical conditions are studied in detail. It is shown that in the general case the identity of the colliding nuclei leads to the appearance of considerable interference maxima and minima in the angular distributions. These depend heavily on the main characteristics of the nuclei: spins, parities, nuclear surface diffusions et al. This can be used as the basis of an original method for the experimental determination of the corresponding characteristics. The theory is specified to magnetic and double Coulomb excitation processes, to the excitation of monopole transitions and to neutron tunnel transfer in the scattering of identical particles. (auth)

30494 CAPTURE OF μ^- MESONS BY NUCLEI. Bunatyan, G. G. Yadern. Fiz., 3: 833-41(May 1966). (In Russian).

The probability of μ^--meson capture by nuclei was calculated for a number of spherical nuclei. The weak (Fermi) interaction is assumed to be universal. The dependence of the μ^--capture probability on the nuclear structure is taken into account according to the finite Fermi-system theory. The theoretical calculations are in agreement with experiments. (auth)

30495 ANALYSIS OF THE ELASTIC SCATTERING OF 6.9-Mev PROTONS BY Ni ISOTOPES AND THE NUCLEAR OPTICAL MODEL. Kashuba, I. E.; Kozin, B. G.; Pasech-

nik, M. V.; Pucherov, N. N.; Chirko, V. I. (Inst. of Physics, Academy of Sciences, Ukrainian SSR). Yadern. Fiz., 3: 842-8(May 1966). (In Russian).

The differential cross sections and polarizations of 6.9 Mev protons, elastically scattered by Ni isotopes, were calculated on the basis of the optical model. It is shown that the model parameters, giving the best agreement between theory and experiment, differ significantly for various Ni isotopes. An uncertainty exists in the choice of the depth and diffusion parameters b and W in the imaginary part of the potential for Wb = const. It is shown, that the uncertainty in the choice of the optimal set of optical model parameters is significantly decreased, if the analysis of the data on elastic scattering takes the angular dependence of the polarization into account, as well as the differential cross section. (auth)

30496 INVESTIGATION OF DISINTEGRATION WITH EMISSION OF FAST He NUCLEI DUE TO HIGH-ENERGY PROTONS. Takibaev, Zh. S.; Shalagina, E. V.; Amankulova, D. S.; Titova, N. S.; Shtern, G. R. (Kazakh State Univ., USSR). Yadern. Fiz., 3: 849-57(May 1966). (In Russian).

The emission of helium nuclei with kinetic energies in the region 100–2500 Mev by stars, produced by 10–20 Bev protons in photoemulsion is investigated. It is shown that ~98% of the double-charged particles are emitted in the disintegration of heavy photoemulsion nuclei. It is noted that the production cross section of the investigated particles and their energy and angular distributions do not depend on the incident proton energy. The average numbers of thin, gray and black tracks are compared in stars with and without helium and the angular distributions of thin, gray and black tracks in these interactions are obtained. The conclusion is made that the emission of fast helium nuclei is connected with a cascade process inside the nucleous. (auth)

30497 DIFFERENTIAL CROSS SECTION FOR THE ELASTIC SCATTERING OF 13.6-Mev DEUTERONS BY Ti, Fe, AND Co NUCLEI. Vereshchagin, A. N.; Sokolov, L. S.; Chernov, I. P.; Tokarevskii, V. V. Yadern. Fiz., 3: 858-60(May 1966). (In Russian).

The differential cross sections for the elastic scattering of 13.6 Mev deuterons by Ti, Fe and Co nuclei were measured. The clear appearance of a third additional maximum is specific for the angular distributions on Ti and Fe. The differential cross sections on ^{59}Co practically coincide with those on ^{60}Ni, indicating that the influence of nuclear structure peculiarities on the form of the angular distributions is small. (auth)

30498 CROSS SECTIONS FOR THE PRODUCTION OF γ-QUANTA IN INELASTIC INTERACTIONS OF 14 Mev NEUTRONS WITH C, O, Al, Fe, AND Pb NUCLEI. Bezotosnyi, V. M.; Vershinin, V. G.; Surov, L. M.; Shvetsov, M. S. Yadern, Fiz., 3: 861-2(May 1966). (In Russian).

Results of cross-section measurements are given for the production of γ-quanta in inelastic interactions of 14 Mev neutrons with C, O, Al, Fe and Pb nuclei. The measurements were performed using a scintillation spectrometer, consisting of an 80 × 80 mm^2 NaI(Tl) crystal, a photoelectron multiplier EFU-1BS, a preamplifier and a 100-channel amplitude pulse analyzer A1-100-1. The energy resolution of the spectrometer for γ-rays from ^{65}Zn (E_γ = 1.12 Mev) is 8%. (auth)

30499 ELASTIC AND INELASTIC SCATTERING OF α PARTICLES BY CARBON NUCLEI. Iferov, G. A.; Matya, P.; Teplov, I. B.; Tulinov, A. F. (Moscow State Univ.). Yadern. Fiz., 3: 863-7(May 1966). (In Russian).

Semiconductor methods are used to measure the angular distributions of α-particles elastically and inelastically scattered by ^{12}C nuclei, for the initial energy changing by 1 Mev steps from 13 to 26 Mev. The cross sections demonstrate a pronounced diffractional structure, varying significantly with the change of the energy. (auth)

30500 KINETIC ENERGIES OF PAIR FRAGMENTS IN THE FISSION OF ^{233}U, ^{235}U, AND ^{238}U BY 12-Mev DEUTERONS. Selitskii, Yu. A.; Solov'ev, S. M.; Eismont, V. P. Yadern. Fiz., 3: 868-73(May 1966). (In Russian).

The energies of pair fragments in the deuteron fission of uranium isotopes were measured using surface-barrier silicon counters. The obtained information was used to determine the dependence of the mean kinetic energy and the energy dispersion of fragments with definite mass, on the nucleon content of the fissile nucleus (and of the fragments). The nature of the observed properties of the fragment kinetic energies is discussed on the basis of the determined relations. (auth)

30501 SLOW MESON PRODUCTION IN THE INTERACTION OF 3.8-Gev π-MESONS WITH PHOTOEMULSION NUCLEI. Lepekhin, F. G.; Makarov, M. M.; Khokhlova, Z. S. (Ioffe Inst. of Physics and Tech., Leningrad). Yadern. Fiz., 3: 874-6(May 1966). (In Russian).

The angular and energy distributions of slow π-mesons (up to 40 Mev), created by a 3.8 Bev π-meson beam on photoemulsion nuclei, were investigated. The dependence of the emission probability and mean π-meson energy on the number of prongs in the parent star was estimated. It was shown that there is no reason to connect the creation of slow mesons with the existence of pion resonances. (auth)

30502 ANGULAR DISTRIBUTION OF INELASTICALLY SCATTERED COMPLEX PARTICLES. Kalinkin, B. N.; Grabowski, J. (Joint Inst. for Nuclear Research, Dubna, USSR). Yadern. Fiz., 3: 880-2(May 1966). (In Russian).

The angular distribution in the inelastic scattering of composite nuclei, accompanied by the excitation of low lying collective levels, is discussed. (auth)

30503 INTERACTIONS OF LIGHT HYPERNUCLEI AND Λ PARTICLES WITH NUCLEI. Kolesnikov, N. N.; Vedrinskii, R. V. Yadern. Fiz., 3: 946-50(May 1966). (In Russian).

The disintegration of light hypernuclei in the Coulomb field of heavy nuclei is investigated in the low- and high-energy approximations and also in the quasiclassical case. The cross section of the process is sensitive to the value of the hypernuclear binding energy B_Λ. For $_\Lambda H^3$, where B_Λ is small, the cross section can become very large, so that the Coulomb disintegration must be taken into account, when analyzing $_\Lambda H^3$ tracks in photoemulsion and of the production of hypertritium. The probability of Λ-particle capture by heavy nuclei, with the formation of heavy hypernuclei and emission of nucleons, is estimated. (auth)

30504 ANGULAR CORRELATIONS IN THE CAPTURE OF π-MESONS BY NUCLEI. Kolybasov, V. M. (Inst. of Theoretical and Experimental Physics, State Atomic Energy Commission, USSR). Yadern. Fiz., 3: 965-73(May 1966). (In Russian).

The capture is considered of stopped π-mesons by α-particle type nuclei (^{12}C, ^{16}O), accompanied by the emission of fast protons, deutrons, tritium nuclei and neutrons. The angular correlations of the final products and the distribution of neutron pairs, with respect to their relative motion energy, are calculated. It is shown that the existing experimental data on the angular correlations of fast particles are in agreement with the assumption, that the pole α-particle graph dominates. (auth)

30505 INVESTIGATION OF THE TIME INVARIANCE OF NUCLEAR FORCES. Krupchitskii, P. A. (Inst. of Theoretical and Experimental Physics, State Atomic Energy Commission, USSR). Yadern. Fiz., 3: 974-7(May 1966). (In Russian).

A method of investigation of the time invariance of nuclear forces is suggested, in which ^{48}Ti nuclei are irradiated by polarized thermal neutrons. If time parity is not conserved, an angular correlation should be observed between the two γ-quanta in the cascade $\frac{1}{2}(E2 + M1)\frac{3}{2}(E2)\frac{1}{2}$, by means of which the excited ^{49}Ti nucleus decays. The observation of the angular correlation reduces to a measurement of the relative probabilities, with which the mentioned γ-quanta are emitted in a plane, perpendicular to the neutron spin, under the angle 45 or 135° with respect to each other, for two opposite spin directions. (auth)

30506 γ-γ ANGULAR CORRELATION OF ^{144}Pr AT 54 TO 80 kev. Beer, H.; Schneider, H. (Justus Liebig-

Univ., Giessen, Ger.). Z. Naturforsch., 21a: 174-5 (Jan.-Feb. 1966). (In German).

The γ-γ angular correlations of ^{144}Pr were measured with a fast-slow coincidence device at 54 to 80 kev. The correlation functions were calculated. With consideration of the space-angle correction the correlation coefficients $A_2 = -0.12 \pm 0.04$ and $4\ A_4 = 0.05 \pm 0.06$ and the angular correlation function $W(\theta) = 1 - (0.12 \pm 0.04)\ P_2(\cos\theta) + (0.05 \pm 0.06)\ P_4(\cos\theta)$ were obtained. The angular correlation coefficient A_2 was determined as a function of the mixing ratio for a spin sequence $1^- \rightarrow 1^- \rightarrow 0^-$ or $0^- \rightarrow 1^- \rightarrow 1^-$. (tr-auth)

30507 ION CHARGE DISTRIBUTION OF UNRETARDED FISSION PRODUCTS. Konecny, E.; Siegert, G. (Justus-Liebig-Univ., Giessen, Ger. Technische Hochschule, Munich). Z. Naturforsch., 21a: 192-6(Mar. 1966). (In German).

An earlier work on the ion charge distribution of fission products (Opower, Z. Naturforsch., 20a: 131(1965)) was supplemented at two points. The fission products of all naturally occurring energies and ion charges were detected and compared with the integral measurements of Lassen. The ion charge distribution was then measured at constant kinetic energy and mass and the dependence of the mean ion charge as a function of the velocity was investigated at constant mass. (tr-auth)

30508 CALCULATION OF THE BINDING ENERGY OF HEAVY NUCLEI WITH NONLOCAL TWO-BODY FORCES. Kistler, S. (Univ., Cologne). Z. Phys., 193: 358-65(1966).

A nonlocal, separable potential which matches the phase shifts up to 320 Mev and gives saturation for nuclear matter in the first order at a Fermi-momentum of $k_F = 1.6f^{-1}$ with an energy per particle of -8 Mev has been constructed by Tabakin. This potential is employed for calculations of finite nuclei using the Fermi-gas model. The binding energy has been minimalized with respect to two parameters b and c (the surface-thickness and the radius of the nucleus). However the calculations show that an arbitrarily sharp surface is possible. (auth)

30509 THEORY OF MULTIPLE SCATTERING. Andreev, I. V. (Lebedev Inst. of Physics, Moscow). Zh. Eksp. Teor. Fiz., 50: 1081-3(Apr. 1966). (In Russian).

An expression for scattering of relativistic electrons at sufficiently large angles is obtained, which takes into account the finite size of the nucleus and the effect of multiple scattering under conditions when the correction to the formula for single scattering is relatively small. (auth)

30510 NUCLEAR MAGNETIC RESONANCE AND ELECTRON SPIN RESONANCE SPECTRA. INDEX FOR 1958-1963. Hershenson, Herbert M. New York, Academic Press, 1965. 112p.

This index includes more than 8000 references to NMR and ESR spectra published in sixty-seven journals and two collections of spectra during 1958-1963. Each reference indicates the journal, volume, and page where an actual spectrum may be found. (J.G.B.)

30511 PRESENT STATUS OF THE THEORY OF NUCLEAR STRUCTURE. Brueckner, Keith A. (Univ. of California, San Diego, La Jolla). pp 152-60 of Many-Body Theory. Kubo, Ryogo (ed.). Tokyo, Syokabo Publishing Co. New York, W. A. Benjamin, Inc., 1966.

The status of the theory of nuclear structure is considered. Nuclear matter, finite nuclei, optical-model parameters, and rotational effects in shell structure are briefly discussed. (D.C.W.)

30512 INELASTIC PROTONS FROM ^4He [Thesis]. Williams, Lawrence Ernest. Minneapolis, Univ. of Minnesota, 1965. 120p.

Two and possibly three resonances were seen in the inelastic proton continuum resulting from a 40-Mev proton bombardment of a NTP ^4He gas cell. A region of ^4He excitation between 19 and 24 Mev was explored over the lab angular range $15° \leq \theta_{lab} \leq 90°$. From knowledge of beam energy and detected particle type and energy, an absolute determination of the resonance Q values was obtained. The first resonance occurs 0.64 ± 0.14 Mev above the onset of the first continuum reaction ($^4He + p \rightarrow 2p + T$) and has a full width Γ_I of 450 ± 70 kev. The 3.5 ± 0.2 Mev broad second resonance lies 2.18 ± 0.14 Mev above p + T onset and is the stronger state throughout the angular range. Using the Q value of -19.82 Mev for the continuum onset excitation energies of 20.46 ± 0.14 Mev for resonance I and 22.00 ± 0.14 Mev for resonance II are obtained. An additional very weak resonance was observable between $26 \leq E^* \leq 28$ Mev at $\theta_{lab} = 15°$ and 25°. No bound states were detected. All resonances were seen to lie upon a background made up of two distinct components: (1) the phase space continua of the various 3-body final states and (2) an experimental flat background due to neutrons and elastic protons, which was independent of excitation at a given scattering angle. Peak I appears to be associated with the $J^\pi = 0^+$ state calculated by Werntz and Meyerhof and has no definite T value. Peak II, an enigma of $^4He(p,p')$ experiments, has, at higher bombardment energies, been explained via quasi-elastic scattering. This experiment may strengthen the argument for it being a true virtual state. The third peak lies in the E^* region previously associated with the $^4He(\gamma,p)T$ resonance and thus may be a $J^\pi = 1^-$ state. (TCO)

30513 THERMAL NEUTRON FISSION OF ^{235}U WITH EMISSION OF LONG-RANGE ALPHA PARTICLES [Thesis]. Schroeder, Ivan Gaston. New York, Columbia Univ., 1965. 66p.

The ratio of binary to ternary fission in ^{235}U was measured using solid state detectors and aluminum absorbers, for two reactor beams having cadmium ratios of 30 to 1 and 200 to 1, and for incident neutron energies of 0.003, 0.0253, 0.08, and 0.3 ev. A new method of measuring this ratio without the use of absorbers is presented. The results obtained show that the binary-to-ternary fission ratio in ^{235}U is a constant to a precision of 3% in the energy region between 0.003 and 0.3 ev. The measurements performed with the two reactor beams, having cadmium ratios of 30 to 1 and 200 to 1, gave for this ratio 518 ± 13 and 512 ± 14 respectively. The measurement performed without an absorber gave a value of 490 ± 20 for the 30 to 1 cadmium ratio beam. The kinetic energy distribution of the fission fragments associated with the emission of long-range alpha particles in the thermal neutron fission of ^{235}U was studied. The results obtained show that the mean energy of the light and heavy fragment peaks in ternary fission are shifted down in energy from the corresponding values for binary fission by $\Delta_l E = 6.8 \pm 0.2$ Mev and $\Delta E_h = 5.3 \pm 0.2$ Mev respectively. The kinetic energy distribution in ternary fission is narrower than the corresponding one for binary fission though the ratio of the peak positions and the relative heights remain the same. The mean total kinetic energy of the ternary fission fragments is displaced down in energy from the corresponding value for the binary process by $\Delta E = 12.7 \pm 0.5$ Mev, and, furthermore, the distribution is narrower. The mean kinetic energy of the long-range alpha particles decreases with increasing total kinetic energy of the associated fission fragments. A descriptive model of ternary fission with emission of long-range alpha particles is described, and its conclusions are correlated to some of the known results in ternary fission. (Dissertation Abstr.)

30514 SPURIOUS STATES IN THE NUCLEAR SHELL MODEL [Thesis]. Seaborn, James Byrd. Charlottesville, Va., Univ. of Virginia, 1965. 111p.

Numerical procedures are established for constructing and eliminating spurious shell model state (in j-j coupling) for double closed shell nuclei. The program is applied to states in ^{16}O with parity, spin and isospin $J^\pi(T) = 0^+(0,1)$, $1^-(0,1)$, $1^+(0)$, $2^+(0)$, $4^+(0,1)$. Energy eigenvalues and eigenvectors and photo- and electro-excitation transition matrix elements are calculated using a zero-range residual interaction. Spin-dependent and spin-independent forces are considered. For the even parity states two particle-two hole, as well as one particle-one hole, excitations are included. The results are compared with the experimental

data available below 20 Mev. The spectrum of $0^+(0)$ and $2^+(0)$ states agrees reasonably well with the observed 0^+ and 2^+ levels. On the other hand, the energies of the $4^+(0)$ levels are much too low. Form factors for inelastic electron scattering are, for the most part, much smaller than the measured values. This is also the case for the lifetime for pair emission from the lowest 0^+ level. The shapes of the form factors appear to be in agreement with experiment. Form factors for the 1^- levels demonstrate the operation of the E1 isospin selection rule for inelastic electron scattering in the T = 0 levels at low momentum transfer. Isospin impurities are introduced phenomenologically and the breakdown of the selection rule is particularly appreciable for the T = 0 level calculated at 23.0 Mev. (Dissertation Abstr.)

30515 NUCLEAR STRUCTURE EFFECTS IN INTERNAL CONVERSION [Thesis]. Seltzer, Edwin Charles. Pasadena, Calif., California Inst. of Tech., 1966. 82p.

Experimental studies of nuclear effects in internal conversion in ^{181}Ta and ^{175}Lu were performed. Nuclear structure effects (penetration effects) in internal conversion are described in general. Calculations of theoretical conversion coefficients are outlined. Comparisons with the theoretical conversion coefficient tables of Rose and Sliv and Band are made. Discrepancies between our results and those of Rose and Sliv are noted. The theoretical conversion coefficients of Sliv and Band are in substantially better agreement with our results than are those of Rose. The ratio of the M1 penetration matrix element to the M1 gamma-ray matrix element, called λ, is equal to $+175 \pm 25$ for the 482-kev transition in ^{181}Ta. The results for the 343-kev transition in ^{175}Lu indicate that λ may be as large as -8 ± 5. These transitions are discussed in terms of the unified collective model. Precision L subshell measurements in ^{169}Tm (130 kev), ^{182}W (100 kev), and ^{181}Ta (133 kev) show definite systematic deviations from the theoretical conversion coefficients. The possibility of explaining these deviations by penetration effects is investigated and is shown to be excluded. Other explanations of these anomalies are discussed. (Dissertation Abstr.)

30516 NUCLEAR CONTRIBUTION TO RADIATIVE PROCESSES [Thesis]. Hubbard, Darryl Franklin. Charlottesville, Va., Univ. of Virginia, 1965. 133p.

The cross section for bremsstrahlung is calculated in the Born approximation, taking into account the emission by the nucleus of the bremsstrahlung photon, as well as the emission of the brensstrahlung photon by the electron. The formal results, which are expressed in terms of various form factors, are applicable to an arbitrary nucleus. Nuclear matrix elements for the specific case of ^{16}O are evaluated in the long wavelength limit, using the j-j coupling particle-hole model. Excited states included in evaluating the summations over intermediate nuclear states are limited to 1-particle, 1-hole configurations coupled by electric dipole transitions to the ground state. Effects in the bremsstrahlung spectrum due to the intrinsic structure of the ^{16}O nucleus are found to be clearly visible in the form of peaks superimposed on the background from electron emission. The relative magnitude of the nuclear effects depends strongly on photon energy, essentially a resonance effect, and varies over a wide range from one nuclear level to another. (Dissertation Abstr.)

30517 NUCLEAR STRUCTURE OF ^{143}Nd, ^{149}Nd, AND ^{151}Nd [Thesis]. Nealy, Carson Louis. Tallahassee, Florida State Univ., 1965. 120p.

Studies of the nuclear structure of ^{143}Nd, ^{149}Nd, and ^{151}Nd were made utilizing the reactions ^{142}Nd(d,p)^{143}Nd, ^{148}Nd (d,p)^{149}Nd, ^{150}Nd(d,t)^{149}Nd, and ^{150}Nd(d,p)^{151}Nd. Protons and tritons resulting from the bombardment of 10- to 12-Mev deuterons incident on separated Nd isotopes were analyzed in a broad-range magnetic spectrograph. The Q values for the (d,p) reactions on ^{142}Nd, ^{148}Nd, and ^{150}Nd are 3902 ± 15, 2702 ± 15, and 3084 ± 15 kev respectively. The Q value for the (d,t) reaction on ^{150}Nd is −1276 ± 20 kev. Angular distributions were determined of the proton groups resulting from the (d,p) reactions on ^{142}Nd and ^{150}Nd. These angular distributions were interpreted in terms of DWBA theory and l values were assigned. In the case of ^{143}Nd some 37 levels up to an excitation energy of 3576 kev were observed and the angular distributions allowed the determination of the l values of 14 of these levels. The interpretation in terms of nuclear models is done using the shell model. Levels were assigned as belonging to the f $7/2$, p $3/2$, h $9/2$, p $1/2$, i $13/2$, and f $5/2$ shell model states. In ^{149}Nd some 15 levels up to an excitation energy of approximately 880 kev were observed in both the (d,p) and (d,t) reactions. It was not possible to make spectroscopic assignments of these levels. Some 49 states in ^{151}Nd were observed up to an excitation energy of 2208 kev and angular distributions allowed the determination of l values of eight of these states. The interpretation is done in terms of the unified model utilizing the theoretical (d,p) stripping cross sections of Satchler. Levels are assigned as belonging to the $5/2$-[523], $3/2$-[521], $1/2$-[530], $5/2$-[512], and $1/2$-[521] rotational bands. (Dissertation Abstr.)

30518 CROSS SECTION FLUCTUATIONS IN THE REACTION ^{32}S(d,p)^{33}S AT BOMBARDING ENERGIES BELOW 3.0 Mev [Thesis]. Wilson, Fred Lee. Lawrence, Kan., Univ. of Kansas, 1965. 118p.

Excitation functions in the differential cross section at 30, 90, and 135° and in the energy range from 1.7 to 3.0 Mev were obtained for the reaction ^{32}S(d,p)^{33}S leading to the ground state, and first, second, third, fifth, and seventh excited states of ^{33}S. The differential cross sections exhibit marked fluctuations and there is little, if any, correlation between the differential cross sections for the final states. Eighteen angular distributions were taken in this energy range and in each case showed noticeable asymmetry about 90° and rapid changes with energy. When the angular distributions were averaged over the energy range of the data, the familiar stripping patterns were obtained in qualitative agreement with the l_n assignments made to the low-lying ^{33}S states. The mean level width Γ determined from correlation functions was in the order of 75 kev. Estimates of the amount of direct reaction present and of the fluctuation damping coefficient N were made from autocorrelation studies and from the probability distributions of the differential cross sections. The values obtained indicated the major portion of the reaction was due to a direct mechanism. (Dissertation Abstr.)

30519 ANGULAR DISTRIBUTIONS AND TOTAL CROSS SECTIONS OF REACTIONS INDUCED BY ^{6}Li,^{7}Li ON ^{10}B,^{11}B AT 3 Mev CENTER OF MASS ENERGY [Thesis]. McGrath, Robert Leslie. Iowa City, Iowa, Univ. of Iowa, 1965. 186p.

Charged particles from four sets of reactions induced by ^{6}Li, ^{7}Li on ^{10}B, ^{11}B targets were observed. The incident beam energy in each case corresponds to 3.05 Mev in the center-of-mass system. A dE/dx, E proportional counter, silicon lithium-drifted detector system coupled to an on-line computer is used to obtain angular distributions and absolute cross sections of p, d, t, ^{3}He, and ^{4}He particles. Evidence for the following unreported energy levels is found: 7.17 ± .07, 7.37, 8.14, 8.54, 8.93, 9.26, and 9.74 Mev in ^{17}N; 8.10, 8.36, 8.83 Mev in ^{16}N; 11.35, 11.60 Mev in ^{14}C; 10.79 ± .03 Mev in ^{14}N (previously reported as 10.71 ± .09 Mev). ^{14}N, ^{15}N, ^{16}N, and ^{13}C are formed in several different reactions. The observed relative cross sections are essentially independent of mode of formation. Cross sections from low-lying states of these nuclei, and ^{12}C, ^{14}C are closely proportional to $(2J_F + 1)$ where J_F is the spin of the residual state. At higher level excitations the yields typically deviate upward from $(2J_F + 1)$ dependence. On this evidence and the lack of qualitative agreement of angular distributions with the shapes expected on the basis of the direct reaction model, it is suggested that the statistical compound nucleus mechanism dominates the cross sections to low lying states. At higher excitations direct reactions evidently supplement the statistical yields. (Dissertation Abstr.)

30520 TOTAL CROSS SECTIONS AND ANGULAR DISTRIBUTIONS OF REACTION PRODUCTS FROM THE

^{6}Li + ^{12}C REACTION. Heikkinen, Dale William. Iowa City, Iowa, Univ. of Iowa, 1965. 183p.

The ^{6}Li + ^{12}C reaction was investigated for bombarding energies in the range 4.5 to 5.5 Mev. Angular distributions and total cross sections were obtained at 100-kev intervals using a dE/dx-E system coupled to a computer. The reaction products studied are proton groups from the ground and first four excited states of ^{17}O, deuterons from the ground and first four excited states of ^{16}O, and alpha particles from the ground and second excited state of ^{14}N. The total cross sections vary with energy in a smooth fashion with no apparent resonances of fluctuations suggestive of compound nucleus formation. However, the angular distributions of certain particle groups do show fluctuations from energy to energy. This is interpreted as due to a non-negligible compound nucleus contribution. This contribution is not observed in the total cross section for reasons discussed. It is also observed that the angular distributions of the excited state deuteron and alpha-particle groups are generally smoothly varying with energy. This can be interpreted in terms of a dominant direct reaction mechanism, which is favored for these states. The relative total cross sections for each particle group can be explained qualitatively in terms of a direct reaction. There is no strong (2J + 1) dependency that would imply a statistical compound nucleus decay. In particular the relative total cross sections of the alpha-particle groups can only be explained by invoking a direct reaction mechanism taking into account the internal structure of ^{6}Li. It is concluded that the transitions to the excited states of ^{16}O and ^{14}N are primarily by a direct reaction. The ground state transitions and the proton groups contain significant compound nucleus contributions. (Dissertation Abstr.)

30521 SHELL MODEL STUDY OF THE TIN ISOTOPES [Thesis]. Kuo, Thomas Tzu Szu. Pittsburgh, Univ. of Pittsburgh, 1964. 194p.

The tin isotopes were studied under the framework of the extended nuclear shell model, in which the nucleus is considered as a collection of interacting quasiparticles defined by the Bogoliubov-Valatin transformation. Instead of the conventional pairing plus quadrupole effective two-nucleon interaction, the Gaussian interaction with standard exchange terms is used. The even isotopes were studied using a modified random phase approximation (RPA), in which the single quasiparticle energies and the occupation numbers were taken directly from experiments rather than calculated from the BCS theory. Results yield a better fit to experiments than the usual BCS-RPA results, particularly for the shapes for the lowest 2^{+} states. This indicates the possibility that the usual BCS-RPA may be improved by including certain self-energy effects. The odd isotopes were studied using the Tamm-Dancoff approximation (TDA) in a subspace of one and three quasiparticles. A more general formulation is also derived; it includes certain backward-going Feynman diagrams that TDA has left out. The effect of these diagrams was found to be small. In both formulations, there exist spurious states that must be projected out. Higher states can be described qualitatively, but not quantitatively by the phonon plus quasiparticle approximation. The agreement between the calculated and experimental energies of the low-lying states is satisfactory. Better wave functions for the odd isotopes are revealed by the calculation of their 1-forbidden M1 transition rates and magnetic dipole moments are obtained. A preliminary calculation using a more realistic effective interaction was performed. This interaction is a non-local interaction given by Tabakin. It fits the two-nucleon scattering data and the saturation properties of nuclear matter and is smooth enough for shell-model calculations. Preliminary results indicated that this interaction is promising for the shell-model description of the tin isotopes. The inclusion of levels outside the conventional filling shell for the tin isotopes was found to be necessary. (Dissertation Abstr.)

30522 DETERMINATION OF FIRST-FORBIDDEN BETA-DECAY MATRIX ELEMENTS WITH THE INCLUSION OF NUCLEAR FINITE SIZE EFFECTS [Thesis]. Manthuruthil, Jose Chacko. Bloomington, Ind., Indiana Univ., 1965. 120p.

Matrix elements were obtained for ^{124}Sb, ^{152}Eu, ^{154}Eu, ^{72}Ga, ^{140}La, ^{186}Re, ^{84}Rb, ^{86}Rb, and ^{170}Tm by analyzing experimental data on beta decay taking into account finite nuclear size effects and finite de Broglie wavelength effects. A predominance of the tensor matrix element over the scalar and vector matrix elements was observed for all the transitions considered. Qualitative explanations of all the decays are given using nuclear models. It is demonstrated that measurements on beta decay can be used to test the predictions of nuclear models. It is also shown that the inclusion of nuclear finite size effects and finite de Broglie wavelength effects can cause a significant deviation of the final results from results obtained using the Konopinski-Uhlenbeck approximation. (TCO)

30523 APPLICATIONS OF THE BRUECKNER MANY-BODY THEORY: THE BOUNDARY CONDITION MODEL IN NUCLEAR MATTER; THE NEUTRON GAS [Thesis]. Hoenig, Milton Maurice. Ithaca, N. Y., Cornell Univ., 1964. 219p.

Brueckner reaction matrix methods are applied to two problems: the calculation of the ground-state properties of nuclear matter using the boundary condition model (BCM) of Feshbach and Lomon for the two-nucleon interaction, and the determination of the ground state energy of the neutron gas. For the first problem it is shown that, upon imposing the BCM condition that the Schroedinger wave function for two nucleons at a relative separation r_0 be described by a set of strictly energy-independent logarithmic derivative parameters, this wave function vanishes in $r < r_0$, and the Bethe-Goldstone wave function for two nucleons in nuclear matter is, likewise, described by the same set of logarithmic derivative parameters. Both wave functions are discontinuous at $r = r_0$, and since the Bethe-Goldstone wave function does not vanish in $r < r_0$, it possesses a complementary set of energy-independent logarithmic derivatives at $r_0 - \epsilon$ ($\epsilon \to 0$), bearing no relation to two-body scattering. For the purpose of solving the Bethe-Goldstone equation and obtaining the Brueckner reaction matrix, the two sets of parameters are replaced by an effective potential acting at r_0. This is combined with the one- and two-meson exchange potential, in $r > r_0$, used in fitting the BCM to the two-body data. The neutron gas is investigated in the region $0.4\ f^{-1} \leq k_F \leq 1.0\ f^{-1}$, using the nucleon-nucleon interaction of Moszkowski and Scott and treating the attractive tail as a Serber force. The difference from a nuclear matter calculation is solely statistical, but this is seen to be sufficient to prevent binding. The separation method of Moszkowski and Scott is used to obtain the reaction matrix. It turns out that the particle spectrum and the average energy per neutron are determined almost entirely by the diagonal matrix elements of the long-range part of the potential in S states. Including a D-state correction, E/A ranges from +1.23 Mev at $k_F = 0.4\ f^{-1}$ to +5.20 Mev at $k_F = 1.0\ f^{-1}$. (TCO)

30524 POLARIZATION OF PROTONS FROM THE D(d,p)T REACTION [Thesis]. Porter, Leonard Edgar. Madison, Wis., Univ. of Wisconsin, 1965. 147p.

The angular dependence of the polarization of D(d,p)T protons was determined at eight laboratory deuteron energies from 2.1 through 14.1 Mev. Symmetry considerations in the reaction of identical particles demand that the polarization be antisymmetric about 90° in the center-of-mass system. Measurements were therefore made only over the first center-of-mass quadrant, at laboratory angles from 10° through 70°. The experiment made use of the double-scattering technique, utilizing gas targets and the deuteron beam from a tandem electrostatic accelerator. The polarization analyzer was scattering from helium at 45°. Protons were detected with a pair of coincident counters in each of two telescopes. The polarization is negative over the first quadrant at 2.1 Mev, but becomes positive in the first half of the quadrant at 3.1 Mev. At 6.1 Mev and higher energies, the polarization is positive over the entire angular range. Extrema occurred near the center of the quadrant. The highest polarization, +0.57 ± 0.05, was observed at 12.1 Mev. The lowest −0.11 ± 0.05, was found at 2.1 Mev. The angular dependence of the product of polarization and differential cross section was fitted for each deuteron energy with the trigonometric series, $\Sigma_k a_k \sin \theta_r \cos^{(2k-1)}\theta_r$.

Satisfactory fits were obtained with the first two terms of the series for deuteron energies below 6.3 Mev. Above this energy the third term was also needed. The results of this experiment were compared with the polarization of $D(d,n)^3He$ neutrons. The proton polarization was observed to be slightly higher, in general. The largest difference was found to occur near a center-of-mass angle of 45° and to increase with deuteron energy. (Dissertation Abstr.)

30525 SHAPE OF NEUTRON YIELD FROM $^7Li(p,n)^7Be$ REACTION NEAR THRESHOLD AND NEUTRON ENERGY DISTRIBUTION NEAR THRESHOLD [Thesis]. Palmer, David Wayne. Madison, Wis., Univ. of Wisconsin, 1965. 98p.

Three aspects of the $^7Li(p,n)^7Be$ reaction were studied: the shape of the neutron yield curve near threshold, the neutron energy distribution near threshold, and the energy of the reaction threshold relative to the energy of the 992-kev $^{27}Al(p,\gamma)^{28}Si$ resonance. Experimental thick-target yield curves were obtained from the reaction for proton energy resolution near 6100. The experimental data are compared to yield curves computed by Monte Carlo techniques using a discrete energy-loss spectrum for the protons supplied by E. Merzbacher. A good fit is obtained, which indicates that the yield rises faster above threshold than is expected when discrete energy losses are ignored. Only the additional assumptions of a reasonable energy resolution and no target contamination were used for the fits. A table of the calculated yield as a function of beam energy and beam resolution is included for use in locating the reaction threshold on experimental data. Neutron energy distributions were calculated for Li targets up to 1900 Å thick at 0, 45, 90, 135, and 180°. The distributions are affected in several ways when account is taken of the discrete nature of energy losses experienced by protons in the target: peaks and long tails appear on the distributions, and the neutron intensity in any direction in the laboratory is seldom equal to the intensity predicted when continuous energy losses are assumed for the protons. The ratio of the $^7Li(p,n)^7Be$ threshold energy and the energy of the 992-kev $^{27}Al(p,\gamma)^{28}Si$ resonance, E_T/E_R, was determined from many experimental yield curves taken in rapid succession from both reactions. The positions of E_T and E_R were determined from fits to the data which accounted for discrete energy losses. The result is $E_T/E_R = 1.89545$ with an average deviation of 0.00006. Errors due to self-heating of resistors in the power supply for the electrostatic analyzer are probably so large that this result will not contribute to an improved experimental value of E_T/E_R. (Dissertation Abstr.)

30526 ANGULAR DISTRIBUTIONS AND CORRELATIONS IN THE $^{12}C(^3He,p)^{14}N$ REACTION [Thesis]. Ludemann, Carl Arnold. College Park, Md., Univ. of Maryland, 1965. 128p.

In an attempt to obtain information concerning the mechanism involved in the $^{12}C(He\text{-}3,p_2)^{14*}N$ reaction, thirteen angular distributions were measured in the energy interval from 2.25 to 3.60 Mev. Excitation curves were also obtained for protons observed at laboratory angles of 5°, 70°, and 150°. Angular correlations between the second-excited state proton group and the subsequent 1.63-Mev γ rays leading to the 2.31-Mev level of ^{14}N were studied as a function of the angle of γ-ray emission for protons emitted at seven angles at the 2.4-Mev resonance. Similar measurements were made "off resonance" at 2.25 Mev at five proton angles. The angular distributions show strong forward and moderate backward peaking with minima at approximately 75°. These features are observed over the entire energy interval. Total cross sections exhibit and confirm the resonance structure observed in the excitation functions at 2.4 and 3.0 Mev. Each distribution was least-squares fitted to an expansion in terms of Legendre polynomials up to P_5. The angular distributions in the region of 2- to 3-Mev incident energy of the second-excited state proton group as well as of the n_0-, p_0-, and p_1-exit channels are compared with predictions based upon a compound nucleus formation calculation. While some interference from higher energy resonances was needed in the interpretation of the p_0- and p_2-group data, the behavior of all groups was achieved primarily by considering three levels in ^{15}O corresponding to resonances in the laboratory system at 2.40 Mev (Γ = 245 kev), 2.69 Mev (Γ = 325 kev), and 2.97 Mev (Γ = 120 kev). The spin and parity assignments are $\frac{3}{2}^-$, $\frac{1}{2}^+$, and $\frac{5}{2}^+$ respectively. The angular correlation functions were least-squares fitted to essentially the expression $W(\theta_p,\theta_\gamma) = A_1(\theta_p) + A_2(\theta_p)\cos 2[\theta_\gamma - \theta_0(\theta_p)]$. The change in position of the symmetry axis of the angular correlations as a function of θ_p cannot be explained in terms of plane wave Born approximation stripping theory. The mean value of the correlations as a function of proton angle was explained in the framework of compound nucleus formation using the parameters found in fitting the p_2-angular distributions. $A_2(\theta_p)$ and $\theta_0(\theta_p)$ are discussed in terms of this model. (Dissertation Abstr.)

30527 THE L-AUGER SPECTRUM OF ^{113}In AS DERIVED FROM THE ELECTRON CAPTURE DECAY OF ^{113}Sn [Thesis]. Krisciokaitis, Raymond John. East Lansing, Mich., Michigan State Univ., 1965. 76p.

The low energy range of the $\pi\sqrt{2}$ iron-free beta spectrometer was extended down to 1 kev by means of electrostatic post-focusing acceleration of the electron beam. It was shown that accurate relative intensity measurements of electron spectra are possible at least down to these energies. The spectrometer data-acquisition system was automated to facilitate more reliable and efficient data taking particularly as this applies to weak low-energy Auger spectra. The L-Auger spectrum of ^{113}In as derived from the electron capture decay of ^{113}Sn (~2 to 4 kev) was measured and the major Auger lines and groups were identified. Order of magnitude of the relative intensities of these lines was also determined. The effective incremental charge ΔZ was determined for the most prominent and important transitions. ΔZ is 0.55 and 0.67 for transitions of the type $L_{1,2,3}\text{-}M_{1,2,3}$, $M_{1,2,3}$, and $L_{1,2,3}\text{-}M_{4,5}M_{4,5}$, respectively. It was shown that the spectrum exhibited intermediate coupling features and that shifts of Auger lines due to double vacancy effects probably exist. (Dissertation Abst.)

30528 ANGULAR CORRELATIONS OF GAMMA RAYS IN THE $^{25}Mg(p,\gamma)^{26}Al$ REACTION [Thesis]. Graber, Harlan Duane. Lawrence, Kan., Univ. of Kansas, 1964. 68p.

Results of an experimental investigation of spin and parity characteristics of excited states in the odd-odd nucleus ^{26}Al as determined by angular correlation measurements of various gamma rays are presented. Angular distribution measurements of significant gamma rays were performed at six prominent resonances in the $^{25}Mg(p,\gamma)^{26}Al$ reaction. These resonances corresponded to proton bombarding energies of 956, 1045, 1242, 1652, 1701, and 1716 kev. Five triple correlation measurements were taken. Targets were prepared by the evaporation of MgO on tantalum discs. A Van de Graaff accelerator provided the source of energetic protons, and the resulting gamma rays were detected with 5-in. scintillation crystal. Pulse sorting was handled with a 256-channel analyzer in the early work and a 400-channel analyzer in more recent work. An IBM 1620 computer was used extensively in analyzing and fitting the data. A program was written that permitted the computer to fit selected portions of the pulse-height spectrum with gamma shapes by the least-squares method to yield gamma intensities. Fitting the data to a series of Legendre polynomials was accomplished by the computer as well as the calculation of theoretical curves as functions of the associated mixing parameters. The results of analysis are $J^\pi = 3^+$ for the 2.07-Mev (T = 0) level and $J^\pi = 3^+$ for the 2.36-Mev level. Resonance levels at 956, 1652, and 1716 kev were found to be 3^-, 4^+ or 4^-, and 4^+ or 4^-, respectively. The computer analysis of the spectra suggests that for several of the resonances studied the decay scheme is more complex than previous hand analysis has revealed. Included in the thesis as appendices are descriptions and actual Fortran listings of programs used in the spectrum fitting and a program for finite solid-angle corrections. Theoretical angular distributions appropriate to channel spins 2 and 3 are included in an appendix. (Dissertation Abstr.)

30529 GAMMA RADIATION FROM THE ALPHA PARTICLE BOMBARDMENT OF ^{12}C. Larson, James Daniel. Pasadena, Calif., California Inst. of Tech., 1965. 124p.

The excitation function of the reaction $^{12}C(\alpha,\gamma)^{16}O$ was studied over the region E_α = 2.8 to 8.3 Mev using a NaI(Tl) detector and enriched ^{12}C targets. Resonances were observed at E_α = 3.24, 3.58, 4.26, 5.81, 7.05, 7.88, and 8.13 Mev, corresponding to ^{16}O states at E_x = 9.59, 9.85, 10.36, 11.52, 12.45, 13.07, and 13.26 Mev. Radiative widths Γ_γ for ground state radiation from the states at 9.59, 9.85, 11.52, and 12.45 Mev were measured to be 0.022 ± 0.005, 0.0059 ± 0.0006, 0.66 ± 0.09, and 7 ± 1 ev, respectively. Radiative widths for cascade radiation from the 9.85- and 10.36-Mev states through intermediate states of ^{16}O were measured to be 0.0012 ± 0.0004 and 0.046 ± 0.006 ev, respectively. Interference effects in ground state radiation from the 13.07-Mev (1^-) state support evidence for an underlying 2^+ state at nearly the same energy. Other information on excited states of ^{16}O is presented. (Dissertation Abstr.)

30530 FOUR-PARAMETER COINCIDENCE STUDIES OF THE REACTION $^6Li(^6Li,\alpha)2\alpha$ [Thesis]. Berkowitz, Edward Howard. Iowa City, Iowa, Univ. of Iowa, 1965. 114p.

The $^6Li(^6Li,\alpha)2\alpha$ reaction was studied at E_{Li} 6 = 2.75 Mev. A four-parameter data acquisition system employing two position-sensitive surface barrier detectors, four pulse height analyzers, and a general purpose computer provided simultaneous measurement of coincident energy spectra for any pair of angles within the 40° angular intervals subtended by each detector. No statistically correlated component appears in the energy or angle correlations. Regions of the coincidence spectra that correspond to the intense continuum observed in singles spectra were found to exhibit pronounced structure, which varied rapidly with angle. Contributions to these spectra from the decay of high-lying excited states of ^8Be provide limited explanations for the observed structure. Angles and energies that satisfy the kinematic conditions for the zero momentum transfer of a deuteron from the incident ^6Li to the target tend to coincide with the highest coincidence rates in the angular range covered, in accord with a simple direct reaction model. These high coincidence rates, localized in energy and angle, are a feature of all of the data and not restricted to any sharp range of momentum transfer. No single hypothesis based upon decay of states of ^8Be or a special reaction mechanism accounts for this structure. (Dissertation Abstr.)

30531 CROSS SECTION RATIOS OF ISOBARS FROM SPALLATION REACTIONS UNDER VARYING CONDITIONS [Thesis]. Forster, William Hull. Davis, Calif., Univ. of California, 1965. 118p.

Natural copper was irradiated with high-energy protons and alpha particles, and the cross section ratios were determined for the following isobaric pairs: $^{45}Ti/^{45}Ca$, $^{48}Cr/^{48}V$, $^{52}Fe/^{52}Mn$, $^{55}Co/^{55}Fe$, and $^{56}Ni/^{56}Co$. Yttrium was irradiated with 300-Mev protons, and the cross section ratios of $^{52}Fe/^{52}Mn$ and $^{55}Co/^{55}Fe$ were determined. Incident protons were varied from 230 to 760 Mev, and incident alpha particle energies were varied from 310 to 880 Mev. Excitation functions were determined for each member of the isobaric pairs for proton and alpha-particle irradiations of copper. Within experimental error, the yield ratios of all the isobaric pairs were found to be independent of the type of incident particle and the incident-particle energy. One member of each pair was formed in much greater yield than the other member. These preferences could be explained on the basis of relative binding energies in the precursor nuclei and on the bases of level densities and shell characteristics of the product nuclei. All of these results are in agreement with an evaporation phase to the mechanism of high-energy nuclear reactions. The yield ratios of the two pairs of isobars determined from yttrium irradiations were about 30% less than the ratios of these isobars determined from copper irradiations, indicating that the isobar with the higher neutron-to-proton ratio is preferentially formed in targets with a higher neutron-to-proton ratio. This result is in agreement with predictions based on the cascade-evaporation model. The absolute excitation functions of the alpha-particle reactions paralleled the excitation functions of proton reactions, but were 1.5 to 2 times as large. The similarity of yield ratios of isobaric pairs in both proton- and alpha-particle-induced reactions is an indication that the evaporation process is very nearly the same for each type of reaction, and the larger cross sections of alpha-particle reactions may be a consequence of a different type of initial interaction. (Dissertation Abstr.)

30532 MOESSBAUER EFFECT IN ^{159}Tb [Thesis]. Woolum, John Carl. Ithaca, N. Y., Cornell Univ., 1965. 80p.

A report of the previously unreported Mössbauer resonance in ^{159}Tb, a measurement of the lifetime of the 58-kev isomeric state displaying the resonance—9.2×10^{-11} sec (compared to 1.3×10^{-10} sec as measured by fast coincidence techniques) corresponding to a linewidth of 0.055°K, and a discussion of the limits provided on the magnitude of hyperfine interactions in Tb metal and oxide are presented. The use of ^{159}Tb in an attempt to observe a 3.4°K optical mode in terbium ethyl sulfate is described. No evidence could be established for this mode by these Mössbauer measurements, and current interpretations of the original thermal resistance and recently measured specific heat data do not require such a mode. (Dissertation Abstr.)

30533 INDEPENDENT FISSION YIELDS OF SOME XENON ISOTOPES. Storms, H. A.; Coryell, C. D. 18p. (CONF-650902–22). ORAU. Gmelin, AED-CONF-65-235-16.

From American Chemical Society, 150th National Meeting, Atlantic City.

Quantitative measurements were made on the fractional independent yields of 5.27-day ^{133}Xe and 9.20-hr ^{135}Xe in fission of ^{235}U and ^{233}U with thermal neutrons and fission of ^{232}Th, ^{235}U, and ^{238}U with 14-Mev deuterons and with 25-Mev helium ions. The independent yields were only slightly dependent on the charge dispersion assumed for the xenon precursors. A Gaussian charge dispersion, $f_i = (\pi C)^{-\frac{1}{2}} \exp[-(Z - Z_P)^2/C]$, with C = 0.94 was assumed for thermal neutron fission and 1.20 for charged-particle fission with energy deposit of 20 Mev. Attempts to correlate Z_P values for charged-particle fission with Z_P for thermal neutron fission using several existing methods were unsuccessful. It was concluded that the charge distribution in charged-particle fission in this mass region is different from the distribution in thermal-neutron fission. The difference may be described as a shortening of fission-product chains in the mass region where they are unusually long in thermal-neutron fission. This is correlated with a general decrease in fine structure in fission with increasing energy deposit rather than with specific effects of the projectile, such as energy deposit and angular momentum. (auth)

30534 KOLLOQUIUM UEBER β-ZERFALL UND SCHWACHE WECHSELWIRKUNGEN, HEIDELBERG, 10. BIS 13. MAERZ 1965. (Conference on Beta Decay and Weak Interactions, Heidelberg, March 10–13, 1965). 330p. 10 DM. (CONF-650329). ORAU.

The 35 papers presented at the Conference on β Decay and Weak Interactions are compiled together with the discussions following each paper. Individual abstracts were prepared for 26 of the papers. Eight papers were previously abstracted for NSA; see: 19: 1391, 23474, 34508, 35114, 35389, 39824, 43012, and 20: 4919. The remaining paper is a general summary on the theory of weak interactions. (L.B.S.)

For abstracts of individual papers see: 3000–3003, 30114, and 30535–30555.

30535 INTERACTIONS IN β DECAY (S = 0) Daniel, H. (Max-Planck-Institut fuer Kernphysik, Heidelberg). pp 44-71 of Kolloquium Ueber β-Zerfall und Schwache

Wechselwirkungen. Heidelberg, Max-Planck-Instituts fuer Kernphysik, 1965. (In German).

Nuclear β decay and the β decay of muons are discussed. V-A interactions, parity violations, time reversal invariance, universal Fermi interactions, and CVC theory are discussed. The question of a partially conserved axial vector current was investigated and double β decay was considered. The nuclear force and intensity of the interactions of neutrons and protons are studied. (J.S.R.)

30536 BETA DECAY AND NUCLEAR STRUCTURE. Deutsch, J. P. (Univ., Louvain, Belg.). pp 72-81 of Kolloquium Ueber β-Zerfall und Schwache Wechselwirkungen. Heidelberg, Max-Planck-Instituts fuer Kernphysik, 1965.

The principal studies undertaken in the last few years in the field of nuclear decay are discussed from the viewpoint of the experimental physicist. The significance of these studies and the areas needed for more intensive study are indicated. (J.S.R.)

30537 TIME-REVERSAL INVARIANCE IN β DECAY OF RaE. Dierker, J.; Wengener, H. (Univ., Erlangen-Nuerberg, Ger.). pp 124-6 of Kolloquium Ueber β-Zerfall und Schwache Wechselwirkungen. Heidelberg, Max-Planck-Instituts fuer Kernphysik, 1965. (In German).

In the study of the time-reversal invariance in the β decay of RaE the θ phase between the eventual complex coupling constants C_A and C_V was calculated. A value of $\theta = 3 \pm 5°$ was obtained. (J.S.R.)

30538 RE-EVALUATION OF THE COUPLING CONSTANT IN BETA DECAY. Buehring, H. (Physikalisches Institut, Heidelberg); Schopper, H. pp 134-41 of Kolloquium Ueber β-Zerfall und Schwache Wechselwirkungen. Heidelberg, Max-Planck-Instituts fuer Kernphysik, 1965.

The f function was calculated for the neutron and ^{14}O on the basis of an exact solution of the Dirac equation. The results obtained are tabulated and compared with those obtained by other methods using various approximations. (J.S.R.)

30539 HOW ARE THE MEASURABLE QUANTITIES IN NUCLEAR BETA DECAY MODIFIED BY THE INDUCED INTERACTIONS? Buehring, W.; Schuelke, L. (Univ., Heidelberg). pp 142-6 of Kolloquium Ueber β-Zerfall und Schwache Wechselwirkungen. Heidelberg, Max-Planck-Instituts fuer Kernphysik, 1965.

The rather generally valid answer to this question is explained in the case of the $0^- \rightarrow 0^+$ transition by consideration of the induced pseudoscalar interaction. (auth)

30540 SHAPES OF THE β SPECTRA FROM ^{143}Pr AND ^{32}P. Persson, B.; Reynolds, J. (Univ. of Lund, Sweden). pp 164-77 of Kolloquium Ueber β-Zerfall und Schwache Wechselwirkungen. Heidelberg, Max-Planck-Instituts fuer Kernphysik, 1965.

The beta spectra of ^{143}Pr and ^{32}P were measured using solid state detectors in approximately 4π-geometry. Deviations from the statistical shape consistent with the experimental results are small, if any. (auth)

30541 NUMERICAL ANALYSIS OF BETA SPECTRA. Loehken, R.; Rebel, H.; Schatz, G. (Univ., Heidelberg). pp 193-7 of Kolloquium Ueber β-Zerfall und Schwache Wechselwirkungen. Heidelberg, Max-Planck-Instituts fuer Kernphysik, 1965. (In German).

A numerical method is proposed to determine nuclear matrix elements from spectrum shape measurements. The procedure is based on the least squares principle and is applied to some first forbidden beta decays. The main result is that only one second order function of the matrix elements is precisely determined whereas each matrix element can vary within wide limits. (auth)

30542 MEASUREMENT OF THE ASYMMETRY COEFFICIENTS OF THE β-γ CIRCULAR POLARIZATION CORRELATION IN PERMITTED β TRANSITIONS. Behrens, H.; Schopper, H. (Technische Hochschule, Karlsruhe, Ger. Kernforschungszentrums, Karlsruhe, Ger.). pp 198-202 of Kolloquium Ueber β-Zerfall und Schwache Wechselwirkungen. Heidelberg, Max-Planck-Instituts fuer Kernphysik, 1965. (In German).

In a device that made it possible to deduce both the statistical and also the systematic errors, the asymmetry coefficients of ^{24}Na, ^{41}Ar, and ^{47}Ca were determined. The results obtained are tabulated. (J.S.R.)

30543 MEASUREMENT OF β-γ CIRCULAR POLARIZATION CORRELATIONS IN THE β TRANSITIONS OF ^{58}Co, ^{95}Zr, ^{95}Nb, AND ^{141}Ce. Collin, W.; Daniel, H.; Mehling, O.; Schmitt, H. (Max-Planck-Institut fuer Kernphysik, Heidelberg). pp 203-12 of Kolloquium Ueber β-Zerfall und Schwache Wechselwirkungen. Heidelberg, Max-Planck-Instituts fuer Kernphysik, 1965. (In German).

The β-γ circular polarization correlations of ^{58}Co, ^{95}Zr, ^{95}Nb, and ^{141}Ce were measured with Compton forward scattering. In ^{58}Co the effect of annihilation radiation was considered. Both β-γ cascade of ^{95}Zr could be separated by suitable discrimination in the β branch. The asymmetry parameter A was obtained as -0.10 ± 0.03 for ^{58}Co, -0.57 ± 0.08 for ^{95}Zr at $\beta 362 - \gamma 760$, -0.41 ± 0.04 for ^{95}Zr at $\beta 396 - \gamma 726$, -0.52 ± 0.10 for ^{95}Nb, and 0.16 ± 0.05 for ^{141}Ce. From the results for ^{58}Co, a ratio X between Fermi and Gamow-Teller contribution was obtained with $X = -0.077 \pm 0.038$. The β transitions for ^{95}Zr and ^{95}Nb are pure Gamow-Teller transitions with $\Delta I = 1$. The mixing ratios $\delta(E2/M1)$ of the γ radiations are 0.08 ± 0.09 or $1.85^{+0.69}_{-0.37}$ for ^{95}Zr at $\gamma 760 - 0.09 \pm 0.04$ or $3.0^{+0.4}_{-0.6}$ for ^{95}Zr at $\gamma 726$ and $0.02^{+0.17}_{-0.23}$ or $-2.1^{+0.8}_{+1.5}$ for ^{95}Nb. In ^{141}Ce the most probable range is $4.5 < X < 6.5$. (tr-auth)

30544 β-γ DIRECTIONAL CORRELATIONS AND β-γ CIRCULAR POLARIZATION CORRELATIONS IN THE SINGLE FORBIDDEN β DECAY OF ^{144}Ce, ^{144}Pr, ^{170}Tm, AND ^{203}Hg. Collin, W.; Daniel, H.; Martin, B.; Schmidlin, P; Schmitt, H. (Max-Planck-Institut fuer Kernphysik, Heidelberg). pp 213-20 of Kolloquium Ueber β-Zerfall und Schwache Wechselwirkungen. Heidelberg, Max-Planck-Instituts fuer Kernphysik, 1965. (In German).

In the single forbidden β transitions of ^{144}Ce, ^{144}Pr, ^{170}Tm, and ^{203}Hg, β-γ directional correlations and β-γ circular polarization correlations were measured. All measured directional correlations have an anisotropy different from 0. In ^{170}Tm the reduced anisotropy coefficient ϵ' is almost energy independent, whereas in ^{203}Hg there is a strong linear dependence. For the asymmetry parameter $\bar{\omega}$ of the polarization correlation in the nonunique transition, the following values were obtained: 0.64 ± 0.25 for ^{144}Ce, -0.18 ± 0.20 for ^{170}Tm and -0.19 ± 0.04 for ^{203}Hg. (tr-auth)

30545 SPECTRAL FORM OF THE 961-kev β TRANSITION AND THE K CONVERSION COEFFICIENT OF THE 412-kev γ RADIATION OF ^{198}Au. Paul, Helmut (Reaktorzentrum, Seibersdorf, Austria. Osterreichische Studiengesellschaft fuer Atomenergie, Seibersdorf, Austria). pp 221-4 of Kolloquium Ueber β-Zerfall und Schwache Wechselwirkungen. Heidelberg, Max-Planck-Instituts fuer Kernphysik, 1965. (In German).

The form factor $1-(0.031 \pm 0.006)w$ was measured using a carefully tested intermediate image spectrometer. The Fermi function of Dzhelepov and Zyrianova was applied to the measurements. The end point energy was 961.0 ± 1.2 kev. By comparison with the surface under the K conversion line, the conversion coefficient was determined as $299 \pm 2 \times 10^{-4}$ in very good agreement with the theoretical value for an E2 conversion coefficient. (tr-auth)

30546 SPECTRAL FORMS OF THE β SPECTRA OF ^{42}K, ^{86}Rb, AND ^{170}Tm. Daniel, H.; Schmitt, H.; Springer, K. (Max-Planck-Institut fuer Kernphysik, Heidelberg). pp 225-9 of Kolloquium Ueber β-Zerfall und Schwache Wechselwirkungen. Heidelberg, Max-Planck-Instituts fuer Kernphysik, 1965. (In German).

The β spectra of ^{42}K, ^{86}Rb, and ^{170}Tm were measured with Heidelberg double lens spectrometer. In the transition $2^- \rightarrow 2^+$ of 2.00 Mev of ^{42}K, a strong deviation of the permitted form was found. The form of the $2^- \rightarrow 2^+$ transition in ^{86}Rb probably also deviates from the permitted form. The unresolved spectrum of ^{170}Tm indicates a low excess of electrons in the medium energy range. (tr-auth)

30547 NONLINEAR DEVIATION FROM THE STATISTICAL β SPECTRUM SHAPE OF THE ^{32}P ALLOWED β DECAY. Coussement, R. (Univ., Louvain, Belg.).

pp 230-6 of Kolloquium Ueber β-Zerfall und Schwache Wechselwirkungen. Heidelberg, Max-Planck-Instituts fuer Kernphysik, 1965.

The spectrum shape of the ^{32}P allowed β-decay was analyzed on the basis of the possibility of large configuration mixing and new experimental results. It was shown that when allowance is made for large configuration mixings, the high ft value and the non-linear spectrum shape of the allowed ^{32}P β decay can easily be explained. (J.S.R.)

30548 PRELIMINARY RESULTS OF RELATIVE MEASUREMENTS OF ELECTRON POLARIZATION OF ^{199}Au AND ^{32}P. Loehken, Rudolf; Rebel, Heinigerd; Schartz, Gerd (Univ., Heidelberg). pp 237-41 of Kolloquium Ueber β-Zerfall und Schwache Wechselwirkungen. Heidelberg, Max-Planck-Instituts fuer Kernphysik, 1965. (In German).

The ratio of longitudinal polarization values of ^{199}Au and ^{32}p β-particles was measured by the double scattering method. The preliminary result is $P(^{199}Au)/P(^{32}P) = 0.86 \pm 0.07$ for the ground state transition of ^{199}Au at 310 kev. (auth)

30549 BETA DECAY OF ^{199}Au AND STRUCTURE OF THE INVOLVED NUCLEAR STATES. De Raedt, J.; Deutsch, J. P. (Univ., Louvain, Belg.) pp 242-51 of Kolloquium Ueber β-Zerfall und Schwache Wechselwirkungen. Heidelberg, Max-Planck-Instituts fuer Kernphysik, 1965.

The beta-gamma directional correlation of the $(3/2+) - (3/2-) - (1/2-)$ and $(3/2+) - (5/2-) - (1/2-)$ cascades of ^{199}Au was measured for several energies of the beta particles. The results and other characteristics of the beta decay of ^{199}Au are compared to the predictions of the extreme single-particle model and to the weak-coupling hypothesis of the excited ^{199}Hg states. (auth)

30550 NONAXIAL MODEL PREDICTIONS ON THE FIRST-FORBIDDEN BETA TRANSITIONS OF ^{188}Re (1$^-$) TO THE GROUND STATE AND TO THE EXCITED 2^+ STATES OF ^{188}Os. PRELIMINARY RESULTS. Grenacs, L.; Hess, R.; Roehmer, F. C.; Rueegg, W. (Federal Inst. of Tech., Zurich, Switzerland). pp 252-6 of Kolloquium Ueber β-Zerfall und Schwache Wechselwirkungen. Heidelberg, Max-Planck-Instituts fuer Kernphysik, 1965.

Beta-gamma directional correlations and beta-gamma circularly polarized correlations were measured in the decay of $^{188}Re \rightarrow {}^{188}Os$, in order to compare the nuclear matrix elements of beta-transitions with the prediction of the nonaxial model. The agreement between the measurements and the calculations of this model seems to be good. (auth)

30551 NUCLEAR MATRIX ELEMENTS OF THE (1–) – (2+) BETA TRANSITION OF ^{194}Ir. Deutsch, J. P. (Univ., Louvain, Belg.); Grenacs, L.; Lehmann, J. pp 257-9 of Kolloquium Ueber β-Zerfall und Schwache Wechselwirkungen. Heidelberg, Max-Planck-Instituts fuer Kernphysik, 1965.

The spectrum-shape of the ^{194}Ir(1–) beta-decay to the first excited (2+) state of ^{194}Pt and the corresponding beta-gamma directional correlation was measured. Using the Konopinski-Uhlenbeck approximation, the values of the nuclear matrix elements are extracted from the experimental results. (auth)

30552 EVIDENCE FOR THE (1$^-$,K = 0) CHARACTER OF ^{176m}Lu THROUGH BETA-DECAY MEASUREMENTS. Deutsch, J. P. (Univ., Louvain, Belg.); Grenacs, L.; Lehmann, J. pp 260-5 of Kolloquium Ueber β-Zerfall und Schwache Wechselwirkungen. Heidelberg, Max-Planck-Instituts fuer Kernphysik, 1965.

Results of different measurements on the first forbidden beta-decay of ^{176m}Lu to the first excited state of ^{176}Hf are described and the individual nuclear matrix elements are determined. The results are in good agreement with both the Alaga selection rules and the $(4,7/2,25)$, $(5,7/2,41)$, K = 0 Nilsson-orbital assignment to the odd proton and neutron of the mother-state. This confirms the anomalous behavior of the rotational band built on this intrinsic state. If the structure of the initial and final nuclear states is supposed to be exactly known, the result confirms with a good accuracy a provision of the CVC theory of weak interactions. (auth)

30553 MEASUREMENT OF THE β-γ CIRCULAR POLARIZATION CORRELATION ON ^{133}Xe AND THE SPIN-DEPENDENT RAYLEIGH SCATTERING. Daniel, H.; Schmitt, H. (Max-Planck-Institut fuer Kernphysik, Heidelberg). pp 266-72 of Kolloquium Ueber β-Zerfall und Schwache Wechselwirkungen. Heidelberg, Max-Planck-Instituts fuer Kernphysik, 1965. (In German).

In an apparatus for the measurement of β-γ circular polarization correlations by Compton forward scattering, the analysis efficiency ϵ was determined at an energy of 81 kev by a measurement on ^{133}Xe. ϵ was measured at 0.018 ± 0.005. A calculated value for 0.0045 was obtained. The discrepancy was traced back to a previously unobserved effect, the spin-dependent Rayleigh scattering. For Z = 26, $\vartheta = 53°$, and $E_\gamma = 81$ kev the spin-dependent part of the differencial cross section of the Rayleigh scattering was obtained from the present measurements as $9.3 \pm 3.5\%$ of the spin-independent fraction, i.e., a cross section of $1.8 \pm 0.7 \times 10^{-26}$ cm^2/atom. (tr-auth)

30554 RECOIL EFFECT IN THE PERTURBED β-γ DIRECTIONAL CORRELATION IN ^{166}Ho. Grenacs, L.; Hess, R. (Federal Inst. of Tech., Zurich). pp 273-7 of Kolloquium Ueber β-Zerfall und Schwache Wechselwirkungen. Heidelberg, Max-Planck-Instituts fuer Kernphysik, 1965.

Attenuation coefficients G_2 were measured in the perturbed beta-gamma directional correlation in ^{166}Ho, using metallic and various insulator sources. A variation of G_2 with the beta energy was found in the Ho_2O_3 finely powdered source, which is explained by the "emanation effect" due to the recoil following the beta decay. (auth)

30555 MOESSBAUER EFFECT INVESTIGATION OF THE SHELL CONVERSION OF ELECTRON CAPTURE. Steichele, E.; Henning, W.; Huefner, S.; Kienle, P. (Technische Hochschule, Darmstadt, Ger.). pp 291-9 of Kolloquium Ueber β-Zerfall und Schwache Wechselwirkungen. Heidelberg, Max-Planck-Instituts fuer Kernphysik, 1965. (In German).

Investigations on the detection of excited shell states of solids and the investigation of their properties are reported. The recoilless γ emission of the short lived 97-kev level of ^{153}Eu was investigated. The isomerism displacement was investigated and the results obtained are graphed. (J.S.R.)

Plasma Physics and Thermonuclear Processes

See also Fluid Physics and Thermodynamics

Refer also to abstracts 29500, 29959, and 30777.

30556 (AD-631993) RESEARCH ON PLASMA DIAGNOSTIC METHODS FOR HIGH-TEMPERATURE PLASMA RESEARCH. Quarterly Report No. 9, April 1, 1965–June 30, 1965. Dougal, A. A. (Texas Univ., Austin). Dec. 1965. Contract AF 33(615)-3224. 73p. (ARL-65-270). CFSTI $3.00 cy, $0.75 mn.

Further investigations on the previously reported utilization of a He–Ne 3.39 micron infrared maser for experimental time-space resolved diagnostics of highly transient, extreme temperature, deuterium plasmas are reported. The infrared maser coupled resonator technique for measurement of electron density was extended such that useful data were obtained for a theta-pinch plasma source operating at 50 Kg compression with 4 and 6 Kg reverse bias magnetic fields at 0.1 Torr initial pressure. Peak electron densities to 3×10^{16} cm^{-3} were observed near the central axis. Electron density time variations as large as 6×10^{16} cm^{-3} μs^{-1} were observed. Measurement of the magnetoplasma Faraday rotation of the plane of polarization of the He–Ne maser infrared radiation by the use of an infrared polarization analyzer

was extended and uncertainties in the measurements were reduced. The signal to noise ratio was reduced, permitting angles as small as 0.05° to be resolved. The determination of electron density has provided further information for obtaining time-space resolved plasma magnetic fields from the Faraday rotation data. Measurements show that the bias magnetic field is trapped within the plasma column throughout the full half-cycle of the compressing field for compression to 17 Kg with 4 Kg reverse bias and 0.1 Torr initial pressure. There are indications that a high β plasma develops following the disappearance of the reverse bias field for 50 Kg compression and 0.1 Torr initial pressure. (M.O.W.)

30557 (AD–633074) AN ELEMENTARY REVIEW OF THE SCATTERING OF PHOTONS BY HIGHLY IONIZED PLASMAS. Osborn, R. K. (Michigan Univ., Ann Arbor. Dept. of Nuclear Engineering). Feb. 1966. Contract DA-31-124-ARO(D)-403. 33p. (AROD–6092: 4). CFSTI $2.00 cy, $0.50 mn.

A theory is developed for the scattering of photons by equilibrium plasmas sufficiently highly ionized that the presence of neutrals can be neglected. The analysis is systematic and self-contained. (M.O.W.)

30558 (AD–633593) INVESTIGATION OF DENSE PLASMA UNDER A STRONG ELECTRIC FIELD. Mendel, Clifford W. Jr. (Illinois Univ., Urbana. Coordinated Science Lab.). May 1966. Contract DA-28-043-AMC-00073(E). 77p. (R–289). CFSTI $3.00 cy, $0.75 mn.

A hydrogen plasma of density $\sim 10^{16}$ cm^{-3} and electron temperature ~200 ev was investigated under electric fields of 100 to 500 v/cm. A pinch of pinch ratio ~3 was found to be hydrodynamically stable for ~2 μs during which the experiment was performed. A sharp burst of runaway electrons of total current of the order of amperes occurred and disappeared shortly after conduction began. Large low-frequency oscillations believed to be ion-acoustic oscillations appear and give rise to very high resistivities in qualitative agreement with recent theories on plasma conductivity. (auth)

30559 (FTI–114/P-044) O KOLEBANIYAKH I NAGREVE MALYKH PLAZMENNYKH SGUSTKOV, NALETAYUSHCHIKH NA AKSIAL'NO-SIMMETRICHNOE MAGNITNOE POLE. (Oscillations and Heating of Small Plasmoids Incident in Axisymmetric Magnetic Fields). Khizhnyak, N. A.; Vodyanitskii, A. A. (Akademiya Nauk Ukrainskoi SSR, Kharkov. Fiziko-Tekhnicheskii Institut). 1965. 10p. Dep. mn.

Azimuthal induction currents are excited in a plasma when plasma bundles strike an axially symmetrical magnetic field. The interaction of these currents with the external magnetic field determines the plasma behavior and the extent of heating in the magnetic field. The system of the equations of motion of an ellipsoidal bundle in a hydrodynamic approximation is represented by the total current in the bundle and its self-induction. In determining the relation between the effective dimensions of the bundle and the thermodynamic quantities such as the temperature and pressure of the plasma, it is assumed that the bundle has a sharp dividing boundary with a zero internal pressure gradient, and that the ideal gas laws are valid. It is assumed that the energy of the coulombic interaction is less than 1% of the average thermal energy ($\Delta E_{coul.}/T < 0.01$). Equations are derived for the radial oscillations of the bundle. It is found that the frequency of the radial oscillations does not depend on the amplitude, that is, the oscillations of the square of the radius are harmonic. Expressions are given for the maximum and minimum temperatures. The equations indicate that the plasma bundle can expand or contract so as to equalize the gas pressure with the magnetic pressure. (TTT)

30560 (LA-DC–7282) REDUCTION OF THE FOKKER-PLANCK EQUATION FOR APPLICATIONS TO PRACTICAL PLASMA DYNAMICS PROBLEMS INVOLVING DEVIATIONS FROM THERMAL EQUILIBRIUM. Oliphant, Thomas A. Jr. (Los Alamos Scientific Lab., Univ. of California, N. Mex.). [1965]. Contract W-7405-eng-36. 42p. Dep. mn. CFSTI $2.00 cy, $0.50 mn.

The Fokker-Planck equation is reduced to a form which is useful from the point of view of doing practical calculations of problems involving configuration space as well as velocity space. The basic technique is a spherical harmonic decomposition in velocity space which reduces the number of independent variables by two. As an example, the method is applied to a problem with θ-pinch geometry. (auth)

30561 (MATT–415) EFFECT OF PRESSURE ON NEGATIVE V'' STELLARATORS. Johnson, John L. (Princeton Univ., N. J. Plasma Physics Lab.). May 1966. Contract AT(30-1)-1238. 11p. Dep. mn. CFSTI $1.00 cy, $0.50 mn.

Stability with respect to hydromagnetic interchanges can be achieved in closed configurations if $V''(\psi) < 0$ with $V''(\psi)$ the volume inside a magnetic surface of flux ψ. A low-pressure expansion is used to examine the effects of plasma currents in a negative V'' configuration which utilizes an $\ell = 2$ shaping field and an $\ell = 1$, $\ell = 3$ corrugating field and in which toroidal curvature is neglected. Numerical calculations indicate that the effect on stability of these currents is small. Since the basic features of all the proposed negative V'' configurations are similar, this strengthens the belief that vacuum field considerations provide an adequate approximation. (auth)

30562 (MPI-PAE–P1/25/66) INHOMOGENEOUS DEVELOPMENT OF A PLASMA THROUGH QUASI-LINEAR THEORY. Bloomberg, H. (Max-Planck-Institut fuer Physik und Astrophysik, Munich (West Germany)). Apr, 1966. 39p. Dep. mn.

A quasi linear perturbation expansion is used to study the evolution of a localized disturbance introduced in a homogeneous plasma characterized by a distribution function having a small "bump" on its tail. For this problem first order theory of the Vlasov equation predicts the development of growing waves. The curtailment of this instability through a plateau development in v space is given through the second order corrections. During the curtailment process the distribution function develops weak time and space dependence. There is shown an energy transfer balance between the growing waves and the particles with bump velocity which are part of the "background" distribution function and those which are second order in the "disturbance" distribution. The plasma is affected by the localized disturbance throughout a much wider region. Comparison with earlier quasi-linear theory is made. (auth)

30563 (NP–16096) TEMPERATURE DISTRIBUTION IN A POISEUILLE PLASMA ARC. Technical Report No. 8. Chuang, Hsing (Harvard Univ., Cambridge, Mass. Div. of Engineering and Applied Physics). July 1964. 44p.

Temperature distribution in an argon and a helium plasma generated in a wall-stabilized arc was studied. Good agreement between temperatures obtained by different methods of measurement was shown. (auth)

30564 (NYO–1480-26) LONGITUDINAL PLASMA OSCILLATIONS. Weitzner, Harold (Courant Inst. of Mathematical Sciences, New York Univ., N. Y.). June 1, 1965. Contract AT(30-1)-1480. 46p. (MF–46). Dep. mn. CFSTI $2.00 cy, $0.50 mn.

The problem of the plane wave oscillation of a one-dimensional plasma is considered. Various asymptotic expansions of the solution for a stable plasma are presented. First, an expansion is given for short time valid for arbitrary wavelengths. Second, expansions are given for long wavelengths valid over a long time interval. The time interval is sufficiently long to observe exponential damping of the plasma oscillations. The mixed initial value-boundary value problem is solved for the case of harmonic time-dependent data given on a wall. It is shown that for stable plasmas the electric field approaches a limiting form in time. The specular reflection boundary condition is solved as a special case. The limiting electric field is characterized by an analyticity condition analogous to those obtained from causality conditions in scattering theory.

Finally, asymptotic expansions are given with results analogous to those described above where the small parameter analogous to wave number is the deviation of the frequency of oscillation from the plasma frequency. (auth)

30565 (STI-PUB-111(Vol.1)) PLASMA PHYSICS AND CONTROLLED NUCLEAR FUSION RESEARCH. VOL. I. Proceedings Series. Proceedings of a Conference Held by the International Atomic Energy Agency, Culham, 6-10 September 1965. (International Atomic Energy Agency, Vienna (Austria)). Apr. 1966. 790p. (CONF-650935(Vol.1)). IAEA: $15.00, S315,-; £4.10.0; F Fr 60,-; DM 52,50.

Separate abstracts were prepared for 27 of the 45 included papers. For abstracts of the remaining 18 papers see the papers under CONF 650935 in the report number index. (M.O.W.)

For abstracts of individual papers see: 30605–30631.

30566 (STI-PUB-111(Vol. 2)) PLASMA PHYSICS AND CONTROLLED NUCLEAR FUSION RESEARCH. VOL. II. Proceedings Series. Proceedings of a Conference Held by the International Atomic Energy Agency, Culham, 6–10 September 1965. (International Atomic Energy Agency, Vienna (Austria)). Apr. 1966. 1014 p. (CONF-650935 (Vol. 2)). IAEA: $21.00; S441,-; £ 6.6.0; F Fr 84,-; DM 73,50.

Separate abstracts were prepared for 34 of the 59 included papers. For abstracts of the remaining 25 papers see CONF-650935(Vol.2) in the report number index. (M.O.W.)

For abstracts of individual papers see: 30632–30665.

30567 (UCRL–14246) THE RANDOM PHASE APPROXIMATION. Bodner, Stephen E. (Lawrence Radiation Lab., Univ. of California, Livermore). June 11, 1965. Contract W-7405-eng-48. 10p. Dep. mn. CFSTI $1.00 cy, $0.50 mn.

Generalized harmonic analysis is used to prove that there is a rapid phase variation in the Fourier transform of functions for which the correlation distance is small compared to the box size. In the limit of infinite box size, the Fourier transform has infinite derivative and zero correlation length in k-space. However, it is shown that one cannot neglect terms in an equation by an appeal to this rapid phase variation. (auth)

30568 NOTE ON GRAVITATIONAL INSTABILITY. Gandhi, J. M. (Univ. of Rajasthan, Jaipur, India); Gupta, G. P. Acta Phys. Austr., 21: 245-7(1966).

It is shown that Jean's Criterion for gravitational instability remains unmodified in the presence of a magnetic field having components $(0,H_y,H_z)$ along the three cartesian coordinates (x,y,z) and H_z is assumed to be stratified along the vertical z direction. (auth)

30569 THEORY OF TRANSVERSE WAVES IN PLASMA. Varma, N. L. (Univ. of Rajasthan, Jaipur, India). Acta Phys. Austr., 21: 262-72(1966).

The Berz's theory of longitudinal plasma waves is extended to the case of transverse waves in classical, hot plasma and it is also applied to the case when a constant external magnetic field B_0 permeates it. It is based on the arbitrary stationary electron velocity distribution and collisions are neglected altogether. Damping and amplification of transverse waves are considered and finally the dispersion relation is discussed. (auth)

30570 ONE-DIMENSIONAL UNSTEADY POTENTIAL MHD FLOW. Cap, F.; Herrnegger, F. (Univ., Innsbruck). Acta Phys. Austr., 21: 298-304(1966).

Plasma one-dimensional MHD flow is considered. Negligible heat conductivity, negligible friction and infinite electric conductivity in the continuous medium are assumed. (J.F.P.)

30571 ELECTROMAGNETIC WAVES IN PLASMA. Varma, N. L. (Univ. of Rajasthan, Jaipur, India). Acta Phys. Austr., 21: 383-8(1966).

The problem of propagation of electromagnetic waves in plasma free from any external electric or magnetic field was studied classically through the use of Boltzmann equation and Maxwell's field equations, following Van Kampen's method of stationary solutions. The dispersion formula for transverse waves is discussed, and the expressions for Landau damping and dielectric constant are obtained. (auth)

30572 OBSERVATIONS ON COLLISIONAL STARK BROADENING IN RADIO-FREQUENCY DISCHARGES. Schlueter, H.; Avila, C. (Univ. of Texas, Austin). Astrophys. J., 144: 785-97(May 1966).

The profiles of low Balmer lines emitted from a r-f discharge ($N_e \approx 10^{13}$ cm^{-3}) are expected to be in the domain of collisional electron Stark broadening, except for the far parts of the line wings. In order to accomplish a more accurate comparison with the modified generalized impact theory and with the quasi-static theory (including shielding and correlation effects) for the ions only, or the ions and electrons, the contributions other than Stark contributions of the observed Hδ-profile are quantitatively evaluated. Thus for the main body of the profile, the electron broadening contribution is found small compared to that of the ions; the half-width is almost accounted for by the ion broadening contribution. However, toward the far parts of the line wing, where a transition to quasi-static electron broadening can be expected, a slow buildup of a considerable electron broadening contribution is observed, finally equaling the ion contribution. (auth)

30573 SEMI-AUTOMATIC DATA SYSTEM FOR PLASMA STUDY. Sinclair, Rolf M.; Grove, Donald J.; Weissenburger, A. W.; Goldberg, Ernest (Princeton Univ., N. J.). ISA (Instrum. Soc. Amer.) Trans., 5: 139-45(Apr. 1966). (MATT–323).

General features of the data system for the Model C stellarator, a facility for studying hot, fully ionized plasmas, are described. The data signals are exhibited on oscilloscopes and photographed. By suitable modification all the oscilloscope settings can be recorded on the photograph, together with a serial number. The control settings of the stellarator are recorded on punched cards. This record forms a complete history of stellarator operations and is used to prepare a final format which combines control-setting information with the data. (auth)

30574 EXPERIMENTS ON SURFACE WAVE PROPAGATION ALONG ANNULAR PLASMA COLUMNS. Paik, S. F. (Northwestern Univ., Evanston, Ill.); Briggs, R. J.; Osepchuk, J. M. Contract DA 36-039-AMC-02362(E). J. Appl. Phys., 37: 247-83(May 1966).

The propagation of surface waves along a plasma column of annular cross section was investigated experimentally. The laboratory plasma used for the experiment was a mercury-vapor d-c discharge. The properties of the experimental discharge tube were examined to show some basic differences between the laboratory plasma and the idealized model of the plasma used for the analysis. In particular, a radially non-uniform density distribution and the variation of the distribution with the applied magnetic field was noted. In spite of the radial-density inhomogeneity, the experimentally determined phase constants of the backward-surface wave are in good agreement with values predicted from the uniform density theory. The attenuation in the absence of the magnetic field is consistent with collisional losses, predominantly with the walls of the container. The effect of an axial magnetic field on the surface-wave characteristics is examined. Experimental results show that in the presence of a magnetic field the attenuation of the backward wave is markedly increased; this enhancement of the damping is not consistent with simple collision theory within the framework of the uniform-density model. (auth)

30575 PRODUCTION OF A THERMALLY IONIZED PLASMA WITH NEGATIVE IONS. von Goeler, S.; Ohe, T.; D'Angelo, N. (Princeton Univ., N. J.). J. Appl. Phys., 37: 2519-20(May 1966). (MATT–357).

Preliminary results of an investigation of producing by surface ionization a plasma which contains a sizable fraction of negative ions are described. The plasma densities and the percentages of negative ions that can be expected from the theory of the thermodynamic equilibrium are dis-

cussed, and experiments are described in which a plasma containing Cs^+ and Cl^- ions is formed. (J.F.P.)

30576 FIELD BOUNDARY OF TWO LINE CURRENTS IN A PLASMA AT UNIFORM PRESSURE. Sozou, C. (Northampton Coll. of Advanced Tech., London). J. Fluid Mech., 24: 689-96(Apr. 1966).

A solution is obtained for the boundary of the magnetic field of two arbitrary line currents immersed in a plasma at uniform pressure. The linear dimensions of the boundary, which are determined for several sets of data, are proportional to the intensity of the line currents (assuming that their ratio is constant) and inversely proportional to the square root of the plasma pressure. The cusps over the boundary, which when the two line currents are equal and opposite are symmetrical with respect to the line currents, move towards the weaker current until they eventually disappear on the line joining the two currents. When the distance between the currents is such that when the cusps disappear the two line currents lie in the same cavity, some plasma gets trapped inside the cavity. When the cavities of two line currents of the same sign touch an abrupt instability is achieved; the plasma is suddenly pushed out by the surface currents and this results in the formation of a larger field cavity. (auth)

30577 "NON-RESONANT" COUPLING OF R.F. POWER TO A PLASMA. Rothman, M. A.; Sinclair, R. M.; Yoshikawa, S. (Princeton Univ., N. J.). J. Nucl. Energy: Pt. C, 8: 241-5(May-June 1966). (MATT-392).

Application of ion cyclotron resonance heating to the Model C stellarator was at first complicated by coupling of power to the plasma through the electric fields associated with the induction coil. This "non-resonant" coupling produced a large influx of impurities that prevented efficient heating of the plasma. Installation of a Faraday shield between the induction coil and the plasma eliminated most of the undesired coupling. (auth)

30578 ENERGY SPECTRUM OF NEUTRAL HYDROGEN ATOMS FROM A COAXIAL PLASMA GUN. Voorhies, H. G.; Ohkawa, T. (General Atomic Div., General Dynamics Corp., San Diego, Calif.). J. Nucl. Energy: Pt. C, 8: 247-53(May-June 1966). (GA-6582).

To measure the energy spectrum of ions in a plasma, one must extract the ions without altering the spectrum. A measure of the ion energy spectrum is given by the energy spectrum of neutral atoms produced by charge-exchange reactions. The neutral atom energy spectrum and the flux of neutral atoms were measured for the hydrogen plasma from a coaxial gun. The measurements are made on the gun axis at 300 cm from the gun using as atom–ion converters both a gas cell and a metal surface. The two methods give for the converted ions spectra of the same shape with energy in the range 60–3000 ev. The maximum hydrogen atom flux is 1.4×10^{15} atoms cm^{-2} sec^{-1} ev^{-1} at 300 ev for the low-energy mode of gun operation and is 3.2×10^{14} atoms cm^{-2} sec^{-1} ev^{-1} at 800 ev for the high-energy mode. (auth)

30579 PLASMA GUIDING BY MEANS OF MULTIPOLE FIELDS. Tuckfield, R. Jr.; Scott, F. R. (General Atomic Div., General Dynamics Corp., San Diego, Calif.). J. Nucl. Energy: Pt. C, 8: 271-81(May-June 1966). (GA-6374).

A hexapole magnetic field was employed for guiding the accelerated plasma from an inductive gun. The properties of the plasma for both a linear and a curved guide field are determined. Results show that the plasma loss as a function of distance from the gun is greatly reduced, and that the purity of the plasma is enhanced after passing through the guide field. There is indication that further purification of the plasma is accomplished by curving the guide field thus reducing the neutral component emanating from the gun along its injection axis. (auth)

30580 UTILIZING RF ELECTRIC FIELD FOR INJECTION-TRAPPING HIGH-ENERGY MOLECULAR IONS IN MIRROR FIELDS. I. Akimune, Hideo; Fujita, Yoshihiro; Suita, Tokuo (Osaka Univ.). J. Nucl. Sci. Technol. (Tokyo), 3: 171-9(May 1966).

A method of using r-f electric field in a device for high-energy injection is described, and the behavior of the molecular ions injected into a system combining r-f and d-c magnetic fields is investigated by calculation and observation. In this method, some of the injected molecular ions are decelerated by the r-f field, and trapped in a small region between the mirror fields, where they are dissociated by collision with the background gas or with the plasma particles, and are thus trapped in the form of atomic ion. The relation between the r-f frequency ω and the Larmor frequencies $\Omega_{H_2^+}$, $\Omega_{H_1^+}$ is given by $\omega = N/2 \cdot \Omega_{H_2^+} = N/4 \cdot \Omega_{H_1^+}$, where N is the number of r-f electrodes. The number N is chosen so that N/2 is an integer and N/4 a non-integer. Calculation shows that the ions injected in a certain favorable phase are stably decelerated despite their initially possessing a precessional motion. This is proven by observation of actual electron behavior. (auth)

30581 INSTABILITY OF VELOCITY DISTRIBUTIONS OF SLIGHTLY IONIZED GASES IN ELECTRIC FIELDS. Stenflo, Lennart (Univ. of Uppsala). J. Nucl. Sci. Technol. (Tokyo), 3: 189-93(May 1966).

If a slightly ionized gas is subject to a constant electric field the (time- and space independent) distribution function for the electrons may be double-humped if the cross section for electron-molecule interactions is changing sufficiently rapidly with velocity. Accordingly "inverse Landau damping" can make the distribution function unstable with respect to longitudinal waves if the collisional damping is not too large. The results of calculations indicate that the plasma can be unstable and parameters involved are estimated in order to get the conditions for instability. (auth)

30582 FORMATION OF ROTATING PLASMA IN CROSSED FIELD. Wasa, Kiyotaka; Hayakawa, Shigeru (Matsushita Electric Industrial Co., Ltd., Osaka). J. Phys. Soc. Jap., 21: 738-43(Apr. 1966).

The formation process of a rotating plasma in a homopolar-like short coaxial-electrode system carried out in a H_2, N_2, or Ar discharge is described. A Kerr cell shutter with a 50 ns exposure time was used for optical records. It is found that the process is divided into two stages; first a negative streamer appears and developes to a spoke, and later the spoke spreads to a disk. The streamer process is hardly affected by the magnetic field. A plausible mechanism by which the spoke spreads to the disk is ionization of neutrals by $E \times B$ drift motion of ions. There is a critical gas pressure above which the spoke never spreads to the disk. The reason is considered to be that ions cannot drift in $E \times B$ direction above the critical pressure due to a large frictional force between ions and neutrals. (auth)

30583 PLASMA-ION OSCILLATION IN A DRIFTED PLASMA. Yoseli, Morihiro; Kato, Kiyoe (Electrotechnical Lab., Tokyo). J. Phys. Soc. Jap., 21: 743-8(Apr. 1966).

The plasma-ion oscillations were observed in a diode-type discharge tube varying the longitudinal magnetic field or the cathode temperature. When the magnetic field strength was increased, the oscillation frequency increased up to a critical value at constant discharge current and the oscillation disappeared at higher magnetic fields. A similar variation in the oscillation was observed when the cathode temperature was decreased. These frequency shifts are qualitatively explained. Considering the electron drift velocity, the excitation mechanism of the plasma-ion oscillation is also discussed using the theory by Fried and Gould. (auth)

30584 CHARGE EXCHANGE LOSS OF HIGH-TEMPERATURE PLASMA CONFINED BY MIRROR MAGNETIC FIELD. Mori, Ichiro; Suita, Tokuo (Osaka Univ.). J. Phys. Soc. Jap., 21: 749-56(Apr. 1966).

Relaxation of the distribution function of ions confined in a mirror field is investigated theoretically taking both the charge exchange and scattering effects into account. The result is compared with experiment. If the particles are not thermalized sufficiently, the ion density decays exponentially due to the charge exchange, but only linearly due to the mirror loss. The lifetime τ_{ex}, is proportional to the ion velocity while that of the mirror loss, τ_m, is propor-

tional to it to the power three. The experiment is performed on the HX-0 device, a mirror machine for high temperature experiments. A decay time of 26 μsec is obtained for high energy protons which are trapped in the mirror magnetic field at the background pressure of 10^{-5} mm Hg. (auth)

30585 NONLINEAR MOTION OF ION STREAMS IN A BACKGROUND OF HIGH-TEMPERATURE ELECTRONS. Yajima, Nobuo; Taniuti, Tosiya; Outi, Akizi (Univ. of Nagoya, Japan). J. Phys. Soc. Jap., 21: 757-64(Apr. 1966).

Nonlinear ion acoustic waves propagating in a plasma of warm electrons and one or more streams of cold ions are investigated. A hydrodynamical model which employs ion fluid streams interacting among themselves through the electron pressure gradient is used, isothermal electrons being assumed. Though the present model assumes charge neutrality, it enables us to show how large amplitude disturbances become steeper, tending to form shocks or inversely how discontinuous initial disturbances are smoothed out. For a single fluid, the behavior is the same as those of isentropic gas with γ equal to unity. However for multicomponent cases there exist conspicuous properties such as multistream instabilities. All these effects for the case of two streams are discussed. Simple waves are obtained by means of the method of characteristics; for the wave propagating faster than all the ions the compression leads to shock formation while the expansion to the instability, for the waves lower than all the ions the expansion leads to the shock formation and at the same time to instability and for the wave propagating with intermediate speed the situation is more complicated. (auth)

30586 PROPAGATION OF HYDROMAGNETIC WAVES IN COLLISIONLESS PLASMA. I. Kato, Yusuke (Kobe Univ., Japan); Tajiri, Masayoshi; Taniuti, Tosiya. J. Phys. Soc. Jap., 21: 765-77(Apr. 1966).

The propagation of hydromagnetic waves in collisionless plasma is investigated on the basis of the Chew-Goldberger-Low approximation. The dispersion relation for weak, plane disturbances in a uniform plasma is derived. It is found that there exist the fast and slow modes of magneto-acoustic waves as well as the Alfvén wave. However, under certain conditions the phase velocities of the slow and the Alfvén waves become imaginary; namely the system is not necessarily totally hyperbolic but can be partially elliptic. The conditions on the elliptic cases are investigated in detail, especially for the slow wave. Then the propagation of a wave diverging from a point source is investigated graphically as well as analytically. The general theory of steady flow is also given, and some discussions are done for the two dimensional aligned field-flow in which the directions of magnetic field and flow are aligned everywhere. (auth)

30587 ANALYSIS OF THE NEGATIVE ABSORPTION OF PLASMA-CAVITY SYSTEM. Idehara, Toshitaka; Terumichi, Yasushi; Takahashi, Isao; Mitani, Kenji (Kyoto Univ.). J. Phys. Soc. Jap., 21: 778-86(Apr. 1966).

A possibility of amplification by a cylindrical cavity of reflection type coaxial with a plasma column along the static magnetic field is discussed. The Q value contributed from the plasma (Q_p) is calculated under the following conditions: the plasma is so tenuous that the perturbation theory may be used, the velocity distribution function for plasma electrons is $f_0 \propto v^q \exp(-bv^3)$, the effective collision frequency for momentum transfer is dominantly due to the collisions of an electron with neutral particles and varies with the speed v as $\nu_c(v) \propto v^h$, and the radius of the plasma is sufficiently smaller than the radius of the cavity. When $Q_p < 0$, the plasma-cavity system has a possibility of amplification or oscillation. This characteristic depends sensibly on the velocity distribution function for plasma electrons. (auth)

30588 TRANSMISSION AND ABSORPTION OF ELECTROMAGNETIC WAVES IN A COLLISIONLESS PLASMA SLAB. Sugihara, Ryo (Univ. of Nagoya, Japan). J. Phys. Soc. Jap., 21: 786-94(Apr. 1966).

An investigation is made of the propagation of electromagnetic waves normal to a plasma slab having a density gradient. The plane of polarization of waves is perpendicular to an external magnetic field. At resonances, a WKB-type approximation does not represent waves and an appreciable absorption appears due to infinitesimal collisions (the so-called resonance absorption). The transmission and absorption coefficients are obtained in the limit of no collisions when in the slab the cutoff is adjacent to the resonance. (auth)

30589 TWO OPERATING MODES OF A PLASMA SOURCE. Popov, S. N. (Lebedev Inst. of Physics, Moscow). JETP Lett. (USSR) (Engl. Transl.), 3: 177-9(Apr. 1, 1966).

Translated from Zh. Eksp. Teor. Fiz., Pis'ma Redaktsiya, 3: 275-9(Apr. 1, 1966).

An investigation is presented on two modes of operation of a titanium plasma source. In one mode (slow), the average ion energy is 150 to 200 ev, and the number of particles with energy 1 kev is smaller by one order of magnitude than the number with the average energy. The second mode (fast) sets in when the main capacitance of the discharge circuit is reduced. In this case the energy spectrum of the ions in the plasma changes, the relative weight of the tails increases, and the average ion energy increases by one order of magnitude. (B.G.D.)

30590 USE OF A LASER OPERATING IN THE SPIKE MODE TO OBTAIN A HIGH-TEMPERATURE PLASMA. Vanyukov, M. P.; Isaenko, V. I.; Lyubimov, V. V.; Serebryakov, V. A.; Shorokhov, O. A. JETP Lett. (USSR) (Engl. Transl.), 3: 205(Apr. 15, 1966).

Translated from Zh. Eksp. Teor. Fiz., Pis'ma Redaktsiya, 3: 316-18(Apr. 15, 1966).

To obtain longer action of the electromagnetic field of light waves on a plasma, an experiment was performed on ionization of air with the aid of radiation from a laser operating in the spike mode with total generation duration of about one millisecond. (B.G.D.)

30591 SUPPRESSION OF LOW-FREQUFNCY OSCILLATIONS IN TWO-STREAM INSTABILITY BY PRIOR MODULATION OF THE ELECTRON BEAM. Kornilov, E. A.; Fainberg, Ya. B, Bolotin, L. I.; Kovpik, O. F. (Inst. of Physics and Tech., Academy of Sciences, Ukrainian SSR). JETP Lett. (USSR)(Engl. Transl.), 3: 229 31(May 1, 1966).

Translated from Zh. Eksp. Teor. Fiz., Pis'ma Redaktsiyu, 3: 354-7(May 1, 1966).

The results of experimental investigations on the development of two-stream instability accompanied by both low- and high-frequency oscillations and by intense ion currents, comparable in magnitude with the electron current of primary beams are presented. The results indicate that the l-f oscillations can be stopped by modulating the beam at a high frequency. The connection between the low and high frequency spectra indicate that the l-f oscillations are brought about by h-f ones. (B.G.D.)

30592 STEADY PLASMA ELECTRIC FIELD AS A FUNCTION OF IONIZATION DEGREE. Okuda, Takayoshi (Nagoya Univ., Japan). Kakuyugo-Kenkyu, 15: 166-78 (Sept. 1965).

The attainment of the fully ionized plasma is restricted by various collision processes resulting in the energy loss, which are dependent on the velocity and density of the particles associated with the process. To establish the self-sustained plasma, the energy loss must be compensated by an externally applied energy, usually given by an electric field. The solution to the present problem may be provided by finding the necessary electric field as a function of the average velocity and density of the particles, i.e., the temperature and ionization degree. The temperature of the constituent, on the other hand, may be a function of the ionization degree. Consequently, the necessary electric field will be described in terms of the ionization degree only. Starting with the transport equation for the three-component system, the numerical value of E as a function of the ionization degree x can be calculated. A typical plot of E as a function of x shows that E is zero at x = 0 and x = 1, and between these two values of x a maximum

E_m appears. It is concluded that the applied electric field must be greater than the maximum electric field E_m to realize the fully ionized plasma. The magnitude of E_m varies from 10^{-1} v/cm to 10^3 v/cm, depending on the dominant processes. (auth)

30593 INSTABILITY OF TWO COLLIDING PLASMA STREAMS. Ohnuma, Toshiro; Hatta, Yoshisuke (Tohoku Univ., Sendai). Kakuyugo-Kenkyu, 16: 95-105(Feb. 1966). (In Japanese).

The instability of two colliding plasma streams with no magnetic field was investigated by means of the graphical solution of the dispersion equation. Unstable regions of electron beam-electron coupling, electron beam-ion coupling, or electron-ion beam coupling, and ion-ion beam coupling were determined as a function of wave number, beam velocity, and phase velocity. The dependence of those regions on beam temperature and beam density was also found. (auth)

30594 SOME EXPERIMENTS FOR SOLIDIFICATION OF CO_2 AND THE DROPPING IN VACUUM. Nakagawa, Hiroshi (Nippon Sanso, Japan); Inoue, Nobuyuki. Kakuyugo-Kenkyu, 16: 106-18(Feb. 1966). (In Japanese).

Some experimental results on the solidification of CO_2 and the dropping in vacuum are presented. It is a preliminary experiment for solid D_2 dropping in vacuum, in order to produce high density and high temperature plasma with a giant pulse laser. (auth)

30595 AN ANALYSIS OF THE TOROIDALLY SHAPED HELIOTRON FIELD. Oshiyama, Hiroshi; Mohri, Akihiro (Kyoto Univ.). Kakuyugo-Kenkyu, 16: 119-32(Feb. 1966). (In Japanese).

An analysis was made of the magnetic field produced by a current following in the toroidally wound Heliotron coils. Under the assumption that a radius of coils is much less than that of a torus, the analysis can resort to the perturbation method in which all quantitites are expanded in K_a, where K is curvature of torus and a is radius of coil. The Heliotron magnetic field is obtained analytically as a function of coil radius, the ratio of adjacent coils, the distance of adjacent coils, and curvature of torus. This field agrees with the experiment results. (auth)

30596 PLASMA DIFFUSION IN MAGNETIC FIELD. Okuda, Takayoshi; Yamamoto, Kenzo. Mem. Fac. Eng. Nagoya Univ., 17: 49-55(May 1965).

The diffusion of plasma across a longitudinal magnetic field was investigated by measuring the diffusion length for a plasma that was formed in a cylindrical glass tube behind the anode of a discharge tube. Measurements were carried out in Ar, He, and Ne. The results show that the classical ambipolar diffusion model is adequate if the magnetic field is not strong. (D.C.W.)

30597 ONE-DIMENSIONAL STEADY FLOW OF A PLASMA. Miyajima, Shigeki. Mem. Fac. Eng. Nagoya Univ., 17: 74-8(May 1965).

The flow of plasma across a confining magnetic field was investigated. (D.C.W.)

30598 MEASUREMENTS OF ELECTRON DRIFT VELOCITY AND COLLISION FREQUENCY IN AN ARGON DISCHARGE. Zelby, L. W.; Mehuron, W. O.; Kalagher, R. J. (Univ. of Pennsylvania, Philadelphia). Phys. Lett., 21: 522-4(June 15, 1966).

The interaction between waves on a helix and a plasma column was used to measure the electron drift velocity in the column. From these measurements, and also from insertion loss measurements, collision frequency was determined. The results are in agreement with each other and with data published elsewhere. (auth)

30599 POTENTIAL OF AVERAGE FORCE IN A PLASMA. Theimer, O. (Institut fuer Plasmaphysik, Munich); Kepple, P. Phys. Rev., 147: 101-8(July 8, 1966).

The potential of average force $W_{1,2}^{qq'}$ experienced by a charge q' at a distance $|r_1 - r_2|$ from a charge q is calculated from the Bogoliubov-Born-Green-Kirkwood-Yvon equations of classical statistical mechanics without linearization or equivalent approximations. Diverging integrals are eliminated by the condition that bound-particle states with negative internal energy, e.g., atoms, excluded from the partition function. The 3-particle distribution functions required for calculating $W_{1,2}^{qq'}$ are obtained as solutions of a nonlinearized Poisson-Boltzmann equation for the average potential in the neighborhood of two charges fixed at r_1 and r_2. For this latter calculation the difference between average potential and potential of average force is neglected. With the help of $W_{1,2}^{qq'}$ the average thermal energy of the plasma is computed and compared with the result of the linearized Debye-Hückel theory. Numerical corrections to the latter theory are presented and it is shown that linearization is a far more significant source of errors than identification of average potential with potential of average force. (auth)

30600 MEASUREMENT OF RECOMBINATION-RATE COEFFICIENT OF He^{++}. Hinnov, Einar (Princeton Univ., N. J.). Phys. Rev., 147: 197-200(July 8, 1966). (MATT-420).

The rate of recombination of doubly ionized helium in the afterglow of a C stellarator discharge is deduced from measured light intensities of He II and He I, emitted by recombining He^{2+} and He^+. The electron temperature and the He^{2+} and He^+ and electron densities are determined from the Saha equations for the highly excited states and the condition of charge neutrality. The electron density is also measured directly with a 4-mm microwave interferometer. The rate of recombination of He^+ is found to be in good agreement with previous measurements, at temperatures <0.25 ev. At higher temperatures, where He^+ and He^{2+} are both present, the recombination rate is found to follow a Z^3 relationship. The measurements appear to be in quite good agreement with the calculations of Bates, Kingston, and McWhirter over the entire range of measurement. (auth)

30601 INTENSITY BEATS IN RESONANCE RADIATION ABSORBED BY A COHERENTLY EXCITED METASTABLE STATE FORMED BY ELECTRON IMPACT. Hadeishi, Tetsuo; Liu, Chung-Heng (Univ. of California, Berkeley). Phys. Rev. Lett., 16: 1035-7(June 6, 1966). (UCRL-16731).

Intensity beats were observed in resonance absorption by coherent excitation of nondegenerate magnetic sublevels of the nonradiative $^3P_2$ metastable state of mercury. This state was formed by the unidirectional low energy electron-impact excitation in a weakly ionized plasma. The method was utilized to overcome an inherent limitation of the optical-pumping technique, the pumping speed. (B.G.D.)

30602 COUPLED WAVE EQUATIONS FOR HOMOGENEOUS GYROTROPIC COMPRESSIBLE WARM PLASMAS. Unz, H. (RAND Corp., Santa Monica, Calif.). Proc. IEEE (Inst. Elec. Electron. Eng.), 54: 393-4(Mar. 1966).

The coupled wave equations for homogeneous gyrotropic compressible warm plasmas are derived from the basic differential equations in the continuum of plasma dynamics for single fluid, warm, compressible magnetoplasma. (B.G.D.)

30603 WAVE EQUATIONS FOR INHOMOGENEOUS GYROTROPIC HOT PLASMAS. Rao, S. S.; Unz, H. (Univ. of Kansas, Lawrence). Proc. IEEE (Inst. Elec. Electron. Eng.), 54: 407-8(Mar. 1966).

The derivation of a wave equation for an inhomogeneous gyrotropic hot plasma, which takes into account the varying magnetostatic field imposed on the plasma and the varying collision frequency is presented. (B.G.D.)

30604 GRAPHICAL REPRESENTATION OF THE IONIZATION TEMPERATURE OF A PLASMA—APPLICATIONS. Berthelot, Ch. A. (EURATOM, Geel, Belg.). Spectrochim. Acta, 22: 829-37(May 1966).

The ionization temperature of a plasma in LTE (local thermodynamic equilibrium) is given by the slope of the straight line:

$$\log\left\{\left(\frac{1\lambda^3}{gf}\right)_{mn}^{(i+1)}\cdot\left(\frac{gf}{1\lambda^3}\right)_{rs}^{(i)}\right\}_x \text{ or } \log\left\{\left(\frac{N}{g}\right)_{m}^{(i+1)}\cdot\left(\frac{g}{N}\right)_{r}^{(i)}\right\}_x ,$$

versus the algebraic sum of energies $\{V^{(i,i+1)} + E_m^{(i+1)} - E_t^{(i)}\}_x$. At least two pairs of emission or absorption lines from two chemical elements are needed for the construction of the curve. (auth)

30605 CONTROLLED NUCLEAR FUSION RESEARCH, SEPTEMBER 1965: REVIEW OF EXPERIMENTAL RESULTS. Spitzer, Lyman Jr. (Princeton Univ., N. J.). pp 3-11 of STI-PUB-111(Vol.1).

A brief summary is presented which discusses the most significant experimental conclusions presented at the conference. (M.O.W.)

30606 CONTROLLED NUCLEAR FUSION RESEARCH, SEPTEMBER 1965: REVIEW OF THEORETICAL RESULTS. Kadomtsev, V. V. (Kurchatov Inst. of Atomic Energy, Moscow). pp 29-32 of STI-PUB-111(Vol.).

A brief summary is presented which discusses the most significant theoretical conclusions presented at the conference. (M.O.W.)

30607 HEATING AND CONTAINMENT OF PLASMA IN THE MAGNETIC WELL IN DECA II. Biguet, A.; Blanc, P.; Gravier, R.; Lacoustey, P.; Luc, H.; Renaud, C.; Tachon, J.; Veron, D. (Centre d'Etudes Nucleaires de Fontenay-aux-Roses, France). pp 69-82 of STI-PUB-111 (Vol.1). (In French).

A jet of deuterium plasma obtained by an induction gun is guided and slowed down adiabatically by an increasing static longitudinal magnetic field. The energetic part of the plasma is captured between a pulsed magnetic barrier and gate, and then adiabatically compressed between two mirrors. A magnetic well configuration is produced by superimposing a pulsed quadrupolar magnetic field. The lifetime of the hot plasma (mean energy 1 kev) is 50 μsec in the simple mirror configuration (in which flute instabilities are observed) and 200 μsec in the magnetic well configuration. The plasma density—determined by microwave interferometry, spectroscopy in the near ultraviolet, or attenuation of a neutral atom beam—lies between 1×10^{13} and 3×10^{14} cm^{-3}, whereas the density deduced from the emission of fast neutral atoms by the plasma (assuming that the plasma is lost only by charge exchange) is substantially lower, being of the order of 10^{10} cm^{-3}. The experimental results do not rule out the hypothesis that the lifetime of the plasma is limited by diffusion in the cone of losses. (auth)

30608 STABILIZATION BY SHEAR AND NEGATIVE V''. Furth, H. P. (Univ. of California, Livermore); Killeen, J.; Rosenbluth, M. N.; Coppi, B. pp 103-26 of STI-PUB-111(Vol.1).

A criterion is derived for the stability against gravitational interchange of toroidal systems by using the hydrodynamic equation with finite resistivity. The stability depends on an expression that reduces to the sign of the second derivative of the volume per unit flux (V'') in the case that the plasma does not surround any "floating" conductors. If this condition is violated, then a "rapid" resistive instability results. If the condition is satisfied, then both the resistive growth rate and the critical β against "ballooning" modes depend on a figure of merit $rR_c\gamma/L^2$ where r is plasma radius, L is length along field lines between "good" and "bad" regions, R_c the mean radius of curvature and γ is a shape factor depending on the design. A similar consideration applies to "kinking" modes. Using the results of numerical calculations, the structure, stability properties and figure of merit of several "stagnation-point" solutions having the negative-V'' property were discussed. The principle here is to create directions of favorable $\tilde{\nabla}B$, then cause the rotational transform to be weakened in the favorable regions (reaching a null at the stagnation point). The negative contributions to V'' are then weighted heavily, becoming infinite at the stagnation point. Three types of solution are considered: (1) Linear periodic-multipole arrays, by using helical l = 2 and 4, or l = 3 "shaping fields" with natural stagnation points; and by superimposing l = 0 and 2, l = 1 and 3, or l = 0 and 3 "corrugating fields," to create favorable $\tilde{\nabla}B$ regions. (2) Helical equilibria, by using gross helical curvature to create the favorable $\tilde{\nabla}B$ regions and stagnating the rotational transform by means of a current on an axial conductor, around which the helical equilibrium flux-tube is wound. (3) Toroidal equilibria, by using the gross toroidal curvature to create the favorable $\tilde{\nabla}B$ regions. The rotational transform is generated by a helical l = 2 winding and stagnated by an auxiliary poloidal field. (auth)

30609 CLOSED MINIMUM-B CONFIGURATIONS. Solov'ev, L. S.; Shafranov, V. D. (Kurchatov Inst. of Atomic Energy, Moscow). pp 169-90 of STI-PUB-111 (Vol.1). (In Russian).

An investigation was made of the possibility of creating closed toroidal magnetic field configurations that satisfy the stability criterion of a low-pressure plasma $V''(\psi) < 0$, where V is the volume bounded by a magnetic surface with the longitudinal flux ψ. Attention is paid mainly to configurations whose magnetic axis is a spatial curve characterized both by curvature k and by torsion (figure-eight systems of the stellarator type). Unlike the "plane" configurations (whose magnetic axis is a plane curve), the spatial configurations satisfying the minimum-B condition $V'' < 0$ are smoother. In such configurations the cross-section of the toroidal magnetic surfaces can be made constant along the length of the system and to differ little from the round cross section. Another important property of such configurations is a finite shift of the magnetic field lines (shear), which gives the configuration a certain stability relative to the perturbations of the magnetic field, and also ensures the elimination of drift instabilities. For the creation of a minimum-B configuration, in addition to the fundamental longitudinal magnetic field, one must superpose on the magnetic axis a transverse component with multipole orders l = 2 (quadrupole field) and l = 3. The simplest representative of the spatial minimum-B configurations is an unclosed helical-axis configuration. The magnetic surfaces in the transverse section that is perpendicular to the magnetic axis in the polar system of coordinates are described by $\rho = \rho_0 - \rho_0\epsilon(\cos 2\theta)/2 - \rho_0^2 q \cos 3\theta$ where ρ_0 is the mean radius of the transverse section of the magnetic surface, ϵ is a dimensionless coefficient smaller than unity, q is a variable parameter having the dimension of reciprocal length, and θ is the vectorial angle made by the principal normal to the magnetic axis. The condition $V'' < 0$ is reduced to the requirement $\epsilon(5/4 + 6q/k) > 1$ that is easily fulfilled for comparatively small values of ϵ and q. Analogous conditions are obtained also for closed spatial configurations, though in this case magnetic surfaces with constant ϵ and q can be obtained only if the stabilizing fields with l = 2 and l = 3 are distributed in a special (non-uniform) way along the system. (auth)

30610 PLASMA CONTAINMENT AND STABILITY IN A MEGAJOULE THETA PINCH EXPERIMENT. Bodin, H. A. B.; Green, T. S.; Newton, A. A.; Niblett, G. B. F.; Reynolds, J. A. (United Kingdom Atomic Energy Authority, Abingdon, Eng.). pp 193-221 of STI-PUB-111(Vol.1).

The application is described of a fast megajoule capacitor bank to the study of plasma production and confinement in the theta-pinch configuration. Deuterium gas at a pressure in the range 10 to 50 m torr is preionized by a transient axial current and subsequently compressed by a sinusoidal magnetic field with a peak value of 76 kG and a half-period of 12 μsec. The single-turn coil used in the experiment is 200 cm long and 10 cm in diameter. Lateral drift of the plasma to the walls of the discharge tube was avoided by reduction of the curvature of confining lines of magnetic force using a parallel strip transmission line between the coil and collector. The origin of a low-amplitude circular motion of the plasma about the central equilibrium axis, the so-called wobble phenomenon, is discussed. The general properties of the discharge were analyzed by comparing the measured values of electron temperature, plasma diamagnetism, radial density distribution, and neutron yield with numerical predictions using the Hain-Roberts hydromagnetic code. The rate of axial plasma loss was determined by means of a wide variety of techniques. These include optical interferometry to measure the total number of trapped particles, an analysis of con-

tinuum emission in the visible spectrum to give the line density as a function of axial position, and miniature piezoelectric pressure probes to estimate the size of the less aperture. The results show that the plasma is subject to magnetic field diffusion in the early stages and to cooling of the electrons either by impurity radiation or by thermal conduction along the field lines. The consequent depression of the plasma β to a value about 0.5 at peak field enlarges the magnetic apertures at the ends of the coil and thus leads to axial escape of plasma. The main problems for the future are therefore the development of a pre-heat system to give a higher temperature plasma at a β of near unity, and the reduction of the rate of electron energy loss. (auth)

30611 ISAR I: FAST MEGAJOULE THETA-PINCH EXPERIMENT WITH EXTREMELY HIGH COMPRESSION FIELDS. Andelfinger, C.; Decker, G.; Fuenfer, E.; Heiss, A.; Keilhacker, M.; Sommer, J.; Ulrich, M. (Institut fuer Plasmaphysik, Garching, Ger.). pp 249-60 of STI-PUB-111(Vol.1).

The megajoule theta-pinch experiment Isar I was put into operation at Garching in January 1965. The maximum energy stored in the condenser bank is 2.5 MJ at 40 kv. The bank can produce peak magnetic fields in 180 kG with a half-period of 20 μsec in a single-turn coil with a length of 150 cm and an internal diameter of 10.6 cm. A linear z-pinch is used to produce a preionized plasma; bias fields up to ±5 kG can be applied. The first experiments were carried out with stored energies of up to 1.5 MJ and initial pressures in the range 5 to 50 m torr D_2. The observed drift of the plasma column (toward the collector) was reduced by improving the homogeneity of the axial magnetic field thus preventing the plasma from striking the tube wall during the first half-cycle. Electron densities of 1 to 2×10^{16} cm^{-3}, electron temperatures of 350 ev and ion temperatures of 3.7 kev, calculated from the neutron yield were measured. The maximum neutron yield per discharge was 1×10^{10}. At the maximum magnetic field the end losses were $dN_{tot}/dt = 3$ to 6×10^{23}. (auth)

30612 PLASMA CONFINEMENT, HEATING AND LOSSES IN PHAROS WITH AN EXTENDED CURRENT PULSE. Kolb, A. C. (Naval Research Lab., Washington, D. C.); Lupton, W. H.; Elton, R. C.; McLean, E. A.; Swartz, M.; Young, M. P.; Griem, H. R.; Hintz, E. pp 261-73 of STI-PUB-111(Vol.1).

The duration of the current in a large theta-pinch experiment was extended to times of ~100 μsec which is now sufficiently long to study the confinement of a hot, dense (~10^{17} cm^{-3}) plasma in a relatively constant, high magnetic field. Measurements of the spatial and temporal distribution of particles and the heating rates were carried out for the case of an initial reverse bias field. Comparing 640-kJ and 1.3-MJ discharges in a closely coupled coil, the loss rate decreases with increasing peak temperature. The confinement time in the 1.3-MJ case is determined by the onset of a rotating flute instability which is caused by the presence of stray transverse fields near the slot. The heating rate and final 900-ev temperature is large compared to that expected from adiabatic compression of a shock-heated plasma. (auth)

30613 FORMATION AND DEVELOPMENT OF HYDROMAGNETIC DISTURBANCES DURING THE IMPLOSION PHASE OF A PREIONIZED THETA PINCH (CARIDDI). Ascoli-Bartoli, U.; Martellucci, S.; Martone, M. (Comitato Nazionale per l'Energia Nucleare, Frascati, Italy). pp 275-86 of STI-PUB-111(Vol.1).

A study was made of the implosion phase of a preionized theta pinch in an initial magnetic field. High-speed optical refractive methods and a miniature magnetic probe were used in order to compare the actual implosion phase behavior, with the calculated one on the basis of the partially ionized and fully ionized models. The thickness ($\lesssim$ 8 mm) of the measured shock front is appreciably smaller than the relevant collision distances, thus indicating a collisionless phenomenon. High-frequency structure is also observed in the shock transition. (auth)

30614 STABLE AND UNSTABLE BEHAVIOR OF PREHEATED PLASMA IN LINEAR AND CUSPED THETA PINCHES. Belitz, R. J.; Bogen, P.; Dippel, K. H.; Jordan, H. L.; Kugler, E.; Miyahara, A.; Noll, P.; Schlueter, J.; Witulski, H. (Association EURATOM-Kernforschungsanlage, Juelich, Ger.). pp 287-300 of STI-PUB-111(Vol.1).

Experiments on the behavior of the magnetic compression of preheated hydrogen plasmas in theta pinches of linear and spindle-cusped geometries were made with the following devices: (1) 5 kJ linear theta pinch, coil diameter 4.5 cm, length 15 cm, B_{max} = 50 kG, $T_{\frac{1}{4}}$ = 1.5 μsec; (2) 600-kJ linear theta pinch, coil diameter 10.5 cm, length 128 cm, B_{max} = 100 kG, $T_{\frac{1}{4}}$ = 17 μsec; (3) 10-kJ spindle cusped theta with B_{max} = 45 kG at point and line cusps, radius 5.2 cm, length 8.5 cm. They all have provisions for preionization by a capacitively coupled low-power r-f transmitter, magnetic bias field of variable strength and polarity, preheating by pulsed oscillating electrodeless ring discharge, and compression of the plasma by a fast capacitor bank. Observations were made by using smear and framing camera photography, optical interferometry with Mach-Zehnder and differential interferometers, spectroscopy in the visible and the soft x-ray regions, and magnetic probes. These methods give information on plasma structure, on density profiles, on the distribution of electron and ion-Doppler temperatures and their development in time. Both stable and unstable plasmas were observed in linear devices. By variation of pressure, bias field, preionization, preheating, and impurity concentration, and by disturbing the symmetry of the discharge tube, information on stable and unstable parameter regions could be obtained. Deviations from the symmetry of the plasma column can occur because of: (1) drifts connected with spatial inhomogeneities of the confining magnetic field; (2) axial motions and contractions in plasmas with trapped antiparallel fields, and rarefaction waves due to end losses; (3) rotations, and deformation oscillations of the cross-section of the plasma; and (4) star-shaped instabilities and eruptions. While drifts and axial motions are directly connected with magnetic field configurations and relatively insensitive to other parameters, cross-sectional distortions and eruptions depend critically on the initial conditions of the plasma, for example preionization, preheating, inhomogeneities of the conductivity, rate of compression, and very sensitively on small changes in impurity concentration. Under apparently stable conditions reasonably good agreement could be obtained between the maximum values of Doppler temperature for ions, electron temperature and mean temperature taken from pressure balance in high-β plasmas obtained by the 5 kJ linear theta pinch. First results obtained in the spindle cusp experiment indicate a stable behavior of the plasma up to initial gas pressures of 0.5 torr H_2. (auth)

30615 DOPPLER SHIFT MEASUREMENTS TO INVESTIGATE PLASMA ROTATION IN THE THETA PINCH. Keilhacker, M. (Institut fuer Plasmaphysik, Munich-Garching, Ger.); Herold, H.; Cooper, J.; Roberts, D. E. pp 315-30 of STI-PUB-111(Vol.1).

Experiments were performed to determine the mass rotational velocity and the related angular momentum from the Doppler shift of impurity lines. As these shifts can be small compared with the line widths, a Fabry-Perot interferometer was used in the first experiments (carried out at Culham Laboratory on 22.5-kJ theta pinch). A suitable line (C II, 4267 Å) was selected by a 10-Å interference filter and the line profile recorded photoelectrically via an eight-channel fiber bundle array which was crossed with one of the Haidinger fringes produced by the Fabry-Perot. The Doppler shifts measured at different positions across the plasma diameter showed the plasma to rotate as a rigid body. The first detectable shift of the C II line, corresponding to an angular velocity of 5×10^4 rev/s, was measured during the first implosion of the plasma. As the C II line was burned out after one microsecond the Doppler shifts of the C V 2271 Å line were measured in a second experiment carried out at Garching on a 32.5-kJ theta pinch. The profiles were recorded using a high resolution monochromator and a profile-dividing mirror system. In this experiment rotation was only observed at pressures below 30 m torr D_2 and was then again in the direction of the ion current. It was possible to induce rotation and instabilities at higher pressures in an otherwise stable

plasma by superimposing a stationary transverse magnetic field. In this case rotation seems to start in the direction of the electron current but the instabilities showing up later still rotate in the ion current direction. On the other hand the tendency of the plasma to rotate (at pressures of D_2 below 30 m torr) can be reduced and rotational instabilities suppressed by superimposing a transverse field of the same polarity that causes "opposite" rotation for a usually non-rotating plasma. The results are discussed in the light of existing theories on the origin of rotation and on instabilities. (auth)

30616 TOROIDAL THETA PINCH WITH SUPERIMPOSED MULTIPOLE FIELD. Von Gierke, G.; Hofmann, F. W.; Lotz, W.; Rau, F.; Remy, E.; Wobig, H.; Wolf, G. H. (Max-Planck-Institut fuer Physik und Astrophysik, Munich). pp 331-40 of STI-PUB-111(Vol.1).

A toroidal theta-pinch discharge with superimposed hexapole field is investigated. The characteristic data of the discharge are: 10 kG maximum field, 50 ev maximum temperature and densities of about 10^{16} cm^{-3}. The loss rates are determined by measurements of continuum radiation. They are by more than an order of magnitude smaller than loss rates expected from a model which accounts for cusp losses, where the slit width of the line cusp is taken to be the ion Larmor radius. The losses are of the same order as expected by resistive diffusion only. Losses due to a slit width of the order of the electron Larmor radius may contribute. Furthermore the results prove that a toroidal theta pinch with superimposed hexapole field provides a stable toroidal high-beta equilibrium configuration. (auth)

30617 INSTABILITY AND RELATED MACROSCOPIC EFFECTS IN TOROIDAL DISCHARGES. Kadomtsev, B. B.; Pogutse, O. P. (Kurchatov Inst. of Atomic Energy, Moscow). pp 365-82 of STI-PUB-111(Vol.1). (In Russian).

The principal types of instability of plasma in toroidal discharges and the macroscopic effects resulting from the non-linear plasma oscillations building up due to the instability are considered. First discussed is the linear problem of the stability of an axially symmetrical discharge (toroidality being simulated by the boundary conditions at the end joints). A classification of the instabilities is given on the basis of the kinetic equation with consideration of the collisions and the finiteness of the ion Larmor radius. The results of the solution of the linear problem are used as a basis for the subsequent discussion of non-linear processes in the discharge. In discussing the non-linear problem attention is paid chiefly to the simpler case of a discharge in a strong longitudinal magnetic field, where the plasma pressure is considerably smaller than the pressure of the magnetic field. When neglecting the non-potentiality of the oscillations, only two instabilities remain—the drift instability and the current-convective instability. The latter instability leads to the development of large numbers of "convection cells" in which heat is transferred by convection. In the case of a very strong magnetic field the "convection cells" overlap and the macroscopic heat and particle fluxes may considerably exceed the classical fluxes determined by binary collisions. When the plasma pressure is increased the convection cells cease to overlap, and the macroscopic effect of the current-convective instability becomes small. If the plasma pressure increases further the nature of the unstable oscillations becomes non-potential, and they are associated with a curvature of the lines of force leading to a rearrangement of the magnetic surfaces. In a low-pressure plasma, the drift instability develops simultaneously with the current-convective instability and was also considered on the basis of non-linear theory. The interaction of the drift oscillations and the convection cells is also discussed. (auth)

30618 ANOMALOUS ESCAPE OF IONS INTO THE "LOSS CONE." Galeev, A. A. (Inst. of Nuclear Physics, Novosibirsk, USSR). pp 393-416 of STI-PUB-111(Vol. 1). (In Russian).

The non-equilibrium characteristics of a plasma contained in a magnetic mirror trap lead to the appearance of the "flute", the "universal" and anisotropic instabilities considerably limiting the containment times of the particles. It is now held that the flute instability can be suppressed by using a special magnetic field design (the minimum B field). The universal instability, which is due to the inhomogeneous plasma distribution across the magnetic field, is eliminated by a relatively small shear of the magnetic lines of force. On the other hand, as was shown recently by Rosenbluth and Post, in a plasma of sufficiently large density, $n \gtrsim 10^{13}$ cm^{-3}, and length, $L \gtrsim 10^4 \lambda D$, (λD being the Debye radius), even the slight anisotropy in the ion velocity distribution associated with the "loss cone" leads to the development of a shortwave instability. A detailed analysis is therefore made of the spectrum of the resulting turbulent motion and of the anomalous transfer processes taking place in the unstable plasma. In traps of finite length L, the anomalously rapid diffusion of particles into the loss cone leads to the filling of this cone, so that the instability is attenuated. This allows the use, for the description of turbulent transfer processes in a plasma, of the quasilinear theory supplemented by the kinetic equation for the energy density of the plasma oscillations. The maximum scale of the pulsations which are built up is determined by the condition of feeble attenuation near the ends of the trap, where the phase velocity becomes comparable to the mean thermal velocity of the electrons. The escape time into the loss cone arising from scattering of the ions mainly at the large-scale pulsations depends essentially on the length of the device ($\Omega_H \tau \approx 10^5 R_H/L$; where R_H is the Larmor radius of the thermal ions). The escape time of the particles from the trap through the magnetic mirrors is determined by the longest of these escape times ($\tau_{r_i} T \approx L/v_i$; v_i being the ion thermal velocity). The results are used to assess the possibility of controlled thermonuclear fusion in a magnetic mirror trap. For the purpose of this evaluation the optimum trap parameters according to Post were used, based on a comparison of the energy losses from a quiescent plasma in a magnetic mirror trap, the losses in the auxiliary systems and the total energy yield of the thermonuclear reaction. The plasma lifetime in such a trap is determined by the transit time of the thermal ions between the magnetic mirrors, and it is not sufficiently long to make possible an economically favorable thermonuclear fusion. (auth)

30619 TOROIDAL EQUILIBRIA IN THE NARROW-TUBE APPROXIMATION. EFFECT OF CURVATURE. Mercier, C. (Centre d'Etudes Nucleaires de Fontenay-aux-Roses, France). pp 417-34 of STI-PUB-111(Vol. 1).

A toroidal plasma centered about a closed curve (Γ) defined by its characteristic coordinates R(s) and T(s) and whose mean radius R_p at every point of Γ is small compared to R(s) can be investigated in the narrow-tube approximation. One can then, in general, neglect the specific effects of the curvature and replace the toroidal plasma of length L by a cylindrical plasma by imposing periodicity conditions at the two ends of a cylinder of length L. However, in certain conditions, especially when the rotational transform $\iota/2\pi$ is nearly constant throughout the plasma and approximates a whole number k, and if the Fourier expansion of $1/R(s) = a_0 + \Sigma_k 2a_k \cos(2k\pi s/L)$ is such that $a_k \neq 0$, the effects of the curvature may become very important. One may thus arrive at configurations whose principal properties are related to the curvature. To represent these configurations one uses the system $(\rho\theta_0 s)$ related to (Γ) for which $dS^2 = d\rho^2 + \rho^2 d\theta_0^2 + [1 - \rho \cos \theta R^{-1}(s)]^2 ds^2$ with $\theta = \theta + \int_0^s ds/T(s)$. If one wishes to disregard the effects of the curvature and twist, it is sufficient to take $1/R = 0$ and $1/T = 0$. If one wishes to investigate specifically the effect of the harmonic k_0 in $1/R(s)$, which is important if $\iota/2\pi$ is close to $\pm k_0$, it is possible to disregard all members of the series a_k except a_{k0} and to retain only the dependence in $t = (2k\pi s/L) + \theta$. The dS^2 may then be considered as the dS^2 in a triorthogonal system related to an axis $\bar{\Gamma}$ whose characteristic equations would be $1/R = a_k$ and $1/T = 1/T(s) - 2k\pi/L$. For example, in the case of a plane curve $\Gamma(1/T = 0)$ the representation of the plasma in this approximation is not a cylindrical plasma but a plasma centered about a helix defined by $1/R = a_k$ and $1/T = -2k\pi/L$ = constant. In the case generalizing the cylindrical symmetry (physical functions in-

dependent of s) one can put $\vec{B} = f\vec{u} + \vec{u} \cdot \vec{\nabla}F$, $\vec{j} = \vec{\nabla} \times \vec{B} = [(-2Kf/g) + \mathscr{S} \cdot F)]\ \vec{u} + \vec{u} \times \vec{\nabla}(-f)$ where F and f are functions of one another, and F is a solution of $\mathscr{S} \cdot F = (2Kf/g) - (df^2/2dF) - (gdp/dF)$. $\mathscr{S}$ is a second-order differential operator, and $K = 2k\pi L$. These properties generalize the cases of rotational symmetry ($k = 0$, $a_k = 1/R$) and of helicoidal symmetry ($a_k = 0$, $k \neq 0$). One can now investigate the configurations represented by these equations in the conditions specified above, and also their stabilities. In rotational symmetry these conditions apply in the neighborhood of a zero longitudinal current. These configurations are distinguished particularly by the sign in front of $d^2(f^2)/dF^2$, at least in the simple case when this sign is constant. One can obtain either configurations having a kind of boundary layer, or configurations with several magnetic axes. (auth)

30620 THERMALIZATION AND ANOMALOUS DIFFUSION OF TURBULENT PLASMAS. Aamodt, R. E.; Drummond, W. E. (General Dynamics Corp., San Diego, Calif.). pp 435-51 of STI-PUB-111(Vol.1).

At the present time, it appears possible to construct plasma devices which are stable to the so-called flute instabilities. However, no device at present appears in addition to be stable to the so-called micro-instabilities, which depend on the local velocity distribution and density gradient for their growth. For many of these instabilities $\gamma/\omega \ll 1$ and the quasi-linear theory applies, where ω is the frequency and γ is the growth rate. The quasi-linear theory predicts the development of a high-amplitude equilibrium spectrum of waves, and a concomitant distortion of the particle distribution function so that the waves in this equilibrium spectrum are neutrally stable. The time development of this equilibrium spectrum arising from the mode coupling terms that are neglected in the quasi-linear theory is discussed. These terms lead to rapid distortion of the equilibrium spectrum and to a damping of the total energy of the spectrum into both electron and ion thermal motion and to the anomalous diffusion of the plasma across magnetic field lines. The mode coupling terms can be divided into two parts: the "resonant" mode coupling terms that represent wave-wave scattering and lead to a distortion of the spectrum but do not change the total energy of the wave spectrum, and the "non-resonant" mode coupling terms that in addition to distorting the spectrum lead to a decay of the total energy in the spectrum via "non-linear Landau damping." This process in addition leads to an anomalous diffusion of plasma across magnetic field lines. (auth)

30621 STABILITY OF A DIFFUSING PLASMA. Bernard, M.; Briffod, C.; Frank, R.; Weisse, J. (Centre d'Etudes Nucleaires de Saclay, France). pp 469-83 of STI-PUB-111(Vol.1). (In French).

In the DAPHNIS experiment the plasma produced by a magnetron source diffuses along a static magnetic field B_0. There will, therefore, be neither a macroscopic current nor a flux of fast electrons through the measuring chamber located about a meter from the source. Since the neutral gas pressure in the chamber may vary from 10^{-2} to 10^{-5} torr it is verified first that the plasma in fact behaves as a true diffusing plasma, namely, that its density increases with B_0 and decreases as the pressure is increased. However, by measuring $D_{a\perp}$, the coefficient of ambiopolar diffusion perpendicular to B_0, it was found that anomalous diffusion takes place. The noise emitted by the plasma was analyzed, and a distinct emission in two clearly defined regions of the spectrum was determined: (a) a UHF noise emitted in two separate bands on either side of the electron cyclotron frequency; (b) an HF noise from 1 to 10 Mc/s whose amplitude is correlated with density fluctuations of frequency equal to some tens of kilocycles per second. But the coefficient of diffusion $D_{a\perp}$ varies as a function of B_0 similarly to the emitted noise intensity. In order to identify the two types of instability responsible for this emission, the velocity distribution function of the electrons in the source and in the measuring chamber were measured. The influence of these instabilities on the particle diffusion perpendicular to B_0 is analyzed in this investigation. (auth)

30622 LANDAU DAMPING OF ELECTRON PLASMA WAVES. Malmberg, J. H.; Wharton, C. B.; Drummond, W. E. (General Dynamics Corp., San Diego, Calif.). pp 485-97 of STI-PUB-111(Vol.1).

The damping of electron plasma waves propagating along a cylindrical plasma column immersed in a magnetic field was measured. The plasma matches the assumptions of the theory, namely, collisions are so rare as to produce negligible damping; the number of particles in a Debye sphere is large, the plasma radius is large compared to the Debye length, and the electron velocity distribution function is Maxwellian. The frequency, wavelength and damping length of the waves are measured. The electron velocity distribution function is measured for electron velocities corresponding to the range of wave phase velocities. One observes heavy exponential damping of the waves in a density range where collisional damping is negligible. The magnitude of the observed damping and its dependence on phase velocity are predicted accurately, without any normalizations, by the theory of Landau. The plasma boundary conditions may be adjusted to remove electrons exceeding a given velocity from the plasma. When the velocity at which the distribution function is truncated is reduced to the phase velocity of the wave, the wave damping decreases dramatically. By making this measurement as a function of wave phase velocity, one establishes that the damping is caused by a very few electrons traveling in the direction of and at the phase velocity of the wave, as expected from theory. (auth)

30623 COLLECTIVE INTERACTION OF MODULATED AND UNMODULATED ELECTRON BEAMS WITH PLASMA. Berezin, A. K.; Fainberg, Ya. B.; Bolotin, L. I.; Berezina, G. P.; Bez'yazchnyi, I. A.; Lyapkalo, Yu. M.; Livshits, V. I. (Inst. of Physics and Tech., Kharkov). pp 515-35 of STI-PUB-111(Vol.1). (In Russian).

Results are presented of experimental investigations of collective interactions of charged particle beams with a plasma. (Beam current 5 to 35 A, energy of beam electrons 8 to 20 kev, pulse length 3.6 to 100 μs, longitudinal magnetic field 600 to 1300 Oe). The plasma was produced by the electron beam. By experiments with initially unmodulated beams the elementary mechanisms responsible for exciting the instability, the conditions of excitation, the frequency spectra and phase velocities of the excited waves, the oscillation growth rates, the electric field strengths, the absolute values and spectral distribution of the power of the excited oscillations, and the electron temperatures were determined. The power lost by the electron beam as a result of collective interaction with the plasma was determined by a calorimetric method, and it is shown that it coincides with the power of the high-frequency oscillations set up by the interaction of the beam with the plasma. The experimental measurements of the frequencies, oscillation growth rates and phase velocities of the oscillations excited in the plasma show good agreement with the calculated values. Modulation of the beam increases the efficiency of its interaction with the plasma. The power of the oscillations excited at the modulation frequency increases by the factor 50; that of the oscillations at other frequencies decreases considerably over a wide range of frequencies. A possibility is therefore presented of eliminating instabilities over a wide range of frequencies. Experiments were carried out to study the transition of the plasma to a turbulent state as a result of the development of beam instabilities. The variations with time of the frequency spectra during the development of instabilities were investigated (from 100 kc/s to 10,000 Mc/s), the correlation functions were determined and the discontinuities in the phase of the excited oscillations were investigated. These measurements, as well as investigations of particles with higher energies appearing during the development of the instabilities, are necessary to determine the main processes and parameters characterizing a turbulent plasma. (auth)

30624 INTERACTION BETWEEN HF WAVES AND PLASMA IN DELTA-2. Breus, S. N.; Kurdyumov, B. N.

(Inst. of Radio. Tech., Moscow). pp 537-47 of STI-PUB-111(Vol.1). (In Russian).

The results are presented of an investigation on the interaction of a dense plasma with the high-frequency field of a magnetic wave traveling along a toroidal discharge chamber (large diameter–700 mm, small diameter–85 mm). The traveling wave is excited at a frequency 2.4 Mc/s by a three-phase automatic generator with a power about 50 Mw and a pulse length about 250 to 350 μs. The range of initial pressures was 0.1 to 0.001 torr and the amplitude of the hf magnetic field on the surface of the plasma attained 500 to 600 Oe. In these circumstances, the main factors determining the interaction are connected with the non-linear effects and, above all, with the appearance of a steady longitudinal component of current that reached values of a few thousand amperes. In the center of the chamber, in the small-field region, the conductivity of the plasma was of the order of 3 to 4×10^{14} esu, which, for close to 100% ionization, corresponds to an electron temperature of 8 to 12 ev. In the strong-field (skin-layer) region, conductivity falls off by more than an order of magnitude, which leads to a sharp increase in the required HF power. In addition to a longitudinal current, the plasma was found to contain a longitudinal quasi-stationary field formed by transverse currents in the plasma. This field has a composite structure and, as shown by theoretical approximations, is possibly due to a toroidal effect. The existence of quasi-stationary magnetic fields apparently has a connection with the plasma oscillations which were observed at 200 to 500 kc/s, corresponding approximately to the natural Alvén oscillations in such fields. The quasi-stationary currents and fields hamper the detachment of the plasma from the walls of the discharge chamber and subsequent compression. By themselves, however, the longitudinal steady waves cannot lead to the development of kinetic instabilities, since the electron velocities corresponding to such instabilities are smaller than the phase velocity of the traveling wave, about 5×10^7 cm/s, which is considerably smaller than the thermal velocity of the electrons. (auth)

30625 INTERACTION BETWEEN UHF RADIATION AND A TURBULENT PLASMA. Kislyakov, A. I.; Larionov, M. M.; Rozhdestvenskii, V. V. (Ioffe Inst. of Physics and Tech., Leningrad). pp 549-68 of STI-PUB-111(Vol.1). (In Russian).

Previous work revealed an anomalously low low-frequency conductivity of plasma in the Alpha apparatus. The purpose here was to determine the uhf conductivity. For the wavelengths 8 and 4 mm, one observes the passage of signals through the plasma, the thermal radiation of the plasma and, because of the plasma, the changed Q-factor of the discharge chamber which is regarded as a large volume resonator. Simultaneously the average plasma density was determined from the attenuation of the beam of hydrogen atoms passing through it. During the active discharge period, the plasma density was between 10^{12} and 10^{11} cm^{-3}, and the electron temperature 20 to 40 ev. A force-free configuration of fields and currents existed in the discharge, and the plasma filled comparatively evenly the discharge chamber of about 6 m^3. In the decaying plasma, following the discharge current, interferometric measurements of the electron concentration agreed with density measurements that used the attenuation of an atomic beam. In the active period of the discharge, interferometric measurements were impossible because of the strong turbulence of the plasma, so the electron concentration was determined from the attenuation of the atomic beam. From the Q-value of the discharge chamber during the discharge, one can determine the absorption coefficient of the uhf signal in the plasma. If the average density is known from the attenuation of the atomic beam, it is possible to find the effective frequency of electron collisions. This may also be found from the d-c conductivity of the plasma, which is determined by electrical measurements. On the other hand, from the observed densities and electron temperatures one can calculate the frequency of electron collisions for a totally ionized hydrogen plasma. Both methods of determining experimentally the effective collision frequency gave much higher values than found by calculation. One may thus assert that there existed in the plasma an electron slowing-down mechanism which was more effective than Coulomb collisions with singly charged ions. This caused the anomalously low conductivity and anomalously high absorption coefficient in the uhf range. As well as measuring the Q-factor, the attenuation of 8 and 4-mm signals passing through the plasma was measured. The signal was strongly attenuated at plasma densities which were far from critical. For example, the power of a 4-mm signal was reduced by 10 decibels on passing through a layer of plasma 1 m thick, whose density was 1.5 to 2.0×10^{13} cm^{-3} whereas the critical density for this range is 7×10^{13} cm^{-3}. Thus, determination of the electron concentration by "cut-off" of the signal gives much higher results. Attenuation of the signal at concentrations far from critical may be caused both by absorption in the plasma and by scattering from non-homogeneous regions of the plasma. Calculation shows that the observed attenuation cannot be explained by absorption, even with the anomalously high measured absorption coefficient. Most likely, attenuation is a result of the scattering of uhf radiation from non-homogeneous regions in a turbulent discharge. A further, more careful study of this scattering may give a method for investigating the turbulent state of the plasma. (auth)

30626 UNIFIED APPROACH TO RESISTIVE AND MICRO-INSTABILITIES. Stringer, T. E. (United Kingdom Atomic Energy Authority, Abingdon, Eng.). pp 571-93 of STI-PUB-111(Vol.1).

The model used is a slab of plasma supported against a gravitational field by a sheared magnetic field. Fluid-type equations are used to describe the mean motion of ions and electrons perpendicular to the magnetic field lines. The motion along field lines is obtained by taking moments of the Vlasov equation, with a BGK collision term. This gives a generalized Ohms law in which collisions and resonant particle effects are included. In the collisional limit the equations give the resistive-g mode and the pressure-driven drift mode, and in the collision-free limit the drift micro-instability and electron inertial instabilities. The quasi-mode forms of some of these instabilities are considered, and the effect of finite Larmor radius corrections on the resistive-g quasi-mode is discussed. Some criteria are given for estimating the relative importance of the different instability mechanisms. (auth)

30627 OSCILLATIONS AND STABILITY OF PLASMA IN AN EXTERNAL HIGH-FREQUENCY ELECTRIC FIELD. Aliev, Yu. M.; Gorbunov, L. M.; Silin, V. I. (Lebedev Inst. of Physics, Moscow). pp 659-71 of STI-PUB-111(Vol.1). (In Russian).

A theory is developed for the oscillations and stability of plasma in a strong external h-f electric field. The kinetic equation with self-congruent reciprocity is linearized for weak deviations from the ground state. Since the latter depends on an external h-f field, the linearized equation obtained has coefficients with a periodic time dependence. From this equation and also from Maxwell's equations there is derived a dispersion equation for plasma oscillations that represents the zero value of the infinite order determinant, and that is solved both for external field frequencies considerably exceeding the electron Langmuir frequency and for frequencies that are less. The external h-f field changes the oscillation branches in a plasma without an external field, and also leads to a new low-frequency oscillation branch. Movement of particles in the h-f field gives spatial dispersion. If the frequency of the field exceeds the electron Langmuir frequency, the plasma oscillations are stable stable. At frequencies less than this level there occurs a build-up of low-frequency oscillations. Here the maximum of the build-up occurs when the external field frequencies approach the electron Langmuir frequency and is equal to the product of the Langmuir frequency and the one-third power of the electron-ion mass ratio. Away from the resonance, the increment of build-up has the same order of magnitude as the ion Langmuir frequency. An external magnetic field increases the number of possible natural plasma oscillations and thereby increases the possibility

of resonance with the external h-f field. Allowance for the thermal motion of the particles enables one to determine the attenuation of the oscillations in question. Expressions for the decrements are derived. The effect of the external h-f field on a plasma in which there are beams is also discussed. An h-f field has a destabilizing effect on a system of this kind, since on the one hand there can be a build-up of fresh, low-frequency oscillation branches (which are in fact characteristic of plasma in an h-f field) and on the other hand the increments are increased and the region of instability is broadened for some waves which could also exist in plasma without an external field. However, an external h-f field stabilizes a plasma in which there is relative motion of electrons and ions by narrowing the region of instability and reducing the increments in wave build-up. (auth)

30628 NON-LINEAR PLASMA WAVE INTERACTION. Gailitis, A.; Gorbunov, L. M. (Lebedev Inst. of Physics, Moscow). pp 673-94 of STI-PUB-111(Vol.1). (In Russian).

By solving the kinetic equation in the "self-consistent field" approximation, a nonlinear material equation was obtained for a plasma and then this equation was used to write the equation for nonlinear electrodynamics. In the event of underdamping, where the waves are almost monochromatic, an equation was obtained which describes the variation of amplitude of these waves. By averaging this equation over the wave phases, which are assumed to be random, one obtains an equation which describes the evolution of electromagnetic field noises in the plasma when account is taken of the nonlinear interaction between waves. Particular attention is paid to the case of isotropic, homogeneous plasma. Nonlinear interaction of two Langmuir waves with the formation of another Langmuir wave can only occur as the result of induced scattering of the waves on particles. The case was investigated where wave scattering on electrons predominates and also the case where scattering on ions plays the greatest part, and in both cases clarified the role played by the transverse field in the interaction of plasma particles. The case where linear damping of the waves is insignificant in comparison with the nonlinear interaction was also investigated. The question of the conservation of energy and the number of gamma quanta in these processes involving nonlinear interaction of Langmuir waves is discussed. Study of the nonlinear interaction of h-f longitudinal waves in plasma with a slow beam shows that in this case energy from the particles can be transformed into wave energy with ensuring nonlinear instability. The nonlinear interaction of a Langmuir and a transverse wave is considered and the contribution which this process makes to energy changes in longitudinal and transverse waves discussed. The process of non-linear interaction of two transverse waves, resulting in the formation of another transverse wave, was investigated. Possible decay and combination processes involving the participation of three and of four Langmuir and transverse waves were investigated. The latter process is of particular interest in cases where decay conditions are not fulfilled in three waves. In a nonisothermic plasma, when the temperature of the electrons exceeds the temperature of the ions in the plasma, yet another branch of oscillations is possible, namely ionic sound. The nonlinear interaction of ionic sound waves resulting both from induced scattering on particles and from combination and decay with Langmuir and transverse waves, paying particular attention to processes involving the participation of four waves, was investigated. (auth)

30629 NONLINEAR INTERACTION OF ELECTROMAGNETIC WAVES IN A MAGNETO-ACTIVE PLASMA. Kropotkin, A. P.; Pustovalov, V. V. (Lebedev Inst. of Physics, Moscow). pp 695-719 of STI-PUB-111(Vol.1). (In Russian).

With a view to constructing a theory of induced scattering of electromagnetic waves on the particles of a magneto-active plasma, recourse was had to the general method of deriving equations describing the nonlinear interaction of waves as used previously by Gorbunov, Pustovalov and Silin for the case of an isotropic plasma. By this means similar equations can be written for a magnetoactive plasma. The plasma ground state distribution function used for this purpose is regarded as constant in time and space. This means disregarding the effect of oscillations on the distribution of the particles, and in a number of cases this is fully justified; at the same time the equations describing wave interaction can be written in closed form. The spectra of the interacting waves are regarded as linear, that is independent of their energy. The induced scattering of electromagnetic waves on particles of an unbounded homogeneous magnetoactive plasma was discussed. Such interaction plays the greatest part, as far as the problem is treated nonlinearly, in cases where the expansion spectrum of the interacting waves do not satisfy the decay conditions. In such a case, in obtaining the starting equations terms up to and including those of the third order must be taken into account for the purpose of expanding the current density in powers of the field. Particular attention was paid to wave interaction in a cold plasma, and also to the interaction of longitudinal waves in nonisothermal and other plasmas with arbitrary electron and ion temperatures. For the case of a cold plasma, general expressions were derived for the tensors determining the matrix elements of interaction, and by means of these expressions equations were obtained describing the evolution in time of the expansion of oscillation energy for various relationships between the frequencies and directions of propagation of the interacting waves and the parameters of the plasma. On the basis of these equations certain estimates were formed of the relaxation times characterizing this particular type of interactions. In studying the interaction of longitudinal waves, it is sufficient, in order to write the appropriate equations, to know the expressions for two scalar magnitudes, namely the convolutions of the tensors constituted by the matrix elements of interaction with the tensors constituted by the wave vector components of the interacting waves. Explicit expressions were found for these magnitudes and so obtained equations describing the induced scattering on particles of waves belonging to the various transparency regions that exist in magnetoactive plasma. By making a number of specific assumptions regarding the initial energy distribution and the frequency ratios of the interacting waves, estimates were obtained of the interaction times. Thanks to their symmetry properties, the explicit form of the kernels of integro-differential equations for the energies of interacting waves makes it possible to judge whether wave energy is being conserved in the particular approximation under consideration. The situation in this respect is in many ways similar to the case of an isotropic plasma. The equations for nonlinear interaction of electromagnetic waves in a magnetoactive plasma were used to calculate the cross sections for the induced scattering of these waves on the plasma particles. The results were not averaged with respect to wave polarization. (auth)

30630 INSTABILITIES IN A CYLINDRICAL INHOMOGENEOUS PLASMA ON THE BASIS OF THE VLASOV EQUATION. Rebut, P. H. (Centre d'Etudes Nucleaires de Fontenay-aux-Roses, Seine, France). pp 721-33 of STI-PUB-111(Vol.1). (In French).

Instabilities in cylindrical rotational geometry in an inhomogeneous medium are investigated on the basis of the Vlasov equations. The approach is similar to that of Mikhailovsky (perturbation in space of the first integrals of the unperturbed motion), and allows one to bring out some general properties of the marginal modes. By applying this method to the special case of the quasi-electrostatic instabilities it is possible to define the various unstable regions, and to unite in a single equation instabilities of such different aspect as the "flute," the "universal" and the "beam" type instabilities. The stabilizing influence of various parameters, such as the curvature, the "shear" and the large Larmor radii, is demonstrated. (auth)

30631 DRIFT INSTABILITIES AND ELECTRON CYCLOTRON OSCILLATIONS FOR ARBITRARY PLASMA PRESSURE. Krall, N. A.; Pearlstein, L. D. (General Atomic Div., General Dynamics Corp., San Diego, Calif.). pp 735-46 of STI-PUB-www(Vol. 1).

Most of the familiar drift instabilities (flute, universal, etc.) were calculated in the limit β = (plasma pressure)/(magnetic pressure) = 0. In this limit the perturbed electric field is electrostatic, and the Vlasov equation is remarkably simplified. The β limit for validity of the electrostatic approximation depends on the particular mode considered and many present experiments fall outside the range. Two well-known low frequency drift instabilities are examined at arbitrary β; the zero-β regime is determined and stability criteria for larger values of β are derived. In addition, the influence of finite β on radiation at the electron cyclotron harmonics is examined. The finite Larmor radius (R) flute instability driven by mirror type curvature of the magnetic field is considered first. The lowest order's ominously large contribution, inversely proportional to R^2, cancels to all orders of β. The leading terms are then independent of R, and are included in the eigenvalue problem; stability criteria are obtained for various ranges of β. Next the universal instability, $\vec{E}$ = Perturbed = $\vec{E}$ (exp $ik_\perp r_\perp$)(exp $ik_{||} r_{||}$), in a uniform magnetic field $\vec{B} = B_0 \hat{i}_{||}$ is considered, with field curvature simulated by a fictitious gravity. Here the zero-β limit is dependent upon wavelengths. If β < (electron mass)/(ion mass), or if $\beta < (k_{||} r_p)^2$ where r_p = plasma radius and $1/k_{||} \geq$ plasma length, the zero-β limit obtains. Since the instability only exists for $(k_{||} r_p)^2 < 0.01$, a modest plasma pressure violates the zero-β limit. The eigenvalue for $\beta > (k_{||} r_p)^2$ is calculated and conditions for cusp stabilization as well as mirror destabilization are obtained. The dominant high frequency nonrelativistic modes of the stable zero-β plasma are longitudinal waves at electron gyrofrequency harmonics. If excited these modes can radiate only if coupled to transverse waves; in zero-β this coupling occurs at a surface or at a local inhomogeneity. Since a prominent effect of finite β is to couple longitudinal and transverse waves, the spectrum and coupling of electron cyclotron oscillations is calculated for arbitrary β. (auth)

30632 PLASMA PRODUCED BY NEUTRAL INJECTION INTO A MAGNETIC MIRROR/WELL GEOMETRY. Bernstein, W.; Chechkin, V. V.; Kuo, L. G.; Murphy, E. G.; Petravic, M.; Riviere, A. C.; Sweetman, D. R. (Culham Lab., United Kingdom Atomic Energy Authority, Abingdon, Eng.). pp 23-44 of STI-PUB-111(Vol.2).

In the PHOENIX IA experiment an 8 mA equivalent, 20 kev H^0 beam is ionized by Lorentz $\vec{v} \times \vec{B}$ field to produce a plasma in simple mirror geometry. In the PHOENIX II experiment a beam of up to 35 mA equivalent at 20 kev is used to produce a plasma in magnetic well geometry formed by combining a mirror and l = 2 stabilizing field. The observations in simple mirror geometry are summarized. An m = 1 hydromagnetic drift instability limits the plasma density to about 3×10^8 particles/cm^3. In addition there are bursts of high frequency oscillation which begin at the ion cyclotron frequency corresponding to the central magnetic field and then drop both in amplitude and frequency, the latter falling by about 5% in a typical case. During these bursts, the ion energy is spread dramatically. The possibility of additional ion loss by scattering into the loss cones cannot be excluded. In the magnetic well condition, the drift instability is absent and there is no evidence for plasma loss by process other than charge exchange. A density an order of magnitude higher than that in the simple mirror case was reached and appears to be limited only by technological considerations. In the well condition the high frequency instability is smaller in amplitude and more intermittent. There is a scatter in frequency, the predominant emission being at the central field ion cyclotron frequency and a value 2.5 to 3.0 Mc/s above. Higher harmonics also appear and at the highest density achieved the emission is predominantly second harmonic. The ion energy spread is considerably less than that in the simple mirror geometry. Complex phenomena occur during the transition from simple mirror to magnetic well geometry. These are discussed in terms of the changes of precessional drift behavior of the ions. The emission of fast neutral atoms from charge exchange of plasma ions is observed with a collimated detector in the median plane. This emission is found to be anomalously high at high plasma density. Several explanations of this effect are under investigation. One possibility is that ionization and consequent trapping of the incident beam by the plasma may be significant. The cross section for this process derived from the observed emission is not inconsistent with known data. (auth)

30633 PRODUCTION OF A HOT PLASMA IN OGRA-II BY THE INJECTION OF FAST HYDROGEN ATOMS INTO A MAGNETIC TRAP. Artemenkov, L. I.; Vasil'ev, R. P.; Galkin, I. V.; (and others) (I. V. Kurchatov Inst., Moscow). pp 45-66 of STI-PUB-111(Vol.2). (In Russian).

The results are presented of plasma production by injecting fast hydrogen atoms into a magnetic mirror trap with a stabilizing hexagonal field. The experiments were carried out at a residual gas pressure of approximately 2×10^{-9} torr and an injected atom stream of up to 15 to 20 mA (equivalent). The duration of the injection was 1.5 s, the energy of the fast atoms was 75 kev, the strength of the main field at the center of the trap was 10 kG, and the mirror ratio was 1.44. The radial mirror ratio varied between 0.95 and 1.15. When the stabilizing field was switched off, a plasma with density limited by non-gas losses to approximately 5×10^6 cm^{-3} accumulated in the trap. In this process the signals from all the detectors undergo sharp fluctuations, low-frequency oscillations are recorded in the plasma at frequencies of 15 to 20 Kc/s and intense radiation, lasting for several seconds after injection has ceased, is observed at the ion cyclotron frequency, 15.5 Mc/s, and at its first harmonic, 31 Mc/s. The energy distribution of the ions confined in the trap is strongly broadened in the direction of higher energies. After injection has ceased the plasma decays non-exponentially: rapid fall-offs and long tails are observed with time constants from 30 to 50 and from 300 to 400 ms, respectively. When the stabilizing field is switched on the oscillograms become smooth while the cyclotron radiation becomes intermittent. Its frequency fluctuates in a random manner between 14 and 18 Mc/s and its amplitude falls by a factor of 30 to 100. The low-frequency oscillations, however, are not suppressed; their frequency falls to 4 to 7 Kc/s and they become irregular, but their amplitude decreases by a factor of only three. In this process there is no strong broadening of the energy distribution of the trapped ions, and the plasma decays exponentially with a gas time of up to 140 ms after injection has ceased. The density of the accumulated plasma is 3×10^7 for a volume of 50 l. From the results obtained no final conclusions can be drawn as to the occurrence of non-gas losses in this process. (auth)

30634 INJECTION OF IONS INTO A MAGNETIC MIRROR MACHINE (M.M.I.I.). Prevot, F.; Bariaud, A.; Dei-Cas, R.; Fumelli, M.; Girard, J. P.; Gourdon, C.; Sledziewski, Z.; Valckx, F. P. G. (Centre d'Etudes Nucleaires, Fontenay-aux-Roses, France). pp 135-51 of STI-PUB-111(Vol.2). (In French).

A plasma was formed by injecting the high-energy molecular ions H_2^+, dissociating them in the residual gas and accumulating them in a static simple magnetic mirror machine (10 kG at center, mirror ratio = 3). The ions were formed in an annular magnetron source of 1 m diameter located in the median plane of the machine. A typical value for the acceleration energy was 70 to 80 kev. The maximum injected current was 200 mA. Confinement times greater than 1 ms were observed for weak injected currents (6 mA). In all cases the measured confinement time was equal to the charge exchange time. The density of the confined fast protons increased in proportion to the injected current, reaching an average of 2×10^8 cm^{-3} in a volume of 700 cm^3. The radial density distribution, measured by the secondary ions formed in the neutral gas, agrees well with the theoretical distribution calculated from the ionic trajectories. The radiation observed at the fundamental and higher harmonics of the ion cyclotron frequency must be attributed to the injected beam, and not to the proton plasma. Within the limits of the experiment no instability, either flute or electrostatic, was detected as a result of the measurements carried out. Pos-

sible reasons for this are discussed. It is shown that the entrapment of the beam and the velocity distribution could be improved considerably by substituting oblique or conical injection, using a Störmer nozzle located near one of the mirrors, for purely transverse injection. Numerical results calculated for the trajectories of particles injected into a machine with a separation distance of 2 m between mirrors are presented. In these conditions the 150 trajectories chosen to represent a real beam have a mean capture length during entrapment, equal to 60 m. The losses are distributed uniformly between the mirrors and the entrance port. The velocities disperse very rapidly. The mean value of $v_{||}^2/v_{\perp}^2$ exceeds 0.5. (auth)

30635 STABILITY OF MIRROR MACHINES. Grad, H. (Courant Inst. of Mathematical Sciences, New York Univ., N. Y.). pp 161-75 of STI-PUB-111(Vol.2).

Stability of confined plasmas has been studied mostly with regard to the effect of variation of the containing magnetic fields, but the injected particle distribution is an equal partner and should also be subject to experimental control. It is found that stability of a guiding center plasma depends on the proper coordination of a field geometry with a particle distribution function. For example, one special distribution function is associated with "minimum B"; another requires "average minimum B"; but there also exist many practical particle distributions which are stable in much less severely constrained magnetic systems. (auth)

30636 INJECTION OF PLASMA BLOBS INTO A MIRROR TRAP WITH ADIABATIC PLASMA COMPRESSION: "ASPA" DEVICE. Babichev, A. P.; Buryak, E. M.; Gorbunova, E. F.; Karchevskii, A. I.; Muromkin, Yu. A. (Kurchatov Inst. of Atomic Energy, Moscow). pp 191-208 of STI-PUB-111(Vol.2). (In Russian).

The main features of the "Aspa" device, designed for studies of the adiabatic compression of plasma in a magnetic mirror trap, are described. The vacuum chamber is housed in a solenoid (4 m in length, 1 m in diameter) on whose axis there is a maximum quasi-stationary driving field of 5000 Oe. A titanium injector or coaxial plasma gun generates the deuterium plasma. The plasma blob is injected along the axis and enters the compression zone—a glass tube 10 cm in diameter. A pulsed mirror magnetic field is formed by two coils 20 cm apart (mirror ratio 1 : 2); the maximum pulsed mirror field is 40 kOe, its rise time approximately 40 μs and decay time 350 μs. The composition and energy distributions of the ion component of the plasma in the titanium and coaxial injectors were investigated by mass spectrometry. A microwave interferometer was used to measure the density of the plasma blob as it moved from the injector to the compression zone. The passage of the plasma blob through the magnetic mirrors at fields up to 20 kOe was also investigated. In some experiments the mirror field was parallel to the driving magnetic field, whereas in others it was anti-parallel; in other words a field of the diverter type, with two regions of zero field, was formed. For both the titanium and the coaxial injectors, the injected plasma blob penetrated comparatively freely the magnetic mirror that was parallel to the guiding magnetic field, whereas it hardly penetrated at all when the field was of the diverter type. The possibility was thus demonstrated of removing the heavy impurities from an injected blob by using a pulsed magnetic gate which forms regions of zero magnetic field and whose magnetic lines lead to the walls of the chamber. In provisional experiments on adiabatic plasma compression in a mirror trap, hard x-radiation (of 30 kev) was found and the effect of the initial magnetic field and the parameters of the plasma blob on the intensity and hardness of this radiation were investigated. (auth)

30637 EXPERIMENTAL STUDIES WITH THE ASTRON FACILITY. Briggs, R. J.; Christofilos, N.; Hester, R. E.; Lauer, E. J.; Weiss, P. B. (Univ. of California, Livermore). pp 211-25 of STI-PUB-111(Vol.2).

Astron experiments are being conducted by injecting very intense pulses of relativistic electrons into a cylindrical azimuthally-symmetric magnetic trap. The beam current is 100 to 120 A at approximately 4 Mev with 0.3-μsec pulse width. Approximately 30% of the injected (2×10^{14}) electrons are irreversibly trapped, forming a cylindrical layer of electrons, known as the E-layer, 60 cm in diameter, 300 to 400 cm in length. The circulating current is in excess of 1000 A and its density is 3 to 4 A cm^{-1}. During the first 100 μsec of the electron confinement time, approximately 50% of the initially trapped particles are lost. The remaining fraction of the electrons are trapped for a lifetime of several milliseconds. If the electrons are injected in eccentric orbits, the E-layer precesses at a frequency $\omega = (n\omega_c/2)$ where ω_c is the cyclotron frequency and $n = (R\partial B/B\partial r)$ is the average value of the field index experienced by the electrons. The oscillations usually damp out at a rate faster than the loss rate of the trapped electrons. The observation that the frequency of the precession is discrete and its phase is constant along a generatrix of the electron cylinder leads to the conclusion that the E-layer behaves like a rigid coil. The self-field radial gradient of the E-layer is much high than the vacuum guide field gradient; thus a "minimum B" configuration is created. When the circulating current fa to a level where the two field gradients are approximately equal and opposite the particles are promptly lost. Injection of a sequence of pulses at a repetition rate of 360 pps has achieved "overlap" of the pulses and resulted in increased trapping efficiency at low pressures (for example 6×10^{-4} torr H_2). A slow buildup of the current density, approximately 1.8 A cm^{-1}, and mean particle lifetimes of 5 to 6 msec were achieved. No destructive velocity-space instabilities were observed to date. While the present rate of injection limits the buildup of the E-layer modifications of the accelerator were undertaken to provide an injection rate of 1440 pps in a sequence of 10 pulses, followed by continuous operation at 60 pps. (auth)

30638 PLASMA WITH RELATIVISTIC ELECTRONS IN A MAGNETIC MIRROR TRAP. Budker, G. I.; Voloso V. I.; Moiseev, S. S.; Pal'chikov, V. E.; Tsel'nik, F. A. (Nuclear Physics Inst., Novosibirsk, USSR). pp 245-58 of STI-PUB-111(Vol.2). (In Russian).

The possibility is discussed of using a plasma with relativistic electrons in magnetic mirror traps. Uniform filling of the trap with particles without resorting to special E-layer magnetic field configurations is assumed. In a similar system the relativistic electrons are used to stabilize the plasma and to heat the ion component. The principal characteristics of a similar system are investigated, such as the elimination of instabilities, the mechanism of heating the ions using the electron energy, the contributions of different types of radiation towards energy losses, the specific instabilities associated with the injection of fast neutrons into the trap. The stabilization arising from relativistic electrons with an energy γmc^2 grows as γ increases for all instability types investigated, and this combines with an improvement in the density criterion in the region of onset of the instability and in the growth rate of the instability. Heating the ions in the electric field of the electron space charge seems to be the most effective method in a system with pulsed electron injection. The special features of this heating mechanism are considered. Estimates indicate that the mechanism for heating the ion component, considered previously in the Astron project, that is, the heating first of the slow electrons and then, using these electrons, of the ion component, is much less effective. When using a plasma of this type to produce a controlled thermonuclear reaction, the mechanism is already uneconomical under steady-state conditions for $\gamma \geq 2$ to 5, owing to the strong magnetic bremsstrahlung. Probably the most interesting practical application of a system using relativistic electrons is, therefore, fast pulsed heating of the plasma ions, other methods being necessary for the further stabilization of the plasma. In producing a similar plasma, difficulties also arise because it is necessary to use beams of monokinetic electrons, which inevitably leads to the development of beam-type instabilities in the trap at relatively small

electron densities. Results are indicated of experiments showing limitation of the electron densities in the trap at densities corresponding to the threshold of development of this instability. (auth)

30639 INTER-DIFFUSION OF PLASMA AND MAGNETIC FIELDS IN PINCH AND HARDCORE DISCHARGES. Reynolds, P.; Lees, D. J.; Bickerton, R. J.; Hardcastle, R. A.; Wetherell, A. T.; White, B. M. (Culham Lab., United Kingdom Atomic Energy Authority, Abingdon, Eng.). pp 279-89 of STI-PUB-111(Vol.2).

The inter-diffusion of plasma and magnetic field is studied in pinch and hardcore discharges in a large bore, linear discharge tube (TIBER). The variation with magnetic field configuration, initial pressure, peak current, pre-heat conditions and rise time is found. The rapid ("anomalous") field diffusion found in the pinch case is due to a hydromagnetic rather than an electrostatic instability. (auth)

30640 PLASMA EQUILIBRIUM IN A TORUS WITH HIGH-FREQUENCY FIELDS AND PLASMA HEATING RESULTING FROM THE DEVELOPMENT OF A POWERFUL BEAM OF "ESCAPING ELECTRONS". Demirkhanov, R. A.; Kirov, A. G.; Stotland, M. A.; Malykh, N. I.; Khorasanov, G. P.; Vishnevskii, N. K.; Gutkin, T. I.; Yampol'skii, I. R. (Inst. of Physics and Tech., Sukhumi, USSR). pp 327-43 of STI-PUB-111(Vol.2). (In Russian).

Experiments conducted on the "RT-0" apparatus are described. It consists of a torus with large diameter 100 cm and with small diameter 10 cm. A toroidal magnetic field about 6 kOe is established along the chamber. The plasma is ignited at $\geq 5 \times 10^{-4}$ torr by means of a longitudinal rotating electric field of f = 8.3 Mc/s. Rotating around the small diameter is a high-frequency (540 kc/s) quadrupole field with H_φ = 200 Oe at the chamber walls. When the low-induction capacitor bank is discharged on the loops located along the torus, a damped vortical electric field with maximum strength E_z = 200 v cm^{-1} and with half-period about 1 μs may be generated within the chamber. The purposes of the experiments were: (1) To explain the equilibrium and stabilization of plasma in a quasi-constant toroidal magnetic field by using rotating multipole high-frequency fields, on the assumption that the toroidal drift force, equal to ~(r/R)nkt, must be compensated by the electromagnetic wave pressure $^2H/8\pi$; and (2) To study the heating of plasma resulting from dissipation of the "beam" instability produced by a powerful beam of "escaping electrons" when the electric fields in the plasma are characterized by $E_z \gg E_c$. The apparatus was used to carry out: (a) Microwave measurements of plasma density, by using an interferometer of wave length λ = 2 mm, and observation of the plasma boundary by the reflected signal on the wave λ = 17 mm; (b) Recording of the behavior of the H_β line in time and scanning of plasma luminescence in time, by using a photoelectric converter; (c) Measurement of the total intensity of the x-radiation in time, by using a scintillation counter; (d) Measurement of the current in the plasma and of the voltage in the bypass. The results show that a high-frequency igniting field of 8.3 Mc/s creates a plasma touching the walls with an average electron density 0.5 to 1×10^{13} cm^{-3} and an electron temperature of the order of a few ev. When a rotating quadrupole high-frequency field is applied, the plasma is forced away from the walls and is localized in the center with an increase in temperature. Attention was also paid to heating by a strong electric field in the absence of a rotating high-frequency quadrupole field. In this case, when the electric field is E_z = 100 to 200 v cm^{-1}, a current J_P = 3 to 5 kA is developed in the plasma; on being strongly damped, this current becomes essentially ohmic in character. At the same time the voltage in the bypass is very strongly damped in comparison with the inactive condition, which indicates effective absorption of the loop energy by the plasma. The energy absorbed by the plasma during the first half-cycle of the current, that is, during about 1 μs, represents about 20 J, and the conductivity of the plasma is anomalously low. When the heating is performed by a strong electric field, an intensive burst of x-radiation with an energy of the order of 100 kev is observed, together with the emission of microwave noises at frequencies close to that of the plasma. (auth)

30641 HOLLOW DYNAMIC PINCH. Maisonnier, Ch.; Haegi, M.; Linhart, J. G. (Comitato Nazionale per l'Energia Nucleare, Frascati, Italy). pp 345-65 of STI-PUB-111(Vol.2).

With the aim of producing very high densities and eventually high temperatures, a hollow linear z pinch of medium size (50 kJ) was built. The initial plasma is obtained by very fast volatilization and ionization of an annular cylindrical shell of $LiAlH_4$ powder that is electrostatically injected. The collapse is symmetrical and the diameter is up to 30 times smaller than the initial diameter. The experimental results, including x-ray and neutron measurements, are discussed; a coherent model is found which explains the main features of the discharge. (auth)

30642 PHENOMENA ASSOCIATED WITH THE BUILDUP OF A NON-CYLINDRICAL FOCUSSED Z PINCH. Filippov, N. V.; Filippova, T. I. (Kurchatov Inst. of Atomic Energy, Moscow). pp 405-16 of STI-PUB-111(Vol.2). (In Russian).

Further investigations of the central region of a discharge in deuterium in a discharge vessel with metallic walls were carried out on a pinch device using a 180-μF capacitor bank. The velocities of the plasma sheath (up to 4×10^7 cm/sec) were determined by streak photography using a slit aperture and by a new technique based on the modulation of the x-rays emitted by the electrode. The quantity (more than 10^{14}) and hardness (100 to 300 kev) of the radiation increases as the intial pressure decreases, while the neutron radiation is inversely dependent with a maximum at p = 1.2 torr. Neutron time of flight measurements showed that, in spite of the axial anisotropy of the velocity, the number of neutrons was virtually independent of this effect. A moving "boiler" mechanism is proposed to explain these facts. A two percent addition of xenon to the deuterium stabilized and increased the neutron yield and the intensity of the soft x-rays. From the splitting of the electrode and away from the discharge, the plasma energy at the focal point of compression was estimated to be ~100 kJ/cm^3, or nT = 10^{23} to 10^{24} ev · cm^{-3}. At a temperature of 1 to 3 kev typical for such discharges, this energy contact corresponds to a plasma concentration of (1 to 3) · 10^{20} cm^{-3} or to pinch radii less than 0.5 mm. (auth)

30643 DENSE PLASMA PRODUCED BY A CUSP INJECTION. Ito, H.; Ishimura, T.; Hirano, K.; Ozaki, A.; Shinano, K.; Goto, S. (Osaka Univ.). pp 419-26 of STI-PUB-111(Vol.2).

Experimental measurements were carried out on the injection of dense plasmas of hydrogen and deuterium into a biconical cusp field by using a plasma gun. In an early stage of the experiment, a simple straight glass cylinder was the vacuum vessel to permit direct observation of the plasma. The axial velocity of the top of the hydrogen plasma measured by a streak camera was larger than 1×10^7 cm/sec and sometimes attained 1×10^8 cm/sec in some conditions. The occurrence of some irreversible process at the stage of plasma trapping was proved by streak pictures. In Kerr cell pictures, it was observed that the trapped plasma was stable and took a clear-cut shape limited by field lines. From the data obtained from the measurement of field variation, it was concluded that the plasma penetrated the entrance cusp at 4 kG magnetic field and was stopped in front of the exit cusp whose field intensity was 10 kG. The intensity of the entrance cusp is $^2/_5$ of that of the exit cusp in order to let the plasma enter easily. Although the magnetic disturbance continued for rather a short time, for example, 20 μsec, this was accidentally nearly the same time in which some macroscopic motion of the plasma existed while the magnetic bottle became full of plasma particles. More energetic injection of deuterium plasma is now going on using a vessel with a bell-shaped ring hump to include the strongest part of the ring cusp inside it. The spectral line profiles of D_β and D_γ were measured as they depend on time. The density of the plasma was estimated by applying some statistical theory of line broadening to these data. A few typical data denote that the peak value of

the density varies from (0.4 to 1) × 10^{16} ions/cm^3 according to changes in the working condition of the gun and these large values persist for about 100 μsec when the field intensity becomes large. The decay of the plasma is slow and it must be emphasized that the density in some conditions is still 1 × 10^{15} ions/cm^3, even 300 μsec after injection. (auth)

30644 CUSP INJECTION EXPERIMENT. Allen, T. K.; Cox, A. J.; Spalding, I. J. (Culham Lab., United Kingdom Atomic Energy Authority, Abingdon, Eng.). pp 427-48 of STI-PUB-111(Vol.2).

A brief survey is given of the characteristics of the $\beta = 1$ cusped configuration and the experimental techniques for establishing hot field-free cusped plasmas. Results from the cusp-compression experiments at the Culham Laboratory are summarized and it is concluded that wall and external plasma effects make it extremely difficult to obtain a cusp hole of size less than an ion gyro-diameter by the compression method. An injection technique is described in which hot field-free plasma is transferred from a conical theta-pinch gun through a uniform magnetic guide field into a cusped field region where directed energy is randomized by collision with counter-streaming plasma. Experimental results are presented on gun development, on the injection of plasma into guide fields and on the stability of flow of plasma "spears" along guide fields. Preliminary measurements on plasma trapping in a cusped region are reported. Experiments on the collision of plasmas in guide field and zero field show the importance of very low magnitude trapped magnetic fields in causing strong interaction and randomization of directed energy. The study of a magnetic mirror plasma formed by colliding plasma spears indicates that thermal conductivity may be the major energy loss process. (auth)

30645 FLUTE CHARACTERISTICS OF AND MICROWAVE EMISSION FROM A PLASMA IN A MIRROR. Scott, F. R.; Jensen, T. H.; Wharton, C. B. (General Atomic Div., General Dynamics Corp., San Diego, Calif.). pp 463-82 of STI-PUB-111(Vol.2).

A pulsed mirror was constructed to study the stability of a plasma of modest energy. The 70-ev plasma is piped from a gun to the mirror by a linear octopole guide field. The mirror field is turned on in a plasma transit time. Plasma densities of 10^{13} electrons/cm^3 are observed in the central plane of the mirror. Two distinct modes of operation are observed and depend only on conditions established in the guide field. In the first mode the plasma in the mirror appears flute stable, most of the plasma escapes axially, a slow anomalous radial diffusion is observed and microwave emission occurs at the electron cyclotron harmonics ranging from n = 1 to at least n = 19. The microwave emission is not compatible with the electron branch of the Harris instability. The stability of this mode is attributed to line tieing by cold plasma effusing from the guide field region. Densities above 10^{11} electrons/cm^3 were observed for 200 μsec in the region between the mirror and the guide field. With the addition of an axially symmetric cylinder in the guide field, this density is decreased. Measurements show plasma densities below 10^{11} cm^{-3} after 40 μsec in this region. The resulting plasma trapped in the mirror exhibits flute instabilities, radial plasma loss, intense erratic microwave emission and rapid density decay. The m = 1 flute is identified and its phase is followed through 4π. The phase velocity is in the direction of the electron B drift. The sign of this phase velocity may be explained by the theory of Krall if the electron energy exceeds the ion energy sufficiently. The addition of conducting plates in the downstream mirror region tempered the violence of the flute instability. This tempering depends only on the surface resistance of these plates. This effect was examined by measuring the frequency spectrum of signals from coated scintillator probes placed near the vacuum envelope. (auth)

30646 ACCELERATION AND REFLECTION OF PLASMA BY THE GRADIENTS OF HF AND STATIC MAGNETIC FIELDS AT THE ELECTRON CYCLOTRON RESONANCE. Consoli, T. (Centre d'Etudes Nucleaires, Saclay, France). pp 483-97 of STI-PUB-111(Vol.2). (In French).

A number of studies of the acceleration, reflection and accumulation of plasma by composite structures formed through the association of hf and static magnetic field gradients are summarized. In these structures the hf electromagnetic field is either a stationary transverse field (TE_{mn} mode) or a progressive field damped in the ionized medium as a result of the electron cyclotron resonance. The static magnetic field is itself the superposition of an inhomogeneous axial field in a magnetic bottle and a multipolar radial field. Three experimental arrangements designed to verify the acceleration, reflection and accumulation of plasma jets are described. The arrangements differ with respect to: type of field (damped progressive or stationary, TE_{mn} modes); power applied (continuous from 1 to 12 kw and pulsed for 100 μsec at 2 Mw); frequencies employed (K, S and L bands); energies and fluxes of beams thus obtained. The object of these different structures, which are designed to verify the scaling laws, is the same: to compare the systems having a stationary hf field with those having a progressive field; to permit axial injection of energetic plasma in a magnetic bottle; to eliminate losses at the mirrors; to confine the plasma accumulated by continuous or pulsed injection. The experimental results obtained in the asymmetric case with a single injector and in the symmetric case with an injector and reflector, and with stationary or damped progressive h-f fields are presented. (M.O.W.)

30647 MOTION OF PLASMOID IN A CURVILINEAR MAGNETIC FIELD. Voitsenya, V. S.; Gorbanyuk, A. G.; Onishchenko, I. N.; Safronov, B. G.; Khizhnyak, N. A.; Shkoda, V. V. (Physico-Technical Inst., Kharkov). pp 545-62 of STI-PUB-111(Vol.2). (In Russian).

The passage of a plasmoid through the magnetic field of a toroidal solenoid and its decontamination from heavy ion impurities were studied theoretically and experimentally. The theoretical analysis was carried out within the framework of a drift approximation. The passage of the plasma is achieved through the closing currents which Sinelnikov assumed to exist. The circuit-closing currents substantially reduce the polarization fields but, as calculations show, do not prevent the drift of heavy ions to the chamber walls. Even in dense plasma, in which $4\pi n_0 Mc^2/H_\theta^2 \gg 1$, the heavy-ion drift is governed by the same laws as in the single-particle approximation. More precise analysis of the field structure shows that, in addition to the polarization field perpendicular to the torus plane, there is a radial electric field directed towards the inner wall of the toroidal chamber. The magnitude of the polarization field is determined essentially by the shorting currents and measurement of the polarization fields therefore confirms indirectly the assumed existence of these currents. Earlier experiments showed that the measured polarization fields agree in order of magnitude with the theoretical predictions. The results of the experimental investigation of the passage and decontamination of fast plasmoids of high density ($n_0 > 10^{13}$ cm^{-3}, $4\pi n_0 Mc^2/H_\theta^2 \approx 5 \times 10^3 \gg 1$) are discussed. A coaxial source with a pulsed gas inlet was used to obtain the plasmoids (1 cm^3 of hydrogen at atmospheric pressure). The 17-μF source bank was charged to 18 kv. After passing through the rectilinear section of the magnetic field (L = 150 cm) the plasma entered the toroidal magnetic field (radius of curvature, 75 cm; angle of deflection, approximately 90°). The magnitude of the pulsed magnetic field reached 10 kOe and remained virtually unchanged during the passage of the plasma (T = 10 ms). A Thompson mass-spectrograph, a transit mass-analyzer, electric and high-frequency probes, calorimeters and a plasmascope were employed in the utilization of the plasmoids. On entry into the toroidal solenoid, the velocity of the plasma fronts of density $n_1 \sim 10^{12}$ cm^{-3} and $n_2 \sim 10^{13}$ cm^{-3} was 7×10^7 cm/s. By photometric measurement of the Thompson parabolas, the mean energy of the H^+ ions was found to exceed 3 kev, while impurities accounted for about 40%. The main impurities were carbon and oxygen ions and the ions of the electrode materials, and their mean energy was higher than that of the hydrogen ions. As the plasmoid moved along the toroidal solenoid,

the energy transferred by the plasma and the total number of charged particles decreased by factors of 5 and 3, respectively, for H = 8000 Oe; at the same time the fraction of fast particles in the H^+ ion spectrum declined and the mean energy fell to 2 or 2.5 kev. The velocity of the density front n_i remained unchanged, while that of the density front n_e fell to approximately 4×10^7 cm/s. The impurities in the fast plasmoid (mainly C^{2+} and O^{2+} ions) accounted for about 5%. The mean energy of the impurity ions passing through the toroidal field was approximately half the initial energy (after passing through the straight solenoid). (auth)

30648 CHARACTERISTICS AND PURIFICATION OF A PLASMA PRODUCED BY A COAXIAL GUN WITH ANNULAR PREIONIZATION. Deschamps, P.; Gravier, R.; Lasry, J.; Vernon, D. (Centre d'Etudes Nucleaires, Fontenay-aux-Roses, France). pp 563-74 of STI-PUB-111(Vol.2). (In French).

A coaxial gun using annular preionization and deuterium injection is described. Using a 2-μF, 22-kv condenser, an inverse-pinch preionizing discharge is struck between the two sections of the central electrode. A plasma ring is then accelerated by striking another discharge between one section of the central electrode and the external electrode, using a condenser bank with low inductance (9 to 18 μF). The plasma gun may be located in an axial magnetic field. By varying the system parameters the characteristics of the fast diamagnetic component of the plasma can be varied within the following (not limiting) regions: mean directed energy, 10 to 40 kev; density, 0.4 to 3×10^{13} ions/cm^3; total number of ions, 0.5 to 6×10^{17}; mean transverse energy, several kev. The plasma is purified (removal of neutrals and heavy ions) by the following methods: it is injected parallel to the tube axis into a metal tube of length 1 m. This tube has two identical oppositely curved end sections, each extending over 1/8 of the circumference (radius of curvature 1 m), followed by a straight section 1 m long whose axis is parallel to that of the injected beam. The diameter of all sections is 30 cm. The maximum longitudinal magnetic field is 10 kG. This configuration was designed to allow the plasma to follow the curvature of the field. The effect of the oppositely directed electric fields set up by the drift of the particles in the curved sections can in fact be compensated by the current flow along the lines of force. Efficient purification of the fastest plasma portion was demonstrated by using a field of 2.5 kG. (auth)

30649 PLASMA-COLUMN EQUILIBRIUM IN TOKAMAK-5. Mukhovatcv, V. S. (I. V. Kurchatov Inst., Moscow). pp 577-93 of STI-PUB-111(Vol.2). (In Russian).

An investigation was made of the conditions of equilibrium of the plasma column in Tokamak-5. This equipment has the following parameters: large radius of the copper casing R = 62.5 cm, small radius b = 25 cm, small radius of the liner = 20 cm, radius of the opening in the diaphragm = 15 cm (the center of the opening in the diaphragm and the center of the cross section of the casing coincide), intensity of the longitudinal magnetic field B_0 = 6 to 12 kOe and current in the plasma J = 15 to 20 kA. The tests were carried out at an initial hydrogen pressure of (1.8 to 5.0) $\times$ 10^{-4} torr. Between the casing and the liner were placed conductors, used to set up within the chamber a transverse magnetic field B_z varying synchronously with the discharge current. Grigorovich and Mukhovatov had demonstrated qualitative agreement of experimental results with the hypothesis that the column is maintained in equilibrium by the copper casing, and had shown that the average electrical conductivity of the plasma over the cross section of the column reaches its maximum if by means of the transverse field B_z the column is arranged concentrically with the opening in the diaphragm. It is shown that in most discharge regimes there is good quantitative agreement between the experimental data and the theory of column equilibrium within the conducting casing. However, in a number of discharge regimes (with low initial gas pressures and high values of displacement $\Delta_B = b^2 B_z c/2J$ directed towards the inner wall of the torus) there is a certain discrepancy between theory and experiment. An attempt was made to assess to what extent the process of cutting off drift current by the conducting diaphragm contributes to maintaining equilibrium of the column in Tokamak. For this purpose the diaphragm was cut into six segments isolated from each other. During a discharge at $B_z = 0$, a polarized voltage appeared between the upper and lower segments; this was almost one order of magnitude higher than the electron temperature calculated from the average electrical conductivity of the plasma. At the optimum value of B_z the potential difference was close to zero, and changed its sign with further increase in B_z. A similar dependence on B_z was observed for the currents flowing between the segments when they were connected by low resistance. Connecting all the segments together did not lead to any noticeable change in the displacement of the column or in the other characteristics of the discharge. The current measured between the segments remained insufficient to explain the discrepancy mentioned above, the more so since the latter also occurred when the segments were isolated. The possible causes of this discrepancy are discussed, together with the reasons for the high potential difference between the segments. (auth)

30650 JOULE HEATING OF PLASMA IN THE TOROIDAL TOKAMAK-3 DEVICE. Artsimovich, L. A.; Afrosimov, V. V.; Gladovskii, I. P.; Mirnov, S. V.; Petrov, M. P.; Strelkov, V. S. (I. V. Kurchatov Inst., Moscow). pp 595-616 of STI-PUB-111(Vol.2). (In Russian).

In Tokamak-3, a hydrogen plasma is formed and heated by an annular electric current of 40 to 60 kA. The time of current flow is 20 to 30 ms. The bulk of the experiments was performed with a 25-kOe stabilizing longitudinal magnetic field. The transverse component of the stray magnetic field was compensated for by using special correcting loops. In the course of the discharge there was no appreciable displacement of the center of the column from the equatorial plane of the torus, and a plasma-column drift "to the outside" (increase of the large radius of the loop) was observed. This motion can be caused by a charge in the radius of the current column, by plasma heating or by the damping of the Foucault currents in the conducting vessel. A macroscopically stable plasma column was obtained in Tokamak-3 under these conditions, but the plasma temperature was lower than should be expected for the case with no anomalous energy losses. The interaction processes between the plasma column and the diaphragm must lead to large energy losses. This interaction was attenuated by applying a diaphragm of special shape and by using the property of the column to shift to the outside in the course of the process. The problem of the investigations was to determine various plasma parameters under these conditions, including electron and ion temperatures. To determine the electron temperature from the change of plasma resistance, it is necessary to know the column-radius changes with time, as well as the electric characteristics of the column. By using a computer to solve a set of equations, including the electrical engineering and the equilibrium equations, one can determine the time-dependence of changes in plasma temperature and density and also in the radius and displacement of the plasma column, making use of experimentally measured time-dependencies of plasma current, voltage and magnetic probe and radio-interferometer signals. The computed temperature function increases during the process and reaches 100 to 200 ev. Spectroscopic measurements of the electron temperature give values close to the computed values. The measured energy distributions of the fast neutral-atom flux fit in well with the assumption that the ion distribution of the plasma resembles a Maxwellian distribution of about 100 ev. A significant departure of this distribution from a Maxwellian is observed in the unstable discharge at the same moments as the characteristic plasma column instabilities. In addition, a perceptible difference is observed in the flux of neutrals from the "upper" and the "lower" portions of the column, which can be explained by ion drift fluxes inside the column that have large transverse velocities. (auth)

30651 HIGHER-MODE INSTABILITIES IN A TOKAMAK DEVICE. Vinogradova, N. D.; Razumova, K. A. (I. V.

Kurchatov Inst., Moscow). pp 617-27 of STI-PUB-111(Vol. 2). (In Russian).

As indicated in previous publications, so-called "stable" regimes (that is, regimes without variations in the integral discharge characteristics—current, bypass voltage, etc.) can be attained in a Tokamak device if optimum parameters are selected. An investigation was made to consider whether magnetohydrodynamic instabilities exist in such regimes or whether they are suppressed up to the highest modes. The plasma column is investigated by streak photography, carried out both with all the visible light and by the light of the spectral lines of hydrogen. In the latter case, interferometric filters with a transmission band of 100 Å are set up in front of the objective lens of the recording instrument. A time resolution of 2 μs is used. Photography is carried out for a transverse section near the diaphragm that limits the plasma. In all the discharge regimes studied, the streak photographs showed a characteristic structure of luminous bands that moved across the plasma column. Comparisons of the photographs taken through the side and lower ports justify the conclusion that the luminous bands are rotating around the discharge axis. In "stable" regimes the bands on the streak photographs resemble a many-turn screw with variable pitch. The relationship between the radius of the screw, the current flowing through the plasma and the strength of the longitudinal magnetic field indicates that this formation is an instability which has developed, with a mode number equal to the number of turns in the screw. A more complicated structure, corresponding to the simultaneous presence of several different modes, may be observed in various regimes. As the experiment shows, high and low unstable modes present at the same time may rotate around the discharge axis in opposite directions. The speed of rotation of the luminous bands changes during discharge, the linear velocity reaching in some cases several times 10^6 cm/s. The appearance of sharp variations in the voltage oscillograms corresponds to the appearance of bright rotating bands on the radius close to the internal radius of the diaphragm. (auth)

30652 ELECTRON DENSITY IN TOKAMAK DEVICES BY THE MICROWAVE METHOD. Gorbunov, E. P. (I. V. Kurchatov Inst., Moscow). pp 629-46 of STI-PUB-111 (Vol.2). (In Russian).

Four years of experiments with the T-2 toroidal device have shown that the electrons leave the plasma with abnormal rapidity. Subsequent tests showed that this abnormally rapid departure may be linked with the breakdown of equilibrium of the plasma loop within the discharge chamber. The microwave interferometer, used to measure electron density, records changes in phase of a wave passing through the plasma. This phase shift is proportional in the linear approximation to the product of the range of the radiowaves in the plasma (the chord length in the cylindrical or toroidal case with transverse probing) and the electron density $\bar{n}_e$ averaged over this range d. Change in the equilibrium position of the plasma loop relative to the probing beam may change the chord length. The effect of "cutting-off" by the diaphragm may lead to a reduction in the small radius of the plasma loop a. In such cases probing of the plasma at one point of its cross section allows determination only of $\bar{n}_e \times d$. To determine n_e, it is necessary to know the value of a at each moment and the position of the axis of the plasma loop relative to the center of the chamber Δ. The present work used the method of probing at several points of the cross section of the plasma column, which makes it possible to determine these values. The values of Δ and a are compared with those for displacement of the center of the current, as calculated from magnetic probe data, and for the radius, as determined by solving the set of equilibrium equations and Ohm's law. In the working range of pressures, the electron density increases linearly with increase in the initial hydrogen pressure. The electron density decay time depends on the magnitude of the stabilizing longitudinal magnetic field, the equilibrium conditions of the plasma column and the state of the chamber walls. In work with hydrogen the maximum electron density is normally 30 to 50% of the initial concentration of hydrogen atoms. In macroscopically stable systems the electron density remains constant throughout the duration of the discharge (about 10 ms). However, the radiointerferometer allows determination only of the lifetime of the plasma, not of the average life of the separate particles. Particle lifetime was determined by two methods: The first determines the energy lifetime as calculated from the energy balance; the second uses the neutral gas pressure in the "jacket" surrounding the plasma column. (auth)

30653 PLASMA ENERGY LOSSES IN THE TOROIDAL CHAMBER TOKAMAK TM-2. Gorelik, L. L.; Razumova, K. A.; Sinitsyn, V. V. (I. V. Kurchatov Inst., Moscow). pp 647-58 of STI-PUB-111(Vol.2). (In Russian).

Experimental results are given for the distribution of plasma energy losses along the liner surface together with experimental data on the basic components of these losses and on the energy balance during discharge. Measurements are carried out with a special bolometric probe, whose basic element is "three-layer" germanium bolometer. It can be set up at various distances from the liner surface and the energy losses due to charged particles studied by comparing bolometer readings (taking into account the solid angle) at two positions: at the liner surface and at a given distance from it (where the bolometer does not record the energies of the charged particles). If the plasma is macroscopically stable (there are no variations in the integral discharge characteristics) energy losses to the liner walls are caused by radiation and neutral particles. These losses are fairly uniformly distributed and make up 20 to 90% of the total losses, depending on circumstances. The remaining energy is lost mainly by being carried to the diaphragm by charged particles. Because of the radiation of impurities dislodged from the diaphragm the energy losses per unit liner surface are several times greater near the diaphragm than at points some distance from it. However, these additional losses are localized near the diaphragm and account for only a small proportion of the total losses (not more than 10%). At a hydrogen pressure $p_0 \sim 2 \times 10^{-4}$ torr ($T_e \sim 30$ to 50 ev) of the energy losses to the liner walls account for 30 to 40%, and at $p_0 \sim 10^{-3}$ torr ($T_e \sim 5$ ev) for 80 to 90% of the total. This was confirmed by measuring the energy lost through being carried directly to the diaphragm. At $p_0 \sim 10^{-3}$ torr up to 30% of the losses may be caused by neutral particles of low energy (up to 50 ev). At $p_0 \sim 2 \times 10^{-4}$ torr ($T_e \sim 50$ ev) energy losses due to neutral particles are considerably less. For an impurity content of up to 30% radiation losses do not account for more than 60%, in agreement with theoretical estimates. An increase is observed in radiation losses as the energy contribution per particle decreases. (auth)

30654 TOROIDAL DISCHARGE IN A VARYING LONGITUDINAL MAGNETIC FIELD. Ivanov, D. P.; Parfenov, D. S. (I. V. Kurchatov Inst., Moscow). pp 659-72 of STI-PUB-111(Vol.2). (In Russian).

Results are presented on the behavior of a current-carrying toroidal plasma column in a strong longitudinal magnetic field whose magnitude is varied (increased) considerably during discharge in order to constrict the plasma column and reduce its interaction with the walls of the discharge chamber. These experiments are a continuation of the work of Ivanov and Razumova and were carried out on Tokamak TM-1, which is similar in its dimensions and main parameters to the Tokamak TM-2. The large radius of its toroidal chamber is R = 40 cm and the small radius a = 10 cm. The discharge current is 9 to 15 kA and lasts 3.2 ms. It is found that the quasi-stationary stabilizing longitudinal magnetic field can vary by 8 kOe over a period of 1 ms at any time during discharge. The total magnetic field reaches 16 kOe. The discharge currrent, the bypass voltage and the displacement of the current column relative to the center of the cross-section of the discharge chamber are measured. In addition, a streak photograph is made of the luminescence of the cross-section of the discharge. Measurements are also made of the density with a microwave radiointerferometer on three channels located at various points

in the cross section of the plasma column. Discharge processes are attained in which plasma conductivity, displacement of the current column and density of the charged particles in the constant magnetic field are weakly dependent on the magnitude of the latter, beginning about 8 kOe. In such processes an increase in the magnetic field during discharge leads to a concentration of the current, the velocity of which is estimated by the jump in bypass voltage at the moment when the field begins to increase and by the change in the displacement of the current column. However, no substantial change in the density distribution over the plasma column cross section is observed, at least when the magnetic field H/H is increasing at rates not in excess of 10^3 s^{-1}. Possible explanations of this plasma behavior are discussed. (auth)

30655 CRYOGENIC MAGNETIC TRAP VGL-2. Borovik, E. S.; Busol, F. I.; Glasov, B. V.; Kovalenko, V. A.; Skibenko, E. I.; Yuferov, V. B. (Physico-Technical Inst., Kharkov). pp 705-18 of STI-PUB-111(Vol.2). (In Russian).

A magnetic trap with strong magnetic field is described whose distinguishing feature is the consistent use of cryogenic techniques in solving the basic technological problems. Calculations performed in connection with the problem of filling the trap with plasma are discussed and data on the parameters of the plasma which is formed through the injection of 30-kev hydrogen atoms are given. The application of cryogenic techniques in creating the VGL-2 trap requires investigation of: solenoids without iron cores, cooled to 78° or 20°K for obtaining strong magnetic fields of long duration; helium and hydrogen condensation pumps for creating and maintaining an ultra high vacuum; ultrasonic jets for creating a charge-exchange target in the fast hydrogen atom injector. Calculations are carried out for filling the VGL-2 trap with plasma by injecting a beam of hydrogen atoms with an energy of 30 kev. If it is assumed that the fraction of atoms captured in the trap as a result of Lorentz ionization amounts to 5×10^{-4}, then at a system pressure of 1×10^{-9} torr, the required differentials can be obtained with an injection "current" of only about 20 mA. The results are given of initial plasma accumulation experiments. For an injection current of 0.3 to 0.5 mA a plasma is obtained whose density is about 3×10^7 cm^{-3} and whose lifetime after injection cut-off is about 5 ms. The measured lifetime corresponds approximately to the charge-exchange lifetime. (auth)

30656 COMPARISON OF ALKALI PLASMA LOSS RATES IN A STELLARATOR AND IN A TOROIDAL DEVICE WITH MINIMUM MEAN-B PROPERTIES. Eckhartt, D.; Von Gierke, G.; Grieger, G. (Max-Planck-Institut fuer Physik und Astrophysik, Munich). pp 719-31 of STI-PUB-111(Vol.2).

The confinement of toroidal low-β plasmas in the absence of ohmic heating currents was studied by using a thermal Cs plasma in a stellarator with l = 3 helical windings. These experiments gave evidence that the surfaces of constant pressure roughly coincided with the surfaces of constant magnitude of B, rather than being identical with the magnetic surfaces as would normally be expected for a stellarator in magnetohydrodynamic equilibrium. These experiments were extended to the stellarator with l = 2 windings which provide a constant rotational transform to all lines of force of the magnetic confining field. Secondary currents as well as macroscopic mass motions along the lines of force are required for equilibrium in a stellarator in which the confining field is mainly azimuthal in direction. In a toroidal device of azimuthal symmetry with a purely meridional magnetic field, however, equilibrium can be achieved without any currents of macroscopic motions along B. In addition, stability against flutes can be provided for low-β plasmas if $\nabla \oint dl/B$ is directed parallel to ∇p. A machine was constructed with the above-mentioned properties. It consists essentially of four current-carrying ring conductors immersed in the plasma (similar to the arrangement of Okhawa, et al.). The conductors are fed by direct currents in order to avoid azimuthally directed electric fields within the plasma. Plasma confinement in this device is studied by using thermal alkali plasmas which are produced by contact ionization. The operating conditions can be chosen so that plasma losses due to "classical" mechanisms (collisional diffusion to the walls and to the ring conductors, particle losses to the supports, volume recombination, etc.) became small compared to the high loss rates ascribed to "pump-out." Preliminary experimental results with the Wendelstein stellarator and with the octopole device indicate that in both arrangements the observed particle loss rates agree quite well with theoretical calculations in which resistive diffusion and surface recombination on supports was assumed. "Pump out" losses would yield particle loss rates one to two orders of magnitude larger than observed. (auth)

30657 INJECTION AND CONFINEMENT OF PLASMA IN A STELLARATOR WITH A MULTIPOLAR (l = 2) HELICAL FIELD. Akulina, D. K.; Batanov, G. M.; Berezhetskii, M. S.; Grebenshchikov, S. E.; Rabinovich, M. S.; Sbitinkova, I. S.; Shpigel, I. S. (Lebedev Inst. of Physics and Tech., Moscow). pp 733-49 of STI-PUB-111(Vol.2). (In Russian).

The results are given of external injection of plasma into a closed magnetic trap and on the investigation of the effect of helical fields on the maintenance of the plasma. The "L-I" apparatus consists of a toroidal magnetic trap of stellarator type with a continuous "double-thread" multipolar (l = 2) helical field. The large diameter of the torus is 120 cm and the diameter of the vacuum chamber section 10 cm. The maximum value of the longitudinal field H is 10^4 Oe. The magnetic field of the stellarator is variable in time, to enable a study of adiabatic heating of the plasma in a trap of this type. The L-I stellarator and low-energy electron beams were used to investigate the structure of the magnetic surfaces. The method made it possible to determine the existence and form of closed magnetic surfaces over a wide range of the ratio of the helical and longitudinal fields. Resonance perturbations of the magnetic surfaces were detected that led to splitting of the latter and the formation of rosettes. Magnetic measurements confirmed the theoretical postulates regarding the magnetic surfaces and the effect of perturbations in resonance and non-resonance cases. Filling of the trap with plasma was effected by injecting plasma jets from spark guns into the transverse magnetic field. The total number of charged particles generated at each injection was $\sim 5 \times 10^{14}$. Injection could be made both while the field was growing, with subsequent adiabatic compression of the plasma, and while the field was quasi-constant. Filling of the trap took place over a time of the order of tens of μs. The initial density of the plasma was $\sim 10^{11}$ cm^{-3}, and the electron temperature ~15 ev. The density of the plasma was measured by the resonance ultra-high-frequency method and its distribution over the section was determined by twin Langmuir probes. The experiments showed the effective influence of a helical field on plasma. In the absence of a helical field, the density distribution was non-symmetrical relative to the center of the chamber and the plasma drifted towards the external wall of the torus; its lifetime was the order of 100 to 200 μs. When a helical field was applied then density distribution was symmetrical about the axis of the chamber and was determined by the form of the magnetic surfaces; the constant of density fall-off time was ~1 to 2 ms. The measured lifetime of the plasma when the apparatus is working as a stellarator cannot be explained by conventional diffusion. The spectrum of oscillations in the plasma electric fields was studied, and the various mechanisms capable of explaining the anomalously high plasma diffusion rates were discussed. (auth)

30658 SCATTERING OF MICROWAVES BY TURBULENT PLASMA. Edwards, S. F.; Stott, P. E. (Univ. of Manchester, Eng. Culham Lab., United Kingdom Atomic Energy Authority, Abingdon, Eng.). pp 765-78 of STI-PUB-111(Vol.2).

A theory is presented to cover the microwave transmission through the turbulent plasma of the Zeta machine, which has fluctuations over a range λ_R of 0 to 10 cm with

low frequency, relative to the microwaves which have a wavelength λ of 1 to 2 mm. The electrons, at say 2.5×10^{14} cm^{-3} have a critical wavelength $\lambda_c = 2$ mm. There are then three lengths λ, λ_c, λ_R and their related magnitudes determine the appropriate theory; for example for $\lambda_R \ll \lambda$ one has wave diffraction, for $\lambda_R \gg \lambda$ geometrical optics. A new method is presented which is designed for the difficult and interesting case of $\lambda_R \sim \lambda \sim \lambda_c$ in which the use of the ratio of these lengths to the mean free path as expansion parameter is replaced by the assumption of the randomness of the fluctuations of the system. A Boltzmann equation is derived for the transport of radiation in which the kernel, analogous to the collision cross section of the usual Boltzmann equation, is derived by this generalization of the random phase approximation. Experimental results are available for the direct transmission and scattering of microwaves in Zeta, and these results are compared with the solution of the theory. (auth)

30659 PLASMA HEATING UNDER BEAM INSTABILITY CONDITIONS. Demirkanov, R. A.; Gevorkov, A. K.; Popov, A. F.; Khorasanov, G. L. (Inst. of Physics and Tech., Sukhumi, USSR). pp 801-13 of STI-PUB-111(Vol.2). (In Russian).

Results are discussed of the interaction of electron beams with a plasma in mirror magnetic fields and the heating of the electron and ion components of the plasma under beam instability conditions. The experiments were carried out in a mirror device with mirror ratio 1.5 and a maximum field of 1500 Oe at the center. An electron beam of 200 to 300 mA and energy up to 4 kev was injected continuously. Plasma was formed by the ionization of the gas (hydrogen or helium) filling the vessel at pressures of 10^{-4} to 10^{-5} torr. As a result of the interaction of the electron beam with the plasma, a broad spectrum of plasma and electromagnetic waves is excited in the system. The spectra of the high- and of the low-frequency oscillations in beam instability conditions were experimentally investigated. A broad spectrum of oscillations in the region of the plasma and cyclotron frequencies was observed. The results are described of the investigations of the systematic low-frequency oscillations excited in the region from 10 to 50 kc/s, and possible mechanisms responsible for the excitation of the oscillations are discussed. The observed absorption of the energy of the high-frequency oscillations in the region of the electron-cyclotron frequency and its harmonics is also considered. The interaction between the plasma particles and the fields of the oscillations excited in the system cause the directed energy of the beam to be transformed into thermal plasma energy. Intense x-radiation from the plasma region was recorded; from its energy distribution, the plasma electron temperature was determined of the order of 20 to 40 kev. The plasma density determined from the x-radiation power was $(1 \text{ to } 2) \times 10^{11}$ cm^{-3}. According to microwave measurements one obtains $n_e \sim (0.7 \text{ to } 1) \times 10^{-12}$ cm^{-3}. The heating of the plasma is also confirmed by spectrometric measurements of the electron temperature from the relative intensity of the helium lines. The ion temperature measured from the Doppler broadening of He(II) lines was of the order of 25 to 35 ev. The plasma containment time determined from the drop of the x-ray intensity with time agrees adequately with the collision times. Provisional results are also reported of investigations of the interaction of a powerful beam of electrons (beam current per pulse 10 to 20 A, beam energy order of 20 kev, pulse length 20 to 500 μs) with a highly ionized plasma injected into a magnetic mirror machine from a titanium plasma gun. The magnetic field at the center was ~5 Oe, at a mirror ratio of 2 to 3. (auth)

30660 PLASMA COMPRESSION BY A MAGNETIC FIELD IN A TOROIDAL-TYPE DEVICE. Golant, V. E.; Kaganskii, M. G.; Ovsyannikov, V. A. (A. F. Ioffe Physico-Technical Inst., Leningrad). pp 829-50 of STI-PUB-111 (Vol.2). (In Russian).

The Tuman device, a racetrack, was built to study the adiabatic compression of a plasma column by an external magnetic field increasing with time, and was designed to carry out two-stage heating of the plasma. Magnetic compression is preceded by ohmic heating of the plasma under conditions analogous to those for the operation of Tokamak. During ohmic heating the longitudinal magnetic field is essentially non-uniform. In the curved toroidal sections the maximum quasi-stationary magnetic field is approximately 40 kOe, and in the straight parts 1 to 2 kOe. The glass discharge chamber is a magnetic force tube, that is, its cross section in the curved sections is $1/20$th the cross section in the straight sections. The plasma must fill the force tube, whose dimensions are set by a diaphragm in the middle of the straight section and by the ratio of field intensities in the straight and curved sections. With this column configuration considerably more power can be introduced into the plasma than in a uniform torus. The plasma volume is approximately 15-l when the plasma column is 250 cm long. Compression must be carried out by increasing the longitudinal magnetic field in the straight sections to 30 kOe. The field build-up time may vary from 30 to 250 μs. The plasma must be compressed in the wide, straight sections to approximately the same cross section as in the curved sections. Compression reduces the volume of plasma by a factor of 10 to 20. All the tests were carried out with hydrogen at pressures from 1×10^{-3} to 5×10^{-2} torr. The toroidal discharge was excited by a transformer. The duration of ohmic heating was 300 μs. The current in the plasma did not normally exceed 1 to 2 kA. With a quasi-stationary magnetic field of 1 to 2 kOe in the curved sections, plasma is obtained with a conductivity of $(1 \text{ to } 2) \times 10^{14}$ esu. Measurements of the diamagnetic moment of the plasma and microwave measurements showed that when the magnetic field in the toroidal sections was increased to 1 or 2 kOe the degree of ionization rose rapidly to 60 or 90%. Preliminary tests were carried out on compressing the plasma with a compressing-field build-up time of 30 μs. On compression the diameter of the plasma column is reduced from 12 cm to 1 or 2 cm. When the quasi-stationary magnetic field in the curved sections is increased above 1 to 2 kOe the conductivity of the plasma decreases and the pulsation amplitude and frequency of the plasma current rise sharply. This effect is enhanced by reducing the pressure. Analysis shows that this is due to a transverse component of the magnetic field in the curved sections. Tests are at present being carried out on ohmic heating and compression of plasma in equipment with an improved magnetic field geometry. (auth)

30661 TURBULENT HEATING OF PLASMA BY A DIRECT-CURRENT DISCHARGE. Babykin, M. V.; Gavrin, P. P.; Zavoiskii, E. K.; Rudakov, L. I.; Skoryupin, V. A. (I. V. Kurchatov Inst., Moscow). pp 851-62 of STI-PUB-111(Vol.2). (In Russian).

Results are reported of experiments on the turbulent heating of plasma by a current from a direct discharge in a magnetic mirror trap. The adiabatic compression of the heated plasma was investigated as well as various other characteristics of the turbulent plasma. The magnetic field increased to 9 kOe in 1.75 msec. At fields of 0.5 to 9 kOe, the trap was filled with a deuterium plasma of density 10^{12} to 10^{13} cm^{-3} from titanium guns; simultaneously the end electrodes were connected to the capacitors for the direct discharge that was variously 0.2, 0.8, and 2.65 μF and at potentials of 10 to 30 kv. The onset of the discharge was timed to coincide with the collision of the plasma jets. The discharge was aperiodic to start with, had a slow current increase, and the oscillograms showed oscillations consistent with instability of the current. The resistance of the plasma determined from the plasma current and potential considerably exceeded the value calculated from the Coulomb collision time. It was 50 to 60 Ω at the outset, and dropped to a few tenths of an ohm as the trap became increasingly filled and the plasma temperature increased. The noise on the current oscillograms vanished, and the discharge became oscillatory. The duration of the aperiodic regime is determined by the time necessary for filling the trap. It follows from measurements of the potential distribution that up to the transition to the oscillatory regime the main potential drop occurs at the center of the trap, in the region of reduced density. In this region the current velocities are maximum and intense turbulence must develop

As a result the plasma develops an anomalous resistance and an appreciable part of the energy stored in the capacitor is absorbed. Intense noise radiation was observed in the range from 10^6 to 4×10^{10} c/s; the noise at very high frequencies persists for longer periods than the low-frequency noise on the current oscillograms. The instability, accordingly, persists even after transition to the oscillatory regime. The plasma temperature, determined from the hardness of the x-ray bremsstrahlung, was 5 to 10 kev. The density was determined by a microwave interferometer. The plasma pressure estimated from the diamagnetic effect was $\sim 10^{17}$ ev cm^{-3}. For $n \gtrsim 2 \times 10^{13}$ cm^{-3} this gives a temperature of ~5 kev, which agrees with other measurements. At a density of the heated plasma of less than 10^{13} cm^{-3} it is compressed adiabatically, remaining stable. The electron temperature after compression attains 200 kev. When the initial plasma density is increased its temperature after heating is lower and no compression occurs. A signal with frequency 3×10^8 c/s was passed through the plasma during the instability of the current. In a strongly turbulent plasma the thickness of the skin layer considerably exceeds c/ω_p and an interpretation of this phenomenon is put forward. The mechanism of plasma heating when there is a current instability is discussed. (auth)

30662 ION CYCLOTRON RESONANCE HEATING OF THE QP PLASMA. Matsuura, K.; Miyahara, A.; Sato, T.; Kuroda, T.; Masuzaki, M.; Fujiwaka, S.; Kojima, C.; Nagao, S. (Nagoya Univ., Japan). pp 863-76 of STI-PUB-111(Vol.2).

It is of importance for a plasma compression experiment to prepare a high temperature plasma that is as quiescent as possible before it is compressed by a magnetic field. Included are descriptions of some experiments of the ion cyclotron resonance heating and the adiabatic compression of plasma in the QP machine, which prepares a highly ionized steady state plasma in a magnetic field by preferentially eliminating the neutral particles from a partially ionized plasma in a PIG discharge. A rather dense plasma (up to 5×10^{12} particles/cm^3 at present) can be obtained in the heating section of the machine by the application of a magnetic field of mirror type in the PIG region that however has a zero field stagnation circle near the anode surface, quite similar to the field in a stellarator diverter at Princeton. A highly ionized and steady plasma stream thus obtained is heated by an induction coil of Stix type or by a pair of electrodes of spiral type at a frequency near the gyrofrequency ω_{ci} of the ions. The induction coil generates ion cyclotron waves whose wavelengths and accompanying magnetic fields are measured accurately by magnetic loops. The cyclotron damping of the waves in the beach field and the shifts of resonant frequencies according to the increase of the plasma density are observed to be as predicted by the theory. Ions in a low density plasma (less than 10^{10} particles/cm^3) are accelerated up to several hundred electron volts by applying through the electrode system an r-f electric field at the frequencies $\omega = n\omega_{ci}$ ($n = 1, 2, 3, \ldots$). However, an anomalous plasma loss was observed at these resonances. (auth)

30663 HEATING OF PLASMA ELECTRONS BY ULTRA-HIGH-FREQUENCY FIELDS IN AN ADIABATIC TRAP. Alikaev, V. V.; Glagolev, V. M.; Morozov, S. A. (I. V. Kurchatov Inst., Moscow). pp 877-99 of STI-PUB-111(Vol.2). (In Russian).

The heating of plasma electrons by ultra-high-frequency fields was investigated in a d-c magnetic field that could be varied for h-f electromagnetic-wave and for plasma-wave propagation. In the experiments the magnetic field was varied between 600 and 1200 Oe; the extreme values correspond to $\omega_H/\omega = \frac{1}{2}$ (parametric resonance) and $\omega_H/\omega = 1$ (electron-cyclotron resonance). The h-f fields in the resonator, excited by a ten-centimeter magnetron generator, were H_{01} oscillations. Along the resonator axis was a quartz tube, 25 mm in diameter, in which a plasma was created. The resonator was in the static field of an adiabatic trap parallel to the quartz-tube axis. In the interaction zone between the h-f field and the plasma, the static field remained practically uniform. Different gases were used at pressures from 10^{-4} to 10^{-3} torr, and the magnetron on-time varied from 10 to 1000 μsec. The h-f power that was scattered in the resonator changed from 30 to 200 kw. At the first stage of the discharge development, a plasma with a concentration of $\sim 10^{11}$ cm^{-3} appeared. Plasma concentration was measured with a uhf phasometer of wavelength 4 mm; the temperature was determined from plasma-diamagnetism measurements. At this stage of the discharge development one observed a slow increase of concentration and an almost constant signal from the magnetic field that was displaced by the plasma, in the course of 20 to 500 μsec (as a function of the initial neutral-gas pressure and the magnetic field). In spite of the low ionization ~1%, the electron temperature was ~400 ev. Simultaneously, a 30-kev roentgen radiation was recorded. Starting from a certain critical value, plasma concentration increased rapidly up to 10^{12} cm^{-3}, and simultaneously one observed an increase of the plasma pressure by several factors, which corresponded to a mean electron energy of 300 ev. The characteristic time for plasma-pressure fall-off in the adiabatic trap, measured after switching off the magnetron generator was 50 μsec. These observations indicate a fast plasma drift at the first stage of the discharge development, which disappears when the plasma concentration passes a certain critical value. After the passage, a plasma forms in the trap, with a velocity distribution that differs strongly from a Maxwellian distribution. The temperature and the concentration of the hot plasma component, which are found from the measurements of pressure fall-off and under the assumption of the coulombic nature of particle drift from the trap, amount to ~2 kev and $\sim 10^{11}$ cm^{-3}, respectively. (auth)

30664 HEATING OF A DENSE PLASMA IN A METALLIC CHAMBER. Shvets, O. M.; Tarasenko, V. F.; Ovchinnikov, S. S.; Tolok, V. T. (Physico-Technical Inst., Kharkov). pp 913-24 of STI-PUB-111(Vol.2). (In Russian).

Experiments are reported on h-f heating of a plasma in an installation consisting of a copper vacuum chamber into which aluminim-tipped feed electrodes are inserted from both ends along the axis. The electrodes are coupled to an h-f generator across an isolating capacitor. The chamber is located within a solenoid magnet that can be regulated smoothly within the range 0 to 2500 Oe. The field configuration was selected to meet the conditions necessary for generating and absorbing the ion-cyclotron waves (the region of maximum magnetic field gradient is at the center of the solenoid). A controlled leak maintains the hydrogen gas at a constant pressure in the range 10^{-4} to 10^{-2} torr. To produce a plasma which is detached from the chamber walls, an h-f discharge is used, because of the properties of the plasma the discharge creates a constant potential difference between the electrodes and the chamber. This leads to the appearance between the electrodes of electrons which oscillate along the force lines of the magnetic field and produce a high degree of ionization in the gas between the electrodes. A shaft of dense plasma, with diameter determined by the diameter of the electrodes, is formed on the axis of the vacuum chamber. The spectrum of the discharge radiation was investigated and the plasma density by the Stark broadening of the H_β line was estimated. The temperature of the plasma electrons was found from the intensity ratio of the singlet and triplet helium lines. The fluxes of fast neutron atoms formed during the charge-exchange of the hydrogen ions on the neutral gas and, with special probes, the transverse energies of the ions as a function of the magnetic field intensity and of other properties were measured. (auth)

30665 HOT-ICE EXPERIMENT. Ascoli-Bartoli, U.; De Michelis, C.; Mazzucato, E. (Comitato Nazionale per l'Energia Nucleare, Frascati, Italy). pp 941-51 of STI-PUB-111(Vol.2).

Plasma was produced by firing a giant-pulse laser onto a solid deuterium pellet. Time-resolved scattering of light, schlieren photography together with time-of-flight measurements have demonstrated a strong anisotropy in the plasma outburst. (auth)

30666 PRODUCTION OF ENERGETIC PLASMA BY LIGHT PULSES. Opower, H.; Press, W. (Technische Hochschule, Munich). Z. Naturforsch., 21a: 344-50(Mar. 1966). (In German).

Light pulses from a Q-switched laser with a peak power of 250 Mw and 3.5 joules were focussed on carbon and LiH targets in a vacuum chamber. A rapidly expanding plasma was formed by this means. The expansion velocities of the electrons and ions were nearly equal. By means of an electric field the electrons were drawn out of the plasma; the ions were detected in a Faraday box. From time-of-flight measurements particles with a maximum energy of 6.3 kev were found for the carbon targets and 1.7 kev for the LiH (average mass number = 4). The high values of the ion energies resulted from an energy transfer from the electrons to the ions during the expansion process. This energy transfer is explained by a simple electrostatic model. If the averaged ion energy is equally distributed to all particles of the plasma (electrons and ions), a mean energy of 340 ev per particle is obtained for a LiH target and 550 ev for a carbon target. These values are 5 times higher than the data previously reported. The number of expanding ions in a solid angle π is determined to be about 2×10^{15} in the case of LiH. The total kinetic energy of these ions is about 0.3 joules. It is hoped, that by an increase of the energy by a factor 4 and the use of a D–T mixture nuclear fusion reactions will be obtained. (auth)

30667 MULTISTAGE ACCELERATION AND HEATING OF PLASMA. Schindler, Heinrich (Siemens-Schuckertwerke AG, Erlangen, Ger.). Z. Naturforsch., 21a: 351-8 (Mar. 1966). (In German).

It was previously shown that with the help of a theta pinch in the symmetry plane of a cusp field a plasma acceleration and, with series circuits of two similar stages, a supplementary acceleration are possible. On a 3-stage installation suitable both for step acceleration and heating of plasma, the discharge was investigated. It was shown that the plasma properties can be varied in a wide range. The ejection velocities behind the individual stages are, according to the selection of the delay times, 0.5 to 1×10^7, 1.5 to 6×10^7, and 2×10^7 to 2×10^8 cm/sec. About 10^{17} to 10^{18} particles were accelerated per discharge. Their density in the guide field was between 10^{13} and 3×10^{15} cm^{-3}. Probe measurements in the vicinity of the cusp symmetry plane gave data on the characteristics of the acceleration processes. (tr-auth)

30668 QUANTIZATION OF AN ELECTROMAGNETIC FIELD IN A DISPERSIVE MEDIUM. Alekseev, A. I.; Nikitin, Yu. P. (Inst. of Engineering Physics, Moscow). Zh. Eksp. Teor. Fiz., 50: 915-25(Apr. 1966). (In Russian).

A free macroscopic electromagnetic field in a homogeneous transparent nonmagnetic dispersive anisotropic medium is quantized by taking into account all types of waves excited in the medium. The Green function and retarded Green function of the electromagnetic field are obtained. The radiation from an impurity atom in an anisotropic dispersive medium is determined on the basis of the method developed. Selection rules for emission of longitudinal quanta are derived. The probability of long wave emission of transverse and longitudinal quanta is calculated for an impurity molecule located in a homogeneous isotropic plasma with spatial dispersion. (auth)

30669 PARAMETRIC RESONANCE IN A PLASMA IN A MAGNETIC FIELD. Aliev, Yu. M.; Silin, V. P.; Watson, C. (Lebedev Inst. of Physics, Moscow). Zh. Eksp. Teor. Fiz., 50: 943-53(Apr. 1966). (In Russian).

A theory of the oscillations and stability of a plasma in high-frequency electric and stationary magnetic spatially homogeneous fields is developed. Small deviations of the state of the system from the ground state, in which, due to the presence of external fields, a relative motion of the electrons and ions occurs, are considered, using a kinetic equation with self-consistent interaction. A dispersion equation for determining the spectrum of potential oscillations of such a system is derived. The equation is solved for the case of a cold plasma. The frequency range of an external magnetic field in which the plasma is unstable is determined. Expressions for the increments of growing potential oscillations are obtained in the instability region. Since the characteristic oscillations of a plasma in a magnetic field occur only in a finite frequency range, the region of instability of a plasma with relatively large increments turns out to be much broader than in the case of a plasma without a magnetic field. The maximum value of the instability increment is plotted as a function of the external-field frequency. (auth)

30670 QUASILINEAR THEORY OF PLASMA CYCLOTRON INSTABILITY. Rowlands, J.; Shapiro, V. D.; Shevchenko, V. I. (Inst. of Physics and Technology, Academy of Sciences, Ukrainian SSR). Zh. Eksp. Teor. Fiz., 50: 979-93(Apr. 1966). (In Russian).

A solution of the quasilinear equations for cyclotron instability is obtained for the case of a one-dimensional spectrum of oscillations. The spectral density of the energy of the electromagnetic oscillations produced in a plasma with anisotropic ion temperatures due to ion-beam interaction with the plasma is determined with the help of the obtained solution. The case of simultaneous excitation of several branches of oscillations is also considered. (auth)

30671 CONTRIBUTION TO THE THEORY OF DECAY OF ELECTROMAGNETIC WAVES IN A MAGNETOACTIVE PLASMA. Rowlands, J.; Sizonenko, V. L.; Stepanov, K. N. (Inst. of Physics and Tech., Academy of Sciences, Ukrainian SSR). Zh. Eksp. Teor. Fiz., 50: 994-1004 (Apr. 1966). (In Russian).

Cherenkov and cyclotron decay of electromagnetic waves in an homogeneous magnetoactive plasma is considered in the quasilinear approximation by taking into account collisions between resonance particles responsible for absorption of the waves and the remaining particles of the plasma. The velocity of the resonance particles along the magnetic field may be of the order of or less than the thermal velocity. For three-dimensional wave packets it is shown that in the absence of collisions the system finally reaches a steady state in which either the oscillation energy vanishes or the distribution function has a plateau. In the case of Cherenkov resonance, diffusion of particles on the waves in velocity space occurs only along the magnetic field, whereas in the case of cyclotron resonance diffusion takes place along, as well as across, the magnetic field. The distribution function is determined in the quasistationary state when particle diffusion on waves is balanced by collisions; the nonlinear decay decrement is determined. (auth)

30672 INSTABILITY OF NONLINEAR STATIONARY POTENTIAL OSCILLATIONS IN ELECTRON-ION BEAMS. Smirnov, V. M. (Inst. of Engineering Physics, Moscow). Zh. Eksp. Teor. Fiz., 50: 1005-12(Apr. 1966). (In Russian).

A simple criterion is found for instability of nonlinear stationary potential oscillations in one-dimensional ion-electron beams emitted from a plane in a restricted volume, the potential difference between the emitter and collector being fixed. It is assumed that close collisions may be neglected. The cases of a monoenergetic electron current in vacuum or in the presence of an ion background are considered in detail. Some conclusions are drawn regarding the instability of nonlinear stationary conditions for arbitrary initial ion and electron distribution functions. (auth)

30673 QUASILINEAR TRANSFORMATION OF WAVES IN AN INHOMOGENEOUS PLASMA. Mikhailovskii, A. B.; Jungwirth, K. Zh. Eksp. Teor. Fiz., 50: 1036-47(Apr. 1966). (In Russian).

Quasilinear equations for an inhomogeneous plasma in a magnetic field are derived, in which convection of charges across the magnetic field is taken into account. The problem of quasilinear pumping of the energy of electron Langmuir oscillations excited in the plasma by an inhomogeneous electron beam into the low frequency spectral range of the oscillations is treated by means of the equations. It is shown that the effect may lead to an appreciable decrease of the Langmuir oscillation energy. (auth)

30674 SCATTERING OF WAVES IN A PLASMA. Gorbunov, L. M.; Silin, V. P. (Lebedev Inst. of Physics, Moscow). Zh. Eksp. Teor. Fiz., 50: 1095-1100 (Apr. 1966). (In Russian).

It is shown that, for a complete description of scattering and transformation of electromagnetic waves in a plasma, besides fluctuations in the electron density, fluctuations of the vortex current should also be taken into account. As an example of application of the general expressions for the cross section, scattering of transverse waves with frequencies greatly exceeding the Langmuir frequency is considered. (auth)

30675 PERTURBATION OF THE DENSITY OF CHARGED PARTICLES AT LARGE DISTANCES FROM A BODY RAPIDLY MOVING IN A PLASMA IN THE PRESENCE OF A MAGNETIC FIELD. Vas'kov, V. V. (Inst. of Geomagnetics, Ionosphere and Radiowave Propagation, Academy of Sciences, USSR). Zh. Eksp. Teor. Fiz., 50: 1124-32 (Apr. 1966). (In Russian).

An analytical expression is obtained for the perturbation of the density of ions (electrons) δN at large distances ($r \gg 2\pi\rho_H V_0/v_i$) from a body rapidly moving with a velocity V_0 in a collisionless plasma ($V_0 \gg v_i$) in the presence of a stationary external magnetic field H_0. The angular dependence $\delta N(r,\theta)$ is calculated in the plane (V_0H_0). In the direction normal to the plane δN rapidly decreases over a distance of the order of the mean Larmor ion radius ρ_H providing $\rho_H \gg R_0$ (R_0 is the body dimension). The result is compared with the perturbation produced by the body without taking into account the effect of a magnetic or electric field on the ion motion. (auth)

30676 DYNAMIC DISSIPATION OF MAGNETIC ENERGY IN THE VICINITY OF A NEUTRAL MAGNETIC FIELD LINE. Syrovatskii, S. I. (Lebedev Inst. of Physics, Moscow). Zh. Eksp. Teor. Fiz., 50: 1133-47 (Apr. 1966).

The deformation of a magnetic field in a compressible conducting medium in the vicinity of zero field lines is considered. It is demonstrated that, on shifting the currents producing the field, regions appear in which an increase of the field gradients is accompanied by a decrease of the density of the medium. Under certain conditions this process leads to violation of the freezing in of the field and to the appearance of strong electric fields which accelerate charged particles in the medium. The process is essentially a nonstationary one and produces the transformation of excessive magnetic energy into kinetic energy of the fast particles. The mechanism may be the cause of generation of fast particles in cosmic conditions and in a laboratory plasma. (auth)

30677 OSCILLATIONS OF A PLASMA IN CONSTANT EXTERNAL ELECTRIC AND MAGNETIC FIELDS. Bakanov, S. P.; Rukhadze, A. A. (Lebedev Inst. of Physics, Moscow). Zh. Tekh. Fiz., 36: 7-12 (Jan. 1966). (In Russian).

The excitation under the influence of a constant electric field of low frequency electromagnetic oscillations in a weakly ionized electron-ion plasma and in the electron-hole plasma of a semiconductor was discussed previously. The influence on these oscillations of a strong external magnetic field parallel to the electric field is considered. It is shown that the magnetic field does not stabilize the noise oscillations that arise in arbitrarily weak electric fields. It is found that in a plasma having unequal numbers of carriers of the two signs there can arise drift waves with a propagation velocity close to the drift velocity. Conditions for the stability of these waves are derived and it is shown that these conditions depend on the longitudinal dimension of the plasma. This phenomenon can be employed to design a semiconductor microwave amplifier. The influence of the magnetic field on the stability of the waves propagating transversely to the drift velocity, the possible existence of which was demonstrated earlier is discussed. (ATD)

30678 PROPAGATION OF ELECTROMAGNETIC WAVES IN A PLASMA LOCATED IN THE MAGNETIC FIELD OF A CONSTANT LINEAR CURRENT. Yashin, Yu. Ya. Zh. Tekh. Fiz., 36: 13-24 (Jan. 1966). (In Russian).

The propagation of electromagnetic waves in an axially symmetric plasma in the presence of the magnetic field due to a constant line current flowing along the symmetry axis is discussed. Only waves propagating in a plane perpendicular to the symmetry axis are considered. The calculations were undertaken rather to disclose general features of the influence of curvature of magnetic lines of force on the propagation of waves in plasmas than because of any significance ascribed to the particular configuration of plasma and field. The calculations are performed in the geometric optics approximation, i.e., it is assumed that the wavelength is long compared with the distance within which the properties of the plasma change significantly and ion motions, collisions, and space dispersion are neglected. From the known expression for the dielectric tensor in this approximation the eikonal equation is derived and is discussed at length. Considerations for the propagation and refraction of the ordinary and extraordinary waves are derived and the locations of the reflection points are found. Some features of the propagation are compared with analogous features for the case of a laminar plasma in an inhomogeneous magnetic field with rectilinear lines of force. It is shown that there can exist propagation channels (regions of transparency) bounded by regions of absorption, even when the magnetic field strength and the plasma density vary monotonically with the space coordinates. Within the propagation channel the energy is propagated along the lines of force of the external magnetic field. (ATD)

30679 KINETIC THEORY OF THE PASSAGE OF ELECTROMAGNETIC WAVES THROUGH A PLASMA LAYER. II. Kondratenko, A. N.; Miroshnichenko, V. I. Zh. Tekh. Fiz., 36: 25-32 (Jan. 1966). (In Russian).

Calculations, based on Maxwell's equations and the kinetic equation for the deviation from Maxwellian form of the distribution function for the plasma electrons, of the reflection, transmission, and absorption of plane electromagnetic waves incident at an arbitrary angle on an infinite plane layer of plasma of finite thickness, the incident waves being polarized with the electric vector normal to the plane of incidence were previously presented. Similar calculations for incident waves polarized with the electric vector in the plane of incidence are presented. There are imposed on the distribution function boundary conditions which correspond to assumption of a fixed probability p for specular reflection of a plasma electron arriving at the plasma-vacuum boundary, an expression is derived for the current in the plasma, and a set of coupled equations is obtained for the spatial Fourier components of the electric field within the plasma. These equations are solved for the case $p = 1$ and arbitrary plasma thickness, and for a thick plasma and arbitrary p, and expressions are derived for the reflection transmission and absorption coefficients of the incident electromagnetic waves. For the case of a thick plasma layer the absorption coefficient is proportional to the electron thermal velocity even when $p = 1$. In the limit of an infinitely thick plasma layer, the expression obtained for the absorption reduces to that given by V. P. Silin and Ye. P. Fetisov. For the case of a thin layer with $p = 1$ the absorption can be considerable, although under these conditions the absorption of waves polarized with the electric vector perpendicular to the plane of incidence is always small. For the case when the plasma layer is thin and p is not too close to unity the reflection and transmission coefficients are derived directly from the expression for the current. The results derived in this case can be obtained phenomenologically in the hydrodynamic approximation by employing an electron collision frequency equal to the ratio of the electron thermal velocity to the thickness of the plasma layer. The penetration into the plasma of the longitudinal wave excited at its surface is also briefly discussed. (ATD)

30680 ON THE THEORY OF THE STABILITY OF AN AXIALLY SYMMETRIC NONUNIFORM PLASMA CARRYING A CURRENT. Lovetskii, E. E. (Inst. of Engineering Physics, Moscow). Zh. Tekh. Fiz., 36: 45-52 (Jan. 1966). (In Russian).

The stability of an axially symmetric nonuniform plasma carrying an azimuthal current and located in an axial magnetic field is discussed in the geometric optics approximation. The calculations were undertaken because of their practical importance in connection with slipping instability in a plasma betatron. From the two-fluid hydrodynamic model there is derived the equation for small potential oscillations of the electromagnetic field, including the term describing the effect of centrifugal force. The eikonal equations of the geometric optics approximation valid in different frequency ranges and the corresponding dispersion equations are derived. The roots of the dispersion equations are discussed at some length and conditions are given for the stability of the corresponding oscillations. Except for oscillations in a narrow resonance band, all the oscillations can be stabilized by magnetic and electric fields that must be strong but can be realized in practice. The unstable resonance oscillations increase in amplitude sufficiently slowly that the resonance region can be passed before the oscillations have time to reach such amplitudes as to endanger the stable operation of the plasma betatron. (ATD)

30681 LOCATION OF MOVING PLASMA BURSTS FROM A COAXIAL INJECTOR. **Il'in, S. D.; Likhachev, V. M.; Petrusev, S. S.; Chernetskii, A. V. Zh. Tekh. Fiz., 36: 53-7(Jan. 1966). (In Russian).**

A microwave Doppler shift radar technique was used to measure the velocities of hydrogen plasma bursts injected at velocities from 3.6×10^6 to 1.5×10^7 cm/sec into a 10-cm diameter 130-cm long glass drift tube by a conical plasma gun powered with a 6 kv 20 μF capacitor bank. The measurements were undertaken to explore the possibilities of the Doppler shift technique. For control purposes the velocities of the plasma bursts were also measured with two microwave transmission cutoff setups located at different positions along the drift tube. Microwaves in the 3-cm range were employed for both the cutoff and the Doppler shift measurements. In the Doppler shift measurements a single dielectric antenna, coupled with a 10-db directional coupler with a directionality of 25 db, was employed for both radiation and reception. In order to determine the influence of the fluctuations of the reflecting surface of the plasma burst on the frequency of the reflected signal, Doppler shift measurements were made at several angles (up to 40°) to the line of flight. Good agreement was obtained among all the velocity measurements, and it is concluded that the Doppler shift technique can be used to measure the velocities of plasma bursts. With further development the method will provide other data, including the time variation of the velocity, the trajectory, the direction of flight, and information concerning the internal structure of the plasma burst. (ATD)

30682 INVESTIGATION OF PLASMA IN THE "TUMAN" INSTALLATION. Golant, V. E.; Kaganskii, M. G.; Ovsyannikov, V. A. (Ioffe Inst. of Physicotechnical, Leningrad). Zh. Tekh. Fiz., 36: 67-79(Jan. 1966). (In Russian).

The first experiments with the "Tuman" installation are reported. The machine is of race-track construction. In the semicircular end sections the diameter of the chamber is small and the longitudinal magnetic field strength is made high to facilitate ohmic heating; in the straightaways the diameter of the chamber is larger and the initial longitudinal magnetic field strength is made low, to facilitate adiabatic magnetic compression of the plasma. The present experiments were undertaken mainly to explore the conditions of electrodeless discharge and ohmic heating. The experiments were performed with a steady flow of hydrogen. With no longitudinal magnetic field, discharge could be effected at pressures down to 0.008 mm Hg, and in the presence of a weak longitudinal magnetic field, at pressures down to 0.002 mm Hg. In both cases an electric field of 1.2 v/cm or higher was required. To effect preliminary ionization at lower hydrogen pressures a 0.5 μF capacitor charged to 5 kv was connected to both diaphragms simultaneously with application of the high frequency pulse; by this means it was possible to reduce the minimum pressure at which ionization could be effected by a factor 2 or 3. Ohmic heating experiments were performed at hydrogen pressures from 0.008 to 0.05 mm Hg and induced emfs from 300 to 1000 v. The maximum plasma current increased rapidly with increasing longitudinal magnetic field strength for fields below about 1 kOe. With further increase of the magnetic field strength the maximum current as well as its duration decreased and the current exhibited strong oscillations. This behavior is ascribed to the influence of a transverse component of the magnetic field. The diamagnetic moment of the plasma was measured with the aid of a pickup coil at the center of one of the semicircular end sections. The emf induced by the longitudinal magnetic field itself was compensated by the emf induced in a second winding located outside the plasma and the self inductance between the pickup coil and the plasma filament was eliminated by making successive measurements with the current in opposite directions. From the diamagnetic moment of the plasma its density and temperature were estimated. At hydrogen pressures of 0.02 to 0.002 mm Hg ionizations of 50 to 90% were achieved with plasma temperatures of 4 to 8 ev. At 0.01 mm Hg hydrogen pressure and magnetic fields from 1 to 2 kOe, a plasma density of 5×10^{14} cm^{-3} was reached. Energy balance considerations indicated that the plasma was confined for approximately 20 μsec. Preliminary magnetic compression experiments were performed, with the field increasing to a maximum of from 4.5 to 18 kOe in from 20 to 30 μsec. High speed photographs showed that the diameter of the plasma filament was decreased by several times. (ATD)

30683 ACCELERATION OF A PLASMA BURST IN A COAXIAL ACCELERATOR WITH ERODING ELECTRODES. **Kolesnikov, P. M. Zh. Tekh. Fiz., 36: 80-4 (Jan. 1966). (In Russian).**

The acceleration of a plasma burst in a rail- or Marshall-type plasma gun is discussed with the effects of electrode erosion and resistance of the unexcited gas ahead of the plasma taken into account. To formulate the equations of motion it is assumed that the mass of material eroded from the electrodes is proportional to the time integral of the square of the current and that of the resistance of the medium is proportional to the square of the velocity of the plasma burst. It is assumed that the eroded material becomes part of the plasma burst and is accelerated with it. The equations of motion were solved with the aid of a computer for a number of values of the relevant parameters, and the solutions are presented graphically and discussed. It is concluded that electrode erosion decreases the maximum velocity of the plasma burst but has relatively little effect on its momentum, and that the resistance of the medium decreases the maximum velocity, particularly of high velocity bursts. In the presence of a resistive medium the plasma burst reaches a certain maximum velocity that it does not exceed. To achieve maximum velocity of the plasma burst and maximum efficiency of the accelerator, the design must be such as to minimize the acceleration time; this can be achieved by optimizing the length of the gun and properly locating the initiating discharge. (ATD)

30684 INVESTIGATION OF THE STANDBY OPERATION OF A COAXIAL PLASMA GUN. **Goncharenko, V. P.; Derepovskii, N. T.; Konovalov, I. I. Zh. Tekh. Fiz., 36: 85-8(Jan. 1966). (In Russian).**

A Thomson mass spectrometer was employed to investigate the composition of hydrogen plasma bursts from a coaxial plasma gun to which the firing potential was applied before the gas was admitted (stand-by operation). Stand-by operation of plasma guns has the advantage of simplicity, and the present investigation was undertaken to determine whether plasmas of adequate purity could be obtained from stand-by operated guns. The plasma gun consisted of two 25-cm long coaxial copper cylinders; the outer diameter of one cylinder was 3.2 cm and the inner diameter of the other was 7.9 cm. The inner cylinder had three slots at 17.5 cm from one end through which hydrogen was admitted by means of an electromagnetic valve operated by discharge of a 300 μF capacitor. The potential on the capacitor operating the valve was varied from 1.3 to 3.0 kv, and the gas pres-

sure behind the valve was varied from 2 to 8 atm; under these conditions the volume of gas admitted to the gun ranged from 0.1 to 3.0 cm^3. The plasma gun was powdered by a 1 μF capacitor charged to 16 kv; the resonant period of the discharge circuit was 1.5 μsec. The discharge of the plasma gun began from 190 to 300 μsec after operation of the valve, depending both on the power applied to the valve and the gas pressure behind it. The velocities of the plasma bursts ranged between 2×10^7 and 3×10^7 cm/sec and, as was shown by cutoff of 8 mm microwaves, their charged particle densities exceeded 10^{13} cm^{-3}. The impurity content of the plasma bursts decreased rapidly with increasing gas pressure behind the valve and potential applied to the valve. With a gas pressure of 2 atm and a valve potential of 1.8 kv the plasma was 48% hydrogen; with a gas pressure of 8 atm and a valve potential of 2.4 kv the plasma was 92% hydrogen. The principal impurity was carbon, but nitrogen, oxygen, fluorine, and copper were also observed in amounts up to 5% or more. The relative importance of carbon as an impurity increased with increasing purity of the plasma: when the total impurity content was 52%, the carbon content was 31%; when the total impurity content was only 8%, the carbon content was 6%. It is concluded that rather pure hydrogen plasmas can be obtained by stand-by operation of a coaxial plasma gun. (ATD)

30685 ACTIVE DIAGNOSIS OF A HOT PLASMA BY MEANS OF NEUTRAL PARTICLES. **Afrosimov, V. V.; Ivanov, B. A.; Kislyakov, A. I.; Petrov, M. P. Zh. Tekh. Fiz., 36: 89-101(Jan. 1966). (In Russian).**

A technique for measuring the charged particle density of a hydrogen plasma with the aid of a beam of high energy (5–20 kev) hydrogen atoms was developed and tested by measuring plasma densities in the "Al'fa" installation. The method has the advantages of good sensitivity, negligible interference with the plasma and independence of the physical state of the plasma and the presence of magnetic fields. The injector consisted of an ion source, accelerating electrodes, electrostatic deflecting electrodes for directing the beam, a charge exchange chamber containing hydrogen at $1-4 \times 10^{-4}$ mm Hg in which some of the ions were neutralized, and a transverse electric field which removed the unneutralized ions. After traversing the plasma the hydrogen atom beam passed through a transverse electric field which cleared it of any charged particles that it might have picked up, and a charge exchange chamber in which some of the atoms became ionized. The ions issuing from the charge exchange chamber were analyzed by means of electric and magnetic fields and those with the proper energy and mass, corresponding to the energy and mass of the initial probe beam particles, were recorded with a scintillation counter. The sensitivity was such that a beam current corresponding to 10^{-10} amp of singly-charged ions could be employed. The injector and detector assemblies were enclosed in iron housings of approximately 1-cm wall thickness for magnetic shielding. The plasma density was calculated from the attenuation of the beam on traversing the plasma. The theoretical discussion is facilitated by the fact that once a beam particle is ionized it is removed from the beam by the ambient magnetic field, so that the possibility of the ion becoming neutralized again does not have to be considered. The most significant beam attenuating process is shown to be resonant charge exchange with plasma protons; ionization by electron impact is also significant, but other processes are negligible. The effect of scattering of beam atoms was partly eliminated by comparing the attenuation of the beam by the plasma with its attenuation by an equivalent mass of unionized gas, and the residual effect of scattering was shown experimentally to be imperceptible. The attenuation of the beam was independent of beam energy over the investigated range from 4 to 20 kev. The attenuation of such high energy beams is nearly independent of the plasma temperature. The decay curve of the plasma in the "Al'fa" machine from 1.5×10^{13} to 0.2×10^{13} cm^{-3} as measured with the hydrogen atom probe agreed within the experimental error with the decay curve measured with a microwave interferometer. It is concluded that with the investigated technique one can make absolute measurements of the ion concentration in a hot hydrogen plasma over the range of plasma thickness from 5×10^{13} cm^{-2}. (ATD)

30686 INVESTIGATION OF THE PLASMA CONCENTRATION IN THE "α" INSTALLATION WITH A PROBE BEAM OF FAST ATOMS. **Afrosimov, V. V.; Ivanov, B. A.; Kislyakov, A. I.; Petrov, M. P. Zh. Tekh. Fiz., 36: 102-10(Jan. 1966). (In Russian).**

A technique of plasma diagnosis with a fast atomic beam was employed to investigate the hydrogen ion concentration in plasmas in the alpha installation over a wide range of operating conditions. The theory of the technique and the apparatus employed were described previously. For the measurements the apparatus was so adjusted as to have a resolving time of 30 μsec. Under all operating conditions the proton density rose rapidly to a maximum value of n_{max} at time t_{max} after initiation of the discharge, decreased less rapidly with irregular fluctuations until the discharge current fell to zero, and subsequently decreased exponentially with the time constant T. The variations with the discharge conditions (the gas pressure P_0 prior to the discharge, the strength H_z of the longitudinal magnetic field, and the potential U on the capacitor bank feeding the eddy winding) of the parameters n_{max}, t_{max}, T, and the time $t_{0.5}$ during which the proton concentration was greater than half its maximum value are presented graphically and are discussed at some length. n_{max} was proportional to P_0 and, for fixed P_0, increased linearly with H_z. Values of n_{max} up to nearly 10^{14} cm^{-3} were observed. The ionization was relatively independent of U and increased from about 42% for H_z = 200 Oe to approximately 85% for H_z = 1 kOe. For U = 10 kv, t_{max} and $t_{0.5}$ reached minimum values of 0.5 and 1.4 millisec, respectively, at about the same value (360 Oe) of H_z. T increased linearly with H_z from approximately 0.25 millisec for H_z = 200 Oe to 0.8 millisec for H_z = 900 Oe. Mechanisms possibly contributing to the plasma decay are discussed and it is concluded that diffusion plays no appreciable part, that drift in the toroidal magnetic field makes the most significant contribution, and that recombination may be important if the plasma temperature at this stage is of the order of 0.2 ev. (ATD)

30687 INVESTIGATION OF THE ENERGY DISTRIBUTION IN THE HYDROGEN PLASMA FROM A COAXIAL PLASMA GUN. **Zolototrubov, I. M.; Rastrepin, A. B.; Skoblik, I. P. Zh. Tekh. Fiz., 36: 111-16(Jan. 1966). (In Russian).**

The energy distribution of hydrogen ions in hydrogen plasmas emitted by a coaxial plasma gun was investigated as a function of the polarity of the potential applied to the gun electrodes and the delay time between admitting the gas and firing the gun in an effort to elucidate the operating mechanism of the plasma gun. The plasma gun was described previously. Approximately 0.8 cm^3 of hydrogen was admitted through an opening in the outer electrode of the gun by an electrodynamic valve that remained open for 80 μsec. The gun was powered by a 20 kv 12 μF capacitor, the resonant period of the circuit being 13 μsec. On the axis of the gun and 1 m from it was the entrance aperture of a mass spectrometer. Plasma ions entering the spectrometer were accelerated by a 15 kv electric field, deflected by a magnetic field, and detected by a scintillation counter. The flight time of each ion from the mouth of the gun to the detector was subtracted from the time at which it was recorded, thus determining the instant of origin. The current through the plasma gun and the potential at each end of it were recorded with an oscillograph. When the delay between opening the valve and firing the gun was short (85 μsec) the energy distribution of the plasma ions was approximately the same, regardless of the polarity of the potential applied to the gun: the energy distribution was bimodal with peaks at 1–2 and 8 kev, ions with energies as high as 20 kev were recorded, and substantially all the ions originated near the instant of maximum current through the plasma gun. When the delay time was increased the high energy peak disappeared, the low energy peak shifted toward lower energies, and the ions originated at later times in the discharge cycle. These shifts were much more pronounced when the inner electrode of the plasma gun was negative than when it was positive. When the delay

was 285 μsec and the inner electrode was positive the peak of the energy distribution was at 0.8 kev and the ions originated at the instant the current through the gun first fell to zero (some 6 μsec after application of the potential); with the same delay time and the inner electrode negative, the peak of the energy distribution was at 0.3 kev and the ions originated some 20–22 μsec after potential was applied to the gun. The observed phenomena are discussed at some length, and it is concluded that the difference between the energy spectra of the ions observed with positive and negative potentials applied to the inner electrode of the gun apparently reflects differences between the physical processes taking place in the two cases. (ATD)

30688 INVESTIGATION OF THE DISCHARGE IN A HOLLOW CATHODE. I. COMPARISON OF THE ELECTRICAL CHARACTERISTICS OF A HOLLOW CATHODE AND A POSITIVE COLUMN. Borodin, V. S.; Kagan, Yu. M. (Leningrad State Univ.). Zh. Tekh. Fiz., 36: 181-5(Jan. 1966). (In Russian).

The electron density and velocity distribution in helium discharge positive columns and in hollow cathode helium discharges were measured using a technique previously employed to measure electron velocity distributions in positive columns. Two hollow cathodes with diameters of 2 and 1 cm and lengths of 5 and 10 cm, respectively, were investigated. The electron density and velocity distribution at the center of the hollow cathode and on the axis of a positive column of equal diameter were derived from the probe characteristics of 0.06-mm diameter 5-mm long cylindrical probes. Measurements were made at helium pressures from 0.9 to 3.5 mm Hg and discharge currents from 20 to 40 mamp. Deviations from the Maxwellian distribution were observed at the higher pressures: in the hollow cathode there was an excess of high-energy electrons, and in the positive column there was a deficiency of high energy electrons. The number of high-energy electrons in the hollow cathode was maximum at a certain optimum pressure that was higher for the smaller cathode than for the larger one. The ratio of the number of electrons with energies from 6 to 13 ev to the number with energies from 19 to 26 ev was nearly independent of pressure for the hollow cathode and was small and exhibited a minimum as a function of pressure for the positive column. The significance of these results for the interpretation of the spectra of the discharges is discussed briefly. (ATD)

30689 LINEAR THEORY OF THE EXCITATION OF OSCILLATIONS IN A PLASMA BY A CHARGED PARTICLE BEAM. Kostyukova, Yu. S.; Nekrasov, F. M. Zh. Tekh. Fiz., 36: 191-3(Jan. 1966). (In Russian).

The initial stages of the excitation by a charged particle beam of oscillations in a plasma that is of limited extent in the direction of the beam and is located in a uniform magnetic field is briefly discussed. The discussion is based on Maxwell's equations and the kinetic equation without collision integral and is limited to times short compared with that required by a plasma particle, owing to its thermal motion, to traverse a distance equal to the wavelength of the excited oscillations. The kinetic equation is first solved by the method of characteristics, and temperature-dependent terms are dropped from the resulting expressions for the charge and current densities. After substitution of these expressions for the charge and current densities into Maxwell's equations, the equations are subjected to a Laplace transformation and their solutions are discussed. It is found that resonant excitation with linear increase of amplitude with time can occur at certain frequencies depending on the system and the initial disturbance. An equation is derived for the resonant frequencies in excitation by an electron beam of the extraordinary wave propagating parallel to the external magnetic field in an electronic plasma. The excitation of these waves is due to the component of the beam velocity perpendicular to the magnetic field. It is suggested that heating of the plasma electrons can result from such excitation of the extraordinary wave and its subsequent absorption as a result of the thermal motions of the electrons. (ATD)

30690 NONLINEAR THEORY OF THE DIPOLE RESONANCE OF A PLASMA BURST AND THE COHERENT ACCELERATION OF PLASMA. Andronov, A. A. Zh. Tekh. Fiz., 36: 196-8(Jan. 1966). (In Russian).

The efficiency of the coherent method of plasma acceleration is considered. A uniform cylinder of radius R and length L small compared with the wavelength is adopted as a model of the plasma burst and all resonances are neglected except the quasistatic dipole resonance at frequency $F = f/2^{\frac{1}{2}}$, where f is the plasma frequency. It is assumed that the electromagnetic wave is circularly polarized with the electric vector perpendicular to the axis of the plasma cylinder, and that the plasma is confined in an axial magnetic field. Results of calculations of the scattering cross section and the polarization phase as functions of the deviation of the frequency from the resonance value and the ratio of the intensity of the wave to the strength of the axial magnetic field are presented graphically, and the hysteresis phenomena that they reveal are discussed. If F is from 3×10^9 to 10^{10} rad/sec, the plasma temperature is $10^{4\circ}$K, the cross section of the accelerator waveguide is $10-50$ cm^2, and the Q factor is 100, hysteresis sets in at powers of the order of several watts. If the radius of the plasma cylinder is 1 cm, the time required for a plasma ion, owing to its thermal velocity, to cross the plasma cylinder is approximately 6×10^{-7} sec. This time is of the same order as that required to accelerate the plasma to 10^8 cm/sec within a length of 50 cm; it may therefore be difficult to achieve resonance conditions. (ATD)

30691 KINETIC THEORY OF OSCILLATIONS OF A NONUNIFORM PLASMA WITH COLLISIONS TAKEN INTO ACCOUNT. Mikhailovskii, A. B.; Pogutse, O. P. Zh. Tekh. Fiz., 36: 205-18(Feb. 1966). (In Russian).

A method for studying the oscillations and stability of an inhomogeneous plasma with collisions is developed. The method is based on the use of the kinetic equation with model collision integral in the Batnagar-Gross-Krook form. The basic emphasis is on obtaining an expression for the permittivity tensor. It is assumed that the plasma is in a helical cylindrically symmetric magnetic field. The density gradient, the magnetic-field gradient, and the radius of curvature of the lines of force are taken into account. The temperature is taken to be uniform. It is taken into consideration that the equilibrium current can flow along the lines of force. The general dispersion equation for oscillations of the longitudinal type is obtained, from which more simple equations for oscillations with small β are found. The effect of collisions on the increment of a drift instability with not too small β and the oscillation of a weakly ionized nonhomogeneous plasma in the presence of a longitudinal current are examined using the obtained equations. (tr-auth)

30692 THEORY OF EXCITATION OF ION PLASMA OSCILLATIONS BY ELECTRON LANGMUIR WAVES. Repalov, N. S.; Khizhnyak, N. A. Zh. Tekh. Fiz., 36: 219-24(Feb. 1966). (In Russian).

An attempt is made to account for the excitation of low-frequency ion oscillations in a plasma by high-frequency electron plasma waves. The one-dimensional oscillations of the plasma electrons excited by a low-amplitude longitudinal traveling electromagnetic wave are treated in a small nonlinearity approximation by a technique of Bogolyubov with the ion motion neglected. The low-frequency motions of the ions excited by the electron oscillations are then calculated after first averaging out the high-frequency ion motions. It is shown that when the frequency of the external wave is close to a harmonic of the electron Langmuir frequency and the amplitude of the wave is close to one of a discrete set of resonance values, there develop beats that can excite low-frequency ion oscillations. Resonance transfer of energy from the electrons to the ions can also occur for other values of the external wave amplitude provided the frequency of the external wave is sufficiently close to a certain resonance value depending on the amplitude; in this case, however, the efficiency of the energy transfer is low. (ATD)

30693 MOTION OF CHARGED PARTICLES IN CONSTANT AND ROTATING MAGNETIC FIELDS. Soldatenkov, T. R. Zh. Tekh. Fiz., 36: 246-9(Feb. 1966). (In Russian).

The motion of a plasma simultaneously in the presence of a constant longitudinal magnetic field and a rotating transverse magnetic field is studied. This problem is of interest in connection with the confinement of plasma in a magnetic mirror system. The plasma motion is treated in the drift approximation under the assumptions that the strength of the transverse rotating component of the magnetic field is small compared with that of the constant longitudinal component and that the field rotation frequency is small compared with the Larmor frequency. It is found that when the rotation frequency of the field exceeds a certain value the motions of both ions and electrons are finite and independent of the direction of rotation of the magnetic field. At lower field rotation frequencies (or higher relative strengths of the rotating field) the motions are finite only when the angular-velocity vector of the rotating field is in the direction of the constant field. In a plasma with a finite number of particles and a sufficiently low collision frequency a condensation of electrons develops in the plane of the rotating component of the field. This condensation rotates with the field and can drag the ions along with it. (ATD)

30694 INTERACTION OF PLANE AND SURFACE ELECTROMAGNETIC WAVES IN A PLASMA. Alanakyan, Yu. R. (Lebedev Inst. of Physics, Moscow). Zh. Tekh. Fiz., 36: 258-65(Feb. 1966). (In Russian).

The interaction of electromagnetic radiation incident on the surface of a plasma with a surface wave is examined. The plasma is assumed isotropic and semi-infinite. It is shown that the amplitude of the surface wave increases or decreases according to an exponential law. Expressions for the fields generated at the combined frequencies are found. (tr-auth)

30695 INTERACTION OF INTENSE HIGH FREQUENCY ELECTROMAGNETIC WAVES WITH LANGMUIR ELECTRON OSCILLATIONS IN A UNIFORM ISOTROPIC PLASMA. Danilkin, I. S. (Lebedev Inst. of Physics, Moscow). Zh. Tekh. Fiz., 36: 266-72(Feb. 1966). (In Russian).

Problems associated with the propagation of an intense h-f wave in an isothermal isotropic uniform plasma are considered. Because of the nonlinearity of the medium for sufficiently large amplitude of the initial electromagnetic wave (with frequency $\omega^{(0)} \gg \omega_L$, where ω_L is the electron Langmuir frequency), this process is accompanied by the formation of a large number of secondary transverse waves at the combination frequencies $\omega^{(n)} = \omega^{(0)} \pm n\omega_L$, n = 1, 2, 3 .... Under the assumption that $\omega^{(0)} \gg \omega_L$, an analytic solution for the amplitudes of the waves with frequency $\omega^{(n)}$ and of the longitudinal wave ω_L is obtained, valid in an interval of distances substantially exceeding the characteristic length of conversion of the initial wave into a wave at the first difference of the combined frequency. It is shown that the intensity of the longitudinal waves remains constant in this case. The case of propagation of two transverse waves with frequencies $\omega^{(0)}$ and $\omega^{(1)} = \omega^{(0)} - \omega_L$ through a plasma, leading to the monotonic growth of intensity of the longitudinal waves, is investigated. (tr-auth)

30696 BEHAVIOR OF THE ELECTROMAGNETIC FIELD IN AN INHOMOGENEOUS MAGNETIZED PLASMA. Dolgopolov, V. V. Zh. Tekh. Fiz., 36: 273-9(Feb. 1966). (In Russian).

Discontinuities of an electromagnetic field in a nonuniform magnetoactive plasma, caused by plasma resonance, are considered. Expressions are obtained for the field in the vicinity of the singularity in the general case. For some frequently occurring cases, a solution is found in a wider range. It is shown that, in the case where the length of the emitted wave is of the order of the thickness of the layer, the presence of singularities leads to the intensity of the radiation from the transparent inhomogeneous medium being of the order of the intensity of radiation from a black body. The possibility of using plasma resonance for heating plasma is evaluated. (tr-auth)

30697 INVESTIGATION OF THE PROCESSES BEHIND A REFLECTED SHOCK WAVE IN AN ELECTROMAGNETIC SHOCK TUBE. Makarov, Yu. V.; Maksimov, A. M. (Inst. of Power Engineering, Moscow). Zh. Tekh. Fiz., 36: 280-93(Feb. 1966). (In Russian).

Results are presented of a study of the process of reflection of a shock wave from a hard wall. The shock wave was formed using an electromagnetic shock tube with a conical discharge chamber. Measurements were carried out in air, argon, and carbon dioxide. The velocities of the reflected shock wave, which agree with calculated values, were measured by photoscanning of the reflection process. Time-resolved scannings of the radiation spectra of the plasma behind the reflected wave were obtained for the various gases. The plasma conductivity behind the shock wave was measured using an oscillatory circuit. The experimental conductivity values are presented and compared with theoretical values and with previous results. The advantages and insufficiencies of the method of conductivity measurement are evaluated. (tr-auth)

30698 DYNAMIC STABILIZATION OF A DIRECT DISCHARGE IN A MAGNETIC FIELD. Andrezen, A. B.; Gordienko, V. P.; Dubovoi, L. V.; Roife, I. M.; Yakovlev, S. P. Zh. Tekh. Fiz., 36: 294-6(Feb. 1966). (In Russian).

The stabilizing effect of a h-f electric field on a high-current pulsed gas discharge in a longitudinal magnetic field was investigated. The discharges took place in a cylindrical quartz tube containing hydrogen at pressures from 10^{-2} to 10^{-4} mm Hg. The discharges were highly unstable; harmonics of the helical instability with a fundamental frequency of about 40 kc were observed. The instability was affected by the magnetic-field and discharge-current strengths and by the location of the glass septa which limited the discharge-column diameter. The stabilizing effect of the h-f electric field was marked only when the h-f component of the current in the discharge column was comparable with or greater than the direct component. The ratio of the h-f to the direct component of the current required to effect a given degree of stabilization decreased for increasing discharge current. Experiments with He and Ar gave similar results. The experiments confirm the predicted stabilization of the current-convective instability of a positive column in a magnetic field. (M.J.T.)

30699 PROPERTIES OF A PLASMA CAPACITOR. Golovanivskii, K. S.; Pogosyan, V. A. (Friendship of Nations Univ., Moscow). Zh. Tekh. Fiz., 36: 297-303 (Feb. 1966). (In Russian).

The response of a plane capacitor partly filled with plasma to the sudden application of a potential which is thereafter maintained constant is calculated. The plasma layer is assumed centered between the capacitor plates and insulated from them by nonconducting dielectrics. The calculations are based on previously derived expressions for the electron and ion densities as functions of position and time. Expressions are derived for the capacitor potential distribution and current. The equation for the transient current is the sum of two terms of which the first (second) decays exponentially with a time constant equal to twice the reciprocal of the ion (electron) collision frequency and oscillates with a frequency close to the ion (electron) Langmuir frequency. By observing the transient current with an oscilloscope, therefore, the collision and Langmuir frequencies of the plasma can be obtained, provided the time constant of the external circuit is small compared with the reciprocal of the Langmuir frequency. The additional steady-state capacity of the capacitor due to the presence of the plasma depends only on geometric factors and the two Debye radii in the plasma. If the electron temperature of the plasma is much higher than the ion temperature, the electron Debye radius can be determined directly by measuring the capacity of the capacitor after the transient has decayed. (ATD)

30700 DETERMINATION OF PLASMA DENSITY DISTRIBUTION BY MICROWAVE REFRACTION. Dushin, L. A.; Kononenko, V. I.; Sizonenko, V. L.; Skibenko, A. I.; Stepanov, K. N. Zh. Tekh. Fiz., 36: 304-12(Feb. 1966). (In Russian).

Fermat's principle is used to calculate the path of a microwave beam in a cylindrical plasma in which the density decreases monotonically with increasing distance from the axis, for the two cases in which the beam lies in a plane containing the axis or in a plane perpendicular to the axis. For each case, an equation is derived giving the plasma density as a function of the distance from the axis implicitly in terms of the position at which the microwave beam leaves the plasma as a function of the angle of incidence. The use of these equations to determine plasma density distributions from microwave refraction measurements was tested by measuring density distributions in decaying hydrogen plasmas at 5×10^{-2} mm Hg in a quartz tube, using 8-mm microwaves. For various positions of the radiating and receiving antennas, the time after plasma excitation at which the refracted wave reached the receiving antenna was recorded. Curves giving the antenna positions as functions of the incidence angle for different times were constructed. From these curves the electron density of the plasma was calculated as a function of time and distance from the axis. Measurements were made both with the beam in a plane containing the axis and with the beam in a plane perpendicular to the axis. Good agreement was obtained between the different measurements. (ATD)

30701 ACHIEVEMENT OF ULTRAHIGH VACUUM IN THE OGRA-1 INSTALLATION. Butuzov, S. S.; Konyaev, V. P.; Maslennikov, E. A.; Pustovoit, Yu. M. Zh. Tekh. Fiz., 36: 316-23(Feb. 1966). (In Russian).

The pumping system of the Ogra-1 magnetic mirror device and improvements made on it since 1958 are described. The system consists of mercury-vapor, ion-sorption, titanium-sorption, and high-speed-diffusion pumps. Results of measurements of the partial pressures of the various residual gases left after evacuation, the evacuation rates, and the maximum vacuums achieved are reported. The effect of a lithium arc on the vacuum is discussed. A satisfactory solution to the problem of maintaining a vacuum of 10^{-10} mm Hg in the Ogra-1 device has not been found. (M.J.T.)

30702 MEASUREMENT OF PROPERTIES OF A PARTIALLY IONIZED GAS WITH A HOT-WIRE ANEMOMETER. Khazen, A. M.; Shuvalov, V. A. (Scientific Research Inst. of Mechanics, Moscow). Zh. Tekh. Fiz., 36: 377-83(Feb. 1966). (In Russian).

A method is proposed for experimentally determining the parameters of a partially ionized gas, based on the use of a hot-wire anemometer which is incorporated at the same time as a Langmuir probe. The use of two orientations of the anemometer wire with respect to the current permits the temperature of the ions, neutral particles, and electrons, the velocity of directed motion, and the charged-particle concentrations to be determined. A theory of the operation of the hot-wire anemometer is developed under the assumption that, besides the electric field, a weak axial magnetic field also acts on the charged particles in the plasma. (The Larmor radius of the ions is taken to be much larger than the probe radius.) (tr-auth)

30703 MEANS FOR PRODUCING A HELICAL MAGNETIC FIELD. Popov, S. N.; Popryadukhin, A. P. (Lebedev Inst. of Physics, Moscow). Zh. Tekh. Fiz., 36: 390-2 (Feb. 1966). (In Russian).

A calculation is carried out of the magnetic field produced by a winding whose shape is given in cylindrical coordinates r, θ, z by the equation $r = r_0\{1 + \delta \cos[n(\theta - \alpha z)]\}$, where n is an integer and r_0, δ, and α are constants. The calculation is performed with the aid of a perturbation expansion in δ, and the first order solution is given. The ratio of the helical component to the uniform longitudinal component of the field can be improved by compensating a portion of the latter with the uniform field of an auxiliary solenoid. By using a sequence of short windings spaced in the z direction and separately adjusting their azimuths, the pitch of the helical field can be adjusted. A wide variety of fields can be obtained by using sequences of short windings constructed with different values of n. (ATD)

30704 KINETIC THEORY OF PASSAGE OF ELECTROMAGNETIC WAVES THROUGH A THIN NONUNIFORM LAYER OF PLASMA. Kondratenko, A. N. Zh. Tekh. Fiz., 36: 398-401(Feb. 1966). (In Russian).

A calculation is carried out of the passage of polarized electromagnetic waves through a plasma layer which is not uniform in the direction normal to its surface and is thin with respect to the distance traveled by an electron due to its thermal motion during one period of the incident wave. Maxwell's equations and the kinetic equation for the electron distribution function are used. Collisions and ion motion are neglected. It is assumed that a constant fraction of the plasma electrons incident on the plasma-layer surface undergo mirror reflection. A solution is obtained, valid for an arbitrary spherically symmetric electron velocity distribution and an arbitrary plasma-density distribution in the direction normal to the plasma layer. Expressions for the reflection and transmission coefficients are derived. (M.J.T.)

30705 DETERMINATION OF ELECTRON TEMPERATURE OF A THETA-PINCHED HYDROGEN PLASMA BY MEANS OF CARBON LINE RADIATION [Thesis]. Ho, Chieh. College Park, Md., Univ. of Maryland, 1965. 120p.

Electron temperatures of a fully ionized hydrogen plasma were determined by means of line radiation emitted by the excited ions of carbon impurities present in the plasma. A model that uses the corona approach along with the assumption that the rate of electron-impact ionization is balanced by the rates of radiative and collisional recombination was used to describe the reaction phenomena in such a plasma. Photoionization was considered unimportant. Hydrogen gas at 50- and 200-micron-of-Hg pressures was heated by the magnetic compression produced by discharging three capacitor banks through a single-turn coil in a Theta-pinch configuration. The intensities of four carbon lines were measured spectroscopically. The electron temperatures were determined by comparing the measured intensity ratios of carbon lines, CV(2277 Å) to CIV(2530 Å) and CIV(2530 Å) to CIII(2297 Å), with the ratios calculated for the semi-corona model. The maximum electron temperatures of the hydrogen plasma were found to be on the order of 570,000°K for the 50-micron case from the intensity ratio of CV and CIV lines, and 91,000°K for the 200-micron case from the intensity ratio of CIV and CIII spectral lines. The coexistence of more than one electron temperature in an inhomogeneous plasma indicates the local nature of these deduced temperatures which, by no means, represents the average temperature of a plasma. The distribution of electron temperature in a plasma can be obtained if spatial resolution of the measured line intensities is achieved. The two-fluid model of magnetohydrodynamics was used to investigate the behavior of the plasma. The spatial distribution of the ion and electron temperatures, the electron density, and the magnetic field were calculated, and the degree of agreement with the experimental results are discussed. (TCO)

30706 COLLISIONLESS DAMPING OF NON-LINEAR PLASMA OSCILLATIONS [Thesis]. O'Neil, Thomas Michael. San Diego, Calif., Univ. of California, 1965. 89p.

The linear theory of collisionless damping is first reviewed. Landau's derivation of the damping coefficient is presented and discussed. J. Dawson's derivation is also presented. A summary of Malmberg and Wharton's recent experiment is presented. It is then shown that the linear theory of collisionless damping for a single wave breaks down in a time of order $\tau = \sqrt{(m/eEk)}$, where E is the amplitude of the electric field and k is the wave number. In the case where linearization breaks down long before one e-folding time, Jacobi elliptic functions are used to solve the nonlinear Vlasov equation, and the damping coefficient is generalized to be valid for times greater than τ. This generalized damping coefficient reduces to the linear result when $t/\tau \ll 1$; it has an oscillatory behavior when t/τ is of order unity; and it phase mixes to zero as t/τ approaches infinity. By considering the electron phase trajectories, these results are all shown to have simple physical interpretations. The time integral of the damping coefficient, $\int_0^\infty \gamma(t)dt$, is obtained by straightforward in-

tegration and checked by using an argument based upon an ergodic theorem and conservation of energy. Since this integral is of order ($\gamma_{Landau}\,\tau$), the change in the amplitude of the electric field is limited to the value $\Delta E \sim E_0(\gamma_{Landau}\,\tau) \ll E_0$. This verifies that the nonlinear effects stop the growth (or damping) of the waves. In the case where many waves are present, there has been previous work on the nonlinear theory of collisionless damping. The relationship between this previous work and the above single-wave problem is discussed. Quasi-linear theory is first reviewed and then shown to suffer from the same breakdown linearization encountered in the single-wave problem. This breakdown of linearization apparently does not change the results of quasi-linear theory. (Dissertation Abstr.)

30707 FLUTE INSTABILITY IN MIRROR MACHINES IN VARIOUS DENSITY REGIMES [Thesis]. Varma, Ram Kumar. San Diego, Calif., Univ. of California, 1965. 180p.

A study of flute instability is made for the low β inhomogeneous plasma equilibria that occur in the inhomogeneous magnetic fields of the mirror machines. An appropriate approximation technique for solving the Vlasov equation is developed, which consists basically of an ordering scheme in which the expansion parameter ϵ = ion Larmor radius/plasma radius $\ll 1$. By this expansion procedure sets of approximate equations appropriate for high and low-density plasmas in both the short fat (radius of the plasma r is of the same order as the radius of curvature of the field line ρ) and the long thin ($r/\rho \sim \epsilon^2$) mirror machines are obtained and their properties are discussed. For a high-density plasma in the long thin machine the finite Larmor radius effects are important. The set of approximate equations for this case and the resulting eigenvalue equation are found to be completely analogous to those for the cylindrical geometry as found by Rosenbluth and Simon. In the low-density regime a variational principle is derived for flute instability for the three-dimensional mirror machine geometry with no space charge in equilibrium and a near δ-function distribution of energy appropriate to neutral injection devices like ALICE and PHOENIX. In general, for given trail functions the variational principle furnishes a dispersion relation that for small electron temperature gives a cubic. Two of the roots of the cubic furnish the stability criterion. The third root describes a density-independent mode of oscillation at a frequency equal to the ion precessional frequency. This is identified with the density-independent mode observed in ALICE. The critical plasma density for the onset of instability is presented as a function of the ratio of the length to the radius of the plasma for some values of the ratio of the radius of the plasma to the radius of curvature of the field line. (Dissertation Abstr.)

30708 EXPERIMENTAL STUDY OF PLASMA MOTION IN A TOROIDAL OCTUPOLE MAGNETIC FIELD [Thesis]. Meade, Dale Michael. Madison, Wis., Univ. of Wisconsin, 1965. 109p.

The filling of a rod-terminated toroidal magnetic octupole containment device was studied experimentally by directing a tenuous ($n = 10^{11}$ cm^{-3}), fast ($v = 2 \times 10^7$ cm/sec) hydrogen plasma stream from a conical pinch gun at the concave region of a toroidal octupole magnetic field. The motion of this collisionless plasma was studied by using Langmuir probes to measure densities and special attenuator probes to measure high-impedance electric fields. The velocity field given by ExB/B^2 can then be compared to the observed density motion. Sensitive Rogowsky loops and magnetic probes were used to detect the small diamagnetic effects of this tenuous plasma. The total number of electrons in the toroidal container was monitored by observing the shift of the resonant frequency of the cavity when plasma was present. It is observed that the plasma easily penetrates the transverse magnetic field as it enters the octupole region by developing an electric polarization field that cancels the average Lorentz force on the particles. Since the magnetic-field lines are closed, the plasma short circuits the polarization field as it attempts to escape. The plasma stream, unable to move in its original direction, now divides into two streams moving in opposite directions around the toroid in the weak-field region. The streams move in the same transverse magnetic octupole field by developing electric octupole fields of opposite polarity. The plasma streams are confined in the low-field region as they travel around the toroidal structure with the same velocity as the original stream. When the streams of plasma meet halfway around the toroid, the resulting interaction of oppositely polarized electric fields both ejects and traps plasma. The motion of the plasma can be described quantitatively in terms of self-consistent first order orbit theory. (Dissertation Abstr.)

30709 COLLISIONAL EFFECTS ON PLASMA STABILITY [Thesis]. Bhadra, Dilip Kumar. San Diego, Calif., Univ. of California, 1965. 209p.

In the framework of kinetic theory, the effect of collision on certain phenomena in a plasma was investigated. By use of Krook-type collision operator, the effect of ion-ion collisions was studied on the propagation of ion sound waves and ion cyclotron waves. It was found that the damping of ion sound waves decreases with the increase of collision frequency. In the case of ion cyclotron waves, the effects of collision on the resonant nature of the mode and on the critical drift velocity were obtained. Also investigated was the effect of electron-ion collisions on the phenomenon of 'Universal' instability in a slightly inhomogeneous plasma. Both Krook and Fokker-Planck collision operators were used. It was noticed that even in the presence of electron-ion collisions, the 'Universal' instability survives though there are interesting differences in the results obtained from using the two different collision operators. Both analytical and numerical calculations were made. (Dissertation Abstr.)

30710 DIFFUSION AND DRIFT LOSSES AND ELECTRON COOLING IN HELIUM AFTERGLOWS CONFINED BY A TOROIDAL MAGNETIC FIELD [Thesis]. Olson, Orlando Duane. Saskatoon, Saskatchewan, Univ. of Saskatchewan, 1964. 96p.

Theoretical and experimental investigations of the decay of electron density and energy in afterglow plasmas confined by a toroidal magnetic field are described. An analysis was carried out on the rate of diffusion of a plasma across a magnetic field, taking into account interactions between all species of particles. The rate of drift of plasma across the magnetic field, due to the inhomogeneity in the field, was also calculated. Measurements of electron density and energy were made in helium afterglows by means of double Langmuir probes. The degree of ionization was high enough so that Coulomb interactions were dominant. For sufficiently weak magnetic field strengths (≤ 0.020 Wb/m^2), diffusion determines the rate of decay of electron density and the observed rate of diffusion agrees with the calculated rate within a factor of two for a wide range of electron densities and energies. At higher magnetic fields, drift in the inhomogeneous magnetic field becomes the dominant loss mechanism; theory and experiment agree within a factor of about two. Observed electron energy decay rates are compared with calculated cooling rates due to elastic collisions with ions and neutral atoms. For sufficiently low discharge power and neutral gas pressure, the agreement is reasonably good. For higher pressures and larger discharge power, the cooling rate is slower than that expected from recoil cooling alone. There is some evidence that this slow cooling is due to heating of the electrons through interactions involving metastable atoms in the afterglow. (Dissertation Abstr.)

30711 RADIATION IN A PLASMA ENVIRONMENT WITH CYLINDRICAL BOUNDARIES [Thesis]. Chen, Hollis Huei-Ching. Syracuse, N. Y., Syracuse Univ., 1965. 89p.

Research work accomplished in four major areas is reported: (1) the introduction of a "compressivity tensor" as a new constitutive parameter for anisotropic and compressible plasma, (2) the decomposition of the fields in a compressible plasma medium into electromagnetic and plasma modes and, in an anisotropic and compressible medium with cylindrical boundaries, into transverse and longitudinal components, (3) the complete solution, both

analytical and numerical, of a radiation problem in an anisotropic environment, and (4) the complete analytical solution of a radiation problem in a compressible environment. The introduction of the compressivity tensor makes possible not only the solution of electromagnetic problems in an anisotropic and compressible medium in a systematic manner but also a plausible and meaningful physical interpretation of a rather complex situation. The decomposition of fields in a compressible plasma into electromagnetic and plasma modes is made formal and systematic; it is independent of the geometrical configuration of the problem. The decomposition of the fields into transverse and longitudinal components in an anisotropic and compressible plasma with cylindrical boundaries simplifies the analytical solution greatly. The radiation patterns of an axially slotted and anisotropic plasma-coated conducting cylinder should be of both theoretical and practical value because they show the dependence of radiation characteristics on the degree of plasma anisotropy. The complete analytical solution of a ring source around a cylindrical column of compressible plasma is new. The formal expressions for both the surface wave and the radiation field have been obtained. It is shown that the radiation pattern depends on the sound velocity in the compressible plasma in a complicated way. (Dissertation Abstr.)

30712 RECOMBINATION, IONIZATION, AND NONEQUILIBRIUM ELECTRICAL CONDUCTIVITY IN SEEDED PLASMAS [Thesis]. Cool, Terrill Alan. Pasadena, Calif., California Inst. of Tech., 1965. 208p.

The theoretical and experimental description of the behavior of dense seeded plasmas under the influence of applied electric fields under steady-state conditions as well as during electronic ionizational and recombinational relaxations is discussed. Measurements were made under conditions of practical importance for proposed MHD energy converters in argon-potassium and helium-potassium plasmas. Translational gas temperatures ranged from 1250 to 2000°K; seed concentrations were varied between 0.1 and 1 mole percent; and the total gas pressure was 1 atmosphere. Extensive steady-state measurements of nonequilibrium electrical conductivity, and the influence upon it of variations in gas temperatures, seed concentrations, atomic cross sections, current densities, electric field strengths, and energy-loss processes were made. This detailed experimental work led to important modifications of existing theory that have enabled an accurate description of the plasma in terms of a simple physical model. Electron temperature measurements provide a conclusive and quantitative verification of the validity of this physical model. The essential theoretical modifications made here are the inclusion of both inelastic and elastic electronic collisional energy loss mechanisms in a manner that accurately reflects the essential physical differences between these two processes in terms of fundamental atomic properties and employs no adjustable parameters. Consideration of the detailed energy dependence of the atomic cross sections and the inclusion of both electron-ion and electron-atom interactions was essential in accurately describing the experimental results. Experimental measurements of recombination rates, ionization rates, and electronic collisional relaxation characteristics of potassium-seeded plasmas were performed. Measured recombination and ionization rates for potassium show good agreement with theoretical calculations based upon a formulation employing the Gryzinski classical inelastic collision cross sections and a simple physical model of the relaxing plasma. (Dissertation Abstr.)

30713 PARTIAL WAVE ANALYSIS OF ELECTROMAGNETIC WAVE PROPAGATION IN INHOMOGENEOUS MEDIA [Thesis]. Mitchell, Ferdinand Haverman Jr. University, Ala., Univ. of Alabama, 1965. 123p.

A solution to several classes of plasma problems was found by applying a technique similar to that used in nonrelativistic quantum mechanics when studying particle scattering by partial waves. In both types of problems it is desired to find out how a varying index of refraction affects the propagation of incident waves. The solutions are represented as sums or integrals of Fourier components which represent the partial waves. When the inhomogeneous medium is removed, the partial waves are known for many cases of interest; when the spatially-varying medium is reintroduced, each of these partial waves will change. It is convenient to define the partial wave phase shifts as the natural logarithm of the ratio of the new to the old partial waves. Perfectly conducting boundaries will always exist in the electromagnetic problem, so that both the regular and irregular solutions must be retained. Since the method of solution depends on the presence of the boundary, the mathematical techniques employed are quite different from those of the quantum case. There is also a difference in the basic wave equations to be solved; the quantum problem involves a scalar wave equation in three dimensions while in the electromagnetic case a vector wave equation must be solved and both two- and three-dimensional models are considered. By using the approach described, an analytic solution to several problems of interest is obtained in the form of an infinite series where successive terms are defined by an integral recursion relation. It should be mentioned that no restrictions are necessary with regard to near and far fields and with regard to the thickness of the medium layer. (TCO)

30714 DIFFUSION OF TEST PARTICLES ACROSS A MAGNETIC FIELD. Eldridge, O. (Culham Lab., Abingdon, Eng.). 23p. (CONF-651126–12; CLM-P-88). ORAU. Gmelin, AED-CONF-65-353-24.

From American Physical Society, 7th Annual Meeting of the Division of Plasma Physics, San Francisco.

A diffusion equation that describes the transport of charged particles across a magnetic field is derived from the first two equations of the BBGKY hierarchy. The overall plasma is spatially uniform but the diffusion is calculated by identifying a group of test particles and following their motion. (auth)

30715 EVOLUTION OF A PLASMA PUFF IN A LONGITUDINAL MAGNETIC FIELD. Moss, S. J. 13p. (CONF-651126–13). ORAU. Gmelin, AED-CONF-65-353-27.

From American Physical Society, 7th Annual Meeting of the Division of Plasma Physics, San Francisco.

The hydromagnetic model of Waelbroeck was used to analyze the plasma puffs produced by a conical pinch gun as the plasmoids pass through a longitudinal magnetic field. Four single-turn magnetic loops surrounding the vacuum chamber and inside the flux conserver were used as diagnostic probes. The model employs the signals induced in the magnetic loops by the passing plasma to extract the characteristic of the puff. The probe signals and the model predictions for the signals agree fairly well except for the first loop signal, where the model predicts a more rapidly decaying pulse than is found experimentally. (A.G.W.)

30716 SCATTERING OF A LASER BEAM BY A HOT ELECTRON PLASMA. Pechacek, R. E.; Trivelpiece, A. W. (Univ. of California, Berkeley). 11p. (CONF-651126–14). ORAU. Gmelin, AED-CONF-65-353-31.

From American Physical Society, 7th Annual Meeting of the Division of Plasma Physics, San Francisco.

By using a relativistically correct differential cross section and Maxwellian distribution and the method of Papas and Lee, the spectrum of radiation scattered from a distribution of electrons at temperatures between 25 and 200 kev is computed for several cases. It is found that the spectrum shifts to shorter wavelengths and broadens with increasing temperatures; e.g., the peak of the power spectrum of light scattered at right angles from a ruby laser beam at 6943 Å by a 200-kev electron distribution is near 1100 Å. The initial slope of the power spectrum curve is such as to yield an approximately constant number of photons per unit bandwidth until the peak of the power curve is reached. The effect of anisotropies in the plasma distribution function is demonstrated by considering scattering from a one-dimensional electron velocity distribution from several directions. The principal effect

accounted for in this relativistic theory, omitted in a non-relativistic treatment, is the tilting of the radiation pattern of a fast particle in the direction of its velocity. This has an influence on the interpretation of laser diagnostics involving hot electron magnetic mirror compression experiments. (auth)

30717 NUCLEAR FUSION BY MAGNETIC ACCELERATION OF A SUPERCONDUCTING SOLENOID. Winterberg, F. (Univ. of Nevada, Reno). 17p. (CONF-651126-15). ORAU. Gmelin, AED-CONF-65-353-25.

From American Physical Society, 7th Annual Meeting of the Division of Plasma Physics, San Francisco.

A recently discovered approach to nuclear fusion consists of accelerating macroscopic solid particles to high velocities and focusing them on a target of liquid or solid T-D. A method for magnetic acceleration of such particles is discussed. In this case, a superconducting solenoid is accelerated by a magnetic traveling wave. It should be possible by this method to accelerate macroparticles with a diameter of the order of 1 cm. With macroparticles of this size the product of particle number density and confinement time for the thermonuclear material can substantially exceed the critical value of 10^{14} sec/cm^3. In addition, the fusion products remain within the reacting volume, resulting in a small fusion explosion. Since velocities up to 10^8 cm/sec are required, the accelerator must have a length of at least 7 km. The big initial investment needed to build such a machine may be justified economically by the immense power output that should be obtainable. (auth)

30718 RECENT ADVANCES IN BEAM-PLASMA AMPLIFIERS. Chorney, P. (Microwave Associates, Inc., Burlington, Mass.). 16p. (CONF-660301-3). ORAU. Gmelin, AED-CONF-66-052-1.

From IEEE International Convention, New York.

The theory of operation of the beam-plasma amplifier (BPA) is reviewed and the potential advantages offered by this device concept are discussed. The most recent results obtained in BPA research are described with regard to high-power operation and millimeter waves. Technological problems that have been solved and those that remain to be solved are discussed. (A.G.W.)

Shielding

30719 (CONF-651109, pp 327-45) SHIELDING CALCULATIONS FOR HIGH-ENERGY ACCELERATORS. Alsmiller, R. G. Jr. (Oak Ridge National Lab., Tenn.).

Shields for high-energy accelerators can be designed adequately and at minimum cost only if detailed calculations of the transport of high-energy particles through matter are available. Some of the existing calculations are discussed with the view of indicating the areas of uncertainty. Shielding studies for electron accelerators must, of necessity, begin with a consideration of the electron-photon cascade induced in matter by high-energy electrons. The calculation of such cascades is discussed. Shielding calculations for both electron and proton accelerators ultimately reduce to a study of the nuclear cascade. To a considerable extent, the accuracy with which nuclear-cascade computations can be carried out is determined by the available data on particle emission from nucleon-nucleus and pion-nucleus collisions. Experimental results are generally lacking so data obtained from theoretical considerations must be used. Calculated data on particle emission from nuclear collisions are discussed and compared with experiment. The nuclear cascade in thick shields is considered and numerical results are compared with experimental values. (M.O.W.)

30720 (CONF-651109, pp 410-16) SHIELDING ASPECTS OF ACCELERATOR FACILITY DESIGN. Barrett, M. J. (Nuclear Utility Services, Inc., Washington, D. C.).

Concepts for designing accelerator shielding are discussed in terms of the following: particle emission efficiency, radiation spectrum, angular distributions, and buildup factors for the shield. (M.O.W.)

30721 (EUR-2778.e) THE BASIC CONCEPTS OF LYRA SYSTEM. Mongini-Tamagnini, C. (European Atomic Energy Community, Ispra (Italy). European Scientific Data Processing Center). 1966. 38p. Dep. mn.

LYRA system consists in the whole of conversion programs which convert multigroup data files from a standard form to the forms suitable to the most used diffusion codes, and vice-versa. In such a way data set suitable to a particular code can be converted, through standard form, into the form suitable to another code. (auth)

30722 (KAPL-M-6497) GROUP CONSTANTS FOR GAMMA-RAY HEATING. Dudley, T. E.; Mendelson, M. R. (Knolls Atomic Power Lab., Schenectady, N. Y.). Nov. 1965. Contract W-31-109-eng-52. 65p. Dep. mn. CFSTI $3.00 cy, $0.75 mn.

A trapezoidal rule quadrature solution of the infinite medium gamma-ray slowing down equation is described, using the Klein-Nishina scattering kernel and cross sections computed from bivariate polynomial expansions. The resulting spectrum was used to weigh few group constants for gamma-ray heating calculations. Comparisons were then made between the modified energy slowing down treatment used in KARE gamma ray heating calculations with a more accurate few group treatment, for several infinite medium problems. It was found that discrepancies of ten to twenty percent in groupwise heating rates may exist in the infinite medium KARE calculations, indicating that spatial calculations might exhibit similar effects and suggesting further research in that area. The derivation of a consistent few-group formulation of gamma transport, as well as a variational approach based upon the use of two overlapping spectra was developed. (auth)

30723 (NAA-SR-11831) THE DTF-II SHIELDING DATA LIBRARY. Green, W. B. (Atomics International, Canoga Park, Calif.). May 25, 1966. Contract AT(11-1)-Gen-8. 80p. Dep. mn. CFSTI $3.00 cy, $0.75 mn.

A new data library is available for use with the DTF-II S_N theory transport code in computing neutron fluxes in shield systems and reactor criticality. Two group structures are available: a 21-group structure with nine energy groups in the 0.41- to 14.9-Mev range (primarily for use in shielding problems) and a 16-group structure (suitable for use in criticality calculations). The epithermal data for both group structures were obtained by group-averaging pointwise data over a typical SNAP spectrum using the GAM-II code (these calculations were performed by personnel at Oak Ridge National Laboratory). Data for the thermal range were taken from previously generated data libraries at Atomics International. A complete listing of the library data is also included. (auth)

30724 (NASA-CR-461) DEVELOPMENT OF EPITAXIAL STRUCTURES FOR RADIATION-RESISTANT SILICON SOLAR CELLS. (Texas Instruments Inc., Dallas). May 1966. Contract NAS-5-3559. 137p. CFSTI $4.00 cy, $1.00 mn.

Experimental silicon drift-field solar cells were produced by means of advanced epitaxial and diffusion technology. Three different approaches were used for producing the drift-field structures and two different procedures were used for cell fabrication. Drift-field structures built by a single-epitaxial-deposit-and-diffusion technique and fabricated into cells by an improved procedure represent the best combination of methods by which a drift-field solar cell may be produced. Excellent reproducibility of cell characteristics and overall high process yields establish the production feasibility of this procedure to build drift-field solar cells. On the basis of a theoretical analysis of drift fields which was made, these sample cells when irradiated should show superior radiation resistance. The theoretical analysis, which took into account the variation of mobility with concentrations, suggests that the ratio of the impurity concentrations in the drift field should not exceed three orders of magnitude. Furthermore, the width of the drift-field probably should not exceed 25 microns. Low carrier lifetime prevents improvement of overall collection efficiency by use of significantly thicker deposited layers. Longer wavelength response was enhanced in some

instances by wider drift fields and by higher initial lifetime (e.g. by use of Lopex silicon or gettering), but the available power after irradiation apparently was not improved. A method developed for determining the concentration profile in a drift-field structure represents an important advance in cell evaluation. (a·th)

30725 (ORNL-3786) EFFECT OF ERROR ON RESULTS OF A LOW-ENERGY INTRANUCLEAR CASCADE CALCULATION. Bertini, Hugo W. (Oak Ridge National Lab., Tenn.). June 1966. Contract W-7405-eng-26. 188p. Dep. mn. CFSTI $5.00 cy, $1.00 mn.

The program used in the intranuclear calculations issued as ORNL-3383 was found to contain an error. Correcting the error results in a better agreement with experiment for the energy dependence of the (p,pn) cross sections previously calculated and in most cases in a better agreement in absolute value as well; however, a disagreement with experiment was found in the shape of the neutron spectrum for the case of 50-Mev protons on lead at 0°. All of the distributed data which were generated using the program that contained the error were replaced by data generated using the corrected program. (auth)

30726 (TID-22964) ADONIS: AN IBM-7090 MONTE CARLO SHIELDING CODE WHICH SOLVES FOR THE TRANSPORT OF NEUTRONS OR GAMMA RAYS IN THREE-DIMENSIONAL RECTANGULAR GEOMETRY. Eisenman, Burton; Hennessy, Elinor (United Nuclear Corp., White Plains, N. Y. Development Div.). Mar. 1963. Contract AT(30-1)-2303. 94p. (UNUCOR-635). Dep. mn. CFSTI $3.00 cy, $0.75 mn.

ADONIS is written in FORTRAN and FAP for IBM-7090. A 32k core and 10 tapes are required. ADONIS calculates the solution to the transport equation for primary neutrons (or gammas) in a three dimensional rectangular geometry. The program computes either neutron or gamma fluxes and their standard deviations in each of up to 80 regions. By use of response functions, dose and secondary gamma ray sources can be generated throughout the configuration. In particular, the code has proved useful in analyzing the penetration of neutrons or gammas through ducted shields. (M.O.W.)

30727 ACCUMULATION OF ELECTRIC CHARGE IN GLASS FOR γ-RAY SHIELDING WINDOW BY γ-RAY IRRADIATION. Asada, Tsunesaburo; Kikuchi, Riichi (Osaka Univ.). Mem. Inst. Sci. Ind. Res. Osaka Univ., No. 22, 85-7 (Mar. 1965).

Gamma-ray shielding nonbrowning glass is often broken by an electric discharge after long periods of exposure to the γ rays. There is no established theory for the nature of the charge traps and the spatial distribution of charge accumulated in the glass. The thermally released current of the γ-irradiated glass vs the glass temperature with the glass being kept in the furnace was measured with an electrometer. The sample materials used in the experiment were NB-36 and NB-25 of Ohara Optical Glass Corp. Both of these materials had two peaks in the released current at the temperatures of about 90–135°C and 140–180°C. The thermoluminescences of the glasses were measured to determine if each of the peaks of thermally released current corresponded to the different depth of charge traps. The thermoluminescence curve was obtained only for NB-25. (auth)

30728 EXPERIMENTAL DETERMINATION OF THE ENERGY DISTRIBUTION OF GAMMA RAYS SCATTERED IN SAND. Alberg, Mary; O'Brien, Keran; McLaughlin, James (Atomic Energy Commission, New York). Nucl. Sci. Eng., 25: 303-5(July 1966).

The differential energy spectra of γ rays from a point isotropic ^{137}Cs source placed in an effectively infinite medium of sand have been determined by scintillation spectrometer measurements that were interpreted with an analytic method based on the Scofield iteration scheme. (B.G.D.)

30729 ENERGY AND ANGULAR DISTRIBUTION OF GAMMA RAYS SCATTERED IN ALUMINUM. Dardis, J. G.; Scofield, N. E. (Naval Radiological Defense Lab., San Francisco). Phys. Rev., 147: 280-7(July 8, 1966).

The energy and angular distribution of plane perpendicular ^{137}Cs gamma rays scattered in 1 through 5 mean free paths of aluminum was measured using a NaI(Tl) spectrometer. The results are compared with distributions calculated from the method of moments and polynomial expansion. For 1 and 2 mean free paths the infinite-medium calculations for multiple scatter are considerably in excess of the experimental results at the distribution peak; otherwise, the spectrum shape is reproduced satisfactorily. For 3, 4, and 5 mean free paths the calculations are in good agreement with experiment. (auth)

30730 APPLICATION OF DIMENSIONAL ANALYSIS TO RADIATION SHIELDING [Thesis]. Assaf, Walid Constantine. Ames, Iowa, Iowa State Univ. of Science and Tech., 1965. 78p.

An application of the method of dimensional analysis to the problem of radiation shielding design is presented. The answers to two questions were sought. First, to what extent is a shield for low-energy gamma radiation a model of one at a higher energy and what are some of the limitations that are involved? The second question concerned the possibility of using dimensional analysis to find a property of the material that is important in radiation shielding design. A series of model tests was conducted using lead, concrete, aluminum, and iron. The answers to the questions, as indicated by the results of the analysis and the subsequent experiments and calculations, are encouraging. Model theory and dimensional analysis can be used successfully as an aid in radiation shielding design if proper efforts are directed toward that end. (Dissertation Abstr.)

30731 ATTENUATION CROSS SECTIONS OF THALLIUM AT 122 kev [Thesis]. Dowe, Ray Michael Jr. University, Ala., Univ. of Alabama, 1965. 83p.

Attenuation cross sections of thallium were measured at 122 kev, using a ^{57}Co source. Cross sections were determined using multiple thicknesses of thin foils, extrapolated graphically to "zero thickness," eliminating absorption effects, and effectively creating disk sources. The ratio of $\tau + \sigma_K(\theta)$ to $\sigma_{free}(\theta)$ was measured using thallium and aluminum equivalent foils, respectively. From this ratio $\tau + \sigma_K(\theta)$ was obtained by use of $\sigma_{free}(\theta)$ computed from the Klein-Nishina formula. $\sigma_K(\theta)$ was measured from coincidences between thallium K-shell x rays and scattered γ rays. Results are $\tau = 967.30 \pm 9.91$ barns/atom; $\sigma_K = 0.94 \pm 0.09$ barns/atom; [$\sigma_K(45°) = 0.042 \pm 0.005$, $\sigma_K(90°) = 0.036^{+0.003}_{-0.004}$, $\sigma_K(135°) = 0.049^{+0.003}_{-0.008}$ barns/electron/steradian] and $\sigma_{Coherent} = 37.07 \pm 13.65$ barns/atom, in agreement with theory, except that $\sigma_K(\theta)$ was larger than atomic form-factor predictions for large angles. (Dissertation Abstr.)

30732 NEUTRON SHIELDING COMPOSITION HAVING GOOD HIGH TEMPERATURE STRENGTH. Bliss, Joseph F.; Gilvary, John P.; Castner, Foster J. (to Union Carbide Corp.). U. S. Patent 3,247,131. Apr. 19, 1966. Filed Apr. 4, 1963.

A composition is provided that is suitable for neutron shielding, which has a high content of olefinically unsaturated hydrocarbon polymer, which is readily fabricated into simple or complex contours, and which exhibits good compressive strength over a wide temperature spectrum. The composition comprises 40 to 80 parts by weight of a particulate olefin polymer per 100 parts by weight of the binder. The binder is made up of from 30 to 90 parts by weight of a polyglycidyl ether of a polyhydric phenol having an epoxy equivalent greater than 1, from 10 to 70 parts by weight of bis (2,3-epoxycyclopenty) ether, and approximately a stoichiometric amount of a hardener. The hardener consists of from 25 to 75 parts by weight of an aliphatic amine and from 25 to 75 parts by weight of a eutectic blend of aromatic amines and bisphenol-A. (B.L.M.)

Solid State Physics

See also CHEMISTRY — Inorganic and Physical Chemistry
METALS, CERAMICS, AND OTHER MATERIALS — Properties and Structure

Refer also to abstracts 29622, 30189, and 30312.

30733 (ORNL-TM-1425) OR GNU: A FORTRAN PROGRAM FOR CALCULATING FREQUENCY-DISTRIBUTION FUNCTIONS OF CUBIC CRYSTALS. Raubenheimer, L. J.; Gilat, G. (Oak Ridge National Lab., Tenn.). June 1966. Contract W-7405-eng-26. 41p. Dep. mn. CFSTI $2.00 cy, $0.50 mn.

A computer program is described which finds the frequency-distribution function of a centrosymmetric cubic solid for which a Born-von-Kármán force model is available. The FORTRAN language is used in order to facilitate modifications necessary for other force models, as well as other crystal structures. Detailed instructions for using the program are included. (auth)

30734 (TID-22970, pp 1-63) CHEMICAL AND SOLID STATE PHYSICS. (Massachusetts Inst. of Tech., Cambridge).

Summaries of investigations are presented concerning solid state theory; structure of solids by x-ray diffraction, neutron diffraction, and electron diffraction; low temperature physics and properties of solids; optical, microwave, and radiofrequency physics; and interatomic and intermollecular forces. (J.R.D.)

30735 (TID-22970, pp 331-73) NATIONAL MAGNET LABORATORY. (Massachusetts Inst. of Tech., Cambridge).

Research and development are summarized on high-field magnets, semiconductor Faraday rotation and optical absorption, for infrared studies, optical spectra of solids, sonic effects in solids, de Haas-van Alphen effect, magnetic measurements, r-f size effects, Mössbauer studies, superconductivity, properties of liquid He, low temperature physics, electron exchange in metals, transport theory, electron polarization in metals, spectra and properties of rare earths, and Bloch electron dynamics. (J.R.D.)

30736 OPTICAL PROPERTIES OF GRAPHITE IN THE INFRARED REGION. Ichikawa, Yoshi H.; Kobayashi, Kenji. Carbon, 3: 401-6(Feb. 1966).

The optical properties of graphite in the infrared region were studied theoretically on the basis of the Slonczewskii-Weiss band model of π-electrons in graphite. The calculated conductivity of graphite with a large value of $\gamma_1 = 0.4$ ev is in good agreement with the experimental result obtained by others through a larger value of γ_1 is not favorable to fit the reflectance previously measured by others. (auth)

30737 ENERGY BAND PARAMETER DETERMINATION IN GRAPHITE. Dresselhaus, Mildred S.; Mavroides, John G. (Massachusetts Inst. of Tech., Lexington). Carbon, 3: 465-73(Feb. 1966).

The results of magnetoreflection experiments in pyrolytic graphite, carried out at low temperatures in the photon energy range $0.06 < \hbar\omega < 0.50$ ev and in the magnetic field range $0 < H < 110$ kG, were interpreted in terms of the Slonczewski-Weiss band model. Interband transmissions associated with point H in the Brillouin zone yielded the parameters γ_0 and $|\Delta|$, while the other set of interband transitions (about point K) yielded values for γ_1, γ_3, and γ_4. The de Haas-van Alphen measurements provided the additional information required to complete the band parameter determination. Using the band parameters obtained by this method, a model of the Fermi surface of graphite was constructed. (auth)

30738 DETERMINATION OF THE STRUCTURE OF La_2TiO_5 WITH X RAYS AND NEUTRONS. Guillen, Marcelo; Bertaut, Erwin Felix (CNRS, Grenoble, France). Compt. Rend., Ser. B, 262: 962-5(Apr. 4, 1966). (In French).

La_2TiO_5 is orthorhombic ($\underline{a}$ = 10.97 Å, $\underline{b}$ = 11.37 Å, c = 3.93 Å, Z = 4) with the space group P nam(D_{2h}^{16}). All the atoms are in special (4 $\underline{c}$) positions. Ti is penta-coordinated by a trigonal bipyramid. (tr-auth)

30739 F-COLORING IN GAMMA- AND D-T NEUTRON-IRRADIATED IONIC CRYSTALS. Nishi, Masato; Ikeda, Masaomi (Hiroshima Univ.). Hiroshima Daigaku Kogakubu Kenkyu Hokoka, 13: No. 2, 11-20(Jan. 1966). (In Japanese).

Measurements were made on the F-coloring in some ionic crystals under ^{60}Co gamma and 14 Mev neutron irradiations. The growth and the decay curves of F-center in gamma irradiated crystals were quite similar to the results reported by others. Under 14 Mev neutron irradiations, the increase in F-coloring of LiF crystals was proportional to the total neutron dose, but in NaCl crystals it was saturated at doses of approximately 4×10^{13} neutrons. During 14 Mev neutron irradiation, the crystals were exposed in the atmosphere to gamma radiation generated near the target, and its intensity was estimated as about 10^2 R/hr. In the crystals colored with gamma rays to the secondary process, a very small amount of F-center was converted to R-centers by neutron irradiation. This conversion was promoted by the short time gamma irradiations. (auth)

30740 ELASTIC EXPLOSIONS IN SOLIDS CAUSED BY RADIATION. Bullough, R.; Gilman, J. J. (Univ. of Illinois, Urbana). J. Appl. Phys., 37: 2283-7(May 1966). (COO-1491-1).

If intense radiation (coherent light, secondary ionization, or sustained fission) is put into a solid in a time δ short compared with the elastic relaxation time, a resulting internal "explosion" may cause multiple fracturing and other damage. It is postulated that at $t = \delta \simeq 0$, the radiation causes a uniform dilation within a cylindrical region of radius a. Solution of the relevant wave equation (continuity preserved at $r = a$) indicates that a rarefaction wave of increasing amplitude moves inward from a with velocity v during the time interval, $0 < t < a/v$. The transient pressure variation at the center demonstrates a negative divergence at $t = a/v$. The pressure field at various times was found by numerical integration. This model accounts for some features of the damage caused by laser beams and other damage processes. (auth)

30741 IONIC DISPLACEMENT IN THE ALKALI HALIDES. Torrens, Ian McC.; Chadderton, Lewis T.; Morgan, D. Vernon (Cavendish Lab., Cambridge, Eng.). J. Appl. Phys., 37: 2395-8(May 1966).

Computer simulations of dynamic radiation damage events in the alkali halides reveal the importance of the focusing of energy in these lattices. Ionic displacement for KCl is most probable in the ⟨110⟩ direction, when the energy is in the region of 30 ev or greater and is least probable in the ⟨100⟩ direction. (auth)

30742 OXYGEN-DEFECT COMPLEXES IN NEUTRON-IRRADIATED GERMANIUM. Whan, R. E. (Sandia Lab., Albuquerque, N. Mex.). J. Appl. Phys., 37: 2435-9(May 1966).

The recovery processes in neutron-irradiated oxygen-doped germanium were studied by measuring the growth and decay of infrared absorption bands associated with oxygen-defect complexes. After a neutron irradiation at −50°C, the absorption band assigned to the stable oxygen-vacancy complex is barely detectable but increases upon annealing to 50°C. These results indicate that additional vacancies are produced by the dissociation of the large defect clusters formed by neutron irradiation. Annealing to higher temperatures produces the same bands in the same sequence as those which developed in the spectra of electron irradiated samples upon annealing. Comparisons of the annealing curves of the absorption bands produced by the two types of irradiations, however, reveal a general shift to higher annealing temperatures for the neutron-irradiated samples. These temperature shifts are inter-

preted as resulting from changes in equilibria of the oxygen-defect complexes caused by the dissociation of clusters into simpler defects. No similar evidence for the presence of clusters above annealing temperatures of 350°C was observed. (auth)

30743 ELECTRICAL CONDUCTION BY OXYGEN IONS IN CERIUM OXIDE. Holverson, E. L.; Kevane, C. J. (Arizona State Univ., Tempe). J. Chem. Phys., 44: 3692-6(May 15, 1966).

Oxygen gas was observed by means of a mass spectrometer to be evolved from calcium-doped ceramic cerium oxide when direct current was passed through it as 450°C. The applied voltage necessary to cause the electrolysis was about 100 v across a sample 4 mm long containing 0.86 at. % calcium. When voltages of 1.0 v or less were applied to ceramic and single-crystal samples there were pronounced transients and nonlinear potential distributions. These latter effects appear to be consistent with a picture of oxygen ions migrating to an electrode where they are at least partially blocked. (auth)

30744 ENERGY LEVELS AND CRYSTAL-FIELD SPLITTINGS OF Nd^{3+} IN YTTRIUM OXIDE. Chang, N. C. (Aerospace Corp., El Segundo, Calif.). Contract AF 04-(695)-669. J. Chem. Phys., 44: 4044-50(May 15, 1966).

Studies of the absorption and fluorescence spectra of Nd^{3+} in yttrium oxide are reported. The three Racah parameters $E^{1,2,3}$ and the spin-orbit parameter ξ giving the best overall agreement between the observed and calculated spectrum are $E^1 = 4853.9$, $E^2 = 24.20$, $E^3 = 471.87$, and $\xi = 877.59\ cm^{-1}$. The Stark splittings of the four levels $^4I_{9/2}$, $^4I_{11/2}$, $^4I_{13/2}$, and $^4I_{15/2}$ are used in a first-order perturbation calculation to determine the crystal-field parameters for Nd^{3+} in the C_2 sites of the Y_2O_3 lattice. The parameters are used to calculate the Stark splitting of 13 excited levels, and the results are compared with experimentally observed values. For 64 Stark components, the calculation predicts the splitting with an average of about 15 cm^{-1}. For the components of the $^2H_{11/2}$ and $^2G_{7/2}$ levels, very large discrepancies are present. (auth)

30745 ONE-PHONON COHERENT SCATTERING OF SLOW NEUTRONS FROM POLYCRYSTALLINE ALUMINUM. Iijima, Shungo (Nippon Atomic Industry Group Co., Japan). J. Nucl. Sci. Technol. (Tokyo), 3: 160-4 (Apr. 1966).

An approximate, closed expression is presented for one-phonon coherent scattering from a polycrystal of cubic Bravais lattice adopting assumptions on the dispersion relations more realistic than the simple Debye type. The multi-phonon process was calculated in incoherent approximation by the UNCLE code, and was added to the one-phonon coherent scattering. The results are found to be in fair agreement with previous measurements for aluminum. (L.B.S.)

30746 LATTICE SPECTRUM AND DIELECTRIC PROPERTIES OF EuF_2. Axe, J. D.; Pettit, G. D. (IBM Watson Research Center, Yorktown Heights, N. Y.). J. Phys. Chem. Solids, 27: 621-4(Apr. 1966).

Measurements at room temperature of the infrared reflectivity, low frequency dielectric constant ($\epsilon_0 = 7.7 \pm 0.2$) and optical index of refraction ($n = 1.555 \pm 0.005$) were carried out on EuF_2. The data were analyzed both by classical dispersion theory and Kramers-Kronig relations to obtain the frequency dependent dielectric dispersion from 50 cm^{-1} to 1400 cm^{-1}. As with other crystals of the fluorite type, a single strong resonant absorption is found. The optical mode frequencies are $\omega_{t0} = 194\ cm^{-1}$; $\omega_{l0} = 347\ cm^{-1}$. The best classical dispersion formula fit to the reflectivity yields the following parameters: $\omega_0 = 195.2\ cm^{-1}$, $4\pi\rho = 5.15$, $\bar{\gamma} = 25.2\ cm^{-1}$. The (Szigeti) effective charge on the Eu^{+2} ion is 1.67 e. These results are used to discuss polarizabilities, covalency, and crystal chemistry of divalent europium compounds within the context of a "shell" model. (auth)

30747 FOURTH ORDER CRYSTAL FIELD SPLITTING IN RARE EARTH(III) IONS. Schumacher, D. P.; Hollingsworth, C. A. (Univ. of Pittsburgh). J. Phys. Chem. Solids, 27: 749-53(Apr. 1966).

The energy level expressions for paramagnetic rare earth (III) ions in cubic crystalline fields are calculated as a function of a perturbing magnetic field applied parallel to the ⟨100⟩ and ⟨111⟩ axes and of a fourth order crystalline field parameter for the Stark effect. The presence in an energy level expression of a $g\mu_B H$ term indicates a permanent moment while an induced moment is indicated by a $g^2\mu_B^2 H^2$ term. (auth)

30748 COLOR CENTERS IN X-RAYED OR ULTRAVIOLET-IRRADIATED POTASSIUM IODIDE. Konitzer, John D.; Hersh, Herbert N. (Zenith Radio Corp., Chicago). J. Phys. Chem. Solids, 27: 771-81(Apr. 1966).

The properties of KI colored by x-rays or ultraviolet rays were studied between 5 and 300°K. The production and properties of F, H, V_1, V_2, R_1, R_2, M, N, O and F′ centers are similar in most respects to analogous centers produced in bromides and chlorides. A notable exception is that each of the trapped hole centers, H, V_1, V_2, exhibits two major absorption bands in the uv-visible region rather than one. In addition to F aggregates, KI also exhibits radiation-produced V center aggregates. The most unusual features noted in KI are the following: color centers (F and V_2) can be easily produced by nonionizing ultraviolet radiation, apparently by an intrinsic excitonic process; although V_k, i.e., I_2^-, centers are not stable centers in pure KI, they exist in some form as the major transient during irradiation; between 90 and 110°K, KI exhibits the following sharp temperature-dependences: F and V_2 center production rates by uv or x-ray increase markedly, characteristic luminescence excited by uv or x rays exhibits a downswing, I_2^- centers become mobile. The H center exhibits an anisotropy in its two absorption bands having its optical dipole moment parallel to the ⟨110⟩ axes of the crystal, a symmetry consistent with I_4^{-3}. The radiation-induced V_2 and V_3 bands are shown to be related to the chemically-produced Mollwo bands with both bands being due to one center (V_2). Based on a photochemical concept of color center formation the model suggested for the radiation-induced V_2 center is an interstitial I_3^- molecule-ion, and for the V_1 center an I_2 molecule. Taking the experimental observations as a whole it is believed possible that an excitonic mechanism may be responsible for vacancy and interstitial production even in an x-rayed crystal. (auth)

30749 ANGULAR DEPENDENCE OF THE ONE-PHONON-NUCLEAR QUADRUPOLE INTERACTIONS. Mahler, R. J. (National Bureau of Standards, Boulder, Colo.). J. Phys. Chem. Solids, 27: 871-9(May 1966).

The angular dependence of the $\Delta m = \pm 1$ and $\Delta m = \pm 2$ nuclear quadrupole-lattice phonon interaction is developed in a crystal with 43m symmetry, assuming a lattice potential $V = f(r)$ and a definite wave number and polarization for the interacting phonons. The results can be used to explain experiments involving the interaction of a nuclear spin system with externally added phonons. (auth)

30750 TEMPERATURE DEPENDENCE OF INTERNAL FIELD AT THE ^{57}Fe NUCLEUS IN NICKEL LATTICE. Bhide, V. G.; Shenoy, G. K. (Inst. of Science, Bombay). J. Phys. Soc. Jap., 21: 625-30(Apr. 1966).

The hyperfine field at the ^{57}Fe nucleus introduced as an impurity in the nickel lattice has been measured at various temperatures, using the Mössbauer resonance technique. The values follow closely but not exactly the saturation magnetization curve of nickel. No internal field is observed above the Curie temperature of nickel. The results indicate that the hyperfine field at the impurity nucleus is dependent on the impurity and host magnetic moments in a complex way. The above measurements are compared with the NMR measurements of the temperature variation of the hyperfine field at the ^{59}Co and ^{61}Ni nuclei in nickel. The nonoverlap of these variations is explained qualitatively. (auth)

30751 OPTICAL PROPERTIES OF CsI:Tl AND CsBr:Tl. Masunaga, Shoji; Morita, Ituo; Ishiguro, Masa-

kazu (Osaka Univ.). J. Phys. Soc. Jap., 21: 638-44(Apr. 1966).

Absorption, excitation, and emission spectra and luminescent decay of CsI: Tl have been investigated over the temperature range from 2 to 300°K. Six absorption bands are observed in contrast with four absorption bands, A, B, C, and D in alkali halide–thallium phosphors having the NaCl structure. There exists no other absorption band having a character of the forbidden line as the B band. At 10°K, four emission bands are observed. The luminescent decay is composed of the fast and slow components and is somewhat complicated. For the purpose of comparison, the experiments on CsBr : Tl are also described. (auth)

30752 EFFECTIVE MAGNETIC FIELD AT THE ^{60}Co NUCLEUS IN THE Co–Pd ALLOY. Alekseevskii, N. E.; Anishchenko, V. N.; Erzinkyan, A. L.; Parfenova, V. P.; Shpinel', V. S. (Moscow State Univ.). JETP Lett. (USSR) (Engl. Transl.), 3: 206-7(Apr. 15, 1966).

Translated from Zh. Eksp. Teor. Fiz., Pis'ma Redaktsiya, 3: 318-20(Apr. 15, 1966).

The effective magnetic field at the ^{60}Co nucleus in an alloy of 0.3 at. % Co with Pd was measured, by determining the anisotropy of the γ radiation of oriented ^{60}Co nuclei. (B.G.D.)

30753 BARIUM STANNATE: A SOURCE FOR THE MEASUREMENT OF THE MOESSBAUER EFFECT ON ^{119}Sn. Plotnikova, M. V.; Mitrofanov, K. P.; Shpinel, V. S. (Moscow State Univ.). JETP Lett. (USSR) (Engl. Transl.), 3: 209-11(Apr. 15, 1966).

Translated from Zh. Eksp. Teor. Fiz., Pis'ma Redaktsiya, 3: 323-6(Apr. 15, 1966).

A discussion is presented on $BaSnO_3$ as a source for measurement of the Mössbauer effect on ^{119}Sn because it possesses simultaneously a high probability of the effect at room temperature and a singlet unbroadened resonance-emission line. Measurements of these two characteristics of $BaSnO_3$ are presented. (B.G.D.)

30754 MULTIPURPOSE RELAXATION APPARATUS FOR MEASURING SIGNS OF ELEMENTARY PROCESSES IN IONIC CRYSTALS SUBJECTED TO IONIZING RADIATION. Belkind, A.; Kalendarev, R.; Tomkus, I. (Inst. of Physics, Academy of Sciences, Latvian SSR). Latv. PSR Zinat. Akad. Vestis, Fiz. Tek. Zinat. Ser., No. 6, 11-18(1965). (In Russian).

The apparatus can be used for investigating nonisothermal relaxation processes and for determining their signs. The apparatus permits the carrying out of absorption thermo- and photo-stimulated luminescence, thermo- and photo-stimulated emission measurements simultaneously. The measurements are made in the region with a constant heating rate. An example of a complex investigation of nonisothermal processes due to the destruction of color centers in NaCl + (Tl) crystals is presented. (auth)

30755 NUCLEAR MAGNETIC RESONANCE IN RARE EARTH FLUORIDES. Saraswati, V.; Vijayaraghavan, R. (Tata Inst. of Fundamental Research, Bombay). Phys. Lett., 21: 363-4(June 1, 1966).

The results of ^{19}F resonance in the rare earth trifluorides are presented and discussed. (auth)

30756 VARIATION OF THE MAGNETIC MOMENT OF COBALT IN $Gd_uY_{1-u}Co_2$ COMPOUNDS. Lemaire, R.; Schweizer, J. (CEN, Grenoble, France). Phys. Lett., 21: 366-8(June 1, 1966). (In French).

The magnetic properties of the compounds $Gd_uY_{1-u}Co_2$ are measured. The magnetic moment of cobalt depends on the parameter u. The compound YCo_2 is not ordered above 2°K. (auth)

30757 MOESSBAUER EFFECT OF THE 99- AND 129-kev TRANSITIONS IN ^{195}Pt. Buyrn, A. B.; Grodzins, L. (Massachusetts Inst. of Tech., Cambridge). Phys. Lett., 21: 389-91(June 1, 1966). (MIT–2098-236).

The Mössbauer effect of the 99 kev transition in ^{195}Pt was studied in various diamagnetic environments and Debye temperatures obtained for Pt in Pt, Be, Cu and Ir. Some negative results on the 129 kev transition are also reported. (auth)

30758 APPARENT LOWERING OF ENERGY LEVELS AS MEASURED BY ORBACH RELAXATION RATES. Young, B. A.; Stapleton, H. J. (Univ. of Illinois, Urbana). Contract SD-131. Phys. Lett., 21: 498-501(June 15, 1966).

Discrepancies are noted among the reported excited state energies of rare-earth ions as measured optically and by electron spin-lattice relaxation techniques. A simple modification to the Orbach relaxation mechanism, involving widths of excited states, seems to account for the data. (auth)

30759 ELECTRON SPIN RESONANCE STUDIES OF ALUMINIUM ION DEFECT PAIRS IN REACTOR-IRRADIATED Al_2O_3. Cox, R. T. (Centre d'Etudes Nucleaires, Grenoble, France). Phys. Lett., 21: 503-4(June 15, 1966).

Alpha-Al_2O_3 irradiated in pile at 77°K gives an electron spin resonance spectrum with ^{27}Al hyperfine structure which is attributed to a paramagnetic pair of Al ions. (auth)

30760 THE CRYSTAL FIELD OF $PrCl_3$. Ellis, M. M.; Newman, D. J. (Queen Mary Coll., London). Phys. Lett., 21: 508-10(June 15, 1966).

A simple model is suggested for the calculation of crystal field parameters of rare earth ions in paramagnetic salts. The results of some calculations on $PrCl_3$ show that this model gives parameters close to those obtained experimentally. (auth)

30761 NUCLEAR MAGNETIC RESONANCE STUDIES OF SOME MATERIALS CONTAINING DIVALENT EUROPIUM. Boyd, E. L. (IBM Watson Research Center, Yorktown Heights, N. Y.). Contract AF49(638)-1230. Phys. Rev., 145: 174-8(May 6, 1966).

The results of a low-temperature NMR experiment on ^{153}Eu in EuO are reported. The data, which are assumed to be linear with magnetization, are compared with calculated values using spin-wave theory. Values of $J_1/k_b = 0.750 \pm 0.0025$°K and $J_2/k_b = -0.0975 \pm 0.004$°K are found to give a good description of EuO. Also the results of NMR studies of the ligands ^{19}F and ^{133}Cs in EuF_2 and $CsEuF_3$ are reported. These experiments indicate that there is a reversal in sign of the unpaired spin density of the europium ion. The same results are obtained with europium-bearing glasses. This effect is discussed in terms of the Freeman-Watson model of Gd^{3+} and in terms of a virtual 5d state in Eu^{2+}. (auth)

30762 EFFECTS OF LATTICE VIBRATIONS ON ANGULAR CORRELATIONS. Tang, L. H. (Univ. of Detroit); Osborn, R. K. Phys. Rev., 146: 695-703(June 17, 1966).

A theory of the influence of the environment on γ-γ angular correlation is presented. The theory is formulated by using the damping theory, and the perturbation factor of the perturbed angular-correlation function, which contains the effects of the changes of the states of the environment on the angular correlation, is obtained. In the solid environment, the effects of the lattice vibrations on the electric quadrupole coupling were analyzed by using the normal-mode expansion of the lattice displacements; and the perturbed angular correlation function is shown to be a function of the crystal temperature. In order to determine the nuclear electric quadrupole moment in an excited state, which cannot be done by the usual microwave methods, a rotational technique is suggested and the theory has been developed for the case of asymmetric fields. For the special case of an axially symmetric crystalline field, the present theory predicts a phase shift in the rotational pattern of anisotropy. (auth)

30763 LOWEST 4f → 5d TRANSITION OF TRIVALENT RARE-EARTH IONS IN CaF_2 CRYSTALS. Loh, Eugene (Hughes Research Labs., Malibu, Calif.). Phys. Rev., 147: 332-5(July 8, 1966).

The lowest 4f → 5d ultraviolet adsorption band of eleven (Ce, Pr, Nd, Sm, Eu, Tb, Dy, Ho, Er, Tm, and Yb) of the fourteen trivalent rare-earth (RE) ions in host CaF_2 crystals was measured. The room temperature absorption cross section [cm^2] and half-width [cm^{-1}] of these bands for the first-half series of RE^{3+} are larger than that of the

second-half series (from Tb^{3+} on), possibly because of some spin-forbiddenness in the transition of the latter. Typically, they are $\sim 5 \times 10^{-18}$ cm^2 and ~ 1700 cm^{-1}, respectively, for the former and $\sim 3 \times 10^{-18}$ cm^2 and ~ 1300 cm^{-1}, respectively, for the latter at typical concentration of $\sim 10^{-4}$. The oscillator strength is estimated to be $\sim 10^{-2}$ for the first half-series and $\sim 4 \times 10^{-3}$ for the second half-series RE^{3+}. At liquid nitrogen temperature the band sharpens and shifts ~ 200 cm^{-1} toward lower wave number, probably because of increasing crystal field in the contracted lattice; a zero-phonon line and some vibrational structure are also developed in Ce^{3+}- and Pr^{3+}-doped CaF_2. The location of the band ranges from $\sim 33{,}000$ cm^{-1} (Ce^{3+}) to $\sim 71{,}000$ cm^{-1} (Yb^{3+}), with that of Gd^{3+} and Lu^{3+} outside ($\gtrsim 80{,}000$ cm^{-1}) of the transparent region of CaF_2 crystal. Compared with the data available for the free ions Ce^{3+}, Pr^{3+}, and Yb^{3+}, the location of the lowest 4f → 5d transition of $(RE)^{3+}$ ions in CaF_2 is found to be lowered $\sim 18{,}000$ cm^{-1} in the crystal environment. The energy of the lowest 4f → 5d transition is described satisfactorily by a formula due to Jørgensen for $4f^n \rightarrow 4f^{n-1}$ 5d transitions in the free ion, decreased by 18,000 cm^{-1}. (auth)

30764 MOESSBAUER STUDY OF ^{83}Kr IN THE COMPOUND KrF_2. Ruby, S. L.; Selig, H. (Argonne National Lab., Ill.). Phys. Rev., 147: 348-54(July 8, 1966).

The compound KrF_2 was studied by use of the techniques of Mössbauer spectroscopy. The results are that (a) the interaction energy is $e^2qQ_g = 130 \pm 4$ mm/sec $= 960 \pm 30$ mHz, (b) the ratio of the nuclear quadrupole moment of the excited state to that of the ground state is $R = Q_e/Q_g = 1.70 \pm 0.02$, and (c) the isomer shift referred to atomic krypton is 1.50 ± 0.10 mm/sec. These results are interpreted as supporting the infrared, Raman, and NMR results which other groups had previously obtained for this compound and as confirming the earlier conclusions reached with the analogous compound XeF_2. The quadrupole moment of the first excited state of ^{83}Kr is found to be 0.459 ± 0.006 b, and the fractional decrease in charge radius between the first excited state and the ground state is approximately 4×10^{-4}. (auth)

30765 NEUTRON INVESTIGATION OF TEMPERATURE EFFECTS IN THE MAGNON SPECTRUM OF MAGNETITE. Dimitrijevic, Z. (Inst. of Nuclear Sciences Boris Kidric, Vinca, Yugoslovakia); Krasnicki, S.; Rzany, H.; Todorovic, J.; Wanic, A. Phys. Status Solidi, 15: 119-22(May 1, 1966).

The diffuse magnon scattering peaks connected with $\tau =$ (111) in magnetite are examined at a number of temperatures using neutrons with $\lambda = 1.314$ Å. The decrease in magnon energies at elevated temperatures is observed and compared with the theory of Mills. Pronounced temperature dependent asymmetry of the magnon low energy peak is found. (auth)

30766 MOESSBAUER EFFECT FOR ^{57}Fe IMPURITY ATOMS. Bara, J. (Jagiellonian Univ., Krakow); Hrynkiewicz, A. Z. Phys. Status Solidi, 15: 205-9(May 1, 1966).

The Debye-Waller factors for the 14.4 kev γ rays of ^{57}Fe atoms as a dilute impurity in 16 crystal lattices are measured at room temperature. The force constants for the host-impurity atoms are found to be almost the same as for the host-host atoms. A correlation between the isomer shifts and the standard electrode potentials is observed. (auth)

30767 THERMOLUMINESCENCE AND THERMOLUMINESCENCE SPECTRA OF CALCIUM FLUORIDE CRYSTALS IRRADIATED BY X RAYS. Ratnam, V. V.; Bose, H. N. (Indian Inst. of Tech., Kharagpur). Phys. Status Solidi, 15: 309-16(May 1, 1966).

The glow curve pattern obtained for CaF_2 crystals irradiated by x rays at room temperature is markedly affected by even a small rise (say 30°C) in the temperature of irradiation. This is presumably due to the neutral fluorine atoms which are produced by the holes trapped by the fluorine ions during x irradiation and which, at elevated temperatures of irradiation, form molecular complexes or diffuse out of the crystal. The spectral composition of the thermoluminescence obtained with samples irradiated at room temperature is similar for the first three glow peaks, except for minor changes in the relative intensities of the emission peaks; for the fourth glow peak however it is markedly different. Further, the first three glow peaks attain saturation with x ray dose similar to the color bands, but no such tendency is observed for the fourth glow peak. These results indicate that the traps and emitting centers responsible for the first three glow peaks are different from those of the fourth glow peak. (auth)

30768 INTERACTION OF MICROWAVE PHONONS WITH IRRADIATION CENTERS IN QUARTZ. Lewis, M. F.; Rosenberg, H. M.; Wigmore, J. K. (Oxford Univ.). Phys. Status Solidi, 15: 317-23(May 1, 1966).

The electron spin resonance spectrum of the paramagnetic centers produced by the irradiation of quartz was investigated at 1.8°K at 10 GHz from well below to above the microwave saturation region. Hypersonics at 10 GHz were then introduced and this reduced the resonance signal. The effect was studied as a function of hypersonic power and frequency, microwave monitoring power and magnetic field orientation. The experimental results suggest that the spin-lattice relaxation time is of the order of 6s at 1.8°K and is determined by cross relaxation processes. (auth)

30769 SIMULTANEOUS DIFFUSION OF ARGON AND KRYPTON IN SINGLE CRYSTALS OF KCl–RbCl. Schmeling, P.; Schroerschwarz, R. (Kernforschungszentrum, Karlsruhe, Ger.). Phys. Status Solidi, 15: 325-9(May 1, 1966).

The simultaneous diffusion of ^{41}Ar and ^{85m}Kr into single crystals containing 30 mole percent of KCl and 70 mole percent of RbCl is studied. The rare gases are created by irradiation with fast neutrons. The diffusion kinetics are similar to those of the systems KCl/Ar and RbCl/Kr. The interesting high temperature region is characterized by activation energies of (0.28 ± 0.035) ev and (0.56 ± 0.035) ev for KCl–RbCl/Ar and KCl–RbCl/Kr, respectively. The diffusion coefficients of argon are about one order of magnitude higher than those of krypton. Comparison with experiments performed after irradiation to high neutron doses shows that these values are not affected by radiation damage. (auth)

30770 PLASMA-TYPE OSCILLATIONS OF KINKED DISLOCATIONS. Alefeld, G. (General Atomic Division, General Dynamics Corp., San Diego, Calif.). Phys. Status Solidi, 15: 331-7(May 1, 1966).

The oscillation frequencies of interacting kinks of both signs are determined taking into account long range interaction between kinks. The frequencies are proportional to the square root of the sum of positive and negative kink densities and are consequently temperature dependent, in contrast to the frequencies of the dislocation string model. The temperature dependence of the relaxation time for the phonon scattering peak is therefore determined not only by the temperature dependence of the damping constant B but also by that of the kink densities. (auth)

30771 RADIATION DEFECTS IN DEUTERON-BOMBARDED CdS CRYSTAL. Schweinberger, W.; Wruck, D. (Physikalisch-Technisches Institut, Deutsche Akademie der Wissenschaften, Berlin. Humboldt Univ., Berlin). Phys. Status Solidi, 15: 355-68(May 1, 1966). (In German).

The dark conductivity, the spectral response of the photoconductivity, the electron lifetime, and the trap distribution in CdS single crystals irradiated with 13.5 Mev deuterons at 150°K are studied. The concentration of In and Sn created by by nuclear transmutations is measured by γ-spectroscopic techniques. From the electrical measurements, it is found that defect levels which are stable at room temperature at $E_c - 0.10$ ev, $E_c - 0.42$ ev, and at $E_c - 0.65$ ev with an introduction rate of approx. 5×10^{-3} cm^{-1} and with electron capture cross sections of 5×10^{-15}, 1×10^{-14}, and 5×10^{-14} cm^2, respectively. The center at $E_c - 0.42$ ev acts both as a donor and a trap. The behavior of the electron lifetime indicates an increase in the concentration of class II recombination cen-

ters at approx. E_v + 0.15 ev. Suggestions are made as to the origin of the bombardment-induced defect levels. (auth)

30772 ^{19}F NUCLEAR RELAXATION TIME IN CaF_2 : Nd. Burnett, R. (Rice Univ., Houston, Tex.). Physica, 32: 433-43(Feb. 1966).

The ^{19}F nuclear spin-lattice relaxation time T_1 was measured in neodymium doped calcium fluoride (0.005 weight-%) in the temperature range 2°K < T < 300°K. Data were obtained by a pulsed nuclear resonance method for the magnetic field aligned along the crystal directions (100) and (110). The experimental results were analyzed by means of a general expression for T_1 valid for diffusion limited and rapid diffusion relaxation as well as for the intermediate case. This expression takes account of the dependence of the barrier for diffusion on temperature and impurity correlation time and can be used to determine the effective correlation time as a function of temperature. The impurity correlation times ρ necessary to explain the observed values of T_1 range from $\rho \approx 10^{-4}$ sec at 2°K to $\rho \approx 10^{-11}$ sec at 300°K. The temperature dependence of ρ can be explained by an Orbach process involving an excited state at approximately 65 cm^{-1}. (auth)

30773 PSEUDO WAVE FUNCTIONS. Singh, N.; Joshi, S. K. (Univ. of Allahabad, India). Physica, 32: 479-83(Feb. 1966).

The pseudo wave function in the Cohen-Heine scheme is expressed in terms of the complete orthonormal set of the wave functions of the original hamiltonian and the expansion coefficients are calculated. The applicability of this scheme is discussed. (auth)

30774 NEW LASER LINE DUE TO ENERGY TRANSFER FROM COLOR CENTERS TO ERBIUM IONS IN CaF_2. Forrester, P. A.; Sampson, D. F. (Royal Radar Establishment, Worcester, Eng.). Proc. Phys. Soc., 88: 199-204(May 1966).

Two new laser lines at 1.5308 μm were observed in single crystals of CaF_2 grown from a melt containing Er_2O_3. The stimulated emission from such crystals is different from those doped with ErF_3, presumably reflecting a difference in the crystalline environment at the site of the impurity ions. The emission only occurs in crystals which have been γ-irradiated; this treatment produces strong absorption bands centered on 3620 and 5520 Å, which arise from a color center associated with the presence of oxygen in the lattice. Absorption in these bands produces excitation which is transferred to the erbium impurity ions, resulting in an enhancement of the fluorescence power. The lines have lower thresholds than previously reported emissions from erbium, but only occur at temperatures in the liquid helium region. The output power shows a saturation effect which is attributed to a rise in the temperature of the lattice during the pumping pulse. (auth)

30775 S-D EXCHANGE INTERACTIONS AND FERMI SURFACE IN NICKEL. Furrer, A.; Schneider, T.; Haelg, W. (Eidgenoessisches Institut fuer Reaktorforschung, Wuerenlingen, Switzerland). Solid State Commun., 4: 99-101(Mar. 1966). (In German).

The dispersion of spin waves in nickel was investigated with polarized thermal neutrons. The anomalies observed in the measurements allow for the following conclusions: The s-d interaction contributes significantly to the exchange. The wave number of the s-electron Fermi surface has a value of 1.48 ± 0.02 $Å^{-1}$ in the (111)-direction. (auth)

30776 CHARACTERISTIC ENERGY LOSSES OF ELECTRONS AND COLOR CENTERS IN LiF, LiCl, AND NaCl. Pradal, F.; Gout, C.; Lahaye, B. (Faculte des Sciences, Toulouse). Solid State Commun., 4: 119-22(Mar. 1966). (In French).

The energy losses of an electron beam of 20 kev passing through thin films of LiF, LiCl, and NaCl are investigated. The excitation energies of some color centers and the energy band gaps are evaluated. The lines of color centers are particularly intense with cleaved samples previously x irradiated. (auth)

30777 PLASMA EXCITATIONS IN LiF. Lynch, David W. (Ames Lab., Ames, Iowa). Solid State Commun., 4: 159-63(Apr. 1966). (IS-1301).

The absorption data of Milgram and Givens on LiF films have been analyzed by means of dispersion integrals. From the plot of $Im(\epsilon^{-1})$ vs. energy the characteristic electron energy loss at 25.3 ev can be identified as a plasma-like excitation very close to a one-electron excitation peak at 23.9 ev. Other possible plasma loss peaks are at 13.4, ~45, and ~50 ev. (auth)

30778 FREE INDUCTION SIGNAL IN EXCHANGE PAIRS. Shubina, R. V. (Inst. of Physics and Tech., Kazan). Zh. Eksp. Teor. Fiz., 50: 936-42(Apr. 1966). (In Russian).

Formulas are derived for the initial amplitude and shape of the free induction signal (FIS). The usual conditions of magnetic resonance are assumed, and the time-dependent solution of the wave equation for the interaction of two coupled spins in fields of arbitrary intensity is employed. The temperature dependence of the signal is taken into account. It is demonstrated that, due to the relaxation terms, the decay of the FIS is of an oscillatory nature. The signal amplitude contains oscillations with a frequency proportional to the interaction constant of the coupled spins of the pair. It is shown that variation of the shape of the FIS depends on the temperature T. Near T = 0 decay of the FIS becomes weaker. The results of the theory are considered for the case of Nd^{3+} pairs in lanthanum ethyl sulfate. (auth)

30779 EFFECT OF INTERELECTRON COLLISIONS ON THE ELECTRON DISTRIBUTION FUNCTION IN A STRONG ELECTRIC FIELD. Levinson, Y. B.; Mazhuolite, G. E. (Inst. of Physics and Mathematics, Academy of Sciences, Lithuanian SSR). Zh. Eksp. Teor. Fiz., 50: 1048-54(Apr. 1966). (In Russian).

The collision frequency of an electron is much greater in the active region $\epsilon > \omega_0$ than in the passive region $\epsilon < \omega_0$ during scattering on optical phonons with a limiting frequency ω_0 and at temperatures $T \ll \omega_0$. Therefore those cases when interelectron collisions are predominant only in the passive region should be distinguished from those when this occurs throughout all momentum space. An examination of the kinetic equation with this circumstance in mind indicates that interelectron collisions lead to a new channel for relaxation of energy and momentum (imparted to the passive electrons by the field) as a result of their transfer to the active region with subsequent transfer to the lattice. In distinction from the ordinary relaxation which occurs upon absorption and instantaneous reemission, such energy relaxation is not connected with dispersion of optical phonons. (auth)

30780 RELAXATION PHENOMENA NEAR THE CRITICAL POINTS. Mori, Hazime (Kyushu Univ., Fukuoka). pp 17-35 of Many-Body Theory. Kubo, Ryogo (ed.). Tokyo, Syokabo Publishing Co. New York, W. A. Benjamin, Inc., 1966.

The anomalous relaxation phenomena near the critical points are reduced to the critical fluctuations of certain variables by expressing the damping constants and the associated transport coefficients in terms of the fluctuations of a set of variables. The spin diffusion in ferromagnets and the line widths of the electron spin resonance in ferro- and antiferro-magnets are discussed as examples, and the mechanisms of their anomalies near the critical points are clarified. (G.O.Y.)

30781 THEORY OF CORRELATED CRYSTALS. Brueckner, Keith A.; Frohberg, T. (Univ. of California, San Diego, La Jolla). Contract DA-31-124-ARO-D-257. pp 134-51 of Many-Body Theory. Kubo, Ryogo (ed.). Tokyo, Syokabo Publishing Co. New York, W. A. Benjamin, Inc., 1966.

The single-particle description of crystals is extended by including correlation effects in the wave function of the system and developing the cluster expansion for the energy. Some approximations to the cluster expansion are considered, and it is shown that the principal features of the ap-

proximate results can be readily derived by a partial summation of the series given by the Rayleigh-Schroedinger perturbation theory. (D.C.W.)

30782 FLUORESCENCE DECAY OF THE Sm^{2+} ION IN LANTHANUM CHLORIDE [Thesis]. Partlow III, William Dempsey. University, Ala., Univ. of Alabama, 1965. 59p.

Sm^{2+} fluorescence has been observed in $LaCl_3$ from ions in two nonequivalent lattice sites. In one site the free-ion degeneracy of the energy levels has been completely removed by the crystalline field. The levels of the other ions, which are in a site with higher symmetry, are partially degenerate. The $^5D_1$ fluorescence line positions of the high-symmetry type are reported. The fluorescence lifetimes of the $^5D_1$ levels in the two locations were measured. The lifetime of the ions in high-symmetry sites was found to be independent of temperature in the region from 4.2°K to 80°K. The lifetime of the $^5D_1$ levels in low-symmetry sites was found to decrease at the higher temperatures, due to population of the $^5D_0$ level of these ions by nonradiative transitions. The nonexponential decay of the $^5D_0$ level was measured, and its behavior supports this conclusion. The temperature dependence of the lifetime of $^5D_1$ level of the ions in the low-symmetry sites was measured from 4.2°K to 80°K, and was attributed to a multiphonon process. A study was made of the influence upon the decay lifetime of the $^5D_0$ level of the low-symmetry ions of the addition of several trivalent rare earth ions to the crystals. Nd^{3+}, Dy^{3+}, Sm^{3+} were found to reduce this lifetime appreciably. (Dissertation Abstr.)

30783 LECTURES ON SOLID STATE PHYSICS DELIVERED AT THE EIGHTH SUMMER MEETING OF PHYSICISTS, SEPTEMBER 1963, HERCEGNOVI, YUGOSLAVIA. VOLUME I. RELAXATION PHENOMENA AND RELATED TOPICS. Blinc, R. (ed.). Yugoslavia, Federal Nuclear Energy Commission [1964]. 316p. (CONF-630910-(Vol.1)). Nuklearni Institut J. Stefan, Ljubljana, Yugoslavia.

Papers (14) are included on the concept of relaxation time, impurity condition, theory of transport for nonspherical and nonparabolic energy bands, nuclear relaxation in solids, hydrogen bond dynamics by NMR methods, nuclear polarizations and relaxation, dielectric relaxation and ice crystals, diffusion processes in ice, hydrogen bond, proton-lattice interactions in hydrogen bonded ferroelectric crystals, isotope effects in hydrogen bonding in solids, theory of polarons, and vortex lines in superconductors. (B.G.D.)

30784 LECTURES ON SOLID STATE PHYSICS DELIVERED AT THE EIGHTH SUMMER MEETING OF PHYSICISTS, SEPTEMBER 1963, HERCEGNOVI, YUGOSLAVIA. VOLUME II. RADIATION DAMAGE AND NEUTRON SCATTERING. Blinc, R. (ed.). Yugoslavia, Federal Nuclear Energy Commission [1964]. pp 311-568. (CONF-630910-(Vol.2)). Nuklearni Institut J. Stefan, Ljubljana, Yugoslavia.

Papers (5) include radiation damage in solids, lattice defects observation by electron microscopy, neutron diffraction studies of magnetic materials, magnetic scattering of neutrons, and inelastic scattering of neutrons. (B.G.D.)

30785 THERMAL CYCLE DEGRADATION OF CHARGE CARRIER LIFETIME AND RESISTIVITY IN SILICON. Walter, F. J.; Bates, D. D. (Nuclear-Chicago Corp., Oak Ridge, Tenn.). 23p. (CONF-660304-11). ORAU. Gmelin, AED-CONF-66-020-4.

From Institute of Electrical and Electronics Engineers, Scintillation and Semiconductor Counter Symposium, Washington, D. C.

Numerous published examples of high-temperature-induced changes in the properties of semiconductors indicate that thermal degradation of charge carrier lifetime may be responsible for excess current and noise in diffused junction radiation detectors. By comparing the noise and current in surface barrier diodes made from silicon subjected to a thermal cycle to the properties of similar diodes made from uncycled material, it is demonstrated that there can be severe degradation of the original material. The relationship between charge carrier lifetime and noise in semiconductor radiation detectors is discussed. Detailed information on changes in resistivity and etch pit density for both p- and n-type silicon from several manufacturers as a function of original resistivity and thermal cycle is presented. Information on excess diode current and noise is available only for the n-type samples. The results are consistent with the previously observed strong dependence on both maximum temperature and rate of temperature change. Large increases in diode current and noise were observed for cycles with peak temperatures as low as 500°C. (auth)

REACTOR TECHNOLOGY

General

Refer also to abstract 29470.

30786 (ANL–7190) REACTOR ENGINEERING DIVISION ANNUAL REPORT, JULY 1, 1964 TO JUNE 30, 1965. (Argonne National Lab., Ill.). Mar. 1966. Contract W-31-109-eng-38. 207p. Dep. mn. CFSTI $6.00 cy, $1.25 mn.

Research and development are summarized in eight sections. Separate abstracts were prepared for six sections. One of the sections for which no abstract was prepared contains a brief discussion of process heat uses, while the other section contains lists of publications for the period. (J.R.D.)

For abstracts of individual sections see: 29374, 29375, 29974, 30787, 30788, and 30875.

30787 (ANL–7190, pp 11-142) REACTOR PROJECTS AND PROGRAMS. (Argonne National Lab., Ill.).

Activities associated with the EBR-II are summarized. Information is included on approach-to-power program, plant improvements, and experimental support. The fast reactor test facility is described, and research in support of this facility is summarized. Information is presented concerning component design and testing, design of in-cell fuel and equipment handling systems, and safety analyses results. The history and status of the Argonne Advanced Research Reactor (AARR) are reviewed. Information is included on design of the AARR and on supporting research and development. Research on the Experimental Boiling Water Reactor is reported under plant modification, inspection, maintenance, and supporting research and development. Stress analysis of the CP-5 vessel coolant distribution plenum is reported. The Argonne nuclear rocket program is described. Information is included on system analysis, fuel element development, operations at the H_2 flow facility, and research on structural mechanics. (J.R.D.)

30788 (ANL–7190, pp 176-88) FAST REACTOR SAFETY RESEARCH AND DEVELOPMENT. (Argonne National Lab., Ill.).

Investigations of reactor Na coolant expulsion are summarized along with studies of reactor control and stability, digital control of EBR-II, and fuel meltdown in TREAT. Design of TREAT experimental facilities are described. A review of radiation damage assessment of pressure vessel steels is presented. Results of tests and calculations on stresses and deflections in reactor core support grid structures are included. (J.R.D.)

30789 (ANL–7204) REACTOR DEVELOPMENT PROGRAM PROGRESS REPORT, APRIL 1966. (Argonne National Lab., Ill.). May 31, 1966. Contract W-31-109-eng-38. 95p. Dep. mn. CFSTI $3.00 cy, $0.75 mn.

Separate abstracts were prepared for the four included sections. (M.O.W.)

For abstracts of individual sections see: 30790–30792 and 30932.

30790 (ANL–7204, pp 1-31) LIQUID-METAL-COOLED REACTORS. (Argonne National Lab., Ill.).

Further developments in liquid-metal cooled reactors are reported on the EBR-II, general fast reactor physics, general fast reactor fuel development, general fast reactor fuel reprocessing development, and sodium technology. (M.O.W.)

30791 (ANL–7204, pp 32-64) GENERAL REACTOR TECHNOLOGY. (Argonne National Lab., Ill.).

Further research developments are reported on experimental reactor and nuclear physics, theoretical reactor physics, instrumentation, high-temperature materials studies, other reactor fuels and materials development, engineering development, and chemical separations. (M.O.W.)

30792 (ANL–7204, pp 74-86) NUCLEAR SAFETY. (Argonne National Lab., Ill.).

Brief summaries of various research dealing with reactor kinetics are presented. The compatibility of W and TaC after heating to 2700°C was investigated. The metal-water reactions associated with the meltdown of Zircaloy-2 clad, Vibra-packed UO_2-core fuel in TREAT were investigated. (M.O.W.)

30793 (IDO–17147) NUCLEAR TECHNOLOGY BRANCHES QUARTERLY REPORT, JULY 1–SEPTEMBER 30, 1965. (Phillips Petroleum Co., Idaho Falls, Idaho. Atomic Energy Div.). Apr. 1966. Contract AT(10-1)-205. 44p. Dep. mn. CFSTI $2.00 cy, $0.50 mn.

Separate abstracts were prepared for the 3 included sections. (M.O.W.)

For abstracts of individual sections see: 30347, 30794, and 30795.

30794 (IDO–17147, pp 1-12) REACTOR ENGINEERING. (Phillips Petroleum Co., Idaho Falls, Idaho. Atomic Energy Div.).

Repeated measurements, conducted over a period of two years, on a selected ETR fuel element have shown that the overall reproducibility of boron assays in the ETRC is 0.0274 g. Irradiation of fuel and cladding materials specified for the ATR in a loop facility in the ETR at conditions prototypical of the ATR have shown apparent satisfactory fuel stability and aluminum corrosion rates in agreement with those measured in an ex-reactor loop. Reduction in corrosion of ATR aluminum fuel plates by electroless nickel coating is being attempted. The nickel coatings showed no significant weight changes after corrosion testing in an autoclave at 350 to 400°F for 61 days. Under dynamic corrosion testing at 325°F and 25 ft/sec, the heat-treated, nickel-coated samples showed superior corrosion resistance to the as-plated specimens. Out of five samples of electroless nickel coatings plated on 6061 aluminum alloy, only one showed diffusion to have occurred as a result of heat treatment. A microprobe study made on this sample revealed three distinct diffusion zones in the heat-treated condition. An electron microscope examination of electroless nickel coatings on aluminum fuel plates showed a good bond was obtained when the aluminum base was roughened by pickling and the aluminum-nickel composite was heat treated for 40 hours at 400°C. (M.O.W.)

30795 (IDO–17147, pp 29-36) MATHEMATICAL ANALYSIS AND MACHINE COMPUTATIONS. (Phillips Petroleum Co., Idaho Falls, Idaho. Atomic Energy Div.).

A number of computer codes were developed and written for the IBM 040 during this period. Preparation continued for replacement of the IBM 1401 by the CDC 3100. (M.O.W.)

30796 (IDO–17177) REVIEW OF THE SPERT SUBASSEMBLY TEST PROGRAM FOR THE CDC AND THE PBF. Grund, J. E. (Phillips Petroleum Co., Idaho Falls, Idaho. Atomic Energy Div.). Aug. 1965. Contract AT(10-1)-205. 159p. (PTR–761). Dep. mn. CFSTI $5.00 cy, $1.00 mn.

A discussion is presented of the in-pile subassembly program that is planned at the SPERT project for the next five years. A review is presented of postulated reactor accidents and accident experience which provides a basis for establishment of the types of accidents to be considered for simulation in the in-pile subassembly program. A review of methods of accident analysis is presented and the information available for use in reactor analysis is discussed. The objectives of the in-pile subassembly program are outlined. A description of the facilities to be used, and the experimental program outline and schedule are included. Detailed descriptions of some typical experiments to be performed early in the program are included. (M.O.W.)

30797 (IITRI–578P21-18) STUDIES OF REACTOR CONTAINMENT. Progress Report, February 1–March 31, 1966. Gallagher, E. V.; Wiedermann, A. H. (IIT Research Inst., Chicago, Ill.). Contract AT(11-1)-578. 37p. (IITRI–T6042-18). Dep. mn. CFSTI $2.00 cy, $0.50 mn.

Work during this period on coolant decompression experiments and analysis for PWR's is reported. A discussion of an analytical model for water decompression is presented. Experimental data for the case of unobstructed flow in the driver section are described. Preliminary experiments with obstructions in the driver section were started. (M.O.W.)

30798 (NP–16043) ANNUAL REPORT, 1965 [ON REACTOR STUDIES]. (Atomic Energy Establishment, Winfrith (England)). 92p. Dep. mn. UKAEA.

Further developments in general reactor technology during this period are reported in the following areas: gas-cooled reactors, steam-generating heavy-water reactors, sodium-cooled fast reactors, reactor assessments and exploratory studies, reactor systems research, technical services, establishment services, and organizations and resources. (M.O.W.)

30799 REPORT ON THE 1965 CONFERENCE ON REACTOR OPERATING EXPERIENCE. Cramer, E. N. Nucl. Safety, 7: 148-59(Winter 1965–1966).

The main trends noted in the papers presented at the conference are summarized, and some of the more significant papers are reviewed. (G.O.Y.)

30800 NOTES ON REACTOR SAFETY IN THE USSR. Nucl. Safety, 7: 159-61(Winter 1965–1966).

The observations of a US delegation to the USSR on the general safety criteria applied at Soviet installations are summarized. (G.O.Y.)

30801 IGNITION AND COMBUSTION OF REACTOR MATERIALS UNDER ACCIDENT CONDITIONS. Peterson, Sigfred. Nucl. Safety, 7: 169-74(Winter 1965–1966).

Some recently obtained information on the oxidation reactions that are pertinent to the nuclear industry is summarized. The ignition of metallic reactor fuels and the oxidation of uranium mononitride, graphite, and structural metals are considered. 62 references. (G.O.Y.)

30802 REACTION OF URANIUM WITH WATER AS INITIATED BY A POWER EXCURSION IN A NUCLEAR REACTOR (TREAT). Ivins, Richard O.; Liimatainen, Robert C.; Testa, Frank J. Nucl. Sci. Eng., 25: 131-40 (1966).

The extent of reaction with water of fuel materials having uranium metal as the major constituent is reported. This chemical reaction occurs as a result of the fission heating and meltdown of these materials during a nuclear transient. Observations of the physical changes that occur are also noted. The technique involved the transient irradiation of fuel samples immersed in water in stainless-steel capsules in the Transient REActor Test Facility (TREAT). Uranium wires, 64 mil diam by 1 in. long; uranium, 5 wt % zirconium, 1.5 wt % niobium alloy pins, 0.2 in. diam by 0.5 in. long (both Zircaloy-2 clad and bare); and clusters of uranium pins, 0.2 in. diam by $5\frac{5}{8}$ in. long were heated under water by the transient neutron pulse of the TREAT reactor. Subsequent measurement of the hydrogen evolved was used to determine the extent of reaction. The extent of reaction was correlated as a function of the fission energy developed in the fuel samples. Unbonded strain-gauge transducers were used to measure the pressure history in the autoclaves that contained the fuel samples. The extent of reaction was determined for energies ranging from 37 to 394 cal/g and reactor periods from 63 to 515 msec. With reactor periods of the order of 100 msec, melting of fuel samples began at a fission energy input of 40 cal/g, and complete melting occurred at 95 cal/g. The extent of reaction varied from a few tenths of a percent for those samples which had not melted appreciably to 4% for those which were completely melted in the experiments conducted in 25°C water (20 psia helium overpressure). Above 95 cal/g, the samples fragmented, and the extent of reaction increased with increasing fission energy to 50% at the highest energy of 394 cal/g. Three experiments were performed in 285°C water (1000 psi steam overpressure). The three samples in 285°C water reacted from two to three times as much as those in the 25°C water at the same energies. The effect of longer reactor periods was to decrease the temperature reached by the samples and thus the extent to which it reacted. Although the samples were of various sizes initially, the average particle size of the samples after the transient was reduced to the order of 15 mil when the fission energy input was above 200 cal/g. A few of the samples were initially irradiated to a burnup of 0.3% of the total uranium atoms prior to the TREAT experiments; however, no effect on the extent of reaction or degree of fragmentation was observed. The effect of original sample size and the presence or absence of cladding were also minor. The results are directly applicable to the analysis of reactor excursion accidents. (auth)

30803 INFLUENCE OF CROSS-SECTIONAL SHAPE ON IRRADIATION-INDUCED STRESSES IN GRAPHITE COLUMNS. Witt, F. J.; Greenstreet, B. L. Nucl. Sci. Eng., 25: 141-51(1966).

Plane-strain linear elastic models with constant shrinkage coefficients were analyzed to determine the relationship of cross-sectional shapes to irradiation-induced stresses in graphite moderator components. If a relaxation factor is known, results of this study can be applied to a system in viscoelastic creep. The geometries considered are cylinders and prisms containing one or more cylindrical holes and sectors of these configurations. Although particular mechanical properties and fast-flux distributions are assumed, the results imply predictions for other conditions. In the study of multihole prisms, little difference in maximum stresses exists; however, some simply connected sectors have almost negligible in-plane stresses. Concentric cylinders and cylindrical sectors exhibit a very significant reduction of stresses when compared with those of the related thick-walled cylinder. (auth)

30804 PHYSICS OF NUCLEAR REACTORS. Jakeman, D. New York, American Elsevier Publishing Company, Inc., 1966. 365p. $10.00.

An introduction to the physics of nuclear reactors is given, assuming previous familiarity with calculus and elementary nuclear physics. Discussions are given of the general behavior of neutrons in nonmultiplying and multiplying media, neutron thermalization and capture, characteristics and calculations of fast and thermal reactors, nuclear fuels, transient behavior and reactivity changes in thermal and fast systems, and reactor control systems. (M.J.T.)

30805 APPARATUS INCLUDING A NUCLEAR REACTOR FOR HEATING INJECTION GASES. Natland, Manley L. (to Richfield Oil Corp.). U. S. Patent 3,246,697. Apr. 19, 1966. Filed Sept. 8, 1958.

An apparatus is described for stripping an oil-bearing formation of its petroleum content, preferably after conventional flowing and pumping methods have ceased to be economical or by recovering the petroleum fluids from a formation in which the petroleum is too heavy and viscous for recoveries in the usual manner. A gas cooled neutronic reactor is interconnected in such a manner that cooling gas passing through the reactor is in heat exchange relationship with the reactive elements of the reactor and removes heat of the fission reaction to heat the cooling gases. The gases heated in this manner are withdrawn from the reactor and passed under pressure by means of a pump down the borehole transversing the oil-bearing formation and then outwardly into the formation. These hot gases raise the temperature of the petroleum in the formation to reduce its viscosity and render it flowable and easily recoverable. (B.L.M.)

Auxiliaries and Components

Refer also to abstracts 29512 and 29578.

30806 (BAW–1280-36) SODIUM-HEATED STEAM GENERATOR DEVELOPMENT. Quarterly Progress Re-

port, January–March 1966. Probert, P. B. (Babcock and Wilcox Co., Barberton, Ohio. Boiler Div.). Apr. 8, 1966. Contract AT(11-1)-1280. 32p. Dep. mn. CFSTI $2.00 cy, $0.50 mn.

The Preliminary Design of the Prototype Steam Generator was completed. Fabrication of the Prototype Steam Generator is approximately 35% complete and on schedule. The present status of the several research and development projects still underway is outlined. (auth)

30807 (ORNL-TM-1485) FEEDFORWARD COMPENSATION OF A TEMPERATURE CONTROL SYSTEM [Thesis]. Whitt, Richard Elmo (Oak Ridge National Lab., Tenn.). June 1966. Contract W-7405-eng-26. 32p. Dep. mn. CFSTI $2.00 cy, $0.50 mn.

Submitted to Auburn Univ., Ala.

The closed-loop control system which regulates the temperature of a nuclear fuel specimen experiment in a nuclear reactor was simulated on an analog computer. All components of the system, except the controller, were represented by linear mathematical models determined from test data. An equivalent analog circuit was developed for each of the component models. Using these circuits and the actual temperature controller, the response of the analog system to a simulated load disturbance was determined. A circuit which compensated the temperature control system for the load disturbance effect was developed and incorporated into the simulation. Simulated neutron flux perturbations were then introduced into the compensated model. Data recorded showed that the compensation circuit reduced the temperature deviations by a factor of ten. (auth)

30808 (WCAP-3269-54) AUTOMATIC CONTROL OF ROD POSITION WITH BORON IN A CHEMICAL SHIM NUCLEAR PLANT. Batenburg, A.; Buis, G. R.; Mangan, M. A.; Strittmatter, J. A. (Westinghouse Electric Corp., Pittsburgh, Pa. Atomic Power Div.). Mar. 1966. Contract AT(30-1)-3269. 43p. Dep. mn. CFSTI $2.00 cy, $0.50 mn.

In order to maintain the control rods of a chemical shim pressurized water reactor within a predetermined band around a specified position, the concentration of boric acid in the reactor coolant system can be controlled. A simple controller of the "on-off" type can be used. Due to the transport time delays in the chemical and volume control system, in many cases the uncompensated controller yields an unstable system. It was shown that the system can be stabilized by inserting a compensator of the feed-forward type. A second order system is sufficient; however, its parameters must be adjusted according to the plant operating conditions. Since variations in the plant parameters can be considered as long-term effects, these adjustments will be infrequent. In the case of a sudden seal failure, followed by a load transient, the control system may start to oscillate. However, manual adjustment will be sufficient to restore stability. (auth)

30809 TELEVISION IN NUCLEAR REACTORS. Oudin, Jacques. Belgicatom, Ass. Belge Develop. Pac. Energ. At., Bull. Inform., 11: No. 60, 19-23(Feb. 1966). (In French).

The use of closed circuit television in highly radioactive areas is considered. The conditions under which the television camera must operate is discussed with the consideration of the selection of materials and the electronic equipment necessary. The special problems encountered in the construction of such television circuits are described and their solutions are indicated. (J.S.R.)

30810 STUDY ON SLIGHT LEAKAGE FROM A REACTOR CONTAINMENT VESSEL. Report of the Sub-Committee on Slight Leakage. Nippon Kikai Gakkaishi, 68: 1321-32(Sept. 1965). (In Japanese).

Test specimens of mild steel, stainless steel, and Al were prepared with leaking holes resembling as closely as possible the actual welding joints in reactor containment vessels to study the mechanism of leaking by gases and liquids. The amount of He, CO_2, N_2, and H_2O leaking through the test specimen at 20–200°C from an atmosphere at a pressure of 1–100 atm into a vacuum was measured by the pressure-increasing method. The cross sectional shape of the holes was found to be a slit rather than a circle. However, with increasing hole size, the cross sectional shape approached a circular cross section. The leakage rate was found to be independent of temperature over the range investigated. The current of gas leaking through the minute holes was nearly molecular in size; however, with increasing hole size, a viscous current becomes involved. The mechanism of H_2O leakage was found to be quite different from that of gases with the vapor state of H_2O being involved. Somewhere along the length of the leaking hole water of evaporation is produced causing a mixed two-phase flow. In smaller holes the vapor-phase flow is predominant; while in the larger holes, the liquid-phase flow predominates. (TCO)

30811 REACTOR PRIMARY-PIPING-SYSTEM RUPTURE STUDIES. Kilsby, E. R. Jr. (General Electric Co., San Jose, Calif.). Nucl. Safety, 7: 185-94; 214(Winter 1965–1966).

An assessment was made of the present understanding of piping failures, and specific problem areas were defined. Research and development programs were recommended. (D.C.W.)

30812 LEAK TESTING OF REACTOR CONTAINMENT SYSTEMS. Robinson, G. C.; Horton, T. R. Nucl. Safety, 7: 194-203; 214-15(Winter 1965–1966).

Some data on the design, leak testing, and leak-rate testing of pressure-tight containment systems are compiled and discussed. (D.C.W.)

30813 STRENGTH OF STEEL CONTAINMENT SHELLS. Merkle, J. G. Nucl. Safety, 7: 204-12; 215-16(Winter 1965–1966).

Some experimental and theoretical research on the bursting strength of thin-walled cylinders with flat ends is summarized. Failure and strength are defined, and the basic equations of plasticity are derived. The results of analytical solutions for thin-walled cylinders with rigid ends are tabulated. (D.C.W.)

30814 VAPOR TRAPS PROTECT LIQUID-METAL SYSTEMS. Thompson, David H. Power Reactor Technol., 8: 259-70(Fall 1965).

The principles of metal-vapor traps for liquid-metal systems are discussed. Some recommendations concerning their use and the need of improved technology for future reactors are considered. Experience with traps for static systems is also discussed briefly in connection with fume traps for melt-refining furnaces for the reprocessing of fuels. (G.O.Y.)

30815 MATERIALS APPLICATIONS FOR NUCLEAR POWER PLANTS FROM THE VIEWPOINT OF AN ENGINEER-CONSTRUCTOR. Bond, G. W.; Dyer, G. H. (Bechtel Corp., San Francisco, Calif.). 27p. (CONF-660319-3). ORAU, Gmelin, AED-CONF-66-041-1.

American Society for Metals Sessions, WESTEC Conference, Los Angeles.

Materials used in containment of nuclear power plants, radioactive waste disposal systems, refueling systems, and shielding are reviewed. Radiation damage to materials and low-temperature brittle fracture are also considered briefly. Tables show properties of steels suitable for containment structures, containment costs for several nuclear power plants, and materials for radioactive waste disposal systems. (A.G.W.)

30816 NEUTRON REFLECTORS FOR NUCLEAR REACTORS. Le Baron, Robert (to Great Lakes Carbon Corp.). British Patent 1,028,248. May 4, 1966. Filed Mar. 29, 1963.

A process is described for the production of graphite bodies containing Be and/or a Be compound that are suitable for use as neutron reflectors in reactors. The bodies can contain 0.3 to 49.5 wt % Be or Be compound and are prepared by mix-mulling reactor-grade carbon particles, if required or desired, a carbonizable binder, and sufficient Be or Be compound to provide the desired proportion of Be; cooling the resulting mixture; milling the cooled mixture; forming a compact body of the mixture; and baking, and optionally, graphitizing the body so formed. (B.L.M.)

30817 IMPROVEMENTS IN OR RELATING TO RETARDING MECHANISMS. Lockett, George Edward; Coast, Geoffrey (to United Kingdom Atomic Energy Authority). British Patent 1,028,886. May 11, 1966. Filed Apr. 6, 1964.

A retarding mechanism for a weight lowering device that comprises a first member arranged to execute linear motion in response to the movement of the weight and forms with a second member a sliding pair is described. The members of the sliding pair are constrained to perform successively relative sliding and screw motion. and an energy absorbing device is driven by this relative screw motion. The first member is preferably carried by the weight or an extension of it and has a projecting cam surface forming one element of the pair. which engages in a slot in the second. follower member. The slot is shaped to constrain the relative sliding movement of the cam in the slot to a linear movement followed by a relative rotation and movement between the cam surfaces and the second member. The first member is restrained against rotational movement. and the second member is rotatably connected to the energy absorbing device. such as a flywheel. All the members of the pair move out of engagement to allow the flywheel to run on when the weight reaches the end of its travel. The mechanism is particularly. but not exclusively. applicable to neutron absorbing rods in a nuclear reactor. (B.L.M.)

30818 IMPROVEMENTS IN OR RELATING TO SPACING GRIDS FOR CLOSELY SPACED ARTICLES. Hooper, Alan Thomas (to Societe Anglo-Belge Vulcain). British Patent 1,029,061. May 11, 1966. Filed Feb. 1, 1963.

A spacing grid for positioning a cluster of closely spaced articles. particularly nuclear fuel rods forming part of a nuclear fuel assembly. comprises a number of sinusoidal strips formed with transverse saw cuts at the points of inflection along their length. Each strip is arranged in a grid defining path and engages saw cuts on other strips at positions so as to form a number of article-receiving pockets bounded by strip portions between the saw cuts. A nuclear fuel element assembly using the spacing grid is patented. (B.L.M.)

30819 IMPROVEMENTS IN OR RELATING TO CHARGE/DISCHARGE MACHINES FOR NUCLEAR REACTORS. Lockett, George Edward; Pugh, John (to United Kingdom Atomic Energy Authority). British Patent 1,029,111. May 11, 1966. Filed Apr. 6, 1964.

A charge machine for a gas cooled reactor is introducible for operation through an opening in the pressure vessel in which the reactor core is housed. The machine comprises a housing arranged to extend into and through the penetration of the pressure vessel. a track hingedly mounted within the housing for a charging trolley. a track extension hingedly mounted on the track. and actuating means operative to unfold the track extension. The track extension is mounted so as to be pivotable between positions in which the extension lies co-extensive with the track in the folded position or to form an extension of the track in an unfolded position. During servicing. a trolley traverses the track to service the core by means of a grapple on the trolley to transfer fuel elements between the core and a location above the lower penetration of the pressure vessel. (B.L.M.)

30820 IMPROVEMENTS IN OR RELATING TO THERMAL INSULATION. Armstrong, Edward (to Darchem Engineering Ltd.). British Patent 1,029,599. May 18, 1966. Filed Dec. 5, 1961.

A device is described to interrupt the upward flow of convection currents between two adjacent thermal insulation panels that consist of a number of metal foils in which alternative layers of foil are plain and dimpled to form spaces between successive foils. The device for interrupting the flow consists of a capping strip of "V" cross section that is coextensive with the edge of the panel and fits snugly between adjacent plain foils near the uppermost edge of the panel. Such thermal shields are used on reactor pressure vessels. (B.L.M.)

30821 FORCED-FLOW, ONCE-THROUGH VAPOUR GENERATOR. Bell, Alan (to Foster Wheeler Ltd.). British Patent 1,029,618. May 18, 1966. Filed June 27, 1963.

A forced-flow. once through vapor generator is described for application to the production of high temperature. high pressure steam from a high temperature. high pressure heating fluid such as the primary coolant from a gas cooled reactor. An upright cylindrical shell contains vertical tube bundles which form one or more evaporating sections and other vertical tube bundles which form superheating sections and which are connected in series with the evaporating sections. A water inlet feed to each of the evaporating sections is provided at the lower end of the shell so that the water is evaporated in an upward pass. The steam is superheated on a downward pass. and an outlet for the steam after superheating is provided at the lower end of the shell. Heating inlet and outlets are provided at the lower end of the shell. and the flow path within the shell between the inlet and outlet connections is determined by baffles so that it is counter-current relative to the flow of heated fluid through the evaporating and superheating sections. Only the heating fluid that has been cooled by indirect heat exchange with the heated fluid comes into contact with the steam generator shell. (B.L.M.)

30822 IMPROVEMENTS IN OR RELATING TO NUCLEAR REACTORS. Gratton, Charles Peter (to United Kingdom Atomic Energy Authority). British Patent 1,029,712. May 18, 1966. Filed Feb. 11, 1964.

A method for controlling a nuclear reactor that includes a fuel region made up of fuel-containing and fuel-free zones is described. The fuel-free zones are bounded by neutron-absorbing material stationary in the core and having neutron-absorbing properties mainly in the thermal energy region. The fuel regions in the core are loaded in such a manner to produce a neutron spectrum having a predominant energy level that is epithermal. and the reactor is controlled by introducing moderating material into selected ones of the fuel free zones that are disposed on concentric annular rows, each equi-distance from the core center. The design is applicable to either liquid or solid moderated reactors and to gas and water cooled reactors. (B.L.M.)

30823 MODERATOR STRUCTURES FOR NUCLEAR REACTORS. Thorn, James Douglas; Rodwell, William; Jobson, Donald Albert (to United Kingdom Atomic Energy Authority). British Patent 1,030,152. May 18, 1966. Filed June 1, 1962.

A graphite moderator structure for a gas cooled reactor is made up of interlocking bricks and tiles of graphite. Both the bricks and tiles are formed in two co-extensive parts with the grain running lengthwise in the bricks and parallel to that of the bricks in the tile. The outer parts of the tiles have surfaces adapted for interlocking engagement with adjacent tiles, and the tiles are radially weakened to provide hoop stress relief. The core structure is so formed that the inner bricks and tiles, which are subject to the severest conditions under reactor operation, are removable without disturbing the entire structure. (B.L.M.)

30824 IMPROVEMENTS IN OR RELATING TO GRAB DEVICES. Hutchinson, William George; Cooper, James Leslie (to United Kingdom Atomic Energy Authority). British Patent 1,030,157. May 18, 1966. Filed Nov. 26, 1962.

A grab device is provided for refuelling a nuclear reactor that operates by means of a weight member adapted for suspension from a grab cable within a casing member. The weight member is movable within the casing along a path having definite limits. Grab fingers are mounted on one of the members and are movable between grab engaging and disengaging positions by movement of the weight member along part of the path and stop means operable to prevent movement of the weight member along part of the path. (B.L.M.)

30825 TRANSFER MECHANISM. Girard, Pierre (to Commissariat a l'Energie Atomique). Canadian Patent 731,014. Mar. 29, 1966. Priority date Dec. 6, 1960, France.

This device is intended primarily for controlling the insertion of an absorber (control) rod into a nuclear reactor, so that it may reach a given position in the least time without rebounding or overshooting. The kinetic energy of the falling rod is transferred to an inertia wheel, a drum and a spring resulting in a large deceleration beginning when the rod has almost reached its pre-determined position. This is accomplished without damage to any of the components. (AECL)

30826 SUPPORT STRUCTURE FOR VERTICALLY-STACKED SOLID MODERATOR RODS OF A NUCLEAR REACTOR. Rouge, Pierre (to Commissariat a l'Energie Atomique). Canadian Patent 731,271. Mar. 29, 1966. Priority date Apr. 14, 1961, France.

The support structure consists of a series of rigid, independent, concentrically arranged supporting moderator rings enclosing a fuel element. These are connected by pins in radial slots so that slight relative movement or deformation of the rings occur. The connection on the inner faces of the rings is completed with flexible metal bellows. A strut resting on the base of the reactor housing supports each stack using heat insulated swivel joints. By these means it is claimed that diametral expansion over a 20-meter span may be compensated. (AECL)

30827 SUPPORT FOR LIQUID COOLED NUCLEAR REACTOR BED. Chauvin, Michel; Margueron, Jean C. (to Commissariat a l'Energie Atomique). Canadian Patent 731,272. Mar. 29, 1966. Priority date Apr. 10, 1961, France.

Leakage between the bed and the vessel of a molten metal-cooled fast reactor is controlled by this device. The bed of the reactor rests on an annular projection on the vessel in such a manner as to cause contact between two plane metallic parts. There is between the bed and vessel a flexible metal skirt of which the two ends folded over each other are rigidly secured one to bed and the other to the vessel. Cavitation is prevented. Calibrated outlets in the skirt allow necessary movement of the metal coolant. (AECL)

30828 REMOVABLE THERMAL SHIELD. Laming, Lindon C. (to Foster Wheeler Corp.). Canadian Patent 731,273. Mar. 29, 1966.

Segmented shield pieces, capable of insertion or withdrawal through the opening for the reactor core assembly are adapted to be locked together within a reactor vessel. One or more shield layers may be used but only the one adjacent to the vessel wall is joined to a plate on the bottom. Chevron or bevel joints are used to avoid rectilinear radiation leakage paths. No welded, rivetted or bolted joints are used. Personnel do not enter the vessel for installation or removal of the shield segments but the handling methods from the outside are not described. (F.S.A.)

30829 DEVICES FOR ADJUSTING THE RELATIVE POSITIONS OF FUEL ELEMENTS WITHIN A NUCLEAR REACTOR. Aranovitch, Eric; Molica, Guido; Bonnaure, Pierre (to Communaute Europeenne de l'Energie Atomique). Canadian Patent 731,274. Mar. 29, 1966. Priority date Sept. 4, 1961, Germany.

A device is designed for changing the lattice spacing of reactor fuel rods or reflectors consists of two guide bars at right angles with articulated rhombuses for altering the distance between adjacent rods. (F.S.A.)

30830 COMPOSITE GUIDE TUBE FOR NUCLEAR REACTORS. Alfille, Lucien; Barriere, Andre; Farges, Guy; Rodier, Georges; Rozenholc, Michel (to Commissariat a l'Energie Atomique). Canadian Patent 731,352. Apr. 5, 1966. Priority date Jan. 31, 1962, France.

In this reactor the pressure tubes are surrounded by heavy water which is not intended to absorb much heat from the fission process. The guide tube inserted inside the pressure tube consists of two concentric tubes with heat insulating material such as magnesium oxide between. During fuel changing, the guide tube carries the weight of the fuel elements, as well as serving as a channel for the coolant and resisting corrosion at operating temperatures. Details of fabrication are given and also methods of joining this composite guide tube to the cooling system. (F.S.A.)

30831 TEMPORARY FIXING DEVICE FOR NUCLEAR REACTOR ELEMENTS. Costes, Didier (to Commissariat a l'Energie Atomique). Canadian Patent 731,772. Apr. 5, 1966. Priority date Aug. 16, 1961, France.

A fuelling mechanism is designed for horizontal reactors in which a shell containing the fuel rod is driven by a ram into the pressure tube. A set of resilient tongues secures the shell and fuel rod temporarily during the fuelling operation so that adequate coolant flow may be maintained. When fuel changing is complete, the shell is withdrawn. (F.S.A.)

30832 CONTROL OF NUCLEAR POWER PLANT. Powell, Elno M.; Argersinger, John I. (to Combustion Engineering, Inc.). U. S. Patent 3,247,069. Apr. 19, 1966. Filed July 13, 1960.

A method is described for operating a nuclear power plant including a reactor having a negative temperature coefficient, a reactor cooling circuit, and a working fluid circuit including a power output device. The circuits are in communication with each other through heat exchanger means. The coolant is circulated through the reactor coolant circuit at a constant flow rate so as to maintain a constant average coolant temperature in the reactor. The fluid in the working circuit of the reactor is superheated in the heat exchanger and transmitted to the power output device in the superheated state. Any variation in the load demand on the power plant is detected, and the flow rate of the fluid in the working fluid circuit is changed by an amount representative of the variation in the load demand in a direction to satisfy the demand. The flow rate of the working fluid is changed by means of variable fluid supply means which control the pressure of the superheated fluid and maintain the level of reactivity of the reactor substantially constant. This change in the flow rate of the fluid in the working fluid circuit acts through the fluid in the reactor coolant circuit to adjust the power level of the reactor since the fluid in the coolant circuit of the heat exchanger is in communication with the reactor. (B.L.M.)

30833 PRESSURE-ABSORBING MEANS FOR NUCLEAR REACTOR STATIONS. Norman, Hans (to Allmanna Svenska Elektriska Aktiebolaget). U. S. Patent 3,248,298. Apr. 26, 1966. Priority date Jan. 24, 1963, Sweden.

A pressure supression chamber for taking up the pressure originating from water vaporizing in the reactor chamber upon reactor breakdown is arranged for communication with the open air rather than being closed and dimensioned for the air volume that is normally present over the water level as well as for the air volume in the reactor chamber. By means of an isolating arrangement, the partly water-filled tank is in communication with at least one chamber, which is in turn in communication with the open air by means of a channel. The isolating arrangement may be either a water lock or a membrane. (B.L.M.)

30834 NUCLEAR REACTOR CORE ASSEMBLY. Junkermann, Wolfgang; Mueller, Arno (to Babcock and Wilcox, Ltd.). U. S. Patent 3,248,299. Apr. 26, 1966. Filed June 12, 1961.

A moderator design is described for a nuclear reactor comprising a cylindrical pressure vessel, a cylindrical shell disposed coaxially with the pressure vessel and a generally cylindrical core assembly axially movable within the cylindrical shell and comprised of a number of moderator blocks. The graphite blocks have side faces parallel to the core axis. Surrounding the radial periphery of the core assembly and closely embracing the outer radial surface of the core assembly are means arranged at the outer surface of the embracing means to act laterally inwardly through the embracing means upon the moderator blocks

perpendicular to the plane side faces to laterally force adjacent blocks against one another. A number of restraint wedges are arranged along and around the outer surface of the embracing means, and a number of compression wedges coact with the restraint wedges and transmit a portion of the lateral reactive force from the moderator blocks to the cylindrical shell and a portion to the longitudinal movement of the shell. The shell is resiliently attached to the pressure vessel to resist the axial movement of the shell within the pressure vessel. (B.L.M.)

30835 SHUTDOWN APPARATUS FOR NUCLEAR REACTORS. Dohm, Arthur J. Jr.; Carlson, David A. (to General Dynamics Corp.). U. S. Patent 3,249,510. May 3, 1966. Filed Aug. 5, 1963.

A control assembly for the emergency shutdown of a nuclear reactor comprises an elongated housing adapted to be moved vertically within and relative to the core of the reactor. The housing has a hollow central portion and an open lower end communicating with the hollow portion. A filler of neutron absorbing material is disposed within the hollow central portion, and an end plug is connected to the lower open end of the housing for releasably containing the filler in the hollow portion of the housing. The end plug is fabricated at least partially of a fusible material that melts when the core temperature exceeds a preselected temperature to allow the filler to be discharged from the housing into the reactor core to shut down the reactor. (B.L.M.)

Criticality Studies

Refer also to abstract 30339.

30836 (BAW-3492-1) LUMPED BURNABLE POISON PROGRAM. Final Report. Clark, R. H.; Batch, M. L.; Pitts, T. G. (Babcock and Wilcox Co., Lynchburg, Va. Critical Experiment Lab.). Jan. 1966. Contract AT(30-1)-3492. 60p. Dep. mn. CFSTI $3.00 cy, $0.75 mn.

A series of critical experiments was conducted to study the physics effects of cylindrically shaped, lumped poison distributed throughout a light-water-moderated nuclear reactor. The lumped poisons were borosilicate glass rods (12.6% B_2O_3) of 0.460- and 0.326-inch diameters, silica glass rods (3.0% B_2O_3) of 0.326-inch diameter, and aluminum-clad B_4C rods. The fuel was 4 and 2.5%-enriched UO_2 rods of 0.475-inch OD. Lattice non-moderator/moderator volume ratios were 0.750. Measurements included critical size and composition, poison rod reactivity worth, $\partial\rho/\partial h$ and excess reactivity, gross power distribution, and thermal flux distribution around the central poison rod. Measurements are tabulated, and results are summarized and discussed. (auth)

30837 (IDO-17169) THE ADVANCED REACTIVITY MEASUREMENT FACILITY II NOISE STUDY. Cloud, L. G.; Brown, R. H.; Wilde, N.; Boland, T. J. (Phillips Petroleum Co., Idaho Falls, Idaho. Atomic Energy Div.). May 1966. Contract AT(10-1)-205. 28p. Dep. mn. CFSTI $2.00 cy, $0.50 mn.

Work performed during the noise study associated with the Advanced Reactivity Measurement Facility II (ARMF-II) at the National Reactor Testing Station is described. The primary objective was the analytical determination of the precision limit for a fixed-time differential reactivity measurement made with the ARMF-II. The major result of the work demonstrates that a precision limit can be determined analytically for any "noisy" differential measurement if the noise spectrum involved in the measurement is known. The analysis is oriented toward nuclear technology; however, the information is applicable to the study of noise problems in general. (auth)

30838 NUMERICAL ANALYSIS OF REACTOR KINETICS BY DIGITAL COMPUTER. Fujiie, Yoichi; Miyasaki, Keiji (Technical Research Lab., Hitachi Zosen, Japan). J. Nucl. Sci. Technol. (Tokyo), 3: 131-9(Apr. 1966).

Numerical analysis of typical reactor kinetics problems is made with a digital computer. In the description of recurrence relation, several equivalent reciprocal periods of time are proposed to reduce difficulty in treating the discontinuity of reactivity and to improve accuracy in computation. A variable time interval corresponding to the prevailing state is also introduced to save machine time. The results obtained show fairly good agreement with rigorous solutions evaluated analytically for step inputs of reactivity, and also incorporate nonlinear effects when referred to the linearized approximation for sinusoidal inputs of reactivity. (auth)

30839 REACTIVITY WORTH OF FUEL ELEMENTS. MEASUREMENT AND PERTURBATION ANALYSIS. Wajima, J. Tsunetaka; Ohnishi, Tadahiro; Kiyokawa, Kazuhiro (Hitachi, Ltd., Japan). J. Nucl. Sci. Technol. (Tokyo), 3: 150-9(Apr. 1966).

Reactivity worths of fuel elements were measured in the Ozenji Critical Facility (OCF) and analyzed with three-group perturbation method. The result shows that the worth of one single fuel pin can be well predicted by calculation over a very wide range of the core spectrum, namely from a lattice of 2.5% enrichment and 0.43 volume ratio to that of 1.5% enrichment and 3.5 volume ratio. The analysis indicates the importance of thermal neutron flux peaking remaining after the removal of a fuel pin. Only by incorporating this effect can the reactivity worth of a fuel pin be correctly evaluated. The neutron spectrum in the water hole where the peaking occurred was assumed to be the same as in the reflector. The reflector spectrum seems to provide better agreement with experiment than the core spectrum. Validity of the analysis was extended to a bundle of sixteen fuel pins by measuring the reactivity worths of bundles of fuel pins as well as the thermal neutron flux distributions. One dimensional diffusion calculations were employed throughout the analysis. (auth)

30840 DISADVANTAGE FACTOR IN A CLOSELY PACKED CYLINDRICAL LATTICE. Fukai, Yuzo (Nippon Atomic Industry Group Co., Japan). J. Nucl. Sci. Technol. (Tokyo), 3: 165-8(Apr. 1966).

Cylindrical two-region lattices composed of fuel with a common radius a = 1 cm and a common cross section $\Sigma_1 = 0.25\ cm^{-1}$, and of a moderator with no absorption were considered in order to reinvestigate the discrepancies observed in the trend of the disadvantage factor $\bar{\phi}_1/\bar{\phi}_0$ for decreasing moderator cross section, decreasing moderator-to-fuel ratio and decreasing volume ratio. Calculations were made for an A-series lattice with changing ν at constant $\Sigma_1 a = 1$ and a B-series with changing $\Sigma_1 a$ at constant $\nu = 1$. The lattice configurations, methods of calculation, and results are discussed. It is concluded that the calculated disadvantage factor by either P_1-Cohen's, P_3-Clendenin's, or Amouyal's method does not always decrease monotonously, and that it can be considered to be a proper trend that $\bar{\phi}_1/\bar{\phi}_0$ has a minimum value. (L.B.S.)

30841 EFFECT OF EPITHERMAL FISSION ON NEUTRON MULTIPLICATION. Yamamoto, Hisashi (Hitachi Ltd., Japan). J. Nucl. Sci. Technol. (Tokyo), 3: 180-3(May 1966).

A formula for the effect of epithermal fission on the neutron multiplication factor is derived with a modified four factor approach. The fraction of neutron multiplication due to epithermal fission is expressed by

$$\frac{\Delta k}{k^0} \simeq \left(1 - \frac{1 + \alpha_3^{25}}{\nu_{eff}}\right)\delta^{25}.$$

The deduction factor sensitively depends on neutron leakage in the fast and the resonance regions through the effective number of neutrons produced per epithermal fission, ν_{eff}. As an example, the effect of the epithermal fission on the neutron multiplication measured in the Hitachi training reactor (HTR) is shown. (auth)

30842 DANCOFF FACTOR IN ARRAYED-TYPE CLADDED FUEL LATTICE. Yasukawa, Shigeru; Shindo, Ruichi (Japan Atomic Energy Research Inst., Tokyo). J. Nucl. Sci. Technol. (Tokyo), 3: 208-9(May 1966).

The equations for the Dancoff factor in an arrayed cladded fuel lattice is developed. (L.B.S.)

30843 XENON STABILITY OF A PARTIALLY DIVIDED SLAB. Stach, Vaclav (Inst. of Nuclear Research, Czechoslovak Academy of Sciences, Rez). Jad. Energ., 12: 50-5(1966). (In Czech).

Absorbing foils, placed in nuclear reactors on the perpendicular axis, can indicate the stability of the reactor with respect to xenon oscillations. This problem was solved using the Randall-St. John method for the first harmonic of the actual neutron current. It was established that, as a result of the dissimilar weights of the absorbing foils for the fundamental distribution and for the first harmonic of the neutron current, there is an area of stabilizing effect and an area for destabilizing effect for the foil in the reactor. For very small absorbing areas, the stabilizing effect comprises the space between the reactor edge and $\frac{1}{3}$ of its height and the range of destabilizing effect is the space between the first and second third of the reactor height. The results obtained make possible the quantitive utilization of focused absorption with other reactor geometries and absorbing organs. (tr-auth)

30844 STATISTICAL THEORY OF REACTORS. Kozik, B. (Zentralinstitut fuer Kernforschung, Rossendorf, Ger.). Kernenergie, 9: 81-7(Mar. 1966). (In German).

Some concrete examples are used to show that all the problems connected with the neutron correlation in nuclear reactors can be uniquely solved on the basis of the correlation theory of neutron multiplication. As was shown earlier the correlation reactor neutron theory is based on nonstationary homogeneous Boltzmann equations for the binary correlation densities, on a system of equations for the binary densities of the second order central moments and on the Boltzmann equation for the mean neutron density. The essential connections are shown, most of the details, definitions, etc., are not given. (auth)

30845 SPACE-DEPENDENT REACTOR KINETICS. Kasten, Paul R. Nucl. Safety, 7: 162-5; 172(Winter 1965–1966).

Space-dependent effects in reactor kinetics are discussed on the basis of some transfer-function calculations, pulsed neutron experiments, and specific kinetics studies. (D.C.W.)

30846 SPECTRUM OF THE ANGULAR NEUTRON FLUX IN A HEAVY-WATER NATURAL-URANIUM LATTICE. Johansson, E.; Jonsson, E. Nucl. Sci. Eng., 25: 157-64(1966).

Using the fast chopper at the Stockholm reactor R1, angular neutron-flux spectra were measured in an arrangement consisting of short uranium rods in heavy water. The rods were mounted in an aluminum container placed in the central vertical channel of the reactor. The axes of the rods were horizontal and approximately located in a vertical plane. The uranium was 29-mm diam, the aluminum can was 1-mm thick, and the spacing was about 140 mm. $\theta(E, r, \Omega)$ was measured in the vertical direction Ω, for various positions r. At 1 ev the results obtained were equal to each other within ±7%, but in the thermal region, they differed considerably. Thus, at 0.01 ev, the highest value measured was as much as 4.5 times the lowest one. In spite of the unclean geometry, the angular-flux spectra were also calculated, starting from scalar-flux spectra obtained from the THERMOS code. The shape of the calculated spectra of the angular flux agreed within a few percent with the experimental spectra. From a combination of calculated and experimental results, the spectrum of the incoming neutron current for a fuel rod was obtained. This current proved to have a neutron temperature about 7°C above the neutron temperature of the flux halfway between two rods. In the low-energy region (around 0.015 ev) the out-flux from a rod showed a wavy variation, believed to depend on Bragg effects in the metal. (auth)

30847 NUMERICAL SOLUTION OF THE REACTOR KINETICS EQUATIONS BY APPROXIMATE EXPONENTIALS. Porsching, T. A. Nucl. Sci. Eng., 25: 183-8 (1966).

A numerical solution of the reactor kinetics equations is given in terms of a difference equation involving an exponential matrix. It is shown that this equation yields a local discretinization error of the order of the time step-size cubed. The exponential of the original equation is approximated by rational matrix functions and a bound for the error resulting from such approximations is established. Three particular rational matrix functions are proposed, and the two problems involving ramp changes in reactivity are solved using them. (auth)

30848 IMPROVED METHOD FOR THE PROMPT-NEUTRON-PERIOD MEASUREMENTS. Chwaszczewski, S.; Szechter, A.; Dybowski, K. (Inst. of Nuclear Research, Warsaw). Nucl. Sci. Eng., 25: 201-2(1966).

A modification of the Rossi-α method for prompt-neutron decay-constant determination is proposed, which extends its usefulness to thermal reactors. An additional gain is the possibility of working with a high counting rate, up to 1000 to 2000 counts/sec. The block diagram of the measuring system is shown. A typical decay curve, together with one obtained using a pulsed-neutron source, is shown for a negative reactivity equal to 0.05 dollars. (L.B.S.)

30849 A NOTE ON MULTIPLICATION METHOD OF REACTIVITY MEASUREMENTS. Bouzyk, J.; Latek, S.; Suwalski, W. (Inst. of Nuclear Research, Swierk, Poland). Nucl. Sci. Eng., 25: 202-4(1966).

Some basic experimental problems in the multiplication method presented by Hogan for reactivity measurements are examined. (L.B.S.)

30850 EFFECT OF DELAYED NEUTRONS IN REACTOR DYNAMICS. Smets, Henri B. Nucl. Sci. Eng., 25: 236-41(July 1966).

A study of linearized reactor dynamic equations shows that delayed neutrons do not always improve the stability of nuclear reactors at power level and that a reactor may be unstable although it is stable when delayed neutrons are neglected. The critical power for instability and the damping of natural oscillations are larger when delayed neutrons are taken into account in the case of low-pass phase lagging reactivity feedbacks, but this property is not true for all types of feedbacks. (auth)

30851 DEFINITION OF NEUTRON DIFFUSION PARAMETERS FOR A UNIFORM REACTOR LATTICE. Stewart, J. D. Nucl. Sci. Eng., 25: 266-74(July 1966).

Two equally valid systems of definitions are given for the neutron diffusion parameters of a reactor lattice, cell-average and cell-surface. In defining the cell-average parameters, a macroscopic flux distribution is imagined to be fixed in space while the lattice is translated with respect to it. In defining the cell-surface parameters, work is done in terms of fluxes and currents on the surface of a cell having the fissile material at its center. Parameters from both systems have been used before; but until recently it lacked complete clarity of definition and the realization that there are two valid systems of parameters that should not be mixed in the one calculation. The early formula, L^2 is equal to the summation over all values of i of $f_i L_i^2$, is for a cell-average thermal diffusion area; L^2 = (outleakage)/B^2 (absorption), applied to a cell with the fissile material at the center, is a cell-surface diffusion area and is less than the summation over all values of i of $f_i L_i^2$ by ≈ (lattice spacing)^2/24. (auth)

30852 VARIATIONAL METHOD FOR PROMPT NEUTRON KINETICS. Koehler, Walter H. (Kernforschungszentrum, Karlsruhe, Ger.). Nukleonik, 8: 203-15(May 1966).

It is shown that the Euler-Lagrange equations of a variational principle are the multigroup diffusion equations for prompt neutrons and their adjoint equations. The Kantorovich method is used to get approximate solutions for the nonseparable flux. The method is applied to a step change in configuration of the fast core of a coupled fast-thermal reactor. (auth)

30853 REACTOR NOISE ANALYSIS BY MEANS OF POLARITY CORRELATION. Dragt, Jan B. (Reactor Centrum Nederland, Petten). Nukleonik, 8: 225-6(May 1966).

The use of the polarity correlation function for direct on-line analysis of reactor noise is briefly discussed and compared with the autocorrelation function. (L.B.S.)

30854 USE OF INTEGRAL TRANSPORT THEORY FOR THE CALCULATION OF THE NEUTRON FLUX DISTRIBUTION IN A WIGNER-SEITZ CELL. Carlvik, Ingvar (Aktiebolaget Atomenergi, Stockholm). Nukleonik, 8: 226-7(May 1966).

The use of transport theory for calculations of flux distribution in a Wigner-Seitz cell is discussed. Results are reported of cell calculations in annular geometry for a typical heavy-water lattice cell, using the one-group transport code, Flurig-3. Calculations were also performed for Thie lattices and the results are compared with those obtained with the K7-Transpo program. Two multigroup programs were written, Flup for annular geometry and Flubag for spherical geometry, by combining the routines for the transport matrix with the Pip-routine for solving the group-fluxes. Three-group calculations on a certain spherical loading of the fast zero-power reactor FR-0 are presented as an example, using a preliminary version of Flubag. (L.B.S.)

30855 DISADVANTAGE FACTOR IN URANIUM/WATER LATTICES. Alvarez Rivas, J. L. (Junta de Energia Nuclear, Madrid). Nukleonik, 8: 229(May 1966).

A comparison is made between recent measurements of the disadvantage factor of cylindrical cells in uranium-water lattices and the values calculated using elementary diffusion theory with a geometry and material dependent effective diffusion coefficient. (L.B.S.)

30856 CRITICAL SIZE AND FLUX DISTRIBUTION OF HOLLOW SPHERICAL AND CYLINDRICAL REACTORS. Bueki, G.; Bede, G. (Polytechnical Univ., Budapest). Period. Polytech., 9: 227-42(1965).

In general, the literature of reactor physics deals with the computation of the flux and of the critical size of compact spherical and cylindrical reactors. Geometrical buckling, flux distribution and critical size of hollow reactors with the one group diffusion method are defined. The procedure is approximative because only by using the transport theory as well as the multigroup diffusion method could the exact values be determined. (The extension of the computation in this direction is planned.) The investigation deals with spherical reactors having a central cavity, as well as with cylindrical reactors having longitudinal and transverse cavities. In each case the results are demonstrated by graphs. (auth)

30857 EVALUATING HEAVY-ATOM CROSS SECTIONS FOR PLUTONIUM-RECYCLE CALCULATIONS. Pennington, Edwin M. Power Reactor Technol., 8: 210-11(Fall 1965).

Some reactivity calculations were made for Yankee critical experiments and for Hanford experiments that involved Pu fuel. The calculational methods used were standard; but large reactivity differences were obtained by using different cross sections in the same computational model. (G.O.Y.)

30858 CRITICAL AND EXPONENTIAL EXPERIMENTS WITH PLUTONIUM. Plumlee, Karl E. Power Reactor Technol., 8: 211-14(Fall 1965).

A brief survey of experiments on plutonium-bearing assemblies is presented. (D.C.W.)

30859 FAST FISSION FACTOR FOR A LATTICE SYSTEM. Yamakoshi, Hisao (Ship Research Inst., Tokyo). Senpaku Gijutsu Kenkyujo, 2: No. 7, 1-17(June 1965).

It is shown that the fast fission factor for heterogeneous reactor can be expressed in terms of fast neutron flux. This expression suggests a new technique which is superior to the conventional one that is described in terms of an averaged quantity, first flight collision probability, because the new technique takes into account the distribution of neutron flux in the fuel region. With the new technique a new definition for fast fission factor is proposed. The new fast fission factor is discussed in accordance with the Soodack's three group idea. It is shown that both the interaction of fast fissions among fuel rods and the slowing down of neutrons through the threshold energy can be calculated by using an approximate solution of an integral type transport equation. A formulation for the new fast fission factor was derived, and a numerical calculation was performed for an infinite system of heavy water and natural uranium slab lattice to compare the difference between two definitions (new and old) by using Soodack's nuclear constants. It was concluded that in case of the new definition, neutron capture in fuel rods under the threshold energy surpasses the multiplication of fast neutrons as the thickness of the fuel slab increases, while the result for the conventional concept of the fast fission factor is just the opposite. (TCO)

30860 APPROXIMATE INVESTIGATION OF THE KINETICS OF A SUBCRITICAL REACTOR DURING A SINUSOIDAL REACTIVITY VARIATION. Dideykin, T. S. Vestsi Akad. Navuk BSSR, Ser. Fiz. Tekh. Navuk, No. 2, 22-8(1965). (In Russian).

The kinetics of a subcritical reactor were investigated during a reactivity variation given by $\Delta k = \Delta k_0 + A \sin \omega t$ where Δk is the magnitude of excess reactivity, and Δk_0 the initial subcritical depth expressed in units of the effective multiplication factor. The system of equations describing the behavior of the instantaneous fission neutron density and of the delayed neutron sources within a reactor existing at the initial instant of time in a subcritical state is given. Expressions determining the phase-frequency characteristics of the subcritical reactor and the relations between the parameters of the sinusoidally varying reactivity with the amplitude and the constant component of neutron density are derived. (ATD)

30861 SPACE-DEPENDENT NEUTRON THERMALIZATION [Thesis]. Sargis, David Albert. Berkeley, Calif., Univ. of California, 1965. 197p.

Various critical parameters or eigenvalues are determined for homogeneous and heterogeneous nuclear fission reactors using neutron thermalization theory. The diffusion theory approximation to the Boltzmann equation is employed along with the heavy monoatomic gas scattering model. The eigenvalues are calculated using the Galerkin variational technique with associated Laguerre polynomials as trial functions. The equivalence of the Galerkin and degenerate kernel solution techniques is shown. Analytic error-estimating techniques are developed to treat integral equation eigenvalue problems arising in neutron transport problems. The methods are derived without restricting the form of the integral equation kernel so that broad classes of integral equations of the second kind may be treated. Error estimates are obtained, with regard to the Wilkins and Wigner-Wilkins kernels, for the homogeneous non-multiplying medium space-decay constant problem. The Feinberg-Galanin source-sink technique is employed in the finite, heterogeneous fission reactor calculations. Approximate eigenvalues are obtained by expanding the neutron flux in associated Laguerre polynomials. (Dissertation Abstr.)

30862 KINETIC THEORY OF THE SPATIAL AND SPECTRAL COUPLING OF THE REACTOR NEUTRON FIELD [Thesis]. Cockrell, Robert Gifford. Gainesville, Fla., Univ. of Florida, 1965. 172p.

A semidirect variational method is used to reduce the integro-differential form of the general Boltzmann neutron transport equation to a coupled set of first-order ordinary time-dependent differential equations. The independent variables in this set of coupled equations are the amplitudes of the neutron flux within each arbitrarily specified region of the core and/or within each arbitrarily specified energy group of the neutron spectrum. A study is made to determine the accuracy of point-model kinetic theory in the prediction of the fundamental prompt neutron decay constant. The results of the study indicate that even the 1-point-model kinetics equation predicts the decay constant to within a few per cent of the exact value. The results of flux calculations for the University of Florida Training Reactor are presented. The results include a set of 18-

group cross sections and graphs of 1- and 2-dimensional calculations of the flux. On the basis of 18-group, 1-dimensional flux calculations the effective delayed neutron fraction is 0.00703 and the mean prompt neutron generation time is 247.5 microseconds. Comparisons of theoretical calculations with experimental measurements show good agreement. In connection with this work several computer codes were developed for use on the University of Florida IBM-709 computer. A brief discussion of these codes is given. The coupled point-model representation of the reactor neutron field should find its greatest applicability in the study of transients and of the propagation of perturbations in a reactor with weakly coupled fuel regions. (Dissertation Abstr.)

30863 ANGULAR CORRELATIONS IN NEUTRON DENSITY FLUCTUATIONS. Akcasu, A. Ziya (Univ. of Michigan, Ann Arbor). 23p. (CONF-660206-5). ORAU. Gmelin, AED-CONF-66-014-3.

From Symposium on Neutron Noise, Waves, and Pulse Propagation, Gainesville, Fla.

Space- and angle-dependent correlations in the fluctuations of neutron density and count rate were investigated using the Langevin technique and the single-collision approximation. The work is confined to an infinite homogeneous multiplying medium with an isotropic scattering in the laboratory system, and delayed neutrons are ignored. The energy dependence is removed by making a one-speed approximation. Physical implications of the results are discussed, and an application to neutron scattering is mentioned. (A.G.W.)

30864 APPROXIMATE TREATMENT OF NEUTRON THERMALIZATION IN HETEROGENEOUS SYSTEMS. Haubert, P. R.; Meyvaert, N. R. (Belgo Nucleaire, Belgium). 17p. (CONF-660204-10). ORAU. Gmelin, AED-CONF-66-017-9.

From American Nuclear Society Meeting, San Diego, Calif.

For the practical study of neutron thermalization, the multigroup approximation is now widely used. An alternative approach is considered, which consists in replacing the integral equation of neutron thermalization by a second order differential equation, as was first proposed by M. Cadilhac. This equation reduces to the Wigner-Wilkins equation for the monoatomic hydrogeneous gas moderator and to the Horowitz equation for the heavy gas moderator, and is thus correct in both limits. For all moderators it is also valid in the limit of infinitely weak absorption. Practically, it gives good results even when strong resonance absorbers, such as Pu-239, are present. The collision probability methods seem to be best suited for the treatment of heterogeneity in relation with the Cadilhac treatment of thermalization. Two ways of using collision probability methods are presented. Both lead to a system of second order differential equations easily solved by usual techniques. (auth)

30865 IMPROVEMENTS IN OR RELATING TO NEUTRON ABSORBER MATERIAL. Nettley, Peter Thomas; Fazackerley, Cecil Henry (to United Kingdom Atomic Energy Authority). British Patent 1,028,221. May 4, 1966. Filed Feb. 20, 1963.

Lithium aluminate is proposed as a burnable poison in a nuclear reactor. The high density lithium aluminate can be compacted into a ceramic form which does not crack under irradiation because of its marked ability to absorb gaseous irradiation products. The aluminate can be disposed as pellets in a hollow rod in the center of a fuel element assembly comprising a cluster of fuel rods. (B.L.M.)

30866 REACTIVITY PULSING DEVICE FOR PULSED FAST REACTORS. Riccobono, Gaetano (to EURATOM). British Patent 1,029,415. May 11, 1966. Filed Apr. 14, 1964.

A pulsing device for a fast nuclear reactor comprises at least one wheel carrying neutron-absorbing material on its periphery. Upon rotation of the wheel, the neutron-absorbing material is carried into and out of the reactor core. One or more voids a region substantially devoid of absorbing material as well as a region of reduced absorption power, is present in the neutron-absorbing material that will also pass into and out of the reactor core. The reactor is designed to be below critical when the absorbing material without a void or voids is in the core and to be at least prompt critical when a void is within the core. (B.L.M.)

30867 NUCLEAR REACTORS REACTIVITY CONTROL. Tollet, Louis H. J.; Maldague, Pierre E. J. M. (to Societe Anglo-Belge Vulcain Societe Anonyme). Canadian Patent 730,779. Mar. 22, 1966. Priority date May 24, 1961, Belgium.

Two liquids having different moderating capacities are employed in this reactor. One moderator is contained in a chamber having flexible walls. By suitable variation of pressure the flexible chamber is caused to expand or contract thus changing the proportion of good to poorer moderator. The moderator composition may be made different at various levels by subdividing the chamber into several compartments. By these methods the reactivity may be closely controlled. (F.S.A.)

Design and Feasibility

30868 IMPROVEMENTS IN OR RELATING TO NUCLEAR REACTORS. Wootton, William Robert (to Babcock and Wilcox Ltd.). British Patent 1,029,836. May 18, 1966. Filed Aug. 15, 1961.

A nuclear reactor is described that has a core contained in a pressure vessel and includes natural U heterogeneously arranged in the core that is moderated and cooled by a mixture of light and heavy water. The volume ratio of water to fuel in the core is substantially greater than that appropriate to a light moderated enriched U core and substantially less than that appropriate to a heavy water moderated natural U core. By variation of the proportion of light water in the mixture of light and heavy water, it is possible to vary the reactivity of the core. (B.L.M.)

30869 IMPROVEMENTS IN OR RELATING TO NUCLEAR REACTORS. Wootton, William Robert (to Babcock and Wilcox Ltd.). British Patent 1,029,837. May 18, 1966. Filed Aug. 25, 1961.

A pressurized water reactor is described that is either light water moderated and cooled, heavy water moderated and cooled, or a mixture of light and heavy water moderated and cooled. The fuel elements are arranged with spaces between them for filler members so that the rate of mass flow of liquid coolant during operation to effect cooling of the fuel elements is reduced. The filler elements exert a moderating influence on the reactor action and may be fluid-tight jackets filled with liquid (the same as the coolant) or solid filled. Alternatively, the jacket may be vented to permit a low rate of flow of fluid into and out of the jacket; in which case the end plugs have apertures of venturi form. The entire assembly of mutually spaced longitudinally extending fuel pins and filler members may be enclosed within an elongated box having a coolant inlet and outlet at respective ends. (B.L.M.)

Fuels

30870 (ORNL-TM-1528) COATED-PARTICLE FUELS DEVELOPMENT AT OAK RIDGE NATIONAL LABORATORY FOR PERIOD NOVEMBER 15, 1965 TO MAY 15, 1966. Coobs, J. H.; Morgan, J. G. (comps.) (Oak Ridge National Lab., Tenn.). May 1966. Contract W-7405-eng-26. 48p. Dep. mn. CFSTI $2.00 cy, $0.50 mn.

Highlights of the development work during the period Nov. 15, 1965, to May 15, 1966, on graphite-base fuel concepts involving pyrolytic-carbon-coated fuel particles for gas-cooled, civilian power reactor applications are reported. The major emphasis was on the testing and evaluation of pyrolytic-carbon-coated oxide fuel particles. A mathematical model for coated-particle behavior was used to guide the irradiation program and to correlate

results from irradiation experiments. The work described includes out-of-reactor characterization of coated-particle materials, irradiation testing, and postirradiation examination. (W.L.G.)

30871 PROBLEMS IN JAPAN'S ACQUISITION OF NUCLEAR FUELS. Haginoya, Toru (Atomic Energy Bureau, Tokyo). Genshiryoku Chosa Jiho (Tokyo), No. 8, 4-10(1965). (In Japanese).

By 1969, 117 tons of 2.3% enriched uranium will be needed in Japan, and 1975, 355 tons (9.2 tons of ^{235}U). The total cumulative amount required up to the end of the latter year from the present is 1435 tons of 2.3% enriched uranium (or 37.1 tons of ^{235}U). By 1975 the total atomic power generation in Japan will be about 4,400,000 Kw. In Japan's policy for the future acquisition of nuclear fuels, because of the lack of promising nuclear fuel resources, two things are important, namely, variety of possible nuclear fuels and of their resources, and the stability in nuclear fuel supplies. For enriched uranium, Japan depends on the U.S.A. Therefore, the treatment of problems of nuclear fuel acquisition are centered about these matters. (TCO)

30872 IMPROVEMENTS IN OR RELATING TO GAS COOLED NUCLEAR REACTORS AND FUEL ELEMENTS THEREFOR. Marien, Pierre Jean Camille Albert (to United Kingdom Atomic Energy Authority). British Patent 1,028,364. May 4, 1966. Filed Jan. 22, 1963.

A nuclear reactor fuel element for a gas cooled reactor includes provision for purging the element of fuel products formed during operation and is made up of at least one annular cartridge of the nuclear fuel-bearing material positioned within an outer casing by means of an inner tubular spine of non-fuel bearing material. Ports in the outer casing communicate with the bore of the tubular spine so as to cooperate with the spine to define a flow path for purge gas. The permeability of the fuel-bearing cartridge to gaseous fission products is considerably greater than that of the outer casing, and the permeability of the tubular spine is equal to or greater than that of the cartridge fuel-bearing material so that fission products formed within the fuel pass preferentially through the walls of the non-fuel bearing spine into the bore of the spine. Taking advantage of the relative permeability diffusivities of the various parts, the parts of the element are so arranged that there is a continuous inward diffusion of the fraction of the gas coolant that serves as a purge gas through the wall of the outer casing into the central purge gas flow path; then the purge gas having entrained the fission products formed during operation is led or transferred to a suitable process plant for the recovery or removal of the fission products. (B.L.M.)

30873 NUCLEAR REACTOR FUEL-CONTROL ROD ASSEMBLY. Tollet, Louis H. J.; Maldague, Pierre E. J. M. (to Societe Anglo-Belge Vulcain Societe Anonyme). Canadian Patent 730,780. Mar. 22, 1966. Priority date Mar. 9, 1961, Belgium.

A reactor is described in which the core consists of a number of self contained units. Each unit combines fuel elements in a support tube, a drive mechanism, a reactivity control member, also an inlet and outlet(s) for moderator and coolant. Each unit may be handled as a united assembly so that changes in the core do not require separate fuel removal. (F.S.A.)

Power and Power-Breeder Reactors

Refer also to abstracts 29080, 29383, 29980, and 30934.

30874 (ACNP–65612) PATHFINDER CORE BORATION AND FLUX MAPPING TEST 313. Smith, J. A.; Kelly, J. P.; Kern, R. C.; Lacy, P. S. (Allis-Chalmers Mfg. Co., Bethesda, Md. Atomic Energy Div.). Mar. 11, 1966. Contract AT(11-1)-589. 116p. Dep. mn. CFSTI $4.00 cy, $0.75 mn.

For Northern States Power Co., Minneapolis, Minn. and Central Utilities Atomic Power Associates.

Test 313 was made to determine the cold core excess reactivity and to provide sufficient flux distributions so that a thorough comparison could be made between measured and calculated distributions. Axial flux shapes in both boiler and superheater, radial flux peaks, the ratio of superheater to boiler flux, and core symmetries were checked. Since k excess and the flux map measurements were made for the cold-borated core rather than for the hot-voided core, the results were used to verify and improve analytical techniques. (M.O.W.)

30875 (ANL–7190, pp 143-55) FAST REACTOR RESEARCH AND DEVELOPMENT. (Argonne National Lab., Ill.).

Research progress is reported on design of 1000-Mwe metal-fueled fast reactors and design of large steam-electric generating units. Summaries of research are included on high-temperature test loops, high-temperature materials testing, and loops for Na sampling and quality measurement. (J.R.D.)

30876 (BAW–1302) INDIAN POINT REACTOR: NUCLEAR INSTRUMENTATION ASYMMETRY RESPONSE VERIFICATION. Ball, R. M.; Batch, M. L.; Pitts, T. G.; Barringer, H. S.; Hostetler, D. R.; Wolfe, G. E. (Babcock and Wilcox Co., Lynchburg, Va.). Jan. 1966. Contract 70-0012. 80p.

A deliberate asymmetric power distribution was induced in the Indian Point Reactor Core A at low power, and the indicated neutron flux on each of 18 power-range chambers outside the pressure vessel was compared with values determined analytically for the same configuration. The test results show that the external power-range detectors respond correctly to an asymmetric power distribution and are capable of indicating such a distribution. The response of the core power distribution and nuclear instrumentation readings as xenon redistributes indicates the degree of power asymmetry. Analytic calculations were within 10% of measured values. (auth)

30877 (CVNA–254) CAROLINAS VIRGINIA NUCLEAR POWER ASSOCIATES, INC. RESEARCH AND DEVELOPMENT PROGRAM. Quarterly Progress Report, October-December 1965. (Westinghouse Electric Corp., Pittsburg, Pa. Atomic Power Div.). Contract AT(30-1)-2286. 101p. Dep. mn. CFSTI $4.00 cy, $0.75 mn.

Brief summaries of the following areas of work during this period on the CVTR research and development program are presented: evaluation of operating logs, primary coolant system pressure drops, reactor transients, radiation analysis, chemistry program, thermal and hydraulic core, plant nuclear evaluation, ultrasonic inspection of pressure tubes, metallurgical examination of CVTR components, high burnup tests, and an organic loop feasibility study. (M.O.W.)

30878 (EURAEC–1516) RESEARCH PROGRAM FOR THE GARIGLIANO NUCLEAR POWER PLANT. Report No. 6. (Ente Nazionale per l'Energia Elettrica, Rome (Italy). Societa Elettronucleare Nazionale, Rome (Italy)). Oct. 1, 1965. Contract 101-63-11-RDI. 12p. (EUR-2668). Dep. mn. CFSTI $1.00 cy, $0.50 mn.

Work Performed under United States–Euratom Joint Research and Development Program.

Further research developments on the data logging computer system and instrumented assemblies are reported. Availability tests and program acceptance tests were performed satisfactorily. To complete the installation there still remains to enlarge the drum memory and to finish the program for the calibration of the in-core chambers. The read-out and the control panels were installed. Other installations of cables and equipment were performed. (M.O.W.)

30879 (GA–6995) 40-MW(E) PROTOTYPE HIGH-TEMPERATURE GAS-COOLED REACTOR POSTCONSTRUCTION RESEARCH AND DEVELOPMENT PROGRAM. Quarterly Progress Report for the Period Ending January 31, 1966. (General Dynamics Corp., San Diego, Calif. General Atomic Div.). Mar. 15, 1966. Contract AT(04-3)-314. 30p. Dep. mn. CFSTI $2.00 cy, $0.50 mn.

Analytical studies in connection with loading and zero-power testing continued. Effort was also applied to analyses relating to experiments to be performed during the approach to power and at power. Studies of the differences between one-dimensional GAZE calculations and two-dimensional GAMBLE calculations of core reactivity and control rod worth continued during the period. Several improvements in the one-dimensional calculations have resulted in closer agreement than that reported in the previous quarterly report; thus many of the calculations required for the zero-power test program can now be performed in one dimension. Calculations to predict the initial reactivity of the core using as-built loadings and dimensions were completed. Primarily because of increased carbon content in the core and reflector, the predicted just-critical loading was reduced from 700 ± 20 elements to 689 ± 20 elements. As a result, 24 additional poisoned dummy elements were prepared and inserted in the dummy core. The insertion of these additional elements was used as a dry-run demonstration of the functions to be performed during test BP-1. Measurements were taken with the three in-core neutron detectors to determine their count rate response as a function of the high voltage applied to the detectors. The previously reported in-core and source-range detector response as a function of distance from the source was used to make a preliminary specification for the location of the in-core detectors and sources for core loading. It is estimated that the detector and source locations will result in more than one-half of the count rate on all the in-core detectors being due to the center source. Fuel transfer machine settings were measured for each of the locations where flux traverses will be made. The flux plotter mechanism was lowered into the auxiliary parking hole; the fuel transfer machine then picked up the flux plotter and indexed it over each core position where a flux traverse will be made. Calculations were made to predict the static or operating power coefficient that will be measured during the approach to power and at power. Results indicate that, if the predicted behavior is confirmed by experiment, automatic control of the reactor can be accomplished primarily by coolant flow changes, and the automatic flux controller will require only small changes in the automatic control rod position to maintain the desired helium outlet temperature. (auth)

30880 (HPR–67) HBWR QUARTERLY PROGRESS REPORT, JANUARY TO MARCH 1966. (Institutt for Atomenergi, Halden (Norway). OECD Halden Reaktor Prosjekt). May 1966. 114p. Dep. mn.

The reactor was operated at about 15 Mw until 12th January. The only interruptions were a short stop on 22nd December for the repair of a slight D_2O leakage from the purification return pump and a scram on 26th December. Recalibration of IFA-3 and IFA-11 was carried out in order to investigate the long term performance of the in-core instruments. The following seven new instrumented test fuel assemblies were loaded: IFA-14 (one of the Project's tubular metallic uranium assemblies), IFA-26 and IFA-27 (German), IFA-29 and IFA-35 (British), IFA-36 (Swedish) and IFA-37 (Norwegian). IFA-37 was replacing IFA-34 which failed. At the same time IFA-20 (British) was unloaded, and also the cadmium oscillator thimble. Some shuffling of elements was also performed. The reactor was restarted and the calibration of the new instrumented fuel assemblies was begun. Due to very unstable flow in the forced circulation assemblies, IFA-26, IFA-29, and IFA-30, which also resulted in a slow scram, the reactor was shut down and cooled. The forced circulation assemblies were rearranged in a more symmetric core pattern and the reactor was restarted. Calibration of the new instrumented test fuel assemblies was then carried out. Dynamics experiments were begun in order to investigate the coupling effects between the tubular metallic natural uranium assemblies, IFA-12, IFA-13, and IFA-14. Operation was continued and attempts to identify the failed assembly were made concurrently with the dynamics experiments. It was confirmed that IFA-27 had failed, and it was suspected also that IFA-26 had failed. A scram was caused by a mains voltage drop. The dynamics experiments and the attempts to localize the failed fuel elements were continued afterwards. All results confirmed that IFA-27 had definitely failed and that IFA-26 and also IFA-21 and IFA-30 had possibly failed. The fission gas pressure on one of the stringers of IFA-27 had increased from the normal 4 ato to 28 ato, which was the reactor pressure, proving that there was a canning leakage in this particular fuel pin. The reactor was then shut down and cooled. This shutdown took place one day earlier than the planned shutdown for installation of new test elements. During the period of fission product release the fission gas collection system was in continuous operation. (M.O.W.)

30881 (NAA-SR–11712) IRRADIATION PERFORMANCE OF PIQUA CORE I FUEL ELEMENTS. Arnold, J. L. (Atomics International, Canoga Park, Calif.). May 25, 1966. Contract AT(11-1)-Gen-8. 42p. Dep. mn. CFSTI $2.00 cy, $0.50 mn.

Destructive examinations were made on two fuel elements from the Piqua Nuclear Power Facility (PNPF) Core I, as part of a continuing fuel performance surveillance program, to determine the effects of the organic-cooled reactor environment on the integrity of the fuel elements, and as an aid in determining the achievable Core I fuel lifetime. The general mechanical condition of the fuel elements, the fuel cylinder dimensional changes, coolant decomposition films on heat transfer surfaces, abnormal coolant decomposition products, and the integrity of fuel-cladding diffusion barrier were the principal areas of evaluation. The peak burnups attained were 0.65×10^{20} and 1.19×10^{20} fissions/cc (1400 and 2550 Mwd/MTU) for Fuel Elements P-1071 and P-1091 respectively. In general, the results of the examinations were very encouraging, in that the fuel elements were in excellent mechanical condition. Fuel dimensional changes were small (<0.8% outer diameter change); surface films on heat transfer surfaces were thin (a maximum thickness of 0.0017 in.); and the fuel-cladding diffusion barrier had maintained its integrity. Decomposed organic coolant deposits were found in the low-flow regions of the inner process tube and in the valve body assembly below it. (auth)

30882 (NUS–264) REACTOR OPERATION'S SAFETY ANALYSIS MONTHLY REPORT NO. 7, NOVEMBER 1, 1965 TO JANUARY 31, 1966. (NUS Corp., Washington, D. C.). Apr. 7, 1966. Contract AT(11-1)-651; Subcontract No. 4. 123p. Dep. mn. CFSTI $4.00 cy, $0.75 mn.

For Rural Cooperative Power Association, Elk River, Minn.

Discussions are presented on the operation and analysis of the following five areas: (1) health physics, waste disposal, and safeguards, (2) chemistry and materials, (3) reactor analysis, (4) instrumentation and control, and (5) reactor plant engineering. The size of the primary demineralizer cartridge necessitates awkward and potentially hazardous maneuvering to remove the spent resin from the unit. Three alternative solutions to this problem are presented along with additional evaluation of resin handling and storage equipment. Re-evaluation of annual average dilution factors for the discharge of gases to the atmosphere was performed utilizing an NUS computer program (WINDIF-3) with input data from the site and alternatively from adjacent meteorological centers. The relationships between oxygen and chlorine concentrations in the primary system with regard to the corrosion of stainless steel in the Elk River Reactor are discussed. As a check on the reactivity loss rate the position of the center control rod was recorded for an extended period. The actual rod positions were then compared to previous predictions of reactivity loss rate with the result that the recorded information correlated well with the predicted trend. The alternative methods of calculating fuel costs were reviewed, including projected costs for several reactor modes. The prediction of center rod worth, including fuel burnup effects was derived using the FLARE calculation and compared with beginning-of-life conditions. A design for modifying the four-rod scram system was developed to

provide redundancy of each reactor plant parameter signal supplied to the four-rod scram relays. This modification also extends the concept of redundancy to the vital scram relay functions (withdraw permit, four-rod insert and four-rod scram). Additional refinements to the system include a provision for testing secondary plant auxiliary relays with scram functions during reactor operation. The modification includes the installation of a sequence monitor to identify the order of receipt of multiple four-rod scram initiation signals. A tool post holder was developed to facilitate the refacing of the previously seal-welded evaporator handholes. In anticipation of converting the No. 2 evaporator handholes from seal-welded closures to a gasket and coverplate type, a more adaptable type of tool post holder was designed. A study was conducted to obtain an understanding of the mechanism and cause(s) of the primary feedwater system hydraulic oscillations. Specifications were developed for a network of insulation block support bands and an aluminum exterior weather cover for the containment vessel. (M.O.W.)

30883 (SAN-570-2) A PROBABILISTIC METHODOLOGY FOR THE SAFETY ANALYSIS OF NUCLEAR POWER REACTORS. VOLUMES 1 AND 2. Technical Final Report No. 1. Mulvihill, R. J. (Planning Research Corp., Los Angeles, Calif.). Feb. 28, 1966. Contract AT(04-3)-570. 430p. (PRC-R-657). Dep. mn. CFSTI $7.30 cy, $2.00 mn.

The methodology superimposes probabilities on a deterministic analysis which includes the best available analytical models for the several stages involved in an accident sequence (e.g., reactor kinetics, heat transfer, fission product transport within the containment, atmospheric transport outside the containment). Consideration was given to reactor design, operation, maintenance, and location parameters and to the effect of engineered safeguards. The overall model was adapted to automatic computation and was applied to an existing pressurized water (PWR) power reactor (Yankee). Its end product is the probability distribution of radiation dose level as a function of time and location with respect to the reactor. There is no inherent limitation to PWR systems in the methodology; however, modifications of the submodels and the input data would be required in the probabilistic safety analysis of other reactor types (e.g., gas-cooled, liquid metal-cooled) to account for significant differences between types (e.g., kinetics, heat transfer). Computer programs for making the calculations are listed. (M.O.W.)

30884 (WCAP-3269-16) LARGE CLOSED-CYCLE WATER REACTOR RESEARCH AND DEVELOPMENT PROGRAM. Progress Report, October 1–December 31, 1965. (Westinghouse Electric Corp., Pittsburgh, Pa. Atomic Power Div.). Contract AT(30-1)-3269. 41p. Dep. mn. CFSTI $2.00 cy, $0.50 mn.

Brief summaries of results are given for each of the following areas of research: fuel and control management, development of nuclear instrumentation system, Zircaloy hydriding in pressurized water, irradiation proof testing of advanced fuel assembly prototypes, irradiation proof testing of advanced fuel assemblies with improved grids, fuel swelling studies, development of advanced RCC canless fuel assembly design, reactor evaluation channel operation and specimen equipment maintenance, out-of-pile corrosion testing, in-pile chemistry testing, and chemical studies of soluble neutron poisons. (M.O.W.)

30885 THE NUCLEAR POWER PLANTS FURNISH IN GREAT BRITAIN ELECTRICITY AT COMPETITIVE PRICES. Cockcroft, John (Cambridge Univ., Eng.). Belgicatom, Ass. Belge Develop. Pac. Energ. At., Bull. Inform., 10: No. 59, 9-15(Dec. 1965). (In French).

The construction of the Oyster Creek in the United States, of the Dungeness "B" in Great Britain, and of the Pickering Reactor in Canada begins the era of competitive prices from nuclear power plants. The characteristics of the Dungeness "B" Reactor that made its power competitive with that of fossil fuel power plants are summarized. The characteristics of the heavy water moderated reactors constructed in Canada are briefly summarized. The program of the United States for the development of competitive nuclear power plants is indicated. A summary is given of the future program of the United Kingdom for the development of power reactors. (J.S.R.)

30886 CANADIAN HEAVY WATER MODERATED, LIGHT WATER COOLED REACTOR. Energ. Nucl., 8: 126-9(Mar.-Apr. 1966). (In French).

The novelties and advantages of reactor cooling with boiling light water are summarized. The characteristics of the tube in-shell fuel element are presented. The parameters and economy of the heavy water-moderated boiling light water-cooled 500 Mw(e) reactor are tabulated. A cost comparison was made of this reactor type with other reactor types. (J.S.R.)

30887 MEASUREMENT OF THE INFINITE MULTIPLICATION CONSTANT OF THE LATINA REACTOR LATTICE BY THE NULL REACTIVITY METHOD. Casali, F. (CNEN, Bologna); Ghilardotti, G. Energ. Nucl. (Milan), 13: 221-32(May 1966).

The measurement of the infinite multiplication factor of the Latina lattice is described, which was carried out in the critical assembly RB-1 of Montecuccolino, Bologna by the null reactivity method. The experimental procedure and the interpretation of the results are given in detail. The value obtained for K_∞ is 1.085, to be compared with 1.079, as calculated by a correlation based on a large set of exponential experiments. (auth)

30888 KRB GUNDREMMINGEN NUCLEAR POWER STATION. Jaerschky, Rudolf; Taurit, Rudolf (Allgemeine Elektrizitaetsegesellschaft, Frankfurt am Main). EuroNuclear, 3: 212-26(May 1966).

The boiling water reactor of the KRB power station is considered. The design and performance data are given. The nuclear steam supply system, the turbine generator set and main heat cycle, control and instrumentation, electric facilities, and nuclear service systems are discussed. (J.F.P.)

30889 AN OUTLINE OF THE DESIGN OF JPDR-II AND ITS TECHNOLOGICAL PROBLEMS. Ishikawa, Michio (Japan Atomic Energy Research Inst., Tokyo). Genshiryoku Kogyo, 11: No. 10, 3-9(Oct. 1965). (In Japanese).

The JPDR-II project aims (partly) at doubling the power output of its predecessor JPDR (boiling-water type, Japan Power Demonstration Reactor), i.e., into approximately 90 Mw, by changing the present natural convection into the forced circulation (leading to a higher power density of the fuel). To achieve this project, in the JAER-I, in June 1965, a JPDR-II project was established and the work initiated. An outline of JPDR-II is presented with the project itself also being described. A comparison of the JPDR characteristics and the design ones for JPDR-II is given. JPDR-II, in addition to the described development of nuclear fuels and technologies, can provide, with its attained high power densities, places of (actual) intense radiations for irradiation of nuclear fuels for light-water reactors to be developed in the future. (auth)

30890 METHOD FOR BURNUP ANALYSIS OF POWER REACTORS IN EQUILIBRIUM OPERATION CYCLES. Nakamura, Shoichiro (Hitachi Works, Japan). J. Nucl. Sci. Technol. (Tokyo), 3: 184-8(May 1966).

A method based on the consistent thermal neutron flux concept for burnup analysis of power reactors in equilibrium operation cycle is described. Radial flux distributions are discussed, as well as the variation of isotopic densities in the fuel, and considerations are given on control rod distribution for maintaining a consistent thermal flux distribution. The present method can be applied to most power reactors like BWR and PWR in which a multiple-batch refueling scheme is adopted. (auth)

30891 NUCLEAR POWER READIED FOR BASE LOADS. Mod. Power Eng., 59: 68-71(Dec. 1965).

The immediate and future power requirements of Ontario are reviewed. CANDU is compared with other reactor types and the experience with NPD examined. Expected results from the Douglas Point station scheduled for opera

tion early in 1966 are considered along those of Pickering which is still in the design stage. Computer control, absorber rods for flux flattening and boiling coolant are discussed. (AECL)

30892 THERMODYNAMIC DESIGN OF REACTOR COOLED BY GAS. Ciszewski, G.; Hediger, W.; Naegelin, R. Neue Tech., 8: 69-79(1966). (In French).

The preparation of a program for a digital computer intended for the thermal design of gas-cooled power reactors is discussed. The program consists of two parts, the first covering the fuel aspect, while the second deals with the secondary circuit comprising the steam generator and the turbine. The equations used are relatively simple, yet the program enables several constructive variants to be treated and the problem to be raised in different forms. (auth)

30893 CASCADE ARRANGEMENT IN SPHERICAL VESSEL DESIGN FOR NUCLEAR POWER REACTORS. Hu, L. W. (Pennsylvania State Univ., University Park); Schutzler, J. C. Nucl. Eng. Design, 3: 412-20(Apr. 1966).

The use of pressure vessels in cascade arrangement instead of the conventional single shell vessels is proposed for nuclear power reactor design, particularly in view of meeting the demand of increasing pressures and temperatures for pressurized-water reactors. The stress analysis and a procedure for the minimum weight design of irradiated cascade spherical shells are presented. A numerical example of two stage spherical shells is given to demonstrate the procedures developed as well as the need for such type of pressure vessels in nuclear power reactor design. (auth)

30894 REQUIREMENTS FOR THE PROPERTIES OF MATERIALS FOR REACTOR PRESSURE VESSELS IN REGARD TO OPERATION AND SAFETY—A REVIEW. Uebing, D. (Technischer Ueberwachungs-Verein Rheinland, Duesseldorf). Nucl. Eng. Design, 3: 421-31(Apr. 1966). (In German).

In view of the stringent requirements for safety and operating reliability of nuclear power plants, considerable attention has to be focused on the structural design of the highly stressed components of the reactor system. The design of reactor pressure vessel and primary piping must comply with most exacting standards. The demands, unprecedented in conventional applications, require additional knowledge on the behavior of materials. The primary objective is to critically review and assess the adequacy of the foundations of mechanical design of steel reactor pressure vessels on the basis of recent German research work, pointing out those aspects which are presently considered essential to be further investigated with the goal of achieving a more adequate quantitative evaluation of structural reliability and safety under various loading conditions. (Neutron-induced changes of the mechanical properties of pressure vessel materials, however, are outside the scope of the present considerations.) The maximum strength of pressure vessels for internal pressure loading is discussed showing that not only the tensile strength σ_B of the steel but also the uniform strain ϵ_G and the true stress at maximum pressure σ_G are of crucial importance for structural safety. At areas of stress concentrations the weakening effect on bursting strength expressed by the reduction factor ν_B in general seems to be covered in a conservative way by the strength reduction factors at the onset of effective yield $\nu_{0.2}$ as they are presently prescribed in Germany for conventional pressure vessel design. However, experimental programs with larger specimens are required. Expected deformations at maximum internal pressure and the significance of material ductility (reduction of cross sectional area at tensile rupture ψ, notch impact toughness a_k) are indicated. The problem of low-cycle fatigue is also considered. Experimental data are given for fluctuating internal pressure, alternating plastic straining at elevated temperatures, alternating low frequency loading in water environments, and for thermal shock. The influence of specimen-size on tensile strength of bars with notches and the influence of multiaxial stress states on the failure characteristics are discussed. (auth)

30895 POST-ACCIDENT PRESSURE AND TEMPERATURE TRANSIENTS IN A DRY CONTAINMENT—A PARAMETRIC STUDY. Voigt, O. (Allgemeine Elektricitaets-Gesellschaft, Frankfurt am Main). Nucl. Eng. Design, 3: 451-66(Apr. 1966).

A parametric study, based on the containment design for the 520 Mw(t) Boiling Water Reactor (KWL) at Lingen, Germany, reveals the influence of uncertainties in basic data and assumptions on design pressure and calculated post accident transients within the containment. The computer program used for the calculations is described. (auth)

30896 FOUNDATION CAISSON PROVIDES UNDERGROUND CONTAINMENT FOR NUCLEAR POWER PLANT. Wahl, Howard W. (Bechtel Corp., San Francisco). Nucl. Eng. Design, 3: 478-94(Apr. 1966).

A reinforced concrete caisson provides an economical underground structure for housing a portion of the Humboldt Bay Nuclear Plant. In addition to housing the nuclear steam supply system, the caisson also serves as part of the pressure suppression containment. The unique differences between this caisson and the conventional marine caissons are pointed out. The caisson was sunk immediately adjacent to an existing steam power plant. Special sinking techniques were used to reduce the surface friction, soil subsidence, and sinking weight. Upon completion, the underground structure served as a foundation for the plant refueling building and 250 ft high ventilation stack. The use of a caisson structure proved to be a sound solution to the varied requirements of plant layout, containment, construction, adjacent foundations, and budget. (auth)

30897 ADMINISTRATION OF RADIATION SAFETY AT THE CVTR. Lewis, Lionel (Carolinas-Virginia Nuclear Power Associates, Inc., Parr, S. C.). Nucl. Safety, 7: 137-48; 159(Winter 1965–1966).

The radiation- and reactor-safety programs at the Carolinas-Virginia Tube Reactor are briefly discussed. Plant operating experience, emergency procedures, and the economics of the health and safety program are considered. (D.C.W.)

30898 HALLAM NUCLEAR POWER FACILITY OPERATING EXPERIENCE. Keller, L. E.; Davidson, R. H. Nucl. Safety, 7: 236-42; 267(Winter 1965–1966).

The significant events in the operating experience of the Hallam Nuclear Power Facility are summarized. Reactivity measurements, activity releases, radiation exposures, and difficulties with plant components are considered. (D.C.W.)

30899 ASSESSMENT OF THE CARBON TRANSPORT PROBLEM IN HIGH TEMPERATURE GAS COOLED REACTORS. Pointud, M. L. (OECD, Paris. Atomic Energy Establishment, Winfrith, Eng.); Roemberg, E. Nukleonik, 8: 179-88(May 1966).

In a high temperature, helium cooled, graphite moderated reactor, (H.T.R.), the inleakage of oxidizing impurities constitutes a problem. Graphite corrosion and carbon deposition may reduce considerably the effective life of the core and the heat exchangers. In order to minimize this problem the oxidizing impurities must be kept in certain limits. In a study, which was carried out in support of the development of the O.E.C.D.—H.T.R. "Dragon," an attempt was made to explain and to detail the carbon transport problem by assessing the importance of the different parameters. Equations are presented relating the maximum permissible corrosion to the attack of the fuel particle coating. Other expressions allow the purification flow or the maximum permissible water inleakage to be estimated, for avoiding excessive graphite corrosion and carbon deposition as function of corrosion rates, heat exchanger reactivities, total flow, thermodynamic equilibria, etc. (auth)

30900 REACTIVITY CHANGES WITH LONG IRRADIATION. Spinrad, Bernard I. Power Reactor Technol., 8: 215-17(Fall 1965).

Fuel-management methods are briefly discussed. Four papers on the measurement and prediction of reactivity variations are summarized, together with operating experience with some reactors. (D.C.W.)

30901 REACTOR CONTROL EXPERIENCE. Harrer, Joseph M. Power Reactor Technol., 8: 221-7(Fall 1965).

The experience with control equipment and the failure analyses that were discussed at the conference on Reactor Operating Experience are summarized. (G.O.Y.)

30902 EFFECT OF HYDRIDING ON ZIRCALOY PROPERTIES. Sutton, C. Roger. Power Reactor Technol., 8: 245-51(Fall 1965).

The dominant factors affecting the amount and rate of hydrogen uptake by Zircaloy are discussed. The effects of hydrides on the alloys' properties are also discussed along with the causes and control of orientation and the significance of the hydride effects. (G.O.Y.)

30903 FUEL ELEMENTS. Power Reactor Technol., 8: 252-8(Fall 1965).

The effects of a boiling-water environment on stainless-steel cladding are discussed along with the differences in cladding behavior in boiling water reactors and pressurized-water reactors. (D.C.W.)

30904 OPERATIONAL PROBLEMS AND SOLUTIONS. Skaardal, Rolf C. Power Reactor Technol., 8: 271-9(Fall 1965).

Some operational difficulties with reactors are discussed. Hydraulically induced vibrations, corrosion, leaks in components, and control-system peculiarities are considered. Some repair methods, control of oxygen in heavy water, and modifications to research-reactor experimental facilities are also considered. (G.O.Y.)

30905 HALLAM OPERATION IN RETROSPECT. Smith, Fred A. Power Reactor Technol., 8: 279-89(Fall 1965).

A brief review of operating experience with the Hallam Nuclear Power Facility is presented. The difficulties encountered are discussed. (D.C.W.)

30906 ADVANCEMENTS IN ORGANIC COOLANTS. Sawyers, J. E. Power Reactor Technol., 8: 290-6(Fall 1965).

Some investigations of organic coolants are summarized. (D.C.W.)

30907 APPLICATION OF NETWORK PLANNING TECHNIQUE IN THE CONSTRUCTION OF NUCLEAR POWER PLANTS. Schamburger, Rudolf (Siemens-Schuckertwerke AG, Erlangen, Ger.); Wille, Horst. VDI (Ver. Deut. Ing.) Z., 108: 633-6(May 1966). (In German).

Due to the complex design of a nuclear power plant and the interdependence of the different operations, the construction of such a plant can profitably be planned and supervised by means of the network planning technique. The application of the CPM-process made it possible to build the nuclear power plant at Karlsruhe (Western Germany) according to schedule. (auth)

30908 CALCULATION OF THE STABILITY CONDITIONS OF A WATER-MODERATED WATER-COOLED BOILING REACTOR. Sergeev, I. P. Vestsi Akad. Navuk BSSR, Ser. Fiz. Tekh. Navuk, No. 2, 16-21(1965). (In Russian).

An attempt was made to predict analytically the possibility of small self-sustaining oscillations of the power of an experimental boiling water reactor (EBWR). The latter is treated as an autonomous nonconservative nonlinear system with many degrees of freedom. In this case, the problem amounts physically and formally to the determination of the conditions under which a self-oscillatory process can be achieved in the system. Since no accurate methods of mathematical analysis of such complex systems exist, an approximate method based on the idea of harmonic linearization was found to be the most suitable. The threshold power, frequency, amplitude, and constant component of the power oscillations of the EBWR reactor were determined. (ATD)

30909 NONUNIFORM BURN-UP IN A REFLECTOR REACTOR. Sergeev, I. V. Vestsi Akad. Navuk BSSR, Ser. Fiz. Tekh. Navuk, No. 2, 29-32(1965). (In Russian).

The variational approach was used previously to investigate the influence of the nonuniform burnup of the fuel and of the poison accumulation on the length of run t_k of nuclear reactors without reflectors. The variational method remains applicable to the case of reflector reactors discussed; however, the formulation of the problem and the intermediate calculations require modifications. Since the active zone and the reflector should be considered as a single system in the eigenvalue calculations, in the single group diffusion approximation the stationary diffusion equation cannot be used as the starting point. The study is based on the nonstationary diffusion equation containing sources. Basic expressions for the calculation of t_k are given in the single group and multigroup approximation. Formulas are also given for various partial capture cross sections. (ATD)

30910 TEPLONOSITELI ENERGETICHESKIKH YADERNYCH USTANOVOK. (Nuclear Power Reactor Coolants). Ulybin, S. A. Moscow, Leningrad, Izdatel'stvo Energiya, 1966. 272p.

Special features of the performance of coolants of nuclear power plants are examined. and material from the literature on the various properties of coolants is systematized. The effect of radiation on the properties of coolants and on the corrosion of construction materials is described. and approximation methods for calculating the radioactivity of the coolant are presented. The thermophysical. corrosion. and other properties of water. organic liquid-metal. and gas coolants are described in detail. Special features of the construction and exploitation of reactors. resulting from the use of one or another form of coolant. are considered. (tr-auth)

30911 IMPROVEMENTS RELATING TO NUCLEAR POWER PLANT. Dahlgren, Joens Arthur. British Patent 1,029,151. May 11, 1966. Priority date Feb. 23, 1962, Sweden.

A nuclear power plant consisting of a pressurized water nuclear reactor. steam generator. heat exchanger. steam superheater. and steam turbine is described. A major portion of the pressurized water is passed through the high temperature side of the steam generator. and the steam produced is passed through the steam superheater to the steam turbine. The major portion of the pressurized water is passed through the heat exchanger. and feed water is passed under pressure through the heat exchanger in heat exchange with the minor portion of the pressurized water. From the heat exchanger. the feed water passes through the steam superheater in heat exchange with the steam passing through the superheater. The feed water is then passed at reduced pressure from the steam superheater to the steam generator. (B.L.M.)

30912 IMPROVEMENTS IN OR RELATING TO NUCLEAR REACTORS. Gratton, Charles Peter; Russell, Albert Henry (to Societe Anglo-Belge Vulcain). British Patent 1,029,485. May 11, 1966. Filed Oct. 21, 1963.

A reactor design is proposed that contributes to more uniform power production of the reactor by replacing fuel in flux depressed localities of the core by the liquid moderator, which also serves as reactor coolant. The reactor core is made up of fuel assemblies, each of which is made up of externally similar components. The components are spaced apart to define passages between them. The greater number of the components are fuel elements, and the remaining components are fuel free and have means for being flooded by the liquid. (B.L.M.)

30913 INTEGRAL BOILER NUCLEAR REACTOR. Ammon, Johannes H.; Sprague, Theodore S. (to Babcock and Wilcox Co.). U. S. Patent 3,245,881. Apr. 12, 1966. Filed July 31, 1962.

A compact integral boiler reactor design is described which incorporates the reactor, the heat exchanger, and its associated vapor-liquid separation equipment within

one vessel. A vessel is provided in which a primary coolant continuously circulates absorbing heat generated in the reactor core and giving up the heat to a secondary coolant flowing through a multiplicity of tubes located within the same vessel. The interior of the vessel is divided into a riser space, a pressurizer space, a downcomer or heat exchanger space, and a vapor-liquid separating space. Heaters arranged within the pressurizer space vaporize a quantity of the primary coolant and pressurize it to the desired level. The core is positioned in the lower part of the riser space, and the heat generated within the core is removed by the primary coolant which then flows upwardly through the riser space. From the riser space the primary coolant flows downwardly transferring its heat to the secondary coolant through the tubes in the downcomer space. The secondary coolant may be either vaporized or superheated by this heat transfer. The separating equipment positioned within the vapor-liquid separating space receives the steam-water mixture of secondary coolant from the tubes and then provides separated vapor to be superheated within certain tubes and separated liquid to be recycled through the remainder of the tubes. (B.L.M.)

30914 FAST BREEDER REACTOR AND METHOD OF OPERATION OF SAME. Schluderberg, Donald C.; Barringer, Howard S. (to Babcock and Wilcox Co.). U. S. Patent 3,247,068. Apr. 19, 1966. Filed Feb. 28, 1963.

A heterogeneous reactor comprises a body of fissionable material arranged as a number of fuel elements in a core to undergo self-sustaining fission-type chain reaction having an operating neutron spectrum energy level substantially above the thermal neutron level and having a positive coolant density coefficient of reactivity. The fuel elements are arranged in a fixed lattice with a number of regular flow channels through the core. A blanket of fertile material and one of neutron reflecting material surround the core. A single phase hydrogen-isotope containing fluid capable of a substantial change in density with a change in heat content is passed through the core, and means are provided for varying the hydrogen isotope in the fluid to control the fission type reaction. This fluid also serves to cool the reactor. (B.L.M.)

30915 NUCLEAR REACTOR AND METHOD OF OPERATING TO VARIABLY MODERATE AND CONTROL SAME. Edlund, Milton C.; Schluderberg, Donald C. (to Babcock and Wilcox Co.). U. S. Patent 3,247,072. Apr. 19, 1966. Filed Dec. 8, 1961.

A heterogeneous reactor and a method of operation is patented in which the reactor has a number of fissionable material-bearing fuel elements arranged in a fixed lattice to undergo a self-sustaining fission-type chain reaction and in which the core has a number of fixed regular flow channels. A single phase hydrogen-isotope-bearing vapor which undergoes a change in density with a change in pressure and enthalpy is introduced to the core. The vapor is circulated independently of the fuel elements through the fixed flow channels to moderate the chain reaction by controllably varying the density of the vapor in the core. The moderating fluid may be chosen from the group including steam, vaporous hydrocarbons, or free hydrogen, or mixtures of any of these with inert gases. (B.L.M.)

30916 MULTI-PASS, VAPOR MODERATED AND COOLED NUCLEAR REACTOR AND METHOD OF OPERATING TO VARIABLY MODERATE AND CONTROL SAME. Schluderberg, Donald C. (to Babcock and Wilcox Co.). U. S. Patent 3,247,073. Apr. 19, 1966. Filed May 23, 1962.

The heterogeneous reactor described in U. S. Pat. 3,247,072 has been modified in design so that separate circuits are not necessary for the hydrogen-isotope-bearing moderating fluid and a cooling fluid that may be the same as the moderating fluid, but that must circulate in separate circuits if the negative temperature coefficient of reactivity is to be maintained. Thermal feedback is introduced into the cooling and moderating vapor to provide the reactor with the negative temperature coefficient of reactivity so that upon slight disturbances in reactivity the reactor is self-compensating. With this thermal feedback the reactor can also be made self-regulating. (B.L.M.)

30917 STEAM COOLED REACTOR ARRANGEMENT. Schluderberg, Donald C.; Ryon, John W.; Carlson, Robert W. (to Babcock and Wilcox Co.). U. S. Patent 3,247,074. Apr. 19, 1966. Filed June 18, 1963.

A reactor is patented that may be variably controlled and moderated by introducing a single phase hydrogen-isotope-bearing moderating fluid capable of a substantial change in density with a change in enthalpy into the core, which is made up of a number of fissionable material-bearing fuel elements arranged to undergo a self-sustaining fission-type chain reaction. The chain reaction is regulated by varying the concentration of the moderating fluid within the core and/or by varying the mixture of fluids. The moderating fluid may be chosen from the group consisting of water, at or near, or even above the critical pressure and temperature, or superheated steam at these pressures, vaporous hydrocarbons, or free hydrogen, or mixtures of any of the aforementioned with inert gases. The pressure vessel of the reactor is divided into at least two sections including a first section disposed substantially centrally of the vessel and a second section extending through the first section but separate and distinct from the first section. The fuel elements are arranged in the second section within a multiplicity of tubes extending between and connected through upper and lower tube sheets, and the coolant fluid is introduced through the second section into the tubes in heat transfer relationship with the fuel elements. The moderating fluid is introduced into the first section and flows downward about the tubes containing the fuel elements into the second section to moderate the chain reaction. (B.L.M.)

30918 NUCLEAR REACTOR OPERATING WITH HYDROGEN-BEARING MODERATOR AND COOLING VAPOR. Ryon, John W.; Schluderberg, Donald C. (to Babcock and Wilcox Co.). U. S. Patent 3,247,075. Apr. 19, 1966. Filed May 23, 1962.

A heterogeneous reactor is patented that employs a hydrogen-bearing moderator and cooling vapor that may be a vaporous hydrocarbon, hydrogen gas, steam, or mixtures of any of these with inert gases. A number of fissionable material bearing fuel elements are arranged in a fixed lattice within a pressure vessel. The fuel elements are divided into two groups, the first of which is enclosed in a shroud that is connected to the moderating and cooling vapor inlet so that the vapor is heated to a moderating density by the heat from the fuel elements. The vapor at the moderating density is passed about all the fuel elements in the core to moderate the fission reaction and then is passed through a second group of fuel elements to be further heated. The second group of fuel elements contains about three times the number of fuel elements as the first group. The upper and lower extents of the moderating space in the pressure vessel are defined by tube sheets suspended from the upper portion of the pressure vessel and supported by the lower portion of the pressure vessel, respectively. (B.L.M.)

30919 INTEGRAL VAPOR GENERATING AND SUPERHEATING NEUTRONIC REACTOR SYSTEM. Tower, Stephen N.; Arnold, William H. Jr. (to Westinghouse Electric Corp.). U. S. Patent 3,249,506. May 3, 1966. Filed Apr. 28, 1961.

An integral vapor generating and superheating nuclear reactor has a pressure tube design through which a flow of high pressure primary coolant can be maintained to transfer heat from the fissile fuel also contained in the pressure tubes. The reactor design minimizes the weight, space requirements, and power requirement for auxiliary equipment by eliminating vapor pumps required to force saturated vapor through separate external vapor superheaters and eliminated heat sources outside the reactor for superheating the saturated vapor. The reactor core is made up of the pressure tubes uniformly spaced in the graphite moderator. The primary coolant contacts the boiling pressure tubes in the center region of the core,

absorbs heat from the fissile material contained in the pressure tubes. and is converted into a steam–water mixture. which is sent to a vapor separator, for example a steam drum. The separated steam. which at this stage is saturated. is sent to the pressure tubes or reactor superheat tubes in another region of the core. The saturated steam flows through the reactor superheat tubes and absorbs heat to become superheated steam. The superheated steam is then sent directly to the turbine to generate electric power. After passing through the turbine. the steam is condensed and returned to the reactor to repeat the cycle. A blanket of an inert gas is maintained in the low pressure reactor vessel containing the graphite moderator during operation to facilitate transfer of the moderator heat back to the pressure tubes. (B.L.M.)

Process Heat Reactors

Refer also to abstract 30880.

Production Reactors

30920 GADOLINIUM NITRATE INJECTION AS AN AUXILIARY SHUTDOWN SYSTEM FOR SAVANNAH RIVER REACTORS. Heinrich, L. A. (E. I. Du Pont de Nemours and Co., Aiken, S. C.). Nucl. Safety, 7: 175-9; 184(Winter 1965–1966). (DPSPU–65-30-14; CONF-650710–4).

An auxiliary shutdown system. which functions by injecting $Gd(NO_3)_3 \cdot D_2O$ directly into the reactor moderator, is described. The results of a test of this system on a reactor operating at power are presented. (G.O.Y.)

30921 LONG LIFETIME NUCLEAR REACTOR. Conley, George H. (to U. S. Atomic Energy Commission). U. S. Patent 3,252,867. May 24, 1966.

This invention relates to a seed blanket reactor wherein a long core lifetime is obtained through the proper selection of seed thicknesses, fissile and fertile fuel mass fractions and compositions, and a suitable geometric arrangement of the fissile and fertile fuel such that the excess reactivity which occurs during the core lifetime is of an amount which is controllable by conventional methods. An optimum range of seed thicknesses and fissile to fertile fuel ratios were determined to produce a reactor having a minimum excess reactivity, yet also having a core lifetime which extends several times as long as present day cores. (Gmelin)

Propulsion and Space

See also ENGINEERING — Space Propulsion

30922 (BRLD–3255) FABRICATION AND TEST OF A FLUERIC POSITION SERVO. Quarterly Report, September 10, 1965–December 10, 1965. (Bendix Corp., Southfield, Mich. Research Labs. Div.). Contract NAS 3-6201. 52p. (NASA-CR–54900).

Further-developments on the pneumatic control drum actuator for a nuclear rocket engine in which the electronics were replaced by flueric devices are reported. The designs of the Position Error Detector Unit and Power Control Valve were completed. Breadboard vortex valves, single input amplifiers and summers were built and tested. The lead-lag circuit was revised and preliminary tests on an early design of the circuit were conducted. (auth)

30923 (LA–3394) RADIATION MEASUREMENTS OF THE EFFLUENT FROM THE NRX A-2 AND NRX A-3 REACTORS. Henderson, R. W.; Larson, O. W. (Los Alamos Scientific Lab., Univ. of California, N. Mex.). Jan. 1966. Contract W-7405-eng-36. 51p. Dep. mn. CFSTI $3.00 cy, $0.50 mn.

Compilation of data resulting from the collection of samples of the effluent clouds from the NRX A-2 and A-3 reactors during full power operation is presented. Data are presented concerning the magnetic and isotopic composition of the airborne and ground deposition material. The environmental impact of these tests was calculated for hypothetical conditions of land use and occupancy, and these data are included. A brief description of equipment and techniques is also given. (auth)

30924 (LA-DC–7636) PROPULSION REACTOR TEMPERATURE CONTROL WITH THE INTERNAL POWER LOOP ELIMINATED. Brown, E. A.; Balcomb, J. D. (Los Alamos Scientific Lab., Univ. of California, N. Mex.); Josephson, J.; Junker, D. W.; Mackey, L. (Westinghouse Electric Corp., Pittsburgh, Pa. Astronuclear Lab.). [1965]. Contract W-7405-eng-36. 11p. (CONF-660608-3). Dep. mn. CFSTI $1.00 cy, $0.50 mn.

From 2nd AIAA Propulsion Joint Specialist Conference, Colorado Springs.

Incremental changes of either temperature or the mass of hydrogen in Rover and NERVA reactors generate natural feedback reactivity which makes the reactor self-stabilizing. An increase in reactivity generated by either rod position or flow rate increases will raise power. This will increase core and gas temperature which decrease reactivity. Thus the system will come to a new balance at slightly higher power and temperatures when the natural reactivity decrease just offsets the increase from rod position or flow rate changes. At 1000 megawatts power and 70 lbs/sec flow rate, the static incremental gains from control rod position and flow rate to average core temperature are 68°R/°θ and 31°R/lbs/sec respectively. The natural reactivity loop also tends to cancel the nonlinear effects of the reactivity-to-power gain dependency on power level, and the core heat exchanger bandwidth dependency on flow rate. Advantage was taken of these core characteristics in developing a new temperature control system which does not have the internal power control loop common to earlier propulsion reactors. The change has resulted in considerably improved temperature control system stability and reliability. (auth)

30925 (LA-DC–7637) COOLED HIGH-TEMPERATURE THERMOCOUPLES FOR PHOEBUS REACTORS. Goodier, Benjamin G. (Los Alamos Scientific Lab., Univ. of California, N. Mex.). [1965]. Contract W-7405-eng-36. 17p. (CONF-660608–5). Dep. mn. CFSTI $1.00 cy, $0.50 mn.

From 2nd AIAA Propulsion Joint Specialist Conference, Colorado Springs.

Thermocouple measurements of high temperatures, around 5000°R, in the Project Rover reactors were quite unreliable. Carbon attack upon the refractory metals and the degradation of the resistivity of the electrical insulators were the chief offenders. Phoebus engine design dictates that a long portion of the thermocouple leads pass through the reactor core to the point of interest. By cooling the thermocouple elements along this length except for a short distance at the tip, electrical shunting and chemical attack are minimized. Cooling of these thermocouples is accomplished by thermally insulating this portion of the thermocouple lead from the surrounding graphite and flowing hydrogen around the lead, then diverting this flow away from the sensing area. This approach was effective in Phoebus-1A exit gas measurements and will be used for both exit gas temperatures and core material temperatures in Phoebus-1B. (auth)

30926 ENERGY SUPPLY ARRANGEMENTS WITH NUCLEAR SOURCES FOR SPACE FLIGHT INSTRUMENTS. Pruschek, R. (Technische Hochschule, Stuttgart). Chem.-Ing.-Tech., 38: 514-25(May 1966). (In German).

For high power and long mission purposes nuclear energy is well suitable especially for the supply of electric systems on board space flight systems. The primary energy released as heat can be derived either from the decay of radionuclides or from small reactors carried along in the satellite. The thermal energy is converted to electrical energy by thermoelectric (especially Ge-Si thermoelements) or turboelectric conversion. A large increase in specific power is expected with thermionic converters, especially when they are operated within the fission zone of the reactor. (tr-auth)

30927 THE NUCLEAR AIRSHIP. Morse, Francis (Univ. of Boston). New Sci., 30: 12-14(Apr. 7, 1966).

A feasible and economic nuclear airship, comprising a nuclear reactor coupled with a large lighter-than-air frame, is proposed. Weight and radiation-safety considerations of hypothetical nuclear airplanes and nuclear airships are compared. The displacement of the proposed nuclear airship is nearly twice that of previous conventional airships. The design speed is 103 mph for 6000 hp. The reactor is ceramic-fueled, lithium-cooled, shielded by a laminate of boron-treated polyethylene and lead, and contained in a pressurized steel sphere. Three engines are provided, the two smaller capable of operating on chemical fuel in case of reactor shutdown. The structural arrangement of the design is shown. A comparison of the characteristics of the proposed nuclear airship and the Hindenburg is given. The advantages of the use of the nuclear airship as an air freighter, especially for low-density freight, and as a luxury 400-passenger carrier are described. (M.J.T.)

30928 STRESSES IN THICK-WALLED CONICAL SHELLS. Hausenbauer, George F.; Lee, George C. (State Univ. of New York, Buffalo). Nucl. Eng. Design, 3: 394-401(Apr. 1966).

The radial, tangential, and axial wall stresses in a thick-walled cone under internal and/or external pressure are determined. The cone is considered to be "long" such that the end effect does not influence the wall stresses. The reason for studying the wall stresses in the thick-walled cone arose in the design of nozzles for pressurizers and steam generators used in the pressurized-water reactor systems of nuclear submarines and aircraft carriers. (auth)

30929 REACTORS: KEY TO LARGE-SCALE UNDERWATER OPERATIONS. Wetch, J. R. (Atomics International, Canoga Park, Calif.). Nucleonics, 24: No. 6, 33-7(June 1966).

The applicability of nuclear power plants in oceanographic research is discussed. It is shown that shielded small reactor power plants weigh less than equivalent chemical systems operating for only a few hours in the megawatt range. The uses to which reactors might be put can be classified into exploitation of the oceans and the underlying soil, off-shore power, transportation, and military. Possible reactor types are discussed, and the small fueled-hydride reactors developed under the SNAP program are suggested as the most promising. A 15-kw(e) system known as NEPTUNE was designed as an underwater power system capable of 5-yr unattended operation with potential for 10 yr. For the 100-kw(e) range the COMPACT reactor was designed. It draws on SNAP technology to simultaneously minimize shielded volume and fuel requirements. Boiling water is used as the coolant. Hermetically sealed, high-speed, water-lubricated rotating machinery is used. The 50 to 500 kw(e) power station is 21 ft long with a 7-ft dia. (M.C.G.)

30930 HEARING BEFORE THE JOINT COMMITTEE ON ATOMIC ENERGY, CONGRESS OF THE UNITED STATES, EIGHTY-NINTH CONGRESS, SECOND SESSION ON NAVAL NUCLEAR PROPULSION PROGRAM, JANUARY 26, 1966. Washington, D. C., Joint Committee on Atomic Energy, 1966. 80p. $0.25 GPO.

The progress and schedule of the naval reactor propulsion program is discussed. The capabilities of various nuclear-powered ships and economic studies of propulsion are considered. (J.F.P.)

30931 COMPACT NUCLEAR STEAM GENERATOR. Purdy, David C.; Schoessow, Earl E. (to Babcock and Wilcox Co.). U. S. Patent 3,245,879. Apr. 12, 1966. Filed Nov. 29, 1963.

A compact once-through steam generating reactor plant is patented that employs forced circulation of the primary coolant through a closed circuit within the reactor itself. The reactor plant is directly concerned with marine propulsion but is equally applicable in land operations where a reactor plant of this type is needed. (B.L.M.)

Research and Test Reactors

30932 (ANL-7204, pp 65-73) ADVANCED SYSTEMS RESEARCH AND DEVELOPMENT. (Argonne National Lab., Ill.).

Various research summaries are reported on the following: Argonne Advanced Research Reactor, Liquid Metal Fast Breeder Reactor, and magnetohydrodynamics. Research on the AARR consisted of measurements on the following: radial and vertical traverses of neutron-detector activity, control-blade calibrations, and reactivity worths of Al and SS followers of control blades, reactivity-control capacities of control-blade absorbers, and a preliminary calibration of the peak absolute thermal neutron-flux levels in the ITC and in the Be reflector. (M.O.W.)

30933 (BNWL-216) HEAT TRANSFER EXPERIMENTS FOR THE ADVANCED TEST REACTOR. Waters, E. D. (Battelle-Northwest, Richland, Wash. Pacific Northwest Lab.). May 1966. Contract AT(45-1)-1830. 109p. Dep. mn. CFSTI $4.00 cy, $0.75 mn.

Heat transfer experiments were conducted with electrically heated test sections which were full scale models of a typical coolant channel of the Advanced Test Reactor (ATR). The test section coolant channel was 2.03 in. wide by 0.070 in. thick by 49.5 in. long. A steady state heat conduction analysis of an ATR fuel channel was used to determine the proper size and shape of the resistance heater bars to produce heat flux distribution typical of the reactor fuel elements. A chopped cosine axial heat flux pattern was used in both test sections, and in one test section a lateral flux peaking factor of 1.36 peak/average was also used. A hydraulic analysis was made for the ATR core with many parallel flow channels. The analysis showed that if the hydraulic demand (pressure drop vs flow) curves for any coolant channel exhibited minima (near boiling) which were greater than the constant core pressure drop, then flow instability would occur in that channel and lead to boiling burnout conditions. Experiments were then performed to verify this analysis. Experiments were first conducted to determine hydraulic demand (ΔP vs flow) curves at constant power input rates to the coolant. Coolant velocities from about 1.5 to 5 ft/sec and 25 to 55 ft/sec were used to simulate reactor shutdown conditions and normal reactor operating conditions, respectively. The pressure drop along the test section was recorded as the flow rate was decreased in small steps by a control valve while power input was held constant. Flow reductions were continued until the channel pressure drop reached a minimum and increased appreciably due to boiling and two-phase flow conditions. The experimental apparatus was then arranged to simulate reactor operation with a constant head supplied to the test section. The power input was then increased slowly until flow instability occurred and initiated film boiling conditions. The transient conditions during flow instability were recorded on high speed recorders. (M.O.W.)

30934 (ORNL-TM-1445) SIMULATORS FOR TRAINING MOLTEN-SALT REACTOR EXPERIMENT OPERATORS. Ball, S. J. (Oak Ridge National Lab., Tenn.). Apr. 5, 1966. Contract W-7405-eng-26. 24p. Dep. mn. CFSTI $1.00 cy, $0.50 mn.

Two on-site reactor kinetics simulators were developed for training operators of the Molten-Salt Reactor Experiment (MSRE) in nuclear startup and power-level operating procedures. Both simulators were set up on general purpose, portable Electronic Associates, Inc., TR-10 analog computers and were connected to the reactor control and instrumentation system. The training program was successfully completed. Also, the reactor control and instrumentation system, the operating procedures, and the rod and radiator-door drives were checked out. Some minor modifications were made to the system as a result of the experience with these simulators. (auth)

30935 OPERATIONAL PROCEDURES FOR NRX AND NRU REACTORS. Breckon, D. G. (Atomic Energy of Canada Ltd., Chalk River, Ont.). Can. Nucl. Technol., 5: 37-41(May-June 1966).

A brief description is given of the organization used at Chalk River Nuclear Laboratories, to operate and maintain the NRX and NRU reactors and reviews the operating experience with particular emphasis on procedures. (auth)

30936 RESEARCH AND TEACHING WITH UNIVERSITY REACTORS. PART II. EuroNuclear, 3: 232-6(May 1966).

The Scottish research reactor center is described, and the design of the reactors is discussed. The external flux available from collimators in the horizontal beam tube is typically 1 $(10)^7$ to 2 $(10)^7$ n/cm^2 sec. The layout of the center and research and teaching using the reactor are discussed. (J.F.P.)

30937 RESEARCH CENTERS IN EUROPE. NO. 17. SWIERK AND ZERAN. EuroNuclear, 3: 237-44(May 1966).

The Polish Institute of Nuclear Research is discussed. The Swierk center is described including the design and experiments for the EWA reactor and radioisotope research. Research at the Zeran center which is mainly concerned with chemical and radiobiological studies is also described. (J.F.P.)

30938 EVALUATION OF THE ^{17}N REACTOR POWER LEVEL MONITOR. Notea, A. (Atomic Energy Commission, Yavne, Israel); Hoffmann, A. P.; Shalev, S. J. Nucl. Energy: Pt. A and B, 20: 371-2(May 1966).

The insensitivity of the ^{17}N reactor power level monitoring technique to local variations in the thermal neutron flux distribution is discussed. (B.G.D.)

30939 THERMAL NEUTRON SPECTRUM MEASUREMENTS FROM THE YUGOSLAV HEAVY-WATER REACTOR. Zivanovic, M. D.; Konstantinovic, J. M.; Jovic, D. M. (Boris Kidric Inst. of Nuclear Sciences, Belgrade). J. Nucl. Energy: Pt. A and B, 20: 376-9(May 1966).

The experimental arrangements and results of thermal neutron spectrum measurements from the Yugoslav heavy-water reactor are presented. Measurements are conducted with a crystal neutron spectrometer provided with a single crystal of lead, orientation (111), in the place of the analyzer. (B.G.D.)

30940 SAFETY ASPECTS OF THREE IN-PILE GAS LOOPS. Zasler, J. Nucl. Safety, 7: 165-9; 172-3(Winter 1965–1966).

The design and hazards reports of three in-pile gas loops are reviewed with regard to the design features provided to ensure the safety of personnel and equipment. (G.O.Y.)

30941 RUPTURE-LOOP FAILURE IN PLUTONIUM RECYCLE TEST REACTOR. Nucl. Safety, 7: 242-7 (Winter 1965–1966).

The failure of the Fuel Element Rupture Test Facility in the Plutonium Recycle Test Reactor is discussed. (G.O.Y.)

30942 ACCURATE REACTOR NOISE MEASUREMENTS IN A LOW POWER CRITICAL REACTOR. Dragt, Jan B, (Reactor Centrum Nederland, Petten). Nukleonik, 8: 188-93(May 1966).

Noise measurements in the critical Argonaut-type reactor LFR, with a one slab core loading, at low power are reported. The noise from an ionization chamber was digitally measured and analyzed in a digital computer. The measurements were completely analyzed in the time-domain (autocorrelation functions). This facilitated the discrimination between the noise caused by the neutron detection process and the noise brought about by fluctuations in neutron density. All results could be interpreted by means of the simple point reactor theory. It proved to be possible to determine from the noise reactor parameters with a rather high accuracy (few %). Parameters determined were: prompt neutron decay constant, delayed neutron fraction and neutron generation time (both these quantities within the limitations of point reactor theory), and the ratio of mean square charge and mean charge collected in the ionization chamber per neutron detected. (auth)

WASTE DISPOSAL AND PROCESSING

See also BIOLOGY AND MEDICINE — Ecology
CHEMISTRY — Radiochemistry
CHEMISTRY — Separation Processes and Procedures
HEALTH AND SAFETY

Refer also to abstracts 29099 and 29332.

30943 (ORNL-TM-1465) WASTE TREATMENT AND DISPOSAL SEMIANNUAL PROGRESS REPORT, JULY–DECEMBER 1965. Blanco, R. E.; Parker, F. L. (Oak Ridge National Lab., Tenn.). June 1966. Contract W-7405-eng-26. 101p. Dep. mn. CFSTI $4.00 cy, $0.75 mn.

Developments are reported for studies on: solidification of high-level wastes-engineering and laboratory studies; incorporation of intermediate-level waste in asphalt; water-recycle process; engineering, economic, and safety evaluations for tank storage; disposal by hydrofracturing; disposal in natural salt formations; soil studies; behavior of radionuclides in the ground; disposal of gases into permeable formations; and safety evaluation. (P.C.H.)

30944 CONSIDERATIONS ARISING FROM THE IAEA SYMPOSIUM ON THE TREATMENT OF LOW AND INTERMEDIATE LEVEL RADIOACTIVE WASTES. Facchini, A. (CESNEF, Milan). Energ. Nucl. (Milan), 13: 257-68 (May 1966). (In Italian).

On the basis of the information reported at the Vienna Symposium of Dec. '65, some aspects of the "separate and isolate" criterion for the treatment of low and intermediate level radioactive wastes are examined. In particular the limits and the methods employed by various nuclear centers in the application of this criterion are examined as well as the capital and the operating costs. The resulting economic framework furnishes conclusions of considerable interest, even though they have only an orientative value. This is due to the experimental character of some of the plants and to the absence of a uniform system of economic evaluation which makes it very difficult to obtain a valid comparison between the various experiences. (auth)

30945 CURRENT DISPOSAL OF RADIOACTIVE WASTES AND ITS PROBLEMS. Ishihara, Takehiko (Japan Atomic Energy Research Inst., Tokyo). Genshiryoku Kogyo, 11: No. 11, 1-40(Nov. 1965). (In Japanese).

The current disposal of radioactive wastes in Japan and its associated problems are discussed in eight articles. These articles deal with: regulations concerning radioactive waste disposal; increased amounts of radioactive wastes; disposal of radioactive wastes; waste disposal area and its basic considerations; treatment of medium- and low-level radioactive waste waters by evaporation-concentration and by condensation-deposition; treatment and disposal of the radioactive wastes from production of radioactive medical chemicals; treatment and disposal of radioactive wastes produced in uranium ore refining; and radioactive waste disposal viewed from the plant builders' viewpoint. (TCO)

30946 CHEMICAL ENGINEERING STUDIES ON THE PROCESSING OF RADIOACTIVE LIQUID WASTES BY EVAPORATION. Yamamoto, Yutaka; Kiyose, Ryohei (Tokyo Univ.). J. Fac. Eng., Univ. Tokyo, No. 3, 42-3 (Nov. 1965). (In Japanese).

For processing radioactive liquid wastes, a multiple-effect evaporation process, which uses a fluidized-bed spray evaporator for final evaporation and solidification, has advantages of avoiding radioactive scale formation in pre-evaporation stages, of improving thermal efficiency and speed of processing, and of minimizing off-gas activity from the process, by using superheated steam as heating and fluidizing medium. To examine the operational characteristics of fluidized-bed spray evaporator, mass and heat transfer from liquid spray into superheated steam was studied, and heat transfer coefficient between fluidized-bed and heater-wall, effective thermal conductivity, and longitudinal dispersion coefficient of fluidized-bed were experimentally estimated. Carry-over of waste salt, elutriation of solid particles from the bed, and agglomeration of particles in the bed were also measured. (auth)

30947 CURRENT PRACTICES IN HANDLING AND STORING SOLID RADIOACTIVE WASTE FROM REACTORS. Stevenson, C. E. (Argonne National Lab., Idaho Falls, Idaho). Nucl. Safety, 7: 231-5(Winter 1965–1966).

A survey of solid-waste generation and handling practices at twenty reactors is summarized. (D.C.W.)

30948 CURRENT PRACTICES IN THE DISPOSAL OF RADIOACTIVE WASTES FROM THE OPERATION OF URANIUM MINES AND MILLS. Stevenson, C. E.; Abrams, C. S.; Beverly, R. G.; Dick, I. B.; Falk, C. F.; Stolzenbach, C. F. 6p. of Nuclear Reactor Wastes. New York, American Inst. of Chemical Engineers, 1964.

For American Standards Association, Subcommittee N5.2 on Radioactive Waste Disposal.

Disposal of radioactive wastes, including solids, liquids, and gases, which result from operation of uranium mines and mills, is reviewed. Mills refers to the plants extracting uranium from ores and producing a concentrated uranium oxide product that is subsequently shipped to uranium refineries for further purification. The disposal of nine waste piles or dumps, mine waters, ventilation discharge from mines, solid uranium mill tailings, liquid effluents from uranium mills, and airborne effluents from uranium mills is described. (M.C.G.)

30949 CURRENT PRACTICES IN DISPOSAL OF WASTE RADIOACTIVE GASES FROM NUCLEAR REACTORS. Stevenson, C. E.; Abrams, C. S.; Beverly, R. G.; Dick, I. B.; Falk, C. F.; Stolzenbach, C. F. 16p. of Nuclear Reactor Wastes. New York, American Inst. of Chemical Engineers, 1964.

For American Standards Association, Subcommittee N5.2 on Radioactive Waste Disposal.

The waste radioactive gases, which may be generated in the operation of nuclear reactors, and the methods used to dispose of them are described. Limitations in the disposal of waste radioactive gases, sources and identity of these gases, factors to be considered in choosing the best disposal method, storage and decay before discharge, dilution and discharge, dispersion in atmosphere, removal of particles from the discharge gas, and separation or concentration of radioactive gases are discussed. Present practices are reviewed. (M.C.G.)

30950 METHOD FOR HEATING MINERALS IN SITU WITH RADIOACTIVE MATERIALS. Robinson, Charles L. U. S. Patent 3,246,695. Apr. 19, 1966. Filed Aug. 21, 1961.

A method is described for using the heat from radioactive materials, particularly waste materials, to reduce the viscosity of underground minerals such as sulfur, paraffin based oils, or asphaltic based oils to render them more readily available for use and simultaneously to dispose of the radioactive waste. The radioactive material is introduced into a cementitious slurry that is then injected into the subsurface formation containing the minerals through a borehole. The concentration of the radioactive material in the slurry is sufficient to furnish the heat adequate to in-

crease the temperature and reduce the viscosity of the minerals through the absorption of radiated energy. (B.L.M.)

30951 METHOD AND PRODUCT FOR THE DISPOSAL OF RADIOACTIVE WASTES. Bixby, Henry D. U. S. Patent 3,249,551. May 3, 1966. Filed June 3, 1963.

A method is described for fixing radioactive wastes in a fired ceramic body so that no aqueous leaching takes place upon disposal. The high-level waste is mixed with clay and fired to a temperature less than the maturity temperature of the clay but sufficiently high to obtain a water absorption value less than that at which moisture is not withdrawn from the clay by a ceramic glaze that is applied to the fired clay mixture where cracks form in the glaze upon drying at room temperature and that is greater than that at which the glaze cracks during firing of the glaze and body to the maturing temperature of the glaze. Heating of the mixture is carried out at a temperature below that at which the mixture bloats, and firing of the clay–waste mixture is carried out in a reducing atmosphere to prevent volatilization of Ru as RuO_2. After coating the fired body with a ceramic glaze, the glaze is fired at a maturing temperature for fusing the glaze upon the ceramic body and making the glaze coating impervious. (B.L.M.)

GENERAL AND MISCELLANEOUS

30952 (LA–3467) LOS ALAMOS STRAIGHT LINE DIAGRAM FOR POWDER PATTERN INDEXING. Coleman, James S.; McInteer, B. B. (Los Alamos Scientific Lab., Univ. of California, N. Mex.). Jan. 1966. Contract W-7405-eng-36. 51p. Dep. mn. CFSTI $3.00 cy, $0.50 mn.

A new graphical method is described which is useful for indexing x-ray powder patterns. The experimental points with various Miller indices are plotted so that the points with the desired indices fall on straight lines. Application is illustrated for all crystal symmetries. Related graphical methods are discussed in the Appendixes. (auth)

30953 (ORNL-TM–1542) ORSEF: A FORTRAN CODE FOR THE CALCULATION OF MULTI-STAGE FLASH EVAPORATION DESALINATION PLANT DESIGNS. Mothershed, C. T. (Oak Ridge National Lab., Tenn.). Mar. 1966. Contract W-7405-eng-26. 130p. Dep. mn. CFSTI $4.00 cy, $1.00 mn.

A program was written for the IBM-7090 that determines the operating characteristics, geometry, and cost of a multi-stage flash desalination plant. The plant contains three major components: the brine heater; the evaporator recovery section; and the evaporator reject section. Using the costs of these components and input unit energy costs, the program can calculate the optimum balance between heat consumption, condenser area, and power usage. The output from the code defines the process parameters, costs, and design features of interest. (auth)

30954 (UCRL–14617) PROPAGATION OF STRESS DISTURBANCES IN ELASTIC-PLASTIC CYLINDERS: ONE-DIMENSIONAL THEORIES. Wasley, R. J. (Lawrence Radiation Lab., Univ. of California, Livermore). Dec. 21, 1965. Contract W-7405-eng-48. 72p. Dep. mn. CFSTI $2.00 cy, $0.75 mn.

One-dimensional analytic treatments of propagation of stress disturbances in elastic-plastic cylinders are reported. When compared with experimental data from impact of solid high explosives, some of these theories are shown to predict in a reasonably satisfactory fashion the gross features of the deformation history. The presentation elucidates the basic mechanics and assumptions associated with the impact process, the understanding of which is a prerequisite to introducing further complexities into an analysis. (auth)

30955 STUDIES ON X AGENT. XLVII. DIURNAL AND ANNUAL FLUCTUATION OF X AGENT REVEALED IN ITS ACTION ON FROSTED GLASS SURFACES. Moriyama, Hideo (Shonan Hygiene Inst., Kamakura, Japan). Yokohama Med. Bull., 17: 1-11(Feb. 1966).

A marked diurnal variation was demonstrated in the apparent change of transmittance of the frosted glass surface of absorption cells which had been left beside a water bottle. The variation was observable whether the water bottle, together with the absorption cells, were placed in a box, enclosed by thick metallic walls, or located on a table outside the box. This indicates that the harder component of X agent was under a direct connection with the sun. In addition to the diurnal variation, an annual variation was observed. Continuous observations from 1961 to 1963 show a pronounced disturbance at the beginning of May that continued for two or three months. This disturbance was not noticed in 1964 and 1965. Instead, a considerable change was found in July, although it was not so strong and so durable as that in the early summer. The periods of non-disturbance in the late winter and in autumn months were evident from 1961 through 1965. (auth)

30956 SUMMARY OF THE STUDIES ON X AGENT. Moriyama, Hideo (Shonan Hygiene Inst., Kamakura, Japan). Yokohama Med. Bull., 17: 31-43(Apr. 1966).

Phenomena that suggest the presence of X-agent, an unknown physical factor that affects both living and non-living materials, are reviewed. The essential property of X-agent consists of its ever-changing character so that experimental data on its effects are not reproducible. The author postulates that X-agent is a range of photons or electromagnetic radiations that are temporarily activated, that it is composed of two factors that are antagonistic in action, that most of the agent is related to γ rays of extremely high energy but also includes energies so low that they are affected by thermal radiation or light, that the agent is readily interchangeable with γ radiation, thermal radiation, light, and radio waves, that X-agent is produced on the earth's surface by the interaction between cosmic ray particles and the geomagnetic field, and that X-agent progresses from south to north. Materials and processes said to be affected by X-agent include bacteria, plant growth, the hemolysis and sedimentation of red blood cells, the cloudiness of protein solutions and bismuth-oxychloride solutions, the turbidity of kaolin suspensions, the transparency of frosted glass surfaces, the color of solutions of methyl red and neutral red, and the sensitivity of photoelectric cells. Differences in various substances in their response to X-agent and fluctuations in response caused by atmospheric pressure, solar radiation, circadian rhythms, annual fluctuations, the earth's revolution, the moon, and changes in the weather are discussed. The faculty of birds and insects to return infallibly to their nests is attributed to the ability of animals to perceive various patterns of X-agent that are characteristic of places and it is suggested that the progress of X-agent from north to south may guide the migration of birds. (66 references.) (C.H.)

30957 AEC AUTHORIZING LEGISLATION FISCAL YEAR 1967. PART 1. HEARINGS BEFORE THE JOINT COMMITTEE ON ATOMIC ENERGY, CONGRESS OF THE UNITED STATES, EIGHTY-NINTH CONGRESS, SECOND SESSION ON SPECIAL NUCLEAR MATERIALS; RAW MATERIALS; REACTOR DEVELOPMENT (EXCEPT CIVILIAN POWER AND COOPERATIVE POWER REACTOR CATEGORIES); AND SPACE NUCLEAR SYSTEMS, JANUARY 25, FEBRUARY 15, AND MARCH 4 AND 8, 1966. Washington, D. C., Joint Committee on Atomic Energy, 1966. 590p. GPO.

The hearings on the Atomic Energy Commission authorizing legislation for the fiscal year 1967 are presented in three parts, with appropriate supporting documentation. The major topical items of part 1 include a general review of the overall AEC budget; special nuclear materials; nuclear weapons; raw materials; and reactor development program. (L.B.S.)

30958 AEC AUTHORIZING LEGISLATION FISCAL YEAR 1967. PART 2. HEARINGS BEFORE THE JOINT COMMITTEE ON ATOMIC ENERGY, CONGRESS OF THE UNITED STATES, EIGHTY-NINTH CONGRESS, SECOND SESSION ON REACTOR DEVELOPMENT (CIVILIAN POWER; COOPERATIVE POWER; AND AEC CONTRACTOR TESTIMONY ON REACTOR DEVELOPMENT PROGRAM), FEBRUARY 16, 17, MARCH 3, 15, AND 16, 1966. Washington, D. C., Joint Committee on Atomic Energy, 1966. 91-1083p. GPO.

The hearings on the Atomic Energy Commission authorizing legislation for the fiscal year 1967 are presented in three parts, with appropriate supporting documentation. The major topical items of part 2 include civilian power reactors; cooperative power reactor demonstration program; and AEC contractor testimony on reactor development program. (L.B.S.)

30959 AEC AUTHORIZING LEGISLATION FISCAL YEAR 1967. PART 3. HEARINGS BEFORE THE JOINT COMMITTEE ON ATOMIC ENERGY, CONGRESS OF THE UNITED STATES, EIGHTY-NINTH CONGRESS, SECOND SESSION ON BIOLOGY AND MEDICINE; ISOTOPES DEVELOPMENT; COMMUNITIES; TRAINING, EDUCATION,

AND INFORMATION; SECURITY; PROGRAM DIRECTION AND ADMINISTRATION; PHYSICAL RESEARCH; PLOWSHARE, FEBRUARY 2, MARCH 8, 9, 10, 11, AND 15, 1966. Washington, D. C., Joint Committee on Atomic Energy, 1966. 1085-1768p. GPO.

The hearings on the Atomic Energy Commission authorizing legislation for the fiscal year 1967 are presented in three parts, with appropriate supporting documentation. The major topical items of part 3 include biology and medicine; isotopes development; communities; training, education, and information; security investigations; and program direction and administration. (L.B.S.)

CORPORATE AUTHOR INDEX

This index contains entries for this period for all report literature and, in addition, for certain published literature items for which it is felt that a corporate approach is especially desirable, e.g., symposia, conference proceedings, and meetings.

Each entry under a corporate author is a shortened version of the title of the publication, followed by the *NSA* volume and abstract number. Report numbers are given in parentheses.

The phrase "Progress report" is abbreviated as "Prog. rpt.," permitting a more rapid and complete alphabetical arrangement of the titles without changing the location of the progress report titles in relation to the other titles.

A

AEROJET-GENERAL NUCLEONICS, SAN RAMON, CALIF.
Bibliography on relation between wetting and boiling Hg heat transfer, 20: 29620 (NP-16046)

AEROSPACE MEDICAL DIV., BROOKS AFB, TEX.
Effects of whole-body irradiation by protons on primates, 20: 28931 (CONF-651109, pp 624-35)
Techniques for determining proton depth dose distribution in primates, 20: 28928 (CONF-651109, pp 417-25)

AKADEMIYA NAUK UKRAINSKOI SSR, KHARKOV. FIZIKO-TEKHNICHESKII INSTITUT.
Oscillations and heating of small plasmoids incident in axisymmetric magnetic fields, 20: 30559 (FTI-114/P-044)

ALLIS-CHALMERS MFG. CO., BETHESDA, MD. ATOMIC ENERGY DIV.
Core boration and flux mapping test 313, 20: 30874 (ACNP-65612)

AMES LAB., IOWA STATE UNIV. OF SCIENCE AND TECH.
Partial molal heat capacities of aqueous rare-earth chloride solutions, 20: 29144 (IS-1355)

ARGONNE CANCER RESEARCH HOSPITAL, CHICAGO, ILL.
High-dose human exposure from 10-Mev linear accelerator, 20: 28929 (CONF-651109, pp 574-98)

ARGONNE NATIONAL LAB., ILL.
Advanced systems research and development, 20: 30932 (ANL-7204, pp 65-73)
Analysis of ANL-CERN spark chamber pictures, 20: 29987 (COO-1261-4)
Correlation of heat transfer properties and ultrasonic transmission properties of bonds, 20: 29386 (ANL-7074)
Education—research activities, 20: 29375 (ANL-7190, pp 193-200)
Elasticity and anelasticity of uranium oxides at room temperature, 20: 29698 (ANL-7101)
Fabrication of spiked-core fuel elements for EBWR, 20: 29658 (ANL-6283)
Fast reactor research and development, 20: 30875 (ANL-7190, pp 143-55)
Fast reactor safety, 20: 30788 (ANL-7190, pp 176-88)
General reactor technology, 20: 30791 (ANL-7204, pp 32-64)
Liquid-metal-cooled reactors, 20: 30790 (ANL-7204, pp 1-31)
Liquid metal heat transfer, 20: 29374 (ANL-7190, pp 156-66)
Magnetohydrodynamics, 20: 29974 (ANL-7190, pp 167-75)
Nuclear safety, 20: 30792 (ANL-7204, pp 74-86)
Numerical integration of ordinary differential equations of various orders, 20: 29612 (ANL-7126)
Pilot-plant gettering system of Ti-metal sponge for removal of N from Ar, 20: 29329 (ANL-7128)
Prog. rpt. on reactor engineering, annual, 7/64–6/65, 20: 30786 (ANL-7190)
Prog. rpt. on reactor development, 4/66, 20: 30789 (ANL-7204)
Pulse-shape discrimination applied to fast neutron dosimetry, 20: 29524 (CONF-651109, pp 647-52)
Radiation environment at zero gradient synchrotron, 20: 29843 (CONF-651109, pp 34-56)
Reactor projects and programs, 20: 30787 (ANL-7190, pp 11-142)
Removal of plutonium hexafluoride from cell exhaust air, 20: 29328 (ANL-7066)
Use of personal monitoring neutron film near 50-Mev injection of, 20: 29523 (CONF-651109, pp 639-46)

ASSOCIATED NUCLEONICS, INC., GARDEN CITY, N. Y.
Marine products development irradiator facility, 20: 29584 (TID-22991)

ATOMIC ENERGY ESTABLISHMENT, WINFRITH (ENGLAND).
Prog. rpt. on reactor studies, annual, 1965, 20: 30798 (NP-16043)

ATOMIC ENERGY OF CANADA LTD., CHALK RIVER (ONTARIO).
APEX: program for analysis of gamma-gamma angular correlation data, 20: 30341 (AECL-2529)
Effect of temperature on micro-indentation properties of zirconium hydride, 20: 29697 (AECL-2538)

ATOMIC ENERGY RESEARCH ESTABLISHMENT, HARWELL (ENGLAND).
Eta and neutron cross sections of ^{235}U from 0.03 to 200 ev, 20: 30342 (AERE-M-1670)
Gamma-ray spectra of pitchblende and monazite, 20: 29079 (AERE-M-1736)

ATOMIC WEAPONS RESEARCH ESTABLISHMENT, ALDERMASTON (ENGLAND).
Blast loading simulator for structural response studies, 20: 29371 (AWRE-E-1/66)

ATOMICS INTERNATIONAL, CANOGA PARK, CALIF.
DTF-II shielding data library, 20: 30723 (NAA-SR-11831)
Energy dependence of radiation damage in Si, 20: 29579 (NAA-SR-11887)
Irradiation performance of Piqua fuel elements, 20: 30881 (NAA-SR-11712)
Zone melting of uranium monocarbide, 20: 29619 (NAA-SR-11813)

AUBURN UNIV., ALA.
Feedforward compensation of temperature control system, 20: 30807 (ORNL-TM-1485)

B

BABCOCK AND WILCOX CO., BARBERTON, OHIO. BOILER DIV.
Prog. rpt. on Na-heated steam generator development, 1–3/66, 20: 30806 (BAW-1280-36)

BABCOCK AND WILCOX CO., LYNCHBURG, VA.
Indian Point Reactor—instrumentation asymmetry response verification, 20: 30876 (BAW-1302)

BABCOCK AND WILCOX CO., LYNCHBURG, VA. ATOMIC ENERGY DIV.
Burnout for flow inside round tubes with nonuniform heat fluxes, 20: 29376 (BAW-3238-9)
Prog. rpt. on nonuniform heat generation, 10-12/65, 20: 29377 (BAW-3238-11)

BABCOCK AND WILCOX CO., LYNCHBURG, VA. CRITICAL EXPERIMENT LAB.
Lumped burnable poison program, 20: 30836 (BAW-3492-1)

BATTELLE MEMORIAL INST., COLUMBUS, OHIO.
Joining of nickel and nickel-base alloys, 20: 29666 (RSIC-484)
Machining and grinding of nickel- and cobalt-base alloys, 20: 29665 (RSIC-482)
Mechanical fastening of nickel-base alloys, 20: 29667 (RSIC-509)
Prog. rpt. on civilian applications, 7/65, 20: 29616 (BMI-1738)
Surface treatments for nickel and nickel-base alloys, 20: 29706 (NASA-TM-X-53448)

BATTELLE-NORTHWEST, RICHLAND, WASH. PACIFIC NORTHWEST LAB.
Heat transfer experiments for Advanced Test Reactor, 20: 30933 (BNWL-216)

Pulse-shape discrimination applied to fast neutron dosimetry, 20: 29524 (CONF-651109, pp 647-52)
Pulsed reactor tests of dosimeters, 20: 29518 (BNWL-SA-27)
System for criticality verification, 20: 29519 (BNWL-SA-31)

BENDIX CORP., SOUTHFIELD, MICH. RESEARCH LABS. DIV.
Prog. rpt. fabrication and test of flueric position servo, 9/10–12/10/65, 20: 30922 (BRLD-3255)

BETTIS ATOMIC POWER LAB., WEST MIFFLIN, PA.
Observations on zirconium and its alloys by transmission electron microscopy, 20: 29716 (WAPD-T-1819)

BORDEAUX UNIV. (FRANCE). LABORATOIRE DE PHYSIQUE THEORIQUE.
Approximation method in study of scattering at high energies, 20: 30086 (CONF-640509(Pt.1), Paper 4)
Conference on theoretical physics, Bordeaux, France, 5/28–6/2/64, 20: 30084 (CONF-640509(Pt.1))
Pole contributions to N-N scattering below pion production, 20: 29985 (CONF-640509(Pt.1), Paper 1)
Production and decay of resonances at a few Bev, 20: 30085 (CONF-640509(Pt.1), Paper 3)
Scattering (π-N), Pt. 1, 20: 29986 (CONF-640509(Pt.1), Paper 2)

BROOKHAVEN NATIONAL LAB., UPTON, N. Y.
Acute cellular effects of heavy charged-particle irradiations, 20: 28930 (CONF-651109, pp 601-16)
Cambridge accelerator fire of July 5, 1965, 20: 29851 (CONF-651109, pp 556-73)
Conference on accelerator radiation dosimetry and experience, Brookhaven National Lab., 11/65, 20: 29841 (CONF-651109)
Determination of quality factor through utilization of balanced, tissue-equivalent, ionization chamber, 20: 29847 (CONF-651109, pp 181-98)
Effects of whole-body irradiation by protons on primates, 20: 28931 (CONF-651109, pp 624-35)
Extracorporeal irradiation of blood, 20: 28927 (BNL-9647)
Fast neutron spectrometry with nuclear emulsions, 20: 29848 (CONF-651109, pp 199-212)
Health physics survey methods for measurement of stray radiation around CERN high-energy accelerators, 20: 29844 (CONF-651109, pp 103-16)
High-dose human exposure from 10-Mev linear accelerator, 20: 28929 (CONF-651109, pp 574-98)
High-energy particle spectrometry using activation detectors, 20: 29521 (CONF-651109, pp 213-23)
Inference of accelerator stray neutron spectra from various measurements, 20: 29522 (CONF-651109, pp 286-305)
Mathematical aspects of kinetic model equations, 20: 30165 (BNL-9254)
Methods and experience acquired in dosimetry at Saturne synchrotron, 20: 29845 (CONF-651109, pp 117-42)
Neutron radiation monitoring using ^{3}He spectrometer, 20: 29846 (CONF-651109, pp 154-60)
Neutron thermalization and diffusion in nonisothermal media, 20: 30322 (BNL-947)
Photochemical decomposition of sodium bromate, 20: 29248 (BNL-9672)
Pulse-shape discrimination applied to fast neutron dosimetry, 20: 29524 (CONF-651109, pp 647-52)
Radiation environment at zero gradient synchrotron, 20: 29843 (CONF-651109, pp 34-56)
Radiation hazards peculiar to a linear accelerator meson factory, 20: 29850 (CONF-651109, pp 472-89)
Radiation levels in and around Nimrod, 20: 29842 (CONF-651109, pp 20-33)
Radiation protection problems at Stanford two-mile linear accelerator, 20: 29849 (CONF-651109, pp 442-58)
Shielding aspects of accelerator facility design, 20: 30720 (CONF-651109, pp 410-16)
Shielding calculations for high-energy accelerators, 20: 30719 (CONF-651109, pp 327-45)
Techniques for determining proton depth dose distribution in primates, 20: 28928 (CONF-651109, pp 417-25)
Use of personal monitoring neutron film near 50-Mev injection of, 20: 29523 (CONF-651109, pp 639-46)

BROWN UNIV., PROVIDENCE, R. I. DIV. OF APPLIED MATHEMATICS.
Mathematical aspects of kinetic model equations, 20: 30165 (BNL-9254)

BRUSSELS UNIV. (BELGIUM).
Prog. rpt. on nuclear medicine, annual, 1964, 20: 28871 (EUR-2636.f,i)

BUREAU OF COMMERCIAL FISHERIES, SEATTLE, WASH. TECHNOLOGICAL LAB.
Prog. rpt. on application of radiation-pasteurization to Pacific crab and flounder, final, 11/64–10/65, 20: 29583 (TID-22515)

C

CALIFORNIA UNIV., BERKELEY. COLL. OF ENGINEERING.
Analytical and experimental study of transient heat transfer for external forced convection, 20: 29379 (SAN-1011)

CAMBRIDGE ELECTRON ACCELERATOR, MASS.
Cambridge accelerator fire of July 5, 1965, 20: 29851 (CONF-651109, pp 556-73)

CENTRAL UTILITIES ATOMIC POWER ASSOCIATES.
Core boration and flux mapping Test 313, 20: 30874 (ACNP-65612)

CENTRALNE LABORATORIUM OCHRONY RADIOLOGICZNEJ, WARSAW (POLAND).
Stronium-90-yttrium-90 measurements using Si counters, 20: 29520 (CLOR-45/D)

CENTRE D'ETUDE DE L'ENERGIE NUCLEAIRE, MOL (BELGIUM).
Prog. rpt. on reprocessing of irradiated fuels, 7-9/65, 20: 29330 (EURAEC-1601)

CENTRE NATIONAL DE RECHERCHES METALLURGIQUES, LIEGE (BELGIUM).
Prog. rpt. on plastic fatigue embrittlement of reactor vessel steels, 10–12/65, 20: 29701 (EURAEC-1547)

CHANTIERS DE L'ATLANTIQUE PENHOET-LOIRE, PARIS (FRANCE).
Prog. rpt. on influence of initial stress on isothermal stress-relief tests, 1–3/66, 20: 29702 (EURAEC-1616)

CHICAGO UNIV., ILL. DEPT. OF MEDICINE.
High-dose human exposure from 10-Mev linear accelerator, 20: 28929 (CONF-651109, pp 574-98)

CHICAGO UNIV., ILL. DEPT. OF RADIOLOGY.
High-dose human exposure from 10-Mev linear accelerator, 20: 28929 (CONF-651109, pp 574-98)

COLUMBIA UNIV., NEW YORK.
High-resolution muonic x-ray studies, 20: 29525 (CONF-660209-9)
Neutron radiation monitoring using ^{3}He spectrometer, 20: 29846 (CONF-651109, pp 154-60)

COMITATO NAZIONALE PER L'ENERGIA NUCLEARE, ROME (ITALY).
Filterability and coalescence time of colloidal solutions of ANN–HNO_3–Hg^{2+}–SiO_2, 20: 29333 (RT-CHI-(65)33)

COMMISSARIAT A L'ENERGIE ATOMIQUE, CADARACHE (FRANCE). CENTRE D'ETUDES NUCLEAIRES.
High-energy particle spectrometry using activation detectors, 20: 29521 (CONF-651109, pp 213-23)

COMMISSARIAT A L'ENERGIE ATOMIQUE, FONTENAY-AUX-ROSES (FRANCE). CENTRE D'ETUDES NUCLEAIRES.
Evaluation of number of free radicals produced in irradiated rat bone, 20: 28898 (CEA-R-2910)
Total ionization intensity near ground and separation of various components, 20: 29404 (CEA-R-2880)

COMMISSARIAT A L'ENERGIE ATOMIQUE, GRENOBLE (FRANCE). CENTRE D'ETUDES NUCLEAIRES.
Irreversible magnetic behavior of superconductors, 20: 30253 (CEA-R-2808)
Prog. rpt. on UC shaping and irradiation, 7–12/65, 20: 29804 (EURAEC-1637)

COMMISSARIAT A L'ENERGIE ATOMIQUE, PARIS (FRANCE).
Prog. rpt. on UC shaping and irradiation, 7–12/65, 20: 29804 (EURAEC-1637)

COMMISSARIAT A L'ENERGIE ATOMIQUE, SACLAY (FRANCE). CENTRE D'ETUDES NUCLEAIRES.
Methods and experience acquired in dosimetry at Saturne synchrotron, 20: 29845 (CONF-651109, pp 117-42)
Reliability of planar silicon transistors exposed to ^{60}Co gamma rays, 20: 29577 (CEA-R-2959)

COMPAGNIE DES ATELIERS ET FORGES DE LA LOIRE, PARIS (FRANCE). DEPARTEMENT DES RECHERCHES.
Prog. rpt. on mechanical properties, of steels, 10–12/65, 20: 29639 (EURAEC-1578)

CORNELL UNIV., ITHACA, N. Y. DEPT. OF ENGINEERING PHYSICS.
Atomic motions in monatomic fluids, 20: 30166 (NYO-3326-13)

CORNELL UNIV., ITHACA, N. Y. DEPT. OF FLORICULTURE AND ORNAMENTAL HORTICULTURE.
Prog. rpt. on loss of materials from above-ground plant parts with special reference to decontamination, 1965-66, 20: 29451 (NYO-2598-29)

COURANT INST. OF MATHEMATICAL SCIENCES, NEW YORK UNIV., N. Y.
Longitudinal plasma oscillations, 20: 30564 (NYO-1480-26)

D

DEPARTMENT OF NATIONAL HEALTH AND WELFARE, OTTAWA (ONTARIO). RADIATION PROTECTION DIV.
Data from Radiation Protection Programs, Vol. 4, No. 2, 20: 29053 (NP-15951)

DIVISION OF BIOLOGY AND MEDICINE (AEC), WASHINGTON, D. C.
Acute cellular effects of heavy charged particle irradiations, 20: 28930 (CONF-651109, pp 601-16)
Cambridge accelerator fire of July 5, 1965, 20: 29851 (CONF-651109, pp 556-73)
Conference on accelerator radiation dosimetry and experience, Brook-

haven National Lab., 11/65, 20: 29841 (CONF-651109)
Determination of quality factor through utilization of balanced, tissue-equivalent, ionization chamber, 20: 29847 (CONF-651109, pp 181-98)
Effects of whole-body irradiation by protons on primates, 20: 28931 (CONF-651109, pp 624-35)
Fast neutron spectrometry with nuclear emulsions, 20: 29848 (CONF-651109, pp 199-212)
Health physics survey methods for measurement of stray radiation around CERN high-energy accelerators, 20: 29844 (CONF-651109, pp 103-16)
High-dose human exposure from 10-Mev linear accelerator, 20: 28929 (CONF-651109, pp 574-98)
High-energy particle spectrometry usiag activation detectors, 20: 29521 (CONF-651109, pp 213-23)
Inference of accelerator stray neutron spectra from various measurements, 20: 29522 (CONF-651109, pp 286-305)
Methods and experience acquired in dosimetry at Saturne synchrotron, 20: 29845 (CONF-651109, pp 117-42)
Neutron radiation monitoring using ^{3}He spectrometer, 20: 29846 (CONF-651109, pp 154-60)
Pulse-shape discrimination applied to fast neutron dosimetry, 20: 29524 (CONF-651109, pp 647-52)
Radiation hazards peculiar to a linear accelerator meson factory, 20: 29850 (CONF-651109, pp 472-89)
Radiation levels in and around Nimrod, 20: 29842 (CONF-651109, pp 20-33)
Radiation protection problems at Stanford two-mile linear accelerator, 20: 29849 (CONF-651109, pp 442-58)
Shielding aspects of accelerator facility design, 20: 30720 (CONF-651109, pp 410-16)
Shielding calculations for high-energy accelerators, 20: 30719 (CONF-651109, pp 327-45)
Techaiques for determining proton depth dose distribution in primates, 20: 28928 (CONF-651109, pp 417-25)
Use of personal monitoring neutron film near 50-Mev injection of, 20: 29523 (CONF-651109, pp 639-46)

DIVISION OF OPERATIONAL SAFETY (AEC), WASHINGTON, D. C.
Acute cellular effects of heavy charged particle irradiations, 20: 28930 (CONF-651109, pp 601-16)
Cambridge accelerator fire of July 5, 1965, 20: 29851 (CONF-651109, pp 556-73)
Conference on accelerator radiation dosimetry and experience, Brookhaven National Lab., 11/65, 20: 29841 (CONF-651109)
Determination of quality factor through utilization of balanced, tissue-equivalent, ionization chamber, 20: 29847 (CONF-651109, pp 181-98)
Effects of whole-body irradiation by protons on primates, 20: 28931 (CONF-651109, pp 624-35)
Fast neutron spectrometry with nuclear emulsions, 20: 29848 (CONF-651109, pp 199-212)
Health physics survey methods for measurement of stray radiation around CERN high-energy accelerators, 20: 29844 (CONF-651109, pp 103-16)
High-dose human exposure from 10-Mev linear accelerator, 20: 28929 (CONF-651109, pp 574-98)
High-energy particle spectrometry using activation detectors, 20: 29521 (CONF-651109, pp 213-23)
Inference of accelerator stray neutron spectra from various measurements, 20: 29522 (CONF-651109, pp 286-305)
Methods and experience acquired in dosimetry at Saturne synchrotron, 20: 29845 (CONF-651109, pp 117-42)
Neutron radiation monitoring using ^{3}He spectrometer, 20: 29846 (CONF-651109, pp 154-60)
Pulse-shape discrimination applied to fast neutron dosimetry, 20: 29524 (CONF-651109, pp 647-52)
Radiation environment at zero gradient synchrotron, 20: 29843 (CONF-651109, pp 34-56)
Radiation hazards peculiar to a linear accelerator meson factory, 20: 29850 (CONF-651109, pp 472-89)
Radiation levels in and around Nimrod, 20: 29842 (CONF-651109, pp 20-33)
Radiation protection problems at Stanford two-mile linear accelerator, 20: 29849 (CONF-651109, pp 442-58)
Shielding aspects of accelerator facility design, 20: 30720 (CONF-651109, pp 410-16)
Shielding calculations for high-energy accelerators, 20: 30719 (CONF-651109, pp 327-45)
Techniques for determining proton depth dose distribution in primates, 20: 28928 (CONF-651109, pp 417-25)
Use of personal monitoring neutron film near 50-Mev injection of, 20: 29523 (CONF-651109, pp 639-46)

DIVISION OF RESEARCH (AEC), WASHINGTON, D. C.
Acute cellular effects of heavy charged-particle irradiations, 20: 28930 (CONF-651109, pp 601-16)
Cambridge accelerator fire of July 5, 1965, 20: 29851 (CONF-651109, pp 556-73)
Conference on accelerator radiation dosimetry and experience, Brookhaven National Lab., 11/65, 20: 29841 (CONF-651109)
Determination of quality factor through utilization of balanced, tissue-equivalent, ionization chamber, 20: 29847 (CONF-651109, pp 181-98)
Effects of whole-body irradiation by protons on primates, 20: 28931 (CONF-651109, pp 624-35)
Fast neutron spectrometry with nuclear emulsions, 20: 29848 (CONF-651109, pp 199-212)
Health physics survey methods for measurement of stray radiation around CERN high-energy accelerators, 20: 29844 (CONF-651109, pp 103-16)
High-dose human exposure from 10-Mev linear accelerator, 20: 28929 (CONF-651109, pp 574-98)
High-energy particle spectrometry using activation detectors, 20: 29521 (CONF-651109, pp 213-23)
Inference of accelerator stray neutron spectra from various measurements, 20: 29522 (CONF-651109, pp 286-305)
Methods and experience acquired in dosimetry at Saturne synchrotron, 20: 29845 (CONF-651109, pp 117-42)
Neutron radiation monitoring using ^{3}He spectrometer, 20: 29846 (CONF-651109, pp 154-60)
Pulse-shape discrimination applied to fast neutron dosimetry, 20: 29524 (CONF-651109, pp 647-52)
Radiation environment at zero gradient synchrotron, 20: 29843 (CONF-651109, pp 34-56)
Radiation hazards peculiar to a linear accelerator meson factory, 20: 29850 (CONF-651109, pp 472-89)
Radiation levels in and around Nimrod, 20: 29842 (CONF-651109, pp 20-33)
Radiation protection problems at Stanford two-mile linear accelerator, 20: 29849 (CONF-651109, pp 442-58)
Shielding aspects of accelerator facility design, 20: 30720 (CONF-651109, pp 410-16)
Shielding calculations for high-energy accelerators, 20: 30719 (CONF-651109, pp 327-45)
Techniques for determining proton depth dose distribution in primates, 20: 28928 (CONF-651109, pp 417-25)
Use of personal monitoring neutron film near 50-Mev injection of, 20: 29523 (CONF-651109, pp 639-46)

DOUGLAS AIRCRAFT CO., INC., SANTA MONICA, CALIF. MISSILE AND SPACE SYSTEMS DIV.
Bonding reaction mechanism in chemically bonded ZrO_2, 20: 29145 (NP-16047)

DUKE UNIV., DURHAM, N. C. DEPT. OF ELECTRICAL ENGINEERING.
Prog. rpt. on superconducting circuitry, 5/66, 20: 30255 (ORO-2430-28)

DYNATECH CORP., CAMBRIDGE, MASS.
Prog. rpt. on boiling flow regimes and critical heat flux, 9/16-12/15/65, 20: 29378 (NYO-3304-7)

E

ENTE NAZIONALE PER L'ENERGIA ELETTRICA, ROME (ITALY).
Prog. rpt. on research program for Garigliano nuclear power plant, 10/65, 20: 30878 (EURAEC-1516)

EUROPEAN ATOMIC ENERGY COMMUNITY.
Basic concepts of LYRA system, 20: 30721 (EUR-2778.e)
Digital comparators for handling of data from nuclear experiments, 20: 29485 (EUR-2799.e)
Elastic scattering of neutrons from natural silicon, 20: 30345 (EUR-2798.e)
In-pile application of strain gages, 20: 29578 (EUR-2649.e)
NEUTOF: program to correct neutron time-of-flight spectra, 20: 30344 (EUR-2779.e)
Prog. rpt. on nuclear medicine, annual, 1964, 20: 28871 (EUR-2636.f,i)

EUROPEAN ATOMIC ENERGY COMMUNITY, GEEL (BELGIUM). CENTRAL NUCLEAR MEASUREMENTS BUREAU.
Digital comparators for handling of data from nuclear experiments, 20: 29485 (EUR-2799.e)
Elastic scattering of neutrons from natural silicon, 20: 30345 (EUR-2798.e)

EUROPEAN ATOMIC ENERGY COMMUNITY, ISPRA (ITALY). EUROPEAN SCIENTIFIC DATA PROCESSING CENTER.
Basic concepts of LYRA system, 20: 30721 (EUR-2778.e)

EUROPEAN ATOMIC ENERGY COMMUNITY, ISPRA (ITALY). JOINT NUCLEAR RESEARCH CENTER.
In-pile application of strain gages, 20: 29578 (EUR-2649.e)
NEUTOF: program to correct neutron time-of-flight spectra, 20: 30344 (EUR-2779.e)

EUROPEAN COMPANY FOR THE CHEMICAL PROCESSING OF IRRADIATED FUELS, MOL (BELGIUM).
Large-scale isotope irradiation in reactors, 20: 29609 (NP-15947)

EUROPEAN ORGANIZATION FOR NUCLEAR RESEARCH, GENEVA (SWITZERLAND).
Capacitor bank (150-kj) for magnetic horn, 20: 29840 (CERN-66-16)

Health physics survey methods for measurement of stray radiation around CERN high-energy accelerators, 20: 29844 (CONF-651109, pp 103-16)
Production and decay of resonances at a few Bev, 20: 30085 (CONF-640509(Pt.1), Paper 3)

F

FIAT, TURIN (ITALY). SEZIONE ENERGIA NUCLEARE.
Dependence on microstructure of high-temperature properties of UO_2–Mo and UO_2–W cermets. I., 20: 29699 (CONF-650674-1)

G

GENERAL DYNAMICS CORP., SAN DIEGO, CALIF. GENERAL ATOMIC DIV.
Prog. rpt. on gas-cooled reactor, 1/31/66, 20: 30879 (GA-6995)
GENERAL ELECTRIC CO., CINCINNATI, OHIO. NUCLEAR MATERIALS AND PROPULSION OPERATION.
Neutron cross sections for ^{244}Cm and ^{233}Pu, 20: 30346 (GEMP-411)
Properties of some refractory metals. IV., 20: 29710 (TID-22986)
GENERAL ELECTRIC CO., RICHLAND, WASH. HANFORD ATOMIC PRODUCTS OPERATION.
Design criteria, plutonium buy-back facility, 20: 29453 (RL-SEP-590)
Welding of stainless steel for corrosive radioactive service, 20: 29661 (HWS-8241(Rev.4))
Welding of stainless steel for corrosive non-radioactive service, 20: 29662 (HWS-8242(Rev.5))
GENERAL ELECTRIC CO., SAN JOSE, CALIF. ADVANCED PRODUCTS OPERATION.
Prog. rpt. on fast ceramic reactor development, 8–10/65, 20: 29618 (GEAP-4982)
GENERAL ELECTRIC CO., SAN JOSE, CALIF. ATOMIC POWER EQUIPMENT DEPT.
Prog. rpt. on Zr alloy, 20: 29660 (GEAP-4960)
GENERAL INSTRUMENT CORP., NEWARK, N. J. THERMOELECTRIC DIV.
Thermoelectric Bi telluride improvement program, 20: 29975 (GIC-3362-4)
GENERAL MOTORS CORP., SANTA BARBARA, CALIF. DEFENSE RESEARCH LABS.
Compressive strain rate tests on four composites. Phase I, 20: 29708 (SC-DC-65-1744)
GOSUDARSTVENNYI KOMITET PO ISPOL'ZOVANIYU ATOMNOI ENERGII SSSR.
Behavior of ^{137}Cs during analysis of atmospheric samples, 20: 29081 (NP-14705)
Fallout of Ce-141, Ce-144, Zr-95 + Nb-95 and Sr-90 on U.S.S.R., 20: 29406 (NP-14719)
Radioactive contamination of oceans, 20: 29405 (NP-14694)
GOSUDARSTVENNYI KOMITET PO ISPOL'ZOVANIYU ATOMNOI ENERGII SSSR, MOSCOW. INSTITUT TEORETICHESKOI I EKSPERIMENTAL'NOI FIZIKI.
Accuracy of particle trajectory location in spark chamber, 20: 29527 (ITEF-341)
Decays ($\eta^0 \rightarrow \pi^0 + e^+\mu^+ + e^-\mu^-$) and violation of CP parity, 20: 29988 (ITEF-356)
Proton elastic scattering on deuterons at large angles, 20: 29989 (ITEF-361)
GRENOBLE UNIV. (FRANCE).
Irreversible magnetic behavior of superconductors, 20: 30253 (CEA-R-2808)

H

HARVARD UNIV., CAMBRIDGE, MASS. DIV. OF ENGINEERING AND APPLIED PHYSICS.
Temperature distribution in a Poiseuille plasma arc, 20: 30563 (NP-16096)
HEALTH AND SAFETY LAB., NEW YORK OPERATIONS OFFICE (AEC), N. Y.
Fast neutron spectrometry with nuclear emulsions, 20: 29848 (CONF-651109, pp 199-212)
Inference of accelerator stray neutron spectra from various measurements, 20: 29522 (CONF-651109, pp 286-305)

I

IIT RESEARCH INST., CHICAGO, ILL.
Prog. rpt. on reactor containment, 2–3/66, 20: 30797 (IITRI-578P21-18)
ILLINOIS UNIV., URBANA.
Elasticity and anelasticity of uranium oxides at room temperature, 20: 29698 (ANL-7101)
Production and decay of resonances at a few Bev, 20: 30085 (CONF-640509(Pt.1), Paper 3)
ILLINOIS UNIV., URBANA. COORDINATED SCIENCE LAB.
Dense plasma under strong electric field, 20: 30558 (AD-633593)
INSTITUT FUER PLASMAPHYSIK, G.M.B.H. GARCHING (WEST GERMANY).
Internal potential drop in MHD generators, 20: 29976 (IPP-3/38)
INSTITUTE OF NUCLEAR PHYSICS, KRAKOW (POLAND).
Computation delta (THETA) according to strong absorption theory given by Frahn and Venter, 20: 30348 (INP-446/PL)
Semiconductor system for charged particles identification, 20: 29526 (INP-444/PL)
INSTITUTE OF NUCLEAR RESEARCH, WARSAW (POLAND).
Phase motion of protons in proton linear accelerator with perturbed axial field, 20: 29852 (INR-640/SLBAL/E)
INSTITUTT FOR ATOMENERGI, HALDEN (NORWAY). OECD HALDEN REAKTOR PROSJEKT.
Prog. rpt. on HBWR, 1–3/66, 20: 30880 (HPR-67)
INTERNATIONAL ATOMIC ENERGY AGENCY, VIENNA (AUSTRIA).
Conference on plasma physics and controlled nuclear fusion research, Culham, 9/65, 20: 30565 (STI-PUB-111(Vol.I))
Conference on plasma physics and controlled nuclear fusion research, Culham, 9/65, 20: 30566 (STI-PUB-111(Vol.2))
INTERNATIONAL CENTRE FOR THEORETICAL PHYSICS, TRIESTE (ITALY).
Cabibbo angle and partial conservation of axial current, 20: 30090 (IC-66/52)
Regge pole behavior in an SL(2,C) model field theory, 20: 30087 (IC-66/46)
Renormalized ω–ϕ mixing angle and $J^\mu = 1^-$ meson decays, 20: 30088 (IC-66/50)
Representations of SL(n,C), 20: 30089 (IC-66/51)
ISOCHEM INC., RICHLAND, WASH.
Criticality safety of fissile materials, 20: 29450 (ISO-270)
ISTITUTO SUPERIORE DI SANITA', ROME (ITALY). LABORATORI DI FISICA.
Spectral distribution of photons scattered by electrons bound in K shell. I., 20: 29912 (ISS-66/6)
Spectral distribution of photons scattered by electrons bound in K shell. II., 20: 29913 (ISS-66/7)
Spectral distribution of photons scattered by electrons bound in K shell. III., 20: 29914 (ISS-66/8)

J

JACKSON AND MORELAND, BOSTON, MASS.
Costs of large fossil fuel fired power plants, 20: 29372 (TID-22978)
JAPAN ATOMIC ENERGY RESEARCH INST., TOKYO.
Seminar on fast-neutron cross sections, 20: 30349 (JAERI-1102)
JOINT INST. FOR NUCLEAR RESEARCH, DUBNA (USSR). LAB OF HIGH ENERGY.
Formation of electron-positron pairs by high-energy gamma quanta, 20: 29990 (JINR-P-2667)
JOINT INST. FOR NUCLEAR RESEARCH, DUBNA (USSR). LAB OF THEORETICAL PHYSICS.
Average field levels of nuclei, 20: 30350 (JINR-P-2682)
Coulomb field and non-relativistic space quantization, 20: 29915 (JINR-P-2627)
Dynamical symmetry and hadron mass spectrum, 20: 30091 (JINR-P-2621)
Problems of quantam theory of scalar field with point sources, 20: 30092 (JINR-P-2700)
Quantum theory of gravity in Heisenberg representation and interaction representation, 20: 30239 (JINR-P-2692)
Relativistic wave packets in space and time. I., 20: 30238 (JINR-P-2691)
Representations 189 and 405 of the group SU(6) and classification of mesonic resonances 2^+, 1^+, and 0^+, 20: 30093 (JINR-P-2701)

K

KAMAN NUCLEAR, COLORADO SPRINGS, COLO.
Gamma fluxes from circular and spherical sources, 20: 30351 (N-65-14857)
KNOLLS ATOMIC POWER LAB., SCHENECTADY, N. Y.
Assessment of inhomogeneity of solid reactor fuels by fission-track counting, 20: 29663 (KAPL-M-6556)
Group constants for gamma-ray heating, 20: 30722 (KAPL-M-6497)
Procedure for quantitative recovery of ^{233}Pa from irradiated thoria, 20: 29331 (KAPL-M-6554)
Thermal expansion and temperature dependence of elastic moduli of polycrystalline hafnium, 20: 29703 (KAPL-3112)

L

LAWRENCE RADIATION LAB., UNIV. OF CALIFORNIA, BERKELEY.
Acute cellular effects of heavy charged-particle irradiations, 20: 2890

(CONF-651109, pp 601-16)
Antiproton annihilation at rest in deuterium, 20: 29992 (UCRL-16717)
Correlations of photons from thermal source, 20: 29827 (UCRL-16824)
Design of atomic- and molecular-beam apparatus, 20: 29918 (UCRL-11670)
Dislocation dipoles in deformed magnesium oxide, 20: 29711 (UCRL-11996)
Do-it-yourself lock-in amplifiers, radio and audio frequency, 20: 29487 (UCRL-16632)
Fluctuations of energy loss in semiconductor detectors, 20: 29531 (UCRL-16715)
Hyperfine-structure anomalies of ^{198}Au and ^{199}Au, 20: 30359 (UCRL-16757)
Mechanical design of regenerative deflector for Berkeley 88-in. cyclotron, 20: 29856 (UCRL-16829)
OMNITRON: medium-energy synchrotron for acceleration of light and heavy ions, 20: 29857 (UCRL-16839)

LAWRENCE RADIATION LAB., UNIV. OF CALIFORNIA, LIVERMORE.
Comparison of analytical and numerical solutions for shock tube problem, 20: 30169 (UCRL-14198)
General phenomenological formalism for reactions with particles of arbitrary spin. I., 20: 30094 (UCRL-14222)
Ions and dissociation products obtained from a hydrogen r-f ion source, 20: 29920 (UCRL-14271)
Neutralization of fast H ions colliding with H_2, CO, CH_4, and H_2O molecules, 20: 29919 (UCRL-14214)
Prog. rpt. on analytical chemistry, 1-12/65, 20: 29083 (UCRL-14767)
Propagation of stress disturbances in elastic-plastic cylinders, 20: 30954 (UCRL-14617)
Random phase approximation, 20: 30567 (UCRL-14246)
Relaxation phenomena and chemical cross section, 20: 29147 (UCRL-14901-T)
Shock compression of Ar, 20: 30170 (UCRL-14251)

LOCKHEED–CALIFORNIA CO., BURBANK.
Space electric power systems, 20: 29977 (N-65-32716)

LONDON UNIV. (ENGLAND). UNIVERSITY COLL.
Scattering (π-N), Pt. 1, 20: 29986 (CONF-640509(Pt.1), Paper 2)

LOS ALAMOS SCIENTIFIC LAB., UNIV. OF CALIFORNIA, N. MEX.
AEC Nuclear Cross Sections Advisory Group meeting, Washington, D. C., 3/66, 20: 30360 (WASH-1068)
Calculation of pulse-height response of Ge(Li) semiconductor counters, 20: 29528 (LA-3456)
Cooled high-temperature thermocouples for Phoebus reactors, 20: 30925 (LA-DC-7637)
Copper-boron carbide control material for Phoebus II, 20: 29664 (LA-DC-7745)
Prompt air fluorescence excited by high-altitude nuclear explosions, 20: 30193 (LA-3409(Suppl.))
Propulsion reactor temperature control with internal power loop eliminated, 20: 30924 (LA-DC-7636)
Radiation measurements of effluent from NRX A-2 and NRX A-3 reactors, 20: 30923 (LA-3394)
Reduction of Fokker-Planck equation for applications to practical plasma dynamics problems, 20: 30560 (LA-DC-7282)
Straight-line diagram for powder pattern indexing, 20: 30952 (LA-3467)
Transistorized liquid-He temperature regulator, 20: 30254 (LA-DC-7209)

M

MASSACHUSETTS INST. OF TECH., CAMBRIDGE.
Chemical and solid state physics, 20: 30734 (TID-22970, pp 1-63)
Electric, magnetic, and optical properties of materials and applications to devices, 20: 29709 (TID-22970, pp 65-119)
Instrumentation Laboratory, 20: 29366 (TID-22970, pp 375-91)
Materials engineering, 20: 29624 (TID-22970, pp 257-329)
Metallurgy and materials science, 20: 29623 (TID-22970, pp 121-256)
National Magnet Laboratory, 20: 30735 (TID-22970, pp 331-73)
Prog. rpt. on neutron and gamma-ray spectroscopy and activation analysis, 20: 29078 (AD-633252)
Prog. rpt. on research in materials science and engineering, annual, 1965–66, 20: 29622 (TID-22970)
Prog. rpt. on simultaneous radiation-heating treatment of precooked marine products, final, 2/65–2/66, 20: 29582 (MIT-3343-26)

MASSACHUSETTS INST. OF TECH., CAMBRIDGE. DEPT. OF METEOROLOGY.
Energy sources for the thermosphere, 20: 30194 (MIT-2241-16)

MATERIALS RESEARCH LAB., INC., RICHTON PARK, ILL.
Prog. rpt. on fracture toughness of reactor pressure vessel steels, 5/65–5/66, 20: 29700 (COO-1477-4)

MAX-PLANCK-INSTITUT FUER PHYSIK UND ASTROPHYSIK, MUNICH (WEST GERMANY).
Inhomogeneous development of a plasma through quasi-linear theory, 20: 30562 (MPI-PAE-P1/25/66)

MEDICAL RESEARCH COUNCIL, LONDON (ENGLAND).
Radiation risks to the population from environmental contamination, 20: 29054 (NP-16119)

MICHIGAN UNIV., ANN ARBOR.
Configuration interaction in two- and three-electron atoms, 20: 29917 (TID-22957)
Measurement of 2^3P fine structure of ^4He, 20: 29911 (COO-1112-21)

MICHIGAN UNIV., ANN ARBOR. DEPT. OF NUCLEAR ENGINEERING.
Scattering of photons by highly ionized plasmas, 20: 30557 (AD-633074)

MICHIGAN UNIV., ANN ARBOR. LAB. FOR FLUID FLOW AND HEAT TRANSPORT PHENOMENA.
Comprehensive cavitation damage data for water, mercury, and lead-bismuth alloy including correlations with material and fluid properties, 20: 29640 (NP-16048)

MINNESOTA MINING AND MFG. CO., ST. PAUL.
Prog. rpt. on fabrication of W alloy tubing, 2–5/66, 20: 29659 (COO-1518-3)

MINNESOTA UNIV., MINNEAPOLIS. SCHOOL OF PHYSICS.
Isobaric spin in stripping and pickup reactions, 20: 30343 (COO-1371-30)

MSA RESEARCH CORP., EVANS CITY, PA.
Mechanical properties tests of 316 SS specimens in 1200 F Na contaminated with O, 20: 29704 (MSAR-66-78)

N

NATIONAL ACADEMY OF SCIENCES–NATIONAL RESEARCH COUNCIL, WASHINGTON, D. C.
Application of nuclear excavation experimentation to highway construction, 20: 29370 (PNE-3003)
Geochronology of North America, 20: 29397 (NAS-NRC-1276)

NATIONAL AERONAUTICS AND SPACE ADMINISTRATION, CLEVELAND, OHIO. LEWIS RESEARCH CENTER.
Boron cross sections as source of discrepancy for capture cross sections in kev region, 20: 30352 (NASA-TR-R-240)

NATIONAL AERONAUTICS AND SPACE ADMINISTRATION, WASHINGTON, D. C.
Solar physics, 1958–64, 20: 29873 (NASA-SP-100)

NAVAL CIVIL ENGINEERING LAB., PORT HUENEME, CALIF.
Potential applications of radioisotopes in Navy, 20: 29581 (AD-633785)

NAVAL RADIOLOGICAL DEFENSE LAB., SAN FRANCISCO, CALIF.
Estimate of effects of fallout beta radiation on insects and associated invertebrates, 20: 28925 (AD-633024)
Transfer of myeloma protein synthesis with RNA from C_3H plasma cell tumor. I., 20: 28926 (AD-633469)

NORTH CAROLINA STATE UNIV., RALEIGH.
Prog. rpt. on convection boiling inside channels, 10-12/64, 20: 29380 (TID-22967)

NORTHERN STATES POWER CO., MINNEAPOLIS, MINN.
Core boration and flux mapping Test 313, 20: 30874 (ACNP-65612)

NUCLEAR MATERIALS AND EQUIPMENT CORP., APOLLO, PA.
Prog. rpt. on development and testing of PuO_2–UO_2 fast reactor fuels, 20: 29621 (NUMEC-3524-17)
Prog. rpt. on irradiation testing of PuO_2–UO_2 fuels, 1–3/66, 20: 29805 (NUMEC-3432-21)

NUCLEAR UTILITY SERVICES, INC., WASHINGTON, D. C.
Shielding aspects of accelerator facility design, 20: 30720 (CONF-651109, pp 410-16)

NUS CORP., WASHINGTON, D. C.
Prog. rpt. on Elk River Reactor operation's safety analysis, 11/65–1/66, 20: 30882 (NUS-264)

O

OAK RIDGE NATIONAL LAB., TENN.
Advanced accelerator development, 20: 29855 (ORNL-3940, pp 33-111)
Development and applications of minerals in radioactive waste disposal, 20: 29332 (ORNL-P-1811)
Effect of error on results of a low-energy intranuclear cascade calculation, 20: 30725 (ORNL-3786)
Experimental nuclear physics, 20: 30353 (ORNL-3940, pp 1-61)
Feedforward compensation of temperature control system, 20: 30807 (ORNL-TM-1485)
Impossible Legendre coefficients, 20: 30355 (ORNL-P-2084)
Measurement of mass attenuation coefficients using x rays, 20: 29707 (ORNL-TM-1457)
Nuclear physics theory, 20: 30354 (ORNL-3940, pp 62-9)
Oak Ridge isochronous cyclotron, 20: 29854 (ORNL-3940, pp 70-82)
OR GNU: FORTRAN program for calculating frequency-distribution functions of cubic crystals, 20: 30733 (ORNL-TM-1425)
ORSEF: code for calculation of flash evaporation desalination plant designs, 20: 30953 (ORNL-TM-1542)
Point-set representation of ^{238}U cross sections; values and a FORTRAN program for computation, 20: 30356 (ORNL-TM-1448)

Positron annihilation in metals, 20: 29991 (ORNL-TM-1443)
Postirradiation examination of high burnup EGCR prototype fuel capsules, 20: 29806 (ORNL-TM-1511)
Prog. rpt. on coated-particle fuels development at ORNL, 11/65–5/66, 20: 30870 (ORNL-TM-1528)
Prog. rpt. on electronuclear division, annual, 1965, 20: 29853 (ORNL-3940)
Prog. rpt. on waste treatment and disposal, semiannual, 7–12/65, 20: 30943 (ORNL-TM-1465)
Safety analysis of radionuclide release to Clinch River, 20: 29452 (ORNL-3721(Suppl.3))
Semi-classical model of photoelectric effects in metals, 20: 29916 (ORNL-TM-1458)
Shielding calculations for high-energy accelerators, 20: 30719 (CONF-651109, pp 327-45)
Simulators for training MSRE operators, 20: 30934 (ORNL-TM-1445)
TRANSFER: program to calculate P_n multigroup scattering matrices, 20: 30323 (ORNL-TM-1537)

OESTERREICHISCHE STUDIENGESELLSCHAFT FUER ATOMENERGIE G.M.B.H., SEIBERSDORF.
Quantitative activation analytical purity determination of rare earth oxides, 20: 29082 (SGAE-CH-27/1966)

OKLAHOMA STATE UNIV., STILLWATER.
Solutions of the flow field produced by shock wave emerging into cross-flow, 20: 30167 (SC-DC-65-1916)
Transient flow field analysis of blast wave intercepting a stationary cone at zero angle of attack, 20: 30168 (SC-DC-66-1329)

P

PARAMETRICS, INC., WALTHAM, MASS.
Prog. rpt. on ultrasonic temperature measuring device, 1-4/66, 20: 29486 (NASA-CR-54964)

PARIS UNIV. (FRANCE).
Total ionization intensity near ground and separation of various components, 20: 29404 (CEA-R-2880)

PARIS UNIV., ORSAY (FRANCE). LABORATOIRE DE PHYSIQUE THEORIQUE ET HAUTES ENERGIES.
Approximation method in study of scattering at high energies, 20: 30086 (CONF-640509(Pt.1), Paper 4)

PARIS UNIV., ORSAY (FRANCE). LABORATOIRE JOLIOT-CURIE DE PHYSIQUE NUCLEAIRE.
Pole contributions to N-N scattering below pion production, 20: 29985 (CONF-640509(Pt.1), Paper 1)

PHILLIPS PETROLEUM CO. IDAHO FALLS, IDAHO., ATOMIC ENERGY DIV.
Mathematical analysis and machine computations, 20: 30795 (IDO-17147, pp 29-36)
Noise study, ARMF-II, 20: 30837 (IDO-17169)
Nuclear technology, 20: 30347 (IDO-17147, pp 13-28)
Prog. rpt. on burnup determination of nuclear fuels, 10-12/65, 20: 29080 (IDO-14676)
Prog. rpt. on nuclear technology, 7–9/65, 20: 30793 (IDO-17147)
Reactor engineering, 20: 30794 (IDO-17147, pp 1-12)
Review of SPERT subassembly test program for CDC and the PBF, 20: 30796 (IDO-17177)

PIEDMONT HOSPITAL, ATLANTA, GA.
Oxygen saturation of tumor cells to increase effect of internal radiation, 20: 29059 (TID-22860)

PISA UNIV. (ITALY).
Prog. rpt. on nuclear medicine, annual, 1964, 20: 28871 (EUR-2626.f,i)

PLANNING RESEARCH CORP., LOS ANGELES, CALIF.
Probabilistic methodology for safety analysis of power reactors. I and II., 20: 30883 (SAN-570-2)

PRINCETON UNIV., N. J. GUGGENHEIM LABS. FOR THE AEROSPACE PROPULSION SCIENCES.
Prog. rpt. on combustion of metals, annual, 7/64–6/65, 20: 29641 (SC-DC-65-1691)

PRINCETON UNIV., N. J. PLASMA PHYSICS LAB.
Effect of pressure on negative V'' stellarators, 20: 30561 (MATT-415)

R

REACTOR GROUP, UNITED KINGDOM ATOMIC ENERGY AUTHORITY, RISLEY (ENGLAND).
Mechanized structural analysis, 20: 29367 (TRG-Report-1089)

REACTOR GROUP, UNITED KINGDOM ATOMIC ENERGY AUTHORITY, SELLAFIELD (ENGLAND).
General-purpose multiple regression program, 20: 29613 (TRG-Report-1198)
Grain boundary holes in irradiated U, 20: 29807 (TRG-Report-325)

RENSSELAER POLYTECHNIC INST., TROY, N. Y.
Fast neutron spectrum program, 20: 29529 (RPI-328-56, pp 94-112)
Low-energy neutron inelastic scattering, 20: 30325 (RPI-328-56, pp 113-34)
Neutron cross sections, 20: 30358 (RPI-328-56, pp 1-48)
Neutron thermalization, 20: 30324 (RPI-328-56, pp 52-93)
Prog. rpt. on linear accelerator project, 1–3/66, 20: 30357 (RPI-328-56)

RURAL COOPERATIVE POWER ASSOCIATION, ELK RIVER, MINN.
Prog. rpt. on Elk River Reactor operation's safety analysis, 11/65–1/66, 20: 30882 (NUS-264)

S

SANDIA CORP., ALBUQUERQUE, N. MEX.
Compressive strain rate tests on four composites. Phase I, 20: 29708 (SC-DC-65-1744)
Prog. rpt. on combustion of metals, annual, 7/64–6/65, 20: 29641 (SC-DC-65-1691)
Prog. rpt. on particle fallout and dispersion in atmosphere, 9-11/65, 20: 29454 (SC-CR-66-2010)
Reaction rates for high-temperature air, 20: 29146 (SC-R-66-885)
Solutions of the flow field produced by shock wave emerging into cross-flow, 20: 30167 (SC-DC-65-1916)
Time-interval measuring circuit, 20: 29530 (SCL-DR-65-13)
Transient flow field analysis of blast wave intercepting a stationary cone at zero angle of attack, 20: 30168 (SC-DC-66-1329)

SOCIETA ELETTRONUCLEARE NAZIONALE, ROME (ITALY).
Prog. rpt. on research program for Garigliano nuclear power plant, 10/65, 20: 30878 (EURAEC-1516)

SOCIETE BELGE POUR L'INDUSTRIE NUCLEAIRE, BRUSSELS.
Prog. rpt. on Pu as fuel in nuclear reactors, 10/1–12/31/65, 20: 29617 (EURAEC-1593)

STANFORD LINEAR ACCELERATOR CENTER, STANFORD UNIV., CALIF.
Radiation protection problems at Stanford two-mile linear accelerator, 20: 29849 (CONF-651109, pp 442-58)

T

TEXAS INSTRUMENTS INC., DALLAS.
Epitaxial structures for radiation-resistant Si solar cells, 20: 30724 (NASA-CR-461)

TEXAS UNIV., AUSTIN.
Prog. rpt. on plasma diagnostic methods, 4–6/65, 20: 30556 (AD-631993)

THERMO ELECTRON ENGINEERING CORP., WALTHAM, MASS.
Prog. rpt. on vacuum foil-type insulation for radioisotope power systems, 2–4/66, 20: 29606 (ALO-3634-1)

TRAVELERS RESEARCH CENTER, INC., HARTFORD, CONN.
Prog. rpt. on particle fallout and dispersion in atmosphere, 9-11/65, 20: 29454 (SC-CR-66-2010)

TRW EQUIPMENT LABS., THOMPSON RAMO WOOLDRIDGE INC., CLEVELAND, OHIO.
Prog. rpt. on long-time creep data on refractory alloys, 12/65–3/66, 20: 29705 (NAS-CR-54973)

U

UNION CARBIDE CORP., OAK RIDGE, TENN. Y-12 PLANT.
Average-radius gage, 20: 29668 (Y-NA-18)

UNITED NUCLEAR CORP., WHITE PLAINS, N. Y. DEVELOPMENT DIV.
ADONIS: IBM-7090 Monte Carlo shielding code in three-dimensional rectangular geometry, 20: 30726 (TID-22964)

UNITED STATES–EURATOM JOINT RESEARCH AND DEVELOPMENT PROGRAM.
Burnout for flow inside round tubes with nonuniform heat fluxes, 20: 29376 (BAW-3238-9)
Prog. rpt. on influence of initial stress on isothermal stress-relief tests, 1–3/66, 20: 29702 (EURAEC-1616)
Prog. rpt. on mechanical properties, of steels, 10–12/65, 20: 29639 (EURAEC-1578)
Prog. rpt. on nonuniform heat generation, 10-12/65, 20: 29377 (BAW-3238-11)
Prog. rpt. on plastic fatigue embrittlement of reactor vessel steels, 10–12/65, 20: 29701 (EURAEC-1547)
Prog. rpt. on Pu as fuel in nuclear reactors, 10/1–12/31/65, 20: 29617 (EURAEC-1593)
Prog. rpt. on reprocessing of irradiated fuels, 7-9/65, 20: 29330 (EURAEC-1601)
Prog. rpt. on research program for Garigliano nuclear power plant, 10/65, 20: 30878 (EURAEC-1516)
Prog. rpt. on UC shaping and irradiation, 7–12/65, 20: 29804 (EURAEC-1637)
Prog. rpt. on Zr alloy, 20: 29660 (GEAP-4960)

V

VANDERBILT UNIV., NASHVILLE, TENN.
Measurement of mass attenuation coefficients using x rays, 20: 29707 (ORNL-TM-1457)
Positron annihilation in metals, 20: 29991 (ORNL-TM-1443)
Semi-classical model of photoelectric effect in metals, 20: 29916 (ORNL-TM-1458)

W

WASHINGTON STATE UNIV., PULLMAN.
Conference on radiocarbon and tritium dating, Sixth International, Washington State University, Pullman, Wash., 6/65, 20: 29438 (CONF-650652)
WESTINGHOUSE ELECTRIC CORP., PITTSBURGH, PA. ASTRONUCLEAR LAB.
Effect of H and temperature on mechanical properties of Ti-5Al-2.5Sn ELI alloy, 20: 29715 (WANL-TME-1287)
Prog. rpt. on weldability and elevated-temperature stability of refractory alloys, 6–9/65, 20: 29712 (WANL-PR-(P)-009)
Prog. rpt. on weldability and elevated-temperature stability of refractory alloys, 9–12/65, 20: 29713 (WANL-PR-(P)-010)
Properties of P-03 graphite, 20: 29714 (WANL-TME-1031)
Propulsion reactor temperature control with internal power loop eliminated, 20: 30924 (LA-DC-7636)
Thermocouple program to investigate relative error, 20: 29488 (WANL-TME-948)
WESTINGHOUSE ELECTRIC CORP., PITTSBURGH, PA. ATOMIC POWER DIV.
Automatic control of rod position with boron in a chemical shim nuclear plant, 20: 30808 (WCAP-3269-54)
Prog. rpt. on CVTR, 10–12/65, 20: 30877 (CVNA-254)
Prog. rpt. on large closed-cycle water reactor program, 10–12/65, 20: 30884 (WCAP-3269-16)
WHITWORTH COLL., SPOKANE, WASH.
Conference on radiocarbon and tritium dating, Sixth International, Washington State University, Pullman, Wash., 6/65, 20: 29438 (CONF-650652)
WOODS HOLE OCEANOGRAPHIC INSTITUTION, MASS.
Biological, chemical, and radiochemical studies of marine plankton. I., 20: 28877 (NYO-1918-124)
Biological, chemical, and radiochemical studies of marine plankton. II., 20: 28878 (NYO-1918-138)

Y

YALE UNIV., NEW HAVEN, CONN.
Radiation hazards peculiar to a linear accelerator meson factory, 20: 29850 (CONF-651109, pp 472-89)

PERSONAL AUTHOR INDEX

Each entry after an author's name is a shortened version of the title of the report or article, followed by the *NSA* volume and abstract number. Report numbers are given in parentheses.

The phrase "Progress report" is abbreviated as "Prog. rpt.," permitting a more rapid and complete alphabetical arrangement of the titles without changing the location of the progress report titles in relation to the other titles.

Because of problems involving the mechanical preparation of this index, all accent marks are omitted. The following changes in spelling have been introduced to reduce some of the confusion which might result from omitting the accents:

ä	becomes	ae
ö		oe
ø		oe
ü		ue (except in transliterated Chinese names)

A

AAMODT, R. E., Thermalization and anomalous diffusion of turbulent plasmas, 20: 30620

ABBASOV, A. R., Frequency spectrum of slowly varying component of solar radio emission, 20: 29908

ABDEL-WAHAB, M. F., Paper electrophoresis of steroids. I., 20: 29132

ABDURAKHMANOV, A. Kh., Ion source of hydrogen ions at low gas pressures, 20: 29925

ABE, Shigeki, Activation analysis of alkali halides by photonuclear reaction, 20: 29112

ABE, Toshihiko, Thermal and radiation oxidations of benzene to phenol in aqueous solutions containing metal ions. VII., 20: 29250

ABEE, H. H., Whole-body counting—an environmental monitoring tool, 20: 28882

ABEL, W. R., Low-temperature heat capacity of liquid ^{3}He, 20: 30283

ABERNATHEY, Robert M., Prog. rpt. on burnup determination of nuclear fuels, 10–12/65, 20: 29080 (IDO-14676)

ABKIN, A. D., Radiation-induced polymerization of tetrafluoroethylene and acrylonitrile at 4.2 K, 20: 29300

ABLYAEV, Sh. A., Absorption effect on surfaces of semiconductors and gels due to effects of radiation, 20: 29815

ABOLINS, M. A., Isospin of the A mesons, 20: 30023

ABOLINS, Maris Arvids, A_1 and A_2 resonance production in 3.7-Bev/c π^--deuterium interactions, 20: 30078

ABRAHAM, B. M., Ultrasonic attenuation in liquid ^{4}He at low temperatures, 20: 30299

ABRAMOVICH, I. I., Uranium in traps of Siberian platform, 20: 29419

ABRAMS, C. S., Current practices in the disposal of radioactive wastes from operation of uranium mines and mills, 20: 30948

ABRAMS, C. S., Current practices in disposal of waste radioactive gases from reactors, 20: 30949

ABRAMS, I., Ionizing gamma-defectoscopy for lead containers, 20: 29388

ACOSTA, V., Evidence for sidereal-time-dependent cosmic-ray signal, 20: 29967

ADACHI, Kazushige, Modification of hematopoietic cell transplantation in mice irradiated with gamma rays. II., 20: 29035

ADACHI, Kazushige, Modification of hematopoietic cell transplantation in mice irradiated with gamma rays. III., 20: 29036

ADAM, J., Behavior of refractory metals in radiation environments, 20: 29820

ADAMCHUK, Yu. V., Total neutron cross sections for heavy Sn isotopes below 10 kev, 20: 30490

ADAMSON, I. Y. R., Structural studies on v.u.v./CO_2 oxidation of graphite, 20: 29733

ADLER, A. W., Search for splitting of gamma-ray photons in electric field of nucleus, 20: 30031

ADLER, S. J., Requirements of a general analytical laboratory in pure materials research, 20: 29141

AFANAS'EV, V. N., Radioisotopic instruments in metallurgy, 20: 29598

AFONIN, V. V., Physical experiments on Kosmos-2 in ionosphere, 20: 30198 (NASA-TT-F-389, pp 202-24)

AFRIKANOVA, L. A., Role of adipose cellular tissue in repair of acute radiation injuries of skin, 20: 28946

AFROSIMOV, V. V., Active diagnosis of hot plasma by means of neutral particles, 20: 30685

AFROSIMOV, V. V., Investigation of plasma concentration in Al'fa with probe beam of fast atoms, 20: 30686

AFROSIMOV, V. V., Joule heating of plasma in toroidal Tokamak-3 device, 20: 30650

AGARWALA, K. S., Effect of nuclear explosions on atmospheric potential gradient near ground, 20: 30227

AGIN, G. P., Nuclear states of ^{103}Rh, 20: 30471

AGUILAR, R., Photonuclear interactions of high-energy muons, 20: 29994

AHABABIAN, N., Daily variation of extensive air showers, 20: 29960

AHMED, Feroz, Neutron lifetime and slowing-down time calculations in beryllium, 20: 30333

AHRLAND, Sten, Fluoride and sulfate complexes of Np(IV), 20: 29148

AKAISHI, Jun, Loss of ^{137}Cs and K by dry ashing and HCl treatment of total diet samples, 20: 29122

AKCASU, A. Ziya, Angular correlations in neutron density fluctuations, 20: 30863

AKERMAN, Karol, Effect of radiation on activity of V catalyst in reaction of sulfur dioxide oxidation, 20: 29291

AKHMANOVA, M. V., Investigation of rare-earth carbonates using infrared spectroscopy, 20: 29447

AKHTYAMOV, O. S., Possible experiment for finding superconductors with different pair multiplicity, 20: 30265

AKIMOVA, T. G., Organic coprecipitants. XXIII., 20: 29135

AKIMUNE, Hideo, Utilizing r-f field for injection trapping of high-energy ions in mirror fields. I., 20: 30580

AKIYAMA, Takashi, Radioactivity in rain water, settled dust and activated sludge observed at Kagoshima District. XIII., 20: 29455

AKOPOV, F. A., Electric conductivity and creep of sintered CeO_2 during reduction, 20: 29739

AKS, Stanley Oelof, Proof that scattering implies production in quantum field theory, 20: 30157

AKULINA, D. K., Injection and confinement of plasma in a stellarator with a multipolar ($l = 2$) helical field, 20: 30657

ALANAKYAN, Yu. R., Interaction of plane and surface electromagnetic waves in a plasma, 20: 30694

ALBERG, Mary, Determination of energy distribution of γ rays scattered in sand, 20: 30728

ALBERTI, Giulio, Spectrofluorimetric trace determination of Tb(III) with K oxalate, 20: 29086

ALBESCU, Ileana, Refractometric investigation on the formation of complex samarium halogenides in aqueous solution, 20: 29204

ALBURGER, D. E., Decay of the 2.34- and 2.71-Mev states of ^{9}B, 20: 30445

ALDER, B. J., Relaxation phenomena and chemical cross section, 20: 29147 (UCRL-14901-T)

ALDER, B. J., Shock compression of Ar, 20: 30170 (UCRL-14251)

ALDERSON, Samuel Weir, Radiotherapy phantom, 20: 29077

ALEFELD, G., Plasma-type oscillations of kinked dislocations, 20: 30770

ALEKSANDROV, G. P., Temperature effect on yield and composition of hexanitrocobaltic rare earths mixed with potassium, 20: 29209

ALEKSANDROVA, M. F., Effect of ACTH of hypophysis on cytolytic activity of the blood and organs of irradiated rats, 20: 29044
ALEKSANDROVA, N. S., Effects of porous structure of lignin carbons on uranium sorption, 20: 29360
ALEKSANDROWICZ, J., Sterilization of bone tissues with gamma radiation in Poland, 20: 28987
ALEKSANYAN, L. M., Magnetometric apparatus of the electron-2 space station, 20: 30236
ALEKSEEV, A. I., Quantization of an EM field in a dispersive medium, 20: 30668
ALEKSEEVA, S. I., Recovery of cells from primary cytogenetic injuries, 20: 29049
ALEKSEEVSKII, N. E., Effective magnetic field at ^{60}Co nucleus in Co–Pd alloy, 20: 30752
ALEKSIEV, E., Content of rare earths in igneous rocks G-1, W-1, and G-B, 20: 29101
ALEKSIEV, E. L., Rare earth elements, 20: 29635
ALFF-STEINBERGER, C., Further results from interference of K_S and K_L in $\pi^+\pi^-$ decay modes, 20: 30026
ALFILLE, Lucien, Composite guide tube for reactors, 20: 30830
ALFORD, W. Parker, Re-examination of spin of ^{45}Sc 378-kev level, 20: 30429
ALI, Sameh Abdel Hadi, Chelate formation of americium and curium with nitrilotriacetic acid, 20: 29195
ALIEV, Yu. M., Oscillations and stability of plasma in external high-frequency electric field, 20: 30627
ALIEV, Yu. M., Parametric resonance in plasma in magnetic field, 20: 30669
ALIKAEV, V. V., Heating of plasma electrons by uhf fields in an adiabatic trap, 20: 30663
ALLEN, Alfred W., Elasticity and anelasticity of uranium oxides at room temperature, 20: 29698 (ANL-7101)
ALLEN, D. D., Elastic scattering (π^--p) at 1.7 Bev/c, 20: 30011
ALLEN, T. K., Cusp injection experiment, 20: 30644
ALMQVIST, E., Method of utilizing nuclear reactions in study of oxide layers, 20: 29817
AL'PERT, Ya. L., Altitudinal-time distribution of electron concentration and nonuniform formations of outer ionosphere, 20: 30197 (NASA-TT-F-389, pp 166-201)
AL'PERT, Ya. L., Conference on space physics, Moscow, 6/65, 20: 30195 (NASA-TT-F-389)
ALSHANOVA, T. M., Cholesterol protein blood complexes of dogs in radiation injury, 20: 28998
ALSMILLER, R. G. Jr., Shielding calculations for high-energy accelerators, 20: 30719 (CONF-651109, pp 327-45)
ALVAREZ RIVAS, J. L., Disadvantage factor in U–H_2O, 20: 30855
AMANKULOVA, D. S., Disintegration with emission of fast He nuclei due to high-energy protons, 20: 30496
AMATO, I., Dependence on microstructure of high-temperature properties of UO_2–Mo and UO_2–W cermets. I., 20: 29699 (CONF-650674-1)
AMBEGAOKAR, Vinay, Ultrasonic attenuation in pure strong-coupling superconductors, 20: 30300
AMBLER, J. F. R., Effect of temperature on micro-identation properties of zirconium hydride, 20: 29697 (AECL-2538)
AMIEL, Jean, Production of Re in powdered form, 20: 29672
AMIEL, Saadia, Determination of ^{18}O by bombardment with alpha particles and detection of liberated neutrons, 20: 29143
AMMON, Johannes H., Integral boiler reactor, 20: 30913
AMOIGNON, J., Present limits of devices for production of low pressures, 20: 29396
ANDANSON, Pierre, Electrostatic collecting of RaA and β emission of RaE formed, 20: 29324
ANDAY, M. C., Nuclear measurement of soil properties, 20: 29506
ANDELFINGER, C., Isar I: fast megajoule theta-pinch experiment with extremely high compression fields, 20: 30611
ANDERSON, A., Far-infrared spectra of crystalline acetylenes C_2H_2 and C_2D_2, 20: 29239
ANDERSON, A. C., Experimental thermal conductivity of ^{3}He, 20: 30282
ANDERSON, A. C., Low-temperature heat capacity of liquid ^{3}He, 20: 30283
ANDERSON, A. R., Gamma-radiolysis of water vapor in the presence of NH_3 and O_2, 20: 29295
ANDERSON, Herbert R. Jr., Isomerization of trans polymers of conjugated dienes by radiation, 20: 29321
ANDERSON, Herbert R. Jr., Rubber products resistant to radiation damage, 20: 29322
ANDERSON, John Lynde, Detecting contamination on surfaces, 20: 29484
ANDERSON, Jorge Carlos, Energy and angular distribution of secondary electrons by protons in N, O, Ne, and Ar, 20: 29951
ANDERSON, R. A., Methods for reducing ^{90}Sr in wheat and milled products, 20: 29473
ANDREEV, I. V., Theory of multiple scattering, 20: 30509
ANDRESEN, E. G., Model level-gauges, 20: 29590
ANDREWS, R. C., Mechanical properties tests of 316 SS specimens in 1200°F Na contaminated with O, 20: 29704 (MSAR-66-78)
ANDREZEN, A. B., Dynamic stabilization of a direct discharge in a magnetic field, 20: 30698
ANDRONIKASHVILI, E. L., Nature of oscillations of He II near surface of vibrating disc, 20: 30308
ANDRONOV, A. A., Dipole resonance of plasma burst and coherent acceleration of plasma, 20: 30690
ANDRONOV, V. D., Estimates of Green's function for Helmholtz equation, 20: 30184
ANISHCHENKO, V. N., Effective magnetic field at ^{60}Co nucleus in Co–Pd alloy, 20: 30752
ANISKIN, E. D., Chemical protection against genetic changes, 20: 29045
ANKARA, Said-Ali, Weather prediction on basis of measurement of diminution of electrical conductivity of air, 20: 29402
ANNA, Yoshitoru, Effects of irradiation on Pinus desiflora and Pinus thunbergii, 20: 28980
ANSELM, A. A., Calculation of Σ^+- and Σ^--hyperon mass difference, 20: 30059
ANTILL, J. E., Oxidation of UN and U(CO) in carbon dioxide, steam, and water, 20: 29645
ANTIPOV, V. V., Chemical protection against genetic changes, 20: 29045
ANTIPOV, V. V., Effects of cosmic flight on Tradescantia paludosa microspores, 20: 28971
ANTONOVA, A. E., Formation of radiation zones as result of particle drift in depths of magnetosphere, 20: 30207 (NASA-TT-F-389, pp 442-53)
ANTONOVA, L. A., Soft electron streams in upper atmosphere at altitudes to 500 km, 20: 30203 (NASA-TT-F-389, pp 288-91)
ANZAI, Ikuro, Practical applications of glass dosimetry, 20: 29547
ARAD, B., Study of nuclear resonant scattering using neutron-capture γ rays, 20: 30467
ARANOVITCH, Eric, Devices for adjusting relative positions of fuel elements in reactor, 20: 30829
ARAS, Nemik K., Nuclear levels of ^{101}Ru populated in decay of ^{101}Rh isomers, 20: 30469
ARGERSINGER, John I., Control of nuclear power plant, 20: 30832
ARIFOV, U. A., Registration of secondary-electron current with scintillation counter, 20: 29538
ARIKAWA, Tetsuo, Momentum compaction in a cyclic accelerator, 20: 29861
ARIPOV, R., Production of slow π^+ mesons by 9-Bev proton interaction with photoemulsion nuclei, 20: 30370
ARMSTRONG, Edward, Improvements in or relating to thermal insulation, 20: 30820
ARNOLD, J. I., Irradiation performance of Piqua fuel elements, 20: 30881 (NAA-SR-11712)
ARNOLD, S. V., Production of tungsten sheet bars by zone refining of cemented tungsten-base alloys, 20: 29688
ARNOLD, William H. Jr., Integral vapor generating and superheating reactor system, 20: 30919
ARNTZEN, J. D., Pilot-plant gettering system of Ti-metal sponge for removal of N from Ar, 20: 29329 (ANL-7128)
ARONOV, D. A., Absorption effect on surfaces of semiconductors and gels due to effects of radiation, 20: 29815
ARONSON, S., Bonding energy in Cs-graphite compounds, 20: 29744
ARONSON, S., Mechanism of bromine exchange in bromine–graphite lamellar compounds, 20: 29182
AR-RASHID, Harun, Regge pole behavior in an SL(2,C) model field theory, 20: 30087 (IC–66/46)
ARSENAULT, R. J., Thermally activated deformation in tantalum and tantalum-base alloys, 20: 29724
ARTEMENKOV, L. I., Production of a hot plasma in Ogra-II by injection of fast H atoms into magnetic trap, 20: 30633
ARTEMOV, Yu. M., Use of standard in solid phase for quantitative argon determination by method of isotope dilution, 20: 29102
ARTLEY, John L., Prog. rpt. on superconducting circuitry, 5/66, 20: 30255 (ORO-2430-28)
ARTSIMOVICH, L. A., Joule heating of plasma in toroidal Takamak-3 device, 20: 30650
ARUJA, E., Electron-single-scatter-gage, 20: 29600
ASADA, Tsunesaburo, Accumulation of electric charge in glass for γ shielding window by γ irradiation, 20: 30727
ASCOLI-BARTOLI, U., Formation and development of hydromagnetic disturbances during implosion phase of a preionized theta pinch (Cariddi), 20: 30613
ASCOLI-BARTOLI, U., Hot-ice experiment, 20: 30665
ASSAF, Walid Constantine, Application of dimensional analysis to radiation shielding, 20: 30730
ASTAKHOV, K. V., Cerium nitrilotriacetates, 20: 29228
ASTAKHOV, K. V., Complex formation of rare earths with EDTA, 20: 29222
ATKINS, A. G., Friction and hardness of refractory compounds, 20: 29771
ATKINS, H. L., Scanning of liver, spleen and bone marrow with colloidal ^{99m}Tc, 20: 29065

AU, Guenther F., Research on electric drives for space vehicles, 20: 29394
AUCHAMPAUGH, G. F., Neutron total cross section of ^{242}Pu, 20: 30465
AUER-WELSBACH, H., Quantitative activation analytical purity determination of rare earth oxides, 20: 29082 (SGAE-CH-27/1966)
AVAKYAN, V. A., Effect of x-irradiation on yield of potatoes, 20: 28966
AVDYUSHIN, S. I., Recording cosmic rays on Cosmos-17 satellite, 20: 29966
AVILA, C., Collisional Stark broadening in r-f discharges, 20: 30572
AXE, J. D., Lattice spectrum and dielectric properties of EuF_2, 20: 30746
AYVAZYAN, Yu. M., Emission of point charged particle passing along axis of semi-infinite waveguide, 20: 29828
AZIMOV, M. A., Differential cross section of charge exchange of 4.8-Bev/c π^- mesons with protons, 20: 29998
AZIMOV, S. A., Azimuthal angular distribution of slow particles produced by nuclear interactions with heavy emulsion nuclei at high energies, 20: 30371
AZIMOV, S. A., Production of slow π^+ mesons by 9-Bev proton interaction with photoemulsion nuclei, 20: 30370
AZZONI, A., Ratemeter for variable flow measurements, 20: 29535

B

BAARLI, J., Health physics survey methods for measurement of stray radiation around CERN high-energy accelerators, 20: 29844 (CONF-651109, pp 103-16)
BABAEV, A. I., Experimental investigation of chemical reactions involving muonium, 20: 29247
BABAL'YANTS, V. F., Ion source of hydrogen ions at low gas pressures, 20: 29925
BABCOCK, S. G., Compressive strain rate tests on four composites, Phase I, 20: 29708 (SC-DC-65-1744)
BABICHEV, A. P., Injection of plasma blobs into mirror trap with adiabatic plasma compression: Aspa device, 20: 30636
BABYKIN, M. V., Turbulent heating of plasma by direct-current discharge, 20: 30661
BACCHETTI, Silvio, Recovery from x-ray-induced sub-lethal damage in Saccharomyces cerevisiae cells of different ploidy, 20: 28961
BACHMANN, O., Separation of ^{14}C-compounds in gaseous phase, 20: 29089
BAECHMANN, K., Use of high-voltage electrophoresis for the separation of radionuclides, 20: 29356
BAECKSTROEM, G., Positrons and conversion electrons from ^{90}Mo decay, 20: 30388
BAEZ, Juan N., Separation of ^{90}Sr and ^{90}Y in the presence of Ca by paper chromatography, 20: 29349
BAGNALL, K. W., Chemistry of selenium, tellurium and polonium, 20: 29235
BAGRAMYAN, E. R., Metabolism of exogenous ACTH in normal and irradiated rats, 20: 29005
BAHCALL, John N., Absorption lines in the spectra of distant sources, 20: 29890
BAILEY, J. M., Muonium chemistry, 20: 29177
BAISCH, Roderich, Power supply system for Siemens-Schuckert Research Centre, 20: 29368
BAKAKIN, V. V., Crystallochemical properties of cubic-shaped hydrated uranium tetrafluoride, 20: 29231
BAKANIDZE, I. G., Therapeutic effectiveness of antibiotics on cystamine action during radiation sickness, 20: 29051
BAKANOV, S. P., Oscillations of plasma in constant external electric and magnetic fields, 20: 30677
BAKER, L. Jr., Isothermal reaction of U with steam between 400 and 1600°C, 20: 29188
BAKER, Louis Jr., Nonisothermal reaction of uranium with water by the condenser discharge method, 20: 29189
BAKSHT, F. G., Removal of energy from plasma of a thermoelectric converter, 20: 29981
BAKUNOV, V. S., Electric conductivity and creep of sintered CeO_2 during reduction, 20: 29739
BALAKAEVA, T. A., Thorium orthophosphates, 20: 29160
BALATS, M. Ya., Experimental investigation of chemical reactions involving muonium, 20: 29247
BALCOMB, J. D., Propulsion reactor temperature control with internal power loop eliminated, 20: 30924 (LA-DC-7636)
BALDERMAN, J., Study of nuclear resonant scattering using neutron-capture γ rays, 20: 30467
BALDIN, A. M., Electromagnetic interactions in quark model, 20: 30112
BALKAREI, Yu. M., Lattice stability in phononless mechanism of superconductivity, 20: 30264
BALL, G. C., J dependence in $(^3He,\alpha)$ reaction and assignments in ^{14}N and ^{13}C, 20: 30438
BALL, R. M., Indian Point Reactor—instrumentation asymmetry response verification, 20: 30876 (BAW-1302)
BALL, S. J., Simulators for training MSRE operators, 20: 30934 (ORNL-TM-1445)
BALLESTRACCI, Regis, Sulfide compounds of rare earths and silver of type $AgTS_2$, 20: 29158
BALYASNYI, N. D., Statistical errors in determining concentrations of radioactive elements in rocks using γ-threshold and differential spectrometers, 20: 29421
BANKSTON, Charles A. Jr., Fluid friction, heat transfer turbulence, and interchannel flow stability in transition from turbulent to laminar flow in tubes, 20: 29384
BANNER, M., Search for an isobar of isotopic spin $T = 5/2$, 20: 30022
BANYAI, L., Irreducible tensors for group SU_3, 20: 30102
BANYAI, L., One-particle-exchange model for bootstrap, 20: 30035
BARA, J., Moessbauer effect for ^{57}Fe impurity atoms, 20: 30766
BARANGER, E., Shell-model calculations using realistic interactions, 20: 30384
BAREGAMYAN, V. A., Radiation from electrons moving parallel to metal grid located on edge of uniaxial crystal of finite thickness, 20: 29995
BARGER, V., Forward elastic scattering at high energy in SU(3) Regge-pole model, 20: 30039
BARGERY, J., Leak detection in ultra-high vacuum systems attaining 10^{-8} to 10^{-12} torr, 20: 29496
BARIAUD, A., Injection of ions into a magnetic mirror machine (M.M.I.I.), 20: 30634
BARKER, S. M., Resistivities and lattice parameters of Pd and Nb alloys, 20: 29766
BARKOV, V. I., Coronal solar radiation in continuous spectrum, 20: 29904
BARNABA, P., Main-chain scission and ESR spectra of irradiated polytetrafluoroethylene oxide, 20: 29267
BARNABY, C. F., Liquid scintillatiors based on medicinal paraffin for use in whole-body counters, 20: 29541
BARNES, C. Jr., Isothermal reaction of U with steam between 400 and 1600°C, 20: 29188
BARON, N., Inelastic α-particle excitation in even tin isotopes, 20: 30468
BAR-OR, A., Pearlite reaction in some U–Cr alloys, 20: 29747
BARR, L. W., Effect of surface evaporation on diffusion measured by isotopic exchange reactions, 20: 29731
BARR, R. Q., Recent developments in technology of arc-cast Mo, 20: 29756
BARRETT, M. J., Shielding aspects of accelerator facility design, 20: 30720 (CONF-651109, pp 410-16)
BARRIERE, Andre, Composite guide tube for reactors, 20: 30830
BARRINGER, H. S., Indian Point Reactor—instrumentation asymmetry response verification, 20: 30876 (BAW-1302)
BARRINGER, Howard S., Fast breeder reactor and method of operation, 20: 30914
BARRY, Edward G., Radiation resistant lubricating oil, 20: 29323
BARSCHALL, H. H., Scattering of neutrons by α particles, 20: 30390
BARSUKOV, K. A., Radiation of charge moving above an anisotropically conducting plane, 20: 29836
BART, Carol A., Stability of Drosophila chromosomes to radioactive decay of incorporated ^{32}P, 20: 28955
BARTON, G., Neutron-proton mass difference according to bound-state model, 20: 30042
BASOVA, E. N., Differential cross section of charge exchange of 4.8-Bev/c π^- mesons with protons, 20: 29998
BASSANI, G., Spectroscopic information on samarium isotopes from analog-state experiments, 20: 30430
BASSO, Michael J., Charge-carrier collection from inside and outside the space-charge region, 20: 29550
BASSON, R. A., Yields and rate constants of precursors of hydrogen in radiolysis of n-propanol, 20: 29286
BATALIN, V. A., Pierce optics of beam with finite phase volume, 20: 29871
BATANOV, G. M., Injection and confinement of plasma in a stellarator with a multipolar ($l = 2$) helical field, 20: 30657
BATCH, M. L., Indian Point Reactor—instrumentation asymmetry response verification, 20: 30876 (BAW-1302)
BATCH, M. L., Lumped burnable poison program, 20: 30836 (BAW-3492-1)
BATENBURG, A., Automatic control of rod position with boron in a chemical shim nuclear plant, 20: 30808 (WCAP-3269-54)
BATES, D. D., Thermal cycle degradation of charge carrier lifetime and resistivity in Si, 20: 30785
BATSANOV, S. S., Solid phases of $NH_4F–UO_3–H_2O$ systems, 20: 29200
BAUSCH, R., Motion laws of unclosed quantum systems, 20: 30249
BAVETTA, Lucien A., Collagen and hexosamine changes in subcutaneous granuloma irradiated locally with ^{60}Co source, 20: 28917
BAYANOV, A. P., Distribution of erbium in molten Al–Cd, Al–Pb, and Al–Bi alloys, 20: 29797
BAYBARZ, R. D., Preparation of Cm hydroxide sol-gel spheres as intermediate to CmO_2 microsphere preparation, 20: 29165
BAYLY, Russell J., Labeled compounds in medical diagnosis, 20: 29066
BAYMAN, B. F., Isobaric spin in stripping and pickup reactions, 20: 30343

(COO-1371-30)
BAYUKOV, Yu. D., Accuracy of particle trajectory location in spark chamber, 20: 29527 (ITEF-341)
BAYUKOV, Yu. D., Proton elastic scattering on deuterons at large angles, 20: 29989 (ITEF-361)
BEALS, Robert J., Elasticity and anelasticity of uranium oxides at room temperature, 20: 29698 (ANL-7101)
BEAN, C. H., Fabrication of spiked-core fuel elements for EBWR, 20: 29658 (ANL-6283)
BEAN, C. P., Effect of thermal-neutron irradiation on superconducting properties of Nb_3Al and V_3Si doped with fissionable impurities, 20: 30260
BEATTY, R. A., Fabrication of spiked-core fuel elements for EBWR, 20: 29658 (ANL-6283)
BEAUMARIAGE, M. L., Content of catecholamines of heart and superarenals of rat after irradiation, 20: 28964
BEAVER, W. W., Development of intermetallic compounds for aerospace applications, 20: 29770
BECHER, H. J., Systems Ni–Be–B and Co–Be–B, 20: 29795
BECK, G., Pulse-radiolysis studies on reactivity of catalase with hydrated electrons and free OH radicals, 20: 29279
BECKER, E., Common radiation sources for crude structure tests, 20: 29390
BECKER, J. A., Low-lying states of ^{33}S, 20: 30455
BEDE, G., Critical size and flux distribution of hollow spherical and cylindrical reactors, 20: 30856
BEDER, Douglas Stanley, Two studies of dynamical calculations in two meson systems, 20: 30161
BEDNAROVA-NOVAKOVA, Bohumila, Method of forecasting geomagnetic activity and its practical try-out, 20: 30226
BEER, H., Gamma-γ angular correlation of ^{144}Pr at 54 to 80 kev, 20: 30506
BEGLEY, R. T., Precipitation hardening Nb–Hf–N alloys, 20: 29759
BEGZHANOV, R. B., E2 transitions from 3⁺ level of even-even nuclei, 20: 30372
BEHRENS, H., Asymmetry coefficients of β-γ circular polarization correlation, 20: 30542
BEIDLER, E. A., Fluoride tungsten, 20: 29687
BELITZ, R. J., Stable and unstable behavior of preheated plasma in linear and cusped theta pinches, 20: 30614
BELKIND, A., Multipurpose relaxation apparatus for measuring signs of elementary processes in ionic crystals subjected to ionizing radiation, 20: 30754
BELL, Alan, Forced-flow, once-through vapor generator, 20: 30821
BELL, Eric Brayton, Measurement of concentration of liquid components of mixture of liquids by nuclear radiation, 20: 29570
BELOOZEROV, V. N., Method of images in magnetostatic problems involving a spherical superconductive boundary, 20: 30310
BELOTE, T. A., Reaction $^{42}Ca(d,p)^{43}Ca$ at 7.0 and 7.2 Mev, 20: 30452
BELTRAM, C., Development of ThO_2 pellet fabrication, 20: 29657
BEL'TYUKOVA, S. V., Determination of yttrium and rare earth elements of yttrium subgroup in ores, 20: 29134
BELYAEV, V. A., Measurement of cross sections of ion-atom collisions at low energies by overtaking beams, 20: 29932
BELYAEVSKII, A. I., Possible antimatter nature of micrometeors, 20: 29895
BEM, Ya., Formation of electron-positron pairs by high-energy gamma quanta, 20: 29990 (JINR-P-2667)
BEN-DAVID, G., Study of nuclear resonant scattering using neutron-capture γ rays, 20: 30467
BENESOVSKY, F., Oxygen determination in high-melting metals, 20: 29108
BENESOVSKY, F., Plansee proceedings, 1964, Reutte/Tyrok, 6/64, 20: 29680
BENESOVSKY, F., Processes for degassing of niobium and tantalum, 20: 29633
BENESOVSKY, F., Protective layer problems with high-temperature materials, 20: 29650
BENESOVSKY, F., Protective coatings for niobium and its alloys, 20: 29651
BENEZECH, G., High-energy particle spectrometry using activation detectors, 20: 29521 (CONF-651109, pp 213-23)
BENNETT, E. W., Prompt air fluorescence excited by high-altitude nuclear explosions, 20: 30193 (LA-3409(Suppl.))
BENNETT, Edgar F., Electron multiplication process in proportional counters, 20: 29554
BEONE, G., Filterability and coalescence time of colloidal solutions of $ANN–HNO_3–Hg^{2+}–SiO_2$, 20: 29333 (RT-CHI-(65)33)
BERESTETSKY, V. B., C-parity violation and neutral particles production in colliding electron-positron beams, 20: 30012
BEREZHETSKII, M. S., Injection and confinement of plasma in a stellarator with a multipolar (l = 2) helical field, 20: 30657
BEREZIN, A. K., Collective interaction of modulated and unmodulated electron beams with plasma, 20: 30623
BEREZINA, G. P., Collective interaction of modulated and unmodulated electron beams with plasma, 20: 30623
BEREZNYAK, N. G., Visual solidification of He isotope solutions, 20: 30307
BERGHEZAN, A., Deformation properties of Nb, 20: 29761
BERGLES, A. E., Prog. rpt. on boiling flow regimes and critical heat flux, 9/16–12/15/65, 20: 29378 (NYO-3304-7)
BERGMAN, C., Positrons and conversion electrons from ^{99}Mo decay, 20: 30388
BERGSNOV-HANSEN, B., Absorption, degassing, and solution equilibrium in the N–Nb system at ultrahigh vacuum and high temperature, 20: 29178
BERK, Sigmund, Radiation backscattering and radiation-induced x rays for measuring surface composition and structure, 20: 29754
BERKOWITZ, Edward Howard, Four-parameter coincidence studies of reaction $^6Li(^6Li,\alpha)2\alpha$, 20: 30530
BERLIN, I. K., Reduction of tantalum from tantalum pentoxide by the carbothermal method, 20: 29678
BERLOVSKII, A. Ya., Calculation of doses in x and gamma irradiations through screens, 20: 29056
BERMAN, A. S., Flow and self-diffusion of gases in capillaries. I., 20: 30174
BERMAN, A. S., Flow and self-diffusion of gases in capillaries. II., 20: 30175
BERMANIS, H. L., Boron assay in stainless steel, 20: 29117
BERNARD, M., Stability of a diffusing plasma, 20: 30621
BERNASHEVSKII, G. A., Plasma and electron uhf amplifiers and generators, 20: 29500
BERNSTEIN, W., Plasma produced by neutral injection into magnetic mirror/well geometry, 20: 30632
BERONIUS, Per, Kinetic studies of moderately rapid isotopic exchange reactions, 20: 29207
BERTAUT, Erwin Felix, Determination of the structure of La_2TiO_5 with x rays and neutrons, 20: 30738
BERTHELOT, Ch. A., Graphical representation of ionization temperature of plasma applications, 20: 30604
BERTINI, Hugo W., Effect of error on results of a low-energy intranuclear cascade calculation, 20: 30725 (ORNL-3786)
BERTMAN, B., Surface currents magnetization of hysteretic superconductors, 20: 30269
BERTMAN, B., Susceptibility transition (a-c) in type-II superconductors and surface critical currents, 20: 30293
BERTOLINI, G., Time resolution measurements with fast photomultipliers, 20: 29568
BERTRAM, W., Production of antiprotons by high-energy photons, 20: 30432
BESENBRUCH, G., Mass-spectrometric studies at high temperatures. X., 20: 29183
BESSON, Jean, Hydrolysis of U–Th–C alloys rich in C, 20: 29159
BESYADOVSKII, R. A., Damaging effects of underwater nuclear explosion, 20: 29481
BETEV, B., Daily variation of extensive air showers, 20: 29960
BETSER, A. A., Effects of temperature and heat treatment on strength of sintered WC–Co alloys, 20: 29802
BETZ, E. H., Chronic radiation effects: damage of hematopoiesis, 20: 28984
BEVERLY, R. G., Current practices in the disposal of radioactive wastes from operation of uranium mines and mills, 20: 30948
BEVERLY, R. G., Current practices in disposal of waste radioactive gases from reactors, 20: 30949
BEZOTOSNYI, V. M., Cross sections for production of γ-quanta in inelastic interactions of 14-Mev neutrons with C, O, Al, Fe, and Pb, 20: 30498
BEZRUKIKH, V. V., Comparison of simultaneous measurements of magnetic field and positive ion streams within earth's magnetosphere, 20: 30208 (NASA-TT-F-389, pp 457-63)
BEZRUKIKH, V. V., Possible existence of soft electron component in outer radiation zone, 20: 30213 (NASA-TT-F-389, pp 566-8)
BEZ'YAZCHNYI, I. A., Collective interaction of modulated and unmodulated electron beams with plasma, 20: 30623
BHADRA, Dilip Kumar, Collisional effects on plasma stability, 20: 30709
BHAKAR, B. S., Difference of binding energies of ^3H and ^3He nuclei, 20: 30424
BHAKAR, B. S., Mixing model of intermediate vector bosons, 20: 30133
BHANDARI, A. M., Organic compounds of U. I., 20: 29155
BHARGAVA, P. C., Binding and saturation of nuclear matter, 20: 30434
BHASIN, V. S., Difference of binding energies of ^3H and ^3He nuclei, 20: 30424
BHAT, T. R., Rare earth trichloroacetates. I., 20: 29213
BHIDE, V. G., Temperature-dependent lifetimes of nonequilibrium Fe^{3+} ions in CoO from Moessbauer effect, 20: 29833
BHIDE, V. G., Temperature dependence of internal field at ^{57}Fe nucleus in Ni lattice, 20: 30750
BHOWMIK, B., Lambda-binding energies in heavy hyperfragments, 20: 30448
BIALAS, A., Elastic scattering ($p\bar{p}$) at high momentum transfer and the

Orear formula, 20: 30019
BICKERTON, R. J., Inter-diffusion of plasma and magnetic fields in pinch and hardcore discharges, 20: 30639
BIENLEIN, J. K., Future neutrino experiments, 20: 30002
BIERLEIN, Fred, Mechanical design of regenerative deflector for Berkeley 88-in. cyclotron, 20: 29856 (UCRL-16829)
BIGUET, A., Heating and containment of plasma in the magnetic well in Deca II, 20: 30607
BILDSTEIN, H., Quantitative activation analytical purity determination of rare earth oxides, 20: 29082 (SGAE-CH-27/1966)
BILLINGHAM, John, Method of evaluating radiation risks for manned space flights, 20: 29058
BINFORD, Thomas Oriel., Angular distribution and polarization of neutral hyperons produced in association with K^0 mesons, 20: 30071
BIRSAN, E. T., Decontamination of waters containing ^{90}Sr and ^{90}Y with gypsum and bentonites, 20: 29348
BIRSTEIN, L., Energy levels of ^{63}Zn, 20: 30406
BISHARA, R. H., Paper electrophoresis of steroids. I., 20: 29132
BISHOP, J. M., Strangeness-one resonances, 20: 30049
BISWAS, P. K., Integral conservation law in general relativity, 20: 30241
BIXBY, Henry D., Method and product for disposal of radioactive wastes, 20: 30951
BJERREGAARD, J. H., Proton pickup from the even lead nuclei, 20: 30387
BKHATTACHARIYA, Sudkhindra Nath, Radiolysis of concentrated aqueous solutions of isopropyl alcohol in presence of O, 20: 29277
BLACK, W. C., Low-temperature heat capacity of liquid ^3He, 20: 30283
BLAKE, A. R., Gamma radiolysis of carbon suboxide, 20: 29269
BLANC, P., Heating and containment of plasma in the magnetic well in Deca II, 20: 30607
BLANCO, R. E., Prog. rpt. on waste treatment and disposal, semiannual, 7–12/65, 20: 30943 (ORNL-TM-1465)
BLAU, R., Motion of elementary charged particles, 20: 30144
BLAUGHER, R. D., Magnetic instabilities and flux annihilation in grossly inhomogeneous superconductors, 20: 30261
BLAZEJ, A., Analysis of chromic salt solutions by means of β-ray backscattering, 20: 29107
BLECHINGER, F. K., Thermal expansion and temperature dependence of elastic moduli of polycrystalline hafnium, 20: 29703 (KAPL-3112)
BLEULER, E., Interaction π^+-π^- as studied in 12- and 18-Bev pion-nucleon reactions, 20: 30025
BLIN, Andre, Reliability of planar silicon transistors exposed to ^{60}Co gamma rays, 20: 29577 (CEA-R-2959)
BLINC, R., Lectures on solid-state physics. I., 20: 30783
BLINC, R., Lectures on solid-state physics. II., 20: 30784
BLISS, Joseph F., Neutron shielding composition having good high-temperature strength, 20: 30732
BLOCHER, J. M. Jr., Fluoride tungsten, 20: 29687
BLOCK, F. E., Nonmetallic powders coated with tungsten and molybdenum, 20: 29631
BLOKH, Ya. L., Cosmic ray nuclear component on Elektron-2, 20: 29957 (NASA-TT-F-389, pp 693-710)
BLOOD, R. E., Prog. rpt. on Zr alloy, 20: 29660 (GEAP-4960)
BLOOMBERG, H., Inhomogeneous development of a plasma through quasi-linear theory, 20: 30562 (MPI-PAE-P1/25/66)
BLOOMQUIST, C. A. A., Separation of americium and curium by extraction chromatography, 20: 29337
BLUDMAN, S. A., Spontaneously broken symmetries and question of massless particles in model field theory, 20: 30135
BLUM, Pierre L., Hydrolysis of U–Th–C alloys rich in C, 20: 29159
BOBLETER, O., Adsorption of Np(V) on anion exchangers, 20: 29358
BOBLETER, O., Separation of Pu, Np, Zr, Nb, Mo, Tc, Te, and U from fission-product solutions, 20: 29357
BOCHKAREV, V. V., Coefficient of β backscattering from aluminum backing in 2π geometry, 20: 30369
BODENHEIMER, Peter, Studies in stellar evolution. IV., 20: 29884
BODIN, H. A. B., Plasma containment and stability in megajoule theta-pinch experiment, 20: 30610
BODNER, Stephen E., Random phase approximation, 20: 30567 (UCRL-14246)
BOECKER, Bruce Bernard, Thorium inhalation studies, 20: 28897
BOENZI, D., New experimental data on the decontamination of protective clothing, 20: 29477
BOERBOOM, A. J. H., Gross- and partial-ionization cross sections for electrons on water vapor, 20: 29928
BOGART, Donald, Boron cross sections as source of discrepancy for capture cross sections in kev region, 20: 30352 (NASA-TR-R-240)
BOGDANOV, A. P., Certain problems in dynamic and static pressing of metallic powders, 20: 29679
BOGDANOV, E. V., Plasma and electron uhf amplifiers and generators, 20: 29500
BOGEN, P., Stable and unstable behavior of preheated plasma in linear and cusped theta pinches, 20: 30614
BOGOROV, V. G., Radioactive contamination of oceans, 20: 29405 (NP-14694)
BOGOYAVLENSKII, I. V., Visual solidification of He isotope solutions, 20: 30307
BOKOV, O. G., Leptonic decays of baryons in universal V-A theory, 20: 30058
BOKROS, J. C., Deformation and fracture of pyrolytic carbons deposited in fluidized bed, 20: 29736
BOLAND, T. J., Noise study, ARMF-II, 20: 30837 (IDO-17169)
BOLOTIN, H. H., Level structure in ^{52}Cr populated in 5.7-day ^{52}Mn decay, 20: 30458
BOLOTIN, L. I., Collective interaction of modulated and unmodulated electron beams with plasma, 20: 30623
BOLOTIN, L. I., Suppression of low-frequency oscillations in two-stream instability by prior modulation of electron beam, 20: 30591
BOL'SHOV, V. G., Work function of refractory-metal carbides in cesium vapors, 20: 29800
BOLYUNOVA, A. D., Corpuscle investigations on Elektron-1, 20: 30212 (NASA-TT-F-389, pp 551-66)
BOLYUNOVA, A. D., Radioactivity of Cosmos III after explosion of July 9, 1962, 20: 30234
BOND, G. W., Materials applications for nuclear power plants from viewpoint of engineer-constructor, 20: 30815
BONE, L. I., Xenon-sensitized radiolysis of propane, 20: 29266
BONGIOVANNI, Alfred M., Kinetics of calcium metabolism in children utilizing nonradioactive Sr, 20: 28889
BONNAURE, Pierre, Devices for adjusting relative positions of fuel elements in reactor, 20: 30829
BOPP, Fritz, Regularized delta functions, 20: 30152
BORGARDT, A. A., Bosons in the field of plane electromagnetic wave, 20: 30155
BORGESON, M. E., Design criteria, plutonium buy-back facility, 20: 29451 (RL-SEP-590)
BORISOV, S. V., Crystallochemical properties of cubic-shaped hydrated uranium tetrafluoride, 20: 29231
BORN, H. J., Radiochemical separation of ^{18}F from reactor irradiated gold and uranium, 20: 29338
BORODIN, V. S., Discharge in a hollow cathode. I., 20: 30688
BOROVIK, E. S., Cryogenic magnetic trap VGL-2, 20: 30655
BOROVIKOV, A. P., Measurement of λ transition temperature and density of liquid ^4He, 20: 30306
BOSE, H. N., Thermoluminescence spectra of CaF_2 irradiated by x rays, 20: 30767
BOSHART, R. R., Rectification process at metal-Si surface barriers, 20: 29569
BOSSAERT, Walter, Absolute detection efficiencies of cylindrical scintillation gamma-ray detectors, 20: 29562
BOULGER, F. W., Machining and grinding of nickel- and cobalt-base alloys, 20: 29665 (RSIC-482)
BOURKE, W. P., Anomalies in reaction $^{16}O(^3He,\alpha_0)^{15}O$, 20: 30433
BOURNE, J. G., Prog. rpt. on boiling flow regimes and critical heat flux, 9/16–12/15/65, 20: 29378 (NYO-3304-7)
BOUZYK, J., Multiplication method of reactivity measurements, 20: 30849
BOVALLIUS, A., Solubilization of cholinesterase from plaice muscle by bacteria, 20: 28933
BOWMAN, C. D., Neutron total cross section of ^{242}Pu, 20: 30465
BOYADJIEVA, R., Content of rare earths in igneous rocks G-1, W-1, and G-B, 20: 29101
BOYD, E. L., NMR studies of materials containing divalent europium, 20: 30761
BOYD, R. G., Eddy currents in type II superconductors induced by fast-pulsed magnetic fields, 20: 30262
BRADY, Franklin P., Radially collimating window for well-tool orienting instruments, 20: 29517
BRAIER, H. A., Activation analysis for chlorine in petroleum products and related materials, 20: 29116
BRAMSON, P. E., Pulsed reactor tests of dosimeters, 20: 29518 (BNWL-SA-27)
BRANCA, F. Paolo, Safety measures with regard to use of radioisotopes, 20: 29478
BRANCA, G., New experimental data on the decontamination of protective clothing, 20: 29477
BRANDT, Lars, Fluoride and sulfate complexes of Np(IV), 20: 29148
BRANDT, Peter Juergen, Separation and determination of traces of Sr in calcareous media, 20: 29363
BRANDT, Reinhard, Methods for high energy experiments on heavy nuclei using mica detectors, 20: 29551
BRANDT, W., Binding effects in electronic excitations by heavy charged particles, 20: 29936
BRAUER, G., Reactions of zirconium–molybdenum alloys with hydrogen and with nitrogen, 20: 29632
BRAUN, H., Recent developments in technology of arc-cast Mo, 20: 29756
BRAUN, Joann T., Acatalasemic and hypocatalasemic mouse mutants, 20: 28957

BRAUN, M. A., Nonrelativistic theory of scattering on composite particle with low binding energy, 20: 30150
BRAY, K. H., Anomalies in reaction $^{16}O(^3He,\alpha_0)^{15}O$, 20: 30433
BRDAR, B., Resynthesis of DNA and 50-S ribosomal RNA in uv-irradiated E. coli, 20: 28949
BRECKON, D. G., Operational procedures for NRX and NRU reactors, 20: 30935
BREDOV, M. M., Possible antimatter nature of micrometeors, 20: 29895
BREGER, A. Kh., Preparation of ion-exchange membrane by pre-irradiation method, 20: 29308
BREIZY, C. E., Prog. rpt. on fast ceramic reactor development, 8–10/65, 20: 29618 (GEAP-4982)
BRETTHAUER, E. W., Sampling airborne radioiodine in organic compounds, 20: 29467
BREUS, S. N., Interaction between h-f waves and plasma in Delta-2, 20: 30624
BREUS, T. K., Physical experiments on Kosmos-2 in ionosphere, 20: 30198 (NASA-TT-F-389, pp 202-24)
BREZHNEV, B. G., Measurement of cross sections of ion-atom collisions at low energies by overtaking beams, 20: 29932
BRICKA, M., High-energy particle spectrometry using activation detectors, 20: 29521 (CONF-651109, pp 213-23)
BRIENZA, M. J., Hot electron range in thin metal films, 20: 29952
BRIFFOD, C., Stability of a diffusing plasma, 20: 30621
BRIGGS, R. J., Experiments on surface wave propagation along annular plasma columns, 20: 30574
BRIGGS, R. J., Experimental studies with Astron, 20: 30637
BRIGGS, R. J., Stabilization of intense coasting beams in particle accelerators by inductive walls, 20: 29860
BRIL, M. N., X-ray L_{III} spectra of Gd absorption in hydrides, 20: 29162
BRILL, Edward F., Construction of MHD electrical power generator, 20: 29984
BRIXNER, L. H., Segregation coefficients of some rare earth niobates in $SrMoO_4$, 20: 29746
BROOKES, C. A., Friction and hardness of refractory compounds, 20: 29771
BROOKS, F. D., Eta and neutron cross sections of ^{235}U from 0.03 to 200 ev, 20: 30342 (AERE-M-1670)
BROOME, F. H., Average-radius gage, 20: 29668 (Y-NA-18)
BROWN, C. R., Magnetic field repulsion by a superconducting split cylinder, 20: 30276
BROWN, E. A., Propulsion reactor temperature control with internal power loop eliminated, 20: 30924 (LA-DC-7636)
BROWN, I. H., Photochemistry of uridylyl(3′→5′)-uridine, 20: 28910
BROWN, P. S., Prog. rpt. on particle fallout and dispersion in atmosphere, 9–11/65, 20: 29454 (SC-CR-66-2010)
BROWN, R. H., Noise study, ARMF-II, 20: 30837 (IDO-17169)
BROWN, Robert L., L-uncoupling effects on EPR spectra of $^{14}N^{16}O$ and $^{15}N^{16}O$, 20: 29194
BROWN, Robert Theodore, Configuration interaction in two- and three-electron atoms, 20: 29917 (TID-22957)
BRUECKNER, Keith A., Present status of theory of nuclear structure, 20: 30511
BRUECKNER, Keith A., Properties of liquid He-three, 20: 30188
BRUECKNER, Keith A., Theory of correlated crystals, 20: 30781
BRUENING, R., Polarization of neutrons from $^{15}N(d,n)^{16}O$ reaction, 20: 30427
BRUK, M. A., Radiation-induced polymerization of tetrafluoroethylene and acryloniitrile at 4.2 K, 20: 29300
BRUNO, Fred P., Automatic depth-dose acquisition system, 20: 29070
BRUSSEL, M. K., Polarization in the elastic scattering of protons from carbon and nitrogen, 20: 30457
BRYAN, R., Pole contributions to N-N scattering below pion production, 20: 29985 (CONF-640509(Pt.1), Paper 1)
BUCCELLA, F., KN dispersion relations and symmetry groups, 20: 30018
BUCHANAN, R. A., Infrared absorption of Ce^{3+} in LaF_3 and of CeF_3, 20: 29173
BUCK, K. E., Undersea role for isotopic power, 20: 29607
BUCKA, H., Fine and hyperfine structure of 3^2P term in Li, 20: 29939
BUCKEL, W., Developments in connection with superconductors, 20: 30257
BUCKLAND, Ernest Clifford, Improvements in and relating to electric connectors, 20: 29511
BUCKLAND, Ernest Clifford, Improvements in and relating to electrical coupling devices, 20: 29512
BUCKWALTER, G. L., Confirmatory evidence for sidereal-time-dependent neutral component in cosmic rays, 20: 29968
BUCKWALTER, G. L., Evidence for sidereal-time-dependent cosmic-ray signal, 20: 29967
BUDICK, B., Fine and hyperfine structure of 3^2P term in Li, 20: 29939
BUDKER, G. I., Plasma with relativistic electrons in magnetic mirror trap, 20: 30638
BUDYRKO, L. I., Effects of γ- and ultraviolet rays on copper glycocol, 20: 29303
BUECHNER, W. W., Stripping analysis of (d,p) angular distributions from $^{37}Cl(d,p)^{38}Cl$ reaction, 20: 30391
BUECKLE, H., Protective layer problems with high-temperature materials, 20: 29650
BUEHRING, H., Re-evaluation of the coupling constant in β decay, 20: 30538
BUEHRING, W., Measurable quantities in nuclear β decay, 20: 30539
BUEKI, G., Critical size and flux distribution of hollow spherical and cylindrical reactors, 20: 30856
BUESSER, F. W., Polarization of neutrons from $^{15}N(d,n)^{16}O$ reaction, 20: 30427
BUGG, D. V., Nucleon-nucleon total cross sections from 1.1 to 8 Bev/c, 20: 30028
BUIS, G. R., Automatic control of rod position with boron in a chemical shim nuclear plant, 20: 30808 (WCAP-3269-54)
BUJOK, Jozef, Stress-induced variations in spectral distribution of γ radiation transmitted by graphitized carbon, 20: 29809
BUKAREV, V. A., Neutron radiography, 20: 29627
BUKHMAN, N. D., Changes in cholesterol level in blood following irradiation, 20: 28992
BULLOUGH, R., Elastic explosions in solids caused by radiation, 20: 30740
BUNATYAN, G. G., Capture of μ^- mesons by nuclei, 20: 30494
BURBIDGE, G. R., Nature of quasi-stellar objects, 20: 29877
BURGGER, R. M., Slow-neutron scattering by water, 20: 30330
BURLAKOVA, E. B., Free-radical reactions during exposure of model systems to irradiation, 20: 29037
BURLANT, William J., Process of coating exterior surface of articles with polymerizable coating material, 20: 29320
BURNET, George, Surface concentration changes during distillation of liquid metals, 20: 29346
BURNETT, R., Fluorine-19 nuclear relaxation time in $CaF_2:Nd$, 20: 30772
BURNHAM, Charles A., Radiation source measuring apparatus having automatic background subtract means, 20: 29571
BURYAK, E. M., Injection of plasma blobs into mirror trap with adiabatic plasma compression: Aspa device, 20: 30636
BUSCHHORN, G., Production of antiprotons by high-energy photons, 20: 30432
BUSH, S. F., Vibrational spectrum of hydrazine-d_4 and Raman study of hydrogen bonding in hydrazine, 20: 29175
BUSOL, F. I., Cryogenic magnetic trap VGL-2, 20: 30655
BUSS, W., Reaction $^9Be(d,\gamma)^{11}B$, 20: 30393
BUTUZOV, S. S., Achievement of ultrahigh vacuum in Ogra-1, 20: 30701
BUYRN, A. B., Moessbauer effect of 99- and 129-kev transitions in ^{195}Pt, 20: 30757
BYCHKOV, Yu. A., Electron spectrum in one-dimensional system with randomly arranged scattering centers, 20: 30113
BYLINSKII, A. F., Mutagenic efficiency of intermediate neutrons, 20: 29002

C

CALDWELL, D. O., Interaction π^+-π^- as studied in 12- and 18-Bev pion-nucleon reactions, 20: 30025
CALDWELL, Richard L., Method of compensating for iron casing effect in radioactive well logging, 20: 29442
CALDWELL, Richard L., Method of chlorine logging in nonferrous environment, 20: 29446
CALLAHAN, Andrew Charles, Measurement of K^+ decay branching ratios, 20: 30075
CALOGERO, F., Systematic iterative approach to problem of scattering on singular potentials, 20: 30136
CAMPBELL, Lawrence Joseph, Properties of liquid ^3He, 20: 30192
CAP, F., One-dimensional unsteady potential MHD flow, 20: 30570
CAPPS, Richard H., $SU(6)_W$ and meson resonances of even parity, 20: 30048
CARETTO, A. A. Jr., Reactions (p,n) between 100 and 400 Mev, 20: 30464
CAREY, W. M. Jr., Evidence for sidereal-time-dependent cosmic-ray signal, 20: 29967
CARLSON, David A., Shutdown apparatus for nuclear reactors, 20: 30835
CARLSON, Robert W., Steam-cooled reactor arrangement, 20: 30917
CARLVIK, Ingvar, Use of integral transport theory for calculation of neutron flux distribution in Wigner-Seitz cell, 20: 30854
CARMONY, D. D., Isospin of the A mesons, 20: 30023
CARNEIRO, A. R., Mechanical design of regenerative deflector for Berkeley 88-in. cyclotron, 20: 29856 (UCRL-16829)
CARNEVALE, E. H., Prog. rpt. on ultrasonic temperature measuring device, 1–4/66, 20: 29486 (NASA-CR-54964)
CARNICOM, Mina L., Reaction rates for high-temperature air, 20: 29146 (SC-R-66-885)
CARR, W. H., Policies and procedures used in the United States for decontaminating hot cells, 20: 29468
CARROLL, Edward E., Zirconium (n,p) cross section measurements, 20: 30418

CARROLL, J., Production of antiprotons by high-energy photons, 20: 30432
CARROLL, K. J., Automatic superconducting flux pump, 20: 30274
CARTA, Guy Rodney, Mutants of E. coli partially resistant to bacteriophage T1, 20: 29027
CASALI, F., Measurement of infinite multiplication constant of Latina lattice by null reactivity method, 20: 30887
CASPERS, H. H., Infrared absorption of Ce^{3+} in LaF_3 and of CeF_3, 20: 29173
CASS, Thomas Robert, Dislocation dipoles in deformed magnesium oxide, 20: 29711 (UCRL-11996)
CASSAGNOU, Y., Spectroscopic information on samarium isotopes from analog-state experiments, 20: 30430
CASTNER, Foster J., Neutron shielding composition having good high-temperature strength, 20: 30732
CATALA, J., Environmental radioactivity at Valencia during 1964, 20: 29408
CATICHA-ELLIS, S., Table of real part of dispersion correction for x-ray scattering, 20: 29722
CATOIU, E., Decomposition of zirconium silicate with potassium fluosilicate, 20: 29201
CATRINA, J., Factors affecting selective penetration of sodium pentachlorophenolate in wood, 20: 29161
CATTERALL, J. A., Resistivities and lattice parameters of Pd and Nb alloys, 20: 29766
CECCON, Alberto, Racemization and isotopic exchange with $Na^{35}SCN$ of 4-chlorobenzhydryl thiocyanate, 20: 29237
CEJPEK, J., Remark on F. Moringo's formula for amplitude of (d,n) Coulomb stripping, 20: 30426
CELINSKI, Z., Physical processes in magnetohydrodynamic generators, 20: 29979
CERCEK, B., Novel valence states of thallium as studied by pulse radiolysis, 20: 29271
CERMAK, V., Individual efficiency curves for excitation of 2^3S and 2^1S states of He by electron impact, 20: 29926
CERMAK, V., Retarding-potential measurement of kinetic energy of electrons released in Penning ionization, 20: 29927
CERNY, J., J dependence in $(^3He,\alpha)$ reaction and assignments in ^{14}N and ^{13}C, 20: 30438
CERRAI, E., Ionium/U method for the determination of the age of recent minerals, 20: 29441
CESSION-FOSSION, A., Content of catecholamines of heart and suprarenals of rat after irradiation, 20: 28964
CHADDERTON, Lewis T., Ionic displacement in alkali halides, 20: 30741
CHADHA, M. S., Synthesis of potential antiradiation agents. I., 20: 29241
CHAE, Song-cha, Paper partition chromatography of organic halogen compounds, 20: 29123
CHALOV, P. I., Deposition of atmospheric fallout by precipitation in subcloud layer, 20: 29416
CHAMBERLAIN, G. E., Inelastic electron scattering from H_2, 20: 29953
CHAMBERS, E. S., Ions and dissociation products obtained from a hydrogen r-f ion source, 20: 29920 (UCRL-14271)
CHAMBERS, E. S., Neutralization of fast H ions colliding with H_2, CO, CH_4, and H_2O molecules, 20: 29919 (UCRL-14214)
CHAN, Tsiu Chiu, Nonlinear phenomena in propagation of EM waves in weakly ionized gas, 20: 30190
CHANANA, A. D., Extracorporeal irradiation of blood, 20: 28927 (BNL-9647)
CHAND, T., Lambda-binding energies in heavy hyperfragments, 20: 30448
CHANG, Chien-er, Ligand field theory. I., 20: 29205
CHANG, N. C., Energy levels and crystal-field splittings of Nd^{3+} in Y oxide, 20: 30744
CHANG, Tseng-jui, Relation between chemical structure of alkyl dibutyl phosphonates and characteristics of U and Th extraction, 20: 29354
CHANG, Tsung-hsien, Therapeutic effect of single or multiple grafts of homologous marrow and antibiotics upon domestic rabbits after varying amounts of x-ray, 20: 29052
CHANG, Y. A., Thermodynamic considerations in selection of materials for high-temperature applications, 20: 29774
CHANG, Yuan-chin, Fluorescent measurement of negligible amounts of uranium in waste water, 20: 29128
CHAO, Hui-yang, Radiophosphorus in treatment of certain skin diseases, 20: 29072
CHAO, P. J., Fluidized-bed deposition of protective coatings on refractory metals, 20: 29630
CHAPERON, Edward Alfred, Recovery of thymectomized chickens from induced immunological unresponsiveness, 20: 29014
CHAPMAN, K. R., Reaction $d + d \rightarrow {}^4He + 2\pi$ at 1.69 Bev/c, 20: 30010
CHARAKHCH'YAN, A. N., Cosmic-ray generation on sun, 20: 29875 (NASA-TT-F-389, pp 732-9)
CHARAKHCH'YAN, T. N., Cosmic-ray generation on sun, 20: 29875 (NASA-TT-F-389, pp 732-9)
CHARAKHCH'YAN, T. N., Outer radiation zone of the earth and bursts of x-ray radiation in the stratosphere, 20: 30218 (NASA-TT-F-389, pp 616-23)
CHARAKHICH'YAN, A. N., Outer radiation zone of the earth and bursts of x-ray radiation in the stratosphere, 20: 30218 (NASA-TT-F-389, pp 616-23)
CHARBONNIERE, Robert, Effect of ^{60}Co γ radiation on amidon, 20: 29255
CHARLESBY, A., Gamma-ray thermoluminescence in nucleic acid constituents, 20: 28913
CHARLESWORTH, J. P., Superconducting transition temperatures of Nb_3Sn and $NbSn_2$, 20: 30279
CHASE, John W., Decay of ^{133}I to levels in ^{133}Xe, 20: 30473
CHASE, L. F. Jr., Low-lying states of ^{33}S, 20: 30455
CHATTARJI, Dipankar, Applications of symmetric Dirac-Coulomb Hamiltonian, 20: 29949
CHATTERJEE, S. D., Artificial radioactivity in rain-borne dust and in rain water observed in Calcutta during 1962, 20: 29420
CHATTERLEY, F. J., General-purpose multiple regression program, 20: 29613 (TRG-Report-1198)
CHATTERS, Roy M., Conference on radiocarbon and tritium dating, Sixth International, Washington State University, Pullman, Wash., 6/65, 20: 29438 (CONF-650652)
CHATWIN, W. H., Grain boundary holes in irradiated U, 20: 29807 (TRG-Report-325)
CHAUVIN, Michel, Support for liquid-cooled reactor bed, 20: 30827
CHECHKIN, V. V., Plasma produced by neutral injection into magnetic mirror/well geometry, 20: 30632
CHEEVER, D. L., Mechanical fastening of nickel-base alloys, 20: 29667 (RSIC-509)
CHEISHVILI, O. D., State of liquid He in the vicinity of λ line, 20: 30266
CHEN, Augustine Chen-hsin, Convergence of Born series for rearrangenent collisions, 20: 30162
CHEN, Fei-Shian, Coulomb corrections to β decay of ^{14}O, 20: 30443
CHEN, Hollis Huei-Ching, Radiation in a plasma environment with cylindrical boundaries, 20: 30711
CHERNAVSKII, D. S., Cross section of quark generation, 20: 29999
CHERNETSKII, A. V., Location of moving plasma bursts from coaxial injector, 20: 30681
CHERNOV, I. G., Double focusing in mass spectrometers with an inhomogeneous magnetic field, 20: 29493
CHERNOV, I. P., Cross section for elastic scattering of 13.6-Mev deuterons by Ti, Fe, and Co, 20: 30497
CHERNOV, Z. S., Plasma and electron uhf amplifiers and generators, 20: 29500
CHERNYAK, I. V., Radiation-induced polymerization of tetrafluoroethylene and acrylonitrile at 4.2 K, 20: 29300
CHERNYAKOV, E. I., Radiation from electrons moving parallel to metal grid located on edge of uniaxial crystal of finite thickness, 20: 29995
CHERNYAKOV, E. I., Radiation of electromagnetic waves by electron sheet moving above diffraction grating, 20: 30250
CHESTER, Arthur Noble, Regge poles in field theory and criteria for elementarity, 20: 30163
CHEW, G. F., Bootstrapping with the Regge boundary condition, 20: 30066
CHEW, G. F., Nuclear democracy, Regge poles and analytic S-matrix, 20: 30065
CHEZE, J., Search for an isobar of isotopic spin $T = {}^3/_2$, 20: 30022
CHI, Benjamin E., Single-particle energy levels in Nilsson well, 20: 30392
CHIAKI, Hideo, Determination of trace salt by bremsstrahlung x-rays, induced beta particles, and precision analysis of the measurements, 20: 29103
CHIEFFE, John F., Protective lightway for fallout shelters, 20: 29483
CHILOSI, G., Nuclear levels of ^{101}Ru populated in decay of ^{101}Rh isoners, 20: 30469
CHIN, P. H., Transfer of myeloma protein synthesis with RNA from C_3H plasma cell tumor. I., 20: 28926 (AD-633469)
CHIN, Wei-ch'iao, Radiophosphorus in treatment of certain skin diseases, 20: 29072
CHIOTTI, Premo, Crystallographic data for Ce–Zn compounds, 20: 29719
CHIRIKOV, N. P., Cosmic rays in July of 1961, 20: 29961
CHIRKO, V. I., Analysis of elastic scattering of 6.9-Mev protons by Ni isotopes, 20: 30495
CHIZHIKOV, D. M., Thermal disintegration of nitrates of cerium, neodymium, and gadolinium, 20: 29224
CHLENOV, M. A., Radiation chemistry of carbohydrates. VI., 20: 29307
CHOPRA, D. V., Lambda-binding energies in heavy hyperfragments, 20: 30448
CHORNEY, P., Recent advances in beam-plasma amplifiers, 20: 30718
CHOU, C. C., Substitution reaction of 3-ev tritium atoms with methane, 20: 29265
CHOU, Hsing-ch'uar, Chromatographic analysis and liquid-liquid extraction, 20: 29355
CHOU, Mao-heng, Radiophosphorus in treatment of certain skin diseases, 20: 29072
CHOU, Tsu-teh, S-matrix theory of EM interactions, 20: 30164
CHOUDHURY, S. Rai, Difference of binding energies of ^3H and ^3He nuclei,

20: 30424
CHOUGHULEY, A. S. U., Synthesis of potential antiradiation agents. I., 20: 29241
CHRAMEJEWA, N. P., Preparation and properties of anhydrous scandium nitrate and its solvates, 20: 29214
CHRISTIANSEN, J., Polarization of neutrons from $^{15}N(d,n)^{16}O$ reaction, 20: 30427
CHRISTOFILOS, N., Experimental studies with Astron, 20: 30637
CHU, P., Isomers of ^{129}Sn, 20: 30376
CHUANG, Hsing, Temperature distribution in a Poiseuille plasma arc, 20: 30563 (NP-16096)
CHUDAKOV, A. E., Geometric position and particle composition of radiation zones of earth, 20: 30211 (NASA-TT-F-389, pp 535-50)
CHUDAKOV, A. E., Irregular high-energy electron streams near boundary of radiation zones of earth, 20: 30215 (NASA-TT-F-389, pp 576-87)
CHUDAKOV, A. E., Primary cosmic radiation on Elektron-2 and Elektron-4, 20: 29955 (NASA-TT-F-389, pp 678-83)
CHWASZCZEWSKA, J., Semiconductor system for charged particle identification, 20: 29526 (INP-444/PL)
CHWASZCZEWSKI, S., Improved method for prompt-neutron-period measurements, 20: 30848
CIPOLLA, S., Higher-order effects in β-γ correlations involving allowed β transitions, 20: 30470
CISZEWSKI, G., Thermodynamic design of reactor cooled by gas, 20: 30892
CITTADINI, G., Hematoporphyrin and survival test of pan-irradiated mouse, 20: 29042
CLAESON, T., Superconductivity and electronic structure in alloy system Pb–Tl, 20: 30297
CLARE, R., Blast loading simulator for structural response studies, 20: 29371 (AWRE-E-1/66)
CLARIDGE, R. F. C., Reaction intermediates in radiolysis of alkyl halides at 77°K, 20: 29264
CLARK, L. T., Bibliography on relation between wetting and boiling Hg heat transfer, 20: 29620 (NP-16046)
CLARK, R. H., Lumped burnable poison program, 20: 30836 (BAW-3492-1)
CLARKSON, Jack E., Production of nuclides in the region of Z = 126 and N = 184, 20: 30367
CLAWSON, L. G., Prog. rpt. on boiling flow regimes and critical heat flux, 9/16–12/15/65, 20: 29378 (NYO-3304-7)
CLAYTON, E. D., Criticality studies with plutonium solutions, 20: 29471
CLELAND, W. E., Muonium chemistry, 20: 29177
CLORFEINE, A. S., Inductance vs. current characteristics of superconductors, 20: 30303
CLOUD, L. G., Noise study, ARMF-II, 20: 30837 (IDO-17169)
CLOUGHERTY, E. V., Boride compounds for high-temperature applications, 20: 29772
COAST, Geoffrey, Improvements in or relating to retarding mechanisms, 20: 30817
COCCHI, M., Time resolution measurements with fast photomultipliers, 20: 29568
COCHO, G., Regge pole behavior in an SL(2,C) model field theory, 20: 30087 (IC–66/46)
COCKCROFT, John, Nuclear power plants in Great Britain furnish electricity at competitive prices, 20: 30885
COCKRELL, Robert Gifford, Kinetic theory of spatial and spectral coupling of reactor neutron field, 20: 30862
COGLIATI, G., Thermal treatment of U and U–Th oxides obtained by sol-gel process, 20: 29629
COHEN, Bernard L., High-resolution study of $^{54}Fe(t,p)^{56}Fe$ reaction, 20: 30453
COHEN, J. A., Genetic recombination of bacteriophage $\Phi \times 174$ in spheroplasts, 20: 28948
COHEN, Martin Owen, Thermal neutron distributions from anisotropic fast neutron source, 20: 30340
COHEN, S. G., Search for splitting of gamma-ray photons in electric field of nucleus, 20: 30031
COLEMAN, James S., Straight-line diagram for powder pattern indexing, 20: 30952 (LA-3467)
COLEMAN, L. F., Pilot-plant gettering system of Ti-metal sponge for removal of N from Ar, 20: 29329 (ANL-7128)
COLLIER, G., Thermocouple program to investigate relative error, 20: 29488 (WANL-TME-948)
COLLIN, W., Beta-γ directional correlations and β-γ circular polarization correlations in single-forbidden-β decay of ^{144}Ce, ^{144}Pr, ^{170}Tm, and ^{203}Hg, 20: 30544
COLLIN, W., Measurement of β-γ circular polarization correlations in β transitions of ^{58}Co, ^{95}Zr, ^{95}Nb, and ^{141}Ce, 20: 30543
COLLING, F., Digital comparators for handling of data from nuclear experiments, 20: 29485 (EUR-2799.e)
COLLINS, M. A., Electron spin resonance of irradiated glycine at 77°K, 20: 29281
COLOMBO, A., Method for determining H in Magnox Al 80 and Magnox Zr 55 by vacuum sublimation, 20: 29100
COLOMBO, R. L., Dependence on microstructure of high-temperature properties of UO_2–Mo and UO_2–W cermets. I., 20: 29699 (CONF-650674-1)
CONLEY, George H., Long-lifetime reactor, 20: 30921
CONNOLLY, J. I., Experimental thermal conductivity of ^3He, 20: 30282
CONNOR, W. G., Semi-classical model of photoelectric effect in metals, 20: 29916 (ORNL-TM-1458)
CONSOLI, T., Acceleration and reflection of plasma by gradients of h-f and static magnetic fields at electron cyclotron resonance, 20: 30646
CONSTANTINESCU, O., Factors affecting selective penetration of sodium pentachlorophenolate in wood, 20: 29161
COOBS, J. H., Prog. rpt. on coated-particle fuels development at ORNL, 11/65–5/66, 20: 30870 (ORNL-TM-1528)
COOK, James E., Nuclear radiation detecting means and transmission system, 20: 29575
COOL, Terrill Alan, Recombination, ionization, and nonequilibrium electrical conductivity in seeded plasmas, 20: 30712
COOPER, J., Doppler shift measurements to investigate plasma rotation in the theta pinch, 20: 30615
COOPER, James Leslie, Improvements in or relating to grab devices, 20: 30824
COOPS, M. S., Neutron total cross section of ^{242}Pu, 20: 30465
COPPI, B., Stabilization by shear and negative V'', 20: 30608
COPPOLA, M., Elastic scattering of neutrons from natural silicon, 20: 30345 (EUR-2798.e)
CORDISCHI, D., Main-chain scission and ESR spectra of irradiated poly-tetrafluoroethylene oxide, 20: 29267
CORYELL, C. D., Independent fission yields of some xenon isotopes, 20: 30533
COSTES, Didier, Temporary fixing device for reactor elements, 20: 30831
COULSON, C. A., Deformation of graphite lattices by interstitial carbon atoms, 20: 29735
COUSSEMENT, R., Nonlinear deviation from statistical β spectrum shape of ^{32}P allowed β decay, 20: 30547
COVERT, A. S., Assessment of inhomogeneity of solid reactor fuels by fission-track counting, 20: 29663 (KAPL-M-6556)
COVEYOU, R. R., Impossible Legendre coefficients, 20: 30355 (ORNL-P-2084)
COWAN, C. L., Confirmatory evidence for sidereal-time-dependent neutral component in cosmic rays, 20: 29968
COWAN, C. L., Evidence for sidereal-time-dependent cosmic-ray signal, 20: 29967
COWLARD, Frederick Claud, Production of carbonaceous bodies containing carbides, 20: 29692
COWSER, K. E., Safety analysis of radionuclide release to Clinch River, 20: 29452 (ORNL-3721(Suppl.3))
COX, A. J., Cusp injection experiment, 20: 30644
COX, F. G., Some observations on indirect sintering of tungsten, 20: 29684
COX, R. T., ESR studies of Al ion defect pairs in reactor-irradiated Al_2O_3, 20: 30759
CRAIG, Douglas Kenneth, Interactions that occur between radionuclides and aerosols in respirable size range, 20: 29234
CRAIG, P. P., Critical velocities in superfluid He II, 20: 30272
CRAMER, E. N., Report on 1965 conference on reactor operating experience, 20: 30799
CRASTY, R. L., Single-sample potassium-argon ages using the omegatron, 20: 29413
CRAVEN, C. W. Jr., TRANSFER: program to calculate P_n multigroup scattering matrices, 20: 30323 (ORNL-TM-1537)
CRAWFORD, Frank S. Jr., Conversion of gamma rays from the decay $\eta^0 \rightarrow \pi^+ + \pi^- + \gamma$, 20: 30029
CRESPI, H. L., Fluorescence studies on deuterated Chlorella vulgaris, 20: 28872
CRIEGEE, L., Polarization of 6-Bev bremsstrahlung from Hamburg electron synchrotron, 20: 30045
CRONKITE, E. P., Extracorporeal irradiation of blood, 20: 28927 (BNL-9647)
CROSLEY, Philip, Prog. rpt. on fracture toughness of reactor pressure vessel steels, 5/65–5/66, 20: 29700 (COO-1477-4)
CROUCH, H. R. Jr., Photoproduction on H of ρ^0 mesons between threshold and 6 Bev, 20: 30030
CROW, J. E., Transition temperature of superconductors with paramagnetic impurities, 20: 30271
CROWELL, Julian, Positron annihilation in metals, 20: 29991 (ORNL-TM-1443)
CROWLEY, Barbara K., Comparison of analytical and numerical solutions for the shock tube problem, 20: 30169 (UCRL-14198)
CSONKA, Paul L., General phenomenological formalism for reactions with particles of arbitrary spin. I., 20: 30094 (UCRL-14222)
CUEER, P., Interference effects between N*(1236) and K*(891) production, 20: 30009
CUNINGHAME, J. G., Ratio of asymmetric-to-symmetric fission for ^{239}Pu for 30-kev to 14.7-Mev neutrons, 20: 30404

CUNNINGHAM, J. R., Dose distributions in ^{60}Co planar rotation, 20: 29061
CURTIN, D. J., Evidence for sidereal-time-dependent cosmic-ray signal, 20: 29967
CUYPERS, M. Y., Lunar and planetary surface analysis using neutron activation, 20: 29140
CUYPERS, Marc Y., Study of macroscopic distribution of O in steel rod by neutron-activation and vacuum-fusion techniques, 20: 29088
CZYZEWSKI, O., Elastic scattering ($p\bar{p}$) at high momentum transfer and the Orear formula, 20: 30019

D

DAANE, A. H., High-temperature heat contents and related thermodynamic functions of rare-earth metals, 20: 29743
DABROWSKI, A., Strontium-90–yttrium-90 measurements using Si counters, 20: 29520 (CLOR-45/D)
DAGERHAMM, T., Note on the nine-layer hexagonal structure of YAl_3, 20: 29721
DAGONNIER, R., Brownian motion in Fermi fluid, 20: 30263
DAHLBLOM, T. K., Binding and saturation of nuclear matter, 20: 30434
DAHLGREN, Joens Arthur, Improvements relating to nuclear power plant, 20: 30911
DALGARNO, A., Long-range three-body forces between helium and hydrogen atoms, 20: 29933
DALIDCHIK, F. I., Influence of identity of colliding nuclei in inelastic scattering at sub-barrier energies, 20: 30493
DALITZ, R. H., M1 photo-excitation $N \rightarrow N^*$ and SU(6) symmetry, 20: 30043
DALRYMPLE, G. V., Effects of whole-body irradiation by protons on primates, 20: 28931
DANBARA, Hiroshi, Concentration of ^{137}Cs in beef, 20: 28887
DANBARA, Hiroshi, Prevention of contamination of milk by fallout. I., 20: 29459
DANCHEV, V. I., Origin of uranium exogenous deposits and methods for their exploration, 20: 29449
DANETSKAYA, E. V., Effect of ionizing radiation on vitamin C metabolism, 20: 28921
D'ANGELO, N., Production of a thermally ionized plasma with negative ions, 20: 30575
DANIEL, H., Beta-γ directional correlations and β-γ circular polarization correlations in single-forbidden-β decay of ^{144}Ce, ^{144}Pr, ^{170}Tm, and ^{203}Hg, 20: 30544
DANIEL, H., Beta spectra of ^{42}K, ^{86}Rb, and ^{170}Tm, 20: 30546
DANIEL, H., Interaction strengths of neutron and proton, 20: 30001
DANIEL, H., Interactions in β decay (S = 0), 20: 30535
DANIEL, H., Measurement of β-γ circular polarization correlations in β transitions of ^{58}Co, ^{95}Zr, ^{95}Nb, and ^{141}Ce, 20: 30543
DANIEL, H., Measurement of β-γ circular polarization correlation on ^{133}Xe, 20: 30553
DANIELS, B., Magnetic field repulsion by a superconducting split cylinder, 20: 30276
DANILKIN, I. S., Interaction of intense h-f EM waves with Langmuir electron oscillations in plasma, 20: 30695
DANOS, Michael, Eigenchannel theory of nuclear reactions, 20: 30449
DAPOLITO, John A., Manganese-54 in freshwater clams, 20: 29462
DA PROVIDENCIA, J., Corrections to random-phase approximation, 20: 30398
DARDIS, J. G., Energy and angular distribution of γ rays scattered in Al, 20: 30729
DAS, S. K., Artificial radioactivity in rain-borne dust and in rain water observed in Calcutta during 1962, 20: 29420
DATTA, Sunil, Unsteady slip flow over a flat plate under transverse magnetic field, 20: 30180
DAU, Gary J., Gamma-induced electrical conductivity in alumina, 20: 29823
DAUGHTREY, William, Oxygen saturation of tumor cells to increase effect of internal radiation, 20: 29059 (TID-22860)
D'AURIA, John M., Decay scheme of ^{123}Cs, 20: 30403
DAVIDSON, R. H., Hallam Nuclear Power Facility operating experience, 20: 30898
DAVIES, N. F., Energy dependence of radiation damage in Si, 20: 29579 (NAA-SR-11887)
DAVIGNON, Leon, Action of O on Ti, Zr, Hf, V, Nb, and Ta in powdered form, 20: 29644
DAVIS, Donald Robert, Radiolysis of liquid xenon hexane solutions and positive ion chemistry in solid methane, 20: 29314
DAVIS, H. Ted, Brownian motion in Fermi fluid, 20: 30263
DAVIS, Herbert Larkin Jr., Effects of cuferron on frequency of x-ray induced chromosomal aberrations in Tradescantia paludosa, 20: 29028
DAVIS, Howard F., Possible $N^*(1688) \rightarrow K^+\Lambda$ production in 3-Bev $p + p \rightarrow K^+ + \Lambda + p$, 20: 30034
DAVIS, James A., Variational vacuum boundary conditions for P_N approximation, 20: 30116
DAVIS, Monte V., Gamma-induced electrical conductivity in alumina, 20: 29823
DAVYDOV, B. I., Simulation of biological effect of depth dose from monoenergetic proton, 20: 28972
DAVYDOV, E. N., Fallout of Ce-141, Ce-144, Zr-95 + Nb-95 and Sr-90 on U.S.S.R., 20: 29406 (NP-14719)
DAWSON, D. K., Effect of surface evaporation on diffusion measured by isotopic exchange reactions, 20: 29731
DAWSON, H. R., Lifetimes of n = 3 states of H by electron capture during fast H^+ impact on gases, 20: 29930
DAWSON, I. M., Structural studies on v.u.v./CO_2 oxidation of graphite, 20: 29733
DAY, Robert B., Calculation of pulse-height response of Ge(Li) semiconductor counters, 20: 29528 (LA-3456)
DAYTON, Russell W., Prog. rpt. on civilian applications, 7/65, 20: 29616 (BMI-1738)
DE ALFARO, V., Rules for strong interactions, 20: 30020
DEBNEY, Carole W., Stability of Drosophila chromosomes to radioactive decay of incorporated ^{32}P, 20: 28955
DEBOIS, Jean-M., Metabolism of transuranic elements, 20: 28885
DE CASTRO, Elve Monteiro, Studies of solid H_2–D_2 mixtures by nuclear magnetic resonance, 20: 30320
DECKER, G., Isar I: fast megajoule theta-pinch experiment with extremely high compression fields, 20: 30611
DE HEER, F. J., Gross- and partial-ionization cross sections for electrons on water vapor, 20: 29928
DEI-CAS, R., Injection of ions into a magnetic mirror machine (M.M.I.), 20: 30634
DEKABRUN, L. L., Autodyne nuclear magnetic resonance pickups, 20: 29492
DELBOURGO, R., Dynamical origin of SU(6), 20: 30117
DELLA TORRE, E., Acceleration in generalized coordinates, 20: 29834
DEL LITTO, Bernard, Hydrolysis of U–Th–C alloys rich in C, 20: 29159
DELONE, N. L., Effects of cosmic flight on Tradescantia paludosa microspores, 20: 28971
DE MICHELIS, C., Hot-ice experiment, 20: 30665
DEMINA, D. M., Effect of cold and ultraviolet rays on mast cell system, 20: 28944
DEMIRKHANOV, R. A., Plasma equilibrium in torus with high-frequency fields and plasma heating resulting from beam of "escaping electrons", 20: 30640
DEMIRKHANOV, R. A., Plasma heating under beam instability conditions, 20: 30659
DEMKOV, YU. N., Non-steady problems of quantum mechanics and Laplace transform, 20: 30240 (BNL-tr-67)
DE NERCY, A. Bussiere, Scattering of 40.5-Mev α particles by ^{12}C, ^{13}C, ^{14}N, ^{15}N, ^{16}O, and ^{18}O, 20: 30450
DENG, Zong-hou, Ligand field theory. I., 20: 29205
DENGEL, O., Diffusion of tritons in NH_4F-doped ice single crystals, 20: 29193
DENKINS, R. F., Advanced accelerator development, 20: 29855 (ORNL-3940, pp 83-111)
DENNISON, D. H., High-temperature heat contents and related thermodynamic functions of rare-earth metals, 20: 29743
DENOTKINA, R. G., Solubility of ammonium plutonyl phosphate compounds in aqueous solutions, 20: 29219
DENSCHLAG, H. O., Behavior of recoil atoms in the decay of ^{219}Rn and ^{220}Rn in gases, 20: 29325
DENT, W. A., Extension of non-thermal radio-source spectra to 8000 Mc/s, 20: 29878
DE RAEDT, J., Beta decay of ^{199}Au and structure of involved nuclear states, 20: 30549
DEREPOVSKII, N. T., Standby operation of coaxial plasma gun, 20: 30684
DER MATEOSIAN, E., Limits for lepton-conserving and lepton-nonconserving double β decay in ^{48}Ca, 20: 30461
DESAI, Rashmikant Chimanlal, Atomic motions in monatomic fluids, 20: 30166 (NYO-3326-13)
DESCHAMPS, P., Characteristics and purification of plasma produced by coaxial gun with annular preionization, 20: 30648
DESHPANDE, N. G., Spontaneously broken symmetries and question of massless particles in model field theory, 20: 30135
DESHPANDE, Nilendra Ganesh, Compositeness conditions and broken symmetry in model field theory, 20: 30156
DE STEFANO, M. B., Systematic iterative approach to problem of scattering on singular potentials, 20: 30136
DETOEUF, J. F., Search for an isobar of isotopic spin T = 5/2, 20: 30022
DEUTSCH, J. P., Beta decay and nuclear structure, 20: 30536
DEUTSCH, J. P., Beta decay of ^{199}Au and structure of involved nuclear states, 20: 30549
DEUTSCH, J. P., Evidence for 1^-, K = 0 character of ^{176m}Lu through β-decay measurements, 20: 30552
DEUTSCH, J. P., Nuclear matrix elements of the β transition of ^{194}Ir, 20: 30551

DEVONS, S., High-resolution muonic x-ray studies, 20: 29525 (CONF-660209-9)
DE WAARD, H., Level (27.7 kev) in ^{129}I and use in Moessbauer experiments, 20: 30474
DEY, Arun K., Spectrophotometric study of chelates of ammonium aurintricarboxylate with Sc, Y, and La, 20: 29180
DICK, I. B., Current practices in the disposal of radioactive wastes from operation of uranium mines and mills, 20: 30948
DICK, I. B., Current practices in disposal of waste radioactive gases from reactors, 20: 30949
DIDEYKIN, T. S., Approximate investigation of kinetics of subcritical reactor during sinusoidal reactivity variation, 20: 30860
DIERKER, J., Time-reversal invariance in β decay of RaE, 20: 30537
DIEZ, R., Environmental radioactivity at Valencia during 1964, 20: 29408
DI LAZZARO, M. A., Spectral distribution of photons scattered by electrons bound in K shell. I., 20: 29912 (ISS-66/6)
DI LAZZARO, M. A., Spectral distribution of photons scattered by electrons bound in K shell. II., 20: 29913 (ISS-66/7)
DI LAZZARO, M. A., Spectral distribution of photons scattered by electrons bound in K shell. III., 20: 29914 (ISS-66/8)
DILLON, I. G., Densities and critical properties of alkali metals, 20: 29742
DIMITRIJEVIC, Z., Neutron investigation of temperature effects in magnon spectrum of magnetite, 20: 30765
DI NOVI, Roberta Ann, Correlation of heat transfer properties and ultrasonic transmission properties of bonds, 20: 29386 (ANL-7074)
DIPPEL, K. H., Stable and unstable behavior of preheated plasma in linear and cusped theta pinches, 20: 30614
DISSELHORST, B. F., Irradiation of graphite impregnated with furfuryl alcohol, 20: 29813
DISTENFELD, Carl H., Determination of quality factor through utilization of balanced, tissue-equivalent, ionization chamber, 20: 29847 (CONF-651109, pp 181-98)
DIXON, C. F., Uranium alloy development for non-nuclear application, 20: 29803
DOBROV, N. N., Chemical protection against genetic changes, 20: 29045
DOBSON, Peter N. Jr., Zero-effective-range analysis of pion-nucleon reactions near η^0 production threshold, 20: 30033
DODD, L. R., Divergence of distorted-wave Born series for rearrangement scattering, 20: 30120
DODD, L. R., Rigorous solution of three-body scattering processes in distorted-wave formalism, 20: 30121
DODIN, D. A., Uranium in traps of Siberian platform, 20: 29419
DOE, B. R., Source of Pb and Sr in deep geothermal brines underlying the Salton Sea geothermal area, 20: 29414
DOHM, Arthur J. Jr., Shutdown apparatus for nuclear reactors, 20: 30835
DOI, Toshio, Studies of hard superconductors. I., 20: 29784
DOI, Toshio, Studies of hard superconductors. II., 20: 29785
DOI, Toshio, Studies of hard superconductors. III., 20: 29787
DOI, Toshio, Studies of hard superconductors. IV., 20: 29788
DOLEZAL, J., Silica gel in separation of Th from Zr, 20: 29344
DOLGINOV, Sh. Sh., Comparison of simultaneous measurements of magnetic field and positive ion streams within earth's magnetosphere, 20: 30208 (NASA-TT-F-389, pp 457-63)
DOLGINOV, Sh. Sh., Earth's magnetosphere in radiation zone region ($3\text{-}6R_e$), 20: 30209 (NASA-TT-F-389, pp 464-82)
DOLGOPOLOV, V. V., Behavior of the EM field in an inhomogeneous magnetized plasma, 20: 30696
DOLIAS, M., High-energy particle spectrometry using activation detectors, 20: 29521 (CONF-651109, pp 213-23)
DOLIDZE, G. M., Kinetics of radiation-induced isotope exchange between deuterium and silica gel hydroxyl groups, 20: 29276
DOLIN, P. I., Steady state in radiolysis of neutral aqueous solutions of oxygen, 20: 29257
DOMKE, A., Cybernetic studies on radiation effects on yeast cells. I., 20: 28950
DONALDSON, R. E., Coherent neutron scattering amplitudes of ^{10}B and ^{11}B, 20: 30335
DONNELLY, I. J., Exchange energy of semi-infinite nuclear matter, 20: 30395
DORENBUSCH, W. E., Reaction ^{42}Ca(d,p)^{43}Ca at 7.0 and 7.2 Mev, 20: 30452
DORMAN, L. I., Cosmic ray nuclear component on Elektron-2, 20: 29957 (NASA-TT-F-389, pp 693-710)
DOROFEEV, V. M., Thermal and anaphylactoid edema in acute radiation sickness, 20: 29001
DOTTI, D., Ratemeter for variable flow measurements, 20: 29535
DOUGAL, A. A., Prog. rpt. on plasma diagnostic methods, 4–6/65, 20: 30556 (AD-631993)
DOUGHTY, B. M., Lifetimes of n = 3 states of H by electron capture during fast H^+ impact on gases, 20: 29930
DOUGLAS, John H., Mesonic (K$^-$) x rays and anti $\bar{K}$-N scattering lengths, 20: 29938
DOUGLASS, D. L., Oxidation of oxygen-deficient zirconia, 20: 29648
DOUZOU, Pierre, Photoionization and biphotonic processes of nucleic acids derivatives in frozen solutions, 20: 28914
DOWE, Roy Michael Jr., Attenuation cross sections of Tl at 122 kev, 20: 30731
DRAGT, Jon B., Accurate reactor noise measurements in low-power critical reactor, 20: 30942
DRAGT, Jon B., Reactor noise analysis by means of polarity correlation, 20: 30853
DRAKE, John W., Ultraviolet mutagenesis in bacteriophage T4. I., 20: 28969
DRAKULIC, M., Resynthesis of DNA and 50-S ribosomal RNA in uv-irradiated E. coli, 20: 28949
DRAWERT, F., Separation of ^{14}C-compounds in gaseous phase, 20: 29089
DRESSELHAUS, Mildred S., Energy band parameter determination in graphite, 20: 30737
DREWES, Patricia Ann, Protein synthesis in Ehrlich mouse ascites tumor cells in vitro, and effect of x irradiation, 20: 28923
DRITTLER, K., Radiation damage caused by neutrons in metals, 20: 29819
DROBINSKI, J. C. Jr., Radiocarbon in environment, 20: 29472
DROUILLARD, Thomas F., Ultrasonic inspection of critical components and weldments for pressure and nuclear vessels, 20: 29389
DRUMMOND, W. E., Landau damping of electron plasma waves, 20: 30622
DRUMMOND, W. E., Thermalization and anomalous diffusion of turbulent plasmas, 20: 30620
DRUYVESTEYN, W. F., Distribution of direct transport current in sheets of type-II superconductors, 20: 30273
DUBE, S. S., High-frequency titrimetric study of the reaction between thorium and alkali molybdate, 20: 29092
DUBININ, N. P., Radiation aspects of genetic cell differentiation and problem of malignant growth, 20: 28920
DUBOIS, Emmanuel, Electrostatic collecting of RaA and β emission of RaE formed, 20: 29324
DUBOVOI, L. V., Dynamic stabilization of a direct discharge in a magnetic field, 20: 30698
DU CHATENIER, F. J., Heat capacity below 1°K of some dilute alloys, 20: 29791
DUDEK, Alicja, Computation delta (θ) according to strong absorption theory given by Frahn and Venter, 20: 30348 (INP-446/PL)
DUDLEY, T. E., Group constants for gamma-ray heating, 20: 30722 (KAPL-M-6497)
DUFFY, R. J., Critical temperatures and critical fields of multiple superconducting and normal-conducting films, 20: 30291
DUMAZET, G., Fluctuations of differential polarization of particles emitted in nuclear reactions, 20: 30397
DUMONTET, P., Application of Fano-Racah formalism to a kinematic study of nuclear reactions, 20: 30396
DUNCAN, R. H., Signal produced in monopole antenna by gamma flux from nuclear explosion, 20: 29580
DUNLAP, Henry F., Shielding system for chlorine logging apparatus, 20: 29443
DUNLAY, J. B., Prog. rpt. on vacuum foil-type insulation for radioisotope power systems, 2–4/66, 20: 29606 (ALO-3634-1)
DUNLOP, J. I., Determination of amino acid quantum efficiencies by difference spectrophotometry, 20: 28915
DUPEN, D. W., Stanford's long, long beam, 20: 29862
DURAND III, Loyal, Coulomb corrections to β decay of ^{14}O, 20: 30443
DURASOVA, S. A., Crystallochemical properties of cubic-shaped hydrated uranium tetrafluoride, 20: 29231
DURIG, J. R., Vibrational spectrum of hydrazine-d_4 and Raman study of hydrogen bonding in hydrazine, 20: 29175
DUSHIN, L. A., Determination of plasma density distribution by microwave refraction, 20: 30700
DUTREIX, A., Relative biological efficiency of a beam of 20-Mev electrons as function of depth, 20: 28963
DUTT, Yog, Studies in complex formation of metal ions with tropolones. III., 20: 29179
DUYCKAERTS, G., Determination of trace copper in high-purity arsenic by neutron activation, 20: 29087
DVORAK, Robert F., Radiation environment at zero-gradient synchrotron, 20: 29843 (CONF-651109, pp 34-56)
DYATLOV, I. T., Calculation of Σ^+- and Σ^--hyperon mass difference, 20: 30059
DYBOWSKI, K., Improved method for prompt-neutron-period measurements, 20: 30848
DYER, G. H., Materials applications for nuclear power plants from viewpoint of engineer-constructor, 20: 30815
DYKHNE, A. M., Electron spectrum in one-dimensional system with randomly arranged scattering centers, 20: 30113
DYOS, M. W., Utility of the statistical treatment of resonance absorption in the unresolved resonance region, 20: 30420

DYRSSEN, David, Extraction of $^{233}U(VI)$ by DBP and TBP or TOPO, 20: 29334
DYSON, D. J., Orientation relationship and growth direction of Mo_2C in ferrite, 20: 29726
DZHAPARIDZE, Sh. A., Nature of oscillations of He II near surface of vibrating disc, 20: 30308
DZHELEPOV, B. S., Gamma radiation of 12.3-year ^{152}Eu, 20: 30487

E

EANDI, R., Production of antiprotons by high-energy photons, 20: 30432
EARL, John Alfred, Insulating coating for electrical conductors, 20: 29636
EBERHARDT, P., Mass spectrum of fission Xe in Pasamonte meteorite, 20: 29892
EBERLE, L., Thermodynamic observations on reactions of high-melting carbides, 20: 29729
EBERLE, S. H., Chelate formation of americium and curium with nitrilotriacetic acid, 20: 29195
EBERLEIN, Walter R., Kinetics of calcium metabolism in children utilizing nonradioactive Sr, 20: 28889
EBERT, M., Novel valence states of thallium as studied by pulse radiolysis, 20: 29271
ECKHARTT, D., Comparison of alkali plasma loss rates in a stellarator and in toroidal device with minimum mean-B properties, 20: 30656
ECKSTEIN, Y., Ultrasonic attenuation in liquid ^4He at low temperatures, 20: 30299
EDA, Bunzo, Electron spin resonance of irradiated thiophene 2-carboxylic acid, 20: 29284
EDDY, N. W., Resonant electron capture in small-angle collisions of Ar^+ on Ar and Ne^+ on Ne, 20: 29944
EDLIN, V., Bonding reaction mechanism in chemically bonded ZrO_2, 20: 29145 (NP-16047)
EDLUND, Milton C., Reactor and method of operating to variably moderate and control, 20: 30915
EDMAN, J. R., Physical and chemical properties of hydroxyflavones. V., 20: 29240
EDMONDS, Frank N., Evidence for oscillatory component in solar granulation brightness fluctuations, 20: 29886
EDWARDS, S. F., Scattering of microwaves by turbulent plasma, 20: 30658
EELES, W. T., Annealing studies of boron-doped graphite by electron microscopy and x-ray diffraction, 20: 29625
EFIMOVA, E. I., Forms in which can be found radioactive elements in Fe–Mn concretions, 20: 29426
EFIMOVA, E. I., Radiochemical composition of Fe–Mn concretions and manganese ores, 20: 29425
EFRYUSHINA, N. P., Absorption-spectrophotometric determination of rare earths in tributylphosphate extracts, 20: 29125
EGAN, J. J., Free energies of formation of inorganic fluorides, 20: 29215
EGELHOFER, J. A., Gamma irradiation facility of Frankfurt Research Reactor, 20: 29341
EGOROV, B. B., Effects of cosmic flight on Tradescantia paludosa microspores, 20: 28971
EGUCHI, Hiroko, Low temperature resistivity, magnetic susceptibility, and superconducting transition temperature in La, 20: 29753
EICHLER, Eugene, Decay of ^{133}I to levels in ^{133}Xe, 20: 30473
EIDUS, L. Kh., Radiation damage of protein molecules and molecular protective mechanisms, 20: 29040
EISENBERG, Eugene, Effects of androgens, estrogens, and corticoids on Sr kinetics in mann, 20: 28890
EISENMAN, Burton, ADONIS: IBM-7090 Monte Carlo shielding code in three-dimensional rectangular geometry, 20: 30726 (TID-22964)
EISMONT, V. P., Energies of pair fragments in tission of ^{238}U, ^{235}U, and ^{233}U, by 12-Mev deuterons, 20: 30500
ELDRIDGE, O., Diffusion of test particles across a magnetic field, 20: 30714
ELIAS, Horst, Kinetics of homogeneous isotope exchange between isopropyl chloride and chloride ions in dimethylformamide, 20: 29156
ELIAS, Horst, Kinetics of homogeneous isotope exchange between cycloalkyl chlorides and chloride ions in dimethyl sulfoxide, 20: 29157
ELION, Herbert A., Instrument and chemical analysis aspects of electron microanalysis and macroanalysis, 20: 29119
ELLI, Raffaello, Recovery from x-ray-induced sub-lethal damage in Saccharomyces cerevisiae cells of different ploidy, 20: 28961
ELLINGTON, J. P., Mechanized structural analysis, 20: 29367 (TRG-Report-1089)
ELLIOTT, R. V., Proton scattering from ^{27}Al from 3.5 to 11.3 Mev, 20: 30415
ELLIS, M. M., Crystal field of $PrCl_3$, 20: 30760
ELLSWORTH, L. D., Nuclear states of ^{103}Rh, 20: 30471
ELO, Don, Mechanical design of regenerative deflector for Berkeley 88-in. cyclotron, 20: 29856 (UCRL-16829)
ELSNER, B., Interaction π^+-π^- as studied in 12- and 18-Bev pion-nucleon reactions, 20: 30025
ELTON, R. C., Plasma confinement, heating, and losses in Pharos with an extended current pulse, 20: 30612
EMANUEL, N. M., Free-radical reactions during exposure of model systems to irradiation, 20: 29037
ENDERBY, J. A., Mechanized structural analysis, 20: 29367 (TRG-Report-1089)
ENDRES, G. W. R., Pulsed reactor tests of dosimeters, 20: 29518 (BNWL-SA-27)
ENDT, P. M., Gamma decay of ^{40}Ca levels measured with $^{39}K(p,\gamma)^{40}Ca$ reaction, 20: 30482
ENGELMANN, R., Inelastic Σ^-p interactions at low momenta, 20: 30024
ENGEWALD, W., Hydrogen isotope exchange reactions of nonbenzoid aromatics. II., 20: 29245
ENGLE, G. B., Irradiation of graphite impregnated with furfuryl alcohol, 20: 29813
ENGLESSON, George Anthony, Superconducting coils for shielding in space, 20: 30317
ENKOVSKI, L., Representations 189 and 405 of the group SU(6) and classification of mesonic resonances 2^+, 1^+, and 0^+, 20: 30093 (JINR-P-2701)
ERASTOV, E. M., Measurement of cross sections of ion-atom collisions at low energies by overtaking beams, 20: 29932
ERDMANN, Robert C., Time-dependent monoenergetic neutron transport in two adjacent semi-infinite media, 20: 30339
ERIKSON, Herman E., Radiation detection device with an intensifier screen, 20: 29573
ERNE, F. C., Shell-model calculations on odd-parity levels of nuclei in the range ^{33}S to ^{41}Ca, 20: 30407
ERNST, S., Behaviour and structure of uranyl nitrate in organic solvents. III., 20: 29184
ERNST, Valentin, Information loss in theory of small-angle multiple scattering, 20: 30151
EROSHENKO, E. G., Comparison of simultaneous measurements of magnetic field and positive ion streams within earth's magnetosphere, 20: 30208 (NASA-TT-F-389, pp 457-63)
EROSHENKO, E. G., Earth's magnetosphere in radiation zone region ($3\text{-}6R_e$), 20: 30209 (NASA-TT-F-389, pp 464-82)
EROSHENKO, E. G., Magnetometric apparatus of the electron-2 space station, 20: 30236
ERSHKOVICH, A. I., Formation of radiation zones as result of particle drift in depths of magnetosphere, 20: 30207 (NASA-TT-F-389, pp 442-53)
ERSKINE, J. R., Reaction $^{182}W(d,p)^{183}W$ at 7.5 and 12 Mev, 20: 30475
ERVIN, G. Jr., Zone melting of uranium monocarbide, 20: 29619 (NAA-SR-11813)
ERWIN, A. R., Search for evidence of a K^+K^+ resonance, 20: 30047
ERWIN, A. R., Strangeness-one resonances, 20: 30049
ERZINKYAN, A. L., Effective magnetic field at ^{60}Co nucleus in Co–Pt alloy, 20: 30752
ETHERTON, R. C., Excited states in ^{82}Kr populated by decay of 35-h ^{82}Br, 20: 30410
EULER, J., Modification of conductivity of $Ni(OH)_2$ and CdO by irradiation, 20: 29821
EVANS, B., Absorption, degassing, and solution equilibrium in the N–Nb system at ultrahigh vacuum and high temperature, 20: 29178
EVANS, F. D., Comparison of pressed and sintered and arc-cast billets for refractory metal forgings, 20: 29683
EVANS, J. S., Negative-parity levels in even-even mercury isotopes, 20: 30435
EVANS, R. M., Joining of nickel and nickel-base alloys, 20: 29666 (RSIC-484)
EWING, David, Method of evaluating radiation risks for manned space flights, 20: 29058
EYRE, B. L., Behavior of refractory metals in radiation environments, 20: 29820

F

FACCHINI, A., Treatment of low- and intermediate-level radioactive wastes, 20: 30944
FADDEEV, L. D., S-matrix potential in Schroedinger one-dimensional equation, 20: 30248
FADEEVA, L. A., Determination of yttrium and rare earth elements of yttrium subgroup in ores, 20: 29134
FAIN, E. A., Calculation of doses in x and gamma irradiations through screens, 20: 29056
FAINBERG, Ya. B., Collective interaction of modulated and unmodulated electron beams with plasma, 20: 30623
FAINBERG, Ya. B., Suppression of low-frequency oscillations in two-stream instability by prior modulation of electron beam, 20: 30591
FAIRBANK, Henry A., Sound measurements in liquid and solid ^3He, ^4He, and ^3He–^4He mixtures, 20: 30288
FALCHETTI, Roberto, Recovery from x-ray-induced sub-lethal damage in Saccharomyces cerevisiae cells of different ploidy, 20: 28961

FALCKENBERG, H. R., Electron-single-scatter-gage, 20: 29600
FALK, C. F., Current practices in the disposal of radioactive wastes from operation of uranium mines and mills, 20: 30948
FALK, C. F., Current practices in disposal of waste radioactive gases from reactors, 20: 30949
FANELLI, Robert, Microwave absorption in normal-conducting films on superconducting substrates, 20: 30289
FARGES, Guy, Composite guide tube for reactors, 20: 30830
FARIAS, Nestor, Separation of ^{90}Sr and ^{90}Y in the presence of Ca by paper chromatography, 20: 29349
FASTOVSKII, U. V., Comparison of simultaneous measurements of magnetic field and positive ion streams within earth's magnetosphere, 20: 30208 (NASA-TT-F-389, pp 457-63)
FASTOVSKII, U. V., Magnetometric apparatus of the electron-2 space station, 20: 30236
FAUDROWICZ, Adam, Astronomical observations of high-energy gamma rays, 20: 29969
FAYOUX, M. L., Search for an isobar of isotopic spin $T = 5/2$, 20: 30022
FAZACKERLEY, Cecil Henry, Improvements in or relating to neutron neutron absorber material, 20: 30865
FAZIO, G. G., Cosmic black-body radiation, high-energy electrons, and origin of isotropic x-ray and γ radiation, 20: 29958
FEARING, Harold W., Radiative muon capture and the giant dipole resonance in ^{40}Ca, 20: 30451
FEATES, F. S., Structural studies on v.u.v./CO_2 oxidation of graphite, 20: 29733
FEDOROV, A. F., Radioactivity of organisms of Norwegian Sea, 20: 29424
FEDOROV, V. B., Proton elastic scattering on deuterons at large angles, 20: 29989 (ITEF-361)
FEDOROVA, A. V., Influence of chemical uptake of radioactive substances on lipid and cholesterol levels in blood, 20: 28994
FEINBERG, E. L., Cross section of quark generation, 20: 29999
FEINE, U., Nephrogram with ^{125}I-labeled hippuran in infancy and childhood, 20: 29063
FEINSTEIN, Robert N., Acatalasemic and hypocatalasemic mouse mutants, 20: 28957
FELINGER, A. K., Radioisotopic instruments in metallurgy, 20: 29598
FELTEN, James Edgar, Inverse Compton photons and cosmic electrons in particle astrophysics, 20: 29972
FENDEL, H., Nephrogram with ^{125}I-labeled hippuran in infancy and childhood, 20: 29063
FERGUSON, Robert L., Nuclear charge distribution in fission: ^{92}Kb and ^{93}Rb independent yields, 20: 30477
FERRARI, E., Two-pion decay modes of K mesons, 20: 30015
FERRELL, J. K., Prog. rpt. on convection boiling inside channels, 10-12/64, 20: 29380 (TID-22967)
FETTER, A. L., Stability of a lattice of superfluid vortices, 20: 30286
FETTER, Alexander L., Energy of a lattice of quantized flux lines, 20: 30287
FILIPPOV, N. V., Phenomena associated with buildup of non-cylindrical focused Z pinch, 20: 30642
FILIPPOVA, T. I., Phenomena associated with buildup of non-cylindrical focused Z pinch, 20: 30642
FILIPPOVICH, A. S., Mutagenic efficiency of intermediate neutrons, 20: 29002
FILONENKO, A. P., Radiation effects on catalytic activity of platinum during hydrogenation, 20: 29304
FILTHUTH, H., Inelastic $\Sigma^- p$ interactions at low momenta, 20: 30024
FINAEV, Yu. A., Temperature measurements in studies of combustion of solid fuel particles, 20: 29495
FINCLE, Robert L., Process for coating radioactive spheroids with pyrolytic graphite, 20: 29638
FINK, William C., Radio gas chromatography peak analyzer, 20: 29105
FINTELMANN, D., Exo- and chemical electron emission, 20: 29561
FIRSOV, O. B., Breakup of fast negative ions in inert gases, 20: 29947
FIRSOV, V. G., Experimental investigation of chemical reactions involving muonium, 20: 29247
FISCHER, J., Generalized spherical functions for the noncompact rotation groups, 20: 29614
FISENKO, L. P., Organic coprecipitants. XXIII., 20: 29135
FISHER, G. P., Elastic scattering (π^--p) at 1.7 Bev/c, 20: 30011
FITE, Lloyd E., Study of macroscopic distribution of O in steel rod by neutron-activation and vacuum-fusion techniques, 20: 29088
FITI, Maria, Radiolysis of acetylene in solution. III., 20: 29293
FITZGERALD, Lawrence T., Automatic depth-dose acquisition system, 20: 29070
FLAGELLA, P. N., Properties of some refractory metals. IV., 20: 29710 (TID-22986)
FLAKS, I. P., Charge exchange and ionization in collisions of Ne atoms and ions with CO, 20: 29948
FLEETWOOD, M. J., Diffusion of Cr into Ni-thoria alloys, 20: 29748
FLEISCHER, R. L., Effect of thermal-neutron irradiation on superconducting properties of Nb_3Al and V_3Si doped with fissionable impurities, 20: 30260
FLEISCHHAUER, G., Manufacture of nuclear reactor fuel elements and their coating with pyrolytic carbon, 20: 29670
FLEITMAN, A. H., Boiling Hg corrosion of certain refractory metals and stainless steels from 593 to 703°C, 20: 29646
FLEMING, Gordon Neeld, Contributions of elastic unitarity to three-pion scattering, 20: 30077
FLETCHER, Emery, Quasars—a minority report, 20: 29896
FLOSS, H. G., Simple method for ^{15}N determination, 20: 29131
FLYNN, K. F., Mass distribution in fission of ^{229}Th, 20: 30373
FLYNN, T. M., Nuclear spin relaxation in liquid hydrogen, 20: 30181
FODOR-CSANYI, P., Significance of phosphorescence in measurement of low-energy beta isotopes with liquid scintillator and single-channel counter, 20: 29084
FOMIN, A. A., Polyphase cylindrical inductor with a multipole field, 20: 29835
FORD, J. L. C. Jr., Elastic and inelastic proton scattering from ^{106}Pd and ^{108}Pd, 20: 30462
FORLANO, Roberto J., Elasticity and anelasticity of uranium oxides at room temperature, 20: 29698 (ANL-7101)
FORRESTER, P. A., New laser line due to energy transfer from color centers to erbium ions in CaF_2, 20: 30774
FORSCHER, F., Development of ThO_2 pellet fabrication, 20: 29657
FORSTER, William Hull, Cross section ratios of isobars from spallation reactions under varying conditions, 20: 30531
FOSSAN, D. B., Low-lying states of ^{33}S, 20: 30455
FOSTER, Billy Evon, Measurement of mass attenuation coefficients using x rays, 20: 29707 (ORNL-TM-1457)
FOUARGE, J., Determination of trace copper in high-purity arsenic by neutron activation, 20: 29087
FOWLER, William A., Integrated flux distributions in neutron capture in stars, 20: 29887
FRADKIN, M. I., Cosmic ray nuclear component on Elektron-2, 20: 29957 (NASA-TT-F-389, pp 693-710)
FRADKIN, M. I., Primary cosmic-ray research, 20: 29954 (NASA-TT-F-389, pp 657-77)
FRADKIN, M. I., Transient increases of flux of heavy nuclei accompanied by bursts of x radiation, 20: 29965
FRANK, R., Stability of a diffusing plasma, 20: 30621
FRANK, Richard B., Automatic sample changer for radioactive samples, 20: 29572
FRANKEL, Philip, Space electric power systems, 20: 29977 (N-65-32716)
FREEDMAN, M. S., Level structure in ^{52}Cr populated in 5.7-day ^{52}Mn decay, 20: 30458
FREEDMAN, M. S., Low-intensity branches in ^{45}Ti decay, 20: 30456
FREEMAN, K. B., Photochemistry of uridylyl-(3′→5′)-uridine, 20: 28910
FREINDL, L., Semiconductor system for charged particle identification, 20: 29526 (INP-444/PL)
FRENTROP, Arthur H., Neutron generating discharge tube, 20: 29444
FREUND, F., Phosphidation of compact zirconium metal, 20: 29642
FRIAR, James L., Transverse inelastic form factors in ^{12}C from continuum model, 20: 30411
FRIDMAN, A., Interference effects between N*(1236) and K*(891) production, 20: 30009
FRIDMAN, Sh. D., Statistical errors in determining concentrations of radioactive elements in rocks using γ-threshold and differential spectrometers, 20: 29421
FRIDMAN, Yu. D., Formation and thermal dissociation of yttrium fluorides and carbonates, 20: 29223
FRITZE, K., Ratio of asymmetric-to-symmetric fission for ^{239}Pu for 30-kev to 14.7-Mev neutrons, 20: 30404
FROHBERG, T., Theory of correlated crystals, 20: 30781
FROMM, E., Processes for degassing of niobium and tantalum, 20: 29633
FRONSDAL, C., Representations of SL(n,C), 20: 30089 (IC-66/51)
FRONTAS'EV, V. P., Temperature effects on electron polarization variations in ordinary and heavy water molecules, 20: 29230
FROSCH, R. F., Structure of the α particle from elastic electron scattering, 20: 30439
FRY, Edward S., Calculation of pulse-height response of Ge(Li) semiconductor counters, 20: 29528 (LA-3456)
FUBINI, S., Rules for strong interactions, 20: 30020
FUCHS, H., Discrepancies in proton-transfer reactions to states with different isobaric spin, 20: 30481
FUECHTBAUER, Walter, Kinetics of uv-induced dimerization of thymine in frozen solutions, 20: 28916
FUEKI, Kenji, Radiation-induced cis-trans isomerization of stilbene in methanol solution, 20: 29287
FUENFER, E., Isar I: fast megajoule theta-pinch experiment with extremely high compression fields, 20: 30611
FUJII, Yahei, Ultrasonic attenuation and relaxation times in water vapor and heavy water vapor, 20: 29172
FUJIIE, Yoichi, Numerical analysis of reactor kinetics by digital computer, 20: 30838

FUJIMOTO, Yoshiyuki, Effects of irradiation on Pinus desiflora and Pinus thunbergii, 20: 28980
FUJIMURA, Tadato, Embrittlement of reactor structural steels by neutron irradiation, 20: 29825
FUJISAWA, Hisao, Movement of radioactive calcium in brain slices, 20: 28891
FUJITA, Akira, Studies on fallout particles. V., 20: 29423
FUJITA, Minoru, Loss of ^{137}Cs and K by dry ashing and HCl treatment of total diet samples, 20: 29122
FUJITA, Yoshihiro, Utilizing r-f field for injection trapping of high-energy ions in mirror fields. I., 20: 30580
FUJIWAKA, S., Ion cyclotron resonance heating of QP plasma, 20: 30662
FUKAI, Yuzo, Disadvantage factor in closely packed cylindrical lattice, 20: 30840
FUKUDA, Satoshi, Multilayer Nb–Sn superconducting wire, 20: 29781
FULINSKI, Andrzej, Scattering of slow neutrons in an acoustical field, 20: 30256
FULMER, C. B., Advanced accelerator development, 20: 29885 (ORNL-3940, pp 83-111)
FULTZ, S. C., Neutron total cross section of ^{242}Pu, 20: 30465
FUMELLI, M., Injection of ions into a magnetic mirror machine (M.M.I.), 20: 30634
FUQUA, P. A., Biologic effects of human radiation exposure, 20: 28970
FURDYNA, J. K., Resistive transition near H_{c2} in high field superconductors, 20: 30270
FURLAN, G., Rules for strong interactions, 20: 30020
FURRER, A., S-D exchange interactions and Fermi surface in Ni, 20: 30775
FURTH, H. P., Stabilization by shear and negative V″, 20: 30608
FURUDATE, Masayori, Balneological studies using ^{59}Fe, 20: 28892
FURUSETH, Sigrid, Systems Re–As, Re–Sb, Re–Bi, Re–Te, and Nb–Sb–Te, 20: 29717
FUTRELL, J. H., Xenon-sensitized radiolysis of propane, 20: 29266

G

GABAY, Jack J., Manganese-54 in freshwater clams, 20: 29462
GABRIELLI, Italo, Scattering of α particles by ^{52}Cr, ^{53}Cr, and ^{51}V, 20: 30460
GACHECHILADZE, R. G., Question of anomalous absorption in polar cap, 20: 30225
GACHOK, V. P., Problem of moments in quantum field theory, 20: 30105
GAGARINSKII, Yu. V., Crystallochemical properties of cubic-shaped hydrated uranium tetrafluoride, 20: 29231
GAILITIS, A., Nonlinear plasma wave interaction, 20: 30628
GAILLARD, P., Application of Fano-Racah formalism to a kinematic study of nuclear reactions, 20: 30396
GALE, H. J., Calculating pulse height distribution at output of scintillation counter, 20: 29542
GALEA, V., Decontamination of waters containing ^{90}Sr and ^{90}Y with gypsum and bentonites, 20: 29348
GALEEV, A. A., Anomalous escape of ions into the "loss cone", 20: 30618
GALINDO, A., Electromagnetic form factor normalization, 20: 30096
GALINDO, A., Transformations (P, C, T) for Dirac fields, 20: 30097
GALKIN, I. V., Production of a hot plasma in Ogra-II by injection of fast H atoms into magnetic trap, 20: 30633
GALLAGHER, E. V., Prog. rpt. on reactor containment, 2–3/66, 20: 30797 (IITRI-578P21-18)
GALLAHER, D. F., Coupled-state calculations of H^+-H scattering, 20: 29940
GAL'PERIN, Yu. I., Corpuscle investigations on Elektron-1, 20: 30212 (NASA-TT-F-389, pp 551-66)
GAMTSEMLIDZE, G. A., Nature of oscillations of He II near surface of vibrating disc, 20: 30308
GANDHI, J. M., Gravitational instability, 20: 30568
GANDHI, J. M., Orientation of magnetic field in Rayleigh-Taylor's instability, 20: 30172
GANDHI, J. M., Waves in incompressible conducting fluid in magnetic field, 20: 30171
GANGRSKII, Yu. P., Coulomb excitation of levels in ^{152}Sm and ^{186}W, 20: 30488
GANGULY, B. N., Pressure effects on transition temperature of superconductors, 20: 30259
GARCIA, A., Environmental radioactivity at Valencia during 1964, 20: 29408
GARCIA, R., Cavitation damage data for water, mercury, and lead–bismuth alloy, 20: 29640 (NP-16048)
GARDNER, L. B., Potential applications of radioisotopes in Navy, 20: 29581 (AD-633785)
GAREEV, F. A., Average field levels of nuclei, 20: 30350 (JINR-P-2682)
GARIBYAN, D. V., Pigment mutations in Anacystis nidulans, 20: 28958
GASIOROWICZ, S., Sum rule connecting mesonic and photonic matrix elements and the rate for $\omega^0 \to \pi^0 + \gamma$, 20: 30036
GASIOROWICZ, S., Sum-rule calculation of isovector form factor, 20: 30037
GATTO, R., Current algebras and magnetic moments, 20: 30118
GAUTHERIN, G., New type of high-frequency mass spectrometer with two electrodes, 20: 29126
GAVRIN, P. P., Turbulent heating of plasma by direct-current discharge, 20: 30661
GAWIN, Jerzy, Method of individual location of axes of extensive air showers of cosmic radiation, 20: 29970
GAZZARRINI, F., Ionium/U method for the determination of the age of recent minerals, 20: 29441
GDALEVICH, G. L., Physical experiments on Kosmos-2 in ionosphere, 20: 30198 (NASA-TT-F-389, pp 202-24)
GEAR, C. W., Numerical integration of ordinary differential equations of various orders, 20: 29612 (ANL-7126)
GEBAUHR, W., Separation process for use in activation analysis. II., 20: 29120
GEBHARDT, E., Processes for degassing of niobium and tantalum, 20: 29633
GEDEONOV, L. I., Behavior of ^{137}Cs during analysis of atmospheric samples, 20: 29081 (NP-14705)
GEHEM, L., Large-scale isotope irradiation in reactors, 20: 29609 (NP-15947)
GEISLER, Philip H., Effects of radiations on coagulation of blood, 20: 28985
GEISS, J., Mass spectrum of fission Xe in Pasamonte meteorite, 20: 29892
GENNES, P. G., Landau-Ginsburg equations and properties of type II superconductors, 20: 30313
GEORGE, R. F., Nucleon-nucleon total cross sections from 1.1 to 8 Bev/c, 20: 30028
GERE, E. A., Channel (4096) 50-Mc/s servo stabilized analog-to-digital converter, 20: 29567
GERNHARDT, C., Survival times of rabbits after irradiation of left upper brain hemisphere, 20: 29011
GERRY, Ronald J., Protected refractory articles, 20: 29696
GERSTEIN, I. S., Chiral algebra, configuration mixing, and magnetic moments, 20: 30143
GERSTENBERG, D., Properties of anodic films formed on reactively sputtered Ta, 20: 29745
GEVORKOV, A. K., Plasma heating under beam instability conditions, 20: 30659
GEVORKYAN, V. A., Investigation of luminescence of acetyl acetonates of samarium, europium, and terbium, 20: 29238
GHATAK, A. K., Neutron lifetime and slowing-down time calculations in beryllium, 20: 30333
GHEORGHE, M., Factors affecting selective penetration of sodium pentachlorophenolate in wood, 20: 29161
GHILARDOTTI, G., Measurement of infinite multiplication constant of Latina lattice by null reactivity method, 20: 30887
GHIORSO, Albert, Omnitron: medium-energy synchrotron for acceleration of light and heavy ions, 20: 29857 (UCRL-16839)
GHIORSO, Albert, Production of nuclides in the region of Z = 126 and N = 184, 20: 30367
GHOSE, A. M., Cross sections (n,p) of some low-Z nuclei for 14.8-Mev neutrons, 20: 30394
GHOSH, Ashish K., Fluorescence studies on deuterated Chlorella vulgaris, 20: 28872
GIBERSON, R. C., Reaction of nuclear graphite with water vapor. I., 20: 29626
GIBSON, J. A. B., Calculating pulse height distribution at output of scintillation counter, 20: 29542
GIESCH, M., Capacitor bank (150-kj) for magnetic horn, 20: 29840 (CERN-66-16)
GIL, D., Interactions of 12.8-Bev protons in nuclear emulsions. III., 20: 30364
GIL, G., Reconstruction of events produced in interior of bubble chambers, 20: 29533
GILAT, G., OR GNU: FORTRAN program for calculating frequency-distribution functions of cubic crystals, 20: 30733 (ORNL-TM-1425)
GILBERT, R. W., Radiation damage produced in Cu, Au, and Al during ion bombardments, 20: 29808
GILBOY, W. B., Absence of structure in fission cross section of ^{235}U at 380 to 620 kev, 20: 30425
GILLETTE, Edward LeRoy, Morphology of bovine epididymal spermatozoa after x-irradiation of testes, 20: 29013
GILMAN, H. P., Resonant electron capture in small-angle collisions of Ar^+ on Ar and Ne^+ on Ne, 20: 29944
GILMAN, J. J., Elastic explosions in solids caused by radiation, 20: 30740
GILVARY, John P., Neutron shielding composition having good high-temperature strength, 20: 30732
GINGERICH, K. A., Phosphidation of compact zirconium metal, 20: 29642
GINSBERG, D. M., Superconducting transitions of amorphous bismuth alloys,

20: 30298
GINZBURG, V. L., Primary cosmic-ray research, 20: 29954 (NASA-TT-F-389, pp 657-77)
GINZBURG, V. L., Significance of coherent plasma radiowave emission for quasi-stellar radio objects and supernovae remnants, 20: 29880
GIRARD, J. P., Injection of ions into a magnetic mirror machine (M.M.I.I.), 20: 30634
GIRARD, Pierre, Transfer mechanism, 20: 30825
GLADOVSKII, I. P., Joule heating of plasma in toroidal Tokamak-3 device, 20: 30650
GLAGOLEV, V. M., Heating of plasma electrons by uhf fields in an adiabatic trap, 20: 30663
GLASHOW, S. L., Mass formulae in SU(3) and SU(6), 20: 30111
GLASOV, B. V., Cryogenic magnetic trap VGL-2, 20: 30655
GLASSMAN, I., Prog. rpt. on combustion of metals, annual, 7/64–6/65, 20: 29641 (SC-DC-65-1691)
GLAUDEMANS, P. W. M., Comparison of effective two-nucleon interaction with surface delta interaction, 20: 30423
GLAZMAN, I. M., Direct methods of qualitative spectral analysis of singular differential operators, 20: 29615
GLAZUNOV, P. Ya., Radiation-induced reactions of hydrogen atoms and hydroxyl radicals in aqueous solutions, 20: 29262
GLENDENIN, L. E., Mass distribution in fission of ^{229}Th, 20: 30373
GLENDENNING, N. K., Coupled-channel calculation of inelastic scattering based on a microscopic nuclear description, 20: 30437
GLENN, E. E., Solar simulation testing of nuclear test detection spacecraft, 20: 29440
GLEV, David N., Process for isotope concentration, 20: 29611
GLOVER, I. T., Carbon-14 isotope effects in Beckmann rearrangement, 20: 29242
GODDEN, G., Elastic scattering (π^--p) at 1.7 Bev/c, 20: 30011
GODNEV, I. N., Heat of formation of gaseous uranium fluorides, 20: 29171
GODSHALL, J. L., Precipitation hardening Nb–Hf–N alloys, 20: 29759
GOEKSEL, Selahattin Adil, Toxicity of ^{90}Sr in monkey skeleton, 20: 28896
GOLANT, V. E., Investigation of plasma in Tuman installation, 20: 30682
GOLANT, V. E., Plasma compression by a magnetic field in a toroidal-type device, 20: 30660
GOLD, Louis, Strength of cosmic radio sources, 20: 29898
GOLD, Raymond, Electron multiplication process in proportional counters, 20: 29554
GOLDBERG, E. D., Thorium and uranium isotopes in seawater and sediments, 20: 29412
GOLDBERG, Ernest, Semi-automatic data system for plasma study, 20: 30573
GOLDBLITH, S. A., Prog. rpt. on simultaneous radiation-heating treatment of precooked marine products, final, 2/65–2/66, 20: 29582 (MIT-3343-26)
GOL'DENBERG, A. L., Effect of stabilizers on irradiated polypropylene, 20: 29290
GOLDHABER, M., Limits for lepton-conserving and lepton-nonconserving double β decay in ^{48}Ca, 20: 30461
GOLDMAN, I. L., Radiation aspects of genetic cell differentiation and problem of malignant growth, 20: 28920
GOLDMAN, K. L., Solar simulation testing of nuclear test detection spacecraft, 20: 29440
GOLDMAN, L., Effect of repeated exposure to laser beams, 20: 28936
GOLDSMITH, Mark, Spin polarization and age of neutrons in water, 20: 30329
GOLDSTEIN, G., Partial half life for β decay of ^{36}Cl, 20: 30375
GOLOVANIVSKII, K. S., Properties of a plasma capacitor, 20: 30699
GOLOVIN, B. M., Identification of high-energy particles, 20: 30053
GOLOVIN, D. I., Effect of uranium nitrate on thyroid gland of rat, 20: 28884
GOLOWICH, Eugene, Study of low-energy meson-baryon dynamics, 20: 30070
GOLUB, V. A., Complexing of serine with rare earth elements in aqueous solutions, 20: 29208
GOMEZ, J. L., Interactions of 12.8-Bev protons in nuclear emulsions. III., 20: 30364
GONCHARENKO, V. P., Standby operation of coaxial plasma gun, 20: 30684
GONCHAROV, I. N., Anomalous behavior of j_c(H,T) of heat-treated Nb–75 percent Zr alloys, 20: 30267
GONCHAROV, I. V., Catalytic action of copper ammoniate during oxidation of uranium dioxide, 20: 29199
GONCHAROV, I. V., Kinetics of U(IV) oxidation in carbonate solution by atmospheric oxygen, 20: 29198
GOO, Zion, Ligand field theory. I., 20: 29205
GOODALL, M. C., Relation between Poincare group and exceptional Lie group G_2, 20: 30115
GOODIER, Benjamin G., Cooled high-temperature thermocouples for Phoebus reactors, 20: 30925 (LA-DC-7637)
GOODMAN, L. S., System for suppressing large, nonstatistical noise bursts in digital averaging, 20: 29556
GORBANYUK, A. G., Motion of plasmoid in a curvilinear magnetic field, 20: 30647
GORBUNOV, E. P., Electron density in Tokamak devices by microwave method, 20: 30652
GORBUNOV, L. M., Nonlinear plasma wave interaction, 20: 30628
GORBUNOV, L. M., Oscillations and stability of plasma in external high-frequency electric field, 20: 30627
GORBUNOV, L. M., Scattering of waves in a plasma, 20: 30674
GORBUNOVA, E. F., Injection of plasma blobs into mirror trap with adiabatic plasma compression: Aspa device, 20: 30636
GORDIENKO, V. P., Dynamic stabilization of a direct discharge in a magnetic field, 20: 30698
GORDUS, Adon A., Radio gas chromatography peak analyzer, 20: 29105
GORELIK, L. L., Plasma energy losses in toroidal chamber Tokamak TM-2, 20: 30653
GORIN, A. I., Radiation damages in deoxyribonucleoproteins at molecular and supermolecular levels, 20: 28908
GOROKHOV, S. D., Formation and thermal dissociation of yttrium fluorides and carbonates, 20: 29223
GOROZHANKIN, B. N., Physical experiments on Kosmos-2 in ionosphere, 20: 30198 (NASA-TT-F-389, pp 202-24)
GOSHAW, A. T., Strangeness-one resonances, 20: 30049
GOSHEN, R. J., Fine and hyperfine structure of 3^2P term in Li, 20: 29939
GOTO, S., Dense plasma produced by a cusp injection, 20: 30643
GOTODA, Masao, Initiation and propagation in γ-radiation-induced polymerization of ethylene, 20: 29275
GOULD, Robert J., Temperature of intergalactic matter, 20: 29879
GOURDON, C., Injection of ions into a magnetic mirror machine (M.M.I.I.), 20: 30634
GOUT, C., Characteristic energy losses of electrons and color centers in LiF, LiCl, and NaCl, 20: 30776
GOVINDJEE, Fluorescence studies on deuterated Chlorella vulgaris, 20: 28872
GOWOREK, T., Directional correlations of γ rays in ^{147}Sm, 20: 30362
GOYAL, D. P., Lambda-binding energies in heavy hyperfragments, 20: 30448
GRABER, Harlan Duane, Angular correlations of γ rays in ^{25}Mg(p,γ)^{26}Al reaction, 20: 30528
GRABOVSKII, Ya., Average field levels of nuclei, 20: 30350 (JINR-P-2682)
GRABOWSKI, J., Angular distribution of inelastically scattered complex particles, 20: 30502
GRABOWSKI, Z. W., Higher-order effects in β-γ correlations involving allowed β transitions, 20: 30470
GRACHEV, S. A., β decay of bromine isotopes for synthesis of krypton compounds, 20: 29327
GRAD, H., Stability of mirror machines, 20: 30635
GRADER, R. J., X-ray spectra from three cosmic sources, 20: 29901
GRADY, Charlotte, Oxygen saturation of tumor cells to increase effect of internal radiation, 20: 29059 (TID-22860)
GRADY, Edgar D., Oxygen saturation of tumor cells to increase effect of internal radiation, 20: 29059 (TID-22860)
GRADY, T. K., Nuclear spin relaxation in liquid hydrogen, 20: 30181
GRAEFFE, G., Alpha decay of ^{219}Fr and ^{215}At, 20: 30374
GRAEVSKAYA, B. M., Disturbance in catecholamine metabolism induced by radiation, 20: 28940
GRAEVSKII, E. Ya., Radioprotective mechanisms, 20: 29039
GRAEVSKII, E. Ya., Temperature effect on cysteamine accumulation in cells and its radioprotecting activity, 20: 29057
GRAFF, R. A., Kinetics of high temperature oxidation of refractory materials, 20: 29656
GRASHCHENKOV, N. I., Adrenaline and noradrenaline, 20: 29032
GRASHCHENKOV, N. I., Alterations in content of adrenaline-like substances in blood of dogs during acute and sub-acute radiation sickness, 20: 28941
GRASHCHENKOV, N. I., Disturbance in catecholamine metabolism induced by radiation, 20: 28940
GRASHCHENKOV, N. I., Role of sympathetic influences in genesis of stressed organism reactions to ionizing radiation, 20: 28939
GRATTON, Charles Peter, Improvements in or relating to nuclear reactors, 20: 30822
GRATTON, Charles Peter, Improvements in or relating to reactors, 20: 30912
GRAVIER, R., Characteristics and purification of plasma produced by coaxial gun with annular preionization, 20: 30648
GRAVIER, R., Heating and containment of plasma in the magnetic well in Deca II, 20: 30607
GRAY, Thomas A., Alpha radiation gaging technique as applied to basis weight measurement, 20: 29601
GREBENSHCHIKOV, S. E., Injection and confinement of plasma in a stellarator with a multipolar (l = 2) helical field, 20: 30657
GREEN, A. M., Odd-parity states of ^{16}O with a realistic nucleon-nucleon interaction, 20: 30412

GREEN, Derek, Extrusion apparatus, 20: 29693
GREEN, Derek, Forming of materials by extrusion, 20: 29691
GREEN, S. J., Compressive strain rate tests on four composites, Phase I, 20: 29708 (SC-DC-65-1744)
GREEN, T. S., Plasma containment and stability in megajoule theta-pinch experiment, 20: 30610
GREEN, W. B., DTF-II shielding data library, 20: 30723 (NAA-SR-11831)
GREENBERG, Joseph, Radiomimetic properties of 2-aminopurine in E. coli, 20: 29041
GREENBERG, M. L., Extracorporeal irradiation of blood, 20: 28927 (BNL-9647)
GREENSLADE, Walter Percival, Illuminated telephone dial, 20: 29605
GREENSPAN, J., High-pressure isostatic pressing and pressureless sintering of metal powder compacts, 20: 29681
GREENSTREET, B. L., Influence of cross-sectional shape on irradiation-induced stresses in graphite columns, 20: 30803
GREIDER, K. R., Divergence of distorted-wave Born series for rearrangement scattering, 20: 30120
GREIDER, K. R., Rigorous solution of three-body scattering processes in distorted-wave formalism, 20: 30121
GREINER, Walter, Eigenchannel theory of nuclear reactions, 20: 30449
GRENACS, L., Evidence for 1^-, K = 0 character of ^{176m}Lu through β-decay measurements, 20: 30552
GRENACS, L., Nonaxial model predictions on first-forbidden β transitions of ^{188}Re, 20: 30550
GRENACS, L., Nuclear matrix elements of the β transition of ^{194}Ir, 20: 30551
GRENACS, L., Recoil effect in perturbed β-γ directional correlation in ^{166}Ho, 20: 30554
GREVET, Philippe, Total ionization intensity near ground and separation of various components, 20: 29404
GRIBOV, V. N., Consequences from vector current conservation, 20: 30008
GRIEGER, G., Comparison of alkali plasma loss rates in a stellarator and in toroidal device with minimum mean-B properties, 20: 30656
GRIEM, H. R., Plasma confinement, heating, and losses in Pharos with an extended current pulse, 20: 30612
GRIFFIN, Peter Allan, Electronic thermal conductivity and other properties of gapless superconductors, 20: 30321
GRIFFITH, T. C., Measurement of the spin-rotation parameter β in proton-^{4}He scattering at 48 Mev, 20: 30441
GRIFFY, T. A., Neutron form factors from study of inelastic electron spectra in electrodisintegration of deuterium, 20: 30027
GRINEV, A. N., Loss of hypotensive activity by derivatives of 5-hydroxyindole when animals are irradiated, 20: 29050
GRINGAUZ, K. I., Comparison of simultaneous measurements of magnetic field and positive ion streams within earth's magnetosphere, 20: 30208 (NASA-TT-F-389, pp 457-63)
GRINGAUZ, K. I., Outermost zone of charged particles, 20: 30220 (NASA-TT-F-389, pp 633-52)
GRINGAUZ, K. I., Physical experiments on Kosmos-2 in ionosphere, 20: 30198 (NASA-TT-F-389, pp 202-24)
GRINGAUZ, K. I., Possible existence of soft electron component in outer radiation zone, 20: 30213 (NASA-TT-F-389, pp 566-8)
GRISARU, M. T., Three-particle contributions to elastic scattering, 20: 30129
GRISHIN, V. G., Formation of electron-positron pairs by high-energy gamma quanta, 20: 29990 (JINR-P-2667)
GRISSOM, J. T., Decay of ^{141}Nd. II., 20: 30416
GRITCHENKO, Z. G., Behavior of ^{137}Cs during analysis of atmospheric samples, 20: 29081 (NP-14705)
GROBMAN, Warren D., Persistent currents in many-boson systems, 20: 30140
GROCE, D. E., Neutron-proton total cross sections near 20, 24, and 28 Mev, 20: 30004
GRODZINS, L., Moessbauer effect of 99- and 129-kev transitions in ^{195}Pt, 20: 30757
GRODZINSKII, D. M., Natural radioactivity of plants and soils, 20: 29437
GROMOV, V. F., Radiation-induced polymerization of tetrafluoroethylene and acrylonitrile at 4.2 K, 20: 29300
GROSJEAN, Carl C., Absolute detection efficiencies of cylindrical scintillation gamma-ray detectors, 20: 29562
GROSSMAN, L. N., Niobium–Al_2O_3 reactions yielding condensed and volatile products, 20: 29174
GROSSMAN, Ronald A., Conversion of gamma rays from the decay $\eta^0 \rightarrow \pi^+ + \pi^- + \gamma$, 20: 30029
GROVE, Donald J., Semi-automatic data system for plasma study, 20: 30573
GROVES, D. J., Coherent neutron scattering amplitudes of ^{10}B and ^{11}B, 20: 30335
GROZDOV, S. P., Catecholamine metabolism in acute ^{210}Po lesions, 20: 28886
GRUEHN, R., Modifications of Nb pentoxide, 20: 29728
GRUHN, C. R., Proton spectra from reactions induced by 30.5-Mev α particles, 20: 30472
GRUND, J. E., Review of SPERT subassembly test program for CDC and the PBF, 20: 30796 (IDO-17177)
GRZELEWSKI, L., Sterilization of bone tissues with gamma radiation in Poland, 20: 28987
GSCHNEIDNER, K. A. Jr., High-temperature heat contents and related thermodynamic functions of rare-earth metals, 20: 29743
GUENTHER, H., Simple method for ^{15}N determination, 20: 29131
GUENTHER, John Richard, Production of cured resin bodies by radiation pre-gelling and hot curing, 20: 29637
GUILBOT, Andre, Effect of ^{60}Co γ radiation on amidon, 20: 29255
GUILLEN, Marcelo, Determination of the structure of La_2TiO_5 with x rays and neutrons, 20: 30738
GUIMARD, M., Thermal creep and inelastic behavior of artificial graphite, 20: 29734
GUKASYAN, L. A., Effect of x-irradiation on yield of potatoes, 20: 28966
GULYAMOV, U. G., Differential cross section of charge exchange of 4.8-Bev/c π^- mesons with protons, 20: 29998
GULYAMOV, U. G., Production of slow π^+ mesons by 9-Bev proton interaction with photoemulsion nuclei, 20: 30370
GUNDERMAN, William, Field evaluation of nuclear gages used in compaction control of embankments, 20: 29507
GUPTA, G. P., Gravitational instability, 20: 30568
GUPTA, G. P., Waves in incompressible conducting fluid in magnetic field, 20: 30171
GURKLIS, J. A., Machining and grinding of nickel- and cobalt-base alloys, 20: 29665 (RSIC-482)
GURLAND, J., Effects of temperature and heat treatment on strength of sintered WC–Co alloys, 20: 29802
GUSEV, Yu. K., β decay of bromine isotopes for synthesis of krypton compounds, 20: 29327
GUSEYNOV, O. H., Collapsed stars in binaries, 20: 29889
GUSYNIN, V. I., Effect of an electric field on liquid-hydrocarbon radiolysis, 20: 29263
GUSZAVIN, V. M., Boson resonance at 1.63 Bev in π^-p interactions, 20: 30021
GUTKIN, T. I., Plasma equilibrium in torus with high-frequency fields and plasma heating resulting from beam of "escaping electrons", 20: 30640
GUTMANN, V., Formation of azides of Pr(III) and Nd(III), 20: 29166
GYLFE, J. D., Nuclear power systems for advanced high-power communications satellites, 20: 29608

H

HAASE, Joachim, Atomic scattering amplitudes for fast electrons, 20: 29945
HACHISUKA, Takeji, Effect of Mo on the oxidation of TiC–No–Mo alloys, 20: 29653
HACKSTEIN, K., Manufacture of nuclear reactor fuel elements and their coating with pyrolytic carbon, 20: 29670
HADDOCK, F. T., Extension of non-thermal radio-source spectra to 8000 Mc/s, 20: 29878
HADEISHI, Tetsuo, Intensity beats in resonance radiation absorbed by excited metastable state, 20: 30601
HADEN, C. R., High-frequency residual losses in superconductors, 20: 30304
HAEBERLI, W., Polarization in p-α scattering from 17 to 27 Mev, 20: 30389
HAEGI, M., Hollow dynamic pinch, 20: 30641
HAELG, W., S-D exchange interactions and Fermi surface in Ni, 20: 30775
HAENSGEN, H., Study of Be with polarized neutrons of energy 2.60 to 2.77 Mev, 20: 30414
HAEUSLER, W., Influence of γ-radiation on gasification of lignite, 20: 29586
HAFNER, H., Scalar interaction and conformal space, 20: 30361
HAGE, K. D., Prog. rpt. on particle fallout and dispersion in atmosphere, 9–11/65, 20: 29454 (SC-CR-66-2010)
HAGEE, G. R., Weak α and electron-capture decay in ^{208}Po and ^{209}Po, 20: 30405
HAGINOYA, Toru, Problems in Japan's acquisition of nuclear fuels, 20: 30871
HAGIWARA, Miyuki, Initiation and propagation in γ-radiation-induced polymerization of ethylene, 20: 29275
HAHN, K., Radiation control concentration changes of free amino acid in blood plasma of man, 20: 28979
HAHN, R. L., Interactions of ^{3}He particles with ^{9}Be, ^{12}C, ^{16}O, and ^{19}F, 20: 30444
HAKURA, Y., Development of polar geomagnetic disturbance and PCA event on 2/11/58, 20: 30230
HALEY, Thomas J., Acute radiation effects: damage of hematopoiesis, 20: 28981
HALKO, A., Study of water radiolysis and hydrogen peroxide formation using radioactive ^{15}O, 20: 29315
HALL, A. M., Surface treatments for nickel and nickel-base alloys, 20: 29706 (NASA-TM-X-53448)

HALL, E. J., Routine dosimetry with ^{182}Ta and ^{192}Ir wires, 20: 29456
HALL, Hugh E. Jr., Scintillation-type well logging device with two crystals, 20: 29445
HALTRICH, Walter, Elimination of both P isotopes ^{31}P and ^{32}P from domestic waste water, 20: 29353
HAMA, Masaharu, Preserved hematopoietic tissues for treatment of mice lethally irradiated with gamma rays. II., 20: 29033
HAMA, MASAHARU, Preserved hematopoietic tissues for treatment of mice lethally irradiated with gamma rays. III., 20: 29034
HAMADA, Masayuki, Improvements in ^{14}C assay of organic compounds by dry combustion, 20: 29085
HAMEL, J. L., Search for an isobar of isotopic spin $T = 5/2$, 20: 30022
HAMILTON, J., Scattering (π-N), Pt. 1, 20: 29986 (CONF-640509(Pt.1), Paper 2)
HAMMEL, E. F., Automatic superconducting flux pump, 20: 30274
HAMMER, D. C., Viscosity coefficients for liquid ^{3}He, 20: 30275
HAMMITT, F. G., Cavitation damage data for water, mercury, and lead–bismuth alloy, 20: 29640 (NP-16048)
HAMPE, E., Sintering of uranium of extremely oxide-free surface, 20: 29673
HANDEL, Neil E., Device for producing a modulated beam of beta or x-radiation, 20: 29516
HANFFSTENGEL, K. v., Air locks for safe escape in nuclear reactors, 20: 29465
HANNA, A. E., Potential applications of radioisotopes in Navy, 20: 29581 (AD-633785)
HANSEL, J. G., Prog. rpt. on combustion of metals, annual, 7/64–6/65, 20: 29641 (SC-DC-65-1691)
HANSEN, Ole, Proton pickup from the even lead nuclei, 20: 30387
HANSEN, Ole, Reaction $^{42}Ca(d,p)^{43}Ca$ at 7.0 and 7.2 Mev, 20: 30452
HANSEN, P. G., Sign and magnitude of Coriolis coupling between the $5/2^-[532]$ and $7/2^-[523]$ orbitals in ^{161}Tb, 20: 30401
HARA, Akio, Properties of sintered WC–Co alloys, 20: 29778
HARARI, H., W spin for any spin, 20: 30126
HARCHOL, M., Energy levels of ^{63}Zn, 20: 30406
HARDCASTLE, R. A., Inter-diffusion of plasma and magnetic fields in pinch and hardcore discharges, 20: 30639
HARDY, Kenneth A., Techniques for determining proton depth dose distribution in primates, 20: 28928 (CONF-651109, pp 417-25)
HARDY, Walter G., Radiotherapeutic effects on mammalian tumor cells. I., 20: 28962
HARGRAVE, D. P., Some observations on indirect sintering of tungsten, 20: 29684
HARGRAVES, R., Photoproduction on H of ρ^0 mesons between threshold and 6 Bev, 20: 30030
HARGREAVES, G., Technique for gamma radiation graft polymerization, 20: 29316
HARLAN, Jerry W., Effect of irradiation temperature on organoleptic, physical and chemical properties of beef, 20: 29602
HARLASS, Eberhard, Paragenetic position of U pitchblende in hydrothermal deposits of West Erzgebirge, 20: 29448
HARMELIN, Miroille, Thermal decomposition of trihydrated lutetium iodate, 20: 29097
HARMISON, Lowell Thomas, Derivative neutron activation analysis of zinc, 20: 29136
HARRAR, J. E., Prog. rpt. on analytical chemistry, 1–12/65, 20: 29083 (UCRL-14767)
HARRER, Joseph M., Reactor control experience, 20: 30901
HART, H. R. Jr., Effect of thermal-neutron irradiation on superconducting properties of Nb_3Al and V_3Si doped with fissionable impurities, 20: 30260
HARTE, John, Composite-particle model with application to Ω^- decay, 20: 30069
HARTING, D., Interaction π^+-π^- as studied in 12- and 18-Bev pion-nucleon reactions, 20: 30025
HARTNETT, James P., Advances in heat transfer. Vol. 3, 20: 29381
HARVEY, B. G., Scattering of 40.5-Mev α particles by ^{12}C, ^{13}C, ^{14}N, ^{15}N, ^{16}O, and ^{18}O, 20: 30450
HARVEY, Bernard G., Scattering of α particles by ^{52}Cr, ^{53}Cr, and ^{51}V, 20: 30460
HASAI, Hiromi, Fast double or triple coincidence circuit, 20: 29537
HASHIMOTO, Hitoshi, Transfer of oxygen atom of water in aqueous solution of iron and copper sulfates, 20: 29153
HASHIMOTO, Yuichi, Movement of radioactive calcium in brain slices, 20: 28891
HATANO, Yoshihiko, Photolysis of cis-2-butene and its implications for radiation chemistry, 20: 29251
HATTA, Yoshisuke, Instability of two colliding plasma streams, 20: 30593
HAUBERT, P. R., Approximate treatment of neutron thermalization in heterogeneous systems, 20: 30864
HAUGHTON, Geoffrey, Variation of antigenic characteristics between mouse lymphomas induced by Moloney virus, 20: 28873
HAUSCHILD, J., Sample furnace for experiments on neutron scattering, 20: 29106
HAUSENBAUER, George F., Stresses in thick-walled conical shells, 20: 30928
HAYAKAWA, Akira, Radiation preservation of fruits and vegetables, 20: 29597
HAYAKAWA, Kiyoshi, Dose estimation of electron beam by glass method, 20: 29283
HAYAKAWA, Shigeru, Formation of rotating plasma in crossed field, 20: 30582
HAYAMI, Tadashi, Spectrophotometric determination of F with a PAC–Th complex, 20: 29091
HAYASHI, Koichiro, Radiation-induced solid-state copolymerization of maleic anhydride and acenaphthylene, 20: 29274
HAYASHI, Kozi, Influence of TiC on some properties of sintered WC–Co alloys, 20: 29779
HAYASHI, Miyoko, Dose rate measurements of low-level x-rays having less than 35 kev energies, 20: 29553
HAYASHI, Satoshi, Dose rate measurements of low-level x-rays having less than 35 kev energies, 20: 29553
HEDGE, C. E., Source of Pb and Sr in deep geothermal brines underlying the Salton Sea geothermal area, 20: 29414
HEDIGER, W., Thermodynamic design of reactor cooled by gas, 20: 30892
HEEGER, D., Release of stored energy and electric resistivity changes in neutron-irradiated Cu, 20: 29824
HEIDEMAN, H. G. M., Inelastic electron scattering from H_2, 20: 29953
HEIER, K. S., Thorium, U and K concentrations in granites and gneisses of Rum Jungle Complex, Northern Territory, Australia, 20: 29415
HEIKKINEN, Dale William, Total cross sections and angular distributions of reaction products from $^{6}Li + ^{12}C$ reaction, 20: 30520
HEILIGMAN, Fred, Development of radiation-sterilized seafood products. I., 20: 29603
HEILIGMAN, Fred, Effect of irradiation temperature on organoleptic, physical and chemical properties of beef, 20: 29602
HEINRICH, L. A., Gadolinium nitrate injection as auxiliary shutdown system for Savannah River Reactors, 20: 30920
HEISS, A., Isar I: fast megajoule theta-pinch experiment with extremely high compression fields, 20: 30611
HELENE, Claude, Photoionization and biphotonic processes of nucleic acids derivatives in frozen solutions, 20: 28914
HELFAND, E., Temperature and purity dependence of superconducting critical field, H_{c2}. II., 20: 30295
HELFAND, E., Temperature and purity dependence of superconducting critical field, H_{c2}. III., 20: 30296
HELM, J. W., Radiation effects in graphite at high temperature, 20: 29812
HENDERSON, R. W., Radiation measurements of effluent from NRX A-2 and NRX A-3 reactors, 20: 30923 (LA-3394)
HENDRIE, David L., Scattering of α particles by ^{52}Cr, ^{53}Cr, and ^{51}V, 20: 30460
HENGLEIN, A., Pulse-radiolysis studies on reactivity of catalase with hydrated electrons and free OH radicals, 20: 29279
HENNESSY, Elinor, ADONIS: IBM-7090 Monte Carlo shielding code in three-dimensional rectangular geometry, 20: 30726 (TID-22964)
HENNING, W., Moessbauer effect investigation of shell conversion of electron capture, 20: 30555
HEPP, V., Inelastic Σ^-p interactions at low momenta, 20: 30024
HEREMANS, R., Relative problems of design of pilot plants for reprocessing by volatilization, 20: 29364
HERLEY, P. J., Photochemical decomposition of sodium bromate, 20: 29248 (BNL-9672)
HERMANN, G., Behavior of recoil atoms in the decay of ^{219}Rn and ^{220}Rn in gases, 20: 29325
HERMANN, Robert, Group representations and creation operators, 20: 30099
HERMANN, Robert, Representation of groups containing the Poincare group. I., 20: 30098
HERNADY, T., Radiosensitivity of red cell catalase in vitro, 20: 28911
HEROLD, H., Doppler shift measurements to investigate plasma rotation in the theta pinch, 20: 30615
HERRAEZ, M. A., Deformation of graphite lattices by interstitial carbon atoms, 20: 29735
HERRMANN, Guenter, Volatilization of U fission products in H, Ni, and O, 20: 29211
HERRNEGGER, F., One-dimensional unsteady potential MHD flow, 20: 30570
HERSH, Herbert N., Color centers in x- or uv-irradiated KI, 20: 30748
HERSHENSON, Herbert M., Nuclear magnetic resonance and electron spin resonance spectra, 20: 30510
HERZ, A. J., Particle detectors. I., 20: 29534
HESS, R., Nonaxial model predictions on first-forbidden β transitions of ^{188}Re, 20: 30550
HESS, R., Recoil effect in perturbed β-γ directional correlation in ^{166}Ho, 20: 30554
HESTER, R. E., Experimental studies with Astron, 20: 30637

HEUER, W., Further results from interference of K_S and K_L in $\pi^+\pi^-$ decay modes, 20: 30026
HEUS, R. J., Free energies of formation of inorganic fluorides, 20: 29215
HEWITT, Roger Roy, Metabolism of protectant doses of L-cysteine by rat and guinea pig, 20: 29024
HIBNER, Juliusz, Method of individual location of axes of extensive air showers of cosmic radiation, 20: 29970
HIISMAEKI, P., Crossing and anticrossing signals of ^1H and ^2H atoms in uniform magnetic field, 20: 29935
HILL, C. R., Polonium-210 content of human tissues in relation to dietary habit, 20: 28894
HILL, R. W., X-ray spectra from three cosmic sources, 20: 29901
HILTZ, R. H., Mechanical properties tests of 316 SS specimens in 1200°F, Na contaminated with O, 20: 29704 (MSAR-66-78)
HINDEL, Robert, Radiation source measuring apparatus having automatic background subtract means, 20: 29571
HINDS, S., Proton pickup from the even lead nuclei, 20: 30387
HINNOV, Einar, Measurement of recombination-rate coefficient of He^{++}, 20: 30600
HINTZ, E., Plasma confinement, heating, and losses in Pharos with an extended current pulse, 20: 30612
HIRAKI, Keizo, Fluorometric determination of Y with 5,7-dichlorooxine, 20: 29094
HIRANO, K., Dense plasma produced by a cusp injection, 20: 30643
HIRATSUKA, Satoshi, Metabolism of serum proteins in rats, 20: 28954
HIRAYAMA, Toru, Radiation-induced addition of hydrogen chloride to ethylene, 20: 29252
HISLOP, J. S., Lunar and planetary surface analysis using neutron activation, 20: 29140
HITTERMAN, R. L., Crystal structure of thorium nitrate pentahydrate by neutron diffraction, 20: 29151
HO, Chieh, Determination of electron temperature of a theta-pinched H plasma by means of C line radiation, 20: 30705
HOANG, Tran Duc, Radiative transition probability from $3/2^+$ to $3/2^-$ state in ^5He, 20: 30386
HODGSON, K. E., Gamma radiolysis of carbon suboxide, 20: 29269
HOENIG, Milton Maurice, Applications of Brueckner many-body theory, 20: 30523
HOFFMANN, A. P., Evaluation of the ^{17}N reactor power level monitor, 20: 30938
HOFFMANN, W., Evaluation of activity determination of biological materials with electronic computer, 20: 29121
HOFFSWELL, R. A., Isobaric analog states by (p,n) reactions, 20: 30480
HOFMANN, F. W., Toroidal theta pinch with superimposed multipole field, 20: 30616
HOFSTADTER, R., Neutron form factors from study of inelastic electron spectra in electrodisintegration of deuterium, 20: 30027
HOHENBERG, P. C., Stability of a lattice of superfluid vortices, 20: 30286
HOHENBERG, P. C., Temperature and purity dependence of superconducting critical field, H_{c2}. III., 20: 30296
HOLLAND, M. G., Lorenz number of graphite at low temperatures, 20: 29750
HOLLAND, R. F., Prompt air fluorescence excited by high-altitude nuclear explosions, 20: 30193 (LA-3409(Suppl.))
HOLLINGSWORTH, C. A., Fourth-order crystal field splitting in rare earth(III) ions, 20: 30747
HOLVERSON, E. L., Electrical conduction by oxygen ions in cerium oxide, 20: 30743
HOLZAPFEL, H., Preparation and structure of rare earth titanates and of europium(II) zirconate, 20: 29212
HONDA, Takao, Nuclear fission model with core, 20: 30380
HONDA, Yutaka, Microhardness and plastic deformation of uranium dioxide, 20: 29786
HOOP, B. Jr., Scattering of neutrons by α particles, 20: 30390
HOOPER, Alan Thomas, Improvements in or relating to spacing grids for closely spaced articles, 20: 30818
HOREN, D. J., Scattering of 40.5-Mev α particles by ^{12}C, ^{13}C, ^{14}N, ^{15}N, ^{16}O, and ^{18}O, 20: 30450
HORN, D., W spin for any spin, 20: 30126
HORTON, T. R., Leak testing of reactor containment systems, 20: 30812
HORWITZ, E. P., Separation of americium and curium by extraction chromatography, 20: 29337
HORWITZ, E. P., Sorption of certain transplutonium ions on amorphous zirconium phosphate, 20: 29340
HOSODA, Tadashi, Deoxidation of Mo during arc melting, 20: 29675
HOSTETLER, D. R., Indian Point Reactor—instrumentation asymmetry response verification, 20: 30876 (BAW-1302)
HOTTA, Hiroshi, Thermal and radiation oxidations of benzene to phenol in aqueous solutions containing metal ions. VII., 20: 29250
HOTTA, Hiroshi, Transfer of oxygen atom of water in aqueous solution of iron and copper sulfates, 20: 29153
HOUYVET, A., Future of refractory ceramics in the nuclear field, 20: 29732
HOVI, V., Deuteron magnetic resonance in single crystals of ND_4Cl and ND_4Br, 20: 29191
HOWARD, Judith B., Acatalasemic and hypocatalasemic mouse mutants, 20: 28957
HOWARTH, Sheila, Increase in frequency of ultraviolet-induced mutation in Salmonella typhimurium, 20: 28977
HOWE, L. M., Radiation damage produced in Cu, Au, and Al during ion bombardments, 20: 29808
HOWELL, L. N., Advanced accelerator development, 20: 29885 (ORNL-3940, pp 83-111)
HOYLE, F., Nature of quasi-stellar objects, 20: 29877
HROVAT, M., Spherical pressed-graphite fuel elements for high-temperature reactors, 20: 29669
HRYNKIEWICZ, A. Z., Moessbauer effect for ^{57}Fe impurity atoms, 20: 30766
HSIEH, Lie-Hsiang, Asymmetrical configuration of trapped region and some correlated aeronomical phenomena, 20: 30224
HSIUNG, Chi-hua Wu, Mathematical study of gas-phase hot-atom reactions, 20: 29233
HSU, Hsiao-pei, Oxidation of lanthanum hexaboride in air at 800 and 1000°C, 20: 29163
HU, Kuo-chen, Colorimetric micro-determination of U by EDTA-nitrosonaphthol-azoarsine I, 20: 29130
HU, L. W., Cascade arrangement in spherical vessel design for power reactors, 20: 30893
HUANG, Kerson, Incoherent droplet model of high-energy large-angle scattering, 20: 30038
HUBBARD, Darryl Franklin, Nuclear contribution to radiative processes, 20: 30516
HUBBARD, R. T. J., Protective coatings for niobium and its alloys, 20: 29651
HUDSON, W. R., Flux pinning in superconducting niobium thin films, 20: 30278
HUEBNER, R., Production of antiprotons by high-energy photons, 20: 30432
HUEFNER, S., Moessbauer effect investigation of shell conversion of electron capture, 20: 30555
HUGHES, E. B., Neutron from factors from study of inelastic electron spectra in electrodisintegration of deuterium, 20: 30027
HUGHES, L. B., Neutron separation energies of ^{143}Nd–^{144}Nd, ^{149}Sn–^{150}Sm, and ^{164}Dy–^{165}Dy, 20: 30366
HUGHES, L. B., Reaction $^{197}Au(n,\gamma)^{198}Au$, 20: 30409
HUGHES, R. H., Lifetimes of n = 3 states of H by electron capture during fast H^+ impact on gases, 20: 29930
HUGHES, V. W., Muonium chemistry, 20: 29177
HUKE, Kozuo, Momentum compaction in a cyclic accelerator, 20: 29861
HULL, R. L., Fast-neutron activation analysis using small accelerators, 20: 29139
HULSTON, J. R., Isotope abundance and content of sulfur in meteorites, 20: 29893
HUNTER, James H. Jr., Quasars—a minority report, 20: 29896
HURT, William D., Techniques for determining proton depth dose distribution in primates, 20: 28928 (CONF-651109, pp 417-25)
HUSCHKA, H., Manufacture of nuclear reactor fuel elements and their coating with pyrolytic carbon, 20: 29670
HUTCHINSON, William George, Improvements in or relating to grab devices, 20: 30824
HUTCHISON, Charles Strachan, Calibration of thermoluminescence measurements, 20: 29400
HYAM, E. D., Grain boundary holes in irradiated U, 20: 29807 (TRG-Report-325)

I

IBRAGIMOV, A. P., Radiochemical properties of certain peptides, 20: 29301
ICHIKAWA, Yoshi H., Optical properties of graphite in the infrared region, 20: 30736
IDEHARA, Toshitaka, Analysis of negative absorption of plasma-cavity system, 20: 30587
IFEROV, G. A., Elastic and inelastic scattering of α particles by C, 20: 30499
IGAMBERDIEV, K. R., Differential cross section of charge exchange of 4.8-Bev/c π^- mesons with protons, 20: 29998
IIJIMA, Shungo, One-phonon coherent scattering of slow neutrons from polycrystalline aluminum, 20: 30745
IKEDA, Masaomi, F coloring in γ- and neutron-irradiated ionic crystals, 20: 30739
IKEDA, Mineo, Elementary particles and bound states, 20: 30145
IL'IN, S. D., Location of moving plasma bursts from coaxial injector, 20: 30681
ILLY, H., Vapor pressure of solid D_2O, 20: 29149
IL'YUCHENOK, T. Yu., Loss of hypotensive activity by derivatives of 5-hydroxyindole when animals are irradiated, 20: 29050

IL'YUKEVICH, L. A., Effects of γ- and ultraviolet rays on copper glycocol, 20: 29303
IMAMURA, Rikizo, Studies of graft copolymerization onto viscose rayon. III., 20: 29294
IMRIE, D. C., Measurement of the spin-rotation parameter β in proton-^{4}He scattering at 48 Mev, 20: 30441
INGRAM, H. Vernon, Lasers and ultrasonics, 20: 28951
INOPIN, E. V., Equality of polarization and asymmetry in inelastic scattering, 20: 30492
INOUE, Yasushi, Chemistry of Pa. I., 20: 29335
IOFFE, B. L., Check on T invariance in $\pi^+ \to e^+ + \nu + \gamma$ decay, 20: 29997
IOFFE, B. L., Consequences from vector current conservation, 20: 30008
IONESCU-PALLAS, N. J., Scalar interaction and conformal space, 20: 30361
IOSSIFIDES, Ioulios A., Effects of radiations on coagulation of blood, 20: 28985
IPPOLITOVA, E. A., High-temperature x-ray phase analysis of U–O system from $UO_{2.50}$ to $UO_{2.67}$, 20: 29799
IRVINE, Thomas F. Jr., Advances in heat transfer. Vol. 3, 20: 29381
IRVING, C. D., Impossible Legendre coefficients, 20: 30355 (ORNL-P-2084)
ISAENKO, V. I., Use of laser operating in spike mode to obtain high-temperature plasma, 20: 30590
ISENHOUR, Thomas Lee, Activation analysis using neutron capture and delayed gamma-ray spectrometry, 20: 29137
ISHIBASHI, Nobuyoshi, Effect of radiations on propagation of root-knot nematodes, Meloidogyne incognita Chitwood, 20: 28942
ISHIDA, Humihiko, Studies of hard superconductors. II., 20: 29785
ISHIDA, Humihiko, Studies of hard superconductors. III., 20: 29787
ISHIDA, Humihiko, Studies of hard superconductors. IV., 20: 29788
ISHIGURO, Masakazu, Optical properties of CsI : Tl and CsBr : Tl, 20: 30751
ISHIGURO, Yoshio, Rapid colorimetric determination of beryllium in Al–Mg–Be alloys, 20: 29111
ISHIHARA, Katsumi, Superconducting Nb–10Zr alloy, 20: 29789
ISHIHARA, Takehiko, Disposal of radioactive wastes and problems, 20: 30945
ISHIHARA, Takehiko, Radiation damage to TBP–kerosene solvent. II., 20: 29272
ISHII, Bunpei, High-temperature oxidation mechanism on 2.5Sn–Zr alloy, 20: 29652
ISHII, Yogoro, Gamma radiography with a large ^{60}Co source, 20: 29596
ISHIKAWA, Michio, Design of JPDR-II and technological problems, 20: 30889
ISHIMURA, T., Dense plasma produced by a cusp injection, 20: 30643
ISHINO, Toshio, Preparation of Th carbides, 20: 29676
ISTOMIN, V. G., Radiofrequency mass spectrometer for the Electron satellites, 20: 29545
ITAYA, Mitsuo, Shell model studies of 1f-shell nuclei. I., 20: 30365
ITO, H., Dense plasma produced by a cusp injection, 20: 30643
ITO, Shozo, Deposition velocity of ^{131}I, 20: 29479
IVANNIK, B. P., Radiation damages in deoxyribonucleoproteins at molecular and supermolecular levels, 20: 28908
IVANOV, A. E., Inflammation and penetrating ionizing radiation, 20: 28943
IVANOV, B. A., Active diagnosis of hot plasma by means of neutral particles, 20: 30685
IVANOV, B. A., Investigation of plasma concentration in Al$^+$fa with probe beam of fast atoms, 20: 30686
IVANOV, D. P., Toroidal discharge in a varying longitudinal magnetic field, 20: 30654
IVANOV, K. V., Damaging effects of underwater nuclear explosion, 20: 29481
IVANOV, V. S., Synthesis of high molecular compounds by radiation polymerization methods, 20: 29298
IVANOVA, E. I., Effects of γ radiation on structure of epoxy resins and resin-base metallic polymers, 20: 29296
IVANOVA, E. I., X-ray study of epoxido-dianic ED-5 resin irradiated with ^{60}Co and metallopolymers on its base, 20: 29297
IVANOVA, G. F., Effect of γ-rays from ^{60}Co on certain metabolic processes in pea plants, 20: 28909
IVANOVA, O. M., Thorium tetrasulfate compounds, 20: 29218
IVANOVA, O. M., Thorium penta- and hexasulfate compounds, 20: 29226
IVANOV-KHOLODNYI, G. S., Electron concentration in ionosphere at altitudes of 100-300 km, 20: 30199 (NASA-TT-F-389, pp 248-58)
IVINS, Richard O., Reaction of U with water as initiated by power excursion in TREAT, 20: 30802
IWAMOTO, Jenko, Loss of ^{137}Cs and K by dry ashing and HCl treatment of total diet samples, 20: 29122
IWASAKI, Machio, Free radicals produced by irradiation. II., 20: 29282
IYATA, Gihi, Momentum compaction in a cyclic accelerator, 20: 29861
IZAWA, Masumi, Concentration of radionuclides in sea water by metal sulfide-ion exchange resins, 20: 29345
IZAWA, Masumi, Separation of ^{90}Sr and ^{90}Y by paper electrophoresis, 20: 29336
IZVEKOVA, A. V., Secondary disease in irradiated animals treated with bone marrow, 20: 29006

J

JAARMA, Mairo, Influence of ionizing radiation on proline content of potato tubes, 20: 28932
JAARMA, Mairo, Influence of γ irradiation on β-fructofuranosidase in potato tubers, 20: 28934
JAARMA, Mairo, Influence of γ irradiation on UDPglucose-fructose glucosyltransferase in potato tubers, 20: 28935
JACKOMIS, William N., Transient flow field analysis of blast wave intercepting a stationary cone at zero angle of attack, 20: 30168 (SC-DC-66-1329)
JACKSON, C. M., Surface treatments for nickel and nickel-base alloys, 20: 29706 (NASA-TM-X-53448)
JACKSON, Earle W., Determination of asphalt contents in a paving mixture by thermal neutrons, 20: 29509
JACKSON, Earle W., Effects of type of material on nuclear density measurements, 20: 29505
JACKSON, Earle W., Field evaluation of nuclear gages used in compaction control of embankments, 20: 29507
JACKSON, Earle W., Meeting on nuclear measurements, 1/64, 20: 29504
JACKSON, Earle W., Nuclear measurement of soil properties, 20: 29506
JACKSON, Earle W., Nuclear surface gages for determining soil moisture and density, 20: 29508
JACKSON, H. E., High-energy γ spectra from neutron capture in Hf isotopes, 20: 30466
JACKSON, J. D., Production and decay of resonances at a few Bev, 20: 30085 (CONF-640509(Pt.1), Paper 3)
JACKSON, J. L., Tensile fracture strain of graphite determined during neutron irradiation, 20: 29811
JACOBS, E., Diffusion of tritons in NH_4F-doped ice single crystals, 20: 29193
JACQUOT, A., Fast neutron scattering cross sections of iron, 20: 30417
JAECH, J. L., Prog. rpt. on Zr alloy, 20: 29660 (GEAP-4960)
JAENNE, J., The effect of erythemal reaction caused by ultraviolet irradiation on mast cell degranulation in the skin, 20: 28937
JAERSCHKY, Rudolf, KRB Gundremmingen nuclear power station, 20: 30888
JAFAR, J. D., Reaction $d + d \to {}^4He + 2\pi$ at 1.69 Bev/c, 20: 30010
JAFFE, A. A., Energy levels of ^{63}Zn, 20: 30406
JAGUSZTYN, M., Strontium-90–yttrium-90 measurements using Si counters, 20: 29520 (CLOR-45/D)
JAIN, D. V., Spectrophotometric and conductometric study of UO_2(II) complex of quinizarin-2-sulphonic acid, 20: 29181
JAKEMAN, D., Physics of nuclear reactors, 20: 30804
JAKLY, G., Vapor pressure of solid D_2O, 20: 29149
JAKOB, D., Processes for degassing of niobium and tantalum, 20: 29633
JAKSIC, B., Analytic structure in λ of S matrix for strongly singular potentials, 20: 30100
JALENQUES, F., Leak detection in ultra-high vacuum systems attaining 10^{-8} to 10^{-12} torr, 20: 29496
JANSZ, H. S., Genetic recombination of bacteriophage Φ × 174 in spheroplasts, 20: 28948
JASANI, B. M., Liquid scintillators based on medicinal paraffin for use in whole-body counters, 20: 29541
JASKOLA, M., Energy levels of ^{8}Be from $^{11}B(n,\alpha)^8Li \to {}^8Be$ process, 20: 30363
JAUHO, P., Crossing and anticrossing signals of ^{1}H and ^{2}H atoms in uniform magnetic field, 20: 29935
JENKINS, T. M., Radiation protection problems at Stanford two-mile linear accelerator, 20: 29849 (CONF-651109, pp 442-58)
JENSEN, M. Anthony, Superconductivity in transition metals at very low temperatures, 20: 30318
JENSEN, T. H., Flute characteristics of and microwave emission from a plasma in a mirror, 20: 30645
JERNER, R. Craig, Thermionic properties of polycrystalline Zr, Be, and Zr beryllides, 20: 29801
JESSEN, P. L., New developments in neutron activation systems for analysis of O in steel, 20: 29138
JEZOWSKA-TRZEBIATOWSKA, B., Behaviour and structure of uranyl nitrate in organic solvents. III., 20: 29184
JHAVERI, A. K., Resonant electron capture in small-angle collisions of Ar^+ on Ar and Ne^+ on Ne, 20: 29944
JIN, Y.S., Bootstrap conditions in soluble model, 20: 30127
JIRBERG, R. J., Flux pinning in superconducting niobium thin films, 20: 30278
JIRKOVSKY, Rudolf, Study of beta backscattering for application in analytical chemistry, 20: 29110
JOBSON, D. A., Mechanized structural analysis, 20: 29367 (TRG-Report-1089)

JOBSON, Donald Albert, Moderator structures for nuclear reactors, 20: 30823
JOEL, D. D., Extracorporeal irradiation of blood, 20: 28927 (BNL-9647)
JOEST, Karl-Heinz, General dispersion law of linear Boltzmann equation, 20: 30338
JOHANNESSEN, Steen, Tanderil in treatment of radiation cystitis, 20: 29060
JOHANSSON, E., Spectrum of angular neutron flux in D_2O–U lattice, 20: 30846
JOHNS, H. E., Photochemistry of uridylyl-(3′→5′)-uridine, 20: 28910
JOHNSON, Hugh M., Sky near the brightest x-ray source in Scorpius, 20: 29882
JOHNSON, James E., Appearance of ^{131}I and ^{140}Ba–La in fallout due to second Chinese test, 20: 29429
JOHNSON, James E., Availability of fallout ^{137}Cs to dairy cattle from different types of feed, 20: 29463
JOHNSON, John L., Effect of pressure on negative V^- stellarators, 20: 30561 (MATT-415)
JOHNSON, L. V., Reaction $^{197}Au(n,\gamma)^{198}Au$, 20: 30409
JOHNSON, Noah R., Decay of ^{133}I to levels in ^{133}Xe, 20: 30473
JOHNSON, Ralph E., Fractionated total-body irradiation in patients with leukemia and disseminated lymphomas, 20: 29069
JOHNSON, Ralph E., Radiotherapeutic effects on mammalian tumor cells. I., 20: 28962
JOINER, W. C. H., Magnetic instabilities and flux annihilation in grossly inhomogeneous superconductors, 20: 30261
JOKL, V., Paper electrophoresis of complexes of rare earths with hydroxy-amino acids, 20: 29343
JOLLY, J. E., Eta and neutron cross sections of ^{235}U from 0.03 to 200 ev, 20: 30342 (AERE-M-1670)
JONES, C. K., Ultrasonic investigation of energy-gap anisotropy in superconducting rhenium, 20: 30281
JONES, Delbert Merle, Superconducting transition temperatures of Zr and Zr isotopes, 20: 30316
JONES, K. C., Partial molal heat capacities of aqueous rare-earth chloride solutions, 20: 29144 (IS-1355)
JONES, L. H., Isobaric analog states by (p,n) reactions, 20: 30480
JONES, L. W., Interaction π^+-π^- as studied in 12- and 18-Bev pion-nucleon reactions, 20: 30025
JONES, P. R., Resonant electron capture in small-angle collisions of Ar^+ on Ar and Ne^+ on Ne, 20: 29944
JONES, R. E., New developments in neutron activation systems for analysis of O in steel, 20: 29138
JONSSON, E., Spectrum of angular neutron flux in D_2O–U lattice, 20: 30846
JORDAN, H. L., Stable and unstable behavior of preheated plasma in linear and cusped theta pinches, 20: 30614
JOSEPHSON, J., Propulsion reactor temperature control with internal power loop eliminated, 20: 30924 (LA-DC-7636)
JOSHI, D. P., Spectrophotometric and conductometric study of UO_2(II) complex of quinizarin-2-sulphonic acid, 20: 29181
JOSHI, G. C., Mixing model of intermediate vector bosons, 20: 30133
JOSHI, S. K., Pseudo wave functions, 20: 30773
JOST, K., Measurement of great polarization effects at low-energy electron scattering, 20: 29937
JOUQUET, G., Thermal creep and inelastic behavior of artificial graphite, 20: 29734
JOVIC, D. M., Thermal neutron spectrum measurements from Yugoslav heavy water reactor, 20: 30939
JUEL, Leslie H., Nuclear reactors operating with substantially isotropic graphitized bodies, 20: 29694
JUENKER, D. W., Hot electron range in thin metal films, 20: 29952
JUNGWIRTH, K., Quasi-linear transformation of waves in inhomogeneous plasma, 20: 30673
JUNKER, D. W., Propulsion reactor temperature control with internal power loop eliminated, 20: 30924 (LA-DC-7636)
JUNKERMANN, Wolfgang, Nuclear reactor core assembly, 20: 30834
JUZA, J., Contribution to problem of thermodynamic similarity of H_2O and D_2O, 20: 30182

K

KABAKCH, A. M., X-ray study of epoxido-dianic ED-5 resin irradiated with ^{60}Co and metallopolymers on its base, 20: 29297
KABAKCHI, S. A., Steady state in radiolysis of neutral aqueous solutions of oxygen, 20: 29257
KACHUR, V., Properties of P-03 graphite, 20: 29714 (WANL-TME-1031)
KADENATSI, B. M., Radiation-induced catalytic conversion of methanol at a small surface coverage, 20: 29278
KADOMTSEV, B. B., Instability and related macroscopic effects in toroidal discharges, 20: 30617
KADOMTSEV, V. V., Controlled nuclear fusion research, Sept. 1965: review of theoretical results, 20: 30606
KADYKOV, B. I., Arteriosclerosis in white rats exposed to wholebody x irradiation, 20: 28996
KADYKOV, B. I., Changes in cholesterol level in blood following irradiation, 20: 28992
KADYKOV, B. I., Influence of variable fat content diet on course of radiation sickness, 20: 28993
KADYKOV, B. I., Influence of chemical uptake of radioactive substances on lipid and cholesterol levels in blood, 20: 28994
KADYKOV, B. I., Influence of various diets and x radiation on cholesterol level in tissues, 20: 28995
KAESER, Ernst K., Construction of MHD electrical power generator, 20: 29984
KAGAL, S. A., Physical and chemical properties of hydroxyflavones. V., 20: 29240
KAGAN, Yu. M., Discharge in a hollow cathode. I., 20: 30688
KAGANSKII, M. G., Investigation of plasma in Tuman installation, 20: 30682
KAGANSKII, M. G., Plasma compression by a magnetic field in a toroidal-type device, 20: 30660
KAGIYA, Tsutomu, Initiation and propagation in γ-radiation-induced polymerization of ethylene, 20: 29275
KAJIKAWA, Kozo, Movement of radioactive calcium in brain slices, 20: 28891
KALACHEVA, V. Ya., Uncoupling of oxidation and phosphorylation in mitochondria of plants after x-ray irradiation, 20: 28947
KALAGHER, R. J., Measurements of electron drift velocity and collision frequency in an argon discharge, 20: 30598
KALENDAREV, R., Multipurpose relaxation apparatus for measuring signs of elementary processes in ionic crystals subjected to ionizing radiation, 20: 30754
KALININ, Yu. D., Structure of solar corpuscular stream interaction with magnetosphere, 20: 30210 (NASA-TT-F-389, pp 499-517)
KALINKIN, B. N., Angular distribution of inelastically scattered complex particles, 20: 30502
KALINKIN, B. N., Average field levels of nuclei, 20: 30350 (JINR-P-2682)
KALIS, Kh., Ionizing gamma-defectoscopy for lead containers, 20: 29388
KALISTRATOV, G. V., Body distribution and elimination of ^{35}S-labeled 2-mercaptopropylamine in mice, 20: 28888
KALLIO, A., Odd-parity states of ^{16}O with a realistic nucleon-nucleon interaction, 20: 30412
KAMETANI, Katsuaki, Radiochemical tests of industrial waste water. I., 20: 29099
KAMIGAITO, Ichiro, Spectrochemical analysis of Zr and its alloys. II., 20: 29114
KAMINSKAYA, O. V., Hydrolysis of rare earth metal dicarbides, 20: 29220
KAMOUN, G., Determination of brittle-ductile transition temperatures in Mo and W, 20: 29757
KANA'AN, A. S., Mass-spectrometric studies at high temperatures. X., 20: 29183
KANDROR, V. I., Role of sympathetic influences in genesis of stressed organism reactions to ionizing radiation, 20: 28939
KANEKO, Masahito, Practical applications of glass dosimetry, 20: 29547
KANEKO, Yoshikiko, Time-dependent thermalization in multiplying systems, 20: 30327
KANEVSKII, E. A., Catalytic action of copper ammoniate during oxidation of uranium dioxide, 20: 29199
KANEVSKII, E. A., Kinetics of U(IV) oxidation in carbonate solution by atmospheric oxygen, 20: 29198
KANG, Kyungsik, Bootstrap conditions in soluble model, 20: 30127
KANNO, Akira, Gamma radiography with a large ^{60}Co source, 20: 29596
KANSARA, Mohan, Measuring density with nuclear back-scatter method, 20: 29594
KAPITSA, S. P., Continuous operation microtron, 20: 29858
KAPLAN, I. R., Isotopic abundance and content of sulfur in meteorites, 20: 29893
KAPOOR, R. N., Organic compounds of U. I., 20: 29155
KARAGOD, N. A., Fallout of Ce-141, Ce-144, Zr-95 + Nb-95 and Sr-90 on U.S.S.R., 20: 29406 (NP-14719)
KARAMYAN, S. A., Chemical analysis using heavy ion scattering at large angles, 20: 29090
KARASEV, A. L., Formation of peroxide radicals in irradiated palmitic acid and potassium palmitate, 20: 29309
KARCHEVSKII, A. I., Injection of plasma blobs into mirror trap with adiabatic plasma compression: Aspa device, 20: 30636
KARCZ, W., Semiconductor system for charged particle identification, 20: 29526 (INP-444/PL)
KARLE, J., Evaluation of phases for structure determination by neutron diffraction, 20: 29720
KARMANN, W., Pulse-radiblysis studies on reactivity of catalase with hydrated electrons and free OH radicals, 20: 29279
KARPENKO, D. Ya., Bosons in the field of plane electromagnetic wave, 20: 30155
KARPENKO, L. I., Determination of yttrium and rare earth elements of yttrium subgroup in ores, 20: 29134

KARPOV, V. L., Inhibiting effects of solid impurities on radiation chemistry processes, 20: 29306
KASANG, G., Wilzbach tritiation of an alkyne-2-acid with high specific activity, 20: 29243
KASHIWABARA, SHIZUO, Observing apparatus of geomagnetic micropulsations, 20: 30229
KASHUBA, I. E., Analysis of elastic scattering of 6.9-Mev protons by Ni isotopes, 20: 30495
KASINSKI, Leszek, Proton scattering in tube of electrostatic accelerator, 20: 29866
KASTEN, Paul R., Space-dependent reactor kinetics, 20: 30845
KASTLER, Daniel, Conserved currents and associated symmetries; Goldstone's theorem, 20: 30101
KATAOKA, Iwao, Numerical integration of the neutron transport equation in slab geometry, 20: 30326
KATO, Kiyoe, Plasma-ion oscillation in a drifted plasma, 20: 30583
KATO, Sadatake, Synthesis of radioactive sodium 3,5-diiodofluorescein (3,5-^{131}I), 20: 29236
KATO, Yusuke, Propagation of hydromagnetic waves in collisionless plasma. I., 20: 30586
KATSURA, Masahiro, System U–C–N, 20: 29749
KATZ, J. J., Fluorescence studies on deuterated Chlorella vulgaris, 20: 28872
KATZ, O. M., Observations on zirconium and its alloys by transmission electron microscopy, 20: 29716 (WAPD-T-1819)
KAUFFMAN, F. Leo, Effect of irradiation temperature on organoleptic, physical and chemical properties of beef, 20: 29602
KAUFMAN, L., Boride compounds for high-temperature applications, 20: 29772
KAURANEN, P., Alpha decay of ^{219}Fr and ^{215}At, 20: 30374
KAVLAKOV, S., Daily variation of extensive air showers, 20: 29960
KAWAGUCHI, Takehiko, Spectrochemical analysis of Zr and its alloys. II., 20: 29114
KAWAGUCHI, Takehiko, Spectrochemical analysis of Zr and its alloys. III., 20: 29115
KAWAMURA, MAKOTO, Observing apparatus of geomagnetic micropulsations, 20: 30229
KAWAMURA, Shoichi, Separation of ^{90}Sr and ^{90}Y by paper electrophoresis, 20: 29336
KAWANO, Eiko, Improvements in ^{14}C assay of organic compounds by dry combustion, 20: 29085
KAWARABAYASHI, Ken, Scalar densities in current commutation relations and partially-conserved-axial-vector-current hypothesis, 20: 30138
KAWASAKI, Masayuki, Embrittlement of reactor structural steels by neutron irradiation, 20: 29825
KAWASAKI, Sho, Experimental studies on influence of hormones in x-irradiated animals. II., 20: 29043
KAWASAKI, Sho, Influence of hormones in x-irradiated animals. III., 20: 28912
KAWASAKI, Sho, Influence of hormones in x-irradiated animals. I., 20: 28978
KAZACHEVSKAYA, T. V., Electron concentration in ionosphere at altitudes of 100-300 km, 20: 30199 (NASA-TT-F-389, pp 248-58)
KAZACHEVSKAYA, T. V., Soft electron streams in upper atmosphere at altitudes to 500 km, 20: 30203 (NASA-TT-F-389, pp 288-91)
KAZMIN, V. N., Distribution of U and Th content in effusive and intrusive formations of northeastern Balkhash Foreland, 20: 29418
KEANE, A., Estimate of the decrease in the effective resonance integral due to resonance overlap, 20: 30421
KEIL, R. W., Copper–boron carbide control material for Phoebus II, 20: 29664 (LA-DC-7745)
KEILHACKER, M., Doppler shift measurements to investigate plasma rotation in the theta pinch, 20: 30615
KEILHACKER, M., Isar I: fast megajoule theta-pinch experiment with extremely high compression fields, 20: 30611
KEITH, Johnnie R., Gamma fluxes from circular and spherical sources, 20: 30351 (N-65-14857)
KELLER, K., Phenomenological nuclear cluster model with shell structure, 20: 30377
KELLER, L. E., Hallam Nuclear Power Facility operating experience, 20: 30898
KELLY, J. P., Core boration and flux mapping Test 313, 20: 30874 (ACNP-65612)
KELLY, W. H., Excited states in ^{82}Kr populated by decay of 35-h ^{82}Br, 20: 30410
KEMMLER-SACK, S., Ternary oxides. V. Systems PbO–Ta_2O_5, PbO–Nb_2O_5, and PbO–U_2O_5, 20: 29794
KENDALL, B., Photoproduction on H of ρ^0 mesons between threshold and 6 Bev, 20: 30030
KENDALL, E. G., New class of hypereutectic carbide composites, 20: 29727
KENNEDY, Lawrence A., Steady-state exothermal hydromagnetic discontinuity for arbitrarily orientated magnetic field, 20: 30177
KENNES, F., X irradiation effects on mouse proteins, 20: 28899
KENNETT, T. J., Neutron separation energies of ^{143}Nd–^{144}Nd, ^{149}Sm–^{150}Sm, and ^{164}Dy–^{165}Dy, 20: 30366
KENNETT, T. J., Reaction ^{197}Au(n,γ)^{198}Au, 20: 30409
KENT, R. A., Mass-spectrometric studies at high temperatures. X., 20: 29183
KEOWN, S. R., Orientation relationship and growth direction of Mo_2C in ferrite, 20: 29726
KEPPLE, P., Potential of average force in plasma, 20: 30599
KERKIS, Yu. Ya., Mutagenic action of extracts from various organs of irradiated mice, 20: 28959
KERN, R. C., Core boration and flux mapping Test 313, 20: 30874 (ACNP-65612)
KERN, W., Production of antiprotons by high-energy photons, 20: 30432
KERSHAW, Herbert Arthur, Improvements in thermal engines, 20: 29395
KESSIE, R. W., Removal of plutonium hexafluoride from cell exhaust air, 20: 29328 (ANL-7066)
KESSLER, J., Measurement of great polarization effects at low-energy electron scattering, 20: 29937
KETCHUM, Bostwick H., Biological, chemical, and radiochemical studies of marine plankton. I., 20: 28877 (NYO-1918-124)
KETCHUM, Bostwick H., Biological, chemical, and radiochemical studies of marine plankton. II., 20: 28878 (NYO-1918-138)
KETTERSON, J. B., Ultrasonic attenuation in liquid ^{4}He at low temperatures, 20: 30299
KEVANE, C. J., Electrical conduction by oxygen ions in cerium oxide, 20: 30743
KHACHATURYAN, M. N., Differential cross section of charge exchange of 4.8-Bev/c π^- mesons with protons, 20: 29998
KHALFIN, L. A., Contribution to quantum theory of unstable elementary particles, 20: 30107
KHALIKOV, A. Kh., Registration of secondary-electron current with scintillation counter, 20: 29538
KHAMIDOV, O. Kh., Laves phases in systems containing Re and rare-earth metals, 20: 29792
KHARITONOV, F. Ya., Strength of ceramics made of pure oxides, 20: 29740
KHARKEVICH, G. I., Parity nonconservation in radiative transition of ^{175}Lu, 20: 30381
KHAZEN, A. M., Measurement of properties of a partially ionized gas with a hot-wire anemometer, 20: 30702
KHELASHVILI, A. A., Leptonic decays of baryons in universal V-A theory, 20: 30058
KHIMCHENKO, Yu. I., Effects of γ radiation on structure of epoxy resins and resin-base metallic polymers, 20: 29296
KHIZHNYAK, N. A., Motion of plasmoid in a curvilinear magnetic field, 20: 30647
KHIZHNYAK, N. A., Oscillations and heating of small plasmoids incident in axisymmetric magnetic fields, 20: 30559 (FTI-114/P-044)
KHIZHNYAK, N. A., Theory of excitation of ion plasma oscillations by electron Langmuir waves, 20: 30692
KHOCHOLAVA, G. M., Question of anomalous absorption in polar cap, 20: 30225
KHODYREVA, M. A., Effect of detergents on the penetration of ^{90}Sr through animal skin, 20: 29461
KHOKHLOV, M. Z., Outermost zone of charged particles, 20: 30220 (NASA-TT-F-389, pp 633-52)
KHOKHLOVA, Z. S., Slow meson production in interaction of 3.8-Bev π^- mesons with emulsion nuclei, 20: 30501
KHOMIKOVSKII, P. M., Radiation-induced polymerization of tetrafluoroethylene and acrylonitrile at 4.2 K, 20: 29300
KHOMSKII, D. I., Lattice stability in phononless mechanism of superconductivity, 20: 30264
KHORANA, S., Isotopic exchange and annealing of recoil damage in Co complexes, 20: 29259
KHORASANOV, G. L., Plasma heating under beam instability conditions, 20: 30659
KHORASANOV, G. P., Plasma equilibrium in torus with high-frequency fields and plasma heating resulting from beam of "escaping electrons", 20: 30640
KHOVANSKII, V. D., Proton elastic scattering on deuterons at large angles, 20: 29989 (ITEF-361)
KHOZHAINOV, A. I., Turbulent flow of liquid metals in MHD channels of circular section, 20: 30183
KHUKHAREVA, I. S., Anomalous behavior of j_c(H,T) of heat-treated Nb–75 percent Zr alloys, 20: 30267
KHUSSAR, U., Autoradiographic study of thymus gland in acute irradiation sickness, 20: 28997
KHUSSAR, Yu. P., Protective action of cystamine on thyroid gland tissues in case of acute radiation disease, 20: 29047
KIANG, Yuan-sun, Ligand field theory. I., 20: 29205
KIBBLE, T. W. B., Refraction of electron beams by intense electromagnetic waves, 20: 30046

KIDSON, G. V., Diffusion processes in zirconium and its alloys, 20: 29737
KIEFFER, B. F., Current Nb alloy technology in the United States, 20: 29763
KIEFFER, B. F., Properties of tungsten–rhenium alloys, 20: 29765
KIEFFER, R., New Ta, Nb, impregnated, or sintered alloys and compound materials with graphite, 20: 29764
KIENLE, P., Moessbauer effect investigation of shell conversion of electron capture, 20: 30555
KIKNADZE, L. V., State of liquid He in the vicinity of λ line, 20: 30266
KIKUCHI, Riichi, Accumulation of electric charge in glass for γ shielding window by γ irradiation, 20: 30727
KILEZHENKO, V. P., Radioactivity of organisms of Norwegian Sea, 20: 29424
KILLEEN, J., Stabilization by shear and negative V'', 20: 30608
KILSBY, E. R. Jr., Reactor primary-piping-system rupture studies, 20: 30811
KIL'YANOV, Yu. N., Autodyne nuclear magnetic resonance pickups, 20: 29492
KIM, C. W., Elementary-particle treatment of muon capture in ^{16}O, 20: 30447
KIM, H. C., Yielding and strain ageing of niobium crystals, 20: 29790
KIM, Joe-rock, Synthesis of 5-bromouracil-^{82}Br, 20: 29244
KIM, Y. S., Analysis of ANL–CERN spark chamber pictures, 20: 29987 (COO-1261-4)
KIM, You-sun, Paper partition chromatography of organic halogen compounds, 20: 29123
KIMBLE, S. G., Energy dependence of radiation damage in Si, 20: 29579 (NAA-SR-11887)
KIMURA, Hirozo, Electron-beam refining of niobium, 20: 29634
KINGSLEY, P. S., Welding of stainless steel for corrosive radioactive service, 20: 29661 (HWS-8241(Rev.4))
KINGSLEY, P. S., Welding of stainless steel for corrosive non-radioactive service, 20: 29662 (HWS-8242(Rev.5))
KINOSHITA, Toichiro, High energy behavior of forward scattering amplitude, 20: 30109
KIRCHNER, H., Diffusion of fission products in overlapping chemical reactions, 20: 29190
KIRDINA, G. A., Radiation intensity in earth's radiation belts, 20: 30235
KIRIN, I. S., β decay of bromine isotopes for synthesis of krypton compounds, 20: 29327
KIRKPATRICK, Kim Allen, Electromagnetic radiation from extended sources, 20: 30252
KIROUAC, G. J., Inelastic scattering cross sections for polyethylene and water in gas transition region, 20: 30334
KIROV, A. G., Plasma equilibrium in torus with high-frequency fields and plasma heating resulting from beam of "escaping electrons", 20: 30640
KIRSCHLER, L. H., Mechanical properties tests of 316 SS specimens in 1200°F Na contaminated with O, 20: 29704 (MSAR-66-78)
KIRTADZE, M. G., Kinetics of radiation-induced isotope exchange between deuterium and silica gel hydroxyl groups, 20: 29276
KISLOV, V. Ya., Plasma and electron uhf amplifiers and generators, 20: 29500
KISLYAKOV, A. I., Active diagnosis of hot plasma by means of neutral particles, 20: 30685
KISLYAKOV, A. I., Interaction between uhf radiation and a turbulent plasma, 20: 30625
KISLYAKOV, A. I., Investigation of plasma concentration in Al'fa with probe beam of fast atoms, 20: 30686
KISLYUK, M. M., Mutations in cereals induced by ionizing radiations, 20: 28960
KISS, I., Vapor pressure of solid D_2O, 20: 29149
KISS-IMREH, Gabriela, Spectrophotometric study of uranyl nitrate-salicylaldoxime system, 20: 29202
KISTEMAKER, J., Gross- and partial-ionization cross sections for electrons on water vapor, 20: 29928
KISTENEV, E. P., Formation of electron-positron pairs by high-energy gamma quanta, 20: 29990 (JINR-P-2667)
KISTLER, S., Calculation of binding energy of heavy nuclei with nonlocal two-body forces, 20: 30508
KITAHARA, Keid, Radioactivity in rain water, settled dust and activated sludge observed at Kagoshima District. XIII., 20: 29455
KITANO, Hitoshi, Properties of high-zirconium wrought copper base alloys, 20: 29782
KITANO, Hitoshi, Properties of sintered WC–Co alloys, 20: 29778
KIYOKAWA, Kazuhiro, Reactivity worth of fuel elements, 20: 30839
KIYOSE, Ryohei, Chemical engineering studies on processing of radioactive liquid wastes by evaporation, 20: 30946
KJEKSHUS, Arne, Systems Re–As, Re–Sb, Re–Bi, Re–Te, and Nb–Sb–Te, 20: 29717
KLAIDMAN, S. L., Prog. rpt. on ultrasonic temperature measuring device, 1–4/66, 20: 29486 (NASA-CR-54964)
KLAINER, Stanley M., Monitoring of gaseous contaminants in atmosphere using radioactive clathrate techniques, 20: 29142
KLAMUT, C. J., Boiling Hg corrosion of certain refractory metals and stainless steels from 593 to 703°C, 20: 29646
KLEIN, C. A., Lorenz number of graphite at low temperatures, 20: 29750
KLEIN, Eva, Variation of antigenic characteristics between mouse lymphomas induced by Moloney virus, 20: 28873
KLEIN, George, Variation of antigenic characteristics between mouse lymphomas induced by Moloney virus, 20: 28873
KLEIN, R., Muon capture in heavy nuclei, 20: 30454
KLEINKNECHT, K., Further results from interference of K_S and K_L in $\pi^+\pi^-$ decay modes, 20: 30026
KLEPFER, H. H., Prog. rpt. on Zr alloy, 20: 29660 (GEAP-4960)
KLEPIKOV, N. P., Phenomenology of certain inelastic reactions involving particles with spin, 20: 30149
KLIGER, G. K., Boson resonance at 1.63 Bev in π^-p interactions, 20: 30021
KLOCHKOV, V. P., X-ray study of epoxido-dianic ED-5 resin irradiated with ^{60}Co and metallopolymers on its base, 20: 29297
KLUGE, E., Inelastic Σ^-p interactions at low momenta, 20: 30024
KMONICEK, V., Contribution to problem of thermodynamic similarity of H_2O and D_2O, 20: 30182
KNIGHT, B., Gamma-radiolysis of water vapor in the presence of NH_3 and O_2, 20: 29295
KNITTER, H.-H., Elastic scattering of neutrons from natural silicon, 20: 30345 (EUR-2798.e)
KNOLL, G. F., Absence of structure in fission cross section of ^{235}U at 300 to 620 kev, 20: 30425
KNORRE, K. G., Use of standard in solid phase for quantitative argon determination by method of isotope dilution, 20: 29102
KNOWLES, H. B., Radiation hazards peculiar to a linear accelerator meson factory, 20: 29850 (CONF-651109, pp 472-89)
KNUTH, R., High-energy particle event observed by Sputnik III, 20: 29962
KOBAKCHI, A. M., Effects of γ radiation on structure of epoxy resins and resin-base metallic polymers, 20: 29296
KOBAYASHI, Kenji, Optical properties of graphite in the infrared region, 20: 30736
KOBAYASHI, Tetsuji, Gamma spectra of fission products observed with lithium-drifted germanium detectors, 20: 30379
KOBER, K. J., Air locks for safe escape in nuclear reactors, 20: 29465
KOBOZEV, N. I., Radiation effects on catalytic activity of platinum during hydrogenation, 20: 29304
KOCH, R., ESR study on irradiated sulfur-containing and sulfur-free pyridoxine derivatives, 20: 28901
KOCH, Siegfried, Ash content of bituminous coal, 20: 29127
KOCHAROV, G. E., Determining small quantities of ^{37}Ar and tritium, 20: 29559
KOCHERGINSKAYA, L. L., Preparation of ion-exchange membrane by pre-irradiation method, 20: 29308
KOCHETOV, N. K., Radiation chemistry of carbohydrates. VI., 20: 29307
KOEHLER, D. R., Decay of ^{141}Nd. II., 20: 30416
KOEHLER, Walter H., Variational method for prompt neutron kinetics, 20: 30852
KOETZ, U., Production of antiprotons by high-energy photons, 20: 30432
KOGAN, L. M., Radiolysis of hexachlorocyclopentadiene, 20: 29256
KOGAN, R. M., Recording cosmic rays on Cosmos-17 satellite, 20: 29966
KOGAN, R. M., Statistical errors in determining concentrations of radioactive elements in rocks using γ-threshold and differential spectrometers, 20: 29421
KOGAN, V. I., Registration of secondary-electron current with scintillation counter, 20: 29538
KOHN, W., New formulation of inhomogeneous electron gas problem, 20: 30189
KOJIMA, C., Ion cyclotron resonance heating of QP plasma, 20: 30662
KOJOIAN, Gabriel, Antiproton annihilation at rest in deuterium, 20: 29992 (UCRL-16717)
KOLB, A. C., Plasma confinement, heating, and losses in Pharos with an extended current pulse, 20: 30612
KOLBANOVSKII, Yu. A., Kinetics of radiation-induced isotope exchange between deuterium and silica gel hydroxyl groups, 20: 29276
KOL'CHIN, O. P., Kinetics of combined carbothermal reduction of niobium and tungsten, 20: 29677
KOLCHIN, O. P., Reduction of tantalum from tantalum pentoxide by the carbothermal method, 20: 29678
KOLESNIK, V. G., Differential cross section of charge exchange of 4.8-Bev/c π^- mesons with protons, 20: 29998
KOLESNIKOV, N. N., Interactions of light hypernuclei and Λ particles, 20: 30503
KOLESNIKOV, P. M., Acceleration of plasma burst in coaxial accelerator with eroding electrodes, 20: 30683
KOLGANOV, V. Z., Boson resonance at 1.63 Bev in π^-p interactions, 20: 30021
KOLOMENSKII, A. A., Quasilinear acceleration of particles by transverse electromagnetic wave, 20: 29867

KOLYBASOV, V. M., Angular correlations in capture of π^- mesons, 20: 30504
KOMATA, Toranosuke, Superconducting Nb–10Zr alloy, 20: 29789
KOMISSAROVA, L. N., Reaction of manganese and scandium oxides in air, 20: 29168
KOMISSAROWA, L. N., Preparation and properties of anhydrous scandium nitrate and its solvates, 20: 29214
KONDO, Masao, Effect of Mo on the oxidation of TiC–Ni–Mo alloys, 20: 29653
KONDRATENKO, A. N., Kinetic theory of passage of EM waves through plasma layer. II., 20: 30679
KONDRATENKO, A. N., Kinetic theory of passage of EM waves through a thin nonuniform layer of plasma, 20: 30704
KONDRAT'EV, K. Ya., Interpretation of radiation data from meteorological satellites, 20: 30221 (NASA-TT-F-389, pp 741-57)
KONDRATYUK, L. A., Photon bremsstrahlung in scattering of vector mesons on each other, 20: 30057
KONECNY, E., Ion charge distribution of unretarded fission products, 20: 30507
KONITZER, John D., Color centers in x- or uv-irradiated KI, 20: 30748
KONONENKO, L. I., 1,10-Phenanthrolinethenoyltrifluoroacetone complexes of rare earth elements, 20: 29221
KONONENKO, V. I., Determination of plasma density distribution by microwave refraction, 20: 30700
KONOVALOV, I. I., Standby operation of coaxial plasma gun, 20: 30684
KONSTANTINOV, B. P., Possible antimatter nature of micrometeors, 20: 29895
KONSTANTINOV, P. A., Chemical protection against genetic changes, 20: 29045
KONSTANTINOVA, M. M., Temperature effect on cysteamine accumulation in cells and its radioprotecting activity, 20: 29057
KONSTANTINOVIC, J. M., Thermal neutron spectrum measurements from Yugoslav heavy water reactor, 20: 30939
KONYAEV, V. P., Achievement of ultrahigh vacuum in Ogra-1, 20: 30701
KOONZ, R., Isothermal reaction of U with steam between 400 and 1600°C, 20: 29188
KOPELMAN, J. B., Elastic scattering (π^--p) at 1.7 Bev/c, 20: 30011
KOPYLOVA, D. K., Experimental separation of interactions with free protons, 20: 30083
KORDUBA, B. M., Application of straight line method coupled with method of integral transformations to problem of electrostatic fields with axial symmetry, 20: 29497
KOREN, Kristian, Cesium-137 in milk, meat, and man in Norway, 20: 29432
KORNILOV, E. A., Suppression of low-frequency oscillations in two-stream instability by prior modulation of electron beam, 20: 30591
KOROL', V. S., Nuclear magnetic resonance methods, 20: 29498
KORSUNSKII, M. I., Focusing characteristics of electrostatic mirror with cylindrical field, 20: 29868
KOS, E., Resynthesis of DNA and 50-S ribosomal RNA in uv-irradiated E. coli, 20: 28949
KOSAREV, E. L., Electron-bunching accelerator, 20: 29859
KOSHIJIMA, Tetsuo, Radiation grafting of methyl methacrylate onto lignin, 20: 29288
KOSHIKA, M., Effect of storage at ambient temperature on the volatile components of irradiated beef, 20: 29589
KOSMACHEV, O. S., Focusing characteristics of electrostatic mirror with cylindrical field, 20: 29868
KOSOLAPOVA, T. Ya., Hydrolysis of rare earth metal dicarbides, 20: 29220
KOSS, P., Fluidized-bed coating of fuel particles with pyrocarbon layers, 20: 29671
KOST, M. E., X-ray L_{III} spectra of Gd absorption in hydrides, 20: 29162
KOSTYUKOVA, Yu. S., Linear theory of excitation of oscillations in a plasma by a charged particle beam, 20: 30689
KOTAMSKI, Andrzej, Diagonalization of helicity-crossing matrices, 20: 30095
KOTFILA, R. J., Comparison of pressed and sintered and arc-cast billets for refractory metal forgings, 20: 29683
KOTHARI, D. S., Waves in incompressible conducting fluid in magnetic field, 20: 30171
KOTOV, A. G., Radiation effects on formation of free radicals in frozen $CH_3OH + CCl_4$ solutions, 20: 29305
KOVALENKO, N. A., Hydrolysis of rare earth metal dicarbides, 20: 29220
KOVALENKO, V. A., Cryogenic magnetic trap VGL-2, 20: 30655
KOVALEV, G. V., Nuclear magnetic resonance methods, 20: 29498
KOVALEVA, N. E., Effect of ionizing radiation on nuclear reorganization processes in Paramaecium putrinum. I., 20: 29007
KOVALEVSKII, A. K., Dependence of radioactivity and content of chemical elements on mechanical composition of sedimentary rocks, 20: 29417
KOVBA, L. M., Binary uranium and molybdenum oxides, 20: 29798
KOVBA, L. M., High-temperature x-ray phase analysis of U–O system from $UO_{2.50}$ to $UO_{2.67}$, 20: 29799
KOVBA, L. M., New double oxides of uranium and tungsten, 20: 29170
KOVPIK, O. F., Suppression of low-frequency oscillations in two-stream instability by prior modulation of electron beam, 20: 30591
KOYANAGI, Taku, Concentration of radionuclides in sea water by metal sulfide-ion exchange resins, 20: 29345
KOZAK, Zdzislaw, Effect of radiation on activity of V catalyst in reaction of sulfur dioxide oxidation, 20: 29291
KOZHUSHKO, N. N., Mutations in cereals induced by ionizing radiations, 20: 28960
KOZIK, B., Correlation function of random breeding-type processes, 20: 30052
KOZIK, B., Statistical theory of reactors, 20: 30844
KOZIN, B. G., Analysis of elastic scattering of 6.9-Mev protons by Ni isotopes, 20: 30495
KOZLOV, V. A., Chemical protection against genetic changes, 20: 29045
KOZLOV, V. T., Radical formation in radiolysis of hard rubber, 20: 29299
KRABBENHOFT, Kenneth Louis, Significance of pigments in radiation resistance of Micrococcus radiodurans, 20: 29016
KRAEVSKII, N. A., Inflammation and penetrating ionizing radiation, 20: 28943
KRAINOV, V. P., Pairing correlations and masses of spherical nuclei, 20: 30491
KRALL, N. A., Drift instabilities and electron cyclotron oscillations for arbitrary plasma pressure, 20: 30631
KRAMER, W. C., Fabrication of spiked-core fuel elements for EBWR, 20: 29658 (ANL-6283)
KRASIL'NIKOV, D. D., Investigation of cosmic ray variations in Yakutsk, 20: 29963
KRASIL'NIKOVA, M. K., Chemisorption of ethylene on yttrium oxide, 20: 29186
KRASNICKI, S., Neutron investigation of temperature effects in magnon spectrum of magnetite, 20: 30765
KRASOVITSKII, V. B., Interaction between electromagnetic waves and two level system, 20: 29837
KRASOVSKII, V. I., Conference on space physics, Moscow, 6/65, 20: 30195 (NASA-TT-F-389)
KRASOVSKII, V. I., Upper atmosphere physics and space near earth, 20: 30196 (NASA-TT-F-389, pp 8-25)
KREFT, R., Studies with animals on germ injury with ionizing radiation, 20: 29019
KRESHKOV, A. P., Analysis of rare earth alloys in nonaqueous solutions, 20: 29133
KREY, Philip W., Gamma activity in surface air: 80th meridian network, 1–3/65, 20: 29430
KRIMIGIS, Stamatios Mike, Interplanetary diffusion model for time behavior of intensity in solar cosmic-ray event, 20: 29973
KRISCIOKAITIS, Raymond John, L-Auger spectrum of ^{113}In as derived from electron capture decay of ^{113}Sn, 20: 30527
KRIVOVA, A. A., Heat resistance of rabbit blood serum in ultraviolet radiation, 20: 29004
KRIZHANSKII, L. M., Sign of change of charge radius of ^{119}Sn nucleus, 20: 30382
KROCK, R. H., Elastic and plastic deformation of dispersed phase-liquid phase sintered W composite materials, 20: 29686
KROEGER, F. A., Search for a defect model for UO_2, 20: 29796
KROLIKOWSKI, W., Cabibbo angle and partial conservation of axial current, 20: 30090 (IC–66/52)
KROLL, H., Paper electrophoresis of complexes of rare earths with hydroxyamino acids, 20: 29343
KROPOTKIN, A. P., Nonlinear interaction of electromagnetic waves in a magneto-active plasma, 20: 30629
KRUGLYAKOVA, K. E., Free-radical reactions during exposure of model systems to irradiation, 20: 29037
KRUPCHITSKII, P. A., Investigation of time invariance of nuclear forces, 20: 30505
KRUTZIK, Siegfried, Kinetics of homogeneous isotope exchange between cycloalkyl chlorides and chloride ions in dimethyl sulfoxide, 20: 29157
KRYLOVA, I. V., Radiation effects on catalytic activity of platinum during hydrogenation, 20: 29304
KRYMSKII, G. F., Cosmic rays in July of 1961, 20: 29961
KRYMSKII, G. F., Investigation of cosmic ray variations in Yakutsk, 20: 29963
KUBAL, I., Use of delayed development process in film dosimetry, 20: 29557
KUBO, Ryogo, Breakdown of quasi-particle approximation in metals, 20: 30312
KUBO, Ryogo, Elementary excitations in homogeneous Bose liquid, with application to He II, 20: 30187
KUBO, Ryogo, Fluctuation-dissipation theorem and Brownian motion, 20: 30186
KUBO, Ryogo, Landau-Ginsburg equations and properties of type II superconductors, 20: 30313
KUBO, Ryogo, Lectures in theoretical physics. I., 20: 29838
KUBO, Ryogo, New formulation of inhomogeneous electron gas problem,

20: 30189
KUBO, Ryogo, New mechanism for superconductivity, 20: 30311
KUBO, Ryogo, Properties of liquid He-three, 20: 30188
KUBO, Ryogo, Relaxation phenomena near the critical points, 20: 30780
KUBO, Ryogo, Theory of correlated crystals, 20: 30781
KUBOSE, Don A., Cobalt-60 gamma radiolysis of deuterium–oxygen mixtures, 20: 29285
KUBOTA, Tadashi, Effect of void volume variation on pressure buildup in vibratory-compacted UO_2 fuel element, 20: 29818
KUBYSHKIN, V. V., Solar activity and pressure variations in troposphere, 20: 30237
KUCHERENKO, N. E., Nucleic acid content in guinea pig brain in dynamics of acute radiation sickness, 20: 28919
KUCHUMOVA, A. N., Thorium orthophosphates, 20: 29160
KUDO, Yasuo, Spectrochemical analysis of Zr and its alloys. III., 20: 29115
KUDRYASHOV, L. I., Radiation chemistry of carbohydrates. VI., 20: 29307
KUEHN, S. H., Effects of type of material on nuclear density measurements, 20: 29505
KUEHNER, J. A., Method of utilizing nuclear reactions in study of oxide layers, 20: 29817
KUGLER, E., Stable and unstable behavior of preheated plasma in linear and cusped theta pinches, 20: 30614
KUGLER, M., Perturbation methods in dispersion theory, 20: 30124
KUGLER, M., W spin for any spin, 20: 30126
KUGOT, P. L., Therapeutic effectiveness of antibiotics on cystamine action during radiation sickness, 20: 29051
KUHN, Gerard, Irreversible magnetic behavior of superconductors, 20: 30253 (CEA-R-2808)
KUKHTIN, V. V., Representations 189 and 405 of the group SU(6) and classification of mesonic resonances 2^+, 1^+, and 0^+, 20: 30093 (JINR-P-2701)
KUKUSHKIN, Yu. V., Fission-generated γ radiation during h-a explosion over Johnston Island, 7/9/62, 20: 30233
KULAGIN, Yu. M., Radiation intensity in earth's radiation belts, 20: 30235
KULIKOVA, L. G., Radiation damages in deoxyribonucleoproteins at molecular and supermolecular levels, 20: 28908
KULYUKINA, L. A., Identification of high-energy particles, 20: 30053
KUMAHARA, Tadashi, FET preamplifier for cooled semiconductor detectors, 20: 29548
KUO, Chien-chung, Problem in statistical theory of nuclear fission, 20: 30486
KUO, K'o-hsin, Oxidation of lanthanum hexaboride in air at 800 and 1000°C, 20: 29163
KUO, L. G., Plasma produced by neutral injection into magnetic mirror/well geometry, 20: 30632
KUO, P. K., Radiative corrections to electron-induced processes, 20: 30478
KUO, Thomas Tzu Szu, Shell-model study of tin isotopes, 20: 30521
KUPPERMANN, Aron, Energy threshold for $D + H_2 \rightarrow DH + H$ reaction, 20: 29176
KURATA, Kunio, Synthesis of radioactive sodium 3,5-diiodofluorescein (3,5-^{131}I), 20: 29236
KURDYUMOV, B. N., Interaction between h-f waves and plasma in Delta-2, 20: 30624
KURI, Zen'ichiro, Radiation-induced cis-trans isomerization of stilbene in methanol solution, 20: 29287
KURILKO, V. I., Interaction between electromagnetic waves and two level system, 20: 29837
KURILOVA-NAVRATILOVA, L., Uranyl complexes with phenolic ligands. VI, 20: 29096
KURIR, A., Possibility of control of termites with atomic waste, 20: 29587
KURNOSOVA, L. V., Cosmic ray nuclear component on Elektron-2, 20: 29957 (NASA-TT-F-389, pp 693-710)
KURNOSOVA, L. V., Primary cosmic-ray research, 20: 29954 (NASA-TT-F-389, pp 657-77)
KURNOSOVA, L. V., Transient increases of flux of heavy nuclei accompanied by bursts of x radiation, 20: 29965
KURODA, T., Ion cyclotron resonance heating of QP plasma, 20: 30662
KUS, Joseph E., Automatic sample changer for radioactive samples, 20: 29572
KUSEMANN, D., Evaluation of activity determination of biological materials with electronic computer, 20: 29121
KUSTOV, V. V., Endogenous formation of carbon monoxide, 20: 28880
KUYATT, C. E., Inelastic electron scattering from H_2, 20: 29953
KUYKENDALL, W. E., Lunar and planetary surface analysis using neutron activation, 20: 29140
KUZIN, A. M., Effect of fast neutrons on DNA synthesis in seedlings, 20: 28989
KUZIN, I. A., Effects of porous structure of lignin carbons on uranium sorption, 20: 29360
KUZ'MIN, A. I., Cosmic rays in July of 1961, 20: 29961
KUZ'MIN, A. I., Investigation of cosmic ray variations in Yakutsk, 20: 29963
KUZMINSKII, P. N., Effect on rabbits on incorporation or radioactive acetate in cholesterol, 20: 28895
KUZNETS, E. D., Tritium content in atmospheric fallout over Moscow during 1962–1963, 20: 29409
KUZNETSOV, S. N., Irregular high-energy electron streams near boundary of radiation zones of earth, 20: 30215 (NASA-TT-F-389, pp 576-87)
KUZNETSOV, S. N., Time changes in outer radiation zone of earth, 20: 30214 (NASA-TT-F-389, pp 569-75)
KUZNETSOV, V. I., Organic coprecipitants. XXIII., 20: 29135
KUZNETSOVA, N. E., Alterations in content of adrenaline-like substances in blood of dogs during acute and sub-acute radiation sickness, 20: 28941
KUZNETSOVA, Z. M., Solid phases of $NH_4F–UO_3–H_2O$ systems, 20: 29200
KYLE, M. L., Pilot-plant gettering system of Ti-metal sponge for removal of N from Ar, 20: 29329 (ANL-7128)

L

LABZINA, N. G., Recovery of cells from primary cytogenetic injuries, 20: 29049
LACHENAUD, R., Determination of brittle-ductile transition temperatures in Mo and W, 20: 29757
LACOUSTEY, P., Heating and containment of plasma in the magnetic well in Deca II, 20: 30607
LACY, P. S., Core boration and flux mapping Test 313, 20: 30874 (ACNP-65612)
LADD, I. R., Kinetics of high temperature oxidation of refractory materials, 20: 29656
LADNER, H. A., Radiation control concentration changes of free amino acid in blood plasma of man, 20: 28979
LAGUCHEVA, R. M., Inhibiting effects of solid impurities on radiation chemistry processes, 20: 29306
LAHAYE, B., Characteristic energy losses of electrons and color centers in LiF, LiCl, and NaCl, 20: 30776
LAKSHMINARAYANA, V., Absolute photoelectric cross sections of 320 kev gamma rays, 20: 29924
LAKSHMINARAYANA, V., Influence of electron binding on incoherent scattering of low-energy γ rays, 20: 29923
LAMBERT, M., Application of Fano-Racah formalism to a kinematic study of nuclear reactions, 20: 30396
LAMBERT, M., Fluctuations of differential polarization of particles emitted in nuclear reactions, 20: 30397
LAMERS, Kenneth W., Do-it-yourself lock-in amplifiers, radio and audio frequency, 20: 29487 (UCRL-16632)
LAMING, Lindon C., Removable thermal shield, 20: 30828
LANDER, R. L., Isospin of the A mesons, 20: 30023
LANDERS, Mary K., Development of radiation-sterilized seafood products. I., 20: 29603
LANDMAN, A., Fine and hyperfine structure of 3^2P term in Li, 20: 29939
LANDSBERG, A., Nonmetallic powders coated with tungsten and molybdenum, 20: 29631
LANGE, R. C., Weak α and electron-capture decay in ^{208}Po and ^{209}Po, 20: 30405
LANZL, Lawrence H., High-dose human exposure from 10-Mev linear accelerator, 20: 28929 (CONF-651109, pp 574-98)
LAPIN, B. A., Radiation sickness in Macacus rhesus, 20: 28986
LAPSHOV, Yu. K., Complex alloys based on molybdenum disilicide and boron carbonitride, 20: 29169
LAQUER, H. L., Automatic superconducting flux pump, 20: 30274
LARIONOV, M. M., Interaction between uhf radiation and a turbulent plasma, 20: 30625
LARSON, James Daniel, Gamma radiation from the α-particle bombardment of ^{12}C, 20: 30529
LARSON, O. W., Radiation measurements of effluent from NRX A-2 and NRX A-3 reactors, 20: 30923 (LA-3394)
LASER, M., Diffusion of fission products in overlapping chemical reactions, 20: 29190
LASKER, M. F., Mixed conduction in ThO_2 and $ThO_2–Y_2O_3$ solutions, 20: 29216
LASKORIN, B. N., Extraction of U and associated elements with D2EHPPA, 20: 29361
LASRY, J., Characteristics and purification of plasma produced by coaxial gun with annular preionization, 20: 30648
LASSMANN, G., ESR studies of self-radiolysis ^{3}H-labeled amino and dicarboxylic acids, 20: 29311
LASSNER, E., Oxygen determination in high-melting metals, 20: 29108
LATEK, S., Multiplication method of reactivity measurements, 20: 30849
LATYSHEV, V. K., Radioisotopic instruments in metallurgy, 20: 29598
LAUBERT, R., Binding effects in electronic excitations by heavy charged particles, 20: 29936

LAUCH, J., Nuclear electrons: relay-controlled pulse generator for testing nuclear electronics, 20: 29544
LAUER, E. J., Experimental studies with Astron, 20: 30637
LAUER, R. S., Absorption-spectrophotometric determination of rare earths in tributylphosphate extracts, 20: 29125
LAVRENCHIK, V. N., Global fallout products of nuclear explosions, 20: 29407 (AEC-tr-6666)
LAVRENT'EV, L. N., Arteriosclerosis in white rats exposed to wholebody x irradiation, 20: 28996
LAZUTIN, L. L., Outer radiation zone of the earth and bursts of x-ray radiation in the stratosphere, 20: 30218 (NASA-TT-F-389, pp 616-23)
LAZZARINI, E., Correlation between isomeric effect in Szilard-Chalmers recoil and chemical constitution of target studied on 13 Co(III) complexes, 20: 29258
LEAL, M., Deformation of graphite lattices by interstitial carbon atoms, 20: 29735
LE BARON, Robert, Neutron reflectors for nuclear reactors, 20: 30816
LEBECK, Donald F., Production of nuclides in the region of Z = 126 and N = 184, 20: 30367
LEBEDEV, A. N., Quasilinear acceleration of particles by transverse electromagnetic wave, 20: 29867
LEBEDEV, A. V., Boson resonance at 1.63 Bev in π^-p interactions, 20: 30021
LEBEDEV, V. I., Collective processes in gravitating systems. I., 20: 29902
LEBEDEVA, M. A., Effect of ionizing radiation on vitamin C metabolism, 20: 28921
LE BER, Jacques, Reliability of planar silicon transistors exposed to ^{60}Co gamma rays, 20: 29577 (CEA-R-2959)
LECAILLE, Claude, Production of Re in powdered form, 20: 29672
LEDRUT, J. H. T., Finkelstein reaction for measuring partial organic retention during irradiation of alkyl bromides, 20: 29292
LEE, B. W., Chiral algebra, configuration mixing, and magnetic moments, 20: 30143
LEE, Benjamin W., Algebra of currents and form factors at finite momentum transfer, 20: 30137
LEE, C. W., Shell-model calculations using realistic interactions, 20: 30384
LEE, George C., Stresses in thick-walled conical shells, 20: 30928
LEE, William R., Stability of Drosophila chromosomes to radioactive decay of incorporated ^{32}P, 20: 28955
LEE, Y. K., Moessbauer effect measurements in first and second excited states of ^{155}Gd, 20: 30422
LEENHOUTS, H. P., Gamma decay of ^{40}Ca levels measured with ^{39}K(p,γ)^{40}Ca reaction, 20: 30482
LEES, D. J., Inter-diffusion of plasma and magnetic fields in pinch and hardcore discharges, 20: 30639
LEGGETT, A. J., Theory of superfluid Fermi liquid. II., 20: 30284
LEHMANN, J., Evidence for 1^-, K = 0 character of ^{176m}Lu through β-decay measurements, 20: 30552
LEHMANN, J., Nuclear matrix elements of the β transition of ^{194}Ir, 20: 30551
LEHR, S. N., Solar simulation testing of nuclear test detection spacecraft, 20: 29440
LEIBBRANDT, F., Reactions of zirconium–molybdenum alloys with hydrogen and with nitrogen, 20: 29632
LEIGH, J. L., APEX: program for analysis of gamma-gamma angular correlation data, 20: 30341 (AECL-2529)
LEITMANN, O., Formation of azides of Pr(III) and Nd(III), 20: 29166
LEJEUNE, C., New type of high-frequency mass spectrometer with two electrodes, 20: 29126
LEKSIN, G. A., Accuracy of particle trajectory location in spark chamber, 20: 29527 (ITEF-341)
LEKSIN, G. A., Proton elastic scattering on deuterons at large angles, 20: 29989 (ITEF-361)
LELLOUCH, J., Relative biological efficiency of a beam of 20-Mev electrons as function of depth, 20: 28963
LEMAIRE, R., Variation of magnetic moment of Co in $Gd_uY_{u-1}Co_2$ compounds, 20: 30756
LEMBERG, I. Kh., Coulomb excitation of levels in ^{152}Sm and ^{186}W, 20: 30488
LENSKII, L. A., Measuring activity of tritiated water preparations by means of flow counter, 20: 29098
LEONARD, Brian Phillip, Hall currents and electron temperature effects in MHD shock waves, 20: 30191
LEONARD, R. F., Inelastic α-particle excitation in even tin isotopes, 20: 30468
LEONARDI, R., Isospin quintuplets in A = 16 nuclei, 20: 30440
LEPEKHIN, F. G., Slow meson production in interaction of 3.8-Bev π^- mesons with emulsion nuclei, 20: 30501
LEPEKHIN, V. P., Loss of hypotensive activity by derivatives of 5-hydroxyindole when animals are irradiated, 20: 29050
LESSMANN, G. G., Prog. rpt. on weldability and elevated-temperature stability of refractory alloys, 6–9/65, 20: 29712 (WANL-PR-(P)-009)
LESSMANN, G. G., Prog. rpt. on weldability and elevated-temperature stability of refractory alloys, 9–12/65, 20: 29713 (WANL-PR-(P)-010)
LEUNG, K. T., Changes in vaginal smears after therapeutic irradiation, 20: 29076
LEVANOV, E. I., One-dimensional self-similar motion of thermally and electrically conducting gas in magnetic field, 20: 30185
LEVAY, B., Significance of phosphorescence in measurement of low-energy beta isotopes with liquid scintillator and single-channel counter, 20: 29084
LEVENKO, P. I., Effect of γ-radiation on leathers, 20: 29588
LEVENKO, P. I., Effect of γ-radiation on physical-mechanical properties of chromium-tanned leather, 20: 29592
LEVENKO, P. I., The effect of γ-radiation on chrome-tanned shoe upper leather, 20: 29591
LEVENTHAL, Jacob Joseph, Energetic and angular studies of D_2H^+ formation in D_2^+–H_2 collisions, 20: 29950
LEVI, C., Spectroscopic information on samarium isotopes from analog-state experiments, 20: 30430
LEVIN, M. L., Method of images in magnetostatic problems involving a spherical superconductive boundary, 20: 30310
LEVINSON, Y. B., Effect of interelectron collisions on the electron distribution function in a strong electric field, 20: 30779
LEVY, M., Approximation method in study of scattering at high energies, 20: 30086 (CONF-640509(Pt.1), Paper 4)
LEVY, P. W., Photochemical decomposition of sodium bromate, 20: 29248 (BNL-9672)
LEWIS, Lionel, Administration of radiation safety at CVTR, 20: 30897
LEWIS, M. F., Interaction of microwave phonons with irradiation centers in quartz, 20: 30768
LEWIS, R. E., High-specific-activity ^{198}Au low in ^{199}Au, 20: 29610
LIEBEROTH, Juergen, Classical derivation of effective differential scattering cross section for neutrons in monatomic gas, 20: 30337
LIELPETER, Ya. Ya., Electrodynamic forces and Joule losses in conducting layers in traveling magnetic fields, 20: 29830
LIEM, Djiet Hay, Extraction of ^{233}U(VI) by DBP and TBP or TOPO, 20: 29334
LIESER, K. H., Investigations on corrosion of Zr in electrolytic solutions by use of radionuclides, 20: 29649
LIFSITZ, Jacob Robert, Measurement of 2^3P fine structure of ^{4}He, 20: 29911 (COO-1112-21)
LIIMATAINEN, Robert C., Reaction of U with water as initiated by power excursion in TREAT, 20: 30802
LIKHACHEV, V. M., Location of moving plasma bursts from coaxial injector, 20: 30681
LIMIC, N., Analytic structure in λ of the S matrix for strongly singular potentials, 20: 30100
LIN, Hung-Hsi, Effect of γ-rays from ^{60}Co on certain metabolic processes in pea plants, 20: 28909
LINDSAY, I. R., Effects of whole-body irradiation by protons on primates, 20: 28931 (CONF-651109, pp 624-35)
LINDSAY, J. D. G., Transistorized liquid-He temperature regulator, 20: 30254 (LA-DC-7209)
LINEKIN, D. M., Measurements of mutual-friction parameter B′ rotating He II, 20: 30285
LINHART, J. G., Hollow dynamic pinch, 20: 30641
LINZMAIER, Josef, Power supply system for Siemens-Schuckert Research Centre, 20: 29368
LIPKIN, H. J., W spin for any spin, 20: 30126
LIU, Chung-Heng, Intensity beats in resonance radiation absorbed by excited metastable state, 20: 30601
LIU, Jo-chuang, Ligand field theory. I., 20: 29205
LIU, Lun-yu, Fluorescent measurement of negligible amounts of uranium in waste water, 20: 29128
LIVSHITS, V. V., Collective interaction of modulated and unmodulated electron beams with plasma, 20: 30623
LLEO, A., Interactions of 12.8-Bev protons in nuclear emulsions. III., 20: 30364
LLOYD, Owen, Improvements in or relating to vacuum gages, 20: 29513
LLOYD, R. C., Criticality studies with plutonium solutions, 20: 29471
LOBANOV, Yu. N., Capture of electrons into betatron orbits, 20: 29869
LOBASHOV, V. M., Parity nonconservation in radiative transition of ^{175}Lu, 20: 30381
LOCK, W. O., Particle detectors. I., 20: 29534
LOCKETT, George Edward, Improvements in or relating to retarding mechanisms, 20: 30817
LOCKETT, George Edward, Improvements in or relating to charge/discharge machines for nuclear reactors, 20: 30819
LODIN, H., Experiences with "infusion urography" in children, 20: 29062
LOEHKEN, R., Numerical analysis of β spectra, 20: 30541
LOEHKEN, Rudolf, Relative measurements of electron polarization of ^{199}Au and ^{32}P, 20: 30548
LOEWE, W. E., Beta-backscatter techniques for measurement of layer thick-

ness in multilayer coating, 20: 29391
LOGACHEV, V. I., Cosmic ray nuclear component on Elektron-2, 20: 29957 (NASA-TT-F-389, pp 693-710)
LOGACHEV, Yu. I., Irregular high-energy electron streams near boundary of radiation zones of earth, 20: 30215 (NASA-TT-F-389, pp 576-87)
LOGACHEV, Yu. I., Primary cosmic radiation on Elektron-2 and Elektron-4, 20: 29955 (NASA-TT-F-389, pp 678-83)
LOGINOV, V. A., Absorption spectra of PtH and PtD, 20: 29934
LOH, Eugene, Lowest 4f → 5d transition of trivalent rare-earth ions in CaF_2 crystals, 20: 30763
LOMKAZI, G. S., Boson resonance at 1.63 Bev in π^- p interactions, 20: 30021
LOMON, E. L., Additional radiation correction to wide-angle pair production, 20: 30013
LOMTEVA, E. V., Therapeutic effectiveness of antibiotics on cystamine action during radiation sickness, 20: 29051
LONATI, R. Dugnani, Ionium/U method for the determination of the age of recent minerals, 20: 29441
LONCKE, P., Isospin quintuplets in A = 16 nuclei, 20: 30440
LONG, E. L. Jr., Postirradiation examination of high burnup EGCR prototype fuel capsules, 20: 29806 (ORNL-TM-1511)
LONGO, C. V., Acceleration in generalized coordinates, 20: 29834
LOOKER, J. H., Physical and chemical properties of hydroxyflavones. V., 20: 29240
LOPANTSEVA, G. B., Breakup of fast negative ions in inert gases, 20: 29947
LOPATO, L. M., Phase diagram of system Sc_2O_3–Cr_2O_3, 20: 29167
LOPEZ, Arturo, Series development of solution of eigenvalue problem, 20: 29993
LOPEZ-MENCHERO, E., Large-scale isotope irradiation in reactors, 20: 29609 (NP-15947)
LORD, W. B. H., Development of beryllium for use in aircraft, 20: 29767
LORIO, P. M., Neutron radiation monitoring using ^{3}He spectrometer, 20: 29846 (CONF-651109, pp 154-60)
LOTT, Bryan G., Crystallographic data for Ce–Zn compounds, 20: 29719
LOTZ, W., Toroidal theta pinch with superimposed multipole field, 20: 30616
LOVETSKII, E. E., Theory of stability of axially symmetric nonuniform plasma carrying current, 20: 30680
LUBAN, Marshall, Persistent currents in many-boson systems, 20: 30140
LUC, H., Heating and containment of plasma in the magnetic well in Deca II, 20: 30607
LUCHKINA, L. A., Radiation damages in deoxyribonucleoproteins at molecular and supermolecular levels, 20: 28908
LUCIUS, J. L., TRANSFER: program to calculate P_n multigroup scattering matrices, 20: 30323 (ORNL-TM-1537)
LUDEMANN, Carl Arnold, Angular distributions and correlations in ^{12}C(^{3}He,p)^{14}N reaction, 20: 30526
LUKHOVITSKII, V. I., Inhibiting effects of solid impurities on radiation chemistry processes, 20: 29306
LUKYANOV, A., Calculation of neutron activation cross sections for ^{51}V, ^{55}Mn, ^{63}Cu, ^{65}Cu, and ^{127}I at 0.1 to 14 Mev, 20: 30378
LUKYANOV, A. T., Kinetics of radiation-induced isotope exchange between deuterium and silica gel hydroxyl groups, 20: 29276
LUND, L. M., Flow and self-diffusion of gases in capillaries. I, 20: 30174
LUND, L. M., Flow and self-diffusion of gases in capillaries. II., 20: 30175
LUNDIN, S. J., Solubilization of cholinesterase from plaice muscle by bacteria, 20: 28933
LUPTON, W. H., Plasma confinement, heating, and losses in Pharos with an extended current pulse, 20: 30612
LUSH, G. J., Measurement of the spin-rotation parameter β in proton-^{4}He scattering at 48 Mev, 20: 30441
LUSIGNOLI, M., KN dispersion relations and symmetry groups, 20: 30018
LUTHRA, Jagdish, Radiation blistering: observations of oxides, silicon, and metals, 20: 29816
LUTOMIRSKI, R. F., Exact nonlinear electromagnetic whistler modes, 20: 29899
LUTTINGER, J. M., New mechanism for superconductivity, 20: 30311
LUTZ, G., Polarization of 6-Bev bremsstrahlung from Hamburg electron synchrotron, 20: 30045
L'VOVA, M. A., Coefficient of β backscattering from aluminum backing in 2π geometry, 20: 30369
L'VOVA, T. S., Synergistic effects of ionizing radiation and vibration upon animal organism, 20: 28968
LYAPKALO, Yu. M., Collective interaction of modulated and unmodulated electron beams with plasma, 20: 30623
LYMAN, John T., Acute cellular effects of heavy charged particle irradiations, 20: 28930 (CONF-651109, pp 601-16)
LYNCH, David W., Plasma excitations in LiF, 20: 30777
LYNDIN, V. V., Radioisotopic instruments in metallurgy, 20: 29598
LYNN, J. E., Ratio of asymmetric-to-symmetric fission for ^{239}Pu for 30-kev to 14.7-Mev neutrons, 20: 30404
LYNNWORTH, L. C., Prog. rpt. on ultrasonic temperature measuring device, 1–4/66, 20: 29486 (NASA-CR-54964)
LYONS, C. J., Fluoride tungsten, 20: 29687
LYONS, Charles, Collagen and hexosamine changes in subcutaneous granuloma irradiated locally with ^{60}Co source, 20: 28917
LYUBIMOV, V. B., Experimental separation of interactions with free protons, 20: 30083
LYUBIMOV, V. V., Use of laser operating in spike mode to obtain high-temperature plasma, 20: 30590
LYUBOSHITS, V. L., Decays in a mixed ensemble of neutral K mesons, 20: 30055

M

MA, Shang-kang, Correlations of photons from thermal source, 20: 29827 (UCRL-16824)
MACAROVICI, Const. Gh., Bis-acetylacetone-ethylenediimines of zirconium and thorium, 20: 29203
MACCABEE, Howard D., Fluctuations of energy loss in semiconductor detectors, 20: 29531 (UCRL-16715)
MACFARLANE, A. J., Dirac matrices and Dirac matrix description of Lorentz transformations, 20: 30103
MACHENSCHALK, R., Flow turning of refractory metals, 20: 29682
MACHI, Sueo, Initiation and propagation in γ-radiation-induced polymerization of ethylene, 20: 29275
MACHIDA, Tadao, Error in density measurement of compressed stock coal by back-scattering gamma-ray density meter, 20: 29491
MACKEY, L., Propulsion reactor temperature control with internal power loop eliminated, 20: 30924 (LA-DC-7636)
MAC PHERSON, R. D., Impossible Legendre coefficients, 20: 30355 (ORNL-P-2084)
MADIEVSKII, Yu. M., Heat resistance of rabbit blood serum in ultraviolet radiation, 20: 29004
MADSHUS, Kjell, Cesium-137 in milk, meat, and man in Norway, 20: 29432
MAECK, William J., Prog. rpt. on burnup determination of nuclear fuels, 10–12/65, 20: 29080 (IDO-14676)
MAEKAWA, Takayoshi, Elementary particles and bound states, 20: 30145
MAEKAWA, Tatsuo, High-temperature oxidation mechanism on 2.5Sn–Zr alloy, 20: 29652
MAGIN, George B. Jr., Radioisotopes in oceanographic research, 20: 29401
MAHLER, R. J., Angular dependence of one-phonon-nuclear quadrupole interactions, 20: 30749
MAHONEY, J., Scattering of 40.5-Mev α particles by ^{12}C, ^{13}C, ^{14}N, ^{15}N, ^{16}O, and ^{18}O, 20: 30450
MAHONEY, James R., Energy sources for the thermosphere, 20: 30194 (MIT-2241-16)
MAHONEY, Jeannette, Scattering of α particles by ^{52}Cr, ^{53}Cr, and ^{51}V, 20: 30460
MAIANI, L., Current algebras and magnetic moments, 20: 30118
MAIDEN, C. J., Compressive strain rate tests on four composites, Phase I, 20: 29708 (SC-DC-65-1744)
MAIER, H. J., Excited states of ^{22}Na by ^{20}Ne(^{3}He,p2)^{22}Na reaction, 20: 30400
MAIER, John Gail, Patho-physiologic aspects of radiation nephritis, 20: 29025
MAILLIE, Hugh David, Effects of x irradiation on renal hemodynamic functions of dog, 20: 29026
MAIN, Robert M., Omnitron: medium-energy synchrotron for acceleration of light and heavy ions, 20: 29857 (UCRL-16839)
MAISIN, J. R., X irradiation effects on mouse proteins, 20: 28899
MAISONNIER, Ch., Hollow dynamic pinch, 20: 30641
MAJER, J., Paper electrophoresis of complexes of rare earths with hydroxyamino acids, 20: 29343
MAKAROV, A. A., Current-generated algebras and form factors, 20: 30146
MAKAROV, M. M., Slow meson production in interaction of 3.8-Bev π^- mesons with emulsion nuclei, 20: 30501
MAKAROV, Yu. V., Processes behind reflected shock wave in an EM shock tube, 20: 30697
MAKSIMENKO, V. M., Cross section of quark generation, 20: 29999
MAKSIMOV, A. M., Processes behind reflected shock wave in an EM shock tube, 20: 30697
MAKSUMOV, M. N., Collective processes in gravitating systems. I., 20: 29902
MALAKHOV, S. G., Fallout of Ce-141, Ce-144, Zr-95 + Nb-95 and Sr-90 on U.S.S.R., 20: 29406 (NP-14719)
MALANICHEV, F. G., Complex formation of rare earths with EDTA, 20: 29222
MALANIFY, J. J., Neutron-deuteron polarization at 22.7 Mev, 20: 30442
MALDAGUE, Pierre E. J. M., Reactor reactivity control, 20: 30867
MALDAGUE, Pierre E. J. M., Reactor fuel-control rod assembly, 20: 30873
MALECKI, Henryk, Proton scattering in tube of electrostatic accelerator,

20: 29866
MAL'KOVA, T. V., Neodymium and erbium bromide complexes, 20: 29225
MALMBERG, J. H., Landau damping of electron plasma waves, 20: 30622
MALOYAN, A. G., Gamma radiation of 12.3-year ^{152}Eu, 20: 30487
MALYKH, N. I., Plasma equilibrium in torus with high-frequency fields and plasma heating resulting from beam of "escaping electrons", 20: 30640
MALYSHEV, A. B., Radiation intensity in earth's radiation belts, 20: 30235
MAMALADZE, Yu. G., State of liquid He in the vicinity of λ line, 20: 30266
MAMDAPUR, V. R., Synthesis of potential antiradiation agents. I., 20: 29241
MAMURO, Tetsuo, Radioactive fallout particles from nuclear detonation in China, 20: 29466
MAMURO, Tetsuo, Studies on fallout particles. V., 20: 29423
MANDEL'SHTAM, S. L., Transient increases of flux of heavy nuclei accompanied by bursts of x radiation, 20: 29965
MANDEVILLE, C. E., Nuclear states of ^{103}Rh, 20: 30471
MANDL, V., Time resolution measurements with fast photomultipliers, 20: 29568
MANELI, R. M., Properties of objects produced from lanthanum and yttrium hexaborides by sintering in vacuum, 20: 29738
MANGAN, M. A., Automatic control of rod position with boron in a chemical skim nuclear plant, 20: 30808 (WCAP-3269-54)
MANHARTSBERGER, H., Quantitative activation analytical purity determination of rare earth oxides, 20: 29082 (SGAE-CH-27/1966)
MANIAR, G. N., Effect of increased Ni content on intergranular corrosion of alloy 20Cb, 20: 29643
MANLEY, Oscar P., Free-free emission as source of galactic x rays, 20: 29881
MANSON, Neil, Lasers and ultrasonics, 20: 28951
MANTHURUTHIL, Jose Chacko, Determination of first-forbidden β-decay matrix elements with inclusion of nuclear finite size effects, 20: 30522
MARBLE, Georges, Evaluation of number of free radicals produced in irradiated rat bone, 20: 28898 (CEA-R-2910)
MARBLE, Georges, Production of long-lived free radicals by irradiation in bones of rat, 20: 28906
MARCHUK, G. I., Application of the decomposition method to radiation transfer equations, 20: 30063
MARGOLIN, D. D., Radiochemical properties of certain peptides, 20: 29301
MARGRAVE, J. L., Mass-spectrometric studies at high temperatures. X., 20: 29183
MARGUERON, Jean C., Support for liquid-cooled reactor bed, 20: 30827
MARIEN, Pierre Jean Camille Albert, Improvements in gas-cooled reactors and fuel elements, 20: 30872
MARINESCU, N., Irreducible tensors for group SU_3, 20: 30102
MARINESCU, N., One-particle-exchange model for bootstrap, 20: 30035
MARINSKY, J. A., Isomers of ^{129}Sn, 20: 30376
MARKL, Ilse, Adsorption of Np(V) on anion exchangers, 20: 29358
MARKL, Ilse, Separation of Pu, Np, Zr, Nb, Mo, Tc, Te, and U from fission-product solutions, 20: 29357
MARKOE, Arnold M., Determination of quality factors through utilization of balanced, tissue-equivalent, ionization chamber, 20: 29847 (CONF-651109, pp 181-98)
MARKS, S., Biologic effects of human radiation exposure, 20: 28970
MAROCHNIK, L. S., Collective processes in gravitating systems. I., 20: 29902
MARRUS, Richard, Atomic-beam study of Stark effect in Cs and Rb D lines, 20: 29941
MARSHAK, R. E., Mass difference (K^+-K^0), 20: 30016
MARSHAK, R. E., Present status of weak interactions, 20: 30067
MARSHALL, L., Elastic scattering (π^--p) at 1.7 Bev/c, 20: 30011
MARTELL, Arthur E., Interaction of Th(IV) with pyrocatechol-3,5-disulfonate at a 1:1.5 molar ratio, 20: 29093
MARTELLI, G., Reaction d + d → ^4He + 2π at 1.69 Bev/c, 20: 30010
MARTELLUCCI, S., Formation and development of hydromagnetic disturbances during implosion phase of a preionized theta pinch (Cariddi), 20: 30613
MARTERSTOCK, R., Air locks for safe escape in nuclear reactors, 20: 29465
MARTH, W., Magnetic methods for measuring maximum temperature of irradiated samples, 20: 29387
MARTIN, B., Beta-γ directional correlations and β-γ circular polarization correlations in single-forbidden-β decay of ^{144}Ce, ^{144}Pr, ^{170}Tm, and ^{203}Hg, 20: 30544
MARTIN, D. C., Joining of nickel and nickel-base alloys, 20: 29666 (RSIC-484)
MARTIN, D. C., Mechanical fastening of nickel-base alloys, 20: 29667 (RSIC-509)
MARTIN, Robert F., Stability of Drosophila chromosomes to radioactive decay of incorporated ^{32}P, 20: 28955
MARTIN, Samuel W., Nuclear reactors operating with substantially isotropic graphitized bodies, 20: 29694
MARTON, L., Advances in electronics and electron physics, Vol. 21, 20: 29499
MARTONE, M., Formation and development of hydromagnetic disturbances during implosion phase of a preionized theta pinch (Cariddi), 20: 30613
MARTYNOV, E. V., Radiation damages in deoxyribonucleoproteins at molecular and supermolecular levels, 20: 28908
MARTYNOVICH, T. L., Application of straight line method coupled with method of integral transformations to problem of electrostatic fields with axial symmetry, 20: 29497
MASAITIS, V. L., Uranium in traps of Siberian platform, 20: 29419
MASLENNIKOV, E. A., Achievement of ultrahigh vacuum in Ogra-1, 20: 30701
MASLOV, B. V., Radiochemical properties of certain peptides, 20: 29301
MASLOV, P. G., Heat of formation of thorium, protactinium, uranium, neptunium, and americium halides, 20: 29229
MASLOV, Yu. P., Heat of formation of thorium, protactinium, uranium, neptunium, and americium halides, 20: 29229
MASSUCCI, Maria Antonietta, Spectrofluorimetric trace determination of Tb(III) with K oxalate, 20: 29086
MASUNAGA, Shoji, Optical properties of CsI:Tl and CsBr:Tl, 20: 30751
MASUNOV, E. S., Photon bremsstrahlung in scattering of vector mesons on each other, 20: 30057
MASUYAMA, Toshio, Radiation damage of low-permeability graphite and hard carbon, 20: 29822
MASUZAKI, M., Ion cyclotron resonance heating of QP plasma, 20: 30662
MATHE, G., Effect of irradiation on immunity, 20: 28983
MATHE, Georges, Total-body irradiation injury: disorders of blood and hematopoietic tissues, 20: 28982
MATHUR, B. S., Rare earth trichloroacetates. I., 20: 29213
MATHUR, P. K., Isotopic exchange and annealing of recoil damage in Co complexes, 20: 29259
MATHUR, R. B., Orientation of magnetic field in Rayleigh-Taylor's instability, 20: 30172
MATHUR, V. S., Mass difference (K^+-K^0), 20: 30016
MATHUR, V. S., Two-pion decay modes of K mesons, 20: 30015
MATOBA, Toshio, Deoxidation of Mo during arc melting, 20: 29675
MATSUI, Masakazu, Coprecipitation behavior of strontium with calcium oxalate by precipitation from a homogeneous system, 20: 29154
MATSUMURA, Tetsuo, Spectrochemical analysis of zirconium and its alloys. I., 20: 29113
MATSUMURA, Tetsuo, Spectrochemical analysis of Zr and its alloys. III., 20: 29115
MATSUNAMI, Tadao, Studies on fallout particles. V., 20: 29423
MATSUOKA, Saburo, Diffusion of nucleotides into outer medium from non-irradiated and gamma-irradiated Euglena cells, 20: 28904
MATSUURA, K., Ion cyclotron resonance heating of QP plasma, 20: 30662
MATSUURA, T., Separation of recoiling Cr(II) ion from neutron-irradiated Cr(III) ion, 20: 29261
MATT, R. E., Development of silver infiltrated tungsten nozzles for uncooled rocket motors, 20: 29685
MATTHEWS, P. W., Magnetic field repulsion by a superconducting split cylinder, 20: 30276
MATVEEV, G. M., Strength of ceramics made of pure oxides, 20: 29740
MATVEEV, M. A., Strength of ceramics made of pure oxides, 20: 29740
MATVEEV, V. A., Current-generated algebras and form factors, 20: 30146
MATYA, P., Elastic and inelastic scattering of α particles by C, 20: 30499
MAUDERLI, Walter, Automatic depth-dose acquisition system, 20: 29070
MAURER, G., Interference effects between N*(1236) and K*(891) production, 20: 30009
MAURO, Francesco, Recovery from x-ray-induced sub-lethal damage in Saccharomyces cerevisiae cells of different ploidy, 20: 28961
MAVROIDES, John G., Energy band parameter determination in graphite, 20: 30737
MAYEUR, C., π^+-Mesonic decays of hypernuclei, 20: 30485
MAZHUOLITE, G. E., Effect of interelectron collisions on the electron distribution function in a strong electric field, 20: 30779
MAZUR, Peter, Kinetics of uv-induced dimerization of thymine in frozen solutions, 20: 28916
MAZZUCATO, E., Hot-ice experiment, 20: 30665
MC CALL, Richard C., Radiation protection problems at Stanford two-mile linear accelerator, 20: 29849 (CONF-651109, pp 442-58)
MC CARTHY, J. T., Weak α and electron-capture decay in ^{208}Po and ^{209}Po, 20: 30405
MC COLM, Douglas, Atomic-beam study of Stark effect in Cs and Rb D lines, 20: 29941
MC COLM, Douglas, Design of atomic- and molecular-beam apparatus, 20: 29918 (UCRL-11670)
MC CREA, W. H., Interpretation of observations of quasi-stellar objects, 20: 29876
MC CUAIG, F. D., Fabrication of spiked-core fuel elements for EBWR, 20: 29658 (ANL-6283)

MC CULLOUGH, James R., Evidence for oscillatory component in solar granulation brightness fluctuations, 20: 29886
MC CULLOUGH, W. L., Properties of some refractory metals. IV., 20: 29710 (TID-22986)
MC DONALD, J. D., Mass-spectrometric studies at high temperatures. X., 20: 29183
MC DONALD, R. E., Low-lying states of ^{33}S, 20: 30455
MC FADDEN, Lynne, Optical-model analysis of scattering of 24.7-Mev α particles, 20: 30413
MC GEE, Ian J., Coulomb corrections to β decay of ^{14}O, 20: 30443
MC GRATH, Robert Leslie, Angular distributions and total cross sections of reactions induced by ^{6}Li,^{7}Li on ^{10}B,^{11}B at 3 Mev, 20: 30519
MC GRORY, J. B., Comparison of effective two-nucleon interaction with surface delta interaction, 20: 30423
MC GURN, J. F., Radiation damage produced in Cu, Au, and Al during ion bombardments, 20: 29808
MC INTEER, B. B., Straight-line diagram for powder pattern indexing, 20: 30952 (LA-3467)
MC KIBBEN, J. Malvyn, Performance of mild steel in D_2O moderator-coolant in HWCTR, 20: 29654
MC LAUGHLIN, James, Determination of energy distribution of γ rays scattered in sand, 20: 30728
MC LAUGHLIN, James, Inference of accelerator stray neutron spectra from various measurements, 20: 29522 (CONF-651109, pp 286-305)
MC LAUGHLIN, James E., Fast neutron spectrometry with nuclear emulsions, 20: 29848 (CONF-651109, pp 199-212)
MC LEAN, E. A., Plasma confinement, heating, and losses in Pharos with an extended current pulse, 20: 30612
MC MURRY, H. L., Slow-neutron scattering by water, 20: 30330
MC NEIL, D. A. C., Pairwise trapping in γ-irradiated sodium nitroprusside, 20: 29280
MC NULTY, Peter J., Muon-nucleon inelastic interactions, 20: 30076
MC VITTIE, G. C., Spherically symmetric motions in general relativity, 20: 30244
MEADE, Dale Michael, Experimental study of plasma motion in toroidal octupole magnetic field, 20: 30708
MEDVEDEV, B. V., S-matrix in Heisenberg's representation, 20: 30104
MEERSON, G. A., Properties of objects produced from lanthanum and yttrium hexaborides by sintering in vacuum, 20: 29738
MEHLING, O., Measurement of β-γ circular polarization correlations in β transitions of ^{58}Co, ^{95}Zr, ^{95}Nb, and ^{141}Ce, 20: 30543
MEHRISHI, J. N., Effect of ionizing radiations on electrophoretic mobility of mammalian cells, 20: 28905
MEHURON, W. O., Measurements of electron drift velocity and collision frequency in an argon discharge, 20: 30598
MEISSNER, Hans, Calculation of low-temperature microwave resistance of a thin metal film on bulk substrate, 20: 30290
MEISSNER, Hans, Critical temperatures and critical fields of multiple superconducting and normal-conducting films, 20: 30291
MEISSNER, Hans, Microwave absorption in normal-conducting films on superconducting substrates, 20: 30289
MEISSNER, Hans, Thermal conductivity of lead films for study of surface superconductivity, 20: 30294
MELE, A., Main-chain scission and ESR spectra of irradiated polytetrafluoroethylene oxide, 20: 29267
MELESHEVICH, A. P., Effects of γ radiation on structure of epoxy resins and resin-base metallic polymers, 20: 29296
MELESHEVICH, A. P., X-ray study of epoxido-dianic ED-5 resin irradiated with ^{60}Co and metallopolymers on its base, 20: 29297
MELIK-MUS'YAN, A. B., Histochemical investigation of glycogen in rabbit retina, 20: 28907
MELLOR, A. M., Prog. rpt. on combustion of metals, annual, 7/64–6/65, 20: 29641 (SC-DC-65-1691)
MEL'NIKOV, V. V., Recording charged particle with energy of 0.1 to 10 kev with spherical electrostatic analyzer, 20: 29532 (NASA-TT-F-389, pp 518-25)
MELTON, C. E., Mass spectrometric evidence for H_3O, HD_2O, and D_3O, 20: 29104
MELYUKOV, A. N., Irradiation of animals with ultraviolet rays, 20: 29020
MENDEL, Clifford W. Jr., Dense plasma under strong electric field, 20: 30558 (AD-633593)
MENDELSON, M. R., Group constants for gamma-ray heating, 20: 30722 (KAPL-M-6497)
MENHINICK, Edward F., Strontium-90 plaques for beta radiation studies, 20: 28879
MERCER, E. E., Vibrational spectrum of hydrazine-d_4 and Raman study of hydrogen bonding in hydrazine, 20: 29175
MERCIER, C., Toroidal equilibria in narrow-tube approximation. Effect of curvature, 20: 30619
MERIWETHER, J. R., Scattering of 40.5-Mev α particles by ^{12}C, ^{13}C, ^{14}N, ^{15}N, ^{16}O, and ^{18}O, 20: 30450
MERIWETHER, John R., Scattering of α particles by ^{52}Cr, ^{53}Cr, and ^{51}V, 20: 30460
MERKLE, J. G., Strength of steel containment shells, 20: 30813
MERZ, J. L., Thermoluminescent emission of irradiated rare earth ions in CaF_2, 20: 29318
MESHITSUKA, Gisuke, Radiolysis of aqueous solutions of potassium iodide, 20: 29253
MESHKOV, S., W spin for any spin, 20: 30126
MESROBIAN, Robert B., Production of cured resin bodies by radiation pregelling and hot curing, 20: 29637
MEYVAERT, N. R., Approximate treatment of neutron thermalization in heterogeneous systems, 20: 30864
MEZHLUMYAN, P. G., Investigation of luminescence of acetyl acetonates of samarium, europium, and terbium, 20: 29238
MICHALON, A., Interference effects between N*(1236) and K*(891) production, 20: 30009
MICHIE, Alexander J., Kinetics of calcium metabolism in children utilizing nonradioactive Sr, 20: 28889
MIDDELKOOP, W. C., Interaction π^+-π^- as studied in 12- and 18-Bev pion-nucleon reactions, 20: 30025
MIDDLETON, R., Proton pickup from the even lead nuclei, 20: 30387
MIDDLETON, Roy, High-resolution study of $^{54}Fe(t,p)^{56}Fe$ reaction, 20: 30453
MIEDEMA, A. R., Heat capacity below 1°K of some dilute alloys, 20: 29791
MIHUL, El. K., Peripheral mechanism in $\pi^- + n \rightarrow p + \pi^- + \pi^-$ reaction, 20: 30081
MIKELSON, Yu. Yo., Electrodynamic forces and Joule losses in conducting layers in traveling magnetic fields, 20: 29830
MIKHAILOV, V. A., Solvent extraction of products of uranyl nitrate hydrolysis by alpha-n-amylpyridine-N-oxide, 20: 29359
MIKHAILOVSKII, A. B., Kinetic theory of oscillations of a nonuniform plasma with collisions taken into account, 20: 30691
MIKHAILOVSKII, A. B., Quasi-linear transformation of waves in inhomogeneous plasma, 20: 30673
MILAEV, S. M., Analysis of rare earth alloys in nonaqueous solutions, 20: 29133
MILLER, C. E., Nuclear spin relaxation in liquid hydrogen, 20: 30181
MILLER, David, Highlights of 8th National Heat Transfer Conference, 20: 29383
MILLER, G. L., Channel (4096) 50-Mc/s servo stabilized analog-to-digital converter, 20: 29567
MILNER, A., Prog. rpt. on fabrication of W alloy tubing, 2–5/66, 20: 29659 (COO-1518-3)
MILONE, C., Reactions $^{7}Li+d$, 20: 30402
MINER, George Kenneth, Fast neutron irradiation experiments with strontium titanate single crystals, 20: 29826
MINGLE, J. O., Semiconductor radiation detector measurements of gaseous diffusion coefficients, 20: 29510
MINTON, C. D. T., Protective coatings for niobium and its alloys, 20: 29651
MIR-KASIMOV, R. M., Coulomb field and non-relativistic space quantization, 20: 29915 (JINR-P-2627)
MIRMAN, R., Transformation properties of electromagnetic field, 20: 30243
MIRNOV, S. V., Joule heating of plasma in toroidal Tokamak-3 device, 20: 30650
MIROSHNICHENKO, V. I., Kinetic theory of passage of EM waves through plasma layer. II., 20: 30679
MISHCHENKO, O. A., Radiolysis of isooctyl and heptyl hydroperoxide solutions in hydrocarbons, 20: 29302
MISHCHENKO, V. T., Absorption-spectrophotometric determination of rare earths in tributylphosphate extracts, 20: 29125
MISHENKO, V. M., Statistical errors in determining concentrations of radioactive elements in rocks using γ-threshold and differential spectrometers, 20: 29421
MISSONI, G., Spectral distribution of photons scattered by electrons bound in K shell. I., 20: 29912 (ISS-66/6)
MISSONI, G., Spectral distribution of photons scattered by electrons bound in K shell. II., 20: 29913 (ISS-66/7)
MISSONI, G., Spectral distribution of photons scattered by electrons bound in K shell. III., 20: 29914 (ISS-66/8)
MISTLER, T. E., Semiconductor radiation detector measurements of gaseous diffusion coefficients, 20: 29510
MITANI, Kenji, Analysis of negative absorption of plasma-cavity system, 20: 30587
MITANI, Masao, Studies of hard superconductors. I., 20: 29784
MITCHELL, Ferdinand Haverman Jr., Partial wave analysis of EM wave propagation in inhomogeneous media, 20: 30713
MITCHELL, J. G., Single-sample potassium-argon ages using the omegatron, 20: 29413
MITCHELL, John C., Techniques for determining proton depth dose distribution in primates, 20: 28928 (CONF-651109, pp 417-25)
MITOMI, Mamoru, Antileucopenic action of marinamycin in case of x-ray irradiation, 20: 29055
MITRA, B., Cross sections (n,p) of some low-Z nuclei for 14.8-Mev neutrons,

20: 30394
MITRA, S. N., Effect of nuclear explosions upon ionosphere, 20: 30228
MITROFANOV, K. P., Barium stannate: source for measurement of Moessbauer effect on ^{119}Sn, 20: 30753
MITSUHASHI, Toshihiko, Concentration of ^{137}Cs in beef, 20: 28887
MITTAL, M. L., High-frequency titrimetric study of the reaction between thorium and alkali molybdate, 20: 29092
MITTELSTAEDT, P., Equivalent nonlocal nucleon-nucleon potentials, 20: 30061
MITTLEMAN, M. H., Electron-alkali atom scattering: nonadiabatic approach, 20: 29942
MITTLEMAN, Marvin H., Resonances in multichannel scattering, 20: 29943
MITTLER, Sidney, Adenosine triphosphate: protection against radiation-induced chromosome loss in Drosophila, 20: 29046
MIWA, Hisayoshi, Spectrochemical analysis of zirconium and its alloys. I., 20: 29113
MIYACHI, Yoshihiko, Elementary particles and bound states, 20: 30145
MIYAHARA, A., Ion cyclotron resonance heating of QP plasma, 20: 30662
MIYAHARA, A., Stable and unstable behavior of preheated plasma in linear and cusped theta pinches, 20: 30614
MIYAJIMA, Shigeki, One-dimensional steady flow of plasma, 20: 30597
MIYAMOTO, Goro, Momentum compaction in a cyclic accelerator, 20: 29861
MIYAMOTO, Susumu, Prevention of contamination of milk by fallout. I., 20: 29459
MIYASAKI, Keiji, Numerical analysis of reactor kinetics by digital computer, 20: 30838
MIYATA, Haruo, Spectrophotometric determination of F with a PAC–Th complex, 20: 29091
MIYAUCHI, David, Prog. rpt. on application of radiation-pasteurization to Pacific crab and flounder, final, 11/64–10/65, 20: 29583 (TID-22515)
MIYOSHI, Satoshi, Spectrochemical analysis of Zr and its alloys. II., 20: 29114
MIZUTANI, J., Effect of storage at ambient temperature on the volatile components of irradiated beef, 20: 29589
MKRTCHYAN, A. R., Autodyne nuclear magnetic resonance pickups, 20: 29492
MOBLEY, R. M., Muonium chemistry, 20: 29177
MOCCIA, A., Filterability and coalescence time of colloidal solutions of ANN–HNO_3–Hg^{2+}–SiO_2, 20: 29333 (RT-CHI-(65)33)
MOENIG, H., ESR study on irradiated sulfur-containing and sulfur-free pyridoxine derivatives, 20: 28901
MOGILEVSKII, E. I., Structure of solar corpuscular stream interaction with magnetosphere, 20: 30210 (NASA-TT-F-389, pp 499-517)
MOHANTY, S. R., Kinetics of annealing in irradiated barium nitrate, 20: 29814
MOHRI, Akihiro, Analysis of toroidally shaped Heliotron field, 20: 30595
MOISEEV, S. S., Plasma with relativistic electrons in magnetic mirror trap, 20: 30638
MOIZHES, G. Yu., Removal of energy from plasma of a thermoelectric converter, 20: 29981
MOLCHANOVA, I. V., Effects of Fe on ^{91}Y behavior in turfy-meadow soil, 20: 28881
MOLICA, Guido, Devices for adjusting relative positions of fuel elements in reactor, 20: 30829
MOLODKIN, A. K., Thorium orthophosphates, 20: 29160
MOLODKIN, A. K., Thorium tetrasulfate compounds, 20: 29218
MOLODKIN, A. K., Thorium penta- and hexasulfate compounds, 20: 29226
MONGINI-TAMAGNINI, C., Basic concepts of LYRA system, 20: 30721 (EUR-2778.e)
MONROE, R. E., Joining of nickel and nickel-base alloys, 20: 29666 (RSIC-484)
MONROE, R. E., Mechanical fastening of nickel-base alloys, 20: 29667 (RSIC-509)
MOORE, A., Development of beryllium for use in aircraft, 20: 29767
MOORE, J. H., Properties, availability, and applications of Ta-base alloys, 20: 29760
MOORE, Norman Clement, Production of carbonaceous bodies containing carbides, 20: 29692
MOORE, W. E., Inelastic scattering cross sections for polyethylene and water in gas transition region, 20: 30334
MORAVCSIK, Michael J., General phenomenological formalism for reactions with particles of arbitrary spin. I., 20: 30094 (UCRL-14222)
MORGAN, D. Vernon, Ionic displacement in alkali halides, 20: 30741
MORGAN, J. G., Postirradiation examination of high burnup EGCR prototype fuel capsules, 20: 29806 (ORNL-TM-1511)
MORGAN, J. G., Prog. rpt. on coated-particle fuels development at ORNL, 11/65–5/66, 20: 30870
MORI, Hazime, Relaxation phenomena near the critical points, 20: 30780
MORI, Ichiro, Ambipolar potential in magnetoactive cold plasma, 20: 29978
MORI, Ichiro, Charge exchange loss of high-temperature plasma confined by mirror magnetic field, 20: 30584
MORITA, Ituo, Optical properties of CsI:Tl and CsBr:Tl, 20: 30751
MORIYAMA, Hideo, Studies on X agent. XLVII., 20: 30955
MORIYAMA, Hideo, Summary of the studies on X agent, 20: 30956
MORIZE, P., Beryllium oxide in the nuclear industry, 20: 29810
MOROZ, B. B., Catecholamine metabolism in acute ^{210}Po lesions, 20: 28886
MOROZNMI, Shotaro, Beryllium as cladding material, 20: 29777
MOROZOV, S. A., Heating of plasma electrons by uhf fields in an adiabatic trap, 20: 30663
MOROZOV, V. S., Simulation of biological effect of depth dose from monoenergetic proton, 20: 28972
MORRISON, G. C., Discrepancies in proton-transfer reactions to states with different isobaric spin, 20: 30481
MORSE, Francis, Nuclear airship, 20: 30927
MORTON, Jane I., Influence of deuteration on circulating antibody levels in mouse, 20: 28988
MOSHKINA, V. A., Formation and thermal dissociation of yttrium fluorides and carbonates, 20: 29223
MOSKALEV, S. S., Total neutron cross sections for heavy Sn isotopes below 10 kev, 20: 30490
MOSKVIN, A. I., Solubility of ammonium plutonyl phosphate compounds in aqueous solutions, 20: 29219
MOSLEY, Wilbur Clanton Jr., Electron spin resonances in x-irradiated silver nitrate, 20: 29310
MOSS, S. J., Evolution of plasma puff in longitudinal magnetic field, 20: 30715
MOTHERSHED, C. T., ORSEF: code for calculation of flash evaporation desalination plant designs, 20: 30953 (ORNL-TM-1542)
MOTIU, Emilia, Bis-acetylacetone-ethylenediimines of zirconium and thorium, 20: 29203
MOTT, W. E., Activation analysis for chlorine in petroleum products and related materials, 20: 29116
MOTZ, H. T., AEC Nuclear Cross Sections Advisory Group meeting, Washington, D. C., 3/66, 20: 30360 (WASH-1068)
MOTZ, J. W., Projected requirements in radiation dosimetry, 20: 29482
MOTZ, Robin O., Magnetohydrodynamic drag on oscillating sphere, 20: 30179
MOUSTACCHI, E., Relative biological efficiency of a beam of 20-Mev electrons as function of depth, 20: 28963
MOUSTAFA, H. R., Gross- and partial-ionization cross sections for electrons on water vapor, 20: 29928
MOVCHET, J., Search for an isobar of isotopic spin $T = 5/2$, 20: 30022
MOVSESYAN, M. E., Investigation of luminescence of acetyl acetonates of samarium, europium, and terbium, 20: 29238
MUELLER, Arno, Nuclear reactor core assembly, 20: 30834
MUELLER, H., Hydrogen isotope exchange reactions of nonbenzoid aromatics. II., 20: 29245
MUELLER, M. H., Crystal structure of thorium nitrate pentahydrate by neutron diffraction, 20: 29151
MUKHERJI, Anil K., Simultaneous spectrophotometric determination of thorium and rare earths with xylenol orange, 20: 29109
MUKHOVATOV, V. S., Plasma-column equilibrium in Tokamak-5, 20: 30649
MUKHTAROV, A., Electron-positron pair production during scattering of gamma quanta in nuclear field, 20: 29996
MULLER, Harry Dierks, Physiological responses and implications of genetic transmission after embryonic x irradiation of fowl, 20: 29015
MULVIHILL, R. J., Probabilistic methodology for safety analysis of power reactors. I and II., 20: 30883 (SAN-570-2)
MULYARCHIK, T. M., Investigations of softer corpuscular particles by Cosmos III and Cosmos V, 20: 29964
MULYARCHIK, T. M., Variations in soft component of electron energy spectrum, 20: 30201 (NASA-TT-F-389, pp 277-81)
MUMINOV, V. A., Ion source of hydrogen ions at low gas pressures, 20: 29925
MUNDIS, Robert L., Radiation environment at zero-gradient synchrotron, 20: 29843 (CONF-651109, pp 34-56)
MUNSHI, Kailash N., Spectrophotometric study of chelates of ammonium aurintricarboxylate with Sc, Y, and La, 20: 29180
MURADYAN, H. V., Total neutron cross sections for heavy Sn isotopes below 10 kev, 20: 30490
MURAKAMI, Yukito, Interaction of Th(IV) with pyrocatechol-3,5-disulfonate at a 1:1.5 molar ratio, 20: 29093
MURAKI, Einosuke, Radiation grafting of methyl methacrylate onto lignin, 20: 29288
MURASHOV, E. P., Multipoint control of radiation levels, 20: 29458
MURATA, Kenji, Pulse-analysis method of light elements. I., 20: 29124
MURAYAMA, N., Radioactive fallouts from three nuclear explosions of late 1964 and early 1965, 20: 29422
MURIN, A. N., β decay of bromine isotopes for synthesis of krypton compounds, 20: 29327
MUROMKIN, Yu. A., Injection of plasma blobs into mirror trap with adiabatic plasma compression: Aspa device, 20: 30636
MURPHY, C. M., Progress summary of nuclear safety research and development projects, 20: 29470

MURPHY, E. G., Plasma produced by neutral injection into magnetic mirror/well geometry, 20: 30632

MUSAMOV, L. S., Possible existence of soft electron component in outer radiation zone, 20: 30213 (NASA-TT-F-389, pp 566-8)

MUSATOV, L. S., Comparison of simultaneous measurements of magnetic field and positive ion streams within earth's magnetosphere, 20: 30208 (NASA-TT-F-389, pp 457-63)

MUSKOVAC, Nicholas G., Nuclear radiation detecting means and transmission system, 20: 29575

MUZZARELLI, R. A. A., Separation of traces of manganese and cobalt from iron, 20: 29342

MYASISHCHEVA, G. C., Experimental investigation of chemical reactions involving muonium, 20: 29247

MYATT, B. L., Oxidation of UN and U(CO) in carbon dioxide, steam, and water, 20: 29645

MYERS, D. K., Nucleic acid synthesis in x-irradiated thymocytes, 20: 28953

N

NABICHVRISHVILI, V. A., Coulomb excitation of levels in ^{152}Sm and ^{186}W, 20: 30488

NACHBAR, H. U., Nuclear electrons: relay-controlled pulse generator for testing nuclear electronics, 20: 29544

NADLER, R. A., Effect of H and temperature on mechanical properties of Ti–5Al–2.5Sn ELI alloy, 20: 29715 (WANL-TME-1287)

NADZHAFOV, I., Electron-positron pair production during scattering of gamma quanta in nuclear field, 20: 29996

NAEGELIN, R., Thermodynamic design of reactor cooled by gas, 20: 30892

NAGAI, Hiroyuki, Shell model studies of 1f-shell nuclei. I., 20: 30365

NAGAI, M., Development of polar geomagnetic disturbance and PCA event on 2/11/58, 20: 30230

NAGAO, S., Ion cyclotron resonance heating of QP plasma, 20: 30662

NAGARAJAN, G., Molecular constants and thermodynamic functions of linear symmetrical molecules, 20: 29921

NAGASHIMA, Kozo, Chemical studies of minerals containing rarer elements from Far East District. LX., 20: 29399

NAGATA, Sadayoshi, Microhardness and plastic deformation of uranium dioxide, 20: 29786

NAGUIB, K., Calculation of neutron activation cross sections for ^{51}V, ^{55}Mn, ^{63}Cu, ^{65}Cu, and ^{127}I at 0.1 to 14 Mev, 20: 30378

NAIDENOV, V. O., Determining small quantities of ^{37}Ar and tritium, 20: 29559

NAIDU, P. S., Theoretical considerations of ion optics of mass spectrometer ion source. I., 20: 29489

NAIDU, P. S., Theoretical considerations of ion optics of mass spectrometer ion source. II., 20: 29490

NAKAGAWA, Hiroshi, Experiments for solidification of CO_2 and the dropping in vacuum, 20: 30594

NAKAMURA, Shoichiro, Burnup analysis of power reactors in equilibrium operation cycles, 20: 30890

NAKANISHI, Jun, Radiation-induced addition of hydrogen chloride to ethylene, 20: 29252

NAKAO, Fusofumi, Characteristics of hot cathode magnetron gage for measurement of ultrahigh vacuum. I., 20: 29494

NAMBU, Y., Electromagnetic properties of the baryon, 20: 29922

NAMENSON, A., High-energy γ spectra from neutron capture in Hf isotopes, 20: 30466

NAQVI, M. A., Exchange energy of semi-infinite nuclear matter, 20: 30395

NARYSHKINA, L. G., Radiation of charge moving above an anisotropically conducting plane, 20: 29836

NASER, H. M., Higher-order effects in β-γ correlations involving allowed β transitions, 20: 30470

NATANSON, E. M., Effects of γ radiation on structure of epoxy resins and resin-base metallic polymers, 20: 29296

NATANSON, E. M., X-ray study of epoxido-dianic ED-5 resin irradiated with ^{60}Co and metallopolymers on its base, 20: 29297

NATANSON, L., Energy levels of ^{8}Be from ^{11}B(n,α)^{8}Li → ^{8}Be process, 20: 30363

NATH, Amar, Isotopic exchange and annealing of recoil damage in Co complexes, 20: 29259

NATHAN, O., Proton pickup from the even lead nuclei, 20: 30387

NATLAND, Manley L., Apparatus including a nuclear reactor for heating injection gases, 20: 30805

NAUMANN, R. A., Negative-parity levels in even-even mercury isotopes, 20: 30435

NAZARENKO, V. L., Parity nonconservation in radiative transition of ^{175}Lu, 20: 30381

NAZAROVA, M. N., Radiation intensity in earth's radiation belts, 20: 30235

NAZAROVA, M. N., Recording cosmic rays on Cosmos-17 satellite, 20: 29966

NAZIROV, N. N., Influence of gamma-rays on content of ascorbic acid and reduced glutathione in cotton plants, 20: 28999

NEAGU, D., Decay ($K^0_2 \rightarrow \pi^+\pi^-$) probability in sloped K^0_2-meson beam, 20: 30056

NEAL, R. B., Electrons accelerated to the 10- to 20-Bev range, 20: 29864

NEALY, Carson Louis, Nuclear structure of ^{143}Nd, ^{149}Nd, and ^{151}Nd, 20: 30517

NECHITAYLO, N. A., Effect of stabilizers on irradiated polypropylene, 20: 29290

NEED, John L., Inelastic α-particle excitation in even tin isotopes, 20: 30468

NE'EMAN, Y., Algebra and symmetries, 20: 30110

NEFEDOV, V. D., β decay of bromine isotopes for synthesis of krypton compounds, 20: 29327

NEGOVSKII, V. A., Radiation sickness in Macacus rhesus, 20: 28986

NEIDHARD, H., Systems Ni–Be–B and Co–Be–B, 20: 29795

NEIL, V. K., Stabilization of intense coasting beams in particle accelerators by inductive walls, 20: 29860

NEKRASOV, F. M., Linear theory of excitation of oscillations in a plasma by a charged particle beam, 20: 30689

NEKRASOVA, I. V., Temperature effect on cysteamine accumulation in cells and its radioprotecting activity, 20: 29057

NELSON, D. C., Design criteria, plutonium buy-back facility, 20: 29453 (RL-SEP-590)

NELSON, P. A., Densities and critical properties of alkali metals, 20: 29742

NELSON, Richard F., Variation in radiosensitivity of mice with time of day, 20: 28938

NEMCHINSKII, V. A., Removal of energy from plasma of a thermoelectric converter, 20: 29981

NESTERIN, M. F., Influence of variable fat content diet on course of radiation sickness, 20: 28993

NESTEROV, V. E., Cosmic rays during flights of spacecrafts-satellites and Kosmos, 20: 29956 (NASA-TT-F-389, pp 684-91)

NESTEROV, V. E., Earth's outer radiation zone at low altitudes, 20: 30216 (NASA-TT-F-389, pp 588-606)

NESTEROV, V. E., Inner and artificial radiation zones of earth at low altitudes, 20: 30217 (NASA-TT-F-389, pp 607-15)

NESTEROV, V. E., Radiation safety problems in space flights, 20: 30222 (NASA-TT-F-389, pp 758-63)

NETTLEY, Peter Thomas, Improvements in or relating to neutron absorber material, 20: 30865

NEUDACHIN, V. G., Investigation of the electron states of atoms, molecules, and solids, 20: 29931

NEUMANN, Horschel, Third-order perturbation calculation of deuteron parameters, 20: 30068

NEWCOMBE, C. L., Estimate of effects of fallout beta radiation on insects and associated invertebrates, 20: 28925 (AD-633024)

NEWMAN, D. J., Crystal field of $PrCl_3$, 20: 30760

NEWTON, A. A., Plasma containment and stability in megajoule theta-pinch experiment, 20: 30610

NGUYEN VAN HIEU, Current-generated algebras and form factors, 20: 30146

NGUYEN VAN HIEU, Leptonic decays of baryons in universal V-A theory, 20: 30058

NGUYEN VAN HIEU, Representations 189 and 405 of the group SU(6) and classification of mesonic resonances 2+, 1+, and 0+, 20: 30093 (JINR-P-2701)

NIBLETT, G. B. F., Plasma containment and stability in megajoule theta-pinch experiment, 20: 30610

NICHOLS, D. K., Range of photoparticle recoil atoms in solids, 20: 30479

NICHOLS, L. L., Pulse-shape discrimination applied to fast neutron dosimetry, 20: 29524 (CONF-651109, pp 647-52)

NICKERSON, J. T. R., Prog. rpt. on simultaneous radiation-heating treatment of precooked marine products, final, 2/65–2/66, 20: 29582 (MIT-3343-26)

NICOLATO, A., Changes in lymphocytes of laterocervical lymph nodes of Cavia Cobaya after x irradiation, 20: 28976

NIEBERGALL, F., Polarization of neutrons from ^{15}N(d,n)^{16}O reaction, 20: 30427

NIEDERLE, J., Generalized spherical functions for the noncompact rotation groups, 20: 29614

NIEDZWIEDZIUK, Kazimierz, Proton scattering in tube of electrostatic accelerator, 20: 29866

NIEH, H. T., Broken U(3) symmetry and semileptonic weak interactions, 20: 30123

NIEH, H. T., Electromagnetic masses of pseudoscalar mesons, 20: 30032

NIELSEN, H. L., Sign and magnitude of Coriolis coupling between the 5/2$^-$[532] and 7/2$^-$[523] orbitals in ^{161}Tb, 20: 30401

NIESCHMIDT, E. B., Nuclear states of ^{103}Rh, 20: 30471

NIESSEN, A. K., Distribution of direct transport current in sheets of type-II superconductors, 20: 30273

NIEWODNICZANSKI, H., Reactions ^{40}Ca(d,d), (d,d'), and (d,p) with 12.8-Mev deuterons, 20: 30459

NIHOUL, J., EPR in neutron-irradiated DPPH, 20: 29289

NIHOUL, J., Influence of neutron irradiation on superconductive properties of Sn and In foils, 20: 30301

NIIMI, Yoshinobu, Rapid colorimetric determination of beryllium in Al–Mg–Be alloys, 20: 29111

NIJBOER, B. R. A., Time expansion of correlation functions and theory of slow neutron scattering, 20: 30336

NIKITIN, Yu. P., Quantization of an EM field in a dispersive medium, 20: 30668

NIKOLAEV, D. S., Forms in which can be found radioactive elements in Fe–Mn concretions, 20: 29426

NIKOLAEV, D. S., Radiochemical composition of Fe–Mn concretions and manganese ores, 20: 29425

NIKOLOTOVA, Z. I., Extraction properties of organic compounds. II., 20: 29347

NIMNI, Marcel E., Collagen and hexosamine changes in subcutaneous granuloma irradiated locally with ^{60}Co source, 20: 28917

NIR, Aharon, Determination of ^{18}O by bombardment with alpha particles and detection of liberated neutrons, 20: 29143

NISHI, Masato, F coloring in γ- and neutron-irradiated ionic crystals, 20: 30739

NISHIKAWA, Yasuharu, Fluorometric determination of Y with 5,7-dichloro-oxine, 20: 29094

NISHIMURA, Tomio, Effect of Mo on the oxidation of TiC–Ni–Mo alloys, 20: 29653

NISHIZAKI, Kyoji, Spectrochemical analysis of zirconium and its alloys. I., 20: 29113

NISHIJIMA, K., Unsubtracted dispersion relations in weak interactions and unitary symmetry, 20: 30134

NITSEVICH, E. A., Formation and thermal dissociation of yttrium fluorides and carbonates, 20: 29223

NIXDORF, J., Thermodynamic observations on reactions of high-melting carbides, 20: 29729

NIZET, G., Determination of trace copper in high-purity arsenic by neutron activation, 20: 29087

NODGORETSKII, M. I., Experimental separation of interactions with free protons, 20: 30083

NOHARA, Tadahide, Effect of void volume variation on pressure buildup in vibratory-compacted UO_2 fuel element, 20: 29818

NOLAN, Thomas R., Oxygen saturation of tumor cells to increase effect of internal radiation, 20: 29059 (TID-22860)

NOLAND, R. A., Fabrication of spiked-core fuel elements for EBWR, 20: 29658 (ANL-6283)

NOLL, P., Stable and unstable behavior of preheated plasma in linear and cusped theta pinches, 20: 30614

NOREL, G., Application of x rays to measure porosities and saturations in porous media, 20: 29595

NORMAN, Hans, Pressure-absorbing means for nuclear reactor stations, 20: 30833

NORMAN, Jack Clifford, Abundance and distribution of Sc in rocks and particle competition in nuclear de-excitation, 20: 29436

NORRIS, Andrew E., Nuclear charge distribution in fission: ^{92}Y, ^{93}Y, ^{94}Y, and ^{95}Y independent yields, 20: 30476

NORRIS, Andrew E., Nuclear charge distribution in fission: ^{92}Rb and ^{93}Rb independent yields, 20: 30477

NORRIS, J. E., Solar simulation testing of nuclear test detection spacecraft, 20: 29440

NORWOOD, W. D., Biologic effects of human radiation exposure, 20: 28970

NOTEA, A., Evaluation of the ^{17}N reactor power level monitor, 20: 30938

NOVACU, V., One-particle-exchange model for bootstrap, 20: 30035

NOVAK, M., Peripheral proton–nucleon interactions at 9 Bev, 20: 30080

NOVICK, R., Fine and hyperfine structure of 3^2P term in Li, 20: 29939

NOVIKOV, G. I., Pressure and composition of saturated vapor in NaCl–$LaCl_3$ system, 20: 29227

NOVIKOVA, M. I., Radiation sickness in Macacus rhesus, 20: 28986

NOVOZHILOV, Yu. V., Symmetry of elementary particles in nonuniform group theory, 20: 30106

NOWEIR, T. M., Isobaric analog states by (p,n) reactions, 20: 30480

NOWOTNY, H., New Ta, Nb, impregnated, or sintered alloys and compound materials with graphite, 20: 29764

NUNDOME, Koichi, Dose estimation of electron beam by glass method, 20: 29283

NURZYNSKI, J., Anomalies in reaction $^{16}O(^3He,\alpha_0)^{15}O$, 20: 30433

NURZYNSKI, J., Reactions ^{40}Ca(d,d), (d,d′) and (d,p) with 12.8-Mev deuterons, 20: 30459

NUSSIS, Nicolas, Separation of ^{90}Sr and ^{90}Y in the presence of Ca by paper chromatography, 20: 29349

NYSTROM, R. E., Cavitation damage data for water, mercury, and lead–bismuth alloy, 20: 29640 (NP-16048)

O

O'BRIEN, Keran, Determination of energy distribution of γ rays scattered in sand, 20: 30728

O'BRIEN, Keran, Fast neutron spectrometry with nuclear emulsions, 20: 29848 (CONF-651109, pp 199-212)

O'BRIEN, Keran, Inference of accelerator stray neutron spectra from various measurements, 20: 29522 (CONF-651109, pp 286-305)

OBUKHOV, Yu. V., Experimental investigation of chemical reactions involving muonium, 20: 29247

ODEN, Carol K., Stability of Drosophila chromosomes to radioactive decay of incorporated ^{32}P, 20: 28955

ODLAND, Lawrence Thomas, Hematopoietic system in dogs exposed to varying doses of x-irradiation, 20: 29029

OEHLER, H., Inelastic scattering of 1-Mev photoneutrons on medium nuclei, 20: 30383

OEHME, H., Sample furnace for experiments on neutron scattering, 20: 29106

OEHME, R., Saturation of SU(3) algebra of current densities, 20: 30119

OGIEVETSKII, V. I., Quantum theory of gravity in Heisenberg representation and interaction representation, 20: 30239 (JINR-P-2692)

OGURTSOV, G. N., Charge exchange and ionization in collisions of Ne atoms and ions with CO, 20: 29948

OHE, T., Production of a thermally ionized plasma with negative ions, 20: 30575

OHI, Yoshihiro, Movement of radioactive calcium in brain slices, 20: 28891

OHKAWA, T., Energy spectrum of neutral hydrogen atoms from coaxial plasma gun, 20: 30578

OHNISHI, Tadahiro, Reactivity worth of fuel elements, 20: 30839

OHNUKI, Yuji, Liquid hydrogen target for experiments of high-energy nuclear reactions, 20: 29863

OHNUMA, Toshiro, Instability of two colliding plasma streams, 20: 30593

OI, Noboru, Gamma spectra of fission products observed with lithium-drifted germanium detectors, 20: 30379

OKADA, Isao, Isotope effect in electromigration of sodium ions in fused sodium nitrate, 20: 29185

O'KELLEY, G. Davis, Decay of ^{133}I to levels in ^{133}Xe, 20: 30473

O'KELLEY, G. Davis, Nuclear levels of ^{101}Ru populated in decay of ^{101}Rh isomers, 20: 30469

OKHLOPKOV, V. P., Primary cosmic radiation on Elektron-2 and Elektron-4, 20: 29955 (NASA-TT-F-389, pp 678-83)

OKONOV, E. O., Decay ($K^0_2 \rightarrow \pi^+\pi^-$) probability in sloped K^0_2-meson beam, 20: 30056

OKUDA, Takayoshi, Plasma diffusion in magnetic field, 20: 30596

OKUDA, Takayoshi, Steady plasma electric field as function of ionization degree, 20: 30592

OKUNEWICK, James Philip, Red cell carbonic anhydrase following x irradiation, 20: 28922

OLIPHANT, Thomas A. Jr., Reduction of Fokker-Planck equation for applications to practical plasma dynamics problems, 20: 30560 (LA-DC-7282)

OLIVER, R., Routine dosimetry with ^{182}Ta and ^{192}Ir wires, 20: 29456

OLLERHEAD, R. W., Method of utilizing nuclear reactions in study of oxide layers, 20: 29817

OLOFSON, C. T., Machining and grinding of nickel- and cobalt-base alloys, 20: 29665 (RSIC-482)

OLSON, Edwin A., Conference on radiocarbon and tritium dating, Sixth International, Washington State University, Pullman, Wash., 6/65, 20: 29438 (CONF-650652)

OLSON, Orlando Duane, Diffusion and drift losses and electron cooling in He afterglows confined by a toroidal magnetic field, 20: 30710

OLSSON, M., Forward elastic scattering at high energy in SU(3) Reggepole model, 20: 30039

OMNES, Roland, Finite range of strong interactions and analyticity properties in momentum transfer, 20: 30131

O'NEIL, Thomas Michael, Collisionless damping of nonlinear plasma oscillations, 20: 30706

ONISHCHENKO, I. N., Motion of plasmoid in a curvilinear magnetic field, 20: 30647

ONKEN, K. O., Histopathological effects after x irradiation of developing chick embryos, 20: 29012

ONO, Hironori, Error in density measurement of compressed stock coal by back-scattering gamma-ray density meter, 20: 29491

ONO, Shusuke, Galvanomagnetic properties of graphite at low temperatures, 20: 29751

OPALOVSKII, A. A., Solid phases of NH_4F–UO_3–H_2O systems, 20: 29200

OPOWER, H., Production of energetic plasma by light pulses, 20: 30666

ORLANDINI, K. A., Low-intensity branches in ^{45}Ti decay, 20: 30456

ORLANDINI, K. A., Separation of americium and curium by extraction chromatography, 20: 29337

ORLOVA, L. P., Investigation of rare-earth carbonates using infrared spectroscopy, 20: 29447

OSAKIEWICZ, W., Energy levels of ^{8}Be from ^{11}B(n,α)^{8}Li $\rightarrow$ ^{8}Be process, 20: 30363

OSBORN, R. K., Effects of lattice vibrations on angular correlations, 20: 30762

OSBORN, R. K., Scattering of photons by highly ionized plasmas, 20: 30557 (AD-633074)
OSBORNE, M. F., Postirradiation examination of high burnup EGCR prototype fuel capsules, 20: 29806 (ORNL-TM-1511)
OSEPCHUK, J. M., Experiments on surface wave propagation along annular plasma columns, 20: 30574
OSHIRO, Lyndon Satoru, Natural resistance mechanisms to neoplastic diseases in mice, 20: 29017
OSHIYAMA, Hiroshi, Analysis of toroidally shaped Heliotron field, 20: 30595
OSKAM, H. J., Hollow-cathode glow discharge in hydrogen and noble gases, 20: 30173
OSTERTAG, Werner, Rare earth tungsten bronzes, 20: 29164
OSTRACH, Simon, Principle of exchange of stabilities for MHD thermal stability problem in completely confined fluids, 20: 30178
OSTROVSKII, E. K., Shaping of small bunches in linear electron accelerator, 20: 29870
OSTROWSKI, K., Sterilization of bone tissues with gamma radiation in Poland, 20: 28987
OTIS, DAVID R., Computation and measurement of Hall potentials and flow-field perturbations, 20: 30176
OUDIN, Jacques, Television in nuclear reactors, 20: 30809
OUTI, Akizi, Nonlinear motion of ion streams in a background of high-temperature electrons, 20: 30585
OVADIA, J., Study of water radiolysis and hydrogen peroxide formation using radioactive ^{15}O, 20: 29315
OVCHINNIKOV, S. S., Heating of dense plasma in a metallic chamber, 20: 30664
OVSYANNIKOV, V. A., Investigation of plasma in Tuman installation, 20: 30682
OVSYANNIKOV, V. A., Plasma compression by a magnetic field in a toroidal-type device, 20: 30660
OXLEY, J. H., Fluoride tungsten, 20: 29687
OYOSHI, Akira, Studies on focusing chromatography separation of ^{239}Np from neutron-irradiated U, 20: 29351
OYOSHI, Emiko, Studies on focusing chromatography separation of ^{239}Np from neutron-irradiated U, 20: 29351
OZAKI, A., Dense plasma produced by a cusp injection, 20: 30643
OZERNOI, L. M., Significance of coherent plasma radiowave emission for quasi-stellar radio objects and supernovae remnants, 20: 29880
OZHDYANI, M., Detection of ^{113}Cd isomer by means of γ radiation from ^{60}Co, 20: 30489

P

PAIK, S. F., Experiments on surface wave propagation along annular plasma columns, 20: 30574
PAINE, R. M., Development of intermetallic compounds for aerospace applications, 20: 29770
PAKVASA, S., Parity-violating nonleptonic decay and Cabibbo current, 20: 30041
PAL'CHIKOV, V. E., Plasma with relativistic electrons in magnetic mirror trap, 20: 30638
PALMER, David Wayne, Shape of neutron yield from $^{7}Li(p,n)^{7}Be$ reaction near threshold and neutron energy distribution near threshold, 20: 30525
PALMS, John M., Calculation of pulse-height response of Ge(Li) semiconductor counters, 20: 29528 (LA-3456)
PANASYUK, V. D., Complexing of serine with rare earth elements in aqueous solutions, 20: 29208
PANCHENKO, I. D., Polarographic study of rare earth elements, 20: 29210
PANDIT, L. K., Mass difference (K^+-K^0), 20: 30016
PANDIT, L. K., Two-pion decay modes of K mesons, 20: 30015
PANKOVE, J. I., New effect at superconducting contacts, 20: 30277
PANOFSKY, W. K. H., Electrons accelerated to the 10- to 20-Bev range, 20: 29864
PANTUEV, V. S., Differential cross section of charge exchange of 4.8-Bev/c π^- mesons with protons, 20: 29998
PAPINEAU, L., Spectroscopic information on samarium isotopes from analog-state experiments, 20: 30430
PAPROCKI, Stan J., Prog. rpt. on civilian applications, 7/65, 20: 29616 (BMI-1738)
PARAMONOVA, V. I., Complex formation of uranyl ion with salicylic acid. III., 20: 29197
PARFENOV, D. S., Toroidal discharge in a varying longitudinal magnetic field, 20: 30654
PARFENOVA, V. P., Effective magnetic field at ^{60}Co nucleus in Co–Pd alloy, 20: 30752
PARIKH, N. M., Production of tungsten sheet bars by zone refining of cemented tungsten-base alloys, 20: 29688
PARK, R. S., Fluoride tungsten, 20: 29687
PARKER, F. L., Prog. rpt. on waste treatment and disposal, semiannual, 7–12/65, 20: 30943 (ORNL-TM-1465)
PARKMAN, M. F., Bibliography on relation between wetting and boiling Hg heat transfer, 20: 29620 (NP-16046)
PARKS, R. D., Transition temperature of superconductors with paramagnetic impurities, 20: 30271
PARTHASARADHI, K., Absolute photoelectric cross sections of 320 kev gamma rays, 20: 29924
PARTLOW III, William Dempsey, Fluorescence decay of the Sm^{2+} ion in $LaCl_3$, 20: 30782
PASCUAL, P., Baryonic current ($\Delta S = 0$) coupled to the muonic current, 20: 30141
PASCUAL, P., Electromagnetic form factor normalization, 20: 30096
PASCUAL, P., Transformations (P, C, T) for Dirac fields, 20: 30097
PASCUAL, Ramon, Baryonic current ($\Delta S = 0$) coupled to the muonic current, 20: 30141
PASECHNIK, M. V., Analysis of elastic scattering of 6.9-Mev protons by Ni isotopes, 20: 30495
PASTERNAK, R. A., Absorption, degassing, and solution equilibrium in the N–Nb system at ultrahigh vacuum and high temperature, 20: 29178
PATY, M., Photonuclear interactions of high-energy muons, 20: 29994
PAUL, Helmut, Spectral form of the 961-kev β transition and the K conversion coefficient of the 412-kev γ radiation of ^{198}Au, 20: 30545
PAULUS, K. F. G., Question of superconductivity in organic molecules, 20: 30268
PAULY, Helmut, Direct and indirect radiation effects on enzymes in the cell, 20: 28902
PAULY, Helmut, Temperature dependence and activation energy in direct radiation effects, 20: 28903
PAVLIKOV, V. N., Phase diagram of system Sc_2O_3–Cr_2O_3, 20: 29167
PAWAR, Vijay N., Pocket dosimeter using a phosphor and photocathode, 20: 29576
PEARLSTEIN, L. D., Drift instabilities and electron cyclotron oscillations for arbitrary plasma pressure, 20: 30631
PEARSON, J. H., Fluoride tungsten, 20: 29687
PEARSON, R. K., Coherent neutron scattering amplitudes of ^{10}B and ^{11}B, 20: 30335
PEARSON, Richard Jr., Radio gas chromatography peak analyzer, 20: 29105
PECHACEK, R. E., Scattering of laser beam by hot electron plasma, 20: 30716
PEDRICK, Robert A., Radioisotopes in oceanographic research, 20: 29401
PELROY, Gretchen, Prog. rpt. on application of radiation-pasteurization to Pacific crab and flounder, final, 11/64–10/65, 20: 29583 (TID-22515)
PELTE, D., Excited states of ^{22}Na by $^{20}Ne(^{3}He,p2)^{22}Na$ reaction, 20: 30400
PEMSLER, J. P., Kinetics of oxidation of Hf at high temperatures, 20: 29647
PENKALO, I. I., Polarographic study of rare earth elements, 20: 29210
PENNINGTON, Edwin M., Evaluating heavy-atom cross sections for plutonium-recycle calculations, 20: 30857
PENZIEN, K., Structure elucidation and identification of organic substances by "electron burning." II., 20: 29326
PERELOMOV, A. M., Casimir operators for groups U(n) and SU(n), 20: 30147
PEREYASLOVA, N. K., Recording cosmic rays on Cosmos-17 satellite, 20: 29966
PEREZ, R., Environmental radioactivity at Valencia during 1964, 20: 29408
PERKINS, R. B., Neutron-deuteron polarization at 22.7 Mev, 20: 30442
PERNEGR, J., Peripheral proton–nucleon interactions at 9 Bev, 20: 30080
PERRY, D. R., Radiation levels in and around Nimrod, 20: 29842 (CONF-651109, pp 20-33)
PERSHAN, P. S., Thermoluminescent emission of irradiated rare earth ions in CaF_2, 20: 29318
PERSSON, B., Shapes of β spectra from ^{143}Pr and ^{32}P, 20: 30540
PERTE, Eugenia, Bis-acetylacetone-ethylenediimines of zirconium and thorium, 20: 29203
PERVAYA, T. I., Recording charged particles with energy of 0.1 to 10 kev with spherical electrostatic analyzer, 20: 29532 (NASA-TT-F-389, pp 518-25)
PESHKOV, V. P., Measurement of λ transition temperature and density of liquid ^{4}He, 20: 30306
PETERS, P. C., Perturbations in the Schwarzschild metric, 20: 30246
PETERSON, G. A., Excitation of collective states in ^{208}Pb by inelastic electron scattering, 20: 30436
PETERSON, Sigfred, Ignition and combustion of reactor materials under accident conditions, 20: 30801
PETRAVIC, M., Plasma produced by neutral injection into magnetic mirror/well geometry, 20: 30632
PETREKOVA, J., Silica gel in separation of Th from Zr, 20: 29344
PETRENKO, I. E., Recording cosmic rays on Cosmos-17 satellite, 20: 29966
PETRICK, Michael, Liquid-metal MHD topping cycles, 20: 29980
PETROSYAN, R. A., Effect of irradiation on adsorption and antibodies formation by recticular and endothelial systems, 20: 28965

PETROV, K. A., Extraction properties of organic compounds. II., 20: 29347
PETROV, M. P., Active diagnosis of hot plasma by means of neutral particles, 20: 30685
PETROV, M. P., Investigation of plasma concentration in Al²fa with probe beam of fast atoms, 20: 30686
PETROV, M. P., Joule heating of plasma in toroidal Tokamak-3 device, 20: 30650
PETROV, N. T., Decay ($K_2^0 \to \pi^+\pi^-$) probability in sloped K_2^0-meson beam, 20: 30056
PETROVNINA, E. N., Catecholamine metabolism in acute ^{210}Po lesions, 20: 28886
PETRUSEV, S. S., Location of moving plasma bursts from coaxial injector, 20: 30681
PETRY, R. F., Negative-parity levels in even-even mercury isotopes, 20: 30435
PETTERSSON, H., Positrons and conversion electrons from ^{90}Mo decay, 20: 30388
PETTIT, G. D., Lattice spectrum and dielectric properties of EuF_2, 20: 30746
PFEIFER, V. F., Methods for reducing ^{90}Sr in wheat and milled products, 20: 29473
PFISTER, Helmut, Direct and indirect radiation effects on enzymes in the cell, 20: 28902
PHILLIPS, Peter R., Is the graviton a Goldstone Boson?, 20: 30247
PHILLIPS, R. J. N., Byers-Yang model for NN and $\bar{N}N$ charge exchange, 20: 30014
PICCIONI, O., Isospin of the A mesons, 20: 30023
PIERINI, G., Relative problems of design of pilot plants for reprocessing by volatilization, 20: 29364
PIHL, Alexander, Decay of radiation induced radicals and the yield of thermoluminescence, 20: 29249
PIKAEV, A. K., Radiation-induced reactions of hydrogen atoms and hydroxyl radicals in aqueous solutions, 20: 29262
PILATOV, U. U., Absorption effect on surfaces of semiconductors and gels due to effects of radiation, 20: 29815
PINCUS, P., Stability of a lattice of superfluid vortices, 20: 30286
PINES, David, Elementary excitations in homogeneous Bose liquid, with application to He II, 20: 30187
PISARENKO, N. F., Cosmic rays during flights of spacecrafts-satellites and Kosmos, 20: 29956 (NASA-TT-F-389, pp 684-91)
PISARENKO, N. F., Earth's outer radiation zone at low altitudes, 20: 30216 (NASA-TT-F-389, pp 588-606)
PISARENKO, N. F., Inner and artificial radiation zones of earth at low altitudes, 20: 30217 (NASA-TT-F-389, pp 607-15)
PISARENKO, N. F., Radiation safety problems in space flights, 20: 30222 (NASA-TT-F-389, pp 758-63)
PISUT, J., Consistency of Wolf pion-pion phase shifts with dispersion relations for forward scattering, 20: 30017
PITTILLO, J. Dan, Accumulation of radioisotopes in Juniperus virginiana L, 20: 29410
PITT-PLADDY, R. A., Effect of surface evaporation on diffusion measured by isotopic exchange reactions, 20: 29731
PITTS, T. G., Indian Point Reactor—instrumentation asymmetry response verification, 20: 30876 (BAW-1302)
PITTS, T. G., Lumped burnable poison program, 20: 30836 (BAW-3492-1)
PJERROU, Gerold Michael, Properties of Ξ^- and Ξ^0 hyperons, 20: 30072
PLACHENOV, T. G., Effects of porous structure of lignin carbons on uranium sorption, 20: 29360
PLATONOV, G. F., Cosmic ray nuclear component on Elektron-2, 20: 29957 (NASA-TT-F-389, pp 693-710)
PLATUNOVA, N. B., Complex formation of uranyl ion with salicylic acid. III., 20: 29197
PLETNEV, V. D., Penetration processes into magnetosphere of earth, 20: 30205 (NASA-TT-F-389, pp 386-425)
PLOTNIKOVA, M. V., Barium stannate: source for measurement of Moessbauer effect on ^{119}Sn, 20: 30753
PLUMLEE, Karl E., Critical and exponential experiments with plutonium, 20: 30858
PLUMMER, Gayther L., Accumulation of radioisotopes in Juniperus virginiana L, 20: 29410
PLUNTKE, A., Gamma irradiation facility of Frankfurt Research Reactor, 20: 29341
PLYUSHCHEV, V. E., Stability of metal-alloy bond in rare earths phthalocyanines, 20: 29217
PNIEWSKI, J., Two decays of mass-seven hyperfragments, 20: 30368
PNIEWSKI, T., Two decays of mass-seven hyperfragments, 20: 30368
PODLAHA, M., Kinematical and dynamical principles of relativity, 20: 30242
POESCHEL, E., Thermodynamic observations on reactions of high-melting carbides, 20: 29729
POETSCH, J., Induction of extramutative radiation effects on periclinal chimeras, 20: 29018
POGOSYAN, V. A., Properties of a plasma capacitor, 20: 30699
POGUTSE, O. P., Instability and related macroscopic effects in toroidal discharges, 20: 30617
POGUTSE, O. P., Kinetic theory of oscillations of a nonuniform plasma with collisions taken into account, 20: 30691
POHLIT, W., Cybernetic studies on radiation effects on yeast cells. I., 20: 28950
POINT, J. J., Finkelstein reaction for measuring partial organic retention during irradiation of alkyl bromides, 20: 29292
POINTUD, M. L., Carbon transport problem in high-temperature gas-cooled reactors, 20: 30899
POKROVSKII, V. I., Reaction of manganese and scandium oxides in air, 20: 29168
POLAK, L. S., Effect of stabilizers on irradiated polypropylene, 20: 29290
POLAK, L. S., Kinetics of radiation-induced isotope exchange between deuterium and silica gel hydroxyl groups, 20: 29276
POLEZHAEV, L. V., Mechanism of recovery of regenerative capacity inhibited by x irradiation, 20: 29038
POLIN, F., Dependence on microstructure of high-temperature properties of UO_2–Mo and UO_2–W cermets. I., 20: 29699 (CONF-650674-1)
POLOSUKHINA, T. I., Cholesterol protein blood complexes of dogs in radiation injury, 20: 28998
POLUBARINOV, I. V., Quantum theory of gravity in Heisenberg representation and interaction representation, 20: 30239 (JINR-P-2692)
POLUBARINOV, I. V., Relativistic wave packets in space and time. 1., 20: 30238 (JINR-P-2691)
POLUBOYARINOV, D. N., Electric conductivity and creep of sintered CeO_2 during reduction, 20: 29739
POLUEKTOV, N. S., Absorption-spectrophotometric determination of rare earths in tributylphosphate extracts, 20: 29125
POLUEKTOV, N. S., 1,10-Phenanthrolinethenoyltrifluoroacetone complexes of rare earth elements, 20: 29221
POLUPAN, P. N., Investigation of chromospheric limb flare, 20: 29905
POLUSHKIN, B. V., Thermal and anaphylactoid edema in acute radiation sickness, 20: 29001
POPOV, A. F., Plasma heating under beam instability conditions, 20: 30659
POPOV, G. V., Sign of change of charge radius of ^{119}Sn nucleus, 20: 30382
POPOV, N. I., Radioactive contamination of oceans, 20: 29405 (NP-14694)
POPOV, S., Two decays of mass-seven hyperfragments, 20: 30368
POPOV, S. N., Means for producing a helical magnetic field, 20: 30703
POPOV, S. N., Two operating modes of plasma source, 20: 30589
POPOV, V. S., Casimir operators for groups U(n) and SU(n), 20: 30147
POPOVA, A. M., Elastic scattering of 14-Mev neutrons by deuterons, 20: 30050
POPRYADUKHIN, A. P., Means for producing a helical magnetic field, 20: 30703
PORILE, N. T., Inelastic-scattering model for (p,xn) and (p,p(x-1)n) reactions at intermediate energies, 20: 30446
PORSCHING, T. A., Solution of reactor kinetics equations by approximate exponentials, 20: 30847
PORT, J. H., Developments in Re and Re alloy technology, 20: 29768
PORTER, F. T., Low-intensity branches in ^{45}Ti decay, 20: 30456
PORTER, F. T., Low structure in ^{52}Cr populated in 5.7-day ^{52}Mn decay, 20: 30458
PORTER, Leonard Edgar, Polarization of protons from the D(d,p)T reaction, 20: 30524
PORYADKOVA, N. A., Recovery of cells from primary cytogenetic injuries, 20: 29049
POSE, H., Inelastic scattering of 1-Mev photoneutrons on medium nuclei, 20: 30383
POSE, H., Study of Be with polarized neutrons of energy 2.60 to 2.77 Mev, 20: 30414
POTAPOV, B. P., Corpuscle investigations on Elektron-1, 20: 30212 (NASA-TT-F-389, pp 551-66)
POTENZA, R., Reactions ^{7}Li+d, 20: 30402
POTNIS, V. R., Nuclear states of ^{103}Rh, 20: 30471
POTTER, S. B., Total cross sections of Gd for fast neutrons, 20: 30419
POWELL, Elno M., Control of nuclear power plant, 20: 30832
POWELL, R. W., Room-temperature thermal conductivity of the rare-earth metals gadolinium, terbium, and dysprosium, 20: 29741
POZDNYAKOVA, L. E., Effect of x-irradiation on thiamine phosphorylation, 20: 29003
POZHAROV, S. L., Double focusing in mass spectrometers with an inhomogeneous magnetic field, 20: 29493
POZHIDAEV, E. A., Correlation of sexes in offspring of female and male rats irradiated at different periods of ontogenesis, 20: 28952
PRADAL, F., Characteristic energy losses of electrons and color centers in LiF, LiCl, and NaCl, 20: 30776
PRADAL, J., Isospin quintuplets in A = 16 nuclei, 20: 30440
PRATT, P. L., Yielding and strain ageing of niobium crystals, 20: 29790
PREISS, Ivor L., Decay scheme of ^{123}Cs, 20: 30403
PREPARATA, G., Current algebras and magnetic moments, 20: 30118

PRESS, W., Production of energetic plasma by light pulses, 20: 30666
PRESTWICH, W. V., Neutron separation energies of $^{143}Nd-^{144}Nd$, $^{149}Sm-^{150}Sm$, and $^{164}Dy-^{165}Dy$, 20: 30366
PRESTWICH, W. V., Reaction $^{197}Au(n,\gamma)^{198}Au$, 20: 30409
PREVOT, F., Injection of ions into a magnetic mirror machine (M.M.I.), 20: 30634
PRICE, Keith Robinson, Uptake of ^{131}I from the soil as related to root distribution and phenology in sagebrush vegetation, 20: 28883
PRICE, LeRoy R., Conversion of gamma rays from the decay $\eta^0 \rightarrow \pi^+ + \pi^- + \gamma$, 20: 30029
PRICE, R. J., Deformation and fracture of pyrolytic carbons deposited in fluidized bed, 20: 29736
PRIKHOD'KO, G. P., Effects of γ radiation on structure of epoxy resins and resin-base metallic polymers, 20: 29296
PRIKHOD'KO, G. P., X-ray study of epoxido-dianic ED-5 resin irradiated with ^{60}Co and metallopolymers on its base, 20: 29297
PRIMAK, William, Radiation blistering: observations of oxides, silicon, and metals, 20: 29816
PRIMROSE, Russell Adrian, Separation of mixture of H and C dioxide by gaseous diffusion, 20: 29362
PRINCE, A., Neutron cross sections for ^{244}Cm and ^{238}Pu, 20: 30346 (GEMP-411)
PRITCHARD, J. Paul Jr., Superconducting thin-film technology and applications, 20: 30258
PRITCHETT, William C., Shielding system for chlorine logging apparatus, 20: 29443
PROBERT, P. B., Prog. rpt. on Na-heated steam generator development, 1–3/66, 20: 30806 (BAW-1280-36)
PRONKO, J. G., Excited states of ^{22}Na by $^{20}Ne(^3He,p2)^{22}Na$ reaction, 20: 30400
PRUSAK, Leonard P., Effects of ionizing radiation on gelatin fractions. III., 20: 29273
PRUSCHEK, R., Energy supply arrangements with nuclear sources for space flight instruments, 20: 30926
PRZYBORSKI, W., Semiconductor system for charged particle identification, 20: 29526 (INP-444/PL)
PSHEZHETSKII, S. Ya., Radiation effects on formation of free radicals in frozen $CH_3OH + CCl_4$ solutions, 20: 29305
PUCHEROV, N. N., Analysis of elastic scattering of 6.9-Mev protons by Ni isotopes, 20: 30495
PUGH, John, Improvements in or relating to charge/discharge machines for nuclear reactors, 20: 30819
PURDY, David C., Compact nuclear steam generator, 20: 30931
PUSCHKINA, G. J., Preparation and properties of anhydrous scandium nitrate and its solvates, 20: 29214
PUSTOVALOV, V. V., Nonlinear interaction of electromagnetic waves in a magneto-active plasma, 20: 30629
PUSTOVOIT, L. T., Hydrolysis of rare earth metal dicarbides, 20: 29220
PUSTOVOIT, Yu. M., Achievement of ultrahigh vacuum in Ogra-1, 20: 30701
PUSTYL'NIKOV, L. M., Kinetics of radiation-induced isotope exchange between deuterium and silica gel hydroxyl groups, 20: 29276
PYATENKO, V. S., Recovery of cells from primary cytogenetic injuries, 20: 29049
PYUN, Hyung-chick, Synthesis of 5-bromouracil-^{82}Br, 20: 29244
PYYKKOE, P., Deuteron magnetic resonance in single crystals of ND_4Cl and ND_4Br, 20: 29191

Q

QUETS, J. M., Kinetics of high temperature oxidation of refractory materials, 20: 29656

R

RAAEN, V. F., Carbon-14 isotope effects in Beckmann rearrangement, 20: 29242
RABINOVICH, B. N., Thermal disintegration of nitrates of cerium, neodymium, and gadolinium, 20: 29224
RABINOVICH, M. S., Injection and confinement of plasma in a stellarator with a multipolar ($l = 2$) helical field, 20: 30657
RABOVSKAYA, N. S., Radiolysis of hexachlorocyclopentadiene, 20: 29256
RACHEV, V. V., High-temperature x-ray phase analysis of U–O system from $UO_{2.50}$ to $UO_{2.67}$, 20: 29799
RACZKA, R., Generalized spherical functions for the noncompact rotation groups, 20: 29614
RADFORD, H. E., L-uncoupling effects on EPR spectra of $^{14}N^{16}O$ and $^{15}N^{16}O$, 20: 29194
RADWAN, Zofia, Determination of small concentrations of lanthanum and neodymium in pure cerium oxide, 20: 29095
RAFAL'SON, A. E., Radiofrequency mass spectrometer for the Electron satellites, 20: 29545
RAHMAN, A., Time expansion of correlation functions and theory of slow neutron scattering, 20: 30336
RAJEWSKY, Boris, Direct and indirect radiation effects on enzymes in the cell, 20: 28902
RAJU, Mudundi, R., Fluctuations of energy loss in semiconductor detectors, 20: 29531 (UCRL-16715)
RAKAUSKAS, Yu. K., Use of Pb amplifying screens in electroradiography, 20: 29628
RAKOVITSKII, S. L., E2 transitions from 3^+ level of even-even nuclei, 20: 30372
RALSTON, H. H., Nuclear measurement of soil properties, 20: 29506
RAMAMURTHY, V. S., Shell model and stochastic theory of fission, 20: 30428
RAMAN, K., Current algebras and generalized Ward-Takahashi identities, 20: 30006
RAMANNA, R., Shell model and stochastic theory of fission, 20: 30428
RAMASWAMI, D., Removal of plutonium hexafluoride from cell exhaust air, 20: 29328 (ANL-7066)
RAMSAY, William, Temperature of intergalactic matter, 20: 29879
RAND, R. E., Structure of the α particle from elastic electron scattering, 20: 30439
RAO, J. Rama, Influence of electron binding on incoherent scattering of low-energy γ rays, 20: 29923
RAO, N. B. S. N., Radiolytic oxidation of naphthalene in aerated organic solvents, 20: 29260
RAO, P. S., Radiolytic oxidation of naphthalene in aerated organic solvents, 20: 29260
RAO, P. V. Ramana, Influence of electron binding on incoherent scattering of low-energy γ rays, 20: 29923
RAO, S. S., Wave equations for inhomogeneous gyrotropic hot plasmas, 20: 30603
RAPAPORT, J., Stripping analysis of (d,p) angular distributions from $^{37}Cl(d,p)^{38}Cl$ reaction, 20: 30391
RAPP, Robert A., Mixed conduction in ThO_2 and $ThO_2-Y_2O_3$ solutions, 20: 29216
RAPPENEAU, J., Thermal creep and inelastic behavior of artificial graphite, 20: 29734
RASMUSSEN, Norman C., Prog. rpt. on neutron and gamma-ray spectroscopy and activation analysis, final, 1/61–1/66, 20: 29078 (AD-633252)
RASS, I. T., Radiation injury of thymus in mice, 20: 29008
RAST, H. E., Infrared absorption of Ce^{3+} in LaF_3 and of CeF_3, 20: 29173
RASTREPIN, A. B., Energy distribution in hydrogen plasma from coaxial plasma gun, 20: 30687
RASULKULOV, M. S., Azimuthal angular distribution of slow particles produced by nuclear interactions with heavy emulsion nuclei at high energies, 20: 30371
RASZILLIER, I., Irreducible tensors for group SU_3, 20: 30102
RATNAM, V. V., Thermoluminescence spectra of CaF_2 irradiated by x rays, 20: 30767
RAU, F., Release of stored energy and electric resistivity changes in neutron-irradiated Cu, 20: 29824
RAU, F., Toroidal theta pinch with superimposed multipole field, 20: 30616
RAU, Robert C., Crystal structure of Eu_3O_4, 20: 29718
RAUBENHEIMER, L. J., OR GNU: FORTRAN program for calculating frequency-distribution functions of cubic crystals, 20: 30733 (ORNL-TM-1425)
RAVA, G., Determination of 17-ketosteroid and of 11-oxycorticoid in irradiated guinea pig, 20: 28975
RAVINDRAN, N., Mass distribution in fission of ^{229}Th, 20: 30373
RAWITSCHER, G. H., Effect of stripping channels on elastic scattering of deuterons, 20: 30431
RAYNE, J. A., Ultrasonic investigation of energy-gap anisotropy in superconducting rhenium, 20: 30281
RAYNOR, D., Orientation relationship and growth direction in Mo_2C in ferrite, 20: 29726
RAYNOR, J. B., Pairwise trapping in γ-irradiated sodium nitroprusside, 20: 29280
RAZORENOV, L. A., Cosmic ray nuclear component on Elektron-2, 20: 29957 (NASA-TT-F-389, pp 693-710)
RAZORENOV, L. A., Primary cosmic-ray research, 20: 29954 (NASA-TT-F-389, pp 657-77)
RAZORENOV, L. A., Transient increases of flux of heavy nuclei accompanied by bursts of x radiation, 20: 29965
RAZUMOVA, K. A., Higher-mode instabilities in Tokamak device, 20: 30651
RAZUMOVA, K. A., Plasma energy losses in toroidal chamber Tokamak TM-2, 20: 30653
REAVEY, Thomas C., Distribution of radionuclides in dairy products from two milk processing plants, 20: 29464
REBEL, H., Numerical analysis of β spectra, 20: 30541
REBEL, Heinigerd, Relative measurements of electron polarization of ^{199}Au and ^{32}P, 20: 30548
REBHOLZ, M. J., Application of Be on the Agena, 20: 29393

REBUT, P. H., Instabilities in cylindrical inhomogeneous plasma on basis of Vlasov equation, 20: 30630
REDDY, M. P., Radiolytic oxidation of naphthalene in aerated organic solvents, 20: 29260
REDFERN, Bernard, Production of carbonaceous bodies containing carbides, 20: 29692
REED, Dale H., Shielding system for chlorine logging apparatus, 20: 29443
REED, P. E., Criticality safety of fissile materials, 20: 29450 (ISO-270)
REICHERT, John Douglas, High-energy scattering processes with cuts in angular momentum plane, 20: 30160
REID, George W., Determination of asphalt contents in a paving mixture by thermal neutrons, 20: 29509
REIN, James E., Prog. rpt. on burnup determination of nuclear fuels, 10–12/65, 20: 29080 (IDO-14676)
REINFELDS, J., Application of approximate solution of partial-wave dispersion relations to Yukawa potential scattering, 20: 30128
REMY, E., Toroidal theta pinch with superimposed multipole field, 20: 30616
RENAUD, C., Heating and containment of plasma in the magnetic well in Deca II, 20: 30607
RENGEVICH, V. B., Catalytic action of copper ammoniate during oxidation of uranium dioxide, 20: 29199
RENGEVICH, V. B., Kinetics of U(IV) oxidation in carbonate solution by atmospheric oxygen, 20: 29198
RENNE, O. S., Statistical errors in determining concentrations of radioactive elements in rocks using γ-threshold and differential spectrometers, 20: 29421
RENNER, B., Existence of axial-vector mesons, 20: 30007
REPALOV, N. S., Theory of excitation of ion plasma oscillations by electron Langmuir waves, 20: 30692
RERIKH, K. V., Leptonic decays of baryons in universal V-A theory, 20: 30058
REVINA, A. A., Formation of peroxide radicals in irradiated palmitic acid and potassium palmitate, 20: 29309
REYNOLDS, J., Shapes of β spectra from ^{143}Pr and ^{32}P, 20: 30540
REYNOLDS, J. A., Plasma containment and stability in megajoule theta-pinch experiment, 20: 30610
REYNOLDS, P., Inter-diffusion of plasma and magnetic fields in pinch and hardcore discharges, 20: 30639
RHODES, J. M., Thorium, U and K concentrations in granites and gneisses of Rum Jungle Complex, Northern Territory, Australia, 20: 29415
RIAZUDDIN, Algebra of currents and form factors at finite momentum transfer, 20: 30137
RICCI, E., Interactions of ^{3}He particles with ^{9}Be, ^{12}C, ^{16}O, and ^{19}F, 20: 30444
RICCOBONO, Gaetano, Reactivity pulsing device for pulsed fast reactors, 20: 30866
RICHARDS, P., Scanning of liver, spleen and bone marrow with colloidal ^{99m}Tc, 20: 29065
RICHEY, C. R., Criticality studies with plutonium solutions, 20: 29471
RICHFIELD, D. F., Effect of repeated exposure to laser beams, 20: 28936
RIECK, G. D., Thermal diffusion of oxygen in refractory metals, 20: 29769
RIEHL, N., Diffusion of tritons in NH_4F-doped ice single crystals, 20: 29193
RILEY, K. F., Nucleon-nucleon total cross sections from 1.1 to 8 Bev/c, 20: 30028
RILEY, W. C., New class of hypereutectic carbide composites, 20: 29727
RINGLAND, G. A., Byers-Yang model for NN and $\bar{N}N$ charge exchange, 20: 30014
RIPAN, Raluca, Spectrophotometric study of uranyl nitrate-salicylaldoxime system, 20: 29202
RIPLING, E. J., Prog. rpt. on fracture toughness of reactor pressure vessel steels, 5/65–5/66, 20: 29700 (COO-1477-4)
RISING, F. L., System for criticality verification, 20: 29519 (BNWL-SA-31)
RISTIC, M., Equivalent nonlocal nucleon-nucleon potentials, 20: 30061
RITCHIE, R. H., Positron annihilation in metals, 20: 29991 (ORNL-TM-1443)
RITCHIE, R. H., Semi-classical model of photoelectric effect in metals, 20: 29916 (ORNL-TM-1458)
RITTENBERG, V., Irreducible tensors for group SU_3, 20: 30102
RITTENBERG, V., One-particle-exchange model for bootstrap, 20: 30035
RIVERS, R. J., Renormalized ω–ϕ mixing angle and $J^P = 1^-$ meson decays, 20: 30088 (IC–66/50)
RIVIERE, A. C., Plasma produced by neutral injection into magnetic mirror/well geometry, 20: 30632
RIZAEV, Kh., Experimental separation of interactions with free protons, 20: 30083
RIZAEV, Kh. A., Production of slow π^+ mesons by 9-Bev proton interaction with photoemulsion nuclei, 20: 30370
ROB, L., Charge assymetry of mesons created in proton–neutron interactions, 20: 30082
ROBBINS, Donald E., Method of evaluating radiation risks for manned space flights, 20: 29058
ROBBINS, L. A., Measurement of the spin-rotation parameter β in proton-^{4}He scattering at 48 Mev, 20: 30441
ROBERSON, A. H., Nonmetallic powders coated with tungsten and molybdenum, 20: 29631
ROBERTS, A., Analysis of ANL–CERN spark chamber pictures, 20: 29987 (COO-1261-4)
ROBERTS, D. E., Doppler shift measurements to investigate plasma rotation in the theta pinch, 20: 30615
ROBINSON, Charles L., Method for heating minerals in situ with radioactive materials, 20: 30950
ROBINSON, Derek W., Conserved currents and associated symmetries; Goldstone's theorem, 20: 30101
ROBINSON, G. C., Leak testing of reactor containment systems, 20: 30812
ROBINSON, M. N., Energy dependence of radiation damage in Si, 20: 29579 (NAA-SR-11887)
ROBINSON, R. L., Elastic and inelastic proton scattering from ^{106}Pd and ^{108}Pd, 20: 30462
ROBINSON, Thomas Kneeland Jr., Telemetering from magnetically suspended rotors, 20: 29369
ROCHE, Jean, Electrostatic collecting of RaA and β emission of RaE formed, 20: 29324
ROCHOW, H., Thermodynamic observations on reactions of high-melting carbides, 20: 29729
RODGERS, S. J., Mechanical properties tests of 316 SS specimens in 1200°F Na contaminated with O, 20: 29704 (MSAR-66-78)
RODIER, Georges, Composite guide tube for reactors, 20: 30830
RODWELL, William, Moderator structures for nuclear reactors, 20: 30823
ROEBKE, W., Pulse-radiolysis studies on reactivity of catalase with hydrated electrons and free OH radicals, 20: 29279
ROEDER, Erhard, Volatilization of U fission products in H, Ni, and O, 20: 29211
ROEHMER, F. C., Nonaxial model predictions on first-forbidden β transitions of ^{188}Re, 20: 30550
ROEMBERG, E., Carbon transport problem in high-temperature gas-cooled reactors, 20: 30899
ROESCH, W. C., Pulse-shape discrimination applied to fast neutron dosimetry, 20: 29524 (CONF-651109, pp 647-52)
ROGANOV, V. S., Experimental investigation of chemical reactions involving muonium, 20: 29247
ROGINSKII, V. A., Radiation effects on formation of free radicals in frozen $CH_3OH + CCl_4$ solutions, 20: 29305
ROGOZEV, B. I., Sign of change of charge radius of ^{119}Sn nucleus, 20: 30382
ROHRBACH, F., High-voltage electrostatic separators, 20: 29865
ROIFE, I. M., Dynamic stabilization of a direct discharge in a magnetic field, 20: 30698
ROLFS, C., Excited states of ^{22}Na by ^{20}Ne(^{3}He,p2)^{22}Na reaction, 20: 30400
ROMAN, J., Strontium-90–yttrium-90 measurements using Si counters, 20: 29520 (CLOR-45/D)
ROMAN, O. V., Certain problems in dynamic and static pressing of metallic powders, 20: 29679
ROMANCHUK, P. R., Formation of sunspots and solar magnetic fields. II., 20: 29906
ROMANO, A. J., Boiling Hg corrosion of certain refractory metals and stainless steels from 593 to 703°C, 20: 29646
ROMANOWSKI, T. A., Analysis of ANL–CERN spark chamber pictures, 20: 29987 (COO-1261-4)
ROMANTSEV, E. F., Body distribution and elimination of ^{35}S-labeled 2-mercaptopropylamine in mice, 20: 28888
ROMANTSEV, M. F., Radiolysis of isooctyl and heptyl hydroperoxide solutions in hydrocarbons, 20: 29302
RONCA, L. B., Thermoluminescence as function of climate and temperature, 20: 29398
ROOS, J. P., Prog. rpt. on boiling flow regimes and critical heat flux, 9/16–12/15/65, 20: 29378 (NYO-3304-7)
ROOT, Allen W., Kinetics of calcium metabolism in children utilizing nonradioactive Sr, 20: 28889
ROOT, G. S., Properties of tungsten–rhenium alloys, 20: 29765
ROSE, R. M., Low-temperature electrical resistivity of lattice defects in deformed tungsten single crystals, 20: 29723
ROSEN, S. P., Parity-violating nonleptonic decay and Cabibbo current, 20: 30041
ROSENBERG, H. M., Interaction of microwave phonons with irradiation centers in quartz, 20: 30768
ROSENBLUTH, M. N., Stabilization by shear and negative V″, 20: 30608
ROSENBLYUM, N. D., Preparation of ion-exchange membrane by pre-irradiation method, 20: 29308
ROSENWALD, David, Theory of solid ^{3}He, 20: 30319
ROSNER, Manfred, Magnetohydrodynamic generator, 20: 29983
ROSSETTI, G., Rules for strong interactions, 20: 30020
ROTA, A., Time resolution measurements with fast photomultipliers, 20: 29568

ROTHBERG, J. E., Muonium chemistry, 20: 29177
ROTHE, William E., Gross alpha radioactivity of human bones and teeth, 20: 29476
ROTHMAN, M. A., Non-resonant coupling of r-f power to a plasma, 20: 30577
ROUGE, Pierre, Support structure for vertically-stacked solid moderator rods of a nuclear reactor, 20: 30826
ROUSSEAU, C., Fast neutron scattering cross sections of iron, 20: 30417
ROUX, D. P., Nuclear transducers, 20: 29549
ROWAN, Floyd R., Automatic sample changer for radioactive samples, 20: 29572
ROWE, M. W., Solar nucleosynthesis of extinct ^{129}I, 20: 29891
ROWENHORST, D. D., Prog. rpt. on fabrication of W alloy tubing, 2–5/66, 20: 29659 (COO-1518-3)
ROWLAND, F. S., Substitution reaction of 3-ev tritium atoms with methane, 20: 29265
ROWLANDS, J., Quasilinear theory of plasma cyclotron instability, 20: 30670
ROWLANDS, J., Theory of decay of EM waves in magnetoactive plasma, 20: 30671
ROY, D. P., Study of the reactions $p\bar{p} \rightarrow Y\bar{Y}$ by Regge-pole exchange model, 20: 30044
ROZANOV, A. Ya., Effect of x-irradiation on thiamine phosphorylation, 20: 29003
ROZANOVA, O. N., Binary uranium and molybdenum oxides, 20: 29798
ROZANOVA, O. N., New double oxides of uranium and tungsten, 20: 29170
ROZEN, A. N., Extraction properties of organic compounds. II., 20: 29347
ROZENFELD, Martin L., High-dose human exposure from 10-Mev linear accelerator, 20: 28929 (CONF-651109, pp 574-98)
ROZENHOLC, Michel, Composite guide tube for reactors, 20: 30830
ROZHDESTVENSKII, V. V., Interaction between uhf radiation and a turbulent plasma, 20: 30625
RUBBIA, C., Further results from interference of K_S and K_L in $\pi^+\pi^-$ decay modes, 20: 30026
RUBIN, Morton, Dispersion relations for three-particle scattering amplitudes. I., 20: 30132
RUBINSTEIN, H. R., Nucleon-antinucleon annihilation in quark model, 20: 30005
RUBISCH, O., Graphite in space travel, 20: 29773
RUBY, S. L., Moessbauer study of ^{83}Kr in KrF_2, 20: 30764
RUDAKOV, L. I., Turbulent heating of plasma by direct-current discharge, 20: 30661
RUDOLPH, P. S., Mass spectrometric evidence for H_3O, HD_2O, and D_3O, 20: 29104
RUDY, E., Thermodynamic considerations in selection of materials for high-temperature applications, 20: 29774
RUEDORFF, W., Ternary oxides. V. Systems PbO–Ta_2O_5, PbO–Nb_2O_5, and PbO–U_2O_5, 20: 29794
RUEEGG, W., Nonaxial model predictions on first-forbidden β transitions of ^{188}Re, 20: 30550
RUKHADZE, A. A., Oscillations of plasma in constant external electric and magnetic fields, 20: 30677
RUMYANTSEV, A. P., Damaging effects of underwater nuclear explosion, 20: 29481
RUSAKOV, V. A., Decay ($K_2^0 \rightarrow \pi^+\pi^-$) probability in sloped K_2^0-meson beam, 20: 30056
RUSSELL, Albert Henry, Improvements in or relating to reactors, 20: 30912
RUSSELL, G. J., Slow-neutron scattering by water, 20: 30330
RYABCHENKO, N. I., Radiation damages in deoxyribonucleoproteins at molecular and supermolecular levels, 20: 28908
RYAN, D. F., Confirmatory evidence for sidereal-time-dependent neutral component in cosmic rays, 20: 29968
RYAN, D. F., Evidence for sidereal-time-dependent cosmic-ray signal, 20: 29967
RYAN, H. F., Observations of dislocations in high-angle boundaries in tungsten, 20: 29725
RYAZANOV, M. A., Activity coefficients in multicomponent systems. III., 20: 29196
RYBAKOV, N. I., Chemical protection against genetic changes, 20: 29045
RYBCHINSKII, R. E., Physical experiments on Kosmos-2 in ionosphere, 20: 30198 (NASA-TT-F-389, pp 202-24)
RYON, John W., Nuclear reactor operating with H-bearing moderator and cooling vapor, 20: 30918
RYON, John W., Steam-cooled reactor arrangement, 20: 30917
RYSHKEWITCH, E., Oxide-metal compound ceramics, 20: 29689
RYTHER, John H., Biological, chemical, and radiochemical studies of marine plankton. I., 20: 28877 (NYO-1918-124)
RYTHER, John H., Biological, chemical, and radiochemical studies of marine plankton. II., 20: 28878 (NYO-1918-138)
RYU, Norio, Fast circuits for neutron detection, 20: 29536
RYZHOV, N. V., Multipoint control of radiation levels, 20: 29458
RZANY, H., Neutron investigation of temperature effects in magnon spectrum of magnetite, 20: 30765

S

SAASTAMOINEN, J., Thermal-neutron spectrum in water with temperature discontinuity, 20: 30331
SACCHI, Ada, Recovery from x-ray-induced sub-lethal damage in Saccharomyces cerevisiae cells of different ploidy, 20: 28961
SACH, R. S., Structural studies on v.u.v./CO_2 oxidation of graphite, 20: 29733
SACHS, Volkmar, Nuclear hematology and blood transfusion, 20: 28893
SACTON, J., π^+-Mesonic decays of hypernuclei, 20: 30485
SADCHIKOVA, E. N., Biochemical indices in innervation disturbances of motor apparatus induced by ionizing radiation, 20: 28974
SAENKO, L. F., Parity nonconservation in radiative transition of ^{175}La, 20: 30381
SAFARYAN, F. P., Investigation of luminescence of acetyl acetonates of samarium, europium, and terbium, 20: 29238
SAFRONOV, B. G., Motion of plasmoid in a curvilinear magnetic field, 20: 30647
SAHA, G. B., Inelastic-scattering model for (p,xn) and (p,p(x-1)n) reactions at intermediate energies, 20: 30446
SAITO, Nobufusa, Isotope effect in electromigration of sodium ions in fused sodium nitrate, 20: 29185
SAITO, Takesi, Unsubtracted dispersion relations in weak interactions and Reggeization, 20: 30125
SAKAI, Eiji, FET preamplifier for cooled semiconductor detectors, 20: 29548
SAKSONOV, P. P., Chemical protection against genetic changes, 20: 29045
SALAITA, George N., Method of chlorine logging in nonferrous environment, 20: 29446
SALAM, A., Dynamical origin of SU(6), 20: 30117
SALPETER, E. E., Absorption lines in the spectra of distant sources, 20: 29890
SALTER, D. C., Nucleon-nucleon total cross sections from 1.1 to 8 Bev/c, 20: 30028
SALTER, F. O., System for suppressing large, nonstatistical noise bursts in digital averaging, 20: 29556
SALVAT, M., Internal potential drop in MHD generators, 20: 29976 (IPP-3/38)
SALZANO, F. J., Bonding energy in Cs-graphite compounds, 20: 29744
SALZANO, F. J., Mechanism of bromine exchange in bromine–graphite lamellar compounds, 20: 29182
SAMOILOVA, K. A., Changes in fat and glycogen contents in paramecium caudatum after uv treatment, 20: 28918
SAMPLES, J. T., Decay of the 2.34- and 2.71-Mev states of ^{9}B, 20: 30445
SAMPSON, D. F., New laser line due to energy transfer from color centers to erbium ions in CaF_2, 20: 30774
SANAEV, B., Radiochemical properties of certain peptides, 20: 29301
SANDERS, R., Level (27.7 kev) in ^{129}I and use in Moessbauer experiments, 20: 30474
SANDOR, T., Daily variation of extensive air showers, 20: 29960
SANGAL, Satendra P., Spectrophotometric study of chelates of ammonium aurintricarboxylate with Sc, Y, and La, 20: 29180
SANIN, P. I., Effect of stabilizers on irradiated polypropylene, 20: 29290
SANNA, Robert, Fast neutron spectrometry with nuclear emulsions, 20: 29848 (CONF-651109, pp 199-212)
SANNA, Robert, Inference of accelerator stray neutron spectra from various measurements, 20: 29522 (CONF-651109, pp 286-305)
SANNER, Tore, Decay of radiation induced radicals and the yield of thermoluminescence, 20: 29249
SANNIKOV, S. S., Resonance in the e-p system, 20: 30054
SANO, Tadao, System U–C–N, 20: 29749
SANO, Yukizo, Morphological study on sudden commencements of magnetic storms and sudden impulses. IV., 20: 30231
SANO, Yukizo, Recurrence time pattern (27-day) of Σ Kp and the geometry of solar plasma, 20: 29894
SANTHOLZER, Vilem, Radioactive debris from nuclear explosions and world experience with atmospheric fallout, 20: 29411
SANTOS, E., Deformation of graphite lattices by interstitial carbon atoms, 20: 29735
SANTUS, Rene, Photoionization and biphotonic processes of nucleic acids derivatives in frozen solutions, 20: 28914
SAPEZHINSKII, I. I., Free-radical reactions during exposure of model systems to irradiation, 20: 29037
SARAEVA, V. V., Radiolysis of concentrated aqueous solutions of isopropyl alcohol in presence of O, 20: 29277
SARAEVA, V. V., Radiolysis of isooctyl and heptyl hydroperoxide solutions in hydrocarbons, 20: 29302
SARASWATI, V., Nuclear magnetic resonance in rare earth fluorides, 20: 30755
SARAVIA, Luis R., Table of real part of dispersion correction for x-ray scattering, 20: 29722

SARDA, Ram Prasad, Relation of chromosomal bridges at anaphase to exchanges at metaphase, 20: 29031
SARGIS, David Albert, Space-dependent neutron thermalization, 20: 30861
SARUP, S., Isotopic exchange and annealing of recoil damage in Co complexes, 20: 29259
SASAKI, T., Separation of recoiling Cr(II) ion from neutron-irradiated Cr(III) ion, 20: 29261
SASAKI, Yasuo, Electron-beam refining of niobium, 20: 29634
SASLAW, W. C., Distribution of quasi-stellar radio sources in steady state cosmology, 20: 29897
SASSEN, A., X irradiation effects on mouse proteins, 20: 28899
SATCHLER, G. R., Elastic and inelastic proton scattering from ^{106}Pd and ^{108}Pd, 20: 30462
SATCHLER, G. R., Optical-model analysis of scattering of 24.7-Mev α particles, 20: 30413
SATCHLER, G. R., Reactions ^{40}Ca(d,d), (d,d'), and (d,p) with 12.8-Mev deuterons, 20: 30459
SATO, T., Ion cyclotron resonance heating of QP plasma, 20: 30662
SATO, Taichi, Extraction of U(VI) from HCl solutions by TOA, 20: 29339
SATO, Testuo, Properties of high-zirconium wrought copper base alloys, 20: 29782
SAVENKO, I. A., Cosmic rays during flights of spacecrafts-satellites and Kosmos, 20: 29956 (NASA-TT-F-389, pp 684-91)
SAVENKO, I. A., Earth's outer radiation zone at low altitudes, 20: 30216 (NASA-TT-F-389, pp 588-606)
SAVENKO, I. A., Inner and artificial radiation zones of earth at low altitudes, 20: 30217 (NASA-TT-F-389, pp 607-15)
SAVENKO, I. A., Measurement results on Kosmos-41 in outer radiation zone, 20: 30219 (NASA-TT-F-389, pp 623-9)
SAVENKO, I. A., Radiation safety problems in space flights, 20: 30222 (NASA-TT-F-389, pp 758-63)
SAVENKO, I. A., Recording charged particles with energy of 0.1 to 10 kev with spherical electrostatic analyzer, 20: 29532 (NASA-TT-F-389, pp 518-25)
SAVIN, B. I., Recording charged particles with energy of 0.1 to 10 kev with spherical electrostatic analyzer, 20: 29532 (NASA-TT-F-389, pp 518-25)
SAVITSKII, E. M., Laves phases in systems containing Re and rare-earth metals, 20: 29792
SAVITSKII, I. V., Effect of x-irradiation on thiamine phosphorylation, 20: 29003
SAVITSKII, Yu. M., Effect of interstitial impurities on structure and properties of W single crystals, 20: 29793
SAWAI, Takeshi, Radical yields in the radiolysis of neutral aqueous solutions, 20: 29254
SAWAI, Takeshi, Radiolysis of aqueous solutions of potassium iodide, 20: 29253
SAWYER, J. C., Prog. rpt. on long-time creep data on refractory alloys, 12/65–3/66, 20: 29705 (NAS-CR-54973)
SAWYERS, J. E., Advancements in organic coolants, 20: 30906
SAX, N. Irving, Manganese-54 in freshwater clams, 20: 29462
SAYASOV, Yu. S., Influence of identity of colliding nuclei in inelastic scattering at sub-barrier energies, 20: 30493
SAYRES, A., Neutron radiation monitoring using ^{3}He spectrometer, 20: 29846 (CONF-651109, pp 154-60)
SBITINKOVA, I. S., Injection and confinement of plasma in a stellarator with a multipolar (l = 2) helical field, 20: 30657
SCADRON, Michael D., General phenomenological formalism for reactions with particles of arbitrary spin. I., 20: 30094 (UCRL-14222)
SCHAEFER, G., Paramagnetic resonance of Er^{3+} in Y_2O_3, 20: 29192
SCHAEFER, Harald, Modifications of Nb pentoxide, 20: 29728
SCHAMBURGER, Rudolf, Application of network planning technique in construction of nuclear power plants, 20: 30907
SCHARF, H., Paper electrophoresis of complexes of rare earths with hydroxyamino acids, 20: 29343
SCHARF, Karl, Steady-state response of silicon radiation detectors of diffused p-n junction type to x rays. II., 20: 29540
SCHARFSTEIN, L. R., Effect of increased Ni content on intergranular corrosion of alloy 20Cd, 20: 29643
SCHARMANN, A., Modification of conductivity of $Ni(OH)_2$ and CdO by irradiation, 20: 29821
SCHARZ, Gerd, Relative measurements of electron polarization of ^{199}Au and ^{32}P, 20: 30548
SCHATZ, G., Numerical analysis of β spectra, 20: 30541
SCHELLER, S., Paramagnetic resonance of Er^{3+} in Y_2O_3, 20: 29192
SCHIBY, B., Interference effects between N*(1236) and K*(891) production, 20: 30009
SCHIFFER, L., Scanning of liver, spleen, and bone marrow with colloidal ^{99m}Tc, 20: 29065
SCHIFFER, L. M., Extracorporeal irradiation of blood, 20: 28927 (BNL-9647)
SCHILDKNECHT, H., Structure elucidation and identification of organic substances by "electron burning." II., 20: 29326
SCHINDLER, Heinrich, Multistage acceleration and heating of plasma, 20: 30667
SCHIRMER, G., Study of Be with polarized neutrons of energy 2.60 to 2.77 Mev, 20: 30414
SCHLESINGER, Y., Study of nuclear resonant scattering using neutron-capture γ rays, 20: 30467
SCHLUDERBERG, Donald C., Fast breeder reactor and method of operation, 20: 30914
SCHLUDERBERG, Donald C., Multi-pass, vapor-moderated and cooled reactor, 20: 30916
SCHLUDERBERG, Donald C., Nuclear reactor operating with H-bearing moderator and cooling vapor, 20: 30918
SCHLUDERBERG, Donald C., Reactor and method of operating to variably moderate and control, 20: 30915
SCHLUDERBERG, Donald C., Steam-cooled reactor arrangement, 20: 30917
SCHLUETER, H., Collisional Stark broadening in r-f discharges, 20: 30572
SCHLUETER, J., Stable and unstable behavior of preheated plasma in linear and cusped theta pinches, 20: 30614
SCHMELING, P., Simultaneous diffusion of Ar and Kr in single crystals of KCl–RbCl, 20: 30769
SCHMETS, J., Relative problems of design of pilot plants for reprocessing by volatilization, 20: 29364
SCHMIDLIN, P., Beta-γ directional correlations and β-γ circular polarization correlations in single-forbidden-β decay of ^{144}Ce, ^{144}Pr, ^{170}Tm, and ^{203}Hg, 20: 30544
SCHMITT, H., Beta-γ directional correlations and β-γ circular polarization correlations in single-forbidden-β decay of ^{144}Ce, ^{144}Pr, ^{170}Tm, and ^{203}Hg, 20: 30544
SCHMITT, H., Beta spectra of ^{42}K, ^{86}Rb, and ^{170}Tm, 20: 30546
SCHMITT, H., Measurement of β-γ circular polarization correlations in β transitions of ^{58}Co, ^{95}Zr, ^{95}Nb, and ^{141}Ce, 20: 30543
SCHMITT, H., Measurement of β-γ circular polarization correlation on ^{133}Xe, 20: 30553
SCHMITT, J. M., Monoalkyl phosphoric acid extraction of cesium and strontium values, 20: 29365
SCHMITT, R. A., Range of photoparticle recoil atoms in solids, 20: 30479
SCHMUESER, P., Production of antiprotons by high-energy photons, 20: 30432
SCHNAPPAUF, Hp., Extracorporeal irradiation of blood, 20: 28927 (BNL-9647)
SCHNEIDER, H., Gamma-γ angular correlation of ^{144}Pr at 54 to 80 kev, 20: 30506
SCHNEIDER, T., S-D exchange interactions and Fermi surface in Ni, 20: 30775
SCHNEIDER, V., Production of radioactive gold preparations for medical purposes, 20: 29075
SCHOEB, Virginia Rowland, Stability constants of rare earths with some carboxylic acids, 20: 29232
SCHOESSOW, Earl E., Compact nuclear steam generator, 20: 30931
SCHOMBERG, M. G., Eta and neutron cross sections of ^{235}U from 0.03 to 200 ev, 20: 30342 (AERE-M-1670)
SCHOPPER, H., Asymmetry coefficients of β-γ circular polarization correlation, 20: 30542
SCHOPPER, H., Re-evaluation of the coupling constant in β decay, 20: 30538
SCHOVANEC, K., Contribution to problem of thermodynamic similarity of H_2O and D_2O, 20: 30182
SCHREINER, H., Sintered semiconductors for thermoelectric current generation and cooling, 20: 29690
SCHRIEFFER, J. Robert, Breakdown of quasi-particle approximation in metals, 20: 30312
SCHROEDER, Ivan Gaston, Thermal neutron fission of ^{235}U with emission of long-range α particles, 20: 30513
SCHROERSCHWARZ, R., Simultaneous diffusion of Ar and Kr in single crystals of KCl–RbCl, 20: 30769
SCHUELKE, L., Measurable quantities in nuclear β decay, 20: 30539
SCHUETZ, R., Formation of azides of Pr(III) and Nd(III), 20: 29166
SCHUETZEL, Heinz, Paragenetic position of U pitchblende in hydrothermal deposits of West Erzgebirge, 20: 29448
SCHULTE, F., Modifications of Nb pentoxide, 20: 29728
SCHULTZ, W. W., Assessment of inhomogeneity of solid reactor fuels by fission-track counting, 20: 29663 (KAPL-M-6556)
SCHULTZE, K., Future neutrino experiments, 20: 30002
SCHULZ, H. D., Polarization of 6-Bev bremsstrahlung from Hamburg electron synchrotron, 20: 30045
SCHUMACHER, B. W., Electron-single-scatter-gage, 20: 29600
SCHUMACHER, D. P., Fourth-order crystal field splitting in rare earth(III) ions, 20: 30747
SCHURCLIFF, William A., Radiation dosimeter, 20: 29574
SCHUTTEN, J., Gross- and partial-ionization cross sections for electrons on water vapor, 20: 29928
SCHUTZ, Gerhard, Safety devices for use with radioactive measuring apparatus, 20: 29515

SCHUTZLER, J. C., Cascade arrangement in spherical vessel design for power reactors, 20: 30893
SCHWARTZ, J. J., Re-examination of spin of ^{45}Sc 378-kev level, 20: 30429
SCHWARZ, E., Behavior of recoil atoms in the decay of ^{219}Rn and ^{220}Rn in gases, 20: 29325
SCHWEINBERGER, W., Radiation defects in deuteron-bombarded CdS crystal, 20: 30771
SCHWEITZER, D. G., Surface currents magnetization of hysteretic superconductors, 20: 30269
SCHWEIZER, J., Variation of magnetic moment of Co in $Gd_xY_{x-1}Co_2$ compounds, 20: 30756
SCIAMA, D. W., Distribution of quasi-stellar radio sources in steady state cosmology, 20: 29897
SCIARRONE, Bartley J., Effects of ionizing radiation on gelatin fractions. III., 20: 29273
SCOFIELD, N. E., Energy and angular distribution of γ rays scattered in Al, 20: 30729
SCOTT, F. R., Flute characteristics of and microwave emission from a plasma in a mirror, 20: 30645
SCOTT, F. R., Plasma guiding by means of multipole fields, 20: 30579
SCRIBANO, A., Further results from interference of K_S and K_L in $\pi^+\pi^-$ decay modes, 20: 30026
SCRIMGER, J., Positioning circuit for anatomical marking on gamma-camera scintiphotos, 20: 29067
SEABORN, James Byrd, Spurious states in the nuclear shell model, 20: 30514
SEAHOLM, John E., Acatalasemic and hypocatalasemic mouse mutants, 20: 28957
SEAMAN, G. V. F., Effect of ionizing radiations on electrophoretic mobility of mammalian cells, 20: 28905
SEARS, R., Elastic scattering (π^--p) at 1.7 Bev/c, 20: 30011
SEBACHER, Daniel I., Primary and afterglow emission from gaseous nitrogen excited by electrons, 20: 29929
SEDLACEK, F., Danger of unintentional diagnostic irradiation of fetus in routine x-ray practice, 20: 29068
SEDRAKYAN, D. M., Emission of point charged particle passing along axis of semi-infinite waveguide, 20: 29828
SEEGER, Philip A., Integrated flux distributions in neutron capture in stars, 20: 29887
SEEMANN, K. W., Inelastic scattering cross sections for polyethylene and water in gas transition region, 20: 30334
SEGARCEANU, T., Decomposition of zirconium silicate with potassium fluosilicate, 20: 29201
SEHGAL, Bal Raj, Neutron thermalization and diffusion in nonisothermal media, 20: 30322 (BNL-947)
SEIDEL, T., Thermal conductivity of lead films for study of surface superconductivity, 20: 30294
SEKIZAWA, Kazuko, Magnetic properties of rare earth compounds in Gd(Ag,Cd,In) and Gd(Cu,Ag,Au) systems, 20: 29752
SELIG, H., Moessbauer study of ^{83}Kr in KrF_2, 20: 30764
SELITSKII, Yu. A., Energies of pair fragments in fission of ^{238}U, ^{235}U, and ^{233}U, by 12-Mev deuterons, 20: 30500
SELLIN, I., Binding effects in electronic excitations by heavy charged particles, 20: 29936
SELTMANN, Hans, Safety devices for use with radioactive measuring apparatus, 20: 29515
SELTZER, Edwin Charles, Nuclear structure effects in internal conversion, 20: 30515
SEMCHYSHEN, M., Recent developments in technology of arc-cast Mo, 20: 29756
SEMENOV, L. F., Radiation sickness in Macacus rhesus, 20: 28986
SEMMLER, R. A., Beta-backscatter techniques for measurement of layer thickness in multilayer coating, 20: 29391
SENBA, Kei, Elementary particles and bound states, 20: 30145
SENENT, F., Photonuclear interactions of high-energy muons, 20: 29994
SENENT, F., Reconstruction of events produced in interior of bubble chambers, 20: 29533
SENENT, S., Deformation of graphite lattices by interstitial carbon atoms, 20: 29735
SEN GUPTA, P. R., Effect of nuclear explosions upon ionosphere, 20: 30228
SEPEL, T., Uranyl complexes with phenolic ligands. VI., 20: 29096
SEPTIER, A., New type of high-frequency mass spectrometer with two electrodes, 20: 29126
SEREBRENNIKOV, V. V., Distribution of erbium in molten Al–Cd, Al–Pb, and Al–Bi alloys, 20: 29797
SEREBRYAKOV, V. A., Use of laser operating in spike mode to obtain high-temperature plasma, 20: 30590
SERGEEV, I. P., Calculation of stability conditions of water-moderated water-cooled boiling reactor, 20: 30908
SERGEEV, I. V., Nonuniform burnup in a reflector reactor, 20: 30909
SETTER, Lloyd R., Cesium-137 in food, 20: 29475
SETTER, Lloyd R., Strontium-90 in food, 20: 29433
SETTI, G., Local hypothesis for the quasi-stellar objects, 20: 29888
SEWARD, F. D., X-ray spectra from three cosmic sources, 20: 29901
SHABANSKII, V. P., Formation of radiation zones as result of particle drift in depths of magnetosphere, 20: 30207 (NASA-TT-F-389, pp 442-53)
SHADURSKII, K. S., Loss of hypotensive activity by derivatives of 5-hydroxyindole when animals are irradiated, 20: 29050
SHAFER, G. V., Cosmic rays in July of 1961, 20: 29961
SHAFER, Yu. G., Cosmic rays in July of 1961, 20: 29961
SHAFER, Yu. G., Investigation of cosmic ray variations in Yakutsk, 20: 29963
SHAFRANOV, V. D., Closed minimum-B configurations, 20: 30609
SHAGISUL, G. A., Effects of γ- and ultraviolet rays on copper glycocol, 20: 29303
SHALAGINA, E. V., Disintegration with emission of fast He nuclei due to high-energy protons, 20: 30496
SHALEV, S., Evaluation of the ^{17}N reactor power level monitor, 20: 30938
SHALIMOV, V. I., Charged-particle motion in a magnetic dipole field. I., 20: 29829
SHALITOV, V. P., Penetration processes into magnetosphere of earth, 20: 30205 (NASA-TT-F-389, pp 386-425)
SHAL'NEV, B. I., Changes in conditioned reflex activity of dogs under influence of ^{24}Na, 20: 29009
SHAMASOV, R. G., Absorption effect on surfaces of semiconductors and gels due to effects of radiation, 20: 29815
SHAPIRO, E. Ya., Electric conductivity and creep of sintered CeO_2 during reduction, 20: 29739
SHAPIRO, V. D., Quasilinear theory of plasma cyclotron instability, 20: 30670
SHAPKIN, G. N., β decay of bromine isotopes for synthesis of krypton compounds, 20: 29327
SHAPLYGIN, I. S., Reaction of manganese and scandium oxides in air, 20: 29168
SHARPATYI, V. A., Radiochemical properties of certain peptides, 20: 29301
SHARVINA, K. N., Inner and artificial radiation zones of earth at low altitudes, 20: 30217 (NASA-TT-F-389, pp 607-15)
SHASHKOV, V. S., Simulation of biological effect of depth dose from monoenergetic proton, 20: 28972
SHAVRIN, P. I., Cosmic rays during flights of spacecrafts-satellites and Kosmos, 20: 29956 (NASA-TT-F-389, pp 684-91)
SHAVRIN, P. I., Earth's outer radiation zone at low altitudes, 20: 30216 (NASA-TT-F-389, pp 588-606)
SHAVRIN, P. I., Inner and artificial radiation zones of earth at low altitudes, 20: 30217 (NASA-TT-F-389, pp 607-15)
SHAVRIN, P. I., Measurement results on Kosmos-41 in outer radiation zone, 20: 30219 (NASA-TT-F-389, pp 623-9)
SHAVRIN, P. I., Radiation safety problems in space flights, 20: 30222 (NASA-TT-F-389, pp 758-63)
SHAW, K. B., Radiation levels in and around Nimrod, 20: 29842 (CONF-651109, pp 20-33)
SHCHEDRINA, R. N., Disturbance in catecholamine metabolism induced by radiation, 20: 28940
SHEA, Frederick L. Jr., Nuclear reactors operating with substantially isotropic graphitized bodies, 20: 29694
SHEELEY, N. R. Jr., Measurements of solar magnetic fields, 20: 29885
SHEELEY, Neil Rolfson Jr., Measurements of solar magnetic fields, 20: 29910
SHEINBERG, H., Copper–boron carbide control material for Phoebus II, 20: 29664 (LA-DC-7745)
SHEKHTER, L. Sh., Phenomenology of certain inelastic reactions involving particles with spin, 20: 30149
SHEKHTER, V. M., Consequences from vector current conservation, 20: 30008
SHELEST, V. P., Equations for scattering matrix elements in relativistic three-body problem, 20: 30148
SHELTON, Frank H., Gamma fluxes from circular and spherical sources, 20: 30351 (N-65-14857)
SHENOY, G. K., Temperature-dependent lifetimes of nonequilibrium Fe^{3+} ions in CoO from Moessbauer effect, 20: 29833
SHENOY, G. K., Temperature dependence of internal field at ^{57}Fe nucleus in Ni lattice, 20: 30750
SHEPSTONE, B. J., Routine dosimetry with ^{182}Ta and ^{192}Ir wires, 20: 29456
SHERMAN, L. G., Influence of various diets and x radiation on cholesterol level in tissues, 20: 28995
SHERMAN, Michael, Principle of exchange of stabilities for MHD thermal stability problem in completely confined fluids, 20: 30178
SHERMAN, Warren V., Solute effects in radiolysis of cyclohexane solutions. II., 20: 29270
SHESTAKOV, S. V., Pigment mutations in Anacystis nidulans, 20: 28958
SHESTOPALOV, V. P., Radiation from electrons moving parallel to metal grid located on edge of uniaxial crystal of finite thickness, 20: 29995
SHESTOPALOV, V. P., Radiation of electromagnetic waves by electron

sheet moving above diffraction grating, 20: 30250
SHEVCHENKO, V. B., Solubility of ammonium plutonyl phosphate compounds in aqueous solutions, 20: 29219
SHEVCHENKO, V. I., Quasilinear theory of plasma cyclotron instability, 20: 30670
SHEVCHENKO, Yu. V., Temperature effect on yield and composition of hexanitrocobaltic rare earths mixed with potassium, 20: 29209
SHIDA, Shoji, Photolysis of cis-2-butene and its implications for radiation chemistry, 20: 29251
SHIER, J. S., Superconducting transitions of amorphous bismuth alloys, 20: 30298
SHIFRIN, I. G., Effect of γ-radiation on leathers, 20: 29588
SHIFRIN, I. G., Effect of γ-radiation on physical-mechanical properties of physical-mechanical properties of chromium-tanned leather, 20: 29592
SHIFRIN, I. G., The effect of γ-radiation on chrome-tanned shoe upper leather, 20: 29591
SHIGEMATSU, Tsunenobu, Fluorometric determination of Y with 5,7-dichloroxine, 20: 29094
SHIH, Li-lan, Relation between chemical structure of alkyl dibutyl phosphonates and characteristics of U and Th extraction, 20: 29354
SHILOVSKII, P. P., Origin of uranium exogenous deposits and methods for their exploration, 20: 29449
SHIMIZU, Akira, Radiation-induced solid-state copolymerization of maleic anhydride and acenaphthylene, 20: 29274
SHIMIZU, Ryuichi, Pulse-analysis method of light elements. I., 20: 29124
SHIMOISHI, Yasuaki, Spectrophotometric determination of F with a PAC–Th complex, 20: 29091
SHINAGAWA, Mutsuaki, Studies on focusing chromatography separation of ^{239}Np from neutron-irradiated U, 20: 29351
SHINANO, K., Dense plasma produced by a cusp injection, 20: 30643
SHINDO, Ruichi, Dancoff reactor in arrayed-type cladded fuel lattice, 20: 30842
SHINODA, Gunji, Pulse-analysis method of light elements. I., 20: 29124
SHINOZAKI, Yoshiharu, Radiolysis of aqueous solutions of potassium iodide, 20: 29253
SHIROISHI, Masahide, Radiation preservation of fruits and vegetables, 20: 29597
SHIROKOV, M. I., Problems of quantum theory of scalar field with point sources, 20: 30092 (JINR-P-2700)
SHKLOVER, L. P., Stability of metal-alloy bond in rare earths phthalocyanines, 20: 29217
SHKODA, V. V., Motion of plasmoid in a curvilinear magnetic field, 20: 30647
SHMEL'KOVA, N. I., Effect of γ-rays from ^{60}Co on certain metabolic processes in pea plants, 20: 28909
SHOHNO, Naomi, Elementary particles and bound states, 20: 30145
SHOROKHOV, O. A., Use of laser operating in spike mode to obtain high-temperature plasma, 20: 30590
SHPIGEL, I. S., Injection and confinement of plasma in a stellarator with a multipolar (l = 2) helical field, 20: 30657
SHPIGUN, A. A., X-ray study of epoxido-dianic ED-5 resin irradiated with ^{60}Co and metallopolymers on its base, 20: 29297
SHPINEL, V. S., Barium stannate: source for measurement of Moessbauer effect on ^{119}Sn, 20: 30753
SHPINEL', V. S., Effective magnetic field at ^{60}Co nucleus in Co–Pd alloy, 20: 30752
SHRAIBER, L. S., Temperature effects on electron polarization variations in ordinary and heavy water molecules, 20: 29230
SHTAN, A. S., Neutron radiography, 20: 29627
SHTERN, G. R., Disintegration with emission of fast He nuclei due to high-energy protons, 20: 30496
SHU, Yung-Lan, Asymmetrical configuration of trapped region and some correlated aeronomical phenomena, 20: 30224
SHUBIN, V. N., Steady state in radiolysis of neutral aqueous solutions of oxygen, 20: 29257
SHUBINA, R. V., Free induction signal in exchange pairs, 20: 30778
SHUKOVSKY, H. B., Low-temperature electrical resistivity of lattice defects in deformed tungsten single crystals, 20: 29723
SHUKUROV, Yu., Chemical analysis using heavy ion scattering at large angles, 20: 29090
SHULGINA, N. S., Sorption and separation of zirconium and hafnium on native anionites, 20: 29352
SHUMILOVSKII, N. N., Nuclear magnetic resonance methods, 20: 29498
SHUSHEVICH, S. I., Effect on rabbits on incorporation of radioactive acetate in cholesterol, 20: 28895
SHUTOVA, G. A., Neodymium and erbium bromide complexes, 20: 29225
SHUVALOV, V. A., Measurement of properties of a partially ionized gas with a hot-wire anemometer, 20: 30702
SHUYSKAYA, F. K., Corpuscle investigations on Elektron-1, 20: 30212 (NASA-TT-F-389, pp 551-66)
SHUYSKAYA, F. K., One anomaly in electron pitch distributions, 20: 30200 (NASA-TT-F-389, pp 273-6)
SHVACHUNOV, I. N., Charged particle motion in a magnetic dipole field. I., 20: 29829
SHVACHVONOV, I. N., Penetration processes into magnetosphere of earth, 20: 30205 (NASA-TT-F-389, pp 386-425)
SHVAREV, V. V., Conference on space physics, Moscow, 6/65, 20: 30195 (NASA-TT-F-389)
SHVETS, O. M., Heating of dense plasma in a metallic chamber, 20: 30664
SHVETSOV, M. S., Cross sections for production of γ-quanta in inelastic interactions of 14-Mev neutrons with C, O, Al, Fe, and Pb, 20: 30498
SHYUTTE, N. M., Physical experiments on Kosmos-2 in ionosphere, 20: 30198 (NASA-TT-F-389, pp 202-24)
SIECK, L. W., Xenon-sensitized radiolysis of propane, 20: 29266
SIEGEL, Benjamin V., Influence of deuteration on circulating antibody levels in mouse, 20: 28988
SIEGERT, G., Ion charge distribution of unretarded fission products, 20: 30507
SIELER, J., Preparation and structure of rare earth titanates and of europium(II) zirconate, 20: 29212
SIEMSSEN, R. H., Discrepancies in proton-transfer reactions to states with different isobaric spin, 20: 30481
SIEMSSEN, R. H., Reaction $^{182}W(d,p)^{183}W$ at 7.5 and 12 Mev, 20: 30475
SIFNER, O., Contribution to problem of thermodynamic similarity of H_2O and D_2O, 20: 30182
SIIMES, M., The effect of erythermal reaction caused by ultraviolet irradiation on mast cell degranulation in the skin, 20: 28937
SIKKELAND, Torbjorn, Production of nuclides in the region of Z = 126 and N = 184, 20: 30367
SILIN, V. I., Oscillations and stability of plasma in external high-frequency electric field, 20: 30627
SILIN, V. P., Parametric resonance in plasma in magnetic field, 20: 30669
SILIN, V. P., Scattering of waves in a plasma, 20: 30674
SILKOS, O., Preparation of trichloroethylene labeled with ^{36}Cl and application to study of corrosion, 20: 29655
SILVER, A. H., Flux entry in macroscopic superconducting rings, 20: 30305
SILVERMAN, M. S., Transfer of myeloma protein synthesis with RNA from C_3H plasma cell tumor. I., 20: 28926 (AD-633469)
SILVERT, William, Surface superconductivity at high temperatures, 20: 30302
SIL'VESTROV, L. V., Differential cross section of charge exchange of 4.8-Bev/c π^- mesons with protons, 20: 29998
SIMAK, V., Peripheral proton–nucleon interactions at 9 Bev, 20: 30080
SIMMONS, J. E., Neutron-deuteron polarization at 22.7 Mev, 20: 30442
SIMMONS, J. H., Flux pinning in superconducting niobium thin films, 20: 30278
SIMMONS, Leonard Micojah Jr., Partial wave dispersion relations for pion–nucleon scattering, 20: 30073
SIMON, H., Simple method for ^{15}N determination, 20: 29131
SIMON, Morris, Development of radiation-sterilized seafood products. I., 20: 29603
SIMON-REUSS, I., Effect of ionizing radiations on electrophoretic mobility of mammalian cells, 20: 28905
SINCLAIR, R. M., Non-resonant coupling of r-f power to a plasma, 20: 30577
SINCLAIR, Rolf M., Semi-automatic data system for plasma study, 20: 30573
SINEL'NIKOV, V. M., Altitudinal-time distribution of electron concentration and nonuniform formations of outer ionosphere, 20: 30197 (NASA-TT-F-389, pp 166-201)
SINGH, B. B., Gamma-ray thermoluminescence in nucleic acid constituents, 20: 28913
SINGH, N., Pseudowave functions, 20: 30773
SINGH, R. P., Studies in complex formation of metal ions with tropolones. III., 20: 29179
SINHA, K. P., Pressure effects on transition temperature of superconductors, 20: 30259
SINITSINA, V. G., Cosmic ray nuclear component on Elektron-2, 20: 29957 (NASA-TT-F-389, pp 693-710)
SINITSYN, R. V., Problems in the design and selection of technical parameters for teletherapy units, 20: 29064
SINITSYN, V. V., Plasma energy losses in toroidal chamber Tokamak TM-2, 20: 30653
SINNHUBER, R. O., Development of radiation-sterilized seafood products. I., 20: 29603
SIROVICH, Lawrence, Mathematical aspects of kinetic model equations, 20: 30165 (BNL-9254)
SISAKYAN, I. N., Cross section of quark generation, 20: 29999
SISAKYAN, I. Sh., Effect of x-irradiation on yield of potatoes, 20: 28966
SISAKYAN, N. M., Uncoupling of oxidation and phosphorylation in mitochondria of plants after x-ray irradiation, 20: 28947
SISOEV, E. A., Boson resonance at 1.63 Bev in π^-p interactions, 20: 30021
SITE, A. Delle, Main-chain scission and ESR spectra of irradiated polytetrafluoroethylene oxide, 20: 29267
SIZMANN, R., Magnetic methods for measuring maximum temperature of irradiated samples, 20: 29387

SIZONENKO, V. L., Determination of plasma density distribution by microwave refraction, 20: 30700
SIZONENKO, V. L., Theory of decay of EM waves in magnetoactive plasma, 20: 30671
SKAARDAL, Rolf C., Operational problems and solutions, 20: 30904
Skala, Stephen F., Magnetic methods and apparatus for manipulating beam of charged particles, 20: 29872
SKATKIN, V. M., Multipoint control of radiation levels, 20: 29458
SKEEN, D. R., Criticality studies with plutonium solutions, 20: 29471
SKELLY, H. M., Uranium alloy development for non-nuclear application, 20: 29803
SKIBENKO, A. I., Determination of plasma density distribution by microwave refraction, 20: 30700
SKIBENKO, E. I., Cryogenic magnetic trap VGL-2, 20: 30655
SKOBLIK, I. P., Energy distribution in hydrogen plasma from coaxial plasma gun, 20: 30687
SKORYUPIN, V. A., Turbulent heating of plasma by direct-current discharge, 20: 30661
SKOTNIKOV, A. S., Extraction properties of organic compounds. II., 20: 29347
SKOTNIKOVA, G. A., Thorium tetrasulfate compounds, 20: 29218
SKOTNIKOVA, G. A., Thorium penta- and hexasulfate compounds, 20: 29226
SKOV, Kirsten, Nucleic acid synthesis in x-irradiated thymocytes, 20: 28953
SKRIPIN, G. V., Cosmic rays in July of 1961, 20: 29961
SKRIPKO, A. L., Nuclear magnetic resonance methods, 20: 29498
SKRONN, H. J., Production of antiprotons by high-energy photons, 20: 30432
SKRYPIN, G. V., Investigation of cosmic ray variations in Yakutsk, 20: 29963
SKURIDIN, G. A., Conferences on space physics, Moscow, 6/65, 20: 30195 (NASA-TT-F-389)
SKURIDIN, G. A., Penetration processes into magnetosphere of earth, 20: 30205 (NASA-TT-F-389, pp 386-425)
SLADE, D. H., Summary of measurements of dispersion from quasi-instantaneous sources, 20: 29403
SLAPA, M., Semiconductor system for charged particle identification, 20: 29526 (INP-444/PL)
SLAUGHTER, J. I., New class of hypereutectic carbide composites, 20: 29727
SLEDZIEWSKI, Z., Injection of ions into a magnetic mirror machine (M.M.I.I.), 20: 30634
SLUTSKII, M. E., Radiofrequency mass spectrometer for the Electron satellites, 20: 29545
SMALLEY, A. K., Zone melting of uranium monocarbide, 20: 29619 (NAA-SR-11813)
SMART, Desmond, Lasers and ultrasonics, 20: 28951
SMETS, Henri B., Effect of delayed neutrons in reactor dynamics, 20: 30850
SMIRNOV, V. F., Extraction of U and associated elements with D2EHPPA, 20: 29361
SMIRNOV, V. M., Instability of nonlinear stationary potential oscillations in electron-ion beams, 20: 30672
SMIRNOV, Yu. F., Investigation of the electron states of atoms, molecules, and solids, 20: 29931
SMITH, Bob H., Omnitron: medium-energy synchrotron for acceleration of light and heavy ions, 20: 29857 (UCRL-16839)
SMITH, D. G., Gain variations in some channel multipliers, 20: 29543
SMITH, Donald, Cesium-137 in food, 20: 29475
SMITH, Donald, Strontium-90 in food, 20: 29433
SMITH, E. E., Time-interval measuring circuit, 20: 29530 (SCL-DR-65-13)
SMITH, Fred A., Hallam operation in retrospect, 20: 30905
SMITH, J., Application of approximate solution of partial-wave dispersion relations to Yukawa potential scattering, 20: 30128
SMITH, J. A., Core boration and flux mapping Test 313, 20: 30874 (ACNP-65612)
SMITH, Robert C., Radiative transition probability from $3/2^+$ to $3/2^-$ state in ^{5}He, 20: 30386
SMITH, William Hayden, Far-infrared spectra of crystalline acetylenes C_2H_2 and C_2D_2, 20: 29239
SMITHER, R. K., High-energy γ spectra from neutron capture in Hf isotopes, 20: 30466
SMOLJANKIN, V. T., Boson resonance at 1.63 Bev in π^-p interactions, 20: 30021
SMORODINSKII, Ya. A., Current-generated algebras and form factors, 20: 30146
SMOTRITSKII, L. M., Parity nonconservation in radiative transition of ^{175}Lu, 20: 30381
SMUROVA, V. S., High-temperature x-ray phase analysis of U–O system from $UO_{2.50}$ to $UO_{2.67}$, 20: 29799
SMYSLOV, A. A., Uranium in traps of Siberian platform, 20: 29419
SNYDER, H. A., Measurements of mutual-friction parameter B′ in rotating He II, 20: 30285
SNYDER, W. S., Safety analysis of radionuclide release to Clinch River, 20: 29452 (ORNL-3721(Suppl.3))
SOBOLEVA, V. I., Radiation sickness in Macacus rhesus, 20: 28986
SOEDA, Momoo, Antileucopenic action of marinamycin in case of x-ray irradiation, 20: 29055
SOFIA, Sabatino, Quasars—a minority report, 20: 29896
SOKOLOV, A. P., Boson resonance at 1.63 Bev in π^-p interactions, 20: 30021
SOKOLOV, I. A., Possible antimatter nature of micrometeors, 20: 29895
SOKOLOV, L. S., Cross section for elastic scattering of 13.6-Mev deuterons by Ti, Fe, and Co, 20: 30497
SOKOLOVA, L. N., Accuracy of particle trajectory location in spark chamber, 20: 29527 (ITEF-341)
SOKOLOVA, N. V., Reactions of hematopoietic system in guinea pigs to effects of radiation in small doses, 20: 28945
SOLDATENKOV, T. R., Motion of charged particles in constant and rotating magnetic fields, 20: 30693
SOLIMAN, Moustafa, Analytical and experimental study of transient heat transfer for external forced convection, 20: 29379 (SAN-1011)
SOLOMATINA, E. K., Comparison of simultaneous measurements of magnetic field and positive ion streams within earth's magnetosphere, 20: 30208 (NASA-TT-F-389, pp 457-63)
SOLOMATINA, E. K., Possible existence of soft electron component in outer radiation zone, 20: 30213 (NASA-TT-F-389, pp 566-8)
SOLOV'EV, L. S., Closed minimum-B configurations, 20: 30609
SOLOV'EV, S. M., Energies of pair fragments in fission of ^{238}U, ^{235}U, and ^{233}U, by 12-Mev deuterons, 20: 30500
SOLOV'EV, V. V., Decays ($\eta^0 \to \pi^0 + e^+\mu^+ + e^-\mu^-$) and violation of CP parity, 20: 29988 (ITEF-356)
SOLOV'EV, Yu. N., Effect of cold and ultraviolet rays on mast cell system, 20: 28944
SOMAYAJULU, B. L. K., Thorium and uranium isotopes in seawater and sediments, 20: 29412
SOMMER, J., Isar I: fast megajoule theta-pinch experiment with extremely high compression fields, 20: 30611
SOMMER, L., Uranyl complexes with phenolic ligands. VI., 20: 29096
SOMOGYI, A., Daily variation of extensive air showers, 20: 29960
SOOD, P. C., Non-local potential for optical-model analysis of proton scattering, 20: 30408
SOPIN, E. F., Nucleic acid content in guinea pig brain in dynamics of acute radiation sickness, 20: 28919
SOROKINA, V. A., Reactions of hematopoietic system in guinea pigs to effects of radiation in small doses, 20: 28945
SOSNOVETS, E. N., Irregular high-energy electron streams near boundary of radiation zones of earth, 20: 30215 (NASA-TT-F-389, pp 576-87)
SOSNOVETS, E. N., Time changes in outer radiation zone of earth, 20: 30214 (NASA-TT-F-389, pp 569-75)
SOWERBY, B. D., Neutron-proton total cross sections near 20, 24, and 28 Mev, 20: 30004
SOWERBY, M. G., Eta and neutron cross sections of ^{235}U from 0.03 to 200 ev, 20: 30342 (AERE-M-1670)
SOWMAN, H. G., Prog. rpt. on fabrication of W alloy tubing, 2–5/66, 20: 29659 (COO-1518-3)
SOZOU, C., Field boundary of two line currents in a plasma at uniform pressure, 20: 30576
SPACU, P., Refractometric investigation on the formation of complex samarium halogenides in aqueous solution, 20: 29204
SPALDING, I. J., Cusp injection experiment, 20: 30644
SPALEK, J., Beta-backscatter techniques for measurement of layer thickness in multilayer coating, 20: 29391
SPARROW, Julian H., Steady-state response of silicon radiation detectors of diffused p-n junction type to x rays. II., 20: 29540
SPEAR, R. H., Proton scattering from ^{27}Al from 3.5 to 11.3 Mev, 20: 30415
SPECTOR, Mozart, Cesium-137 in food, 20: 29475
SPECTOR, Mozart, Strontium-90 in food, 20: 29433
SPEDDING, F. H., Partial molal heat capacities of aqueous rare-earth chloride solutions, 20: 29144 (IS-1355)
SPENCE, N. S., Uranium alloy development for non-nuclear application, 20: 29803
SPENER, G., Spherical pressed-graphite fuel elements for high-temperature reactors, 20: 29669
SPERLICH, Diether, Equilibria for inversions induced by x rays in isogenic strains of Drosophila pseudoobscura, 20: 28956
SPIGT, Cornelis Ludovicus, Hydraulic characteristics of boiling water channel with natural circulation, 20: 29385
SPINELLI, John, Prog. rpt. on application of radiation-pasteurization to Pacific crab and flounder, final, 11/64–10/65, 20: 29583 (TID-22515)
SPINRAD, Bernard I., Reactivity changes with long irradiation, 20: 30900
SPITKOVSKII, D. M., Radiation damages in deoxyribonucleoproteins at molecular and supermolecular levels, 20: 28908
SPITSYN, Vikt. I., Radiation-induced reactions of hydrogen atoms and hydroxyl radicals in aqueous solutions, 20: 29262
SPITZER, Lyman Jr., Controlled nuclear fusion research, Sept. 1965:

review of experimental results, 20: 30605
SPITZIN, V. I., Preparation and properties of anhydrous scandium nitrate and its solvates, 20: 29214
SPRAGUE, Theodore S., Integral boiler reactor, 20: 30913
SPRINGER, K., Beta spectra of ^{42}K, ^{86}Rb, and ^{170}Tm, 20: 30546
SPROUL, James Andrew Jr., Degenerative and aging changes in rats influenced by radiations, 20: 29030
SPRUNG, D. W. L., Binding and saturation of nuclear matter, 20: 30434
SRB, Vladimir, Changes in cellular permeability induced by low-dose x irradiation, 20: 28900
STAAS, F. A., Distribution of direct transport current in sheets of type-II superconductors, 20: 30273
STACH, Vaclav, Xenon stability of a partially divided slab, 20: 30843
STAEHLI, G., Investigations of integral doses in section radiography, 20: 29073
STAFFORD, G. H., Nucleon-nucleon total cross sections from 1.1 to 8 Bev/c, 20: 30028
STAGG, M. S., Annealing studies of boron-doped graphite by electron microscopy and x-ray diffraction, 20: 29625
STAHL, Wolfgang J., Determination of isotope ratios and model ages of Bolivian Andes lead ores, 20: 29439
STAMP, A. P., Strong-coupling approximation for double stripping reactions, 20: 30399
STANTON, H. E., Potential applications of radioisotopes in Navy, 20: 29581 (AD-633785)
STAPLETON, H. J., Apparent lowering of energy levels as measured by Orbach relaxation rates, 20: 30758
STARODUBTSEV, S. V., Double focusing in mass spectrometers with an inhomogeneous magnetic field, 20: 29493
STARODUBTSEV, S. V., E2 transitions from 3^+ level of even-even nuclei, 20: 30372
STARODUBTSEV, S. V., Ion source of hydrogen ions at low gas pressures, 20: 29925
STARYI, I. B., X-ray L_{III} spectra of Gd absorption in hydrides, 20: 29162
STASYUK, Kh. A., Preparation of ion-exchange membrane by pre-irradiation method, 20: 29308
STEBEN, J. D., Polarization in the elastic scattering of protons from carbon and nitrogen, 20: 30457
STECH, Berthold, Theory of weak interactions, 20: 30114
STECKER, F. W., Cosmic black-body radiation, high-energy electrons, and origin of isotropic x-ray and γ radiation, 20: 29958
STEELE, Thomas A., Use of personal monitoring neutron film near 50-Mev injection of, 20: 29523 (CONF-651109, pp 639-46)
STEFAN, Muscalu, Elastic scattering of 14-Mev neutrons by deuterons, 20: 30050
STEFFEN, R. M., Higher-order effects in β-γ correlations involving allowed β transitions, 20: 30470
STEICHELE, E., Moessbauer effect investigation of shell conversion of electron capture, 20: 30555
STEIGERWALD, E. A., Prog. rpt. on long-time creep data on refractory alloys, 12/65–3/66, 20: 29705 (NAS-CR-54973)
STEIN, G., Effect of ionizing radiations on electrophoretic mobility of mammalian cells, 20: 28905
STEINBERG, M., Fission recoil synthesis, 20: 29317
STEINBERGER, J., Further results from interference of K_S and K_L in $\pi^+\pi^-$ decay modes, 20: 30026
STELSON, P. H., Elastic and inelastic proton scattering from ^{106}Pd and ^{108}Pd, 20: 30462
STENFLO, Lennart, Instability of velocity distributions of slightly ionized gases in electric fields, 20: 30581
STEPANOV, K. N., Determination of plasma density distribution by microwave refraction, 20: 30700
STEPANOV, K. N., Theory of decay of EM waves in magnetoactive plasma, 20: 30671
STEPANYAN, E. D., Effect of irradiation on adsorption and antibodies formation by recticular and endothelial systems, 20: 28965
STEPIEN, Kazimierz, X rays in astronomy, 20: 29900
STERN, H., Broken symmetry, sum rules, and collective modes in many-body systems, 20: 30139
STERN, H., Nucleon-antinucleon annihilation in quark model, 20: 30005
STEVENS, C. A., Utility of the statistical treatment of resonance absorption in the unresolved resonance region, 20: 30420
STEVENS, R. R. Jr., Moessbauer effect measurements in first and second excited states of ^{155}Gd, 20: 30422
STEVENSON, C. E., Current practices in handling and storing solid radioactive waste from reactors, 20: 30947
STEVENSON, C. E., Current practices in the disposal of radioactive wastes from operation of uranium mines and mills, 20: 30948
STEVENSON, C. E., Current practices in disposal of waste radioactive gases from reactors, 20: 30949
STEWART, H. F., Availability of fallout ^{137}Cs to dairy cattle from different types of feed, 20: 29463
STEWART, J. D., Definition of neutron diffusion parameters for uniform reactor lattice, 20: 30851
STEWART, W. M., Inelastic α-particle excitation in even tin isotopes, 20: 30468
STICKLER, R., Precipitation hardening Nb–Hf–N alloys, 20: 29759
STIEFEL, U., Thermal investigations on rod-cluster elements, 20: 29382
STIER, Robert, Power supply system for Siemens-Schuckert Research Centre, 20: 29368
STOCKER, W., Modified separation method for nuclear potentials, 20: 30060
STODDART, Hugh F., Radiation source measuring apparatus having automatic background subtract means, 20: 29571
STOELZL, D., Magnetic methods for measuring maximum temperature of irradiated samples, 20: 29387
STOLETOV, V. N., Pigment mutations in Anacystis nidulans, 20: 28958
STOLL, Nancy, Prog. rpt. on application of radiation-pasteurization to Pacific crab and flounder, final, 11/64–10/65, 20: 29583 (TID-22515)
STOLPOVSKII, V. G., Irregular high-energy electron streams near boundary of radiation zones of earth, 20: 30215 (NASA-TT-F-389, pp 576-87)
STOLPOVSKII, V. G., Time changes in outer radiation zone of earth, 20: 30214 (NASA-TT-F-389, pp 569-75)
STOLZENBACH, C. F., Current practices in the disposal of radioactive wastes from operation of uranium mines and mills, 20: 30948
STOLZENBACH, C. F., Current practices in disposal of waste radioactive gases from reactors, 20: 30949
STONE, Leonard R., Nuclear radiation detecting means and transmission system, 20: 29575
STONEHOUSE, A. J., Development of intermetallic compounds for aerospace applications, 20: 29770
STONER, D. R., Prog. rpt. on weldability and elevated-temperature stability of refractory alloys, 6–9/65, 20: 29712 (WANL-PR-(P)-009)
STONER, D. R., Prog. rpt. on weldability and elevated-temperature stability of refractory alloys, 9–12/65, 20: 29713 (WANL-PR-(P)-010)
STOOKSBERRY, Robert W., Zirconium (n,p) cross section measurements, 20: 30418
STORMS, H. A., Independent fission yields of some xenon isotopes, 20: 30533
STOTLAND, M. A., Plasma equilibrium in torus with high-frequency fields and plasma heating resulting from beam of "escaping electrons", 20: 30640
STOTT, P. E., Scattering of microwaves by turbulent plasma, 20: 30658
STOYANOV, D. C., Equations for scattering matrix elements in relativistic three-body problem, 20: 30148
STOYANOV, D. Ts., Dynamical symmetry and hadron mass spectrum, 20: 30091 (JINR-P-2621)
STRAIN, J. E., Use of neutron generators in activation analysis, 20: 29118
STRAKHOV, I. P., Effect of γ-radiation on leathers, 20: 29588
STRAKHOV, I. P., Effect of γ-radiation on physical-mechanical properties of chrome-tanned leather, 20: 29592
STRAKHOV, I. P., The effect of γ-radiation on chrome-tanned shoe upper leather, 20: 29591
STRATHDEE, J., Dynamical origin of SU(6), 20: 30117
STRAUB, W. D., Lorenz number of graphite at low temperatures, 20: 29750
STRECKER, Helmut, Kinetics of homogeneous isotope exchange between isopropyl chloride and chloride ions in dimethylformamide, 20: 29156
STRELKOV, A. S., Fission-generated γ radiation during h-a explosion over Johnston Island, 7/9/62, 20: 30233
STRELKOV, V. S., Joule heating of plasma in toroidal Takamak-3 device, 20: 30650
STREL'TSOV, V. N., Experimental separation of interactions with free protons, 20: 30083
STRELYANOV, N. P., Origin of uranium exogenous deposits and methods for their exploration, 20: 29449
STRICOS, D. P., Procedure for quantitative recovery of ^{233}Pa from irradiated thoria, 20: 29331 (KAPL-M-6554)
STRINGER, T. E., Unified approach to resistive and microinstabilities, 20: 30626
STRITTMATTER, J. A., Automatic control of rod position with boron in a chemical shim nuclear plant, 20: 30808 (WCAP-3269-54)
STRIZHOV, V. P., Use of standard in solid phase for quantitative argon determination by method of isotope dilution, 20: 29102
STROMBERG, Thorsten Frederick, Superconducting properties of high-purity Nb, 20: 30315
STROMME, Aksel, Cesium-137 in milk, meat, and man in Norway, 20: 29432
STRONGIN, Myron, Susceptibility transition (a-c) in type-II superconductors and surface critical currents, 20: 30293
STRUB, R., Interference effects between N*(1236) and K*(891) production, 20: 30009
STRYCKMANS, P. A., Extracorporeal irradiation of blood, 20: 28927 (BNL-9647)
STRZALKOWSKI, A., Model of excited core of the nucleus, 20: 30484
STRZALKOWSKI, A., $^{40}Ca(d,d)$, (d,d'), and (d,p) with 12.8-Mev deuterons, 20: 30459

STRZYZEWSKA, Bozena, Determination of small concentrations of lanthanum and neodymium in pure cerium oxide, 20: 29095
STUART, Bruce Owen, Radioprotection of Saccharomyces cerevisiae by cystamine, 20: 29023
STURGES, D. J., Hollow-cathode glow discharge in hydrogen and noble gases, 20: 30173
SUBBOTINA, E. A., Thermal disintegration of nitrates of cerium, neodymium, and gadolinium, 20: 29224
SUDAN, R. N., Exact nonlinear electromagnetic whistler modes, 20: 29899
SUDARSHAN, E. C. G., Current algebras and generalized Ward-Takahashi identities, 20: 30006
SUDARSHAN, E. C. G., Parity-violating nonleptonic decay and Cabibbo current, 20: 30041
SUESS, Hans E., Theory of origin of atomic nuclei of our solar system, 20: 29909
SUFFREDINI, C. S., Range of photoparticle recoil atoms in solids, 20: 30479
SUGAR, Robert, Dispersion relations for three-particle scattering amplitudes. I., 20: 30132
SUGAWARA, Tadashi, Low temperature resistivity, magnetic susceptibility, and superconducting transition temperature in La, 20: 29753
SUGIHARA, Ko, Galvanomagnetic properties of graphite at low temperatures, 20: 29751
SUGIHARA, Ryo, Transmission and absorption of electromagnetic waves in collisionless plasma slab, 20: 30588
SUGIMOTO, Emiko, Practical applications of glass dosimetry, 20: 29547
SUGITA, Tohru, Gamma spectra of fission products observed with lithium-drifted germanium detectors, 20: 30379
SUGIYAMA, Masataka, Influence of TiC on some properties of sintered WC–Co alloys, 20: 29779
SUGIYAMA, Masataka, Properties of sintered WC–Co alloys, 20: 29778
SUGIYAMA, Masataka, Properties of sintered WC–10% Co alloy in relation to particle size and composition of binder-phase, 20: 29780
SUGIYAMA, Masataka, Properties of high-zirconium wrought copper base alloys, 20: 29782
SUITA, Tokuo, Ambipolar potential in magnetoactive cold plasma, 20: 29978
SUITA, Tokuo, Charge exchange loss of high-temperature plasma confined by mirror magnetic field, 20: 30584
SUITA, Tokuo, Utilizing r-f field for injection trapping of high-energy ions in mirror fields. I., 20: 30580
SUITER, J., Observations of dislocations in high-angle boundaries in tungsten, 20: 29725
SUKHANOV, A. D., S-matrix in Heisenberg's representation, 20: 30104
SULCEK, Z., Silica gel in separation of Th from Zr, 20: 29344
SULLIVAN, A. H., Health physics survey methods for measurement of stray radiation around CERN high-energy accelerators, 20: 29844 (CONF-651109, pp 103-16)
SULLIVAN, H. F., Prog. rpt. on combustion of metals, annual, 7/64–6/65, 20: 29641 (SC-DC-65-1691)
SULTANGAZIN, U. M., Application of the decomposition method to radiation transfer equations, 20: 30063
SUMAROKOVA, N. V., Kinetics of combined carbothermal reduction of niobium and tungsten, 20: 29677
SUN, Chia-chung, Ligand field theory. I., 20: 29205
SUND, R. E., Gamma rays from short-lived fission-fragment isomers, 20: 30463
SURA, J., Phase motion of protons in proton linear accelerator with perturbed axial field, 20: 29852 (INR-640/SLBAL/E)
SUROV, L. M., Cross sections for production of γ-quanta in inelastic interactions of 14-Mev neutrons with C, O, Al, Fe, and Pb, 20: 30498
SUSLOV, A. A., Cosmic ray nuclear component on Elektron-2, 20: 29957 (NASA-TT-F-389, pp 693-710)
SUTHERLAND, D. G., M1 photo-excitation N → N* and SU(6) symmetry, 20: 30043
SUTTON, C. Roger, Effect of hydriding on Zircaloy properties, 20: 30902
SUWALSKI, W., Multiplication method of reactivity measurements, 20: 30849
SUZUKI, Hisashi, Influence of TiC on some properties of sintered WC–Co alloys, 20: 29779
SUZUKI, Hisashi, Properties of sintered WC–Co alloys, 20: 29778
SUZUKI, Hisashi, Properties of sintered WC–10% Co alloy in relation to particle size and composition of binder-phase, 20: 29780
SUZUKI, Hisashi, Properties of high-zirconium wrought copper base alloys, 20: 29782
SUZUKI, Nobutake, Thermal and radiation oxidations of benzene to phenol in aqueous solutions containing metal ions. VII., 20: 29250
SUZUKI, Nobutake, Transfer of oxygen atom of water in aqueous solution of iron and copper sulfates, 20: 29153
SUZUKI, Shin, Chemistry of Pa. I., 20: 29335
SVERDLIN, A. S., Heat of formation of gaseous uranium fluorides, 20: 29171
SVIDSKII, P. M., Radiation intensity in earths radiation belts, 20: 30225
SVIDSKII, P. M., Recording cosmic rays on Cosmos-17 satellite, 20: 29966
SWAIN, Robert W., Radiotherapeutic effects on mammalian tumor cells. I., 20: 28962
SWALLOW, A. J., Novel valence states of thallium as studied by pulse radiolysis, 20: 29271
SWAMI, Jnanananda, Absolute photoelectric cross sections of 320 kev gamma rays, 20: 29924
SWANK, L. J., Unsubtracted dispersion relations in weak interactions and unitary symmetry, 20: 30134
SWANSON, B. S., Densities and critical properties of alkali metals, 20: 29742
SWARTZ, M., Plasma confinement, heating, and losses in Pharos with an extended current pulse, 20: 30612
SWARTZ, P. S., Effect of thermal-neutron irradiation on superconducting properties of Nb_3Al and V_3Si doped with fissionable impurities, 20: 30260
SWEETMAN, D. R., Plasma produced by neutral injection into magnetic mirror/well geometry, 20: 30632
SWENSON, L. W., Proton spectra from reactions induced by 30.5-Mev α particles, 20: 30472
SWIECA, Andre, Conserved currents and associated symmetries; Goldstone's theorem, 20: 30101
SYMONS, M. C. R., Pairwise trapping in γ-irradiated sodium nitroprusside, 20: 29280
SYROS, Constantin, Solution (P_1) of transport equation for thermal neutrons, 20: 30328
SYROVATSKII, S. I., Dynamic dissipation of magnetic energy near a neutral magnetic field line, 20: 30676
SYROVATSKII, S. I., Primary cosmic-ray research, 20: 29954 (NASA-TT-F-389, pp 657-77)
SZECHTER, A., Improved method for prompt-neutron-period measurements, 20: 30848
SZEKELY, Zoltan, Spectrophotometric study of uranyl nitrate-salicylaldoxime system, 20: 29202
SZIRMAI, E., Acute radiation effects: damage of hematopoiesis, 20: 28981
SZIRMAI, E., Chronic radiation effects: damage of hematopoiesis, 20: 28984
SZIRMAI, E., Effect of irradiation on immunity, 20: 28983
SZIRMAI, E., Effects of radiations on coagulation of blood, 20: 28985
SZIRMAI, E., Nuclear hematology, 20: 28874
SZIRMAI, E., Nuclear hematology: based on experience with atomic explosions, 20: 28876
SZIRMAI, E., Nuclear hematology and blood transfusion, 20: 28893
SZIRMAI, E., Problems of bone marrow transplantation in radiation damage, 20: 28875
SZIRMAI, E., Total-body irradiation injury: disorders of blood and hematopoietic tissues, 20: 28982

T

TACHIKAWA, Kyoji, Multilayer Nb–Sn superconducting wire, 20: 29781
TACHON, J., Heating and containment of plasma in the magnetic well in Deca II, 20: 30607
TAGUCHI, Shigetoshi, Effect of radiations on propagation of root-knot nematodes, Meloidogyne incognita Chitwood, 20: 28942
TAI, Shu-shan, Ligand field theory. I., 20: 29205
TAJIRI, Masayoshi, Propagation of hydromagnetic waves in collisionless plasma. I., 20: 30586
TAKAAI, Tetsuya, Electron-beam melting of refractory metals. IV., 20: 29674
TAKAAI, Tetsuya, Electron-beam melting of refractory metals. V., 20: 29783
TAKAHASHI, Isao, Analysis of negative absorption of plasma-cavity system, 20: 30587
TAKAHASHI, Shuichiro, Effect of void volume variation on pressure buildup in vibratory-compacted UO_2 fuel element, 20: 29818
TAKAHASHI, Shuichiro, Microhardness and plastic deformation of uranium dioxide, 20: 29786
TAKAO, Zenichiro, Spectrochemical analysis of Zr and its alloys. II., 20: 29114
TAKAYANAGI, Sei-ichi, Gamma spectra of fission products observed with lithium-drifted germanium detectors, 20: 30379
TAKEDA, Gyo, Algebra and symmetries, 20: 30110
TAKEDA, Gyo, Bootstrapping with the Regge boundary condition, 20: 30066
TAKEDA, Gyo, High-energy behavior of forward scattering amplitude, 20: 30109
TAKEDA, Gyo, Lectures in theoretical physics. II., 20: 30064
TAKEDA, Gyo, Mass formulae in SU(3) and SU(6), 20: 30111
TAKEDA, Gyo, Nuclear democracy, Regge poles and analytic S-matrix, 20: 30065
TAKEDA, Gyo, Present status of weak interactions, 20: 30067
TAKEDA, Tatsuoki, Momentum compaction in a cyclic accelerator, 20: 29861

TAKETANI, Kiyoaki, Behavior of crystals and voids in centrally heated UO_2 green pellets, 20: 29776
TAKEUCHI, Kiyoshi, Numerical integration of the neutron transport equation in slab geometry, 20: 30326
TAKHTAMYSHEV, G. G., Decay ($K_2^0 \rightarrow \pi^+\pi^-$) probability in sloped K_2^0-meson beam, 20: 30056
TAKIBAEV, Zh. S., Disintegration with emission of fast He nuclei due to high-energy protons, 20: 30496
TAL'ROZE, V. L., Effect of an electric field on liquid-hydrocarbon radiolysis, 20: 29263
TAMBASCO, Daniel James, Crossing relations and prediction of symmetries, 20: 30159
TAMURA, Hideo, Preparation of Th carbides, 20: 29676
TAMURA, Tsuneo, Development and applications of minerals in radioactive waste disposal, 20: 29332 (ORNL-P-1811)
TANAKA, Mitsuo, Superconducting Nb–10Zr alloy, 20: 29789
TANG, Au-chin, Ligand field theory. I., 20: 29205
TANG, C. H., Electromagnetic cavity resonances in accelerated systems, 20: 29831
TANG, L. H., Effects of lattice vibrations on angular correlations, 20: 30762
TANIUTI, Tosiyo, Nonlinear motion of ion streams in a background of high-temperature electrons, 20: 30585
TANIUTI, Tosiyo, Propagation of hydromagnetic waves in collisionless plasma. I., 20: 30586
TANNENBAUM, M. J., Further results from interference of K_S and K_L in $\pi^+\pi^-$ decay modes, 20: 30026
TANOVA, L. A., Effects of γ- and ultraviolet rays on copper glycocol, 20: 29303
TAO, S. J., Positron annihilation in materials under ionizing radiation, 20: 29268
TAPPER, R. J., Nucleon-nucleon total cross sections from 1.1 to 8 Bev/c, 20: 30028
TARANTIN, N. I., Magnetic spectrometer with field alterations, 20: 29558
TARASENKO, A. G., Temperature effect on cysteamine accumulation in cells and its radioprotecting activity, 20: 29057
TARASENKO, V. F., Heating of dense plasma in a metallic chamber, 20: 30664
TARASOVA, Z. N., Radical formation in radiolysis of hard rubber, 20: 29299
TARDY-JOUBERT, Ph., Methods and experience acquired in dosimetry at Saturne synchrotron, 20: 29845 (CONF-651109, pp 117-42)
TARLOV, Alvin R., High-dose human exposure from 10-Mev linear accelerator, 20: 28929 (CONF-651109, pp 574-98)
TARREGA, P., Interactions of 12.8-Bev protons in nuclear emulsions. III., 20: 30364
TATARU, Sever, Influence of certain ions on adsorption of U by ion exchange resins, 20: 29350
TAURIT, Rudolf, KRB Gundremmingen nuclear power station, 20: 30888
TAUSHKANOV, V. P., Effects of porous structure of lignin carbons on uranium sorption, 20: 29360
TAVKHELIDZE, A. N., Leptonic decays of baryons in universal V-A theory, 20: 30058
TAYLOR, C. D., Signal produced in monopole antenna by gamma flux from nuclear explosion, 20: 29580
TAYLOR, Denis, Measuring density with nuclear back-scatter method, 20: 29594
TAYLOR, J. C., Crystal structure of thorium nitrate pentahydrate by neutron diffraction, 20: 29151
TAYLOR, Kenneth M., Refractory bodies and method of making same, 20: 29695
TEIGER, J., Search for an isobar of isotopic spin $T = 3/2$, 20: 30022
TEL'TSOV, M. V., Inner and artificial radiation zones of earth at low altitudes, 20: 30217 (NASA-TT-F-389, pp 607-15)
TEL'TSOV, M. V., Measurement results on Kosmos-41 in outer radiation zone, 20: 30219 (NASA-TT-F-389, pp 623-9)
TELYUKOVA, T. M., Properties of objects produced from lanthanum and yttrium hexaborides by sintering in vacuum, 20: 29738
TEMNYI, V. V., Corpuscle investigations on Elektron-1, 20: 30212 (NASA-TT-F-389, pp 551-66)
TEMNYI, V. V., Spatial distribution of trapped corpuscles based on data from "Kosmos-2" and "Kosmos-5", 20: 30202 (NASA-TT-F-389, pp 281-7)
TEMPLETON, David H., Crystal structure of thorium nitrate pentahydrate by x-ray diffraction, 20: 29150
TENG, Po, Microdetermination of rare earths in uranium compounds by a spectrographic method, 20: 29129
TENYAKOVA, N., Electron-positron pair production during scattering of gamma quanta in nuclear field, 20: 29996
TEPLOV, I. B., Elastic and inelastic scattering of α particles by C, 20: 30499
TEPPER, F., Mechanical properties tests of 316 SS specimens in 1200°F Na contaminated with O, 20: 29704 (MSAR-66-78)
TERAKAWA, Akira, Radiation-induced addition of hydrogen chloride to ethylene, 20: 29252
TERENT'EV, I. A., Symmetry of elementary particles in nonuniform group theory, 20: 30106
TERESI, J. D., Estimate of effects of fallout beta radiation on insects and associated invertebrates, 20: 28925 (AD-633024)
TERUMICHI, Yasushi, Analysis of negative absorption of plasma-cavity system, 20: 30587
TESTA, Frank J., Reaction of U with water as initiated by power excursion in TREAT, 20: 30802
TETERIN, E. G., Extraction properties of organic compounds. II., 20: 29347
TETERINA, V. I., Reactions of hematopoietic system in guinea pigs to effects of radiation in small doses, 20: 28945
TEVIKYAN, R. V., Quantum theory of particle with electric and magnetic charge, 20: 30153
THEIMER, O., Potential of average force in plasma, 20: 30599
THOMAS, Bruce Robert, Threshold behavior in N/D calculations without arbitrary parameters, 20: 30158
THOMPSON, David H., Vapor traps protect liquid-metal systems, 20: 30814
THOMPSON, J. C. Jr., Variability of fluid milk consumption and relationship to radionuclide intake, 20: 29474
THOMPSON, M. A., Strangeness-one resonances, 20: 30049
THOMPSON, Theos J., Prog. rpt. on neutron and gamma-ray spectroscopy and activation analysis, final, 1/61–1/66, 20: 29078 (AD-633252)
THORN, James Douglas, Moderator structures for nuclear reactors, 20: 30823
THORNE, Kip Stephen, Geometrodynamics of cylindrical systems, 20: 30251
THURBER, James K., Mathematical aspects of kinetic model equations, 20: 30165 (BNL-9254)
THURLBECK, Arthur, Improvements in or relating to temperature recorders, 20: 29514
THYS, W., Influence of neutron irradiation on superconductive properties of Sn and In foils, 20: 30301
TIDMAN, Derek A., Damping of interstellar plasma waves by cosmic-ray gas, 20: 29959
TIETZ, T., Low energy electron-atom scattering cross section in Thomas-Fermi theory, 20: 29946
TIKTOPOULOS, George, Dispersion relations for three-particle scattering amplitudes. I., 20: 30132
TILLER, Hans, Total cross sections of Gd for fast neutrons, 20: 30419
TIMM, U., Polarization of 6-Bev bremsstrahlung from Hamburg electron synchrotron, 20: 30045
TINDO, I. P., Measurement of solar x-ray radiation intensity by Elektron-2, 20: 29874 (NASA-TT-F-389, pp 714-31)
TINDO, I. P., Transient increases of flux of heavy nuclei accompanied by bursts of x radiation, 20: 29965
TINNIS, Walentin, Detection and measurement of radioactivity in pulp, 20: 29427
TISCHER, P., Release of stored energy and electric resistivity changes in neutron-irradiated Cu, 20: 29824
TISHCHENKO, M. A., 1,10-Phenanthrolinethenoyltrifluoroacetone complexes of rare earth elements, 20: 29221
TITOVA, N. S., Disintegration with emission of fast He nuclei due to high-energy protons, 20: 30496
TITTEL, K., Further results from interference of K_S and K_L in $\pi^+\pi^-$ decay modes, 20: 30026
TIUNOV, L. A., Endogenous formation of carbon monoxide, 20: 28880
TKACHEV, L. G., Current-generated algebras and form factors, 20: 30146
TOBIAS, Cornelius A., Fluctuations of energy loss in semiconductor detectors, 20: 29531 (UCRL-16715)
TODOROV, I. T., Dynamical symmetry and hadron mass spectrum, 20: 30091 (JINR-P-2621)
TODOROVIC, J., Neutron investigation of temperature effects in magnon spectrum of magnetite, 20: 30765
TOEI, Kyoji, Spectrophotometric determination of F with a PAC-Th complex, 20: 29091
TOELGYESSY, J., Analysis of chromic salt solutions by means of β-ray backscattering, 20: 29107
TOIVANEN, Timo, Self-adjoint variational principle for deriving vacuum and interface boundary conditions in spherical harmonics method, 20: 30332
TOKAREVSKII, V. V., Cross section for elastic scattering of 13.6-Mev deuterons by Ti, Fe, and Co, 20: 30497
TOKARSKAYA, V. I., Effect of fast neutrons on DNA synthesis in seedlings, 20: 28989
TOLLET, Louis H. J., Reactor reactivity control, 20: 30867
TOLLET, Louis H. J., Reactor fuel-control rod assembly, 20: 30873
TOLMACHEVA, V. D., Pressure and composition of saturated vapor in NaCl–$LaCl_3$ system, 20: 29227
TOLOK, V. T., Heating of dense plasma in a metallic chamber, 20: 30664
TOMITA, Isao, Isotope effect in electromigration of sodium ions in fused sodium nitrate, 20: 29185

TOMKUS, I., Multipurpose relaxation apparatus for measuring signs of elementary processes in ionic crystals subjected to ionizing radiation, 20: 30754

TOMPKINS, Donald R., Equivalent representations in symmetrized tensors, 20: 30142

TONELLATO, Umberto, Racemization and isotopic exchange with $Na^{35}SCN$ of 4-chlorobenzhydryl thiocyanate, 20: 29237

TONGIORGI, E., Ionium/U method for the determination of the age of recent minerals, 20: 29441

TOOR, A., X-ray spectra from three cosmic sources, 20: 29901

TOPCHIEVA, K. V., Chemisorption of ethylene on yttrium oxide, 20: 29186

TORGOV, V. G., Solvent extraction of products of uranyl nitrate hydrolysis by alpha-n-amylpyridine-N-oxide, 20: 29359

TORIKAI, Ayako, Radiation-induced cis-trans isomerization of stilbene in methanol solution, 20: 29287

TORIYAMA, Kazumi, Free radicals produced by irradiation. II., 20: 29282

TOROPTSEV, I. V., Reactions of hematopoietic system in guinea pigs to effects of radiation in small doses, 20: 28945

TORRENS, Ian McC., Ionic displacement in alkali halides, 20: 30741

TORTI, M. L., Properties, availability, and applications of Ta-base alloys, 20: 29760

TOWER, Stephen N., Integral vapor generating and superheating reactor system, 20: 30919

TRAEGER, Richard Kieth, Effects of gamma radiation on viscoelastic properties of polymers, 20: 29313

TRESVYATSKII, S. G., Phase diagram of system Sc_2O_3–Cr_2O_3, 20: 29167

TRET'YAKOV, O. A., Radiation from electrons moving parallel to metal grid located on edge of uniaxial crystal of finite thickness, 20: 29995

TRET'YAKOV, O. A., Radiation of electromagnetic waves by electron sheet moving above diffraction grating, 20: 30250

TREYTL, W. J., Reactions (p,n) between 100 and 400 Mev, 20: 30464

TRIPATHY, Kishor C., Radiative decays of bosons and $SU(6)_w$ symmetry, 20: 30040

TRIVELPIECE, A. W., Scattering of laser beam by hot electron plasma, 20: 30716

TRKA, Z., Experimental separation of interactions with free protons, 20: 30083

TROITSKII, N. A., Mutagenic efficiency of intermediate neutrons, 20: 29002

TRUNOV, V. K., Binary uranium and molybdenum oxides, 20: 29798

TRUNOV, V. K., New double oxides of uranium and tungsten, 20: 29170

TS'AI, Ch'i-hsiu, Chromatographic analysis and liquid-liquid extraction, 20: 29355

TSARAPKIN, L. S., Recovery of cells from primary cytogenetic injuries, 20: 29049

TSAROW, G. L., Effect of interstitial impurities on structure and properties of W single crystals, 20: 29793

TSEITLIN, P. I., Radiation damages in deoxyribonucleoproteins at molecular and supermolecular levels, 20: 28908

TSELISHCHEV, S. P., Effect of γ-rays from ^{60}Co on certain metabolic processes in pea plants, 20: 28909

TSEL'NIK, F. A., Plasma with relativistic electrons in magnetic mirror trap, 20: 30638

TSETSKHLADZE, T. V., Kinetics of radiation-induced isotope exchange between deuterium and silica gel hydroxyl groups, 20: 29276

TSEVELEV, M. A., Deposition of atmospheric fallout by precipitation in subcloud layer, 20: 29416

TSIEN, K. C., Dose distributions in ^{60}Co planar rotation, 20: 29061

TSINGISTER, V. A., Inhibiting effects of solid impurities on radiation chemistry processes, 20: 29306

TSIONSKII, V. M., Tritium content in atmospheric fallout over Moscow during 1962–1963, 20: 29409

TSUBOTA, Hiroyuki, Concentration of radionuclides in sea water by metal sulfide-ion exchange resins, 20: 29345

TSUJINO, Takeshi, Radiation damage to TBP-kerosene solvent. II., 20: 29272

TSUKROVITZ, A., Energy levels of ^{63}Zn, 20: 30406

TSYRAN, N. I., Thermal and anaphylactoid edema in acute radiation sickness, 20: 29001

T'U, T'ung-yuan, Syntheses of isotopically labeled compounds. III., 20: 29246

TUBIANA, M., Relative biological efficiency of a beam of 20-Mev electrons as function of depth, 20: 28963

TUCHSCHEERER, T., Activation during radiation conservation of food, 20: 29599

TUCKFIELD, R. Jr., Plasma guiding by means of multipole fields, 20: 30579

TUDOR, Lucio, Radiolysis of acetylene in solution. III., 20: 29293

TUKEY, H. B. Jr., Prog. rpt. on loss of materials from above-ground plant parts with special reference to decontamination, 1965–66, 20: 29451 (NYO-2598-29)

TULINOV, A. F., Elastic and inelastic scattering of α particles by C, 20: 30499

TULINOVA, N. I., Capture of electrons into betatron orbits, 20: 29869

TULLY, G. R. Jr., Irradiation of graphite impregnated with furfuryl alcohol, 20: 29813

TUMANOV, G. V., Therapeutic effectiveness of antibiotics on cystaine action during radiation sickness, 20: 29051

TUMANYAN, M. A., Secondary disease in irradiated animals treated with bone marrow, 20: 29006

TUNG, Hui-chen, Syntheses of isotopically labeled compounds. III., 20: 29246

TUNG, Shaohua, Radiophosphorus in treatment of certain skin diseases, 20: 29072

TURKIEWICZ, J., Energy levels of ^8Be from $^{11}B(n,\alpha)^8Li \rightarrow {}^8Be$ process, 20: 30363

TURNBULL, J. A., Annealing studies of boron-doped graphite by electron microscopy and x-ray diffraction, 20: 29625

TURUSOV, V. S., Effects of β irradiation of skin on cancerogenesis caused by 7,12-dimethylbenz-a-anthracene, 20: 28973

TVERSKAYA, L. V., Earth's outer radiation zone at low altitudes, 20: 30216 (NASA-TT-F-389, pp 588-606)

TVERSKOY, B. A., Anomalous diffusion of charged particles in radiation zones of earth, 20: 30206 (NASA-TT-F-389, pp 426-42)

TYLER, Lynn D., Solutions of the flow field produced by shock wave emerging into crossflow, 20: 30167 (SC-DC-65-1916)

TYLKINA, M. A., Laves phases in systems containing Re and rare-earth metals, 20: 29792

U

U, Raymond, Adenosine triphosphate: protection against radiation-induced chromosome loss in Drosophila, 20: 29046

UEBING, D., Materials for reactor pressure vessels, 20: 30894

UEHARA, Sigeaki, Electron-beam refining of niobium, 20: 29634

UEKI, Tatzuo, Crystal structure of thorium nitrate pentahydrate by x-ray diffraction, 20: 29150

UEMURA, Teiji, Measurement of α particles by use of a p-n junction semiconductor detector, 20: 29552

UHER, M., Analysis of chromic salt solutions by means of β-ray back-scattering, 20: 29107

UHLIR, M., Current-generated algebras and form factors, 20: 30146

UL'BERG, Z. R., Effects of γ radiation on structure of epoxy resins and resin-base metallic polymers, 20: 29296

UL'BERG, Z. R., X-ray study of epoxido-dianic ED-5 resin irradiated with ^{60}Co and metallopolymers on its base, 20: 29297

ULBRICH, Carlton Wilbur, Theory of superconductive energy gap and thermal conductivity of impure Sn, 20: 30314

ULLMAIER, H. A., Influence of surface currents on alternating-current loss of hard superconductors, 20: 30280

ULRICH, M., Isar I: fast negajoule theta-pinch experiment with extremely high compression fields, 20: 30611

ULYBIN, S. A., Nuclear power reactor coolants, 20: 30910

UMEDA, Keiji, Radiation preservation of fruits and vegetables, 20: 29997

UMEDA, Taketeru, Properties of sintered WC–10% Co alloy in relation to particle size and composition of binder-phase, 20: 29780

UMEZAWA, Tadashi, Studies of hard superconductors. I., 20: 29784

UMEZAWA, Tadashi, Studies of hard superconductors. II., 20: 29785

UMEZAWA, Tadashi, Studies of hard superconductors. III., 20: 29787

UMEZAWA, Tadashi, Studies of hard superconductors. IV., 20: 29788

UNZ, H., Coupled wave equations for homogeneous gyrotropic compressible warm plasmas, 20: 30602

UNZ, H., Wave equations for inhomogeneous gyrotropic hot plasmas, 20: 30603

UPADHYAY, S. R., Kinetics of annealing in irradiated barium nitrate, 20: 29814

URAKUBO, Goro, Radiochemical tests of industrial waste water. I., 20: 29099

URAY, Ildiko, Decontamination of waters containing ^{90}Sr and ^{90}Y with gypsum and bentonites, 20: 29348

URCH, D. S., Role of scavengers in gas-phase recoil tritium reactions, 20: 29206

URZHENKO, A. V., Mutagenic action of extracts from various organs of irradiated mice, 20: 28959

USAKOVSKAYA, T. S., Radiation damages in deoxyribonucleoproteins at molecular and supermolecular levels, 20: 28908

V

VAGI, J. J., Joining of nickel and nickel-base alloys, 20: 29666 (RSIC-484)

VAIL, Charles R., Prog. rpt. on superconducting circuitry, 5/66, 20: 30255 (ORO-2430-28)

VAINSHTEIN, A. I., Check on T invariance in $\pi^+ \rightarrow e^+ + \nu + \gamma$ decay, 20: 29997

VAINSHTEIN, E. E., X-ray L_{III} spectra of Gd absorption in hydrides, 20: 29162
VAKULOV, P. V., Geometric position and particle composition of radiation zones of earth, 20: 30211 (NASA-TT-F-389, pp 535-50)
VAKULOV, P. V., Influence of satellites on radiation intensity in radiation zones, 20: 30223 (NASA-TT-F-389, pp 817-21)
VAKULOV, P. V., Irregular high-energy electron streams near boundary of radiation zones of earth, 20: 30215 (NASA-TT-F-389, pp 576-87)
VAKULOV, P. V., Primary cosmic radiation on Elektron-2 and Elektron-4, 20: 29955 (NASA-TT-F-389, pp 678-83)
VALCKX, F. P. G., Injection of ions into a magnetic mirror machine (M.N.I.), 20: 30634
VALDERAS, Ramon, Evaluation of number of free radicals produced in irradiated rat bone, 20: 28898 (CEA-R-2910)
VALDERAS, Ramon, Production of long-lived free radicals by irradiation in bones of rat, 20: 28906
VALLARIO, Edward J., Why and how of nuclear accident dosimetry, 20: 29469
VALTONEN, E. J., The effect of erythemal reaction caused by ultraviolet irradiation on mast cell degranulation in the skin, 20: 28937
VAN AUDEKERCKE, R., EPR in neutron-irradiated DPPH, 20: 29289
VANDEN BOUT, Paul Adian, Hyperfine-structure anomalies of ^{198}Au and ^{199}Au, 20: 30359 (UCRL-16757)
VAN DER LINDE, H. J., Yields and rate constants of precursors of hydrogen in radiolysis of n-propanol, 20: 29286
VAN DER MEER, S., Capacitor bank (150-kj) for magnetic horn, 20: 29840 (CERN-66-16)
VAN DYK, G., Resonant electron capture in small-angle collisions of Ar^+ on Ar and Ne^+ on Ne, 20: 29944
VAN HOVE, L., S-matrix at very high energy, 20: 30108
VAN ITTERBEEK, A., EPR in neutron-irradiated DPPH, 20: 29289
VAN ITTERBEEK, A., Influence of neutron irradiation on superconductive properties of Sn and In foils, 20: 30301
VAN LINT, V. A. J., Range of photoparticle recoil atoms in solids, 20: 30479
VAN OOSTRUM, K. J., Structure of the α particle from elastic electron scattering, 20: 30439
VAN POUCKE, L., Influence of neutron irradiation on superconductive properties of Sn and In foils, 20: 30301
VAN ROSSUM, L., Search for an isobar of isotopic spin $T = 5/2$, 20: 30022
VAN ROTTERDAM, C., Genetic recombination of bacteriophage $\Phi \times 174$ in spheroplasts, 20: 28948
VAN STEVENINCK, J., Influence of metal ions on hydrolysis of polyphosphates, 20: 29152
VAN THIEL, M., Shock compression of Ar, 20: 30170 (UCRL-14251)
VAN WELY, F. E., High-energy-rate forming of molybdenum, 20: 29758
VAN WYK, Justus M., Study of macroscopic distribution of O in steel rod by neutron-activation and vacuum-fusion techniques, 20: 29088
VANYUKOV, M. P., Use of laser operating in spike mode to obtain high-temperature plasma, 20: 30590
VARFOLOMEEV, A. A., Induced scattering of photons on photons, 20: 30062
VARMA, Man Mohan, Determination of asphalt contents in a paving mixture by thermal neutrons, 20: 29509
VARMA, N. L., Electromagnetic waves in plasma, 20: 30571
VARMA, N. L., Theory of transverse waves in plasma, 20: 30569
VARMA, Ram Kumar, Flute instability in mirror machines in various density regimes, 20: 30707
VASAVADA, Kashyap, Partial-wave dispersion relations for pionic disintegration of deuteron, 20: 30074
VASIL'EV, A. N., Violation of symmetry in Wightman axiomatic scheme, 20: 30154
VASIL'EV, R. P., Production of a hot plasma in Ogra-II by injection of fast H atoms into magnetic trap, 20: 30633
VASILOVA, R. N., Cosmic rays during flights of spacecrafts-satellites and Kosmos, 20: 29956 (NASA-TT-F-389, pp 684-91)
VAS'KOV, V. V., Perturbation of density of charged particles from body moving in plasma in presence of magnetic field, 20: 30675
VASVARI, G., Testing of a drilled-hole scintillometer embedded in plastic, 20: 29546
VASYUTINSKAYA, E. M., Change in the activity of glucosophosphate-isomerase and aldolase under effect of a radiomimetic nembutal preparation, 20: 29048
VAYSBERG, O. L., Corpuscle investigations on Elektron-1, 20: 30212 (NASA-TT-F-389, pp 551-66)
VAYSBERG, O. L., One anomaly in electron pitch distributions, 20: 30200 (NASA-TT-F-389, pp 273-6)
VDOVENKO, V. M., Activity coefficients in multicomponent systems. III., 20: 29196
VEDRINSKII, R. V., Interactions of light hypernuclei and Λ particles, 20: 30503
VEEN, Hans Herbert, Thorium-230/^{238}U and ^{234}U/^{238}U ages of elevated pleistocene coral reefs, 20: 29435
VENET, P., Manufacture of nuclear reactor fuel elements and their coating with pyrolytic carbon, 20: 29670
VERBRAAK, C. A., High-energy-rate forming of molybdenum, 20: 29758
VERDAN, G., NEUTOF: program to correct neutron time-of-flight spectra, 20: 30344 (EUR-2779.e)
VERENIKIN, V. B., Cerium nitrilotriacetates, 20: 29228
VERENIKIN, V. B., Complex formation of rare earths with EDTA, 20: 29222
VERES, A., Detection of ^{113}Cd isomer by means of γ radiation from ^{60}Co, 20: 30489
VERESHCHAGIN, A. N., Cross section for elastic scattering of 13.6-Mev deuterons by Ti, Fe, and Co, 20: 30497
VERNOV, S. N., Earth's outer radiation zone at low altitudes, 20: 30216 (NASA-TT-F-389, pp 588-606)
VERNOV, S. N., Geometric position and particle composition of radiation zones of earth, 20: 30211 (NASA-TT-F-389, pp 535-50)
VERNOV, S. N., Irregular high-energy electron streams near boundary of radiation zones of earth, 20: 30215 (NASA-TT-F-389, pp 576-87)
VERNOV, S. N., Measurement results on Kosmos-41 in outer radiation zone, 20: 30219 (NASA-TT-F-389, pp 623-9)
VERNOV, S. N., Outer radiation zone of the earth and burst of x-ray radiation in the stratosphere, 20: 30218 (NASA-TT-F-389, pp 616-23)
VERNOV, S. N., Primary cosmic radiation on Elektron-2 and Elektron-4, 20: 29955 (NASA-TT-F-389, pp 678-83)
VERNOV, S. N., Recording charged particles with energy of 0.1 to 10 kev with spherical electrostatic analyzer, 20: 29532 (NASA-TT-F-389, pp 518-25)
VERNOV, S. N., State of and prospects for studying the radiation zones of the earth, 20: 30204 (NASA-TT-F-389, pp 375-86)
VERNOV, Yu. S., Ratio of real and imaginary parts of p-d and $\bar{p}$-d scattering amplitudes, 20: 30051
VERON, D., Characteristics and purification of plasma produced by coaxial gun with annular preionization, 20: 30648
VERON, D., Heating and containment of plasma in the magnetic well in Deca II, 20: 30607
VERSHININ, V. G., Cross sections for production of γ-quanta in inelastic interactions of 14-Mev neutrons with C, O, Al, Fe, and Pb, 20: 30498
VETLITSKY, I. A., Boson resonance at 1.63 Bev in π^-p interactions, 20: 30021
VEVERIS, O., Ionizing gamma-defectoscopy for lead containers, 20: 29388
VICTOR, G. A., Long-range three-body forces between helium and hydrogen atoms, 20: 29933
VIGNOS, J. H., Ultrasonic attenuation in liquid ^{4}He at low temperatures, 20: 30299
VIGNOS, James H., Sound measurements in liquid and solid ^{3}He, ^{4}He, and ^{3}He–^{4}He mixtures, 20: 30288
VIJAYARAGHAVAN, R., Nuclear magnetic resonance in rare earth fluorides, 20: 30755
VIKTOROV, S. V., Determining small quantities of ^{37}Ar and tritium, 20: 29559
VILAIN, P., π^+-Mesonic decays of hypernuclei, 20: 30485
VILCHES, O. E., Experimental thermal conductivity of ^{3}He, 20: 30282
VILLAR, E., Interactions of 12.8-Bev protons in nuclear emulsions. III., 20: 30364
VINAROV, I. V., Sorption and separation of zirconium and hafnium on native anionites, 20: 29352
VINOGRADOVA, N. D., Higher-mode instabilities in Tokamak device, 20: 30651
VIOLINI, G., KN dispersion relations and symmetry groups, 20: 30018
VISHNEVSKII, N. K., Plasma equilibrium in torus with high-frequency fields and plasma heating resulting from beam of "escaping electrons", 20: 30640
VITKUN, R. A., 1,10-Phenanthrolinethenoyltrifluoroacetone complexes of rare earth elements, 20: 29221
VLADIMIROVA, V. I., Radiation-induced catalytic conversion of methanol at a small surface coverage, 20: 29278
VLADMANIS, Ya. Ya., Electrodynamic forces and Joule losses in conducting layers in traveling magnetic fields, 20: 29830
VODYANITSKII, A. A., Oscillations and heating of small plasmoids incident in axisymmetric magnetic fields, 20: 30559 (FTI-114/P-044)
VOGEL, D. L., Thermal diffusion of oxygen in refractory metals, 20: 29769
VOGT, R. H., Gamma spectra of ^{124}Te, ^{164}Dy, ^{178}Hf and ^{183}W from radiative capture of neutrons at resonances, 20: 30385
VOHLER, O., Graphite in space travel, 20: 29773
VOIGT, E.-D., Influence of ionizing radiation on metabolism in human erythrocytes, 20: 28924
VOIGT, O., Post-accident pressure and temperature transients in dry containment, 20: 30895
VOITSENYA, V. S., Motion of plasmoid in a curvilinear magnetic field, 20: 30647
VOL'DMAN, M. A., Kinetics of combined carbothermal reduction of niobium and tungsten, 20: 29677
VOLKOV, M. N., Chemical protection against genetic changes, 20: 29045

VOLOSEVICH, P. P., One-dimensional self-similar motion of thermally and electrically conducting gas in magnetic field, 20: 30185
VOLOSOV, V. I., Plasma with relativistic electrons in magnetic mirror trap, 20: 30638
VONDRA, B. L., Development of ThO_2 pellet fabrication, 20: 29657
VON GIERKE, G., Comparison of alkali plasma loss rates in a stellarator and in toroidal device with minimum mean-B properties, 20: 30656
VON GIERKE, G., Toroidal theta pinch with superimposed multipole field, 20: 30616
VON GOELER, S., Production of a thermally ionized plasma with negative ions, 20: 30575
VON HIPPEL, Frank, Mesonic (K⁻) x rays and anti K-N scattering lengths, 20: 29938
VON ROOS, Oldwig, Electromagnetic scattering from inhomogeneous dielectrics of finite extent, 20: 29832
VOORHIES, H. G., Energy spectrum of neutral hydrogen atoms from coaxial plasma gun, 20: 30578
VOROB'EV, D. S., Proton elastic scattering on deuterons at large angles, 20: 29989 (ITEF-361)
VOTAVA, E., Mechanical properties of high-purity niobium single crystals, 20: 29762

W

WACHSMUTH, H. W., Possibility of measurement of muon polarization in neutrino experiments, 20: 30003
WADA, Walter W., Scalar densities in current commutation relations and partially-conserved-axial-vector-current hypothesis, 20: 30138
WAEFFLER, H., Reaction $^{9}Be(d,\gamma)^{11}B$, 20: 30393
WAGNER, Carl, Oxidation of oxygen-deficient zirconia, 20: 29648
WAGNER, E., Preparation of trichloroethylene labeled with ^{36}Cl and application to study of corrosion, 20: 29655
WAGNER, F. Jr., Level structure in ^{52}Cr populated in 5.7-day ^{52}Mn decay, 20: 30458
WAGNER, F. Jr., Low-intensity branches in ^{45}Ti decay, 20: 30456
WAHL, Arthur C., Nuclear charge distribution in fission: ^{92}Rb and ^{93}Rb independent yields, 20: 30477
WAHL, Arthur C., Nuclear charge distribution in fission: ^{92}Y, ^{93}Y, ^{94}Y, and ^{95}Y independent yields, 20: 30476
WAHL, Howard W., Foundation caisson provides underground containment for nuclear power plant, 20: 30896
WAINERDI, R. E., Lunar and planetary surface analysis using neutron activation, 20: 29140
WAINERDI, Richard E., Study of macroscopic distribution of O in steel rod by neutron-activation and vacuum-fusion techniques, 20: 29088
WAJIMA, J. Tsunetaka, Reactivity worth of fuel elements, 20: 30839
WALDRON, M. B., Behavior of refractory metals in radiation environments, 20: 29820
WALKER, J. C., Moessbauer effect measurements in first and second excited states of ^{155}Gd, 20: 30422
WALKER, J. P., Reaction of nuclear graphite with water vapor. I., 20: 29626
WALKER, W. D., Search for evidence of a K^+K^+ resonance, 20: 30047
WALKER, W. D., Strangeness-one resonances, 20: 30049
WALL, B. J., Neutron separation energies of ^{143}Nd–^{144}Nd, ^{149}Sm–^{150}Sm, and ^{164}Dy–^{165}Dy, 20: 30366
WALLACE, W. P., Irradiation of graphite impregnated with furfuryl alcohol, 20: 29813
WALSH, P. N., Kinetics of high temperature oxidation of refractory materials, 20: 29656
WALSH, W. J., Surface concentration changes during distillation of liquid metals, 20: 29346
WALTER, F. J., Rectification process at metal-Si surface barriers, 20: 29569
WALTER, F. J., Thermal cycle degradation of charge carrier lifetime and resistivity in Si, 20: 30785
WALTER, R. L., Neutron-deuteron polarization at 22.7 Mev, 20: 30442
WALTON, R. B., Gamma rays from short-lived fission-fragment isomers, 20: 30463
WAMBERSIE, A., Relative biological efficiency of a beam of 20-Mev electrons as function of depth, 20: 28963
WANIC, A., Neutron investigation of temperature effects in magnon spectrum of magnetite, 20: 30765
WARD, Gerald M., Appearance of ^{131}I and ^{140}Ba–La in fallout due to second Chinese test, 20: 29429
WARD, Gerald M., Availability of fallout ^{137}Cs to dairy cattle from different types of feed, 20: 29463
WARGA, J. J., Comparison of pressed and sintered and arc-cast billets for refractory metal forgings, 20: 29683
WARGA, J. J., Development of silver infiltrated tungsten nozzles for uncooled rocket motors, 20: 29685
WARNOCK, Robert Lee, Matrix N/D method with arbitrary inelasticity, 20: 30130
WARREN, Gary J., Radiation protection problems at Stanford two-mile linear accelerator, 20: 29849 (CONF-651109, pp 442-58)
WASA, Kiyotaka, Formation of rotating plasma in crossed field, 20: 30592
WASHBURN, D. F., Thermal expansion and temperature dependence of elastic moduli of polycrystalline hafnium, 20: 29703 (KAPL-3112)
WASHIJIMA, Shigeo, Studies of graft copolymerization onto viscose rayon. III., 20: 29294
WASLEY, R. J., Propagation of stress disturbances in elastic-plastic cylinders, 20: 30954 (UCRL-14617)
WASSON, Hodge R., Why and how of nuclear accident dosimetry, 20: 29469
WATANABE, Misao, Effects of irradiation on Pinus desiflora and Pinus thunbergii, 20: 28980
WATANABE, Susumu, Nuclear hematology: based on experience with atomic explosions, 20: 28876
WATARI, Kazuo, Concentration of radionuclides in sea water by metal sulfide-ion exchange resins, 20: 29345
WATERS, E. D., Heat transfer experiments for Advanced Test Reactor, 20: 30933 (BNWL-216)
WATSON, C., Parametric resonance in plasma in magnetic field, 20: 30669
WAUGH, J. S., Nuclear spin relaxation in liquid hydrogen, 20: 30181
WAWRYSZCZUK, J., Directional correlations of γ rays in ^{147}Sm, 20: 30382
WEBELER, R. W. H., Viscosity coefficients for liquid ^{3}He, 20: 30275
WEBER, J., Gravitational shielding and absorption, 20: 30245
WEBER, William G. Jr., Nuclear surface gages for determining soil moisture and density, 20: 29508
WEBSTER, C. B., Ratio of asymmetric-to-symmetric fission for ^{239}Pu for 30-kev to 14.7-Mev neutrons, 20: 30404
WEBSTER, J. Wallace, Point-set representation of ^{238}U cross sections; values and a FORTRAN program for computation, 20: 30356 (ORNL-TM-1448)
WEGE, E., Time factor in the graphite coating process, 20: 29730
WEGENER, H., Time-reversal invariance in β decay of RaE, 20: 30537
WEINBERG, A., Search for evidence of a K^+K^+ resonance, 20: 30047
WEINBERG, A., Strangeness-one resonances, 20: 30049
WEISS, C., Hydrogen isotope exchange reactions of nonbenzoid aromatics. II., 20: 29245
WEISS, P. B., Experimental studies with Astron, 20: 30637
WEISSE, J., Stability of a diffusing plasma, 20: 30621
WEISSENBURGER, A. W., Semi-automatic data system for plasma study, 20: 30573
WEITKAMP, W. G., Polarization in p-α scattering from 17 to 27 Mev, 20: 30389
WEITZNER, Harold, Longitudinal plasma oscillations, 20: 30564 (NYO-1480-26)
WELCH, M. J., Role of scavengers in gas-phase recoil tritium reactions, 20: 29206
WELTEVREDEN, P., In-pile application of strain gages, 20: 29578 (EUR-2649.e)
WENSEL, A., Gamma irradiation facility of Frankfurt Research Reactor, 20: 29341
WENZ, W., Thorotrast tumors, 20: 29022
WENZEL, M., Wilzbach tritiation of an alkyne-2-acid with high specific activity, 20: 29243
WENZL, H., Release of stored energy and electric resistivity changes in neutron-irradiated Cu, 20: 29824
WERHAHN, P., Gynaecological individual radium dosimetry in situ using x ray stereoscopy, 20: 29074
WERTENBACH, H., Investigations on corrosion of Zr in electrolytic solutions by use of radionuclides, 20: 29649
WERTHAMER, N. R., Nonlinear self-coupling of Josephson radiation in superconducting tunnel junctions, 20: 30292
WERTHAMER, N. R., Temperature and purity dependence of superconducting critical field, H_{c2}. II., 20: 30295
WERTHAMER, N. R., Temperature and purity dependence of superconducting critical field, H_{c2}. III., 20: 30296
WEST, Roger Karl, Effect of radiation on synthesis of ammonia, 20: 29312
WESTMAN, S., Note on the nine-layer hexagonal structure of YAl_3, 20: 29721
WESTPHAL, K. O., Theoretical considerations of ion optics of mass spectrometer ion source. I., 20: 29489
WESTPHAL, K. O., Theoretical considerations of ion optics of mass spectrometer ion source. II., 20: 29490
WETCH, J. R., Reactors: key to large-scale underwater operations, 20: 30929
WETHERELL, A. T., Inter-diffusion of plasma and magnetic fields in pinch and hardcore discharges, 20: 30639
WETHERILL, J. M., Gamma irradiation of food, 20: 29585
WHAN, R. E., Oxygen-defect complexes in neutron-irradiaged Ge, 20: 30742
WHARTON, C. B., Flute characteristics of and microwave emission from a plasma in a mirror, 20: 30645
WHARTON, C. B., Landau damping of electron plasma waves, 20: 30622
WHEATLEY, J. C., Experimental thermal conductivity of ^{3}He, 20: 30282
WHEATLEY, J. C., Low-temperature heat capacity of liquid ^{3}He, 20: 30283

WHEELER, Robert V., Radiation environment at zero-gradient synchrotron, 20: 29843 (CONF-651109, pp 34-56)
WHIFFEN, D. H., Electron spin resonance of irradiated glycine at 77°K, 20: 29281
WHIFFEN, David H., Electron spin resonance of irradiated thiophene-2-carboxylic acid, 20: 29284
WHITE, B. M., Inter-diffusion of plasma and magnetic fields in pinch and hardcore discharges, 20: 30639
WHITE, D. E., Source of Pb and Sr in deep geothermal brines underlying the Salton Sea geothermal area, 20: 29414
WHITE, John M., Energy threshold for D + H_2 → DH + H reaction, 20: 29176
WHITEMAN, J. A., Orientation relationship and growth direction of Mo_2C in ferrite, 20: 29726
WHITT, Richard Elmo, Feedforward compensation of temperature control system, 20: 30807 (ORNL-TM-1485)
WHITTAKER, E. L., Sampling airborne radioiodine in organic compounds, 20: 29467
WHITTEMORE, W. L., Small neutron beam chopper, 20: 29555
WICK, E. L., Effect of storage at ambient temperature on the volatile components of irradiated beef, 20: 29589
WICKSTROM, C. J., Total cross sections of Gd for fast neutrons, 20: 30419
WIDMAN, H., Experiences with "infusion urography" in children, 20: 29062
WIEDERMANN, A. H., Prog. rpt. on reactor containment, 2–3/66, 20: 30797 (IITRI-578P21-18)
WIESNER, L., Methods for use of radioactive radiation sources, 20: 29593
WIESNER, L., Preparation of trichloroethylene labeled with ^{36}Cl and application to study of corrosion, 20: 29655
WIGMORE, J. K., Interaction of microwave phonons with irradiation centers in quartz, 20: 30768
WIKTOR, S., Two-nucleon exchange reactions in nuclear structure investigations, 20: 30483
WILDE, N., Noise study, ARMF-II, 20: 30837 (IDO-17169)
WILDENTHAL, B. H., Comparison of effective two-nucleon interaction with surface delta interaction, 20: 30423
WILETS, L., Coupled-state calculations of H^+-H scattering, 20: 29940
WILKINSON, D. H., Decay of the 2.34- and 2.71-Mev states of ^9B, 20: 30445
WILKNISS, P., Radiochemical separation of ^{18}F from reactor irradiated gold and uranium, 20: 29338
WILLARD, J. E., Reaction intermediates in radiolysis of alkyl halides at 77°K, 20: 29264
WILLE, Horst, Application of network planning technique in construction of nuclear power plants, 20: 30907
WILLIAMS, D., Gamma-ray spectra of pitchblende and monazite, 20: 29079 (AERE-M-1736)
WILLIAMS, James B., Radiation source measuring apparatus having automatic background subtract means, 20: 29571
WILLIAMS, Lawrence Ernest, Inelastic protons from ^4He, 20: 30512
WILLIAMS, M. M. R., Multi-velocity corrections in the theory of neutron-detecting foils, 20: 29539
WILLIAMSON, S. J., Resistive transition near H_{c2} in high field superconductors, 20: 30270
WILSKY, K., Sign and magnitude of Coriolis coupling between the 5/2⁻[523] and 7/2⁻[523] orbitals in ^{161}Tb, 20: 30401
WILSON, Daniel W., Appearance of ^{131}I and ^{140}Ba–La in fallout due to second Chinese test, 20: 29429
WILSON, Fred Lee, Cross section fluctuations in $^{32}S(d,p)^{33}S$ reaction at energies below 3.0 Mev, 20: 30518
WILSON, J. R., Structure of liquid metals and alloys, 20: 29755
WILSON, O. C., Stellar convection zones, chromospheres, and rotation, 20: 29883
WILSON, R. E., Isothermal reaction of U with steam between 400 and 1600°C, 20: 29188
WINDELBAND, Rolf, Ash content of bituminous coal, 20: 29127
WINDISCH, S., New Ta, Nb, impregnated, or sintered alloys and compound materials with graphite, 20: 29764
WINTER, J. A., Gamma-radiolysis of water vapor in the presence of NH_3 and O_2, 20: 29295
WINTER, K., Two-pion decay of K_2^0 mesons, 20: 30000
WINTERBERG, F., Nuclear fusion by magnetic acceleration of superconducting solenoid, 20: 30717
WINTERNITZ, P., Current-generated algebras and form factors, 20: 30146
WITHERS, H. RODNEY, Dose-response relationship for epithelial cells of skin, 20: 28990
WITKIN, Evelyn M., Radiation-induced mutations and their repair, 20: 28991
WITT, F. J., Influence of cross-sectional shape on irradiation-induced stresses in graphite columns, 20: 30803
WITTERS, J., EPR in neutron-irradiated DPPH, 20: 29289
WITULSKI, H., Stable and unstable behavior of preheated plasma in linear and cusped theta pinches, 20: 30614
WOBIG, H., Toroidal theta pinch with superimposed multipole field, 20: 30616
WOLF, G. H., Toroidal theta pinch with superimposed multipole field, 20: 30616
WOLFE, G. E., Indian Point Reactor—instrumentation asymmetry response verification, 20: 30876 (BAW-1302)
WOLTJER, L., Local hypothesis for the quasi-stellar objects, 20: 29888
WONG, J. L., Mechanical design of regenerative deflector for Berkeley 88-in. cyclotron, 20: 29856 (UCRL-16829)
WOOD, D. E., New developments in neutron activation systems for analysis of O in steel, 20: 29138
WOOLUM, John Carl, Moessbauer effect in ^{159}Tb, 20: 30532
WOOTTON, William Robert, Improvements in or relating to reactors, 20: 30868
WOOTTON, William Robert, Improvements in or relating to reactors, 20: 30869
WORCESTER, S. A., Current Nb alloy technology in the United States, 20: 29763
WORCESTER, S. A., Properties of tungsten–rhenium alloys, 20: 29765
WORONA, Valentin, Field evaluation of nuclear gages used in compaction control of embankments, 20: 29507
WRIGHT, D. J., Dose distributions in ^{60}Co planar rotation, 20: 29061
WRIGHT, J. P., Cosmic black-body radiation, high-energy electrons, and origin of isotropic x-ray and γ radiation, 20: 29958
WRUCK, D., Radiation defects in deuteron-bombarded CdS crystal, 20: 30771
WU, Pao-sun, Radiophosphorus in treatment of certain skin diseases, 20: 29072
WU, Tsung-fan, Decay ($K_2^0 \rightarrow \pi^+\pi^-$) probability in sloped K_2^0-meson beam, 20: 30056
WULFF, J., Low-temperature electrical resistivity of lattice defects in deformed tungsten single crystals, 20: 29723
WURM, Joseph G., Plant for electrolytic refining of nuclear metals, 20: 29373
WYATT, M. E., Range of photoparticle recoil atoms in solids, 20: 30479

X

XUONG, Nguyen-Huu, Isospin of the A mesons, 20: 30023

Y

YAJIMA, Nobuo, Nonlinear motion of ion streams in a background of high-temperature electrons, 20: 30585
YAKIMENKO, L. M., Tritium content in atmospheric fallout over Moscow during 1962–1963, 20: 29409
YAKOVKIN, N. A., Investigation of chromospheric limb flare, 20: 29905
YAKOVLEV, S. P., Dynamic stabilization of a direct discharge in a magnetic field, 20: 30698
YAMADA, Kazunari, Ultrasonic attenuation and relaxation times in water vapor and heavy water vapor, 20: 29172
YAMAGUCHI, Yushin, Inverted SC in the low latitude regions, 20: 30232
YAMAKOSHI, Hisao, Fast fission factor for a lattice system, 20: 30859
YAMAMOTO, Hisashi, Effect of epithermal fission on neutron multiplication, 20: 30841
YAMAMOTO, Kenzo, Plasma diffusion in magnetic field, 20: 30596
YAMAMOTO, Takaharu, Properties of sintered WC–Co alloys, 20: 29778
YAMAMOTO, Yutaka, Chemical engineering studies on processing of radioactive liquid wastes by evaporation, 20: 30946
YAMPOL'SKII, I. R., Plasma equilibrium in torus with high-frequency fields and plasma heating resulting from beam of "escaping electrons", 20: 30640
YAN, Go-sen, Ligand field theory. I., 20: 29205
YANKOVSKII, A. V., Effect of ionizing radiation on nuclear reorganization processes in Paramaecium putrinum. I., 20: 29007
YANOVA, K. G., Radiochemical properties of certain peptides, 20: 29301
YAO, Tu-ch'ing, Syntheses of isotopically labeled compounds. III., 20: 29246
YAROVENKO, A. N., Analysis of rare earth alloys in nonaqueous solutions, 20: 29133
YASHIN, Yu. Ya., Propagation of EM waves in plasma located in magnetic field of a constant linear current, 20: 30678
YASNOVA, L. N., Mutagenic action of extracts from various organs of irradiated mice, 20: 28959
YASUKAWA, Shigeru, Dancoff factor in arrayed-type cladded fuel lattice, 20: 30842
YASUKOCHI, Ko, Magnetic properties of rare earth compounds in Gd(Ag,Cd,In) and Gd(Cu,Ag,Au) systems, 20: 29752
YATSIMIRSKII, K. B., Neodymium and erbium bromide complexes, 20: 29225
YAVIN, A. I., Isobaric analog states by (p,n) reactions, 20: 30480
YEARIAN, M. R., Neutron form factors from study of inelastic electron spectra in electrodisintegration of deuterium, 20: 30027
YEARIAN, M. R., Structure of the α particle from elastic electron scattering,

20: 30439
YELLIN, Joseph, Atomic-beam study of Stark effect in Cs and Rb D lines, 20: 29941
YENNIE, D. R., Radiative corrections to electron-induced processes, 20: 30478
YGER, P. M., Isospin of the A mesons, 20: 30023
YILDIZ, Asim, Electromagnetic cavity resonances in accelerated systems, 20: 29831
YOSELI, Morihiro, Plasma-ion oscillation in a drifted plasma, 20: 30583
YOSHIDA, Hiroshi, Movement of radioactive calcium in brain slices, 20: 28891
YOSHIDA, Yoshikazu, Radiation control for radioactive facilities, 20: 29460
YOSHIKAWA, Kazuko, Studies on fallout particles. V., 20: 29423
YOSHIKAWA, S., Non-resonant coupling of r-f power to a plasma, 20: 30577
YOSHIZAWA, Yasuo, Practical applications of glass dosimetry, 20: 29547
YOUNG, B. A., Apparent lowering of energy levels as measured by Orbach relaxation rates, 20: 30758
YOUNG, F. J., Inductance vs. current characteristics of superconductors, 20: 30303
YOUNG, M. P., Plasma confinement, heating, and losses in Pharos with an extended current pulse, 20: 30612
YU, Chuan-tsan, Problem in statistical theory of nuclear fission, 20: 30486
YU, T. C., Development of radiation-sterilized seafood products. I., 20: 29603
YUAN, Ch'eng-yeh, Chromatographic analysis and liquid-liquid extraction, 20: 29355
YUAN, Ch'eng-yeh, Relation between chemical structure of alkyl dibutyl phosphonates and characteristics of U and Th extraction, 20: 29354
YUDKEVICH, I. S., Radiation intensity in earth's radiation belts, 20: 30235
YUFEROV, V. B., Cryogenic magnetic trap VGL-2, 20: 30655
YUSUPOV, A. A., Effect of strontium on the functional state of thyroid gland in dogs, 20: 29000

Z

ZACHAROV, B., Interaction π^+-π^- as studied in 12- and 18-Bev pion-nucleon reactions, 20: 30025
ZADNEPROVSKII, G. M., Crystallochemical properties of cubic-shaped hydrated uranium tetrafluoride, 20: 29231
ZAITSEV, R. O., Boundary conditions and surface superconductivity, 20: 30309
ZAITSEV, V. V., Theory for type II bursts of solar radio emission, 20: 29903
ZAITSEV, Yu. M., Accuracy of particle trajectory location in spark chamber, 20: 29527 (ITEF-341)
ZAKRZEWSKI, J., Two decays of mass-seven hyperfragments, 20: 30368
ZALKIN, Allan, Crystal structure of thorium nitrate pentahydrate by x-ray diffraction, 20: 29150
ZAMPIERI, Antonio, Radiomimetic properties of 2-aminopurine in E. coli, 20: 29041
ZAPOL'SKAYA, N. A., Influence of chemical uptake of radioactive substances on lipid and cholesterol levels in blood, 20: 28994
ZARET, M. M., Laser hazard, 20: 29457
ZARKHIN, B. I., Radiofrequency mass spectrometer for the Electron satellites, 20: 29545
ZARNOWIECKI, K., Sterilization of bone tissues with gamma radiation in Poland, 20: 28987
ZARUBAILO, T. Yu., Mutations in cereals induced by ionizing radiations, 20: 28960
ZASHKVARA, V. V., Focusing characteristics of electrostatic mirror with cylindrical field, 20: 29868
ZASLER, J., Safety aspects of three in-pile gas loops, 20: 30940
ZATSEPIN, V. I., Primary cosmic radiation on Elektron-2 and Elektron-4, 20: 29955 (NASA-TT-F-389, pp 678-83)
ZATYURYUKIN, V. G., Therapeutic effectiveness of antibiotics on cystamine action during radiation sickness, 20: 29051
ZAVOISKII, E. K., Turbulent heating of plasma by direct-current discharge, 20: 30661
ZAWADZKI, Aleksander, Effects of depth of proton interactions on recording penetrating components in atmospheric showers, 20: 29971
ZAZUNOV, L. G., Resonance in the e-p system, 20: 30054
ZECH, G., Interference effects between N*(1236) and K*(891) production, 20: 30009
ZEIDMAN, B., Discrepancies in proton-transfer reactions to states with different isobaric spin, 20: 30481
ZELBY, L. W., Measurements of electron drift velocity and collision frequency in an argon discharge, 20: 30598
ZELDOVICH, Ya. B., Collapsed stars in binaries, 20: 29889
ZELLER, E. J., Thermoluminescence as function of climate and temperature, 20: 29398
ZHABROVA, G. M., Radiation-induced catalytic conversion of methanol at a small surface coverage, 20: 29278
ZHELEZNYAKOV, V. V., Origin of Jovian radio emission, 20: 29907
ZHERBIN, E. A., Damaging effects of underwater nuclear explosion, 20: 29481
ZHERNOV, V. S., Multipoint control of radiation levels, 20: 29458
ZHEVNER, V. D., Pigment mutations in Anacystis nidulans, 20: 28958
ZHILKINA, M. I., Behavior of ^{137}Cs during analysis of atmospheric samples, 20: 29081 (NP-14705)
ZHITKOVA, L. G., Preparation of ion-exchange membrane by pre-irradiation method, 20: 29308
ZHUKOVSKII, N. N., Gamma radiation of 12.3-year ^{152}Eu, 20: 30487
ZHUKOV-VEREZHNIKOV, N. N., Chemical protection against genetic changes, 20: 29045
ZHUNUSOV, R. S., Change in chemical composition when plants are irradiated at various periods of ontogenesis depending on climatic factors, 20: 28967
ZHUZGOV, L. N., Comparison of simultaneous measurements of magnetic field and positive ion streams within earth's magnetosphere, 20: 30208 (NASA-TT-F-389, pp 457-63)
ZHUZGOV, L. N., Earth's magnetosphere in radiation zone region (3-6R_e), 20: 30209 (NASA-TT-F-389, pp 464-82)
ZHUZGOV, L. N., Magnetometric apparatus of the electron-2 space station, 20: 30236
ZIDRASHKO, T. M., Effect of uranium nitrate on thyroid gland of rat, 20: 28884
ZIEGLER, B., Reaction ^{9}Be(d,γ)^{11}B, 20: 30393
ZIEGLER, J. F., Excitation of collective states in ^{208}Pb by inelastic electron scattering, 20: 30436
ZIELINSKI, Mieczyslaw, Kinetic isotope effects accompanying oxidation of CO, H_2, and CH_4, 20: 29187
ZIETEN, Willy, Power supply system for Siemens-Schuckert Research Centre, 20: 29368
ZIMMERMAN, J. E., Flux entry in macroscopic superconducting rings, 20: 30305
ZIMMERMAN, Robert L., Construction of an equivalent Lagrangian for interacting Fermion-Boson fields, 20: 30122
ZIMMERMANN, M., Effects of x rays on excitation conduction of nerves of cold blooded animals, 20: 29021
ZIMMERMANN, W., Efficiency of multiple plate ion chamber for relative activity measurements of γ emitters, 20: 29560
ZIMMERMANN, W., Polarization of 6-Bev bremsstrahlung from Hamburg electron synchrotron, 20: 30045
ZIVANOVIC, M. D., Thermal neutron spectrum measurements from Yugoslav heavy water reactor, 20: 30939
ZLOTNIKOV, L. M., Phenomenology of certain inelastic reactions involving particles with spin, 20: 30149
ZMBOV, K. F., Mass-spectrometric studies at high temperatures. X., 20: 29183
ZOLOTOTRUBOV, I. M., Energy distribution in hydrogen plasma from coaxial plasma gun, 20: 30687
ZSEBOEK, Z., Radiosensitivity of red cell catalase in vitro, 20: 28911
ZSEMBERY, J., Search for an isobar of isotopic spin T = 5/2, 20: 30022
ZUMWALT, Glen W., Solutions of the flow field produced by shock wave emerging into cross flow, 20: 30167 (SC-DC-65-1916)
ZUMWALT, Glen W., Transient flow field analysis of blast wave intercepting a stationary cone at zero angle of attack, 20: 30168 (SC-DC-66-1329)
ZWANZGER, G., Influence of ionizing radiation on liver blood circulation of rabbits, 20: 29010
ZWILLENBERG, M., Prog. rpt. on combustion of metals, annual, 7/64–6/65, 20: 29641 (SC-DC-65-1691)
ZYLICZ, J., Sign and magnitude of Coriolis coupling between the 5/2-[532] and 7/2-[523] orbitals in ^{161}Tb, 20: 30401

SUBJECT INDEX

Main entries in this index are generally specific materials, things, and processes. These are followed by modifiers that describe the properties of, and processes applied to, the main entries.

The number preceding the colon is the *NSA* volume number, and the number following is the abstract number. The designation (R) following the abstract number indicates that the abstract is of a progress report; (P) indicates a patent; and (T) indicates a translation. Abstracts for reports other than progress reports carry no letter designation. References to report numbers, where appropriate, are included after the abstract number of the citation. Published literature (journal article or book) is identifiable by the absence of a report number.

The user should bear in mind that the ideas presented in the original literature, rather than key words, have been indexed. The indexers have tried to select what seemed the most probable and logical place to look for typical information. Since it is not possible to anticipate where a user would look for information, numerous cross references are included in cumulative indexes to assist him in his search.

Experience in using an index of this type will be the best guide in obtaining the desired information, and a consideration of synonymous or closely related terms will prove valuable.

Information must be so indexed as to be of the greatest use to the greatest number of users. This requires that a topic be indexed to headings that most specifically describe it and not ordinarily to the headings that describe its ultimate use, nor to the general class headings that include the specific headings. For example, information on the treatment of thyroid disease with I-131 would be indexed under Thyroid Gland and under Iodine Isotopes I-131, but not necessarily under Radiotherapy. A study of the effects of x radiation on hair would be indexed under both X Radiation and Hair. However, the information would not be indexed under the experimental animal, e.g., Rats, unless the report discusses the effects on rat hair as compared with the effect on the hair of other animals.

The broad, general class headings are used only for general information or for comprehensive reports or articles.

Subject Heading Styles

Generally, the direct form of subject entry is used rather than inverted headings, e.g., Amino Acids rather than Acids, Amino; Helium Isotopes He-4 rather than Helium—Isotopes He-4 or Helium—He-4 isotopes. Note, however, that in some cases parenthetic modifying terms or inverted headings of the form Neutrons, Fast are used in preference to a direct entry that would result in the scattering of information. Organic compounds are usually entered in the index in the inverted form so that substituted compounds can be listed near the parent compound; e.g., Benzene, Bromo- rather than Bromobenzene. In general, the style of nomenclature used is that of Chemical Abstracts, except that some items listed in that publication as subheadings are elevated to form part of the main heading; e.g., Butyric Acid, Methyl Ester rather than Butyric Acid—methyl ester.

Alphabetization

Main headings are alphabetized word-by-word. A parenthetic qualifier following a main heading is disregarded in alphabetizing unless there are two or more headings identical except for the parenthetic qualifier, in which case the qualifier determines the order. Headings involving Greek letters are arranged as if the names of the letters were spelled out.

Examples:

M-Capture
  see Electron Capture
Magnesium
Magnesium Alloys
Manganese Fluorides
Manganese(II) Fluorides
Mesons
Mesons (π)
Mesons (ρ)
3-Pentanol, 2,4-Dimethyl-
2-Pentanol, 2-Methyl-
2-Pentanol, 4-Methyl-

Nomenclature of Inorganic Compounds

Inorganic compounds are indexed in the direct form, listing cations in the order of increasing valence in the case of polycationic salts of varying valence and in alphabetic order for polycationic salts in which all cations have the same valence; e.g., Sodium Aluminum Silicates and Potassium Sodium Sulfates.

Multicomponent Alloys and Other Systems

Multicomponent alloys, except well-known trade names, are indexed under a main heading in the form "element alloy" for each element in the alloy. The modifier begins with element symbols for each component arranged alphabetically as if the English name for the element were spelled out.

Example: Copper-Gold Alloy is indexed
  Copper Alloys
    Cu-Au...
  Gold Alloys
    Cu-Au...

Well-known alloys such as Zircaloy-2 are indexed directly to the trade name; cross references referring from each component of the alloy to the entry for the trade name appear in cumulative indexes.

Multicomponent systems of non-metallic elements are indexed in a manner similar to alloys except the main heading used contains the word "Systems" in place of "Alloys."

Example: Silicon–Tungsten Systems are indexed
  Silicon Systems
    Si-W...
  Tungsten Systems
    Si-W...

Multicompound systems and mixtures of compounds are indexed under the main heading for each component com-

pound; the modifiers begin with an alphabetical listing of compound formulas.

Example: Lead Titanate–Lead Zirconate is indexed
Lead Titanates
$PbTiO_3$-$PbZrO_3$ . . .
Lead Zirconates
$PbTiO_3$-$PbZrO_3$ . . .

A mixed system of compounds and elements is indexed using a combined form of the above conventions, e.g., a dispersion of copper and alumina would be indexed

Aluminum Oxides
Al_2O_3-Cu . . .
Copper Systems
Al_2O_3-Cu . .

Physical States and Configurations of Materials

Specification of the physical state, if other than normal, or geometric configuration of the material is included in the modifying phrase, i.e., liquid metals would be indexed to the metal with "liquid" in the modifier, and carbon crucibles would be indexed to Carbon with "crucibles" appropriately placed in the modifier and also to Crucibles if appropriate.

Modifying Phrases

The modifiers appearing under a main heading are written specifically to describe the relation of the item being indexed to that main heading. The modifier, therefore, will generally contain more useful information about that relation than will a title or a phrase written to be used under every main heading assigned to the item. Effort is exerted to begin the modifier with the word judged to be of greatest use to the greatest number of users; this, however, does not obviate the need to consider all modifiers under the main heading(s) of interest.

Modifiers are usually intended to form a meaningful phrase when combined with the main heading. Some are intended to be read following the main heading, e.g., the entry Hydrogen—sorption by charcoal is read "hydrogen sorption by charcoal"; however, as a result of placing the important word first, many modifiers must be arranged for smooth reading, e.g., Formaldehyde—yields in radiolysis of ethyl ether, effects of deuterium on is read "effects of deuterium on formaldehyde yields in radiolysis of ethyl ether" and Uranium—crystal structure of, effect of cooling rate on allotropic transformations in is read "effect of cooling rate on allotropic transformations in crystal structure of uranium." Prepositions are sometimes omitted if no ambiguity results.

Special characters are added to modifiers in the field of physics; if the modifier does not establish the experimental or theoretical character of a reference, a symbol (E), (T), or (E/T) is placed immediately after the modifying phrase and before the journal reference number. The value of this identification has been established by the American Institute of Physics.

A

ACCELERATOR TUBES
beam scattering in electrostatic proton, 20: 29866
ACCELERATORS
beam bunching in electron, 20: 29859
beam stabilization in, using inductive walls, 20: 29860
radiation dosimetry of, quality factor determination using ionization chambers, 20: 29847 (CONF-651109, pp 181-98)
radiation environment of CERN, measurement of, 20: 29844 (CONF-651109, pp 103-16)
shielding calculations for high-energy, review of, 20: 30719 (CONF-651109, pp 327-45)
shielding of, design concepts for, 20: 30720 (CONF-651109, pp 410-16)
ACCIDENTS
radiation exposure in criticality, effects on man, 20: 28970
ACENAPHTHYLENE
radioinduced solid-state polymerization with maleic anhydride, gamma, 20: 29274
ACETANILIDE
analysis for carbon-14 by dry combustion methods, 20: 29085
ACETANILIDE, 5-ETHYL-2-PROPYL-
analysis for carbon-14 by dry combustion methods, 20: 29085
ACETATES
effects of nicotinic acid on uptake of carbon-14-labeled, by cholesterol in rabbit liver, 20: 28895
ACETIC ACID
acetic acid–methanol, deuterium exchange between, and azulene, 20: 29245
ACETIC ACID, 2-(1,8-DIHYDROXY-3,6-DISULFO-2-NAPHTHYLAZO)-PHENOXY-
complexes with thorium, uses in spectrophotometric determination of fluoride ions, 20: 29091
ACETIC ACID, (ETHYLENEDIAMINE) TETRA-
with rare earths, preparation, composition, and stability of, 20: 29222
arsenazo I–EDTA–nitrosonaphthol, uses for colorimetric micro-determination of uranium, 20: 29130
ACETIC ACID, (ETHYLENEDIAMINE) TETRA-, SODIUM SALTS
complexes with cobalt, isotope exchange in radiocobalt divalent ion-doped, 20: 29259
complexes with cobalt, radioinduced recoil damage in, thermal annealing of neutron, 20: 29259
ACETIC ACID, [(2-HYDROXYETHYL)IMINO]DI-
complexes with rare earths, composition and stability of, 20: 29343
ACETIC ACID, NITRILOTRI- COMPLEXES
with americium and curium, stability of, 20: 29195
with cerium, preparation and stability of, 20: 29228
ACETIC ACID, TRICHLORO-
Solvesso 100–trichloroacetic acid, radiation effects on clarification and coalescence time of reactor fuel solutions in nitrated, 20: 29333 (RT-CHI-(65)33)
ACETIC ACID, TRICHLORO-, CERIUM SALTS
preparation and thermal decomposition of, in air and in nitrogen, 20: 29213
ACETIC ACID, TRICHLORO-, DYSPROSIUM SALTS
preparation and thermal decomposition of, in air and in nitrogen, 20: 29213
ACETIC ACID, TRICHLORO-, ERBIUM SALTS
preparation and thermal decomposition of, in air and in nitrogen, 20: 29213
ACETIC ACID, TRICHLORO-, EUROPIUM SALTS
preparation and thermal decomposition of, in air and in nitrogen, 20: 29213
ACETIC ACID, TRICHLORO-, GADOLINIUM SALTS
preparation and thermal decomposition of, in air and in nitrogen, 20: 29213
ACETIC ACID, TRICHLORO-, HOLMIUM SALTS
preparation and thermal decomposition of, in air and in nitrogen, 20: 29213
ACETIC ACID, TRICHLORO-, LANTHANUM SALTS
preparation and thermal decomposition of, in air and in nitrogen, 20: 29213
ACETIC ACID, TRICHLORO-, LUTETIUM SALTS
preparation and thermal decomposition of, in air and in nitrogen, 20: 29213
ACETIC ACID, TRICHLORO-, NEODYMIUM SALTS
preparation and thermal decomposition of, in air and in nitrogen, 20: 29213
ACETIC ACID, TRICHLORO-, PRASEODYMIUM SALTS
preparation and thermal decomposition of, in air and in nigrogen, 20: 29213
ACETIC ACID, TRICHLORO-, RARE EARTH SALTS
preparation and thermal decomposition of, in air and in nitrogen, 20: 29213
ACETIC ACID, TRICHLORO-, SAMARIUM SALTS
preparation and thermal decomposition of, in air and in nitrogen, 20: 29213
ACETIC ACID, TRICHLORO-, TERBIUM SALTS
preparation and thermal decomposition of, in air and in nitrogen, 20: 29213
ACETIC ACID, TRICHLORO-, THULIUM SALTS
preparation and thermal decomposition of, in air and in nitrogen, 20: 29213
ACETIC ACID, TRICHLORO-, YTTERBIUM SALTS
preparation and thermal decomposition of, in air and in nitrogen, 20: 29213
ACETIC ACID, TRICHLORO-, YTTRIUM SALTS
preparation and thermal decomposition of, in air and in nitrogen, 20: 29213
ACETIC ACID, VINYL ESTER
radioinduced polymerization with lignin, gamma, 20: 29288
ACETONE
effects on electric conductivity of anhydrous uranyl nitrate, 20: 29184
yields from gamma radiolysis of aqueous solutions of 2-propanol, 20: 29254
ACETONE, THENOYLTRIFLUORO-
1,10-phenanthroline–thenoyltrifluoroacetone, complexes with rare earths, preparation and composition of, 20: 29221
ACETOPHENONE
oxime of, Beckmann rearrangement of, effects of carbon-14 on, 20: 29242
ACETYLENE
helium atom reactions with, electron kinetic energy from ionization in, (E), 20: 29927
radiolysis of aqueous solutions of, effects of hydrogen and oxygen on gamma, 20: 29293
spectra of polycrystalline films of, effects of deuterium on far-infrared, 20: 29239
yields of, from hydrolysis of rare earth carbides, 20: 29220
ACETYLENE, DIPHENYL-
reactions with muonium, (E), 20: 29247
ACIDS
radiation effects on total volatile, in fish, gamma, 20: 29583(R) (TID-22515)
ACOUSTIC WAVES
neutron scattering by ideal gases in field of, total cross sections for, 20: 30256
ACRYLIC ACID
radioinduced polymerization with nylon, 20: 29316
ACRYLONITRILES
radioinduced graft polymerization with viscose rayon, gamma, 20: 29294
radioinduced polymerization of, at 4.2°K, 20: 29300
radioinduced polymerization with nylon, 20: 29316
ACTINIDES
separation of, by high-voltage electrophoresis, 20: 29356
ACTINIUM ISOTOPES Ac-227
alpha spectra, (E), 20: 30347(R) (IDO-17147, pp 13-28)
production of, economics of reactor, 20: 29609 (NP-15947)
ACTIVATION ANALYSIS
computer programs for use in, 20: 29137
development of, for use in routine quality control, 20: 29138
equipment and method for neutron, 20: 29137
method for determining trace amounts of zinc using derivative neutron activation, 20: 29136
neutron generator uses in, 100- to 400-kv, 20: 29118
separation processes for use in, 20: 29120
use for high-energy particle spectrometry, (E/T), 20: 29521 (CONF-651109, pp 213-23)
use in determining ionic composition of intracellular medium in children, 20: 28871(R) (EUR-2636.f,i)
use of silver, for neutron flux measurements, corrections for, 20: 29539
uses in lunar surface analysis, 20: 29140
ADDITION COMPOUNDS
use of krypton-85-labeled hydroquinone for monitoring gaseous contamination in atmosphere, 20: 29142
ADENINE
radiation effects on thermoluminescence of, gamma, 20: 28913
radiation effects on, ESR and thermoluminescence studies of, 20: 29249
radiosensitivity effects on leukopenia in rabbits, 20: 29055
ADENOSINE
radiation effects on thermoluminescence of, gamma, 20: 28913
radiation effects on fluorescence and phosphorescence spectra of, at 77°K, gamma, 20: 28914
ADENOSINEPHOSPHORIC ACIDS
effects of cupferron and, on frequency of radioinduced chromosome aberrations in Tradescantia, 20: 29028

radiation effects on thermoluminescence of, gamma, 20: 28913
radiation effects on, ESR and thermoluminescence studies of, 20: 29249
radioinduced leakage of, from Euglena cells, γ, 20: 28904
radiosensitivity effects on Drosophila, 20: 29046
spectra of nitrogen-15 in, effects of magnesium and zinc on, 20: 29083(R) (UCRL-14767)

ADHESIVES
development of epoxy, for gyro fabrication, 20: 29366(R) (TID-22970, pp 375-91)

ADRENAL GLANDS
radiation effects on metabolism in rat, 20: 28939
radiation effects on metabolism in mouse, 20: 28940
radiation effects on catecholamine content of rat, x, 20: 28964

ADRENALINE
physiological effects in man, 20: 29032
radiation effects on content of, in rabbits, alpha, 20: 28886
radiation effects on metabolism in rats, 20: 28939
radiation effects on metabolism in mice, 20: 28940
radiation effects on content in dog blood, x, 20: 28941
radiation effects on content in rat tissues, x, 20: 28964

ADRENOCORTICOTROPIC HORMONE
effects on leukolytic activity in blood and organs of rats, 20: 29044
effects on radiation effects on heme synthesis in rabbit bone marrow, 20: 28912
radiation effects on metabolism of exogenous, in rat, 20: 29005
radiosensitivity effects on mice, 20: 28978
radiosensitivity effects on erythropoiesis in rats, iron-59 tracer study on, 20: 29043
radiosensitivity effects on rats, 20: 29044

ADVANCED REACTIVITY MEASUREMENT FACILITY
aluminum and water reactivity worth measurement in, 20: 30347(R) (IDO-17147, pp 13-28)
reactivity worth measurements in, noise effects on, 20: 30837 (IDO-17169)

ADVANCED TEST REACTOR
fuel irradiation testing for, aluminum–uranium, 20: 30794(R) (IDO-17147, pp 1-12)
heat transfer analysis for, 20: 30933 (BNWL-216)

AEROSOLS
sorptive properties of iron oxide, for iodine-131, 20: 29234

AGE ESTIMATION
of Pleistocene coral reefs using thorium-230 and uranium isotope ratios, 20: 29435
potassium–argon method for, using neutron irradiation, 20: 29413
thorium-230–uranium method of, for recent volcanic minerals, 20: 29441

AGING
effects of polonium-210 on, in rats, 20: 29030

AIR
analysis for trace gases by radioactive clathrate techniques, 20: 29142
effects on radioinduced polymerization of solid methane, 20: 29314
ionization intensity in, near ground, measurement of, (E), 20: 29404 (CEA-R-2880)
laser beam reactions with, high-temperature plasma from spike-mode, (E), 20: 30590(T)
radioactive iodine contamination of, methods for removing, 20: 29467
reactions of nitrogen and oxygen species in, 20: 29146 (SC-R-66-885)
reactions with molybdenum–nickel–titanium carbide cermets at 600 to 1300°C, effects of molybdenum content on, 20: 29653
reactions with sulfur dioxide, effects of irradiated silicon dioxide–silver sulfate–vanadium oxide catalyst on, 20: 29291
separation of plutonium hexafluoride from cell exhaust, by hydrolysis and filtration, 20: 29328 (ANL-7066)
shock-wave reflection in, in em shock tube, (E), 20: 30697
air–water, density disturbances in flow of, 20: 29375(R) (ANL-7190, pp 193-200)

ALBITES
grinding of, size distribution from ball-mill, 20: 29623(R) (TID-22970, pp 121-256)

ALBUMINS
intestinal sorption of, measurement of, 20: 28871(R) (EUR-2636.f,i)

ALCOHOLS
analysis and determination of carbon-14-labeled, by gas chromatography and radiometric methods, 20: 29089
content in irradiated beef, effects of storage at ambient temperature on, 20: 29589
yields from radiolysis of hydroperoxides in hydrocarbons, 20: 29302

ALDEHYDES
analysis and determination of carbon-14-labeled, by gas chromatography and radiometric methods, 20: 29089

ALGAE
radio- and chemically induced pigment mutations in *Anacystis nidulans*, 20: 28958

ALKALI METAL HALIDES
light scattering from crystalline, measurement of, 20: 30734(R) (TID-22970, pp 1-63)
radiation effects on, color centers in ionic, effect of F centers from gamma and neutron, 20: 30739

ALKALI METALS
density of, at critical temperatures, radiometric techniques for measuring critical, 20: 29742
electron scattering on, nonadiabatic method for, 20: 29942
separation of, by high-voltage electrophoresis, 20: 29356

ALKALINE EARTH FLUORIDES
crystal structure and dielectric properties of, 20: 29709(R) (TID-22970, pp 65-119)

ALKALINE EARTH METALS
separation of, by high-voltage electrophoresis, 20: 29356

ALKALOIDS
effects on calcium-45 movement in guinea pig brain slices, 20: 28891

ALKANES
content in irradiated beef, effects of storage at ambient temperature on, 20: 29589
molecular dissociation following tritium beta decay in, calculation of, 20: 29233

ALKENES
content in irradiated beef, effects of storage at ambient temperature on, 20: 29589

ALLOYS
analysis of, by beta backscattering methods, 20: 29110
superconductivity of transition metal, down to 0.02°K, (E), 20: 30318
thermodynamic properties of solid, at high temperatures, 20: 29623(R) (TID-22970, pp 121-256)
topology of Fermi surfaces in, 20: 29623(R) (TID-22970, pp 121-256)

ALPHA PARTICLES
angular distributions from deuteron reactions (d,α) with lithium-7 at 0.8 and 1 Mev and helium-5 decay, (E), 20: 30402
angular distributions from helium-3 reactions (He-3,α) with oxygen-16 at 9.8 to 11.8 Mev, (E), 20: 30433
angular distributions from lithium-6 reactions with carbon-12, (E), 20: 30520
charge distribution from electron inelastic scattering by helium-4 at 100 to 900 Mev, (E), 20: 30439
detection and measurement of, using p-n semiconductor detector, 20: 29552
detection using p-n semiconductor detectors, charge-carrier collection in, 20: 29550
effects on aging processes in rats after polonium-210 injection, 20: 29030
effects on isomerization of *trans* polymers of conjugated dienes, 20: 29321(P)
emission of long-range, in uranium-235 fission, (E), 20: 30513
interactions with protons at 17.5 to 27 Mev, polarization in, (E), 20: 30389
interactions with neutrons at 6 to 30 Mev, differential cross sections for, (E), 20: 30390
reactions (α,γ) with carbon-12 at 2.8 to 8.3 Mev, resonances from, 20: 30529
reactions (α,He-3) with zirconium-90, -91, and -92 at 66 Mev, cross sections for, (E/T), 20: 30353(R) (ORNL-3940, pp 1-61)
reactions (α,n) with oxygen-18 for analytical use, 20: 29143(P)
reactions (α,p) with nuclei at 30.5 Mev, proton spectra from, (E), 20: 30472
reactions with copper, cross section ratios of isobars from, 20: 30531
reactions with p-n semiconductors at 4.98 Mev, charge-carrier production by, 20: 29550
scattering by carbon-12 at 13 to 26 Mev, cross sections for elastic and inelastic, (E), 20: 30499
scattering by chromium-52, level spins and parities from, (E/T), 20: 30460
scattering by chromium-53 and vanadium-51 at 50 Mev, energy levels from, (E/T), 20: 30460
scattering by nickel-58 at 21 Mev, angular distributions from, (E/T), 20: 30353(R) (ORNL-3940, pp 1-61)
scattering by nuclei at 24.7 Mev, optical-model analysis of elastic, (E/T), 20: 30413
scattering by nuclei at 40.5 Mev, angular distributions for elastic and inelastic, (E), 20: 30450
scattering by tin-116, -118, -120, and -122 at 40 Mev, angular distributions and energy levels from inelastic, (E), 20: 30468

ALPHA SOURCES
content in bones and teeth of American and German subjects, 20: 29476
uses in gages for basis weight measurement, 20: 29601

ALUMINUM
atomic structure of liquid and solid, 20: 29623(R) (TID-22970, pp 121-256)
beta backscattering from, in 2π geometry, (E), 20: 30369

determination in aqueous solutions, design of oxyacetylene burner for measuring sensitivity of spectrophotometric, 20: 29083(R) (UCRL-14767)
determination in graphite and basalts by neutron activation methods, 20: 29140
determination in petroleum, activation, 20: 29139
determination in Zircaloy-2, spectrographic, 20: 29113
effects on copper or silver infiltrants in graphite, 20: 29764
fabrication of powder compacts of, by isostatic pressing and sintering, 20: 29681
gamma scattering at 100 to 280 kev, electron binding effects on incoherent, (E/T), 20: 29923
gamma scattering by, energy and angular distribution of, 20: 30729
helium ion reactions at 25 to 50 kev, K x-ray production cross sections from, (E), 20: 29936
hydrogen ion reactions at 25 to 50 kev, K x-ray production cross sections from, (E), 20: 29936
iron-57 Mössbauer spectra in, 20: 30766
neutron scattering by polycrystalline, one-phonon coherent slow-, (T), 20: 30745
radiation damage in, ion-beam, 20: 29808
reactivity worth of, measurement of, (E), 20: 30347(R) (IDO-17147, pp 13-28)
separation from phosphoric acid solutions by solvent extraction using bis(2-ethylhexyl) ester of pyrophosphoric acid, 20: 29361
use as radiation shielding, model tests of, 20: 30730
x-ray attenuation in type 1100, measurement of, 20: 29707 (ORNL-TM-1457)

ALUMINUM ALLOYS
erosion of types 1100, 2024, and 6061, by water at 70°F, cavitation, 20: 29640 (NP-16048)
Al–Be–Mg, analysis for beryllium, colorimetric, 20: 29111
Al–Bi, diffusion of erbium in molten, at 700°C, 20: 29797
Al–Cd, diffusion of erbium in molten, at 700°C, 20: 29797
Al–Cr–Co–Fe–Mo–Ni–Ti, joining of Udimet 500 and 700, by mechanical fastening, 20: 29667 (RSIC-509)
Al–Cr–Co–Fe–Mo–Ni–Ti, surface treatments for Udimet 500 and 700, coating and mechanical, 20: 29706 (NASA-TM-X-53448)
Al–Cr–Co–Mo–Ni–Ti, joining of M-252, by mechanical fastening, 20: 29667 (RSIC-509)
Al–Cr–Co–Mo–Ni–Ti, surface treatments for Astroloy, coating and mechanical, 20: 29706 (NASA-TM-X-53448)
Al–Cr–Co–Mo–Ni–Ti–V–Zr, surface treatments for IN-100, coating and mechanical, 20: 29706 (NASA-TM-X-53448)
Al–Cr–Co–Ni–Nb–Ti–W, surface treatments for Mar-M 200, coating and mechanical, 20: 29706 (NASA-TM-X-53448)
Al–Cr–Fe–Mo–Ni–Ti–W, joining of D-979, by mechanical fastening, 20: 29667 (RSIC-509)
Al–Cr–Ni–Ti, corrosion by trichloroethylene, tracer studies of, 20: 29655
Al–Cu–Nb, phase studies on, 20: 29764
Al–Cu–Ta, phase studies on, 20: 29764
Al–Nb, intermetallic compounds in, properties of, for use in aerospace technology, 20: 29770
Al–Nb, radiation effects on superconducting properties of boron- and uranium-doped, thermal neutron, (E), 20: 30260
Al–Ni–Nb, crystal structure of M-phase, (E/T), 20: 30734(R) (TID-22970, pp 1-63)
Al–Ni–U, corrosion by steam, 20: 30794(R) (IDO-17147, pp 1-12)
Al–Pb, diffusion of erbium in molten, at 700°C, 20: 29797
Al–Sn–Ti, mechanical properties at –320 to 200°F, effects of hydrogen content on, 20: 29715 (WANL-TME-1287)
Al–Sn–Ti, sorptive properties for hydrogen at 200 to 925°F, 20: 29715 (WANL-TME-1287)
Al–Ta, intermetallic compounds in, properties of, for use in aerospace technology, 20: 29770
Al–Ti, analysis for carbon by induction furnace combustion method, 20: 29083(R) (UCRL-14767)
Al–U, irradiation testing of, 20: 30794(R) (IDO-17147, pp 1-12)
Al–U, metallographic tests on arc melted, 20: 29775
Al–U, reactions with steam at 400 to 1600°C, kinetics of isothermal, 20: 29188
Al–U, x-ray attenuation in, measurement of, 20: 29707 (ORNL-TM-1457)
Al–Y, crystal structure of intermetallic compound YAl_3 in, 20: 29721
Cr–U, precipitation of chromium needles following beta-to-alpha transformation in, 20: 29747

ALUMINUM FLUORIDES
thermodynamic properties of, emf measurements of, 20: 29215

ALUMINUM HYDROXIDES
sorptive properties for fission products in waste solutions, 20: 29332 (ORNL-P-1811)

ALUMINUM IONS
electron spin resonance spectra of, radioinduced defect pairs of, in alpha-aluminum oxides, 20: 30759

ALUMINUM ISOTOPES Al-26
energy levels from magnesium-25 (d,n) and (He-3,d) reactions, 20: 30481
energy levels of, parity and spin of, (E), 20: 30528

ALUMINUM ISOTOPES Al-27
neutron reactions (n,p) at 14.8 Mev, cross sections for, (E), 20: 30394
proton scattering at 3.5 to 11.3 Mev, excitation functions for, (E), 20: 30415

ALUMINUM NITRATES
effects on clarification and coalescence time of fuel elements during processing in organic solvents, 20: 29333 (RT-CHI-(65)33)

ALUMINUM OXIDES
coating of, effects of, on oxidation resistance of graphite, 20: 29773
coating with molybdenum or tungsten by chloride and oxide processes, 20: 29631
content in thalenites from Japan, 20: 29399
effects on fluorination of uranium dioxide in hydrofluoric acid–chlorine trifluoride–fluorine cycle, 20: 29330(R) (EURAEC-1601)
microstructure, 20: 29623(R) (TID-22970, pp 121-256)
oxygen diffusion in, 20: 29623(R) (TID-22970, pp 121-256)
properties of, for use as protective coating on niobium and its alloys, 20: 29651
radiation effects on, 20: 29623(R) (TID-22970, pp 121-256)
radiation effects on electric conductivity of, gamma, 20: 29823
radioinduced aluminum-ion defect pairs in alpha, ESR spectra of, 20: 30759
radioinduced blistering of, ion, (E), 20: 29816
reactions with niobium at 1800 to 2200°K, kinetics of, 20: 29174
sorptive properties for fission products in waste solutions, 20: 29332 (ORNL-P-1811)
Al_2O_3–B_2O_3–EuO, boron-11 NMR in, (E), 20: 30761
Al_2O_3–ZrO_2, fabrication of, method for, 20: 29695(P)

ALUMINUM SYSTEMS
Al–Cr–Si, properties of, for use as protective coating on niobium and its alloys, 20: 29651
Al–Si, properties of, for use as protective coating on niobium and its alloys, 20: 29651
Al–Si–U, radiation effects on clarification and coalescence time during processing of, in organic solvents, 20: 29333 (RT-CHI-(65)33)
Al–U_3O_8, fabrication of Zircaloy-2-clad fuel elements of, 20: 29658 (ANL-6283)
Al–U_3O_8, irradiation testing of, 20: 30794(R) (IDO-17147, pp 1-12)

AMAZON RIVER
effects of outflow of, on biology, chemistry, and hydrography of Atlantic Ocean, 20: 28878 (NYO-1918-138)

AMERICIUM
separation from berkelium, californium, cerium, curium, europium, and uranium by ion exchange on zirconium phosphate, 20: 29340
separation from curium by extraction chromatography using a quaternary ammonium nitrate, 20: 29337

AMERICIUM BROMIDES
heat of formation, 20: 29229

AMERICIUM CHLORIDES
heat of formation, 20: 29229
with nitrilotriacetic acid, stability of, 20: 29195

AMERICIUM FLUORIDES
heat of formation, 20: 29229

AMERICIUM IODIDES
heat of formation, 20: 29229

AMERICIUM ISOTOPES Am-241
metabolism of, 20: 28885
production of, economics of reactor, 20: 29609 (NP-15947)

AMETHOPTERIN
effects on immune response in γ-irradiated mice transplanted with bone marrow, 20: 29035

AMIDE POLYMERS
mechanical properties of composites of phenolic nylon, 20: 29708 (SC-DC-65-1744)
radioinduced polymerization of monomers to, 20: 29316

AMINES
determination in atmosphere using radioactive clathrate techniques, 20: 29142

AMINO ACIDS
content in blood plasma of normal and tumor-bearing mice, 20: 28923
content in blood plasma, effects of radiotherapy of gynecological tumors on, 20: 28979
metabolism of, measurement of, *in vivo* by internal counting, 20: 28871(R) (EUR-2636.f,i)
radiation effects on, quantum efficiency of uv, 20: 28915
radiolysis of tritium-labeled, ESR spectra of radicals from self-, 20: 29311

AMMONIA

complexes with copper, effects of, on oxidation of uranium dioxide by oxygen in carbonate solutions, catalytic, 20: 29199
complexes with rhenium chlorides, production of powdered rhenium from, 20: 29672
content in Amazon River, effects on biology, chemistry, and hydrography of Atlantic Ocean, 20: 28878 (NYO-1918-138)
content in Atlantic Ocean, measurements on, 20: 28877 (NYO-1918-124)
content in Atlantic Ocean, measurements on, 20: 28878 (NYO-1918-138)
production of hydrazine from liquid, fissio-chemical process for, 20: 29319(P)
radiation effects on synthesis of, gamma, 20: 29312
NH_3–H_2O, radiolysis of, hydrogen yields from gamma, 20: 29295
NH_3–O–H_2O, radiolysis of, hydrogen yields from gamma, 20: 29295

AMMONIUM BROMIDES
deuteron magnetic resonance in single crystals of deuterated, 20: 29191
properties and structure of single-crystal, ultrasonic studies of, (E/T), 20: 30734(R) (TID-22970, pp 1-63)

AMMONIUM CHLORIDES
deuteron magnetic resonance in single crystals of deuterated, 20: 29191
effects on frequency of radioinduced chromosome aberrations in Tradescantia, 20: 29028
hypersonic attenuation near critical point of, 20: 30734(R) (TID-22970, pp 1-63)
properties and structure of single-crystal, ultrasonic studies of, (E/T), 20: 30734(R) (TID-22970, pp 1-63)

AMMONIUM COMPOUNDS, QUATERNARY
chlorine-36 exchange between, and isopropyl chloride, kinetics of, 20: 29156
solvent properties of Aliquat-336 nitrate for americium and curium, 20: 29337

AMMONIUM FLUORIDES
effects on corrosion of zirconium by hydrochloric acid, 20: 29649
effects on triton diffusion in ice single crystals, 20: 29193
NH_4F–UO_2–H_2O, properties of solid phases in, chemical and physical, 20: 29200

AMMONIUM PLUTONYL PHOSPHATES
solubility of, in aqueous solutions at pH 1.0 to 6.4, 20: 29219

AMMONIUM THORIUM PHOSPHATES
preparation and properties of, 20: 29160

AMMONIUM THORIUM SULFATES
preparation and properties of, 20: 29226
preparation and properties of, 20: 29218

AMPLIFIERS
book: *Plasma and Electron uhf Amplifiers and Generators*, (E/T), 20: 29500
calibration of, design of relay-controlled pulse generator for, 20: 29544
design and performance of field-effect transistor, 20: 29548
design of lock-in, for audio and radio frequency, 20: 29487 (UCRL-16632)
design of semiconductor microwave, electromagnetic oscillation theory for, 20: 30677
development of beam-plasma, for millimeter waves, 20: 30718

ANALYSIS
equipment and procedures for, in pure materials research, 20: 29141
heavy-ion scattering at large angles for, 20: 29090

ANEMIA
radioinduced in man, erythropoietin content for diagnosing, 20: 28871(R) (EUR-2636.f,i)
radioinduced, effects of dose on, 20: 28982

ANEMOMETERS
design of wind recording system, 20: 29502
operation of hot-wire, for diagnostics of partially ionized plasma, (E/T), 20: 30702

ANIMAL CARE
radiation effects on electrophoretic mobility of, in suspensions, γ and x, 20: 28905

ANIMAL CELLS
radiation effects on, heavy-ion, 20: 28930 (CONF-651109, pp 601-16)
radiation effects on protein synthesis in Ehrlich mouse ascites tumor cells, x, 20: 28923
radiation effects on growth kinetics of leukemic, x, 20: 28962
radiation effects on skin epithelial, x, 20: 28990
radiation effects on mouse thymic, methods for evaluating, 20: 29008
radiosensitivity of, effects of cysteamine on, 20: 29057
transplantation of bone marrow, dosage, preservation, and survival in, 20: 28875

ANIMAL REPRODUCTION
radiation effects in embryonic stage in chickens, 20: 29015

ANIMALS
enzyme activity in, effects of nembutal and radiomimetic substances on, 20: 29048
fallout shelters for, design of, 20: 29392
radiation effects on blood coagulation in, review, 20: 28985
radiation effects on health of domestic, uv, 20: 29020
radiation effects on nerve action potentials in cold-blooded, x, 20: 29021
radiosensitivity of, variations in, 20: 28981

ANION EXCHANGE MATERIALS
properties of anionites for separation of hafnium and zirconium, 20: 29352
sorptive properties of metal sulfide, for radioisotopes in sea water, 20: 29345

ANOXIA
radiosensitivity effects on Ehrlich ascites carcinoma and mouse spleen, mechanism for, 20: 29039

ANTENNAS
radiation effects on signals from monopole, gamma, 20: 29580

ANTHRACENE
reactions with muonium, (E), 20: 29247

ANTIBIOTICS
effects of injected, on irradiated rabbits, 20: 29052
effects on radiation sickness in rabbits, 20: 29051
radiosensitivity effects of marinamycin, on leukopenia in rabbits, 20: 29055

ANTIBODIES
content in circulating mouse blood, effects of deuteration on, 20: 28988
radiation effects on formation of, in rabbits, 20: 28965
synthesis in mice, induction by injected lymphoid cell RNA, 20: 28926 (AD-633469)

ANTIFERROMAGNETIC MATERIALS
electron spin resonance in, line width of, (T), 20: 30780
magnetic spin correlations in, 20: 29623(R) (TID-22927, pp 121-256)

ANTIGENS
radiation effects on response of thymectomized chickens to, 20: 29014

ANTIMONY
determination in petroleum, activation, 20: 29139
evaporation of, from irradiated uranium(IV-VI) oxides at 900 to 1500°C in flowing hydrogen, nitrogen, or oxygen, 20: 29211
neutron capture cross section measurement at 80 to 200 kev, errors in using boron monitors for, (E), 20: 30352 (NASA-TR-R-240)
neutron inelastic scattering cross sections at 1 Mev, (E), 20: 30383

ANTIMONY ALLOYS
Sb–Bi, superconducting transition temperature of amorphous, (E), 20: 30298
Sb–Re, phase studies, 20: 29717
Sb–Zn, thermoelectric properties of intermetallic compound in, 20: 29709(R) (TID-22970, pp 65-119)

ANTIMONY ISOTOPES Sb-121
energy levels from neutron inelastic scattering at 1 Mev, spin of, 20: 30383

ANTIMONY ISOTOPES Sb-123
energy levels from neutron inelastic scattering at 1 Mev, spin of, 20: 30383

ANTIMONY ISOTOPES Sb-124
beta decay of, matrix elements for first-forbidden, (E/T), 20: 30522

ANTIMONY SYSTEMS
Sb–Nb–Te, phase studies, 20: 29717

ANTINEUTRINOS
interactions with protons, vector current conservation in, (T), 20: 30008

ANTINUCLEONS
interactions with nucleons, quark model for annihilation, 20: 30005

ANTIPROTONS
annihilation at rest in deuterium, analysis of, (E), 20: 29992 (UCRL-16717)
interaction with protons, Regge-pole exchange model for $Y\bar{Y}$ production in, 20: 30044
interactions with protons, Regge cuts in high-energy elastic, (T), 20: 30160
interactions with protons at 3.0 Bev/c, Byers-Yang model for charge-exchange, 20: 30014
interactions with protons at high momentum transfer, cross section for elastic, (T), 20: 30019
interactions with protons at 5 to 20 Bev/c, meson-exchange model for forward elastic, 20: 30039
interactions with deuterons at high energies, amplitudes for elastic, (T), 20: 30051
photo production on hydrogen and nitrogen at 4.1 to 6.2 Bev, (E), 20: 30432

ARCHAEOLOGICAL SPECIMENS
age estimation of, use of carbon-14 for, 20: 29438 (CONF-650652)

ARGON
alkali-metal negative-ion dissociation in, cross sections for, (T), 20: 29947
analysis for impurities, mass spectrometric, 20: 29083(R) (UCRL-14767)
argon-ion scattering at 200 ev to 4 kev, resonant electron capture in, (E), 20: 29944
determination as impurity in ultrapure gases, mass spectrometric, 20: 29083(R) (UCRL-14767)

determination by isotope dilution methods, use of standard in solid phase for, 20: 29102
effect on production of powdered rhenium from rhenium tetrammine chloride, 20: 29672
effects on melting points of plutonia–urania, 20: 29621(R) (NUMEC-3524-17)
electron drift velocity and collision frequency in plasma column of, (E), 20: 30598
electron scattering at 40 to 120 kev, calculation of amplitudes for, 20: 29945
hydrogen ion reactions with, lifetime of n = 3 hydrogen states from, (E), 20: 29930
hydrogen negative-ion dissociation in, cross sections for, (T), 20: 29947
magnetohydrodynamic flow of axisymmetric free plasma jet of, flow-field and Hall potentials perturbation's in, (E/T), 20: 30176
neutron scattering by liquid, analysis of slowdown in, (T), 20: 30166 (NYO-3326-13)
production of rotating plasma of, in crossed fields, (E), 20: 30582
proton reactions at 50 to 200 kev, secondary electron emission in, (E), 20: 29951
reactions with calcium, magnesium, molybdenum, tantalum, and zirconium, combustion, 20: 29641(R) (SC-DC-65-1691)
separation of nitrogen impurity from, use of titanium-metal sponge as gettering agent for, · 20: 29329 (ANL-7128)
shock compression of liquid, (E/T), 20: 30170 (UCRL-14251)
shock-wave reflection in, in em shock tube, (E), 20: 30697
stabilization of high-current pulsed discharge in, using h-f electric field, (E), 20: 30698
temperature distribution in arc produced plasma of, 20: 30563 (NP-16096)

ARGON IONS
scattering by argon at 200 ev to 4 kev, resonant electron capture in, (E), 20: 29944

ARGON ISOTOPES
abundance ratio determination of, using Omegatron, 20: 29413

ARGON ISOTOPES Ar-36
energy levels of, spin of, (T), 20: 30360 (WASH-1068)

ARGON ISOTOPES Ar-37
determination of, design and performance of small proportional counters for, 20: 29559

ARGON ISOTOPES Ar-39
diffusion in potassium chloride–rubidium chloride single crystals, 20: 30769

ARGON ISOTOPES Ar-40
uses of ion beams of, for chemical and isotopic analysis, 20: 29090

ARGON ISOTOPES Ar-41
beta decay of, β-γ circular polarization correlation from, (E), 20: 30542
diffusion in potassium chloride–rubidium chloride single crystals, 20: 30769

ARGON SYSTEMS
Ar–He, glow discharges at 1 to 25 torr; between planar anode and hollow cathode, 20: 30173

ARGONNE ADVANCED RESEARCH REACTOR
design and component testing, summary for July 1964 to June 1965, 20: 30787(R) (ANL-7190, pp 11-142)
reactivity measurements for, 20: 30932(R) (ANL-7204, pp 65-73)

ARGONNE FAST REACTOR EXPERIMENT TEST
design and component testing, summary for July 1964 to June 1965, 20: 30787(R) (ANL-7190, pp 11-142)

ARGONNE NATIONAL LAB., LEMONT, ILL.
environs monitoring, 1965, 20: 29434

ARGONNE RESEARCH REACTOR
coolant distribution plenum stress analysis, 20: 30787(R) (ANL-7190, pp 11-142)

ARGONNE SYNCHROTRON
radiation environment of, measurement of, 20: 29843 (CONF-651109, pp 34-56)
radiation monitoring of, performance of neutron film for, · 20: 29523 (CONF-651109, pp 639-46)

ARSENAZO III
precipitation of protactinium with, in acid solutions in presence of crystal violet, 20: 29135

ARSENIC
analysis of, for traces of copper, activation, 20: 29087
evaporation of, from irradiated uranium(IV-VI) oxides at 900 to 1500°C in flowing hydrogen, nitrogen, or oxygen, 20: 29211

ARSENIC FLUORIDES
spectra of, infrared and Raman, (E/T), 20: 30734(R) (TID-22970, pp 1-63)

ARSENIC ISOTOPES As-75
proton reactions (p,α) with, selenium-76 level widths from, (E/T), 20: 30360 (WASH-1068)

ARSENIC SYSTEMS
As–Re, phase studies, 20: 29717

ASBESTOS
mechanical properties of composites of phenolic, 20: 29708 (SC-DC-65-1744)

ASCORBIC ACID
effects of dietary, on guinea pigs and rats, 20: 28921
radiation effects on content of, in cotton plants, γ, 20: 28999

ASPHALT
content in bituminous paving mixture, thermal neutron bombardment-counting technique for determining, 20: 29509
radioactive waste disposal in, 20: 30943(R) (ORNL-TM-1465)

ASTATINE ISOTOPES At-215
alpha decay, 20: 30374

ATHEROSCLEROSIS
effects on catecholamine metabolism in man, 20: 29032
radiation effects on pathology of rat, x, 20: 28996

ATLANTIC OCEAN
analysis for carbon, chlorophyll, dissolved oxygen, inorganic nutrients, nitrogen, and salinity, · 20: 28878 (NYO-1918-138)
analysis for chlorine, chlorophyll, dissolved oxygen, inorganic nutrients, and silicates, · 20: 28877 (NYO-1918-124)
distribution of phytoplankton in, · 20: 28878 (NYO-1918-138)
effects of Amazon River outflow on biology, chemistry, and hydrography of, · 20: 28878 (NYO-1918-138)
radioactive contamination of, from fallout and waste disposal, 20: 29405 (NP-14694)
temperature of, along northeastern coast of South America, 20: 28878 (NYO-1918-138)

ATMOSPHERE
analysis for fallout using gamma spectrometer, behavior of cesium-137 in, 20: 19081 (NP-14705)
analysis for fluorine and hydrofluoric acid, apparatus for, 20: 29330(R) (EURAEC-1601)
carbon-14 content in, 1963 and 1964, 20: 29472
electric conductivity of, weather prediction determinations from, 20: 29402
electron energy spectra in, variations of soft, 20: 30201(T) (NASA-TT-F-389, pp 277-81)
electron intensity distributions at altitudes <1600 km, 20: 30200(T) (NASA-TT-F-389, pp 273-6)
electron reactions in, x-ray production from, 20: 30218(T) (NASA-TT-F-389, pp 616-23)
fallout monitoring of, along 80th meridian W, Jan. through March 1965, 20: 29430
fluorescence in, from nuclear explosions, calculation of prompt, (T), 20: 30193 (LA-3409(Suppl.))
particle dispersion in, from quasi-instantaneous sources, 20: 29403
particle fallout and dispersion in, model for, · 20: 29454(R) (SC-CR-66-2010)
potential gradient of ground-level, effects of nuclear explosions on, 20: 30227
properties of upper, review of, 20: 30196(T) (NASA-TT-F-389, pp 8-25)
radioactivity levels in upper, after July 9, 1962, explosion, (E), 20: 30234

ATOMIC BEAMS
production of, apparatus design considerations for, 20: 29918 (UCRL-11670)

ATOMIC ENERGY COMMISSION
legislation for fiscal year 1967, hearings before Joint Committee on Atomic Energy, Part 1, 20: 30957
legislation for fiscal year 1967, hearings before Joint Committee on Atomic Energy, Part 2, 20: 30958
legislation for fiscal year 1967, hearings before Joint Committee on Atomic Energy, Part 3, 20: 30959

ATOMIC EXPLOSIONS
blast waves from, design of shock tube for simulation of, 20: 29371 (AWRE-E-1/66)
effects of fallout from, on populations in United Kingdom, 20: 29054 (NP-16119)
effects on atmospheric potential gradient near ground, 20: 30227
effects on ionosphere, 20: 30228
effects on survivors, hematologic, 20: 28876
fallout formation and global distribution from, · 20: 29407(T) (AEC-tr-6666)
fallout from Chinese test in rainwater, settled dust, and sewage sludge in Japan, 20: 29455
fallout from Chinese, May 1965, 20: 29429
fallout from 1964 Chinese, radionuclide fractionation in, 20: 29423
fallout from, composition and transport of, 20: 29411
fallout from, in Japan, 1964 and 1965, 20: 29422
fallout particle detection in the Osaka, Japan, region from the Chinese, in October, 1964, 20: 29466
gamma flux effects on monopole antenna signals, 20: 29580
use for highway construction, 20: 29370 (PNE-3003)

ATOMIC PHYSICS
spectral studies of atomic resonances using infrared lasers, 20: 30734(R) (TID-22970, pp 1-63)
ATOMICS INTERNATIONAL, CANOGA PARK, CALIFORNIA
environs monitoring, 1965, 20: 29434
ATOMS
coupling scheme for, in ligand field theory, 20: 29205
electron scattering by, Thomas-Fermi theory for cross sections for, 20: 29946
energy level determination for two- and three-electron, using configuration interaction, (T), 20: 29917 (TID-22957)
energy levels of, 20: 29931(T)
energy spectra of recoil, from photonuclear reactions in solids, (E), 20: 30479
ion reactions at low energies, method for measuring cross sections for, (E/T), 20: 29932(T)
photon scattering by K-shell electrons of, spectral distributions from, (E/T), 20: 29912 (ISS-66/6)
photon scattering by K-shell electrons of, spectral distributions from, (E/T), 20: 29913 (ISS-66/7)
photon scattering by K-shell electrons of, spectral distributions from, (E/T), 20: 29914 (ISS-66/8)
reactions of excited, with thermal molecules, mathematical model for, 20: 29233
ATTAPULGITES
sorptive properties for fission products in waste solutions, 20: 29332 (ORNL-P-1811)
AUGER ELECTRONS
spectra of indium-113, measurement of, (E), 20: 30527
AURINTRICARBOXYLIC ACID, AMMONIUM SALTS
complexes with lanthanum, scandium, and yttrium, composition and stability of, spectrophotometric studies of, 20: 29180
AUSTRALIA
potassium, thorium, and uranium abundances in gneisses and granites of Rum Jungle Complex, 20: 29415
AZULENE
deuterium exchange between, and acetic acid–methanol solutions, 20: 29245

B

BACTERIA
biochemistry, ecology, taxonomy, and ultrastructure of nitrifying, in ocean water, 20: 28878 (NYO-1918-138)
effects on uv radiation damage on DNA in *E. coli*, 20: 28991
radiation effects on, in fish, γ, 20: 29583(R) (TID-22515)
radiation effects on solubilization of cholinesterase from plaice muscles by, 20: 28933
radiosterilization effects on, in precooked marine products, 20: 29582(R) (MIT-3343-26)
BACTERIOPHAGES
infectivity of DNA isolated from, 20: 28948
radiation effects on, genetic uv, 20: 28969
radiation effects on genetic recombination in, uv and x, 20: 28948
radioinduced in *E. coli*, protective effects of AET and MEA against x, 20: 29045
resistance of radioinduced mutants of *E. coli* to T1, 20: 29027
BARIUM
determination in aqueous solutions, design of oxyacetylene burner for measuring sensitivity of spectrophotometric, 20: 29083(R) (UCRL-14767)
determination in petroleum, activation, 20: 29139
BARIUM ISOTOPES Ba-140
effects on blood and hematopoietic system, 20: 28982
BARIUM NITRATES
radiation effects on, isothermal-annealing kinetics of gamma, 20: 29814
BARIUM STANNATES
use as source for Mössbauer effect measurements on tin-119, 20: 30753(T)
BARIUM TITANATES
spectra of single-crystal, Raman, (E/T), 20: 30734 (TID-22970, pp 1-63)
BARLEY
radioinduced mutations of, γ and neutron, 20: 28960
BARRIERS
materials for carbon dioxide–hydrogen separation, 20: 29362
BARYONS
decay of, universal V-A theory for leptonic, 20: 30058
electromagnetic form factors from saturation of SU(3) algebra of current densities, 20: 30119
electromagnetic properties of, composite-particle model for, (T), 20: 30069
electromagnetic properties, (T), 20: 29922
interactions with mesons at low energies, (T), 20: 30070
interactions with mesons, current algebras for, 20: 30006
magnetic moments in current algebra, 20: 30118
mass spectra of, dynamical symmetry for, 20: 30091 (JINR-P-2621)
symmetry model for, configuration mixing and magnetic moments from, 20: 30143
BARYONS, RESONANCE
photoproduction of N* on protons, SU(6) symmetry predictions for, 20: 30043
production and decay of, (T), 20: 30085 (CONF-640509(Pt.1), Paper 3)
production of N*(1236), in meson (K⁻)-proton interactions at 1.45 Bev/c, (E), 20: 30009
production of N*(1688), in proton-proton interactions at 3 Bev, (T), 20: 30034
production of T = ½ isobar in meson (π⁺)-proton interactions at 1.84 Bev/c, (E), 20: 30022
properties of Ξ*, (E), 20: 30072
BASES
radiation effects on total volatile, in fish, gamma, 20: 29583(R) (TID-22515)
BASTNAESITES
crystal structure of, effects of ignition on, 20: 29447
spectra of, infrared, 20: 29447
thorium alpha decay in, structural changes from, 20: 29447
BATTERIES
development for space power, 20: 29977 (N-65-32716)
BAUXITE
sorptive properties for fission products in waste solutions, 20: 29332 (ORNL-P-1811)
BEARINGS
development of gas, 20: 29366(R) (TID-22970, pp 375-91)
development of stainless steel, 20: 29366(R) (TID-22970, pp 375-91)
protective coatings for, 20: 29366(R) (TID-22970, pp 375-91)
BENTONITES
properties for ion exchange separation of strontium-90 and yttrium-99 from water, 20: 29348
BENZAMIDE
analysis for carbon-14 by dry combustion methods, 20: 29085
BENZANTHRACENE
7,12-dimethyl-, effects on skin of mice, protective effects of pre-irradiation by beta particles against carcinogenetic, 20: 28973
BENZENE
effects on oxygen-18 exchange between water and copper and iron sulfates, 20: 29153
effects on radioinduced isomerization of stilbene, 20: 29287
oxidation in aqueous solutions to phenol, deuterium isotope effects and tracer studies on, 20: 29250
radioinduced oxidation of, to phenol in aqueous solutions, tracer studies on, 20: 29250
reactions with muonium, (E), 20: 29247
BENZENE, BROMO-
reactions with muonium, (E), 20: 29247
BENZENE, CHLORO-
reactions with muonium, (E), 20: 29247
BENZENEARSONIC ACID, DERIVATIVES
precipitation of protactinium in acid solutions with, in presence of crystal violet, 20: 29135
BENZENEARSONIC ACID, *o*-(1,8-DIHYDROXY-3,6-DISULFO-2-NAPHTHYLAZO)-
precipitation of protactinium in acid solutions with, in presence of crystal violet, 20: 29135
arsenazo I–EDTA–nitrosonaphthol, uses for colorimetric micro-determination of uranium, 20: 29130
***m*-BENZENEDISULFONIC ACID, 4,5-DIHYDROXY-, SODIUM SALT**
uses in potentiometric determination of thorium, 20: 29093
BENZIMIDAZOLETHIOL
effects on radiation effects on polypropylene, 20: 29290
BENZOIC ACID
analysis for carbon-14 by dry combustion methods, 20: 29085
BENZOIC ACID, *p*-AMINO-
analysis for carbon-14 by dry combustion methods, 20: 29085
BENZOIC ACID, (*p*-BROMOPHENYL) ESTERS
analysis for carbon-14 by dry combustion methods, 20: 29085
BERKELIUM
separation from americium, californium, cerium, curium, europium, and uranium by ion exchange on zirconium phosphate, 20: 29340
BERYLLIUM
determination in aqueous solutions, design of oxyacetylene burner for measuring sensitivity of spectrophotometric, 20: 29083(R) (UCRL-14767)
determination in aluminum–beryllium–magnesium alloys, colorimetric, 20: 29111
determination of, Weibull function for pulse-height distribution from

x-ray micro-, (T), 20: 29124
effects on copper or silver infiltrants in graphite, 20: 29764
fabrication of powder compacts of, by isostatic pressing and sintering, 20: 29681
iron-57 Mössbauer spectra in, 20: 30766
mechanical properties of, at −196 to 700°C for use in aircraft, 20: 29767
neutron age and slowing-down time in, (T), 20: 30333
neutron flux in moderators of, multi-velocity corrections in activation measurements of, 20: 29539
platinum-195 Mössbauer effect in, (E), 20: 30757
properties as fuel cladding for carbon dioxide-cooled reactors, 20: 29777
protective coatings for, anodic, 20: 29366(R) (TID-22970, pp 375-91)
thermionic properties, 20: 29801
use on Agena-D spacecraft, 20: 29393

BERYLLIUM ALLOYS
Al–Be–Mg, analysis for beryllium, colorimetric, 20: 29111
Be–Mo, intermetallic compounds in, properties of, for use in aerospace technology, 20: 29770
Be–Nb, intermetallic compounds in, properties of, for use in aerospace technology, 20: 29770
Be–Ni, analysis for impurities in, development of electron microprobe for, 20: 29083(R) (UCRL-14767)
Be–Ta, intermetallic compounds in, properties of, for use in aerospace technology, 20: 29770
Be–Ti, intermetallic compounds in, properties of, for use in aerospace technology, 20: 29770
Be–U, metallographic tests on arc melted, 20: 29775
Be–Zr, intermetallic compounds in, properties of, for use in aerospace technology, 20: 29770
Be–Zr, thermionic properties, 20: 29801

BERYLLIUM ISOTOPES Be-8
energy levels from lithium-6 (Li-6,α) reactions, (E), 20: 30530
energy levels of, from lithium-8 beta decay, 20: 30363
energy spectra of 1p shell, determination using Hamada-Johnston potential, (T), 20: 30354(R) (ORNL-3940, pp 62-9)

BERYLLIUM ISOTOPES Be-9
deuteron reactions (d,γ) at 0.4 to 1.4 Mev, angular distributions and cross sections for, (E), 20: 30393
deuteron reactions (d,n) with, boron-10 spectroscopic factors from, 20: 30481
energy spectra of 1p shell, determination using Hamada-Johnston potential, (T), 20: 30354(R) (ORNL-3940, pp 62-9)
helium-3 reactions (He-3,n) at 3 to 10 Mev, excitation functions for, (E), 20: 30444
helium-3 reactions (He-3,d), boron-10 spectroscopic factors from, 20: 30481
neutron elastic scattering at 2.60 to 2.77 Mev, polarization from, (E), 20: 30414

BERYLLIUM ISOTOPES Be-10
energy levels from neutron elastic scattering by beryllium-9 at 2.60 to 2.77 Mev, parity and spin of, (E), 20: 30414
neutron reactions (n,γ) with, cross sections for thermal, (E), 20: 30347(R) (IDO-17147, pp 13-28)

BERYLLIUM OXIDES
analysis for contamination in fuel tubes of, development of electron microprobe for, 20: 29083(R) (UCRL-14767)
dimensional stability under loads, 20: 29366(R) (TID-22970, pp 375-91)
properties for use in nuclear reactors, chemical, mechanical, neutronic, and thermal, 20: 29810
radiation effects on mechanical and thermal properties of, neutron, 20: 29810
thermionic properties, 20: 29801
Be–BeO, fabrication of, for use at high temperatures, 20: 29689
BeO–PuO_2–ThO_2, development as reactor fuel, 20: 29616(R) (BMI-1738)
BeO–UO_2, fission-product distribution in irradiated, 20: 29616(R) (BMI-1738)
BeO–UO_2, properties as fuel material, 20: 29810
BeO–UO_2, radiation effects on microstructure of, 20: 29616(R) (BMI-1738)
BeO–W, fabrication of sintered, 20: 29689

BERYLLIUM SYSTEMS
Be–B–Co, crystal structure of compounds in, 20: 29795
Be–BeO, fabrication of, for use at high temperatures, 20: 29689
Be–B–Ni, crystal structure of compounds in, 20: 29795
Be-graphite, fabrication of reactor reflectors from, 20: 30816(P)
Be–Mo–Si, compounds in, properties of, for use in aerospace technology, 20: 29770

BETA DECAY
conference, 20: 30534
interactions in, induced pseudoscalar, (T), 20: 30539
matrix elements for first-forbidden, determination of, (E/T), 20: 30522
measurement of, nuclear structure from, 20: 30536
theory of meson (μ) and nuclear, 20: 30535

BETA PARTICLES
detection and measurement in fallout in Osaka, Japan, October, 1964, 20: 29466
dose to monkey skeletons from ingested strontium-90, 20: 28896
effects of pre-irradiation by, on skin carcinogenesis induced by 7,12-dimethylbenzanthracene, 20: 28973
effects of strontium-90, on cholesterol and lipid content in rat blood, 20: 28994
effects of, from fallout on development, mortality, and sterility of insects and invertebrates, 20: 28925 (AD-633024)
effects on conditioned reflexes of dogs, 20: 29009
effects on Drosophila, genetic, 20: 28955
effects on gelling of resin-impregnated substrates, 20: 29637(P)
effects on thyroid activity in dogs, 20: 29000
polarization from gold-198 and phosphorus-32, relative, (E), 20: 30548
reactions with organic compounds in water-s_2, atomic structure determinations by, 20: 29326
scattering from aluminum in 2π geometry, (E), 20: 30369
scattering of, analysis of chromic salt solutions by back-, 20: 29107
scattering of, uses of, in chemical analysis, 20: 29110
use in measurement of layer thickness in multilayer coating, 20: 29391
use in therapy of skin diseases, 20: 29072

BETA SOURCES
activity of bismuth-210, prepared by polonium-218 electrostatic collection, 20: 29324
design for production of modulated beam, 20: 29516(P)
preparation of strontium-90, for use in radioecology studies, 20: 28879
uses in vacuum gages, 20: 29600

BETA SPECTRA
analysis of, matrix elements from numerical, 20: 30541

BETA SPECTROMETERS
design and performance of $\pi\sqrt{2}$ iron-free, 20: 30527

BETATRONS
beam injection current and pulse duration effects on output of, 20: 29869
stability of plasma, theory for slipping, 20: 30680

BIBLIOGRAPHIES
on boiling, surface tension, and wetting of mercury, 20: 29620 (NP-16046)
on effects of fallout beta radiation on insects and invertebrates, 20: 28925 (AD-633024)
on geochronology of North America, 20: 29397 (NAS-NRC-1276)
on oxidation reactions of reactor materials, 20: 30801
on partial molal thermal capacities of aqueous rare earth chloride solutions at 25°C, 20: 29144 (IS-1355)
on radioinduced inflammation, 20: 28943
on radioinduced polymerization of organic compounds, 20: 29298
on reaction rates for high-temperature air, 20: 29146 (SC-R-66-885)
on reactor engineering, 20: 30786(R) (ANL-7190)
on structure of liquid metals and alloys, 20: 29755
on weak interactions, 20: 30067

BINDERS
preparation of aluminide, 20: 29623(R) (TID-22970, pp 121-256)

BINDING ENERGY
calculation for heavy nuclei with nonlocal two-body forces, 20: 30508

BIOLOGICAL MATERIALS
carbon-14 content in, 1963 and 1964, 20: 29472
effects of radioprotective compounds on damaged, molecular mechanisms for, 20: 29040
radioactivity of, computer program for evaluating determinations of, 20: 29121

BIOLOGICAL MODELS
for iodine metabolism, 20: 28871(R) (EUR-2636.f,i)
properties of, 20: 28871(R) (EUR-2636.f,i)
radiation injuries in, effects of free radical reactions on, 20: 29037
transfer functions of dynamic, 20: 28871(R) (EUR-2636.f,i)

BIPYRIDINES
complexes with cobalt, isotope exchange in radiocobalt divalent ion-doped, 20: 29259
complexes with cobalt, radioinduced recoil damage in, thermal annealing of neutron, 20: 29259

BISMUTH
iron-57 Mössbauer spectra in, 20: 30766

BISMUTH ALLOYS
Al–Bi, diffusion of erbium in molten, at 700°C, 20: 29797
Bi–Cd, distillation of liquid, surface concentration changes in, 20: 29346
Bi–In, electron spectra of, effects of magnetic fields on, (E), 20: 30735(R) (TID-22970, pp 331-73)
Bi–Pb, erosive effects on heat-resisting alloys at 500 and 1500°F, cavitation, 20: 29640 (NP-16048)
Bi–Pb, magnetic hysteresis in type II superconductors of, surface current effects on, (E), 20: 30269

Bi–Pb, superconducting transition temperature of amorphous, (E), 20: 30298
Bi–Pb, surface critical currents and a-c susceptibility transition in superconducting, (E), 20: 30293
Bi–Re, phase studies, 20: 29717
Bi–Tl, annealing and deformation effects on intermetallic compound in, 20: 29623(R) (TID-22970, pp 121-256)
Bi–Tl, superconducting transition temperature of amorphous, (E), 20: 30298
Sb–Bi, superconducting transition temperature of amorphous, (E), 20: 30298

BISMUTH ISOTOPES Bi-208
energy levels from polonium-208 decay, 20: 30405

BISMUTH ISOTOPES Bi-209
energy levels from polonium-209 decay, 20: 30405
meson (μ^-) capture by, x-ray spectra from, (E), 20: 29525 (CONF-660209-9)
neutron scattering at 4.0 Mev, polarization angular distributions from, (E), 20: 30360 (WASH-1068)

BISMUTH ISOTOPES Bi-210
beta activity of, from electrostatic collection of polonium-218, 20: 29324
beta decay of, time-reversal invariance in, 20: 30537

BISMUTH TELLURIDES
performance for thermoelectric power generation, analysis of, 20: 29975 (GIC-3362-4)
radiation effects on, proton, 20: 29623(R) (TID-22970, pp 121-256)

BITUMINOUS MATERIALS
asphalt content in paving mixture of, thermal neutron bombardment-counting technique for determining, 20: 29509

BLADDER
radioinduced cystitis in, treatment with tanderil, 20: 29060

BLOOD
radiation effects on, extracorporeal-exposure, 20: 28927 (BNL-9647)
radiation effects on adrenaline content of dog, x, 20: 28941
radiation effects on, review of immediate, 20: 28982
radiation effects on cholesterol content of rat, x, 20: 28992
radiation effects on cholesterol and lipid content of rat, strontium-90, 20: 28994
radiation effects on cholesterol-protein complexes in dog, 20: 28998
radiation exposure of, extracorporeal, 20: 28927 (BNL-9647)
radioactivity of, computer program for evaluating determinations of, 20: 29121

BLOOD CELLS
pathology, physiology, and morphology, 20: 28874
radiation effects on activity and synthesis of carbonic anhydrase in, x, 20: 28922
radiation effects on, factors affecting, 20: 28981
radiation effects on iron uptake by dog, x, 20: 29029

BLOOD CIRCULATION
measurement of cerebral, using krypton-85, 20: 28871(R) (EUR-2636.f,i)
radiation effects on rabbit, x, 20: 29010
rate of coronary, measurement of, using krypton-85 and rubidium-86, 20: 28871(R) (EUR-2636.f,i)

BLOOD COAGULATION
radiation effects on patterns of, review of γ, neutron, and x, 20: 28985

BLOOD FORMATION
radiation effects on, effects of fractionated exposure on γ, neutron, or x, 20: 28984

BLOOD PICTURE
radiation effects on, in survivors of nuclear bombings, 20: 28876
radiation effects on guinea pig, chronic low-dose x, 20: 28945

BLOOD PLASMA
amino acid content of, effects of radiotherapy of gynecological tumors on, 20: 28979
amino acid content in, of normal and tumor-bearing mice, 20: 28923
radiation effects on proteins in rabbit, uv, 20: 29004
radiation effects on iron clearance rates in dog, x, 20: 29029

BLOOD PLATELETS
radiation effects on, 20: 28981

BLOOD PRESSURE
radiosensitivity of rat, effects of serotonin compounds on, 20: 29050

BLOOD SERUM
antibody content in mouse, effects of deuteration on, 20: 28988
radiation effects on proteins in mouse, x, 20: 28899

BLOOD TRANSFUSIONS
radiosensitivity effects of, 20: 28893
use in removing radioactive materials from tissues, 20: 28893

BLOOD VESSELS
effects of bleeding from, on serum protein metabolism in rats, 20: 28954

BOILERS
design for pressurized water reactors, 20: 30911(P)
design of forced-flow, once-through, 20: 30821(P)
design of sodium-heated, 20: 30806(R) (BAW-1280-36)
design of, integral with nuclear reactor, 20: 30913(P)
inspection of PWR, 20: 29616(R) (BMI-1738)
nozzle design for, stress analysis for, (T), 20: 30928

BOILING
burnout in annular spray flow, probe techniques for analyzing, 20: 29378(R) (NYO-3304-7)
burnout in nonuniformly heated annular tubes, (E/T), 20: 29377(R) (BAW-3238-11)
burnout in tubular flow with nonuniform heat fluxes, (E/T), 20: 29376 (BAW-3238-9)
pressure drop in uniformly heated channel flow, (E/T), 20: 29380(R) (TID-22967)

BOILING REACTORS
coolant flow stability in channels of, 20: 29385
fuel-element cladding in, use of stainless steel as, 20: 30903
stability of, effects of steam voids on, 20: 29375(R) (ANL-7190, pp 193-200)

BOLIVIA
lead ores from Andes in, age estimation and lead isotopic ratio measurements of, 20: 29439

BONDING
properties in brazed and rolled, correlation of heat transfer and ultrasonic transmission, 20: 29386 (ANL-7074)

BONE MARROW
effects of injected, on irradiated rabbits, 20: 29052
effects of transplanted, following whole-body radiation exposure, 20: 28875
radiation doses to, by strontium-90 uptake in bones, 20: 29054 (NP-16119)
radiation effects on immune reactions to transplants of, in mice, 20: 29606
radiation effects on heme synthesis in rabbit, effects of hormones on, 20: 28912
radiography of, use of colloidal technetium-99m in, 20: 29065
radiosensitivity effects of preserved homologous, in mice, gamma, 20: 29033
radiosensitivity effects in mice treated with AET, γ, 20: 29036
transplantation of, experimental and theoretical problems in, 20: 28875
transplants in γ-irradiated mice, effects of methotrexate on, 20: 29035

BONES
alpha radioactivity in human, from America and Germany, 20: 29476
radioinduced free radicals in rat, EPR study of, 20: 28898 (CEA-R-2910)
radioinduced free radicals in rat, γ, 20: 28906
radiosterilization of, for use as grafts, 20: 28987

BORON
determination in stainless steel by neutron cross section measurements, 20: 29117
determination of, by neutron activation methods, 20: 29078(R) (AD-633252)
determination of, Weibull function for pulse-height distribution from x-ray micro-, (T), 20: 29124
effects on ductility of molybdenum, 20: 29675
effects on structure of annealed graphite, electron microscopy and x-ray-diffraction studies on, 20: 29625
performance of, as deoxidizer during arc-melting of molybdenum, 20: 29675

BORON CARBIDES
coating of, effects of, on oxidation resistance of graphite, 20: 29773
effects of lumped, on reactor criticality, 20: 30836 (BAW-3492-1)
hardness and surface friction of, effects of temperature on, 20: 29771
properties for uses as control materials in nuclear reactors, 20: 29732
B_4C–Cu, fabrication and mechanical properties of sheets of, 20: 29664 (LA-DC-7745)

BORON CARBONITRIDES
BCN–$MoSi_2$, preparation and properties, 20: 29169

BORON FLUORIDES
performance in square-tube proportional counters for neutron detection, 20: 30347(R) (IDO-17147, pp 13-28)

BORON ISOTOPES B-9
energy level decay from helium-3 reactions (He-3,α) with boron-10, proton emission in, (E), 20: 30445

BORON ISOTOPES B-10
energy levels from beryllium-9 (d,n) and (He-3,d) reactions, 20: 30481
energy spectra of 1p shell, determination using Hamada-Johnston potential, (T), 20: 30354(R) (ORNL-3940, pp 62-9)
helium-3 reactions (He-3,α) with, proton emission from boron-9 levels from, (E), 20: 30445
lithium-6 and -7 reactions at 3 Mev, angular distributions and total cross sections for, (E), 20: 30519
neutron capture cross sections at 10.7 to 247.0 kev, (E), 20: 30360 (WASH-1068)
neutron cross section measurements for, errors in, (E), 20: 30352

(NASA-TR-R-240)
neutron reactions (n,n'γ) at 2 to 15 Mev, gamma spectra from, (E), 20: 30358(R) (RPI-328-56, pp 1-48)
neutron scattering by, amplitude for coherent, 20: 30335
nitrogen-14 reactions (N-14,N-13) at 8 to 16 Mev, cross sections for, (E/T), 20: 30353(R) (ORNL-3940, pp 1-61)

BORON ISOTOPES B-11
energy spectra of 1 p shell, determination using Hamada-Johnston potential, (T), 20: 30354(R) (ORNL-3940, pp 62-9)
lithium-6 and -7 reactions at 3 Mev, angular distributions and total cross sections for, (E), 20: 30519
neutron reactions (n,α) at 14.2 Mev, lithium-8 production in, (E), 20: 30363
neutron scattering by, amplitude for coherent, 20: 30335
nuclear magnetic resonance in aluminum oxides–boron oxide–europium oxide system, (E), 20: 30761

BORON NITRIDES
spectra of, infrared, (E/T), 20: 30734(R) (TID-22970, pp 1-63)

BORON OXIDES
Al_2O_3–B_2O_3–EuO, boron-11 NMR in, (E), 20: 30761

BORON SYSTEMS
Be–B–Co, crystal structure of compounds in, 20: 29795
Be–B–Ni, crystal structure of compounds in, 20: 29795

BOROSILICATE GLASS
effects of lumped, on reactor criticality, 20: 30836 (BAW-3492-1)

BOSONS
decays of, $SU(6)_w$ symmetry for radiative, 20: 30040
interactions of many-body-systems of, persistent currents in, 20: 30140
interactions of W, cross sections for photon production in, 20: 30057
interactions with fermions, lagrangian density for, 20: 30122
model of intermediate vector, mixing, 20: 30133
symmetry for, relation between Poincare group and exceptional lie group G(2), 20: 30115
wave equations of, in plane electromagnetic field, Kemmer, 20: 30155

BRAIN
blood flow in, measurement of, using krypton-85, 20: 28871(R) (EUR-2636.f,i)
calcium-45 metabolism in slices of guinea pig, effects of alkaloids on, 20: 28891
nucleic acid content in guinea pig, effects of radiation sickness on, 20: 28919
radiation effects on mutagenic properties of tissue extracts from mouse, x, 20: 28959
radiation effects on rabbit, pathological x, 20: 29011
ultrasonic wave effects on, laser-generated, 20: 28951

BRAKES
design for reactor control rods, 20: 30817(P)

BRASS
transformation in rapidly cooled, 20: 29623(R) (TID-22970, pp 121-256)

BREASTS
cancer of, hormone dependence of, 20: 28871(R) (EUR-2636.f,i)

BREEDER REACTORS
design of long-lifetime seed-blanket, 20: 30921(P)
design of 1000-Mw(e) fast, 20: 30875(R) (ANL-7190, pp 143-55)

BREMSSTRAHLUNG
emission in radiative processes, nuclear contribution to, (T), 20: 30516
interactions with protons at threshold to 6 Bev, meson (ρ^0) production, in, (E), 20: 30030
polarization of 6-Bev coherent, 20: 30045
production of relativistic E1, 20: 29949
reactions with nuclei in solids, range of recoil atoms from, (E), 20: 30479

BRITISH REACTORS
development, 20: 30798(R) (NP-16043)
development of power, 20: 30885
development of sodium-cooled fast, 20: 30798(R) (NP-16043)
development of steam-generating heavy-water, 20: 30798(R) (NP-16043)

BROMIDE COMPLEXES
with erbium and neodymium, composition and stability of, 20: 29225

BROMINE
determination in petroleum, activation, 20: 29139
determination of, by neutron activation methods, 20: 29078(R) (AD-633252)
diffusion in potassium bromides, surface evaporation effects on, (E), 20: 29731

BROMINE ISOTOPES
beta decay of, for synthesis of krypton compounds, 20: 29327

BROMINE ISOTOPES Br-80
recoil reactions with alkanes, yields from, 20: 29233

BROMINE ISOTOPES Br-82
beta decay of, krypton-82 levels from, (E), 20: 30410
exchange between bromine–graphite lamellar compounds and bromine, kinetics of, 20: 29182
incorporation in 5-bromouracil by isotopic exchange method, 20: 29244

BROMINE SYSTEMS
Br–butane, tritium reactions with gas-phase, scavenging effects on hot and thermal recoil, 20: 29206
Br–ethane, tritium reactions with gas-phase, scavenging effects on hot and thermal recoil, 20: 29206

BROMOFORM
reactions with muonium, (E), 20: 29247

BROMOORGANIC COMPOUNDS
radiolysis of, Finkelstein reaction for measuring partial organic retention in, 20: 29292

BROWNIAN MOVEMENT
theory of, fluctuation-dissipation theorem in, 20: 30186

BUBBLE CHAMBERS
particle track photographs from, reconstruction of events from, 20: 29533

BUILDING MATERIALS
flaws in, uses of gamma sources for detection of, 20: 29390
properties of fibrous, 20: 29624(R) (TID-22970, pp 257-329)

BURNS
effects of, in irradiated rats, 20: 29001

BUTADIENE POLYMERS
radioinduced *trans-cis* isomerization of, 20: 29321(P)
polybutadiene–polystyrene, radiation effects on viscoelastic properties of, gamma, 20: 29313

BUTANE
helium atom reactions with, electron kinetic energy from ionization in, (E), 20: 29927
Br–butane, tritium reactions with gas-phase, scavenging effects on hot and thermal recoil, 20: 29206
butane–I, tritium reactions with gas-phase, scavenging effects on hot and thermal recoil, 20: 29206

BUTANE, 1-BROMO-
radioinduced reactions with tin, 20: 29616(R) (BMI-1738)
radiolysis of, at 77°K, reaction intermediates in gamma, 20: 29264

BUTANE, 1-CHLORO-
radioinduced formation from hydrogen chloride and ethylene, 20: 29252
radiolysis of, at 77°K, reaction intermediates in gamma, 20: 29264

BUTANE, 1-IODO-
radiolysis of, at 77°K, reaction intermediates in gamma, 20: 29264

BUTANE, 2-IODO-
radiolysis of, at 77°K, reaction intermediates in gamma, 20: 29264

2-BUTANONE
effects on electric conductivity of anhydrous uranyl nitrate, 20: 29184

2-BUTENE
photolysis of, kinetics of, 20: 29251
radiolysis of, kinetics of, 20: 29251

BUTYL PHOSPHATES
solvent properties for uranium, synergistic effects of trioctylphosphine oxide on, 20: 29334
solvent properties for uranium, 20: 29355
kerosene–TBP, radiation effects on solvent properties for uranium and thorium in nitrate solutions, 20: 29272
Shellsol T–TBP, radiation effects on clarification and coalescence time of reactor fuel solutions in, 20: 29333 (RT-CHI-(65)33)
TBP–trioctylphosphine oxide, solvent properties for uranium, effects of electronegative groups on, 20: 29347

C

CADMIUM
determination in petroleum, activation, 20: 29139
evaporation of, from irradiated uranium(IV-VI) oxides at 900 to 1500°C in flowing hydrogen, nitrogen, or oxygen, 20: 29211
gamma scattering at 100 to 280 kev, electron binding effects on incoherent, (E/T), 20: 29923
neutron inelastic scattering cross sections at 1 Mev, (E), 20: 30383
uses as neutron absorber in production of gold-198, 20: 29610

CADMIUM ALLOYS
Al–Cd, diffusion of erbium in molten, at 700°C, 20: 29797
Bi–Cd, distillation of liquid, surface concentration changes in, 20: 29346
Cd–Gd, magnetic properties of, 20: 29752

CADMIUM ISOTOPES Cd-108
energy level widths, (E/T), 20: 30360 (WASH-1068)

CADMIUM ISOTOPES Cd-110
triton reactions (t,p) at 7.2 Mev, strong coupling approximation method for studying, (T), 20: 30399

CADMIUM ISOTOPES Cd-111
neutron inelastic scattering at 14.07 to 14.78 Mev, activation cross sections for, (E), 20: 30360 (WASH-1068)

CADMIUM ISOTOPES Cd-113
gamma scattering by, production of isomeric levels by, (E), 20: 30489

CADMIUM ISOTOPES Cd-114
neutron scattering at 4.0 Mev, polarization angular distributions from, (E),

20: 30360 (WASH-1068)
CADMIUM OXIDES
radiation effects on electric conductivity of, neutron, 20: 29821
CdO–Sc_2O_3, phase studies, 20: 29168
CADMIUM SELENIDES
spectra of, infrared, (E/T), 20: 30734(R) (TID-22970, pp 1-63)
CADMIUM SULFIDES
dissolution kinetics, 20: 29623(R) (TID-22970, pp 121-256)
electric properties of single-crystal and thin-film, 20: 29709(R) (TID-22970, pp 65-119)
radioinduced defects in single crystals of, 13.5-Mev deuteron, 20: 30771
CADMIUM TELLURIDES
optical properties of, 20: 29709(R) (TID-22970, pp 65-119)
CALCITES
thermoluminescence of, effects of climate and temperature on natural, 20: 29398
CALCIUM
content in foods, 20: 29433
determination in aqueous solutions, design of oxyacetylene burner for measuring sensitivity of spectrophotometric, 20: 29083(R) (UCRL-14767)
effects in diet on strontium-90 content of milk in cattle, 20: 29459
effects on separation of strontium from yttrium by paper chromatography, 20: 29349
reactions in gaseous mixtures, combustion, 20: 29641(R) (SC-DC-65-1691)
separation from strontium by ion exchange, 20: 29363
CALCIUM FLUORIDES
defect equilibra and deformation of, 20: 29623(R) (TID-22970, pp 121-256)
fluorine-19 nuclear spin-lattice relaxation time in neodymium-doped crystals of, 20: 30772
radioinduced laser lines in erbium-doped single crystals of, gamma, (E), 20: 30774
radioinduced thermoluminescence of rare earth ions in, 20: 29318
radioinduced thermoluminescence in single crystals of, temperature effects on, 20: 30767
rare-earth ion absorption spectra in, trivalent, 20: 30763
CALCIUM ISOTOPES Ca-40
deuteron elastic scattering at 34.4 Mev, angular distributions from, (E/T), 20: 30353(R) (ORNL-3940, pp 1-61)
deuteron elastic scattering at 11 and 12.8 Mev, stripping channel effects on cross sections for, (E), 20: 30431
deuteron reactions (d,d), (d,d′), and (d,p) at 12.8 Mev, cross sections for, (E), 20: 30459
energy levels from potassium-39 (p,γ) reactions at 0.5 to 2.9 Mev, (E), 20: 30482
energy levels from deuteron inelastic acattering at 12.8 Mev, (E), 20: 30459
meson (μ^-) capture by, giant dipole resonance model for radiative, 20: 30451
nitrogen-14 reactions (N-14,N-13) at 8 to 16 Mev, cross sections for, (E/T), 20: 30353(R) (ORNL-3940, pp 1-61)
proton elastic scattering at 40 Mev, cross sections for, (E/T), 20: 30353(R) (ORNL-3940, pp 1-61)
triton reactions (t,p) at 7.2 Mev, strong coupling approximation method for studying, (T), 20: 30399
CALCIUM ISOTOPES Ca-41
energy levels from deuteron reactions (d,p) with calcium-40 at 12.8 Mev, (E), 20: 30459
CALCIUM ISOTOPES Ca-42
deuteron reactions (d,p) at 7.0 and 7.2 Mev, angular distributions from, (E), 20: 30452
energy levels of, shell-model calculation using realistic interactions for, 20: 30384
CALCIUM ISOTOPES Ca-43
energy levels from deuteron reactions (d,p) with calcium-42 at 7.0 and 7.2 Mev, (E), 20: 30452
CALCIUM ISOTOPES Ca-44
helium-3 reactions (He-3,d) with, scandium-45 levels from, (E/T), 20: 30429
CALCIUM ISOTOPES Ca-45
metabolism in guinea pig brain slices, effects of drugs on, 20: 28891
yield in alpha and proton reactions with copper, 20: 30531
CALCIUM ISOTOPES Ca-47
beta decay of, β-γ circular polarization correlation from, (E), 20: 30542
CALCIUM ISOTOPES Ca-48
beta decay of, limits for lepton-conserving and -nonconserving double, (E), 20: 30461
CALCIUM NITRATES
$Ca(NO_3)_2$–$UO_2(NO_3)_2$–H_2O, activity coefficients of, at 25°C, 20: 29196
CALCIUM OXALATES
precipitation of strontium oxalate with, 20: 29154
CALCIUM OXIDES
content in thalenites from Japan, 20: 29399
CALDER HALL REACTORS
economics of Dungeness B, 20: 30885
CALIFORNIA
lead and strontium abundances and isotopic compositions in brines under Salton Sea area, 20: 29414
radioactivity in water supplies, 1965, 20: 29434
CALIFORNIUM
separation from americium, berkelium, cerium, curium, europium, and uranium by ion exchange on zirconium phosphate, 20: 29340
spectra of, 20: 29083(R) (UCRL-14767)
CALIFORNIUM ISOTOPES Cf-252
metabolism of, 20: 28885
CALORIMETERS
design of adiabatic, for measuring specific heats of aqueous solutions at 25°C, 20: 29144 (IS-1355)
performance of high-temperature, for solutions, 20: 29623(R) (TID-22970, pp 121-256)
CAMBRIDGE SYNCHROTRON
safety guides from July 1965 explosion and fire analysis, 20: 29851 (CONF-651109, pp 556-73)
CAMERAS
radiation detector device for use with, 20: 29573(P)
CANADA
fallout monitoring in, 1966, 20: 29053 (NP-15951)
radiation protection in, program for, 20: 29053 (NP-15951)
CANADIAN REACTORS
economics of heavy water, power, 20: 30885
power requirements evaluation, 20: 30891
CANDU REACTOR
environs monitoring, January 1966, 20: 29053 (NP-15951)
power requirements evaluation, 20: 30891
CAPILLARIES
gas transport and self-diffusion in, model for, 20: 30174
gas transport in, (E/T), 20: 30175
CARBAMIC ACID, DIETHYLDITHIO-, SODIUM SALTS
radiosensitivity effects on phage induction in *E. coli*, x, 20: 29045
CARBAMIC ACID, DITHIO-, AMMONIUM SALTS
radiosensitivity effects on phage induction in *E. coli*, x, 20: 29045
CARBIDES
analysis for oxygen in cemented, method for, 20: 29108
CARBON
content in Atlantic Ocean, measurements on, 20: 28878 (NYO-1918-138)
deposition on fuel particles in fluidized bed, process variables for, 20: 29671
deposition on thorium uranium dicarbide fuel particles, 20: 29670
determination in aluminum–titanium alloys, carbon steel, and titanium by combustion method, 20: 29083(R) (UCRL-14767)
determination of, Weibull function for pulse-height distribution from x-ray micro-, (T), 20: 29124
effects of impurities of, on mechanical properties and structure of tungsten single crystals, 20: 29793
effects of interstitial atoms of, on deformation of graphite, 20: 29735
effects on ductility of electron-beam-melted molybdenum, 20: 29783
gamma scattering at 100 to 280 kev, electron binding effects on incoherent, (E/T), 20: 29923
mechanical properties of composites of phenolic, 20: 29708 (SC-DC-65-1744)
mechanical properties and structure of pyrolytic, deposited in fluidized bed, 20: 29736
molecular constants and thermodynamic functions of, triatomic, (T), 20: 29921
neutron spectra in, (T), 20: 30326
performance of, as deoxidizer during arc-melting of molybdenum, 20: 29675
plasma production on, by light pulses from laser, 20: 30666
production of carbide-containing vitreous, method for, 20: 29692(P)
properties of pyrolytic coatings of, on reactor fuel particles, 20: 30870(R) (ORNL-TM-1528)
proton elastic scattering at 12.8 to 13.4 Mev, angular distribution of polarization from, (E), 20: 30457
radiation effects on dimensions, permeability, and thermal conductivity of hard, reactor, 20: 29822
reactions with tantalum in sputtering, properties of films formed by, 20: 29745
thermal diffusion in refractory metals, 20: 29769
CARBON COMPOUNDS
decomposition, distribution, and production in ocean water, 20: 28878 (NYO-1918-138)
CARBON DIOXIDES
decomposition of, using fission fragment recoil energy, 20: 29317
determination as impurity in ultrapure gases, mass spectrometric, 20: 29083(R) (UCRL-14767)

diffusion coefficients of, measurement by tracer technique, 20: 29510
effects of vacuum ultraviolet irradiated, on oxidation of graphite, structural studies on, 20: 29733
electron energy levels of, determination of, using infrared lasers, (E), 20: 30734(R) (TID-22970, pp 1-63)
helium atom reactions with, electron kinetic energy from ionization in, (E), 20: 29927
leakage in pressure vessels, mechanism and rate of, 20: 30810
molecular dissociation following carbon-14 beta decay in, calculation of, 20: 29233
radiosensitivity effects on organoleptic properties of fish, gamma, 20: 29583(R) (TID-22515)
reactions with calcium, magnesium, molybdenum, tantalum, and zirconium, combustion, 20: 29641(R) (SC-DC-65-1691)
reactions with uranium nitride and uranium carbide oxides at 500 to 1000°C, 20: 29645
separation from hydrogen by gaseous diffusion, 20: 29362
shock-wave reflection in, in em shock tube, (E), 20: 30697
solidification and dropping in vacuum for plasma production, 20: 30594

CARBON IONS
spectra in hydrogen plasma, use in electron temperature measurements, 20: 30705

CARBON ISOTOPES C-12
alpha elastic and inelastic scattering at 40.5 Mev, angular distributions for, (E), 20: 30450
alpha elastic and inelastic scattering at 13 to 26 Mev, cross sections for, (E), 20: 30499
alpha reactions (α,γ) at 2.8 to 8.3 Mev, resonances from, 20: 30529
deuteron elastic scattering at 34.4 Mev, angular distributions from, (E/T) 20: 30353(R) (ORNL-3940, pp 1-61)
deuteron reactions (d,Li-7) at 34.4 Mev, angular distributions from, (E), 20: 30353(R) (ORNL-3940, pp 1-61)
electron inelastic scattering by, excitation in, (E), 20: 30360 (WASH-1068)
electron inelastic scattering by, transverse form factors for, (T), 20: 30411
energy spectra of 1 p shell, determination using Hamada-Johnston potential, (E/T), 20: 30354(R) (ORNL-3940, pp 62-9)
helium-3 reactions (He-3,p) at 2.25 to 3.60 Mev, angular correlations and distributions in, (E), 20: 30526
helium-3 reactions (He-3,α), (He-3,d), and (He-3,n) at 3 to 10 Mev, excitation functions for, (E), 20: 30444
lithium-6 reactions with, angular distributions and total cross sections for, (E), 20: 30520
oxygen-16 reactions (O-16,α) at 20 to 40 Mev, cross sections for, (E/T), 20: 30353(R) (ORNL-3940, pp 1-61)
production in lithium-6 and -7 reactions with boron-10 and -11, 20: 30519
proton elastic scattering at 40 Mev, cross sections for, (E/T), 20: 30353(R) (ORNL-3940, pp 1-61)
uses of ion beams of, for chemical and isotopic analysis, 20: 29090

CARBON ISOTOPES C-13
alpha elastic and inelastic scattering at 40.5 Mev, angular distributions for, (E), 20: 30450
deuteron reactions (d,n) with, nitrogen-14 spectroscopic factors from, 20: 30481
effects on oxidation of carbon monoxide by copper oxide and iodine pentoxide, 20: 29187
energy levels from helium-3 reactions (He-3,α) with carbon-14 at 44.8 Mev, (E), 20: 30438
helium-3 reactions (He-3,d), nitrogen-14 spectroscopic factors from, 20: 30481
production in lithium-6 and -7 reactions with boron-10 and -11, 20: 30519

CARBON ISOTOPES C-14
beta emission of, backscattering from aluminum in 2π geometry, (E), 20: 30369
content in foods and man, 1963 and 1964, 20: 29472
determination by liquid scintillation counting, role of phosphorescence in, 20: 29084
determination in organic compounds by dry combustion methods, 20: 29085
effects in Beckmann rearrangement of phenyl-2-propanone oxime and acetophenone oxime, 20: 29242
effects on oxidation of methane by copper oxides, 20: 29187
energy levels from lithium-6 and -7 reactions with boron-10 and -11, 20: 30519
fixation in Atlantic Ocean, 20: 28878 (NYO-1918-138)
helium-3 reactions (He-3,α) at 44.8 Mev, carbon-13 levels from, (E), 20: 30438
incorporation in insecticides, 20: 29246
production in lithium-6 and -7 reactions with boron-10 and -11, 20: 30519
use in age estimation in archeology, geology, and hydrology, 20: 29438 (CONF-650652)
uses of ion beams of, for chemical and isotopic analysis, 20: 29090

CARBON MONOXIDES
determination as impurity in ultrapure gases, mass spectrometric, 20: 29083(R) (UCRL-14767)
effects on oxidation of graphite by vacuum ultraviolet irradiated carbon dioxide, 20: 29733
evolution from liquid iron, kinetics of, 20: 29623(R) (TID-22970, pp 121-256)
formation and functions in closed ecological systems, endogenous, 20: 28880
helium reactions with, electron kinetic energy from ionization in, (E), 20: 29927
hydrogen ion reactions with molecular, at 1 to 55 kev, particle production cross sections for, 20: 29919 (UCRL-14214)
oxidation by copper oxides and iodine pentoxide, effects of carbon-13 in, 20: 29187
reactions with neon atoms and ions, charge-exchange cross sections for, (E), 20: 29948
separation from hydrogen and methane by selective oxidation, isotope effects in, 20: 29187
yields from gamma radiolysis of frozen carbon tetrachloride–methanol solutions, 20: 29305

CARBON OXIDES
radiolysis of C_3O_2, gamma, 20: 29269

CARBON STEEL
analysis for carbon by induction furnace combustion method, 20: 29083(R) (UCRL-14767)
erosion by mercury and water, cavitation, 20: 29640 (NP-16048)

CARBON SYSTEMS
C–Cr, phase studies, stabilities, and thermodynamics of, at high temperatures, 20: 29774
C–Cr–Mo, phase studies and thermodynamics of, for use at high temperatures, 20: 29774
C–Cr–W, phase studies and thermodynamics of, for use at high temperatures, 20: 29774
C–Hf, fabrication of hypereutectic composites of, with high thermal shock resistance, 20: 29727
C–Hf–Ta, availability, properties, and uses of, 20: 29760
C–Hf–Ta–W, availability, properties, and uses of, 20: 29760
C–Hf–Ta–W, creep properties of T-222, 20: 29705(R) (NAS-CR-54973)
C–Hf–Ta–W, erosion of T-222, by mercury, water, and bismuth–lead alloy, cavitation, 20: 29640 (NP-16048)
C–Hf–Ta–W, tensile properties of T-222, effects of welds on, 20: 29712(R) (WANL-PR-(P)-009)
C–Hf–Ta–W, weldability of T-222, effects of oxygen contamination on, 20: 29712(R) (WANL-PR-(P)-009)
C–Mo, phase studies, stabilities, and thermodynamics of, at high temperatures, 20: 29774
C–Mo–Nb, phase studies and thermodynamics of, for use at high temperatures, 20: 29774
C–Mo–Nb–W–Zr, evaluation of protective coatings for, 20: 29651
C–Mo–Ta, phase studies and thermodynamics of, for use at high temperatures, 20: 29774
C–Mo–Ti–Zr, creep properties of TZC, 20: 29705(R) (NAS-CR-54973)
C–Mo–Ti–Zr, properties at high temperatures, 20: 29756
C–Mo–V, phase studies and thermodynamics of, for use at high temperatures, 20: 29774
C–Nb–W, phase studies and thermodynamics of, for use at high temperatures, 20: 29774
C–Nb–W–Y–Zr, tensile properties of D-43Y, effects of welds on, 20: 29712(R) (WANL-PR-(P)-009)
C–Nb–W–Zr, evaluation of protective coatings for, 20: 29651
C–Nb–W–Zr, fabricability, strength, and weldability of, 20: 29763
C–Nb–W–Zr, tensile properties of D-43, effects of welds on, 20: 29712(R) (WANL-PR-(P)-009)
C–N–V, phase studies, 20: 29749
C–Ta–W, phase studies and thermodynamics of, for use at high temperatures, 20: 29774
C–ThC, fabrication of vitreous, 20: 29692(P)
C–Th–U, hydrolysis of, production of methane during, 20: 29159
C–Ti, fabrication of hypereutectic composites of, with high thermal shock resistance, 20: 29727
C–U, metallographic tests on arc melted, 20: 29775
C–UC, fabrication of vitreous, 20: 29692(P)
C–W, phase studies, stabilities, and thermodynamics of, at high temperatures, 20: 29774
C–W–V, phase studies and thermodynamics of, for use at high temperatures, 20: 29774
C–Zr, fabrication of hypereutectic composites of, with high thermal shock resistance, 20: 29727

CARBON TETRACHLORIDE
effects on metabolism of serum proteins in rats, 20: 28954
effects on radioinduced isomerization of stilbene, 20: 29287
effects on radioinduced polymerization of solid methane, 20: 29314

reactions with muonium, (E), 20: 29247
carbon tetrachloride–methanol, radiolysis of frozen, free radical formation in gamma, 20: 29305
CARBONATE IONS
effects on sorption of uranium by ion exchange resins, 20: 29350
CARBONYL SULFIDE
helium atom reactions with, electron kinetic energy from ionization in, (E), 20: 29927
CARCINOGENESIS
effects of 7,12-dimethylbenzanthracene on, on mouse skin, 20: 28973
radioinduced in man by nuclear explosions, 20: 28876
CARCINOMAS
radiotherapy of, preparation of gold-198 colloids and platinum-coated gold-198 particles for, 20: 29075
CARIBBEAN SEA
distribution of phytoplankton in, 20: 28878 (NYO-1918-138)
CAROLINAS-VIRGINIA TUBE REACTOR
criticality studies for, 20: 30877(R) (CVNA-254)
development and research program, Oct.–Dec. 1965, 20: 30877(R) (CVNA-254)
safety programs, 20: 30897
CASCADE SHOWERS
calculation for accelerator shielding, review of, 20: 30719 (CONF-651109, pp 327-45)
calculation of, effects of mathematical errors in, (T), 20: 30725 (ORNL-3786)
CATALASES
radiolysis of, reactions of hydrated electrons and hydroxide radicals in pulse, 20: 29279
radiosensitivity of erythrocyte, x, 20: 28911
reactions with hydrated electrons and hydroxide radicals in pulse radiolysis, 20: 29279
CATALYSTS
analysis for water by titration, handling methods for, 20: 29083(R) (UCRL-14767)
molecular diffusion in porous, 20: 29624(R) (TID-22970, pp 257-329)
CATIONS
effects as impurities on radiation chemistry processes, 20: 29306
CATTLE
cesium-137 content in muscles in, effects of diet on, 20: 28887
cesium-137 in commercial feeds for, 20: 29463
iodine-131 content in thyroid glands of, 1965, 20: 29428
radiation effects on epididymal spermatozoa in testes of, x, 20: 29013
CAVES
decontamination of, procedures for, 20: 29468
CAVITY RESONATORS
electromagnetic field theory of, in rotating systems, 20: 29831
electron bunching in cylindrical, (T), 20: 29859
microwave absorption by plasma in, negative, (T), 20: 30587
CELLULOSE ACETATES
permeability to carbon dioxide–hydrogen mixtures, 20: 29362
radioinduced graft polymerization with acrylonitriles, gamma, 20: 29294
CERAMIC COATINGS
deposition on fired mixture of clay and radioactive wastes for disposal, 20: 30951(P)
CERAMIC MATERIALS
fabrication of ceramic–metal compounds for use at high temperatures, 20: 29689
mechanical properties of high-purity oxide, effects of crystal structure on, 20: 29740
properties for uses in nuclear industry, 20: 29732
CERIUM
determination in rocks, chemical spectrographic method for, 20: 29083(R) (UCRL-14767)
determination in standard igneous rocks G-1, W-1, and G-B by x-ray fluorescence, 20: 29101
determination in uranium compounds, spectrographic, 20: 29129
polarographic properties of, on fused potassium acid sulfate electrolyte, 20: 29210
separation from americium, berkelium, curium, europium, and uranium by ion exchange on zirconium phosphate, 20: 29340
spectra of, in cerium and lanthanum fluorides, infrared, 20: 29173
CERIUM ALLOYS
Ce–La, electric conductivity, magnetic susceptibility, and superconducting transition temperatures of, 20: 29753
Ce–Zn, crystal structure of intermetallic compounds in, 20: 29719
CERIUM CARBIDES
hydrolysis of, gaseous products from, 20: 29220
CERIUM COMPLEXES
hexanitrocobaltate, preparation and composition of, effects of temperature on, 20: 29209
with nitrilotriacetic acid, preparation and stability of, 20: 29228
with serine, stability of, 20: 29208
CERIUM FLUORIDES
spectra of cerium ions in, infrared, 20: 29173
CERIUM IONS
effects on radiolysis of naphthalene, 20: 29260
energy levels in lanthanum chlorides, Orbach relaxation mechanism for excited, 20: 30758
CERIUM ISOTOPES Ce-137
content in pulp for photographic paper, 20: 29427
CERIUM ISOTOPES Ce-141
beta decay of, β-γ circular polarization correlations in, (E), 20: 30543
content in fallout in USSR, 1962, 20: 29406 (NP-14719)
CERIUM ISOTOPES Ce-144
beta decay of, β-γ directional and circular polarization correlations in, (E), 20: 30544
content in fallout in USSR, 1962, 20: 29406 (NP-14719)
content in juniper trees in Georgia, 20: 29410
content in pulp for photographic paper, 20: 29427
separation from sea water by sorption by metal sulfide-ion exchange resins, 20: 29345
uses as power sources for underwater applications, 20: 29607
CERIUM NIOBATES
distribution in strontium molybdate single crystals, coefficients of, 20: 29746
CERIUM NITRATES
thermal decomposition, 20: 29224
CERIUM OXIDES
analysis for trace amounts of lanthanum and neodymium, spectrographic, 20: 29095
creep properties of, during reduction from CeO_2 to $CeO_{1.9}$, 20: 29739
electric conductivity of, at 20 to 1100°C, during reduction from CeO_2 to $CeO_{1.9}$, 20: 29739
electrolysis of calcium-doped ceramic and single-crystal, oxygen ion evolution during, (E), 20: 30743
CeO_2–UO_2, testing as reactor fuels, 20: 29616(R) (BMI-1738)
CERIUM TITANATES
preparation and crystal structure of, 20: 29212
CERMETS
coating of, effects of, on oxidation resistance of graphite, 20: 29773
CESIUM
density of, at critical temperature, radiometric techniques for measuring critical, 20: 29742
energy losses from plasma of, in arc-mode thermionic cells, (T), 20: 29981
particle losses from minimum-B confined, (E/T), 20: 30656
separation from aqueous solutions by solvent extraction using mono-alkyl ester of phosphoric acid, 20: 29365(P)
spectra of, Stark effect on optical, 20: 29941
CESIUM BROMIDES
luminescent decay and spectra of thallium-doped, at 2 to 300°K, 20: 30751
CESIUM EUROPIUM(II) FLUORIDES
cesium-133 NMR in, (E), 20: 30761
fluorine-19 NMR in, (E), 20: 30761
CESIUM IODIDES
luminescent decay and spectra of thallium-doped, at 2 to 300°K, 20: 30751
CESIUM IONS
dissociation of fast negative, in rare gases, (T), 20: 29947
CESIUM ISOTOPES Cs-123
decay scheme, (E), 20: 30403
CESIUM ISOTOPES Cs-133
nuclear magnetic resonance in cesium europium fluorides, (E), 20: 30761
CESIUM ISOTOPES Cs-134
determination in spent fuel elements, 20: 29078(R) (AD-633252)
CESIUM ISOTOPES Cs-137
content in beef cattle, effects of diet on, 20: 28887
content in cattle feed, 20: 29463
content in Colorado milk samples, May 1965, 20: 29429
content in human placenta, 20: 28894
content in juniper trees in Georgia, 20: 29410
content in man, meat, and milk in Norway, 1962 through 1965, 20: 29432
content in milk and milk products, 20: 29464
content in milk in U. S., 1962, 20: 29474
content in seal meat samples, 20: 29053 (NP-15951)
content in U. S. foods, 1962 and 1963, 20: 29475
desorption from soils, effects of sodium acetate on, 20: 30943(R) (ORNL-TM-1465)
determination in spent fuel elements, 20: 29078(R) (AD-633252)
effects on gamma spectrometric analysis of atmospheric fallout samples, 20: 29081 (NP-14705)
gamma spectra of, solid-state detectors for energy resolution of, 20: 29078(R) (AD-633252)
loss from diet samples during dry ashing and hydrochloric acid treatment,

20: 29122
radiation dose from, in persons using Clinch River water, 20: 29452 (ORNL-3721(Suppl.3))
separation from sea water by sorption by metal sulfide-ion exchange resins, 20: 29345
solubility in hydrochloric and hydrofluoric acid systems with nitric acid, 20: 29081 (NP-14705)
sorption from waste solutions by clay minerals, 20: 29332 (ORNL-P-1811)
use as gamma source for measuring density of stock coal, errors in, 20: 29491
uses as gamma source for detection of flaws in steel foils and plates, 20: 29390
uses as power sources for underwater applications, 20: 29607

CESIUM SAMARIUM CHLORIDES
preparation, 20: 29204

CESIUM SYSTEMS
Cs–Cl, production of thermally ionized plasma of, with negative ions, 20: 30575
Cs–graphite, bonding energy in, model for, 20: 29744

CESIUM THORIUM SULFATES
preparation and properties of, 20: 29226
preparation and properties of, 20: 29218

CHARGED PARTICLE BEAMS
focusing of, apparatus and method for, 20: 29872(P)
focusing of, electrostatic mirror with circular field for, 20: 29868
interactions with plasma, oscillation excitations from, (T), 20: 30689
production of constant-diameter finite-phase-volume, Pierce optics for, (T), 20: 29871

CHARGED PARTICLES
acceleration by transverse plane electromagnetic wave, quasilinear, (T), 20: 29867
acceleration from magnetic-energy dissipation near zero field lines in plasma, (T), 20: 30676
diffusion across magnetic fields, equations for, 20: 30714
emission from semi-infinite waveguides, (T), 20: 29828
emission in yttrium-87 formation by nuclear de-excitation with neutron emission, (T), 20: 29436
energy-loss spectra in semiconductor detectors, fluctuations of, (E/T), 20: 29531 (UCRL-16715)
identification of, semiconductor system for, 20: 29526 (INP-444/PL)
intensities in Van Allen radiation belts, (E), 20: 30235
motion in constant longitudinal and rotating transverse magnetic fields, (T), 20: 30693
motion in magnetic-dipole field in external homogeneous magnetic field, (T), 20: 29829
motion in magnetosphere, trapped-region asymmetrical configuration determination from, (T), 20: 30224
motion of elementary, Coulomb field from, (T), 20: 30144
scattering by nuclei, computer program for differential cross sections for elastic, 20: 30348 (INP-446/PL)
stabilization in accelerators using inductive walls, 20: 29860

CHEMICAL ANALYSIS
book: *Instrument and Chemical Analysis Aspects of Electron Microanalysis and Macroanalysis*, 20: 29119
laboratories for, equipment for automation of, 20: 29083(R) (UCRL-14767)

CHEMISTRY
book: *Chemistry of Selenium, Tellurium, and Polonium*, 20: 29235
cross sections and relaxation phenomena in, computer calculations of, 20: 29147 (UCRL-14901-T)
research on, center for, 20: 30937

CHICKENS
radiation effects on embryos of, pathological x, 20: 29012
radiation effects on immune response of thymectomized, x, 20: 29014
radiation effects in embryonic stage on body weights, growth patterns, and reproduction of, 20: 29015

CHINA
nuclear test in, effects on radioactivity of Colorado milk, 20: 29429

CHLORELLA
spectral properties of deuterated *C. vulgaris*, absorption and fluorescence, 20: 28872

CHLORIDE IONS
determination in sodium bromides by bremsstrahlung-activation methods, 20: 29112
effects on sorption of uranium by ion exchange resins, 20: 29350

CHLORINE
content in Atlantic Ocean, measurements on, 20: 28877 (NYO-1918-124)
detection by radioactive well logging, method for elimination of interference of iron casing in, 20: 29442(P)
detection in subsurface formations, gamma-neutron well logging equipment for, 20: 29446(P)
determination in atmosphere using radioactive clathrate techniques, 20: 29142
determination in borehole formations, shielding away for logging equipment for, 20: 29443(P)
determination in petroleum products and related materials by neutron activation methods, 20: 29116
determination in petroleum, activation, 20: 29139

CHLORINE FLUORIDES
determination in atmosphere using radioactive clathrate techniques, 20: 29142
ClF_3–F–HF, effects on fluorination of uranium dioxide, 20: 29330(R) (EURAEC-1601)

CHLORINE IONS
effects as substituent on solvent properties of organic phosphorus compounds for uranium, 20: 29347

CHLORINE ISOTOPES Cl-36
beta decay of, partial half life for, 20: 30375
exchange between cycloalkyl chlorides and lithium chlorides in dimethyl sulfoxide, kinetics of, 20: 29157
exchange between isopropyl chloride and tetrabutylammonium chloride, kinetics of, 20: 29156
incorporation in trichloroethylene for corrosion studies, 20: 29655

CHLORINE ISOTOPES Cl-37
deuteron reactions (d,p) at 7.5 Mev, chlorine-38 levels from, (E), 20: 30391
neutron reactions (n,p) at 14.8 Mev, cross sections for, (E), 20: 30394

CHLORINE ISOTOPES Cl-38
energy levels from deuteron reactions (d,p) with chlorine-37 at 7.5 Mev, (E), 20: 30391

CHLORINE SYSTEMS
Cs–Cl, production of thermally ionized plasma of, with negative ions, 20: 30575

CHLOROFORM
reactions with muonium, (E), 20: 29247

CHLOROORGANIC COMPOUNDS
analysis and determination of, by radio paper partition chromatography, 20: 29123

CHLOROPHYLLS
content in Atlantic Ocean, measurements on, 20: 28877 (NYO-1918-124)
content in Atlantic Ocean, measurements on, 20: 28878 (NYO-1918-138)

CHOLESTEROL
complexes with protein in dog blood, radiation effects on, 20: 28998
content in rat tissues, effects of diet on, 20: 28995
effects of nicotinic acid on content and radioactivity of, in rabbit liver, 20: 28895
radiation effects on, ESR and thermoluminescence studies of, 20: 29249
radiation effects on content in rat blood, x, 20: 28992
radiation effects on content in rat blood, strontium-90, 20: 28994
radiation effects on content in rat tissues, x, 20: 28995

CHOLINESTERASES
radiation effects on solubilization of, from plaice muscles by bacteria, 20: 28933

CHROMATOGRAPHY
chromatograph design for gas, of gases, 20: 29083(R) (UCRL-14767)
radioactivity measurements in gas, equipment for, 20: 29105

CHROMIUM
abundance and distribution in rocks, 20: 29436
deposition by vapor plating from chromium fluoride, 20: 29650
determination in chromic salt solutions by beta backscattering, 20: 29107
diffusion in nickel–5 thoria alloy for corrosion protection, 20: 29748
effects on copper or silver infiltrants in graphite, 20: 29764
neutron diffraction pattern of, 20: 30360 (WASH-1068)

CHROMIUM ALLOYS
Al–Cr–Co–Fe–Mo–Ni–Ti, joining of Udimet 500 and 700, by mechanical fastening, 20: 29667 (RSIC-509)
Al–Cr–Co–Fe–Mo–Ni–Ti, surface treatments for Udimet 500 and 700, coating and mechanical, 20: 29706 (NASA-TM-X-53448)
Al–Cr–Co–Mo–Ni–Ti, joining of M-252, by mechanical fastening, 20: 29667 (RSIC-509)
Al–Cr–Co–Mo–Ni–Ti, surface treatments for Astroloy, coating and mechanical, 20: 29706 (NASA-TM-X-53448)
Al–Cr–Co–Mo–Ni–Ti–V–Zr, surface treatments for IN-100, coating and mechanical, 20: 29706 (NASA-TM-X-53448)
Al–Cr–Co–Ni–Nb–Ti–W, surface treatments for Mar-M 200, coating and mechanical, 20: 29706 (NASA-TM-X-53448)
Al–Cr–Fe–Mo–Ni–Ti–W, joining of D-979, by mechanical fastening, 20: 29667 (RSIC-509)
Al–Cr–Ni–Ti, corrosion by trichloroethylene, tracer studies of, 20: 29655
Cr–Cu, thermal capacity below 1°K, 20: 29791
Cr–Fe–Zr, corrosion by steam, effects of fabrication process and nitride content on, 20: 29660(R) (GEAP-4960)
Cr–Fe–Zr, microstructure of, effects of heat treatments on, 20: 29660(R) (GEAP-4960)
Cr–Mo–Ni, compatibility with plutonium and uranium carbides, 20: 30790(R) (ANL-7204, pp 1-31)

Cr–Ni, corrosion by trichloroethylene, tracer studies of, 20: 29655
Cr–Ni–Stainless steel 304, corrosion in Saxton steam generator, 20: 30884(R) (WCAP-3269-16)
Cr–Re, effects of interstitial nitrogen on, 20: 29616(R) (BMI-1738)
Cr–U, metallographic tests on arc melted, 20: 29775
Cr–U, radioinduced grain boundary cavitation and cracking in, neutron, 20: 29807 (TRG-Report-325)

CHROMIUM BROMIDES
nuclear magnetic resonance in ferromagnetic, (E/T), 20: 30734(R) (TID-22970, pp 1-63)

CHROMIUM COMPOUNDS
analysis of aqueous solutions of, for chromium by beta backscattering, 20: 29107
radiation effects on, role of recoils in, 20: 29261

CHROMIUM IONS
effects on spinel properties, 20: 29709(R) (TID-22970, pp 65-119)
separation of recoiling divalent, from neutron-irradiated trivalent chromium ions, 20: 29261

CHROMIUM ISOTOPES Cr-48
yield in alpha and proton reactions with copper, 20: 30531

CHROMIUM ISOTOPES Cr-52
alpha scattering by, level spins and parities from, (E/T), 20: 30460
deuteron elastic scattering at 34.4 Mev, angular distributions from, (E/T), 20: 30353(R) (ORNL-3940, pp 1-61)
energy level structure from manganese-52 beta decay, (E), 20: 30458
neutron reactions (n,p) at 14.8 Mev, cross sections for, (E), 20: 30394

CHROMIUM ISOTOPES Cr-53
alpha scattering at 50 Mev, level spins and parities from, (E/T), 20: 30460

CHROMIUM OXIDES
CrO_3–Sc_2O_3, phase diagrams, 20: 29167

CHROMIUM SYSTEMS
Al–Cr–Si, properties of, for use as protective coating on niobium and its alloys, 20: 29651
C–Cr, phase studies, stabilities, and thermodynamics of, at high temperatures, 20: 29774
C–Cr–Mo, phase studies and thermodynamics of, for use at high temperatures, 20: 29774
C–Cr–W, phase studies and thermodynamics of, for use at high temperatures, 20: 29774
Cr–Mo–Si, properties of, for use as protective coating on niobium and its alloys, 20: 29651
Cr–Si–Ti, properties of, for use as protective coating on niobium and its alloys, 20: 29651
Cr–Si–W, properties of, for use as protective coating on niobium and its alloys, 20: 29651

CHROMOSOMES
aberrations in mouse cornea, induced by tissue extracts from x-irradiated donors, 20: 28959
radiation effects on, relation of DNA damage to, 20: 28908
radiation effects on paramecia, x, 20: 29007
radiation effects on anaphase bridges in, fast-neutron and x, 20: 29031
radioinduced aberrations in Tradescantia, effects of cupferron on frequency of x, 20: 29028
radioinduced breaks in onion, RBE for 200-kev fast-neutron, 20: 29002
radioinduced mutations of Drosophila, β, 20: 28955

CIRCUIT NOISE
suppression of large nonstatistical bursts of, digital noise filter for, 20: 29556

CIRCUITS
analysis of autodyne pickup, for NMR measurement in solids, 20: 29492
design and fabrication of digital noise filter, for scalers, 20: 29556
development of thin-film superconducting, 20: 30255(R) (ORO-2430-28)

CLAYS
effects of content of, on radioactivity of sedimentary rocks, 20: 29417
porosity and saturation of, x-ray or gamma absorption measurements of, 20: 29595
sorptive properties for fission products in waste solutions, 20: 29332 (ORNL-P-1811)
waste fixation in fired, ceramic-coated, 20: 30951(P)

CLINCH RIVER
radioactivity of, effects on radiation dose to downstream populations, 20: 29452 (ORNL-3721(Suppl.3))
strontium-90 effects on human skeleton by water ingestion from, 20: 30943(R) (ORNL-TM-1465)

COAL
analysis for ash content by gamma attenuation, 20: 29127
analysis of, for ash content by beta backscattering methods, 20: 29110
density of compressed stock, errors in gamma-scattering measurements on, 20: 29491

COATINGS
deposition of pyrolytic graphite, on radioactive spheroids, 20: 29638(P)
preparation of insulating, for electric conductors, 20: 29636(P)
properties of, for protection of niobium and its alloys, 20: 29651
thickness of layers in, beta-backscatter techniques for measuring, 20: 29391

COBALT
abundance and distribution in rocks, 20: 29436
content in rocks, effects of clay content on, 20: 29417
determination in Zircaloy-2, spectrographic, 20: 29113
deuteron elastic scattering at 13.6 Mev, cross section for, (E), 20: 30497
gamma reactions in electric field of, photon-pair production from, (E), 20: 30031
nuclear polarization in, (E/T), 20: 30734(R) (TID-22970, pp 1-63)
separation of traces of, from iron by paper chromatography, tracer studies of, 20: 29342

COBALT ALLOYS
corrosion of Stellite-6, in Saxton steam generator, 20: 30884(R) (WCAP-3269-16)
machining properties of, 20: 29665 (RSIC-482)
Al–Cr–Co–Fe–Mo–Ni–Ti, joining of Udimet 500 and 700, by mechanical fastening, 20: 29667 (RSIC-509)
Al–Cr–Co–Fe–Mo–Ni–Ti, surface treatments for Udimet 500 and 700, coating and mechanical, 20: 29706 (NASA-TM-X-53448)
Al–Cr–Co–Mo–Ni–Ti, joining of M-252, by mechanical fastening, 20: 29667 (RSIC-509)
Al–Cr–Co–Mo–Ni–Ti, surface treatments for Astroloy, coating and mechanical, 20: 29706 (NASA-TM-X-53448)
Al–Cr–Co–Mo–Ni–Ti–V–Zr, surface treatments for IN-100, coating and mechanical, 20: 29706 (NASA-TM-X-53448)
Al–Cr–Co–Ni–Nb–Ti–W, surface treatments for Mar-M 200, coating and mechanical, 20: 29706 (NASA-TM-X-53448)
Co–Gd–Y, magnetic properties of, 20: 30756
Co–Pd, effective magnetic field at cobalt nucleus in, (E), 20: 30752(T)

COBALT COMPLEXES
isotope exchange in radiocobalt divalent ion-doped, 20: 29259
radioinduced recoil damage in, thermal annealing of neutron, 20: 29259
Szilard-Chalmers reactions in, effect of chemical composition on isomeric effect in, 20: 29258
with potassium nitrate and rare earth nitrates, preparation and composition of, effects of temperature on, 20: 29209

COBALT FLUORIDES
thermodynamic properties of, emf measurements of, 20: 29215

COBALT ISOTOPES Co-55
yield in alpha and proton reactions with copper, 20: 30531
yield in proton reactions with yttrium, 20: 30531

COBALT ISOTOPES Co-56
yield in alpha and proton reactions with copper, 20: 30531

COBALT ISOTOPES Co-58
beta decay of, β-γ circular polarization correlations in, (E), 20: 30543

COBALT ISOTOPES Co-59
deuteron elastic scattering at 13.6 Mev, cross section for, (E), 20: 30497
neutron inelastic scattering by, level spin assignments from, (E), 20: 30360 (WASH-1068)
neutron reactions (n,γ) with gamma spectra from, (E), 20: 30360 (WASH-1068)
neutron scattering at 4.0 Mev, polarization angular distributions from, (E), 20: 30360 (WASH-1068)
proton elastic scattering at 40 Mev, cross sections for, (E/T), 20: 30353(R) (ORNL-3940, pp 1-61)

COBALT ISOTOPES Co-60
beta emission of, backscattering from aluminum in 2π geometry, (E), 20: 30369
Szilard-Chalmers recoil, isomeric effect in, 20: 29258
use of 50-Curie gamma source for radiography, 20: 29596
uses as gamma source for detection of flaws in steel foils and plates, 20: 29390
uses as power sources for underwater applications, 20: 29607
uses of waste, to control termite colonies, 20: 29587

COBALT NITRATES
reactions with potassium nitrate and rare earth nitrates, 20: 29209

COBALT OXIDES
Mossbauer effect in, lifetime of nonequilibrium trivalent iron ions from, 20: 29833
CoO–Sc_2O_3, phase studies, 20: 29168

COBALT SYSTEMS
Be–B–Co, crystal structure of compounds in, 20: 29795
Co–TaC–WC, preparation and properties of cermets of, 20: 29778
Co–TiC–WC, properties of cermets of, effects of titanium carbide content on, 20: 29779
Co–WC, properties of cermets of, effects of binder phase composition and grain size on, 20: 29780
Co–WC, strength of sintered, effects of heat treatments and temperature on, 20: 29802

COCAINE
effects on calcium-45 movement in guinea pig brain slices, 20: 28891

COINCIDENCE CIRCUITS
design of double or triple, for neutron scattering experiments, 20: 29537
COLLAGEN
radiation effects on content of, in rat subcutaneous granulomas, γ, 20: 28917
COLLOIDS
radiation effects on sorptive properties of surfaces of, (T), 20: 29815
COMETS
antimatter nature, (E/T), 20: 29895
COMPLEXES
properties of polyanion-polycation, 20: 29624(R) (TID-22970, pp 257-329)
COMPUTER PROGRAMS
AARDVARK, for use in activation analysis, 20: 29137
ADONIS, for gamma and neutron transport, FAP and FORTRAN for IBM 7090, 20: 30726 (TID-22964)
development for reactor technology, 20: 30795(R) (IDO-17147, pp 29-36)
FLUBAG, for neutron multigroup calculations in spherical geometry, 20: 30854
FLUP, for nuetron multigroup calculations in annular geometry, 20: 30854
FLURIG-3, for neutron flux distribution in annular geometry, 20: 30854
for analysis of fast rocket reactors, 20: 30787(R) (ANL-7190, pp 11-142)
for charged particle elastic scattering differential cross sections, 20: 30348 (INP-446/PL)
for cubic crystal frequency distribution functions, FORTRAN 63 for CDC 1604-A, 20: 30733 (ORNL-TM-1425)
for evaluation of radioactivity determinations in biological materials using IBM-705, 20: 29121
for fitting of gamma angular correlation data, FORTRAN for IBM 1620, 20: 30528
for gamma-gamma angular correlation analysis, in APEX, 20: 30341 (AECL-2529)
for neutron cross section calculations, 20: 30791(R) (ANL-7204, pp 32-64)
for neutron cross sections for uranium-238, in FORTRAN, 20: 30356 (ORNL-TM-1448)
for neutron flux calculations in reactors, for IBM 709, 20: 30862
for power reactor safety analysis, 20: 30883 (SAN-570-2)
for solving polynomial equations, for IBM 7090, 20: 29613 (TRG-Report-1198)
for thermocouple relative error analysis, 20: 29488 (WANL-TME-948)
for thermodynamic design of gas-cooled reactors, 20: 30892
GRID-FRAME, for mechanized structural analysis, FORTRAN IV for IBM 7090, 20: 29367 (TRG-Report-1089)
HAF, for prompt air fluorescence from nuclear explosions, 20: 30193 (LA-3409(Suppl.))
HARAC, for prompt air fluorescence from nuclear explosions, 20: 30193 (LA-3409(Suppl.))
LYRA, for conversion of nuclear diffusion programs into standard form, 20: 30721 (EUR-2778.e)
MOCINGBIRD, for thermal neutron distribution in water, FORTRAN for IBM 7094, 20: 30340
NEUTOF, for correcting neutron time-of-flight spectra, in FORTRAN II, 20: 30344 (EUR-2779.e)
ORSEF, for determining cost, geometry, and operating characteristics of multi-stage flash desalination plant, FORTRAN for IBM-7090, 20: 30953 (ORNL-TM-1542)
SADDLE, for comparing data smoothing and differentiation functions, 20: 29083(R) (UCRL-14767)
SEARCH, for analytical data retrieval, FORTRAN 400 for CDC-3600, 20: 29083(R) (UCRL-14767)
TRANSFER, for P_n multigroup scattering matrices, FORTRAN, 20: 30323 (ORNL-TM-1537)
COMPUTERS
circuitry for, development of thin-film superconducting, 20: 30255(R) (ORO-2430-28)
design of digital, for nuclear data comparisons, 20: 29485 (EUR-2799.e)
programming for solid;state physics, 20: 29623(R) (TID-22970, pp 121-256)
use for radiotherapy depth-dose calculations, 20: 29070
use in calculation of equilibrium constants for rare earth complexes, 20: 29232
CONCRETES
density and thickness of, radiometric methods of measuring, 20: 29581 (AD-633785)
mechanical properties, 20: 29624(R) (TID-22970, pp 257-329)
use as radiation shielding, model tests of, 20: 30730
use of reinforced, for underground containment caisson for Humbolt Bay Power Reactor, 20: 30896
CONCRETIONS
radium, thorium, and uranium chemical forms in iron–manganese, 20: 29426
radium, thorium, and uranium ratios in iron–manganese, 20: 29425
CONDENSERS
design of injecting, for magnetohydrodynamic cells, 20: 29974(R) (ANL-7190, pp 167-75)
CONES
stress in thick-walled shells of long, for nozzel design, (T), 20: 30928
CONFERENCES
see also introduction to Report Number Index
Metals for the Space Age, Fifth Plansee Seminar, Reutte, Tyrol, June 22–26, 1964, 20: 29680
Nuclear Measurements, Washington, D. C., Jan. 13-17, 1964, 20: 29504
CONNECTIVE TISSUE
radiation effects on mast cells in mouse, uv, 20: 28937
radiation effects on mast cells in rat, effects of low temperatures on uv, 20: 28944
CONNECTORS (ELECTRIC)
design for reactor fuel elements, 20: 29512(P)
design for use in nuclear reactors, 20: 29511(P)
COPPER
alpha reactions with, cross section ratios of isobars from, 20: 30531
coating thickness on, use of beta-particle backscattering for measuring Mylar, 20: 29754
determination in copper ore leach solutions, method for, 20: 29083(R) (UCRL-14767)
determination in petroleum, activation, 20: 29139
determination of traces of, in arsenic, activation, 20: 29087
effects as infiltrant on properties of graphite containing carbides and metals, 20: 29764
effects on radiation effects on epoxido-dianic ED-5 resin, 20: 29297
effects on radioinduced changes in structure of epoxy resins, 20: 29296
erosion by water at 70°F, effects of annealing on cavitation, 20: 29640 (NP-16048)
fabrication of powder compacts of, by isostatic pressing and sintering, 20: 29681
gamma reactions in electric field of, photon-pair production from, (E), 20: 30031
gamma scattering at 100 to 280 kev, electron binding effects on incoherent, (E/T), 20: 29923
iron-57 Mössbauer spectra in, 20: 30766
microwave absorption in, on normal and superconducting tin, (T), 20: 30290
neutron inelastic scattering cross sections at 1 Mev, (E), 20: 30383
platinum-195 Mössbauer effect in, (E), 20: 30757
proton reactions with, cross section ratios of isobars from, 20: 30531
radiation damage in, ion-beam, 20: 29808
radiation effects on, electric conductivity changes and stored energy release in neutron, 20: 29824
surface composition and structure of, beta-particle backscattering method of measuring, 20: 29754
surface friction at high temperatures, 20: 29624(R) (TID-22970, pp 257-329)
COPPER ALLOYS
Al–Cu–Nb, phase studies on, 20: 29764
Al–Cu–Ta, phase studies on, 20: 29764
Cr–Cu, thermal capacity below 1°K, 20: 29791
Cu–Au, analysis of, development of electron microprobe for, 20: 29083(R) (UCRL-14767)
Cu–Au, crystal structure of intermetallic compound in, 20: 29623(R) (TID-22970, pp 121-256)
Cu–Gd, magnetic properties of, 20: 29752
Cu–Mn, thermal capacity below 1°K, 20: 29791
Cu–Ni, erosion by water at 70°F, effects of annealing on cavitation, 20: 29640 (NP-16048)
Cu–Ni–Nb, phase studies on, 20: 29764
Cu–Ni–Ta, phase studies on, 20: 29764
Cu–Ni–W, properties of composite-type, 20: 29624(R) (TID-22970, pp 257-329)
Cu–U, metallographic tests on arc melted, 20: 29775
Cu–Zn, erosion by water at 70°F, effects of annealing on cavitation, 20: 29640 (NP-16048)
Cu–Zr, development of age- and dispersion-hardened copper-base, 20: 29782
COPPER CHLORIDES
effects on corrosion of zirconium by hydrochloric acid, 20: 29649
COPPER COMPLEXES
with ammonia, effects of, on oxidation of uranium dioxide by oxygen in carbonate solutions, catalytic, 20: 29199
with glycine, radiolysis of, mechanisms of gamma and uv, 20: 29303
COPPER COUPLES
Cu/Sn, critical field and temperature of superconducting, (E), 20: 30291
Cu/Sn, microwave absorption in superconducting, proximity effects on, (E), 20: 30289

COPPER IONS
oxidation of monovalent, in carbonate solutions by oxygen, kinetics of, 20: 29198
COPPER ISOTOPES Cu-63
deuteron elastic scattering at 34.4 Mev, angular distributions from, (E/T), 20: 30353(R) (ORNL-3940, pp 1-61)
neutron reactions (n,γ) at 0.1 to 14 Mev, cross sections for, (T), 20: 30378
proton reactions (p,n) with copper-63 at 4 to 9 Mev, zinc-63 levels from, (E), 20: 30406
COPPER ISOTOPES Cu-65
deuteron elastic scattering at 34.4 Mev, angular distributions from, (E/T), 20: 30353(R) (ORNL-3940, pp 1-61)
neutron reactions (n,γ) at 0.1 to 14 Mev, cross sections for, (T), 20: 30378
COPPER OXIDES
radioinduced blistering of polycrystalline, helium and hydrogen ion, (E), 20: 29816
reactions with carbon monoxide, hydrogen, and methane, isotope effects in, 20: 29187
COPPER SULFATES
oxygen-18 exchange with water, effects of benzene and oxygen on, 20: 29153
COPPER SYSTEMS
B_4C–Cu, fabrication and mechanical properties of sheets of, 20: 29664 (LA-DC-7745)
Cu–Si, effects on wetting of graphite at high temperatures, 20: 29764
CORROSION
research programs on metal, 20: 29623(R) (TID-22970, pp 121-256)
CORROSION LOOPS
design and operation of 1200°F–sodium, 20: 30875(R) (ANL-7190, pp 143-55)
CORTICOSTERONES
radiosensitivity effects on mice, 20: 28978
CORTISONE
radiosensitivity effects on mice, 20: 28978
COSMIC ELECTRONS
density in galactic clusters and halos and metagalaxy, 20: 29972
energy spectra, (E), 20: 29964
COSMIC MESONS
intensity variations at Yakutsk on 9-20 July 1961, effects of galacto-magnetic and solar phenomena on, 20: 29961
COSMIC MESONS (μ)
intensity of, sidereal-time dependence of, (E), 20: 29967
intensity of, sidereal-time dependence of, (E), 20: 29968
COSMIC NEUTRONS
intensity variations at Yakutsk on 9-20 July 1961, effects of galacto-magnetic and solar phenomena on, 20: 29961
COSMIC PARTICLES
intensities outside of Van Allen radiation belts, as function of L co-ordinate, (E), 20: 29966
intensity increases at heavy, accompanied by solar x-ray bursts, 20: 29965
intensity of high-energy, Sputnik III measurement of, 20: 29962
reactions with heavy emulsion nuclei at high energies, slow particle production in, 20: 30371
COSMIC PHOTONS
flux distribution, (E/T), 20: 29969
intensities outside of Van Allen radiation belts, as function of L co-ordinate, (E), 20: 29966
production of high-energy, by inverse Compton process, 20: 29972
COSMIC PROTONS
interaction depth in atmosphere, effect on recording of penetrating component of extensive air, (T), 20: 29971
COSMIC RADIATION
conference on high-energy physics, Tihany, Sept. 1962, 20: 30079
detection and measurement of nuclear component of, 20: 29957(T) (NASA-TT-F-389, pp 693-710)
effects on microspores of *Tradescantia* during satellite flight, 20: 28971
effects on space flights, 20: 30222(T) (NASA-TT-F-389, pp 758-63)
effects on wave propagation in interstellar medium and supernova remnant, damping, (T), 20: 29959
electron interactions at high energies with black-body, inverse Compton gamma- and x-ray flux from, (T), 20: 29958
intensities outside of Van Allen radiation belts, as function of L co-ordinate, (E), 20: 29966
intensity of solar events, model for time behavior of, 20: 29973
intensity of, sidereal-time dependence of, (E), 20: 29967
intensity of, sidereal-time dependence of, (E), 20: 29968
intensity variations of, 20: 29955(T) (NASA-TT-F-389, pp 678-83)
intensity variations of, performance of gas discharge counter for measuring, 20: 29956(T) (NASA-TT-F-389, pp 684-91)
intensity variations at Yakutsk on 9-20 July 1961, analysis of, 20: 29961
measurements at Yakutsk, analysis of two-year, (E/T), 20: 29963
origin of isotropic gamma and x, (T), 20: 29958
research on, problems and prospects of, 20: 29954(T) (NASA-TT-F-389, pp 657-77)
source models for gamma and x rays, 20: 29972
COSMIC SHOWERS
intensities outside of Van Allen radiation belts, as function of L co-ordinate, (E), 20: 29966
intensity variations of extensive, diurnal, 20: 29960
intensity variations at Yakutsk on 9-20 July 1961, effects of galacto-magnetic and solar phenomena on, 20: 29961
intensity variation at Yakutsk, two-years, (E/T), 20: 29963
particle distributions in extensive, method for locating axes of, 20: 29970
proton interaction depth in extensive, effect on recording of penetrating component, 20: 29971
COSMOLOGY
cylindrical models in, geometrodynamics of, 20: 30251
COTTON
radiation effects on content of ascorbic acid and glutathione in plants of, γ, 20: 28999
***p*-CRESOL, 2,6-DI-*tert*-BUTYL-**
effects on radiation effects on crosslinking in polypropylene, 20: 29290
CRITICAL ASSEMBLIES
control system design and operating experience, 20: 30901
criticality of water-moderated urania-fueled cylindrical, lumped poison effects on, 20: 30836 (BAW-3492-1)
neutron Doppler measurements in ZPR-6 assembly 4Z, 20: 30790(R) (ANL-7204, pp 1-31)
neutron fluctuations in homogeneous, angular correlations in, (T), 20: 30863
reactivity measurements in, multiplication method for, 20: 30849
CRITICALITY STUDIES
of plutonium nitrate in stainless steel spheres, 20: 29471
reactivity calculations for aluminum–plutonium, uranium dioxide, and plutonium dioxide–uranium dioxide lattices, 20: 30857
reactivity of plutonium-bearing lattices, 20: 30858
CROSS SECTIONS
research on, (E/T), 20: 30360 (WASH-1068)
CRYOGENICS
instrumentation development for, use of superconductors in, 20: 30258
CRYOSTATS
design of helium-3, 20: 30316
instrumentation for regulating liquid helium, design of transistorized, 20: 30254 (LA-DC-7209)
CRYSTAL STRUCTURE
defects in, equipment and procedures for examining, 20: 29141
defects in, lectures on, 20: 30784
determination by x-ray diffraction, (E/T), 20: 30734(R) (TID-22970, pp 1-63)
frequency distribution functions for cubic, computer program for, 20: 30733 (ORNL-TM-1425)
lattice parameters, method for powder pattern indexing for, 20: 30952 (LA-3467)
x-ray scattering studies of, dispersion correction for, 20: 29722
CRYSTAL VIOLET
effects on protactinium precipitation with dyes in acid solutions, 20: 29135
CRYSTALLOGRAPHY
angular distribution in films, foils, and sheets, pole figure facility for measuring, 20: 29083(R) (UCRL-14767)
CRYSTALS
electron distribution function in strong electric field in, effect of inter-electron collisions on, (T), 20: 30779
fracture of, effects of interatomic forces on, 20: 29624(R) (TID-22970, pp 257-329)
growth of, stabilizing parameters in, 20: 29623(R) (TID-22970, pp 121-256)
hydrogen bond dynamics in, lectures on, 20: 30783
impurity states in ionic, theory of, 20: 29709(R) (TID-22970, pp 65-119)
nuclear relaxation phenomena in, lattice phonon-quadrupole interactions in, (T), 20: 30749
nuclear spin-spin coupling in, free induction signal from, (T), 20: 30778
photon scattering by, effects of motion on coherent, (E/T), 20: 30734(R) (TID-22970, pp 1-63)
preparation of, methods for, 20: 29709(R) (TID-22970, pp 65-119)
properties of, correlation effects in single-particle description of, (T), 20: 30781
proton-lattice interactions in, hydrogen bonded ferroelectric, 20: 30783
radioinduced relaxation in, apparatus for study of photon and thermal, 20: 30754
structure of, neutron scattering studies of, 20: 29720

CULTURE MEDIA
effects on pigment content and radiosensitivity of *Micrococcus radiodurans*, 20: 29016
CUPFERRON
effects on frequency of radioinduced chromosome aberrations in Tradescantia, 20: 29028
CURIUM
metabolism of, 20: 28885
separation from americium by extraction chromatography using a quaternary ammonium nitrate, 20: 29337
separation from americium, berkelium, californium, cerium, europium, and uranium by ion exchange on zirconium phosphates, 20: 29340
CURIUM CHLORIDES
with nitrilotriacetic acid, stability of, 20: 29195
CURIUM ISOTOPES Cm-242
production of, economics of reactor, 20: 29609 (NP-15947)
CURIUM ISOTOPES Cm-244
neutron reactions at 1 kev to 14 Mev, cross sections for, (T), 20: 30346 (GEMP-411)
production of, economics of reactor, 20: 29609 (NP-15947)
CURIUM OXIDES
preparation of microspheres of, sol-gel process for, 20: 29165
CYCLOHEPTANE, CHLORO-
chlorine-36 exchange between, and lithium chloride, in dimethyl sulfoxide, kinetics of, 20: 29157
CYCLOHEPTATRIENONES
complexes with molybdenum, thorium, and zirconium, composition of, spectrophotometric studies of, 20: 29179
CYCLOHEXANE
reactions with muonium, (E), 20: 29247
CYCLOHEXANE, CHLORO-
chlorine-36 exchange between, and lithium chloride, in dimethyl sulfoxide, kinetics of, 20: 29157
CYCLOHEXANONE
radiolysis of, effects of aromatics and nitrous oxide on hydrogen yields from, 20: 29270
CYCLOHEXENE
hydrogenation of, effects of uv radiation on catalytic activity of platinum in, 20: 29304
reactions with muonium, (E), 20: 29247
CYCLOOCTANE, CHLORO-
chlorine-36 exchange between, and lithium chloride, in dimethyl sulfoxide, kinetics of, 20: 29157
CYCLOPENTADIENE, HEXACHLORO-
radiolysis of, mechanism and yields in gamma, 20: 29256
CYCLOPENTANE, CHLORO-
chlorine-36 exchange between, and lithium chloride, in dimethyl sulfoxide, kinetics of, 20: 29157
CYCLOTRONS
beam deflector for Berkeley 88-inch, design of regenerative, 20: 29856 (UCRL-16829)
beam momentum compaction in, 20: 29861
development of 1000-Mev proton, 20: 29855(R) (ORNL-3940, pp 83-111)
performance characteristics of continuous operation microtron, (T), 20: 29858
radiation monitoring at Nevis 400-Mev, helium-3 spectrometer for neutron, 20: 29846 (CONF-651109, pp 154-60)
CYLINDERS
geometrodynamics of cylindrical systems, 20: 30251
stress disturbances in elastic-plastic, propagation of, (T), 20: 30954 (UCRL-14617)
CYSTEINE
metabolism in guinea pigs and rats, 20: 29024
radiation effects on metabolism of, by rats, 20: 29024
CYSTINE
analysis for sulfur by hydrogen reduction, 20: 29083(R) (UCRL-14767)
CYTOLOGY
cloning mouse skin epithelial cells for radiation dose-response study, 20: 28990
radiation effects on vaginal, therapeutic-dose, 20: 29076
CYTOSINE
radiation effects on thermoluminescence of, gamma, 20: 28913
radiation effects on, ESR and thermoluminescence studies of, 20: 29249

D

DATA RECORDING SYSTEMS
design of remotely operating temperature, 20: 29514(P)
DATA TABULATIONS
efficiencies of cylindrical scintillation gamma detectors, (T), 20: 29562
nuclear energy levels in Nilsson potential, 20: 30392
DECONTAMINATING SOLUTIONS
effectiveness for removal of strontium-90 from wheat, 20: 29473
efficiency of, for fission product, uranium, and thorium removal from cotton protective clothing, 20: 29477
DENSITOMETERS
radiometric, performance of back-scatter, for soil density measurements, 20: 29594
safety device for radiometric, 20: 29515(P)
uses of radiometric, review of Navy, 20: 29581 (AD-633785)
DENSITY
measurement of salt deposition on electric insulators, fluorescent x-ray method for, 20: 29103
measurements on compressed stock coal, errors in radiometric method for, 20: 29491
DETERGENTS
effects on uptake of strontium-90 by rabbit skin, 20: 29461
DEUTERIUM
deuteron reactions (d,p) at 2.1 to 14.1 Mev, proton polarization in, (E), 20: 30524
diagnostics of plasma of, using laser beams, 20: 30556(R) (AD-631993)
effects on absorption and fluorescence spectra of *Chlorella vulgaris*, 20: 28872
effects on far-infrared spectra of acetylene, 20: 29239
effects on oxidation of benzene to phenol, 20: 29250
exchange between azulene and acetic acid–methanol solutions, 20: 29245
exchange between hydrocarbons or hydrogen sulfide and heavy water, 20: 29611(P)
incorporation in hydroxyflavones, 20: 29240
laser beam reactions with, plasma production in, 20: 30665
light scattering at level crossings in, cross sections for polarized, 20: 29935
nuclear magnetic resonance of solid, at 1.10 to 4.2°K, (E), 20: 30320
pinch discharge in plasma of, properties from noncylindrical focused Z, (E), 20: 30642
production of dense plasma of, by cusp field injection, (E), 20: 30643
radioinduced exchange with hydroxyl ions on silica gel, 20: 29276
reactions of atomic, with molecular hydrogen, energy threshold for, 20: 29176
DEUTERIUM HYDRIDES
angular and energy distribution of ions of, from deuterium ion-hydrogen reactions, 20: 29950
DEUTERIUM IONS
reactions with hydrogen, angular and energy distribution of deuterium hydride ions from, 20: 29950
DEUTERIUM SYSTEMS
D–H, nuclear magnetic resonance of solid, (E), 20: 30320
D–O, radiation effects on, yields from gamma, 20: 29285
DEUTERONS
angular distributions from reactions of lithium-6 and -7 with boron-10 and -11, 20: 30519
angular distributions from lithium-6 reactions with carbon-12, (E), 20: 30520
binding energy of, (T), 20: 30060
effects on cadmium sulfide single crystals at 13.5 Mev, defects from, 20: 30771
effects on oxides and silicon, blistering from, (E), 20: 29816
interactions with antiprotons at rest, analysis of annihilation, (E), 20: 29992 (UCRL-16717)
interactions with mesons (π), p-wave dispersion relations for disintegration, (T), 20: 30074
interactions with mesons (π^-) at 3.7 Bev/c, A_1 and A_2 resonance production in, (E), 20: 30078
interactions with protons, cross sections for elastic, (T), 20: 29989 (ITEF-361)
interactions with electrons, neutron form factors from inelastic, (E), 20: 30027
interactions with protons at 1.1 to 8 Bev/c, total cross sections for, (E), 20: 30028
interactions with antiprotons and protons at high energies, amplitudes for elastic, (T), 20: 30051
interactions with deuterons at 1.69 Bev/c, of helium-4 momentum spectra and total cross sections for, 20: 30010
interactions with neutrons at 14 Mev, differential cross sections for elastic, (T), 20: 30050
nuclear magnetic resonance in deuterated ammonium bromide and chloride single crystals, 20: 29191
properties of ground-state, calculation using third-order perturbation theory, 20: 30068
reactions (d-He-3) and (d,t) with nuclei, isobaric spin in, (T), 20: 30343 (COO-1371-30)
reactions (d,α) and (d,n) with lithium-7 at 0.8 and 1 Mev, spectra and angular distributions from, (E), 20: 30402
reactions (d,d), (d,d'), and (d,p) at 12.8 Mev, cross sections for, (E), 20: 30459
reactions (d,γ) with beryllium-9 at 0.4 to 1.4 Mev, angular distributions

and cross sections for, (E), 20: 30393
reactions (d,Li-7) with carbon-12 at 34.4 Mev, angular distributions from, (E), 20: 30353(R) (ORNL-3940, pp 1-61)
reactions (d,n) with nuclei, amplitudes for, (T), 20: 30426
reactions (d,n) with nitrogen-15 at 1.6 to 3.0 Mev, neutron polarization from, (E), 20: 30427
reactions (d,n) with tritium at 6.6 Mev, polarization function for, (E), 20: 30442
reactions (d,n) with beryllium-9, carbon-13, and magnesium 25, spectroscopic factors for boron-10, nitrogen-14, and aluminum-26 from, 20: 30481
reactions (d,pf) with plutonium-239, fission probability and fragment anisotropies for, 20: 30360 (WASH-1068)
reactions (d,p) and (d,t) with neodymium isotopes at 10 to 12 Mev, energy levels from, (E), 20: 30517
reactions (d,p) with calcium-42 at 7.0 and 7.2 Mev, angular distributions from, (E), 20: 30452
reactions (d,p) with silicon-28, gamma angular correlations from, (E), 20: 30360 (WASH-1068)
reactions (d,p) with chlorine-37 at 7.5 Mev, chlorine-38 levels from, (E), 20: 30391
reactions (d,p) with deuterium at 2.1 to 14.1 Mev, proton polarization in, (E), 20: 30524
reactions (d,p) with sulfur-32 at 3.20 Mev, sulfur-33 levels from, (E), 20: 30455
reactions (d,p) with tungsten-182 at 7.5 and 12 Mev, angular distributions from, (E), 20: 30475
reactions (d,p) with sulfur-32 at 1.7 to 3.0 Mev, cross sections for, (E), 20: 30518
reactions with thorium-232 and uranium-235 and -238, yields of xenon-133 and -135 from fission, 20: 30533
reactions with uranium-233, -235, and -238 at 12 Mev, fission fragment kinetic energies from, (E), 20: 30500
scattering by calcium-40 at 11 and 12.8 Mev, stripping channel effects on cross sections for elastic, (T), 20: 30431
scattering by cobalt-59 and nickel-60 at 13.6 Mev, cross sections for elastic, 20: 30497
scattering by cobalt, iron, and titanium at 13.6 Mev, cross sections for elastic, 20: 30497
scattering by mercury-202 and thallium-203, angular distributions and levels from elastic, (T), 20: 30484
scattering by nuclei at 34.4 Mev, cross sections for, (E/T), 20: 30353(R) (ORNL-3940, pp 1-61)
scattering by tungsten-182 at 12 Mev, angular distributions from elastic and inelastic, (E), 20: 30475

DICARBOXYLIC ACIDS
radiolysis of tritium-labeled, ESR spectra of radicals from self-, 20: 29311

DIELECTRICS
electromagnetic wave scattering by, 20: 29832
use in accelerator walls for beam stabilization, 20: 29860

DIES
design of non-metallic, for extruding metals, 20: 29693(P)

DIET
analysis for cesium-137 and potassium-40, losses during dry ashing and hydrochloric acid treatment for, 20: 29122
cesium-137 content in cattle, 20: 29463
effects on cesium-137 content in beef cattle in Japan, 20: 28887
effects on cholesterol content in blood of irradiated rats, 20: 28992
effects on cholesterol content in rat tissues, 20: 28995
effects on pathology of atherosclerosis in rats, 20: 28996
radioactivity in, contribution of milk and milk products to, 20: 29464
radiosensitivity effects on intestinal secretory function in dogs, 20: 28993

DIFFERENTIAL EQUATIONS
integration of ordinary, numerical methods for, 20: 29612 (ANL-7126)

DIFFRACTION GRATINGS
electron sheet motion above, electromagnetic wave emission from, (T), 20: 30250

DIFFUSION
research on, of metals, in nonvalatile materials, 20: 29623(R) (TID-22970, pp 121-256)

DIODES
electric potential of silicon carbide, 20: 29709(R) (TID-22970, pp 65-119)

DISASTERS
radiation dosimetry in, instruments and procedures for, 20: 29469

DISEASES
measurement of insalinemia, 20: 28871(R) (EUR-2636.f,i)
radiotherapy of skin, beta, 20: 29072

DISULFIDE, 2-(3-AMINOPROPYL)-
dihydrobromide, radiosensitivity effects on phage induction in *E. coli*, x, 20: 29045

DOGS
effects of ethanol on conditioned reflexes of, 20: 29009
radiation effects on adrenaline content of blood in, 20: 28941
radiation effects on intestinal secretory function in, effects of dietary fatty acids on x, 20: 28993
radiation effects on cholesterol-protein blood complexes in, 20: 28998
radiation effects on thyroid activity in, β, 20: 29000
radiation effects on conditioned reflexes of, beta, 20: 29009
radiation effects on kidney function and morphology of, x, 20: 29025
radiation effects on renal hemodynamic functions of, x, 20: 29026
radiation effects on hematopoietic system of, lower-body, upper-body, and whole-body x, 20: 29029

DOSIMETERS
design for use in nuclear accidents, 20: 29469
design of gamma G-M probe, 20: 29563
design of personnel-type, with modifying elements, 20: 29574(P)
design using phosphor and photocathode, 20: 29576(P)
development for determining proton depth dose distribution in primates, 20: 28928 (CONF-651109, pp 417-25)
development for nuclear accidents monitoring, using activation detectors, (E/T), 20: 29521 (CONF-651109, pp 213-23)
development for Saturne Synchrotron environs monitoring, 20: 29845 (CONF-651109, pp 117-42)
film, delayed development process in, 20: 29557
performance of film and silicon diode, for gammas and neutrons, 20: 29518 (BNWL-SA-27)
performance of phosphate glass, 20: 29547
performance of, fluence response functions for evaluating, 20: 29482
properties of scintillation, pulse shape discrimination in, 20: 29524 (CONF-651109, pp 647-52)

DROSOPHILA
radiation effects on, genetic x, 20: 28956
radiation effects on, effects of ATP on genetic, 20: 29046
radioinduced mutations of, β, 20: 28955

DUSTS
cylindrical clouds of, effects of gravitation on, 20: 30251
energy of cloud of incoherent, conservation law in general relativity for total proper, 20: 30241
radioactivity of rain-borne, Calcutta, India, 1962, 20: 29420
radioactivity of settled, in Japan after Chinese nuclear explosion of 1964, 20: 29455

DYSPROSIUM
determination in minerals and ores, spectrometric, 20: 29134
determination in rocks, chemical spectrographic method for, 20: 29083(R) (UCRL-14767)
determination in standard igneous rocks G-1, W-1, and G-B by x-ray fluorescence, 20: 29101
determination in TBP extracts, spectrophotometric, 20: 29125
determination in uranium compounds, spectrographic, 20: 29129
thermal conductivity of, at room temperatures, mechanisms for, 20: 29741
thermodynamic properties at 0°C to melting point, 20: 29743

DYSPROSIUM ALLOYS
Dy–La, electric conductivity, magnetic susceptibility, and superconducting transition temperatures of, 20: 29753

DYSPROSIUM CHLORIDES
thermal capacity of aqueous solutions of, at 25°C, 20: 29144 (IS-1355)

DYSPROSIUM COMPLEXES
with 1,10-phenanthroline–thenoyltrifluoroacetone, preparation and composition of, 20: 29221

DYSPROSIUM IONS
effects on fluorescence decay of samarium ions in lanthanum chloride crystals, 20: 30782

DYSPROSIUM ISOTOPES Dy-161
neutron capture by, gamma spectra from, 20: 29078(R) (AD-633252)

DYSPROSIUM ISOTOPES Dy-162
neutron capture by, gamma spectra from, 20: 29078(R) (AD-633252)

DYSPROSIUM ISOTOPES Dy-163
neutron capture at 1 to 5 ev, gamma spectra from, (E), 20: 30385

DYSPROSIUM ISOTOPES Dy-164
energy level transistions from dysprosium-163 neutron capture, (E), 20: 30385
neutron capture by, neutron separation energy determination from, (E), 20: 30366
neutron capture by, gamma spectra from, 20: 29078(R) (AD-633252)

DYSPROSIUM ISOTOPES Dy-165
neutron capture by, gamma spectra from, 20: 29078(R) (AD-633252)
production from neutron capture by dysprosium-164, neutron separation energy determination from, (E), 20: 30366

DYSPROSIUM NIOBATES
distribution in strontium molybdate single crystals, coefficients of, 20: 29746

E

ECOLOGY
carbon monoxide formation and function in closed ecological systems, 20: 28880
studies of, preparation of beta sources for use in, 20: 28879
ELASTOMERS
testing for pressure seals in spacecraft, 20: 29366(R) (TID-22970, pp 375-91)
ELECTRIC CHARGES
accumulation in glass gamma shielding windows, 20: 30727
electromagnetic radiation from extended, covariant treatment of, (T), 20: 30252
radiation from, moving above anisotropically conducting plane, (T), 20: 29836
ELECTRIC CONDENSERS
design and operation of 150 kJ, for CERN Neutrino Experiment, 20: 29840 (CERN-66-16)
sensitivity of plasma-filled, to electric potential, (T), 20: 30699
ELECTRIC CONDUCTORS
coatings for, preparation of insulating oxide, 20: 29636(P)
ELECTRIC DISCHARGE
electron density and velocity distribution in helium hollow-cathode, (E), 20: 30688
plasma diffusion from, in magnetic fields, (E/T), 20: 30639
plasma heating by h-f, in metallic chambers, (E), 20: 30664
plasma stability in megajoule, theta-pinch, (E/T), 20: 30610
plasma turbulent heating in d-c, mirror-confined, 20: 30661
stabilization of high-current pulsed gas, in magnetic field using h-f electric field, (E), 20: 30698
ELECTRIC FIELDS
dynamics of Bloch electrons in, (T), 20: 30735(R) (TID-22970, pp 331-73)
effects on dense hydrogen plasma, (E), 20: 30558 (AD-633593)
effects on hydrogen yields from radiolysis of liquid hydrocarbons, 20: 29263
plasma stability in external h-f, (T), 20: 30627
strength for establishing self-sustaining plasma, determination of, 20: 30592
ELECTRIC GENERATORS
design of superconducting flux pump, 20: 30274
power cycles for nuclear power plants using liquid-metal MHD, 20: 29980
ELECTRIC INSULATORS
analysis for trace salt deposits on, x-ray fluorescent method for, 20: 29103
ELECTRIC POTENTIAL
measurement in magnetically suspended rotors, telemetering system for, 20: 29369
ELECTRIC POWER
generation of, design of MHD-device for, 20: 29984(P)
ELECTRIC PROBES
development for analysis of boiling flow regimes, 20: 29378(R) (NYO-3304-7)
use of cylindrical Langmuir, for electron concentration and temperature measurements in ionosphere, 20: 30198(T) (NASA-TT-F-389, pp 202-24)
ELECTRODES
operation modes of glass, 20: 29623(R) (TID-22970, pp 121-256)
surface properties of thermionic, 20: 29624(R) (TID-22970, pp 257-329)
ELECTRODYNAMICS
S-matrix theory for, 20: 30164
ELECTROLYSIS
current and potential distribution in controlled-potential, 20: 29083(R) (UCRL-14767)
ELECTROLYTIC CELLS
design of, for reactor metal refining, 20: 29373(P)
ELECTROMAGNETIC FIELDS
distribution in nonuniform plasma in magnetic field, resonance-induced discontinuities in, (T), 20: 30696
quantization of free macroscopic, in homogeneous dispersive medium, (T), 20: 30668
transformation properties of, relativistic, 20: 30243
ELECTROMAGNETIC LENSES
use in manipulation of charged-particle beams for irradiation of oddly shaped objects, 20: 29872(P)
ELECTROMAGNETIC SHIELDING
design for space vehicles, using superconducting coils, 20: 30317
ELECTROMAGNETIC WAVES
damping in homogeneous magnetoactive plasma, Cherenkov and cyclotron, (T), 20: 30671
electron motion in field of whistler-mode, 20: 29899
electron refraction by, 20: 30046
emission by electric charge moving above anisotropically conducting plane, (T), 20: 29836
emission from electron sheet motion above diffraction grating, (T), 20: 30250
excitation in anisotropic plasma by ion-beam interactions, (T), 20: 30670
excitation in plasma, strong magnetic field effects on, (T), 20: 30677
interactions in magneto-plasma, nonlinear, (T), 20: 30629
interactions in plasma, nonlinear, (T), 20: 30628
interactions of intense h-f, with Langmuir electron waves in uniform isotropic plasma, (T), 20: 30695
interactions with surface waves of plasma, (T), 20: 30694
propagation in axially symmetric plasma, magnetic field line curvature effects on, (T), 20: 30678
propagation in collisionless plasma, (T), 20: 30588
propagation in hot collisionless plasma, (T), 20: 30569
propagation in inhomogeneous media, partial wave analysis of, 20: 30713
propagation in plasma layer, kinetic theory for, 20: 30679
propagation in plasma, (T), 20: 30571
propagation in weakly ionized gases, nonlinear phenomena in, 20: 30190
propagation through thin nonuniform plasma layer, (T), 20: 30704
radiation from extended sources, covariant treatment of, (T), 20: 20252
reflection of monochromatic resonance-frequency, from nonlinear half-space, (T), 20: 29837
scattering by finite inhomogeneous dielectrics, 20: 29832
scattering in plasma, (T), 20: 30674
use of transverse, for quasilinear acceleration of charged particles, (T), 20: 29867
ELECTROMAGNETISM
cylindrical systems of, geometrodynamics of, 20: 30251
ELECTRON BEAMS
book: *Advances in Electronics and Electron Physics, Vol. 21*, 20: 29499
book: *Instrument and Chemical Analysis Aspects of Electron Microanalysis and Macroanalysis*, 20: 29119
dosimetry of accelerator, use of glass for, 20: 29283
effects of 10-Mev, on man, 20: 28929 (CONF-651109, pp 574-98)
effects on bacteria and yeast, effects of depth in irradiated medium on biological, 20: 28963
effects on l-f oscillations in two-stream plasma, (E), 20: 30591(T)
interactions magnetic mirror confined plasma, instabilities from, (E), 20: 30659
interactions with plasma, analysis of collective, (E), 20: 30623
interactions with plasma, quasilinear transformations of waves from, (T), 20: 30673
interactions with plasma, microwave amplification by, 20: 30718
refraction by electromagnetic waves, 20: 30046
stability of potential oscillations in electron-ion beams, (T), 20: 30672
use for amplification and generation of uhf oscillations, (E/T), 20: 29500
uses in vacuum gages, 20: 29600
ELECTRON-DIFFRACTION ANALYSIS
book: *Instrument and Chemical Analysis Aspects of Electron Microanalysis and Macroanalysis*, 20: 29119
ELECTRON LENSES
book: *Instrument and Chemical Analysis Aspects of Electron Microanalysis and Macroanalysis*, 20: 29119
electrostatic fields of axially symmetric, straight line method for calculating, 20: 29497
ELECTRON MICROSCOPY
book: *Instrument and Chemical Analysis Aspects of Electron Microanalysis and Macroanalysis*, 20: 29119
development, 20: 29499
historical development, 20: 28874
ELECTRON PAIRS
photoproduction at 10 to 5000 Mev, positron to gamma energy ratios for, (E), 20: 29990 (JINR-P-2667)
photoproduction on carbon at wide angles, radiative corrections to, (T), 20: 30013
production by gamma conversion in hydrogen from meson (γ^0) decay, (E), 20: 30029
production in gamma scattering by nuclei, (E/T), 20: 29996
ELECTRON PHOTOGRAPHY
amplification factor of lead screens for, 20: 29628
ELECTRON PROBES
development of, for analysis of ceramics and metals, 20: 29083(R) (UCRL-14767)
ELECTRON TUBES
properties for measurement of ultrahigh vacuum, 20: 29494
ELECTRONIC EQUIPMENT
book: *Advances in Electronics and Electron Physics, Vol. 21*, 20: 29499
design for anatomical marking of γ scintiphotos, 20: 29067

design for time resolution measurements of fast photomultipliers, 20: 29568
development of, for space, 20: 29622(R) (TID-22970)

ELECTRONS

bunching in cylindrical cavity resonators, (T), 20: 29859
capture in small-angle ion-atom scattering, resonance, (E), 20: 29944
capture into n = 3 hydrogen states, relative cross sections for, (E), 20: 29930
content in ionosphere at altitudes of 100–300 km, variations in, 20: 30199(T) (NASA-TT-F-389, pp 248-58)
content in ionosphere, with energies less than 0.1 Mev, (E), 20: 30203(T) (NASA-TT-F-389, pp 288-91)
content in outer Van Allen belts, 20: 30213(T) (NASA-TT-F-389, pp 566-8)
density and energy in helium afterglow plasma, in toroidal magnetic fields, (E/T), 20: 30710
density and temperature in helium discharge in C Stellarator, 20: 30600
detection and measurement of secondary, total-current scintillation method for, 20: 29538
detection of, design of proportional counter for, 20: 29561
diffusion in Van Allen belts, 20: 30206(T) (NASA-TT-F-389, pp 426-42)
distribution in magnetosphere, spatial, 20: 30207 (NASA-TT-F-389, pp 442-53)
distribution in magnetosphere, energy, spatial, and temporal, 20: 30220(T) (NASA-TT-F-389, pp 633-52)
distribution in outer ionosphere, altitude and time dependence of, 20: 30197(T) (NASA-TT-F-389, pp 166-201)
distribution in outer Van Allen belts, spatial, 20: 30215(T) (NASA-TT-F-389, pp 576-87)
distribution in outer Van Allen belts, energy and spatial, 20: 30219(T) (NASA-TT-F-389, pp 623-9)
distribution in Van Allen belts, energy, spatial, and temporal, 20: 30204(T) (NASA-TT-F-389, pp 375-86)
distribution in Van Allen belts, analysis of spatial, 20: 30211(T) (NASA-TT-F-389, pp 535-50)
distribution of geomagnetically trapped, spatial, 20: 30202(T) (NASA-TT-F-389, pp 281-7)
distribution of geomagnetically trapped, spatial, 20: 30212(T) (NASA-TT-F-389, pp 551-66)
distributions in Brazilian magnetic anomaly at 250 to 400 km, spatial and temporal, 20: 30217(T) (NASA-TT-F-389, pp 607-15)
dynamics in electric and magnetic fields, (E/T), 20: 30735(R) (TID-22970, pp 331-73)
effects of pulsed, on sulfuric acid solutions of ferric sulfate, 20: 29262
effects of pulses of, on aqueous solutions of thallium sulfate, 20: 29271
effects on catalase, reactions of hydrated electrons and hydroxide radicals in, 20: 29279
effects on gelatin, ESR studies of, 20: 29273
effects on isomerization of *trans* polymers of conjugated dienes, 20: 29321(P)
effects on liquid hydrocarbons,, 20: 29263
effects on polymerization of vinyl coatings on exterior surfaces, 20: 29320(P)
effects on reactions of hydrogens and hydroxyl radical in aqueous solutions, 20: 29262
effects on water, tracer studies of, 20: 29315
emission in proton reactions with argon, neon, nitrogen, and oxygen at 50 to 200 kev, (E), 20: 29951
emission of, theory of chemical- and exo-, 20: 29561
energy of Dirac, in Coulomb potential, (T), 20: 29949
energy spectra in one-dimensional system with randomly arranged scattering centers, 20: 30113(T)
energy spectra of atmospheric soft, variations in, 20: 30201(T) (NASA-TT-F-389, pp 277-81)
energy states in solids, pseudo wave functions for, 20: 30773
intensities in Van Allen radiation belts, (E), 20: 30235
intensity distributions at altitudes <1600 km, 20: 30200(T) (NASA-TT-F-389, pp 273-6)
intensity of low-energy, satellite measurements of, 20: 29532(T) (NASA-TT-F-389, pp 518-25)
interactions with protons at 2 Bev, cross sections for resonance production in, (T), 20: 30054
interactions with electrons, effects on lattice stability in superconductivity, 20: 30264(T)
interactions with phonons in metals, strong, (T), 20: 30312
interactions with positrons, C-parity violation and neutral vector meson production in, (T), 20: 30012
interactions with electrons in crystal lattice, effect on electron distribution, (T), 20: 30779
interactions with ions in plasma, effects on plasma stability, (T), 20: 30709
interactions with black-body cosmic radiation at high energies, inverse Compton gamma- and x-ray flux from, (T), 20: 29958
interactions with deuterons, neutron form factors from inelastic, (E), 20: 30027
kinetic energy in Penning ionization, retarding-potential measurement of, 20: 29927
laser beam scattering by plasma of, relativistic theory of, 20: 30716
motion above diffraction grating, electromagnetic wave emission from, (T), 20: 30250
motion above surface of uniaxial crystal with metal grating, radiation emission by, 20: 29995
motion in field of whistler-mode electromagnetic wave, 20: 29899
motion in Van Allen belts, effects on geomagnetic field variations, 20: 30209(T) (NASA-TT-F-389, pp 464-82)
multiplication in proportional counters, 20: 29554
photon scattering by K-shell, spectral distributions from, (E/T), 20: 29912 (ISS-66/6)
photon scattering by K-shell, distribution from, 20: 29913 (ISS-66/7)
photon scattering by K-shell, distribution from, 20: 29914 (ISS-66/8)
photoproduction from metallic surfaces on satellites, measurement of, 20: 30198(T) (NASA-TT-F-389, pp 202-24)
polarization in heavy water and water molecules, effects of temperature on, 20: 29230
polarization of, in metals, theory of, 20: 30735(R) (TID-22970, pp 331-73)
ranges in thin metal films, 20: 29952
reactions (e,2e) with atoms, molecules, and solids, energy levels from, 20: 29931(T)
reactions in atmosphere, x-ray production from, 20: 30218(T) (NASA-TT-F-389, pp 616-23)
reactions of hydrated, with catalase in pulse radiolysis, 20: 29279
reactions of, radiative corrections for nuclear excitation and production, (T), 20: 30478
reactions with helium atoms, efficiency curves for (2^3s) and (2^1s) excitation in, 20: 29926
reactions with nitrogen at 10 kev, primary and afterglow emission from, 20: 29929
reactions with water vapor at 0.1 to 20 kev, ionization cross sections for, (E), 20: 29928
scattering by argon and uranium at 40 to 120 kev, calculation of amplitudes for, 20: 29945
scattering by atoms, Thomas-Fermi theory for cross sections for, 20: 29946
scattering by carbon-12, transverse inelastic form factors for, (T), 20: 30411
scattering by helium-4 at 100 to 900 Mev, alpha charge structure from elastic, (E), 20: 30439
scattering by hydrogen, resonances in multichannel elastic, (T), 20: 29943
scattering by hydrogen at 13.7 to 50.7 ev, inelastic, (E), 20: 29953
scattering by lead-208, collective level excitation in inelastic, (E), 20: 30360 (WASH-1068)
scattering by lead-208 at 62.8 Mev, excitation of collective states in inelastic, (E), 20: 30436
scattering by mercury at low energies, polarization effects in elastic, (E), 20: 29937
scattering by nuclei, level excitation in, (E), 20: 30360 (WASH-1068)
scattering by nuclei at relativistic energies, multiple, (T), 20: 30509
scattering on alkali metals, nonadiabatic method for, 20: 29942
spin susceptibility of gaseous, 20: 29709(R) (TID-22970, pp 65-119)
temperature measurement in hydrogen plasma using carbon line radiation, 20: 30705
temperature variations in MHD shock waves, 20: 30191
theory of inhomogeneous gas of interacting, 20: 30189
transmission in alkali halide thin films, color centers and energy losses from, (E), 20: 30776
velocity distribution in electric field in slightly ionized gases, instability of, 20: 30581

ELECTROSTATIC ANALYZERS

design and performance of spherical, for satellite measurements at 0.1 to 10 kev, 20: 29532(T) (NASA-TT-F-389, pp 518-25)

ELECTROSTATIC FIELDS

calculation of, coupled straight line-integral transformation method for, 20: 29497

ELECTROSTATIC GENERATORS

beam scattering in tubes of proton, 20: 29866

ELECTROSTATIC LENSES

charge-particle focusing properties of electrostatic mirror with circular field, 20: 29868
design of high-voltage, 20: 29865

ELEMENTARY PARTICLES

book: *High Energy Physics*, 20: 30064
bound states of, review of, 20: 30145
charge identification and detection of, system for automatic, 20: 30053
classification of, representations of SU(6,6) for, 20: 30099
conference on high-energy physics, Tihany, Sept. 1962, 20: 30079

correlation functions for random breeding-type processes of, 20: 30052
current commutation relations for scalar densities of, PCAC hypothesis for, 20: 30138
elementarity criteria for, 20: 30163
field theory for scalar, quantum, 20: 30092 (JINR-P-2700)
field theory for, regularized delta functions in, 20: 30152
form factors at finite momentum transfer and algebra of currents for, 20: 30137
form factors for, normalization of electromagnetic, 20: 30096
interaction amplitudes for, diagonalization of helicity-crossing matrices for, 20: 30095
interactions at high energies, SU(3) Regge pole model for forward elastic, 20: 30039
interactions in many-body systems of, broken symmetry, sum rules, and collective modes for, 20: 30139
interactions in quark model, electromagnetic, 20: 30112(T)
interactions involving spin of, inelastic, (T), 20: 30149
interactions of composite, with low binding energies, 20: 30150
interactions of, analytic S-matrix theory of strong, 20: 30065
interactions of, approximations for high-energy, (T), 20: 30086 (CONF-640509(Pt.1), Paper 4)
interactions of, Cabibbo angle and partial conservation of axial current for, 20: 30090 (IC-66/52)
interactions of, current-generated algebras and form factors for, 20: 30146
interactions of, convergence of Born series for rearrangement collisions, 20: 30162
interactions of, current algebras and generalized Ward-Takahashi identities for, 20: 30006
interactions of, crossing relations and prediction of symmetries in, (T), 20: 30159
interactions of, conference of weak, 20: 30534
interactions of, finite range of strong, 20: 30131
interactions of, lectures on weak, 20: 30067
interactions of, model for high-energy large-angle, 20: 30038
interactions of, model of broken U(3) symmetry for semileptonic weak, 20: 30123
interactions of, phenomenological formalism for arbitrary spin, (T), 20: 30094 (UCRL-14222)
interactions of, research on, (T), 20: 30084 (CONF-640509(Pt.1))
interactions of, SL(2,c) analysis for strong vertex, 20: 30087 (IC-66/46)
interactions of, S-matrix theory for electromagnetic, 20: 30164
interactions of, sum rules for strong, 20: 30020
interactions of, theory of weak, 20: 30114
interactions of, unsubstracted dispersion relations and Reggeization for weak, 20: 30125
interactions of, unitary symmetry and unsubstracted dispersion relations for weak, 20: 30134
interactions of, use of bubble chamber photographs in reconstructing, 20: 29533
Lorentz transformations for, Dirac matrices and Dirac matrix description of, 20: 30103
mass formulas in SU(3) and SU(6) symmetry, (T), 20: 30111
model for, bootstrap, (T), 20: 30066
model for, bootstrap conditions in Lee, 20: 30127
motion of charged, Coulomb field from, (T), 20: 30144
production and decay of, (T), 20: 30085 (CONF-640509(Pt.1), Paper 3)
production in quantum field theory, 20: 30157
production of quarks in nucleon-proton interactions, (T), 20: 29999(T)
properties of, Zachariasen model for, 20: 30156
quantum theory of, with electric and magnetic charges, 20: 30153
scattering at high energy, S-matrix for, (T), 20: 30108
spin of, $SU(6)_W$ group for W, 20: 30126
symmetries for, conserved currents in associated, 20: 30101
symmetries of strongly interacting, (T), 20: 30110
symmetry for, 20: 30142
symmetry for, irreducible tensors for SU(3), 20: 30102
symmetry for, origin of SU(6), 20: 30117
symmetry for, relation between Poincare group and exceptional lie group G(2), 20: 30115
symmetry for, representations of groups containing Poincare group in, 20: 30098
symmetry group for, representations of SL(n,C), 20: 30089 (IC-66/51)
symmetry group for, decomposition of 189- and 495-plet of SU(6), 20: 30093 (JINR-P-2701)
symmetry groups for, eigenvalues of Casimir operators for, 20: 30147
symmetry of, nonuniform group theory for, 20: 30106
theory of unstable, quantum, 20: 30107

ELEMENTS
crystal structure of, dispersion correction for x-ray scattering studies of, 20: 29722
electron structure and spectra of group V., 20: 29709(R) (TID-22970, pp 65-119)
origin of, in solar system, (T), 20: 29909

ELK RIVER POWER REACTOR
safety analysis of, 20: 30882(R) (NUS-264)

EMBRYOS
radiation effects on chick, pathological x, 20: 29012
radiosensitivity of chicken, x, 20: 29015

ENDOCRINE GLANDS
effect of removal of, on erythropoiesis in x-irradiated rats, 20: 29043
effects of removal of, on radiosensitivity of mice, 20: 28978

ENGINEERING TEST REACTOR
fuel elements of, reproductibility of boron measurements in, 20: 30794(R) (IDO-17147, pp 1-12)

ENGINES
design of thermal, with motive fluid heating chamber, 20: 29395(P)

ENZYMES
activity in animals, effects of nembutal and radiomimetic substances on, 20: 29048
radiation effects on activity of, effects of temperature on, 20: 28903
radiation effects on activity of UDPglucose-fructose glucosyltransferase in potato tubers, 20: 28935
radiation effects on activity of carbonic anhydrase *in vivo*, x, 20: 28922
radioinduced inactivation of, effects of moisture on, 20: 28902

EPITHELIUM
radiation effects on mouse skin, dose-response relations for x, 20: 28990

EQUIPMENT AND PROCEDURES
for decontamination of, hot cells, 20: 29468

ERBIUM
determination in minerals and ores, spectrometric, 20: 29134
determination in rocks, chemical spectrographic method for, 20: 29083(R) (UCRL-14767)
determination in standard igneous rocks G-1, W-1, and G-B by x-ray fluorescence, 20: 29101
determination in TBP extracts, spectrophotometric, 20: 29125
determination in uranium compounds, spectrographic, 20: 29129
diffusion in molten aluminum–bismuth, aluminum–cadmium, and aluminum–lead alloys at 700°C, 20: 29797
thermodynamic properties at 0°C to melting point, 20: 29743

ERBIUM ALLOYS
Er–La, electric conductivity, magnetic susceptibility, and superconducting transition temperatures of, 20: 29753
Er–Re, crystal structure of, laves phase in, 20: 29792(T)

ERBIUM CHLORIDES
thermal capacity of aqueous solutions of, at 25°C, 20: 29144 (IS-1355)

ERBIUM COMPLEXES
bromide, composition and stability of, 20: 29225
with EDTA, preparation, composition, and stability of, 20: 29222

ERBIUM IONS
electron paramagnetic resonance spectra of trivalent, in yttrium oxide single crystals, 20: 29192
energy levels in lanthanum chlorides, Orbach relaxation mechanism for excited, 20: 30758

ERBIUM NIOBATES
distribution in strontium molybdate single crystals, coefficients of, 20: 29746

ERYTHROCYTES
radiation effects on metabolism in, x, 20: 28924
radiation effects on, 20: 28981
radiosensitivity of catalase in, x, 20: 28911

ERYTHROPOIESIS
radiation effects on rat, effects of endocrine gland removal and hormones on, 20: 29043

ERYTHROPOIETIN
use in diagnosing anemia in irradiated subjects, 20: 28871(R) (EUR-2636.f,i)

ERZ-GEBIRGE–BOHEMIA AREA (GERMANY)
pitchblende formation and paragenetic position in hydrothermal deposits of, 20: 29448

ESCHERICHIA COLI
effects of 2-aminopurine in, radiomimetric, 20: 29041
radiation effects on DNA and RNA synthesis in, uv, 20: 28949
radiation effects on DNA in, uv, 20: 28991
radiation effects on, effects of depth in irradiated medium on electron-beam, 20: 28963
radioinduced mutants of, resistance of uv-, to bacteriophage T1, 20: 29027
radioinduced mutations in, RBE for neutron-induced reversions of, 20: 29002
radioinduced phage induction in, RBE for 200-kev fast-neutron, 20: 29002
radioinduced phage in, protective effects of AET and MEA against x, 20: 29045

ESTERS
analysis and determination of carbon-14-labeled, by gas chromatography and radiometric methods, 20: 29089

β-keto, reactions with uranium pentaethoxide, 20: 29155

ESTRADIOL
effects on radiation effects on heme synthesis in rabbit bone marrow, 20: 28912

ESTROGENS
radiosensitivity effects on erythropoiesis in rats, iron-59 tracer study on, 20: 29043

ETHANE
helium atom reactions with, electron kinetic energy from ionization in, (E), 20: 29927
molecular dissociation following carbon-14 beta decay in, calculation of, 20: 29233
yields of, from hydrolysis of rare earth carbides, 20: 29220
Br–ethane, tritium reactions with gas-phase, scavenging effects on hot and thermal recoil, 20: 29206
ethane–O, tritium reactions with gas-phase, scavenging effects on hot and thermal recoil, 20: 29206

ETHANE, BROMO-
radiolysis of, Finkelstein reaction for measuring partial organic retention in, 20: 29292

ETHANE, CHLORO-
radioinduced formation from hydrogen chloride and ethylene, 20: 29252

ETHANE, DIBROMO-
radiolysis of, Finkelstein reaction for measuring partial organic retention in, 20: 29292

ETHANE, 1,2-DICHLORO-1,1,2,2-TETRAFLUORO-
heat transfer near critical point of, 20: 29375(R) (ANL-7190, pp 193-200)

ETHANE, IODO-
radiolysis of, at 77°K, reaction intermediates in gamma, 20: 29264

ETHANETHIOL, 2-AMINO-
radioprotective effects of, effects of temperature on, 20: 29057
radiosensitivity effects on rats, 20: 29047
radiosensitivity effects on phage induction in *E. coli*, x, 20: 29045

ETHANOL
effects on conditioned reflexes of dogs, 20: 29009
radiosensitivity effects on dogs, 20: 29009

ETHYLAMINE, 2,2'-DITHIOBIS-
radiosensitivity effects on *Saccharomyces cerevisiae*, 20: 29023
radiosensitivity effects on rabbits, 20: 29051

ETHYLENE
radioinduced polymerization of, kinetics of gamma, 20: 29275
radioinduced reactions with hydrogen chloride, gamma, 20: 29252
reactions with muonium, cross sections for, 20: 29177
sorption by yttrium oxide, effects of water on, 20: 29186
yields of, from hydrolysis of rare earth carbides, 20: 29220

ETHYLENE, DICHLORO-
reactions with muonium, (E), 20: 29247

ETHYLENE GLYCOL POLYMERS
Antarox DM-970–sodium hexametaphosphate–sodium dodecyl sulfate–sodium nitrates–sulfosalicylic acid, efficiency of, as radioactivity decontamination solution for cotton protective clothing, 20: 29477

ETHYLENE OXIDE, TETRAFLUORO-, POLYMERS
radioinduced main-chain scission in, ESR spectra from gamma, 20: 29267

ETHYLENE POLYMERS
neutron inelastic scattering at 0.238 to 0.570 ev, cross sections for fast, (E), 20: 30325(R) (RPI-328-56, pp 113-34)
neutron inelastic scattering at 0.83 to 1.8 ev, differential cross sections for, (E), 20: 30334
neutron spectra in, time-dependent, (E), 20: 30324(R) (RPI-328-56, pp 52-93)
neutron spectra in, (T), 20: 30326
properties of, determination of, by column fractionation, 20: 29624(R) (TID-22970, pp 257-329)

ETHYLENE, TETRAFLUORO-
radioinduced polymerization of, at 4.2°K, 20: 29300

ETHYLENE, TRICHLORO-
effects on metals, tracer studies of corrosive, 20: 29655
labeling with chlorine-36 for corrosion studies, 20: 29655

ETHYLENEDIIMINE
ethylenediimine–2,4-pentanedione, complexes with thorium, and zirconium, preparation and structure of, 20: 29203

EUGLENA
radiation effects on nucleotide diffusion from, γ, 20: 28904

EUROPIUM
determination in rocks, chemical spectrographic method for, 20: 29083(R) (UCRL-14767)
determination in standard igneous rocks G-1, W-1, and G-B by x-ray fluorescence, 20: 29101
determination in TBP extracts, spectrophotometric, 20: 29125
determination in uranium compounds, spectrographic, 20: 29129
determination of trace amounts of, in gadolinium by activation methods, 20: 29082 (SGAE-CH-27/1966)
gamma spectra, (E), 20: 30353(R) (ORNL-3940, pp 1-61)
polarographic properties of, on fused potassium acid sulfate electrolyte, 20: 29210
separation from americium, berkelium, californium, cerium, curium, and uranium by ion exchange on zirconium phosphate, 20: 29340

EUROPIUM COMPLEXES
with serine, stability of, 20: 29208
with 1,10-phenanthroline–thenoyltrifluoroacetone, preparation and luminescence of, 20: 29221
with 2,4-pentanedione, luminescence spectra of, (E), 20: 29238

EUROPIUM FLUORIDES
crystal and dielectric properties of EuF_2, 20: 30746
fluorine-19 NMR in, (E), 20: 30761

EUROPIUM ISOTOPES Eu-147
decay of, gamma directional correlations from, (E), 20: 30362

EUROPIUM ISOTOPES Eu-149
energy levels, (E), 20: 30353(R) (ORNL-3940, pp 1-61)
energy levels from proton scattering by samarium-148, (E), 20: 30430

EUROPIUM ISOTOPES Eu-151
energy levels from proton scattering by samarium-150, (E), 20: 30430

EUROPIUM ISOTOPES Eu-152
beta decay of, higher-order effects in β-γ correlations from, 20: 30470
beta decay of, matrix elements for first-forbidden, (E/T), 20: 30522
decay scheme and gamma spectra, (E), 20: 30487

EUROPIUM ISOTOPES Eu-153
energy level transitions from gadolinium-153 decay, Mössbauer studies of, (E), 20: 30555
energy levels from proton scattering by samarium-152, (E), 20: 30430
nuclear magnetic resonance in europium oxides, (E), 20: 30761

EUROPIUM ISOTOPES Eu-154
beta decay of, higher-order effects in β-γ correlations from, 20: 30470
beta decay of, matrix elements for first-forbidden, (E/T), 20: 30522

EUROPIUM NIOBATES
distribution in strontium molybdate single crystals, coefficients of, 20: 29746

EUROPIUM OXIDES
crystal structure of Eu_2O_4, 20: 29718
europium-153 NMR in, (E), 20: 30761
Al_2O_3–B_2O_3–EuO, boron-11 NMR in, (E), 20: 30761

EUROPIUM TITANATES
preparation and crystal structure of, 20: 29212

EUROPIUM ZIRCONATES
preparation and crystal structure of, 20: 29212

EVAPORATORS
use of fluidized-bed spray, for processing radioactive waste solutions, 20: 30946

EXPERIMENTAL BOILING WATER REACTOR
development for use in plutonium recycle programs, 20: 30787(R) (ANL-7190, pp 11-142)
fuel element fabrication, spiked-core, 20: 29658 (ANL-6283)
power oscillations of, small self-sustaining, (T), 20: 30908

EXPERIMENTAL BREEDER REACTOR-II
operation and maintenance, April 1966, 20: 30790(R) (ANL-7204, pp 1-31)
operation and performance, summary for July 1964 to June 1965, 20: 30787(R) (ANL-7190, pp 11-142)

EXPERIMENTAL GAS COOLED REACTOR
fuel elements for, radiation effects on, 20: 29806 (ORNL-TM-1511)

EXTRUSION
equipment design for, of tubes, 20: 29691(P)
equipment for hydrostatic, 20: 29693(P)

EYES
chromosomal aberrations in cornea of mouse, induced by tissue extracts from x-irradiated donors, 20: 28959
radiation effects on glycogen metabolism in rabbit, 20: 28907
radiation effects on, laser, 20: 28936
radiation injury by lasers, 20: 29457
ultrasonic wave effects on, laser-generated, 20: 28951

F

FALLOUT
composition and transport of atmospheric, from nuclear explosions, 20: 29411
contamination of milk by, effects of dietary calcium on, 20: 29459
content in cattle feed, 20: 29463
content in oceans, effects of, on populations, 20: 29405 (NP-14694)
determination in atmosphere using gamma spectrometer, behavior of cesium-137 in, 20: 29081 (NP-14705)
dispersion in atmosphere, model for, 20: 29454(R) (SC-CR-66-2010)
effects on development, mortality, and sterility of insects and invertebrates, 20: 28925 (AD-633024)
formation and global distribution of, 20: 29407(T) (AEC-tr-6666)
fractionation in, from Chinese nuclear tests in 1964, 20: 29423

hazards from, to population of United Kingdom, 20: 29054 (NP-16119)
leaching from food plants, 20: 29451(R) (NYO-2598-29)
measurement in Valencia, 1964, 20: 29408
measurements of, in atmospheric precipitation, 20: 29416
monitoring in Canada, 1966, 20: 29053 (NP-15951)
monitoring in North America, 1965, 20: 29434
monitoring in North America, 1965, 20: 29431
monitoring in rainwater, settled dust, and sewage sludge in Japan, 1964, 20: 29455
monitoring in surface air along 80th meridian W, Jan. through March 1965, 20: 29430
monitoring in U. S., 1965, 20: 29428
monitoring in United States, 1965, 20: 29434
monitoring in United States, 1965, 20: 29431
monitoring in USSR, 1962, 20: 29406 (NP-14719)
monitoring of Chinese test, in Colorado, May 1965, 20: 29429
monitoring of, in Japan, 1964 and 1965, 20: 29422
particle size of, in Osaka, Japan, from Chinese nuclear explosion of October, 1964, 20: 29466
prediction of, from tropospheric and stratospheric data, 20: 29407(T) (AEC-tr-6666)
protection of domestic animals from, shelters for, 20: 29392
sample analysis and collection, 20: 29407(T) (AEC-tr-6666)
shelters against, lightway for, 20: 29483(P)
tritium content of, in rain and snow, Moscow, 1961 to 1963, 20: 29409

FAST REACTORS
coolant leakage between bed and vessel of liquid-metal cooled, device for control of, 20: 30827(P)
design of power breeder, with steam (D_2O, H_2O, or D_2O–H_2O) coolant and moderator, 20: 30914(P)
design of 1000-Mw(e) breeder, 20: 30875(R) (ANL-7190, pp 143-55)
development of British sodium-cooled, 20: 30798(R) (NP-16043)
fuel development for liquid metal-cooled, 20: 30790(R) (ANL-7204, pp 1-31)
fuel element design for, effects of cross section uncertainties on ceramic, 20: 29618(R) (GEAP-4982)
reactivity pulsing device for, design of, 20: 30866(P)

FATS
radiation effects on content of, in paramecia, uv, 20: 28918

FATTY ACIDS
effects of dietary, on radioinduced changes in intestinal secretory function in dogs, 20: 28993

FEED MATERIALS PRODUCTION FACTILITY, WELDON SPRINGS, MISSOURI
environs monitoring, 1964, 20: 29434

FERGUSONITES
analysis for yttrium, fluorometric, 20: 29094

FERMIONS
Brownian motion in liquids, (T), 20: 30263
interactions with bosons, lagrangian density for, 20: 30122
superfluidity of liquids of, collective oscillations in, 20: 30284

FERRITES
photon-pumped magnon instabilities in, 20: 29709(R) (TID-22970, pp 65-119)

FERROMAGNETIC MATERIALS
effects on magnetic fields in polyphase cylindrical inductors, (T), 20: 29835
magnetic spin correlations in, 20: 29623(R) (TID-22970, pp 121-256)
photon-pumped magnon instabilities in, 20: 29709(R) (TID-22970, pp 65-119)
spin diffusion in, (T), 20: 30780
uses in temperature measurements on irradiated materials, 20: 29387

FERTILIZERS
preparation of, using fission fragment recoil energy, 20: 29317

FIBRINOGEN
use of iodine-131-labeled, for tumor and metastasis diagnosis, 20: 28871(R) (EUR-2636.f,i)

FIELD THEORY
current algebras and form factors at finite momentum transfer, 20: 30137
current commutation relations and PCAC hypothesis in, scalar densities in, 20: 30138
current densities in, saturation of SU(3) algebra of, 20: 30119
Dirac fields in, CPT transformations for, 20: 30097
elementary particle weak interactions in, Reggeization conditions for, 20: 30125
elementary particle production and scattering in quantum, (T), 20: 30157
many-body problem in, broken symmetry and sum rules for, 20: 30139
properties of scalar, quantum, 20: 30092 (JINR-P-2700)
quantum, moments problem in, 20: 30105
Regge poles in, 20: 30163
S-matrix for quantum theory of gravity, 20: 30239 (JINR-P-2692)
symmetry breakdown and massless particles in model, spontaneous, 20: 30135
symmetry violation in Wightman axiomatic scheme, 20: 30154
Zachariasen model of, broken symmetry and compositeness conditions in, 20: 30156

FILMS
properties of magnetic, 20: 29623(R) (TID-22970, pp 121-256)
research on thin conductive, 20: 29709(R) (TID-22970, pp 65-119)

FISH
nucleotide content in tissues of, method for measuring, 20: 29583(R) (TID-22515)
radiosterilization effects on precooked, 20: 29582(R) (MIT-3343-26)
radiosterilization of cod and halibut patties, 20: 29603
strontium-90 uptake by marine, hazards to mass from, 20: 29405 (NP-14694)

FISSION
effects of epithermal, on multiplication factor in reactors, 20: 30841
model for, core, 20: 30380
theory as Markov process, shell model corrections for, 20: 30428
theory of, statistical, 20: 30486

FISSION CHAMBERS
design of mica-uranium, for high-energy proton reactions, 20: 29551
use for neutron-flux measurements in reactors, 20: 29549

FISSION FRAGMENTS
charge distribution of, from uranium-235 thermal fission, (E), 20: 30476
charge distribution in uranium-235 thermal fission, 20: 30477
effect on liquid ammonia, hydrazine formation in, 20: 29319(P)
effects on mechanical properties of molybdenum, 20: 29820
gamma emission by isomeric, from neutron fission of uranium-235 and plutonium-239, (E), 20: 30463
kinetic energy of, from uranium-235 fission, (E), 20: 30513

FISSION PRODUCTS
diffusion from plutonia–urania fuels, effects of grain growth and preparation procedure on gaseous, 20: 29805(R) (NUMEC-3432-21)
diffusion of gaseous, from carbon-coated urania particles, 20: 29616(R) (BMI-1738)
diffusion of, in graphite, (T), 20: 29190
effects on man, pathological, 20: 29407(T) (AEC-tr-6666)
energy of recoil, chemical compound synthesis using, 20: 29317
evaporation of, from irradiated uranium(IV-VI) oxides at 900 to 1500°C in flowing hydrogen, nitrogen, or oxygen, 20: 29211
gamma flux from circular and spherical configuration of, analysis of, (T), 20: 30351 (N-65-14857)
gamma radiation from nuclear-explosion, 20: 30233
gamma spectra of natural uranium, (E), 20: 30379
ion charge distribution of unretarded, 20: 30507
mass distributions from thorium-229, 20: 30373
removal of, from cotton protective clothing, solution for, 20: 29477
separation from nitrate solutions using kerosene–TBP, radiation effects in, 20: 29272
separation of molybdenum, neptunium, niobium, plutonium, technetium, tellurium, uranium, and zirconium from solutions of, by ion exchange, 20: 29357
sorption from waste solutions by clay minerals, 20: 29332 (ORNL-P-1811)

FISSIONABLE MATERIAL
criticality of, neutron detectors for verification of, 20: 29519 (BNWL-SA-31)
neutron scattering by, technique for measuring resonance, 20: 30358(R) (RPI-328-56, pp 1-48)
safety controls in receiving and shipping, procedures for, 20: 29450 (ISO-270)

FISSIUM
effects on fluorination of uranium dioxide in hydrofluoric acid–chlorine trifluoride–fluorine cycle, 20: 29330(R) (EURAEC-1601)
fissium–Pu–U, fission product release from irradiated, 20: 30790(R) (ANL-7204, pp 1-31)
fissium–U, thermal conductivity of irradiated, as function of burnup, 20: 30791(R) (ANL-7204, pp 32-64)

FLAMES
use of laminar-flow oxyacetylene, for atomic absorption spectrophotometry, 20: 29083(R) (UCRL-14767)

FLAVONES
labeling with deuterium, 20: 29240

FLUID FLOW
boiling burnout in tubular, with nonuniform heat fluxes, (E/T), 20: 29376 (BAW-3238-9)
boiling burnout in nonuniformly heated annular tubes, (E/T), 20: 29377(R) (BAW-3238-11)
boiling burnout in annular spray, probe techniques for analyzing, 20: 29378(R) (NYO-3304-7)
design and performance for variable flows, 20: 29535
heat transfer in external forced convection, (E/T), 20: 29379 (SAN-1011)
of conducting fluids over flat porous plates in transverse magnetic field, 20: 30180

pressure drop in uniformly heated two-phase, (E/T), 20: 29380(R) (TID-22967)
stability in boiling water channels with natural circulation, 20: 29385
two-phase sodium, measurements of adiabatic, 20: 29374(R) (ANL-7190, pp 156-66)

FLUIDIZATION
use of fluidized-bed spray evaporator for processing radioactive waste solutions, 20: 30946
use of fluidized-bed process for deposition of silicon coating on refractory metals, 20: 29630

FLUIDS
atomic motions in monatomic, analysis of, (T), 20: 30166 (NYO-3326-13)
Brownian motion in Fermi, (T), 20: 30263
development of, for gyro damping, 20: 29366(R) (TIR-22970, pp 375-91)
energy loss from expansion of perfect, conservation law in general relativity for total proper, 20: 30241
hydrostatics and stability of cylinders composed of perfect, 20: 30251
magnetohydrodynamic drag on oscillating dielectric sphere in incompressible conducting, (T), 20: 30179
relaxation phenomena in molecular, computer calculations of, 20: 29147 (UCRL-14901-T)
sound waves in, lifetime and velocity of hypersonic, (E), 20: 30734(R) (TID-22970, pp 1-63)
stability in magnetic field, variational methods for Rayleigh-Taylor, (T), 20: 30172
thermal stability for confined, exchange principle for MHD, 20: 30178

FLUOPHOSPHORIC ACID
bonding and chemical reactions with magnesium and zirconium oxides, mechanism of, 20: 29145 (NP-16047)

FLUORESCEIN, DIIODO-
sodium, labeling with iodine-131, 20: 29236

FLUORESCENCE
methods and reagents for spectrophotofluorimetry, 20: 29083(R) (UCRL-14767)

FLUORIDE COMPLEXES
with neptunium, properties and stability of, 20: 29148

FLUORIDE IONS
determination using thorium complex with 2-(1,8-dihydroxy-3,6-disulfo-2-naphthylazo)phenoxyacetic acid, spectrophotometric, 20: 29091

FLUORIDE VOLATILITY PROCESSES
fuel element reprocessing by, pilot plant design problems for, 20: 29364

FLUORINE
determination in atmosphere, design of apparatus for, 20: 29330(R) (EURAEC-1601)
determination in atmosphere using radioactive clathrate techniques, 20: 29142
determination in petroleum, activation, 20: 29139
determination of, by neutron activation methods, 20: 29078(R) (AD-633252)
separation from irradiated gold and uranium by distillation, 20: 29338

FLUORINE IONS
determination using thorium complex with 2-(1,8-dihydroxy-3,6-disulfo-2-naphthylazo)phenoxyacetic acid, spectrophotometric, 20: 29091

FLUORINE ISOTOPES F-18
production by neutron irradiation of gold or uranium, 20: 29338

FLUORINE ISOTOPES F-19
helium-3 reactions (He-3,α) and (He-3,αn) at 3 to 10 Mev, excitation functions for, (E), 20: 30444
neutron reactions (n,p) at 14.8 Mev, cross sections for, (E), 20: 30394
neutron scattering differential cross sections, (E), 20: 30360 (WASH-1068)
nuclear magnetic resonance in rare earth trifluorides, 20: 30755
nuclear magnetic resonance in cesium europium fluorides and europium fluorides, (E), 20: 30761
nuclear spin-lattice relaxation time in neodymium-doped calcium fluoride crystals, 20: 30772
triton reactions (t,α) with, alpha angular distributions from, (E), 20: 30360 (WASH-1068)

FLUORINE SYSTEMS
ClF_3–F–HF, effects on fluorination of uranium dioxide, 20: 29330(R) (EURAEC-1601)

FLUOROORGANIC COMPOUNDS
analysis and determination of, by radio paper partition chromatography, 20: 29123

FOILS
development for use as thermal shields on pressure vessels, 20: 30820(P)

FOLIC ACID
effects on metabolism of vitamin C in guinea pigs and rats, 20: 28921

FOOD
carbon-14 content in, 1963 and 1964, 20: 29472
cesium-137 content in U. S., 1962 and 1963, 20: 29475
radiation control of insects infesting, 20: 29585
radiation processing of, effects on wholesomeness, 20: 29585
radiation processing of, radioactivity induced in, 20: 29599
radioactivity in, 1965 fallout, 20: 29428
radiosterilization effects on precooked marine products, 20: 29582(R) (MIT-3343-26)
radiosterilization of marine products, design of facility for, 20: 29584 (TID-22991)
radiosterilization of cod and halibut patties, 20: 29603
strontium-90 content in, 1962 and 1963, 20: 29433

FORESTS
nutrient leaching and recycling in tropical, 20: 29451(R) (NYO-2598-29)

FOSSILS
age estimation of Pleistocene coral, 20: 29435

FRANCIUM ISOTOPES Fr-219
alpha decay, 20: 30374

FREE RADICALS
electron spin resonance and thermoluminescence of, in irradiated biochemicals, 20: 29249
production of, during radiolysis of rubber at –196°C, ESR studies on, 20: 29299
radioinduced in fluorinated carboxylic acid, ESR spectra of, 20: 29282
radioinduced in pyridoxine derivatives, uv and v, 20: 28901
radioinduced in rat bones, EPR study of, 20: 28898 (CEA-R-2910)
radioinduced in rat bone, γ, 20: 28906
radioinduced in 2-thiophenecarboxylic acid, ESR spectra of, 20: 29284
radioinduced, reactions of, 20: 29037
role in radiation injuries, 20: 29037
yields from gamma radiolysis of frozen carbon tetrachloride–methanol solutions, 20: 29305

FRICTION
in transition from turbulent to laminar gas flow in tubes, 20: 29384

FRUITS
radiation control of insects in chestnuts, 20: 29597
radiopreservation of chestnuts, oranges, and persimmons, gamma, 20: 29597

FUEL CELLS
development for space power, 20: 29977 (N-65-32716)

FURFURYL ALCOHOLS
effects as impregnant on radiation effects on graphite, 20: 29813

FURNACES
design of high-vacuum, for neutron diffraction experiments, 20: 29106

G

GADOLINIUM
analysis of, for traces of europium by activation methods, 20: 29082 (SGAE-CH-27/1966)
determination in aqueous solutions, design of oxyacetylene burner for measuring sensitivity of spectrophotometric, 20: 29083(R) (UCRL-14767)
determination in minerals and ores, spectrometric, 20: 29134
determination in rocks, chemical spectrographic method for, 20: 29083(R) (UCRL-14767)
determination in standard igneous rocks G-1, W-1, and G-B by x-ray fluorescence, 20: 29101
determination in TBP extracts, spectrophotometric, 20: 29125
determination in uranium compounds, spectrographic, 20: 29129
gamma spectra, (E), 20: 30353(R) (ORNL-3940, pp 1-61)
neutron total cross sections at 2.4 to 15.7 Mev, (E), 20: 30419
polarographic properties of, on fused potassium acid sulfate electrolyte, 20: 29210
thermal conductivity of, at room temperatures, mechanisms for, 20: 29741
thermodynamic properties at 0°C to melting point, 20: 29743

GADOLINIUM ALLOYS
Cd–Gd, magnetic properties of, 20: 29752
Co–Gd–Y, magnetic properties of, 20: 30756
Cu–Gd, magnetic properties of, 20: 29752
Gd–Ag, magnetic properties of, 20: 29752
Gd–Au–Ag, magnetic properties of, 20: 29752
Gd–In, magnetic properties of, 20: 29752
Gd–In–Ag, magnetic properties of, 20: 29752
Gd–In–La, superconducting transition temperature, (E), 20: 30271
Gd–La, electric conductivity, magnetic susceptibility, and superconducting transition temperatures of, 20: 29753
Gd–Re, crystal structure of, laves phase in, 20: 29792(T)

GADOLINIUM CARBIDES
hydrolysis of, gaseous products from, 20: 29220

GADOLINIUM HYDRIDES
spectra of, x-ray-absorption, 20: 29162

GADOLINIUM IONS
radioinduced thermoluminescence of, in calcium fluoride, 20: 29318

GADOLINIUM ISOTOPES Gd-148
alpha spectra, (E), 20: 30353(R) (ORNL-3940, pp 1-61)

GADOLINIUM ISOTOPES Gd-149
alpha spectra, (E), 20: 30353(R) (ORNL-3940, pp 1-61)
energy level transitions in, conversion coefficients for, (E), 20: 30353(R) (ORNL-3940, pp 1-61)
GADOLINIUM ISOTOPES Gd-153
decay of, Mössbauer studies of 97-kev level of europium-153 from, (E), 20: 30555
GADOLINIUM ISOTOPES Gd-155
Mössbauer effect in, level quadrupole splitting and spins from, (E), 20: 30422
GADOLINIUM ISOTOPES Gd-161
beta decay of, terbium-161 levels and Coriolis coupling parameter from, 20: 30401
GADOLINIUM NIOBATES
distribution in strontium molybdate single crystals, coefficients of, 20: 29746
GADOLINIUM NITRATES
thermal decomposition, 20: 29224
use in shutdown system for Savannah River Production Reactor, 20: 30920(P)
GADOLINIUM TITANATES
preparation and crystal structure of, 20: 29212
GAGES
alpha sources for, for basis weight measurements, 20: 29601
design and performance of radiometric, for soil density and moisture content determinations, 20: 29507
efficiency of radiometric, for soil density and moisture content determinations, 20: 29506
performance of radiometric surface, for soil density and moisture content determinations, 20: 29508
use for soil density and moisture content determinations, conference on, 20: 29504
GALAXIES
formation, (T), 20: 29879
processes in, oscillation dispersion in collective, 20: 29902(T)
x-ray emission from discrete sources in, free-free emission model for, 20: 29881
GALLIC ACID, PROPYL ESTER
effects on radiation damage in DNA, 20: 29037
GALLIUM
determination in petroleum, activation, 20: 29139
determination of, by neutron activation methods, 20: 29078(R) (AD-633252)
electric conductivity of single-crystal, effects of temperatures less than 10°K on, (E/T), 20: 30734(R) (TID-22970, pp 1-63)
electron spectra of, effects of magnetic fields on, (E/T), 20: 30735(R) (TID-22970, pp 331-73)
geometric resonances in single-crystal, measurement of, (E), 20: 30734(R) (TID-22970, pp 1-63)
specific heat, (E), 20: 30734(R) (TID-22970, pp 1-63)
superconducting transitions in single-crystal, (E), 20: 30734(R) (TID-22970, pp 1-63)
GALLIUM FERRATES (III)
magnetic moments in high magnetic fields, (E/T), 20: 30735(R) (TID-22970, pp 331-73)
GALLIUM ISOTOPES Ga-72
beta decay of, matrix elements for first-forbidden, (E/T), 20: 30522
GAMMA CAMERAS
anatomical markers for, design of electronic, 20: 29067
GAMMA RADIATION
angular correlation analysis for, computer program for, 20: 30341 (AECL-2529)
angular correlation perturbation in solids, effects of lattice vibrations on, 20: 30762
angular correlations of praseodymium-144, 54 to 80 kev, (E), 20: 30506
angular distribution from helium-3 reactions (He-3,p) with carbon-12, (E), 20: 30526
attenuation by thallium at 122 kev, cross sections for, (E), 20: 30731
detection and measurement of, response of lithium-drifted germanium semiconductors for, (T), 20: 29528 (LA-3456)
detection and measurement of, efficiency of multiple-plate ion chamber for, 20: 29560
detection and measurement of, photographic film detector with intensifier screen for, 20: 29573(P)
detection of, design of ion chamber for in-cell, 20: 29564
detection of, design and sensitivity of parallel-plate ion chamber for, 20: 29565
detection of, detector for, 20: 29969
detection of, table of efficiencies of cylindrical scintillation detectors for, (T), 20: 29562
dose rates of, in irradiations through grids, 20: 29056
dosimetry of, automatic system for, 20: 29070
dosimetry of, design of G-M probe for, 20: 29563
dosimetry of, from therapeutic radium implants, 20: 29074
dosimetry of, performance of film and silicon diodes for, 20: 29518 (BNWL-SA-27)
dosimetry of, using glass, 20: 29283
effects on alkyl halides at 77°K, 20: 29264
effects on ammonia–water and ammonia–oxygen–water systems, hydrogen yields from, 20: 29295
effects on barium nitrate, isothermal-annealing kinetics of, at 200 to 275°C, (E/T), 20: 29814
effects on barley, oat, and wheat seed and shoots, 20: 28960
effects on blood, extracorporeal-exposure, 20: 28927 (BNL-9647)
effects on catalytic conversion of methanol on silica gel, 20: 29278
effects on chemical and physical properties of polypropylene with stabilizer additives, 20: 29290
effects on chrome-tanned upper shoe leather, 20: 29591
effects on content of ascorbic acid and glutathione in cotton plants, 20: 28999
effects on copper–glycine complexes, 20: 29303
effects on electric conductivity in aluminum oxides, 20: 29823
effects on electrophoretic mobility of animal cells in suspensions, 20: 28905
effects on F centers in alkali metal halide crystals, 20: 30739
effects on gasification of lignite, 20: 29586
effects on glass-shielding windows, electric charge accumulation from, 20: 30727
effects on heating in nuclear reactors, group constants for, 20: 30722 (KAPL-M-6497)
effects on hematopoiesis, effects of fractionated exposure on, 20: 28984
effects on mechanical and physical properties of tanned leather, 20: 29588
effects on mechanical and physical properties of chromium-tanned goat leather, 20: 29592
effects on metabolism in pea plants, 20: 28909
effects on metabolism of vitamin C in guinea pigs and rats, 20: 28921
effects on metabolic processes in plants, effects of growth phase on, 20: 28967
effects on mice, protective effects of preserved homologous bone marrow against, 20: 29033
effects on mice, protective effects of homografts in methotrexate-treated mice on, 20: 29035
effects on mice, protective effects of preserved homologous fetal liver against, 20: 29034
effects on mice, protective effects of AET combined with bone-marrow-transplants against, 20: 29036
effects on microstructure of silicon transistors, energy dependence of, 20: 29579 (NAA-SR-11887)
effects on nucleotide diffusion from Euglena, 20: 28904
effects on Pacific coast fishery products, 20: 29583(R) (TID-22515)
effects on palmitic acid and potassium palmitate, EPR studies of, 20: 29309
effects on pollen germination of *Pinus desiflora* and *Pinus thunbergii*, 20: 28980
effects on polycrystalline powders of fluorinated carboxylic acids, free radicals produced by, 20: 29282
effects of nuclear explosion flux of, on monopole antenna signal, 20: 29580
effects on activity of β-fructofuranosidase in potato tubers, 20: 28934
effects on activity of transferase in potato tubers, 20: 28935
effects on aqueous solutions of potassium iodide, 20: 29253
effects on aqueous solutions of 2-propanol in presence electron scavengers, 20: 29254
effects on aqueous solutions of oxygen, steady state reactions in, 20: 29257
effects on aqueous solutions of acetylene, 20: 29293
effects on β-benzyl, β-methyl-, and β-phenyl glucosides, 20: 29307
effects on blood coagulation, 20: 28985
effects on carbon suboxide, 20: 29269
effects on collagen and hexosamine content in rat subcutaneous granulomas, 20: 28917
effects on cyclohexane, 20: 29270
effects on deuterium–oxygen mixtures, yields from, 20: 29285
effects on DNA synthesis in pea seedlings, 20: 28989
effects on epoxido-dianic ED-5 resin, 20: 29297
effects on erbium-doped calcium fluoride single crystals, laser lines from, (E), 20: 30774
effects on formation of free radicals in rubber at −196°C, ESR studies on, 20: 29299
effects on frozen carbon tetrachloride–methanol solutions, 20: 29305
effects on grafting of monomers to nylon, 20: 29316
effects on hexachlorocyclopentadiene, mechanism and yields in, 20: 29256
effects on isomerization of stilbene in methanol solution, 20: 29287
effects on man, biological, 20: 28970

effects on monkeys, pathological, 20: 28986
effects on nitroprusside crystals, ESR studies of pairwise trapping from, 20: 29280
effects on organoleptic, chemical, and physical properties of beef at 20 to −196°C, 20: 29602
effects on poly(tetrafluoroethylene oxide), ESR study of main-chain scission from, 20: 29267
effects on polymerization of ethylene, 20: 29275
effects on polymerization of methyl methacrylate with lignin, 20: 29288
effects on polymerization grafting of acrylonitriles with viscose rayon, 20: 29294
effects on polymerization of acrylonitrile and tetrafluoroethylene at 4.2°K, 20: 29300
effects on positron-annihilation lifetime spectra in tritiated ice and water, 20: 29268
effects on proline content in potato tubers, 20: 28932
effects on rat bones, chemical, 20: 28898 (CEA-R-2910)
effects on reactions of hydrogen chloride with thylene, 20: 29252
effects on root-knot nematode propagation in sweet potatoes, 20: 28942
effects on seeds and seedlings of peas, effects of radioprotective compounds on, 20: 29049
effects on serum protein metabolism in rats, 20: 28954
effects on silicon planar transistor reliability, 20: 29577 (CEA-R-2959)
effects on solid-state polymerization of maleic anhydride with acenaphthylene, 20: 29274
effects on solvent properties of kerosene–TBP for fission product, thorium, and uranium, 20: 29272
effects on structure of epoxy resins, 20: 29296
effects on synthesis of ammonia, 20: 29312
effects on thermoluminescence of nucleic acid constituents, 20: 28913
effects on uv photolysis of sodium bromate, kinetics of, 20: 29248 (BNL-9672)
effects on viscoelastic properties of silicone and styrene–butadiene rubbers, 20: 29313
effects on x-ray-diffraction spectra of maize and potato amidones, 20: 29255
effects on 1-propanol, yields of hydrogen precursors in, 20: 29286
effects on 2-thiophenecarboxylic acid, ESR spectral studies on, 20: 29284
emission by fission-fragment isomers from neutron fission of uranium-235 and plutonium-239, (E), 20: 30463
free radical induction in rat bone, 20: 28906
hazards from, from underwater nuclear explosions, 20: 29481
intensity of fission-fragment-generated, during high-altitude nuclear explosion, 20: 30233
internal conversion in hydrogen from meson (η^0) decay, (E), 20: 30029
origin of cosmic isotropic, (T), 20: 29958
reactions in electric field of copper and cobalt nuclei, photon-pair production from, (E), 20: 30031
reactions in food, radioactivity from, 20: 29599
reactions with atoms at 320 kev, absolute electron emission cross sections for, (E), 20: 29924
scattering by aluminum, energy and angular distribution of, 20: 30729
scattering by atoms at 100 to 280 kev, electron binding effects on incoherent, (E/T), 20: 29923
scattering by cadmium 113, production of isomeric levels by, (E), 20: 30489
scattering by compressed stock coal, errors in density measurements by, 20: 29491
scattering by nuclei, electron-pair production by, (E/T), 20: 29996
scattering by nuclei, cross sections for neutron-capture resonant, (E), 20: 30467
scattering by sand, energy distribution from, (E), 20: 30728
transmission through graphite, stress-induced variations in spectral distribution of, 20: 29809
transport in three-dimensional rectangular geometry, computer program for, 20: 30726 (TID-22964)
transport of, standardization of computer programs for, 20: 30721 (EUR-2778.e)
use for soil density and moisture-content determinations, efficiency of air-gap and direct-transmission methods for, 20: 29505
use for soil density and moisture content determinations, for efficiency of probes, 20: 29506
use for sterilization of bone graft tissues, 20: 28987
use in paving-mixture and soil density and moisture determinations, conference on, 20: 29504
use in well logging for chlorine in subsurface formations, 20: 29446(P)
uses for detection of flaws in steel foils and plates, 20: 29390
uses in determining ash content of bituminous coal, 20: 29127
uses in measurement of porosities and saturations in porous media, 20: 29595
uses in preservation of fresh fruits and vegetables, 20: 29597

GAMMA SHIELDING
design of, model use in, 20: 30730
GAMMA SOURCES
calibration of, detector for, 20: 29571(P)
development of cylindrical, for lead shipping container testing, 20: 29388
dose distribution from, computer analysis of, 20: 29061
dose from iridium-192 and tantalum-182 wire, computer calculations for, 20: 29456
flux from circular and spherical, analysis of, (T), 20: 30351 (N-65-14857)
parameters for teletherapy, 20: 29064
use of 50-Curie cobalt-60 as, for radiography, 20: 29596
GAMMA SPECTRA
use of neutron-capture, in activation analysis, 20: 29137
GAMMA SPECTROMETERS
development of lithium-drifted solid-state, 20: 29078(R) (AD-633252)
GAMMA SPECTROSCOPY
errors in, for radium, thorium, and uranium determinations in rocks, 20: 29421
GARIGLIANO POWER REACTOR
development and research program, 20: 30878(R) (EURAEC-1516)
GARNETS
electric and magnetic properties of, 20: 29709(R) (TID-22970, pp 65-119)
magnetic resonance of europium–iron, at 77°K, (E), 20: 30735(R) (TID-22970, pp 331-73)
nuclear resonances of iron-57 in rare earth, (E/T), 20: 30734(R) (TID-22970, pp 1-63)
properties of single-crystal iron–yttrium, anelastic and magnetoelastic, 20: 29709(R) (TID-22970, pp 65-119)
spectra of europium–gallium, optical, (E), 20: 30735(R) (TID-22970, pp 331-73)
GAS COOLED REACTORS
boiler for, forced-flow once-through, 20: 30821(P)
control method for, 20: 30822(P)
core assembly design for graphite-moderated, 20: 30834(P)
design of fast power breeder, with steam (D_2O, H_2O, or D_2O–H_2O) coolant and moderator, 20: 30914(P)
design of steam-cooled and -moderated power, 20: 30917(P)
design of variably moderated and controlled, 20: 30915(P)
design of, computer programming for thermodynamics, 20: 30892
fuel cladding material for, properties of beryllium as, 20: 29777
fuel element design for, 20: 30872(P)
loading apparatus for, 20: 30819(P)
moderator for, design of interlocking graphite brick and tile, 20: 30823(P)
use as heat source for recovering petroleum from oil-bearing formations, 20: 30805(P)
GAS FLOW
in tubes, transition from turbulent to laminar flow in, 20: 29384
magnetohydrodynamic, one-dimensional self-similar, 20: 30185
GAS TURBINE ENGINES
design of, with motive fluid heating chamber, 20: 29395(P)
GASEOUS DIFFUSION PROCESS
development of, for carbon dioxide–hydrogen separation, 20: 29362
GASES
analysis for impurities, mass spectrometric, 20: 29083(R) (UCRL-14767)
analysis of, design of chromatograph for, 20: 29083(R) (UCRL-14767)
diffusion coefficients of, measurement by tracer technique, 20: 29510
electromagnetic wave propagation in weakly ionized, nonlinear phenomena in, 20: 30190
electron velocity distributions in electric fields in slightly ionized, instability of, 20: 30581
flow of adsorbed, in porous media, 20: 29624(R) (TID-22970, pp 257-329)
heat from high-temperature, uses of, 20: 30786(R) (ANL-7190)
hydromagnetic discontinuity in arbitrarily oriented magnetic field, steady-state exothermal, (T), 20: 30177
kinetic theory for, mathematical aspects of, 20: 30165 (BNL-9254)
neutron diffusion and thermalization in heavy, (T), 20: 30322 (BNL-947)
neutron scattering by, in acoustical fields, (T), 20: 30256
neutron scattering by monatomic, differential cross sections for, (T), 20: 30337
performance as power-reactor coolant, 20: 30910
shock wave propagation in ideal, analysis of, (E/T), 20: 30169 (UCRL-14198)
theory of inhomogeneous electron, 20: 30189
transport and self-diffusion in capillaries, model for, 20: 30174
transport in capillaries, (E/T), 20: 30175
GEIGER-MUELLER TUBES
performance for measuring low-level x-ray doses, 20: 29553
GELATIN
radiation effects on, ESR studies of, 20: 29273
GENETICS

radiation effects in embryonic stage on progeny of survivors, in chickens, 20: 29015

GEOLOGY
age estimations in, use of carbon-14 and tritium for, 20: 29438 (CONF-650652)
geochronology of North America, 20: 29397 (NAS-NRC-1276)

GEOMAGNETIC FIELDS
activity of, method using solar chromospheric structure for forecasting, 20: 30226
electron and proton spatial distribution in, 20: 30202(T) (NASA-TT-F-389, pp 281-7)
electron and proton spatial distribution in, trapped, 20: 30212(T) (NASA-TT-F-389, pp 551-66)
intensity of, satellite-based magnetometers for measuring, 20: 30236
intensity variations of, 27-day recurrence pattern of, 20: 29894
interaction of positive ion streams with, 20: 30208(T) (NASA-TT-F-389, pp 457-63)
properties of, review of, 20: 30196(T) (NASA-TT-F-389, pp 8-25)
pulsations in, apparatus for observing micro-, 20: 30229
variations in, from electron and proton motion in Van Allen belts, 20: 30209(T) (NASA-TT-F-389, pp 464-82)

GEOMAGNETIC STORMS
commencement in low latitude regions, classification of sudden, 20: 30232
development of, solar-flare effects on, 20: 30230
structure of sudden-impulse, 20: 30231

GEORGIA
radioisotope uptake by junipers in, 20: 29410

GERMANIUM
evaporation of, from irradiated uranium(IV-VI) oxides at 900 to 1500°C in flowing hydrogen, nitrogen, or oxygen, 20: 29211
molecular constants and thermodynamic functions of, triatomic, (T), 20: 29921
performance of lithium-drifted, for muonic x-ray spectra, 20: 29525 (CONF-660209-9)
performance of lithium-drifted, for determining gamma spectra of monazite and pitchblende, 20: 29079 (AERE-M-1736)
radiation damage recovery in oxygen-doped, oxygen-defect complexes for determining neutron, (E), 20: 30742
response of lithium-drifted, to gamma rays, (T), 20: 29528 (LA-3456)
spectra of, infrared, (E), 20: 30735(R) (TID-22970, pp 331-73)

GERMANY
uranium paragenetic position in hydrothermal deposits of West Erzgebirge, 20: 29448

GLASS
crystallization and phase separation in, 20: 29623(R) (TID-22970, pp 121-256)
determination in iridium–platinum alloys, development of electron microprobe for, 20: 29083(R) (UCRL-14767)
properties, 20: 29623(R) (TID-22970, pp 121-256)
radiation effects on shielding window, gamma, 20: 30727
use in electron beam and gamma dosimetry in linear accelerator, 20: 29283

GLASS TEXTILES
permeability to carbon dioxide–hydrogen mixtures, 20: 29362

GLAZES
deposition on silicon carbide-coated graphite, 20: 29696(P)

GLOW DISCHARGES
properties in hydrogen and noble gases at 1 to 25 torr, between planar anode and hollow cathode, 20: 30173

GLUCOSE
metabolism of, *in vitro* measurement of, 20: 28871(R) (EUR-2636.f,i)
yields from gamma radiolysis of β-benzyl-, β-methyl-, and β-phenyl glucosides, 20: 29307

GLUTATHIONE
radiation effects on content of, in cotton plants, γ, 20: 28999

GLYCERIDES
intestinal sorption of, measurement of, 20: 28871(R) (EUR-2636.f,i)

GLYCINE
complexes with copper, radiolysis of, mechanisms of gamma and uv, 20: 29303
radiation effects on, ESR and thermoluminescence studies of, 20: 29249
radiolysis of, ESR spectra of radicals from x, 20: 29281

GLYCINE, *N,N*-BIS(2-HYDROXYETHYL)-
complexes with rare earths, composition and stability of, 20: 29343

GLYCOGEN
effects of nicotinic acid on composition of, in rabbit liver, 20: 28895
radiation effects on metabolism of, in rabbit eyes, 20: 28907
radiation effects on content of, in paramecia, uv, 20: 28918

GLUCOSIDE, β-BENZYL-D-
radiolysis of, yields from gamma, 20: 29307

GLUCOSIDE, β-PHENYL-D-
radiolysis of, yields from gamma, 20: 29307

GOLD
diffusion in, mechanics of strain-induced self-, 20: 29623(R) (TID-22970, pp 121-256)
iron-57 Mössbauer spectra in, 20: 30766
microwave absorption in, on normal and superconducting tin, (T), 20: 30290
neutron capture cross sections at 30 to 1500 kev, (E), 20: 30360 (WASH-1068)
photon scattering by K-shell electrons of, spectral distributions from, (E/T), 20: 29912 (ISS-66/6)
photon scattering by K-shell electrons of, spectral distributions from, (E/T), 20: 29913 (ISS-66/7)
photon scattering by K-shell electrons of, spectral distributions from, (E/T), 20: 29914 (ISS-66/8)
radiation damage in, ion-beam, 20: 29808
separation of fluorine from irradiated, by distillation, 20: 29338

GOLD ALLOYS
Au–Fe, analysis of, for iron, development of electron microprobe for, 20: 29083(R) (UCRL-14767)
Au–Fe, thermal capacity below 1°K, 20: 29791
Au–Mn, thermal capacity below 1°K, 20: 29791
Au–Ni, elastic constants of single-crystal, effects of pressure on, 20: 29623(R) (TID-22970, pp 121-256)
Au–Sn, atomic structure of liquid and solid, 20: 29623(R) (TID-22970, pp 121-256)
Cu–Au, analysis of, development of electron microprobe for, 20: 29083(R) (UCRL-14767)
Cu–Au, crystal structure of intermetallic compound in, 20: 29623(R) (TID-22970, pp 121-256)
Gd–Au–Ag, magnetic properties of, 20: 29752

GOLD COUPLES
Au/Sn, critical field and temperature of superconducting, (E), 20: 30291
Au/Sn, microwave absorption in superconducting, proximity effects on, (E), 20: 30289

GOLD ISOTOPES Au-197
neutron activation cross sections for, (E), 20: 30360 (WASH-1068)
neutron capture by, production of high-specific-activity gold-198 in, 20: 29610
neutron capture cross section measurement at 80 to 200 kev, errors in using boron monitors for, (E), 20: 30352 (NASA-TR-R-240)
neutron reactions (n,γ) at thermal energies, gold-198 levels from, (E), 20: 30409

GOLD ISOTOPES Au-198
beta decay of, polarization in, (E), 20: 30548
beta spectra and K-conversion coefficient for, (E), 20: 30545
effects on blood and hematopoietic tissue, 20: 28982
energy levels from thermal neutron reactions (n,γ) with gold-197, (E), 20: 30409
hyperfine structure anomalies of, (E/T), 20: 30359 (UCRL-16757)
preparation of colloids of, for medical purposes, 20: 29075
production of high-specific-activity, by epithermal neutron capture by gold-197, 20: 29610

GOLD ISOTOPES Au-199
beta decay of, mercury-199 level structure from, (E), 20: 30549
hyperfine structure anomalies of, (E/T), 20: 30359 (UCRL-16757)

GONADS
radiation effects on epididymal spermatozoa in bovine testes, x, 20: 29013
radiation effects on germ cells of rabbit, x, 20: 29019

GOODYEAR ATOMIC CORP., PIKETON, OHIO
environs monitoring, Jan. to July 1965, 20: 29428

GRANITES
analysis of standard G-1 and G-B, for rare earths, by x-ray fluorescence, 20: 29101
potassium, thorium, and uranium abundances in, Rum Jungle Complex, Australia, 20: 29415

GRAPHITE
analysis for aluminum, iron, magnesium, oxygen, and silicon by neutron activation methods, 20: 29140
coatings for oxidation resistance of, development of carbide, cermet, oxide, and silicide, 20: 29773
coatings of, effects of temperature and time on properties of, 20: 29730
deformation of crystals of, by interstitial carbon atoms, 20: 29735
deposition of pyrolytic, on radioactive spheroids, process for, 20: 29638(P)
deposition on thorium uranium carbide fuel particles by pressing, 20: 29669
design of interlocking bricks and tiles, 20: 30823(P)
diffusion of fission products in, (T), 20: 29190
elastic properties and thermal creep in artificial, 20: 29734
electric conductivity at low temperatures, 20: 29750
electron energy band parameters in pyrolytic, 20: 30737
fabrication of bodies of isotropic, 20: 29694(P)

fabrication of corrosion-resistant, with silicon carbide coating and glaze covering, 20: 29696(P)
gamma transmission through, stress-induced variations in spectral distribution of, 20: 29809
magnetic resonance at low temperatures, (E/T), 20: 30735(R) (TID-22970, pp 331-73)
mechanical and thermal properties of type P-03, 20: 29714 (WANL-TME-1031)
neutron flux in moderators of, multi-velocity corrections in activation measurements of, 20: 29539
neutron thermalization in, time-dependent, (E/T), 20: 30327
optical properties of, in infrared region, 20: 30736
oxidation by carbon dioxide, equipment for studying kinetics of high-temperature, 20: 29656
oxidation by vacuum ultraviolet irradiated carbon dioxide, structural studies on, 20: 29733
oxidation by water vapor in presence of hydrogen, rate of, 20: 29626
preparation and structure of annealed boron-activated, electron microscopy and x-ray-diffraction studies on, 20: 29625
properties of, at low temperatures, galvanomagnetic, 20: 29751
properties of, effects of carbides, metals, and copper and silver infiltrants on, 20: 29764
radiation effects on tensile-fracture strain in EGCR-type neutron, 20: 29811
radiation effects on coke-type, at 425 to 1200°C, 20: 29812
radiation effects on dimensional changes in furfuryl alcohol-impregnated, fast neutron, 20: 29813
radiation effects on dimensions and thermal conductivity of low-permeability, reactor, 20: 29822
radioinduced stresses in moderator columns of, effect of cross-sectional shape on, 20: 30803
thermal conductivity at low temperatures, 20: 29750

GRAPHITE BROMIDES
bromine-82 exchange with, kinetics of, 20: 29182

GRAPHITE MODERATED REACTORS
core assembly design for gas-cooled, 20: 30834(P)
design of integral vapor-generating and superheating, 20: 30919(P)

GRAPHITE SYSTEMS
Be-graphite, fabrication of reactor reflectors from, 20: 30816(P)
Cs–graphite, bonding energy in, model for, 20: 29744
graphite–U, neutron thermalization in, time-dependent, (E/T), 20: 30327

GRAVITATION
field theory for, Heisenberg and interaction representations for, 20: 30239 (JINR-P-2692)
field theory of massive gravitons, 20: 30163
gravitational absorption and shielding in, general relativity theory for, 20: 30245
gravitons in, Goldstone boson model of, 20: 30247
radiation of, geometrodynamics of cylindrical systems of, 20: 30251
Schwarzschild metric for general relativistic field equations in, 20: 30246

GROUND
waste disposal in, by hydrofracturing, 20: 30943(R) (ORNL-TM-1465)

GROUND WATERS
lead and strontium abundances and isotopic compositions in brines under Salton Sea area, California, 20: 29414

GROWTH
radiation effects in embryonic stage on chickens, 20: 29015

GUANINE
radiation effects on thermoluminescence of, gamma, 20: 28913
radiation effects on content of, in DNA in guinea pig brain, 20: 28919
radiation effects on, ESR and thermoluminescence studies of, 20: 29249

GUANOSINE
radiation effects on thermoluminescence of, gamma, 20: 28913
radiation effects on fluorescence and phosphorescence spectra of, at 77°K, gamma, 20: 28914
radioinduced leakage of, from Euglena cells, γ, 20: 28904

GUANYLIC ACID
radiation effects on thermoluminescence of, gamma, 20: 28913

GUINEA PIGS
calcium-45 metabolism in brain slices from, effects of alkaloids on, 20: 28891
cysteine metabolism by, 20: 29024
nucleic acid content in brain in, effects of radiation sickness on, 20: 28919
radiation effects on vitamin C metabolism in, γ and x, 20: 28921
radiation effects on hemopoietic system in, x, 20: 28945
radiation effects on steroid content in, x, 20: 28975
radiation effects on lymphocytes in lymph nodes of, 20: 28976

GUNDREMMINGEN POWER REACTOR
design and performance, 20: 30888

GYPSUMS
properties for ion exchange separation of strontium-90 and yttrium-99 from water, 20: 29348

H

HAFNIUM
determination in zirconium and zirconium alloys, 20: 29115
determination in zirconium and zirconium alloys, 20: 29114
elastic modulus of polycrystalline, at 70 to 900°F, 20: 29703 (KAPL-3112)
oxidation kinetics, 20: 29644
oxidation of, at 850 to 1400°C, kinetics of film growth in, 20: 29647
separation from zirconium by ion exchange using anionites, 20: 29352
thermal expansion of polycrystalline, at 70 to 1400°F, 20: 29703 (KAPL-3112)

HAFNIUM ALLOYS
Hf–Nb–Ti, fabricability, strength, and weldability of, 20: 29763
Hf–Nb–W–Y, fabricability, strength, and weldability of, 20: 29763
Hf–Nb–W–Y, tensile properties of C-129Y, effects of welds on, 20: 29712(R) (WANL-PR-(P)-009)
Hf–Ta–W, availability, properties, and uses of, 20: 29760
Hf–Ta–W, creep properties of T-111, 20: 29705(R) (NAS-CR-54973)
Hf–Ta–W, erosion of T-111, by mercury, water, and bismuth–lead alloy, cavitation, 20: 29640 (NP-16048)
Hf–Ta–W, tensile properties of T-111, effects of welds on, 20: 29712(R) (WANL-PR-(P)-009)
Hf–Ta–W, weldability of T-111, effects of oxygen contamination on, 20: 29712(R) (WANL-PR-(P)-009)

HAFNIUM BORIDES
fabrication and properties of, for use at high temperatures, 20: 29772

HAFNIUM CARBIDES
fabrication and properties, 20: 29727

HAFNIUM ISOTOPES
neutron reactions (n,γ) with, gamma spectra and energy levels from thermal, (E), 20: 30466

HAFNIUM ISOTOPES Hf-170
energy level transitions in, conversion coefficients for, (E), 20: 30353(R) (ORNL-3940, pp 1-61)

HAFNIUM ISOTOPES Hf-178
energy levels from thermal neutron reactions (n,γ) with hafnium-177, (E), 20: 30466
neutron capture at 1 to 5 ev, gamma spectra from, (E), 20: 30385

HAFNIUM ISOTOPES Hf-179
energy level transitions from hafnium-178 neutron capture, (E), 20: 30385
energy levels from thermal neutron reactions (n,γ) with hafnium-178, (E), 20: 30466

HAFNIUM ISOTOPES Hf-180
energy levels from thermal neutron reactions (n,γ) with hafnium-179, (E), 20: 30466

HAFNIUM ISOTOPES Hf-181
energy levels from thermal neutron reactions (n,γ) with hafnium-180, (E), 20: 30466

HAFNIUM SYSTEMS
C–Hf, fabrication of hypereutectic composites of, with high thermal shock resistance, 20: 29727
C–Hf–Ta, availability, properties, and uses of, 20: 29760
C–Hf–Ta–W, availability, properties, and uses of, 20: 29760
C–Hf–Ta–W, creep properties of T-222, 20: 29705(R) (NAS-CR-54973)
C–Hf–Ta–W, erosion of T-222, by mercury, water, and bismuth–lead alloy, cavitation, 20: 29640 (NP-16048)
C–Hf–Ta–W, tensile properties of T-222, effects of welds on, 20: 29712(R) (WANL-PR-(P)-009)
C–Hf–Ta–W, weldability of T-222, effects of oxygen contamination on, 20: 29712(R) (WANL-PR-(P)-009)
Hf–Nb–N, precipitation hardening in, effects of heat treatments on, 20: 29759

HALDEN BOILING REACTOR
development and operation, Jan.–Mar. 1966, 20: 30880(R) (HPR-67)
fuel irradiation testing for, 20: 30880(R) (HPR-67)
neutron flux distribution in, measurement of, 20: 30880(R) (HPR-67)

HALL EFFECT
effects on MHD shock wave structure, 20: 30191

HALLAM POWER REACTOR
operating experience, 20: 30898
operating experience, 20: 30905

HALOORGANIC COMPOUNDS
analysis and determination of, by radio paper partition chromatography, 20: 29123
effects on radiation resistance of, rubber products, 20: 29322(P)

HANDLING AND STORAGE
equipment design for FARET fuel, 20: 30787(R) (ANL-7190, pp 11-142)
equipment operation for AARR fuel, 20: 30787(R) (ANL-7190, pp 11-142)

HANFORD WORKS, RICHLAND, WASH.
environs monitoring, Jan. to July 1965, 20: 29431

HARWELL SYNCHROTRON
radiation levels around and in, measurement of, 20: 29842 (CONF-651109, pp 20-33)
HASTELLOY B
joining by brazing, soldering, or welding, 20: 29666 (RSIC-484)
surface treatments for, coating and mechanical, 20: 29706 (NASA-TM-X-53448)
HASTELLOY C
joining by brazing, soldering, or welding, 20: 29666 (RSIC-484)
machining properties of, 20: 29665 (RSIC-482)
HASTELLOY D
joining by brazing, soldering, or welding, 20: 29666 (RSIC-484)
HASTELLOY F
joining by brazing, soldering, or welding, 20: 29666 (RSIC-484)
machining properties of, 20: 29665 (RSIC-482)
HASTELLOY R235
joining by brazing, soldering, or welding, 20: 29666 (RSIC-484)
joining by mechanical fastening, 20: 29667 (RSIC-509)
machining properties of, 20: 29665 (RSIC-482)
HASTELLOY X
compatibility with plutonium and uranium carbides, 20: 30790(R) (ANL-7204, pp 1-31)
joining by brazing, soldering, or welding, 20: 29666 (RSIC-484)
machining properties of, 20: 29665 (RSIC-482)
reactions with urania at 1250°C, 20: 29621(R) (NUMEC-3524-17)
surface treatments for, coating and mechanical, 20: 29706 (NASA-TM-X-53448)
HAYNES STELLITE NO. 31
machining properties of, 20: 29665 (RSIC-482)
HAYNES 25 ALLOY
machining properties of, 20: 29665 (RSIC-482)
HAYNES 56 ALLOY
compatibility with plutonium and uranium carbides, 20: 30790(R) (ANL-7204, pp 1-31)
HEALTH PHYSICS
equipment for personnel, 20: 29478
radiation control program on, at Japan Atomic Energy Research Institute, 20: 29460
HEART
blood-flow rate in, measurement of, using krypton-85 and rubidium-86, 20: 28871(R) (EUR-2636.f,i)
radiation effects on catecholamine content of rat, x, 20: 28964
HEAT EXCHANGERS
heat transfer in double-pipe liquid-metal, 20: 29374(R) (ANL-7190, pp 156-66)
vapor traps for liquid-metal, 20: 30814
HEAT-RESISTING ALLOYS
creep-rupture properties to 3000°C, equipment and techniques for measuring, 20: 29710 (TID-22986)
weld stability at high temperatures in niobium- and tantalum-base, 20: 29713(R) (WANL-PR-(P)-010)
weldability of niobium- and tantalum-base, effects of oxygen contamination on, 20: 29713(R) (WANL-PR-(P)-010)
HEAT TRANSFER
book: *Advances In Heat Transfer, Vol. III*, 20: 29381
correlation with ultrasonic transmission in brazed and rolled bonds, 20: 29386 (ANL-7074)
in forced convection flows, external, (E/T), 20: 29379 (SAN-1011)
in MHD cells, analysis of, 20: 29974(R) (ANL-7190, pp 167-75)
in reactor cooling systems, conference on, 20: 29383
in transition from turbulent to laminar gas flow in tubes, 20: 29384
in two-phase flow systems, research programs on, 20: 29375(R) (ANL-7190, pp 193-200)
production of alternating, by MHD cells, 20: 29974(R) (ANL-7190, pp 167-75)
research on liquid-metal, 20: 29374(R) (ANL-7190, pp 156-66)
HEAT TREATMENT
use with beta radiation for preparing resin bodies, 20: 29637(P)
HEAVY WATER REACTORS
design, 20: 30869(P)
design using mixed heavy and light water as moderator-coolant, 20: 30868(P)
development of British steam-generating, 20: 30798(R) (NP-16043)
economics of Canadian power, 20: 30885
neutron spectrum measurements from Yugoslav, thermal, 20: 30939
HELIUM
alkali-metal negative-ion dissociation in, cross sections for, (T), 20: 29947
analysis for impurities, mass spectrometric, 20: 29083(R) (UCRL-14767)
atomic forces in three-body systems of, long-range, (T), 20: 29933
attenuation of sound waves by normal and superfluid, (E), 20: 30734(R) (TID-22970, pp 1-63)
electric discharge in, electron density and velocity distribution in hollow-cathode, (E), 20: 30688
electric discharges in C Stellerator, recombination rates in afterglow of, 20: 30600
electron density and energy in afterglow plasma of, in toroidal magnetic fields, (E/T), 20: 30710
electron reactions with atomic, efficiency curves for (2^3s) and (2^1s) excitation in, 20: 29926
emission in proton reactions with heavy emulsion nuclei at 10 to 20 Bev, (E), 20: 30496
friction parameter in rotating liquid II, mutual, (E), 20: 30285
glow discharges at 1 to 25 torr, between planar anode and hollow cathode, 20: 30173
hydrogen ion reactions with, lifetime of n = 3 hydrogen states from, (E), 20: 29930
hydrogen negative-ion dissociation in, cross sections for, (T), 20: 29947
leakage in pressure vessels, mechanism and rate of, 20: 30810
oscillations of liquid II, near surface of vibrating disk, (E/T), 20: 30308
properties of liquid, (E), 20: 30735(R) (TID-22970, pp 331-73)
properties of liquid, near λ line, (T), 20: 30266(T)
quasi-particle excitations in liquid II, (T), 20: 30187
reactions with plutonium nitride at 700 to 1000°C, 20: 29616(R) (BMI-1739)
stabilization of high-current pulsed discharge in, using h-f electric field, (E), 20: 30698
superfluid critical velocities in liquid II, (T), 20: 30272
temperature distribution in arc produced plasma of, 20: 30563 (NP-16096)
temperature regulator system for liquid, design of transistorized, 20: 30254 (LA-DC-7209)
vortex lattices in superfluid liquid II, hydrodynamic stability of, 20: 30286
vortex-line formation and decay in rotating liquid II, (E), 20: 30285
x-ray spectra of K-mesic atoms of, effects of $\bar{K}$-N interactions on, 20: 29938
HELIUM IONS
effects on metals oxides and silicon, blistering from, (E), 20: 29816
reactions with aluminum and magnesium at 25 to 50 kev, K x-ray production cross sections for, (E), 20: 29936
reactions with thorium-232 and uranium-235 and -238, yields of xenon-133 and -135 from fission, 20: 30533
recombination rate of divalent, in C Stellerator discharges, 20: 30600
HELIUM ISOTOPES
solidification of mixture of, visual, 20: 30307
HELIUM ISOTOPES He-3
angular distributions from reactions of lithium-6 and -7 with boron-10 and -11, 20: 30519
binding energies of, 20: 30424
Brownian motion in liquid, (T), 20: 30263
performance in detectors for monitoring neutron radiation levels near cyclotrons, 20: 29846 (CONF-651109, pp 154-60)
properties of liquid, (T), 20: 30188
properties of liquid, (T), 20: 30192
properties of solid, single-particle-model calculation of, 20: 30319
reactions (He-3,α) and (He-3,p) with oxygen-16 at 3 to 10 Mev, excitation functions for, (E), 20: 30444
reactions (He-3,α) with oxygen-16 at 9.8 to 11.8 Mev, angular distributions from, (E), 20: 30433
reactions (He-3,α) with nitrogen-15 at 39.8 Mev, nitrogen-14 levels from, (E), 20: 30438
reactions (He-3,α) with carbon-14 at 44.8 Mev, carbon-13 levels from, (E), 20: 30438
reactions (He-3,α), (He-3,d) and (He-3,n) with carbon-12 at 3 to 10 Mev, excitation functions for, (E), 20: 30444
reactions (He-3,α) and (He-3,αn) with fluorine-19 at 3 to 10 Mev, excitation functions for, (E), 20: 30444
reactions (He-3,α) with boron-10, proton emission from boron-9 levels from, (E), 20: 30445
reactions (He-3,d) with calcium-44, scandium-45 levels from, (E/T), 20: 30429
reactions (He-3,d) with beryllium-9, carbon-13, and magnesium-25, spectroscopic factors from, 20: 30481
reactions (He-3,He-4) with oxygen-17, use of, for oxygen diffusion studies in zirconium oxides, 20: 29817
reactions (He-3,n) with beryllium-9 at 3 to 10 Mev, excitation functions for, (E), 20: 30444
reactions (He-3,p) with carbon-12 at 2.25 to 3.60 Mev, angular correlations and distributions in, (E), 20: 30526
reactions (He-3,3,pγ) with neon-20 at 5.35 Mev, sodium-22 levels from, (E), 20: 30400
sound measurements in liquid and solid, 20: 30288
thermal capacity of liquid, (T), 20: 30283
thermal conductivity of liquid, (E), 20: 30282
viscosity coefficients for, at 0.36 to 2.6°K, 20: 30275

He-3–He-4, sound measurements in liquid and solid, 20: 30288
HELIUM ISOTOPES He-4
angular distributions from reactions of lithium-6 and -7 with boron-10 and -11, 20: 30519
currents in liquid, model of interacting bosons for persistent, 20: 30140
electron elastic scattering at 100 to 900 Mev, alpha charge structure from, (E), 20: 30439
energy levels of, fine structure of n = 2 triplet P-state, (E), 20: 29911 (COO-1112-21)
momentum spectra from deuteron-deuteron interactions at 1.69 Bev/c, 20: 30010
proton elastic scattering at 48 Mev, spin rotation parameter from, (E), 20: 30441
proton inelastic scattering at 40 Mev, continuum resonances in, (E), 20: 30512
sound measurements in liquid and solid, 20: 30288
temperatures of density maximum and lambda transition of liquid, (E), 20: 30306
ultrasonic attenuation in liquid, frequency and temperature dependence of, (E), 20: 30299
He-3–He-4, sound measurements in liquid and solid, 20: 30288
HELIUM ISOTOPES He-5
decay of, alpha angular distributions from, (E), 20: 30402
energy level transitions in, probability of $\frac{3}{2}^+ \rightarrow \frac{3}{2}^-$, (T), 20: 30386
HELIUM SYSTEMS
Ar–He, glow discharges at 1 to 25 torr, between planar anode and hollow cathode, 20: 30173
He–H, long-range three-body forces between atoms in, (T), 20: 29933
HEMATOLOGY
book: *Nuclear Hematology*, 20: 28874
radiation dosimetry in, methods for, 20: 28981
transfusion serology in immune, 20: 28893
HEMATOPOIETIC SYSTEM
pathology, physiology, and morphology, 20: 28874
radiation effects on guinea pig, chronic low-dose x, 20: 28945
radiation effects on, 20: 28981
radiation effects on, review of immediate, 20: 28982
radiation effects on, effects of dose on, 20: 28982
radiation effects on, effects of fractionated exposure on γ, neutron, or x, 20: 28984
radiation effects on dog, lower-body, upper-body, and whole-body x, 20: 29029
2-HEPTANONE
effects on electric conductivity of anhydrous uranyl nitrate, 20: 29184
3-HEPTANONE, 6-(DIMETHYLAMINO)-4,4-DIPHENYL-
radiation effects on structure of, γ, 20: 29255
HETEROGENEOUS REACTORS
design of fast power breeder, with steam (D_2O, H_2O, or D_2O–H_2O) coolant and moderator, 20: 30914(P)
design of multi-pass, vapor moderated and cooled power, 20: 30916(P)
design of variably moderated and controlled, 20: 30915(P)
design of variably moderated and controlled power, with hydrogen-isotope-bearing moderator and cooling vapor, 20: 30917(P)
design using natural uranium fuel and heavy water–light water moderator-coolant, 20: 30868(P)
design with hydrogen-bearing moderator and cooling vapor, 20: 30918(P)
neutron thermalization in, approximate treatment of, 20: 30864
reactivity of, calculations of fast fission factor for, 20: 30859
HEXANE
hexane–Xe, radiolysis of, charge transfer in, 20: 29314
2-HEXEN-1-OL
analysis for carbon-14 by dry combustion methods, 20: 29085
HEXOSAMINES
radiation effects on content of, in rat subcutaneous granulomas, γ, 20: 28917
HIGH-ALTITUDE EXPLOSIONS
effects of July 9, 1962, on radioactivity levels on Cosmos-3, (E), 20: 30234
fluorescence from nuclear, calculation of prompt, (T), 20: 30193 (LA-3409(Suppl.))
gamma radiation during, fission-fragment-generated, 20: 30233
HIGH TEMPERATURE GAS COOLED REACTOR EXPERIMENT
carbon transport and graphite corrosion in, 20: 30899
development of Dragon, 20: 30798(R) (NP-16043)
HIGH-TEMPERATURE OXIDATION
kinetics of, stagnation-flow reactor for studying, 20: 29656
HIROSHIMA
bomb survivors of, hematological disorders in, 20: 28876
HOLMIUM
determination in aqueous solutions, design of oxyacetylene burner for measuring sensitivity of spectrophotometric, 20: 29083(R) (UCRL-14767)
determination in minerals and ores, spectrometric, 20: 29134
determination in rocks, chemical spectrographic method for, 20: 29083(R) (UCRL-14767)
determination in standard igneous rocks G-1, W-1, and G-B by x-ray fluorescence, 20: 29101
determination in TBP extracts, spectrophotometric, 20: 29125
determination in uranium compounds, spectrographic, 20: 29129
thermodynamic properties at 0°C to melting point, 20: 29743
HOLMIUM ALLOYS
Ho–La, electric conductivity, magnetic susceptibility, and superconducting transition temperatures of, 20: 29753
HOLMIUM ISOTOPES Ho-165
neutron capture by, gamma spectra from, 20: 29078(R) (AD-633252)
neutron reactions (n,γ) with, cross sections for, (E), 20: 30360 (WASH-1068)
HOLMIUM ISOTOPES Ho-166
beta decay of, recoil effect in perturbed β-γ directional correlation from, (E), 20: 30554
neutron capture by, gamma spectra from, 20: 29078(R) (AD-633252)
HOLMIUM NIOBATES
distribution in strontium molybdate single crystals, coefficients of, 20: 29746
HORMONES
effect on erythropoiesis in x-irradiated rats, iron-59 tracer study on, 20: 29043
effects on x-radiation effects on heme synthesis in rabbit bone marrow, 20: 28912
radiosensitivity effects on mice, 20: 28978
HOSPITALS
radiotherapy facility planning, 20: 29071
HUMBOLDT BAY POWER REACTOR
containment for, design of reinforced concrete foundation caisson for underground, 20: 30896
HUMIDITY
measurement using NMR method, 20: 29498
HYDRAZINE
preparation of, using fission fragment recoil energy, 20: 29317
production from liquid ammonia, fissio-chemical process for, 20: 29319(P)
spectra of deuterated, infrared and Raman, 20: 29175
HYDRAZOIC ACID
spectra of, rotational for infrared, (E/T), 20: 30734(R) (TID-22970, pp 1-63)
HYDRAZYL, DIPHENYLPICRYL-
radiation effects on, EPR studies of neutron, 20: 29289
reactions with muonium, (E), 20: 29247
HYDRIODIC ACID
separation of protactinium from solutions of, by precipitation with arsenazo dyes, induline, and rhodamine B, 20: 29135
HYDROAROMATIC COMPOUNDS
effects on hydrogen yields from gamma radiolysis of cyclohexane, 20: 29270
HYDROBIOTITES
sorptive properties for fission products in waste solutions, 20: 29332 (ORNL-P-1811)
HYDROBROMIC ACID
separation of protactinium from solutions of, by precipitation with arsenazo dyes, induline, and rhodamine B, 20: 29135
HYDROCARBON POLYMERS
fabrication of neutron shielding composition containing olefinically unsaturated, 20: 30732(P)
HYDROCARBONS
deuterium exchange with heavy water, 20: 29611(P)
radiolysis of liquid, effects of electric field on hydrogen yields from, 20: 29263
HYDROCHLORIC ACID
effects on zirconium, tracer studies of corrosive, 20: 29649
radioinduced reactions with ethylene, gamma, 20: 29252
separation of protactinium from solutions of, by precipitation with arsenazo dyes, induline, and rhodamine B, 20: 29135
yields from gamma radiolysis of frozen carbon tetrachloride–methanol solutions, 20: 29305
HCl–HNO_3, solvent properties for cesium-137 in fallout samples, 20: 29081 (NP-14705)
HYDROCYANIC ACID
preparation of, using fission fragment recoil energy, 20: 29317
HYDROFLUORIC ACID
determination in atmosphere, design of apparatus for, 20: 29330(R) (EURAEC-1601)
ClF_3–F–HF, effects on fluorination of uranium dioxide, 20: 29330(R) (EURAEC-1601)
HF–HNO_3, solvent properties for cesium-137 in fallout samples, 20: 29081 (NP-14705)
HYDROGEN
analysis for impurities, mass spectrometric, 20: 29083(R) (UCRL-14767)

atom energy spectra in plasma of, neutral, 20: 30578
atomic forces in three-body systems of, long-range, (T), 20: 29933
atomic structure of, Coulomb field and nonrelativistic space quantization in, (T), 20: 29915 (JINR-P-2627)
charged-particle density in hot plasma of, technique for measuring, 20: 30685
compression of plasma of, in toroidal magnetic fields, (E), 20: 30660
density distribution of plasma of, microwave refraction for determining, (E), 20: 30700
determination as impurity in ultrapure gases, mass spectrometric, 20: 29083(R) (UCRL-14767)
determination in type-Al-80 and -Zr-55 Magnox alloys, 20: 29100
deuterium ion reactions with, angular and energy distribution of deuterium hydride ions from, 20: 29950
effect on production of powdered rhenium from rhenium tetrammine chloride, 20: 29672
effects of flowing, on volatilization of fission products from irradiated uranium(IV-VI) oxides, 20: 29211
effects of, on gamma radiolysis of aqueous solutions of acetylene, 20: 29293
effects on mechanical properties of titanium–5 aluminum–2.5 tin alloy at –320 to 200°F, 20: 29715 (WANL-TME-1287)
effects on rate of graphite oxidation by water vapor, 20: 29626
electric field effects on dense plasma of, strong, (E), 20: 30558 (AD-633598)
electron capture into n = 3 states of, relative cross sections for, (E), 20: 29930
electron elastic scattering by, resonances in multichannel, 20: 29943
electron inelastic scattering at 13.7 to 50.7 ev, (E), 20: 29953
energy distribution in coaxial plasma jets of, (E), 20: 30687
energy levels of diatomic, 20: 29931(T)
energy levels of molecular, excitation cross sections for, (E), 20: 29953
glow discharges at 1 to 25 torr, between planar anode and hollow cathode, 20: 30173
hydrogen ion reactions with molecular, at 1 to 55 kev, particle production cross sections for, 20: 29919 (UCRL-14214)
hyperfine structure, (T), 20: 29922
ion density in plasma of, (E), 20: 30686
ion energy spectra in plasma of, 20: 30578
light scattering at level crossings in, cross sections for polarized, 20: 29935
neutron diffusion and thermalization in gaseous, (T), 20: 30322 (BNL-947)
nuclear magnetic resonance of solid, at 1.10 to 4.2°K, (E), 20: 30320
nuclear spin relaxation in liquid, effects of *ortho* and *para* concentrations on, (E), 20: 30181
oxidation by copper oxide, effects of tritium on, 20: 29187
photon reactions (γ,p) at 4.1 to 6.2 Bev, (E), 20: 30432
production of dense plasma of, by cusp field injection, (E), 20: 30643
production of plasma of, by hydrogen atom injection in cryogenic magnetic trap VGL-2, 20: 30655
production of plasma of, by neutral injection in magnetic mirror/well geometry, (E), 20: 30632
production of plasma of, by neutral hydrogen injection in Ogra II, 20: 30633
production of plasma of, by molecular ion injection in magnetic mirror machines, (E), 20: 30634
production of rotating plasma of, in crossed fields, (E), 20: 30582
proton reactions at low energies, charge-exchange cross sections for, (E), 20: 29932(T)
proton scattering by atomic, coupled-state calculations of, 20: 29940
radioinduced reactions with hydroxyl radicals in aqueous solutions, rate constants of, 20: 29262
radon-219 and radon-220 decay in, properties of recoils from, 20: 29325
reactions of molecular, with atomic deuterium, energy threshold for, 20: 29176
reactions with molybdenum–zirconium alloys, hydride formation in, 20: 29632
reactions with tantalum in sputtering, properties of films formed by, 20: 29745
reduction of tungsten hexafluoride, production of fluoride tungsten by, 20: 29687
separation from carbon dioxide by gaseous diffusion, 20: 29362
separation from carbon monoxide and methane by selective oxidation, isotope effects in, 20: 29187
sorption by titanium–5 aluminum–2.5 tin at 200 to 925°F, 20: 29715 (WANL-TME-1287)
spectra from r-f discharge plasma of, collisional Stark broadening in, (E), 20: 30572
stabilization of high-current pulsed discharge in, using h-f electric field, (E), 20: 30698
use of liquid, as target for high-energy nuclear reactions, 20: 29863
velocities of plasma bursts of, Doppler shift technique for measuring, 20: 30681
x-ray emission from hot fully ionzed plasma of, (T), 20: 29881
yield rate constants in radiolysis of 1-propanol, 20: 29286
yields from gamma radiolysis of aqueous potassium iodide solutions, 20: 29253
yields from gamma radiolysis of aqueous solutions of 2-propanol, 20: 29254
yields from gamma radiolysis of frozen carbon tetrachloride–methanol solutions, 20: 29305
yields from radiolysis of liquid hydrocarbons, effects of electric field on, 20: 29263
yields of, from hydrolysis of rare earth carbides, 20: 29220

HYDROGEN IONS
analysis of, design of mass spectrometer for, 20: 29126
dissociation in collisions with hydrogen molecules, (E), 20: 29920 (UCRL-14271)
dissociation of fast negative, in rare gases, (T), 20: 29947
production of, at low pressure, 20: 29925
reactions with aluminum and magnesium at 25 to 50 kev, K x-ray production cross sections for, (E), 20: 29936
reactions with carbon monoxide, hydrogen, methane, and water molecules at 1 to 55 kev, particle production cross sections for, 20: 29919 (UCRL-14214)
sorption by hematite and rutile, 20: 29623(R) (TID-22970, pp 121-256)

HYDROGEN MODERATED REACTORS
design of hydrogen cooled, with variable control and moderation for power production, 20: 30915(P)
design of hydrogen-cooled power, 20: 30917(P)
design of hydrogen-cooled power, with variable control and moderation, 20: 30918(P)
design of multi-pass hydrogen cooled, with variable control and moderation for power production, 20: 30916(P)

HYDROGEN PEROXIDES
decomposition of, effects of uv radiation on catalytic activity of platinum in, 20: 29304
effects on gamma radiolysis of aqueous solutions of 2-propanol, 20: 29254
preparation of, using fission fragment recoil energy, 20: 29317
yields from gamma radiolysis of aqueous potassium iodide solutions, 20: 29253
yields from gamma radiolysis of aqueous solutions of 2-propanol, 20: 29254
yields in gamma radiolysis of aqueous solutions of oxygen, 20: 29257

HYDROGEN SULFIDES
deuterium exchange with heavy water, 20: 29611(P)

HYDROGEN SYSTEMS
D–H, nuclear magnetic resonance of solid, (E), 20: 30320
He–H, long-range three-body forces between atoms in, (T), 20: 29933
H–N, effects on melting points of plutonia–urania, 20: 29621(R) (NUMEC-3524-17)
H–U, metallographic tests on arc melted, 20: 29775

HYDROGEN TRITIDES
molecular dissociation following tritium beta decay in, calculation of, 20: 29233

HYDROLOGY
age estimations in, use of carbon-14 and tritium for, 20: 29438 (CONF-650652

HYDROMAGNETIC WAVES
propagation in collisionless plasma, (T), 20: 30586
propagation in gases in arbitrarily oriented magnetic fields, discontinuity in steady-state exothermal, (T), 20: 30177
propagation in heavy viscous liquids, with variable density, (T), 20: 30171

HYDROPEROXIDES
radiolysis of, in hydrocarbons, 20: 29302

HYDROXYL IONS
radioinduced isotopic exchange of, with deuterium, on silica gel, 20: 29276
yields from gamma radiolysis of aqueous solutions of 2-propanol, 20: 29254

HYDROXYL RADICAL
radioinduced reactions with hydrogen atoms in aqueous solutions, rate constants of, 20: 29262
reactions with catalase in pulse radiolysis, 20: 29279

HYPERFRAGMENTS
decay of ${}_{\Lambda}He^{7}$ and ${}_{\Lambda}Li^{7}$, 20: 30368
decay of, emission of mesons (π^{-}) in, 20: 30485
hyperon (Λ) binding energy in $35 \lesssim A \lesssim 80$, (E), 20: 30448
reactions of ${}_{\Lambda}H^{3}$ in Coulomb field of heavy nuclei, (T), 20: 30503

HYPERONS
decay of, Cabibbo current theory for parity-violating nonleptonic, 20: 30041

HYPERONS (Λ)
binding energy in $35 \lesssim A \lesssim 80$ hyperfragments, (E), 20: 30448
capture by heavy nuclei, hypernuclei production and nucleon emission in, (T), 20: 30503
polarization from hyperon (Σ^-) interactions with protons at 105 to 165 Mev/c, (E), 20: 30024
HYPERONS (Λ^0)
magnetic moment of, measurement using emulsions, 20: 29534
polarization from meson (π^-)-proton interactions at 1.17 Bev/c, (E), 20: 29987 (COO-1261-4)
production in meson (π^-)-proton interactions at 1128 to 1326 Mev/c, (E), 20: 30071
HYPERONS (Ω^-)
decay properties of, calculation using composite-particle model, (T), 20: 30069
HYPERONS (Σ^-)
interactions with protons at 105 to 165 Mev/c, cross sections and hyperon (Λ) polarization from, (E), 20: 30024
mass relative to hyperons (Σ^+), electromagnetic, (T), 20: 30059
HYPERONS (Σ^0)
polarization from meson (π^-)-proton interactions at 1.17 Bev/c, (E), 20: 29987 (COO-1261-4)
production in meson (π^-)-proton interactions at 1128 to 1326 Mev/c, (E), 20: 30071
HYPERONS (Σ^+)
mass relative to hyperons (Σ^-), electromagnetic, (T), 20: 30059
HYPERONS (Ξ^-)
properties, (E), 20: 30072
HYPERONS (Ξ^0)
properties, (E), 20: 30072

I

ICE
deformation mechanisms in, 20: 29623(R) (TID-22970, pp 121-256)
dielectric relaxation and diffusion processes in, lectures on, 20: 30783
triton diffusion in single crystals of, effects of ammonium fluoride on, 20: 29193
ICE-t_2
radiation effects on positron-annihilation lifetime spectra in, gamma, 20: 29268
IGNEOUS ROCKS
analysis of basalts, for aluminum, iron, magnesium, oxygen, and silicon by neutron activation methods, 20: 29140
analysis of standard W-1, for rare earths, by x-ray fluorescence, 20: 29101
ILLITES
sorptive properties for fission products in waste solutions, 20: 29332 (ORNL-P-1811)
ILMENITES
age estimation of, by thorium-230–uranium method, 20: 29441
IMMUNE REACTIONS
effects of extracorporeal blood irradiation on, to tissue transplants, 20: 28927 (BNL-9647)
effects of methotrexate on mouse homograft, 20: 29035
induction of antibody synthesis with RNA in mice, 20: 28926 (AD-633469)
radiation effects on rabbit, 20: 28965
radiation effects on, to bone marrow transplants in mice, 20: 29006
radiation effects on, in thymectomized chickens, 20: 29014
transfusion serology in hematologic, 20: 28893
variations in, to virus-induced tumors in mice, 20: 28873
IMMUNITY
radiation effects on, review, 20: 28983
IN-PILE LOOPS
safety aspects of gas-cooled, 20: 30940
INCOLOY
joining of type 901, by mechanical fastening, 20: 29667 (RSIC-509)
machining properties of, 20: 29665 (RSIC-482)
properties of type 800, as cladding for plutonia–urania fuels, 20: 29617(R) (EURAEC-1593)
INCONEL
corrosion of type 600, in Saxton steam generator, 20: 30884(R) (WCAP-3269-16)
joining by brazing, soldering, or welding, 20: 29666 (RSIC-484)
joining of types 700, 718, and X-750, by mechanical fastening, 20: 29667 (RSIC-509)
machining properties of, 20: 29665 (RSIC-482)
surface treatments for types 600, 713C, 718, and X-750, coating and mechanical, 20: 29706 (NASA-TM-X-53448)
INDENE
complexes with cobalt, isotope exchange in radiocobalt divalent ion-doped, 20: 29259
complexes with cobalt, radioinduced recoil damage in, thermal annealing of neutron, 20: 29259
INDEXES
on ESR and NMR spectra, 1958 to 1963, 20: 30510
INDIA
radioactivity in rain, Calcutta, 1962, 20: 29420
INDIAN POINT POWER REACTOR
neutron flux distribution in, detector asymmetry response verification for, 20: 30876 (BAW-1302)
INDIUM
radiation effects on superconducting properties of, neutron, 20: 30301
superconducting transitions in single-crystal, (E), 20: 30734(R) (TID-22970, pp 1-63)
INDIUM ALLOYS
Bi–In, electron spectra of, effects of magnetic fields on, (E), 20: 30735(R) (TID-22970, pp 331-73)
Gd–In–La, superconducting transition temperature, (E), 20: 30271
In–Gd, magnetic properties of, 20: 29752
In–Gd–Ag, magnetic properties of, 20: 29752
In–La, superconducting transition temperatures of, containing paramagnetic impurities, (E), 20: 30271
In–Pb, superconducting current distribution in sheets of, 20: 30273
In–Zn, distillation of liquid, surface concentration changes in, 20: 29346
INDIUM ISOTOPES In-113
electron spectra of, measurement of Auger L, 20: 30527
neutron inelastic scattering cross sections, (E), 20: 30360 (WASH-1068)
neutron reactions (n,γ) with, cross sections for, (E), 20: 30360 (WASH-1068)
INDIUM ISOTOPES In-115
neutron capture cross section measurement at 80 to 200 kev, errors in using boron monitors for, (E), 20: 30352 (NASA-TR-R-240)
neutron inelastic scattering cross sections, (E), 20: 30360 (WASH-1068)
neutron reactions (n,γ) with, cross sections for, (E), 20: 30360 (WASH-1068)
neutron scattering at 4.0 Mev, polarization angular distributions from, (E), 20: 30360 (WASH-1068)
INDOLE, 3-(2-AMINOETHYL)-α-METHYL-
hydrochloride, effects on edema and blood serotonin in irradiated rats, 20: 29001
5-INDOLOL, 3-(2-AMINOETHYL)-
content in blood of rats, effects of burns and irradiation on, 20: 29001
derivatives of, effects on blood pressure in rats, 20: 29050
radiosensitivity effects on Ehrlich ascites carcinoma and mouse spleen, mechanism for, 20: 29039
INDUCED RADIOACTIVITY
levels in radiation processed foods, 20: 29599
INDUCTORS
conducting layer in traveling magnetic field of two-sided symmetrical, higher space harmonic effects on, (T), 20: 29830
magnetic field strength in polyphase cylindrical, with multipole field, (T), 20: 29835
INDULINE DYES
precipitation of protactinium in acid solutions with, in presence of crystal violet, 20: 29135
INDUSTRIAL HYGIENE
laser system handling rules, 20: 29480
INFLAMMATION
radioinduced cystitis, treatment with tanderil, 20: 29060
radioinduced, pathology of, 20: 28943
INFRARED RADIATION
absorption by semiconductors, (E), 20: 30734(R) (TID-22970, pp 1-63)
INFRARED SPECTROSCOPY
methods for molecules with anharmonic potential functions, (E/T), 20: 30734(R) (TID-22970, pp 1-63)
INOR-8
joining by brazing, soldering, or welding, 20: 29666 (RSIC-484)
INSECTICIDES
labeling with carbon-14 and phosphorus-32, 20: 29246
INSECTS
control of termites using atomic waste, 20: 29587
radiation control of, infesting foods, 20: 29585
radiation control of, in chestnuts, 20: 29597
radiation effects from fallout on development, mortality, and sterility of, beta, 20: 28925 (AD-633024)
INSTRUMENTATION
design and testing of FARET, 20: 30787(R) (ANL-7190, pp 11-142)
development for solar research, 20: 29873 (NASA-SP-100)
INSTRUMENTS
book: *Radioisotopic Instruments in Metallurgy*, 20: 29598
INSULIN
effects on tissues, 20: 28871(R) (EUR-2636.f,i)

INTERMETALLIC COMPOUNDS
fabrication and properties of, for use in space technology, 20: 29680
fabrication and properties of sintered, for use as thermoelectric cooling plates and generators, 20: 29690
properties of, for use in aerospace technology, 20: 29770
INTERMOLECULAR FORCES
determination of, by beam scattering and gaseous diffusion, (E/T), 20: 30734(R) (TID-22970, pp 1-63)
INTERNAL CONVERSION
nuclear structure effects in, 20: 30515
INTESTINE
radiation effects on secretory function of dog, effects of dietary fatty acids on, 20: 28993
sorption of albumin, triglycerides, and xylose by, measurement of, 20: 28871(R) (EUR-2636.f,i)
INVERTASE
radiation effects on activity of, in potato tubers, 20: 28934
INVERTEBRATES
radiation effects from fallout on development, mortality, and sterility of, beta, 20: 28925 (AD-633024)
IODIDE IONS
determination in sodium bromides and chlorides by bremsstrahlung-activation methods, 20: 29112
iodine-131 exchange between, and methyl iodide, kinetic studies of, 20: 29207
IODINE
separation from airborne organic compounds using electric sparks and ion exchange resins, 20: 29467
yields from gamma radiolysis of aqueous potassium iodide solutions, 20: 29253
IODINE ISOTOPES I-125
use in kidney function tests, 20: 29063
IODINE ISOTOPES I-127
neutron capture cross section measurement at 80 to 200 kev, errors in using boron monitors for, (E), 20: 30352 (NASA-TR-R-240)
neutron reactions (n,γ) at 0.1 to 14 Mev, cross sections for, (T), 20: 30378
neutron scattering at 4.0 Mev, polarization angular distributions from, (E), 20: 30360 (WASH-1068)
IODINE ISOTOPES I-128
recoil reactions with alkanes and haloalkanes, yields from, 20: 29233
IODINE ISOTOPES I-129
energy levels from beta decay of tellurium-129, properties of 27.7-kev, (E), 20: 30474
origin of extinct, in meteorites, 20: 29891
IODINE ISOTOPES I-131
content in bovine thyroid glands, 1965, 20: 29428
content in milk and milk products, 20: 29464
content in milk in Colorado, May 1965, from Chinese nuclear test, 20: 29429
deposition in Japan in 1959, 20: 29479
determination in industrial waste water, method for, 20: 29099
effects on blood and hematopoietic system, 20: 28982
exchange between iodide ions and iodomethane, kinetics of, 20: 29207
incorporation in sodium diiodofluorescein, 20: 29236
movement in soils, 20: 30943(R) (ORNL-TM-1465)
sorption by iron oxide aerosols, effects of particle size on, 20: 29234
uptake by sagebrush roots, relation of, to phenology and root distribution, 20: 28883
uptake by thyroid gland in dogs, effects of strontium-90 on, 20: 29000
use in identification of steroids using paper electrophoresis, 20: 29132
use in method for detecting radioactive surface contamination, 20: 29484(P)
use of fibrinogen-incorporated, for tumor and metastasis diagnosis, 20: 28871(R) (EUR-2636.f,i)
IODINE ISOTOPES I-132
movement in soils, 20: 30943(R) (ORNL-TM-1465)
IODINE ISOTOPES I-133
beta decay of, xenon-133 level scheme from, (E), 20: 30473
half life, 20: 30473
IODINE OXIDES
reactions with carbon monoxide, effects of carbon-13 in, 20: 29187
IODINE SYSTEMS
butane–I, tritium reactions with gas-phase, scavenging effects on hot and thermal recoil, 20: 29206
IODOORGANIC COMPOUNDS
analysis and determination of, by radio paper partition chromatography, 20: 29123
separation of iodine from, using electric sparks and ion exchange resins, 20: 29467
ION BEAMS
effects on structure of aluminum, copper, and gold at 20°K, 20: 29808
injection and trapping in mirror fields, use of r-f field for high-energy, 20: 30580
interactions with plasma, electromagnetic-wave excitation in, (T), 20: 30670
stability of potential oscillations in electron-ion beams, (T), 20: 30672
transmission efficiency in mass spectrometers, (T), 20: 29490
ION EXCHANGE MATERIALS
performance of zeolite, 20: 29624(R) (TID-22970, pp 257-329)
preparation of, by pre-irradiation method, 20: 29308
structures of Zeolites, neutron- and x-ray-diffraction studies on, (E/T), 20: 30734(R) (TID-22970, pp 1-63)
ION EXCHANGE PROCESSES
for separation of strontium from calcareous media, 20: 29363
ION SOURCES
design of low-pressure hydrogen, 20: 29925
ion trajectories in multiple-slit, component effects on, (T), 20: 29489
ions and dissociation products from hydrogen r-f, (E), 20: 29920 (UCRL-14271)
IONIZATION
cross sections for electron, method of measuring, 20: 29709(R) (TID-22970, pp 65-119)
IONIZATION CHAMBERS
design and performance for radiation field quality factor determination, 20: 29847 (CONF-651109, pp 181-98)
design and sensitivity of parallel-plate gamma, 20: 29565
design for gamma in-cell monitoring, 20: 29564
efficiency of multiple-plate, for gamma measurements, 20: 29560
gamma compensation for neutron-flux measurements in reactors, 20: 29549
IONOSPHERE
absorption in polar-cap region of, during chromospheric flare, 20: 30225
disturbances in, solar-flare effects on, 20: 30230
electron and ion concentrations and temperatures in, measurement of, 20: 30198(T) (NASA-TT-F-389, pp 202-24)
electron content at altitudes of 100–300 km variations in, 20: 30199(T) (NASA-TT-F-389, pp 248-58)
electron content in, with energies less than 0.1 Mev, 20: 30203(T) (NASA-TT-F-389, pp 288-91)
electron density of, effects of nuclear explosion on, 20: 30228
electron distribution in outer, altitude and time dependence of, 20: 30197(T) (NASA-TT-F-389, pp 166-201)
energy sources for thermosphere, (T), 20: 30194 (MIT-2241-16)
IONS
content in ionosphere, variations in, 20: 30198(T) (NASA-TT-F-389, pp 202-24)
distribution in magnetosphere, energy, spatial, and temporal, 20: 30220(T) (NASA-TT-F-389, pp 633-52)
effects on mammalial cells, 20: 28930 (CONF-651109, pp 601-16)
energy spectra in hydrogen plasma, measurement of, 20: 30578
injection and trapping in mirror fields, use of r-f field for high-energy, 20: 30580
intensity of low-energy, satellite measurements of, 20: 29532(T) (NASA-TT-F-389, pp 518-25)
interaction of positive streams of, with geomagnetic fields, 20: 30208(T) (NASA-TT-F-389, pp 457-63)
interactions in plasma, effects on plasma stability and wave propagation, (T), 20: 30709
motion in electric and magnetic fields, (T), 20: 29489
reactions with atoms at low energies, method for measuring cross sections for, (E/T), 20: 29932(T)
reactions with gases, lifetimes of n = 3 hydrogen states from, (E), 20: 29930
scattering by metallic surfaces, 20: 29499
IPRONIAZID
effects on edema and blood serotonin in irradiated rats, 20: 29001
IRIDIUM
iron-57 Mössbauer spectra in, 20: 30766
platinum-195 Mössbauer effect in, (E), 20: 30757
properties of, at 2000°C, for use in thermionic converters, 20: 29729
radiation effects on, for use as sensor material, 20: 29486(R) (NASA-CR-54964)
IRIDIUM ALLOYS
Ir–Pt, analysis for glassy inclusion in, development of electron microprobe for, 20: 29083(R) (UCRL-14767)
IRIDIUM ISOTOPES Ir-191
neutron capture by, gamma spectra from, 20: 29078(R) (AD-633252)
IRIDIUM ISOTOPES Ir-192
gamma dose from wires of, computer calculations for, 20: 29456
uses as gamma source for detection of flaws in steel foils and plates, 20: 29390
IRIDIUM ISOTOPES Ir-193
neutron capture by, gamma spectra from, 20: 29078(R) (AD-633252)
IRIDIUM ISOTOPES Ir-194

beta transition of, nuclear matrix elements of, (E), 20: 30551
IRON
abundance and distribution in rocks, 20: 29436
carbon monoxide desorption from liquid, 20: 29623(R) (TID-22970, pp 121-256)
content in Amazon River, effects on biology, chemistry, and hydrography of Atlantic Ocean, 20: 28878 (NYO-1918-138)
content in Atlantic Ocean, measurements on, 20: 28878 (NYO-1918-138)
determination in copper ore leach solutions, method for, 20: 29083(R) (UCRL-14767)
determination in gold–iron alloys, development of electron microprobe for, 20: 29083(R) (UCRL-14767)
determination in graphite and basalts by neutron activation methods, 20: 29140
determination in petroleum, activation, 20: 29139
deuteron elastic scattering at 13.6 Mev, cross section for, (E), 20: 30497
effects on radiometric well logging of boreholes, method for eliminating, 20: 29442(P)
effects on yttrium absorption in turfy-meadow soil, 20: 28881
fabrication of powder compacts of, by isostatic pressing and sintering, 20: 29681
fracture initiation in, mechanisms of, 20: 29623(R) (TID-22970, pp 121-256)
iron-57 Mössbauer spectra in, 20: 30766
magnetization of, distribution of internal, (T), 20: 30734(R) (TID-22970, pp 1-63)
neutron capture by, energy resolution of gamma spectra from, 20: 29078(R) (AD-633252)
neutron elastic and inelastic scattering at 0.45 to 2.28 Mev, cross sections for, (E), 20: 30417
neutron inelastic scattering at 5.0 Mev, Q values for, (E), 20: 30360 (WASH-1068)
neutron reactions (n,n′γ) at 2 to 15 Mev, gamma spectra from, (E), 20: 30358(R) (RPI-328-56, pp 1-48)
nuclear resonances of iron-57 in, (E/T), 20: 30734(R) (TID-22970, pp 1-63)
pressing of powder of, for plate and sheet fabrication, 20: 29679
radiation effects on plasma clearance rate and red cell uptake in dogs, x, 20: 29029
separation from phosphoric acid solutions by solvent extraction using bis(2-ethylhexyl) ester of pyrophosphoric acid, 20: 29361
separation of traces of cobalt and manganese from, by paper chromatography, tracer studies of, 20: 29342
sorptive properties of liquid, for nitrogen, 20: 29623(R) (TID-22970, pp 121-256)
use as radiation shielding, model tests of, 20: 30730
IRON ALLOYS
defects in, formation of clustered vacancy, 20: 29623(R) (TID-22970, pp 121-256)
Al–Cr–Co–Fe–Mo–Ni–Ti, joining of Udimet 500 and 700, by mechanical fastening, 20: 29667 (RSIC-509)
Al–Cr–Co–Fe–Mo–Ni–Ti, surface treatments for Udimet 500 and 700, coating and mechanical, 20: 29706 (NASA-TM-X-53448)
Al–Cr–Fe–Mo–Ni–Ti–W, joining of D-979, by mechanical fastening, 20: 29667 (RSIC-509)
Au–Fe, analysis of, for iron, development of electron microprobe for, 20: 29083(R) (UCRL-14767)
Au–Fe, thermal capacity below 1°K, 20: 29791
Cr–Fe–Zr, corrosion by steam, effects of fabrication process and nitride content on, 20: 29660(R) (GEAP-4960)
Cr–Fe–Zr, microstructure of, effects of heat treatments on, 20: 29660(R) (GEAP-4960)
Fe–Ag, properties of composite-type, 20: 29624(R) (TID-22970, pp 257-329)
Fe–Mn–Ni, martensitic reaction nucleation rate in, 20: 29623(R) (TID-22970, pp 121-256)
Fe–Ni–W, deformation properties of dispersed and sintered composites of, elastic and plastic, 20: 29686
Fe–Ni–W, properties of composite-type, 20: 29624(R) (TID-22970, pp 257-329)
Fe–Ni–W, zone refining of cemented, production of tungsten sheet bars by, 20: 29688
Fe–Ti, strengthening of, by strain hardening, theory of, 20: 29623(R) (TID-22970, pp 121-256)
Fe–U, metallographic tests on arc melted, 20: 29775
IRON CARBIDES
electronic bonding in, 20: 29623(R) (TID-22970, pp 121-256)
Mössbauer effect in, 20: 29623(R) (TID-22970, pp 121-256)
IRON(III) CHLORIDES
corrosive effects on austenitic and austeno-ferritic stainless steels, stress-, 20: 29639(R) (EURAEC-1578)
effects on corrosion of zirconium by hydrochloric acid, 20: 29649
effects on radioinduced isomerization of stilbene, 20: 29287
IRON IONS
effects on radiolysis of naphthalene, 20: 29260
lifetime of nonequilibrium trivalent, from Mossbauer effect in cobalt oxides, 20: 29833
IRON ISOTOPES Fe-52
yield in alpha and proton reactions with copper, 20: 30531
yield in proton reactions with yttrium, 20: 30531
IRON ISOTOPES Fe-54
deuteron elastic scattering at 34.4 Mev, angular distributions from, (E/T), 20: 30353(R) (ORNL-3940, pp 1-61)
proton elastic scattering at 40 Mev, cross sections for, (E/T), 20: 30353(R) (ORNL-3940, pp 1-61)
proton inelastic scattering at 40 Mev, cross sections for, (E/T), 20: 30353(R) (ORNL-3940, pp 1-61)
triton reactions (t,p) at 12 Mev, iron-56 levels from, (E), 20: 30453
IRON ISOTOPES Fe-55
yield in alpha and proton reactions with copper, 20: 30531
yield in proton reactions with yttrium, 20: 30531
IRON ISOTOPES Fe-56
energy levels from triton reactions (t,p) with iron-54 at 12 Mev, 20: 30453
IRON ISOTOPES Fe-57
hyperfine field in nickel lattice, temperature dependence of, 20: 30750
Mössbauer spectra of, in crystal lattices, 20: 30766
nuclear resonances in iron and rare earth garnets, (E/T), 20: 30734(R) (TID-22970, pp 1-63)
IRON ISOTOPES Fe-59
uptake by mouse skin from bath water, 20: 28892
use as tracer in studies on radiation effects on erythropoiesis in rats, 20: 29043
IRON NITRIDES
Mössbauer effect in, 20: 29623(R) (TID-22970, pp 121-256)
IRON OXIDES
hydrogen ion sorption by, 20: 29623(R) (TID-22970, pp 121-256)
sorptive properties of aerosols of, for iodine-131, 20: 29234
IRON(III) OXIDES
content in thalenites from Japan, 20: 29399
neutron magnetic scattering by alpha, 20: 30360 (WASH-1068)
IRON SILICIDES
preparation of, method for, 20: 29650
IRON(II) SULFATES
oxygen-18 exchange with water, effects of benzene and oxygen on, 20: 29153
IRON(III) SULFATES
oxygen-18 exchange with water, effects of benzene and oxygen on, 20: 29153
radiolysis of sulfuric acid solutions of, kinetics of pulse, 20: 29262
IRON SYSTEMS
Fe–Mo_2C, growth and orientation of carbide precipitates in ferrite matrix, 20: 29726
Fe–Si–V, crystal structure of D-phase, (E/T), 20: 30734(R) (TID-22970, pp 1-63)
IRRADIATION FACILITIES
design for irradiating oddly shaped objects with charged-particle beams, 20: 29872(P)
design of cobalt-60, for marine products, 20: 29584 (TID-22991)
operation of EBR-II, 20: 30787(R) (ANL-7190, pp 11-142)
IRRADIATION TECHNIQUES
extracorporeal blood, 20: 28927 (BNL-9647)
ISOTHIOCYANIC ACID
spectra of, rotational for infrared, (E/T), 20: 30734(R) (TID-22970, pp 1-63)
ISOTOPE EFFECTS
of carbon-14 on Beckmann rearrangement of phenyl-2-propanone oxime and acetophenone oxime, 20: 29242
of deuterium on far-infrared spectra of acetylene, 20: 29239
of deuterium on oxidation of benzene to phenol, 20: 29250
on oxidation of carbon monoxide, hydrogen, and methane, 20: 29187
on superconducting transition temperatures of zirconium, 20: 30316
ISOTOPIC EXCHANGE
between azulene and deuterated acetic acid and methanol, 20: 29245
between bromine and bromine–graphite lamellar compounds, 20: 29182
between chlorine-36-labeled isopropyl chloride and tetrabutylammonium chloride, kinetics of, 20: 29156
between cycloalkyl chlorides and lithium chlorides in dimethyl sulfoxide, kinetics of, 20: 29157
between hydrocarbons or hydrogen sulfide and heavy water, 20: 29611(P)
between methyl iodide and iodide ions, kinetic studies of, 20: 29207
between water and cupric, ferric, and ferrous sulfates, 20: 29153
between 4-chlorobenzhydryl thiocyanate and sodium thiocyanate, 20: 29237
between 5-bromouracil and ammonium bromide or bromine, 20: 29244
radioinduced, between deuterium and hydroxyl ions on silica gel, 20: 29276

J

JAPAN
fallout monitoring in Osaka, October 1964, 20: 29466
fallout monitoring in, 1964 and 1965, 20: 29422
JAPANESE POWER DEMONSTRATION REACTOR II
design, 20: 30889

K

KAOLINITES
hardening of, mechanisms of reversible-shear, 20: 29624(R) (TID-22970, pp 257-329)
sorptive properties for fission products in waste solutions, 20: 29332 (ORNL-P-1811)
KEROSENE
kerosene–TBP, radiation effects on solvent properties for uranium and thorium in nitrate solutions, 20: 29272
KETENE
effects on oxidation of graphite by vacuum ultraviolet irradiated carbon dioxide, 20: 29733
KIDNEYS
function tests on, of children, use of iodine-125 for, 20: 29063
measurement of glomerular filtration in, effects of tracer de-iodination on, 20: 28871(R) (EUR-2636.f,i)
radiation effects on function and morphology of dog, x, 20: 29025
radiation effects on hemodynamic functions of dog, x, 20: 29026
radiography of, in children, 20: 29062
KRYPTON
alkali-metal negative-ion dissociation in, cross sections for, (T), 20: 29947
hydrogen negative-ion dissociation in, cross sections for, (T), 20: 29947
KRYPTON FLUORIDES
krypton-83 Mössbauer effect in, (E), 20: 30764
preparation by beta decay of bromine isotopes in bromine fluorides, 20: 29327
KRYPTON ISOTOPES Kr-82
energy levels from bromine 82 decay, (E), 20: 30410
KRYPTON ISOTOPES Kr-83
Mössbauer effect in, in krypton fluorides, (E), 20: 30764
KRYPTON ISOTOPES Kr-85
diffusion in potassium chloride–rubidium chloride single crystals, 20: 30769
use in measuring cerebral blood flow, 20: 28871(R) (EUR-2636.f,i)
KRYPTON OXIDES
preparation by beta decay of bromine isotopes in bromine fluorides, 20: 29327

L

LABORATORIES
automation of, equipment for, 20: 29083(R) (UCRL-14767)
LANTHANUM
determination in pure cerium oxide, spectrographic, 20: 29095
determination in rocks, chemical spectrographic method for, 20: 29083(R) (UCRL-14767)
determination in standard igneous rocks G-1, W-1, and G-B by x-ray fluorescence, 20: 29101
polarographic properties of, on fused potassium acid sulfate electrolyte, 20: 29210
LANTHANUM ALLOYS
Ce–La, electric conductivity, magnetic susceptibility, and superconducting transition temperatures of, 20: 29753
Dy–La, electric conductivity, magnetic susceptibility, and superconducting transition temperatures of, 20: 29753
Er–La, electric conductivity, magnetic susceptibility, and superconducting transition temperatures of, 20: 29753
Gd–In–La, superconducting transition temperature, (E), 20: 30271
Gd–La, electric conductivity, magnetic susceptibility, and superconducting transition temperatures of, 20: 29753
Ho–La, electric conductivity, magnetic susceptibility, and superconducting transition temperatures of, 20: 29753
In–La, superconducting transition temperatures of, containing paramagnetic impurities, (E), 20: 30271
La–Nd, electric conductivity, magnetic susceptibility, and superconducting transition temperatures of, 20: 29753
La–Pr, electric conductivity, magnetic susceptibility, and superconducting transition temperatures of, 20: 29753
La–Sm, electric conductivity, magnetic susceptibility, and superconducting transitiontemperatures of, 20: 29753
La–Tb, electric conductivity, magnetic susceptibility, and superconducting transition temperatures of, 20: 29753
LANTHANUM BORIDES
oxidation of LaB_6 in air at 800 and 1000°C, kinetics of, 20: 29163
porosity and mechanical properties of vacuum-sintered, 20: 29738
LANTHANUM CARBIDES
hydrolysis of, gaseous products from, 20: 29220
LANTHANUM CHLORIDES
cerium ion energy levels in, Orbach relaxation mechanism for excited, 20: 30758
ion energy levels in, Orbach relaxation mechanism for excited, 20: 30758
samarium ion energy levels in, Orbach relaxation mechanism for excited, 20: 30758
samarium ion fluorescence decay in, 20: 30782
thermal capacity of aqueous solutions of, at 25°C, 20: 29144 (IS-1355)
$LaCl_3$–NaCl, compound formation in saturated vapor of, at 1100 to 1350°C, 20: 29227
LANTHANUM COMPLEXES
hexanitrocobaltate, preparation and composition of, effects of temperature on, 20: 29209
with Aluminon, composition and stability of, spectrophotometric studies of, 20: 29180
with carboxylic acids, stability constants of, 20: 29232
with serine, stability of, 20: 29208
with 1,10-phenanthroline–thenoyltrifluoroacetone, preparation and composition of, 20: 29221
LANTHANUM ETHYL SULFATES
neodymium ion spin-spin coupling in, free induction signal from, (T), 20: 30778
LANTHANUM FLUORIDES
heat of sublimation and sublimation pressure of, mass spectrometric studies of, 20: 29183
spectra of cerium ions in, infrared, 20: 29173
LANTHANUM ISOTOPES La-140
beta decay of, matrix elements for first-forbidden, (E/T), 20: 30522
effects on blood and hematopoietic system, 20: 28982
LANTHANUM NIOBATES
distribution in strontium molybdate, 20: 29746
LANTHANUM TITANATES
crystal structure, (E), 20: 30738
preparation and crystal structure of, 20: 29212
LATINA POWER REACTOR
neutron multiplication factor of, null-reactivity measurement of infinite, 20: 30887
LAURIC ACID
dibutyl ester of, analysis for tin, 20: 29083(R) (UCRL-14767)
LEAD
abundance and isotopic compositions of, in brines under Salton Sea area, California, 20: 29414
abundance in stars, mechanism for, (T), 20: 29887
amplification factor of screens of, for electron photography, 20: 29628
determination in Zircaloy-2, spectrographic, 20: 29113
effects on radiation effects on epoxido-dianic ED-5 resin, 20: 29297
effects on radioinduced changes in structure of epoxy resins, 20: 29296
gamma spectra in, at 0.2 to 6 Mev, 20: 30722 (KAPL-M-6497)
neutron inelastic scattering by liquid, analysis of, (T), 20: 30347(R) (IDO-17147, pp 13-28)
neutron scattering law for liquid, 20: 30360 (WASH-1068)
photoelectric cross sections at 320 kev, absolute, (E), 20: 29924
photon reactions (γ,n) with, fast neutron spectra from, (E), 20: 29529(R) (RPI-328-56, pp 94-112)
superconducting transitions in single-crystal, (E), 20: 30734(R) (TID-22970, pp 1-63)
testing of shipping containers of, gamma radiographic, 20: 29388
thermal conductivity of thick films of, surface superconducting properties from, 20: 30294
use as radiation shielding, model tests of, 20: 30730
Pb–Tl, superconductivity and electronic structure of, 20: 30297
LEAD ALLOYS
Al–Pb, diffusion of erbium in molten, at 700°C, 20: 29797
Bi–Pb, erosive effects on heat-resisting alloys at 500 and 1500°F, cavitation, 20: 29640 (NP-16048)
Bi–Pb, magnetic hysteresis in type II superconductors of, surface current effects on, (E), 20: 30269
Bi–Pb, superconducting transition temperature of amorphous, (E), 20: 30298
Bi–Pb, surface critical currents and a-c susceptibility transition in superconducting, (E), 20: 30293
In–Pb, superconducting current distribution in sheets of, 20: 30273
Pb–U, metallographic tests on arc melted, 20: 29775
LEAD FLUORIDES
thermodynamic properties of, emf measurements of, 20: 29215
LEAD ISOTOPES
abundance ratios of, in lead ores from Bolivian Andes, 20: 29439
LEAD ISOTOPES Pb-204

energy levels from polonium-208 decay, (E), 20: 30405
triton reactions (t,α) at 13.5 Mev, thallium-203 levels from, (E), 20: 30387

LEAD ISOTOPES Pb-205
energy levels from polonium-209 decay, (E), 20: 30405

LEAD ISOTOPES Pb-206
triton reactions (t,α) at 13.5 Mev, thallium-205 levels from, (E), 20: 30387

LEAD ISOTOPES Pb-208
electron inelastic scattering by, collective level excitation in, (E), 20: 30360 (WASH-1068)
electron inelastic scattering at 62.8 Mev, excitation of collective states in, (E), 20: 30436
proton elastic scattering at 40 Mev, cross sections for, (E/T), 20: 30353(R) (ORNL-3940, pp 1-61)
triton reactions (t,α) at 13.5 Mev, thallium-207 levels from, (E), 20: 30387

LEAD ORES
age estimation of, in Bolivian Andes, 20: 29439
lead isotope abundances in, in Bolivian Andes, 20: 29439

LEAD OXIDES
$PbO–Nb_2O_5$, phase studies, 20: 29794
$PbO–Ta_2O_5$, phase studies, 20: 29794
$PbO–U_2O_5$, phase studies, 20: 29794

LEAD SELENIDES
electron structure and spectra of, 20: 29709(R) (TID-22970, pp 65-119)
electron structure and spectra of group V., 20: 29709(R) (TID-22970, pp 65-119)

LEAD SULFIDES
electron structure and spectra of, 20: 29709(R) (TID-22970, pp 65-119)

LEAD TELLURIDES
production of epitaxial films of, 20: 29709(R) (TID-22970, pp 65-119)

LEAK DETECTORS
mass spectrometer design for use in ultra-high vacuum, 20: 29496
mass spectrometer design for use as, 20: 29126

LEAKS
testing of reactor containment systems, 20: 30812

LEATHER
radiation effects on mechanical and physical properties of tanned, 20: 29588
radiation effects on chrome-tanned, for shoe uppers, gamma, 20: 29591
radiation effects on mechanical and physical properties of chromium-tanned goat, gamma, 20: 29592

LEAVES
radioisotope uptake by juniper, 20: 29410

LECTURES
book: *High Energy Physics*, 20: 30064
book: *Many-Body Theory*, 20: 29838
on solid state physics, 20: 30783
on solid state physics, 20: 30784
on space electric power systems, 20: 29977 (N-65-32716)

LEUKEMIA
radiation effects on growth kinetics of cells of, x, 20: 28962
radiotherapy using fractionated whole-body exposures, x, 20: 29069
therapy of, use of extracorporeal blood irradiation for, 20: 28927 (BNL-9647)

LEUKOCYTES
radiation effects on cultured, morphological, 20: 28920
radiation effects on guinea pig, x, 20: 28976
radiation effects on, 20: 28981
radiation effects on lymphocyte count in dogs, x, 20: 29029
radioinduced lysis of rat, effects of ACTH on, 20: 29044

LEUKOPENIA
radioinduced in rabbits, protective effects of chemical agents against x, 20: 29055
radioinduced, effects of dose on, 20: 28982

LEVEL INDICATORS
design and operation of liquid sodium, 20: 30875(R) (ANL-7190, pp 143-55)
nuclear, design and testing of, 20: 29590

LIGHT
effects on phytosynthesis rate in marine phytoplankton, 20: 28878 (NYO-1918-138)
intensity measurements of, design of photometer for low-level, 20: 29503
interactions with light beams, cross sections for induced, (T), 20: 30062
modulation device for, 20: 30734(R) (TID-22970, pp 1-63)
scattering by deuterium and hydrogen atoms in magnetic field, cross section for polarized, 20: 29935
scattering by homogeneous dielectric sphere, 20: 29832

LIGHT SOURCES
design using tritium and phosphor-coated, for illumination of telephone dials, 20: 29605(P)
photon emission from, amplitude and emission correlations for, (T), 20: 29827 (UCRL-16824)

LIGNIN
radioinduced polymerization with methyl methacrylate, styrene, and vinyl acetate, gamma, 20: 29288
sorptive properties for uranium, effects of pore structure on, 20: 29360

LIGNITES
radiation effects on gasification of, gamma, 20: 29586

LIMESTONE
thermoluminescence of, effects of climate and temperature on natural, 20: 29398
thermoluminescence measurements in, calibration of, 20: 29400

LINEAR ACCELERATORS
beam bunch shaping in electron, methods for, 20: 29870
beam phase motion in proton, with perturbed axial field, (T), 20: 29852 (INR-640/SLBAL/E)
radiation hazards of high-energy meson factory, 20: 29850 (CONF-651109, pp 472-89)

LINGEN POWER REACTOR
containment for, post-accident pressure and temperature transients in dry, (T), 20: 30895

LIPIDS
effects of nicotinic acid on composition of, in rabbit liver, 20: 28895
radiation effects on content in rat blood, strontium-90, 20: 28994
radiation effects on metabolism in rats, x, 20: 28996

LIQUID METAL COOLED REACTORS
coolant expulsion from sodium-cooled, mechanisms of, 20: 30788(R) (ANL-7190, pp 176-88)
coolant leakage between bed and vessel of fast, device for control of, 20: 30827(P)
development of British sodium, 20: 30798(R) (NP-16043)
fuel development for fast, 20: 30790(R) (ANL-7204, pp 1-31)
vapor traps for gas systems of, 20: 30814

LIQUIDS
concentration of components in mixture of, radiometric device for measuring, 20: 29570(P)
hydromagnetic wave propagation in heavy viscous, with variable density, (T), 20: 30171
level of, nuclear gages for measuring, 20: 29590
quasi-particle excitations in homogeneous Bose, (T), 20: 30187
stability in magnetic field, variational methods for Rayleigh-Taylor, (T), 20: 30172
theory of superfluid Fermi, collective oscillations in, 20: 30284

LITHIUM
density of, at critical temperature, 20: 29742
determination of, by neutron activation methods, 20: 29078(R) (AD-633252)
energy level determination for, using configuration interaction, (T), 20: 29917 (TID-22957)

LITHIUM ALLOYS
Li–Mg, protective coatings for, anodic, 20: 29366(R) (TID-22970, pp 375-91)

LITHIUM ALUMINATES
use as a neutron absorber material, 20: 30865(P)

LITHIUM CHLORIDES
chlorine-36 exchange between, and cycloalkyl chlorides in dimethyl sulfoxide, kinetics of, 20: 29157
electron transmission in thin films of, energy losses and color centers from, (E), 20: 30776

LITHIUM FLUORIDES
electron transmission in thin films of, energy losses and color centers from, (E), 20: 30776
plasma excitations in films of, 20: 30777
radiation effects on, color centers in ionic, effects of F centers from gamma and neutron, 20: 30739

LITHIUM HYDRIDES
plasma production on, by light pulses from laser, 20: 30666

LITHIUM IODIDES
use of europium-activated, in scintillation-type well logging device, 20: 29445(P)

LITHIUM IONS
dissociation of fast negative, in rare gases, (T), 20: 29947

LITHIUM ISOTOPES Li-5
energy levels from proton scattering by helium-4, parity and spin of, (E), 20: 30389

LITHIUM ISOTOPES Li-6
energy spectra of 1p shell, determination using Hamada-Johnston potential, (T), 20: 30354(R) (ORNL-3940, pp 62-9)
lithium-6 reactions (Li-6,α) with, four-parameter coincidence studies of, (E), 20: 30530
neutron capture cross sections at 10.7 to 102.0 kev, (E), 20: 30360 (WASH-1068)
neutron cross sections, (E), 20: 30360 (WASH-1068)
reactions with boron-10 and -11 at 3 Mev, angular distributions and total cross sections for, (E), 20: 30519

reactions with carbon-12, angular distributions and total cross sections for, (E), 20: 30520
LITHIUM ISOTOPES Li-7
deuteron reactions (d,α) and (d,n) with lithium-7 at 1 Mev, spectra and angular distributions from, (E), 20: 30402
energy spectra of 1p shell, determination using Hamada-Johnston potential, (T), 20: 30354(R) (ORNL-3940, pp 62-9)
neutron cross sections, (E), 20: 30360 (WASH-1068)
proton reactions (p,n) near threshold, neutron energy distributions and yields from, (E), 20: 30525
reactions with boron-10 and -11 at 3 Mev, angular distributions and total cross sections for, (E), 20: 30519
structure of 3^2P term in, fine and hyperfine, (E/T), 20: 29939
LITHIUM ISOTOPES Li-8
beta decay of, beryllium-8 levels from, (E), 20: 30363
LIVER
effects of nicotinic acid on cholesterol and specific radioactivity of rabbit, 20: 28895
radiography of, use of colloidal technetium-99m in, 20: 29065
radiosensitivity effects of preserved homologous fetal, in mice, gamma, 20: 29034
LOOPS
design for liquid metal heat transfer at 2100°F, 20: 29374(R) (ANL-7190, pp 156-66)
design for sodium analysis and sampling, 20: 30875(R) (ANL-7190, pp 143-55)
design of hot-hydrogen, for rocket reactor fuel testing, 20: 30787(R) (ANL-7190, pp 11-142)
oscillations in two-phase-flow natural circulation, 20: 29375(R) (ANL-7190, pp 193-200)
LUBRICANTS
development of, for vacuum uses, 20: 29366(R) (TID-22970, pp 375-91)
development of, for space uses, 20: 29366(R) (TID-22970, pp 375-91)
preparation of radiation-resistant, 20: 29323(P)
LUNGS
radiotherapy of tumors of rabbit, effects of hyperbaric oxygen, 20: 29059 (TID-22860)
thorium content in rat, after inhalation, 20: 28897
LUTETIUM
determination in minerals and ores, spectrometric, 20: 29134
determination in rocks, chemical spectrographic method for, 20: 29083(R) (UCRL-14767)
determination in standard igneous rocks G-1, W-1, and G-B by x-ray fluorescence, 20: 29101
determination in uranium compounds, spectrographic, 20: 29129
determination of trace amounts of, in ytterbium by activation methods, 20: 29082 (SGAE-CH-27/1966)
thermodynamic properties at 0°C to melting point, 20: 29743
LUTETIUM IODATES
thermal decomposition of trihydrated, 20: 29097
LUTETIUM ISOTOPES Lu-170
energy levels, (E), 20: 30353(R) (ORNL-3940, pp 1-61)
LUTETIUM ISOTOPES Lu-175
energy level transitions in, parity nonconservation of, (E), 20: 30381(T)
internal conversion in, nuclear structure effects in, (E/T), 20: 30515
LUTETIUM ISOTOPES Lu-176
beta decay of, nuclear matrix elements from, (E), 20: 30552
LUTETIUM NIOBATES
distribution in strontium molybdate single crystals, coefficients of, 20: 29746
LUTETIUM PERIODATES
production in thermal decomposition of trihydrated lutetium iodates, 20: 29097
LYMPH CELLS
radiosensitivity of, 20: 28927 (BNL-9647)

M

MACHINING
inspection gage for average radius, 20: 29668 (Y-NA-18)
MAGNESIUM
alpha elastic scattering at 24.7 Mev, optical-model analysis of, (E/T), 20: 30413
determination in aqueous solutions, design of oxyacetylene burner for measuring sensitivity of spectrophotometric, 20: 29083(R) (UCRL-14767)
determination in graphite and basalts by neutron activation methods, 20: 29140
determination in Zircaloy-2, spectrographic, 20: 29113
effects on spectra of nitrogen-15 in ATP, 20: 29083(R) (UCRL-14767)
helium ion reactions at 25 to 50 kev, K x-ray production cross sections from, (E), 20: 29936
hydrogen ion reactions at 25 to 50 kev, K x-ray production cross sections from, (E), 20: 29936
iron-57 Mössbauer spectra in, 20: 30766
reactions in gaseous mixtures, combustion, 20: 29641(R) (SC-DC-65-1691)
MAGNESIUM ALLOYS
Al–Be–Mg, analysis for beryllium, colorimetric, 20: 29111
Li–Mg, protective coatings for, anodic, 20: 29366(R) (TID-22970, pp 375-91)
MAGNESIUM CERIUM NITRATES
specific heat of, low-temperature, (E), 20: 30283
MAGNESIUM CHLORIDES
corrosive effects on austenitic and austeno-ferritic stainless steels, stress-, 20: 29639(R) (EURAEC-1578)
MAGNESIUM ISOTOPES Mg-25
deuteron reactions (d,n) with, aluminum-26 spectroscopic factors from, 20: 30481
helium-3 reactions (He-3,d), aluminum-26 spectroscopic factors from, 20: 30481
proton reactions (p,γ) at 0.956 to 1.716 Mev, gamma angular correlations from, (E), 20: 30528
MAGNESIUM NITRATES
$Mg(NO_3)_2$–$UO_2(NO_3)_2$–H_2O, activity coefficients of, at 25°C, 20: 29196
MAGNESIUM OXIDES
bonding and chemical reactions with fluophosphoric acid, mechanism of, 20: 29145 (NP-16047)
coating with molybdenum or tungsten by chloride and oxide processes, 20: 29631
content in thalenites from Japan, 20: 29399
cracks in single-crystals, nucleation of, 20: 29624(R) (TID-22970, pp 257-329)
deformation of, dislocation substructures formed during plastic, 20: 29711 (UCRL-11996)
radiation effects on, 20: 29623(R) (TID-22970, pp 121-256)
radioinduced blistering of, ion, (E), 20: 29816
MAGNETIC FIELDS
charged-particle diffusion across, equations for, 20: 30714
charged-particle motion in constant longitudinal and rotating transverse, 20: 30693
charged-particle motion in dipole, in external homogeneous magnetic field, (T), 20: 29829
conducting layer in traveling, higher-space-field harmonic effects on, (T), 20: 29830
dynamics of Bloch electrons in, (T), 20: 30735(R) (TID-22970, pp 331-73)
effects on electromagnetic oscillations in plasma, (T), 20: 30677
effects on electromagnetic wave propagation in plasma, (T), 20: 30678
effects on neutrons, (T), 20: 30734(R) (TID-22970, pp 1-63)
effects on surface wave propagation along annular mercury plasma column, (E), 20: 30574
effects on type-II superconductors, eddy currents from, 20: 30262
effects on ultrasonic attenuation by superconductors, (E/T), 20: 30735(R) (TID-22970, pp 331-73)
electron density and energy in helium afterglow plasma in toroidal, (E/T), 20: 30710
energy dissipation to charged particles near zero field lines in plasma, (T), 20: 30676
fluid stability in, variational methods for Rayleigh-Taylor, (T), 20: 30172
interactions with plasma, h-f, (T), 20: 30624
measurement of solar, 20: 29910
plasma acceleration and reflection by h-f and static, at electron cyclotron resonance, 20: 30646
plasma compression in toroidal, adiabatic, (E), 20: 30660
plasma containment in closed minimum-B, analysis of, 20: 30609
plasma diffusion and thermalization in, turbulent, (T), 20: 30620
plasma diffusion across, equations for, 20: 30714
plasma diffusion across longitudinal, (E/T), 20: 30596
plasma diffusion in, from hard-core and pinch discharges, (E), 20: 30639
plasma electron heating by h-f, adiabatically confined, (E), 20: 30663
plasma flow across, one-dimensional, (T), 20: 30597
plasma injection and compression in cusped, (E), 20: 30644
plasma loss rates in toroidal minimum-B, alkali, (E/T), 20: 30656
plasma motion in toroidal octupole, (E), 20: 30708
plasma production by injection in cusp, dense, (E), 20: 30643
plasma puffs in longitudinal, hydromagnetic model for, 20: 30715
plasma stability in toroidal discharges, (T), 20: 30617
plasma stability in toroidal, (E), 20: 30640
plasmoid heating and oscillation in axisymmetric, (T), 20: 30559 (FTI-114/P-044)
plasmoid motion in curvilinear, (E/T), 20: 30647
production in toroidal Heliotron, 20: 30595
production of helical, coil shape for, (T), 20: 30703
radiofrequency skin depth in d-c, nonresonant changes in, (E/T), 20: 30734(R) (TID-22970, pp 1-63)

strength in circular cylinder, ferromagnetic material effects on, (T), 20: 29835
transport of solar, from spot and bipolar regions, (T), 20: 29906(T)
use of multipole, in plasma injection control, 20: 30579

MAGNETIC MATERIALS
relaxation phenomena near critical points, 20: 30780

MAGNETIC MIRROR MACHINES
design of cryogenic VGL-2, 20: 30655
magnetic field production in toroidal Heliotron, 20: 30595
plasma compression in, adiabatic, 20: 30636
plasma containment and heating in DECA II, 20: 30607
plasma flute instability in, effects of density on, (T), 20: 30707
plasma heating under electron beam instability conditions, (E), 20: 30659
plasma ion losses through charge exchange in, 20: 30584
plasma production by molecular hydrogen ion injection in, (E), 20: 30634
plasma properties in, relativistic electron, (T), 20: 30638
plasma stability in, (T), 20: 30635
vacuum system for Ogra-1, ultrahigh, 20: 30701

MAGNETIC MIRRORS
molecular ion injection and trapping in, use of r-f field for, 20: 30580
plasma ion losses from, analysis of, (T), 20: 30618
plasma production by neutral hydrogen injection in well geometry of, (E), 20: 30632

MAGNETIC RESONANCE
book: *Nuclear Magnetic Resonance and Electron Spin Resonance Spectra. Index for 1958–1963*, 20: 30510

MAGNETISM
research programs on, at low temperatures, 20: 30735(R) (TID-22970, pp 331-73)

MAGNETITES
magnon spectra of, temperature effects on, (E), 20: 30765

MAGNETOHYDRODYNAMIC CELLS
book: *Physical Processes in Magnetohydrodynamic Generators*, 20: 29979
design of large scale, 20: 29984(P)
design of, with provision for removing sulfur oxide from exhaust gas, 20: 29982(P)
design with semi-open operating cycle, 20: 29983(P)
electric potential drop in, analysis of, (T), 20: 29976 (IPP-3/38)
performance using magnetoactive cold plasma with ambipolar potential, (E), 20: 29978
power cycles for nuclear power plants using liquid-metal, 20: 29980
power generation by liquid-metal, evaluation for central-station, 20: 29974(R) (ANL-7190, pp 167-75)

MAGNETOHYDRODYNAMICS
fluid flow over flat porous plate in transverse field, (T), 20: 30180
gas flow in magnetic fields, electrically and thermally conducting, 20: 30185
hydromagnetic discontinuity in gases in, combustible adiabatic for, (T), 20: 30177
liquid metal flow resistance in circular channels, (T), 20: 30183
plasma jet flow-field perturbations and Hall potentials in, axisymmetric, (E/T), 20: 30176
plasma one-dimensional unsteady flow in, (T), 20: 30570
shock wave structure in, effects of electron temperature and Hall currents on, 20: 30191

MAGNETOMETERS
design and operation of search-coil, for satellite measurements of geomagnetic fields, 20: 30236

MAGNETOSPHERE
charged-particle motion in deformed, trapped-region asymmetrical configuration determination from, (T), 20: 30224
charged-particle penetration processes in, 20: 30205(T) (NASA-TT-F-389, pp 386-425)
electron and proton drift in, formation of Van Allen belts from, 20: 30207 (NASA-TT-F-389, pp 442-53)
electron, proton, and ion energy, spatial, and temporal distribution in, 20: 30220(T) (NASA-TT-F-389, pp 633-52)
solar wind interactions with, 20: 30210(T) (NASA-TT-F-389, pp 499-517)

MAGNETS
development of high-field, 20: 30735(R) (TID-22970, pp 331-73)
Mössbauer effects in, (E/T), 20: 30735(R) (TID-22970, pp 331-73)
potting compounds for, 20: 29366(R) (TID-22970, pp 375-91)

MAGNOX ALLOYS
analysis of type-Al-80, for hydrogen, 20: 29100
analysis of type-Zr-55, for hydrogen, 20: 29100

MAIZE
radiation effects on x-ray diffraction spectra of amidones in, γ, 20: 29255

MALEIC ANHYDRIDE
radioinduced solid-state polymerization with acenaphthylene, gamma, 20: 29274

MAN
cesium-137 content in Norwegian, 1962 through 1965, 20: 29432
effects of fallout on, pathological, 20: 29407(T) (AEC-tr-6666)
hazards to, from eating fish contaminated with radioisotopes, 20: 29405 (NP-14694)
ionic composition of intracellular medium in, determined by activation analysis, 20: 28871(R) (EUR-2636.f,i)
radiation dose to skeleton in, from strontium-90 content in river water, 20: 30943(R) (ORNL-TM-1465)
radiation effects on, 10-Mev electron, 20: 28929 (CONF-651109, pp 574-98)
radiation effects on blood picture in, nuclear explosion, 20: 28876
radiation effects on, from criticality accidents, γ and neutron, 20: 28970
radiation effects on, physiological, 20: 28974
radiation effects on blood coagulation in, review, 20: 28985
radiation effects on, review, 20: 29478
radiation hazards to, in space flight, 20: 29058

MANGANESE
content in rocks, effects of clay content on, 20: 29417
determination in Zircaloy-2, spectrographic, 20: 29113
neutron capture by, energy resolution of gamma spectra from, 20: 29078(R) (AD-633252)
neutron scattering cross sections at 700 to 1200 kev, (E), 20: 30360 (WASH-1068)
separation of traces of, from iron by paper chromatography, tracer studies of, 20: 29342

MANGANESE ALLOYS
Au–Mn, thermal capacity below 1°K, 20: 29791
Cu–Mn, thermal capacity below 1°K, 20: 29791
Fe–Mn–Ni, martensitic reaction nucleation rate in, 20: 29623(R) (TID-22970, pp 121-256)
Mn–Ag, thermal capacity below 1°K, 20: 29791
Mn–U, metallographic tests on arc melted, 20: 29775

MANGANESE ISOTOPES Mn-52
beta decay of, chromium-52 level structure from, (E), 20: 30458
yield in alpha and proton reactions with copper, 20: 30531
yield in proton reactions with yttrium, 20: 30531

MANGANESE ISOTOPES Mn-54
content in freshwater clams, 20: 29462
content in juniper trees in Georgia, 20: 29410

MANGANESE ISOTOPES Mn-55
neutron reactions (n,γ) with, cross sections for, (E), 20: 30360 (WASH-1068)
neutron reactions (n,γ) at 0.1 to 14 Mev, cross sections for, (T), 20: 30378

MANGANESE ORES
radium, thorium, and uranium abundance ratios in, 20: 29425

MANGANESE OXIDES
content in thalenites from Japan, 20: 29399
Mn_2O_3–Sc_2O_3, magnetic susceptibility, 20: 29168
Mn_2O_3–Sc_2O_3, phase studies, 20: 29168
MnO–Sc_2O_3, phase studies, 20: 29168

MANGANESE STEEL
radiation effects on SA 302 B, 20: 30788(R) (ANL-7190, pp 176-88)

MARITIME REACTORS
design for once-through steam generation, 20: 30931(P)
development of, Joint Committee hearing on, 20: 30930
nozzle design for pressurized water, stress analysis for, (T), 20: 30928

MARTENSITES
fracture of, effects of atomic displacements on, 20: 29623(R) (TID-22970, pp 121-256)
strengthening of, by strain tempering, 20: 29623(R) (TID-22970, pp 121-256)

MASERS (OPTICAL)
beam effects on solids, elastic explosions from, (T), 20: 30740
beam reactions with deuterium, plasma production in, 20: 30665
beam reactions with air, high-temperature plasma production from spike-mode, (E), 20: 30590(T)
beam scattering by hot electron plasma, relativistic theory of, 20: 30716
hazards evaluation of, in industry and research, 20: 29480
monitoring in industry and research, 20: 28936
radiation effects of, pathological, 20: 28936
radiation effects of, pathological, 20: 29457
ultrasonic wave generation from, effects of, on neurological and retinal changes, 20: 28951
use for plasma diagnostics, 20: 30556(R) (AD-631993)

MASS SPECTROGRAPHY
development of, for ruthenium isotope yield analysis in uranium burnup, 20: 29080(R) (IDO-14676)

MASS SPECTROMETERS
design, 20: 29709(R) (TID-22970, pp 65-119)
design and performance of r-f, for satellite measurements of atmospheric

composition, 20: 29545
design of high-frequency, 20: 29126
head attachment design for use in ultra-high vacuum leak detector, 20: 29496
ion beam double focusing in, with inhomogeneous magnetic field, 20: 29493
ion beam transmission efficiency for, (T), 20: 29490
ion optics for, (T), 20: 29489
MASS TRANSFER
book: *Advances In Heat Transfer, Vol. III*, 20: 29381
MATERIALS TESTING
bonded joint, correlation of heat transfer and ultrasonic transmission properties for, 20: 29386 (ANL-7074)
creep-rupture properties of refractory metals, equipment and techniques for, 20: 29710 (TID-22986)
equipment for high-temperature tensile, 20: 30875(R) (ANL-7190, pp 143-55)
equipment for radiometric, safety device for, 20: 29515(P)
fracture toughness of reactor pressure vessel steels, methods development for, 20: 29700(R) (COO-1477-4)
methods for pressure vessels, 20: 29389
temperature measurements on irradiated materials, magnetic method for, 20: 29387
use of neutron radiography in nondestructive, review of, 20: 29627
MATHEMATICS
book: *Direct Methods of Qualitative Spectral Analysis of Singular Differential Operators*, 20: 29615
boundary conditions for P_N approximation in, variational vacuum, 20: 30116
equations in, multiple regression computer program for solving polynomial, 20: 29613 (TRG-Report-1198)
formula for fallout distribution calculations, 20: 29407(T) (AEC-tr-6666)
groups in, Casimir operators for U(n) and SU(n), 20: 30147
representations of noncompact rotation group in, generalized spherical functions for, 20: 29614
MATTER
binding energy of nuclear, saturation, 20: 30434
exchange energy of semi--infinite nuclear, (T), 20: 30395
properties of nuclear, calculation using boundary-condition model, 20: 30523
MEATS
cesium-137 content in seal, 20: 29053 (NP-15951)
cesium-137 content in Norwegian, 1962 through 1965, 20: 29432
radiation effects on organoleptic, chemical, and physical properties of beef at 20 to −196°C, gamma, 20: 29602
volatile compounds in irradiated beef, effects of storage at ambient temperatures on, 20: 29589
MECONIC ACID
complexes with uranium, equilibrium constants for, 20: 29096
MEMBRANES
development of semipermeable, 20: 29624(R) (TID-22970, pp 257-329)
MEMORY DEVICES
development, 20: 29499
development of thin magnetic films for, 20: 29709(R) (TID-22970, pp pp 65-119)
MENTHOL
atomic structure of, "electron burning" method of determination of, 20: 29326
MERCAPTO GROUP
radiosensitivity effects of, 20: 29039
MERCURY
boiling, surface tension, and wetting of, review on, 20: 29620 (NP-16046)
corrosive effects on refractory metals and stainless steels at 593 to 703°C, 20: 29646
determination in petroleum, activation, 20: 29139
electron elastic scattering at low energies, polarization effects in, (E), 20: 29937
electron impact excitation in plasma of, resonance absorption from, 20: 30601
erosive effects on metals and alloys at 70 and 500°F, cavitation, 20: 29640 (NP-16048)
neutron reactions (n,γ) near 5 Mev, gamma spectra from, (E), 20: 30358(R) (RPI-328-56, pp 1-48)
wave propagation along annular column of plasma of, surface, (E), 20: 30574
MERCURY IONS
effects on radiolysis of naphthalene, 20: 29260
MERCURY ISOTOPES Hg-194
energy levels from thallium-194 decay, negative parity, (E), 20: 30435
MERCURY ISOTOPES Hg-196
energy levels from thallium-196 decay, negative-parity, (E), 20: 30435
MERCURY ISOTOPES Hg-198
energy levels from thallium-198 decay, negative-parity, (E), 20: 30435
MERCURY ISOTOPES Hg-199
energy level structure from gold-199 beta decay, (E), 20: 30549
MERCURY ISOTOPES Hg-202
deuteron and proton elastic scattering by, angular distributions and levels from, (T), 20: 30484
MERCURY ISOTOPES Hg-203
beta decay of, β-γ directional and circular polarization correlations in, (E), 20: 30544
MESIC ATOMS
x-ray spectra from K-mesic helium, effects of $\bar{K}$-N interactions on, 20: 29938
MESONS
binding forces for two-body pseudoscalar, dynamical calculations on, 20: 30161
decay of spin 1⁻, mixing angles for, 20: 30088 (IC-66/50)
electromagnetic properties of, composite-particle model for, (T), 20: 30069
interactions of neutral pseudoscalar, with static spin-1 source, (T), 20: 30159
interactions of vector, cross sections for photon production in, 20: 30057
interactions of zero-mass, Regge poles in, 20: 30163
interactions with baryons at low energies, (T), 20: 30070
interactions with baryons, current algebras for, 20: 30006
mass spectra of, dynamical symmetry for, 20: 30091 (JINR-P-2621)
mass splittings of, dynamical calculations on electromagnetic, 20: 30161
masses of pseudoscalar, electromagnetic, 20: 30032
production of vector, in electron interactions with positrons, (T), 20: 30012
symmetry for, relation between Poincare group and exceptional lie group G(2), 20: 30115
theory for axial-vector, 20: 30007
MESONS, RESONANCE
classification in SU(6) group, 20: 30093 (JINR-P-2701)
mass differences of K* (885), electromagnetic, (T), 20: 30161
production and decay of, (T), 20: 30085 (CONF-640509(Pt.1), Paper 3)
production and properties of A_1 and A_2, from meson (π) interactions with nucleons, (E/T), 20: 30023
production of A_1 and A_2, in deuteron-meson (π^-) interactions, (E), 20: 30078
production of K*(891), in meson (K⁻)-proton interactions at 1.45 Bev/c, (E), 20: 30009
production of K^+K^+* (1280) from meson (K^+)-proton interactions at 3.535 Bev/c, 20: 30047
production of $\pi^+\pi^-\pi^-$ (1630), in meson (π^-)-proton interactions at 4.7 Bev/c, 20: 30021
production of strangeness +1, in meson (K^+)-proton interactions at 3.54 Bev/c, 20: 30049
properties of, in $SU(6)_W$, 20: 30048
spin of A_1 and A_2, (E), 20: 30078
symmetry for, origin of SU(6), 20: 30117
theory of A_1(1072) and K_C(1215), as axial-vector mesons, 20: 30007
MESONS (η^0)
decay of, CP violation in, 20: 29988 (ITEF-356)
decay of, gamma conversion in hydrogen from, (E), 20: 30029
production in meson (π) interactions with nucleons, zero-effective-range analysis of, 20: 30033
MESONS (K)
interactions with protons, Regge cuts in high-energy elastic, (T), 20: 30160
interactions with nucleons, dispersion relations and symmetry groups for, 20: 30018
production in antiproton-annihilation at rest in deuterium, (E), 20: 29992 (UCRL-16717)
MESONS (K^-)
capture by emulsion nuclei, meson (π^+) emissions from, 20: 30485
interactions with protons, properties of hyperons (Ξ^-) and (Ξ^0) from, (E), 20: 30072
interactions with protons at 1.45 Bev/c, K*(891) and N*(1236) production in, (E), 20: 30009
interactions with protons at 5 to 20 Bev/c, meson-exchange model for forward elastic, 20: 30039
reactions with emulsion nuclei at 1.5 Bev, Λ-hyperfragment production in, (E), 20: 30448
reactions with heavy emulsion nuclei at 1.5 Bev/c, $_{\Lambda}He^7$ and $_{\Lambda}Li^7$ production in, 20: 30368
MESONS (K^0)
decay modes of, current algebra for 2π, 20: 30015
decay of K_1^0, Cabibbo current theory for parity-violating nonleptonic, 20: 30041
decay of $K_{2\gamma}^0$, probability of 2π, (E), 20: 30056
decay of K_2^0, CP violation in 2π, (E), 20: 30000
decay of, interference of K_S and K_L in $\pi^+\pi^-$, (E), 20: 30026

decays of, CP violation in 2π, (T), 20: 30055
mass relative to K^+, 20: 30016
MESONS (K^+)
decay of, branching ratios and form factors for, (E), 20: 30075
decay of, Cabibbo current theory for parity-violating nonleptonic, 20: 30041
interactions with protons at 5 to 20 Bev/c, meson-exchange model for forward elastic, 20: 30039
interactions with protons at 3.535 Bev/c, production of K^+K^{+*} (1280) from, 20: 30047
interactions with protons at 3.54 Bev/c, production of strangeness +1 resonances from, 20: 30049
mass relative to K^0, 20: 30016
MESONS (μ)
beta decay, (T), 20: 30535
interactions with nucleons, inelastic, (T), 20: 30076
interactions with nucleons, cross sections for, (E/T), 20: 29994
production in neutrino interactions, polarization measurement of, 20: 30003
MESONS (μ^-)
capture by calcium-40, giant dipole resonance model for radiative, 20: 30451
capture by nuclei, x-ray spectra from, (E), 20: 29525 (CONF-660209-9)
capture by nuclei, $\Delta S = 0$ neutron current coupling in, 20: 30141
capture by oxygen-16, elementary-particle treatment of, 20: 30447
capture by spherical nuclei, (T), 20: 30494
capture rates in heavy nuclei, closure approximation for, 20: 30454
MESONS (ω)
decay of, mixing angles for, 20: 30088 (IC-66/50)
decay of, $SU(6)_w$ symmetry for radiative, 20: 30040
decay properties of, calculation using composite-particle model, (T), 20: 30069
width of, calculation from elastic unitarity equation, 20: 30077
MESONS (ω')
decay rate of, sum rule for, 20: 30036
MESONS (ϕ)
decay of, mixing angles for, 20: 30088 (IC-66/50)
MESONS (π)
electroproduction amplitude at finite momentum transfer, 20: 30137
interactions of, contributions of elastic unitarity to three-body, (T), 20: 30077
interactions with nucleons, p-wave dispersion relations for, (T), 20: 30073
interactions with deuterons, p-wave dispersion relations for disintegration, (T), 20: 30074
interactions with meson (ρ), elastic unitarity in, (T), 20: 30077
interactions with nucleons, N/D calculations of p-wave amplitudes for, (T), 20: 30158
interactions with protons, Regge cuts in high-energy elastic, (T), 20: 30160
interactions with nucleons, amplitudes for, (T), 20: 29986 (CONF-640509(Pt.1), Paper 2)
interactions with nucleons, amplitudes for, 20: 30006
interactions with mesons (π), phase shifts and dispersion relations for forward, 20: 30017
interactions with mesons (ρ), sum rules for strong, 20: 30020
interactions with nucleons, production and properties of mesons A_1 and A_2 from, (E/T), 20: 30023
interactions with nucleons, zero-effective-range analysis for meson (η^0) production in, 20: 30033
interactions with mesons (π) OPE model for bootstrap for, 20: 30035
production in meson (μ)-nucleon interactions, (T), 20: 30076
production of pairs of, in meson (π^-) interactions with nucleons at 12 and 18 Bev, (E), 20: 30025
production of slow, in meson (π^-) reactions with emulsion nuclei at 3.8 Bev, 20: 30501
MESONS (π^-)
capture by nuclei, angular correlations of particles from, (T), 20: 30504
interactions with protons at 1.17 Bev/c, hyperon (Λ^0) and (Σ^0) polarization in, (E), 20: 29987 (COO-1261-4)
interactions with protons at 1128 to 1326 Mev/c neutral hyperon production, (E), 20: 30071
interactions with deuterons and nucleons at 3.7 Bev/c, A_1 and A_2 resonance production in, (E), 20: 30078
interactions with neutrons, peripheral mechanisms in, (T), 20: 30081
interactions with protons at 6.8 Bev/c, criterion for separating products of elastic, (E/T), 20: 30083
interactions with protons at 180 to 500 Mev/c, criterion for separating products of inelastic, (E/T), 20: 30083
interactions with protons at 4.8 Bev/c, differential cross sections for charge-exchange, (E), 20: 29998(T)
interactions with protons at 1.7 Bev/c, differential cross sections for elastic, (E), 20: 30011
interactions with protons at 4.7 Bev/c, production of meson resonance (1630) in, (E), 20: 30021
interactions with protons at 5 to 20 Bev/c, meson-exchange model for forward elastic, 20: 30039
interactions with nucleons at 12 and 18 Bev, meson (ρ^0) and dipion production in, (E), 20: 30025
production in proton interactions with neutrons and protons in nuclear emulsions, charge asymmetry of, (E), 20: 30082
reactions with emulsion nuclei at 3.8 Bev, slow meson (π) production in, (E), 20: 30501
MESONS (π^+)
decay of, T invariance in, 20: 29997(T)
emission in decay of hypernuclei, 20: 30485
interactions with protons at 1.840 Bev/c, search for $T = \frac{5}{2}$ isobar in, (E), 20: 30022
interactions with protons at 5 to 20 Bev/c, meson-exchange model for forward elastic, 20: 30039
production in proton interactions with neutrons and protons in nuclear emulsions, charge asymmetry of, (E), 20: 30082
production of slow, in proton reactions with emulsion nuclei at 9 Bev, (E), 20: 30370
MESONS (ρ)
decay of, $SU(6)_w$ symmetry for radiative, 20: 30040
exchange in meson (π) interactions, OPE model for bootstrap for, 20: 30035
interactions with mesons (π), elastic unitarity in, (T), 20: 30077
interactions with mesons (π), sum rules for strong, 20: 30020
mass differences of, electromagnetic, (T), 20: 30161
MESONS (ρ^0)
production in bremsstrahlung reactions with protons at threshold to 6 Bev, (E), 20: 30030
production in meson (π^-) interactions with nucleons at 12 and 18 Bev, (E), 20: 30025
MESONS (X)
decay of, $SU(6)_w$ symmetry for radiative, 20: 30040
METABOLISM
measurement *in vivo* by external counting of iodine-131-labeled albumin as a function of iodine labeling intensity, 20: 28871(R) (EUR-2636.f,i)
serum protein, in rats, effects of carbon tetrachloride, radiation, and venous bleeding on, 20: 28954
METAL-FOIL DETECTORS
performance for xenon stability determinations in reactors, 20: 30843
METAL POWDERS
pressing of, for plate and sheet fabrication, 20: 29679
METALLIC FILMS
electron ranges in thin, 20: 29952
microwave absorption in, on normal and superconducting tin, (T), 20: 30290
METALLURGY
book: *Radioisotopic Instruments in Metallurgy*, 20: 29598
developments in high-temperature, 20: 29623(R) (TID-22970, pp 121-256)
effects on iodine-131 deposition in urban districts in Japan, 20: 29479
METALS
analysis of, by beta backscattering methods, 20: 29110
atomic structure and properties of liquid, review of, 20: 29755
condensation to liquid, electromagnetic rate control of, 20: 29974(R) (ANL-7190, pp 167-75)
crystal structure and growth kinetics of undercooled, 20: 29623(R) (TID-22970, pp 121-256)
current rectification processes at semiconductor contacts with, 20: 29569
electron interband transport in, quantum theory of, 20: 30735(R) (TID-22970, pp 331-73)
electron polarization in, theory of conduction, 20: 30735(R) (TID-22970, pp 331-73)
electron-phonon interactions in, strong, (T), 20: 30312
extrusion through non-metallic dies, equipment for, 20: 29693(P)
heat transfer by liquid, 20: 29381
ion scattering by surfaces of, 20: 29499
magnetohydrodynamic flow resistance of liquid, in circular channels section, 20: 30183
performance of liquid, as reactor coolant, 20: 30910
photoelectric effect in, model for analysis of, (T), 20: 29916 (ORNL-TM-1458)
positron annihilation in, analysis of, (T), 20: 29991 (ORNL-TM-1443)
radiation effects on, review of neutron, 20: 29819
refining of reactor, electrolytic cell design for, 20: 29373(P)
research on control of solidification in, 20: 29623(R) (TID-22970, pp 121-256)
specific heat at low temperatures, continuous warming method of measuring, (E), 20: 30734(R) (TID-22970, pp 1-63)
METASTASES

radiodiagnosis of, using iodine-131-labeled fibrinogen, 20: 28871(R) (EUR-2636.f,i)

METEORITES
iodine-129 in, origin of extent, 20: 29891
sulfur content and isotopic abundances in, 20: 29893
xenon isotope abundances in Pasamonte, fission-produced, 20: 29892

METEOROLOGICAL INSTRUMENTS
design of wind recording system, 20: 29502

METEOROLOGY
effects of climate on iodine-131 uptake by sagebrush, 20: 28883
radiation data for, interpretation of satellite, 20: 30221(T) (NASA-TT-F-389, pp 741-57)
weather prediction from atmospheric electric conductivity measurements, 20: 29402

METEORS
antimatter nature of micro-, from showers, (E/T), 20: 29895

METHACRYLIC ACID, METHYL ESTER
radioinduced polymerization with lignin, gamma, 20: 29288

METHACRYLIC ACID, METHYL ESTER POLYMERS
erosion of plexiglass, by mercury and water at 70°F, cavitation, 20: 29640 (NP-16048)
reactions with muonium, (E), 20: 29247

METHANE
determination as impurity in ultrapure gases, mass spectrometric, 20: 29083(R) (UCRL-14767)
effects on oxidation of graphite by vacuum ultraviolet irradiated carbon dioxide, 20: 29733
helium atom reactions with, electron kinetic energy from ionization in, (E), 20: 29927
hydrogen ion reactions with molecular, at 1 to 55 kev, particle production cross sections for, 20: 29919 (UCRL-14214)
neutron scattering by gaseous and solid deuterated, (E), 20: 30360 (WASH-1068)
oxidation by copper oxide, effects of carbon-14 on, 20: 29187
production during hydrolysis of thorium uranium carbides, 20: 29159
radioinduced polymerization of solid, positive ion chemistry in, 20: 29314
radon-219 and radon-220 decay in, properties of recoils from, 20: 29325
separation from carbon monoxide and hydrogen by selective oxidation, isotope effects in, 20: 29187
tritium reactions with, at 3 ev, 20: 29265
yields from gamma radiolysis of frozen carbon tetrachloride–methanol solutions, 20: 29305

METHANE, DIIODO-
reactions with muonium, (E), 20: 29247

METHANE, IODO-
iodine-131 exchange between, and iodide ions, kinetic studies of, 20: 29207

METHANE, TRICHLOROFLUORO-
flow in high-pressure loops, two-phase, 20: 29375(R) (ANL-7190, pp 193-200)

METHANOL
radioinduced catalytic conversion of, on silica gel, 20: 29278
reactions with muonium, (E), 20: 29247
acetic acid–methanol, deuterium exchange between, and azulene, 20: 29245
carbon tetrachloride–methanol, radiolysis of frozen, free radical formation in gamma, 20: 29305

METHYL SULFOXIDE
effects of cupferron and, on frequency of radioinduced chromosome aberrations in Tradescantia, 20: 29028
effects on frequency of radioinduced chromosome aberrations in Tradescantia, 20: 29028

MICA
properties as detector in high-energy proton reactions, 20: 29551
sorptive properties for fission products in waste solutions, 20: 29332 (ORNL-P-1811)

MICE
antibody levels in circulating blood of, effects of deuteration on, 20: 28988
chromosomal aberrations in cornea of, induced by tissue extracts from x-irradiated donors, 20: 28959
homograft immunity in γ-irradiated, effects of methotrexate on, 20: 29035
iron-59 uptake by skin of, from bath water, 20: 28892
lymphomas in, antigenic characteristics of virus-induced, 20: 28873
radiation effects on blood serum proteins in, x, 20: 28899
radiation effects on synthesis of blood plasma proteins induced by injected lymphoid cells in, 20: 28926 (AD-633469)
radiation effects on mast cells in skin of, uv, 20: 28937
radiation effects on catecholamine metabolism in, 20: 28940
radiation effects on, genetic x, 20: 28957
radiation effects on, synergistic effects of vibration with, 20: 28968
radiation effects on survival of, depth-dose factor in 120-Mev proton, 20: 28972
radiation effects on skin in, protection by, against effects of 7,12-dimethylbenzanthracene, 20: 28973
radiation effects on skin epithelial cells, dose-response relations for x, 20: 28990
radiation effects on thiamine metabolism in, x, 20: 29003
radiation effects on thymus cells in, methods for evaluating, 20: 29008
radiation effects on, protective effects of preserved homologous bone marrow against gamma, 20: 29033
radiation effects on immune reactions to bone marrow transplants in, 20: 29006
radiation effects on resistance to Ehrlich ascites tumors of, 20: 29017
radiation effects on, protective effects of preserved homologous fetal liver against gamma, 20: 29034
radiation effects on, protective effects of AET combined with bone marrow transplants against, γ, 20: 29036
radioinduced skin lesions in, role of adipose tissue in repair of x, 20: 28946
radiosensitivity of, effects of time of day on x, 20: 28938
radiosensitivity of, effects of hormones on, 20: 28978
radiosensitivity of, effects of removal of endocrine glands on, 20: 28978
radiosensitivity of, effects of porphyrins on, 20: 29042
2-mercaptopropylamine metabolism in, tracer study, 20: 28888

MICROANALYSIS
book: *Instrument and Chemical Analysis Aspects of Electron Microanalysis and Macroanalysis*, 20: 29119
electron microprobe for, development of, 20: 29083(R) (UCRL-14767)

MICROORGANISMS
radiation effects on populations of, in fish, gamma, 20: 29583(R) (TID-22515)
radiosensitivity of *Micrococcus radiodurans*, effects of pigments on, 20: 29016

MICROWAVE EQUIPMENT
charged-particle emission from semi-infinite waveguides, (T), 20: 29828
design of semiconductor amplifier, electromagnetic oscillation theory for, 20: 30677
development of ferrites for, 20: 29709(R) (TID-22970, pp 65-119)

MICROWAVES
absorption by metal films on tin at low temperatures, (T), 20: 30290
absorption by plasma, in cavity resonator, negative, (T), 20: 30587
absorption in copper–tin and gold–tin superconductors, proximity effects in, (E), 20: 30289
amplification by electron beam-plasma interactions, 20: 30718
emission from magnetic mirror plasma, properties of, (E), 20: 30645
production and amplification in plasma, 20: 29499
refraction in cylindrical plasma, plasma density from, (E/T), 20: 30700
scattering by turbulent plasma, (E/T), 20: 30658

MILK
cesium-137 content in Colorado, May 1965, 20: 29429
cesium-137 content in Norwegian, 1962 through 1965, 20: 29432
consumption in U. S., 1962, effects on radionuclide intake, 20: 29474
iodine-131 content in Colorado, May 1945, from Chinese nuclear test, 20: 29429
radioactivity in, and milk products, 20: 29464
radioactivity in, 1965 fallout, 20: 29428
strontium-90 content in, effects of dietary calcium on, 20: 29459
strontium-90 transfer from mother to baby monkeys by, 20: 28896

MINERALS
analysis for rare earths, spectrometric, 20: 29134
heating *in situ* with radioactive materials, process for, 20: 30950(P)

MITOCHONDRIA
radiation effects on uncoupling of oxidation and phosphorylation in, of green plants, x, 20: 28947(T)
radiation effects on guinea pig, x, 20: 28976

MITOMYCINS
radiosensitivity effects on leukopenia in rabbits, 20: 29055

MOLECULAR BEAMS
injection and trapping in mirror fields, use of r-f field for high-energy, 20: 30580
production of, apparatus design considerations for, 20: 29918 (UCRL-11670)
scattering of, use of, in intermolecular force studies, (E/T), 20: 30734(R) (TID-22970, pp 1-63)

MOLECULAR PROPERTIES
spectral studies of resonance, using infrared lasers, 20: 30734(R) (TID-22970, pp 1-63)

MOLECULES
coupling scheme for, in ligand field theory, 20: 29205
energy levels of, 20: 29931(T)
reactions with solid surfaces, 20: 29624(R) (TID-22970, pp 257-329)

MOLLUSKS
manganese-54 content in freshwater clams, 20: 29462

MOLTEN SALT REACTOR EXPERIMENT

operation of, personnel training simulators for, 20: 30934 (ORNL-TM-1445)
MOLYBDENUM
analysis for oxygen, method for, 20: 29108
brittle-ductile transition temperature in, method for determining, 20: 29757
compatibility of coating of, with uranium carbide–zirconium carbide thermionic diode at 1800 to 2500°C, 20: 29820
compatibility with plutonium carbides at 1200 to 1400°C, 20: 29820
corrosion by mercury at 593 to 703°C, 20: 29646
creep properties of arc-cast at 2200°C, 20: 29710 (TID-22986)
deformation of recrystallized polycrystalline and single-crystal, 20: 29758
deposition on refractory metal–nonmetal powders by chloride and oxide processes, 20: 29631
determination in Zircaloy-2, spectrographic, 20: 29113
determination of, by neutron activation methods, 20: 29078(R) (AD-633252)
ductility of electron-beam-melted, effects of carbon, titanium, or zirconium additions on, 20: 29783
ductility of, effects of boron additions on, 20: 29675
effects on properties of graphite, with and without copper and silver infiltration, 20: 29764
electron ranges in thin films of, 20: 29952
evaporation of, from irradiated uranium(IV-VI) oxides at 900 to 1500°C in flowing hydrogen, nitrogen, or oxygen, 20: 29211
forging of, comparison of arc-cast, pressed, and sintered billets for, 20: 29683
iron-57 Mössbauer spectra in, 20: 30766
melting of, electron-beam, 20: 29674
melting of, properties of boron, carbon, and titanium hydride as deoxidizers during arc-, 20: 29675
production and properties of low-carbon unalloyed, arc-cast, evaluation of, 20: 29756
properties as high-temperature coating, 20: 29650
properties of, at 2000°C, for use in thermionic converters, 20: 29729
radiation effects on mechanical properties of, fission fragment and neutron, 20: 29820
radiation effects on, for use as sensor material, 20: 29486(R) (NASA-CR-54964)
reactions in gaseous mixtures, combustion, 20: 29641(R) (SC-DC-65-1691)
separation from fission product solutions by ion exchange, 20: 29357
MOLYBDENUM ALLOYS
Al–Cr–Co–Fe–Mo–Ni–Ti, joining of Udimet 500 and 700, by mechanical fastening, 20: 29667 (RSIC-509)
Al–Cr–Co–Fe–Mo–Ni–Ti, surface treatments for Udimet 500 and 700, coating and mechanical, 20: 29706 (NASA-TM-X-53448)
Al–Cr–Co–Mo–Ni–Ti, joining of M-252, by mechanical fastening, 20: 29667 (RSIC-509)
Al–Cr–Co–Mo–Ni–Ti, surface treatments for Astroloy, coating and mechanical, 20: 29706 (NASA-TM-X-53448)
Al–Cr–Co–Mo–Ni–Ti–V–Zr, surface treatments for IN-100, coating and mechanical, 20: 29706 (NASA-TM-X-53448)
Al–Cr–Fe–Mo–Ni–Ti–W, joining of D-979, by mechanical fastening, 20: 29667 (RSIC-509)
Be–Mo, intermetallic compounds in, properties of, for use in aerospace technology, 20: 29770
Cr–Mo–Ni, compatibility with plutonium and uranium carbides, 20: 30790(R) (ANL-7204, pp 1-31)
Mo–Nb, crystal structure and electric conductivity of, 20: 29766
Mo–Nb–Ti, evaluation of protective coatings for, 20: 29651
Mo–Nb–Ti–Zr, creep properties of niobium-modified TZM, 20: 29705(R) (NAS-CR-54973)
Mo–Nb–V, fabricability, strength, and weldability, 20: 29763
Mo–Nb–V–Zr, tensile properties of B-66, effects of welds on, 20: 29712(R((WANL-PR-(P)-009)
Mo–Pd, crystal structure and electric conductivity of, 20: 29766
Mo–Re, fabrication, properties, and uses of, 20: 29768
Mo–Ta–W, availability, properties, and uses of, 20: 29760
Mo–Ti, coating with silicon by fluidized-bed process, 20: 29630
Mo–Ti, erosion by mercury, water, and bismuth–lead alloy, cavitation, 20: 29640 (NP-16048)
Mo–Ti, melting of, effects of composition on electron-beam, 20: 29674
Mo–Ti–Zr, creep properties of TZM, 20: 29705(R) (NAS-CR-54973)
Mo–Ti–Zr, production and properties of sheets of, 20: 29756
Mo–U, casting of, testing of products from, 20: 29803
Mo–U, mechanical properties, 20: 29803
Mo–U, mechanical properties, metallography, and structure of, 20: 29775
Mo–Zr, melting of, effects of composition on electron-beam, 20: 29674
Mo–Zr, reactions with hydrogen and nitrogen, 20: 29632
MOLYBDENUM CARBIDES
properties of, at 2000°C, for use in thermionic converters, 20: 29729
MOLYBDENUM CHLORIDES
Fe–Mo_2C, growth and orientation of carbide precipitates in ferrite 20: 29726
MOLYBDENUM COMPLEXES
with α-carboxy-β-methyltropolone, composition of, spectrophotometric studies of, 20: 29179
MOLYBDENUM ISOTOPES Mo-99
decay of, conversion electron and positron spectra from, (E), 20: 30388
MOLYBDENUM OXIDES
MoO_3–UO_2–UO_3, phase studies at 750°C, 20: 29798
MOLYBDENUM SILICIDES
coating of, effects of, on oxidation resistance of graphite, 20: 29773
hardness and surface friction of, effects of temperature on, 20: 29771
properties as high-temperature coating, 20: 29650
BCN–$MoSi_2$, preparation and properties, 20: 29169
MOLYBDENUM STEEL
radiation effects on SA 212 B, 20: 30788(R) (ANL-7190, pp 176-88)
MOLYBDENUM SYSTEMS
Be–Mo–Si, compounds in, properties of, for use in aerospace technology, 20: 29770
C–Cr–Mo, phase studies and thermodynamics of, for use at high temperatures, 20: 29774
C–Mo, phase studies, stabilities, and thermodynamics of, at high temperatures, 20: 29774
C–Mo–Nb, phase studies and thermodynamics of, for use at high temperatures, 20: 29774
C–Mo–Nb–W–Zr, evaluation of protective coatings for, 20: 29651
C–Mo–Ta, phase studies and thermodynamics of, for use at high temperatures, 20: 29774
C–Mo–Ti–Zr, creep properties of TZC, 20: 29705(R) (NAS-CR-54973)
C–Mo–Ti–Zr, properties at high temperatures, 20: 29756
C–Mo–V, phase studies and thermodynamics of, for use at high temperatures, 20: 29774
Cr–Mo–Si, properties of, for use as protective coating on niobium and its alloys, 20: 29651
Mo–Ni–TiC, oxidation of, by air at 600 to 1300°C, effects of molybdenum content on, 20: 29653
Mo–Si, effects on wetting of graphite at high temperatures, 20: 29764
Mo–UO_2, electric conductivity at 25 to 1300°C, effects of composition and fabrication process on, 20: 29699 (CONF-650674-1)
MONAZITES
gamma spectra of, performance of germanium detectors for determining, 20: 29079 (AERE-M-1736)
MONEL
joining by brazing, soldering, or welding, 20: 29666 (RSIC-484)
machining properties of, 20: 29665 (RSIC-482)
surface treatments for types 400 and K-500, coating and mechanical, 20: 29706 (NASA-TM-X-53448)
MONKEYS
radiation dosimetry in *Mucaca mulatta*, proton, 20: 28928 (CONF-651109, pp 417-25)
radiation effects on *Macaca mulatta*, whole-body proton, 20: 28931 (CONF-651109, pp 624-35)
radiation effects on, pathological γ, 20: 28986
strontium-90 content and distribution in skeletons of, after intravenous and oral administration, 20: 28896
MONTE CARLO METHOD
for calculating fast neutron attenuation and thermalization in water, 20: 30340
MONTMORILLONITES
sorptive properties for fission products in waste solutions, 20: 29332 (ORNL-P-1811)
MOON
analysis of surface of, neutron activation methods for, 20: 29140
MOTORS
stators for electric, development of glass-coated, 20: 29366(R) (TID-22970, pp 375-91)
MULTIPLICATION FACTOR
effect of epithermal fission on, (E/T), 20: 30841
MUONIUM
chemical properties of, methods for studying, 20: 29177
reactions with ethylene, nitrous oxide, and oxygen, cross sections for, 20: 29177
reactions with organic compounds and mixtures, (E), 20: 29247
MUSCLES
radiation effects on solubilization of cholinesterase from plaice, by bacteria, 20: 28933
MUTATIONS
induced by nitrosomethylurea in Anacystis pigments, 20: 28958
radioinduced Anacystis pigment, uv and x, 20: 28958
radioinduced in barley, oats, and wheat, γ and neutron, 20: 28960
radioinduced in bacteriophage, uv, 20: 28969
radioinduced in Drosophila, 20: 28955

radioinduced in Drosophila, x, 20: 28956
radioinduced in *E. coli*, RBE for neutron-induced reversions, 20: 29002
radioinduced in mice, x, 20: 28957
radioinduced in plants, x, 20: 29018
radioinduced in *Salmonella typhimurium*, uv, 20: 28977

N

NAGASAKI
bomb survivors of, hematological disorders in, 20: 28876
NAPHTHALENE
radiolysis of, effects of metal ions and temperature on, 20: 29260
NAPHTHOL
yields from radiolysis of naphthalene, effects of metal ions and temperature on, 20: 29260
1-NAPHTHOL, 2-NITROSO-
arsenazo I–EDTA–nitrosonaphthol, uses for colorimetric microdetermination of uranium, 20: 29130
2-NAPHTHYLAMINE, *N*-PHENYL-
effects on radiation effects on polypropylene, 20: 29290
NATIONAL REACTOR TESTING STATION
environs monitoring, 1965, 20: 29434
NAVAL REACTORS
propulsion of, Joint Committee hearing on nuclear, 20: 30930
NEBULAE
radio emission from Crab, coherent plasma mechanism for, 20: 29880
NEMATODES
radiation effects on propagation of root-knot, in sweet potatoes, 20: 28942
NEODYMIUM
analysis of, for traces of praseodymium by activation methods, 20: 29082 (SGAE-CH-27/1966)
determination in pure cerium oxide, spectrographic, 20: 29095
determination in rocks, chemical spectrographic method for, 20: 29083(R) (UCRL-14767)
determination in standard igneous rocks G-1, W-1, and G-B by x-ray fluorescence, 20: 29101
determination in TBP extracts, spectrophotometric, 20: 29125
determination in uranium compounds, spectrographic, 20: 29129
NEODYMIUM ALLOYS
La–Nd, electric conductivity, magnetic susceptibility, and superconducting transition temperatures of, 20: 29753
NEODYMIUM AZIDES
preparation, 20: 29166
NEODYMIUM CARBIDES
hydrolysis of, gaseous products from, 20: 29220
NEODYMIUM CHLORIDES
thermal capacity of aqueous solutions of, at 25°C, 20: 29144 (IS-1355)
NEODYMIUM COMPLEXES
bromide, composition and stability of, 20: 29225
hexanitrocobaltate, preparation and composition of, effects of temperature on, 20: 29209
with EDTA, preparation, composition, and stability of, 20: 29222
with serine, stability of, 20: 29208
with 1,10-phenanthroline–thenoyltrifluoroacetone, preparation and composition of, 20: 29221
NEODYMIUM IONS
effects on fluorescence decay of samarium ions in lanthanum chloride crystals, 20: 30782
energy levels and crystal-field splittings in yttrium oxides, 20: 30744
spin-spin coupling in lanthanum ethyl sulfates, free induction signal from, (T), 20: 30778
NEODYMIUM ISOTOPES Nd-141
decay of, praseodymium-141 levels from, (E), 20: 30416
NEODYMIUM ISOTOPES Nd-142
deuteron reactions (d,p) at 10 to 12 Mev, energy levels from, (E), 20: 30517
meson (μ^-) capture by, x-ray spectra from, (E), 20: 29525 (CONF-660209-9)
NEODYMIUM ISOTOPES Nd-143
energy levels from neodymium-142 (d,p) reactions, (E), 20: 30517
energy levels of, (T), 20: 30350 (JINR-P-2682)
neutron capture by, neutron separation energy determination from, (E), 20: 30366
NEODYMIUM ISOTOPES Nd-144
meson (μ^-) capture by, x-ray spectra from, (E), 20: 29525 (CONF-660209-9)
production from neutron capture by neodymium-143 neutron separation energy determination from, (E), 20: 30366
NEODYMIUM ISOTOPES Nd-146
meson (μ^-) capture by, x-ray spectra from, (E), 20: 29525 (CONF-660209-9)
NEODYMIUM ISOTOPES Nd-148
deuteron reactions (d,p) at 10 to 12 Mev, energy levels from, (E), 20: 30517
NEODYMIUM ISOTOPES Nd-149
energy levels from neodymium-148 (d,p) and neodymium-150 (d,t) reactions, (E), 20: 30517
NEODYMIUM ISOTOPES Nd-150
deuteron reactions (d,p) and (d,t) at 10 to 12 Mev, energy levels from, (E), 20: 30517
NEODYMIUM ISOTOPES Nd-151
energy levels from neodymium-150 (d,p) reactions, (E), 20: 30517
NEODYMIUM NIOBATES
distribution in strontium molybdate single crystals, coefficients of, 20: 29746
NEODYMIUM NITRATES
thermal decomposition, 20: 29224
NEODYMIUM TITANATES
preparation and crystal structure of, 20: 29212
NEON
alkali-metal negative-ion dissociation in, cross sections for, (T), 20: 29947
glow discharges at 1 to 25 torr, between planar anode and hollow cathode, 20: 30173
hydrogen negative-ion dissociation in, cross sections for, (T), 20: 29947
neon–ion scattering at 200 ev to 4 kev, resonant electron capture in, (E), 20: 29944
proton reactions at 50 to 200 kev, secondary electron emission in, (E), 20: 29951
reactions with carbon monoxide, charge-exchange cross sections for, (E), 20: 29948
NEON IONS
reactions with carbon monoxide, charge-exchange cross sections for, (E), 20: 29948
scattering by neon at 200 ev to 4 kev, resonant electron capture in, (E), 20: 29944
NEON ISOTOPES Ne-20
helium-3 reactions (He-3,pγ) at 5.35 Mev, sodium-22 levels from, (E), 20: 30400
NEPTUNIUM
separation from aqueous and alcohol-containing hydrochlorine acid solutions by ion exchange, 20: 29358
separation from fission product solutions by ion exchange, 20: 29357
separation from irradiated uranium dioxide in chlorine trifluoride by volatilization, 20: 29330(R) (EURAEC-1601)
NEPTUNIUM BROMIDES
heat of formation, 20: 29229
NEPTUNIUM CHLORIDES
heat of formation, 20: 29229
NEPTUNIUM COMPLEXES
with fluorides and sulfates, properties and stability of, 20: 29148
NEPTUNIUM FLUORIDES
heat of formation, 20: 29229
NEPTUNIUM IODIDES
heat of formation, 20: 29229
NEPTUNIUM ISOTOPES Np-237
alpha emission from, use of p-n semiconductor detector for measuring, 20: 29552
metabolism of, 20: 28885
NEPTUNIUM ISOTOPES Np-239
electrophoretic properties, 20: 29351
separation from neutron-irradiated uranium using focusing chromatography, 20: 29351
NERVES
radiation effects on action potentials of, in cold-blooded animals, x, 20: 29021
NERVOUS SYSTEM
effects of ethanol on conditioned reflexes of dog, 20: 29009
radiation effects on conditioned reflexes in dogs, β, 20: 29009
NEUTRINOS
effects on biological processes, 20: 29402
interactions of, measurement of meson (μ) polarization from, 20: 30003
reactions of, experiments on, 20: 30002
NEUTRON BEAMS
collimating tube design for AARR, 20: 30787(R) (ANL-7190, pp 11-142)
effects on blood coagulation, 20: 28985
effects on solids, elastic explosions from, (T), 20: 30740
production of pulsed, design and operation of rotating mechanical chopper for, (E), 20: 29555
NEUTRON CROSS SECTIONS
calculation of, computer program development for, 20: 30791(R) (ANL-7204, pp 32-64)
calculation of, impossible Legendre coefficients in, 20: 30355 (ORNL-

P-2084)
library of, for reactor and shielding transport calculations, 20: 30723 (NAA-SR-11831)
measurement using boron monitors, errors in, (E), 20: 30352 (NASA-TR-R-240)
research on, (E/T), 20: 30360 (WASH-1068)
research on fast, review of, (E/T), 20: 30349 (JAERI-1102)
NEUTRON-DIFFRACTION ANALYSIS
furnace for, design of high-vacuum, 20: 29106
lectures on magnetic materials, 20: 30784
uses for phase evaluation for structure determination, 20: 29720
NEUTRON PHOTOGRAPHY
review, 20: 29627
NEUTRON SOURCES
design of discharge-tube, for well logging, 20: 29444(P)
design of, for use in activation analysis of petroleum products for chlorine, 20: 29116
use in age estimation by potassium–argon method, 20: 29413
use in well logging for chlorine in subsurface formations, 20: 29446(P)
use of, measurement methods for, 20: 29593
uses of 100- to 400-kv, in activation analysis, 20: 29118
NEUTRON SPECTRA
errors in time-of-flight, computer program for correcting, 20: 30344 (EUR-2779.e)
measurement of fast, from photon reactions with lead and uranium-238, (E), 20: 29529(R) (RPI-328-56, pp 94-112)
measurement using Bonner sphere and nuclear emulsions, performance for, 20: 29522 (CONF-651109, pp 286-305)
measurement using nuclear emulsions, techniques for fast, 20: 29848 (CONF-651109, pp 199-212)
NEUTRON SPECTROMETERS
chopper design and operation for, rotating mechanical, 20: 29555
data readout system for time-of-flight, design of, 20: 29566
operation of fast chopper, 20: 30325(R) (RPI-328-56, pp 113-34)
performance of Bonner sphere and nuclear emulsion, 20: 29522 (CONF-651109, pp 286-305)
performance of helium-3, for cyclotron environs monitoring, 20: 29846 (CONF-651109, pp 154-60)
NEUTRONS
absorption by lithium aluminate as burnable reactor poison, 20: 30865(P)
absorption by sodium, resonance, 20: 30358(R) (RPI-328-56, pp 1-48)
absorption by tungsten isotopes, resonance parameters from, 20: 30358(R) (RPI-328-56, pp 1-48)
absorption by uranium-235 at 0.1 to 2.3 ev, spin dependence of cross sections for, (E), 20: 30360 (WASH-1068)
absorption in unresolved resonance region, statistical treatment of, 20: 30420
age and slowing-down time in beryllium, (T), 20: 30333
age to absorption in water, calculation of average, 20: 30340
angular distributions from deuteron reactions (d,n) with lithium-7 at 0.8 and 1 Mev, (E), 20: 30402
capture by boron-10 and lithium-6 at 10.7 to 247.0 Bev, cross sections for, (E), 20: 30360 (WASH-1068)
capture by gold at 30 to 1500 kev, cross sections for, (E), 20: 30360 (WASH-1068)
capture by nuclei at 1 to 5 ev, gamma spectra from, (E), 20: 30385
capture by nuclei, neutron separation energy determination from, (E), 20: 30366
capture by rhenium-185 and -187, cross sections and resonance parameters for, (E), 20: 30360 (WASH-1068)
capture in stars, integrated flux distributions for, 20: 29887
density fluctuations in homogeneous multiplying media, angular correlations in, (T), 20: 30863
detection and measurement near Argonne ZGS, film for, 20: 29523 (CONF-651109, pp 639-46)
detection of, fast circuits for, 20: 29536
diffusion in nonisothermal media, (T), 20: 30322 (BNL-947)
diffusion parameters for uniform reactor matrices, (T), 20: 30851
disadvantage factor in uranium-water lattices, (E/T), 20: 30855
dosimetry of, performance of film and silicon diodes for, 20: 29518 (BNWL-SA-27)
effects of magnetic fields on, (T), 20: 30734(R) (TID-22970, pp 1-63)
effects on alkyl bromides, Finkelstein reaction for measuring partial organic retention in, 20: 29292
effects on barley, oat, and wheat seed and shoots, 20: 28960
effects on catalytic activity of silicon dioxide–silver sulfate–vanadium oxide in oxidation of sulfur dioxide, 20: 29291
effects on cobalt complexes, thermal annealing of recoil damage from, 20: 29259
effects on coke-type graphite at 425 to 1200°C, 20: 29812
effects on copper, electric conductivity changes and stored energy release in, 20: 29824
effects on density of uranium monocarbide at 750°C, 20: 29804(R) (EURAEC-1637)
effects on diphenylpicrylhydrazyl, EPR studies of, 20: 29289
effects on electric conductivity of cadmium oxide and nickel hydroxide, 20: 29821
effects on embrittlement of reactor structural steels, 20: 29825
effects on F centers in alkali metal halide crystals at 14 Mev, 20: 30739
effects on grain boundary cavitation and cracking in uranium, 20: 29807 (TRG-Report-325)
effects on hematopoiesis, effects of fractionated exposure on, 20: 28984
effects on man, biological, 20: 28970
effects on mechanical properties of molybdenum, 20: 29820
effects on metals, 20: 29819
effects on microstructure of plutonia–urania fuels, effects of preparation procedures on, 20: 29805(R) (NUMEC-3432-21)
effects on oxygen-doped germanium, oxygen-defect complexes for determining recovery from, (E), 20: 30742
effects on resistance strain gages, in-pile, 20: 29578 (EUR-2649.e)
effects on superconducting properties of indium and tin foils, 20: 30301
effects on tensile-strain fracture in EGCR-type graphite, 20: 29811
emission in proton reactions (p,n) with lithium-7 near threshold, (E), 20: 30525
energy of system of interacting, ground-state, (T), 20: 30523
flux densities in heterogeneous reactors, calculation of fast fission factor for, 20: 30859
flux distribution in Wigner-Seitz cell, transport codes for, 20: 30854
flux in Univ. of Florida Training Reactor, calculations of, 20: 30862
flux measurement using silver activation foils, corrections for, 20: 29539
form factors from inelastic electron interactions with deuterons, (E), 20: 30027
interaction strengths of, (T), 20: 30001
interactions with polarized protons at 23 Mev, spin correlation coefficients for, (E), 20: 30360 (WASH-1068)
interactions with mesons (π^-), peripheral mechanism in, (T), 20: 30081
interactions with protons in nuclear emulsions, mesons (π^+) and (π^-) charge asymmetry from, (E), 20: 30082
interactions with alpha particles at 6 to 30 Mev, differential cross sections for, (E), 20: 30390
interactions with protons at 20 to 28 Mev, total cross sections for, (E), 20: 30004
interactions with protons, total cross sections for, (E/T), 20: 30028
interactions with protons at 5 to 20 Bev/c, meson-exchange model for forward elastic, 20: 30039
interactions with mesons (K^+) at 5 to 20 Bev/c, meson-exchange model for forward elastic, 20: 30039
interactions with antiprotons at 5 to 20 Bev/c, meson-exchange model for forward elastic, 20: 30039
interactions with deuterons at 14 Mev, differential cross sections for elastic, (T), 20: 30050
kinetics in reactors, statistical theory of, 20: 30844
mass relative to protons, bound-state model for, 20: 30042
polarization from deuteron reactions (d,n) with tritium at 6.6 Mev, (E), 20: 30442
polarization in deuteron reactions (d,n) with nitrogen-15 at 1.6 to 3.0 Mev, (E), 20: 30427
reactions (n,α) with boron-11 at 14.2 Mev, lithium-8 production in, (E), 20: 30363
reactions (n,γ) with mercury near 5 Mev, gamma spectra from, (E), 20: 30358(R) (RPI-328-56, pp 1-48)
reactions (n,γ) with gold-197 and yttrium-89, cross sections for, (E), 20: 30360 (WASH-1068)
reactions (n,γ) with indium-113 and -115, cross sections for, (E), 20: 30360 (WASH-1068)
reactions (n,γ) with cobalt-59, gamma spectra from, (E), 20: 30360 (WASH-1068)
reactions (n,γ), with vanadium-51, manganese-55, copper-63, copper-65, and iodine-127 at 0.1 to 14 Mev, cross sections for, (T), 20: 30378
reactions ($n,n'\gamma$) with boron-10 and iron at 2 to 15 Mev, gamma spectra from, (E), 20: 30358(R) (RPI-328-56, pp 1-48)
reactions with curium-244 and plutonium-238 at 1 kev to 14 Mev, cross sections for, (T), 20: 30346 (GEMP-411)
reactions with lithium-6 and -7, cross sections for, (E), 20: 30360 (WASH-1068)
reactions with niobium, resonance parameters for, (E), 20: 30360 (WASH-1068)
reactions with oxygen isotopes, reactor power level monitoring with nitrogen-17 from, 20: 30938
reactions with plutonium-242, resonances and total cross sections for, (E), 20: 30360 (WASH-1068)
reactions with plutonium-241 at 20 to 74 ev, fission and resonance widths and cross sections for, (E), 20: 30360 (WASH-1068)
reactions with plutonium-240, resonances in, (E), 20: 30360 (WASH-1068)

reactions with thorium-230, resonance parameters for, (E), 20: 30360 (WASH-1068)
reactions with uranium-235 at 0.04 to 1.0 Mev, prompt neutron yields from fission, (E), 20: 30360 (WASH-1068)
reactions with uranium-235 at 0.01 to 40 ev, fission cross sections for, (E), 20: 30360 (WASH-1068)
reactions with uranium-235 at 1 to 20 ev, capture-to-fission ratios for, (E), 20: 30360 (WASH-1068)
reactions with uranium-233, capture and fission cross sections for, (E), 20: 30358(R) (RPI-328-56, pp 1-48)
reactions with uranium-238, computer program for calculating cross sections for, 20: 30356 (ORNL-TM-1448)
reactions with uranium-235 at 0.03 to 200 ev, cross sections for, (E/T), 20: 30342 (AERE-M-1670)
reactions with vanadium-50 at 3 to 60 kev, resonance parameters and total cross sections for, (E), 20: 30360 (WASH-1068)
resonance escape probability in arrayed cladded fuel lattice, Dancoff factor for, 20: 30842
reactions (n,n′γ) with aluminum, carbon, iron, lead, and oxygen at 14 Mev, cross sections for, 20: 30498
reactions (n,p) with nuclei at 14.8 Mev, cross sections for, (E), 20: 30394
reactions (n,p) with zirconium isotopes, cross sections for, (E), 20: 30418
reactions in food, radioactivity from, 20: 29599
reactions with even-even tin isotopes, total cross sections for, (E), 20: 30490
reactions with plutonium-239 at 30 kev to 14.7 Mev, ratio of asymmetric to symmetric fission in, (E), 20: 30404
reactions with plutonium-242 at 0.02 to 400 ev, total cross sections for, (E), 20: 30465
reactions with uranium-235 at 380 to 620 kev, fission cross sections for, (E), 20: 30425
resonance absorption integrals of, effects of resonance overlap on, 20: 30421
scattering by antimony, cadmium, copper, and tin at 1 Mev, cross sections for inelastic, (E), 20: 30383
scattering by beryllium-9 at 2.60 to 2.77 Mev, polarization from elastic, (E), 20: 30414
scattering by boron-10 and -11 in boron oxides, amplitudes for coherent, 20: 30335
scattering by cobalt-59, level spin assignments from, (E), 20: 30360 (WASH-1068)
scattering by fluorine-19, differential cross sections for, (E), 20: 30360 (WASH-1068)
scattering by gaseous and solid deuterated methane, (E), 20: 30360 (WASH-1068)
scattering by indium-113 and -115, cross sections for inelastic, (E), 20: 30360 (WASH-1068)
scattering by iron at 0.45 to 2.28 Mev, cross sections for elastic and inelastic, (E), 20: 30417
scattering by liquid lead, (E), 20: 30360 (WASH-1068)
scattering by liquid lead, analysis of inelastic, (T), 20: 30347(R) (IDO-17147, pp 13-28)
scattering by magnetite, temperature effects on magnon spectra from, (E), 20: 30765
scattering by manganese at 700 to 1200 kev, cross sections for, (E), 20: 30360 (WASH-1068)
scattering by monatomic gases, differential cross sections for, (T), 20: 30337
scattering by nuclei, technique for measuring resonance, 20: 30358(R) (RPI-328-56, pp 1-48)
scattering by polyethylene and water at 0.83 to 1.8 ev, differential cross sections for inelastic, (E), 20: 30334
scattering by silicon at 0.57 to 2.28 Mev, cross sections for elastic, (E/T), 20: 30345 (EUR-2798.e)
scattering of, lectures on inelastic and magnetic, 20: 30784
shielding of, fabrication of organic materials for, 20: 30732(P)
slowdown in liquid argon, analysis of, (T), 20: 30166 (NYO-3326-13)
spectra in heavy water and polyethylene, time-dependent, (E), 20: 30324(R) (RPI-328-56, pp 52-93)
spectra in heavy-water natural uranium lattice, angular, (E), 20: 30846
thermalization in nonisothermal media, (T), 20: 30322 (BNL-947)
thermalization in reactors, space-dependent, (T), 20: 30861
thermalization in heterogeneous systems, approximate treatment of, 20: 30864
thermalization in graphite and graphite-moderated enriched uranium systems, time-dependent, (E/T), 20: 30327
thermalization of, research on, 20: 30324(R) (RPI-328-56, pp 52-93)
transport in adjacent semi-infinite media, time-dependent monoenergetic, (T), 20: 30339
transport in reactor systems, 20: 30804
transport in reactors, equations for, 20: 30862
transport in slab geometry, numerical integration of equations for, 20: 30326
transport in three-dimensional rectangular geometry, computer program for, 20: 30726 (TID-22964)
transport of, computer program for P_n multigroup scattering matrices in, 20: 30323 (ORNL-TM-1537)
transport of, standardization of computer programs for, 20: 30721 (EUR-2778.e)
transport theory for, vacuum boundary conditions for spherical harmonic method in, 20: 30332
transport theory for, dispersion law of linear Boltzmann equation in, 20: 30338
use for soil density and moisture content determinations, for efficiency of probes, 20: 29506
use for soil density and moisture-content determinations, efficiency of air-gap and direct-transmission methods for, 20: 29505
use in paving-mixture and soil density and moisture determinations, conference on, 20: 29504

NEUTRONS, DELAYED
effects on reactor stability, (T), 20: 30850

NEUTRONS, FAST
attenuation and thermalization in water, (E/T), 20: 30340
detection and measurement of, instrumentation development for, 20: 29529(R) (RPI-328-56, pp 94-112)
dosimetry, 20: 29078(R) (AD-633252)
dosimetry of, performance of film and silicon diodes for, 20: 29518 (BNWL-SA-27)
dosimetry of, pulse shape discrimination in scintillator, 20: 29524 (CONF-651109, pp 647-52)
effects of 200-kev, on phage induction in *E. coli*, RBE for, 20: 29002
effects of 200-kev, on chromosomes, RBE for, 20: 29002
effects on chromosomal bridges at anaphase in barley seeds and Tradescantia, 20: 29031
effects on cracking in type 347 stainless steel, 20: 29618(R) (GEAP-4982)
effects on dimensional changes in furfuryl alcohol-impregnated graphite, 20: 29813
effects on DNA synthesis in pea seedlings, 20: 28989
effects on fission-gas-generation and temperature in plutonia–urania, profiles of, 20: 29618(R) (GEAP-4982)
effects on mechanical and thermal properties of beryllium oxides, 20: 29810
effects on single crystals of strontium titanate, 20: 29826
effects on structure of plutonia–urania, 20: 29618(R) (GEAP-4982)
effects on temperature of plutonia–urania, effects of diametral gap size on, 20: 29618(R) (GEAP-4982)
photoproduction on lead and uranium-238, spectra of, (E), 20: 29529(R) (RPI-328-56, pp 94-112)
reactions with gadolinium at 2.4 to 15.7 Mev, total cross sections for, (E), 20: 30419
reactions with niobium-93 at 1.7 and 2.1 Mev, differential gamma production cross sections for, (E/T), 20: 30360 (WASH-1068)
reactions with nuclei, review of cross section research on, (E/T), 20: 30349 (JAERI-1102)
reactions with plutonium-239 and uranium-235 and -238 at 1.09, 1.7, and 2.1 Mev, gamma spectra from, (E), 20: 30360 (WASH-1068)
scattering by cadmium-111 at 14.07 to 14.78 Mev, activation cross sections for, (E), 20: 30360 (WASH-1068)
scattering by iron at 0.45 to 2.28 Mev, cross sections for elastic and inelastic, (E), 20: 30417
scattering by nuclei at 4.0 Mev, polarization angular distributions from, (E), 20: 30360 (WASH-1068)
scattering by polyethylene and zirconium hydride at 0.238 to 0.570 ev, cross sections for inelastic, (E), 20: 30325(R) (RPI-328-56, pp 113-34)
spectroscopy of, performance of nuclear emulsions for, 20: 29848 (CONF-651109, pp 199-212)

NEUTRONS, FISSION
age in water, effects of spin polarization on, 20: 30329
effects on microstructure of silicon transistors, energy dependence of, 20: 29579 (NAA-SR-11887)

NEUTRONS, PROMPT
decay constants for, method for measurement of, 20: 30848
decay constants of, prediction by point-model kinetic theory, 20: 30862
kinetics in fast core of fast-thermal reactor, variational method for, 20: 30852
yields from uranium 235 neutron fission, (E), 20: 30360 (WASH-1068)

NEUTRONS, THERMAL
capture by gold-197, production of high-specific-activity gold-198 in, 20: 29610
distribution in water, from anisotropic fast source, (E/T), 20: 30340
effects on fission-gas-generation and temperature in plutonia–urania, profiles of, 20: 29618(R) (GEAP-4982)

effects on stainless steel-clad urania fuel elements, 20: 29806 (ORNL-TM-1511)
effects on superconducting properties of aluminum–niobium alloys and vanadium silicides, (E), 20: 30260
reactions (n,γ) with mercury near 5 Mev, gamma spectra from, (E), 20: 30358(R) (RPI-328-56, pp 1-48)
reactions (n,γ) with tungsten isotopes, gamma spectra from, (E), 20: 30360 (WASH-1068)
reactions (n,γ) with beryllium-10, cross sections for, (E), 20: 30347(R) (IDO-17147, pp 13-28)
reactions (n,γ) with gold-197, gold-198 levels from, (E), 20: 30409
reactions (n,γ) with hafnium isotopes, gamma spectra and energy levels from, (E), 20: 30466
reactions (n,γ) with titanium-48, time invariance of nuclear forces from, 20: 30505
reactions with thorium-229, product mass distribution from fission, 20: 30373
reactions with uranium-235 at 0.003 to 0.3 ev, fission, (E), 20: 30513
reactions with uranium-233 and -235, yields of xenon-133 and -135 from fission, 20: 30533
scattering by ideal gases in acoustical fields, total cross sections for, (T), 20: 30256
scattering by polycrystalline aluminum, one-phonon coherent, (T), 20: 30745
scattering by water, model for, (E/T), 20: 30330
scattering of, time-dependent correlation functions for, (T), 20: 30336
spectra in water near temperature discontinuity, (E/T), 20: 30331
spectra in Yugoslav heavy water reactor, 20: 30939
transport equation for, P_1 analytical solution of energy- and space-dependent, 20: 30328
use for asphalt-content determination in paving mixture, bombardment-counting-technique for, 20: 29509

NICKEL
alpha elastic scattering at 24.7 Mev, optical-model analysis of, (E/T), 20: 30413
content in rocks, effects of clay content on, 20: 29417
effects on copper or silver infiltrants in graphite, 20: 29764
effects on intergranular corrosion of 20Cb stainless steel, 20: 29643
erosion by water at 70°F, effects of annealing on cavitation, 20: 29640 (NP-16048)
fatigue of cold-rolled, α-ray-diffraction studies of, 20: 29623(R) (TID-22970, pp 121-256)
hyperfine field at iron-57 nuclei in lattice of, temperature dependence of, 20: 30750
magnetization of, distribution of internal, (T), 20: 30734(R) (TID-22970, pp 1-63)
spin wave dispersion in, s-d interaction and Fermi surface for, 20: 30775
surface treatments for, coating and mechanical, 20: 29706 (NASA-TM-X-53448)

NICKEL ALLOYS
joining by brazing, soldering, or welding, 20: 29666 (RSIC-484)
joining by mechanical fastening, 20: 29667 (RSIC-509)
machining properties of, 20: 29665 (RSIC-482)
surface treatments for, coating and mechanical, 20: 29706 (NASA-TM-X-53448)
Al–Cr–Co–Fe–Mo–Ni–Ti, joining of Udimet 500 and 700, by mechanical fastening, 20: 29667 (RSIC-509)
Al–Cr–Co–Fe–Mo–Ni–Ti, surface treatments for Udimet 500 and 700, coating and mechanical, 20: 29706 (NASA-TM-X-53448)
Al–Cr–Co–Mo–Ni–Ti, joining of M-252, by mechanical fastening, 20: 29667 (RSIC-509)
Al–Cr–Co–Mo–Ni–Ti, surface treatments for Astroloy, coating and mechanical, 20: 29706 (NASA-TM-X-53448)
Al–Cr–Co–Mo–Ni–Ti–V–Zr, surface treatments for IN-100, coating and mechanical, 20: 29706 (NASA-TM-X-53448)
Al–Cr–Co–Ni–Nb–Ti–W, surface treatments for Mar-M 200, coating and mechanical, 20: 29706 (NASA-TM-X-53448)
Al–Cr–Fe–Mo–Ni–Ti–W, joining of D-979, by mechanical fastening, 20: 29667 (RSIC-509)
Al–Cr–Ni–Ti, corrosion by trichloroethylene, tracer studies of, 20: 29655
Al–Ni–Nb, crystal structure of M-phase, (E/T), 20: 30734(R) (TID-22970, pp 1-63)
Al–Ni–U, corrosion by steam, 20: 30794(R) (IDO-17147, pp 1-12)
Au–Ni, elastic constants of single-crystal, effects of pressure on, 20: 29623(R) (TID-22970, pp 121-256)
Be–Ni, analysis for impurities in, development of electron microprobe for, 20: 29083(R) (UCRL-14767)
Cr–Mo–Ni, compatibility with plutonium and uranium carbides, 20: 30790(R) (ANL-7204, pp 1-31)
Cr–Ni, corrosion by trichloroethylene, tracer studies of, 20: 29655
Cr–Ni–stainless steel 304, corrosion in Saxton steam generator, 20: 30884(R) (WCAP-3269-16)
Cu–Ni, erosion by water at 70°F, effects of annealing on cavitation, 20: 29640 (NP-16048)
Cu–Ni–Nb, phase studies on, 20: 29764
Cu–Ni–Ta, phase studies on, 20: 29764
Cu–Ni–W, properties of composite-type, 20: 29624(R) (TID-22970, pp 257-329)
Fe–Mn–Ni, martensitic reaction nucleation rate in, 20: 29623(R) (TID-22970, pp 121-256)
Fe–Ni–W, deformation properties of dispersed and sintered composites of, elastic and plastic, 20: 29686
Fe–Ni–W, properties of composite-type, 20: 29624(R) (TID-22970, pp 257-329)
Fe–Ni–W, zone refining of cemented, production of tungsten sheet bars by, 20: 29688
Ni–U, metallographic tests on arc melted, 20: 29775

NICKEL FLUORIDES
thermodynamic properties of, emf measurements of, 20: 29215

NICKEL HYDROXIDES
radiation effects on electric conductivity of, neutron, 20: 29821

NICKEL IONS
effects on hydrolysis of polyphosphates, 20: 29152

NICKEL ISOTOPES
proton elastic scattering at 6.9 Mev, differential cross sections and polarization from, (T), 20: 30495

NICKEL ISOTOPES Ni-56
yield in alpha and proton reactions with copper, 20: 30531

NICKEL ISOTOPES Ni-58
alpha scattering at 21 Mev, angular distributions from, (E/T), 20: 30353(R) (ORNL-3940, pp 1-61)
electron inelastic scattering by, level excitation in, (E), 20: 30360 (WASH-1068)
proton elastic scattering at 40 Mev, cross sections for, (E/T), 20: 30353(R) (ORNL-3940, pp 1-61)
proton inelastic scattering at 40 Mev, cross sections for, (E/T), 20: 30353(R) (ORNL-3940, pp 1-61)

NICKEL ISOTOPES Ni-60
deuteron elastic scattering at 34.4 Mev, angular distributions from, (E/T), 20: 30353(R) (ORNL-3940, pp 1-61)
deuteron elastic scattering at 13.6 Mev, cross section for, (E), 20: 30497
electron inelastic scattering by, level excitation in, (E), 20: 30360 (WASH-1068)
proton elastic scattering at 40 Mev, cross sections for, (E/T), 20: 30353(R) (ORNL-3940, pp 1-61)
proton inelastic scattering at 40 Mev, cross sections for, (E/T), 20: 30353(R) (ORNL-3940, pp 1-61)
proton inelastic scattering at 17.8 Mev, cross sections for, (T), 20: 30437

NICKEL ISOTOPES Ni-62
neutron scattering at 4.0 Mev, polarization angular distributions from, (E), 20: 30360 (WASH-1068)

NICKEL ISOTOPES Ni-64
proton reactions (p,n) at 100 to 400 Mev, excitation functions for, 20: 30464

NICKEL OXIDES
radioinduced blistering of polycrystalline, helium ion, (E), 20: 29816
NiO–Sc_2O_3, phase studies, 20: 29168

NICKEL SYSTEMS
Be–B–Ni, crystal structure of compounds in, 20: 29795
Mo–Ni–TiC, oxidation of, by air at 600 to 1300°C, effects of molybdenum content on, 20: 29653
Ni–ThO_2, diffusion of chromium in, for corrosion protection, 20: 29748
Ni–ThO_2, joining by brazing, soldering, or welding TD nickel, 20: 29666 (RSIC-484)
Ni–ThO_2, surface treatments for TD nickel, coating and mechanical, 20: 29706 (NASA-TM-X-53448)

NICOTINIC ACID
effects on cholesterol and specific radioactivity in rabbit liver, 20: 28895

NIMONIC-75
joining by brazing, soldering, or welding, 20: 29666 (RSIC-484)
machining properties of, 20: 29665 (RSIC-482)

NIMONIC-80
joining by brazing, soldering, or welding, 20: 29666 (RSIC-484)
machining properties of, 20: 29665 (RSIC-482)

NIMONIC-90
joining by brazing, soldering, or welding, 20: 29666 (RSIC-484)
machining properties of, 20: 29665 (RSIC-482)

NIOBIUM
analysis of oxygen, method for, 20: 29108
coatings for, evaluation of protective, 20: 29651
compatibility of coating of, with uranium carbide–zirconium carbide thermionic diode at 1800 to 2500°C, 20: 29820
compatibility with plutonium carbides at 1200 to 1400°C, 20: 29820
current density in contact points of oxidized wires of superconducting, (E),

20: 30277
deformation properties of, electron microscopic study of plastic, 20: 29761
determination in aqueous solutions, design of oxyacetylene burner for measuring sensitivity of spectrophotometric, 20: 29083(R) (UCRL-14767)
magnetic flux pinning in superconducting thin films of, (E), 20: 30278
magnetic properties of superconducting, effects of lattice defects on, 20: 30253 (CEA-R-2808)
mechanical properties of single-crystal, as function of orientation, 20: 29762
neutron resonance parameters, (E), 20: 30360 (WASH-1068)
oxidation kinetics, 20: 29644
properties as high-temperature coating, 20: 29650
properties of, at 2000°C, for use in thermionic converters, 20: 29729
radiation effects on, for use as sensor material, 20: 29486(R) (NASA-CR-54964)
reactions with aluminum oxides at 1800 to 2200°K, kinetics of, 20: 29174
refining in electron-beam melting furnace, 20: 29634
separation from fission product solutions by ion exchange, 20: 29357
separation from irradiated uranium dioxide in chlorine trifluoride by volatilization, 20: 29330(R) (EURAEC-1601)
separation of nitrogen and oxygen from, degasification processes for, 20: 29633
sorptive properties for nitrogen at 10^{-5} to 10^{-8} torr and 1400 to 1900°K, 20: 29178
strain aging and London yielding of single crystals of, impurity effects on, 20: 29790
superconducting properties of high-purity, (E), 20: 30315
thermal diffusion of oxygen in, 20: 29769

NIOBIUM ALLOYS
Mo–Nb–V, fabricability, strength, and weldability of, 20: 29763
Al–Cr–Co–Ni–Nb–Ti–W, surface treatments for Mar-M 200, coating and mechanical, 20: 29706 (NASA-TM-X-53448)
Al–Cu–Nb, phase studies on, 20: 29764
Al–Nb, intermetallic compounds in, properties of, for use in aerospace technology, 20: 29770
Al–Nb, radiation effects on superconducting properties of boron- and uranium-doped, thermal neutron, (E), 20: 30260
Al–Ni–Nb, crystal structure of M-phase, (E/T), 20: 30734(R) (TID-22970, pp 1-63)
Be–Nb, intermetallic compounds in, properties of, for use in aerospace technology, 20: 29770
Cu–Ni–Nb, phase studies on, 20: 29764
Hf–Nb–Ti, fabricability, strength, and weldability of, 20: 29763
Hf–Nb–W–Y, fabricability, strength, and weldability of, 20: 29763
Hf–Nb–W–Y, tensile properties of C-129Y, effects of welds on, 20: 29712(R) (WANL-PR-(P)-009)
Mo–Nb, crystal structure and electric conductivity of, 20: 29766
Mo–Nb–Ti, evaluation of protective coatings for, 20: 29651
Mo–Nb–Ti–Zr, creep properties of niobium-modified TZM, 20: 29705(R) 20: 29705(R) (NAS-CR-54973)
Mo–Nb–V–Zr, tensile properties of B-66, effects of welds on, 20: 29712(R) (WANL-PR-(P)-009)
Nb–Pd, crystal structure and electric conductivity of, 20: 29766
Nb–Sn, preparation of multilayer continuous intermediate phase wires of, 20: 29781
Nb–Sn, superconductivity of multilayer continuous intermediate phase wires of, effects of heat treatments on, 20: 29781
Nb–Sn, superconducting transition temperatures of $NbSn_2$ and Nb_6Sn_5, 20: 30279
Nb–Ta, deformation in tantalum-base, mechanisms of thermally activated, 20: 29724
Nb–Ta, superconducting current distribution in sheets of, 20: 30273
Nb–Ta–V, availability, properties, and uses of, 20: 29760
Nb–Ta–W, tensile properties of SCb-291, effects of welds on, 20: 29712(R) (WANL-PR-(P)-009)
Nb–Ta–W–Zr, fabricability, strength, and weldability of, 20: 29763
Nb–Ta–W–Zr, tensile properties of FS-85, effects of welds on, 20: 29712(R) (WANL-PR-(P)-009)
Nb–Ta–W–Zr, weldability of FS-85, effects of oxygen contamination on, 20: 29712(R) (WANL-PR-(P)-009)
Nb–Ti–Zr, phase studies on, at 570 to 1100°C, 20: 29785
Nb–Ti–Zr, superconductivity of, effects of composition on, 20: 29784
Nb–Ti–Zr, superconductivity of, effects of cold working and heat treatments on, 20: 29787
Nb–Ti–Zr, superconductivity of, effects of microstructure on, 20: 29788
Nb–U, casting of, testing of products from, 20: 29803
Nb–U, mechanical properties, 20: 29803
Nb–U, metallographic tests on arc melted, 20: 29775
Nb–W–Zr, fabricability, strength, and weldability of, 20: 29763
Nb–W–Zr, tensile properties of Cb-752, effects of welds on, 20: 29712(R) (WANL-PR-(P)-009)
Nb–Zn, properties as high-temperature coating, 20: 29650
Nb–Zr, coating with silicon by fluidized-bed process, 20: 29630
Nb–Zr, corrosion by mercury at 593 to 703°C, 20: 29646
Nb–Zr, crystal structure and electric conductivity of, 20: 29766
Nb–Zr, erosion by mercury, water, and bismuth–lead alloy, cavitation, 20: 29640 (NP-16048)
Nb–Zr, superconductivity of, effects of cold working and heat treatments on, 20: 29787
Nb–Zr, superconductivity of, effects of microstructure on, 20: 29788
Nb–Zr, superconductivity of, effects of cold working and heat treatments on, 20: 29789
Nb–Zr, superconducting critical current density of wires of, (E), 20: 30267(T)
Nb–Zr, superconducting critical fields of, angular dependence of upper, (E), 20: 30270
Nb–Zr, surface current effects in superconducting, 20: 30280

NIOBIUM BORIDES
fabrication and properties of, for use at high temperatures, 20: 29772

NIOBIUM CARBIDES
effects on properties of graphite, with and without copper and silver infiltration, 20: 29764
properties of, at 2000°C, for use in thermionic converters, 20: 29729
reactions with niobium oxide–tungsten oxide and niobium oxide–tungsten carbide to form niobium–tungsten alloy, 20: 29677
thermoelectric emission in cesium vapor, 20: 29800

NIOBIUM ISOTOPES Nb-90
energy levels from molybdenum-90 decay, multipolarity, parity, and spin of, (E), 20: 30388

NIOBIUM ISOTOPES Nb-91
energy levels in, from proton reactions (p,n) with zirconium-91 at 12.35 Mev, 20: 30480

NIOBIUM ISOTOPES Nb-93
neutron reactions at 1.7 and 2.1 Mev, differential gamma production cross sections for, (E/T), 20: 30360 (WASH-1068)
neutron scattering at 4.0 Mev, polarization angular distributions from, (E), 20: 30360 (WASH-1068)

NIOBIUM ISOTOPES Nb-95
beta decay of, β-γ circular polarization correlations in, (E), 20: 30543
content in fallout in USSR, 1962, 20: 29406 (NP-14719)
content in fallout from Chinese nuclear tests, 20: 29423

NIOBIUM OXIDES
crystal structures of, Nb_2O_5, 20: 29728
Nb_2O_5–WC, reduction to niobium–tungsten alloy by niobium carbide, 20: 29677
Nb_2O_5–WO_3, reduction to niobium–tungsten alloy by niobium carbide, 20: 29677
PbO–Nb_2O_5, phase studies, 20: 29794

NIOBIUM SYSTEMS
C–Mo–Nb, phase studies and thermodynamics of, for use at high temperatures, 20: 29774
C–Mo–Nb–W–Zr, evaluation of protective coatings for, 20: 29651
C–Nb–W, phase studies and thermodynamics of, for use at high temperatures, 20: 29774
C–Nb–W–Y–Zr, tensile properties of D-43Y, effects of welds on, 20: 29712(R) (WANL-PR-(P)-009)
C–Nb–W–Zr, evaluation of protective coatings for, 20: 29651
C–Nb–W–Zr, fabricability, strength, and weldability of, 20: 29763
C–Nb–W–Zr, tensile properties of D-43, effects of welds on, 20: 29712(R) (WANL-PR-(P)-009)
Hf–Nb–N, precipitation hardening in, effects of heat treatments on, 20: 29759
Sb–Nb–Te, phase studies, 20: 29717

NITRATES
content in Amazon River, effects on biology, chemistry, and hydrography of Atlantic Ocean, 20: 28878 (NYO-1918-138)
content in Atlantic Ocean, measurements on, 20: 28877 (NYO-1918-124)
content in Atlantic Ocean, measurements on, 20: 28878 (NYO-1918-138)

NITRIC ACID
HCl–HNO_3, solvent properties for cesium-137 in fallout samples, 20: 29081 (NP-14705)
HF–HNO_3, solvent properties for cesium-137 in fallout samples, 20: 29081 (NP-14705)

NITRITE IONS
yields from gamma radiolysis of aqueous solutions of 2-propanol, 20: 29254

NITRITES
content in Atlantic Ocean, measurements on, 20: 28877 (NYO-1918-124)
content in Atlantic Ocean, measurements on, 20: 28878 (NYO-1918-138)

NITRO COMPOUNDS
reduction of, effects of uv radiation on catalytic activity of platinum in, 20: 29304

NITROGEN
content in Atlantic Ocean, measurements on, 20: 28878 (NYO-1918-138)

determination as impurity in ultrapure gases, mass spectrometric, 20: 29083(R) (UCRL-14767)
determination in petroleum, activation, 20: 29139
determination of, by neutron activation methods, 20: 29078(R) (AD-633252)
effect on production of powdered rhenium from rhenium tetrammine chloride, 20: 29672
effects of flowing, on volatilization of fission products from irradiated uranium(IV-VI) oxides, 20: 29211
effects of impurities of, on mechanical properties and structure of tungsten single crystals, 20: 29793
effects of, on corrosion of zirconium-base alloy by steam, 20: 29660(R) (GEAP-4960)
electron reactions with, primary and afterglow emission from, 20: 29929
helium reactions with, electron kinetic energy from ionization in, (E), 20: 29927
hydrogen ion reactions with, lifetime of n = 3 hydrogen states from, (E), 20: 29930
leakage in pressure vessels, mechanism and rate, 20: 30810
photon reactions (γ,p) at 4.1 to 6.2 Bev, (E), 20: 30432
production of rotating plasma of, in crossed fields, (E), 20: 30582
proton elastic scattering at 12.6 to 13.6 Mev, angular distribution of polarization from, (E), 20: 30457
proton reactions at 50 to 200 kev, secondary electron emission in, (E), 20: 29951
radiosensitivity effects on organoleptic properties of fish, gamma, 20: 29583(R) (TID-22515)
radon-219 and radon-220 decay in, properties of recoils from, 20: 29325
reactions with air species above 1000°K, 20: 29146 (SC-R-66-885)
reactions with calcium, magnesium, molybdenum, tantalum, and zirconium, combustion, 20: 29641(R) (SC-DC-1691)
reactions with molybdenum–zirconium alloys, nitride formation in, 20: 29632
reactions with tantalum in sputtering, properties of films formed by, 20: 29745
separation from niobium and tantalum, degasification processes for, 20: 29633
separation from rare gases, use of tritium-metal sponge as gettering agent for, 20: 29329 (ANL-7128)
sorption by liquid iron, effects of surface-active elements on, 20: 29623(R) (TID-22970, pp 121-256)
sorption by niobium at 10^{-5} to 10^{-8} torr and 1400 to 1900°K, 20: 29178
thermal diffusion in refractory metals, 20: 29769

NITROGEN ISOTOPES N-13
energy spectra of 1 p shell, determination using Hamada-Johnston potential, (E/T), 20: 30354(R) (ORNL-3940, pp 62-9)

NITROGEN ISOTOPES N-14
alpha elastic and inelastic scattering at 40.5 Mev, angular distributions for, (E), 20: 30450
energy levels from helium-3 reactions (He-3,α) with nitrogen-14 at 39.8 Mev, (E), 20: 30438
energy levels from carbon-13 (d,n) and (He-3,d) reactions, 20: 30481
energy levels from lithium-6 and -7 reactions with boron-10 and -11, 20: 30519
energy spectra of 1 p shell, determination using Hamada-Johnston potential, (E/T), 20: 30354(R) (ORNL-3940, pp 62-9)
production in lithium-6 and -7 reactions with boron-10 and -11, 20: 30519
reactions (N-14,N-13) with boron-10 and calcium-40 at 8 to 16 Mev, cross sections for, (E/T), 20: 30353(R) (ORNL-3940, pp 1-61)
scattering by samarium-152 and tungsten-186, Coulomb excitation from inelastic, (E), 20: 30488

NITROGEN ISOTOPES N-15
alpha elastic and inelastic scattering at 40.5 Mev, angular distributions for, (E), 20: 30450
determination in inorganic and organic compounds, mass-spectrometric, 20: 29131
deuteron reactions (d,n) at 1.6 to 3.0 Mev, neutron polarization from, (E), 20: 30427
energy levels of, (E/T), 20: 30353(R) (ORNL-3940, pp 1-61)
helium-3 reactions (He-3,α) at 39.8 Mev, nitrogen-14 levels from, (E), 20: 30438
production in lithium-6 and -7 reactions with boron-10 and -11, 20: 30519
spectra in ATP, effects of magnesium and zinc on, 20: 29083(R) (UCRL-14767)

NITROGEN ISOTOPES N-16
energy levels from lithium-6 and -7 reactions with boron-10 and -11, 20: 30519
production in lithium-6 and -7 reactions with boron-10 and -11, 20: 30519

NITROGEN ISOTOPES N-17
energy levels from lithium-6 and -7 reactions with boron-10 and -11, 20: 30519

NITROGEN OXIDES
determination in atmosphere using radioactive clathrate techniques, 20: 29142
effects on hydrogen yields from gamma radiolysis of cyclohexane, 20: 29270
effects on radioinduced polymerization of solid methane, 20: 29314
electron energy levels of, determination of, using infrared lasers, (E), 20: 30734(R) (TID-22970, pp 1-63)
helium atom reactions with, electron kinetic energy from ionization in, (E), 20: 29927
reactions with muonium, cross sections for, 20: 29177
reactions with scandium chlorides, 20: 29214
spectra of, *L*-uncoupling effects on EPR, 20: 29194

NITROGEN SYSTEMS
C–N–V, phase studies, 20: 29749
Hf–Nb–N, precipitation hardening in, effects of heat treatments on, 20: 29759
H–N, effects on melting points of plutonia–urania, 20: 29621(R) (NYMEC-3524-17)
N–U, metallographic tests on arc melted, 20: 29775

NORTH AMERICA
fallout monitoring, 1965, 20: 29428
fallout monitoring, 1965, 20: 29431
fallout monitoring, 1965, 20: 29434
geochronology, 20: 29397 (NAS-NRC-1276)

NORWAY
cesium-137 content in man, meat, and milk in, 1962 through 1965, 20: 29432

NORWEGIAN SEA
radioactivity of organisms at bottom of, variations in, 20: 29424

NOZZLES
design for pressurizers and steam generators, stress analysis for, (T), 20: 30928
testing converging-diverging, 20: 29974(R) (ANL-7190, pp 167-75)

NPD REACTOR
performance evaluation, 20: 30891

NRU REACTOR
operation procedures for, 20: 30935

NRX REACTOR
operation procedures for, 20: 30935

NUCLEAR AIRCRAFT
design of lighter-than-air, (T), 20: 30927

NPD REACTOR
environs monitoring, January 1966, 20: 29053 (NP-15951)

NUCLEAR EMULSIONS
cosmic-particle reactions with heavy nuclei in, slow particle production in high-energy, 20: 30371
meson (K$^-$) reactions at 1.5 Bev/c with heavy nuclei in, $_{\Lambda}He^7$ and $_{\Lambda}Li^7$ production in, 20: 30368
meson (π^-) reactions at 3.8 Bev, slow meson (π) production in, (E), 20: 30501
mesons (K$^-$) reactions at 1.5 Bev, Λ-hyperfragment production in, (E), 20: 30448
performance for fast neutron spectra measurements, 20: 29848 (CONF-651109, pp 199-212)
performance for particle detection, 20: 29534
performance for stray neutron spectra, 20: 29522 (CONF-651109, pp 286-305)
proton reactions at 12.8 Bev with heavy nuclei in, angular distributions of secondaries from, (E), 20: 30364
proton reactions at 9 Bev with, slow meson (π^+) production from, (E), 20: 30370
proton reactions at 10 to 20 Bev with, emission of fast helium nuclei, (E), 20: 30496
use in measurement of hyperon (Λ^0) magnetic moment, 20: 29534

NUCLEAR MAGNETIC RESONANCE
book: *Nuclear Magnetic Resonance Methods*, 20: 29498
measurement in solids, stable autodyne pickup circuit for, 20: 29492

NUCLEAR MODELS
description of, combining cluster model and shell model, 20: 30377
for energy level E2 transitions of even-even nuclei, 20: 30372
theory for excited-core, 20: 30484

NUCLEAR MODELS (SHELL)
energy levels in, fractional parentage coefficients for f^3 and f^4 configurations of, 20: 30365
energy levels in, elimination of spurious, 20: 30514
fission theory as Markov process in, corrections for, 20: 30428
nucleon interactions in $2s_{1/2}1d_{3/2}$ shell, surface delta interaction approximation of, 20: 30423
reaction matrix for, calculation of effective, 20: 30354(R) (ORNL-3940, pp 62-9)
use in description of tin isotopes, (T), 20: 30521

NUCLEAR POWER
uses in industrial processes, 20: 30786(R) (ANL-7190)

NUCLEAR POWER PLANTS
construction of, use of network planning technique in, 20: 30907
containment costs for, 20: 30815
containment system for, pressure-suppression, 20: 30833(P)
control system for, load-response, 20: 30832(P)
cost studies on large steam-electric, 20: 30875(R) (ANL-7190, pp 143-55)
design for once-through steam generation, 20: 30931(P)
design using pressurized water reactor and steam generator, 20: 30911(P)
development and economics of, for communications satellites, 20: 29608
development in United States, 20: 30885
efficiency using liquid-metal MHD power cycles, 20: 29980
materials for, review, 20: 30815
NUCLEAR REACTIONS
data comparators for analyzing, design of digital, 20: 29485 (EUR-2799.e)
kinematic study of, Fano-Racah formalism for, 20: 30396
nucleon transfer in, isobaric spin in, (T), 20: 30343 (COO-1371-30)
particle production in, fluctuations in differential polarizations of, (T), 20: 30397
theory for two nucleon pickup and stripping, 20: 30483
theory of inelastic scattering of identical nuclei, 20: 30493
theory of, eigenchannel, 20: 30449
NUCLEAR SPIN
relaxation of, stochastic equations for, 20: 30249
NUCLEAR STRUCTURE
analysis from beta decay measurements, 20: 30536
theory of, status of, 20: 30511
NUCLEAR THEORY
baryonic–muonic current interactions in, $\Delta S = 0$, 20: 30141
energy level E2 transitions of even-even nuclei, 20: 30372
forces in, nuclear reaction method for time invariance of, 20: 30505
potentials for binding and saturation of nuclear matter, 20: 30434
NUCLEI
alpha elastic scattering at 4.7 Mev, optical-model analysis of, (E/T), 20: 30413
alpha reactions (d,p) at 30.5 Mev, proton spectra from, (E), 20: 30472
beta decay, (T), 20: 30535
beta decay of, conference on, 20: 30534
beta decay of, matrix elements for first-forbidden, (E/T), 20: 30522
beta decay of, nuclear structure from, 20: 30536
binding energies of heavy, nonlocal potential calculation of, 20: 30508
bremsstrahlung emission by, contribution to radiative processes, (T), 20: 30516
charged particle elastic scattering by, computer program for differential cross sections for, 20: 30348 (INP-446/PL)
decay of, calculation of gamma-gamma angular correlations for, (T), 20: 30341 (AECL-2529)
deuteron reactions (d-He-3) and (d,t) with, isobaric spin in, (T), 20: 30343 (COO-1371-30)
deuteron reactions (d,n) with, amplitudes for, (T), 20: 30426
electron multiple scattering at relativistic energies, (T), 20: 30509
energy levels in A = 16, isospin quintuplet, 20: 30440
energy levels in Nilsson potential, (T), 20: 30392
energy levels of, (T), 20: 30350 (JINR-P-2682)
energy levels of even-even, E2 transitions from 3^+, (E/T), 20: 30372
energy levels of $16 \leq Z \leq 20$, shell-model calculations of odd-parity, 20: 30407
energy levels of, random-phase approximation for particle-hole, (T), 20: 30398
gamma resonant scattering by, cross sections for neutron-capture, (E), 20: 30467
gamma scattering by, electron-pair production in, (E/T), 20: 29996
hyperfragment and hyperon (Λ) reactions with heavy, (T), 20: 30503
intensity increases of heavy cosmic, accompanied by solar x-ray bursts, 20: 29965
masses and nucleon pairing correlations for spherical, 20: 30491
meson (K^-) reactions with heavy, at 1.5 Bev/c, hyperfragments from, 20: 30368
meson (μ^-) capture rates in heavy, closure approximation for, 20: 30454
meson (μ^-) capture by spherical, (T), 20: 30494
meson (π^-) capture by, angular correlations of particles from, (T), 20: 30504
mesons (μ^-) capture by, $\Delta S = 0$ neutron current coupling in, 20: 30141
neutron reactions with, review of cross section research on, (E/T), 20: 30349 (JAERI-1102)
neutron scattering by, technique for measuring resonance, 20: 30358(R) (RPI-328-56, pp 1-48)
nucleon binding in, potentials for saturation, 20: 30434
nucleon interactions in, nonlinear field equation for, 20: 30361
nucleon interactions in $2s_{1/2}1d_{3/2}$ shell, surface delta interaction approximation of, 20: 30423
origin of, in solar system, (T), 20: 29909
particle inelastic scattering by, polarization and asymmetry in inelastic, (T), 20: 30492
photon reactions at 10 to 5000 Mev, electron pair production in, (E), 20: 29990 (JINR-P-2667)
production of, in N = 184 and Z = 126 region, (T), 20: 30367
properties of, calculation using boundary-condition model, (T), 20: 30523
proton reactions (p,xn) and (p,p(x-1)n) at 40 to 100 Mev, inelastic scattering model for, 20: 30446
proton scattering by, nonlocal potential for optical-model analysis of, 20: 30408
reactions of identical, theory of inelastic, 20: 30493
relaxation phenomena in crystals, lattice phonon-quadrupole interactions in, (T), 20: 30749
scattering of complex, angular distributions from inelastic, 20: 30502
NUCLEI (CELLS)
radiation effects on, in cultured leukocytes, 20: 28920
radiation effects on paramecia, x, 20: 29007
radiation effects on guinea pig, x, 20: 28976
NUCLEIC ACIDS
molecular structure of, (E/T), 20: 30734(R) (TID-22970, pp 1-63)
radiation effects on synthesis in rat thymus, x, 20: 28953
NUCLEONS
exchange in pickup and stripping reactions, two-body, (T), 20: 30483
form factor for, sum rule calculation of isovector, 20: 30037
interactions in nuclei, nonlinear field equation for, 20: 30361
interactions in oxygen-16, properties of odd-parity states from effective, 20: 30412
interactions in $2s_{1/2}1d_{3/2}$ shell nuclei, surface delta interaction of, 20: 30423
interactions of, nonsingular energy-dependent potential for, 20: 30060
interactions of, nonlocal potential for, 20: 30061
interactions with mesons (π), p-wave dispersion relations for, (T), 20: 30073
interactions with mesons (μ), inelastic, (T), 20: 30076
interactions with mesons (π^-) at 3.7 Bev/c, A_1 and A_2 resonance production in, (E), 20: 30078
interactions with protons at 9 Bev, peripheral model for, (E/T), 20: 30080
interactions with mesons (π), N/D calculations of p-wave amplitudes for, (T), 20: 30158
interactions with nucleons at 0 to 300 Mev, pole contributions to, (T), 20: 29985 (CONF-640509(Pt.1), Paper 1)
interactions with mesons (π), amplitudes for, (T), 20: 29986 (CONF-640509(Pt.1), Paper 2)
interactions with mesons (μ), cross sections for, (E/T), 20: 29994
interactions with protons, quark production in, (T), 20: 29999(T)
interactions with antinucleons, quark model for annihilation, 20: 30005
interactions with mesons (π), amplitudes for, 20: 30006
interactions with mesons (K), dispersion relations and symmetry groups for, 20: 30018
interactions with mesons (π^-) at 12 and 18 Bev, meson (ρ^0) and dipion production in, (E), 20: 30025
interactions with mesons (π), zero-effective-range analysis for meson (η^0) production in, 20: 30033
interactions with mesons (π), production and properties of mesons A_1 and A_2 from, (E/T), 20: 30023
interactions with photons, SU(6) symmetry predictions for N* production in, 20: 30043
pairing in spherical nuclei, (T), 20: 30491
NUCLEOPROTEINS
desoxyribo-, radiation effects on, at molecular and supermolecular levels, 20: 28908
NUCLEOTIDES
content in fish tissue, methods for measurement of, 20: 29583(R) (TID-22515)
NUCLEOTIDES, PYRIDINE DIPHOSPHATE
radiation effects on, ESR and thermoluminescence studies of, 20: 29249
NUTRIENTS
leaching and recycling in plants and forests, 20: 29451(R) (NYO-2598-29)

O

OAK RIDGE NATIONAL LAB., TENN.
waste disposal in Clinch River, effects on radiation dose to downstream populations, 20: 29452 (ORNL-3721(Suppl.3))
OATS
radioinduced mutations of, γ and neutron, 20: 28960
OCEANOGRAPHY
radioisotope uses in research in, 20: 29401
OCTANE
reactions with muonium, (E), 20: 29247
2-OCTYNOIC ACID

labeling with tritium, to high specific activity, Wilzbach method for, 20: 29243
ODOR
yield from irradiated beef, effects of storage at ambient temperature on, 20: 29589
OILS
analysis for chlorine by neutron activation methods, 20: 29116
OLIVINES
magnetic properties of transition-metal, 20: 29709(R) (TID-22970, pp 65-119)
ONIONS
radiation effects on cellular permeability in epidermal cells of, x, 20: 28900
radioinduced chromosome breaks in, RBE for 200-kev fast-neutron, 20: 29002
OPTICAL MATERIALS
radiation effects on, 20: 29366(R) (TID-22970, pp 375-91)
ORES
analysis for rare earths, spectrometric, 20: 29134
ORGANIC ACIDS
analysis and determinations of carbon-14-labeled, by gas chromatography and radiometric methods, 20: 29089
complexes with rare earths, stability constants of, 20: 29232
radiation effects on fluorinated, free radical production in gamma, 20: 29282
ORGANIC COMPOUNDS
analysis and determination of carbon-14-labeled, by gas chromatography and radiometric methods, 20: 29089
analysis for carbon-14 by dry combustion methods, 20: 29085
analysis for sulfur by hydrogen reduction, 20: 29083(R) (UCRL-14767)
atomic structure of, "electron burning" method of determination of, 20: 29326
decomposition, distribution, and production in ocean water, 20: 28878 (NYO-1918-138)
performance as power-reactor coolant, 20: 30910
radioinduced polymerization of, review of, 20: 29298
spectra of four-membered-ring, infrared, (E/T), 20: 30734(R) (TID-22970, pp 1-63)
ORGANIC COOLED REACTORS
design of multi-pass organic vapor moderated, variably controlled and moderated, 20: 30916(P)
design of organic-moderated, for power production, 20: 30912(P)
design of variably moderated and controlled power, 20: 30915(P)
design of variably controlled and moderated power, using hydrogen-isotope-bearing moderator vapor, 20: 30917(P)
design of variably moderated and cooled heterogeneous power, using organic vapor as moderator and coolant, 20: 30918(P)
ORGANIC MODERATED REACTORS
design of multi-pass organic vapor cooled, with variable control and moderation for power production, 20: 30916(P)
design of organic-cooled, for power production, 20: 30912(P)
design of power, with organic vapor coolant, 20: 30917(P)
design of variably controlled and moderated organic vapor cooled, for power production, 20: 30915(P)
design of variably moderated and cooled heterogeneous power, using organic vapor as moderator and coolant, 20: 30918(P)
ORGANISMS
radioactivity of, at bottom of Norwegian Sea, 20: 29424
strontium-90 uptake by marine, hazards to mass from, 20: 29405 (NP-14694)
ORGANS
radioactivity of, computer program for evaluating determinations of, 20: 29121
ORNL HIGH FLUX ISOTOPE REACTOR
neutron beam leakage spectra from, measurement of, 20: 30791(R) (ANL-7204, pp 32-64)
ORNL RELATIVISTIC ISOCHRONOUS CYCLOTRON
development and operations, 20: 29854(R) (ORNL-3940, pp 70-82)
OXIDES
coatings of, for electric conductors, 20: 29636(P)
mechanical properties of high-purity ceramic, effects of crystal structure on, 20: 29740
properties for uses as thermal insulators in nuclear reactors, 20: 29732
OXIME COMPLEXES
with uranyl nitrate, composition and stability of, spectrophotometric studies of, 20: 29202
OXONIUM IONS
analysis of deuterated, mass spectrometric, 20: 29104
OXYGEN
content of dissolved, in Atlantic Ocean, 20: 28877 (NYO-1918-124)
content of dissolved, in Atlantic Ocean, 20: 28878 (NYO-1918-138)
corrosive effects on zirconium–2.5 tin alloy at 850°C, mechanisms of, 20: 29652
determination as impurity in ultrapure gases, mass spectrometric, 20: 29083(R) (UCRL-14767)
determination in alloys, metals, and refractory materials, methods for, 20: 29108
determination in graphite and basalts by neutron activation methods, 20: 29140
determination in plutonium and uranium, sample preparation for vacuum fusion, 20: 29083(R) (UCRL-14767)
determination in petroleum, activation, 20: 29139
determination in steels, activation, 20: 29138
determination in steel rods by neutron-activation and vacuum-fusion techniques, 20: 29088
determination of, Weibull function for pulse-height distribution from x-ray micro-, (T), 20: 29124
diffusion in aluminum oxide, 20: 29623(R) (TID-22970, pp 121-256)
diffusion in zirconium oxide layers on zirconium metal, nuclear reaction study of, 20: 29817
effects of flowing, on volatilization of fission products from irradiated uranium(IV-VI) oxides, 20: 29211
effects of impurities of, on mechanical properties and structure of tungsten single crystals, 20: 29793
effects of, on gamma radiolysis of aqueous solutions of acetylene, 20: 29293
effects on weldability of FS-85, T-111, and T-222 refractory alloys, 20: 29712(R) (WANL-PR-(P)-009)
proton reactions at 50 to 200 kev, secondary electron emission in, (E), 20: 29951
radiolysis of aqueous solutions of, steady state in gamma, 20: 29257
radiosensitivity effects on lung tumors in rabbits, 20: 29059 (TID-22860)
radiosensitivity effects of cystamine and, on *Saccharomyces cerevisiae*, 20: 29023
reactions of, with hafnium, niobium, tantalum, titanium, vanadium, and zirconium, kinetics of, 20: 29644
reactions with air species above 1000°K, 20: 29146 (SC-R-66-885)
reactions with calcium, magnesium, molybdenum, tantalum, and zirconium, combustion, 20: 29641(R) (SC-DC-65-1691)
reactions with copper and uranium ions in carbonate solutions, kinetics of, 20: 29198
reactions with hafnium at 850 to 1400°C, kinetics of film growth in, 20: 29647
reactions with muonium, cross sections for, 20: 29177
reactions with tantalum in sputtering, properties of films formed by, 20: 29745
reactions with uranium dioxide in carbonate solutions, catalytic effects of copper ammoniate on, 20: 29199
reactions with zirconium and oxygen–deficient zirconia, 20: 29648
separation from niobium and tantalum, degasification processes for, 20: 29633
thermal diffusion in refractory metals, 20: 29769
thermal diffusion in niobium and β-zirconium, 20: 29769
yields from gamma radiolysis of aqueous potassium iodide solutions, 20: 29253
NH_3–O–H_2O, radiolysis of, hydrogen yields from gamma, 20: 29295
OXYGEN IONS
emission from calcium-doped cerium oxides during electrolysis, 20: 30743
OXYGEN ISOTOPES O-14
beta decay of, Coulomb corrections to, 20: 30443
beta decay of, coupling constant in, 20: 30538
OXYGEN ISOTOPES O-15
energy levels of, parity and spin of, (E), 20: 30526
OXYGEN ISOTOPES O-16
alpha elastic and inelastic scattering at 40.5 Mev, angular distributions for, (E), 20: 30450
bremsstrahlung emission from, nuclear matrix elements for, 20: 30516
deuteron elastic scattering at 34.4 Mev, angular distributions from, (E/T), 20: 30353(R) (ORNL-3940, pp 1-61)
deuteron reactions (d,He-3) at 43.3 Mev, angular distributions from, (E/T), 20: 30353(R) (ORNL-3940, pp 1-61)
energy levels from alpha reactions (α,γ) with carbon-12 at 2.8 to 8.3 Mev, 20: 30529
energy levels in, isospin quintuplet, 20: 30440
energy levels of, effective nucleon interaction for properties of odd-parity, 20: 30412
energy levels of, spurious shell model states analysis of, (T), 20: 30514
helium-3 reactions (He-3,α) at 9.8 to 11.8 Mev, angular distribution from, (E), 20: 30433
helium-3 reactions (He-3,p) and (He-3mα) at 3 to 10 Mev, excitation functions for, (E), 20: 30444
meson (μ^-) capture by, elementary-particle treatment of, 20: 30447
neutron reactions (n,p) at 14.8 Mev, cross sections for, (E), 20: 30394
photon reactions (γ,n) with, neutron polarization and spectra from, (E), 20: 30360 (WASH-1068)

reactions (O-16,α) with carbon-12 at 20 to 40 Mev, cross sections for, (E/T), 20: 30353(R) (ORNL-3940, pp 1-61)
triton reactions (t,p) at 6.8 to 10.0 Mev, strong coupling method for studying, (T), 20: 30399

OXYGEN ISOTOPES O-17
helium-3 reactions (He-3,He-4) with, use of, for oxygen diffusion studies in zirconium oxides, 20: 29817
neutron reactions (n,p) with, use for reactor power level monitoring, 20: 30938

OXYGEN ISOTOPES O-18
alpha elastic and inelastic scattering at 40.5 Mev, angular distributions for, (E), 20: 30450
determination of, using alpha-particle bombardment, 20: 29143(P)
energy levels from fluorine-18 (t,α) reactions, (E), 20: 30360 (WASH-1068)
energy levels of, shell-model calculation using realistic interactions for, 20: 30384
exchange between water and cupric, ferric, and ferrous sulfates, 20: 29153
neutron reactions (n,d) with, use for reactor power level monitoring, 20: 30938

OXYGEN SYSTEMS
D–O, radiation effects on, yields from gamma, 20: 29285
ethane–O, tritium reactions with gas-phase, scavenging effects on hot and thermal recoil, 20: 29206
O–U, metallographic tests on arc melted, 20: 29775

OZONE
determination in atmosphere using radioactive clathrate techniques, 20: 29142
preparation of, using fission fragment recoil energy, 20: 29317

P

PACIFIC OCEAN
radioactive contamination of, from fallout and waste disposal, 20: 29405 (NP-14694)

PACKAGING
design criteria for purified reactor-grade plutonium, for buy-back facility, 20: 29453 (RL-SEP-590)

PALLADIUM
iron-57 Mössbauer spectra in, 20: 30766

PALLADIUM ALLOYS
Co–Pd, effective magnetic field at cobalt nucleus in, (E), 20: 30752(T)
Mo–Pd, crystal structure and electric conductivity of, 20: 29766
Nb–Pd, crystal structure and electric conductivity of, 20: 29766
Pd–Zr, crystal structure and electric conductivity of, 20: 29766

PALLADIUM ISOTOPES Pd-104
energy level widths, (E/T), 20: 30360 (WASH-1068)

PALLADIUM ISOTOPES Pd-106
proton elastic and inelastic scattering at 12 and 13 Mev, cross sections and energy levels from, (E), 20: 30462

PALLADIUM ISOTOPES Pd-108
proton elastic and inelastic scattering at 12 and 13 Mev, cross sections and energy levels from, (E), 20: 30462

PALMITIC ACID
radiolysis of, EPR studies of peroxide radical formation in gamma, 20: 29309

PALMITIN
radiolysis of, EPR studies of peroxide radical formation in gamma, 20: 29309

PAPER
industry, conference on instrumentation for control and measurement in, 20: 29604
radioactivity of photographic, detection and measurement of, 20: 29427
weight of, alpha absorption techniques for measuring, 20: 29601

PARAFFIN
scintillation efficiency of systems of liquid medicinal, for use in whole-body counters, 20: 29541

PARAMECIUM
radiation effects on fat and glycogen content in, uv, 20: 28918
radiation effects on nuclear reorganization in, x, 20: 29007

PARTICLE BEAMS
scattering by nuclei, polarization and asymmetry in inelastic, (T), 20: 30492

PARTICLE STATISTICS
book: *Many-Body Theory*, 20: 29838
many-body problem in, random phase approximation for, (T), 20: 30567 (UCRL-14246)

PARTICLE TRACKS
photographs of bubble-chamber, reconstruction of events from, 20: 29533

PARTICLE TRAJECTORIES
determination in spark chambers, accuracy of, 20: 29527 (ITEF-341)

PARTICLES
acceleration in generalized coordinates, 20: 29834
acceleration of macro-, for thermonuclear reactions, (T), 20: 30717
dispersion and fallout of, in atmosphere, model for, 20: 29454(R) (SC-CR-66-2010)
dispersion in atmosphere, from quasi-instantaneous sources, 20: 29403
oscillations in collisionless gravitating systems of, dispersion equations for, 20: 29902(T)

PEACH BOTTOM POWER REACTOR
coolant flow transients in, 20: 30879(R) (GA-6995)
development and research program, 20: 30879(R) (GA-6995)
reactivity analysis of, 20: 30879(R) (GA-6995)

PEAS
radiation effects on metabolism in plants of, γ, 20: 28909
radiation effects on DNA synthesis in seedlings of, γ and fast neutron, 20: 28989
radiosensitivity of seeds and seedlings of, effects of chemical and biological compounds on, 20: 29049

PENTANE, 1-IODO-
radiolysis of, at 77°K, reaction intermediates in gamma, 20: 29264

2,4-PENTANEDIONE
complexes with cobalt, isotope exchange in radiocobalt divalent ion-doped, 20: 29259
complexes with cobalt, radioinduced recoil damage in, thermal annealing of neutron, 20: 29259
ethylenediimine–2,4-pentanedione, complexes with thorium, and zirconium, preparation and structure of, 20: 29203

2,4-PENTANEDIONE COMPLEXES
with europium, luminescence spectra of, (E), 20: 29238
with samarium, luminescence spectra of, (E), 20: 29238
with terbium, luminescence spectra of, (E), 20: 29238

2-PENTANONE, 4-METHYL-
effects on electric conductivity of anhydrous uranyl nitrate, 20: 29184

PENTOBARBITAL SODIUM
effects on enzyme activity in animals, 20: 29048

PEPTIDES
radiolysis of aqueous solutions of, role of radicals in, 20: 29301

PERMEABILITY
measurement in barrier materials for carbon dioxide–hydrogen separation, apparatus for, 20: 29362

PEROVSKITES
dielectric properties, 20: 29709(R) (TID-22970, pp 65-119)

PEROXIDES
yields from radiolysis of hydroperoxides in hydrocarbons, 20: 29302

PERSONNEL
radiation doses to, automation and centralization of systems for measuring and controlling, 20: 29458
radiation protection devices for, 20: 29478
safety of, in reactor operation, air locks for, 20: 29465

PERTURBATION THEORY
use of third-order in calculation of parameters of ground-state deuterons, 20: 30068

PETROLEUM
analysis for chlorine by neutron activation methods, 20: 29116
analysis for trace elements, activation, 20: 29139
heating deposits of, *in situ* with radioactive materials, process for, 20: 30950(P)
prospecting for, by radiometric well logging, equipment for, 20: 29445(P)
recovery from oil-bearing formations using reactor-heated gases, 20: 30805(P)

PHANTOMS
design and fabrication of skull and torso, for radiotherapy dosimetry, 20: 29077(P)
gamma dosimetry in, computer analysis of, 20: 29061
proton reactions with primates at 32 to 2200 Mev, depth dose distribution in, 20: 28928 (CONF-651109, pp 417-25)

PHASE STUDIES
thermodynamics of metastable and stable-phase alloys, 20: 29623(R) (TID-22970, pp 121-256)

PHENANTHRENE
analysis for carbon-14 by dry combustion methods, 20: 29085

1,10-PHENANTHROLINE
1,10-phenanthroline–thenoyltrifluoroacetone, complexes with rare earths, preparation and composition of, 20: 29221

PHENOL, DINITRO-
effects of cupferron and, on frequency of radioinduced chromosome aberrations in Tradescantia, 20: 29028

PHONONS
effects on nuclear relaxation phenomena in crystals, (T), 20: 30749
interactions with electrons in metals, strong, (T), 20: 30312
interactions with radioinduced paramagnetic centers in quartz, 20: 30768

PHOSPHATE GLASS
performance as dosimeters, 20: 29547

PHOSPHATES

content in Amazon River, effects on biology, chemistry, and hydrography of Atlantic Ocean, 20: 28878 (NYO-1918-138)
content in Atlantic Ocean, measurements on, 20: 28877 (NYO-1918-124)
content in Atlantic Ocean, measurements on, 20: 28878 (NYO-1918-138)
properties of fused, structure-sensitive, 20: 29623(R) (TID-22970, pp 121-256)

PHOSPHATIDES
effects of dietary, on chlolesterol content in blood of irradiated rats, 20: 28992

PHOSPHINE OXIDE, TRIOCTYL-
effects on solvent extraction of uranium from sulfuric acid solutions using dibutyl phosphate, synergistic, 20: 29334
TBP–trioctylphosphine oxide, solvent properties for uranium, effects of electronegative groups on, 20: 29347

PHOSPHONIC ACID, ALKYL-, DIBUTYL ESTERS
solvent properties for thorium and uranium, 20: 29354

PHOSPHORESCENCE
effects on measurement of soft beta emitters by liquid scintillation techniques, 20: 29084

PHOSPHORIC ACID, ALKYL ESTERS
solvent properties for cesium and strontium, 20: 29365(P)

PHOSPHORODITHIOIC ACID, DIOCTADECYL ESTER
barium salt of, effects on radiation effects on polypropylene, 20: 29290

PHOSPHORS
reactions of, with tritium, illumination of telephone dials by, 20: 29605(P)
scintillation efficiency of medicinal paraffin-based, liquid, for use in whole-body counters, 20: 29541

PHOSPHORUS
content in Amazon river, effects on biology, chemistry, and hydrography of Atlantic Ocean, 20: 28878 (NYO-1918-138)
content in Atlantic Ocean, measurements on, 20: 28877 (NYO-1918-124)
content in Atlantic Ocean, measurements on, 20: 28878 (NYO-1918-138)
determination in petroleum, activation, 20: 29139
reactions with zirconium at 500 to 1000°C, 20: 29642
separation from waste solutions by activated sludge methods, 20: 29353

PHOSPHORUS FLUORIDES
spectra of, infrared and Raman, (E/T), 20: 30734(R) (TID-22970, pp 1-63)

PHOSPHORUS ISOTOPES P-32
beta decay of, energy release in, 20: 28955
beta decay of, polarization in, (E), 20: 30548
beta decay of, statistical spectrum shape of allowed, (E), 20: 30547
beta spectra of, shape of, (E), 20: 30540
effects on blood and hematopoietic tissue, 20: 28982
energy levels of, spin of, (T), 20: 30360 (WASH-1068)
incorporation in insecticides, 20: 29246
incorporation in sperm of Drosophila, 20: 28955
use in therapy of skin diseases, 20: 29072

PHOTOELECTRIC CELLS
development and economics of, for communications satellites, 20: 29608
development of materials and technology for, 20: 29709(R) (TID-22970, pp 65-119)

PHOTOELECTRIC EFFECT
analysis of, in metals, model for, (T), 20: 29916 (ORNL-TM-1458)

PHOTOGRAPHIC FILM
development process for radiation dosimetry, delayed, 20: 29557
radioactive contamination of, detection and measurement of, 20: 29427

PHOTOGRAPHIC FILM DETECTORS
design with intensifier screen for use with cameras, 20: 29573(P)
performance for gamma and neutron dosimetry, 20: 29518 (BNWL-SA-27)
performance for neutron monitoring near Argonne ZGS, 20: 29523 (CONF-651109, pp 639-46)

PHOTOMETERS
design for low-level sources, 20: 29503

PHOTOMETRY
use of flame, for strontium determination, 20: 29363

PHOTOMULTIPLIER TUBES
gain variations in channel, 20: 29543
time resolution limits of fast, (E/T), 20: 29568

PHOTONS
absorption by semiconductors in crossed electric-magnetic fields, (E/T), 20: 30735(R) (TID-22970, pp 331-73)
effects on sodium chloride crystals, color centers from, 20: 30754
emission from thermal sources, amplitude and intensity correlations for, (T), 20: 29827 (UCRL-16824)
exchange of virtual, in meson (μ)-nucleon interactions, (T), 20: 30076
interactions with photons in electromagnetic field, cross sections for, (T), 20: 30062
interactions with photons, eigenvalue problem for, 20: 29993
interactions with nucleons, SU(6) symmetry predictions for N* production in, 20: 30043
production in interactions of vector mesons, 20: 30057
reactions (γ,n) with lead and uranium-238, fast neutron spectra from, (E), 20: 29529(R) (RPI-328-56, pp 94-112)
reactions (γ,p) with hydrogen and nitrogen at 4.1 to 6.2 Bev, (E), 20: 30432
reactions with nuclei at 10 to 5000 Mev, electron pair production in, (E), 20: 29990 (JINR-P-2667)
reactions with nuclei, radiative corrections to wide-angle pair production by, 20: 30013
reactions with solid surfaces, 20: 29624(R) (TID-22970, pp 257-329)
scattering by highly ionized plasma, analysis of, (T), 20: 30557 (AD-633074)
scattering by K-shell electrons, spectral distributions from, (E/T), 20: 29912 (ISS-66/6)
scattering by K-shell electrons, spectral distributions from, (E/T), 20: 29913 (ISS-66/7)
scattering by K-shell electrons, spectral distributions from, (E/T), 20: 29914 (ISS-66/8)

PHOTOSYNTHESIS
reactions in marine phytoplankton, effects of light on rate of, 20: 28878 (NYO-1918-138)

PHYSICS
book: *Many-Body Theory*, 20: 29838
book: *Potential Theory*, 20: 29839

PHYSIOLOGY
effects of weather on, solar neutrino production as mechanism for, 20: 29402

PICKERING POWER REACTOR
design and economic aspects, 20: 30886
power requirements evaluation, 20: 30891

PIGMENTS
effects on radiosensitivity of *Micrococcus radiodurans*, 20: 29016

PINACOL
yields from gamma radiolysis of aqueous solutions of 2-propanol, 20: 29254

PINCH DEVICES
design and operation of hollow linear Z, 20: 30641
design and performance of Isar 1, 20: 30611
plasma confinement, heating, and losses in Pharos, 20: 30612

PINCH EFFECT
plasma containment and stability in theta, (E/T), 20: 30610
plasma diffusion from, in magnetic fields, (E/T), 20: 30639
plasma hydromagnetic instabilities during implosive phase of theta-, 20: 30613
plasma losses from toroidal theta, with superimposed hexapole field, 20: 30616
plasma rotation in theta-, Doppler measurements of, 20: 30615
plasma stability in cusped and linear theta, 20: 30614
properties of noncylindrical focused Z, in deuterium plasma, (E), 20: 30642

PINELLAS PENINSULA PLANT, FLA.
environs monitoring, Jan. to July 1965, 20: 29431

PIPERIDINE
effects on radioinduced isomerization of stilbene, 20: 29287

PIPES
rupture in reactor cooling systems, research program on, 20: 30811

PIQUA POWER REACTOR
fuel element irradiation testing and inspection for, 20: 30881 (NAA-SR-11712)

PITCHBLENDES
formation and paragenetic position of, in hydrothermal deposits of West Erzgebirge, Germany, 20: 29448
gamma spectra of, performance of germanium detectors for determining, 20: 29079 (AERE-M-1736)

PLACENTA
cesium-137 content in human, 20: 28894
polonium-210 content in human, 20: 28894

PLANETS
radio emission from Jupiter, origin of, (T), 20: 29907(T)

PLANKTON
content, distribution, and growth in Amazon, effects on biology, chemistry, and hydrography of Atlantic Ocean, 20: 28878 (NYO-1918-138)
culture and physiology of marine, 20: 28878 (NYO-1918-138)
distribution in Atlantic Ocean and western Caribbean Sea, 20: 28878 (NYO-1918-138)
effects on chlorophyll content in Atlantic Ocean, 20: 28877 (NYO-1918-124)
photosynthesis in marine, effects of light on rate of, 20: 28878 (NYO-1918-138)

PLANT CELLS
radiation effects on cellular permeability in onion, x, 20: 28900

PLANT METABOLISM
radiation effects on, γ, 20: 28909

radiation effects on, effects of growth phase on γ, 20: 28967

PLANTS

book: *Natural Radioactivity of Plants and Soils*, 20: 29437
fallout removal from, 20: 29451(R) (NYO-2598-29)
metabolite leaching from, tracer studies, 20: 29451(R) (NYO-2598-29)
radiation effects on uncoupling of oxidation and phosphorylation in mitochondria of green, x, 20: 28947(T)
radiation effects on content of ascorbic acid and glutathione in cotton, γ, 20: 28999
radiation effects on *Abutilon hydridum* and *Pelargonium zonale*, genetic, 20: 29018
strontium-89 in food, removal of, 20: 29451(R) (NYO-2598-29)

PLASMA

acceleration and heating of, theta pinch for multistage, 20: 30667
acceleration and reflection by h-f and static magnetic fields at electron cyclotron resonance, 20: 30646
charged-particle beam interactions with, oscillation excitations from, (T), 20: 30689
charged-particle density far from moving body in collisionless, in magnetic field, (T), 20: 30675
charged-particle density in hot hydrogen, technique for measuring, 20: 30685
compression by toroidal magnetic fields, adiabatic, (E), 20: 30660
compression in magnetic mirror machines, adiabatic, 20: 30636
compressivity tensor in anisotropic compressible, 20: 30711
containment and heating in Pharos, 20: 30612
containment and heating in DECA II, 20: 30607
containment and stability in megajoule theta-pinch, (E/T), 20: 30610
containment in closed minimum-B configurations, analysis of, 20: 30609
containment in stellerators with multipolar helical fields, 20: 30657
density distribution of cylindrical, microwave refraction for determining, (E/T), 20: 30700
diagnostics of deuterium, using laser beams, 20: 30556(R) (AD-631993)
diagnostics of partially ionized, hot-wire anemometer for, (E/T), 20: 30702
diffusion across longitudinal magnetic fields, (E/T), 20: 30596
diffusion across magnetic fields, equations for, 20: 30714
diffusion and thermalization of turbulent, in magnetic fields, (T), 20: 30620
diffusion in magnetic fields of hard-core and pinch discharges, (E/T), 20: 30639
electric conductivity of turbulent, uhf, (E), 20: 30625
electric conductivity of, behind reflected shock wave in em shock tube, (E), 20: 30697
electric conductivity of seeded, nonequilibrium, (E/T), 20: 30712
electric field effects on dense hydrogen, strong, (E), 20: 30558 (AD-633593)
electromagnetic field quantization in homogeneous dispersive, (T), 20: 30668
electromagnetic wave interactions in, nonlinear, (T), 20: 30628
electromagnetic wave interactions in magneto-, nonlinear, (T), 20: 30629
electromagnetic wave damping in homogeneous magneotactive, (T), 20: 30671
electromagnetic wave propagation in axially symmetric, magnetic field line curvature effects on, (T), 20: 30678
electromagnetic wave propagation through layer of, kinetic theory for, 20: 30679
electromagnetic wave propagation in inhomogeneous, partial wave analysis of, 20: 30713
electromagnetic wave propagation in hot collisionless, (T), 20: 30569
electromagnetic wave propagation in, (T), 20: 30571
electromagnetic wave propagation in collisionless, (T), 20: 30588
electromagnetic-field discontinuities from resonance in nonuniform, in magnetic field, (T), 20: 30696
electromagnetic-wave propagation through thin nonuniform layer of, (T), 20: 30704
electromagneticwave scattering in, (T), 20: 30674
electron beam interactions with, analysis of collective, (E), 20: 30623
electron beam interactions with magnetic mirror confined, instabilities from, (E), 20: 30659
electron cyclotron oscillations in arbitrary pressure, (T), 20: 30631
electron density and velocity in helium hollow-cathode discharge, (E), 20: 30688
electron density and energy in helium afterglow, in toroidal magnetic fields, (E/T), 20: 30710
electron density measurement in Tokamak, using microwave method, 20: 30652
electron drift velocity and collision frequence in argon discharge, (E), 20: 30598
electron heating by h-f fields in adiabatic traps, (E), 20: 30663
electron impact excitation in mercury, resonance absorption from, 20: 30601
electron temperature measurement in hydrogen, using carbon line radiation, 20: 30705
electron velocity distributions in electric fields in slightly ionized, instability of, 20: 30581
electron wave propagation in, Landau damping of, (E/T), 20: 30622
energy losses from cesium, in arc-mode thermionic cells, (T), 20: 29981
energy losses in toroidal-chamber Tokamak TM-2, (E), 20: 30653
field decomposition in anisotropic compressible, 20: 30711
flow across magnetic fields, one-dimensional, (T), 20: 30597
flow of, MHD one-dimensional unsteady potential, (T), 20: 30570
forces in, potential of average, 20: 30599
heating by electron beam emission from toroidal, (E), 20: 30640
heating by ion cyclotron resonance, power coupling to plasma in, 20: 30577
heating in axisymmetric magnetic fields, (T), 20: 30559 (FTI-114/P-044)
heating in toroidal Tokamak-3, (E), 20: 30650
heating of dense by h-f discharge in a metallic chamber, (E), 20: 30664
heating of mirror-confined, by d-c discharges, turbulent, 20: 30661
hydromagnetic instabilities during implosion of theta-pinch, 20: 30613
hydromagnetic model for puffs of, in longitudinal magnetic fields, 20: 30715
hydromagnetic wave propagation in collisionless, (T), 20: 30586
injection and compression in cusped field regions, (E), 20: 30644
injection of, multipole magnetic guide fields for, (E), 20: 30579
interactions with electron beams, microwave amplification by, 20: 30718
ion acoustic wave propagation in high temperature electron, nonlinear, (T), 20: 30585
ion cyclotron resonance heating of QP, (E), 20: 30662
ion density in hydrogen, (E), 20: 30686
ion energy spectra in hydrogen, measurement of, 20: 30578
ion losses from magnetic mirror confined, analysis of, (T), 20: 30618
ion losses through charge exchange in mirror-confined, (E/T), 20: 30584
ion oscillations in drifted, (E), 20: 30583
ion-wave excitation by h-f electron Langmuir waves in, low-frequency, (T), 20: 30692
ionization and recombination in seeded, (E/T), 20: 30712
ionization temperature of, in local thermodynamic equilibrium, 20: 30604
Langmuir waves in uniform isotropic, interactions with intense h-f electromagnetic waves, (T), 20: 30695
laser beam scattering by hot electron, relativistic theory of, 20: 30716
magnetic energy dissipation near zero field lines in, charged-particle accelerations from, (T), 20: 30676
magnetic field boundary of line currents in, at uniform pressure, 20: 30576
magnetic wave interactions with, h-f, (T), 20: 30624
microwave absorption in cavity resonator containing, negative, (T), 20: 30587
microwave emission from magnetic mirror confined, properties of, (E), 20: 30645
microwave scattering by turbulent, (E/T), 20: 30658
motion in toroidal octupole magnetic fields, (E), 20: 30708
oscillations and stability of, in h-f electric and stationary magnetic fields, (T), 20: 30669
oscillations in inhomogeneous, with collisions, kinetic theory of, 20: 30691
oscillations in two-stream, suppression of l-f, (E), 20: 30591(T)
oscillations in, analysis of longitudinal, (T), 20: 30564 (NYO-1480-26)
oscillations in, collisionless damping of nonlinear, (T), 20: 30706
oscillations in, in axisymmetric magnetic field, (T), 20: 30559 (FTI-114/P-044)
oscillations in, quasilinear theory of cyclotron instability of, 20: 30670
oscillations in, strong magnetic field effects on, (T), 20: 30677
particle density in, random phase approximation for, (T), 20: 30567 (UCRL-14246)
particle losses from toroidal theta pinch with superimposed hexapole field, 20: 30616
particle losses from minimum-B confined, (E/T), 20: 30656
particle motion in, in constant longitudinal and rotating transverse magnetic fields, (T), 20: 30693
photon scattering by highly ionized, analysis of, (T), 20: 30557 (AD-633074)
pinch discharge in deuterium, properties from noncylindrical focused Z, (E), 20: 30642
plasmoid motion in curvilinear magnetic fields, (E/T), 20: 30647
production by coaxial gun with annular preionization, 20: 30648
production by hydrogen atom injection in cryogenic magnetic trap VGL-2, 20: 30655
production by molecular hydrogen ion injection in magnetic mirror machines, (E), 20: 30634
production by neutral hydrogen injection in magnetic mirror/well geometry, (E), 20: 30632
production in hollow linear Z pinch discharge, 20: 30641
production in Ogra II, by neutral hydrogen injection, 20: 30633
production of dense, by cusp field injection, (E), 20: 30643

production of deuterium, using laser irradiation, 20: 30665
production of high-energy, by light pulses from lasers, 20: 30666
production of high-temperature, by laser operating in spike mode, (E), 20: 30590(T)
production of rotating argon, hydrogen, and nitrogen, in crossed fields, (E), 20: 30582
production of self-sustaining, determination of electric field strength for, 20: 30592
production of thermally ionized cesium and chlorine, containing negative ions, 20: 30575
production of, studies on carbon dioxide solidification and dropping in vacuum for, 20: 30594
properties in Tuman device, 20: 30682
properties of relativistic electron, in magnetic mirror machines, (T), 20: 30638
properties of toroidal, with longitudinal varying magnetic field, 20: 30654
properties of, effects of multipole guide fields on, (E), 20: 30579
properties of, reduction of Fokker–Planck equation for determining, (T), 20: 30560 (LA-DC-7282)
radiation patterns in anisotropic compressible, with cylindrical boundaries, 20: 30711
radiation spectrum from, behind reflected shock wave, (E), 20: 30697
sensitivity to electric potential in capacitors, (T), 20: 30699
shock propagation in theta-pinch, analysis using Fokker–Planck method, (T), 20: 30560 (LA-DC-7282)
source of, operational modes of titanium, 20: 30589(T)
spectra from r-f discharge hydrogen, collisional Stark broadening in, (E), 20: 30572
stability in cusped and linear theta pinches, 20: 30614
stability in external h-f electric field, (T), 20: 30627
stability in magnetic mirror machines, (T), 20: 30635
stability in magnetic mirror machines, effects of density on flute, (T), 20: 30707
stability in negative V″ stellarators, pressure effects on, (T), 20: 30561 (MATT-415)
stability in Tokamak-5, (E/T), 20: 30649
stability in Tokamak device, higher-mode, (E), 20: 30651
stability in toroidal discharges, (T), 20: 30617
stability of arbitrary pressure, drift, (T), 20: 30631
stability of axially symmetric nonuniform, with current, (T), 20: 30680
stability of colliding streams of, graphical solution of dispersion equation for, 20: 30593
stability of cylindrical inhomogeneous, analysis using Vlasov equation, (T), 20: 30630
stability of diffusing, (E), 20: 30621
stability of inhomogeneous, with collisions, kinetic theory of, 20: 30691
stability of inhomogeneous, quasi-linear theory for, 20: 30562 (MPI-PAE-P1/25/66)
stability of potential oscillations in electron-ion beams, (T), 20: 30672
stability of theta-pinch, Doppler measurement of rotational, 20: 30615
stability of toroidal in narrow tube approximation, effect of curvature on, (T), 20: 30619
stability of toroidal confined, (E), 20: 30640
stability of toroidal, gravitational interchange effects on, (T), 20: 30608
stability of, collision effects on, (T), 20: 30709
stability of, gravitational, (T), 20: 30568
stability of, unified approach to micro- and resistive, (T), 20: 30626
surface waves of, interactions with incident electromagnetic waves, (T), 20: 30694
temperature distribution in arc produced, 20: 30563 (NP-16096)
use for amplification and generation of uhf oscillations, (E/T), 20: 29500
use for generation and amplification of microwaves, 20: 29499
use of magnetoactive cold, in MHD cells, 20: 29978
wave equation for inhomogeneous gyrotropic hot, 20: 30603
wave equations for homogeneous gyrotropic compressible warm, coupled, 20: 30602
wave propagation along annular column of mercury, surface, (E), 20: 30574
wave propagation in interstellar, cosmic ray damping effects on, (T), 20: 29959
wave transformation in inhomogeneous magnetoactive, quasilinear, (T), 20: 30673
x-ray emission from hot fully ionized hydrogen, (T), 20: 29881

PLASMA JETS
acceleration and dipole resonance of, nonlinear theory for coherent, 20: 30690
design and operation of coaxial gun with annular preionization, 20: 30648
design and performance of coaxial, 20: 30684
energy distribution in coaxial hydrogen, (E), 20: 30687
magnetohydrodynamic flow of axisymmetric free argon, flow-field perturbations and Hall potentials in, (E/T), 20: 30176
performance of coaxial, with eroding electrodes, 20: 30683
velocities of hydrogen, Doppler shift technique for measuring, 20: 30681

PLASTIC COATINGS
radioinduced polymerization of, on exterior surfaces, electron, 20: 29320(P)

PLASTICS
wave propagated stress disturbances in cylindrical, theories for, 20: 30954 (UCRL-14617)

PLATES
fluid flow over flat porous, MHD, 20: 30180

PLATINUM
iron-57 Mössbauer spectra in, 20: 30766
photoelectric cross sections at 320 kev, absolute, (E), 20: 29924
platinum-195 Mössbauer effect in, (E), 20: 30757
radiation effects on catalytic activity of, uv, 20: 29304

PLATINUM ALLOY COUPLES
Pt/Pt–Rh, performance of thermocouples of, 20: 29495

PLATINUM ALLOYS
Ir–Pt, analysis for glassy inclusion in, development of electron microprobe for, 20: 29083(R) (UCRL-14767)

PLATINUM COUPLES
Pt/Pt–Rh, performance of thermocouples of, 20: 29495

PLATINUM HYDRIDES
spectra of deuterated and normal, absorption, (E), 20: 29934(T)

PLATINUM ISOTOPES Pt-195
Mossbauer effect on 99- and 129-kev transitions in, (E), 20: 30757

PLUTONIUM
inhalation and resorption of, 20: 28885
metabolism of, 20: 28885
preparation of samples of, for vacuum fusion analysis, 20: 29083(R) (UCRL-14767)
receiving and repackaging purified reactor-grade, design criteria for buyback facility for, 20: 29453 (RL-SEP-590)
separation from fission product solutions by ion exchange, 20: 29357
spectra of, emission lines in, 20: 29083(R) (UCRL-14767)

PLUTONIUM ALLOYS
fissium–Pu–U, fission product release from irradiated, 20: 30790(R) (ANL-7204, pp 1-31)

PLUTONIUM BROMIDES
heat of formation, 20: 29229

PLUTONIUM CARBIDES
compatibility with molybdenum, niobium, tantalum, tungsten, vanadium, and zirconium for use in SNAP devices, 20: 29820
PuC–UC, compatibility with potential cladding materials, 20: 30790(R) (ANL-7204, pp 1-31)

PLUTONIUM CHLORIDES
heat of formation, 20: 29229

PLUTONIUM FLUORIDES
heat of formation, 20: 29229

PLUTONIUM(IV) FLUORIDES
reactions in lithium chloride–potassium chloride eutectic, preparation of plutonium dioxide by, 20: 29330(R) (EURAEC-1601)

PLUTONIUM(VI) FLUORIDES
separation from cell exhaust air by hydrolysis and filtration, 20: 29328 (ANL-7066)

PLUTONIUM HYDRIDES
heat of formation, 20: 29229

PLUTONIUM IODIDES
heat of formation, 20: 29229

PLUTONIUM ISOTOPES
production of, economics of reactor, 20: 29609 (NP-15947)

PLUTONIUM ISOTOPES Pu-238
neutron reactions at 1 kev to 14 Mev, cross sections for, (T), 20: 30346 (GEMP-411)
uses as power sources for underwater applications, 20: 29607

PLUTONIUM ISOTOPES Pu-239
deuteron reactions (d,pf) with, fission probability and fragment anisotrophies for, 20: 30360 (WASH-1068)
effects on blood and hematopoietic system, 20: 28982
neutron fission at 30 kev to 14.7 Mev, ratio of asymmetric to symmetric, (E), 20: 30404
neutron fission of, delayed gamma emission from, (E), 20: 30463
neutron reactions at 1.09, 1.7, and 2.1 Mev, gamma spectra from, (E), 20: 30360 (WASH-1068)
photofission of, delayed gamma emission from, (E), 20: 30463
triton reactions (t,pf) with, fission probability and fragment anisotropies for, 20: 30360 (WASH-1068)

PLUTONIUM ISOTOPES Pu-240
neutron resonances of, (E), 20: 30360 (WASH-1068)
triton reactions (t,pf) with, fission probability and fragment anisotropies for, 20: 30360 (WASH-1068)

PLUTONIUM ISOTOPES Pu-241

neutron fission and resonance widths and cross sections at 20 to 74 ev, (E), 20: 30360 (WASH-1068)
PLUTONIUM ISOTOPES Pu-242
neutron resonances and total cross sections for, (E), 20: 30360 (WASH-1068)
neutron total cross sections at 0.02 to 400 ev, (E), 20: 30465
PLUTONIUM NITRATES
criticality studies on solutions of, in stainless steel spheres, 20: 29471
PLUTONIUM NITRIDES
reactions with helium at 700 to 1000°C, 20: 29616(R) (BMI-1738)
thermal conductivity at 250 to 1400°C, 20: 29616(R) (BMI-1738)
PLUTONIUM(IV) OXIDES
preparation by reactions of plutonium tetrafluoride in lithium chloride–potassium chloride eutectic, 20: 29330(R) (EURAEC-1601)
$BeO–PuO_2–ThO_2$, development as reactor fuel, 20: 29616(R) (BMI-1738)
$PuO_2–UO_2$, development as reactor fuel, 20: 29617(R) (EURAEC-1593)
$PuO_2–UO_2$, fabrication of pellets of, process development for, 20: 29621(R) (NUMEC-3524-17)
$PuO_2–UO_2$, fission gas diffusion from, effects of grain growth and preparation procedure on, 20: 29805(R) (NUMEC-3432-21)
$PuO_2–UO_2$, melting points of, effects of argon and nitrogen–hydrogen atmospheres on, 20: 29621(R) (NUMEC-3524-17)
$PuO_2–UO_2$, phase studies, 20: 29618(R) (GEAP-4982)
$PuO_2–UO_2$, radiation effects on microstructure of, effects of preparation procedure on neutron, 20: 29805(R) (NUMEC-3432-21)
$PuO_2–UO_2$, radiation effects on structure of, fast-neutron, 20: 29618(R) (GEAP-4982)
$PuO_2–UO_2$, radioinduced fission-gas-generation and temperature profiles in, fast- and thermal-neutron, 20: 29618(R) (GEAP-4982)
$PuO_2–UO_2$, radioinduced melting in, effects of diametral gap size on fast-neutron, 20: 29618(R) (GEAP-4982)
$PuO_2–UO_2$, reactions with sodium at 750°C, effects of fuel stoichiometry on, 20: 29618(R) (GEAP-4982)
$PuO_2–UO_2$, reactivity of water-moderated lattices of, 20: 29617(R) (EURAEC-1593)
PLUTONIUM RECYCLE TEST REACTOR
fuel-element rupture test loop in, failure of, 20: 30941
POLAND
research centers in, Swierk and Zeran, 20: 30937
POLAROGRAPHS
development of transistorized, controlled-potential differential, 20: 29083(R) (UCRL-14767)
POLARONS
theory of, lectures on, 20: 30783
POLLEN
radiation effects on germination and tube growth of, in *Pinus desiflora* and *Pinus thunbergii*, 20: 28980
POLONIUM
book: *Chemistry of Selenium, Tellurium, and Polonium*, 20: 29235
POLONIUM ISOTOPES Po-208
decay of, alpha and electron-capture, (E), 20: 30405
POLONIUM ISOTOPES Po-209
decay of, alpha and electron-capture, (E), 20: 30405
POLONIUM ISOTOPES Po-210
alpha emission from, use of p-n semiconductor detector for measuring, 20: 29552
content in human placenta, 20: 28894
effects of injected, on aging processes in rats, 20: 29030
effects on blood and hematopoietic system, 20: 28982
effects on catecholamine metabolism in rabbits, 20: 28886
uses as power sources for underwater applications, 20: 29607
POLONIUM ISOTOPES Po-218
collection of, bismuth-210 beta activity from, 20: 29324
POLYENES
superconductivity in, 20: 30268
POLYMERIZATION
radioinduced, of condensed alkanes, mechanism of, 20: 29314
radioinduced, review of, 20: 29298
POLYMERS
fabrication and mechanical properties of, 20: 29624(R) (TID-22970, pp 257-329)
gas transport in glassy amorphous, 20: 29624(R) (TID-22970, pp 257-329)
radiation effects on creep rates of, 20: 29624(R) (TID-22970, pp 257-329)
POLYPHENYLS
properties for use as reactor coolants, research on, 20: 30906
POLYPHOSPHATES
effects on radiopreserved seafood, 20: 29583(R) (TID-22515)
hydrolysis of, effects of nickel and uranyl ions on, 20: 29152
POPULATIONS
radiation dose to, downstream from Clinch River, 20: 29452 (ORNL-3721 (Suppl.3))
radiation hazards to United Kingdom, from fallout, 20: 29054 (NP-16119)
POROSITY
measurement of, by gamma or x-ray absorption, 20: 29595
PORPHYRINS
radiosensitivity effects on mice, 20: 29042
POSITRONIUM
annihilation of, series development for eigenvalues for, 20: 29993
POSITRONS
annihilation in metals, analysis of, (T), 20: 29991 (ORNL-TM-1443)
annihilation lifetime spectra in tritiated ice and water, gamma radiation effects on, 20: 29268
interactions with electrons, C-parity violation and neutral vector meson production in, (T), 20: 30012
POTASSIUM
abundance in gneisses and granites of Rum Jungle Complex, Australia, 20: 29415
content in foods, 20: 29475
density of, at critical temperature, radiometric techniques for measuring critical, 20: 29742
determination of, by neutron activation methods, 20: 29078(R) (AD-633252)
POTASSIUM BROMIDES
diffusion of bromine in, surface evaporation effects on, (E), 20: 29731
POTASSIUM CHLORIDES
effects on calcium-45 movement in guinea pig brain slices, 20: 28891
radioinduced damage in, computer simulation of ionic displacement, 20: 30741
KCl–RbCl, argon-39, -41, and krypton-85 diffusion in, 20: 30769
POTASSIUM COMPLEXES
hexanitrocobaltate, preparation and composition of, effects of temperature on, 20: 29209
with salicylic acid, preparation and composition of, 20: 29197
POTASSIUM FLUOSILICATES
uses in decomposition of zirconium silicate, 20: 29201
POTASSIUM IODIDES
radioinduced color centers in, uv or x, (E), 20: 30748
radiolysis of aqueous solutions of, yields from gamma, 20: 29253
POTASSIUM IONS
dissociation of fast negative, in rare gases, (T), 20: 29947
POTASSIUM ISOTOPES K-39
proton reactions (p,γ) at 0.5 to 2.9 Mev, calcium-40 levels from, (E), 20: 30482
POTASSIUM ISOTOPES K-40
content in juniper trees in Georgia, 20: 29410
loss from diet samples during dry ashing and hydrochloric acid treatment, 20: 29122
POTASSIUM ISOTOPES K-42
beta spectra, (E), 20: 30546
POTASSIUM NITRATES
effects on gamma radiolysis of aqueous solutions of 2-propanol, 20: 29254
reactions with cobalt nitrate and rare earth nitrates, 20: 29209
POTASSIUM OXALATES
uses in spectrofluorimetric determination of terbium, 20: 29086
POTASSIUM PALMITATES
radiolysis of, EPR studies of peroxide radical formation in gamma, 20: 29309
POTASSIUM SAMARIUM BROMIDES
preparation, 20: 29204
POTASSIUM SAMARIUM CHLORIDES
preparation, 20: 29204
POTASSIUM THORIUM HYDROXIDE PHOSPHATES
preparation and properties of, 20: 29160
POTASSIUM THORIUM SULFATES
preparation and properties of, 20: 29218
POTATOES
radiation effects on activity of β-fructofuranosidase in, 20: 28934
radiation effects on activity of transferase in, 20: 28935
radiation effects on sprouting and yield of, x, 20: 28966
radiation effects on x-ray diffraction spectra of amidones in, γ, 20: 29255
radiation effects on proline content of, 20: 28932
POWDER COMPACTS
fabrication of aluminum, beryllium, copper, and iron, by isostatic pressing and sintering, 20: 29681
POWER BREEDER REACTORS
design of fast, with steam (D_2O, H_2O, or $D_2O–H_2O$) coolant and moderator, 20: 30914(P)
POWER CYCLES
efficiency of liquid-metal MHD, for nuclear power plants, 20: 29980
POWER PLANTS
economics of large fossil-fuel, 20: 29372 (TID-22978)
POWER REACTORS

control system design and operating experience, 20: 30901
coolants for, performance of, 20: 30910
design of graphite-moderated integral vapor-generating and superheating, 20: 30919(P)
design of liquid cooled and moderated, 20: 30912(P)
design of multi-pass variably moderated and controlled, vapor moderated and cooled heterogeneous, 20: 30916(P)
design of pressurized water, with steam generator, 20: 30911(P)
design of variably moderated and controlled heterogeneous, 20: 30915(P)
design of variably controlled and moderated heterogeneous, using hydrogen-isotope-bearing moderator and cooling vapor, 20: 30917(P)
design of variably moderated and controlled heterogeneous, with hydrogen-bearing vapor as moderator and coolant, 20: 30918(P)
development and research program for large closed-cycle water cooled, 20: 30884(R) (WCAP-3269-16)
development for underwater applications, 20: 30929
development of British, 20: 30885
economics of Canadian heavy water, 20: 30885
fuel burnup analysis for equilibrium operation cycles of, method for, 20: 30890
heat-transfer technology for, conference on, 20: 29383
operating experience, review of, 20: 30904
pressure vessels for pressurized-water, design and stress analysis of cascade arrangement of, 20: 30893
pressure vessels for, design and strength requirements of steel, 20: 30894
reactivity variations with burnup, 20: 30900
safety analysis of, probabilistic methodology for, 20: 30883 (SAN-570-2)

POWER SUPPLIES
description of power system of Siemens-Schuckert Research Center, 20: 29368
design of regulated, 20: 29501
development for large manned orbital space station, 20: 29977 (N-65-32716)
development of isotopic, for underwater uses, 20: 29607
survey of, for communications satellites, 20: 29608

PRASEODYMIUM
determination in rocks, chemical spectrographic method for, 20: 29083(R) (UCRL-14767)
determination in standard igneous rocks G-1, W-1, and G-B by x-ray fluorescence, 20: 29101
determination in TBP extracts, spectrophotometric, 20: 29125
determination in uranium compounds, spectrographic, 20: 29129
determination of trace amounts of, in neodymium by activation methods, 20: 29082 (SGAE-CH-27/1966)

PRASEODYMIUM ALLOYS
La–Pr, electric conductivity, magnetic susceptibility, and superconducting transition temperatures of, 20: 29753

PRASEODYMIUM AZIDES
preparation, 20: 29166

PRASEODYMIUM CARBIDES
hydrolysis of, gaseous products from, 20: 29220

PRASEODYMIUM CHLORIDES
crystal field parameters of, 20: 30760

PRASEODYMIUM COMPLEXES
hexanitrocobaltate, preparation and composition of, effects of temperature on, 20: 29209
with EDTA, preparation, composition, and stability of, 20: 29222
with serine, stability of, 20: 29208

PRASEODYMIUM IONS
crystal field parameters of trivalent, in praseodymium chlorides, 20: 30760

PRASEODYMIUM ISOTOPES Pr-141
energy levels from neodymium-141 decay, (E), 20: 30416

PRASEODYMIUM ISOTOPES Pr-143
beta spectra of, shape of, (E), 20: 30540

PRASEODYMIUM ISOTOPES Pr-144
beta decay of, β-γ directional and circular polarization correlations in, (E), 20: 30544
gamma emission at 54 to 80 kev, angular correlations in, (E), 20: 30506

PRASEODYMIUM NIOBATES
distribution in strontium molybdate single crystals, coefficients of, 20: 29746

PRASEODYMIUM TITANATES
preparation and crystal structure of, 20: 29212

PRECIPITATION, ATMOSPHERIC
fallout deposition in, effects of cloud formation on, 20: 29416
radioactivity in, 1965 fallout, 20: 29428

PREGNANCY
radiography during early, danger of diagnostic, 20: 29068

PRESSURE
effects on rate of synthesis of ammonia, 20: 29312

PRESSURE VESSELS
design and strength requirements of steel, 20: 30894
design and stress analysis of cascade arrangement of spherical, for pressurized-water power reactors, 20: 30893
embrittlement of steels for, plastic fatigue, 20: 29701(R) (EURAEC-1547)
fracture toughness of steels in reactor, development of test procedures for, 20: 29700(R) (COO-1477-4)
inspection of steel, methods for, 20: 29389
leak rates in, gas and liquid, 20: 30810
leak testing for reactor containment, 20: 30812
materials for reactor, review, 20: 30815
radiation effects on steels for, 20: 30788(R) (ANL-7190, pp 176-88)
strength of steel, for reactor containment, 20: 30813
testing of EBWR, nondestructive, 20: 30787(R) (ANL-7190, pp 11-142)
thermal shields for, design of, 20: 30820(P)

PRESSURIZED WATER REACTORS
control rod positioning by boron addition in chemical shim, 20: 30808 (WCAP-3269-54)
coolant blowdown in, analysis of, (E/T), 20: 30797(R) (IITRI-578P21-18)
design for nuclear power plant, 20: 30911(P)
fuel assembly for, 20: 30869(P)
nozzle design for maritime and aircraft, stress analysis for, (T), 20: 30928
pressure vessels for power, design and stress analysis of cascade arrangement of, 20: 30893

PRESSURIZERS
nozzle design for, stress analysis for, (T), 20: 30928

PROLINE
radiation effects on content of, in potato tubers, 20: 28932

PROMETHIUM
determination in uranium compounds, spectrographic, 20: 29129

PROMETHIUM ISOTOPES Pm-147
use as beta source for vacuum gage, 20: 29600
uses as power sources for underwater applications, 20: 29607
uses for determining surface composition and structure of copper, 20: 29754
uses for measuring Mylar film thickness on copper, 20: 29754

PROPANE
helium atom reactions with, electron kinetic energy from ionization in, (E), 20: 29927
radiolysis of, ion and free radical interceptor effects on xenon-sensitized x, 20: 29266

PROPANE, 2-CHLORO-
chlorine-36 exchange between, and tetrabutylammonium chloride, kinetics of, 20: 29156

2-PROPANETHIOL, 1-AMINO-
hydrochloride, radiosensitivity effects on phage induction in *E. coli*, x, 20: 29045
metabolism in mice, tracer study, 20: 28888

1-PROPANOL
radiolysis of, yields and rate constants of percursors of hydrogen in gamma, 20: 29286

2-PROPANOL
radolysis of aqueous solutions of, effects of electron scavengers on yields from gamma, 20: 29254
radiolysis of aqueous solutions of, in presence of oxygen, 20: 29277

2-PROPANONE, PHENYL-
oxime of, Beckmann rearrangement of, effects of carbon-14 on, 20: 29242

PROPENE POLYMERS
radiation effects on chemical and physical properties of, effects of stabilizers on gamma, 20: 29290

PROPORTIONAL DETECTORS
design and performance for gaseous argon-37 and tritium determinations, 20: 29559
design for electrons, 20: 29561
efficiency for tritium determination in water, 20: 29098
electron multiplication process in, 20: 29554
performance of helium-3, for cyclotron environs monitoring, 20: 29846 (CONF-651109, pp 154-60)

PROPULSION
design of nuclear airship, (T), 20: 30927
development of electric and nuclear-electric, 20: 29394
nuclear, development of reactors for underwater, 20: 30929

PROTACTINIUM
separation from acid solutions by precipitation with arsenazo dyes, induline, and rhodamine B, 20: 29135
separation of, from irradiated thorium dioxide by solvent extraction and anion exchange, 20: 29335
separation of, from impurities by solvent extraction and anion exchange, 20: 29335

PROTACTINIUM BROMIDES
heat of formation, 20: 29229

PROTACTINIUM CHLORIDES
heat of formation, 20: 29229
PROTACTINIUM FLUORIDES
heat of formation, 20: 29229
PROTACTINIUM IODIDES
heat of formation, 20: 29229
PROTACTINIUM ISOTOPES Pa-233
preparation, 20: 29335
separation from irradiated thoria, method for, 20: 29331 (KAPL-M-6554)
PROTECTIVE CLOTHING
decontamination solutions for, 20: 29477
PROTEINS
complexes with cholesterol in dog blood, radiation effects on, 20: 28998
metabolism of serum, in rats, effects of carbon tetrachloride, radiation, and venous bleeding on, 20: 28954
radiation effects on mouse blood serum, x, 20: 28899
radiation effects on synthesis of, in blood cells, x, 20: 28922
radiation effects on metabolism in rats, tracer study, 20: 28997
radiation effects on rabbit blood plasma, uv, 20: 29004
radiation effects on synthesis in Ehrlich mouse ascites tumor cells *in vitro*, x, 20: 28923
radiation effects on, role of free radicals in, 20: 29037
radiation effects on induced synthesis of blood plasma, in mice, 20: 28926 (AD-633469)
synthesis of, natural systems for, 20: 30734(R) (TID-22970, pp 1-63)
PROTONS
angular distributions from reactions of lithium-6 and -7 with boron-10 and boron-11, 20: 30519
angular distributions from lithium-6 reactions with carbon-12, (E), 20: 30520
angular distribution from helium-3 reactions (He-3,p) with carbon-12, (E), 20: 30526
diffusion in Van Allen belts, 20: 30206(T) (NASA-TT-F-389, pp 426-42)
distribution in magnetosphere, spatial, 20: 30207 (NASA-TT-F-389, pp 442-53)
distribution in magnetosphere, energy, spatial, and temporal, 20: 30220(T) (NASA-TT-F-389, pp 633-52)
distribution in outer Van Allen belts, energy and spatial, 20: 30219(T) (NASA-TT-F-389, pp 623-9)
distribution in Van Allen belts, analysis of spatial, 20: 30211(T) (NASA-TT-F-389, pp 535-50)
distribution in Van Allen belts, energy, spatial, and temporal, 20: 30204(T) (NASA-TT-F-389, pp 375-86)
distribution of geomagnetically trapped, spatial, 20: 30202(T) (NASA-TT-F-389, pp 281-7)
distribution of geomagnetically trapped, spatial, 20: 30212(T) (NASA-TT-F-389, pp 551-66)
distributions in Brazilian magnetic anomaly at 250 to 400 km, spatial and temporal, 20: 30217(T) (NASA-TT-F-389, pp 607-15)
effects of 120-Mev, on survival of mice, depth-dose factor in, 20: 28972
effects on bismuth telluride at 7.5 Mev, 20: 29623(R) (TID-22970, pp 121-256)
effects on isomerization of *trans* polymers of conjugated dienes, 20: 29321(P)
effects on *Macaca mulatta*, whole-body exposure, 20: 28931 (CONF-651109, pp 624-35)
effects on metals oxides and silicon, blistering from, (E), 20: 29816
emission by boron-9 from helium-3 reactions (He-3,α) with boron-10, (E), 20: 30445
emission during solar flares, 20: 29875(T) (NASA-TT-F-389, pp 732-9)
intensities in Van Allen radiation belts, (E), 20: 30235
interaction strengths of, (T), 20: 30001
interactions with polarized neutrons at 23 Mev, spin correlation coefficients for, (E), 20: 30360 (WASH-1068)
interactions with mesons(π^-) at 1.17 Bev/c, hyperon (Λ^0) and (Σ^0) polarization in, (E), 20: 29987 (COO-1261-4)
interactions with electrons at 2 Bev, cross sections for resonance production in, (T), 20: 30054
interactions with mesons (π^-) at 1128 to 1326 Mev/c, neutral hyperon production in, (E), 20: 30071
interactions with mesons (K-), properties of hyperons (Ξ^-) and (Ξ^0) from, (E), 20: 30072
interactions with nucleons at 9 Bev, peripheral model for, (E/T), 20: 30080
interactions with neutrons in nuclear emulsions, mesons (π^+) and (π^-) charge asymmetry from, (E), 20: 30082
interactions with protons in nuclear emulsions, mesons (π^+) and (π^-) charge asymmetry from, (E), 20: 30082
interactions with mesons (π^-) at 6.8 Bev/c, criterion for separating products of elastic, (E/T), 20: 30083
interactions with mesons (π^-) at 180 to 500 Mev/c, criterion for separating products of inelastic, (E/T), 20: 30083
interactions with antiprotons, mesons (κ), mesons (π), and protons, Regge cuts in high-energy elastic, (T), 20: 30160
interactions with alpha particles at 17.5 Mev, polarization in, (E), 20: 30389
interactions with deuterons, cross sections for elastic, (T), 20: 29989 (ITEF-361)
interactions with nucleons, quark production in, (T), 20: 29999(T)
interactions with neutrons at 20 to 28 Mev, total cross sections for, (E), 20: 30004
interactions with antineutrinos, vector current conservation in, (T), 20: 30008
interactions with mesons (π^-) at 1.7 Bev/c, differential cross sections for elastic, (E), 20: 30011
interactions with antiprotons and neutrons at 3.0 Bev/c, Byers-Yang model for charge-exchange, 20: 30014
interactions with antiprotons at high momentum transfer, cross section for elastic, (T), 20: 30019
interactions with mesons (π^-) at 4.7 Bev/c, production of meson resonance (1630) in, (E), 20: 30021
interactions with mesons (π^+) at 1.840 Bev/c, search for T = ½ isobar in, (E), 20: 30022
interactions with hyperons (Σ^-) at 105 to 165 Mev/c, cross section and hyperon (Λ) polarization from, (E), 20: 30024
interactions with protons and deuterons at 1.1 to 8 Bev/c, total cross sections for, (E), 20: 30028
interactions with neutrons, total cross sections for, (E/T), 20: 30028
interactions with bremsstrahlung at threshold to 6 Bev, meson (ρ^0) production in, (E), 20: 30030
interactions with protons, model for high-energy large-angle, 20: 30038
interactions with mesons (π^0), (K±), neutrons, and protons at 5 to 20 Bev/c, meson-exchange model for, 20: 30039
interactions with antiprotons, Regge-pole exchange model for $Y\bar{Y}$ production in, 20: 30044
interactions with deuterons at high energies, amplitudes for elastic, (T), 20: 30051
interactions with mesons (K-) at 1.45 Bev/c, K*(891) and N*(1236) production in, (E), 20: 30009
interactions with mesons (K+) at 3.54 Bev/c, production of strangeness +1 resonances from, 20: 30049
interactions with mesons (π^-) at 4.8 Bev/c, differential cross sections for charge-exchange, (E), 20: 29998(T)
interactions with protons at 3 Bev, N*(1688) production in, (T), 20: 30034
interactions with mesons (K+) at 3.535 Bev/c, production of K+K+* (1280) from, 20: 30047
mass relative to neutrons, bound-state model for, 20: 30042
motion in Van Allen belts, effects on geomagnetic field variations, 20: 30209(T) (NASA-TT-F-389, pp 464-82)
polarization in deuteron reactions (d,p) with deuterium at 2.1 to 14.1 Mev, (E), 20: 30524
reactions (p,α) with nuclei, compound nucleus level widths from, (E/T), 20: 30360 (WASH-1068)
reactions (p,α) with yttrium-89 and zirconium-90 at 20.2 Mev, alpha spectra from, (E/T), 20: 30353(R) (ORNL-3940, pp 1-61)
reactions (p,d) with yttrium-89 and zirconium-90 at 36 Mev, deuteron spectra from, (E/T), 20: 30353(R) (ORNL-3940, pp 1-61)
reactions (p,γ) with potassium-39 at 0.5 to 2.9 Mev, calcium-40 levels from, (E), 20: 30482
reactions (p,γ) with magnesium-25 at 956 to 1716 kev, gamma angular correlations from, (E), 20: 30528
reactions (p,n) with copper-63 at 4 to 9 Mev, zinc-63 levels from, (E), 20: 30406
reactions (p,n) with nuclei at 100 to 400 Mev, excitation functions for, 20: 30464
reactions (p,n) with zirconium-91 at 12.35 Mev, niobium-91 levels in proton emission from, 20: 30480
reactions (p,n) with lithium-7 near threshold, neutron energy distributions and yields from, (E), 20: 30525
reactions (p,xn) and (p,p(x-1)n) with nuclei at 40 to 100 Mev, inelastic scattering model for, 20: 30446
reactions with argon, neon, nitrogen, and oxygen, secondary electron in, (E), 20: 29951
reactions with copper and yttrium, cross section ratios of isobars from, 20: 30531
reactions with emulsion nuclei at 9 Bev, slow meson (π^+) production from, (E), 20: 30370
reactions with heavy emulsion nuclei at 12.8 Bev, angular distributions of secondaries from, (E), 20: 30364
reactions with heavy nuclei, detector for instrumenting, 20: 29551
reactions with heavy emulsion nuclei at 10 to 20 Bev, emission of fast helium nuclei from, (E), 20: 30496
reactions with hydrogen atoms at low energies, charge-exchange cross sections for, (E), 20: 29932(T)

reactions with primates at 32 to 2200 Mev, depth dose distribution in, 20: 28928 (CONF-651109, pp 417-25)
scattering by aluminum-27 at 3.5 to 11.3 Mev, excitation functions for, (E), 20: 30415
scattering by atomic hydrogen, coupled-state calculations of, 20: 29940
scattering by carbon at 12.8 to 13.4 Mev, angular distribution of polarization from elastic, (E), 20: 30457
scattering by helium-4 at 48 Mev, spin-rotation parameter from elastic, (E), 20: 30441
scattering by helium-4 at 40 Mev, continuum resonances in, (E), 20: 30512
scattering by mercury-202 and thallium-203, angular distributions and levels from elastic, (T), 20: 30484
scattering by nickel-60 at 17.8 Mev, cross sections for inelastic, (T), 20: 30437
scattering by nickel isotopes at 6.9 Mev, differential cross sections and polarization from, (T), 20: 30495
scattering by nitrogen at 12.6 to 13.6 Mev, angular distribution of polarization from elastic, (E), 20: 30457
scattering by nuclei at 40 Mev, cross sections for, (E/T), 20: 30353(R) (ORNL-3940, pp 1-61)
scattering by nuclei, nonlocal potential for optical-model analysis of, 20: 30408
scattering by palladium-106 and -108 at 12 and 13 Mev, cross sections and energy levels from, (E), 20: 30462
scattering by samarium isotopes at 9.98 to 10.60 Mev, europium isotope analog states from elastic and inelastic, (E), 20: 30430
scattering by tungsten-183 at 12 Mev, angular distributions from, (E), 20: 30475

PSEUDOUREA, 2-(2-AMINOETHYL)-2-THIO-
radiosensitivity effects on mice, 20: 28972
radiosensitivity effects in mice transplanted with bone marrow, γ, 20: 29036
radiosensitivity effects on phage induction in *E. coli*, x, 20: 29045

PULSE ANALYZERS
analog-to-digital converter for 4096-channel, design of servo-stabilized, 20: 29567
calibration of, design of relay-controlled pulse generator for, 20: 29544

PULSE GENERATORS (ELECTRONICS)
book: *Plasma and Electron uhf Amplifiers and Generators*, (E/T), 20: 29500
design of relay-controlled, for checking linear amplifiers and pulse-height analyzers, 20: 29544

PURINE
radiation effects on fluorescence and phosphorescence spectra of, at 77°K, gamma, 20: 28914

PURINES
2-amino-, radiomimetic properties in *E. coli*, 20: 29041

PYRIDINE, 2-PENTYL-, 1-OXIDE
solvent properties for products of uranyl nitrate hydrolysis, 20: 29359

PYRIDOXINE
radioinduced free radicals in sulfur-containing and sulfur-free derivatives of, uv and x, 20: 28901

PYROCATECHOL
amine derivatives of, content and metabolism of, in acute polonium-210 lesions in rabbits, 20: 28886
amine derivatives, radiation effects on metabolism in rats, 20: 28939
amine derivatives, radiation effects on content in rat adrenal glands and heart, 20: 28964
amine derivatives, determination in biological fluids, 20: 29032
amine derivatives, radiation effects on metabolism in mice, 20: 28940
amine derivatives, physiological effects in man, 20: 29032

4-PYRONE, 5-HYDROXY-2-(HYDROXYMETHYL)-
complexes with uranium, equilibrium constants for, 20: 29096

PYROPHOSPHORIC ACID, BIS(2-ETHYLHEXYL) ESTERS
solvent properties for aluminum, iron, thorium, and uranium, 20: 29361

Q

QUALITY CONTROL
inspection gage for average radius of machined parts, 20: 29668 (Y-NA-18)
neutron activation analysis in, 20: 29138

QUANTUM ELECTRODYNAMICS
theory of interband transitions, 20: 30735(R) (TID-22970, pp 331-73)

QUANTUM MECHANICS
chemical cross sections in, computer calculations of, 20: 29147 (UCRL-14901-T)
equation for, solution of non-steady Schroedinger, 20: 30240(T) (BNL-tr-67)
oscillators in, stochastic equation of motion for damped harmonic, 20: 30249
S-matrix potential in one-dimensional Schroedinger equation, (T), 20: 30248
spectral analysis of singular differential operators in, direct methods for, 20: 29615
wave packets in, relativistic space and time, 20: 30238 (JINR-P-2691)

QUARTZ
radioinduced paramagnetic centers in, microwave phonon reactions with x, 20: 30768

QUINIZARIN-2-SULFONIC ACID
complexes with uranium, composition and stability of, conductometric and spectrophotometric studies of, 20: 29181

8-QUINOLINOL, 5,7-DIBROMO-
use in determination of zinc, 20: 29136

R

RABBITS
effects of nicotinic acid on cholesterol and specific radioactivity in liver in, 20: 28895
radiation effects on catecholamine metabolism in, alpha, 20: 28886
radiation effects on glycogen metabolism in eyes of, 20: 28907
radiation effects on heme synthesis in bone marrow in, effects of hormones on, 20: 28912
radiation effects on immune reactions in, 20: 28965
radiation effects on blood plasma proteins in, uv, 20: 29004
radiation effects on brain of, pathological x, 20: 29011
radiation effects on germ cells of, x, 20: 29019
radiation effects on blood circulation in, x, 20: 29010
radiation injuries in, effects of antibiotics and bone marrow grafts on x, 20: 29052
radioinduced leukopenia in, protective effects of chemical agents against x, 20: 29055
radiosensitivity of, effects of cystamine on, 20: 29051
radiotherapy of lung tumors in, using internally deposited yttrium-90 particles, effects of hyperbaric oxygen, 20: 29059 (TID-22860)
strontium-90 uptake by skin of, effects of detergent treatment on, 20: 29461

RADIATION
dosimetry of, fluence response functions for equipment in, 20: 29482
effects on acceptance of tissue transplants, 20: 28983
effects on animals, effects of bone marrow transplants on, 20: 28875
effects on blood picture, effects of bone marrow transplants on recovery from, 20: 28981
effects on blood pressure of rats, 20: 29050
effects on catecholamide metabolism in rats, 20: 28939
effects on catecholamine metabolism in mice, 20: 28940
effects on catecholamine metabolism in man, 20: 29032
effects on clarification and coalescence time of reactor fuel solutions during processing in organic solvents, 20: 29333 (RT-CHI-(65)33)
effects on cysteine metabolism by rats, 20: 29024
effects on dimensions and thermal conductivity of low-permeability graphite, 20: 29822
effects on enzyme activity, effects of temperature on, 20: 28903
effects on glycogen metabolism in rabbit eyes, 20: 28907
effects on human body, review, 20: 29478
effects on immune reactions in mice, 20: 28926 (AD-633469)
effects on immune reactions in rabbits, 20: 28965
effects on immune reactions to bone marrow transplants in mice, 20: 29006
effects on immunity and para-immune defenses, 20: 28983
effects on leukolytic activity in blood and organs of rats, 20: 29044
effects on man, physiological, 20: 28974
effects on metabolism of exogenous ACTH in rats, 20: 29005
effects on metal wires for use as sensor materials, 20: 29486(R) (NASA-CR-54964)
effects on mice, synergistic effects of vibration with, 20: 28968
effects on mouse thymus cells, methods for evaluating, 20: 29008
effects on potassium chloride crystals, computer simulation of ionic displacement from, 20: 30741
effects on pressure vessel steels, 20: 30788(R) (ANL-7190, pp 176-88)
effects on rubber products, effects of halogenated organic compounds on, 20: 29322(P)
effects on sex ratio in rats, prenatal exposure, 20: 28952
effects on sorptive properties of surfaces of gels and semiconductors, (T), 20: 29815
effects on stresses in graphite columns, effect of cross-sectional shape on, 20: 30803
effects on yeast reproduction, 20: 28950
emission by anisotropic compressible plasma, patterns of, 20: 30711
emission by electrons moving above surface of uniaxial crystal with metal grating, 20: 29995
transport equations for, decomposition method for, 20: 30063
transport in plane parallel medium, decomposition method for equations

of, 20: 30063
use in satellite meteorology, 20: 30221(T) (NASA-TT-F-389, pp 741-57)
RADIATION CHEMISTRY
chemonuclear process for producing gaseous products from liquid reactants, 20: 29319(P)
mathematical model for gas-phase hot-atom reactions, 20: 29233
radiolysis of condensed alkanes, positive ion reactions in, 20: 29314
reaction kinetics in, effects of solid impurities on, 20: 29306
uses in preparation of ion-exchange membranes, 20: 29308
RADIATION DETECTION INSTRUMENTS
description of, for neutron-flux measurements in reactors, 20: 29549
design for criticality verification, 20: 29519 (BNWL-SA-31)
design for gamma source calibration, 20: 29571(P)
design for remote monitoring, 20: 29575(P)
design of whole-body, 20: 28871(R) (EUR-2636.f,i)
use of whole-body counters in environmental monitoring, 20: 28882
RADIATION DETECTION INSTRUMENTS (PULSE TYPE)
circuits for, design of fast, 20: 29536
performance for measuring secondary-electron current, 20: 29538
performance of gas discharge, for cosmic ray intensity measurements, 20: 29956(T) (NASA-TT-F-389, pp 684-91)
performance of square boron trifluoride, for neutrons, 20: 30347(R) (IDO-17147, pp 13-28)
RADIATION DETECTORS
book: *Instrument and Chemical Analysis Aspects of Electron Microanalysis and Macroanalysis*, 20: 29119
calibration technique for fast neutron, 20: 29529(R) (RPI-328-56, pp 94-112)
operation of high-energy gamma, 20: 29969
sample changer for, design of automatic, 20: 29572(P)
RADIATION INJURIES
effects of endocrine gland removal and hormones on, in mice, 20: 28978
effects of free radical reactions on, model studies of, 20: 29037
hemotherapy of, tranfusion methods for, 20: 28893
pathology of laser-induced, 20: 28936
pathology of, after exposure in criticality accident, 20: 28970
protection against, using hematoporphyrin in mice, 20: 29042
protection against, using cystamine in rabbits, 20: 29051
protection against, using antibiotics and bone marrow grafts in rabbits, 20: 29052
recovery from, in yeast, effects of ploidy on, 20: 28961
RADIATION MONITORING
use of whole-body counters in environmental, 20: 28882
RADIATION PROTECTION
control system for, for personnel, multipoint, 20: 29458
program in Canada, 20: 29053 (NP-15951)
program on, at Japan Atomic Energy Research Institute, 20: 29460
reactor personnel air lock for, 20: 29465
RADIATION-SCATTERING ANALYSIS
book: *Instrument and Chemical Analysis Aspects of Electron Microanalysis and Macroanalysis*, 20: 29119
RADIATION SICKNESS
edema associated with, in rats, 20: 29001
effects on nucleic acid content in guinea pig brain, 20: 28919
etiology of, in monkeys, 20: 28986
pathology of associated inflammation, 20: 28943
therapy of, using antibiotics, 20: 29051
RADIATION SOURCES
use of, measurement methods for, 20: 29593
RADIATION TARGETS
design of liquid hydrogen, 20: 29863
RADIO WAVES
emission from Crab nebula source, quasi-stellar objects, and supernovae remnants, coherent plasma mechanism for, 20: 29880
emission from Jupiter, origin of, (T), 20: 29907(T)
emission from solar corona, shock propagation mechanism for type-II, (T), 20: 29903(T)
emission from sun, frequency spectrum of slowly varying component of, 20: 29908
emission in continuous spectrum from solar corona, flux in isothermal model for, 20: 29904(T)
RADIOACTIVE CONTAMINATION
detection on surfaces, tracer technique for, 20: 29484(P)
hazards from, from underwater nuclear explosions, 20: 29481
RADIOACTIVE MATERIALS
removal from tissues by exchange transfusion, 20: 28893
use for heating minerals *in situ*, 20: 30950(P)
RADIOACTIVITY
book: *Natural Radioactivity of Plants and Soils*, 20: 29437
induced in foods during radiation processing, 20: 29599
measurement of environmental, in Valencia, 1964, 20: 29408
measurement of natural, near ground level, (E), 20: 29404 (CEA-R-2880)
measurement of, in gas chromatography, 20: 29105
measurements in rocks, 20: 29417
monitoring in rainwater, settled dust, and sewage sludge in Japan, 1964, 20: 29455
monitoring of particulate fallout for, in Osaka, Japan, October, 1964, 20: 29466
RADIOBIOLOGY
research on, center for, 20: 30937
RADIOCHEMICAL PROCESSING PLANTS
safety controls in receiving and shipping fissionable materials, procedures for, 20: 29450 (ISO-270)
RADIODIAGNOSIS
method for hematologic, using extracorporeal irradiation, 20: 28893
radioisotope-labeled compounds in, 20: 29066
technetium-99m uses in, 20: 29065
RADIOFREQUENCY SPECTROMETERS
design of NMR, 20: 29498
RADIOGRAPHY
dosimetry in section, 20: 29073
incidence of diagnostic, during early pregnancy, 20: 29068
method for kidney, in children, 20: 29062
performance of 50-Curie cobalt-60 gamma source for, 20: 29596
RADIOISOTOPES
book: *Radioisotopic Instruments in Metallurgy*, 20: 29598
determination of beta-emitting, by liquid scintillation counting, role of phosphorescence in, 20: 29084
movement in soils, 20: 30943(R) (ORNL-TM-1465)
production of, economics of reactor, 20: 29609 (NP-15947)
research on, center for, 20: 30937
separation of, by high-voltage electrophoresis, 20: 29356
use as space power source, 20: 30926
use in power systems for communications satellites, 20: 29608
uses as power sources for underwater applications, 20: 29607
uses in medical diagnosis, 20: 29066
uses in Naval Shore Establishment, review of potential, 20: 29581 (AD-633785)
uses in oceanographic research, 20: 29401
uses of waste, to control termite colonies, 20: 29587
RADIOMETRIC ANALYSIS
equipment for determining liquid component concentrations in mixture, 20: 29570(P)
RADIOMIMETIC SUBSTANCES
effects on enzyme activity in animals, 20: 29048
RADIOPROTECTIVE COMPOUNDS
action of, on biological materials, molecular mechanisms for, 20: 29040
effects on Ehrlich ascites carcinoma and mouse spleen, mechanism for, 20: 29039
effects on seeds and seedlings of peas, 20: 29049
efficiency of rhodanine derivatives as, 20: 29241
RADIOSENSITIVITY
effects of hyperbaric oxygen on lung tumor, 20: 29059 (TID-22860)
effects of time of day on mouse, 20: 28938
of *Micrococcus radiodurans*, effects of pigments on, 20: 29016
RADIOSTERILIZATION
effects on precooked marine products, 20: 29582(R) (MIT-3343-26)
effects on wholesomeness of foods, 20: 29585
facility for marine product, design of, 20: 29584 (TID-22991)
methods of, for cod and halibut patties, 20: 29603
RADIOTHERAPY
dose measuring system for, design of automatic, 20: 29070
dosimetry in, design and fabrication of, phantom for, 20: 29077(P)
effects on amino acid content in blood plasma, 20: 28979
effects on vaginal cytology, 20: 29076
facility planning, 20: 29071
gold-198 for use in, preparation of colloidal and platinum-coated, 20: 29075
method for hematologic, using extracorporeal irradiation, 20: 28893
radiation doses in grid, 20: 29056
radiation source design for γ, 20: 29064
use of internally deposited yttrium-90 for, 20: 29059 (TID-22860)
RADIUM
content and chemical form in iron–manganese concretions, 20: 29426
content in iron–manganese concretions and manganese ores, 20: 29425
determination in rocks by gamma spectroscopy, errors in, 20: 29421
dosimetry of therapeutic implants of, 20: 29074
effects on blood and hematopoietic system, 20: 28982
RADIUM ISOTOPES Ra-226
production of, economics of reactor, 20: 29609 (NP-15947)
RADON ISOTOPES Rn-219
decay of, distribution in electric field of products from, 20: 29325
decay of, in hydrogen, methane, and nitrogen, properties of recoils from, 20: 29325
RADON ISOTOPES Rn-220
decay of, in hydrogen, methane, and nitrogen, properties of recoils from,

20: 29325
RAIN WATER
radioactivity of, in Japan in 1964, 20: 29455
radioactivity of, Calcutta, India, 1962, 20: 29420
tritium content of, Moscow, Dec. 1961 to Dec. 1963, 20: 29409
RARE EARTH ALLOYS
analysis of, by dissolution in hydrobromic acid and titration in non-aqueous solutions, 20: 29133
RARE EARTH CARBIDES
hydrolysis of, gaseous products from, 20: 29220
RARE EARTH COMPLEXES
with carboxylic acids, stability constants of, 20: 29232
with EDTA, preparation, composition, and stability of, 20: 29222
with *N,N*-bis(2-hydroxyethyl)glycine and *N*-2-hydroxyethyliminodiacetic acid, composition and stability of, 20: 29343
with serine, stability of, 20: 29208
with 1,10-phenanthroline–thenoyltrifluoroacetone, preparation and composition of, 20: 29221
RARE EARTH FLUORIDES
fluorine-19 NMR in, 20: 30755
RARE EARTH IONS
energy levels for paramagnetic trivalent, fourth order crystal field splitting of, (T), 20: 30747
radioinduced thermoluminescence of, in calcium fluoride, 20: 29318
spectra of trivalent, in calcium fluoride crystals, uv absorption, 20: 30763
RARE EARTH NIOBATES
distribution in strontium molybdate single crystals, coefficients of, 20: 29746
RARE EARTH NITRATES
reactions with cobalt nitrate and potassium nitrate, 20: 29209
RARE EARTH OXIDES
analysis of, for trace impurities by activation methods, 20: 29082 (SGAE-CH-27/1966)
magnetic moments in high magnetic fields, (E/T), 20: 30735(R) (TID-22970, pp 331-73)
properties for uses as control materials in nuclear reactors, 20: 29732
RARE EARTH PHTHALOCYANINES
stability of, electron absorption spectra studies of, 20: 29217
RARE EARTH TITANATES
preparation and cyrstal structure of, 20: 29212
RARE EARTH TUNGSTEN BRONZE
preparation, properties, and structure of, 20: 29164
RARE EARTHS
analysis of, for terbium using potassium oxalate, spectrofluorimetric, 20: 29086
book: *Rare Earth Elements*, 20: 29635
determination in standard igneous rocks G-1, W-1, and G-B by x-ray fluorescence, 20: 29101
determination in TBP extracts, spectrophotometric, 20: 29125
determination in uranium compounds, spectrographic, 20: 29129
determination of, in presence of thorium, spectrophotometric, 20: 29109
electron interband mixing model for, 20: 30735(R) (TID-22970, pp 331-73)
polarographic properties of, on fused potassium acid sulfate electrolyte, 20: 29210
properties of, relations of, with band structure and Fermi surfaces, (T), 20: 30735(R) (TID-22970, pp 331-73)
separation by paper electrophoresis, 20: 29343
separation of, by high-voltage electrophoresis, 20: 29356
single crystal preparation, (E), 20: 30735(R) (TID-22970, pp 331-73)
thermodynamic properties at 0°C to melting point, 20: 29743
RARE GASES
separation of nitrogen impurity from, use of titanium-metal sponge as gettering agent for, 20: 29329 (ANL-7128)
transport coefficients in dense systems of, computer calculations of, 20: 29147 (UCRL-14901-T)
RATE METERS
design and performance for variable flow measurements, 20: 29535
design using phosphor and photocathode, 20: 29576(P)
RATS
aging processes in, effects of polonium-210 on, 20: 29030
blood pressure of, effects of radioprotective compounds on, 20: 29050
cholesterol content in tissues of, effects of diet on, 20: 28995
cysteine metabolism by, 20: 29024
effects of injected thorotrast in, carcinogenic, 20: 29022
leukolytic activity in blood and organs of, effects of ACTH on, 20: 29044
metabolism of serum proteins in, effects of carbon tetrachloride, radiation, and venous bleeding on, 20: 28954
radiation effects on collagen and hexosamine contents in subcutaneous granulomas of, γ, 20: 28917
radiation effects on vitamin C metabolism in, γ and x, 20: 28921
radiation effects on catecholamine metabolism in, 20: 28939
radiation effects on nucleic acid synthesis in thymus cells of, x, 20: 28953
radiation effects on catecholamine and tyramine activity in tissues of, x, 20: 28964
radiation effects on cholesterol content in tissues of, x, 20: 28995
radiation effects on pathology of atherosclerosis in, 20: 28996
radiation effects on protein metabolism in, tracer study, 20: 28997
radiation effects on metabolism of exogenous ACTH in, 20: 29005
radiation effects on cysteine metabolism by, 20: 29024
radiation effects on mast cells of connective tissue of, effects of low temperatures on uv, 20: 28944
radiation effects on sex ratio in, prenatal exposure, 20: 28952
radiation effects on cholesterol and lipid content of blood of, strontium-90, 20: 28994
radiation effects on erythropoiesis in, effects of endocrine gland removal and hormones on, 20: 29043
radiation effects on leukolytic activity in blood and organs of, 20: 29044
radiation effects on blood pressure of, 20: 29050
radiation sickness in, edema during, 20: 29001
radioinduced free radicals in bones of, EPR study of, 20: 28898 (CEA-R-2910)
radioinduced free radicals in bones of, γ, 20: 28906
radioinduced skin lesion in, role of adipose tissue in repair of x, 20: 28946
radiosensitivity of thyroid gland of, effects of cystamine on, 20: 29047
thorium distribution and excretion in, after inhalation, 20: 28897
thyroid activity and morphology in, uranium nitrate effects on, 20: 28884
REACTION MECHANISMS
chemical cross section and relaxation phenomena in, computer calculations of, 20: 29147 (UCRL-14901-T)
REACTOR BREEDING BLANKETS
design, 20: 30921(P)
REACTOR COMPONENTS
design and testing of FARET, 20: 30787(R) (ANL-7190, pp 11-142)
design and testing of AARR, 20: 30787(R) (ANL-7190, pp 11-142)
performance of safety-system, 20: 30901
testing deflections and stresses in core support grids, 20: 30788(R) (ANL-7190, pp 176-88)
REACTOR CONTROL ELEMENTS
design of combination control-fuel rod assembly, 20: 30873(P)
REACTOR CONTROL RODS
brake design for, 20: 30817(P)
drive mechanism for insertion control of, design of, 20: 30825(P)
performance in EBR-II, 20: 30787(R) (ANL-7190, pp 11-142)
REACTOR CONTROL SYSTEMS
analysis of temperature, analog simulation for feedforward compensation for, 20: 30807 (ORNL-TM-1485)
design and operating experience, 20: 30901
design for liquid or solid moderated reactors, 20: 30822(P)
position servo for, fabrication and testing of flueric, 20: 30922(R) (BRLD-3255)
rod positioning by boron addition in chemical shim of PWR, 20: 30808 (WCAP-3269-54)
shutdown apparatus using neutron-absorbing filler, design of, 20: 30835(P)
use of lithium aluminate as burnable poison in, 20: 30865(P)
REACTOR COOLANTS
book: *Nuclear Power Reactor Coolants*, 20: 30910
properties of organic, research on, 20: 30906
REACTOR COOLING SYSTEMS
heat transfer in, conference on, 20: 29383
pipe rupture in, research program on, 20: 30811
temperature in liquid-metal, equations for, 20: 29374(R) (ANL-7190, pp 156-66)
testing of EBWR, nondestructive, 20: 30787(R) (ANL-7190, pp 11-142)
vapor traps for liquid-metal, 20: 30814
REACTOR ENGINEERING
bibliography on, 20: 30786(R) (ANL-7190)
REACTOR EXPERIMENTAL FACILITIES
failure of PRTR fuel-element rupture test loop, 20: 30941
REACTOR FUEL ELEMENTS
analysis of spent, 20: 29078(R) (AD-633252)
cladding for boiling-water, use of stainless-steel, 20: 30903
cladding for, hydridation effects on Zircaloy, 20: 30902
cladding material for, properties of beryllium as, 20: 29777
design for gas-cooled reactors, 20: 30872(P)
design for water-cooled and -moderated reactors, 20: 30869(P)
design of assembly of, with spacing grid, 20: 30818(P)
design of combination control-fuel rod assembly, 20: 30873(P)
electric coupling device for, design of, 20: 29512(P)
fabrication of cermet, for AARR, 20: 30787(R) (ANL-7190, pp 11-142)
handling device for, design of, 20: 30824(P)
neutron resonance escape probability in arrayed cladded, Dancoff factor for, 20: 30842

performance in EBR-II, 20: 30787(R) (ANL-7190, pp 11-142)
processing of irradiated, pilot plant design problems for fluoride-volatility, 20: 29364
testing urania, for hydrogen-propelled rocket reactors, 20: 30787(R) (ANL-7190, pp 11-142)
thermal properties of rod-cluster, 20: 29382

REACTOR FUEL ELEMENTS (CERAMIC)
burnup ratio in plutonia–urania, method for determination of, 20: 29617(R) (EURAEC-1593)
design for fast reactors, effects of cross section uncertainties on, 20: 29618(R) (GEAP-4982)
development of Incoloy 800-clad plutonia–urania, 20: 29617(R) (EURAEC-1593)
fabrication of carbide-containing vitreous carbon, 20: 29692(P)
fission-gas pressure buildup in uranium dioxide, effects of void volume variation on, 20: 29818
thermal performance of plutonia–urania, effects of plutonia segregation on, 20: 29617(R) (EURAEC-1593)

REACTOR FUEL ELEMENTS (DISPERSION)
fabrication of pressed graphite, 20: 29669

REACTOR FUEL PINS
reactivity worth of, perturbation analysis of, (E), 20: 30839

REACTOR FUEL RODS
arrangement of, design of device for, 20: 30829(P)

REACTOR FUELS
acquisition in Japan, problems of, 20: 30871
burnup in reflected reactor, nonuniform, (T), 20: 30909
coating of particulate, with pyrolytic graphite, process for, 20: 29638(P)
development for fast liquid metal-cooled reactors, 20: 30790(R) (ANL-7204, pp 1-31)
development of pyrolytic carbon-coated particulate, 20: 30870(R) (ORNL-TM-1528)
preparation of fine particles of thorium carbide for, 20: 29676
processing in Shellsol T-TBP and Solvesso 100–TCAN solvents, radiation effects on clarification and coalescence time during, 20: 29333 (RT-CHI-(65)33)
radiation effects on pyrolytic-carbon-coated particulate, 20: 30870(R) (ORNL-TM-1528)
reactivity variations with burnup, in power reactors, 20: 30900
testing of coated urania and uranium carbide particulate, 20: 29616(R) (BMI-1738)
testing stainless steel-clad ceria–urania and urania–zirconia, 20: 29616(R) (BMI-1738)

REACTOR MATERIALS
development for fast breeder reactors, 20: 30875(R) (ANL-7190, pp 143-55)
oxidation reactions of, research on, 20: 30801
radiation effects on embrittlement of steel, neutron, 20: 29825
refining of, electrolytic cell for, 20: 29373(P)

REACTOR MATRICES
analysis of water-moderated plutonia–urania, 20: 29617(R) (EURAEC-1593)
design of, 20: 30818(P)
design of EBWR, for plutonium recycle programs, 20: 30787(R) (ANL-7190, pp 11-142)
neutron diffusion parameters for uniform, (T), 20: 30851
neutron disadvantage factor in closely packed cylindrical, 20: 30840
neutron disadvantage factor in uranium-water, (E/T), 20: 30855
neutron flux spectra in heavy-water natural-uranium lattice, angular, (E), 20: 30846
neutron resonance escape probability in arrayed cladded, Dancoff factor for, 20: 30842
neutron thermalization in heterogeneous, approximate treatment of, 20: 30864
reactivity calculations for aluminum–plutonium, uranium dioxide, and plutonium dioxide–uranium dioxide, 20: 30857
reactivity of plutonium-bearing, 20: 30858

REACTOR MODERATORS
design of graphite-block, 20: 30834(P)
design of interlocking brick and tile, 20: 30823(P)
neutron transport in adjacent semi-infinite, time-dependent monoenergetic, (T), 20: 30339
radioinduced stresses in, effect of cross-sectional shape on, 20: 30803
support structure for vertically stacked solid, design of, 20: 30826(P)

REACTOR REFLECTORS
fabrication of beryllium-containing graphite matrix, 20: 30816(P)

REACTOR SAFETY
analysis for AARR, 20: 30787(R) (ANL-7190, pp 11-142)
analysis for FARET facilities, 20: 30787(R) (ANL-7190, pp 11-142)
design of pressure-suppression chamber for reactor plant, 20: 30833(P)
oxidation of reactor materials, research on, 20: 30801
programs and standards in Soviet Union, 20: 30800
research programs on, 20: 29470

REACTOR SAFETY EXPERIMENTS
accident analysis for, SPERT subassembly test program for, 20: 30796 (IDO-17177)
fuel meltdown studies in TREAT, metal-water reactions from, 20: 30792(R) (ANL-7204, pp 74-86)
meltdown loops in TREAT, design and operation of, 20: 30788(R) (ANL-7190, pp 176-88)
neutron flux profile in TREAT, effects of cadmium filter on, 20: 29618(R) (GEAP-4982)
power excursion in TREAT, uranium-water reactions from, 20: 30802

REACTOR SIMULATORS
design for training MSRE operators, 20: 30934 (ORNL-TM-1445)

REACTOR SOLUTIONS
processing in Shellsol T-TBP and Solvesso 100–TCAN solvents, radiation effects on clarification and coalescence time during, 20: 29333 (RT-CHI-(65)33)

REACTORS
accident analysis for, SPERT subassembly test program for, 20: 30796 (IDO-17177)
book: *Physics of Nuclear Reactors*, 20: 30804
ceramic material uses in, review of, 20: 29732
containment air locks for personnel safety in, 20: 29465
containment systems for, leak testing of, 20: 30812
containment vessels for, strength of steel, (T), 20: 30813
control and stability of, methods for predicting, 20: 30788(R) (ANL-7190, pp 176-88)
control of liquid or solid moderated, method for, 20: 30822(P)
core design for, 20: 30873(P)
critical size of hollow cylindrical and spherical, (T), 20: 30856
design with integral heat exchanger and associated vapor-liquid separating equipment, 20: 30913(P)
development, 20: 30789(R) (ANL-7204)
fuel burnup and poison accumulation in reflected, (T), 20: 30909
gamma heating in, group constants for, 20: 30722 (KAPL-M-6497)
kinetic equations for, numerical solution of, 20: 30847
kinetics of, computer analysis of, 20: 30838
kinetics of, space-dependent, 20: 30845
loading of, design of guide tube for, 20: 30830(P)
loading of, design of fixing device for, 20: 30831(P)
loading systems for, materials for, 20: 30815
neutron buckling and flux distribution for hollow cylindrical and spherical, one-group diffusion method for, 20: 30856
neutron fields in, kinetic theory of spatial and spectral coupling of, 20: 30862
neutron kinetics in fast core of fast-thermal, variational method for prompt, 20: 30852
neutron multiplication in, correlation theory of, 20: 30844
neutron thermalization in, space-dependent, (T), 20: 30861
neutron transport calculations for, cross section library for, 20: 30723 (NAA-SR-11831)
neutron-flux measurements in, instruments for, 20: 29549
operating experience and procedures, conference on, 20: 30799
reactivity control for, 20: 30867(P)
reactivity measurements in, multiplication method for, 20: 30849
reactivity noise analysis using polarity correlation function, 20: 30853
reactivity of subcritical, kinetics during sinusoidal variation of, 20: 30860
shield design for, thermal, 20: 30828(P)
shutdown of, design of apparatus for, 20: 30835(P)
stability of, effects of delayed neutrons on, (T), 20: 30850
use as space power sources, 20: 30926
use for production of radioisotopes, economics of, 20: 29609 (NP-15947)
waste disposal methods for radioactive solids from, 20: 30947
waste disposal of gases from, 20: 30949
xenon stability in, absorbing foil determination of, 20: 30843

RECOIL IONS
mathematical model for chemical reactions involving, 20: 29233
ranges in solids, (E), 20: 30479

REFRACTORY MATERIALS
coating with silicon by fluidized-bed process, 20: 29630
fabrication and properties of, for use in space technology, 20: 29680
fabrication of corrosion-resistant, with low thermal neutron capture cross section, 20: 29696(P)
fabrication of high-strength bodies of, method for, 20: 29695(P)
fabrication of, by flow turning, 20: 29682
thermal diffusion of carbon, nitrogen, and oxygen in, review on, 20: 29769

RELATIVITY THEORY
field equations in general, perturbed Schwarzschild metric for, 20: 30246

gravitational absorption and shielding in general, 20: 30245
Lorentz transformation in, 20: 30242
motion in general, spherically symmetric, 20: 30244
of cylindrical systems, general, 20: 30251

RENÉ-41
joining by brazing, soldering, or welding, 20: 29666 (RSIC-484)
joining by mechanical fastening, 20: 29667 (RSIC-509)
machining properties of, 20: 29665 (RSIC-482)
surface treatments for, coating and mechanical, 20: 29706 (NASA-TM-X-53448)

RENÉ-62
joining by mechanical fastening, 20: 29667 (RSIC-509)
machining properties of, 20: 29665 (RSIC-482)

RESEARCH REACTORS
design and experimental program of Scottish, 20: 30936
design and experiments for EWA, 20: 30937
experimental facilities of, modifications to, 20: 30904
experimental facilities of, safety aspects of gas-cooled in-pile loops for, 20: 30940
gamma irradiation facility of Frankfurt, 20: 29341
neutron flux in Univ. of Florida Training Reactor, calculations of, 20: 30862
neutron multiplication factor in Hitachi, effect of epithermal fission on, (E/T), 20: 30841
reactivity noise measurement in LFR, 20: 30942

RESINS
analysis for water by titration, handling methods for, 20: 29083(R) (UCRL-14767)
development of epoxy, for electronic equipment potting, 20: 29366(R) (TID-22970, pp 375-91)
preparation of cured bodies of, by hot curing and radiation pre-gelling, 20: 29637(P)
radiation effects on epoxido-dianic ED-5, effects of copper and lead on, 20: 29297
radioinduced changes in structure of epoxy, effects of copper and lead on gamma, 20: 29296
sorptive properties of metal sulfide-ion exchange, for radioisotopes in sea water, 20: 29345
use of ion-exchange, for strontium separation from calcareous media, 20: 29363

RESISTANCE FURNACES
design of, for measuring creep-rupture of refractory metals to 3000°C, 20: 29710 (TID-22986)

RETICULO-ENDOTHELIAL SYSTEM
radiation effects on function of rabbit, 20: 28965

RHENIUM
compatibility of coating of, with uranium carbide–zirconium carbide thermionic diode at 1800 to 2500°C, 20: 29820
effects on properties of graphite, with and without copper and silver infiltration, 20: 29764
electron ranges in thin films of, 20: 29952
iron-57 Mössbauer spectra in, 20: 30766
magnetic properties of superconducting, effects of lattice defects on, 20: 30253 (CEA-R-2808)
production of powdered, from rhenium tetrammine chloride, effects of inert atmosphere on, 20: 29672
properties and uses of, 20: 29768
properties of, at 2000°C, for use in thermionic converters, 20: 29729
radiation effects on, for use as sensor material, 20: 29486(R) (NASA-CR-54964)
superconducting energy gap in, anisotropy of, (E), 20: 30281

RHENIUM ALLOYS
Bi–Re, phase studies, 20: 29717
Cr–Re, effects on interstitial nitrogen on, 20: 29616(R) (BMI-1738)
Er–Re, crystal structure of, laves phase in, 20: 29792(T)
Gd–Re, crystal structure of, laves phase in, 20: 29792(T)
Mo–Re, fabrication, properties, and uses of, 20: 29768
Re–Ta–W, availability, properties, and uses of, 20: 29760
Re–Tb, crystal structure of, laves phase in, 20: 29792(T)
Re–W, extrusion of tubing of, development of process for, 20: 29659(R) (COO-1518-3)
Re–W, fabrication, properties, and uses of, 20: 29768
Re–W, tensile properties of sheets and wires of, 20: 29765
Sb–Re, phase studies, 20: 29717

RHENIUM COMPLEXES
chloride, thermal decomposition of, production of powdered rhenium from, 20: 29672

RHENIUM ISOTOPES Re-185
neutron capture cross sections and resonance parameters, (E), 20: 30360 (WASH-1068)

RHENIUM ISOTOPES Re-186
beta decay of, matrix elements for first-forbidden, (E/T), 20: 30522

RHENIUM ISOTOPES Re-187
neutron capture cross sections and resonance parameters, (E), 20: 30360 (WASH-1068)

RHENIUM ISOTOPES Re-188
beta transitions of, nonaxial model prediction on first-forbidden, (E/T), 20: 30550

RHENIUM SYSTEMS
As–Re, phase studies, 20: 29717
Re–Te, phase studies, 20: 29717
Re–ThO_2–W, fabrication, properties, and uses of, 20: 29768

RHODAMINE B
precipitation of protactinium with, in acid solutions in presence of crystal violet, 20: 29135

RHODANINE
radiosensitivity effects and preparation of, 20: 29241

RHODANINE, 5-CARBO XYMETHYL-
radiosensitivity effects and preparation of, 20: 29241

RHODANINE, 5-CARBOXYMETHYLIDENE-
radiosensitivity effects and preparation of, 20: 29241

RHODANINE, 5-ETHYL-
radiosensitivity effects and preparation of, 20: 29241

RHODANINE, 5-ETHYLIDENE-
radiosensitivity effects and preparation of, 20: 29241

RHODANINE, 5-(1-METHYLCARBOXYMETHYL)-
radiosensitivity effects and preparation of, 20: 29241

RHODANINE, 5-(1-METHYLCARBOXYMETHYLIDENE)-
radiosensitivity effects and preparation of, 20: 29241

RHODIUM ALLOY COUPLES
Pt/Pt–Rh, performance of thermocouples of, 20: 29495

RHODIUM ISOTOPES Rh-101
decay of isomeric, ruthenium-101 energy levels from, (E), 20: 30469

RHODIUM ISOTOPES Rh-103
energy level transitions from ruthenium-103 decay, K conversion coefficients for, (E), 20: 30471
neutron capture by, gamma spectra from, 20: 29078(R) (AD-633252)
proton reactions (p,α) with, palladium-104 level widths from, (E/T), 20: 30360 (WASH-1068)
proton reactions (p,n) at 100 to 400 Mev, excitation functions for, 20: 30464

RHODIUM ISOTOPES Rh-104
neutron capture by, gamma spectra from, 20: 29078(R) (AD-633252)

RIBONUCLEIC ACID
content of, in guinea pig brain, effects of radiation sickness on, 20: 28919
effects of nicotinic acid on composition of, in rabbit liver, 20: 28895
effects on recovery of regenerative capacity in axolotl limbs exposed to x irradiation, 20: 29038
induction of antibody synthesis in mice by injected, 20: 28926 (AD-633469)
radiation effects on thermoluminescence of, gamma, 20: 28913
radiation effects on synthesis in *E. coli*, uv, 20: 28949

RIBONUCLEIC ACID, DESOXY-
content of, in guinea pig brain, effects of radiation sickness on, 20: 28919
infectivity of bacteriophage, 20: 28948
radiation effects on, relation of chromosome damage to, 20: 28908
radiation effects on thermoluminescence of, gamma, 20: 28913
radiation effects on synthesis in *E. coli*, uv, 20: 28949
radiation effects on, ESR and thermoluminescence studies of, 20: 29249
radiation effects on synthesis in pea seedlings, y and neutron, 20: 28989
radiation effects on, role of free radicals in, 20: 29037

RIBOSE
radiation effects on thermoluminescence of, gamma, 20: 28913

ROCKET MOTOR NOZZLES
fabrication of silver-infiltrated tungsten, by compaction and sintering, 20: 29685
production of tungsten, by flow turning, 20: 29682

ROCKET MOTORS
design of, with motive fluid heating chamber, 20: 29395(P)

ROCKET REACTORS
control system for, fabrication and testing of flueric position servo for, 20: 30922(R) (BRLD-3255)
design of metal-fueled fast, 20: 30787(R) (ANL-7190, pp 11-142)
radiation hazards from NRX A-2 and A-3 tests, 20: 30923 (LA-3394)

ROCKET REACTORS (KIWI)
control system for, temperature, 20: 30924 (LA-DC-7636)
temperature measurements in, cooled thermocouples for, 20: 30925 (LA-DC-7637)

ROCKETS
design of Agena-D, using beryllium, 20: 29393

ROCKS
analysis for radium, thorium, and uranium by gamma spectroscopy, errors in, 20: 29421
potassium, thorium, and uranium abundances in gneisses, Rum Jungle

Complex, Australia, 20: 29415
radioactivity of, effects of clay content on, 20: 29417
scandium abundance and distribution in, 20: 29436
thorium and uranium contents of, in northeastern Balkhash foreland, USSR, 20: 29418
uranium content in traprock formation of, Siberian platform, USSR, 20: 29419
ROOTS
iodine-131 uptake by sagebrush, 20: 28883
ROTORS
measurements in magnetically suspended, telemetering system for, 20: 29369
RUBBER
deformation bands in sheet, 20: 29624(R) (TID-22970, pp 257-329)
preparation of vulcanized radiation-resistant, 20: 29322(P)
radiolysis of hard, at −196°C, ESR studies on formation of free radicals in, 20: 29299
RUBIDIUM
density of, at critical temperature, radiometric techniques for measuring critical, 20: 29742
spectra of, Stark effect on optical, 20: 29941
RUBIDIUM CHLORIDES
KCl–RbCl, argon-39, -41, and krypton-85 diffusion in, 20: 30769
RUBIDIUM IONS
dissociation of fast negative, in rare gases, (T), 20: 29947
RUBIDIUM ISOTOPES Rb-84
beta decay of, matrix elements for first-forbidden, (E/T), 20: 30522
RUBIDIUM ISOTOPES Rb-86
beta decay of, matrix elements for first-forbidden, (E/T), 20: 30522
beta spectra, (E), 20: 30546
use in measuring coronary blood-flow rate, 20: 28871(R) (EUR-2636.f,i)
RUBIDIUM ISOTOPES Rb-92
half life, 20: 30477
yields from uranium-235 thermal fission, (E), 20: 30477
RUBIDIUM ISOTOPES Rb^{95}
half life, (E), 20: 30477
yields from uranium-235 thermal fission, (E), 20: 30477
RUBIDIUM MANGANESE FLUORIDES
magnetic properties of, 20: 29709(R) (TID-22970, pp 65-119)
RUBIDIUM SAMARIUM BROMIDES
preparation, 20: 29204
RUBIDIUM SAMARIUM CHLORIDES
preparation, 20: 29204
RUBIDIUM THORIUM SULFATES
preparation and properties of, 20: 29218
RUSSIAN REACTORS
safety programs and standards, 20: 30800
RUTHENIUM
evaporation of, from irradiated uranium(IV-VI) oxides at 900 to 1500°C in flowing hydrogen, nitrogen, or oxygen, 20: 29211
separation from irradiated uranium dioxide in chlorine trifluoride by volatilization, 20: 29330(R) (EURAEC-1601)
RUTHENIUM ISOTOPES Ru-101
energy levels from rhodium-101 decay, (E), 20: 30469
yields from uranium-233 and -235 fission, (E), 20: 29080(R) (IDO-14676)
RUTHENIUM ISOTOPES Ru-102
yields from uranium-233 and -235 fission, (E), 20: 29080(R) (IDO-14676)
RUTHENIUM ISOTOPES Ru-103
beta decay of, K conversion coefficient for, (E), 20: 30471
content in fallout from Chinese nuclear tests, 20: 29423
RUTHENIUM ISOTOPES Ru-104
yields from uranium-233 and -235 fission, (E), 20: 29080(R) (IDO-14676)
RUTHENIUM ISOTOPES Ru-106
content in juniper trees in Georgia, 20: 29410
content in pulp for photographic paper, 20: 29427
movement in soils, 20: 30943(R) (ORNL-TM-1465)
separation from sea water by sorption by metal sulfide-ion exchange resins, 20: 29345
yields from uranium-233 and -235 fission, (E), 20: 29080(R) (IDO-14676)

S

SACLAY PROTON SYNCHROTRON
radiation dosimetry of, methods for, 20: 29845 (CONF-651109, pp 117-42)
SAFETY
design of device for, in radioactive measuring apparatus, 20: 29515(P)
procedures for receiving and shipping fissionable materials, 20: 29450 (ISO-270)
research programs on nuclear, 20: 29470
SALAMANDERS
radiation effects on regenerative capacity of axolotl limbs, effects of RNA on recovery from, 20: 29038
SALICYLATE COMPLEXES
with uranium, preparation and composition of, 20: 29197
with uranyl nitrate, composition and stability of, spectrophotometric studies of, 20: 29202
SALICYLIC ACID
reactions with uranyl ions, 20: 29197
SALICYLIC ACID, SULFO-
Antarox DM-970–sodium hexametaphosphate–sodium dodecyl sulfate–sodium nitrates–sulfosalicylic acid, efficiency of, as radioactivity decontamination solution for cotton protective clothing, 20: 29477
SALMONELLA
radioinduced mutations of, uv, 20: 28977
SALT DEPOSITS
waste disposal in, 20: 30943(R) (ORNL-TM-1465)
SALTS
deposition on electric insulators, x-ray fluorescent method for measuring, 20: 29103
SAMARIUM
determination in rocks, chemical spectrographic method for, 20: 29083(R) (UCRL-14767)
determination in standard igneous rocks G-1, W-1, and G-B by x-ray fluorescence, 20: 29101
determination in TBP extracts, spectrophotometric, 20: 29125
determination in uranium compounds, spectrographic, 20: 29129
SAMARIUM ALLOYS
La–Sm, electric conductivity, magnetic susceptibility, and superconducting transition temperatures of, 20: 29753
SAMARIUM COMPLEXES
hexanitrocobaltate, preparation and composition of, effects of temperature on, 20: 29209
with EDTA, preparation, composition, and stability of, 20: 29222
with serine, stability of, 20: 29208
with 1,10-phenanthroline–thenoyltrifluoroacetone, preparation and luminescence of, 20: 29221
with 2,4-pentanedione, luminescence spectra of, (E), 20: 29238
SAMARIUM ETHYL SULFATES
samarium ion energy levels in, Orbach relaxation mechanism for excited, 20: 30758
SAMARIUM IONS
energy levels in lanthanum chlorides, Orbach relaxation mechanism for excited, 20: 30758
energy levels in samarium ethyl sulfates, Orbach relaxation mechanism for excited, 20: 30758
fluorescence decay in lanthanum chloride crystals, 20: 30782
SAMARIUM ISOTOPES Sm-147
energy levels from europium-147 decay, multipolarity and spin of, (E), 20: 30362
SAMARIUM ISOTOPES Sm-148
proton scattering at 9.98 to 10.50 Mev, europium-149 analog states from elastic and inelastic, (E), 20: 30430
SAMARIUM ISOTOPES Sm-149
neutron capture by, neutron separation energy determination from, (E), 20: 30366
SAMARIUM ISOTOPES Sm-150
production from neutron capture by samarium-149, neutron separation energy determination from, (E), 20: 30366
proton scattering at 10.30 to 10.55 Mev, europium-151 analog states from elastic and inelastic, (E), 20: 30430
SAMARIUM ISOTOPES Sm-152
nitrogen-14 inelastic scattering by, Coulomb excitation from, (E), 20: 30488
proton scattering at 10.3 to 10.6 Mev, europium-153 analog states from elastic, 20: 30430
SAMARIUM NIOBATES
distribution in strontium molybdate single crystals, coefficients of, 20: 29746
SANDS
gamma scattering by, energy distribution from, (E), 20: 30728
SATELLITES
effects on charged-particle intensity in Van Allen belts, 20: 30223(T) (NASA-TT-F-389, pp 817-21)
power plants for communications, survey of, 20: 29608
radioactivity of Cosmos-3, after July 9, 1962, explosion, (E), 20: 30234
testing of Nuclear Test Detection, solar simulation, 20: 29440
SAVANNAH RIVER COMPONENTS TEST REACTOR
steel corrosion by heavy water coolant-moderator in, 20: 29654
SAVANNAH RIVER PLANT
environs monitoring, Jan. to July 1965, 20: 29431
SAVANNAH RIVER PRODUCTION REACTORS
shutdown system using injection of gadolinium nitrate, 20: 30920(P)
SAXTON POWER REACTOR
boiler corrosion testing in, 20: 30884(R) (WCAP-3269-16)
fuel element irradiation testing in, 20: 30884(R) (WCAP-3269-16)
SCALERS

noise filter for, 20: 29556
SCANDIUM
abundance and distribution in rocks, 20: 29436
thermodynamic properties at 0°C to melting point, 20: 29743
SCANDIUM CHLORIDES
reactions with nitrogen oxides, 20: 29214
SCANDIUM COMPLEXES
with Aluminon, composition and stability of, spectrophotometric studies of, 20: 29180
SCANDIUM FLUORIDES
heat of sublimation and sublimation pressure of, mass spectrometric studies of, 20: 29183
SCANDIUM ISOTOPES Sc-45
energy levels from calcium-44 (He-3,d) reactions, parity and spin of 378-kev, (E/T), 20: 30429
energy levels from beta decay of titanium-45, (E), 20: 30456
neutron capture by, gamma spectra from, 20: 29078(R) (AD-633252)
proton reactions (p,n) at 100 to 400 Mev, excitation functions for, 20: 30464
SCANDIUM ISOTOPES Sc-46
neutron capture by, gamma spectra from, 20: 29078(R) (AD-633252)
SCANDIUM NIOBATES
distribution in strontium molybdate single crystals, coefficients of, 20: 29746
SCANDIUM NITRATES
preparation and properties of, 20: 29214
SCANDIUM OXIDES
$CdO–Sc_2O_3$, phase studies, 20: 29168
$CoO–Sc_2O_3$, phase studies, 20: 29168
$CrO_3–Sc_2O_3$, phase diagrams, 20: 29167
$Mn_2O_3–Sc_2O_3$, magnetic susceptibility, 20: 29168
$Mn_2O_3–Sc_2O_3$, phase studies, 20: 29168
$MnO–Sc_2O_3$, phase studies, 20: 29168
$NiO–Sc_2O_3$, phase studies, 20: 29168
$Sc_2O_3–ZnO$, phase studies, 20: 29168
SCARS
radioinduced in mice and rats, x, 20: 28946
SCATTERING
amplitude for high-energy, forward, (T), 20: 30109
amplitude for three-body rearrangement, distorted-wave Born approximation for, 20: 30120
amplitude for three-body, solution in distorted-wave formalism for, 20: 30121
amplitudes for elastic, three-particle contributions to, 20: 30129
amplitudes for finite-range-potential, analyticity properties of, 20: 30131
amplitudes for singular potential, iterative method for partial wave, 20: 30136
amplitudes for three-particle, dispersion relations for, 20: 30132
amplitudes for Yukawa potential, 20: 30128
amplitudes for, N/D calculations of p-wave, (T), 20: 30158
approximation methods for high-energy, (T), 20: 30086 (CONF-640509(Pt.1), Paper 4)
dispersion relations for πN, partial-wave, (T), 20: 30073
dispersion theory for, perturbation methods in, 20: 30124
elementary particle production in quantum field theory, 20: 30157
matrix elements in relativistic three-body problem, equations for, 20: 30148
matrix N/D method with arbitrary inelasticity for, 20: 30130
Regge cuts in angular momentum plane of high-energy, (T), 20: 30160
Regge poles in, 20: 30163
S-matrix for high-energy, (T), 20: 30108
S-matrix for strongly singular potentials in, analytic structure in, 20: 30100
S-matrix in Heisenberg representation for, 20: 30104
S-matrix potential in one-dimensional Schroedinger equation, (T), 20: 30248
theory of elastic small-angle multiple, information loss in, 20: 30151
vacuum boundary conditions for P_N approximation for, variational, 20: 30116
SCINTILLATION DETECTORS
design of, for neutron-gamma well logging, 20: 29445(P)
efficiencies of cylindrical sodium-iodide (thallium) gamma-ray, table of, (T), 20: 29562
efficiency of drilled-hole scintillometer, embedded in plastic, 20: 29546
efficiency of medicinal, paraffin-based, liquid whole-body, 20: 29541
pulse height distribution at output of, methods for calculating, 20: 29542
pulse shape discrimination in fast neutron dosimetry, 20: 29524 (CONF-651109, pp 647-52)
uses in measurement of soft beta emitters, 20: 29084
SEA WATER
analysis for chlorine, chlorophyll, dissolved oxygen, inorganic nutrients, and silicates, methods for, 20: 28877 (NYO-1918-124)
decomposition, distribution, and production of organic compounds in, 20: 28878 (NYO-1918-138)
desalination plant for, computer program for determining cost, geometry, and operating characteristics of, 20: 30953 (ORNL-TM-1542)
separation of radioisotopes from, by sorption by metal sulfide-ion exchange resins, 20: 29345
thorium isotope abundances in, 20: 29412
uranium isotope abundances in, 20: 29412
SEAFOOD
radiopreservation of pacific coast, gamma, 20: 29583(R) (TID-22515)
SEALING MATERIALS
development of, for magnetic materials, 20: 29366(R) (TID-22970, pp 375-91)
SEALS AND GLANDS
testing elastomeric, for spacecraft, 20: 29366(R) (TID-22970, pp 375-91)
SEED
radiation effects on pea, γ, 20: 28909
radiation effects on chromosomal bridges at anaphase in barley, fast-neutron and x, 20: 29031
radiosensitivity of pea, effects of chemical and biological compounds on, 20: 29049
SEEDLINGS
radiation effects on DNA synthesis in pea, γ and neutron, 20: 28989
radiosensitivity of pea, effects of chemical and biological compounds on, 20: 29049
SELENIUM
book: *Chemistry of Selenium, Tellurium, and Polonium*, 20: 29235
determination in petroleum, activation, 20: 29139
pair distribution function for, 20: 29623(R) (TID-22970, pp 121-256)
SELENIUM ISOTOPES Se-76
energy level widths, (E/T), 20: 30360 (WASH-1068)
SELENIUM ISOTOPES Se-80
neutron scattering at 4.0 Mev, polarization angular distributions from, (E), 20: 30360 (WASH-1068)
SEMICONDUCTOR DETECTORS
charge carrier lifetime and resistivity in silicon, thermal cycling effects on, 20: 30785
charge-carrier collection of p-n, for 4.98-Mev alpha particles, 20: 29550
charged particle energy-loss spectra in, fluctuations of, (E/T), 20: 29531 (UCRL-16715)
design for charged-particle identification, 20: 29526 (INP-444/PL)
development of, for gamma spectroscopy, 20: 29078(R) (AD-633252)
efficiency of silicon *p-n* junction, for x-ray measurements, 20: 29540
performance for measuring alpha particles from polonium-210 and neptunium-237, 20: 29552
performance of germanium, for muonic x-ray spectra, 20: 29525 (CONF-660209-9)
performance of germanium, for determining monazite and pitchblende gamma spectra, 20: 29079 (AERE-M-1736)
performance of silicon diode, for gamma and neutron dosimetry, 20: 29518 (BNWL-SA-27)
performance of silicon, for beta spectra measurements on strontium-90–yttrium-90, 20: 29520 (CLOR-45/D)
preamplifier for cooled, field-effect transistor, 20: 29548
response of lithium-drifted germanium, to gamma rays, (T), 20: 29528 (LA-3456)
use in measurement of gaseous diffusion coefficients, 20: 29510
SEMICONDUCTORS
current rectification processes at metal contacts with, 20: 29569
development by crystallochemical methods, 20: 29623(R) (TID-22970, pp 121-256)
electromagnetic wave propagation in, (E/T), 20: 30735(R) (TID-22970, pp 331-73)
electron interband transport in, quantum theory of, 20: 30735(R) (TID-22970, pp 331-73)
electron recombination with donors in, 20: 29623(R) (TID-22970, pp 121-256)
fabrication and properties of sintered, for use as thermoelectric cooling plates and generators, 20: 29690
infrared absorption by, (E), 20: 30734(R) (TID-22970, pp 1-63)
phonon processes in, theory of Franz-Keldysh effect on, 20: 29709(R) (TID-22970, pp 65-119)
photon absorption by, effects of crossed electric and magnetic fields on, (E/T), 20: 30735(R) (TID-22970, pp 331-73)
plasma oscillations in, strong magnetic field effects on electron-hole, (T), 20: 30677
radiation effects on sorptive properties of surfaces of, (T), 20: 29815
surface properties, 20: 29623(R) (TID-22970, pp 121-256)
SEPARATION PROCESSES
development of, for use in activation analysis, 20: 29120
SERINE
complexes with rare earths, stability of, 20: 29208
radiation effects on incorporation of, by blood cells, x, 20: 28922
SEWAGE

radioactivity in sludge from, in Japan in 1964, 20: 29455
SEX
radiation effects on ratios of rat, prenatal exposure, 20: 28952
SHEETS
angular distribution of crystal planes in, pole figure facility for measuring, 20: 29083(R) (UCRL-14767)
SHELLS
strength of steel, for reactor containment, 20: 30813
stress in thick-walled long conical, for nozzle design, (T), 20: 30928
SHELLSOL
Shellsol T–TBP, radiation effects on clarification and coalescence time of reactor fuel solutions in, 20: 29333 (RT-CHI-(65)33)
SHELTERS
design criteria for animal, 20: 29392
fallout, protective lightway for, 20: 29483(P)
SHIELDED CONTAINERS
testing of lead, gamma radiographic, 20: 29388
SHIELDING
cascade shower calculations for, effects of mathematical errors on, (T), 20: 30725 (ORNL-3786)
design of array of, for chlorine logging apparatus, 20: 29443(P)
design of, use of dimensional analysis and model theory in, 20: 30730
materials for nuclear power plant, 20: 30815
neutron transport calculations for, cross section library for, 20: 30723 (NAA-SR-11831)
SHIELDING MATERIALS
preparation of olefinically unsaturated hydrocarbon polymer, for neutrons, 20: 30732(P)
radiation effects on glass, charge accumulation from gamma, 20: 30727
SHIPPINGPORT ATOMIC POWER STATION, PENNA.
environs monitoring, Jan. to July 1965, 20: 29431
SHIPPINGPORT PRESSURIZED WATER REACTOR
inspection of boiler from, 20: 29616(R) (BMI-1738)
SHOCK TUBES
design for nuclear blast simulation, 20: 29371 (AWRE-E-1/66)
SHOCK WAVES
hazards from, from underwater nuclear explosions, 20: 29481
interactions of crossflow, flow field analysis of, (T), 20: 30167 (SC-DC-65-1916)
interactions with stationary cone, transient flow field analysis of, (T), 20: 30168 (SC-DC-66-1329)
propagation in ideal gases, analysis of, (E/T), 20: 30169 (UCRL-14198)
propagation in solar corona, type-II r-f emission from, (T), 20: 29903(T)
propagation in theta-pinch plasma, analysis using Fokker–Planck method, (T), 20: 30560 (LA-DC-7282)
propagation of hydromagnetic, in gases in arbitrarily oriented magnetic fields, (T), 20: 30177
reactions with liquid argon, compression in, (E/T), 20: 30170 (UCRL-14251)
reflection in em shock tube, (E), 20: 30697
structure of MHD, effects of electron temperature and Hall currents on, 20: 30191
SILICATES
content in Atlantic Ocean, measurements on, 20: 28877 (NYO-1918-124)
content in Atlantic Ocean, measurements on, 20: 28878 (NYO-1918-138)
SILICON
absorption of infrared radiation by semiconducting, (E), 20: 30735(R) (TID-22970, pp 331-73)
deposition on refractory metals by fluidized-bed process, 20: 29630
determination in graphite and basalts by neutron activation methods, 20: 29140
determination in petroleum, activation, 20: 29139
efficiency of *p-n* junctions of, in x-ray measurements, 20: 29540
iron-57 Mössbauer spectra in, 20: 30766
molecular constants and thermodynamic functions of, triatomic, (T), 20: 29921
neutron elastic scattering at 0.57 to 2.28 Mev, cross sections for, (E/T), 20: 30345 (EUR-2798.e)
performance for gamma and neutron dosimetry, 20: 29518 (BNWL-SA-27)
performance for measuring beta spectra from strontium-90–yttrium-90, 20: 29520 (CLOR-45/D)
properties of semiconducting, thermal cycling effects on, 20: 30785
radiation damage in transistors of, energy dependence of fission-neutron and gamma, 20: 29579 (NAA-SR-11887)
radiation effects on planar transistors of, gamma, 20: 29577 (CEA-R-2959)
radioinduced isotopic exchange of hydroxyl ions on colloidal, with deuterium, 20: 29276
reactions of diffused impurities in, 20: 29709(R) (TID-22970, pp 65-119)
surface properties in semiconductors, 20: 29569
thermal cycling effects on surface barrier diodes of, 20: 30785
SILICON CARBIDES
coating of, effects of, on oxidation resistance of graphite, 20: 29773
electric potential of diodes of, 20: 29709(R) (TID-22970, pp 65-119)
glaze for coating of, on graphite, 20: 29696(P)
hardness and surface friction of, effects of temperature on, 20: 29771
properties of, at 2000°C, for use in thermionic converters, 20: 29729
SILICON CHLORIDES
properties, 20: 29623(R) (TID-22970, pp 121-256)
SILICON ISOTOPES Si-28
deuteron reactions (d,p) with, gamma angular correlations from, (E), 20: 30360 (WASH-1068)
energy levels from proton scattering by aluminum-27 at 3.5 to 11.3 Mev, width of, (E), 20: 30415
neutron reactions (n,p) at 14.8 Mev, cross sections for, (E), 20: 30394
proton elastic scattering at 40 Mev, cross sections for, (E/T), 20: 30353(R) (ORNL-3940, pp 1-61)
proton inelastic scattering at 40 Mev, cross sections for, (E/T), 20: 30353(R) (ORNL-3940, pp 1-61)
SILICON ISOTOPES Si-29
energy level transitions from silicon-28 (d,p) reactions, angular correlations for, (E), 20: 30360 (WASH-1068)
SILICON OXIDES
coating of, effects of, on oxidation resistance of graphite, 20: 29773
content in Amazon River, effects on biology, chemistry, and hydrography of Atlantic Ocean, 20: 28878 (NYO-1918-138)
content in thalenites from Japan, 20: 29399
mechanical properties of composition of phenolic refrasil, 20: 29708
SiO_2–Ag_2SO_4–V_2O_5, radiation effects on catalytic activity of, in oxidation of sulfur dioxide by air, 20: 29291
SILICON SYSTEMS
Al–Cr–Si, properties of, for use as protective coating on niobium and its alloys, 20: 29651
Al–Si, properties of, for use as protective coating on niobium and its alloys, 20: 29651
Al–Si–U, radiation effects on clarification and coalescence time during processing of, in organic solvents, 20: 29333 (RT-CHI-(65)33)
Be–Mo–Si, compounds in, properties of, for use in aerospace technology, 20: 29770
Cr–Mo–Si, properties of, for use as protective coating on niobium and its alloys, 20: 29651
Cr–Si–Ti, properties of, for use as protective coating on niobium and its alloys, 20: 29651
Cr–Si–W, properties of, for use as protective coating on niobium and its alloys, 20: 29651
Cu–Si, effects on wetting of graphite at high temperatures, 20: 29764
Fe–Si–V, crystal structure of D-phase, (E/T), 20: 30734(R) (TID-22970, pp 1-63)
Mo–Si, effects on wetting of graphite at high temperatures, 20: 29764
Si–U, metallographic tests on arc melted, 20: 29775
SILICONE RUBBERS
permeability to carbon dioxide–hydrogen mixtures, 20: 29362
radiation effects on viscoelastic properties of, gamma, 20: 29313
SILTS
thorium isotope abundances in ocean, 20: 29412
uranium isotope abundances in, 20: 29412
SILVER
determination of, by neutron activation methods, 20: 29078(R) (AD-633252)
effects as infiltrant on properties of graphite containing carbides and metals, 20: 29764
iron-57 Mössbauer spectra in, 20: 30766
neutron capture cross section measurement at 80 to 200 kev, errors in using boron monitors for, (E), 20: 30352 (NASA-TR-R-240)
use for neutron flux measurements, multi-velocity corrections in, 20: 29539
SILVER ALLOYS
Ag–W, fabrication of rocket motor nozzle of, 20: 29685
Fe–Ag, properties of composite-type, 20: 29624(R) (TID-22970, pp 257-329)
Gd–Ag, magnetic properties of, 20: 29752
Gd–Au–Ag, magnetic properties of, 20: 29752
Gd–In–Ag, magnetic properties of, 20: 29752
Mn–Ag, thermal capacity below 1°K, 20: 29791
SILVER DYSPROSIUM SULFIDES
crystal structure, 20: 29158
SILVER ERBIUM SULFIDES
crystal structure, 20: 29158
SILVER GADOLINIUM SULFIDES
crystal structure, 20: 29158
SILVER HOLMIUM SULFIDES
crystal structure, 20: 29158
SILVER ISOTOPES Ag-107
proton reactions (p,α) with, cadmium-108 level widths from, (E/T), 20: 30360 (WASH-1068)
SILVER NITRATES

radiation effects at 77°K on, ESR studies of x, 20: 29310

SILVER SAMARIUM SULFIDES
crystal structure, 20: 29158

SILVER SULFATES
SiO_2–Ag_2SO_4–V_2O_5, radiation effects on catalytic activity of, in oxidation of sulfur dioxide by air, 20: 29291

SILVER TERBIUM SULFIDES
crystal structure, 20: 29158

SILVER THULIUM SULFIDES
crystal structure, 20: 29158

SILVER YTTERBIUM SULFIDES
crystal structure, 20: 29158

SILVER YTTRIUM SULFIDES
crystal structure, 20: 29158

SINGLE CRYSTALS
analysis of pure, equipment and procedures for, 20: 29141
preparation of rare earth, methods for, (E/T), 20: 30735(R) (TID-22970, pp 331-73)
properties of, dielectric and optical, 20: 29709(R) (TID-22970, pp 65-119)

SINTERING
mechanisms in, research on, 20: 29623(R) (TID-22970, pp 121-256)

SIOUX FALLS POWER REACTOR
neutron flux mapping in borated core of, (E/T), 20: 30874 (ACNP-65612)

SKELETON
radiation dose to human, from strontium-90 content in river water, 20: 30943(R) (ORNL-TM-1465)
strontium-90 content and distribution in monkey, after intravenous and oral administration, 20: 28896
thorium content in rat, after inhalation, 20: 28897

SKIN
effects of irradiation by beta particles prior to application of 7,12-dimethyl-, benzanthracene on, 20: 28973
iron-59 uptake by mouse, from bath water, 20: 28892
radiation effects on cellular permeability in onion, x, 20: 28900
radiation effects on mast cells in mouse, uv, 20: 28937
radiotherapy of diseases of, beta, 20: 29072
strontium-90 uptake by rabbit, effects of detergent treatment on, 20: 29461

SKIN GRAFTING
radiation effects on response of thymectomized chickens to, 20: 29014

SKIN LESIONS
radioinduced in mice and rats, role of adipose tissue in repair of x, 20: 28946

SNOW
tritium content of, Moscow, Dec. 1961 to Dec. 1963, 20: 29409

SODIUM
density of, at critical temperature, radiometric techniques for measuring critical, 20: 29742
effects of oxygen-contaminated, on mechanical properties of type 316 stainless steel at 1200°F, 20: 29704 (MSAR-66-78)
flow of liquid, loop experiments on two-phase adiabatic, 20: 29374(R) (ANL-7190, pp 156-66)
level indicator for liquid, 20: 30875(R) (ANL-7190, pp 143-55)
neutron resonance absorption measurements for, 20: 30358(R) (RPI-328-56, pp 1-48)
reactions with plutonia–urania at 750°C, effects of fuel stoichiometry on, 20: 29618(R) (GEAP-4982)

SODIUM ACETATES
effects on cesium-137 desorption from soils, 20: 30943(R) (ORNL-TM-1465)

SODIUM BROMATES
photolysis of gamma-irradiated and normal, kinetics of, 20: 29248 (BNL-9672)

SODIUM BROMIDES
analysis for chloride and iodide ions by bremsstrahlung-activation methods, 20: 29112

SODIUM CARBONATES
reactions with yttrium fluorides at 550 to 700°C, 20: 29223

SODIUM CHLORIDES
analysis for iodide ions by bremsstrahlung-activation methods, 20: 29112
color centers in thallium-doped, equipment for measuring relaxation of, 20: 30754
corrosive effects on austenitic and austeno-ferritic stainless steels, stress-, 20: 29639(R) (EURAEC-1578)
effects on radiopreserved seafood, 20: 29583(R) (TID-22515)
electron transmission in thin films of, energy losses and color centers from, (E), 20: 30776
radiation effects on, color centers in ionic, effect of F centers from gamma and neutron, 20: 30739
radioinduced color centers in thallium-doped, photon and thermal, (E), 20: 30754
slip mechanisms of rock salt, 20: 29624(R) (TID-22970, pp 257-329)
$LaCl_3$–NaCl, compound formation in saturated vapor of, at 1100 to 1350°C, 20: 29227

SODIUM DODECYL SULFATES
Antarox DM-970–sodium hexametaphosphate–sodium dodecyl sulfate–sodium nitrates–sulfosalicylic acid, efficiency of, as radioactivity decontamination solution for cotton protective clothing, 20: 29477

SODIUM IODIDES
efficiencies in cylindrical scintillation gamma detectors, table of, (T), 20: 29562
use of thallium-activated, in scintillation-type well logging device, 20: 29445(P)

SODIUM IONS
dissociation of fast negative, in rare gases, (T), 20: 29947
migration in fused sodium nitrate, isotope effect in, 20: 29185

SODIUM ISOTOPES Na-22
effects on sodium electromigration in fused sodium nitrate, 20: 29185
energy levels from helium-3 reactions (He-3,$p\gamma$) with neon-20 at 5.35 Mev, (E), 20: 30400

SODIUM ISOTOPES Na-23
neutron inelastic scattering at 5.0 Mev, Q values for, (E), 20: 30360 (WASH-1068)
neutron reactions (n,γ) with, cross sections for, (E), 20: 30360 (WASH-1068)
neutron reactions (n,p) at 14.8 Mev, cross sections for, (E), 20: 30394

SODIUM ISOTOPES Na-24
beta decay of, β-γ circular polarization correlation from, (E), 20: 30542
effects on blood and hematopoietic system, 20: 28982
effects on catecholamine metabolism in rats, 20: 28939
effects on conditioned reflexes of dogs, 20: 29009
uses as gamma source for detection of flaws in steel foils and plates, 20: 29390

SODIUM MOLYBDATES
uses in titrimetric determination of thorium, 20: 29092

SODIUM NITRATES
sodium ion electromigration in fused, isotope effect in, 20: 29185
Antarox DM-970–sodium hexametaphosphate–sodium dodecyl sulfate–sodium nitrates–sulfosalicylic acid, efficiency of, as radioactivity decontamination solution for cotton protective clothing, 20: 29477

SODIUM NITROPRUSSIDE
radiation effects on crystals of, ESR studies of pairwise trapping from gamma, 20: 29280

SODIUM OXIDES
content in thalenites from Japan, 20: 29399

SODIUM, (PENTACHLOROPHENOXY)-
penetration in wood, radioactivation determination of factors affecting selective, 20: 29161

SODIUM PHOSPHATES
Antarox DM-970–sodium hexametaphosphate–sodium dodecyl sulfate–sodium nitrates–sulfosalicylic acid, efficiency of, as radioactivity decontamination solution for cotton protective clothing, 20: 29477

SODIUM SAMARIUM BROMIDES
preparation, 20: 29204

SODIUM SAMARIUM CHLORIDES
preparation, 20: 29204

SODIUM SILICATES
crystallization and melting kinetics of, 20: 29623(R) (TID-22970, pp 121-256)

SODIUM THIOCYANATES
sulfur-35 exchange between, and 4-chlorobenzhydryl thiocyanate, 20: 29237

SODIUM THORIUM HYDROXIDE PHOSPHATES
preparation and properties of, 20: 29160

SODIUM THORIUM PHOSPHATES
preparation and properties of, 20: 29160

SODIUM THORIUM SULFATES
preparation and properties of, 20: 29218

SOILS
book: *Natural Radioactivity of Plants and Soils*, 20: 29437
cesium-137 desorption from, effects of sodium acetate on, 20: 30943(R) (ORNL-TM-1465)
density and moisture content determinations using radiometric gages, conference on, 20: 29504
density and moisture content of, radiometric methods for determining, 20: 29505
density and moisture content determinations for, efficiencies of radiometric devices for, 20: 29506
density and moisture content in, performance of radiometric gages for determining, 20: 29507
density and moisture content of, radiometric surface gages for determining, 20: 29508
density of, radiation back-scattering methods for measuring, 20: 29594
effects on iodine-131 uptake by sagebrush, 20: 28883
moisture content and surface density of compacted, radiometric methods

for measuring, 20: 29581 (AD-633785)
radioisotope movement in, 20: 30943(R) (ORNL-TM-1465)
sorptive properties of turfy-meadow, for yttrium, effects of iron on, 20: 28881

SOLAR BATTERIES
development for space power, 20: 29977 (N-65-32716)
development of epitaxial structures for silicon, (E/T), 20: 30724 (NASA-CR-461)

SOLAR FLARES
effects of chromospheric, on polar-cap-region anomalous absorption, 20: 30225
effects on geomagnetic storm development and ionospheric disturbances, 20: 30230
effects on space flights, 20: 30222(T) (NASA-TT-F-389, pp 758-63)
effects on tropospheric pressure variations, (E), 20: 30237(T)
hazards of, in manned space flights, 20: 29058
properties of chromospheric limb, (T), 20: 29905(T)
radiation emission from, 20: 29875(T) (NASA-TT-F-389, pp 732-9)

SOLAR POWER
development and economics of, for communications satellites, 20: 29608

SOLAR RADIATION
bursts of x-ray, short intensity increases of heavy cosmic nuclei accompanying, 20: 29965
effects of solar wind on Van Allen belts, 20: 30204(T) (NASA-TT-F-389, pp 375-86)
effects on Nuclear Test Detection Satellites, simulation testing of, 20: 29440
emission during solar flares, 20: 29875(T) (NASA-TT-F-389, pp 732-9)
emission of coronal r-f, in continuous spectrum, 20: 29904(T)
frequency spectrum of slowly varying component of r-f, 20: 29908
intensity variations of x, 20: 29874(T) (NASA-TT-F-389, pp 714-31)
interactions of solar wind with magnetosphere, 20: 30210(T) (NASA-TT-F-389, pp 499-517)
penetration of charge particles into magnetosphere, processes in, 20: 30205(T) (NASA-TT-F-389, pp 386-425)
spectra of u-v and x, 20: 29873 (NASA-SP-100)

SOLENOIDS
design of superconducting, for shielding of space vehicles, 20: 30317
size effects in superconducting, r-f, (E), 20: 30735(R) (TID-22970, pp 331-73)
use of superconducting, in macroparticle acceleration for nuclear fusion, (T), 20: 30717

SOLIDS
dislocation kinks in, oscillations of, 20: 30770
electron ejection from, 20: 29499
electron energy levels in, 20: 29931(T)
electron energy levels in, pseudo wave functions for, 20: 30773
gamma angular correlation perturbation in, effects of lattice vibrations on, 20: 30762
hydrogen bonding in, lectures on isotope effects on, 20: 30783
nuclear relaxation in, lectures on, 20: 30783
photonuclear reactions in, range of recoil atoms from, (E), 20: 30479
radiation damage in, lectures on, 20: 30784
radioinduced elastic explosions in, laser and neutron beam, (T), 20: 30740

SOLVENTS
development of, for cured epoxy resins, 20: 29366(E) (TID-22970, pp 375-91)

SOLVESSO
Solvesso 100–trichloroacetic acid, radiation effects on clarification and coalescence time of reactor fuel solutions in nitrated, 20: 29333 (RT-CHI-(65)33)

SOUTH AMERICA
fallout monitoring, 1965, 20: 29428

SOUTHWEST EXPERIMENTAL FAST OXIDE REACTOR
core design and fission traverse rates for, 20: 30790(R) (ANL-7204, pp 1-31)

SOVIET UNION
fallout in atmospheric precipitation in, effects of cloud formation on, 20: 29416
fallout monitoring in, 1962, 20: 29406 (NP-14719)
reactor safety programs and standards, 20: 30800
thorium and uranium contents of effusive and intrusive formations of northeastern Balkhash foreland, 20: 29418
tritium content of rain and snow in Moscow, Dec. 1961 to Dec. 1963, 20: 29409
uranium content in traprock formation of Siberian platform, 20: 29419

SPACE
conference on space research, 20: 30195(T) (NASA-TT-F-389)
gas temperature in intergalactic, (T), 20: 29879
wave propagation in interstellar, cosmic ray damping effects on, (T), 20: 29959
x-ray sources in, properties of Scorpius, (E), 20: 29882

SPACE FLIGHT
effects on microspores of *Tradescantia*, 20: 28971
power systems for, lectures on, 20: 29977 (N-65-32716)
radiation hazards of, 20: 30222(T) (NASA-TT-F-389, pp 758-63)
radiation hazards in manned, method of evaluating, 20: 29058

SPACE VEHICLES
life support in, role of carbon monoxide in, 20: 28880
materials for, fabrication and properties of, 20: 29680
power sources for, radioisotope and reactor, 20: 30926
propulsion systems for, ion and electromagnetic review of, 20: 29394
shielding design for manned, using superconducting coils, 20: 30317

SPAIN
fallout monitoring in Valencia, 1964, 20: 29408

SPARK CHAMBERS
particle trajectory location in, accuracy of, (T), 20: 29527 (ITEF-341)

SPECIFIC HEAT
measurement in metals, methods for, (E), 20: 30734(R) (TID-22970, pp 1-63)

SPECTRA
book: *Nuclear Magnetic Resonance and Electron Spin Resonance Spectra. Index for 1958–1963*, 20: 30510

SPECTROMETERS
development of magnetic-particle, with field alterations, 20: 29558

SPECTROPHOTOMETRY
methods and reagents for spectrophotofluorimetry, 20: 29083(R) (UCRL-14767)
oxyacetylene burner for atomic absorption, design of laminar-flow, 20: 29083(R) (UCRL-14767)

SPECTROSCOPY
development of high-energy, using activation detectors, (E/T), 20: 29521 (CONF-651109, pp 213-23)

SPERM
radiation effects on bovine epididymal, x, 20: 29013

SPHERES
criticality studies of plutonium nitrate, 20: 29471
magnetohydrodynamic drag on oscillating, in conducting fluid, (T), 20: 30179

SPINELS
properties of chromium-doped, 20: 29709(R) (TID-22970, pp 65-119)
radioinduced blistering of, ion, (E), 20: 29816

SPLEEN
effects of removal of, on radiation response of hematopoietic system of dogs, 20: 29029
radiography of, use of colloidal technetium-99m in, 20: 29065
transplants in γ-irradiated mice, effects of methotrexate on, 20: 29035

STAINLESS STEEL
analysis for boron by neutron cross section measurements, 20: 29117
compatibility of type 304, with plutonium and uranium carbides, 20: 30790(R) (ANL-7204, pp 1-31)
corrosion of austenitic and austeno-ferritic, by chloride solutions, stress-, 20: 29639(R) (EURAEC-1578)
corrosion of types 304 and 403, in Saxton steam generator, 20: 30884(R) (WCAP-3269-16)
corrosion of types 304 and 410, by mercury at 593 to 703°C, 20: 29646
corrosion of 20Cb, effects of increased nickel content in intergranular, 20: 29643
development of, for ball bearings, 20: 29366(R) (TID-22970, pp 375-91)
erosion of types 304 and 316, by mercury, water, and bismuth–lead alloy, cavitation, 20: 29640 (NP-16048)
heat treatment of type 347, effects on composition on, 20: 29616(R) (BMI-1738)
mechanical properties of type 316, effects of oxygen-contaminated sodium on, at 1200°F, 20: 29704 (MSAR-66-78)
radiation effects on stress-rupture properties of type 304L, 20: 30790(R) (ANL-7204, pp 1-31)
radiation effects on type 304, cladding on uranium fuel elements, thermal-neutron, 20: 29806 (ORNL-TM-1511)
radioinduced cracking in type 347, fast-neutron, 20: 29618(R) (GEAP-4982)
tensile properties of type 310, at 1300°F, effects of heat treatments on, 20: 29618(R) (GEAP-4982)
use as fuel-element cladding for boiling-water reactors, 20: 30903
welding specifications for structural quality welds for mildly corrosive nonradioactive service, 20: 29662 (HWS-8242(Rev.5))
welding specifications for process quality welds for mildly corrosive radioactive service, 20: 29661 (HWS-3241(Rev.4))
x-ray attenuation in types 304 and 307, measurement of, 20: 29707 (ORNL-TM-1457)
Cr–Ni–stainless steel 304, corrosion in Saxton steam generator, 20: 30884(R) (WCAP-3269-16)
stainless steel-UO_2, fabrication for AARR fuel, 20: 30787(R) (ANL-7190, pp 11-142)

STANFORD LINEAR ACCELERATOR
design and experimental program for, 20: 29862
operation of, 20: 29864
radiation hazards, 20: 29849 (CONF-651109, pp 442-58)
STARS
chromospheric properties and rotation of main-sequence, (E), 20: 29883
distances and luminosities of quasars, 20: 29896
distribution of quasi-stellar radio sources in steady state cosmology, 20: 29897
evolution and radiation mechanism of neutron, from supernova, 20: 29900
evolution of pre-main-sequence, initial condition effects on, (T), 20: 29884
existence of collapsed, in binaries, (T), 20: 29889
lead abundance in, mechanism for, (T), 20: 29887
mass of quasi-stellar objects, 20: 29888
neutron capture in, integrated flux distributions for, 20: 29887
origin of quasi-stellar objects, (T), 20: 29877
properties of quasi-stellar objects, models for, 20: 29876
properties of Scorpius x-ray source, (E), 20: 29882
properties of x-ray source, 20: 29900
radio emission from Crab nebula source, quasi-stellar, and supernova-remnant, coherent plasma mechanism for, 20: 29880
radio spectra of 3C273 A and B, strength of, 20: 29898
spectra of distant quasi-stellar objects, mechanisms for absorption, (T), 20: 29890
spectra of nonthermal radio-sources, 20: 29878
wave propagation in supernova remnant plasma, cosmic ray damping effects on, (T), 20: 29959
x-ray spectra of Cyg XR-1, Tau XR-1, and Sco XR-1, 20: 29901
STEAM
corrosive effects on nickel-coated aluminum fuel plates, 20: 30794(R) (IDO-17147, pp 1-12)
corrosive effects on zirconium–chromium–iron alloy, effects of fabrication process and nitride content on, 20: 29660(R) (GEAP-4960)
generator for, forced-flow once-through, 20: 30821(P)
reactions with uranium nitride and uranium carbide oxides at 200 to 1000°C, 20: 29645
reactions with uranium and aluminum–uranium alloys at 400 to 1600°C, kinetics of isothermal, 20: 29188
superheating of, integral boiler reactor design for, 20: 30913(P)
STEEL
analysis for oxygen, activation, 20: 29138
analysis of rods of, for oxygen, by neutron-activation and vacuum-fusion techniques, 20: 29088
corrosion by heavy water in Savannah River Components Test Reactor, 20: 29654
corrosion of austenitic and ferritic, by trichloroethylene, tracer studies of, 20: 29655
embrittlement of reactor pressure vessel, plastic fatigue, 20: 29701(R) (EURAEC-1547)
flaws in, uses of gamma sources for detection of, 20: 29390
fracture initiation in, mechanisms of, 20: 29623(R) (TID-22970, pp 121-256)
fracture toughness of reactor pressure vessel, development of test procedures for, 20: 29700(R) (COO-1477-4)
inspection of, ultrasonic, 20: 29389
properties as reactor containment material, 20: 30815
radiation effects on low-temperature brittleness of, 20: 30815
radiation effects on embrittlement of reactor structural, neutron, 20: 29825
strength of reactor containment shells of, 20: 30813
strength requirements of pressure vessel, 20: 30894
stress-relaxation at 650°C of low-alloy, effects of prior deformation on, 20: 29702(R) (EURAEC-1616)
thickness of in-place sheets of, radiometric methods of measuring, 20: 29581 (AD-633785)
STELLARATORS
plasma injection and confinement in multipolar helical-field, 20: 30657
plasma loss rates in minimum-B, alkali, (E/T), 20: 30656
plasma stability in negative V″, pressure effects of, (T), 20: 30561 (MATT-415)
STELLARATORS (C)
data recording and display system for, development of semi-automatic, 20: 30573
electric discharges in, recombination rate of doubly ionized helium in, 20: 30600
plasma heating in, by ion cyclotron resonance, 20: 30577
STEROIDS
identification of, using radiochemical paper electrophoresis of the hydrazones of, 20: 29132
radiation effects on content in guinea pigs, x, 20: 28975
STILBENE
radioinduced isomerization of, in methanol solutions, effects of additives on gamma, 20: 29287
STRAIN GAGES
radiation stability of in-pile resistance, 20: 29578 (EUR-2649.e)
STRESS ANALYSIS
of mechanical structures, computer program for, 20: 29367 (TRG-Report-1089)
of wave-propagated disturbances in elastic-plastic cylinders, 20: 30954 (UCRL-14617)
STRONTIUM
abundance and isotopic compositions of, in brines under Salton Sea area, California, 20: 29414
determination in calcareous media by flame photometry, 20: 29363
metabolism in children and adolescents, 20: 28889
metabolism in man, 20: 28890
separation from aqueous solutions by solvent extraction using monoalkyl ester of phosphoric acid, 20: 29365(P)
separation from calcium and magnesium by ion exchange, 20: 29363
separation from dilute solutions by precipitation with calcium oxalate using dimethyl oxalate, 20: 29154
separation from water by ion exchange using bentonite and gypsum, 20: 29348
separation from yttrium by paper electrophoresis, 20: 29336
separation from yttrium by paper chromatography, effects of calcium on, 20: 29349
STRONTIUM ISOTOPES Sr-85
movement in soils, 20: 30943(R) (ORNL-TM-1465)
separation from sea water by sorption by metal sulfide-ion exchange resins, 20: 29345
STRONTIUM ISOTOPES Sr-86
energy levels of, (E/T), 20: 30353(R) (ORNL-3940, pp 1-61)
STRONTIUM ISOTOPES Sr-89
effects on blood and hematopoietic tissue, 20: 28982
STRONTIUM ISOTOPES Sr-90
beta emission of, backscattering from aluminum in 2π geometry, (E), 20: 30369
beta spectra from, silicon counters for measuring, 20: 29520 (CLOR-45/D)
content and distribution in monkey skeletons after intravenous and oral administration, 20: 28896
content and distribution in oceans, 20: 29405 (NP-14694)
content in fallout in USSR, 1962, 20: 29406 (NP-14719)
content in foods, 1962 and 1963, 20: 29433
content in milk and milk products, 20: 29464
content in milk in cattle, effects of dietary calcium on, 20: 29459
content in milk in U. S., 1962, 20: 29474
content in wheat, effects of washing with decontaminating solutions on, 20: 29473
effects of dietary, on cholesterol and lipid content of rat blood, 20: 28994
effects on blood and hematopoietic tissue, 20: 28982
effects on bone marrow by uptake in bones, 20: 29054 (NP-16119)
effects on radiation dose to human skeleton from content in river water, model for predicting, 20: 30943(R) (ORNL-TM-1465)
effects on thyroid activity in dogs, 20: 29000
leaching from food plants, 20: 29451(R) (NYO-2598-29)
movement in soils, 20: 30943(R) (ORNL-TM-1465)
preparation of, for radioecological studies, 20: 28879
radiation dose to skeleton from, in persons using Clinch River water, 20: 29452 (ORNL-3721(Suppl.3))
sorption from waste solutions by clay minerals, 20: 29332 (ORNL-P-1811)
uptake by rabbit skin, effects of detergent treatment on, 20: 29461
uses as power sources for underwater applications, 20: 29607
uses of waste, to control termite colonies, 20: 29587
STRONTIUM ISOTOPES Sr-94
half life, 20: 30476
STRONTIUM ISOTOPES Sr-95
half life, 20: 30476
STRONTIUM MOLYBDATES
distribution coefficients of rare earth niobates in single crystals of, 20: 29746
STRONTIUM NITRATES
$Sr(NO_3)_2$–$UO_2(NO_3)_2$–H_2O, activity coefficients of, at 25°C, 20: 29196
STRONTIUM OXALATES
precipitation with calcium oxalate using dimethyl oxalate, 20: 29154
STRONTIUM TITANATES
diffusion in, self-, 20: 29623(R) (TID-22970, pp 121-256)
radiation effects on single crystals of, neutron, 20: 29826
STRUCTURES
stress analysis of, computer program for, 20: 29367 (TRG-Report-1089)
STYRENE
radioinduced polymerization with lignin, gamma, 20: 29288

STYRENE POLYMERS
permeability to carbon dioxide–hydrogen mixtures, 20: 29362
reactions with muonium, (E), 20: 29247
polybutadiene–polystyrene, radiation effects on viscoelastic properties of, gamma, 20: 29313
SULFAMIC ACID
analysis for sulfur by hydrogen reduction, 20: 29083(R) (UCRL-14767)
SULFATE COMPLEXES
with neptunium, properties and stability of, 20: 29148
SULFATE IONS
effects on sorption of uranium by ion exchange resins, 20: 29350
SULFIDES
crystal structure of intermetallic-phase, 20: 29623(R) (TID-22970, pp 121-256)
thermodynamic properties of, 20: 29623(R) (TID-22970, pp 121-256)
SULFUR
content in meteorites, 20: 29893
determination in organic compounds by hydrogen reduction, 20: 29083(R) (UCRL-14767)
heating deposits of, *in situ* with radioactive materials, process for, 20: 30950(P)
SULFUR DIOXIDES
determination in atmosphere using radioactive clathrate techniques, 20: 29142
oxidation of, effects of irradiated vanadium oxide–silicon dioxide–silver sulfate catalyst on, 20: 29291
separation from exhaust gases in MHD generator, method for, 20: 29982(P)
SULFUR FLUORIDES
light scattering by, effects of density and temperature on, 20: 30734(R) (TID-22970, pp 1-63)
SULFUR ISOTOPES S-32
deuteron (d,p) reactions at 1.7 to 3.0 Mev, cross sections for, (E), 20: 30518
deuteron reactions (d,p) at 3.20 Mev, sulfur-33 levels from, (E), 20: 30455
SULFUR ISOTOPES S-33
content in meteorites, 20: 29893
energy levels from deuteron reactions (d,p) with sulfur-32 at 3.20 Mev, (E), 20: 30455
energy levels from sulfur-32 (d,p) reactions, (E), 20: 30518
energy levels of, spin of, (T), 20: 30360 (WASH-1068)
SULFUR ISOTOPES S-34
content in meteorites, 20: 29893
SULFUR ISOTOPES S-35
exchange between 4-chlorobenzhydryl thiocyanate and sodium thiocyanate, 20: 29237
SUN
activity of, effects on tropospheric pressure variations, (E), 20: 30237(T)
brightness fluctuations of, oscillatory component in granulation, (T), 20: 29886
chromospheric structure and filaments in, geomagnetic activity prediction method using, 20: 30226
effects on galactic cosmic radiation intensity, 20: 29973
magnetic field measurements, (E), 20: 29885
magnetic field transport outward from spot and bipolar regions of, (T), 20: 29906(T)
magnetic fields of, measurement of, 20: 29910
plasma streams from, 27-day recurrence pattern of, 20: 29894
radio emission from shock propagation in corona of, type-II, (T), 20: 29903(T)
radio wave emission from, frequency spectrum of slowly varying component of, 20: 29908
SUPERCONDUCTIVITY
mechanism of, lattice stability in electron-electron interaction, 20: 30264(T)
of transition metals and alloys down to 0.02°K, (E), 20: 30318
properties of surface, thermal conductivity measurements for, 20: 30294
research programs on, 20: 30735(R) (TID-22970, pp 331-73)
theory for polyenes, 20: 30268
theory of surface, at high temperatures, 20: 30302
theory of transition with Cooper pair formation, 20: 30311
SUPERCONDUCTORS
boundary conditions for interfaces of, Ginzburg-Landau-Gorkov, 20: 30309
critical current density of niobium–zirconium wires, (E), 20: 30267(T)
critical fields and temperatures of multiple, (E), 20: 30291
critical fields of niobium–zirconium alloy, angular dependence of upper, (E), 20: 30270
critical fields of type-II, temperature and purity dependence of, 20: 30295
critical fields of type-II, electron spin and spin-orbit effects on, 20: 30296
current density in contact points of oxidized niobium wires, (E), 20: 30277
current distribution in sheets of type II, magnetic field effects on, (E), 20: 30273
current-inductance characteristics of, 20: 30303
development by crystallochemical methods, 20: 29623(R) (TID-22970, pp 121-256)
development of thin-film, for computer circuitry, 20: 30255(R) (ORO-2430-28)
eddy currents in type-II, fast-pulsed magnetic field induced, 20: 30262
electron spin-pairing in vanadium silicide, (E/T), 20: 30734(R) (TID-22970, pp 1-63)
energy gap in rhenium, anisotropy of, (E), 20: 30281
energy losses in, h-f residual, 20: 30304
Gibbs free energy of bulk type-II, (T), 20: 30287
magnetic field repulsion by split cylinders of, (E), 20: 30276
magnetic fields in, method of images for, (T), 20: 30310
magnetic flux annihilation pulses in grossly inhomogeneous, reversed field, 20: 30261
magnetic flux density of bulk type-II, (T), 20: 30287
magnetic flux in macroscopic rings of, (E), 20: 30305
magnetic flux pinning in thin-film niobium, (E), 20: 30278
magnetic flux pump for, design of, 20: 30274
magnetic hysteresis in type II, surface current effects on, (E), 20: 30269
magnetic properties of type I, effects of lattice defects on, 20: 30253 (CEA-R-2808)
microwave absorption in copper–tin and gold–tin, proximity effects on, (E), 20: 30289
pair multiplicity of, Josephson method for finding, 20: 30265(T)
properties and uses of type-II, 20: 30257
properties of high-purity niobium, (E), 20: 30315
properties of type II, (T), 20: 30313
radiation effects on properties of indium and tin, neutron, 20: 30301
radiation effects on properties of boron- and uranium-doped aluminum–niobium alloy and vanadium silicides, (E), 20: 30260
surface critical currents and a-c susceptibility transition in bismuth–lead, (E), 20: 30293
surface current effects in niobium–zirconium, 20: 30280
thermal conductivity of tin, (T), 20: 30314
thermal conductivity of gapless, calculation of electronic, (T), 20: 30321
transition points in single-crystal gallium, indium, and lead, (E), 20: 30734(R) (TID-22970, pp 1-63)
transition temperatures of, pressure dependence of, 20: 30259
transition temperatures of indium–lanthanum alloy, containing paramagnetic impurities, (E), 20: 30271
transition temperatures of niobium–tin intermetallic compound, 20: 30279
transition temperature of zirconium and zirconium isotopes, (E), 20: 30316
tunneling current in Josephson junction, electromagnetic radiation from, 20: 30292
ultrasonic attenuation by, effects of magnetic fields on, (E/T), 20: 30735(R) (TID-22970, pp 331-73)
ultrasonic attenuation in pure strong-coupling, (T), 20: 30300
use in macroparticle acceleration for nuclear fusion, (T), 20: 30717
use in magnetic shielding of space vehicles, 20: 30317
use of thin-film, in cryogenic devices, 20: 30258
vortex lattices in type-II, hydrodynamic stability of, 20: 30286
vortex lines in, lectures on, 20: 30783
SUPERFLUIDITY
critical velocities in helium II, (T), 20: 30272
properties of helium, near λ line, 20: 30266(T)
theory of Fermi-liquid, collective oscillations in, 20: 30284
ultrasonic attenuation in helium, frequency and temperature dependence of, (E), 20: 30299
SURFACE WATERS
distribution of waste solutions in, use of iodine-131 for tracer studies on, 20: 29099
radioactivity in, 1965 fallout, 20: 29428
SURFACES
contamination of, tracer technique for detecting, 20: 29484(P)
reactions at fluid–solid, effects of ions on, 20: 29623(R) (TID-22970, pp 121-256)
reactions of gas molecules and photons with, 20: 29624(R) (TID-22970, pp 257-329)
SWEET POTATOES
radiation effects on propagation of root-knot nematodes in, 20: 28942
SWIMMING POOL REACTORS
neutron multiplication factor in Hitachi, effect of epithermal fission on, (E/T), 20: 30841
power level monitoring using nitrogen-17, sensitivity of, 20: 30938
SWITCHES
development of superconducting thin film cryotrons, 20: 30258
SYNCHROTRONS

design of Omnitron, for light and heavy ions, 20: 29857 (UCRL-16839)
SYNERGISTIC ACTION
radiation–vibration, in mice, 20: 28968
SYSTEMS FOR NUCLEAR AUXILIARY POWER
development of, for underwater uses, 20: 29607
insulation development for radioisotope, vacuum foil-type thermal, 20: 29606(R) (ALO-3634-1)
use underwater, 20: 30929

T

TANDERIL
use in treatment of radioinduced cystitis, 20: 29060
TANKS
radioactive waste disposal in, economics and safety of, 20: 30943(R) (ORNL-TM-1465)
TANTALUM
analysis of oxygen, method for, 20: 29108
compatibility of coating of, with uranium carbide–zirconium carbide thermionic diode at 1800 to 2500°C, 20: 29820
compatibility with plutonium carbides at 1200 to 1400°C, 20: 29820
corrosion by mercury at 593 to 703°C, 20: 29646
deformation in, mechanisms of thermally activated, 20: 29724
electron ranges in thin films of, 20: 29952
iron-57 Mössbauer spectra in, 20: 30766
magnetic properties of superconducting, effects of lattice defects on, 20: 30253 (CEA-R-2808)
oxidation kinetics, 20: 29644
photoelectric cross sections at 320 kev, absolute, (E), 20: 29924
preparation of, by carbothermal reduction of tantalum pentoxide, 20: 29678
properties as high-temperature coating, 20: 29650
properties of, at 2000°C, for use in thermionic converters, 20: 29729
radiation effects on, for use as sensor material, 20: 29486(R) (NASA-CR-54964)
reactions in gaseous mixtures, combustion, 20: 29641(R) (SC-DC-65-1691)
separation of nitrogen and oxygen from, degasification processes for, 20: 29633
sputtering of, properties of anodic films formed in reactive, 20: 29745
TANTALUM ALLOYS
availability, properties, and uses of, 20: 29760
Al–Cu–Ta, phase studies on, 20: 29764
Al–Ta, intermetallic compounds in, properties of, for use in aerospace technology, 20: 29770
Be–Ta, intermetallic compounds in, properties of, for use in aerospace technology, 20: 29770
Cu–Ni–Ta, phase studies on, 20: 29764
Hf–Ta–W, availability, properties, and uses of, 20: 29760
Hf–Ta–W, creep properties of T-111, 20: 29705(R) (NAS-CR-54973)
Hf–Ta–W, erosion of T-111, by mercury, water, and bismuth–lead alloy, cavitation, 20: 29640 (NP-16048)
Hf–Ta–W, tensile properties of T-111, effects of welds on, 20: 29712(R) (WANL-PR-(P)-009)
Hf–Ta–W, weldability of T-111, effects of oxygen contamination on, 20: 29712(R) (WANL-PR-(P)-009)
Mo–Ta–W, availability, properties, and uses of, 20: 29760
Nb–Ta, deformation in tantalum-base, mechanisms of thermally activated, 20: 29724
Nb–Ta, superconducting current distribution in sheets of, 20: 30273
Nb–Ta–V, availability, properties, and uses of, 20: 29760
Nb–Ta–W, tensile properties of SCb-291, effects of welds on, 20: 29712(R) (WANL-PR-(P)-009)
Nb–Ta–W–Zr, fabricability, strength, and weldability of, 20: 29763
Nb–Ta–W–Zr, tensile properties of FS-85, effects of welds on, 20: 29712(R) (WANL-PR-(P)-009)
Nb–Ta–W–Zr, weldability of FS-85, effects of oxygen contamination on, 20: 29712(R) (WANL-PR-(P)-009)
Re–Ta–W, availability, properties, and uses of, 20: 29760
Ta–W, availability, properties, and uses of, 20: 29760
Ta–W, deformation in tantalum-base, mechanisms of thermally activated, 20: 29724
Ta–W, tensile properties of, effects of welds on, 20: 29712(R) (WANL-PR-(P)-009)
Ta–W–Zr, availability, properties, and uses of, 20: 29760
TANTALUM BORIDES
fabrication and properties of, for use at high temperatures, 20: 29772
TANTALUM CARBIDES
compatibility with tungsten at 2700°C, 20: 30792(R) (ANL-7204, pp 74-86)
dielectric properties of films of, on sputtered tantalum, 20: 29745
effects on properties of graphite, with and without copper and silver infiltration, 20: 29764
preparation from tantalum pentoxide, 20: 29678
properties of, at 2000°C, for use in thermionic converters, 20: 29729
thermoelectric emission in cesium vapor, 20: 29800
Co–TaC–WC, preparation and properties of cermets of, 20: 29778
TANTALUM HYDRIDES
dielectric properties of films of, on sputtered tantalum, 20: 29745
TANTALUM ISOTOPES Ta-181
internal conversion in, nuclear structure effects in, (E/T), 20: 30515
neutron capture cross section measurement at 80 to 200 kev, errors in using boron monitors for, (E), 20: 30352 (NASA-TR-R-240)
TANTALUM ISOTOPES Ta-182
gamma dose from wires of, computer calculations for, 20: 29456
TANTALUM NITRIDES
dielectric properties of films of, on sputtered tantalum, 20: 29745
TANTALUM OXIDES
dielectric properties of films of, on sputtered tantalum, 20: 29745
reduction of Ta_2O_5 by carbothermal method, 20: 29678
PbO–Ta_2O_5, phase studies, 20: 29794
TANTALUM SILICIDES
properties of, for use in aerospace technology, 20: 29770
TANTALUM SYSTEMS
C–Hf–Ta, availability, properties, and uses of, 20: 29760
C–Hf–Ta–W, availability, properties, and uses of, 20: 29760
C–Hf–Ta–W, creep properties of T-222, 20: 29705(R) (NAS-CR-54973)
C–Hf–Ta–W, erosion of T-222, by mercury, water, and bismuth–lead alloy, cavitation, 20: 29640 (NP-16048)
C–Hf–Ta–W, tensile properties of T-222, effects of welds on, 20: 29712(R) (WANL-PR-(P)-009)
C–Hf–Ta–W, weldability of T-222, effects of oxygen contamination on, 20: 29712(R) (WANL-PR-(P)-009)
C–Mo–Ta, phase studies and thermodynamics of, for use at high temperatures, 20: 29774
C–Ta–W, phase studies and thermodynamics of, for use at high temperatures, 20: 29774
TAURINE
excretion by guinea pigs and rats after cysteine administration, 20: 29024
radioinduced hypertaurinuria in rats, effects of cysteine on, 20: 29024
TECHNETIUM
separation from fission product solutions by ion exchange, 20: 29357
separation from irradiated uranium dioxide in chlorine trifluoride by volatilization, 20: 29330(R) (EURAEC-1601)
TECHNETIUM ISOTOPES Tc-99
uses of 6-hr isomer of, in scintillation scanning of bone marrow, liver, and spleen, 20: 29065
TECHNICAL REPORTS
lists of M.I.T., on metallurgy and materials science, 20: 29623(R) (TID-22970, pp 121-256)
lists of M.I.T., on materials engineering, 20: 29624(R) (TID-22970, pp 257-329)
lists of M.I.T., on electric and optical properties of materials, 20: 29709(R) (TID-22970, pp 65-119)
lists of M.I.T., on chemical and solid-state physics, 20: 30734(R) (TID-22970, pp 1-63)
TEETH
alpha radioactivity in human, from America and Germany, 20: 29476
TELEMETERING SYSTEMS
design for measurements in magnetically suspended rotors, 20: 29369
TELEVISION EQUIPMENT
design for use in nuclear reactors, 20: 30809
TELLURIUM
book: *Chemistry of Selenium, Tellurium, and Polonium*, 20: 29235
evaporation of, from irradiated uranium(IV-VI) oxides at 900 to 1500°C in flowing hydrogen, nitrogen, or oxygen, 20: 29211
separation from fission product solutions by ion exchange, 20: 29357
separation from irradiated uranium dioxide in chlorine trifluoride by volatilization, 20: 29330(R) (EURAEC-1601)
TELLURIUM ISOTOPES Te-123
neutron capture at 1 to 5 ev, gamma spectra from, (E), 20: 30385
TELLURIUM ISOTOPES Te-124
energy level transitions from tellurium-123 neutron capture, (E), 20: 30385
TELLURIUM ISOTOPES Te-129
beta decay of, properties of iodine-129 27.7-kev level from, (E), 20: 30474
TELLURIUM ISOTOPES Te-130
proton reactions (p,n) at 100 to 400 Mev, excitation functions for, 20: 30464
TELLURIUM SYSTEMS
Re–Te, phase studies, 20: 29717
Sb–Nb–Te, phase studies, 20: 29717
TEMPERATURE
effects of storage, on shelf life of seafood, 20: 29583(R) (TID-22515)

effects of storage at ambient, on volatile compounds in irradiated beef, 20: 29589
effects on rate of synthesis of ammonia, 20: 29312
measurement in irradiated samples, magnetic method for, 20: 29387
measurement in magnetically suspended rotors, telemetering system for, 20: 29369
measurement of, development of ultrasonic device for, 20: 29486(R) (NASA-CR-54964)
measurements in Atlantic Ocean, 20: 28877 (NYO-1918-124)
radiosensitivity effects on rat mast cells, 20: 28944

TENNESSEE RIVER SYSTEM
radioactivity of, effects of waste disposal in Clinch River on, 20: 29452 (ORNL-3721(Suppl.3))

TERBIUM
determination in minerals and ores, spectrometric, 20: 29134
determination in rocks, chemical spectrographic method for, 20: 29083(R) (UCRL-14767)
determination in standard igneous rocks G-1, W-1, and G-B by x-ray fluorescence, 20: 29101
determination in uranium compounds, spectrographic, 20: 29129
determination using potassium oxalate, effects of other rare earths on spectrofluorimetric, 20: 29086
thermal conductivity of, at room temperatures, mechanisms for, 20: 29741
thermodynamic properties at 0°C to melting point, 20: 29743

TERBIUM ALLOYS
La–Tb, electric conductivity, magnetic susceptibility, and superconducting transition temperatures of, 20: 29753
Re–Tb, crystal structure of, laves phase in, 20: 29792(T)

TERBIUM COMPLEXES
with 2,4-pentanedione, luminescence spectra of, (E), 20: 29238

TERBIUM ETHYL SULFATES
Mössbauer studies of, using terbium-159, 20: 30532

TERBIUM ISOTOPES Tb-159
energy levels of, lifetime of 58-kev isomeric, 20: 30532
Mössbauer effect in, (E), 20: 30532

TERBIUM ISOTOPES Tb-160
beta decay of, higher-order effects in β-γ correlations from, 20: 30470

TERBIUM ISOTOPES Tb-161
energy levels from gadolinium-161 decay, 20: 30401

TERBIUM NIOBATES
distribution in strontium molybdate single crystals, coefficients of, 20: 29746

TEREPHTHALIC ACID, ETHYLENE POLYMER ESTERS
film thickness of, on copper, use of beta-particle backscattering for measuring, 20: 29754

TESTOSTERONE
radiosensitivity effects on erythropoiesis in rats, iron-59 tracer study on, 20: 29043

TEXTILES
properties of fibers for, 20: 29624(R) (TID-22970, pp 257-329)

THALENITE
chemical composition and properties of, in Japan, 20: 29399

THALLIUM
gamma attenuation cross sections at 122 kev, (E), 20: 30731
spectra of, absorption, 20: 29271
Pb–Tl, superconductivity and electronic structure of, 20: 30297

THALLIUM ALLOYS
Bi–Tl, annealing and deformation effects on intermetallic compound in, 20: 29623(R) (TID-22970, pp 121-256)
Bi–Tl, superconducting transition temperature of amorphous, (E), 20: 30298

THALLIUM ISOTOPES Tl-194
decay of isomeric, mercury-194 negative-parity levels from, (E), 20: 30435

THALLIUM ISOTOPES Tl-196
decay of isomeric, mercury-196 negative-parity levels from, (E), 20: 30435

THALLIUM ISOTOPES Tl-198
decay of isomeric, mercury-198 negative-parity levels from, (E), 20: 30435

THALLIUM ISOTOPES Tl-203
deuteron and proton elastic scattering by, angular distributions and levels from, (T), 20: 30484
energy levels from triton reactions (t,α) with lead-204 at 13.5 Mev, (E), 20: 30387

THALLIUM ISOTOPES Tl-204
beta emission of, backscattering from aluminum in 2π geometry, (E), 20: 30369

THALLIUM ISOTOPES Tl-205
energy levels from triton reactions (t,α) with lead-206 at 13.5 Mev, (E), 20: 30387

THALLIUM ISOTOPES Tl-207
energy levels from triton reactions (t,α) with lead-208 at 13.5 Mev, (E), 20: 30387

THALLIUM SULFATES
radiolysis of aqueous solutions of, electron-pulse, 20: 29271

THERMAL CYCLING
effects on properties of silicon surface barrier diodes, 20: 30785

THERMAL INSULATION
development of vacuum foil-type, for radioisotope power systems, 20: 29606(R) (ALO-3634-1)
properties of, for use in nuclear reactors, 20: 29732

THERMAL RADIATION SHIELDING
design of metal foil panels for use as, on reactor pressure vessels, 20: 30820(P)

THERMIONIC CELLS
development for space power, 20: 30926
development for space power, 20: 29977 (N-65-32716)
energy losses from cesium-plasma arc-mode, (T), 20: 29981
materials selection for, 20: 29729

THERMOCOUPLES
development for ultrasonic temperature measurements, 20: 29486(R) (NASA-CR-54964)
error analysis of, model for relative, (T), 20: 29488 (WANL-TME-948)
performance of cooled, in Phoebus reactors, 20: 30925 (LA-DC-7637)
performance of platinum/platinum–rhodium, for high-temperature measurements, 20: 29495
recorder for, design of, 20: 29514(P)

THERMODYNAMICS
Helmholtz equation in, Green's function for, 20: 30184

THERMOELECTRIC CELLS
development and economics of, for communications satellites, 20: 29608
development for space power, 20: 30926
development for space power, 20: 29977 (N-65-32716)
development of, for underwater uses, 20: 29607
performance of bismuth tellurides, analysis of, 20: 29975 (GIC-3362-4)

THERMOELECTRIC MATERIALS
fabrication and properties of sintered semiconductors for use as, 20: 29690

THERMOLUMINESCENCE
measurements in minerals, calibration of, 20: 29400

THERMONUCLEAR EXPLOSIONS
data on, announced Feb. 1966, 20: 29434
data on, announced Dec. 1965, 20: 29428
data on, announced Jan. 1966, 20: 29431
effects on survivors, hematologic, 20: 28876
fallout formation and global distribution from, 20: 29407(T) (AEC-tr-6666)

THERMONUCLEAR REACTIONS
particle acceleration for, using superconducting solenoids, (T), 20: 30717
research on, review of, (E), 20: 30605
research on, review of, (T), 20: 30606

THERMONUCLEAR REACTORS
design and performance of Tuman device, 20: 30682
operation of Astron, 20: 30637
plasma bunch injection in Aspa, properties of, 20: 30636
plasma electron density measurement in Tokamak, using microwave method, 20: 30652
plasma energy losses in toroidal chamber of Tokamak TM-2, 20: 30653
plasma heating in toroidal Tokamak-3, 20: 30650
plasma ion density in alpha, hydrogen, 20: 30686
plasma production in Ogra II, by neutral hydrogen injection, 20: 30633
plasma properties in Tokamak TM-1, 20: 30654
plasma stability in Tokamak, higher-mode, (E), 20: 30651
plasma-column equilibrium in Tokamak-5, (E/T), 20: 30649

THERMOSTATS
design for regulating liquid helium temperatures, 20: 30254 (LA-DC-7209)

THICKNESS GAGES
safety device for radiometric, 20: 29515(P)
uses of radiometric, review of Navy, 20: 29581 (AD-633785)

THIOCYANIC ACID
separation of protactinium from solutions of, by precipitation with arsenazo dyes, induline, and rhodamine B, 20: 29135

THIOCYANIC ACID, 4-CHLOROBENZHYDRYL ESTER
racemization of, tracer studies of, 20: 29237
sulfur-35 exchange between, and sodium thiocyanate, 20: 29237

THIOLS
radiosensitivity effects on Ehrlich ascites carcinoma and mouse spleen, mechanism for, 20: 29039

2-THIOPHENECARBOXYLIC ACID
radiation effects on, ESR spectral studies on, 20: 29284

THORIUM
abundance in gneisses and granites of Rum Jungle Complex, Australia, 20: 29415
alpha decay in bastnaesites, structural changes from, 20: 29447

content and chemical form in iron–manganese concretions, 20: 29426
content in effusive and intrusive formations of northeastern Balkhash foreland, USSR, 20: 29418
content in iron–manganese concretions and manganese ores, 20: 29425
determination by potentiometric titration using pyrocatechol-3,5-disulfonate, 20: 29093
determination in rocks by gamma spectroscopy, errors in, 20: 29421
determination of, in presence of rare earths, spectrophotometric, 20: 29109
determination using sodium molybdate, titrimetric, 20: 29092
distribution and excretion of inhaled, in rats, 20: 28897
distribution in nuclear fuels, fission-track method for measurement of, 20: 29663 (KAPL-M-6556)
removal of, from cotton protective clothing, solution for, 20: 29477
separation from aqueous solutions by solvent extraction using alkyl dibutyl phosphonates, effects of structure of alkyl group on, 20: 29354
separation from nitrate solutions using kerosene–TBP, radiation effects in, 20: 29272
separation from phosphoric acid solutions by solvent extraction using bis(2-ethylhexyl) ester of pyrophosphoric acid, 20: 29361
separation from zirconium by selective adsorption on silica gel, 20: 29344

THORIUM BROMIDES
heat of formation, 20: 29229

THORIUM CARBIDES
preparation of fine particles of, 20: 29676
C–ThC, fabrication of vitreous, 20: 29692(P)
ThC–UC, coating with graphite by pressing, 20: 29669
ThC–UC, development of pyrolytic-carbon-coated, 20: 30870(R) (ORNL-TM-1528)
ThC_2–UC_2, production of pyrolytic-carbon-coated fuel particles of, 20: 29670

THORIUM CHLORIDES
heat of formation, 20: 29229

THORIUM COMPLEXES
with acetylacetone–ethylenediimines, preparation and structure of, 20: 29203
with α-carboxy-β-methyltropolone, composition of, spectrophotometric studies of, 20: 29179
with 2-(1,8-dihydroxy-3,6-disulfo-2-naphthylazo)phenoxyacetic acid, uses in spectrophotometric determination of fluoride ions, 20: 29091

THORIUM FLUORIDES
heat of formation, 20: 29229

THORIUM(IV) FLUORIDES
thermodynamic properties of, emf measurements of, 20: 29215

THORIUM IODIDES
heat of formation, 20: 29229

THORIUM ISOTOPES Th-228
abundance in sea water and sediments, 20: 29412

THORIUM ISOTOPES Th-229
neutron fission of, product mass distribution from thermal, 20: 30373

THORIUM ISOTOPES Th-230
abundance in Pleistocene coral reefs, age estimation by, 20: 29435
abundance in sea water and sediments, 20: 29412
abundance ratio to uranium in ilmenite and zirconia, 20: 29441
content and chemical form in iron–manganese concretions, 20: 29426
content in iron–manganese concretions and manganese ores, 20: 29425
neutron resonance parameters, (E), 20: 30360 (WASH-1068)

THORIUM ISOTOPES Th-232
abundance in sea water and sediments, 20: 29412
deuteron fission at 14 Mev, yields of xenon-133 and -135 from, 20: 30533
helium ion fission at 25 Mev, xenon-133 and -135 yields from, 20: 30533

THORIUM NITRATES
crystal structure of petahydrate of, x-ray diffraction studies of, 20: 29150
crystal structure of pentahydrate of, neutron diffraction studies of, 20: 29151

THORIUM(IV) OXIDES
carcinogenic effects in rats, 20: 29022
content in thalenites from Japan, 20: 29399
electric conductivity of solutions of, electronic and ionic components of, 20: 29216
fabrication of pellets of, 20: 29657
grain growth and sintering of, 20: 29623(R) (TID-22970, pp 121-256)
separation of protactinium-233 from irradiated, method for, 20: 29331 (KAPL-M-6554)
separation of protactinium from irradiated, 20: 29335
BeO–PuO_2–ThO_2, development as reactor fuel, 20: 29616(R) (BMI-1738)
Ni–ThO_2, diffusion of chromium in, for corrosion protection, 20: 29748
Ni–ThO_2, joining by brazing, soldering, or welding TD nickel, 20: 29666 (RSIC-484)
Ni–ThO_2, surface treatments for TD nickel, coating and mechanical, 20: 29706 (NASA-TM-X-53448)
Re–ThO_2–W, fabrication, properties, and uses of, 20: 29768
ThO_2–UO_2, heat treatments of, 20: 29629
ThO_2–UO_2, homogeneity of, fission-track method for measurement of, 20: 29663 (KAPL-M-6556)
ThO_2–UO_2, vapor pressure, 20: 29616(R) (BMI-1738)
ThO_2–Y_2O_3, electric conductivity of solutions of, electronic and ionic components of, 20: 29216

THORIUM PHOSPHATES
preparation and properties of, 20: 29160

THORIUM SYSTEMS
C–Th–U, hydrolysis of, production of methane during, 20: 29159

THRESHOLD DETECTORS
performance of, in fast neutron spectra measurements, 20: 29078(R) (AD-633252)

THULIUM
determination in minerals and ores, spectrometric, 20: 29134
determination in rocks, chemical spectrographic method for, 20: 29083(R) (UCRL-14767)
determination in standard igneous rocks G-1, W-1, and G-B by x-ray fluorescence, 20: 29101
determination in uranium compounds, spectrographic, 20: 29129
thermodynamic properties at 0°C to melting point, 20: 29743

THULIUM ISOTOPES Tm-169
internal conversion coefficients, (E/T), 20: 30515

THULIUM ISOTOPES Tm-170
beta decay of, β-γ directional and circular polarization correlations in, (E), 20: 30544
beta decay of, matrix elements for forst-forbidden, (E/T), 20: 30522
beta spectra, (E), 20: 30546
uses as gamma source for detection of flaws in steel foils and plates, 20: 29390

THULIUM NIOBATES
distribution in strontium molybdate single crystals, coefficients of, 20: 29746

THYMINE
radiation effects on thermoluminescence of, gamma, 20: 28913
radiation effects on content of, in DNA in guinea pig brain, 20: 28919
radiation effects on, ESR and thermoluminescence studies of, 20: 29249
radioinduced dimerization of, at −5 to −70°C, kinetics of uv, 20: 28916

THYMUS GLAND
radiation effects on nucleic acid synthesis in rat, x, 20: 28953
radiation effects on cells in mouse, methods for evaluating, 20: 29008
radiation effects on immune response of thymectomized chickens, 20: 29014

THYROID GLAND
activity and morphology of rat, effects of uranium nitrate on, 20: 28884
iodine-131 content of bovine, 1965, 20: 29428
iodine-131 uptake by dog, effects of strontium-90 on, 20: 29000
radiation effects on activity of dog, beta, 20: 29000
radiosensitivity of rat, effects of cystamine on, 20: 29047

THYROXINE
effects on radiation effects on heme synthesis in rabbit bone marrow, 20: 28912
radiosensitivity effects on mice, 20: 28978
radiosensitivity effects on erythropoiesis in rats, iron-59 tracer study on, 20: 29043

TIMING CIRCUITS
design, 20: 29530 (SCL-DR-65-13)

TIN
determination in dibutyl laurate catalyst for silastic polymer, 20: 29083(R) (UCRL-14767)
determination in petroleum, activation, 20: 29139
effects on copper or silver infiltrants in graphite, 20: 29764
energy levels of, existence of 2.0-min and 1-hr isomeric, 20: 30376
evaporation of, from irradiated uranium(IV-VI) oxides at 900 to 1500°C in flowing hydrogen, nitrogen, or oxygen, 20: 29211
iron-57 Mössbauer spectra in, 20: 30766
neutron inelastic scattering cross sections at 1 Mev, (E), 20: 30383
radiation effects on superconducting properties of, neutron, 20: 30301
radioinduced reactions with 1-bromobutane, 20: 29616(R) (BMI-1738)
thermal conductivity of normal and superconducting, (T), 20: 30314
Au–Sn, atomic structure of liquid and solid, 20: 29623(R) (TID-22970, pp 121-256)

TIN ALLOYS
Al–Sn–Ti, mechanical properties at −320 to 200°F, effects of hydrogen content on, 20: 29715 (WANL-TME-1287)
Al–Sn–Ti, sorptive properties for hydrogen at 200 to 925°F, 20: 29715 (WANL-TME-1287)
Nb–Sn, preparation of multilayer continuous intermediate phase wires of, 20: 29781
Nb–Sn, superconductivity of multilayer continuous intermediate phase wires of, effects of heat treatments on, 20: 29781
Nb–Sn, superconducting transition temperatures of $NbSn_2$ and Nb_6Sn_5, 20: 30279

Sn–Zn, distillation of liquid, surface concentration changes in, 20: 29346
Sn–Zr, oxidation of, at 850°C, mechanisms of breakaway, 20: 29652
TIN COUPLES
Au/Sn, critical fields and temperatures of superconducting, (E), 20: 30291
Au/Sn, microwave absorption in superconducting, proximity effects on, (E), 20: 30289
Cu/Sn, critical fields and temperatures of superconducting, (E), 20: 30291
Cu/Sn, microwave absorption in superconducting, proximity effects on, (E), 20: 30289
TIN ISOTOPES
energy level properties from shell model, (T), 20: 30521
neutron cross sections for even-even, below 10 kev, (E), 20: 30490
TIN ISOTOPES Sn-113
electron capture decay of, indium-113 Auger electron spectrum from, (E), 20: 30527
TIN ISOTOPES Sn-116
alpha inelastic scattering at 40 Mev, angular distributions and energy levels from, (E), 20: 30468
neutron total cross section below 10 kev, (E), 20: 30490
TIN ISOTOPES Sn-118
alpha inelastic scattering at 40 Mev, angular distributions and energy levels from, (E), 20: 30468
neutron scattering at 4.0 Mev, polarization angular distributions from, (E), 20: 30360 (WASH-1068)
neutron total cross section below 10 kev, (E), 20: 30490
TIN ISOTOPES Sn-119
charge radius change of, (E/T), 20: 30382(T)
Mössbauer effect on, barium stannate source for measuring, 20: 30753(T)
TIN ISOTOPES Sn-120
alpha inelastic scattering at 40 Mev, angular distributions and energy levels from, (E), 20: 30468
neutron total cross section below 10 kev, (E), 20: 30490
proton elastic scattering at 40 Mev, cross sections for, (E/T), 20: 30353(R) (ORNL-3940, pp 1-61)
TIN ISOTOPES Sn-122
alpha inelastic scattering at 40 Mev, angular distributions and energy levels from, (E), 20: 30468
neutron total cross section below 10 kev, (E), 20: 30490
TIN ISOTOPES Sn-124
neutron total cross section below 10 kev, (E), 20: 30490
TIN SULFIDES
thermodynamic properties, 20: 29623(R) (TID-22970, pp 121-256)
TISSUE TRANSPLANTS
immune reactions to, effects of extracorporeal blood irradiation on, 20: 28927 (BNL-9647)
immunity in mice to bone marrow and spleen cell, effects of methotrexate on, 20: 29035
radiation effects on acceptance of, 20: 28983
TISSUES
radiation effects on regenerative capacity of axolotl, effects of RNA on recovery from, 20: 29038
radioactivity of, computer program for evaluating determinations of, 20: 29121
radiosterilization of bone graft, 20: 28987
role of adipose, in recovery processes in irradiated mice and rats, 20: 28946
TITANIUM
analysis for carbon by induction furnace combustion method, 20: 29083(R) (UCRL-14767)
deposition by vapor plating from titanium iodide, 20: 29650
determination in petroleum, activation, 20: 29139
determination in Zircaloy-2, spectrographic, 20: 29113
deuteron elastic scattering at 13.6 Mev, cross section for, (E), 20: 30497
effects on ductility of electron-beam-melted molybdenum, 20: 29783
iron-57 Mössbauer spectra in, 20: 30766
oxidation kinetics, 20: 29644
performance as gettering agent for nitrogen separation from rare gases, 20: 29329 (ANL-7128)
plasma source of, operational modes of, 20: 30589(T)
TITANIUM ALLOYS
Al–Cr–Co–Fe–Mo–Ni–Ti, joining of Udimet 500 and 700, by mechanical fastening, 20: 29667 (RSIC-509)
Al–Cr–Co–Fe–Mo–Ni–Ti, surface treatments for Udimet 500 and 700, coating and mechanical, 20: 29706 (NASA-TM-X-53448)
Al–Cr–Co–Mo–Ni–Ti, joining of M-252, by mechanical fastening, 20: 29667 (RSIC-509)
Al–Cr–Co–Mo–Ni–Ti, surface treatments for Astroloy, coating and mechanical, 20: 29706 (NASA-TM-X-53448)
Al–Cr–Co–Mo–Ni–Ti–V–Zr, surface treatments for IN-100, coating and mechanical, 20: 29706 (NASA-TM-X-53448)
Al–Cr–Co–Ni–Nb–Ti–W, surface treatments for Mar-M 200, coating and mechanical, 20: 29706 (NASA-TM-X-53448)
Al–Cr–Fe–Mo–Ni–Ti–W, joining of D-979, by mechanical fastening, 20: 29667 (RSIC-509)
Al–Cr–Ni–Ti, corrosion by trichloroethylene, tracer studies of, 20: 29655
Al–Sn–Ti, mechanical properties at –320 to 200°F, effects of hydrogen content on, 20: 29715 (WANL-TME-1287)
Al–Sn–Ti, sorptive properties for hydrogen at 200 to 925°F, 20: 29715 (WANL-TME-1287)
Al–Ti, analysis for carbon by induction furnace combustion method, 20: 29083(R) (UCRL-14767)
Be–Ti, intermetallic compounds in, properties of, for use in areospace technology, 20: 29770
Fe–Ti, strengthening of, by strain hardening, theory of, 20: 29623(R) (TID-22970, pp 121-256)
Hf–Nb–Ti, fabricability, strength, and weldability of, 20: 29763
Mo–Nb–Ti, evaluation of protective coatings for, 20: 29651
Mo–Nb–Ti–Zr, creep properties of niobium-modified TZM, 20: 29705(R) (NAS-CR-54973)
Mo–Ti, coating with silicon by fluidized-bed process, 20: 29630
Mo–Ti, erosion by mercury, water, and bismuth–lead alloy, cavitation, 20: 29640 (NP-16048)
Mo–Ti, melting of, effects of composition on electron-beam, 20: 29674
Mo–Ti–Zr, creep properties of TZM, 20: 29705(R) (NAS-CR-54973)
Mo–Ti–Zr, production properties of sheets of, 20: 29756
Nb–Ti–Zr, phase studies on, at 570 to 1100°C, 20: 29785
Nb–Ti–Zr, superconductivity of, effects of composition on, 20: 29784
Nb–Ti–Zr, superconductivity of, effects of cold working and heat treatments on, 20: 29787
Nb–Ti–Zr, superconductivity of, effects of microstructure on, 20: 29788
Ti–U, casting of, testing of products from, 20: 29803
Ti–U, mechanical properties, 20: 29803
Ti–V, creep rate testing and thermal expansivity of, 20: 30790(R) (ANL-7204, pp 1-31)
TITANIUM BORIDES
coating of, effects of, on oxidation resistance of graphite, 20: 29773
fabrication and properties of, for use at high temperatures, 20: 29772
TITANIUM CARBIDES
analysis for oxygen, method for, 20: 29108
coating of, effects of, on oxidation resistance of graphite, 20: 29773
fabrication and properties, 20: 29727
hardness and surface friction of, effects of temperature on, 20: 29771
properties of, at 2000°C, for use in thermionic converters, 20: 29729
Mo–Ni–TiC, oxidation of, by air at 600 to 1300°C, effects of molybdenum content on, 20: 29653
TiC–$TiSi_2$, coating of, effects of, on oxidation resistance of graphite, 20: 29773
TITANIUM CHLORIDES
crystal growth by vapor deposition of, 20: 29623(R) (TID-22970, pp 121-256)
TITANIUM HYDRIDES
performance of, as deoxidizer during arc-melting of molybdenum, 20: 29675
TITANIUM ISOTOPES Ti-45
beta decay of, scandium-45 levels from, (E), 20: 30456
yield in alpha and proton reactions with copper, 20: 30531
TITANIUM ISOTOPES Ti-48
deuteron elastic scattering at 34.4 Mev, angular distributions from, (E/T), 20: 30353(R) (ORNL-3940, pp 1-61)
neutron reactions (n,γ) at thermal energies, time invariance of nuclear forces from, 20: 30505
TITANIUM ISOTOPES Ti-49
deuteron elastic scattering at 34.4 Mev, angular distributions from, (E/T), 20: 30353(R) (ORNL-3940, pp 1-61)
TITANIUM ISOTOPES Ti-50
deuteron elastic scattering at 34.4 Mev, angular distributions from, (E/T), 20: 30353(R) (ORNL-3940, pp 1-61)
TITANIUM ISOTOPES Ti-51
deuteron elastic scattering at 34.4 Mev, angular distributions from, (E/T), 20: 30353(R) (ORNL-3940, pp 1-61)
TITANIUM OXIDES
hardness and surface friction of, effects of temperature on, 20: 29771
hydrogen ion sorption by, 20: 29623(R) (TID-22970, pp 121-256)
TITANIUM SILICIDES
coating of, effects of, on oxidation resistance of graphite, 20: 29773
TiC–$TiSi_2$, coating of, effects of, on oxidation resistance of graphite, 20: 29773
TITANIUM SYSTEMS
C–Mo–Ti–Zr, creep properties of TZC, 20: 29705(R) (NAS-CR-54973)
C–Mo–Ti–Zr, properties at high temperatures, 20: 29756
Co–TiC–WC, properties of cermets of, effects of titanium carbide content on, 20: 29779

Cr–Si–Ti, properties of, for use as protective coating on niobium and its alloys, 20: 29651
C–Ti, fabrication of hypereutectic composites of, with high thermal shock resistance, 20: 29727
TOLUENESULFONAMIDE
N,N-dimethyl-*p*-, analysis for sulfur by hydrogen reduction, 20: 29083(R) (UCRL-14767)
TRACER TECHNIQUES
use in hematologic diagnosis, 20: 28893
use in measurement of gaseous diffusion coefficients, 20: 29510
use in nuclear hematology, 20: 28874
TRACER TECHNIQUES (MEDICINE)
for kidney function tests, 20: 29063
TRADESCANTIA
radiation and space-flight effects on microspores of, 20: 28971
radiation effects on chromosomal bridges at anaphase in, fast-neutron and x, 20: 29031
radioinduced chromosome aberrations in, effects of cupferron on frequency of x, 20: 29028
TRANSCURIUM ELEMENTS
production of, in N = 184 and Z = 126 region, (T), 20: 30367
TRANSDUCERS
properties of magnetostrictive and piezoelectric, for operation in extensional and shear wave modes, 20: 29486(R) (NASA-CR-54964)
TRANSFORMATION TEMPERATURES
relaxation phenomena near, (T), 20: 30780
TRANSISTORS
radiation effects on silicon planar, gamma, 20: 29577 (CEA-R-2959)
use of field-effect, in preamplifier for semiconductor detectors, 20: 29548
TRANSITION METAL OXIDES
dielectric properties of, 20: 29709(R) (TID-22970, pp 65-119)
TRANSITION METALS
deformation of bcc, 20: 29624(R) (TID-22970, pp 257-329)
superconductivity of, down to 0.02°K, (E), 20: 30318
thermal diffusion of carbon, nitrogen, and oxygen in, review on, 20: 29769
TRANSURANIC ELEMENTS
metabolism and toxicity of, review on, 20: 28885
TRAPS
development of sodium vapor, 20: 30875(R) (ANL-7190, pp 143-55)
TREES
radiation effects on pollen germination of *Pinus desiflora* and *Pinus thunbergii*, gamma, 20: 28980
radioisotope uptake by *Juniperus virginiana*, in Georgia, 20: 29410
TRIMETHYLAMINE
radiation effects on production in fish, gamma, 20: 29583(R) (TID-22515)
TRIOCTYLAMINE
solvent properties for uranium, 20: 29339
TRITIUM
binding energies of, 20: 30424
content in rain and snow in Moscow, Dec. 1961 to Dec. 1963, 20: 29409
decay of, in amino and dicarboxylic acids, ESR spectra of radicals from self-radiolysis in, 20: 29311
determination by liquid scintillation counting, role of phosphorescence in, 20: 29084
determination in water, efficiency of flow counter for, 20: 29098
determination of, design and performance of small proportional counters for, 20: 29559
deuteron reactions (d,n) at 6.6 Mev, polarization function for, (E), 20: 30442
effects on oxidation of hydrogen by copper oxide, 20: 29187
incorporation in 2-octynoic acid to high specific activity, Wilzbach method for, 20: 29243
molecular dissociation following tritium beta decay in, calculation of, 20: 29233
reactions of 3-ev atoms of, with methane, 20: 29265
reactions of, with phosphors, illumination of telephone dials by, 20: 29605(P)
reactions with gaseous hydrocarbons, scavenger effects of labeled product distribution from, 20: 29206
recoil reactions with alkanes and haloalkanes, yields from, 20: 29233
use in age estimation in geology and hydrology, 20: 29438 (CONF-650652)
TRITONS
angular distributions from reactions of lithium-6 and -7 with boron-10 and -11, 20: 30519
diffusion in ice single crystals, effects of ammonium fluoride on, 20: 29193
reactions (t,α) with fluorine-alpha angular distributions from, (E), 20: 30360 (WASH-1068)
reactions (t,pf) with plutonium-239 and -240, fission probability and fragment anisotropies for, 20: 30360 (WASH-1068)
reactions (t,p) with oxygen-16, calcium-40, and cadmium-110, strong coupling approximation method for studying, (T), 20: 30399
reactions (t,p) with iron-54 at 12 Mev, iron-56 levels from, (E), 20: 30453
reactions with lead-204, -206, and -207 at 13.5 Mev, thallium-203, -205, and -207 levels from, (E), 20: 30387
TROPOSPHERE
pressure variations in, solar activity effects on, (E), 20: 30237(T)
TRYPTOPHAN
effects on edema and blood serotonin in irradiated rats, 20: 29001
radiation effects on, quantum efficiency of uv, 20: 28915
TUBES
boiling burnout in round, with nonuniform heat fluxes, (E/T), 20: 29376 (BAW-3238-9)
boiling burnout in nonuniformly heated annular, (E/T), 20: 29377(R) (BAW-3238-11)
extrusion of, apparatus for, 20: 29691(P)
gas flow in, transition from turbulent to laminar, 20: 29384
TUMORS
antigenic characteristics of virus-induced mouse lymphomas, 20: 28873
hormone dependence of breast, 20: 28871(R) (EUR-2636.f,i)
radiation effects on collagen and hexosamine content in rat subcutaneous granulomas, γ, 20: 28917
radiation effects on protein synthesis in cells of Ehrlich mouse ascites, x, 20: 28923
radiation effects on response of mice to injected RNA from, 20: 28926 (AD-633469)
radiation effects on resistance of mice to Ehrlich ascites, 20: 29017
radiodiagnosis of, using iodine-131-labeled fibrinogen, 20: 28871(R) (EUR-2636.f,i)
radioinduced by thorotrast in rats, 20: 29022
radiosensitivity of rabbit lung, effects of hyperbaric oxygen on, 20: 29059 (TID-22860)
radiotherapy of lymphomas using fractionated whole-body exposures, x, 20: 29069
radiotherapy of gynecological, amino acid variations in blood plasma during, 20: 28979
radiotherapy using internally deposited yttrium-90 particles, 20: 29059 (TID-22860)
TUNGSTEN
analysis for oxygen, method for, 20: 29108
brittle-ductile transition temperature in, method for determining, 20: 29757
compatibility of coating of, with uranium carbide–zirconium carbide thermionic diode at 1800 to 2590°C, 20: 29820
compatibility with tantalum carbides at 2700°C, 20: 30792(R) (ANL-7204, pp 74-86)
compatibility with plutonium carbides at 1200 to 1400°C, 20: 29820
corrosion by mercury at 593 to 703°C, 20: 29646
creep properties of arc-cast and vapor-deposited, 20: 29705(R) (NAS-CR-54973)
deposition on refractory metal–nonmetal powders by chloride and oxide processes, 20: 29631
determination in aqueous solutions, design of oxyacetylene burner for measuring sensitivity of spectrophotometric, 20: 29083(R) (UCRL-14767)
dislocations in high-angle boundaries in, 20: 29725
effects on properties of graphite, with and without copper and silver infiltration, 20: 29764
electric conductivity of single-crystal, effects of deformation on, 20: 29723
forging of, comparison of arc-cast, pressed, and sintered billets for, 20: 29683
iron-57 Mössbauer spectra in, 20: 30766
mechanical properties and structure of single crystals of, effects of carbon, nitrogen, and oxygen impurities on, 20: 29793
oxidation by carbon dioxide and oxygen, equipment for studying kinetics of high-temperature, 20: 29656
production by hydrogen reduction of tungsten hexafluoride, 20: 29687
production of nozzle of, by flow turning, 20: 29682
production of sheet bars of, by zone refining of cemented tungsten-base alloys, 20: 29688
properties as high-temperature coating, 20: 29650
properties of, at 2000°C, for use in thermionic converters, 20: 29729
radiation effects on, for use as sensor material, 20: 29486(R) (NASA-CR-54964)
reactions of adsorbed layers on, effects of mechanical stress on, 20: 29624(R) (TID-22970, pp 257-329)
sintering of compacts of, factors affecting indirect, 20: 29684
TUNGSTEN ALLOYS
Ag–W, fabrication of rocket motor nozzle of, 20: 29685
Al–Cr–Co–Ni–Nb–Ti–W, surface treatments for Mar-M 200, coating and mechanical, 20: 29706 (NASA-TM-X-53448)
Al–Cr–Fe–Mo–Ni–Ti–W, joining of D-979, by mechanical fastening,

20: 29667 (RSIC-509)
Cu–Ni–W, properties of composite-type, 20: 29624(R) (TID-22970, pp 257-329)
Fe–Ni–W, deformation properties of dispersed and sintered composites of, elastic and plastic, 20: 29686
Fe–Ni–W, properties of composite-type, 20: 29624(R) (TID-22970, pp 257-329)
Fe–Ni–W, zone refining of cemented, production of tungsten sheet bars by, 20: 29688
Hf–Nb–W–Y, fabricability, strength, and weldability of, 20: 29763
Hf–Nb–W–Y, tensile properties of C-129Y, effects of welds on, 20: 29712(R) (WANL-PR-(P)-009)
Hf–Ta–W, availability, properties, and uses of, 20: 29760
Hf–Ta–W, creep properties of T-111, 20: 29705(R) (NAS-CR-54973)
Hf–Ta–W, erosion of T-111 by mercury, water, and bismuth–lead alloy, cavitation, 20: 29640 (NP-16048)
Hf–Ta–W, tensile properties of T-111, effects of welds on, 20: 29712(R) (WANL-PR-(P)-009)
Hf–Ta–W, weldability of T-111, effects of oxygen contamination on, 20: 29712(R) (WANL-PR-(P)-009)
Mo–Ta–W, availability, properties, and uses of, 20: 29760
Nb–Ta–W, tensile properties of SCb-291, effects of welds on, 20: 29712(R) (WANL-PR-(P)-009)
Nb–Ta–W–Zr, fabricability, strength, and weldability of, 20: 29763
Nb–Ta–W–Zr, tensile properties of FS-85, effects of welds on, 20: 29712(R) (WANL-PR-(P)-009)
Nb–Ta–W–Zr, weldability of FS-85, effects of oxygen contamination on, 20: 29712(R) (WANL-PR-(P)-009)
Nb–W–Zr, fabricability, strength, and weldability of, 20: 29763
Nb–W–Zr, tensile properties of Cb-752, effects of welds on, 20: 29712(R) (WANL-PR-(P)-009)
Re–Ta–W, availability, properties, and uses of, 20: 29760
Re–W, extrusion of tubing of, development of process for, 20: 29659(R) (COO-1518-3)
Re–W, fabrication, properties, and uses of, 20: 29768
Re–W, tensile properties of sheets and wires of, 20: 29765
Ta–W, availability, properties, and uses of, 20: 29760
Ta–W, deformation in tantalum-base, mechanisms of thermally activated, 20: 29724
Ta–W, tensile properties of, effects of welds on, 20: 29712(R) (WANL-PR-(P)-009)
Ta–W–Zr, availability, properties, and uses of, 20: 29760

TUNGSTEN CARBIDES
analysis for oxygen, method for, 20: 29108
hardness and surface friction of, effects of temperature on, 20: 29771
properties of, at 2000°C, for use in thermionic converters, 20: 29729
Co–TaC–WC, preparation and properties of cermets of, 20: 29778
Co–WC, properties of cermets of, effects of binder phase composition and grain size on, 20: 29780
Nb_2O_5–WC, reduction to niobium–tungsten alloy by niobium carbide, 20: 29677

TUNGSTEN FLUORIDES
reduction of WF_6 by hydrogen, production of tungsten by, 20: 29687

TUNGSTEN ISOTOPES W-182
deuteron elastic and inelastic scattering at 12 Mev, angular distributions from, 20: 30475
deuteron reactions (d,p) at 7.5 and 12 Mev, angular distributions from, (E), 20: 30475
internal conversion coefficients, (E/T), 20: 30515
neutron reactions (n,γ) with, gamma spectra from thermal, (E), 20: 30360 (WASH-1068)
neutron resonance parameters for, 20: 30358(R) (RPI-328-56, pp 1-48)

TUNGSTEN ISOTOPES W-183
energy level transitions from tungsten-182 neutron capture, (E), 20: 30360 (WASH-1068)
neutron capture at 1 to 5 ev, gamma spectra from, (E), 20: 30385
neutron reactions (n,γ) with, gamma spectra from thermal, (E), 20: 30360 (WASH-1068)
neutron resonance parameters for, 20: 30358(R) (RPI-328-56, pp 1-48)
proton scattering at 12 Mev, angular distributions from, (E), 20: 30475

TUNGSTEN ISOTOPES W-184
energy level transitions from tungsten-183 neutron capture, (E), 20: 30360 (WASH-1068)
energy level transitions from tungsten-183 neutron capture, (E), 20: 30385
neutron reactions (n,γ) with, gamma spectra from thermal, (E), 20: 30360 (WASH-1068)
neutron resonance parameters for, 20: 30358(R) (RPI-328-56, pp 1-48)

TUNGSTEN ISOTOPES W-185
energy level transitions from tungsten-184 neutron capture, (E), 20: 30360 (WASH-1068)

TUNGSTEN ISOTOPES W-186
neutron reactions (n,γ) with, gamma spectra from thermal, (E), 20: 30360 (WASH-1068)
neutron resonance parameters for, 20: 30358(R) (RPI-328-56, pp 1-48)
nitrogen-14 inelastic scattering by, Coulomb excitation from, (E), 20: 30488
proton reactions (p,n) at 100 to 400 Mev, excitation functions for, 20: 30464

TUNGSTEN ISOTOPES W-187
energy level transitions from tungsten-186 neutron capture, (E), 20: 30360 (WASH-1068)

TUNGSTEN OXIDES
reactions with niobium carbide to form niobium–tungsten alloy, 20: 29677
reactions with uranium dioxide, 20: 29170
Nb_2O_5–WO_3, reduction to niobium–tungsten alloy by niobium carbide, 20: 29677

TUNGSTEN SILICIDES
properties of, for use in aerospace technology, 20: 29770

TUNGSTEN SYSTEMS
BeO–W, fabrication of sintered, 20: 29689
C–Cr–W, phase studies and thermodynamics of, for use at high temperatures, 20: 29774
C–Hf–Ta–W, availability, properties, and uses of, 20: 29760
C–Hf–Ta–W, creep properties of T-222, 20: 29705(R) (NAS-CR-54973)
C–Hf–Ta–W, erosion of T-222, by mercury, water, and bismuth–lead alloy, cavitation, 20: 29640 (NP-16048)
C–Hf–Ta–W, tensile properties of T-222, effects of welds on, 20: 29712(R) (WANL-PR-(P)-009)
C–Hf–Ta–W, weldability of T-222, effects of oxygen contamination on, 20: 29712(R) (WANL-PR-(P)-009)
C–Mo–Nb–W–Zr, evaluation of protective coatings for, 20: 29651
C–Nb–W, phase studies and thermodynamics of, for use at high temperatures, 20: 29774
C–Nb–W–Y–Zr, tensile properties of D-43Y, effects of welds on, 20: 29712(R) (WANL-PR-(P)-009)
C–Nb–W–Zr, evaluation of protective coatings for, 20: 29651
C–Nb–W–Zr, fabricability, strength, and weldability of, 20: 29763
C–Nb–W–Zr, tensile properties of D-43, effects of welds on, 20: 29712(R) (WANL-PR-(P)-009)
Co–TiC–WC, properties of cermets of, effects of titanium carbide content on, 20: 29779
Co–WC, strength of sintered, effects of heat treatments and temperature on, 20: 29802
Cr–Si–W, properties of, for use as protective coating on niobium and its alloys, 20: 29651
C–Ta–W, phase studies and thermodynamics of, for use at high temperatures, 20: 29774
C–W, phase studies, stabilities, and thermodynamics of, at high temperatures, 20: 29774
C–W–V, phase studies and thermodynamics of, for use at high temperatures, 20: 29774
Re–ThO_2–W, fabrication, properties, and uses of, 20: 29768
W–UO_2, electric conductivity at 25 to 1300°C, effects of composition fabrication process on, 20: 29699 (CONF-650674-1)
W–ZrO_2, fabrication, 20: 29689

TYRAMINE
radiation effects on content in rat tissues, x, 20: 28964

TYROSINE
radiation effects on, quantum efficiency of uv, 20: 28915

U

ULCERS
radioinduced in mice and rats, x, 20: 28946

ULTRASONICS
attenuation in liquid helium, frequency and temperature dependence of, (E), 20: 30299
attenuation in pure strong-coupling superconductors, (T), 20: 30300
transmission in brazed and rolled bonds, correlation of heat transfer and, 20: 29386 (ANL-7074)

ULTRAVIOLET RADIATION
effects on amino acids, quantum efficiency, 20: 28915
effects on Anacystis pigments, mutagenic, 20: 28958
effects on bacteriophage, genetic, 20: 28948
effects on bacteriophage, genetic, 20: 28969
effects on blood plasma proteins in rabbits, 20: 29004
effects on carbon dioxide effects on oxidation of graphite, 20: 29733
effects on catalytic activity of platinum, 20: 29304
effects on copper–glycine complexes, 20: 29303
effects on dimerization of thymine at −5 to −70°C, kinetics of, 20: 28916
effects on DNA and RNA synthesis in *E. coli*, 20: 28949
effects on *E. coli*, mutations from, 20: 28991
effects on fat and glycogen content in paramecia, 20: 28918
effects on fluorescence and phosphorescence spectra of nucleic acid derivatives at 77°K, 20: 28914

effects on gamma-irradiated and normal sodium bromate, kinetics of, 20: 29248 (BNL-9672)
effects on health of domestic animals, 20: 29020
effects on mast cells in mouse skin, 20: 28937
effects on mast cells of rat connective tissue, effects of low temperatures on, 20: 28944
effects on phosphorus-32-labeled uridylyluridine, 20: 28910
effects on potassium iodides, color center formation from, (E), 20: 30748
effects on properties of pyridoxine derivatives, 20: 28901
effects on resistance of *E. coli* to bacteriophage T1, 20: 29027
effects on *Salmonella typhimurium*, genetic, 20: 28977
UNDERGROUND EXPLOSIONS
data on, announced Feb. 1966, 20: 29434
data on, announced Dec. 1965, 20: 29428
data on, announced Jan. 1966, 20: 29431
use for highway construction, 20: 29370 (PNE-3003)
UNDERWATER EXPLOSIONS
hazards from, review of gamma, radioactive-contamination, and shock-wave, 20: 29481
UNION CARBIDE NUCLEAR CO., PADUCAH PLANT, KY.
environs monitoring, Jan. to July 1965, 20: 29428
UNION CARBIDE NUCLEAR CO. Y-12 PLANT, OAK RIDGE, TENN.
environs monitoring, Jan. to July 1965, 20: 29428
UNITED KINGDOM
radiation hazards to population of, from fallout, 20: 29054 (NP-16119)
UNITED STATES
fallout monitoring, 1965, 20: 29434
fallout monitoring, 1965, 20: 29428
fallout monitoring, 1965, 20: 29431
URACIL
radiation effects on thermoluminescence of, gamma, 20: 28913
radiation effects on, ESR and thermoluminescence studies of, 20: 29249
URACIL, 5-BROMO-
labeling with bromine-82 by isotopic exchange method, 20: 29244
URANATES
spectra of, optical, (E), 20: 30735(R) (TID-22970, pp 331-73)
URANIUM
abundance in gneisses and granites of Rum Jungle Complex, Australia, 20: 29415
abundance ratio to thorium-230 in ilmenite and zirconia, 20: 29441
aquisition in Japan, problems of, 20: 30871
analysis for rare earths, spectrographic, 20: 29129
content and chemical form in iron–manganese concretions, 20: 29426
content in effusive and intrusive formations of northeastern Balkhash foreland, USSR, 20: 29418
content in iron–manganese concretions and manganese ores, 20: 29425
content in traprock formations of Siberian platform, USSR, 20: 29419
deposition and mineralization of, in hydrothermal deposits of West Erzgebirge, Germany, 20: 29448
determination in rocks by gamma spectroscopy, errors in, 20: 29421
determination of trace amounts of, in waste water, fluorescence, 20: 29128
determination using arsenazo I–EDTA–nitrosonaphthol, colorimetric micro-, 20: 29130
distribution in nuclear fuels, fission-track method for measurement of, 20: 29663 (KAPL-M-6556)
electron scattering at 40 to 120 kev, calculation of amplitudes for, 20: 29945
neutron reactions with, fission product gamma spectra from thermal, (E), 20: 30379
photon scattering by K-shell electrons of, spectral distributions from, (E/T), 20: 29912 (ISS-66/6)
photon scattering by K-shell electrons of, spectral distributions from, (E/T), 20: 29913 (ISS-66/7)
photon scattering by K-shell electrons of, spectral distributions from, (E/T), 20: 29914 (ISS-66/8)
preparation of samples of, for vacuum fusion analysis, 20: 29083(R) (UCRL-14767)
radioinduced grain boundary cavitation and cracking in, neutron, 20: 29807 (TRG-Report-325)
reactions with steam at 400 to 1600°C, kinetics of isothermal, 20: 29188
reactions with water, reactor-excursion initiation of, 20: 30802
reactions with water, condenser discharge method for nonisothermal, 20: 29189
removal of, from cotton protective clothing, solution for, 20: 29477
separation from americium, berkelium, californium, cerium, curium, and europium by ion exchange on zirconium phosphate, 20: 29340
separation from aqueous solutions by solvent extraction using alkyl dibutyl phosphonates, effects of structure of alkyl group on, 20: 29354
separation from aqueous solutions by liquid-liquid extraction and chromography using butyl phosphates, 20: 29355
separation from fission product solutions by ion exchange, 20: 29357
separation from hydrochloric acid solutions by solvent extraction using trioctylamine, 20: 29339
separation from nitrate solutions using kerosene–TBP, radiation effects in, 20: 29272
separation from nitric acid solutions by solvent extraction using organic phosphorus compounds, effects of electronegative groups on, 20: 29347
separation from phosphoric acid solutions by solvent extraction using bis(2-ethylhexyl) ester of pyrophosphoric acid, 20: 29361
separation from solutions by sorption on lignins, effects of pore structure on, 20: 29360
separation from sulfuric acid solutions by solvent extraction using dibutyl phosphate, synergistic effects of tributyl phosphate and trioctylphosphine oxide on, 20: 29334
separation of fluorine from irradiated, by distillation, 20: 29338
separation of neptunium-239 from, 20: 29351
sintering of oxide-free powders of, 20: 29673
sorption by ion-exchange resins, effects of carbonate, chloride, and sulfate ions on, 20: 29350
URANIUM ALLOYS
Al–Ni–U, corrosion by steam, 20: 30794(R) (IDO-17147, pp 1-12)
Al–U, irradiation testing of, 20: 30794(R) (IDO-17147, pp 1-12)
Al–U, metallographic tests on arc melted, 20: 29775
Al–U, reactions with steam at 400 to 1600°C, kinetics of isothermal, 20: 29188
Al–U, x-ray attenuation in, measurement of, 20: 29707 (ORNL-TM-1457)
Be–U, metallographic tests on arc melted, 20: 29775
Cr–U, metallographic tests on arc melted, 20: 29775
Cr–U, precipitation of chromium needles following beta-to-alpha transformation in, 20: 29747
Cr–U, radioinduced grain boundary cavitation and cracking in, neutron, 20: 29807 (TRG-Report-325)
Cu–U, metallographic tests on arc melted, 20: 29775
Fe–U, metallographic tests on arc melted, 20: 29775
fissium–Pu–U, fission product release from irradiated, 20: 30790(R) (ANL-7204, pp 1-31)
fissium–U, thermal conductivity of irradiated, as function of burnup, 20: 30791(R) (ANL-7204, pp 32-64)
Mn–U, metallographic tests on arc melted, 20: 29775
Mo–U, casting of, testing of products from, 20: 29803
Mo–U, mechanical properties, 20: 29803
Mo–U, mechanical properties, metallography, and structure of, 20: 29775
Nb–U, casting of, testing of products from, 20: 29803
Nb–U, mechanical properties, 20: 29803
Nb–U, metallographic tests on arc melted, 20: 29775
Ni–U, metallographic tests on arc melted, 20: 29775
Pb–U, metallographic tests on arc melted, 20: 29775
Ti–U, casting of, testing of products from, 20: 29803
Ti–U, mechanical properties, 20: 29803
U–V, casting of, testing of products from, 20: 29803
U–V, mechanical properties, 20: 29803
U–Y, metallographic tests on arc melted, 20: 29775
U–Zr, casting of, testing of products from, 20: 29803
U–Zr, mechanical properties, 20: 29803
URANIUM BROMIDES
heat of formation, 20: 29229
URANIUM CARBIDE OXIDES
oxidation by carbon dioxide, steam, and water, 20: 29645
URANIUM CARBIDES
coating of fuel particles of, with pyrolytic graphite, process for, 20: 29638(P)
development of pyrolytic-carbon-coated, 20: 30870(R) (ORNL-TM-1528)
melting of, zone, 20: 29619 (NAA-SR-11813)
production of single-crystal, by zone melting, 20: 29619 (NAA-SR-11813)
properties for uses as reactor fuel, 20: 29732
properties of, at 2000°C, for use in thermionic converters, 20: 29729
radiation effects on density of, irradiated at 750°C, neutron, 20: 29804(R) (EURAEC-1637)
C–UC, fabrication of vitreous, 20: 29692(P)
PuC–UC, compatibility with potential cladding materials, 20: 30790(R) (ANL-7204, pp 1-31)
ThC–UC, coating with graphite by pressing, 20: 29669
ThC–UC, development of pyrolytic-carbon-coated, 20: 30870(R) (ORNL-TM-1528)
ThC_2–UC_2, production of pyrolytic-carbon-coated fuel particles of, 20: 29670
UC–ZrC, compatibility of thermionic diodes of, with refractory metal coatings at 1800 to 2500°C, 20: 29820
UC–ZrC, thermoelectric emission in cesium vapor, 20: 29800
URANIUM CHLORIDES
heat of formation, 20: 29229
URANIUM COMPLEXES
with kojic and meconic acids, equilibrium constants for, 20: 29096
with quinizarin-2-sulfonic acid, composition and stability of, con-

ductometric and spectrophotometric studies of, 20: 29181
with salicylic acid, preparation and composition of, 20: 29197
URANIUM COMPOUNDS
analysis for rare earths, spectrographic, 20: 29129
URANIUM DEPOSITS
book: *Origin of Uranium Exogenous Deposits and Methods for Their Exploration*, 20: 29449
URANIUM ETHOXIDES
reactions with β-keto esters, 20: 29155
URANIUM FLUORIDES
heat of formation, 20: 29229
heat of formation of gaseous, 20: 29171
URANIUM(III) FLUORIDES
thermodynamic properties of, emf measurements of, 20: 29215
URANIUM(IV) FLUORIDES
density of hydrated, effects of crystal structure on, 20: 29231
reactions in lithium chloride–potassium chloride eutectic, preparation of uranium dioxide by, 20: 29330(R) (EURAEC-1601)
URANIUM(VI) FLUORIDES
preparation by fluorination of uranium dioxide in hydrofluoric acid–chlorine trifluoride–fluorine cycle, 20: 29330(R) (EURAEC-1601)
URANIUM HYDRIDES
heat of formation, 20: 29229
URANIUM IODIDES
heat of formation, 20: 29229
URANIUM IONS
oxidation of tetravalent, in carbonate solutions by oxygen, kinetics of, 20: 29198
URANIUM ISOTOPES
abundance in sea water and sediments, 20: 29412
URANIUM ISOTOPES U-233
deuteron fission at 12 Mev, pair fragment kinetic energies from, (E), 20: 30500
fission of, ruthenium isotope yields from, (E), 20: 29080(R) (IDO-14676)
neutron fission, yields of xenon-133 and -135 from thermal, 20: 30533
neutron reactions with, capture and fission cross sections for, (E), 20: 30358(R) (RPI-328-56, pp 1-48)
URANIUM ISOTOPES U-234
abundance in Pleistocene coral reefs, age estimation by, 20: 29435
URANIUM ISOTOPES U-235
deuteron fission at 12 Mev, pair fragment kinetic energies from, (E), 20: 30500
deuteron fission at 14 Mev, yields of xenon-133 and -135 from, 20: 30533
fission of, ion charge distribution of unretarded products from, 20: 30507
fission of, ruthenium isotope yields from, (E), 20: 29080(R) (IDO-14676)
helium ion fission at 25 Mev, xenon-133 and -135 yields from, 20: 30533
neutron absorption cross section at 0.1 to 2.3 ev, spin dependence of, (E), 20: 30360 (WASH-1068)
neutron capture-to-fission ratios at 1 to 20 ev, (E), 20: 30360 (WASH-1068)
neutron fission at 0.04 to 1.0 Mev, prompt neutron yields from, (E), 20: 30360 (WASH-1068)
neutron fission at 0.003 to 0.3 ev, (E), 20: 30513
neutron fission cross sections at 0.01 to 40 ev, (E), 20: 30360 (WASH-1068)
neutron fission cross sections at 380 to 620 kev, (E), 20: 30425
neutron fission of, delayed gamma emission from, (E), 20: 30463
neutron fission of, fragment charge distribution in thermal, (E), 20: 30476
neutron fission of, fragment charge distribution from thermal, (E), 20: 30477
neutron reactions at 1.09, 1.7, and 2.1 Mev, gamma spectra from, (E), 20: 30360 (WASH-1068)
neutron reactions at 0.03 to 200 ev, cross sections for, (E/T), 20: 30342 (AERE-M-1670)
photofission of, delayed gamma emission from, (E), 20: 30463
URANIUM ISOTOPES U-238
abundance in Pleistocene coral reefs, age estimation by, 20: 29435
deuteron fission at 12 Mev, pair fragment kinetic energies from, (E), 20: 30500
deuteron fission at 14 Mev, yields of xenon-133 and -135 from, 20: 30533
helium ion fission at 25 Mev, xenon-133 and -135 yields from, 20: 30533
meson (μ^-) capture by, x-ray spectra from, (E), 20: 29525 (CONF-660209-9)
neutron cross sections for, computer program for calculating, 20: 30356 (ORNL-TM-1448)
neutron reactions at 1.09, 1.7, and 2.1 Mev, gamma spectra from, (E), 20: 30360 (WASH-1068)
photofission of, delayed gamma emission from, (E), 20: 30463
photon reactions (γ,n) with, fast neutron spectra from, (E), 20: 29529(R) (RPI-328-56, pp 94-112)
URANIUM NITRATES
effects on thyroid activity in rats, 20: 28884
separation from nitric acid solutions by solvent extraction using organic phosphorus compounds, effects of electronegative groups on, 20: 29347
URANIUM NITRIDES
oxidation by carbon dioxide, steam, and water, 20: 29645
URANIUM ORE PROCESSING PLANTS
waste disposal from, 20: 30948
URANIUM ORES
book: *Origin of Uranium Exogenous Deposits and Methods for Their Exploration*, 20: 29449
mining and processing of, disposal of wastes from, 20: 30948
URANIUM OXIDES
elastic modulus at 25°C, effects of density and microstructure on, 20: 29698 (ANL-7101)
phase studies at 20 to 1100°C, 20: 29799
phase studies of, in composition interval from $UO_{2.50}$ to $UO_{2.67}$ at 20 to 900°C, 20: 29799
properties for uses as reactor fuel, 20: 29732
URANIUM OXIDES (Zr ALLOY CLAD)
meltdown in TREAT, 20: 30792(R) (ANL-7204, pp 74-86)
URANIUM(IV) OXIDES
content in thalenites from Japan, 20: 29399
crystal structure and stoichiometry of, defect models for, 20: 29796
development of pyrolytic-carbon-coated, 20: 30870(R) (ORNL-TM-1528)
elastic modulus at 25°C, 20: 29698 (ANL-7101)
fluorination by hydrofluoric acid–trifluoride–fluorine cycle, effects of alumina and fissium on, 20: 29330(R) (EURAEC-1601)
hardness and plastic deformation of single-crystal, at 25 to 500°C, 20: 29786
heat treatments of, 20: 29629
meltdown of Zircaloy-clad, in TREAT, 20: 30792(R) (ANL-7204, pp 74-86)
microstructure of centrally heated green pellets of, 20: 29776
oxidation by oxygen in carbonate solutions, catalytic effects of copper ammoniate on, 20: 29199
preparation by reactions of plutonium tetrafluoride in lithium chloride–potassium chloride eutectic, 20: 29330(R) (EURAEC-1601)
radiation effects on stainless steel-clad fuel elements of, thermal-neutron, 20: 29806 (ORNL-TM-1511)
reactions with Hastelloy X at 1250°C, 20: 29621(R) (NUMEC-3524-17)
reactions with tungsten oxides and uranyl tungstates, 20: 29170
testing for fueling hydrogen-propelled rocket reactors, 20: 30787(R) (ANL-7190, pp 11-142)
void volume variation in vibratory-compacted, effect on pressure buildup in fuel element of, 20: 29818
BeO–UO_2, fission-product distribution in irradiated, 20: 29616(R) (BMI-1738)
BeO–UO_2, properties as fuel material, 20: 29810
BeO–UO_2, radiation effects on microstructure of, 20: 29616(R) (BMI-1738)
CeO_2–UO_2, testing as reactor fuels, 20: 29616(R) (BMI-1738)
MoO_3–UO_2–UO_3, phase studies at 750°C, 20: 29798
Mo–UO_2, electric conductivity at 25 to 1300°C, effects of composition and fabrication process on, 20: 29699 (CONF-650674-1)
PuO_2–UO_2, development as reactor fuel, 20: 29617(R) (EURAEC-1593)
PuO_2–UO_2, fabrication of pellets of, process development for, 20: 29621(R) (NUMEC-3524-17)
PuO_2–UO_2, fission gas diffusion from, effects of grain growth and preparation procedure on, 20: 29805(R) (NUMEC-3432-21)
PuO_2–UO_2, melting points of, effects of argon and nitrogen–hydrogen atmospheres on, 20: 29621 (NUMEC-3524-17)
PuO_2–UO_2, phase studies, 20: 29618(R) (GEAP-4982)
PuO_2–UO_2, radiation effects on structure of, fast-neutron, 20: 29618(R) (GEAP-4982)
PuO_2–UO_2, radiation effects on microstructure of, effects of preparation procedure on neutron, 20: 29805(R) (NUMEC-3432-21)
PuO_2–UO_2, radioinduced fission-gas-generation and temperature profiles in, fast- and thermal-neutron, 20: 29618(R) (GEAP-4982)
PuO_2–UO_2, radioinduced melting in, effects of diametral gap size on fast-neutron, 20: 29618(R) (GEAP-4982)
PuO_2–UO_2, reactions with sodium at 750°C, effects of fuel stoichiometry on, 20: 29618(R) (GEAP-4982)
PuO_2–UO_2, reactivity of water-moderated lattices of, 20: 29617(R) (EURAEC-1593)
stainless steel-UO_2, fabrication for AARR fuel, 20: 30787(R) (ANL-7190, pp 11-142)
ThO_2–UO_2, heat treatments of, 20: 29629
ThO_2–UO_2, homogeneity of, fission-track method for measurement of, 20: 29663 (KAPL-M-6556)
ThO_2–UO_2, vapor pressure, 20: 29616(R) (BMI-1738)
UO_2–ZrO_2, fission-product distribution in irradiated, 20: 29616(R) (BMI-1738)
UO_2–ZrO_2, testing as reactor fuels, 20: 29616(R) (BMI-1738)
W–UO_2, electric conductivity at 25 to 1300°C, effects of composition

and fabrication process on, 20: 29699 (CONF-650674-1)
URANIUM(IV-VI) OXIDES
evaporation of fission products from irradiated, at 900 to 1500°C in flowing hydrogen, nitrogen, or oxygen, 20: 29211
Al–U_3O_8, fabrication of Zircaloy-2-clad fuel elements of, 20: 29658 (ANL-6283)
Al–U_3O_8, irradiation testing of, 20: 30794(R) (IDO-17147, pp 1-12)
URANIUM(V) OXIDES
PbO–U_2O_5, phase studies, 20: 29794
URANIUM(VI) OXIDES
MoO_3–UO_2–UO_3, phase studies at 750°C, 20: 29798
NH_4F–UO_2–H_2O, properties of solid phases in, chemical and physical, 20: 29200
URANIUM SYSTEMS
Al–Si–U, radiation effects on clarification and coalescence time during processing of, in organic solvents, 20: 29333 (RT-CHI-(65)33)
C–N–V, phase studies, 20: 29749
C–Th–U, hydrolysis of, production of methane during, 20: 29159
C–U, metallographic tests on arc melted, 20: 29775
graphite-U, neutron thermalization in, time-dependent, (E/T), 20: 30327
H–U, metallographic tests on arc melted, 20: 29775
N–U, metallographic tests on arc melted, 20: 29775
O–U, metallographic tests on arc melted, 20: 29775
Si–U, metallographic tests on arc melted, 20: 29775
U-H_2O, neutron disadvantage factor for, 20: 30855
U–O_2O, calculation of fast fission factor for, 20: 30859
URANIUM TUNGSTATES
preparation by reactions of uranium dioxide with tungsten oxide or uranyl tungstates, 20: 29170
URANYL IONS
determination using kojic and meconic acids, spectrophotometric, 20: 29096
effects on hydrolysis of polyphosphates, 20: 29152
effects on radiolysis of naphthalene, 20: 29260
reactions with salicylic acid, 20: 29197
URANYL NITRATE COMPLEXES
with salicylaldoxime, composition and stability of, spectrophotometric studies of, 20: 29202
URANYL NITRATES
electric conductivity of anhydrous, in ketones, 20: 29184
hydrolysis of, use of *α-n*-amylpyridine-*N*-oxide for solvent extraction of products from, 20: 29359
$Ca(NO_3)_2$–$UO_2(NO_3)_2$–H_2O, activity coefficients of, at 25°C, 20: 29196
$Mg(NO_3)_2$–$UO_2(NO_3)_2$–H_2O, activity coefficients of, at 25°C, 20: 29196
$Sr(NO_3)_2$–$UO_2(NO_3)_2$–H_2O, activity coefficients of, at 25°C, 20: 29196
$UO_2(NO_3)_2$–H_2O–$Zn(NO_3)_2$, activity coefficients of, at 25°C, 20: 29196
URANYL TUNGSTATES
reactions with uranium dioxide, 20: 29170
UREA, 1-METHYL-1-NITROSO-
effects on Anacystis pigments, mutagenic, 20: 28958
URIDINE
radiation effects on thermoluminescence of, gamma, 20: 28913
radioinduced leakage of, from Euglena cells, γ, 20: 28904
uridylyl-, radiation effects on, tracer studies of uv, 20: 28910
URIDYLIC ACID
radiation effects on thermoluminescence of, gamma, 20: 28913
radiation effects on content of, in RNA in guinea pig brain, 20: 28919
URINE
radioactivity of, computer program for evaluating determinations of, 20: 29121

V

VACUUM GAGES
design of electron-single-scatter, for 10^{-5} to 1 torr, 20: 29600
design of ionization-type, 20: 29513(P)
mass spectrometer design for use in, 20: 29496
properties of hot cathode magnetron, 20: 29494
VACUUM PUMPS
design of, for sample furnace for neutron diffraction experiments, 20: 29106
performance of, contamination effects and limits for, 20: 29396
VACUUM SYSTEMS
design and performance for Ogra-1 magnetic mirror machine, 20: 30701
performance of enclosures in, contamination effects and limits for, 20: 29396
VAGINA
radiation effects on cytology of, therapeutic dose, 20: 29076
VAN ALLEN RADIATION BELTS
charged-particle diffusion in, 20: 30206(T) (NASA-TT-F-389, pp 426-42)
charged-particle intensity in, effects of satellites on, 20: 30223(T) (NASA-TT-F-389, pp 817-21)
charged-particle intensities in, (E), 20: 30235
effects on space flights, 20: 30222(T) (NASA-TT-F-389, pp 758-63)
electron and proton energy, spatial, and temporal distribution in, 20: 30204(T) (NASA-TT-F-389, pp 375-86)
electron and proton motion in outer, effects on geomagnetic field variations, 20: 30209(T) (NASA-TT-F-389, pp 464-82)
electron and proton spatial distribution in, analysis of, 20: 30211(T) (NASA-TT-F-389, pp 535-50)
electron and proton distributions in Brazilian magnetic anomaly at 250 to 400 km, spatial and temporal, 20: 30217(T) (NASA-TT-F-389, pp 607-15)
electron and proton energy and spatial distribution in, 20: 30219(T) (NASA-TT-F-389, pp 623-9)
electron content in outer, 20: 30213(T) (NASA-TT-F-389, pp 566-8)
electron spatial distribution in outer, 20: 30215(T) (NASA-TT-F-389, pp 576-87)
formation of, effects of electron and proton drift in magnetosphere on, 20: 30207 (NASA-TT-F-389, pp 442-53)
intensity variations in outer, nocturnal, 20: 30214(T) (NASA-TT-F-389, pp 569-75)
properties of outer, at low altitudes, 20: 30216(T) (NASA-TT-F-389, pp 588-606)
properties of, review of, 20: 30196(T) (NASA-TT-F-389, pp 8-25)
properties of, survey on, 20: 30204(T) (NASA-TT-F-389, pp 375-86)
VANADIUM
compatibility with plutonium carbides at 1200 to 1400°C, 20: 29820
determination in aqueous solutions, design of oxyacetylene burner for measuring sensitivity of spectrophotometric, 20: 29083(R) (UCRL-14767)
determination in petroleum, activation, 20: 29139
determination in Zircaloy-2, spectrographic, 20: 29113
iron-57 Mössbauer spectra in, 20: 30766
oxidation kinetics, 20: 29644
properties of, for use in furnace for neutron diffraction experiments, 20: 29106
VANADIUM ALLOYS
Al–Cr–Co–Mo–Ni–Ti–V–Zr, surface treatments for IN-100, coating and mechanical, 20: 29706 (NASA-TM-X-53448)
Mo–Nb–V, fabricability, strength, and weldability of, 20: 29763
Mo–Nb–V–Zr, tensile properties of B-66, effects of welds on, 20: 29712(R) (WANL-PR-(P)-009)
Nb–Ta–V, availability, properties, and uses of, 20: 29760
Ti–V, creep rate testing and thermal expansivity of, 20: 30790(R) (ANL-7204, pp 1-31)
U–V, casting of, testing of products from, 20: 29803
U–V, mechanical properties, 20: 29803
VANADIUM ISOTOPES V-48
yield in alpha and proton reactions with copper, 20: 30531
VANADIUM ISOTOPES V-50
neutron resonance parameters and total cross sections at 3 to 60 kev, (E), 20: 30360 (WASH-1068)
VANADIUM ISOTOPES V-51
alpha scattering at 50 Mev, level spins and parities from, (E/T), 20: 30460
neutron reactions (n,γ) at to 14 Mev, cross sections for, (T), 20: 30378
neutron reactions (n,p) at 14.8 Mev, cross sections for, (E), 20: 30394
VANADIUM OXIDES
SiO_2–Ag_2SO_4–V_2O_5, radiation effects on catalytic activity of, in oxidation of sulfur dioxide by air, 20: 29291
VANADIUM SILICIDES
electron spin-pairing in superconducting, (E/T), 20: 30734(R) (TID-22970, pp 1-63)
radiation effects on superconducting properties of boron- and uranium-doped, thermal neutron, (E), 20: 30260
VANADIUM SYSTEMS
C–Mo–V, phase studies and thermodynamics of, for use at high temperatures, 20: 29774
C–W–V, phase studies and thermodynamics of, for use at high temperatures, 20: 29774
Fe–Si–V, crystal structure of D-phase, (E/T), 20: 30734(R) (TID-22970, pp 1-63)
VIBRATIONS
radiosensitivity effects on mice, synergistic, 20: 28968
VINYL COMPOUNDS
radioinduced polymerization of coatings of, on exterior surfaces, 20: 29320(P)
VIRUSES
lymphomas induction in mice by, 20: 28873
VITAMIN B
radiation effects on metabolism in mice, x, 20: 29003
VITAMIN B_{12}
isotope exchange in radiocobalt divalent ion-doped, 20: 29259
radioinduced recoil damage in, thermal annealing of neutron, 20: 29259

VITAMIN C
radiation effects on metabolism of, in guinea pigs and rats, γ and x, 20: 28921
VOLATILITY SEPARATION PROCESSES
fuel element reprocessing by, pilot plant design problems for, 20: 29364

W

WASPALOY
joining by brazing, soldering, or welding, 20: 29666 (RSIC-484)
joining by mechanical fastening, 20: 29667 (RSIC-509)
machining properties of, 20: 29665 (RSIC-482)
surface treatments for, coating and mechanical, 20: 29706 (NASA-TM-X-53448)
WASTE DISPOSAL
deep well, of radioactive materials for heating minerals *in situ*, 20: 30950(P)
fixation in ceramic-coated clay, method for, 20: 30951(P)
methods and problems of, in Japan, 20: 30945
methods for radioactive solid, from reactors, 20: 30947
methods for, developments in studies on, 20: 30943(R) (ORNL-TM-1465)
methods of, for gaseous, liquid, and solid wastes from uranium mines and mills, 20: 30948
methods of, for radioactive gases from nuclear reactors, 20: 30949
radioactive, ocean contamination by, 20: 29405 (NP-14694)
systems for, materials for nuclear power plant, 20: 30815
WASTE PROCESSING
activated sludge methods, 20: 29353
criteria for, of low and intermediate level wastes, 20: 30944
evaporation of radioactive liquids in fluidized bed, 20: 30946
methods for, developments in studies on, 20: 30943(R) (ORNL-TM-1465)
WASTE SOLUTIONS
analysis for trace amounts of uranium, fluorescence, 20: 29128
distribution in rivers, use of iodine-131 determination for studying, 20: 29099
evaporation of radioactive, in fluidized bed, 20: 30946
separation of fission products from, by sorption using clay minerals, 20: 29332 (ORNL-P-1811)
separation of phosphorus from, by activated sludge methods, 20: 29353
WATER
analysis for tritium, efficiency of flow counter for, 20: 29098
content in soil, radiometric methods for determining, 20: 29505
content in thalenites from Japan, 20: 29399
determination in catalyst and silastic resin, by titration, handling methods for, 20: 29083(R) (UCRL-14767)
determination in compacted soils, radiometric methods for, 20: 29581 (AD-633785)
effects on chemisorption of ethylene by yttrium oxide, 20: 29186
effects on oxygen-18 exchange between water and copper and iron sulfates, 20: 29153
electron polarization in molecules of, effects of temperature on, 20: 29230
erosive effects on metals and alloys at 70°F, cavitation, 20: 29640 (NP-16048)
gamma spectra in, at 0.2 to 6 Mev, 20: 30722 (KAPL-M-6497)
hydrogen ion reactions with molecular, at 1 to 55 kev, particle production cross sections for, 20: 29919 (UCRL-14214)
leakage in pressure vessels, mechanism and rate, 20: 30810
neutron attenuation and thermalization in, fast, (E/T), 20: 30340
neutron flux in moderators of, multi-velocity corrections in activation measurements of, 20: 29539
neutron inelastic scattering at 0.83 to 1.8 ev, differential cross sections for, (E), 20: 30334
neutron scattering by, model for thermal, (E/T), 20: 30330
neutron slowing down in, effects of spin polarization on age of fission, 20: 30329
neutron spectra in, (T), 20: 30326
neutron spectra near temperature discontinuity in, thermal, (E/T), 20: 30331
oxygen-18 exchange with cupric, ferric, and ferrous sulfates, 20: 29153
performance as power-reactor coolant, 20: 30910
radiolysis of, tracer studies of kinetics of electron, 20: 29315
reactions with uranium nitride and uranium carbide oxides at 80 to 300°C, 20: 29645
reactions with uranium, reactor excursion initiation, 20: 30802
reactions with uranium, condenser discharge method for nonisothermal, 20: 29189
reactivity worth of, measurement of, (E), 20: 30347(R) (IDO-17147, pp 13-28)
separation of strontium-90 and yttrium-90 from, by ion exchange using bentonites and gypsum, 20: 29348
thermodynamic properties of, (E), 20: 30182
air–water, density disturbances in flow of, 20: 29375(R) (ANL-7190, pp 193-200)
$Ca(NO_3)_2$–$UO_2(NO_3)_2$–H_2O, activity coefficients of, at 25°C, 20: 29196
$Mg(NO_3)_2$–$UO_2(NO_2)_2$–H_2O, activity coefficients of, at 25°C, 20: 29196
NH_4F–UO_2–H_2O, properties of solid phases in, chemical and physical, 20: 29200
NH_3–H_2O, radiolysis of, hydrogen yields from gamma, 20: 29295
NH_3–O–H_2O, radiolysis of, hydrogen yields from gamma, 20: 29295
$Sr(NO_3)_2$–$UO_2(NO_3)_2$–H_2O, activity coefficients of, at 25°C, 20: 29196
U-H_2O, neutron disadvantage factor for, 20: 30855
$UO_2(NO_3)_2$–H_2O–$Zn(NO_3)_2$, activity coefficients of, at 25°C, 20: 29196
WATER-*d*
vapor pressure of, at –40 to 0°C, 20: 29149
WATER-d_2
corrosive effects on steel in Savannah River Components Test Reactor, 20: 29654
deuterium exchange with hydrocarbons or hydrogen sulfide, 20: 29611(P)
effects of, on circulating antibody levels in mice, 20: 28988
electron polarization in molecules of, effects of temperature on, 20: 29230
neutron spectra in, time-dependent, (E/T), 20: 30324(R) (RPI-328-56, pp 52-93)
production of, process for, 20: 29611(P)
thermodynamic properties of, (E), 20: 30182
ultrasonic attenuation and relaxation time in vapor, 20: 29172
vapor pressure of, at –40 to 0°C, 20: 29149
U–O_2O, calculation of fast fission factor for, 20: 30859
WATER-t_2
radiation effects on positron-annihilation lifetime spectra in, gamma, 20: 29268
tritium beta decay in, atomic structure studies of organic compounds by, 20: 29326
WATER COOLED REACTORS
control method for, 20: 30822(P)
design of graphite-moderated steam-generating and superheating, 20: 30919(P)
design of heterogeneous steam-moderated power, 20: 30918(P)
design of multi-pass vapor moderated, for power production, 20: 30916(P)
design of steam moderated power reactors, 20: 30915(P)
design of variably controlled and moderated power, using hydrogen-isotope-bearing moderator vapor, 20: 30917(P)
design of water-moderated, 20: 30869(P)
design of water-moderated, for power production, 20: 30912(P)
design using mixed heavy and light water as moderator-coolant, 20: 30868(P)
development and research program for large closed-cycle, 20: 30884(R) (WCAP-3269-16)
reactivity of, effects of stainless steel- and zirconium-clad fuel loading on, 20: 30884(R) (WCAP-3269-16)
WATER MODERATED REACTORS
design of heterogeneous steam-cooled power, 20: 30918(P)
design of multi-pass steam cooled, for power production, 20: 30916(P)
design of steam cooled power reactors, 20: 30915(P)
design of steam-cooled power, 20: 30917(P)
design of water-cooled, 20: 30869(P)
design of water-cooled, for power production, 20: 30912(P)
design using mixed heavy and light water as moderator-coolant, 20: 30868(P)
WATER VAPOR
decomposition of, using fission fragment recoil energy, 20: 29317
electron reactions at 0.1 to 20 kev, ionization cross sections for, (E), 20: 29928
oxidation of graphite by, in presence of hydrogen, rate of, 20: 29626
radiolysis of, hydrogen yields from gamma, 20: 29295
reactions with calcium, magnesium, molybdenum, tantalum, and zirconium, combustion, 20: 29641(R) (SC-DC-65-1691)
ultrasonic attenuation and relaxation times in, 20: 29172
WELDED JOINTS
inspection of steel, methods for, 20: 29389
leakage rate in pressure vessel gas and liquid, 20: 30810
WELDING
effects on properties of metals, 20: 29623(R) (TID-22970, pp 121-256)
WELL LOGGING
equipment for chlorine detection in a non-ferrous environment, neutron-gamma, 20: 29446(P)
equipment for neutron-gamma, scintillation-type detector for, 20: 29445(P)
equipment shielding for neutron–gamma for chlorine determination, 20: 29443(P)
method for radiometric, elimination of interference of iron casing effect in, 20: 29442(P)
neutron source for, design of, 20: 29444(P)
WELLS

tool orienting in, radially collimating window for instruments for, 20: 29517(P)
WHEAT
radioinduced mutations of, γ and neutron, 20: 28960
strontium-90 content in, effects of washing with decontaminating solutions on, 20: 29473
WHISTLERS
modes for, equations for exact nonlinear electromagnetic, 20: 29899
WHITESHELL REACTOR NO. 1
environs monitoring, January 1966, 20: 29053 (NP-15951)
WINDOWS
design of radially collimating, for well-tool orienting instruments, 20: 29517(P)
radiation effects on shielding, charge accumulation from gamma, 20: 30727
WINDSCALE ADVANCED GAS COOLED REACTOR
development, 20: 30798(R) (NP-16043)
WIRES
radiation effects on, for use as sensors, 20: 29486(R) (NASA-CR-54964)
WOOD
penetration of sodium pentachlorophenolate in, radioactivation analysis of, 20: 29161

X

X AGENT
flux of, annual and diurnal fluctuations in, 20: 30955
studies on, summary of, 20: 30956
X RADIATION
attenuation in reactor materials, measurement of, 20: 29707 (ORNL-TM-1457)
bursts of solar, short intensity increases of heavy cosmic nuclei accompanying, 20: 29965
detection and measurement of, using silicon p-n junction detectors operated as photodiodes, 20: 29540
detection and measurement of, photographic film detector with intensifier screen for, 20: 29573(P)
dose distribution measurements, 20: 29073
dose rate measurements of low-level, modification of Geiger-Mueller counter for, 20: 29553
dose rates of, in irradiations through grids, 20: 29056
dosimetry of, automatic system for, 20: 29070
effects of, on lymphocytes in guinea pig lymph nodes, 20: 28976
effects on activity and synthesis of red-cell carbonic anhydrase *in vivo*, 20: 28922
effects on adrenaline content in blood of dogs, 20: 28941
effects on adrenaline content in rats, 20: 28964
effects on Anacystis pigments, mutagenic, 20: 28958
effects on bacteriophage, genetic, 20: 28948
effects on biochemicals, ESR and thermoluminescence studies of, 20: 29249
effects on blood coagulation, 20: 28985
effects on blood circulation in rabbits, 20: 29010
effects on blood, extracorporeal-exposure, 20: 28927 (BNL-9647)
effects on brain of rabbits, pathological, 20: 29011
effects on calcium fluoride single crystals, temperature dependence of thermoluminescence from, 20: 30767
effects on catecholamines content of rat adrenal glands and heart, 20: 28964
effects on cellular permeability in onions, effects of dose on, 20: 28900
effects on chick embryos, pathological, 20: 29012
effects on chicken embryos and post-hatching growth of survivors, 20: 29015
effects on cholesterol content in rat blood, 20: 28992
effects on cholesterol content in rat tissues, 20: 28995
effects on cholesterol-blood complexes in dogs, 20: 28998
effects on chromosomal bridges at anaphase in barley seeds and Tradescantia, 20: 29031
effects on desoxyribonucleoproteins at molecular and supermolecular levels, 20: 28908
effects on Drosophila, genetic, 20: 28956
effects on Drosophila, effects of ATP on genetic, 20: 29046
effects on electrophoretic mobility of animal cells in suspensions, 20: 28905
effects on electron-induced color centers in alkali halides, (E), 20: 30776
effects on enzyme activity, effects of moisture on, 20: 28902
effects on epididymal spermatozoa in bovine testes, 20: 29013
effects on erythropoiesis in rats, effects of endocrine gland removal and hormones on, 20: 29043
effects on function and morphology of dog kidneys, 20: 29025
effects on germ cells in rabbits, 20: 29019
effects on glycine, ESR spectra of radicals in, 20: 29281
effects on growth kinetics of leukemia cells, 20: 28962
effects on hematopoiesis, effects of fractionated exposure on, 20: 28984
effects on hematopoietic systems of dogs, lower-body, upper-body, and whole-body, 20: 29029
effects on heme synthesis in rabbit bone marrow cells, effects of hormones on, 20: 28912
effects on hemopoietic system in guinea pigs, chronic low-dose, 20: 28945
effects on immune response of thymectomized chickens, 20: 29014
effects on intestinal secretory functions in dogs, effects of dietary fatty acids on, 20: 28993
effects on leukocytes in culture, morphological, 20: 28920
effects on lipid metabolism in rats, effects of phosphatides on, 20: 28992
effects on metabolism of vitamin C in guinea pigs and rats, 20: 28921
effects on metabolism in erythrocytes, 20: 28924
effects on mice, effects of time of day on lethal, 20: 28938
effects on mice, genetic, 20: 28957
effects on mouse skin epithelial cells, dose-response relations for, 20: 28990
effects on mutagenic properties of tissue extracts, 20: 28959
effects on nerve action potentials in cold-blooded animals, 20: 29021
effects on nuclear reorganization in paramecia, 20: 29007
effects on nucleic acid synthesis in rat thymus cells, 20: 28953
effects on pathology of atherosclerosis in rats, 20: 28996
effects on phage induction in *E. coli*, protective effects of AET and MEA against, 20: 29045
effects on plants, genetic, 20: 29018
effects on potassium iodides, color center formation from, (E), 20: 30748
effects on propane, decomposition yields from, 20: 29266
effects on properties of pyridoxine derivatives, 20: 28901
effects on protein synthesis in Ehrlich mouse ascites tumor cells, 20: 28923
effects on protein metabolism in rats, tracer study, 20: 28997
effects on quartz, microwave phonon reactions with paramagnetic centers formed in, 20: 30768
effects on rabbits, pathological, 20: 29051
effects on red cell catalase in nitro, 20: 28911
effects on regenerative capacity of axolotl limbs, effects of RNA on recovery from, 20: 29038
effects on renal hemodynamic functions of dogs, 20: 29026
effects on resistance of mice to Ehrlich ascites tumor cells, 20: 29017
effects on root-knot nematode propagation in sweet potatoes, 20: 28942
effects on *Saccharomyces cerevisiae*, effects of ploidy on, 20: 28961
effects on serum proteins in mice, 20: 28899
effects on silver nitrate at 77°K, ESR studies of, 20: 29310
effects on skin of mice and rats, role of adipose tissue in repair of, 20: 28946
effects on solubilization of cholinesterase from plaice muscle by bacteria, 20: 28933
effects on sprouting and yield of potatoes, 20: 28966
effects on steroid content in guinea pigs, 20: 28975
effects on thermoluminescence of rare earth ions in calcium fluoride, 20: 29318
effects on thiamine metabolism in mice, 20: 29003
effects on thyroid gland in rats, 20: 29047
effects on Tradescantia, effects of cupferron on frequency of chromosome aberrations in, 20: 29028
effects on uncoupling of oxidation and phosphorylation in mitochondria of green plants, 20: 28947(T)
emission from (K^-) mesic atoms of helium, effects of $\bar{K}$-N interactions on, 20: 29938
emission from galactic sources, free-free emission model for discrete, 20: 29881
emission from hot fully ionized hydrogen plasma, (T), 20: 29881
intensity variations of solar, 20: 29874(T) (NASA-TT-F-389, pp 714-31)
origin of cosmic isotropic, (T), 20: 29958
production in electron reactions in atmosphere, 20: 30218(T) (NASA-TT-F-389, pp 616-23)
scattering by xenon, form factors for, (T), 20: 29949
scattering in amorphous materials, theory of multiple, 20: 30734(R) (TID-22970, pp 1-63)
sources of cosmic, stellar, 20: 29900
spectra of Cyg XR-1, Tau XR-1, and Sco XR-1, 20: 29901
use of fractionated-dose whole-body, for therapy, 20: 29069
uses in measurement of porosities and saturations in porous media, 20: 29595
X-RAY BEAMS
production of modulated, 20: 29516(P)
X-RAY-DIFFRACTION ANALYSIS
crystal structure determination by, table for dispersion corrections in, 20: 29722
X-RAY FLUORESCENCE ANALYSIS
method for measuring salt deposits on electric insulators, 20: 29103

use of, for light elements, Weibull function for pulse-height distributions from, 20: 29124
X-RAY SPECTRA
measurement of muonic, performance of germanium detectors for, 20: 29525 (CONF-660209-9)
X-RAY SPECTROSCOPY
book: *Instrument and Chemical Analysis Aspects of Electron Microanalysis and Macroanalysis*, 20: 29119
XENON
alkali-metal negative-ion dissociation in, cross sections for, (T), 20: 22947
buildup in reactors, absorbing foil determination of, 20: 30843
effects on propane radiolysis, 20: 29266
effects on radioinduced polymerization of solid methane, 20: 29314
hydrogen negative-ion dissociation in, cross sections for, (T), 20: 29947
x-ray scattering form factors, (T), 20: 29949
hexane–Xe, radiolysis of, charge transfer in, 20: 29314
XENON FLUORIDES
molecular constants and thermodynamic functions of, (T), 20: 29921
XENON ISOTOPES Xe-123
energy levels from cesium-123 decay, (E), 20: 30403
XENON ISOTOPES Xe-129
content in meteorites, origin of, 20: 29891
XENON ISOTOPES Xe-131
abundance of fission-produced, in Pasamonte meteorite, 20: 29892
XENON ISOTOPES Xe-132
abundance of fission-produced, in Pasamonte meteorite, 20: 29892
XENON ISOTOPES Xe-133
beta decay of, β-γ circular polarization correlation in, (E), 20: 30553
energy level scheme from iodine-133 beta decay, (E), 20: 30473
yields from fission of thorium-232, and uranium-233, -235, and -238, 20: 30533
XENON ISOTOPES Xe-134
abundance of fission-produced, in Pasamonte meteorite, 20: 29892
XENON ISOTOPES Xe-135
yields from fission of thorium-232 and uranium-233, -235, and -238, 20: 30533
XENON ISOTOPES Xe-136
abundance of fission-produced, in Pasamonte meteorite, 20: 29892
XENOTIMES
analysis for yttrium, fluorometric, 20: 29094
XYLOSE
intestinal sorption of, measurement of, 20: 28871(R) (EUR-2636.f,i)

Y

YANKEE POWER REACTOR
safety analysis of, probabilistic methodology for, 20: 30883 (SAN-570-2)
YEASTS
radiation effects on reproduction of, 20: 28950
radiation effects on *Saccharomyces cerevisae*, effects of depth in irradiated medium on electron-beam, 20: 28963
radiation injuries in, effects of ploidy on recovery from x, 20: 28961
radiosensitivity of *Saccharomyces cerevisiae*, effects of cystamine on, 20: 29023
YTTERBIUM
analysis of, for trace amounts of lutetium by activation methods, 20: 29082 (SGAE-CH-27/1966)
determination in minerals and ores, spectrometric, 20: 29134
determination in rocks, chemical spectrographic method for, 20: 29083(R) (UCRL-14767)
determination in standard igneous rocks G-1, W-1, and G-B by x-ray fluorescence, 20: 29101
determination in TBP extracts, spectrophotometric, 20: 29125
determination in uranium compounds, spectrographic, 20: 29129
YTTERBIUM CHLORIDES
thermal capacity of aqueous solutions of, at 25°C, 20: 29144 (IS-1355)
YTTERBIUM NIOBATES
distribution in strontium molybdate single crystals, coefficients of, 20: 29746
YTTRIUM
determination in aqueous solutions, design of oxyacetylene burner for measuring sensitivity of spectrophotometric, 20: 29083(R) (UCRL-14767)
determination in fergusonites and xenotimes, fluorometric, 20: 29094
determination in minerals and ores, spectrometric, 20: 29134
determination in rocks, chemical spectrographic method for, 20: 29083(R) (UCRL-14767)
determination in standard igneous rocks G-1, W-1, and G-B by x-ray fluorescence, 20: 29101
polarographic properties of, on fused potassium acid sulfate electrolyte, 20: 29210
proton reactions with, cross section ratios of isobars from, 20: 30531
separation from strontium by paper electrophoresis, 20: 29336
separation from strontium by paper chromatography, effects of calcium on, 20: 29349
separation from water by ion exchange using bentonite and gypsum, 20: 29348
sorption by turfy-meadow soil, effects of iron on, 20: 28881
YTTRIUM ALLOYS
Al–Y, crystal structure of intermetallic compound YAl_3 in, 20: 29721
Co–Gd–Y, magnetic properties of, 20: 30756
Hf–Nb–W–Y, fabricability, strength, and weldability of, 20: 29763
Hf–Nb–W–Y, tensile properties of C-129Y, effects of welds on, 20: 29712(R) (WANL-PR-(P)-009)
U–Y, metallographic tests on arc melted, 20: 29775
YTTRIUM BORIDES
porosity and mechanical properties of vacuum-sintered, 20: 29738
YTTRIUM CARBIDES
hydrolysis of, gaseous products from, 20: 29220
YTTRIUM CARBONATES
thermal decomposition at 155 to 700°C, 20: 29223
YTTRIUM COMPLEXES
with Aluminon, composition and stability of, spectrophotometric studies of, 20: 29180
with carboxylic acids, stability constants of, 20: 29232
with 1,10-phenanthroline–thenoyltrifluoroacetone, preparation and composition of, 20: 29221
YTTRIUM FLUORIDES
heat of sublimation and sublimation pressure of, mass spectrometric studies of, 20: 29183
reactions with sodium carbonate at 550 to 700°C, 20: 29223
thermal decomposition at 450 to 800°C, 20: 29223
YTTRIUM ISOTOPES Y-87
energy levels of, (E/T), 20: 30353(R) (ORNL-3940, pp 1-61)
formation by nuclear de-excitation with neutron emission, charged-particle emission in, (T), 20: 29436
YTTRIUM ISOTOPES Y-89
neutron activation cross sections for, (E), 20: 30360 (WASH-1068)
neutron inelastic scattering at 5.0 Mev, Q values for, (E), 20: 30360 (WASH-1068)
proton reactions (p,α) with, zirconium-90 level widths from, (E/T), 20: 30360 (WASH-1068)
proton reactions (p,d) at 36 Mev, deuteron spectra from, (E/T), 20: 30353(R) (ORNL-3940, pp 1-61)
proton reactions (p,α) at 20.2 Mev, alpha spectra from, (E/T), 20: 30353(R) (ORNL-3940, pp 1-61)
YTTRIUM ISOTOPES Y-90
beta emission of, backscattering from aluminum in 2π geometry, (E), 20: 30369
beta spectra from, silicon counters for measuring, 20: 29520 (CLOR-45/D)
movement in soils, 20: 30943(R) (ORNL-TM-1465)
preparation of, for radioecological studies, 20: 28879
use of internally deposited particles of, for cancer therapy, 20: 29059 (TID-22860)
YTTRIUM ISOTOPES Y-91
effects on blood and hematopoietic system, 20: 28982
YTTRIUM ISOTOPES Y-92
yields from uranium 235 thermal fission, (E), 20: 30476
YTTRIUM ISOTOPES Y-93
yields from uranium 235 thermal fission, (E), 20: 30476
YTTRIUM ISOTOPES Y-94
yields from uranium 235 thermal fission, (E), 20: 30476
YTTRIUM ISOTOPES Y-95
yields from uranium 235 thermal fission, (E), 20: 30476
YTTRIUM NIOBATES
distribution in strontium molybdate single crystals, coefficients of, 20: 29746
YTTRIUM OXIDES
content in thalenites from Japan, 20: 29399
electron paramagnetic resonance spectra of trivalent erbium ions in single crystals of, 20: 29192
neodymium ion energy levels and crystal-field splittings in, 20: 30744
sorptive properties for ethylene, effects of water on, 20: 29186
ThO_2–Y_2O_3, electric conductivity of solutions of, electronic and ionic components of, 20: 29216
YTTRIUM SYSTEMS
C–Nb–W–Y–Zr, tensile properties of D-43Y, effects of welds on, 20: 29712(R) (WANL-PR-(P)-009)

Z

ZINC
content in rocks, effects of clay content on, 20: 29417

determination of trace amounts of, by derivative neutron activation, 20: 29136
determination of, by neutron activation methods, 20: 29078(R) (AD-633252)
effects on copper or silver infiltrants in graphite, 20: 29764
effects on spectra of nitrogen-15 in ATP, 20: 29083(R) (UCRL-14767)
iron-57 Mössbauer spectra in, 20: 30766

ZINC ALLOYS
Ce–Zn, crystal structure of intermetallic compounds in, 20: 29719
Cu–Zn, erosion by water at 70°F, effects of annealing on cavitation, 20: 29640 (NP-16048)
In–Zn, distillation of liquid, surface concentration changes in, 20: 29346
Nb–Zn, properties as high-temperature coating, 20: 29650
Sb–Zn, thermoelectric properties of intermetallic compound in, 20: 29709(R) (TID-22970, pp 65-119)
Sn–Zn, distillation of liquid, surface concentration changes in, 20: 29346

ZINC ISOTOPES
radiation effects on incorporation of, by blood cells, x, 20: 28922

ZINC ISOTOPES Zn-63
energy levels from proton reactions (p,n) with copper-63 at 4 to 9 Mev, (E), 20: 30406

ZINC ISOTOPES Zn-68
proton elastic scattering at 40 Mev, cross sections for, (E/T), 20: 30353(R) (ORNL-3940, pp 1-61)

ZINC NITRATES
$UO_2(NO_3)_2$–H_2O–$Zn(NO_3)_2$, activity coefficients of, at 25°C, 20: 29196

ZINC OXIDES
Sc_2O_3–ZnO, phase studies, 20: 29168

ZINC SELENIDES
dissolution kinetics, 20: 29623(R) (TID-22970, pp 121-256)

ZINC SULFIDES
dissolution kinetics, 20: 29623(R) (TID-22970, pp 121-256)

ZIRCALOY-2
analysis for impurities, spectrographic, 20: 29113
fabrication of fuel element cladding of, 20: 29658 (ANL-6283)
hydridation of, effects on mechanical properties, 20: 30902
radiation effects on tensile properties at room and 650°F temperatures, 20: 30884(R) (WCAP-3269-16)
x-ray attenuation in, measurement of, 20: 29707 (ORNL-TM-1457)

ZIRCALOY-3
hydridation of, effects on mechanical properties, 20: 30902

ZIRCALOY-4
fretting-wear studies in water at 550°F, 20: 29616(R) (BMI-1738)
hydridation of, effects on mechanical properties, 20: 30902
microstructure of cold-worked tubing of, effects of annealing on, 20: 29716 (WAPD-T-1819)
microstructure of, effects of cold-working on, 20: 29716 (WAPD-T-1819)

ZIRCONIUM
analysis for hafnium, 20: 29114
analysis for hafnium, 20: 29115
compatibility with plutonium carbides at 1200 to 1400°C, 20: 29820
corrosion by hydrochloric acid, tracer studies of effects of ammonium fluorides, copper chlorides, and iron chlorides on, 20: 29649
determination in aqueous solutions, design of oxyacetylene burner for measuring sensitivity of spectrophotometric, 20: 29083(R) (UCRL-14767)
diffusion of oxygen in zirconium oxides on, nuclear reaction study of, 20: 29817
diffusion processes in, review of solute and self-, 20: 29737
effects on ductility of electron-beam-melted molybdenum, 20: 29783
gamma spectra in, at 0.2 to 6 Mev, 20: 30722 (KAPL-M-6497)
oxidation kinetics, 20: 29644
oxidation of, kinetics of, 20: 29648
reactions in gaseous mixtures, combustion, 20: 29641(R) (SC-DC-65-1691)
reactions with phosphorus at 500 to 1000°C, 20: 29642
separation from fission product solutions by ion exchange, 20: 29357
separation from hafnium by ion exchange using anionites, 20: 29352
separation from thorium by selective adsorption on silica gel, 20: 29344
superconducting transition temperature, (E), 20: 30316
thermal diffusion of oxygen in β-, method for measuring, 20: 29769
thermionic properties, 20: 29801

ZIRCONIUM ALLOYS
analysis for hafnium, 20: 29114
analysis for hafnium, 20: 29115
diffusion processes in, review of solute and self-, 20: 29737
Al–Cr–Co–Mo–Ni–Ti–V–Zr, surface treatments for IN-100, coating and mechanical, 20: 29706 (NASA-TM-X-53448)
Be–Zr, intermetallic compounds in, properties of, for use in aerospace technology, 20: 29770
Be–Zr, thermionic properties, 20: 29801
Cr–Fe–Zr, corrosion by steam, effects of fabrication process and nitride content on, 20: 29660(R) (GEAP-4960)
Cr–Fe–Zr, microstructure of, effects of heat treatments on, 20: 29660(R) (GEAP-4960)
Cu–Zr, development of age- and dispersion-hardened copper-base, 20: 29782
Mo–Nb–Ti–Zr, creep properties of niobium-modified TZM, 20: 29705(R) (NAS-CR-54973)
Mo–Nb–V–Zr, tensile properties of B-66, effects of welds on, 20: 29712(R) (WANL-PR-(P)-009)
Mo–Ti–Zr, creep properties of TZM, 20: 29705(R) (NAS-CR-54973)
Mo–Ti–Zr, production and properties of sheets of, 20: 29756
Mo–Zr, melting of, effects of composition on electron-beam, 20: 29674
Mo–Zr, reactions with hydrogen and nitrogen, 20: 29632
Nb–Ta–W–Zr, fabricability, strength, and weldability of, 20: 29763
Nb–Ta–W–Zr, tensile properties of FS-85, effects of welds on, 20: 29712(R) (WANL-PR-(P)-009)
Nb–Ta–W–Zr, weldability of FS-85, effects of oxygen contamination on, 20: 29712(R) (WANL-PR-(P)-009)
Nb–Ti–Zr, phase studies on, at 570 to 1100°C, 20: 29785
Nb–Ti–Zr, superconductivity of, effects of composition on, 20: 29784
Nb–Ti–Zr, superconductivity of, effects of cold working and heat treatments on, 20: 29787
Nb–Ti–Zr, superconductivity of, effects of microstructure on, 20: 29788
Nb–W–Zr, fabricability, strength, and weldability of, 20: 29763
Nb–W–Zr, tensile properties of Cb-752, effects of welds on, 20: 29712(R) (WANL-PR-(P)-009)
Nb–Zr, coating with silicon by fluidized-bed process, 20: 29630
Nb–Zr, corrosion by mercury at 593 to 703°C, 20: 29646
Nb–Zr, crystal structure and electric conductivity of, 20: 29766
Nb–Zr, erosion by mercury, water, and bismuth–lead alloy, cavitation, 20: 29640 (NP-16048)
Nb–Zr, superconductivity of, effects of cold working and heat treatments on, 20: 29787
Nb–Zr, superconductivity of, effects of microstructure on, 20: 29788
Nb–Zr, superconductivity of, effects of cold working and heat treatments on, 20: 29789
Nb–Zr, superconducting critical current density of wires of, (E), 20: 30267(T)
Nb–Zr, superconducting critical fields of, angular dependence of upper, (E), 20: 30270
Nb–Zr, surface current effects in superconducting, 20: 30280
Pd–Zr, crystal structure and electric conductivity of, 20: 29766
Sn–Zr, oxidation of, at 850°C, mechanisms of breakaway, 20: 29652
Ta–W–Zr, availability, properties, and uses of, 20: 29760
U–Zr, casting of, testing of products from, 20: 29803
U–Zr, mechanical properties, 20: 29803

ZIRCONIUM BORIDES
coating with molybdenum or tungsten by chloride and oxide processes, 20: 29631
fabrication and properties of, for use at high temperatures, 20: 29772

ZIRCONIUM CARBIDES
coating of, effects of, on oxidation resistance of graphite, 20: 29773
coating with molybdenum or tungsten by chloride and oxide processes, 20: 29631
fabrication and properties, 20: 29727
properties of, at 2000°C, for use in thermionic converters, 20: 29729
thermoelectric emission in cesium vapor, 20: 29800
UC–ZrC, compatibility of thermionic diodes of, with refractory metal coatings at 1800 to 2500°C, 20: 29820
UC–ZrC, thermoelectric emission in cesium vapor, 20: 29800

ZIRCONIUM COMPLEXES
with acetylacetone–ethylenediimines, preparation and structure of, 20: 29203
with α-carboxy-β-methyltropolone, composition of, spectrophotometric studies of, 20: 29179

ZIRCONIUM HYDRIDES
hardness at 25 to 225°C, 20: 29697 (AECL-2538)
neutron inelastic scattering at 0.238 to 0.570 ev, cross sections for fast, (E), 20: 30325(R) (RPI-328-56, pp 113-34)

ZIRCONIUM ISOTOPES Zr-90
alpha reactions (α,He-3) at 66 Mev, cross sections for (E/T), 20: 30353(R) (ORNL-3940, pp 1-61)
energy level widths, (E/T), 20: 30360 (WASH-1068)
neutron reactions (n,p) at 3.55 to 15 Mev, cross sections for, (E), 20: 30418
proton elastic scattering at 40 Mev, cross sections for, (E/T), 20: 30353(R) (ORNL-3940, pp 1-61)
proton reactions (p,d) at 36 Mev, deuteron spectra from, (E/T), 20: 30353(R) (ORNL-3940, pp 1-61)
proton reactions (p,α) at 20.2 Mev, alpha spectra from, (E/T), 20: 30353(R) (ORNL-3940, pp 1-61)

superconducting transition temperature, (E), 20: 30316

ZIRCONIUM ISOTOPES Zr-91

alpha reactions (α,He-3) at 66 Mev, cross sections for, (E/T), 20: 30353(R) (ORNL-3940, pp 1-61)

deuteron elastic scattering at 34.4 Mev, angular distributions from, (E/T), 20: 30353(R) (ORNL-3940, pp 1-61)

energy levels of, (T), 20: 30350 (JINR-P-2682)

neutron reactions (n,p) at 4.32 to 6.02 Mev, cross sections for, (E), 20: 30418

proton reactions (p,n) at 12.35 Mev, niobium-91 levels in proton emission from, 20: 30480

ZIRCONIUM ISOTOPES Zr-92

alpha reactions (α,He-3) at 66 Mev, cross sections for, (E/T), 20: 30353(R) (ORNL-3940, pp 1-61)

energy levels of, shell-model calculation using realistic interactions for, 20: 30384

neutron reactions (n,p) at 6.0 Mev, cross sections for, (E), 20: 30418

superconducting transition temperature, (E), 20: 30316

ZIRCONIUM ISOTOPES Zr-94

neutron reactions (n,p) at 6.0 Mev, cross sections for, (E), 20: 30418

superconducting transition temperature, (E), 20: 30316

ZIRCONIUM ISOTOPES Zr-95

beta decay of, β-γ circular polarization correlations in, (E), 20: 30543

content in fallout in USSR, 1962, 20: 29406 (NP-14719)

content in fallout from Chinese nuclear tests, 20: 29423

content in juniper trees in Georgia, 20: 29410

content in pulp for photographic paper, 20: 29427

determination in spent fuel elements, 20: 29078(R) (AD-633252)

separation from sea water by sorption by metal sulfide-ion exchange resins, 20: 29345

ZIRCONIUM OXIDES

age estimation of, by thorium-230–uranium method, 20: 29441

bonding and chemical reactions with fluophosphoric acid, mechanism of, 20: 29145 (NP-16047)

coating of, effects of, on oxidation resistance of graphite, 20: 29773

coating with molybdenum or tungsten by chloride and oxide processes, 20: 29631

diffusion of oxygen in layers of, on zirconium metal, 20: 29817

oxidation of oxygen-deficient, at 450 to 900°C, kinetics of, 20: 29648

Al_2O_3–ZrO_2, fabrication of, method for, 20: 29695(P)

UO_2–ZrO_2, fission-product distribution in irradiated, 20: 29616(R) (BMI-1738)

UO_2–ZrO_2, testing as reactor fuels, 20: 29616(R) (BMI-1738)

W–ZrO_2, fabrication, 20: 29689

ZIRCONIUM PHOSPHATES

properties as ion exchange for separation of americium, berkelium, californium, and curium, 20: 29340

ZIRCONIUM SILICATES

decomposition of, using potassium fluosilicate, 20: 29201

ZIRCONIUM SILICIDES

coating of, effects of, on oxidation resistance of graphite, 20: 29773

ZIRCONIUM SYSTEMS

C–Mo–Nb–W–Zr, evaluation of protective coatings for, 20: 29651

C–Mo–Ti–Zr, creep properties of TZC, 20: 29705(R) (NAS-CR-54973)

C–Mo–Ti–Zr, properties at high temperatures, 20: 29756

C–Nb–W–Y–Zr, tensile properties of D-43Y, effects of welds on, 20: 29712(R) (WANL-PR-(P)-009)

C–Nb–W–Zr, evaluation of protective coatings for, 20: 29651

C–Nb–W–Zr, fabricability, strength, and weldability of, 20: 29763

C–Nb–W–Zr, tensile properties of D-43, effects of welds on, 20: 29712(R) (WANL-PR-(P)-009)

C–Zr, fabrication of hypereutectic composites of, with high thermal shock resistance, 20: 29727

REPORT NUMBER INDEX

Reports, conference papers and proceedings, numbered translations, and patents abstracted during the period are included in this index. Each item is listed by report number; this is followed by the abstract number and a brief notation regarding public availability. The index entries show which reports are on file in the depository libraries, which reports have been published in open-literature journals (journal citation given), and which reports can be purchased (source and price). Whenever a report is identified by more than one number, cross references from secondary to primary report numbers are cited.

The report number codes apply to AEC reports unless designated otherwise. Non-AEC reports are identified by parenthetical notes after the report codes; e.g., (non-AEC), (British), (Canadian), (French). The note (Misc.) identifies those codes used for both USAEC and non-AEC reports. Patents are listed under the heading "PATENTS"; the country of origin is included in parentheses.

A comprehensive listing of both AEC and non-AEC report codes is contained in TID-8505(5th Rev.), *Report Number Series Used by the Division of Technical Information in Cataloging Reports*. This information is also included in the Cumulative Report Number Index (issued annually).

Public Availability of USAEC Reports

All USAEC reports abstracted in *NSA* are available to the public through one or more of the following sources:

(1) Depository libraries in the United States, in other countries, and in international agencies. A list of these depositories appears on the inside covers of each issue of *NSA*.

(2) Scientific and technical journals or other publications.

(3) Microcard Editions, Inc., in Microcard and micronegative form. Orders and inquiries should be sent to: Accounting and Shipping Department, West Salem, Wisconsin 54669.

(4) Clearinghouse for Federal Scientific and Technical Information, U. S. Department of Commerce, Springfield, Virginia 22151.

(5) Superintendent of Documents, U.S. Government Printing Office, Washington, D. C. 20402.

Public Availability of Non-AEC Reports

U. S. Reports. Many reports of U. S. Government agencies are available to the public from the Clearinghouse for Federal Scientific and Technical Information (CFSTI). This availability is given when known. Such reports should be ordered by AD number or NASA-N number. If availability is not shown, inquiries may be directed to CFSTI. In the case of NP numbers, inquiries should be by title and author.

Non-U. S. Reports. Many reports of atomic energy establishments of other countries are deposited in the libraries listed on the inside covers of each issue of *NSA*.

Additionally, the following have made their reports available as indicated.

AUSTRALIA

Australian Atomic Energy Commission Research Establishment. Available upon request from the Library, Australian Atomic Research Establishment, Private Mail Bag, Sutherland, New South Wales, Australia.

BELGIUM

Centre d'Étude de l'Énergie Nucléaire. Available upon request to individuals and organizations, from the Centre d'Étude de l'Énergie Nucléaire (CEN), 31, Rue Belliard, Bruxelles, Belgium.

CANADA

Atomic Energy of Canada Limited. For sale by the Technical Information Officer, Atomic Energy of Canada Limited, Chalk River, Ontario, Canada. Copies are also deposited in libraries in the United Kingdom.

National Research Council of Canada. Available from the National Research Council of Canada, Ottawa 2, Ontario, Canada.

DENMARK

Atomic Energy Commission Research Establishment, Risø. Available on exchange from the Library, Danish Atomic Energy Commission, Risø, Roskilde, Denmark. Also for sale by Jul. Gjellerup, Booksellers, 87 Sölvgade, København K., Denmark.

Danatom. Available on loan from Research Establishment, Risø, Roskilde, Denmark. Copies are available from Danatom, Aurehøjvej 2, Hellerup, Denmark.

EURATOM

Reports from the Commission of the European Atomic Energy Community are available from: Presses academiques europeennes, 98, chaussee de Charleroi, Brussels 6, Belgium; and Office central de vente des publications des Communautes eurodeennes 2, place de Metz, Luxemburg.

FRANCE

Commissariat à l'Énergie Atomique. Inquiries for reports numbered 1-2199 should be addressed to Commissariat à l'Énergie Atomique, Service Central de Documentation, Centre d'Études Nucléaires de Saclay, Boite Postale No. 2, Gif-sur-Yvette (S. et O.), France. Reports numbered 2200 and above are available from La Documentation Francaise, 16 Rue Lord-Byron, Paris VIII, France.

Service Central de Protection contre les Rayonnements Ionisants. Copies are available from Ministère de la Santé Publique, Service Central de Protection contre les Rayonnements Ionisants, B. P. n° 35—LE VESINET (S. et O.), France.

GERMANY

Deutsches Elektronen-Synchrotron DESY. Copies are available from Deutsches Elektronen-Synchrotron Desy, Dokumentation, 2000 Hamburg-Gr. Flottbek 1, Notkestieg 1, Germany.

Gesellschaft für Kernforschung mbH (KFK). Copies are available from Gesellschaft für Kernforschung mbH, 75 Karlsruhe, Postfach 947, Germany. Copies are also deposited in many national nuclear centers in the world.

Kernforschungsanlage. Copies may be ordered from Zentralbibliothek der Kernforschungsanlage Jülich, Jülich, Bundesrepublik Deutschland.

Hahn-Meitner-Institute für Kernforschung. Available without charge from Hahn-Meitner-Institute für Kernforschung Berlin, Bibliothek, Glienicker Strasse 100, 1 Berlin

39, Germany. Copies are deposited in many national nuclear centers in the world.

Johann-Wolfgang-Goethe Universität, Frankfurt Am Main, Institut für Kernphysik, (IKF). Copies are available from Gmelin Institut, 40-42 Varrentrappstrasse, Frankfurt (Main), West Germany.

ISRAEL

Israel Atomic Energy Commission. Available without charge from Ministry of Defence/Atomic Energy Commission, Soreq Research Establishment, Yavne, Israel. Copies are deposited in libraries in Israel and in other countries.

ITALY

Centro Informazioni Studi Esperienze (CISE). For sale at CISE Press Office, Casella Postale 3986, Milano, Italy. Copies are deposited in libraries in Italy.

Comitato Nazionale per l'Energia Nucleare. Copies are available from Comitato Nazionale per l'Energia Nucleare, Divisione Affari Internazionali e Studi Economici, Ufficio Pubblicazioni, Via Belisario, 15, Roma, Italy.

JAPAN

Japan Atomic Energy Research Institute (JAERI). Available from the Staff Supply Cooperative of Japan Atomic Energy Research Institute (JAERI), 1-1 Tamura-Cho, Shiba, Minato-Ku, Tokyo, Japan. Copies are deposited in depositories in Tokyo, Nagoya, and Osaka.

Nagoya University. Copies are available from Research Information Center, Institute of Plasma Physics, Nagoya University, Nagoya, Japan.

University of Tokyo. Available free of charge from Institute for Nuclear Study, University of Tokyo, Tanashi-Machi, Kitatama-gun, Tokyo, Japan.

NETHERLANDS

Reactor Centrum Nederland. For sale by Reactor Centrum Nederland, 112 Scheveningseweg, 's-Gravenhage, The Netherlands. Copies are deposited in university libraries in Holland and in many national nuclear centers in the world.

NEW ZEALAND

Institute of Nuclear Sciences. Copies are available from Librarian, Institute of Nuclear Sciences, D.S.I.R., Private Bag, Lower Hutt, New Zealand. Copies are deposited in other countries.

NORWAY

Forsvarets Forskningsinstitutt. Copies available from Norwegian Defence Research Establishment, Library, P. O. Box 25, Kjeller, Norway.

Institutt for Atomenergi. "KR" reports are available on an exchange basis from the Library, Institutt for Atomenergi, Box 40, Kjeller, Norway. Other series are not generally available to the public.

Norwegian Reactor School. Copies are available from The Library, Institutt for Atomenergi, P. O. Box 40, Kjeller, Norway.

PAKISTAN

Atomic Energy Center. Copies are available from Atomic Energy Center, P. O. Box 658, Lahore, (West Pakistan).

POLAND

Reports of the Polish nuclear institutes are published by the Nuclear Energy Information Center of the Government Commissioner for Use of Nuclear Energy. Copies are available from Ośrodek Informacji o Energii Jądrowej, Warszawa, PKiN, Poland.

SPAIN

Junta de Energia Nuclear. "JEN" reports are available without charge from Servicio de Documentation, Junta de Energia Nuclear, Ciudad Universitaria, Madrid (3), Spain.

SWEDEN

Aktiebolaget Atomenergi. "AE" reports are for sale from Aktiebolaget Atomenergi, Library Section, Box 43041, Stockholm 43, Sweden. Bibliographies and literature surveys of the VDDIT- series may be obtained from Aktiebolaget Atomenergi, Information Office, Scientific and Technical Information, Box 43041, Stockholm 43, Sweden. Other series are not generally available to the public. Organizations in the atomic energy field may obtain copies from Aktiebolaget Atomenergi. Microcopy of AE reports is available from the International Documentation Centre, Tumba, Sweden.

SWITZERLAND

CERN European Organization for Nuclear Research. Available without charge from CERN European Organization for Nuclear Research, Geneva 23, Switzerland. Copies are deposited in libraries in 13 countries.

Eidgenössisches Institut für Reaktorforschung. "EIR" reports are available from Eidgenössiches Institut für Reaktorforschung, c/o Bibliothek, Würenlingen/Ag, Switzerland.

TURKEY

Turkish Atomic Energy Commission. Copies are available free of charge from T.A.E.C., Çekmece Nuclear Research Center, P. O. Box 1, Airport, Istanbul, Turkey.

UNITED KINGDOM

United Kingdom Atomic Energy Authority. Some reports are for sale in the United States by the British Information Service (BIS), 845 Third Avenue, New York, N. Y. 10022. United Kingdom reports generally may be purchased from Her Majesty's Stationery Office, London. Copies not for sale by Her Majesty's Stationery Office may be purchased in microcopy form from Micro Methods Limited, East Ardsley, Wakefield, Yorks, England. Report copies are deposited in a large number of libraries in England, depositories of the USAEC in the United States and abroad, and in most national nuclear centers throughout the world.

Conferences

Published conference proceedings as well as individual unpublished papers from conferences are included in this index. A CONF number is assigned to the conference if published proceedings are received and also if only a single paper is received. The base number used is year-month-sequence. Thus, the number CONF-650101 would indicate that the conference was held in 1965, in January, and that this was the first January 1965 conference so received. This number would be assigned to complete published proceedings, or if individual papers are received, the base number would be extended to include a paper number, i.e., CONF-650101-1. As additional papers are received, they will be assigned consecutive numbers in the series, CONF-650101-1, 2, 3, 4, etc. This numbering system ensures that all papers received from a conference will be associated with that conference in this index.

If published proceedings are received after the receipt of individual papers, the complete proceedings will be abstracted and the abstract number will appear in this index with the base CONF number.

Abbreviations Used in Availability Column

AECL	For sale by Atomic Energy of Canada Ltd., Chalk River, Ontario, Canada.
BIS	For sale by British Information Service, 845 Third Avenue, New York, N. Y. 10022
CFSTI	For sale by the Clearinghouse for Federal Scientific and Technical Information, U.S. Department of Commerce, Spring-

field, Virginia 22151. The symbol "cy" indicates that the format of the item sold may be either a printed document or a photographic reproduction (two-thirds of original size) depending upon the availability of printed stock. The indicated price is for either format. The symbol "mn" is used to indicate that copy is also available in the form of micronegatives (microfiche).

Dep. — AEC reports: Full-size copy is on deposit in the depository libraries both inside and outside the United States. These reports are also for sale by Microcard Editions, Inc., Accounting and Shipping Department, West Salem, Wisconsin 54669.

Non-AEC reports: Full-size copy on deposit in the depository libraries in the United States only.

Dep.(mc) — Same as for Dep., except copy is in Microcard form.

Dep.(mn) — Same as for Dep., except copy is in micronegative (microfiche) form.

DSIR — For sale by the National Lending Library for Science and Technology (D.S.I.R.), Boston Spa, Yorkshire, England.

DTI Extension — Available from the U. S. Atomic Energy Commission, Division of Technical Information Extension, P. O. Box 62, Oak Ridge, Tennessee 37830.

EM — Blueprints and microcopy of AEC engineering drawings are available from Clearinghouse for Federal Scientific and Technical Information, U. S. Department of Commerce, Springfield, Virginia 22151. Current prices of the CAPE- packages may be obtained from this address. TID-4100, available from the Division of Technical Information Extension, P. O. Box 62, Oak Ridge, Tennessee 37831, contains information on all the CAPE- packages for sale.

Gmelin — Available at a nominal charge and under the AED- number shown from Atomic Energy Documentation Center, Gmelin Institute, 40-42 Varrentrappstrasse Frankfurt (Main), West Germany.

GPO — For sale by the Superintendent of Documents, Government Printing Office, Washington, D. C. 20402.

HMSO — Her Majesty's Stationery Office, London.

IAEA — Available from the International Atomic Energy Agency, Vienna, Austria, and from its sales agencies in various countries throughout the world. A list of these agencies is found in each STI/DOC and STI/PUB publication.

JCL — For sale by the Special Libraries Association Translation Center, John Crerar Library, 35 West 33rd Street, Chicago, Illinois 60616.

LC — For sale by the Library of Congress, Photoduplication Service, Washington, D. C. 20540.

NAS — National Academy of Sciences, National Research Council, Washington, D. C. 20418.

NRC — For sale by the National Research Council of Canada, Ottawa, Ontario, Canada.

ORAU — Available on interlibrary loan from the Library, Oak Ridge Associated Universities, Post Office Box 117, Oak Ridge, Tennessee 37830.

ORINS — See ORAU.

UKAEA, London — Available from United Kingdom Atomic Energy Authority, 11 Charles II Street, London, S. W. 1.

UN — United Nations Bookshop, United Nations Headquarters, New York, New York.

USGS — Available free of charge from the U. S. Geological Survey, Washington, D. C. 20242.

[The symbols "ph," "mf," and "fs" are used to designate that copy is available only in photostat, microfilm, or facsimile form. The symbol **"mn"** is used to designate that copy is available in micronegative (microfiche) form. The symbol **"cy"** is used to designate full size or photographically enlarged copy (two-thirds of original size).]

Report No.	Abstract No.	Availability
AAEC-TM–	**(Australian)**	
296	20-30421	Nucl. Sci. Eng., 25: 296-8(1966)
ACNP	**(Misc.)**	
65612	20-30874	Dep. mn; CFSTI $4.00 cy, $0.75 mn
AD–	**(Misc.)**	
631993	20-30556	CFSTI $3.00 cy, $0.75 mn
633024	20-28925	CFSTI $3.00 cy, $0.75 mn
633074	20-30557	CFSTI $2.00 cy, $0.50 mn
633252	20-29078	CFSTI $5.00 cy, $1.00 mn
633469	20-28926	CFSTI $1.00 cy, $0.50 mn
633593	20-30558	CFSTI $3.00 cy, $0.75 mn
633785	20-29581	CFSTI $2.00 cy, $0.50 mn
AEC-tr–	**(For complete listing see TID-4025)**	
6666	20-29407	Dep. mn; CFSTI $5.00 cy, $1.00 mn
AECL	**(Canadian)**	
2529	20-30341	Dep. mn; AECL $1.00
2538	20-29697	Dep. mn; AECL $0.50
AERE-M–	**(British)**	
1670	20-30342	Dep. mn
1736	20-29079	Dep. mn; BIS $0.50; HMSO 2s. 6d.
AERE-R–	**(British)**	
5067	20-29542	J. Sci. Instrum., 43: 224-8(1966)
AFCRL	**(Non-AEC)**	
66-135	20-29078	See AD-633252
ALO–		
3634-1	20-29606	Dep. mn; CFSTI $2.00 cy, $0.50 mn
AN–	**(Misc.)**	
147	20-29584	See TID-22991
ANL–		
6283	20-29658	Dep. mn; CFSTI $3.00 cy, $0.50 mn
7066	20-29328	Dep. mn; CFSTI $3.00 cy, $0.75 mn
7074	20-29386	Dep. mn; CFSTI $1.00 cy, $0.50 mn
7101	20-29698	Dep. mn; CFSTI $3.00 cy, $0.75 mn
7126	20-29612	Dep. mn; CFSTI $2.00 cy, $0.50 mn
7128	20-29329	Dep. mn; CFSTI $2.00 cy, $0.50 mn
7190	20-20786	Dep. mn; CFSTI $6.00 cy, $1.25 mn
7204	20-30789	Dep. mn; CFSTI $3.00 cy, $0.75 mn
ARL–	**(Non-AEC)**	
65-270	20-30556	See AD-631993
AROD–	**(Misc.)**	
6092:4	20-30557	See AD-633074
AWRE-E–	**(British)**	
1/66	20-29371	Dep. mn; BIS $1.40; HMSO 7s. 0d.
BAW–	**(Misc.)**	
1280-36	20-30806	Dep. mn; CFSTI $2.00 cy, $0.50 mn
1302	20-30876	
3238-9	20-29376	Dep. mn; CFSTI $4.00 cy, $0.75 mn
3238-11	20-29377	Dep. mn; CFSTI $2.00 cy, $0.50 mn
3492-1	20-30836	Dep. mn; CFSTI $3.00 cy, $0.75 mn
BLG–	**(Belgian)**	
358	20-29364	See CONF-650964-2
BMI–	**(Misc.)**	
1738	20-29616	Dep. mn; CFSTI $1.00 cy, $0.50 mn
BN–	**(Misc.)**	
6602-02	20-29617	See EURAEC-1593
BNL–		
947	20-30322	Dep. mn; CFSTI $1.00 cy, $0.50 mn
9210	20-29065	Nucl. Appl., 2: 27-32(1966)
9254	20-30165	Dep. mn; CFSTI $2.00 cy, $0.50 mn
9456	20-29182	J. Inorg. Nucl. Chem., 28: 1343-53(1966)
9647	20-28927	Dep. mn; CFSTI $2.00 cy, $0.50 mn
9672	20-29248	Dep. mn; CFSTI $1.00 cy, $0.50 mn
9768	20-29744	J. Chem. Phys., 44: 4320-6(1966)
9791	20-30461	Phys. Rev., 146: 810-15(1966)
9857	20-30293	Phys. Rev., 147: 268-72(1966)
9872	20-30445	Phys. Rev., 146: 662-70(1966)
9899	20-29215	Z. Phys. Chem. (Frankfurt), 49: 38-43(1966)
9939	20-30269	Phys. Lett., 21: 361-2(1966)
BNL-tr–		
67	20-30240	Dep. mn; CFSTI $1.00 cy, $0.50 mn; JCL $1.60 fs, $0.80 mf
BNWL–		
216	20-30933	Dep. mn; CFSTI $4.00 cy, $0.75 mn
BNWL-SA–		
27	20-29518	Dep. mn; CFSTI $1.00 cy, $0.50 mn
31	20-29519	Dep. mn; CFSTI $1.00 cy, $0.50 mn
232	20-29471	Nucl. Sci. Eng., 25: 165-73(1966)
BRLD–	**(Non-AEC)**	
3255	20-30922	
CALT–		
68-63	20-30138	Phys. Rev., 146: 1209-17(1966)
CAPE–		
1337	20-29501	EM
1341	20-29564	EM
1343	20-29502	EM
1345	20-29566	EM
1346	20-29563	EM
1347	20-29565	EM
1348	20-29503	EM
CEA-R–	**(French)**	
2808	20-30253	Dep. mn
2880	20-29404	Dep. mn
2910	20-28898	Dep. mn
2959	20-29577	Dep. mn
CERN–	**(European Organization for Nuclear Research)**	
66-16	20-29840	Dep. mn
CLM-P–	**(British)**	
88	20-30714	See CONF-651126-12
CLOR–	**(Polish)**	
45/D	20-29520	Dep.
CONF-378–	19-18096 20-29504	**(43rd Annual Meeting, Highway Research Board, Washington, D. C., Jan. 1964) NAS $1.80 as NAS-NRC-Pub-1250**
CONF-517–	20-29680	**(5th Plansee Seminar-Reutte, Tyrol, Austria, June 1964)**
CONF-620905–	20-30079	**(International Conference on High Energy Physics, Tihany, Hungary, Sept. 25–30, 1962)**
CONF-630910–	**(8th Summer Meeting of Physicists, Hercegnovi, Yugoslavia, Sept. 1963)**	
Vol. 1	20-30783	Nuklearni Institut J. Stefan, Ljubljana, Yugoslavia
Vol. 2	20-30784	Nuklearni Institut J. Stefan, Ljubljana, Yugoslavia
CONF-640503–	20-29604	**(5th International Pulp and Paper Symposium, Vancouver, B. C., May 18–24, 1964)**
CONF-640509–	**(Colloquium on Theoretical Physics, Bordeaux, May 1964)**	
Pt. 1	20-30084	Dep. mn
CONF-640513–	**(American Petroleum Institute's Div. of Refining, 29th Midyear Meeting, Session on Activation Analysis, St. Louis, Mo., May 12, 1964)**	
1	20-29139	ORAU
CONF-640632–	20-29839	**(International Conference on the Theory of Potential, Orsay, France, June 22–26, 1964)**

Report No.	Abstract No.	Availability
CONF-650329--	20-30534	(Conference on β Decay and Weak Interactions, Heidelberg, Mar. 10–13, 1965) ORAU
CONF-650643--		(3rd International Vacuum Congress, Stuttgart, June 28–July 2, 1965)
2	20-29600	ORAU
CONF-650652--	20-29438	(6th International Conference on Radiocarbon and Tritium Dating, Pullman, Wash., June 7–11, 1965) Dep. mn; CFSTI $8.00 cy, $3.25 mn
CONF-650672--	20-30195	(Transactions of the All-Union Conference on Space Physics, Moscow, June 10–16, 1965) See NASA-TT-F-389
CONF-650674--		(International Conference on Mechanical and Physico-Chemical Properties of Refractories at High Temperature, Paris, June 18–July 1, 1965)
1	20-29699	Dep. mn
CONF-650710--	19-43507	(American Nuclear Society, Meeting on Reactor Operating Experience, Jackson Lake Lodge, Wyo., July 28–30, 1965)
4	20-30920	See DPSPU-65-30-14
CONF-650819--		(American Electron Microscopy Society, 23rd Annual Meeting, New York, Aug. 25–28, 1965)
2	20-29716	See WAPD-T-1819
CONF-650841--		(Conference of Metallurgists, Ottawa, Aug. 30–Sept. 1, 1965)
2	20-29803	ORAU. Gmelin, AED-CONF-65-277-5
CONF-650902--		(American Chemical Society, 150th National Meeting, Atlantic City, Sept. 12–17, 1965)
22	20-30533	ORAU. Gmelin, AED-CONF-65-235-16
24	20-29602	ORAU. Gmelin, AED-CONF-65-235-6
CONF-650935--		(2nd IAEA Conference on Plasma Physics and Controlled Nuclear Fusion Research, Culham, England, Sept. 6–10, 1965)
Vol. 1	20-30565	See STI-PUB-111(Vol.1)
Vol. 2	20-30566	See STI-PUB-111(Vol.2)
CONF-650964--		(Symposium on Design and Construction Problems of Pilot Plants for Recycling Irradiated Fuels, Turin, Sept. 23–24, 1965)
2	20-29364	ORAU
CONF-650972--		(European Atomic Energy Society Symposium on Irradiation Experiments, Hague, The, Sept. 20–22, 1965)
1	20-29609	See NP-15947
CONF-651004--		(9th Conference on Analytical Chemistry in Nuclear Technology, Gatlinburg, Tenn., Oct. 12, 1965)
13	20-29141	ORAU
CONF-651070--		(18th Annual Gaseous Electronics Conference, Minneapolis, Oct. 20–22, 1965)
5	20-29953	ORAU. Gmelin, AED-CONF-65-395-13
CONF-651101--	20-3647 20-9102	(American Nuclear Society, Winter Meeting, Washington, D. C., Nov. 15–18, 1965. Revised 11–8–65)
39	20-30329	See WAPD-T-1844
75	20-29657	ORAU. Gmelin, AED-CONF-65-332-40
CONF-651109--	20-29841	(1st Symposium on Accelerator Radiation Dosimetry and Experience, Upton, N. Y., Nov. 3–5, 1965) Dep. mn; CFSTI $6.75 cy, $2.75 mn
CONF-651126		(American Physical Society, 7th Annual Meeting of the Division of Plasma Physics, San Francisco, Nov. 8–11, 1965)
12	20-30714	ORAU. Gmelin, AED-CONF-65-353-24
13	20-30715	ORAU. Gmelin, AED-CONF-65-353-27
14	20-30716	ORAU. Gmelin, AED-CONF-65-353-31
15	20-30717	ORAU. Gmelin, AED-CONF-65-353-25
CONF-660107--		(American Physical Society Meeting, New York, Jan. 26–29, 1966)
7	20-29318	ORAU. Gmelin, AED-CONF-66-003-6
CONF-660201--		(Conference on Analytical Chemistry and Applied Spectroscopy, Pittsburgh, Feb. 1966)
2	20-29138	ORAU
CONF-660204--		(American Nuclear Society Meeting, San Diego, Calif., Feb. 7–9, 1966)
10	20-30864	ORAU. Gmelin, AED-CONF-66-017-9
CONF-660206--		(Symposium on Neutron Noise, Waves, and Pulse Propagation, Gainesville, Feb. 14–16, 1966)
5	20-30863	ORAU. Gmelin, AED-CONF-66-014-3
CONF-660207--		(Radioisotope Applications in Aerospace Symposium, Dayton, Ohio, Feb. 15–17, 1966)
9	20-29140	ORAU. Gmelin, AED-CONF-66-011-13
14	20-29142	ORAU. Gmelin, AED-CONF-66-011-8
CONF-660209--		(Conference on Intermediate Energy Physics, Williamsburg, Va., Feb. 9–11, 1966)
9	20-29525	Dep. mn; CFSTI $2.00 cy, $0.50 mn
CONF-660212--		(Radiation Research Society. 14th Annual Meeting, Coronado, Calif., Feb. 13–16, 1966)
1	20-29315	ORAU. Gmelin, AED-CONF-66-016-5
3	20-29482	ORAU. Gmelin, AED-CONF-66-016-2
6	20-29058	ORAU. Gmelin, AED-CONF-66-016-6
CONF-660213--		(Technical Assn. of the Pulp and Paper Industry, 51st Annual Meeting, New York, Feb. 20–24, 1966)
1	20-29601	ORAU. Gmelin, AED-CONF-66-042-1
CONF-660214--		(American Chemical Society, 1st Middle Atlantic Regional Meeting, Philadelphia, Feb. 3–4, 1966)
1	20-29316	ORAU. Gmelin, AED-CONF-66-039-1
CONF-660301--		(IEEE International Convention, New York, Mar. 21–25, 1966)
3	20-30718	ORAU. Gmelin, AED-CONF-66-052-1
CONF-660303--		(American Physical Society, Conference of Neutron Cross Section Technology, Washington, D. C., Mar. 22–24, 1966)
30	20-30355	See ORNL-P-2084
CONF-660304--		(Institute of Electrical and Electronics Engineers, Scintillation and Semiconductor Counter Symposium, Washington, D. C., Mar. 2–4, 1966)
10	20-29569	ORAU. Gmelin, AED-CONF-66-020-3
11	20-30785	ORAU. Gmelin, AED-CONF-66-020-4
12	20-29531	See UCRL-16715
13	20-29568	ORAU. Gmelin, AED-CONF-66-020-8
14	20-29567	ORAU. Gmelin, AED-CONF-66-020-12
CONF-660306--		(American Physical Society, Conference on Isobaric Spin, Tallahasee, Mar. 17–19, 1966)
8	20-30343	See COO-1371-30
CONF-660319--		(American Society for Metals Sessions, WESTEC Conference, Los Angeles, Mar. 1966)
3	20-30815	ORAU. Gmelin, AED-CONF-66-041-1
CONF-660322--		(Society for Nondestructive Testing, Spring Convention, Los Angeles, Mar. 7–10, 1966)
1	20-29391	ORAU. Gmelin, AED-CONF-66-018-4
CONF-660324--		(26th Annual Conference on Physical Electronics, Cambridge, Mass., Mar. 21–23, 1966)
3	20-29952	ORAU. Gmelin, AED-CONF-66-036-1
CONF-660506--		(American Inst. of Chemical Engineers, Nuclear Engineering Div. Symposium, Columbus, Ohio, May 15, 1966)
2	20-29510	ORAU
3	20-29317	ORAU
4	20-29656	ORAU
CONF-660510--		(International Conference on Isochronous Cyclotrons,

Report No.	Abstract No.	Availability
	Gatlinburg, Tenn., May 2–5, 1966)	
2	20-29857	See UCRL-16839
5	20-29856	See UCRL-16829
CONF-660517–	**(AIAA Communications Satellite Systems Conference, Washington, D. C., May 2–4, 1966)**	
1	20-29608	ORAU
CONF-660519–	**(Design Engineering Conference and Show, Chicago, May 9–12, 1966)**	
1	20-29802	ORAU
CONF-660601–	**(International Clay Conference, Jerusalem, Israel, June 20–24, 1966)**	
2	20-29332	See ORNL-P-1811
CONF-660608–	**(2nd AIAA Propulsion Joint Specialist Conference, Colorado Springs, June 13–17, 1966)**	
3	20-30924	See LA-DC-7636
5	20-30925	See LA-DC-7637
CONF-660609–	**(International Symposium on Food Irradiation Meeting, Karlsruhe, Germany, June 6–10, 1966)**	
2	20-29603	ORAU
CONF-660701–	**(International Symposium on Reaction Mechanisms of Inorganic Solids, Aberdeen, Scotland, July 11–16, 1966)**	
1	20-29248	See BNL-9672
COO–		
7-0393	20-30390	Nucl. Phys., 83: 65-79(1966)
7-0394	20-30389	Nucl. Phys., 83: 46-63(1966)
274-69	20-29952	See CONF-660324
881-57	20-30039	Phys. Rev., 146: 1080-91(1966)
1112-21	20-29911	Dep. mn; CFSTI $5.00 cy, $1.00 mn
1198-318	20-30282	Phys. Rev., 147: 86-93(1966)
1198-328	20-30283	Phys. Rev., 147: 111-19(1966)
1261-4	20-29986	Dep. mn; CFSTI $2.00 cy, $0.50 mn
1371-21	20-30412	Nucl. Phys., 84: 161-76(1966)
1371-25	20-30037	Phys. Rev., 146: 1071-4(1966)
1371-26	20-30036	Phys. Rev., 146: 1067-71(1966)
1371-30	20-30343	Dep. mn; CFSTI $1.00 cy, $0.50 mn
1477-4	20-29700	Dep. mn; CFSTI $1.00 cy, $0.50 mn
1491-1	20-30740	J. Appl. Phys., 37: 2283-7(1966)
1505-6	20-30446	Phys. Rev., 146: 687-91(1966)
1518-3	20-29659	Dep. mn; CFSTI $1.00 cy, $0.50 mn
CRT–	**(Canadian)**	
1231	20-30341	See AECL-2529
CVNA–	**(Misc.)**	
254	20-30877	Dep. mn; CFSTI $4.00 cy, $0.75 mn
DPSPU–		
65-30-14	20-30920	Nucl. Safety, 7: 175-184(1965–1966)
DUBNA REPORTS		
See JINR (Russian)		
EANDC-US–	**(European-American Nuclear Data Committee)**	
85U	20-30360	See WASH-1068
ETR–	**(Belgian)**	
178	20-29609	See NP-15947
EUR–	**(European Atomic Energy Community)**	
2636.f,i	20-28871	Dep. mn
2649.e	20-29578	Dep. mn
2668	20-30878	See EURAEC-1516
2689	20-29701	See EURAEC-1547
2778.e	20-30721	Dep. mn
2779.e	20-30344	Dep. mn
2798.e	20-30345	Dep. mn
2799.e	20-29485	Dep. mn
2807	20-29639	See EURAEC-1578
2814	20-29617	See EURAEC-1593
2819	20-29330	See EURAEC-1601
2829	20-29702	See EURAEC-1616
2839	20-29804	See EURAEC-1637
EURAEC–		
1516	20-30878	Dep. mn; CFSTI $1.00 cy, $0.50 mn
1538	20-29660	See GEAP-4960
1547	20-29701	Dep. mn; CFSTI $2.00 cy, $0.50 mn
1554	20-29377	See BAW-3238-11
1578	20-29639	Dep. mn; CFSTI $3.00 cy, $0.75 mn
1593	20-29617	Dep. mn; CFSTI $4.00 cy, $0.75 mn
1601	20-29330	Dep. mn; CFSTI $2.00 cy, $0.50 mn
1616	20-29702	Dep. mn; CFSTI $1.00 cy, $0.50 mn
1637	20-29804	Dep. mn; CFSTI $1.00 cy, $0.50 mn
1640	20-29376	See BAW-3238-9
FTI–	**(Non-AEC)**	
114/P-044	20-30559	Dep. mn
GA–	**(Misc.)**	
6374	20-30579	J. Nucl. Energy: Pt. C, 8: 271-81(1966)
6582	20-30578	J. Nucl. Energy: Pt. C, 8: 247-53(1966)
6670	20-29813	Carbon, 3: 543-4(1966)
6995	20-30879	Dep. mn; CFSTI $2.00 cy, $0.50 mn
GEAP–	**(Misc.)**	
4960	20-29660	Dep. mn; CFSTI $2.00 cy, $0.50 mn
4982	20-29618	Dep. mn; CFSTI $3.00 cy, $0.75 mn
GEMP–	**(Misc.)**	
411	20-30346	Dep. mn; CFSTI $3.00 cy, $0.75 mn
GIC–		
3362-4	20-29975	Dep. mn: CFSTI $3.00 cy, $0.75 mn
HPR–	**(Norwegian)**	
67	20-30880	Dep. mn
HWS–		
8241(Rev.4)	20-29661	Dep. mn; CFSTI $1.00 cy, $0.50 mn
8242(Rev.5)	20-29662	Dep. mn; CFSTI $1.00 cy, $0.50 mn
IBJ–	**(Polish)**	
See INR		
IC–	**(Misc.)**	
66/46	20-30087	Dep. mn
66/50	20-30088	Dep. mn
66/51	20-30089	Dep. mn
66/52	20-30090	Dep. mn
IDO–		
14676	20-29080	Dep. mn; CFSTI $2.00 cy, $0.50 mn
17147	20-30793	Dep. mn; CFSTI $2.00 cy, $0.50 mn
17169	20-30837	Dep. mn; CFSTI $2.00 cy, $0.50 mn
17177	20-30796	Dep. mn; CFSTI $5.00 cy, $1.00 mn
IFJ–	**(Polish)**	
See INP		
IITRI–	**(Misc.)**	
578P21-18	20-30797	Dep. mn; CFSTI $2.00 cy, $0.50 mn
T6042-18	20-30797	See IITRI-578P21-18
INDC(US)–		
3U	20-30360	See WASH-1068
INP–	**(Polish)**	
444/PL	20-29526	Dep.
446/PL	20-30348	Dep.
INR–	**(Non-AEC)**	
640/SLBAL/E	20-29852	Dep.
IPP–	**(Non-AEC)**	
3/38	20-29976	Dep. mn
IPST–	**(Russian)**	
2146	20-29615	Israel Program for Scientific Translations, Jerusalem, 1965
IS–		
1047	20-29346	Nucl. Sci. Eng., 25: 227-35(1966)
1151	20-29719	Acta Crystallogr., 20: 733-8(1966)
1301	20-30777	Solid State Commun., 4: 159-63(1966)
1355	20-29144	Dep. mn; CFSTI $3.00 cy, $0.75 mn
ISO–		

Report No.	Abstract No.	Availability
270	20-29450	Dep. mn; CFSTI $1.00 cy, $0.50 mn
ISS–	**(Italian)**	
66/6	20-29912	Dep. mn
66/7	20-29913	Dep. mn
66/8	20-29914	Dep. mn
ITEF–	**(Russian)**	
341	20-29527	Dep. mn
356	20-29988	Dep. mn
361	20-29980	Dep. mn
J&M–		
636	20-29372	See TID-22978
JAERI–	**(Japanese)**	
1102	20-30349	Dep. mn
JINR–	**(Russian)**	
P-2621	20-30091	Dep. mn
P-2627	20-29915	Dep. mn
P-2667	20-29990	Dep. mn
P-2682	20-30350	Dep. mn
P-2691	20-30238	Dep. mn
P-2692	20-30239	Dep. mn
P-2700	20-30092	Dep. mn
P-2701	20-30093	Dep. mn
K-L–		
6077-1R	20-30174	J. Appl. Phys., 37: 2489-95(1966)
6077-2R	20-30175	J. Appl. Phys., 37: 2496-2508(1966)
KAPL–		
3112	20-29703	Dep. mn; CFSTI $2.00 cy, $0.50 mn
KAPL-M–		
6497	20-30722	Dep. mn; CFSTI $3.00 cy, $0.75 mn
6554	20-29331	Dep. mn; CFSTI $1.00 cy, $0.50 mn
6556	20-29663	Dep. mn; CFSTI $1.00 cy, $0.50 mn
KN–	**(Non-AEC)**	
691-64-5	20-30351	See N-65-14857
LA–		
3394	20-30923	Dep. mn; CFSTI $3.00 cy, $0.50 mn
3409(Suppl.)	20-30193	Dep. mn; CFSTI $3.00 cy, $0.75 mn
3456	20-29528	Dep. mn; CFSTI $2.00 cy, $0.50 mn
3467	20-30952	Dep. mn; CFSTI $3.00 cy, $0.50 mn
LA-DC–		
6721	20-30442	Phys. Rev., 146: 632-7(1966)
7209	20-30254	Dep. mn; CFSTI $1.00 cy, $0.50 mn
7282	20-30560	Dep. mn; CFSTI $2.00 cy, $0.50 mn
7442	20-29887	Astrophys. J., 144: 822-4(1966)
7636	20-30924	Dep. mn; CFSTI $1.00 cy, $0.50 mn
7637	20-30925	Dep. mn; CFSTI $1.00 cy, $0.50 mn
7720	20-30274	Phys. Lett., 21: 397-8(1966)
7745	20-29664	Dep. mn; CFSTI $2.00 cy, $0.50 mn
LR–	**(Misc.)**	
17558	20-29977	See N-65-32716
MATT–		
323	20-30573	ISA (Instrum. Soc. Amer.) Trans., 5: 139-45(1966)
357	20-30575	J. Appl. Phys., 37: 2519-20(1966)
392	20-30577	J. Nucl. Energy: Pt. C, 8: 241-5(1966)
415	20-30561	Dep. mn; CFSTI $1.00 cy, $0.50 mn
420	20-30600	Phys. Rev., 147: 197-200(1966)
MF–	**(Misc.)**	
46	20-30564	See NYO-1480-26
MIT–	**(Misc.)**	
2098-172	20-30391	Nucl. Phys., 83: 80-96(1966)
2098-212	20-30472	Phys. Rev., 146: 886-98(1966)
2098-214	20-30452	Phys. Rev., 146: 734-8(1966)
2098-216	20-30391	See MIT-2098-172
2098-236	20-30757	Phys. Lett., 21: 389-91(1966)
2241-16	20-30194	Dep. mn; CFSTI $6.00 cy, $1.25 mn
3343-26	20-29582	Dep. mn; CFSTI $3.00 cy, $0.50 mn

Report No.	Abstract No.	Availability
MITNE–	**(Misc.)**	
70	20-29078	See AD-633252
MSAR–	**(Misc.)**	
66-78	20-29704	Dep. mn; CFSTI $4.00 cy, $0.75 mn
N–	**(Misc.)**	
65-14857	20-30351	
65-32716	20-29977	
NAA-SR–		
11712	20-30881	Dep. mn; CFSTI $2.00 cy, $0.50 mn
11813	20-29619	Dep. mn; CFSTI $2.00 cy, $0.50 mn
11831	20-30723	Dep. mn; CFSTI $3.00 cy, $0.75 mn
11887	20-29579	Dep. mn; CFSTI $3.00 cy, $0.50 mn
NAS-CR–	**(Non-AEC)**	
54973	20-29705	
NAS-NRC–	**(Non-AEC)**	
1276	20-29397	National Academy of Sciences, Washington, D. C. $6.00
NASA-CR–	**(Misc.)**	
461	20-30724	CFSTI $4.00 cy, $1.00 mn
54900	20-30922	See BRLD-3255
54923	20-29712	See WANL-PR-(P)-009
54964	20-29486	
54975	20-29713	See WANL-PR-(P)-010
NASA-SP–	**(Misc.)**	
100	20-29873	GPO $0.50
NASA-TM–	**(Misc.)**	
X-53441	20-29667	See RSIC-509
X-53446	20-29665	See RSIC-482
X-53447	20-29666	See RSIC-484
X-53448	20-29706	
NASA-TR–	**(Non-AEC)**	
R-240	20-30352	CFSTI $1.00 cy, $0.50 mn
NASA-TT–	**(Non-AEC)**	
F-389	20-30195	CFSTI $8.35 cy, $3.50 mn
NP–	**(AEC File No. for Non-AEC Reports)**	
14694	20-29405	Dep. mn
14705	20-29081	Dep. mn
14719	20-29406	Dep. mn
15947	20-29609	Dep. mn; CFSTI $1.00 cy, $0.50 mn
15951	20-29053	Dep. mn
16043	20-30798	Dep. mn; UKAEA
16046	20-29620	
16047	20-29145	
16048	20-29640	
16096	20-30563	
16119	20-29054	Dep. mn; BIS $0.30; HMSO 1s. 9d.
NUMEC–		
3432-21	20-29805	Dep. mn; CFSTI $2.00 cy, $0.50 mn
3524-17	20-29621	Dep. mn; CFSTI $1.00 cy, $0.50 mn
NUS–	**(Misc.)**	
264	20-30882	Dep. mn; CFSTI $4.00 cy, $0.75 mn
NYO–		
1480-26	20-30564	Dep. mn; CFSTI $2.00 cy, $0.50 mn
1918-124	20-28877	Dep. mn; CFSTI $5.00 cy, $1.00 mn
1918-138	20-28878	Dep. mn; CFSTI $5.00 cy, $1.00 mn
1932-105	20-30124	Phys. Rev., 146: 1026-30(1966)
2262-107	20-30127	Phys. Rev., 146: 1058-67(1966)
2262-114	20-30030	Phys. Rev., 146: 994-1000(1966)
2598-29	20-29451	Dep. mn; CFSTI $1.00 cy, $0.50 mn
3304-7	20-29378	Dep. mn; CFSTI $1.00 cy, $0.50 mn
3326-13	20-30166	Dep. mn; CFSTI $3.00 cy, $0.75 mn
3399-46	20-30041	Phys. Rev., 146: 1118-22(1966)
3399-64	20-30006	Phys. Lett., 21: 450-2(1966)
ORNL–		
3721(Suppl.3)	20-29452	Dep. mn; CFSTI $4.00 cy, $0.75 mn
3786	20-30725	Dep. mn; CFSTI $5.00 cy, $1.00 mn
3940	20-29853	Dep. mn; CFSTI $4.00 cy, $0.75 mn

Report No.	Abstract No.	Availability
ORNL-P–	**(Misc.)**	
1180	20-28879	Health Phys., 12: 973-9(1966)
1284	20-30375	J. Inorg. Nucl. Chem., 28: 937-9(1966)
1464	20-29724	Acta Met., 14: 831-8(1966)
1614	20-28916	Photochem. Photobiol., 5: 323-35(1966)
1811	20-29332	Dep. mn; CFSTI $2.00 cy, $0.50 mn
1829	20-30473	Phys. Rev., 146: 899-906(1966)
1880	20-30413	Nucl. Phys., 84: 177-200(1966)
1888	20-30469	Phys. Rev., 146: 869-76(1966)
1936	20-30444	Phys. Rev., 146: 650-9(1966)
1940	20-30462	Phys. Rev., 146: 816-23(1966)
1955	20-30459	Phys. Rev., 146: 799-803(1966)
2084	20-30355	Dep. mn; CFSTI $1.00 cy, $0.50 mn
2143	20-29165	Inorg. Nucl. Chem. Lett., 2: 129-32(1966)
ORNL-TM–		
1425	20-30733	Dep. mn; CFSTI $2.00 cy, $0.50 mn
1443	20-29991	Dep. mn; CFSTI $5.00 cy, $1.00 mn
1445	20-30934	Dep. mn; CFSTI $1.00 cy, $0.50 mn
1448	20-30356	Dep. mn; CFSTI $2.00 cy, $0.75 mn
1457	20-29707	Dep. mn; CFSTI $3.00 cy, $0.50 mn
1458	20-29916	Dep. mn; CFSTI $3.00 cy, $0.75 mn
1465	20-30943	Dep. mn; CFSTI $4.00 cy, $0.75 mn
1485	20-30807	Dep. mn; CFSTI $2.00 cy, $0.50 mn
1511	20-29806	Dep. mn; CFSTI $2.00 cy, $0.50 mn
1528	20-30870	Dep. mn; CFSTI $2.00 cy, $0.50 mn
1537	20-30323	Dep. mn; CFSTI $2.00 cy, $0.50 mn
1542	20-30953	Dep. mn; CFSTI $4.00 cy, $1.00 mn
ORO–		
2430-28	20-30255	Dep. mn; CFSTI $1.00 cy, $0.50 mn
PAN–	**(Polish)**	**(This series of reports was terminated in 1965. Subsequent reports are identified by the code INR)**
PATENTS	**(British)**	**(4s. 6d. each, U. K. Patent Office)**
730,779	20-30867	
1,023,325	20-29636	
1,025,962	20-29077	
1,026,751	20-29511	
1,026,752	20-29512	
1,027,350	20-29513	
1,027,479	20-29319	
1,027,692	20-29691	
1,028,192	20-29514	
1,028,197	20-29570	
1,028,221	20-30865	
1,028,248	20-30816	
1,028,364	20-30872	
1,028,556	20-29515	
1,028,886	20-30817	
1,029,061	20-30818	
1,029,111	20-30819	
1,029,151	20-30911	
1,029,245	20-29692	
1,029,347	20-29982	
1,029,415	20-30866	
1,029,485	20-30912	
1,029,599	20-30820	
1,029,618	20-30821	
1,029,712	20-30822	
1,029,836	20-30868	
1,029,837	20-30869	
1,029,840	20-29395	
1,030,141	20-29605	
1,030,152	20-30823	
1,030,157	20-30824	
PATENTS	**(Canadian)**	
727,029	20-29611	
730,780	20-30873	
731,014	20-30825	
731,126	20-29373	
731,271	20-30826	
731,272	20-30827	
731,273	20-30828	
731,274	20-30829	
731,352	20-30830	
731,772	20-30831	
PATENTS	**(U. S.)**	**($0.50 each, U. S. Patent Office)**
3,243,985	20-29693	
3,245,879	20-30931	
3,245,880	20-29694	
3,245,881	20-30913	
3,246,054	20-29637	
3,246,147	20-29872	
3,246,150	20-29571	
3,246,152	20-29442	
3,246,156	20-29572	
3,246,157	20-29443	
3,246,191	20-29444	
3,246,564	20-29483	
3,246,695	20-30950	
3,246,697	20-30805	
3,247,000	20-29695	
3,247,008	20-29638	
3,247,012	20-29320	
3,247,068	20-30914	
3,247,069	20-30832	
3,247,072	20-30915	
3,247,073	20-30916	
3,247,074	20-30917	
3,247,075	20-30918	
3,247,088	20-29321	
3,247,131	20-30732	
3,247,160	20-29322	
3,247,376	20-29516	
3,247,377	20-29445	
3,247,378	20-29573	
3,247,379	20-29574	
3,247,380	20-29143	
3,247,381	20-29446	
3,247,384	20-29517	
3,247,385	20-29484	
3,247,405	20-29983	
3,248,298	20-30833	
3,248,299	20-30834	
3,248,546	20-29575	
3,248,578	20-29984	
3,249,460	20-29696	
3,249,506	20-30919	
3,249,510	20-30835	
3,249,542	20-29323	
3,249,551	20-30951	
3,249,755	20-29576	
3,252,867	20-30921	
3,258,315	20-29365	
PNE–		
3003	20-29370	Dep. mn; CFSTI $1.00 cy, $0.50 mn
PRC-R–		
657	20-30883	See SAN-570-2
PTR–		
761	20-30796	See IDO-17177
R–	**(Misc.)**	
103	20-29699	See CONF-650674-1
289	20-30558	See AD-633593
445	20-29581	See AD-633785
RL-SEP–		
590	20-29453	Dep. mn; CFSTI $1.00 cy, $0.50 mn
RLO–		
1062-664	20-30468	Phys. Rev., 146: 861-8(1966)
1927-3	20-28988	Proc. Soc. Exp. Biol. Med., 122: 305-7(1966)
RPI–	**(Misc.)**	
328-56	20-30357	Dep. mn; CFSTI $4.00 cy, $1.00 mn
RSIC–	**(Non-AEC)**	
482	20-29665	
484	20-29666	
509	20-29667	
513	20-29706	See NASA-TM-X-53448
RT-CHI–	**(Italian)**	
(65)33	20-29333	Dep. mn

Report No.	Abstract No.	Availability
SAN–		
570-2	20-30883	Dep. mn; CFSTI $7.30 cy, $2.00 mn
1011	20-29379	Dep. mn; CFSTI $6.00 cy, $1.25 mn
SC-CR–		
66-2010	20-29454	Dep. mn; CFSTI $3.00 cy, $0.50 mn
SC-DC–		
65-1691	20-29641	Dep. mn; CFSTI $2.00 cy, $0.50 mn
65-1744	20-29708	Dep. mn; CFSTI $4.00 cy, $1.00 mn
65-1916	20-30167	Dep. mn; CFSTI $5.00 cy, $1.00 mn
66-1329	20-30168	Dep. mn; CFSTI $5.00 cy, $1.00 mn
SC-R–		
66-885	20-29146	Dep. mn; CFSTI $3.00 cy, $0.50 mn
SCL-DR–		
65-13	20-29530	Dep. mn; CFSTI $1.00 cy, $0.50 mn
SGAE-CH–	(Austrian)	
27/1966	20-29082	Dep. mn
SM–	(Misc.)	
45974	20-29145	See NP-16047
STI-PUB–	(International Atomic Energy Agency)	
111(Vol.1)	20-30565	IAEA $15.00; S 315,-; 4.10.0; F.Fr. 60,-; DM 52,50
111(Vol.2)	20-30566	IAEA $21.00; S 441,-; 6.6.0; F.Fr. 84,-; DM 73,50
TID–		
22515	20-29583	Dep. mn; CFSTI $4.00 cy, $1.00 mn
22691	20-29940	Phys. Rev., 147: 13-20(1966)
22835	20-30423	Phys. Lett., 21: 427-9(1966)
22860	20-29059	Dep. mn; CFSTI $1.00 cy, $0.50 mn
22957	20-29917	Dep. mn; CFSTI $4.00 cy, $1.00 mn
22964	20-30726	Dep. mn; CFSTI $3.00 cy, $0.75 mn
22967	20-29380	Dep. mn; CFSTI $2.00 cy, $0.50 mn
22970	20-29622	Dep. mn; CFSTI $7.40 cy, $2.00 mn
22978	20-29372	Dep. mn; CFSTI $4.00 cy, $1.00 mn
22986	20-29710	Dep. mn; CFSTI $2.00 cy, $0.50 mn
22991	20-29584	Dep. mn; CFSTI $2.00 cy, $0.50 mn
TM–	(Misc.)	
65-5-10	20-29710	See TID-22986
TRG-Report–	(British)	
325	20-29807	Dep.; BIS $1.00; HMSO 5s.
1089	20-29367	Dep.; BIS $1.10; HMSO 5s. 6d.
1198	20-29613	Dep.; BIS $0.30; HMSO 1s. 9d.
UCD-CNL–		
38	20-30120	Phys. Rev., 146: 671-5(1966)
43	20-30121	Phys. Rev., 146: 675-86(1966)
UCRL–		
11670	20-29918	Dep. mn; CFSTI $1.00 cy, $0.50 mn
11996	20-29711	Dep. mn; CFSTI $4.00 cy, $1.00 mn
12379	20-30465	Phys. Rev., 146: 840-3(1966)
12379(Rev.1)	20-30465	See UCRL-12379
14198	20-30169	Dep. mn; CFSTI $2.00 cy, $0.50 mn
14214	20-29919	Dep. mn; CFSTI $1.00 cy, $0.50 mn
14222	20-30094	Dep. mn; CFSTI $4.00 cy, $0.75 mn
14246	20-30567	Dep. mn; CFSTI $1.00 cy, $0.50 mn
14251	20-30170	Dep. mn; CFSTI $2.00 cy, $0.50 mn
14271	20-29920	Dep. mn; CFSTI $1.00 cy, $0.50 mn
14301	20-30335	Phys. Rev., 146: 660-1(1966)
14407(Rev.1)	20-29860	J. Nucl. Energy: Pt. C, 8: 255-69(1966)
14591	20-29942	Phys. Rev., 147: 69-72(1966)
14617	20-30954	Dep. mn; CFSTI $2.00 cy, $0.75 mn
14636	20-29943	Phys. Rev., 147: 73-6(1966)
14732	20-29901	Science, 152: 1499-1504(1966)
14767	20-29083	Dep. mn; CFSTI $2.00 cy, $0.50 mn
14901-T	20-29147	Dep. mn; CFSTI $1.00 cy, $0.50 mn
16438	20-29150	Acta Crystallogr., 20: 836-41(1966)
16518	20-30460	Phys. Rev., 146: 804-10(1966)
16541	20-29941	Phys. Rev., 147: 55-9(1966)
16573	20-30450	Phys. Rev., 146: 712-22(1966)
16628	20-30125	Phys. Rev., 146: 1048-51(1966)
16632	20-29487	Dep. mn; CFSTI $3.00 cy, $0.75 mn
16684	20-30029	Phys. Rev., 146: 993-4(1966)
16715	20-29531	Dep. mn; CFSTI $1.00 cy, $0.50 mn
16717	20-29992	Dep. mn; CFSTI $3.00 cy, $0.75 mn
16731	20-30601	Phys. Rev. Lett., 16: 1035-7(1966)
16757	20-30359	Dep. mn; CFSTI $3.00 cy, $0.75 mn
16824	20-29827	Dep. mn; CFSTI $4.00 cy, $0.75 mn
16829	20-29856	Dep. mn; CFSTI $1.00 cy, $0.50 mn
16839	20-29857	Dep. mn; CFSTI $1.00 cy, $0.50 mn
16841	20-30437	Phys. Lett., 21: 549-50(1966)
UNUCOR–		
635	20-30726	See TID-22964
UR–		
875-142	20-30016	Phys. Lett., 21: 563-7(1966)
875-143	20-30015	Phys. Lett., 21: 560-3(1966)
USC–		
113P13-1	20-28917	Proc. Soc. Exp. Biol. Med., 122: 134-7(1966)
USNRDL-TR–	(Misc.)	
982	20-28925	See AD-633024
1005	20-28926	See AD-633469
WANL-PR–	(Misc.)	
P-009	20-29712	
P-010	20-29713	
WANL-TME–	(Misc.)	
948	20-29488	Dep. mn; CFSTI $1.00 cy, $0.50 mn
1031	20-29714	Dep. mn; CFSTI $3.00 cy, $0.75 mn
1287	20-29715	Dep. mn; CFSTI $2.00 cy, $0.50 mn
WAPD-T–		
1730	20-30418	Nucl. Sci. Eng., 25: 285-90(1966)
1819	20-29716	Dep. mn; CFSTI $3.00 cy, $0.75 mn
1844	20-30329	Nucl. Sci. Eng., 25: 242-7(1966)
1848	20-30116	Nucl. Sci. Eng., 25: 189-97(1966)
WASH–		
1068	20-30360	Dep. mn; CFSTI $6.00 cy, $1.25 mn
WCAP–	(Misc.)	
3269-16	20-30884	Dep. mn; CFSTI $2.00 cy, $0.50 mn
3269-54	20-30808	Dep. mn; CFSTI $2.00 cy, $0.50 mn
Y-NA–		
18	20-29668	Dep. mn; CFSTI $1.00 cy, $0.50 mn
YALE–		
2726H-78	20-30403	Nucl. Phys., 84: 37-48(1966)

DEPOSITORIES OF USAEC REPORTS

In Countries Other than the U.S.

ARGENTINA
Buenos Aires, Comisión Nacional de Energía Atómica
AUSTRALIA
Canberra, Australian National Library
Sutherland, New South Wales, Australian Atomic Energy Commission
AUSTRIA
Vienna, Zentral Bibliothek der Physikalischen Institute der Universität
BELGIUM
Mol-Donk, Centre d'Etude de l'Energie Nucleaire
BOLIVIA
La Paz, Comisión Nacional de Energiá Nuclear
BRAZIL
Rio de Janeiro, Instituto Brasileiro de Bibliografia e Documentacao
São Paulo, Instituto de Energia Atomica, Cidade Universitaria São Paulo
BURMA
Rangoon, Union of Burma Applied Research Institute, Atomic Energy Center Library
CANADA
Hamilton, McMaster University
Ottawa, National Research Council Library
Vancouver, University of British Columbia
CHILE
Santiago, Instituto de Fisica y Matematicas, Universidad de Chile
CHINA
Hsinchu, Taiwan, Free China, National Tsing Hua University
COLOMBIA
Bogota, Instituto De Asuntos Nucleares
COSTA RICA
San Pedro, University of Costa Rica Library
DENMARK
Risö, Danish Atomic Energy Commission
ECUADOR
Quito, Escuela Politécnica Nacional
EL SALVADOR
San Salvador, Universidad de El Salvador, Biblioteca de Energia Nuclear
FINLAND
Helsinki, Teknillisen Korkeakoulun Kirjasto
FRANCE
Gif-sur-Yvette, Centre d'Etudes Nucléaires de Saclay
Paris, Académie des Sciences
GERMANY
Berlin, Hahn-Meitner-Institut für Kernforschung Berlin
Frankfurt/Main, Gmelin-Institut
Munich, Technische Hochschule, Bibliothek
GHANA
Accra, University College of Ghana
GREECE
Athens, Nuclear Research Center "Democritus"
GUATEMALA
Guatemala, Comisión Nacional de Energía Nuclear
INDIA
Bombay, Department of Atomic Energy
IRAN
Tehran, Tehran University Nuclear Centre
IRAQ
Baghdad, Iraqi Atomic Energy Commission
IRELAND
Dublin, University College
ISRAEL
Rehovoth, Israel Atomic Energy Commission
ITALY
Rome, Centro di Studi Nucleari della Casaccia
Rome, Comitato Nazionale per l'Energia Nucleare
JAPAN
Tokyo, National Diet Library
KOREA
Seoul, Office of Atomic Energy
LEBANON
Beirut, Lebanese National Council for Scientific Research
LUXEMBOURG
Luxembourg, Ministry of Transport and Electricity
MALAYSIA
Kuala Lumpur, University of Malaysia
MEXICO
Mexico, D.F., Comisión Nacional de Energía Nuclear
NETHERLANDS
The Hague, Reactor Centrum Nederland
NEW ZEALAND
Lower Hutt, Institute of Nuclear Sciences
NIGERIA
Ibadan, University of Ibadan
NORWAY
Lillestrøm, Institutt för Atomenergi
PAKISTAN
Lahore, West Pakistan, Atomic Energy Centre
PERU
Lima, Junta de Control de Energia Atomica
PHILIPPINE REPUBLIC
Manila, Philippine Atomic Energy Commission
POLAND
Warsaw, Biura Pelnomocnika Rzadu do Spraw Wykorzystania Energii Jadrowej
PORTUGAL
Sacavem, Junta de Energía Nuclear
REPUBLIC OF SOUTH AFRICA
Pretoria, Atomic Energy Board Library
REPUBLIC OF THE CONGO
Leopoldville, Université Lovanium
SPAIN
Madrid, Junta de Energía Nuclear, Biblioteca Documentación y Publicaciones, Ciudad Universitaria
SWEDEN
Nyköping, Aktiebolaget Atomenergi
SWITZERLAND
Zürich, Eidgenössische Technische Hochschule, Bibliothek
THAILAND
Bangkok, Office of the Thai Atomic Energy Commission, Department of Science
TURKEY
Ankara, Turkish Atomic Energy Commission, Atomic Energy Library
UNITED ARAB REPUBLIC
Cairo, Atomic Energy Commission
UNITED KINGDOM
Birmingham, Central Library
Boston Spa, National Lending Library for Science and Technology
Kingston upon Hull, Central Library
Liverpool, Central Library
London, Central Library, Acton
London, National Reference Library
London, Science Museum Library, South Kensington
Manchester, Central Library
Newcastle upon Tyne, Central Library
Nottingham, Central Library
Sheffield, Central Library
URUGUAY
Montevideo, Comision Nacional de Energia Atomica
VENEZUELA
Caracas, Instituto Venezolano de Investigaciones Científicas
VIET-NAM
Saigon, Atomic Energy Office
YUGOSLAVIA
Belgrade, Federal Commission for Nuclear Energy

In International Agencies

AUSTRIA
Vienna, International Atomic Energy Agency
BELGIUM
Brussels, La Bibliotheque EURATOM
FRANCE
Paris, European Nuclear Energy Agency, O.E.C.D.
ITALY
Ispra, EURATOM Research Center
SWITZERLAND
Geneva, United Nations Library

UNITED STATES
GOVERNMENT PRINTING OFFICE
DIVISION OF PUBLIC DOCUMENTS
WASHINGTON, D.C. 20402

OFFICIAL BUSINESS

POSTAGE AND FEES PAID
U.S. GOVERNMENT PRINTING OFFICE

TECHNICAL PROGRESS REVIEWS

The Division of Technical Information, U. S. Atomic Energy Commission, also publishes the Technical Progress Reviews, a series of five quarterly journals on nuclear technology. These journals, compiled by specialists and recognized authorities, summarize, evaluate, and reference the progress of development in five important fields.

Isotopes and Radiation Technology P. S. Baker, A. F. Rupp, and associates, Oak Ridge National Laboratory. Reviews AEC-sponsored projects and related significant worldwide developments in radioisotopes and radiation technology.

Nuclear Safety Wm. B. Cottrell, W. H. Jordan, and associates, Oak Ridge National Laboratory. Covers topics relevant to the analysis and control of hazards associated with nuclear reactors and with operations involving fissionable materials and the products of nuclear fission.

Power Reactor Technology Argonne National Laboratory. Reviews research, development, design practices, and operating experiences associated with power reactors, including aerospace applications.

Reactor Fuel Processing Stephen Lawroski and associates, Argonne National Laboratory. Reviews all aspects of the fuel-processing field, including aqueous and nonaqueous processing and waste disposal.

Reactor Materials R. W. Dayton, E. M. Simons, and associates, Battelle Memorial Institute. Covers the properties, behavior, and fabrication processes of materials used in nuclear reactors and associated equipment.

MIAMI UNIVERSITY LIBRARY

Availability

SUBSCRIPTION RATE: The Technical Progress Reviews may be purchased from the Superintendent of Documents, U. S. Government Printing Office, Washington, D. C. 20402, at $2.50 per year for each subscription or $0.70 per issue.

POSTAGE: Postpaid within the United States, Canada, Mexico, and all Central and South American countries except Argentina, Brazil, British and French Guiana, Surinam, and British Honduras. For these Central and South American countries and all other countries, add $0.75 per year or $0.20 per single issue.

REMITTANCE: Payment should be by check, money order, or document coupons and MUST accompany order. Remittances from foreign countries should be made by international money order or draft on an American bank payable to the Superintendent of Documents or by UNESCO book coupons.